University of Agronomic Sciences
and Veterinary Medicine of Bucharest
Faculty of Land Reclamation
and Environmental Engineering

SCIENTIFIC PAPERS

Series E

LAND RECLAMATION, EARTH OBSERVATION & SURVEYING, ENVIRONMENTAL ENGINEERING

Volume XIV



2025
BUCHAREST

SCIENTIFIC PAPERS

Series E

LAND RECLAMATION, EARTH OBSERVATION &
SURVEYING, ENVIRONMENTAL ENGINEERING

Volume XIV



University of Agronomic Sciences
and Veterinary Medicine of Bucharest
Faculty of Land Reclamation
and Environmental Engineering

SCIENTIFIC PAPERS

Series E

LAND RECLAMATION, EARTH OBSERVATION & SURVEYING, ENVIRONMENTAL ENGINEERING

Volume XIV

2025
BucharesT

EDITORIAL BOARD

General Editor: Razvan Ionut TEODORESCU

Executive Editor: Ana VIRSTA

Managing Editor: Augustina Sandina TRONAC

Members: Maria Jose ORUNA CONCHA, Radu Claudiu FIERASCU, Jana ŠIC ŽLABUR, Maria POPA, Fulvio CELICO, Catalina ITICESCU, Rupesh Kumar SINGH, Jelena LUBURA STOŠIĆ, Petrica VIZUREANU, Orhan ERCAN, Denis MIHAILESCU, Deodato TAPETE, Lucian COPOLOVICI, Jesus SIMAL-GANDARA, Alina ORTAN

PUBLISHERS:
University of Agronomic Sciences and Veterinary Medicine of Bucharest, Romania - Faculty of Land Reclamation and Environmetal Engineering
Address: 59 Marasti Blvd, District l, Zip code 011464, Bucharest, Romania
Phone: + 40 213 1830 75, E-mail: conference@fifim.ro, Webpage: www.fifim.ro

CERES Publishing House
Address: 106 Izbiceni Street, District 1, Bucharest, Romania
E-mail: edituraceres@yahoo.com, Webpage: www.editura-ceres.ro

Copyright 2025
To be cited: Scientific Papers. Series E. LAND RECLAMATION, EARTH OBSERVATION & SURVEYING, ENVIRONMENTAL ENGINEERING, Vol. XIV, 2025

The publishers are not responsible for the content of the scientific papers and opinions published in the Volume. They represent the authors' point of view.

Print ISSN 2285-6064, CD-ROM ISSN 2285-6072, Online ISSN 2393-5138, ISSN-L 2285-6064

International Database Indexing:
Web of Science Core Collection (Emerging Sources Citation Index)
Index Copernicus; Ulrich's Periodical Directory (ProQuest); PNB (Polish Scholarly Bibliography); Scientific Indexing Service; Cite Factor (Academic Scientific Journals) Scipio; OCLC; Research Bible

SCIENTIFIC & REVIEW COMMITTEE

SCIENTIFIC CHAIRMAN
Prof. univ. dr. Sorin Mihai CIMPEANU

MEMBERS*

- Stefano CASADEI – University of Perugia, Italy
- Carmen CIMPEANU – University of Agronomic Sciences and Veterinary Medicine of Bucharest, Romania
- Sorin Mihai CIMPEANU – University of Agronomic Sciences and Veterinary Medicine of Bucharest, Romania
- Andrea DOMINIJANNI – Politecnico di Torino, Italy
- Claudiu DRAGOMIR - University of Agronomic Sciences and Veterinary Medicine of Bucharest/ National Institute for Research and Development - URBAN-INCERC, Bucharest, Romania
- Eric DUCLOS-GENDREU – Spot Image GEO-Information Services, France
- Jean-Luc HORNICK – Université de Liège, Belgium
- Hossein KAZEMI – GUASNR, Gorgan, Iran
- Bela KOVACS – University of Debrecen, Hungary
- Raluca MANEA – University of Agronomic Sciences and Veterinary Medicine of Bucharest, Romania
- Tamara van OMMEREN-MYSLYVA – Ministry of Spatial Planning and Environment of Suriname
- Jovan Br. PAPIC – Ss. Cyril and Methodius University, Skopje, R. N. Macedonia
- Nelson PÉREZ-GUERRA – University of Vigo, Spain
- Nicolae PETRESCU – Valahia University Targoviste, Romania
- Dorin Dumitru PRUNARIU – Romanian Space Agency, Romania
- Andrei Victor SANDU – „Gheorghe Asachi" Technical University of Iași, Romania
- Mirela Alina SANDU – University of Agronomic Sciences and Veterinary Medicine of Bucharest, Romania
- Umut Gunes SEFERCIK – Gebze Technical University, Turkey
- Ando SHIN – Tokyo University of Science, Japan
- Marisanna SPERONI – Centro di Ricerca Zootecnia e Acquacoltura, Consiglio per la Ricerca in Agricoltura e L'analisi Dell'economia Agraria (CREA), Italy
- Razvan Ionut TEODORESCU – University of Agronomic Sciences and Veterinary Medicine of Bucharest, Romania
- Péter UDVARDY – Óbuda University, Hungary
- Neven VOĆA – University of Zagreb, Croatia

**alphabetically ordered by family name*

CONTENTS

ENVIRONMENTAL SCIENCE AND ENGINEERING

1 EVALUATION OF CHEMICAL COMPOSITION OF ESSENTIAL OIL AND TOXIC METAL ACCUMULATION OF TARRAGON (*ARTEMISIA DRACUNCULUS* L.) CULTIVATED ON METAL-CONTAMINATED SOILS - **Violina ANGELOVA** ……. 17

2 EVALUATION OF WASTE BIOMASS FROM AROMATIC PLANTS FOR ENERGY PURPOSES - **Violina ANGELOVA** 24

3 DETECTION AND MONITORING OF HYDROCARBON POLLUTION SOURCES IN THE PETROMIDIA REFINERY AREA - **Sorin ANGHEL** 30

4 INVESTIGATING CURRENTS, FLOW VELOCITIES, AND RIVERBED MORPHOLOGY - AN ADCP-CENTRIC APPROACH TO UNDERSTANDING HYDRODYNAMICS AND EROSION PATTERNS - **Maxim ARSENI, Adrian ROȘU, Nina-Nicoleta LAZĂR, Mădălina CĂLMUC, Mihail VESTE, Cătălina ITICESCU** 37

5 STRUCTURAL ANALYSIS OF SLUDGE FROM THE ARAD WASTEWATER TREATMENT PLANT: REDUCING QUANTITY AND ENHANCING ITS POTENTIAL AS FERTILIZER - **Denisa BACALU-RUS, Lucian COPOLOVICI, Dana COPOLOVICI, Ioan BOTH, Maria MIHĂILESCU** 44

6 DEVELOPMENT AND VALIDATION OF A GC-MS/MS METHOD FOR THE DETECTION OF ORGANOCHLORINE AND ORGANOPHOSPHATE PESTICIDES IN COMPOST AND SOIL - **Silviu-Laurențiu BADEA, Carmen CONSTANTIN, Liliana BĂDULESCU** 52

7 PRELIMINARY RESULTS VALIDATION ON THE THEORETICAL AND EXPERIMENTAL APPROACH FOR USING SPENT GARNET RESIDUES OF ROMANIAN LOCAL INDUSTRIES IN CONSTRUCTION MATERIALS - **Cornelia BAERĂ, Aurelian GRUIN, Ana-Cristina VASILE, Bogdan BOLBOREA, Alexandru ION, Luiza VARGA, Alexandra Marina BARBU** …… 59

8 STRUCTURAL INTEGRITY IN EARTHEN ARCHITECTURE WITH NDT METHODS - **Bogdan BOLBOREA, Cornelia BAERĂ, Aurelian GRUIN, Sorin DAN, Ana-Cristina VASILE** ……... 73

9 EVALUATING AGGREGATE CONTENT AND ITS EFFECT ON CLAY MORTAR PERFORMANCE - **Aurelia BRADU, Alexandrina-Elena ANDON, Alexandra-Marina BARBU, Claudiu-Sorin DRAGOMIR** 81

10 INTEGRATION OF UAV-BASED LIDAR, PHOTOGRAMMETRY, AND SLAM TECHNOLOGIES FOR THE COMPLETE ABOVE AND BELOW GROUND MAPPING OF MOUNTAINOUS HYDRO-TECHNICAL INFRASTRUCTURE - **Simion BRUMA, Catalin-Stefanel SABOU, Ioana POP, Florica MATEI, Paul SESTRAS, Mircea NAP, Elemer-Emanuel SUBA, Tudor SALAGEAN** 87

11 CLAY APPLICATION IN THE REMEDIATION OF NICKEL RICH SOIL – **Teuta BUSHI, Aida BANI, Selma MYSILHAKA, Franz OTTNER, Ilaria COLZI, Isabella BETTARINI, Seit SHALLARI** 99

12 A PIONEERING STUDY ON THE INVESTIGATION OF MICROPLASTIC POLLUTION IN THE WATER OF THE SOMOVA-PARCHEȘ LACUSTRINE COMPLEX, ROMANIA - **Mădălina CĂLMUC, Valentina Andreea CĂLMUC, Nina Nicoleta LAZĂR, Marius IVANOV, Puiu-Lucian GEORGESCU, Cătălina ITICESCU** 105

13 INVESTIGATION OF THE PHARMACEUTICALS PRESENCE IN THE SOMOVA-PARCHEȘ AQUATIC COMPLEX - **Valentina Andreea CĂLMUC, Mădălina CĂLMUC, Carmen CHITESCU, Silvia DRĂGAN, Cătălina ITICESCU, Puiu-Lucian GEORGESCU** 112

14 VALIDATION OF A UHPLC-HRMS METHOD FOR THE ASSESSMENT OF PER AND POLY-FLUOROALKYL SUBSTANCES (PFAS) IN BIOTA - **Andreea-Miruna CODREANU, Ștefania-Adelina MILEA, Valentina Andreea CĂLMUC, Justinian-Andrei TOMESCU, Alin Constantin DÎRȚU, Cătălina ITICESCU, Puiu-Lucian GEORGESCU** 119
15 INDICATORS OF THE STRUCTURAL AND COMPOSITIONAL DIVERSITY OF STANDS ON DEGRADED LANDS IN THE VRANCEA AREA - **Cristinel CONSTANDACHE, Ciprian TUDOR, Laurențiu POPOVICI** 125
16 GROUND MOTION DATA QUALITY ASSURANCE: FUNDAMENTAL REQUIREMENTS AND THEIR PRACTICAL IMPLEMENTATION WITHIN THE NATIONAL NETWORK FOR THE SEISMIC MONITORING AND PROTECTION OF BUILDING STOCK, NIRD URBAN-INCERC, ROMANIA **- Iolanda-Gabriela CRAIFALEANU, Claudiu-Sorin DRAGOMIR, Daniela DOBRE, Emil-Sever GEORGESCU, Alexandra-Marina BARBU** 133
17 COMPREHENSIVE ANALYSIS OF PARTICULATE MATTER VARIABILITY IN AN URBAN ENVIRONMENT USING Rapid-E MONITORING - **Mădălin CRISTEA, Adrian ROȘU, Bogdan ROȘU, Daniel-Eduard CONSTANTIN, Simona CONDURACHE-BOTA, Mirela VOICULESCU, Cătălina ITICESCU, Puiu- Lucian GEORGESCU, Silvia DRĂGAN** 143
18 THE IMPACT OF LAND USE CHANGES ON NATURAL PROTECTED AREAS IN THE OLTEȚ PIEDMONT (ROMANIA) - **Raluca Lucia DINCULOIU, Daniel SIMULESCU, Carmen Otilia RUSĂNESCU, Mihaela BEGEA, Gigel PARASCHIV, Sorin Ștefan BIRIȘ, Maria CIOBANU** 152
19 A CRITICAL REVIEW OF SUSTAINABLE APPROACHES FOR REDUCING THE ENVIRONMENTAL IMPACT OF PLASTIC PRODUCTION - **Andreea DOROFTE, Ira-Adeline SIMIONOV, Ștefan-Mihai PETREA, Cătălin PLATON, Puiu-Lucian GEORGESCU, Cătălina ITICESCU** 159
20 MONITORING THE INACTIVE LANDFILL STABILITY IN GORJ COUNTY - **Silvia Alexandra DREGHICI, Levente DIMEN, Mircea RÎȘTEIU, Tudor BORȘAN, Florin FAUR** 169
21 SOIL FLUX AND SOIL GAS MONITORING OF A NATURAL LABORATORY FOR THE STUDY OF CO_2 LEAKAGE - **Alexandra-Constanța DUDU, Corina AVRAM, Gabriel IORDACHE, Constantin-Ștefan SAVA, Lia STELEA, Andrei-Gabriel DRAGOȘ** 180
22 POSSIBILITIES FOR THE RECOVERY OF AGRICULTURAL VEGETABLE WASTE - **Timea GABOR, Andreea HEGYI, Stelian COSTE, Alina Iuliana CADAR, Cristian PETCU, Carmen FLOREAN, Ioana Monica SUR** 186
23 GROUND AIR MICROFLORA STUDY USING A CASCADE IMPACTOR - **Bilyana GRIGOROVA-PESHEVA, Asen PESHEV** 196
24 POSSIBILITIES OF SURFACE TREATMENT OF PLASTERS BASED ON CLAY **- Andreea HEGYI, Cristian PETCU, Claudiu Sorin DRAGOMIR, Gabriela CĂLĂTAN, Alexandra CSAPAI** 202
25 EVALUATION OF THE POSSIBILITIES OF USING CLAY SOILS FOR THE REALIZATION OF VERNACULAR CONSTRUCTIONS - **Andreea HEGYI, Gabriela CĂLĂTAN, Cristian PETCU, Stefan BAKOS, Alexandra CSAPAI** 218
26 HIERARCHY OF ALTERNATIVES FOR THE REHABILITATION OF ASBESTOS WATER SUPPLY NETWORKS BASED ON ENVIRONMENTAL CRITERIA - **Iulian IANCU, Sorin PERJU, Ioan BICA, Alexandru-Nicolae DIMACHE** 231
27 AFFORESTATION OF SANDY SOILS OF OLTENIA - A REVIEW - **Paula IANCU, Marin SOARE, Mariana NICULESCU** 239
28 CURRENT TRENDS AND INSTITUTIONAL FRAMEWORKS IN CLIMATE CHANGE RESEARCH: A EUROPEAN AND NATIONAL PERSPECTIVE - **Ionela-Alexandra ION, Carmen Otilia RUSĂNESCU, Sabrina-Maria BĂLĂNESCU** 246
29 BEHAVIOR OF ASPHALT MIXTURES MANUFACTURED WITH RECYCLED MATERIALS AND THEIR *IN SITU* PERFORMANCE LEVEL - **Nicoleta-Adaciza IONESCU, Daniela DOBRE**... 252
30 SOLUTIONS FOR THE RESTORATION IN THE NATURAL CIRCUIT OF CONTAMINATED SITES FROM THE PETROLEUM INDUSTRY - **Cristian Mugurel IORGA, Lucian-Gabriel ZAMFIR**, **Alina Ceoromila CANTARAGIU** 260

31 ASSESSMENT OF IRON, COPPER, AND ZINC IN THE MUSCLE OF PONTIC SHAD: INFLUENCE OF YEAR, WEIGHT, AND LENGTH - **Nina-Nicoleta LAZĂR, Mădălina CĂLMUC, Ira-Adeline SIMIONOV, Maxim ARSENI, Mihaela TIMOFTI, Puiu-Lucian GEORGESCU, Cătălina ITICESCU, Violeta DOMNITEANU** 268
32 SUSTAINABLE GEOPOLYMER BINDERS: MECHANICAL AND DURABILITY INSIGHTS INTO FLY ASH-BASED COMPOSITES - **Adrian-Victor LAZARESCU, Brăduț-Alexandru IONESCU, Mihail CHIRA, Tudor-Panfil TOADER, Alexandra CSAPAI, Andreea HEGYI, Carmen-Teodora FLOREAN** 274
33 THERMAL CONDUCTIVITY OF SILTY SOILS IN THE SOUTH-EAST REGION OF ROMANIA - **Daniel-Marcel MANOLI, Cristian-Ştefan BARBU, Mihaela-Elena STAN, Manole-Stelian ŞERBULEA, Alina TATOMIR, Oana-Cristina CARAŞCA, Ruxandra-Irina ERBASU, Andrei-Dan SABAU** 284
34 DISTRIBUTION OF HEAVY METALS IN THE DANUBE RIVER ECOSYSTEM AND THE IMPACT ON THE ENVIRONMENT. A REVIEW - **Maria Daniela (IONICA) MIHAILA, Valentina Andreea CĂLMUC, Cătălin PLATON, Puiu-Lucian GEORGESCU, Cătălina ITICESCU** 292
35 EXPLORING THE QuEChERS - GAS CHROMATOGRAPHY APPROACH FOR SEDIMENT PESTICIDE ANALYSIS - **Stefania-Adelina MILEA, Maria Daniela (IONICA) MIHAILA, Valentina Andreea CĂLMUC, Cătălina ITICESCU, Puiu-Lucian GEORGESCU, Alin-Constantin DIRTU, Cătălin Eugen PLATON** 305
36 MATHEMATICAL MODEL FOR PREDICTION OF NO_2 CONCENTRATION IN THE SOUTHEASTERN REGION OF ROMANIA, USING RECURSIVE LEAST SQUARES FILTER METHODS - **Gabriel MURARIU, Sorin FRASINA, Adrian ROȘU, Corneliu DOROFTEI, Iulian RACOVIȚĂ, Bogdan ROȘU, Cătălin FETECĂU, Mirela VOICULESCU, Cătălin NEGOIȚĂ** 312
37 PLANT RESPONSE TO SOIL WATERLOGGING: PHYSIOLOGICAL, MORPHOLOGICAL AND BIOCHEMICAL ADAPTATIONS - A REVIEW - **Senad MURTIĆ, Adnan HADŽIĆ** 318
38 HEAVY METAL ACCUMULATION IN FOOD CROPS CULTIVATED IN CONTAMINATED SOILS IN ALBANIA - **Selma MYSLIHAKA, Aida BANI, Teuta BUSHI, Dorina XHULAJ, Eugen SKURA, Irena DUKA** 330
39 BIOMOLECULE PRODUCTION BY MICROORGANISMS ISOLATED FROM SALINE ENVIRONMENTS - **Simona NEAGU, Mihaela Marilena STANCU** 337
40 ENERGY-ENVIRONMENT INTERACTIONS FOR AN IMPROVED SUSTAINABILITY OF DÂMBOVIȚA COUNTY - THE ROLE OF INNOVATION AND TECHNOLOGY TRANSFER FROM UNIVERSITIES - **Otilia NEDELCU, Ioan Corneliu SALISTEANU, Iulian UDROIU, Aurora DIACONEASA, Claudia GILIA, Daniel DUNEA** 346
41 THE SWELLING PRESSURE OF ACTIVE CLAYS ACCORDING TO VARIOUS TECHNICAL NORMS AND PROCEDURES - **Ernest Daniel OLINIC** 356
42 THE SHEAR STRENGTH PARAMETERS OF SOIL-ROOT SYSTEMS - **Tatiana OLINIC** 362
43 BIOACCUMULATION OF CADMIUM, LEAD, ZINC AND COPPER IN RED FESCUE (*FESTUCA RUBRA* L.) GROWN IN POLLUTED MEADOWS IN COPȘA MICĂ - **Bogdan Ștefan OPREA, Dumitru-Marian MOTELICĂ, Nicoleta Olimpia VRÎNCEANU, Vera CARABULEA, Georgiana Iuliana PLOPEANU, Mihaela COSTEA** 368
44 CHEMICAL STATE AND ECOLOGICAL ASSESSMENT OF ATMOSPHERIC AIR QUALITY - **Georgi PATRONOV, Diana KIRIN, Petya ZAHARIEVA, Radoslava ZAHARIEVA, Dimitrinka KUZMANOVA** 377
45 ECOMONITORING STUDIES OF GROUNDWATER AND SOIL FOR POLLUTION WITH OIL AND PETROLEUM PRODUCTS - **Georgi PATRONOV, Diana KIRIN, Radoslava ZAHARIEVA, Petya ZAHARIEVA, Marian VARBANOV** 384
46 ANALYSIS OF GROUNDWATER RESOURCES IN STARA ZAGORA DISTRICT, BULGARIA: QUALITY AND ENVIRONMENTAL RISKS - **Alexander PETROV, Svetla STOYKOVA, Diyana DERMENDZHIEVA, Gergana KOSTADINOVA, Milen STOYANOV, Georgi PETKOV, Stefka BOYANOVA, Georgi BEEV** 391

47 ASSESSMENT OF SOIL CONTAMINATION BY POLYCYCLIC AROMATIC HYDROCARBONS (PAH_S) IN BUCHAREST: SOURCES AND DISTRIBUTION - **Mihaela PREDA, Veronica TĂNASE, Nicoleta Olimpia VRÎNCEANU, Florența JAFRI, Mihaela COSTEA, Bogdan-Ștefan OPREA** 402
48 THE EFFECTS OF AIR POLLUTION WITH PARTICULATE MATTER ON HUMAN HEALTH - **Elena-Denisa PREDESCU, Carmen Otilia RUSĂNESCU, Irina Aura ISTRATE, Roxana-Elena FRÎNCU, Sabrina Maria BĂLĂNESCU** 412
49 ASSESSMENT OF SUSPENDED SEDIMENT CONCENTRATION AND GRANULOMETRY USING AQUASCAT 1000S ON THE SULINA BRANCH OF THE DANUBE RIVER - **Adrian ROȘU, Mădălin CRISTEA, Bogdan ROȘU, Maxim ARSENI, Mihai Ștefan PETREA, Cătălina ITICESCU, Puiu-Lucian GEORGESCU, Silvia DRĂGAN** 418
50 ADVANCING URBAN AIR POLLUTION MONITORING WITH REMOTE SENSING AND LOW-COST SENSOR TECHNOLOGIES - **Adrian ROȘU, Daniel-Eduard CONSTANTIN, Maxim ARSENI, Mirela VOICULESCU, Cătălina ITICESCU, Puiu-Lucian GEORGESCU, Ionuț Cornel BEJAN, Sorin FRĂSINĂ, Silvia DRĂGAN, Mădălin CRISTEA** 429
51 HYDROTHERMAL ASSESSMENT OF MAIN AGRICULTURAL AREAS IN SOUTHERN ROMANIA AND NORTHERN BULGARIA - **Nadezhda SHOPOVA, Desislava SLAVCHEVA-SIRAKOVA** 439
52 FIRE SAFETY OF ETICS BASED ON EPS TYPE POLYSTYRENE - **Adrian SIMION, Claudiu-Sorin DRAGOMIR** 447
53 DEVELOPMENT AND APPLICATION OF AN OPTIMIZED TD-GC/MS METHOD FOR MONITORING VOLATILE ORGANIC COMPOUNDS (VOCs) IN AMBIENT AIR - **Alexandru-Florin SIMION, Angela-Nicoleta GĂMAN, Sorin SIMION, Marius KOVACS** 453
54 NUMERICAL STUDY OF THE CYLINDRICAL SHAFT'S BEHAVIOUR USING 3D FINITE ELEMENT METHOD - **Elena-Mihaela STAN, Horațiu POPA, Daniel MANOLI** 465
55 AMBIENT AIR POLLUTION: A GLOBAL HEALTH CRISIS - **Svetla STOYKOVA, Diyana DERMENDZHIEVA, Gergana KOSTADINOVA, Miroslava IVANOVA, Milen STOYANOV, Georgi PETKOV, Lilko DOSPATLIEV, Georgi BEEV** 472
56 STUDY ON THE DYNAMICS OF CEREALS CULTIVATED IN TULCEA COUNTY IN THE CONTEXT OF CLIMATE CHANGE - **Traian Ciprian STROE, Oana MIHAI-FLOREA, Liliana MIRON** 486
57 STUDIES AND MEASUREMENTS FOR THE IDENTIFICATION OF NOISE AND VIBRATION LEVELS IN A SITE IN BUCHAREST - CASE STUDY - **Marta Cristina ZAHARIA, Daniela DOBRE, Claudiu-Sorin DRAGOMIR** 496

DISASTER RESILIENCE AND SUSTAINABLE DEVELOPMENT

1 INCREASING THE SAFETY LEVEL CONSIDERING SOIL-STRUCTURE INTERACTION IN HIGH SEISMIC HAZARD-PRONE AREAS - **Stefan Florin BALAN, Bogdan Felix APOSTOL** 506
2 DURABILITY AND SUSTAINABILITY OF MOUNTAIN FARMS IN ROMANIA WITH A FOCUS ON AGRICULTURAL DIVERSIFICATION - **Daniela-Mihaiela BOCA, Tudor Panfil TOADER, Andreea HEGYI, Marius VLADU** 518
3 INTEGRATING VEGETABLE WASTE IN CLAY COMPOSITIONS: A SUSTAINABLE PATH FOR ECO CONSTRUCTION - **Aurelia BRADU, Alexandrina-Elena ANDON, Alexandra-Marina BARBU, Claudiu-Sorin DRAGOMIR** 528
4 THE IMPACT OF EXTREME WEATHER PHENOMENA ON THE MANAGEMENT OF CONIFEROUS STANDS - **Ghiță Cristian CRAINIC** 534
5 UPGRADING THE TRADITIONAL DATABASE THROUGH BIM-BASED SHM VISION - **Daniela DOBRE, Claudiu-Sorin DRAGOMIR, Iolanda-Gabriela CRAIFALEANU, Cornelia-Florentina DOBRESCU, Emil-Sever GEORGESCU** 548

6 RISK OF WINDTHROWS STANDS WITH VARIOUS STRUCTURES USING VERTICAL DIFFERENTIATION INDEX - **Lucian Sorin DOROG** 555
7 InSAR TECHNOLOGY FOR RISK MANAGEMENT AND NATURAL DISASTER IMPACT ASSESSMENT IN BUCHAREST - **Ana-Maria GLOD-LENDVAI, Iuliana ARMAȘ, Razvan TEODORESCU, Aurora DIACONEASA, Virgil MOISE, Daniel DUNEA** 562
8 FLOOD IMPACT ASSESSMENT ON RAILWAY INFRASTRUCTURE USING NUMERICAL MODELLING: CASE STUDY OF NĂDAB, ROMANIA - **Dorian HAUSLER COZMA, Teodor Eugen MAN, Robert Florin BEILICCI, Erika BEILICCI** 569
9 NATURE-BASED SOLUTIONS FOR THE SUSTAINABLE DEVELOPMENT OF GREEN AND BLUE INFRASTRUCTURE IN ROMANIA - **Andreea Catalina POPA, Teodora UNGUREANU, Claudiu-Sorin DRAGOMIR, Antonio-Valentin TACHE** 578
10 COMPATIBILITY BETWEEN NATURAL AGRO-INDUSTRIAL BY-PRODUCTS AND SYNTHETIC MATERIALS, A BASIC ELEMENT IN OBTAINING BIOCOMPOSITE MATERIALS WITH POTENTIAL FOR USE IN CONSTRUCTION - **Irina POPA, Vasilica VASILE, Alexandrina MUREȘANU** 586
11 THE INTEGRATION OF CERAMIC WASTE AS A PARTIAL SUBSTITUTE OF NATURAL AGGREGATES IN EXPERIMENTAL CONCRETE RECIPES - **Mircea SĂLCUDEAN, Maria POPA** 594

WATER RESOURCES MANAGEMENT

1 IMPACT OF FLOOD DISCHARGE ON WATER QUALITY IN DANUBE RIVER BIFURCATIONS AND SELECTED LAKES (GORGOVA-UZLINA HYDROGRAPHIC UNIT) - **Irina CATIANIS, Dumitru GROSU, Laura DUTU, Albert SCRIECIU, Andrei TOMA, Ana Bianca PAVEL, Ovidiu BORZAN, Gabriel IORDACHE** 601
SPATIAL DISTRIBUTION OF TOTAL ORGANIC MATTER IN RECENT SEDIMENTS OF DANUBE DELTA LAKES (GORGOVA-UZLINA HYDROGRAPHIC UNIT) **- Irina CATIANIS, Ion STANESCU, Dumitru GROSU, Ana Bianca PAVEL, Albert SCRIECIU, Ovidiu BORZAN, Andrei TOMA, Florin DUTU, Gabriel IORDACHE** 613
3 ADAPTING ROMANIA'S IRRIGATION INFRASTRUCTURE TO CLIMATE CHANGE: OPPORTUNITIES AND CHALLENGES - **Mihai Teopent CORCHEȘ** 623
4 DRIP IRRIGATION'S INFLUENCE ON CHERNOZEM SOIL: ELECTROPHYSICAL AND SALINITY DYNAMICS - **Yurii DEHTIAROV, Zinaida DEHTIAROVA** 630
5 WATER RESOURCE MANAGEMENT IN FRUIT AND VEGETABLE PRODUCTION USING ALTERNATIVE MULCHES - **Gary L. HAWKINS** 644
6 ASSESSMENT OF GROUNDWATER QUALITY AND POLLUTION RISKS NEAR A HYDROCARBON POWER PLANT **- Ramona-Carmen HĂRȚĂU, Simona GAVRILAȘ, Claudiu-Ștefan URSACHI, Simona PERȚA-CRIȘAN, Florentina-Daniela MUNTEANU** 650
7 METAL CONTAMINATION IN THE SYSTEM WATER - SEDIMENTS – *PERCA FLUVIATILIS* LINNAEUS, 1758 AND *EUSTRONGYLIDES EXCISUS* JÄGERSKIÖLD*,* 1909 LARVAE - **Nikolina ILIEVA, Diana KIRIN** 663
8 CONTAMINATION OF POLLUTANTS IN *ABRAMIS BRAMA* (LINNAEUS, 1758), BIOINDICATION AND ECOLOGICAL RISK ASSESSMENT OF THE WETLAND MANDRA-PODA, BULGARIA - **Nikolina ILIEVA, Diana KIRIN** 670
9 SEDIMENT TRANSPORT MODELING WITH ADVANCE HYDRAULICS SOFTWARE - **Dorina Gabriela IONESCU, Robert Florin BEILICCI, Erika Beata Maria BEILICCI, Mihai NEGURA, Mirela Laura IEREMCIUC** 676
10 ECOLOGICAL MONITORING OF THE PARVENETSKA RIVER, PART OF THE MARITSA RIVER WATERSHED - **Diana KIRIN, Radoslava ZAHARIEVA, Petya ZAHARIEVA, Marian VARBANOV, Georgi PATRONOV, Gergana METODIEVA** 684

11 ECOLOGICAL ASSESSMENT OF THE BOROVITSA RIVER, EAST AEGEAN SEA BASIN - **Diana KIRIN, Petya ZAHARIEVA, Radoslava ZAHARIEVA, Georgi PATRONOV, Marian VARBANOV, Gergana METODIEVA, Dimitrinka KUZMANOVA** 690
12 ADVANCED HYDRAULIC MODELINGOF IRRIGATION CHANNEL - **Mihai NEGURA, Robert Florin BEILICCI, Erika Beata Maria BEILICCI, Mirela Laura IEREMCIUC, Dorina Gabriela IONESCU** 696
13 WATER USE EFFICIENCY IN IRRIGATED AGRICULTURE IN ROMANIA: OPTIMIZATION STRATEGIES IN THE CONTEXT OF CLIMATE CHANGE - **Oana Alina NIȚU, Ionuț Ovidiu JERCA, Mihaela BĂLAN, Elena Ştefania IVAN** 705
14 ASSESSMENT OF SURFACE WATER QUALITY IN THE SFÂNTU GHEORGHE BRANCH OF THE DANUBE DELTA - **Ana Bianca PAVEL, Laura DUTU, Florin DUTU, Irina CATIANIS, Gabriel IORDACHE, Catalina GAVRILA** 711
15 PHYSICO-CHEMICAL CHARACTERISTICS OF SURFACE WATER SAMPLES FROM THE GORGOVA-UZLINA DEPRESSION AND THE IZMAIL AND SF. GHEORGHE CONFLUENCES (SEPTEMBER–OCTOBER 2024) - **Ana Bianca PAVEL, Irina CATIANIS, Laura DUTU, Gabriel IORDACHE, Catalina GAVRILA** 729
16 ASSESSMENT OF SURFACE WATER QUALITY ACROSS SELECTED DANUBE RIVER SECTORS BASED ON PHYSICO-CHEMICAL PARAMETERS AND HYDROCARBON LEVELS - **Ana Bianca PAVEL, Andrei TOMA, Albert SCRIECIU, Catalina GAVRILA, Irina CATIANIS** 749
17 EVALUATION OF THE DEGREE OF MICROBIOLOGICAL CONTAMINATION OF GROUNDWATER IN GORJ COUNTY - **Emil Cătălin ȘCHIOPU, Roxana Gabriela POPA, Irina Ramona PECINGINĂ, Ramona Violeta CAZALBAȘU, Marinela Florica BODOG** 766
18 ECOLOGICAL STATUS ASSESSMENT OF MECHKA RIVER WATER (MARITSA RIVER BASIN) - **Petya ZAHARIEVA, Radoslava ZAHARIEVA, Diana KIRIN** 776
19 ECOLOGICAL ASSESSMENT OF THE KAYALIIKA RIVER WITHIN THE MARITSA RIVER WATERSHED USING MACROZOOBENTHOS AS A BIOINDICATOR - **Radoslava ZAHARIEVA, Petya ZAHARIEVA, Diana KIRIN** 782

REMOTE SENSING AND GEOINFORMATICS

1 THE EFFECTS OF APPLYING THE LAW IN CADASTRE ACTIVITY – A COMPARATIVE STUDY OF THE RESOLUTIONS THAT CAN BE ADOPTED FOR THE REGISTRATION OF REAL ESTATE PROPERTIES IN THE LAND REGISTRY - **Andreea BEGOV-UNGUR, Ioana Aurica BERINDEIE, Levente DIMEN** 788
2 THE APPLICABILITY OF GIS TECHNOLOGY IN THE STUDY OF RIVERBED DYNAMICS AND MORPHOLOGY - **Gabriela BIALI, Maria Catalina PASTIA, Paula COJOCARU, Carmen Elena MAFTEI** 794
3 CASE STUDY ON THE USE OF SCANNING EQUIPMENT UAV IN ORDER TO DRAW UP A MULTIFUNCTIONAL DATABASE, IN CÂRȚIȘOARA LOCALITY, SIBIU COUNTY - **Jenica CĂLINA, Aurel CĂLINA, Marius MILUȚ** 802
4 STUDY ON THE IMPACT OF THE APPLICATION OF INFORMATION SYSTEMS ON THE EFFICIENCY AND PRECISION OF TOPO-CADASTRAL WORKS IN THE PREPARATION OF DOCUMENTATION FOR A ROAD IN DOLJ COUNTY - **Jenica CĂLINA, Aurel CĂLINA, Alin CROITORU** 816
5 TECHNICAL METHODOLOGIES FOR CADASTRAL PLAN DEVELOPMENT USING GNSS AND UAV TECHNOLOGIES: A CASE STUDY IN PIETROASA, ROMANIA - **Flavia Mălina CIOFLAN, Flavius IRIMIE, Nicu Cornel SABĂU** 827
6 ASSESSMENT OF LAND USE CHANGES IN NON-COLLECTIVIZED AREAS USING GEOMATIC APPLICATIONS: A CASE STUDY IN VÎRFURILE, ROMANIA - **Flavia Mălina CIOFLAN** 839

7 ACCURACY IN VERTICAL ASSESSMENT OF TELECOMMUNICATIONS TOWERS THROUGH 3D SCANNING - **Andreea Diana CLEPE, Sorin HERBAN, Clara-Beatrice VÎLCEANU, George CRISTIAN** 851
8 FLOOD SUSCEPTIBILITY ASSESSMENT IN THE NERA RIVER BASIN USING GIS: IMPACTS ON LAND USE AND LAND COVER **- Loredana COPĂCEAN, Luminița COJOCARIU** 858
9 ADVANCING CADASTRAL UPDATES AND GIS SPATIAL ANALYSIS FOR FORESTED AREAS - **Iulia COROIAN, Silvia CHIOREAN, Rodica SOBOLU, Diana FICIOR, Paul SESTRAS, Luca-Pavel RUS, Catalin-Stefanel SABOU, Luisa ANDRONIE** 868
10 INTEGRATING UAS, LiDAR, AND GROUND-BASED SURVEYING FOR PRECISE DEMOLITION VOLUME ASSESSMENT: A CASE STUDY OF THE DOLJ CHIM INDUSTRIAL COMPLEX - **George CRISTIAN, Sorin HERBAN, Carmen GRECEA, Clara-Beatrice VÎLCEANU, Andreea Diana CLEPE** 878
11 THE USE OF THE GIS TECHNIQUE IN HIGHLIGHTING THE HUMAN PRESSURE ON THE ENVIRONMENT IN OLTEȚ PIEDMONT (SOUTHERN ROMANIA) - **Raluca Lucia DINCULOIU, Daniel SIMULESCU, Carmen Otilia RUSĂNESCU, Irina Aura ISTRATE, Gabriel Alexandru CONSTANTIN, Mihaela BEGEA, Edmond MAICAN, Gheorghe VOICU, Maria CIOBANU** 886
12 ASPECTS RELATING TO THE POSITIONING BY THE SEMI-KINEMATIC METHOD (STOP AND GO) OF DETAIL CHARACTERISTIC POINTS, NECESSARY FOR THE DESIGN OF COMMUNICATION WAYS - **Călin Ioan IOVAN, Tudor Andrei FLORIȘ, Georgiana Denisa BOJINCĂ** 894
13 SPATIAL POSITIONING OF TOPOGRAPHIC DETAILS WITH INTEGRATED MODERN TECHNOLOGIES, IN AREAS WITH FOREST VEGETATION - **Călin Ioan IOVAN, Tudor Andrei FLORIȘ, Georgiana Denisa BOJINCĂ, Călin Gheorghe PĂȘCUȚ** 904
14 SPATIAL POSITIONING WITH COMBINED METHODS OF TOPOGRAPHIC POINTS NECESSARY FOR ACCESSIBILITY OF FORESTS IN MOUNTAIN AREA - **Flavius IRIMIE** 914
15 APPLICATION OF HIGH-RESOLUTION SATELLITE IMAGERY FOR EVAPOTRANSPIRATION ESTIMATION - A SCIENTIFIC REVIEW - **Vanya IVANOVA, Zhulieta ARNAUDOVA, Rossitza MERANZOVA** 925
16 ANALYZING THE INFLUENCE OF TEMPERATURE ON NDVI FOR A POTATO CROP IN BRAȘOV AREA - **Mihai IVANOVICI, Maria ȘTEFAN, Angel CAȚARON, Adrian GHINEA, Gheorghe OLTEANU** 933
17 ENGINEERING AN INTERACTIVE MAP OF STATUES AND MONUMENTS FROM CLUJ-NAPOCA - **Florica MATEI, Tudor SĂLĂGEAN, Ioana POP, Elemer-Emanuel ŞUBA, Mircea-Emil NAP, Silvia CHIOREAN, Paul SESTRAŞ, Simion BRUMĂ, Ştefan BORCAN-CONȚEVICI, Cristian MĂLINAŞ, Lucia-Adina TRUȚĂ** 940
18 HYBRID MODELLING APPROACHES FOR LAND USE/LAND COVER CHANGE PREDICTION AND CARBON DYNAMICS IN MAROWIJNE, SURINAME - **Tamara MYSLYVA, Christiaan Max HUISDEN, Marek MROZ, Nataliia TSUMAN, Yurii BILYAVSKYI** 951
19 DETERMINATION OF LAND VALUATION FACTORS FOR THE PROCESS OF LAND CONSOLIDATION - A CASE STUDY IN SASCHIZ ADMINISTRATIVE UNIT IN ROMANIA - **Vlad PAUNESCU, Divyani KOHLI, Raluca MANEA, Mariana (CALIN) CIOLACU, Alexandru Iulian ILIESCU** 964
20 INVESTIGATION BETWEEN VEGETATION INDICES, METEOROLOGICAL DATA AND PHENOLOGY OF WINE GRAPE VARIETIES - **Anelia POPOVA, Zhulieta ARNAUDOVA** 976
21 RIVER CORRIDOR CHANGE DETECTION USING SATELLITE IMAGERY AND LIDAR DATA: A CASE STUDY OF THE SIRET RIVER NEAR CORBU VECHI VILLAGE - **Catalin-Stefanel SABOU, Simion BRUMA, Ioana POP, Florica MATEI, Paul SESTRAS, Jutka DEAK, Silvia CHIOREAN, Tudor SALAGEAN** 985

22 A GIS-BASED MULTICRITERIA APPROACH FOR IDENTIFYING OPTIMAL REFUGE LOCATIONS FOR SEVERE STORMS: A CASE STUDY IN CLUJ COUNTY, ROMANIA - **Paul SESTRAS, Ioana POP, Florica MATEI, Catalin-Stefanel SABOU, Simion BRUMA, Silvia CHIOREAN, Elemer Emanuel SUBA, Mircea NAP, Iulia COROIAN, Jutka DEAK, Tudor SALAGEAN** 994
23 MONITORING DIFFERENT GRASS VARIETIES USING MULTISPECTRAL IMAGERY BASED ON DIFFERENT IRRIGATION REGIMES - **Elemer-Emanuel SUBA, Tudor SALAGEAN, Ioana Delia POP, Florica MATEI, Silvia CHIOREAN, Mircea-Emil NAP, Paul SESTRAS, Simion BRUMA, Catalin-Stefanel SABOU, Vlad PAUNESCU, Valentin-Sebastian DAN, Ferencz VAKAR** 1006
24 GIS-BASED SUITABILITY ANALYSIS FOR SKI RESORT DEVELOPMENT IN THE BRAN–RÂȘNOV AREA, BRAȘOV COUNTY, ROMANIA - **Cornel Cristian TEREȘNEU** 1020

MISCELLANEOUS

1 TRENDS AND INSIGHTS IN MACHINE LEARNING FOR WASTE MANAGEMENT: A DECADE OF BIBLIOMETRIC ANALYSIS - **Sneha BASKARAN, Ezhilmaran DEVARASAN** 1028
2 ANALYSIS OF DIAMETER AND HEIGHT GROWTH OF SCOTS PINE SAPLINGS PLANTED IN 2023 ON THE STERILE DUMPS OF RECEA ȘUNCUIUȘ QUARRY, BIHOR COUNTY - **Bogdan BODEA, Cristian Mihai ENESCU, Ovidiu Ioan HÂRUȚA, Camelia Elena MOGA, Ruben BUDĂU, Adrian Ioan TIMOFTE** 1044
3 FIRE CHANGES IN SOIL FERTILITY AND MICROBIAL DYNAMICS IN NORTHWESTERN BULGARIA - **Simeon BOGDANOV, Bilyana GRIGOROVA-PESHEVA** 1052
4 EUROPEAN UNIVERSITY STUDENTS' ATTITUDES TOWARD THE EUROPEAN GREEN DEAL: A COMPARATIVE STUDY - **Mihai Dan CARMIHAI, Nicoleta RADU, Zina PARASCHIV, Francisca BLANQUEZ CANO, Oksana MULESA, Adrián SILVA, Razvan TEODORESCU** 1063
5 CHANGES OF PLANKTON COMPOSITION IN WINTER CONDITIONS IN AN URBAN LAKE - **Larisa FLORESCU, Mirela MOLDOVEANU, Ioana ENACHE, Rodica CATANA** 1070
6 EVALUATION OF CURRENT Li-Ion BATTERY RECYCLING TECHNOLOGIES - **Roxana-Elena FRÎNCU, Carmen Otilia RUSĂNESCU, Gheorghe VOICU, Gabriel Alexandru CONSTANTIN, Elena-Denisa PREDESCU, Sabrina Maria BĂLĂNESCU** 1085
7 STUDY OF MICROBIOLOGICAL STATUS OF SOILS IN BEECH PLANTATIONS - **Bilyana GRIGOROVA-PESHEVA, Yordan IVANOV** 1093
8 H_2S GAS LEAK EMERGENCY PREPAREDNESS AND COMMUNITY RESPONSE: A CRITICAL REVIEW OF BEHAVIORAL FACTORS AND GAPS - **Saeed KARIMI, Ehsan TALEBI, Saeed GIVEHCHI** 1100
9 RESTORATION ACTIVITIES AND BIODIVERSITY SURVEY OF WEST STUPINI MIRE IN THE BÂRSA DEPRESSION: BASELINE FOR NATURA 2000 CONSERVATION - **Anca MANOLE, Ana-Maria MOROȘANU, Attila MÁTIS, Anna SZABÓ, Georgiana-Roxana NICOARĂ, Florența-Elena HELEPCIUC, Mihnea VLADIMIRESCU, Ioana Cătălina PAICA, Mihaela CIOBOTĂ, Daniela Elena MOGÎLDEA, Constantin-Ciprian BÎRSAN, Constanța-Mihaela ION, Tiberiu SAHLEAN, Sorin ȘTEFĂNUȚ** 1112
10 THE DEGREE OF THE ROOTING AND ADAPTABILITY OF CORMOFLORA ON THE WASTE DUMPS OF THE BAIA NOUĂ QUARRY (MEHEDINȚI COUNTY) - **Mariana NICULESCU, Florina GRECU** 1122
11 FIBONACCI'S SEQUENCE IN NATURE, SCIENCE AND ARTS. THE GOLDEN RATIO - **Cosmin-Constantin NIȚU, Anca ROTMAN** 1128
12 DIMENSIONING OF UNDERGROUND PIPE NETWORKS OF IRRIGATION PLOTS. CASE STUDY – FÂNTÂNELE-SAGU IRRIGATION PLOT, ARAD COUNTY - **Antonia Mariana PASC, Teodor Eugen MAN, Robert Florin BEILICCI, Erika BEILICCI, Mircea VISESCU** 1139

13 ATTITUDES OF EUROPEAN GRADUATE STUDENTS REGARDING THE ROLE OF ADVANCED TECHNOLOGIES IN ENERGY AND INDUSTRY FOR A GREEN ENVIRONMENT IN THE CONTEXT OF CLIMATE CHANGE AND THE EUROPEAN GREEN DEAL - **Nicoleta RADU, Mihai Dan CARAMIHAI, Francisca BLANQUEZ CANO, Oksana MULESA, Adrian SILVA, Razvan TEODORESCU** 1148
14 EXPERT PERCEPTIONS ON DIGITAL EDUCATION TOOLS AND ASSESSMENT STRATEGIES UNDER THE EUROPEAN GREEN DEAL FRAMEWORK - **Nicoleta RADU, Mihai Dan CARAMIHAI, Francisca BLANQUEZ CANO, Montserrat Sarrà ADROGUER, Oksana MULESA, Adrian SILVA, Razvan TEODORESCU** 1155
15 ROLE OF GRASSLANDS IN CARBON SEQUESTRATION: A HYPOTHETICAL RESEARCH APPROACH - **Ioan ROTAR, Florin PĂCURAR, Marcel DÎRJA, Anca PLEȘA, Alina ȘUTEU, Ioana GHEȚE, Ferencz VAKAR** 1162
16 AN ARDUINO-PYTHON INTEGRATED PREDICTIVE DATA ACQUISITION SYSTEM FOR ENVIRONMENTAL MONITORING - **Georgian ROTARU, Gabriel PREDUȘCĂ, Liana Denisa CÎRCIUMĂRESCU, Emil DIACONU** 1168
17 REPURPOSING SAND-WASHING SLUDGE AS A SUSTAINABLE GROWTH MEDIUM FOR NON-FRUIT BEARING PLANT CULTIVATION - **Sally SALEHI, Farid Gholamreza FAHIMI, Masoud Kia DALIRI, Ahmad TAVANA, Keyvan SAEB** 1179
18 VIRTUAL LABS IN ENGINEERING EDUCATION: ENHANCING LEARNING OUTCOMES - **Mirela Alina SANDU, Veronica IVANESCU** 1193
19 THE INFLUENCE OF MUSIC ON PLANT GROWTH IN A SMART GREENHOUSE USING IoT TECHNOLOGY - **Cristian STĂNESCU, Gabriel PREDUȘCĂ, Liana Denisa CÎRCIUMĂRESCU** 1201
20 VEGETATION SURVEYS FOR MONITORING CO_2 GEOLOGICAL STORAGE SITES: A CASE STUDY FROM TWO ANALOGUE SITES FROM ROMANIA - **Lia STELEA, Alexandra-Constanța DUDU, Corina AVRAM, Gabriel IORDACHE, Constantin-Ștefan SAVA** 1210
21 STUDIES SUPPORTING THE DESIGNATION OF A NEW NATURA 2000 SITE: BAHNELE BANCULUI NORD - **Sorin ȘTEFĂNUȚ, Florența-Elena HELEPCIUC, Constantin-Ciprian BÎRSAN, Georgiana-Roxana NICOARĂ, Tiberiu SAHLEAN, Gabriela TAMAS, Gabriel-Mihai MARIA, Viorel-Dumitru GAVRIL, Miruna-Maria ȘTEFĂNUȚ, Larisa-Isabela FLORESCU, Mirela-Mădălina MOLDOVEANU, Constanța-Mihaela ION, Ana-Maria MOROȘANU** 1218
22 PRELIMINARY BIODIVERSITY SURVEY IN A NEWLY PROPOSED SITE OF COMMUNITY IMPORTANCE: THE AVRIG PEAT BOG - **Sorin ȘTEFĂNUȚ, Miruna-Maria ȘTEFĂNUȚ, Tiberiu SAHLEAN, Ana-Maria MOROȘANU, Florența-Elena HELEPCIUC, Georgiana-Roxana NICOARĂ, Constantin-Ciprian BÎRSAN, Gabriel-Mihai MARIA, Mihnea VLADIMIRESCU, Anca MANOLE, Constanța-Mihaela ION** 1229
23 INDOOR IoT SEEDLING NURSERY DEVELOPMENT - **Peter UDVARDY, Matyas Csongor KOVACS, Levente DIMEN** 1236
24 BIBLIOMETRIC ANALYSIS OF SOIL POLLUTION RESEARCH BASED ON WEB OF SCIENCE **- Bao-Zhong YUAN** 1245

Scientific Papers. Series E. Land Reclamation, Earth Observation & Surveying, Environmental Engineering. Vol. XIV, 2025
Print ISSN 2285-6064, CD-ROM ISSN 2285-6072, Online ISSN 2393-5138, ISSN-L 2285-6064

EVALUATION OF CHEMICAL COMPOSITION OF ESSENTIAL OIL AND TOXIC METAL ACCUMULATION OF TARRAGON (*ARTEMISIA DRACUNCULUS* L.) CULTIVATED ON METAL-CONTAMINATED SOILS

Violina ANGELOVA

Agricultural University - Plovdiv, 12 Mendeleev Blvd, 4000, Plovdiv, Bulgaria

Corresponding author email: vileriz@yahoo.com

Abstract

This study evaluates the quality of tarragon essential oil, toxic metals content, and the growth potential of tarragon on heavy metal-contaminated soils. Tarragon demonstrated tolerance to toxic metals and can be cultivated on highly polluted soils. The levels of toxic metals in tarragon essential oil were below the Maximum Permissible Concentrations. Based on translocation and bioconcentration coefficients, tarragon is a Cd, Pb, Zn and Hg excluder and suitable for phytostabilization. Tarragon essential oil exhibits a mixed sabinene/elemicin/isoelemicin/methyleugenol chemotype and could be used in the pharmaceutical, cosmetic, and related industries.

Key words*: essential oil, phytoremediation, polluted soils, tarragon, toxic metals.*

INTRODUCTION

Artemisia dracunculus L., commonly known as tarragon, is a perennial plant belonging to the Asteraceae family. Tarragon is widespread across North America, Europe, Southeastern Russia, Central Asia, Turkey, and Mongolia (Aglarova et al., 2008; Fildan et al., 2019; Sharopov et al., 2020). It is cultivated in Europe, Russia, Asia, Africa, and North America and is widely used in food flavoring, medicine, and perfumery (Obolskiy et al., 2011; Fildan et al., 2019; Sharopov et al., 2020).

Tarragon is a small perennial shrub that grows 120-150 cm tall. Its alternate leaves measure 2-6 cm in length and 1-8 mm in width, often covered with fine hairs and featuring smooth or slightly toothed edges. The plant produces small yellow flowers with whitish petals, arranged in globose, inclined baskets that form broom-shaped racemes. The entire herb is green and mossy, with a pleasant aroma and taste, and flowers in the second half of summer. Tarragon thrives in various environments but produces the highest yields in moist, sandy loam soils with an alkaline reaction. Depending on the variety, it can be propagated by seed (Russian tarragon) or rhizome cuttings (French and German tarragon). In Europe, plantings are established in April, with cuttings placed 60 cm apart and covered with a thin layer of soil. The first harvest occurs in the same year, and in subsequent years, up to three harvests per season are possible. The harvested material is dried using natural air circulation or heated to 35°C before the leaves are separated from the stems (Aglarova et al., 2008; Obolskiy et al., 2011).

Tarragon essential oil, a pale yellow to amber liquid with a spicy scent, is extracted from the plant's aerial parts during flowering (Fildan et al., 2019). Traditionally, it has been valued for a wide range of therapeutic properties, including antioxidant, antimicrobial, antidiabetic, and anti-inflammatory effects (Obolskiy et al., 2011; Fildan et al., 2019; Sharopov et al., 2020).

Certain medicinal plants, such as mint, St. John's wort, and sage, are known to accumulate significant amounts of toxic heavy metals in their tissues. These plants can be used for phytoremediation, serving as an alternative to food crops grown in contaminated conditions. The concentrations of plant by-products depend on growing conditions, influencing metabolic pathways responsible for the synthesis of natural compounds (Akula & Ravishankar, 2011). Heavy metals can significantly alter the chemical composition of secondary metabolites in aerial plant parts, affecting the quality, safety, and efficacy of plant-derived products.

Although the composition of tarragon essential oil is well studied, limited information is available on toxic metal accumulation in tarragon's aboveground biomass and essential oil when grown on contaminated soils.

This study aims to conduct a comparative analysis to determine heavy metal accumulation, macro- and trace element deposition in the vegetative organs of tarragon, and the quality of its essential oil. Additionally, this study explores the feasibility of cultivating tarragon on heavy metal-contaminated soils.

MATERIALS AND METHODS

This experiment was conducted on an agricultural field contaminated with Zn, Pb, and Cd, located 0.5 km from the Non-Ferrous Metals Plant (NFMW) near Plovdiv, Bulgaria.

Tarragon seedlings were purchased and planted in the spring at sites 0.5 km from the pollution source. In the second and third years after planting, plants were collected and analyzed. Tarragon was hand-harvested at the flowering stage in late August. After transport to the laboratory, plants were separated into individual organs (roots, stems, leaves, and flowering tops) using scissors. Samples were air-dried at room temperature until reaching a stable dry mass, followed by further drying at 35ºC. The concentrations of metals in different plant parts - roots, aboveground mass (stems and leaves), and flowering tops - were determined.

Tarragon essential oil was extracted under laboratory conditions via steam distillation for 2 hours using a Clevenger-type apparatus.

The pseudo-total metal content of soils was determined following ISO 11466. The microwave mineralization method was used to measure metal concentrations in tarragon and its essential oil. Quantitative measurements were performed using ICP (Jobin Yvon Emission - JY 38 S, France). Hg content was analyzed without sample pretreatment using a mercury analyzer. The accuracy and performance of the ICP and mercury analyzer were validated using standard reference material from apple leaves (SRM 1515, National Institute of Standards and Technology, NIST).

The chemical composition of the essential oil (diluted in hexane, 1:1000) was analyzed using an Agilent 7890A gas chromatography (GC) system equipped with an FID detector and an Agilent 5975C mass spectrometer. Compounds were identified by comparing retention times and Kovats retention indices (RI) with standard substances and mass spectral data from the NIST'08 library (National Institute of Standards and Technology, USA).

RESULTS AND DISCUSSIONS

Soil Characteristics

The soils in the study area have a neutral to slightly alkaline reaction (pH = 7.5), with moderate organic matter content (2.1%) and average nutrient levels (P, K). The total Zn, Pb, and Cd concentrations are significantly elevated, measuring 2423.9 mg/kg Zn, 2509.1 mg/kg Pb, and 63.7 mg/kg Cd, far exceeding the maximum permissible concentrations (MPC) of 400 mg/kg Zn, 100 mg/kg Pb, and 3.0 mg/kg Cd (Table 1).

Table 1. The total content of Pb, Zn, Cd (mg/kg) and Hg (µg/kg) in soils

Element	Pb	Zn	Cd	Hg
Total, x±sd	2509.1±6.5	2423.9±4.5	63.7±1.8	488.0±13
MPC	100	400	3.0	1.5

x = mean value (mg/kg) from five repetitions; sd = standard deviation

Metal content in tarragon

Table 2 presents the results obtained for the toxic metals and nutrient contents in the organs of the essential oil crop studied. The Pb content in tarragon roots reached 141.8 mg/kg, while Zn, Cd, Hg, Cu, Fe, and Mn levels were 50.9 mg/kg, 3.9 mg/kg, 48.3 µg/kg, 7.1 mg/kg, 157.8 mg/kg, and 5.6 mg/kg, respectively. These results can be attributed to tarragon's anatomical and biological characteristics. The plant's rhizomatous root system consists of thick, lignified, serpentine rhizomes with a dense network of thin, branched roots extending 30-45 cm deep. This structure enhances nutrient and water absorption, allowing tarragon to thrive in various soil conditions.

The movement and accumulation of toxic metals in tarragon's vegetative organs varied significantly. Notably, Pb was highly accumulated in the aerial parts, reaching 1144.1 mg/kg in leaves. Typically, plants

absorb only a small fraction of Pb from soil, with most Pb retained in the roots. However, findings suggest that tarragon efficiently translocates Pb to aboveground tissues, likely due to its anatomical and morphological features. Leaf hairs may contribute to Pb fixation from airborne pollutants.

Cadmium, known for its high mobility in plants, was present at 39.0 mg/kg in tarragon leaves, exceeding the toxic threshold of 5.0 mg/kg (Kabata-Pendias, 2001). Similarly, Hg accumulation in tarragon was attributed primarily to aerosol deposition, as leaves are the primary uptake site, with soil absorption being secondary. Hg concentrations were higher in the aerial parts and flowering tops than in the roots.

The Zn content in tarragon leaves reached 556.1 mg/kg, below the phytotoxic threshold of 500-1500 mg/kg (Kabata-Pendias, 2001). The Cu concentration in leaves was 74.3 mg/kg, exceeding the toxic range for most plants (25-40 mg/kg). Fe accumulated mainly in leaves (396.3 mg/kg), surpassing normal plant values (50-250 mg/kg), while Mn levels (56.5 mg/kg) remained well below phytotoxic thresholds (400-2000 mg/kg).

Most macroelements accumulated in tarragon's aerial parts. In leaves, P, K, Mg, and Ca levels reached 1590.1 mg/kg, 9843.0 mg/kg, 540.4 mg/kg, and 2387.0 mg/kg, respectively. In flowering tops, these concentrations were significantly higher: 5062.1 mg/kg P, 24,233.6 mg/kg K, 2536.6 mg/kg Mg, and 16,915.4 mg/kg Ca.

Despite accumulating heavy metals at levels exceeding critical toxicity thresholds, tarragon exhibited no visible symptoms of heavy metal toxicity, indicating a high level of tolerance. Heavy metal and nutrient accumulation was significantly higher in flowering tops than in leaves, except for Pb and Zn. In flowering tops, Pb reached 932.8 mg/kg, Zn 304.8 mg/kg, Cd 35.1 mg/kg, and Hg 78.2 µg/kg.

Overall, metal distribution in tarragon was selective, primarily depending on the plant organ and its surface characteristics. Heavy metals and micro- and macroelements were predominantly accumulated in leaves and flowering tops (Figure 1).

Table 2. Content of toxic metals and nutrients (mg/kg) in tarragon

	Roots	Stems	Leaves	Flowering tops
Pb	148.8±1.2	45.3±0.3	1084.7±2.6	932.8±2.0
Cd	3.9±0.1	15.5±0.2	39.0±0,,5	35.1±0.5
Zn	50.9±1.3	68.5±1.5	556.1±8.7	304.6±4.6
Cu	7.1±0.8	13.3±1.0	74.3±3.5	79.5±3.8
Fe	57.8±0.8	166.9±3.4	396.3±4.6	4790.1±8.9
Mn	5.6±'0.5	16.0±1.0	56.5±1.8	232.2±2.6
P	493.0±5.5	675.8±5.9	1590.1±9.8	5062.1±12.7
Ca	1420.4±8.8	2387.0±10.8	16915.3±25.0	19226.8±26.0
Mg	216.7±1.9	540.4±2.8	2536.6±10.6	4616.8±12.7
K	5751.5±8.7	9843.0±9.8	24233.6±23.0	36562.5±26.9
Hg*	48.3±3.8	45.0±4.5	284.7±10.0	78.2±7.1

x - average value (mg/kg) from 5 repetitions; sd - mean standard deviation; *- µg/kg.

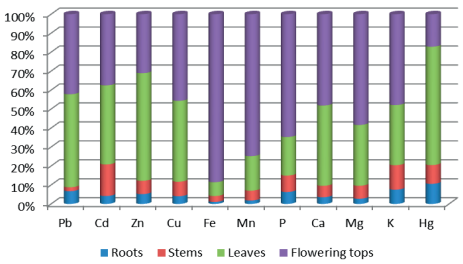


Figure 1. Distribution of toxic metals and nutrients in tarragon

Toxic Metal Content in Tarragon Essential Oil

The toxic metal content of tarragon essential oil was also analyzed. The results indicate that most metals present in flowering tops do not transfer into the oil during distillation. Consequently, their concentrations in the oil are significantly lower. The Pb content in tarragon essential oil reached 0.27 mg/kg, and Zn 1.09 mg/kg, while Cd and Hg levels were below the detection limits of the analytical method.

These findings strongly suggest that a substantial portion of metals present in tarragon flowering tops does not pass into the essential oil. Furthermore, the levels in the oil remain below the accepted maximum limits for an environmentally safe product (5 mg/kg Pb, 1 mg/kg Cd, 0.1 mg/kg Hg) as per the Council of Europe (2021).

These results confirm previous findings by Angelova et al. (2015), which demonstrated that the heavy metal content in essential oils remains minimal, regardless of soil contamination levels. This is primarily due to the high molecular weight and non-volatile nature of heavy metals, preventing their concentration during the distillation process.

Phytoremediation potential of tarragon

The phytoremediation efficiency of tarragon was evaluated using the Bioaccumulation Factor (BCF) and Translocation Factor (TF). These indices are commonly used to assess plant-based remediation potential and depend on factors such as soil conditions, plant species, and heavy metal bioavailability.

The coefficients were calculated using the following equations:

- Translocation Factor (TF):

$$TF = \frac{Cshoots}{\text{Croots}}$$

where:

- *Cshoots* represents the heavy metal content (mg/kg) in the aerial parts (stems, leaves, flowering tops);
- *Croots* represents the concentration in the roots (mg/kg).

- Bioaccumulation Factor (BCF):

$$BCF = \frac{Cplant\ parts}{\text{Csoil}}$$

where:

- *Cplant parts* represents the heavy metal content (mg/kg) in various plant organs (roots, stems, leaves, flowering tops);
- *Csoil* represents the heavy metal concentration in the corresponding soil (mg/kg).

A plant species is considered suitable for phytoextraction when its translocation factor (TF) > 1. If TF < 1, the plant is more suitable for phytostabilization.

The results indicate that tarragon exhibits high translocation potential for heavy metals: Pb: TF = 8.15; Cd: TF = 9.96; Zn: TF = 10.93; Hg: TF = 5.89.

The bioaccumulation factor for roots (BCFroots) was calculated as follows: Pb: BCFroots = 0.059; Cd: BCFroots = 0.061; Zn: BCFroots = 0.021; Hg: BCFroots = 0.099 and is presentet in Tabel 3.

Table 3. Bioaccumulation (BCF) and translocation (TF) factors for tarragon

	TF	BCFroots	BCFleaves	BCF tops
Pb	8.15	0.059	0.43	0.37
Cd	9.96	0.061	0.61	0.55
Zn	10.93	0.021	0.22	0.13
Hg	5.89	0.0995	0.58	0.16

For flowering tops, the BCF values were all below 1, indicating limited metal accumulation in this plant part (Table 4).

Table 4. Composition of tarragon oil (%)

	Component	RI	% of TIC
1	α-Thujene	924	0.233
2	α-Pinene	939	0.428
3	**Sabinene**	969	**21.414**
4	β-Pinene	979	0.671
5	β-Myrcene	991	1.615
6	α-Phellandrene	1005	0.119
7	α-Terpinene	1018	0.412
8	p-Cymene	1026	0.191
9	Limonene	1029	0.963
10	β-Phellandrene	1032	0.146
11	cis-beta-Ocimene	1040	2.244
12	trans-beta-Ocimene	1050	3.529
13	γ-Terpinene	1062	0.745
14	cis-Sabinene hydrate	1065	0.363
15	Terpinolene	1086	2.342
16	beta-Linalool	1097	0.179
17	trans-Verbenol	1141	0.068
18	Terpinene-4-ol	1177	0.761
19	Estragol	1186	0.446
20	β-Citronellol	1211	0.227
21	Citronellyl acetate	1354	2.565
22	Geranyl acetate	1383	1.411
23	**Methyleugenol**	1402	**13.107**
24	β-Caryophyllene	1419	0.236
25	α-Humulene	1454	0.115
26	γ-Curcumene	1481	0.382
27	Germacrene D	1484	3.923
28	Methyl isoeugenol	1490	2.734
29	Bicyclogermacrene	1500	2.597
30	**Elemicin**	1557	**17.429**
31	trans-Nerolidol	1563	0.587
32	**Isoelemicin**	1570	**15.259**
33	(-)-Spathulenol	1578	1.076
34	Caryophyllene oxide	1581	0.162
35	α-Cadinol	1652	0.136
36	Farnesol	1722	0.244
Total			99.059
Oil content, %			1.1

RI - Kovacs relative indices

BCF for leaves reflects the plant's ability to absorb and transfer metals to the leaves, which can be harvested for remediation purposes. The classification of plants based on BCF values is as follows: BCF < 1: Excluder; BCF = 1: Indicator; 1 < BCF < 10: Accumulator; BCF > 10: Hyperaccumulator. The BCF values for tarragon leaves were: Pb: 0.43; Cd: 0.61; Zn: 0.23; Hg:0.58. These results suggest that tarragon functions as an excluder of Cd, Pb, Zn, and Hg when grown in contaminated soils.

Previous studies support the findings of Kocaman (2022) classified tarragon as an accumulator of Pb and Cd (1<Cd-Pb<10) and an excluder of Hg (Hg<1). Ghasemidehkordi et al. (2018) reported Pb bioaccumulation in Artemisia dracunculus L. in Iran. Ozyigit et al. (2018) found that tarragon accumulates low levels of Cd and has not been identified as a heavy metal accumulator.

Essential oil quality

The quantity and composition of tarragon essential oil are influenced by genetic factors, phenological stage, and environmental conditions (e.g., soil composition and light intensity).

The essential oil yield varied between 0.15% and 3.1%, with the highest concentrations occurring at the beginning of flowering (Fildan et al., 2019). The results from this study align with previous reports.

In total, 36 components were identified in tarragon essential oil, primarily belonging to the terpene group (monoterpenes and sesquiterpenes) and phenylpropanoids, which together accounted for 99.059% of total oil composition (Table 4). The dominant compounds (>10%) were: Sabinene (21.414%), Elemicin (17.429%) Isoelemicin (15.259%), Methyleugenol (13.107%).

Based on functional group classification, tarragon oil was composed of:

- Phenylpropanoids: 48.975%
- Monoterpene hydrocarbons: 35.052%
- Sesquiterpene hydrocarbons: 7.253%
- Oxygenated monoterpenes: 5.574%
- Oxygenated sesquiterpenes: 2.205%.

The main phenylpropanoids in essential oil are elemicin (17.429%), isoelemicin (15.259%), methyleugenol (13.107%), methyl isoeugenol (2.734%). The amount of phenylpropanoid compounds in tarragon oils varies widely (25.4% (Sharopov et al., 2020), 36.41% (Fildan et al., 2019), 51.93% (Varban et al., 2023), 52.2%, (Lopez-Lutz et al.,2008), 62.2% (Zawislak and Dzida, 2012), 73.3% (Fraternale et al., 2015).

Variation in methyleugenol composition was found (0.2% (Fraternale et al., 2015), 6.2% (Zawislak and Dzida, 2012), 9.09% (Fildan et al., 2019), 13.107% (this study) 29.19% (Varban et al., 2023). The content of methyleugenol depends on the phenophase, with the highest content identified in *A. dracunculus* in mass flowering (Khodakov et al. 2009). The content of elemicin also varies widely (7.95% (Fildan et al., 2019), 11.43% (Varban et al., 2023), 17.429% (this study), 56.0% (Zawislak and Dzida, 2012). Elemicin has antimicrobial, antioxidant, antiviral and psychoactive effects, and there is no significant difference in its content at the growth stages of tarragon (Varban et al., 2023). Significant differences were also found in the content of estragole (methyl chavicol) (phenylpropanoid compound) (0.446% (this study), 3.9% (Russia), 16.2% (Canada) (Obolskiy et al., 2011), 24.6% (Sharopov et al., 2020), 73.3% (Italy, Fraternale et al., 2015), 82% (USA, Obolskiy et al., 2011). This compound is considered a key component of French tarragon oil (>80%) (Sharopov et al., 2020). Monoterpenes belong to the second primary chemical class of oil constituents, which reach 40.626% of the total oil composition. The amount of monoterpene hydrocarbons reaches 35.052%, of which sabinene (21.414%), trans-beta-ocimene (3.529%), terpinolene (2.342%), cis-beta-ocimene (2.244%), β-myrcene (1.615%).

Sabinene is a significant component in tarragon essential oils from different geographical origins (Sharopov et al., 2020). It was found in high concentrations in the essential oil of *A. dracunculus* growing in Tibet (China| (19.2%, Liu et al., 2018), Lithuania (14-25%, Sharopov et al., 2020), Romania (9.44-42.4%, Fildan et al., 2019; Varban et al., 2023), Kazakhstan (20.2%, Suleimenov et al., 2010), Poland (20.9%, Zawislak and Dzida, 2012), Tajikistan (29.1%, Sharopov et al., 2020), while in India – trace amount (Verma et al., 2010).

The number of oxygenated monoterpenes reaches 5.574 % of the total composition of the oil. The main oxygenated monoterpenes are citronellyl acetate (2.565%) and geranyl acetate (1.411%).

The sesquiterpenes reach 9.458%. The amount of sesquiterpene hydrocarbons reaches 7.253%. Germacrene D (3.923%) and bicyclogermacrene (2.597%) are the main components that predominate in this group.

The amount of oxygenated sesquiterpenes reaches 2.205% of the total oil composition.

The oil contains (> 1.0 %) caryophyllene oxide (1.076%).

The results show significant differences in the composition of oils obtained from different geographical locations. Studies have shown significant differences in the composition of tarragon essential oil. These differences in the chemical composition of the essential oil extracted from the aerial parts of *A. dracunculus* may be due to environmental conditions (Fildan et al., 2019), habitat, soil pH, plant part used, extraction method applied, and other factors such as genotypes and ontogeny (Obolskiy et al., 2011; Fraternale et al., 2015; Fildan et al., 2019). According to Ekiert et al. (2021), the main components in the essential oil of *A. dracunculus* are estragole (40-85%), sabinene (up to 35%), methyleugenol (up to 25%) and elemicin (up to 57%). The essential oil of tarragon from Tajikistan is characterised mainly by sabinene (29.1%), and estragole (24.6%), the oil from Turkey contains Z anethole (81.0%) (Kordali et al., 2005), the oil from Cuba - elemicin (53.0%) and methyleugenol (17.6%) (Pino et al., 1996), the oil from Iran - anethole (21.2%), E-(β)-ocimene (22.6%) and limonene (12.4%) (Sayyah et al., 2004). The Russian tarragon oil is rich in sabinene (39.4%), elemicin (16.0%), methyl eugenol (14.7%) and iso-elemicin (7.7%), while the French tarragon oil has the main component methyl chavicol (68.6%) (Arabhosseini et al., 2006).

Based on 30 components of 105 essential oils of different geographical origins, Sharopov et al. (2020) established 7 main chemotypes of tarragon essential oil. The results show that the essential oil of *A. dracunculus* belongs to the mixed chemotype variation without a dominant component. Tarragon essential oil is characterised by a mixed sabinene/elemicin/isoelemicin/methyleugenol chemotype.

CONCLUSIONS

Based on the results obtained, the following key conclusions can be drawn:

1. Toxic metal tolerance and phytoremediation: Tarragon is tolerant to toxic metals and can be cultivated on highly contaminated soils (2423.9 mg/kg Zn, 2509.1 mg/kg Pb, and 63.7 mg/kg Cd). It is effective for phytoremediation of soils contaminated with heavy metals.
2. Heavy metal excluder: Tarragon functions as a Cd, Pb, Zn and Hg excluder when grown in contaminated environments.
3. Metal and nutrient uptake: There is a distinct pattern in the absorption and distribution of heavy metals, microelements, and macroelements between the vegetative and reproductive organs of tarragon
4. Essential oil safety: The levels of Pb, Cd, Zn, and Hg in tarragon essential oil, cultivated 0.5 km from NFMW-Plovdiv, were below the Maximum Permissible Concentrations. This makes the oil suitable for use in the pharmaceutical, cosmetic, and related industries.
5. Essential oil composition: phenylpropanoids (48.975%) are the predominant components in tarragon oil, followed by monoterpene hydrocarbons (35.052%), sesquiterpene hydrocarbons (7.253%), oxygenated monoterpenes (5.574%), and oxygenated sesquiterpenes (2.205%).
6. Chemotype classification: Tarragon essential oil from the NFMW-Plovdiv region exhibits a mixed sabinene/elemicin/isoelemicin/methyleugenol chemotype.

ACKNOWLEDGEMENTS

This research was supported by the Bulgarian National Science Fund [grant number KP-06-H54/7].

REFERENCES

Aglarova, A. M., Zilfikarov, I. N., & Severtseva, O. V. (2008). Biological characteristics and useful properties of tarragon (*Artemisia dracunculus* L.) (review). *Pharm. Chem. J*., *42*(2), 81–86.

Angelova, V., Grekov, D., Kisyov, V., & Ivanov, K. (2015). Potential of lavender (*Lavandula vera* L.) for phytoremediation of soils contaminated with heavy metals. International *Journal of Biological, Biomolecular, Agricultural, Food and Biotechnological Engineering*, *9*(5), 522-529.

Akula, R., & Ravishankar, G.A. (2011). Influence of abiotic stress signals on secondary metabolites in plants. *Plant signaling and behavior*, *6*, 1720-1731.

Arabhosseini, A., Padhye, S., van Beek, T.A., van Boxtel, A.J.B., Huisman, W., Posthumus, M.A. & Muller, J. (2006). Loss of essential oil of tarragon

Artemisia dracunculus L. due to drying. *J. Sci. Food Agric.*, *86,* 2543-2550.

Council of Europe. (2021). European Pharmacopoeia 10th Edition (with supplements 10.6-10.7-10.8). Strasbourg

Ekiert, H., Swiatkowska, J., Knut, E., Klin, P., Rzepiela, A., Tomczyk, M., & Szopa, A. (2021). *Artemisia dracunculus* (Tarragon): A Review of its traditional uses, phytochemistry and pharmacology. *Front. Pharmacol*., *12*, 653993.

Fildan, A. P., Pet, I., Stoin, D., Bujanca, G., Lukinich-Gruia, A.T., Jianu, C., Jianu, A.M., Radulescu, M., & Tofolean, D.E. (2019). *Artemisia dracunculus* essential oil. chemical composition and antioxidant properties. *Rev.Chim. (Bucharest), 70*(12), 59-62.

Fraternale, D., Flamini, G., & Ricci, D. (2015). Essential oil composition and antigermination activity of *Artemisia dracunculus* (tarragon). *Nat Prod Commun.*, *10*(8),1469-1472.

Ghasemidehkordi, B., Malekirad, A.A., Nazem, H., Fazilati, M., Salavati, H., & Shariatifar, N. (2018). Concentration of lead and mercury in collected vegetables and herbs from Markazi province, Iran: a non-carcinogenic risk assessment. *Food and chemical toxicology*, *113*, 204-210.

ISO 11466 (1995). Soil Quality-Extraction of Trace Elements Soluble in Aqua Regia.

Kabata-Pendias, A. (2001). *Trace Elements in Soils and Plants*. 3rd ed. CRC Press LLC, Boca Raton, 2001.

Khodakov, G.V., Kotikov, I.V., & Pankovetskii, V.N. (2009). Component Composition of Essential Oil from *Artemisia abrotanum* and *A. dracunculus*. *Chem. Nat. Compd*., *45*, 905-908.

Kocaman, P. (2022). Assessment of the use of *Artemisia Dracunculus* L. and *Erigeron Canadensis* in the remediation of heavy metal contaminated soils and their ability to phytoextraction and biomass yield. *Ayhan Turkiss journal of nature and science*, *11*(4), 1-10.

Kordali, S., Kotan, R., Mavi, A. Cakir, A., Ala, A. & Yildirim, A. (2005). Determination of the chemical composition and antioxidant activity of the essential oil of *Artemisia dracunculus* and of the antifungal and antibacterial activities of Turkish *Artemisia absinthiumm, A. dracunculus, Artemisia santonicum*, and *Artemisia spicigera* essential oils. *J. Agric. Food Chem*., *53*, 9452-9458.

Liu, T., Lin, P., & Bao, T. (2018). Essential oil composition and antimicrobial activity of *Artemisia dracunculus* L. var. qinghaiensis Y. R. Ling (Asteraceae) from Qinghai-Tibet Plateau. *Ind Crops Prod*., *125*, 1-4.

Lopez-Lutz, D., Alviano D.S., Alviano, C., & Kolodziejczyk P.P. (2008). Screening of chemical compo sition, antimicrobial and antioxidant activities of Artemisia essential oils. *Phytochemistry*, *69*, 1732-1738.

Obolskiy, D., Pischel, I., Feistel, B., Glotov, N., & Heinrich, M. (2011). *Artemisia dracunculus* L. (tarragon): a critical review of its traditional use, chemical composition, pharmacology, and safety. *J. Agric. Food Chem*., 59 (21), 11367–11384.

Ozyigit, I., Yalcin, B., Turan, S., Saracoglu, I.A., Karadeniz, S., & Yalcin, I.E. (2018). Investigation of heavy metal level and mineral nutrient status in widely used medicinal plants' leaves in Turkey: Insights into health implications. *Biological trace element research*, *182*(2), 387-406.

Pino, J.A., Rosado, A., Correa, M.T. & Fuentes, V. (1996). Chemical composition of the essential oil of *Artemisia dracunculus* L. from Cuba. *J. Essent. Oil Res*., 8, 563-676.

Sayyah, M., Nadjafnia, L., & Kamalinejad, M. (2004). Anticonvulsant activity and chemical composition of *Artemisia dracunculus* L. essential oil. *Journal of Ethnopharmacology*, *94*(2-3), 283-287.

Sharopov, S., Salimov, A., Numonov, S., Bakri, M., Sangov, Z., Habasi, M., Aisa, H.A., & Setzer, W.N. (2020). Phytochemical study on the essential oils of tarragon (*Artemisia dracunculus* L.) growing in Tajikistan and its comparison with the essential oil of the species in the rest of the world. *Natural Product Communications, 15*(12), 1–7.

Suleimenov, E.M., Tkachev, A.V., & Adekenov, S.M. (2010). Essential oil from Kazakhstan *Artemisia* species. *Chem Nat Compd*., 46(1),135-139.

Varban, D., Zahan, M., Crisan, I., Pop, C.R., Gal, E., Stefan, R., Rotar, A.M., Musca, A.S., Mesesan, D., & Horga, V. (2023). Unraveling the potential of organic oregano and tarragon essential oils: profiling composition, FT-IR and Bioactivities. *Plants, 12*, 4017.

Verma, M. K., Anand, R., Chisti, A.M., Kitchlu, S., Chandra, S., Shawl, A.S., & Khajuria, R.K. (2010). Essential oil composition of *Artemisia dracunculus* L. (Tarragon) growing in Kashmir India, *Journal of Essential Oil Bearing Plants*, *13*(3), 331-335.

Zawislak, G., & Dzida, K. (2012). Composition of essential oils and content of macronutrients in herbage of tarragon (*Artemisia Dracunculus* L.) grown in southeastern *Poland. J. Elem. S*. 721–729.

Scientific Papers. Series E. Land Reclamation, Earth Observation & Surveying, Environmental Engineering. Vol. XIV, 2025
Print ISSN 2285-6064, CD-ROM ISSN 2285-6072, Online ISSN 2393-5138, ISSN-L 2285-6064

EVALUATION OF WASTE BIOMASS FROM AROMATIC PLANTS FOR ENERGY PURPOSES

Violina ANGELOVA

Agricultural University - Plovdiv, 12 Mendeleev Blvd, 4000, Plovdiv, Bulgaria

Corresponding author email: vileriz@yahoo.com

Abstract

This study aims to evaluate the feasibility of obtaining energy from waste biomass. The potential of waste biomass from aromatic plants, left after the production of essential oils, was assessed. The calorific value, ash content, volatile compounds, and moisture content were determined. Elemental analysis of the waste biomass was conducted to measure the C, H, N, and S contents. The results indicate that residual waste has significant potential as a quality feedstock for solid biofuel production. Compared to coal, the calculated emission factors demonstrate a reduction in CO and CO2 emissions by up to 30%, NOx by up to 80%, SO2 by up to 99%, and dust by up to 67%, depending on the waste used. When selecting suitable waste for energy production, it's essential to balance calorific value and emission factors. If energy efficiency is the priority, lavender, tansy, and thyme waste may be preferred. However, for sustainability and lower environmental impact, common sage waste could be the better choice. It's important to consider the specific context, including regulations and energy needs, when making a final decision.

Key words*: biofuel, elemental analysis, emission factors, waste.*

INTRODUCTION

In recent years, alternative energy sources characterized by low emissions, including greenhouse gases and dust particles, have been increasingly sought after (Kimming et al., 2015; Obernberger et al., 2017). Waste plays a crucial role in the European Commission's strategy for energy security and greenhouse gas (GHG) emission reduction. As a renewable energy source, the use of waste biomass has been expanding worldwide, primarily for household heating as an alternative to fossil fuels (Lasek et al., 2018; Pastorello et al., 2011). The demand for plants with high productivity, low nutrient requirements, and valuable biological composition for various bioeconomic applications is of utmost importance. Perennial plants, in particular, offer advantages by reducing production costs and energy inputs compared to annual field preparation and planting. Additionally, such a biomass production system can enhance ecosystem services and support soil conservation, aligning with the concept of "low energy consumption and high output" regarding energy investments and additional costs. Essential oil crops are primarily cultivated for their essential oils (Duce et al., 2017; Giacometti et al., 2018; Kant & Kumar, 2022). The area dedicated to essential oil production in the European Union is steadily increasing, reaching approximately 80,000 hectares (Maj et al., 2020). In recent years, global trade in medicinal and aromatic plants has grown by 10-12% annually (Chandra & Sharma, 2019). Consequently, waste generation in this industry has also increased, reaching up to 30 million tons annually (Wei et al., 2022).

A substantial amount of waste biomass is generated during harvesting, pre-processing, drying, collection of harvested crops, and plant feedstock processing. After essential oil extraction, solid residue remains, which can be utilized for fuel energy production through pyrolysis, gasification, or hydrothermal carbonization processes (Mastellone, 2015). Despite containing valuable substances, these residues are often discarded through stockpiling, landfilling, or open field burning, leading to resource waste and significant environmental pollution (Wei et al., 2022; Marcelino et al., 2023).

Despite the strong economic potential of utilizing plant biomass waste, limited research has focused on the calorific value of these residues (Maj et al., 2020; Chakyrova & Doseva, 2021; Pulidori et al., 2023).

This study aims to evaluate the energy potential of residues obtained after the steam distillation of essential oils from lavender, tansy, thyme, yarrow, and common sage. Additionally, it examines the emission factors of toxic exhaust components and explores the feasibility of using these residues for energy production.

MATERIALS AND METHODS

Aromatic plants, including lavender, tansy, thyme, yarrow, and common sage, were collected from southern Bulgaria at the flowering stage. After essential oil extraction via steam distillation, the plant residues were dried in an oven at 105°C and ground using a laboratory grinder. The physico-chemical characterization of the plant residues was conducted based on calorific value, ultimate analysis, and proximate analysis.

The heating value was determined following the ISO standard (BDS EN ISO 18125:2017) using an IKA C6000 oxygen bomb calorimeter (IKA Werke GmbH, Germany).

The samples were analyzed according to standard methods: moisture content (BDS EN ISO 18134-3:2015), ash content (BDS EN ISO 18122:2015), volatile matter (BDS EN ISO 18123:2015).

Total carbon, hydrogen, nitrogen, and sulfur contents were determined by dry combustion using a Vario Macro CHNS analyzer (Elementar GmbH, Germany) (BDS EN ISO 16948:2015).

Using the results from the ultimate analysis, emission factors for CO, CO_2, NO_x, SO_2, and dust emissions were estimated through equations (1)-(7) (Borycka, 2008):

CO emission factor

$$\mathrm{CO} = \frac{28}{12} x\ \mathrm{Ec}\ x\ (C_CO/C) \quad (1)$$

Emission factor of chemically pure coal

$$Ec = c.uc \quad (2)$$

CO_2 emission factor

$$CO_2 = \frac{44}{12} x\ (Ec - \frac{12}{28}\ x\ CO - \frac{12}{16}\ x\mathrm{ECH_4} - \frac{26.4}{31.4} x\ ENMVOC) \quad (3)$$

Methane emission factor:

$$ECH4 = \frac{16}{12} xEc \times \left(\frac{C_{CH4}}{C}\right) \quad (4)$$

NOx emission factor

$$NOx = \frac{46}{14} \times Ec \times \frac{N}{C} \times \left(\frac{N_{NOx}}{N}\right) \quad (5)$$

Emission factor of SO_2

$$\mathrm{SO_2} = \frac{2S}{100} \quad (6)$$

Dust emissions:

$$Edust = 1.5 \times A \times \frac{100 - \eta 0}{100 - k} \quad (7)$$

RESULTS AND DISCUSSIONS

Proximate and ultimate analysis

The proximate and ultimate analysis results for essential oil plant waste are presented in Tables 1 and 2. According to CEN/TS 14961, biomass for solid biofuels is categorized into three main groups: woody biomass, herbaceous biomass, and fruit biomass. Essential oil plant waste falls under the herbaceous biomass group - specifically, agricultural and garden herbs.

Table 1. Proximate analysis and heating values of plant waste

Plant waste	M, %	Ash, %	FC, %	VM, %	LHV, MJ/kg	HHV, MJ/kg
Lavender	8.42	7.28	11.5	80.08	17.41	19.23
Tansy	7.31	8.35	12.69	80.0	18.16	19.78
Thyme	7.08	8.24	14.42	78.5	17.85	19.17
Yarrow	6.22	8.79	16.48	77.3	16.7	17.96
Commom sage	8.95	6.22	13.46	77.59	16.24	18.06
ISO 17225-6	≤12 - 15	≤ 6-10	-	-	≥14.5	-
CEN/TS 14961-1Harvest (July - Oct.)	-	6.5 (2.5-10)	-	-	16.6	-

M - moisture, FC- fixed carbon, VM - volatile matter, LHV - lower heating value, HHV - higher heating value

The key parameters of biomass waste were compared against the requirements of the ISO 17225-6 standard for herbaceous biomass and data from other studies.

Heating Value and Energy Potential: The LHV (Lower Heating Value) is a crucial parameter for evaluating biomass as a biofuel. According to ISO 17225-6, the standard LHV for solid fuel is ≥14.5 MJ/kg. The LHV of the tested plant waste ranged from 16.24 MJ/kg (common sage) to 18.16 MJ/kg (tansy). The tested biomass meets or exceeds ISO 17225-6 standards for LHV (≥14.5 MJ/kg), indicating good energy potential.

The HHV (Higher Heating Value), which represents the total energy content, ranged from 17.96 MJ/kg (yarrow) to 19.78 MJ/kg (tansy). Tansy waste shows the highest energy efficiency (19.78 MJ/kg HHV), making it an excellent candidate for biofuel. Conversely, the lower HHV of common sage implies reduced energy potential. These values align with previous studies, such as Pulidori et al. (2023) for lavender waste (19.2 MJ/kg) and thyme waste (17.8 MJ/kg), Maj et al. (2020) for mint waste (15.90-16.64 MJ/kg), and Zając et al. (2019) for miscanthus (17.99 MJ/kg), wood (18.35 MJ/kg), and rapeseed straw (15.97 MJ/kg).

Moisture Content and Ash Content: Moisture content significantly affects combustion efficiency, as lower moisture levels lead to better energy performance. The tested biomass had moisture content ranging from 6.22% (yarrow waste) to 8.95% (common sage waste), which complies with ISO 17225-6 (≤12-15%).

Ash content is a critical parameter in biomass fuel quality, as higher ash levels can reduce combustion efficiency and cause operational challenges. The tested samples contained 6.22% (common sage) to 8.79% (yarrow) ash, which is within the acceptable ISO 17225-6 range (≤6-10%). Moisture and ash contents are within acceptable ranges, ensuring good combustion properties. These values are comparable to previous findings for lavender waste (6.7-7.8%) (Chakyrova & Doseva, 2021) andmint waste (7.23-10.29%) (Maj et al., 2020).

Fixed Carbon and Volatile Matter: Fixed carbon content is a positive attribute of biomass, as it determines combustion stability and burning duration. While ISO 17225-6 does not specify a standard for fixed carbon, the values in this study ranged from 11.5% (lavender) to 16.48% (yarrow), with yarrow showing the highest combustion stability. Similar values were reported for mint waste: 9.40-15.77% (Maj et al., 2020) andlavender waste: 15.3% (Chakyrova & Doseva, 2021).

Volatile matter plays a key role in biomass combustion, with higher volatile content leading to easier ignition and more intense burning. Fixed carbon and volatile matter values indicate stable burning characteristics. Biomass typically contains 60-80% volatile matter, and the tested biomass samples ranged from 77.3% (yarrow) to 80.08% (lavender). These values align with mint waste (64.99-70.36%) (Maj et al., 2020), miscanthus (72.5%) and rapeseed straw (73.5%) (Zając et al., 2019).

Table 2 presents the results of the ultimate analysis of the tested wastes. These values are compared with the requirements of ISO 17225-6 and with findings from other studies. The main components of solid biofuels are carbon (C), hydrogen (H), and oxygen (O). During combustion, C and H undergo oxidation in exothermic reactions, forming CO_2 and H_2O, which impact the gross calorific value of the fuel (Clarke & Preto, 2011). Higher C content indicates a greater energy potential for biomass, making it more viable as a renewable energy source. The total C content in the tested samples ranged from 46.9% to 49.3%, with lavender waste exhibiting the highest values. Similar C content has been reported for mint waste (44.82-47.05%) (Maj et al., 2020), lavender (45.4-48.1%) (Chakyrova & Doseva, 2021), willow biomass (50.84%) (Szczukowski et al., 2015), and wood (49.80%) (Kajda-Szczesniak, 2013). Hydrogen content ranged from 3.8% (tansy waste) to 5.53% (common sage waste). Comparable H content has been observed in mint waste (5.54-5.76%) (Maj et al., 2020), lavender waste (5.8-6.77%) (Chakyrova and Doseva, 2021), willow biomass (5.86%) (Szczukowski et al., 2015), and wood (6.30%) (Kajda-Szczesniak, 2013). These values are also close to those of wheat, barley, flax, and timothy straw (6.1-6.4%). Oxygen content negatively affects the energy value. The O content of the tested biomass ranged from 37.81% to 41.00%, with no significant differences among the samples. These values are similar to those of wheat, barley, flax, and timothy straw (44.4-52.1%) but lower than those reported for mint waste (29.14-36.09%) (Maj et al., 2020) and lavender waste (37.8%) (Chakyrova & Doseva, 2021). According to Vassilev et al. (2010), the elemental composition of biomass is a key factor in estimating heating values, combustion air requirements, and the composition of flue gases. Knowledge of elemental composition also helps assess gaseous emissions from fuel combustion. From an environmental

perspective, N and S contribute to greenhouse gas emissions and are considered undesirable in biomass fuels. During combustion, N leads to NOx emissions, while S contributes to SOx emissions, which can cause particulate pollution, acid rain, and corrosion (Clarke & Preto, 2011). The N content in the tested biomass ranged from 0.178% (lavender waste) to 0.36% (tansy waste), remaining well below the 1.5-2% limit set by ISO 17225-6. Lower nitrogen levels improve the suitability of biomass for combustion. Comparable N values have been reported for mint waste (0.23-0.70%) (Maj et al., 2020) and lavender (1.3%) (Chakyrova & Doseva, 2021).

Sulfur content in biomass is generally low but still plays a role in emissions. The sulfur levels in the tested samples ranged from 0.0334% (lavender waste) to 0.0784% (yarrow waste), remaining well below the 0.2-0.3% standard limit. Comparable S content has been reported for lavender waste (0.1%) (Chakyrova & Doseva, 2021) and mint waste (0.0-0.19%) (Maj et al., 2020). Low S content minimizes the risk of releasing SO_2 during combustion, reducing environmental impact.

Table 2. Ultimate analysis of tested wastes

Waste	N, %	S, %	Cl, %	C, %	H, %	O, %
Lavender	0.178	0.0334	0.0220	49.3	5.40	37.81
Tansy	0.360	0.0738	0.0895	49.2	3.80	38.22
Thyme	0.240	0.0593	0.0358	48.5	3.80	39.16
Yarrow	0.250	0.0784	0.2121	46.9	4.60	39.38
Common sage	0.198	0.0500	0.0148	47.0	5.53	41.00
ISO 17225-6	1.5-2	0.2- 0.3	0.1-0.3	-	-	-
CEN/TS 14961-1 Harvest (July-Oct.)	1.3	0.1 (0.1-0.2)	0.5 (0.2-0.6)	46	5.7	40

Chlorine levels ranged from 0.0148% (common sage) to 0.2121% (yarrow), staying within the allowable limits for solid fuels. Lower chlorine content is beneficial as it reduces the potential for corrosion and harmful emissions.

Emission factors

Determining emission factors is essential for estimating the levels of pollutants emitted during fuel combustion. To determine these factors, it's crucial to understand the physicochemical characteristics of the waste being used. The emission factors for CO, CO_2, NOx, SO_2, and dust emissions from the plant waste studied are presented in Table 3, along with data for coal emissions for comparison.

Table 3. Emission factors (kg/mg) for analysed waste and coal

Waste	CO	CO_2	NOx	$S0_2$	Edust
Lavender	60.74	1487.07	0.63	0.067	9.20
Tansy	60.61	1484.05	1.27	0.148	10.55
Thyme	59.75	1462.94	0.85	0.119	10.41
Yarrow	57.78	1414.66	0.88	0.157	11.10
Common sage	57.90	1417.68	0.70	0.100	7.86
Hard coal	82.01	1969	4,09	5,2	23,57

No significant differences were observed in the carbon monoxide (CO) emission levels of the investigated plant wastes. The highest CO emission rate was observed for lavender (60.74 kg/mg), while the lowest was for yarrow (57.78 kg/mg), with a difference of up to 3%.

The Nox emissions ranged from 0.6289 kg/mg for lavender waste to 1.27 kg/mg for tansy waste.

The CO_2 emission factor was highest for tansy waste (1484.05 kg/mg) and lowest for yarrow waste (1414.66 kg/mg).

SO_2 emissions ranged from 0.067 kg/mg for lavender waste to 0.118 kg/mg for thyme waste. Dust emissions were highest for yarrow waste (11.10 kg/mg) and lowest for common sage (7.86 kg/mg).

The emission factors show that the tested wastes exhibit similar emission levels to those of mint waste (Maj et al., 2020), Eucalyptus globulus tree (Mateos et al., 2019), and larch needles (Maj, 2018). Overall, emissions are comparable to other waste types, and the SO_2 content in the wastes is minimal. CO and CO_2 emission factors are similar to those for mint (Maj et al., 2020), larch needles (Maj, 2018), and hazelnut husk and leaves (Maj, 2018; Borkowska et al., 2024).

Plant wastes have significantly lower NOx emissions compared to straw pellets, sunflower stalks, corn stalks, and wood pellets (Krugly et al., 2014), as well as Eucalyptus globulus (Mateos et al., 2019).

Wastes from lavender, thyme, and yarrow showed higher particulate emissions similar to those from mint waste (9.14-13.0%) (Maj et al., 2022), tree leaves (10.80%) (Maj, 2018), and hazelnut waste (10.95%) (Borkowska et al., 2024). The high dust emissions are associated with the high ash content of the tested wastes, so technological solutions to reduce these

emissions (e.g., using additional filters to capture emitted dust) should be considered.

The emission method for determining gas and dust emissions allows for an assessment of the environmental impact of plant waste when used for energy purposes, without requiring specialized analytical equipment. This method enables quick estimation of biofuel emissivity, which is often overlooked when assessing biomass suitability for energy.

Differences in emissions among the tested wastes may influence selection decisions, especially when considering environmental aspects and incineration efficiency. Based on the emission factors, common sage waste is characterized by low emissions. Higher emission factors for CO and CO_2 were found for lavender and tansy waste. Using common sage waste as a source of energy can contribute to reduction in GHG emissions.

Using waste from essential oil crops results in emission reductions compared to coal (Borycka et al., 2008). Emission levels decreased by 26-30% for CO, 24-28% for CO_2, 68-84% for NOx, 97-99% for SO_2, and 53-67% for dust, depending on the type of waste used. Therefore, utilizing these wastes as fuel provides real environmental benefits.

CONCLUSIONS

Significant differences were found between the plant wastes in terms of calorific value. Lavender waste (17.40 MJ/kg; 19.23 MJ/kg), tansy waste (18.16 MJ/kg; 19.78 MJ/kg), and thymewate (17.85 MJ/kg; 19.17 MJ/kg) showed higher lower and higher heating values, making them an excellent candidate for biofuel compared to yarrow waste (16.7 MJ/kg; 17.96 MJ/kg) and common sage (16.24 MJ/kg; 18.06 MJ/ kg).

The chemical composition of plant wastes affects their energy value and emission factors. The common sage waste is characterised by a higher moisture content (8.95%), which negatively affects the energy value of the waste.

The type of waste mainly influences the amount of emissions from waste incineration. Higher emissions of CO (60.61 and 60.76 kg/mg) and CO_2 (1484.05-1487.07 kg/mg) were found for tansy and lavender waste, NOx - for tansy waste (1.26 kg/mg), while for yarrow there are higher dust emissions (11.10 kg/mg).

When selecting suitable waste for energy production, it's essential to balance calorific value and emission factors. If energy efficiency is the priority, lavender, tansy, and thyme waste may be preferred. However, for sustainability and lower environmental impact, common sage waste could be the better choice. It's important to consider the specific context, including regulations and energy needs, when making a final decision.

ACKNOWLEDGEMENTS

This research work has been carried out in the framework of the National Science Program "Critical and Strategic Raw Materials for a Green Transition and Sustainable Development", approved by the Resolution of the Council of Ministers № 508/18.07.2024 and funded by the Ministry of Education and Science (MES) of Bulgaria.

REFERENCES

BDS EN ISO 16948 (2015). Solid biofuels. Determination of total content of carbon, hydrogen and nitrogen.

BDS EN ISO 18122 (2015). Solid biofuels. Determination of ash content.

BDS EN ISO 18123 (2015). Solid biofuels. Determination of the content of volatile matter.

BDS EN ISO 18125 (2017). Solid biofuels. Determination of calorific value.

BDS EN ISO 18134-3 (2015). Solid biofuels. Determination of moisture content. Oven dry method. Moisture in general analysis sample.

Borkowska, A., Klimek, K.E., Maj, G., Kapłan, M. (2024). Analysis of the Energy–Carbon Potential of the Pericarp Cover of Selected Hazelnut Varieties. *Energies*, 17, 3899.

Borycka, B. (2008). Commodity Study on Food and Energy Utilization of Rich-Food Waste of the Fruit and Vegetables Industry. Monograph; *Radom University of Technology: Radom*, Poland, 2008.

CEN/TS 14961 (2010). Biomass standards - Fuel specifications and classes.

Chakyrova, D., & Doseva, N. (2021). Analysis of the energy recovery possibilities of energy from lavender straws after a steam distillation process, IOP Conference Series: Materials Science and Engineering, 1032 012023

Chandra, P., & Sharma, V. (2019). Marketing information system and strategies for sustainable and competitive medicinal and aromatic plants trade. *Inf. Dev.*, 35, 806–818.

Clarke, S., & Preto, F. (2011). *Biomass Burn Characteristics*. Factsheet, ISSN 1989-712X.

Duce, C., Vecchio Ciprioti, S., Spepi, A., Bernazzani, L., & Tine, M.R. (2017). Vaporization kinetic study of lavender and sage essential oils.*J. Therm. Anal. Calorim.*, *130,* 595–604.

Giacometti, J., Bursac Kovacevic, D., Putnik, P., Gabric, D., Bilusic, T., Kresic, G., Stulic, V., Barba, F.J., Chemat, F., & Barbosa-Canovas, G. (2018). Extraction of bioactive compounds and essential oils from mediterranean herbs by conventional and green innovative techniques: *A review. Food Res. Int*., *113*, 245–262.

ISO 17225-6 (2014). Solid biofuels. Fuel specifications and classes. Part 6: Graded non-woody pellets.

Kajda-Szcześniak, M. (2013). Evaluation of the basic properties of the wood waste and wood-based wastes. *Arch. J. Waste Manag. Environ. Prot*., *15*, 2–10.

Kant, R., & Kumar, A. (2022). Review on essential oil extraction from aromatic and medicinal plants: Techniques, performance and economic analysis. *Sustain. Chem. Pharm*., *30*, 100829.

Kimming, M., Sundberg, C., Nordberg, A.A., Baky, A., Bernesson, S., & Hansson, P.A. (2015). Replacing fossil energy for organic milk production–potential biomass sources and greenhouse gas emission reductions. *g*, *106*, 400–407.

Krugly, E., Martuzevicius, D., Puida, E., Buinevicius, K., Stasiulaitiene, I., Radziuniene, I.; Minikauskas, A., & Kliucininkas, L. (2014). Characterization of gaseous-and particle-phase emissions from the combustion of biomass-residue-derived fuels in a small residential boiler. *Energy Fuel*, *28*, 5057–5066.

Lasek, J. A., Matuszek, K., Hrycko, P., & Piechaczek, M. (2018). Adaptation of hard coal with high sinterability for solid fuel boilers in residential heating systems. *Fuel*, *215*, 239-248.

Maj, G. (2018). Emission Factors and Energy Properties of Agro and Forest Biomass in aspect of sustainability of energy sector. *Energies*, 11, 1516.

Maj, G., Najda, A., Klimek, K., & Balant, S. (2020). Estimation of energy and emissions properties of waste from various species of mint in the herbal products industry. *Energies, 13*, 55.

Maj, G., Klimek, K., Kapłan, M., & Wrzesińska-Jędrusiak, E. (2022). Using wood-based waste from grapevine cultivation for energy purposes. *Energies*, *15*, 890.

Marcelino, S., Gaspar, P.D., & Paco, A. (2023). Sustainable waste management in the production of medicinal and aromatic plants - A systematic review. *Sustainability*, 15, 13333.

Mastellone, M.L. (2015). *Waste management and clean energy production from municipal solid waste*. Nova Science Publishers, Inc. New York, NY, USA, 2015.

Mateos, E., & Ormaetxea, L. (2019). Sustainable renewable energy by means of using residual forest biomass. *Energies*, *12*, 13.

Obernberger, I., Brunner, T., Mandl, C., Kerschbaum, M., & Svetlik, T. (2017). Strategies and technologies towards zero emission biomass combustion by primary measures. *Energy Procedia*, 120, 681–688.

Pastorello, C., Caserini, S., Galante, S., Dilara, P., & Galletti, F. (2011). Importance of activity data for improving the residential wood combustion emission inventory at regional level. *Atmospheric Environment, 45*(17), 2869-2876.

Pulidori, E., Gonzalez-Rivera, J., Pelosi, C., Ferrari, C., Bernazzani, L., Bramanti, E., Tine, M.R., & Duce, C. (2023). Thermochemical evaluation of different waste biomasses (citrus peels, aromatic herbs, and poultry feathers) towards their use for energy production. *Thermo*, *3*, 66–75.

Szczukowski, S., Tworkowski, J., Stolarski, M., & Krzyżaniak, M. (2015). The energy efficiency of willow biomass production in Poland - A comparative study. *Pap. Glob. Chang*. IGBP, 22, 123–130.

Vassilev, S.V., Baxter, D., Andersen, L.K., & Vassileva, C.G. (2010). An overview of the chemical composition of biomass. *Fuel,* 89, 913–933.

Wei, L.S., Goh, K.W., Abdul Hamid, N.K., Abdul Kari, Z., Wee, W., & Van Doan, H. (2022). A mini-review on co-supplementation of probiotics and medicinal herbs: Application in aquaculture. *Front. Vet. Sci*., *9,* 1–10.

Zając, G., Szyszlak-Bargłowicz, J., & Słowik, T. (2019). Comparison and assessment of emission factors for toxic exhaust components during combustion of biomass fuels, *RocznikOchronaŚrodowiska*, *21*, 378-394

Scientific Papers. Series E. Land Reclamation, Earth Observation & Surveying, Environmental Engineering. Vol. XIV, 2025
Print ISSN 2285-6064, CD-ROM ISSN 2285-6072, Online ISSN 2393-5138, ISSN-L 2285-6064

DETECTION AND MONITORING OF HYDROCARBON POLLUTION SOURCES IN THE PETROMIDIA REFINERY AREA

Sorin ANGHEL

National Institute for Research and Development on Marine Geology and Geoecology -GeoEcoMar, 23-25 Dimitrie Onciul, District 2, Bucharest, Romania

Corresponding author email: soanghel@geoecomar.ro

Abstract

The detection and spatiotemporal monitoring of hydrocarbon contamination in the geological environment (soil, geological formations, and groundwater) represent the main objective of the study, conducted during the period of 2023-2024. The study focused on areas adjacent to the Petromidia refinery with industrial activity exceeding five decades, located in the vicinity of the city of Navodari. Both `classic` geophysical techniques (VES - Vertical Electrical Sounding, IP - Induced Polarization) and recently introduced techniques on a global scale (GPR - Ground Penetrating Radar) were employed. Electrical and electromagnetic measurements were complemented by magnetic investigations, drilling works, and geological and hydrogeological observations. The most effective geophysical measurements, both for detecting and monitoring underground hydrocarbon contamination, were the geoelectrical resistivity ones, due to the significant contrast in electrical resistivity between the highly resistive pollutant substances and the affected geological environment, consisting of rocks and fluids with much higher electrical conductivity. The geological and hydrogeological data from shallow boreholes were used for the correct interpretation of geophysical anomalies, while the results of magnetic measurements indicated the routes of buried pipelines, and potential sources of pollution.

Key words*: electrometry, hydrocarbon, pollution, soil.*

INTRODUCTION

Contamination with hydrocarbons of the land and groundwater in the vicinity of refineries, fuel depots, oil wells, and even transportation pipelines, constitutes one of the significant environmental protection issues (Onutu & Tita, 2018). The localization and determination of the spatial-temporal distribution of contamination currently rely exclusively on the use of direct methods of biochemical analysis of soil and water samples taken from the surface or from boreholes.

The information obtained in this way is point-based and therefore cannot provide an overall picture of land and groundwater contamination. Analyses are costly and require an extended period for observations to be made.

The integration of point-based information into a three-dimensional spatial-temporal image of areas contaminated with hydrocarbons and residual waters becomes possible through the appropriate use of geophysical methods, supported by hydrogeological information.

The main objective of the geophysical investigation was to develop a geophysical monitoring of hydrocarbon contamination resulting from refining, storage, and transportation activities of petroleum products in the vicinity of refinery located in the area of the city of Navodari.

MATERIALS AND METHODS

1. Physical-geographical characterization

The objective under analysis is located on the coastal strip separating the Black Sea from the Gargalac (Corbu) and Tașaul lakes, an integral part of the Central Dobrogea Platform.

The relief generally exhibits the characteristics of a high hilly plain, with wide valleys and terraces, reaching heights of up to 100 meters.

The average relief energy is 50 meters. Genetically, the area represents a paneplain (nearly flat land surface resulting from long - continental erosion and denudation) of the Caledonian mountains (Green Shale Formation), covered in the Quaternary by a loess cover.

Beneath this cover of aeolian deposits, patches of eroded Jurassic limestone emerge, featuring karstic landforms such as caves and gorges.

Towards the coastal zone, the relief is lower, featuring lagoons, fluvio-marine estuaries, and sandy coastal barriers.
The climate is typically continental, with the sea exerting its influence over a coastal strip 10-15 kilometres wide. The basin of Lake Taşaul is situated on the contact zone between Jurassic limestone and the Proterozoic substrate of the Green Shale Formation. Along this stratigraphic contact, the course of the Casimcea River has insinuated itself, more active during cold, glacial periods of the Quaternary (Chitea, 2011). From a geomorphological perspective, the studied objective is situated on the "complex barrier beach" (barrier beach) of Taşaul - Corbu, which extends southward to the Mamaia complex barrier beach.

2. Aspects of historical hydrocarbon contamination in the Petromidia refinery area

The pollution phenomenon with petroleum products from industrial areas related to the extraction, transportation, and processing of oil in Romania, noted in the last 40 years, especially through its harmful effects on the quality of some drinking and surface water sources, as well as on the productivity of soil in some agricultural lands, has been the subject of special research initiated in the 1960s.
These studies were prioritized through hydrogeological and geophysical investigations conducted in the vicinity of refineries and fuel transportation pipelines by ISPIF Bucharest and the University of Bucharest starting from 1975.
The contamination with hydrocarbons of land, groundwater, and surface water near major pollution sources (refineries, fuel depots, oil and fuel transportation pipelines, oil extraction rigs, petroleum residue ponds, etc.) represents one of the largest and most challenging environmental protection issues in Romania (Paraschiv, 1979).

The placement near Navodari city of the country's most important sources of petroleum pollution (the Petromidia refinery, petroleum and fuel depots, and petroleum product transportation pipelines) makes this area the subject of numerous research endeavours and the primary motivation for selecting this perimeter for implementing hydro-geophysical research (Figure 1).



Figure 1. Petromidia refinery

The pollution sources in the Petromidia refinery area are classified as follows:
- systematic losses of petroleum products in the technological processes of extraction, transportation, and storage;
- accidental losses of petroleum products in the transportation and refining processes (explosions, fires, pipeline corrosion, earthquakes, technical accidents, pipeline breakages for fuel theft);
- slow leaks of products through cracks in pipelines, tanks, ponds, basins, sewers;
- losses of petroleum products during long-distance transportation of pollutants through watercourses, rainwater, and wind.

The migration of hydrocarbons, immiscible with water, occurs in two ways:
a) In unsaturated conditions, under the influence of gravity and meteoric waters (within refinery);
b) In saturated conditions, at the surface of groundwater in the form of a laminar contamination plume, laterally advancing in the direction of groundwater flow (outside refinery, in the direction of groundwater flow).
An example of contamination in saturated conditions at the level of the groundwater table is represented by the area southeast of the Petrobrazi refinery, where the boundary of the spread of groundwater contamination with petroleum products covered an area of approximately 11 km^2 in January 1981, separated into two distinct sectors according to the degree of pollution:
A central sector, affected by intense pollution, with significant concentrations of pollutants in the form of a lens-shaped layer above the groundwater, ranging from 1 cm to 5 m in thickness, predominantly spreading within the refinery premises and extending south-eastward

to approximately 2.5 km away; A sector with reduced pollution, with thin films, iridescence, or a specific petroleum smell in the groundwater, with the boundary located approximately 3.5 km from the refinery. In the Petromidia refinery case, the depths of the petroleum layer were frequently recorded at values of 2-6 m and are variable over time, depending on the vertical oscillation of local groundwater levels. The general propagation direction of the petroleum pollution front is similar to that of the predominant groundwater flow (NW - SE), but the advancement speed differs from that of water, being slower in the case of petroleum pollutants due to the different physical-mechanical characteristics (higher viscosity and adhesion of petroleum products) and the specific horizontal and vertical migration mechanism of petroleum products (depending on the action of capillary forces in the porous medium).

3. Geoelectric detection of hydrocarbon contamination

The use of various geoelectrical techniques for detecting underground hydrocarbon pollution is an efficient and non-invasive method for soil investigation in search of contamination. Among these techniques are VES (Vertical Electrical Sounding), IP (Induced Polarization), ERT (Electrical Resistivity Tomography), and GPR (Ground Penetrating Radar). Measurements of VES (Vertical Electrical Sounding) conducted with instruments such as AGI MINISTING (Figure 2) is extremely useful in identifying zones of hydrocarbon contamination.

VES involves measuring the electrical resistance of the soil in a vertical manner, allowing for the determination of the vertical distribution of the electrical properties of the subsurface. These techniques are particularly effective when placed on profiles that traverse areas of interest, such as refineries or other potential sources of hydrocarbon pollution.

By combining data obtained from various geoelectrical techniques, a more comprehensive picture of the distribution and characteristics of subsurface contamination can be obtained, which can better guide strategies for remediation and environmental monitoring (Greenhouse, 1993).

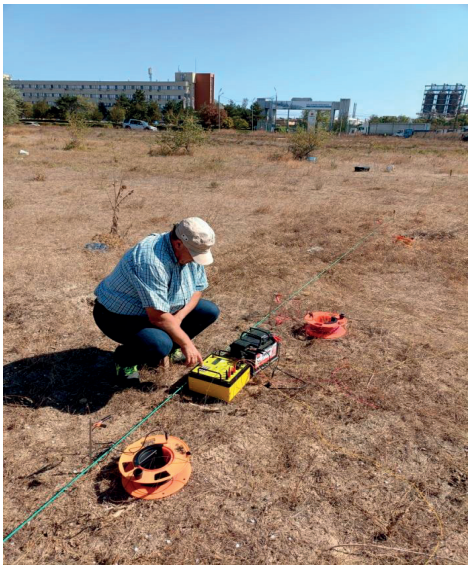


Figure 2. Geoelectric data acquisition using Ministing system from AGI

The observation data has been processed and interpreted using specialized software such as Res_2DInv, EarthImager, as well as programs developed by the research team members. Analysing the curves of the vertical electrical soundings conducted in the area of the four refineries, it was observed that from a geoelectric standpoint, two main modes of electrical resistivity distribution in depth can be distinguished in the investigated region (Figure 3):

- VES curves representative of type H (for example-yellow colour) in the northeastern area, where the Petromidia refinery is located;
- VES curves representative of type K (for example-blue colour) in the southwestern area, where the Petromidia refinery is located.

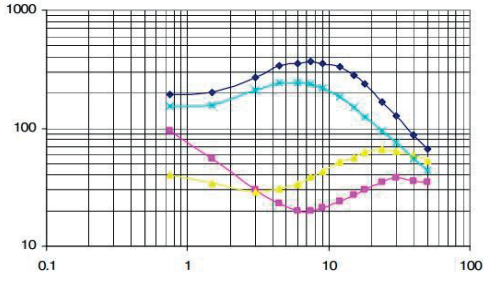


Figure 3. Representative VES curves

The main difference between the two separately identified sectors, with distinct variations in electrical resistivity, lies in the presence of a clay layer electrically conductive at the upper part of the geological structure in the northeastern part of investigated area (type H VES curves), a layer absent in the south-western part of investigated area (type K VES curves). The mentioned clay layer, intercepted in shallow boreholes, largely protects the northeastern area, with hydrocarbon contamination significantly lower compared to the southwestern area. The rapid increase in electrical resistivity in the electrical soundings conducted in the investigated area is due to the presence at shallow depths (1.5-4 m) of the resistive layer containing the pollutant film and geological formations impregnated with petroleum products. The processing and quantitative interpretation of VES data have resulted in obtaining resistivity sections down to a depth of 4 meters along the profiles in the investigated areas. The outlined anomalies of maximum resistivity (Figure 4 - red colour) illustrate the presence of hydrocarbon contamination plumes at depth.

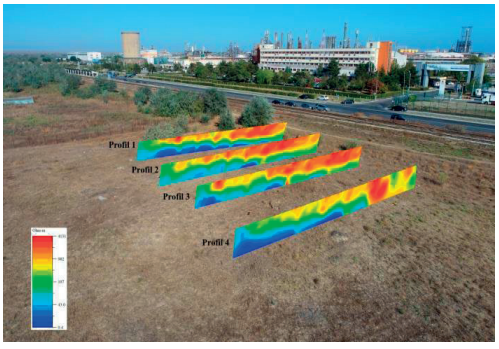


Figure 4. Apparent resistivity sections - Perimeter I

Figure 4 shows the distribution of electrical resistivity along profiles I, II, III and IV (Perimeter I), which traverses the north-south direction of the pollution zone associated with the Petromidia refinery. The elongated anomaly of maximum resistivity located at depths of 1.5-3 meters is interpreted as being due to the presence of the hydrocarbon contamination plume located at the aquifer's surface. Interruptions or variations in the thickness of the resistive layer are interpreted as being caused by variations in the compaction of the contaminated gravel (Berkowitz, 2008).

The thickness of the resistive layer (Figure 4– red colour), greater than the contaminant film at the aquifer's surface, also includes that of the gravel impregnated with hydrocarbons during seasonal variations in the hydrostatic level (historical contamination). The interpretation of these resistivity anomalies was supported by direct information from recently executed hydrogeological boreholes and from artisanal excavations present in the immediate vicinity of the investigated perimeters (McNeill, 1980).

In order to obtain detailed information on the distribution of resistivity in depth in areas significant for understanding the relationships between the contaminant and the polluted geological environment, VES measurements were conducted on Perimeter II (Figure 5).

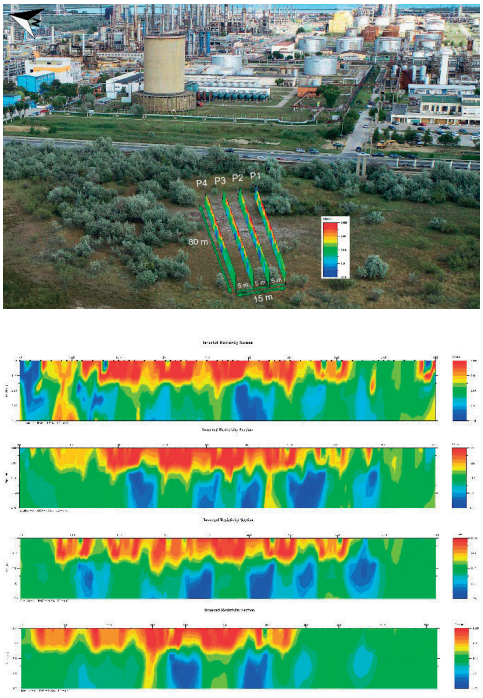


Figure 5. Apparent resistivity sections-Perimeter II

The electrical resistivity section obtained down to a depth of 4 meters illustrates details of anomalies of maximum resistivity associated with the hydrocarbon contamination plume on each profile. Variations in the intensity of resistivity anomalies can be interpreted as

variations in contaminant concentration, while interruptions in the major resistivity maximum anomaly can be attributed to the effects of local tectonic accidents.

4. Georadar detection of hydrocarbon contamination

The georadar investigation at the Petromidia refinery in the southeastern sector revealed some interesting findings. The underground limit interpreted as the water table suggests the presence of groundwater at that depth. Additionally, the zones of weak electromagnetic signal could indicate the presence of a hydrocarbon plume within the upper aquifer. This suggests the possibility of hydrocarbon contamination in the groundwater, which is a concern for environmental and remediation efforts. Further investigation and monitoring would likely be necessary to assess the extent of the contamination and develop appropriate mitigation measures (Fuente, 2021).

In the Petromidia refinery area, 10 longitudinal profiles and 6 transverse profiles were continuously recorded using a 100 MHz antenna (Figure 6).

The analysis of the recordings on the longitudinal profiles shows the existence of a well-defined geophysical boundary located at 0.75 m (Figure 7). The detected interface is practically continuous along the entire length of the measurement profiles. Correlating these observations with archive data obtained from previous boreholes, the following values for velocity and permittivity are obtained:

- a velocity of 6.5-7.6 cm/ns for the medium above the first georadar limit, considering this interface as the water level;
- the permittivity varies in the range of 15.58-21.30 (Kapicka, 1997).

Considering that the permittivity of a sandy medium saturated with water is around 25, and the reflection sign is negative, we can conclude that the interface encountered at 0.75 m (Figure 7) is due to the level of petroleum product. Electric permittivity (or dielectric constant) is a quantity, denoted by ε, which indicates the resistance to electric polarization of a dielectric material (Tezkan, 2005).

In practice, a dimensionless quantity expressed by the ratio of the permittivity of a medium to that of vacuum is used. The groundwater level is located at depths of 1.5-2 m. Below the first detected georadar limit, the value of electromagnetic wave velocity decreases due to the presence of water in the propagation medium. By decreasing the velocity, the travel time of the wave increases.

Areas where reflection coefficients have high values and do not allow the delimitation of a reference radar horizon have been interpreted as being due to hydrocarbon intrusions (yellow zones - Figure 8).



Figure 6. Georadar acquisition data with 100MHz antenna

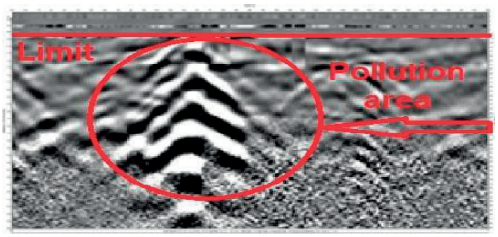


Figure 7. Georadar data (radargram) in the Petromidia refinery area

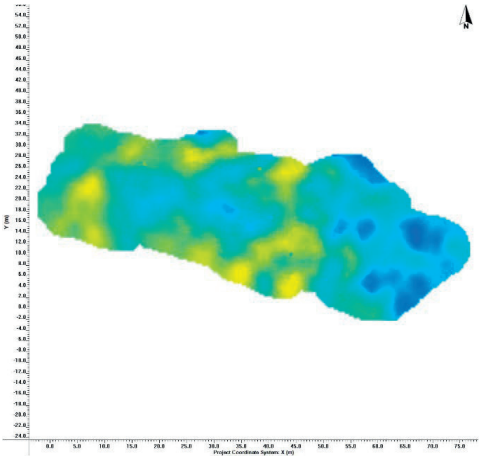


Figure 8. Georadar section

RESULTS AND DISCUSSIONS

Geophysical monitoring of the temporal and spatial evolution of hydrocarbon contamination plumes has been studied in the Petromidia refinery area. The hydrocarbon contamination plume, resulting from the temporal overlay of historical contamination with current contamination, is largely influenced by the regional dynamics of the aquifer. Geoelectrical VES measurements conducted for monitoring has investigated the central part of perimeter I and II.

The results of monitoring measurements were analysed in the form of resistivity pseudo sections to avoid disturbances caused by quantitative interpretation programs. The observed changes in resistivity during monitoring, considered for interpretation, are due to variations in moisture in surface layers (soil, paleosol, loess), fluctuations in the water table level, and some quantities of pollutants recently introduced into the geological environment in the refinery area (Figures 3, 4 and 5). The fragmentation of the major resistivity maximum anomaly is due to active processes of surface water infiltration along a fault system, which affects the geological structure and the soil layer (Figures 3, 4 and 5).

The results obtained from the georadar investigation were presented in the form of radargrams or depth sections, which can highlight geological structures at shallow depths, including the localization of tectonic features with local significance, as well as the delineation between hydrocarbon-saturated and unsaturated zones (Manescu, 1994).

CONCLUSIONS

The results of geophysical investigations dedicated to the detection and monitoring of hydrocarbon contamination plumes near the Petromidia refinery have shown that VES geoelectrical resistivity measurements are the most effective. Elongated anomalies of maximum electrical resistivity, located at depths where the first aquifer is localized, illustrate the presence of contamination plumes due to the hydrocarbon film and the geological environment impregnated with contaminants during seasonal variations in the water table level. Interruptions in the maximum resistivity anomalies are due to variations in the compaction of gravel or local tectonic accidents. The geoelectric monitoring of hydrocarbon contamination plumes was conducted using vertical electrical soundings, through the sequential analysis of resistivity pseudo sections. The geoelectric effect of hydrocarbon contamination is evident even under significantly different seasonal climatic variations, with the maximum resistivity anomaly determined by the presence of hydrocarbons being well delineated through repeated geophysical measurements.

This resilience in detection is particularly significant in delineating the maximum resistivity anomaly associated with subsurface hydrocarbon contamination (Allred, 2010). Repeated geophysical measurements serve as a reliable tool in accurately mapping out these anomalies, aiding in the assessment and management of hydrocarbon contamination in diverse environmental conditions. It's interesting to hear that geophysical investigations near the Petromidia refinery have identified VES (Vertical Electrical Sounding) geoelectrical resistivity measurements as the most effective method for detecting and monitoring hydrocarbon contamination plumes. Geophysical methods play a crucial role in environmental studies, especially when dealing with issues such as pollution and contamination. VES involves measuring the electrical resistivity of subsurface materials at different depths using a vertical electrode array. In the context of hydrocarbon contamination, variations in resistivity can be indicative of changes in the subsurface caused by the presence of hydrocarbons (Vafidis et al., 2014). Here are some reasons why VES geoelectrical resistivity measurements might be effective in this scenario:

Contrast in Resistivity - hydrocarbons generally have a lower electrical resistivity than the surrounding soil or rock. This contrast allows for the detection of hydrocarbon plumes in the subsurface.

Depth Profiling - VES provides information at different depths, allowing for a vertical profile of subsurface resistivity. This can help in understanding the depth and extent of the contamination plumes.

Spatial Resolution - VES can offer good spatial resolution, helping to map the lateral extent of contamination. This information is crucial for effective remediation strategies.
Cost-Effectiveness - compared to some other geophysical methods, VES can be relatively cost-effective, making it a practical choice for large-scale monitoring projects.
Non-Invasive Nature - geoelectrical methods are non-invasive, meaning they don't require drilling or excavation. This minimizes disturbance to the site and provides a more environmentally friendly approach.
Real-Time Monitoring - VES measurements can be conducted periodically, allowing for real-time monitoring of changes in subsurface resistivity. This is important for tracking the dynamic nature of contamination plumes.
It's essential to note that the effectiveness of geophysical methods can vary based on site-specific conditions. Additionally, integrating multiple geophysical techniques can provide a more comprehensive understanding of subsurface conditions.
If VES has proven to be the most effective in this case, it demonstrates the importance of selecting the right geophysical tools for the specific challenges posed by hydrocarbon contamination near the Petromidia refinery. The GPR data was obtained using a NOGGIN system with 100, 250, and 500 MHz antennas. The 100 and 250 MHz antennas provided the best results in terms of spatial resolution and depth, while the shallow groundwater level provided excellent conditions for GPR.

ACKNOWLEDGEMENTS

This research work was carried out with the support of Ministry of Innovation and Digitalization, and also was financed from CORE PROGRAM PN IV - Project PN 23300403.

REFERENCES

Allred, B.J. (2010). Agricultural Geophysics: Past, Present and Future. *23rd EEGS Symposium on the Application of Geophysics to Engineering and Environmental Problems,* 10.3997/2214-4609-pdb.175.SAGEEP023

Berkowitz, I., Yaron, B. (2008). *Contaminant Geochemistry. Interactions and Transport in the Subsurface Environment*, Springer-Verlag, Berlin, Heidelberg, ISBN 978-3-642-54776-8, DOI 10.1007/978-3-642-54777-5

Chitea, F., Georgescu P., Ioane D. (2011). Geophysical detection of marine intrusions in Black Sea coastal areas (Romania) using VES and ERT data. *Geo-Eco-Marina, 17*(17), 95-102, 10.5281/zenodo.56903

Fuente, J.V. (2021), Detection and Delineating of Hydrocarbon Contaminants by Using Time and Frequency Analysis of Ground Penetrating Radar, *Journal of Geoscience and Environment Protection, 9*(12.), 10.4236/gep.2021.912003

Greenhouse, J., Brewster, M., Schnider,G., Redman D., Annan,P., Olhoeft, G., Lucius, J., Sander, K., Mazzella A. (1993). Geophysics and solvents: The Borden experiment, *The Leading Edge, 12*(4), https://doi.org/10.1190/1.1436946

Kapicka, A., Petrovsky, E., Jordanova, N. (1997), Comparison of in situ field measurements of soil magnetic susceptibility with laboratory data. *Studia Geoph. Geod., 41*, 391–395, https://doi.org/10.1023/A:1023363502016

Manescu, M., Bica, I., Stan, I. (1994). La pollution d'eau soutterraine avec des produits petroliers dans la zone de Ploiesti, *Proceedings of the International Hydrogeological* Symposium, Bucharest University Press, pp. 364–388.

McNeill, J.D. (1980). Electromagnetic terrain conductivity measurement at low induction numbers. *Tech. Note TN-6, Geonics Ltd., Mississauga.*

Onutu, I. & Tita, M. (2018). Soil contamination with petroleum compounds and heavy metals - case study. *Scientific Papers. Series E. Land Reclamation, Earth Observation & Surveying, Environmental Engineering, VII*, 140-145, Print ISSN 2285-6064.

Paraschiv, D. (1979). *Romanian oil and gas fields, Institute of Geology and Geophysics*. Technical and Economical Studies, 13, pp. 382, Editor, Institute of Geology and Geophysics, ISSN 0557-4536.

Tezkan, B., Georgescu, P., Fauzi, U. (2005). Radiomagnetotelluric survey on an oil-contaminated area near the Brazi refinery, Romania. *Geophysical Prospecting, 53*, 311-323, https://doi.org/10.1111/j.1365-2478.2005.00475.x

Vafidis, A., Soupios, P., Economou, N., Hamdan, H., Andronikidis, N., Kritikakis, G., Panagopoulos, G., Manoutsoglou, E., Steiakakis, M., Candansayar, E., Schafmeister, M. (2014). Seawater intrusion imaging at Tybaki, Crete, using geophysical data and joint inversion of electrical and seismic data. *First Break Journal, 32*(8), 107–114, https://doi.org/10.3997/1365-2397.32.8.76970

Scientific Papers. Series E. Land Reclamation, Earth Observation & Surveying, Environmental Engineering. Vol. XIV, 2025
Print ISSN 2285-6064, CD-ROM ISSN 2285-6072, Online ISSN 2393-5138, ISSN-L 2285-6064

INVESTIGATING CURRENTS, FLOW VELOCITIES, AND RIVERBED MORPHOLOGY - AN ADCP-CENTRIC APPROACH TO UNDERSTANDING HYDRODYNAMICS AND EROSION PATTERNS

Maxim ARSENI[1, 2], Adrian ROȘU[1, 2], Nina-Nicoleta LAZĂR[2], Mădălina CĂLMUC[2], Mihail VESTE[3], Cătălina ITICESCU[1, 2]

[1]"Dunărea de Jos" University of Galați, 47 Domnească Street, 800201, Galați, Romania
[2]REXDAN Research Infrastructure, "Dunărea de Jos" University of Galaţi,
98 George Coșbuc Blvd, 800223, Galați, Romania
[3]SC PRINTDREAM REAL S.R.L., 15 Cetățianu Ioan Street, 800264, Galați, Romania

Corresponding author email: maxim.arseni@ugal.ro

Abstract

The sediment movement on a river plays a crucial role in safe navigation and economic activities on navigable channels. Environmental changes in time are given by the morphological characteristics of the riverbed during seasonal water variation on the Danube River. This study presents a comprehensive assessment of the Danube River`s velocity and current characteristics based on Acoustic Doppler Current Profiler measurements. The correlation between flow velocities and depths helps to understand the factors that influence sediment patterns and provides insights into the sustainable management of the river system. The study was conducted along a 71-kilometer length of the Sulina Branch from the Danube River, where ADCP measurements were collected at multiple locations and over periods. The data collected included water depth, flow velocity, and current direction. By clustering the column depth cell velocities it revealed significant spatial and temporal variations in the velocity and current patterns, influenced by factors such as river morphology, discharge, and seasonal changes.

Key words*: ADCP survey, currents direction, Danube discharge, hydro-morphology, water flow velocities.*

INTRODUCTION

The Danube River divides into 2 branches at Patlageanca Village. Chilia - the first branch, flows in the North-East direction. The second one flows to the East, and after at, the Tulcea city is divided into two other branches, Sulina respectively Sfantu Gheorghe (Figure 1).

The Sulina branch is the main waterway of Romania, for the ships with a maximum 7.01 m ± 10-15 cm draught, from the Black Sea up to Braila city (Cociasu et al., 1996; Giosan et al., 2006; Kuhl, 1891).

The rectification of the Sulina arm was carried out during the 1868-1902 period, shortened this branch by about 25% (83.8 km before the cut-offs and only 69 km today) (Cociasu et al., 1996; Giosan et al., 2006; Kuhl, 1891; Panin & Jipa, 1998).

This cut-off program induced a redistribution of water and sediment discharge among the delta distributaries.

The Sulina discharge increased from 7-9% up to 16-17% in 1921 and to about 18-20% of the total Danube discharge at present (Panin & Jipa, 1998).

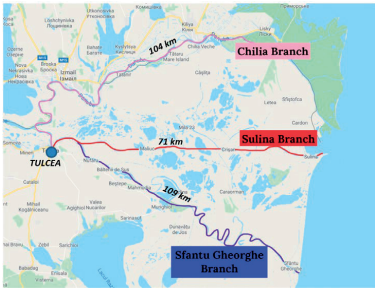


Figure 1. The main branches of the Danube River

The Sulina Channel, one of the branches of the Danube River, has specific dimensions: a length of 71 kilometers, a maximum width of 50 meters, a maximum depth of 18 meters, and a minimum depth of 7.32 meters (Banescu et al., 2020a). This arm of the Danube has been regulated and channelized, allowing for maritime navigation of seagoing vessels with a draft of up to 7 meters. The maintenance and

management of this waterway fall under the responsibility of the Lower Danube River Administration (AFDJ), based in Galati, the largest city along the Romanian stretch of the Danube. It is noteworthy that the Sulina Channel, also referred to as the Sulina arm, is the shortest and most direct branch of the Danube, flowing directly into the Black Sea near the town of Sulina. Sulina is the easternmost settlement within the European Community.

The Sulina branch carries a significant amount of sediment, particularly during flood events, which can lead to the deposition and accumulation of sediments Danube Delta. Sediment transport and deposition in the Sulina Channel can affect water depths and navigation channels, necessitating periodic dredging operations to maintain the required depths for maritime traffic. The management of sediment transport and dredging activities in the Sulina Channel is crucial for maintaining navigation and preventing potential blockages or shallow areas that could hinder vessel movement. Monitoring and modeling of sediment transport patterns, as well as implementing appropriate sediment management strategies, are essential for the sustainable management of the Sulina Channel and the Danube Delta region.

At the same time, the sediment deposition influences the stock of heavy metals on the Danube River (Popa et al., 2018; Teodorof et al., 2021). According to Lazăr (2024), the heavy metals from sediments and water in the Danube River are ingested directly by biota, especially in the *Alosa immaculata* fish. According to the study conducted by Burada (2015), hydro-morphological parameters are important for identifying the areas where the speed of flow currents decreases because sedimentation increases in these areas, and with it the accumulation of pollutants (heavy metals) also occurs. This suggests that the morphology of the riverbed and the hydrodynamics of the river are key factors in identifying areas vulnerable to contamination, and can be achieved by accurate ADCP measurements.

The present study aims to investigate the relationship between hydro-morphological parameters surveyed on the Sulina branch from the Danube River. The physical characteristics and dynamic parameters help to understand the patterns of erosion, underwater forms, and turbulence in the study area.

STUDY AREA

The study area is focused on the Sulina branch of the Danube River. There are 6 points of observation. Each of them is located downstream of Partizani, Maliuc, Gorgova, Crisan, and Sulina villages (Figure 2), and one at an intermediate point between Crisan and Sulina.

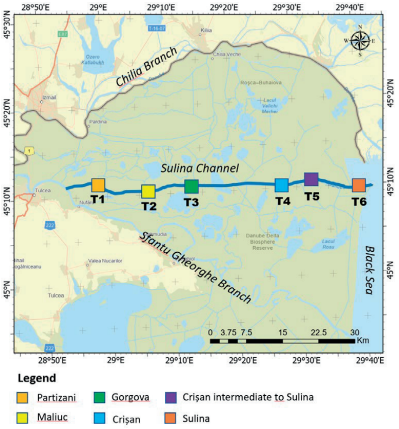


Figure 2. Study area map located on the Sulina navigable channel from the Danube Delta area

The points labeled T1 through T6 mark specific cross-sections where Acoustic Doppler Current Profiler (ADCP) data are collected. These six cross-sections are conveniently located along one of the main tributaries of the Danube River, the Sulina arm.

The corresponding ADCP cross-sections measured in July 2023 and August 2023 from this transects are crucial to understanding how riverine discharge, velocity profiles, and sediment deposition are influenced across the river continuum, particularly in the tidal junction near the mouth of the river (Banescu et al., 2020b; Pomázi & Baranya, 2025).

MATERIALS AND METHODS

To better understand the flow dynamics of the Sulina channel, which is an arm supposed to hydrotechnical development works, it is important to measure the hydro-morphological

parameters in different hydrological periods of the channel.

Thus, we can assess whether sediments are transported from one section to another. Along with the transport of sediments, the minor channel bed is also modified, but also their deposition by favouring the increase in the surface area of the Danube Delta.

To obtain a detailed picture of the hydro-morphological parameters on the Sulina branch, several measurement campaigns were carried out. These aimed to evaluate the spatial and temporal variability of current speeds and flows, essential information for determining the sediment transport regime. Within these campaigns, ADCP (Acoustic Doppler Current Profiler) technology was used, a modern instrument for measuring water current speeds in three dimensions, at different depths (Figure 3). The device used was the RiverSurveyor M9 model produced by SonTek, a high-performance equipment designed specifically for river measurements.

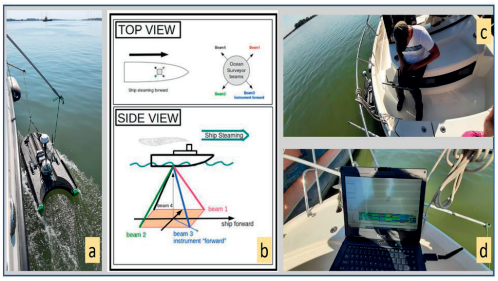


Figure 3. The Sontek M9 ADCP work principle: a - mounting on a moving boat; b - beam spread principle (Deogade et al., 2023); c, d - main setting applying and real-time display data

The ADCP works based on the Doppler effect: it emits sound waves in the water, which, when reflected from suspended particles, change their frequency according to the relative motion of these particles. By analyzing this frequency change, the instrument can calculate the speed of the current in different layers of the water column, according to equation 1 (Liu et al., 2024).

$$v = (\Delta f \times c) / (2 \times f_0 \times cos(\theta)) \quad (1)$$

where:

- v represents particle (water current) velocity in the direction of the sound beam [m/s];
- Δf represents Doppler frequency difference (f_r - f_0), i.e. the difference between speed of sound in water (approximately 1500 m/s);
- c represents frequency of the signal emitted by the ADCP [Hz];
- θ - angle between the acoustic beam and the vertical direction.

In addition to the basic hydromorphological parameters measured, it is important to determine the energy in each flow section. The calculation of the current energy (or kinetic energy of flowing water) in a section measured with an ADCP is based on the application of fluid mechanics principles, in particular the formula for the kinetic energy of a volume of water moving at a given speed. Equation 2 represents the calculation of the energy flow on a river cross-section measured with ADCP equipment (Guseva et al., 2021).

$$E = \frac{1}{2} \cdot \rho \cdot Q \cdot v^2 \quad (2)$$

where:

- E represents current energy (mechanical power) [W – watts, i.e. J/s];
- ρ represents water density [kg/m³] (usually ≈ 1000 kg/m³ for fresh water);
- Q represents water volume flow or disgharge [m³/s], obtained directly from ADCP data;
- v represents average current velocity [m/s], measured by ADCP.

RESULTS AND DISCUSSIONS

The monitoring of sediment transport comprises suspended sediments, a well as bedload. To understand, to assess, and to give potential solutions for sediment-related problems in the Danube River, especially on the Sulina Branch, the amount of transported sediments, varying both in time and space, has to be known. For this purpose, ADCP cross-sections are measured during two different campaigns, in July and August 2023. The results of ADCP cross-sections at T1 to T6 monitoring points are represented in Figure 4.

The ADCP measurement from both survey campaigns shows a well-distributed water velocity in the middle of the cross-section. The water velocity decreases near the left and right banks in all cases.

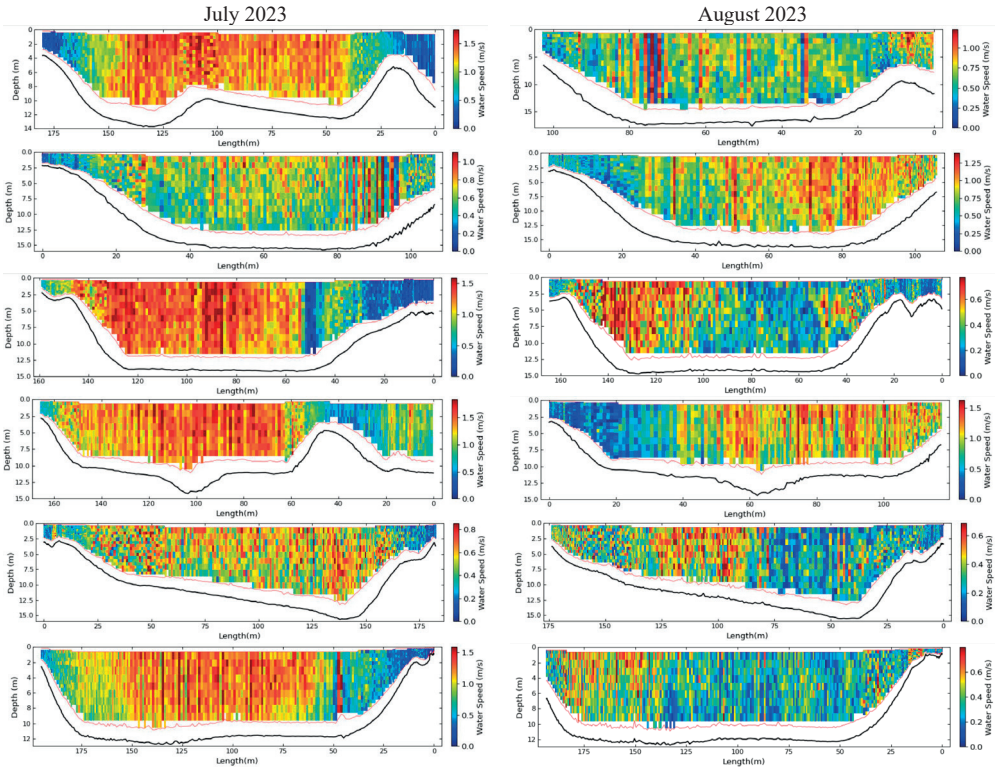


Figure 4. The ADCP velocity representation on the T1 to T6 cross-section

The maximum of 1.13 m/s water velocity was recorded at T1 section in July 2023, and 0.988 m/s at T2 section in the August campaign.

Figures 5 and 6 highlight a vector representation of the flow currents in the cross-sections T1-T6. The orientation or angle of inclination of the black vectors indicates the flow currents' direction, and the length of the vectors shows the intensity of the flow currents.

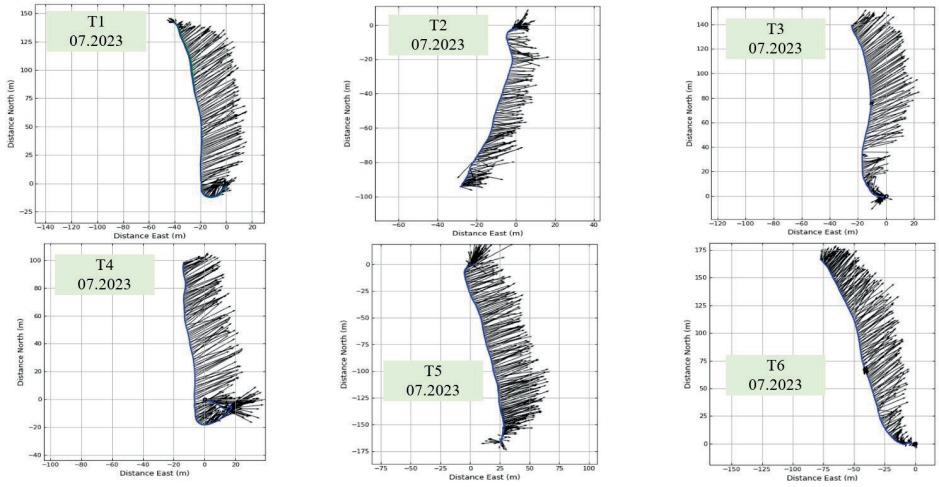


Figure 5. Comparison of flow patterns, directions, and intensities of currents for the July survey across T1-T6 transects

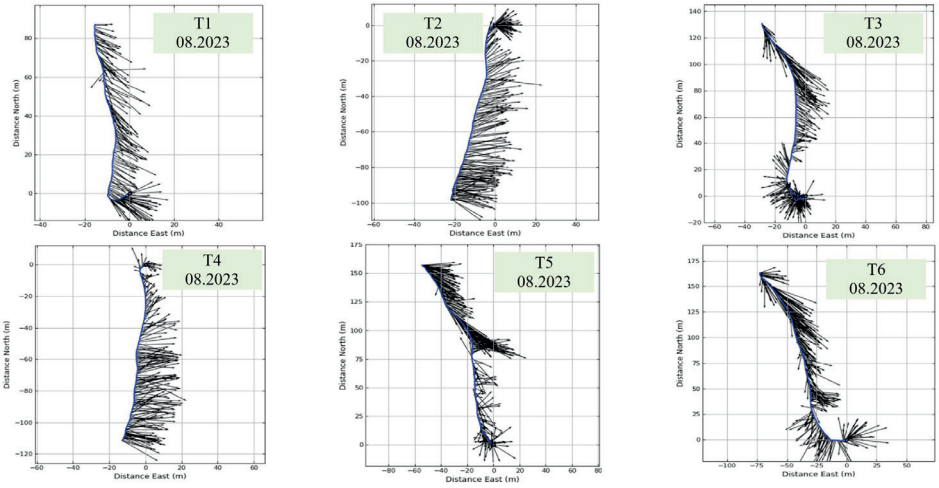


Figure 6. Comparison of flow patterns, directions, and intensities of currents for the August survey across T1-T6 transects

If we analyse the data in the context of the riverbed morphology of the Sulina channel, we can mention that in the sections T3 and T4, we have a series of eddy currents that favor the engagement of sediments in the water suspension and their transport from upstream to downstream.

Figure 7 shows a decrease in water velocity downstream of the Sulina channel. Compared to discharges, it can be mentioned that these parameters are influenced directly by water velocity.

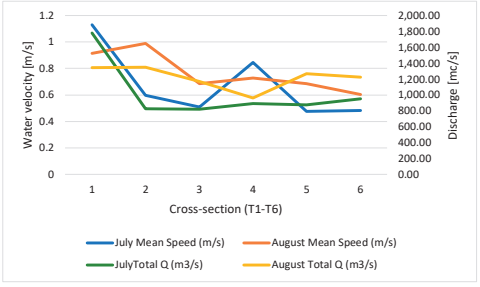


Figure 7. The water velocity average values in each cross-section are compared to the total discharge at two different survey times

The calculated energy values increase from upstream to downstream of the river, and it is higher for the August survey campaign when the discharges are also higher (Figure 8).

In the assumption that the sediment suspended concentration is calculated by Equation 3, the total suspended sediment concentration (SSC) on each vertical profile from each cross-section was calculated (Boldt, 2015).

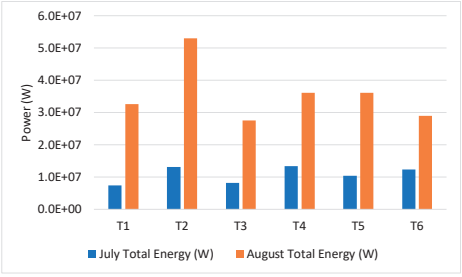


Figure 8. The total energy power of T1 to T6 cross-section

$$log_{10}(SSC) = log_{10}(a \cdot 10^{b \cdot DB}) \quad (3)$$

The a=0.005, and b=0.01 are the coefficients averaged from different scientific sources, related to Danube River SSC values. According to Baranya and Józsa (2013), in the Danube River, a 125 mg/l average SSC was measured. The SSC estimated from the SWAT method in the Danube River Basin by Vigiak (2017) was about 80 mg/l.

Between the T1 and T6 transects in July 2023, significant variations in the SSC values are given across transect length (Figure 9).

In the T1, T2, and T5 sections, where the currents are stronger, the average SSC is: 53.5 mg/l, 69.7 mg/l, and 50.8 mg/l,

respectively. This suggests a higher transport of sediment from one section to another.

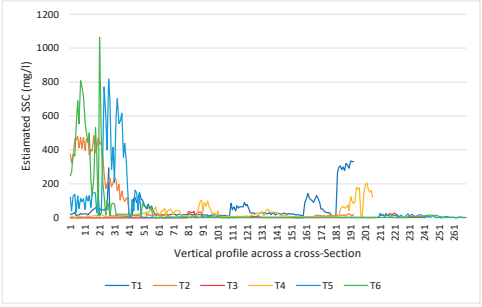


Figure 9. Suspended sediment concentration estimation based on backscatter signal (dB) on the July 2023 survey

In section T6, with the maximum value of SSC concentrations of 1064.59 mg/l, it is demonstrated that all sediments are transported downstream to the mouth of the Black Sea, more precisely, the "Bara Sulina" area.
Analyzing Figure 10, we observe an increase in the SSC value for transects T5 and T6.

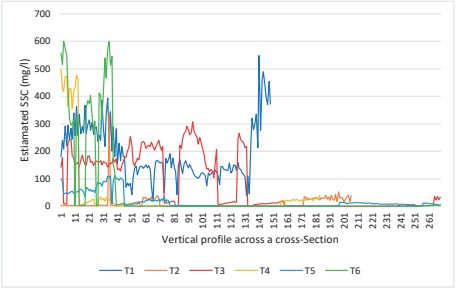


Figure 10. Suspended sediment concentration estimation based on backscatter signal (dB) on the August 2023 survey

These only confirm the fact that the sediments are transported in large quantities downstream in the area of Sulina, where the intensity of the current gradually decreases and their storage takes place. In section T1, the highest mean value of the EFS of 193.2 mg/l and a high standard deviation (100.1 mg/l) were estimated. This denotes the fact that the hydrodynamic conditions in this area are varied and with strong suspended sediment entrainment. In the T6 section, the maximum of 941.5 mg/l suggests the presence of intense sedimentary accumulation events.

CONCLUSIONS

The research study carried out for the monitoring of flow currents by the ADCP method helps to determine the phenomenon of sediment transport in fluvial environments.
The high values of the SSC concentration in July 2023 (1064.5 mg/l) and August 2023 (941.4 mg/l) in section T6 show the presence of sediment transport processes towards the confluence with the Black Sea, and their deposition in the "Bara Sulina" area.
The hydrodynamic parameter E (energy), increased in value especially in August 2023, in the upstream sections T1 (3.3×10^7 W) and T2 (5.3×10^7 W), and decreased in value in the T6 section in both months, indicates the erosion trend from upstream to downstream.
Applying the method of estimating the SSC from the backscattering of the ADCP signal, we concluded that the largest amounts of sediments are in the downstream area of the Sulina channel.
The effect of sediment transport from upstream to downstream only increases the clogging of the Sulina channel at the confluence with the Black Sea. Thus, continuous monitoring and investigation of currents and flow velocities by the ADCP method is mandatory. The ADCP and SSC estimation method offers an integrated approach to measuring hydro-morphological parameters and correlating with sediment transport processes, helping to plan hydrotechnical maintenance works and emergency interventions on the maritime-river navigation infrastructure in the respective area.

ACKNOWLEDGEMENTS

The studies based on which this work was carried out were carried out within the project 101094070 - DALIA - Danube Region Water Lighthouse Action, HORIZON-MISS-2021-OCEAN-02-02, implemented in the REXDAN Research Infrastructure.

REFERENCES

Banescu, A., Arseni, M., Georgescu, L.P., Rusu, E., & Iticescu, C., 2020a. Evaluation of different simulation methods for analyzing flood scenarios in the Danube Delta. *Applied Sciences*, 10, 8327.

Banescu, A., Arseni, M., Georgescu, L.P., Rusu, E., & Iticescu, C., 2020b. Evaluation of different simulation methods for analyzing flood scenarios in the Danube Delta. *Applied Sciences,* 10, 8327.

Baranya, S., & Józsa, J., 2013. Estimation of Suspended Sediment Concentrations with Adcp in Danube River. *Journal of Hydrology and Hydromechanics,* 61, 232–240. https://doi.org/10.2478/johh-2013-0030

Boldt, J.A., 2015. From mobile ADCP to high-resolution SSC: a cross-section calibration tool, in: *3rd Joint Federal Interagency Conference on Sedimentation and Hydrologic Modeling.* pp. 1258–1260.

Burada, A., Topa, C.M., Georgescu, L.P., Teodorof, L., Nastase, C., Seceleanu-Odor, D., & Iticescu, C., 2015. Heavy Metals Environment Accumulation in Somova-Parches Aquatic Complex from the Danube Delta Area. *Rev. Chim.*Buchar.Orig. Ed 66, 48–54.

Cociasu, A., Dorogan, L., Humborg, C., & Popa, L., 1996. Long-term ecological changes in Romanian coastal waters of the Black Sea. *Marine Pollution Bulletin,* 32, 32–38.

Deogade, R.B., Khandagale, H.R., & Someshwara, M., 2023. Performance Testing of Acoustic Doppler Current Profiler Used for Stream Flow Measurement. https://doi.org/10.26077/369C-74C5

Giosan, L., Donnelly, J.P., Constantinescu, S., Filip, F., Ovejanu, I., Vespremeanu-Stroe, A., Vespremeanu, E., & Duller, G.A., 2006. Young Danube delta documents stable Black Sea level since the middle Holocene: Morphodynamic, paleogeographic, and archaeological implications. *Geology,* 34, 757–760.

Guseva, S., Aurela, M., Cortés, A., Kivi, R., Lotsari, E., MacIntyre, S., Mammarella, I., Ojala, A., Stepanenko, V., Uotila, P., Vähä, A., Vesala, T., Wallin, M.B., & Lorke, A., 2021. Variable Physical Drivers of Near-Surface Turbulence in a Regulated River. *Water Resources Research*, 57, e2020WR027939. https://doi.org/10.1029/2020WR027939

Kuhl, C.H.L., 1891. The Sulina branch of the Danube. (includes plate and appendices). Minutes of the Proceedings of the Institution of Civil Engineers, 106, 238–247. https://doi.org/10.1680/imotp.1891.20256

Lazăr, N.-N., Simionov, I.-A., Petrea, Ștefan-M., Iticescu, C., Georgescu, P.-L., Dima, F., & Antache, A., 2024. The influence of climate changes on heavy metals accumulation in *Alosa immaculata* from the Danube River Basin. *Marine Pollution Bulletin*, 200, 116145. https://doi.org/10.1016/j.marpolbul.2024.116145

Liu, P., Liu, B., Zhu, X., Chen, P., & Li, Y., 2024. Noise Reduction of Velocity Measured by Frequency-Supervised Combined Doppler Sonar Using an Adaptive Sliding Window and Kalman Filter. *Journal of Marine Science and Engineering, 12*, 2320. https://doi.org/10.3390/jmse12122320

Panin, N., & Jipa, D., 1998. Danube river sediment input and its interaction with the north-western Black Sea: results of EROS-2000 and EROS-21 projects. National Institute of Marine Geology and Geo-ecology GeoEcoMar.

Pomázi, F., & Baranya, S., 2025. Simulation-Based Assessment of Fine Sediment Transport to Support River Restoration Measures. *River Research & Apps,* 41, 367–381. https://doi.org/10.1002/rra.4378

Popa, P., Murariu, G., Timofti, M., Georgescu, L.P., 2018. Multivariate statistical analyses of water quality of Danube River at Galati, Romania. *Environ. Eng. Manag. J*., 17, 491–509.

Teodorof, L., Ene, A., Burada, A., Despina, C., Seceleanu-Odor, D., Trifanov, C., Ibram, O., Bratfanof, E., Tudor, M.-I., & Tudor, M., 2021. Integrated assessment of surface water quality in Danube River Chilia Branch. *Applied Sciences,* 11, 9172.

Vigiak, O., Malagó, A., Bouraoui, F., Vanmaercke, M., Obreja, F., Poesen, J., Habersack, H., Fehér, J., & Grošelj, S., 2017. Modelling sediment fluxes in the Danube River Basin with SWAT. *Science of the Total Environment,* 599, 992–1012.

Scientific Papers. Series E. Land Reclamation, Earth Observation & Surveying, Environmental Engineering. Vol. XIV, 2025
Print ISSN 2285-6064, CD-ROM ISSN 2285-6072, Online ISSN 2393-5138, ISSN-L 2285-6064

STRUCTURAL ANALYSIS OF SLUDGE FROM THE ARAD WASTEWATER TREATMENT PLANT: REDUCING QUANTITY AND ENHANCING ITS POTENTIAL AS FERTILIZER

Denisa BACALU-RUS[1], Lucian COPOLOVICI[1, 2], Dana COPOLOVICI[2], Ioan BOTH[3], Maria MIHĂILESCU[4]

[1]"Aurel Vlaicu" University of Arad, Interdisciplinary School of Doctoral Studies, 2 Elena Drăgoi Street, 310330, Arad, Romania
[2]"Aurel Vlaicu" University of Arad, Faculty of Food Engineering, Tourism and Environmental Protection, Institute of Interdisciplinary Research, 2 Elena Drăgoi Street, 310330, Arad, Romania
[3]Politehnica University of Timișoara, Faculty of Civil Engineering, 1st Ioan Curea Street, 300226, Timișoara, Romania
[4]Politehnica University of Timișoara, Research Institute for Renewable Energy, 138 Gavriil Musicescu Street, 300774, Timișoara, Romania

Corresponding author email: lucian.copolovici@uav.ro

Abstract

Sludge from sewage treatment plants is a byproduct of wastewater treatment processes, consisting of solid particles, microorganisms, and organic and inorganic substances. It is generated during sedimentation and digestion processes to remove contaminants such as organic matter, heavy metals, and chemicals from water. Before storage or disposal, sludge is typically treated to reduce its volume and eliminate pathogens. Standard treatment methods include dehydration, biological stabilization, and incineration. Depending on its composition, treated sludge can be repurposed for agricultural use as fertilizer, provided it meets strict regulatory standards to prevent soil and groundwater contamination. In Romania, sewage sludge is generally classified as waste under European and national legislation. According to the European Union Waste Directive 2008/98/EC, sludge is considered waste if it cannot be safely treated, recovered, or reused. Studies have explored its potential environmental risks, including soil contamination and its suitability as a fertilizer. This article presents a structural sludge analysis, focusing on its physicochemical properties and moisture content. Experiments were conducted to evaluate the behavior of sludge samples under varying temperatures, exposure durations, and drying conditions. Results showed that evaporation rates increased with temperature, with significant differences observed between ventilated and non-ventilated drying environments. At temperatures ranging from 50°C to 100°C, sludge mass consistently decreased, with the lowest masses recorded in ventilated drying processes at 100°C. In non-ventilated conditions, the percentage of evaporation increased progressively with prolonged heat treatment. Additionally, heavy metal concentrations in the sludge were experimentally determined and found to be below the limits imposed by national legislation. These results confirm that the analyzed sludge samples are suitable for agricultural use, aligning with regulatory requirements.

Key words*: chemical composition, heavy metals, sludge, unventilated currying, ventilated heat currying.*

INTRODUCTION

During the pre-accession period to the European Union (EU), various strategies for sludge management were formulated, though their execution differed among countries. A primary strategy involved aligning national legislation with EU directives, specifically the Urban Wastewater Treatment Directive (91/271/EEC) and the Sewage Sludge Directive (86/278/EEC), which set forth regulations for sludge treatment, monitoring, and land application (Council of the European Communities, 1991; Council of the European Communities, 1986). Simultaneously, investments were directed towards enhancing wastewater treatment infrastructure to upgrade facilities and optimize sludge handling processes. Various disposal and valorisation strategies have been investigated in light of the rising sludge production. Land application in agriculture is advocated as a sustainable practice, contingent upon the sludge adhering to strict criteria concerning heavy metal levels

and pathogen reduction (Fytili & Zabaniotou, 2008). Due to constrained treatment capacities, numerous countries have opted for landfilling or temporary storage, contrary to the EU's long-term goal of minimizing sludge disposal in landfills. Composting and co-composting are promoted as methods for transforming sludge into a beneficial soil amendment for agricultural, landscaping, and land reclamation purposes (Smith, 2009). The exploration of anaerobic digestion as a method for reducing sludge volume and generating biogas for renewable energy production was initiated. However, the adoption of this technology was limited at that time (Yaser et al., 2022). In addition to these technical strategies, public awareness campaigns and institutional capacity-building initiatives were launched to inform stakeholders, such as municipalities, farmers, and industries, about the safe and effective management of sludge (Benedetti et al., 2008; Vinayagam et al., 2024). The initial strategies established a foundation for developing more sophisticated sludge management policies after EU accession. Thus, only 0.2% of the sludge was used on agricultural land (Ministerul Mediului și Pădurilor, Direcția Generală AM POS Mediu, 2011).

Accumulated sewage sludge is essentially wet matter, which can currently be stored on special platforms equipped with drainage systems or directly on the ground (Qasim & Shareefdeen, 2022), subsequently finding a solution to remove it, to make room for another amount of sludge, or it can be used in some branches of agriculture, to improve the quality of soils, through the content of phosphorus and nitrogen (Shi et al., 2021).

Sludge recovery is not the main objective of the urban wastewater treatment process. Still, it should be considered as a means of removing sludge from the treatment plant area without having a negative impact on the environment. Therefore, it is crucial to balance the amount of sludge generated and recovered through effective sludge management (Andreoli et al., 2015).

Unfortunately, significant amounts of dewatered sewage sludge are stored in improper conditions, causing the sludge to become a source of pollution (Iacob & Deac, 2021).

The peculiarities of the circular economy (CE) in the management of municipal wastewater and sewage sludge in the specific context of local conditions, such as those in Poland, were analyzed by Kacprzak (Kacprzak & Kupich, 2021) and Lipińska (Lipińska, 2018), with a focus on clean and ecological technologies. From the perspective of the circular economy, in addition to the recovery, collection, and use of biogas as an energy source, the recovery of materials resulting from the purification process, such as gravel, or the extraction of phosphorus from sludge or ash (piles) can also be considered (Domini et al., 2022).

Russian Federation researchers conducted a preliminary assessment of the possible uses of biogas from sewage sludge in the Water - Wastewater - Sludge and Circular Economy sector. They used a computational model for biogas and biomethane, MCBioCH$_4$, comparing the results with laboratory tests on sewage sludge fermentation (Kiselev et al., 2019).

Bratina et al. (2016) carried out a study in which it presented a method of drying the sludge in a vacuum at low temperatures, as well as treating the sludge by reducing heavy metals with nanoparticles covered with chitosan.

MATERIALS AND METHODS

To analyze the influence of temperature on the drying of dewatered sludge under different ventilation conditions, 14 sludge samples were collected from the sewage treatment plant in the Municipality of Arad. They were dried in an oven and weighed at regular intervals. The purpose of the determinations was to evaluate the efficiency of the drying process according to its duration. As part of the experiment, tests were carried out using sludge samples with known moisture, exposed to drying for different periods. The drying time was divided into three intervals: 30 minutes, 60 minutes, and 100 minutes.

To study the evaporation phenomenon in more detail, the impact of temperature on the drying process of dewatered sludge was also investigated, using two distinct temperatures: 50°C and 100°C. Before and after drying, the samples were weighed using Petri dishes and a

high-precision analytical balance Kern Adb 100-4. After measuring the initial mass of the dewatered sludge samples (m_1) and the final mass (m_2) after drying, the degree of evaporation (GE) was calculated, which represents the evaporated mass concentration, expressed as a percentage (Olsson & Newell, 2015), which was later used to evaluate the degree of evaporation of the sludge samples analyzed in this research using the calculation formula:

$$GE = ((m_1 - m_2) / m_1)) \cdot 100\ [\%] \quad (1)$$

Experiments were conducted under both ventilated and unventilated conditions to assess the impact of airflow on the drying process. Additionally, heavy metal content was determined using flame and electrothermal atomic absorption spectrometry (FAAS/ETAAS) to evaluate the potential environmental risks associated with sludge re-use (ISO 11047:1998).

The collected sludge was subjected to a physicochemical analysis to check if the samples meet the necessary parameters for use in other fields, according to the requirements established in the experimental research.

RESULTS AND DISCUSSIONS

The dehydrated sludge at 50°C under unventilated conditions

To carry out the experiments in non-ventilated conditions of the drying space, three of the 14 samples taken and prepared by weighing will be used. Sampling was performed in duplicate, and the estimated value is the average of the two measurements. Dewatered sludge with a solids (SS) content of 22% was the source from which the samples were selected for the experiments. The three samples will be introduced simultaneously into the drying space at a temperature of 50°C. Samples will be drawn at 30, 60, and 100 minute intervals. After each draw, the samples will be weighed immediately to determine the percentage of water evaporated.

It is assumed that all parameters are identical, namely the size of the drying space, the temperature, and the absence of ventilation. Table 1 shows the values obtained by calculation, according to formula (1), for the three samples subjected to drying in a non-ventilated space at 50°C for 30, 60, and 100 minutes.

Table 1. Results for 50°C - unventilated

Time [min]	Initial mass m_1 [g]	Final mass m_2 [g]	Petri dish [g]	Evaporation rate [%]
30	15.32	14.16	36.2	7.57
60	16.12	14.33	36.2	11.10
100	17.23	13.51	36.2	21.59

It can be seen from Table 1 that after 30 minutes, the percentage of humidity decrease is 7.57%. After 60 minutes, the humidity decreases by 11.10%, increasing to 21.59% at a holding time of 100 minutes.

In order to determine the optimal temperature at which sludge drying is effective, another 3 (three) samples from the remaining 11 samples were used.

The dehydrated sludge at 100°C under unventilated conditions

The research was carried out under the same conditions (unventilated closed space), increasing the working temperature from 50°C to 100°C. For this set of experiments, the conditions of the previous experiment were maintained in terms of periods.

The parameter change is only the temperature, which has increased from 50°C to 100°C. In conditions where the workspace is not ventilated, the parameter that influences the degree of evaporation is the temperature, which increases from 50°C to 100°C.

This experiment was done to show how water evaporation is influenced by increasing temperature. The first experiment showed how water evaporation is influenced by holding time to dry. Also, through the graphic representation in the temperature-time coordinates, it is possible to see how the holding time for drying influences the evaporation of water under conditions where the working temperature doubles. The results align with findings from other researchers, who reported that proper air circulation prevents water vapor from recondensing on sludge, enhancing drying efficiency (Santos et al., 2020).

Table 2 shows the values resulting from the calculations according to the calculation formula (1), results obtained for the three samples subjected to drying in a non-ventilated space, at a temperature of 100°C, for time intervals of 30, 60 and 100 minutes.

Table 2. Results for 100°C - unventilated

Time [min]	Initial mass m_1 [g]	Final mass m_2 [g]	Petri dish [g]	Evaporation rate [%]
30	16.32	12.06	36.2	26.10
60	16.58	10.15	36.2	38.78
100	17.05	5.21	36.2	69.44

Table 2 shows that, in the case of the sample subjected to the thermal treatment of 100°C, after 30 minutes, the percentage of moisture decrease is 26.10%. After 60 minutes, the humidity decreases by 38.78%; after 100 minutes, the decrease reaches 69.44%.
The graphical representation in Figure 1 illustrates the evolution of evaporation as the temperature increases from 50°C to 100°C. Thus, water evaporation rises from 7.57% after 30 minutes at 50°C, reaching 21.59% after 100 minutes.

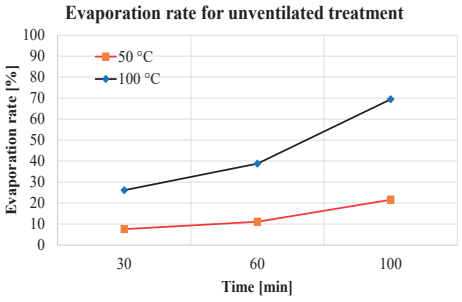


Figure 1. Evaporation rate for unventilated treatment.

The evaporation phenomenon significantly intensifies when the temperature is increased from 50°C to 100°C, reaching 26.10% after 30 minutes and 79.44% after 100 minutes.

The dehydrated sludge at 50°C under ventilation conditions

In order to highlight the influence of ventilation on the drying process, experiments were carried out under the same temperature and time conditions, replacing the non-ventilated drying space with a ventilated one.
The three samples were simultaneously introduced into the drying space at a temperature of 50°C. The first sample was left in the drying space for 30 minutes, the second was dried for 60 minutes, and the third was dried for 100 minutes. After each time interval, each sample was weighed to compare the weight of the dried sample with its weight before drying. The difference in weight was considered equal to the weight of the amount of water evaporated following drying.
Table 3 shows the values obtained by calculation, according to formula (1), for the three samples subjected to drying in a ventilated space at 50°C for 30, 60, and 100 minutes.

Table 3. Results for 50°C - ventilated

Time [min]	Initial mass m_1 [g]	Final mass m_2 [g]	Petri dish [g]	Evaporation rate [%]
30	16.77	13.26	36.2	20.93
60	17.12	10.13	36.2	40.83
100	18.02	7.11	36.2	60.54

Table 3 shows the decrease in humidity after 30 minutes, at a temperature of 50°C, in a ventilated space, by 20.93% for the first sample. After 60 minutes, under the same conditions, the degree of evaporation increases to 40.83%, and after a period of 100 minutes in the drying space, the evaporation reaches 60.54%.
These experiments highlight how the phenomenon of water evaporation from the dewatered sludge is influenced by the holding time, under the conditions of a ventilated drying space, at a temperature of 50°C.

The dehydrated sludge at 100°C under ventilation conditions

The research was conducted under the same conditions (ventilated closed space), but the working temperature increased from 50°C to 100°C. Three other samples were used for the second set of experiments (at a temperature of 100°C).
In these experiments, the conditions of the first set were kept unchanged, the only change being

the temperature increase from 50°C to 100°C. The purpose of these experiments was to highlight how temperature influences the evaporation of water during the heating process.

Table 4 shows the values obtained by calculations, according to formula (1), for the three samples subjected to drying in a ventilated space at a temperature of 100°C for 30, 60, and 100 minutes. The results presented in Table 4 indicate that, under the conditions of drying in a ventilated space, at a temperature of 100°C, the evaporation of water is 47.76% after 30 minutes. After 60 minutes, at the same temperature, the degree of evaporation reaches 62.43%, and after 100 minutes, at a temperature of 100°C, in the ventilated space, the degree of evaporation reaches 78.24%.

Table 4. Results for 100°C - ventilated

Time [min]	Initial mass m_1 [g]	Final mass m_2 [g]	Petri dish [g]	Evaporation rate [%]
30	15.62	8.16	36.2	47.76
60	16.29	6.12	36.2	62.43
100	16.13	3.51	36.2	78.24

Ventilation of the drying space significantly increases the efficiency of the drying process. Figure 2 shows that the drying differences between 50°C and 100°C (which are very large in the case of drying without ventilation) are greatly reduced when using ventilated spaces. Proper ventilation of the space can reduce the drying temperature while maintaining the efficiency of the drying process.

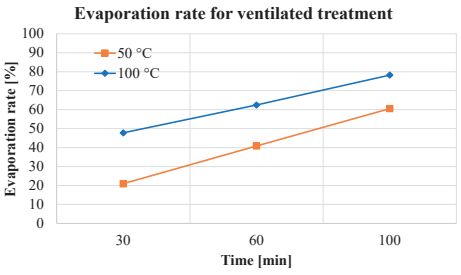


Figure 2. Evaporation rate for ventilated treatment

Interpreting the results offers multiple solutions and combinations of temperatures, drying spaces, and time that can optimize the drying process. One can analyze the degree of increase in evaporation percentage under different temperature conditions and the same time conditions to identify the most efficient settings. The results in Figures 3 and 4 highlight the optimal conditions of time, temperature, and drying space necessary to ensure efficient drying of the dehydrated sludge originating from the wastewater treatment process in the treatment plants.

Moreover, in the case of non-ventilation of the drying space, a progressive increase in the percentage of evaporation was observed, which increased as the heat treatment progressed. This phenomenon suggests that, in the absence of ventilation, the evaporation process continues progressing as the drying time increases, but with a lower efficiency than in ventilated conditions.

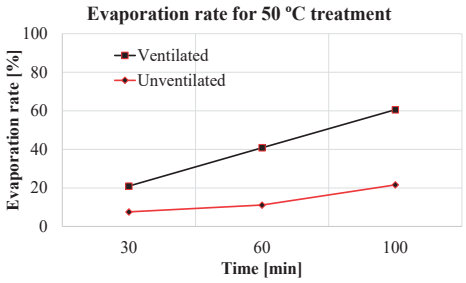


Figure 3. Evaporation rate for 50°C treatment.

The investigated dewatered sludge samples were subjected to a chemical analysis to determine the composition of the elements in the sludge, to identify the presence of heavy metals, which may constitute a risk of environmental pollution (Suciu et al., 2008).

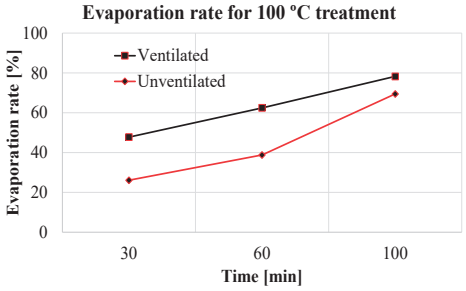


Figure 4. Evaporation rate for 100°C ventilated treatment

The dewatered sludge was chemically analyzed for heavy metals in accordance with ISO 11047:1998.

Table 5 shows the results of the analyses. Chemical: dry matter, organic matter, heavy metals (ISO 11047:1998), total nitrogen (ISO 13878:1998). The analyses were mainly conducted to determine the heavy metals in the dewatered sludge. The percentage of these elements in the dewatered sludge is essential in determining the final destination of the dewatered and dried sludge.

The nutrient content of experimentally determined sludge (ISO 11047:1998) is of remarkable importance when the sludge is utilized as an agricultural fertilizer or used to improve soil conditions. They enrich the soil with substances essential for plant growth, making dewatered sludge a useful resource in agriculture. Also, the use of sludge in agriculture is conditioned by the presence and amount of heavy metals (copper, zinc, lead, chromium, etc.), which have a high degree of toxicity and accumulate in the soil (ISO 11047:1998).

Table 5. Chemical analyses performed on the sludge sample

Determined parameters	UM	The value obtained	Analysis method	Maximum limit*
Dry substance (DS)	[%]	17	STAS12586-87	
Organic Substance	[%]	82,5	STAS12586-87	
Manganese	[mg/kg DS]	283	ISO 11047/1999	
Copper	[mg/kg DS]	337	SR EN ISO 11047/1999	*500
Zinc	[mg/kg DS	988	SR EN ISO 11047/1999	*2000
Crom	[mg/kg SU]	181	SR EN ISO 11047/1999	*500
Lead	[mg/ kg DS]	34	SRENISO 11047/1999	*300
Total nitrogen	[% DS]	5.19	ISO 13878:1998	-
Cobalt	[mg/kg DS]	110	SR EN ISO 11885:2009	*50
Calciu	[%]	2.88	EPA7000B	-
Potasiu	[%]	0.61	EPA7000B	-

Suppose urban sludge contains low amounts of heavy metals, generally below the permissible limits. In that case, sludge resulting from the combined treatment of domestic and industrial water may have higher concentrations of heavy metals, depending on the industry profile. Therefore, periodic chemical analysis of sludges is required to monitor and control their levels.

CONCLUSIONS

The comparative graphic representation of the results of drying the samples at a temperature of 50°C and 100°C (without ventilation) shows a linear increase in water evaporation from 7.57% after 30 minutes at 50°C, reaching a value of 21.59% after 100 minutes. The phenomenon of evaporation intensifies as the temperature increases from 50°C to 100°C. After 30 minutes, the percentage of evaporation is 26.10%. After 100 minutes, the value is 79.44%.

Following these experiments, it was highlighted how the evaporation of water is influenced by the temperature and the time allocated to the drying process in the conditions of a non-ventilated drying space. The increase in the degree of evaporation from 7.57% to 26.10% after 30 minutes, with the increase in temperature from 50°C to 100°C, represents a 3.4-fold increase. After 60 minutes, the increase is from 11.10% to 38.78%, representing a 3.4-fold increase. After 100 minutes, the evaporation percentage increases from 21.59% to 69.44%, a 3.2-fold increase.

The drying process is carried out in the non-ventilated drying space without evenly distributing the heat throughout the sludge mass. Lack of ventilation causes water vapor released during drying to condense and return to the dried sludge.

The ventilation of the drying space significantly increases the efficiency of the drying process. The drying differences between 50°C and 100°C, which are very large in the case of drying in non-ventilated spaces, are greatly reduced when using ventilation spaces with an increasing trajectory, but a linear trajectory.

In contrast, in the ventilated drying space, at a temperature of 50°C and a drying time of 30

minutes, the degree of dehydration is 20.93%. Raising the temperature to 100°C and keeping the drying time the same results in an evaporation rate of 47.76%, a 2.2-fold increase. After 60 minutes, the degree of dehydration increases from 40.83% to 62.43%, a 1.5-fold increase. After 100 minutes, the degree of evaporation is 60.54% at 50°C, and at 100°C it increases to 78.24%, a 1.3-fold increase. The rate of increase in evaporation remains relatively constant, and the increase is more uniform in the case of ventilation of the drying space, as opposed to drying in unventilated spaces.

Water vapor returning to the sludge negates dewatering efforts. Moreover, these vapors can be toxic and, by accumulation, become dangerous. Sludge drying should only be done in properly ventilated areas that allow evaporation to be controlled and vapors to be directed to safe areas for condensation and disposal without endangering the safety of the work area.

Experiments carried out in unventilated spaces have shown that sludge drying is possible with higher temperatures and longer times. Still, the uncontrolled presence of vapors in the working space constitutes a significant risk and prevents the process from being carried out on an industrial scale. The degree of evaporation remains relatively constant during drying. The lack of homogeneity of temperature in the drying space, caused by the absence of ventilation, leads to high evaporation rates.

The values obtained from these experiments highlighted the correlation between temperature, drying time, and the degree of evaporation.

With the increase in the drying temperature, a constant increase in the evaporation percentage was observed, which increased as the heat treatment increased. This phenomenon indicates that evaporation continues to occur in the absence of ventilation as drying time increases, but at a lower efficiency compared to ventilated drying conditions. Following the analysis of the chemical substances from the sludge samples from the Arad Wastewater Treatment Plant, especially the heavy metals, it was proven that they are far below the limits allowed by the standards in force (Directive 86/278/CEE), which means that it can be used as a fertilizer for plants and used on agricultural land, without affecting the ecological balance.

Future research will focus on finding safe areas for the use of dewatered and dried sludge so that in the near future, sludge will be viewed not as a colossal waste but as an inexhaustible resource.

REFERENCES

Andreoli, C.V., Von Sperling, M., & Fernandes, F. (2015). Sludge Treatment and Disposal. *Water Intelligence Online, 6*(0), 9781780402130-9781780402139. doi:10.2166/9781780402130.

Benedetti, L., Dirckx, G., Bixio, D., Thoeye, C., & Vanrolleghem, P. A. (2008). Environmental and economic performance assessment of the integrated urban wastewater system. *Journal of Environmental Management, 88*(4), 1262-1272. doi:https://doi.org/10.1016/j.jenvman.2007.06.020.

Bratina, B., Šorgo, A., Kramberger, J., Ajdnik, U., Zemljič, L. F., Ekart, J., & Šafarič, R. (2016). From municipal/industrial wastewater sludge and FOG to fertilizer: A proposal for economic sustainable sludge management. *Journal of Environmental Management, 183*, 1009-1025. doi:10.1016/j.jenvman.2016.09.063.

Council of the European Communities (1991). Council Directive 91/271/EEC of 21 May 1991 concerning urban waste-water treatment. *Official Journal of the European Communities*, L 135, 40–52.

Council of the European Communities (1986). Council Directive 86/278/EEC of 12 June 1986 on the protection of the environment, and in particular of the soil, when sewage sludge is used in agriculture. *Official Journal of the European Communities*, L 181, 6–12.

Domini, M., Bertanza, G., Vahidzadeh, R., & Pedrazzani, R. (2022). Sewage Sludge Quality and Management for Circular Economy Opportunities in Lombardy. *Applied Sciences, 12*(20), 10391. doi:10.3390/app122010391.

Fytili, D., & Zabaniotou, A. (2008). Utilization of sewage sludge in EU application of old and new methods - A review. *Renewable and Sustainable Energy Reviews, 12*(1), 116-140. doi:https://doi.org/10.1016/j.rser.2006.05.014.

Iacob, C., & Deac, A. (2021). Study Regarding the Negative Effects of Industrial Wastewater Discharges. *Revista Romana de Inginerie Civila/Romanian Journal of Civil Engineering, 13*(1), 97-106. doi:10.37789/rjce.2022.13.1.12.

ISO 11047:1998. Soil quality - Determination of cadmium, chromium, cobalt, copper, lead, manganese, nickel and zinc - Flame and electrothermal atomic absorption spectrometric methods. (1998).

ISO 13878:1998 Soil quality - Determination of total nitrogen content by dry combustion ("elemental analysis"). (1998).

Kacprzak, M.J., & Kupich, I. (2021). The specificities of the circular economy (CE) in the municipal wastewater and sewage sludge sector - local circumstances in Poland. *Clean Technologies and Environmental Policy*. doi:10.1007/s10098-021-02178-w.

Kiselev, A., Magaril, E., Magaril, R., Panepinto, D., Ravina, M., & Zanetti, M.C. (2019). Towards Circular Economy: Evaluation of Sewage Sludge Biogas Solutions. *Resources, 8*(2), 91. doi:10.3390/resources8020091.

Lipińska, D. (2018). The Water-wastewater-sludge Sector and the Circular Economy. *Comparative Economic Research. Central and Eastern Europe, 21*(4), 121-137. doi:10.2478/cer-2018-0030.

Ministerul Mediului și Pădurilor, Direcția Generală AM POS Mediu (2011). *Strategia națională de gestionare a nămolurilor, Partea I.* București: Ministerul Mediului și Pădurilor.

Olsson, G., & Newell, B. (2015). Wastewater Treatment Systems: Modelling, Diagnosis and Control. *Water Intelligence Online, 4*(0), 9781780402864-9781780402869. doi:10.2166/9781780402864.

Qasim, M., & Shareefdeen, Z. (2022). *Advances in Waste Collection, Storage, Transportation, and Disposal.* In (pp. 135-166): Springer International Publishing.

Santos, F.A., Santos, P.C., Matos, M.A., Cardoso, O., & Quina, M.J. (2020). Effect of Thermal Drying and Chemical Treatments with Wastes on Microbiological Contamination Indicators in Sewage Sludge. *Microorganisms, 8*(3), 376.

Shi, W., Healy, M.G., Ashekuzzaman, S.M., Daly, K., Leahy, J.J., & Fenton, O. (2021). Dairy processing sludge and co-products: A review of present and future re-use pathways in agriculture. *Journal of Cleaner Production, 314*, 128035. doi:10.1016/j.jclepro.2021.128035.

Smith, S.R. (2009). A critical review of the bioavailability and impacts of heavy metals in municipal solid waste composts compared to sewage sludge. *Environment International, 35*(1), 142-156. doi:https://doi.org/10.1016/j.envint.2008.06.009.

Suciu, I., Cosma, C., Todică, M., Bolboacă, S.D., & Jäntschi, L. (2008). Analysis of Soil Heavy Metal Pollution and Pattern in Central Transylvania. *International Journal of Molecular Sciences, 9*(4), 434-453. doi:10.3390/ijms9040434.

Vinayagam, V., Sikarwar, D., Das, S., & Pugazhendhi, A. (2024). Envisioning the innovative approaches to achieve circular economy in the water and wastewater sector. *Environmental Research, 241*, 117663. doi:https://doi.org/10.1016/j.envres.2023.117663.

Yaser, A.Z., Lamaming, J., Suali, E., Rajin, M., Saalah, S., Kamin, Z., Safie, N.N., Aji, N.A.S., Wid, N. (2022). Composting and Anaerobic Digestion of Food Waste and Sewage Sludge for Campus Sustainability: A Review. *Current Progress in Anaerobic Digestion and Composting Processes,* (1), 6455889. doi:https://doi.org/10.1155/2022/6455889.

Scientific Papers. Series E. Land Reclamation, Earth Observation & Surveying, Environmental Engineering. Vol. XIV, 2025
Print ISSN 2285-6064, CD-ROM ISSN 2285-6072, Online ISSN 2393-5138, ISSN-L 2285-6064

DEVELOPMENT AND VALIDATION OF A GC-MS/MS METHOD FOR THE DETECTION OF ORGANOCHLORINE AND ORGANOPHOSPHATE PESTICIDES IN COMPOST AND SOIL

Silviu-Laurenţiu BADEA, Carmen CONSTANTIN, Liliana BĂDULESCU

University of Agronomic Sciences and Veterinary Medicine of Bucharest,
Research Center for Studies of Food Quality and Agricultural Products,
59 Mărăşti Blvd, District 1, 011464, Bucharest, Romania

Corresponding author email: silviu.badea@qlab.usamv.ro

Abstract

Many legacy and emerging chemicals pose significant environmental concerns due to their persistence, bioaccumulation potential, toxicity, and widespread presence in environment. Among those, are organochlorine (OCs) and organophosphate (OPs) pesticides. This study aimed to develop a GC-MS/MS method for the targeted analysis of selected OCs (1,2,3,4,5,6-hexachlorocyclohexane (HCH) isomers, aldrin, and chlordecone) and OPs (dichlorvos, chlorpyrifos, and chlorpyrifos-methyl). The linearity of the developed method was assessed for selected organochlorine and organophosphate pesticides, yielding good R^2 values (≥ 0.98) for all target compounds except chlordecone. Furthermore, a spiking procedure in sol and compost was developed for OCs and OPs. To quantify OCs and OPs in soil and compost, Soxhlet extraction with toluene was used, followed by clean-up with silica-based chromatographic columns. Good recoveries were obtained for aldrin and chlorpyrifos-methyl. Lower correlation with spiked concentrations for some compounds was likely due to matrix effects. The results showed that GC-MS/MS is an efficient method for the quantification of OCs, and OPs, in complex matrices as soil and compost, highlighting their applicability for environmental monitoring and contamination assessment.

Key words*: GC-MS/MS, compost, soil, clean-up.*

INTRODUCTION

Spiking organic chemicals into soil enables controlled and reproducible experiments to study their interactions with the soil matrix and to validate analytical methods. In the same time, spiking can be used to validate analytical methods for detecting chemicals in soil (Brinco, Guedes, Gomes da Silva, Mateus, & Ribeiro, 2023). High-volume spiking facilitates homogenous distribution of compounds in samples, enhancing reproducibility and analytical method validation (Keighley, Ramwell, Werner & Sinclair, 2021). Furthermore, it is a technique commonly used in environmental science, soil chemistry, and ecotoxicology that is introducing relatively large concentrations of specific organic compounds (van Hall & van Gestel, 2025). In the same time, high-volume spiking ensures a uniform and known concentration across samples, improving reproducibility of lab-based experiments (Brinch, Ekelund & Jacobsen, 2002; Northcott & Jones, 2000). The ageing process of organic chemicals in soil reduces their bioavailability and extractability, influencing their environmental fate and toxicity (Alexander, 2000; Hatzinger & Alexander, 1995; Wang, Schlenk & Gan, 2019). This phenomenon is particularly important for understanding the environmental fate, persistence, and toxicity of pollutants such as pesticides, polycyclic aromatic hydrocarbons (PAHs) (Preda, Mocanu & Tănase, 2024), and other hydrophobic organic compounds (Duan et al., 2015). Many organic chemicals may diffuse into micropores or become tightly associated with soil organic matter, making them harder to extract or degrade (Barriuso, Benoit & Dubus, 2008; Jespersen, Trapp & Kästner, 2024; Ukalska-Jaruga et al., 2023). Furthermore, some organic contaminants can form non-extractable residues through covalent or strong non-covalent interactions with humic substances in soil (Loeffler et al., 2020). For this reason, in order to avoid the formation of non-extractable residues it is recommended that for some organic contaminants, the tests or the analysis with the

spiked soils to be performed no longer than several weeks after the spiking procedures (Northcott & Jones, 2000).

Organochlorine pesticides (OCs), such as HCH isomers, aldrin, and chlordecone, are persistent synthetic compounds previously used in agriculture and now recognized for their environmental persistence and toxicity (Micuți et al., 2018; Pang et al., 2022). Among them, the 1,2,3,4,5,6-hexachlorocyclohexanes (HCHs). HCHs can be considered as model compounds since they are persistent, global pollutants that were banned by the Stockholm Convention (Liu et al., 2017). Other priority organochlorine pesticides are: aldrin, and the chlordecone a synthetic organochlorine pesticide, extensively used in banana plantations of the French West Indies from 1972 to 1993 and which therefore was detected in pumpkin and zucchini in the French Region Aquitaine (Chevallier et al., 2018). Comparing with the HCHs, the persistence of chlordecone in the environment is higher due to its bis-homocubane structure (Momtaz & Khan, 2024) numerous chlorine atoms. Organophosphate pesticides (OPs) are a group of synthetic chemicals used to control insects on crops, animals, and in homes. Among them, dichlorvos is an is an insecticide and acaricide, while chlorpyrifos and chlorpyrifos-methyl are acetylcholinesterase inhibitors and they were extensively used to control insect pests on various crops and in stored grain (Kunwar et al., 2021; Mazari et al., 2020). Reliable quantification of OCs and OPs in complex matrices such as soil and compost requires advanced analytical methods with high sensitivity and specificity. In the case of contaminants suitable for gas chromatography-mass spectrometry methods, the used of tandem mass spectrometry using triple quadrupole analysers (GC-QQQ-MS) is employing the development of multiple reaction monitoring (MRM) methods. MRM method development involves three critical steps: (1) selection of precursor ions, (2) optimization of collision energy, and (3) adjustment of dwell time to balance sensitivity. A higher dwell time increases the sensitivity but also decreases the number of points available for each target peak (Badea, Geana, Niculescu & Ionete, 2020). GC-QQQ-MS is considered a highly sensitive technique for targeted and trace-level analysis (pg to fg range on-column). GC-QQQ-MS allows for the selection of a specific precursor ion, its fragmentation in the collision cell, and the subsequent selection of a fragment ion for detection, significantly reducing chemical noise and enhancing the signal-to-noise ratio. In spite of its sensitivity, the linearity domain of the MRM methods is somewhat limited and depends on the sensitivity of the mass spectrometer, as well on the ionization efficiency of the compound and on matrix effects (Vijaykumar et al., 2025). Usually, the linearity domain of the MRM methods is ranged from sub-ng/mL to µg/mL, depending on the compound and method sensitivity.

This study aims to develop and validate a GC-MS/MS method for quantifying selected organochlorine and organophosphate pesticides in soil and compost. The method includes assessment of linearity, recovery rates, and matrix effects in both sample types.

MATERIALS AND METHODS

Chemicals. Most of the target chemicals (α-HCH (analytical purity: 99%, β-HCH (99 %), γ-HCH (97 %), δ-HCH (99 %), hexachlorobenzene (HCB) (99 %), dichlorvos (99 %) and chlordecone (99 %) were obtained from Sigma-Aldrich (Darmstadt, Germany), while aldrin (99%), chlorpyrifos (99%) and chlorpyrifos-methyl (99%) and triphenyl phosphate (TPP) (99%) were purchased from Dr. Ehrenstorfer (Germany).

Linearity domain test. To evaluate the linearity, two calibration mixtures - one for OCs and one for Ops - were prepared in dichloromethane (DCM).

Table 1. The concentration domains of OCs and OPs tested in the linearity test.

Compound	Tested concentration range (ng/mL)
Aldrin	54-8130
α-HCH	45-6750
β-HCH	57-8625
γ-HCH	58-8700
δ-HCH	45-6825
Chlordecone	50-8812
Dichlorvos	49-7481
Chlorpyrifos	59-8850
Chlorpyrifos-methyl	50-7620

HCB (505 ng/mL) and TPP (505 ng/mL) were used as internal standards for OCs and OPs, respectively. The range of concentration range for OCs and OPs is summarized in Table 1.

Spiking of soil and compost. Approximately 60 g of soil and 60 g of compost were spiked with 25 mL of an acetone solution containing the target OCs and OPs (excluding dichlorvos and chlordecone). Samples were homogenized manually, to accelerate acetone evaporation. The theoretical concentration for the target compound in soil were: 0.09 µg/g for aldrin, 0.08 µg/g for α-HCH 0.04 µg/g for β-HCH, 0.05 µg/g for γ-HCH, 0.05 µg/g for δ-HCH, 0.10 µg/g for chlorpyrifos and 0.09 µg/g for chlorpyrifos-methyl while the theoretical concentration for the target compounds in compost were 0.09 µg/g for aldrin, 0.08 µg/g for α-HCH 0.05 µg/g for β-HCH, 0.05 µg/g for γ-HCH, 0.06 µg/g for δ-HCH, 0.11 µg/g for chlorpyrifos and 0.09 µg/g for chlorpyrifos-methyl.

Extraction and clean-up of the soil and compost samples. Triplicate 10 g portions of each spiked matrix were extracted via Soxhlet using toluene for 24 hours. Internal standards (100 µL of 100 µg/mL HCB for OCs and 100 µL of 100 µg/mL TPP for OPs) were added prior to extraction. Upon evaporation, the clean-up of the extracts was performed both with 3 x 3 mL of n-hexane on SPE columns containing 500 mg silica (55 µm, 70 Å) and with 120 mL hexane on 8 g of silica gel deactivated with 10% water (w/w) packed on glass columns. About 1 ml of toluene was added to the eluates followed by the evaporation of n-hexane. Before GC-MS analysis, the recovery standard (RS), consisting of heptachlor was added.

GC-MS analysis. The target compounds were analysed using an Agilent 7890B gas chromatograph (GC) coupled to Agilent 7010 triple quadrupole mass spectrometer (Agilent Technology, Palo Alto, USA) operated in positive electron ionization (EI) mode (70 eV) and configured in multiple reaction monitoring (MRM). The samples (volume: 1 µL) were injected at 225°C into a PTV injector operated in split less mode, while the flow rate of carrier gas (helium) was 1 mL/min. The target compounds were separated on a Agilent HP-5MS (5% Phenyl Polysilphenylene-siloxane) capillary column (30 m × 0.25 mm × 0.25 µm), using the following oven program: initial temperature of 40°C (5 min isothermal), ramp with 5°C min^{-1} to 110°C (0 min), 20°C min^{-1} to 180°C (0 min), 5°C min^{-1} to 230°C (0 min) and 20°C min^{-1} to 310°C (3 min isothermal).

RESULTS AND DISCUSSIONS

Assessment of linearity domains. The linearity domains across two orders of magnitude concentrations were assessed. The respective domains were assessed as linear if the R-Square values (R^2) of the linear regressions were at least 0.98 or higher. For aldrin, linearity was observed in the concentration range of 54–1622 ng/mL ($R^2 \geq 0.98$). Higher concentrations (2710 ng/mL and 8130 ng/mL) fell outside the linear range (Figure 1).

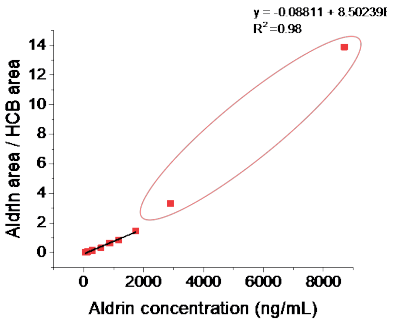


Figure 1. Linearity domain of the aldrin for developed GC-MS-MS method

Assessment of linearity domains for hexachlocylohexanes (HCHs) is presented in Figure 2. The linearity domain for α-HCH was calculated in the range 45-1347 ng/mL, while the concentrations of 2250 ng/mL and 6750 ng/mL were considered as outside of linear domain (Figure 2A). The linearity domain for β-HCH was defined in the range 57-1721 ng/mL, while the concentrations of 2875 ng/mL and 8625 ng/mL were outside of the linear domain (Figure 2B). The linearity domain for lindane (γ-HCH) was measured in the range 58-1736 ng/mL, while the concentrations of 2900 ng/mL and 8700 ng/mL were considered as outside of linear domain (Figure 2C). Also, the linearity domain for δ-HCH was defined in the range 45-1362 ng/mL, while the concentrations of 2275 ng/mL and 6825 ng/mL were outside of the

linearity domain (Figure 2D). Overall, similar linear ranges were observed for all HCH isomers, likely due to their comparable molecular structures and physicochemical properties. The assessment of linear domain for chlordecone in the range 58-2937 ng/mL gave a week R-square value (R^2 = 0.786) comparing with the other OCs, even upon exclusion of its higher concentration of 8812 ng/mL (data not shown). This indicates that hexachlorobenzene is not a good internal standard for chlordecone in GC-MS-MS determinations and Hexabromobenzene (HBB) or TPP may be preferred. The assessment of linearity domains for OPs is presented in Figure 3. Dichlorvos gave a good linearity domain in the range 49-2493 ng/mL (R^2 = 0.99) showing the highest linearity domain from all the target compounds (Figure 3A). This may be attributable to its lower molecular weight (M.W = 220.97) comparing with the rest of the target compounds. The linearity domain for chlorpyrifos was calculated in the range 59-1177 ng/mL, while the last three concentrations of 1766 ng/mL, 2950 ng/mL, 2540 ng/mL and 8850 ng/mL were considered as outside of linear domain (Figure 3B). The linearity domain for chlorpyrifos-methyl was defined in the narrow range 254-1520 ng/mL, while both the last two lowest concentrations (50 ng/mL and 101 ng/mL) and last highest concentration (7620 ng/mL) being calculated as outside linear domain (Figure 3C). Overall, the results of the linearity test shown extensively linearity domain for all the target compounds and this shown that the developed GC-MS-MS method was validated from linearity point of view.

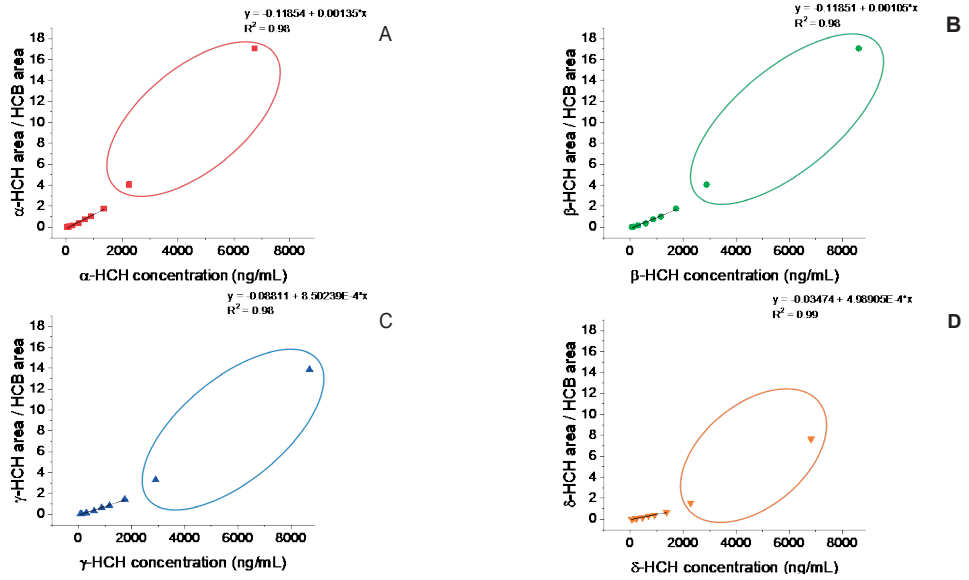


Figure 2. Linearity domain for α-HCH (■))(A), β-HCH (●) (B), γ-HCH (▲) (C) and δ-HCH (▼) (D) for the developed GC-MS-MS method

Assessment of concentrations in soil and compost. The concentrations of OCs and OPs in soil samples are presented in Table 2 and those values are comparing with those of the theoretical spiked concentrations.

Aldrin (117.20%) and chlorpyrifos-methyl (116.08%) recoveries in soil were consistent with their theoretical concentrations, indicating effective extraction and minimal matrix interference for these compounds.

For the rest of the OCs and OPs the concordance with the spiked concentration is weak (Table 2). The high recoveries may indicate a strong matrix enhancement for some compounds (e.g. γ-HCH).

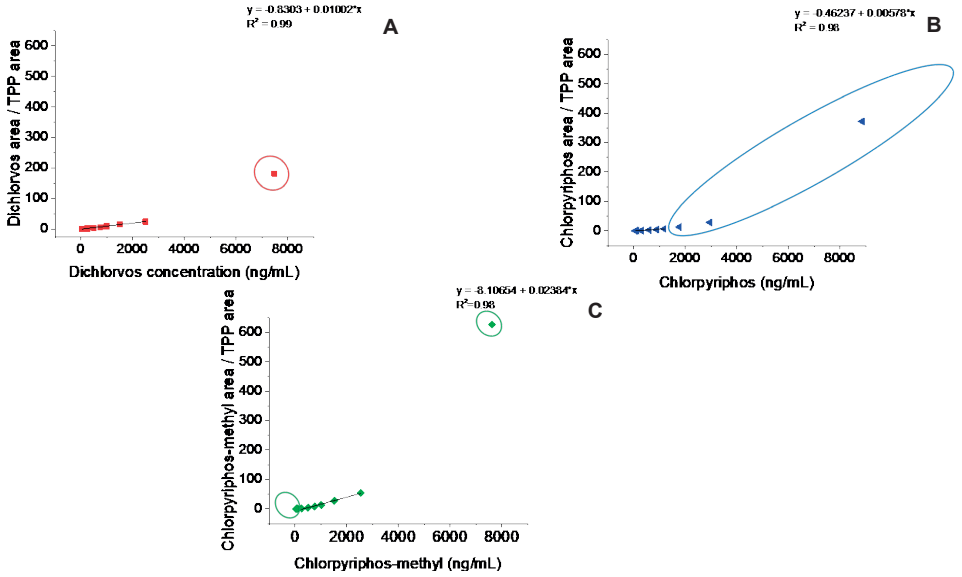


Figure. 3. Linearity domain for diclorvos (■) (A), chlorpyrifos (◀) (B), and chlorpyrifos-methyl (♦) (C) for the developed GC-MS-MS method

Table 2. Concentration of OCs and OPs pesticides determined in soil

Compound	Theoretical concentration (µg/g)	Measured concentration in sol (µg/g)	Recovery (%)
Aldrin	0.09	0.11 ± 0.002	117.20
α-HCH	0.08	0.05 ± 0.004	60.50
β-HCH	0.04	0.06 ± 0.01	134.86
γ-HCH	0.05	0.16 ± 0.01	314.24
δ-HCH	0.05	0.07 ± 0.01	127.66
Chlorpyrifos	0.10	0.15 ± 0.11	150.03
Chlorpyrifos-methyl	0.09	0.10 ± 0.05	116.08

Table 3. Concentration of OCs and OPs pesticides determined in compost

Compound	Theoretical concentration (µg/g)	Measured concentration in compost (µg/g)	Recovery (%)
Aldrin	0.10	0.08 ± 0.01	84.07
α-HCH	0.08	0.05 ± 0.002	66.50
β-HCH	0.05	0.07 ± 0.002	141.36
γ-HCH	0.05	0.08 ± 0.01	136.49
δ-HCH	0.06	0.07 ± 0.01	124.20
Chlorpyrifos	0.11	0.39 ± 0.01	363.68
Chlorpyrifos-methyl	0.09	0.11 ± 0.004	119.51

The discrepancies between measured and spiked concentrations, particularly in compost, are likely attributable to matrix effects such as co-extracted interferences causing ion suppression or enhancement in the mass spectrometer. (Wu & Ding, 2023). These effects can suppress or enhance the ionization of target OCs and OPs in the mass spectrometer detector, leading to inaccurate results. The concentrations of OCs and OPs in compost samples are presented in Table 3 and those values are comparing too with those of the theoretical spiked concentrations. Here too, the concentration of aldrin (0.08 ± 0.01 µg/g, recovery of 84.07%) and chlorpyrifos-methyl (0.11 ± 0.004 µg/g, recovery of 119.51%) are in good concordance with spiked concentrations. For the rest of the OCs and OPs, the concordance of measured concentrations with spiked concentrations is weak too, probably due to matrix effects. Non-isotopically labelled internal standards may be insufficient to fully correct for matrix effects and losses during sample preparation. Isotopically labelled analogues are recommended for improved quantification accuracy, as supported by prior studies (Badea, Lundstedt, Liljelind & Tysklind, 2013) (Peña, Sosa, Hilber, Escobar & Bucheli, 2024).

CONCLUSIONS

A GC-MS/MS method was successfully developed and applied for the quantification of selected organochlorine and organophosphate

pesticides in soil and compost. The evaluation of linearity domains gave good R^2 values for all the target compounds excepting for chlordecone. Dichlorvos exhibited the broadest linear range, likely due to its lower molecular weight and favourable ionization characteristics. Overall, the results of the linearity test shown extensively linearity domain for all the target compounds. With respect of solid matrices analyses, aldrin and chlorpyrifos-methyl showed recoveries consistent with their theoretical spiked levels in both matrices, indicating reliable quantification under the proposed method. Deviations in recovery for other analytes were attributed to matrix effects, highlighting the need for more robust internal standardization. In order to overcome those matrix effects, the use of isotopic labelled internal standards (contains atoms of ^{2}H, ^{13}C) is expecting to lead to higher accurate concentration values for a variety of OCs and OPs. Overall, the study demonstrates the feasibility of applying a GC-MS/MS method for multi-residue pesticide analysis in complex environmental matrices.

ACKNOWLEDGEMENTS

This study was performed within the project PNRR-III-C9-2022-I9, contract no. 760265/06.03.2024, entitled “New Paradigms in Compound Specific Isotope Analysis for Assessment of Environmental Fate of Emerging Contaminants” - CF34/19.12.2023 (“Postdoctoral Fellowships”) funded by Ministry of Research, Innovation and Digitalization (MCID), through Romania's National Recovery and Resilience Plan (PNRR).

REFERENCES

Alexander, M. (2000). Aging, Bioavailability, and Overestimation of Risk from Environmental Pollutants. *Environmental Science & Technology, 34*(20), 4259-4265. doi:10.1021/es001069+

Badea, S.-L., Geana, E.-I., Niculescu, V.-C., & Ionete, R.-E. (2020). Recent progresses in analytical GC and LC mass spectrometric based-methods for the detection of emerging chlorinated and brominated contaminants and their transformation products in aquatic environment. *Science of The Total Environment, 722*, 137914. doi:https://doi.org/10.1016/j.scitotenv.2020.137914

Badea, S.-L., Lundstedt, S., Liljelind, P., & Tysklind, M. (2013). The influence of soil composition on the leachability of selected hydrophobic organic compounds (HOCs) from soils using a batch leaching test. *Journal of Hazardous Materials, 254-255*, 26-35. doi:https://doi.org/10.1016/j.jhazmat.2013.03.019

Barriuso, E., Benoit, P., & Dubus, I. G. (2008). Formation of Pesticide Nonextractable (Bound) Residues in Soil: Magnitude, Controlling Factors and Reversibility. *Environmental Science & Technology, 42*(6), 1845-1854. doi:10.1021/es7021736

Brinch, U. C., Ekelund, F., & Jacobsen, C. S. (2002). Method for spiking soil samples with organic compounds. *Appl Environ Microbiol, 68*(4), 1808-1816. doi:10.1128/aem.68.4.1808-1816.2002

Brinco, J., Guedes, P., Gomes da Silva, M., Mateus, E. P., & Ribeiro, A. B. (2023). Analysis of pesticide residues in soil: A review and comparison of methodologies. *Microchemical Journal, 195*, 109465. doi:https://doi.org/10.1016/j.microc.2023.109465

Chevallier, M. L., Cooper, M., Kümmel, S., Barbance, A., Le Paslier, D., Richnow, H. H., . . . Adrian, L. (2018). Distinct Carbon Isotope Fractionation Signatures during Biotic and Abiotic Reductive Transformation of Chlordecone. *Environmental Science & Technology, 52*(6), 3615-3624. doi:10.1021/acs.est.7b05394

Duan, L., Naidu, R., Liu, Y., Palanisami, T., Dong, Z., Mallavarapu, M., & Semple, K. T. (2015). Effect of ageing on benzo[a]pyrene extractability in contrasting soils. *Journal of Hazardous Materials, 296*, 175-184. doi:https://doi.org/10.1016/j.jhazmat.2015.04.050

Hatzinger, P. B., & Alexander, M. (1995). Effect of Aging of Chemicals in Soil on Their Biodegradability and Extractability. *Environmental Science & Technology, 29*(2), 537-545. doi:10.1021/es00002a033

Jespersen, C., Trapp, S., & Kästner, M. (2024). Non-extractable residues (NER) in persistence assessment: effect on the degradation half-life of chemicals. *Environmental Sciences Europe, 36*(1), 206. doi:10.1186/s12302-024-01025-1

Keighley, N., Ramwell, C., Werner, D., & Sinclair, C. (2021). Analytical method development and validation for the quantification of metaldehyde in soil. *MethodsX, 8*, 101482. doi:https://doi.org/10.1016/j.mex.2021.101482

Kunwar, P. S., Parajuli, K., Badu, S., Sapkota, B., Sinha, A. K., De Boeck, G., & Sapkota, K. (2021). Mixed toxicity of chlorpyrifos and dichlorvos show antagonistic effects in the endangered fish species golden mahseer (Tor putitora). *Comparative Biochemistry and Physiology Part C: Toxicology & Pharmacology, 240*, 108923. doi:https://doi.org/10.1016/j.cbpc.2020.108923

Liu, Y., Bashir, S., Stollberg, R., Trabitzsch, R., Weiß, H., Paschke, H., . . . Richnow, H.-H. (2017). Compound Specific and Enantioselective Stable Isotope Analysis as Tools To Monitor Transformation of Hexachlorocyclohexane (HCH) in a Complex Aquifer System. *Environmental Science & Technology, 51*(16), 8909-8916. doi:10.1021/acs.est.6b05632

Loeffler, D., Hatz, A., Albrecht, D., Fligg, M., Hogeback, J., & Ternes, T. A. (2020). Determination of non-extractable residues in soils: Towards a standardised approach. *Environmental Pollution, 259*, 113826. doi:https://doi.org/10.1016/j.envpol.2019.113826

Micuți, M.M., Bădulescu, L., Burlacu, A., & Israel-Roming, Fl. (2018). Activity of peroxidase and catalase in soils as influenced by some insecticides and fungicides. *AgroLife Scientific Journal, 7*(2), 99-104. https://agrolifejournal.usamv.ro/index.php/agrolife/article/view/232

Mazari, A. K., Amel, B. A., Fatma, B., Nadia, B., Youcef, A., & Nawel, K. (2020). Application effects of chlorpyrifos-ethyl and malathion on the lichen Xanthoria parietina and the moss Funaria hygrometrica. *AgroLife Scientific Journal, 9*(2).

Momtaz, M., & Khan, M. S. (2024). Analysis of Chlorpyrifos Pesticide Residue in Locally Grown Cauliflower, Cabbage, and Eggplant Using Gas Chromatography–Mass Spectrometry (GC-MS) Technique: A Bangladesh Perspective. *Foods, 13*(11), 1780.

Northcott, G. L., & Jones, K. C. (2000). Spiking hydrophobic organic compounds into soil and sediment: A review and critique of adopted procedures. *Environmental Toxicology and Chemistry, 19*(10), 2418-2430. doi:https://doi.org/10.1002/etc.5620191005

Pang, S., Lin, Z., Li, J., Zhang, Y., Mishra, S., Bhatt, P., & Chen, S. (2022). Microbial Degradation of Aldrin and Dieldrin: Mechanisms and Biochemical Pathways. *Front Microbiol, 13*, 713375. doi:10.3389/fmicb.2022.713375

Peña, B., Sosa, D., Hilber, I., Escobar, A., & Bucheli, T. D. (2024). Validation of a modified QuEChERS method for the quantification of residues of currently used pesticides in Cuban agricultural soils, using gas chromatography tandem mass spectrometry. *Environmental Science and Pollution Research, 31*(23), 33623-33637. doi:10.1007/s11356-024-33237-6

Preda, M., Mocanu, V., & Tănase, V. (2024). Polychlorinated biphenyls and polycyclic aromatic hydrocarbons in soils from Danube Delta. *AgroLife Scientific Journal, 13*(2), 210-217. doi:10.17930/AGL2024219

Ukalska-Jaruga, A., Bejger, R., Smreczak, B., Weber, J., Mielnik, L., Jerzykiewicz, M., . . . Bekier, J. (2023). The Interaction of Pesticides with Humin Fractions and Their Potential Impact on Non-Extractable Residue Formation. *Molecules, 28*(20), 7146.

van Hall, B. G., & van Gestel, C. A. M. (2025). The influence of soil organic matter content on the toxicity of pesticides to the enchytraeid Enchytraeus crypticus. *Environmental Pollution, 368*, 125825. doi:https://doi.org/10.1016/j.envpol.2025.125825

Vijaykumar, L. K., Krishnegowda, D. N., Judith, S., Shankarappa, L. T., Mayanna, A., Sanganal, J. S., & Hegde, R. (2025). Method validation and quantification of 188 pesticides in animal liver using QuEChERS and GC-MS/MS. *Toxicologie Analytique et Clinique, 37*(1), 62-76. doi:https://doi.org/10.1016/j.toxac.2024.07.002

Wang, J., Schlenk, D., & Gan, J. (2019). A Direct Method for Quantifying the Effects of Aging on the Bioavailability of Legacy Contaminants in Soil and Sediment. *Environmental Science & Technology Letters, 6*(3), 148-152. doi:10.1021/acs.estlett.8b00661

Wu, X., & Ding, Z. (2023). Evaluation of matrix effects for pesticide residue analysis by QuEChERs coupled with UHPLC-MS/MS in complex herbal matrix. *Food Chemistry, 405*, 134755. doi:https://doi.org/10.1016/j.foodchem.2022.134755

Scientific Papers. Series E. Land Reclamation, Earth Observation & Surveying, Environmental Engineering. Vol. XIV, 2025
Print ISSN 2285-6064, CD-ROM ISSN 2285-6072, Online ISSN 2393-5138, ISSN-L 2285-6064

PRELIMINARY RESULTS VALIDATION ON THE THEORETICAL AND EXPERIMENTAL APPROACH FOR USING SPENT GARNET RESIDUES OF ROMANIAN LOCAL INDUSTRIES IN CONSTRUCTION MATERIALS

Cornelia BAERĂ[1, 2], Aurelian GRUIN[1, 3], Ana-Cristina VASILE[1, 3], Bogdan BOLBOREA[1, 3], Alexandru ION[1], Luiza VARGA[4], Alexandra Marina BARBU[5]

[1]National Institute for Research and Development in Construction, Urban Planning and Sustainable Spatial Development - URBAN-INCERC, Timișoara Branch, 2 Traian Lalescu Street, 300223, Timișoara, Romania
[2]Politehnica University of Timișoara, Faculty of Management in Production and Transportation, 14 Remus Street, 300191, Timișoara, Romania
[3]Politehnica University of Timișoara, Faculty of Civil Engineering, 2 Traian Lalescu Street, 300223, Timișoara, Romania
[4]West University of Timișoara, Faculty of Arts and Design, 4 Oituz Street, 300086, Timișoara, Romania
[5]National Institute for Research and Development in Construction, Urban Planning and Sustainable Spatial Development - URBAN-INCERC, Bucharest Branch, 266 Pantelimon Road, 021652, District 2, Bucharest, Romania

Corresponding author email: cornelia.baera@upt.ro

Abstract

Waterjet cutting is an industrial method that uses high-pressure water jets to cut a variety of materials such as metals, concrete, wood, ceramic, stone, rubber, foams, plastic, etc. For improving the procedure performance, in terms of speed and cutting accuracy, abrasive agents like red garnet sand is mixed with the water, generating the Abrasive Water Jet (AWJ) methodology. This is known to present environmental drawbacks, including the production of wastewater, garnet sludge and corresponding dried wastes, and microscopic particles from the cut materials, still disposed in household landfills, which generate severe environmental issues. Using Garnet Sand (SG) wastes in cementitious materials (mortars and concrete) as partial aggregate substitution is an innovative approach to enhance sustainability in construction, offering several benefits like increased strength, durability performance, etc., reduced production costs due to the re-using material approach and ecological protection as well. Preliminary studies in this direction were conducted in the last years within NIRD URBAN – INCERC, Timişoara branch, showing encouraging results in the proposed aggregate substitution proposal in the regular mortar mixes, in accordance with initial international studies in the field. The current paper aims to confirm the initial results by specific extension of the research area, reaching some critical parameters, like SG material source variation, as a mandatory validation procedure of preliminary conclusion and foundation of further specific studies regarding the viability of the SGs recycling opportunities in construction products and their effective use.

Keywords*: aggregate substitution, Circular Economy (CE), green building design, recycling, Spent Garnet (SG).*

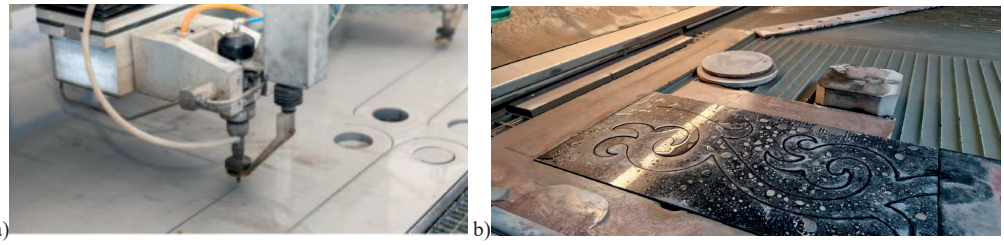
INTRODUCTION

Abrasive waterjet (AWJ) cutting is an advanced, non-thermal machining technique that utilizes a high-pressure jet of water mixed with abrasive particles - primarily Garnets - to cut a wide range of materials with precision. The AWJ cutting technique is widely used in various industries due to its ability to accurately process a diverse range of materials (metals, ceramics and glass, composites, stone and marble, metals and other hard materials, etc.) without inducing thermal damage or structural distortion (Figure 1). Garnets, the most versatile abrasive material for the AWJ process, represents a group of silicate minerals known for their crystalline structure and diverse chemical compositions; the general chemical formula is $X_3Y_2(SiO_4)_3$, where X and Y are various metal cations, such as calcium, magnesium, aluminium, iron, and manganese (Chassé et al., 2018). The chemical composition flexibility of Garnets determines their wide range of varieties, each with distinct

physical and optical properties. The most common colour of Garnets is red (reddish-pink range of colours), but they can also be green, orange, yellow, or even black, depending on their specific type (Figure 2). Garnet varieties include (Bucher et al., 2019; Usman et al., 2021; Skanavi & Dovydenko, 2018; Vasile et al., 2024):

- Almandine (iron - aluminum, $Fe_3Al_2(SiO_4)_3$, of red to reddish-brown colour, represents the most widespread of Garnets, with a wide range of use in abrasive applications;
- Pyrope (magnesium - aluminum, $Mg_3Al_2(SiO_4)_3$), of deep red colour;
- Spessartine (manganese - aluminum): Orange to reddish-brown;
- Grossular (calcium - aluminum): Green, yellow, or colorless;
- Andradite (calcium - iron): Green, yellow, or black, etc.

Garnets are preferred for AWJ cutting procedures due to their hardness (6.5-7.5 on the Mohs scale), angular particle shape, and chemical stability, which facilitate efficient cutting while minimizing equipment wear (Baeră et al., 2023; Cornelia B. et al., 2023; Vasile et al., 2024). Garnet production varies globally, with several countries, like India, Australia, United States, China, South Africa, etc., leading the extraction and processing and also dominating the global Garnet market, as raw materials suppliers for industries such as waterjet cutting and sandblasting (https://pubs.usgs.gov/periodicals/mcs2024/mcs2024-garnet.pdf). According to Precision Business Insights (https://www.precisionbusinessinsights.com/market-reports/garnet-market) "the global Garnet market size was valued at approximately $892.8 million in 2024 and is projected to grow at a compound annual growth rate (CAGR) of 7.2% from 2025 to 2031", which predicts a corresponding growth of the industries connected to AWJ processes.



a) b)

Figure 1. Abrasive waterjet cutting device for material processing: a) specific AWJ equipment (Vasile et al., 2024); b) metal piece processed by AWJ operations (TimCut SRL, Timisoara, Romania)



a) b)

Figure 2. Garnet sands: a) Garnet sand deposits, Long Island Sound in Madison, Connecticut, USA; b) Garnet sand grains (aspect and colour variation) (https://fredmhaynes.com/2021/03/11/a-sea-of-garnet-sand/)

In abrasive waterjet (AWJ) cutting operations utilizing Garnets (Figure 1), the process produces Garnet slurries as the initial waste, consisting of a liquid suspension of water mixed with smaller, altered Garnet particles of varying size distribution (Cornelia B. et al.,

2023; Vasile et al., 2024). Typically gathered in a container positioned beneath the cutting equipment, the Garnet slurries are periodically removed at irregular intervals and, through natural drying, form waste piles (Figure 3). Discarding spent Garnet sands (SGs) in landfills generates environmental pollution and increases waste management costs. Integrating sustainable materials and innovative techniques in civil engineering contributes to environmental protection while enhancing resource efficiency and structural reliability, which requires sustainable solutions (Longobardi et al., 2024; Olinic et al., 2024). Research performed in the last decade shows the potential of SG materials as a fine aggregate replacement in construction materials, mortar and concrete. This can be seen as an eco-friendly alternative to natural sand, which represents an exhaustible, natural resource. In this context, garnet waste, a byproduct of abrasive waterjet cutting in the material processing industry, can be effectively repurposed in the construction sector. It holds significant potential for use in cement-based (Budiea et al., 2021; Ab Kadir et al., 2019; Kanta & Ponnada, 2021; Lim et al., 2020; Kunchariyakun & Sukmak, 2020; Jamaludin et al., 2021) or alkali-activated concrete (Huseien et al., 2019; Muttashar et al., 2018a; 2018b) and mortars, plaster, fibre-reinforced composites, and other building materials (Cornelia B. et al., 2023; Vasile et al., 2024). The use of SG waste as a replacement for fine aggregates in cement-based materials, such as mortar and concrete, has been explored to enhance sustainability in construction. Experimental studies performed worldwide indicated that incorporating spent Garnets (SGs) in the concrete or mortar mixture can improve their physical and mechanical properties, such as densities and workability, flexural and compressive strength, while also contributing to environmental sustainability.

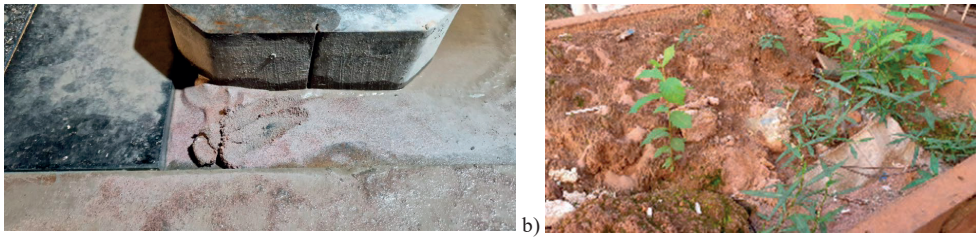


Figure 3 . AWJ processes waste generation: a) Waterjet sludge collected in recipients (TimCut SRL, Timisoara); b) Garnet waste dry slurry collected in outside recipients for medium-term storage (National Research & Development Institute for Welding and Material Testing - ISIM Timisoara, Romania) (Vasile et al., 2024)

Overview of ongoing research

Over the past decade, the rapid growth of the AWJ industry and the associated waste generation have driven an increasing need for research on SG waste management, particularly its integration into construction materials. This demand has led to a proportional rise in studies focused on repurposing SG in the building materials industry, in accordance with the Circular Economy approach: innovative transformation of potential waste into new products with distinct life cycles. In this context, SGs generated from abrasive waterjet material processing can be repurposed as a valuable by-product through improved industrial process control. The SG wastes can therefore be effectively integrated into various building materials, mortar and concrete as well (Baeră et al., 2023). Early studies conducted by Malaysian researchers explored the potential of garnet waste in alkali-activated mortars and concrete (Muttashar et al., 2018a; 2018b), while parallel research efforts investigated its application in cementitious composites as part of spent Garnet valorisation (Budiea et al., 2021; Ab Kadir et al., 2019; Kanta & Ponnada., 2021; Lim et al, 2020; Kunchariyakun & Sukmak, 2020; Jamaludin et al., 2021; Huseien et al., 2019). A common methodology in these studies involves developing a reference mortar or concrete mix, followed by testing variations with incremental sand replacement levels of

25%, 50%, 75%, and 100%. The findings consistently highlight the viability of sand substitution by SG material for cement-based mixes.

The present study was developed within the research project PN 23 35 04 01 of Nucleu Programme of the National Research Development and Innovation Plan 2022-2027, "ECODIGICONS", supported by the Ministry of Research, Innovation and Digitalization, with focus on waste management implementation, environmental protection and natural resources saving (Baeră et al., 2023; Cornelia B. et al., 2023; Vasile et al., 2024) and is consistent to the previously mentioned experimental methodology: a standard cementitious mortar was first developed as the reference mix (R). Subsequently, the conventional sand was partially replaced with SG waste material, sourced from two local companies. The first stages of the study (Baeră et al., 2023; Cornelia B. et al., 2023; Vasile et al., 2024) evaluated as favourable the compatibility of Garnet waste material with cement-based materials, by the means of comparative analysis of fresh and hardened state properties (fresh state appearance, cohesivity of the mixture, material consistency and fresh state density, etc., together with hardening age and typical mechanical performance, 7-day and 28-day flexural and compressive strength, etc.) in substitution mortars relative to the reference. The focus of this phase is the validation of the previous conclusion and evaluation of its consistency, with respect to the viability of the proposed substitution procedure. The current natural aggregate substitution was conducted by weight, following guidelines from previous studies on the subject, with replacement levels of 10%, 30% and 50% of the sand (S) content in the reference mix.

MATERIALS AND METHODS

The current experimental procedures are performed to validate the previous conclusions of the initial stages of the study. Consequently, the SG material used in this study, derived from two local providers: SG 1 and SG 3 were provided from the National Research & Development Institute for Welding and Material Testing (ISIM) (Ionescu et al., 2014; Perianu et al., 2017), but they were collected at different times - SG 1 in April 2022 and SG 3 in August 2023, over a year apart (Vasile et al., 2024). This time gap is considered significant for assessing the consistency of preliminary findings, as it allows for an evaluation of waste dynamics in terms of both material properties and compositional performance when integrating SG 1 and SG 3. Additionally, another SG source is considered, namely the local company SC Tim Cut SRL Timisoara, Romania, specializing in AWJ material processing technology (https://www.timcut.ro/); the material they provided is denoted SG 5.

The comparative evaluation is performed in terms of mechanical behaviour, of the modified mortars with respect to the reference, namely flexural and compressive strength recorded at early ages (7 days) and also the regular age of 28 days. The control mixes (R1 and R2) consist of conventional mortars, while the test mixes incorporate SG materials (SG 1, SG 3 and SG 5) as a partial replacement for sand in the reference mix (R). The substitution is performed at 10%, 30% and 50% by mass, following the standard methodology established in previous studies, and the mixing procedure is in accordance with EN 196-1 and 1015-11.

Raw materials

The Reference and the SG mixes were produced with locally available raw materials (Figure 4):

- Portland Cement, CEM II/A-LL 42.5 R (C) (Figure 4a);
- granular class 0/4 Natural sand (S), (Figure 4b);
- Spent Garnet sand (SG), from by two distinct local sources: SG 1 (Source 1 (ISIM), sampling: April 2022), (Figure 4c); SG 3 (Source 1 (ISIM), sampling: August 2023, (Figure 4d); e) SG 5 (Source 2 (Tim Cut SRL) (Figure 4c), sampling: 2023, (Figure 4e);
- Water (tap water);
- Free additives mixtures.



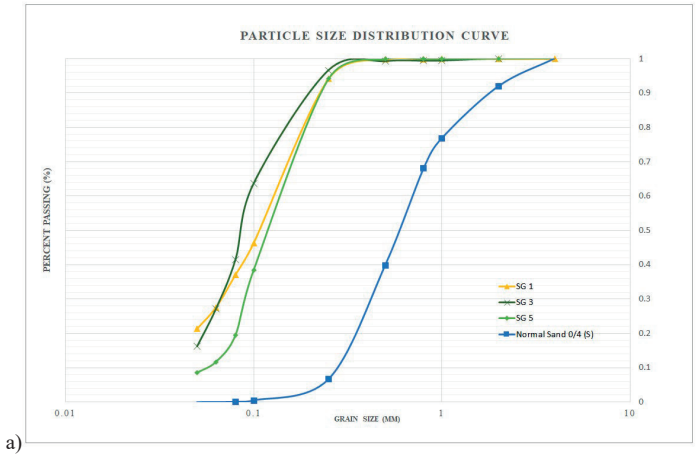
Figure 4. Raw materials: a) Portland Cement; b) Natural sand (0/4), S; c); SG 1 (Source 1 (ISIM), sampling: April 2022); d) SG 3 (Source 1 (ISIM), sampling: August 2023); e) SG 5 (Source 2 (Tim Cut SRL), sampling: 2023)

Preliminary experimental procedure - Granulometric analysis

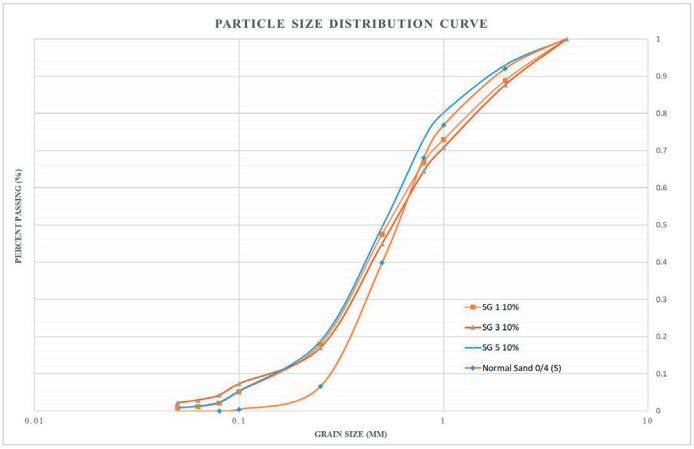
The sieving analysis is performed according to EN 933-1 method for the usual sand 0/4 (S), for the considered substitution SG materials, SG 1, SG 3 and SG 5 and additionally for the S+SG blended aggregate, containing 10%, 30% and 50% replacement levels of the sand (S). The graphical representation of the sieving analysis is presented in Figures 5 and 6 (Vasile et al., 2024).



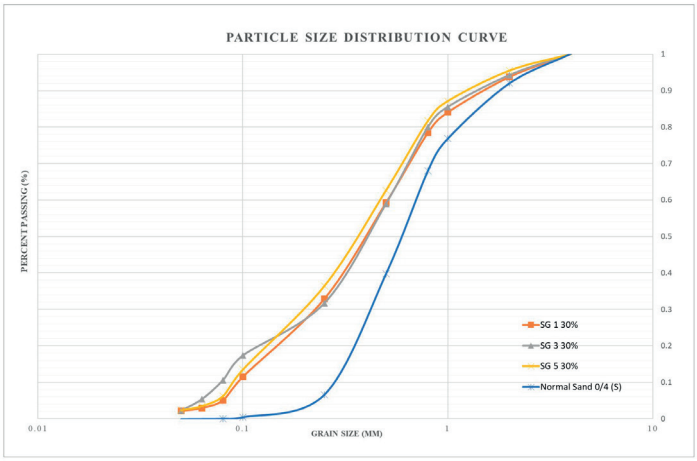
Figure 5. Determination of particle size distribution for SG 1 50% mixture: a) component materials, S+ SG 1, before mixing; b) S+SG 1, after mixing; c) particle size fractions (retained on sieve) resulting from the sieving operation



b)



c)



d)

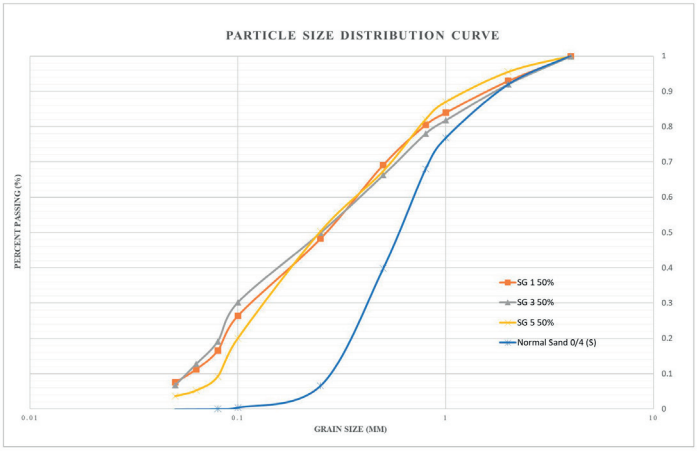


Figure 6. Aggregate grading: a) Natural sand 0/4 (S), SG 1, SG 3 and SG 5; b) Natural sand 0/4 (S), blended aggregate mixture of S+SG (1, 3 or 5) (10%); c) Natural sand 0/4 (S), blended aggregate mixture of S+SG (1, 3 or 5) (30%); d) Natural sand 0/4 (S), blended aggregate mixture of S+SG (1, 3 or 5) (50%)

Mix proportion and specimen preparation

The reference mortar mixes, R1 ((W/C) 0.61) and R2 ((W/C) 0.56), were developed with classic raw materials: regular sand 0/4 (S), cement and water are produced (Cornelia B. et al., 2023; Vasile et al., 2024). The S+SG mortar mixes were produced by SG material incremental replacement, by mass, of the usual aggregate (S), with SG additions (10%, 30% and 50%). The 10% sand replacement presents reduced economic significance for real use purposes, but it serves as important data for completing the perspective regarding the incremental growth and the corresponding mortar performance.

The mortar mix design follows the approach used in the preliminary studies (Cornelia B. et al., 2023; Vasile et al., 2024), the mixing process performed in accordance with the SR EN 196-1 and SR EN 1015-11 standards. Similarly, the casting of prismatic specimens (40 × 40 × 160 mm) and their conditioning before mechanical testing remain consistent with previous research (Baera et al., 2021; 2022; 2023; Vasile et al., 2024). The SG mortars incorporate blended aggregate mixes, with SG materials replacing the natural 0/4 sand at predetermined substitution levels of 10%, 30% and 50%. The water-to-cement (W/C) ratio for SG mortars is maintained at 0.56, aligning with R2. The mix proportions for both the reference mortars (R1 and R2) and the SG-modified mixes are standardized relative to the cement content (C = 1.0) and are detailed in Table 1. Figure 7 emphasises some relevant stages of the mortar specimen development process and testing procedures, as well.

Table 1. Mix proportions of the considered mortar mixtures: References and SG mixtures

Ingredients / Mixtures	C	S 0/4	SG	W/C	A/C
R1-1	1	3	-	0.56	3
R2-1	1	3	-	0.61	3
SG 1-1 10%	1	2.10	0.90	0.56	3
SG 1-1 30%	1	2.70	0.30	0.56	3
SG 1-1 50%	1	1.50	1.50	0.56	3
R1	1	3	-	0.56	3
R2	1	3	-	0.61	3
SG 1 10%	1	2.10	0.90	0.56	3
SG 1 30%	1	2.70	0.30	0.56	3
SG 1 50%	1	1.50	1.50	0.56	3
SG 3 10%	1	2.10	0.90	0.56	3
SG 3 30%	1	2.70	0.30	0.56	3
SG 3 50%	1	1.50	1.50	0.56	3
SG 5 10%	1	2.10	0.90	0.56	3
SG 5 30%	1	2.70	0.30	0.56	3
SG 5 50%	1	1.50	1.50	0.56	3



Figure 7. Specimen preparation and testing: a) fresh state aspect of the mortar during mixing sequences; b) fresh mortar casted in the prismatic mold; c) SG 5 50% mix specimen after removal from the mold, 24 h after casting and specific conditioning (air, high moisture (>95%)); d) Specimen placement in the 3PB testing equipment; e) Compression testing; f) Specimens after 3PB and compressive testing

After mixing and fresh state evaluation, the mortars were cast into the 40 x 40 x 160 (mm) prismatic, metallic molds (Figure 7b), cured for 24 h at the temperature T (20±1)°C and relative humidity RH (90±5)%. The hardened specimens (Figure 7c) were removed from the molds after 24 hours, visually evaluated and placed in water at the temperature T (20±1)°C, until the testing age, 7days and 28 days, respectively.

Hardened state evaluation of the SG mixes: validation of early and regular age mechanical performance

The validation stage of the SG substitution mortars (Table 1) is performed based on the mechanical characteristics of the developed mixes, namely the compressive and flexural strength, at early age (7 days) and regular age of 28 days.

The mechanical performance of the mortars is evaluated via bending tensile strength (three-point bending, 3PB) and compression strength, determined on the 40 x 40 x 160 mm prismatic specimens (Figure 7d), at early age (7 day-strength) and further at 28 days, in accordance with EN 1015-11 and EN 196-1 specifications. The flexural strength was determined using the three-point bending (3PB) test performed on whole specimens (Figure 7d), followed by the compression test on the resulting half-prism specimens (Figure 7e).

RESULTS AND DISCUSSIONS

Aggregate grain size distribution

The natural sand 0/4 (S) has a lower fine grain content, as anticipated. Replacing 10% natural sand (S) with SG material does not influence the overall grain size distribution (Figure 6b), but 30% and 50% sand replacement by SG (Figure 6c and 6d) helps balance the aggregate grading curve. All SG materials exhibit a consistent grain size distribution pattern (Figure 6a, Figure 8), with minimal variation, enhancing the reliability of the proposed substitution.

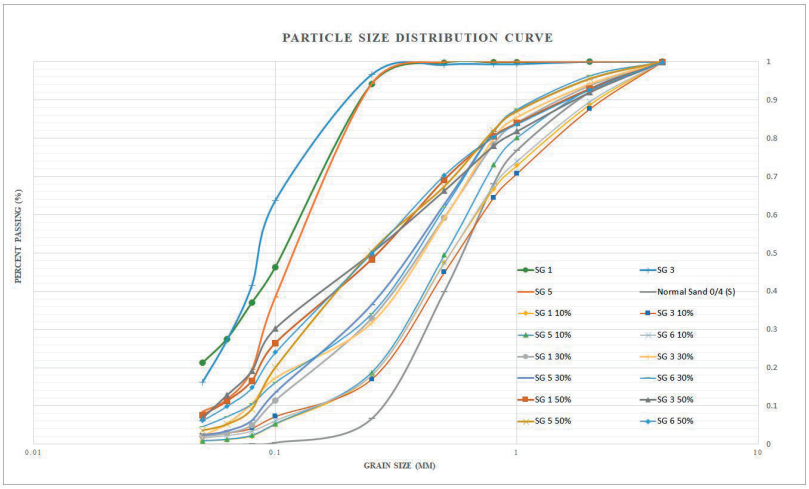


Figure 8. Aggregate grading: Natural sand 0/4 (S), SG 1, SG 3, SG 5 and blended aggregate mixture of S+SG (1, 3 or 5) (10%, 30% and 50%)

Mechanical performance

The physico-mechanical performances at early ages (7 days), bending tensile strength (3PB) and compressive strength, respectively, are essential parameters in evaluating the primary compatibility of the considered SG admixture with the cementitious matrix. Their evaluation, highlighted in Table 2, confirms the previously identified trends of overall improvement in material performance by using SG inert mineral aggregate as a partial aggregate substitute.

Table 2. Mechanical performances of SG mortars and References at young age (7 days) and regular, 28 days: flexural strength and compressive strength

Mechanical strength	7-day 3PB Flexural resistance				7-day 3PB Flexural resistance			
Age	Early age (7-day strength)		28-day strength		Early age (7-day strength)		28-day strength	
Mixtures	Strength (MPa)	Strength gain/loss vs R2 (%)	Strength (MPa)	Strength gain/loss vs R2 (%)	Strength (MPa)	Strength gain/loss vs R2 (%)	Strength (MPa)	Strength gain/loss vs R2 (%)
R1-1	5.9	-15.7	7.2	-14.3	22.0	-7.6	32.2	-11.3
R2-1	**7.0**	**0.0**	**8.4**	**0.0**	**23.8**	**0.0**	**36.3**	**0.0**
SG 1-1 10%	6.6	-5.7	8.0	-4.8	24.2	1.7	38.2	5.2
SG 1-1 30%	7.9	12.9	8.3	-1.2	29.5	23.9	40.6	11.8
SG 1-1 50%	7.6	8.6	8.5	1.2	33.0	38.7	39.5	8.8
R1	**5.7**	**-5.0**	**6.6**	**-4.3**	**25.4**	**-8.6**	**33.0**	**-3.8**
R2	***6.0***	***0.0***	***6.9***	***0.0***	***27.8***	***0.0***	***34.3***	***0.0***
SG 1 10%	6.3	5.0	6.6	-4.3	29.2	5.0	35.1	2.3
SG 1 30%	6.1	1.7	7.6	10.1	32.4	16.5	45.6	32.9
SG 1 50%	6.7	11.7	7.4	7.2	36.4	30.9	38.5	12.2
R1	**5.7**	**-5.0**	**6.6**	**-4.3**	**25.4**	**-8.6**	**33**	**-3.8**
R2	***6.0***	***0.0***	***6.9***	***0.0***	***27.8***	***0.0***	***34.3***	***0.0***
SG 3 10%	5.5	-8.3	7.2	4.3	28.7	3.2	37.2	8.5
SG 3 30%	6.4	6.7	6.8	-1.4	33.2	19.4	40.7	18.7
SG 3 50%	7.1	18.3	7.3	5.8	35.2	26.6	38.9	13.4
R1	**5.7**	**-5.0**	**6.6**	**-4.3**	**25.4**	**-8.6**	**33**	**-3.8**
R2	***6.0***	***0.0***	***6.9***	***0.0***	***27.8***	***0.0***	***34.3***	***0.0***
SG 5 10%	5.6	-6.7	7.7	11.6	29	4.3	39.6	15.5
SG 5 30%	6.8	13.3	6.6	-4.3	36.3	30.6	31.5	-8.2
SG 5 50%	7.3	21.7	7.7	11.6	34.5	24.1	43.5	26.8

Legend:

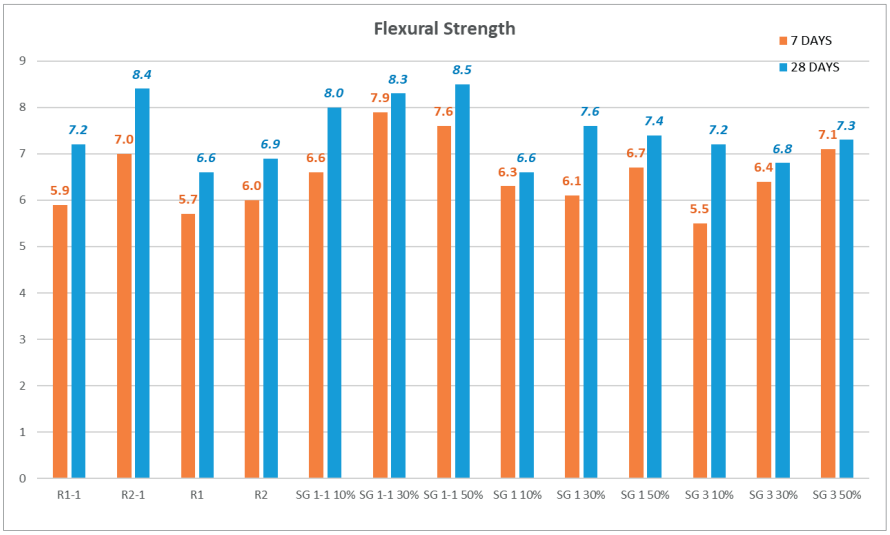
- **R1-1 and R2-1:** Reference mortars produced during the initial mechanical testing of SG 1 material (source 1, ISIM Timisoara, initial sampling) – PRELIMINARY STAGE
- **SG 1-1 10%, SG 1-1 30%, SG 1-1 30%:** Substitution mortars produced during the initial mechanical testing of SG 1 material (source 1, ISIM Timisoara, initial sampling) – PRELIMINARY STAGE
- **R1 and R2:** Reference mortars produced during the secondary mechanical testing of SG 1 material (source 1, ISIM Timisoara, initial sampling), SG 3 (source 1, ISIM Timisoara, secondary sampling); SG 5 (source 2, Tim Cut SRL, Timisoara, initial sampling) – VALIDATION STAGE
- **SG 1, SG 2, SG 3 (10%, 30%, 50 %)**: Substitution mortars produced during secondary mechanical testing of SG 1 material (source 1, ISIM Timisoara, initial sampling), SG 3 (source 1, ISIM Timisoara, secondary sampling); SG 5 (source 2, Tim Cut SRL, Timisoara, initial sampling) – VALIDATION STAGE.

The validation phase of the research confirms the initial results and implicitly the derived conclusions regarding the viability of the concept of partial substitution of fine aggregate (sand) in usual cement-based mortars by SG waste derived from AWJ processes. The credibility of the initial studies is confirmed in the secondary stage by the comparative analysis of the R1-1, R2-1 and SG1-1 samples, with similar compositions, developed with the same raw material, but more than 1 year later. The variation of the R1-1 vs R1 and R2-1 vs. R2, respectively, is sensitive for both 3PB flexural strength and compressive strength, at 7 and 28 days, and is within the usual variational limits, typical of cementitious composites, characterized by heterogeneity (Table 2, Figure 9). Simultaneously, the performance of the substitution mortars (SG1-1, SG 1 and SG 3), developed considering the percentage variation of the substitution of 0/4 natural sand 0/4 by SG material, from 10%, to 30% and 50%, confirms the trend traced by the R references, through sensible variations in the comparative analysis in Figure 8. At the same time, the results confirm the similarity of the SG material performance in cement-based material, considering the two distinct sampling

procedures (SG 1 and SG 3), sourced from the same AWJ cutting operator. The variation of the AWJ cutting operations (processed material, equipment processing, conditioning, etc.) seems to produce a negligible effect on the SG waste performance when added to usual mortars. The SG grading curve (SG1 vs SG3), (Figure 6a and Figure 8) also confirms this assumption, in terms of physical characteristics.

The validation conclusions can be further expanded by including the SG 5 material, sourced from Tim Cut SRL Timisoara (Table 2, Figure 10). A common behavior pattern of SG waste in cement-based materials as partial sand replacement can be sketched, due to small variations recorded while comparative analyses are extended by SG 5 mortar inclusions.

a)



b)

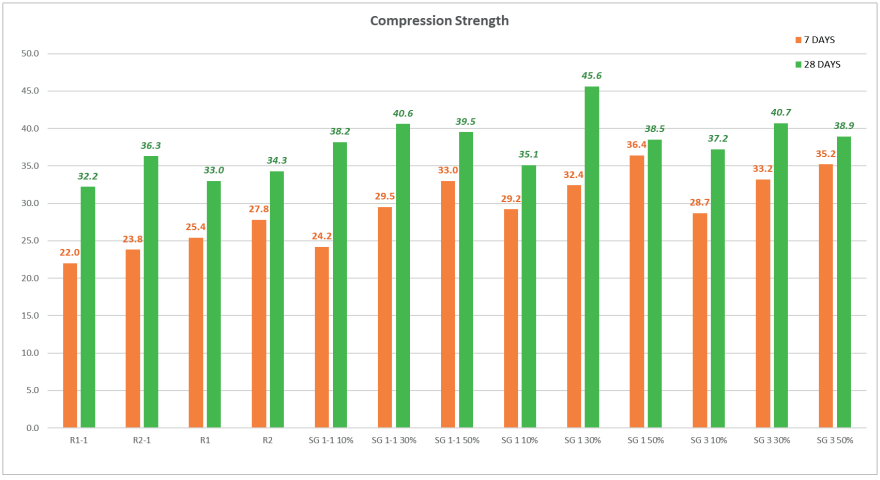
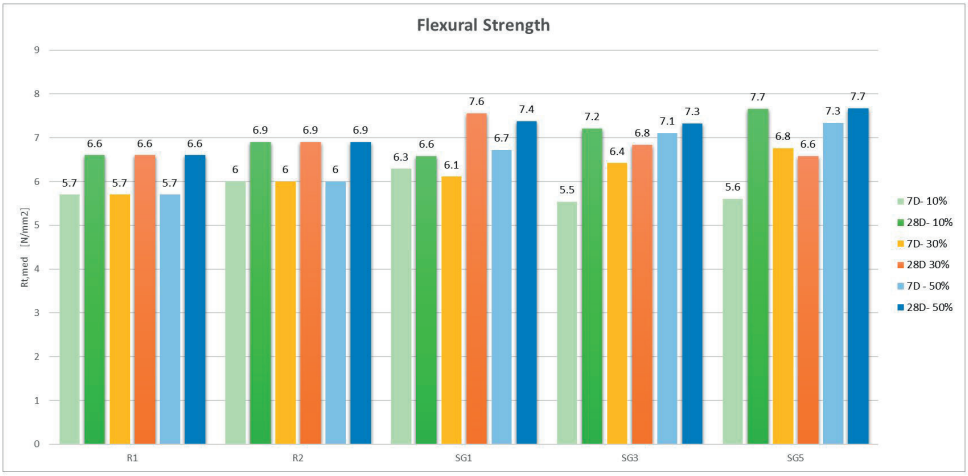
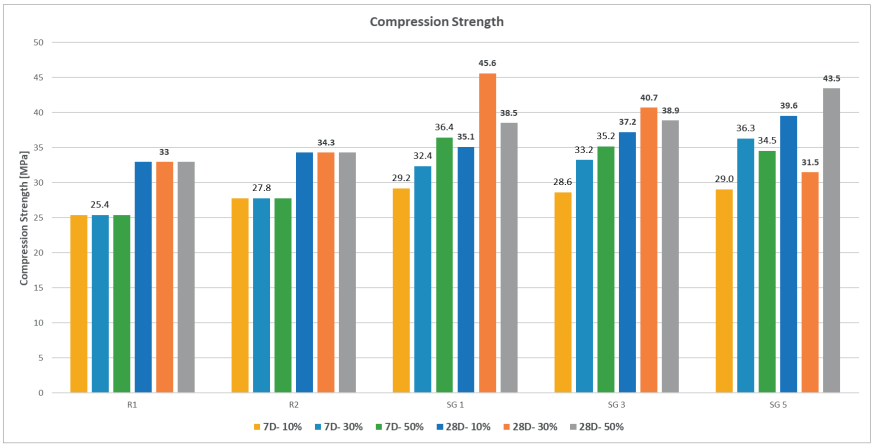


Figure 9. Validation stage - mechanical strength evaluation for the SG material sourced 1 (SG1 and SG 3) and Reference: a) 7-day and 28-day flexural strength; b) 7-day and 28-day compression strength

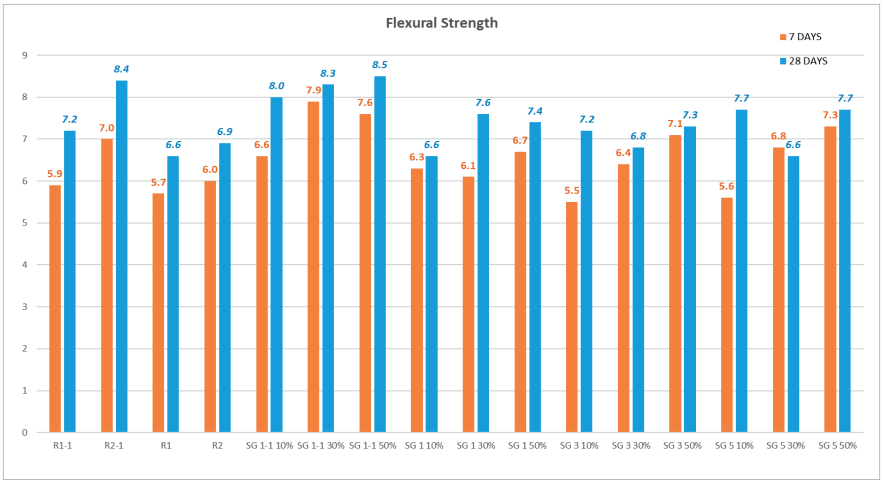
a)

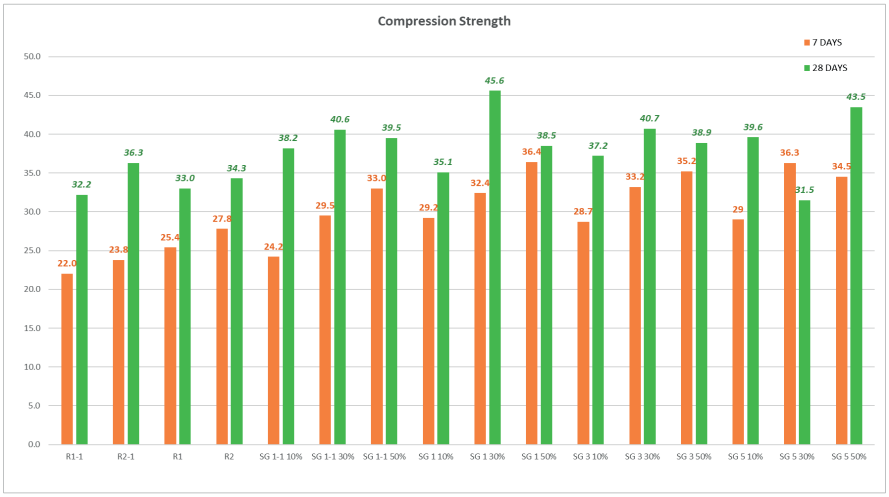

Flexural Strength
Rf,med [N/mm2]
R1
R2
SG1
SG3
SG5
7D- 10%
28D- 10%
7D- 30%
28D 30%
7D - 50%
28D- 50%

b)


Compression Strength
Compression Strength [MPa]
R1
R2
SG 1
SG 3
SG 5
7D- 10%
7D- 30%
7D- 50%
28D- 10%
28D- 30%
28D- 50%

c)


Flexural Strength
7 DAYS
28 DAYS
R1-1
R2-1
R1
R2
SG 1-1 10%
SG 1-1 30%
SG 1-1 50%
SG 1 10%
SG 1 30%
SG 1 50%
SG 3 10%
SG 3 30%
SG 3 50%
SG 5 10%
SG 5 30%
SG 5 50%



d)

Figure 10. Comparative analysis of mechanical strength evaluation for the SG material sourced 1 (SG 1 and SG 3), sourced 2 (SG 5) and Reference: a), c) 7-day and 28-day flexural strength; b), d)7-day and 28-day compression strength

CONCLUSIONS

The experimental research program of compositional development of SG partially substituted preliminary mixtures, established in line with previous studies, conducted internationally (Muttashar et al., 2018a; 2018b) as well as in the laboratory (Cornelia B. et al., 2023; Vasile et al., 2024), generated 9 SG compositions, considering the operation of a specific screening in the area of substitution percentages used in the initial studies. This leads to the identification of the following as relevant values for assessing the efficiency of the substitution process:

a) 10% substitution;
b) 30% substitution;
c) 50% substitution.

Hardened state determinations and comparative performance evaluation lead to the identification of SG 30% and SG 50% compositions as prototype SG Mortar. The SG 10% compositions do not offer dramatic changes, and the percentage of substitution, 10% substitution is reduced to generate potential for technology transfer in the compositional area of common mortars and micro mortars. The SG 10% type compositions, though, have the role of confirming the identified trend and identifying possible compositional anomalies that may occur in the mix design.

In addition, the initial SG waste source is extended to a second one. (source 2). At the same time, new samplings are made from the original source 1 (ISIM Timisoara), thus extending the investigation area towards the validation of the initial conclusion and insurance of the robustness of the proposed concept. Ongoing research is offering valuable data regarding the compositional drawbacks and optimisation possibilities, related to the considered direct field of applicability, namely development of paving blocks for the innovative integration of SG into concrete mixes. Development of prefabricated paving products is considered an initial, practical, and more accessible use of SG substitution, with lower health risks for the population due to the outdoor placement of the products.

This field of application is particularly promising given the growing demand for paving products in the local Romanian market, driven by current infrastructure needs in both urban and rural areas. The approach also aligns with Circular Economy principles, by preventing Garnet sand waste and reintegrating it into new life cycles - specifically in building materials and products - while also contributing to the conservation of natural resources such as natural aggregates.

ACKNOWLEDGEMENTS

This work was carried out within the Nucleu Programme of the National Research Development and Innovation Plan 2022-2027, supported by MCID, "ECODIGICONS" project no. PN 23 35 04 01: “Fundamental-applied research into the sustainable development of construction products (materials, elements, and structures, as well as methods and technologies) that utilizes current national resources to enhance the eco-innovative and durable aspects of Romania's civil and transport infrastructure”, financed by the Romanian Government.

REFERENCES

Ab Kadir, M. A., Khiyon, M. I., Sam, A. R. M., Kueh, A. B. H., Lim, N. H. A. S., Mastor, M. N. M. A., Zuhan, N., & Mohamed, R. N. (2019). Performance of spent garnet as a sand replacement in high-strength concrete exposed to high temperature, *Journal of Structural Fire Engineering, 10*(4), 468-481, 10.1108/JSFE-10-2018-0025

Budiea, A. M. A., Sek, W. Z., Mokhatar, S. N., Muthusamy, K., & Yusoff, A. R. M. (2021). Structural Performance Assessment of High Strength Concrete Containing Spent Garnet under Three Point Bending Test, IOP Conference Series: *Materials Science and Engineering 1144*(1), 10.1088/1757-899X/1144/1/012018.

Bucher, K., Weisenberger, T. B., Klemm, O., & Weber, S. (2019). Decoding the complex internal chemical structure of garnet porphyroblasts from the Zermatt area, *Western Alps. Journal of metamorphic Geology, 37*(9), 1151-1169, https://doi.org/10.1111/jmg.12506.

Baera, C., Gruin, A., Enache, F., Bolborea, B., Chendes, R. V., Ciobanu, A., ... & Corbu, O. (2023). Opportunities regarding the innovative conservation of the Romanian vernacular urbanistic heritage. *International Journal of Conservation Science, 14*(3), 913-936, DOI: 10.36868/IJCS.2023.03.09.

Chassé, M., Griffin, W. L., Alard, O., O’Reilly, S. Y., & Calas, G. (2018). Insights into the mantle geochemistry of scandium from a meta-analysis of garnet data. *Lithos, 310-311*, 409-421, 10.1016/j.lithos.2018.03.026.

Cornelia, B., Gruin, A., Bolborea, B., Chendeș, R., Burduhos-Nergiș, D. D., & Varga, L. (2023). Experimental Approach Regarding the Potential of Spent Garnets Use as Mineral Addition in Cement-Based Construction Products. *In Olympiad in Engineering Science (pp. 566-584). Cham: Springer Nature Switzerland.*

EN 196-1. Methods of testing cement - Part 1: Determination of strength.

EN 1015-11. Methods of test for mortar for masonry - Part 11: Determination of flexural and compressive strength of hardened mortar.

Huseien, G. F., Sam, A. R. M., Shah, K. W., Budiea, A. M. A., & Mirza, J. (2019). Utilizing spent garnets as sand replacement in alkali-activated mortars containing fly ash and GBFS, *Construction and Building Materials, 225,* 132-145*,* 10.1016/j.conbuildmat.2019.07.149.

Ionescu D., Serbanescu S. I., Perianu, I. A. - Patent No. 1. 129363 of 2014, Procedure for obtaining a mortar-type construction material from abrasive material waste, Oficiul de Stat pentru Mărci și Invenții, București, România BOPI 12 (2016).

Jamaludin, N. F. A., Muthusamy, K., Isa, N. N., Jaafar, M. F. M, & Ghazali, N. (2021) Use of spent garnet in industry: A review. *Materials Today: Proceedings, 48*(9), 10.1016/j.matpr.2021.02.210.

Kanta, N. R., & Ponnada, M. R. (2021). Performance of spent garnet sand and used foundry sand as fine aggregate in concrete, World *Journal of Engineering,* 10.1108/WJE-10-2020-0514.

Lim, N. H. A. S., & Alladin, N. F. N, Mohammadhosseini, H., Ariffin, N.F., Mazlan, A. N. (2020). Properties of Mortar Incorporating Spent Garnet as Fine Aggregates Replacement, *International Journal of Integrated Engineering 12*(9), 96-102. 10.30880/ijie.2020.12.09.012.

Longobardi, G., Moșoarca, M., Gruin, A., Ion, A., & Formisano, A. (2024). An innovative, lightweight, and sustainable solution for the integrated seismic energy retrofit of existing masonry structures, *Sustainability 16(11),* https://doi.org/10.3390/su16114791

Kunchariyakun, K., & Sukmak, P. (2020). Utilization of garnet residue in radiation shielding cement mortar, *Construction and Building Materials, 262,* 10.1016/j.conbuildmat.2020.120122.

Muttashar, H. L., Ariffin, M. A. M., Hussein, M. N., Hussin M. W., & Ishaq, S. B. (2018a). Self-compacting geopolymer concrete with spent garnet as sand replacement. *Journal of Building Engineering, 15,* 85-94, https://doi.org/10.1016/j.jobe.2017.10.007.

Muttashar, H. L., Ali, N. B., Ariffin, M. A. M., & Hussin, M. W. (2018b). Microstructures and physical properties of waste garnets as a promising construction material, *Case studies in construction materials, 8*, 87-96, https://doi.org/10.1016/j.cscm.2017.12.001.

Olinic, T., Olinic, E. D., & Butcaru, A. C. (2024). Integrating Geosynthetics and Vegetation for Sustainable Erosion Control Applications. *Sustainability, 16*(23), https://doi.org/10.3390/su162310621.

Perianu I. A., D. Ionescu, & V. Verbitchi. (2017) Method of measuring the abrasive-water jet diameter, for the cutting process control, *Welding and Material Testing – BID, 1*.

Skanavi, N., & Dovydenko, T. (2018, June). The use of waterjet cutting wastes in the production of building materials. In *IOP Conference Series: Materials Science and Engineering*, *365*(3), 10.1088/1757-899X/365/3/032025.

Usman, K. R., Hainin, M. R., Satar, M. K. I. M., Warid, M. N. M., Usman, A., Al-Saffar, Z. H., & Bilema, M. A. (2021). A comparative assessment of the physical

and microstructural properties of waste garnet generated from automated and manual blasting process, Case Studies in *Construction Materials, 14* e00474.

Vasile, A. C., Baeră, C., Gruin, Perianu, I. A., Petrisor K.I. & Ion A. (2024). Experimental Study on Spent Garnets for Fine Grain Aggregate, a Partial Substitution in Cement Based Mortars: Validation of Preliminary Research. *Condferece Proceedings of "Innovative Technologies for Joining Advanced Materials" TIMA25, November 06-07, 2025 Timişoara, Romania (accepted for publication)*

https://pubs.usgs.gov/periodicals/mcs2024/mcs2024-garnet.pdf (accesesed at 15.03.2025);

https://fredmhaynes.com/2021/03/11/a-sea-of-garnet-sand/ (accesesed at 15.03.2025);

https://www.precisionbusinessinsights.com/market-reports/garnet-market (accesesed at 15.03.2025);

Scientific Papers. Series E. Land Reclamation, Earth Observation & Surveying, Environmental Engineering. Vol. XIV, 2025
Print ISSN 2285-6064, CD-ROM ISSN 2285-6072, Online ISSN 2393-5138, ISSN-L 2285-6064

STRUCTURAL INTEGRITY IN EARTHEN ARCHITECTURE WITH NDT METHODS

Bogdan BOLBOREA[1, 2], Cornelia BAERĂ[1, 3], Aurelian GRUIN[1, 2], Sorin DAN[2], Ana-Cristina VASILE[1, 2]

[1]National Institute for Research and Development in Construction,
Urban Planning and Sustainable Spatial Development - URBAN-INCERC, Timișoara Branch,
2 Traian Lalescu Street, 300223, Timișoara, Romania
[2]Politehnica University of Timișoara, Faculty of Civil Engineering,
2 Traian Lalescu Street, 300223, Timișoara, Romania
[3]Politehnica University of Timișoara, Faculty of Management in Construction and Transportation,
14 Remus Street, 300191, Timișoara, Romania

Corresponding author email: bogdan.bolborea@incd.ro

Abstract

The resurgence of earthen construction highlights the environmental, economic, and aesthetic benefits of natural materials. Non-Destructive Testing (NDT) methods are important for assessing the integrity and performance of earthen structures without physical damage. This article reviews key NDT techniques, including ultrasonic testing, electrical resistivity tomography, nuclear magnetic resonance, time domain reflectometry, infrared thermography, and acoustic emission testing, emphasizing their role in evaluating moisture content, mechanical properties, and thermal performance. Despite their advantages, challenges such as material variability, lack of standardized protocols, and specialized training persist. Future efforts must focus on standardization, advanced technologies, and improved data interpretation to maximize NDT's potential. By overcoming these obstacles, the construction industry can ensure the structural integrity and sustainability of earthen materials, promote broader acceptance of earthen construction and foster resilient, eco-friendly building solutions.

Key words*: NDT, Earthen Constructions, Structural Integrity, Structural Health Monitoring.*

INTRODUCTION

Earthen architecture, widely acknowledged as a sustainable and ecologically responsible construction practice, has played a pivotal role in human habitation for millennia, utilizing naturally available soil as a primary building material (Mousourakis et al., 2020). This architectural tradition encompasses a diverse range of construction techniques, including adobe, rammed earth, and compressed stabilized earth blocks (CSEBs), each of which is distinguished by its unique material composition and construction methodology. These techniques have been extensively lauded not only for their minimal environmental impact - characterized by low embodied energy and thermal efficiency - but also for their profound cultural and historical significance in various regions worldwide (Bui & Morel, 2014).

Despite the numerous advantages associated with earthen construction, the long-term structural stability of such buildings remains a significant challenge due to their inherent vulnerability to environmental degradation. Exposure to climatic factors, including fluctuations in moisture levels, temperature variations, and seismic activity, often accelerates material deterioration, compromising the mechanical integrity and durability of these structures over time (Campiani et al., 2019). As a result, the development and implementation of effective assessment methodologies have become imperative to ensure the preservation and continued use of earthen buildings.

Among the various approaches employed to evaluate the condition and mechanical performance of earthen structures, non-destructive testing (NDT) techniques have gained considerable traction due to their ability to provide critical diagnostic insights without inflicting damage on the material. In particular, Ultrasonic Pulse Velocity (UPV) testing has

emerged as a highly effective method for assessing key material properties such as density, porosity, and compressive strength, offering valuable data for both conservation specialists and structural engineers engaged in the maintenance and restoration of earthen heritage and contemporary constructions. This approach not only facilitates the preservation of these culturally significant structures but also enhances our understanding of their material properties and performance over time (Charif et al., 2024).

Ultrasonic Pulse Velocity testing involves sending ultrasonic waves through a material and measuring the time it takes for the waves to travel through it. The velocity of these waves is influenced by the material's density, elasticity, and internal structure, making UPV a valuable indicator of the material's quality and strength. In the context of earthen architecture, the relationship between UPV and compressive strength is particularly significant. Numerous studies have established a correlation between the two, indicating that higher ultrasonic velocities typically correspond to greater compressive strength. For example, Kim et al. (2022) demonstrated that ultrasonic pulse velocity can effectively predict the compressive strength of concrete across varying aggregate types, reinforcing the applicability of UPV in assessing earthen materials. Similarly, Hong et al. (2020) provided empirical evidence of the correlation between UPV and compressive strength, proposing a predictive equation based on their findings.

The compressive strength of earthen materials is an important factor in determining their load-bearing capacity and overall durability. Factors such as the composition of the soil, moisture content, and the presence of stabilizers can significantly influence both the compressive strength and the UPV measurements. For instance, the addition of stabilizers like lime or cement can enhance the mechanical properties of earthen materials, leading to improved performance underload (Mohammad, 2011). Ni et al. (2024) highlighted that various factors, including mix proportions and aggregate types, affect both the strength development of concrete and ultrasonic pulse velocity, emphasizing the need for careful consideration of these variables in earthen architecture.

Recent advancements in ultrasonic pulse velocity (UPV) testing methodologies have significantly expanded its applicability within the domain of earthen architecture, offering enhanced capabilities for the non-destructive evaluation of material properties. In particular, the integration of machine learning techniques into UPV data analysis represents a transformative development, as these approaches facilitate more precise predictive modelling of compressive strength by incorporating a broader spectrum of input variables (Boukhelkhal & Guermazi, 2018). Such advancements not only improve the reliability of UPV-based assessments but also contribute to the refinement of diagnostic frameworks for evaluating structural stability in historical and contemporary earthen constructions.

Moreover, the synergistic application of UPV testing with complementary non-destructive testing (NDT) techniques, such as rebound hammer tests, has been increasingly recognized as a robust strategy for achieving a more comprehensive characterization of material properties (Lee et al., 2014). By integrating multiple diagnostic approaches, researchers can mitigate the limitations inherent in individual testing methods, thereby enhancing the accuracy of assessments related to mechanical performance and long-term durability. These methodological innovations underscore the growing potential of UPV testing as an important tool in the preservation, maintenance, and structural analysis of earthen architecture, reinforcing its role in both academic research and practical engineering applications (Lee et al., 2014).

The use of Ultrasonic Pulse Velocity testing represents an important advancement in the assessment of structural integrity in earthen architecture. By establishing a reliable correlation between UPV and compressive strength, this non-destructive method offers a practical solution for monitoring the health of earthen structures. As the demand for sustainable building practices continues to grow, the preservation of earthen architecture through effective assessment techniques will play an essential role in safeguarding this valuable cultural heritage for future generations.

This research paper explores the potential of

using Ultrasonic Pulse Velocity (UPV) as a dependable method for evaluating the structural integrity of earthen constructions.

MATERIALS AND METHODS

In this study, a series of experiments were conducted to evaluate the mechanical properties of various earthen mixtures, focusing on the relationship between Ultrasonic Pulse Velocity (UPV) measurements and compressive strength. For this purpose, 44 mixtures were developed (Table 1) with materials that included different soil types, sand, water, and various additives such as lignin, deflocculants, and lime. These components were selected based on their potential to influence the mechanical properties of earthen materials, particularly in enhancing compressive strength and durability. The mixtures were cast into 40 x 40 x 160 mm prisms.

The earthen mixtures were formulated using a systematic approach, where different recipes were created by varying the ratios of soil, sand, and water, along with the incorporation of specific additives. The soil used in the mixtures was sourced from local deposits, ensuring that it was representative of typical earthen materials used in construction. The sand was selected for its grain size distribution, which is known to affect the overall strength of the mixture. The water content was adjusted to achieve optimal workability while maintaining the desired consistency of the mixtures.

Additives were introduced to enhance the properties of the mixtures. Lignin, a natural polymer, was included to improve the binding characteristics of the mixtures, while deflocculants were used to reduce the viscosity of the slurry, facilitating better mixing and compaction. Lime was added as a stabilizer, known for enhancing the compressive strength of earthen materials through pozzolanic reactions.

Table 1. Earth-based materials mix design

	Clay C1	Clay C2	Clay C3	Sand 0-1	Sand 0-2	Sand 0-4	Clay plaster	Water	Lime	Straws	Deflocculant	Lignin
M1	x							x				
M2	x			x				x	x			
M3	x			x	x			x				
M4	x			x	x			x				
M5	x			x	x			x				
M6	x			x	x			x				
M7	x			x				x	x			
M8	x			x				x				
M9			x					x			x	
M10		x						x			x	
M11			x					x			x	
M12		x						x			x	
M13			x					x			x	
M14		x						x			x	
M15		x						x			x	
M16			x					x			x	
M17		x						x			x	
M18			x					x			x	
M19		x						x			x	
M20	x					x		x			x	
M21		x				x		x			x	
M22			x			x		x			x	
M23	x					x		x			x	
M24		x				x		x			x	
M25			x			x		x			x	
M26		x				x		x			x	
M27			x			x		x			x	
M28	x					x		x			x	
M29		x				x		x			x	
M30			x			x		x			x	

	Clay C1	Clay C2	Clay C3	Sand 0-1	Sand 0-2	Sand 0-4	Clay plaster	Water	Lime	Straws	Deflocculant	Lignin
M31	x					x		x	x	x		x
M32	x					x		x	x			x
M33	x						x	x				x
M34	x						x	x				x
M35	x						x	x				x
M36	x						x	x				x
M37	x						x	x				x
M38	x						x	x				x
M39	x						x	x				x
M40	x						x	x				x
M41	x						x	x				x
M42	x						x	x				
M43	x						x	x				
M44	x						x	x				

Ultrasonic pulse velocity (UPV)

The initial phase of the experimental investigation focused on the application of Ultrasonic Pulse Velocity (UPV) testing as a means of evaluating the quality, homogeneity, and structural integrity of the prepared earthen material mixtures. This non-destructive testing procedure was conducted utilizing a portable ultrasonic testing device, which was equipped with transducers operating at a frequency of 150 kHz. These transducers were responsible for generating and transmitting ultrasonic waves through the test specimens, facilitating the assessment of their internal consistency and mechanical performance.

The selection of transducers with a 150 kHz frequency was informed by established technical guidelines, which recommend their use for assessing relatively thin structural elements - specifically those with dimensions of less than 50 mm. This frequency range has been demonstrated to provide an optimal balance between wave penetration depth and resolution, thereby enabling the precise detection of internal inconsistencies, voids, or heterogeneities within the tested materials. By employing UPV testing in this manner, the study aimed to generate a reliable dataset for characterizing the physical and mechanical behaviour of the prepared mixtures, ultimately contributing to a more comprehensive understanding of their suitability for use in earthen construction applications (NP137-2014). The time taken for the waves to traverse the material was recorded, and the velocity was calculated. This measurement provided insights into the density and elastic properties of the mixtures, which are closely related to their compressive strength. For these types of specimens with dimensions of 40x40x160 mm, the UPV testing was conducted at two points on each sample, as shown in Figure 1. In Figure 2 a cross section with the positioning of the transducers can be observed. This positioning of the transducers was chosen due to the fact that the specimens were tested destructively to determine the flexural strength, thus each specimen resulting in 2 samples to be tested for compressive strength. Prior to the destructive testing, each specimen was weighed to determine an air-dry density.

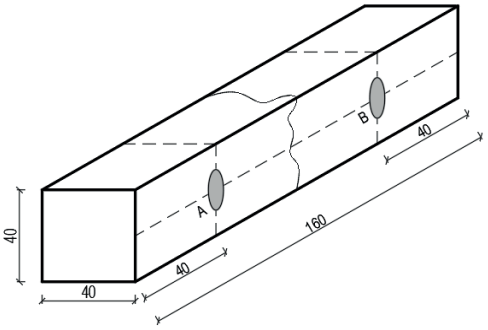


Figure 1. Transducers positioning on the prismatic specimens

Destructive testing for compressive strength

Following the UPV assessments, the same samples were subjected to compressive strength testing to obtain definitive mechanical property data.

The compressive strength tests were performed following standard testing procedures, using a hydraulic press to apply axial loads until failure

occurred. The maximum load recorded during the test was used to calculate the compressive strength of each mixture, allowing for a direct comparison with the UPV results.

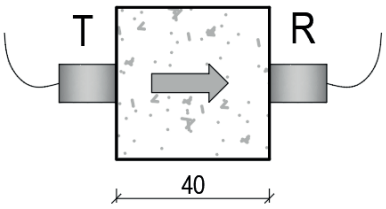


Figure 2. Cross section of the specimens with the positioning of the transducers

RESULTS AND DISCUSSIONS

Correlation between UPV and density

The mean values of the UPV were correlated with the mean values of the air-dry density determined by measuring and weighing each specimen to determine a correlation between them. The UPV values ranged from 0.645 km/s to 1.435 km/s, while density values varied between 1409 kg/m³ and 1782 kg/m³. These measurements indicate a diverse set of materials, with varying degrees of compactness and internal structure. The ultrasonic velocity (UPV) is generally influenced by factors such as elasticity, stiffness, and porosity of the material, while density is determined by the mass per unit volume.

A preliminary dataset analysis suggests a weak correlation between UPV and density, indicating that materials with higher densities tend to exhibit higher ultrasonic velocities. This relationship could be explained by the fact that denser, more compact and cohesive materials offer greater resistance to the propagation of ultrasonic waves. In contrast, lower-density materials, which may contain more voids and less internal cohesion, could allow ultrasonic waves to propagate more easily, resulting in lower UPV values. Figure 3 presents a graphical representation of the correlation between UPV and density. From these values, some trends can be identified:

- Higher UPV values (e.g. 1.252 km/s, 1.383 km/s, 1.435 km/s) are often associated with higher densities (e.g., 1622 kg/m³, 1619 kg/m³, 1603 kg/m³);
- Lower UPV values (e.g., 0.626 km/s, 0.645 km/s, 0.649 km/s) tend to correspond to lower or moderate densities (e.g., 1516 kg/m³, 1591 kg/m³, 1473 kg/m³).

The observed correlation between UPV and density, however, is not linear, as there is some variation in the data. For instance, some samples with relatively high UPV values (e.g., 1.186 km/s) have lower densities (e.g., 1502 kg/m³), which could indicate the presence of other factors influencing the UPV, such as differences in soil composition or structure. Further statistical analysis and experimental studies would be necessary to fully quantify this relationship and account for additional variables.

Correlation between UPV and compressive strength

The ultrasonic velocity values obtained through non-destructive testing (NDT) and the corresponding compressive strength values obtained through destructive testing (DT) were analyzed to identify a correlation between the two (Figure 4). The relationship between ultrasonic pulse velocity (UPV) and compressive strength in the studied soil mixtures reveals significant variations, indicating the influence of material composition and structural characteristics on mechanical performance. The recorded UPV values range from approximately 0.472 km/s to 1.626 km/s, while the compressive strength values exhibit a broader spectrum, from 0.419 MPa to 7.421 MPa.

An initial observation highlights that higher UPV values tend to correspond to increased compressive strength, which aligns with the general principle that denser and more compact materials facilitate faster ultrasonic wave propagation and exhibit greater strength. However, exceptions exist, particularly in cases where relatively low UPV values are associated with remarkably high compressive strengths. For instance, a UPV of 0.759 km/s is linked to a compressive strength of 2.837 MPa, while another instance with a similar UPV of 0.731 km/s reaches 3.970 MPa.

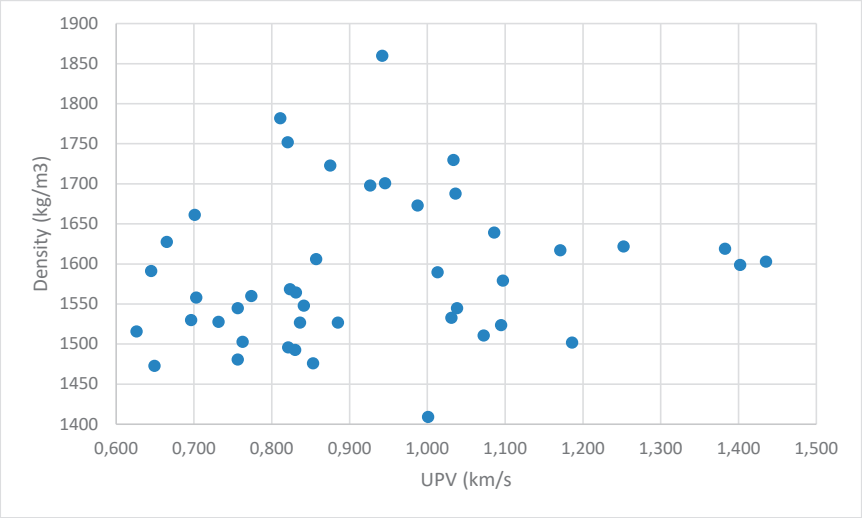


Figure 3. Correlation between UPV and density

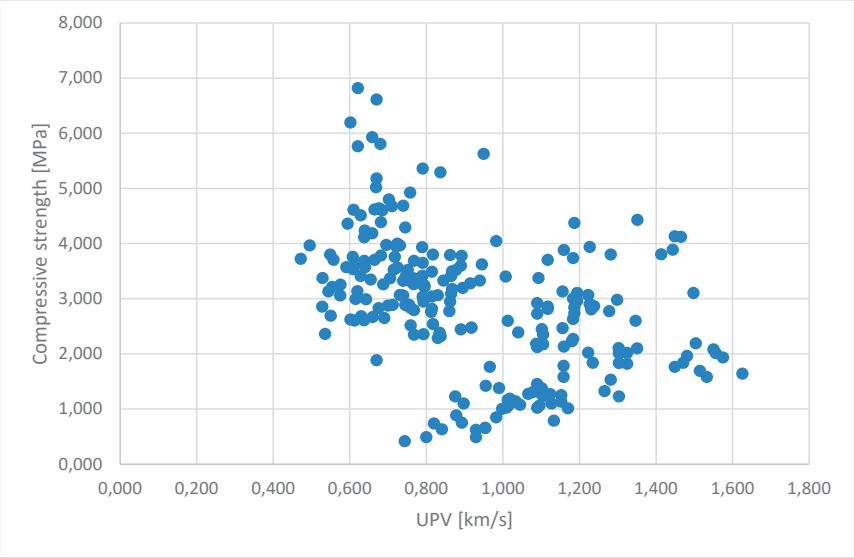


Figure 4. Correlation between UPV and compressive strength

This suggests that factors beyond wave velocity, such as bonding properties and granular arrangement, play an important role in determining compressive strength.

In the lower UPV range (below 0.8 km/s), the compressive strength fluctuates significantly. Some samples exhibit moderate values (e.g., 0.744 km/s corresponding to 0.419 MPa), whereas others demonstrate much higher strengths (e.g., 0.629 km/s associated with 4.513 MPa). These variations imply that certain compositions enable substantial strength development even at relatively low wave velocities, possibly due to optimized particle packing and binder interactions.

Conversely, in the upper UPV range (above 1.2 km/s), compressive strength values remain predominantly higher. For example, a UPV of 1.498 km/s corresponds to a compressive strength of 3.108 MPa, while another instance with 1.303 km/s reaches 2.109 MPa. The consistency in this range suggests that well-

compacted and structurally sound mixtures promote both enhanced wave transmission and mechanical resistance.

Notably, some outliers indicate a deviation from the expected trend. For instance, a UPV of 0.670 km/s corresponds to a remarkably high compressive strength of 6.613 MPa, demonstrating that under specific conditions, even materials with relatively low ultrasonic velocities can exhibit superior values of compressive strength. These anomalies may arise from unique microstructural formations or particular curing processes that enhance cohesion and load-bearing capacity.

Overall, the data suggest a general positive correlation between UPV and compressive strength, albeit with notable exceptions influenced by material-specific properties. The findings highlight the complexity of soil-based materials and underscore the necessity for a comprehensive understanding of both physical and chemical factors when evaluating their mechanical performance.

CONCLUSIONS

The first part of the analysis focused on the relationship between UPV and density. A general trend was observed, where higher UPV values tended to correspond to higher densities. This is consistent with the fundamental principles of material science, as denser materials typically allow sound waves to propagate more quickly due to their compact and homogeneous structure. For example, samples with UPV values above 1.0 km/s often exhibited densities exceeding 1600 kg/m³, while lower UPV values (e.g., 0.626 km/s) were associated with lower densities (e.g., 1409 kg/m³). However, exceptions to this trend were noted, indicating that factors such as soil composition, porosity, and moisture content also play a significant role in influencing UPV independently of density.

The second part of the analysis examined the relationship between UPV and compressive strength. The data revealed a general trend where higher UPV values tend to correspond to higher compressive strengths. This aligns with the fundamental principles of material science, as materials with greater density and compactness typically exhibit faster ultrasonic wave propagation and higher resistance to compressive forces. For instance, samples with UPV values exceeding 1.0 km/s often demonstrated compressive strengths above 1.0 MPa, with some reaching up to 4.136 MPa. This trend supports the hypothesis that UPV can serve as an indirect indicator of compressive strength in soil and similar materials.

Despite the general trend, the dataset exhibited significant variability and several outliers. Some samples with relatively low UPV values (e.g., 0.629 km/s) displayed unexpectedly high compressive strengths (e.g., 4.513 MPa), while others with moderate UPV values (e.g., 0.930 km/s) showed low compressive strengths (e.g., 0.491 MPa). These anomalies highlight the influence of additional factors, such as soil composition, moisture content, curing conditions, and the presence of binding agents, which can significantly alter the mechanical properties of the material independently of UPV.

Combining the insights from both analyses, it is evident that density, UPV, and compressive strength are interrelated but not solely dependent on one another. Higher density generally contributes to both higher UPV and higher compressive strength, but the relationships are not strictly linear or deterministic. For example, some samples with moderate densities exhibited high UPV but low compressive strength, while others with lower densities showed high compressive strength due to factors such as strong internal bonding or optimal moisture content. This highlights the complexity of the interactions between these variables.

ACKNOWLEDGEMENTS

This work was carried out within the Nucleus Programme of the National Research Development and Innovation Plan 2022-2027, supported by MCID, "ECODIGICONS" project no. PN 23 35 04 01: “Fundamental-applied research into the sustainable development of construction products (materials, elements, and structures, as well as methods and technologies) that utilizes current national resources to enhance the eco-innovative and durable aspects of Romania's civil and transport infrastructure”, financed by the Romanian Government.

REFERENCES

Bui, Q., & Morel, J. (2014). First exploratory study on the ageing of rammed earth material. *Materials*, 8(1), 1-15.

Boukhelkhal, D. and Guermazi, M. (2018). The use of non-destructive tests to estimate self-compacting concrete compressive strength. *Matec Web of Conferences*, 149, 01036.

Campiani, A., Lingle, A., & Lercari, N. (2019). Spatial analysis and heritage conservation: leveraging 3-D data and GIS for monitoring earthen architecture. *Journal of Cultural Heritage*, 39, 166-176.

Charif, H. B., Zerlenga, O., & Iaderosa, R. (2024). Low-cost photogrammetry for detailed documentation and condition assessment of earthen architectural heritage: the ex-hotel oasis rouge in Timimoun as a case study. *Buildings*, 14(10), 3292.

Hong, S., Yoon, S., Kim, J., Lee, C., Kim, S., & Lee, Y. (2020). Evaluation of condition of concrete structures using ultrasonic pulse velocity method. *Applied Sciences*, 10(2), 706.

Kim, W., Jeong, K., Choi, H., & Lee, T. (2022). Correlation analysis of ultrasonic pulse velocity and mechanical properties of normal aggregate and lightweight aggregate concretes in 30–60 MPa range. *Materials*, 15(8), 2952.

Lee, Y., Hong, S., Kim, S., & Park, J. (2014). Estimation of compressive strength of concrete member using ultrasonic pulse velocity method. *Key Engineering Materials*, 605, 143-146.

Mohammad, I. (2011). Non-destructive testing for concrete: dynamic modulus and ultrasonic velocity measurements. *Advanced Materials Research*, 243-249, 165-169.

Mousourakis, A., Arakadaki, M., Kotsopoulos, S., Sinamidis, I., Mikrou, T., Frangedaki, E., & Lagaros, N. D. (2020). Earthen architecture in Greece: traditional techniques and revaluation. *Heritage*, 3(4), 1237-1268.

Ni, L., Zheng, D., Yang, H., Ding, X. (2024). Effect of pouring time on the integrity of pulverized fuel ash concrete. *Applied Sciences*, 14(4), 1332.

NP137. Normative for *in situ* evaluation of the concrete compressive strength of the existing constructions. 2014.

Scientific Papers. Series E. Land Reclamation, Earth Observation & Surveying, Environmental Engineering. Vol. XIV, 2025
Print ISSN 2285-6064, CD-ROM ISSN 2285-6072, Online ISSN 2393-5138, ISSN-L 2285-6064

EVALUATING AGGREGATE CONTENT AND ITS EFFECT ON CLAY MORTAR PERFORMANCE

Aurelia BRADU[1], Alexandrina-Elena ANDON[1], Alexandra-Marina BARBU[1], Claudiu-Sorin DRAGOMIR[2]

[1]National Institute for Research and Development in Construction, Urban Planning and Sustainable Spatial Development - URBAN-INCERC, 266 Pantelimon Road, 021652, District 2, Bucharest, Romania
[2]University of Agronomic Sciences and Veterinary Medicine of Bucharest, 59 Mărăşti Blvd, 011464, District 1, Bucharest, Romania

Corresponding author email: aurelia.bradu@incd.ro

Abstract

The most commonly used material in the construction sector is arguably cement, the production of which generates massive amounts of greenhouse gases, contributing approximately 5-8% of global CO_2 emissions. A potential solution in this context is the use of inorganic binders from local sources, a trend that is gaining momentum in research studies within the construction materials industry. Clay-based masonry mortar represents a viable, eco-friendly, and cost-effective solution, with its components being abundantly available worldwide. Clay has demonstrated its effectiveness as a binder over centuries. In its natural, calcined, or modified forms, clay serves as an important alternative to cement, offering sustainable material development at lower costs and with reduced environmental impact. Clay is a sedimentary rock, whose main ingredient is aluminium silicate, characterized by its colloidal appearance and binding properties. The primary feature of clay is its ability to absorb large amounts of water, transforming into a pasty, ductile mass that can be easily shaped into any form.

Key words*: clay composite, local materials, mortar.*

INTRODUCTION

Global demand for cement and concrete products has increased significantly in recent years, due to the development of economies and the continuous growth of the world population (Kouakou et al., 2009; Berriel et al., 2016). According to the report published by CEMBUREAU (2023), in 2022 about 4.1 billion tons of cement were produced, the largest share being attributed to China - 51.1%.

The total quantity of cement that was imported in 2022 to Europe increased almost fourfold compared to 2016, the values of the quantities of imported tons are illustrated in Figure 1 (Andrew, 2018). Romania has witnessed a 459% increase in cement imports during this period, from 204,264 t in 2016 to 1,142,932 t in 2022 (CEMBUREAU, 2023). This has contributed to the expansion of various concrete-related industries, from the extraction of raw materials to the increased consumption of fossil fuels for material processing and cement production (Memon et al., 2012). At the same time, it should be noted that the impact of increased demand is reflected in the increase in cement prices by over 150% in the last decade and threatens significant environmental impacts, phenomena that need to be mitigated (Ahmad et al., 2011). Thus, improving the sustainability of the construction sector has become a major concern for researchers in this field.

A significant percentage of construction materials contain cement, which represents a hydraulic binder developed through an energy-intensive process. Cement production process emits large amounts of greenhouse gases and contributes approximately 5-8% to global CO_2 emissions.

According to estimates, this share could reach 10-15% if stringent measures are not taken to decarbonize the construction industry (Schneider et al., 2011). In this regard, significant progress has been made in the field of making construction products more efficient and there is a considerable increase in the level of involvement, awareness and engagement in projects to reduce environmental impact

(Kajaste et al., 2016). The automation of lime production in modern kilns and the use of alternative fuel resources represent an important step towards reducing energy consumption and CO_2 emissions (Deja et al., 2010), but these solutions are being outpaced by the exponential growth of demand, which is driving the development of new ways to reduce environmental impact and costs.

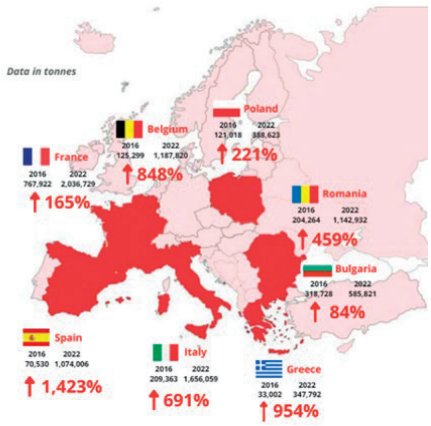


Figure 1. Quantity of tons of cement imported into Europe (CEMBUREAU, 2023)

Among the classic solutions to reduce the need for cement in the shrinkage materials industry, one can mention the partial substitution of cement by using industrial by-products such as fly ash and blast furnace slag, but its applicability is limited by the generation capacity of power plants or blast furnace industries (Alujas et al., 2015; Teklay et al., 2016).

Currently, in the construction sector, there is a growing demand for sustainable materials and products, with ecological characteristics, obtained through non-polluting processes and with increasingly lower energy consumption (Mircea et al., 2021). In order to gain a secure market, being in competition with traditional construction materials/products, made through energy-consuming and polluting processes, materials with ecological properties must have comparable or superior characteristics and durability (Calatan et al., 2020).

The use of natural materials in the production of various construction products is one of the solutions with high potential to achieve the aforementioned goals, and clay is one of these materials (Hegyi et al., 2023).

Clay represents a natural, sustainable, cheap and widely available material worldwide. Since the earliest times of the development of human civilization, clay has been used to obtain various materials and products for construction, either with a non-structural role, such as clay walls and floors, or even with a structural role, namely tiles for making roofs, bricks or clay blocks (Hegyi et al., 2016).

Clay is a sedimentary rock, whose main ingredient is aluminium silicate, characterized by its colloidal appearance and binding properties. The primary feature of clay is its ability to absorb large amounts of water, transforming into a pasty, ductile mass that can be easily shaped into any form (Petcu et al., 2023).

Clay-based construction materials and products are increasingly used at the national level, with the benefits of clay recognized not only for the technical characteristics it imparts to construction materials and products but also for its contribution to enhancing the durability of construction elements over time. The growing adoption of clay in Romanian construction, alongside other traditional natural materials, reflects the industry's alignment with sustainable development principles through the application of environmentally friendly technologies. Additionally, it supports the creation of a healthier environment and contributes to reducing climate change caused directly by human activities.

This study evaluates the influence of aggregate content on the performance of clay-based mortar which can be used to create eco masonry for sustainable buildings.

MATERIALS AND METHODS

The clay composite utilized in this study was prepared using locally sourced materials, including sand fractions of 0-1 mm and 0-4 mm, coarse aggregates of 4-8 mm, and clayey soil characterized by a composition of 53% clay, 44% silt, and 3% sand. The water content required for each formulation was determined experimentally to achieve optimal workability. The compositions analysed in the study are detailed in Table 1.

Table 1. Tested clay compositions

`Constituents	Units	R1	R2	R3
Sand 0-1	g	439	366	293
Sand 0-4	g	4578	3851	3052
Aggregates 4-8 mm	g	4204	3503	2803
Clay soil	g	6148	7684	9221
Water/clay soil ratio		0.52	0.48	0.52
Clay soil/aggregates ratio		0.40	0.50	0.60

The consistency of the fresh mixture was evaluated in accordance with the standard SR EN 1015-3:2001/A2:2007, which specifies the procedure for determining the consistency of masonry mortars using the flow table method. As illustrated in Figure 2, the test involved placing a conical mould on a circular table and filling it with the fresh clay-based mortar in two layers. Each layer was compacted using a standardized metal tamper. Following the removal of the mould, 15 consecutive drops of the table were performed within 15 seconds, after which the average spread diameter of the sample was measured.



Figure 2. Determination of the consistency of the fresh clay mixture

The fresh clay mortar was then cast into standardized metallic moulds with dimensions of 160 × 40 × 40 mm (Figure 3). After a curing period of three days, the specimens were demoulded and stored under controlled laboratory conditions at a temperature of 20 ± 2°C and relative humidity of 65 ± 5% until testing at 28 days.

The performance of the hardened clay mortar was assessed based on density, flexural strength, and compressive strength. The density of the material was influenced by the granulometric distribution, which governed the packing efficiency of the particles and the proportion of voids within the composite.



Figure 3. Casting fresh clay mixture in metal moulds

The internal structure of the clay-based material played a significant role in determining its mechanical performance and durability, as extensively examined in previous studies under various operational conditions.

The density of the hardened mixture was determined with the relationship:

$$D = \frac{m}{V} \qquad (1)$$

where:

D - density of hardened mixture, kg/m^3;

m - mass of the specimen, kg;

V - volume determined by measurement, m^3.

Flexural strength testing was conducted according to the SR EN 1015-11:2020 standard, which outlines the procedures for evaluating the mechanical performance of hardened masonry mortars. The specimens were positioned on support rollers, and a controlled load was applied at a rate of 10-50 N/s until failure occurred within a time frame of 30 to 90 seconds. The flexural strength was determined using the following equation:

$$R_f = \frac{1.5 \cdot F_f \cdot l}{bd^2} \qquad (2)$$

where:

R_f - bending strength, MPa;

b - prism width, mm;

d - prism height, mm;

F_f - load applied in the middle of the prism at rupture, N;

l - distance between the support rollers, mm.

Compressive strength, a fundamental parameter in the assessment of mortars, was also determined in accordance with SR EN 1015-11:2020. The test was conducted on the halves of the specimens obtained from the flexural strength test. Prior to testing, the specimens

were measured to ensure dimensional accuracy, and their surfaces were verified for parallelism to minimize experimental errors. The load-bearing surfaces of the testing apparatus were cleaned using a dry textile before securing the samples. The specimens were positioned to ensure uniform load distribution, with a clearance of 16 ± 1 mm from the nearest support edge. The compressive load was applied gradually, within a controlled range of 50 N/s to 500 kN/s, ensuring failure occurred within 30 to 90 seconds.

Compressive strength was determined with the formula:

$$R_c = \frac{F_c}{1600} \qquad (3)$$

where:

R_c - compressive strength, MPa;

F_c - maximum load at the moment of rupture, N;

1600 - area of the plates (40 x 40 mm), mm^2.

RESULTS AND DISCUSSIONS

The clay-based mortar formulations achieved optimal workability at a spread diameter of 105 ± 1 mm. As illustrated in Figure 4, mixtures with a lower spread exhibited reduced cohesion and workability, forming a stiff, low-fluidity mass. In contrast, mixtures with excessive spread exhibited a paste-like consistency with excessive stickiness.

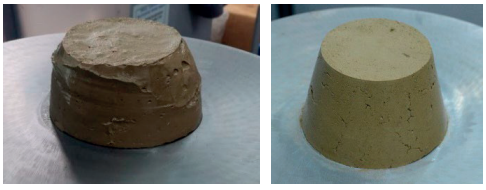


Figure 4. Different consistency of the fresh clay mixture

Density of clay mortar

Higher-density clay mixtures displayed a more compact internal structure, with enhanced particle bonding and lower porosity, whereas lower-density mixtures exhibited improved thermal properties. The uniformity of the clay mortar mixtures was confirmed by the low coefficient of variation (COV), which remained below 1%, indicating a consistent internal structure. The mean density values at 28 days were 1914 kg/m³ for recipe R1 (COV = 0.24), 1939 kg/m³ for R2 (COV = 0.08), and 1961 kg/m³ for R3 (COV = 0.24). The increase in aggregate content led to higher densities due to the greater specific weight of the aggregates compared to the clay matrix, promoting a denser packing arrangement where fine clay particles occupied the voids between aggregates. The aggregate distribution for recipe R2 is depicted in Figure 5.



Figure 5. Aggregate distribution for R2

Flexural Strength

The flexural strength results, determined in accordance with SR EN 1015-11:2020, ranged from 1.06 MPa for recipe R1 (50% clay) to 1.17 MPa for recipe R3 (60% clay). The correlation between density and flexural strength at 28 days is presented in Figure 6. The binding role of clay was evident, as its proportion directly influenced the mechanical performance.

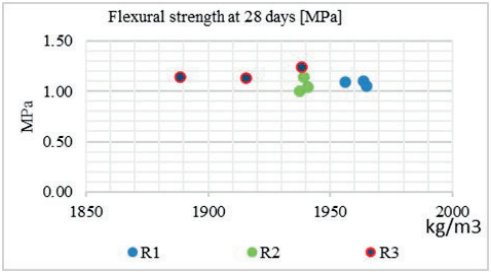


Figure 6. Correlation between density and flexural strength at 28 days

To achieve optimal strength, the clay content must be sufficient to completely coat the aggregate surfaces, facilitating the development of a cohesive and structurally stable matrix. The increased flexural strength observed in mixtures

with higher clay content can be attributed to the formation of silico-aluminate bonds, which enhance the mechanical integrity of the composite. The failure mode of the specimens under flexural testing is shown in Figure 7. The coefficient of variation for flexural strength ranged from 2.19% to 6.53%, further confirming the homogeneity of the material.



Figure 7. The mode of failure of the sample subjected to bending

Compressive Strength

Compressive strength was evaluated using the prism halves obtained from the flexural strength test (Figure 8). The failure mechanism of the material under uniaxial compression was associated with the transverse tensile stresses generated at the aggregate-matrix interface. The primary factors influencing compressive strength included the quality and proportion of the constituent materials, adhesion between the clay matrix and aggregates, compaction state, curing conditions, and specimen age.



Figure 8. Compressive strength of the prism halves

The average compressive strengths recorded at 28 days were 2.98 MPa for R1 (40% clay), 3.72 MPa for R2 (50% clay), and 3.79 MPa for R3 (60% clay), with coefficients of variation ranging from 4.22% to 5.77%. The distribution of compressive strength results is shown in Figure 9. The results indicated that the recipe R3, containing 60% clay marked highest compressive strength, representing a 27% increase compared to the Recipe R1 with 40% clay content. The higher clay content contributed to improved compressive strength due to enhanced bonding between the matrix and aggregates. However, excessive clay content may lead to reduced permeability, which could affect the long-term durability of the material.

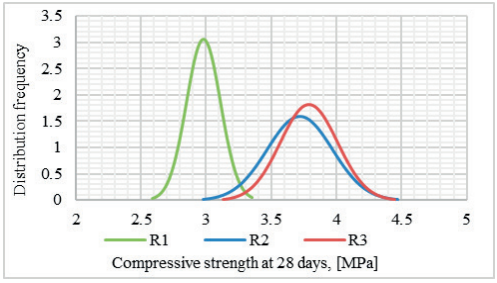


Figure 9. Distribution of 28-day compressive strength results

CONCLUSIONS

The increasing demand for sustainable materials and products in the construction sector contributes to the development of environmentally friendly materials, which contribute to reducing the consumption of natural resources, increasing the energy efficiency of buildings and protecting the environment.

Preliminary results have marked a promising performance of the prototypes, confirming their potential to replace traditional masonry mortar with a high ecological footprint. In addition, the use of local and economically accessible materials supports the development of a circular economy, while contributing to the sustainability of rural communities and reducing production costs

Thus, following the analysis of the results obtained, the R3 recipe containing 60% of the total amount of aggregates showed superior results, both in the case of flexural strength - 1.17 MPa, with a coefficient of variation of

5.19%, and in the case of compressive strength - 3.79 MPa, and a coefficient of variation of 5.77%.

ACKNOWLEDGEMENTS

This paper was supported by the Program Advanced research on the development of eco-innovative solutions, composite materials, technologies and services, in the concept of a circular economy and increased quality of life, for a sustainable digitized infrastructure in a built and urban environment resilient to climate change and disasters, "ECODIGICONS", Program code: PN 23 35 03 01: "Integrated system of development and scientific research of constructions and vital infrastructures exposed to extreme seismic and climatic environmental actions and the exploitation of sustainable resources of materials and energy", financed by the Romanian Government.

REFERENCES

Ahmad, S., Barbhuiya, S., Elahi, A., & Iqbal, J. (2011). Effect of Pakistani bentonite on properties of mortar and concrete. *Clay Minerals,* 46(1), 85–92

Alujas, A., Fernández, R., Quintana, R., Scrivener, K. L., & Martirena, F. (2015). Pozzolanic reactivity of low grade kaolinitic clays: Influence of calcination temperature and impact of calcination products on OPC hydration. *Applied Clay Science, 108,* 94–101.

Andrew, R. M. (2018). Global CO_2 emissions from cement production. *Earth System Science Data Discussions, 10*, 195–217.

Berriel, S. S., Favier, A., Domínguez, E. R., Machado, I. S., Heierli, U., Scrivener, K., Hernández, F. M., & Habert, G. (2016). Assessing the environmental and economic potential of Limestone Calcined Clay Cement in Cuba. *Journal of Cleaner Production, 124*, 361–369

Calatan, G., Hegyi, A., Dico, C., & Szilagyi, H. (2020). Opportunities regarding the use of adobe-bricks within contemporary architecture. *Procedia Manufacturing*, 46, 150–157

CEMBUREAU, Activity report 2022. *The European Cement Association*, 2023, Brussel.

Deja, J., Uliasz-Bochenczyk, A., & Mokrzycki, E. (2010). CO_2 emissions from Polish cement industry. *International Journal of Greenhouse Gas Control*, *4*(4), 583–588.

Hegyi, A., Dico, C., & Calatan, G. (2016). Construction sustainability with adobe bricks type elements. *Urbanism. Arhitectura. Constructii*, *7*(2), 147.

Hegyi, A., Petcu, C., Ciobanu, A. A., Calatan, G., & Bradu, A. (2023). Development of Clay-Composite Plasters Integrating Industrial Waste. *Materials*, *16*(14), 4903.

Kajaste, R., & Hurme, M. (2016). Cement industry greenhouse gas emissions - Management options and abatement cost. *Journal of Cleaner Production, 112*, 4041–4052.

Kouakou, C., & Morel, J. C. (2009). Strength and elasto-plastic properties of non-industrial building materials manufactured with clay as a natural binder. *Applied Clay Science, 44*(1), 27–34.

Memon, S. A., Arsalan, R., Khan, S., & Lo, T. Y. (2012). Utilization of Pakistani bentonite as partial replacement of cement in concrete. *Construction and Building Materials, 30*, 237–242.

Mircea, C., Toader, T.-P., Hegyi, A., Ionescu, B.-A., & Mircea, A. (2021). Early Age Sealing Capacity of Structural Mortar with Integral Crystalline Waterproofing Admixture. *Materials*, *14*(17), 4951.

Petcu, C., Dobrescu, C. F., Dragomir, C. S., Ciobanu, A. A., Lăzărescu, A. V., & Hegyi, A. (2023). Thermophysical Characteristics of Clay for Efficient Rammed Earth Wall Construction. *Materials*, *16*(17), 6015

Schneider, M., Romer, M., Tschudin, M., & Bolio, H. (2011). Sustainable cement production - Present and future. *Cement and Concrete Research, 41*(7), 642–650.

Teklay, A., Yin, C., & Rosendahl, L. (2016). Flash calcination of kaolinite rich clay and impact of process conditions on the quality of the calcines: A way to reduce CO2 footprint from cement industry. *Applied Energy*,*162,* 1218–1224.

SR EN 1015-3:2001/A2:2007, Methods of test for mortar for masonry - Part 3: Determination of consistence of fresh mortar (by flow table).

SR EN 1015-11:2020. Methods of test for mortar for masonry - Part 11: Determination of flexural and compressive strength of hardened mortar.

Scientific Papers. Series E. Land Reclamation, Earth Observation & Surveying, Environmental Engineering. Vol. XIV, 2025
Print ISSN 2285-6064, CD-ROM ISSN 2285-6072, Online ISSN 2393-5138, ISSN-L 2285-6064

INTEGRATION OF UAV-BASED LIDAR, PHOTOGRAMMETRY, AND SLAM TECHNOLOGIES FOR THE COMPLETE ABOVE AND BELOW GROUND MAPPING OF MOUNTAINOUS HYDRO-TECHNICAL INFRASTRUCTURE

Simion BRUMA[1, 2], Catalin-Stefanel SABOU[1, 2], Ioana POP[1], Florica MATEI[1], Paul SESTRAS[1, 3], Mircea NAP[1], Elemer-Emanuel SUBA[1], Tudor SALAGEAN[1, 2, 4]

[1]University of Agricultural Sciences and Veterinary Medicine Cluj-Napoca, 3-5 Calea Mănăștur, 400372, Cluj-Napoca, Romania
[2]Technical University of Civil Engineering Bucharest, Doctoral School, 122-124 Lacul Tei Blvd, District 2, 020396, Bucharest, Romania
[3]Academy of Romanian Scientists, 3 Ilfov Street, District 5, 050044, Bucharest, Romania
[4]Technical Sciences Academy of Romania, 26 Dacia Blvd, District 2, 030167, Bucharest, Romania

Corresponding author emails: paul.sestras@usamvcluj.ro, tudor.salagean@usamvcluj.ro

Abstract

The comprehensive mapping and inspection of both underground and above-ground terrain in mountainous environments pose significant challenges for engineering projects, particularly those involving legacy infrastructure. This study presents an integrated geospatial methodology for the rehabilitation and modernization of the Tomesti micro-hydropower station in Timiș County, Romania. By combining GNSS-based control networks, UAV photogrammetry, airborne LiDAR, and handheld SLAM scanning, the project achieved high-resolution data acquisition across complex topographies and inaccessible subsurface structures. Ground control points were established using total stations to ensure millimetric precision and consistent georeferencing of all datasets. The workflow delivered orthophotos, digital surface and terrain models, detailed topographic plans, and 3D reconstructions of the interior hydro-technical gallery. These outputs formed the foundation for updated technical documentation and supported engineering analyses for structural rehabilitation and eco-friendly water intake systems. The results confirm that modern geomatics, when anchored in classical surveying practices, provides a robust framework for accurate assessment, design, and environmental integration. This case study underscores the value of multi-sensor approaches in repurposing abandoned infrastructure for sustainable energy production and demonstrates their practical relevance in mountainous terrain.

Key words*: 3D, LiDAR, SLAM, topographic mapping, UAV.*

INTRODUCTION

Accurate land surveying is a cornerstone of complex engineering projects, especially in rugged or inaccessible terrain (Sestras et al., 2025). Infrastructure and energy development rely on precise topographic data, spatial modelling, and georeferenced planning to minimize risk, control costs, and ensure environmental sustainability. This becomes even more critical in projects involving legacy infrastructure or underground features, where outdated or missing data can cause technical and environmental issues (Langhammer et al., 2018). In response, modern surveying integrates advanced technologies, GNSS, UAV LiDAR, photogrammetry and SLAM, that have reshaped terrain analysis, rehabilitation strategies, and design processes (Nap et al., 2023). These tools not only support but significantly enhance the resolution, speed, and precision of early-stage decision-making.

This study centers on the revival of the Tomesti micro-hydropower station in Timiș County, Romania, combining geospatial innovation with sustainable energy goals. Initially launched before 1989, the site includes upstream intakes, an underground gallery, and a partially built hydroelectric cavern. Work was halted, leaving behind incomplete and poorly documented infrastructure. With renewed emphasis on renewable energy and national energy security, reassessing and completing this project using modern technical and

environmental standards has become a strategic priority.

To guide the design, rehabilitation, and environmental compliance of this complex project, a comprehensive geospatial survey was carried out. The methodology integrated total stations and GNSS-based control networks for spatial accuracy, UAV-based LiDAR for detailed surface modelling, and SLAM technology for high-precision scanning of underground tunnels (Liu et al., 2024). These combined approaches produced orthophotos, DSM/DTM models, topographic plans, and 3D reconstructions of the subterranean system, forming the technical foundation for feasibility assessments and future planning.

While geospatial technologies like UAV photogrammetry, LiDAR, and SLAM have advanced rapidly, classical instruments such as GNSS receivers and total stations remain essential in complex terrain (Sălăgean et al., 2019; Sestras, 2021). Their precision is unmatched when defining geodetic control networks - critical for survey accuracy. GNSS, particularly in RTK or PPK mode, enables fast, accurate 3D positioning across large areas, while total stations offer high angular accuracy in areas with limited satellite visibility, such as valleys or forested regions.

Classical surveying instruments are essential in establishing Ground Control Points (GCPs) and Independent Check Points (ICPs), which are critical for georeferencing UAV imagery and validating products like orthophotos, DSMs, and DTMs (Stöcker et al., 2020). Regardless of technological advancements, airborne systems depend on precise ground data for calibration and accuracy. UAV and SLAM outputs achieve their full potential only when tied to a solid geodetic network established via GNSS and total stations.

As highlighted in both the literature and the present methodology, relying solely on aerial or mobile sensors can lead to positional drift, systematic errors, or reduced accuracy in dense vegetation or occluded zones. Total stations and GNSS provide consistent benchmarks and validation points across the survey area, mitigating these limitations.

Given the complexity of terrain in engineering surveys, no single method suffices in isolation (Bilașco et al., 2021). A multi-sensor approach, especially combining UAV-based LiDAR and photogrammetry, proves far more effective in achieving full spatial coverage and accuracy.

Structure-from-Motion (SfM) photogrammetry reconstructs 3D surfaces from drone-captured images (Khanal et al., 2020), excelling in open areas with visible features like buildings or roads. It offers affordability, high visual detail, and easy interpretation. However, in vegetated areas, it struggles to capture ground surfaces (Popescu et al., 2024). LiDAR, by contrast, penetrates vegetation to provide accurate terrain data, even in low-light conditions (Oniga et al., 2023). Still, it may miss finer architectural elements and demands more advanced equipment and processing (You & Lee, 2020).

By integrating LiDAR and photogrammetry, surveyors harness the strengths of both systems while mitigating their individual limitations. LiDAR accurately captures terrain beneath vegetation, whereas photogrammetry excels at rendering visible structures. Combined, they offer a more complete and balanced view of the landscape (Sestras et al., 2025a).

This integrated approach is especially valuable for infrastructure projects like hydropower development, where natural topography and built features must be mapped with precision. Generating detailed topographic outputs, 3D models, and full site documentation facilitates improved decision-making, risk evaluation, and design planning (Coroian et al., 2024).

Simultaneous Localization and Mapping (SLAM) has become a crucial technology in areas where GNSS or total stations are less effective (Chio & Hou, 2021). Using LiDAR sensors and inertial units (IMUs), SLAM continuously tracks scanner movement while generating accurate 3D point clouds. Its portability allows surveyors to collect data in confined, GPS-denied spaces like underground infrastructure, interiors, or dense forests (Keitaanniemi et al., 2021).

In our case study, SLAM was essential for mapping the abandoned hydro-technical gallery in Tomesti. The underground sewer system, unreachable by GNSS and unsuited for static scanning, was navigated on foot with a handheld SLAM unit. This enabled both 3D data collection and real-time video inspection, producing a reliable model of the tunnel's

condition and revealing critical information for structural evaluation.

The application of SLAM in rugged environments highlights its value in engineering projects where complex geometries, poor visibility, and restricted access make traditional surveying difficult (Urban et al., 2024). In this project, integrating SLAM data with UAV-derived surface models and geodetic networks created a seamless spatial database, essential for feasibility studies and rehabilitation planning. SLAM emerges not merely as a complementary tool, but as a key technology in multi-sensor surveying, enabling accurate and efficient mapping in the most challenging conditions.

The combined use of photogrammetry and LiDAR greatly improves the quality and flexibility of modern surveys, especially in difficult terrain (Rogers et al., 2020). While these technologies increase coverage and speed, classical instruments like GNSS and total stations remain vital for providing the precision needed for georeferencing and validation. This hybrid approach ensures high-resolution, standards-compliant data that supports reliable infrastructure planning and environmental assessment.

The Tomesti project exemplifies how outdated hydro-infrastructure can be revitalized through a balanced mix of advanced geomatics and traditional methods. It addresses both technical demands and broader goals like sustainable energy and responsible land use in mountainous regions. This case stands out for its interdisciplinary methodology, reliance on accurate data, and strong potential for replication. The following sections outline the geospatial workflow, equipment used, survey results, and how this integrated strategy informs rehabilitation and energy planning.

MATERIALS AND METHODS

Study area and desideratum

The study focuses on a hydro-technical site in eastern Timiș County, within the administrative boundaries of Tomești commune, Romania (Figure 1). Timiș is Romania's largest county, covering about 8,696.7 km² or 3.65% of the national territory. Located in the historical Banat region, it borders Hungary to the west and Serbia to the southwest. The county's capital, Timișoara, situated on the Bega River, is the main urban and administrative centre.

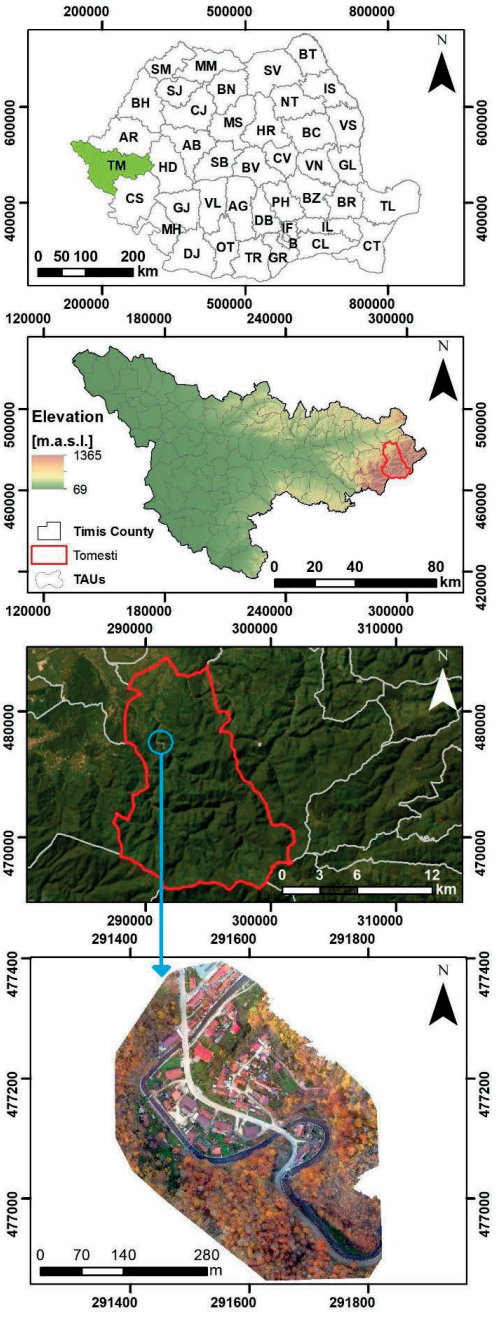


Figure 1. Location of the study area in Timiș County, Romania, showing elevation context, satellite view, and orthophoto of the Tomești micro-hydropower site

Tomești commune lies on the northern slopes of the Poiana Ruscă Mountains, covering 140.94 km² and comprising six villages, including its namesake seat. As of the 2021 census, the population totals 1,879, continuing a declining trend. The area features steep, forested terrain shaped by the upper Bega River and its tributaries, which provide favourable conditions for hydro-technical development due to the region's geomorphological and hydrological profile.

This site was part of a larger hydropower initiative begun during the communist era, which included partial construction of a 9.4 km underground tunnel, two water intakes, and a cavern for a micro-hydropower station. Abandoned before completion, the infrastructure has since deteriorated without maintenance.

The current investment project aims to modernize and finalize the original development using advanced surveying and design tools. Given the complex terrain, outdated documentation, and limited access, technologies such as GNSS, UAV-based LiDAR, and SLAM scanning are essential for georeferencing, surface modelling, and underground inspection.

Aligned with Romania's renewable energy strategy, the project seeks to sustainably harness the site's hydropower potential while ensuring all planning and design stages are based on precise geospatial data. This initiative not only supports technical feasibility and environmental evaluation but also demonstrates how modern methods can breathe new life into legacy infrastructure.

Methodological framework

This study presents an integrated methodological framework for the accurate mapping and inspection of both surface and subsurface components of a previously abandoned micro-hydropower project in Tomești commune, Timiș County. Due to the site's challenging terrain, partial hydro-technical infrastructure, and renewed national focus on renewable energy, the campaign aimed to develop a high-resolution spatial and technical database to support the project's redesign and revitalization.

The need for intervention stems from the deteriorated and outdated state of the original infrastructure. Initially planned before 1989, the project includes two upstream concrete intakes on Bega River tributaries, an underground gallery, and a partially excavated hydroelectric cavern. With no recent surveys or technical evaluations, these structures have experienced extensive environmental and structural degradation. The adopted workflow is outlined in Figure 2.

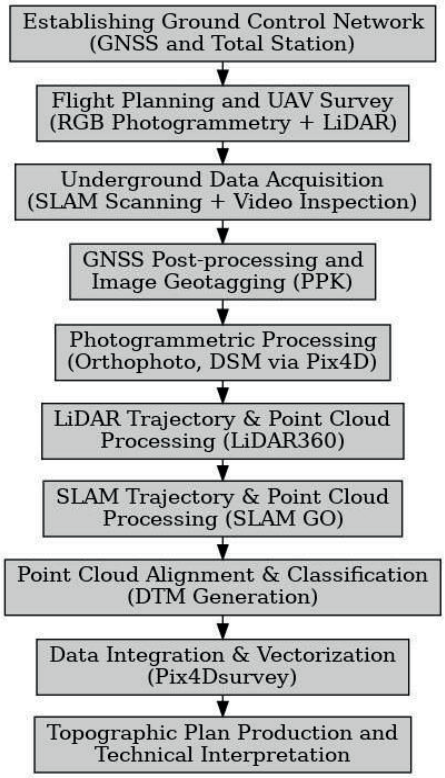


Figure 2. Methodological workflow

To address the complex demands of this project, the methodological framework combined traditional geodetic surveying with advanced remote sensing and 3D scanning techniques. Initially, a ground control network was established using GNSS receivers and total stations, forming a stable reference system for all subsequent data collection and ensuring spatial consistency across datasets.

UAV-based photogrammetry was then performed using drones with high-resolution RGB cameras to produce orthophotos and digital surface models (DSM). These were

refined using LiDAR sensors mounted on UAV platforms, which provided detailed elevation data, even in vegetated or inaccessible zones, enabling the generation of accurate digital terrain models (DTMs) for hydrological and engineering analyses.

To map the underground gallery and associated structures, SLAM (Simultaneous Localization and Mapping) technology was employed. A handheld SLAM unit enabled the collection of 3D point clouds in GPS-denied tunnel environments while also capturing video for visual inspection of structural conditions such as cracks, sedimentation, or collapses.

This hybrid methodology produced robust deliverables tailored for engineering and environmental applications, including:

- High-resolution orthophotos;
- Precise DSMs and DTMs;
- Cross-sectional terrain and tunnel profiles;
- Integrated 3D models;
- Video records of underground conditions.

By providing reliable spatial data, this approach supports feasibility and safety assessments for completing the hydroelectric project in alignment with Romania's energy policy. The method also offers a replicable model for other complex or partially completed infrastructure projects.

Surveying instrumentation and equipment overview

In the Tomești micro-hydropower station rehabilitation project, a suite of advanced surveying instruments was deployed to ensure high-precision data acquisition across diverse terrains and structural challenges. These technologies enabled comprehensive spatial analyses essential for design and planning.

■ GNSS Technology: UniStrong G10 Receiver

To establish the Stereographic 1970 projection, the UniStrong G10 GNSS receiver was used in both static and RTK modes. Supporting GPS, GLONASS, BeiDou, and Galileo constellations, the G10 ensures high positional accuracy. Its tilt compensator auto-corrects based on pole orientation, and its cloud capabilities offer real-time monitoring, updates, and triple data storage for secure acquisition.

■ Total Station: Leica TS16P

In mountainous zones with poor satellite visibility, the Leica TS16P robotic total station was used to densify the control network. This self-learning instrument auto-adjusts to site conditions, offering high-accuracy measurements, a 5-inch touch display, and AutoHeight functionality for automated instrument height reading. It also includes LOC8 technology for remote locking and tracking.

■ UAV-Based Surveying

A DJI Matrice M200 drone with a Zenmuse X4S camera and TOPODRONE 200+ LiDAR system captured aerial data (Figure 3). The LiDAR system, based on the Hesai XT32M2X sensor, offers 200 m range, triple return mode, and 3–5 cm XYZ accuracy. Its built-in 200 Hz IMU and GNSS receiver enable precise georeferencing. Flight planning was performed via Map Pilot Pro, maintaining a steady altitude of 120 m AGL for optimal coverage.



Figure 3. UAV system and GNSS

■ SLAM Technology: Feima SLAM100 Handheld Imaging LiDAR Scanner

The complex water intake structure, which includes underground components, required additional scanning using Simultaneous Localization and Mapping (SLAM) technology (Figure 4). The Feima SLAM100 handheld LiDAR scanner was used for mobile mapping in GNSS-denied environments like tunnels, delivering high-resolution 3D point clouds critical for evaluating the geometry and condition of subterranean infrastructure.

The strategic integration of these advanced surveying instruments ensured the acquisition of precise and comprehensive data, necessary for the effective rehabilitation of the Tomesti micro-hydropower station. Each technology addressed specific challenges posed by the project's diverse terrains and structural intricacies, collectively contributing to a robust

geospatial framework for informed decision-making.



Figure 4. SLAM and TS mapping; video inspection

Geospatial Data Processing and Integration

Following field data acquisition, a structured processing workflow was implemented to ensure data accuracy and integration across UAV photogrammetry, airborne LiDAR, and mobile SLAM sources. Each dataset was processed independently, followed by a unified integration and vectorization stage to produce final deliverables.

UAV imagery was first geotagged using TOPODRONE Post Processing, which synchronized GNSS trajectories with image metadata for high-precision PPK georeferencing. Images were then processed in Pix4Dmapper using a Structure-from-Motion (SfM) pipeline, including alignment, sparse and dense point cloud generation, and surface modelling. The result was a high-resolution orthophoto mosaic accurately referenced to the national coordinate system.

Airborne LiDAR data was refined through several stages to reconstruct the sensor's trajectory and generate a georeferenced 3D point cloud. Using TOPODRONE LiDAR Post Processing, GNSS and IMU data were merged to define the flight path (Figure 5), while the Cloud Generation module converted raw data into spatial coordinates.

To correct internal misalignments, boresight calibration was performed in GreenValley LiDAR360. Manual adjustments of Roll, Pitch, and Heading were made via Stepwise Geometric calibration, using cross-sectional analysis of overlapping flight lines. This was followed by automated strip alignment through least-squares matching for improved spatial coherence.

Ground classification was completed using the Cloth Simulation Filter (CSF), effectively separating terrain from vegetation and infrastructure, resulting in a reliable Digital Terrain Model (DTM).

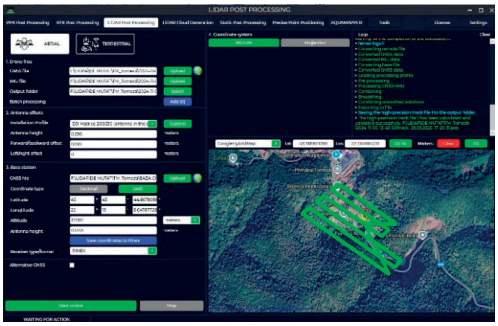


Figure 5. LiDAR postprocessing

SLAM (Simultaneous Localization and Mapping) was performed using the Feima SLAM100 handheld scanner, equipped with a Hensai XT16 LiDAR sensor offering 360° horizontal and 270° vertical coverage. This was essential for mapping the hydro-technical gallery's interior, where GNSS was unavailable. Georeferencing was achieved by aligning SLAM data with Ground Control Points (GCPs) previously measured via total stations, ensuring consistency with the national coordinate system.

Raw SLAM data was processed in SLAM GO software for trajectory reconstruction, noise filtering, and initial alignment. The resulting point cloud was imported into LiDAR360, where the Cloth Simulation Filter (CSF) algorithm classified ground and non-ground points to extract underground terrain and structural elements. All datasets, LiDAR, photogrammetry, SLAM, and total station measurements, were integrated in Pix4Dsurvey, enabling vector extraction and cross-validation. This harmonized geospatial environment allowed accurate digitization of infrastructure features, later exported to AutoCAD for engineering design.

The fusion of classical surveying tools with advanced scanning technologies ensured precise documentation of both surface and subsurface structures, supporting the rehabilitation planning of the Tomesti hydro-technical system.

RESULTS AND DISCUSSIONS

Integrated survey outputs and geospatial products

The integrated survey campaign carried out for the Tomesti micro-hydropower station rehabilitation produced a comprehensive suite of geospatial deliverables essential to the project's technical and environmental planning. These outputs include orthophotos, digital terrain and surface models (DTM/DSM), dense point clouds, topographic layouts, and detailed cross-sections, each contributing to a deeper understanding of both surface and underground conditions.

Figure 6 illustrates a detailed three-dimensional topographic rendering of the Tomesti site, showcasing elevation through dense contour lines. The layout captures the steep and complex terrain of the valley, essential for hydrotechnical planning. Superimposed vector elements such as roads, hydro-technical structures, and land parcel outlines are integrated into the model, allowing for precise spatial analysis and elevation profiling. This visualization supports slope analysis, infrastructure alignment, and drainage assessment, forming a key tool in the rehabilitation planning process of the micro-hydropower system.

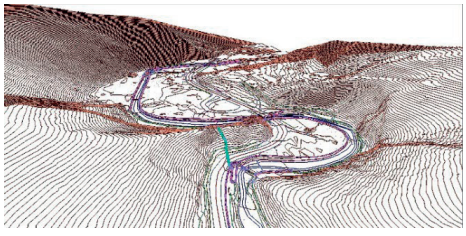


Figure 6. 3D terrain representation with contour lines

Figure 7 presents a high-resolution Digital Elevation Model (DEM) of the Tomesti study area, visualized using a hue-saturation-value (HSV) shader to depict elevation changes. The colour gradient, from red (higher elevations) to blue and green (lower elevations), clearly outlines the valley's terrain morphology, built structures, and hydrological features. The DEM was derived from UAV-based LiDAR data, offering fine detail necessary for slope analysis, hydrological modelling, and infrastructure planning. This product is essential for understanding elevation variability and guiding technical designs within the hydropower rehabilitation project.

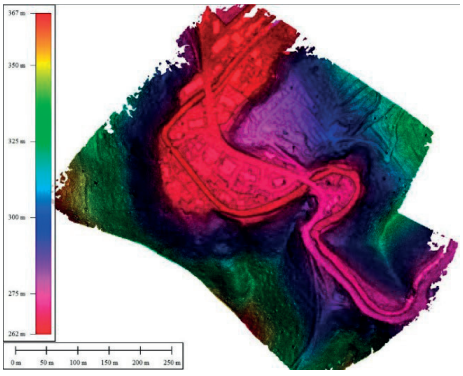


Figure 7. Digital Elevation Model (DEM) with HSV Shading

Figure 8 illustrates a Triangulated Irregular Network (TIN) model overlaid with vector data and geospatial control points. The TIN surface, derived from LiDAR and photogrammetric inputs, represents detailed terrain morphology through irregular triangle meshes. Superimposed vector lines denote features such as roads, hydrological networks, and infrastructure elements, while coloured pins mark field-verified geospatial targets or control points. This combined visualization supports 3D terrain analysis, infrastructure alignment, and engineering planning within the Tomesti hydropower site.

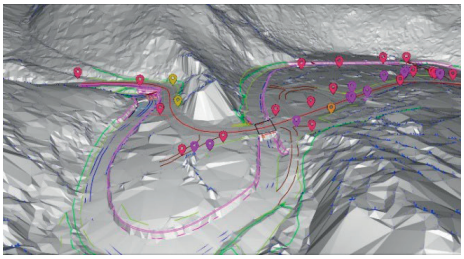


Figure 8. TIN surface with vector overlay and markers

Figure 9 presents a cross-section profile extracted from LiDAR data, corresponding to the yellow transect line shown on the elevation-coloured orthophoto. The upper image provides spatial context within the Tomesti site, while the lower section displays elevation values along the transect. The profile distinctly captures both surface terrain, including road infrastructure and vegetation, as well as the outline of the underground hydrotechnical tunnel. This dual-layer representation offers valuable insights into the vertical spatial relationships between above-ground features and subsurface infrastructure.

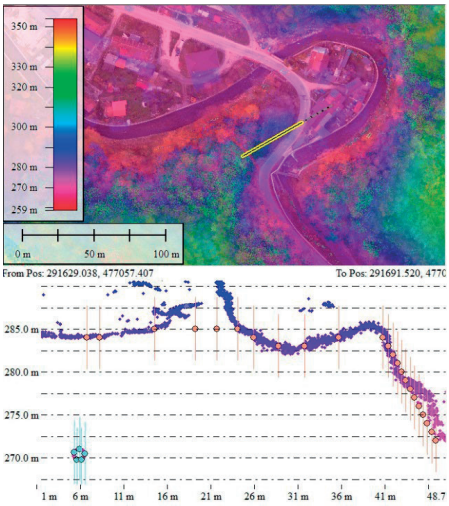


Figure 9. LiDAR and SLAM derived cross-section profile

Figure 10 displays a high-resolution UAV-derived orthophoto of the Tomesti site, overlaid with the traced alignment of the underground tunnel.

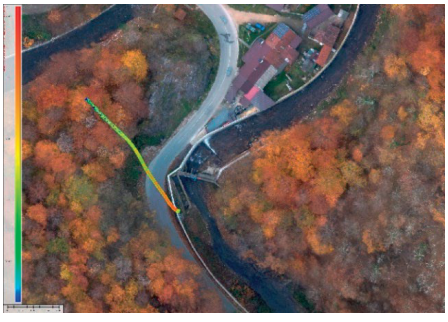


Figure 10. Orthophoto with tunnel overlay

The tunnel path is color-coded by elevation, allowing clear visualization of its trajectory beneath the terrain and infrastructure. The overlay facilitates precise spatial correlation between the subsurface gallery and surface features, proving essential for engineering assessment and future rehabilitation planning.

Topographic mapping and layout plan

Topographic plans are essential tools in civil engineering, infrastructure development, and environmental management. These scaled cartographic outputs accurately represent terrain through elevation contours, hydrography, vegetation, and man-made structures such as roads or utilities. They are critical for understanding slope dynamics, drainage paths, construction feasibility, and site access, particularly in mountainous terrain like the Tomesti study area.

Beyond visual representation, topographic plans integrate data from GNSS, total station, UAV photogrammetry, and LiDAR to provide georeferenced context for all design and modelling efforts.

In modern workflows, these plans are derived from dense point clouds and processed in platforms such as Pix4Dsurvey or AutoCAD Civil 3D, allowing precise integration with engineering and environmental analyses. Their role extends from initial assessment to ongoing monitoring, making them a central deliverable in multidisciplinary survey projects.

The Topographic Plan (Figure 11) marks the culmination of the Tomesti survey campaign, merging LiDAR and photogrammetric data with vector features derived from total station observations. It depicts both natural and built elements, offering a comprehensive layout for hydrotechnical assessment and design. Contour lines extracted from the DTM illustrate slope variations and elevation changes crucial for hydrological planning and infrastructure layout. The alignment of the underground gallery, catchment structures, forested zones, roads, and open terrain are all vectorized and overlaid on an orthophoto mosaic, enabling precise visual correlation with real-world imagery.

This detailed and multi-layered plan provides the spatial foundation for modelling, engineering design, and environmental evaluations, supporting the informed rehabilitation of the Tomesti micro-hydropower system.

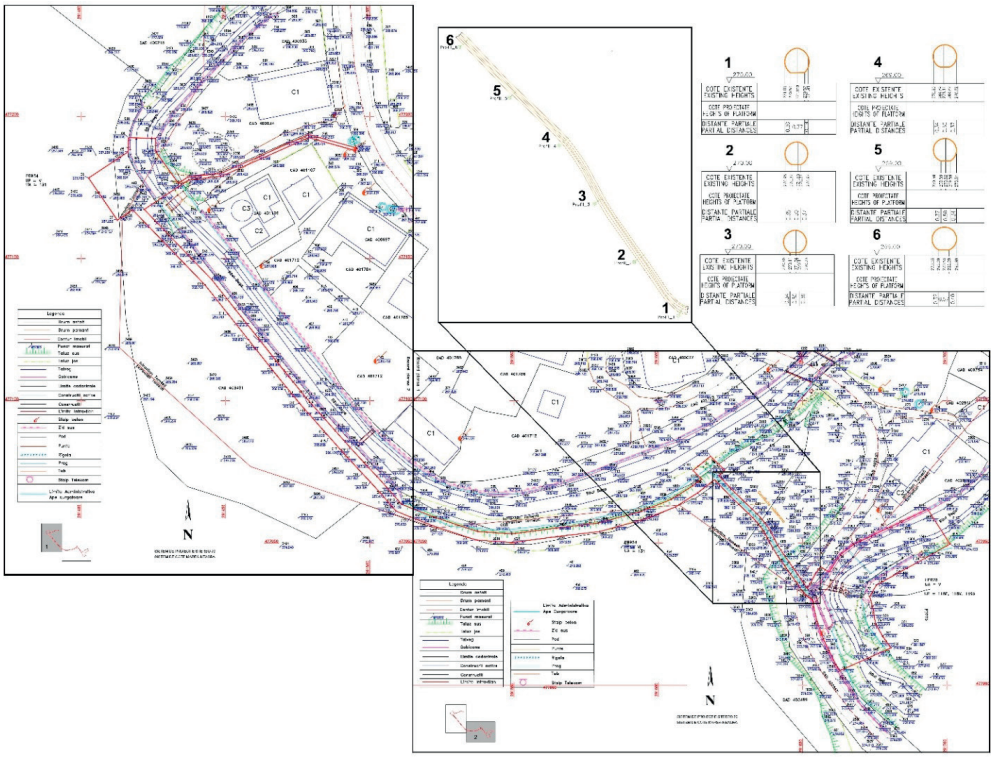


Figure 11. Topographic plan of Tomesti study area with integrated elevation, hydrography, and infrastructure data

SLAM data accuracy assessment and control point validation

Accuracy assessment is a critical element in geospatial data acquisition, especially when merging outputs from multiple sensors like SLAM and total stations (Figure 12). In complex engineering projects, spatial precision underpins reliable design, structural analysis, and implementation. While SLAM excels in GNSS-denied environments such as tunnels, it is prone to positional drift and trajectory errors from motion instability and sensor noise. To ensure spatial integrity, SLAM point clouds must be validated against high-accuracy control points, best obtained using total stations, which offer millimetric precision in areas where GNSS is ineffective. Comparing SLAM outputs with total station-derived control points allows for the identification and correction of spatial discrepancies, ensuring the dataset is accurately aligned within the project's coordinate system. This process is essential for hydrotechnical rehabilitation, where accurate underground alignment and modelling are vital. Ultimately, such accuracy checks enhance the reliability of final products and support confident, data-driven decisions.



Figure 12. SLAM point cloud with GCPs (G6–G11) used for spatial alignment and accuracy validation in the national coordinate system

The table presents an accuracy assessment comparing SLAM (Simultaneous Localization and Mapping) data with control point coordinates measured via total station. It includes six control points (G6 to G11), showing both coordinate sets to evaluate SLAM's spatial precision in inaccessible environments. For each point, residual errors in X, Y, and Z axes are provided (Table 1), with D_{XY} representing horizontal deviation and D_Z the vertical difference. D_{XY} errors range from 0.021 to 0.052 m, while D_Z values remain below ±0.02 m, indicating strong vertical consistency.

Table 1. Residual errors for each GCP, with overall accuracy assessment

Control point (m)				Measurement Coordinates (m)			Residual Error (m)			
GCP Name	East X	North Y	Up Z	Measurement X	Measurement Y	Measurement Z	DX	DY	DXY	DZ
G 8	291671.593	477060.581	272.453	291671.570	477060.582	272.473	0.023	-0.001	0.023	-0.020
G 9	291653.152	477030.348	274.453	291653.147	477030.320	274.469	0.005	0.028	0.029	-0.016
G 10	291664.952	477032.59	272.710	291664.900	477032.587	272.712	0.052	0.003	0.052	-0.002
G 11	291691.226	477045.855	271.724	291691.207	477045.884	271.727	0.019	-0.029	0.034	-0.003
G 7	291661.634	477099.282	270.974	291661.625	477099.263	270.997	0.009	0.019	0.021	-0.023
G 6	291637.355	477123.85	270.088	291637.383	477123.871	270.087	-0.028	-0.021	0.035	0.001
Mean Error							0.013	0.000	0.032	-0.010
RMSE							0.027	0.020	0.034	0.014

Also included are the mean error and Root Mean Square Error (RMSE), with an RMSE of ~0.027 m, validating the system's high accuracy, remarkable for a GNSS-denied, subterranean environment. This confirms SLAM's ability to achieve centimeter-level precision when anchored to total station benchmarks. For the Tomesti project, SLAM delivered reliable 3D documentation that met engineering standards for structural evaluation and design planning.

Rehabilitation strategy and hydro-technical design proposals

The revitalization of the Tomesti micro-hydropower station represents a strategic fusion of modern geospatial technologies and sustainable energy objectives. Originally planned decades ago but left incomplete, the site remains viable due to its existing underground infrastructure and favorable hydrological context. The current project outlines a full rehabilitation strategy, aligning with present-day technical, environmental, and policy standards.

Based on high-resolution topographic and 3D mapping using GNSS, LiDAR, and SLAM, the proposed works address both surface and underground hydro-technical components. This geospatial data provided accurate terrain models, structural detail, and precise spatial alignment to guide engineering analysis and updated documentation.

Rehabilitation efforts focus on the adduction gallery and water intake systems. The pre-existing tunnel, though unused, was digitally reconstructed via SLAM scanning, allowing for condition evaluation and targeted actions such as consolidation, alignment correction, and sealing, ensuring long-term functionality under varying flow regimes.

At the surface, the intake structures on Bega River tributaries will be redesigned to meet modern hydropower standards. The updated system integrates ecological flow control, sediment handling, and durability improvements, using adjustable sluices and fish-friendly features to guide water safely into the rehabilitated gallery.

Further downstream, the incomplete power cavern will be fitted with automated turbines and linked to the national grid. The upgraded facility aims to deliver efficient, low-impact renewable energy, contributing to local sustainability goals.

The 3D rendering of the intake structure illustrates the planned upgrades derived from our integrated survey campaign (Figure 13). Key rehabilitation targets include degraded concrete components such as the overflow weir, sluice niches, retaining walls, and loading chamber. These will be cleaned and reinforced using mesh and sprayed concrete to restore structural integrity.

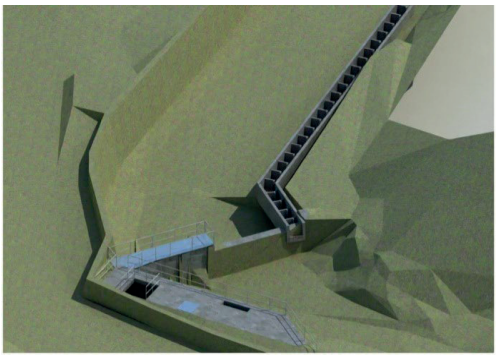


Figure 13. 3D rendering of the rehabilitated water intake structure, designed based on topographic and LiDAR measurements, showing the restored weir, retaining walls, and access elements integrated into the terrain

Interior and exterior reinforcements will be connected to enhance cohesion (Figure 14). The proposed design aligns precisely with terrain data extracted from UAV photogrammetry and SLAM scans, ensuring accurate positioning and minimal landscape alteration.

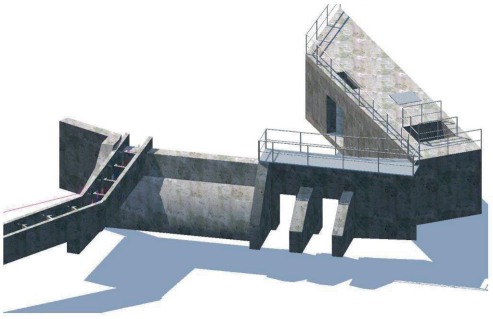


Figure 14. Detailed 3D model of the rehabilitated intake structure, highlighting spillway elements, intake gates, and access platforms, reconstructed based on precise geospatial data

Crucially, all interventions are designed to comply with national energy and environmental regulations. The project embraces a low-impact philosophy, reusing existing structures, minimizing deforestation, and preserving the visual integrity of the mountainous landscape. As such, the Tomesti initiative illustrates how legacy hydro-infrastructure can be repurposed using contemporary tools, offering a replicable model for future sustainable energy projects in similar terrains.

CONCLUSIONS

This study demonstrates the critical importance of integrating modern geospatial technologies with traditional surveying methods for complex infrastructure projects situated in rugged, forested, and geologically challenging environments. The revitalization of the Tomesti micro-hydropower station, a legacy project abandoned decades ago, required not only technical innovation but also methodological precision and environmental sensitivity. Through the combined use of GNSS-based control networks, total station measurements, UAV photogrammetry, airborne LiDAR, and SLAM scanning, a comprehensive spatial dataset was generated, one capable of supporting both engineering design and environmental compliance.

The resulting geospatial products, including orthophotos, DSMs, DTMs, 3D tunnel reconstructions, and a detailed topographic plan, provide a unified spatial framework for decision-making and technical validation. Accuracy assessments between SLAM-derived outputs and total station control points confirmed the reliability of the multi-sensor workflow, with sub-decimetric residuals ensuring confidence in the datasets used for design.

The case of Tomesti highlights how modern geomatics can breathe new life into dormant infrastructure by bridging outdated documentation with current spatial realities. The proposed rehabilitation, grounded in this high-fidelity survey campaign, encompasses both structural restoration and environmentally conscious hydrotechnical design. If implemented, this initiative will not only contribute to local renewable energy production, but also serve as a replicable model for similar projects across Romania and other mountainous regions. This work underlines the evolving role of geomatics in sustainable development, where multi-sensor integration, precision mapping, and terrain intelligence converge to enable resilient, future-ready engineering solutions.

ACKNOWLEDGEMENTS

This research was carried out with the support of the Ministry of Education and was financed

through the CNFIS-FDI-2024-F-0195 project, funded by the National Council for Financing Higher Education (CNFIS).

REFERENCES

Bilașco, Ș., Roșca, S., Vescan, I., Fodorean, I., Dohotar, V., & Sestras, P. (2021). A GIS-based spatial analysis model approach for identification of optimal hydrotechnical solutions for gully erosion stabilization. Case Study. *Applied Sciences*, *11*(11), 4847.

Chio, S. H., & Hou, K. W. (2021). Application of a hand-held lidar scanner for the urban cadastral detail survey in digitized cadastral area of taiwan urban city. *Remote Sensing*, *13*(24), 4981.

Coroian, I., Ficior, D., Sălăgean, T., Chiorean, S., Pop, I. D., Nap, M. E., & Șuba, E. E. (2024). 3d Modeling of the Campus of the University of Agricultural Sciences and Veterinary Medicine Cluj-Napoca Using Arcgis Pro. *Scientific Papers. Series E. Land Reclamation, Earth Observation & Surveying, Environmental Engineering*, *13*, 786-793. Print ISSN 2285-6064.

Keitaanniemi, A., Virtanen, J. P., Rönnholm, P., Kukko, A., Rantanen, T., & Vaaja, M. T. (2021). The combined use of SLAM laser scanning and TLS for the 3D indoor mapping. *Buildings*, *11*(9), 386.

Khanal, M., Hasan, M., Sterbentz, N., Johnson, R., & Weatherly, J. (2020). Accuracy comparison of aerial lidar, mobile-terrestrial lidar, and UAV photogrammetric capture data elevations over different terrain types. *Infrastructures*, *5*(8), 65.

Langhammer, J., Janský, B., Kocum, J., & Minařík, R. (2018). 3-D reconstruction of an abandoned montane reservoir using UAV photogrammetry, aerial LiDAR and field survey. *Applied geography*, *98*, 9-21.

Liu, S., Sun, E., & Dong, X. (2024). SLAMB&MAI: a comprehensive methodology for SLAM benchmark and map accuracy improvement. *Robotica*, *42*(4), 1039-1054.

Nap, M. E., Chiorean, S., Cira, C. I., Manso-Callejo, M. Á., Păunescu, V., Șuba, E. E., & Sălăgean, T. (2023). Non-destructive measurements for 3D modeling and monitoring of large buildings using terrestrial laser scanning and unmanned aerial systems. *Sensors*, *23*(12), 5678.

Oniga, V. E., Loghin, A. M., Macovei, M., Lazar, A. A., Boroianu, B., & Sestras, P. (2023). Enhancing LiDAR-UAS derived digital terrain models with hierarchic robust and volume-based filtering approaches for precision topographic mapping. *Remote Sensing*, *16*(1), 78.

Popescu, G., Popescu, C. A., Dragomir, L. O., Herbei, M. V., Horablaga, A., Țenche-Constantinescu, A. M., ... & Sestras, P. (2024). Utilizing UAV technology and GIS analysis for ecological restoration: A case study on Robinia pseudoacacia L. in a mine waste dump landscape rehabilitation. *Notulae Botanicae Horti Agrobotanici Cluj-Napoca*, *52*(4), 13937-13937.

Rogers, S. R., Manning, I., & Livingstone, W. (2020). Comparing the spatial accuracy of digital surface models from four unoccupied aerial systems: Photogrammetry versus LiDAR. *Remote Sensing*, *12*(17), 2806.

Sălăgean, T., Șuba, E.E., Pop, I.D., Matei, F., Deak, J. (2019). Determining Stockpile Volumes Using Photogrammetric Methods. *Scientific Papers-Series E-Land Reclamation Earth Observation & Surveying Environmental Engineering*, *8*, 114-119. Print ISSN 2285-6064.

Sestras, P. (2021). Methodological and on-site applied construction layout plan with batter boards stake-out methods comparison: A case study of Romania. *Applied Sciences*, *11*(10), 4331.

Sestras, P., Badea, G., Badea, A. C., Salagean, T., Roșca, S., Kader, S., & Remondino, F. (2025b). Land surveying with UAV photogrammetry and LiDAR for optimal building planning. *Automation in Construction*, 173, 106092.

Stöcker, C., Nex, F., Koeva, M., & Gerke, M. (2020). High-quality UAV-based orthophotos for cadastral mapping: Guidance for optimal flight configurations. *Remote sensing*, *12*(21), 3625.

Urban, R., Štroner, M., Braun, J., Suk, T., Kovanič, Ľ., & Blistan, P. (2024). Determination of accuracy and usability of a SLAM scanner GeoSLAM Zeb Horizon: A bridge structure case study. *Applied Sciences*, *14*(12), 5258.

You, R. J., & Lee, C. L. (2020). Accuracy improvement of airborne lidar strip adjustment by using height data and surface feature strength information derived from the tensor voting algorithm. *ISPRS International Journal of Geo-Information*, *9*(1), 50.

Scientific Papers. Series E. Land Reclamation, Earth Observation & Surveying, Environmental Engineering. Vol. XIV, 2025
Print ISSN 2285-6064, CD-ROM ISSN 2285-6072, Online ISSN 2393-5138, ISSN-L 2285-6064

CLAY APPLICATION IN THE REMEDIATION OF NICKEL RICH SOIL

Teuta BUSHI[1], Aida BANI[1], Selma MYSILHAKA[2], Franz OTTNER[3], Ilaria COLZI[4], Isabella BETTARINI[4], Seit SHALLARI[1]

[1]Agricultural University of Tirana, Kodër Kamëz, 1029, Tirana, Albania
[2]University "Aleksander Xhuvani", Rruga Ismail Zyma, 3000, Elbasan, Albania
[3]Institute of Applied Geology, Department of Civil Engineering and Natural Hazar, 8010, Graz, Austria
[4]University of Florence, Department of Biology, 12 Via del Proconsolo, 50122, Florence, Italy

Corresponding author email: teuta.halilaj@ubt.edu.al

Abstract

The objective of this study was to evaluate the ability of clay (nano- montmorillonite) to the remediation of natural (Ni) rich soils, having the nickel hyperaccumulator Odontarrhena calchidica test plant. The experiment was conducted in a greenhouse in a completely randomized design, with three replicates. The experiment was conducted in 2 kg plastic plot. We used four doses of clays: 0.0, 21.4, 44.3 and 64g kg^{-1}, corresponding to 0, 30, 60 and 90 t ha^{-1}, respectively. Throughout the experiment, the plants were regularly irrigated, and NPK fertilization was applied to ensure optimal growth conditions. After 60 days, the soil analyzed for total nickel in XRF and available nickel $_{DTPA}$ extraction in Atomic Absorption. The BFP and BFR of Odontarrhena chalcidica decreased significantly as a function of increasing doses of nano-montmorillonite, indicating an increase in the adsorption of nickel in the soil. However, the BFP and BFR values were high, indicating hyperaccumulation potential of O. chalcidica. Based on the results, the application of clay in agricultural nickel rich soils favors their improvement.

Key words*: clay, nano-montmorillonite, hyperaccumulator, Odontarrhena calchidica, XRF.*

INTRODUCTION

Nickel (Ni) is an essential micronutrient for plant growth but when present in high concentrations it can become toxic to both plants and the environment (Seregin & Kozhevnikova, 2006; Chen et al., 2009). Serpentine soils, which are naturally rich in nickel and derived from ultramafic rocks are particularly challenging for agriculture (Kazakou et al., 2008). These soils can lead to excessive nickel accumulation in food crops, raising health concerns and reducing agricultural productivity. Excess nickel slows plant growth, lowers yields and decreases the nutritional value of food (Marschner, 2012). Therefore, finding effective strategies to manage nickel-rich soils is crucial for sustainable farming.

A notable example of this challenge is the Tropoja region in northeastern Albania, where serpentine soils contain naturally high levels of nickel, posing risks to both the environment and local agriculture (Bani et al., 2015). Existing remediation methods, such as phytoremediation (using plants to absorb nickel) and chemical stabilization, have limitations.

Phytoremediation is a slow process, while chemical treatments can introduce new environmental risks (Kumpiene et al., 2008). To reduce nickel availability in soil remediation techniques such as the use of adsorbent materials, particularly clay minerals have been explored (Ghorbel-Abid et al., 2010; Uddin, 2017). These materials are readily available, environmentally friendly and effective at immobilizing heavy metals (Uddin, 2017). This occurs through processes such as adsorption and ion exchange, where nickel ions are replaced by other ions on the clay surface (Bhattacharyya & Gupta, 2008).

Nano-montmorillonite, a type of clay predominantly composed of smectite (90%), has proven effective in reducing the bioavailability of heavy metals, thereby limiting their uptake by plants (Wang et al., 2015).

Due to its high surface area and cation exchange capacity, nano-montmorillonite can be incorporated into soil as a conditioner to improve

chemical and physical properties, particularly in sandy soils (Tako, 2015).

The objective of this study was to evaluate the ability of clay minerals to improve naturally nickel-rich soils, using the nickel hyperaccumulator plant *Odontarrhena chalcidica* as a test species. We use as amendment clay minerals extracted from soil of a distinct ultramafic regions of Albania, from Domosdova field, Prrenjas (Tako, 2015).

This research also aims to contribute to the development of sustainable and cost-effective methods for managing nickel-contaminated farmland while enhancing our understanding of nickel dynamics in soil-plant systems.

MATERIALS AND METHODS

Experimental Materials and Treatment

The study was conducted under greenhouse conditions at Sila Company, Fushe-Kruje, Tirane to investigate the effects of clay amendments on nickel availability and plant accumulation. Experiments were performed using the nickel hyperaccumulator plant *Odontarrhena chalcidica* native plant in serpentine soil of Albania. The soil collected from the ultramafic soil of Tropoja region in northeastern Albania (0-20 cm depth). From previous study we know that this soil was rich in nickel. Seeds of *O. chalcidica* came from native plants that grow up in ultramafic site of Tropoja. The experiments were conducted in 2 kg plastic containers. The plots were designed according to a randomized complete block design. The experiment was organized with four replicates for each treatment.

Each experimental unit received four doses of clay: 0.0, 21.4, 44.3, and 64 g kg^{-1}, corresponding to 0, 30, 60, and 90 t ha^{-1}, respectively. The clay was sourced from clayey soil from the main serpentine clay deposit in Domosdova field, southeast of Albania (Tako, 2015). The clay was thoroughly mixed with the soil to ensure uniform distribution (Uddin, 2017). The X-ray diffractogram of the clay minerals was performed in the Institute of Soil Research, University of Natural Resources and Life Sciences, Vienna, Austria and it is presented in Figure 1. The soil was conditioned in plastic containers, irrigated to field capacity, and incubated for 20 days. After incubation, *O. chalcidica* seeds were sown on March 1, 2024. Plant seeds were sown using a broadcast method and covered with a thin layer of soil on the surface. Throughout the growth period, water was periodically supplemented using the weighing method to maintain soil moisture at 60~70% of field capacity. Eight days after emergence, thinning was performed to maintain two plants per container. Fertilization was applied at rates of 3g of 20N: 20P: 20K to ensure adequate nutrient supply.

Soil and plant sample analyses

After 60 days of growth, plants were harvested, and soil and plant samples were collected. The plants aboveground parts and root systems were cleaned and weighed separately. The aerial parts and roots were separated, washed with deionized water, oven-dried at 80°C until a constant weight was achieved, and weighed to determine dry biomass of plants (Kazakou et al., 2008).

The dried soil and plant samples were finely pulverized and ground for subsequent analysis. The soil samples were air dried and passed through a 2 mm nylon sieve to determine soil physico- chemical properties; its pH, organic matter content, cation exchange capacity (CEC), available nickel was analysed in the Laboratory of the Department of Environment and Natural Resources at the Agricultural University of Tirana. Available nickel in the soil was extracted using DTPA and quantified via AAS (Lindsay & Norvell, 1978). Total heavy metals concentrations in soil and heavy metals in plant analyzed using X-ray fluorescence (XRF) in the Laboratory of the Department of Biology at the University of Florence, Italy.

The following parameters were assessed for plants: Bioaccumulation Factor in Plant (BFP) was calculated as the ratio of nickel concentration in the aerial parts to that in the soil (Bani et al., 2024). Bioaccumulation Factor in Root (BFR) was calculated as the ratio of nickel concentration in the roots to that in the soil (Kidd et al., 2018). Translocation Factor (TF) was calculated as the ratio of nickel concentration in the aerial parts to that in the roots (Bani et al., 2015).

Statistical Analysis

Data was analyzed using analysis of variance (ANOVA) with an F-test to assess treatment

effects (Clay doses effects on BFP, BFR and Shoot Dry Biomass) (Kumpiene et al., 2008).

RESULTS AND DISCUSSIONS

Bulk mineralogy of the clay from source Domosdova field, south-east of Albania is dominated by the group of layer silicates.
We count to this group mica and all clay minerals. Accessory minerals are feldspars, pyroxenes, talc, serpentine minerals and traces of quartz (Figure 1). This clay could be the weathering product of ultramafic rocks. Semiquantitative results of clay mineralogy <2µm told us that this clay mineral is a nano-montmorillonite, absolutely dominated by smectite with about 90 %. All the other clay minerals are present in very small amounts. In this sample, the diffractograms from the various treatments are not definitive; some indicate the presence of smectite, while others also suggest the presence of vermiculite. The observed peaks are characteristic of smectite clays, serpentine as well as layer silicates, quartz and feldspars. This mineral will show a very high absorption capacity independently if it is smectite or vermiculite.

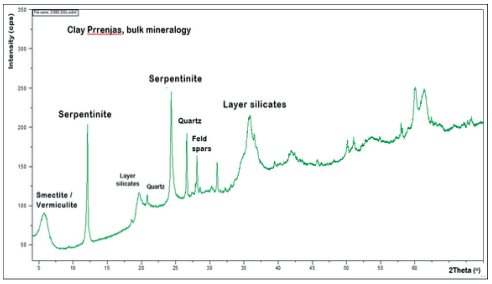


Figure 1: X-ray diffractogram of clay from Domosdova field, bulk mineral composition. The most important peaks are marked

Soil characteristics

The serpentine soil from the Tropoja region was analyzed to determine its physicochemical properties which are essential for understanding its suitability for plant growth, particularly for hyperaccumulator plants. Table 1 presents the soil properties, including pH, organic matter, texture and concentrations of essential nutrients and heavy metals.
The soil pH was neutral (7.0) that is in the adequate range for this hyperaccumulating species (Bani et al., 2014, Kukier et al., 2004). The soil of Tropoja shows a CEC of 20.6 cmol kg^{-1}, this because had a considerable clay content in the soil (27.5%).

Table 1. pH, Physicochemical properties (Mean values ± SD) of serpentine soil of Tropoja

Physicochemical properties	Mean values ± SD
pH	7
Organic matter (%)	4.5
CEC (cmol kg^{-1})	20.6
EC (µs/cm)	27.6
Sand (%)	9.95
silt (%)	62.5
Clay (%)	27.5
K (mg kg^{-1})	1442 ± 330
P (mg kg^{-1})	1859 ± 240
Ca (mg kg^{-1})	8645 ± 250
Mg (mg kg^{-1})	21867 ± 370
Cr (mg kg^{-1})	475 ± 79
Mn (mg kg^{-1})	1728 ± 13
Fe (mg kg^{-1})	96338 ± 3340
Co (mg kg^{-1})	170 ± 33
Ni (mg kg^{-1})	1739 ± 36
Cu (mg kg^{-1})	25 ± 3
Zn (mg kg^{-1})	123 ± 8
Pb (mg kg^{-1})	34 ± 4

*SD - standard deviation

Total P and K concentrations in the soil were low respectively 1442 mg kg^{-1} for P and 1859 mg kg^{-1} for K. In general, serpentine soils are deficient in K and P total contents (Bonifacio & Barberis, 1999), which is a major cause of poor agricultural yields of main crops. The use of fertilizers and organic amendments improved soil fertility.
The organic matter content was 4.5% that is satisfactory for agronomic purposes (Fenton et al., 2008). Total Ca (8645mg kg^{-1}) concentrations in the soil were lower than Mg (21867 mg kg^{-1}), and soil has elevated levels of total metals like Ni, Co, Cr, Mn and Fe that are typical of ultramafic soils. Total Ni concentration is high 1739 mg kg^{-1}, higher than those considered toxic to normal plants by Allen et al. (1974), Kabata-Pendias (1984), and Brooks (1987).

Nickel availability in soil

The application of nano- montmorillonites clay significantly reduced the bioavailability of nickel in the serpentine soil of Tropoja. As

shown in Table 2, the available nickel concentration decreased with increasing clay doses.

Table 2. The available nickel in serpentine soil of Tropoja for the different clay treatments

Treatment (Clay Dose) (g/kg)	Nickel available in soil (mg/kg)
0	88.7
30	69.9
60	33.6
90	27.9

Thus, the available nickel content in the Tropoja soil, where clay from the Domosdova field was applied and nickel hyperaccumulator plants were cultivated, decreased by 68.5%, from 88.7 mg/kg to 27.9 mg/kg.
This reduction is attributed to the adsorption and ion exchange properties of nano-montmorillonites which immobilize nickel ions due to its high surface area and cation exchange capacity (CEC).

Nickel Concentrations in Plants and Roots

The dry biomass of the aerial part (shoot) of the *O. calchidica* was adjusted to a linear model as a function of increasing doses of clay mineral (Figure 2) ranged from 3.1 g (0 t ha^{-1} clay mineral) to 5.4 g (90 t ha^{-1} clay mineral), corresponding to an increase of 1.74 times higher in the highest dose compared to control.

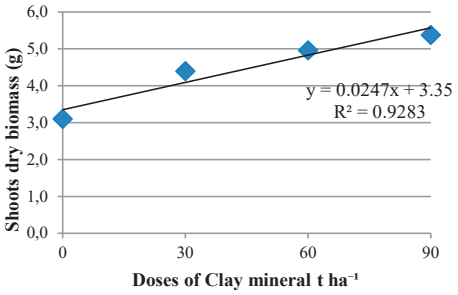


Figure 2. Dry biomass of the shoots for *O. calchidica* cultivated in serpentine soil of Tropoja for the different nano-montmorillonite clay treatments

The positive effect of nano-montmorillonite clay addition on plant growth may be due to its positive effect on the water retention capacity (Wang et al., 2015) and the growth of surface area, increasing the metal cation adsorption capacity present in the soil (Tako, 2015) and consequently decreasing the concentration in the plant parts.
The nickel concentration in the shoot and in the roots of radish was significantly influenced by applying nano-montmorillonite clay (Figure 3). The linear behavior of the nickel concentration in shoots and roots of plants, shows the decrease of Ni concentration with increasing doses of nano- montmorillonite clay ranging from 16545 to 9078 mg kg^{-1} in the shoot (Figure 3A) and ranging to 1993 to 2660 mg kg^{-1} in the roots (Figure 3B) occurring a decrease of 31.47% and 25%, respectively, the control regarding the higher dose.

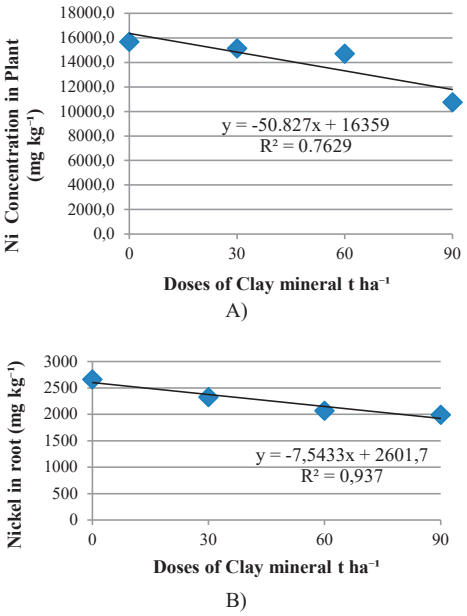


Figure 3. Nickel concentration in the shoots (A) and roots (B) of *O. calchidica* cultivated in serpentine soil of Tropoja for the different nano-montmorillonite clay treatments

The reduction of Ni concentration in this hyperaccumulator plant is explained by the reduction of the availability of the nickel in the soil with the increase of clay doses from 0 to 90 t ha^{-1}. This decrease is likely attributable to the adsorption of nickel by nano-montmorillonite. The ability of a plant to accumulate metals from soil can be estimated using the bioaccumulation potential in plant (BFP) and/or in root (BFR). These factors can be used to estimate a potential

plant for phytoremediation purposes. The BFP and BFR of *O. calchidica* decreased significantly by increasing doses of nano-montmorillonite soil (Tables 1, 3) indicating an increase in the adsorption of nickel in the soil, decreasing the concentration in the plant parts.
This behavior is beneficial since clay minerals such as nano- montmorillonite have a great potential to adsorb pollutants due to their large specific surface area, the layered structure, and high cation exchange capacity (Bhattacharyya & Gupta, 2008).
According to Figure 4, the BFP and BFR ranged from 9 to 6.17 and from 1.52 to 1.14 showing a reduction of 31% and 25%, respectively. The BFP and BFR values were high, indicating high hyperaccumulation potential of *O. calchidica*, for Ni. Application of nano- montmorillonite reduced BFP and BFR values indicating reduced nickel uptake. These results suggest that nano-montmorillonite is an effective amendment for reducing nickel bioavailability in nickel-rich soils.

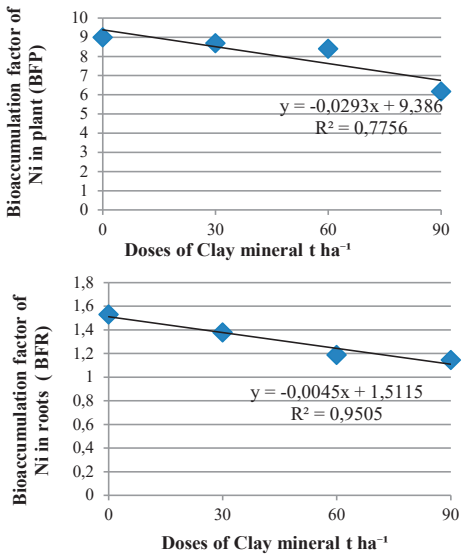


Figure 4. Bioaccumulation factor of nickel in plant (BFP) and in root (BFR) of O. calchidica for the different nano-montmorillonite clay treatments

The translocation factor (TF) gives the shoot/root nickel concentration and showed the ability of our plant for nickel translocation from roots to shoots at our experiment with different doses of clay minerals.

Table 3. Clay doses effects on BFP, BFR and Shoot Dry Biomass tested one-way ANOVA

Variable	F-value	P-value	F crit
BFP	25.61	0.000187	4.066
BFR	118.01	5.82E-07	4.066
Shoot Dry Biomass	46.9	2.02E-05	4.066

The TF varied from 7.1 to 5.89 showing a reduction of 17% depending on Clay doses. However, TF values were high, indicating high nickel translocation potential of *O. calchidica* plant.

CONCLUSIONS

Nano-montmorillonite in nickel-rich soil significantly enhanced the shoot development of *Odontarrhena calchidica* and promoted nickel retention in the soil, as evidenced by reduced nickel concentrations in the plant's shoots and roots. It also contributed to the reduction of bioaccumulation factors of nickel.
This study highlights the vital role of nano-montmorillonite clay in making nickel-rich soils safer and more productive. By applying this clay, the bioavailability of nickel is significantly reduced, protecting crops and the food chain from harmful accumulation.
The notably high nickel concentrations in the aerial parts of *O. calchidica* further confirm its strong hyperaccumulation ability, making it highly suitable for phytoremediation.
These findings are not only scientifically significant but also offer practical solutions for farmers and communities dealing with nickel-rich soils.
By improving soil health and reducing nickel toxicity, this approach supports healthier crops, sustainable agriculture, and public health. Future research should examine the long-term effects of clays and the use of *Odontarrhena calchidica* to enhance remediation efforts.

ACKNOWLEDGEMENTS

Special thanks to the technical staff of the three laboratories that assisted us with all analyses presented in this paper: the Laboratory of the Department of Environment and Natural Resources at the Agricultural University of Tirana, the Laboratory of the Institute of

Applied Geology, Department of Civil Engineering and Natural Hazards in Austria, and the Laboratory of the Department of Biology at the University of Florence, Italy.

REFERENCES

Allen, S. E., Grimshaw, H. M., Parkinson, J. A., & Quarmby, C. (1974). *Chemical analysis of ecological materials*. Blackwell Scientific Publications.

Bani, A., Echevarria, G., Pelletier, E. M., Gjoka, F., Sulçe, S., & Morel, J. L. (2014). Pedogenesis and nickel biogeochemistry in a typical Albanian ultramafic toposequence. *Environmental Monitoring and Assessment, 186*, 4431–4442. https://doi.org/10.1007/s10661-014-3723-8

Bani, A., Echevarria, G., Sulçe, S., & Morel, J. L. (2015). Improving the agronomy of *Alyssum murale* for extensive phytomining: A five-year field study. *International Journal of Phytoremediation, 17*(2), 117–127. https://doi.org/10.1080/15226514.2013.862204

Bani, A., Alvarez-López, V., Prieto-Fernandez, A., Miho, L., Shahu, E., Echevarria, G., & Kidd, P. (2024). Designing cropping systems for nickel agromining on ultramafic land in Albania. *Ecological Research, 1–18*. https://doi.org/10.1111/1440-1703.12525

Bhattacharyya, K. G., & Gupta, S. S. (2008). Adsorption of a few heavy metals on natural and modified kaolinite and montmorillonite: A review. *Advances in Colloid and Interface Science, 140*(2), 114–131. https://doi.org/10.1016/j.cis.2007.12.008

Bonifacio, E., & Barberis, E. (1999). Phosphorus dynamics during pedogenesis on serpentinite. *Soil Science, 164*(12), 960–968. https://doi.org/10.1097/00010694-199912000-00006

Brooks, R. (1987). *Serpentine and its vegetation (a multidisciplinary approach)*. Dioscorides Press.

Chen, C., Huang, D., & Liu, J. (2009). Functions and toxicity of nickel in plants: Recent advances and future prospects. *Clean – Soil, Air, Water, 37*(4-5), 304–313. https://doi.org/10.1002/clen.200800199

Fenton, M., Albers, C., & Ketterings, Q. (2008). *Soil organic matter*. Nutrient Management Spear Program, Cornell University. Retrieved from http://nmsp.cals.cornell.edu/publications/factsheets/factsheet41.pdf

Ghorbel-Abid, I., Galai, K., & Trabelsi-Ayadi, M. (2010). Adsorption of heavy metals on clay minerals: A review. *Journal of Environmental Chemistry and Ecotoxicology, 2*(6), 98–105. Retrieved November 3, 2018, from www.journalwebsite.com/resource

Kabata-Pendias, A., & Pendias, H. (1984). *Trace elements in soils and plants*. CRC Press.

Kazakou, E., Adamidis, G. C., Baker, A. J. M., Reeves, R. D., Godino, M., & Dimitrakopoulos, P. G. (2008). Growth, reproduction and nickel accumulation by the nickel hyperaccumulator *Alyssum lesbiacum*. *Plant and Soil, 314*(1-2), 227–238. https://doi.org/10.1007/s11104-008-9720-3

Kidd, P. S., Álvarez-López, V., & Becerra-Castro, C. (2018). Nickel hyperaccumulation in *Odontarrhena* species: A review. *Plant and Soil, 423*(1-2), 1–19. https://doi.org/10.1007/s11104-017-3494-4

Kukier, U., Peters, C. A., Chaney, R. L., Angle, J. S., & Roseberg, R. J. (2004). The effect of pH on metal accumulation in two *Alyssum* species. *Journal of Environmental Quality, 33*(6), 2090–2102. https://doi.org/10.2134/jeq2004.2090

Kumpiene, J., Lagerkvist, A., & Maurice, C. (2008). Stabilization of As, Cr, Cu, Pb, and Zn in soil using amendments – A review. *Waste Management, 28*(1), 215–225. https://doi.org/10.1016/j.wasman.2006.12.012

Lindsay, W. L., & Norvell, W. A. (1978). Development of a DTPA soil test for zinc, iron, manganese, and copper. *Soil Science Society of America Journal, 42*(3), 421–428. https://doi.org/10.2136/sssaj1978.03615995004200030009x

Marschner, H. (2012). *Mineral nutrition of higher plants* (3rd ed.). Academic Press.

Seregin, I. V., & Kozhevnikova, A. D. (2006). Physiological role of nickel and its toxic effects on higher plants. *Russian Journal of Plant Physiology, 53*(2), 257–277. https://doi.org/10.1134/S1021443706020178

Tako, E. (2015). *Studimi i ekuilibrave të adsorbimit në argjilat montmorillonite të disa metaleve të rëndë*. Universiteti i Tiranës, Fakulteti i Shkencave të Natyrës, Departamenti i Kimisë Industriale, Tiranë, Shqipëri. https://unitir.edu.al/wp-content/uploads/2015/07/Doktoratura-Edlira-Tako-Fakulteti-i-Shkencave-i-Natyrore-Departamenti-i-Kimise-Industriale.pdf

Uddin, M. K. (2017). A review on the adsorption of heavy metals by clay minerals, with special focus on the past decade. *Chemical Engineering Journal, 308*, 438–462. https://doi.org/10.1016/j.cej.2016.09.029

Wang, L., Wang, Y., Ma, F., Tankpa, V., Bai, S., Guo, X., & Wang, X. (2015). Mechanisms and reutilization of modified biochar used for removal of heavy metals from wastewater: A review. *Science of the Total Environment, 668*, 1298–1309. https://doi.org/10.1016/j.scitotenv.2019.03.011

Scientific Papers. Series E. Land Reclamation, Earth Observation & Surveying, Environmental Engineering. Vol. XIV, 2025
Print ISSN 2285-6064, CD-ROM ISSN 2285-6072, Online ISSN 2393-5138, ISSN-L 2285-6064

A PIONEERING STUDY ON THE INVESTIGATION OF MICROPLASTIC POLLUTION IN THE WATER OF THE SOMOVA-PARCHEȘ LACUSTRINE COMPLEX, ROMANIA

Mădălina CĂLMUC[1], Valentina Andreea CĂLMUC[1], Nina Nicoleta LAZĂR[1], Marius IVANOV[3], Puiu-Lucian GEORGESCU[1, 2], Cătălina ITICESCU[1, 2]

[1]"Dunărea de Jos" University of Galați, REXDAN Research Centre,
98 George Coșbuc Blvd, 800223, Galați, Romania
[2]"Dunărea de Jos" University of Galați, Faculty of Sciences and Environment,
111 Domnească Street, 800201, Galați, Romania
[3]ALTFACTOR S.R.L, 8 Martie Street, no. 29, 800258, Galați, Romania

Corresponding author email: madalina.calmuc@ugal.ro

Abstract

Although the presence of microplastics in the oceans was first reported in the 1970s, the first studies on lakes were published in 2011. This pioneering study aims to determine the presence of microplastics in the Somova-Parches lacustrine complex, situated in the predeltaic territory of the Danube Delta Biosphere Reserve. The Pollution Load Index (PLI) was also calculated to assess the microplastic pollution level in water. The microplastics concentrations in the water of the 6 investigated lakes varied in the 0.15 - 0.65 particles·m^{-3} range. The PLI index values indicated a low level of microplastic pollution (level 1). The results of the micro-FTIR analyses highlighted the predominant presence of polyethylene and polypropylene polymers in the composition of the collected microplastics. The present study contributes to bridging the knowledge gap regarding the occurrence of microplastics in freshwater.

Key words*: emerging pollutant, freshwater, Lower Danube water, micro-FT-IR.*

INTRODUCTION

In recent years, due to their versatility, the production and consumption of plastic products have increased significantly worldwide. According to predictions, global production could reach 25 billion tons by 2050 (Liu et al., 2025). In addition, total plastic waste production could be estimated at 12 000 million tons by 2050 (Zhang et al., 2024). The mismanagement of plastic waste contributes to its release into the environment, where it is fragmented into microplastics (MPs) (Gan et al., 2025). Microplastics are considered hazardous substances in the environment due to their composition (e.g. additives), irregular shape, small size and their ability to carry other pollutants that can have a harmful impact on biota (Nguyen et al., 2023).

Although most research has focused on microplastics in marine ecosystems, recent studies have shown that microplastic pollution in inland waters can be 20 times higher than in marine ecosystems (Horton et al., 2017; Pol et al., 2023). Human activity and terrestrial ecosystems are strongly connected to inland waters. Therefore, their pollution has a direct impact not only on aquatic and terrestrial biota, but also on human health (Luo et al., 2024). Lentic ecosystems serve as indicators of watershed health due to their capacity to accumulate pollutants (Dusaucy et al., 2021). For these reasons, it is essential to monitor microplastics in lakes.

The main aim of this study is to evaluate for the first time the presence of microplastics in six lakes from the Somova-Parcheș aquatic complex, Romania. In addition, the pollution level of lake water with microplastics was determined by calculating the Pollution Load Index (PLI).

Somova-Parcheș lacustrine complex is situated in the western part of the Danube Delta, near Tulcea City. The lakes in this complex are fed with water from the Danube River, especially in high-flow seasons (e.g., spring) (Burada et al., 2015). The water quality of the Danube and its tributaries in Romania has been physico-chemical evaluated in numerous articles by calculating the Water Quality Index (WQI).

According to the obtained results, it was mostly classified in class II - "good" (Frîncu, 2021). Regarding microplastic pollution, according to the study conducted by Procop et al., 2024 the Danube water transports approximately 46-51 tons of microplastics per year on the territory of Romania.

MATERIALS AND METHODS

The area investigated in this study is important because the Danube Delta has been part of the UNESCO (United Nations Educational, Scientific and Cultural Organization) World Heritage Site Biosphere Reserve since 1991 (Popa et al., 2018). In Figure 1, the 6 lakes from which the microplastics were taken can be localized: Morun Lake, Babele Lake, Parcheș Lake, Potica Lake, Câșla Lake, and Somova Lake.

The microplastics were collected from the water with a 150 µm mesh size with a mechanical flow meter that quantifies the volume of filtered water.

The sample preparation, i.e., the isolation of microplastics from organic matter and dense impurities, was carried out according to the method presented in the article by Calmuc et al., 2023.

Microplastics were filtered on Polyvinylidene Fluoride (PVDF) membrane filters with 0.45 µm pore size and 47 mm diameter.

The microplastic filters were analysed using the Spotlight 400 FT-IR Imaging System, PerkinElmer equipment, to identify the polymers in the composition.

The analyses were performed with a resolution of 16 cm^{-1}, a spatial resolution of 6.25 µm, and a spectral range between 4000 -750 cm^{-1}.

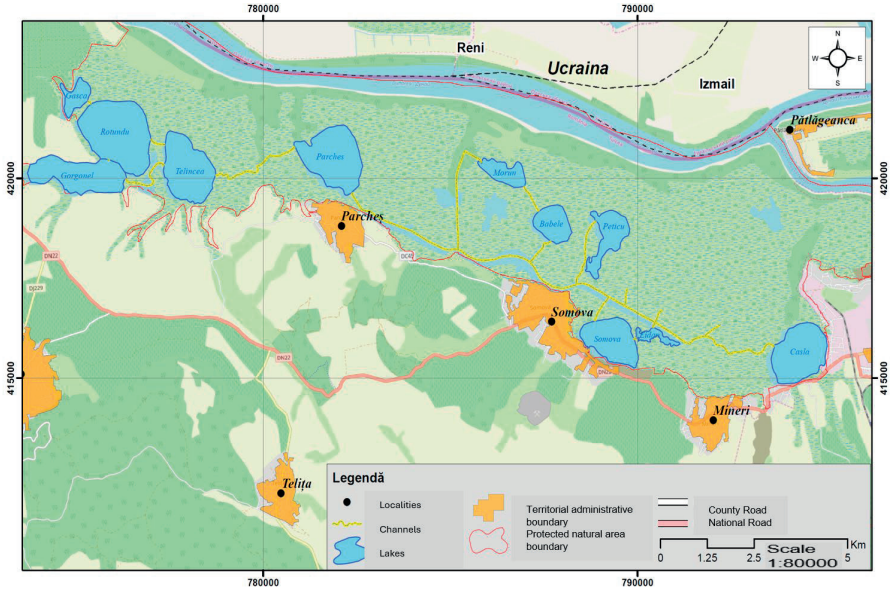


Figure 1. Location of lakes investigated

The Pollution Load Index (PLI) is used to assess the degree of microplastic pollution in the environment and can be calculated according to formulae 1 and 2 (Qiu et al., 2023; Zhou et al., 2024):

$$PLI = \sqrt{CFi} \quad (1)$$

$$CF_i = \frac{Ci}{C0} \quad (2)$$

were:

- CF_i = MPs contamination index;
- C_i = MPs abundance in monitoring stations;
- C_0 = MPs background value (in this study, C_0 represents the lowest MPs concentration recorded in investigated lakes, respectively 0.15 particles·m^{-3}.

According to Table 1, the degree of MPs pollution can be divided into four levels depending on the PLI index score.

Table 1. Pollution Load Index classes
(Qiu et al., 2023; Zhou et al., 2024)

PLI values	Pollution Level
0-10	I – Low
11-20	II – Medium
21-30	III – High
>30	IV – Extremely high

RESULTS AND DISCUSSIONS

Figure 2 illustrates the abundance of microplastic particles recorded in each of the 6 lakes investigated. Particle concentrations ranged from 0.15-0.65 particles·m^{-3}, with the highest abundance recorded in Somova Lake. The main sources of pollution with MPs would be the Danube River that supplies the lakes with water, fishing, tourism, and anthropogenic activities that take place in the localities near the lakes. For example, the village of Somova is located on one of the banks of Somova Lake (where the maximum value was recorded).

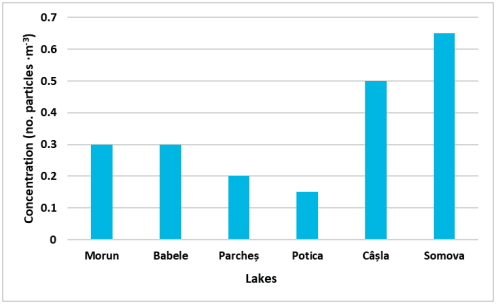


Figure 2. Microplastics concentration in the investigated lakes

Studies showed that MPs concentration in freshwater depends on anthropogenic factors such as population density (Jian et al., 2020). The density of the Somova commune, which includes the villages of Somova, Parcheș, and Mineri, is low, at 33.65 people·km^{-2} (2021) (www.citypopulation.de). Similar results were observed in the study conducted by (Fischer et al., 2016), where concentrations of 2.68 to 3.36 particles·m^{-3} and 0.82 to 4.42 particles·m^{-3} were identified in the surface water from Chiusi Lake and Bolsena Lake, respectively (central Italy). High concentrations of MPs (2425 – 7050 particles·m^{-3}) were observed in the surface water of 20 lakes in the urban area of Changsha, China (Yin et al., 2019).

Based on the morphological classification, MPs collected were film, fragment, and fiber. Fragment and fiber shapes dominate the six lakes, which indicates different sources of pollution (Figure 3) (Li et al., 2021).

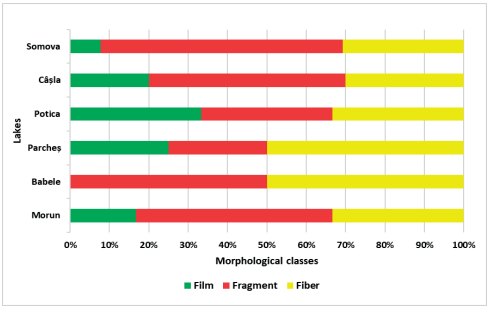


Figure 3. Morphological classification of microplastics

Visible images of MPs particles collected from the six lakes of different colors (green, blue, red), irregular shapes (film - a, fragment - b, fiber - c, d), and sizes are illustrated in Figure 4. An irregular shape suggests that the larger particles' fragmentation can be the source (Rosal, 2021). The sharp edges of irregular shapes can cause physical damage to the stomach wall of fish ingesting MPs (Hossain et al., 2019).

The size classes of microplastics are plotted in Figure 5. In the Somova, Câșla, and Babele lakes, MPs were collected from all four size categories (<150 µm, 150 - 500 µm, 500 - 1000 µm, and 1000 - 5000 µm), while in the Potica and Parcheș lakes, only the 500 - 1000 µm and 1000 - 5000 µm classes were found. The size of microplastics is another important morphological parameter. The presence of larger particle sizes is a source for the secondary of smaller fragments, thus favoring an increase in concentration. Smaller sizes are more bioaccessible and have a higher surface-to-volume ratio, making them more harmful (Sutkar et al., 2023). The polymer composition is another essential parameter of microplastics that provides valuable information for identifying pollution sources. Figure 6 illustrates the image obtained after micro-FT-IR analysis of a microplastic sample on a PVDF filter. Variations in absorbance intensity can be observed, with higher intensities corresponding to greater thickness of the MPs particles.

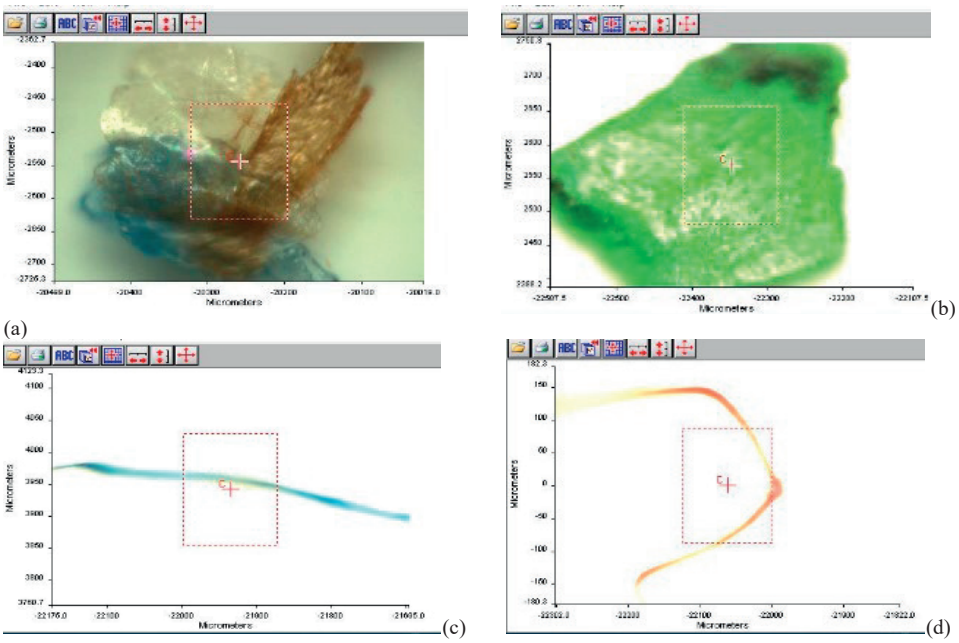


Figure 4. Visible images of microplastics: a) film; b) fragment c); d) fiber

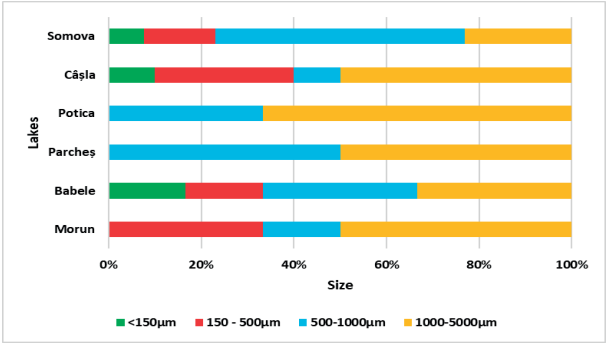


Figure 5. Microplastics size categories

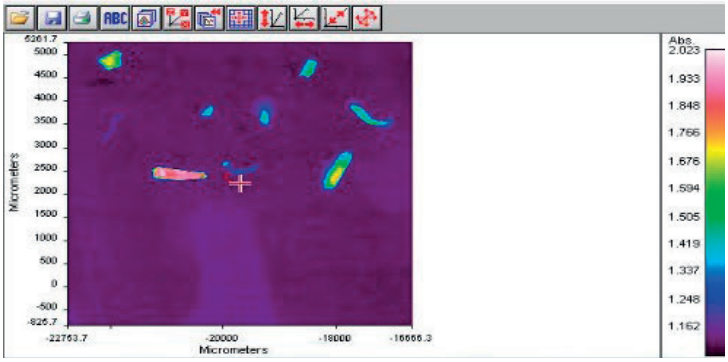


Figure 6. Micro-FT-IR spectral image of microplastics

The IR spectra were extracted from the obtained images (Figure 7) and based on a comparison with the Spectra Databases for Polymers - S.T.Japan Europe GmbH, the polymers composing the microplastics were identified.

The ubiquitous polymer identified in greatest abundance was polyethylene (PE) (Figure 8). The highest polymer diversity was found in Somova and Câșla lakes, where the highest concentrations were recorded. This result is explained by the fact that PE is the most widely used polymer in plastics production (https://www.britannica.com/science/polyethylene.). The second polymer observed was polypropylene (PP), which is one of the most widely used polymers worldwide for packaging (Fernández-González et al., 2021). Polyester (PES), polyacrylonitrile (PAN), and rayon were identified in the fiber composition. Microfiber pollution is caused by fishing nets, rope from lakes, and textiles, in particular by their presence in the air and domestic washing machine effluents (Salvador Cesa et al., 2017).

PVC (polyvinyl chloride) was found in the Somova Lake, which could originate from the degradation of building materials and insulation of cables based on this polymer (Akovali, 2012). In addition, a hydroxyl functional polyester–based paint particle was collected from Somova Lake, which could come from the boat paint. According to the report "Plastic Paints the Environment", published in 2022 by Environmental Action in Switzerland, paints account for 58% of microplastics in the world's oceans and waterways (Paruta et al., 2022).

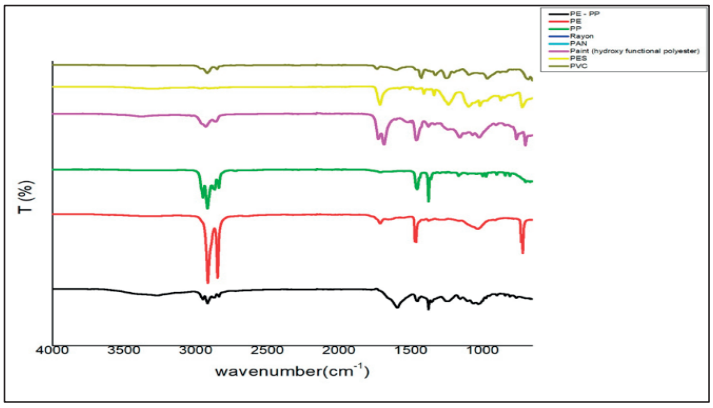


Figure 7. IR spectra of the identified polymers

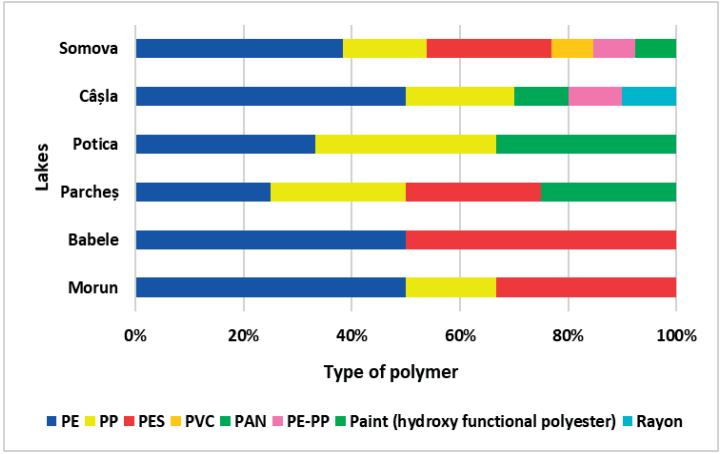


Figure 8. Polymer composition of microplastics

Another aim of the present paper was to assess the level of microplastic pollution in the 6 lakes by calculating the PLI index. The index values are plotted in Figure 9 and are in the range 0.86-1.80, indicating a low level of microplastic pollution (category risk I). Low MPs pollution load was observed in high-altitude glacier lakes in Northern Anatolia, water PLI values ranging from 1.00 to 2.65 (Akdemir et al., 2025).



Figure 9. PLI index values

CONCLUSIONS

In this paper, the presence of microplastics in 6 lakes from the Somova-Parcheș lacustrine complex was studied for the first time. The MPs concentrations in the water of the 6 investigated lakes varied in the 0.15-0.65 particles·m^{-3} range. A variety in the shape, size, and polymer composition of the MPs in the collected samples was observed, indicating the diversity of pollution sources. The MPs shapes identified were fragment>fiber>film. The results of the micro-FT-IR analyses highlighted the presence of PE>PP>PES>PAN>PVC>Paint (hydroxyl functional polyester) polymers in the composition of the collected microplastics. PLI values of all the lakes showed minor contamination with microplastics in the risk I category. This pioneering research fills a knowledge gap, providing valuable information on microplastic pollution of previously unexplored freshwater ecosystems.

ACKNOWLEDGEMENTS

This research was supported by the project "Integrated research and sustainable solutions to protect and restore Lower Danube Basin and coastal Black Sea ecosystems" (ResPonSE), contract no. 760010/30.12.2022. The experimental results have been obtained within the REXDAN Research Infrastructure developed within the project An Integrated System for Research and Monitoring of the Complex Environment in the Danube River Area, REXDAN, SMIS code 127065, co-financed by the European Regional Development Fund through the Competitiveness Operational Program 2014-2020, contract no. 309/10.07.2021.

REFERENCES

Akdemir, T., Terzi, Y., Gündoğdu, S., Öztürk, R. Ç., Gedik, K. (2025). Microplastic contamination in high-altitude glacier lakes in Northern Anatolia. *Environmental Sciences Europe, 37*, 92. https://doi.org/10.1186/s12302-025-01139-0

Akovali, G. (2012). Plastic materials: Polyvinyl chloride (PVC). In F. Pacheco-Torgal, S. Jalali, & A. Fucic (Eds.), *Toxicity of building materials* (pp. 23–53). Woodhead Publishing. https://doi.org/10.1533/9780857096357.23

Burada, A., Topa, C. M., Georgescu, L. P., Teodorof, L., Nastase, C., Seceleanu-Odor, D., & Iticescu, C. (2015). Heavy metals environment accumulation in Somova – Parches aquatic complex from the Danube Delta area. *Revista de Chimie, 66*(1), 48–54.

Calmuc, M., Calmuc, V. A., Condurache, N. N., Arseni, M., Simionov, I.-A., Timofti, M., Georgescu, P.-L., & Iticescu, C. (2023). Study on microplastics occurrence in the Lower Danube River water. *Scientific Papers. Series E. Land Reclamation, Earth Observation & Surveying, Environmental Engineering, 12*.

Dusaucy, J., Gateuille, D., Perrette, Y., & Naffrechoux, E. (2021). Microplastic pollution of worldwide lakes. *Environmental Pollution, 284*, 117075. https://doi.org/10.1016/j.envpol.2021.117075

Fernández-González, V., Andrade-Garda, J. M., López-Mahía, P., & Muniategui-Lorenzo, S. (2021). Impact of weathering on the chemical identification of microplastics from usual packaging polymers in the marine environment. *Analytica Chimica Acta, 1142*, 179–188. https://doi.org/10.1016/j.aca.2020.11.002

Fischer, E. K., Paglialonga, L., Czech, E., & Tamminga, M. (2016). Microplastic pollution in lakes and lake shoreline sediments: A case study on Lake Bolsena and Lake Chiusi (central Italy). *Environmental Pollution, 213*, 648–657. https://doi.org/10.1016/j.envpol.2016.03.012

Frîncu, R.-M. (2021). Long-Term Trends in Water Quality Indices in the Lower Danube and Tributaries in Romania (1996–2017). *International Journal of Environmental Research and Public Health*, *18*(4), 1665. https://doi.org/10.3390/ijerph18041665

Gan, Y., Zhao, Y., Yu, Y., Gai, Y., Nie, Z., Li, C., Ukwattage, N., & Wang, R. (2025). Aquaculture activities influence the distribution and environmental behavior of microplastics in lakes. *Process Safety and*

Environmental Protection, 198, 107117. https://doi.org/10.1016/j.psep.2025.107117

Horton, A. A., Walton, A., Spurgeon, D. J., Lahive, E., & Svendsen, C. (2017). Microplastics in freshwater and terrestrial environments: Evaluating the current understanding to identify the knowledge gaps and future research priorities. *Science of the Total Environment, 586*, 127–141. https://doi.org/10.1016/j.scitotenv.2017.01.190

Hossain, M. S., Sobhan, F., Uddin, M. N., Sharifuzzaman, S. M., Chowdhury, S. R., Sarker, S., & Chowdhury, M. S. N. (2019). Microplastics in fishes from the Northern Bay of Bengal. *Science of the Total Environment, 690*, 821–830. https://doi.org/10.1016/j.scitotenv.2019.07.065

Jian, M., Zhang, Y., Yang, W., Zhou, L., Liu, S., & Xu, E. G. (2020). Occurrence and distribution of microplastics in China's largest freshwater lake system. *Chemosphere, 261*, 128186. https://doi.org/10.1016/j.chemosphere.2020.128186

Li, C., Gan, Y., Zhang, C., He, H., Fang, J., Wang, L., Wang, Y., & Liu, J. (2021). "Microplastic communities" in different environments: Differences, links, and role of diversity index in source analysis. *Water Research, 188*, 116574. https://doi.org/10.1016/j.watres.2020.116574

Liu, Y., Wang, K., Shi, X., Chen, L., & Li, H. (2025). Analysis of microplastic sources in Wuliangsuhai Lake, China: Implications to microplastic deposition in cold, arid region lakes. *Journal of Hazardous Materials, 492*, 138135. https://doi.org/10.1016/j.jhazmat.2025.138135

Luo, S., Wu, H., Xu, J., Wang, X., He, X., & Li, T. (2024). Effects of lakeshore landcover types and environmental factors on microplastic distribution in lakes on the Inner Mongolia Plateau, China. *Journal of Hazardous Materials, 465*, 133115. https://doi.org/10.1016/j.jhazmat.2023.133115

Nguyen, M.-K., Rakib, M. R. J., Lin, C., Hung, N. T. Q., Le, V.-G., Nguyen, H.-L., Malafaia, G., & Idris, A. M. (2023). A comprehensive review on ecological effects of microplastic pollution: An interaction with pollutants in the ecosystems and future perspectives. *TrAC Trends in Analytical Chemistry, 168*, 117294. https://doi.org/10.1016/j.trac.2023.117294

Paruta, P., Pucino, M., & Boucher, J. (2022). Plastic paints the environment. Environmental Action.

Pol, W., Stasińska, E., Żmijewska, A., Więcko, A., & Zieliński, P. (2023). Litter per liter – Lakes' morphology and shoreline urbanization index as factors of microplastic pollution: Study of 30 lakes in NE Poland. *Science of the Total Environment, 881*, 163426. https://doi.org/10.1016/j.scitotenv.2023.163426

Polyethylene (PE) | Properties, structures, uses, & facts. (n.d.). In *Encyclopedia Britannica*. Retrieved April 21, 2025, from https://www.britannica.com/science/polyethylene

Popa, P., Murariu, G., Timofti, M., & Georgescu, L. P. (2018). Multivariate statistical analyses of Danube River water quality at Galati, Romania. *Environmental Engineering and Management Journal, 17*, 1249–1266. https://doi.org/10.30638/eemj.2018.124

Procop, I., Calmuc, M., Pessenlehner, S., Trifu, C., Ceoromila, A. C., Calmuc, V. A., Fetecău, C., Iticescu, C., Musat, V., & Liedermann, M. (2024). The first spatio-temporal study of the microplastics and meso–macroplastics transport in the Romanian Danube. *Environmental Sciences Europe, 36*, 154. https://doi.org/10.1186/s12302-024-00969-8

Qiu, Y., Zhou, S., Zhang, C., Qin, W., & Lv, C. (2023). A framework for systematic microplastic ecological risk assessment at a national scale. *Environmental Pollution, 327*, 121631. https://doi.org/10.1016/j.envpol.2023.121631

Rosal, R. (2021). Morphological description of microplastic particles for environmental fate studies. *Marine Pollution Bulletin, 171*, 112716. https://doi.org/10.1016/j.marpolbul.2021.112716

Salvador Cesa, F., Turra, A., & Baruque-Ramos, J. (2017). Synthetic fibers as microplastics in the marine environment: A review from textile perspective with a focus on domestic washings. *Science of the Total Environment, 598*, 1116–1129. https://doi.org/10.1016/j.scitotenv.2017.04.172

Somova (Tulcea, Romania) - Population statistics, charts, map, location, weather and web information. (n.d.). Retrieved April 22, 2025, from https://www.citypopulation.de/en/romania/tulcea/_/161302__somova/

Sutkar, P. R., Gadewar, R. D., & Dhulap, V. P. (2023). Recent trends in degradation of microplastics in the environment: A state-of-the-art review. *Journal of Hazardous Materials Advances, 11*, 100343. https://doi.org/10.1016/j.hazadv.2023.100343

Yin, L., Jiang, C., Wen, X., Du, C., Zhong, W., Feng, Z., Long, Y., & Ma, Y. (2019). Microplastic pollution in surface water of urban lakes in Changsha, China. *International Journal of Environmental Research and Public Health, 16*, 1650. https://doi.org/10.3390/ijerph16091650

Zhang, F., Guo, X., Zhang, J., & Zhang, Z. (2024). Microplastics in Qinghai-Tibet Plateau and Yunnan-Guizhou Plateau lakes, China. *Science of the Total Environment, 915*, 169978. https://doi.org/10.1016/j.scitotenv.2024.169978

Zhou, Y., Zhang, Z., Bao, F., Du, Y., Dong, H., Wan, C., Huang, Y., & Zhang, H. (2024). Considering microplastic characteristics in ecological risk assessment: A case study for China. *Journal of Hazardous Materials, 470*, 134111. https://doi.org/10.1016/j.jhazmat.2024.134111

Scientific Papers. Series E. Land Reclamation, Earth Observation & Surveying, Environmental Engineering. Vol. XIV, 2025
Print ISSN 2285-6064, CD-ROM ISSN 2285-6072, Online ISSN 2393-5138, ISSN-L 2285-6064

INVESTIGATION OF THE PHARMACEUTICALS PRESENCE IN THE SOMOVA-PARCHEȘ AQUATIC COMPLEX

Valentina Andreea CĂLMUC[1], Mădălina CĂLMUC[1], Carmen CHITESCU[1], Silvia DRĂGAN[2], Cătălina ITICESCU[1], Puiu-Lucian GEORGESCU[1]

[1]"Dunărea de Jos" University of Galați, REXDAN Research Centre,
98 George Coșbuc Blvd, 800223, Galați, Romania
[2]EnviroEcoSmart SRL, 3 Nufărului Street, 800298, Galați, Romania

Corresponding author email: valentina.calmuc@ugal.ro

Abstract

The Somova-Parcheș Aquatic Complex is part of the Danube Delta Biosphere Reserve and hosts a wide variety of fauna and flora species of community importance. This complex is fed with a significant volume of water from the Danube River, thus influencing the quality of the lake ecosystems. For this reason, the present study aims to investigate the presence of certain classes of pharmaceutical residues in water sampled from 6 lakes, namely Somova, Parcheș, Morun, Potica, Babele, Câșla, as well as their ability to accumulate in the tissues of fish collected from the same study area. Extraction of pharmaceutical compounds was performed using the solid phase extraction method for water samples and the QuEChERS method for fish tissues. Results obtained from analyses using high-performance liquid chromatography coupled with high-resolution mass spectrometry revealed the presence of the pharmaceutical compound caffeine in most water samples and its tendency to accumulate in some fish organs, such as the gills.

Key words*: Somova-Parcheș Aquatic Complex, pharmaceutical residues, water, fish tissue.*

INTRODUCTION

The Danube River supplies water to the Somova-Parches Aquatic Complex, thus facilitating the entry of various contaminants into the lakes. Numerous studies have been carried out on the Danube River, which have shown that, in general, the water falls into class quality II (Good) (Mănoiu & Crăciun, 2021). However, a wide variety of chemical and physical compounds have been identified which, in certain concentrations, can have toxic effects on the aquatic environment, such as: nutrients (Malagó et al., 2017; Popa et al., 2018), gross alpha and gross beta activities (Pintilie-Nicolov et al., 2021), heavy metals (Lazăr et al., 2024; Mîndrescu et al., 2022), pharmaceutical compounds (Chitescu et al., 2015), microplastics (Procop et al., 2024), pesticides (Đurišić-Mladenović et al., 2024), etc.
To date, studies have been conducted in the Somova-Parcheș Aquatic Complex area to evaluate the quality of aquatic ecosystems, considering the common parameters regulated by Order 161/2006. Among the most frequently analyzed compounds in this study area are heavy metals, oxygen regime, and nutrients (Burada et al., 2015; Catianis et al., 2019). This study aims to investigate, for the first time in this area, a class of emerging pollutants represented by pharmaceutical residues. The main pollution sources of the Danube river with pharmaceutical residues are conventional wastewater treatment plants and animal farms (Kock et al., 2023; Radović et al., 2012).
The analysis of this type of contaminants in aquatic environments is very important, as they can have direct toxic effects on aquatic biota and can accumulate in biotic tissues depending on their concentration and the physicochemical properties of each pharmaceutical substance (Khan et al., 2020; Rojo et al., 2021; Williams et al., 2009). For this reason, the present research focuses on investigating the presence of different classes of pharmaceuticals in various organs of the *Carassius gibelio* fish species collected from the Somova-Parcheș Aquatic Complex.

MATERIALS AND METHODS

To study the presence of pharmaceutical compounds in the Somova-Parcheș Aquatic Complex, four water samples were collected

from different areas (inlet, middle and outlet) of each lake, namely Somova, Parcheş, Morun, Potica, Babele and Câşla (Figure 1).

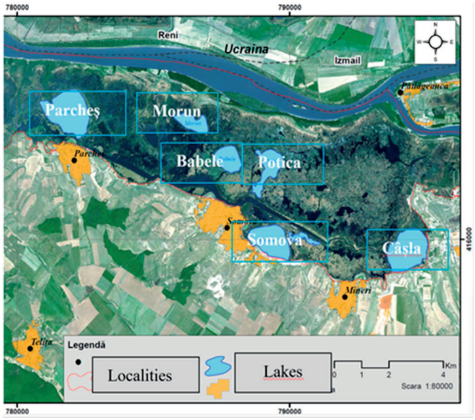


Figure 1. Map of the studied lakes in the Somova-Parcheş Aquatic Complex

Extraction of pharmaceutical residues from water samples was performed with a Dionex AutoTrace 280 Thermo Scientific automated solid phase extraction system (Figure 2).



Figure 2. Automated solid phase extraction system

To extract the target compounds from fish tissues, the QuEChERS (Quick, Easy, Cheap, Effective, Rugged, and Safe) technique was used. This method involved the extraction of contaminants from the matrix into the solvent acetonitrile in the presence of the following salt mixture: 6 g anhydrous magnesium sulfate, 5 g sodium chloride, 1.5 g disodium citrate dihydrate, and 0.75 g trisodium citrate sesquihydrate. To remove fats, lipids, and pigments from the extract, a purification step was performed using the dispersive solid-phase extraction (d-SPE) method in the presence of sorbent materials (PSA – primary secondary amine, C18, and GCB – graphitized carbon) (Figure 3).



Figure 3. QuEChERS extraction steps

The extraction step was followed by the analysis of pharmaceutical substances from the obtained extracts using high-performance liquid chromatography coupled with high-resolution mass spectrometry.

The following pharmaceutical compounds were investigated in water and fish tissue samples: metformin, carbamazepine, clindamycin, ciprofloxacin, clarithromycin, trimethoprim, sulfamethoxazole, amoxicillin, ketoprofen, diclofenac, and caffeine. To quantify these compounds, the internal standards were used depending on the class of pharmaceutical substances they belong to, as follows: enrofloxacin for antibiotics, dihydrocarbamazepine for carbamazepine, fenoprop for anti-inflammatories, phenacetin for metformin and caffeine (Figure 4).

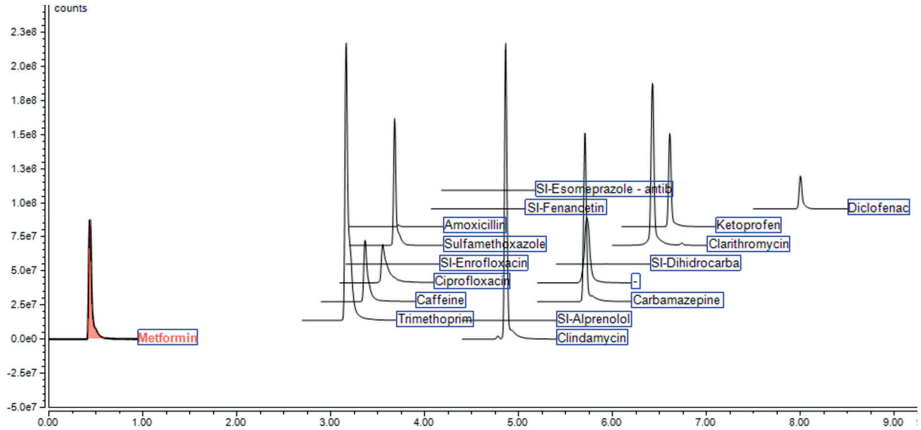


Figure 4. Chromatogram of the analyzed pharmaceutical compounds

RESULTS AND DISCUSSIONS

Spatial distribution of pharmaceutical compounds identified in water samples taken from lakes in the Somova-Parcheş Aquatic Complex

From all the 6 lakes studied in this paper, water samples were taken from 4 different stations, and the presence of different pharmaceutical substances was investigated. Of the 11 compounds monitored in water samples, only caffeine and the internal standards added to the samples for compound quantification were identified in all sampling stations (Figure 5).

Caffeine is found in beverages, foods, and medications that are consumed in significant quantities worldwide. For this reason, it is considered a significant pollutant in the class of active pharmaceutical compounds that is found with high frequency in the environment (Li et al., 2020).

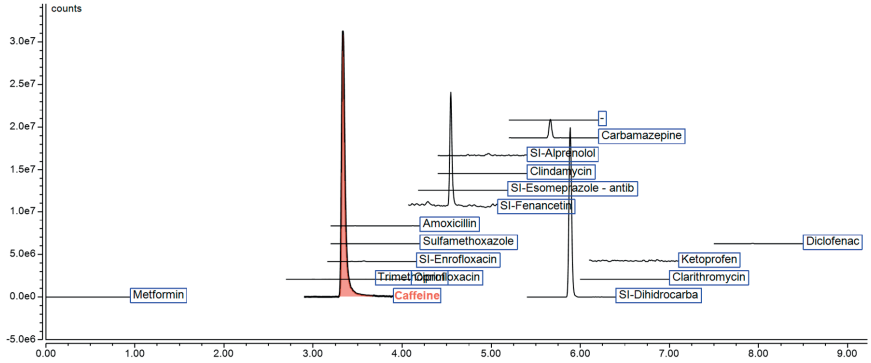


Figure 5. Chromatogram example of compounds in a water sample analyzed from lakes

In the lakes analyzed in the present study, caffeine concentrations varied between 15 ng/L and 65 ng/L. The highest values of the caffeine compound were identified in Somova lake, the mean concentration being 55 ng/L. The lowest concentrations were obtained in water samples collected from Morun lake, where a mean concentration of 20 ng/L was recorded. In most lakes, slight variations in caffeine concentrations were observed from one sampling station to another (Figure 6). The main contamination source of the aquatic environment with this psychoactive compound is anthropogenic,

generally represented by municipal wastewater (Vieira et al., 2022).

The presence of this compound in the aquatic environment can be explained by its pseudo-persistent character, caused by its long half-life. This substance also exhibits high resistance to chemical and biological degradation in the environment, has low volatility, and its low octanol-water partition coefficient (log Kow = -0.07) explains its high solubility in water (Rodrigues et al., 2025). In the aquatic environment, this alkaloid can have direct toxic effects on biota and can even induce behavioral disorders in fish at environmentally relevant concentrations (Cerveny et al., 2022).

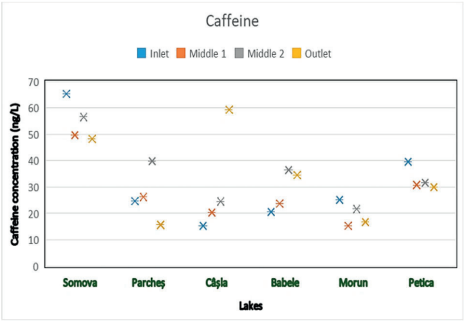


Figure 6. Spatial distribution of caffeine in the Somova-Parcheș Aquatic Complex lakes

The caffeine compound was also identified at high frequency in the Danube River in the territory of the Novi Sad, Serbia with concentrations varying from 3.10 to 621 ng/L (Milić et al., 2018).

On the territory of Romania, there is a limited number of studies that have focused on the analysis of pharmaceutical residues in the aquatic environment.

Chitescu et al., identified the following compounds in water samples taken from the Danube River: sulfamethoxazole, trimethoprim, enilconazole, carbamazepine, and tylosin. Pharmaceutical residues such as sulfamethoxazole, diclofenac, trimethoprim, carbamazepine, piroxicam and ketoprofen were quantified in the Olt, Argeș and Siret tributaries. A smaller number of pharmaceutical substances were identified in water samples taken from the Danube Delta, including sulfamethoxazole and carbamazepine (Chitescu et al., 2015).

Investigation of the pharmaceutical compounds presence in fish specimens of the species Carassius gibelio

The fish species *Carassius gibelio* is found abundantly in the Danube River basin and is considered the most consumed local freshwater fish (Raita and Georgescu, 2019). To identify the presence of pharmaceutical compounds in the species *Carassius gibelio*, 3 fish specimens were taken for analysis and extractions were made from muscle tissue, liver tissue, gills and eggs. Of all the investigated compounds, caffeine was the one that was found in all the organs analyzed from the 3 fish, with mean values ranging from 0.77 ng/g to 2.42 ng/g (Figure 7). Table 1 shows that the highest average concentration of caffeine was identified in the gills. This can be explained by the fact that the gills are in direct contact with water and can more easily accumulate pollutants found in the aquatic environment (Nikolić et al., 2020). However, it can be noted that traces of caffeine were identified even in the fish eggs analyzed in this study.

The obtained results show that the same compound identified in water samples from the Somova-Parcheș Aquatic Complex, represented by caffeine, accumulated also in the organs of fish collected from the same study area.

Table 1. Concentration levels of pharmaceuticals in fish specimens of the species *Carassius gibelio* – the values are expressed as mean ± standard deviation

Pharmaceutical compound identified	Fish organs analyzed	Mean concentration ± std (ng/g)
Caffeine	Muscle tissue	1.04 ± 0.19
	Liver tissue	1.60 ± 0.23
	Gills	2.42 ± 1.10
	Eggs	0.77 ± 0.30

In the literature, there are laboratory studies that monitored the behaviour and physiology of fish exposed to caffeine and it was highlighted that, even in relatively low concentrations, this compound can cause liver enlargement and anxiety of fish (Bikker et al., 2024). There are also studies reporting accumulations of the caffeine compound in the organs of different fish species. For example, Wang and Gardinali reported the presence of caffeine in the fish species *Gambusia holbrooki* at a mean concentration of 1.3 ng/g (Wang & Gardinali, 2012).

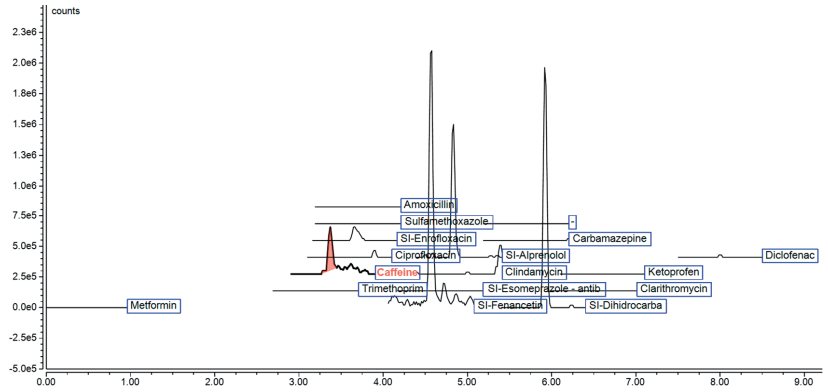


Figure 7. Chromatogram example of compounds identified in fish tissue from the species *Carassius gibelio*

In the panga fish (*Pterogymnus laniarus*) caffeine was detected in the intestine, liver and gills with a concentration of 2.03 ng/g (Ojemaye and Petrik, 2019). Caffeine was also identified in the fish species Common Silver biddy (*Gerres oyena*), Golden snapper (*Lutjanus johni*), Emperor fish (*Lethrinus, nebulosus*), Nile Tilapia (*Oreochromis niloticus*), and Milk fish (*Chanos chanos*) (Ali et al., 2018).
No results have been reported in the specialized literature regarding the presence of pharmaceutical residues in the fish species *Carassius gibelio*.

CONCLUSIONS

Due to their high toxicity, it is important to monitor the emerging contaminant class represented by pharmaceutical compounds in all water bodies.
The present study emphasizes that a wide variety of pharmaceutical substances were not found in the lakes of the Somova-Parcheș Aquatic Complex. This may be due to the fact that there are no direct sources of pollution in the area. This may also be influenced by the low concentrations of these compounds in the Danube water, which may undergo various processes of accumulation, degradation, dilution until they reach the lakes of the Somova-Parcheș Aquatic Complex.
However, the psychoactive substance caffeine was identified in all water samples analyzed. A possible explanation could be that it is generally found in higher concentrations in the aquatic environment compared to the other pharmaceutical compounds analyzed and can therefore reach even areas far from direct sources of pollution.
This study also highlights the ability of the caffeine compound to accumulate in aquatic biota. Low concentrations of caffeine were identified in the organs of the fish analyzed from the species *Carassius gibelio*.

ACKNOWLEDGEMENTS

This work was supported by the REXDAN Infrastructure developed within the project An Integrated System for Research and Monitoring of the Complex Environment in the Danube River Area, REXDAN, SMIS code 127065, co-financed by the European Regional Development Fund through the Competitiveness Operational Program 2014-2020, contract no. 309/10.07.2021.
This research was supported by the project "Integrated research and sustainable solutions to protect and restore Lower Danube Basin and coastal Black Sea ecosystems" (ResPonSE), contract no. 760010/30.12.2022.

REFERENCES

Ali, A. M., Rønning, H. T., Sydnes, L. K., Alarif, W. M., Kallenborn, R., & Al-Lihaibi, S. S. (2018). Detection of PPCPs in marine organisms from contaminated coastal waters of the Saudi Red Sea. *Science of The Total Environment, 621,* 654–662. https://doi.org/10.1016/j.scitotenv.2017.11.298

Bikker, J., MacDougall-Shackleton, H., Bragg, L. M., Servos, M. R., Wong, B. B. M., & Balshine, S. (2024). Impacts of caffeine on fathead minnow behaviour and

physiology. *Aquatic Toxicology, 273,* 106982. https://doi.org/10.1016/j.aquatox.2024.106982

Burada, A., Topa, C. M., Georgescu, L. P., Teodorof, L., Năstase, C., Seceleanu-Odor, D., & Iticescu, C. (2015). Heavy metals environment accumulation in Somova-Parches aquatic complex from the Danube Delta area. *Revista de Chimie, 66,* 48–54.

Catianis, I., Pojar, I., Grosu, D., & Pavel, A. B. (2019). Investigation of the surface water quality parameters in the predeltaic area of the Danube Delta in 2017. Study case: Somova-Parcheș aquatic complex lakes. *Scientific Annals of the Danube Delta Institute,* 139–146. https://doi.org/10.7427/DDI.24.15

Cerveny, D., Cisar, P., Brodin, T., McCallum, E. S., & Fick, J. (2022). Environmentally relevant concentration of caffeine - effect on activity and circadian rhythm in wild perch. *Environmental Science and Pollution Research, 29,* 54264–54272. https://doi.org/10.1007/s11356-022-19583-3

Chitescu, C. L., Kaklamanos, G., Nicolau, A. I., & Stolker, A. A. M. (Linda). (2015). High sensitive multiresidue analysis of pharmaceuticals and antifungals in surface water using U-HPLC-Q-Exactive Orbitrap HRMS. Application to the Danube river basin on the Romanian territory. *Science of The Total Environment, 532,* 501–511. https://doi.org/10.1016/j.scitotenv.2015.06.010

Đurišić-Mladenović, N., Živančev, J., Antić, I., Rakić, D., Buljovčić, M., Pajin, B., Llorca, M., Farre, M., 2024. Occurrence of contaminants of emerging concern in different water samples from the lower part of the Danube River Middle Basin – A review. *Environmental Pollution 363*, 125128. https://doi.org/10.1016/j.envpol.2024.125128

Khan, H. K., Rehman, M. Y. A., & Malik, R. N. (2020). Fate and toxicity of pharmaceuticals in water environment: An insight on their occurrence in South Asia. *Journal of Environmental Management, 271,* 111030. https://doi.org/10.1016/j.jenvman.2020.111030

Kock, A., Glanville, H.C., Law, A.C., Stanton, T., Carter, L.J., Taylor, J.C., 2023. Emerging challenges of the impacts of pharmaceuticals on aquatic ecosystems: A diatom perspective. *Science of The Total Environment 878,162939.*

https://doi.org/10.1016/j.s env.2023.162939

Lazăr, N.-N., Simionov, I.-A., Petrea, Ș.-M., Iticescu, C., Georgescu, P.-L., Dima, F., & Antache, A. (2024). The influence of climate changes on heavy metals accumulation in *Alosa immaculata* from the Danube River Basin. *Marine Pollution Bulletin, 200,* 116145. https://doi.org/10.1016/j.marpolbul.2024.116145

Li, S., Wen, J., He, B., Wang, J., Hu, X., & Liu, J. (2020). Occurrence of caffeine in the freshwater environment: Implications for ecopharmacovigilance. *Environmental Pollution, 263,* 114371. https://doi.org/10.1016/j.envpol.2020.114371

Malagó, A., Bouraoui, F., Vigiak, O., Grizzetti, B., Pastori, M., 2017. Modelling water and nutrient fluxes in the Danube River Basin with SWAT. *Science of The Total Environment, 603–604*, 196–218. https://doi.org/10.1016/j.scitotenv.2017.05.242

Mănoiu, V.-M., Crăciun, A.-I., 2021. Danube river water quality trends: A qualitative review based on the open access web of science database. *Ecohydrology & Hydrobiology 21,* 613–628. https://doi.org/10.1016/j.ecohyd.2021.08.002

Mîndrescu, M., Haliuc, A., Zhang, W., Carozza, L., Carozza, J.-M., Groparu, T., Valette, P., Sun, Q., Nian, X., Gradinaru, I., 2022. A 600 years sediment record of heavy metal pollution history in the Danube Delta. *Science of The Total Environment, 823*, 153702. https://doi.org/10.1016/j.scitotenv.2022.153702

Milić, N., Milanović, M., Radonić, J., Turk Sekulić, M., Mandić, A., Orčić, D., Mišan, A., Milovanović, I., Grujić Letić, N., & Vojinović Miloradov, M. (2018). The occurrence of selected xenobiotics in the Danube River via LC-MS/MS. *Environmental Science and Pollution Research, 25,* 11074–11083. https://doi.org/10.1007/s11356-018-1401-z

Nikolić, D., Skorić, S., Rašković, B., Lenhardt, M., & Krpo-Ćetković, J. (2020). Impact of reservoir properties on elemental accumulation and histopathology of European perch (*Perca fluviatilis*). *Chemosphere, 244,* 125503. https://doi.org/10.1016/j.chemosphere.2019.1

Order 161/2006 of Romanian Ministry of Environment and Water Management regarding norms for surface water classification in order to establish ecological state of water bodies. (2006). Romanian Official Monitor: Bucharest, Romania. Available online: http://www.legex.ro/Ordin-161-2006-71706.aspx (accessed on May 15, 2025).

Ojemaye, C. Y., & Petrik, L. (2019). Occurrences, levels and risk assessment studies of emerging pollutants (pharmaceuticals, perfluoroalkyl and endocrine disrupting compounds) in fish samples from Kalk Bay harbour, South Africa. *Environmental Pollution, 252,* 562–572. https://doi.org/10.1016/j.envpol.2019.05.091

Pintilie-Nicolov, V., Georgescu, P.-L., Iticescu, C., Moraru, D. I., & Pintilie, A. G. (2021). The assessment of the annual effective dose due to ingestion of radionuclides from drinking water consumption: Calculation methods. *Journal of Radioanalytical and Nuclear Chemistry, 327,* 49–58. https://doi.org/10.1007/s10967-020-07438-5

Popa, P., Murariu, G., Timofti, M., & Georgescu, L. P. (2018). Multivariate statistical analyses of Danube River water quality at Galati, Romania. *Environmental Engineering and Management Journal, 17,* 1249–1266.

Procop, I., Calmuc, M., Pessenlehner, S., Trifu, C., Ceoromila, A.C., Calmuc, V.A., Fetecău, C., Iticescu, C., Musat, V., Liedermann, M., 2024. The first spatio-temporal study of the microplastics and meso–macroplastics transport in the Romanian Danube. *Environmental Sciences Europe, 36*, 154. https://doi.org/10.1186/s12302-024-00969-8

Radović, T., Grujić, S., Dujaković, N., Radišić, M., Vasiljević, T., Petković, A., Boreli-Zdravković, D., Dimkić, M., & Laušević, M. (2012). Pharmaceutical residues in the Danube River Basin in Serbia—a two-year survey. *Water Science and Technology, 66,* 659–665. https://doi.org/10.2166/wst.2012.225

Raita, S. M., & Georgescu, M. (2019). Monitoring *Carassius gibelio* muscle tissue quality under black cumin oil fortification and typical cold storage. *Scientific Works. Series C. Veterinary Medicine, LXV,* 21–28.

Rodrigues, S., Alves, R. S., & Antunes, S. C. (2025). Impact of caffeine on aquatic ecosystems: Assessing trophic-level biological responses. *Journal of Xenobiotics, 15,* 86. https://doi.org/10.3390/jox15030086

Rojo, M., Cristos, D., González, P., López-Aca, V., Dománico, A., & Carriquiriborde, P. (2021). Accumulation of human pharmaceuticals and activity of biotransformation enzymes in fish from two areas of the lower Rio de la Plata Basin. *Chemosphere, 266,* 129012. https://doi.org/10.1016/j.chemosphere.2020.129012

Vieira, L. R., Soares, A. M. V. M., & Freitas, R. (2022). Caffeine as a contaminant of concern: A review on concentrations and impacts in marine coastal systems. *Chemosphere, 286,* 131675. https://doi.org/10.1016/j.chemosphere.2021.131675

Wang, J., & Gardinali, P. R. (2012). Analysis of selected pharmaceuticals in fish and the fresh water bodies directly affected by reclaimed water using liquid chromatography-tandem mass spectrometry. *Analytical and Bioanalytical Chemistry, 404,* 2711–2720. https://doi.org/10.1007/s00216-012-6139-8

Williams, M., Ong, P. L., Williams, D. B., & Kookana, R. S. (2009). Estimating the sorption of pharmaceuticals based on their pharmacological distribution. *Environmental Toxicology and Chemistry, 28,* 2572–2579. https://doi.org/10.1897/08-587.1

Scientific Papers. Series E. Land Reclamation, Earth Observation & Surveying, Environmental Engineering. Vol. XIV, 2025
Print ISSN 2285-6064, CD-ROM ISSN 2285-6072, Online ISSN 2393-5138, ISSN-L 2285-6064

VALIDATION OF A UHPLC-HRMS METHOD FOR THE ASSESSMENT OF PER AND POLY-FLUOROALKYL SUBSTANCES (PFAS) IN BIOTA

Andreea-Miruna CODREANU[1], Ștefania-Adelina MILEA[1], Valentina Andreea CĂLMUC[1], Justinian-Andrei TOMESCU[2, 3], Alin Constantin DÎRȚU[1, 4], Cătălina ITICESCU[1, 5], Puiu-Lucian GEORGESCU[1, 5]

[1]"Dunărea de Jos" University of Galați, REXDAN Research Infrastructure, 98 George Coșbuc Blvd, 800223, Galați, Romania
[2]SC Hofigal Export Import SA, 2 Intrarea Serelor Street, District 4, 042124, Bucharest, Romania
[3]National University of Science and Technology Politehnica Bucharest, Faculty of Chemical Engineering and Biotechnologies, Department Bioresources and Polymer Sciences, 1-7 Gh. Polizu Street, 011061, District 1, Bucharest, Romania
[4]"Alexandru Ioan Cuza" University of Iași, Faculty of Chemistry, Kogălniceanu Entrance, Building A (UAIC), 11 Carol I Street, 700506, Iași, Romania
[5]"Dunărea de Jos" University of Galați, Faculty of Sciences and Environment, 111 Domnească Street, 800201, Galați, Romania

Corresponding author email: miru.an@yahoo.com

Abstract

PFAS are present in freshwater fish in the Danube River, posing concerns about aquatic ecosystem contamination and adverse effects on human health. These substances also referred to as "forever chemicals" have the potential to accumulate in the food chain and provoke several health issues, including hormonal imbalance and cancer. In this work, the QuEChERS extraction and clean-up method combined with UHPLC-HRMS (Ultra-High-Performance Liquid Chromatography – High-Resolution Mass Spectrometry) was applied for the determination of 18 PFAS in muscle tissue of freshwater fish (European wels catfish – Silurus glanis). The method was validated in terms of Specificity, Linearity, Precision (% RSD), Recovery, and Accuracy (mean spike recovery, %) at two levels of concentration: 0.1 and 5 ng. Additionally, the study assessed the impact of matrix effects on PFAS detection in fish tissue.

Key words*: Danube River, freshwater fish, mass spectrometry, PFAS, QuEChERS.*

INTRODUCTION

Per and poly-fluoroalkyl substances (PFAS) are a class of thousands of environmental contaminants that contain carbon-fluorine bonds, known in organic chemistry as one of the strongest chemical bonds (Figure 1) (*Per- and Polyfluoroalkyl Substances (PFAS) - ECHA*, n.d.). They have been detected in freshwater fish from European rivers, the contamination with these substances is mainly the result of bioaccumulation in aquatic food chains (*PFAS Pollution in European Waters*, 2024). Given the increased anthropogenic pressures on aquatic ecosystems, fish meat and fish products have been observed to accumulate various contaminants, which can pose toxicity risks if transferred to humans via consumption (Panda et al., 2023). PFAS can accumulate in fish via two pathways: direct uptake from contaminated water and indirect uptake through the consumption of contaminated sediments and feed. In time, this can lead to bioaccumulation especially in vulnerable fish species tissue, causing disruption of the aquatic ecosystem.

The Danube River, one of the most important rivers in Europe, has been exposed to environmental pollutants like PFAS mainly through agriculture, industrial processes and wastewater discharges. In the Danube River Basin, a comprehensive study has focused on the occurrence and distribution of 4,777 PFAS in river water, wastewater, groundwater, and biota samples. Results revealed the presence of 82 PFAS, with perfluorooctanoic acid (PFOA) and perfluorooctanesulfonic acid (PFOS) being widespread in surface water. Furthermore, the risk assessment led to identifying 18 PFAS of environmental concern, highlighting the

ubiquity of these substances throughout the river basin (Ng et al., 2022). Another study conducted in the Lower Danube River region focused on the occurrence of PFAS in surface water and ground water from two sites. PFAS concentrations were mostly low with the exception of PFOA concentrations that exceeded 10 ng/L at one site (Obeid et al., 2023).

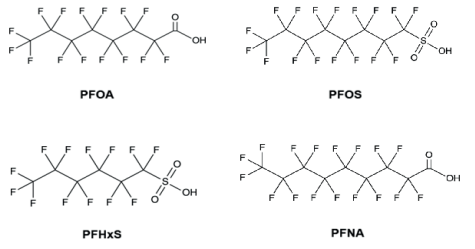


Figure 1. Chemical structure of the most studied PFAS

In the literature (Chaudhary et al., 2024), it is found that the absorption of PFAS at the level of biota depends on several factors that characterize water quality, e.g. heavy metals. It is necessary to associate studies on heavy metals from sensitive areas (Burada et al., 2015) with studies including statistical processing of the results of physicochemical determinations from surface ecosystems (Popa et al., 2018) and determinations of certain pollutants in biota.

As a consequence, regulations regarding PFAS are increasingly strict in Europe due to growing concern about their environmental and health impacts. The European Union has proposed restrictions on the use for specific PFAS under the REACH (Registration, Evaluation, Authorisation, and Restriction of Chemicals) regulation (*REACH Annex XVII: REACH Restricted Substance List 2023*, n.d.). In addition, the European Chemicals Agency (ECHA) is actively identifying and imposing limitations for the use of PFAS substances of high concern (*Per and Polyfluoroalkyl Substances (PFAS) - ECHA*, n.d.). These restrictions will have as an impact an increased demand for targeted assessment of PFAS in different environmental matrices, like water, sediment and biota. Moreover, researchers and environmental agencies will update their monitoring strategies to comply with these regulations with focus on the most harmful and widespread PFAS.

The aim of the present work was to develop and validate a method for the determination of 18 PFAS in fish muscle using QuEChERS (Quick, Easy, Cheap, Effective, Rugged and Safe) extraction and clean-up followed by UHPLC-HRMS (Ultra-High-Performance Liquid Chromatography – High-Resolution Mass Spectrometry) analysis.

MATERIALS AND METHODS

The fish tissue used in this validation study was muscle from three different wels catfish (*Silurus glanis*). The fish were purchased from a local fisherman in the Lower Danube River Region, Galați. 5 grams of each homogenized tissue (wet weight) were submitted to the QuEChERS extraction and dSPE (dispersive solid-phase extraction) clean-up. PFAS compounds were extracted from the fish tissue using acetonitrile and extraction salts (6.0 g $MgSO_4$ and 1.5 g Na-acetate). The resulted extract was submitted to clean-up (150 mg $MgSO_4$, 50 mg Primary and Secondary Amines) and concentrated under a gentle nitrogen flow. All resulted extracts were stored in polypropylene vials to prevent sample contamination. Figure 2 depicts the general workflow for the PFAS analysis in fish samples. For the method validation, spiked samples of 0.1 and 5 ng PFAS were also prepared in triplicate using the same protocol.

The final extracts were separated on Accucore aQ C18 (100 mm x 2.1 mm, 2.6 μm) analytical column in a gradient mode, and the mobile phase consisted of methanol and ultrapure water, both acidified with 0.1% formic acid. The flow rate was 0.5 mL/min. The temperature of the autosampler was 6°C and the analytical column temperature was set to 45°C. Furthermore, the extracts were analysed using a Thermo Fisher Scientific Chromatographic System consisting of Vanquish Flex Liquid Cromatograph coupled to Orbitrap Exploris 120 Mass Spectrometer with heated electrospray ionization (H-ESI II), operated in Full Scan at 120,000 (FWHM) at m/z 200, negative ion mode. The mass measurement accuracy was 5ppm. The chromatographic separation and detection were

performed within 21 min of analysis time. All chromatograms were processed using Chromeleon 7.3 software.

Table 1 contains a list of the target analytes; their acronyms and chemical formula and they are presented in their elution order. Also, the table presents the negative monitored ion (MS Quantitation peak) for each of the 18 PFAS.

The following validation parameters were tested according to Commission Decision 657/2002: specificity, linearity, precision, recovery, accuracy and matrix effects (*Decision - 2002/657 - EN - EUR-Lex*, n.d.). The obtained data represent a helpful tool in evaluating the reliability of the analytical method, in particular for low concentrations quantification of compounds in environmental samples.

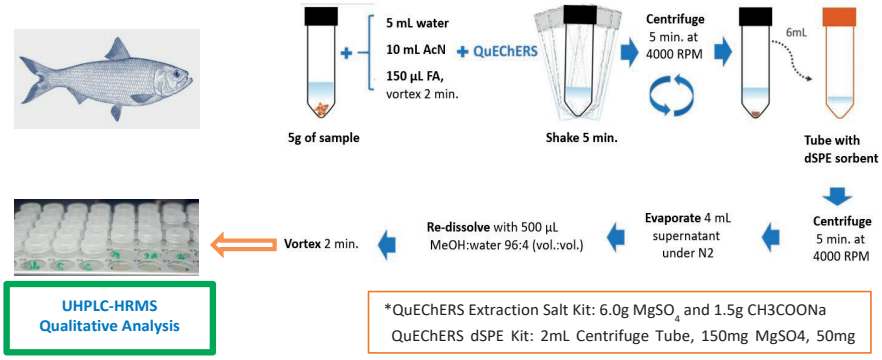


Figure 2. General targeted PFAS analysis workflow in biota samples

RESULTS AND DISCUSSIONS

The specificity of the method was investigated by injecting standard solution and solvent (a mixture of methanol and ultrapure water). Also, a chromatogram of the mobile phase was analysed. The obtained chromatograms demonstrated the absence of interference in the analyte elution. Figure 3 and 4 show a Total Ion Chromatogram (TIC), respectively an Extracted Ion Chromatogram of the PFAS standard mixture at a concentration of 100 ng/mL.

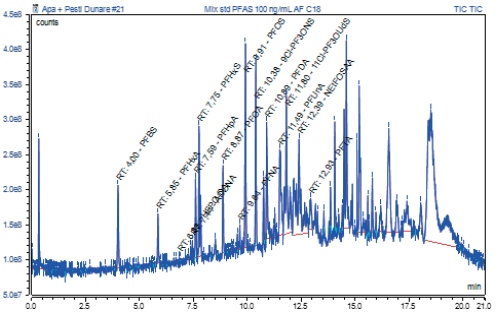


Figure 3. Total Ion Chromatogram of the PFAS standard mixture at 100 ng/mL

They both show a good separation of the compounds which is an indicator for an appropriate choice of the mobile phase, gradient and chromatographic column.

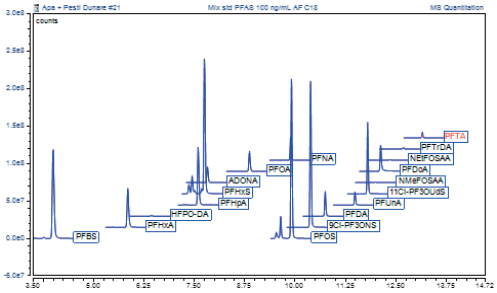


Figure 4. Extracted Ion Chromatogram of the PFAS standard mixture at 100 ng/mL

Linearity of the method was evaluated by testing calibration standards of PFAS on 8 concentration levels. These were prepared by dilutions of the stock standard solution prepared in 96%: 4% methanol: ultrapure water (vol./vol.) and comprise a mixture of target analytes in a calibration range of 0.5-100 ng/mL for most analytes, except for HFPO-DA (5-100 ng/mL).

The coefficient of determination was R^2>0.995, which complies with the acceptance criteria (Table 2). This indicates a strong linear relationship between the measured concentration and expected concentration in the method used for analysis.

Precision was measured as %Relative Standard Deviation. Higher RSD values indicate lower precision, while lower values suggest less variability in measurements. 2 levels of spike were tested: 0.1 and 5 ng. The analysis was performed in triplicate for each spike level. Results for most compounds were reasonably low, especially for the 0.1ng spike. Precision values range from about 2.74% to 18.62% for different compounds and are below 20%. (Tabel 2). For example, PFBS at the 0.1 ng spike has an RSD of 8.14% and at the 5 ng spike of 8.13%, which indicates that the measurements are consistent. Some compounds like PFOS have a relatively low % RSD of 3.11 at 5 ng, indicating good precision, while others like HFPO-DA have higher % RSD values of 18.06 at 0.1 ng, which suggests poorer precision in the measurements at lower concentrations.

Recovery represents a measure of the analytical method efficiency in detecting the spiked compound and it is the measured concentration compared to the spiked concentration, expressed as a percentage. The recovery for some compounds at the 0.1 ng spike is lower than ideal (100%). For example, PFH x A has a recovery of 66.53% at the 0.1 ng spike, suggesting that the method may not be as efficient at detecting lower concentrations. Many compounds (e.g., PFHpA, PFDA, NMeFOSAA) have recoveries slightly lower than 100% at the 5 ng spike, which indicates that the method has good efficiency at higher concentrations.

Accuracy, measured as mean spike recovery %, shows how close a result is to the true value. The obtained results are presented in Table 2. % RSD of the % recovery was within a range of 1.97 to 16.15%.

Table 1. Targeted analytes list

Compound name	Acronym	Chemical formula	Retention Time, min	MS quantitation peal
Perfluoro-1-butanesulfonic Acid	PFBS	C4HF9O3S	3.72	298.94300
Perfluorohexanoic Acid	PFHxA	C6HF11O2	5.59	268.98370
Undecafluoro-2-methyl-3-oxahexanoic Acid	HFPO-DA	C5HF11O	6.17	284.97790
Perfluoroheptanoic Acid	PFHpA	C7HF13O2	7.34	318.97849
Perfluorohexanesulfonic Acid	PFHxS	C6HF13O3S	7.47	398.93660
2,2,3-trifluoro-3-[1,1,2,2,3,3-hexafluoro-3 (trifluoromethoxy) propoxy] propanoic Acid	ADONA	C7H2F12O4	7.59	376.96890
Pentadecafluorooctanoic Acid Hydrate, Linear	PFOA	C8HF15O2	8.59	412.96640
9-chlorohexadecafluoro-3-oxanone-1-sulfonic Acid, K Salt Unlabeled As Free Acid	PFNA	C9HF17O2	9.63	462.96320
Perfluorooctanesulfonic Acid	PFOS	C8HF17O3S	9.63	498.93020
Perfluorononanoic Acid	9Cl-PF3ONS	C8HClF16O4S	10.11	530.89510
Perfluorodecanoic Acid	PFDA	C10HF19O2	10.50	512.96000
Potassium 11-chloroeicosafluoro-3-oxaundecane-1-sulfonate As Free Acid	PFUnA	C11HF21O2	11.24	562.95680
N-methyl Perfluorooctanesulfonamidoacetic Acid	11Cl-PF3OUdS	C10HClF20O4S	11.55	630.88920
Perfluoroundecanoic Acid	NMeFOSAA	C11H6F17NO4S	11.85	569.96730
N-ethyl Perfluorooctanesulfonamidoacetic Acid	PFDoA	C12HF23O2	11.90	612.95370
Perfluorododecanoic Acid	NEtFOSAA	C12H8F17NO4S	12.21	583.98300
Perfluorotridecanoic Acid	PFTrDA	C13HF25O2	12.47	662.95050
Perfluorotetradecanoic Acid	PFTA	C14HF27O2	12.97	712.94730

Table 2. Method validation results for the target PFAS evaluated in wels catfish muscle

Compound name	Coeff. of determination	Precision (%RSD)		Recovery (%)			
		Spike 0.1 ng	Spike 5 ng	Spike 0.1 ng	RSD, %	Spike 5 ng	RSD, %
PFBS	0.9993	8.14	4.16	71.75	8.13	97.48	4.16
PFHxA	0.9989	10.45	7.81	66.53	10.43	92.53	7.80
HFPO-DA	0.9951	18.06	12.19	77.89	12.06	87.13	9.19
PFHpA	0.9991	9.93	15.49	82.26	9.92	102.19	15.48
PFHxS	0.9991	5.63	16.16	72.27	5.62	78.82	16.15
ADONA	0.9989	11.66	15.71	89.84	11.66	98.58	15.71
PFOA	0.9986	6.74	9.26	118.55	5.92	135.21	8.71
PFNA	0.9989	6.66	5.18	113.47	5.84	127.43	4.86
PFOS	0.9991	18.62	14.12	89.23	3.11	87.78	7.44
9Cl-PF3ONS	0.9975	6.55	2.74	68.13	6.55	78.76	2.74
PFDA	0.9993	16.10	7.73	92.82	7.48	119.43	5.01
PFUnA	0.9990	7.99	6.57	115.82	4.41	131.70	4.91
11Cl-PF3OUdS	0.9979	7.68	2.86	67.96	7.68	81.36	2.86
NMeFOSAA	0.9984	15.06	6.71	124.60	14.67	110.64	6.65
PFDoA	0.9992	16.34	12.50	102.55	3.11	128.71	1.97
NEtFOSAA	0.9982	10.07	5.88	98.83	10.07	131.55	5.88
PFTrDA	0.9992	16.07	7.14	127.79	8.21	121.02	4.89
PFTA	0.9992	4.79	7.67	103.74	3.54	128.05	6.62

Matrix effects were significantly reduced by the Orbitrap 120 Mass Spectrometer due to its high resolution, sensitivity, and accurate mass measurements, along with its ability to optimize ionization conditions, whereas in traditional quadrupole MS, matrix effects can lead to ion suppression or enhancement, causing inaccurate quantification and reduced sensitivity due to interference from co-eluting compounds in the sample. Therefore, the proposed method is well-suited for environmental testing, such as analysing fish extracts for contaminants.

The carryover effect was evaluated by injecting two solvent blanks right after the analysis of the highest calibration standard concentration. There was no carryover effect observed.

CONCLUSIONS

An optimized analytical method based on QuEChERS extraction and UHPLC-HRMS analysis of PFAS was successfully validated. However, there are some limitations to this method. While it demonstrates high sensitivity and specificity, it may not detect all PFAS, particularly those with low ionization. Future research could focus on expanding its scope by refining extraction protocols or incorporating complementary extraction techniques. Additionally, further validation on a broader range of environmental matrices would also be valuable for improving the method's practical applications in monitoring PFAS contamination.

The proposed method is highly suitable for the accurate quantification of PFAS in biota samples, offering accurate measurement of these contaminants in fish. This makes it an effective tool for environmental monitoring, risk assessment, and studies on the bioaccumulation and potential health impacts of PFAS exposure in ecosystems and human populations. PFAS determinations in biota are part of the quality indicators for surface aquatic ecosystems and must be included in integrative systems such as the Water Quality Index (Iticescu et al., 2016) due to their persistence, bioaccumulation potential, and widespread distribution in aquatic ecosystems. This will give a correct global picture of the interactions between the different pollutants in complex systems such as the Danube.

ACKNOWLEDGEMENTS

The technical support was provided by the Rexdan Research Infrastructure, created

through the project An Integrated System for the Complex Environmental Research and Monitoring in the Danube River Area, REXDAN, SMIS code 127065, project co-financed by the European Regional Development Fund through the Competitiveness Operational Programme 2014-2020, contract no. 309/10.07.2020.

REFERENCES

Burada, A., Topa, M.C., Georgescu, L., Teodorof, L., Despina (Nastase), C., Seceleanu-Odor, D., & Iticescu, C. (2015). Heavy Metals Environment Accumulation in Somova-Parches Aquatic Complex from the Danube Delta Area. *Revista de Chimie - Bucharest - Original Edition*, *66*, 48–54.

Chaudhary, A., Usman, M., Cheng, W., Haderlein, S., Boily, J.-F., & Hanna, K. (2024). Heavy-Metal Ions Control on PFAS Adsorption on Goethite in Aquatic Systems. *Environmental Science & Technology*, *58*(45), 20235–20244. https://doi.org/10.1021/acs.est.4c10068

Decision - 2002/657 - EN - EUR-Lex. (n.d.). Retrieved February 24, 2025, from https://eur-lex.europa.eu/eli/dec/2002/657/oj/eng

Iticescu, C., Murariu, G., Georgescu, L., Burada, A., & Topa, M.C. (2016). Seasonal Variation of the Physico-chemical Parameters and Water Quality Index (WQI) of Danube Water in the Transborder Lower Danube Area. *Revista de Chimie -Bucharest-Original Edition*, *67*(9), https://revistadechimie.ro/Articles.asp?ID=5199

Ng, K., Alygizakis, N., Androulakakis, A., Galani, A., Aalizadeh, R., Thomaidis, N., & Slobodnik, J. (2022). Target and suspect screening of 4,777 per and polyfluoroalkyl substances (PFAS) in river water, wastewater, groundwater and biota samples in the Danube River Basin. *Journal of Hazardous Materials*, *436*, 129276. https://doi.org/10.1016/j.jhazmat.2022.129276

Obeid, A. A., Oudega, T. J., Zoboli, O., Gundacker, C., Blaschke, A. P., Zessner, M., Saracevic, E., Devau, N., Stevenson, M. E., Krlovic, N., Liu, M., Nagy-Kovács, Z., László, B., Lindner, G., & Derx, J. (2023). *Occurrence and Distribution of PFAS in the River and Groundwater at Two Danube Sites*. EGU-11264. EGU General Assembly Conference Abstracts. https://doi.org/10.5194/egusphere-egu23-11264.

Panda, B. P., Mohanta, Y. K., Parida, S. P., Pradhan, A., Mohanta, T. K., Patowary, K., Wan Mahari, W. A., Lam, S. S., Ghfar, A. A., Guerriero, G., Verma, M., & Sarma, H. (2023). Metal pollution in freshwater fish: A key indicator of contamination and carcinogenic risk to public health. *Environmental Pollution*, *330*, 121796. https://doi.org/10.1016/j.envpol.2023.121796

Per and polyfluoroalkyl substances (PFAS)-ECHA. (n.d.). Retrieved February 17, 2025, from https://echa.europa.eu/hot-topics/perfluoroalkyl-chemicals-pfas

PFAS pollution in European waters. (2024, December 9). https://www.eea.europa.eu/en/analysis/publications/ pfas-pollution-in-european-waters

Popa, P., Murariu, G., Mihaela, T., Georgescu, L., & Iticescu, C. (2018). Multivariate statistical analyses of water quality of Danube river at Galati, Romania. *Environmental Engineering and Management Journal*, *17*(5), https://doi.org/10.30638/eemj.2018.124

REACH Annex XVII: REACH Restricted Substance List 2023. (n.d.). Retrieved July 18, 2024, from https://www.chemsafetypro.com/Topics/EU/REACH_annex_xvii_REACH_restricted_substance_list.html

Scientific Papers. Series E. Land Reclamation, Earth Observation & Surveying, Environmental Engineering. Vol. XIV, 2025
Print ISSN 2285-6064, CD-ROM ISSN 2285-6072, Online ISSN 2393-5138, ISSN-L 2285-6064

INDICATORS OF THE STRUCTURAL AND COMPOSITIONAL DIVERSITY OF STANDS ON DEGRADED LANDS IN THE VRANCEA AREA

Cristinel CONSTANDACHE[1], Ciprian TUDOR[1, 2], Laurenţiu POPOVICI[1]

[1]"Marin Drăcea" National Institute for Research and Development in Forestry,
128 Eroilor Street, 077190, Voluntari, Ilfov, Romania
[2]"Transilvania" University of Braşov, Interdisciplinary Doctoral School, Romania
29 Eroilor Blvd, 500036, Braşov, Romania

Corresponding author emails: ciprian.tudor@icas.ro, ciprian.tudor@unitbv.ro

Abstract

The ecological reconstruction of degraded lands was based on the predominant use of pine species (Pinus nigra and Pinus sylvestris), resulting in pure stands or sometimes mixed with deciduous trees, with a fragile structure, prone to damage. The research was carried out during 2023-2024, in 18 research areas located on degraded lands in the Vrancea area, in stands of different ages with the aim of the knowledge of compositional and structural indicators that reflect the intensity of competitive processes. The results indicate a pronounced predisposition to disturbances in pure young stands, with a high level of compositional homogeneity and relative abundances of Scots pine. The relationship between the structural diversity index (Gini) and the coefficient of variation allowed the determination of the structure type of the stand, the correlation coefficient being significant (r=0.9923). Research has shown that mixed stands are more structurally stable than pure stands, promoting mixed species being essential in increasing the resistance of stands. The results are useful for decision-makers, the goal being to create stands with structures resistant to the action of damaging factors.

Key words*: structural and compositional diversity, pine species, degraded lands.*

INTRODUCTION

Forest biodiversity is closely correlated with the diversified horizontal and vertical structures of the component stands, and the so-called silviculture (silvotechnics) close to nature is largely based on observations and measurements carried out either in strict research plots located in the improvement perimeters, in the case of degraded stands or in forests affected by disasters (natural disasters due to climatic factors, anthropogenic degradation, etc.) (Seidl, 2017).

Global-scale studies highlight a consistent positive relationship between tree species diversity and productivity, using tree species richness as a proxy for biodiversity, as taxonomic diversity is considered to incorporate other traits, such as those of a functional, phylogenetic, or genomic nature (Liang et al., 2016). Studies from North America and Europe also indicate a positive relationship between species richness and tree productivity, while addressing the influence on the environment and climate (Ruiz-Benito et al., 2017). Other studies highlight that the role of biodiversity tends to be stronger in harsher climates (arid or boreal lands) (Ratcliffe et al., 2017).

Because both productivity and biodiversity depend on a wide range of factors, controlled or not by forest management, the scientific hypotheses of various researchers have mostly supported the role of forests in capturing and storing carbon but also as shelters for the protection of biodiversity (Bodin & Wiman, 2007). An important challenge for forest management and conservation is to achieve an appropriate balance between biodiversity and aboveground biomass in order to support forest managers and decision-makers in developing sustainable management plans in relation to the intended purpose (e.g. conservation, increasing forest resilience, and so on) (Silva et al., 2017).

Within stands on degraded lands, their evolution over time is influenced by harmful abiotic and biotic factors, which destabilize the structure of

the stands and endanger the dynamic balance (Giurgiu, 2004). The ecological reconstruction of degraded lands was achieved through repeated afforestation interventions and the predominant use of pine species (*Pinus nigra* and *Pinus sylvestris*), resulting in stands with a fragile structure, prone to damage, in which there is a risk of diminishing eco-protective functions. (Constandache et al., 2015). The installation of protective forestry crops is made difficult in most situations due to difficult environmental conditions, consisting of lands affected by complex degradation processes, which requires the use of special techniques for arranging/consolidating the respective lands. (Constandache & Nistor, 2008).

The role of forestry crops established through ecological reconstruction consists of limiting surface erosion, increasing infiltration, and improving internal drainage (Sandu et al., 2015), soil improvement and so on. Protective forest crops installed on degraded lands, consisting of pine species, associated with various deciduous species (sycamore, ash, cherry, alder, oak, sea buckthorn, and so on) have demonstrated their hydrological and anti-erosional efficiency, but also their increased resistance to the action of disturbing factors. Many stands are affected by drying, breakage, and so on, due to climate change on the one hand (Vlad et al., 2019), or improper application of silvicultural operations on the other hand (Nistor & Constandache, 2013).

The specific conditions in which each stand develops show that it is necessary to abandon the application of rigid, template measures at stand level. To this end, it is necessary to know the inter- and intraspecific relationships that are established between trees, more precisely, specific indicators, estimators and descriptors of the structure of stands (Ciubotaru & Păun, 2014). These parameters can constitute the basic elements for creating models of stands structures appropriate to environmental conditions, stable and resistant to the action of harmful factors, which can properly fulfill their protective functions (Cristinel et al., 2024).

The research conducted aimed to determine indicators of compositional and structural diversity of stands on degraded lands. These indicators, expressed in measurable/evaluable and comparable units, are necessary to ensure sustainable management of forestry ecosystems installed on degraded lands. The results were obtained based on research on monitoring stands on degraded lands carried out in the period 2023-2024.

MATERIALS AND METHODS

The research was carried out in permanent research plots (SEP), located in representative situations of stands on degraded lands in three experimental perimeters in the Vrancea area (Figure 1):

Caciu-Bârsești (CB), Pârâul Sărat-Valea Sării (PS) and Roșoiu-Andreiașu (RA), located from a phytoclimatic point of view in the hilly storey of sessile oak, beech and sessile oak-beech codified as FD_3.



Figure 1. Location of the study (marked on the map with red dots). Source: www.wikipedia.org

The research consisted in observations, measurements, field data collection, processing and interpretation. The working methodology consisted of applying empirical equations to determine compositional and structural diversity indices at the stand level (Giurgiu & Drăghiciu, 2004; Ciubotaru & Păun, 2014).

In the first stage, to determine the indexes, it was necessary to collect raw field data that include the dimensional characteristics of the trees, which enter into the empirical equations, namely: compositional diversity indices: Shannon index (H), compositional diversity index (A), equity index (Pielou) (E), Simpson index (D); structural diversity indices: Camino index (C), Gini index (G), density index (Id), density index (IG).

The Shannon diversity index (H) measures the diversity of species within a stand.

The compositional diversity index (A) is an indicator of biodiversity, based on the relative abundance of species in a stand (Jaehne & Dohrenbusch, 1997).

The Pielou-Equity index (E). Evenness (E) shows the relationships between the abundances of species or categories of species. In the case of similar relative abundances, the equity will have a unitary value, and if most observations belong to a single category, it tends to value zero. Equity represents a form of standardization of the Shannon index, as the ratio between observed diversity and maximum diversity (Pielou, 1969; Lexerod & Eid, 2006).

The Simpson index (D) expresses the probability that two observations drawn at random from the analyzed perimeter belong to the same category. It is strongly influenced by the abundance of categories and little sensitive to the number of categories (Simpson, 1949).

The analysis of the type of structure and homogeneity of pine stands on degraded lands was carried out using the Camino and Gini indices, which have as their scientific basis the variability of experimental values on Lorenz curves. The indices were calculated using the Gini-Lorenz statistical application (Popa, 1999), implemented through Microsoft Excel. The Camino index shows the trend of structural diversification over time, even for even-aged stands. Research has shown that homogeneity provides information on the type and intensity of interventions in stands: if extractions are performed in the upper storey, homogeneity is reduced, while interventions in the middle and lower storey increase homogeneity (Cenuşă et al., 2002).

The Gini index (G) determined according to the basal area is calculated as the ratio between the area determined by the Lorenz curve and the reference line on the one hand and the area of the triangle formed by the reference line with the abscissa and the parallel to the ordinate through the intersection point between the Lorenz curve and the reference line, on the other hand (Katholnig, 2012; Duduman, 2011). Gini coefficient values range between 0 and 1, with a value of 1 indicating maximum biodiversity or maximum heterogeneity (Roibu, 2010).

The density index (Id) expresses the ratio between the actual number of trees per unit area and the optimal number of trees according to the production tables (Giurgiu & Drăghiciu, 2004) in relation to the species and production class.

The density index (GI), also called the basal area index or area index (Rădulescu, 1956), is calculated as the ratio between the actual basal area per hectare and that in the production tables, considered normal for a stand in conditions similar to the one analyzed. The analysis of the relationships between the dimensional variables was carried out based on modelling the linear regression equations of the form $y = a \cdot x + b$, where y is the analyzed parameter, x-the considered independent variable; a, b- the coefficients of the regression equation. The significance testing of the Pearson r-correlation coefficient was performed at a coverage probability of 95% (α=5%).

RESULTS AND DISCUSSIONS

The trees on the degraded lands (strongly to very strongly eroded and ravined in the analyzed perimeters, are mostly made up of a mixture of Scots pine and black pine (Figure 2), sometimes mixed with deciduous species, with an age between 42 and 69 years (Table 1).



Figure 2. Scots pine grove mixed with black pine, on very heavily eroded land (SEP 11, Caciu-Bârseşti perimeter)

Analysis of compositional diversity indices

Information on the characteristics of the current structure of stands is provided by the *Shannon index (H).*

The H-index is an index of diversity and takes into account species richness and evenness of species distribution (E) (Shannon, 1948), so its value increases with the number of species. At the experimental plot level, calculated in relation to the frequencies of individuals and species (for the tree layer) it is between 0.32 (PS 9) and 1.03 (PS 1). These values, compared to the maximum value that can be reached in each sample area (ln(k) - where k is the abundance of species), signal a high level of compositional homogeneity, the ratio being between 29.13 and 93.75%, this aspect indicating that the differences between the relative frequencies of species in the composition of each stand are relatively small. The most diverse structures are found in mixtures of pine with deciduous trees where this index shows higher values (Table 1). *The compositional diversity (A)* at the experimental surface level is between 1.25 (PS 9) and 2.30 (CB 11). The values within this range are mainly determined by the maximum relative abundance of the main species in the stand composition.

Table 1. Indicators of structural and compositional diversity

PA	SEP	Composition after N Composition after G	Age (years)	N·ha^{-1} G·ha^{-1}	I_d I_G	H	A	E	D
Caciu-Bârsești (CB)	3	52Pi 38Pi.n 10Dt 59Pi 33 Pi.n 8Dt	49	1577 42.03	1.17 1.29	0.48	1.98	0.34	0.42
	4	42Pi 57Pi.n 1Mj 40Pi 60Pi.n	49	1753 37.27	1.31 1.19	0.68	1.90	0.49	0.50
	5	42Pi 55Pi.n 3 An.a 44Pi 53Pi.n 3An.a	49	3127 60.37	2.22 1.90	0.80	2.09	0.58	0.48
	6	29Pi 69Pi.n 2Dt 44Pi 55Pi.n 1Dt	49	1933 33.66	1.37 1.11	0.70	1.71	0.50	0.56
	7	84Pi 14 Pi.n 2Mj 90 Pi 8Pi.n 2Mj	49	1423 24.42	1.09 0.71	0.51	1.74	0.37	0.73
	9	26Pi 73Pi.n 1Sc 31Pi 69Pi.n	50	1860 24.71	1.34 0.91	0.63	1.69	0.45	0.60
	8	89Pi 11Pi.n 93Pi 7Pi.n	49	1854 24.49	1.37 0.72	0.35	1.54	0.25	0.80
	10	37Pi 53Pi.n 10Mj 45Pi 52Pi.n 3Mj	50	1232 23.30	0.87 0.78	0.93	2.05	0.85	0.43
	11	28Pi 72Pi.n 33Pi 67Pi.n	50	2030 41.16	1.54 1.27	0.57	2.30	0.41	0.62
	12	75Pi 25Pi.n 84Pi 16Pi.n	42	1682 44.08	1.27 1.20	0.56	2.27	0.41	0.63
	13	64Pi 28Pi.n 8An.a 76Pi 12Pi.n 12An.a	42	800 27.69	0.71 0.76	0.86	1.76	0.62	0.51
Pr. Sărat-Vl. Sării (PS)	1	39Pi 44Pi.n 17 Dt 44Pi 48Pi.n 8 Dt	67	925 39.06	0.95 1.10	1.03	2.22	0.74	0.37
	9	6Pi 92Pi.n 2Vi.t 8Pi 92 Pi.n	69	1515 81.40	1.66 2.29	0.32	1.25	0.23	0.85
Roșoiu-Andreiașu (RA)	4	66Pi 32Pi.n 2 Ci 79Pi 20Pi.n 1 Ci	63	630 25.23	0.62 0.70	0.72	1.39	0.52	0.54
	7	20 Pi 80 Pa 34 Pi 66 Pa	63	783 33.89	0.94 1.02	0.50	1.57	0.36	0.68
	9	8Pi 74 Pi.n 18Dt 9Pi 85 Pi.n 6Dt	63	678 29.26	0.68 0.76	0.74	1.51	0.53	0.58
	10	83 Pi 17 Dt 93 Pi 7 Dt	62	470 26.78	0.51 0.66	0.46	1.36	0.33	0.71

Symbols: PA - improvement perimeter; SEP - permanent experimental plot;.N - number of trees; G - basal area; Id - density index according to number of trees; IG - density index according to basal area; H - Shannon index; A - compositional diversity index; E - equity index (Pielou); D - Simpson index; Composition (forest species) Pi - Scots pine; Pi.n - black pine; Dt - various hardwoods; Pa - sycamore; Ci - cherry; Vi.t - Turkish sour cherry; An.a - white alder; Mj - manna ash; Sc - locust.

The relative abundance of a species represents the proportion between the number and/or biomass of individuals (specimens) of a species in relation to the other species, at a given time. Abundance can be expressed both by the number of individuals and by their biomass, in order to obtain undistorted information regarding the structure of the biocenosis (Sava, 2012).

Evenness (E) ranges between 0.23 (CB 9) and 0.85 (CB 10), indicating that most stands exhibit maximum relative abundances belonging to a single category. For example, in the case of the stand in the Caciu-Bârsești perimeter, SEP 8 (CB 8), Scots pine has maximum relative abundance, the value being close to 0 (zero). The values tend towards the unitary value when there is similarity between the relative abundances. In the case of the stand in CB 10, the similarity is reflected by the close relative abundances of the two pine species (Scots pine and black pine) in the composition.

The Simpson index (D) expresses the probability that two observations randomly drawn from the analyzed surfaces belong to the same category. It ranges between 0.37 (PS 1) and 0.85 (PS 9). Given that the stands are predominantly made up of main species (Scots pine and black pine), there is a high probability that two extracted observations belong to these species, being correlated with their abundance.

Analysis of structural diversity indices

In the case of younger stands less than 50 years old (Caciu-Bîrsești perimeter), *the Camino index (C)* has values ranging from 2.90 (CB 6) to 6.47 (CB 11), which indicates that most of the analyzed stands have an even-aged structure (Figure 4). The exception is the stand in CB 10, where the structure is relatively even aged, and the stands in CB 6 and CB 13, where the structure is relatively plurien.

The types of structure reflected by *the Gini index (G)* are similar. This indicator ranges between 0.25 (CB 5) and 0.46 (CB 6) and additionally indicates the homogeneity of the structures based on the distributions of *the Lorenz curves* (Figure 3 a, b). *The Gini index* was determined separately for each species (Table 2). This results in bimodal structures, with *the Gini index* ranging from 0.17 (CB 9) to 0.36 (CB 12) for Scots pine, and from 0.22 (CB 8) to 0.48 (CB 12) for Scots pine. The closer the *Gini index* values are to the straight line, the more homogeneous the structures are (*Gini* tends to take the value 0 in this case).

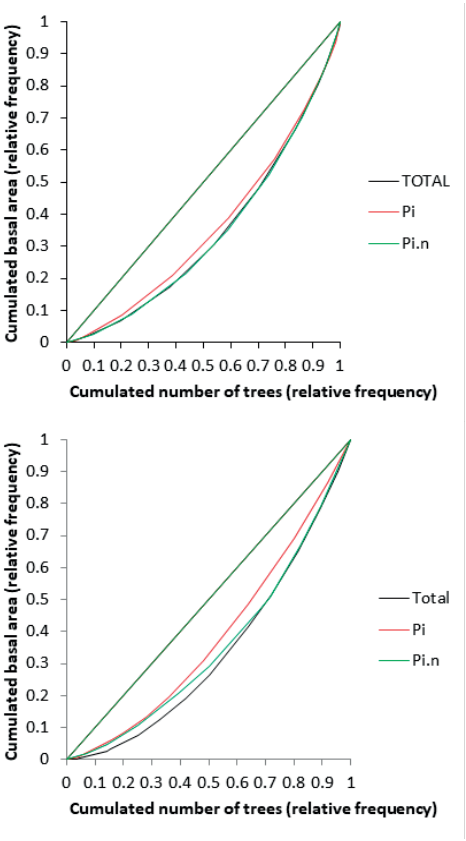


Figure 3. Lorenz curves generated by the Gini index and structural homogeneity analysis after Camino (a - CB11; b - PS1)

The density indexes (ID and IG) (Table 1) reflect the horizontal structure of the stands.

The density index according to the number of trees (Id) is between 0.71 (CB 13) and 2.22 (CB 5), being determined by the actual number of trees per hectare, as well as by the proportion of species in the composition of the stand and the production class. Values lower than 1 indicate a lower number of trees than normal. These indices correspond to a minimum real number of 800 trees per hectare (Id = 0.71), respectively a maximum real number of 3127 trees per hectare (Id = 2.22 which represents a real number of trees, 2.22 times higher than the normal number), the explanation being the dense

planting scheme but also the failure to carry out silvitechnical works.

The density index according to basal area (IG) is between 0.71 (CB 7) and 1.90 (CB 5) and expresses the quality of the stands in relation to the development of their horizontal structure. The basal area expressed per hectare is between 23.30 and 60.37 m^2 (Table 1) indicating a very high variability, especially within stands with a relatively multi-year structure, where the coefficients of variation for the diameter characteristic show high values (CV > 30%) (Figure 4).

Table 2. Structure types according to Camino and Gini indices for young stands predominantly composed of main pine species in the Caciu-Bârsești PA (CB)

SEP	3	4	5	6	7	8	9	10	11	12	13
DEG	R	R	E_3	E_3	E_3	E_3	E_3	E_3	E_3	E_3	E_3
(C)-total	4.485	4.259	6.445	2.900	4.992	5.554	4.488	4.070	6.465	4.810	3.420
(C)-Pi	4.075	4.336	6.893	2.770	5.389	5.372	7.809	3.895	6.300	6.358	4.120
(C)- Pi.n	12.260	4.259	6.422	3.343	3.209	17.823	4.102	3.131	6.919	2.440	2.460
(G)-total	0.277	0.298	0.252	0.455	0.319	0.333	0.280	0.340	0.318	0.335	0.410
(G)-Pi	0.267	0.305	0.225	0.357	0.295	0.334	0.172	0.304	0.285	0.268	0.330
(G)-Pi.n	0.261	0.288	0.267	0.430	0.369	0.223	0.307	0.362	0.322	0.484	0.450
Structure type after C	E	E	E	RP	E	E	E	RE	E	E	RP
Structure type after G	E	E	E	RP	E	E	E	RE	E	E	RP

Symbols: PA - improvement perimeter; SEP - permanent experimental area; DEG - form and intensity of degradation; R - ravine; E3 - very strong erosion; (C) - Camino index; (G) - Gini index; Pi - Scots pine; Pi.n - black pine; Structure type: E = even aged trees; RP = relatively pluriennial; RE = relatively even

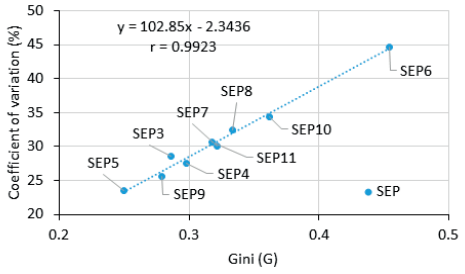


Figure 4. Pearson's r-correlation between the Gini homogeneity index and the coefficients of variation (%)

In the case of older stands (62-69 years old), the Camino index (C) per total stand has values between 2.72 (RA 4) and 4.75 (PS 9), which indicates that most of the analyzed stands present different structures (from even-aged to relatively multi-aged) determined both by the growth conditions and by the action of damaging factors (Figure 5).

The types of structure reflected by the Gini index (G) are similar. This indicator ranges between 0.23 (RA 10) and 0.37 (RA 4). The Gini index determined separately by species indicates bimodal structures, with values ranging between 0.08 (PS 9) and 0.31 (RA 9) for Scots pine, respectively between 0.27 (PS 9) and 0.44 (RA 4) for Scots pine.

The closer the Gini index values are to the straight line, the more homogeneous the structures are (the Gini index tends to take the value 0. In this case, populations formed mainly by Scots pine are more homogeneous than those made up of its competitor, the black pine (Figure 3 a, b).

The density index according to the number of trees (Id) and the density index according to the basal area (IG) reflect the horizontal structure of the stands. *The density index (Id) has ranges between 0.51 (RA 10) and 1.66 (PS 9).* In general, the density of older stands is lower, compared to young ones, the thinning being caused, in most cases, by damage caused by wind and snow at the age of 30-40 years, sometimes by drying but also by natural elimination, etc. These indices correspond to a minimum real number of 470 trees per hectare, respectively a maximum real number of 1515 trees per hectare. The higher values of *the density index* (over-unit) in older stands are the result of the use of small planting schemes (1.0-

1.5 x 1.0 m), the high participation proportion of pine trees (over 90%) but also the failure to carry out silvitechnical works.

The density index (IG) is between 0.66 (RA 10) and 2.29 (PS 9), corresponding to the basal area per hectare, between 26.78 and 81.40 m^2.

These values indicate a reduced variability of stands with even and relatively even structure, where the coefficients of variation for the diameter characteristic show values below 30% (Figure 5).

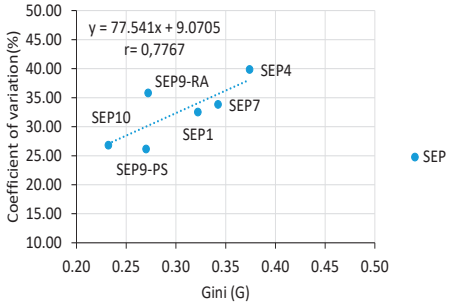


Figure 5. Pearson's r-correlation between the Gini homogeneity index and the coefficients of variation (%)

CONCLUSIONS

The structural and qualitative assessment of stands on degraded lands in the context of climate scenarios provides useful scientific information for the monitoring and sustainable management of forestry ecosystems on degraded lands.

By applying specific data processing methods, indices/parameters regarding the state and structure of stands were obtained. These parameters reflect the intensity of physiological and competitive processes at the tree and stand level (growth, natural pruning, natural elimination, regeneration and so on), having different variability in relation to the composition (component species) and age of the stands, the environmental conditions (form and intensity of degradation) but also to the damage caused by harmful abiotic factors. By the exercise of a optimal functional efficiency throughout their entire evolution period, stands installed on degraded lands require careful supervision and intervention with specific silvotechnical works in relation to their condition, stage of evolution, component species and environmental conditions in which they evolve.

From the point of view of the Shannon compositional diversity index, the analyzed stands present a high level of compositional homogeneity. This aspect derives from the relatively small differences between the relative frequencies of species in the compositions of each stand.

From the point of view of the Gini structural index (G), most of the stands, especially the youngest ones, present an even structure in terms of the distribution of the number of trees and the basal area by diameter classes. The homogeneity of stands is more pronounced especially in stands where the relative abundance of a species (especially Scots pine) is maximum. The exception is made by the older stands with a higher proportion of mixed species (deciduous), where the variability of diameters is high, even if the specimens correspond to the same age class, being determined by competitive and natural elimination processes.

The structure of stands can be easily identified if the coefficients of variation of the actual basal diameters of trees in a population and the Gini index of the respective population are known. From the Gini-coefficient of variation relationship, the correlation coefficients r was obtained, which indicate a high level of significance at a 95% coverage probability, the correlative links being direct and positive for the analyzed cases.

The density indices (Id and IG), determined by the actual number of trees and the basal area per hectare, capture the horizontal structure of the studied stands. In **younger stands**, due to the relatively high number of real trees per hectare and the active development of growth in the basal diameter of the trees, the two indicators present values above unity. In **older stands**, thinned as a result of damage caused by wind and/or snow, the same indicators present values below unity.

Considering the aforementioned conclusions, the following recommendations can be drawn:

1) *Sustainable management of forest ecosystems on degraded lands is ensured by knowing the variability of structural and compositional diversity indices of stands.*

2) *Planning silvicultural works, based on these indicators, establishes urgent measures to*

regulate the homogeneity of stands in order to create optimal and stable structures necessary to ensure resistance to the action of damaging factors.

ACKNOWLEDGEMENTS

This research activity was carried out within the NUCLEU Research Program through Project PN 23090203/2024.

REFERENCES

Bodin, P., & Wiman, B. L. (2007). The usefulness of stability concepts in forest management when coping with increasing climate uncertainties. *Forest Ecology and Management*, *242*(2-3), 541-552.

Cenuşă, R., Popa, C., & Teodosiu, M. (2002). Cercetări privind relaţia structură-funcţie şi evoluţia ecosistemelor forestiere naturale din nordul ţării. *Anale ICAS, 45*, 9-19.

Ciubotaru, A., & Păun, M. (2014). *Structura arboretelor.* Braşov, RO: Editura Universităţii "Transilvania".

Constandache, C., & Nistor, S. (2008). *Reconstrucţia ecologică a terenurilor ravenate şi alunecătoare din zona Subcarpaţilor de Curbură şi a Podişului Moldovei.* Bucureşti, RO*:* Seria a II-a, Editura Silvică.

Constandache C., Vlad, R., & Popovici, L. (2015). Dinamica unor parametrii structurali în arborete de pin silvestru instalate pe terenuri degradate. *Revista Pădurilor, 1-2.*

Cristinel, C, Ciprian, T., Popovici, L., Radu, V., Crişan, V., & Dincă, L.C. (2024). Structural Characteristics of the Pine Stands on Degraded Lands in the South-East of Romania, in the Context of Climate Changes. *Applied Sciences, 14*(18), 8127.

Duduman, G. (2011). A forest management planning tool to create highly diverse uneven-aged stands. *Forestry, 84*(3), 301-314.

Giurgiu, V. (2004). Silvologie, vol III B, *Gestionarea durabilă a pădurilor Romaniei*. Bucureşti, RO: Editura Academiei Române.

Giurgiu V., & Drăghiciu D. (2004). *Modele matematico-auxologice şi tabele de producţie pentru arborete.* Bucureşti, RO: Editura Ceres.

Jaehne, S., & Dohrenbusch, A. (1997). Ein Verfahren zur Beurtielung der Bestandesdiversität. A method to evaluate forest stand diversity. *Forstwissenshhaftliches Centralblatt,* 116, 333-345.

Katholnig, L. (2012). *Growth dominance and Gini-Index in even-aged and in uneven-aged forests*. Vienna, Austria: Master Thesis submitted by Institute of Forest Growth and Yield Research, University of Natural Resources and Applied Life Sciences, Department of Forest and Soil Sciences.

Lexerod, N.L., & Eid, T. (2006). An evaluation of different diameter diversity indices based on criteria related to forest management planning. *Forest Ecology and Management* 222, 17–28.

Liang, J., Crowther, T. W., Picard, N., Wiser, S., Zhou, M., Alberti, G., & Reich, P. B. (2016). Positive biodiversity-productivity relationship predominant in global forests. *Science*, *354*(6309), aaf8957.

Nistor, S., & Constandache, C., (2013). Consideraţii asupra eficienţei lucrărilor silvotehnice în arboretele de pe terenuri degradate. *Revista Pădurilor, 6,* 19-27.

Pielou, E.C. (1969). *An Introduction to Mathematical Ecology.* New York, USA: Wiley-Interscience Publishing House.

Popa, I. (1999). Aplicaţii informatice utile în silvicultură, Programul Carota şi programul PROARB. *Revista Pădurilor, 2,* 41-42.

Rădulescu, A.V. (1956). *Silvicultura generală*. Bucureşti, RO: Editura Agro-silvică de stat.

Ratcliffe, S., Wirth, C., Jucker, T., van Der Plas, F., Scherer-Lorenzen, M., Verheyen, K., ... & Baeten, L. (2017). Biodiversity and ecosystem functioning relations in European forests depend on environmental context. *Ecology letters*, *20*(11), 1414-1426.

Roibu, C. (2010). *Cercetări dendrometrice, auxologice şi dendrocronologice în arborete de fag din Podişul Sucevei*. Suceava, RO*:* Teză de doctorat, manuscris, Universitatea Ştefan cel Mare Suceava.

Ruiz-Benito, P., Ratcliffe, S., Jump, A. S., Gómez-Aparicio, L., Madrigal-González, J., Wirth, C., & Zavala, M. A. (2017). Functional diversity underlies demographic responses to environmental variation in European forests. *Global Ecology and Biogeography*, *26*(2), 128-141.

Sava, A. (2012). Abundenţa relativă a speciilor, indicator al biodiversităţii. *Revista de Silvicultură şi Cinegetică, 30,* 93-97.

Sandu, T., Trofin, A. E., Bernardis, R. R., & Paraschiv, N. L. (2015). Issues regarding the ecological forestry reconstruction of the degraded land inside Podu-Iloaiei forest district, Iaşi county. *Scientific Papers, Agriculture "Ion Ionescu de la Brad" Iasi,* 58*(2),* 155-158.

Seidl, R., Thom, D., Kautz, M., Martin-Benito, D., Peltoniemi, M., Vacchiano, G., & Reyer, C. P. (2017). Forest disturbances under climate change. *Nature climate change*, *7*(6), 395-402. Shannon, C. E. (1948). A Mathematical Theory of Communication" PDF). *Bell System Technical Journal*, *27*(3), 379-423.

Silva, P. M., Rammer, W., & Seidl, R. (2017). Disentangling the effects of compositional and structural diversity on forest productivity. *Journal of Vegetation Science*, *28*(3), 649-658.

Simpson, E. H. (1949). Measurement of diversity. *Nature, 163*(4148), 688-688.

Vlad, R., Constandache, C., Dinca, L., Tudose, N. C., Sidor, C. G., Popovici, L., & Ispravnic, A. (2019). Influence of climatic, site and stand characteristics on some structural parameters of scots pine (*Pinus sylvestris*) forests situated on degraded lands from east Romania. *Range Management and Agroforestry*, *40*(1), 40-48.

Scientific Papers. Series E. Land Reclamation, Earth Observation & Surveying, Environmental Engineering. Vol. XIV, 2025
Print ISSN 2285-6064, CD-ROM ISSN 2285-6072, Online ISSN 2393-5138, ISSN-L 2285-6064

GROUND MOTION DATA QUALITY ASSURANCE: FUNDAMENTAL REQUIREMENTS AND THEIR PRACTICAL IMPLEMENTATION WITHIN THE NATIONAL NETWORK FOR THE SEISMIC MONITORING AND PROTECTION OF BUILDING STOCK, NIRD URBAN-INCERC, ROMANIA

Iolanda-Gabriela CRAIFALEANU[3, 1], Claudiu-Sorin DRAGOMIR[1, 2], Daniela DOBRE[3, 1], Emil-Sever GEORGESCU[1], Alexandra-Marina BARBU[1]

[1]National Institute for Research and Development in Constructions, Urbanism and Sustainable Spatial Development - URBAN-INCERC, 266 Pantelimon Blvd, District 2, Bucharest, Romania
[2]University of Agronomic Sciences and Veterinary Medicine of Bucharest, 59 Mărăști Blvd, District 1, Bucharest, Romania
[3]Technical University of Civil Engineering Bucharest, 122-124 Lacul Tei Blvd, District 2, Bucharest, Romania

Corresponding author email: i.craifaleanu@gmail.com

Abstract

The participation of the National Network for the Seismic Monitoring and Protection of Building Stock (RNMPSPC) at NIRD URBAN-INCERC in EPOS ERIC, the pan-European Research Infrastructure for Solid Earth Science, requires a rigorous framework for ensuring high-quality seismic data. This paper presents key criteria for seismic data quality assurance and their implementation within RNMPSPC, which operates a strong-motion network of 64 stations across Romania. We detail modern methodologies for seismic data acquisition, processing, and validation, emphasizing compliance with international standards. The practical application of these methods is illustrated using records from a recent ML 5.4 earthquake in the Vrancea seismogenic zone. The study highlights ongoing improvements in equipment, software integration, and data management to enhance the accuracy and reliability of ground motion records. These advancements support seismic hazard assessment and structural safety, reinforcing Romania's contribution to global seismological research.

Key words*: seismic data, quality assurance, seismic network, Romania, research infrastructure.*

INTRODUCTION

Seismic monitoring is a key activity in informing pre-earthquake seismic hazard assessments, rapid identification of seismic damage in instrumented buildings and assisting post-earthquake decision making. From a broader perspective, data acquired from recording ground motions and the response of buildings to these actions provide an essential basis for advancing earthquake engineering science. Seismic networks have already a long history, dating from the late 1800s, when the British geologist, engineer and seismologist John Milne deployed the first international network of seismograph stations, consisting eventually of 30 instruments that recorded ground motion on photographic paper (ISC, 2018; Tripathy-Lang & Bohon, 2022a). Nowadays, seismographic networks maintained by organizations from various countries cover most of the Earth's surface and, given the advancements of sensor technology, not only provide data on ground motions and issue earthquake early warnings, but they are also used in tsunami warning systems (Tripathy-Lang & Bohon, 2022a). Strong-motion networks, equipped with accelerographs and developed from the need of recording potentially damaging ground motions, were first installed in the early 1930s, in the United States (USGS, 2025). Gradually, more and more countries deployed their own strong-motion networks. At present, thousands of accelerographs are deployed all over the world.
In Romania, the first seismographic station was installed in 1895, on Filaret Hill in Bucharest, by the physicist, astronomer and meteorologist Ștefan Hepites (INFP Archive, 2025). The first strong-motion network in Romania was established in 1967 by the National Institute for Building Research, INCERC. Starting from

2009, INCERC is part of the National Institute for Research and Development in Constructions, Urbanism and Sustainable Spatial Development - URBAN-INCERC. This seismic network has been in continuous operation since its establishment and provides ground motion records, as well as data from the monitoring of instrumented buildings. A history of the evolution of strong-motion networks in Romania is provided in (Craifaleanu et al., 2010).

At present, the strong-motion network of URBAN-INCERC consists of 64 digital accelerometers, located according to the main seismicity patterns of the country. Of these, 31 are Kinemetrics (U.S.) instruments and 33 are from GeoSIG (Switzerland), almost 80% being permanently connected online to the Data Center of the seismic network, by using transmission lines from the Romanian Special Telecommunications Service (STS) and from local GSM operators. The URBAN-INCERC seismic network is the central infrastructure of the National Network for the Seismic Monitoring and Protection of Building Stock (RNMPSPC), established in 2017, and which also includes components for experimental testing of building materials, elements and structures. In 2023, in recognition of its importance for a seismic country like Romania, RNMPSPC was granted the status of Infrastructure / Special Objective of National Interest (I.O.S.I.N.), which entitled it for receiving, from the Romanian Ministry of Education and Research, annual funding for maintenance, operation and exploitation.

Given its long existence, the seismic network of URBAN-INCERC has developed, over the years, durable relations with several universities, academic institutions and organizations in Romania and abroad. One of the most significant is collaboration, based on complementarity, with the National Research and Development Institute for Earth Physics, INCDFP, which also owns and operates a large national seismic network, with a focus on seismology. With worldwide recognition in its field, INCDFP is a member of the European Research Infrastructure Consortium EPOS (European Plate Observing System, https://www.epos-eu.org/epos-eric, the pan-European Research Infrastructure for Solid Earth Science), coordinating its Romanian branch, EPOS-RO (https://epos-ro.infp.ro/). EPOS ERIC has currently 19 member countries, and one country, Germany, participating as an observer. The Romanian branch, EPOS-RO, includes five research and development institutes and two universities.

At present, RNMPSPC provides seismic data to the EIDA node (www.orfeus-eu.org/eida) of INCDFP, which is directly connected to the EPOS data portal. The number of connected stations is expected to increase progressively.

Participation in the EPOS Consortium, as well as the need for providing accurate and standardized seismic data, imply, for RNMPSPC, conforming with several requirements, such as hardware and software performance, compatibility with similar worldwide infrastructures, rigorous procedures for seismic data recording, processing and archiving, connectivity with the EPOS data portal, and a structured management of the entire infrastructure. The actions conducted recently in this respect are presented below, with a particular focus on those dedicated to the quality assurance of seismic data. Additional insights into ongoing research and development activities at RNMPSPC can be found in (Dragomir et al., 2023; Mărmureanu et al., 2021).

MATERIALS AND METHODS

In recent years, numerous studies have focused on quality assurance in seismic data, driven by the growing importance of global seismological networks, the interconnection of earthquake monitoring infrastructures, and the increasing demand for high-quality ground motion data. These advancements are essential for seismology, earthquake engineering, and global seismic hazard assessment.

With the advancement of ground motion sensor technology and the automation of recorded data processing, even though human involvement has remained a necessity, the search for methodologies adapted to the automatic screening and quality verification of large amounts of data gained significant momentum. A review of common data processing techniques has revealed several aspects that can lead to distortions or unrealistic features in the

processed signal. Several key studies (Douglas, 2003; Boore & Bommer, 2005; Akkar & Bommer, 2006; Akkar & Boore, 2009; Casey et al., 2018; Ravizza et al., 2019; 2021; Di Giulio et al., 2021) have identified critical issues in seismic data processing and proposed best practices to mitigate these errors. More recently, modern technologies such as machine learning and advanced signal processing techniques have been integrated to assist in the large-scale processing of seismic data (Bellagamba, 2019). Many of the findings of these studies were implemented within complex projects aimed at creating reference ground motion databases and leveraging international collaboration in the field, like RESORCE (https://www.resorce-portal.eu/; Akkar et al, 2013), NERA (Luzi et al., 2016) or SERA (http://www.sera-eu.org/en/home/index.html; Crowley et al., 2018). One of the most significant achievements in the field of seismic data infrastructures is ORFEUS (Observatories and Research Facilities for European Seismology), (https://www.orfeus-eu.org/), the European Infrastructure for seismic waveform data in EPOS. The EIDA data centres connect twelve European data archives, totalling 450 TB of data from almost 300 seismic networks (11000 seismic stations) (Strollo et al., 2021). Within EPOS, seismic data quality assurance is considered an essential prerequisite, covering all steps of the data recording, processing, archiving and distribution. The EIDA nodes and the associated seismological observatories are responsible for implementing their own procedures of data and metadata quality control, complying at the same time with the best international standards and practices (ORFEUS documentation, 2023; Schaeffer et al., 2024).

To comply with the requirements coming from the participation of RNMPSPC in the EPOS-RO/ EPOS ERIC consortium, several actions were taken in the recent period, as presented in the following. These actions are in line with the requirements of the ORFEUS Quality Assurance (QA) documentation (ORFEUS, 2023).

1. Extending and upgrading the infrastructure

a) The seismic network was extended with new stations and accelerometers in existing stations are being gradually replaced with state-of-the-art equipment, with superior capabilities. The accelerometers used in the network come from worldwide trusted manufacturers (Kinemetrics, GeoSIG). Best practices are followed for the placement of accelerometers, typically in small buildings, with low influence on recorded signal. For instrumented buildings, at least two sensors are placed (bottom and top of the building), accompanied, when possible, by a free-field type station, following the COSMOS Guidelines (COSMOS, 2001). It should be noted that instrument deployment must be first agreed with the owner of the space, which induces some restrictions on location selection.

b) Starting from 2023, the year when RNMPSPC received the status of Special Installation/Objective of National Interest (IOSIN), funding for maintenance and reparation of existing equipment, as well as retrofitting of the spaces of the Data Centre is provided, in a large measure, by the Executive Unit for Financing Higher Education, Research, Development and Innovation (UEFISCDI), within the Programme "Research Infrastructures", PN-IV-P5.5-IOSIN-1. Figure 1 shows the newly retrofitted RNMPSPC Data Centre.

c) Most of the data transmission equipment is installed and maintained by the Romanian Special Telecommunication Service. For some additional seismic stations, data transmission is made over GMS lines. All communication channels are functional 24/7 and potential issues are promptly addressed by the providers.

d) The SeisComP (https://www.gempa.de/products/seiscomp/) seismological software for data acquisition, processing, distribution and interactive analysis was implemented at the RNMPSPC Data Centre in Bucharest, starting from 2021. SeisComP uses the SeedLink protocol for communication, a protocol which today practically represents a worldwide standard. With the upgrading of ground motion recording and telecommunication equipment, RNMPSPC stations are gradually connected to SeisComP and to the EIDA node of EPOS. In addition, the *sigma* module (gempa GmbH) is used for advanced data processing, mapping, visualisation and interpretation.

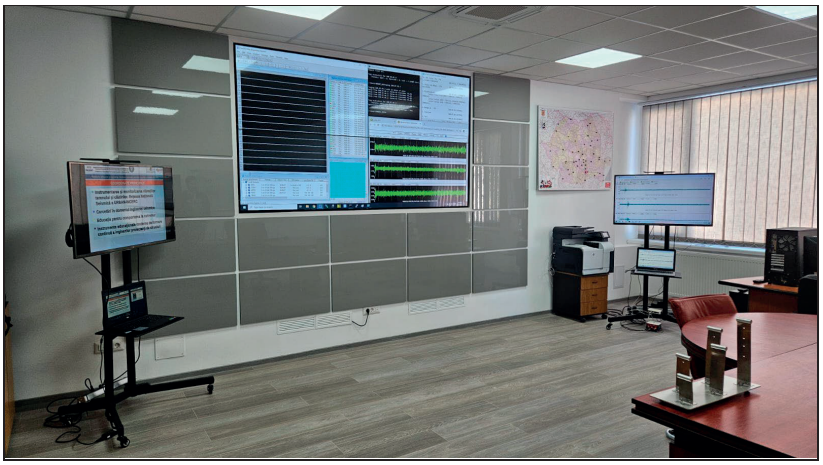


Figure 1. The RNMPSPC Data Centre, with real-time monitoring of seismic activity

2. Seismic data and station metadata curation, storage, archival and dissemination

a) A key condition for data quality assurance is the rigorous specification of station metadata, which ensures accurate interpretation of recorded data. The configuration of stations connected to the SeisComP system was done providing detailed specifications of digitizer and sensor characteristics, locations and orientations. The IRIS DMC Library of Nominal Responses for Seismic Instruments was used, as available in the Station Management Portal created by gempa (https://smp.gempa.de/). The information already available in the seismic station database maintained at the RNMPSPC Data Centre was also used, for all stations. The upgrading and extension of the seismic network were done concomitantly with the upgrading and revision of both databases.

b) The recorded seismic data is stored on NAS (Network-Attached Storage) units and backed-up on a regular basis. In addition, the own data storage system of SeisComP, SDS, is used for the stations connected to this software. Storage capacities are extended as necessary.

c) The seismic network of RNMPSPC was registered at the International Federation of Digital Seismograph Networks, FDSN (https://www.fdsn.org/), with the RQ code (Figure 2).

d) The dissemination of data and research results is done by publishing in peer-reviewed journals, as those mentioned in the "Introduction" section of this article.

3. Structured management of operations

The structured management of seismic network operations was implemented ever since its establishment and evolved continuously with its expansion and modernization. The organization gained additional momentum with the acquirement of the IOSIN status, which imposed the implementation of rigorous procedures for management and reporting.

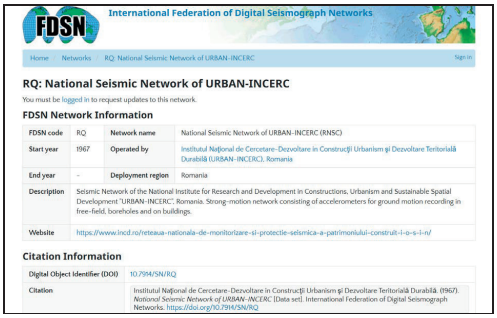


Figure 2. The seismic network of RNMPSPC, as displayed on the FDSN website

An important role in leveraging the activities dedicated to the assurance of the quality of seismic data is played by the various research projects conducted by the RNMPSPC team. The requirements imposed by these projects, as well as the development possibilities they provide, represent an additional incentive. One of the most recent projects is PN 23 35 01 01, aimed at the development of an integrative digital concept for recording, transmitting, processing and analysing data resulting from seismic

monitoring of territory and buildings, based on the implementation of state-of-the-art hardware and software tools, in order to efficiently and operationally identify the destructive potential of earthquakes occurring in Romania and adjacent regions, and at the creation of an open access database for instrumented buildings, set up in accordance with the Open Access, Open Data and FAIR principles and following the best practice models of similar European infrastructures.

RESULTS AND DISCUSSIONS

To demonstrate the practical application of the previously discussed principles, the following section presents examples from recent activities within the seismic network.

Figure 3 displays a screenshot from the SeisComP software, showcasing tests conducted to verify the operational accuracy of seismic stations. The BTH station, featured in the figure, is installed on an instrumented building and is complemented by a free-field accelerometer nearby. This setup is located at the Faculty of Biotechnologies, University of Agronomic Sciences and Veterinary Medicine of Bucharest. Several tests of this type are performed on a regular basis at RMPSPC, for all instruments. For the stations connected to the SeisComP system, values are checked in parallel in SeisComP and in the software applications provided by the instrument manufacturers.

The most important result of quality assurance activities consists in obtaining accurate seismic data and information. The following figures provide an illustration of ground motion records and of seismic data processing and mapping for the largest-magnitude event recorded in Romania in 2024, i.e. the ML=5.4 Vrancea earthquake of September 16th, 14:40:22 UTC.

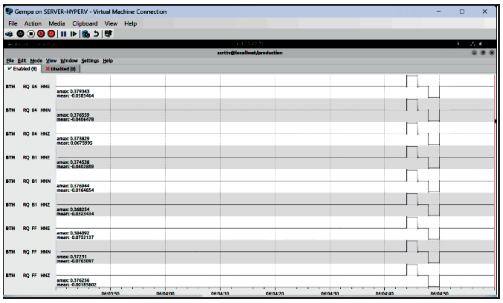


Figure 3. Tests for the verification of station operation. Station BTH (Faculty of Biotechnologies, USAMV, Bucharest). Screenshot taken from SeisComP software

Figure 4 presents a map of the RNMPSPC stations that recorded the ML 5.4 Vrancea earthquake on September 16, 2024, generated using the *sigma* module.

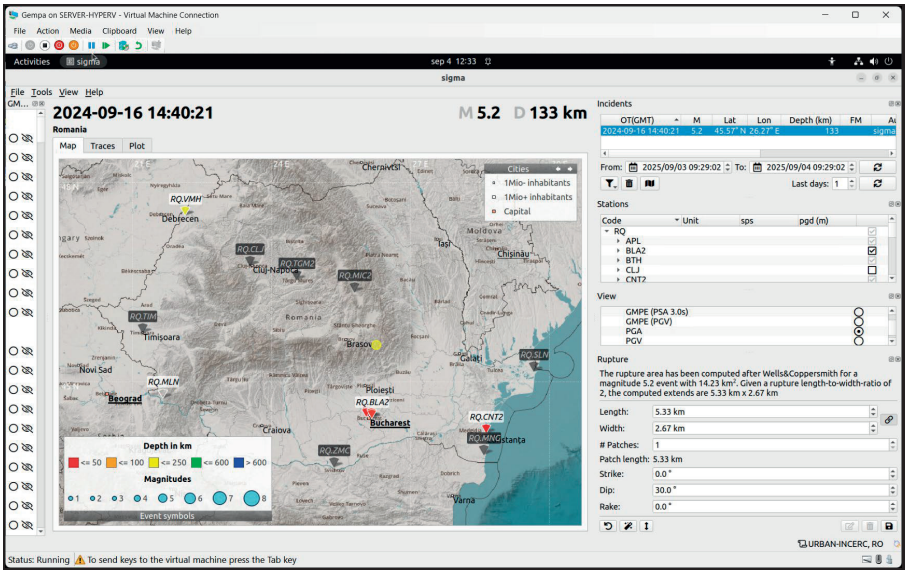


Figure 4. Map of the RNMPSPC stations that recorded the 16.09.2024 Vrancea earthquake, created with the *sigma* module

Figures 5 and 6 display the seismic records from this event and their subsequent processing, both performed with the *sigma* module, ensuring accurate data visualization and analysis. Figure 7 shows the spectrogram representation of the INC6 record from the ML5.4 Vrancea earthquake on September 16, 2024, processed using the *sigma* module. The displayed magnitude is that of the initial estimation in FDSN-SW.



Figure 5. Records of the 16.09.2024 Vrancea earthquake, visualised with the sigma module

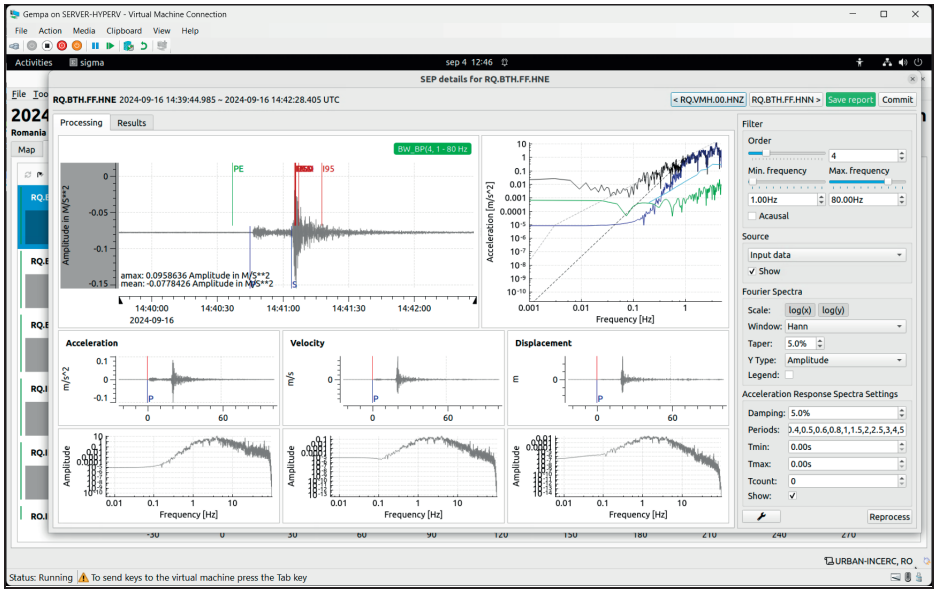


Figure 6. Processing of the 16.09.2024 Vrancea earthquake BTH record, performed with the sigma module



Figure 7. Spectrogram representation of the INC6 record of the 16.09.2024 Vrancea earthquake, obtained with the *sigma* module

Additionally, Figures 8, 9 and 10 illustrate the seismic data recorded at station FOC6, located in Focșani, near the earthquake's epicentre. These figures present the raw seismic record in Figure 8, the acceleration response spectra computed for the three components in Figure 9, and the FFT magnitude plots corresponding to the same record in Figure 10.

The recorded data, acquired using a GMS-18 accelerometer, was processed with the GeoDAS software from GeoSIG, the instrument manufacturer, ensuring high accuracy and compliance with seismic data processing standards.

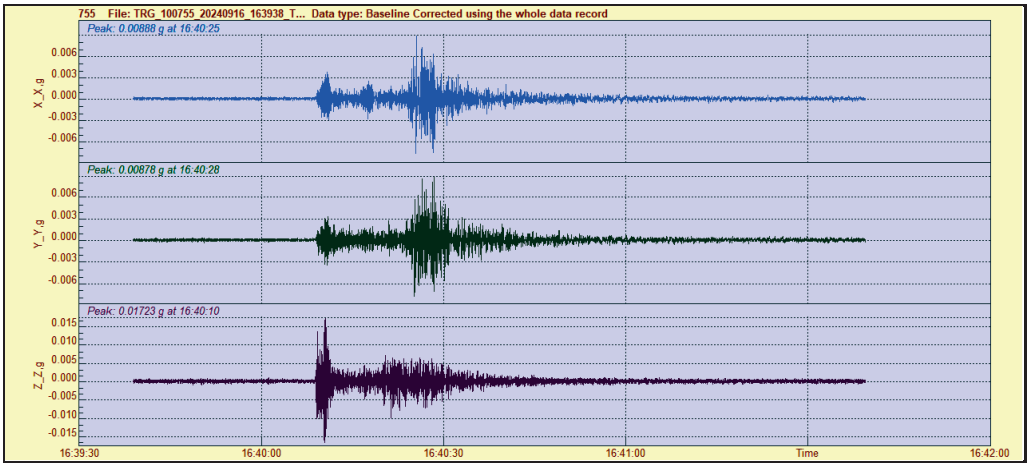


Figure 8. Acceleration record from the M_L=5.4 Vrancea earthquake on 16.09.2024. Station FOC6

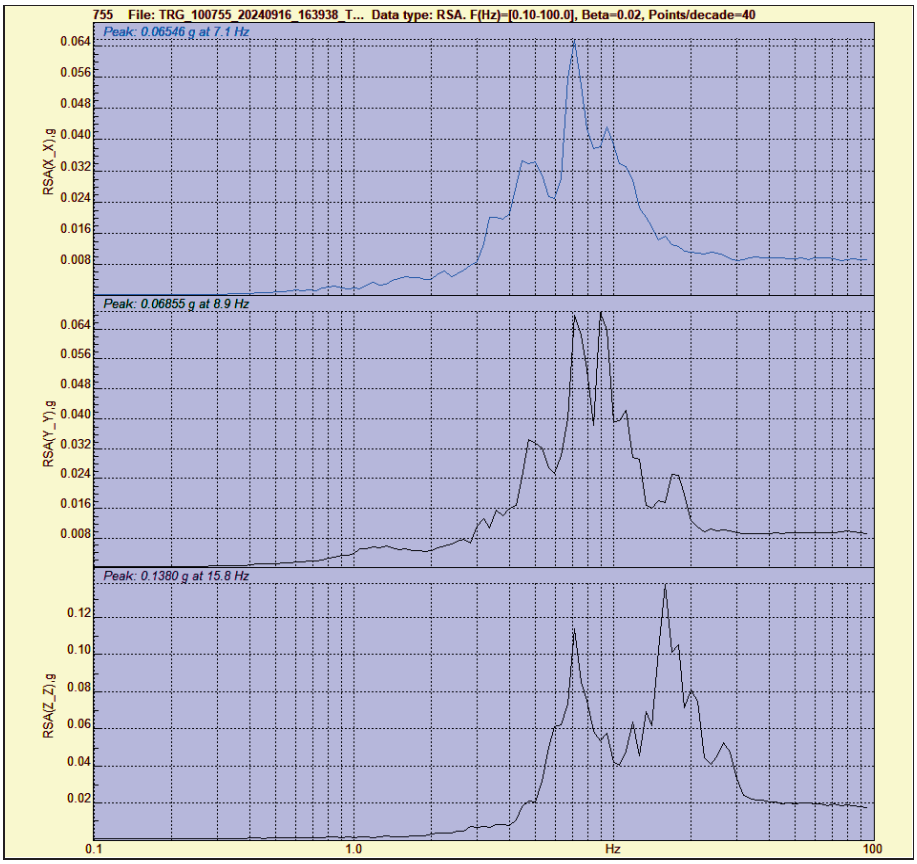


Figure 9. Acceleration response spectra for the three components of the FOC6 ground motion record. Event: 16.09.2024 Vrancea earthquake



Figure 10. FFT magnitude plots for the FOC6 ground motion record. Event: 16.09.2024 Vrancea earthquake

CONCLUSIONS

This study provided an overview of the fundamental principles of seismic data quality assurance, highlighting their significance in the context of major international research initiatives. The implementation of these quality assurance measures within the National Network for the Seismic Monitoring and Protection of Building Stock (RNMPSPC) at the National Research and Development Institute URBAN-INCERC was examined, detailing compliance with international standards and best practices. The role of RNMPSPC as a Special Installation / Objective of National Interest (IOSIN) within the EPOS European Research Infrastructure Consortium was also emphasized.

Furthermore, the study demonstrated the practical application of these methodologies through the recent ML 5.4 Vrancea earthquake (2024), showcasing the effectiveness of the current seismic monitoring infrastructure, including state-of-the-art software and hardware solutions. These findings reinforce the critical importance of continuous advancements in data acquisition, processing, and validation to enhance the reliability of seismic records and contribute to global earthquake research and hazard assessment.

ACKNOWLEDGEMENTS

This work referred some of the results obtained at INCD URBAN-INCERC within the project PN 23-35 01 01 "*Integrative concept of digital analysis of data from large-scale seismic monitoring of the national territory and the built environment, aimed for the rapid identification of the destructive potential of seismic events occurring in Romania and in the adjacent regions*", funded by the Romanian Ministry of Education and Research in the framework of the "Nucleu" Programme code PN 23-35, acronym "ECODIGICONS". The financial support for the publication of this work is gratefully acknowledged.

The maintenance, operation and exploitation of the RNMPSPC (IOSIN) infrastructure benefits from annual funding from the Executive Unit for Financing Higher Education, Research, Development and Innovation (UEFISCDI), Romania, within the Programme "Research Infrastructures", PN-IV-P5.5-IOSIN-1.

REFERENCES

Akkar, S., & Bommer, J. J. (2006). Influence of long-period filter cut-off on elastic spectral displacements. *Earthquake Engineering & Structural Dynamics*, 35(9), 1145-1165.

Akkar, S., & Boore, D. M. (2009). On baseline corrections and uncertainty in response spectra for baseline variations commonly encountered in digital accelerograph records. *Bulletin of the Seismological Society of America*, 99(3), 1671-1690.

Akkar, S., Sandıkkaya, M. A., M. Şenyurt, A. Azari Sisi, Ay, B. Ö., Traversa, P., Godey, S. (2013). Reference database for seismic ground-motion in Europe (RESORCE). *Bulletin of Earthquake Engineering*, 12(1), 311–339. https://doi.org/10.1007/ s10518-013-9506-8

Bellagamba, X., Lee, R., & Bradley, B. A. (2019). A neural network for automated quality screening of ground motion records from small magnitude earthquakes. *Earthquake Spectra*, 35(4), 1637-1661.

Boore, D. M., & Bommer, J. J. (2005). Processing of strong-motion accelerograms: needs, options and consequences. *Soil Dynamics and Earthquake Engineering*, 25(2), 93-115.

Casey, R., Templeton, M. E., Sharer, G., Keyson, L., Weertman, B. R., & Ahern, T. (2018). Assuring the quality of IRIS data with MUSTANG. *Seismological Research Letters*, 89(2A), 630-637.

COSMOS (2001). *Guidelines for Installation of Advanced National Seismic System Strong-Motion Reference Stations*. Consortium of Organizations for Strong-Motion Observation Systems Retrieved February 2025 from https://www.strongmotion.org/archive/publications/guidelines/Guidelines_ANSS.pdf

Craifaleanu, I. G., Borcia, I. S., Prăun, I. C. (2010). Strong-Motion Networks in Romania and Their Efficient Use in the Structural Engineering Applications. Chapter 17 in: *Earthquake Data in Engineering Seismology. Predictive Models, Data Management and Networks*, S. Akkar, P. Gülkan, & T. van Eck (Eds.), Springer, 275 p., pp. 247-259. DOI: 10.1007/978-94-007-0152-6_17

Crowley, H., Rodrigues, D., Silva, V., Despotaki, V., Romão, X., Castro, J., … Wenzel, M. (2018). Towards a uniform earthquake risk model for Europe. Proc. of the 16th European Conference on Earthquake Engineering, Thessaloniki, 18-21 June 2018.

Di Giulio, G., Cultrera, G., Cornou, C., Bard, P. Y., & Al Tfaily, B. (2021). Quality assessment for site characterization at seismic stations. Bulletin of Earthquake Engineering, 19(10), 4643-4691.

Douglas, J. (2003). What is a poor quality strong-motion record? Bulletin of Earthquake Engineering, 1(2), 141-156.

Dragomir, C.-S., Craifaleanu, I.-G., Dobre, D., Georgescu, E.-S. (2023). Spatial data resulting from the automation of the permanent seismic monitoring system. *Scientific Papers, Series E: Land*

Reclamation, Earth Observation & Surveying, Environmental Engineering, 12, 199-204.

ISC (2018). John Milne. International Seismological Centre. Retrieved February 22, 2025, from isc.ac.uk website: https://www.isc.ac.uk/about/history/milne/

INFP (2025). Archive INFP. Retrieved February 2025, from Infp.ro website: http://archive.infp.ro/

Luzi, L., Puglia, R., Russo, E., D'Amico, M., Felicetta, C., Pacor, F., Lanzano, G., Çeken, U., Clinton, J., Costa, G., Duni, L., Farzanegan, E., Gueguen, P., Ionescu, C., Kalogeras, I., Özener, H., Pesaresi, D., Sleeman, R., Strollo, A., Zare, M. (2016). The Engineering Strong-Motion Database: A Platform to Access Pan-European Accelerometric Data. *Seismological Research Letters*, 87(4), 987–997. https://doi.org/10.1785/0220150278

Mărmureanu, A., Ionescu, C., Grecu, B., Toma-Danila, D., Tiganescu, A., Neagoe, C., Toader, V., Craifaleanu, I. G., Dragomir, C. S., Meita, V., Liashchuk, O. I., Dimitrova, L., Ilies, I. (2021). From National to Transnational Seismic Monitoring Products and Services in the Republic of Bulgaria, Republic of Moldova, Romania, and Ukraine. *Seismological Research Letters*, 92(3), 1685–1703. DOI: 10.1785/0220200393.

Ravizza, G., Ferrari, R., Rizzi, E., Dertimanis, V., & Chatzi, E. N. (2019). Denoising corrupted structural vibration response: critical comparison and assessment of related methods. In COMPDYN 2019-7th ECCOMAS Thematic Conference on Computational Methods in Structural Dynamics and Earthquake Engineering.

ORFEUS (2023). Quality Assurance — ORFEUS documentation. Retrieved February 2025, from Readthedocs.io website: https://orfeus.readthedocs.io/en/latest/overview.html

Ravizza, G., Ferrari, R., Rizzi, E., & Dertimanis, V. (2021). On the denoising of structural vibration response records from low-cost sensors: a critical comparison and assessment. *Journal of Civil Structural Health Monitoring*, 11(5), 1201-1224.

Schaeffer, J., Pedersen, H., Bienkowski, J., Evangelidis, C., Petrakopoulos, V., Quinteros, J., Strollo, A., & ORFEUS-EIDA Technical Committee and Management Board. (2024). Data Delivery Indicators in EIDA: Designing a Consistent Metrics System in a Distributed Services Environment. *Data Science Journal*, 23, 51. https://doi.org/10.5334/dsj-2024-051

Strollo, A., Cambaz, D., Clinton, J., Danecek, P., Evangelidis, C. P., Marmureanu, A., … Kaestli, P. (2021). EIDA: The European Integrated Data Archive and Service Infrastructure within ORFEUS. *Seismological Research Letters*, *92*(3), 1788–1795. https://doi.org/10.1785/0220200413

Tripathy-Lang, A., Bohon, W. (2022a). Global seismographic networks part I: A brief history. SAGE. Retrieved February 2025, from iris.edu website: https://dev.iris.edu/hq/science_highlights/global_seismographic_networks_part_i_a_brief_history

Tripathy-Lang, A., Bohon, W. (2022b). Global seismographic networks part II: A slew of studies. SAGE. Retrieved February 2025, from iris.edu website: https://dev.iris.edu/hq/science_highlights/global_seismographic_networks_part_ii_a_slew_of_studies

USGS (2025). NSMP History. Retrieved February 2025, from usgs.gov website: https://earthquake.usgs.gov/monitoring/nsmp/history/

Data centres of the European Integrated Data Archive, Retrieved from www.orfeus eu.org/eida

https://www.gempa.de/products/sigma/

https://smp.gempa.de/

https://www.fdsn.org/

https://www.resorce-portal.eu/

http://www.sera-eu.org/en/home/index.html

https://www.orfeus-eu.org/

Scientific Papers. Series E. Land Reclamation, Earth Observation & Surveying, Environmental Engineering. Vol. XIV, 2025
Print ISSN 2285-6064, CD-ROM ISSN 2285-6072, Online ISSN 2393-5138, ISSN-L 2285-6064

COMPREHENSIVE ANALYSIS OF PARTICULATE MATTER VARIABILITY IN AN URBAN ENVIRONMENT USING Rapid-E MONITORING

Mădălin CRISTEA[1], Adrian ROȘU[1, 2], Bogdan ROȘU[1], Daniel-Eduard CONSTANTIN[1, 2], Simona CONDURACHE-BOTA[1], Mirela VOICULESCU[1, 2], Cătalina ITICESCU[1, 2], Puiu-Lucian GEORGESCU[1, 2], Silvia DRĂGAN[3]

[1]"Dunărea de Jos" University of Galați, Faculty of Sciences and Environment, Department of Chemistry, Physics and Environment, 111 Domnească Street, Galați, Romania
[2]"Dunărea de Jos" University of Galați, REXDAN Research Infrastructure, 98 George Coşbuc Blvd, Galați, Romania
[3]EnviroEcoSmart S.R.L., 189 Tecuci Street, Galați, Romania

Corresponding author emails: rosu_adrian_90@yahoo.ro, adrian.rosu@ugal.ro

Abstract

Fine particulate matter (PM) pollution is a significant environmental and public health concern in urban areas. This study presents an extensive assessment of PM concentrations in Galați, Romania, using the RAPID-E monitoring system. The equipment was deployed at the RI REXDAN (Research Infrastructure REXDAN – George Coşbuc no. 98) to continuously measure PM concentrations at 0.3, 0.5, 1, and 5 µm from December 31, 2023 (22:00) to December 30, 2024 (22:00). The collected data were analysed to determine temporal variations in particulate matter, including monthly means, daily averages, weekday versus weekend patterns, and variations between working days and weekends. By identifying key pollution trends and fluctuations over the monitoring period, this study provides insights into the dynamics of urban air quality and potential emission sources. The findings contribute to a better understanding of PM pollution variability and support the development of effective air quality management strategies in urban environments.

Key words: *air pollution, particulate matter, urban monitoring, RAPID-E, PM variability, temporal analysis, air quality assessment.*

INTRODUCTION

In recent decades, air quality has become a significant global issue, raising concerns about its impact on public health, the environment and ecosystems. The pollutants that influence air quality are SO_2, NO_2, CO, CO_2, O_3 and particulate matter (Constantin et al., 2013; Dragomir et al., 2015; Meier et al., 2017). SO_2, NO_2 and particulate matter arise from the combustion of fossil fuels (Constantin et al., 2020; Merlaud et al., 2018; 2020; Roșu et al., 2020; 2021; 2023). Particulate matter air pollution is a serious problem, especially when we are dealing with fine and ultrafine particles, between 0.3 and 5 µm (Sanda et al., 2023; Iordache, 2017). These particles, often invisible to the naked eye, can penetrate deep into the respiratory tract and even enter the bloodstream, posing significant health risks. Primary sources of these particles include industrial activities, road traffic and natural phenomena such as volcanic eruptions and desert dust (Baldacchini et al., 2019; Lonati & Giugliano, 2006; Ramgolam et al., 2008). The size of these particles determines their ability to reach the lungs and bloodstream, increasing the risk of respiratory and cardiovascular diseases. Prolonged exposure to air polluted with fine particles can exacerbate pre-existing conditions such as asthma and chronic lung disease and may even contribute to reduced life expectancy (Alemayehu et al., 2020; Kelly et al., 2017). Vulnerable groups, such as children, the elderly, and people with compromised immune systems, are particularly susceptible (Kirešová et al., 2023; Pétremand et al., 2022). The economic burden of air pollution, including healthcare costs and loss of working productivity, further underscores the urgency of addressing this issue (Conte et al., 2020; Zoran et al., 2023). Air pollution also has a wider environmental impact, including contamination of water sources, soil degradation, and

disruption of ecosystems. The European Commission has set air quality limit values for particulate matter (PM10) and requires the collection of PM2.5 data to protect public health. However, data on finer particles, such as $PM_{0.5}$, PM_1, and PM_5, are less available. To address this gap, the Rapid E+ equipement, the successor of Rapid E and PA-300, has emerged as a crucial tool for measuring fine particles in the air (Aït-Khaled et al., 2009; Šaulienė et al., 2019). This device uses optical detection technology and laser illumination to measure particles in the 0.3-5 µm range with high accuracy (Boldeanu et al., 2021; Tešendić et al., 2020). Rapid E+ provides a fast and accurate method for continuous monitoring of particle concentrations in a variety of environments, from polluted urban areas to industrial and natural environments (Crawford et al., 2023; Yanagi et al., 2023) . In this study we present the results of one year (2024) of data analysis from our Rapid E+ equipment installed at RI REXDAN (Galați city, Romania).

MATERIALS AND METHODS

Study area and localization

For our study, we conducted continuous dust measurements in the city of Galați, one of the largest urban areas in Romania. The measurements were carried out over a whole year, from January 1, 2024, to December 30, 2024, at the specific location at George Coșbuc Blvd, no. 98 (coordinates: 45°26'6.66"N 28° 2'14.02"E). This location was chosen because it is an area with intense traffic and urban activity. It is also important to note that during this period, significant infrastructure repair works were underway in the area, which could have affected air quality. To collect accurate and reliable data on particle levels, we used the Rapid-E+ equipment, which was placed in the courtyard of the RI Rexdan. The location of the Rapid-E+ device is shown in Figure 1. The aim of this study was to analyse particulate levels in the context of ongoing construction activities and urban development.



Figure 1. Location of the deployment of the measuring equipment (REXDAN)

Equipment and data used

Rapid-E+ is an advanced bioaerosol sensor that uses proprietary laser technology to analyze individual aerosol particles in real time. Its integration with GPU (Graphics Processing Unit) acceleration significantly improves the speed of data acquisition and processing, providing exceptional performance in tracking and identifying aerosols in complex environments. The sensor continuously monitors and characterizes airborne particles ranging in diameter from 0.3 to 100 µm. Values of 0.3 µm indicate particles with sizes between 0.3 and 100 µm, while values of 0.5 µm refer to particles between 0.5 and 100 µm. Also, values of 1 µm cover particles between 1 and 100 µm, and values of 5 µm include particles between 5 and 100 µm. Backed by years of continuous measurements, Plair technology combines scattered light pattern analysis and fluorescence spectroscopy, ensuring reliable, real-time monitoring of ambient air. Rapid-E+ operates

autonomously and remotely, giving users access to data anytime, anywhere. Detailed characteristics of the device (Rapid-E+) are provided in the following table, Table 1, which outlines its specifications and key features of the equipment (https://www.plair.ch/rapid-e.html).

Table 1. Specification of the intelligent bioaerosol sensor Rapid-E+ used for data collection in the city of Galați throughout the year 2024

Parameter	Value	Details
Particle size range, micrometers (µm)	0.3-100	-
UV laser wavelength, nanometers (nm)	337 ± 5	-
Scattering laser wavelength (nm)	447 ± 5	-
Imaging laser wavelength (nm)	637 ± 5	-
Fluorescence spectral range (nm)	390-570 ± 5	12 nm per pixel
Fluorescence spectral ranges of lifetime module (nm)	375-397 ± 5 415-450 ± 5 467-487 ± 5	1 photodetector per spectral range
Fluorescence decay resolution, nanoseconds (ns)	1	For each spectral range
Sample airflow, liters per minute (LPM)	5	-
Maximum counts (scattering only), Maximum counts (fully analysed)	1,000,000 4.800	Particles per minute
Power supply (Volts AC)	90-240	-
Power consumption (watts)	less than 200	Maximum value
Size (H x W x D), centimeters	40 x 34 x 55	-
Operating temperature (°C)	-10 ... +40	Temperature range can be extended with an outdoor box
Humidity (%)	0-95	Without condensation
Weight (kg)	25	-

Rapid-E+ comes with an online platform or dashboard called PlairGrid, which allows users to visualize data collected in the field. PlairGrid is a free, easy-to-use tool that allows users to explore raw data and create a machine learning model capable of classifying particles in real time. This advanced functionality is designed to help users accelerate their data analysis processes, giving them the ability to take full control of their experiments and projects. With these tools, users can start working with their data immediately and easily, without the need for complex setup or additional software. The device was designed to meet the growing need for efficient, accurate, and real-time monitoring of bioaerosols, which include particles such as pollen, bacteria, and fungal spores, among others. By enabling continuous and accurate data collection, Rapid-E+ helps users better understand the dynamics of airborne particles, which can have a significant impact on health, environmental quality, and various research areas. Its design allows researchers, healthcare professionals, and environmental specialists to detect, classify, and analyse these particles in real time, making it a powerful tool for studying air quality, biological hazards, and public health risks. The integration of machine learning and real-time data visualization improves the overall efficiency and effectiveness of experiments, ensuring that users have the flexibility to adapt their approaches and make informed decisions quickly.



Figure 2. Image of REXDAN RI Rapid-E+ equipment

RESULTS AND DISCUSSIONS

Using the detailed data collected by the Rapid-E+ sensor, we have created a series of complex graphs that highlight the average values of airborne particle concentrations throughout

2024. We have separated each category of particles data, so we were able to organize the values so that they showed the values for different categories i.e. 0.3μm (particles between 0.3μm and 0.5μm), 0.5μm (0.5-1μm), 1μm (1-5μm), and 5μm (5-100μm), respectively. These results of data analysis are structured for each day of the week, for particle size interval in the air: 0.3, 0.5, 1 and 5 μm. Analysis of these data allows for a detailed assessment of daily variations in fine particle concentrations, providing valuable information about the behaviour and distribution of aerosols in the atmosphere over an entire year. These observations are essential for understanding the factors that influence air quality that could affect public health and the environment, especially regarding the sizes of respirable particles that can have significant effects on human health. We also present the σ = RMSA to determine the errors that may arise from external conditions, measurement errors, and systematic errors. In this formula, σ represents the standard error, and RMS (Root Mean Square) measures the average magnitude of the errors, calculated by the square root of the average of the squares of the differences between the estimated and actual values. All data representation was created using python code i.e. using matplotlib a native Matlab ploting library implemented with python code via the open-source IDE Spyder (Scientific Python Development Environment).

As can be seen in Figure 3, the values increase exponentially with the size of the particles included in that range. This phenomenon is due to the fact that small particles (below 1 μm) persist longer in the air, due to their small mass and the reduced influence of gravity on them (Casale et al., 2009). Thus, they are suspended for a longer period of time and can be transported over long distances by winds and atmospheric currents. In contrast, larger particles (above 5 μm) settle more quickly due to their greater weight and rapid sedimentation in the atmosphere.

In the analysed graphs, the size range 5-100 μm does not exceed values over 4 thousand per hour, which suggests that larger particles are fewer, because they sediment quickly. In contrast, particles in the range 0.3-0.5 μm can reach concentrations of up to 1.5 million particles per hour, since they are more numerous and remain suspended longer in the air.

As can be seen in the seven graphs presented, the values corresponding to particles of 0.3 and 0.5 μm are represented on the vertical axis on the left, and the data are collected periodically, at one-hour intervals. These values reflect the particle concentrations in a specific period, and the collection interval allows for a detailed observation of their variability over time. On the other hand, the values corresponding to particles of 1 and 5 μm are displayed on the vertical axis on the right, and the scale of this axis varies from one day to the next, depending on the distribution of larger particles. As we progress further into the week, we notice that the values increase slowly but progressively, with Mondays having relatively low values due to the break period of the weekend, when traffic was reduced and work-related activities were at lower end, and Fridays having the highest values of the week and some of the most visible fluctuations in the measured parameters.

On October 19, 2024, between 10:00 and 11:00, a significant and sudden increase in the values of particles in the size range of 1-5 μm was observed in the monitoring carried out on the PlairGrid online platform. This increase was remarkable, with values exceeding by more than 100 times the average values recorded in previous reference periods. Moreover, this fluctuation not only had an immediate impact on the data from that period, but also affected the annual average of Saturday, causing an unusual increase in the values recorded for this day compared to other Saturdays of the year. The significant change in the annual average underlines the importance of a detailed analysis to identify the causes of this abnormal behaviour.

As for the possible causes of this phenomenon, they may include a technical error in the measuring equipment. Another possible cause may be temporary contamination of the environment or equipment. If an external source of contamination was active at that time, this could have led to a punctual accumulation of particles, influencing the measurements, without affecting the entire monitoring time frame.

To facilitate the observation of the differences between weekdays and weekends, we have created two distinct graphs. The first graph includes the average values for weekdays (Monday-Friday), and the second graph presents the average values for weekend days (Saturday and Sunday).

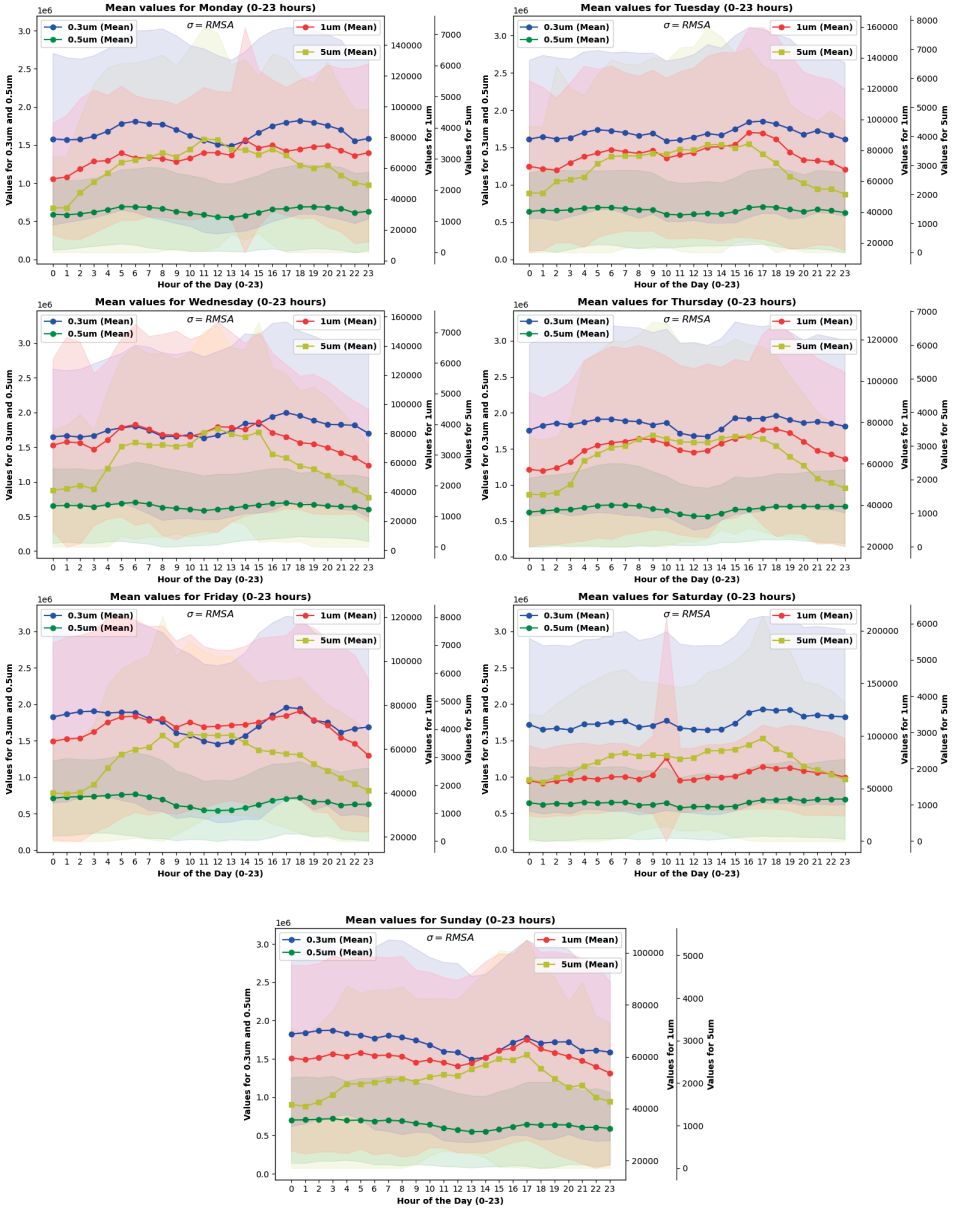


Figure 3. Mean value for each day of the week

These graphs allow a clear visual comparison of the trends and variability characteristic of each category of days, facilitating the identification of possible anomalies or

significant differences in the behaviour of particle values depending on the week period (Figure 4).

By comparing the two data sets, it is possible to observe fluctuations that could be attributed to external factors specific to weekdays or weekends, such as changes in industrial activities, transportation, weather conditions or other environmental influences that may vary depending on the day of the week.

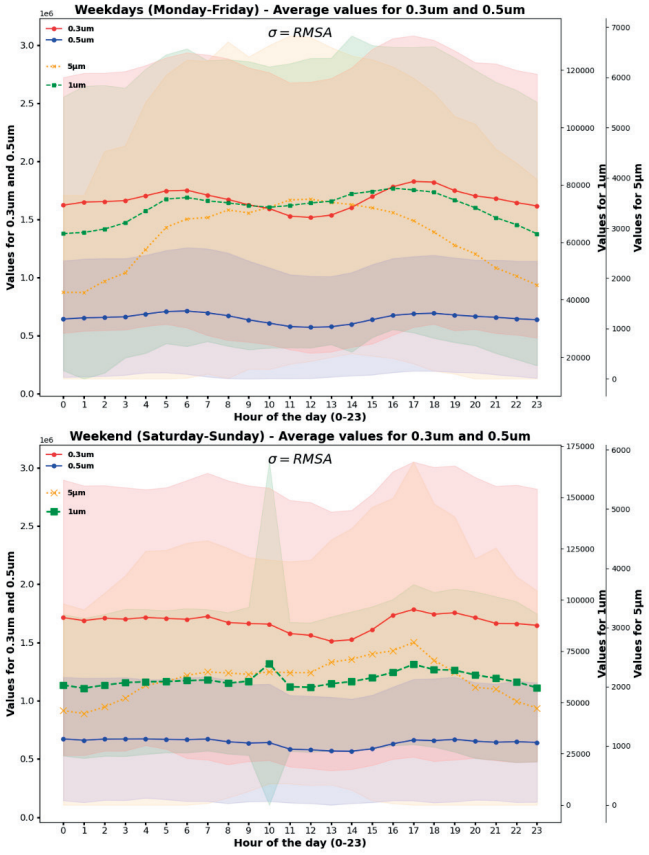


Figure 4. Mean value for workdays and weekend

Analysing the 2 graphs presented in Figure 4, a clear trend of variation of the measured values of particulate matter depending on the time of day is observed, with significant particularities on weekdays compared to weekends. During the week, the data reveal notable fluctuations, with substantial increases in the values around peak hours (6:00 and 17:00), intervals in which, usually, the highest values can be attributed the peak of human activity or intensified traffic. These peaks are significant, indicating moments of increased traffic or other activities related to the daily schedule of employees or workers.

In contrast, on weekends, the data show a relative stability of the values, without notable fluctuations, with only a few isolated exceptions that do not reach the intensity of those observed on weekdays. This behaviour suggests that, on weekends, activity is more constant and less influenced by the rigid schedule of weekdays, making it possible that variation factors are reduced and the activities carried out are more uniform. A significant external factor that can influence these variations on weekdays is represented by the road restoration projects carried out near the measurement area during the respective period.

Considering that infrastructure works involve periodic interventions that can affect the traffic flow or the schedule of activities, we can hypothesize that the significant decrease in the values around 12:00 on weekdays can be attributed to the lunch breaks of the workers involved in these projects. Thus, during the mentioned time interval, the activity of the workers is considerably reduced, which implicitly leads to a decrease in the measured values, even if the values are related to traffic, economic activities or other variables. It can be seen that particles larger than 5 μm do not follow the same rule as particles below 5 μm, as they do not have their maximums during peak hours of the day, but at 12:00 when small particles decrease in number. Another significant difference between weekdays and weekends is made by particles over 1 μm, which during the week reach values of over 80 thousand particles per hour, while during the weekend they do not exceed values of 75 thousand particles.

CONCLUSIONS

The results of this study demonstrate that the Rapid-E+ device is a complex and useful tool for local urban monitoring of airborne particulate matter as we presented in the results of measurements made throughout 2024 at REXDAN RI located at no 98 George Coșbuc Blvd, Galati, Romania. The main advantage of this device is the accuracy of its measurements on an extended scale (0.3-100 μm) and the ease with which the data can be recorded and processed. By making continuous measurements for particulate matter, we can more easily observe the dynamics of these pollutants and determine the factors that influence these parameters and the main sources (traffic, constructions and other natural or anthropogenic factors). The main objective of this research was to determine the average values of some air parameters over a whole year, with a particular focus on monitoring particulate matter. During the analysis, we observed that the factor that most influences the variation of pollutants is human activity, especially construction-related activities. These activities contribute significantly to fluctuations in particulate matter concentrations, especially during peak periods of the day. The most pronounced pollution values were observed during peak hours, when the number of construction sites and associated activities are increasing. This trend suggests that particulate matter emissions generated by such activities have a significant impact on air quality and public health. It is also important to note that these fluctuations are much more evident in urban areas, where economic activity and construction are at a high level. The next study will analyse the diurnal and nocturnal variations of particulate matter, as well as their changes according to the seasons (spring, summer, autumn, winter), using the Rapid-E+ device. This method will provide us with detailed information on how pollutant concentrations fluctuate throughout the day and at different times of the year. Thus, we will be able to observe the differences between day and night, but also how the seasons influence the level of particulate matter in the air. This analysis will contribute to a clearer understanding of the behaviour of pollution under different temporal conditions, providing essential data for long-term air quality management.

ACKNOWLEDGEMENTS

The authors acknowledge the support of the project “Support for the operation of Romania's facilities within the ACTRIS ERIC research infrastructure”, MySMIS code 309113, funding contract No. 309010/19.12.2024. The equipment used for this study are part of REXDAN Research Infrastructure (REXDAN RI).

REFERENCES

Aït-Khaled, N., Pearce, N., Anderson, H. R., Ellwood, P., Montefort, S., Shah, J., Asher, M. I., Beasley, R., Björkstén, B., Brunekreef, B., Crane, J., Foliaki, S., García-Marcos, L., Keil, U., Lai, C. K. W., Mallol, J., Robertson, C. F., Mitchell, E. A., Odhiambo, J., … Wong, G. (2009). Global map of the prevalence of symptoms of rhino-conjunctivitis in children: The International Study of Asthma and Allergies in Childhood (ISAAC) Phase Three. *Allergy: European Journal of Allergy and Clinical Immunology, 64*(1), 123–148. https://doi.org/10.1111/j.1398-9995.2008.01884.x

Alemayehu, Y. A., Asfaw, S. L., & Terfie, T. A. (2020). Exposure to urban particulate matter and its

association with human health risks. *Environmental Science and Pollution Research, 27*(27), 27491–27506. https://doi.org/10.1007/s11356-020-09132-1

Baldacchini, C., Sgrigna, G., Clarke, W., Tallis, M., & Calfapietra, C. (2019). An ultra-spatially resolved method to quali-quantitative monitor particulate matter in urban environment. *Environmental Science and Pollution Research, 26*(19), 18719–18729. https://doi.org/10.1007/s11356-019-05160-8

Boldeanu, M., Marin, C., Ene, D., Marmureanu, L., Cucu, H., & Burileanu, C. (2021). Mars: The first Romanian pollen dataset using a Rapid-E particle analyzer. *2021 11th International Conference on Speech Technology and Human-Computer Dialogue (SpeD 2021)*, 145–150. https://doi.org/10.1109/SpeD53181.2021.9587447

Casale, F., Nieddu, G., Burdino, E., Vignati, D. A. L., Ferretti, C., & Ugazio, G. (2009). Monitoring of submicron particulate matter concentrations in the air of Turin City, Italy: Influence of traffic limitations. *Water, Air, and Soil Pollution, 196*(1), 141–149. https://doi.org/10.1007/s11270-008-9763-3

Constantin, D. E., Voiculescu, M., & Georgescu, L. (2013). Satellite observations of NO trend over Romania. *The Scientific World Journal, 2013*, Article 261634. https://doi.org/10.1155/2013/261634

Constantin, D. E., Bocăneala, C., Voiculescu, M., Roşu, A., Merlaud, A., Van Roozendael, M., & Georgescu, P. L. (2020). Evolution of SO_2 and NOx emissions from several large combustion plants in Europe during 2005–2015. *International Journal of Environmental Research and Public Health, 17*(10), 3630. https://doi.org/10.3390/ijerph17103630

Conte, R., De Rosa, G., Cavallo, A., & Fico, A. (2020). Low cost air quality monitors to evaluate nanosized particulate matter: A pilot study. *International Journal of Nano Dimension, 11*(4), 356–367. https://oiccpress.com/ijnd/article/download/4290/12393

Crawford, I., Bower, K., Topping, D., Di Piazza, S., Massabò, D., Vernocchi, V., & Gallagher, M. (2023). Towards a UK airborne bioaerosol climatology: Real-time monitoring strategies for high time resolution bioaerosol classification and quantification. *Atmosphere, 14*(8), 1214. https://doi.org/10.3390/atmos14081214

Dragomir, C. M., Constantin, D. E., Voiculescu, M., Georgescu, L. P., Merlaud, A., & Van Roozendael, M. (2015). Modeling results of atmospheric dispersion of NO_2 in an urban area using METI–LIS and comparison with coincident mobile DOAS measurements. *Atmospheric Pollution Research, 6*(3), 503–510. https://doi.org/10.5094/APR.2015.056

Iordache, S., Dunea, D., Ianache, C., Predescu, L., & Dumitru, D. (2017). Assessment of outdoor pollution with submicrometric and fine particulate matter in Ploiesti City, Romania. *Revista de Chimie (Bucharest), 68*(4), 811–817. https://www.plair.ch/Rapid-E.html

Kelly, K. E., Whitaker, J., Petty, A., Widmer, C., Dybwad, A., Sleeth, D., Martin, R., & Butterfield, A. (2017). Ambient and laboratory evaluation of a low-cost particulate matter sensor. *Environmental Pollution, 221*, 491–500. https://doi.org/10.1016/j.envpol.2016.12.039

Kirešová, S., Guzan, M., & Sobota, B. (2023). Using low-cost sensors for measuring and monitoring particulate matter with a focus on fine and ultrafine particles. *Atmosphere, 14*(2), 324. https://doi.org/10.3390/atmos14020324

Lonati, G., & Giugliano, M. (2006). Size distribution of atmospheric particulate matter at traffic exposed sites in the urban area of Milan (Italy). *Atmospheric Environment, 40*(13), 264–274. https://doi.org/10.1016/j.atmosenv.2005.11.077

Meier, A. C., Schönhardt, A., Bösch, T., Richter, A., Seyler, A., Ruhtz, T., Constantin, D.-E., Shaiganfar, R., Wagner, T., Merlaud, A., Van Roozendael, M., Belegante, L., Nicolae, D., Georgescu, L., & Burrows, J. P. (2017). High-resolution airborne imaging DOAS measurements of NO_2 above Bucharest during AROMAT. *Atmospheric Measurement Techniques, 10*(5), 1831–1857. https://doi.org/10.5194/amt-10-1831-2017

Merlaud, A., Tack, F., Constantin, D., Georgescu, L., Maes, J., Fayt, C., Mingireanu, F., Schuettemeyer, D., Meier, A. C., Schönardt, A., Ruhtz, T., Bellegante, L., Nicolae, D., Den Hoed, M., Allaart, M., & Van Roozendael, M. (2018). The Small Whiskbroom Imager for atmospheric composition monitoring (SWING) and its operations from an unmanned aerial vehicle (UAV) during the AROMAT campaign. *Atmospheric Measurement Techniques, 11*(1), 551–567. https://doi.org/10.5194/amt-11-551-2018

Merlaud, A., Belegante, L., Constantin, D.-E., Den Hoed, M., Meier, A. C., Allaart, M., Ardelean, M., Arseni, M., Bösch, T., Brenot, H., Calcan, A., Dekemper, E., Donner, S., Dörner, S., Balanica Dragomir, M. C., Georgescu, L., Nemuc, A., Nicolae, D., Pinardi, G., … Van Roozendael, M. (2020). Satellite validation strategy assessments based on the AROMAT campaigns. *Atmospheric Measurement Techniques, 13*(11), 5513–5535. https://doi.org/10.5194/amt-13-5513-2020

Pétremand, R., Suárez, G., Besançon, S., Dil, J. H., & Canu, I. G. (2022). A real-time comparison of four particulate matter size fractions in the personal breathing zone of Paris subway workers: A six-week prospective study. *Sustainability, 14*(10), 5999. https://doi.org/10.3390/su14105999

Ramgolam, K., Chevaillier, S., Marano, F., Baeza-Squiban, A., & Martinon, L. (2008). Proinflammatory effect of fine and ultrafine particulate matter using size-resolved urban aerosols from Paris. *Chemosphere, 72*(9), 1340–1346. https://doi.org/10.1016/j.chemosphere.2008.04.025

Roşu, A., Constantin, D. E., Voiculescu, M., Arseni, M., Merlaud, A., Van Roozendael, M., & Georgescu, P. L. (2020). Observations of atmospheric NO_2 using a new low-cost MAX-DOAS system. *Atmosphere, 11*(2), 129. https://doi.org/10.3390/atmos11020129

Roşu, A., Constantin, D. E., Voiculescu, M., Arseni, M., Roşu, B., Merlaud, A., Van Roozendael, M., & Georgescu, P. L. (2021). Assessment of NO_2 pollution level during the COVID-19 lockdown in a

Romanian city. *International Journal of Environmental Research and Public Health, 18*(2), 544. https://doi.org/10.3390/ijerph18020544

Roșu, A., Arseni, M., Constantin, D. E., Roșu, B., Petrea, S. M., Voiculescu, M., & Georgescu, L. P. (2023). Study of air pollution level in an urban area using low-cost sensor system onboard mobile platform. *Scientific Papers. Series E. Land Reclamation, Earth Observation & Surveying, Environmental Engineering, 12*(1), 124–133.

Sanda, M., Dunea, D., Iordache, S., Predescu, L., Predescu, M., Pohoata, A., & Onutu, I. (2023). Recent urban issues related to particulate matter in Ploiesti City, Romania. *Atmosphere, 14*(4), 746. https://doi.org/10.3390/atmos14040746

Šaulienė, I., Šukienė, L., Daunys, G., Valiulis, G., Vaitkevičius, L., Matavulj, P., Brdar, S., Panić, M., Sikoparija, B., Clot, B., Crouzy, B., & Sofiev, M. (2019). Automatic pollen recognition with the Rapid-E particle counter: The first-level procedure, experience and next steps. *Atmospheric Measurement Techniques, 12*(5), 3435–3452. https://doi.org/10.5194/amt-12-3435-2019

Tešendić, D., Boberić Krstićev, D., Matavulj, P., Brdar, S., Panić, M., Minić, V., & Šikoparija, B. (2020). RealForAll: Real-time system for automatic detection of airborne pollen. *Enterprise Information Systems*, 1–17. https://doi.org/10.1080/17517575.2020.1793391

Yanagi, U., Fukushima, N., Nagai, H., Ye, H., & Kano, M. (2023). Bioaerosol sensor for in situ measurement: Real-time measurement of bioaerosol particles in a real environment and demonstration of the effectiveness of air purifiers to reduce bioaerosol particle concentrations at hot spots. *Atmosphere, 14*(11), 1769. https://doi.org/10.3390/atmos14111656

Zoran, M., Savastru, R., Savastru, D., Tautan, M., & Tenciu, D. (2023). Linkage between airborne particulate matter and viral pandemic COVID-19 in Bucharest. *Microorganisms, 11*(10), 2531. https://doi.org/10.3390/microorganisms11102531

Scientific Papers. Series E. Land Reclamation, Earth Observation & Surveying, Environmental Engineering. Vol. XIV, 2025
Print ISSN 2285-6064, CD-ROM ISSN 2285-6072, Online ISSN 2393-5138, ISSN-L 2285-6064

THE IMPACT OF LAND USE CHANGES ON NATURAL PROTECTED AREAS IN THE OLTEȚ PIEDMONT (ROMANIA)

Raluca Lucia DINCULOIU[1], Daniel SIMULESCU[2], Carmen Otilia RUSĂNESCU[1], Mihaela BEGEA[1], Gigel PARASCHIV[1], Sorin Ștefan BIRIȘ[1], Maria CIOBANU[1]

[1]National University of Science and Technology Politehnica Bucharest,
Faculty of Biotechnical Systems Engineering, 313 Splaiul Independenţei, District 6,
060042, Bucharest, Romania
[2]University of Craiova, Faculty of Sciences, Geography Department,
13 A. I. Cuza Street, Craiova, Romania

Corresponding authors emails: daniel.simulescu@edu.ucv.ro, rusanescuotilia@gmail.com

Abstract

The identification and assessment of the pressures and threats to which protected areas are subjected is crucial in order to plan, implement and assess conservation actions. Our study aimed to assess the spatio-temporal dynamics of land use/land cover changes that occurred in the Olteț Piedmont between 2012 and 2018 and identify the main threats that anthropogenic activities pose to natural protected areas. The major changes in land use that took place between 2012 and 2018 had a great impact on the landscape. The disappearance of large surfaces of vineyards (–8150 ha), orchards (–2400 ha), watercourses (–700 ha), beaches, dunes and sand plains (–140 ha) and inland marshes (–40 ha) are the most significant. These terrains were occupied by complex crops (+4350 ha), deciduous forests (+2900 ha) and transitional woodland shrub (+750 ha). Also, the built-up areas, especially near cities like Craiova, Filiași, Balș and Drăgășani, had an increase in surface. The results revealed that the expansion of arable land and urban areas have a great impact in the conservation of biodiversity in natural protected areas from the Olteț Piedmont.

Key words*: land use, land cover changes, natural protected areas*, *Olteț Piedmont, Romania*

INTRODUCTION

Land is a three-dimensional, dynamic, and complex system, developed through the interaction of lithology, structure, drainage, climate, vegetation, and geomorphological processes operating over time (Laha, 2023). As a fundamental natural resource, it underpins diverse economic, social, and ecological functions (Phuong & Thien, 2023).

Within this context, land use and land cover (LULC) emerge as interrelated dimensions that describe both the ways land is utilized and the distribution of vegetation and surface features. Transformations in LULC not only reshape landscapes but also intensify global challenges such as climate change, biodiversity loss, and broader environmental crises (Bairwa et al., 2025).

LULC effects and dynamics vary from one region to another according to the type of vegetation cover and activities (Mesmin et al., 2025). Land use and land cover changes (LULCCs), driven by deforestation, forest degradation, and the expansion of human activities - such as agriculture, infrastructure development, and fuelwood extraction - have historically led to widespread land cover loss on both local and global scales (Nkinda et al., 2025). These changes have an impact on a wide range of environmental and landscape attributes, including the quality of water, land and air resources, ecosystem processes and function, and ecosystem quality (Yogesha et al., 2025; Shastri et al., 2020).

Changes in land cover and land use caused by human activities have modified the plant cover (Valea, 2024), forest ecosystems (Prăvălie et al., 2022), deforestation can lead to excessive soil erosion (Nigussie et al., 2025) and even landslide occurrence (Jurchescu et al., 2023).

Protected areas were "invented" and then established all over the world in order to protect the most outstanding values of biological and geological diversity, as well as exceptional cultural values.

The management of protected areas must ensure measures to prevent threats that may

destroy them in the future and if they can reduce the effects of the many pressures that exist today.

The development of urbanization around the world may have a negative impact on some existing plant and animal species (Ives et al., 2016). Nature plays an important role for human health, therefore measures must be taken to preserve biodiversity (Kowarik et al., 2020).

Biodiversity must be approached in relation to the characteristics of the urban and rural environment, plants, animals, the interaction and the pressure people put on nature for their own existence (Elmqvist et al., 2013; Opoku, 2019; Güneralp & Seto, 2013; Aronson et al., 2014).

The role of protected areas in conserving biodiversity and landscape is very important due to global environmental changes and climate change. For an adequate management there is a need to create corridors to link them in order to reduce human impact (Geacu et al., 2012).

In the context of sustainable development of cities and rural communities, it is necessary to find solutions to stop the loss of plant and animal species and maintain restore biodiversity.

Land use change is one of the issues which intensifies environmental problems because of the growing demand for natural capital and the increasingly anthropogenic interference; it threatens ecosystems on which human livelihoods rely upon. So, understanding the magnitude of land use change, drivers, and implications is very crucial in a successful management of land resource (Mekonnen, 2025).

MATERIALS AND METHODS

Study area

The Olteț Piedmont, located in the eastern subunit of the Getic Plateau, represents a geomorphological unit strongly influenced by both morphodynamic processes and anthropogenic activities dating back to the 17th-19th centuries. The region covers approximately 3,771 km² and has a predominant north-south orientation (Figure 1). Intensified human impact, particularly from the late 19th to the early 20th century, disrupted the natural balance through widespread deforestation to create land for cereal crops, orchards, vineyards, pastures, hayfields, as well as through the expansion of rural and urban settlements.

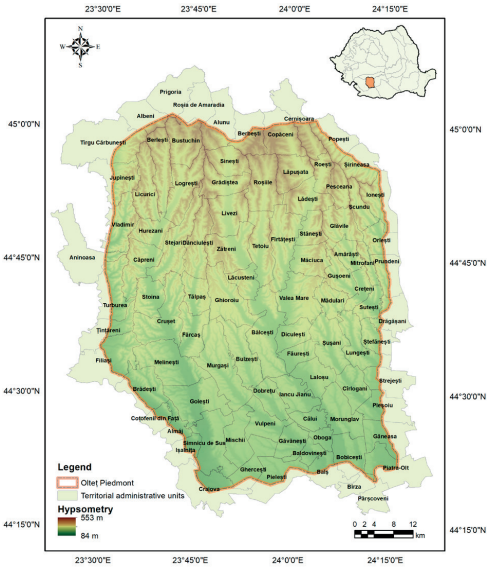


Figure 1. Study area - Olteț Piedmont (Romania)

During the past century, the Romanian agricultural lands underwent deep transformations primarily under the impact of political and socio-economic factors and less, of the biophysical and climatic ones (Bălteanu & Popovici, 2010; Popovici et al., 2013).

Given the major and ongoing spatial, structural and functional transformations of the post-communist period, a substantial body of literature has focused on the social and economic consequences of the Land Reform of 1991 (Urșanu et al., 2024; Dogaru et al., 2024). This reform (Law no. 18/1991) shifted the ownership of land from state to private individuals, small-scale farms appearing and fragmenting the agricultural land, which in time became vulnerable to anthropogenic pressure and climate changes (Prăvălie et al., 2021).

For monitoring land dynamics, the CORINE Land Cover (CLC) project, initiated in 1985, provides a harmonized inventory of land cover across Europe, structured into 44 classes. Building on this, the Copernicus Land Monitoring Service (CLMS), launched in 2012

by the European Environment Agency (EEA) and the European Commission's DG Joint Research Centre, supplies geospatial information on land cover and land-use changes, vegetation state, the water cycle, and Earth surface energy variables for a wide range of terrestrial applications.

In this study, we employed land use/land cover (LULC) databases provided by the EEA for the years 2012 and 2018. This period was selected as it captures the most significant changes in LULC, largely driven by anthropogenic activities. Notably, rising living standards spurred the rapid urbanization of rural areas near cities, where populations increasingly purchased land for residential purposes, particularly secondary homes used on weekends as retreats from urban environments.

Additionally, shapefiles of Romania's natural protected areas were obtained from the Ministry of Environment, Waters and Forests, along with management plans and other relevant data for the five protected areas located within the Olteț Piedmont. These sites were declared under the provisions of OUG 57/2007 and Law 5/2000. Using ArcGIS 10.7, the data for the study area were extracted (via the *Clip* feature), enabling a detailed analysis of how LULC changes affect these protected natural areas.

RESULTS AND DISCUSSIONS

The classified LULC categories comprised built-up areas, farmland, bare land, grassland, forests, wetlands, shrubland, and water bodies. Using ArcGIS 10.7, we extracted and reclassified 21 land use/land cover categories identified within the Olteț Piedmont. The results were represented through cartographic outputs (Figures 2 and 3) for the two reference years of the study, 2012 and 2018.

The period between 2012 and 2018 is marked by major changes in several land use categories (Table 1). Notably, there was a significant reduction in the areas occupied by vineyards (−8,150 ha), orchards (−2,400 ha), watercourses (−700 ha), beaches, dunes, and sand plains (−140 ha), as well as inland marshes (−40 ha). The decline observed in the latter three categories can largely be attributed to flood protection works implemented along most rivers crossing the piedmont.

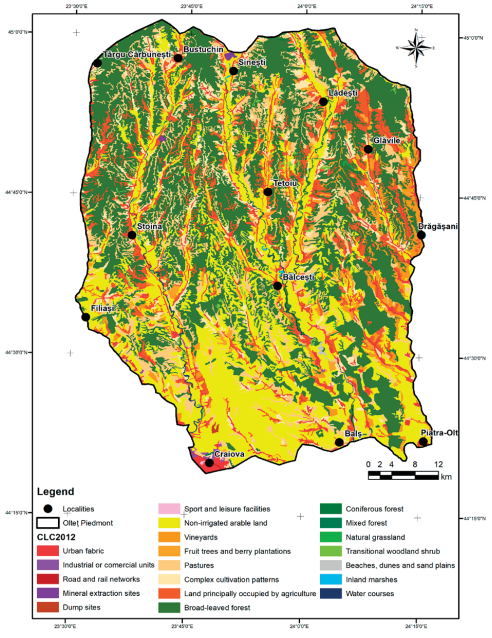


Figure 2. Olteț Piedmont - Corine Land Cover, 2012

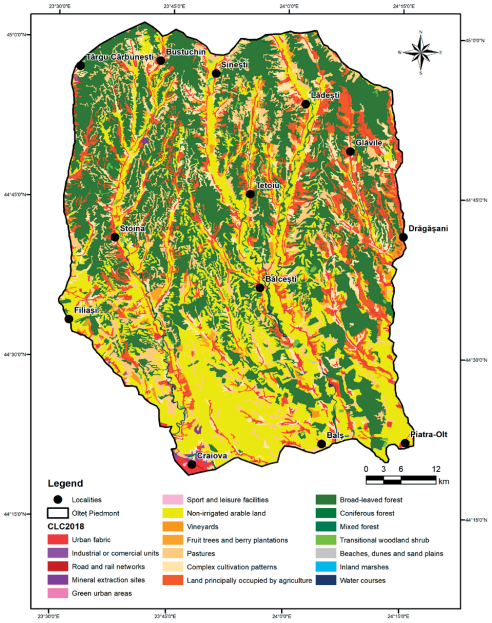


Figure 3. Olteț Piedmont - Corine Land Cover, 2018

The terrains occupied by vineyards and orchards were transformed mainly into areas with complex crops (+4350 ha), deciduous forests (+2900 ha) and transitional woodland shrub (+750 ha). Also, the built-up surface

increased by 610 ha, mainly by the extension of urban areas around major cities like Craiova, Filiași, Balș and Drăgășani.

The constant depopulation of the rural areas within the Olteț Piedmont and the expansion of the periurban areas around major cities have influenced the major changes in land use/land cover between 2006 and 2018. These changes affect not only its population but also the environment.

The influence of human activities has been manifested in all geographical regions of Romania. These have significantly influenced the rate, intensity and pattern of land use/cover changes. Important agricultural areas in the Romanian Plain have become fragmented and gradually abandoned but also subjected to (sub)urbanization processes (Urșanu (Popovici) et al., 2024).

Land use has been seriously influenced by urbanization and by the conversion from one category to another. This has led to the degradation of vegetal associations, the almost destruction of the wild flora and fauna in areas suitable to cultivation (Popovici et al., 2010).

Tabel 1. Land use in the Olteț Piedmont between 2012 and 2018

Land use	Area 2012 (ha)	Area 2018 (ha)
Urban fabric	18105.71	18715.64
Industrial or commercial units	578.45	643.63
Road and rail networks	130.84	130.62
Mineral extraction sites	277.95	237.79
Dump sites	151.62	-
Green urban areas	-	4.40
Sport and leisure facilities	37.44	37.44
Non-irrigated arable land	106522.92	107085.46
Vineyards	12551.88	4370.34
Fruit trees and berry plantations	7894.80	5492.06
Pastures	36379.22	36750.09
Complex cultivation patterns	19823.28	24170.46
Land principally occupied by agriculture	31274.33	33208.10
Broad-leaved forest	139633.92	142516.62
Coniferous forest	142.25	142.25
Mixed forest	53.88	53.88
Natural grassland	96.08	-
Transitional woodland shrub	1257.81	2070.48
Beaches, dunes and sand plains	213.26	77.26
Inland marshes	126.49	85.48
Water courses	1903.59	1363.71

The southern part of Romania was continuously exposed to strong human pressure since early times through extensive/intensive agricultural use, industrialization, urbanization/suburbanization processes. Therefore, the primeval vegetation has been massively transformed, and forests have been significantly fragmented and reduced to even smaller surface (Geacu et al., 2018).

In the study area there are 5 natural protected areas - 3 of national interest and 2 Natura2000 sites (Figure 4): 2.451 Locul fosilifer Valea Desului (1 ha), 2.796 Pădurea Tisa Mare (50 ha), 2.797 Pădurea Silea (25 ha), ROSCI0168 Pădurea Sarului (6768 ha) and ROSCI0296 Dealurile Drăgășaniului (7265 ha).

The International Union for Conservation of Nature (IUCN) defines a protected area as "a clearly delimited geographical space, recognized, designated and managed on the basis of legal acts or by other effective means, with the aim of achieving the long-term conservation of nature as well as of environmental services and associated cultural values".

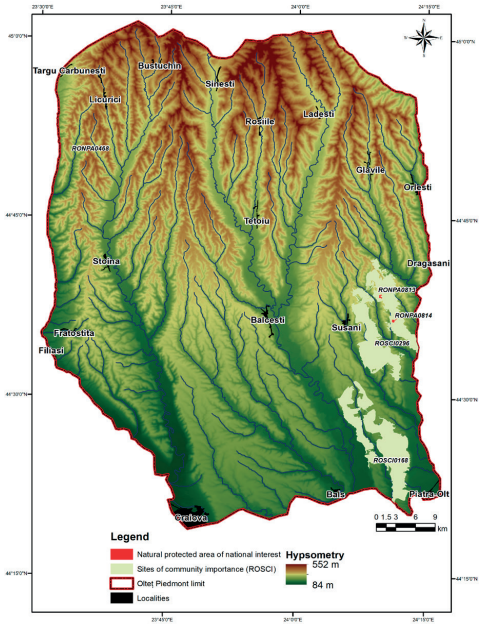


Figure 4. Olteț Piedmont - natural protected areas

Protected areas must guarantee and allow the following:
- conservation of biodiversity by maintaining within the perimeter of protected areas some species and ecosystems in their natural or very close to natural state;
- scientific substantiation of management methods and procedures that allow for the sustainable use of natural resources;
- scientific substantiation of the process of reconstruction and rehabilitation of ecological systems;
- maintenance of ecological services by conserving ecosystems;
- protection of cultural values and landscapes.

2.451 Locul fosilifer Valea Deșului fossil site is a protected area of national interest corresponding to IUCN category IV (paleontological nature reserve), protecting remains of Levantine fossil fauna.

2.796 Pădurea Tisa Mare is a protected natural area corresponding to IUCN category IV (mixed nature reserve) and represents a protection zone for trees of the species sessile oak (*Quercus petraea*) and hornbeam (*Carpinus betulus*) and shrubs of the species tulichine (*Daphne mezereum*) or thorn (of the species *Ruscus aculeatus*).

2.797 Silea Forest is a protected natural area that corresponds to IUCN category IV (mixed nature reserve) and represents the forested area on the two banks of the Silea stream that preserves natural habitats with tree species of sessile oak (*Quercus petraea*) and hornbeam (*Carpinus betulus*), as well as a rare shrub species, known as thorn (*Ruscus aculeatus*).

ROSCI0296 Dealurile Drăgășaniului includes 3 types of protected habitats: 9130, 91M0 and 91Y0.

ROSCI0168 Pădurea Sarului includes only 1 type of protected habitat, 91M0.

These protect a large number of species of conservation importance: over 30 species of mammals, over 90 species of birds, 1 species of plant and 8 species of amphibians and reptiles.

The important changes in land use and the constant increase in urbanization can have a major impact on these natural protected areas by: the use of pesticides and chemical fertilizers in agriculture, in the vicinity of these areas, the existence and spread of invasive plants and water pollution with plastic, glass, household or construction waste. Also, illegal deforestation and poaching represent a major threat to the integrity of natural protected areas.

We have managed to identify the main anthropogenic activities that may have a negative impact:
- harvesting of wild animals (legal/poaching);
- harvesting of mushrooms and berries;
- harvesting of live snails;
- logging activities (legal/illegal) in the funds managed by the Forest Districts;
- development of water and wastewater infrastructure;
- reconstruction works of communal roads, which cross protected natural areas.

These pressures and threats to which protected natural areas are subject must be considered when we study how land use/land cover changes affect the environment because they are an integrant part of a sustainable development for the population in this area.

CONCLUSIONS

The environment constitutes an essential prerequisite for human existence, so its protection and conservation is very important.

The predominance of agricultural activities in the southern part of the Olteț Piedmont, mainly in the rural localities, had a major impact in the land use changes that occurred in the last 20 years.

The major changes in land use, especially after 2012, have put a great pressure on the environment, modifying the landscape and making it more vulnerable to the effects of human activities and even climate change.

To preserve the protected habitats and species in these natural protected areas, administrators and decision-makers should consider the following measures:

- limit the use of pesticides and fertilizers in the vicinity of these sites and using insecticides only in the affected areas, not preventively;
- use of biological control as much as possible and preserve natural regulation mechanisms;
- limit access into the forest only on arranged trails and carrying out picnics and open fires only in designated areas;
- stop illegal deforestation;
- preserve, especially near wetlands, fallen trees or stumps, to boost the biological activity of insects;
- carry out actions to sanitize temporary ponds and waters within the perimeter of these sites;
- preserve open forest areas with shrub and grass vegetation, etc.
- prevent and stop activities with potential negative effects on the natural and cultural values in the protected areas;
- informing and raising awareness among stakeholders and the general public about the importance of biodiversity conservation, by promoting sustainable development models and involving local communities in the management of protected areas.

Future studies should focus on the effectiveness of protected natural areas management and minimizing anthropogenic impact on their territory in order to achieve a better conservation and protection.

REFERENCES

Aronson, M. F. J., La Sorte, F. A., Nilon, C. H., Katti, M., Goddard, M. A., Lepczyk, C. A., Warren, P. S., Williams, N. S. G., Cilliers, S., Clarkson, B., et al. (2014). A global analysis of the impacts of urbanization on bird and plant diversity reveals key anthropogenic drivers. *Proceedings of the Royal Society B: Biological Sciences, 281*(1780), 2013330. https://doi.org/10.1098/rspb.2013.3330

Bălteanu, D., & Popovici, E. A. (2010). Land use changes and land degradation in post-socialist Romania. *Romanian Journal of Geography, 54*(2), 95–107.

Bairwa, B., Sharma, R., Kundu, A., Sammen, S. Sh., Alshehri, F., Pande, C. B., Orban, Z., & Salem, A. (2025). Predicting changes in land use and land cover using remote sensing and land change modeller. *Frontiers in Environmental Science, 13*, 1540140. https://doi.org/10.3389/fenvs.2025.1540140

Dogaru, D., Petrișor, A. I., Angearu, C. V., Lupu, L., & Bălteanu, D. (2024). Land governance and fragmentation patterns of agricultural land use in Southern Romania during 1990–2020. *Land, 13*(6), 1084. https://doi.org/10.3390/land14071473

EEA (European Environmental Agency). (2012, 2018). *Copernicus land monitoring service – Corine land cover*. https://land.copernicus.eu/pan-european/corine-landcover

Elmqvist, T., Fragkias, M., Goodness, J., Güneralp, B., Marcotullio, P. J., & McDonald, R. I. (2013). *Urbanization, biodiversity and ecosystem services: Challenges and opportunities – A global assessment*. Springer.

Geacu, S., Dumitrașcu, M., & Maxim, I., (2012). The evolution of the natural protected areas network in Romania. *Revue Roumaine de Géographie/Romanian Journal of Geography, 56*(1), 33–41.

Geacu, S., Dumitrașcu, M., & Grigorescu, I. (2018). On the Biogeographical Significance of Protected Forest Areas in Southern Romania. *Sustainability, 10*(7), 2282. https://doi.org/10.3390/su10072282

Güneralp, B., & Seto, K. C. (2013). Futures of global urban expansion: Uncertainties and implications for biodiversity conservation. *Environmental Research Letters, 8*(1), 014025. https://doi.org/10.1088/1748-9326/8/1/014025

Ives, C. D., Lentini, P. E., Threlfall, C. G., Ikin, K., Shanahan, D. F., Garrard, G. E., Bekessy, S. A., Fuller, R. A., Mumaw, L., Rayner, L., et al. (2016). Cities are hotspots for threatened species. *Global Ecology and Biogeography, 25*(1), 117–126. https://doi.org/10.1111/geb.12404

International Union for Conservation of Nature (IUCN). (n.d.). Retrieved August 19, 2025, from https://iucn.org/

Jurchescu, M., Kucsicsa, G., Micu, M., Bălteanu, D., Sima, M., & Popovici, E.-A. (2023). Implications of future land-use/cover pattern change on landslide susceptibility at a national level: A scenario-based analysis in Romania. *CATENA, 231*, 107330. https://doi.org/10.1016/j.catena.2023.107330

Kowarik, I., Fischer, L. K., & Kendal, D. (2020). Biodiversity conservation and sustainable urban development. *Sustainability, 12*(12), 4964. https://doi.org/10.3390/su12124964

Laha, M. (2023). Change detection analysis using Landsat images on Balurghat Municipality, West Bengal, India. *Forum geografic, XXII*(1), 67–77. https://doi.org/10.5775/fg.2023.022.i

Legea nr. 5/2000 privind aprobarea Planului de amenajare a teritoriului național – Secțiunea a III-a – zone protejate. (2000). *Monitorul Oficial al României*. https://legislatie.just.ro/Public/DetaliiDocument/21860

Ministerul Mediului, Apelor și Pădurilor. (n.d.). *Arii naturale protejate de interes național și internațional*. https://mmediu.ro/portal-gis/date-spatiale/arii-naturale-protejate-de-interes-national-si-international

Mekonnen, A. (2025). Land use and land cover change analysis in Choke Mountain, Ethiopia (2013–2023). *Asian Journal of Environmental Research, 2*(2), 189–205. https://doi.org/10.69930/ajer.v2i2.343

Mesmin, T., Frédéric, S., Eric, V., Fendoung, P. M., Makak, R. N., Ismaël, I., & Frédéric, S. T. (2025). Land use and land cover changes in the Centre Region of Cameroon. *Journal of Advance Research in Social Science and Humanities, 10*(9), 36–70. https://doi.org/10.61841/ta2n8a56

Nkinda, R., Ojija, F., Bacaro, G., & Malunguja, G. (2025). Land-use/land-cover change in the Ngerengere River Catchment, Tanzania: Insights from 2004 to 2034. *Asian Journal of Water, Environment and Pollution*. https://doi.org/10.36922/AJWEP025180137

Opoku, A. (2019). Biodiversity and the built environment: Implications for the Sustainable Development Goals (SDGs). *Resources, Conservation and Recycling, 141*, 1–7. https://doi.org/10.1016/j.resconrec.2018.10.011

Ordonanță de urgență nr. 57/2007 privind regimul ariilor naturale protejate, conservarea habitatelor naturale, a florei și faunei sălbatice. (2007). *Monitorul Oficial al României*. https://legislatie.just.ro/Public/DetaliiDocument/83289

Prăvălie, R., Patriche, C., Borrelli, P., Panagos, P., Roșca, B., Dumitrașcu, M., Niță, I.-A., Săvulescu, I., Birsan, M.-V., & Bandoc, G. (2021). Arable lands under the pressure of multiple land degradation processes: A global perspective. *Environmental Research, 194*, 110697. https://doi.org/10.1016/j.envres.2020.110697

Prăvălie, R., Sîrodoev, I., Niță, I.-A., Patriche, C., Dumitrașcu, M., Roșca, B., Tișcovschi, A., Bandoc, G., Săvulescu, I., Mănoiu, V., & Birsan, M.-V. (2022). NDVI-based ecological dynamics of forest vegetation and its relationship to climate change in Romania during 1987–2018. *Ecological Indicators, 136*, 108629. https://doi.org/10.1016/j.ecolind.2022.108629

Popovici, E. A., Bălteanu. D., Dumitrașcu. M., & Sima. M. (2010). Land use and human pressure in the Getic Piedmont. *In Proceeding of BALWOIS, Conference on Water Observation and Information Systems for Decision Support*, Ohrid, Macedonia.

Popovici, E. A., Bălteanu, D., & Kucsicsa, G. (2013). Assessment of changes in land-use and land-cover pattern in Romania using Corine land cover database. *Carpathian Journal of Earth and Environmental Sciences, 8*(4), 195–208.

Phuong, V., & Thien, B. (2023). A multi-temporal Landsat data analysis for land-use/land-cover change in the Northwest mountains region of Vietnam using remote sensing techniques. *Forum geografic, XXII*(1), 54–66. https://doi.org/10.5775/fg.2023.030.i

Shastri, S., Singh, P., Verma, P., Rai, P., & Singh, A. (2020). Assessment of spatial changes of land use/land cover dynamics, using multi-temporal Landsat data in Dadri Block, Gautam Buddh Nagar, India. *Forum geografic, XIX*(1), 72–77. https://doi.org/10.5775/fg.2020.063.i

Urşanu (Popovici), E. A., Grigorescu, I., Dumitrică, C., Kucsicsa, G., Mitrică, B., Roznovietchi (Mocanu), I., Dumitrașcu, M., & Ciubuc, C. (2024). Long-term changes of agricultural land over the last century in Romania: The showcase of Romanian plain. *Anthropocene, 48*, 100449. https://doi.org/10.1016/j.ancene.2024.100449

Urşanu, E. A., Grigorescu, I., & Roznovietchi, I. (2024). Land reform catalysts of capitalism and communism: 150 years of agricultural change in Romania. *Journal of Historical Geography, 86*, 326–340. https://doi.org/10.1016/j.jhg.2024.10.013

Valea, F. (2024). Spatio-temporal dynamics of land use and land cover in the commune of Po, Burkina Faso. *Forum geografic, XXIII*(2), 245–255. https://doi.org/10.5775/fg.2024.2.3641

Yogesha, D. S., Sandeep, N., & Umesh, C. (2025). Assessing the land use/land cover changes due to urbanization in Mangalore, Karnataka, India. *International Journal of Environmental Sciences, 11*(8s), 891–903. https://doi.org/10.64252/w570hc50

Scientific Papers. Series E. Land Reclamation, Earth Observation & Surveying, Environmental Engineering. Vol. XIV, 2025
Print ISSN 2285-6064, CD-ROM ISSN 2285-6072, Online ISSN 2393-5138, ISSN-L 2285-6064

A CRITICAL REVIEW OF SUSTAINABLE APPROACHES FOR REDUCING THE ENVIRONMENTAL IMPACT OF PLASTIC PRODUCTION

Andreea DOROFTE[1], Ira-Adeline SIMIONOV[1, 2], Ștefan-Mihai PETREA[1, 2], Cătălin PLATON[3], Puiu-Lucian GEORGESCU[1, 4], Cătălina ITICESCU[1, 4]

[1]"Dunărea de Jos" University of Galați, REXDAN Research Centre,
98 George Coșbuc Blvd, 800223, Galați, Romania
[2]"Dunărea de Jos" University of Galați, Faculty of Food Science and Engineering,
111 Domnească Street, 800201, Galați, Romania
[3]ROMFISH National Fish Farmers Association, 12 Nicolae Iorga Blvd, 700583, Iasi, Romania
[4]"Dunărea de Jos" University of Galați, Faculty of Sciences and Environment,
111 Domnească Street, 800201, Galați, Romania

Corresponding author email: andreea.dorofte@ugal.ro

Abstract

The production of plastics in the context of global warming contributes to water pollution by microplastic particles. Consequently, a shift towards sustainable practices in the field of plastic production is crucial. This paper aims to address the main concerns related to plastic and microplastic pollution and to identify environmentally sustainable strategies applied in the production sector. A particular focus is placed on biodegradable, eco-friendly materials as alternatives to conventional plastics, with an emphasis on their environmental impact. For example, food waste has emerged as a promising alternative for plastic packaging production, offering a sustainable solution, valorization of by-products, and mitigating environmental impacts. The paper also focuses on the potential of using waste to create biodegradable materials, highlighting the importance of a zero-waste approach to enhance the economic value of by-products, while promoting a cleaner environment and waste management presented in environmental contexts. Through its comparative analysis, this study contributes to a deeper understanding of waste management and supports the advancement of a sustainable circular economy.

Key words: *biodegradable, by-products, microplastics, pollution, sustainable.*

INTRODUCTION

Conventional plastics made from petroleum have a significant impact on the environment, contributing to water pollution, global warming, resource depletion, and the spread of microplastics. This makes the search for durable and sustainable alternatives increasingly critical (Mutmainna et al., 2025; Saleem et al., 2023). Alarmingly, plastic pollution is now ubiquitous - plastic particles have been discovered in the deep sea, rainwater, and even in the human placenta and bloodstream (Stoett et al., 2024). Although the stability of conventional plastics is often cited as an advantage (Xuyang et al., 2025), it also becomes a major drawback due to their persistence and accumulation in the environment.

Globally, the average plastic consumption per person is 20.9 kg per year (Khan et al., 2025), with production projected to rise from 464 Mt in 2020 to 884 Mt by 2050 (Dokl et al., 2024). Equally concerning is that approximately 79% of plastic waste ends up either in landfills or the natural environment, while only 9% is recycled and 12% is incinerated (Kumar M. et al., 2024; Wojnowska-Baryła et al., 2022). Plastics derived from fossil fuels (crude oil, gas, and coal) are a substantial environmental threat, not only due to their long lifespan but also because they emit greenhouse gases, contributing to global temperature rise (Nicholson et al., 2021; Sharma et al., 2023).

Microplastics (MPs), defined as plastic particles smaller than 5 mm, are formed through the gradual degradation of larger plastic items, typically triggered by ultraviolet (UV) radiation (Lee et al., 2025; Niu et al., 2024; Xuyang et al., 2025). Microplastics are a complex pollutant, ubiquitous in freshwater, with negative effects

that can affect the function and health of the entire ecosystem (Garfansa et al., 2025). MP can enter rivers through sources such as atmospheric deposition, surface runoff, in-stream activities, and wastewater discharge (Graham et al., 2024). Also, river receive MP from direct dumping of garbage, the confluence of small streams into the main river, effluents from the cosmetic and textile industries and fishing activities, rivers contribute about 80% of ocean pollution. Rivers also discharge 1.6- 2.3 MMT of MP into the ocean annually (Choudhary et al., 2025). Filtration methods using materials such as sand or activated carbon materials are applied in municipal wastewater treatment to remove MPs. MPs removal efficiency varies depending on particle size, adhesion to the surface of the filter medium, and filtration technique (Garfansa et al., 2025). However, these techniques are largely ineffective at removing MPs, allowing them to continue threatening aquatic environments (Lee et al., 2025; Niu et al., 2024).

In recent years, global attention has increasingly focused on the circular plastic economy and sustainable development. A truly sustainable approach seeks to meet the needs of the present without compromising the resources of future generations - one of the core objectives of of waste management and supports progress toward a sustainable circular economy.

IMPACT OF PLASTIC POLLUTION: ENVIRONMENTAL SIGNIFICANCE AND HUMAN HEALTH

Plastics pose a serious threat to ecosystems, biodiversity, and human health, while also contributing to climate change (Schmidt et al., 2024). Popa et al. (2015) observed that the anthropogenic footprint on the water quality of the Danube, was highlighted in the summer, under the action of the human, trophic factor and the impact of anthropogenic activities. MPs are considered emerging pollutants of increasing concern due to their ubiquitous presence and toxic potential in the aquatic ecosystem (Călmuc et al., 2022).

Water resource management is a major issue, being a very important transporter of pollutants (Pintilie et al., 2016), rivers contributing to approximately 80% of plastic pollution in the oceans, and 20% coming from marine activities sustainable development (Xuyang et al., 2025). Poor plastic waste management exacerbates environmental degradation and health hazards while also contributing to climate change (Roy & Chakraborty, 2024). The growing interest in bio-based alternatives, particularly in the food industry, reflects a shift toward sustainable, efficient, and safer packaging systems compared to those made from petroleum-derived polymers (Dorofte et al., 2023). Biodegradable plastics are now applied across various sectors, and even oil-producing nations are supporting initiatives that promote circularity within the plastic economy (Fei et al., 2024; Saxena, 2025).

The aim of this study is to provide a critical perspective on replacing petroleum-based plastics with sustainable alternatives, while promoting the circular economy and principles of sustainable development. This review offers a comprehensive synthesis of the current literature on the environmental impacts of plastics, as well as strategies for leveraging natural resources and waste to produce biodegradable materials. Emphasis is placed on the zero-waste approach, which adds economic value to by-products and fosters improved waste management. Through a comparative and critical lens, the study enhances understanding (Kumar M. et al., 2024). MPs enter the aquatic environment through wastewater discharges, industrial operations, excessive vehicle use, and human activities (Xuyang et al., 2025). Population and distance from residential areas influence the effects of anthropogenic activity on MPs abundance, urban lakes being more affected by MPs contamination than rural lakes (Anagha et al., 2023; Pierdomenico et al., 2024). China currently records the highest level of surface water microplastic pollution globally, with a concentration of 34 MP/L detected in Lake Poyang (Tran-Nguyen et al., 2024).

In Romania, areas near the confluence of the Siret and Prut rivers with the Danube show particularly high pollutant concentrations, largely due to agricultural and industrial activity and the absence of effective water treatment systems (Iticescu et al., 2014). In marine environments, plastics reduce light and oxygen levels, diminishing biodiversity and affecting marine life through ingestion, suffocation and reduced mobility (Roy & Chakraborty, 2024). Plastics facilitate the bioaccumulation of heavy

metals in aquatic systems. Heavy metals, after being released from microplastics, enter the food chain, accumulating in fish and subsequently affecting human health through biomagnification processes (Bolea et al., 2025). The ecotoxicological effects of MP depend on concentration, types, degradation process, environmental longevity and specific organisms affected (Shi et al., 2024). The presence of MPs has been reported in human saliva, feces, and blood (Saleem et al., 2023). MPs contain harmful chemicals, such as phthalates, bisphenol A (BPA), which can disrupt hormone regulation, interfere with reproductive health and increase the risk of cancer, developmental disorders, and have adverse effects on the immune, nervous, and cardiovascular system (Roy & Chakraborty, 2024; Schmidt et al., 2024). MPs generate toxicity in living organisms by disrupting the defense mechanism against oxidative stress, genotoxicity, neurotoxicity, growth and metabolic diseases, but they can also be vectors of transport in aquatic ecosystems by adsorbing potentially toxic elements (mercury, cadmium, lead and aluminum, copper, nickel, zinc, chromium or arsenic) on their surface (Kumar et al., 2024; Simionov et al., 2023). Exposure and accumulation of heavy metals in the human body has been linked to cognitive impairment, endocrine disruption, developmental abnormalities, and cancer (Simfukwe et al., 2025). As a result, bioplastics have emerged as a promising alternative, offering the potential to mitigate both health risks and environmental degradation associated with conventional plastic use (Kumar et al., 2024).

Biodegradation in soil is considered the best option due to the microorganisms present in the environment. Biodegradation in aquatic environments is usually more complex and limited due to nutrient content, temperature, pH, microbial diversity and density, which reduce the biodegradation capacity of bioplastics (Negrete-Bolagay & Guerrero, 2024).

Biodegradation is a process that depends largely on environmental conditions, such as temperature, humidity, pH, and many other abiotic factors. Biodegradable plastics show mass losses of 23-100%, with higher degradation efficiencies than petroleum- based plastics. PLA biodegradation is complete within 1-3 months in marine environments in Hong Kong, but not all bioplastics degrade completely in these marine environments. Fragmentation of biodegradable plastics requires special attention as it can contribute to microplastic pollution, which is a challenge for in situ studies as the fragments may be too small to be recovered or further biodegraded (Cheung & Not, 2024). Microplastics generated by incomplete biodegradation of biodegradable plastics may persist in environments, affect aquatic microbial communities, plant adaptability, and animal physiology, with their toxicity increasing upon degradation, but knowledge of the effects of biodegradable microplastics, in the aquatic environment remains limited (Shi et al., 2024).

CONVENTIONAL PLASTIC

Conventional plastics, also referred to as petroleum-based, are the most widely used form of plastic. They exist in various physical forms - such as fragments, foams, films, fibers, filaments, pellets, spheres, and particles - and come in a wide range of colors, including red, green, blue, white, transparent, black, and yellow (Chen et al., 2024; de Deus et al., 2024). Depending on size, there are five distinct categories of plastics: nanoplastics (< 0.001 mm), microplastics (0.001-5 mm), mesoplastics (5-25 mm), macroplastics (> 25 mm) and megaplastics (> 1 m) (de Deus et al., 2024).

Microplastics (MPs) are further classified by origin: *primary MPs* are manufactured intentionally for industrial or domestic applications, while *secondary MPs* result from the degradation of larger plastic debris, often due to improper waste disposal or environmental breakdown (Acarer, 2023; Xuyang et al., 2025; Zhuo et al., 2024).

Packaging accounts for approximately 40% of global plastic production, with 60% of that used specifically for food and beverage applications (Ceballos-Santos et al., 2024). Conventional plastics such as polyvinyl chloride (PVC), polypropylene (PP), polystyrene (PS), polyethylene terephthalate (PET or PETE), low-density polyethylene (LDPE) or high-density polyethylene (HDPE) contain additives (stabilizers, plasticizers, foaming agents, colorants, etc.) which, although improving the properties of the material, are known to be

endocrine disruptors and carcinogens (Rajvanshi et al., 2023). Additionally, many plastics contain environmentally harmful compounds such as flame retardants, phthalates, bisphenol A (BPA), and heavy metals (e.g., lead and cadmium), which can leach into the soil, contaminate ecosystems, and bioaccumulate in living organisms (Martínez-Narro et al., 2024).

Conventional plastics are advantageous for storage, use and transport, but not for disposal, as they degrade slowly, in approximately 500 years (Martínez-Narro et al., 2024). Currently, petroleum-based plastics are more cost-effective than those derived from renewable sources, but when external costs and future optimization are taken into account, the price of fossil-based polymers is expected to increase by 44% compared to bio-based polymers (Jiao et al., 2024).

In terms of environmental impact, conventional MPs degrade slowly and thus have a lower immediate impact on soil microorganisms; however, this same persistence increases their potential for long-term bioaccumulation and toxicity in soil fauna (Fei et al., 2024). Although petroleum-based plastics are known for their accessibility, durability, and adaptability, their widespread use continues to fuel the generation of persistent environmental pollutants and the ongoing accumulation of plastic waste (Jiao et al., 2024).

BIOPLASTIC, AN ALTERNATIVE TO CONVENTIONAL PLASTICS: SUSTAINABLE STRATEGIES

Recognizing the complexity and emerging concerns surrounding biodegradable microplastics, it is important to understand their impact on the environment (Shi et al., 2024). Bioplastics are polymers derived from natural or renewable sources that can be either *biodegradable* or *non-biodegradable* (Kumar et al., 2024). Importantly, bioplastics are not exclusively based on biological sources; they may also originate from fossil fuels. As such, there are four main categories (Jiao et al., 2024; Vigneswari et al., 2024):

- Bio-based biodegradable;
- Bio-based non-biodegradable;
- Fossil-based biodegradable;
- Fossil-based non-biodegradable.

Not all bioplastics are entirely composed of natural materials or guaranteed to be biodegradable. Therefore, understanding their classification is essential when evaluating their environmental benefits. An overview of the major classes of bioplastics is presented in Figure 1, which summarizes their source materials and degradation characteristics.

The four major bioplastic categories include:

- Bio-based biodegradable bioplastics such as polylactic acid (PLA), polyhydroxyalkanoates (PHA), polyhydroxybutyrate (PHB), and starch blends.
- Fossil-based biodegradable bioplastics such as poly(butylene adipate-co-terephthalate) (PBAT), polycaprolactone (PCL), poly(butylene succinate) (PBS), poly(butylene succinate-co-adipate) (PBSA), and polyvinyl alcohol (PVA).
- Bio-based non-biodegradable bioplastics including bio-based polyethylene (PE), polyethylene furanoate (PEF), polytrimethylene terephthalate (PTT), and polyethylene terephthalate (PET).

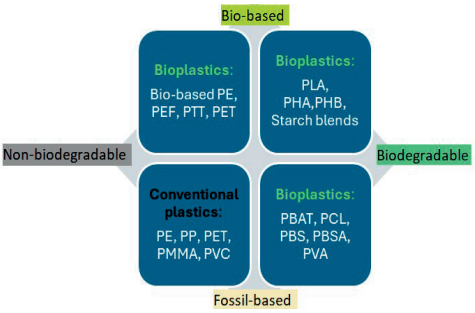


Figure 1. Classification of plastics based on their origin and degradability. Adapted from Shi et al. (2024) and Vigneswari et al. (2024)

In line with current trends, the development of eco-friendly plastics increasingly focuses on low-cost and renewable raw materials as a sustainable alternative to conventional petroleum-based plastics. These bio-based materials show great potential for application across multiple sectors, including packaging, agriculture, and biomedical industries (Rajvanshi et al., 2023).

Table 1 summarizes various biodegradable alternatives to conventional plastics, outlining their applications, key advantages, and limitations.

The primary advantages of bio-based polymers stem from their renewable and low-cost sources. However, cost feasibility is a challenge for the commercial viability of bioplastics. For example, the use of PHA in various applications remains limited due to the high production costs and the high cost of substrates for PHA production (refined carbon origins, sugars, oils, organic acids and fatty acids). Current studies present methods to reduce the cost of PHA production such as the use of renewable substrates, the use of cheaper carbon sources from industries (biodiesel, agriculture, dairy and animal processing). Less expensive substrates for PHA synthesis must be accessible, available in sufficient quantities, stable and resistant to microbial spoilage, and easy to store (Hadri et al., 2025).

Bioplastics derived from biological materials—such as starch, cellulose, vegetable oils, fats, and microorganisms—are generally non-toxic, easier to recycle, and faster to degrade than conventional plastics. They contribute to energy savings, reduce waste volume and landfill space requirements, and help lower greenhouse gas emissions, making them promising solutions due to their abundance and biodegradability (Khan et al., 2025; Mutmainna et al., 2025; Vigneswari et al., 2024).

Table 1. Alternative bio-based for conventional plastics

Biodegradable materials	Advantages	Disadvantages	Applications	References
PLA	Biocompatibility, resistance to fragmentation and good processability, good mechanical properties, simple and rapid degradation mechanism, gas barrier comparable to that of polystyrene and low-density polyethylene (LDPE).	Low degradability in water. Can increase oxidative stress of organisms, cause metabolic disorders, growth limitations; can adsorb heavy metals; higher gas barrier than PET. The cytotoxicity in human cell lines remains limited.	Packaging materials, tissue engineering, drug delivery, 3D printing, face masks.	(Burada et al., 2015; Fei et al., 2024; Hadri et al., 2025; Jiao et al., 2024; Kumar S. et al., 2024; Niu et al., 2024; Rajvanshi et al., 2023; Wen et al., 2025)
PBS	Crystallinity, mechanical performance equivalent to PP/PE, good processability, thermal stability, simple and rapid degradation mechanism.	Requires specific conditions for biodegradation. Weaker mechanical and physical properties. The cytotoxicity in human cell lines remains limited.	Packaging materials, compost bags, biomedical materials and hygiene products.	(Fei et al., 2024; Hadri et al., 2025; Kaur et al., 2025)
PCL	Elastomeric, relatively crystalline and suitable for modification, mechanical properties comparable to other basic plastics.	Requires specific conditions for biodegradation.	Mulch films, tissue engineering, dressings, drug delivery.	(Fei et al., 2024; Hadri et al., 2025; Kaur et al., 2025)
PBAT	High flexibility and toughness, biocompatibility, good processability.	Requires specific conditions for biodegradation. The cytotoxicity in human cell lines remains limited.	Mulch sheets, packaging materials and shopping bags.	(Fei et al., 2024; Mutmainna et al., 2025; Wen et al., 2025)
PHA	Eco-friendly, biocompatible, biodegradable, moisture and heat resistant, good gas barrier properties, rigid.	Requires specific conditions for biodegradation.	Packaging, bags, containers, drug delivery, pens and hygiene products.	(Mutmainna et al., 2025; Vigneswari et al., 2024)
PGA (Polyglycolic acid)	Crystalline, thermal stability, good degradability and biocompatibility.	The cytotoxicity of new degradable polymers in human cell lines remains limited.	Materials for drug delivery and packaging.	(Chia et al., 2020; Hadri et al., 2025; Mogany et al., 2024)

One of the disadvantages of biodegradable MPs is that they can accumulate cadmium, could support certain microbial communities or could inhibit microbial activity, could negatively affect plant adaptability and animal physiology, and their toxicity may increase with their degradation (Shi et al., 2024). In addition, biodegradable plastics require specific conditions for their mineralization (humidity, temperature, pH, oxygen, light and the presence of functional microorganisms) (Rajvanshi et al., 2023), and failure to meet the conditions turns bioplastics into a source of pollution (Shi et al., 2024), with prolonged periods being required for the biodegradation process (Fei et al., 2024). Biodegradable MPs have a higher adsorption capacity and exhibit greater mobility than conventional MPs, thus they promote the transport of contaminants, affecting ecosystems (Fei et al., 2024). Compared to conventional plastics, bioplastics have poorer mechanical and barrier properties, which limits their commercial use (Dorofte et al., 2025; Kumar et al., 2024).

Recent studies also challenge the notion that all bioplastics are inherently biodegradable. They emphasize limitations such as the need for

equivalence in production volumes relative to conventional plastics and the requirement of specific conditions for effective degradation. Nevertheless, microbial degradation technologies offer promising, environmentally friendly avenues for managing bioplastic waste sustainably (Roy & Chakraborty, 2024).

WASTE MANAGEMENT AND FOOD PACKAGING INNOVATION FOR SUSTAINABILITY

Urbanization has led to a significant increase in food waste generation from various sources. In this context, biomaterials derived from food waste have emerged as promising alternatives for plastic production due to their biodegradability, biocompatibility, bio-stability, and biofunctionality. Adopting a zero-waste approach enhances both the sustainability and the economic value of these by-products, while contributing to a cleaner environment through more effective food waste management (Mutmainna et al., 2025).

One such example is vegetable starch, a biodegradable biopolymer presents in various food waste streams, which can be processed into functional, environmentally friendly bioplastics such as PLA (Hadri et al., 2025; Li & Chen, 2024; Mutmainna et al., 2025). Similarly, whey proteins, a by-product of the cheese manufacturing industry, are being utilized to develop biodegradable packaging materials. Their low cost, high biodegradability, flexibility, and neutral taste and aroma make them ideal for food applications (Dorofte et al., 2025).

Waste from the meat and poultry processing industry (bones, blood, eggshells, skin, tendons, etc.) is used to produce polymers such as collagen, chitin, PHA and gelatin, and waste generated from dairy processing, grain processing and fruit and vegetable processing industries are also widely used for PHA production (Rajvanshi et al., 2023). Also, food waste from agriculture, fruits, vegetables and plant by-products (banana peels, pineapple peels, avocado seeds and durian seeds) offer a sustainable solution to reduce plastic pollution (Mutmainna et al., 2025). Other industrial by-products such as glycerol, cellulosic materials, molasses and waste oil are also used as alternative raw materials for bioplastic production (Rajvanshi et al., 2023).

The research trajectory is moving towards new biodegradable and sustainable food packaging solutions as alternatives to conventional packaging, which can provide safe and quality food, so mixing essential oils with bioplastics, alternative to chemical preservatives, is a growing trend for creating antimicrobial films to conventional plastic used as packaging in the food industry (Dorofte et al., 2024; Kumar et al., 2024). Whey films functionalized with essential oils have high potential for use on various foods due to their antimicrobial and antioxidant activities (Lanciu Dorofte et al., 2023). Microbial polymers such as yeast and fungal biomass, exopolymers such as kefiran from kefir culture, bacterial cellulose, gellan and levan, are capable of forming films, being used as packaging materials (Bleoanca et al., 2025).

Despite their benefits, bioplastics derived from plant waste often exhibit inferior mechanical properties compared to conventional plastics. However, these limitations can be mitigated through innovative enhancements, such as the incorporation of materials like chitosan, polyvinyl alcohol (PVA), nanoparticles, or the application of ultrasound treatments, which significantly improve the structural and functional performance of bioplastics (Mutmainna et al., 2025).

CIRCULAR ECONOMY, SUSTAINABILITY AND PLASTIC POLLUTION MANAGEMENT STRATEGIES

Plastic waste management is one of the imperative components of the circular economy concept. This model seeks to transform the traditional linear plastic economy - characterized by a "take, make, dispose" approach - into a more sustainable system by eliminating unnecessary plastic use, fostering innovation, and promoting material recirculation. This transformation aims to reduce plastic leakage into the environment while enhancing long-term sustainability (Mehta et al., 2025).

The efficiency of the circular economy is supported by the integration of recyclable materials and the transition to a circular

economy is a central pillar of European sustainable development to achieve successful European goals (Georgescu et al., 2025). Among its key objectives is tackling plastic pollution by promoting recycling and reducing waste generation (Buruiana et al., 2023).

The linear economy model is one in which products are manufactured, used and disposed of as waste, but the circular approach emphasizes the importance of closing the loop by recycling and reusing at every stage, to create a sustainable system that maximizes resource efficiency and minimizes environmental pollution (Saxena, 2025).

Currently, mechanical recycling is still the main plastic recycling process in Europe (Hsu et al., 2022). Although waste-to-energy processes (pyrolysis and gasification) convert plastic waste into fuels or chemicals, promoting a circular economy, the disadvantage is that they generate carbon, a solid residue often deposited (Khan et al., 2025). Compared to conventional plastics, bioplastics can be completely degraded under controlled conditions, reducing CO_2 emissions. Recycling helps conserve resources, reduce energy consumption and minimize the carbon footprint associated with plastic production (Fayshal, 2024).

However, several barriers hinder the widespread adoption of recycling and circular strategies. These include techno-economic challenges such as the high cost and reduced quality of recycled plastics, as well as legislative, social, and cultural obstacles (Xuyang et al., 2025). An emerging solution is the biodegradation of plastics using microorganisms isolated from landfills, which can break down plastics into carbon dioxide, water, and biomass in an environmentally friendly manner (Hsu et al., 2022; Roy & Chakraborty, 2024).

Although recycling recovers valuable petrochemicals, recycled plastics have disadvantages, such as significant emissions that could be produced during transportation, lower quality compared to new products, and energy consumption. By using bioplastics, reducing the use of unnecessary packaging, and adopting environmentally friendly materials, the negative environmental impact caused by plastics can be effectively mitigated (Jiao et al., 2024).

Circular approach measures such as using reusable products, transforming plastic waste into value-added products to improve socio-economic conditions, or adopting a "zero waste" lifestyle contribute to the transition towards adopting sustainable practices, which is a complex but necessary one (Bertolazzi et al., 2024; Kaplan Sarısaltık et al., 2025; Roy & Chakraborty, 2024).

CONCLUSIONS

Plastic and microplastic pollution in the aquatic environment are one of the most urgent global challenges, as it represents an undeniable threat to marine ecosystems and human health. This study presents an overview of the use of sustainable bioplastics over conventional plastics, with the aim of reducing the total consumption of fossil-based plastics and their waste, minimizing the devastating impact on the environment and mitigating the harmful effects of microplastic pollution.

Implementing sustainable strategies for the use and disposal of synthetic polymers is essential, as these materials are major contributors to environmental contamination through the continuous release of microplastics. While bio-based materials offer a promising solution - being more sustainable, durable, and aligned with the zero-waste approach - their widespread adoption still faces significant hurdles.

Addressing the challenges related to the properties of bioplastics, their costs and their biodegradability are essential for their widespread adoption.

This review highlights both the advantages and limitations of conventional plastics and bio-based alternatives. Future research and innovation in the field of bioplastic development, biodegradation technologies, and circular economy practices will be critical for improving bioplastics' market performance and environmental impact. These efforts will play a pivotal role in tackling the global plastic pollution crisis and in advancing the broader goals of sustainability and circular economy adoption. Based on this review work, the following ideas for future work are recommended: exploring the development of biodegradable plastic formulations with better degradation efficiency in various environments, streamlining the production costs of bio-based

materials, and improving waste management systems.

ACKNOWLEDGEMENTS

This research was supported by the project "Integrated research and sustainable solutions to protect and restore Lower Danube Basin and coastal Black Sea ecosystems" (ResPonSE), contract no. 760010/30.12.2022.

REFERENCES

Acarer, S. (2023). Microplastics in wastewater treatment plants: Sources, properties, removal efficiency, removal mechanisms, and interactions with pollutants. *Water Science and Technology*, *87*(3), 685–710. https://doi.org/10.2166/wst.2023.022

Anagha, P. L., Viji, N. V., Devika, D., & Ramasamy, E. V. (2023). Distribution and abundance of microplastics in the water column of Vembanad Lake–A Ramsar site in Kerala, India. *Marine Pollution Bulletin*, *194*, 115433. https://doi.org/10.1016/j.marpolbul.2023.115433

Bertolazzi, S., Cuttitta, A., & Pipitone, V. (2024). Addressing marine plastic pollution: A systematic literature review. *Current Opinion in Environmental Sustainability*, *68*, 101428. https://doi.org/10.1016/j.cosust.2024.101428

Bleoanca, I., Turturica, M., Aprodu, I., Stan, F., Fetecau, C., & Borda, D. (2025). Influence of Glycerol and Tween on Yeast Films Functionalized with Cinnamon and Lavender Essential Oils. *Coatings*, *15*(2), Article 2. https://doi.org/10.3390/coatings15020118

Bolea, E., Brunetti, L. S., Abad-Alvaro, I., Cellini, E., Ruffolo, S. A., La Russa, M. F., & Laborda, F. (2025). Release of heavy metals during in vitro fish gastrointestinal digestion from microplastics collected at Calabrian coasts. *Marine Pollution Bulletin*, *217*, 118080. https://doi.org/10.1016/j.marpolbul.2025.118080

Burada, A, Topa, C.M., Georgescu, L. P., Teodorof, L, Nastase, C., Seceleanu-Odor, D. & Iticescu, C. (2015). Heavy Metals Environment Accumulation in Somova - Parches Aquatic Complex from the Danube Delta Area; *Revista de chimie*, *66*(1), 48-54.

Buruiana, D. L., Georgescu, P. L., Carp, G. B., & Ghisman, V. (2023). Recycling micro polypropylene in modified hot asphalt mixture. *Scientific Reports*, *13*(1), 3639. https://doi.org/10.1038/s41598-023-30857-9

Călmuc, V. A., Maxim, A., Simionov, I. A., Antache, A., Apetrei, C., Georgescu, P. L. & Iticescu C. (2022). Identification and characterization of plastic particles found in the lower Danube River. *Scientific Papers. Series E. Land Reclamation, Earth Observation Surveying, Environmental Engineering, 11*, Print ISSN 2285-6064, 332-337.

Ceballos-Santos, S., de Sousa, D. B., García, P. G., Laso, J., Margallo, M., & Aldaco, R. (2024). Exploring the environmental impacts of plastic packaging: A comprehensive life cycle analysis for seafood distribution crates. *The Science of the Total Environment*, *951*, 175452. https://doi.org/10.1016/j.scitotenv.2024.175452

Chen, L., Zhou, S., Zhang, Q., Su, B., Yin, Q., & Zou, M. (2024). Global occurrence characteristics, drivers, and environmental risk assessment of microplastics in lakes: A meta-analysis. *Environmental Pollution*, *344*, 123321. https://doi.org/10.1016/j.envpol.2024.123321

Cheung, C. K. H., & Not, C. (2024). Degradation efficiency of biodegradable plastics in subtropical open-air and marine environments: Implications for plastic pollution. *Science of The Total Environment*, *938*, 173397. https://doi.org/10.1016/j.scitotenv.2024.173397

Chia, W. Y., Ying Tang, D. Y., Khoo, K. S., Kay Lup, A. N., & Chew, K. W. (2020). Nature's fight against plastic pollution: Algae for plastic biodegradation and bioplastics production. *Environmental Science and Ecotechnology*, *4*, 100065. https://doi.org/10.1016/j.ese.2020.100065

Choudhary, A., George, L., Mandal, A., Biswas, A., Ganie, Z. A., & Darbha, G. K. (2025). Assessment of microplastics and associated ecological risk in the longest river (Godavari) of peninsular India: A comprehensive source-to-sink analysis in water, sediment and fish. *Marine Pollution Bulletin*, *212*, 117560. https://doi.org/10.1016/j.marpolbul.2025.117560

de Deus, B. C. T., Costa, T. C., Altomari, L. N., Brovini, E. M., de Brito, P. S. D., & Cardoso, S. J. (2024). Coastal plastic pollution: A global perspective. *Marine Pollution Bulletin*, *203*, 116478. https://doi.org/10.1016/j.marpolbul.2024.116478

Dokl, M., Copot, A., Krajnc, D., Fan, Y. V., Vujanović, A., Aviso, K. B., Tan, R. R., Kravanja, Z., & Čuček, L. (2024). Global projections of plastic use, end-of-life fate and potential changes in consumption, reduction, recycling and replacement with bioplastics to 2050. *Sustainable Production and Consumption*, *51*, 498–518. https://doi.org/10.1016/j.spc.2024.09.025

Dorofte, A. L., Bleoanca, I., Bucur, F. I., Mustatea, G., Borda, D., Stan, F., & Fetecau, C. (2025). Biocomposite Active Whey Protein Films with Thyme Reinforced by Electrospun Polylactic Acid Fiber Mat. *Foods (Basel, Switzerland)*, *14*(1), 119. https://doi.org/10.3390/foods14010119

Dorofte, A. L., Dima, C., Bleoanca, I., Aprodu, I., Alexe, P., Kharazmi, M. S., Jafari, S. M., Dima, Ş., & Borda, D. (2024). Mechanism of β–cyclodextrin - thyme nanocomplex formation and release: *In silico* behavior, structural and functional properties. *Carbohydrate Polymer Technologies and Applications*, *7*, 100422. https://doi.org/10.1016/j.carpta.2024.100422

Fayshal, M. A. (2024). Current practices of plastic waste management, environmental impacts, and potential alternatives for reducing pollution and improving management. *Heliyon*, *10*(23), e40838. https://doi.org/10.1016/j.heliyon.2024.e40838

Fei, J., Bai, X., Jiang, C., Yin, X., & Ni, B.-J. (2024). A state-of-the-art review of environmental behavior and potential risks of biodegradable microplastics in soil ecosystems: Comparison with conventional microplastics. *The Science of the Total Environment*, *954*, 176342. https://doi.org/10.1016/j.scitotenv.2024.176342

Garfansa, M. P., Zalizar, L., Husen, S., Triwanto, J., Iswahyudi, I., Bakhtiar, A., Lasaksi, P., & Ekalaturrahmah, Y. A. C. (2025). Addition of biochar based-activated carbon into sand filtration columns to improved removal efficiency microplastic from water. *Bioresource Technology Reports*, *30*, 102099. https://doi.org/10.1016/j.biteb.2025.102099

Georgescu, L. P., Barbuta Misu, N., Antohi, V. M., Fortea, C., & Zlati, M. L. (2025). Approaches and perspectives on the transition to the circular economy in the European Union. *Frontiers in Environmental Science*, *13*. https://doi.org/10.3389/fenvs.2025.1533776

Graham, P. M., Pattinson, N. B., Bakir, A., McGoran, A. R., & Nel, H. A. (2024). Determination of microplastics in sediment, water, and fish across the Orange-Senqu River basin. *Water Research*, *266*, 122394.

Hadri, S. H., Tareen, N., Hassan, A., Naseer, M., Ali, K., & Javed, H. (2025). Alternatives to conventional plastics: Polyhydroxyalkanoates (PHA) from microbial sources and recent approaches – A review. *Process Safety and Environmental Protection*, *195*, 106809. https://doi.org/10.1016/j.psep.2025.106809

Hsu, W.-T., Domenech, T., & McDowall, W. (2022). Closing the loop on plastics in Europe: The role of data, information and knowledge. *Sustainable Production and Consumption*, *33*, 942–951. https://doi.org/10.1016/j.spc.2022.08.019

Jiao, H., Ali, S. S., Alsharbaty, M. H. M., Elsamahy, T., Abdelkarim, E., Schagerl, M., Al-Tohamy, R., & Sun, J. (2024). A critical review on plastic waste life cycle assessment and management: Challenges, research gaps, and future perspectives. *Ecotoxicology and Environmental Safety*, *271*, 115942. https://doi.org/10.1016/j.ecoenv.2024.115942

Kaplan Sarısaltık, A., Gulden, T., & Boks, C. (2025). A visual scoping review of plastic consumption in everyday life. *Cleaner and Responsible Consumption*, *16*, 100248. https://doi.org/10.1016/j.clrc.2024.100248

Kaur, S., Okoffo, E. D., Thomas, K. V., & Rauert, C. (2025). Unearthing the hidden plastic in garden compost. *Science of The Total Environment*, *973*, 179153. https://doi.org/10.1016/j.scitotenv.2025.179153

Khan, N., Sudhakar, K., & Mamat, R. (2025). Biodegradable plastics from marine biomass: A solution to marine plastic pollution. *Journal of Hazardous Materials Advances*, *17*, 100559. https://doi.org/10.1016/j.hazadv.2024.100559

Kumar, M., Bhujbal, S. K., Kohli, K., Prajapati, R., Sharma, B. K., Sawarkar, A. D., Abhishek, K., Bolan, S., Ghosh, P., Kirkham, M. B., Padhye, L. P., Pandey, A., Vithanage, M., & Bolan, N. (2024). A review on value-addition to plastic waste towards achieving a circular economy. *Science of The Total Environment*, *921*, 171106. https://doi.org/10.1016/j.scitotenv.2024.171106

Kumar, S., Dubey, N., Kumar, V., Choi, I., Jeon, J., & Kim, M. (2024). Combating micro/nano plastic pollution with bioplastic: Sustainable food packaging, challenges, and future perspectives. *Environmental Pollution*, *363*, 125077. https://doi.org/10.1016/j.envpol.2024.125077

Iticescu, C., Georgescu, L., Topa M. C., Murariu, G. (2014). Monitoring the Danube water quality near the Galati city. *Journal of Environmental Protection and Ecology*. 15. 30-38.

Lanciu Dorofte, A., Dima, C., Ceoromila, A., Botezatu, A., Dinica, R., Bleoanca, I., & Borda, D. (2023). Controlled Release of β-CD-Encapsulated Thyme Essential Oil from Whey Protein Edible Packaging. *Coatings*, *13*(3), Article 3. https://doi.org/10.3390/coatings13030508

Lee, S. H., Han, S.-J., & Wee, J.-H. (2025). A mini review of recent advances in environmentally friendly microplastic removal technologies in water systems. *Journal of Contaminant Hydrology*, *269*, 104485. https://doi.org/10.1016/j.jconhyd.2024.104485

Li, Z., & Chen, Y. (2024). Behavioral effects of polylactic acid microplastics on the tadpoles of *Pelophylax nigromaculatus*. *Ecotoxicology and Environmental Safety*, *285*, 117146. https://doi.org/10.1016/j.ecoenv.2024.117146

Martínez-Narro, G., Hassan, S., & Phan, A. N. (2024). Chemical recycling of plastic waste for sustainable polymer manufacturing – A critical review. *Journal of Environmental Chemical Engineering*, *12*(2), 112323. https://doi.org/10.1016/j.jece.2024.112323

Mehta, J., Dilbaghi, N., Deep, A., Hai, F. I., Hassan, A. A., Kaushik, A., & Kumar, S. (2025). Plastic waste upcycling into carbon nanomaterials in circular economy: Synthesis, applications, and environmental aspects. *Carbon*, *234*, 119969. https://doi.org/10.1016/j.carbon.2024.119969

Mogany, T., Bhola, V., & Bux, F. (2024). Algal-based bioplastics: Global trends in applied research, technologies, and commercialization. *Environmental Science and Pollution Research*, *31*(26), 38022–38044. https://doi.org/10.1007/s11356-024-33644-9

Mutmainna, I., Gareso, P. L., Suryani, S., & Tahir, D. (2025). Can agriculture and food waste be a solution to reduce environmental impact of plastic pollution? Zero-waste approach for sustainable clean environment. *Bioresource Technology*, *420*, 132130. https://doi.org/10.1016/j.biortech.2025.132130

Negrete-Bolagay, D., & Guerrero, V. H. (2024). Opportunities and Challenges in the Application of Bioplastics: Perspectives from Formulation, Processing, and Performance. *Polymers*, *16*(18), Article 18. https://doi.org/10.3390/polym16182561

Nicholson, S. R., Rorrer, N. A., Carpenter, A. C., & Beckham, G. T. (2021). Manufacturing energy and greenhouse gas emissions associated with plastics consumption. *Joule*, *5*(3), 673–686. https://doi.org/10.1016/j.joule.2020.12.027

Niu, Z., Curto, M., Le Gall, M., Demeyer, E., Asselman, J., Janssen, C. R., Dhakal, H. N., Davies, P., Catarino,

A. I., & Everaert, G. (2024). Accelerated fragmentation of two thermoplastics (polylactic acid and polypropylene) into microplastics after UV radiation and seawater immersion. *Ecotoxicology and Environmental Safety*, *271*, 115981. https://doi.org/10.1016/j.ecoenv.2024.115981

Pierdomenico, M., Morgana, S., & Chiocci, F. L. (2024). First report of microplastics in water and sediments of the alkaline Bagno dell'Acqua Lake (Pantelleria Island, southern Italy). *Environmental Pollution (Barking, Essex: 1987)*, *362*, 124962. https://doi.org/10.1016/j.envpol.2024.124962

Pintilie, V., Ene, A., Georgescu, L., Moraru, L., Iticescu, C. (2016). Measurements of gross alpha and beta activity in drinking water from Galati region, Romania. *Romanian Reports in Physics*, 68, 1208–1220.

Popa, P., Murariu, G., Mihaela, T., Georgescu, L., Iticescu, C. (2015). Multivariate statistical analyses of water quality of Danube river at Galati, Romania. *Environmental engineering and management journal,* 10.30638/eemj.2018.124.

Rajvanshi, J., Sogani, M., Kumar, A., Arora, S., Syed, Z., Sonu, K., Gupta, N. S., & Kalra, A. (2023). Perceiving biobased plastics as an alternative and innovative solution to combat plastic pollution for a circular economy. *Science of The Total Environment*, *874*, 162441. https://doi.org/10.1016/j.scitotenv.2023.162441

Roy, A., & Chakraborty, S. (2024). A comprehensive review on sustainable approach for microbial degradation of plastic and it's challenges. *Sustainable Chemistry for the Environment*, *7*, 100153. https://doi.org/10.1016/j.scenv.2024.100153

Saleem, J., Tahir, F., Baig, M. Z. K., Al-Ansari, T., & McKay, G. (2023). Assessing the environmental footprint of recycled plastic pellets: A life-cycle assessment perspective. *Environmental Technology & Innovation*, *32*, 103289. https://doi.org/10.1016/j.eti.2023.103289

Saxena, S. (2025). Pyrolysis and beyond: Sustainable valorization of plastic waste. *Applications in Energy and Combustion Science*, *21*, 100311. https://doi.org/10.1016/j.jaecs.2024.100311

Schmidt, C., Kühnel, D., Materić, D., Stubenrauch, J., Schubert, K., Luo, A., Wendt-Potthoff, K., & Jahnke, A. (2024). A multidisciplinary perspective on the role of plastic pollution in the triple planetary crisis. *Environment International*, *193*, 109059. https://doi.org/10.1016/j.envint.2024.109059

Sharma, S., Sharma, V., & Chatterjee, S. (2023). Contribution of plastic and microplastic to global climate change and their conjoining impacts on the environment - A review. *Science of The Total Environment*, *875*, 162627. https://doi.org/10.1016/j.scitotenv.2023.162627

Shi, C., Zhang, Y., Shao, Y., Ray, S. S., Wang, B., Zhao, Z., Yu, B., Zhang, X., Li, W., Ding, J., Liu, Z., & Zhang, H. (2024). A review on the occurrence, detection methods, and ecotoxicity of biodegradable microplastics in the aquatic environment: New cause for concern. *TrAC Trends in Analytical Chemistry*, *178*, 117832. https://doi.org/10.1016/j.trac.2024.117832

Simfukwe, K., Jere, W. W. L., & Msukwa, A. V. (2025). Heavy metal contamination in riverine fish from the Lilongwe River, Malawi: Implications for human health risk. *Environmental Pollution and Management*, *2*, 163–171. https://doi.org/10.1016/j.epm.2025.06.003

Simionov, I.-A., Călmuc, M., Iticescu, C., Călmuc, V., Georgescu, P.-L., Faggio, C., & Petrea, Ș.-M. (2023). Human health risk assessment of potentially toxic elements and microplastics accumulation in products from the Danube River Basin fish market. *Environmental Toxicology and Pharmacology*, *104*, 104307. https://doi.org/10.1016/j.etap.2023.104307

Stoett, P., Scrich, V. M., Elliff, C. I., Andrade, M. M., de M. Grilli, N., & Turra, A. (2024). Global plastic pollution, sustainable development, and plastic justice. *World Development*, *184*, 106756. https://doi.org/10.1016/j.worlddev.2024.106756

Tran-Nguyen, Q. A., Le, T. M., Nguyen, H. N. Y., Nguyen, Q. T., & Trinh-Dang, M. (2024). Microplastics in the surface water of urban lakes in central Vietnam: Pollution level, characteristics, and ecological risk assessment. *Case Studies in Chemical and Environmental Engineering*, *9*, 100622. https://doi.org/10.1016/j.cscee.2024.100622

Vigneswari, S., Kee, S. H., Hazwan, M. H., Ganeson, K., Tamilselvan, K., Bhubalan, K., Amirul, A.-A., & Ramakrishna, S. (2024). Turning agricultural waste streams into biodegradable plastic: A step forward into adopting sustainable carbon neutrality. *Journal of Environmental Chemical Engineering*, *12*(2), 112135. https://doi.org/10.1016/j.jece.2024.112135

Wen, L., Hu, Q., Lv, Y., Ding, W., Yin, T., Mao, H., & Wang, T. (2025). Environmental release behavior, cell toxicity and intracellular distribution of novel biodegradable plastic materials. *Environmental Pollution*, *367*, 125554. https://doi.org/10.1016/j.envpol.2024.125554

Wojnowska-Baryła, I., Bernat, K., & Zaborowska, M. (2022). Plastic Waste Degradation in Landfill Conditions: The Problem with Microplastics, and Their Direct and Indirect Environmental Effects. *International Journal of Environmental Research and Public Health*, *19*(20), 13223. https://doi.org/10.3390/ijerph192013223

Xuyang, W., Khalil, K., Zhuo, T., Keyan, C., Nazir, M. Y. M., Aqma, W. S., & Hong, N. Q. (2025). Addressing the plastisphere: Sustainable approaches to combat plastic pollution. *Science of The Total Environment*, *959*, 178105. https://doi.org/10.1016/j.scitotenv.2024.17810`5

Zhuo, M., Chen, Z., Liu, X., Wei, W., Shen, Y., & Ni, B.-J. (2024). A broad horizon for sustainable catalytic oxidation of microplastics. *Environmental Pollution*, *340*, 122835. https://doi.org/10.1016/j.envpol.2023.122835.

Scientific Papers. Series E. Land Reclamation, Earth Observation & Surveying, Environmental Engineering. Vol. XIV, 2025
Print ISSN 2285-6064, CD-ROM ISSN 2285-6072, Online ISSN 2393-5138, ISSN-L 2285-6064

MONITORING THE INACTIVE LANDFILL STABILITY IN GORJ COUNTY

Silvia Alexandra DREGHICI[1], Levente DIMEN[1], Mircea RÎȘTEIU[1], Tudor BORȘAN[1], Florin FAUR[2]

[1]"1 Decembrie 1918" University of Alba Iulia, 5 Gabriel Bethlen, 510009, Alba Iulia, Romania
[2]University of Petroșani, University Street, 332006, Petroșani, Romania

Corresponding author email: ldimen@uab.ro

Abstract

Monitoring landfill stability is critical in mining operations to prevent failures that could have significant environmental and safety implications. Site characterization is a comprehensive approach to monitoring landfill stability in order to conduct detailed geological assessments to understand the composition, structure, and physical properties of the tailing material, to perform laboratory tests to assess the engineering properties, all these correlated with geodetic repeated measurements. Techniques and instruments used in geodetic monitoring are chosen depending on the type of surveyed displacement and level of accuracy required. Photogrammetric and remote sensing technologies play an essential role in the detection and monitoring displacements and deformations, providing crucial support in the rapid and effective management of these emergencies. These techniques allow for large-scale, continuous monitoring of slope movements without requiring direct contact with the slope. This way, it ensures precise deformation monitoring, validates theoretical models, enhances predictive capabilities, and supports safety, regulatory compliance, and environmental protection efforts. A well-designed monitoring system not only ensures compliance with environmental regulations but also provides valuable insights for designing effective mitigation and rehabilitation strategies.

Key words*: displacement and deformation, environmental protection, geotechnical assessment, monitoring landfill stability, photogrammetric and remote sensing technologies.*

INTRODUCTION

Precise spatial measurement, a surveyor's most traditional and well-known expertise, is crucial not only for monitoring climate change impacts but also for developing adaptation strategies. Detailed topographic mapping, fundamental for land use planning and deformation monitoring, can be achieved through conventional surveying techniques, laser scanning, or digital image analysis. The construction of new engineering infrastructure to support climate change adaptation depends on geodetic measurements - such as levelling, total stations, and GNSS technologies – complemented by visual assessments and geotechnical data (Hannah et al., 2014).

At the 2002 World Summit on Sustainable Development, nine key societal benefits of Earth observations were identified (United Nations publication, 2002): disaster management (minimizing loss of life and property from natural and human-made disasters), health (analysing environmental factors affecting human well-being), energy resources (enhancing energy resource management), climate (assessing, predicting, mitigating, and adapting to climate variability and change), water (improving water resource management by understanding the water cycle), weather (enhancing forecasting and warning systems), ecosystems (better management and protection of terrestrial, coastal, and marine ecosystems), agriculture (promoting sustainable farming and combating desertification), and biodiversity (monitoring, preserving, and understanding biodiversity).

Romania adheres to Decision No. 766 of November 21, 1997, which governs the monitoring of construction behaviour during operation, investment phases, and post-usage. Published in the Official Gazette No. 352 on December 10, 1997, this law applies to all types of constructions and aims to evaluate their technical condition while ensuring their continued suitability for use. In the field of construction and civil engineering, a tailings landfill is a designated site for storing mine

tailings, which are the residual materials left after valuable minerals have been extracted from ore. These tailings, typically consisting of fine rock particles, water, and chemicals, are often disposed of in large, controlled piles or ponds.

Monitoring the stability of tailings landfill slopes is essential in mining operations to prevent failures that could lead to severe environmental and safety consequences. Quality in the construction sector is maintained through the following measures (Hannah et al., 2014; Caldera et al., 2016):

- Monitoring construction behaviour during operation to ensure structural stability and enable early detection of potential degradations.
- Interventions involving construction work aimed at maintaining or enhancing operational efficiency.
- Post-usage management, including safe demolition or in-situ abandonment, efficient material recovery, environmental restoration, and sustainability assurance.

The security and sustainability of a tailings landfill are evaluated based on two key engineering and environmental factors (Hannah et al., 2014; Caldera et al., 2016; CRED, 2016; VicRoads, 2021):

- Geotechnical stability: Engineering design must ensure that the tailings landfill remains structurally safe, preventing catastrophic failures such as tailings dam collapses.
- Environmental impact: Effective management of tailings landfills is crucial to prevent pollution of nearby water sources, soil contamination, and harm to wildlife. In some cases, monitoring is necessary to detect the release of hazardous substances like heavy metals or cyanide.

A comprehensive approach to assessing landfill slope stability involves site characterization (Hannah et al., 2014; Caldera et al., 2016; CRED, 2016; VicRoads, 2021):

- Geological surveys: Conducting thorough geological assessments to determine the composition, structure, and physical properties of the tailing's material.
- Soil and rock testing: Performing laboratory analyses (e.g., shear strength, consolidation, and permeability tests) to evaluate the engineering properties of the tailings.

MATERIALS AND METHODS

Monitoring tailings landfills – large accumulations of waste materials from mining operations – is essential to ensuring environmental safety, structural stability, and regulatory compliance. Slope stability assessment relies on two complementary approaches: the geotechnical approach (analytical) and the parametric approach (measurable). A comprehensive and realistic evaluation of tailings landfill stability requires considering both perspectives (Caldera et al., 2016; CRED, 2016; Gilbert Gedeon, 2021; VicRoads, 2021). Slope stability and landslide monitoring involve identifying specific parameters and tracking their variations over time. The two primary factors in this process are groundwater levels and displacement. Slope displacement is analysed based on failure plane depth, direction, magnitude, and rate, with one or more of these aspects being continuously monitored.

Traditional slope monitoring employs either a single method or a combination of techniques. Piezometers measure water levels, while tools such as surveyed surface monuments, extensometers, inclinometers, and tiltmeters provide insights into slope movement direction, rate, depth, and failure plane extent. Extensometers specifically help quantify displacement magnitude. For long-term slope monitoring, manually operated probe inclinometers are the most widely used instrument (Caldera et al., 2016; CRED, 2016; Gilbert Gedeon, 2021; VicRoads, 2021). Effective waste landfill management requires a combination of monitoring activities and interventions to ensure both stability and sustainability.

These approaches are divided into invasive and non-invasive methods. Invasive methods involve direct physical interaction with the landfill mass, such as drilling, excavation, or other intrusive processes. Non-invasive methods enhance and assess landfill stability without disturbing the waste mass, using remote sensing, surface-based techniques, and indirect monitoring measures. By integrating both invasive and non-invasive strategies, tailings landfills can be efficiently monitored and stabilized, promoting long-term environmental

and structural sustainability (Caldera et al., 2016; CRED, 2016; Gilbert Gedeon, 2021; VicRoads, 2021).
The typical workflow for tailings landfill monitoring focuses on:

1. PLANNING AND PREPARATION
The monitoring of tailings landfills starts with a site assessment, which involves identifying specific risks related to the landfill, such as its composition, size, slope, and proximity to sensitive areas like water bodies or nearby communities. This phase also includes defining the monitoring objectives, which may focus on detecting seepage, evaluating slope stability, tracking dust emissions, or ensuring compliance with safety regulations (Popa, 2012; CRED, 2016).

2. DATA COLLECTION
The data collection process employs a combination of manual and automated techniques to monitor various environmental and structural conditions of the tailings landfill (Figure 1). Routine monitoring is a systematic process focused on assessing the technical condition of the land or structures. Its primary goal is to ensure stability during operation. If certain parameters exceed predefined thresholds, special monitoring must be implemented. This involves conducting regular, periodic investigations on specific parameters to assess deformations in the land, structures, or specific components. Special monitoring activities are typically defined during the project planning phase or determined through technical expertise (UTCB, 2009; Popa, 2012; Buchmayer et al., 2021).

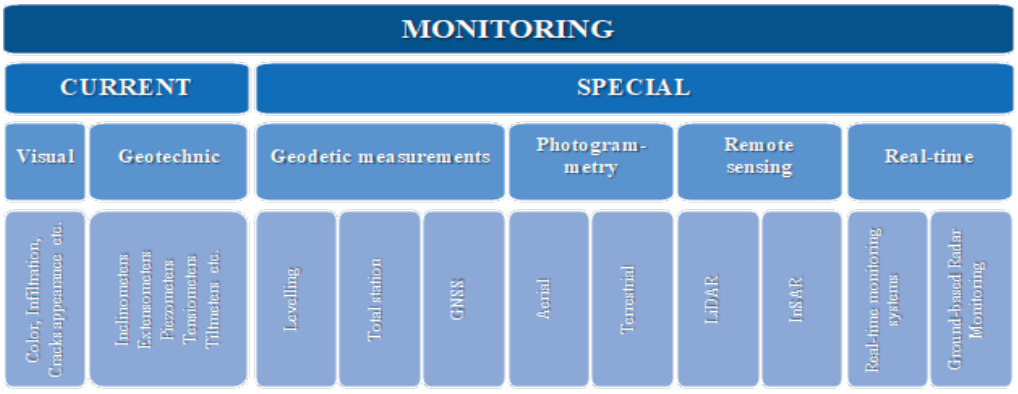


Figure 1. Monitoring methods and instruments - classification by monitoring aspects

Visual Monitoring
Regular field inspections and surveys play a crucial role in supplementing instrument-based monitoring. Visual inspections help identify early warning signs of instability, such as the formation or expansion of surface cracks, changes in vegetation or water drainage patterns (which may indicate subsurface movement or shifts in stability), and surface subsidence or slumping. These issues are particularly common in carbonate deposits due to karst features or weathering (UTCB, 2009).

Geotechnical Monitoring
Geotechnical monitoring utilizes various instruments to continuously or periodically measure ground movements, stresses, and other factors influencing slope stability.
The geotechnical parameters essential for ensuring construction stability and safety can be categorized into two main groups (UTCB, 2009):

- Environmental factors: These include water levels, air temperature, water temperature at various depths, solar radiation, and seismic activity.
- Structural response measurements: These depend on the type of construction. For tailings landfills, key monitored parameters include: absolute and relative displacements of the landfill and geotechnical characteristics, particularly vertical settlements during construction and operation, displacement between structural

elements, temperature variations within the landfill body, deformation and stress conditions, crack development, infiltration rates and the position of the infiltration curve, pore water pressure within earthen sealing elements, effective and total stress conditions, and slope displacements and infiltration through slopes.

Monitoring instruments must be deployed in adequate numbers and at appropriate intervals to detect abnormal behaviour. When irregularities are observed, the data collected – combined with field inspections – should enable the identification of underlying causes. In some cases, additional monitoring tools may be required (UTCB, 2009).

Advancements in technology, particularly the Internet of Things (IoT), have significantly enhanced traditional monitoring methods, overcoming challenges such as low measurement frequency and time-intensive data collection. IoT-based systems enable real-time and precise tracking of changes in enclosure structures, allowing for dynamic adjustments to construction parameters and techniques (Figure 2). This adaptive monitoring approach provides critical technical support by assessing the stability of surrounding rock formations, evaluating the reliability of primary supports and secondary linings, refining support system designs based on real-time data, determining optimal timing for secondary lining installation, and adjusting construction methods to enhance overall structural safety and efficiency. By integrating modern monitoring technologies, construction teams can proactively address stability concerns, ensuring the long-term safety and sustainability of tailings landfills (Buchmayer et al., 2021).

Global investigations focus on determining the geophysical structure and geotechnical characteristics of a tailings landfill, as well as detecting water circulation within the landfill and its surrounding environment. Piezometers are used to measure pore water pressure within weak soil layers, particularly inside slopes. Installed in boreholes within the landfill or slope, these instruments monitor fluctuations in water pressure within carbonate rock formations. Elevated pore pressure can reduce effective stress, potentially leading to slope instability. In carbonate deposits, water infiltration through fractures or karst formations can further contribute to slope failures. Piezometer data is essential for tracking groundwater conditions and assessing stability risks (UTCB, 2009; Buchmayer et al., 2021.

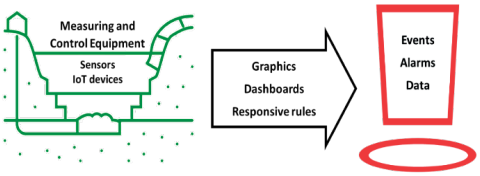


Figure 2. The use of modern technologies in monitoring activities

In addition to geotechnical monitoring instruments, seismic activity monitoring is critical for tailings landfills. Seismometers record ground movement, measuring velocity and acceleration, while seismographs track acceleration over time. For comprehensive seismic monitoring, devices should have three measurement components and be installed at three levels at least: the crest elevation of the tailings landfill, the foundation level, and the open field reference point. The interpretation of seismic data and application of results must be conducted by qualified specialists to ensure accurate risk assessments and effective mitigation strategies (UTCB, 2009; Buchmayer et al., 2021).

Geodetic Measurements

Field surveys are commonly conducted using geodetic methods and instruments such as levelling, total stations, and GNSS systems, which enable the detection of surface movements over time. The Monitoring Geodetic Network (MGN) consists of two main categories of points (Figure 3) (Popa, 2012):

- Reference points: These are further classified into three types: survey points – directly used for monitoring the targeted structure, control points – assess the stability of survey points, and orientation points – provide geodetic network alignment. Reference points must meet several essential criteria: ensure long-term stability and reliability, be strategically positioned to enable precise and accurate data collection, be placed on solid, stable geological formations to prevent movement-related distortions, and be located in areas

where groundwater levels do not compromise stability.

- Object points: These points must also fulfil specific requirements: they should be embedded within the load-bearing components of the structure, and their placement should align with the foundation's geometry and load distribution to ensure accurate monitoring.

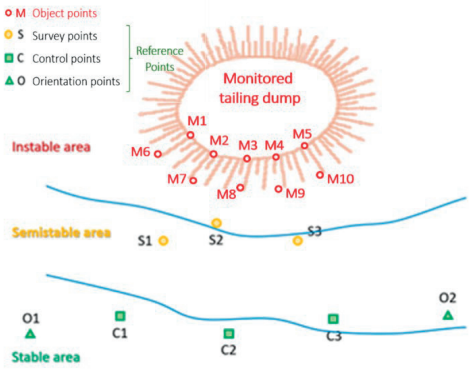


Figure 3. The monitoring geodetic network

Techniques and instruments used in geodetic monitoring are chosen depending on the type of surveyed displacements and deformations, and level of accuracy required.

Photogrammetry

Photogrammetry plays a significant role in slope stability monitoring by providing accurate, detailed, and often real-time measurements of changes in the surface geometry of slopes, being preferred over traditional methods. Photogrammetry contributes to surface change detection (comparing models over time, deformations, cracks, subsidence, or bulging can be revealed – key signs of instability). Photogrammetry allows the surveying of extensive or dangerous terrains without needing physical access, ensuring safety while capturing critical data. The outputs of repeated surveys can be integrated into Geographic Information Systems (GIS) for more advanced geotechnical analyses and risk mapping. Photogrammetry is an effective method for monitoring terrain displacement, particularly useful for generating 3D models of slopes through photographic imagery. Multiple aerial or ground-based photos are combined to create detailed models of the landfill slope. By comparing models taken at different times, any changes in the slope can be identified. This technique is particularly useful for detecting surface cracks, erosion, and slumping in carbonate deposits (Hannah et al., 2014; Dimen et al., 2024).

Photogrammetry combines precise visual data with geospatial analysis, making it ideal for both large-scale and localized environmental monitoring projects (Hannah et al., 2014; Dimen et al., 2024).

Photogrammetry and unmanned aerial vehicles (UAVs) are closely linked, with UAVs enhancing photogrammetry by providing a versatile and efficient platform for capturing aerial imagery, which serves as the foundation for photogrammetric analysis (Hannah et al., 2014).

A UAV (drone) can operate autonomously or be controlled remotely. Equipped with technologies like GNSS, cameras, sensors, and specialized software for tasks such as collecting data from hard-to-reach areas, UAVs are increasingly utilized in monitoring (Hannah et al., 2014).

The imagery captured by UAVs is processed using photogrammetry software to create 3D models, orthomosaics, and contour maps. Advanced algorithms use overlapping images to triangulate points and generate accurate spatial data, which is then correlated with other field-collected information (Hannah et al., 2014).

Though, there are a few challenges which should be kept in mind. Photogrammetry requires good lighting and clear views (vegetation can be a problem), while accuracy depends heavily on ground control points and the camera quality and processing software. Photogrammetry mostly tracks surface movement, not internal slope deformations (for subsurface issues, photogrammetric surveys still need to be correlated with geotechnical measurements).

Remote Sensing

Modern remote sensing technologies play a crucial role in detecting and monitoring displacements and deformations in tailings landfills. These technologies support rapid and effective management, enabling large-scale, continuous monitoring of slope movements without direct contact. This is especially

valuable for monitoring expansive landfill slopes in mining operations (Hannah et al., 2014; Dimen et al., 2024).
When satellite data is combined with aerial imagery and field measurements, it provides an accurate and comprehensive view of the monitored area. This data is crucial for coordinating adaptation strategies, responding to emergencies, and optimizing resource allocation. It also aids in planning operational measures and predicting future behaviour (Dimen et al., 2024).

Real-time Monitoring

A real-time monitoring system continuously collects data and provides alerts for any significant changes. The goal of such systems, especially for mining waste landfills, is to ensure safety, environmental compliance, and operational efficiency. Real-time data helps detect even small, progressive slope movements before they escalate into major failures, allowing for prompt mitigation actions in cases of structural instability, excessive seepage, or environmental contamination (UTCB, 2009; Buchmayer et al., 2021).
In addition to geotechnical, hydrological, and environmental sensors, real-time monitoring systems should include GNSS and total stations for precise surface movement monitoring.
These sensors continually collect data on various parameters, with wireless communication networks (e.g., 4G/5G, LoRaWAN, or satellite links) transmitting the information in real-time to central monitoring stations or cloud-based platforms. Specialized software analyses incoming data to identify anomalies and trends. Machine learning algorithms or predefined thresholds can trigger automated alarms when critical conditions are detected (Buchmayer et al., 2021).
The data is displayed on user-friendly dashboards featuring charts, maps, and 3D visualizations. Stakeholders are notified via SMS, email, or other notification systems when thresholds are exceeded. Real-time data is also integrated with weather monitoring, geological models, and remote sensing data (such as from drones or satellites) for a comprehensive analysis (UTCB, 2009; Buchmayer et al., 2021).
Interpretative algorithms are absolutely crucial when it comes to predicting landfill slope failures, especially when working with large, complex datasets. Modern monitoring methods produce huge datasets (e.g. point clouds, images, displacement maps). Algorithms process, analyse, and filter this data efficiently, identifying meaningful patterns or anomalies that humans would miss. There could be early warning signs, like subtle slope movements (millimetres of displacement), that can be an early indicator of impending failure. Algorithms can detect these small changes over time, often earlier and more accurately than manual inspections. By learning historical deformation patterns, algorithms can predict future behaviour, recognizing acceleration trends that precede a collapse. Moreover, algorithms can combine various factors (e.g. displacement rates, rainfall data, soil type, slope angle) to quantify failure probabilities, turning subjective assessments into objective risk metrics, aiding decision-making. Interpretative algorithms interpret incoming data in real time. If critical thresholds are crossed (e.g. displacement rate suddenly doubles), the system can trigger alarms immediately (Buchmayer et al., 2021).
By continuously monitoring the landfill, real-time systems enable proactive risk management, providing ongoing insights into structural, environmental, and operational conditions. This technology supports sustainable, safe management practices, reduces risks to human life and the environment, and improves decision-making (Caldera et al., 2016; CRED, 2016).

3. DATA TRANSMISSION AND MANAGEMENT

Data from different type of sensors and monitoring devices are consolidated within a centralized system, often referred to as a Supervisory Control and Data Acquisition (SCADA) system or a similar platform. This system enables real-time monitoring and triggers alerts in response to abnormal readings, such as unusual seepage or deformation (Figure 4) (Buchmayer et al., 2021).

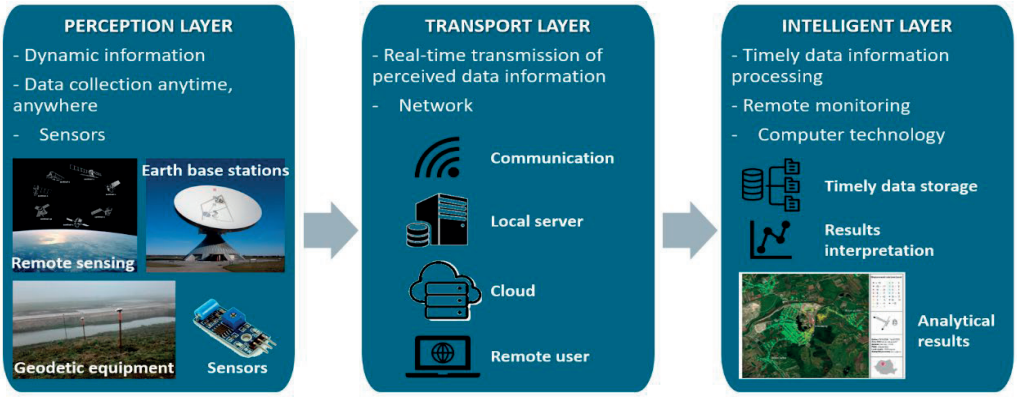


Figure 4. Layers of a real-time monitoring system

4. DATA ANALYSIS

For thorough analysis and interpretation, field-collected data is integrated by combining outputs from various instruments using specialized software designed for analysis and stability assessments. The data is then processed and interpreted to uncover patterns, trends, and potential issues. To create a 3D model of the tailings landfill for further analysis, the collected data must be processed using specific modelling software. Interpolation techniques are often required due to challenges in data acquisition and the limited number of measurement points. Most modelling software provides users with various interpolation methods to choose from. Before selecting the most suitable spatial interpolation technique, it is essential to evaluate the assumptions and characteristics of each approach, along with the spatial properties and analysis of the data (Herban & Alionescu, 2012).

Several factors influence the accuracy of Digital Elevation Models (DEMs), including sampling density for contour derivation, the vertical spacing of contours, the grid cell size of the DEM, field complexity, and spatial filtering. Advances in terrestrial measurement technology have significantly improved accuracy, enabling the development of models that can be utilized in deformation analysis and predicting the future behaviour of the tailings landfill (Figure 5) (Herban & Alionescu, 2012).

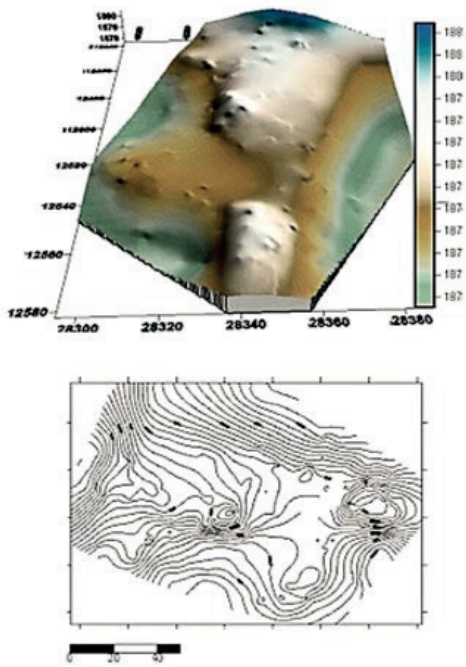


Figure 5. Digital elevation model and contour lines (Herban & Alionescu, 2012)

Data Quality Control

Data cleaning is essential to eliminate outliers or erroneous values, often caused by sensor malfunctions. The validated data must align with known benchmarks and expected ranges for parameters like pH, temperature, and deformation (Welsch & Heunecke, 2005; Popa, 2012).

The relation between geotechnical parameters (e.g., pH, temperature) and landfill slope stability is indirect but significant, because they influence the geotechnical behaviour of the waste material, leachate chemistry, and biological activity, all of which affect how stable the landfill slope is. Low pH accelerates the breakdown of organic materials leads to weaker waste material, and, therefore, higher risk of slope failures. On the other side, a neutral or high pH leads to more chemically stable environment and more stable slopes. High temperatures are more often met in case of waste weakening and could be an early sign for slope instability.

Statistical and Geospatial Analysis

Statistical methods, such as regression and trend analysis, are applied to detect significant changes in tailings behaviour, including gradual slope shifts or sudden seepage spikes. Environmental conditions, like rainfall or temperature, are correlated with variations in tailings characteristics, such as water chemistry and seepage rates. Geographic Information System (GIS) software enables mapping of monitoring points to visualize spatial patterns, like areas of excessive settling or deformation. By overlaying environmental data—groundwater and surface water quality—onto topographical maps, risks of contamination can be assessed (Welsch & Heunecke, 2005; Popa, 2012).

During analysis, the tailings landfill is treated as a unified system, fully monitored to identify displacements and deformations over time. Repeated measurements relative to the surrounding environment form the basis for determining absolute displacements (Welsch & Heunecke, 2005; Popa, 2012).

To forecast future evolution with maximum accuracy, displacement and deformation models are developed by analysing changes over time and space. These models incorporate causal forces, such as internal or external stresses, which drive the displacements and deformations (Nikolić, 2009).

A practical method involves integrating observation-based analyses to study displacements and deformations. This includes geometric state analysis and physical interpretations that identify dynamic processes. "Integrated analysis" refers to merging geometric evaluations with predictive models (Welsch & Heunecke, 2005).

The synergy between geodetic repeated measurements and parametric modelling is pivotal for effective tailings landfill monitoring and management. Geodetic measurements yield high-resolution spatial data on deformations, while parametric models contextualize these measurements, integrating geotechnical and environmental factors. By combining these approaches, deformation trends can be precisely analysed, risks predicted, and future behaviours simulated under varying conditions (Welsch & Heunecke, 2005; Popa, 2012).

This integrated framework validates theoretical models while enhancing safety compliance and environmental stewardship. It enables proactive identification of hazards - like seepage or slope failures - that may lead to contamination or ecological damage. Ultimately, the correlation fosters a robust risk assessment strategy, supporting informed decision-making and resource optimization to protect human lives, infrastructure, and the surrounding ecosystem (Welsch & Heunecke, 2005; Popa, 2012).

Predictive Modelling, Alarm Systems and Thresholds

Historical data is utilized to develop predictive models that can anticipate issues such as tailings dam failure, seepage migration, or structural shifts. These models support proactive management and the establishment of early warning systems. Key parameters, such as maximum allowable pore pressure or ground displacement, are assigned thresholds. If these thresholds are exceeded, alarms are triggered to alert the management team to potential risks (Welsch & Heunecke., 2005).

5. REPORTING AND DECISION MAKING

Reporting involves generating regular summaries of monitoring data and analysis. These reports typically include visual representations, such as graphs, charts, and maps, alongside an assessment of trends and anomalies. Recommendations for mitigation measures or further monitoring are also provided. Ensuring regulatory compliance involves meeting environmental regulations, standards, and submitting the necessary reports

to local authorities or regulatory bodies (Welsch & Heunecke, 2005; Caldera et al., 2016; CRED, 2016).

Based on these analyses, the management team may implement actions such as modifying the operation of the tailing's facility, strengthening the structure, or initiating deeper investigations. After each monitoring cycle, it is crucial to review the system's effectiveness. This review assesses whether the data collected is sufficient and accurate, prompting adjustments to the monitoring strategy where needed—for example, adding sensors or altering data collection intervals (Welsch & Heunecke, 2005; Caldera et al., 2016; CRED, 2016).

As technologies advance, adopting new monitoring tools and analytical techniques should be considered to enhance accuracy and efficiency in the monitoring process.

RESULTS AND DISCUSSIONS

Ensuring the stability of landfill slopes in carbonate deposits requires a combination of instrumentation, remote sensing, and geotechnical modelling. The unique characteristics of carbonate formations - such as fractures, karst features, and susceptibility to water infiltration - necessitate a comprehensive monitoring approach to maintain safety and stability. Continuous data collection from these methods enables the early detection of potential failures, allowing for proactive mitigation (Welsch & Heunecke, 2005; Caldera et al., 2016; CRED, 2016).

A multi-faceted approach is essential for monitoring tailings landfill slope stability, integrating traditional geotechnical techniques with modern technology. By implementing a robust monitoring program, mining operations can significantly reduce risks associated with tailings storage, enhancing both safety and environmental protection (Welsch & Heunecke, 2005; Caldera et al., 2016; CRED, 2016).

Integrating geodetic repeated measurements with parametric modelling plays a critical role in monitoring tailings landfills, which serve as storage areas for mining waste. This integration delivers precise, timely, and actionable insights into the structural stability, integrity, and environmental impact of the landfill. Key advantages of this correlation include (Welsch & Heunecke, 2005; Caldera et al., 2016; CRED, 2016; Gilbert Gedeon, 2021; VicRoads, 2021):

- Geodetic measurements provide high-precision spatial data on geometric displacements, while parametric modelling aids in understanding the behaviour of the landfill. Together, they enable the detection of deformation trends and early identification of anomalies signalling potential instability. Combining high-precision geodetic tools (e.g. GNSS, LiDAR) with robust modelling and uncertainty analysis is crucial in early warning systems. Thus, minor inaccuracies in measurement or modelling can mask critical pre-failure displacements, especially in systems like landfills where early deformations may be subtle but significant. Small but persistent inaccuracies can lead to misinterpretation of long-term trends, such as poor resolution or incorrect model calibration that may suggest stability even when precursors to failure exist.
- Discrepancies between observed measurements and model predictions can highlight areas for model improvement or uncover hidden risk factors. Geodetic deformation analysis helps validate parametric models, while tailings landfill conditions and responses are simulated based on their characteristics.
- Localized geodetic displacements may indicate risks, such as slope failures or seepage. By considering material properties, loading conditions, and environmental factors, this approach develops a complete risk profile, combining empirical observations with theoretical assessments for more informed decision-making.
- Regular monitoring and reporting are often required to meet regulatory standards. Incorporating geodetic monitoring within parametric models enhances communication with regulators and stakeholders by providing evidence-based assurances of safety and stability. This practice minimizes the risk of overdesigning stabilization measures or underestimating risks, ensuring optimized resource allocation.
- A general monitoring strategy for tailings landfills should support sustainable mining by addressing environmental hazards proactively. Monitoring displacement

patterns can reveal potential pathways for seepage or contamination. Simulating environmental impacts enables the development of effective containment strategies, further reinforcing environmental stewardship.

CONCLUSIONS

Romania complies with legislation regarding the monitoring of construction behaviour throughout all phases of its life cycle – pre-usage, exploitation, and end-of-life. In case of inactive landfills, as construction in the third life cycle phase, a long-term stability assessment is still required, in order to ensure residual waste continuity to settle safely without causing surface deformation or failure, while environmental monitoring involves continuous tracking of groundwater, air quality, and leachate for decades.

Therefore, monitoring through all life cycle phases ensures the landfill does not become a long-term environmental or structural hazard. It protects ecosystems, human health, and investments while enabling informed decision-making.

Monitoring a landfill using both geodetic methods and geotechnical parameter measurements is essential because each approach provides complementary information crucial for understanding and managing stability risks. This approach brings more benefits, such as a comprehensive understanding of landfill stability, early warning and risk mitigation, improvement in data reliability and confidence in decision-making, more accurate predictive modelling for stability assessments, and ensuring compliance and enhancing public and environmental safety.

A range of sensors, including vibrating wire piezometers, electrolytic bubble inclinometers, and tiltmeters, are commonly used to monitor groundwater levels and ground movement for slope stability assessments. Recent advances in electronic technology, coupled with reduced costs, have made remote monitoring a highly efficient and cost-effective tool for evaluating slope stability.

The workflow for monitoring tailings landfills is a multi-step process involving meticulous planning, the use of advanced monitoring equipment, systematic data collection, comprehensive analysis, and ongoing reporting. This structured approach helps identify risks early, enabling prompt action to prevent environmental damage and ensure community safety.

In summary, the integration of geodetic repeated measurements with parametric modelling establishes a synergistic framework for tailings landfill monitoring. This integration provides accurate deformation assessments, validates theoretical models, improves predictive capabilities, and bolsters efforts in safety, regulatory compliance, and environmental protection.

Environmental monitoring for water, air, and soil should follow an integrated approach rather than operating separately. This ensures a holistic management strategy through:

- Identifying relationships between pollutants across water, air, and soil systems.
- Utilizing real-time data to detect contamination at an early stage and prevent its spread.
- Implementing actions like containment barriers for water and soil, dust suppression systems for air, water treatment methods such as filtration, reverse osmosis, or chemical neutralization, and soil rehabilitation through phytoremediation or amendments.

Monitoring tailings landfills is crucial for minimizing environmental and public health risks. A thoughtfully designed monitoring system not only ensures compliance with environmental regulations but also provides valuable insights to develop effective mitigation and rehabilitation strategies. Continuous evaluation of environmental conditions allows stakeholders to preserve ecological balance and promote sustainable mining practices.

REFERENCES

Buchmayer, F., Monsberger, C., & Lienhart, W. (2021). Advantages of tunnel monitoring using distributed fibre optic sensing. *Journal of Applied Geodesy*. 15. 1-12. DOI: 10.1515/jag-2019-0065.

Caldera, H. J., Wirasinghe, S. C., & Zanzotto, L. (2016). An approach to classification of natural disasters by severity. *5th International Natural Disaster Mitigation Specialty Conference, CSCE Annual Conference*, *NDM-528,* 1-10.

Dimen, L., Borşan, T., Dreghici, A., & Sânzâiană, Gh. (2024). The Use of GIS in the Management of Forest Fire Extinguishing, *6th International Conference on Central European Critical Infrastructure Protection, Hungary.*

Gilbert Gedeon, P.E. (2021). "Slope stability", PhD online course EM 1110-2-1902 www.cedengineering.com.

Hannah, J. (Ed.), Boateng, I., Dalyot, S., Enemark, S., Friesecke, F., Mitchell, D., van der Molen, P., Pearse, M., Sutherland, M., & Vranken, M. (2014). The surveyor's role in monitoring, mitigating and adapting to climate change. *FIG publication No. 65*, International Federation of Surveyors (FIG). https://www.fig.net/resources/publications/figpub/pub65/figpub65.asp.

Herban, I.S., & Alionescu, A. (2012). 3-Dimensional Modeling for Assessment of the Touristic Potential, *12th International Multidisciplinary Scientific Geoconference SGEM 2012*, Vol. II, 933-938, DOI: 10.5593/SGEM2012/S09.V2002.

Nikolić, B. (2009). Projektovanje Kontrolne Geodetske Mreže Za Prćenje Deformacija U Kojoj Se Merenja Izvode GPS Tehnoligijom, Univerzitet U Beogradu, Građevinski Fakultet, Katedra Za Geodeziju I Geoinformatiku.

Popa, A. (2012). Contribuţii privind automatizarea procesului de prelucrare şi interpretare a datelor în vederea determinării deplasărilor şi deformaţiilor, PhD Thesys, Technical University of Civil Engineering Bucharest.

Welsch, W., & Heunecke, O. (2005). Models and Terminology for the Analysis of Geodetic Monitoring Observations, Official Report of the Ad-Hoc Committee of FIG Working Group 6.1, *FIG Publication No. 25.*

***CRED (2016). "EMDAT- International Disaster Database: Centre for Research on the Epidemiology of Disasters" www.emdat.be.

***Technical University of Civil Engineering Bucharest (UTCB) (2009). Ghid privind echiparea construcţiilor hidrotehnice de retenţie cu aparatură de măsură şi control - Faza 1, Contract no. 437/2009.

***United Nations publication (2002). Report of the World Summit on Sustainable Development, *United Nations publication*, A/CONF.199/20, ISBN 92-1-104521-5.

***VicRoads (2021). Monitoring slope stability. *Technical Note TN79.*

Scientific Papers. Series E. Land Reclamation, Earth Observation & Surveying, Environmental Engineering. Vol. XIV, 2025
Print ISSN 2285-6064, CD-ROM ISSN 2285-6072, Online ISSN 2393-5138, ISSN-L 2285-6064

SOIL FLUX AND SOIL GAS MONITORING OF A NATURAL LABORATORY FOR THE STUDY OF CO_2 LEAKAGE

Alexandra-Constanţa DUDU, Corina AVRAM, Gabriel IORDACHE, Constantin-Ștefan SAVA, Lia STELEA, Andrei-Gabriel DRAGOȘ

National Institute for Research and Development on Marine Geology and Geoecology - GeoEcoMar, 23-25 Dimitrie Onciul Street, 024053, District 2, Bucharest, Romania

Corresponding author email: alexandra.dudu@geoecomar.ro

Abstract

Carbon capture and storage (CCS) is a technology designed to reduce greenhouse gas emissions by capturing CO_2 from industrial processes or power generation and securely storing it in geological formations. Băile Lăzărești serves as a promising natural laboratory for studying the environmental effects of potential CO_2 leakage from an anthropogenic CO_2 storage site and for testing monitoring solutions. One effective method for environmental monitoring of CO_2 geological storage involves soil flux and soil gas surveys, which can identify potential CO_2 leakage points by determining the natural variability of CO_2 flux. Since 2019, several soil flux surveys have been conducted at Băile Lăzărești across different seasons, combined with soil-gas measurements. By analyzing seasonal CO_2 variation along with geological knowledge, we have determined the natural variability of post-volcanic emissions and important for monitoring CO_2 geological storage sites, aiding in the identification and understanding of potential leakage in the near-surface environment.

Key words: *CO_2 geological storage, monitoring, natural laboratory, soil flux surveys, soil gas-surveys, leakage detection.*

INTRODUCTION

Carbon capture and storage is an important tool for reducing CO_2 emissions (IPCC, 2022; IPCC, 2023) and it is expected to be deployed large-scale to achieve the climate targets. From all the components of the CCS chain, the storage seems to be the most debated since there are some public concerns related to the risks of storing CO_2 underground, although the storage occurs in the deep environment at more than 800 m depth. Environmental monitoring in this respect is very important since it can easily demonstrate the absence of leakage and its undesirable effects in the environment (West et al., 2005; Beaubien et al., 2008; Ziogou et al., 2013). One important monitoring method which has been successfully applied at all the current and past storage projects is soil flux monitoring (Beaubien et al., 2008). Its application was also demonstrated on natural laboratories (Beaubien et al., 2008; Ziogou et al., 2013), sites where CO_2 is leaking naturally, mostly related with volcanic or post-volcanic activity. The study of these sites can provide valuable insights on the natural variability of soil fluxes and on the migration pathways of CO_2 in the near-surface (Beaubien et al., 2008).

In Romania, a promising natural laboratory can be considered Băile Lăzărești site (Harghita County). The site is located at approximately 16 km north-east from Băile Tușnad and it is renowned for its post-volcanic activity (Pricăjan, 1974; 1985; Karátson et al., 2022).
The site was selected for further research as a natural analogue for CO_2 leakage in 2019 (Dudu et al., 2021; Dudu et al., 2024) in the context of a national research project. Several soil flux and soil gas surveys have been conducted in the following years in order to determine the natural variability of CO_2 soil fluxes and concentrations and to highlight migration pathways, contributing to the understanding of CO_2 leakage mechanisms in the environment and therefore to the design of monitoring for future CO_2 storage sites. During the last 6 years, the site underwent significant landscaping projects, which also complicated its assessment.

MATERIALS AND METHODS

Study area

The Gurghiu-Harghita post-eruptive chain represents the most intense post-volcanic manifestation in the Eastern Carpathians, with a significant release of gases. The ascent of

volcanic gases to the surface is favoured by deep tectonics, through a complex crustal, regional, and local fracture system, of which regional and local fractures have different degrees of current mobility (Airinei & Pricăjan, 1972). The post-volcanic emissions in the Lăzărești area propagate along a system of deep fractures, which are then taken over by surface faults. These emissions are redistributed with varying intensity throughout the entire sedimentary volume of the Cretaceous flysch (Airinei & Pricăjan, 1972).

From a lithostratigraphic perspective, the post-volcanic emissions in the Lăzărești area traverse a series of deposits, starting with the Cretaceous flysch (Sânmartin-Bodoc strata, Barremian-Albian) at the base, continuing with terrace deposits (Mutihac, 1990). The Cretaceous flysch (Barremian-Albian) is characterized by accentuated flysch features (pronounced rhythmic alternations of rusty grey sandstones, often bituminous, and shales), while lacking marl-limestones. The flysch, with its low permeability due to the alternating layers of shale and sandstone, can act as a barrier, limiting the free migration of gases. However, tectonic activity and the presence of fractures within the flysch can create pathways for volcanic emissions to reach the surface. These fractures and fault systems essentially create a "stratigraphic screen," which can either trap or channel gases depending on their alignment and mobility. Quaternary deposits are terrace deposits, composed of coarse sediments, locally or at the base of the slopes covered with finer alluvium, such as fine sands and sandy shales, marls, and grey shales. The formation of carbonated mineral water deposits in the region results from the interaction of moffetic carbon dioxide with the aquifer layers within the mentioned geological formations. Additionally, the specific hydrodynamic characteristics of the known springs (sulfonated, ferruginous, etc.) are directly influenced by the chemical composition of the volcanic, flysch, Neogene and Quaternary formations through which the groundwater flows.

In 2019 several gas measurements were made near important elements such as the dry and wet mofettes, mineral spring and therapeutic bath. The level of CO_2 emissions was determined to reach more than 85% inside the dry mofette cabin (Dudu et al., 2021). From the measurements made across several location across the site, it was decided to divide it into two perimeters, completely different considering the level of emissions and the presence and number of the gas vents (Figure 1).

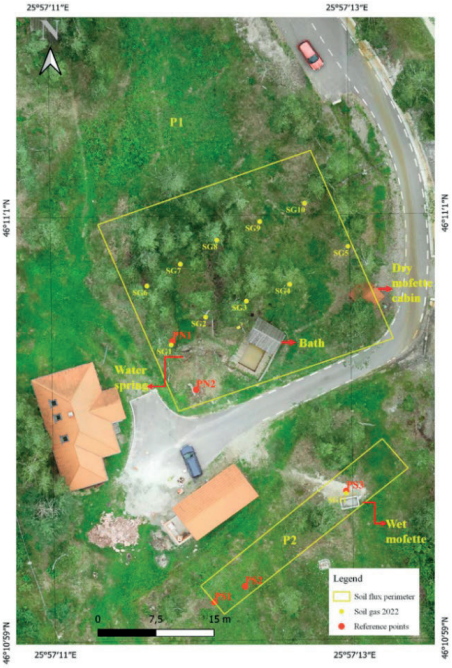


Figure 1. Location of study perimeters, reference points, soil gas sample points and touristic features

The northern perimeter (P1) presents high CO_2 emissions and many wet and dry gas vents, including most of the touristic features such as the baths used for therapeutic purposes and the dry mofette. The southern perimeter (P2) presents much lower emissions and includes a wet mofette and some dry gas vents reduced in intensity and area. This perimeter also was mostly affected by an extensive landscaping process over the years (see example in Figure 2 and Figure 3).



Figure 2. Wet mofette from P2 (PS3) in 2020



Figure 3. Wet mofette in P2 (PS3) in 2024

Soil flux surveys

Starting with 2020, several field campaigns of soil flux measurements have been conducted in the dry (summer) and wet (autumn and spring) seasons of 2020, 2022 and partially in 2024 (after the site underwent an extensive landscaping project).

The most extensive surveys were made in 2022 (Figure 1). Several key points (reference points in Figure 1) were monitored during all this time to see the flux variation in time and its dependence on hydrological regime. The soil flux measurements were made using the closed chamber accumulation method and were conducted with a West Systems portable fluxmeter equipped with CO_2, H_2S and CH_4 sensors (Figure 4).



Figure 4. Soil flux survey conducted with West Systems portable fluxmeter in October 2022

The raw data was processed with FluxRevision software and the calculated flux values were interpolated using ArcGIS software to obtain the maps showing the flux variation.

Soil gas surveys

Soil gas surveys were also implemented on selected sample locations in 2020 and 2022.

In 2020, the soil gas measurements were done during July and focused mainly around the identified wet and dry mofettes of the site.

In 2022, the soil gas measurements were done mostly on 2 selected profiles from P1 (including a reference point) and on a reference point from P2 located around the wet mofette. The measurements were done using the Gas Data GFM 436 portable gas analyser coupled with a hardened steel probe from Durridge (Figure 7). This ensemble allows measuring CO_2 concentrations at different depths, in this case 25, 50 and 75 cm.

RESULTS AND DISCUSSIONS

Soil flux surveys

The extensive soil flux surveys from 2022, conducted in the summer (dry) and autumn (wet) season, shown a significant difference in the level of CO_2 fluxes, most probably due to the difference in the hydrological regime.

In the summer (July for P1 and August for P2), the CO_2 flux varied on P1 between 0.43 and 185 mol/m^2/day and on P2 between 0.20 and 178 mol/m^2/day (Figure 5). The highest CO_2 fluxes

on P1 were measured next north of the therapeutic bath (where several smaller baths exist), near the water spring and on the alignment of the dry mofette cabin. On P2 the maximum CO_2 fluxes were measured near the wet mofette and on the alignment of the water spring.

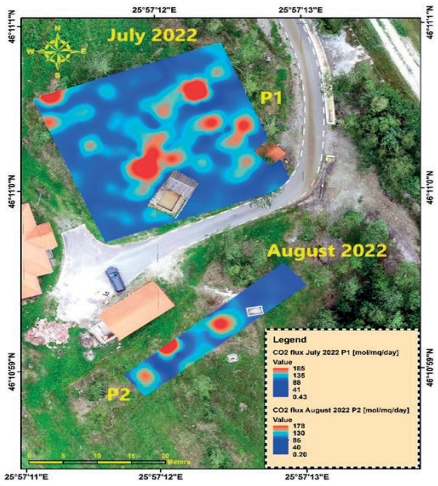


Figure 5. CO_2 soil flux variation in July and August 2022

In October 2022 (Figure 6), CO_2 flux shows much larger values, between 0.17 and 893 mol/m^2/day on P1 and between 0.27 and 625 mol/m^2/day on P2. The maximum values are located, as in the summer, around the water spring, wet and dry mofettes on P1 and on the alignment of water spring and bath and near the wet mofette on P2.

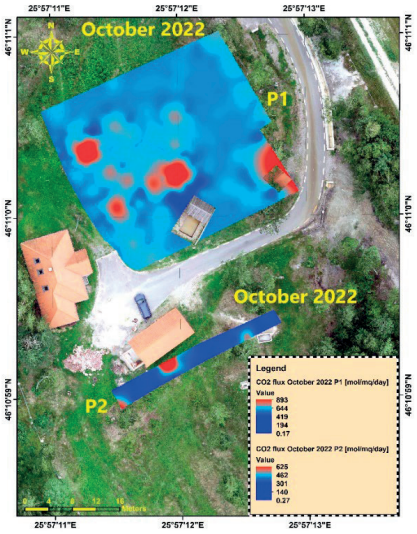


Figure 6. CO_2 soil flux variation in October 2022

The variation of fluxes recorded for the reference points in 2020, 2022 and 2024, show a clear difference between summer and autumn seasons (Table 1).

Table 1. CO_2 flux values in the reference points measured in the surveys from 2020, 2022 and 2024

Ref. point	CO_2 flux October 2020 (mol/m^2/day)	CO_2 flux July/August 2022 (mol/m^2/day)	CO_2 flux October 2022 (mol/m^2/day)	CO_2 flux September 2024 (mol/m^2/day)
PN1	130.2	1.994	262.1	323.3
PN2	32.25	1.898	51.71	60.64
PS1	2.092	3.017	3.17	9.985
PS2	6.688	2.309	12.29	13.78
PS3	1.532	0.939	4.103	2.877

Soil gas surveys

As mentioned before, soil gas surveys from July 2020 have focused around the wet and dry gas vents identified at the site. Two of the sample stations measured then are corresponding with the reference points PN2 (near the water spring) and PS3 (near the wet mofette). For PN2, the measured CO_2 concentrations were 30.6% at 25 cm depth, 16.8% at 50 cm depth and 13.4% at 75 cm depth. For PS3, the measured CO_2 concentrations were 33.3% at 25 cm depth, 31.5% at 50 cm depth and 4.7% at 75 cm depth. The drop in CO_2 concentration with depth, opposite to what have been expected, can be explained with the water ascension in the steel probe. At 25 cm depth, the measurement time was stopped at 2 minutes, but for larger depths, the measurement was stopped at 1 minute due to water intake.

The same situation was encountered also in October 2022 (Table 2), especially near the water spring (SG 1), the smaller wet mofettes (SG2 and SG3) from P1 and near the wet mofette from P2 (SG11).

Table 2. CO_2 soil concentrations in October 2022

Point	CO_2 conc. (%) 25 cm depth	CO_2 conc. (%) 50 cm depth	CO_2 conc. (%) 75 cm depth
SG1	95.6	97.1	n.d.
SG2	9.5	2.2	95.9
SG3	97.2	22	4.6
SG4	1	16.8	2.4
SG5	11.9	2.7	3.6
SG6	0.7	0.3	80
SG7	8.7	96.3	96.7
SG8	13.3	96	27
SG9	35.8	38.8	11.8
SG10	2.3	7.2	12.3
SG11	71.2	0.3	0.1

For SG1, due to water intake, the CO_2 concentration could not be measured at 75 cm depth, considering the specifics of the used equipment. For SG6 and SG7, located north of the water spring and very close to PN 1 (where large CO_2 fluxes have been measured), the increase of CO_2 concentration with depth is clear, having a normal variation in the absence of water at depth.

For SG8 and SG9, the increase of CO_2 concentration was measured at 50 cm depth, but decreased rapidly at 75 cm depth together with the water ascension. SG10, located north of the dry mofette cabin, shows an increase of CO_2 concentration with depth in the absence of water. The most drastic drop of CO_2 concentration with depth can be seen for SG11 (Figure 7), where water intake was higher than in any other point.



Figure 7. Soil gas survey using Gas Systems portable gas analyser and Durridge hardened steel probe next to a wet mofette (SG 11) in October 2022

CONCLUSIONS

During the 2022 campaign, measurements highlighted significant fluctuations in CO_2 flux, both in terms of intensity (concentration) and diffusion area. During the dry season (July-August), CO_2 emissions were relatively low. In contrast, during the wet season (October), CO_2 fluxes increased significantly.

These measurements suggest a correlation between CO_2 emissions and the water regime, with higher emission tendencies in the wet season and lower ones in the dry season. The diffusion of carbon dioxide occurs both at the level of Cretaceous aquifer complexes (a succession of sandstones, marls, and clays) and Quaternary formations, as well as in non-aquifer levels that generate dry mofettes.

Soil moisture plays an important role in how CO_2 diffuses through the soil. In wetter soils, water aids in CO_2 transfer, as moisture appears to facilitate CO_2 mobility, allowing it to migrate more easily to the surface. In wet soils (such as the marshy areas in the northern perimeter - P1), porosity is higher, enabling better CO_2 circulation. As a result, CO_2 concentrations in the soil can increase since it can migrate more easily to the surface. Conversely, in dry soils (during the dry season), porosity may be lower, restricting CO_2 mobility, which leads to the accumulation of CO_2 at deeper levels.

The arrangement of the maximum fluxes mapped, could be possibly associated with migration pathways of CO_2 in the near environment. Possible paths are distinctly highlighted on a north to south direction on the alignment of the water spring, of the therapeutic baths and on the alignment of the dry mofette cabin.

The soil gas surveys revealed a rather strange correlation of CO_2 concentration with depth. In the dry sample locations, the CO_2 concentration increased with depth. In wet locations, the water intake at 50 to 75 cm depth in soil decreased due to water intake.

The studies conducted so far showed the importance of determining the seasonal variability of CO_2 fluxes and concentrations for establishing future monitoring solutions. Apart from this seasonal variability, the hydrological regime and landscaping can play very important roles.

ACKNOWLEDGEMENTS

The research leading to these results was made within the projects PN19 20 05 03 "The study of natural CO_2 emission sites in Banat and Harghita for accession to the European ECCSEL network (Studiul siturilor cu emisii naturale de CO_2 din Banat și Harghita în vederea aderării la rețeaua europeană ECCSEL)" and PN 23 30 04 04 "Development of an environmental monitoring methodology for potential CO_2 storage sites in Romania (Dezvoltarea unei metodologii de monitorizare de mediu pentru potențialele situri de stocare de CO_2 din România)", both financed by the Ministry of Research, Innovation and Digitalization of Romania through the Core Program.
The authors would like to acknowledge and to thank for the support of town hall of Cozmeni who facilitated the access to the site and the smooth running of the campaigns.
We also thank the anonymous reviewers for all suggestions provided for improving the manuscript.

REFERENCES

Airinei, S., & Pricăjan, A. (1972). Correlations between the deep geological structure and the mofetic aureole in Harghita County, regarding the areas of occurrence of carbonated mineral waters (Corelații între structura geologică adâncă și aureola mofetică din județul Harghita, cu privire la zonele de apariție a apelor minerale carbogazoase). *Geological, Geophysical, Geographical Studies and Research, Geology Series*, *2*, 245-258.

Beaubien, S. E., Ciotoli, G., Coombs, P., Dictor, M. C., Kruger, M., Lombardi, S., Pearce, J. M., & West, J. M. (2008). The impact of a naturally occurring CO_2 gas vent on the shallow ecosystem and soil chemistry of a Mediterranean pasture (Latera, Italy). *International Journal of Greenhouse Gas Control 2*(3).

Dudu, A., Avram, C., Sava, C. S., & Caraban, I. (2021). Natural laboratories for the study of CO_2 geological storage in Romania. *Proceedings of the 15th Greenhouse Gas Control Technologies Conference*, 15-18, March 2021, SSRN. https://doi.org/10.2139/ssrn.3812176

Dudu, A.-C., Pavel, A. B., Avram, C., Catianis, I., Iordache, G., Rădulescu, F., Lupașcu, N., Dragoș, A.-G., Dobre, O., Sava, C. S. (2024). Environmental assessment of the area with natural CO_2 emissions in Băile Lăzărești. *Scientific Papers. Series E. Land Reclamation, Earth Observation & Surveying, Environmental Engineering, 13*.

Karátson, D., Veres, D., Gertisser, R., Magyari, E. K., Jánosi, C., & Hambach, U. (2022). *Ciomadul (Csomád), The Youngest Volcano in the Carpathians.* Cham, CH: Springer Nature Switzerland.

Mutihac, V. (1990). *Structura geologică a teritoriului României*. Bucharest, RO: Tehnică Publishing House.

Pricăjan, A. (1974). The dowry of mineral waters and natural gas of Harghita County. (Zestrea de ape minerale și gaze mofetice a Județului Harghita). *Natural Therapeutic Factors from Harghita County*, 7-42.

Pricăjan, A. (1985). *Therapeutic Mineral Substances of Romania (Substanțele minerale terapeutice din România)*. Bucharest, RO: Scientific and Encyclopedia Publishing House.

West, J. M., Pearce, J., Bentham, M., & Maul, P. (2005). Issue Profile: Environmental issues and the geological storage of CO_2. *European Environment, 15*: 250-259.

Ziogou, F., Gemeni, V., Koukouzas, N., de Angelis, D., Libertini, S., Beaubien, S. E., Lombardi, S., West, J. M., Jones, D. G., Coombs, P., Barlow, T. S., Gwosdz, S., Kruger, M. (2013). Potential environmental impacts of CO_2 leakage from the study of natural analogue sites in Europe. *Energy Procedia, 37*: 3521-3528.

***IPCC (2022). Climate Change 2022: Mitigation of Climate Change. Contribution of Working Group III to the Sixth Assessment Report of the Intergovernmental Panel on Climate Change [P.R. Shukla, J. Skea, R. Slade, A. Al Khourdajie, R. van Diemen, D. McCollum, M. Pathak, S. Some, P. Vyas, R. Fradera, M. Belkacemi, A. Hasija, G. Lisboa, S. Luz, J. Malley, (eds.)]. Cambridge University Press, Cambridge, UK and New York, NY, USA. doi: 10.1017/9781009157926.002.

***IPCC (2023). Sections. In: Climate Change 2023: Synthesis Report. Contribution of Working Groups I, II and III to the Sixth Assessment Report of the Intergovernmental Panel on Climate Change [Core Writing Team, H. Lee and J. Romero (eds.)]. IPCC, Geneva, Switzerland, pp. 35-115. doi: 10.59327/IPCC/AR6-9789291691647.

Scientific Papers. Series E. Land Reclamation, Earth Observation & Surveying, Environmental Engineering. Vol. XIV, 2025
Print ISSN 2285-6064, CD-ROM ISSN 2285-6072, Online ISSN 2393-5138, ISSN-L 2285-6064

POSSIBILITIES FOR THE RECOVERY OF AGRICULTURAL VEGETABLE WASTE

Timea GABOR[1], Andreea HEGYI[1, 2], Stelian COSTE[1], Alina Iuliana CADAR[1], Cristian PETCU[2], Carmen FLOREAN[1, 2], Ioana Monica SUR[1]

[1]Technical University of Cluj-Napoca, 103-105 Muncii Blvd, 400641, Cluj-Napoca, Romania
[2]National Institute for Research and Development in Construction, Urban Planning and Sustainable Spatial Development - URBAN-INCERC, 266 Pantelimon Road, District 2, 021652, Bucharest, Romania

Corresponding author email: andreea.hegyi@gmail.com

Abstract

Agricultural activities generate substantial volumes of waste and by-products annually, primarily of plant origin, which are either underutilized or not utilized at all. Through partial pyrolysis, these waste materials can be transformed into a product known as "biochar (BCH)," which has potential applications in both agriculture and innovative construction materials. This paper presents a comparative study examining the impact of BCH utilization in these two fields. Research findings demonstrated beneficial effects on soil quality and crop yield improvement. Additionally, studies conducted on cementitious composites incorporating 5-15% biochar revealed reduced density, increased open porosity, maintained mechanical strength parameters, and thermal conductivity values that suggest the possibility of developing innovative mortars with enhanced thermal resistance or suitable for manufacturing paving elements. Through this dual approach, this paper aims to highlight the potential of transforming agricultural waste into valuable materials that benefit both agriculture and the development of new, innovative, and environmentally friendly construction materials.

Key words*: agricultural sub-products, benefits for agriculture, biochar, innovative cementitious composites.*

INTRODUCTION

Globally, there is an ongoing transition from the linear economic model of "EXTRACT – PRODUCE – CONSUME – DISPOSE", now considered obsolete, to a circular model. This new approach focuses on reintegrating industrial and agricultural waste and/or by-products into the production cycle, emphasizing increased product durability and extended operational lifespans (Ricciardi et al., 2020; Kebaili et al., 2022). This transition addresses two key challenges: first, the need to find valorization solutions for the large volume of biomass generated by agricultural activities, and second, the necessity to develop new, innovative, and environmentally friendly sustainable materials and technologies to reduce the construction industry's environmental impact (Androutsopoulos et al., 2020). Using agro-industrial waste, which would otherwise be destined for landfills or incineration (Madurwar et al., 2013), presents an opportunity to prevent increased greenhouse gas emissions. The International Biochar Initiative (IBI) defines biochar (BCH) as "a solid material obtained by biomass carbonization" (Cha et al., 2016). Specifically, BCH is a sterile vegetable charcoal produced through thermochemical biomass processing – pyrolysis at 400-900ºC under limited oxygen conditions – which could address both identified challenges. BCH contains 75-90% carbon and is characterized by extremely high porosity and superior adsorption capacity. Its applications include use as an agricultural soil amendment to enhance fertility, an additive in animal feed, and a filtering medium for air, gases, and water (Chan et al., 2007).

Currently, researchers are investigating BCH's potential in developing carbon-neutral concrete, leveraging its ability to store atmospheric CO_2 (Winters et al., 2022; Gupta & Kua, 2018a; Choi et al., 2012; Zhao et al., 2019; Cuthbertson et al., 2019; Gupta & Kua, 2017).

Some research shows that the rich pore structure of BCH causes it to absorb a large amount of water during the concrete preparation stage, which it then releases during the cement hydration-hydrolysis stage. This process

promotes the secondary hydration reaction and additional hardening, thereby increasing the mechanical performance of cementitious composites (Maljaee et al., 2021; Gupta et al., 2018b; Chen et al., 2022a).

However, international research results remain controversial.

Generally, it is reported that the beneficial effect of biochar-type materials in cementitious composites is optimal at a maximum addition of 5% in the composition, with higher quantities hurting the composite's performance (Song et al., 2023).

Some studies limit the mass percentage of BCH addition in cementitious composites to 2% (Maljaee et al., 2021), while others suggest that it's possible to partially substitute up to 10% of cement with BCH while maintaining the physical-mechanical performance indicators of both the cementitious composite (Hylton et al., 2024) and cement-based agglomerated boards (Chen et al., 2022b).

Regarding the effect of using BCH in agricultural soils, studies have shown that poor nutrient content and accelerated mineralization of soil organic matter are the two major constraints currently encountered in sustainable agriculture (Zheng et al., 2010).

In recent years, there has been much evidence that BCH is not only more stable than other soil amendments but also that soil nutrient content is higher compared to the effects of other fertilizers (Lehmann & Joseph, 2009).

Numerous studies have reported improvements in water capacity and retention when a rate of 0.5% BCH was applied, modifying porosity and facilitating the formation of bonds and complexes of cations and anions with metals and elements in the soil, which improves nutrient retention capacity (Suarau et al., 2016), while reducing soil density (Mukherjee & Lal, 2013).

The increase in soil fertility also results from the fact that the basic cations contained in BCH are discharged into the soil, replacing Al and H+ and thus improving the cation exchange capacity (CEC) of the soil (Cha et al., 2016), but also through the influence on the dynamics of Soil Organic Carbon (SOC), inhibiting the degradation process and increasing the mean residence time (MRT) in which organic carbon remains in the soil, respectively, increasing the processes of stabilization and retention of SOC (Suarau et al., 2016). At the same time, studies have reported an increase, from 50% to 72%, of biological nitrogen fixation in the soil and increases in the yield of agricultural crops (Suarau et al., 2016).

A recent statistical meta-analysis of global results (Hartley et al., 2016; Zhang et al., 2016) indicates a significant positive effect on agricultural production yield, namely an increase of 12%, simultaneously showing a significant impact on soil performance indicators (Schmidt et al., 2016).

For example, an analysis carried out on the use of inorganic fertilizers in the cultivation systems of small farmers in Africa shows that they often become ineffective due to increased sensitivity to fertilizer application.

The use of BCH, alone or in combination with classical fertilizers (urea or di-ammonium phosphate), had no effects on macrofauna, such as beetles, centipedes, millipedes, termites and ants, but attracted earthworms and led to taxonomic enrichment of species as well as increased corn production yield in the first 2 growing seasons, with no subsequent significant effects in seasons 3 and 4 (Kamau et al., 2019).

Other studies (Mikajlo et al., 2024; Kammann et al., 2016) indicate that good results were obtained for soil treatment intended for lettuce growth. Thus, it is shown that BCH applied by simply spreading on the surface does not necessarily lead to an improvement in soil quality, but composted BCH, or BCH applied in a mixture with compost, can lead to 3-6 times higher growth of lettuce plants compared to untreated soil. The study also indicates more obvious results in soils with lower iron content.

Therefore, in recent years the use of BCH in agriculture has become increasingly common, as evidenced by countries such as Portugal, Spain, Germany, Austria and Switzerland (Calotescu, 2016; Zmaranda, 2019; Schmidt et al., 2016), where very large quantities of biochar are used to replace chemical fertilizers and pesticides. Countries such as Belize, Cameroon, Chile, Costa Rica, Egypt, India, Kenya, Mongolia, and Vietnam are implementing similar projects as discussed at the Biochar 2018 conference (IBI, 2018).

In this context, the purpose of this paper is to present a parallel study on the possibilities of using BCH in two apparently unrelated fields

which, in this case, have in common the possibility of implementing circular economy principles on biomass residues.

MATERIALS AND METHODS

The research methodology followed two parallel directions. Thus, on one hand, cementitious composites with BCH addition were prepared, and on the other hand, the development of three plant species was monitored: radish (*Raphanus sativus*), spinach (*Spinacia oleracea*), and garden lettuce (*Lactuca sativa*) on a plot of land located in Sălaj County, where the soil was enriched with BCH. The BCH used was obtained from vegetable waste, produced by Explocom GK through the slow pyrolysis process (temperature of 500ºC, residence time of 15 minutes) and is characterized by the following parameters: granulation 0-20 mm, pH 9, carbon content 70-76%, volatile substances content 8-19%, ash content 3-6%, and water content max. 12%. To analyze the influence of BCH addition on the performance of cementitious composites, 4 compositions were prepared: one control and three compositions with BCH addition, using Portland cement CEM I 52.5 R, water, and standardized polygranular sand (Table 1).

Table 1. Ratio of raw materials for the preparation of cementitious compositions

Sample code	Cement (g)	Ratio water/ cement	Polygranular sand (g)	BCH (% based on cement quantity)
R-M	450	0.5	860	0
R-5BCH				5
R-10BCH				10
R-15BCH				15

The indicators for quantifying the influence of BCH on the performance of cementitious composites were: density in the hardened state, according to EN 1015-10:2002+A1:2007; water absorption according to EN 1339:2004+AC:2006; compressive strength and flexural tensile strength determined according to EN 1015-11:2020; and wear resistance (EN 1339:2004+AC:2006). At the same time, an analysis of the influence of BCH on the durability of cementitious composites was carried out, namely an analysis in terms of behavior after 25 freeze-thaw cycles (EN 1339:2004+AC:2006) and 25 wet-dry cycles (a wet-dry conditioning cycle was performed by completing 8 h of air conditioning at a temperature of 21±2°C and 16 h of immersion in 3% NaCl solution at a temperature of 21±2°C). All tests were performed under laboratory conditions, on sets of 3 prismatic specimens 40x40x160 mm each, made by casting in metal molds. After casting, the samples were kept for 24 h in high humidity conditions (90%), at room temperature (23°C), then demolded, deburred, and kept under controlled temperature and humidity conditions in the climatic chamber until reaching the age of 28 days from casting. Finally, the influence of BCH on the thermal performance of cementitious composites was evaluated by following the variation of the thermal conductivity coefficient λ (W/m·K). For this purpose, 300x300x20 mm plates made by casting from cementitious composites and conditioned under conditions similar to the prismatic specimens were used. Using the hot plate method, a FOX 314 conductivity meter was used for testing at a temperature difference between the plates of 10°C, according to EN 12667:2002.

The research conducted to identify the influence of BCH on plant growth performance was carried out using soil collected from an agricultural area in Sângeorgiu de Meseș locality, Buciumi commune, Sălaj county. The soil falls into the class of clinohydromorphic black soils, with a concave appearance, having a high humus content, a dark brown to black color, and being slightly stony. This soil was prepared for planting seeds of radish (*Raphanus sativus*), spinach (*Spinacia oleracea*), and garden lettuce (*Lactuca sativa*), by adding 5%, 10%, 15%, and 20% BCH (mass percentages in relation to the amount of soil). BCH was used in the soil in combination with Bio-pyrolytic condensate - a biopyrolytic distilled product, representing a solution of organic fertilizer (pyrolinic acid - humic acid), a commercially purchased nutrient intended for use on all soil types, dosed at 1ml/l water/container, applied in odd weeks of growth. An experimental greenhouse-type stand was built in which containers with a capacity of 1l were placed, 3 for each type of plant and each type of soil sample, with a set of 3 containers for each type of plant being filled with soil without the addition of BCH and considered as control. In each container, purchased commercially, 5 seeds of the same type were planted and watered

with 100 ml of water. Subsequently, at equal intervals of 2 days, each sample was watered with 50 ml of water, continuously monitoring the temperature in the greenhouse, which was kept constant at 25±2ºC, and the degree of sunlight was ensured equally for all samples by their location. Plant growth monitoring was carried out for 9 weeks from planting until they reached a degree of development that no longer allowed cultivation in the containers used. The quantifiable monitoring indicator was the height of the plants, measured using a graduated ruler with a minimum division of 1 mm, reporting average values of all plants of a species developed in the 3 pots with the same type of soil. The samples were assigned codes (Table 2).

Table 2. Sample coding system for plants grown with different BCH concentrations

	BCH 0%	BCH 5%	BCH 10%	BCH 15%	BCH 20%
Radish	CR	R5	R10	R15	R20
Spinach	CS	S5	S10	S15	S20
Garden lettuce	CSV	SV5	SV10	SV15	SV20

RESULTS AND DISCUSSIONS

Regarding the influence of BCH addition on the performance indicators of cementitious composites, the experimental results indicate a progressive reduction in apparent density, with an increase in the amount of BCH, by 4.8%-5.8% compared to the control sample.
Based on these results, a first benefit of using BCH can be identified: reducing the mortar density (Figure 1) therefore, in the case of its use as a construction material, reducing the load on the construction's resistance structure.

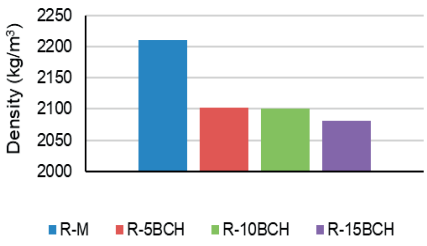


Figure 1. Hardened bulk density of cementitious composites

Regarding water absorption (Figure 2), the results indicate increases in this indicator following the addition of BCH, without being able to identify a direct correlation with the amount of BCH added to the composite.

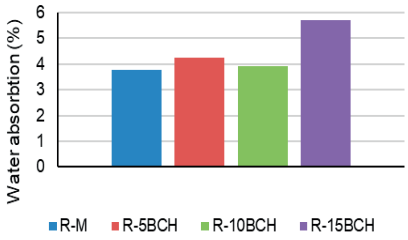


Figure 2. Water absorption of cementitious composites

However, correlating this information with the variation of apparent density in the hardened state, it can be concluded that both directions provide indications leading to the hypothesis of increased open porosity in mortars with the introduction of BCH in the composition.
On the other hand, correlating the experimentally obtained results with the references in standards EN 1338, EN 1339, and EN 1340, which indicate a maximum water absorption of 6% for prefabricated elements such as tiles, pavers, and curbs, it can be noted that, from this point of view, the analyzed mortars successfully satisfy the condition of resistance and durability to climatic factors required for use in the production of such elements.
These results correlate with the literature which indicates the possibility of increasing the total water absorption by up to 28% compared to the control samples (Song et al., 2023).
From the point of view of BCH addition's influence on the mechanical strengths of cementitious composites (Figure 3) the results indicate reductions of 30-40% in tensile bending strength (from 10.4 N/mm² to min. 6.2 N/mm²), and 26-47% in compressive strength (from 71.3 N/mm² to min. 37.9 N/mm²), while maintaining sufficient performance to be classified as M35 or M50 masonry mortars according to EN 998-2 specifications.
Comparing the experimental results with other findings reported in the literature (30-50 N/mm²) (Roychand et al., 2023), it can be said that they are consistent, with some cases where the compressive strength of the laboratory-tested cementitious composite is even better.

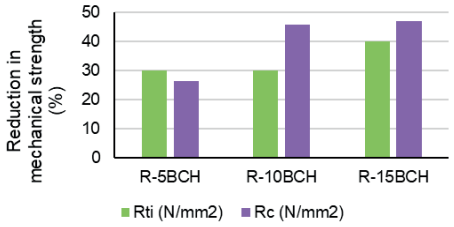


Figure 3. Reduction in mechanical strength of cementitious composites with BCH, compared to the control sample

Although negative influences of BCH addition on mechanical strength are identified under laboratory conditions when cementitious composites are subjected to freeze-thaw cycles (Figure 4), a first beneficial effect is observed: the reduction in mechanical strength following freeze-thaw action occurs only in the control composition, while composites with BCH show slight increases in strength indicators. This behavior suggests the possibility of improving the durability of cementitious composites through BCH addition.

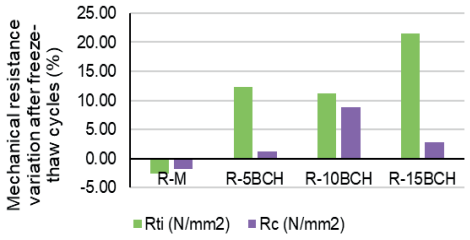


Figure 4. Increase in mechanical strength of control and BCH cementitious composites after 25 freeze-thaw cycles

Similarly, the action of wet-dry alternation cycles combined with the action of chlorine ions in the immersion phase (wet), leads to a reduction in mechanical strength only for the control composition, supporting the possibility of improving durability by using BCH (Figure 5).
According to the literature (Chen et al., 2023), a possible explanation for this phenomenon could be found as a result of several processes that occur when BCH is introduced into the composite matrix:
- the incorporation of biochar into the cementitious composite improves the pore structure, dimensions, and distribution, which leads to a reduction in capillary porosity. At the same time, the macropore structure becomes more independent, providing more space for frozen water (this being the main factor that induces internal stresses in the composite matrix upon freezing), thus reducing the internal stresses in the freezing phase and the loss of mechanical strength (Gupta et al., 2020; Jia et al., 2023; Qin et al., 2016);

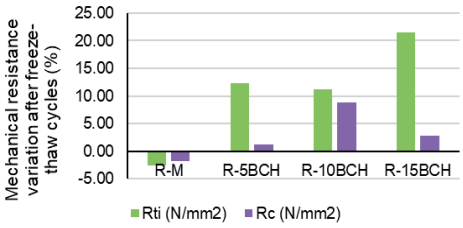


Figure 5. Increase in mechanical strength of control and BCH cementitious composites after 25 wet-dry cycles

- on the other hand, the porous structure of BCH can store and, when necessary, slowly release an amount of water necessary to reduce the self-shrinkage of the cement paste, promoting the hydration reactions of the partially or unreacted cement granules, densifying the material and thus improving long-term properties and durability (Mo et al., 2019). Additionally, it has been shown that the BCH-cement paste transition zone (ITZ) can be superior to that characteristic of sand particles, which increases the yield of hydration product formation (Mrad & Chehab, 2019);
- at the same time, studies have shown that the incorporation of BCH into the composite matrix strongly contributes to increasing the possibilities of storing CO_2 and forming stable calcium carbonate precipitates through rapid reaction with the main compounds of non-hydrated cement, tricalcium silicate (C_3S) and calcium hydrogen silicate (C-S-H) inside the cement matrix, while promoting the process through its function as a nucleating agent. Subsequently, through the precipitation of calcium carbonate, BCH will cause the filling of pores and the reduction of the carbonation depth (Liu et al., 2022), a similar effect being probably possible on the penetration of liquids in the freeze-thaw or wet-dry process in the presence of chloride. This CO_2 absorption capability could also improve indoor air quality, as recent

studies have shown that CO2 levels in multifamily buildings often exceed recommended thresholds for a health-safe indoor environment (Magurean & Petran, 2023). The mass loss due to abrasion stresses is reduced by modifying the mortar composition as a result of the addition of organic waste subjected to thermal treatments (mass loss of 13.6-17.2% for samples with BCH, compared to 19.6% for the control sample). However, given that the addition of organic waste subjected to thermal treatments results in a reduction in the density of the material, it is considered that this indicator is inconclusive and could lead to an erroneous conclusion indicating an increase in wear resistance. Therefore, two other indicators were analyzed: the height loss of the sample and its volume loss (Figure 6).

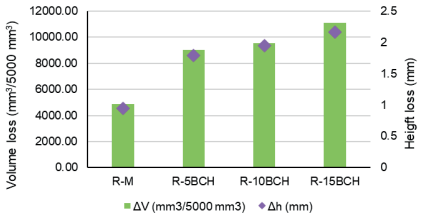


Figure 6. Height/volume loss of specimens subjected to abrasion stress

It is thus demonstrated that with the addition of BCH, the wear resistance of the mortars decreases, increasing the height losses and volume losses of the specimens. However, analyzing the experimentally obtained results in correlation with the series of standards EN 1338, EN 1339, and EN 1340, specific to prefabricated elements such as tiles, pavers, and curbs, it can be said that mortars with the addition of BCH meet the acceptability criteria in terms of wear resistance, with maximum height and volume loss limits being 2 mm and 11080 mm^3 / 5000 mm^3, respectively.

It should be noted that the specialized literature restricts the amount of heat-treated organic waste to 1-2%, a maximum 5% mass percentage, and the tests carried out addressed substantially larger amounts of used waste. This approach, assuming the risk of reducing some physical-mechanical performance indicators, allowed demonstrating the achievement of the acceptability criteria specific to a specified field of use, in this case, masonry mortars or compositions intended for the manufacture of paving elements. At the same time, corroborating the indicators relating to the apparent density and water absorption that lead to an increasing porosity with the addition of BCH, with the thermal conductivity coefficient (Figure 7), it is appreciated that the addition of BCH contributes to improving the thermal performance of the composites. Thus, a possibility is foreseen to produce cementitious composites similar to adhesive mortars intended for the production of ETICS thermal insulation systems whose thermal conductivity coefficient generally falls within the range of 0.08-0.11 W/mK. At the same time, for cementitious composites containing BCH, the mechanical strength indicators support this possibility of defining a field of use in the area of adhesive mortars intended for the creation of ETICS thermal insulation systems.

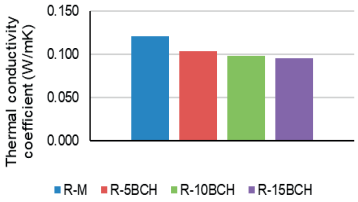


Figure 7. Thermal conductivity of cementitious composites

Regarding the results of the program analyzing the influence of BCH on plant growth, several key elements were highlighted. After the first week following seed planting (Figure 8), it was observed that the control containers showed a germination rate of 60% (3 shoots out of 5 seeds), while in containers with BCH-enriched soil, the germination rate was 80-100% (4-5 shoots out of 5 seeds).



Figure 8. Plant development - week 1

During the 9 weeks of monitoring, more accelerated plant development was recorded, regardless of plant type, in the soil enriched with BCH (Figures 9-11).



Figure 9. Plant development - week 5

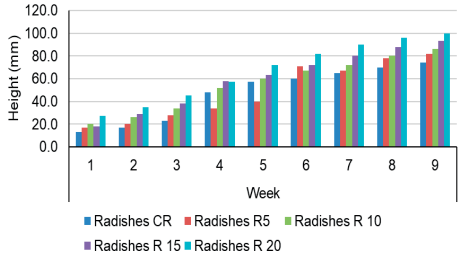


Figure 10. Plant development - week 9

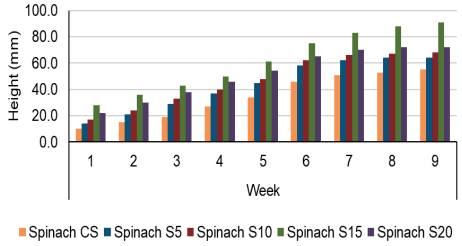
Compared to the control sample, radishes showed a 6-fold more intense growth after 9 weeks with just 5% BCH addition, and for additions of 10-20% BCH in the soil, the height increase was 16.2%, 25.7%, and 35.1% more intense.

In the case of spinach, a Gaussian evolution of the benefit was observed, quantified by the increase in plant height. In the range of 5-15% BCH addition to the soil, after 9 weeks, compared to the control, the plants were taller by 16.4%, 23.6%, and 65.5%, respectively, while for soil with 20% BCH, this indicator was 30.9%. This Gaussian evolution was maintained throughout all weekly measurements, indicating that a 20% BCH addition to the soil is not beneficial, with the limit in the analyzed case being 15% BCH.

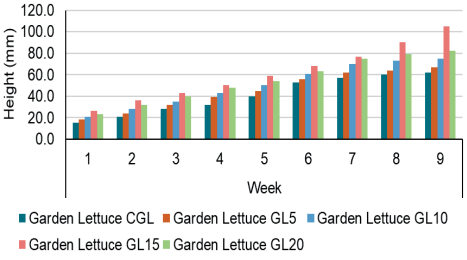
A similar evolution to spinach development was also recorded in lettuce plants. For 5-15% BCH, the plant heights were 8.1%, 21%, and 69.4% higher compared to the control after 9 weeks, while for soil with 20% BCH, this indicator was 32.3% higher compared to the control. Again, this Gaussian-type evolution was maintained throughout all 9 weeks, similarly indicating a limitation of 15% for BCH addition to the soil.



a)



b)



c)

Figure 11. Evolution of plant height during the 9 weeks of analysis, based on the amount of BCH used: a) radishes (R); b) spinach (S); c) garden lettuce

Similar results were also obtained by Goldan E. and Nedefe V. (Goldan & Nedeff, 2020) in their experimental research on winter barley plants in open fields.

CONCLUSIONS

The purpose of this study was to analyze, in parallel, possible directions for using plant waste treated by partial pyrolysis, specifically a biochar-type product, in two independent fields: construction materials and agriculture. Based on the experimental results presented, regarding the

influence of BCH addition in cementitious composites, the following can be stated:
- reductions in apparent density in the hardened state were recorded simultaneously with increases in water absorption, which could be considered indicators suggesting an increase in open porosity. Additionally, reductions in mechanical resistance to compressive, flexural, and abrasion stresses were recorded. However, by correlating the obtained results with the specific conformity indicators for tiles, pavers, and curbs specified in the product standards EN 1338, EN 1339 and EN 1340, a preliminary direction for identifying the field of use can be determined, as cementitious composites with BCH addition satisfy these criteria;
- analyzing the durability indicators, namely the loss of mechanical resistance following exposure to freeze-thaw cycles and wet-dry cycles under the action of chlorine ions, the experimental results indicate a performance improvement. More specifically, mechanical resistance increases in cementitious composites with BCH addition, unlike the control sample whose mechanical performance is, as expected, reduced following exposure to the test cycles. Possible explanations can be found in the scientific literature, which identifies a significant influence of BCH on the porosity of cementitious composites, on the hydration-hydrolysis mechanism of cement granules, on the structure of the interfacial transition zone (ITZ) between the cement paste and BCH granules, and the potential for CO_2 storage and formation of stable calcium carbonate precipitate. This precipitate forms through rapid reaction with the main compounds of non-hydrated cement and could fill the pores or even the microcracks that appeared during the stress period of the test cycles;
- regarding the influence of BCH on the thermal conductivity coefficient, this indicator showed improvement compared to the control sample, which, correlated with the reduction in apparent density and sufficient mechanical resistance, can support the identification of a new research direction, namely, the development of adhesive mortars intended for ETICS thermal insulation systems of building facades.

Therefore, although the literature restricts the amount of heat-treated organic waste to 1-2%, with a maximum of 5% mass percentage, the tests carried out addressed substantially larger amounts of waste. This approach, while assuming the risk of reducing some physical-mechanical performance indicators, allowed the demonstration of achieving acceptability criteria specific to a particular field of use, in this case, masonry mortars, compositions intended for the manufacture of paving elements, or even adhesive mortars specific to ETICS thermal insulation systems.

Based on the experimental results presented, regarding the influence of BCH addition to agricultural soil, a positive influence was also identified on the development of some food consumption plants: radish (*Raphanus sativus*), spinach (*Spinacia oleracea*), and garden lettuce (*Lactuca sativa*). The experimental results indicated an increase in germination rate from 60% recorded for the control samples to 80-100% recorded for the soil samples with BCH addition. Additionally, more accelerated plant development was recorded, regardless of plant type, in the soil enriched with BCH, noting that, for the same development time interval, the evolution of plant height depending on the amount of BCH used in the soil can be Gaussian-type, depending on the cultivated plant type. Overall, a maximum limit of 15% BCH amount is recorded, exceeding it (samples with 20% BCH) may lead to reduced benefits in terms of plant development (spinach and lettuce).

In conclusion, based on the experimental results, in addition to several benefits that prove the possibility of valorizing plant waste and using BCH in construction and agriculture, several future research directions can be identified:
- analysis of the influence of introducing BCH into cementitious composite matrices not as an addition but as a raw material substitute;
- identification of maximum acceptable limits for BCH use in cementitious composites, depending on the expected field of use;
- identification of correlations between soil nature and characteristics, plant type, and optimal BCH amount used to obtain maximum benefits.

REFERENCES

Androutsopoulos, A., Geissler, S., Charalambides, A. G., Escudero, C. J., Kyriacou, O., & Petran, H. (2020). Mapping the deep renovation possibilities of European buildings. In IOP Conference Series: Earth and Environmental Science (Vol. 410, No. 1, p. 012056). *IOP Publishing*.

Calotescu, T. (2016). Biochar şi gazogen din resturi vegetale. *Agromedia.*

Cha, J. S., Park, S. H., Jung, S. C., Ryu, C., Jeon, J. K., Shin, M. C., & Park, Y. K. (2016). Production and utilization of biochar: A review. *Journal of Industrial and Engineering Chemistry*, *40*, 1-15.

Chan, K. Y., Van Zwieten, L., Meszaros, I., Downie, A., & Joseph, S. (2007). Agronomic values of greenwaste biochar as a soil amendment. *Soil Research*, *45*(8), 629-634.

Chen, L., Yuying, Z., Claudia, L., Lei W., Shaoqin, R., Chi, S. P., Yong, S. O. & Daniel, C. W. T. (2022a). Carbon-negative cement-bonded biochar particleboards. *Biochar, 4*(1), 58.

Chen, L., Zhang, Y., Wang, L., Ruan, S., Chen, J., Li, H. & Yang, J. (2022b). Biochar-augmented carbon-negative concrete. *Chemical Engineering Journal, 431*, 133946.

Chen, L., Zhou, T., Yang, J., Qi, J., Zhang, L., Liu, T., Dai, S., Zhao, Y., Huang, Q., Liu, Z. & Li, B. (2023). A review on the roles of biochar incorporated into cementitious materials: Mechanisms, application and perspectives. *Construction and Building Materials*, *409*, 134204.

Choi, W. C., Do Yun, H., Lee J. Y. (2012). Mechanical Properties of Mortar Containing Biochar from Pyrolysis. *Journal Korea Institute for Structural Maintenance and Inspection*, *16*, 67–74.

Cuthbertson, U., Berardi, C., Briens, F. & Berruti, B. (2019). Biochar from residual biomass as a concrete filler for improved thermal and acoustic properties. *Biomass Bioenergy, 120*, 77–83, https://doi.org/10.1016/j.biombioe.2018.11.007.

EN 12667:2002 Thermal performance of building materials and products. Determination of thermal resistance by means of guarded hot plate and heat flow meter methods. Products of high and medium thermal resistance.

EN 1015-10:2002+A1:2007 Methods of test for mortar for masonry - Part 10: Determination of dry bulk density of hardened mortar

EN 1015-11:2020 Methods of test for mortar for masonry - Part 11: Determination of flexural and compressive strength of hardened mortar

EN 1338:2004/AC:2006 Concrete paving blocks - Requirements and test methods

EN 1339:2004+AC:2006 Concrete paving flags - Requirements and test methods

EN 1340:2004 Concrete kerb units - Requirements and test methods

EN 998-2:2016 Specification for mortar for masonry. Masonry mortar

Goldan E. & Nedeff V., (2020). *Studii şi cercetări privind posibilitățile de utilizare ca fertilizatori a deșeurilor organice tratate*. Teza de doctorat, Bacau, Romania.

Gupta, S. & Kua, H. W. (2017). Factors Determining the Potential of Biochar as a Carbon Capturing and Sequestering Construction Material: Critical Review. *Journal of Materials in Civil Engineering, 29,* 04017086, https://doi.org/10.1061/(asce)mt.1943-5533.0001924.

Gupta, S. & Kua, H.W. (2018a). Effect of water entrainment by pre-soaked biochar particles on strength and permeability of cement mortar. *Construction and Building Materials*, *159*, 107–125, https://doi.org/10.1016/j.conbuildmat.2017.10.095

Gupta, S., Kua, H. W. & Pang S. D. (2018b). Biochar-mortar composite: manufacturing, evaluation of physical properties and economic viability. *Construction and Building Materials*, *167*, 874–889.

Gupta, S., Kua, H. W. & Pang S. D. (2020). Effect of biochar on mechanical and permeability properties of concrete exposed to elevated temperature. *Construction and Building Materials*, *234*, 117338, https://doi.org/10.1016/j.conbuildmat.2019.117338.

Hartley, W., Riby, P., & Waterson, J. (2016). Effects of three different biochar's on aggregate stability, organic carbon mobility and micronutrient bioavailability. *Journal of Environmental Management*, *181*, 770-778.

Hylton, J., Hugen, A., Rowland, S. M., Griffin, M., & Tunstall, L. E. (2024). Relevant biochar characteristics influencing compressive strength of biochar-cement mortars. *Biochar, 6*(1), 1-27.

International Biochar Initiative. (2018, August 20–23). Biochar 2018: The carbon link in watershed ecosystem services *Conference. Wilmington*, DE. Retrieved from https://biochar-international.org/event/biochar-2018/.

Jia, Y., Li, H., He, X., Li, P. & Wang, Z. (2023). Effect of biochar from municipal solid waste on mechanical and freeze–thaw properties of concrete. *Construction and Building Materials, 368*, 130374, https://doi.org/10.1016/j.conbuildmat.2023.130374.

Kamau, S., Karanja, N. K., Ayuke, F. O., & Lehmann, J. (2019). Short-term influence of biochar and fertilizer-biochar blends on soil nutrients, fauna and maize growth. *Biology and Fertility of Soils*, *55*, 661-673.

Kammann, C, Glaser, B. & Schmidt, H. P. (2016). *Combining biochar and organic amendments in biochar in European soils and agriculture: science and practice*. Routledge, England.

Kebaili, F.K., Baziz-Berkani, A., Aouissi, H.A., Mihai, F.C., Houda, M., Ababsa, M., Azab, M., Petrisor, A.I., & Fürst C. (2022). Characterization and Planning of Household Waste Management: A Case Study from the MENA Region. *Sustainability*, *14*(9), 5461. https://doi.org/10.3390/su14095461

Lehmann, J., & Joseph, S. (2009). *Biochar for Environmental Management: An Introduction*, Chapter 1, 1-12, www.books.google.com.

Liu, J., Guang L., Weizhuo Z., Zhenlin L., Feng X. & Luping T. (2022). Application potential analysis of biochar as a carbon capture material in cementitious composites: A review. *Construction and Building Materials*, *350*, 128715.

Madurwar, M.V., Ralegaonkar, R.V. & Mandavgane, S.A. (2013). Application of agro-waste for sustainable construction materials: A review. *Construction and Building Materials*, *38*, 872–878.

Magurean, A. M., & Petran, H. A. (2023). Analysis of Measured CO2 Levels through Long-Term Monitoring in Renovated Multifamily Buildings: A Common Case. *Buildings*, *13*(8), 2113.

Maljaee, H., Madadi, R., Paiva, H., Tarelho, L. & Ferreira, V. M. (2021). Incorporation of biochar in cementitious materials: a roadmap of biochar selection. *Construction and Building Materials,* 283, 122757.

Mikajlo, I., Lerch, T. Z., Louvel, B., Hynšt, J., Záhora, J., & Pourrut, B. (2024). Composted biochar versus compost with biochar: effects on soil properties and plant growth. *Biochar, 6*(1), 85.

Mo, L., Fang, J., Huang, B., Wang, A. & Deng, M. (2019). Combined effects of biochar and MgO expansive additive on the autogenous shrinkage, internal relative humidity and compressive strength of cement pastes, *Construction and Building Materials. 229*, 116877. https://doi.org/10.1016/j.conbuildmat.2019.116877.

Mrad, R. & Chehab, G. (2019). Mechanical and microstructure properties of biochar-based mortar: an internal curing agent for PCC. *Sustainability 11*(9), 2491, https://doi.org/10.3390/su11092491.

Mukherjee, A. & Lal, R., (2013). Biochar Impacts on Soil Physical Properties and Greenhouse Gas Emissions. *Agronomy*, *3*, 313-339.

Qin, X. Meng, S. Cao, D., Tu, Y. Sabourova, N., Grip, N., Ohlsson, U., Blanksvard, T., Sas, G. & Elfgren, L. (2016). Evaluation of freeze-thaw damage on concrete material and prestressed concrete specimens. *Construction and Building Materials*, *125*, 892–904, https://doi.org/10.1016/j.conbuildmat.2016.08.098.

Ricciardi, P., Cillari, G., Carnevale Miino, M. & Collivignarelli, M. C. (2020). Valorization of agro-industry residues in the building and environmental sector: A review. *Waste Management & Research*, *38*(5), 487-513.

Roychand, R., Li, J., Kilmartin-Lynch, S., Saberian, M., Zhu, J., Youssf, O. & Ngo, T. (2023). Carbon sequestration from waste and carbon dioxide mineralisation in concrete–A stronger, sustainable and eco-friendly solution to support circular economy. *Construction and Building Materials*, *379,* 131221.

Schmidt, H. P., Bucheli, T., Kammann, C., Glaser, B., Abiven, S. & Leifeld, J. (2016). *European biochar certificate-guidelines for a sustainable production of biochar.*

Song, N., Li, Z., Wang, S. & Li, G. (2023). Biochar as internal curing material to prepare foamed concrete. *Construction and Building Materials*, *377*, 131030.

Suarau, O., Oreva, O., & Aliku, O., (2016). *Biochar Technology for Sustainable Organic Farming*, Biochar book, Chapter 6., DOI: 10.5772/61440,

Winters, D., Boakye, K. & Simske, S. (2022). Toward Carbon-Neutral Concrete through Biochar–Cement–Calcium Carbonate Composites: A Critical Review. *Sustainable*, *14*, 4633. https://doi.org/10.3390/SU14084633;

Zhang, D., Yan, M., Niu, Y., Liu, X., Zwieten, L., Chen, D. & Pan, G. (2016). Is current biochar research addressing global soil constraints for sustainable agriculture? *Agriculture, ecosystems & environment, 226*, 25-32.

Zhao, M., Jia, Y., Yuan, L., Qiu, J. & Xie, C. (2019). Experimental study on the vegetation characteristics of biochar-modified vegetation concrete, *Construction and Building Materials, 206*, 321–328, https://doi.org/10.1016/j.conbuildmat.2019.01.238.

Zheng, W., Sharma, B. K. & Rajagopalan, N. (2010). Using Biochar as a Soil Amendment for Sustainable Agriculture, *Sustainable Agriculture Grant Program Illinois* Department of Agriculture, Champaign, France.

Zmaranda, L. (2019). Biocharul și sănătatea solului, *Agrotehnica,* 18 aprilie.

Scientific Papers. Series E. Land Reclamation, Earth Observation & Surveying, Environmental Engineering. Vol. XIV, 2025
Print ISSN 2285-6064, CD-ROM ISSN 2285-6072, Online ISSN 2393-5138, ISSN-L 2285-6064

GROUND AIR MICROFLORA STUDY USING A CASCADE IMPACTOR

Bilyana GRIGOROVA-PESHEVA, Asen PESHEV

University of Forestry, 10 Kliment Ohridski Blvd, 1797 Sofia, Bulgaria

Corresponding author email: b.pesheva@ltu.bg

Abstract

Urban air pollution poses significant public health risks, with airborne microorganisms contributing to air quality concerns and respiratory illnesses. This study investigates the distribution of airborne microflora using a six-stage cascade impactor. Samples were collected from three urban hotspots, three park areas, and a natural control site in Sofia, Bulgaria. Microbial counts were analyzed across six particle size fractions to determine spatial distribution patterns. Hotspots showed significantly higher microbial loads, especially in larger particle fractions (>7 µm, 4.7- 7 µm), whereas densely forested green areas exhibited lower microbial levels with a shift toward finer fractions (2.1- 3.3 µm, 1.1-2.1 µm). Parks with minimal vegetation showed microbial patterns similar to hotspots. These findings underscore the role of urban vegetation in mitigating microbial air pollution and highlight the importance of incorporating forested green spaces into urban planning to enhance air quality and public health.

Key words*: air microorganisms, air microflora, cascade impactor, green zone, hotspots.*

INTRODUCTION

Clean air is essential for human and environmental health. Urbanization and anthropogenic activities have significantly degraded air quality, with particulate matter (PM) serving as an indicator of complex pollutant mixtures. Recent studies suggest a correlation between PM levels and airborne microbial content (Mansour et al., 2014; Palladino et al., 2021). Historically, air quality studies focused on inorganic contaminants due to their abundance; however, interest in organic components, including airborne microbial biota, has grown (Friedlander et al., 2000).

Airborne microorganisms - including bacteria, micromycetes, actinomycetes, and viruses - can remain suspended either freely or attached to dust particles (Stetzenbach, 2009; Lighthart, 1997). Larger dust particles tend to harbor more microorganisms (Meklin et al., 2002). Research conducted by Tignat-Perrier et al. (2019) has shown that airborne microbial communities are influenced by ecosystem types and meteorological conditions. Their concentrations vary with air pollution levels, influenced by factors such as dust storms, fog, biomass burning, and traffic emissions. Seasonal and diurnal patterns in bioaerosol levels often reflect human activity, and studies have found correlations between microbial concentrations and the Air Quality Index (AQI). Shammi et al. (2021) observed distinct seasonal and diurnal variations in bioaerosol concentrations that closely reflect patterns of human activity in densely populated urban areas. Similarly, Yan et al. (2019) reported a strong correlation between bacterial and micromycete concentrations and the Air Quality Index (AQI). Their findings indicated that micromycete concentrations gradually increased when the AQI was below 200, whereas bacterial concentrations rose when the AQI exceeded 200. However, the mechanisms underlying the increase in bioaerosols - particularly aerophilic microorganisms - in response to air pollution remain unclear. One hypothesis is that elevated or extreme pollution levels primarily influence the diversity and composition of airborne microbial communities (Fan et al., 2019). The viability of microorganisms within bioaerosols depends on various environmental factors, including climate and atmospheric chemistry (Gong et al., 2020). Consequently, understanding the microbiological structure and composition of particulate matter is essential for identifying potential disease transmission pathways and assessing risks to human health (Wang et al., 2019).

The primary objective of this study is to examine the dynamics of airborne microflora across three urban hotspots and three park areas in Sofia,

Bulgaria, along with one control site located in the Vitosha Mountain. Specifically, the study quantifies the total number of airborne microorganisms in each sample and assesses their distribution across six particle size fractions, as determined by a cascade impactor.

MATERIALS AND METHODS

The study was conducted in early November 2024 at various locations in Sofia, Bulgaria, and the Vitosha Mountain region. Three urban park areas, their adjacent hotspots, and one site in Vitosha Mountain were selected to compare the composition of airborne microorganisms across different environments. The Vitosha Mountain site was chosen based on Kadinov's research, which highlighted its exposure to anthropogenic pollution - particularly during summer, when slope winds transport pollutants from Sofia (Kadinov, 2021a). However, Kadinov (2019) also reported that the fine dust in Vitosha originates mainly from background sources, with less than 1% attributed to Sofia, and that particulate matter (PM) deposition remains below critical levels. Seasonal PM trends show summer peaks in Vitosha Mountain, in contrast to the winter peaks observed in Sofia (Kadinov, 2021b).

The sampling sites included:

- TA1: Borisova Gradina – green area; coordinates: 42°41′15″N, 23°20′16″E
- TA2: Orlov Most intersection – hotspot; coordinates: 42°41′23″N, 23°20′17″E
- TA3: Voenna Academia Park – green area; coordinates: 42°41′30″N, 23°20′42″E
- TA4: Voenna Academia intersection – hotspot; coordinates: 42°41′33″N, 23°20′39″E
- TA5: Studentski Grad Park – green area; coordinates: 42°39′09″N, 23°21′09″E
- TA6: 8 Dekemvri St. and Rosario St. intersection – hotspot; coordinates: 42°39′06″N, 23°21′16″E
- TA7: Vitosha Mountain – nature park; coordinates: 42°36′34″N, 23°19′34″E

The geographic distribution of all sampling locations is illustrated in Figure 1, providing a visual overview of the selected green areas, urban hotspots, and the control site in Vitosha Mountain.

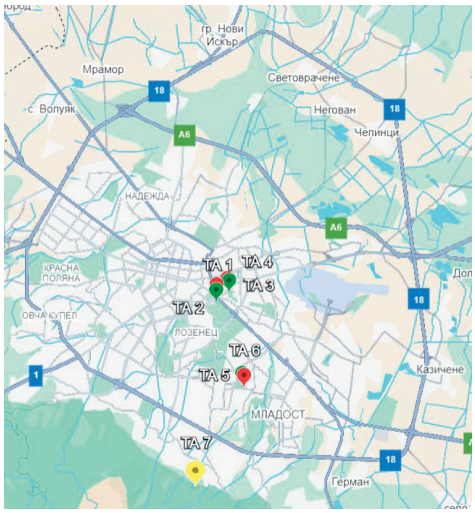


Figure 1. Map of the sampling locations

Air microflora sampling and analysis

Airborne microbial abundance was analyzed using a six-stage cascade impactor, which separates particles by aerodynamic diameter as follows:

- Stage 1: > 7 µm;
- Stage 2: 4.7-7 µm;
- Stage 3: 3.3-4.7 µm;
- Stage 4: 2.1-3.3 µm;
- Stage 5: 1.1-2.1 µm;
- Stage 6: 0.65-1.1 µm.

Petri dishes with appropriate nutrient media were placed on each stage. One cubic meter of air passed through the impactor at a constant flow rate. The microorganisms collected on each plate were then cultured and counted.

Microbial cultivation and identification

Microbial colonies were cultured under controlled conditions using the following nutrient media:

- Meat-Peptone Agar (MPA): bacterial growth at 28°C for 48 hours.
- Starch-Ammonia Agar (SAA): bacterial growth at 28°C for 10 days.
- Czapek Dox Agar Medium: fungal growth at 28°C for 7 days.

Sampling conditions and data processing

Sampling was conducted on a dry day following five consecutive precipitation-free days to minimize the influence of weather on airborne microbial concentrations.

Average atmospheric conditions during sampling:

- temperature: 4°C;
- relative humidity: 92%;
- atmospheric pressure: 1009 millibars;
- wind speed: 9 km/h (southwest direction).

Statistical analysis of the microbiological data was performed using StatSoft Statistica 12. Results are presented as the means of three replicates with corresponding standard deviations. A 95% confidence level was used to determine statistical significance.

RESULTS AND DISCUSSIONS

The results of the experiments are presented in colony-forming units (CFU) × 10²/m³. The total levels of airborne microorganisms are shown in Figure 2, while Figure 3 illustrates the distribution of microorganisms across the different stages of the cascade impactor. Unlike our previous studies (Peshev et al., 2024), the current study revealed that not all green areas exhibited lower microbial loads compared to their adjacent hotspots.

Table 1 provides a summary of microbial abundance across various particle size fractions for each location. The overall microbial load observed in this study is notably lower than that reported in studies conducted during the winter season. This difference is likely related to the increased concentration of fine particulate matter (PM) in winter. As Azis et al. (2018) noted, fine PM serves as a core for the accumulation of airborne microorganisms. Accordingly, microbial levels are expected to increase during the winter months, driven by increased PM concentrations due to the continued widespread use of solid fuels for heating in Sofia.

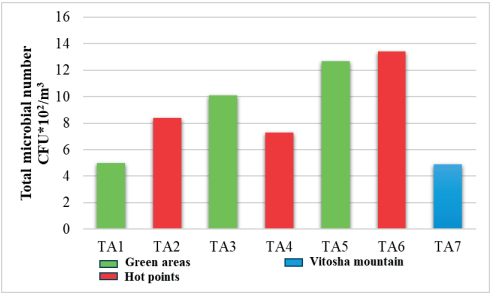


Figure 2. Total number of airborne microorganisms (CFU × 10²/m³) measured across all sampling sites

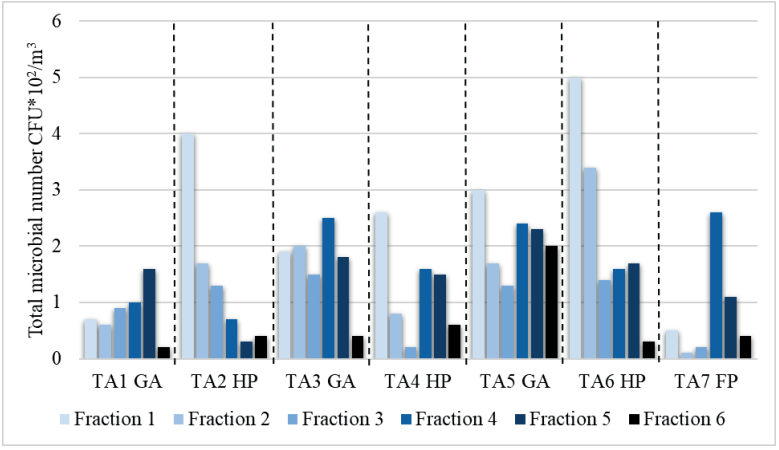


Figure 3. Total microbial number of airborne microorganisms from each of the stage of air Separator

According to the World Health Organization (WHO), air pollution is the greatest environmental health risk globally, affecting both developed and developing countries (WHO, 2017). However, no current WHO guideline specifically addresses the health impacts of airborne microorganisms in outdoor environments. Most WHO documentation on air quality and respiratory health focuses on non-organic hazards such as ozone, carbon dioxide, and fine particulate matter.

Table 1. Microbial abundance at different sites (CFU $\times 10^2/m^3$)

Location	Microbial count (CFU x $10^2/m^3$)	Dominant particle size fraction	Observations
Hotspot (TA2-Orlov most)	8.4 ± 3.25	>7 µm, 4.7-7 µm	Hight traffic, PM accumulation
Hotspot (TA4-Voenna Academia	7.3 ± 3.25	>7 µm, 4.7-7 µm	Hight vehicle emissions
Hotspot (TA6 – Studentski grad	13.4 ± 3.25	>7 µm	Construction activities contributing to PM
Green Area (TA1 – Borisova Gradina)	5.0 ± 3.92	2.1-3.3 µm, 1.1-2.1 µm	Dense tree cover, reduce PM levels
Green Area (TA3 – Voenna Academia Park	10.1 ± 3.92	3.3-4.7 µm, 2.1-3.3 µm	Lower elevation, direct PM exposure from traffic
Green area (TA5 – Studentski grad Par)	13.4 ± 3.92	> 7 µm, 4.7-7 µm	Minimal tree cover, resembling hotspots
Vitosha mountain – Nature Park	4.9	2.1-3.3 µm, 1.1-2.1 µm	Nature forest, the lowest load with microorganisms

When microorganisms are considered, the emphasis is typically on indoor air quality. Nevertheless, the 2021 WHO guidelines on particulate matter acknowledge the importance of analyzing the effects of organic aerosols on human health, alongside combustion particles and secondary inorganic aerosols (WHO, 2021). Many studies highlight the role of green spaces in mitigating air pollution (Givoni, 1991; Cohen et al., 2014). Chiesura (2004) found that urban parks improve air quality, particularly in large cities, while Dadvand et al. (2023) documented the positive health effects of tree vegetation.

Our study clearly shows that the location and forest cover of park areas matter.

Our study clearly demonstrates that both the location and forest cover of park areas significantly influence airborne microbial levels. TA1 – Borisova Gradina, one of the largest parks in Sofia with dense tree and shrub vegetation, recorded the lowest levels of airborne microorganisms. These findings are consistent with previous research (Mhuireach et al., 2016). The timing of the sampling - late autumn - likely contributed to these results, as trees retained a substantial portion of their leaf mass, aiding in particle filtration.

Interestingly, TA3, another green area, showed higher microbial concentrations than its adjacent hotspot, TA4. This discrepancy underscores the importance of both vegetation and location. TA3 is situated at a lower elevation than the nearby boulevard, making it more susceptible to direct dust and PM exposure from traffic. This highlights the need for careful urban planning that incorporates principles of "Environmental Hygiene". As Robinson et al. (2019) suggest, expanding research in this area is vital given the growing recognition of urban green spaces as essential to public health.

The data for TA5 further emphasizes the importance of vegetation type. This green area, dominated by grass with minimal tree cover, exhibited microbial levels comparable to its nearby hotspot, TA6. These findings, supported by the trends in Figure 2, suggest that grassland-type parks do not effectively reduce PM or associated microbial loads.

In hotspots, microorganisms were primarily concentrated in the upper stages of the cascade impactor (Stage 1: >7 µm; Stage 2: 4.7-7 µm), indicating association with larger PM particles. In contrast, green areas with substantial woody vegetation exhibited a greater concentration of microorganisms in the finer particle stages. TA5 again deviated from this trend due to its lack of trees, resulting in microbial distributions more similar to those observed in hotspots.

Moreover, notable differences in microbial loads among hotspots were observed. TA2, despite being one of the busiest intersections in Sofia, had lower microbial concentrations than TA6, a residential neighbourhood. This can be attributed to the influence of wind and air mass

movement. Additionally, ongoing excavation work in the TA6 area at the time of sampling likely increased dust levels, contributing to higher microbial counts. These findings support the conclusion that construction and renovation activities significantly deteriorate ambient air quality by increasing both PM and microbial content.

Our study reinforces the need for more urban green spaces that mimic natural forests, rather than purely aesthetic, meadow-type landscapes. Tree vegetation, even with reduced leaf mass during autumn, remains effective in capturing particulate matter and the microorganisms it carries. In hotspots, microbial concentrations were highest in the coarser PM fractions, whereas in green areas with tree cover, microorganisms were more prevalent in finer fractions (Stages 4 and 5). The control site in Vitosha Mountain demonstrated the lowest microbial levels, comparable only to Borisova Gradina, further affirming the role of dense forest vegetation in limiting airborne microflora.

CONCLUSIONS

The main objective of this study was to conduct a preliminary analysis of airborne microbial abundance across selected urban and natural locations and to assess the distribution of microorganisms in relation to different particulate matter (PM) size fractions. The results revealed that green areas do not always exhibit lower microbial loads than their adjacent urban hotspots. This variation is largely influenced by the type of vegetation cover and the specific location of the green spaces.

Park areas dominated by grass and with limited woody vegetation displayed microbial patterns similar to nearby high-traffic zones. In contrast, parks with dense tree covers showed a more favorable profile, with lower microbial concentrations. Additionally, areas with strong air mixing due to moving air masses demonstrated a reduction in microbial presence, even in busy hotspots.

Our findings suggest that both busy intersections and green spaces situated near active construction or renovation zones should be approached with caution, as they pose elevated health risks due to increased microbial and particulate loads. In hotspots and grass-dominated green areas, microorganisms were mainly associated with larger PM fractions. Conversely, in tree-rich parks, microbial abundance shifted toward finer particle fractions.

These insights underscore the importance of integrating principles of "Environmental Hygiene" into urban planning. Efforts should focus on minimizing particulate and microbial exposure to improve respiratory health among urban populations. This study provides a foundation for further research and can inform the development of detailed urban design strategies aimed at optimizing air quality and public health outcomes.

ACKNOWLEDGEMENTS

This research work was carried out with the support of Research Fund of Ministry of Education and Science in Bulgaria, project №: КП-06-Н74/5 „Relationships between the amount of fine particulate matter and airborne microorganisms in "hot spots", park areas, urban background areas and control forest areas''.

REFERENCES

Azis, A., Lee, K., Park, B., Park, H., Park, K., Choi, I., & Chang, I. (2018). Comparative study of the airborne microbial communities and their functional composition in fine particulate matter (PM2.5) under non-extreme and extreme PM2.5 conditions. *Atmospheric Environment, 194*, 82–89.

Chiesura, A. (2004). The role of urban parks for the sustainable city. *Landscape and Urban Planning, 68*(1), 121–138.

Cohen, P., Potchter, O., & Schnell, I. (2014). The impact of an urban park on air pollution and noise levels in the Mediterranean city of Tel-Aviv, Israel. *Environmental Pollution, 195*, 73–83.

Dadvand, P., Vries, S., Bauer, N., & Triguero-Mas, M. (2023). The health and wellbeing effects of forests, trees and green space. In *Forests and Trees for Human Health: Pathways, Impacts, Challenges and Response Options – A Global Assessment Report* (pp. 77–125). International Union of Forest Research Organizations (IUFRO). https://www.iufro.org/science/special/spdc/netw/for-health/

Fan, X.-Y., Gao, J.-F., Pan, K.-L., Li, D.-C., Dai, H.-H., & Li, X. (2019). More obvious air pollution impacts on variations in bacteria than fungi and their co-occurrences with ammonia-oxidizing microorganisms in PM2.5. *Environmental Pollution, 251*, 668–680. https://doi.org/10.1016/j.envpol.2019.05.004

Friedlander, S. K. (2000). *Smoke, dust and haze: Fundamentals of aerosol dynamics* (2nd ed.). Oxford University Press.

Givoni, B. (1991). Impact of planted areas on urban environment quality: A review. *Atmospheric Environment, 25B* (3), 289–299.

Gong, J., Qi, J. E. B., Yin, Y., & Gao, D. (2020). Concentration, viability and size distribution of bacteria in atmospheric bioaerosols under different types of pollution. *Environmental Pollution, 257*, 113485. https://doi.org/10.1016/j.envpol.2019.113485

Lighthart, B. (1997). The ecology of bacteria in the alfresco atmosphere. *FEMS Microbiology Ecology, 23*(4), 263–274. https://doi.org/10.1111/j.1574-6941.1997.tb00408.x

Kadinov, G. (2019). Quantitive Assessment of the Importance of the Atmospheric Environment on Air Pollutant Concentrations at Regional and Local Scales in Sofia“. *Ecologia Balcanica, Special Edition, 2*, 63–70.

Kadinov, G. (2021a). Comparative Assessment of Tropospheric Ozone Loads of Two Fagus sylvatica Sites. *Journal of Balkan Ecology, 24*(2), 157-172.

Kadinov, G. (2021b). Dynamics of Dust Concentration in Atmosphere above Sofia for Last 10 Years. *Journal of Balkan Ecology, 24*(3), 285–305.

Mansour, A., Shamy, M., Redal, M., Khoder, M., Awad, A., & Elserougy, S. (2014). Microorganisms associated with particulate matter: A preliminary study. *Science of the Total Environment, 479–480*, 109–116.

Meklin T, Reponen T, Toivola M, Koponen V, Husman T, Hyvärinen A, & Nevalainen A. (2002) Size distributions of airborne microbes in moisture-damaged and reference school buildings of two construction types. *Atmos Environ*, 36, 39–40.

Mhuireach, G., Johnson, B. R., Altrichter, A. E., Ladau, J., Meadow, J. F., Pollard, K. S., & Green, J. L. (2016). Urban greenness influences airborne bacterial community composition. *Science of the Total Environment, 571*, 680–687. https://doi.org/10.1016/j.scitotenv.2016.07.037

Palladino, G., Morozzi, P., Biagi, E., Brattich, E., Turroni, S., Rampelli, S., Tositti, L., & Candel, M. (2021). Particulate matter emission sources and meteorological parameters combine to shape the airborne bacteria communities in the Ligurian coast, Italy. *Scientific Reports, 11*, Article 175. https://doi.org/10.1038/s41598-020-80336-2

Peshev, A., Grigorova-Pesheva, B., Malcheva, B., & Kadinov, G. (2024). Microflora of the ground air from "hot points" and park areas. *Scientific Papers. Series E. Land Reclamation, Earth Observation & Surveying, Environmental Engineering, 13*, 182–188.

Robinson, M., & Breed, F. (2019). Green prescriptions and their co-benefits: Integrative strategies for public and environmental health. *Challenges, 10*(1), 9. https://doi.org/10.3390/challe10010009

Shammi, M., Rahman, M. M., & Tareq, S. M. (2021). Distribution of bioaerosols in association with particulate matter: A review on emerging public health threat in Asian megacities. *Frontiers in Environmental Science, 9*, 698215. https://doi.org/10.3389/fenvs.2021.698215

Stetzenbach, L. D. (2009). Airborne infectious microorganisms. In M. Schaechter (Ed.), *Encyclopedia of Microbiology* (pp. 175–182). Academic Press. https://doi.org/10.1016/B978-012373944-5.00177-2

Tignat-Perrier, R., Dommergue, A., Thollot, A., Keuschnig, C., Magand, O., Vogel, T. M., & Larose, C. (2019). Global airborne microbial communities controlled by surrounding landscapes and wind conditions. *Scientific Reports, 9*, 14441. https://doi.org/10.1038/s41598-019-51073-4

Wang, Z., Li, J., Qian, L., Liu, L., Qian, J., Lu, B., & Guo, Z. (2019). Composition and distribution analysis of bioaerosols under different environmental conditions. *Journal of Visualized Experiments, 143*, e58795. https://doi.org/10.3791/58795

World Health Organization. (2017). *Evolution of WHO air quality guidelines: Past, present and future*. WHO Regional Office for Europe. https://www.euro.who.int/en/publications/abstracts/evolution-of-who-air-quality-guidelines-past,-present-and-future-2017

World Health Organization. (2021). *WHO global air quality guidelines: Particulate matter (PM2.5 and PM10), ozone, nitrogen dioxide, sulfur dioxide and carbon monoxide*. https://www.who.int/publications/i/item/9789240034228

Yan, X., Qiu, D., Zheng, S., Yang, J., Sun, H., Wei, Y., Han, J., Sun, J., & Su, X. (2019). Distribution characteristics and noncarcinogenic risk assessment of culturable airborne bacteria and fungi during winter in Xinxiang, China. *Environmental Science and Pollution Research, 26*(36), 36698–36709. https://doi.org/10.1007/s11356-019-06720-8

Scientific Papers. Series E. Land Reclamation, Earth Observation & Surveying, Environmental Engineering. Vol. XIV, 2025
Print ISSN 2285-6064, CD-ROM ISSN 2285-6072, Online ISSN 2393-5138, ISSN-L 2285-6064

POSSIBILITIES OF SURFACE TREATMENT OF PLASTERS BASED ON CLAY

Andreea HEGYI[1], Cristian PETCU[1], Claudiu Sorin DRAGOMIR[1, 2], Gabriela CĂLĂTAN[3], Alexandra CSAPAI[1]

[1]National Institute for Research and Development in Construction, Urban Planning and Sustainable Spatial Development - URBAN-INCERC, 266 Pantelimon Road, District 2, 021652, Bucharest, Romania
[2]University of Agronomic Sciences and Veterinary Medicine of Bucharest, 59 Mărăşti Blvd, District 1, 011464, Bucharest, Romania
[3]Office of Pedological and Agrochemical Studies Cluj-Napoca, 1 Fagului Street, 400524, Cluj-Napoca, Romania

Corresponding author email: alexandra.csapai@incerc-cluj.ro

Abstract

One of the key challenges associated with traditional buildings constructed from vernacular materials is their response to climatic agents and microorganisms. These present a significant challenge also for the surface of constructions based on unbaked clay elements. This paper presents the possibility of creating plasters based on clay, lime and other additives, their behaviour in response to mould growth, and the potential for coating treatments to enhance their resistance to the harmful action of microorganisms. The antifungal treatment was conducted with the objective of exploring the potential for recycling expired non-food household and medical products. The experimental results indicated the initial development of colonies of Penicillium notatum and Aspergillus niger and subsequently demonstrated the potential for enhancing resistance to mould action through pellicular treatment and/or surface impregnation. It can therefore be concluded that not only is it possible to create clay-based plasters with enhanced performance, but also that this represents an original contribution to the implementation of the concept of the circular economy.

Key words*: antifungal treatment, circular economy, clay soil, plaster mortar, vernacular constructions.*

INTRODUCTION

Vernacular architecture is a foundational model for contemporary energy-efficient construction, given its capacity to adapt to local microclimates and environmental conditions. Recent studies have demonstrated its exceptional energy conservation performance, often exceeding initial scholarly assumptions (Abdelrazek & Yılmaz, 2020; Martinovic et al., 2023). In Romania, earth-based constructions, primarily adobe and wattle-and-daub, account for approximately 32.9% of buildings nationwide, predominantly as single-story structures built before 1992, with a higher prevalence in lowland counties where timber resources are less abundant compared to hilly and mountainous areas (INCD URBAN-INCERC). Structures built with unfired loamy soil represent some of the earliest forms of building technology. A variety of construction techniques have been utilised across the globe over time, including the construction of rammed earth walls, cob walls, and walls constructed from naturally dried unfired clay bricks. These techniques have been preserved and continue to be employed in various regions, exhibiting regional variations influenced by local resources and traditional building practices. These constructions present numerous advantages: they contribute to a healthy indoor environment by maintaining thermal stability and consistent humidity levels, while emitting no toxic substances - a critical factor in reducing the risk of respiratory diseases and allergies, they are cost-effective to construct, require minimal specialist labour, have a low environmental impact due to the limited use of raw materials, integrate harmoniously with local architectural traditions, and have a minimal impact on the surrounding landscape. These specific elements have the capacity to exert a considerable influence on the enhancement of hygiene and health standards for occupants, whilst

concurrently effecting the mitigation of energy consumption and pollutant emissions. This, in turn, results in a contribution to environmental sustainability (Androutsopoulos et al., 2020; Măgurean & Petran, 2023). There are many studies in the literature that demonstrate the benefits of building with clay using indigenous techniques in different geographical and climatic conditions (Minke, 2006; Bui, 2009a Ciurileanu & Bucur, 2011). However, the main challenge with these constructions is the high risk of cracking during the drying process and their low resistance to water and weathering, which often requires frequent surface repairs and maintenance (Vural et al., 2007; Bui et al., 2009a; Kiroff & Roedel, 2010;). The scientific literature indicates that clay soils used for earthworks must contain a minimum of 15-16% clay to ensure the plasticity and workability required for proper handling (Vural et al., 2007; Kiroff & Roedel, 2010). In addition, to effectively control the risk of cracking, the acceptable linear shrinkage should be in the range of 3-12% for soft mixes and 0.4-2% for drier mixes (Minke, 2006; Jayasinghe & Kamaladasa, 2007). A variety of organic or inorganic additives of plant, animal or industrial origin may be used to achieve these indicators (Bahobail, 2012). However, increasing the resistance of the exposed surface to climatic or biological factors remains a challenge, although these additives can significantly improve the bulk performance of the clay composite. Research aimed at identifying surface treatment solutions for clay surfaces has been reported in the literature, with some researchers analysing the possibility of developing sol-gel solutions based on TiO_2 (Calabria et al., 2010) while others have focused their attention on more traditional solutions, such as natural oil-based waterproofing agents of vegetable or animal origin, sodium silicate, silicon nanoparticles, titanium dioxide, silica nanoparticles, silane-siloxane, beeswax, ethyl silicate, organic polymer products, lime-based paints and others (Ferron, 2007; Li et al., 2009; Ferron & Matero, 2011; Pacheco et al., 2016; Stazi et al., 2016; Lanzón et al., 2017; Camerini et al., 2019; Elert et al., 2019; Rescic et al., 2023**)**.

On the other hand, the cosmetics, pharmaceuticals and other non-food household products industries are experiencing rapid growth in correlation with the demands of modern society. The cosmetics market tends to grow year on year, making it the third fastest growing market, with the global beauty and self-care industry estimated to be worth USD 341 billion in 2020, USD 565 billion in 2022, USD 758 billion in 2025 and USD 480.4 billion in 2030 (Nciri et al., 2022; Morganti et al., 2023). It is therefore of interest to find solutions for the recovery and recycling of expired non-food household products, cosmetics, pharmaceuticals, various aromatic oils, etc., so that they no longer pose a pollution risk when disposed of in sewers or landfills (Juliano & Magrini, 2017; Cinelli et al., 2019; Bashir et al., 2021; Silletta et al., 2024**)**. Research has shown that, in addition to specific functional ingredients, cosmetic products, for example, are rich in phenolic compounds, flavonoids and organic acids known for their antimicrobial properties, preservatives and bioactive molecules for the treatment of skin conditions (such as dermatitis, atopic eczema, atopic dermatitis or acne) (Varvaresou et al., 2009; Houston et al., 2017; Halla et al., 2018; Hamrita et al., 2022; Sandle, 2022).

A distinctive attribute of cosmetic products is the homogeneity of their component formulations, which is characterised by minimal variation in size, extending down to the nanometric level, even for mineral-derived products (Silletta et al., 2024).

The utilisation of non-food household products in the domain of construction has been documented in the extant literature. For instance, a group of researchers from the Department of Civil Engineering, PVPIT Budhgaon, Maharashtra, India (Patil et al., 2021) demonstrated the potential use of an aqueous soap solution to induce a high volume of pores in the cementitious matrix, enabling the production of concrete with a density lower than 1000 kg/m³, commonly referred to as "floating concrete". Moreover, other studies have emphasised the advantageous properties of soap, along with soap precursors such as oils or fats, in enhancing the performance of unfired clay bricks, particularly in terms of their resistance to water (Browne, 2009; Bahobail, 2012).

A group of researchers from Korea University of Technology & Education (Nciri et al., 2022)

demonstrated that cosmetic waste can be integrated into the creation of green, sustainable road pavements. Specifically, the incorporation of cosmetic waste, such as lipstick (completely soluble at temperatures above 50ºC) or other cosmetic products containing oils, fats, emulsifiers, wax, fillers, mica, silicon, titanium oxide, or zinc oxide, into asphalt mixtures can act as additive materials that improve rheological properties, viscosity, and elasticity. This contributes to reducing fatigue-induced cracking, enhancing aging resistance, and improving durability, including through the influence of crystallization/hardening mechanisms.

This exploratory study aims to assess the potential reuse of expired cosmetic-pharmaceutical products for protecting clay surfaces against mould growth, which can act as a trigger for allergies. While the permeability of these compounds through clay materials represents an important consideration that may affect treatment effectiveness and durability, this initial investigation focuses on surface application effects. The method employed for repurposing these expired products involved their integration as functional additive raw materials in formulations designed for surface application, resulting in a protective coating with increased resistance to microbial activity. It is important to note that the scope of this research does not extend to evaluating the potential health implications associated with the utilisation of these products for construction purposes beyond the specified scope, nor does it include in-depth analysis of treatment permeability through the clay matrix - aspects that deserve further investigation in future studies. Therefore, the aim of the present study is to analyse the feasibility of recycling non-food household waste (namely cosmetic-pharmaceutical products) through the development of a protective and finishing coating aimed at enhancing the resistance of unfired clay construction surfaces to biological agents.

MATERIALS AND METHODS

The raw materials utilised in the fabrication of clay-based plaster mortar composites for the protection and finishing of vernacular construction surfaces comprised the following: clay soil (named "clay") extracted from Valea Drăganului, Cluj-Napoca, Romania, hydraulic lime with the commercial designation RÖFIX NHL5, with an apparent density of 520 kg/m³ and a minimum compressive strength of 5 N/mm², river sand with a maximum grain size of 4 mm, and water.

To characterise the clay that was utilised in this study, an XRF analysis was conducted (Table 1).

Table 1. The oxide composition of the clay, determined through XRF analysis

Oxides	SiO_2	Al_2O_3	Fe_2O_3	CaO
Content [%]	74.17	12.74	4.38	0.7
Oxides	MgO	K_2O	Na_2O	TiO_2
Content [%]	1.0	1.43	0.73	0.05

This non-destructive analytical technique utilises the measurement of characteristic secondary X-rays to determine the elemental composition and concentration of materials, through the exposure of a sample to high-energy X-rays or gamma rays, which results in the emission of secondary X-rays due to the excitation of inner-shell electrons. The subsequent analysis of the resultant data enabled the determination of the clay's oxide composition and enabled prediction of its classification according to the standard mineralogical nomenclature. The analysis revealed that the clay in question belonged to the clay loam domain (Figure 1), as indicated by its specific mineralogical composition (Figure 2).

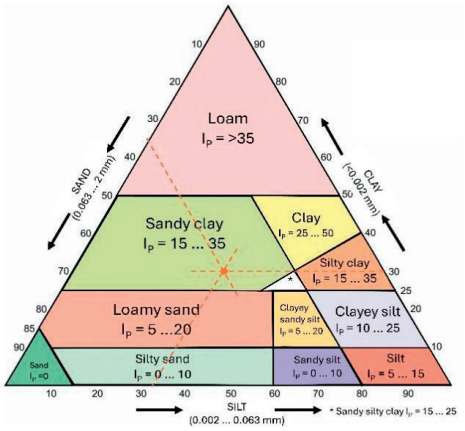


Figure 1. Characterization of the clay as a raw material – classification within the ternary diagram

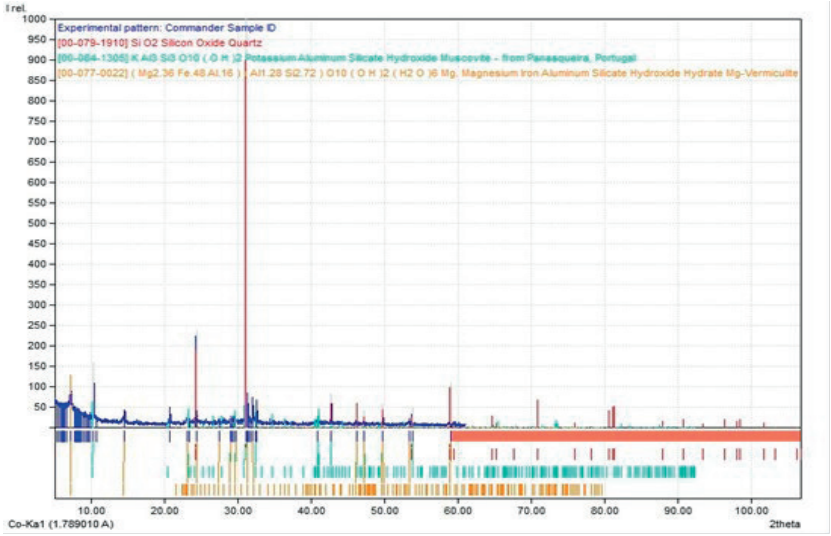


Figure 2. Mineralogical analysis of the clay used as a raw material

From a mineralogical perspective (Figure 2), experimental tests revealed the presence of predominant minerals, including quartz with approximately two-thirds of the composition, muscovite accounting for nearly one-third, and a minor fraction of vermiculite, along with montmorillonite, illite and kaolinite. (Minke, 2006; Niroumand et al., 2013; Dormohamadi & Rahimnia, 2020; Muñoz et al., 2020; Ige & Danso, 2022). In accordance with existing literature on the subject, these characteristics support the assessment that this raw material is suitable for use in the construction sector.

The selection of the hydraulic binder (hydraulic lime) was based on preliminary experimental tests and existing literature highlighting its beneficial effects (Minke, 2006; Pacheco-Torgal, 2015; Ige & Danso, 2022; Rescic et al., 2023) particularly the additional contribution of calcium oxide in mitigating drying shrinkage and reducing the risk of cracking. The water used in the preparation process was carefully dosed to maintain a consistent fresh mix consistency within a controlled range of 95 ± 5 mm.

In order to evaluate and analyse the performance of clay-based compositions intended for plastering applications, a series of mixtures were formulated and prepared under controlled laboratory conditions.

The proportional composition of the raw materials, together with the corresponding sample codes, is shown in Table 2.

Table 2. The ratio of raw materials in composites intended for use as plaster mortar

Sample code	Clay (%*)	Hydraulic Lime (%*)	Sand (%*)
P1	60	0	40
P2	57	3	40
P3	55	5	40
P4	50	10	40
P5	45	15	40
P6	40	20	40
P7	35	25	40
P8	30	30	40
P9	25	35	40
P10	20	40	40
P11	10	50	40
P12	0	60	40

*Note: It should be noted that the percentage indicated is that by weight of the total dry material.

For each clay-based composite, a number of indicators were evaluated to characterise the material and confirm its suitability for use as a rendering mortar, in particular:

- apparent density in the hardened state, according to the standardised method EN 1015-10;
- axial shrinkage, according to the standardised method STAS 2634;
- presence of drying cracks, assessed on visual inspection;
- flexural tensile strength and compressive strength, according to the standardised method EN 1015-11;

- adhesion to the substrate, tested on ceramic bricks and unfired clay masonry units, according to the standard method EN 1015-12.

The experimental evaluation of the physical and mechanical performance was conducted under laboratory conditions using prismatic specimens of 40×40×160 mm, formed in metal moulds and demoulded 72 hours after preparation. To assess substrate adhesion, flat specimens were prepared by applying a 3-5 mm thick layer of the clay-based composite to the selected substrates. All samples were stored for 40 days until a constant mass was reached, which was taken as an indicator of full maturation and drying of the material. The samples were stored under controlled laboratory conditions at 23±2°C and 65±1% relative humidity, and then subjected to experimental testing. In order to ensure the repeatability of the experimental determinations, a minimum of three samples were prepared for each case and the values reported represent the arithmetic mean of the individual measurements.

Subsequently, to analyse the resistance to microbiological attack, a test scheme was designed for four clay-based composites selected on the basis of their physical and mechanical performance. The test procedure consisted of three stages:

- evaluation of the behaviour of plastering mortars in an environment contaminated with mould spores;
- design, preparation and application of a protective product on the clay surface;
- validation of the antifungal performance by evaluating the behaviour in an environment contaminated with mould spores.

Samples were selected on the basis of minimum thresholds for four indicators identified in correlation with references from the literature: (Minke, 2006; Pacheco-Torgal, 2015; Muñoz et al., 2020; Eslami et al., 2022; Azalam et al., 2024):

- absence of drying cracks;
- adhesion to substrate: minimum 0.5 N/mm²;
- compressive strength: at least 2.5 N/mm²;
- bending tensile strength: minimum 1.5 N/mm².

In addition, a batch of clay-based composites without hydraulic lime content (P1) was subjected to a comparative analysis.

The analysis of the resistance of the clay-based composites to microbiological attack was carried out by exposing the samples to a highly contaminated cross-infection environment with *Penicillium notatum* (PN) and *Aspergillus niger* (AN) spores. For this purpose, individual culture systems were prepared for each sample type. A disc-shaped specimen, 15 mm in diameter and 3 mm thick, prepared in the same way as the prismatic specimens used for the determination of physical and mechanical tests, was placed in a Petri dish on a potato dextrose agar (PDA) nutrient substrate (prepared by dissolving 39 g/L of granular substance in warm water). The test sample and the culture medium were sprayed vertically from a distance of 100 mm with a solution containing *Penicillium notatum* (PN) and *Aspergillus niger* (AN) spores (10 µl PN + 10 µl AN/20 ml distilled water). The entire system was then sealed and incubated at a constant temperature (23±1°C) in a BIOBASE BOV-D30 incubator. At predetermined time intervals, the systems were evaluated by observing the appearance and development of mould and the degree of surface coverage on the material sample. The evaluation was performed by microscopic examination using a LEICA SAPO microscope. The results were quantified using two indicators: one to assess fungal growth (Table 3) and the other to estimate product performance (Table 4).

Table 3. Fungal growth assessment

Class	Fungal Growth Evaluation
Class 0	No fungal growth is visible upon microscopic examination.
Class 1	The growth is invisible to the naked eye but is clearly visible under a microscope.
Class 2	Visible growth to the naked eye, covering up to 25% of the surface area that was tested.
Class 3	Visible growth to the naked eye, covering up to 50% of the surface area that was tested.
Class 4	Visible growth to the naked eye, with a surface coverage of more than 50%.
Class 5	Heavy growth, with complete coverage of the tested surface.

Table 4. Product performance estimation

Category	Product Performance Estimation
0	The material is characterised as being inert or fungistatic, thereby serving as an unsuitable nutrient medium for microorganisms.
1	The material contains minimal nutrients or is minimally contaminated, resulting in restricted microbial growth.
2-3	The material demonstrates susceptibility to microbial attack and contains nutrients that facilitate microorganism growth.

The surface treatment solutions were prepared using expired non-food household products (cosmetic-pharmaceutical products) together with dispersion matrices. The raw materials used were:

- dispersion matrices:
  - commercially available liquid wax, natural beeswax dispersed in water, manufactured by Borma Wachs, Italy;
  - rabbit skin glue solution, made from rabbit skin glue granules (manufacturer: Divolo, Italy, commercially available) dissolved in warm water at a ratio of 1:10 by mass (one part glue to ten parts water).
- cosmetic-pharmaceutical products:
  - liquid pharmaceutical product for the treatment and prevention of fungal infections of the mucous membranes, particularly in the oral cavity, based on glycerine. It is an over-the-counter solution available in pharmacies that combines the properties of glycerine, borax (B) (sodium tetraborate, a substance with antiseptic and antifungal properties) and nystatin (NT) (a broad-spectrum antifungal agent that inhibits the growth and spread of fungi by disrupting their cell membrane);
  - liquid antifungal pharmaceutical product for the treatment of fungal infections of the skin and nails. It is available over the counter and contains the active ingredient naftifine (NF), which belongs to the class of allylamines with antifungal and antimicrobial properties. Naftifine inhibits enzymes involved in the formation of fungal cell membranes, thereby affecting their growth and survival. It is effective against several types of fungi, including yeasts and moulds;
  - hand cream for dry skin, made in Romania (contains 15% glycerine);
  - lipstick, produced in Romania (contains 50% glycerine);
  - lavender oil, produced by Ecoland Production SRL, Romania.

The selection of these raw materials was driven by the following criteria:

- representation of waste materials for which potential reuse solutions are being explored;
- affordability, accessibility, and absence of health risks to users;
- capability to serve as natural treatment solutions suitable for vernacular construction applications;
- liquid wax has been demonstrated to reduce the water sensitivity of clay surfaces by filling pores and forming a water-repellent sealing film, thereby enhancing resistance to water exposure and climatic agents. When utilised in an efficient manner during the mixing process, it functions as an effective dispersion medium for fine powdered substances and lavender oil;
- rabbit skin glue solution is recognised as an effective surface treatment material, frequently used in furniture and painting restoration, as well as in traditional and eco-friendly construction works. The formation of a varnish-like film is the result of the interaction of the glue with the substrate, and this results in strong adhesion. It is expected that this will enhance surface resistance to water exposure and climatic agents. The solution's application as an aqueous medium facilitates the dissolution of other raw materials (e.g., expired pharmaceutical products) while ensuring the effective dispersion of fine powdered substances;
- lavender oil is renowned for its antiseptic, antifungal, antimycotic, and antibacterial properties, as well as its effectiveness as a natural insect repellent. Its efficacy in treating contamination caused by *E. coli*, *P. aeruginosa*, *S. aureus*, *P. vulgaris*, *E.s faecalis*, *L. monocytogenes*, *B. subtilis*, *A. niger*, *P. chrysogenum*, and *C. albicans* has been well-documented (de Elguea-Culebras et al., 2016; Vasileva et al., 2018; Silletta et al., 2024);
- the improper disposal of expired cosmetic pharmaceutical products in household settings represents a significant environmental concern, as these materials have the potential to contaminate water sources and soil. The selected products are intended for external use, are available without medical restrictions, and do not present risks associated with use by children, pregnant women, or breastfeeding individuals. Furthermore, the glycerine content present in these products has been demonstrated to

enhance the flexibility of the protective film (for rabbit skin glue film, the required glycerine content is 5%). Finally, while some of these materials function exclusively as treatment agents to enhance resistance to mould growth, others can readily serve as pigments, thereby enabling a broad spectrum of colours and shades in the protective coating.

The evaluation of coating coverage uniformity was conducted by applying the treatment solutions to a white cementitious substrate characterised by a smooth surface (specimens fabricated from white cement paste, aged two years post-casting). Preliminary tests demonstrated that, under constant exposure and lighting conditions, the coatings were more visible on the white cementitious substrate compared to the clay substrate. The coding and composition of the treatment solutions are presented in Table 5.

Following the preparation stage, the treatment solutions were applied by brushing onto the surface of the selected clay-based composite specimens in two layers, with a 24-hour interval between applications.

Table 5. Ratio of raw materials utilised in the formulation of clay surface treatment solutions.

Sample code	Liquid wax (ml)	Rabbit skin glue solution (ml)	B+NT+NF Total content (%)	Cosmetics (g hand cream/g lipstick)	Lavender oil (ml)
S1	100	-	0.0017	10/7	1
S2	50	50			
S3	-	100			

Following the application of the second layer, the specimens were left to dry for a period of seven days. Thereafter, the contamination exposure procedure described earlier was employed to test the specimens. Figure 3 provides a schematic representation of the experimental research methodology.

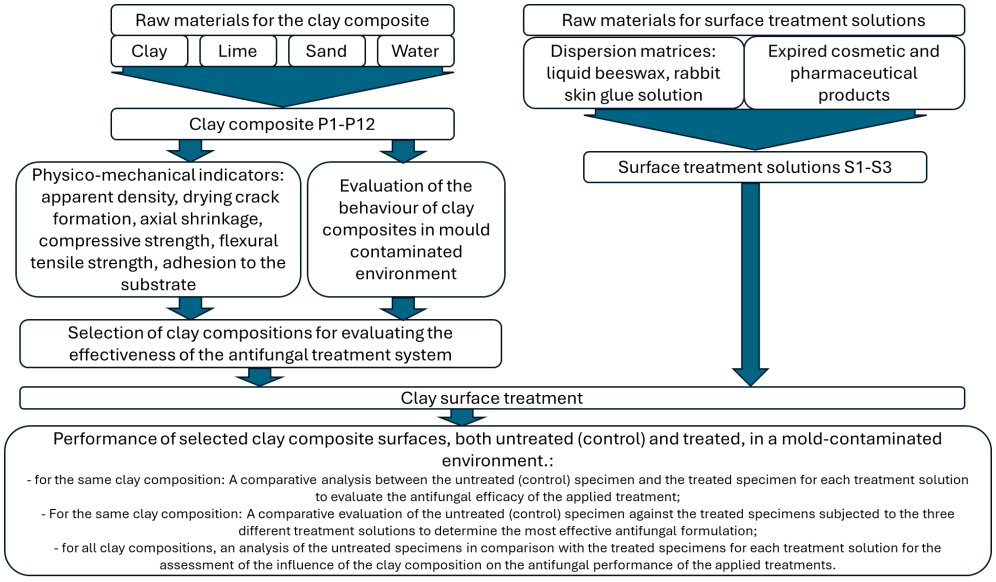


Figure 3. Schematic representation of the experimental research methodology

RESULTS AND DISCUSSIONS

The experimental results obtained in this study demonstrate that, in relation to physical and mechanical indicators, an increase in the hydraulic lime content in the composition results in a decrease in apparent density (Figure 4) and a reduction in axial shrinkage (Figure 5). These outcomes are particularly favourable for such materials, as they are accompanied by the absence of cracks.

However, it is crucial to acknowledge the unfavourable consequence of elevated hydraulic lime content, namely the decrease in mechanical strength, both in compression and flexural tensile resistance, which underscores the

necessity for the identification of the optimal hydraulic lime content in each instance where the composition of the clay material is subject to alteration (Figure 6).

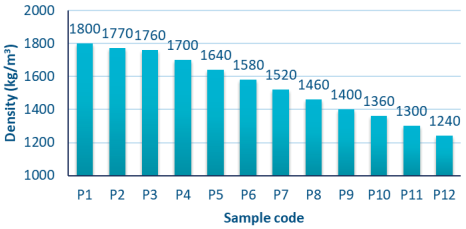


Figure 4. Bulk density of clay composites in their hardened state

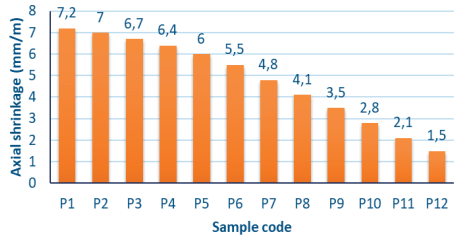


Figure 5. Axial shrinkage of clay composites

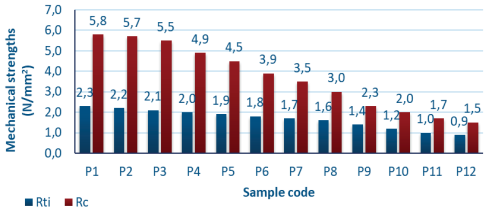


Figure 6. Mechanical strengths of clay composites

Concerning the adhesion of clay-based composites to the substrate, a Gaussian trend was observed (see Figure 7).

In particular, an increase in hydraulic lime content, coupled with a reduction in clay content (while maintaining a constant sand proportion in the total dry mix), resulted in enhanced adhesion to both adobe brick and fired ceramic brick surfaces. This adhesion exhibited a peak at composition P8 (30% clay, 30% hydraulic lime, 40% sand). Conversely, compositions where the lime content exceeds the clay content (P9-P12) exhibited a decline in adhesion to the substrate. It is therefore essential to establish the optimal hydraulic lime content to achieve a sustainable balance between its benefits and potential drawbacks.

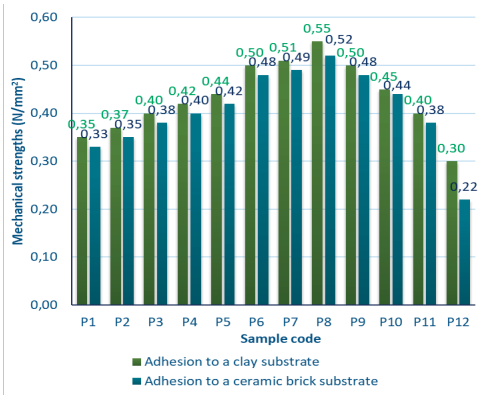


Figure 7. Adherence of clay composites to the substrate

The experimental results regarding the evaluation of the resistance of clay-based compositions under cross-contamination conditions with *Penicillium notatum* and *Aspergillus niger* revealed the following:

- All clay-based compositions invariably allowed the growth of one or both types of mould on their surface, although at different rates. The initial indications of mould growth (3 days after contamination) manifested in compositions with a reduced lime content, thereby validating the advantageous and sanitizing effect of lime.
- Following a period of seven days of exposure to the contaminated environment, all compositions exhibited indications of fungal growth, which was classified as Class 1 according to the classification system (i.e. invisible to the naked eye but clearly visible under a microscope). According to the performance estimation indicator (Table 4), all compositions were categorised as Category 1 (i.e. the material contains very few nutrients or is minimally contaminated, allowing only very limited fungal growth).
- During the exposure period of 7 to 33 days in the contaminated environment, visual and microscopic evaluations of the clay surfaces indicated varied behaviours. Some compositions exhibited a more intense development of PN (*Penicillium notatum*) colonies, while others showed a more pronounced growth of AN (*Aspergillus niger*) colonies. Additionally, the extent of

surface coverage by the microbiological film varied depending on the composition. Consequently, the analysis of the results has not permitted the establishment of a clear correlation between the clay composition and the predominant type of mould growth.

- The final evaluation, conducted 33 days after exposure to the contaminated environment (see Figure 8), revealed the following classification based on fungal growth: Class 1 (invisible to the naked eye but clearly visible under a microscope) for compositions P8-P12 (minimum 30% lime content), Class 2 (visible growth covering up to 25% of the tested surface) for compositions P3-P7 (minimum 5% lime content), and Class 3 (visible growth covering up to 50% of the tested surface) for compositions P1 and P2 (0% or 3% lime content in the dried material). In terms of product performance estimation, the P3-P12 compositions were classified as Category 1. The rationale behind this categorisation is that these materials contain negligible nutrients or minimal contaminants, which precludes substantial fungal growth. Conversely, the compositions with minimal or no lime content (P2 - 3% lime and P1 - 0% lime) were classified as Category 2. This classification is attributed to the fact that these materials lack the resilience to microbial attacks and contain nutrients that facilitate microorganism growth. One potential explanation for these results is the presence of residual organic content in the clay soil, despite the processing of the soil through sorting and sieving to remove vegetative materials prior to use. Consequently, in order to enhance the durability and hygienic properties of clay surfaces, the implementation of an appropriate surface treatment is considered beneficial.

The selection criteria for the clay-based compositions (absence of drying cracks; adhesion to the substrate of at least 0.5 N/mm²; compressive strength of at least 2.5 N/mm²; flexural tensile strength of at least 1.5 N/mm²) as identified in Figure 9 were applied, and three compositions that met all these requirements were selected for validation testing of the antifungal treatment through surface coating. These selected compositions are: P6 (40% clay, 20% lime, 40% sand), P7 (35% clay, 25% lime, 40% sand) and P8 (30% clay, 30% lime, 40% sand).

The protective and surface treatment solutions for clay-based surfaces, as prepared (Figure 10), were found to be homogeneous, easy to apply by brushing, and demonstrated good surface coverage. The most homogeneous solution was the one prepared with liquid wax (S1). However, with the addition of rabbit skin glue, the dispersion of raw materials derived from the recycling of expired cosmetic products became more challenging.

Despite this, the resulting coatings were found to be smooth, continuous, and uniform, ensuring adequate surface coverage. However, it was observed that the presence of rabbit skin glue in the treatment solution had a slightly negative effect on coating coverage capacity. This effect was particularly noticeable on the white cementitious substrate, which remained slightly visible beneath the treatment film, especially in the case of solution S3, where rabbit skin glue was used exclusively as the dispersion matrix (Figure 10d).

In relation to the investigation of the resistance exhibited by clay-based composites following treatment with a liquid beeswax-based solution, observations made after a seven-day exposure period (see Figure 11) indicate that the surface remains impermeable when exposed to a mould-contaminated environment. The moisture generated by the mould's metabolic processes manifests as water droplets, thereby supporting the hypothesis of the surface's hydrophobic nature. No signs of mould growth were present on the surface of the specimens. Furthermore, the testing systems exhibited a slight inhibition halo around the clay-based specimens, with the halo size ranging from 1 to 5 mm from the edge of the specimen, forming a circular pattern around it, as exemplified in Figure 11b-c. In accordance with the fungal growth evaluation system and product performance estimation criteria (Tables 3 and 4), it can be concluded that treating clay surfaces with solution S1 resulted in their classification under: Class 0 (No signs of fungal growth upon microscopic examination),
Category 0 (The material does not serve as a nutrient medium for microorganisms – it is inert or fungistatic).

The results of the 7-day exposure period in a highly contaminated environment demonstrated

the treatment solution's high efficacy and a significant improvement in fungal resistance. The treatment of clay surfaces with solution S2, which uses a liquid beeswax and rabbit skin glue mixture (1:1 mass ratio) as the dispersion matrix, resulted in a loss of surface hydrophobicity compared to specimens treated with solution S1 after seven days of exposure to a contaminated environment (Figure 12).

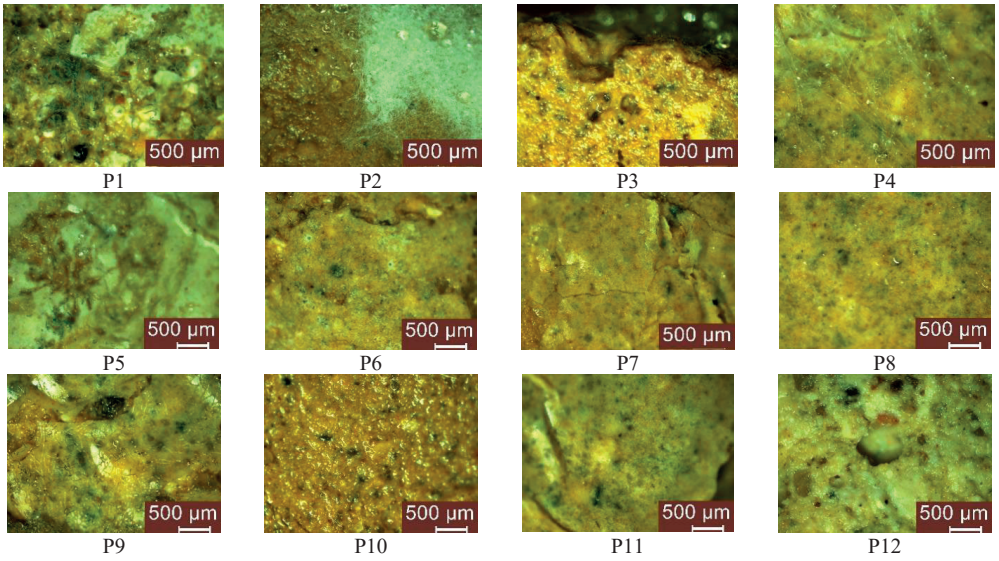


Figure 8. Optical microscopy images depicting the behaviour of clay composites in a mould-contaminated environment following 33 days of exposure.

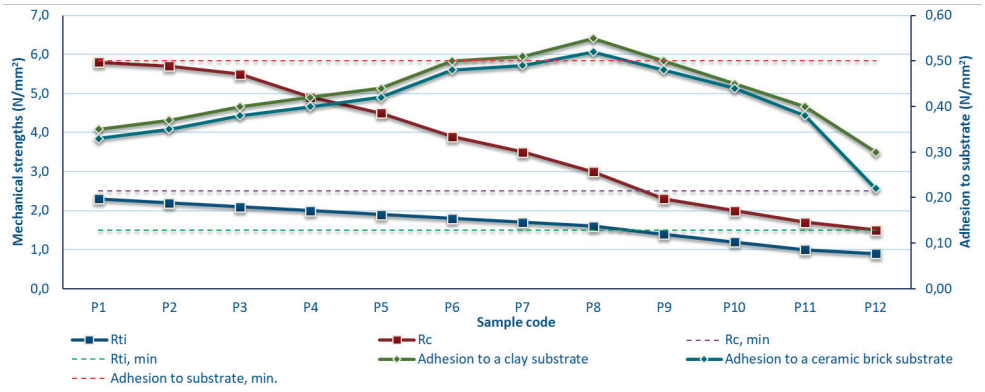


Figure 9. Selection of compositions for testing the efficacy of the antifungal treatment system.

It is noteworthy that no mould development was detected on the surfaces of any of the specimens. According to the fungal growth evaluation system and product performance criteria (Tables 3 and 4), treatment with solution S2 classified high-lime-content compositions (P7 and P8) in Class 0/Category 0 (no fungal growth detected, inert or fungistatic).

In contrast, the control (P1) and the 20% lime composition (P6) were placed in Class 1/Category 1 (microscopic fungal growth with minimal contamination).

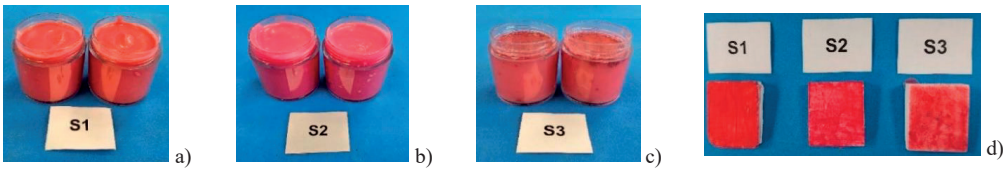


Figure 10. Representative images of protective and surface treatment solutions and their coating appearance on a white cementitious substrate

Therefore, the efficacy of solution S2 was clearly influenced by the nature of the clay substrate to which it was applied. The treatment of clay surfaces with solution S3, in which rabbit skin glue was used exclusively as the dispersion matrix, yielded the poorest results in terms of protection and coating durability after seven days of exposure in a contaminated environment (Figure 13). Exposure to moisture from mould growth compromised the integrity of the rabbit skin glue matrix, leading to the softening, dissolution, and absorption of the coating into the clay substrate. Consequently, only minimal traces of glycerine-based cosmetic products remained on the surface, appearing as dispersed lipstick residues. Additionally, a mucilaginous layer formed on the clay surface, with a more distinct and continuous film observed in compositions with higher lime content. This suggests that the mucilaginous film, likely containing traces of glycerine and rabbit skin glue, was less readily absorbed into the clay matrix as the lime content increased.

The analysis revealed the loss of inhibition halo formation, surface hydrophobicity, and visible moisture, suggesting its absorption into the system, which contributed to the dissolution of the rabbit skin glue coating and the formation of a mucilaginous film.

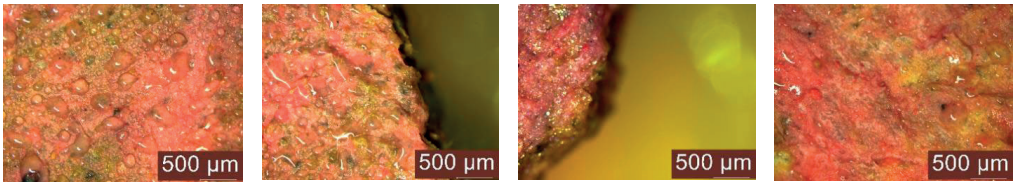
Clear signs of mould proliferation were observed, particularly in specimens with lower lime content, such as the control (P1) and sample P6. Quantitative evaluation based on fungal growth assessment criteria and product performance indicators confirmed the ineffectiveness of solution S3, with specimens classified as Class 1 (microscopic fungal growth) and Category 1 (minimal contamination allowing limited growth).

The final evaluation of the clay specimens treated with solutions S1-S3, conducted 33 days after exposure in a contaminated environment, demonstrated good resistance in the specimens treated with the beeswax-based solution (S1) (Figure 14). No fungal growth was observed on the specimens, and the coating maintained its hydrophobic properties. Although the inhibition halo previously observed at shorter exposure durations was no longer present, microscopic evaluation of the specimen surfaces confirmed their classification as: Class 0 (no signs of fungal growth under microscopic examination), Category 0 (the material does not serve as a nutrient medium for microorganisms – it is inert or fungistatic).

As rabbit skin glue was incorporated into the dispersion matrix (S2 and S3), the coatings on the clay specimens demonstrated diminished resistance to the contaminated environment (Figures 15 and 16). In the case of treatment solution S2, a decline in hydrophobicity was observed, accompanied by distinct indications of mould growth on the control specimen (P1) and the low-lime-content clay specimen (P6). Furthermore, the presence of fungal growth was detected in the cracks that formed on the surfaces of the high-lime-content specimens (P7 and P8). Utilising the product performance estimation criteria outlined in Tables 3 and 4, the treatment of clay surfaces with solution S2 led to the classification of the high-lime-content compositions (P7 and P8) as: Class 1 (Growth invisible to the naked eye but clearly visible under a microscope), Category 1 (The material contains very few nutrients or is minimally contaminated, allowing only very limited fungal growth). In contrast, the control composition (P1) and the composition with 20% lime content (P6) exhibited behaviour classified as Class 2 (visible growth covering up to 25% of the tested surface) and Category 2 (the material does not resist microbial attacks; it contains nutrients that support microorganism growth).

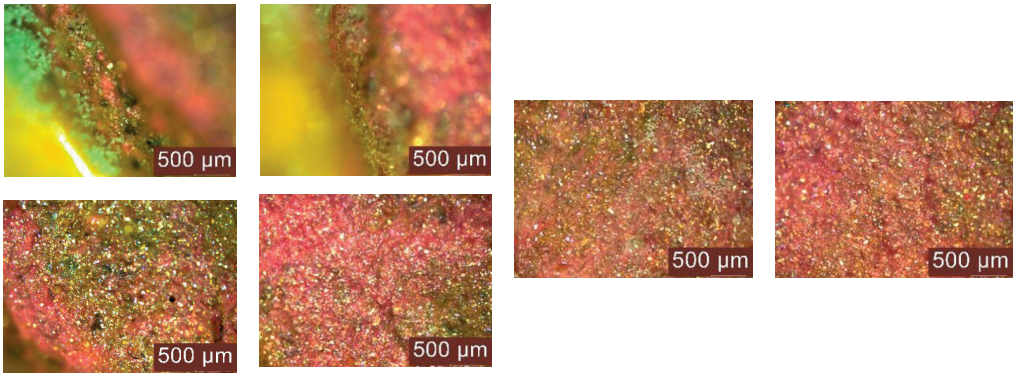
For treatment solution S3 (100% rabbit skin glue dispersion matrix), microscopic examination confirmed significant mould growth on all clay surfaces, resulting in a loss of colour and a transition to a mucilaginous state. The

classification results are outlined below: P1: Class 3/Category 2 (Visible growth covering up to 50% of the tested surface; material supports microbial growth); P6-P7: Class 2/Category 2 (Visible growth covering up to 25% of the tested surface; material allows microorganism development); P8 (highest lime content): Class 1/Category 1 (Growth invisible to the naked eye but clearly visible under a microscope; very limited fungal development). As illustrated in Table 6, a comprehensive overview of the temporal progression of quantification indicators, contingent on the nature and implementation of treatment, was provided. It is evident that surface treatment resulted in an enhancement of resistance within the contaminated environment, with an increase ranging from 1 to 3 classes and 1 to 2 categories, depending on the treatment modality and the clay composition. This is particularly influenced by the presence and proportion of lime in the mixture.



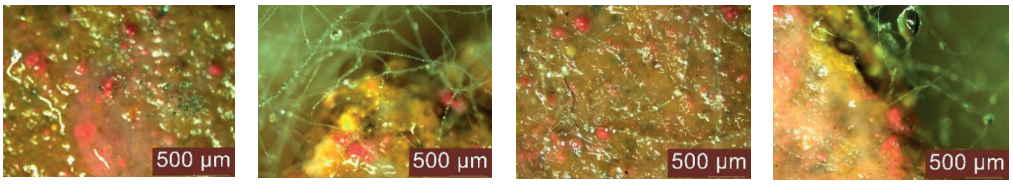
a) P1 b) P6 c) P7 d) P8

Figure 11. Optical microscopy images depicting the performance of clay composites treated with solution S1 in a mould-contaminated environment following 7 days of exposure



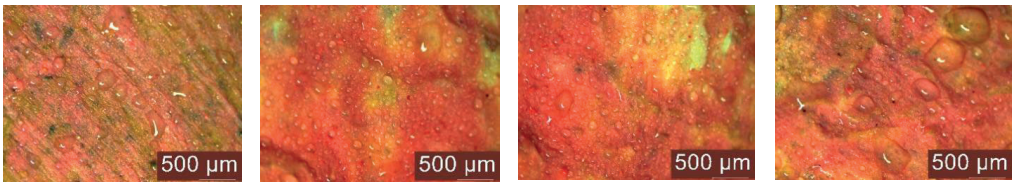
a) P1 b) P6 c) P7 d) P8

Figure 12. Optical microscopy images depicting the performance of clay composites treated with solution S2 in a mould-contaminated environment following 7 days of exposure



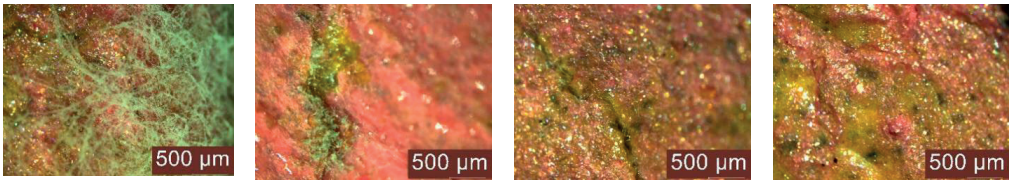
a) P1 b) P6 c) P7 d) P8

Figure 13. Optical microscopy images depicting the performance of clay composites treated with solution S3 in a mould-contaminated environment following 7 days of exposure



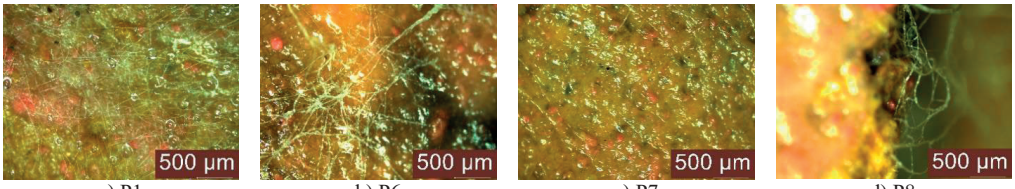
a) P1 b) P6 c) P7 d) P8

Figure 14. Optical microscopy images depicting the performance of clay composites treated with solution S1 in a mould-contaminated environment (33 days of exposure)



a) P1 b) P6 c) P7 d) P8

Figure 15. Optical microscopy images depicting the performance of clay composites treated with solution S2 in a mould-contaminated environment (33 days of exposure).



a) P1 b) P6 c) P7 d) P8

Figure 16. Optical microscopy images depicting the performance of clay composites treated with solution S3 in a mould-contaminated environment (33 days of exposure)

Table 6. The evolution of quantification indicators over time, with a focus on the impact of clay composition, the existence of treatment, and the nature of the treatment itself

Sample code - Treatment		P1				P6				P7				P8			
Exposure time	Quantification indicator	P1	P1-S1	P1-S2	P1-S3	P6	P6-S1	P6-S2	P6-S3	P7	P7-S1	P7-S2	P7-S3	P8	P8-S1	P8-S2	P8-S3
7 days	Class	1	0	1	1	1	0	1	1	1	0	0	1	1	0	0	1
	Category	1	0	1	1	1	0	1	1	1	0	0	1	1	0	0	1
33 days	Class	3	0	2	3	2	0	2	2	2	0	1	2	1	0	1	1
	Category	2	0	2	2	1	0	2	2	1	0	1	2	1	0	1	1

Although equal amounts of expired non-food household cosmetic-pharmaceutical products were used in all three prepared solutions - some selected for their fat content, others for their antifungal properties, and some only as colour pigments - only the beeswax-based solution proved fully effective. This solution imparted hydrophobic properties to the clay surface and utilised the antifungal effect of the non-food household additives, as evidenced by the formation of an inhibition halo around the specimen in the test system.

The beeswax-based surface treatment resulted in more favourable classifications in both fungal growth evaluation and product performance estimation compared to untreated surfaces. In contrast, the rabbit skin glue solution reduced the antifungal efficiency of the non-food household products.

The addition of rabbit skin glue to the mixture, even when combined with beeswax, resulted in only modest outcomes in terms of clay surface protection. The nature of the clay substrate also influenced the outcomes, with a higher lime content in the clay composition contributing to slightly improved outcomes.

CONCLUSIONS

Vernacular constructions, which frequently comprise unfired clay walls, offer a number of advantages, including enhanced indoor air quality, minimal environmental impact, and a beneficial role in preserving and promoting local identity. However, these structures are not without vulnerability; a primary concern pertains to their diminished resilience to Vernacular constructions, which frequently comprise unfired clay walls, offer a number of advantages, including enhanced indoor air quality, minimal environmental impact, and a beneficial role in preserving and promoting local identity. However, these structures are not without vulnerability; a primary concern pertains to their diminished resilience to biological and environmental factors. The objective of this experimental research was to investigate the feasibility of repurposing non-food household waste and minimally processed products through the development of surface treatment solutions aimed at enhancing the durability of unfired clay-based wall surfaces against mould growth.

The experimental research yielded the following conclusions:

- The composition and ratio of raw materials utilised in clay-based composites significantly impact the physical and mechanical performance, resistance, and durability. Among the 12 analysed clay compositions, three were identified as having the most suitable clay-to-lime ratio for the intended application: P6, P7, and P8, which are characterized by the following ranges of raw materials: 30-40% clay, 20-30% lime, and 40% sand.
- With regard to resistance to mould growth (*Penicillium notatum* and *Aspergillus niger*), it was found that all clay compositions ultimately permitted the development of one or both types of mould on their surface. The initial signs of mould appeared earliest (3 days after contamination) in compositions with lower lime content, thereby confirming the beneficial and sanitizing effect of lime.
- The efficacy of surface treatment in enhancing the resistance of clay surfaces to contamination is dependent on the nature of the treatment solution.
- The enhancement of clay surfaces through surface treatment has been shown to occur within a range of 1 to 3 classes and 1 to 2 categories. The most effective performance was observed in the clay composite with the highest lime content (P8), treated with the solution using a 100% liquid beeswax dispersion matrix (S1). The replacement of beeswax with rabbit skin glue (S2) led to a reduction in the antifungal efficacy of the surface treatment for all clay surfaces that were tested, including the composition with the highest lime content (P8). Furthermore, when beeswax was entirely substituted with rabbit skin glue (S3), this decline in antifungal protection persisted.
- Rabbit skin glue (S3) functions as a dispersion matrix, yet it does not yield a substantial beneficial effect in terms of enhancing mould resistance on clay surfaces. In comparison, liquid beeswax has been demonstrated to be a significantly more effective dispersion matrix.

In conclusion, based on the findings presented, new research hypotheses can be formulated, focusing on the use of liquid beeswax as a dispersion matrix while exploring and identifying new expired non-food household products that could be repurposed to develop surface treatment solutions for unfired clay surfaces in construction, with the aim of enhancing their resistance and durability.

REFERENCES

Abdelrazek, H., & Yılmaz, Y. (2020). Methodology Toward Cost-Optimal and Energy-Efficient Retrofitting of Historic Buildings. *Journal of Architectural Engineering*, 26(4). https://doi.org/10.1061/(asce)ae.1943-5568.0000433.

Androutsopoulos, A., Geissler, S., Charalambides, A. G., Escudero, C. J., Kyriacou, O., & Petran, H. (2020). Mapping the deep renovation possibilities of European buildings. *In IOP Conference Series: Earth and Environmental Science*, 410(1), 012056. IOP Publishing.

Azalam, Y., Alioui, A., Benfars, M., Mabrouki, M., & Bendada, E. M. (2024). Physical and mechanical properties of adobe bricks reinforced by natural additives, a case study of alfalfa fibers. *EUREKA: Physics and Engineering,* (4), 144-159.

Bahobail, M. A. (2012). The mud additives and their effect on thermal conductivity of adobe bricks. *Journal of Engineering Sciences*, 40(1), 21-34.

Bashir, S. M., Kimiko, S., Mak, C. W., Fang, J. K. H., & Gonçalves, D. (2021). Personal care and cosmetic

products as a potential source of environmental contamination by microplastics in a densely populated Asian city. *Frontiers in Marine Science*, 8, 683482.

Browne, G. (2009). Stabilised interlocking rammed earth blocks: alternatives to cement stabilisation. In 11th International Conference on Non-conventional Materials and Technologies (NOCMAT, 2009), 6th-9th September 2009, Bath University, 25-26.

Bui, Q. B., Morel, J. C., Hans, S., & Meunier, N. (2009a). Compression behaviour of non-industrial materials in civil engineering by three scale experiments: the case of rammed earth. *Materials and structures*, 42, 1101-1116.

Bui, Q. B., Morel, J. C., Reddy, B. V., & Ghayad, W. (2009b). Durability of rammed earth walls exposed for 20 years to natural weathering. *Building and Environment*, 44(5), 912-919.

Calabria, J., Vasconcelos, W. L., Daniel, D. J., Chater, R., McPhail, D., & Boccaccini, A. R. (2010). Synthesis of sol–gel titania bactericide coatings on adobe brick. *Construction and Building Materials*, 24(3), 384-389.

Camerini, R., Chelazzi, D., Giorgi, R., & Baglioni, P. (2019). Hybrid nano-composites for the consolidation of earthen masonry. *Journal of colloid and interface science,* 539, 504-515.

Cinelli, P., Coltelli, M. B., Signori, F., Morganti, P., & Lazzeri, A. (2019). Cosmetic packaging to save the environment: Future perspectives. *Cosmetics*, 6(2), 26.

Ciurileanu, G. T., & Bucur Horvath, I. (2011). The new vernacular based architecture. *JAES Sect. Civil. Eng. Inst*, 1, 27-34.

de Elguea-Culebras, G. O., Sánchez-Vioque, R., Santana-Méridas, O., Herraiz-Peñalver, D., Carmona, M., & Berruga, M. I. (2016). In vitro antifungal activity of residues from essential oil industry against Penicillium verrucosum, a common contaminant of ripening cheeses. *Lwt*, 73, 226-232.

Dormohamadi, M., & Rahimnia, R. (2020). Combined effect of compaction and clay content on the mechanical properties of adobe brick. *Case Studies in Construction Materials*, 13, e00402.

Elert, K., Bel-Anzué, P., Monasterio-Guillot, L., & Pardo, S. (2019). Performance of alkaline activation for the consolidation of earthen architecture. *Journal of Cultural Heritage*, 39, 93-102.

Eslami, A., Mohammadi, H., & Banadaki, H. M. (2022). Palm fiber as a natural reinforcement for improving the properties of traditional adobe bricks. *Construction and Building Materials*, 325, 126808.

Ferron, A. (2007). The consolidation of earthen surface finishes: a study of disaggregating plasters at Mesa Verde National Park (Doctoral dissertation, University of Pennsylvania).

Ferron, A., & Matero, F. G. (2011). A comparative study of ethyl-silicate–based consolidants on earthen finishes. *Journal of the American Institute for Conservation*, 50(1), 49-72.

Halla, N., Fernandes, I.P., Heleno, S.A., Costa, P., Boucherit-Otmani, Z., Boucherit, K., Rodrigues, A.E., Ferreira, I.C. & Barreiro, M.F. (2018). Cosmetics preservation: a review on present strategies. *Molecules*, 23(7), 1571.

Hamrita, B., Emira, N., Papetti, A., Badraoui, R., Bouslama, L., Ben Tekfa, M.I., Hamdi, A., Patel, M., Elasbali, A.M., Adnan, M. & Ashraf, S.A. (2022). Phytochemical Analysis, Antioxidant, Antimicrobial, and Anti-Swarming Properties of *Hibiscus sabdariffa* L. Calyx Extracts: *In Vitro* and In Silico Modelling Approaches. *Evidence-Based Complementary and Alternative Medicine*, 1, 1252672.

Houston, D. M., Bugert, J., Denyer, S. P., & Heard, C. M. (2017). Anti-inflammatory activity of *Punica granatum* L. (Pomegranate) rind extracts applied topically to ex vivo skin. *European Journal of Pharmaceutics and Biopharmaceutics*, 112, 30-37.

Ige, O., & Danso, H. (2022). Experimental characterization of adobe bricks stabilized with rice husk and lime for sustainable construction. *Journal of Materials in Civil Engineering*, 34(2), 04021420.

Jayasinghe, C., & Kamaladasa, N. (2007). Compressive strength characteristics of cement stabilized rammed earth walls. *Construction and Building Materials*, 21(11), 1971-1976.

Juliano, C., & Magrini, G. A. (2017). Cosmetic ingredients as emerging pollutants of environmental and health concern. A mini-review. *Cosmetics*, 4(2), 11.

Kiroff, L., & Roedel, H. (2010). Sustainable construction technologies: Earth buildings in New Zealand. In Second International Conference of Sustainable Constructions Materials and Technologies, Ancona, Italy (pp. 349-360).

Lanzón, M., Madrid, J. A., Martínez-Arredondo, A., & Mónaco, S. (2017). Use of diluted Ca (OH) 2 suspensions and their transformation into nanostructured $CaCO_3$ coatings: A case study in strengthening heritage materials (stucco, adobe and stone). *Applied Surface Science*, 424, 20-27.

Li, Z. X., Zhao, L. Y., & Sun M. (2009). Deterioration of earthen sites and consolidation with PS material along silk road of China [J]. Chinese *Journal of Rock Mechanics and Engineering*, 28(5), 1047-1054.

Martinovic, S., N. Zecevic, & A. Salihbegović. 2023. Vernacular Residential Architecture in the Context of Sustainability - Case Study of Svrzo's House Complex. *Journal of Sustainable Architecture and Civil Engineering* 32 (1): 19–40. https://doi.org/10.5755/j01.sace.32.1.32753.

Măgurean, A. M., & Petran, H. A. (2023). Analysis of Measured CO_2 Levels through Long-Term Monitoring in Renovated Multifamily Buildings: A Common Case. *Buildings*, 13(8), 2113.

Minke, G. (2006). Building with earth: design and technology of a sustainable architecture. De Gruyter.

Morganti, P., Lohani, A., Gagliardini, A., Morganti, G., & Coltelli, M. B. (2023). Active ingredients and carriers in nutritional eco-cosmetics. *Compounds*, 3(1), 122-141.

Muñoz, P., Letelier, V., Muñoz, L., & Bustamante, M. A. (2020). Adobe bricks reinforced with paper & pulp wastes improving thermal and mechanical properties. *Construction and Building Materials*, 254, 119314.

Nciri, N., Kim, N., & Caron, A. (2022). Unlocking the Hidden Potential of Cosmetics Waste for Building

Sustainable Green Pavements in the Future: A Case Study of Discarded Lipsticks. *Molecules*, 27(5), 1697.

Niroumand, H., Zain, M. F. M., & Jamil, M. (2013). A guideline for assessing of critical parameters on Earth architecture and Earth buildings as a sustainable architecture in various countries. *Renewable and sustainable energy reviews*, 28, 130-165.

Pacheco, G., Pozzi-Escot, D., Cappai, M., Malpartida, S., & Petrick, S. (2016). Productos orgánicos para la conservación de pintura mural. *In Proceedings of the XII World Congress on Earthen Architecture Terra* Lyon, France, 11-14 July, Craterre: Villefontaine, 33–137, ISBN 9791096446117.

Pacheco-Torgal, F. (2015). Introduction to eco-efficient masonry bricks and blocks. *In Eco-Efficient Masonry Bricks and Blocks* (pp. 1-10). Woodhead Publishing.

Patil, A., Mulani, S., Kokare, M., & Kumbhar, R. (2021). An experimental study on floating concrete using soap solution, plywood dust & thermocol. *International Research Journal of Engineering and Technology (IRJET)*, 8(6).

Rescic, S., Mattone, M., Fratini, F., & Luvidi, L. (2023). Conservation of Earthen Bricks in Architecture: An Experimental Campaign to Test Different Treatments on Vernacular Built Heritage. *Heritage*, 6(2), 1541-1566.

Sandle, T. (2022). EU GMP Annex 1: Manufacture of Sterile Medicinal Products. European Commission: Brussels, Belgium.

Silletta, A., Mancuso, A., d'Avanzo, N., Cristiano, M. C., & Paolino, D. (2024). Antimicrobial Compounds from Food Waste in Cosmetics. *Cosmetics*, 11(5), 151.

Stazi, F., Nacci, A., Tittarelli, F., Pasqualini, E., & Munafò, P. (2016). An experimental study on earth plasters for earthen building protection: The effects of different admixtures and surface treatments. *Journal of Cultural Heritage*, 17, 27-41.

Varvaresou, A., Papageorgiou, S., Tsirivas, E., Protopapa, E., Kintziou, H., Kefala, V., & Demetzos, C. (2009). Self-preserving cosmetics. *International Journal of cosmetic science*, 31(3), 163-175.

Vasileva, I., Denkova, R., Chochkov, R., Teneva, D., Denkova, Z., Dessev, T., ... & Slavov, A. (2018). Effect of lavender (*Lavandula angustifoli*a) and melissa (*Melissa officinalis*) waste on quality and shelf life of bread. *Food Chemistry*, 253, 13-21.

Vural, N., Vural, S., Engin, N., & Sümerkan, M. R. (2007). Eastern Black Sea Region - A sample of modular design in the vernacular architecture. *Building and environment*, 42(7), 2746-2761.

Scientific Papers. Series E. Land Reclamation, Earth Observation & Surveying, Environmental Engineering. Vol. XIV, 2025
Print ISSN 2285-6064, CD-ROM ISSN 2285-6072, Online ISSN 2393-5138, ISSN-L 2285-6064

EVALUATION OF THE POSSIBILITIES OF USING CLAY SOILS FOR THE REALIZATION OF VERNACULAR CONSTRUCTIONS

Andreea HEGYI[1], Gabriela CĂLĂTAN[2], Cristian PETCU[1], Stefan BAKOS[2], Alexandra CSAPAI[1]

[1]National Institute for Research and Development in Construction, Urban Planning and Sustainable Spatial Development - URBAN-INCERC, 266 Pantelimon Road, District 2, Bucharest, Romania
[2]Office of Pedological and Agrochemical Studies from Cluj-Napoca, 1 Fagului Street, 400524, Cluj-Napoca, Romania

Corresponding author email: cristian.petcu@yahoo.com

Abstract

Since time immemorial, mankind has sought solutions to the problem of creating sustainable living spaces that provide thermal comfort and good indoor air quality. One of the most prevalent techniques has been the construction of buildings from clay-based materials. Nevertheless, even at the present time, this method is still insufficiently regulated by generalised regulations. The principal issue is the diversity of raw material characteristics, which necessitates a considerable number of preliminary tests and a lengthy period of time. This paper puts forward an interdisciplinary methodology for the analysis of clayey earth, with a view to determining the potential applications of this material in the production of adobe-brick masonry elements and plastering mortars for vernacular construction. The research methodology entailed a pedological analysis of 30 clay soil samples sourced from Mârgău and Ciucea region, Cluj, followed by an evaluation of their suitability for construction applications. The experimental findings have indicated the potential for establishing limiting conditions regarding the clay, sand, and dust content of the soils, in conjunction with pH, humus, and carbonate levels.

Key words*: vernacular constructions; clay soil; pedological analysis; adobe-brick, plaster mortar*

INTRODUCTION

The construction sector is responsible for approximately 40% of global energy consumption, 40% of raw material usage, 50% of greenhouse gas emissions, and 60% of total waste generation, with only 20-30% of this waste being recycled (Măgurean & Petran, 2023; Papadaki et al., 2022; Asif et al., 2007; Santamouris et al., 2015; Papadaki et al., 2019; Mollaei et al., 2023; Munaro et al., 2020). This issue has been widely recognised on a global level, leading to an increased focus on identifying strategies to mitigate and reduce its adverse environmental impact (Androutsopoulos et al., 2020), a significant initiative in this regard being the European Green Deal (Ak et al., 2024; Montanarella & Panagos, 2021; Kotseva-Tikova & Dvorak, 2022).

Recent studies have increasingly concentrated on formulating solutions that support sustainability objectives in the construction industry. One such approach involves the resurgence of traditional construction practices, with a focus on the development and optimisation of clay-based building techniques to preserve their benefits while mitigating their limitations.

A substantial body of documenttation on this subject is available in the scientific literature. Evidence of the growing research interest in this field is illustrated by a query of the Web of Science Core Collection using the keyword "adobe brick", which yielded 518 publications, of which 39% were classified under Construction Building Technology, 38.8% under Civil Engineering, and 25% under Materials Science Multidisciplinary.

This distribution underscores the increasing emphasis on the development of environmentally sustainnable construction materials, with a notable surge in research publications after the year 2000 (Figure 1).

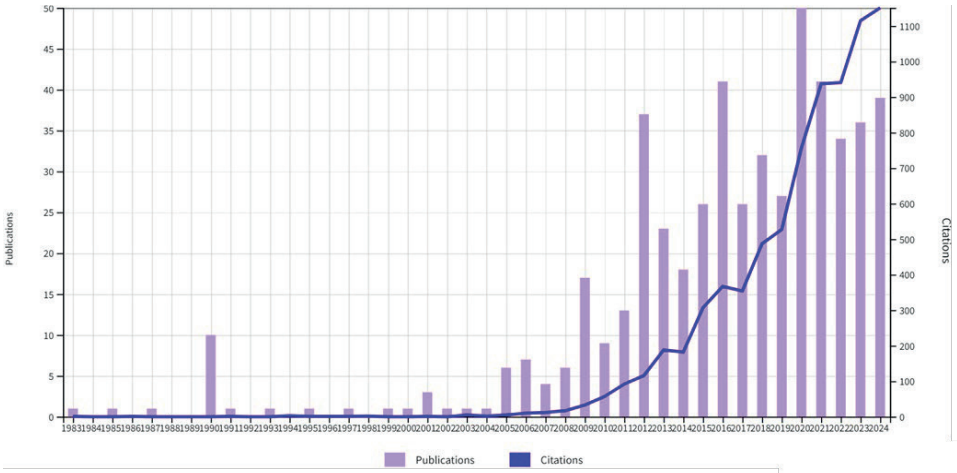


Figure 1. Evolution of publications and citations, according to WOS, of scholarly works identified using the keyword "adobe brick"

Notwithstanding the advantages inherent in unfired clay-based constructions, it is important to acknowledge their inherent limitations. Niroumand et al. (Niroumand et al., 2013) emphasise that one of the most critical drawbacks of earth-based structures is their inadequate mechanical strength, which hinders their utilisation to the same extent as conventional construction materials. However, contemporary research endeavours are actively addressing this limitation by enhancing the mechanical performance of these materials through the application of composite material principles. These advancements involve the incorporation of additive raw materials, such as lime, fly ash, bitumen, asphalt, or dispersed reinforcing fibres, to improve their structural integrity and durability.

Despite the fact that the field of earth-based construction remains a minimally regulated and standardised field, largely due to the high heterogeneity of its primary raw material, clay soil, a review of the scientific literature identifies several guiding principles that support its potential for sustainable building applications. The most notable regulatory frameworks include the German Earth Building Code, which was established in 1944 and laid the foundation for the development of DIN 18951. In addition, New Zealand has introduced relevant standards (NZS 4297:1998; NZS 4298:1998; NZS 4299:1998), and specific regulations exist in Australia, New Mexico and Zimbabwe. Furthermore, various guidelines, instructional documentation and specialised educational programmes have been developed, particularly within Europe, to promote and standardise earth-based construction practices (Pacheco-Torgal & Jalali, 2012). Therefore, given the existence of regional variations based on geographical location, several criteria have been established to determine the suitability of clay soil for the production of adobe bricks. The most fundamental requirements, irrespective of the geographical location of the experimental area, include the absence of organic matter (Pacheco-Torgal & Jalali, 2012) and the implementation of a sampling method that ensures soil collection from a minimum depth of 150 mm below the surface. This approach is designed to minimise the presence of organic residues, such as vegetal or animal matter (Giada et al., 2019). Furthermore, G. Minke advances the argument that a minimum sampling depth of 400 mm may be required to ensure the material's suitability for construction applications (Minke, 2005). From a chemical, oxide, and mineralogical composition standpoint, which are challenging to assess in the field without access to specialised laboratories, the scientific literature (Salih et al., 2020) highlights a predominance of silicon dioxide (SiO_2) in the range of 50-60%, followed by aluminium oxide (Al_2O_3) at approximately 10%. These elements contribute to the structural quality of adobe bricks. Additionally, the presence of ferric oxide

(Fe_2O_3), generally not exceeding 10%, is noted, with its hydrated form responsible for the characteristic brown-reddish soil colouration. However, ferric oxide has also been implicated in the development of efflorescence, which may have a detrimental effect on the material's durability and performance.

Limitation of the calcium oxide (CaO) concentration to a maximum of 10% is another critical aspect. When not chemically bound to SiO_2, CaO can have detrimental effects, including swelling in the presence of water and carbonation, which leads to the formation of $CaCO_3$, a compound characterised by low mechanical strength and reduced durability. In terms of granulometric composition, clay functions as the primary binding agent, while silt, sand, and aggregates act as fillers that influence the material's mechanical and structural properties. The scientific literature suggests that the aggregate fraction should not exceed 10% for particles larger than 2 mm, while the sand content should range between 40% and 80%, with particle sizes between 0.063 and 2 mm. Furthermore, the recommended silt content varies between 10% and 30%, with grain sizes between 0.002 and 0.063 mm, whereas the clay fraction typically ranges from 20% to 50% (grain sizes between 0.002-0.063 mm) (Salih et al., 2020; Giada et al.,2019). However, older references indicate that clay content should not fall below 15%, as it plays a crucial role in maintaining the structural integrity and cohesion of the material (Laaroussi et al., 2013; Boduroglu, 1989). From a mineralogical standpoint, the predominant minerals present in clay soils may be associated with a high silicon content or be characteristic of clay-rich compositions. The most commonly identified minerals include quartz, calcite, feldspars, illite, kaolinite, chlorite, smectite, and montmorillonite. The presence of calcite is often indicative of soil alkalinity (Dormohamadi & Rahimnia, 2020; Demir, 2008).

From a physico-mechanical perspective, the assurance of optimal thermal insulation and substantial thermal inertia - facilitating the accumulation of heat during warm periods and its subsequent release during colder seasons – necessitates that the bulk density of the mixture falls within the range of 1800-2000 kg/m³ (Burroughs, 2008). From a structural performance standpoint, the ASTM D1633-00 standard (New Mexico) stipulates a minimum compressive strength of 2.07 N/mm² for earthen wall materials. In a similar fashion, the Zimbabwean code for rammed earth walls establishes a minimum compressive strength of 1.5 N/mm² for single-story structures with 400 mm thick walls and 2.0 N/mm² for two-story buildings. In Australia, the relevant standard prescribes a minimum compressive strength of 1.15 N/mm², while the ASTM International E2392/E2392M-10e1-2010 standard mandates a threshold of 2.068 N/mm². Additionally, the ACI Materials Journal Committee has reported that compressive strength varies based on soil composition, with values ranging from 2.76 to 6.89 N/mm² for sandy soils and from 1.72 to 4.14 N/mm² for clay-rich soils. Moreover, the Peruvian Standard E.080 stipulates a minimum compressive strength of 1.2 N/mm² and a minimum tensile strength of 0.4 N/mm², thereby underscoring the heterogeneity of regulatory approaches to earthen construction materials (Pacheco-Torgal & Jalali, 2012; Vega et al., 2011).

During the preparation process, clay soil is typically mixed with water, thereby initiating the delamination of clay particles. Ensuring adequate plasticity and workability is crucial; however, it is important to recognize that an excessive water content increases the risk of cracking and significant axial shrinkage. Achieving crack-free final elements is imperative, and it is considered acceptable for bricks produced using soft mixture technologies to exhibit a linear shrinkage between 3% and 12%. Conversely, drier mixtures should exhibit a linear shrinkage ranging from 0.4% to 2% (Minke, 2005).

The physico-mechanical properties of clay-based materials vary significantly depending on the characteristics of the clay soil, the preparation and testing methods employed, and the type and proportion of additives incorporated. The scientific literature reports a wide range of values for these parameters, reflecting the diversity of experimental approaches1. Specifically, the compressive strength has been documented to range from 0.5 MPa to over 7 MPa (Dormohamadi & Rahimnia, 2020), while the flexural strength has been reported to vary between 0.25 MPa and 1.25

MPa (Dormohamadi & Rahimnia, 2020). Furthermore, Silveira et al. (Silveira et al., 2013) reported a tensile strength of 0.16 MPa for adobe bricks. The parameters under consideration – namely, particle size distribution, density, mixing water content, and consistency – are relatively straightforward to analyse and assess, particularly in situ, where access to a specialized laboratory for chemical and mineralogical analysis may be limited. However, for a comprehensive evaluation, it is essential to incorporate both physical and chemical testing methodologies to ensure a thorough characterization. The objective of this study was to assess, through chemical and pedological analysis, the potential suitability of clay soils from the Mârgău and Ciucea regions in Cluj County for the production of adobe masonry elements.

MATERIALS AND METHODS

The study aimed to assess the feasibility of rapidly determining the suitability of clay soils from the selected locations – Mârgău, Cluj County (46°44′35″N 22°57′51″E), and Ciucea, Cluj County (46°57′13″N 22°48′27″E) – for construction applications through chemical and pedological analysis methods was carried out by collecting soil samples at variable depths, up to a maximum of 1200 mm, using a transversal sampling method with a soil probe. The sampling process was carried out while maintaining the depth of the pedogenetic soil horizon in order to preserve the integrity of the analysed profiles. The soil sample batch was selected on the basis of pedological analysis requests submitted to OSPA (Office for Soil and Agrochemical Studies) by external clients, specifically landowners, in 2024. Each collected soil sample was assigned a unique identification code and subjected to pedological analysis under controlled laboratory conditions using standardized methods recognised in Romania. The analysis focused on key soil properties, including texture and skeletal fraction, clay content, sand content and granulometry, determined according to STAS 7184/10-79, pH value, determined according to the standardized method described in SR 7184-13:2001, humus concentration, determined according to STAS 7184/21-82, and $CaCO_3$ content determined according to the standardized method described in STAS 7184/16-80. 169 samples were collected from the Mârgău and Ciucea areas and coded as follows: M1–M114 for those collected from the Mârgău area, C1–C55 for those from the Ciucea area, and VD for the sample collected from Valea Drăganului.

In order to evaluate the potential applicability of the selected clay soils, a series of working hypotheses were formulated based on insights from the scientific literature (Figure 2). Following the pedological characterisation of the collected clay soil samples, a systematic multi-step selection process was implemented (Figure 3), wherein samples that did not meet the predefined criteria were excluded.

This methodological framework was applied to both the clay soil samples collected from the Mârgău area, Cluj County, and those from the Ciucea area, Cluj County. Subsequently, the selected soil samples were subjected to laboratory analysis in order to evaluate their physico-mechanical properties and to compare them with a reference set of indicators derived from specimens produced using clay soil collected from the Valea Drăganului area, Cluj County (46°54′10″N 22°49′53″E).

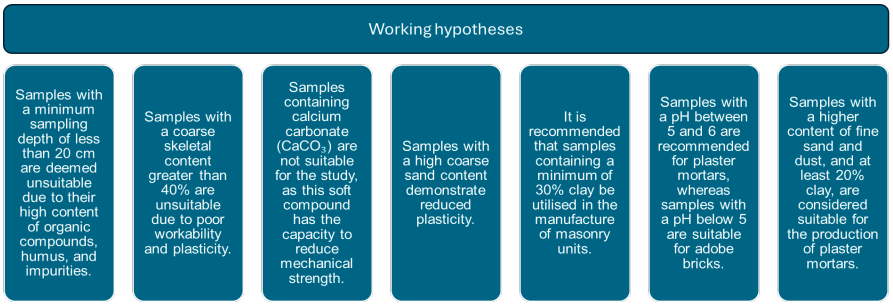


Figure 2. Working assumptions based on references found in the literature

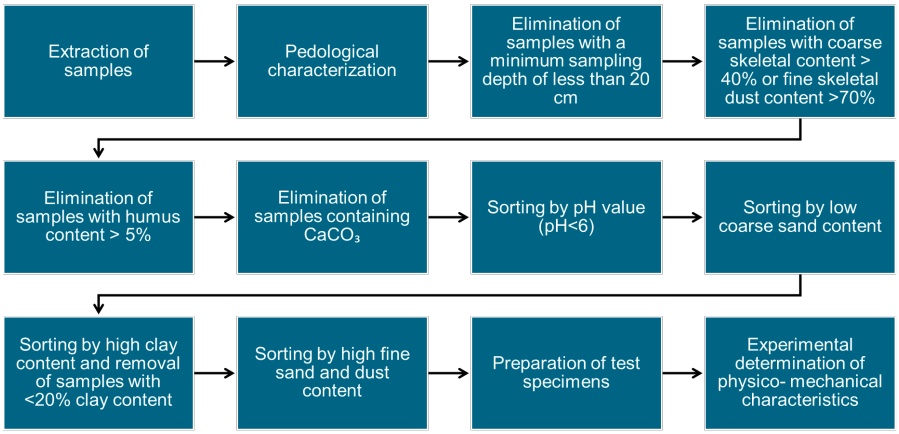


Figure 3. Clay soil sample selection scheme

The suitability of Valea Drăganului soil for adobe brick production had previously been established through experimental testing and documented findings in the scientific literature (Calatan et al., 2017; Hegy et al., 2016; Hegyi et al., 2023; Calatan et al., 2016; Călătan et al., 2020).

The present study therefore set out to validate the selection methodology applied through a comparative assessment of the soil samples.

The physico-mechanical performance of the specimens was assessed by the fabrication of prismatic specimens (40×40×160 mm) from each batch of collected and selected clay soil, as detailed below:

- the clay soil was mixed with a precise quantity of water in order to maintain consistent workability, as measured by a spread diameter of 95±5 mm;
- the freshly prepared clay-water mixture was subsequently introduced into metal moulds, with the internal dimensions of 40×40×160 mm;
- the moulded specimens were stored under controlled laboratory conditions at a temperature of 23 ± 2°C and a relative humidity of 65 ± 2% for a period of three days, after which they were demoulded for subsequent analysis;
- the clay-based specimens were then subjected to the same temperature and humidity conditions until they had attained a constant mass, which was considered an indicator of uniform drying;
- for each clay soil type selected for laboratory analysis, a set of three identical specimens was prepared to ensure the repeatability and reproducibility of the experimental results.

The physico-mechanical performance characterisation tests were conducted under controlled laboratory conditions using standardised methodologies. Thus, the analysis included the determination of apparent density in the hardened state, in accordance with EN 1015-10, and axial shrinkage, as specified by STAS 2634. Axial shrinkage represents the reduction in a material's length along its longitudinal axis during the processes of drying or curing, flexural tensile strength is defined as a material's resistance to bending stress before fracture, and compressive strength is represented as its ability to withstand axial loads without failure. Furthermore, flexural tensile strength and compressive strength were evaluated following the procedures outlined in EN 1015-11. The risk of cracking was monitored through visual examination throughout the conditioning and drying process in order to assess the material's structural integrity.

The experimental results were analysed comparatively, in relation to existing data reported in the scientific literature, as well as to the findings obtained for clay soil samples collected from the Valea Drăganului area (VD).

RESULTS AND DISCUSSIONS

In the course of the study, 114 soil samples were collected in the Mârgău area. Following the application of the sampling depth criteria, 52 samples were excluded. A similar process was followed in the Ciucea area, where 18 out of 55

samples were excluded after meeting the same selection criteria (Figure 4).

The experimental analysis of the soil texture from the predefined sampling locations revealed a wide distribution on the ternary diagram (Figure 5). As evidenced by the analysis, the soil samples from the Valea Drăganului area are classified within the L (loam) zone, having a medium-textured (M) profile.

In contrast, the soil samples collected from the Mârgău area displayed a heterogeneous distribution, with a predominant LP (loamy sand) texture, though some samples were also situated within adjacent zones, including S (sand), SS (sandy loam), SP (sandy clay loam), TP (clay loam), and AP (silty clay loam).

A similar distribution of soil samples was observed in the Ciucea area, with the majority of samples falling within the LP zone, and a smaller number positioned in the SS, SP, TP, and AP zones.

Following the selection process based on soil texture, an additional seven samples from the Mârgău batch were excluded due to their classification within the AP zone. Furthermore, ten additional samples were eliminated as they had a dust content exceeding 70%, coupled with a low clay content. Similarly, within the Ciucea batch, one additional sample (C9) was removed, as its fine particle composition rendered it more suitable for plaster mortar or finishing coat preparation rather than for adobe brick production.

Following the elimination of samples that did not meet the sampling depth criteria, the texture analysis of the remaining soil samples revealed the necessity for further exclusions. Specifically, additional samples (M14, M20, M52 from the Mârgău batch and C19, C43, C54 from the Ciucea batch) were excluded on the basis that their coarse skeletal content exceeded 40% (Figure 6).

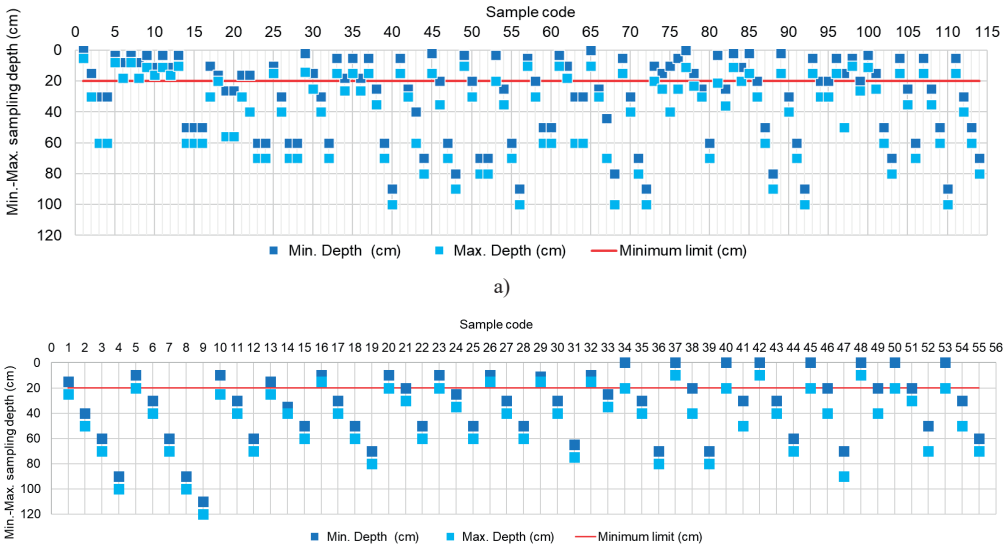
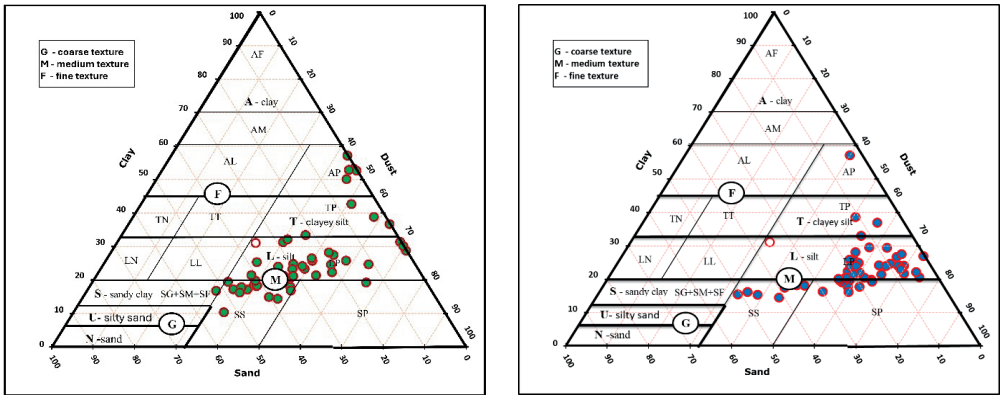


Figure 4. Sampling depth for: a) samples taken from Mârgău area; b) samples taken from Ciucea area

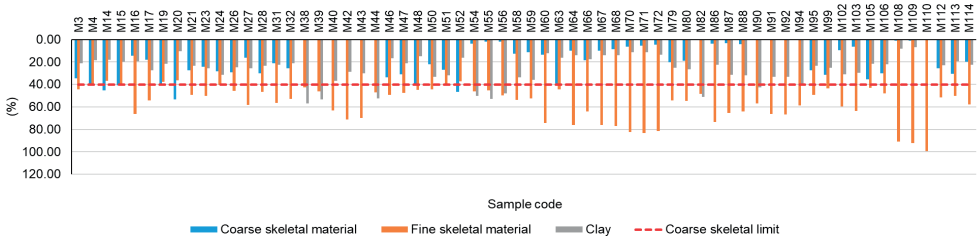


a) Texture of soil samples from Mârgău area (green) compared to soil samples from Valea Drăganului area (white)

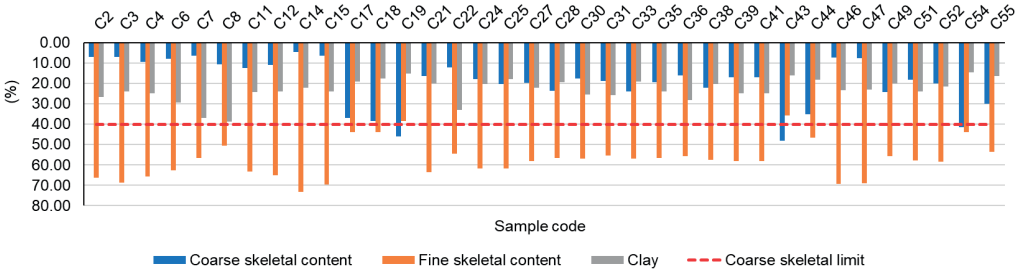
b) Texture of the soil samples from Ciucea (blue) compared to the soil samples from Valea Drăganului (white)

Figure 5. A graphical comparison between the texture of the soils sampled for analysis and that of the soil sampled in Valea Drăganului locality

Note: Coarse Texture: N - Sand (NG - Coarse sand, NM – Medium sand, NF - Fine sand), U - Loamy sand (UG - Coarse loamy sand, UM - Medium loamy sand, UF - Fine loamy sand); Medium Texture: LN - Sandy-clayey loam, LL - Medium loam, L - Loam, LP - Silty loam, SG - Coarse sandy loam, SM - Medium sandy loam, SF - Fine sandy loam, SS - Silty sandy loam, SP - Silt; Fine Texture: AF - Fine clay, A - Clay, AM - Medium clay, AL - Loamy clay, AP = Silty clay, TN - Sandy clay, TT - Medium clayey loam, TP - Silty-clayey loam, T - Clayey loam (Ministerul Agriculturii, Academia de Științe Agricole și Silvice, ICPA, 1987)



a)



b)

Figure 6. Comparative soile texture analysis for: a) samples procured in the Mârgău area; b) samples procured in the Ciucea area

From a chemical analysis perspective, the experimental results indicated that the remaining soil samples from the Mârgău batch, after selection based on textural criteria, had a humus content ranging between 0% and 12.16% (Figure 7a). Moreover, a total of 12 samples were found to have CaCO3 concentrations ranging from 0.06% to 10.19%, which consequently prompted the exclusion of an additional 19 soil samples from the batch. Conversely, the Ciucea batch had a humus content ranging from 0% to 3.32%, with no

detectable levels of $CaCO_3$ in any of the samples. Consequently, all soil samples from this batch were retained for subsequent analysis (Figure 7b).

The analysis of acidity revealed that the pH values of the Mârgău soil samples ranged between 4.12 and 6.73 (Figure 8a), while those of the Ciucea soil samples varied from 3.75 to 5.50 (Figure 8b). Following the analysis, the distribution of pH values exhibited by the clay soils under consideration enabled the grouping of the samples into three categories.:

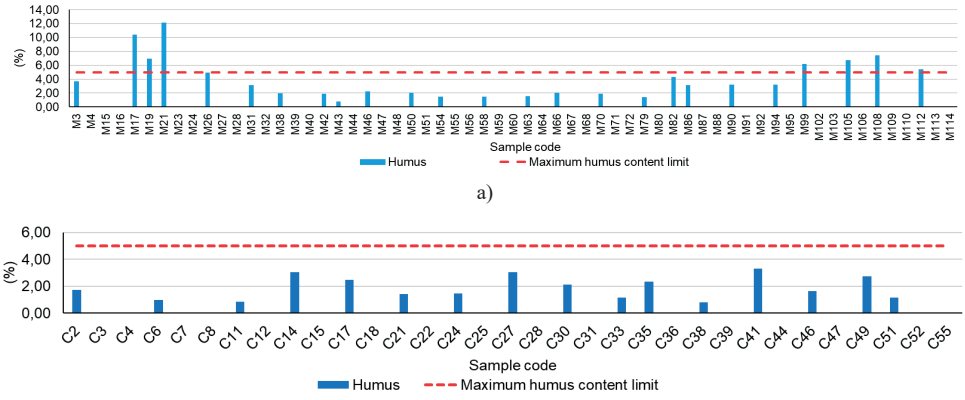
I. soil samples with a pH greater than 6 – excluded at this stage of the analysis;

II. soil samples with a pH ranging between 5 and 6 – deemed suitable for use in plaster mortar production but not recommended for adobe brick manufacturing;

III. soil samples with a pH of 5 or lower – identified as being appropriate for adobe brick production.

Following this analysis, the Mârgău batch was reduced to 25 soil samples with a pH below 6, of which six samples had a pH ranging from 4.12 to 4.99 (≤5).

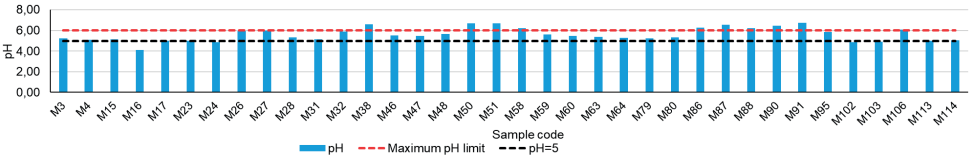
A similar reduction process was applied to the Ciucea batch, which was reduced to 21 soil samples, all with a pH between 3.75 and 4.99 (≤5).



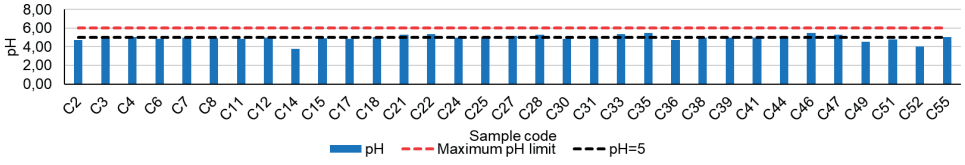
a)

b)

Figure 7. Comparative humus content analysis for: a) samples procured in the Mârgău area; b) samples procured in the Ciucea area



a)



b)

Figure 8. Comparative pH valuea analysis for: a) samples procured in the Mârgău area; b) samples procured in the Ciucea area

A subsequent evaluation of the clay content and its proportional relationship to sand and silt, conducted as part of the selective elimination process, revealed that an additional nine samples from the Mârgău batch did not meet the established criteria. These samples (M16, M113, M4, M15, M64, M43, M60, M46, and M48) had clay content values ranging from 12.32% to 19.75%, rendering them unsuitable under the predetermined selection parameters.

A similar analysis of the Ciucea batch indicated that two of the remaining 21 samples had a clay content below 20% (C17: 19.05% and C44: 18.30%). As a result, these samples were excluded from further evaluation.

Following the selection process, 16 samples remained from the Mârgău batch. Of these, two samples (M24: 31.27% clay content, pH 4.87; M102: 30.8% clay content, pH 4.88) had a clay content exceeding 30% and a pH below 5, making them suitable for adobe brick production. The remaining 14 samples had clay contents ranging from 20 to 30%, with fine sand content exceeding 40%, making them more appropriate for plaster mortar and finishing coat applications (Figure 9a). Of particular note were samples M102 and M103, which had a coarse sand content below 10% (9.48% and 6.58%, respectively). Of additional significance is the observation that sample M102, in addition to having a pH below 5, also had a clay content in excess of 30%, thus rendering it suitable for utilisation in adobe brick production. Similarly, sample M103 had a clay content close to 30% (29.70%) and a pH below 5, which also suggested its suitability for adobe brick manufacturing.

Of the 19 remaining samples from the Ciucea batch, two samples (C8: 38.7% clay content; C7: 37.05% clay content) had a clay content of at least 30%, rendering them suitable for adobe brick production (Figure 9). Among the remaining 17 samples, which contained 20–30% clay, all had a fine sand content exceeding 50%, suggesting their compatibility for use in plaster mortar and finishing coat production (Figure 10). However, particular attention is drawn to samples C2, C3, C6, C7, C14, and C15, which were characterized by a coarse sand content ranging from 4.51% to 7.86%, with sample C14 having the lowest coarse sand content at 4.51%. Moreover, sample C7 is noteworthy for its low coarse sand content (6.44%), high fine sand content (56.51%), and clay content exceeding 30% (37.05%). These characteristics suggest that this clay soil has the potential to be utilised for the manufacturing of adobe bricks and plaster mortar.

Following the stepwise selection process, the soil samples selected for further investigation and physico-mechanical performance analysis were as follows: from the Mârgău batch: M24 (31.27% clay, 28.51% coarse sand), M102 (30.8% clay, 9.48% coarse sand), and M103 (29.7% clay, 6.58% coarse sand) and from the Ciucea batch: C7 (37.05% clay, 6.44% coarse sand) and C8 (38.7% clay, 10.82% coarse sand). The selection of these samples was based on their compositional properties, ensuring their suitability for subsequent experimental analyses. In consideration of the findings presented, and given the number of soil samples collected from a minimum depth of 20 cm at each location (62 samples from the Mârgău batch and 37 samples from the Ciucea batch), as well as the fact that, following the selection process, it was found that only three samples from Mârgău and two samples from Ciucea met the predefined criteria for adobe brick production. This indicates that the Ciucea area exhibits slightly greater potential than the Mârgău area in terms of identifying clay soils with properties that are compatible with the intended application. A subsequent investigation into the properties of the sample batch, with a focus on its compatibility with plaster mortars, fine plasters, and finishing coats, revealed that the 15 selected samples from the Ciucea batch exhibited higher compatibility with these applications when compared to the 14 samples selected from the Mârgău batch, indicating a potentially superior performance in these specific contexts.

The experimental results of the physico-mechanical tests conducted on prismatic specimens, produced by casting the selected soil samples, demonstrated that, in terms of apparent density (Figure 11), the recorded values were higher than those observed for the reference sample from Valea Drăganului.

In addition, these values correspond to the optimal range suggested in the scientific literature (1800-2000 kg/m³) to ensure adequate thermal inertia (Burroughs, 2008).

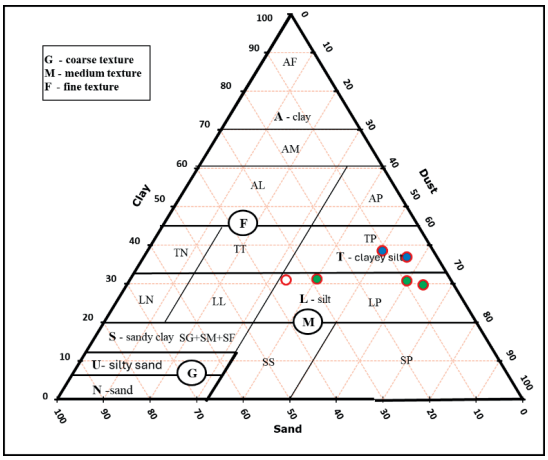


Figure 9. Humus content for: a) samples collected from Mârgău area; b) samples collected from Ciucea area

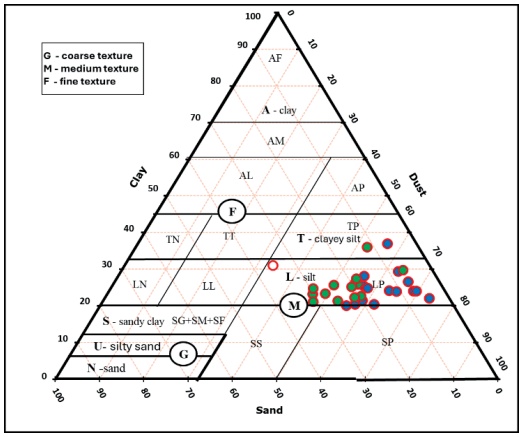


Figure 10. Texture of the soils sampled for analysis, selected for the realization of mortars for plastering, tinctures or plasters, Mârgău (green), Ciucea (blue), compared with the texture of the soil sampled in Valea Drăganului

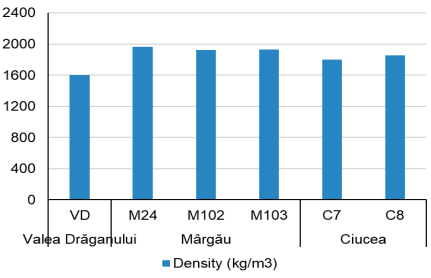


Figure 11. Graphical representation of the apparent density for a reference sample from Valea Drăganului, compared to samples M24, M102, and M103 (from Mârgău), and samples C7 and C 8 (from Ciucea)

With regard to axial shrinkage, the selected clay soil samples exhibited values within the recommended range of 3-12%, as documented in the scientific literature (Minke, 2005) (Figure 12). However, it was observed that sample M102 exceeded the upper limit of this range by 15%, suggesting an increased susceptibility to cracking during the drying process. In order to mitigate this risk, the scientific literature indicates that various additive materials, such as bone glue, salt (NaCl), or vegetable oils, may be employed to improve the material's dimensional stability.

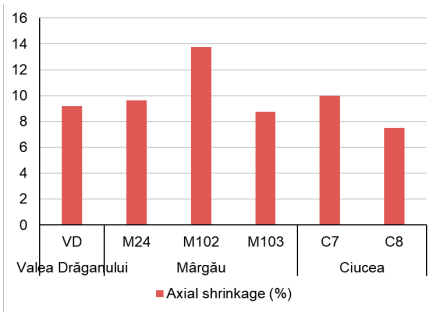


Figure 12. Graphical representation of the axial shrinkage for a reference sample from Valea Drăganului, compared to samples M24, M102, and M103 (from Mârgău), and samples C7 and C 8 (from Ciucea)

The analysis of mechanical strength under compressive and flexural tensile stresses indicates that the performance of the selected clay soil samples is comparable in magnitude to that of the reference sample from Valea Drăganului (Figure 13). Considering the previous experimental studies conducted on clay soil from Valea Drăganului (Calatan et al., 2017; Hegyi et al., 2016; Hegyi et al., 2023; Calatan et al., 2016; Călătan et al., 2020), it can be inferred that the selected clay soils from the Mârgău and Ciurila batches could also be effectively utilised for a variety of applications. These include the development of fiber-reinforced compositions incorporating dispersed vegetable fibers, as well as compositions intended for the production of construction elements, plaster mortars, and masonry mortars. Furthermore, these materials may serve as a base for incorporating performance-enhancing additives or for the integration of waste-derived raw materials, thereby contributing to the exploration of novel recycling strategies.

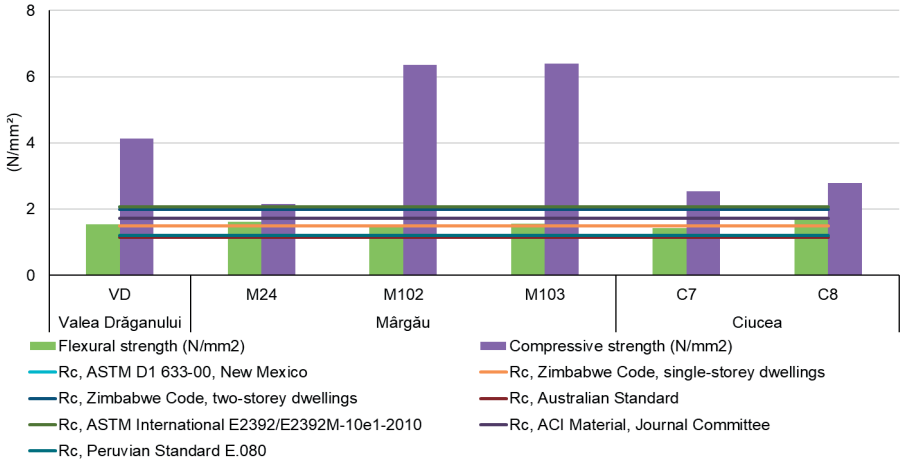


Figure 13. Analysis of flexural strength and compressive strength for a reference sample from Valea Drăganului, samples M24, M102, and M103 (from Mârgău), and samples C7 and C8 (from Ciucea), compared to relevant standards from New Mexico (ASTM D1 633-00, blue), Zimbabwe (dark blue - two stories' dwellings and orange - one story dwellings), ASTM International E2392/E2392M-10e-1-2010 (dark green), ACI Material (purple), and the Peruvian E.080 Standard (turquoise)

Furthermore, a comparison of the mechanical strength indicators with the minimum thresholds established by international standards, including ASTM D1633-00 (New Mexico), the Zimbabwean Code for Rammed Earth Walls, ASTM International E2392/E2392M-10e1-2010, and Peruvian Standard E.080, indicates that the selected and analysed samples satisfy the requirements for use in the construction of residential building walls. The findings of this study suggest that the materials can be effectively utilised in various construction techniques, facilitating the development of both single-story and multi-story structures.

CONCLUSIONS

The objective of this study was to assess the viability of utilising chemical and pedological analysis techniques to determine the prospective

suitability of clay soils from the Mârgău and Ciucea regions in Cluj County for the fabrication of adobe brick masonry components. The experimental research programme was conducted on two distinct batches of soil samples: one collected from the Mârgău area and the other from the Ciucea area, both of which are located in Cluj County. The study was designed to encompass two primary phases:

I. Selection of clay soil samples, conducted in accordance with a set of predefined criteria, which were established in alignment with the specifications outlined in the scientific literature.

II. Validation of the clay soil selection methodology is based on physico-mechanical indicators obtained through experimental testing, with a comparative analysis against references from the scientific literature. The characteristics of a clay soil sample from Valea Drăganului are also presented, and this sample had previously been investigated in a comprehensive experimental research programme.

The selection process involved the reduction of the initial 62 soil samples from the Mârgău batch and 37 soil samples from the Ciucea batch, all collected from a minimum depth of 20 cm at each location, to a final selection of three soil samples from the Mârgău batch (M24, M102, M103) and two soil samples from the Ciucea batch (C7, C8).

The validation phase, which was conducted via experimental testing, established that the selected clay soil samples had an apparent density ranging from 1798 to 1965 kg/m^3, thereby satisfying the critical mass criterion necessary to ensure optimal thermal inertia. The axial shrinkage values generally fell within the recommended range of 3-12%, with the exception of sample M102, which exceeded the upper limit by 15%, indicating a heightened risk of cracking during the drying process. The mechanical strength assessments yielded values that exceeded the minimum thresholds stipulated by international standards and were comparable in magnitude to those of the reference sample from Valea Drăganului, with compressive strength ranging from 2.54 to 6.39 N/mm² and flexural tensile strength between 1.43 and 1.69 N/mm².

In conclusion, the proposed methodology for assessing the suitability of clay soils for adobe brick production demonstrates promising potential benefits. While further refinement of the experimental protocol is necessary to fully validate the soil selection approach, it is anticipated that by integrating current knowledge in the field with rapidly obtainable data through fundamental laboratory testing in soil pedology or cost-effective on-site evaluations, the following advantages can be realised:

- enhanced comprehension of a soil horizon's capacity for a specific application;
- reduced evaluation times in comparison to conventional methodologies. In the case of conventional methods, clay soil undergoes processing, adobe bricks are fabricated, and a prolonged conditioning period is required (achieving constant mass necessitates several days under controlled temperature and humidity conditions) before being tested using physico-mechanical methods;
- the mitigation of risk associated with the selection of soil with unsuitable properties for the intended application, with a consequent minimisation of resource inefficiencies and the reduction of material and time wastage.

REFERENCES

Ak, Ş., Aytekin, O., Kuşan, H., & Zorluer, İ. (2024). Environmental sustainability of building materials in Turkey: Reference information recommendations for European Green Deal declarations. *Buildings, 14*(4), 889.

Androutsopoulos, A., Geissler, S., Charalambides, A. G., Escudero, C. J., Kyriacou, O., & Petran, H. (2020). Mapping the deep renovation possibilities of European buildings. *IOP Conference Series: Earth and Environmental Science, 410*(1), 012056. IOP Publishing.

Asif, M., Muneer, T., & Kelley, R. (2007). Life cycle assessment: A case study of a dwelling home in Scotland. *Building and Environment, 42*(3), 1391–1394.

Boduroglu, M. H. (1989). Rural buildings in Turkey that have suffered damages in recent earthquakes: Their main causes. *Bulletin of the International Institute of Seismology and Earthquake Engineering, 23*, 359–380.

Burroughs, S. (2008). Soil property criteria for rammed earth stabilization. *Journal of Materials in Civil Engineering, 20*(3), 264–273.

Călătan, G., Hegyi, A., Dico, C., & Mircea, C. (2016). Determining the optimum addition of vegetable materials in adobe bricks. *Procedia Technology, 22*, 259–265.

Călătan, G., Hegyi, A., Dico, C., & Mircea, C. (2017). Experimental research on the recyclability of the clay material used in the fabrication of adobe bricks type masonry units. *Procedia Engineering, 181*, 363–369.

Călătan, G., Hegyi, A., Grebenișan, E., & Mircea, A. C. (2020, December). Possibilities of recovery of industrial waste and by-products in adobe-brick-type masonry elements. *Proceedings, 63*(1), 1.

Demir, I. (2008). Effect of organic residues addition on the technological properties of clay bricks. *Waste Management, 28*(3), 622–627.

Dormohamadi, M., & Rahimnia, R. (2020). Combined effect of compaction and clay content on the mechanical properties of adobe brick. *Case Studies in Construction Materials, 13*, e00402.

Giada, G., Caponetto, R., & Nocera, F. (2019). Hygrothermal properties of raw earth materials: A literature review. *Sustainability, 11*(19), 5342.

Hegyi, A., Dico, C., & Călătan, G. (2016). Construction sustainability with adobe bricks type elements. *Urbanism. Arhitectura. Constructii, 7*(2), 147–156.

Hegyi, A., Petcu, C., Ciobanu, A. A., Călătan, G., & Bradu, A. (2023). Development of clay-composite plasters integrating industrial waste. *Materials, 16*(14), 4903.

Laaroussi, N., Cherki, A., Garoum, M., Khabbazi, A., & Feiz, A. (2013). Thermal properties of a sample prepared using mixtures of clay bricks. *Energy Procedia, 42*, 337–345.

Măgurean, A. M., & Petran, H. A. (2023). Analysis of measured CO2 levels through long-term monitoring in renovated multifamily buildings: A common case. *Buildings, 13*(8), 2113.

Ministerul Agriculturii, Academia de Științe Agricole și Silvice, & ICPA (1987). *Metodologia elaborării studiilor pedologice. Partea I, II, III.* București.

Minke, G. (2005). *Building with earth: Design and technology of a sustainable architecture.* Basel: Birkhäuser.

Mollaei, A., Bachmann, C., & Haas, C. (2023). Assessing the impact of policy tools on building material recovery. *Resources, Conservation and Recycling, 198*, 107188.

Montanarella, L., & Panagos, P. (2021). The relevance of sustainable soil management within the European Green Deal. *Land Use Policy, 100*, 104950.

Munaro, M. R., Tavares, S. F., & Bragança, L. (2020). Towards circular and more sustainable buildings: A systematic literature review on the circular economy in the built environment. *Journal of Cleaner Production, 260*, 121134.

Niroumand, H., Zain, M. F. M., & Jamil, M. (2013). A guideline for assessing critical parameters on earth architecture and earth buildings as sustainable architecture in various countries. *Renewable and Sustainable Energy Reviews, 28*, 130–165.

Standards New Zealand. (1998a). *NZS 4297: Engineering design and earth buildings.* Wellington, NZ: Standards New Zealand.

Standards New Zealand. (1998b). *NZS 4298: Materials and workmanship for earth buildings.* Wellington, NZ: Standards New Zealand.

Standards New Zealand. (1998c). *NZS 4299: Earth buildings not requiring specific design.* Wellington, NZ: Standards New Zealand.

Pacheco-Torgal, F., & Jalali, S. (2012). Earth construction: Lessons from the past for future eco-efficient construction. *Construction and Building Materials, 29*, 512–519.

Papadaki, D., Foteinis, S., Binas, V., Assimakopoulos, M. N., Tsoutsos, T., & Kiriakidis, G. (2019). A life cycle assessment of PCM and VIP in warm Mediterranean climates and their introduction as a strategy to promote energy savings and mitigate carbon emissions. *AIMS Materials Science, 6*(6), 944–959.

Papadaki, D., Nikolaou, D. A., & Assimakopoulos, M. N. (2022). Circular environmental impact of recycled building materials and residential renewable energy. *Sustainability, 14*(7), 4039.

Salih, M. M., Osofero, A. I., & Imbabi, M. S. (2020). Critical review of recent development in fiber reinforced adobe bricks for sustainable construction. *Frontiers of Structural and Civil Engineering, 14*, 839–854.

Santamouris, M., Cartalis, C., Synnefa, A., & Kolokotsa, D. (2015). On the impact of urban heat island and global warming on the power demand and electricity consumption of buildings - A review. *Energy and Buildings, 98*, 119–124.

Silveira, D., Varum, H., & Costa, A. (2013). Influence of the testing procedures in the mechanical characterization of adobe bricks. *Construction and Building Materials, 40*, 719–728.

Vega, P., Juan-Valdés, A., Ignacio Guerra, M., Morán, J., Aguado, P., & Llamas, B. (2011). Mechanical characterization of traditional adobes from the north of Spain. *Construction and Building Materials, 25*(7), 3020–3023.

Scientific Papers. Series E. Land Reclamation, Earth Observation & Surveying, Environmental Engineering. Vol. XIV, 2025
Print ISSN 2285-6064, CD-ROM ISSN 2285-6072, Online ISSN 2393-5138, ISSN-L 2285-6064

HIERARCHY OF ALTERNATIVES FOR THE REHABILITATION OF ASBESTOS WATER SUPPLY NETWORKS BASED ON ENVIRONMENTAL CRITERIA

Iulian IANCU, Sorin PERJU, Ioan BICA, Alexandru-Nicolae DIMACHE

Technical University of Civil Engineering of Bucharest,
122-124 Lacul Tei Blvd, District 2, 020396, Bucharest, Romania

Corresponding author email: alexandru.dimache@utcb.ro

Abstract

Asbestos water supply networks are not believed to represent a significant hazard to public health in normal use. However, repair, rehabilitation and removal of asbestos pipes involve cutting, and demolition, can release asbestos fibers into the air, posing risks to public health. Many water utilities currently have significant portions of their water mains composed of asbestos pipes that need to be rehabilitated. This paper focuses on the evaluation of four different alternatives to rehabilitate/remove of asbestos pipes, considering the impact on the environment, respectively the total air emissions generated by the activities involved in this rehabilitation. A very performant model, EMEP/EEA air pollutant emission inventory guidebook 2023, was used for this assessment. Results indicate that the replacement of asbestos-cement pipes with no-dig, pipe-bursting technology, which involves laying the new pipe on the inside of the existing pipe, which is broken but remains underground, will have the lowest environmental impact.

Key words*: water supply networks, asbestos-cement pipes, emissions of pollutants.*

INTRODUCTION

Produced and widely used in the construction of water supply networks, asbestos cement pipes were, during the 1950s-1970s, the main type of material used for the design and execution of water distribution networks (Coufal et al., 2014).

Asbestos is an extremely cost-effective material with high tensile strength and good compressive strength. It can withstand alkaline environments, corrosion, heat, electrical conductivity, and bad weather (Pini et al., 2021). The reinforcing properties of Chrysotile fibers greatly increase durability and allow thinner and lighter pipes to be made (World Health Organization, 2011).

The use of asbestos-cement pipes brought several advantages for water operators, thus explaining the wide development of asbestos-cement networks:

- reduced production costs;
- easy installation;
- low weight compared to steel or cast iron;
- resistance to electrochemical erosion;
- relatively low roughness, so low hydraulic load losses;
- low thermal conductivity;
- durability, relatively long-life span.

However, over time it was found that using this material in water supply networks also has some disadvantages, among which are significant:

- risk to human health due to the content of asbestos fibers;
- fragility of pipes; tendency to crack under bending stress;
- difficulties in repairing degraded pipes;
- reduced resistance to vibrations generated by traffic.

Although exposure to asbestos is potentially dangerous, health risks can be minimized. In most cases, the fibers are only released if the asbestos-containing material (asbestos cement) is broken or crumbled (Logsdon, 1983). The product, non-crushed materials containing asbestos, such as water pipes, do not pose health risk. The mere presence of asbestos does not mean that the health of people working with asbestos is threatened. Asbestos is harmless in water because the problem is not ingesting the fibers but inhaling them (Qldwater, 2014).

The natural dissolution of asbestos-containing minerals in the surrounding environment implies the existence of asbestos fibers in water, and research has indicated that most waters, distributed or not through asbestos-cement pipes, contain asbestos fibers (Qldwater, 2014).

Fiber in drinking water consists almost entirely of short fibers, which are considered to pose little risk to public health.

Compared to the reduced health risk associated with the ingestion of asbestos released into drinking water, the repair, rehabilitation and replacement of water mains is of increased health concern as it involves pipe cutting, demolition, transport and disposal, resulting in emissions of very fine asbestos particles into the atmosphere, that could be inhaled (Wang et al., 2010).

Currently, within the urban water infrastructure, the problem of the existence of asbestos-cement pipes is increasingly topical, from the perspective of restrictions on use but also related to the difficulties of decommissioning them from drinking water transport and distribution systems, in which asbestos-cement pipes have been used a long time (Zavašnik et al., 2022). The fact that many of these works have reached the end of their life cycle requires their replacement and rehabilitation.

Asbestos pipe replacement technologies

The potential technologies considered for the replacement of asbestos pipes, which are the subject of this study, are:

- T1 - Replacement of asbestos pipes by placing the new pipe in an open excavation on a route parallel to the replaced pipe and leaving the existing pipe underground by filling it with concrete.
- T2 - Replacement of asbestos-cement pipes by supported open excavation and laying of the new pipe on the same route as the replaced pipe, using a temporary pipe until the new pipe is put into operation; this technology involves the evacuation of the existing pipe from the ground and its transport to an authorized waste landfill having a waste storage cell containing asbestos.
- T3 - Replacement of asbestos pipes by laying the new pipe through horizontal drilling directed along a route parallel to the replaced pipe and leaving the existing pipe underground by filling it with concrete.
- T4 - Replacement of asbestos pipes by no-dig, pipe-bursting technology, which involves laying the new pipe on the inner area of the existing pipe, which is broken, but remains underground.

The carrying out of the works to replace the asbestos-cement pipelines constitutes, on the one hand, a source of dust emissions, and on the other hand, a source of emissions of pollutants specific to the combustion of fuels (distilled petroleum products – petrol and diesel) both in the engines of the necessary machines carrying out the works, as well as the vehicles used to transport the materials (Gottesfeld, 2024).

Dust emissions, which occur during the execution of works specific to the four technologies for replacing asbestos-cement pipes, are generally associated with excavation works, transportation and putting into operation. Dust released into the atmosphere often varies substantially from day to day, depending on the level of activity, specific operations, and weather conditions (Zhang et al., 2002). The temporary nature of the asbestos pipeline replacement works, the specifics of the various execution phases, the continuous modification of the work fronts clearly differentiate the emissions specific to these works from other undirected sources of dust, both in terms of estimation and control of emissions.

The main pollutants associated with the release of dust into the atmosphere from the execution of the construction works are suspended dust - TSP, PM_{10} and $PM_{2.5}$.

As regards the emission sources of pollutants specific to the combustion of fuels, they are differentiated, according to the specifics of the machines, into two categories: heavy construction equipment (construction machinery) and material transport vehicles.

The activity of heavy construction equipment includes, in general, the work that is performed on the pipeline section that is being rehabilitated. The pollution specific to the activity of the machines is assessed according to their type, fuel consumption, period of operation and the area in which they carry out activities.

The main pollutants associated with fuel combustion in engines are CO, NMVOC, NO_x, N_2O, NH_3, SO_2 (Mitra et al., 2002). The amounts of pollutants emitted into the atmosphere by construction machinery depend mainly on the following factors:

- technological level of the engine;
- engine power;
- fuel consumption per power unit;
- machine capacity;

- age of engine/machinery, equipped with pollution reduction devices.

It is obvious that pollutant emissions decrease as the performance of the engine is more advanced, the trend in the world being the manufacture of engines with the lowest possible consumption per unit of power and with the most restrictive control of emissions. It is estimated that the pollution specific to the activities of refueling, maintenance and repair of machinery is reduced because these activities will be carried out mainly in filling stations and specialized repair bases.

The circulation of material transport means can represent an important source of pollution associated with asbestos-cement pipeline replacement technologies. Pollution specific to vehicle traffic is assessed by fuel consumption (polluting substances - NO_x, CO, NMVOC, NO_x, N_2O, NH_3, SO_2, material particles from fuel combustion, etc.) and the distances traveled.

MATERIALS AND METHODS

The evaluation of pollutant emissions into the atmosphere from the activities of replacing asbestos pipes was carried out starting from a series of general calculation assumptions or associated with each technology of replacing pipes separately.

Thus, it was considered:

- the length of the replaced asbestos-cement pipe: 100 m;
- several connections on the new pipe: 10 connections;
- an average transport distance of earth from excavations for disposal: 20 km (round trip);
- an average transport distance of construction materials: 15 km (round trip);
- an average transport distance of asbestos cement waste disposed of at the hazardous waste landfill: 220 km - nearest hazardous waste landfill from Bucharest (round trip);
- fuels used for heavy construction equipment/construction machinery (bulldozer, motor compressor, generator, horizontal directional drilling machine, etc.) and transport vehicles (dump truck, concrete mixer, etc.): diesel (density 860 kg/m^3) and/or gasoline (density 750 kg/m^3);
- fuel consumption was evaluated depending on the transport distances, the volumes of transported materials and the number of operating hours of each construction machine;
- location of construction works – Bucharest, Romania.

As a function of the rehabilitation technology profile, for heavy construction equipment/construction machinery and material transport vehicles used for the replacement of asbestos-cement pipelines, their number and operating time were considered within the activities carried out for each of the four technologies presented. The duration of the works to replace the asbestos-cement pipes, as well as the volumes of excavated earth and the volumes required to restore the filling layers for the length of 100 linear meters of replaced pipe are presented in Table 1.

Table 1. Durations of execution, volumes of excavated earth and volumes required to restore fill layers

Potential technologies	T1	T2	T3	T4
Construction period (days)	3	3	4	4
Volume of excavated soil (m^3)	164	160	92	64
Sand (m^3)	49.2	48	22.8	17.76
Gravel (m^3)	8.2	8	3.8	2.96
Crushed stone (m^3)	8.2	8	3.8	2.96
Asphalt mixture (m^3)	8.2	8	3.8	2.96

Based on the assumptions and the data presented, the emissions of pollutants into the atmosphere were calculated for the four categories of emissions:

- dust/particle emissions resulting from the construction activity itself;
- emissions of dust/particles resulting from the transport of materials;
- emissions of pollutants resulting from the combustion of fuels in the engines of construction machinery;
- emissions of pollutants resulting from the combustion of fuels in the engines of material transport vehicles.

Emissions associated with asbestos pipe replacement technologies

The dust/particle emissions from the asbestos-cement pipe replacement activities themselves, for 100 linear m of asbestos-cement pipe replaced, were calculated with the relation (U.S. E.P.A., 1986):

$$EM_{PM_{10}} = EF_{PM_{10}} \times A_{affected} \times d \times (1 - CE) \times \frac{24}{PE} \times \frac{s}{9\%}$$

where:

$EF_{PM_{10}}$ - the corresponding emission factor for PM_{10}

$A_{affected}$ - the area affected by the works

d - the duration of construction works, d = *3 days = 0.00822 years*

CE - coefficient regarding the efficiency of emission control works, *CE = 0*

PE - the Thornthwaite coefficient of precipitation-evapotranspiration, *PE = 49.47*

s - the dust content of the soil, s = *32%*.

The results of calculations for dust/particle emissions from the actual asbestos pipe replacement activities, for 100 linear m of asbestos pipe, by the four technologies are presented in Table 2.

Table 2. Dust/particles emissions from asbestos-cement pipe replacement activities

Technology	T1	T2	T3	T4
Affected area [m^2]	320	300	176	162
Duration [days]	3	3	4	4
Total suspended particles – TSP [kg]	1.316	1.234	0.965	0.888
Suspended particles with d<10 µm – PM_{10} [kg]	0.390	0.366	0.286	0.263
Suspended particles with d<2.5 µm – $PM_{2.5}$ [kg]	0.039	0.037	0.029	0.026

Dust/particle emissions from the transport of materials on public roads were calculated per km traveled by a transport vehicle, using the formula (European Environment Agency, 2023):

$$E = k \times 1.7 \times \left(\frac{s}{12}\right) \times \left(\frac{S}{48}\right) \times \left(\frac{W}{2.7}\right)^{0,7} \times \left(\frac{w}{4}\right) \times \left(\frac{365-p}{365}\right)$$

for which it was considered:

- multiplication factor for the particle size:
  - 0.35 for PM_{10};
  - 0.053 for $PM_{2.5}$.;
- s - dust content of the road surface, s = *3*;
- S - average speed of vehicles, S = *30 km/h*;
- W - weight of vehicles, $W \approx 20$ *t*;
- w - number of wheels, w = *6*;
- p - number of dry days, p = *132* (for Romania).

The results of the calculations for dust/particle emissions from the transport of materials on public roads, for the four technologies, are presented in Table 3.

Table 3. Emissions of dust/particles resulting from the transport of materials on public roads

Technology	T1	T2	T3	T4
Distance [km]	575	745	330	240
Suspended particles with d<10 µm – PM_{10} [kg]	207.93	449.02	119.34	86.79
Suspended particles with d<2.5 µm – $PM_{2.5}$ [kg]	31.49	67.99	18.07	13.14

The total emissions of pollutants resulting from the combustion of fuels in the engines of heavy construction equipment and in the engines of vehicles transporting construction materials, used for the replacement activities of asbestos-cement pipes (100 linear m of pipe) were calculated based on the "EMEP/EEA" guide air pollutant emission inventory guidebook 2023, 1.A.3.b. Combustion - Road transport, with the relationship (European Environment Agency, 2023):

$$E_i = \sum_j \left(\sum_m \left(FC_{j,m} \times EF_{i,j,m} \right) \right)$$

in which:

E_i - emission of the pollutant i [gr];

$FC_{j,m}$ - fuel consumption of vehicle category j using the fuel m [kg];

$EF_{i,j,m}$ - emission factor for the pollutant i, for the vehicle of category j using the fuel m [gr/kg].

The results of the calculations for the total emissions of combustion fuels in the engines of construction machinery and in the engines of construction material transport vehicles for the four technologies are presented in Table 4.

Table 4. Total emissions resulting from the combustion of fuels in the engines of construction machinery

Technology	T1	T2	T3	T4
NMVOC [kg]	5.107	5.201	1.493	1.340
NO_x [kg]	15.320	16.955	11.759	11.173
PM [kg]	0.497	0.543	0.343	0.325
N_2O [kg]	0.0250	0.0275	0.0183	0.0173
NH_3 [kg]	0.0078	0.0084	0.0049	0.0047
SO_2 [kg]	0.0030	0.0033	0.0022	0.0021
CO [kg]	19.48	19.85	5.76	5.18
CO_2 [kg]	1536.8	1692.0	1132.5	1074.6

RESULTS AND DISCUSSIONS

Following the calculations performed and the results obtained and represented graphically in Figure 1, it is found that the emissions of dust/particle matter for T4 technology for the

replacement of asbestos-cement pipes are lower than in the other three technologies, as follows:

- T1 – 1.48 times higher than T4;
- T2 – 1.39 times higher than T4;
- T3 – 1.09 times higher than T4.

This is mainly due to the smaller land areas affected by T4 technology.

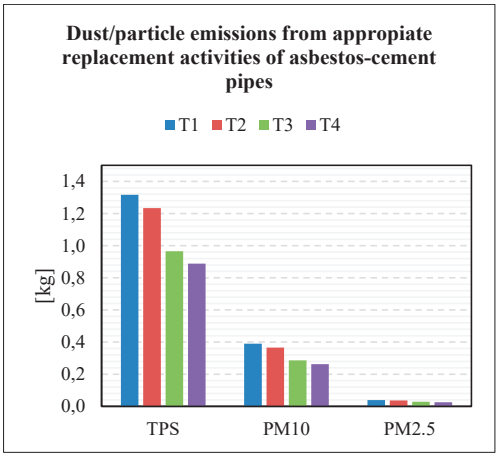


Figure 1. Emissions of dust/particles from the activities of replacing the appropriate asbestos-cement pipes, through the four technologies

For the emissions of dust/particle matter in suspension, generated from the transport of construction materials, shown graphically in Figure 2, it is found that the values obtained for the T4 technology for the replacement of asbestos-cement pipes are lower than the values obtained for the other three technologies, as follows:

- T1 – 2.40 times higher than T4;
- T2 – 5.17 times higher than T4;
- T3 – 1.38 times higher than T4.

The value of dust/particle emissions from the transport of construction materials for T2 technology for the replacement of asbestos-cement pipes, are very high due to the disposal of the disused asbestos-cement pipe at a hazardous waste landfill.

In terms of total emissions of combustion fuels in the engines of heavy construction equipment and construction material transport vehicles, they also vary from one technology to another for the replacement of asbestos-cement pipes, but also from one activity to another.

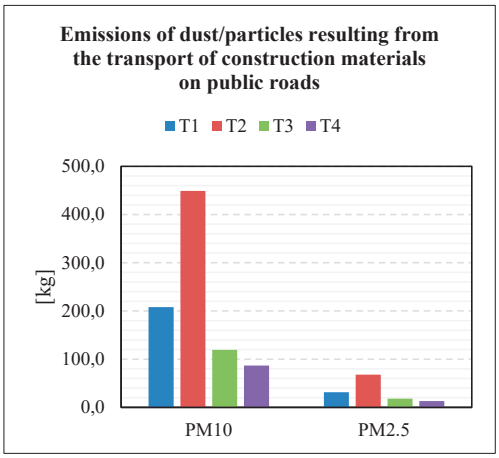


Figure 2. Emissions of dust/particles resulting from the transport of construction materials on public roads, through the four technologies

In comparison, Figure 3 and Figure 4 show, for the four technologies of replacing asbestos-cement pipes, the main emissions (NMVOC, NO_x, PM, N_2O, NH_3 and SO_2) from combustion in the engines of heavy construction equipment.

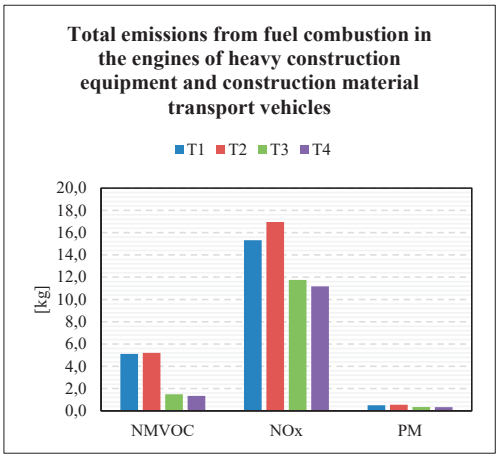


Figure 3. Total NMVOC, NOx and PM emissions resulting from fuel combustion

Analyzing the obtained values, it is found that again the technology with the lowest level of pollutants resulting from fuel combustion is T4 technology (smaller volumes of excavations, shorter transport distances, non-recovery of the replaced asbestos-cement pipe).

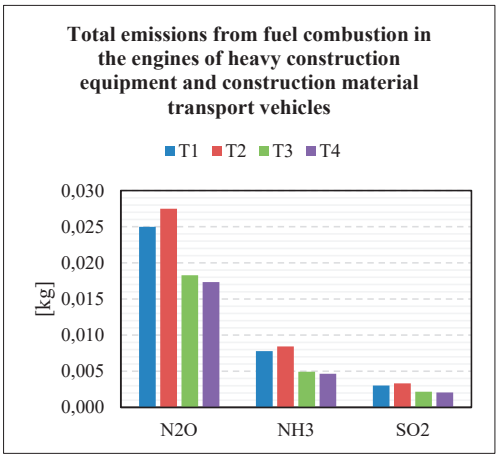


Figure 4. Total N_2O, NH_3 and SO_2 emissions from fuel combustion

It is also found that T4 technology has the lowest levels of pollutants, for the same reasons, both for the CO emission values represented graphically in Figure 5 and for the CO_2 emission values graphically represented in Figure 6.

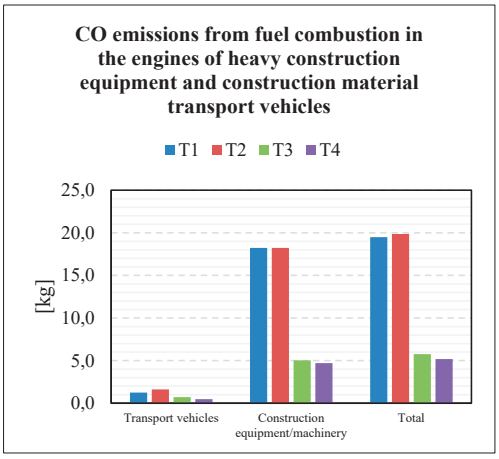


Figure 5. CO emissions [kg], resulting from fuel combustion

The comparative analysis of dust/particle emissions from the actual asbestos pipeline replacement activities, through the four technologies, highlights for any of the four evaluated factors, namely TSP, PM_{10}, $PM_{2.5}$, the fact that the lowest values of them are recorded for T3 and T4 technologies. Technologies T1 and T2 have high values, in the order in which they are listed. Overall, dust/particle emissions for the T4 asbestos-cement pipe replacement technology are lower than the other three technologies.

The emissions of dust/particle matter (PM_{10}, $PM_{2.5}$) from the transport of construction materials for the T4 technology are lower than in the other three technologies.

Emissions from the transport of construction materials for the T2 technology are very high, this fact results from the need to dispose of asbestos pipe waste at a hazardous waste landfill.

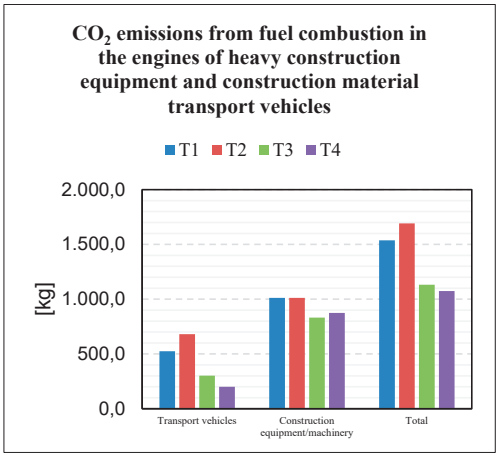


Figure 6. CO_2 emissions [kg], resulting from fuel combustion

NO_x emissions from the combustion of fuels in the engines of heavy construction equipment/construction machinery and vehicles transporting construction materials (NMVOC, NO_x, PM, N_2O, NH_3 and SO_2) also vary from one technology to another, proposed to replace pipelines of asbestos, but also from one activity to another.

The emissions resulting from the combustion of fuels in the engines of heavy construction equipment, for technologies T3 and T4 have the lowest values.

The level of emissions associated with the T2 technology for replacing asbestos pipes is 3.41 times higher than that of the technology with the lowest levels of NO_x emissions T4.

The other two technologies, T1 and T3 record values of 2.63 and 1.51 times higher than technology T4, respectively.

Table 5. Air pollutant emissions associated with the four asbestos-cement pipe replacement technologies

Type of emissions	Emissions			
	T1	T2	T3	T4
Dust/particle emissions from the appropriate asbestos pipe replacement activities, for 100 linear m of asbestos pipe [kg]				
Total suspended particles – TSP	1.316	1.234	0.965	0.888
Suspended particles with d < 10 µm – PM_{10}	0.390	0.366	0.286	0.263
Suspended particles with d < 2.5 µm – $PM_{2.5}$	0.039	0.037	0.029	0.026
Emissions of dust/particles resulting from the transport of materials on public roads [kg]				
Suspended particles with cu d < 10 µm – PM_{10}	207.93	449.02	119.34	86.79
Suspended particles with d < 2.5 µm – $PM_{2.5}$	31.49	67.99	18.07	13.14
Total emissions of pollutants resulting from the fuel combustion in the engines of heavy construction equipment and vehicles transporting construction materials [kg]				
Carbon monoxide – CO	19.48	19.85	5.76	5.18
Non-methane volatile organic compounds – NMVOC	5.107	5.201	1.493	1.340
Nitrogen oxides – NO_x	15.320	16.955	11.759	11.173
Suspended particles – PM	0.497	0.543	0.343	0.325
Nitrous oxide – N_2O	0.0250	0.0275	0.0183	0.0173
Ammonia – NH_3	0.0078	0.0084	0.0049	0.0047
Sulfur dioxide – SO_2	0.0030	0.0033	0.0022	0.0021
Carbon dioxide – CO_2	1536.78	1692.00	1132.53	1074.60

The emission levels of the four technologies were compared by assigning standardized scores to each emission type.

These scores were normalized to a common scale within the [0,1] interval using the following formula:

$$Score_{[0,1]} = 1 - \frac{E - max(E_i)}{max(E_i) - min(E_i)}$$

in which:

E - the emission for a certain type of pollutant;

max(Eᵢ) - the maximum value of the pollutant emission, from the four technologies;

min(Eᵢ) - the minimum pollutant emission value, from the four technologies.

A value of "0" was assigned to the highest emission level, while a value of "1" was assigned to the lowest. Based on this approach, Table 6 presents the standardized scores for each technology and type of atmospheric emission, corresponding to the four asbestos–cement pipe replacement methods.

Table 6. Standardized scores by technology and type of atmospheric emissions associated with the four asbestos-cement pipe replacement technologies

Type of emissions	Standardized scores according to technology and type of emissions			
	T1	T2	T3	T4
Dust/particulate emissions from appropriate asbestos pipe replacement activities, for 100 linear m of asbestos pipe				
Total suspended particles – TSP	0	0.19	0.82	1
Suspended particles with d<10 µm – PM_{10}	0	0.19	0.82	1
Suspended particles with d<2.5 µm – $PM_{2.5}$	0	0.19	0.82	1
Final grade (arithmetic average):	0	0.19	0.82	1
Emissions of dust/particles resulting from the transport of materials on public roads				
Suspended particles with d<10 µm – PM_{10}	0.67	0	0.91	1
Suspended particles with d<2.5 µm – $PM_{2.5}$	0.67	0	0.91	1
Final grade (arithmetic average):	0.67	0	0.91	1
Total emissions of pollutants resulting from the fuel combustion in the engines of heavy construction equipment and vehicles transporting construction materials				
Carbon monoxide – CO	0.03	0	0.96	1
Non-methane volatile organic compounds – NMVOC	0.02	0	0.96	1
Nitrogen oxides – NO_x	0.28	0	0.90	1
Suspended particles – PM	0.21	0	0.92	1
Nitrous oxide – N_2O	0.25	0	0.91	1
Ammonia – NH_3	0.17	0	0.92	1
Sulfur dioxide – SO_2	0.24	0	0.91	1
Carbon dioxide – CO_2	0.25	0	0.91	1
Final grade (arithmetic average):	**0.18**	**0**	**0.92**	**1**

CONCUSIONS

The analysis elements presented for the four options highlight the diversity of rehabilitation technologies, respectively their impact on the environment, in particular the emissions of pollutant substances and particles in the atmosphere. At the same time, it was noted that there is still no definitive (dominant) opinion at the international level regarding the solutions applied, or applicable, each country oscillating between various possible options.

Synthesizing the results obtained based on the calculations performed for the emissions of pollutants in the atmosphere highlights the fact that the T1 and T2 technologies have major effects on the environment. However, it can be noted that the T2 technology has higher values of emissions compared to the T1 technology by approximately 18%. T3 and T4 technologies have relatively equal minimum values (slightly better for T4 technology, but the difference is insignificant).

Comparing the scores obtained for the four technologies based on the standardization and normalization of atmospheric emissions in the interval [0,1], various rankings can be made, giving different weights to the three categories of emissions:

- dust/particle emissions from the actual asbestos pipeline replacement activities,
- emissions of dust/particles resulting from the transport of materials on public roads,
- total emissions of pollutants resulting from the combustion of fuels in the engines of heavy construction equipment and vehicles transporting construction materials,

all considered for the replacement of 100 linear m of asbestos-cement pipe.

Regardless of the weightings chosen, technology T4 – replacement of asbestos pipes by no-dig, pipe-bursting technology will get the highest score, and technology T2 – replacement and removal of asbestos pipes by supported open excavation and laying the new pipe on the same route as replaced pipe – will get the lowest score.

REFERENCES

Coufal, M., Václavík, V., & Dvorský, T. (2014). Rehabilitation of asbestos cement water mains for potable water in the Czech Republic. *SGEM2014 Conference Proceedings*, *B31*(S12.075). https://doi.org/10.5593/SGEM2014/B31/S12.075

European Environment Agency. (2023). *EMEP/EEA air pollutant emission inventory guidebook 2023*. https://www.eea.europa.eu/en/analysis/publications/emep-eea-guidebook-2023

Gottesfeld, P. (2024). Exposure hazards from continuing use and removal of asbestos cement products. *Annals of Work Exposures and Health*, *68*(1), 8-18. https://doi.org/10.1093/annweh/wxad066

Logsdon, G. S. (1983). Engineering and operating approaches for controlling asbestos fibers in drinking water. *Environmental Health Perspectives*, *53,* 169 – 176, https://doi.org/10.1289/ehp.8353169

Mitra, A. P., Morawska, L., Sharma, C., & Zhang, J. (2002). Methodologies for characterisation of combustion sources and for quantification of their emissions. *Chemosphere*, *49*(9), 903-22, https://doi.org/10.1016/s0045-6535(02)00236-9

Pini, M., Scarpellini, S., Rosa, R., Neri, P., Gualtieri, A. F., & Ferrari, A. M. (2021). Management of asbestos containing materials: A detailed LCA comparison of different scenarios comprising first time asbestos characterization factor proposal. *Environmental Science & Technology*, *55*(18), https://doi.org/10.1021/acs.est.1c02410

Qldwater. (2014). *Cutting, handling and disposal of asbestos cement (AC) pipe guidelines* (Rev. 1). Queensland Water Directorate. http://www.qldwater.com.au

World Health Organization. (2011). *Guidelines for drinking-water quality* (4th ed.). WHO Library Cataloguing-in-Publication Data.

Wang, D. L., Hu, Y., & Chowdhury, R. (2010). Safety and waste management of asbestos cement pipes. *ASCE Pipeline Conference*, Keystone, Colorado, USA.

U.S. Environmental Protection Agency. (1986). *AP-42: Compilation of air emissions factors from stationary sources*. https://www.epa.gov/air-emissions-factors-and-quantification/ap-42-compilation-air-emissions-factors

Zavašnik, J., Šestan, A., & Škapin, S. (2022). Degradation of asbestos-reinforced water supply cement pipes after long-term operation. *Chemosphere*, *287*(1), https://doi.org/10.1016/j.chemosphere.2021.131977

Zhang, J. J., & Morawska, L. (2002). Combustion sources of particles: 2. Emission factors and measurement methods. *Chemosphere*, *49*(9), 1059-74, https://doi.org/10.1016/s0045-6535(02)00240-0

Scientific Papers. Series E. Land Reclamation, Earth Observation & Surveying, Environmental Engineering. Vol. XIV, 2025
Print ISSN 2285-6064, CD-ROM ISSN 2285-6072, Online ISSN 2393-5138, ISSN-L 2285-6064

AFFORESTATION OF SANDY SOILS OF OLTENIA - A REVIEW -

Paula IANCU, Marin SOARE, Mariana NICULESCU

University of Craiova, 13 Libertății Street, 200583, Craiova, Romania

Corresponding author email: soare_marin@yahoo.com

Abstract

Oltenia is the region in southwestern Romania facing significant challenges related to desertification, especially in Dolj County. Sandy soils from this area present specific characteristics due to the low water retention, low nutrient content and limited organic matter typically found in these types of soils. Afforestation could be an essential solution to prevent desertification in this region, which faces significant risks related to land degradation. Afforestation of sandy soils, however, requires a multifaceted approach, combining soil improvement techniques, careful species selection, water management and continuous monitoring. With the right strategies, it is possible to restore ecological functions and to improve fertility of these types of soils. The key to success lies in understanding the specific challenges of sandy soils and adapting techniques accordingly to promote the growth and sustainability of forested areas.

Key words*: afforestation, aridity, desertification, Oltenia region, sandy soils.*

INTRODUCTION

Afforestation is the process of planting trees on lands that were not previously forested. Key features of afforestation refer to the plantation of entirely new forested areas and often involve the use of native or fast-growing species. In the context of Oltenia, where there are challenges like sandy soils, desertification, and degraded agricultural land, afforestation could address land degradation and create new forest ecosystems in areas which became unsuitable for agriculture.

Agroforestry is also a technique which could be effective in the area because utilizes the integration of trees with farming systems to stabilize soils and improve livelihoods. This system has considerable potential to mitigate climate change (Doelman et al., 2020).

The afforestation projects of degraded terrains must be carried out in accordance with the technical norms issued by the ministry responsible for forest management. Afforestation can bring numerous ecological and economic benefits, contributing significantly to their stabilization.

Afforestation of sandy soils is an essential measure to combat desertification and stabilize affected lands. Oltenia is facing an alarming phenomenon of desertification, which is seriously affecting which once were fertile soils. Oltenia is the region in southwestern Romania that encompasses a varied relief and diverse soils, influenced by specific climatic and geological conditions. This area is characterized by a combination of plains, hills and mountains, which significantly influences the types of soils and their use in agriculture. It is also home to the largest area of sands and sandy soils. These are arranged in longitudinal dunes oriented from west to east, in the direction of the dominant wind (Prioteasa, 2021). Yield potential of these soils is low and requires measures to stem deflation, increase in the content of humus in the soil, mineral and organic fertilizer application and preservation of forest areas (Stanila et al., 2020). Fertilization becomes essential for sandy soils, the main practice being inorganic fertilization, but also organic manures can supply nutrients in slowly available forms which improve soil physico-chemical properties. The incorporation of organic manures deeper into the soil or spreading a carpet-like layer (at least 1 cm thick) improves water storage, biological activity, and nutrient status (https://www.fao.org/soils-portal). Under current conditions (drought and extreme temperatures), fertilization combined with appropriate irrigation practices, becomes even

more important to ensure a constant supply of nutrients, thereby ensuring good crop development (Nițu et al., 2024). Another technique is applying mulch in order to reduce evaporation. Crop residues from the soil surface reduce evaporation losses, decrease the range between maximum and minimum soil temperature, and wind erosion. There are authors which sustain that mulching improves yield (ex. sweet potato) by maintaining soil temperature and moisture, increasing plant growth, and leading to higher tuber numbers and weight. Also, influence their quality, by increasing total soluble solids, starch, and vitamin C content in the tubers. But, the effectiveness of mulching can vary depending cultivar and mulch type (Dinu et al., 2022).

To combat the advance of sand and revitalize this type of soil, planting trees or forest curtains to stabilize them and create a favorable micro-climate can be a solution. The implementation of new agricultural technologies based on reducing resource consumption contributes to reducing the impact of agriculture on the environment (Coca et al., 2020).

As in the specific context of Oltenia, afforestation is a key strategy to combat soil desertification, the purpose of this work is to present the advantages of this action and how it can help reduce the vulnerability to the drought and to the current or future climatic changes.

MATERIALS AND METHODS

The sandy soils occupy a significant surface in Oltenia, especially in its south and have become difficult for agriculture due to the high permeability and the low water retention capacity. However, their afforestation can transform this useless land into some productive ones, income generators. The presentation of this process was carried out by consulting relevant materials, such as books, scientific articles, conference works, reports or online databases. The objectives of the documentation focused on identifying the context of desertification, the benefits and challenges of afforestation actions in the context of current climate change by attempting to address the following aspects:

- advantages;
- challenges;
- techniques;
- recommended trees.
- afforestation projects in Oltenia region.

RESULTS AND DISCUSSIONS

Advantages of afforestation action

- *Reducing soil erosion*. Forests help to fix the soil through tree roots, which hold soil particles together. This reduces the risk of erosion, a common phenomenon in areas with sandy soils, where wind and water can quickly carry soil particles (Akca et al., 2010). Erosion usually affects soil fertility because removes the fertile layers in the upper horizons, which contain a large amount of organic matter and nutrients (Bălan et al., 2024).
- *Improving soil quality and structure*. Afforestation helps improve soil structure and fertility. Fallen leaves and organic matter in the forest decompose, enriching the soil with essential nutrients and increasing its water-holding capacity. Tree roots help form a dense root system, which can improve the texture of sandy soil by creating channels for water and other components.
- *Regulation of the hydrological cycle*. Forests positively influence the local hydrological regime. They contribute to increasing soil moisture and reducing flood risks by absorbing excess water. This is crucial in areas with sandy soils, which have a low water retention capacity.
- *Creating a favorable microclimate*. By shading the land and through plant transpiration, forests contribute to creating a more stable microclimate, which can favor the development of other plant and animal species. This microclimate helps maintain humidity and reduce extreme temperatures. Forests contribute to better infiltration of water into the soil, which helps prevent droughts and improve the availability of water for crops and other plants.
- *Diversification of fauna and flora*. Planting tree species contributes to creating a habitat for various animal and plant species, increasing local biodiversity (Jorge et al., 2022).
- *Carbon sequestration*. Forests are essential in sequestering carbon, thus contributing to combating climate change. Through the process of photosynthesis, trees absorb carbon dioxide from the atmosphere, which helps reduce greenhouse gases.

- *Economic and social benefits*. Afforestation can generate economic opportunities through the development of eco-tourism and sustainable forestry activities. Local communities also benefit from the creation of jobs in forest management and sustainable agriculture (Akca et al., 2010). Afforestation of degraded land is not an end in itself but a national necessity (Crăciunescu et al., 2014).

Challenges regarding afforestation

- *Low precipitation*. Oltenia is characterized by a low annual precipitation rate, which has been recorded as low as 262.7 mm in certain years.
- *Water scarcity*. Sandy soils typically have low water retention capacity, making it challenging to sustain newly planted trees during dry periods. Effective water management practices are essential for success (Mingyuan, 2024).
- *Drought sensitivity*. In southern Romania, frequent droughts can affect the success of tree planting and development, necessitating additional irrigation and seedling protection strategies. Oltenia region is highly sensitive to drought conditions, which are exacerbated by climate change.
- *Soil characteristics*. Sandy soils in Oltenia are prone to erosion and have poor nutrient retention capabilities. These factors make it challenging for trees to obtain the necessary nutrients for growth, leading to higher mortality rates among afforested species.
- *Long-term maintenance*. Continuous monitoring and management are required to ensure the health of afforested areas, especially in terms of pest control and competition among species (Jorge et al., 2022).
- *Conflict with agricultural land use*. In areas where sandy lands are used for agriculture, afforestation may conflict with economic interests related to crops.
- *Lack of funds and infrastructure*. Afforestation projects can be expensive and require considerable financial resources for implementation and long-term maintenance.

Recently, the Ministry of Environment has launched initiatives to expand the forested area in southwestern Romania, with the aim of combating desertification and improving the local ecosystem.

Afforestation of the sands in this region can bring numerous ecological, economic and social benefits, essential for combating desertification and improving living conditions in the region.

As afforestation techniques, the following can be used:

- **planting on degraded lands**: in the plain regions of southern Romania, it is essential to plant forest species on lands degraded due to erosion or excessive exploitation. Planting should be done in a way that maximizes the success of the seedlings (e.g., using irrigation systems, protecting the seedlings from strong winds);
- **silvopasture**: this involves combining forest with animal grazing, with the aim of conserving the soil and efficiently using natural resources. Also, in some areas, to increase the efficiency of afforestation, methods such as mixed plantations (using combinations of tree and shrub species to create a stable and diversified ecosystem) or the use of local species (in some cases, native plants are preferred to ensure better adaptation to the ecological conditions in Oltenia) can be used;
- **Miyawaki method**: this technique involves planting a dense mix of native species in a small area, which helps create a self-sustaining forest ecosystem quickly. The method emphasizes biodiversity and can improve soil quality rapidly;
- **patch planting**: instead of uniform planting, creating patches of vegetation can help gather surface runoff and improve local moisture levels, facilitating better growth conditions for the trees (Mingyuan, 2024).

Tree species suitable for afforestation of sandy soils

For the afforestation of sandy soils, several species of trees and shrubs are recommended that adapt well to the specific conditions of these soils. These are:

- Acacia (*Robinia pseudoacacia*) is a drought-resistant species that grows well on sandy soils and helps fix nitrogen in the soil.
- Oak (*Quercus robur*) is a hardy tree that can help stabilize soils and can grow on poorer soils. In the Oltenia Plain the Turkey Oak occupies 10061.9 ha, and the Hungarian Oak 4655.0 ha (Cojoacă et al., 2020).
- Poplar (*Populus* spp.). Poplars are often used in reforestation projects in lowland areas

because they grow quickly and can tolerate sandy soils.

- Pine trees (*Pinus* spp.). Various species of pine are well-suited to sandy soils due to their deep root systems and drought tolerance. Research from Turkey demonstrates that afforestation of sand dunes with pine (specifically Stone Pine, *Pinus pinea*), along with other species, increases soil organic matter, phosphorus content, and socio-economic value within several decades. Pines not only stabilize sandy soils and reduce erosion but can also serve as sources of timber, nuts, and other products, benefiting local communities (Akca et al., 2010). Planting trees such as *Pinus sylvestris* and *Ulmus pumila* has been shown to enrich soil nutrients in the surface layers, improve soil structure, and reduce bulk density, which enhances overall soil health (Guo et al., 2024).
- *Casuarina* spp. (Sheoak). These trees are drought-resistant and can fix nitrogen, improving soil quality.
- *Hakea* spp. An Australian native that adapts well to sandy soils and is drought-tolerant.
- *Grevillea* spp. Another Australian native that flourishes in sandy conditions, known for its unique flowers and deep root system.
- Olive Tree (*Olea europaea*). Drought-tolerant and well-adapted to nutrient-poor soils, making it ideal for sandy environments.
- *Telopea* spp. (Tree Waratah): Known for vibrant flowers and hardiness in poor soil conditions.
- Bald Cypress (*Taxodium distichum*): Thrives in wet or dry sandy conditions and is known for its resilience.
- Sand grass or perennial grass species - they can be used as short-term cover plants to help stabilize the soil until the trees become mature enough.

In addition to these, a number of other species can also be used such as: juniper, sea buckthorn, willow, weeping willow, etc., and shrubs that can also be used for the afforestation of degraded lands (Enescu, 2015, 2018). Among best shrubs or other plants:

- *Lavandula angustifolia* (Lavender): Excellent for sandy soils due to its drought resistance and ability to thrive in poor nutrients.
- *Rudbeckia* spp. (Black-Eyed Susan): A flowering plant that does well in full sun and sandy conditions.
- *Salvia* spp.: These plants are hardy and can tolerate dry, sandy soils.
- *Buddleja* spp. (Butterfly Bush): Thrives in sunny, dry locations with sandy soil.
- *Juniperus* spp. (Junipers): Adaptable shrubs that can withstand drought and poor soil.

Choosing the right species for afforestation in sandy soils is essential for ensuring successful growth and sustainability of the forest ecosystem. The mentioned species are well-suited to cope with the challenges posed by sandy environments, making them ideal candidates for afforestation projects (https://www.rhs.org.uk/plants/for-places/sandy-soils).

The lands from the Oltenia area were gradually subjected to changes induced by intensive agricultural use, so that on large areas of forest it was intervened in numerous stages of afforestation and deforestation (Iordache & Ciuinel, 2013). In the last three decades over 4300 hectares of forests and vineyards areas in sandy dunes perimeter were lost (Prăvălie, 2013). The absence of irrigation and the uncontrolled deforestation of protection belts accelerated the extension of desertification of sandy soils, leading to depleted arable-land productivity and, in time, abandonment of these lands (Bălteanu et al., 2013). The impact of climate change in the sandy soil areas of Sadova, Bechet, Corabia, Apele Vii, etc. leaded to intense aridity phenomena and tends to enhance desertification on larger surfaces. Therefore, there is an urgent need to cover and protect the soil from Apele Vii, Mârşani, Daneţi, Celaru, Castranova, etc. communes which also falls into the high drought-affected sandy soils of the Leu-Rotunda Plain. Recent studies suggest that the combination of black locust (*Robinia pseudoacacia*) and bird cherry (*Prunus padus*) is optimal for afforestation in this region. These species are favored due to their rapid growth rates and ability to stabilize shifting sands within five years. They are also economically viable, as their seedlings are easy to produce and affordable (Enescu, 2019; Răducă et al., 2022). Black locust is an important non-native tree species used mostly for sandy soil and sterile dump afforestation for its ornamental role, but also for its wood (lumber, poles, firewood) and honey production (Buzatu-Goanță et al., 2020).

Few years ago, in Radovan (medium fertility soil), Tâmburești (sandy soil, irrigation) and Işalnița (antropomorphic soil formed from coal ash), an experiment with SRC willow crop of was initiated considering the specie a sustainable source of biomass because of its potential to fix carbon (C) in the soil and also, short-term crops could be an option for solving the demand for bioenergy (Păniță et al., 2017).
Salix genus includes many species with various uses - wood production, biomass, animal feed, source of salicylic acid, land reclamation, biofuel, etc. (Corneanu et al., 2022).
In Dolj county there is a natural forest in Bratovoiești, which occupies a large part Oltenia Plain, of the Valley Jiu with three types of natural habitats and plant communities rich in mesophyle, mesohygrophyle and hygrophyle species (Cojoacă & Niculescu, 2018).
Juglans regia L. is also a specie which is growing well in temperate climate areas. Oltenia is a region known for walnut diversity because its various eco-geographical areas (Cosmulescu & Botu, 2012).
The challenges of afforestation of Oltenia region necessitate careful planning and the selection of drought-resistant tree species for afforestation projects. Strategies must include efficient water management practices and soil improvement techniques to enhance the viability of afforestation efforts in this vulnerable region.
The zoning and micro-zoning of the potential forest vegetation can be the base of the selection of species that optimally harness the stationary potential in the case of the extension of the forest land to the agricultural land unfit for agricultural use, and the extension of forest protection curtains in territories where their design has not been carried out (Bercea & Dinucă, 2018).

Recent afforestation initiatives

The increase of areas covered by forest vegetation and the necessity to take actions against drought, aridity and land degradation is a priority of the national strategy for preventing and control of these (MMAP, 2008).
Romania has implemented several afforestation programs, such as the "National Afforestation Program", which encourages the rehabilitation of degraded lands, including sandy soils in the south of the country. These projects are carried out in collaboration with local authorities and environmental organizations and aim to protect soils and improve ecosystems.
MMAP (2017) emitted a National Forest Strategy for 2018-2027 was published, putting an emphasis on sustainable management of the national forest fund.
Generally, funding is a problem of afforestation in Romania. Along time, afforestation projects were supported mainly through different funding mechanisms: Special Accession Program for Agriculture and Rural Development (SAPARD) (Law no. 316/2001), the Environmental Fund (Law no. 73/2000, completed by Government Emergency Ordinance no. 196/2005 and the European Union funding instruments implemented through the National Program for Rural Development (PNDR) actions (Government Decision no. 1.284/2008 for 2007-2013 and no. 226/2015 for 2014-2020) (PNDR, 2017) (Palaghianu & Dutca, 2017).
Afforestation projects implementation is hindered by the lack of cadastre and funds. Also, to the population and the landowners it must be explained the importance of forest protection belts for the improvement of environment and living conditions, for the gradual diminishing of drought effects and for the enhancement of agricultural production (Achim et al., 2012).
PNDR, 2014-2020, through Measure 8.1 for afforestation by the concept of transferable carbon credits could potentially contribute to increasing forest area in Romania and carbon sequestration projects such as PCF, could represent viable opportunities for future afforestation (Palaghianu & Dutca, 2017).
123 Measure "Increasing the added value of agricultural and forestry products" has as general objectives to increase the competitiveness of agrifood and forestry processing enterprises by improving the general performance of enterprises in the processing and marketing sector of agricultural and forestry products, through better use of human resources and other factors of production (Vladu et al., 2018).
A large part of the budget for afforestation funds from the National Plan for Recovery and Resilience (PNRR) is being allocated to the south of the country, where it is most needed. 70 hectares of sand from the Oltenia Sahara were afforested with acacia, elm and mulberry.

Another 2500 hectares of sandy land will be afforested to protect localities and crops.
In 2023, Romania added 3,159 hectares of new forests, bringing the total forested area to 6.45 million hectares. This increase is largely due to reforestation efforts on pastures, afforestation of degraded lands, and inclusion of new areas in the national forest fund.
Key contributors to this growth include:
- Government and EU-funded initiatives focusing on afforestation and reforestation.
- NGOs and private projects, such as the Tomorrow's Forest Foundation and Mossy Earth, which restore forests and combat illegal deforestation. Their projects in Dolj County, for instance, aim to restore ecosystems and support local communities. There were also some reforestation initiatives made by students, teachers and volunteers' communities in order to contribute to climate change mitigation efforts.
Afforestation efforts are increasing, but deforestation still poses challenges, especially in areas affected by illegal logging or land-use changes. Sustainable forest management remains a key priority. The afforestation of degraded sandy soils is seen as a valuable opportunity to expand the national forest fund, providing ecological benefits and supporting local communities.

CONCLUSIONS

Oltenia is a region with significant agricultural potential due to the diversity of its soils. However, the challenges related to desertification require innovative solutions to maintain the viability of agriculture in this area. Adapting agricultural techniques to local conditions will be essential for the future of the region.
Afforestation of sandy soils helps stabilize them, but also contributes to improving the quality of the environment, having a positive impact on biodiversity. Also, can be a viable solution for ecological restoration and sustainable land management. By carefully selecting appropriate species, employing effective planting techniques, and managing resources wisely, it is possible to transform degraded sandy landscapes into productive ecosystems that benefit both the environment and local communities.
For the afforestation of sandy soils, species capable of stabilizing the soil, reducing erosion and contributing to improving environmental quality are recommended.

REFERENCES

Achim, E., Manea, G., Vijulie, I., Cocoș, O., Tîrlă, L. (2012). Ecological reconstruction of the plain areas prone to climate aridity through forest protection belts. Case study: Dăbuleni town, Oltenia Plain, Romania. *Procedia Environmental Sciences, 14*, 154-163, https://doi.org/10.1016/j.proenv.2012.03.015.

Akca, E., Kapur, S., Tanaka, Y., Kaya, Z., Bedestenci, H.C., Yakti, S. (2010). Afforestation Effect on Soil Quality of Sand Dunes. *Polish J. of Environ. Stud., 19*(6), 1109-1116. https://www.pjoes.com/pdf-88489-22348?filename=22348.pdf.

Bercea, I., Dinucă, N.C. (2018). Considerations on zoning and micro-zoning of the Dolj County area for potential forest vegetation in the context of anthropic changes in forest lands and climatic changes. *Analele Universităţii din Craiova, Seria Agricultură – Montanologie – Cadastru (Annals of the University of Craiova - Agriculture, Montanology, Cadastre Series). XLVIII*, 18-34.

Buzatu-Goanță, C., Corneanu, M., Nețoiu, C., Buzatu, A., Lăcătușu, A-R., Cojocaru, L. (2020) Black locust stand structure on the sterile dump in the middle basin ofJiu River (Romania). *Reforesta, 9*, 9-18. DOI:https://dx.doi.org/10.21750/REFOR.9.02.76.

Bălan, M., Nițu, O.A., Popescu C. (2024). The evolution of soil agrochemical properties, under the influence of mineral fertilisation and water erosion, on a natural grassland located at the Preajba Experimental Centre in the Gorj county. *Scientific Papers. Series A. Agronomy, LXVII*(1), 25-31.

Bălteanu, D., Dragotă, C-S., Popovici, A., Dumitrașcu. M., Kucsicsa, Gh., Grigorescu, I. (2013). Land use and crop dynamics related to climate change signals during the post-communist period in the South Oltenia, Romania. *Proc. Rom. Acad., Series B, 15(3)*, p. 265-278.

Coca, O., Mironiuc, M., Pânzaru, R.L., Crețu, A., Ștefan, G. (2020). Exploring the statistical association between the economic, environmental and innovative areas of performance: the case of European Union agriculture. *Romanian Agricultural Research*, *37*, 253-261, ISSN 1222–4227.

Cojoacă, F.D., Gheorghe, I.L., Băru, E., Niculescu Mariana, 2020. The distribution of soils and forest sites in the turkey oak and hungarian oak stands of Oltenia plain. *Analele Universităţii din Craiova, seria Agricultură – Montanologie – Cadastru (Annals of the University of Craiova - Agriculture, Montanology, Cadastre Series),* L. 78-86.

Cojoacă, F.D., Niculescu, M. (2018). Divesity, distribution and ecology of the forest natural haitats in the Bratovoești forest, Dolj county. *Scientific Papers. Series A. Agronomy, LXI*(1)*,* 453-457.

Corneanu, M., Buzatu-Goanță, C., Hollerbach, W., Horvat, A. (2022). Interspecific variability of some accessions of *Salix sp*. collected from Oltenia region, Romania. *Analele Universităţii din Craiova, seria Agricultură – Montanologie – Cadastru (Annals of the University of Craiova - Agriculture, Montanology, Cadastre Series)*. 52/1, p. 492-499.

Cosmulescu S., Botu M. (2012). Walnut biodiversity in south-western Romania-resource for perspective cultivars. *Pak. J. Bot., 44*(1), 307-311, https://mail.pakbs.org/pjbot/PDFs/44(1)/44.pdf

Crăciunescu, A., Moatăr Mihaela, Stanciu, S. (2014). Considerations regarding the afforestation fields. *Journal of Horticulture, Forestry and Biotechnology, 18*(1), 108- 111, https://www.usab-tm.ro/Journal-HFB/romana/2014/Lista%20lucrari%20PDF/Vol%2018(1)%20PDF/17Craciunescu%20Adam%202.pdf

Dinu, M., Soare, R., Poulianiti, K., Karageorgou, I., Bozinou, E., Makris, D.P., Lalas, S., Botu, M. (2022). Mulching Effect on Quantitative and Qualitative Characteristics of Yield in Sweet Potatoes. *Horticulturae, 8*(3), 271, https://doi.org/10.3390/horticulturae8030271.

Doelman, J.C., Stehfest, E., van Vuuren, D.P., Tabeau, A., Hof, A.F., Braakhekke, M.C., Gernaat, D.E.H.J., van den Berg, M., van Zeist, W.-J., Daioglou, V., van Meijl, H., Lucas, P.L. (2020). Afforestation for climate change mitigation: Potentials, risks and trade-offs. *Glob. Chang. Biol., 26*, 1576-1591, https://doi.org/10.1111/gcb.14887

Enescu, C.M. (2019). Sandy soils from Oltenia and Carei plains: a problem or an opportunity to increase the forest fund in Romania? *Scientific Papers Series Management, Economic Engineering in Agriculture and Rural Development*, *19*(3), 203-206.

Enescu, C.M. (2018). Which shrub species should be used for the establishment of field shelterbelts in Romania? *Scientific Papers. Series A. Agronomy, LXI*(1), 464-469.

Enescu, C.M. (2015). Shrub and tree species used for improvement by afforestation of degraded lands in Romania. *Forestry ideas*, *21*, 1(49), 3-15, https://forestry-ideas.info/issues/issues_Index.php?journalFilter=53

Guo, X., Yang, G., Ma, Y., Qiao, S. (2024). Effects of different sand fixation plantations on soil properties in the Hunshandake Sandy Land, Eastern Inner Mongolia, China. *Sci Rep., 14*(1), 27904. doi: 10.1038/s41598-024-78949-4.

Iordache, C., Ciuinel, A.M. (2013). The impact of human intervention on the forest fund within the southern part of Dolj county. *Muzeul Olteniei Craiova. Oltenia. Studii şi comunicări. Ştiinţele Naturii. Tom*., *29*(2), 268-273.

Mongil-Manso, J., Navarro-Hevia, J., & San Martín, R. (2022). Impact of Land Use Change and Afforestation on Soil Properties in a Mediterranean Mountain Area of Central Spain. *Land, 11*(7), 1043, https://doi.org/10.3390/land11071043.

Mingyuan, W. (2024). The Theory of Sandy Land Soil Hydrology and Mode of Low Coverage Afforestation in Northwest China. *International Journal of Plant, Animal and Environmental Sciences*, *14*, 42-58, https://fortuneonline.org/articles/the-theory-of-sandy-land-soil-hydrology-and-mode-of-low-coverage-afforestation-in-northwest-china.html

Nițu, O.A., Gheorghe, M., Ivan, E.Ș., Bălan, M. (2024). Optimizing drip irrigation yield in grain maize cultivation in Eastern Romania. *Scientific Papers. Series A. Agronomy, Vol. LXVII*(2), 307-313.

Palaghianu, C., Dutca, I. (2017). Afforestation and reforestation in Romania: History, current practice and future perspectives. *Reforesta*, *4*, 54-68. https://dx.doi.org/10.21750/REFOR.4.05.44.

Păniță, O., Soare, M., Corneanu, M., Iancu, P. (2017). The variability study of morphological characters on some *Salix* spp. genotypes. *Analele Universităţii din Craiova, seria Agricultură – Montanologie – Cadastru (Annals of the University of Craiova - Agriculture, Montanology, Cadastre Series), XLVII*, 209-216.

Prioteasa, A. M. (2021). *Evoluția potențialului productiv al terenurilor nisipoase nivelate și nenivelate din stânga Jiului.* Editura Universitaria, Craiova.

Prăvălie, R. (2013). Spatio-temporal changes of forest and vineyard surfaces in areas with sandy soils from southern Oltenia. *Scientific Annals of Ştefan cel Mare of Suceava, Geography Series*, *22*(1), 30-37.

Răducă, C., Boengiu, S., Mititelu-Ionuș, O., Simulescu, M., Enache, C. (2022). Sandy soils-geomorphology relationships in Jiana Plain (South-Western Romania). *Rev. Roum. Géogr. /Rom. Journ. Geogr., 66*(1), 45–56, București.

Stanila, A.L., Simota, C.C., Dumitru, M. (2020). Contributions to the Knowledge of Sandy Soils from Oltenia Plain. *Rev. Chem*., *71*(1), 192-200. http://www.revistadechimie.ro.

Vladu, M., Pânzaru, R.L., Săvescu, P., Matei, G. (2018). Studies on the situation of investments made with public funds under 123 measure "Increasing the added value of agricultural and forestry products" of the National Rural Development Program, in the South-West Oltenia development region in Romania. *Romanian Agricultural Research*, *35*, 275-281.www.incda-fundulea.ro/new4/images/rar/nr35/rar3532.pdf.

***https://www.rhs.org.uk/plants/for-places/sandy-soils (accessed 04.02.2025)

***https://www.fao.org/soils-portal/soil-management (accessed 13.02.2025)

***Ministerul Mediului, Apelor și Pădurilor - MMAP (2017). Strategia forestieră națională 2018-2027, www.mmediu.ro/app/webroot/uploads/files/2017-10-27_Strategia_forestiera_2017.pdf (accessed 17.02.2025).

***Ministerul Mediului, Apelor și Pădurilor – MMAP (2008). Strategia Națională privind reducerea efectelor secetei, prevenirea și combaterea degradării terenurilor și deșertificării, pe termen scurt, mediu și lung, 15.04.2008, https://old.madr.ro/pages/strategie/strategie_antisecet a_update_09.05.2008.pdf (accessed 17.02.2025).

Scientific Papers. Series E. Land Reclamation, Earth Observation & Surveying, Environmental Engineering. Vol. XIV, 2025
Print ISSN 2285-6064, CD-ROM ISSN 2285-6072, Online ISSN 2393-5138, ISSN-L 2285-6064

CURRENT TRENDS AND INSTITUTIONAL FRAMEWORKS IN CLIMATE CHANGE RESEARCH: A EUROPEAN AND NATIONAL PERSPECTIVE

Ionela-Alexandra ION, Carmen Otilia RUSĂNESCU, Sabrina-Maria BĂLĂNESCU

National University of Science and Technology Politehnica Bucharest,
Faculty of Biotechnical Systems Engineering, 313 Splaiul Independenţei,
District 6, 060042, Bucharest, Romania

Corresponding author: ionionelaalexandra@yahoo.com

Abstract

Research on climate change has become a cornerstone of the global scientific and political response to one of the most pressing environmental crises. This paper provides an overview of major climate research directions, with a focus on international, European, and national institutional frameworks. Based on the analysis of strategic documents and institutional sources, the paper identifies key trends, structural gaps, and opportunities for advancing national climate research in Romania. It highlights the need for interdisciplinary approaches and stronger links between science and public policy as critical components of effective climate action.

Key words**:** *adaptation, climate change, climate research, mitigation, science-policy interface.*

INTRODUCTION

Climate change has evolved from an environmental concern to an emerging issue on global political, economic, and scientific agendas. The manifestations of climate instability, ranging from extreme weather events to shifts in precipitation patterns and rising sea levels, pose direct risks to biodiversity, public health, water availability, and infrastructure.

What distinguishes current climate dynamics from previous geological or meteorological shifts is the speed, scale, and underlying anthropogenic influence. A growing body of evidence confirms that human activities, particularly fossil fuel combustion, deforestation, and industrial agriculture, have drastically altered atmospheric composition, leading to global warming and associated feedback effects (IPCC, 2021; IPCC, 2022).

Since the late 20th century, climate science has matured as an interdisciplinary field, integrating atmospheric physics, oceanography, ecology, geography, and socio-economic analysis.

The European Union (EU) has played a significant role in coordinating climate research and funding programmes, which will be further detailed in subsequent sections.

Over the past two decades, scientific research has emerged as both a diagnostic and a prescriptive tool in addressing climate change. It not only deepens our understanding of physical and ecological systems but also informs the design of mitigation and adaptation strategies. As the climate crisis intersects with challenges such as urbanisation, food security, and energy transition, there is an increasing demand for interdisciplinary and problem-oriented approaches to climate research (Bai et al., 2016). This article contributes to the scientific dialogue by reviewing the current state of climate change research. It identifies dominant research directions, maps institutional ecosystems at global and European levels, and reflects on Romania's position within this broader context.

MATERIALS AND METHODS

This study adopts a qualitative research approach, based on documentary analysis and thematic synthesis. Primary sources include official reports from international organisations such as the Intergovernmental Panel on Climate Change (IPCC) (IPCC, 2021), the World Meteorological Organization (WMO) (WMO, 2023), the European Environment Agency (EEA) (EEA, 2025), and the European Commission (EC) (European Commission, 2020). These sources were selected based on four key criteria: (i) credibility and institutional authority, (ii) thematic relevance to climate science and policy, (iii) recency (2015–2024),

and (iv) open-access availability to ensure transparency and replicability.

To structure the analysis, a thematic framework was applied, comprising the following four axes:

1. institutional structure and governance – this axis explore the key actors involved in climate change research at the international, European, and national levels, as well as their mandates, coordination mechanisms, and roles in policy support;
2. major scientific trends and innovations – here, the focus is on the evolving directions of climate research, including technological innovation, modelling capacities, and interdisciplinary shifts;
3. science–policy integration – this axis investigates how scientific knowledge is used to inform climate legislation, adaptation planning, and multilevel governance;
4. regional and national disparities – the final axis assesses asymmetries in research infrastructure, funding availability, institutional capacities, and participation in transnational programmes.

The Romanian research context was examined through national policy strategies, websites of public research institutes, and academic literature (National Meteorological Administration; The Ministry of Research, Innovation and Digitalisation) and recent integrative approaches on local governance in climate strategy (Drăghici et al., 2024). Particular emphasis was placed on identifying structural gaps in funding, digital infrastructure, scientific collaboration, and stakeholder engagement. The data analysis process was descriptive-interpretive, aimed at identifying systemic patterns and practical recommendations.

While qualitative documentary analysis is an effective tool for mapping institutional and thematic trends, its limitations must also be acknowledged. The method does not allow for empirical testing of hypotheses or for generalisation of findings across all EU member states. Furthermore, the reliance on official publications may overlook grey literature or localised research initiatives not captured in mainstream data repositories. However, the method is justified by the study's exploratory and comparative objectives, and by the need to establish a foundational understanding of systemic structures in climate research.

RESULTS AND DISCUSSIONS

International climate change research is coordinated through established institutions with distinct but complementary mandates. The IPCC synthesises scientific literature and provides assessment reports that inform global climate policy (IPCC, 2021). The WMO ensures access to harmonised meteorological datasets, which are essential for modelling and forecasting (WMO, 2023). The UNEP facilitates knowledge transfer, particularly for low- and middle-income countries (UNEP, 2023). These organisations increasingly collaborate to align climate science with policy and capacity-building efforts, contributing to a more integrated global research ecosystem.

At the European level, climate research is supported through a combination of strategic frameworks, legislative instruments, and dedicated funding programmes aimed at fostering innovation, scientific collaboration, and evidence-based policymaking. The European Commission's Joint Research Centre and EEA produce decision-support tools, vulnerability indices, and thematic maps used by national authorities (European Commission, 2020; EEA, 2025).

Table 1 presents a selection of key international and European institutions involved in climate change research, highlighting their primary areas of focus and the roles they play in supporting scientific advancement, policy development, and global coordination efforts.

Thematic evolution in climate research reveals a broadening scope that transcends disciplinary boundaries. Early scientific efforts focused on climatology and atmospheric chemistry, but the current landscape includes socio-economic vulnerability, policy innovation, technological transitions, and public engagement. One area is impact assessment, which quantifies climate effects on agriculture, infrastructure, public health, and water security. The development of mitigation strategies, including renewable energy, and sustainable transport, is equally prominent. Research into adaptation measures has gained ground, especially regarding nature-based solutions, climate-resilient infrastructure, and community-based planning (IPBES and IPCC, 2021; Raymond et al., 2017).

Table 1. Key Climate Research Institutions

Institution	Main Focus	Role
Intergovernmental Panel on Climate Change	Assessment of climate science and policy recommendations	Provides scientific basis for international climate negotiations
World Meteorological Organization	Meteorological observations and climate monitoring	Coordinates global weather and climate data systems
United Nations Environment Programme	Environmental policy and sustainable development	Supports climate initiatives and policy in developing countries
European Environment Agency	Environmental indicators and data for EU policy	Publishes key reports on EU environmental status
Joint Research Centre	Scientific support for EU policies	Develops tools and models for EU policy design

Despite these advances, significant asymmetries persist across regions. Romania illustrates some of the structural challenges facing Eastern European countries in aligning with EU and global research frameworks. Although institutions like the National Meteorological Administration (ANM), the National Institute for Earth Physics (INCDFP), and several universities contribute to climate research, their efforts are often isolated and underfunded. Participation in European projects remains low, and the country lacks integrated databases and interdisciplinary networks. Scientific findings are seldom used in policymaking, and there is little institutional capacity to bridge the gap between research and decision-making (Sarkki et al., 2015).

Key challenges include weak coordination between ministries and research bodies, insufficient digital tools, lack of long-term funding, and limited incentives for interdisciplinary collaboration. Yet, Romania's integration into European research frameworks presents a significant opportunity for capacity building, especially if local research agendas are aligned with EU priorities.

To consolidate these observations, a SWOT analysis was developed to outline the key strengths, weaknesses, opportunities, and threats influencing Romania's climate research system. This strategic overview (Figure 1) highlights internal capabilities and limitations, as well as external drivers that may either support or constrain future development.

In order to synthesise the structural challenges and strategic potential of Romania's climate research system, a SWOT analysis was conducted (Figure 1). This structured approach highlights internal and external factors influencing the national research environment and supports the identification of priority areas for capacity development.

Among the strengths, Romania benefits from an increasing academic interest in climate-related themes, with several universities and research institutes such as ANM actively engaged in monitoring and scientific studies.

However, the analysis also identifies significant weaknesses. The national research landscape remains fragmented and underfunded, with minimal strategic coordination between relevant ministries, academic bodies, and public authorities. The lack of open-access, interoperable data infrastructures, such as climate risk maps or national research repositories, limits both the visibility and the applicability of scientific work in national decision-making.

On the opportunity side, Romania has the potential to improve its position by leveraging available European funding mechanisms, responding to growing political and societal awareness of climate risks, and investing in interdisciplinary collaboration and innovation (OECD, 2021). The ongoing push for green transition policies, resilience planning, and sustainable development can serve as entry points for strengthening institutional research frameworks.

Nevertheless, several threats persist. These include continued underinvestment in research and development, the emigration of qualified researchers, administrative complexity in accessing funding, and the limited use of scientific evidence in policymaking processes. If left unaddressed, these factors could deepen existing gaps between Romania and more research-intensive EU Member States.

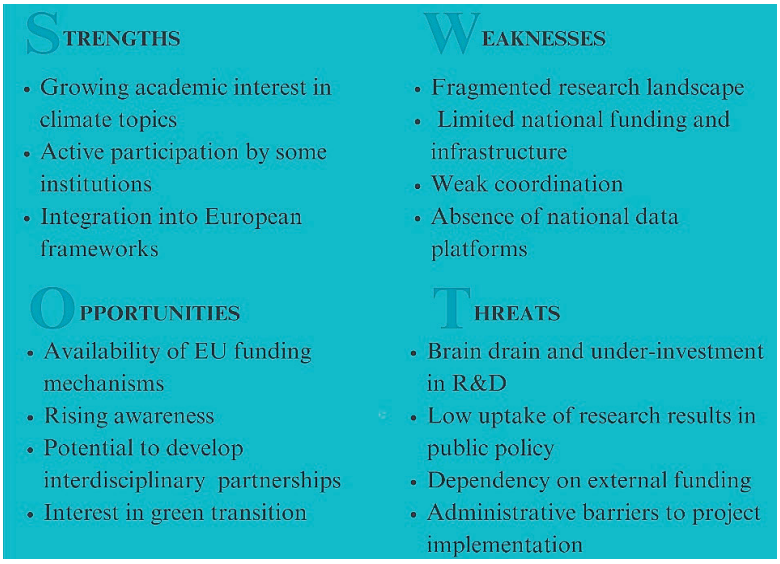


Figure 1. National-level capacity: SWOT Perspective on Romania's climate research landscape

This SWOT analysis reinforces the need for a national strategic vision that bridges science, policy, and practice, while supporting long-term investment in knowledge systems capable of responding to complex climate challenges.

Moreover, aligning Romania's research directions with foresight-based strategic planning is essential to strengthen institutional resilience and adaptive governance mechanisms. As highlighted by the European Commission's Strategic Foresight Report (European Commission, 2023), placing sustainability and wellbeing at the centre of strategic autonomy can help bridge the divide between knowledge production and societal needs. This implies not only more inclusive research agendas but also the mobilisation of innovation ecosystems around climate adaptation, mitigation, and environmental equity.

Recent studies underscore the importance of iterative, reflexive science-policy interfaces to support climate action in complex governance systems.

Sarkki et al. (2015) propose a dynamic framework that integrates credibility, relevance, legitimacy, and "iterativity" as dimensions that influence the effectiveness of science-based decision-making. Such frameworks could inspire improvements in Romania's institutional settings, particularly in strengthening the integration of scientific knowledge in local and national planning processes.

Additionally, climate science in Romania would benefit from adopting anticipatory and transdisciplinary methodologies. As Bai et al. (2016) argue, envisioning plausible and desirable futures in the Anthropocene requires transformative research agendas that go beyond problem identification and focus on systems innovation. This involves deeper collaboration between public authorities, academic institutions, and civil society, as already piloted in some local contexts.

Ultimately, strengthening Romania's position in the global climate research landscape requires both institutional transformation and alignment with forward-looking EU policy priorities.

Integrating foresight, innovation, and co-designed research can help Romania better generate and apply climate knowledge in support of public needs.

CONCLUSIONS

This article has outlined the evolving landscape of climate change research, with a particular focus on institutional structures, thematic directions, and regional disparities. Globally, the institutional architecture supporting climate science has matured through well-established organisations, as discussed earlier in the paper.

In Europe, the combination of policy instruments, dedicated research programmes, and technological platforms has fostered a dynamic research environment with increasingly integrated outputs.

Romania, however, continues to face structural challenges in aligning with this evolving framework.

As evidenced by the SWOT analysis, the national climate research ecosystem suffers from weak institutional coordination, inadequate funding, and a lack of digital infrastructure. Although several public research institutes have longstanding expertise, their efforts remain disconnected from policy processes and broader European initiatives.

Despite these weaknesses, Romania has the potential to strengthen its position through targeted reforms and strategic investments.

Opportunities include aligning national priorities with European foresight frameworks. Romania could also strengthen its participation in international research consortia and foster closer ties between academia, public institutions, and civil society. Lessons from countries with successful integration into EU research ecosystems could offer useful models for institutional reform.

Overall, strengthening climate resilience and adaptation capacities requires more than scientific output, it calls for coherent strategies that link research, governance, and innovation.

The insights presented here serve as a stepping stone for continued doctoral research and contribute to the broader understanding of how science can inform robust climate action, especially in structurally underrepresented regions like Romania.

Moreover, as climate research increasingly intersects with areas such as urban resilience, health, biodiversity, and digital innovation, the capacity to develop integrated, cross-sectoral responses becomes essential. Romania's future progress will depend not only on scientific excellence but also on the ability to embed research findings into operational decision-making, local planning, and national policy frameworks.

Finally, the institutional landscape must be supported by a long-term vision that promotes continuity, transparency, and collaboration. Establishing dedicated national programmes for climate knowledge co-production, incentivising open data sharing, and creating platforms for public-private partnerships can serve as catalysts for systemic change.

As climate risks intensify, the need for responsive, inclusive, and adaptive research systems will grow. This calls for a cultural shift in how research is prioritised, communicated, and leveraged, transforming climate science from an academic pursuit into a cornerstone of societal transformation.

REFERENCES

Bai, X., van der Leeuw, S., Robinson, J., Maasen, S., Guimaraes Pereira, A., Jäger, J., et al. (2016). Plausible and desirable futures in the Anthropocene: A new research agenda. *Global Environmental Change, 39*, 351–362. https://doi.org/10.1016/j.gloenvcha.2015.09.017

European Commission: Directorate-General for Research and Innovation (2020). *A new ERA for research and innovation*. https://data.europa.eu/doi/10.2777/605834

European Commission (2023). *Strategic foresight report 2023*.

European Environment Agency (EEA) (2025). *Climate change impacts, risks and adaptation*. https://www.eea.europa.eu

Intergovernmental Science-Policy Platform on Biodiversity and Ecosystem Services (IPBES), & Intergovernmental Panel on Climate Change (IPCC) (2021). *Biodiversity and climate change*. https://doi.org/10.5281/zenodo.4782538

IPCC (2021). *Climate change 2021: The physical science basis. Contribution of Working Group I to the Sixth Assessment Report of the Intergovernmental Panel on Climate Change* (V. Masson-Delmotte, P. Zhai, A. Pirani, S. L. Connors, C. Péan, S. Berger, ... B. Zhou, Eds.). Cambridge University Press. https://doi.org/10.1017/9781009157896

IPCC (2022). *Climate change 2022: Impacts, adaptation and vulnerability. Contribution of Working Group II to the Sixth Assessment Report of the Intergovernmental Panel on Climate Change*. Cambridge University Press

National Meteorological Administration (ANM). (n.d.). *Despre ANM*. Retrieved from https://www.meteoromania.ro

Organisation for Economic Co-operation and Development (OECD). (2021). *Addressing climate change through innovation: OECD green growth papers*. https://doi.org/10.1787/aa98ed53-en

Raymond, C. M., Frantzeskaki, N., Kabisch, N., Berry, P., Breil, M., Nita, M. R., et al. (2017). A framework for assessing and implementing the co-benefits of nature-based solutions in urban areas. *Environmental Science & Policy, 77*, 15–24. https://doi.org/10.1016/j.envsci.2017.07.008

Ministry of Research, Innovation and Digitalisation. (n.d.). *Strategii și politici*. Retrieved from https://www.mcid.gov.ro

Sarkki, S., Tinch, R., Niemelä, J., Heink, U., Waylen, K., Timaeus, J., et al. (2015). Adding 'iterativity' to the credibility, relevance, legitimacy: A novel scheme to highlight dynamic aspects of science-policy interfaces. *Environmental Science & Policy, 54*, 505–512. https://doi.org/10.1016/j.envsci.2015.02.016

United Nations Environment Programme (UNEP) (2023). *Emissions gap report 2023*. Nairobi: UNEP.

World Meteorological Organization (WMO) (2023). *State of the global climate 2022*. Geneva: WMO

Scientific Papers. Series E. Land Reclamation, Earth Observation & Surveying, Environmental Engineering. Vol. XIV, 2025
Print ISSN 2285-6064, CD-ROM ISSN 2285-6072, Online ISSN 2393-5138, ISSN-L 2285-6064

BEHAVIOR OF ASPHALT MIXTURES MANUFACTURED WITH RECYCLED MATERIALS AND THEIR *IN SITU* PERFORMANCE LEVEL

Nicoleta-Adaciza IONESCU[1], Daniela DOBRE[1, 2]

[1]National Institute for Research and Development in Construction,
Urban Planning and Sustainable Spatial Development - URBAN-INCERC,
266 Pantelimon Road, District 2, 021652, Bucharest, Romania
[2]Technical University of Civil Engineering of Bucharest,
122-124 Lacul Tei Blvd, District 2, 020396, Bucharest, Romania

Corresponding author email: adaionescu2002@yahoo.co.uk

Abstract

In the context of several solutions that can be used to improve the performance of asphalt mixtures during their service life, the paper presents a case study in which asphalt mixtures are manufactured using some recycled materials such as glass, plastic and rubber. The level of performance will be quantified both by the rheological properties measured by conventional tests (viscosity, permanent deformation etc.), but also by some tests that take into account the change in response over time and that lead to variation curves for the stiffness modulus, yielding and fatigue resistance etc. Asphalt mixtures with different percentages of recycled materials will be studied and the results obtained from dynamic and rheological tests before and after the aging process will be compared and interpreted. Determining the degree of influence of recycled materials on the aging resistance of modified asphalt mixtures and characterizing the dynamic and rheological properties can lead to optimizing the percentages of additions and choosing the most advantageous solution based on multi-criteria analyses in different climatic and stress conditions.

Key words*: asphalt mixtures, performances, recycled materials, service life.*

INTRODUCTION

In the context of reducing the irrational use of resources and reducing the level of pollution, the use of waste or secondary materials instead of natural materials can have great benefits, of an economic and environmental nature, with a relatively low energy consumption (Gheorghe et al., 2008; Croitoru, 2016; Dobrescu et al., 2016; Radu et al., 2017; Dobrescu & Calarasu, 2019; Petcu & Racanel, 2024; Saca et al., 2023; 2024).

The choice of materials used for asphalt mixtures depends on the traffic and climate conditions for which the respective asphalt mixture is designed. When designing the asphalt mixture recipe, it is important to consider the ways in which the raw material can affect the performance of asphalt mixtures during the exploitation period, as well as how it will affect the performance of the mixture and the service life of the road structure.

In order to obtain durable, cheap, high-quality asphalt mixtures, with physical-mechanical and dynamic characteristics comparable to those of existing asphalt mixtures, consideration will be given to improving the qualities of bitumen, as well as the use of recyclable materials (glass, recycled mixture, slag aggregates, recycled plastic, recycled rubber, industrial waste, oils), which will replace part of the quantity of aggregates and fillers.

The following research directions outline the development of solutions and formulations incorporating specific dosages of recycled materials.

Use of industrial waste powders in asphalt mixtures

By using power plant ash in asphalt mixtures, the Marshall stability determined for temperatures higher than the test temperature by 10°C, respectively 20°C, due to the higher conductivity and specific heat for the asphalt mixture containing a significant percentage of ash in the mixture (7.5%, 10%), decreases by approximately 5% compared to 30% for the mixture containing limestone filler in the mixture (Paul Marc, 2011).

Use of bio-oil as a substitute for bituminous binder in asphalt mixtures

Replacing 25% bitumen with bio-oil, at the current production price of the asphalt mixture, will result in a production saving of 5%. If the reduction of mixing and compaction temperature are taken into account, the economic opportunity in using this technology is greater (Perlata, 2013).

Use of bituminous binders modified with industrial waste and bio-oil in asphalt mixtures

Regarding the fatigue behavior of asphalt mixtures with polymer-modified bitumen, the fatigue resistance of the studied asphalt mixtures highlights the fact that the working temperature in the laboratory must be correlated with the *in situ* atmospheric temperature. An increase in temperature by 10°C corresponds to an increase in specific deformation by almost 280% (Burlacu & Răcănel, 2014).

Use of crushed glass in asphalt mixtures

In the study on the performance of asphalt mixtures (paving asphalt), in which a finely divided aggregate is replaced by crushed glass, it was found that the performance of the aggregate is not affected for crushed glass percentages of up to 30% of the aggregate mass, a combination of 3% rubber polymer plus 2% glass powder can considerably improve the mechanical properties of the asphalt mixture and that asphalt mixture layers containing 10-15% ground glass in surface mixtures performed satisfactorily (Issa, 2016).

Use of recycled construction aggregates in asphalt mixtures

Asphalt mixtures containing recycled construction aggregates (roads, concrete) have the problem of high bitumen absorption. The effects of glass on bitumen absorption and volumetric properties of asphalt mixtures containing 25% and 50% recycled aggregates are demonstrated through laboratory investigations. Three glass contents of 0%, 10% and 20% in terms of the total weight of fine aggregates are used in the mix design to prepare 100 mm diameter samples containing 0%, 25% and 50% recycled aggregates, under 120 rotation cycles. The results indicate that waste glass can be a viable material for improving the problem of high bitumen absorption of asphalt mixtures containing recycled aggregates (Tahmoorian et al., 2018).

The use of compounds obtained by processing industrial waste in ecological asphalt mixtures

The partial replacement of quarry mineral aggregates with steel mill slag considerably influences the physical-mechanical characteristics of the asphalt mixture. The addition of certain materials derived from industrial waste can bring benefits to the quality of the asphalt mixture, e.g. the behavior of adding power plant ash as a substitute for the usual limestone filler that leads to the stiffening of the asphalt mixture, giving it properties that can be compared to the use of polymers/elastomers in the composition of the bituminous mixture (Lixandru et al., 2018).

Use of aggregates from recycled asphalt mixtures

These mixtures were prepared with two filler additives, steel mill slag and silica fume, at four different percentages of the aggregate weight. A total of 234 mixtures were tested. The laboratory results indicated the effectiveness of using such additives as fillers. Marshall stability showed an improvement for mixtures prepared with steel slag ranging from 11.73 to 32.73 kN as the dosage of recovered asphalt aggregates increased; high stability was recorded for a dosage of 75% recovered asphalt pavement aggregates with a mixture of 50% steel slag. On the other hand, silica fume showed variations in its strength, however the maximum load value of 31.02 kN was for a dosage of 75% recovered asphalt aggregates with 100% silica fume (Naser et al., 2023).

Finite element modelling of asphalt mixture

An advanced area of research and testing aims to assess deformations and stress distributions under specific static and dynamic loading conditions for asphalt mixtures, both homogeneous and inhomogeneous. This approach incorporates the use of recyclable materials and employs modelling through the finite element method within a multidisciplinary framework that includes

chemistry, engineering, and finite element analysis (Ionescu et al., 2024).

MATERIALS AND METHODS

Testing the physical and mechanical properties according to normative standards

Given the importance of asphalt mixtures' performances, this paper highlights the behavior of classic asphalt mixtures, as well as those modified by introducing a recycled material, used in the base, binding and wear layers.

The physical-mechanical characteristics of the asphalt mixtures were determined on Marshall specimens made from the asphalt mixture prepared in the laboratory to establish the optimal dosages of materials: aggregates, filler, bitumen and fiber (according to the requirements of Normative AND 605).

To prepare the asphalt mixtures in the laboratory, all materials were heated to a temperature of 180°C in an oven. After that, they were mixed for homogenization for 5 minutes in the laboratory mixer. Marshall samples were compacted at 170-180°C using an impact hammer stand (Marshall press), by applying a compaction effort on each side of the specimen 50 blows or 75 blows (for SMA).

The following physical and mechanical characteristics were determined on the specimens made with the Marshall press:

- apparent density, according to SR EN 12697-6;
- Marshall stability, at 60°C, according to SR EN 12697-34;
- flow index, at 60°C, according to SR EN 12697-34;
- void volume, according to SR EN 12697-8;
- water sensitivity, according to SR EN 12697-12;
- water absorption, Normative AND 605:2016;

After obtaining the optimal bitumen dosage, the following tests were performed:

- on specimens made with a rotary press;
- modulus of rigidity, SR EN 12697-26;
- fatigue resistance, SR EN 12 697-24;
- resistance to permanent deformations by cyclic compression (dynamic creep), SR EN 12 697-25;
- resistance to permanent deformations (tracking), SR EN 12697- 22.

RESULTS AND DISCUSSIONS

Experimental data analysis for different classic asphalt mixtures

To highlight the behavior of mixtures with different percentages of bitumen (behavior of interest in the case of the action of external agents such as traffic, or atmospheric phenomena), some representations will be presented based on the results of the tests carried out (Figures 1, 2 and 3), for the following types of asphalt mixtures:

- wear layer:
  - asphalt mixture with high mastic content using modified bitumen with a maximum grain size of 16 mm - SMA 16 (bitumen PmB 45/80-80);
  - asphalt mixture with high mastic content using simple bitumen type 50/70 with a maximum grain size of 16 mm - SMA 16 (bitumen 50/70);
  - asphalt concrete with crushed gravel with a maximum grain size of 16 mm - BAPC 16 (Bitumen 50/70);
  - asphalt concrete with a maximum grain size of 11.2 mm - BA 11.2;
  - asphalt concrete with crushed gravel with a maximum grain size of 8 mm - BAPC 8;
  - asphalt concrete with a maximum grain size of 8 mm - BA 8;
  - asphalt concrete with crushed gravel with a maximum grain size of 31.5 mm - BAPC 31.5.
- binder layer:
  - asphalt concrete with modified bitumen and a maximum grain size of 22.4 - BAD 22.4 (Bitumen PmB45/80-65)
- base layer:
  - bituminous asphalt with a maximum grain size of 31.5 mm - AB 31.5;
  - bituminous asphalt with a maximum grain size of 22.4 mm - AB 22.4.

Bitumen is part of an asphalt mixture in a proportion of 5-7% of its mass and the optimal dosage must be chosen depending on the physical and mechanical characteristics considered.

High stability for approx. 5.3 % percentage of bitumen is shown in Figure 1.
An inverse dependence, i.e. bitumen content increases, water absorption decreases, is observed in Figure 2.
In Figure 3, density is mainly influenced by the source of aggregates (i.e. their density).
The characterization of asphalt mixtures through dynamic laboratory tests is presented in Figures 4, 5 and 6.

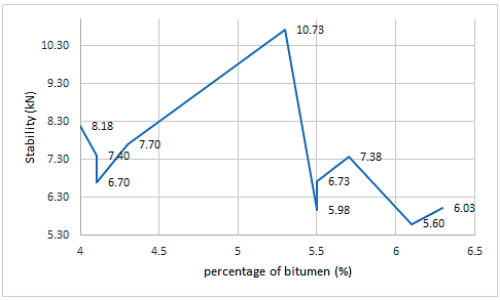


Figure 1. Graphical representation of Stability - the percentage of bitumen

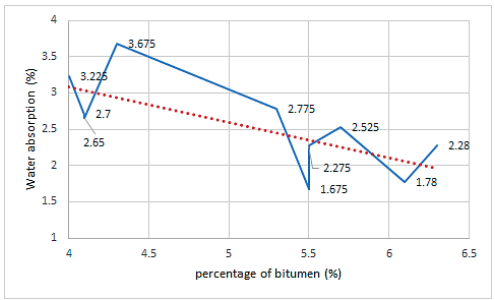


Figure 2. Graphical representation of water absorption - percentage of bitumen

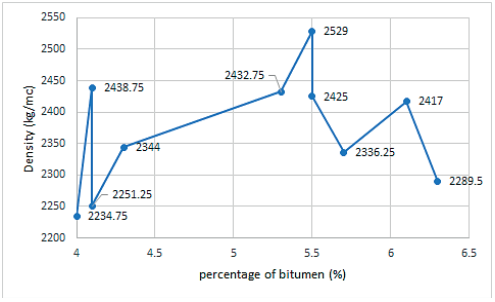


Figure 3. Graphical representation of Density-percentage of bitumen

The modulus of rigidity is higher for asphalt mixtures used in base layers (Figure 4).

The lower the dynamic creep, the more resistant the mixture is under traffic (Figure 5). It is important that the tracking resistance is below 5 min. cycles to cracking at 15°C to avoid undulations under traffic (Figure 6).

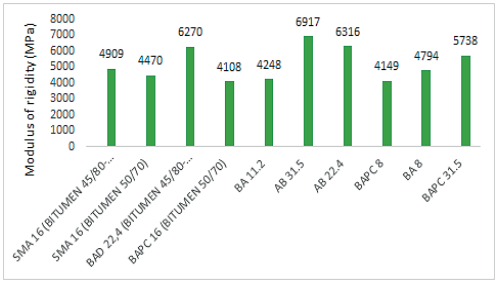


Figure 4. Graphical representation of the modulus of rigidity

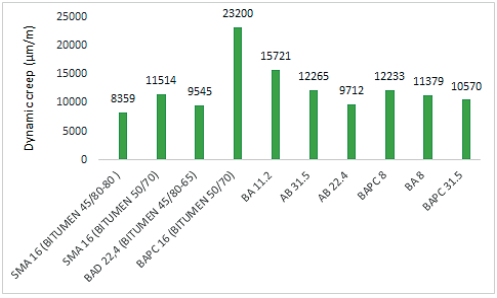


Figure 5. Graphical representation of the resistance to permanent deformations – dynamic creep - deformation at 50°C, 300 kPa and 10000 impulses

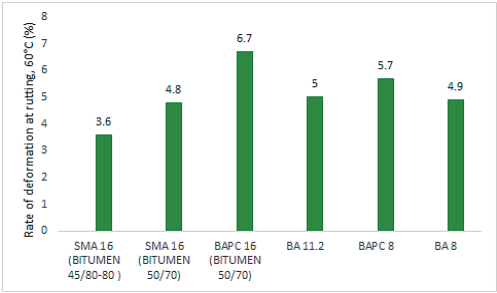


Figure 6. Graphical representation of the rate of deformation at tracking at 60°C

Description of different types of asphalt mixtures, including those with recycled materials

As a case study, the asphalt mixture type SMA 16 is presented, prepared in two variants in which different conventional raw materials and recycled materials were used:

- asphalt mixture prepared with quarry aggregates, filler, fibre and road bitumen type 50/70 modified with 15% recycled rubber (MA1);
- asphalt mixture prepared with recycled asphalt mixture, quarry aggregates, filler, fibre and bitumen PmB45/80-50 (MA2).

The two asphalt mixtures were designed in accordance with the requirements of the documents: Normative AND 605:2016 and SR EN 13108-5:2016.

Bitumen modified with a polymer (in our case recycled rubber) and which consists of two distinct phases, can be considered in three situations (Brule, 1993; Dony, 2014):

• The polymer content is low (below 4%), the bitumen constitutes the continuous phase of the system in which the polymer phase is dispersed (Figure 7a). The dispersed polymer phase improves the properties at high service temperature and at low temperatures.

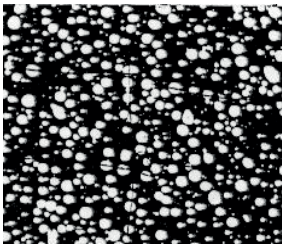


Figure 7a. The polymer phase is dispersed (Dony, 2014)

• The polymer content is high (above 7%), the polymer phase constitutes the matrix of the system (Figure 7b). In this case the polymer is plasticized by the oils in the bitumen in which the heavy fractions of the initial binder are dispersed. The properties of this system are fundamentally different from those of a bitumen and depend largely on the properties of the polymer.

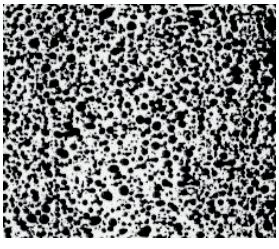


Figure 7b. The polymer is plasticized by the oils in the bitumen (Dony, 2014)

• The polymer content is around 5%, microstructures are obtained in which the two phases are continuous and interpenetrated (Figure 7c). However, this system presents stability problems, being difficult to control.

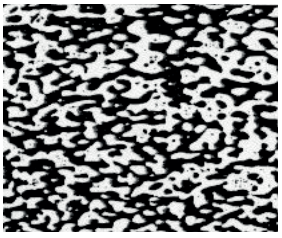


Figure 7c. Microstructures are obtained in which the two phases are continuous and interpenetrated (Dony, 2014)

The rheological properties of modified bitumen are strongly influenced by the polymer content (Tudose, 1982). For a low polymer content (3%) the behavior of modified bitumen remains close to that of plain bitumen, and for modified bitumen with a high polymer content (e.g. higher than 6%) the rheological behavior changes fundamentally. These rheological properties are highlighted in (Background of SUPERPAVE asphalt binder test methods, 1994), which selects the measurement of the bitumen's contribution to improving the resistance to permanent deformation. This methodology demonstrates that the bitumen must have both a high complex modulus and high elasticity at the maximum temperature that the asphalt pavement can withstand.

Dynamic shear and bending tests on plain and modified bitumen have revealed the dynamic shear modulus (G, Pa), and the phase angle (δ, deg). For a given complex shear modulus, low values of the phase angle are found, so better resistance to permanent deformations and better fatigue resistance (Tudose, 1982). There is an influence of the styrene-butadiene-styrene type polymer (rubber) on the complex modulus and the phase shift angle (Tudose, 1982), a decrease in the phase shift with the increase in the values of the complex shear modulus.

The graphical representation of Complex shear modulus-temperature shows a plateau with a high modulus that varies little with temperature (low temperature susceptibility), resulting in good resistance to permanent deformation (Tudose, 1982).

In Figure 8, two asphalt mixtures used for thewear layer are presented in comparison: MA1-asphalt mixture (prepared with bitumen type 50/70 modified with 15% rubber powder) and MA2-asphalt mixture (prepared with modified bitumen type PmB45/80-50). The results for the tracking test by monitoring are the deformation rate at 50°C, 300 kPa and 10000 pulses (mm/10000 cycles) and the rut depth % of the initial thickness of the sample.
Bitumen modified with rubber powder is obtained in bitumen modification installation or laboratory, by introducing a recycled material into the bitumen mass, in this case recycled rubber.

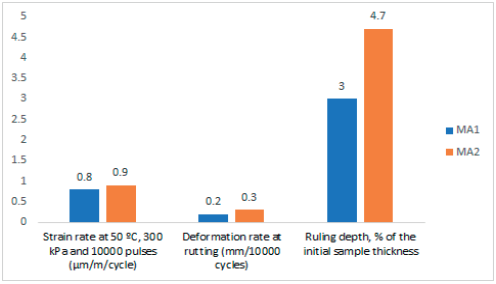


Figure 8. Comparative representation of MA1 and MA2

The performance of the two asphalt mixtures MA1 and MA2 in operation was also monitored, by performing *in situ* tests on two road sections, 6 months after laying (Table 1).

Table 1. Results of *in situ* tests

Determined characteristics	Values			Test method
	Obtained		Imposed by Normative AND 605	
	MA1	MA2		
Roughness (with SRT pendulum), SRT units at 1 m from axis at 3 m from axis	90 87	83 81	min. 80	SR EN 13036-4
Roughness (volumetric method), mm at 1 m from the axis at 3 m from the axis	1.6 1.5	1.3 1.2	min. 1.2	SR EN 13036-1
Resistance to permanent deformation at 60°C (tracking) determined on cores taken from the road: -rut depth, mm/% of the initial sample thickness -tracking deformation rate, mm/10000 cycles	3.56 0.23	4.87 0.35	max. 5 max. 0.5	SR EN 12697-22 +A1

The behavior of the two mixtures in terms of roughness and deformations can be compared using Figures 9 and 10. The asphalt mixture with recycled rubber shows greater roughness but also a high resistance to permanent deformation at 60°C, as illustrated in Figure 10.

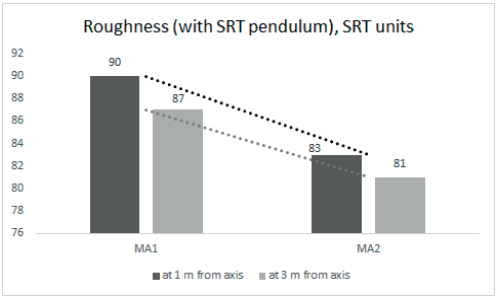


Figure 9. Variation of roughness between asphalt mixtures (MA1 and MA2)

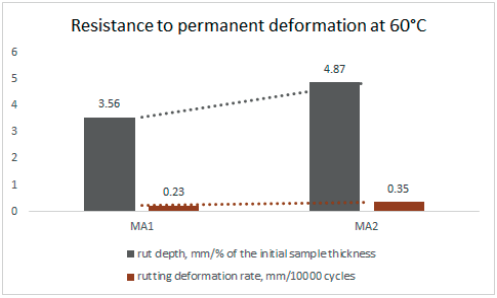


Figure 10. Variation of resistance to deformations between asphalt mixtures (MA1 and MA2)

CONCLUSIONS

The service life of road structures is very important, starting from the date of execution and commissioning until the decision to rehabilitate or reconstruct is made.
From the presented study it can be concluded that recycled materials used in the preparation of asphalt mixtures can have better performance compared to classic asphalt mixtures, important for the road‘s service life. To carry out durable and high-performance works, it is important to test the physical-mechanical and dynamic characteristics of the resulting asphalt mixture. It is also important to declare the performance of asphalt mixtures under the requirements of Regulation (EU) No. 305/2011 and the harmonized European standards (often referred to as "CE marking").

The trend of studying the potential of some additions of animal waste and agro-industrial by-products for use in the construction field should be sustained at the level of exploratory research also in the direction of additions in asphalt mixtures (only for temporary roads, no heavy traffic) (Popa et al., 2021; 2023).

ACKNOWLEDGMENTS

This research work was done within the "Nucleu" Programme in PNCDI 2022-2027, with the support of MCDI, Project PN 2335.

REFERENCES

Brule, B. (1993). Les bitumes - polymeres, notion de base, *Revue generale des routes et aerodromes no. 711*.

Burlacu, A. & Racanel, C. (2014). Reducing costs of infrastructure works using new technologies. *Split, Croatia*, Tiskara Zelina, pp. 189-195.

Croitoru G. & Garaz, C. (2016). Study of asphalt coatings with addition of recycled rubber granules. *Conference Current Issues in Urbanism and Land Management*, V3, pp 65-70. Repository.utm.md.

Dobrescu, C.F., Calaraşu, E.A., Ungureanu, V.V. (2016). Systematic studies on defining interaction process of clay minerals for achieving synthetic mixtures as composite materials applied in stabilization works. *3rd International Conference Structural and Physical Aspects of Construction Engineering*, Štrbské Pleso (High Tatras), Slovacia.

Dobrescu C.F. & Calaraşu E.A. (2019). Engineering and environmental benefits of using construction wastes in ground improvement works. MATEC Web of Conferences 310, 00024 (2020), *4th International Scientific Conference Structural and Physical Aspects of Construction Engineering* (SPACE 2019), Proceedings Paper, Doi: 10.1051/matecconf/ 202031000024.

Dony, A. (2014). Liants bitumes-polymeres. *Serie chaussees CR15*. ERLPC-CR-LCPC-CR15.pdf.

Gheorghe, M., Radu, L., Saca, N. (2008). Aspects on dimensional stability and mechanical strength of E waste glass addition concrete, *Scientific Bulletin*, *1*, 40-53, ISSN -1224-628X.

Ionescu, N.A., Dobre, D., Dragomir, C.S. (2024). Modeling the Structural Behavior of a CNC Bearing Member Subjected to Static and Dynamic Loads. *Scientific Papers. Series E. Land Reclamation, Earth Observation & Surveying, Environmental Engineering*, *13*, 425-430, Print ISSN 2285-6064.

Issa, Yazan. (2016). Effect of Adding Crushed Glass to Asphalt Mix. *Archives of Civil Engineering*. Doi: 62. 10.1515/ace-2015-0063.

Lixandru, C., Dicu, M., Grisic, G., Andrei, B. (2018). The Use of Industrial Waste as a Replacement for the Filler Commonly Used in Asphalt Mixtures. *15th National Congress of Roads and Bridges*, Issue Environment and Climate Change.

Marc, P. T. (2011). Design and construction of high-performance road structures. *Politehnica Publishing House*, Timisoara.

Naser, M., Abdel-Jaber, M., Al-Shamayleh, R., Ibrahim, R., Louzi, N., AlKhrissat, T. (2023). Improving the mechanical properties of recycled asphalt pavement mixtures using steel slag and silica fume as a filler. *Buildings, 13*, *132*. https://doi.org/10.3390/buildings 13010132.

Perlata, E.J.F. (2013). Micro-Analysis of psysicichemical interaction between the components of asphalt mixture with rubber. *Ames*, Iowa: Iowa State University.

Petcu, C. & Racanel, C. (2024). Estimation of asphalt mixture fatigue behaviour using the two-point bending test. *Journal of Applied Engineering Sciences*, *14(27),* 153-160, ISSN: 2247-3769 / e-ISSN: 2284-7197.

Popa, I., Petcu, C., Muresanu, A. (2023). Durability of multifunctional coatings made with additions of animal waste and agro-industrial by-products. *Chem. Proc., 13*(1), 22. https://doi.org/10.3390/chemproc2023013022.

Popa, I., Petcu, C., Mureşanu, A. (2021). Sunflower seed shells and sheep wool, starting points for innovative coatings with thermal insulation properties. *Proceedings of XXIth International Multidisciplinary Scientific GeoConference Surveying, Geology and Mining, Ecology and Management – SGEM* 2021, Section Green Buildings Technologies and Materials, ISBN 978-619-7408-13-3, ISSN 1314-2704.

Radu, L., Saca, N., Gheorghe, M., Mazilu, C., Fugaru, V. (2017). Concretes with gamma radiation shielding capacity for special construction applications. *Romanian Materials Journal, 47*(3), 322-327. https://api.semanticscholar.org/CorpusID:198923094.

Saca, N., Radu, L., Trusca, R., Calota, R., Dobre, D., Nastase, I. (2023). Assessment of properties and microstructure of concrete with cotton textile waste and crushed bricks, *Materials, 16*(20), 6807. https://doi.org/10.3390/ma16206807

Saca, N., Radu, L., Stoleriu, S., Dobre, D., Calota, R., Trusca, R. (2024). Investigation of physical-mechanical properties and microstructure of mortars with perlite and thermal-treated materials. *Materials, 17*(14), 3412. https://doi.org/10.3390/ ma17143412

Saca, N., Radu, L., Calota, R., Mitran, R.A., Romanitan, C., Trusca, R., Racanel, C., Radu, I. (2024). An investigation of the physic-mechanical properties of the expanded perlite mortars with thermal-activated concrete waste and microencapsulated paraffin. *Heliyon, 10*(21), e39720, https://doi.org/10.1016/j. heliyon.2024.e39720

Tahmoorian, F., Samali, B., Yeaman, J., Crabb, R. (2018). The Use of Glass to Optimize Bitumen Absorption of Hot Mix Asphalt Containing Recycled Construction Aggregates. *Materials, 11. 1053.* Doi: 10.3390/ma11071053.

Tudose, R.Z., Volintiru, T., Asandei, N., Lungu, M., Ivan, G. (1982). Rheology of macromolecular

compounds. Introduction to rheology (in Romanian). *Technical Publishing House*, Bucharest.

***Normative for hot-mixed asphalt mixtures. Technical conditions for design, preparation and commissioning of asphalt mixtures. Indicative AND 605-2016, published in the Official Monitor Part I no. 126 of 09.02.2018

***SR EN 13108-5:2016 Asphalt mixtures. Specifications for materials. Part 5: Asphalt concrete with high mastic content published in the Catalog of Romanian Standardization Association (ASRO)

***U.S. Department of Transportation, Federal Highway Administration (1994). Background of SUPERPAVE asphalt binder test methods. National Asphalt Training Center Demonstration Project 101.

Scientific Papers. Series E. Land Reclamation, Earth Observation & Surveying, Environmental Engineering. Vol. XIV, 2025
Print ISSN 2285-6064, CD-ROM ISSN 2285-6072, Online ISSN 2393-5138, ISSN-L 2285-6064

SOLUTIONS FOR THE RESTORATION IN THE NATURAL CIRCUIT OF CONTAMINATED SITES FROM THE PETROLEUM INDUSTRY

Cristian Mugurel IORGA[1], Lucian-Gabriel ZAMFIR[2], Alina Ceoromila CANTARAGIU[3]

[1]"Dunărea de Jos" University of Galaţi, Faculty of Sciences and Environment,
111 Domnească Street, 800201, Galaţi, Romania
[2]National Institute of Research and Development in Chemistry and Petrochemistry - ICECHIM,
Biotechnology and Bioanalysis Department, 202 Splaiul Independenţei,
060021, District 6, Bucharest, Romania
[3]"Dunărea de Jos" University of Galaţi, Cross-border Faculty,
47 Domnească Street, 800008, Galaţi, Romania

Corresponding author email: cristian.iorga@ugal.ro

Abstract

The restoration of sites contaminated by the petroleum industry aims to mitigate negative effects on the environment, and human health, and facilitate the reuse of significant land areas. In addition to reducing soil contaminant concentrations, another objective of restoration is the rehabilitation of the vegetation layer. The use of sewage sludge in decontamination processes can provide nutrients and microorganisms, potentially forming the basis for vegetation layer regeneration. However, the application of sewage sludge can also have negative environmental impacts due to high concentrations of heavy metals and the presence of various pathogenic microbiota. This study presents an experimental investigation into the potential use of sewage sludge for remediating petroleum-contaminated sites and regenerating the vegetation layer. Lawn grass was sown in the remediated soil treated with sewage sludge to study its development. Using combined SEM-EDX and electrochemical methods, we analysed the plant microstructure and the distribution of chemical elements to evaluate turf growth. The results obtained are promising and open new research perspectives for the use of sewage sludge in the remediation of sites contaminated by the oil industry.

Key words*: bioremediation, environment, petroleum, pollution, sewage sludge.*

INTRODUCTION

Contaminated sites from the petroleum industry represent a mosaic in the world's geographical landscape, occupying large areas of land. Restoring the natural environment with the aim of reusing land has become a global concern of humanity, but with the optimization of restoration activities and minimizing costs. A current approach to the remediation of contaminated sites is based on the assessment of associated risks, so that the return to the natural cycle does not pose risks to the environment and human health.

The present study is a continuation of the research on the restoration of contaminated sites from the petroleum industry using sewage sludge. Previous studies have shown the bioremediation potential of sewage sludge for lands polluted with petroleum hydrocarbons. In addition to the nutrient and microorganism content of sewage sludge that helps in the bioremediation process, it also comes with a contribution of mineral matter that, when mixed with the soil it has bioremediated, can to a certain extent complete the need for filling material in excavated areas, thus minimizing the use of natural resources. By using sewage sludge in the bioremediation processes of soils contaminated with petroleum hydrocarbons, it was found that there is a double recovery of two materials with harmful effects on the environment: sewage sludge and contaminated soil from the petroleum industry, thus reducing the disposal of hazardous waste (Iorga et al., 2025). Previous research has shown that petroleum hydrocarbons contaminated soil and bioremediated with sewage sludge can be the basis for the development of a fertile layer for plant growth (Iorga et al., 2024). Both the high content of heterotrophic bacteria and filamentous fungi identified by microbiological analyses the soil microstructure and the distribution of chemical elements with a role in

plant growth were identified in petroleum hydrocarbon contaminated soils and bioremediated with sewage sludge.

In the present study, the microstructure and elemental analysis of the soil-sewage sludge/ plant systems were studied using a scanning electron microscope coupled with an energy dispersive X-ray analyzer (SEM-EDX) method. The morphological and elemental characteristics of the control soil were presented before (Iorga et al., 2024). Therefore, the results of these two research papers will be correlated to validate them.

Nitrite monitoring in soil is essential as these compounds have a significant impact on agriculture and human health. Nitrite is part of the nitrogen cycle and eutrophication, and its accumulation in soil can lead to high toxic effects on plants and animals. Furthermore, nitrites and nitrates are used as additives in food processing and as inhibitors of the growth of microorganisms, and their overexpression in the body can affect the transport of oxygen in the blood and generate methemoglobinemia, which is known to cause death (Beeckman et al., 2018; Zdolec et al., 2022). In this regard, electrochemical detection methods were used because they have high sensitivity and rapidity in detection. Electrochemical sensors based on carbon nanomaterials were developed for the sensitive and rapid determination of nitrite from soil solution samples extracted with low-volume suction lysimeters. The techniques used in this study were cyclic voltammetry (CV) and amperometry.

MATERIALS AND METHODS

The analyzed samples come from three mixtures made from soil contaminated with petroleum products bioremedied with sewage sludge (S: N v/v), in three different proportions S2:N1 (2:1 v/v), S1:N1 (1:1 v/v), and S1:N2 (1:2 v/v). The soil mixtures were introduced separately into pots and sown with turf. The analysis of the samples was carried out both from each bioremedied soil mixture and from each pot, two months after the development of the plants. The turf was sown on the last day of January 2024, during a period of the year when seed germination cannot occur under natural conditions. The pots were kept in the free atmosphere of the laboratory, at a temperature of approximately 22-24°C (Iorga et al., 2024).

SEM images were captured using TESCAN VEGA microscope (Brno, Czech Republic), from CC-ITI laboratory "Dunărea de Jos" University of Galati. Prior to imagistic evaluation, the organic samples were thin metal layered by means of pulverization method (SPI Supplies, West Chester, USA) (Iorga et al., 2024). The powdered and grass samples were dried, then fixed onto aluminium stub using double adhesive carbon tape, as described by Caprita et al. (2021). The low-vacuum pressure (60 Pa) and electron accelerating voltage of 10 kV allowed to identify many chemical elements as possible, at two different magnifications (260X and 1400X). SEM-EDX results were obtained on randomly selected areas from the surface, for major and trace elements quantification and spatially mapping. Electrochemical measurements were performed with a portable Potentiostat/Galvanostat from Metrohm Dropsens, and data recording was performed using the DropView8400 software. The sensors used in this study were commercial, screen-printed, carbon paste electrochemical sensors DRP-110 (SPE) from Metrohm Dropsense, which consisted of three electrodes, the working electrode made of carbon paste, the reference electrode made of Ag, and the auxiliary electrode made of graphite. Cyclic voltammetry measurements were performed in stationary solution, by sweeping the potential between -0.2 and 1.0 V, with a scan rate of 0.05 V/sec. Amperometric measurements were performed in stirred solution, all working potentials being referenced to the reference electrode made of Ag/AgCl. Amperometric detection of NO_2^- concentration in soil solutions was performed with the portable bipotentiostat, at different applied potentials, depending on the pH of the soil solution (Gurban et al., 2023).

Preparation of nanomaterial-modified sensors

To determine the NO_2^- concentration, the sensors were functionalized by depositing on the active surface of the SPE electrodes a volume ranging from 5 to 20 µL of the multi-walledcarbon nanotubes (MWCNTs) suspension made in a 0.5% low molecular weight Chitosan solution (CS, molecular weight =

50-190 kDa) in 2% acetic acid. The sensors obtained and labelled with MC/SPE were stored at room temperature, protected from light.

Measurements on real soil samples

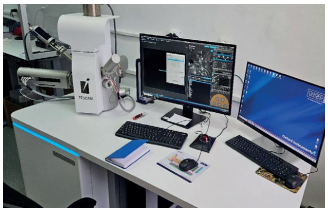
Small volume suction lysimeters from Hanna Instruments, 30 cm, were used to collect the soil solutions that were analyzed. Nitrite concentrations were determined by amperometric measurements using the nanomaterial-modified screen-printed sensors.

Electrochemical characterization of the sensors

Cyclic Voltammetry (CV) Studies were performed using the sensors obtained by MC/SPE (MWCNT-CS nanomaterial-based sensors) in a stationary solution of phosphate buffer electrolyte (PBS) 0.1 M, pH=7, in the absence and presence of 5 mM $NaNO_2$ (Figure 1). The potential was swept in a range between -0.2 V and 1.0 V vs. Ag/AgCl, with a scan rate of 0.05 V/sec, for a single scan cycle.



Sample metallization



SEM EDX analysis



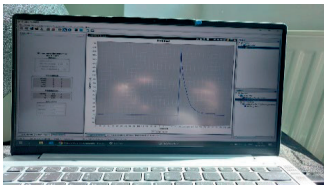
Electrochemical determination



Lysimeter extraction of uncultivated bioremedied soil solution



Lysimeter extraction of bioremedied soil solution cultivated with grass



Data recording

Figure 1. Soil sample analysis steps

The voltammograms were recorded using the MC/SPE sensor, and it was observed that the shape of the cyclic voltammograms for both the simple electrolyte and the 5 mM nitrite solution underwent changes (Figure 2).

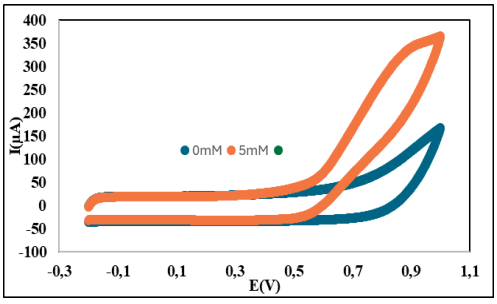


Figure 2. Influence of nitrite concentration on the oxidizing character

Cyclic voltammograms recorded at the surface of the sensor modified with MWCNTs, MC/SPE (PBS, 0.1 M, pH = 7): in the absence and in the presence of the analyte at different nitrite concentrations.

In the case of voltammograms recorded using the MC/SPE sensor, an increase in the intensity of the anodic current peak can be observed with the increase in nitrite concentration from 1 to 5 mM (Table 1).

Table 1. Influence of nitrite concentration on oxidation current and potential

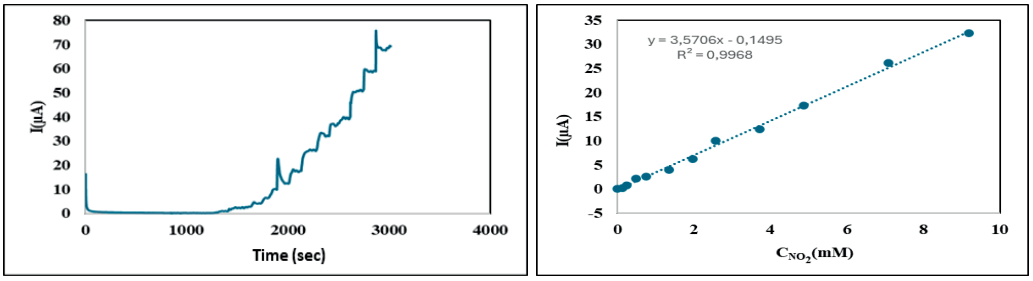
$[NO_2^-]$ (mM)	I (μA)	E (V)
0	-	-
1	145.682	0.832
2	198.581	0.904
5	292.962	0.890

The increase in the intensity of the anodic peak current with increasing nitrite concentration demonstrates the synergistic effect of multi-walled carbon nanotubes and chitosan. The

sensors based on MWCNTs-CS showed high electrocatalytic behavior for nitrite oxidation, the stability of the nanomaterial on the sensor surface being considerably improved by using the chitosan solution.
The potential value of 0.65 V was selected for performing amperometric studies of nitrite detection in order to ensure increased sensitivity and selectivity.

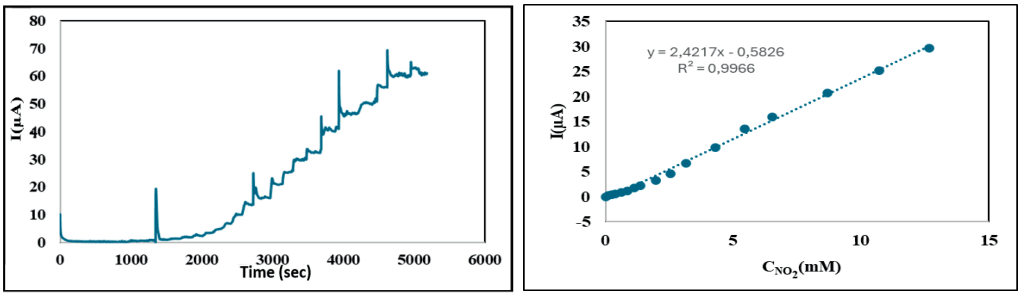
Amperometric determination of nitrite using MC/SPE-based sensors. Considering the previous CV studies, the working conditions for amperometric detection of nitrite were optimized by using MWCNT-CS/SPE sensors at an applied potential of 0.65 V, using PBS (pH of 7-7.5) (Figure 3A and Figure 4A). Sensor calibration was performed at room temperature in stirred 0.1 M phosphate buffer saline (PBS) electrolyte solution, pH 7 (Figure 3A) and pH 7.5 (Figure 4A), respectively, by applying a potential of 0.65 V vs Ag/AgCl and successively injecting increasing volumes of 0.1 M nitrite standard solution.

The analytical performances of the MWCNTs-CS sensors at different pH values were obtained from the calibration curves using linear regressions shown in Figure 3B (pH 7) and Figure 4B (pH 7.5), respectively. Table 2 shows the analytical parameters obtained from the calibration curves for nitrite detection.
After the development and electrochemical characterization of the sensors modified with MWCNTs, using the analytical parameters obtained from the calibration curves, they were further used to determine the nitrite content in solutions of bioremedied soils.
To collect the soil solutions, lysimeters were used that were introduced into the bioremedied soil before and after turf cultivation. The sensors were introduced into the soil solution in these lysimeters. The determination of the nitrite content was performed for each sample volume by interpolating the values of the currents recorded on the calibration curves for the used sensors, using the provided portable potentiostat



A B

Figure 3. Amperogram (A) and calibration curve (B) obtained in PBS support electrolyte solution, 0.1 M, pH 7, for nitrite detection using the MC/SPE sensor



A B

Figure 4. Amperogram (A) and calibration curve (B) obtained in PBS support electrolyte solution, 0.1 M, pH 7.5, for nitrite detection using the MC/SPE sensor

Table 2. Analytical performances of MWCNTs - Chitosan based sensors for nitrite determination

pH	Linear Domain (mM)	R^2	Sensitivity (μA/mM)	Specific sensitivity (μA/mM·cm^2)
7	0-9.194	0.996	3.570	28.42
7.5	0-12.664	0.996	2.421	19.275

RESULTS AND DISCUSSIONS

Morphological and chemical characterization

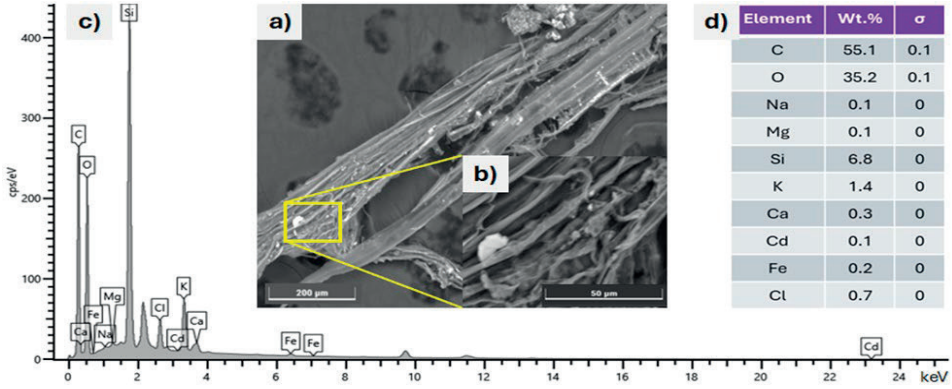
Microstructure, variability and distribution of chemical elements in plants which are developed under un-treated and treated soil systems were investigated by means of SEM-EDX combined method (Figures 5-7).

Morphological and elemental characteristics of control soil were presented by (Iorga, et al.2024). Therefore, the results from these two research papers will be corelated to validate them. The microstructure of root's lawn grass grew up from uncontaminated soil was imagistic explored at two scale bars – 200 μm (total view) and 50 μm (detail) (Figure 5a-b). Mineral compounds can be distinguished by varied shapes and gray shades, attached on the plant cellular tissue. The presence of natural elements was marked out by semi-quantitative and qualitative X-ray analysis (Figure 5c-d). Higher carbon content (55.1 wt.%) has a component derived from carbon tape, as fixation tool. The macro / micro-elements and nutrients identified from roots have very low concentrations compared to that from soil, as presented by Iorga et al. in 2024. This could be explained by the soil fertilization deficiency during these experiments, which can slow down the vegetal growing process and affect root evolution (the case of phosphorous). Figure 6a shows the mapping of macro / micro and trace of elements in the sewage sludge powder.

It is known that sewage sludge has high content in organic compounds and lower in nutrients. Usually, 2.39 wt.% of carbon in soil is comparable with the European average for the soil upper horizon (2.48 wt.%) (Salminen et al., 2005). However, higher C value of 11.03 wt.% in sludge is due to the presence of carbonates. Heavy metals were identified as minor elements in sludge, around 1 wt.%. The bioremediation effect of sewage sludge on vegetal layer is here discussed in terms of macro and micro-elements, and nutrients, respectively. SEM micrographs of underside plants developed in three soil-sludge systems are shown in Figure 7 a-c. After experimental soil remediation, a lot of necessary elements were identified in roots, with increasing concentration. So, we can remark the stimulating effect of sewage sludge, attributed to large amounts of nutrients (Mg, P, S, Na, Ca), as showed (Kominko et al., 2022). For example, P content increased from 0 wt.% (S1:N1 v/v) to 1.7 wt.% (S2:N1 v/v); Ca varied from 5.5 wt.% (S1:N1 v/v) to 9.9 wt.% (S2:N1 v/v); Fe is almost constant (2.16 wt.%). At the same time, some heavy elements (Al, Ni, Mn, Cu, Zr, Cr, Cd) from sludge (Figure 7b) are accumulated in roots. Aluminium is one of the toxic elements which has been found decreasing from 2.6 wt.% (S1:N1 v/v) to 1.9 wt.% (S2:N1 v/v) and the others are trace of element (< 0.5 wt.%). Thus, we can conclude that S2:N1 v/v mixture of soil and sewage sludge could be a promising solution for natural fertilizer of contaminated sites.

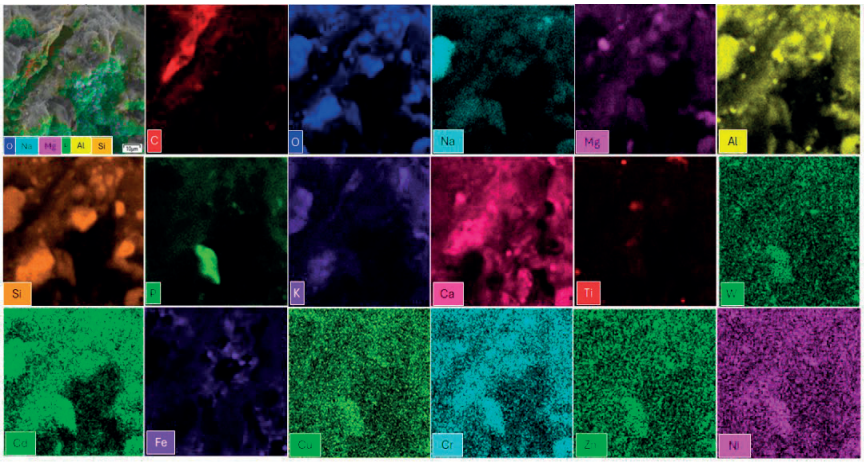
Amperometric detection of nitrite in real soil samples using MWCNTs/SPE sensors

MWCNTs/SPE sensors were used to detect nitrite content in different soil samples. Using lysimeters, a sufficient amount of soil solutions was extracted and transferred to new containers. The electrode was placed in a horizontal position and for amperometric detection, 200 μL of sample was taken and injected directly onto the sensor surface. The actual detection took place and the nitrite amounts in the samples were determined by interpolating the values of the currents recorded on the calibration curves obtained for the pH values 7, respectively 7.5 corresponding to the soil samples. Table 3 shows the results obtained from amperometric studies on soil samples. From the soil samples without plants analyzed, it is observed that at pH 7 in the S2:N1(v/v) mixture, the lowest nitrite concentration value was recorded (0.023 g/L).



Element	Wt.%	σ
C	55.1	0.1
O	35.2	0.1
Na	0.1	0
Mg	0.1	0
Si	6.8	0
K	1.4	0
Ca	0.3	0
Cd	0.1	0
Fe	0.2	0
Cl	0.7	0

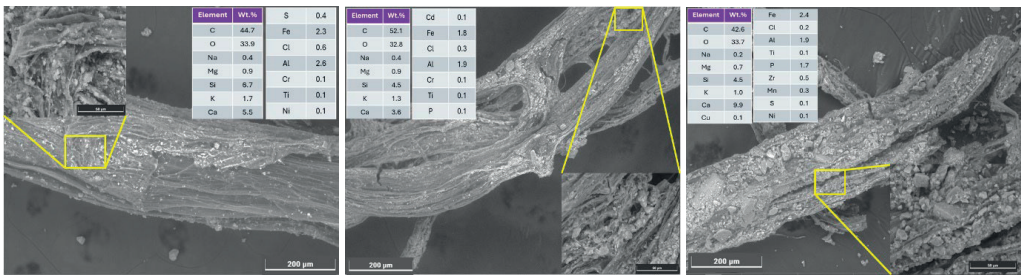
Figure 5. SEM images (a-b), X-ray spectrum (c) and semi-quantitative EDX results (d) of root's lawn grass, developed under uncontaminated soil conditions



Element	Wt.%
C	11.03
O	31.32
Na	5.35
Mg	2.98
Al	11.15
Si	16.03
P	3.47
K	1.83
Ca	9.08
Ti	0.51
W	1.05
Cd	1.59
Fe	1.49
Cu	0.3
Cr	1.31
Zn	1.31
Ni	1.29

a b

Figure 6. Elemental distribution map (a) and concentration (wt.%) (b) of sewage sludge sample, before soil mixing process



a) b) c)

Figure 7. Imagistic and chemical composition results of root's lawn grass tested in three soil-sewage sludge/plant systems: a) S1:N1; b) S1:N2; c) S2:N1

Table 3. Nitrite concentration determined from soil samples

Sample	pH	Soil without plants		pH	Soil with plants	
		mM	g/L		mM	g/L
S2-N1	7	0.491	0.023	7.5	0.471	0.022
S1-N1	7.5	0.532	0.024	7.5	0.491	0.023
S1-N2	7.5	0.880	0.040	7.5	0.749	0.034

In the mixtures where a slight increase in pH 7.5 was observed, an increase in nitrite concentration values was also observed as the amount of sludge increased from 0.024 g/L in S1:N1 (v/v) to 0.040 g/L in S1:N2 (v/v). At the time of determination, from the analysis of the results of the soil samples with plants, it is observed that at pH 7.5 of the S2:N1 mixture, the determined nitrite concentration is lower than in the initial S2:N1 mixture. For the other mixtures, the pH values did not change, remaining at 7.5, but the nitrite concentration values decreased from 0.024 g/L in S1:N1 without plants to 0.023 g/L in the S1:N1 sample with plants, respectively from 0.040 g/L (S1:N2 without plants) to 0.034 g/L (S1:N2 with plants). The results are predictable, as it is known that some nitrites are absorbed by plant roots. Considering the pH variation in the analyzed samples, a determination over time was carried out on samples of mixtures cultivated with turf, for a period of 32 days, the results being presented in the following Table 4. Sample S1-N1 had a relatively constant pH of 7.5, except for a decrease to pH 7 after 7 days. Sample S1-N2 showed a small decrease in pH from 7.5 to 7 after one week and then increased to 7.5 after 19 days, remained at 7.5 after 29 days and increased slightly to pH 8 on day 32. Sample S2-N1 showed pH variations between 7 and 7.5 over the course of 29 days, then increased to pH 8 after 32 days. Electrochemical determinations were performed as a function of pH.

Table 4. pH values recorded over time for the analysed soil samples

Time period between tests (days)	pH		
	S1-N1	S1-N2	S2-N1
0	7.5	7.5	7
7	7	7	7.5
19	7.5	7.5	7
29	7.5	7.5	7.5
32	7.5	8	8

CONCLUSIONS

The use of sewage sludge for remediating petroleum-contaminated sites and regeneration of vegetation was studied. The stimulating effect of the sewage sludge on plant growth is attributed to the presence of a large amounts of nutrients in the sludge which is confirmed by SEM-EDX analysis. Electrochemical sensors modified with MWCNTs-CS nanomaterials were used for the amperometric detection of nitrite in real soil samples collected using lysimeters, showing a decrease of nitrite concentrations due to plant growth and thus, a bioremediation effect.

ACKNOWLEDGEMENTS

The support was provided by the Ministry of Research, Innovation, and Digitization through Core Program PN 23.06.01.01.

REFERENCES

Beeckman, F., Motte, H., & Beeckman, T. (2018). Nitrification in agricultural soils: impact, actors and mitigation. *Current Opinion in Biotechnology*, *50*, 66–173.

Caprita, A., Ene, A., & Cantaragiu Ceoromila A. (2021). Valorification of ulva rigida algae in pulp and paper industry for improved paper characteristics and wastewater heavy metal filtration. *Sustainability, 13*(19), 10763.

Gurban, A.M., Zamfir, L.G., Epure, P., Şuică-Bunghez, I.R., Senin, R.M., Jecu, M.L., Jinga, M.L., & Doni M. (2023). Flexible Miniaturized Electrochemical Sensors Based on Multiwalled Carbon Nanotube-Chitosan Nanomaterial for Determination of Nitrite in Soil Solutions. *Chemosensors, 11*(224).

Iorga, C.M., Ţopa, C.M., Ghisman, G, Ceoromila Cantaragiu, A., & Stancu, M.M. (2024). Vegetal layer restoration of contaminated sites from petroleum industry using sewage sludge. *Annals of "Dunărea de Jos" University of Galaţi, mathematics, physics, theoretical mechanics, fascicle II, year XVI (XLVII)*, (1), 17–23.

Iorga, C.M., Georgescu, L.P., Ungureanu, C., Stancu, & M.M. (2025). Sustainable remediation of polluted soils from the oil industry using sludge from municipal wastewater treatment plants. *Processes, 13*, 245.

Kominko, H., Gorazda, K., & Wzorek, Z. (2022). Effect of sewage sludge-based fertilizers on biomass growth and heavy metal accumulation in plants. *Journal of Environmental Management*, *305*, 114417.

Salminen, R., Reeder, S., De Vivo, B., Demetriades, A., Pirc, S., Batista, M.J., Marsina, K., Ottesen, R.T., O'Connor, P.J., Bidovec, M., Lima, A., Siewers, U., Smith, B., Taylor, H., Shaw, R., Salpeteur, I., Gregorauskiene, V., Halamic, J., Slaninka, I., Lax, K., Gravesen, P., Birke, M., Breward, N., Ander, E.L., Jordan, G., Duris, M., Klein, P., Locutura, J., Bel-lan, A., Pasieczna, A., Lis, J., Mazreku, A., Gilucis, A., Heitzmann, P., Klaver, G., & Petersell, V *FOREGS Geochemical Atlas of Europe, Part 1: Background Information, Methodology and Maps*. Available from: https://www.researchgate.net/publication/259290724_FOREGS_Geochemical_Atlas_of_Europe_Part_1_Background_Information_Methodology_and_Maps#fullTextFileContent [accessed Mar 24, 2025].

Zdolec N., Bogdanović T., Severin K., Dobranić V., Kazazić S., Grbavac J., Pleadin J., Petričević S., Kiš M. (2022). Biogenic amine content in retailed cheese varieties produced with commercial bacterial or mold cultures, *Processes*, *10*(1), 10

Scientific Papers. Series E. Land Reclamation, Earth Observation & Surveying, Environmental Engineering. Vol. XIV, 2025
Print ISSN 2285-6064, CD-ROM ISSN 2285-6072, Online ISSN 2393-5138, ISSN-L 2285-6064

ASSESSMENT OF IRON, COPPER, AND ZINC IN THE MUSCLE OF PONTIC SHAD: INFLUENCE OF YEAR, WEIGHT, AND LENGTH

Nina-Nicoleta LAZĂR[1], Mădălina CĂLMUC[1], Ira-Adeline SIMIONOV[1, 3], Maxim ARSENI[1, 2], Mihaela TIMOFTI[1, 2], Puiu-Lucian GEORGESCU[1, 2], Cătălina ITICESCU[1, 2], Violeta DOMNITEANU[4]

[1]"Dunărea de Jos" University of Galați, REXDAN Research Centre,
98 George Coșbuc Street, 800223, Galați, Romania
[2]"Dunărea de Jos" University of Galați, Faculty of Sciences and Environment,
111 Domnească Street, 800201, Galați, Romania
[3]"Dunărea de Jos" University of Galați, Faculty of Food Science and Engineering,
111 Domnească Street, 800201, Galați, Romania
[4]Software Republic S.R.L., Șivita Village, Tulucești Commune,
4 Trandafirilor Street, 800204, Galați, Romania

Corresponding author email: nina.condurache@ugal.ro

Abstract

This study aimed to analyze the concentrations of iron (Fe), copper (Cu), and zinc (Zn) in pontic shad (Alosa immaculata) and assess the influence of factors such as capture year, length, and weight on these concentrations. Fish samples were collected during the 2023 and 2024 fishing seasons. After recording the length and weight of each specimen, the muscle underwent acidic digestion. The concentrations of Fe, Cu, and Zn were then determined using a Total Reflection X-ray Fluorescence (TXRF) spectrometer. The results revealed an overall increase in chemical elements concentrations from 2023 to 2024. While Cu levels showed no correlation with length or weight, Fe and Zn exhibited strong correlations with these parameters.

Key words*: Alosa immaculata, chemical elements, correlation, Total Reflection X-ray Fluorescence (TXRF).*

INTRODUCTION

Fish size may influence the concentration of some important metals in its tissues. But does this association apply to all chemical elements? Copper (Cu), zinc (Zn) and iron (Fe) are chemical elements that are vital to all living species, including fish, and play important roles in cellular metabolic processes. However, high concentrations of these substances may produce more harm than benefits (Simionov et al., 2023; Dinu (Iacob) et al., 2024). For instance, redox activity of Cu and Fe can produce harmful free radicals that can react with biomolecules including lipids, proteins, and DNA. The oxidation of these compounds can cause cellular damage, damage normal biological functioning, and contribute to the development of a variety of disorders (Bury, 2003; Kozlowski et al., 2009; Wang et al., 2024). In fish, these compounds can enter the body in two main ways: through the intestines from food or through the gills from the water (Bury, 2003). According to Kumar et al. (2024), many factors impact the concentrations of Fe, Cu, and Zn in fish, including age, size, sex, swimming behavior, the environment, and eating behaviors. Since larger fish generally have more body mass and muscle tissue, they tend to have higher concentrations of certain chemical elements compared to smaller fish, although the concentration per unit of muscle may be lower than in smaller fish. Additionally, larger fish are often older and may have accumulated more chemical elements due to longer exposure to their environment, particularly if those metals are present in the water, sediment, or food (Jezierska & Witeska, 2006; Łuczyńska & Tonska, 2006; Has-Schön et al., 2015; Balzani et al., 2022).

Alosa immaculata (Bennett, 1835), commonly referred to as the pontic shad, is a marine teleost fish native to the Black Sea. It belongs to the *Clupeidae* family, along with the herrings, sardines and sprats. As an anadromous

migratory species, it inhabits the sea but migrates to coastal lakes and lower sections of rivers (such as the Danube, Dniester, and Prut) to spawn in the springtime. It is predominantly a predator and a secondary macrophage that feeds solely in saltwater habitats, consuming small fish and crustaceans. It does not feed in freshwater (https://fish-commercial-names.ec.europa.eu/; https://fishbase.se/).

In Romania, the Pontic shad is an economically valuable fish species, with its population in decline (Milea et al., 2023). For this reason, the Pontic shad has been added to the IUCN Red List of Threatened Species (Lazăr et al., 2024).

In the scientific literature there are several studies on the presence of heavy metals in the transition zone of the Pontic shad, the presence of these heavy metals being characteristic of the Lower Danube area (Burada et al., 2015).

Considering that the Pontic shad is not a fish species as extensively studied as others, yet it holds significant importance for Romanian traditions, customs, gastronomy, and economy, the aim of this study was:

- The use of the TXRF method for precise determination of the Fe, Cu, and Zn.
- The analysis of Fe, Cu, and Zn content in *Alosa immaculata* captured in 2023 and 2024.
- The preliminary investigation of the correlations between fish length, weight, and the concentrations of these metals.

MATERIALS AND METHODS

Chemicals and reagents

The following reagents were used: Gallium (Ga) standard solution purchased from SCP Science (Canada); polyvinyl alcohol (PVA), Suprapur nitric acid 65% (HNO_3), and perhydrol 30% (H_2O_2) purchased from Sigma-Aldrich (Germany), and silicone solution in isopropanol purchased from Serva Electrophoresis GmbH (Germany).

Sample preparation

Three Pontic shad specimens were collected during each fishing season (April-May) in 2023 and 2024, utilizing traditional methods associated with commercial fishing in the Lower Danube Basin. Following capture, they were transported to the REXDAN Research Infrastructure, at the "Dunărea de Jos" University of Galați, Romania. After having measured the total length and weight, the fish were washed with ultrapure water, dissected, and muscle tissue samples were taken for analysis. Each muscle sample was subsequently digested using a microwave digestion procedure, as described by Simionov et al. (2023), with a mixture of 65% HNO_3 and 30% H_2O_2 in a 9:1 ratio. Following digestion, the samples were diluted to 50 mL with ultrapure type I water and stored in Falcon tubes for further analysis using TXRF (Figure 1).

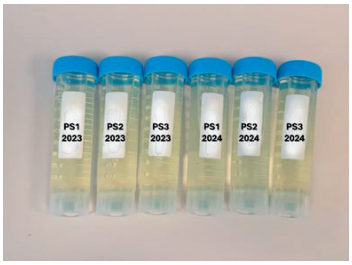


Figure 1. Digested samples of pontic shad

TXRF analysis

The sample preparation process included mixing the digested samples with a 0.3 g/L PVA solution at a 10:1 ratio and incorporating an internal standard. In our study, gallium (Ga) was used as the internal standard at concentrations ranging from 50 to 100 µg/L, depending on the sample matrix. Subsequently, 10 µL of each prepared sample was transferred onto a siliconized quartz carrier and dried on a hot plate at 50°C for 5 min. Measurements were conducted in triplicate for 1000 sec per sample, using a Bruker S4 T-Star spectrometer (Bruker AXS Microanalysis GmbH, Billerica, MA, USA) illustrated in Figure 2. The results were reported as the mean ± standard deviation of the triplicates. The elemental concentrations in the samples were calculated using the following equation:

$$Ci = CIS \cdot Ni \cdot SIS/NIS \cdot Si$$

where:

- Ci represents the element concentration;
- CIS is the Ga concentration;
- Ni is the element net count rate;
- NIS is the Ga net count rate,
- Si is the element sensitivity factor;
- SIS is the Ga sensitivity factor.

Before measurements, the equipment was calibrated as described by Lazăr et al. (2025).

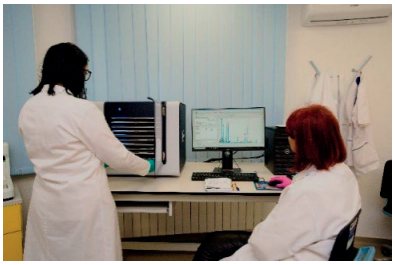


Figure 2. Sample analyzis using Bruker S4 T-Star spectrometer at REXDAN Research Infrastructure

Statistical Analysis

The data were analyzed using descriptive statistics (mean and standard deviation), inferential statistics (ANOVA), and exploratory and relational analysis (correlation matrices), employing Minitab 17 software and Microsoft Excel.

RESULTS AND DISCUSSIONS

Understanding fish weight, length, and metals' concentrations offers essential information for managing fish populations, protecting human health, and ensuring environmental sustainability. These factors contribute to the responsible use of fishery resources while protecting aquatic ecosystems and public health. Table 1 shows the length and weight ranges of the pontic shad specimens captured and analysed in our study. The lengths of the fish from 2023 ranged between 26.70 cm and 32.40 cm, while for those of 2024 varied between 27.90 cm and 31.60 cm. The weight of the fish captured in 2023 varied from 144.10 g to 206.17 g, while for the specimens from 2024 varied between 200.58 g and 273.21 g, with a mean weight of 226.76 ± 40.33 g. Stroe et al. (2024) reported a mean weight of 223.5 ± 44.95 g and a mean length of 29.53 ± 1.79 cm for the Pontic shad specimens captured during March-June 2023 between 169-197 river km along the Danube.

In our study, it can be noted that the Pontic shad specimens captured in 2024 were larger in terms of weight compared to the specimens captured in 2023, which may suggest a possible greater food availability or favorable environmental factors.

Table 1. Biometric data of the analyzed pontic shad specimens

Fish specimen	Length (cm)	Weight (g)
PS 1 (2023)	29.30	206.17
PS 2 (2023)	32.40	179.42
PS 3 (2023)	26.70	144.10
PS 1 (2024)	27.90	206.50
PS 2 (2024)	28.70	200.58
PS 3 (2024)	31.60	273.21

Figure 3 illustrates the average metal concentrations in the muscle tissue of pontic shad, along with their standard deviations. The highest Fe concentration was observed in PS1 captured in 2024. The highest Cu concentrations were identified in PS2 from 2024. The highest Zn concentration was observed in PS3 from 2024.

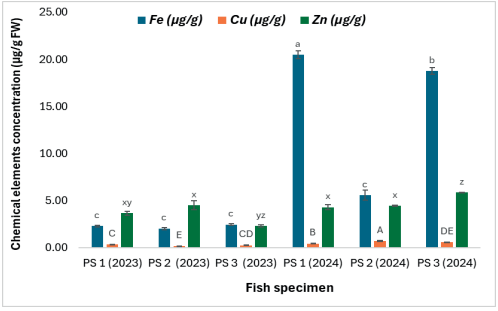


Figure 3. Concentration of Fe, Cu, and Zn in pontic shad. Statistical differences in Fe concentrations are indicated by lowercase letters (a-c), in Cu by uppercase letters (A-E), and in Zn concentrations by lowercase letters (x-z). Values that share the same letter are not significantly different ($p > 0.05$)

Numerous studies have analyzed heavy metal concentrations in fish from the Danube River, yet few have focused on the pontic shad. Stancheva et al. (2014) reported Fe concentrations of 9.00 ± 1.00 µg/g wet weight in pontic shad from the Bulgarian coast of the Black Sea, captured in 2010. Jitar et al. (2015) documented Cu concentrations ranging from 0.73 to 2.10 µg/g wet weight and Zn concentrations between 2.22 and 4.12 µg/g wet weight in specimens collected along the Romanian coastline of the Black Sea, between 2011 and 2012. Makedonski et al. (2017) identified Cu concentrations of 0.45 ± 0.03 µg/g wet weight and Zn concentrations of 9.00 ± 1.00 µg/g wet weight in Pontic shad from the Bulgarian coast, also from 2010. Bat et al.

(2018) reported a Cu concentration of 2.25 ± 0.81 µg/g wet weight in the muscle tissue of Pontic shad fished from Turkish waters of the Black Sea in 2016. More recently, Simionov et al. (2021) reported Cu concentrations of 0.40 ± 0.10 µg/g wet weight in Pontic shad from both the Black Sea and the Danube River. They also recorded Zn concentrations of 4.00 ± 0.40 µg/g wet weight in specimens from the Black Sea and 3.60 ± 0.30 µg/g wet weight from the Danube River. Additionally, Fe concentrations were reported at 10.50 ± 1.60 µg/g wet weight in Pontic shad from the Black Sea, and 6.00 ± 1.00 µg/g wet weight from the Danube River.

Comparing our results with previous studies on metals' accumulation in pontic shad highlights both similarities and differences across various geographic areas and years, providing insight into potential environmental and ecological influences.

Furthermore, beyond concentration levels, it is also crucial to explore how these metals relate to the biometric characteristics of the specimens. Figures 4 and 5 present the correlation between the concentrations of metals identified in the muscle of the pontic shad fished in 2023 and 2024, and their biometric data. In the case of the specimens from 2023, both negative and positive correlations can be observed. For instance, between Fe and Zn, a strong negative correlation can be observed with a value of -0.96. Fe also showed a strong negative correlation with a value of -0.99 with the length, and a moderate negative correlation with the weight of the fish. Zn has a strong positive correlation with the length (0.98) and moderate positive correlation with the weight (0.67). Cu has a moderate positive correlation with Fe (0.69), suggesting that these metals may be regulated similarly in the body. Cu also showed a negative correlation with length (-0.62), indicating a possible dilution of copper in larger fish. Weight and length are somewhat positively correlated, with a value of 0.52, suggesting allometric growth (not necessarily proportional between length and weight).

In the case of the pontic shad caught in 2024, a strong negative correlation between Fe and Cu (-0.85) was also observed. Fe showed a low correlation with the length and Zn concentration, but a high correlation with weight.

	Fe (µg/g)	Cu (µg/g)	Zn (µg/g)	L (cm)	G (g)
Fe (µg/g)	1				
Cu (µg/g)	0.691987871	1			
Zn (µg/g)	-0.963653642	-0.473975182	1		
L (cm)	-0.996288626	-0.62728103	0.983073	1	
G (g)	-0.449639507	0.33367145	0.671922	0.524854	1

Figure 4. Correlation matrix of Fe, Cu, Zn, and biometric data of the pontic shad from 2023. Green color - highest value; yellow color - average value; red color - lowest value

	Fe (µg/g)	Cu (µg/g)	Zn (µg/g)	L (cm)	G (g)
Fe (µg/g)	1				
Cu (µg/g)	-0.847525735	1			
Zn (µg/g)	0.333034566	0.218200625	1		
L (cm)	0.207227518	0.343602444	0.99146	1	
G (g)	0.469863086	0.070296626	0.988828	0.960946	1

Figure 5. Correlation matrix of Fe, Cu, Zn, and biometric data of the pontic shad from 2024. Green color - highest value; yellow color - average value; red color - lowest value

Zn had very strong correlations with the length (0.99) and weight (0.99). In addition, the length (L) and weight (G) had a very strong correlation (0.96). This fact confirms that as fish grow in length, they also increase in weight, but not necessarily in a linear manner (possible allometric growth as already stated by other authors).

In our study, Fe and Cu had an antagonistic relationship in both data sets, with strong negative correlations. This suggests a biological competition between the two metals, either at the level of absorption or in the tissue distribution of the fish. On the other hand, Zn was strongly correlated with length and weight in both cases indicating that Zn is an essential element for fish growth, as it is involved in the metabolic and structural processes of the fish. In correlation with weight and length, fish growth does not seem to be directly proportional to the accumulation of Fe, Zn, Cu. In a similar study, a positive correlation between Zn content and biometric data of pike and negative correlation between Zn and weight and length of perch was reported (Łuczyńska & Tonska, 2006). Positive correlations between the Cu and Zn concentrations and the length of fish were reported in various species of fish from Yangtze River in China (Yi & Zhangm, 2012). Contrary to our study, other authors observed a negative correlation between Cu concentrations and fish length and weight (Balzani et al., 2022; Kaçar, 2022). Furthermore, a positive correlation

between Fe and the length of *S. glaris* captured in Arno river in Italy was reported (Balzani et al., 2022).

To address the initial question raised at the beginning of the manuscript, fish size and weight can affect the bioaccumulation of certain elements, while having no impact on others. As previously stated, the concentration of metals in fish is influenced by multiple factors, such as age, size, sex, swimming behaviour, the environment, and feeding habits. Therefore, a more in-depth study is necessary to fully understand the process of bioaccumulation in fish.

CONCLUSIONS

Our research highlighted variations in Fe, Cu, and Zn concentrations among Pontic shad specimens. Zn was positively associated with fish growth, while Fe and Cu showed an inverse relationship, suggesting that the metal metabolism and absorption in fish are complex and primarily influenced by interactions between metals rather than by size. These findings contribute to sustainable fisheries management, ensuring both environmental protection and public health. However, further research is needed to fully understand bioaccumulation mechanisms and their potential effects on fish health and human consumption. Studies on biota can be associated with studies on the quality of surface aquatic ecosystems that include the determination of the presence of heavy metals, studies that use statistical methods of integration of major pollutants with an impact on biodiversity (Popa et al., 2018).

For future research, we aim to address Lower Danube areas located in the cross-border area of Romania, Ukraine and the Republic of Moldova, where, due to various anthropogenic factors, the presence of certain pollutants in surface waters has an important impact on the ichthyofauna (Iticescu et al., 2016).

ACKNOWLEDGEMENTS

This research is part of the project *"Innovative sediment management framework for a SUstainNable DANube black Sea system (SUNDANSE)",* co-funded by the European Union. Views and opinions expressed are however those of the author(s) only and do not necessarily reflect those of the European Union or the European Climate, Infrastructure and Environment Executive Agency. Neither the European Union nor the granting authority can be held responsible for them.

REFERENCES

Alosa immaculata (n.d.). Retrieved February 11, 2025, from https://fish-commercial-names.ec.europa.eu/fish-names/species/alosa-immaculata_ro

Alosa immaculata summary page (n.d.). *FishBase*. Retrieved February 11, 2025, from https://www.fishbase.us/summary/Alosa-immaculata.html

Balzani, P., Kouba, A., Tricarico, E., Kourantidou, M., & Haubrock, P. J. (2022). Metal accumulation in relation to size and body condition in an all-alien species community. *Environmental Science and Pollution Research, 29*(17), 25848–25857. https://doi.org/10.1007/s11356-021-17621-0

Bat, L., Öztekin, A., & Şahin, F. (2018). Trace metals amounts and health risk assessment of *Alosa immaculata* Bennett, 1835 in the Southern Black Sea. *Discovery Science, 14*, 109-116

Burada, A., Topa, C. M., Georgescu, L. P., Teodorof, L., Nastase, C., Seceleanu-Odor, D., & Iticescu, C. (2015). Heavy metals environment accumulation in Somova-Parcheş aquatic complex from the Danube Delta area. *Revista de Chimie, 1*.

Bury, N. (2003). Iron acquisition by teleost fish. *Comparative Biochemistry and Physiology Part C: Toxicology & Pharmacology, 135*(2), 97–105. https://doi.org/10.1016/S1532-0456(03)00021-8

Dinu (Iacob), A., Bounegru, A.V., Iticescu, C., Georgescu, L.P., & Apetrei, C. (2024). Electrochemical detection of Cd^{2+}, Pb^{2+}, Cu^{2+} and Hg^{2+} with sensors based on carbonaceous nanomaterials and Fe_3O_4 nanoparticles. *Nanomaterials, 14*(8), Article 8. https://doi.org/10.3390/nano14080702

Has-Schön, E., Bogut, I., Vuković, R., Galović, D., Bogut, A., & Horvatić, J. (2015). Distribution and age-related bioaccumulation of lead (Pb), mercury (Hg), cadmium (Cd), and arsenic (As) in tissues of common carp (*Cyprinus carpio*) and European catfish (*Silurus glanis*) from the Buško Blato reservoir (Bosnia and Herzegovina). *Chemosphere, 135*, 289–296. https://doi.org/10.1016/j.chemosphere.2015.04.015

Iticescu, C., Murariu, G., Georgescu, L. P., Burada, A., & Topa, C. M. (2016). Seasonal variation of the physico-chemical parameters and water quality index (WQI) of Danube water in the transborder Lower Danube area. *Revista de Chimie, 67*(9). https://revistadechimie.ro/Articles.asp?ID=5199.

Jezierska, B., & Witeska, M. (2006). The metal uptake and accumulation in fish living in polluted waters. In I. Twardowska, H. E. Allen, M. M. Häggblom, & S. Stefaniak (Eds.), *Soil and water pollution monitoring, protection and remediation* (pp. 107–114). Springer Netherlands. https://doi.org/10.1007/978-1-4020-4728-2_6

Jitar, O., Teodosiu, C., Oros, A., Plavan, G., & Nicoara, M. (2015). Bioaccumulation of heavy metals in marine organisms from the Romanian sector of the Black Sea. *New Biotechnology, 32*(3), 369–378. https://doi.org/10.1016/j.nbt.2014.11.004

Kaçar, E. (2022). Relationship of concentrations of some heavy metals with fish size in muscle tissue of *Carassius gibelio* (Bloch, 1782) from the Tigris River (Turkey). *Erzincan Üniversitesi Fen Bilimleri Enstitüsü Dergisi, 15*(2), 475–481. https://doi.org/10.18185/erzifbed.959413

Kozlowski, H., Janicka-Klos, A., Brasun, J., Gaggelli, E., Valensin, D., & Valensin, G. (2009). Copper, iron, and zinc ions homeostasis and their role in neurodegenerative disorders (metal uptake, transport, distribution and regulation). *Coordination Chemistry Reviews, 253*(21), 2665–2685. https://doi.org/10.1016/j.ccr.2009.05.011

Kumar, M., Singh, S., Jain, A., Yadav, S., Dubey, A., & Trivedi, S. P. (2024). A review on heavy metal-induced toxicity in fishes: Bioaccumulation, antioxidant defense system, histopathological manifestations, and transcriptional profiling of genes. *Journal of Trace Elements in Medicine and Biology, 83*, 127377. https://doi.org/10.1016/ j.jtemb.2023. 127377

Lazăr, N.N., Simionov, I.A., Petrea, Șt.-M., Iticescu, C., Georgescu, P.L., Dima, F., & Antache, A. (2024). The influence of climate changes on heavy metals accumulation in *Alosa immaculata* from the Danube River Basin. *Marine Pollution Bulletin, 200*, 116145. https://doi.org/10.1016/j.marpolbul.2024.116145

Lazăr, N.N., Simionov, I.A., Călmuc, M., Călmuc, V.A., Iticescu, C., Georgescu, P.L., Timofti, M., & Drăgan, S. (2025). Cross-regional elemental comparison of mussels using total reflection X-ray fluorescence (TXRF). *Molecules, 30*(2), Article 2. https://doi.org/10.3390/molecules30020283

Łuczyńska, J., & Tonska, E. (2006). The effect of fish size on the content of zinc, iron, copper, and manganese in the muscles of perch (*Perca fluviatilis* L.) and pike (*Esox lucisus* L.). *Archives of Polish Fisheries, 14*, 5–13.

Makedonski, L., Peycheva, K., & Stancheva, M. (2017). Determination of heavy metals in selected Black Sea fish species. *Food Control, 72*, 313–318. https://doi.org/10.1016/j.foodcont.2015.08.024

Milea, Ștefania-A., Lazăr, N.N., Simionov, I.A., Petrea, Ștefan-M., Călmuc, M., Călmuc, V., Georgescu, P.L., & Iticescu, C. (2023). Effects of cooking methods and co-ingested foods on mercury bioaccessibility in pontic shad (*Alosa immaculata*). *Current Research in Food Science, 7*, 100599. https://doi.org/10.1016/j.crfs.2023.100599

Popa, P., Murariu, G., Timofti, M., & Georgescu, L.P. (2018). Multivariate statistical analyses of Danube River water quality at Galati, Romania. *Environmental Engineering and Management Journal, 17*(5), 1249–1266. https://doi.org/10.30638/eemj.2018.124

Simionov, I.A., Cristea, D.S., Petrea, S.M., Mogodan, A., Nicoara, M., Plavan, G., Baltag, E.S., Jijie, R., & Strungaru, S.A. (2021). Preliminary investigation of lower Danube pollution caused by potentially toxic metals. *Chemosphere, 264*, 128496. https://doi.org/10.1016/j.chemosphere.2020.128496

Simionov, I.-A., Călmuc, M., Iticescu, C., Călmuc, V., Georgescu, P.-L., Faggio, C., & Petrea, Șt.-M. (2023). Human health risk assessment of potentially toxic elements and microplastics accumulation in products from the Danube River Basin fish market. *Environmental Toxicology and Pharmacology, 104*, 104307. https://doi.org/10.1016/j.etap.2023.104307

Stancheva, M., Makedonski, L., & Peycheva, K. (2014). Determination of heavy metal concentrations of most consumed fish species from Bulgarian Black Sea coast.

Stroe, D.M., Cretu, M., Tenciu, M., Dima, F.M., Patriche, N., Tiganov, G., & Dediu, L. (2024). Age, growth, and mortality of pontic shad, *Alosa immaculata* Bennett, 1835, in the Danube River, Romania. *Fishes, 9*(4), Article 4. https://doi.org/10.3390/fishes9040128

Wang, L., Wang, H., Gao, C., Wang, C., Yan, Y., & Zhou, F. (2024). Dietary copper for fish: Homeostasis, nutritional functions, toxicity, and affecting factors. *Aquaculture, 587*, 740875. https://doi.org/10.1016/j.aquaculture.2024.740875

Yi, Y. J., & Zhang, S. H. (2012). The relationships between fish heavy metal concentrations and fish size in the upper and middle reach of Yangtze River. *Procedia Environmental Sciences, 13*, 1699–1707. https://doi.org/10.1016/j.proenv.2012.01.163

Scientific Papers. Series E. Land Reclamation, Earth Observation & Surveying, Environmental Engineering. Vol. XIV, 2025
Print ISSN 2285-6064, CD-ROM ISSN 2285-6072, Online ISSN 2393-5138, ISSN-L 2285-6064

SUSTAINABLE GEOPOLYMER BINDERS: MECHANICAL AND DURABILITY INSIGHTS INTO FLY ASH-BASED COMPOSITES

Adrian-Victor LAZARESCU, Brăduț-Alexandru IONESCU, Mihail CHIRA, Tudor-Panfil TOADER, Alexandra CSAPAI, Andreea HEGYI, Carmen-Teodora FLOREAN

National Institute for Research and Development in Construction, Urban Planning and Sustainable Spatial Development - URBAN-INCERC, 266 Pantelimon Road, District 2, Bucharest, Romania

Corresponding author email: alexandra.csapai@incerc-cluj.ro

Abstract

Geopolymers can be regarded as a type of sustainable and green building material, with the potential to significantly reduce carbon emissions when compared with conventional alternatives. The present study analyses the performance of geopolymeric binder-based composites that have been obtained by means of alkaline activation of fly ash, which is an abundant industrial waste. The present research is centred upon the evaluation of mechanical properties, such as compressive strength and flexural strength, as main characteristics of their durability. A further objective of the project was to investigate the influences of various factors on the final properties of the material. The experimental findings suggest that the optimised mixture displays enhanced performance with regard to durability and sustainability. This suggests that the material has considerable potential for use in a variety of construction applications. The study provides detailed insight into the potential of this innovative material, which contributes to the development of environmentally friendly construction technologies.

Key words*: alkaline activator, Circular Economy, fly ash, geopolymer binder.*

INTRODUCTION

The increasing environmental concerns surrounding the excessive use of Portland cement (PC) in construction have led researchers to explore alternative, sustainable binders with lower carbon footprints (Provis & Bernal, 2014; Davidovits, 2015). The utilisation of geopolymer binders as a substitute for conventional materials has been identified as a potential solution for mitigating climate change, with their capacity to incorporate industrial by-products such as fly ash, blast furnace slag and metakaolin, leading to a substantial reduction in carbon dioxide (CO_2) emissions (Duxson et al., 2007; Zhang et al., 2009). Of particular interest are fly ash-based geopolymers, which have proven to be a subject of considerable interest due to their widespread availability and favourable mechanical and durability characteristics (Temuujin et al., 2009; Heah et al., 2011). It is estimated that Protland cement production is responsible for approximately 8% of global CO_2 emissions. This is primarily attributable to the limestone calcination process and the significant amount of energy consumption inherent in manufacturing processes (Gartner & Hirao, 2015; Andrew, 2018). In contrast, the synthesis of geopolymeric binders entails the alkaline activation of aluminosilicate-rich precursors, resulting in the formation of a three-dimensional amorphous network, which exhibits enhanced mechanical and chemical properties (Xu & van Deventer, 2000; Chindaprasirt et al., 2007). The use of fly ash, a by-product of coal combustion, further enhances sustainability by diverting waste materials from landfills while reducing the demand for virgin resources (Van Riessen et al., 2013; Abhishek et al., 2020).

Geopolymerization is a chemical process involving the dissolution of aluminosilicate precursors in an alkaline medium, followed by the formation of oligomers that subsequently condense into a rigid network (Phair & van Deventer, 2001; Fernández-Jiménez et al., 2005). The reaction kinetics and final properties of geopolymer composites are influenced by factors such as the precursor composition, activator type and concentration, curing temperature, and water-to-solid ratio

(Provis & van Deventer, 2009; Zhang et al., 2009). The amorphous to semi-crystalline nature of geopolymer binders provides excellent mechanical strength, chemical resistance, and long-term durability (Kumar et al., 2010; Fernández-Jiménez et al., 2019). Fly ash-based geopolymer composites exhibit high compressive strength, reaching up to 80 MPa depending on the synthesis conditions (Sathonsaowaphak et al., 2009; Ryu et al., 2013). Their mechanical performance is attributed to the compact microstructure and strong bonding within the aluminosilicate gel matrix (Lloyd & Rangan, 2010; Sukmak et al., 2013). In addition, geopolymer composites demonstrate enhanced flexural and tensile strength compared to PC-based counterparts due to their dense microstructure and reduced porosity (Lee & van Deventer, 2004; Deb et al., 2014).

Durability is a critical parameter for assessing the long-term performance of construction materials. Fly ash-based geopolymers exhibit superior resistance to sulfate attack, acid corrosion, and freeze-thaw cycles compared to conventional cementitious materials (Bakharev, 2005; Olivia & van Riessen, 2011). The low calcium content and dense matrix of geopolymers hinder the formation of expansive ettringite, thus mitigating degradation due to sulfate exposure (Lloyd et al., 2012; Ismail et al., 2013). Additionally, their reduced permeability and high resistance to chloride penetration make them suitable for marine and aggressive environments (Pan et al., 2012; Pasupathy et al., 2021).

The integration of geopolymer binders into the circular economy framework is crucial for achieving sustainable construction practices. Circular economy principles emphasize the reduction, reuse, and recycling of materials to minimize environmental impact and resource depletion (Ghisellini et al., 2016; Kirchherr et al., 2017). Fly ash-based geopolymers align with this concept by utilizing industrial waste as raw materials, thereby reducing landfill disposal and promoting the valorization of secondary resources (Pacheco-Torgal et al., 2012). Moreover, the long service life and recyclability of geopolymer composites contribute to a closed-loop material flow, further enhancing sustainability (Rahman & Rasul, 2020). By adopting circular economy strategies, the construction industry can significantly decrease its reliance on virgin materials while improving environmental and economic performance. Despite the notable strides made in the field of developing fly ash-based geopolymer binders, challenges persist in the optimisation of their formulation, the assessment of their long-term performance, and the expansion of their production capacities for large-scale implementation (Bernal et al., 2011; Provis, 2018). The present article aims to provide a comprehensive analysis of the mechanical and durability characteristics of fly ash-based geopolymer composites, utilising various types of aggregates. The article places particular emphasis on recent advancements in synthesis techniques, performance evaluation, and factors that influence the mechanical properties of the material. The discussion will contribute to the ongoing efforts to promote geopolymer technology as a sustainable alternative to traditional cement-based materials using Romanian local raw materials.

MATERIALS AND METHODS

The raw materials used in this study were sourced from local Romanian industries to promote sustainability and regional resource utilization. The primary aluminosilicate precursor, fly ash (FA), was obtained from a Romanian coal-fired power plant. The chemical composition of the fly ash was analyzed using X-ray fluorescence (XRF) (Table 1).

Table 1. Fly ash sample chemical composition

Oxides	Percentage (%)
SiO_2	46.94
Al_2O_3	23.83
Fe_2O_3	10.08
CaO	10.72
MgO	2.625
SO_3	0.45
Na_2O	0.62
K_2O	1.645
P_2O_5	0.25
TiO_2	0.92
Cr_2O_3	0.02
Mn_2O_3	0.06
ZnO	0.02
SrO	0.03
L.O.I.	2.105

The cumulative distribution of fly ash particles from a Romanian thermal power plant was determined using a HELOS RODOS/L, R5 instrument (Sympatec, Germany) in order to analyse the particle size of the material utilised in the development of alkali-activated geopolymers. The physical characteristics of the fly ash are presented in Figure 1 (Particle size distribution) and Figure 2 (Distribution density of the particles), offering a better visualisation representation.

In order to obtain the alkaline activator (AA) solution, a commercially purchased sodium silicate (Na_2SiO_3) solution was combined with a sodium hydroxide (NaOH) solution (purity ≥ 98%) of 6M, 8M, and 10M molar concentrations in various mass ratios at room temperature. Following the completion of the preparatory stage, the alkaline activator solution was stored under laboratory conditions (23°C) in a closed container for a period of 24 hours in order to allow maturation. In this study, two types of fine aggregates were utilised in the preparation of geopolymer samples: polygranular sand and recycled glass aggregates with a diameter of 0/4 mm (Figure 3). Each aggregate was used independently to evaluate its influence on the material's performance. The selected aggregates were thoroughly mixed with the binder to ensure uniform distribution and proper interaction within the geopolymer matrix. The use of recycled glass aimed to enhance sustainability while maintaining the structural integrity of the material. The activation process and curing conditions were optimized to promote effective geopolymerization and achieve a stable hardened structure.

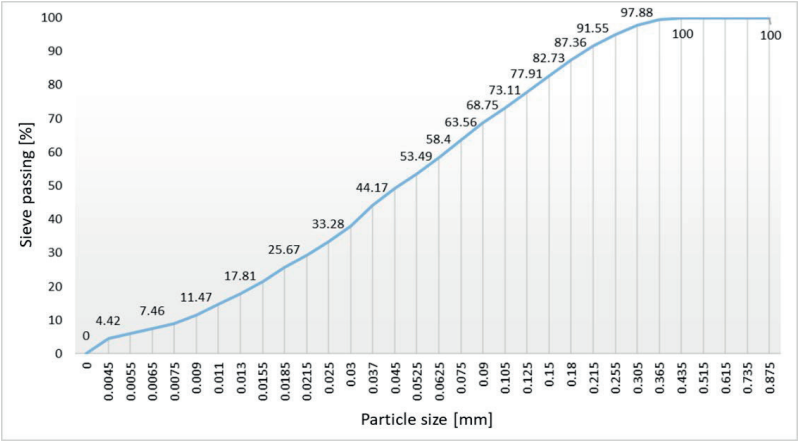


Figure 1. Fly ash particle size distribution

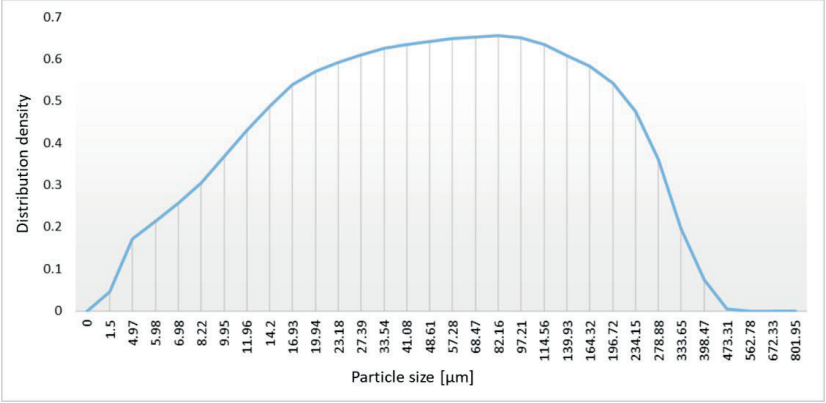


Figure 2. Fly ash distribution density of the particles

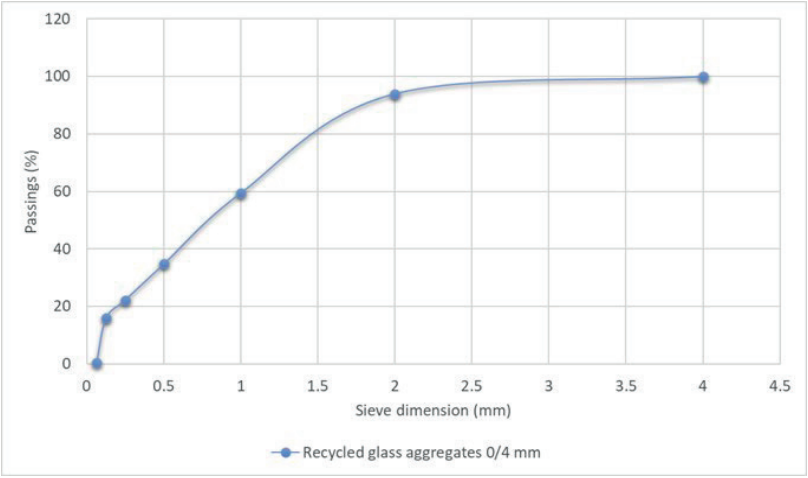


Figure 3. Particle size analysis of the recycled glass aggregates (granular class 0/4 mm)

The geopolymer samples were formulated using two different binder-to-aggregate ratios of 1:1 and 1.25:1 to assess their influence on the material's properties. In the alkaline activation system, sodium silicate (Na_2SiO_3) was dissolved in a solution of sodium hydroxide (NaOH), at a ratio of 2:1 and 1:2, respectively.

To evaluate the influence of alkalinity on the geopolymerisation process, the NaOH solution was prepared in a range of molar concentrations: 6M, 8M, and 10M. The fly ash-to-alkaline activator ratio was fixed at 0.9 to ensure a consistent binder composition. The prepared mixtures were homogenized to achieve a uniform consistency before being cast into molds and subjected to curing under controlled conditions (70°C for 24 hours).

The specimens were demolded after 24 hours and cured at elevated temperatures to study the impact of thermal curing on strength development. Based on preliminay research, curing conditions were optimized to achieve maximum compressive strength and durability resistance (Lăzărescu et al., 2020).

The mix design ratios of the geopolymer samples are presented in Table 2 (samples produced using polygranular standardized sand - PS and samples produced using recycled glass agreggates - GA). For each mixture, a color coding was considered. Each result was obtained from the combination of a minimum of three independently tested samples.

All tests were conducted at the age of 7 days, primarily because geopolymer samples typically gain most of their strength and resistance during this period, particularly due to the heat treatment applied. Research indicates that heat curing accelerates the polymerization process, allowing geopolymers to reach their maximum strength within the first week (Lăzărescu et al., 2024). This time frame was critical for evaluating the material's early-stage properties, as the heat treatment enhances the formation of the geopolymer matrix and strengthens the material. Compressive strength was selected as the main parameter for evaluation due to its direct correlation with the material's structural integrity.

RESULTS AND DISCUSSIONS

The results are presented in graphical form, with each graph, with specific colour code representing different mixtures. The colour coding facilitated the identification of variations in the mixture. Throughout the analysis, the molar concentration of the NaOH solution remained constant, ensuring that the observed differences in the results are solely attributable to the variations in the other components of the mixture (Figures 4-6).

Table 2. Mix design ratio of the alkali-activated geopolymer samples

Type of aggregate	Code	Code colour	NaOH solution concentration	Binder:Aggregate ratio	Na_2SiO_3 / NaOH ratio
Polygranular standardized sand (PS)	P1(PS)		10M	1:1	1:2
	P2(PS)				2:1
	P3(PS)			1.25:1	1:2
	P4(PS)				2:1
	P5(PS)		8M	1:1	1:2
	P6(PS)				2:1
	P7(PS)			1.25:1	1:2
	P8(PS)				2:1
	P9(PS)		6M	1:1	1:2
	P10(PS)				2:1
	P11(PS)			1.25:1	1:2
	P12(PS)				2:1
Recycled glass Granular class 0/4 mm (RG)	P1(RG)		10M	1:1	1:2
	P2(RG)				2:1
	P3(RG)			1.25:1	1:2
	P4(RG)				2:1
	P5(RG)		8M	1:1	1:2
	P6(RG)				2:1
	P7(RG)			1.25:1	1:2
	P8(RG)				2:1
	P9(RG)		6M	1:1	1:2
	P10(RG)				2:1
	P11(RG)			1.25:1	1:2
	P12(RG)				2:1

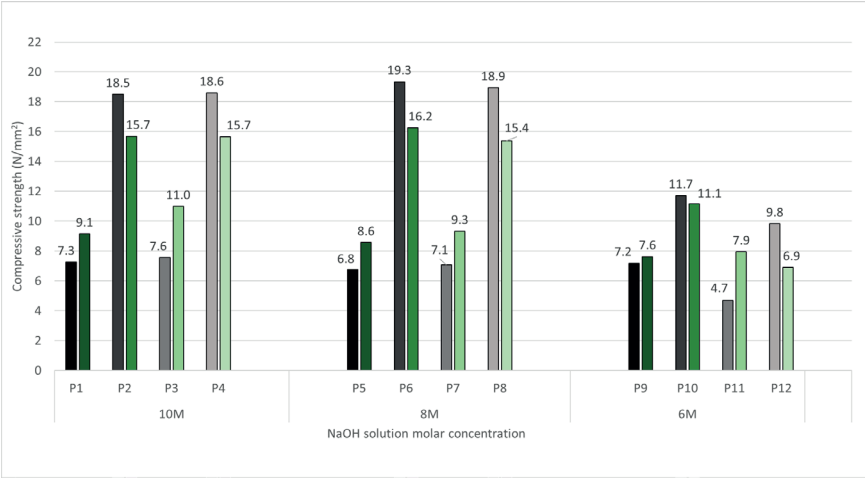


Figure 4. Graphical representation of the compressive strength variation in alkali-activated geopolymer samples (10M, 8M, and 6M)

The performance of the geopolymer samples, particularly in terms of compressive strength, was found to be significantly affected by the incorporation of polygranular sand, as indicated by the results of mechanical tests (Figure 4). Samples with Na_2SiO_3/NaOH ratio of 2:1 (P2(PS), P4(PS) -10M, P6(PS), P8(PS) – 8M and P10(PS), P12(PS) – 6M) exhibited higher values of compressive strength than those with a ratio of 1: 2, suggesting that a higher content of sodium silicate contributes to a better consolidated and denser geopolymer matrix. Regarding the influence of the molar concentration of the NaOH solution, a significant increase in compressive strength between 6M and 8M can be observed, but above this threshold, samples produced with 10M NaOH solution do not show an improvement in compressive strength, which indicates reaching a saturation level in the alkaline activation process.

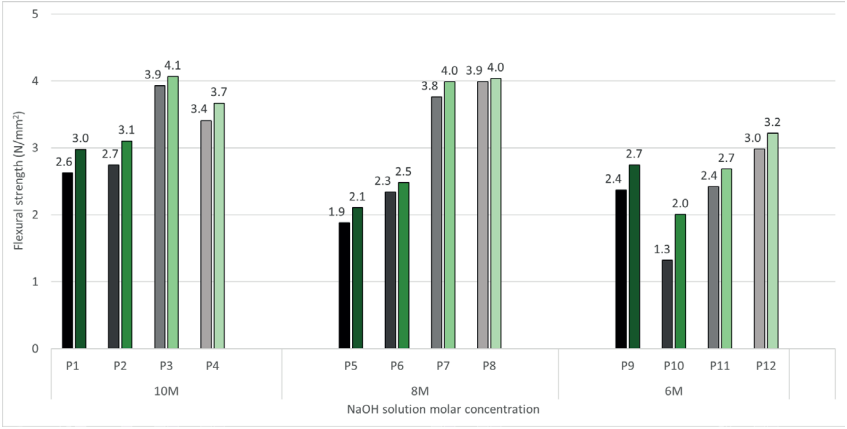


Figure 5. Graphical representation of the flexural strength variation in the alkali-activated geopolymer samples (10M, 8M, and 6M)

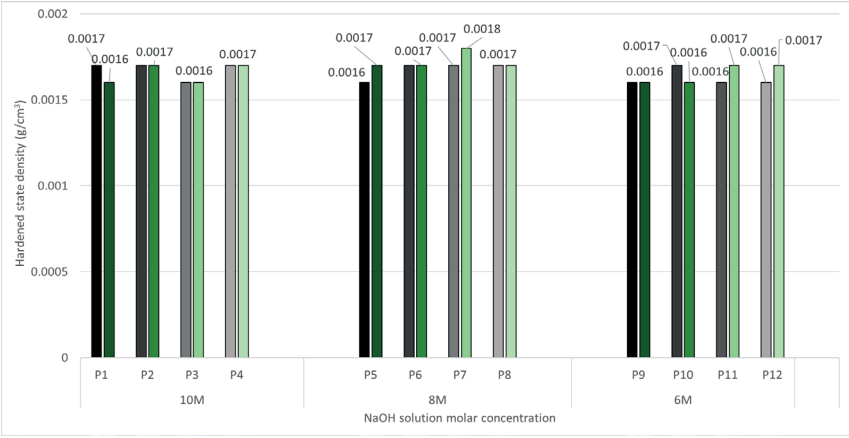


Figure 6. Graphical representation of the hardened state density variation in the alkali-activated geopolymer samples (10M, 8M, and 6M)

However, the flexural strength test results did not follow the same trend (Figure 5). Although the samples with an activator ratio of 2:1 had better compressive strength, the values obtained for flexural strength did not show a direct correlation with this ratio. This difference suggests that although a denser geopolymer matrix favors compressive behavior, the mechanisms of cracking and crack propagation under tensile stress are influenced by additional factors such as pore distribution, microstructure of the gel formed, and interfacial adhesion between component phases.

The mechanical performance of the samples exhibited variation depending on the type of aggregate utilised. Recycled glass aggregates demonstrated distinct behaviour in both compressive and flexural strength when compared to polygranular sand. For the 1:2 activator ratio, samples incorporating recycled glass (P1(RG), P3(RG) – 10M, P5(RG), P7(RG) – 8M, and P9(RG), P11(RG) – 6M) demonstrated higher compressive strength values. The enhancement in strength is attributed to the improved compaction of the geopolymer matrix, a consequence of the morphology of the glass particles, and the potential contribution of an additional pozzolanic reaction involving the glass particles. However, the general trend was maintained, and the samples with 2:1 activator ratio continued to show the best compressive performance regardless of the type of aggregate used.

In terms of the influence of the molar concentration of NaOH, the same significant increase was observed between 6M and 8M, with no significant improvements when using 10M NaOH solution.

However, the tensile behavior was different from that observed in compression. In contrast to the samples with polygranular sand, those with recycled glass aggregates exhibited higher values of tensile strength, for all the mixtures (P1-P12(RG)).

This result suggests that glass aggregates may contribute to improve the ability of the geopolymer to respond to tensile stresses, possibly through a more favorable stress distribution in the matrix and a more efficient interface between the binder and the aggregates. Despite the smooth surface of the glass particles, which could reduce interfacial adhesion, it is possible that this effect could be compensated by a better interaction at the microstructural level, limiting crack initiation and propagation under tensile stress.

Moreover, optimising the molar concentration of NaOH within the 6M to 8M range, where mechanical performance improvements become negligible beyond this threshold, may have significant sustainability implications. This optimisation enables a reduction in the quantity of alkaline substances required for geopolymer activation, thereby minimising both the consumption of chemical resources and the environmental impact associated with their production and handling. Within the framework of the circular economy, geopolymers emerge as a viable and environmentally friendly alternative to conventional building materials, as their mechanical properties benefit from the incorporation of recycled aggregates. This approach not only enhances material performance but also contributes to effective glass waste management.

A key aspect highlighted by this study is that, although the mechanical performance of the samples differs depending on the type of aggregates used and the activator ratios, the density in the hardened state remains relatively constant for all samples (Figure 6). This result is extremely important, as it suggests that the improvement in mechanical properties observed in some samples is not due to a simple variation in density, but to a complex interaction between the geopolymer matrix and the aggregates. Thus, optimization of material performance is achieved by changing the chemical composition and type of aggregates without significantly affecting the final density. This observation further supports the potential of using recycled aggregates in the development of sustainable geopolymers. Should the density remain consistent, irrespective of the type of aggregate utilised, it can be deduced that recycled glass has the potential to serve as a substitute for conventional aggregates without altering the material's fundamental characteristics. Additionally, the observation that recycled glass samples exhibited higher tensile strength values suggests that these aggregates contribute to a more uniform stress distribution and reduce premature cracking. These phenomena, if substantiated, may enhance the durability of constructed structures.

Furthermore, the consistency in sample density suggests that incorporating additional functionalization, such as the integration of TiO_2 nanoparticles, is unlikely to alter the material's density but rather enhance its functional properties. Thus, the utilisation of geopolymer materials as a medium for the creation of intelligent and environmentally sustainable solutions has been demonstrated to result in a dual effect, with a reduction in ecological impact through the reutilisation of discarded materials and an improvement in the functionality of these solutions, including self-cleaning properties and antibacterial protection. It is clear that the constant density of these materials offers a significant technological advantage. Indeed, these materials can be manufactured in a manner that does not demand substantial adjustments to existing processes. Consequently, the shift towards sustainable and intelligent geopolymers becomes a viable and readily implementable solution. This transformation has the potential to redefine the building materials industry by promoting structures that are more sustainable, efficient and environmentally friendly.

CONCLUSIONS

This study emphasises the considerable influence of aggregate type and activator ratios on the mechanical performance and durability of geopolymers, thereby validating their potential as a sustainable substitute for conventional building materials. Previous studies have shown that geopolymer concrete has higher initial costs due to the price of alkali activators and specialized production processes. However, due to its superior durability, low maintenance costs and significantly lower environmental impact, it is becoming a sustainable and cost-effective alternative to traditional concrete in the long term. A specific cost assessment can only be made on a case-by-case basis, considering both initial costs and long-term benefits. Furthermore, studies have shown that, when compared to ordinary Portland cement with similar mechanical properties, geopolymer concrete reduces CO_2 equivalent (CO_2eq) emissions by up to 50-60%, due to the use of industrial waste and the elimination of the Portland cement production process (Lăzărescu et al., 2024). Thus, in the long term, geopolymer concrete not only offers the benefits of durability and low maintenance but also contributes significantly to the goals of sustainability and reduced environmental impact.

This study has shown that, the use of recycled glass aggregates was found to be beneficial, improving the tensile strength and, in the case of an activator ratio of 1:2, even the compressive strength compared to polygranular sand. These results highlight that the right choice of aggregates can lead to optimized performance of geopolymeric materials, thus facilitating the transition towards more sustainable and environmentally friendly solutions. Furthermore, the recovery of waste glass contributes directly to reducing the impact on natural resources, promoting a circular economy model.

The study also demonstrated that the ratio of activators to NaOH molar concentration plays a crucial role in the formation of a stable and efficient geopolymer network. The significance of sodium silicate in establishing a compact structure is substantiated by the attainment of optimal mechanical strengths at an activator ratio of 2:1. An analysis of molar concentration of NaOH revealed a significant increase between 6M and 8M, with no such improvement observed at 10M, thus indicating the attaining of a saturation point in the activation process. This finding carries significant implications for sustainability as it facilitates optimisation of chemical consumption, leading to a reduction in costs and a diminished environmental impact within the manufacturing process.

It is anticipated that future research on geopolymer materials will concentrate on mechanical properties and sustainability. In addition, however, there is a growing recognition of the importance of exploring the development of smart, eco-innovative materials that can provide enhanced benefits to meet evolving efficiency and performance demands. The integration of titanium dioxide (TiO_2) nanoparticles has been identified as a potentially significant solution in this regard. This integration has the capacity to impart self-cleaning, antibacterial, and antimicrobial properties to geopolymers, thereby enhancing their applicability in environments subject to contamination or within urban infrastructure. The incorporation of TiO_2 into geopolymer materials has been shown to yield a photocatalytic property, enabling the degradation of organic pollutants when exposed to light. This property has the potential to mitigate the environmental impact of buildings, positioning geopolymers as a promising alternative to conventional materials. The functionalization of geopolymers with TiO_2 could lead to their advancement as smart materials that actively contribute to environmental protection and safety.

In this context, geopolymers are evolving beyond their traditional role as a sustainable alternative to conventional cement. They are increasingly recognised as a pivotal component in the development of innovative materials characterised by advanced, adaptable and environmentally friendly properties. The integration of the principles of the circular economy, utilising recycled aggregates, with cutting-edge nanomaterials-based technologies is pivotal in shaping a genuine transition towards smart, eco-innovative materials. These

materials have the potential to redefine standards in the domains of construction and infrastructure. This will not only reduce environmental impact, but also increase the durability, functionality, and safety of built structures, thus contributing to a more sustainable and smarter future.

ACKNOWLEDGEMENTS

This research was funded by the Romanian Government Ministry of Research, Innovation and Digitalization, project No. PN 23 35 05 01 *Innovative sustainable solutions to implement emerging technologies with cross- cutting impact on local industries and the environment, and to facilitate technology transfer through the development of advanced, eco- smart composite materials in the context of sustainable development of the built environment.*

REFERENCES

Abhishek, A., Sharma, R., Patel, V., & Singh, K. (2020). Sustainable materials for construction. *Materials Science and Engineering.*

Andrew, R.M. (2018). Global CO_2 emissions from cement production. *Earth System Science Data*.

Bakharev, T. (2005). Durability of geopolymer materials. *Cement and Concrete Resea*rch, 35(7), 1244–1256.

Bernal, S.A., Provis, J.L., Mejía de Gutiérrez, R., Rose, V., & van Deventer, J.S.J. (2011). Activation of fly ash in geopolymerization. *Cement and Concrete Composites*, 33(1), 1–8.

Chindaprasirt, P., Chareerat, T., & Sirivivatnanon, V. (2007). Microstructure and strength of geopolymer composites. *Cement and Concrete Research*, 37(2), 227–233.

Davidovits, J. (2015). *Geopolymer chemistry and applications* (4th ed.). Institut Géopolymère.

Deb, P.S., Nath, P., & Sarker, P.K. (2014). Mechanical behavior of geopolymer composites. *Journal of Materials Science*, 49(15), 5841–5852.

Duxson, P., Fernández-Jiménez, A., Provis, J.L., Lukey, G.C., Palomo, A., & van Deventer, J.S.J. (2007). The role of Al and Si in geopolymer formation. *Journal of the American Ceramic Society*, 90(12), 3811–3816.

Fernández-Jiménez, A., Garcia-Lodeiro, I., & Palomo, A. (2019). Advances in geopolymer durability. *Construction and Building Materials*, 211, 737–748.

Fernández-Jiménez, A., Palomo, A., & Criado, M. (2005). Chemical characterization of geopolymers. *Cement and Concrete Research*, 35(5), 780–787.

Gartner, E.M., & Hirao, H. (2015). Future cements. *Cement and Concrete Research*, 114, 2–26.

Ghisellini, P., Cialani, C., & Ulgiati, S. (2016). A review on circular economy: The expected transition to a balanced interplay of environmental and economic systems. *Journal of Cleaner Production*, 114, 11–32.

Heah, C.Y., Kamarudin, H., Bnhussain, M., Luqman, M., Nizar, I.K., Lee, B.C., & Ruzaidi, C.M. (2011). Properties of fly ash geopolymers. *Construction and Building Materials*, 25(12), 4179–4185.

Ismail, I., Bernal, S. A., Provis, J.L., Nicolas, R.S., Hamdan, S., & van Deventer, J.S.J. (2013). Sulfate resistance of geopolymers. *Materials and Structures*, 46(3), 473–490.

Kirchherr, J., Reike, D., & Hekkert, M. (2017). Conceptualizing the circular economy: An analysis of 114 definitions. *Resources, Conservation and Recycling,* 127, 221–232.

Kumar, S., Kumar, R., Alex, T.C., Bandopadhyay, A., & Mehrotra, S.P. (2010). Factors influencing geopolymer strength. *Construction and Building Materials*, 24(8), 1515–1523.

Lăzărecu, A.-V., Hegyi, A. & Florean, C. (2024). Smart eco-innovative composite materials with self-cleaning capability and enchanced resistance to microorganisms. *Scientific Papers. Series E. Land Reclamation, Earth Observation Surveying, Environmental Engineering*, 13, 125–136.

Lăzărescu, A.-V., Szilagyi, H., Baeră, C., & Hegyi, A. (2020). Parametric Studies Regarding the Development of Alkali-Activated Fly Ash-Based Geopolymer Concrete Using Romanian Local Raw Materials. *Proceedings*, 63(1), 11.

Lee, W.K.W., & van Deventer, J.S.J. (2004). Role of calcium in geopolymerization. *Cement and Concrete Research*, 34(4), 599–610.

Lloyd, N. A., & Rangan, B.V. (2010). Strength of geopolymer concrete. *ACI Materials Journal*, 107(6), 579–586.

Lloyd, R.R., Provis, J.L., & van Deventer, J.S.J. (2012). Acid resistance of inorganic polymer binders. 1. Corrosion rate. *Materials and Structures,* 45(1-2), 1–14.

Olivia, M., & van Riessen, A. (2011). Acid resistance of geopolymers. *Materials and Structures*, 44(2), 399–411.

Pacheco-Torgal, F., Ding, Y., & Jalali, S. (2012). Properties and durability of concrete containing polymeric wastes (review). *Construction and Building Materials*, 30, 714–724.

Pan, Z., Sanjayan, J.G., Rangan, B.V., & Hardjito, D. (2012). Chloride penetration in geopolymer concrete. *Construction and Building Materials*, 42, 273–279.

Pasupathy, K., Sanjayan, J.G., Rajeev, P., & Wilson, J. (2021). Long-term performance of geopolymers. *Materials Today*, 46(3), 212–219.

Phair, J. W., & van Deventer, J. S. J. (2001). Effect of silicate activator pH on the leaching and material characteristics of waste-based inorganic polymers. *Minerals Engineering,* 14(3), 289–304.

Provis, J.L. (2018). Alkali-activated materials. *Cement and Concrete Research,* 114, 40–48.

Provis, J.L., & Bernal, S.A. (2014). Geopolymers and alkali-activated materials. *Cement and Concrete Research*, 57, 1–9.

Provis, J.L., & van Deventer, J.S.J. (Eds.). (2009). Geopolymers: Structures, processing, properties and

industrial applications. Cambridge, UK: Woodhead Publishing.

Rahman, M.M., & Rasul, M.G. (2020). The circular economy and the construction industry: A review of strategies, implementation, and the role of digital technologies. *Resources, Conservation and Recycling*, 156, 104632.

Ryu, G.S., Lee, Y.B., Koh, K.T., & Chung, Y.S. (2013). The mechanical properties of fly ash-based geopolymer concrete with alkaline activators. *Construction and Building Materials,* 47, 409–418.

Sathonsaowaphak, A., Chindaprasirt, P., & Pimraksa, K. (2009). Workability and strength of lignite bottom ash geopolymer mortar. *Journal of Hazardous Materials,* 168(1), 44–50.

Sukmak, P., Horpibulsuk, S., & Shen, S. (2013). Strength development in clay-fly ash geopolymer. *Contr. Build. Mater.,* 40, 566–574.

Temuujin, J., van Riessen, A., & Williams, R. (2009). Influence of calcium compounds on the mechanical properties of fly ash geopolymer pastes. *J. Hazard. Mater.*, 167, 82–88.

Van Riessen, A., Chen-Tan, N.W., & Ly, C.V. (2013). Beneficial recycling of industrial waste residues: Fly ash-based geopolymers. *Materials*, 6(8), 2952–2968.

Xu, H., & Van Deventer, J.S.J. (2000). The Geopolymerisation of Alumino-Silicate Minerals. *International Journal of Mineral Processing*, 59, 247–266.

Zhang, Z., Yao, X., Zhu, H., & Chen, Y. (2009). Role of water in the synthesis of calcined kaolin-based geopolymer. *Applied Clay Science,* 43(2), 218–223.

Scientific Papers. Series E. Land Reclamation, Earth Observation & Surveying, Environmental Engineering. Vol. XIV, 2025
Print ISSN 2285-6064, CD-ROM ISSN 2285-6072, Online ISSN 2393-5138, ISSN-L 2285-6064

THERMAL CONDUCTIVITY OF SILTY SOILS IN THE SOUTH-EAST REGION OF ROMANIA

Daniel-Marcel MANOLI, Cristian-Ștefan BARBU, Mihaela-Elena STAN, Manole-Stelian ȘERBULEA, Alina TATOMIR, Oana-Cristina CARAȘCA, Ruxandra-Irina ERBASU, Andrei-Dan SABAU

Technical University of Civil Engineering of Bucharest,
122-124 Lacul Tei Blvd, District 2, 020396, Bucharest, Romania

Corresponding author email: daniel.manoli@utcb.ro

Abstract

The thermal properties of loess soil are essential for the distribution of heat generated by electrical cables in wind turbines. In these systems, where high-intensity electrical flow induces conductor heating through the Joule effect, the ability of the soil to facilitate heat transfer has a direct impact on the energy efficiency, operational safety and the durability of the electrical infrastructure, as inefficient thermal diffusion can lead to conductor overheating, affecting electrical resistance, degrading insulation and reducing cable lifespan. This study investigates the effects of density and moisture content on the thermal conductivity of silty soils at different compaction levels. Experimental tests were conducted on loessial soil samples compacted to 85-90% of the maximum dry density determined by the modified Proctor test. All measurements included the determination of dry-out curves to observe the variations of thermal conductivity with a gradual decrease in moisture content. The results indicate an increase in thermal conductivity with higher degree of compaction due to reduced porosity and improved particle contact.

Key words*: dry-out curve, loess, thermal conductivity.*

INTRODUCTION

Wind power is considered as one of the most efficient and sustainable forms of renewable electricity, contributing significantly to the reduction of greenhouse gas emissions and global dependence on fossil fuels. As global energy consumption continues to rise, the integration of renewable energy sources such as wind power is becoming a strategic necessity to long-term environmental and energy security challenges. Wind energy systems are clean, widely available and can be implemented on a large scale.

The rapid development of renewable energy technologies has led to a significant expansion of wind energy infrastructure across different terrains and climates. In this evolving energy landscape, the reliability and durability of underground electrical systems, particularly those associated with wind turbines are critical to maintaining overall system performance and longevity. These systems play a vital role in the safe and efficient transmission of electrical power from turbines to substations and the main power grid.

One of the technical challenges associated with underground power cable systems is the thermal management of conductors that carry high-intensity currents and generate heat through the Joule effect. This heat must be effectively dissipated into the surrounding ground to prevent overheating. The ability of the ground to transfer this thermal energy - determined primarily by its thermal conductivity - is a key factor in preventing excessive temperatures, minimising energy losses and extending the operational life of electrical components such as insulation materials and cable sheaths (Wang et al., 2024). Loess is thought to be derived mainly from glacial or periglacial material transported by wind after glaciers have retreated. However, loess can also be formed from other sources, resulting from the accumulation of eroded material in dry continental conditions, either cold or warm, which has subsequently been transported and deposited by the wind. Volcanic ash carried by the wind over long distances from its source can also be a significant contributor.

In many areas, loess is eroded by precipitation and runoff and then redeposited in accumulations similar to the original, but losing

its aeolian character through sedimentation (Dragomir, 2002).

Loess a wind-deposited, fine-grained soil is common in many regions with large-scale wind energy projects. It forms extensive sedimentary layers that often underlie wind turbine foundations and cable routes. Its physical properties, such as porosity, moisture retention capacity, and mineral composition, vary significantly with compaction and environmental conditions, affecting its thermal behaviour. The inherent variability in the structure and composition of loess presents a challenge to the design of consistent and safe cable installations. Inadequate thermal conductivity in such soils can lead to conductor overheating, insulation degradation and a reduction in the reliability of the underground cable system (Sangprasat et al., 2024). For this reason, a thorough investigation of the thermal conductivity of loess is essential.

In this study, soil samples were collected from a construction site near Medgidia, Constanța County, at a depth between 1 to 2 meters. The site was selected based of its typical loessial profile, which is common in south-eastern Romania and representative of the conditions encountered in wind farm development. The testing was conducted at the Geotechnical Laboratory of the Technical University of Civil Engineering Bucharest. The soil was identified as loessial, characterised by fine texture, high capillarity and moderate to high water retention, making it suitable for detailed thermal analysis.

The aim of this work is to provide insight into the optimisation of underground electrical design in wind energy applications by highlighting the influence of soil properties, in particular moisture content and maximum dry density on thermal conductivity. This approach is in line with the wider aims of improving renewable energy infrastructure through innovations in materials science and geotechnical engineering.

MATERIALS AND METHODS

Methods for thermal conductivity measurements

The most relevant thermal parameter of the earth is the thermal conductivity λ, as it directly influences the heat transfer processes in underground applications. For the preliminary design of complex energy foundations, the detailed sizing of standard geothermal systems and the engineering layout of underground electrical cables in wind energy infrastructure, thermal conductivity can be reasonably estimated using empirical diagrams that correlate with water content, saturation density and soil texture. This approach provides a practical and sufficiently accurate basis for early-stage thermal analysis in geotechnical and energy systems applications (Brandl, 2006).

In the laboratory, the experimental procedure was carefully designed to avoid any disturbance of the internal structure of the loess soil samples or alterations to the local thermal environment. Ensuring minimal disturbance is essential to preserve the native properties of the soil, which directly affect the accuracy of the thermal conductivity measurements. To achieve this, no pushing or mechanical insertion forces were applied to the thermal needle during installation (ASTM D5334-14 STM, 2014) (Figure 1).

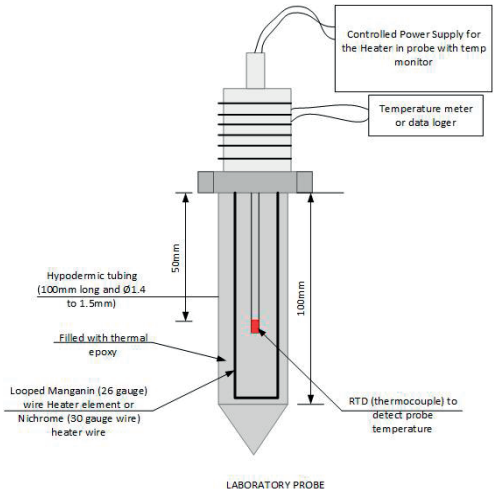


Figure 1. Thermal needle apparatus (IEEE Std 442™, 2017)

Instead, a precise pre-drilling method was used to create an access path within the sample, see Figure 2, allowing the thermal needle to be placed in direct contact with the soil along its entire length without causing deformation or compaction. This technique ensures uniform thermal contact between the probe and the surrounding material, which is essential to

replicate in-situ conditions and avoid artificial thermal gradients. Pre-drilling also helped to eliminate potential sources of mechanical heat that could interfere with the temperature readings during the test.



Figure 2. Pre-drilled soil sample

To further minimise errors, special attention was given to thermal stabilisation prior to measurement. The sample and instrumentation were allowed sufficient time to reach thermal equilibrium with the laboratory environment. This stabilisation period ranged from a few minutes to over an hour, depending on initial temperature differences and environmental factors such as air flow or sample moisture content levels. The thermal conductivity measurement cycles were not initiated until a stable temperature had been reached and maintained.

The entire test protocol strictly followed the methodology outlined in IEEE Std 442™, (2017) – "IEEE Guide for Thermal Resistivity Measurements of Soils and Backfill Materials". This standard prescribes installation procedures, measurement timing, calibration requirements and data interpretation techniques necessary to ensure reliable and repeatable results in assessing soil thermal resistivity. Adherence to this guide will ensure consistency in the evaluation of loess soil behaviour under thermal stress conditions typically encountered in energy infrastructure projects.

Methods for laboratory measurements

The thermal needle probe is primarily used to determine the effects of variations in density and moisture content on the thermal resistivity of the soil. This method is widely recognised in geotechnical and electrical engineering for its accuracy and adaptability to various soil types. It operates by applying a controlled and localised heat pulse and measuring the resulting temperature change over time, allowing the determination of soil thermal properties through analytical modelling.

The probe can be used to both undisturbed and reconstituted soil samples compacted using the Modified Proctor test. Undisturbed samples preserve the natural structure and stratification of the soil, while reconstituted soil samples allow controlled variations in compaction and moisture for comparative studies. The ASTM D1557-12 (2021) standard was used to determine the maximum dry density and optimum moisture content required for soil compaction. This standard is particularly relevant for the evaluation of soils used in civil engineering applications, such as backfill around buried utilities.

For this study, test samples were compacted to 85% and 90% of the Modified Proctor maximum dry density. These values represent realistic field conditions encountered after backfilling and compaction of soil in cable trenches. Compaction was carried out in five uniform layers using mechanical energy equivalent to 2700 kNm/m³, ensuring homogeneous sample preparation and consistent test conditions. The layered approach helps to minimise void heterogeneity and improve the reproducibility of thermal measurements.

After compaction, the soil samples were allowed to equilibrate with the laboratory temperature for a period to eliminate transient thermal effects. This step is essential to ensure that the initial thermal state of the sample does not bias the results, particularly given the sensitivity of thermal resistance to moisture migration and temperature gradients.

In practical field applications, particularly in wind energy infrastructure, foundation soils are compacted after cable installation to achieve densities ranging between 85% and 90% of the Modified Proctor maximum along the entire underground cable route. Ensuring consistent soil compaction is not only vital for mechanical stability but also has a significant impact on the thermal performance of the buried cables. Poorly compacted soil can retain air voids which act as thermal insulators, reducing the ability of

soil to dissipate heat effectively and creating a risk of conductor overheating. Therefore, replicating these field conditions in the laboratory provides an accurate representation of operational scenarios and helps in the design of optimised cable burial systems.

Analysis of thermal conductivity test results

The analytical model for calculating thermal resistance has been developed based on the assumption of an infinite linear heat source dissipating heat in an infinite homogeneous medium. Under these idealised conditions, the thermal resistivity (ρ) (IEEE Std 442™, 2017) can be calculated using the following equation:

$$\rho = \frac{4\pi(T_2 - T_1)}{q \ln\left(\frac{t_2}{t_1}\right)} \quad (1)$$

where:

r is thermal resistivity (K·m/W);

T_1 - temperature measured at some arbitrary elapsed time (K);

T_2 - temperature measured at another arbitrary elapsed time (K);

q - dissipated per unit length (W/m);

t_1 - elapsed time at which temperature T1 is recorded (min);

t_2 - elapsed time at which temperature T2 is recorded (min).

Initial thermal transients occur due to the finite diameter of the thermal probe and are not representative of the ideal line source model. Similarly, boundary effects can occur due to the finite size of the soil sample container, leading to distortions in the measured thermal profile at later times. To ensure accurate calculations, the measured data must be carefully filtered to exclude these non-linear periods.

A standard approach is to plot the recorded temperature against the logarithm of time. The linear portion of this semi-log plot is identified as the valid interval for analysis. Data points within this region reflect stable thermal diffusion unaffected by the probe transients or edge boundary conditions.

Deviations at the beginning or end of the curve indicate either insufficient thermal stabilisation or the onset of confounding factors such as heat reflection from sample boundaries or moisture redistribution.

To simplify the calculation process and increase reliability an alternative form of the equation is often used. If the temperature change (ΔT) is measured over a complete logarithmic cycle, the resistivity can be approximated as (IEEE Std 442™, 2017):

$$\rho = \frac{4\pi}{2.303q}\Delta T \quad (2)$$

This formulation allows a simpler interpretation of the linear segment and is endorsed by the IEEE Std 442™ (2017) for thermal resistivity assessments. The use of these analytical techniques provides a robust framework for comparing thermal behaviour under varying moisture and compaction conditions. Three determinations were made for each sample (Figure 3).

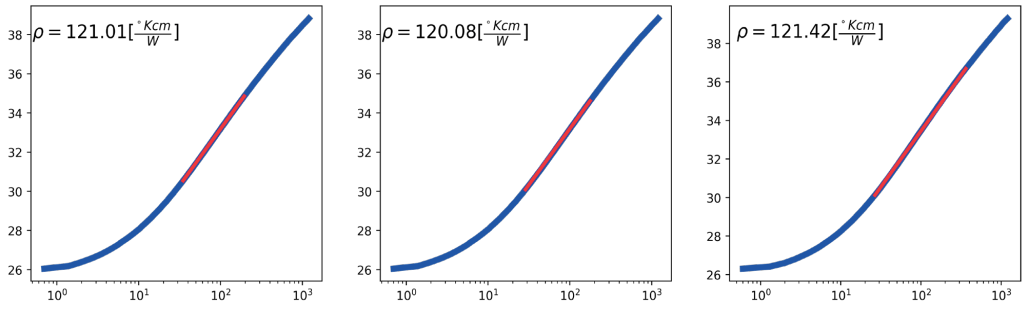


Figure 3. Thermal Resistivity Curves

Analysis of the geotechnical parameters of the soil

In order to characterise the investigated soil, a comprehensive programme of geotechnical laboratory tests was conducted to determine the physico-mechanical properties of the material. These tests were designed to provide essential data to evaluate the behaviour of the soil under different conditions, particularly for applications involving thermal performance, degree of compaction and load-bearing capacity. An understanding of these parameters is essential for the integration of thermal conductivity knowledge into practical design. Granulometric (particle-size) analysis indicated that the soil samples tested fell within the classification range of silty clay to clayey silt, as shown in Figure 4.

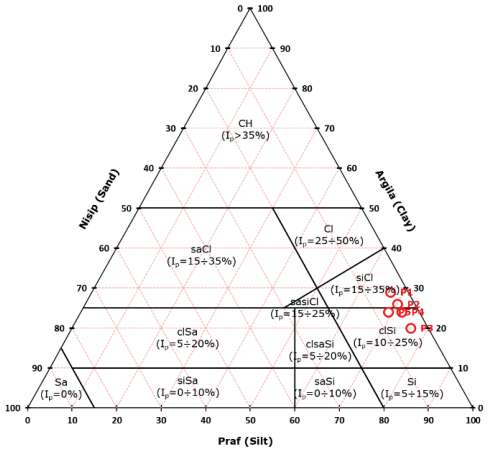


Figure 4. Ternary diagram of the soils

This classification suggests a fine-grained soil composition, which is typically associated with moderate permeability and relatively high-water retention capacity. Such properties have a direct influence on the thermal conductivity of the soil, as finer particles and higher moisture content levels can either promote or inhibit heat flow depending on their spatial arrangement and degree of saturation ration.

The Atterberg limits were determined to evaluate the soil's plasticity characteristics. The measured liquid and plastic limits indicate a medium plasticity index, indicating that the soil has a moderate deformation potential under variable moisture conditions (Figure 5). This plasticity range is important in determining how the soil content to seasonal changes in moisture, affecting both its thermal and mechanical stability. Soils with medium to high plasticity tend to be workable in the field, but their sensitivity to moisture variations requires careful consideration in the design of earthworks.

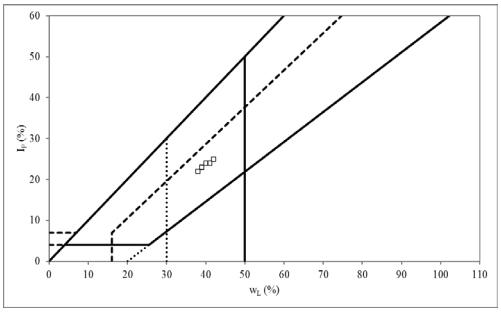


Figure 5. Soil plasticity

To further assess the quality and potential performance of the soil, the organic matter content was also determined. Laboratory results indicate that the organic content is between 2% and 3%. Although this level is not excessively high, it may still influence the soil's compaction behaviour, strength, and long-term stability. Organic materials tend to reduce dry density and increase water retention, which can alter thermal conductivity and pose risks in load-bearing applications, especially when the soil is used as backfill material.

To determine the optimum compaction parameters, Modified Proctor tests were performed on all tested samples in accordance with ASTM D1557. The test results helped identify the optimum moisture content and the corresponding maximum dry density necessary for achieving maximum density under in-situ conditions. The Modified Proctor curve (Figure 6) shows a clear peak, indicating the optimum moisture content at which soil particles are in the denseness state, minimising air voids and maximising thermal conduction potential.

In addition, California Bearing Ratio (CBR) tests were carried out in accordance with ASTM D1883 (2021) to assess the strength and bearing capacity of the soil. The CBR test results (Figure 7) provide critical information for assessing the mechanical performance of the soil, particularly the suitability of the subgrade material.

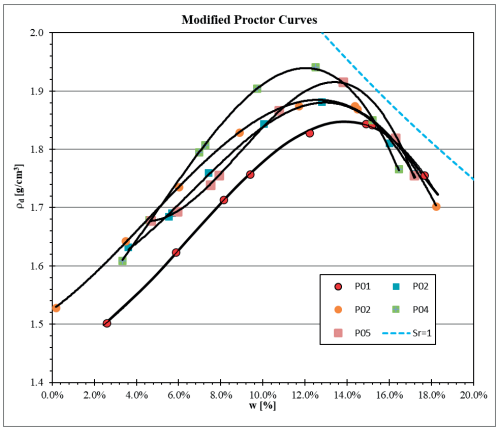


Figure 6. Modified Proctor Curves

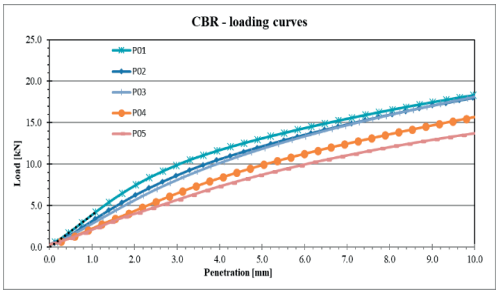


Figure 7. CBR Curves

Table 1 shows the compiled optimum compaction parameters, including the optimum water content (w_{opt}), the maximum dry density ($\gamma_{d,max}$) and CBR values for each of the conditions tested.

Table 1. Optimal compaction parameters

w_{opt}	$\gamma_{d,max}$	CBR	
		1	2
[%]	[g/cm^3]	[%]	
13.9	1.85	66.53	65.59
13.0	1.88	57.24	60.96
12.6	1.88	52.94	59.41
12.0	1.94	41.48	49.5
13.4	1.92	36.62	43.62

RESULTS AND DISCUSSIONS

The testing programme involved preparing samples at different Modified Proctor compaction levels, specifically 85% and 90%, to replicate field conditions typically encountered during the backfilling process (Olinic & Olinic, 2016) at underground cable installations. Each soil sample was meticulously prepared under controlled laboratory conditions to ensure repeatability and reliability of results. Compaction was carried out in successive layers to maintain a uniform density distribution throughout the soil sample volume.

All samples were pre-drilled along the vertical axis to accommodate the thermal needle probe, ensuring optimum thermal contact and minimising disturbance to the compacted matrix. This pre-drilling procedure is critical for accurate thermal conductivity measurements as it prevents deformation around the probe and eliminates artificial voids that could distort temperature readings.

Three independent resistivity tests were carried out on each sample at different moisture contents, allowing conductivity trends to be observed as a function of moisture content. The range of moisture contents tested ranged from near optimum compaction values to air-dried conditions. This enabled a detailed drying curve to be constructed, characterising how thermal resistivity evolves with progressive moisture loss.

Three independent resistivity tests were carried out on each sample at different moisture contents, allowing conductivity trends to be observed as a function of moisture content. The range of moisture contents tested ranged from near optimum compaction values to air-dried conditions. This enabled a detailed drying curve to be constructed, characterising how thermal resistivity evolves with progressive moisture loss

Figure 8 shows the variation in thermal conductivity over the range of moisture contents for both 85% and 90% compacted samples.

A comparative analysis of the curves highlights the significant effect of the degree of compaction level on thermal performance.

This observed behaviour confirms the critical role of both moisture content and dry density in optimising heat dissipation around underground conductors. The results reinforce the importance of proper site preparation and moisture control to ensure efficient thermal management in wind energy infrastructure.

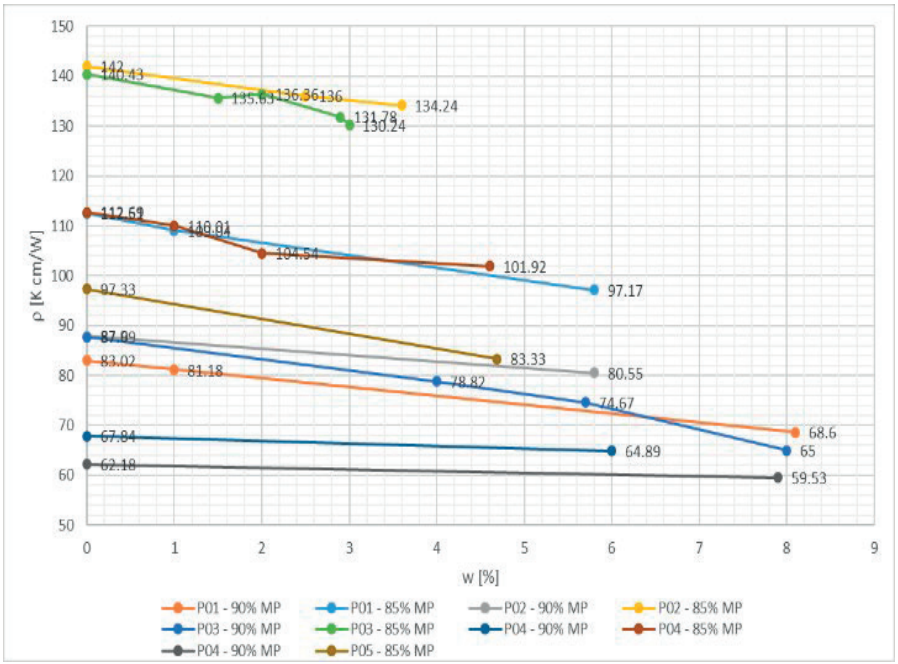


Figure 8. Thermal conductivity of tested soil

CONCLUSIONS

The experimental results clearly demonstrate that moisture content is a primary factor controlling the thermal conductivity of loess soils. The relationship between water content and heat transfer efficiency is non-linear and subject to threshold behaviour, influenced by soil microstructure and particle interactions (Nikiforova et al., 2013).

Three main regimes were identified:

- Dry state (low moisture content): In the absence of sufficient moisture, loess has very low thermal conductivity. This is mainly due to the dominance of air-filled pores which act as thermal insulators and significantly reduce the rate of heat transfer through the soil matrix.
- Moderate saturation (10–20%): As water content increases, capillary bridges begin to form between particles, allowing more efficient heat transfer. This is the optimum range for thermal conductivity where the combined effects of the higher thermal conductivity of water and increased interparticle contact significantly reduce the resistivity.
- High saturation (>40%): Surprisingly, thermal conductivity does not continue to increase indefinitely with moisture content. At high saturation levels, water tends to occupy voids in a discrete manner, forming capillary barriers. These restrict heat flow and can reduce conductivity by disrupting of continuous solid-liquid pathways.

The generation of drying curves proved to be an essential tool for understanding how progressive moisture loss affects thermal performance. These curves provide a dynamic perspective on how loess soils behave under real environmental conditions, particularly after compaction which is typical of wind farm installations.

In particular, below 8% moisture content, the thermal conductivity of remoulded loess samples prepared using the modified Proctor test showed inconsistent or subdued responses. Only when a stable temperature was achieved and maintained, the thermal conductivity measurement cycles were initiated. This variation is likely to be related to irregularities in void ratio and uneven moisture distribution within the soil matrix at very low water contents. Additionally, the degree of compaction level plays an important role in determining thermal

conductivity. At densities above 85–90% of the maximum dry density (according to Modified Proctor), the reduction in pore air volume significantly improves heat transfer through the soil. The denser particle arrangement creates more efficient conductive pathways, which is critical in preventing overheating of buried electrical systems (Mostafa et al., 2018).

In conclusion, the synergy between moisture content and dry density must be carefully considered in the thermal design of underground electrical installations. Loess soils, although generally suitable due to their fine structure and moisture retention properties, require site-specific assessment and control of compaction and drainage conditions to ensure reliable performance.

To improve thermal properties (Martinez et al. 2019), a mixture was proposed that exchanged heat more effectively than soil particle contact points, and a linear relationship was obtained between $CaCO_3$ content and thermal conductivity. The thermal conductivity increased by 50% when the $CaCO_3$ content exceeded 8%.

Further research is recommended to investigate long-term thermal behaviour under cyclic moisture conditions and to quantify the influence of soil anisotropy and mineralogical variability on thermal conductivity.

ACKNOWLEDGEMENTS

This paper was made possible through the contribution of the research grant, “Evaluation of the Thermal Conductivity of Soil and Injection Material in Geothermal Boreholes” (GeoThermo) awarded to the authors by the Technical University of Civil Engineering from Bucharest under the ARUST2024 research program.

REFERENCES

ASTM International (2014). ASTM D5334-14 Standard Test Method for Determination of Thermal Conductivity of Soil and Soft Rock by Thermal Needle Probe Procedure, United States of America.

ASTM International (2021). ASTM D1557-12 Standard Test Methods for Laboratory Compaction Characteristics of Soil Using Modified Effort (56,000ft-lbf/ft^3 (2,700 kN-m/m^3)), United States of America.

ASTM International (2021). ASTM D1883-21 Standard Test Method for California Bearing Ratio (CBR) of Laboratory-Compacted Soils, United States of America.

Brandl, H. (2006). *Geotechnique*, London: The institution of civil engineers.

Dragomir, B.P. (2002). *Geologie fizică*. Bucureşti: Editura Universitatii din Bucuresti.

IEEE Std 442™. (2017). The Institute of Electrical and Electronics Engineers Guide for Thermal Resistivity. Measurements of Soils and Backfill Materials. United States of America.

Olinic, T., & Olinic, E. (2016). The Effect of Quicklime Stabilization on Soil Properties. *Agriculture and agricultural science Procedia, 10,* 444-451.

Martinez, A., Huang, L., & Gomez, M. (2019). Thermal conductivity of MICP-treated sands at varying degrees of saturation. *Géotechnique Letters, 8*, 1-7.

Mostafa, M., Anwar, M.B., & Radwan, A. (2018). Application of electrical resistivity measurement as quality control test for calcareous soil. *HBRC Journal, 14*(3), 379-384.

Nikiforova, T., Savytskyi, M., Limam, K., Bosschaerts, W., Belarbi, R. (2013). Methods and results of experimental researches of thermal conductivity of soils. *Energy Procedia, 42,* 775-783.

Sangprasat, K., Puttiwongrak, A., & Inazumi, S. (2024). Comprehensive analysis of correlations between soil electrical resistivity and index geotechnical properties. *Results in engineering*, *23*.

Wang, J., Deng, J., Zheng, J., Wang, T., & Yu, Y. (2024). Thermal Conductivity of Loess: Experimental Studies and Empirical Model. *KSCE Journal of Civil Engineering, 28*(2), 644-654.

Scientific Papers. Series E. Land Reclamation, Earth Observation & Surveying, Environmental Engineering. Vol. XIV, 2025
Print ISSN 2285-6064, CD-ROM ISSN 2285-6072, Online ISSN 2393-5138, ISSN-L 2285-6064

DISTRIBUTION OF HEAVY METALS IN THE DANUBE RIVER ECOSYSTEM AND THE IMPACT ON THE ENVIRONMENT. A REVIEW

Maria Daniela (IONICA) MIHAILA[1, 2], Valentina Andreea CĂLMUC[2], Cătălin PLATON[3], Puiu-Lucian GEORGESCU[1, 2], Cătălina ITICESCU[1, 2]

[1]"Dunărea de Jos" University of Galaţi, Faculty of Sciences and Environment,
111 Domnească Street, 800201, Galaţi, Romania
[2]"Dunărea de Jos" University of Galaţi, REXDAN Research Centre,
98 George Coşbuc Blvd, 800223, Galaţi, Romania
[3]ROMFISH National Fish Farmers Association, 12 Nicolae Iorga Blvd, 700583, Iaşi, Romania

Corresponding author email: maria.mihaila@ugal.ro

Abstract

The Danube Basin collects water from nineteen countries and is exposed to significant amounts of pollutants. Heavy metals such as lead (Pb), cadmium (Cd), mercury (Hg), arsenic (As), chromium (Cr), nickel (Ni), zinc (Zn), copper (Cu), aluminum (Al) are considered critical contaminants of aquatic ecosystems, given their high predilection to enter and accumulate in food chains. The primary sources of heavy metal pollution consist of discharges from agricultural waste, industrial and urban wastewater into the aquatic environment, as well as mining activities. Given their persistence in the environment, it is required to conduct studies on heavy metal concentrations to understand their implications for aquatic life and to assess biomagnification through food chains. For this purpose, various pollution indices are utilised to evaluate the chemical speciation of metals within the environmental system. Shortly, it is essential to prioritize the development of technologies that can facilitate the recovery of harmful heavy metals, while mitigating potential risks to the environment.

Key words*: bioaccumulation, Danube River, heavy metals.*

INTRODUCTION

The Danube River is one of the most essential in Europe, covering around 2.860 kilometres and crossing ten countries: Germany, Austria, Slovakia, Hungary, Croatia, Serbia, Romania, Bulgaria, Moldova, and Ukraine. It is an important river for the economy, transportation, drinking water, agriculture, and biodiversity (Popa et al., 2018).

The Danube Delta Biosphere Reserve (UNESCO protected area) forms at the mouth of the Danube into the Black Sea, making it one of the world's largest deltas and the second largest in Europe. It is also one of Europe's largest wetlands and a refuge for numerous bird, fish, and plant species. This area is ecologically, economically and geographically important, having a significant impact on the environment and economy of the riparian regions since it is an important place for fishing and tourism (Mîndrescu et al., 2022).

The Danube has numerous important tributaries coming from different regions of Central, Eastern and South-Eastern Europe, such as Inn, Morava, Drava, Sava, Tisa, Iskar, Olt, Siret, Prut and Velika Morava, which play an important role in supplying the river with water, but also with pollutants, significantly influencing water quality and disrupting the ecological equilibrium (Culicov et al., 2022). Sources of pollution with these metals can be natural or anthropogenic. The natural sources can include volcanic eruptions, weathering, wildfires, while anthropological sources can be mining, chemical and metallurgical industries, industrial waste discharges, agriculture (using pesticides and fertilizers), and through transportation or construction activities (Benhadji et al., 2025). Human activity in river basins and deltas causes pollutants to be released into the air, soil and water. The principal pollutants found in aquatic systems include volatile organic compounds, pharmaceutical compounds, plant nutrients, suspended solids, microbial pathogens, and parasites (Paul, 2017). Among these pollutants are also heavy metals (HMs), which are chemical elements with a high density that can

pose serious risks to both human health and the ecosystem, such as lead (Pb), cadmium (Cd), mercury (Hg), arsenic (As), chromium (Cr), nickel (Ni), zinc (Zn), copper (Cu), aluminium (Al) (Zaynab et al., 2022). Because of their widespread distribution, toxicity, persistence in the environment and capacity for bioaccumulation, heavy metals represent a critical contaminant of aquatic ecosystems (Jarić et al., 2011). In the past years, monitoring heavy metals in the aquatic environment has become a priority for authorities. The presence of heavy metals can be examined by inductively coupled plasma optical emission spectroscopy (ICP-OES) (Mikala Okouyi et al., 2024), inductively coupled plasma mass spectrometry (ICP-MS) (Calmuc et al., 2021), atomic absorption spectrometry (Lazarević et al. 2022), atomic fluorescence spectrometry (AFS), X-ray absorption spectroscopy (XAS) and X-ray fluorescence spectrometry (XRF) (He et al., 2024).
This study assesses the heavy metal concentration of the surface water, sediment, and biota of the Danube River, as well as the environmental impact.

MATERIALS AND METHODS

Sources of heavy metals

Aluminum (Al) is one of the most abundant metallic elements in the Earth's crust and occurs naturally only in the +3-oxidation state (Al^{3+}), typically in combination with elements such as oxygen, silicon, and fluorine. Al^{3+} is a key component of various minerals, including mica, feldspars, and clays. Aluminum enters the environment through natural processes such as rock weathering and volcanic activity, as well as anthropogenic activities, including aluminum production, coal combustion, mining, waste incineration, motor vehicle emissions, fireworks, packaging, toothpaste, vaccines, antiperspirants, and certain pharmaceuticals such as buffered aspirin and antacids (Alasfar & Isaifan, n.d.; Briffa et al., 2020; Closset et al., 2022).
Arsenic (As) is a crystalline metalloid that occurs naturally in the environment. It originates from both natural processes - such as wildfires, pedogenesis, dust storms, volcanic and geothermal activity - and anthropogenic sources including electroplating, smelting, fossil fuel combustion, production of glass, pharmaceuticals, insecticides, pesticides, fertilizers, electronics, mining, and wood preservation (Briffa et al., 2020; Byeon et al., 2021; Liu et al., 2022; Zhang et al., 2022; Wang et al., 2023; Sevak & Pushkar, 2024). In aquatic systems, the dominant and most toxic inorganic forms are arsenate (As^{5+}) and arsenite (As^{3+}) (Jeong et al., 2023).
Cadmium (Cd) is a highly toxic heavy metal found abundant in Earth's crust, usually in combination with ores of copper, zinc and lead. Natural cadmium emissions arise from rock weathering, volcanic eruptions, dust transport, marine aerosols, forest fires, and soil erosion (Khan et al., 2022; Jeong et al., 2023; Oladimeji et al., 2024). Anthropogenic sources include electroplating, metal coatings, mining, plastics stabilization, cement manufacturing, paint pigments, battery production, fossil fuel combustion, pesticide and fertilizer use, as well as incineration of municipal and sewage sludge (Briffa et al., 2020; Khan et al., 2022; Jeong et al., 2023; Oladimeji et al., 2024).
Chromium (Cr) particularly in the Cr^{+3} and Cr^{+6} oxidation states, is one of the most toxic heavy metals naturally present in water and soil due to geological processes like weathering. Anthropogenic contributions include metal processing, chromate production, leather tanning, stainless steel welding, electroplating, cement and pigment manufacturing, textile dyeing, mining, coal and oil combustion, fertilizer application, thermal power generation, and the paper industry (Briffa et al., 2020; He et al., 2020; Tumolo et al., 2020; Ayele & Godeto, 2021; Kolarova & Napiórkowski, 2021; Prasad et al., 2021; Jeong et al., 2023).
Copper (Co) is naturally present in the form of sulphide and oxide ores, salt minerals, and native copper deposits. It is released into the environment via volcanic activity, geological deposits, and the weathering and erosion of rocks and soils (Rehman et al., 2019). Copper contamination of water can occur through corrosion of pipes and plumbing fixtures (Alkhanjaf et al., 2024). Human-induced sources include mining, smelting, metal and electronics manufacturing, discharge of industrial wastewater, wood preservatives, antifouling paints, fossil fuel combustion, urban runoff, fertilizers, fungicides, and pesticides

(Rehman et al., 2019; Briffa et al., 2020; Izydorczyk et al., 2021; Jeong et al., 2023).

Lead (Pb) is a trace metal found naturally in reduced quantities in the environment, with unknown role in cells, but extremely toxic even at low concentrations, which can be bioaccumulated by aquatic organisms (Valová et al., 2010). It can be found in galena and can be generated by volcanic activities, weathering and erosion (Briffa et al., 2020; Jeong et al., 2023), but it is predominantly produced due to anthropogenic sources such as metal processing, battery production industry, lead-based paints, lead in gasoline, mining, smelting, automobiles production, metal plating, agricultural fertilizers, insecticides, pesticides, waste disposal (batteries and electronics), unsuitable industrial waste, ammunitions and projectiles, lead crystal glass, pipes, glass screens, cable covers (Briffa et al., 2020; Jeong et al., 2023; Raj & Das, 2023; Oladimeji et al., 2024).

Mercury (Hg) is a non-essential, persistent, and highly toxic metal that bioaccumulates and biomagnifies in aquatic ecosystems. Naturally, mercury is emitted from the Earth's crust, wildfires, erosion of mercury-containing rocks, volcanic activity, geothermal processes, weathering, and evaporation from surface water (Budnik & Casteleyn, 2019; de Almeida Rodrigues et al., 2019; Jeong et al., 2023; 2024) Anthropogenic sources include chlor-alkali and thermal power plants, manufacturing of batteries, thermometers, and fluorescent lamps, ore smelting, agriculture, fossil fuel combustion, sewage, industrial wastewater, and cultural practices such as fish-based diets (Budnik & Casteleyn, 2019; de Almeida Rodrigues et al., 2019; Briffa et al., 2020; Kolarova & Napiórkowski, 2021; Jeong et al., 2023; 2024). Mercury exists in elemental (Hg^0), inorganic (Hg^+, Hg^{2+}), and organic forms (e.g., methylmercury – $MeHg^+$) (Kumar et al., 2024; Tsui et al., 2025).

Nickel (Ni) is a potentially toxic element commonly present in soil and aquatic systems. Natural inputs include rock weathering, wildfires, and volcanic activity (Gauthier et al., 2021), while anthropogenic sources include alloy manufacturing, pigment production, tannery wastewater, fossil fuel combustion, stainless steel manufacturing, battery production, electroplating, automobile and refinery emissions (Briffa et al., 2020; Wang et al., 2020; El-Naggar et al., 2021).

Zinc (Zn) is an abundant trace element in the Earth's crust, primarily found in sulphide minerals like sphalerite (Zn, Fe) S. Anthropogenic sources of zinc include metal processing, mining, municipal wastewater discharges, galvanization, smelting, electroplating, cosmetics, sunblock, deodorants, and vitamin supplements (Seto et al., 2013; Briffa et al., 2020; Jeong et al., 2023).

These pollutants mainly come from metallurgical, chemical, mining industries and urban wastewater, having a major impact on water quality and aquatic ecosystems (Simionov et al., 2021a). Identifying the sources of contamination is essential for developing effective monitoring, control and remediation strategies.

In ***Austria***, the city of Linz serves as a major industrial centre where metallurgical and chemical processes are potential sources of contamination (Winkler et al., 2018). This is further compounded by the Inn River, which traverses Switzerland, Austria, and Germany, and receives industrial runoff from regions such as Bavaria, where lead (Pb), zinc (Zn), and copper (Cu) have been detected in elevated concentrations (Saeed et al., 2023). In ***Slovakia***, the industrial area near the capital Bratislava includes oil refineries and chemical facilities that may release hazardous substances into nearby watercourses (Culicov et al., 2022), with additional input from the Morava River, which transports agro-industrial pollutants and legacy contaminants from former industrial facilities in Slovakia (Vesković et al., 2024). In ***Hungary***, the accumulation of industrial residues from bauxite processing, particularly in the form of "red mud", poses a major environmental threat, owing to elevated concentrations of aluminium (Al), iron (Fe), and cadmium (Cd), with implications for both ecosystem integrity and public health (Winkler et al., 2018). The capital Budapest hosts active industrial and port areas, contributing to the metal load of the Danube, mainly through metallurgical and chemical activities (Culicov et al., 2022). The Drava River, which flows through Hungary as well as Italy, Austria, Slovenia, and Croatia, adds further contamination originating from mining, agriculture, and industry (Šorša et al., 2022). In

Serbia, heavy industrial activity along the Danube in Belgrade is a key source of contaminants, with metal processing facilities discharging trace elements such as lead and zinc directly into the river (Subotić et al., 2013). The Sava River, Serbia's most significant tributary, passes through major industrial cities like Zagreb and Belgrade, transporting both metallic and organic pollutants (Vuković et al., 2012; Jovanović et al., 2017). Further inland, the Velika Morava River carries industrial effluents from central Serbia's densely populated areas (Culicov et al., 2022). In ***Romania***, the city of Galați, with one of the country's largest steel producers, is a major source of industrial emissions (Ioniță et al., 2014; Iticescu et al., 2014; Georgescu et al., 2023). Although industrial activity in Turnu Măgurele has diminished, the persistence of contaminants from former chemical plants continues to raise ecological concerns. Similarly, Drobeta-Turnu Severin presents industrial activities, such as shipyard operations, that may continue to influence water quality (Georgescu et al., 2023). The Tisza, flowing through five countries including Romania, has been affected by pollution by mining-related accidents in Maramureș that released cyanide and metal contaminants downstream (Kraft et al., 2006). The Olt River has been affected by longstanding pollution from the chemical and mining sectors around Râmnicu Vâlcea (Iordache et al., 2022), while the Siret and Prut Rivers are influenced by both agriculture and urban development across Ukraine, Moldova, and Romania (Calmuc et al., 2021; Burdenyuk et al., 2023; Georgescu et al., 2023). In ***Bulgaria***, the industrial cities of Ruse and Vidin host chemical and metallurgical facilities whose discharges further burden the Danube's ecological balance (Culicov et al., 2022). Similarly, the Iskar River carries pollutants from industrial areas in Sofia and northern Bulgaria into the Danube (Angelova et al., 2020).

These tributaries highlight the complexity and scale of the challenges related to heavy metal pollution in the Danube basin.

Analytical Techniques for Heavy Metals Determination

Several analytical techniques are available for detecting and quantifying heavy metals in environmental samples, each with specific advantages and limitations depending on the matrix and target elements. ICP-OES and AAS are commonly used for water, sediment, and biota analysis, both providing detection limits around 0.1-10 ppb. ICP-OES enables simultaneous multi-element analysis, high throughput, and reduced matrix effects compared to AAS, though spectral interferences may occur in complex samples (Mikala Okouyi et al., 2024). AAS is a well-established method offering high precision for single-element determinations, though it is limited to sequential analysis and requires complete digestion of solid matrices (Lazarević et al., 2022). ICP-MS offers exceptional sensitivity (0.001-0.1 ppb), supporting ultra-trace analysis, wide dynamic range, and applications in isotopic and speciation studies, though it may be affected by polyatomic and isobaric interferences (Burada et al., 2015; Calmuc et al., 2021). AFS, with detection limits between 0.01 and 1 ppb, is highly sensitive for select elements such as Hg, As, and Se, offering good selectivity and low background noise, although its applicability is limited to a narrow range of elements and can be influenced by molecular and matrix interferences (Abdelmonem et al., 2025). For elemental speciation and oxidation state determination, XAS provides detailed structural information in solid, liquid, and biological samples. This non-destructive, element-specific technique requires advanced facilities and complex data interpretation (Hu et al., 2020). Lastly, XRF allows rapid, non-destructive analysis of solid matrices like sediments and dried biota, with detection limits of 1-10 ppm. While effective for screening and minimal sample preparation, it offers lower sensitivity for trace-level elements and is less suitable for light elements or complex organic matrices (Lu et al., 2023).

RESULTS AND DISCUSSIONS

Status of heavy metal in Danube River water, sediments and biota

Extensive studies have been carried out by several researchers on heavy metal pollution of river Danube (Table 1). A research group (Saeed et al., 2023) studied the concentrations of arsenic, chromium, copper, nickel, lead and zinc

in the water of the river Danube at Dunaföldvár, Baja and Hercegszántó (Hungary) between 2013 and 2019 and reported temporal and spatial variations in heavy metal distribution. Concentrations of Zn reached up to 19.39 $\mu g \cdot L^{-1}$, Cu up to 4.4 $\mu g \cdot L^{-1}$, and Ni exceeded 3 $\mu g \cdot L^{-1}$ in some sites. Other study presents (Popescu et al., 2022) the levels of As, Cd, Hg, Pb and Zn in several Romanian sites along the Danube during 2020. It was found that arsenic levels, though low (0.09-0.14 $\mu g \cdot L^{-1}$), were present throughout all sampling stations, while Pb concentrations ranged from 0.21 to 0.31 $\mu g \cdot L^{-1}$ and Zn levels were notably high, up to 21.1 $\mu g \cdot L^{-1}$. Simionov and his team (Simionov et al., 2021b) also conducted an important study on the concentrations of As, Cd, Cu, Ni, Pb and Zn in surface waters collected from Galați and Tulcea. The highest recorded values were for Zn (57 $\mu g \cdot L^{-1}$), Cu (6.7 $\mu g \cdot L^{-1}$), and Ni (8.2 $\mu g \cdot L^{-1}$) around Galați, while Pb reached up to 3.1 $\mu g \cdot L^{-1}$ and Cd 0.14 $\mu g \cdot L^{-1}$. These values significantly exceeded those reported in upstream areas and reflect strong anthropogenic influence, likely related to industrial and urban discharge. A seasonal assessment was performed in Croatia (Redžović et al., 2023) at Medsave and Jarun, where Al, Cd, Cr, Cu, Ni, Pb and Zn were monitored in water samples. Aluminum levels reached 3.94 $\mu g \cdot L^{-1}$, and Cd was found up to 0.030 $\mu g \cdot L^{-1}$.

Table 1. Concentrations of heavy metals in water of the Danube River and adjacent areas

Sampling area/Country	Survey period	Heavy metals									References
		Al ($\mu g \cdot L^{-1}$)	As ($\mu g \cdot L^{-1}$)	Cd ($\mu g \cdot L^{-1}$)	Cr ($\mu g \cdot L^{-1}$)	Cu ($\mu g \cdot L^{-1}$)	Hg ($\mu g \cdot L^{-1}$)	Ni ($\mu g \cdot L^{-1}$)	Pb ($\mu g \cdot L^{-1}$)	Zn ($\mu g \cdot L^{-1}$)	
Dunaföldvár, Hungary	April - September (2013-2019)	-	1.21	-	1.45	4.29	-	2.55	1.22	16.45	Saeed et al., 2023
		-	1.27	-	1.3	4.17	-	2.64	1.61	14.78	
		-	1.34	-	1.42	4.4	-	2.64	1.42	17.66	
Baja, Hungary		-	1.35	-	1.8	3.48	-	3.1	1.14	12.93	
Hercegszántó, Hungary		-	1.37	-	1.11	3.74	-	2.87	1.2	11.98	
		-	1.20	-	1.49	4.11	-	2.86	1.45	14.38	
		-	1.31	-	1.44	4.03	-	2.27	1.14	16.8	
Dunaföldvár, Hungary	October - March (2013-2019)	-	1.30	-	1.07	3.33	-	2.41	0.93	14.35	
		-	1.27	-	0.93	3.37	-	2.29	1.37	14.44	
		-	1.45	-	1.01	3.71	-	2.71	1.03	16.25	
Baja, Hungary		-	1.28	-	1.58	3.81	-	2.45	1.3	12.79	
Hercegszántó, Hungary		-	1.46	-	1.42	3.62	-	2.3	1.12	16.13	
		-	1.70	-	1.83	3.79	-	2.6	1.55	15.8	
		-	1.60	-	1.65	4.17	-	2.8	1.34	19.39	
Baziaș, Romania	July-September 2020	-	0.09	0.004	-	-	0.011	-	0.21	21.1	Popescu et al., 2022
Divici, Romania		-	0.12	0.009	-	-	0.017	-	0.24	18.5	
Coronini, Romania		-	0.12	0.008	-	-	0.012	-	0.28	20.1	
Liborajdea, Romania		-	0.14	0.012	-	-	0.014	-	0.21	18.5	
Svinița, Romania		-	0.10	0.014	-	-	0.011	-	0.21	17.9	
Dubova, Romania		-	0.11	0.008	-	-	0.009	-	0.22	19.1	
Gura Văii, Romania		-	0.09	0.0011	-	-	0.010	-	0.22	19.7	
Drobeta - Turnu Severin, Romania		-	0.11	0.042	-	-	0.009	-	0.22	19.4	
Țigănași, Romania		-	0.14	0.088	-	-	0.015	-	0.31	18.1	
Galati, Romania	April 2018	-	2.8	0.14	-	6.7	-	8.2	3.1	57	Simionov et al., 2021b
Tulcea, Romania		-	2.7	0.05	-	4.1	-	4.4	1.4	3	
Pietrei pond, Romania		-	3.9	0.004	-	0.5	-	1.1	0.7	0.5	
Barcaz Lake, Romania		-	1.7	0.02	-	2.6	-	2.9	0.8	5	
Soschi Lake, Romania		-	2.4	0.01	-	1.1	-	1	0.5	8	
Black Sea Sf. Gheorghe, Romania		-	1	0.06	-	1.8	-	7	1	4	
Black Sea Perisor, Romania		-	0.4	0.04	-	1.4	-	11	0.9	2	
Medsave, Croatia	Winter 2018	2.11	-	0.013	< 0.060	0.696	-	0.80	0.024	2.75	Redžović et al., 2023
	Spring 2019	1.96	-	0.020	0.396	0.648	-	1.13	0.043	1.64	
	Summer 2019	3.94	-	0.030	0.298	1.46	-	1.61	0.043	2.20	
	Autumn 2019	3.46	-	0.021	0.421	0.838	-	1.06	0.050	1.16	
Jarun, Croatia	Winter 2018	0.38	-	0.013	< 0.060	0.606	-	1.12	0.046	1.23	
	Spring 2019	1.79	-	0.017	0.327	1.17	-	2.03	0.050	1.43	
	Summer 2019	1.69	-	0.012	0.272	0.476	-	1.88	0.049	1.13	
	Autumn 2019	1.73	-	0.023	0.419	1.21	-	2.39	0.039	1.20	

This study emphasized seasonal fluctuations, with higher concentrations typically recorded during summer and autumn months. Heavy metal contamination in sediments is a critical indicator of long-term pollution in riverine ecosystems (Table 2).

Table 2. Concentrations of heavy metals in river and lake sediments along the Danube Basin

Sampling area/Country	Survey period	Heavy metals								References
		Al ($\mu g \cdot g^{-1}$)	As ($\mu g \cdot g^{-1}$)	Cd ($\mu g \cdot g^{-1}$)	Cr ($\mu g \cdot g^{-1}$)	Cu ($\mu g \cdot g^{-1}$)	Ni ($\mu g \cdot g^{-1}$)	Pb ($\mu g \cdot g^{-1}$)	Zn ($\mu g \cdot g^{-1}$)	
Galati, Romania	April 2018	-	11	0.6	23	26	34.9	11	130	Simionov et al., 2021b
Tulcea, Romania		-	7	0.5	18	19	29.7	10	100	
Pietrei pond, Romania		-	10	0.7	26	30	36.7	11	150	
Barcaz Lake, Romania		-	10	0.7	22	40	39.8	12	140	
Soschi Lake, Romania		-	13	0.7	18	34	27.6	8	100	
Black Sea Sf. Gheorghe, Romania		-	2	0.05	8	3	8.9	3	30	
Black Sea Perisor, Romania		-	1.4	0.01	5	2	5.2	2	17	
Tamis, Serbia		-	28.10	1.13	81.76	90.50	40.46	35.22	164.92	Kašanin-Grubin et al., 2023
Tisa, Serbia		-	16.54	2.12	12.69	77.58	60.56	49.22	312.12	
Sava, Serbia		-	9.84	2.57	69.08	28.71	78.49	27.29	149.84	
Danube, Serbia		-	15.05	2.75	14.24	98.79	82.17	91.45	353.91	
Medsave, Croatia	Winter 2018	5310	-	0.045	16.2	5.11	8.69	4.92	14.4	Redžović et al., 2023
	Spring 2019	8300	-	0.063	14.5	5.30	8.14	4.04	18.6	
	Summer 2019	8960	-	0.086	13.6	4.24	7.51	4.86	18.0	
	Autumn 2019	9270	-	0.088	13.1	4.07	7.51	5.11	18.3	
Jarun, Croatia	Winter 2018	5090	-	0.037	19.9	4.58	10.4	3.77	10.4	
	Spring 2019	8790	-	0.051	19.6	5.77	11.2	4.90	16.8	
	Summer 2019	7720	-	0.078	19	5.42	10.2	5.69	15.5	
	Autumn 2019	7660	-	0.070	14.5	4.49	7.50	5.28	15.8	
Danube, Serbia		-	17.8	-	183	56	97	-	328	Culicov et al., 2022
Insula Chici	Autumn 2018	-	-	0.30	-	4.30	16.03	5.90	58.84	Calmuc et al., 2021
Bac 1 (Braila)		-	-	0.59	-	10.72	29.12	8.96	118.54	
Bac 2		-	-	0.74	-	17.39	27.88	12.57	120.76	
Chiscani, Romania		-	-	0.50	-	12.58	22.31	8.49	87.43	
Priza Dunarii, Romania		-	-	0.50	-	12.54	20.53	7.93	84.15	
Siret, Romania		-	-	0.46	-	7.60	14.00	5.17	62.39	
Libertatea, Romania		-	-	0.57	-	11.81	19.99	7.28	84.65	
Cotul Pisicii, Romania		-	-	0.54	-	10.24	22.09	21.14	77.64	
Prut, Romania		-	-	0.54	-	7.89	16.28	4.84	64.48	
Grindu, Romania		-	-	0.76	-	13.42	23.90	7.55	146.23	
Luncavita, Romania		-	-	0.53	-	6.68	24.83	7.83	85.40	
Isaccea, Romania		-	-	0.63	-	9.79	24.76	6.84	96.11	
Somova, Romania	Autumn 2018	-	-	0.75	-	16.64	28.35	8.29	121.38	Calmuc et al., 2021
Vard Amo, Romania		-	-	0.57	-	15.17	38.81	8.11	117.01	
Tulcea, Romania		-	-	0.53	-	9.42	16.94	5.34	69.97	
Insula Chici	Spring 2019	-	-	0.59	-	10.31	20.17	6.02	78.69	
Bac 1 (Braila)		-	-	0.65	-	11.65	19.33	6.05	84.21	
Bac 2		-	-	0.99	-	25.01	35.80	13.78	177.33	
Chiscani, Romania		-	-	0.63	-	8.97	16.04	6.41	73.57	
Priza Dunarii, Romania		-	-	0.57	-	10.08	24.58	5.70	95.67	
Siret, Romania		-	-	0.41	-	7.55	19.09	4.17	71.27	
Libertatea, Romania		-	-	0.46	-	7.47	17.65	5.68	63.21	
Cotul Pisicii, Romania		-	-	0.78	-	19.47	28.49	10.35	131.50	
Prut, Romania		-	-	0.46	-	9.29	17.40	4.31	66.06	
Grindu, Romania		-	-	0.65	-	17.18	27.41	8.33	121.05	
Luncavita, Romania		-	-	0.72	-	27.50	50.46	14.64	161.24	
Isaccea, Romania		-	-	0.77	-	20.75	32.55	9.87	146.53	
Somova, Romania		-	-	0.82	-	23.29	39.03	9.90	154.34	
Vard Amo, Romania		-	-	0.48	-	9.29	25.85	6.76	81.26	
Tulcea, Romania		-	-	0.52	-	10.07	28.13	8.01	86.43	

A collaborative study (Simionov et al., 2021b) analysed sediment samples from Galați, Tulcea, Pietrei Pond, Barcaz Lake, and Soschi Lake in Romania, detecting As, Cd, Cr, Cu, Ni, Pb and Zn at varying levels. The maximum values reached 0.7 $\mu g \cdot g^{-1}$ for Cd, 40 $\mu g \cdot g^{-1}$ for Cu, and 150 $\mu g \cdot g^{-1}$ for Zn, while arsenic was found in concentrations up to 13 $\mu g \cdot g^{-1}$ in Soschi Lake. Recent findings in Serbia (Kašanin-Grubin et al., 2023) highlight significant contamination in sediments from the Danube, Sava, Tisa and Tamiš rivers. In the Danube, Cd reached 2.75 $\mu g \cdot g^{-1}$, Cu up to 98.79 $\mu g \cdot g^{-1}$, and Zn 353.91 $\mu g \cdot g^{-1}$. Lead (Pb) was also present at concerning levels, up to 91.45 $\mu g \cdot g^{-1}$, while Cr measured 14.24 $\mu g \cdot g^{-1}$, indicating severe industrial pollution. A Croatian study (Redžović et al., 2023) conducted a seasonal assessment at Medsave and Jarun. Aluminum concentrations ranged from 5310 to 9270 $\mu g \cdot g^{-1}$, and cadmium reached up to 0.088 $\mu g \cdot g^{-1}$. While heavy metal values were moderate compared to other regions, seasonal variation influenced levels of Cr, Ni, and Zn, with higher concentrations typically observed in spring and summer.

Calmuc et al., 2021 assessed sediment contamination between Braila and Tulcea, Romania. At Grindu, Zn reached up to 146.23 $\mu g \cdot g^{-1}$ and Cu 13.42 $\mu g \cdot g^{-1}$. At Luncavița and Somova, Cd exceeded 0.70 $\mu g \cdot g^{-1}$, and Cu surpassed 27.50 $\mu g \cdot g^{-1}$. Elevated levels of Ni, Pb, and Zn suggest strong anthropogenic input, especially near industrial zones and confluence areas. Heavy metals accumulation in fish provides valuable insight into bioavailability and potential human health risks (Table 3). The investigation performed (Simionov et al., 2021b) focused on several species sampled from Galați, Tulcea, Pietrei Pond, Barcaz Lake, Soschi Lake, Black Sea Sf. Gheorghe, Black Sea Perisor (Romania). They determined that liver tissues generally exhibited higher concentrations of metals than muscle. Notably, Cd reached 0.8 $\mu g \cdot g^{-1}$ in *Cyprinus carpio* liver, while Zn levels peaked at 157 $\mu g \cdot g^{-1}$, indicating significant bioaccumulation. In addition, Jovičić et al., 2024 assessed metal content in *Rutilus rutilus* and *Blicca bjoerkna* from Veliko Ratno Ostrvo and Višnjica (Serbia), identifying the presence of As, Cr, Cu, Hg, Ni, Pb and Zn. Zinc concentrations were the highest, up to 27.64 $\mu g \cdot g^{-1}$, while Cr and Ni also showed moderate levels.

Table 3. Concentrations of heavy metals in biota from Danube Basin

Sampling area/Country	Species	Sample type	Survey period	Heavy metals								References
				As ($\mu g \cdot g^{-1}$)	Cd ($\mu g \cdot g^{-1}$)	Cr ($\mu g \cdot g^{-1}$)	Cu ($\mu g \cdot g^{-1}$)	Hg ($\mu g \cdot g^{-1}$)	Ni ($\mu g \cdot g^{-1}$)	Pb ($\mu g \cdot g^{-1}$)	Zn ($\mu g \cdot g^{-1}$)	
Galati, Romania	*Abramis brama*	muscle	April 2018	-	0.02	-	0.4	-	-	0.025	4.38	Simionov et al., 2021b
		liver		-	0.3	-	10	-	-	0.043	25.6	
	Leuciscus aspius	muscle		-	0.02	-	0.2	-	-	0.005	5.14	
		liver		-	0.24	-	2	-	-	0.27	12.6	
	Alosa immaculata	muscle		-	0.02	-	0.4	-	-	0.01	3.6	
		liver		-	0.11	-	1	-	-	0.02	25.9	
Tulcea, Romania	*Silurus glanis*	muscle		-	0.03	-	0.5	-	-	0.015	7.6	
		liver		-	0.14	-	3	-	-	0.03	20.6	
	Cyprinus carpio	muscle		-	0.15	-	2	-	-	0.013	20.6	
		liver		-	0.73	-	7	-	-	0.03	74.4	
Pietrei pond, Romania	*Silurus glanis*	muscle		-	0.02	-	5.4	-	-	0.005	7.4	
		liver		-	0.17	-	12	-	-	0.015	25.6	
	Cyprinus carpio	muscle		-	0.12	-	5	-	-	0.004	32.9	
		liver		-	0.8	-	8	-	-	0.016	157	
	Carassius gibelio	muscle		-	0.08	-	0.4	-	-	0.013	13.3	
		liver		-	0.03	-	2	-	-	0.16	94.7	
Barcaz Lake, Romania	*Silurus glanis*	muscle		-	0.2	-	1.4	-	-	0.024	4.1	
		liver		-	0.6	-	2.5	-	-	0.012	17.2	
	Cyprinus carpio	muscle		-	0.06	-	1.4	-	-	0.02	37.9	
		liver		-	0.07	-	3	-	-	0.03	133	
	Carassius gibelio	muscle		-	0.02	-	3	-	-	0.014	16.7	
		liver		-	0.015	-	5.4	-	-	0.156	35.9	
Soschi Lake, Romania	*Silurus glanis*	muscle		-	0.006	-	0.5	-	-	0.009	5	
		liver		-	0.06	-	2	-	-	0.013	16.1	
	Cyprinus carpio	muscle		-	0.001	-	1.4	-	-	0.002	7.7	
		liver		-	0.02	-	8	-	-	0.013	34	
	Esox lucius	muscle		-	0.002	-	0.5	-	-	0.003	15	
		liver		-	0.002	-	3.2	-	-	0.015	43	
	Carassius gibelio	muscle		-	0.005	-	2.3	-	-	0.016	31	
		liver		-	0.02	-	5.5	-	-	0.07	72	

Sampling area/Country	Species	Sample type	Survey period	Heavy metals								References
				As ($\mu g \cdot g^{-1}$)	Cd ($\mu g \cdot g^{-1}$)	Cr ($\mu g \cdot g^{-1}$)	Cu ($\mu g \cdot g^{-1}$)	Hg ($\mu g \cdot g^{-1}$)	Ni ($\mu g \cdot g^{-1}$)	Pb ($\mu g \cdot g^{-1}$)	Zn ($\mu g \cdot g^{-1}$)	
Black Sea Sf. Gheorghe, Romania	*Trachurus m. ponticus*	muscle	April 2018	0.4	0.02	-	0.3	-	-	0.015	6	Simionov et al., 2021b
		liver		0.9	0.09	-	2	-	-	0.034	22	
Black Sea Perisor, Romania	*Alosa immaculata*	muscle		0.4	0.02	-	0.4	-	-	0.021	4	
		liver		0.7	0.12	-	2	-	-	0.03	31	
	Mugil cephalus	muscle		0.3	0.05	-	5	-	-	0.021	8	
		liver		2.3	0.62	-	35	-	-	0.06	35	
	Platichtys flesus	muscle		0.5	0.02	-	0.1	-	-	0.013	8	
		liver		0.6	0.17	-	3.2	-	-	0.025	30	
Veliko Ratno Ostrvo, Serbia	*Rutilus rutilus*	muscle	April 2021	0.019	-	0.019	0.264	0.080	0.480	0.023	9.002	Jovičić et al., 2024
	Blicca bjoerkna (Abramis brama)			0.115	-	0.110	0.202	0.109	0.317	0.028	12.935	
Višnjica, Serbia	*Rutilus rutilus*	muscle		0.072	-	0.020	0.566	0.081	0.158	0.029	27.641	
	Blicca bjoerkna (Abramis brama)			0.048	-	0.051	0.269	0.050	0.591	0.024	12.228	
Spačva, Croatia	*Cybister lateralimarginalis*	-	Spring - Summer 2023	420	39	-	-	630	-	40	-	Bjedov et al., 2025
Podravlje, Croatia				510	113	-	-	250	-	150	-	
Mužilovčica, Croatia				530	28	-	-	690	-	80	-	
Strug, Croatia				470	42	-	-	560	-	210	-	
Kopački rit, Croatia				390	19	-	-	520	-	200	-	
Stara Drava, Croatia				1440	29	-	-	360	-	160	-	
Reka, Croatia				570	24	-	-	500	-	640	-	
Zemun, Serbia	*Carassius auratius gibelio*	muscle	October 2013	139	57	-	-	994	-	30	-	Jovanović et al., 2017
	Barbus barbus			189	52	-	-	222	-	48	-	
	Abramis brama			109	21	-	-	110	-	19	-	
	Cyprinus carpio			258	59	-	-	393	-	59	-	
	Stizostedion lucioperca			105	23	-	-	106	-	32	-	
	Silurus glanis			160	68	-	-	208	-	58	-	
Grocka, Serbia	*Carassius auratius gibelio*			172	51	-	-	139	-	40	-	
	Barbus barbus			239	62	-	-	325	-	62	-	
	Abramis brama			154	27	-	-	161	-	28	-	
	Cyprinus carpio			333	82	-	-	466	-	84	-	
	Stizostedion lucioperca			153	36	-	-	162	-	37	-	
	Silurus glanis			211	69	-	-	260	-	69	-	

Effects of heavy metals

Heavy metals present significant ecotoxicological threats to aquatic ecosystems, exerting their toxicity through a variety of mechanisms, including oxidative stress, neurotoxicity, enzymatic inhibition, impaired reproduction, and disruption of metabolic homeostasis. ***Lead*** accumulates in tissues such as gills, muscles, gonads, and digestive glands, where it mimics essential metals like copper, zinc, and iron, disrupting physiological functions (Jeong et al., 2023). Its affinity for sulfhydryl groups leads to enzymatic inhibition, including suppression of heme synthesis and antioxidant defense, resulting in lipid peroxidation, protein degradation, and DNA damage (Raj & Das, 2023; Oladimeji et al., 2024). ***Cadmium***, although not subject to biomagnification, bioaccumulates extensively and replaces essential metals in enzymatic systems, impairing cell signalling and inducing oxidative stress, calcium imbalance, and DNA damage (Khan et al., 2022; Jeong et al., 2023). Its toxicity is evident even at low concentrations, causing growth reduction and neurotoxicity in species such as *Daphnia magna* and *Ostrea edulis* (Abd Elnabi et al., 2023). Moreover, cadmium persists in sediments and alters microbial activity and plant growth, destabilizing ecosystem processes (Kolarova & Napiórkowski, 2021; Oladimeji et al., 2024). ***Mercury***, particularly as methylmercury (MeHg), is one of the most dangerous aquatic pollutants due to its ability to bioaccumulate and biomagnifies along food chains (Jeong et al., 2023). MeHg, formed under anoxic or even oxic

conditions, is readily absorbed by phytoplankton, initiating trophic transfer and causing severe neurotoxicity and structural deformities in fish (Kumar et al., 2024; Tsui et al., 2025). It also crosses the blood-brain barrier, accumulating in organs and impairing immune responses (Briffa et al., 2020). ***Arsenic***, influenced by pH, redox conditions, and organic matter, accumulates in sediments via adsorption to iron and manganese oxides, from where it may be remobilized (Wang et al., 2023). The inorganic form, arsenite (As^{+3}), is particularly toxic and bioavailable, accumulating in the liver and gills and causing oxidative stress, growth inhibition, and apoptosis (Jeong et al., 2023; Sevak & Pushkar, 2024). Although bioreduction is common in food chains, certain arsenic forms, such as arsenobetaines, may undergo biomagnification (Zhang et al., 2022). ***Chromium***, especially as Cr^{+6}, is mutagenic and carcinogenic, affecting fish, invertebrates, and aquatic plants through oxidative stress, reproductive toxicity, and developmental inhibition (He et al., 2020; Ayele & Godeto, 2021). Cr^{+6} reduces photosynthesis in aquatic flora, while Cr^{+3} can cause more severe effects in fish (Prasad et al., 2021; Jeong et al., 2023;). ***Nickel***, although essential for some microorganisms, becomes toxic at high concentrations, accumulating in gills, liver, and kidneys, where it induces respiratory disturbances and ionic imbalance (Gauthier et al., 2021). Sensitivity varies by species, with gastropods and vascular plants being more susceptible than fish or algae (Blewett & Leonard, 2017; Wang et al., 2020). ***Zinc***, an essential trace element, becomes toxic in excess, disturbing calcium metabolism in freshwater fish, leading to hypocalcemia and mortality (Jeong et al., 2023). While phytoplankton may mitigate its toxicity by supporting microbial metabolism, invertebrates often suffer from reduced respiration and excretion, leading to restricted growth (Seto et al., 2013). ***Aluminum***, particularly soluble at low pH, accumulates in tissues such as the brain in species like *Oncorhynchus mykiss*, where it causes neurotoxicity, oxidative stress, inflammation, and acetylcholinesterase inhibition (Closset et al., 2022). Its toxicity is form-dependent, with monomeric inorganic species being most harmful. Finally, ***copper***, though an essential micronutrient, is highly toxic at elevated levels, even exceeding the toxicity of cadmium or lead in some cases (Jeong et al., 2023). Cu disrupts enzymatic activity, reproduction, and neurological function, and may become remobilized from sediments under climate-induced changes, amplifying ecological risks (Izydorczyk et al., 2021; Cui et al., 2024). Its impact is compounded by its widespread use in industry and agriculture and its influence on drinking water toxicity under varying pH and hardness conditions (Rehman et al., 2019).

CONCLUSIONS

Heavy metal pollution in the Danube basin is the result of industrial, urban and agricultural sources, both along the river and from its major tributaries. The use of modern analytical methods and the precise identification of critical areas is essential to understand the dynamics of pollution and to implement coherent monitoring and remediation measures.

ACKNOWLEDGEMENTS

This research was supported by the project "Integrated research and sustainable solutions to protect and restore Lower Danube Basin and coastal Black Sea ecosystems" (ResPonSE), contract no. 760010/30.12.2022.

REFERENCES

Abd Elnabi, M. K., Elkaliny, N. E., Elyazied, M. M., Azab, S. H., Elkhalifa, S. A., Elmasry, S., Mouhamed, M. S., Shalamesh, E. M., Alhorieny, N. A., Abd Elaty, A. E., Elgendy, I. M., Etman, A. E., Saad, K. E., Tsigkou, K., Ali, S. S., Kornaros, M., & Mahmoud, Y. A. G. (2023). Toxicity of Heavy Metals and Recent Advances in Their Removal: A Review. *Toxics, 11*(7). https://doi.org/10.3390/toxics11070580

Abdelmonem, B. H., Kamal, L. T., Elbaz, R. M., Khalifa, M. R., & Abdelnaser, A. (2025). From contamination to detection: The growing threat of heavy metals. *Heliyon, 11*(1). https://doi.org/10.1016/j.heliyon.2025.e41713

Alasfar, R. H., & Isaifan, R. J. (n.d.). Aluminum environmental pollution: the silent killer. https://doi.org/10.1007/s11356-021-14700-0/Published

Alkhanjaf, A. A. M., Sharma, S., Sharma, M., Kumar, R., Arora, N. K., Kumar, B., Umar, A., Baskoutas, S., & Mukherjee, T. K. (2024). Microbial strategies for copper pollution remediation: Mechanistic insights

and recent advances. *Environmental Pollution, 346*. https://doi.org/10.1016/j.envpol.2024.123588

Angelova, I., Ivanov, I., & Venelinov, T. (2020). Origin of Aluminium in the Raw Drinking Water of Sofia City, Bulgaria. *Water, Air, and Soil Pollution, 231*(9). https://doi.org/10.1007/s11270-020-04819-0

Ayele, A., & Godeto, Y. G. (2021). Bioremediation of Chromium by Microorganisms and Its Mechanisms Related to Functional Groups. *Journal of Chemistry, 2021*. https://doi.org/10.1155/2021/7694157

Benhadji, N., Kurniawan, S. B., & Imron, M. F. (2025). Review of mayflies (Insecta Ephemeroptera) as a bioindicator of heavy metals and microplastics in freshwater. *Science of the Total Environment, 958*. https://doi.org/10.1016/j.scitotenv.2024.178057

Bjedov, D., Turić, N., Mikuška, A., Vignjević, G., Kovačić, L. S., Pavičić, A. M., Toth Jakeljić, L., & Velki, M. (2025). The diving beetle, Cybister lateralimarginalis (De Geer, 1774), as a bioindicator for subcellular changes affected by heavy metal(loid) pollution in freshwater ecosystems. *Aquatic Toxicology, 279*. https://doi.org/10.1016/j.aquatox.2025.107258

Blewett, T. A., & Leonard, E. M. (2017). Mechanisms of nickel toxicity to fish and invertebrates in marine and estuarine waters. *Environmental Pollution, 223*, 311–322. https://doi.org/10.1016/j.envpol.2017.01.028

Briffa, J., Sinagra, E., & Blundell, R. (2020). Heavy metal pollution in the environment and their toxicological effects on humans. *Heliyon, 6*(9). https://doi.org/10.1016/j.heliyon.2020.e04691

Budnik, L. T., & Casteleyn, L. (2019). Mercury pollution in modern times and its socio-medical consequences. *Science of the Total Environment, 654*, 720–734. https://doi.org/10.1016/j.scitotenv.2018.10.408

Burada, A., Maria-Catalina, T., Georgescu, L., & Teodorof, L. (2015). Heavy Metals Environment Accumulation in Somova-Parches Aquatic Complex from the Danube Delta Area. https://www.researchgate.net/publication/279316234

Burdenyuk, I., Masykevich, A., Dombrovskiy, K., Rylskyi, O., Masykevich, Y., Deyneka, S., Malovanyy, M., & Tymchuk, I. (2023). Sanitary, Microbiological Condition, and Ecological State of Surface Water Quality in the Upper Siret River Basin (Ukraine). *Ecological Engineering and Environmental Technology, 24*(9), 55–63. https://doi.org/10.12912/27197050/172930

Byeon, E., Kang, H. M., Yoon, C., & Lee, J. S. (2021). Toxicity mechanisms of arsenic compounds in aquatic organisms. *Aquatic Toxicology, 237*. https://doi.org/10.1016/j.aquatox.2021.105901

Calmuc, V. A., Calmuc, M., Arseni, M., Topa, C. M., Timofti, M., Burada, A., Iticescu, C., & Georgescu, L. P. (2021). Assessment of heavy metal pollution levels in sediments and of ecological risk by quality indices, applying a case study: The lower Danube River, Romania. *Water (Switzerland), 13*(13). https://doi.org/10.3390/w13131801

Closset, M., Cailliau, K., Slaby, S., & Marin, M. (2022). Effects of aluminium contamination on the nervous system of freshwater aquatic vertebrates: A review. *International Journal of Molecular Sciences, 23*(1). https://doi.org/10.3390/ijms23010031

Cui, L., Cheng, C., Li, X., Gao, X., Lv, X., Wang, Y., Zhang, H., & Lei, K. (2024). Comprehensive assessment of copper's effect on marine organisms under ocean acidification and warming in the 21st century. *Science of the Total Environment, 927*. https://doi.org/10.1016/j.scitotenv.2024.172145

Culicov, O. A., Trtić-Petrović, T., Nekhoroshkov, P. S., Zinicovscaia, I., & Duliu, O. G. (2022). On the Geochemistry of the Danube River Sediments (Serbian Sector). *International Journal of Environmental Research and Public Health, 19*(19). https://doi.org/10.3390/ijerph191912879

de Almeida Rodrigues, P., Ferrari, R. G., dos Santos, L. N., & Conte Junior, C. A. (2019). Mercury in aquatic fauna contamination: A systematic review on its dynamics and potential health risks. *Journal of Environmental Sciences (China), 84*, 205–218. https://doi.org/10.1016/j.jes.2019.02.018

El-Naggar, A., Ahmed, N., Mosa, A., Niazi, N. K., Yousaf, B., Sharma, A., Sarkar, B., Cai, Y., & Chang, S. X. (2021). Nickel in soil and water: Sources, biogeochemistry, and remediation using biochar. *Journal of Hazardous Materials, 419*. https://doi.org/10.1016/j.jhazmat.2021.126421

Gauthier, P. T., Blewett, T. A., Garman, E. R., Schlekat, C. E., Middleton, E. T., Suominen, E., & Crémazy, A. (2021). Environmental risk of nickel in aquatic Arctic ecosystems. *Science of the Total Environment, 797*. https://doi.org/10.1016/j.scitotenv.2021.148921

Georgescu, P. L., Moldovanu, S., Iticescu, C., Calmuc, M., Calmuc, V., Topa, C., & Moraru, L. (2023). Assessing and forecasting water quality in the Danube River by using neural network approaches. *Science of the Total Environment, 879*. https://doi.org/10.1016/j.scitotenv.2023.162998

He, C., Gu, L., Xu, Z., He, H., Fu, G., Han, F., Huang, B., & Pan, X. (2020). Cleaning chromium pollution in aquatic environments by bioremediation, photocatalytic remediation, electrochemical remediation and coupled remediation systems. *Environmental Chemistry Letters, 18*(3), 561–576. https://doi.org/10.1007/s10311-019-00960-3

He, S., Niu, Y., Xing, L., Liang, Z., Song, X., Ding, M., & Huang, W. (2024). Research progress of the detection and analysis methods of heavy metals in plants. *Frontiers in Plant Science, 15*. https://doi.org/10.3389/fpls.2024.1310328

Hu, H., Zhao, J., Wang, L., Shang, L., Cui, L., Gao, Y., Li, B., & Li, Y. F. (2020). Synchrotron-based techniques for studying the environmental health effects of heavy metals: Current status and future perspectives. *TrAC - Trends in Analytical Chemistry, 122*. https://doi.org/10.1016/j.trac.2019.115721

Ioniță, C., Mititelu, M., & Moroşan, E. (2014). Analysis of heavy metals and organic pollutants from some Danube River fishes. *Farmacia, 62*(2).

Iordache, A. M., Nechita, C., Zgavarogea, R., Voica, C., Varlam, M., & Ionete, R. E. (2022). Accumulation and ecotoxicological risk assessment of heavy metals in surface sediments of the Olt River, Romania. *Scientific Reports, 12*(1). https://doi.org/10.1038/s41598-022-04865-0

Iticescu, C., Georgescu, L., Maria-Catalina, T., & Murariu, G. (2014). Monitoring the Danube water quality near the Galati city. https://www.researchgate.net/publication/289852048

Izydorczyk, G., Mikula, K., Skrzypczak, D., Moustakas, K., Witek-Krowiak, A., & Chojnacka, K. (2021). Potential environmental pollution from copper metallurgy and methods of management. *Environmental Research, 197*. https://doi.org/10.1016/j.envres.2021.111050

Jarić, I., Višnjić-Jeftić, Ž., Cvijanović, G., Gačić, Z., Jovanović, L., Skorić, S., & Lenhardt, M. (2011). Determination of differential heavy metal and trace element accumulation in liver, gills, intestine and muscle of sterlet (*Acipenser ruthenus*) from the Danube River in Serbia by ICP-OES. *Microchemical Journal, 98*(1), 77–81. https://doi.org/10.1016/j.microc.2010.11.008

Jeong, H., Ali, W., Zinck, P., Souissi, S., & Lee, J. S. (2024). Toxicity of methylmercury in aquatic organisms and interaction with environmental factors and coexisting pollutants: A review. *Science of the Total Environment, 943*. https://doi.org/10.1016/j.scitotenv.2024.173574

Jeong, H., Byeon, E., Kim, D. H., Maszczyk, P., & Lee, J. S. (2023). Heavy metals and metalloid in aquatic invertebrates: A review of single/mixed forms, combination with other pollutants, and environmental factors. *Marine Pollution Bulletin, 191*. https://doi.org/10.1016/j.marpolbul.2023.114959

Jovanović, D. A., Marković, R. V., Teodorović, V. B., Šefer, D. S., Krstić, M. P., Radulović, S. B., Ivanović Ćirić, J. S., Janjić, J. M., & Baltić, M. (2017). Determination of heavy metals in muscle tissue of six fish species with different feeding habits from the Danube River, Belgrade—public health and environmental risk assessment. *Environmental Science and Pollution Research, 24*(12), 11383–11391. https://doi.org/10.1007/s11356-017-8783-1

Jovičić, K., Djikanović, V., Santrač, I., Živković, S., Dimitrijević, M., & Vranković, J. S. (2024). Effects of trace elements on the fatty acid composition in Danubian fish species. *Animals, 14*(6). https://doi.org/10.3390/ani14060954

Kašanin-Grubin, M., Gajić, V., Veselinović, G., Stojadinović, S., Antić, N., & Štrbac, S. (2023). Provenance and pollution status of river sediments in the Danube watershed in Serbia. *Water (Switzerland), 15*(19). https://doi.org/10.3390/w15193406

Khan, Z., Elahi, A., Bukhari, D. A., & Rehman, A. (2022). Cadmium sources, toxicity, resistance and removal by microorganisms - A potential strategy for cadmium eradication. *Journal of Saudi Chemical Society, 26*(6). https://doi.org/10.1016/j.jscs.2022.101569

Kolarova, N., & Napiórkowski, P. (2021). Trace elements in aquatic environment: Origin, distribution, assessment and toxicity effect for the aquatic biota. *Ecohydrology and Hydrobiology, 21*(4), 655–668. https://doi.org/10.1016/j.ecohyd.2021.02.002

Kraft, C., von Tümpling, W., & Zachmann, D. W. (2006). The effects of mining in Northern Romania on the heavy metal distribution in sediments of the rivers Szamos and Tisza (Hungary). *Acta Hydrochimica et Hydrobiologica, 34*(3), 257–264. https://doi.org/10.1002/aheh.200400622

Kumar, A., Kumar, V., Bakshi, P., Parihar, R. D., Radziemska, M., & Kumar, R. (2024). Mercury in the natural environment: Biogeochemical cycles and associated health risks. *Journal of Geochemical Exploration, 267*. https://doi.org/10.1016/j.gexplo.2024.107594

Lazarević, J., Čabarkapa, I., Rakita, S., Banjac, M., Tomičić, Z., Škrobot, D., Radivojević, G., Kalenjuk Pivarski, B., & Tešanović, D. (2022). Invasive crayfish *Faxonius limosus*: Meat safety, nutritional quality and sensory profile. *International Journal of Environmental Research and Public Health, 19*(24). https://doi.org/10.3390/ijerph192416819

Liu, X., Zeng, B., & Lin, G. (2022). Arsenic (As) contamination in sediments from coastal areas of China. *Marine Pollution Bulletin, 175*. https://doi.org/10.1016/j.marpolbul.2022.113350

Lu, X., Li, F., Yang, W., Zhu, P., & Lv, S. (2023). Quantitative analysis of heavy metals in soil by X-ray fluorescence with improved variable selection strategy and Bayesian optimized support vector regression. *Chemometrics and Intelligent Laboratory Systems, 238*. https://doi.org/10.1016/j.chemolab.2023.104842

Mikala Okouyi, C., Kamdem, M. M., Voua Otomo, P., & Maganga, G. D. (2024). Metal accumulation in fish species of a vast hydrographic network in the Moyen-Ogooué and Haut-Ogooué Provinces of Gabon: Implications for human health. *Toxicology Reports, 13*. https://doi.org/10.1016/j.toxrep.2024.101842

Mîndrescu, M., Haliuc, A., Zhang, W., Carozza, L., Carozza, J. M., Groparu, T., Valette, P., Sun, Q., Nian, X., & Gradinaru, I. (2022). A 600 years sediment record of heavy metal pollution history in the Danube Delta. *Science of the Total Environment, 823*, 153702. https://doi.org/10.1016/j.scitotenv.2022.153702

Oladimeji, T. E., Oyedemi, M., Emetere, M. E., Agboola, O., Adeoye, J. B., & Odunlami, O. A. (2024). Review on the impact of heavy metals from industrial wastewater effluent and removal technologies. *Heliyon, 10*(23). https://doi.org/10.1016/j.heliyon.2024.e40370

Paul, D. (2017). Research on heavy metal pollution of river Ganga: A review. *Annals of Agrarian Science, 15*(2), 278–286. https://doi.org/10.1016/j.aasci.2017.04.001

Popa, P., Murariu, G., Timofti, M., & Georgescu, L. P. (2018). Multivariate statistical analyses of Danube River water quality at Galati, Romania. *Environmental Engineering and Management Journal, 17*(5), 1249–1266. https://doi.org/10.30638/eemj.2018.124

Popescu, F., Trumić, M., Cioabla, A. E., Vujić, B., Stoica, V., Trumić, M., Opris, C., Bogdanović, G., & Trif-Tordai, G. (2022). Analysis of surface water quality and sediments content on Danube Basin in Djerdap-Iron Gate protected areas. *Water (Switzerland), 14*(19). https://doi.org/10.3390/w14192991

Prasad, S., Yadav, K. K., Kumar, S., Gupta, N., Cabral-Pinto, M. M. S., Rezania, S., Radwan, N., & Alam, J. (2021). Chromium contamination and effect on environmental health and its remediation: A sustainable approaches. *Journal of Environmental Management, 285*. https://doi.org/10.1016/j.jenvman.2021.112174

Raj, K., & Das, A. P. (2023). Lead pollution: Impact on environment and human health and approach for a sustainable solution. *Environmental Chemistry and Ecotoxicology, 5*, 79–85. https://doi.org/10.1016/j.enceco.2023.02.001

Redžović, Z., Erk, M., Gottstein, S., Sertić Perić, M., Dautović, J., Fiket, Ž., Brkić, A. L., & Cindrić, M. (2023). Metal bioaccumulation in stygophilous amphipod *Synurella ambulans* in the hyporheic zone: The influence of environmental factors. *Science of the Total Environment, 866*. https://doi.org/10.1016/j.scitotenv.2022.161350

Rehman, M., Liu, L., Wang, Q., Saleem, M. H., Bashir, S., Ullah, S., & Peng, D. (2019). Copper environmental toxicology, recent advances, and future outlook: A review. *Environmental Science and Pollution Research, 26*(18), 18003–18016. https://doi.org/10.1007/s11356-019-05073-6

Saeed, O., Székács, A., Jordán, G., Mörtl, M., Abukhadra, M. R., & Eid, M. H. (2023). Investigating the impacts of heavy metal(loid)s on ecology and human health in the lower basin of Hungary's Danube River: A Python and Monte Carlo simulation-based study. *Environmental Geochemistry and Health, 45*(12), 9757–9784. https://doi.org/10.1007/s10653-023-01769-4

Seto, M., Wada, S., & Suzuki, S. (2013). The effect of zinc on aquatic microbial ecosystems and the degradation of dissolved organic matter. *Chemosphere, 90*(3), 1091–1102. https://doi.org/10.1016/j.chemosphere.2012.09.014

Sevak, P., & Pushkar, B. (2024). Arsenic pollution cycle, toxicity and sustainable remediation technologies: A comprehensive review and bibliometric analysis. *Journal of Environmental Management, 349*. https://doi.org/10.1016/j.jenvman.2023.119504

Simionov, I. A., Cristea, D. S., Petrea, Ștefan M., Mogodan, A., Jijie, R., Ciornea, E., Nicoară, M., Rahoveanu, M. M. T., & Cristea, V. (2021a). Predictive innovative methods for aquatic heavy metals pollution based on bioindicators in support of blue economy in the Danube River Basin. *Sustainability (Switzerland), 13*(16). https://doi.org/10.3390/su13168936

Simionov, I. A., Cristea, D. S., Petrea, S. M., Mogodan, A., Nicoara, M., Plavan, G., Baltag, E. S., Jijie, R., & Strungaru, S. A. (2021b). Preliminary investigation of lower Danube pollution caused by potentially toxic metals. *Chemosphere, 264*. https://doi.org/10.1016/j.chemosphere.2020.128496

Šorša, A., Čeru, T., Kovács, Z., Jordan, G., Dudás, K. M., & Szabó, P. (2022). Assessment of river sediment quality according to the EU Water Framework Directive in lowland fluvial conditions: A case study in the Drava River area, Danube River Basin. *Carpathian Journal of Earth and Environmental Sciences, 17*(2), 459–468. https://doi.org/10.26471/cjees/2022/017/235

Subotić, S., Spasić, S., Višnjić-Jeftić, Ž., Hegediš, A., Krpo-Ćetković, J., Mićković, B., Skorić, S., & Lenhardt, M. (2013). Heavy metal and trace element bioaccumulation in target tissues of four edible fish species from the Danube River (Serbia). *Ecotoxicology and Environmental Safety, 98*, 196–202. https://doi.org/10.1016/j.ecoenv.2013.08.020

Tsui, M. T. K., Wang, S., & Cheng, M. L. H. (2025). Review of mercury pollution research in Southeast Asian marine environments. *Marine Pollution Bulletin, 212*. https://doi.org/10.1016/j.marpolbul.2024.117462

Tumolo, M., Ancona, V., De Paola, D., Losacco, D., Campanale, C., Massarelli, C., & Uricchio, V. F. (2020). Chromium pollution in European water, sources, health risk, and remediation strategies: An overview. *International Journal of Environmental Research and Public Health, 17*(15). https://doi.org/10.3390/ijerph17155438

Valová, Z., Jurajda, P., Janáč, M., Bernardová, I., & Hudcová, H. (2010). Spatiotemporal trends of heavy metal concentrations in fish of the River Morava (Danube Basin). *Journal of Environmental Science and Health - Part A: Toxic/Hazardous Substances and Environmental Engineering, 45*(14), 1892–1899. https://doi.org/10.1080/10934529.2010.520605

Vesković, J., Deršek-Timotić, I., Lučić, M., Miletić, A., Đolić, M., Ražić, S., & Onjia, A. (2024). Entropy-weighted water quality index, hydrogeochemistry, and Monte Carlo simulation of source-specific health risks of groundwater in the Morava River plain (Serbia). *Marine Pollution Bulletin, 201*. https://doi.org/10.1016/j.marpolbul.2024.116277

Vuković, Ž., Vuković, D., Radenković, M., & Stanković, S. (2012). A new approach to the analysis of the accumulation and enrichment of heavy metals in the Danube River sediment along the Iron Gate reservoir in Serbia. *Journal of the Serbian Chemical Society, 77*(3), 381–392. https://doi.org/10.2298/JSC110217169V

Wang, N., Ye, Z., Huang, L., Zhang, C., Guo, Y., & Zhang, W. (2023). Arsenic occurrence and cycling in the aquatic environment: A comparison between

freshwater and seawater. *Water (Switzerland), 15*(1). https://doi.org/10.3390/w15010147

Wang, Z., Yeung, K. W. Y., Zhou, G. J., Yung, M. M. N., Schlekat, C. E., Garman, E. R., Gissi, F., Stauber, J. L., Middleton, E. T., Lin Wang, Y. Y., & Leung, K. M. Y. (2020). Acute and chronic toxicity of nickel on freshwater and marine tropical aquatic organisms. *Ecotoxicology and Environmental Safety, 206*. https://doi.org/10.1016/j.ecoenv.2020.111373

Winkler, D., Bidló, A., Bolodár-Varga, B., Erdő, Á., & Horváth, A. (2018). Long-term ecological effects of the red mud disaster in Hungary: Regeneration of red mud flooded areas in a contaminated industrial region. *Science of the Total Environment, 644*, 1292–1303. https://doi.org/10.1016/j.scitotenv.2018.07.059

Zaynab, M., Al-Yahyai, R., Ameen, A., Sharif, Y., Ali, L., Fatima, M., Khan, K. A., & Li, S. (2022). Health and environmental effects of heavy metals. *Journal of King Saud University - Science, 34*(1). https://doi.org/10.1016/j.jksus.2021.101653

Zhang, W., Miao, A. J., Wang, N. X., Li, C., Sha, J., Jia, J., Alessi, D. S., Yan, B., & Ok, Y. S. (2022). Arsenic bioaccumulation and biotransformation in aquatic organisms. *Environment International, 163*. https://doi.org/10.1016/j.envint.2022.107221

Scientific Papers. Series E. Land Reclamation, Earth Observation & Surveying, Environmental Engineering. Vol. XIV, 2025
Print ISSN 2285-6064, CD-ROM ISSN 2285-6072, Online ISSN 2393-5138, ISSN-L 2285-6064

EXPLORING THE QuEChERS - GAS CHROMATOGRAPHY APPROACH FOR SEDIMENT PESTICIDE ANALYSIS

Stefania-Adelina MILEA[1], Maria Daniela (IONICA) MIHAILA[1, 2], Valentina-Andreea CĂLMUC[2], Cătălina ITICESCU[1, 2], Puiu-Lucian GEORGESCU[1, 2], Alin-Constantin DIRTU[3], Cătălin Eugen PLATON[4]

[1]"Dunărea de Jos" University of Galați, REXDAN Research Centre,
98 George Coșbuc Blvd, 800223, Galați, Romania
[2]"Dunărea de Jos" University of Galați, Faculty of Sciences and Environment,
111 Domnească Street, 800201, Galați, Romania
[3]"Alexandru Ioan Cuza" University of Iași, Faculty of Chemistry,
Kogălniceanu Entrance, Building A (UAIC), 11 Carol I Street, 700506, Iași, Romania
[4]ROMFISH National Fish Farmers Association,
12 Nicolae Iorga Blvd, 700583, Iași, Romania

Corresponding author email: adelina.milea@ugal.ro

Abstract

Pesticides have been classified as the most harmful substances in the world because of their extensive application, toxicity, and persistence. Hydrophobic chemicals, such as pesticides, have a considerable tendency to sorb to organic matter in sediment and soil. Measuring pesticides in sediment is crucial for monitoring their environmental fate and possible toxicity because they are typically found at higher concentrations in sediment. Since many hydrophobic substances do not break down easily, they remain in the environment for a very long time. This study aims to develop an integrated approach to extracting and quantifying pesticides from sediment samples using QuEChERS-gas chromatography techniques. The extraction of organochlorine and organophosphorus pesticides from the sediment sample was achieved by slightly modifying the QuEChERS method. The extracted compounds were identified and quantified by gas chromatography with a triple-quadrupole mass detector. Organochlorine pesticides or their degradation compounds provided the majority of the target substances. Monitoring pesticide content in sediments is essential for understanding bioaccumulation and long-term environmental effects, as well as for promoting sustainable agricultural practices.

Key words*: pesticides, sediments, chromatography, QuEChERS.*

INTRODUCTION

In present-day agriculture, pesticides are crucial for both ensuring global food security and protecting crops from pests (Khurshid et al., 2024). Even though these substances offer several advantages, using them might have major negative effects on the environment and human health. Pesticide residues in food and the environment cause chronic health hazards, such as cancer, endocrine disruption, and neurological diseases (Zhou et al., 2025). Their presence in water, accumulation in sediments and soils, and possible biomagnification in the food chain could harm non-target organisms due to their possible toxicity (Peris et al., 2022). Pesticides that are used carelessly find their way into bottom sediments, where sediment particles absorb them and might eventually constitute a major cause of contamination in aquatic environments (Shah & Parveen, 2023). According to their physicochemical characteristics, such as solubility and octanol-water partition coefficient, pesticides disperse throughout the several aquatic ecosystem compartments (water, suspended materials, and biota) after being released into the environment (Ijzerman et al., 2024). Additionally, entrapped contaminants can be released at any moment through resuspension by natural processes or human intervention (Peris et al., 2022). Some pesticides adsorb onto suspended particles and have stronger affinities for organic materials; these particles subsequently settle and

accumulate in the waterbed (Khurshid et al., 2024).

The presence of hydrophobic pollutants in a waterway may be effectively determined by analyzing contaminants in the sediment and aquatic biota. Hydrophobic compounds have limited solubility in water, but high solubility in lipids. They also tend to accumulate to organic material in soil and sediment and their resistance to degradation makes them very persistent (USGS Fact Sheet, 2000). Over the past 50 years, a large number of pesticides have been detected in sediments, most of them belonging to organochlorine insecticides and their breakdown products.

The most frequently detected pesticides in sediment were DDTs, dieldrin, and chlordane even though some of them had been banned since the 1970s and 1980s (Yang et al., 2015). Studies have shown that sediment pollution has been linked to negative impacts on aquatic life such as hepatic lesions or DNA adducts (Yang et al., 2015). Moreover, hazardous substances present in aquatic ecosystems can accumulate and pose toxic risks when transferred to humans through consumption (Bashir et al., 2020). Pesticide residues were first analyzed using acetonitrile and petroleum ether. Then, acetone was added to prevent partial loss of polar insecticides, whereas salt improved their recovery.

In order to achieve a lower limit of quantification, solid-phase extraction and many other methods (supercritical fluid extraction, accelerated solvent extraction, gel-permeation chromatography, or microwave-assisted extraction) were included (Afify et al., 2022). The introduction of the (QuEChERS) method (quick, easy, cheap, effective, rugged, and safe) was revolutionary, innovative, and applicable to most official analysis methods. The QuEChERS approach is faster, requires less solvents, and produces consistent results (Shendy et al., 2019). Moreover, the combination of gas chromatography and mass spectrometry has proven to be among the best methods for the examination of pesticides from different matrices (Tankiewicz & Berg, 2022). Therefore, the objective of this study is to provide an optimal approach for the simultaneous extraction, determination, and quantification of 27 pesticides from both organochlorine (OCP) and organophosphorus (OPP) categories in sediment samples.

MATERIALS AND METHODS

QuEChERS Extraction

Organochlorine and organophosphorus pesticides were extracted from all sediment samples using a modified QuEChERS (rapid, simple, cheap, effective, robust, and safe) approach. Therefore, the following protocol was carried out, after spiking with different concentrations of the standard mix and the addition of the internal standard mix: 5 g of the sample and 10 mL of ACN (acetic acid 1%) were well homogenized. To begin the extraction stage, 6 g of MgSO4 and 1.5 g NaOAc were added as QuEChERS salts. The final mixture was vigorously shaken for 5 minutes and then centrifuged. A volume of 5 mL from the supernatant was collected and cleaned with different one, or two units of clean-up consisting of 50 mg MgSO4, 25 mg PSA, 25 mg C18, and 5 mg GCB. After a second centrifugation, the liquid part was subjected to evaporation through a nitrogen system and reconstituted with 0.5 mL or 0.250 mL acetonitrile. Even though this extraction method has many advantages, sometimes certain steps need to be particularly optimized because there are also problematic pesticides. Such pesticides are sensitive to pH, which creates strong bonds with other substances, leading to their misquantification. For example, using PSA (Primary Secondary Amine) in the QuEChERS extraction method is not indicated in the case of acidic pesticides that can form acid-base interactions with the sorbent. This combination can lead to the loss of acidic pesticides during the clean-up phase (Musarurwa et al., 2019).

Instrument and Method Setup

A TSQ 9000 Triple quadrupole GC-MS/MS instrument coupled with a Thermo Scientific™ TRACE™ 1310 GC was used to analyze the samples (Figure 1). A Thermo Scientific™ TriPlus™ RSH autosampler was used to inject the sample, and a Thermo Scientific™ TraceGOLD TG-5MS 30 m × 0.25 mm I.D. × 0.25 µm film capillary column was used for chromatographic separation. The instrument

was operated in a splitless mode with a 2 µL injection volume. The GC oven program was set up as follows: initial temperature 80°C with a 0.5 min hold time, from 80°C to 190°C at a rate of 25°C/min, from 130°C to 300°C at a rate of 6°C/min, and the final step, 300°C with a hold time of 10 min. The total run time was about 33 minutes.

Three SRM transitions - two for further ion ratio confirmation and one for quantitation - were utilized to identify each targeted compound. The Chromeleon 7.3 software was used to process and report the data.



Figure 1. TSQ 9000 Evo triple quadrupole mass spectrometer coupled to a Thermo Scientific™ TRACE™ 1310 GC

Analytical standards

- EPA 625/CLP Pest. Mix, 1x1 mL, 2000 µg/mL in hexane:toluene (50:50) containing Aldrin, α-BHC, β-BHC, Lindane, δ-BHC, 4,4′-DDT, Dieldrin, α-Endosulfan, β-Endosulfan, Endosulfan sulfate, Endrin, Endrin aldehyde, Heptachlor, Heptachlor exo-epoxide
- EPA 8270 Organophosphorus Pesticides Mix 2, 1x1 mL, 2000 µg/mL in dichloromethane containing Dimethoate, Disulfoton, Famphur, Parathion, Parathion-methyl, Phorate, Sulfotep, Thionazin, Triethyl thiophosphate. A mixture containing two internal standards (ε-HCH and PCB-143) was used for the calibration curve.

RESULTS AND DISCUSSIONS

Five different samples were prepared to provide an optimal method for the extraction and detection of the target analytes. The first sample (A) is represented by sediment with internal standards. Sample B was obtained by spiking sample A with a standard solution in a concentration of 20 ng/mL. Samples coded C, D, and E represented sediment spiked with 100 ng/mL standard solution, cleaned up and redissolved differently after the concentration step. In this context, the evaluation of specific extraction steps was conducted to achieve the most precise, rapid, and efficient quantification of the compounds, while confirming their presence through three distinct transitions (Table 1).

Table 1. Pesticides retention time and product ions

Compounds	Retention Time	Quant. Ion	Conf. Ion #1	Conf. Ion #2
	min	m/z	m/z	m/z
O, O, O-Triethylphosphoro thioate	3.86	65	93.1	65
Thionazin	6.45	79.1	68	79
Sulfotep	7	202	174	174
Phorate	7.13	65	75	81
d-BHC	7.28	182.9	146.7	146.5
Dimethoate	7.44	42.1	63	79
g-BHC (Lindane)	7.72	145	109	183
a-BHC	7.82	183	146.6	146.2
Disulfoton	8.11	59,8	45	96.9
b-BHC	8.23	145	146.6	183
e-HCH	8.42	181	111	111
Methyl parathion	8.93	109	79	89
Heptachlor	9,.15	236.9	39	65
Aldrin	9.89	192,9	191	298.9
Parathion	9.94	96.9	65,1	81
Heptachlorepoxide Isomer B	10.76	262.9	192,9	264.9
Endosulfan I (a)	11.61	205.9	125	159.4
4,4`-DDE	12.14	176.1	246	248
Dieldrin	12.25	192.9	190.9	227.8
Endrin	12.79	192.9	173	245.3
Endosulfan II (b-Isomer)	13.02	159	205.8	123
PCB-143	13.19	290	325	290
4,4`-DDD	13.21	165.1	199	165
Endrin Aldehyde	13.49	215	317	142
Famphur	13.82	109	63	79
Endosulfan Sulfate	14.11	236.8	234.9	203.9
4,4`-DDT	14.17	165.1	199.5	165

Figure 2 displays the peaks corresponding to each investigated compound. In Figure 3, the final amount of each tested experimental variant is exposed.

As expected, similar values for most of the

organochlorine pesticides were obtained when variants E, D, and C were applied. The common aspect among these three samples is the spiking level, which is 100 ng/mL. The difference lies in the final step of the extraction. However, it is important to mention that variant E was distinguished by better and easier quantification during data processing. Therefore, in addition to a slightly higher final concentration, the peak intensities corresponding to each compound - including the internal standard - were significantly higher than those calculated in the other variants. Even though organochlorine chemicals are banned, their traces can still be found in food and the environment as contaminants (Zohair, 2001).

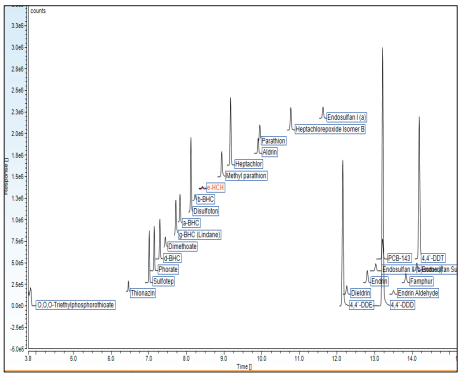


Figure 2. Standard solution (OCP and OPP) chromatogram in MS Quantitation

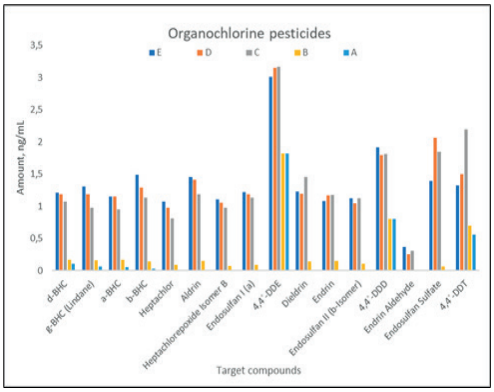


Figure 3. Organochlorine pesticides concentration in each experimental variant

A similar observation can be made for the organophosphorus pesticides in Figure 4. With a few exceptions, the best variant of the extraction is sample E. It seems that redissolving the final extract in a smaller volume of acetonitrile promotes the detection of the compounds. Of course, that in the case of sample B, where the spiking was made with a much lower concentration of pesticides, the final concentration is also much lower than the final amount detected in other samples.

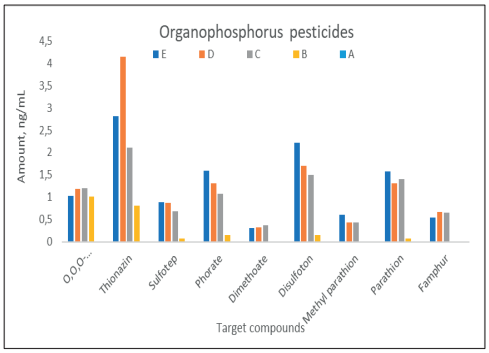


Figure 4. Organophosphorus pesticides concentration in each experimental variant

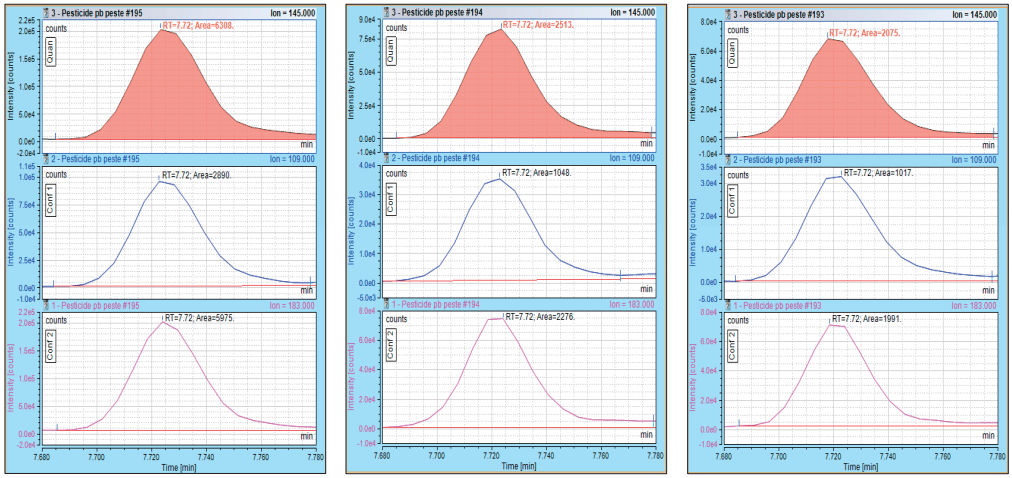
Compared to organochlorines, organophosphorus pesticides are more acutely hazardous, but they have the benefit of being quickly broken down in the environment (Zohair, 2001).

In a study conducted by Khurshid et al., 2024 on pesticide contamination in sediments of 38 water bodies, only one sample was 'pesticide-free' and 3 samples contained a single pesticide.

Figure 5 and Figure 6 confirm the abovementioned idea. As can be observed, an example of a well-known agricultural insecticide, γ-BHC is represented along with its representative ions (Figure 5). The higher intensity peak for this compound highlights variant E compared to Variants D and C. Moreover, an identical situation is valid for the internal standard PCB-143 represented in Figure 6. It is very important to improve the compounds' detection because in most cases they belong to complex matrices. Matrix effects are a major challenge for analyzing low levels of different contaminants using gas chromatography-triple quadrupole mass spectrometry. When examining complex matrices, a practical approach is required due to the complex nature of matrix effects, which can be influenced by various factors such as the

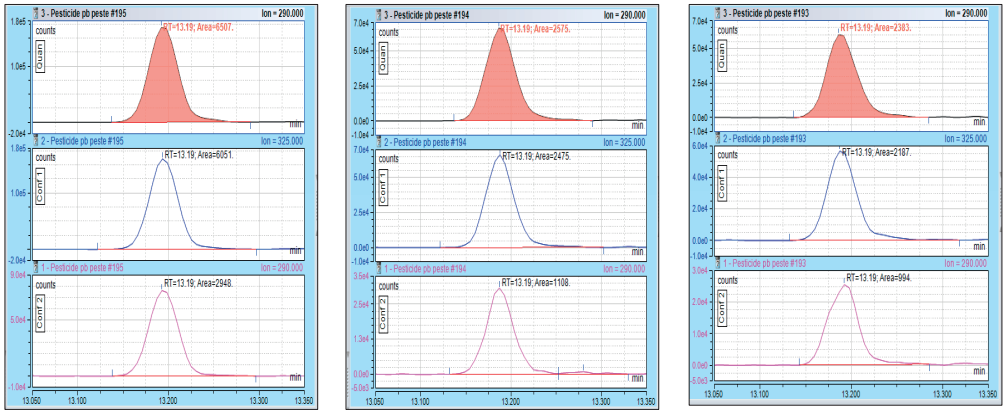
target analyte, sample preparation technique, composition, and instrument selection (Williams et al., 2023). Most often, salts and SPE sorbents are the key components in terms of removing water residues or other matrix interferences (QuEChERS Pesticides, 2011). However, PSA does not apply, for example, to non-polar pigments, and can be replaced or supplemented with GCB (graphitized carbon black). Florisil and low temperature can be used also when fatty matrices are analyzed (Musarurwa et al., 2019).

Moreover, studying residual pesticide compounds in sediments emphasizes the necessity of investigating the immediate and long-term impacts of pesticide use on aquatic systems and, eventually, the need for more ecologically friendly and sustainable farming methods (Khurshid et al., 2024).



a) Variant E b) Variant D c) Variant C

Figure 5. MS Components for g-BHC



a) Variant E b) Variant D c) Variant C

Figure 6. MS Components for PCB-143 (IS)

The screening of these contaminants in sediments is essential to understanding their dynamics and any possible hazards to aquatic life (Peris et al., 2022). Sediments may provide important details about the quality of water and vary considerably in composition, shape, and processes (Brondi et al., 2011).

CONCLUSIONS

The development of a method for determining pesticides in sediment is essential for many reasons, including pollution monitoring, ecosystem protection, identifying contamination sources, evaluating toxicity and bioaccumulation potential, establishing regulations in the field, and assessing the detrimental impact on human health.

QuEChERS approach' short operating time, ease of use, and affordability facilitate the simultaneous analysis of multiclass pesticide residues in sediment samples. Because the QuEChERS approach produces far less waste and requires less hazardous solvents and reagents, it is also consistent with green chemistry.

In the present study, the QuEChERS approach using the 1:5 ratio for the clean-up: liquid extract, as well as the re-dissolution after concentration in a smaller volume of solvent, resulted in better separation and identification of compounds.

There is an increasing demand for validated techniques capable of detecting pesticide residues in sediments, comparable to those used for water and vegetable samples. This is an area that is constantly evolving and demands ongoing research into better, more affordable, quicker, wider-ranging, and environmentally friendly methods.

Protecting and conserving aquatic ecosystems as well as achieving the European Union's goal of zero pollution in soil, air, and water by 2050 (European Commission. Directorate General for Environment. et al., 2021) depend on the understanding of the dynamics and effects of (mixtures of) pesticide residues.

ACKNOWLEDGEMENTS

This research is part of the project `Innovative sediment management framework for a SUstainNable DANube black Sea system (SUNDANSE)', co-funded by the European Union. Views and opinions expressed are however those of the author(s) only and do not necessarily reflect those of the European Union or the European Climate, Infrastructure and Environment Executive Agency. Neither the European Union nor the granting authority can be held responsible for them.

REFERENCES

USGSFact Sheet, 2000, Pesticides in Stream Sediment and Aquatic Biota

Afify, A. S., Abdallah, M., Ismail, S. A., Ataalla, M., Abourehab, M. A. S., Al-Rashood, S. T., & Ali, M. A. (2022). Development of GC–MS/MS method for environmental monitoring of 49 pesticide residues in food commodities in Al-Rass, Al-Qassim region, Saudi Arabia. *Arabian Journal of Chemistry*, *15*(11), 104199. https://doi.org/10.1016/j.arabjc.2022.104199

Bashir, I., Lone, F. A., Bhat, R. A., Mir, S. A., Dar, Z. A., & Dar, S. A. (2020). Concerns and Threats of Contamination on Aquatic Ecosystems. Bioremediation and Biotechnology, 1–26. https://doi.org/10.1007/978-3-030-35691-0_1

Brondi, S. H. G., de Macedo, A. N., Vicente, G. H. L., & Nogueira, A. R. A. (2011). Evaluation of the QuEChERS Method and Gas Chromatography–Mass Spectrometry for the Analysis Pesticide Residues in Water and Sediment. *Bulletin of Environmental Contamination and Toxicology*, *86*(1), 18–22. https://doi.org/10.1007/s00128-010-0176-9

European Commission. Directorate General for Environment., VVA., Toegepast natuurwetenschappelijk onderzoek., Tecnalia., ANOTEC., & Universitat Autònoma de Barcelona. (2021). *Assessment of potential health benefits of noise abatement measures in the EU: Phenomena project.* Publications Office. https://data.europa.eu/doi/10.2779/24566

Ijzerman, M. M., Raby, M., Letwin, N. V., Kudla, Y. M., Anderson, J. D., Atkinson, B. J., Rooney, R. C., Sibley, P. K., & Prosser, R. S. (2024). New insights into pesticide occurrence and multicompartmental monitoring strategies in stream ecosystems using periphyton and suspended sediment. *Science of The Total Environment*, *915*, 170144. https://doi.org/10.1016/j.scitotenv.2024.170144

Khurshid, C., Silva, V., Gai, L., Osman, R., Mol, H., Alaoui, A., Christ, F., Schlünssen, V., Vested, A., Abrantes, N., Campos, I., Baldi, I., Robelot, E., Bureau, M., Pasković, I., Polić Pasković, M., Glavan, M., Hofman, J., Harkes, P., … Geissen, V. (2024). Pesticide residues in European sediments: A significant concern for the aquatic systems? *Environmental Research*, *261*, 119754. https://doi.org/10.1016/j.envres.2024.119754

Musarurwa, H., Chimuka, L., Pakade, V. E., & Tavengwa, N. T. (2019). Recent developments and applications of QuEChERS based techniques on food samples during pesticide analysis. *Journal of Food Composition and Analysis*, *84*, 103314. https://doi.org/10.1016/j.jfca.2019.103314

Peris, A., Barbieri, M. V., Postigo, C., Rambla-Alegre, M., López de Alda, M., & Eljarrat, E. (2022). Pesticides in sediments of the Ebro River Delta cultivated area (NE Spain): Occurrence and risk assessment for aquatic organisms. *Environmental Pollution*, *305*, 119239. https://doi.org/10.1016/j.envpol.2022.119239

QUECHERS PESTICIDE.pdf. (n.d.).

Shah, Z. U., & Parveen, S. (2023). Distribution and risk assessment of pesticide residues in sediment samples from river Ganga, India. *PloS One*, *18*(2), e0279993. https://doi.org/10.1371/journal.pone.0279993

Shendy, A., Eltanany, B., Al-Ghobashy, M., Alla, S., Mamdouh, W., & Lotfy, H. (2019). Coupling of GC-MS/MS to Principal Component Analysis for Assessment of Matrix Effect: Efficient Determination of Ultra-Low Levels of Pesticide Residues in Some Functional Foods. *Food Analytical Methods*, *12*, 1–16. https://doi.org/10.1007/s12161-019-01643-z

Tankiewicz, M., & Berg, A. (2022). Improvement of the QuEChERS method coupled with GC–MS/MS for the determination of pesticide residues in fresh fruit and vegetables. *Microchemical Journal*, *181*, 107794. https://doi.org/10.1016/j.microc.2022.107794

Williams, M. L., Olomukoro, A. A., Emmons, R. V., Godage, N. H., & Gionfriddo, E. (2023). Matrix effects demystified: Strategies for resolving challenges in analytical separations of complex samples. *Journal of Separation Science*, *46*(23), 2300571. ttps://doi.org/10.1002/jssc.202300571

Yang, Y.-Y., Toor, G. S., & Williams, C. F. (2015). Pharmaceuticals and organochlorine pesticides in sediments of an urban river in Florida, USA. *Journal of Soils and Sediments*, *15*(4), 993–1004. https://doi.org/10.1007/s11368-015-1077-7

Zhou, W., Li, M., & Achal, V. (2025). A comprehensive review on environmental and human health impacts of chemical pesticide usage. *Emerging Contaminants*, *11*(1), 100410. https://doi.org/10.1016/j.emcon.2024.100410

Zohair, A. (2001). Behaviour of some organophosphorus and organochlorine pesticides in potatoes during soaking in different solutions. *Food and Chemical Toxicology*, *39*(7), 751–755. https://doi.org/10.1016/S0278-6915(01)00016-3

Scientific Papers. Series E. Land Reclamation, Earth Observation & Surveying, Environmental Engineering. Vol. XIV, 2025
Print ISSN 2285-6064, CD-ROM ISSN 2285-6072, Online ISSN 2393-5138, ISSN-L 2285-6064

MATHEMATICAL MODEL FOR PREDICTION OF NO_2 CONCENTRATION IN THE SOUTHEASTERN REGION OF ROMANIA, USING RECURSIVE LEAST SQUARES FILTER METHODS

Gabriel MURARIU[1], Sorin FRASINA[2] Adrian ROȘU[1], Corneliu DOROFTEI[3], Iulian RACOVIȚĂ[1], Bogdan ROȘU[1], Fetecău CĂTĂLIN[2], Mirela VOICULESCU[1], Cătălin NEGOIȚĂ[1]

[1]"Dunărea de Jos" University of Galați, Faculty of Sciences and Environment, 111 Domnească Street, 800201 Galați, Romania
[2]"Dunărea de Jos" University of Galați, Faculty of Engineering, 111 Domnească Street, 800201 Galați, Romania
[3]"Alexandru Ioan Cuza" University of Iași, Science Research Department, Institute of Interdisciplinary Research, Research Center in Environmental Sciences for the North-Eastern Romanian Region (CERNESIM), 11 Carol I Blvd, 700506, Iași, Romania

Corresponding author email: gabriel.murariu@ugal.ro

Abstract

Nitrogen dioxide is found in the atmosphere as a key ingredient in the photochemical formation of smog and acid rain, nitrogen dioxide is a poisonous gas that is formed during combustion. Toxic at high concentrations, it reacts with moisture in the air to form nitric acid, which is highly corrosive and dangerous to plants and animals. In this study, we present a predictive model for nitrogen dioxide concentrations measured between 2017 and 2024 at ground level in a national network of monitoring stations. The model is based on a statistical approach to measurements from 152 automatic measurement points, with an hourly resolution. The analysis carried out allowed the construction of a mathematical model in order to make an effective prediction. The algorithms used were of the Recursive least squares filter type. The application used was made possible by running a dedicated software in PyCharm. It was found that the model for daytime concentrations depends linearly on a series of parameters monitored by the national network.

Key words*: NO_2, algorithm, RLS, statistical analysis.*

INTRODUCTION

Nitrogen dioxide (NO_2) pollution has emerged as a major environmental and public health concern globally (Moreda-Piñeiro et al., 2021), particularly following efforts to reduce $PM_{2.5}$ concentrations to below regulatory thresholds. There is widespread scientific and regulatory interest in understanding the dynamics of ground-level NO_2, a key atmospheric pollutant, due to its well-documented harmful effects on human health. Research has also highlighted the detrimental impacts of NO_2 on vegetation, contributing to reduced plant growth and crop yields (Pietrogrande et al., 2021). According to the World Health Organization (WHO), strong evidence from both epidemiological and toxicological studies shows that elevated NO_2 concentrations are a primary contributor to adverse respiratory outcomes (Varga-Balogh et al., 2021). These effects range from decreased lung function and aggravated asthma symptoms to increased mortality, particularly among sensitive population groups such as children, the elderly, and individuals with pre-existing respiratory conditions.

Ground-level ozone is a secondary pollutant that results predominantly from the photochemical chain reactions involving nitrogen oxides (NO_X = NO + NO_2), carbon monoxide (CO) and volatile organic compounds (VOCs) using the catalysis of sunlight in the troposphere (Vîrghileanu et al., 2020).

Over the past few decades, greenhouse gas concentrations have increased around the world. With the rapid development of car traffic and the car fleet in particular, air pollution has become increasingly in South-Eastern Europe (Constantin et al., 2017). Since 2017, several legislative actions have been carried out, including the elimination of the environmental tax on vehicle registration. This

fact led to the increase in the level of air pollution in the South-East of Europe.
In this paper, the nitrogen dioxide monitoring data in the South-East of Europe are presented, taking into account a system of 7 automatic air quality monitoring stations within the national network. The data were used to analyse the characteristics of variation and the main causes of the concentration of nitrogen dioxide - NO_2 in the South-East area of Europe in combination with the relationship between different pollutants and meteorological factors.

MATERIALS AND METHODS

Since 2010, a national air quality monitoring network (https://www.calitateaer.ro/) has been established in South-Eastern Europe, which now includes 158 national automatic stations. Data for NO_2 were sourced from seven automatic air quality monitoring stations that are part of Romania's national monitoring network. These stations provided hourly measurements of NO_2 and associated pollutants (e.g., NO, NO_x, O_3, CO, PM), along with meteorological variables such as solar radiation, wind speed, temperature, and humidity, covering the years 2017 to 2024. This high-resolution dataset enabled the examination of NO_2 variability across multiple temporal scales.
To investigate temporal trends, the researchers employed classical statistical techniques, notably one-way Analysis of Variance (ANOVA) and the Kruskal-Wallis test. These methods were applied to assess seasonal, weekly, and diurnal fluctuations in NO_2 concentrations. The statistical tests consistently yielded p-values below 0.001, confirming significant variation in NO_2 levels across different time periods. Seasonal changes likely reflected atmospheric chemistry and heating or traffic patterns, while weekly and hourly patterns pointed to anthropogenic influences such as workweek traffic cycles and photochemical processes during daylight hours.
The data recorded between 2017 and 2025 were used together for data processing in this paper. The equipment of the automatic air quality monitoring stations collects automatically air samples and generates data reports every 30 minutes; then automatically uploads this data to the national database from local environmental protection departments. Table 1 shows the details of the parameters taken into the statistical analysis from each sampling stations, and Table 2 presents the location of the air quality stations used in this study based on their coordinates.

Table 1. Monitored parameters in the network of monitoring points

Parameters	Unit of measurement	Evaluation method	Notatia param.
O3	[µg/m³]	Hourly averaged	P1
CO.	[µg/m³]	Hourly averaged	P2
NO	[µg/m³]	Hourly averaged	P3
NO2	[µg/m³]	Hourly averaged	P4
NOx	[µg/m³]	Hourly averaged	P5
SO2	[µg/m³]	Hourly averaged	P6
Benzene	[µg/m³]	Hourly averaged	P7
Ethylbenzene	[µg/m³]	Hourly averaged	P8
m-Xilene	[µg/m³]	Hourly averaged	P9
o-Xilene	[µg/m³]	Hourly averaged	P10
p-Xilen	[µg/m³]	Hourly averaged	P11
Toluene	[µg/m³]	Hourly averaged	P12
SERIOUS. 10 - PM 10	[µg/m³]	Hourly averaged	P13
SERIOUS. 2.5 - PM 2.5	[µg/m³]	Hourly averaged	P14
LSPM10 - PM 10	[µg/m³]	Hourly averaged	P15
LSPM10 - PM 2.5	[µg/m³]	Hourly averaged	P16
Precipitation	[mm]	Hourly averaged	P17
Air pressure	[mbar]	Hourly averaged	P18
Solar radiation	[W/m²]	Hourly averaged	P19
Air temperature	[°C]	Hourly averaged	P20
Relative humidity	[%]	Hourly averaged	P21
Wind speed	[m/s]	Hourly averaged	P22
Wind direction	[grN]	Hourly averaged	P23

Table 2. Coordinates of monitoring stations

Area	Name	Wide	Long	Altitude
South-eastern part of Romania	GL5	45.82	27.44	31.00
	GL1	45.42	44.02	51.00
	GL4	45.41	44.05	38.00
	BR2	45.26	27.97	19.00
	BZ1	45.15	26.82	98.00
	FP2	45.18	28.77	35.00
	VN1	45.70	27.21	45.00

RESULTS AND DISCUSSIONS

In this section, we will present the results of statistical analysis and the results of numerical simulations using digital fitre (Voipan, Voipan, & Barbu, 2025).

Statistical analysis of the temporal variation of nitrogen dioxide concentration.

Seasonal variation analyses were performed for the concentration of NO_2 in the South-East area of Romania. Figure 1 shows, for example, box plot charts (Afshar-Mohajer et al., 2018) of NO_2 concentration in relation to the season in

question for the set of monitoring stations for 2018.

Obviously, seasonal variation was analyzed using ANOVA methods (Koziel, Pietrenko-Dabrowska, Wójcikowski, & Pankiewicz, 2025). In Table 3 are presented the results obtained for the seasonal variation presented above. It is noted that there is certainly a significant difference between the seasons considered between 2017 and 2024 (Table 3).

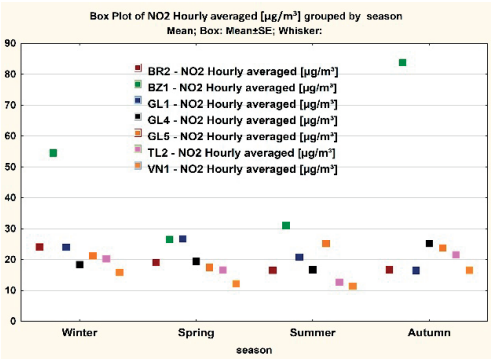


Figure 1. Seasonal variation of NO_2 during 2018

Thus, it is observed that in all cases submitted on NO_2 concentration, values of parameter p – confidence level, both for the analysis of using ANOVA methods one-way and for statistical analysis the Kruskal-Wallis test (KW) (Iticescu et al., 2019), are much smaller than 0.05 (Table 3).

Table 3. results obtained for the seasonal ANOVA method

Name	F value, p - value	H value, p- value
GL5	F(3.8751) = 223.6277, p = 0.0000	KW H(3.8755) = 861.4596, p = 0.0000
GL1	F(3.8751) = 1923.508, p = 0.0000	KW H(3.8755) = 2776.935, p = 0.0000
GL4	F(3.8751) = 186.0061, p = 0.0000	KW H(3.8755) = 995.1096, p = 0.0000
BR2	F(3.8751) = 72.9322, p = 0.0000	KW H(3.8755) = 179.6793, p = 0.0000
BZ1	F(3.8751) = 61.504, p = 0.0000	KW H(3.8755) = 173.5316, p = 0.0000
FP2	F(3.8751) = 133.792, p = 0.0000	KW H(3.8755) = 955.3999, p = 0.0000
VN1	F(3.8751) = 76.092, p = 0.0000	KW H(3.8755) = 424.889, p = 0.0000

Similarly, for all data sets, the weekly variation analysis for NO_2 concentration in the South-East area of Romania was performed.

Figure 2 shows, for example, the box plot graphs (NO_2 concentration in relation to the day of the week) for the set of monitoring stations for 2018 and Table 4 shows the values resulting from the ANOVA and Kruskal-Wallis test. Thus, it is observed that, in all cases, the values of the p parameter are much lower than 0.001, which means significant differences.

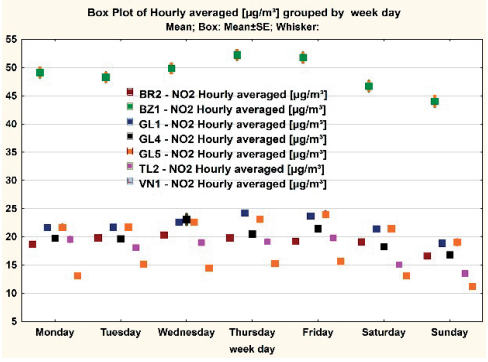


Figure 2. Weekdays variation of NO_2 during 2018

Table 4. Results obtained for weekly ANOVA (for a period of one week)

Name	F value, p – value	H value, p - value
GL5	F(6.8748) = 14.6618, p = 0.0000;	KW H(6.8755) = 118.6725, p = 0.0000
GL1	F(6.8748) = 7.906, p = 0.00000;	KW H(6.8755) = 133.5861, p = 0.0000
GL4	F(6.8748) = 16.3105, p = 0.0000;	KW H(6.8755) = 137.9648, p = 0.0000
BR2	F(6.8748) = 12.5073, p = 0.0000;	KW H(6.8755) = 162.6187, p = 0.0000
BZ1	F(6.8748) = 7.3831, p = 0.00000;	KW H(6.8755) = 239.9735, p = 0.0000
FP2	F(6.8748) = 27.9262, p = 0.0000;	KW H(6.8755) = 306.9294, p = 0.0000
VN1	F(6.8748) = 16.3649, p = 0.0000;	KW H(6.8755) = 138.5051, p = 0.0000

Lastly, we investigated the diurnal variability of NO_2 concentrations in the south-eastern region of Romania.

Figure 3 shows, for example, the box plot charts for the set of monitoring stations for 2018, and Table 5 shows the values for the ANOVA and Kruskal-Wallis test (NO_2 concentration in relation to the hour).

At this stage, the question arises whether a numerical model can be made that can integrate all these statistical data leading to the identification of some essential parameters - NO_x, NO, and solar radiation (Table 1).

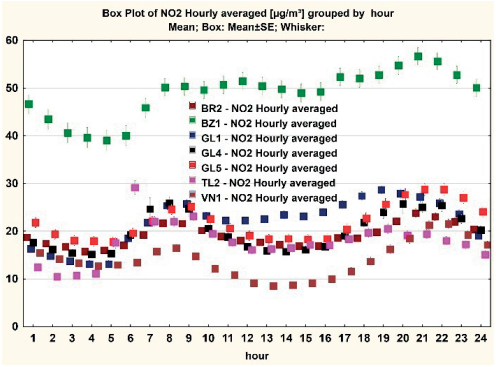


Figure 3. Diurnal variation of NO_2 during 2018

Table 5. Results obtained for daytime ANOVA

Name	F value, p - value	H value, p - value
GL5	F(23.8731) = 15.6522, p = 0.0000;	KW-H(23.8755) = 348.5298, p = 0.0000
GL1	F(23.8731) = 7.2156, p = 0.0000;	KW-H(23.8755) = 448.7269, p = 0.0000
GL4	F(23.8731) = 38.4603, p = 0.0000;	KW-H(23.8755) = 1896.5265, p = 0.0000
BR2	F(23.8731) = 13.8979, p = 0.0000;	KW-H(23.8755) = 680.6765, p = 0.0000
BZ1	F(23.8731) = 12.2314, p = 0.0000;	KW-H(23.8755) = 603.4816, p = 0.0000
FP2	F(23.8731) = 25.2004, p = 0.0000;	KW-H(23.8755) = 770.6485, p = 0.0000
VN1	F(23.8731) = 28.4301, p = 0.0000;	KW-H(23.8755) = 1139.2773, p = 0.0000

In this regard, a multidimensional model was developed to identify the set of physical variables influencing ground-level NO_2 concentration. Table 6 presents the results obtained for the BR2 station in 2017. The statistical model employed a factorial analysis approach, using the parameters listed in Table 1, with the sum of squares (SS) as a key metric.
It is important to note that, for assessing NO_2 conformity, the key parameters comprise NO concentration, NO_x concentration, and ground-level solar radiation values - as indicated in Table 6 (Iticescu et al., 2019).
At this stage, the reliability and robustness of the developed statistical model can be evaluated. Table 7 presents the results for the BR-2 station based on the 2017 dataset, with respect to the model's approximation accuracy. For all other stations considered, the models achieved an R^2 coefficient exceeding 0.90, indicating a high degree of explanatory power.

Table 6. Univariate Tests of Significance, Effect Sizes, and Powers for BR2 - NO_2 Hourly averaged [µg/m³]*

Effect	SS	F	p
Intercept	0.0	0	1.000000
O3 [µg/m³]	0.0	0	1.000000
CO [µg/m³]	0.0	0	1.000000
NO [µg/m³]	**129543.6**	**2854069**	**0.000000***
NOx [µg/m³]	**540546.5**	**11909170**	**0.000000***
SO2 [µg/m³]	0.0	0	1.000000
Benzene [µg/m³]	0.0	0	1.000000
Ethylbenzene [µg/m³]	0.0	0	1.000000
m-Xylene [µg/m³]	0.0	0	1.000000
o-Xylene [µg/m³]	0.0	0	1.000000
p-Xylene [µg/m³]	0.0	0	1.000000
Toluene [µg/m³]	0.0	0	1.000000
Precipitation [mm]	0.0	0	1.000000
Air pressure [mbar]	0.0	0	1.000000
Solar radiation [W/m²]	**0.3**	**6**	**0.012867***
Air temperature [°C]	0.0	0	1.000000
Relative humidity [%]	0.0	0	1.000000
Wind speed [m/s]	0.1	3	0.091114
Error	363.6		

*Sigma-restricted parameterization Effective hypothesis decomposition

Table 7. Test of SS Whole Model vs. SS Residual (BR2 Report 2017)

Dependent variable	Multiple R	Multiple R^2	Adjusted R^2	F	p
BR2 - NO_2 [µg/m³]	**0.999848**	**0.999695**	**0.999694**	**1545295**	**0.00**

Numerical simulation of the temporal variation of nitrogen dioxide concentration.
The specialized literature provides a variety of analysis and interpolation procedures, as well as algorithms, aimed at improving the accuracy of NO_2 estimation and prediction (Koziel et al., 2025). Several highly efficient algorithms implementing difference-based methods have been reported (Koziel et al., 2025). In the present study, we employed a filter with three input parameters and a single output parameter - NO_2 concentration (Figure 4) (Koziel et al., 2025). The algorithm follows the structure of a Recursive Least Squares (RLS) filter (Barbu, 2024). As a result of the iterative process, numerical simulations consistently converged in all cases, with the trace of the covariance matrix reaching its minimum value (Figure 5).

At the same time, the Nyquist diagram (Koziel et al., 2025) shows that the simulation process is stationary, being finally obtained closed trajectories in the right semiplane (Voipan et al., 2025). Finally, the response of the applied filter and the evolution of the estimation error exhibit a clear tendency toward convergence (Figure 6), indicating that the filter operates effectively.



Figure 4. Digital filter configuration

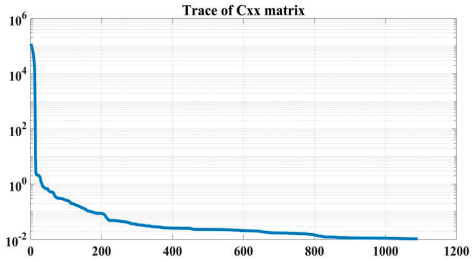


Figure 5. Digital filter covariance matrix trace and evolution towards convergence (matrix trace value versus simulation number)

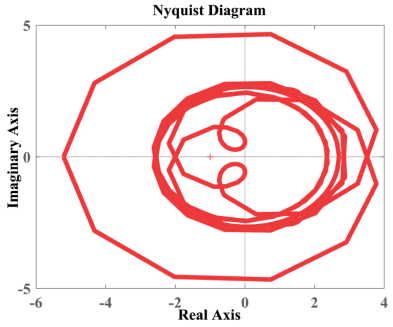


Figure 6. Nyquist filter response diagram

The final output of the filter is illustrated in Figure 7, where the amplification and refinement of the data following the filter's application are evident.

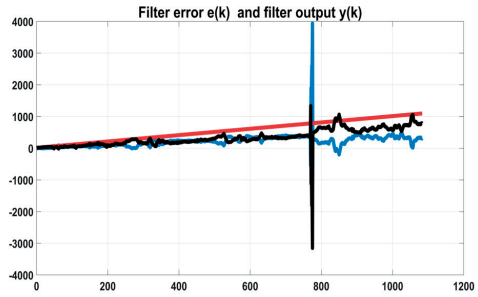


Figure 7. Digital filter response

CONCLUSIONS

Beyond exploratory statistics, the study advanced to multivariate modeling to identify key predictors influencing NO_2 concentrations. Using univariate tests of significance, our work determined that NO, NO_x, and solar radiation were the most impactful variables. These predictors were integrated into a factorial regression model, which showed exceptionally high accuracy, with R^2 values exceeding 0.99 for certain stations, such as BR2. This strong explanatory power highlighted the model's potential for accurate and localized air quality assessments.

The predictive component of the study was based on a Recursive Least Squares (RLS) filter, a numerical algorithm implemented in Python. This digital filter used the key predictors to estimate NO_2 concentrations in real-time, dynamically adjusting to new input data. The RLS model achieved convergence in all test cases, demonstrated by the minimization of the covariance matrix trace and stability confirmed through Nyquist diagram analysis. Model validation revealed high correlation with observed data and RMSE values under 3.5 $\mu g/m^3$, underscoring the model's effectiveness. These results indicate that the proposed approach not only enables reliable NO_2 prediction but also holds promise for cost-effective deployment in air quality monitoring and environmental management.

The corrective analysis and simulation process developed within the group exploited reference data and data provided by the national air quality monitoring network, collected in several locations, regarding the evaluation of the evolution and prediction of the NO_2 concentration. The rigorous verification indicates that the proposed correction technique achieves a very good accuracy of NO_2 monitoring, with a correlation coefficient exceeding 0.88, obtained for the reference data. Simultaneously, the RMSE error remains below 3.5 $\mu g/m^3$. Achieving such very high accuracy confirms the practicality and reliability of NO_2 detection using inexpensive detection devices. Further experiments involving alternative correction configurations emphasize the importance of the algorithmic tools developed in refining the correction scheme. Specifically, the inclusion of additional input variables, and the improvement of global data correlation together increase the accuracy of NO_2 detection.

AKNOWLEDGEMENTS

The work of Gabriel Murariu was supported by a grant of the Ministry of Research, Innovation and Digitization, CNCS/CCCDI - UEFISCDI, project number PN-IV-P8-8.1-PRE-HE-ORG-2024-0212, within PNCDI IV.

REFERENCES

Afshar-Mohajer, N., Zuidema, C., Sousan, S., Hallett, L., Tatum, M., Rule, A. M., & Koehler, K. (2018). Evaluation of low-cost electrochemical sensors for environmental monitoring of ozone, nitrogen dioxide, and carbon monoxide. *Journal of Occupational and Environmental Hygiene, 15*(2), 87–98. https://doi.org/10.1080/15459624.2017.1388918

Barbu, M. (2024). *Modeling, simulation, control and optimization in engineering with applications*. https://www.linkedin.com/posts/mathematics-mdpi_mathematics-activity-7004350949817274368-0UAW

Constantin, D.-E., Merlaud, A., Voiculescu, M., Van Roozendael, M., Arseni, M., Roşu, A., & Georgescu, L. (2017). NO_2 and SO_2 observations in Southeast Europe using mobile DOAS observations. *[Conference paper / report - details to be added if available]*.

Iticescu, C., Georgescu, L. P., Murariu, G., Topa, C., Timofti, M., Pintilie, V., & Arseni, M. (2019). Lower Danube water quality quantified through WQI and multivariate analysis. *Water, 11*(6), 1305. https://doi.org/10.3390/w11061305

Koziel, S., Pietrenko-Dąbrowska, A., Wójcikowski, M., & Pankiewicz, B. (2025). Nitrogen dioxide monitoring by means of a low-cost autonomous platform and sensor calibration via machine learning with global data correlation enhancement. *Sensors, 25*(8), 2352. https://doi.org/10.3390/s25082352

Moreda-Piñeiro, J., Sánchez-Piñero, J., Fernández-Amado, M., Costa-Tomé, P., Gallego-Fernández, N., Piñeiro-Iglesias, M., & Muniategui-Lorenzo, S. (2021). Evolution of gaseous and particulate pollutants in the air: What changed after five lockdown weeks at a Southwest Atlantic European region (Northwest of Spain) due to the SARS-CoV-2 pandemic? *Atmosphere, 12*(5), 562. https://doi.org/10.3390/atmos12050562

Pietrogrande, M. C., Casari, L., Demaria, G., & Russo, M. (2021). Indoor air quality in domestic environments during periods close to Italian COVID-19 lockdown. *International Journal of Environmental Research and Public Health, 18*(8), 4060. https://doi.org/10.3390/ijerph18084060

Varga-Balogh, A., Leelőssy, Á., & Mészáros, R. (2021). Effects of COVID-induced mobility restrictions and weather conditions on air quality in Hungary. *Atmosphere, 12*(5), 561. https://doi.org/10.3390/atmos12050561

Vîrghileanu, M., Săvulescu, I., Mihai, B.-A., Nistor, C., & Dobre, R. (2020). Nitrogen dioxide (NO_2) pollution monitoring with Sentinel-5P satellite imagery over Europe during the coronavirus pandemic outbreak. *Remote Sensing, 12*(21), 3575. https://doi.org/10.3390/rs12213575

Voipan, D., Voipan, A. E., & Barbu, M. (2025). Evaluating machine learning-based soft sensors for effluent quality prediction in wastewater treatment under variable weather conditions. *Sensors, 25*(6), 1692. https://doi.org/10.3390/s25061692

Scientific Papers. Series E. Land Reclamation, Earth Observation & Surveying, Environmental Engineering. Vol. XIV, 2025
Print ISSN 2285-6064, CD-ROM ISSN 2285-6072, Online ISSN 2393-5138, ISSN-L 2285-6064

PLANT RESPONSE TO SOIL WATERLOGGING: PHYSIOLOGICAL, MORPHOLOGICAL AND BIOCHEMICAL ADAPTATIONS – A REVIEW

Senad MURTIĆ, Adnan HADŽIĆ

University of Sarajevo, Faculty of Agriculture and Food Sciences, Department of Plant Physiology, 8 Zmaja od Bosne, 71000, Sarajevo, Bosnia and Herzegovina

Corresponding author email: murticsenad@hotmail.com

Abstract

The phenomenon of global climate change, largely driven by human activities and associated with rising air temperatures, not only leads to intensified and longer-lasting droughts, but also increases the likelihood of extreme precipitation events that may trigger flooding concerns. The stress caused by soil waterlogging is intricate, leading to several concurrent challenges that disrupt normal plant functioning. A key challenge is the oxygen deficiency, which arises from the considerably reduced diffusion rates in floodwater relative to those in the atmosphere. The ability of plants to adapt to waterlogging stress is quite limited primarily because of the partial or complete absence of oxygen in the growth medium. However, certain plant species have evolved specific mechanisms through evolution that allow them to survive for a certain duration in hypoxic or anoxic environments. These mechanisms can be classified into two broad categories: plant morpho-anatomical adaptations to waterlogging stress and the biochemical and physiological responses of plants to such stress. These adaptations are interconnected rather than acting in isolation. Instead, they are intricately connected. This review explores: (i) the impact of soil waterlogging on plant development and function; (ii) current insights into the signal transduction pathways involved in stress recognition and response; and (iii) the key morpho-anatomical and physiological strategies plants use to cope with waterlogged conditions.

Key words*: waterlogging, plant stress, oxygen deficiency, ethylene, adventitious roots, aerenchyma, flooding adaptation.*

INTRODUCTION

Soil waterlogging is a severe abiotic stress that occurs when water saturates the spaces between soil particles, severely limiting oxygen availability to plant roots and leading to hypoxic or anoxic conditions (Walne & Reddy, 2021). Under these conditions, the oxygen diffusion rate is up to ten thousand times lower than in well-drained soils, significantly impairing root function (Manghwar et al., 2024).

When soil becomes waterlogged, oxygen supply to the roots drops sharply, which stunts their growth and reduces the plant's ability to absorb water and nutrients (Abuarab et al., 2019). Excess water also disrupts the metabolism of aerobic soil microorganisms (Siebielec et al., 2020). Without oxygen, these microbes either die off or shift to anaerobic metabolism, producing organic acids that lower soil pH (Abdul Rahman et al., 2021). This acidification encourages harmful microbial activity and accelerates nutrient leaching from the soil's adsorptive complex, further limiting root nutrient uptake (Husson, 2013).

The accumulation of excess water also alters the soil's hydraulic conductivity, reducing water movement and impeding root penetration. In saturated or nearly saturated conditions, the soil's capacity to transmit water is greatly diminished, hindering root penetration through the compacted layer of soil (Jitsuyama, 2017; Luo et al., 2024). Collectively, these effects slow plant metabolism and, if prolonged, may cause wilting.

Although drought stress is more common, waterlogging remains a significant threat - particularly to crops. Poor drainage and excessive rainfall can quickly create oxygen-deficient soil conditions that impair root function (Topali et al., 2024).

Moreover, global climate change - driven by human activities and marked by rising air temperatures - intensifies both droughts and heavy rainfall. Over the last few decades, scientists studying this topic have persistently raised awareness about the problems associated with global climate change (Furtak & Wolińska, 2023; Bolane et al., 2024). The growing frequency of alternating drought and flooding

events confirms their predictions and suggests that crops will face increasing vulnerability to both types of stress in the future.

EFFECTS OF WATERLOGGING STRESS ON PLANTS

Waterlogging stress occurs when oxygen is partially or completely absented from the growth medium, triggering several interconnected challenges that disrupt plant functioning. The primary concern is the impaired respiration, which consequently affects all metabolic processes in the plant that require energy, i.e., adenosine triphosphate (ATP) molecules (Aslam et al., 2023). The negative impact on the plant's metabolism due to low oxygen levels in the growth medium (soil) also leads to competition between the plant's roots and beneficial aerobic microflora. As a result, roots must compete with soil microflora for scarce oxygen, which weakens beneficial microbial nitrification and reduces nutrient uptake (Martínez-Arias et al., 2023). These circumstances pose significant challenges to all aspects of plant development, especially regarding the transition from the vegetative to the generative phase. Prolonged exposure of roots to anaerobic conditions caused by waterlogging prevents flowering, pollination, fertilization, and seed maturation (Insausti & Gorjón, 2013).

Roots are the first to encounter oxygen deprivation and are highly sensitive to it. Numerous studies show that root growth declines significantly when soil oxygen concentration drops below 20% (Tete et al., 2015; Fukao et al., 2019). As oxygen decreases, carbon dioxide (CO_2) concentrations rise, which further hinders root development. For instance, elevated CO_2 in the rhizosphere has been shown to suppress cell division in the root apical meristem (Ben-Noah and Friedman, 2018).

Greenway et al. (2006) have reported that increased soil CO_2 levels adversely affected the growth of the root apical meristem by restricting cell division. This finding agrees with He et al. (2019).

Above-ground symptoms of waterlogging resemble those caused by drought. Although it may seem counterintuitive, waterlogged plants often show signs of water stress. This happens because roots damaged by hypoxia cannot absorb water, prompting the plant to close its stomata to conserve internal moisture (Olorunwa et al., 2022). However, stomatal closure also restricts carbon dioxide uptake, reducing photosynthesis and leading to visible leaf chlorosis (Liu et al., 2022). This deficiency is visually evident through leaf chlorosis, which becomes more pronounced as the anaerobic conditions in the soil last longer.

If the closure of stomata is insufficient in effectively reducing transpiration, the plant may shed its lower leaves to reduce the surface area for transpiration, thereby limiting water loss. However, shedding leaves reduces the plant's ability to produce assimilates, which in turn lowers ATP levels and limits the synthesis of key stress-related metabolites (Chada et al., 2023).

The inability of plants to efficiently perform photosynthesis and respiration during anaerobic stress conditions results in a dysfunction in the mitochondrial electron transport chain and oxidative phosphorylation (Jethva et al., 2022). This, in turn, leads to an increased production of reactive oxygen species (ROS), resulting in oxidative stress. Oxidative stress is a common occurrence in all forms of stress, including waterlogging stress, and it poses a significant threat to plant organisms.

Overproduction of ROS causes severe damage to lipids, proteins and other biomolecules present in cells (Sachdev et al., 2021). Exposure to flooding stress can also lead to osmotic stress in plants, which disrupts all metabolic and physiological processes within plant cells (Li et al., 2025).

Due to the combined effects of oxygen deficiency, nutrient loss, oxidative damage, and metabolic disruption, most plants can only tolerate waterlogging for a limited time. Only those species with specific adaptive strategies can survive extended periods under hypoxic or anoxic conditions.

WATERLOGGING STRESS SIGNAL TRANSMISSION

Roots are the primary plant organs to encounter waterlogging stress, due to their direct exposure to the saturated soil environment. The precise mechanisms by which roots perceive anaerobic

stress and initiate signal transduction remain under active scientific investigation.

Some researchers propose that oxygen deficiency itself is the primary signal (Sasidharan et al., 2018), while others suggest that alterations in the physical or chemical properties of the soil under hypoxic conditions are responsible for triggering the stress response (Setter & Waters, 2003; Rupngam & Messiga, 2024).

Likewise, there is ongoing debate regarding the nature of the primary abiotic stress sensors that detect such signals within plant cells. One school of thought posits that plant cells contain specific oxygen-sensing molecules capable of detecting sharp declines in intracellular oxygen concentrations (Sewelam et al., 2016; León et al., 2021; Selinski et al., 2024). A notable example is Class-1 hemoglobin (Hb), a molecule with high oxygen affinity that allows it to bind oxygen even at extremely low intracellular concentrations (Cochrane et al., 2017).

Conversely, other researchers argue that no dedicated oxygen sensor exists. Instead, they propose that plant cells detect anaerobic stress through disturbances in cellular homeostasis resulting from oxygen deprivation (Schmidt et al., 2018; Kosová et al., 2018; Safavi-Rizi et al., 2020). These disturbances may manifest as changes in cytosolic pH, shifts from aerobic to anaerobic metabolism, fluctuations in the reduced-to-oxidized glutathione ratio, calcium ion (Ca^{2+}) fluxes, or broader disruptions in the cellular redox balance (Rathore et al., 2015).

When plant cells detect anaerobic stress - either directly or through disrupted homeostasis - they activate signaling pathways that produce second messengers, including ethylene, reactive oxygen species (ROS), calcium ions (Ca^{2+}), and nitric oxide (NO). These substances function as essential regulatory components of signaling pathways that transmit signals to transcription factors by activating a series of downstream cascades (Farnese et al., 2016). Ethylene or ROS trigger stress signaling cascades, primarily through MAPKs or calcium-dependent protein kinases. Ultimately, they stimulate the expression of specific defense genes, leading to a comprehensive defensive response (Jagodzik et al., 2018).

Under anaerobic conditions, ethylene serves as a key regulator of plant adaptation by activating ethylene response factors (ERFs). These transcription factors upregulate genes involved in several key adaptive responses, including:

1. the development of aerenchyma in roots,
2. the growth and development of adventitious roots,
3. stem elongation,
4. various morphological or physiological alterations that ultimately improve the plant's ability to adapt to anaerobic stress.

Figure 1 illustrates the general pathway by which plants detect flooding stress and initiate adaptive responses.

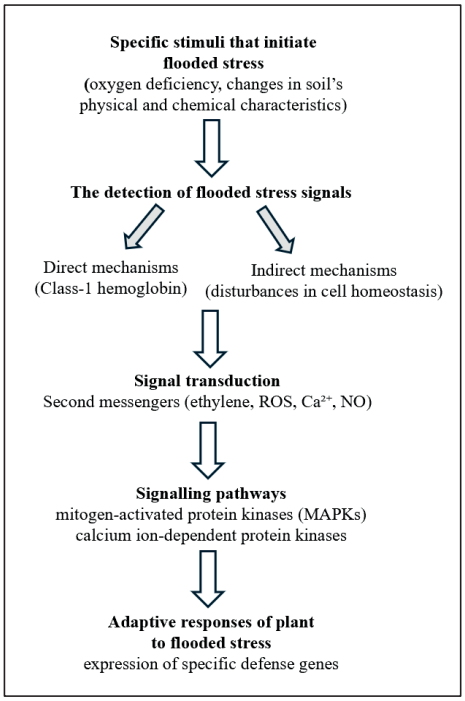


Figure 1. A simple diagram illustrating the pathway from recognizing flooded stress to the plant's response

PLANT MORPHO-ANATOMICAL AND PHYSIOLOGICAL ADAPTIONS TO WATERLOGGING STRESS

The ability of plants to adapt to anaerobic stress, caused by soil waterlogging, is quite limited because of the partial or complete absence of oxygen in the growth medium.

Nevertheless, certain plant species have evolved specific strategies that enable them to tolerate hypoxic or anoxic environments for limited periods. These strategies fall into two major categories: (1) morphological and anatomical adaptations, and (2) physiological modifications (Jia et al., 2021). These categories often operate in parallel; morpho-anatomical adaptations are typically accompanied by physiological changes, together forming an integrated response that enhances plant resilience under flooding stress.

Plant morpho-anatomical adaptations to waterlogging stress

Morphological and anatomical changes resulting from waterlogging primarily affect the root system, which is the first to detect anaerobic conditions in the soil (Lin et al., 2024). Common structural responses include: (1) the growth and development of adventitious roots, (2) the development of hypertrophic lenticels, (3) the formation of aerenchyma within the primary root cortex, and (4) the elongation of stem internodes (Leeggangers et al., 2023).

Growth and development of adventitious roots under soil waterlogging

In response to waterlogging, the plant activates a mechanism for the growth and development of adventitious roots, mainly occurring in the upper part of the root or in the lower part of the stem (Steffens & Rasmussen, 2016). These postembryonic roots are observed in several plant species, including rice, tomato and bittersweet (Sasidharan et al., 2018). When triggered by soil waterlogging, the formation of adventitious roots helps the plant escape hypoxic conditions in the root zone by improving oxygen uptake and increasing its chances of survival.

A plant's ability to promote the formation of adventitious roots is mainly based on the function of the hormone ethylene (Bai et al., 2020). Ethylene plays a significant role as a stress signal in plants affected by flooding, initiating various morphological and metabolic changes that facilitate their adaptation and survival in these challenging conditions. When plants face anaerobic stress, ethylene accumulates in plants underground parts at high levels because its diffusion and consequently its exit from the plant's roots are considerably hindered in these circumstances. During flooding, plant roots synthesize 1-aminocyclopropane-1-carboxylic acid (ACC), the direct precursor of ethylene. ACC is then transported to the stem—an aerobic region—where the enzyme ACC oxidase (ACO) converts it into ethylene, increasing ethylene concentrations in the stem. This rise in ethylene triggers adaptive responses in the submerged stem, initiating the plant's reaction to flooding stress (Khan et al., 2024). This response involves the activation of ethylene-responsive transcription factors (ERFs), which play a key role in regulating plant adaptation to flooding stress. Under anaerobic conditions, ethylene binds to membrane receptors, triggering a conformational change that releases ERFs into the cytosol. These transcription factors then move to the nucleus, where they activate stress-responsive genes essential for the plant's survival under hypoxic conditions (Wang et al., 2025) (Figure 2).

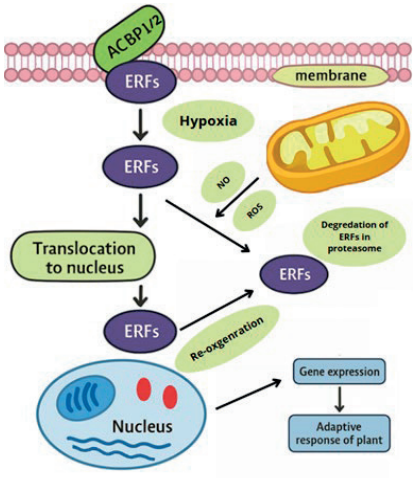


Figure 2. Diagram showing the ethylene-induced signaling pathway in plants facing waterlogging stress

In the context of adventitious root formation, ERF-activated genes are believed to encode enzymes that degrade cells adjacent to meristematic tissue in the root pericycle. This cell breakdown creates the necessary space for root meristem cells to divide and grow, ultimately leading to the emergence of adventitious roots (Roussos, 2023). While ethylene often promotes cell degradation or

death, in this case, the process is beneficial, enabling structural adaptation under stress.
Ethylene's role in enhancing plant adaptation to waterlogging becomes evident under low-oxygen conditions.
In well-aerated environments, ethylene-responsive transcription factors (ERFs) remain inactive. Under these normal conditions, cysteine oxidases - together with reactive oxygen species (ROS) and nitric oxide (NO) - oxidize ERFs, marking them for degradation via the proteasome pathway. ERF activation is therefore tightly regulated and occurs only under stress, with ethylene acting as the primary hormonal trigger (Giuntoli & Perata, 2018).

Formation of hypertrophic lenticels at the stem base

A significant adaptive mechanism that plants utilize to cope with waterlogging stress is the formation of hypertrophic lenticels at the stem base, situated slightly above the water surface (Shimamura et al., 2010). These lenticels function to improve oxygen intake while simultaneously allowing the release of ethanol, methane, and other toxic byproducts that arise from anaerobic metabolic activity. Many scientists note that the formation of hypertrophic lenticels occurs alongside the development of aerenchyma in roots (Thomas et al., 2005; Sou et al., 2021). This is quite reasonable, as it allows the plant to secure a constant influx of oxygen from the atmosphere to its roots.
Although the formation of large cracks (i.e., hypertrophic lenticels) at the stem base is not fully understood, it is generally accepted that the hypertrophy of secondary aerenchyma is responsible for their development. This aerenchyma is formed through successive divisions of the phellogen and is characterized by its white, porous (spongy) tissue. Being of secondary origin, it differs in both morphology and anatomy from the primary cortical aerenchyma (Jackson et al., 2009).

Aerenchyma formation in the root

The typical response of a plant to waterlogging is the development of aerenchyma in its roots. This formation, along with the connection to hypertrophied lenticels, creates a pathway for the roots to interact with the atmosphere. As a result, the plant can supply oxygen from the atmosphere to all root cells, despite being in anaerobic conditions (Evans, 2004). It is important to highlight that a certain amount of oxygen transported to the root aerenchyma is released into the rhizosphere, creating a distinct small zone of aerobic rhizosphere near the roots. This environment promotes the functioning of beneficial aerobic microflora, which greatly improves the roots' survival and, consequently, the plant's ability to withstand flooding (Björn et al., 2022).
Ethylene, a plant hormone, serves as the main mediator in the development of aerenchyma in the primary root cortex. The process through which ethylene promotes aerenchyma formation closely resembles its role in inducing the development of new adventitious roots when faced with anaerobic conditions. Essentially, a higher concentration of ethylene in the root, resulting from the roots' exposure to waterlogging stress, acts as a signal that activates a signaling pathway leading to the disintegration and programmed cell death of certain cells in the primary root cortex (Mergemann & Sauter, 2000). This leads to the formation of a specialized empty space in the primary root cortex i.e., aerenchyma, which serves to store and subsequently distribute oxygen throughout the root.
Recent studies have demonstrated that ethylene is not the only mediator in aerenchyma formation; nitric oxide (NO) and some other reactive oxygen species also fulfill this role (Wany & Gupta, 2018; Basu et al., 2020). The formation of aerenchyma in plant roots experiencing anaerobic stress is further influenced by the activity of certain enzymes that are responsible for the production and deposition of suberin in the cell walls of the root exodermis (Abiko et al., 2012).
Many agricultural species, including corn, tomato, soybean, wheat, and barley, have the ability to develop root aerenchyma under anaerobic stress conditions. Rice also has the capacity to form root cortical aerenchyma, but this process occurs independently of external environmental factors (Yamauchi et al., 2013).

Stem elongation

To cope with soil waterlogging, the plant initiates the development of adventitious roots, hypertrophied lenticels, and root aerenchyma,

while also facilitating the elongation of submerged stem internodes (Jing et al., 2024). The mediator of stem elongation is also ethylene; however, in this instance, its activity will not result in programmed cell death. Instead, it will promote the synthesis of gibberellins, resulting in the stem elongation (Sasidharan & Voesenek, 2015). Thus, the signaling pathways triggered by ethylene can vary significantly depending on the plant species, its demands, and the surrounding environments.

The ethylene-induced signaling pathway that results in the elongation of stem internodes, especially those underwater, consists of the following phases:

(1) ethylene, which accumulates highly in cells under anaerobic stress, binds to a membrane protein receptor associated with an ethylene-responsive factor that contains an APETALA2 (AP2) DNA-binding domain;

(2) the binding of ethylene to the receptor results in a conformational change in the receptor, leading to the release of ethylene-responsive factor, which subsequently initiates the expression of the SK1/SK2 genes in the nucleus;

(3) the expression of the SK1/SK2 gene leads to the production of an enzyme essential for gibberellin synthesis;

(4) the resulting gibberellins subsequently activate signaling pathways that ultimately lead to the elongation of cells, and consequently, the internodes of the submerged stem (Patil et al., 2019) (Figure 3).

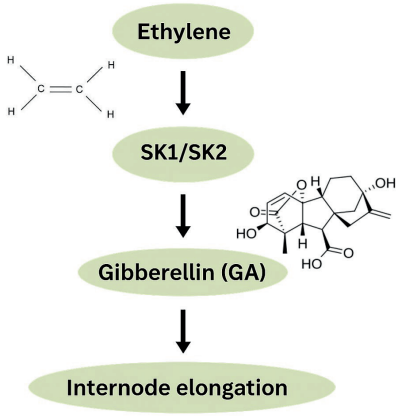


Figure 3. Diagram showing the ethylene-induced signaling pathway that results in the elongation of stem internodes

Plant physiological adaptations to waterlogging stress

In addition to mechanisms based on morpho-anatomical changes, plants strive to adapt to waterlogging stress by altering their metabolic processes. Key adaptations include shifts in respiration, adjustments in photosynthesis, and the synthesis of specific metabolites that enhance the plant's defense against flooding stress (Kato-Noguchi et al., 2003).

Plant respiration under oxygen deficiency

In the absence of oxygen, whether partially or fully, the capacity of plant cells to produce ATP in mitochondria through the Krebs cycle (aerobic metabolism) is limited, necessitating a switch to anaerobic metabolism, where ATP is generated via anaerobic respiration (Meng et al., 2020). From the standpoint of plant life, the greatest challenge of anaerobic respiration lies in its production of an extremely low amount of ATP. During anaerobic respiration, plant cells generate just two ATP molecules for every glucose molecule broken down, indicating that this process is much less efficient than aerobic respiration (2 ATP in glycolysis compared with 36 ATP in the Krebs cycle from one glucose molecule). For these reasons, the plant aims to enhance anaerobic metabolism by intensively producing the enzymes pyruvate decarboxylase and alcohol dehydrogenase within its cells.

The increased activity of these enzymes accelerates anaerobic metabolism, specifically the breakdown of pyruvate generated from glycolysis, leading to a faster production of ATP (Tougou et al., 2012).

Under oxygen deficiency, plant cells switch to anaerobic metabolism via two main pathways. The first pathway is characterized by the activity of the lactate dehydrogenase enzyme (LDH) which catalyzes the conversion of pyruvate into lactate, accompanied by the transformation of NADH into NAD^+. This pathway is referred to as lactic fermentation, enabling plant cells to transform one glucose molecule into two lactate molecules and produce two ATP molecules. Nonetheless, a negative aspect of lactic fermentation is the acidification of the cytoplasm, which adversely influences the metabolic reactions occurring in the cell (Peetermans et al., 2021). The second pathway is marked by the action of the pyruvate

decarboxylase enzyme (PDC), which transforms pyruvate into acetaldehyde. This acetaldehyde is then converted into ethanol by the alcohol dehydrogenase enzyme (ADH). This anaerobic fermentation process, known as alcoholic fermentation, also results in the generation of two ATP molecules.
A visual representation of anaerobic metabolism in plant cells is shown in Figure 4.

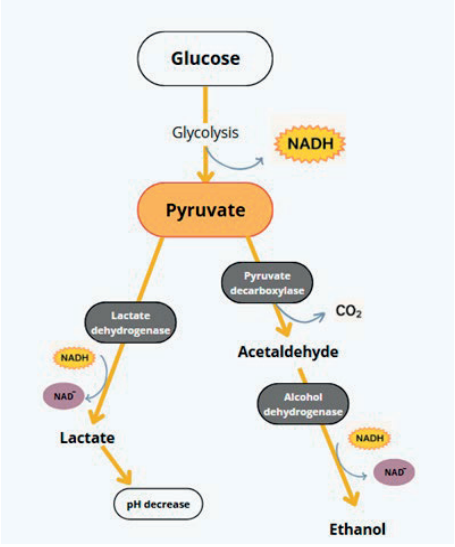


Figure 4. Diagram showing the process of anaerobic respiration in plant cell

Although ATP produced via anaerobic metabolism can offer temporary energy essential for a plant's existence, it is crucial to recognize that this process also generates toxic byproducts like lactate (lactic acid), ethanol, and aldehydes, which can severely disrupt cellular metabolism (Jain et al., 2020). Through anaerobic respiration, the plant cell can temporarily survive without oxygen; however, it cannot serve as a permanent alternative to aerobic metabolism. This means that a plant cell cannot survive for an extended time without oxygen.

Dynamics of photosynthesis under oxygen deficiency

In waterlogging stress conditions, plants cannot take up water through their root systems. Therefore, to maintain their existing water reserves, they must initiate mechanisms that result in stomatal closure. By closing their stomata, plants reduce transpiration but also limit CO_2 intake, which is essential for photosynthesis (Else et al., 2009). Waterlogging stress also negatively affects photosynthesis by limiting the distribution of nutrients, particularly nitrogen, throughout the plant (Zayed et al., 2023). This limitation obstructs chlorophyll synthesis, consequently threatening the plant's ability to absorb photosynthetically active light required for photosynthesis. Waterlogging stress adversely impacts the function of enzymes essential for photosynthesis and disrupts leaf development. This clearly demonstrates that performing photosynthesis under waterlogging stress is highly difficult (Zheng et al., 2009; Muhammad et al., 2021).
To overcome or at least reduce the negative effects of waterlogging stress on photosynthesis, plant cells in the early stages of flooding stress synthesize enzymes essential for converting starch into sucrose, which is then transported to other parts of the plant, particularly to the roots. By relocating assimilates to the roots, the plant aims to enhance root growth, helping it to escape the anaerobic zone of the growth medium and regain its ability to absorb the water and nutrients necessary for photosynthesis (Gangana Gowdra et al., 2025). Nevertheless, prolonged exposure to waterlogging stress can greatly diminish a plant's capacity to generate and transport assimilates to its roots, thereby restricting root growth. Under these conditions, the plant's chances of survival are considerably decreased.

Anaerobic stress-induced metabolites

Multiple studies have shown that plant cells subjected to waterlogging stress tend to either activate or produce significant quantities of specific metabolites, including non-symbiotic hemoglobin (Class-1 Hb) and nitric oxide (NO) (Igamberdiev et al., 2005; Zhao et al., 2008).
A key characteristic of Class-1 Hb is its strong affinity for oxygen, enabling it to effectively bind oxygen in conditions where its concentration in the cell is very low (Singh & Bhatla, 2019). The role of Class-1 Hb in plant cells subjected to anaerobic stress is highly significant: (1) it acts as a signaling molecule that transmits stress signals to target points, i.e., transcription factors; (2) it binds oxygen

necessary for cellular aerobic respiration, thus slowing down the transition of plant cells from aerobic to anaerobic metabolism; and (3) it helps maintain glycolysis in cells facing oxygen deficiency (Riquelme & Hinrichsen, 2015). The research by Hebelstrup et al. (2007) indicates that the synthesis of Class-1 hemoglobin happens whenever the respiratory chain is inhibited, regardless of the oxygen concentration within the cell. This implies that the signal for increased Class-1 Hb production is not solely due to oxygen deficiency in plant cells but also encompasses any situation that results in a significant decrease in ATP synthesis.

Nitric oxide (NO) serves as a vital signaling molecule that regulates plant growth and development under stress conditions such as flooding. It plays a crucial role in enhancing plant resistance to flooding stress through several mechanisms: (1) it interacts with reactive oxygen species (ROS) to control their levels, thereby reducing the harmful effects of oxidative stress on plants; (2) it serves as the mediator in the development of aerenchyma in the primary root cortex; (3) it enhances plant immunity and stress tolerance through the post-translational modification of proteins; (4) it interacts with various plant hormones, playing a significant role in the regulation of plant growth and development under stress conditions (Khan et al., 2023).

It is important to highlight that these two metabolites, Class-1 Hb and NO, work together to alleviate the negative effects of anaerobic stress. In this regard, these metabolites assist in regenerating the enzymatic cofactor NAD^+ from NADH during hypoxia, which is crucial for maintaining glycolysis in plant cells under anaerobic conditions. This synergistic relationship between Class-1 Hb and NO is recognized in scientific literature as the Hb/NO cycle (Dordas et al., 2003) (Figure 5).

Hb/NO cycle initiates with activity of nitrate reductase (NR), which catalyzes the reduction of nitrate (NO_3^-) into nitrite (NO_2^-). Subsequently, NO_2^- is oxidized to nitric oxide (NO) through the activity of nitrite-NO reductase (NiNOR). NO is than reduced to NO3- by oxyhemoglobin ($Hb(Fe^{2+})O_2$), which transforms into methemoglobin ($HbFe^{3+}$), consuming NAD(P)H in the process. In essence, hemoglobin in plant cells helps reduce nitric oxide (NO) levels generated from nitrate during hypoxia. Through the Hb/NO cycle, the plant oxidizes approximately 2.5 moles of NADH for every mole of nitrate (NO_3^-) recycled in the reaction. This cycle is crucial for sustaining redox and energy equilibrium during hypoxia, which in turn reduces the production of ethanol and lactic acid (van Veen et al., 2024).

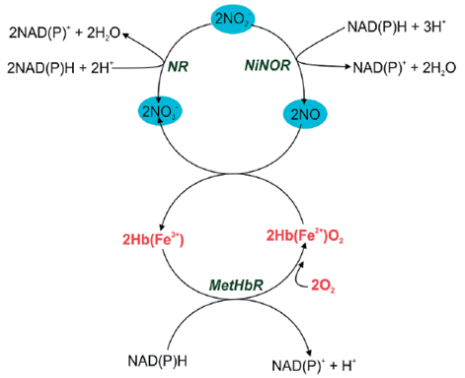


Figure 5. A simple diagram outlining the Hb/NO cycle

In addition to Class-1 Hb and NO, plant cells produce several additional metabolites that serve to strengthen the plant's ability to withstand the negative impacts of this stress. For instance, in response to osmotic stress caused by an excess of water in the growth medium, the plant cells intensively synthesize small organic metabolites (collectively called compatible solutes or osmolytes). Due to their small molecular weight and non-toxic nature, even at elevated concentrations, osmolytes are widely used by plants to alleviate osmotic stress. Among the most prevalent osmolytes in plant cells are amino acids like proline, sugars including mannitol, trehalose, and sorbitol, along with polyamines. This accumulation is beneficial as it enhances tolerance to osmotic stress without disrupting cellular processes. Plant species exhibit varying degrees of tolerance to osmotic stress, which depends on the type and level of osmolyte accumulation during osmotic stress caused by flooding or other stress factors (Chen et al., 2022).

To protect themselves from oxidative damage caused by flooding, plant cells strive to maintain a balance between the production of reactive oxygen species (ROS) and their neutralization.

An imbalance between ROS production and elimination can degrade essential structural and functional biomolecules, ultimately threatening the plant's overall integrity. To counteract these effects, plants deploy a broad array of enzymatic and non-enzymatic antioxidants that play a vital role in neutralizing excess ROS. Among the most prevalent non-enzymatic antioxidants in plant cells are ascorbic acid, tocopherol, glutathione, isoprenoids, carotenoids, flavonoids, ubiquinone and plastoquinone (Rudenko et al., 2023). These antioxidants typically serve as a secondary defense mechanism for plants, protecting them from the harmful effects of reactive oxygen species (ROS). While the mechanisms of action differ among these compounds, they generally function by providing an electron to free radicals, thereby neutralizing their harmful effects (Zandi & Schnug, 2022).

CONCLUSIONS

To address the escalating challenges posed by climate change, it is essential to deepen our understanding of how plants respond to waterlogging stress. This review highlights the complex physiological, morphological, and biochemical responses that plants employ to survive hypoxic conditions caused by soil saturation. Oxygen deprivation disrupts respiration, nutrient uptake, and photosynthesis, severely limiting plant productivity. However, certain species have evolved adaptive traits - such as adventitious root formation, aerenchyma development, and metabolic reprogramming - that enhance their survival under such conditions.

Recognizing these adaptive mechanisms holds significant value for improving agricultural resilience. As climate models predict more frequent and intense rainfall events, crop species will increasingly face alternating periods of drought and flooding. Integrating waterlogging-tolerant traits into breeding programs, particularly for staple crops, can help stabilize yields in flood-prone areas. Moreover, understanding root-zone adaptations can guide the design of land reclamation strategies on poorly drained or flood-affected soils.

In addition, these insights support the development of sustainable land and water management practices, which encompass improving drainage systems, altering planting schedules, and selecting or engineering robust crop varieties.

Ultimately, translating this knowledge into applied practices can help secure food production and maintain soil health in the face of accelerating climate variability.

REFERENCES

Abdul Rahman, N. S. N., & Abdul Hamid, N. W., & Nadarajah K. (2021). Effects of Abiotic Stress on Soil Microbiome. *International Journal of Molecular Sciences, 22*(16), 9036. https://doi.org/10.3390/ijms22169036

Abiko, T., Kotula, L., Shiono, K., Malik, A. I., & Colmer, T. D., & Nakazono, M. (2012). Enhanced formation of aerenchyma and induction of a barrier to radial oxygen loss in adventitious roots of *Zea nicaraguensis* contribute to its waterlogging tolerance as compared with maize (*Zea mays* ssp. mays). *Plant, Cell & Environment, 35*(9), 1618–30. https://doi.org/10.1111/j.1365-3040.2012.02513 .x

Abuarab, M. E., El-Mogy, M. M., Hassan, A. M., Abdeldaym, E. A., Abdelkader, N. H., & El-Sawy, M. B. I. (2019). The Effects of Root Aeration and Different Soil Conditioners on the Nutritional Values, Yield, and Water Productivity of Potato in Clay Loam Soil. *Agronomy, 9*(8), 418. https://doi.org/10.3390/agronomy9080418

Aslam, A., Mahmood, A., Ur-Rehman, H., Li, C., Liang, X., Shao, J., Negm, S., Moustafa, M., Aamer, M., & Hassan, M. U. (2023). Plant Adaptation to Flooding Stress under Changing Climate Conditions: Ongoing Breakthroughs and Future Challenges. *Plants (Basel), 12*(22), 3824. https://doi.org/10.3390/plants12223824

Bai, T., Dong, Z., Zheng, X., Song, S., Jiao, J., Wang, M., & Song, C. (2020). Auxin and Its Interaction with Ethylene Control Adventitious Root Formation and Development in Apple Rootstock. *Frontiers in Plant Science, 11,* 574881. https://doi.org/10.3389/fpls.2020.574881

Basu, S., Kumar, G., Kumari, N., Kumari, S., Shekhar, S., Kumar, S., & Rajwanshi, R. (2020). Reactive oxygen species and reactive nitrogen species induce lysigenous aerenchyma formation through programmed cell death in rice roots under submergence. *Environmental and Experimental Botany, 177,* 104–118. https://doi.org/10.1016/j.envexpbot.2020.104118

Ben-Noah, I., & Friedman, S. P. (2018). Review and evaluation of root respiration and of natural and agricultural processes of soil aeration. *Vadose Zone Journal, 17*, 170119. https://doi.org/10.2136/vzj2017.06.0119

Björn, L. O., Middleton, B. A., Germ, M., & Gaberščik, A. (2022). Ventilation Systems in Wetland Plant Species. *Diversity, 14*(7), 517. https://doi.org/10.3390/d14070517

Bolan, S., Padhye, L. P., Jasemizad, T., Govarthanan, M.,

Karmegam, N., Wijesekara, H., Amarasiri, D., Hou, D., Zhou, P., Biswal, B. K., Balasubramanian, R., Wang, H., Siddique, K. H. M., Rinklebe, J., Kirkham, M. B., & Bolan N. (2024). Impacts of climate change on the fate of contaminants through extreme weather events. *Science of the Total Environment, 909*, 168388. https://doi.org/10.1016/j.scitotenv.2023.168388

Chada, S., Asiedu, S. K., Ofoe, R., & Abbey, L. (2023). An overview of plant morpho-physiology, biochemicals, and metabolic pathways under water stress. *Horticulture International Journal, 7*(4), 115–125. https://doi.org/10.15406/hij.2023.07.00285

Chen, D., Mubeen, B., Hasnain, A., Rizwan, M., Adrees, M., Naqvi, S. A. H., Iqbal, S., Kamran, M., El-Sabrout, A. M., Elansary, H. O., Mahmoud, E. A., Alaklabi, A., Sathish, M., & Din, G. M. U. (2022). Role of Promising Secondary Metabolites to Confer Resistance Against Environmental Stresses in Crop Plants: Current Scenario and Future Perspectives. *Frontiers in Plant Science, 13*, 881032. https://doi.org/10.3389/fpls.2022.881032

Cochrane, D. W., Shah, J. K., Hebelstrup, K. H., & Igamberdiev, A. U. (2017). Expression of phytoglobin affects nitric oxide metabolism and energy state of barley plants exposed to anoxia. *Plant Science, 265*, 124–130. https://doi.org/10.1016/j.plantsci.2017.10.001

Dordas, C., Hasinoff, B., Igamberdiev, A. U., Manac'h, N., Rivoal, J., & Hill, R. D. (2003). Expression of a stress-induced hemoglobin affects NO levels produced by alfalfa under hypoxic stress. *Plant Journal, 35,* 763–770. https://doi.org/10.1046/j.1365-313x.2003.01846.x

Else, M. A., Janowiak, F., Atkinson, C. J., & Jackson, M. B. (2009). Root signals and stomatal closure in relation to photosynthesis, chlorophyll a fluorescence and adventitious rooting of flooded tomato plants. *Annals in Botany, 103*(2), 313–23. https://doi.org/10.1093/aob/mcn208

Evans, D. E. (2004). Aerenchyma formation. *New Phytologist, 161,* 35–49. https://doi.org/10.1046/j.1469-8137.2003.00907.x

Farnese, F. S., Menezes-Silva, P. E., Gusman, G. S., & Oliveira, J. A. (2016). When Bad Guys Become Good Ones: The Key Role of Reactive Oxygen Species and Nitric Oxide in the Plant Responses to Abiotic Stress. *Frontiers in Plant Science, 7*, 471. https://doi.org/10.3389/fpls.2016.00471

Fukao, T., Barrera-Figueroa, B. E., Juntawong, P., & Peña-Castro, J. M. (2019). Submergence and Waterlogging Stress in Plants: A Review Highlighting Research Opportunities and Understudied Aspects. *Frontiers in Plant Science, 10*, 340. https://doi.org/10.3389/fpls.2019.00340

Furtak, K., & Wolińska, A. (2023). The impact of extreme weather events as a consequence of climate change on the soil moisture and on the quality of the soil environment and agriculture – A review. *Catena, 231*, 107378. https://doi.org/10.1016/j.catena.2023.107378

Gangana Gowdra, V. M., Lalitha, B. S., Halli, H. M., Senthamil, E., Negi, P., Jayadeva, H. M., Basavaraj, P. S., Harisha, C. B., Boraiah, K. M., Adavi, S. B., Suresha, P. G., Nargund, R., Mohite, G., & Sammi Reddy, K. (2025). Root growth, yield and stress tolerance of soybean to transient waterlogging under different climatic regimes. *Scientific Reports, 15*, 6968. https://doi.org/10.1038/s41598-025-91780-9

Giuntoli, B., & Perata, P. (2018). Group VII Ethylene Response Factors in Arabidopsis: Regulation and Physiological Roles. *Plant Physiology, 176*(2), 1143–1155. https://doi.org/10.1104/pp.17.01225

Greenway, H., Armstrong, W., & Colmer, T. D. (2006). Conditions leading to high CO_2 (>5 kPa) in waterlogged-flooded soils and possible effects on root growth and metabolism. *Annals of Botany, 98*(1), 9–32. https://doi.org/10.1093/aob/mcl076

He, W., Yoo, G., Moonis, M., Kim, Y., & Chen X. (2019) Impact assessment of high soil CO2 on plant growth and soil environment: a greenhouse study. *PeerJ, 7,* e6311. https://doi.org/10.7717/peerj.6311

Hebelstrup, K. H., Igamberdiev, A. U., & Hill, R. D. (2007). Metabolic effects of hemoglobin gene expression in plants. *Gene, 398*(1-2), 86–93. https://doi.org/10.1016/j.gene.2007.01.039

Husson, O. (2013). Redox potential (Eh) and pH as drivers of soil/plant/microorganism systems: a transdisciplinary overview pointing to integrative opportunities for agronomy. *Plant and Soil, 362,* 389–417. https://doi.org/10.1007/s11104-012-1429-7

Igamberdiev, A. U., Baron, K., Manac'h-Little, N., Stoimenova, M., & Hill, R. D. (2005). The haemoglobin/nitric oxide cycle: involvement in flooding stress and effects on hormone signalling. *Annals in Botany, 96*(4), 557–564. https://doi.org/10.1093/aob/mci210

Insausti, P., & Gorjón, S. (2013). Floods affect physiological and growth variables of peach trees (Prunus persica (L.) Batsch), as well as the postharvest behavior of fruits. *Scientia Horticulturae, 152,* 56–60. https://doi.org/10.1016/j.scienta.2013.01.005

Jackson, M. B., Ishizawa, K., & Osamu, I. (2009). Evolution and mechanisms of plant tolerance to flooding stress. *Annals of Botany, 103*, 137–142. https://doi.org/10.1093/aob/mcn242

Jagodzik, P., Tajdel-Zielinska, M., Ciesla, A., Marczak, M., & Ludwikow, A. (2018). Mitogen-Activated Protein Kinase Cascades in Plant Hormone Signaling. *Frontiers in Plant Science, 9*, 1387. https://doi.org/10.3389/fpls.2018.01387

Jain, M., Aggarwal, S., Nagar, P., Tiwari, R., & Mustafiz, A. (2020). A D-lactate dehydrogenase from rice is involved in conferring tolerance to multiple abiotic stresses by maintaining cellular homeostasis. *Scientific Reports, 10,* 12835. https://doi.org/10.1038/s41598-020-69742-0

Jethva, J., Schmidt, R. R., Sauter, M., & Selinski, J. (2022). Try or Die: Dynamics of Plant Respiration and How to Survive Low Oxygen Conditions. *Plants, 11*(2), 205. https://doi.org/10.3390/plants11020205

Jia, W., Ma, M., Chen, J., & Wu, S. (2021). Plant Morphological, Physiological and Anatomical Adaption to Flooding Stress and the Underlying Molecular Mechanisms. *International Journal of Molecular Sciences, 22*(3), 1088. https://doi.org/10.3390/ijms22031088

Jing, S., Ren, X., Lin, F., Niu, H., Ayi, Q., Wan, B., Zeng, B., & Zhang, X. (2024). Water depth-dependent stem elongation of completely submerged Alternanthera philoxeroides is mediated by intra-internodal growth variations. *Frontiers in Plant Science, 15,* 1323547. https://doi.org/10.3389/fpls.2024.1323547

Jitsuyama, Y. (2017). Hypoxia-Responsive Root Hydraulic Conductivity Influences Soybean Cultivar-Specific Waterlogging Tolerance. *American Journal of Plant Sciences, 8*, 770–790. https://doi.org/10.4236/ajps.2017.84054

Kato-Noguchi, H., Ohashi, C., & Sasaki, R. (2003). Metabolic adaptation to flooding stress in upland and lowland rice seedlings. *Acta Physiologiae Plantarum, 25,* 257–261. https://doi.org/10.1007/s11738-003-0006-3

Khan, M., Ali, S., Al Azzawi, T. N. I., & Yun, B. W. (2023). Nitric Oxide Acts as a Key Signalling Molecule in Plant Development under Stressful Conditions. *International Journal of Molecular Sciences, 24*(5), 4782. https://doi.org/10.3390/ijms24054782

Khan, S., Alvi, A. F., & Khan, N. A. (2024). Role of Ethylene in the Regulation of Plant Developmental Processes. *Stresses, 4*(1), 28–53. https://doi.org/10.3390/stresses4010003

Kosová, K., Vítámvás, P., Urban, M. O., Prášil, I. T., & Renaut, J. (2018). Plant Abiotic Stress Proteomics: The Major Factors Determining Alterations in Cellular Proteome. *Frontiers in Plant Science, 9,* 122. https://doi.org/10.3389/fpls.2018.00122

Leeggangers, H. A. C. F., Rodriguez-Granados, N. Y., Macias-Honti, M. G., & Sasidharan, R. (2023). A helping hand when drowning: The versatile role of ethylene in root flooding resilience. *Environmental and Experimental Botany, 213*, 105422. https://doi.org/10.1016/j.envexpbot.2023.105422

León, J., Castillo, M. C., & Gayubas, B. (2021). The hypoxia–reoxygenation stress in plants. *Journal of Experimental Botany, 72*(16), 5841–5856. https://doi.org/10.1093/jxb/eraa591

Li, Y-K., Zhang, Y-M., Dai, G-Y., Chen, Y-L., Chen, D-K., & Yao, N. (2025). Sphingolipid remodeling in the plasma membrane is essential for osmotic stress tolerance in Arabidopsis. *Plant Physiology, 197*(2), kiaf031. https://doi.org/10.1093/plphys/kiaf031

Lin, C., Zhang, Z., Shen, X., Liu, D., & Pedersen, O. (2024). Flooding-adaptive root and shoot traits in rice. *Functional Plant Biology, 51*, FP23226. https://doi.org/10.1071/FP23226

Liu, C., Wang, Q., Mäkelä, A., Hökkä, H., Peltoniemi, M., & Hölttä, T. (2022). A model bridging waterlogging, stomatal behavior and water use in trees in drained peatland. *Tree Physiology, 42*(9), 1736–1749. https://doi.org/10.1093/treephys/tpac037

Luo, H., Liu, S., Song, Y., Qin, T., Xiao, S., Li, W., Xu, L., & Zhou, X. (2024). Effects of Waterlogging Stress on Root Growth and Soil Nutrient Loss of Winter Wheat at Seedling Stage. *Agronomy, 14*(6), 1247. https://doi.org/10.3390/agronomy14061247

Manghwar, H., Hussain, A., Allam, I., Khoso, M. A., Ali, Q., & Liu, F. (2024). Waterlogging stress in plants: Unraveling the mechanisms and impacts on growth, development, and productivity. *Environmental and Experimental Botany, 224,* 105824. https://doi.org/10.1016/j.envexpbot.2024.105824

Martínez-Arias, C., Witzell, J., Solla, A., Martin, J. A., & Rodríguez-Calcerrada, J. (2022). Beneficial and pathogenic plant-microbe interactions during flooding stress. *Plant, Cell & Environment, 45*(10), 2875–2897. https://doi.org/10.1111/pce.14403

Meng, X., Li, L., Narsai, R., De Clercq, I., Whelan, J., & Berkowitz O. (2020). Mitochondrial signalling is critical for acclimation and adaptation to flooding in Arabidopsis thaliana. *Plant Journal, 103*(1), 227–247. https://doi.org/10.1111/tpj.14724

Mergemann, H., & Sauter, M. (2000). Ethylene induces epidermal cell death at the site of adventitious root emergence in rice. *Plant Physiology, 124*(2), 609–614. https://doi.org/10.1104/pp.124.2.609

Muhammad, I., Shalmani, A., Ali, M., Yang, Q. H., Ahmad, H., & Li, F. B. (2021). Mechanisms Regulating the Dynamics of Photosynthesis Under Abiotic Stresses. *Frontiers in Plant Science, 11,* 615942. https://doi.org/10.3389/fpls.2020.615942

Olorunwa, O. J., Adhikari, B., Brazel, S., Popescu, S. C., Popescu, G. V., & Barickman, T. C. (2022). Short waterlogging events differently affect morphology and photosynthesis of two cucumber (*Cucumis sativus* L.) cultivars. *Frontiers in Plant Science, 13*, 896244. https://doi.org/10.3389/fpls.2022.896244

Patil, V., McDermott, H. I., McAllister, T., Cummins, M., Silva, J. C., Mollison, E., Meikle, R., Morris, J., Hedley, P. E., Waugh, R., Dockter, C., Hansson, M., & McKim, S. M. (2019). APETALA2 control of barley internode elongation. *Development, 146*(11), dev170373. https://doi.org/10.1242/dev.170373

Peetermans, A., Foulquié-Moreno, M. R., & Thevelein, J. M. (2021). Mechanisms underlying lactic acid tolerance and its influence on lactic acid production in Saccharomyces cerevisiae. *Microbial Cell, 8*(6), 111–130. https://doi.org/10.15698/mic2021.06.751

Rathore, S., Datta, G., Kaur, I., Malhotra, P., & Mohmmed, A. (2015). Disruption of cellular homeostasis induces organelle stress and triggers apoptosis like cell-death pathways in malaria parasite. *Cell Death and Disease, 6*(7), e1803. https://doi.org/10.1038/cddis.2015.142

Riquelme, A., & Hinrichsen, P. (2015). Non-symbiotic hemoglobin and its relation with hypoxic stress. *Chilean journal of agricultural research, 75*(1), 80–89. https://doi.org/10.4067/S0718-58392015000300009

Roussos, P. A. (2023). Adventitious Root Formation in Plants: The Implication of Hydrogen Peroxide and Nitric Oxide. *Antioxidants,12*(4), 862. https://doi.org/10.3390/antiox12040862

Rudenko, N. N., Vetoshkina, D. V., Marenkova, T. V., & Borisova-Mubarakshina, M. M. (2023). Antioxidants of Non-Enzymatic Nature: Their Function in Higher Plant Cells and the Ways of Boosting Their Biosynthesis. *Antioxidants (Basel), 12*(11), 2014. https://doi.org/10.3390/antiox12112014

Rupngam, T., & Messiga, A. J. (2024). Unraveling the Interactions between Flooding Dynamics and Agricultural Productivity in a Changing Climate.

Sustainability, 16(14), 6141. https://doi.org/10.3390/su16146141

Sachdev, S., Ansari, S. A., Ansari, M. I., Fujita, M., & Hasanuzzaman, M. (2021). Abiotic Stress and Reactive Oxygen Species: Generation, Signaling, and Defense Mechanisms. *Antioxidants, 10*(2), 277. https://doi.org/10.3390/antiox10020277

Safavi-Rizi, V., Herde, M., & Stöhr, C. (2020). RNA-Seq reveals novel genes and pathways associated with hypoxia duration and tolerance in tomato root. *Scientific Reports, 10*, 1692. https://doi.org/10.1038/s41598-020-57884-0

Sasidharan, R., Hartman, S., Liu, Z., Martopawiro, S., Sajeev, N., van Veen, H., Yeung, E., & Voesenek, L. A. C. J. (2018). Signal Dynamics and Interactions during Flooding Stress. *Plant Physiology, 176*(2), 1106–1117. https://doi.org/10.1104/pp.17.01232

Sasidharan, R., & Voesenek, L. A. C. J. (2015). Ethylene-mediated acclimations to flooding stress. *Plant Physiology, 169*, 3–12. https://doi.org/10.1104/pp.15.00387

Schmidt, R. R., Weits, D. A., Feulner, C. F. J., & van Dongen, J. T. (2018). Oxygen Sensing and Integrative Stress Signaling in Plants. *Plant Physiology, 176*(2), 1131–1142. https://doi.org/10.1104/pp.17.01394

Selinski, J., Frings, S., & Schmidt-Schippers, R. (2024). Perception and processing of stress signals by plant mitochondria. *Plant Journal, 120*(6), 2337–2355. https://doi.org/10.1111/tpj.17133

Setter T. L., & Waters I. (2003). Review of prospects for germplasm improvement for waterlogging tolerance in wheat, barley and oats. *Plant and Soil, 253*, 1–34. https://doi.org/10.1023/A:1024573305997

Sewelam, N., Kazan, K., & Schenk, P. M. (2016). Global Plant Stress Signaling: Reactive Oxygen Species at the Cross-Road. *Frontiers in Plant Science, 7*, 187. https://doi.org/10.3389/fpls.2016.00187

Shimamura, S., Yamamoto, R., Nakamura, T., Shimada, S., & Komatsu, S. (2010). Stem hypertrophic lenticels and secondary aerenchyma enable oxygen transport to roots of soybean in flooded soil. *Annals of Botany, 106*(2), 277–284. https://doi.org/10.1093/aob/mcq123

Siebielec, S., Siebielec, G., Klimkowicz-Pawlas, A., Gałązka, A., Grządziel, J., & Stuczyński, T. (2020). Impact of Water Stress on Microbial Community and Activity in Sandy and Loamy Soils. *Agronomy, 10* (9), 1429. https://doi.org/10.3390/agronomy10091429

Singh, N., & Bhatla, S. C. (2019). Hemoglobin as a probe for estimation of nitric oxide emission from plant tissues. *Plant Methods, 15*, 39. https://doi.org/10.1186/s13007-019-0425-9

Sou, H. D., Masumori, M., Yamanoshita, T., & Tange, T. (2021). Primary and secondary aerenchyma oxygen transportation pathways of Syzygium kunstleri (King) Bahadur & R. C. Gaur adventitious roots in hypoxic conditions. *Scientific Reports, 11*, 4520. https://doi.org/10.1038/s41598-021-84183-z

Steffens, B., & Rasmussen, A. (2016). The Physiology of Adventitious Roots. *Plant Physiology, 170*(2), 603–617. https://doi.org/10.1104/pp.15.01360

Tete, E., Viaud, V., & Walter, C. (2015). Organic carbon and nitrogen mineralization in a poorly-drained mineral soil under transient waterlogged conditions: an incubation experiment. *European Journal of Soil Science, 66,* 427–437. https://doi.org/10.1111/ejss.12234

Thomas, A. L., Guerreiro, S. M., & Sodek, L. (2005). Aerenchyma formation and recovery from hypoxia of the flooded root system of nodulated soybean. *Annals of Botany, 96*(7), 1191–1198. https://doi.org/10.1093/aob/mci272

Topali, C., Antonopoulou, C., & Chatzissavvidis, C. (2024). Effect of Waterlogging on Growth and Productivity of Fruit Crops. *Horticulturae, 10*(6), 623. https://doi.org/10.3390/horticulturae10060623

Tougou, M., Hashiguchi, A., Yukawa, K., Nanjo, Y., Hiraga, S., Nakamura, T., Nishizawa, K., & Komatsu, S. (2012). Responses to flooding stress in soybean seedlings with the alcohol dehydrogenase transgene. *Plant Biotechnology, 29*, 301–305. https://doi.org/10.5511/plantbiotechnology.12.0301a

van Veen, H., Triozzi, P. M., & Loreti, E. (2024). Metabolic strategies in hypoxic plants. *Plant Physiology, 197*(1), kiae564. https://doi.org/10.1093/plphys/kiae564

Walne, C. H., & Reddy, K. R. (2021). Developing Functional Relationships between Soil Waterlogging and Corn Shoot and Root Growth and Development. *Plants, 10*(10), 2095. https://doi.org/10.3390/plants10102095

Wang, X., Wen, H., Suprun, A., & Zhu, H. (2025). Ethylene Signalling in Regulating Plant Growth, Development, and Stress Responses. *Plants, 14*(3), 309. https://doi.org/10.3390/plants14030309

Wany, A., & Gupta, K. J. (2018). Reactive oxygen species, nitric oxide production and antioxidant gene expression during development of aerenchyma formation in wheat. *Plant Signaling & Behavior, 13*(2), e1428515. https://doi.org/10.1080/15592324

Yamauchi, T., Shimamura, S., Nakazono, M., & Mochizuki, T. (2013). Aerenchyma formation in crop species: A review. *Field Crops Research, 152*, 8–16. https://doi.org/10.1016/j.fcr.2012.12.008

Zandi, P., & Schnug, E. (2022). Reactive Oxygen Species, Antioxidant Responses and Implications from a Microbial Modulation Perspective. *Biology (Basel), 11*(2), 155. https://doi.org/10.3390/biology11020155

Zayed, O., Hewedy, O. A., Abdelmoteleb, A., Ali, M., Youssef, M. S., Roumia, A. F., Seymour, D., & Yuan, Z. C. (2023). Nitrogen Journey in Plants: From Uptake to Metabolism, Stress Response, and Microbe Interaction. *Biomolecules, 13*(10), 1443. https://doi.org/10.3390/biom13101443

Zhao, L., Gu, R., Gao, P., & Wang, G. (2008). A nonsymbiotic hemoglobin gene from maize, ZmHb, is involved in response to submergence, high-salt and osmotic stresses. *Plant Cell, Tissue and Organ Culture, 95*, 227–237. https://doi.org/10.1007/s11240-008-9436-3

Zheng, C., Jiang, D., Liu, F., Dai, T., Jing, Q., & Cao, W. (2009). Effects of salt and waterlogging stresses and their combination on leaf photosynthesis, chloroplast ATP synthesis, and antioxidant capacity in wheat. *Plant Science, 176*, 575–582. https://doi.org/10.1016/j.plantsci.2009.01.015

Scientific Papers. Series E. Land Reclamation, Earth Observation & Surveying, Environmental Engineering. Vol. XIV, 2025
Print ISSN 2285-6064, CD-ROM ISSN 2285-6072, Online ISSN 2393-5138, ISSN-L 2285-6064

HEAVY METAL ACCUMULATION IN FOOD CROPS CULTIVATED IN CONTAMINATED SOILS IN ALBANIA

Selma MYSLIHAKA[1], Aida BANI[1], Teuta BUSHI[2], Dorina XHULAJ[1], Eugen SKURA[1], Irena DUKA[1]

[1]Agricultural University of Tirana, Faculty of Agriculture and Environment, 1025 Rruga Paisi Vodica, 1000, Tiranë, Albania
[2]Agricultural University of Tirana, Faculty of Forest Sciences, 1025 Rruga Paisi Vodica, 1000, Tiranë, Albania

Corresponding author email: selma.myslihaka@yahoo.com

Abstract

The consumption of vegetables and fruits is a major pathway for human exposure to heavy metals, especially when these elements accumulate in edible plant parts. This study assessed the accumulation of nickel (Ni), chromium (Cr), zinc (Zn), iron (Fe), and manganese (Mn) in soils and food crops cultivated near a former metallurgical plant in Elbasan, Albania. The analyzed crops included onion, salad, potato, pepper, and strawberry. Bioconcentration factors (BCFs) were calculated to evaluate the capacity of each crop to uptake heavy metals from soil. Available metal concentrations in soil were determined using the Mehlich-1 extraction method and quantified by atomic absorption spectrometry. The results indicated that Mn, Zn, Fe, and Cr concentrations in potatoes, and Fe levels in pepper, were within WHO safety limits. However, Fe levels in onion, salad, and strawberry, Ni in all edible crops, and Cr in onion, salad, strawberry, and pepper exceeded recommended thresholds. The calculated BCFs confirmed notable metal accumulation, particularly for Ni and Cr. These findings highlight the need for regular monitoring of heavy metal levels in both soil and crops to safeguard food safety and public health.

Key words*: accumulation; available metals; bioaccumulation factor plants (BFP*); *food crops; heavy metals.*

INTRODUCTION

Heavy metals are naturally occurring elements with a density greater than 5 g/cm³ and are integral components of the Earth's crust. Their concentration in soil varies depending on the geochemical and mineralogical characteristics of the soil, as well as the extent of anthropogenic pollution. Soil contamination with heavy metals can result from numerous human activities, including mining, metallurgical and smelting processes, the application of organic and inorganic fertilizers, the use of pesticides and insecticides containing metal compounds, emissions from transportation, discharges from chemical plants, runoff, and waste from landfills (Hu et al., 2013; Osmani et al., 2015; Gjoka et al., 2022).

In recent years, the widespread use of heavy metals in industrial applications, and in the production of agrochemicals, has heightened the risk of environmental contamination and their subsequent entry into the food chain (Bradl, 2002). Fruits and vegetables are essential components of the human diet, valued for their rich content of micronutrients, carbohydrates, vitamins, and fiber, all of which contribute positively to human health (Hu et al., 2013). However, elevated concentrations of heavy metals in edible plant parts pose significant health risks. Numerous studies have demonstrated that heavy metals can be absorbed by plant roots and transported to aerial parts, leading to accumulation in edible tissues, even when soil concentrations are relatively low (Jolly et al., 2013; Sharma et al., 2018; Zwolak et al., 2019).

Vegetables grown in agricultural soils located near industrial sites or in regions with naturally elevated metal content are particularly susceptible to contamination.

The metallurgical complex in Elbasan, central Albania, has long been identified as a major source of heavy metal pollution. Spanning an area of 155 hectares, this complex historically processed approximately 800,000 tons of ultramafic minerals (Fe-Ni), releasing an estimated 44.8 tons of toxic dust. Following

significant political and technological changes in the 1990s, many of the complex factories were shut down, and the surrounding area was repurposed for residential and agricultural use. Today, a variety of crops - including vegetables, fruits, and cereals - are cultivated on this land.

As a result of the long-term processing and smelting of Fe-Ni-rich minerals, the soils surrounding the former industrial site are heavily contaminated with several heavy metals, including Fe, Mn, Ni, Zn, and Cr (Shallari et al., 1998; Sallaku et al., 1999; Osmani et al., 2015; Osmani et al., 2018). Despite this known contamination, limited research has been conducted on the accumulation of heavy metals in food crops grown in this area, or on the potential for selecting crop species or cultivars with low metal uptake.

Therefore, the present study aims to fill this gap by (1) investigating the concentration and bioavailability of selected heavy metals in the soils of the study area, and (2) assessing the accumulation of these metals in the edible parts of selected vegetables and fruit cultivated in this industrial region of Elbasan, Albania.

MATERIALS AND METHODS

Study area

This study was conducted in 2024 on contaminated farmland located in the Elbasan region of central Albania. The site, situated near the former metallurgical plant (41°09’18.12"N, 20°04’34.17"E), lies to the west of Elbasan city and is characterized by flat topography (Figure 1). The area where the samples were collected is located about 500 meters from the former Ferro-nickel factory, which has not been operational for years. The local climate is typically Mediterranean, with an average annual temperature ranging between 15 and 16°C.

Sampling of Soil and Vegetables

Samples were collected from farmland adjacent to the metallurgical complex during the spring and summer of 2024. Three subsamples were taken for each of the four vegetable species and one fruit species cultivated in the area. Both soil and edible plant parts were collected.

The plant types and species included in the study are presented in Table 1.

Table 1. Vegetables type and species used in study

Vegetable Type	Vegetable Species
Bulb vegetable	*Allium cepa* (Onion)
Leafy vegetable	*Lactuca sativa* (Salad)
Tuber	*Solanum tuberosum* (Potato)
Fruits	*Fragaria vesca* (Strawberry)
Solanaceous	*Capsicum annuum* (Pepper)

Soil samples were taken from the rhizosphere (root zone) of each plant type, with three repetitions per crop. All samples were placed in clean polyethylene bags, clearly labeled by type, and transported to the Laboratory of the Department of Environment and Natural Resources at the Agricultural University of Tirana (AUT) for analysis.

Soil and Plant sample preparation and analysis

Plant samples were washed thoroughly with distilled water to remove the adhering dust. Soil samples were air-dried at room temperature to a constant weight and then finely ground using a mortar and pestle. The edible plant parts were chopped into small pieces using a pre-cleaned stainless-steel knife and oven-dried at 75°C for three days. Dried samples were then pulverized into a fine powder and stored in clean polyethylene (PE) bags for analysis.

Soil and plant analyses were performed at the Agricultural University of Tirana (AUT) and the University of Pristina in Kosovo. Soil pH was measured using a 0.01 M $CaCl_2$ solution at a 1:2.5 soil-to-solution ratio. Cation exchange capacity (CEC) was determined using the ammonium acetate method.

The Mehlich-1 extractant was used to determine the available concentrations of nickel (Ni) in soil, which were then analyzed using atomic absorption spectrometry (AAS). For total concentrations of macronutrients (P, K, Ca, Mg) and micronutrients (Fe, Mn, Zn, Ni, Cr, Co), 0.5 g of soil was digested in aqua regia (a 1:3 mixture of 65% HNO_3 and 37% HCl) at 200°C for 40 minutes, followed by analysis via AAS. To determine heavy metal concentrations in plant tissues, 0.2 g of dried plant material (edible parts and roots) was digested in a 4:1 mixture of 65% HNO_3 and 30% H_2O_2 using microwave digestion at 200°C for 25 minutes.

Digest solutions were analyzed using Atomic Absorption Spectrophotometry (AAS) with the Analytik Jena AAS 400 instrument. The elements analyzed included iron (Fe), magnesium (Mg), manganese (Mn), nickel (Ni), chromium (Cr), zinc (Zn), and cobalt (Co). The limit of detection (LOD) for each element was defined as three times the standard deviation of the blank signal. We used the slope of the curve (absorbance per mg/L) to convert absorbance units in mg/L. The LOD values (in mg/L) for Fe, Mg, Mn, Zn, Ni, Cr, and Co were 0.009, 0.03, 0.0018, 0.012, 0.015, 0.012, and 0.02, respectively. The calibration ranges used in this study (in mg/L) were as follows: Fe: 0-10, Mg: 0-5, Mn: 0-5, Zn: 0-5, Ni: 0-5, Cr: 0-5, Co: 0-5. Dilution was applied to samples containing element concentrations above the upper limit of the calibration range. Quality control was ensured through the use of blanks and certified reference materials (CRMs), with recovery rates maintained within ±10% of the target values.

Bioconcentration factor (BCF)

The Bioconcentration Factor (BCF) quantifies a plant's ability to accumulate metals from soil. It is calculated as the ratio of the metal concentration in the plant's edible part to its total concentration in the corresponding rhizospheric soil:

$$BCF = C_{plant} / C_{soil}$$

A BCF value below 1 indicates limited metal transfer from soil to plant, while a BCF greater than 1 suggests substantial uptake (Sharma et al., 2018; Ba et al., 2024).

Statistical analysis

Differences in the BCFs of heavy metals (Mn, Zn, Ni, and Cr) among the edible parts of the five crop species were evaluated using one-way ANOVA. A significance level of $p < 0.05$ was used to determine statistical relevance.

RESULTS AND DISCUSSIONS

Soil characteristics

Phosphorus (P) levels in the study soils were within the typical range, between 0.5 and 0.6 g/kg of dry soil. The total potassium (K) content in the upper 0.2 meters of agricultural soil generally ranges from 10 to 20 g/kg (Mandloi et al., 2022); however, in this study, values ranged from 6 to 9.8 g/kg, which is slightly below the expected range.

Calcium (Ca) and Magnesium (Mg), though considered secondary nutrients, are essential for plant growth. In the study soils, Ca concentrations were consistently higher than Mg concentrations. This pattern suggests that the soils do not have a natural ultramafic origin, as ultramafic soils typically show higher Mg levels relative to Ca. Instead, the elevated presence of elements commonly associated with ultramafic rocks - such as Fe, Mg, Ni, Cr, and Co - can likely be attributed to anthropogenic contamination from the long-term processing of ultramafic minerals at the nearby metallurgical complex (Table 2A).

Iron (Fe) concentrations in the soil ranged from 18 to 26 g/kg, aligning with typical background levels reported for agricultural soils (Bodek et al., 1988).

The soils in the study area were found to be contaminated with several heavy metals, including manganese (Mn), zinc (Zn), nickel (Ni), chromium (Cr), and cobalt (Co), as detailed in Tables 2A and 2B. Nickel concentrations in rhizospheric soils ranged from 400 to 610 mg/kg, exceeding both the background level for Albanian agricultural soils (287.15 mg/kg) (Gjoka et al., 2022) and the intervention threshold of 210 mg/kg set by Denneman and Robberse (1990) and the Netherlands Ministry of Housing (1994).

Cobalt concentrations varied between 85 and 111 mg/kg across different sampling sites, also exceeding the background value of 83.10 mg/kg. Chromium levels ranged from 310 to 380 mg/kg, far above the target value of 100 mg/kg and the background level of 131.63 mg/kg reported for Albanian agricultural soils.

These elevated concentrations of Ni, Cr, and Co are consistent with long-term emissions from metallurgical operations that processed ultramafic ores rich in these elements. Zinc concentrations ranged from 75 to 132 mg/kg. While these values are above the background concentration for Zn in Albanian soils (81.80 mg/kg) in the cases of soils under potato, strawberry, and pepper crops, they remain below the intervention threshold of 150-300 mg/kg established by the Council of the European Communities (1986).

As shown in Table 2, soils associated with all sampled crops exhibited elevated concentrations of Ni, Cr, and Co compared to both background levels and intervention thresholds.

Nickel and cobalt exceeded the permissible limits in all plots, with the highest Ni level recorded in strawberry soil (610 mg/kg), nearly three times the intervention threshold. Similarly, chromium levels in onion and strawberry soil surpassed the 360 mg/kg intervention value.

Zinc levels were highest in soils associated with strawberry and pepper but remained below the intervention limit of 300 mg/kg. Manganese concentrations were well below critical thresholds in all plots, though consistently elevated.

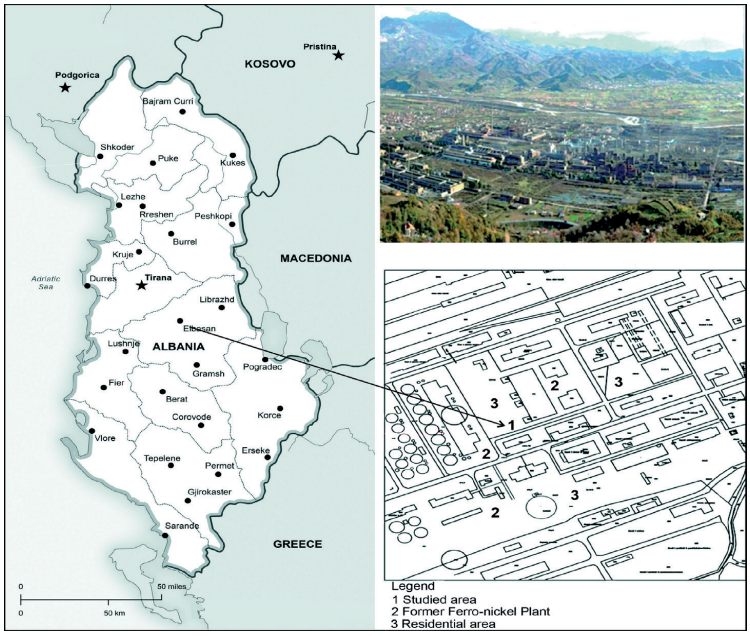


Figure 1. Map of Albania with the location of former Ferro-nickel plant and the study area.

Table 2. Total macronutrients and micronutrients (mean ± SD) in soils of different sampling sites

A) Macronutrients (g/kg dry soil)

Soil of Vegetable	P	K	Ca	Mg	Fe
Onion	0.5 ± 0.04	8.1 ± 1.0	31 ± 2	14 ± 2	26 ± 6
Salad	0.7 ± 0.01	7.2 ± 0.5	29 ± 5	13 ± 3	18 ± 1
Potato	0.6 ± 0.01	9.8 ± 0.5	30 ± 4	14 ± 5	19 ± 5
Strawberry	0.6 ± 0.02	6.0 ± 1.0	41 ± 8	15 ± 4	19 ± 2
Pepper	0.6 ± 0.02	8.1 ± 0.5	30 ± 5	14 ± 4	18 ± 1

B) Micronutrients (mg/kg dry soil)

Soil of Vegetable	Mn	Zn	Ni	Cr	Co
Onion	576 ± 40	75 ± 5	410 ± 7	380 ± 16	75 ± 9
Salad	538 ± 60	90 ± 14	440 ± 13	310 ± 52	74 ± 4
Potato	557 ± 15	122 ± 12	405 ± 10	315 ± 68	74 ± 8
Strawberry	547 ± 30	132 ± 16	610 ± 11	370 ± 62	111 ± 6
Pepper	565 ± 23	123 ± 8	400 ± 20	360 ± 19	85 ± 5

*Intervention Threshold Values (mg/kg): Mn - 1500, Zn - 300, Ni - 210, Cr - 360, Co – 50

Macronutrient data showed moderate variability across sites, with phosphorus ranging from 0.5 to 0.7 g/kg and potassium from 6.0 to 9.8 g/kg. Notably, the strawberry plot had the highest calcium concentration (41 g/kg), suggesting potential input differences or localized soil characteristics.

A soil pH between 6.0 and 7.2 is considered optimal for the growth of most garden crops, although many vegetable and fruit species can tolerate pH values between 7.0 and 8.0 (extension.usu.edu). The pH values in the rhizosphere of crops collected from the contaminated area in Elbasan (Table 3) fall within this acceptable range, suggesting that pH is not a limiting factor for plant growth in these soils.

Cation exchange capacity (CEC) in the studied soils ranged from 15 to 26 cmol/kg, with an average of 20.6 cmol/kg. These values reflect a moderate-to-high nutrient-holding capacity, which is typical of fertile agricultural soils.

While total metal concentrations are useful for identifying long-term contamination and possible sources, they do not accurately represent the portion of metals available for plant uptake. To evaluate bioavailability, the Mehlich-1 extraction method was used to assess the potentially available fractions of Fe, Mn, Zn, Ni, Cr, and Co.

The results indicate that available Fe concentrations ranged from 16 to 58 mg/kg, Mn from 4 to 15 mg/kg, and Ni from 2.4 to 4.5 mg/kg. Notably, Co and Cr showed very low extractable concentrations across all sampled soils, a finding consistent with their limited uptake by plants in this study.

Table 3. Soil pH, CEC, and available metal concentrations (mean values)

Soil of vegetable	pH	CEC (cmol/kg)	Fe (mg/kg)	Mn (mg/kg)	Zn (mg/kg)	Ni (mg/kg)	Cr (mg/kg)	Co (mg/kg)
Onion	7.5	15	38	4	3.8	3.6	0.1	0.2
Salad	8.0	17	57	5	3.0	4.0	0.1	0.2
Potato	7.7	14	16	3	3.7	3.6	0.1	0.2
Strawberry	7.5	16	58	12	2.9	4.5	0.1	0.2
Pepper	7.5	26	28	15	3.9	2.4	0.1	0.2

Nickel concentrations in edible plants and roots of food crops

The mean concentrations of iron (Fe), manganese (Mn), zinc (Zn), nickel (Ni), and chromium (Cr) in the edible parts of the sampled food crops ranged as follows: Fe (99-765 mg/kg), Mn (6.2-90 mg/kg), Zn (3.6-12 mg/kg), Ni (10-26 mg/kg), Cr (0.5-19 mg/kg) (Table 4).

Among these, the Mn, Zn, Fe, and Cr concentrations in potatoes, and Fe in peppers, remained below the permissible limits set by the World Health Organization (WHO). However, Fe levels in onion, salad, and strawberry, Ni concentrations in all edible samples, and Cr concentrations in onion, salad, strawberry, and pepper exceeded the WHO safety thresholds.

Table 4. Heavy Metal concentrations in edible parts of crops (mean ± SD)

Vegetable	Fe (mg/kg)	Mn (mg/kg)	Zn (mg/kg)	Ni (mg/kg)	Cr (mg/kg)
Onion	200 ± 4	6.4 ± 2	8 ± 2	12 ± 2	2.0 ± 0.1
Salad	646 ± 41	25 ± 3	3.6 ± 0.2	16 ± 1	5.0 ± 0.7
Potato	59.5 ± 9	6.2 ± 1	10.0 ± 0.7	10 ± 0.5	0.5 ± 0.3
Strawberry	765 ± 59	90 ± 2	7 ± 0.1	26 ± 3	19.0 ± 3.0
Pepper	99 ± 3	21 ± 4	12 ± 2	15 ± 1	4.0 ± 0.6
WHO Limits	270	300	300	10	1.3

These findings indicate a significant health concern, particularly regarding Ni and Cr accumulation. The order of Ni accumulation in edible parts of the crops was as follows: Strawberry (fruit) > Salad (leafy vegetable) > Pepper (solanaceous) > Onion (bulb) > Potato (tuber). The metal concentrations in the roots of these food crops were significantly higher than in the edible parts, ranging as follows: Fe (1899-2658 mg/kg), Mn (25-97 mg/kg), Zn (6-28 mg/kg), Ni (16-56 mg/kg), Cr (4.2-24 mg/kg) (Table 5).

Table 5. Heavy Metal concentrations in roots of crops from contaminated soil (mean ± SD)

Vegetable	Fe (mg/kg)	Mn (mg/kg)	Zn (mg/kg)	Ni (mg/kg)	Cr (mg/kg)
Onion	2658 ± 4	97 ± 2	26 ± 0.06	56 ± 0.4	21.0 ± 0.1
Salad	2494 ± 41	25 ± 3	6 ± 0.2	16 ± 0.8	23.0 ± 0.7
Potato	2239	87 ± 0.7	20.0 ± 0.7	42 ± 0.5	24.0 ± 0.3
Strawberry	2487 ± 59	70 ± 0.7	11 ± 0.1	27 ± 2.6	12.0 ± 3.0
Pepper	1899 ± 3	41 ± 4	28 ± 2	25 ± 1.2	4.2 ± 0.6

This pattern reflects the bioaccumulation of metals in root tissues and is consistent with the elevated levels of available metals in the rhizospheric soils. In all cases, root concentrations of Fe, Mn, Zn, Ni, and Cr exceeded WHO safety thresholds (FAO/WHO, 2001).

Bioconcentration Factor (BCF)

Bioconcentration Factors (BCFs) are used to evaluate the capacity of food crops to accumulate heavy metals in their edible tissues. The transfer of metals from soil to plants, and specifically into the edible parts, represents the principal route through which potentially toxic elements enter the human food chain. This process is influenced by several factors, including the type and concentration of the metal, plant species, soil physicochemical properties, and environmental conditions (Gebeyehu & Bayissa, 2020).

Figure 2 presents the BCF values calculated for Fe, Mn, Zn, Ni, and Cr in the edible parts of the crops analyzed in this study. Notably, the BCFs for Mn, Ni, and Cr were significantly higher in the fruit crop (strawberry) compared to the four vegetable types, indicating a greater potential for metal accumulation in fruit tissues under similar soil contamination conditions.

In all tested vegetables and fruits, BCF values were below 1.0 when calculated using the total metal concentrations in rhizospheric soil, suggesting that while metals were taken up, the transfer efficiency was relatively low. However, values close to or approaching 1 may still indicate concern when paired with high soil concentrations.

The relative order of metal transfer based on BCFs differed across plant types: Onion (Zn > Ni > Mn > Cr), Salad (Mn > Zn > Ni > Cr), Potato (Zn > Ni > Mn > Cr), Pepper (Zn > Ni > Mn > Cr). These differences highlight species-specific metal uptake mechanisms and the importance of crop selection when cultivating in contaminated areas.

Statistical analysis using one-way ANOVA revealed significant differences ($p < 0.05$) in the BCFs of Mn, Zn, Ni, and Cr among the five food crop types analyzed, as shown in Table 6.

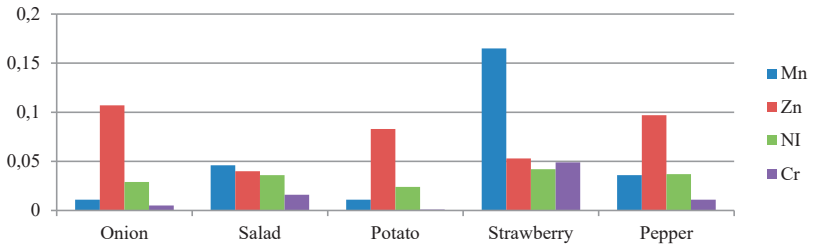


Figure 2. Bioconcentration Factor (BCF) in food plants

Table 6. ANOVA results: Significant differences in BCFs of Heavy Metals among edible parts of five food crops

Metal	Degrees of Freedom (df)	F-value	P-value	Critical F-value
Mn	4	208	0.000	3.47805
Zn	4	16.7	0.0002	3.47805
Ni	4	11.2	0.001	3.47805
Cr	4	153	0.000	3.47805

CONCLUSIONS

This study investigated the accumulation of heavy metals in four vegetable species and one fruit species cultivated on farmland contaminated with iron (Fe), manganese (Mn), zinc (Zn), and nickel (Ni) in Elbasan, Albania. The concentrations of these metals in the soil exceeded the typical background levels reported for Albanian agricultural soils.

Among the edible parts of the analyzed crops, metal concentrations decreased in the following order: Fruit (Strawberry) > Leafy vegetable (Salad) *(except for Zn)*> Solanaceous (Pepper) > Bulb (Onion) > Tuber (Potato). This gradient indicates that certain crop types, particularly fruits and leafy vegetables, are more prone to accumulating heavy metals and may therefore pose greater health risks when grown in contaminated environments.

These findings support the selection of low-accumulator plant species - such as onions and potatoes - for cultivation in areas with known soil contamination. Conversely, high-accumulator species should be avoided or managed carefully to reduce human exposure to toxic metals through the food chain.
Future research should focus on identifying the chemical forms and mineral phases of metals - especially Ni, soil to better understand their bioavailability, environmental mobility, and potential risks. This knowledge will be crucial for developing effective mitigation strategies and improving food safety in contaminated regions.

ACKNOWLEDGEMENTS

The authors extend their sincere thanks to the technical staff of the Laboratory of the Department of Environment and Natural Resources at the Agricultural University of Tirana (AUT), as well as the Laboratory of the University of Pristina in Kosovo, for them invaluable assistance with the analytical work presented in this study.

REFERENCES

Ba, V.N., Thien, B.N., Phuong, H.T., Loan, T.T. H.L., & Anh, T.T. (2024). Bioconcentration and translocation of elements from soil to vegetables and associated health risk. *Journal of Food Composition and Analysis, 132*, 106296.

Bradl, H. (Ed.). (2005). *Heavy metals in the environment: Origin, interaction and remediation* (Vol. 6). Elsevier.

Bodek, I., Lyman, W.J., Reehl, W.F., & Rosenblatt, D.H. (Eds.). (1988). *Environmental inorganic chemistry: Properties, processes, and estimation methods* (Vol. 10). Pergamon Press.

Codex Alimentarius Commission. (2001). *Food additives and contaminants* (ALINORM 01/12). Joint FAO/WHO Food Standards Programme.

Council of the European Communities. (1986). Council Directive of 12 June 1986 on the protection of the environment, and of the soil, when sewage sludge is used in agriculture (86/278/EEC). *Official Journal of the European Communities, L181*, 6–12.

Denneman, C.A., & Robberse, J.G. (1990). Ecotoxicological risk assessment as a base for development of soil quality criteria. In *Contaminated Soil'90: Third International KfK/TNO Conference on Contaminated Soil, 10–14 December 1990, Karlsruhe, Federal Republic of Germany* (pp. 157–164). Springer Netherlands.

Gebeyehu, H.R., & Bayissa, L.D. (2020). Levels of heavy metals in soil and vegetables and associated health risks in Mojo area, Ethiopia. *PLoS ONE, 15*(1), e0227883. https://doi.org/10.1371/ journal.pone. 0227883

Gjoka, F., Duering, R.A., & Siemens, J. (2022). Background concentrations and spatial distribution of heavy metals in Albania's soils. *Environmental Monitoring and Assessment, 194*(2), 115. https://doi.org/10.1007/s10661-022-09749-4

Hu, J., Wu, F., Wu, S., Cao, Z., Lin, X., & Wong, M. (2013). Bioaccessibility, dietary exposure and human risk assessment of heavy metals from market vegetables in Hong Kong revealed with an in vitro gastrointestinal model. *Chemosphere, 91*(4), 455–461, DOI:10.1016/j.chemosphere.2012.11.066

Jolly, Y.N., Islam, A., & Akbar, S. (2013). Transfer of metals from soil to vegetables and possible health risk assessment. *SpringerPlus, 2*, 1–8, https://doi.org/10.1186/2193-1801-2-385

Mandloi, S., Singh, S., & Prajapati, S. (2022). Potassium and its forms in soil. *Agriculture Magazine, 1*(4).

Ministry of Housing, Netherlands. (1994). *Physical Planning and Environmental Conservation Report HSE 94.021*.

Osmani, M., Bani, A., & Hoxha, B. (2015). Heavy metals and Ni phytoextraction in the metallurgical area soils in Elbasan. *Albanian Journal of Agricultural Sciences, 14*(4), 414.

Osmani, M., Bani, A., & Hoxha, B. (2018). The phytomining of nickel from industrial polluted site of Elbasan-Albania. *European Academic Research, 10*, 5347–5364.

Sallaku, F., Shallari, S., Wegener, H. R., & Henningsen, P. F. (1999). Heavy metals in industrial area of Elbasan. *Bulletin of Agricultural Sciences*, *3*, 85–92. *(in Albanian)*

Shallari, S., Schwartz, C., Hasko, A., & Morel, J. L. (1998). Heavy metals in soils and plants of serpentine and industrial sites of Albania. *Science of the Total Environment, 209*(2–3), 133–142, https://doi.org/10.1016/S0048-9697(98)80104-6

Sharma, S., Nagpal, A.K., & Kaur, I. (2018). Heavy metal contamination in soil, food crops and associated health risks for residents of Ropar wetland, Punjab, India and its environs. *Food Chemistry, 255*, 15–22, DOI:10.1016/j.foodchem.2018.02.037

Zwolak, A., Sarzyńska, M., Szpyrka, E., & Stawarczyk, K. (2019). Sources of soil pollution by heavy metals and their accumulation in vegetables: A review. *Water, Air, & Soil Pollution, 230*, 164. https://doi.org/10.1007/s11270-019-4221-y

Scientific Papers. Series E. Land Reclamation, Earth Observation & Surveying, Environmental Engineering. Vol. XIV, 2025
Print ISSN 2285-6064, CD-ROM ISSN 2285-6072, Online ISSN 2393-5138, ISSN-L 2285-6064

BIOMOLECULE PRODUCTION BY MICROORGANISMS ISOLATED FROM SALINE ENVIRONMENTS

Simona NEAGU, Mihaela Marilena STANCU

Institute of Biology Bucharest of Romanian Academy, 296 Splaiul Independenţei, 060031, District 6, Bucharest, P.O. Box 56-53, Romania

Corresponding authors' email: simona.neagu@ibiol.ro, mihaela.stancu@ibiol.ro

Abstract

Saline environments, characterized by extreme conditions, are unique habitats that harbor diverse microorganism communities capable of synthesizing biomolecules, such as extracellular hydrolytic enzymes and carotenoid pigments with significant industrial potential. These biomolecules are important in microorganisms' survival and adaptation to harsh environments. The present study aimed to isolate several new biomolecule-producing microorganisms from two salt wells (Curmătura and Băicoi, Prahova County, Romania). The strains NC18, NC21, NC28, and SB1 were isolated using a selective agar medium supplemented with 3.4 M sodium chloride (NaCl). Specifically, NC18, NC21, and NC28 were obtained from Curmătura, while SB1 was isolated from Băicoi. As a result of their ability to grow on agar medium with 1–5 M NaCl, all the new isolates were included in the extreme halophilic organisms. Based on their phenotypic and molecular characteristics, all these strains were included in the domain Archaea. The four isolates NC18, NC21, NC28, and SB1 were further assessed for their ability to produce extracellular hydrolytic enzymes, including lipase, protease, amylase, cellulase, xylanase, and pectinase, as well as carotenoid pigments. Due to their ability to produce a range of bioactive compounds, the halophilic isolates present promising opportunities for diverse biotechnological applications, such as industrial enzyme production, and the development of bio-based products.

Key words: *carotenoids, exoenzymes, halophiles, saline environment.*

INTRODUCTION

Halophilic Archaea, primarily belonging to the family *Halobacteriaceae*, are extremophiles that thrive in hypersaline environments, where high salt concentrations inhibit the growth of most other organisms. Extreme halophiles typically require NaCl concentrations exceeding 1.5 M for optimal development. They are ubiquitous and are widely distributed in habitats classified as salt lakes, hypersaline soils or sediments, salterns, and salt mines (Oren, 2002). To survive under osmotic stress, these organisms have evolved unique biochemical and physiological mechanisms. Their primary adaptation is the 'salt-in' strategy, maintaining high intracellular K^+ and Cl^- levels. They also possess specialized membrane lipids, an S-layer, and numerous acidic proteins that require high salt concentrations to maintain their native structure (Galinski, 1993; Oren, 1999). These adaptations make them a valuable source of biologically active compounds. Among the most significant compounds produced by halophiles are salt-resistant extracellular enzymes, pigments, and biosurfactants. These biomolecules have broad industrial and environmental applications due to their stability under extreme conditions (Antón et al., 2002; Mnif et al., 2009; Subramanian & Gurunathan, 2020).

Halophilic archaea are known for their ability to produce extracellular hydrolytic enzymes, such as amylases, proteases, and lipases (Qiu et al., 2021; Moopantakath et al., 2022; Song et al., 2023). Due to their remarkable stability and optimal activity under extreme environmental conditions, including high salinity and temperature, these exoenzymes are of both theoretical and practical interest. Their unique properties grant them significant value in industrial applications, such as detergent formulation, biofuel production, and pharmaceutical synthesis (Kasirajan et al., 2020; Schreck et al., 2021). For example, halophilic proteases have been employed in food processing and leather industries due to their catalytic efficiency at high salt concentrations (Antón et al., 2002).

Halophiles frequently produce carotenoid pigments, with bacterioruberin (C50 carotenoid) being the most characteristic in

extremely halophilic archaea. These microorganisms form colonies in shades of pink, orange, or red due to the high accumulation of bacterioruberin and related pigments. Such compounds absorb solar radiation and also protect the cells from photooxidative damage, shielding them against oxidative stress caused by UV exposure and high salinity. Beyond their protective role, C50 carotenoids exhibit strong antioxidant, antimicrobial, and anticancer properties, highlighting their relevance in pharmaceutical and cosmetic applications. Their stability and intense coloration enhance their potential as natural colorants (Antón et al., 2002; Subramanian & Gurunathan, 2020; Bouhamed et al., 2024).

The present study aimed to isolate several new halophilic microorganisms capable of producing biomolecules, including extracellular enzymes and carotenoid pigments, from different saline habitats, with a key role in their survival under extreme conditions.

MATERIALS AND METHODS

The samples used in this study were collected from two salt wells in Curmătura (Latitude: 45°09′25.307″ N, Longitude: 26°09′06.006″ E, Altitude: 213 m) and Băicoi (Latitude: 45°2′34.553″ N, Longitude: 25°53′18.667″ E, Altitude: 265 m), both located in Prahova County, Romania**.** We gathered and examined mud from Curmătura, and soil from the Băicoi salt well.

Isolation and characterization of biomolecule-producing halophiles

For the isolation and cultivation of halophilic microorganisms, we used JCM 168 medium (Rasooli et al., 2016), which contained the following components (g/L): NaCl (200), KCl (2), $MgSO_4 \cdot 7H_2O$ (20), $FeCl_2 \cdot 4H_2O$ (0.036), $MnCl_2 \cdot 4H_2O$ (0.00036), casamino acids (5), yeast extract (5), sodium glutamate (1), trisodium citrate (3), and agar (20)**,** with a final pH of 7.0. Decimal dilutions (10^{-1}-10^{-3}) of the samples were prepared in 3.4 M NaCl solution and inoculated by the pour-plate method (Sanders, 2012) in JCM 168 agar. The Petri plates were incubated at 37 °C up to 20 days. The number of viable microorganisms in samples was expressed as colony-forming units (CFU/g). The newly isolated strains were purified by multiple subculturing on JCM 168 agar medium and stored in glycerol at -80°C for long-term preservation. The new four isolates were further characterized by their phenotypic characteristics, including colony color, growth temperature, salt tolerance (0–5 M NaCl), production of extracellular hydrolytic enzymes, and molecular characteristics, specifically the 16S rRNA gene. Genomic DNA was extracted from isolates using the Pure Link genomic DNA kit (Invitrogen, Carlsbad, CA, USA). The 16S rRNA gene was amplified via polymerase chain reaction (PCR) using extracted genomic DNA, universal primers 27f/1492r (Marchesi et al., 1998) and 20f/1492r (Orphan et al., 2001), alongside GoTaq G2 Hot Start Polymerase (Promega, Madison, WI, USA), as previously described (Stancu, 2020; 2023; 2025). The thermal cycling conditions were carried out on an Eppendorf Mastercycler Pro S thermocycler (Hamburg, Germany) and included an initial denaturation at 94°C for 10 min, followed by 35 cycles of 94°C for 1 min, 55°C for 30 s, and 72°C for 2 min, with a final extension at 72°C for 10 min. The PCR products were visualized onto 1.5% (w/v) agarose gels stained with SYBR Safe (Invitrogen) (Stancu, 2020; 2023; 2025).

The four isolates were screened to produce extracellular hydrolases, including lipase, protease, amylase, cellulase, xylanase, and pectinase, using the plate assay method (Rohban et al., 2008). The composition of the JCM 168 medium was modified by removing casamino acids, and reducing yeast extract to 1 g/L, and supplementing with 1 g/L of specific substrates such as Tween-80, casein, starch, carboxymethylcellulose, xylan, and pectin. Cultures were spot-inoculated onto the surface of the medium and incubated at 37°C for 10 to 20 days. Enzymatic activity was determined based on halo formation around the cultures.

The four isolates were further screened to produce carotenoid pigments. After reaching the stationary phase, the cultures were centrifuged, and the biomass was resuspended in acetone to extract pigments. Carotenoid extracts analysis was conducted using UV-visible spectroscopy, with absorbance measured from 200 to 800 nm (SPECORD 200

UV-Vis spectrophotometer, Analytik Jena, Jena, Germany). Total carotenoid content was determined at 494 nm using an absorption coefficient of 2500 (Hiyama et al., 1969). High-Performance Thin-Layer Chromatography (HPTLC) analysis was further performed using a CAMAG system, with samples applied to silica gel plates and developed in a chloroform-methanol (90:10, v/v) mobile phase (Stancu, 2020). The TLC plates were scanned under UV light (366 nm) for pigments examination. Antimicrobial activity of carotenoid extracts was evaluated using the agar diffusion techniques (Gómez-Villegas et al., 2020). The reference strains tested were *Escherichia coli* ATCC 25922, *Pseudomonas aeruginosa* ATCC 15442, *Staphylococcus aureus* ATCC 25923, and *Candida albicans* ATCC 10231. Tryptic Soy Agar (TSA) plates were inoculated with 0.5 McFarland standard suspension of each pathogen. After drying, pigment extracts (10 µL), were spotted onto the medium. Acetone toxicity was ruled out before testing. Gentamicin (10 µg) and Fluconazole (25 µg) were used as positive controls. Petri Plates were incubated at 37°C for 24 hours.

RESULTS AND DISCUSSIONS

Romania has over 300 salt deposits, located either inside or outside the Carpathian Arc, formed through the evaporation of seawater and later shaped by tectonic processes, leading to the formation of salt massifs, saline springs, and hypersaline lakes (Cavruc & Chiricescu, 2006). Due to their high purity and accessibility, these deposits have been exploited over time for industrial purposes, balneotherapy, and human consumption. To make use of these resources, people have built salt wells, using their water for various food preservation, such as pickles and cheeses. Similar saline wells have been identified in Prahova County, specifically on the outskirts of Curmătura village and Băicoi town. These two saline wells, characterized by distinct physicochemical properties, including salinity exceeding 280 g/L, served as sources for the halophilic microorganisms' isolation (Figure 1.a).

Isolation and characterization of biomolecule-producing halophiles

From Curmătura mud and Băicoi soil we identified a microbial density of 10^4 CFU/g for both samples. Among the 27 isolates obtained in pure culture, four colonies with distinct morphological traits (Table 1) were chosen for further analysis. These colonies were designated as NC18, NC21, and NC28, all isolated from Curmătura mud, while SB1 was obtained from the Băicoi soil sample. Sensitivity tests to chloramphenicol (a broad-spectrum antibiotic) and sodium deoxycholate (a bile salt detergent), showed that all strains were resistant to chloramphenicol. This response differentiates them from typical bacteria and is consistent with established archaeal traits. Unlike bacteria, haloarchaea often exhibit antibiotic resistance patterns, including ampicillin, tetracycline, erythromycin, and chloramphenicol which generally target peptidoglycan synthesis and/or bacterial ribosomal structures (Thombre et al., 2016). Our results showed that all isolates were sensitive to sodium deoxycholate (Table 1), consistent with literature indicating that most non-coccoid halophilic archaea are more susceptible to bile salts than many bacteria. This sensitivity is likely due to structural variations in the membrane and S-layer, which differ among archaeal genera and species (Elevi & Oren, 2008). The four isolates exhibit remarkable salt tolerance, thriving in 1-5 M NaCl. Thus, NC18 grew from 1 up to 4 M salt, while NC21 and NC28 tolerated 1-5 M, and SB1 grew only in 2-5 M NaCl. Such high salt requirements are characteristic of halophilic Archaea. Extreme halophiles typically require over 1.5 M NaCl to develop, with optimal proliferation often at 3.4-5.2 M NaCl (Oren, 2002). Their growth temperature of 37 °C is within the mesophilic range common for many haloarchaeal species which generally grow well at 30-45 °C, with some able to exceed 50°C (Bowers et al, 2011).

Focusing on the amplification of the 16S rRNA gene, PCR-based molecular techniques were employed for the genetic characterization of the four isolates. All strains were successfully amplified using archaeal-specific primers (20f/1492r), confirming their classification within the Archaea domain, with the

characteristic 1472 bp amplicon obtained through PCR (Table 1, Figure 1c). No amplification was observed with bacterial-specific primers (27f/1492r) in any strain except NC28, suggesting the general absence of bacterial DNA. However, the amplification observed in NC28 could be due to horizontal gene transfer, which may have introduced the 16S rRNA gene of bacteria into the archaeal genome.

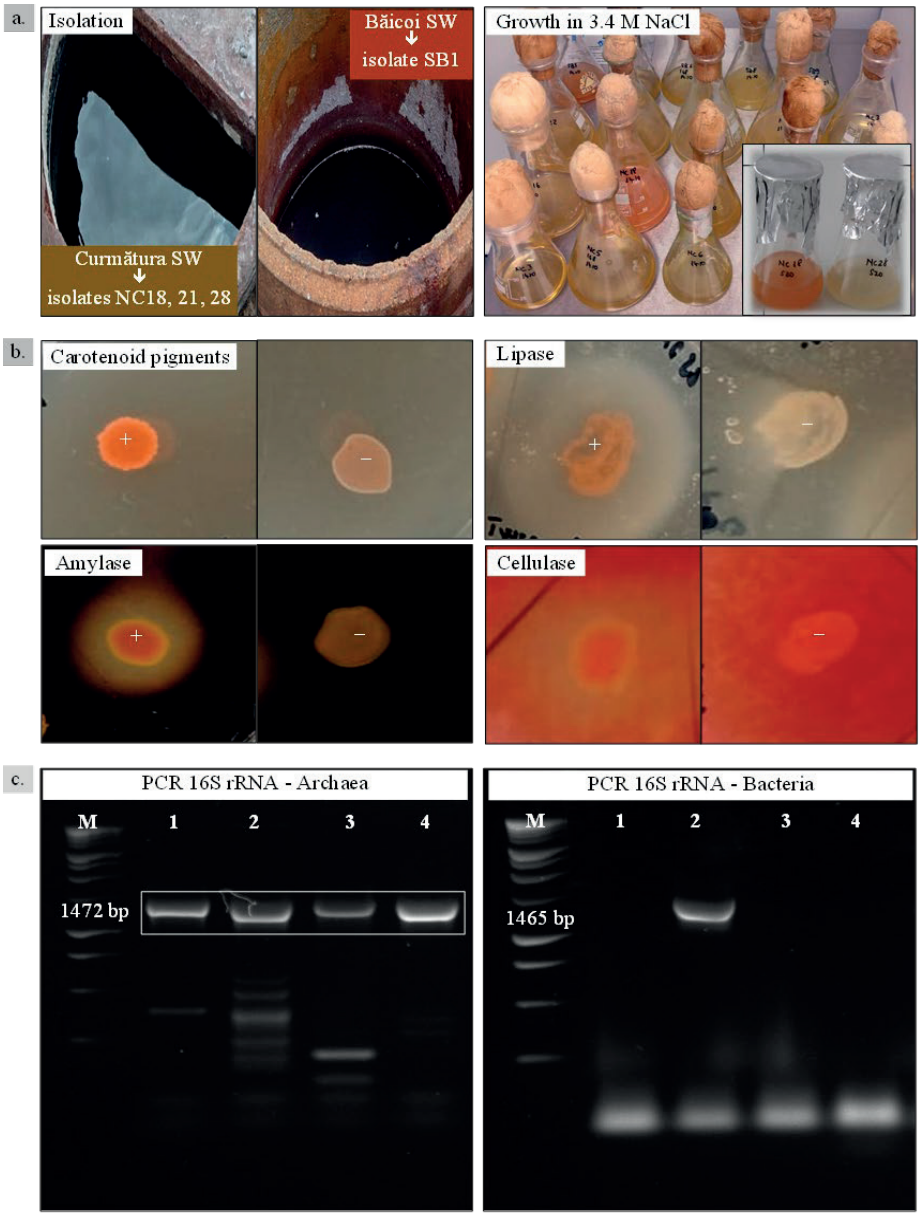


Figure 1. Isolation of halophiles from saline samples and their characterization: a. Curmătura and Băicoi salt well (SW) isolates NC18 (1), NC28 (2), NC21 (3), SB1 (4) grown in JCM168 medium with 3.4 M NaCl; b. isolate characterization, carotenoids, lipase, amylase, and cellulase, positive reaction (+), negative reaction (–); c. PCR of 16S rRNA gene using gDNA extracted from strains NC18 (1), NC28 (2), NC21 (3), SB1 (4), 1 kb DNA ladder (M)

Table 1. Characterization of halophiles isolated from saline samples

Characteristics	Strain			
	NC18	**NC21**	**NC28**	**SB1**
Isolation source	Curmătura mud	Curmătura mud	Curmătura mud	Băicoi soil
Growth on				
JCM168 agar	+	+	+	+
Chloramphenicol	+	+	+	+
Sodium deoxycholate	–	–	–	–
Color of colonies	Red	orange	orange	orange
Temperature growth (°C)	37	37	37	37
Salt tolerance capacity	1–4 M	1–5 M	1–5 M	2–5 M
PCR 16S rRNA gene using primers for				
Archaea (1472 bp)	+	+	+	+
Bacteria (1465 bp)	–	–	–	–
Extracellular hydrolase production				
Lipase (Tween80)	–	+	+	+
Protease (casein)	–	–	–	–
Amylase (starch)	+	+	+	–
Cellulase (carboxymethylcellulose)	–	+	+	+
Xylanase (xylan)	–	–	–	+
Pectinase (pectin)	–	–	–	–
Carotenoid pigments production	+	+	+	+
HPTLC (R_f)	0.07–0.61	0.19–0.69	0.09–0.23	0.22–0.26
Antimicrobial activity				
E. coli ATCC25922	+	+	+	–
P. aeruginosa ATCC 15442	–	–	–	–
S. aureus ATCC25923	–	–	–	–
C. albicans ATCC 10231	+	+	+	–

Positive reaction (+), negative reaction (–).

As confirmed by genetic and physiological characterization, the isolates belonging to the haloarchaea were further examined for their biotechnological potential by testing their ability to produce extracellular enzymes and carotenoid pigments.

Extremophilic enzymes, particularly extracellular ones, have a lot of promise for industrial applications due to their stability in high-salt environments and their ability to function in unconventional conditions (Moopantakath et al., 2022). In this study, the synthesis of six extracellular hydrolytic enzymes by haloarchaea isolates was assayed qualitatively (Table 1, Figure 1b). Several strains exhibited combined enzymatic activities, with NC21 and NC28 isolates capable of synthesizing amylase, lipase, and cellulase, while SB1 isolate synthesized lipase, cellulase, and xylanase. In contrast, NC18 displayed only amylase activity. No strains were capable of producing protease or pectinase. The findings are consistent with existing literature that indicates haloarchaea commonly produce amylase and lipase, which have applications in starch hydrolysis, biofuel production, and biocatalysis (Menasria et al., 2018). Extracellular enzymes, such as cellulase and xylanase, are less commonly found in halophilic Archaea (Zhang et al., 2011). Thus, their presence in certain strains is noteworthy. Our findings highlight the metabolic diversity of the haloarchaea isolates, their capability to produce multiple extracellular enzymes, and their consequent potential for diverse biotechnological applications.

One of the most prominent and conserved phenotypes observed in haloarchaea in their respective natural environments is the ability to produce carotenoids. UV-Vis spectra (in the domain 200-800 nm) of the carotenoid pigments extracted from the strains isolated in this study showed differences in their composition (Figure 2b). The absorbance spectrum of the red pigment extract from the NC18 showed a profile with maxima at 440, 500, and 530 nm. The peaks recorded at 500 and 536 nm are comparable to those documented for bacterioruberin (495 and 530 nm) (Bouhamed et al., 2024), the predominant C_{50} carotenoid in haloarchaea, indicating the potential presence of at least one variant of bacterioruberin.

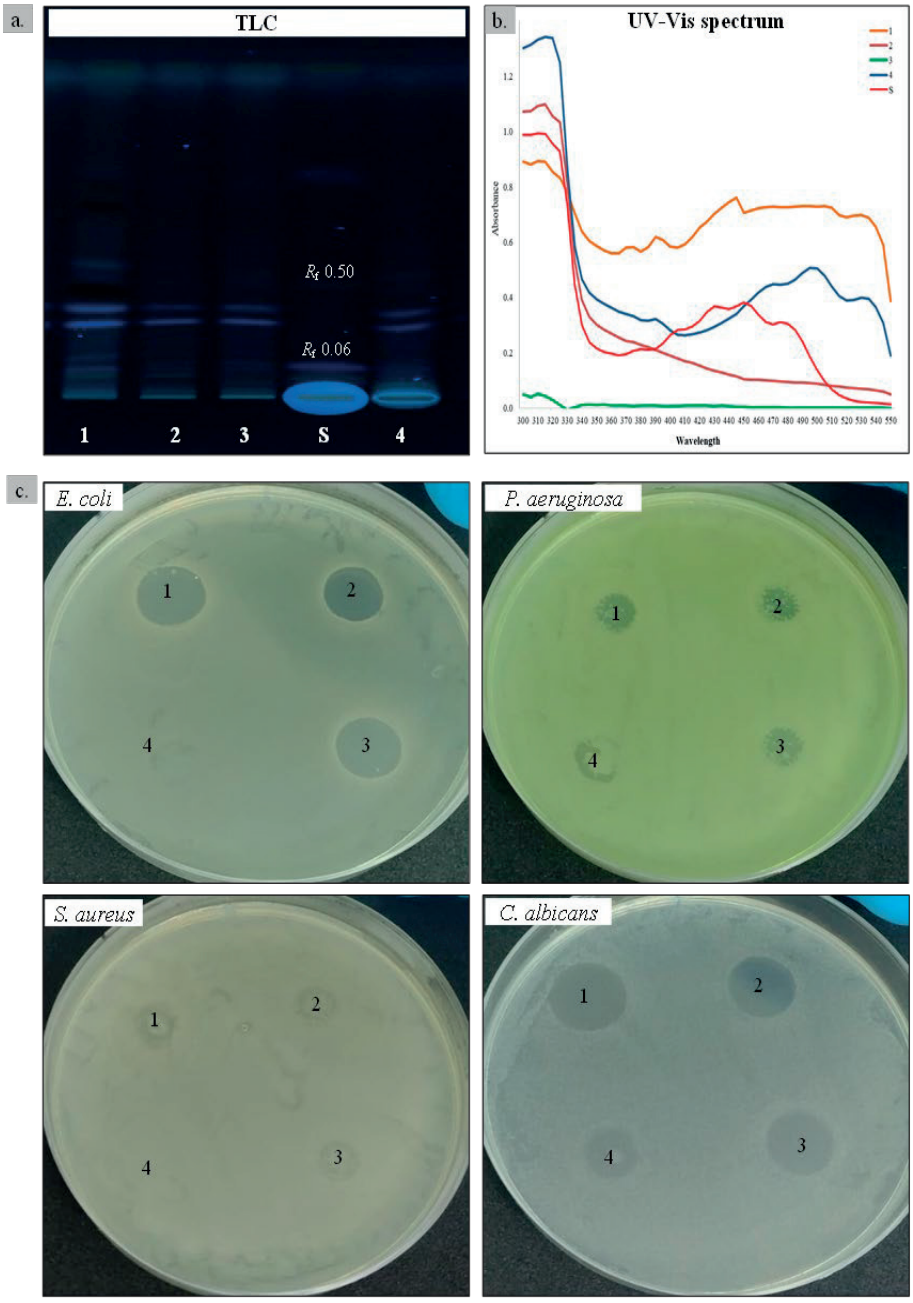


Figure 2. Carotenoid pigments production by halophiles: a. TLC of carotenoids extracted from strains NC18 (1), NC21 (2), NC28 (3), SB1 (4) grown in JCM168 medium with 3.4 M NaCl; retardation factor (Rf), carotenoid standards (S); b. UV-Vis spectrum of carotenoids (300-550 nm); c. antimicrobial activity of carotenoids extracted from strains NC18 (1), NC21 (2), NC28 (3), SB1 (4) on references pathogenic microorganisms

Given its known roles in photoprotection, membrane stability, and oxidative stress resistance, bacterioruberin presence may contribute to the survival and adaptation of these archaea in extreme environments. Additionally, its industrial potential in

biotechnology and pharmaceuticals further underscores the relevance of these results. The orange pigment extract from the SB1 also displayed three distinct absorption peaks at 470, 495, and 530 nm. This aligns with the findings of Kesbiç et al. (2023), who reported bacterioruberin absorption maxima at 467, 494, and 527 nm, values closely matching those observed in SB1. In contrast, the NC21 and NC28 did not exhibit peaks at these wavelengths (440-530 nm). However, all strains showed a peak at ~310 nm, likely corresponding to carotenoid precursors present in the cells, such as phytoene or phytofluene. Although no absorption peak in the visible range was identified for extracts from NC21 and NC28, HPTLC analysis revealed several visible bands in all the halophiles extracts, confirming the presence of carotenoid pigments with distinct R_f values ranging from 0.07 and 0.69 (Table 1, Figure 2a). The superior sensitivity of TLC, which may separate trace pigments undetectable by UV-Vis spectroscopy, may be responsible for this discrepancy. For better understanding of carotenoid production, the total carotenoid concentrations were further determined. NC18 and SB1 were the highest carotenoid producers, yielding 585.2 µg/mL and 406.2 µg/mL, respectively, while NC21 (84.2 µg/mL) and NC28 (52.0 µg/mL) produced significantly lower amounts, consistent with our previous results.

The antimicrobial activity of the carotenoid pigment extracts was assessed against the pathogenic reference strains *E. coli*, *S. aureus*, *P. aeruginosa,* and *C. albicans*. Our results revealed that the carotenoid extracts from NC18, NC21, and NC28 exhibited inhibitory effects against *E. coli* and *C. albicans*, but not against *P. aeruginosa* or *S. aureus* (Figure 2c). Interestingly, the SB1 pigment extract had no antimicrobial activity against any of the pathogens tested, despite the high carotenoid concentration. According to our results, stability, bioavailability, and composition of pigments are important factors in antibacterial activity. These results indicate that pigment stability, bioavailability, and composition are key to antimicrobial efficacy. The specific chemical structures of the pigments from NC18, NC21, and NC28 might interact more effectively with the membranes or metabolic pathways of *E. coli* and *C. albicans,* while the inherent resistance mechanisms in *P. aeruginosa* and *S. aureus* could inhibit these interactions. Moreover, the lack of activity in the SB1 extract shows that a high carotenoid concentration alone is not sufficient for antimicrobial action.

This underscores the necessity for an in-depth investigation of haloarchaeal carotenoids, particularly their structural and functional properties, to explore their potential in biotechnological applications. Halophilic microorganisms present sustainable solutions to industrial and environmental challenges, while their distinctive metabolic pathways offer valuable insights into extremophile adaptations, facilitating the development of innovative biotechnological applications (Antón et al., 2002; Subramanian & Gurunathan, 2020; Bouhamed et al., 2024).

CONCLUSIONS

Based on the phenotypic and molecular characteristics, the four newly isolated strains, designed as NC18, NC21, NC28, and SB1, were included in the Archaea domain. Our results highlight the remarkable ability of the halophilic isolates to thrive in extreme environments, making them promising candidates for industrial processes that require stability under harsh conditions. Their capability to synthesize biomolecules, including extracellular hydrolytic enzymes and carotenoid pigments under extreme environmental conditions (NaCl 3.4 M, pH 7.0, and 37 °C) minimizes the dependency on synthetic chemicals, thereby supporting the principles of green technology.

ACKNOWLEDGEMENTS

The study was funded by project no. RO1567-IBB05/2025 from the Institute of Biology Bucharest of Romanian Academy.

REFERENCES

Antón, J., Oren, A., Benlloch, S., Rodríguez-Valera, F., Amann, R., & Rosselló-Móra, R. (2002). *Salinibacter ruber* gen. nov., sp. nov., a novel, extremely halophilic member of the Bacteria from saltern

crystallizer ponds. *International Journal of Systematic and Evolutionary Microbiology*, *52*, 485–491. https://doi.org/10.1099/00207713-52-2-485

Bouhamed, S. B. H., Chaari, M., Baati, H., Zouari, S., & Ammar, E. (2024). Extreme halophilic archaea: *Halobacterium salinarum* carotenoids characterization and antioxidant properties. *Heliyon, 10,* e36832.

Bowers, K. J., & Wiegel, J. (2011). Temperature and pH optima of extremely halophilic archaea: A mini-review. *Extremophiles*, *15*, 119–128. https://doi.org/10.1007/s00792-010-0347-y.

Cavruc, V., & Chiricescu, A. (2006). *Sarea, timpul şi omul*. Sfântu Gheorghe, RO: Angustia. https://www.academia.edu/5093178/Sarea_Timpul_si_Omul.

Elevi, B.R., & Oren, A. (2008). Sensitivity of *Haloquadratum* and *Salinibacter* to antibiotics and other inhibitors: Implications for the assessment of the contribution of Archaea and Bacteria to heterotrophic activities in hypersaline environments. *FEMS Microbiology Ecology, 63*(3), 309–315. https://doi.org/10.1111/j.1574-6941.2007.00433.x.

Galinski, E. A. (1993). Compatible solutes of halophilic eubacteria: Molecular principles, water-solute interaction, stress protection. *Experientia, 49*, 487–496.

Gómez-Villegas, P., Vigara, J., Vila, M., Varela, J., Barreira, L., & Léon, R. (2020). Antioxidant, antimicrobial, and bioactive potential of two new haloarchaeal strains isolated from Odiel Salterns (Southwest Spain). *Biology*, *9*, 298.

Hiyama, T., Nishimura, M., & Chance, B. (1969). Determination of carotenes by thin-layer chromatography. *Analytical Biochemistry*, *29*, 339–342.

Kasirajan, L., & Maupin-Furlow, J. A. (2021). Halophilic archaea and their potential to generate renewable fuels and chemicals. *Biotechnology and Bioengineering*, *118*(3),1066–1090.

Kesbiç, F. I., Metin, H., Fazio, F., Parrino, V., & Kesbiç, O. S. (2023). Effects of bacterioruberin-rich haloarchaeal carotenoid extract on the thermal and oxidative stabilities of fish oil. *Molecules*, *28*(24), 8023. https://doi.org/10.3390/molecules28248023.

Marchesi, J. R., Sato, T., Weightman, A. J., Martin, T. A., Fry, J. C., Hiom, S. J., & Wade, W. G. (1998). Design and evaluation of useful bacterium-specific PCR primers that amplify genes coding for bacterial 16S rRNA. *Applied and Environmental Microbiology, 64*, 795–799.

Menasria, T., Aguilera, M., Hocine, H., Benammar, L., Ayachi, A., Si Bachir, A., Dekak, A., & Monteoliva-Sánchez M. (2018). Diversity and bioprospecting of extremely halophilic archaea isolated from Algerian arid and semi-arid wetland ecosystems for halophilic-active hydrolytic enzymes. *Microbiological Research,* 207, 289–298.

Mnif, S., Chamkha, M., & Sayadi, S. (2009). Isolation and characterization of *Halomonas* sp strain C2SS100, a hydrocarbon-degrading bacterium under hypersaline conditions. *Journal of Applied Microbiology*, *107*, 785–794. https://doi.org/10.1111/j.1365-2672.2009.04251.x.

Moopantakath, J., Imchen, M., Anju, V. T., Busi, S., Dyavaiah, M., Martínez-Espinosa, R. M., & Kumavath, R. (2023). Bioactive molecules from haloarchaea: Scope and prospects for industrial and therapeutic applications. *Frontiers in Microbiology, 14,* 1113540.

Oren, A. (1999). Bioenergetic aspects of halophilism. *Microbiology and Molecular Biology Reviews, 63*(2), 334–348. https://doi.org/10.1128/MMBR.63.2.334-348.1999

Oren, A. (2002). Diversity of halophilic microorganisms: environments, phylogeny, physiology, and applications. *Journal of Industrial Microbiology and Biotechnology, 28*, 56–63.

Orphan, V. J., Hinrichs, K. U., Ussler, W., Paull, C. K., Taylor, L. T., Sylva, S. P., Hayes, J. M., & Delong, E. F. (2001). Comparative analysis of methane-oxidizing archaea and sulfate-reducing bacteria in anoxic marine sediments. *Applied and Environmental Microbiology, 67*, 1922–1934.

Qiu, J., Han, R., & Wang, C. (2021). Microbial halophilic lipases: A review. *Journal of Basic Microbiology, 61(*7), 594–602.

Rasooli, M., Amoozegar, M. A., Sepahy, A. A., Babavalian, H., & Tebyanian, H. (2016). Isolation, identification and extracellular enzymatic activity of culturable extremely halophilic archaea and bacteria of IncheBoroun Wetland. *International Letters of Natural Sciences,* 56*,* 40–51.

Rohban, R., Amoozegar, M. A., & Ventosa, A. (2009). Screening and isolation of halophilic bacteria producing extracellular hydrolyses from Howz Soltan Lake, Iran. *Journal of Industrial Microbiology and Biotechnology,* 36*,* 333–340.

Sanders, E. R. (2012). Aseptic laboratory techniques: plating methods. *Journal of Visualized Experiments,* 63*,* e3064.

Schreck, S. D., & Grunden, A. M. (2014). Biotechnological applications of halophilic lipases and thioesterases. *Applied Microbiology and Biotechnology,* 98(3), 1011–1021.

Singh, A., & Singh, A. K. (2017). Haloarchaea: Worth exploring for their biotechnological potential. *Biotechnology Letters,* 39*,* 1793–1800.

Song, P., Zhang, X., Wang, S., Xu, W., Wang, F., Fu, R., & Wei, F. (2023). Microbial proteases and their applications. *Frontiers in Microbiology, 14,* 1236368. https://doi.org/10.3389/fmicb.2023.123636

Stancu, M.M. (2020). Kerosene tolerance in *Achromobacter* and *Pseudomonas* species. *Annals of Microbiology,* 70*,* 8. https://doi.org/10.1186/s13213-020-01543-2.

Stancu, M.M. (2023). Characterization of new diesel-degrading bacteria isolated from freshwater sediments. *International Microbiology,* 26*,* 109–122.

Stancu, M. M. (2025). Investigating the potential of native soil bacteria for diesel biodegradation. *Microorganisms, 13*(3), 564.

Subramanian, P., & Gurunathan, J. (2020). Differential production of pigments by halophilic bacteria under the effect of salt and evaluation of their antioxidant activity. *Applied Biochemistry and Biotechnology, 190*(3), 391–409. https://doi.org/10.1007/s12010-019-03107-w

Thombre, R. S., Shinde, V., Thaiparambil, E., Zende, S., & Mehta, S. (2016). Antimicrobial activity and mechanism of inhibition of silver nanoparticles against extreme halophilic archaea. *Frontiers in Microbiology, 7,* 1424.

Zhang, T., Datta, S., Eichler, J., Ivanova, N., Axen, S. D., Kerfeld, C. A., & Chen, F., Kyrpides, N., Hugenholtz, P., Cheng, J. F., Sale, K. L., Simmons, B., & Rubin, E. (2011). Identification of a haloalkaliphilic and thermostable cellulase with improved ionic liquid tolerance. *Green Chemistry, 13*, 2083–2090.

Scientific Papers. Series E. Land Reclamation, Earth Observation & Surveying, Environmental Engineering. Vol. XIV, 2025
Print ISSN 2285-6064, CD-ROM ISSN 2285-6072, Online ISSN 2393-5138, ISSN-L 2285-6064

ENERGY-ENVIRONMENT INTERACTIONS FOR AN IMPROVED SUSTAINABILITY OF DÂMBOVIȚA COUNTY - THE ROLE OF INNOVATION AND TECHNOLOGY TRANSFER FROM UNIVERSITIES

Otilia NEDELCU[1], Ioan Corneliu SALISTEANU[1], Iulian UDROIU[1], Aurora DIACONEASA[1], Claudia GILIA[2], Daniel DUNEA[3]

[1]Valahia University of Târgoviște, Faculty of Electrical Engineering, Electronics and Information Technology, 13 Sinaia Alley, 130004, Târgoviște, Romania
[2]Valahia University of Târgoviște, Faculty of Law and Administrative Sciences, 13 Sinaia Alley, 130004, Târgoviște, Romania
[3]Valahia University of Târgoviște, Faculty of Environmental Engineering and Food Science, 13 Sinaia Alley, 130004, Târgoviște, Romania

Corresponding author email: dan.dunea@valahia.ro

Abstract

The paper presents an assessment of the status of the sustainability of Dâmbovița County with special attention to the energy and environment interactions. A society seeking sustainable development ideally must utilize only energy resources that cause low or no environmental impact meaning no emissions released to the environment. In this matter, several indicators were analyzed and discussed such as increasing the share of renewable energy sources and low-carbon fuels in the transport sector (electric vehicles), including alternative fuels, and environmental issues in terms of energy conservation and renewable energy technologies, together with limitations on increased energy efficiency, and the relations between energy and sustainable development, and between the environment and sustainable development. To complete this complex approach, the role of innovation and technology transfer from universities actively involved in regional development was briefly discussed.

Key words*: critical analysis, energy efficiency, energy-environment interaction, low emissions, sustainable development goals.*

INTRODUCTION

The 2030 Agenda for Sustainable Development, adopted by all United Nations Member States in 2015, outlines a global vision for peace and prosperity for people and the planet. At the core of this agenda are 17 Sustainable Development Goals (SDGs) and 169 targets, addressing critical issues such as poverty, health, education, clean energy, and climate action (European Commission, 2015).
The European Union (EU) and its member states are fully committed to the 2030 Agenda, implementing it through comprehensive strategies including the 2030 Climate and Energy Framework and the Territorial Agenda 2030 (European Commission, 2020). (https://www.iea.org/policies/1494-2030-climate-and-energy-framework) particularly to These frameworks contribute significantly to SDG 13 (Climate Action) and SDG 7 (Affordable and Clean Energy), with targets to:

- Reduce greenhouse gas emissions by at least 55% by 2030 (compared to 1990 levels);
- Increase the share of renewable energy in gross final energy consumption to at least 42.5%, aiming for 45%;
- Improve energy efficiency by reducing final energy consumption by at least 11.7%.

The EU is implementing various policies and legislation to achieve these targets, aiming to become the first climate-neutral continent by 2050. The Territorial Agenda 2030 focuses on the territorial dimensions of sustainable development across Europe. It aims for an inclusive and sustainable future for all places and people in Europe and emphasizes the importance of strategic spatial planning and strengthening the territorial dimension of sector policies at all levels of governance.
Romania, as an EU member state, has aligned its national policies with the 2030 Agenda through the National Sustainable Development Strategy 2030. This strategy focuses on

economic, social, and environmental dimensions and emphasizes innovation, resilience, and citizen-centered development (FAO, 2018)

Romania's commitment includes:

- *National Sustainable Development Strategy 2030*, which is a central guiding document outlining Romania's framework for implementing the 2030 Agenda and achieving the 17 Sustainable Development Goals (SDGs), focusing on the three dimensions of sustainable development: economic, social, and environmental. The strategy follows a citizen-centered approach, innovation, employment, resilience, and environmental protection.
- *Aligning with the EU Green Deal.* Romania actively participated in the development of the 2030 Agenda and is committed to its implementation at the national level. The National Strategy 2030 directly addresses all 17 SDGs.
- *EU Green Deal Alignment*. As a member of the European Union, Romania is also committed to the EU's Green Deal, which aims to make Europe the first climate-neutral continent by 2050. Romania's national strategies and policies are increasingly aligned with the EU's ambitious climate and environmental targets.
- *Climate Action Commitments*. Romania has ratified key international agreements such as the United Nations Framework Convention on Climate Change (UNFCCC), the Kyoto Protocol, and the Paris Agreement, integrating them into national legislation. The country is working towards the EU's goal of reducing greenhouse gas emissions by at least 55% by 2030 compared to 1990 levels.
- *Renewable Energy and Energy Efficiency*. Romania has made progress in increasing the share of renewable energy in its energy production and is committed to further expanding this sector. Energy efficiency improvements are also a key focus.
- *The Romanian Sustainability Code* aims to promote sustainability and transparency within the Romanian business environment by increasing the number of entities reporting sustainability information, improving the transparency of these reports, and ensuring their comparability.
- *Green Financing Initiatives*: The National Bank of Romania (NBR) has established a working group to stimulate green financing and raise awareness about the importance of sustainability within the financial sector. Measures to incentivize private investment in sustainable projects, such as reduced VAT rates, have also been introduced.
- *Focus on Environmental Protection*: Romania recognizes the importance of environmental protection and is addressing challenges such as waste management, air quality, biodiversity protection, and sustainable forest management. Initiatives like the national afforestation program demonstrate a commitment to a cleaner environment.
- *Urban Sustainable Development*. Strategies are being developed at the urban level to address environmental issues and promote sustainable development in cities.

While Romania has established a strong framework and demonstrated commitment, progress towards achieving all SDGs is ongoing. Some areas where further effort is needed include waste management and recycling by improving recycling rates and waste management systems (it still remains a significant challenge), reducing inequalities (disparities between urban and rural areas need to be addressed to ensure inclusive and equitable growth), policy coherence and implementation (the principles of sustainable development should be reflected throughout the policy framework and effectively implemented at all levels), and data collection and monitoring (strengthening regular reporting mechanisms and data collection for the SDGs for tracking progress) (GR, 2023). Overall, Romania has made significant progress in committing to sustainability and has established a comprehensive framework to guide its efforts towards achieving the goals of the 2030 Agenda (GR, 2023). Continued dedication and effective implementation of policies will be key to realizing a sustainable future for the country.

A strong link between energy, environment, and sustainable development is well-documented (Dincer & Rosen, 1999). At the regional level, Dâmbovița County shows

progress in natural gas distribution and urban infrastructure but remains deficient in household drinking water supply (Davidescu et al., 2020).

From an energy perspective, Dâmbovița County's installed power capacity declined from 596.5 MW in 1989 to 133.2 MW in 2020. The county contributed just 0.7% to the national power system in 2020, with an average energy production of 285 GWh since 2018 (Badita, 2025). A major upcoming development is an 80 MWp solar project in Răscăeți village, led by the Swiss-based MET Group.

In this context, this paper explores key energy and environmental sustainability indicators relevant to Dâmbovița County. It also examines the role of universities, particularly Valahia University of Târgoviște, in supporting regional development through innovation and technology transfer.

MATERIALS AND METHODS

To evaluate the status of energy and environmental sustainability in Romania and Dâmbovița County, data were extracted from the Tempo Online database (http://statistici.insse.ro:8077/tempo-online/), focusing on time series spanning 2008 to 2020. The year 2020 represents the most recent period for which comprehensive data are available.

The assessment of objective achievement within each of the 17 Sustainable Development Goals (SDGs) necessitates measurable targets. Within Romania's SNDDR, 104 such targets have been defined for the 2030 horizon.

To effectively monitor the implementation of this strategy, the national sustainable development indicators - Horizon 2030 - were developed, encompassing 242 unique indicators, of which 99 are designated as core framework. This set received validation from the Sustainable Development Advisory Council on February 14, 2022, during a technical workshop facilitated by the Romanian National Institute of Statistics.

For this study, the analysis concentrated on three SDGs relevant to energy and environment:

- **SDG 7: Affordable and Clean Energy**
- **SDG 11: Sustainable Cities and Communities**
- **SDG 13: Climate Action**

Relevant indicators selected from the Tempo Online database include:

SDG 7: Affordable and Clean Energy

- ZBW0712 (Level 3 - Economic): Romania's foreign trade in electricity.
- ZBY0714 (Level 3 - Environment): Share of renewable energy in gross final energy consumption.
- ZBZ0715 (Level 3 - Environment): Share of electric vehicles in the total fleet.

SDG 11: Sustainable Cities and Communities (Natural Disasters and Climate Change)

- ZCV1111 (Level 3 - Environment): Expenditures for air and climate protection as a percentage of GDP.
- ZCW1112 (Level 3 - Environment): Investments in air and climate protection as a percentage of GDP.
- ZCX1111 (Level 4 - Environment): Production of environmental goods and services.
- ZCZ1113 (Level 4 - Environment): Deaths from respiratory and circulatory diseases.

SDG 13: Climate Action

Natural Disasters and Climate Change

- ZAB1311 (Level 1 - Environment): Greenhouse gas emissions by NACE Rev.2 economic activities.
- ZAG1312 (Level 1 - Environment): Average CO2 emissions per km from new passenger cars.

Education in Climate Change

- ZDP1321 (Level 2 - Environment): Yearly average temperatures in Romania.

Additionally, data reflecting the status of sustainable development in Dâmbovița County and, where unavailable, the South Muntenia Region, were selected to provide context-specific insights. These figures were primarily drawn from national social and economic statistics and include localized indicators on energy consumption, prosumer activity, and environmental health.

RESULTS AND DISCUSSIONS

At the national level, the foreign trade in electricity, corresponding to the ZBW0712,

was shifting towards a higher import in 2019 and 2020, with a corresponding negative trade balance. The average of the period between years 2008 and 2020 for export was 210.6 million euros, while the import was 117.2, and the trade balance was 93.4, respectively (Figure 1).

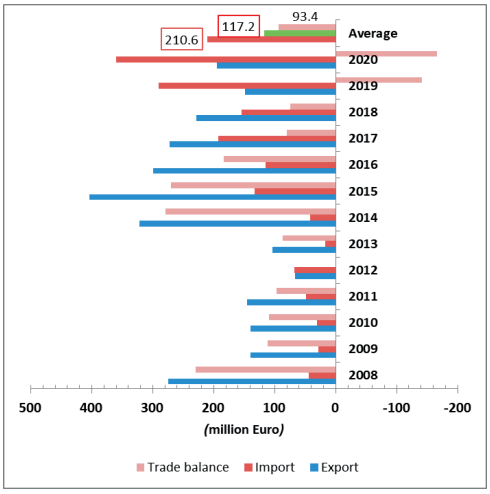


Figure 1. Romania's foreign trade in electricity, corresponding to the ZBW0712 (Data sources: National Institute of Statistics - Romania)

Figure 2 shows the expenditures for air and climate protection and investments for air and climate protection as a percentage of GDP, corresponding to the ZCV1111 and ZCW1112. A decrease in the percentage was observed for the investments starting from 2016 to 2020. The average of the 2008-2020 period was 0.1% of GDP for investments, while the expenditures reached 0.3.

Figure 3 highlights the percentage of renewable energy in gross final energy consumption (%), corresponding to the ZBY0714. A constant increase was observed from 2008 to 2020, with an average of the period of 23.5%. This can be related to the continuous development of new renewable installations.

The efforts of Romania to reduce the emissions from conventional vehicles were combined in a few initiatives, including the Rabla program. Despite the Rabla Program's efforts to promote electric and hybrid vehicle adoption in Romania's public transport and personal car sectors - evidenced by 2021 registrations of 6,903 electric and 38,531 hybrid vehicles, and a total of 26,277 electric vehicles registered in 2022 - the overall presence of these vehicles remains limited.

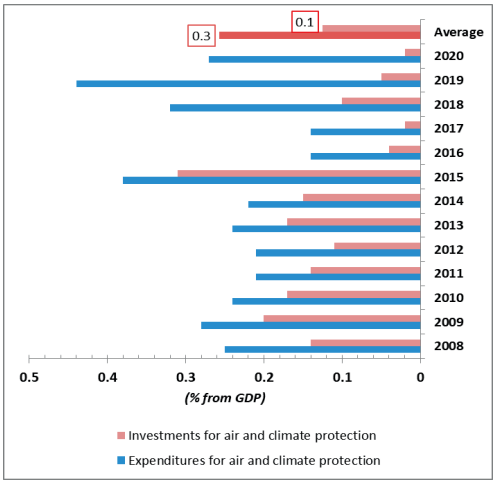


Figure 2. Expenditures for air and climate protection and Investments for air and climate protection as a percentage of GDP, corresponding to the ZCV1111 and ZCW1112, respectively (Data sources: National Institute of Statistics - Romania)

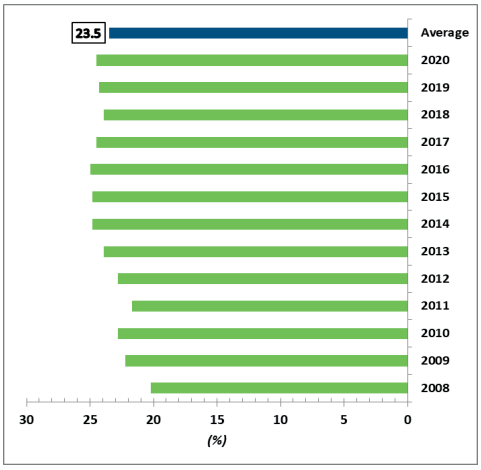


Figure 3. The percentage of renewable energy in gross final energy consumption (%), corresponding to the ZBY0714 (Data sources: Eurostat database - https://ec.europa.eu/)

As of the latest data, electric vehicles constitute a mere 0.07%, and hybrid vehicles 0.44% of the total vehicle count in Romania (GR, 2023). Figure 4 shows the evolution of the percentage of electric vehicles in the total fleet of vehicles from 2008 to 2020.

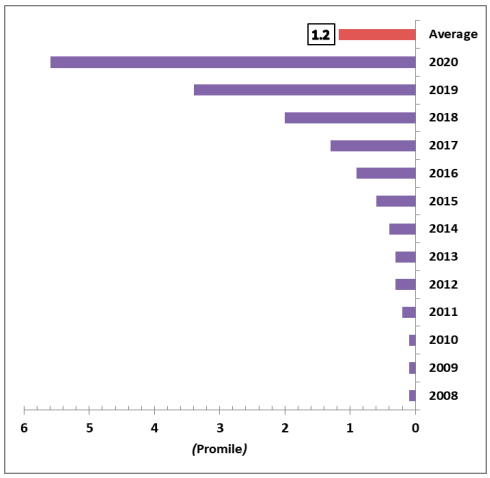


Figure 4. The percentage of electric vehicles in the total fleet of vehicles (promile), corresponding to the ZBZ0715 (Data sources: NIS Statistical survey on registered vehicles in circulation)

Figure 5 provides information regarding the production of environmental goods and services for the protection of the surrounding air and climate in millions of lei, showing a constant decrease and an average of the 2008-2020 period of 21635.1 million lei.

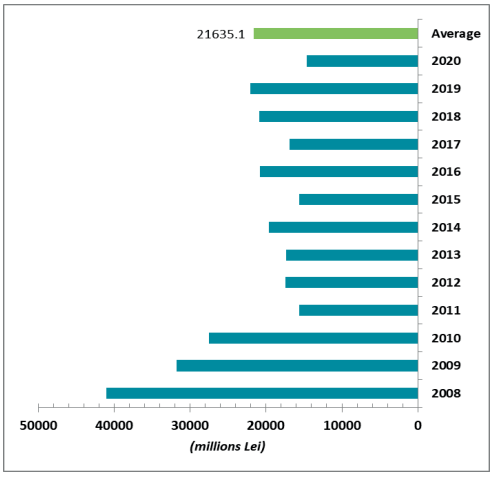


Figure 5. Production of environmental goods and services for the protection of the surrounding air and climate in millions of lei, corresponding to the ZCX1111 (Data sources: National Institute of Statistics - Romania)

Figure 6 shows the deaths from respiratory and circulatory diseases (number of persons), corresponding to the ZCZ1113. An increase in the deaths caused by diseases of the respiratory system occurred especially in 2020, being potentially correlated with air pollution in urban areas and other associated factors such as meteorology and topographical conditions (Dunea et al., 2015; Oprea et al., 2015).

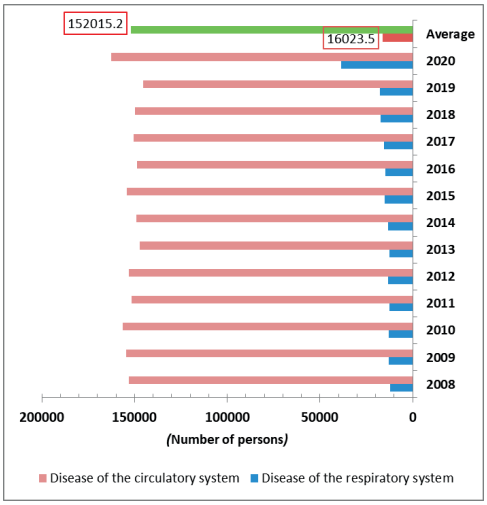


Figure 6. Deaths from respiratory and circulatory diseases (number of persons), corresponding to the ZCZ1113; causes of death are according to the WHO - ICD - 10th revision starting with 1994 (Data sources: National Institute of Statistics - Romania)

Regarding the greenhouse gas emissions by NACE Rev.2 economic activities, as sources of GHG emissions, corresponding to the ZAB1311, a decrease in the emissions can be observed. The average of the 2008-2020 period is 108,545.5 thousand tons of CO_2 equivalent (Figure 7).

On the other hand, the average CO_2 emissions per km from new passenger cars were 140.9 g CO_2/km from 2008 to 2020 (Figure 8).

Figure 9 shows the yearly average temperature recorded at Varfu Omu Meteorological station from the Bucegi Mountains located in the north of Dambovita County. An increase in the annual average temperature is evident compared to the 1901-2000 period, pointing out the effects of climate change (Venturi et al., 2025). This is related to the emissions effect and emphasizes the need for further exploration of the energy-transport-environment interaction in a complex approach and the fulfilment of the corresponding SDGs (Nakhle et al., 2024).

Dâmbovița County is one of the 41 counties of Romania, situated in the south-central part of

the country, within the historical region of Muntenia. Its capital city is Târgoviște, which holds significant historical importance as the former capital of Wallachia province. It covers an area of approximately 4,054 km^2, representing about 1.7% of Romania's total land. As of December 2021, the population of Dâmbovița County was approximately 479,404 inhabitants, making it one of the more densely populated counties in Romania. The county has 7 cities and towns (two of which are municipalities - Târgoviște and Moreni) and 82 communes with 361 villages (NIS, 2024). The county has been focusing on attracting EU funds for various development projects, including infrastructure improvements, tourism development, and environmental protection. The GDP per capita in 2023 was 11,439 euros per capita (NIS, 2024).

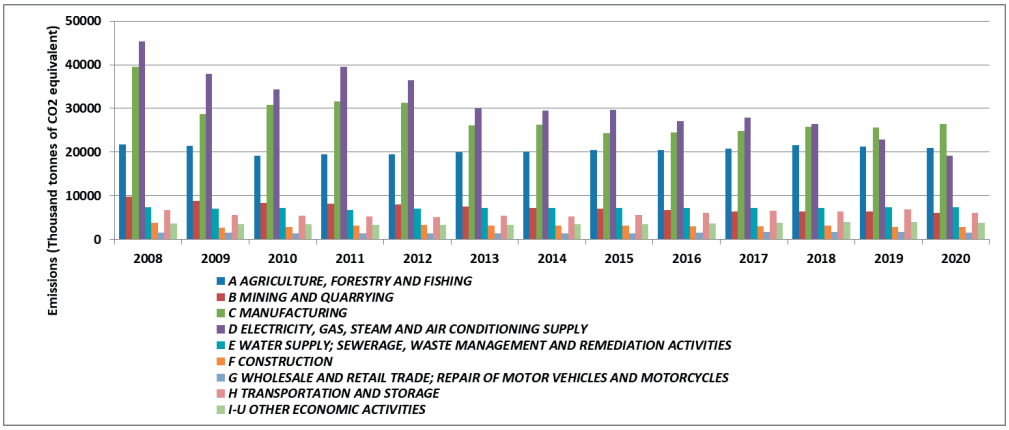


Figure 7. Greenhouse gas emissions by NACE Rev.2 economic activities, as sources of gas emissions, corresponding to the ZAB1311 (Data sources: National Institute of Statistics - Romania)

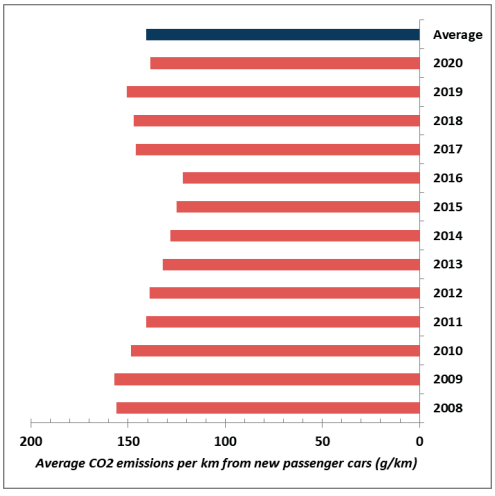


Figure 8. Average CO_2 emissions per km from new passenger cars, corresponding to the ZAG1312 (Data sources: National Institute of Statistics - Romania)

Table 1 shows some characteristics regarding the electricity and natural gas consumption in Dambovita County from 2021 and 2023. Both household and non-household consumption of electricity and natural gas have continuously decreased from one year to another.

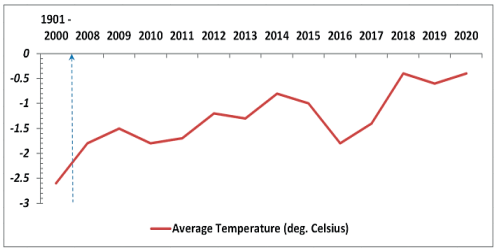


Figure 9. Yearly average temperature recorded at Vârfu Omu Meteorological station from the Bucegi Mountains located in the north of Dâmbovița County, corresponding to the ZDP1321 (Data sources: National Administration of Meteorology)

Furthermore, the number of prosumers increased considerably each year, contributing to the renewable energy production.

Another step for reducing the emissions and the environmental impact was the increase in the number of electric and hybrid vehicles

registered (Figure 10). Both directions contribute to the share of renewable energy and low-carbon fuel used in the transport sector (electric vehicles), including the use of alternative fuels. However, the monitoring of the air pollutants is not sufficient in Dambovita County to be able to quantify the benefits to the environment in urban areas.

Table 1. Details of electricity and natural gas consumption in Dâmboviţa county (Source: https://energymap.ro/en/)

Year	2021	2022	2023
Total Prosumers	200	586	2,258
Household consumption of electricity (MWh)	348,800	326,662	277,430
Non-household consumption of electricity (MWh)	1,062,355	958,503	901,012
Household consumption of natural gas (MWh)	1,026,064	975,523	971,525
Non-household consumption of natural gas (MWh)	1,160,538	1,115,428	936,177

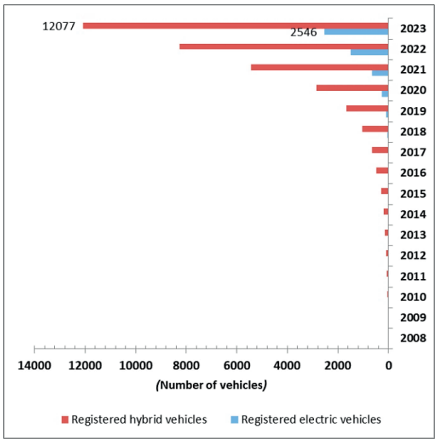


Figure 10. Target 4 - Environment - Number of electric and hybrid vehicles registered (Data sources: Ministry of home affairs - Direction of Driving-licenses Regime and Vehicles Registration)

There are only two urban background monitoring stations located in two towns, i.e., Târgovişte and Fieni. Unfortunately, the data reported from these stations did not meet the data capture criteria, and consequently, there were significant data gaps due to malfunction (Figure 11).

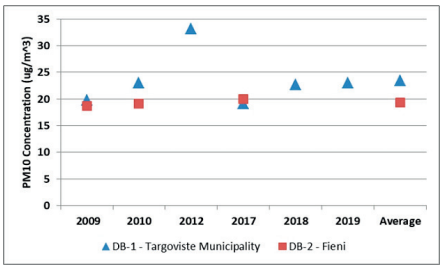


Figure 11. Target 7 - Environment - average annual levels of particulate matter PM10 at urban background monitoring stations, corresponding to the TMP1173 at the two monitoring stations located in Dâmboviţa County (Data sources: National Agency for Environmental Protection)

Furthermore, important pollutants that are responsible for serious adverse effects are not measured (e.g., PM1, PM2.5, PAH, etc.). Therefore, it is difficult to assess the exposure and the effects on human health. Figure 12 presents the number of deaths caused by respiratory and cardiovascular diseases (number of persons) in Dâmboviţa County. An increase in the number of persons affected by respiratory diseases was observed in 2020 and 2021, probably related to the COVID pandemic factors.

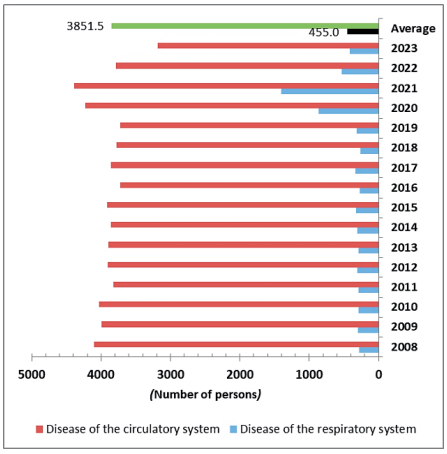


Figure 12. TMK1165 - Target 6 - Environment - number of deaths caused by respiratory and cardiovascular diseases (number of persons) in Dâmboviţa County, causes of death are according to the WHO - ICD - 10th revision starting with 1994 (Data sources: NIS - Statistical survey on mortality)

To establish the intrinsic aspects related to the energy-environment interactions, research

programs and entities should be sustained within a national and regional strategy. It is important to improve the number of employees from research-development activity (Figure 13) and the total expenditure from research-development activity (Figure 14).
Universities and research entities should be key vectors for sustainability, especially through the research results, including scientific articles, patents, and innovation items facilitating the transfer of technology to industry.

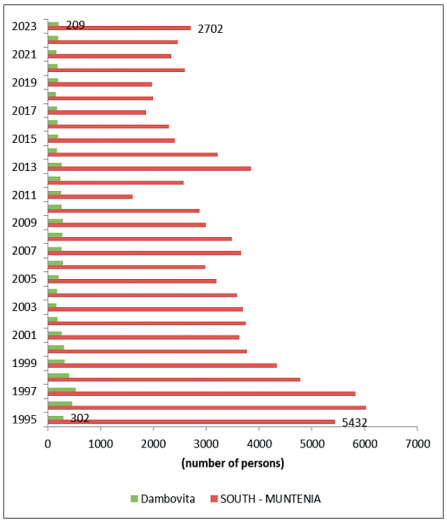


Figure 13. CDP103E - Employees from research - development activity (in full-time equivalent), by macroregions, development regions, and counties – Data for Dâmbovița County and South-Muntenia region (Data sources: National Institute of Statistics - Romania)

Valahia University is committed to contributing to sustainable development through the performed research. Figure 15 shows the research performed at Valahia University on the SDGs based on Scopus-indexed publications in the specific domains. From the 2,609 documents indexed in the Scopus database, 1064 are in Engineering, 200 in Environmental Sciences, and 196 in Energy. Important SDGs are related to SDG 12, SDG 8, SDG 9, SDG 11, SDG 6, and SDG 7. Valahia University is consistently promoting multi- and interdisciplinary research. This is reflected in the Institute of Multidisciplinary Research for Science and Technology, a research-dedicated facility with 36 laboratories with state-of-the-art equipment and spaces for scientific events, offering open access to all academic staff.

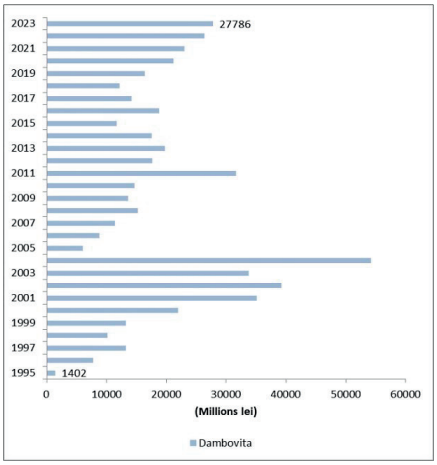


Figure 14. CDP104B - Total expenditure from research-development activity by macroregions, development regions and counties - current prices (millions of lei) – Data for Dâmbovița County (Data sources: National Institute of Statistics - Romania)

Valahia University of Târgoviște (VUT) cooperates with a key regional NGO (www.adrmuntenia.ro/) active in developing the Smart Specialization Strategy of South-Muntenia Region (2021-2027) and other policy documents related to SDGs, and the Management Authority for structural funds projects dedicated to regional development.
The university actively fosters cross-sectoral dialogue on SDGs, particularly through its engagement in projects focused on energy, environmental sustainability, and social inclusion. For instance, its contribution to the E-LAND project (https://elandh2020.eu/) is creating smarter energy systems using solar power and advanced building controls, actively involving energy businesses, regulatory bodies, and local communities. Furthermore, the university drives SDG progress through its research, educational projects, and scientific events centred on air quality, circular design, advanced materials, resource valorisation, food safety, and social inclusion.
This proactive, cross-sectoral approach enables the university to facilitate impactful discussions and contribute significantly to addressing current and future sustainability challenges.

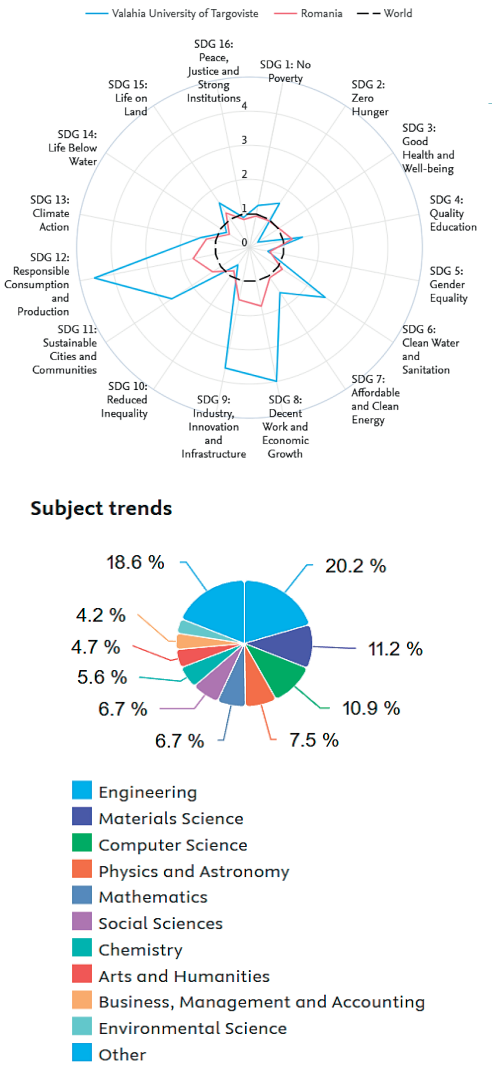


Figure 15. Contributions of the research performed at Valahia University to the SDGs based on Scopus indexed publications in the specific domains (Source: Scopus database)

Recognizing the importance of robust SDG data, VUT actively participates in international collaborations, including the development of the KreativEU university alliance. This alliance strives to be a catalyst for positive transformation at all levels by strategically linking cultural and ecological stewardship with a dedicated effort to gather and measure data relevant to achieving the SDGs.

CONCLUSIONS

In conclusion, the "European 2030 Agenda" is the main framework of the EU's commitment to the UN's 2030 Agenda for Sustainable Development, which includes ambitious climate and energy targets and a focus on territorial cohesion within Europe. Romania, as a member of the European Union, is committed to the Sustainable Development Goals outlined in the 2030 Agenda. The national Sustainable Development Strategy 2030 provides a framework for local and regional efforts. Projects in Dâmbovița County, particularly those funded by the EU, are likely aligned with these national and international sustainability objectives.

Dâmbovița County is engaged in various initiatives that contribute to sustainability, particularly in water management, renewable energy adoption, and the preservation of cultural heritage for sustainable development. These efforts reflect a commitment to both environmental protection and the well-being of its communities within the broader context of national and European sustainability goals. Romanian universities require advanced capacities in the field of interdisciplinary research and innovation for energy-environment interactions, ICT and bioeconomy to provide technology offers and transfer. VUT is actively involved in research and innovation, particularly in energy and sustainability. It has developed advanced Energy Management Systems (EMS) to support decarbonization and energy efficiency, aligning with EU strategies.

Additionally, research efforts have focused on initiatives that support sustainability, human health, and economic efficiency across the entire supply chain. With demonstrated engagement in European projects, VUT plays a vital role in advancing knowledge and innovation in key strategic areas at regional level.

ACKNOWLEDGEMENTS

The research leading to these results received support for publishing from the CNFIS-FDI-2025-F-0421 project financed by the Romanian Ministry of Education and implemented by Valahia University of Târgoviște.

REFERENCES

Badita, C.M. (2025). Electricity production capacities in Dambovita County, Accessed on April 10, 2025 https://romania594.blogspot.com/2020/03/capacitati-de-productie-energiei_10.html

Davidescu, A. A.,Apostu, S.A., Pantilie, A.M., & Amzuica, B.F. (2020). Romania's South-Muntenia Region, towards Sustainable Regional Development. Implications for Regional Development Strategies. *Sustainability*, *12*(14), 5799. https://doi.org/10.3390/su12145799.

Dincer, I., & Rosen, M.A. (1999) Energy, environment and sustainable development. *Applied Energy*, *64*(1–4), 427-440, https://doi.org/10.1016/S0306-2619(99)00111-7

Dunea, D., Iordache, S., & Ianache, C. (2015). Relationship between airborne particulate matter and weather conditions in Targoviste urban area during cold months. *Rev. Roum. Chim, 60*(5-6), 595-601.

EU (2015). Europe 2020 Strategy. Available online: https://www.eesc.europa.eu/sites/default/files/resources/docs/qe-01-14-110-en-c.pdf; (accessed on 10 April 2025).

EU (2020). Delivering on the UN's Sustainable Development Goals – A comprehensive approach https://commission.europa.eu/document/download/1ae1e765-0a3f-4092-b87e-86ecbd1ec0c7_en?filename=delivering_on_uns_sustainable_development_goals_staff_working_document_en.pdf

FAO (2018). Romania's Sustainable Development Strategy 2030. Available online: https://faolex.fao.org/docs/pdf/rom195029.pdf (accessed on 10 April 2025).

Government of Romania (2023). Voluntary National Review - Implementing the 17 SDGs. https://hlpf.un.org/sites/default/files/vnrs/2023/VNR%202023%20Romania%20Report.pdf

Nakhle, P., Stamos, I., Proietti, P., & Siragusa, A. (2024) Environmental monitoring in European regions using the sustainable development goals (SDG) framework. *Environmental and Sustainability Indicators, 21*, 100332.

NIS (2024). Anuarul statistic al județului Dâmbovița, https://dambovita.insse.ro/produse-si-servicii/publicatii-statistice/anuarul-statistic-al-judetului/

Oprea, M., Ianache, C., Mihalache, S.F., Dragomir, E.G., Dunea, D., Iordache, S., & Savu, T. (2015). On the development of an intelligent system for particulate matter air pollution monitoring, analysis and forecasting in urban regions. *19th International Conference on System Theory, Control and Computing*, 711-716.

Venturi, S., Dunea, D., Mateescu, E., Virsta, A., Petrescu, N., & Casadei, S. (2025). SPEI and SPI correlation in the study of drought phenomena in Umbria region (central Italy). *Environmental Science and Pollution Research, 32*(1), 168-188.

Scientific Papers. Series E. Land Reclamation, Earth Observation & Surveying, Environmental Engineering. Vol. XIV, 2025
Print ISSN 2285-6064, CD-ROM ISSN 2285-6072, Online ISSN 2393-5138, ISSN-L 2285-6064

THE SWELLING PRESSURE OF ACTIVE CLAYS ACCORDING TO VARIOUS TECHNICAL NORMS AND PROCEDURES

Ernest Daniel OLINIC

Technical University of Civil Engineering of Bucharest,
122-124 Lacul Tei Blvd, District 2, 020396, Bucharest, Romania

Corresponding author email: ernest.olinic@utcb.ro

Abstract

The main geotechnical parameter indicating the presence of active clays is the swelling pressure, which is globally determined using at least three different methods. In Romania, however, the swelling pressure is determined using only one method (through the compressibility test in oedometer on initially saturated samples). Regardless of the method used, the initial moisture content significantly influences the results. Two types of moisture content are typically considered: natural moisture content (according to STAS 1913/12-88) and the shrinkage limit (according to NP 126-2010). In current practice, the initial moisture content is usually the natural moisture content. However, by saturating the sample, only the swelling characteristics of the soil are identified, not the shrinkage characteristics. This article aims to synthesize the methods for determining the specific properties of active clays, based on international technical standards and norms.

Key words*: active clays, swelling pressure, technical norms, laboratory tests.*

INTRODUCTION

Expansive soils, characterized by their ability to undergo significant volume changes upon moisture variation (to shrink and/or swell), are found across many regions globally. They are particularly prevalent in semi-arid and arid climates, where the formation of smectite clay minerals (montmorillonite and illites) is geologically favoured (Diaz & Tomas, 2025). In Romania, expansive clays are frequently encountered, especially in the southern and eastern regions, where their geotechnical behavior is rigorously classified and evaluated under NP 126-2010, which sets the national standards for identifying and testing swelling pressure.

In geotechnical engineering, the determination of the swelling pressure (p_s, kPa) is critical for the design of shallow and deep foundations, retaining walls, underground structures, and linear infrastructure (Fredlund, 1996). This pressure quantifies the force exerted by a clayey soil when its volume is restrained during wetting (Chen & Ng, 2013).

The swelling pressure (p_s) is defined as the equilibrium pressure required to prevent volumetric expansion of an initially unsaturated clay soil when its moisture content increases to full saturation under constant volume conditions (Jones et al., 2020; BS 1377-5: 1990).

Various laboratory techniques such as: the one-dimensional oedometer (NP 126-2010; Feng et al, 1998), CBR and triaxial tests (Chen & Ng, 2013) are commonly employed to measure p_s directly.

Also, a wide array of empirical and semi-empirical correlations has been developed to estimate p_s from more readily available soil parameters. Extensive research has explored how p_s varies with clay fraction, dry unit weight, water content, liquid limit, and plasticity index (Mowafy & Bauer, 1985), affirming that such index properties can serve as reliable predictors under certain conditions.

The determination of the p_s is essential to reduce construction risks, limit post-construction deformations, and minimize maintenance costs, thereby enhancing the sustainability and safety of engineering projects (Jones et al., 2020).

MATERIALS AND METHODS

This study is based on an extensive review of the scientific literature, supported by a critical analysis of national and international standards and regulations relevant to the geotechnical characterization of expansive soils. Key references include normative documents such as NP 126-2010 (Romania), STAS 8942/1-89, as well as international standards like ASTM

D4546, BS 1377, and other globally recognized testing protocols.

The primary objective is to synthesize the most representative laboratory methods for determining swelling pressure (p_s), focusing particularly on one-dimensional oedometer tests (constant volume and free swell methods), triaxial testing procedures, and empirical correlations derived from index properties. The methodology involves a comparative and integrative analysis of procedures, test conditions, and parameters influencing p_s, as presented in both peer-reviewed scientific publications and engineering practice documents.

Wetting-after-loading tests on multiple specimens

The most complex method for determining the behaviour of active clays is the "wetting-after-loading tests on multiple specimens" or "Deformation versus Vertical Stress, Method A" from ASTM D4546. The tests are performed on several specimens from the same sample which, initially at natural moisture content, are loaded in the oedometer to different pressures and subsequently saturated. The final specific settlements of the sample at natural moisture content and, respectively, after saturation are recorded. Thus, compressibility curves are obtained for the material at natural moisture content (red dotted line from Figure 1) and in the hypothesis that, after being subjected to a certain compression stress (geological load or geological load to which the surcharge is added), it is saturated (blue dotted line from Figure 1). The swelling pressure is obtained at the intersection of the saturated soil compressibility curve with the zero-deformation line.

This method is a very complex one that identifies, in addition to the swelling pressure, the entire behaviour of the soil at natural moisture content, loaded at different pressures and subsequently saturated.

The method has two major disadvantages: (1) long duration or occupation of several oedometric devices and implicitly significant costs and (2) difficulties in taking quasi-identical samples to obtain accurate comparable results.

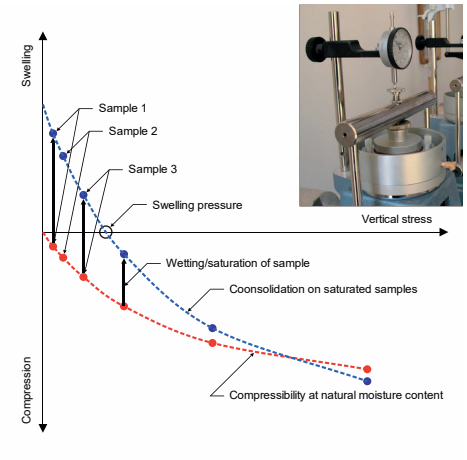


Figure 1. Wetting-after-loading tests on multiple specimens

Wetting-after-loading test on a single specimen

The "Wetting-after-loading test on a single specimen" or "Deformation versus Vertical Stress, Single-Point Test Method B" from ASTM D4546 is a method that only determines the swelling after the sample is loaded with a compression pressure (geological load or geological load to which the surcharge is added) (Figure 2).

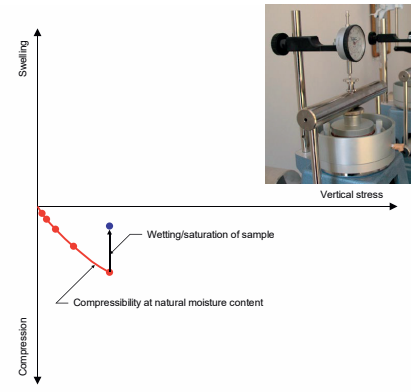


Figure 2. Wetting-after-loading test on a single specimen

This test determines the behaviour of a soil subjected to a certain compression stress and subsequently saturated. Through this test the swelling pressure is not determined.

Loading-wetting-loading test

The "Loading-wetting-loading test" or "Deformation versus Vertical Stress, Loading-after-Wetting Test Method C" from ASTM D4546 is a method in which a soil sample at natural moisture content is loaded to a certain pressure (geological load or geological load to which the surcharge is added) and then saturated and loaded further with different pressures. If the swelling is large enough to exceed the initial height of the sample, the swelling pressure can also be determined at the intersection of the saturated soil compressibility curve with the zero-deformation line (Figure 3).

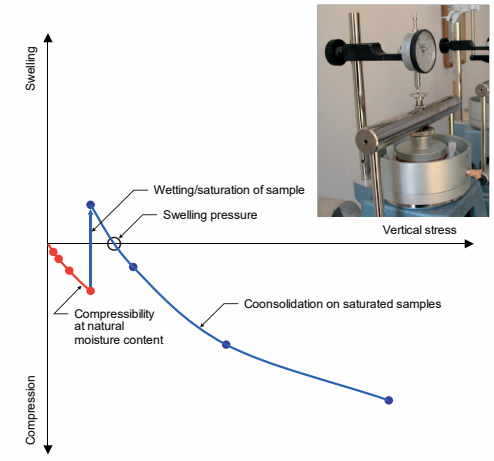


Figure 3. Loading-wetting-loading test

It is a method by which the behaviour of the soil is obtained after it, at natural humidity, is loaded with a certain pressure and subsequently saturated and the loading continues. Basically, it is described the behaviour of a soil loaded with the geological pressure, then saturated and subsequently the construction is built that comes with a certain surcharge.

Loading-after-wetting test

This method is imposed by STAS 1913/12-88 and NP 126-2010 and is almost identical to the "Deformation versus Vertical Stress, Loading-after-Wetting Test Method C" from ASTM D4546, with the difference that the sample is saturated after applying the first loading step, usually equal to 10...25 kPa (Figure 4).

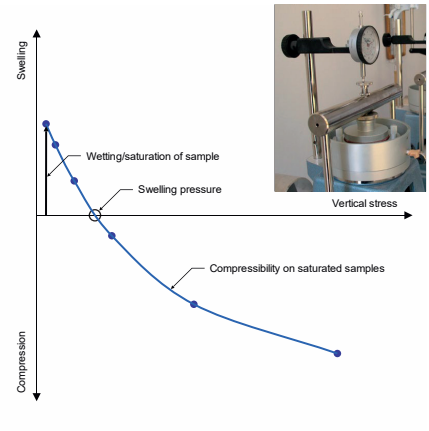


Figure 4. Loading-after-wetting test

According to STAS 1913/12-88 the initial moisture content is the equilibrium moisture content, which is very close to the natural moisture content, while according to NP 126-2010, the initial moisture content should be the shrinkage limit. This technical norm is the only one that refers to the shrinkage limit. In the specialized technical literature, tests are performed starting from the natural moisture content of the sample.

Most likely, the idea behind performing this test starting from the shrinkage limit is to identify the behaviour of the soil after it experiences significant drops in moisture content and subsequently becomes saturated. It is the worst-case scenario, but it does not consider the fact that shrinkage occur both vertically and horizontally (visible by cracks in the soil).

Performing the compressibility test in an oedometer on samples brought to the shrinkage limit involves major difficulties in soil sampling doe to its solid state.

Constant volume test

This method can be applied in two variants: (1) as described in "Deformation versus Vertical Stress, Loading-after-Wetting Test Method C" from ASTM D4546 in which small loading steps are applied to maintain the sample around zero deformations or (2) in a CBR type device through which the sample is kept at constant volume and by means of a dynamometric ring the force that the soil sample develops, following saturation, is measured (Figure 5).

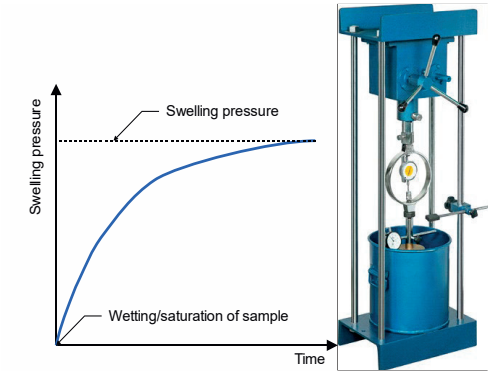


Figure 5. Constant volume

The swelling pressure is an indicator of whether a soil has swelling behaviour when saturated. The strict determination of the swelling pressure does not provide an image of the soil behaviour under different compression stresses which is necessary in order to estimate swelling/settlement.

RESULTS AND DISCUSSIONS

The swelling pressure (p_s) is the pressure required to prevent volumetric expansion of an initially unsaturated clayey soil when its moisture content increases to full saturation. In current practice, it is erroneously considered that if a foundation transmits a pressure greater than or equal to the swelling pressure to the foundation soil, then, in the event of saturation of the foundation soil, no swelling will occur.

In Figure 6 it is presented the scheme for the calculation of the foundation soil settlement, and it is the same scheme that should be applied for the estimation of swelling.

This scheme is taken from NP 125-2010 which is used to determine the additional specific settlement upon wetting of soils sensitive to wetting.

A soil element is initially subjected to a vertical stress equal to the geological stress (σ_{gn}) and, after a construction is built, the vertical stress due to surcharge is added (σ_z) resulting the total vertical stress equal to $p_n = \sigma_z + \sigma_{gn}$. If the foundation soil is saturated the geological stress (σ_{gi}) increases due to the unit weight of the soil increases to saturated unit weight and the total vertical stress becomes $p_i = \sigma_z + \sigma_{gi}$.

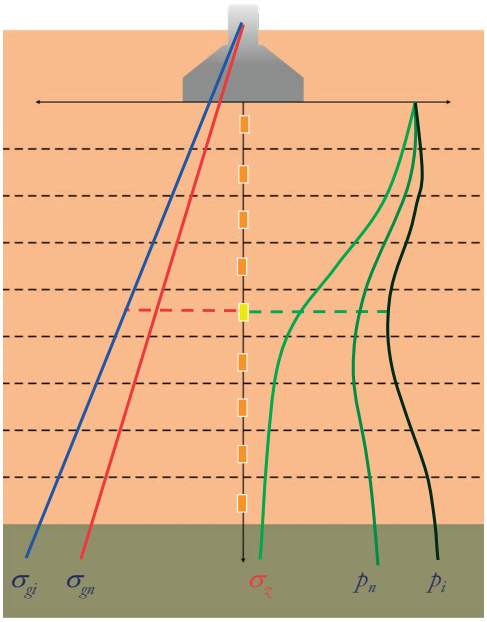


Figure 6. Calculation scheme for foundation soil settlement

In Figure 7 a, b and c are presented different stress-strain curves of soil samples at natural moisture content and initially saturated obtained in different common laboratory tests (cases frequently encountered in current practice).

In Figure 7.a it is presented an example of a soil with a swelling pressure of about 35 kPa.

By estimating the geological load of the elementary layer “i” by intersecting with the stress-strain curve of the soil at natural moisture content, the specific settlement ε_{gz} is determined. This is the initial stress-strain state of the elementary layer “i”. After the execution of a construction, a vertical compression stress equal to p_n is transmitted to the same element and, by intersecting with the stress-strain curve of the sample at natural moisture content, the specific settlement (ε_{pn}) under this load is determined. The difference between ε_{pn} and ε_{gz} is the specific settlement of the elementary layer “i” at natural moisture content.

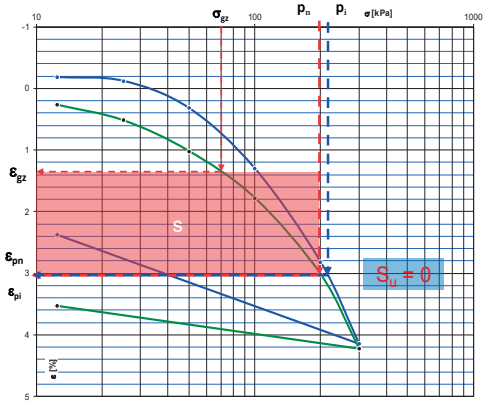
Considering that the foundation soil becomes saturated, at the level of elementary layer "i" the total vertical stress becomes p_i and by intersecting with the stress-strain curve of the initially saturated soil sample the specific settlement ε_{pi} is obtained. The difference

between ε_{pn} and ε_{pi} is the specific settlement or swelling of the elementary layer "i" when saturated.

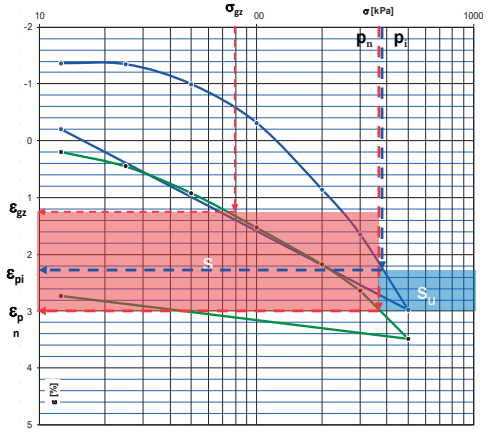
In the case presented in Figure 7.a, it is found that, following the saturation of the foundation soil, neither settlement nor swelling is recorded at the level of the elementary layer "i".

Following the same principle described previously, by which the states of stress and deformation are evaluated from the initial moment, after the execution of the construction, respectively, in the hypothesis of saturation of the foundation soil, Figure 7.b presents a case in which the swelling pressure is equal to 120 kPa but, in the case of saturation of the foundation soil, even at pressures higher than the swelling pressure, a significant swelling of the elementary layer "i" is recorded.

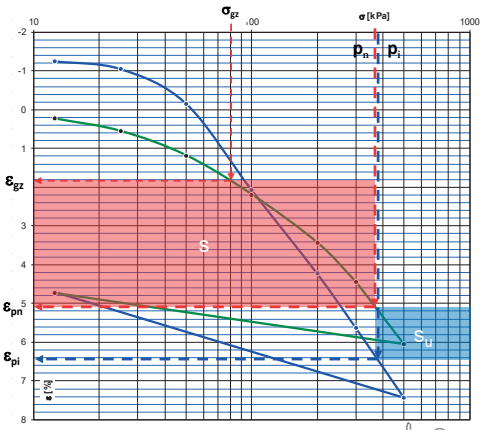
In Figure 7.c, after saturation of the foundation soil, a settlement is recorded.



(a)



(b)



(c)

Figure 7. Stress-strain curves of soil samples at natural moisture content and initially saturated

CONCLUSIONS

The swelling pressure (p_s) is the pressure required to prevent volumetric expansion of an initially unsaturated clayey soil when its moisture content increases to full saturation and is just an indicator of whether a soil has high swelling when saturated.

As in accordance with NP 074-2022, double compressibility tests should be performed on soils with high swelling and shrinkage, on samples at natural moisture content and on samples initially saturated in order to obtain the behaviour of the soil under different vertical loads. The methodology imposed by the Romanian technical norms and standards is very close with the method A from ASTM D4546 but is performed only on two samples, not on minimum 4.

According to the calculation model of additional settlement upon wetting described in NP 125-2010, the stress-strain curves obtained from compressibility in oedometer tests (affected by correction coefficient M_0 used for the calculation of the deformation modulus $E=E_{oed} \cdot M_0$) allow the estimation of the settlement/swelling of the foundation soil.

ACKNOWLEDGEMENTS

This research was funded by the Technical University of Civil Engineering Bucharest, grant number $GnaC^{ARUST}_{2024}$-19 "Contributions to

modelling the behaviour of expansive soils in interaction with structures", acronym: ModUCS.

REFERENCES

Chen, R. & Ng, C. W. W. (2013). Impact of wetting–drying cycles on hydro-mechanical behavior of an unsaturated compacted clay. *Applied clay science*, *86*, 38-46.

Díaz, E. & Tomás, R. (2025). Predicting Clay Swelling Pressure: A Comparative Analysis of Advanced Symbolic Regression Techniques. *Applied Sciences*, *15*(10), 5603. https://doi.org/10.3390/app15105603

Feng, M., Gan, J. K. M., Fredlund, D. G. (1998). A laboratory study of swelling pressure using various test methods. In *Proc. International Conference on Unsaturated Soils, Beijing, China, International Academic Publishers*, VI (pp. 350-355).

Fredlund, D. G. (1996). Geotechnical problems associated with swelling clays. *Developments in Soil Science* (Vol. 24, pp. 499-524). Elsevier.

Jones, L., Banks, V., Jefferson, I. (2020). Swelling and shrinking soils. *Geological Society of London, Engineering Geology Special Publications*, *29*(1), 223-242.

Mowafy, M. Y., Bauer, G. E. (1985). Prediction of swelling pressure and factors affecting the swell behaviour of an expansive soil. *Transportation research record*, *1032*, 23-28.

***BS 1377-5: 1990. Methods of test for Soils for civil engineering purposes - Part 5: Compressibility, permeability and durability tests.

***D4546–08 Standard Test Methods for One-Dimensional Swell or Collapse of Cohesive Soils

***IS 2720-41 (1977): Methods of test for soils, Part 41: Measurement of swelling pressure of soils

***NP 125-2010 Technical norm on foundation of constructions on soils sensitive to wetting

***NP 126-2010 Technical norm on foundation of constructions on swelling-shrinkage soils

***STAS 1913/12-88. Foundation soil. The determination of the physical and mechanical characteristics of the swelling and shrinking soils

Scientific Papers. Series E. Land Reclamation, Earth Observation & Surveying, Environmental Engineering. Vol. XIV, 2025
Print ISSN 2285-6064, CD-ROM ISSN 2285-6072, Online ISSN 2393-5138, ISSN-L 2285-6064

THE SHEAR STRENGTH PARAMETERS OF SOIL-ROOT SYSTEMS

Tatiana OLINIC

University of Agronomic Sciences and Veterinary Medicine of Bucharest,
59 Mărăști Blvd, District 1, Bucharest, Romania

Corresponding author email: tatiana.olinic@fifim.ro

Abstract

The root systems of vegetation are fundamental in enhancing shallow slope stability, with the shear strength of soil-root systems serving as a critical parameter for its assessment. The role of roots in stabilizing shallow slopes has been extensively documented, and the use of vegetation for slope stabilization and soil erosion control is a well-established practice across many regions worldwide. This sustainable approach has even led to the emergence of new research disciplines focused on its development. This review article aims to synthesize and evaluate existing research on the shear strength parameters of soil-root systems across various plant species and soil types. Additionally, it examines how these parameters are affected when plant roots dry out due to hydric stress caused by recent climate change. The study provides insights into the impact of root desiccation on slope stability, highlighting the importance of understanding vegetation`s role in maintaining soil cohesion under changing conditions.

Key words*: shear strength, soil-roots, type of vegetation, age of vegetation.*

INTRODUCTION

Vegetation plays a crucial role in shallow slope stability and erosion control through both mechanical and hydrological mechanisms. Yen, as cited by Cazzuffi, classified root systems into five distinct categories based on their branching patterns: VH-type, H-type, V-type, R-type, and M-type. This classification, originally developed by Yen and later illustrated in Figure 1, highlights the varying effectiveness of root structures in stabilizing slopes (Cazzuffi et al., 2014). Among these, H-type and VH-type roots are particularly effective in combating soil erosion and enhancing slope stability. These root systems extend horizontally and vertically across the soil surface, creating a dense network that provides superior protection against the loss of topsoil. In contrast, R-type and M-type roots, while still beneficial, offer comparatively less resistance to erosion due to their less extensive branching patterns. Yen's analysis underscores the importance of selecting vegetation with H-type and VH-type root systems for optimal erosion control and slope stabilization.

Root networks contribute to hillslope stability through two key mechanisms: root pull-out resistance and enhanced soil cohesion (Wu, 2013; Fan et al., 2021). Key factors modulating this reinforcement include root architecture, soil moisture content, and vegetation type (Olinic et al., 2024). Under climate change, drought-induced root desiccation dynamically alters shear strength parameters, demanding context-specific assessments (Boldrin et al., 2018).

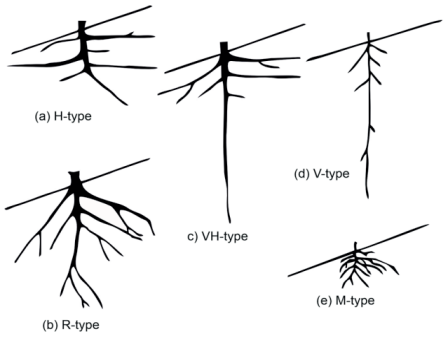


Figure 1. The root structure classified by Yen (recreated figure)

Optimal mitigation of land degradation requires detailed knowledge of site-specific soil materials, weather patterns, and terrain behaviour across diverse regions. Through laboratory testing and FEM simulations, Zhou et al. (2023) assessed how root-soil composite shear resistance varies across plant

developmental stages and influences slope reinforcement mechanisms.

This work aims to: synthesize practical insights on plant species selection for erosion control and slope stability; to evaluate species-specific efficacy in improving mechanical shear strength parameters, and to demonstrate that slope reinforcement by root systems is strongly governed by soil moisture dynamics.

MATERIALS AND METHODS

A systematic literature review was conducted from June 2022 to present, using Web of Science and Scopus databases, covering publications written in English. Primary search terms ('soil-roots system', 'soil erosion', 'shear strength' and 'shallow slope stability') identified candidate studies. Subsequent screening eliminated duplicates and prioritized research aligned with sustainable development principles. This process yielded 3 review articles addressing shear strength parameters of soil-roots applications for soil erosion control and shallow slope stability.

RESULTS AND DISCUSSIONS

Type of vegetation

Based on the critical role of vegetation type in determining erosion control efficacy and slope stabilization performance, key species analyzed in this review - including grasses (*Chrysopogon zizanioides, Elytrigia elongata, Panicum virgatum*) and threes/shrubs (alder - *Alnus* spp., paper Mulberry - *Broussonetia papyrifera*). They demonstrate how root biomechanics, soil adaptability, and hydrological resilience govern their suitability for geoenvironmental applications (Francis et al., 2005; Bischetti et al., 2005; Cazzuffi et al., 2006; Cazzuffi et al., 2014; Fan et al., 2021).

Table 1. The core strengths of various vegetation species, emphasizing their biomechanical properties, environmental adaptability, and erosion control performance (Francis et al., 2005; Bischetti et al., 2005; Cazzuffi et al., 2006; Cazzuffi et al., 2014; Fan et al., 2021)

Plant Species	Key strengths	Tensile strength (MPa)	Root depth	Environmental adaptability	Performance in erosion control
Chrysopogon zizanioides	Highest root density; deep vertical roots; tolerates pollutants/saline soils	25–60	4–5 m	pH 4–11; drought/flood/saline-tolerant	Very good: cohesion gain: ≤15 kPa; rapid stabilization
Cortaderia selloana	Drought-resistant; forms dense root mats; thrives in poor soils	15–23	3–4 m	Sandy/rocky substrates; full sun	Good: 90% survival in drought season; reduces surface erosion
Corylus avellana	Exceptional tensile strength; deep anchoring	≤60	>2 m	Temperate forests; well-drained soils	Good: superior slope reinforcement; high RAR in topsoil
Elytrigia elongata	Robust fibrous roots; high tensile strength per diameter	38–55	3–4 m	Dry, nutrient-poor soils; heat-tolerant	Medium: Good for arid slopes; moderate cohesion gain
Alnus alnobetula	Nitrogen-fixing; improves soil fertility; cold-adapted	~35	1–2 m	Alpine/subalpine zones; resists frost	Medium: enhances soil structure; moderate erosion reduction
Panicum virgatum	Evergreen; saline-tolerant; persistent ground cover	25–70	≤2 m	Coastal/arid regions; full sun	Medium: long-term resilience; slower initial growth
Broussonetia papyrifera	Pioneer species; fast-growing in disturbed soils	Depending on the diameter	≤1 m	Collapsed slopes; low-moisture soils	Low: limited use in saturated soils: strength drops to 64%

Shear strength

Depending on the soil types analysed and the plant species employed in stabilization techniques, an increase in shear strength parameters is consistently observed in root-reinforced soils compared to those without

vegetation. Most commonly, stabilization is applied to soils with inherently low cohesion - such as sandy or silty soils, where the contribution of roots to improved cohesion is particularly evident.

A study conducted by Zhou et al. (2023) confirms that the presence of plant roots substantially increases shear resistance. Direct shear tests on unrooted soil (bare soil) indicated a cohesion (c) of 33.2 kPa and an internal friction angle (φ) of 23.8°. In contrast, the soil-root composite with various plant types - namely *Cynodon dactylon* (Cd), *Magnolia multiflora* (Mm), and a grass-shrub mixture (Gs) recorded significantly higher values: cohesion ranged from 34.1-82.8 kPa (Cd), 49.5-72.9 kPa (Mm), and 36.8-99.8 kPa (Gs), while φ increased up to 39.1°. The maximum of 99.8 kPa (Gs, after 90 days) is three times higher than that of the bare soil, demonstrating the effective contribution of roots to the stabilization of the soil mass.

A study by Olinic & Olinic (2025) investigates the influence of plant roots on the shear strength parameters of sandy soils. Direct shear tests conducted on bare sand (BS) revealed a low cohesion value (c) of 1.24 kPa and an internal friction angle (φ) of 32.94°. They studied a root system composed of *Medicago sativa, Dactylis glomerata, Phleum pratense*, and *Trifolium* species which was growth in greenhouse conditions, cohesion increased to 23.43 kPa, representing a 1790% rise (because of the low value of unrooted soil), while the friction angle remained relatively stable at 32.35°, indicating a substantial reinforcement effect in sandy soils.

In the case of organic soil, a different behaviour was observed. Although the presence of roots reduced cohesion from 36.11 kPa (bare organic soil) to 29.72 kPa (approx. 18% decrease), the internal friction angle improved significantly, rising from 19.57° to 35.21°, an increase of nearly 80%. This pattern suggests that while roots may loosen compact soils, thereby reducing cohesion, they enhance internal friction through the mechanical interlocking effect of dense root networks.

The study further emphasizes that the reinforcement effect is most pronounced in the surface layer (0-5 cm), where root density is highest. For example, cohesion in sand drops to 10.65 kPa at 20-25 cm depth, indicating diminishing reinforcement with depth. These findings highlight the value of using dense-rooted vegetation as a sustainable and effective strategy for shallow slope stabilization and erosion control.

Growth period of vegetation

The type of vegetation and its temporal development dramatically influence reinforcement efficiency. In the study conducted by Zhou et al. (2023), the Gs mixture provided the best performance, owing to its complementary root structure: under a normal stress of 200 kPa, its shear strength was 15-30% higher than that of the other plant types. Furthermore, strength evolved nonlinearly over time, peaking at 90 days after germination (for both cohesion and shear resistance), followed by a slight decrease at 120 days. This pattern highlights the importance of species selection and optimal implementation timing. The effect depends on plant age and species: maximum performance is reached between 90-120 days, and Gs shows clear superiority over monoculture. These conclusions provide a scientific basis for designing ecological slope protection systems.

Also, stability analyses using the finite element method (FEM) validated the practical benefits of plant roots on the factor of safety (FS), resulting in an increase of 1.7-15.7% compared to slopes without vegetation (FS = 1.48).

Specifically, slopes planted with Gs had the highest value (FS = 1.72), followed by those with Mm (FS = 1.66), and those with Cd recorded the lowest value (FS = 1.60).

Hydric stress

Hydric stress (water deficiency or excess) influences plant physiology, root development, and ultimately, soil reinforcement capacity.

Roots improve slope stability via mechanical reinforcement (e.g., tensile strength, soil-root bond strength) and hydrological regulation (Wu et al., 2013; Fan et al., 2021).

Hydric stress significantly alters root architecture, directly impacting soil cohesion (c) and friction angle (ϕ). Under drought conditions, moderate water deficits can enhance deep-rooting in resilient species like *Salix elaeagnos*, increasing root tensile strength

and soil cohesion by up to 25% due to adaptive root elongation, as demonstrated in cyclic drying experiments (Ghestem et al., 2011). Conversely, severe drought triggers root shrinkage and mortality, reducing root density by 50% and diminishing shear strength by 18-22% due to weakened root-soil interlocking, elevating landslide risks (Ng et al., 2016).

Waterlogging equally compromises shear strength through root degradation. Prolonged saturation depletes soil oxygen, causing root rot in sensitive species like *Alnus incana*, which exhibits 35% biomass loss and 40% tensile strength reduction (Francis et al., 2005). Saturated conditions also induce fiber slippage and diminish root-soil friction, leading to 30-50% cohesion loss in root-soil systems, as quantified by Ghestem et al. (2011). These biomechanical failures critically undermine slope stability during extreme hydric events.

Recent studies demonstrate that soil moisture dramatically influences root-soil resistance. Fan et al. (2021) observed a 63.9% decrease in pullout resistance under high moisture conditions (w = 30.6%), compared to low moisture conditions (w = 6.5%). This decline is attributed to reduced soil cohesion and the formation of water films at the root-soil interface. Furthermore, a critical root diameter threshold (3 mm in dry soil vs. 7 mm in wet soil) was identified, determining the transition between failure by breaking versus pullout. Field tests, which account for the intertwining of root hairs with soil, yield values 3-15 times greater than laboratory tests, underscoring the necessity of in situ evaluations. This integration highlights the impact of water stress on slope stabilization mechanisms, providing an empirical basis for risk management recommenddations under extreme climatic conditions

Climate-induced hydric stress (drought/floods) compromises root functionality, escalating landslide risks (Boldrin et al., 2018; Francis et al., 2005).

The use of vegetation in sustainable soil stabilization and erosion control provides numerous benefits, but also presents certain challenges that require careful evaluation. As shown in Figure 2, root systems bind soil particles, increasing shear strength and reducing susceptibility to erosion (creating a natural reinforcement mechanism). As an eco-friendly and cost-effective solution is well known that vegetation-based methods are sustainable, require low maintenance once established, and are generally less expensive than hard engineering solutions (Stokes et al., 2014). Along with the other strengths, the use of vegetation in sustainable soil stabilization and erosion control enhances biodiversity, promotes carbon sequestration, improves soil structure, and regulates hydrological cycles.

The weaknesses of the use of vegetation in soil stabilization and erosion control depend on a required growth period needed for root systems to get mature and effectively stabilize the slope; effectiveness depends on local soil, climate and plant species and requires careful selection and site-specific planning. Also, drought of frost can weaken root systems, reducing stabilization capacity during critical periods (Lüscher et al., 2020).

The use of vegetation in soil stabilization and erosion control can be combined with bioengineering and nature-based solution making an opportunity in order to align with global and EU strategies on climate resilience, land reclamation and disaster risk reduction (Mickovski, 2021, Olinic & Olinic, 2025).

The threats are related to: climate change - increased frequency and intensity of rainfalls which may exceed root system capabilities, triggering shallow landslides (Noviandi et al., 2025), land-use conflicts - when the expansion of urban of agricultural land may limit vegetation-based slope interventions) and invasive species risk - non-native or poorly managed vegetation may disrupt local ecosystems or fail to provide stabilization (Sladonja and Poljuha, 2018).

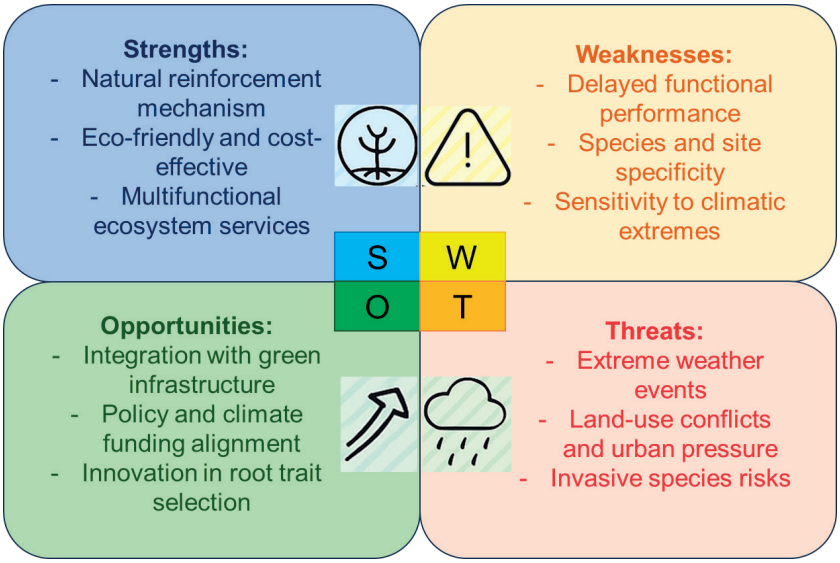


Figure 2. Vegetation for slope stabilization and surface erosion control

CONCLUSIONS

The shear strength parameters of soil-root systems are dynamic and highly sensitive to water stress. Effective slope stabilization strategies must incorporate (1) the selection of plant species based on their eco-physiological tolerance, and (2) the optimization of soil properties to mitigate the impacts of climate change.

Vegetation root systems significantly enhance slope stability through soil-root cohesion, with shear strength parameters serving as critical stability indicators. This review synthesizes global research on soil-root interactions across plant species and soil types, with emphasis on hydraulic stress impacts from climate change. Results demonstrate that root desiccation reduces shear strength by up to 64%, while interspecies variability in drought/flood tolerance dictates survival and reinforcement capacity. We argue that integrating root biomechanics with eco-physiological resilience is essential for sustainable slope management.

Plant roots, especially in the case of grass and shrub mixtures offer a sustainable solution for soil stabilization. Through the combined effect of deep roots (anchoring) and shallow roots (mechanical reinforcement), they reduce erosion and the risk of shallow landslides.

Vegetative root systems contribute to improving soil moisture regulation by facilitating water uptake and retention, thereby mitigating the likelihood of landslides triggered by slope saturation. In contrast to unsaturated, unvegetated slopes, analysing seepage and stability in vegetated terrains necessitates accounting for transpiration-induced variations in matric suction and the modified hydrological behaviour of soils influenced by plant activity.

ACKNOWLEDGEMENTS

This research was financed by the University of Agronomic Sciences and Veterinary Medicine of Bucharest (Grant number: 1068/15.06.2022, Acronym: GeoRoots).

REFERENCES

Bischetti, G. B., Chiaradia, E. A., Simonato, T., Speziali, B., Vitali, B., Vullo, P., Zocco, A. (2007). Root strength and root area ratio of forest species in Lombardy (Northern Italy). *In Eco-and Ground Bio-Engineering: The Use of Vegetation to Improve Slope Stability: Proceedings of the First International Conference on Eco-Engineering* 13-17 September 2004 (pp. 31-41). Springer Netherlands.

Boldrin, D., Leung, A. K., Bengough, A. G. (2018). Effects of root dehydration on biomechanical properties of woody roots of Ulex europaeus. *Plant and Soil, 431*(1), 347-369.

Cazzuffi, D., Corneo, A., Crippa, E. (2006). Slope stabilisation by perennial "gramineae" in Southern Italy: plant growth and temporal performance. *Geotechnical & Geological Engineering, 24(3)*, 429-447.

Cazzuffi, D., Cardile, G., Gioffrè, D. (2014). Geosynthetic engineering and vegetation growth in soil reinforcement applications. *Transportation Infrastructure Geotechnology*, *1*, 262-300.

Fan, C. C., Lu, J. Z., Chen, H. H. (2021). The pullout resistance of plant roots in the field at different soil water conditions and root geometries. *Catena*, *207*, 105593.

Francis, R. A., Gurnell, A. M., Petts, G. E., Edwards, P. J. (2005). Survival and growth responses of Populus nigra, *Salix elaeagnos* and *Alnus incana* cuttings to varying levels of hydric stress. *Forest Ecology and Management*, *210*(1-3), 291-301.

Ghestem, M., Sidle, R. C., Stokes, A. (2011). The influence of plant root systems on subsurface flow: implications for slope stability. *Bioscience, 61*(11), 869-879.

Lüscher, A., Barkaoui, K., Finn, J. A., Suter, D., Suter, M., Volaire, F. (2022). Using plant diversity to reduce vulnerability and increase drought resilience of permanent and sown productive grasslands. *Grass and Forage Science, 77(*4), 235-246.

Mickovski, S. B. (2021). Re-thinking soil bioengineering to address climate change challenges. *Sustainability, 13*(6), 3338.

Ng, C. W. W., Ni, J. J., Leung, A. K., Wang, Z. J. (2016). A new and simple water retention model for root-permeated soils. *Géotechnique Letters, 6(1),* 106-111.

Noviandi, R., Gomi, T., Pratama, G. M., Ritonga, R. P., Fathani, T. F. (2025). Understanding the role of vegetation root systems in the initiation of rainfall-induced shallow landslides: scaling perspectives. *Journal of Forest Research, 30*(3), 165-178.

Olinic, T., Olinic, E. D., Butcaru, A. C. (2024). Integrating Geosynthetics and Vegetation for Sustainable Erosion Control Applications. *Sustainability*, *16*(23), 10621.

Olinic, T., Olinic, E. D. (2025). A sustainable approach to shallow slope stability and erosion control. *In Proceedings of the 4th International Conference on Sustainable Development in Civil, Urban and Transportation Engineering: CUTE 2024, 14–17 October 2024, Wrocław, Poland* (Vol. 418, p. 401). Springer Nature.

Sladonja, B., Poljuha, D. (2018). Non-Native Invasive Species as Ecosystem Service. *Ecosystem services and global ecology, 39*.

Stokes, A., Douglas, G. B., Fourcaud, T., Giadrossich, F., Gillies, C., Hubble, T., Walker, L. R. (2014). Ecological mitigation of hillslope instability: ten key issues facing researchers and practitioners. *Plant and Soil, 377*(1), 1-23.

Wu, T.H., (2013). Root reinforcement of soil: review of analytical models, test results and applications to design. *Canadian Geotechnical Journal, 50*: 259-274.

Zhou, X., Fu, D., Wan, J., Xiao, H., He, X., Li, Z., Deng, Q. (2023). The shear strength of root–soil composites in different growth periods and their effects on slope stability. *Applied Sciences, 13*(19), 2076-3417.

Scientific Papers. Series E. Land Reclamation, Earth Observation & Surveying, Environmental Engineering. Vol. XIV, 2025
Print ISSN 2285-6064, CD-ROM ISSN 2285-6072, Online ISSN 2393-5138, ISSN-L 2285-6064

BIOACCUMULATION OF CADMIUM, LEAD, ZINC AND COPPER IN RED FESCUE (*FESTUCA RUBRA* L.) GROWN IN POLLUTED MEADOWS IN COPŞA MICĂ

Bogdan Ștefan OPREA, Dumitru-Marian MOTELICĂ, Nicoleta Olimpia VRÎNCEANU, Vera CARABULEA, Georgiana Iuliana PLOPEANU, Mihaela COSTEA

National Research and Development Institute for Soil Science, Agrochemistry and Environment, 61 Mărăști Blvd, District 1, Bucharest, Romania

Corresponding author email: carabulea_vera@yahoo.com

Abstract

Studies on the influence of heavy metals are essential because they have a negative impact on human and animal health, the environment, and ecosystems. This work aims to assess the heavy metals content in soil and plant (Festuca rubra L.) samples collected from permanent grasslands in a heavily polluted area during 2023–2024. The total content and DTPA extractable forms of cadmium (Cd), lead (Pb), zinc (Zn), and copper (Cu) in soil and plant were analyzed. The mean value of total Cd content in soil was 5.50 mg/kg dry weight (DW), while the mean values for Pb, Zn and Cu were 201.1 mg/kg DW, 368.7 mg/kg DW and 46.9 mg/kg DW, respectively. In the plant the mean Cd content had the lowest value (0.47 mg/kg DW), the second lowest mean value was recorded for Pb, while the Zn content was the highest (47.6 mg/kg DW). The values of the correlation coefficients showed that heavy metals uptake by Festuca rubra varies according to the type of metal and its form in the soil. The results of this research showed that soils in the Copşa Mică area continue to have a high content of heavy metals, which may have a negative impact on the quality of human and animal life through their accumulation in the food chain.

Key words*: bioaccumulation, Festuca rubra L., heavy metals, meadows, pollution.*

INTRODUCTION

Mining, metal smelting, and agricultural practices are among the main anthropogenic activities that contribute to environmental contamination with heavy metals. Exposure to heavy metals, even in small quantities, through ingestion of contaminated food and water or inhalation of polluted air can lead to numerous health problems (Osman et al., 2019; Briffa et al., 2020; Budi et al., 2022).

Cd is a toxic heavy metal that is non-biodegradable, posing long-term risks to ecosystems and human health. Cd accumulation in plants causes oxidative stress and affects physiological processes (Suhani et al., 2021; Bouida et al., 2022).

Another microelement that can have negative effects in high amounts is Cu. Many studies have shown that Cu assimilation in high quantities can have numerous toxic effects on plants, such as growth inhibition observed through low seed germination rate, disruption of photosynthesis, oxidative stress, or nutrient imbalance (Adrees et al., 2015; Rehman et al., 2019; Mir et al., 2021).

Kuziemska et al. (2021) reported that the use of organic amendaments, especially cattle manure, reduces the bioavailability of Cu in soil. Also, the application of bacterial siderophores also promoted plant growth and improved phytoremediation by reducing metal toxicity (Grobelak et al., 2017).

Tan et al. (2020) reported that Zn plays an important role in plant metabolism.

However, Zn phytotoxicity can affect normal development, photosynthesis and nutrient uptake, but some plants are tolerant to high concentrations and have potential use in phytoremediation (Broadley et al., 2007; Kaur et al., 2021).

Festuca rubra L. is a perennial grass, widespread in various habitats around the world, used in the phytoremediation of contaminated soils due to its well-developed root system, large biomass and high capacity to grow in unfavorable environmental conditions (Gajić et al., 2020).

Phytoremediation is an ecological process of remediation of soils or water polluted with heavy metals. The phytoextraction process refers to the absorption and transfer of contaminants into the aerial parts of plants, while phytostabilization is the immobilization of contaminants in the roots of plants (Hrynkiewicz et al., 2018).

Pusz et al. (2021) analyzed the absorption capacity of heavy metals by red fescue (*Festuca rubra* L.) and reported that it accumulated higher amounts in roots compared to shoots.

Lago-Vila et al. (2015) demonstrated that red fescue can be grown on soils contaminated with heavy metals (Cd, Co, Ni) due to its high phytostabilization capacity.

Niesiobędzka (2023) demonstrated that the concentration of heavy metals in red fescue varies depending on the ecosystem, with the highest concentrations being found in plants grown in urban areas and along roads where the Pb content was above limits.

Red fescue is a species with high potential in phytoremediation of polluted soils, having the ability to retain high amounts of heavy metals in its roots (Gajić et al., 2016).

Mitrović et al. (2008) reported higher Zn concentrations in the roots of *Festuca rubra* compared to the aerial parts indicating a poor mobility of this metal in the plant. On the other hand, the phenomenon of wilting of young leaves was observed, being associated with Cu deficiency.

Wyszkowska et al. (2022) demonstrated that *Festuca rubra* exhibits higher resistance to Cd concentrations compared to Co, and the accumulation factor indicated that this plant has a high potential in the phytoremediation process for lands contaminated with these metals.

The study aims to assess the bioaccumulation of heavy metals (Cd, Pb, Zn, and Cu) by *Festuca rubra* plants from soil of permanent meadows affected by industrial pollution in the Copșa Mică area.

MATERIALS AND METHODS

This study was conducted in the most affected area by industrial pollution in Romania, Copșa Mică, during 2023-2024.

This area became known worldwide for its high pollution levels due to the two factories (Carbosin and Sometra) that operated in the past for approximately 60 years. Plant (aerial part) and soil samples were collected from the studied area to determine the content of heavy metals.

Festuca rubra plant samples harvested were oven dried then milled and treated with nitric acid in a microwave digestion system (Ethos Easy Microwave Dygestion System from Milestone).

Microwave digestion was performed using 10 mL mixture of HNO3 + H2O2 (9 mL HNO3 and 1 mL H2O2) at 210°C for 20 min, method developed in–house.

The measurement of heavy metals content was performed by atomic absorption spectrometry (Flame GBC 932AA to determine Zn and Cu content and Graphite furnace GBC SavanatAAZ to determine Cd and Pb content).

Soil samples were collected from the topsoil (0-20 cm). A soil sample was composed of 13 sub-samples, air-dried at room temperature, crushed, and sifted through a 0.2 mm to remove stones and plant waste.

For the determination of heavy metals content was used atomic absorption spectrometry, after the extraction by the aqua regia-microwave digestion method (Ethos Easy Microwave Dygestion System from Milestone).

Microwave digestion was performed using 10 mL of aqua regia (7.5 mL HCl and 2.5 mL HNO3) at 140°C for 30 min, method developed according to SR ISO 11466:1999.

(DTPA)–extractable heavy metals were extracted from soil (10 g) with 20 ml of extracting solution (0.05 M DTPA (dietilentriaminopentacetic acid), 0.01 M $CaCl_2$ and 0.1 M tetraethylammonium adjusted to pH 7.3), according to SR ISO 14870:2002.

Statistical data processing was performed using Microsoft Excel 2010.

RESULTS AND DISCUSSIONS

Based on the values of the statistical parameters that characterize the central tendency and variability of the total content of Cd, Pb, Zn and Cu in soil (Table 1), it was observed that the contents varied from 0.17 mg/kg DW to 17.74 mg/kg DW for Cd, between 13-692 mg/kg DW for Pb, while the content of Zn and Cu had values ranging between 42-993 mg/kg DW, respectively 12-161 mg/kg DW.

Regarding the median results, the highest value 223 mg/kg DW was recorded for Zn and the second highest in the case of the Pb content (118 mg/kg DW). Cu had a median value of 29 mg/kg DW, while the lowest value was observed for Cd (3.24 mg/kg).

Analyzing the values obtained for the geometric mean, they varied from 3.13 mg/kg DW for Cd to 255.9 mg/kg DW for Zn content. The geometric mean values for Pb and Cu contents were 126.5 mg/kg DW and 36.8 mg/kg DW, respectively.

Table 1. Values of statistical parameters that characterize the central tendency and the variability of the total cadmium, lead, zinc and copper contents in soil (n = 17)

Variable	Minimum	Maximum	Median	Geometric mean	Arithmetic mean	Standard deviation	Coefficient of variation
				mg/kg DW			
Cd_{soil}	0.17	17.74	3.24	3.13	5.50	5.50	100%
Pb_{soil}	13	692	118	126.5	201.1	188	93.5%
Zn_{soil}	42	993	223	255.9	368.7	297.8	80.8%
Cu_{soil}	12	161	29	36.8	46.9	38	81%

DW - dry weight

Regarding the arithmetic mean (Table 1), the heavy metals contents followed the order: Zn>Pb>Cu>Cd. The highest content was recorded by Zn at 368.7 mg/kg DW followed by the Pb content (201.1 mg/kg DW). Cu content had the third highest value (46.9 mg/kg DW) while the lowest content (5.50 mg/kg DW) was recorded for Cd.

According to the Order of the Ministry no. 756/1997 for the approval of the Regulation on the assessment of environmental pollution, the mean values for the Cd and Pb contents exceeded the alert threshold of 3 mg/kg, respectively 50 mg/kg and the intervention threshold of 5 mg/kg and 100 mg/kg for sensitive land use while, the mean values for the Zn and Cu contents remained within normal limits, below the alert thresholds of 300 mg/kg and, respectively, 200 mg/kg.

Muntean et al. (2010) obtained similar results regarding the Cd and Pb content in soil in Copșa Mică area.

Following the results for standard deviation, Cd had the lowest value (5.50 mg/kg DW), while Zn recorded the highest (297.8 mg/kg DW). The standard deviation for Pb was 188 mg/kg DW and for Cu, it was 38 mg/kg DW. A large standard deviation for Pb and Cd indicates that pollution is not evenly distributed.

Analyzing the values obtained for the coefficient of variation (Table 1), it is observed that Cd obtained the highest value (100%) followed by Pb which recorded the second highest result (93.5%). In comparison, the content of Cu and Zn recorded values of 81% and 80.8%, respectively.

The high values of the coefficients of variation indicate an uneven distribution of pollution in the 17 analyzed points suggesting non-uniform pollution.

The studied area is characterized both by a wide variability of soil types and the degree of heavy metal contamination.

Shabbir et al. (2020) reported that the main soil characteristics that influence the mobility and availability of Cu in the soil and uptake by plants are pH and organic matter.

Intrinsic soil factors and environmental variables such as pH, soil organic matter and topographic moisture index influence the spatial variation of heavy metals in soil (Wu et al., 2020).

Analyzing the values of statistical parameters that characterize the central tendency and variability of Cd, Pb, Zn and Cu content in soil – DTPA-extractable forms (Table 2), the order of heavy metals was as follows: Zn>Pb>Cu>Cd except for the values obtained for the coefficient of variation where the metals were ranked as: Pb>Cd>Zn>Cu.

Following the minimum and maximum values for the extractable forms, Cd content ranged from 0.08 mg/kg DW to 15.44 mg/kg DW, Pb varied between 2.7 mg/kg DW and 301 mg/kg

DW, Zn ranged from 2.6 mg/kg DW to 326.8 mg/kg DW, while Cu were between 1.13 mg/kg DW to 23.41 mg/kg DW.
Regarding the median values, Cd had the lowest value (2.28 mg/kg DW), while Zn had the highest (63.2 mg/kg DW). Pb had a median value of 58.8 mg/kg DW, whereas Cu obtained 4.83 mg/kg DW.

Table 2. Values of statistical parameters that characterize the central tendency and the variability of the cadmium, lead, zinc, copper contents in soil – DTPA-extractable forms (n = 17)

Variable	Minimum	Maximum	Median	Geometric mean	Arithmetic mean	Standard deviation	Coefficient of variation
			mg/kg DW				
Cd_{DTPA}	0.08	15.44	2.28	2.31	4.27	4.54	106.3%
Pb_{DTPA}	2.7	301	58.8	39	73	79.2	108.5%
Zn_{DTPA}	2.6	326.8	63.2	51.5	105.2	111.2	105.7%
Cu_{DTPA}	1.13	23.41	4.83	5.22	6.90	6.22	90.1%

DW–dry weight

Analyzing the results for the geometric mean, the highest value was obtained by Zn (51.5 mg/kg DW), Pb had the second highest value (39 mg/kg DW), while Cd and Cu obtained results of 2.31 mg/kg DW and 5.22 mg/kg DW, respectively.
Following the arithmetic mean values, they ranged between 4.27 mg/kg DW for Cd and 105.2 mg/kg DW Zn.
Pb had an arithmetic mean of 73 mg/kg DW, while Cu recorded 6.90 mg/kg DW.
Regarding the standard deviation, the lowest value was obtained for Cd (4.54 mg/kg DW), followed by Cu with a value of 6.22 mg/kg DW.
Pb had a standard deviation of 70.2 mg/kg DW, while Zn had the highest value (111.2 mg/kg DW).
Analyzing the coefficient of variation, the highest result was obtained by Pb (108.5%) and the lowest by Cu (90.1%). For the other metals, the values were 106.3% for Cd and 105.7% for Zn, respectively.
The high values obtained for the coefficient of variation and standard deviation indicate that pollution does not show a uniform distribution and that there are areas where the accumulation of heavy metals is significant. The median values are not influenced by extremes as is the case for the arithmetic mean. At the same time the geometric mean indicates a possibly asymmetric distribution of pollution.
Table 3 shows the statistical parameters that characterize the central tendency and variability of heavy metals content (Cd, Pb, Zn and Cu) in *Festuca rubra* plants.

Table 3. Values of statistical parameters that characterize the central tendency and the variability of the cadmium, lead, zinc, and copper contents in the red fescue (*Festuca rubra* L.) (n = 17)

Variable	Minimum	Maximum	Median	Geometric mean	Arithmetic mean	Standard deviation	Coefficient of variation
			mg/kg DW				
$Cd_{F.rubra}$	0.01	1.64	0.39	0.16	0.47	0.48	102.1%
$Pb_{F.rubra}$	0.09	1.92	0.35	0.36	0.62	0.61	98.4%
$Zn_{F.rubra}$	7.4	89.2	50.1	36.0	47.6	29.5	62%
$Cu_{F.rubra}$	1.19	7.53	3.35	3.44	3.84	1.79	46.6%

DW - dry weight

The ability of *Festuca rubra* to accumulate Cd, Pb, Zn and Cu indicates that it can be used in the phytoremediation of polluted soils (Gajić et al., 2020; Pusz et al., 2021).

Korzeniowska and Stanislawska-Glubiak (2023) demonstrated in a study regarding Zn accumulation in different grass species that *Festuca rubra* compared to *Deschampia caepitosa* is more suitable for phytostabilization than for phytoextraction because it has the ability to retain this element in the roots and limits the translocation to the leaves.

Gołda & Korzeniowska (2016) showed that *Festuca rubra* accumulates high amounts of Cd in the roots and translocates very small amounts to the aerial parts.

Fernández et al. (2017) reported that *Festuca rubra* is an efficient species for phytostabilization of heavy metals especially mercury and arsenic from contaminated areas.

Wyszkowska et al. (2022) investigated the potential use of *Festuca rubra* in phytostabilization of soils contaminated with heavy metals, including Zn and Cu and the results demonstrated that this species efficiently accumulates these metals, being suitable for phytostabilization in contaminated environments.

Based on the minimum and maximum heavy metals content in the plant, Cd levels ranged from 0.01 mg/kg DW to 1.64 mg/kg DW, while Pb varied between 0.09 mg/kg DW and 1.92 mg/kg DW, Zn content ranged from 7.4 mg/kg DW to 89.2 mg/kg DW, while Cu levels were between 1.19 mg/kg DW and 7.53 mg/kg DW.

Analyzing the median values, the highest concentration was obtained by Zn (50.1 mg/kg DW), while Pb had the lowest (0.35 mg/kg DW). The median values for Cd and Cu were 0.39 mg/kg DW and 3.35 mg/kg DW, respectively.

Analyzing the arithmetic mean values, Zn had the highest concentration (47.6 mg/kg DW), followed by Cu (3.84 mg/kg DW). The mean values for Cd and Pb were 0.47 mg/kg DW and 0.62 mg/kg DW respectively.

The arithmetic mean significantly higher than the median in the case of Pb and Cd (0.62 mg/kg DW vs. 0.35 mg/kg DW and 0.47 mg/kg DW vs. 0.39 mg/kg DW, respectively), suggests the presence of potential contamination hotspots while for Cu, the small difference between the mean and the median indicates a more uniform distribution.

Regarding the geometric mean, values ranged from 0.16 mg/kg DW for Cd to 36 mg/kg DW for Zn. The geometric mean values for Pb and Cu were 0.36 mg/kg DW and 3.44 mg/kg DW, respectively.

In a study conducted by Gómez et al. (2016) they showed that *Festuca rubra* tolerates high concentrations of Zn but is sensitive to Pb, especially in the mobile form (Pb-EDTA).

However, in a study by Begonia et al. (2005), the addition of EDTA and acetic acid was shown to enhance Pb uptake in tall fescue by increasing its translocation index, leading to higher Pb concentrations in shoots. This suggests that chelate amendments may improve the efficiency of tall fescue for phytoextraction.

In terms of standard deviation, Cd had the lowest value (0.48 mg/kg DW), the second lowest result was for Pb (0.61 mg/kg DW), followed by Cu with a value of 1.79 mg/kg DW, while Zn obtained the highest value (29.5 mg/kg DW).

Following the coefficient of variation, the highest value was obtained by Cd (102.1%) and the lowest value (46.6%) by Zn. Pb had a value of 98.4% while Cu obtained 62%.

The very high values of the coefficient of variation obtained for Cd and Pb (102.1% and 98.4%, respectively) suggest an extremely non-uniform accumulation of these metals in the plant indicating significant differences between harvesting points while the lower values obtained for Zn and Cu (62% and 46.6% respectively) suggest a more balanced accumulation in the sampled plants.

Following the high values obtained for standard deviation and coefficient of variation suggest that some areas are more affected than others.

Analyzing the log-log diagram for the power regression curves (Figure 1a), it can be observed that the correlation coefficient had distinctly significant value ($r = 0.697^{**}$) indicating a significant positive relationship between total Cd concentration in soil (mg/kg DW) and Cd concentration accumulated in the plant (*Festuca rubra*).

Similarly, the correlation coefficient value for soil Cd content DTPA-extractable form was also distinctly significant ($r = 0.659^{**}$) indicates a statistically significant correlation, but slightly weaker than for total Cd.

This relationship may signal a high mobility of Cd in soil and increased bioavailability, which

makes *Festuca rubra* an effective bioindicator of soil Cd contamination.

In a study conducted by Dong et al. (2019), they reported that tall fescue is effective in phytoremediation of Cd. They demonstrated that plants extract Cd from soil and can excrete it through leaves via hydathodes.

However, to reduce the risk of bioaccumulation it is necessary to add soil amendments that reduce Cd mobility, such as biochar, lime or zeolites.

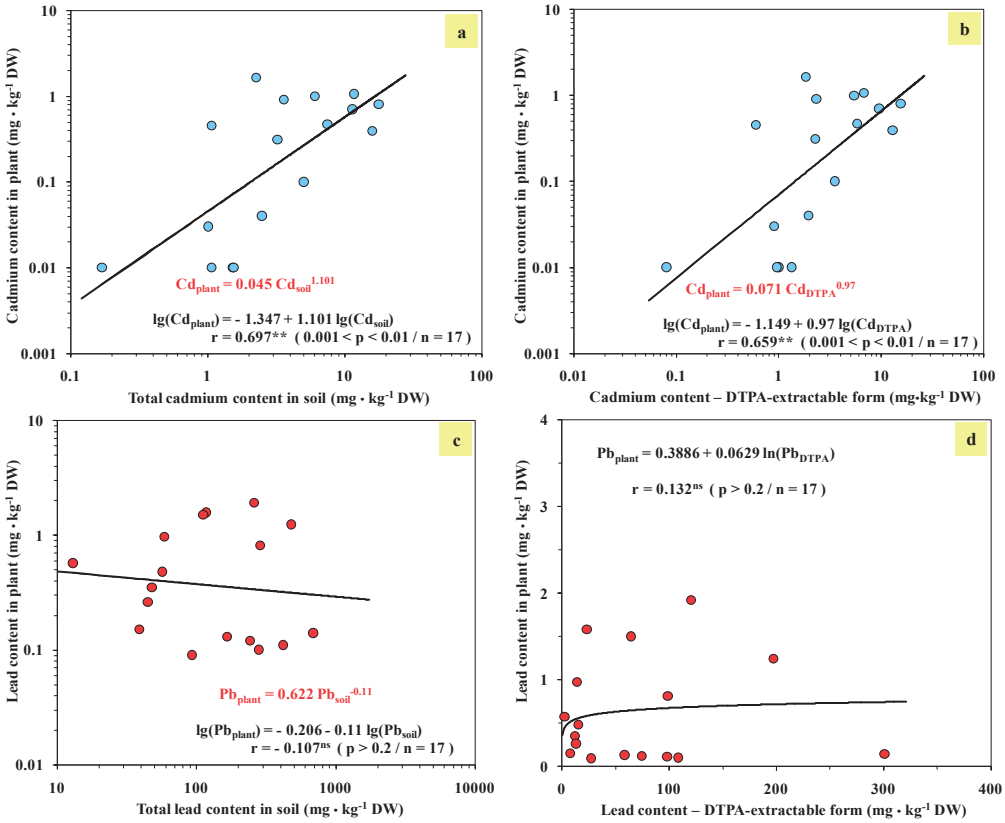


Figure 1. Log-log diagrams for power regression curves that estimate the stochastic dependency between total cadmium content in soil (a), soil cadmium content – DTPA-extractable form (b), total lead content in soil (c), soil lead content – DTPA-extractable form (d) and cadmium/lead contents in *Festuca rubra* plants

Figures 1c, 1d show the relationship between the total Pb and DTPA-extractable form contents in the soil and Pb accumulated in the plant. A very weak correlation is observed suggesting that these parameters are not suitable to assess the accumulation of Pb in aerial parts of *Festuca rubra* plants.

The absorption and toxicity of Pb depends on both time and concentration and affects plants by reducing the rate of seed germination and impairing the ability to absorb nutrients due to its interference with enzymatic activities (Zulfiqar et al., 2019).

According to log-log diagram (Figure 2a) which presents the power regression curves that estimate the stochastic dependence between the total Zn content in soil and Zn content in *Festuca rubra*, the correlation coefficient had a highly significant value (r = 0.826***) indicating a strong correlation.

A highly significant value (r = 0.885***) of the correlation coefficient is also observed for the Zn DTPA–extractable form indicating that bioavailable of this metal is a determining factor for accumulation in the plant.

Wołejko et al. (2013) investigated the impact

of sewage sludge on the accumulation of heavy metals in soil and grass mixtures (*Lolium perenne*, *Festuca rubra* and *Poa pratensis*). They demonstrated that the application of sewage sludge positively influenced the growth of the grass mixture, with Cd, Zn and Cu being more readily assimilated by plants than Pb and Ni.

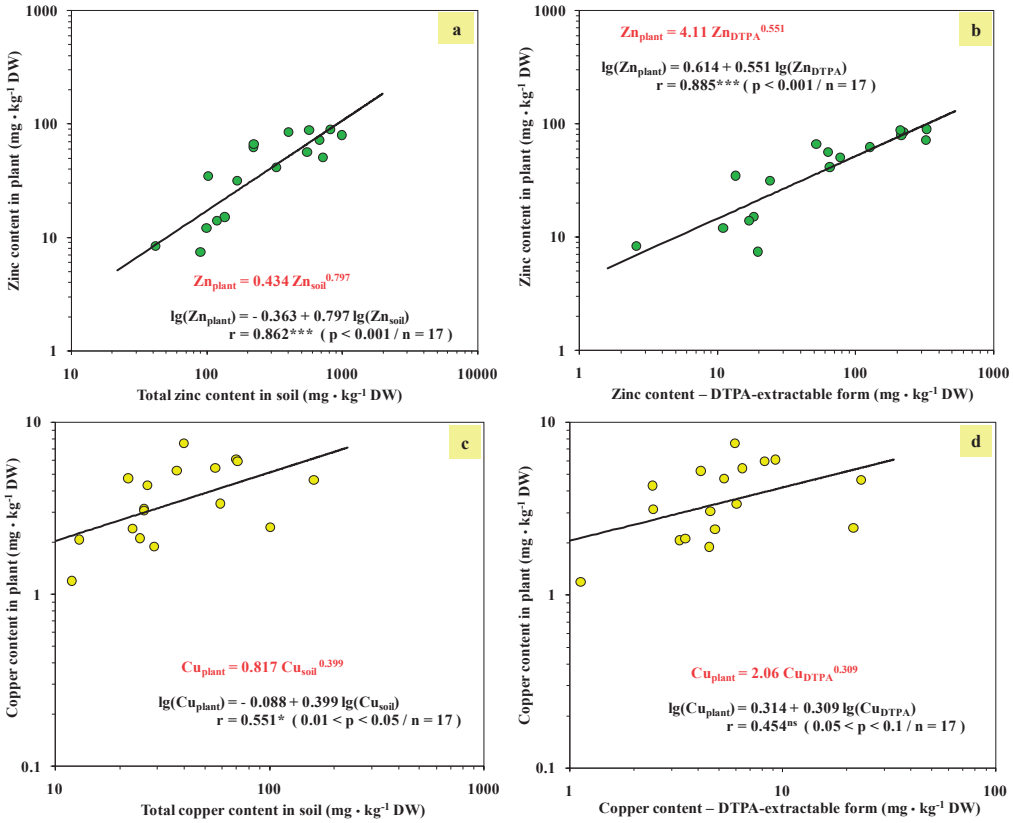


Figure 2. Log-log diagrams for power regression curves that estimate the stochastic dependency between total zinc content in soil (a), soil zinc content – DTPA–extractable form (b), total copper content in soil (c), soil copper content – DTPA–extractable form (d) and zinc/copper contents in *Festuca rubra* plants.

Analyzing the log-log diagram for the power regression curves that estimate the stochastic dependence between total Cu content in the soil and Cu content in plants (Figure 2c), it can be observed that the correlation coefficient value was significant (r = 0.551*). However, in the case of Cu content DTPA-extractable form (Figure 2d), it can be observed that the correlation coefficient value was insignificant (r = 0.454) suggesting a low accumulation rate of bioavailable Cu in the plant.

This could indicate either a higher Cu tolerance or an active uptake-regulating mechanism. Malagoli et al. (2014) reported that *Festuca rubra* accumulates more Cu in its roots than in its aerial parts.

Padmavathiamma and Li. (2009), demonstrated that *Festuca rubra* accumulated high amounts of Cu in the roots indicating that it is a plant that can be successfully used in the phytostabilization process.

CONCLUSIONS

Cd content in soil recorded the lowest mean value (5.50 mg/kg total content and 4.27 mg/kg DTPA-extractable form) while Zn had the highest mean value (368.7 mg/kg total

content and 105.2 mg/kg DTPA-extractable form).

The bioaccumulation of Cd and Zn in aerial parts of the plant (*Festuca rubra*) can be estimated using the total content and DTPA–extractable forms in soil. However, for Cu and Pb, due to their low mobility within the soil–plant system, the studied parameters are not suitable indicators of bioaccumulation.

The results of this research showed that soils in the Copșa Mică area continue to have a high content of heavy metals, which may have a negative impact on the quality of human and animal life through their accumulation in the food chain. Continuous monitoring of areas at risk of heavy metals contamination is needed to assess the dynamics of heavy metals accumulation in soil and plants. Such research is essential for tracking changes in contamination levels and determining the safety of using pastures for livestock farming or using land for crop growing.

ACKNOWLEDGEMENTS

This work was financed by project number PN 23.29.04.01 entitled: "Assessment of heavy metals bioaccumulation in meadows vegetation using the regression analysis to develop a guide of good practices for grazing and animal feedstock in areas affected by industrial pollution" and project number 78/18.12.2024 (NEC): "Contract for non-reimbursable financing for the provision of activities stipulated in Government Decision No. 1300/2024 for the approval of the project regarding the monitoring and periodic reporting of indicators on the impact of air pollution on terrestrial ecosystems, as well as the financing of the project from the Environmental Fund budget".

REFERENCES

Adrees, M., Ali, S., Rizwan, M., Ibrahim, M., Abbas, F., Farid, M., Zia-Ur-Rehman, M., Irshad, M., & Bharwana, S. (2015). The effect of excess copper on growth and physiology of important food crops: a review. *Environmental Science and Pollution Research, 22*, 8148-8162.

Begonia, M. T., Begonia, G. B., Ighoavodha, M., & Gilliard, D. (2005). Lead Accumulation by Tall Fescue (*Festuca arundinacea* Schreb.) Grown on a Lead-Contaminated Soil. International Journal of *Environmental Research and Public Health, 2*(2), 228-233. https://doi.org/10.3390/ijerph2005020005

Bouida, L., Rafatullah, M., Kerrouche, A., Qutob, M., Alosaimi, A., Alorfi, H., & Hussein, M. (2022). A Review on Cadmium and Lead Contamination: Sources, Fate, Mechanism, Health Effects and Remediation Methods. Water.

Briffa, J., Sinagra, E., & Blundell, R. (2020). Heavy metal pollution in the environment and their toxicological effects on humans. Heliyon, 6(9).

Broadley, M., White, P., Hammond, J., Zelko, I., & Lux, A. (2007). Zinc in plants. *The New phytologist, 173*, 677-702.

Budi, H., Opulencia, M., Afra, A., Kamal, W., Abdullaev, D., Majdi, A., Taherian, M., Ekrami, H., & Mohammadi, M. (2022). Source, toxicity and carcinogenic health risk assessment of heavy metals. *Reviews on Environmental Health, 39*, 77 - 90.

Dong, Q., Fei, L., Wang, C., Hu, S., & Wang, Z. (2019). Cadmium excretion via leaf hydathodes in tall fescue and its phytoremediation potential. *Environmental Pollution, 252*, 1406-1411.

Fernández, S., Poschenrieder, C., Marcenò, C., Gallego, J. R., Jiménez-Gámez, D., Bueno, A., & Afif, E. (2017). Phytoremediation capability of native plant species living on Pb-Zn and Hg-As mining wastes in the Cantabrian range, north of Spain. *Journal of Geochemical Exploration*, *174*, 10-20.

Gajić, G., Djurdjević, L., Kostić, O., Jarić, S., Mitrović, M., Stevanović, B., & Pavlović, P. (2016). Assessment of the phytoremediation potential and an adaptive response of *Festuca rubra* L. sown on fly ash deposits: Native grass has a pivotal role in ecorestoration management. *Ecological Engineering, 93*, 250-261.

Gajić, G., Mitrović, M., & Pavlović, P. (2020). Feasibility of *Festuca rubra* L. native grass in phytoremediation. *Phytoremediation potential of perennial grasses*, 115-164.

Gołda, S., & Korzeniowska, J. (2016). Comparison of phytoremediation potential of three grass species in soil contaminated with cadmium. *Environmental Protection and Natural Resources, 27*(1), 8-14.

Gómez, J., Yunta, F., Esteban, E., Carpena, R. O., & Zornoza, P. (2016). Use of radiometric indices to evaluate Zn and Pb stress in two grass species (*Festuca rubra* L. and *Vulpia myuros* L.). *Environmental Science and Pollution Research, 23*, 23239-23248.

Grobelak, A., & Hiller, J. (2017). Bacterial siderophores promote plant growth: Screening of catechol and hydroxamate siderophores. *International journal of phytoremediation*, *19*(9), 825-833.

Hrynkiewicz, K., Złoch, M., Kowalkowski, T., Baum, C., & Buszewski, B. (2018). Efficiency of microbially assisted phytoremediation of heavy-metal contaminated soils. *Environmental Reviews, 26*(3), 316-332.

Kaur, H., & Garg, N. (2021). Zinc toxicity in plants: a review. *Planta, 253*.

Korzeniowska, J., & Stanislawska-Glubiak, E. (2023). The phytoremediation potential of local wild grass versus cultivated grass species for zinc-contaminated soil. *Agronomy*, *13*(1), 160.

Kuziemska, B., Trębicka, J., Wysokiński, A., & Jaremko, D. (2021). Supplementation of Organic Amendments

Improve Yield and Adaptability by Reducing the Toxic Effect of Copper in Cocksfoot Grass (*Dactylis glomerata* L. Cv Amera). *Agronomy, 11*, 791.

Lago-Vila, M., Arenas-Lago, D., Rodríguez-Seijo, A., Andrade Couce, M. L., & Vega, F. A. (2015). Cobalt, chromium and nickel contents in soils and plants from a serpentinite quarry. *Solid earth*, *6*(1), 323-335.

Malagoli, M., Rossignolo, V., Salvalaggio, N., & Schiavon, M. (2014). Potential for phytoextraction of copper by *Sinapis alba* and *Festuca rubra* cv. Merlin grown hydroponically and in vineyard soils. *Environmental Science and Pollution Research, 21*, 3294-3303.

Ministry Order No. 756 from November 3, 1997 for approval of Regulation concerning environmental pollution assessment published in Official Monitor No. 303/6 November 1997

Mir, A., Pichtel, J., & Hayat, S. (2021). Copper: uptake, toxicity and tolerance in plants and management of Cu-contaminated soil. *BioMetals, 34*, 737-759.

Mitrović, M., Pavlović, P., Lakušić, D., Djurdjević, L., Stevanović, B., Kostić, O., & Gajić, G. (2008). The potential of *Festuca rubra* and *Calamagrostis epigejos* for the revegetation of fly ash deposits. *Science of the total environment, 407*(1), 338-347.

Muntean, E., Muntean, N., & Mihăiescu, T. (2010). Cadmium and lead soil pollution in Copsa Mica area in relation with the food chain. *Research Journal of Agricultural Science, 42*, 731-734.

Niesiobędzka, K. (2023). Bioaccumulation of Copper, Lead and Zinc in *Festuca rubra* of Grassy Ecosystems (in Poland). *Current Trends on Biotechnology & Microbiology, 3*(4).

Osman, M., Yang, F., & Massey, I. (2019). Exposure routes and health effects of heavy metals on children. *BioMetals, 32*, 563 - 573.

Padmavathiamma, P. K., & Li, L. Y. (2009). Phytoremediation of metal-contaminated soil in temperate humid regions of British Columbia, Canada. *International Journal of Phytoremediation*, *11*(6), 575-590.

Pusz, A., Wiśniewska, M., & Rogalski, D. (2021). Assessment of the accumulation ability of *Festuca rubra* L. and *Alyssum saxatile* L. tested on soils contaminated with Zn, Cd, Ni, Pb, Cr, and Cu. *Resources, 10*(5), 46.

Rehman, M., Liu, L., Wang, Q., Saleem, M., Bashir, S., Ullah, S., & Peng, D. (2019). Copper environmental toxicology, recent advances, and future outlook: a review. *Environmental Science and Pollution Research, 26*, 18003-18016.

Shabbir, Z., Sardar, A., Shabbir, A., Abbas, G., Shamshad, S., Khalid, S., N., Murtaza, G., Dumat, C., & Shahid, M. (2020). Copper uptake, essentiality, toxicity, detoxification and risk assessment in soil-plant environment. *Chemosphere, 259*, 127436.

Suhani, I., Sahab, S., Srivastava, V., & Singh, R. (2021). Impact of Cadmium Pollution on Food Safety and Human Health. Current Opinion in Toxicology.

Tan, L., Qu, M., Zhu, Y., Peng, C., Wang, J., Gao, D., & Chen, C. (2020). Zinc transporter 5 and Zinc transporter 9 Function Synergistically in Zinc/Cadmium Uptake. *Plant physiology, 183*(3), 1235–1249.

Wołejko, E. L. Ż. B. I. E. T. A., Wydro, U. R. S. Z. U. L. A., Butarewicz, A. N. D. R. Z. E. J., & Łoboda, T. A. D. E. U. S. Z. (2013). Effects of sewage sludge on the accumulation of heavy metals in soil and in mixtures of lawn grasses. *Environment Protection Engineering, 39*(2), 67-76.

Wu, Z., Chen, Y., Han, Y., Ke, T., & Liu, Y. (2020). Identifying the influencing factors controlling the spatial variation of heavy metals in suburban soil using spatial regression models. *Science of the Total Environment*, *717*, 137212.

Wyszkowska, J., Boros-Lajszner, E., & Kucharski, J. (2022). Calorific Value of *Festuca rubra* Biomass in the Phytostabilization of Soil Contaminated with Nickel, Cobalt and Cadmium Which Disrupt the Microbiological and Biochemical Properties of Soil. *Energies, 15*(9), 3445.

Zulfiqar, U., Farooq, M., Hussain, S., Maqsood, M., Hussain, M., Ishfaq, M., Ahmad, M., & Anjum, M. (2019). Lead toxicity in plants: Impacts and remediation. *Journal of environmental management, 250*, 109557.

Scientific Papers. Series E. Land Reclamation, Earth Observation & Surveying, Environmental Engineering. Vol. XIV, 2025
Print ISSN 2285-6064, CD-ROM ISSN 2285-6072, Online ISSN 2393-5138, ISSN-L 2285-6064

CHEMICAL STATE AND ECOLOGICAL ASSESSMENT OF ATMOSPHERIC AIR QUALITY

Georgi PATRONOV[1], Diana KIRIN[2, 3], Petya ZAHARIEVA[3], Radoslava ZAHARIEVA[3], Dimitrinka KUZMANOVA[2]

[1]University of Plovdiv "Paissii Hilendarski", Department of Chemical Technology, 24 Tsar Assen Street, 4000, Plovdiv, Bulgaria
[2]Agricultural University - Plovdiv, 12 Mendeleev Blvd, 4000, Plovdiv, Bulgaria
[3]National Institute of Geophysics, Geodesy and Geography, Hydrology and Water Management Research Centre, Bulgarian Academy of Sciences, Block 3, Acad. G. Bonchev Street, 1113, Sofia, Bulgaria

Corresponding author email: patron@uni-plovdiv.bg

Abstract

Research was conducted on the state of atmospheric air in the region of the village of Voyvodino, Maritsa municipality, and Plovdiv district, Bulgaria, influenced by industrial sources of impact. The indicators of main pollutants of the atmospheric air above populated areas were measured (PM10, SO2, CO, NO2, NO, O3, Benzene, Toluene, m-p-xylene, o-xylene). The research was carried out according to established standards. The chemical and ecological state is presented. The air quality index is analyzed. An ecological assessment of the state of atmospheric air was carried out. The risk to human health, the impact of pollution on living organisms, on protected species, habitats and territories was assessed. Measures to improve the ecological state of the air have been identified.

Key words*: air pollution, air quality index, chemical state, ecological assessment, industrial impact.*

INTRODUCTION

Clean air is a fundamental human right. Air pollution is identified as the biggest environmental threat to health and a leading cause of non-communicable diseases such as heart attack and stroke. According to World Health Organization (WHO), "there are no safe levels of air pollution". The organization identifies air pollution as one of the risk factors for early mortality worldwide (WHO, 2021; EEA, 2024). Article 6 of Directive 2016/2284/EU requires each EU Member State to submit a national air pollution control program (Directive (EU) 2016/2284 of The European Parliament and of the Council, 2016). Air pollution emissions have decreased significantly in recent decades. Nevertheless, problems with pollutant emissions from individual industries persist (Directive (EU) 2024/2881 of the European Parliament and of the Council, 2024; Nunez et al., 2024).

There are different systems for ambient air quality in individual countries and regions. Each system uses its own hazard index, pollution concentration, and time of measurement. This makes it difficult for the average consumer to navigate between the systems of different countries.

The United States Environmental Protection Agency (US-EPA) defines the Air Quality Index (AQI) – a number used to inform the public about the level of air pollution and to predict the expected level of pollution. The AQI is based on measurements of particulate matter emissions (PM2.5 and PM10), ozone, nitrogen dioxide, sulfur dioxide, and carbon monoxide. The AQI values indicate 6 levels of air pollution, each of which is color-coded and provides information on possible health effects (Table 1). The AQI provides the public with important information about the state of air pollution over the past five decades (Sheikh, 2019; Horn & Dasgupta, 2024).

The European Environment Agency is developing and implementing the European Air Quality Index (EAQI) for the countries of the European Union. The (EAQI) is based on the measurement of the following main pollutants in ambient air: PM10, PM2.5, ozone, nitrogen

dioxide and sulphur dioxide. The scale for each pollutant is different, and for PM10 it is presented in Table 2. The individual zones are based on the relative health risk, as defined by the World Health Organization, associated with short-term exposure to the pollutants. The Air Quality Index is not a tool for checking compliance with air quality standards but allows users to orient themselves on the quality of ambient air in populated areas or in places of travel and work.

These indices raise public awareness of the importance of clean air and help build broader support for air quality and emissions regulations. As regulatory constraints change, both indices change, keeping them relevant and alive (Sheikh, 2019; EAQI, 2024).

Table 1. Air Quality Index (AQI) values and corresponding condition color scale

Values	Condition color scale
0-50	good
51-100	moderate
101-150	unhealthy for sensitive individuals
151-200	unhealthy
201-300	very unhealthy
300+	dangerous

Table 2. European Air Quality Index (EAQI) values for PM10 and the corresponding condition color scale

EAQI, PM10, µg/m^3	Condition color scale
0-20	good
20-40	fair
40-50	moderate
50-100	poor
100-150	very poor
150-1200	extremely poor

There is growing interest in the contribution of fine particulate matter to air quality, climate and human health. The negative effects of these particles depend mainly on their chemical composition and physicochemical properties (Lei et al., 2024).

In aerosol science, heavy metal pollution is also a current problem, especially when it comes to road dust in densely populated cities. The main sources of heavy metals in road dust are industrial activities (32.05%), transport (34.90%), and a combination of transport, industrial, and construction activities (33.05%) (Ma et al., 2025).

The increase in public health incidents resulting from air quality, as well as environmental degradation, is prompting authorities and experts to improve and seek new ways to monitor air quality and "adequately" deploy air quality sensors (Chaudhuri & Roy, 2024).

Air pollution continues to have a negative impact on the health of Europeans. A significant part of Europe's population lives in cities where EU air quality standards to protect human health are often exceeded. These health impacts shorten lives, increase economic and medical costs and reduce work productivity. The pollutants with the most serious impact on human health are particulate matter, nitrogen dioxide and ground-level ozone. According to the latest EEA estimates, at least 239,000 deaths in the EU in 2022 were due to exposure to PM2.5 pollution above the WHO recommended limit 5 µg/m^3. 70,000 deaths were due to exposure to ozone pollution, and 48,000 deaths were due to exposure to nitrogen dioxide pollution. These deaths could have been avoided if WHO guidelines had been followed (EEA, 2024a).

For Bulgaria, deaths due to long-term exposure to fine particles decreased by 53% between 2005 and 2022. Yield losses due to ozone exposure at the national level in 2022 were estimated at 1.98% yield loss for wheat and 4.22% yield loss for potatoes. This represents an economic loss of approximately €26 million for wheat and €1.6 million for potatoes (EEA, 2024a).

Air pollution has a negative impact on both terrestrial and aquatic ecosystems, degrading the environment and reducing biodiversity. Different pollutants damage ecosystems in different ways. Ozone (secondary air pollutant) damages crops, forests and plants by reducing growth rates, lowering yields and affecting biodiversity. Reduced yields of wheat and potatoes demonstrate the negative impact of ozone layer, with losses expected to amount to €1.3 billion for wheat and €680 million for potatoes across Europe by 2022.

Nitrogen deposition on land and in water bodies is mainly caused by ammonia from agricultural activities and nitrogen oxides from combustion processes. In water bodies, increased nitrogen content contributes to eutrophication, characterized by algal blooms and less available oxygen due to excess nutrients. In sensitive terrestrial ecosystems, such as grasslands, exceeding critical loads for nitrogen deposition can lead to the loss of sensitive species. At the

same time, species requiring high levels of nitrogen may develop excessively, which can alter the structure and function of the ecosystem. Sulfur dioxide can also have a significant negative impact on ecosystems. Its deposition can lead to changes in the chemical composition of soil, lakes, rivers and seas. This can cause acidification, which disrupts ecosystems and leads to a loss of biodiversity. A major source of SO_2 is coal-based energy.

Heavy metals are toxic pollutants that travel long distances in the atmosphere and are deposited in ecosystems. They accumulate in soils and subsequently bioaccumulate and biomagnify in the food chain (i.e., concentrations of substances in animal tissues increase progressively through the food web). The main sources of heavy metals include the processing and mining industries, energy, and road transport.

Europe's waters continue to be affected by chemicals, mainly from atmospheric pollution from coal-fired power generation and diffuse pollution from agriculture. The main pollutants in surface waters are related to pollution from diffuse sources, such as atmospheric deposition (52%) (Impacts of air pollution on ecosystems in Europe, 2024)

The latest data confirms once again that Europeans remain exposed to concentrations of air pollutants well above the World Health Organization (WHO) recommended levels. Nearly three quarters of European ecosystems are exposed to harmful levels of air pollution (EEA, 2024).

The main indicators characterizing the quality of atmospheric air in the ground layer are suspended particles, fine dust particles, sulfur dioxide, nitrogen dioxide and/or nitrogen oxides, carbon monoxide, ozone, lead (aerosol), benzene, polycyclic aromatic hydrocarbons, heavy metals - cadmium, nickel and mercury, arsenic (RIAA, 2023; 2024).

The present research concerns the region of Plovdiv, Bulgaria. The territory of the city is urbanized, with high density of construction, intensive automobile traffic and industrial activity. The main factors of air pollution are combustion processes, transport, the condition of the road and adjacent infrastructure and finally the industrial sector. During the summer period, construction and repair-construction activities acquire significant importance for atmospheric air pollution.

Specific climatic conditions have a significant impact on the quality of atmospheric air. The Plovdiv Field is alluvial lowland formed by the Maritsa River and its tributaries. There is a so-called trough-shaped morphostructure, at the "bottom" of which the city is located. Plovdiv is located on six syenite hills. These natural features significantly contribute to the adverse meteorological conditions associated with temperature inversions, fogs along the Maritsa River, long periods of drought and a large number of days a year with calm weather, reflecting on the dispersion of locally emitted pollutants. (RIAA, 2023; 2024).

MATERIALS AND METHODS

The measurements were carried out hourly with a Mobile Automatic Station in 2023 in spring (13 days), summer (14 days) and autumn (16 days) (Figure 1). The following main indicators of atmospheric air quality were recorded – Particulate matter, Sulphur dioxide, Carbon monoxide, Nitrogen dioxide, Nitrogen monoxide, Ozone, Benzene, Toluene, m-p-xylene, o-xylene. The main characteristics of these indicators are presented in Table 3. The total number of samples taken is as follows – 3116 for spring, 3240 for summer and 2784 for autumn. The production activities carried out in the study area are in the field of metalworking, chemical and food industry.

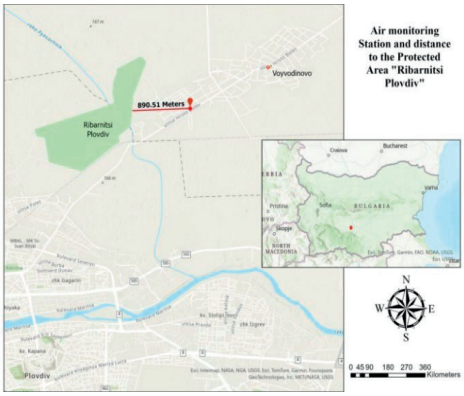


Figure 1. Location of the air monitoring station and the protected area "Ribarnitsi", Plovdiv

The dust emissions formed are of short-term local nature, with a low discharge height and high gravitational deposition velocity (RIAA, 2023; 2024).

Table 3. Main characteristics of the measured indicators

Indicator	Unit of measure	Analysis method	Uncertainty	Standard, μg/m³
Particulate matter	μg/m³	BDS EN 16450:2017	U=14.7%	ADN – 50 AAN – 40
Sulphur dioxide	μg/m³	BDS EN 14212:2012	U=3.70%	AHN – 325 AND – 125
Carbon monoxide	μg/m³	BDS EN 14626:2012	U=3.75%	HHPS – 10
Nitrogen dioxide and Nitrogen oxides	μg/m³	BDS EN 14211:2012	U=3.74%	AHN – 200 AAN – 40
Ozone	μg/m³	BDS EN 14625:2012	U=3.60%	HHPS – 120
Benzene	μg/m³	BDS EN 14662-3:2015	U=4.5%	AAN – 5

Legend: ADN – Average daily norm for the protection of human health; AAN – Average annual norm for the protection of human health; AHN – Average hourly norm for protecting human health; HHPS – Human health protection standard (maximum eight-hour average value within 24 hours); Regulation No. 12 (2010).

The norm for the PM10 indicator is average daily, that is, the registered hourly values during the day are averaged, which does not imply exceedances of the average daily values, due to the fact that the likely intensive transport traffic is in the period 08.00 – 17.00. Based on the results obtained in 2023, an assessment of the pollution levels in the studied area was carried out in accordance with the requirements of the currently current Regulation No. 12 of 2010 (Regulation No. 12, 2010).

RESULTS AND DISCUSSIONS

The measurements in 2023 were carried out with a Mobile Automatic Station in spring, summer and autumn, as indicated in the previous chapter. The choice of the location of the station is in accordance with the requirements of Regulation No. 12 of 2010 (Regulation No. 12, 2010). The monitoring station is a non-urban background station, located more than 5 km from the city of Plovdiv (Figure 1). Point sources of emissions from industrial sites are located more than 5 km from the station area. In the area studied there are both industrial enterprises and residential buildings.

Emission sources can be combustion processes; road transport; other mobile sources and machinery; natural processes - adverse weather conditions that contribute to the accumulation and hinder the dispersion of pollutants.

The results obtained as a range of values are presented in Table 4.

Table 4. Interval of measured daily average concentrations for the reported indicators by season

Indicator	Value range, μg/m³		
	spring	summer	autumn
Particulate matter	9 ÷ 48	15 ÷ 33	23 ÷ 73
Sulphur dioxide	8 ÷ 14	1 ÷ 10	7 ÷ 16
Carbon monoxide	0.1 ÷ 0.4	0.2 ÷ 0.4	0.2 ÷ 0.4
Nitrogen dioxide	7 ÷ 23	9 ÷ 15	10 ÷ 34
Nitrogen monoxide	1 ÷ 8	1 ÷ 2	1 ÷ 12
Ozone	30 ÷ 67	37 ÷ 66	17 ÷ 53
Benzene	0.20 ÷ 0.60	0.12 ÷ 0.25	0.27 ÷ 0.40
Toluene	0.17 ÷ 1.35	0.24 ÷ 0.70	0.39 ÷ 0.58
m-p-xylene	0.14 ÷ 0.67	0.27 ÷ 0.61	0.34 ÷ 2.10
o-xylene	0.06 ÷ 0.23	0.01 ÷ 0.17	0.09 ÷ 0.49

The only exceedances of the average daily concentrations were for PM10 during the autumn period – 56, 61, 70 and 73μg/m³ at a norm of 50μg/m³. All other measured average daily indicators have values in accordance with the regulatory requirements.

The hourly exceedances of the norm for the average daily concentration (50 μg/m³) are only for the PM10 values for the measurement intervals during the 3 seasons (Table 5). Of the total 1032 hourly PM10 values obtained for the measurements made during the spring, summer and autumn seasons, 10.17% (105 values) indicate poor air quality; 1.07% (11 values) indicate very poor air quality, and 0.48% (5 values) indicate extremely poor air quality (Table 5). The main PM10 assessment indicators for ambient air quality are summarized in Table 5.

The lower and upper assessment thresholds for the average daily and annual values are two exceedances of the upper threshold for spring, one for summer and 10 for autumn. The average annual norm of the upper threshold is exceeded based on the results obtained for the three seasons 31.30 μg/m³.

This exceedance is below the average daily norm for the protection of human health (50 μg/m³) and below the average annual norm for the protection of human health (40 μg/m³) from the legislation in Bulgaria (Regulation No. 12, 2010).

With increasing temperatures, PM10 values decrease, which is why lower maximum short-term (60 minutes) single values and average daily values are recorded during summer days.

Table 5. Summarized exceedances of PM10 according to the main assessment standards for ambient air quality

Criteria	Overshoots, µg/m³		
	spring	summer	autumn
Maximum hourly values measured, µg/m³	198 461	57 85 52 88	60 53 94 114 70 84 71 150 55 63 69 139 178 159
Number of hourly exceedances of the average daily norm (over **50** µg/m³)	10	5	107
Average daily norm for the protection of human health - **50** µg/m³ (exceeded no more than 35 times per calendar year)	-	-	56 61 70 73
Lower and upper assessment thresholds - norm **25 – 35** µg/m³ **average daily value** (exceeded no more than 35 times per calendar year)	43, 48	36	43, 47, 56, 47, 61, 40, 42, 49, 70, 73
Lower and upper assessment thresholds - norm **20-28** µg/m³ **average annual value**	**31.30 µg/m³ – upper assessment threshold exceeded for the period spring, summer and autumn**		
Average annual norm for the protection of human health - **40** µg/m³	–		

Legend: EAQI – poor, very poor, extremely poor; Regulation No. 12 (2010).

In calm weather (wind speed < 1.5 m/s) and fog, pollutants are retained and accumulated. The number of days and nights with calm weather during the periods of measurements taken is respectively: 7 in spring, 14 in summer and 15 in autumn. As humidity increases, the levels of pollutants in the air decrease. According to the PM10 indicator, maximum short-term values were not recorded only at 100% relative humidity. Such are only 5 days of the reporting periods. The hourly and daily average exceedances recorded during the autumn period from the measurements of the quality of the ambient air in the range of 20.00-07.00 hours of the day could be the result of the operation of wood and coal-fired heating appliances, although the night temperatures in October and the reporting period are not low, but also as a result of the certain meteorological conditions that hinder the dispersion of pollutants (calm, others). Overall, for the year - the unfavorable climatic conditions in the region - more than 50% days a year with calm weather and over 75% days a year with inversion processes, lead to the retention of the formed relatively high background concentrations of PM10.

The impact of the obtained values of the monitored air quality parameters on the health of the population was assessed on the basis of the Environmental Protection Act, the Clean Air Act, the Health Act, and Regulation No. 12 from 2010 on standards of harmful substances in the ambient air of populated areas. (AAPL, 1996; Law on environmental protection, 2002; Law of Health, 2005; Regulation No. 12, 2010).

The exceeded average daily values indicate acceptable ambient air quality, moderately dangerous for very sensitive people with respiratory diseases. The hourly standards exceed the average daily standard by 1.02 – 9.22 times. Of the total 1032 hourly values for PM10 obtained, 8.72% of the values (90 values) indicate a moderate state of ambient air quality, with a risk for very sensitive people with respiratory diseases; 0.39% (4 values) indicate an unhealthy state of ambient air quality for sensitive groups of the population; 0.1% or 1 value is dangerous for the entire population. Even though the relative share of the results for the most part indicates a good state of AQI (below 50 µg/m3; 90.60%, 937 values), the obtained exceedances are not to be ignored, especially those associated with risks to human health.

PM is not a single substance, but a mixture of pollutants with different chemical properties and varying physical properties such as size and surface area, which has a major impact on the distribution and deposition in the respiratory tract. A significant relationship has been found between high PM concentrations and mortality, hospital admissions for respiratory diseases, and person-days of bronchodilator use.

The resulting exceedances have a negative impact on the health of the population. The increase in PM levels is also expected to affect cultural, household, agricultural and other economic activities. All this requires immediate measures to be taken to eliminate the sources of pollution and provide permanent control by the control bodies, aimed at achieving good

ecological status for PM10 and the overall quality of air.

The protected area BG0002016 "Fisheries Plovdiv" is located near the assessed site (Figure 1; Natura 2000).

The objectives of declaring the protected area are related to the protection and maintenance of the habitats of the bird species specified in the Biodiversity Act to achieve their favorable conservation status, as well as the restoration of the habitats of those bird species for which it is necessary to improve their conservation status (Biodiversity Law, 2002).

Of the total 43 protected species, 39 bird species are concentrated in the protected area (c), 15 species are wintering (w, non-migratory species) and 3 species are breeding in the protected area (r). Two of the species are not sufficiently studied in the protected area but are represented (p; *Ardea cinerea* and *Tachybaptus ruficollis*). Overall, the quality of data on birds in the protected area is good (G), with minor exceptions (2 cases with insufficient study (DD) and one with moderate (M)). Of the 43 protected bird species, the International Red Data Book includes: 33 species with the category Least Concern (LC); 4 species with the category Vulnerable (VU); 5 species with the category Near Threatened (NT). 18 species are included in Appendix 2 of the Bern Convention; 16 species – in Appendix 3 and respectively 2, 23 and 1 species are included in Appendix 1, 2 and 3 of the Bonn Convention. In CITES – Appendices 1 and 2, 1 and 5 species are included respectively, and in the Birds Directive – 16 species in Annex 1 and 3 and in Annex 3. The Red Book of the Republic of Bulgaria includes 28 species with the following protection categories: vulnerable (VU) – 12 species; endangered (EN) – 8 species; critically endangered (CR) – 7 species; near threatened (NT) – 1 species. The Biodiversity Act protects: 16 species included in Annex 2; 26 species included in Annex 3 and 1 species included in Annex 4 (Biodiversity Law, 2002; Biserkov et al., 2015; Golemanski et al., 2015; Red List of Peev et al., 2015; RLTS, 2025;).

Increasing PM10 levels are expected to worsen the living conditions of these species and their ability to inhabit the protected area.

Air pollutants of various anthropogenic origins have an adverse effect on plant and animal life. These effects occur not only at high concentrations, but also at values close to or even below the maximum permissible concentrations. Phytotoxicity depends on many factors such as the type of plants, duration of exposure to pollutants, nature of pollutants, and others. As a result, a number of consequences are observed, such as disruption of normal metabolism, disruptions in the process of photosynthesis, and even death of plants and animals (Chuturkova, 2015).

CONCLUSIONS

The resulting exceedances have a negative impact on the health of the population. The increase in PM levels is expected to also affect the cultural, household, agricultural and other economic activities carried out. All this requires immediate measures to be taken to eliminate the sources of pollution and provide permanent control by the control bodies, aimed at achieving a good ecological status for PM10 and air quality in general.

The increase in PM10 levels is expected to worsen the living conditions of people, plants and animals (including those living in the vicinity of the protected area).

Particulate matter is a serious problem. To reduce the impact of this pollutant on atmospheric air, the following are necessary: modernization and quality maintenance of the road surface; control of construction activities; quality washing of road arteries; landscaping of open areas.

ACKNOWLEDGEMENTS

This research work was carried out with the support of University of Plovdiv „Paissii Hilendarski“, Agricultural University – Plovdiv and National Institute of Geophysics, Geodesy and Geography, Hydrology and Water Management Research Centre, Bulgarian Academy of Sciences, Sofia, Bulgaria.

REFERENCES

AAPL - Atmospheric Air Purity Law. (1996). *State Gazette* No. 45/28.05.1996, last amended and supplemented *State Gazette* No. 1/3.01.2019.

BDS EN 14211:2012. (2012, November 20). *Ambient air – Standard method for the measurement of the*

concentration of nitrogen dioxide and nitrogen monoxide by chemiluminescence.

BDS EN 14212:2012. (2012, November 20). *Ambient air – Standard method for the measurement of the concentration of sulphur dioxide by ultraviolet fluorescence.*

BDS EN 14625:2012. (2012, November 20). *Ambient air – Standard method for the measurement of the concentration of ozone by ultraviolet photometry.*

BDS EN 14626:2012. (2012, November 20). *Ambient air – Standard method for the measurement of the concentration of carbon monoxide by non-dispersive infrared spectroscopy.*

BDS EN 14662-3:2015. (2018, May 17). *Ambient air – Standard method for the measurement of benzene concentrations – Part 3: Automated pumped sampling with in situ gas chromatography.*

BDS EN 16450:2017. (2017, April 18). *Ambient air – Automated measuring systems for the measurement of the concentration of particulate matter (PM10; PM2.5).*

Biodiversity Law. (2002). *State Gazette* No. 77/9.08.2002, last amended and supplemented *State Gazette* No. 88/20.10.2023.

Biserkov, V., et al. (Eds.). (2015). *Red data book of the Republic of Bulgaria* (Vol. 3, Natural habitats). BAS & MEW.

Chaudhuri, S., & Roy, M. (2024). Global ambient air quality monitoring: Can mosses help? A systematic meta-analysis of literature about passive moss biomonitoring. *Environment, Development and Sustainability, 26,* 5735–5773. https://doi.org/10.1007/s10668-023-03043-0

Chuturkova, R. (2015). *Air pollution.* Technical University.

Directive (EU) 2016/2284 of the European Parliament and of the Council of 14 December 2016 on the reduction of national emissions of certain atmospheric pollutants, amending Directive 2003/35/EC and repealing Directive 2001/81/EC, 17.12.2016. *Official Journal of the European Union,* L 344/1.

Directive (EU) 2024/2881 of the European Parliament and of the Council of 23 October 2024 on ambient air quality and cleaner air for Europe, 20.11.2024. *Official Journal of the European Union,* L.

EAQI – European Air Quality Index. (2019, modified 2024, March 12). European Environment Agency. https://www.eea.europa.eu/en/analysis/maps-and-charts/index

EEA – European Environment Agency. (2024a). *Air pollution quick country facts.* https://www.eea.europa.eu/en/topics/in-depth/air-pollution/air-pollution-country-fact-sheets-2024/quick-country-facts

EEA – European Environment Agency. (2024b). *Health and environment impacts of air pollution exposure remain high across Europe* [Press release]. https://www.eea.europa.eu/en/newsroom/news/health-and-environment-impacts-of-air-pollution

Golemanski, V., et al. (Eds.). (2015). *Red data book of the Republic of Bulgaria* (Vol. 2, Animals). BAS & MEW.

Horn, S., & Dasgupta, P. (2024). The Air Quality Index (AQI) in historical and analytical perspective: A tutorial review. *Talanta, 267,* 125260. doi: 10.1016/j.talanta.2023.125260.

Impacts of air pollution on ecosystems in Europe. (2024, December 10; modified 2024, December 12). *European Environment Agency.* https://www.eea.europa.eu/en/analysis/publications/impacts-of-air-pollution-on-ecosystems-in-europe

Law of Health. (2005). *State Gazette* No. 70/10.08.2004, last amended and supplemented *State Gazette* No. 18/27.02.2018.

Law on Environmental Protection. (2002). *State Gazette* No. 91/25.09.2002, last amended and supplemented *State Gazette* No. 42/7.06.2022.

Lei, T., Xiang, W., Zhao, B., Hou, C., Ge, M., & Wang, W. (2024). Advances in analysis of atmospheric ultrafine particles and application in air quality, climate, and health research. *Science of the Total Environment, 949,* 175045. https://doi.org/10.1016/j.scitotenv.2024.175045

Ma, Y., Zhang, Y., & Song, L. (2025). Ecological and health risk assessment and anthropogenic sources analysis of heavy metals in different types of urban road dust. *Process Safety and Environmental Protection, 195,* 106813. https://doi.org/10.1016/j.psep.2025.106813.

Natura 2000. https://natura2000.egov.bg/EsriBg.Natura.Public.Web.App/Home/Map#

Nunez, Y., Benavides, J., Shearston, J., Krieger, E., Daouda, M., Henneman, L., McDuffie, E., Goldsmith, J., Casey, J., & Kioumourtzoglou, M. (2024). An environmental justice analysis of air pollution emissions in the United States from 1970 to 2010. *Nature Communications, 15(1),* 268. doi: 10.1038/s41467-023-43492-9.

Peev, D., et al. (Eds.). (2015). *Red book of the Republic of Bulgaria* (Vol. 1, Plants and fungi). BAS & MEW.

Regulation No. 12 of July 15 (2010). Standards for sulfur dioxide, nitrogen dioxide, fine dust particles, lead, benzene, carbon monoxide and ozone in atmospheric air. (2010). *State Gazette* No. 58/30.07.2010, amended and supplemented *State Gazette* No. 48/16.06.2017; No. 79/08.10.2019.

RIAA – Report on the Influence of the Atmospheric Air on the Health of the Population of "Plovdiv Agglomeration" in 2023. (2024). https://www.riokozpd.com/index/556-dokladi-vuzduh.html

RLTS – Red List of Threatened Species. (2025). *International Union for Conservation of Nature and Natural Resources.* https://www.iucnredlist.org

Sheikh, A. (2019). *Standards for Air Quality Indices in Different Countries (AQI).* https://atmotube.com/blog/standards-for-air-quality-indices-in-different-countries-aqi

World Health Organization. (2021). *WHO global air quality guidelines: Particulate matter (PM2.5 and PM10), ozone, nitrogen dioxide, sulphur dioxide and carbon monoxide (Executive summary).*

Scientific Papers. Series E. Land Reclamation, Earth Observation & Surveying, Environmental Engineering. Vol. XIV, 2025
Print ISSN 2285-6064, CD-ROM ISSN 2285-6072, Online ISSN 2393-5138, ISSN-L 2285-6064

ECOMONITORING STUDIES OF GROUNDWATER AND SOIL FOR POLLUTION WITH OIL AND PETROLEUM PRODUCTS

Georgi PATRONOV[1], Diana KIRIN[2, 3], Radoslava ZAHARIEVA[3], Petya ZAHARIEVA[3], Marian VARBANOV[3]

[1]University of Plovdiv "Paissii Hilendarski", Department of Chemical Technology, 24 Tsar Assen, Plovdiv, 4000, Bulgaria
[2]Agricultural University-Plovdiv, Department of Chemistry, Phytopharmacy and Ecology and Environmental Protection, 12 Mendeleev Blvd, Plovdiv, 4000, Bulgaria
[3]National Institute of Geophysics, Geodesy and Geography, Hydrology and Water Management Research Centre, Bulgarian Academy of Sciences, Acad. G. Bonchev Street, Sofia, 1113, Bulgaria

Corresponding author email: gipatronov@abv.bg

Abstract

The results of ecological monitoring studies of groundwater and soils in the region of the city of Plovdiv, East Aegean Basin, and Ecoregion 7 Eastern Balkans are presented. The studies were necessary as a result of the repair activities carried out on a damaged oil pipeline. The results obtained from the physicochemical monitoring of waters and soils are discussed (electrical conductivity, odour, turbidity, pH, colour, anthracene, aromatic hydrocarbons, acenaphthene, acenaphthylene, benzene, benz(a)pyrene, naphthalene, petroleum pyrene, polycyclic petroleum products, fluorene, fluoranthene, phenanthrene, chrysene), with the application of the existed standards. The exceedances of the monitored indicators of water quality for irrigation of crops, for the adjacent sources of surface water, and these oils are assessed. An ecological assessment of the studied groundwater and soils is presented. The health risks from using anthropogenically influenced groundwater and soils for plants, animals, and humans have been assessed. Measures to improve the ecological state have been identified.

Key words*: chemical state, ecological assessment, groundwater, health risk assessment, pollutions, soils.*

INTRODUCTION

Oil, or petroleum, is a mixture of gaseous, liquid and solid hydrocarbons of varying densities. Petroleum products are derived from crude oil (petroleum) (Walther & Otto, 2005). Oil spills result from the release of oil from tankers, oil platforms, drilling rigs and oil wells, as well as from refined petroleum products (gasoline, diesel) and their by-products (fuel oil). Spilled oil can affect animals and plants in two ways: directly through the oil spills and through the response to the clean-up process (Bautista & Rahman, 2016b; Sarbatly, 2016). There is no clear relationship between the amount of oil in the aquatic environment and the potential impact on biodiversity. A smaller spill in the wrong place or at the wrong season in a sensitive environment can be much more devastating than a larger spill at a different time of year, even in the same environment (Bautista & Rahman, 2016a). Animals can be poisoned or die from oil entering their lungs. Oil spills can degrade air quality (Middlebrook et al., 2011). The constituents of crude oil are mainly hydrocarbons, which contain toxic chemicals such as benzene, toluene, and polycyclic aromatic hydrocarbons (Tidwell et al., 2015). These chemicals have adverse effects when they enter the human body. They can be oxidized in the atmosphere and form fine particles (Li et al., 2013). Clean up and restoration also generates air pollutants, such as nitrogen oxides and ozone (Ehrenhauser et al., 2014; Nance et al., 2016). The impact of oil and oil products on aquatic systems can be expressed in the following directions: some substances dissolved in water are toxic, and their effect on organisms can be lethal; another part accumulates in the tissues and disrupts the physiological activity of organisms; leads to a change in the species composition of aquatic

communities because organisms adapt to oil pollution differently (Velev, 2015).

The study aims to present ecomonitoring results for contamination of anthracene, aromatic hydrocarbons, acenaphthene, acenaphthylene, benzene, benzo(α)pyrene, naphthalene, petroleum pyrene, polycyclic petroleum products, fluorene, fluoranthene, phenanthrene, chrysene, as well as the indicators electrical conductivity, odour, turbidity, pH, colour in groundwater and soil samples from the vicinity of the city of Plovdiv, Bulgaria, provoked by repair activities of a damaged oil pipeline.

MATERIALS AND METHODS

Twenty-three groundwater samples and four soil samples were tested near a damaged oil pipeline (Figure 1) during 2024. Groundwater samples were taken from a 9-10 m depth according to standard BSS ISO 5667-11:2011. Soil samples were taken from two depths: 0-10 cm and 10-20 cm, according to standard BSS ISO 18400-203:2020.

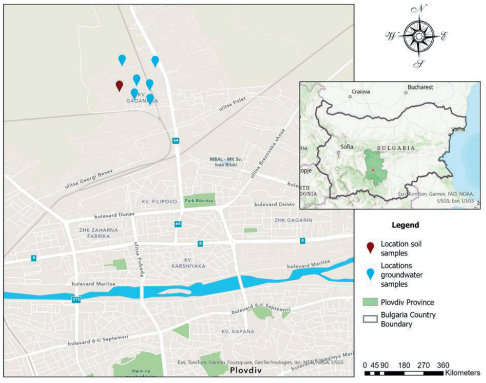


Figure 1. Spatial sampling locations

Chemical analyses were carried out in an accredited laboratory using approved standards: active reaction (pH) - BSS EN ISO 10523:2012; dissolved oxygen (mg/l) - BSS EN ISO 5814:2012; temperature (^{0}C) - BSS 17.1.4.01:1977; electrical conductivity (μS/cm) - BSS EN 27888:2000; petroleum products (μ/l) - BSS EN ISO 9377-2:2004; benzene (μ/l) - BSS EN ISO 15680:2004; benzo(α)pyrene, naphthalene, petroleum pyrene, polycyclic petroleum products, fluorene, fluoranthene, phenanthrene, chrysene - Internal laboratory methodology (ILM 1016/2010). Soil samples were tested for petroleum products according to BSS EN ISO 16703:2011. The results are statistically processed using MS Excel (Microsoft 2010).

RESULTS AND DISCUSSIONS

Chemical analyses were performed to determine the benzene, benzo(α)pyrene, petroleum products, anthracene, acenaphthene, acenaphthylene, naphthalene, pyrene, phenanthrene, fluoranthene, fluorene, chrysene content in the samples of groundwaters (Table 1).

Table 1. Contamination of the samples of groundwater

Pollutants	Mean ± SD (μg/l)
Benzene	79.17 ± 25.38
Benzo(α)pyrene	78.50 ± 6.36
Petroleum products	653.00 ± 386.35
Polycyclic aromatic hydrocarbons:	
Anthracene	0.22 ± 0.06
Acenaphthene	0.80 ± 0.44
Acenaphthylene	0.18 ± 0.07
Naphthalene	25.82 ± 22.24
Pyrene	0.19 ± 0.12
Phenanthrene	1.50 ± 1.73
Fluoranthene	0.17 ± 0.03
Fluorene	5.2 ± 1.19
Chrysene	0.11 ± 0.01

The ecological assessment of the impact of groundwater contaminated with oil and petroleum products on the health of humans, animals and plants is based on the provisions of the Water Directive (Directive 2000/60/EC), the Groundwater Directive (Directive 2006/118/EC), the Environmental Protection Act (EPA), the Water Law, the Health Law. The analysis of the results obtained from the study is based on specific standards regulated by Regulation No.1 of 10 October 2007 on the study, use and protection of groundwater; Regulation No.H-4 of 14 September 2012 on the characterization of surface waters; Regulation No.9 of 16 March 2001 on the quality of water intended for drinking and domestic purposes; Regulation No.8 of 27 May 2009 on the quality of waters for irrigation of crops; Regulation on environmental quality standards for priority substances and certain other pollutants (2010), etc.

Twenty-three groundwater samples were tested by Appendix No.1 of Regulation No.1 (2007)

for the study, use and protection of groundwater. The standards approved under the ordinance are: Benzene – 1.0 µg/l; Benzo(a)pyrene – 0.01 µg/l; Petroleum products – 50 µg/l; Polycyclic aromatic hydrocarbons – 0.10 µg/l.

According to Appendix No.1 to Regulation No.1 (2007) for the study, use and protection of groundwater, polycyclic hydrocarbons are defined as the sum of benzo(b) fluoranthene, benzo(k) fluoranthene, benzo(ghi)perylene and indeno(1,2,3-cd) pyrene, naphthalene, acenaphthene, fluorene, phenanthrene, acenaphthalene, anthracene, pyrene, fluoranthene, and chrysene are polycyclic aromatic hydrocarbons. Measurements on groundwater samples show contamination with petroleum products and related pollutants such as benzene and benzo(a)pyrene, representatives of polycyclic aromatic hydrocarbons.

The highest exceedances compared to the applicable standards were found for benzo(b)pyrene (7400-8300 times), followed by those for benzene (1.9-98 times) and petroleum products (1.7-19.9 times) (Table 2).

Table 2. Exceedance of standards under regulatory documents

Pollutants	Exceedances, Mean ± SD				
	1	2	3	4	5
Benzene	59.94 ± 41.56	55.35 ± 42.66	-	5.83 ± 10.65	1.78 ± 0.18
Benz(a)pyrene	7850 ± 636.39	7850 ± 636.39	-	289.21 ± 21.50	
Petroleum products	12.95 ± 7.63		1.12 - 3.32		
Polycyclic petroleum products				Anthracene 2.15 ± 0.64	

Legend: 1 - Regulation No.1(2007); 2 - Regulation No.9(2001); 3 - Regulation No.18(2009); 4 - Regulation (2010); 5 - Regulation H-4(2012).

The Health Law (2004) and Regulation No.9 (2001) on the quality of water intended for drinking and domestic purposes, promulgated to protect human health from the adverse effects of drinking water pollution, regulate requirements for the quality and safety of drinking water, as well as for improving access to water intended for drinking and domestic purposes. According to Regulation No.9, the maximum values for chemical water quality indicators for drinking and domestic water supply are (µg/l): benzene – 1.0; benzo(a)pyrene – 0.010; polycyclic aromatic hydrocarbons – 0.10 (as the sum of the concentrations of: benzo(b)fluoranthene; benzo(k)fluoranthene; benzo(ghi)perylene; indeno(1,2,3-cd)pyrene). Indicators with indicative significance are: pH ≥6.5≤9.5; Electrical conductivity – 2,000 µS.cm^{-1}; Odour – without significant fluctuations; Turbidity – without significant fluctuations; Colour – without significant fluctuations. The exceedances of the indicators from Regulation No. 9 are as follows: pH – 0.99 times; benzene – from 1.9 to 98 times; benzo(b)pyrene – from 7,400 to 97,400 times. A smell of petroleum products and a visible film were detected (Table 2). Based on these findings, the withdrawal of groundwater for drinking and domestic use is not permitted, regardless of whether wells are constructed for private or industrial purposes, as the studied groundwater poses a risk to human health if used for drinking or other domestic applications. At the same time, no pollutants were detected in the samples from the water supply network for drinking and domestic water supply.

Exceedances of the indicators in Regulation No.18 (2009) on the quality of water for irrigation of crops were established for petroleum products at the MPC of 0.3 mg/dm^3 (= 300 µg/l): from 1.12-3.32 times. Therefore, using water for irrigation of crops from the tested groundwater is unacceptable because it poses a risk to human health, cultivated crops, and animals. The Water Law carries out monitoring of irrigation water, Regulation No.5 (2007) on water monitoring, and Regulation No.18 (2009) on the quality of water for irrigation of crops.

The Regulation on Environmental Quality Standards for Priority Substances and Certain Other Pollutants establishes the environmental quality standards (EQS) for priority substances and certain other pollutants to achieve good chemical status of surface waters by the provisions and objectives of Chapter Ten, Section III of the Water Law (WL). According

to this regulation, the MPC (μg/l) in surface waters for some of the pollutants identified in groundwater from the studied sites are: benz(a)pyrene – 0.27; anthracene – 0.1; naphthalene – 130; fluoranthene – 0.12; benzene – 50. The tests carried out on groundwater samples showed excesses of benzene (from 1.5-30 times), benzo(α)pyrene (from 274-304.41 times), anthracene (from 1.7-2.6 times), and fluoranthene (1.42 times). Therefore, using tested groundwater is unacceptable because it poses a risk to humans, plants, and animals.

Regulation No.H-4 (2012) regulates the procedure and manner for the characterization, classification and presentation of the ecological status/potential of surface water bodies. According to this regulation, the SCC/MPC (μg/l) in surface waters, for comparison with some of the established pollutants in groundwater from the studied sites, are: acenaphthene – 3.8 SCC; 50 MAC; acenaphthylene – 0.64 SCC; fluorene – 3.1 SCC; phenanthrene – 1.3 SCC; pyrene – 0.012 SCC; chrysene – 0.02 SCC; benzene – 10 SCC; 50 MPC; Oil and oil products – without visible film on the surface and without odour. Exceedances of the standards set by Regulation H-4 were found in the tested groundwater samples for benzene (1.5-1.96 times), anthracene (1.7-2.6 times), and chrysene (5.5 times). The established exceedances and changes in the condition and quality of the analysed groundwater (smell of oil products; visible film) make the water abstraction and use of the tested groundwater inadmissible because they pose a risk to humans, animals and plants.

According to Regulation No.4 (2000) on the quality of waters for fish farming and shellfish breeding, the presence of oil products that form a film on the surface of the water or form deposits on the beds of river streams and lakes is not allowed, because they give a petroleum taste to fish and fish products and they have a harmful effect on fish. The deteriorated quality of groundwater affects the quality of surface waters when used to connect with surface waters. The tested soil samples did not show excesses in the oil products indicator. The reported amount is less than the detection limit according to the approved standard (below 15 $\mu g.kg^{-1}$ soil) and the requirements of Regulation No.3 (2008). Deterioration in the condition of terrestrial ecosystems is expected due to water abstraction and use of the studied groundwater, which is unacceptable because it poses a risk to the health of people, animals and plants.

The increase in oil production and its processing, its transportation through pipelines, accidental spills during its transportation, poor storage and manipulation lead to a number of environmental problems. Hydrocarbon pollution of the environment is a huge catastrophe for ecosystems because it leads to lethality and damage to flora and fauna for a long period. Oil and its derivatives penetrating the soil specifically impact the entire environment, the former communities and ecosystems. It has been established that the main reason for the delay in the development or death of plants is due to the deterioration of the water-physical properties of the soil, the blocking of nutrients (Crummer, 1964), the occurrence of oxygen starvation (Odu, 1972) and a complete disruption of biochemical processes (Gaydarova et al., 1990). The extracted groundwater contains oil and many salts (80-90%). Soil contamination occurs most often when corroded pipelines break, resulting oil and salt pollution. Drilling wells are located on vast areas, usually agricultural lands and pastures. The most intensive pollution is about 2.5 km from petrochemical and oil refining enterprises. With a distance of 6-10 km from the source, the content of pollutants decreases, but the range of soil pollution is not less than 20 km (Suleĭmanov et al., 1996).

Crop contamination occurs when groundwater containing petroleum products is used for irrigation. Soil contamination with petroleum products is not limited to the surface horizon. Infiltration is directly dependent on the current humidity. This rate decreases by 6 to 14 times at higher humidity compared to dry soil (Dimitrov et al., 1995). The properties of soils contaminated with petroleum and petroleum products change. Petroleum products are a permanent component of organic environmental pollution. Their presence in the soil significantly disrupts its water-physical, agrochemical and microbiological properties. The changes resulting from pollution with petroleum products are mainly associated with

the disruption of the water-air regime due to filling the pore spaces with petroleum products and the aggregation of soil particles. As a result, the oxidative conditions dominant before the contamination in the soil change to oxidative-reductive and reduction. The emergence of anaerobic conditions leads to the suppression of nitrification and the enhancement of ammonification. An accumulation of ammonia nitrogen of 20-40 $mg \cdot kg^{-1}$ occurs, and the content of nitrate nitrogen remains in traces. The amount of mobile phosphorus decreases (from 2 to 9 times), which is explained by the immobilization of inorganic phosphorus by microorganisms and phosphine formation. With very strong salinization, regardless of the pollution with petroleum products, the content of mobile phosphates can increase. Mineralization increases, and sulphate, chloride, calcium, magnesium, sodium, and potassium ions appear. The amount of trace elements increases - Mn (up to 4 times), Co, Mo, Cu, Zn, Pb, Ni (up to 2 times), the oxidation-reduction potential decreases (up to -340 mW) (Haziev et al., 1987; Gabbasova et al., 1997).

Oil and oil products have a toxic effect on soil microorganisms. Fungi are relatively resistant to pollution. Their resistance to higher concentrations of oil products and the increase in saprophytic fungi is related to the fact that the pH in some of the studied contaminated soils is in the acidic range, favouring fungi development. Fungi use the hydrocarbons as a source of "carbon" nutrition, and thanks to the high enzymatic activity, they decompose oil into low-molecular compounds quite quickly. Of the algae, the most resistant to oil pollution is blue-green algae. When components of oil pollutants penetrate the aquifer, specific microorganisms settle which are difficult to be purified. The number of one of the most important participants in soil-forming processes - the earthworm, decreases almost twice near the source of pollution (Molodova, 1978). Oil and petroleum products have a detrimental effect on the metabolism of plants, with some lighter fractions entering them directly (Markov, 2009).

CONCLUSIONS

The studied groundwater is significantly contaminated with petroleum products. Environmental monitoring studies show excess petroleum products and/or related indicators such as benzene, benzo(α)pyrene, and representatives of polycyclic aromatic hydrocarbons. According to environmental legislation, the excesses range from several times to tens and thousands of times as deviations from the standards. On this basis, water withdrawal and water use from the studied groundwater for personal or industrial purposes, drinking and domestic needs, water use for irrigation of crops and other needs is inadmissible because it poses a risk to people, plants and animals until their decontamination.

ACKNOWLEDGEMENTS

This research work was carried out with the support of Agricultural University – Plovdiv and National Institute of Geophysics, Geodesy and Geography, Hydrology and Water Management Research Centre, Bulgarian Academy of Sciences, Sofia, Bulgaria.

REFERENCES

Bautista, H., & Rahman, K. M. M. (2016a). Effects of Crude Oil Pollution in the Tropical Rainforest Biodiversity of Ecuadorian Amazon Region. *Journal of Biodiversity and Environmental Sciences*, *8*(2). 249–254.

Bautista, H., & Rahman, K. M. M. (2016b). Review on the Sundarbans Delta Oil Spill: Effects on Wildlife and Habitats. *International Research Journal*, 1(43) *2*. 93–96.

BSS ISO 5667-11:2011 Water quality - Sampling - Part 18: Guidance on sampling of groundwater at contaminated sites.

BSS ISO 18400-203:2020 Soil quality - Sampling - Part 203: Investigation of potentially contaminated sites.

BSS EN ISO 10523:2012. Water quality - Determination of pH.

BSS EN ISO 5814:2012. Water quality. Determination of dissolved oxygen. Electrochemical method with electrode.

BSS 17.1.4.01:1977. Nature conservation. Hydrosphere. Water quality indicators. Method for determining odour, colour and temperature.

BSS EN 27888:2000. Water quality - Determination of electrical conductivity.

BSS EN ISO 9377-2:2004. Water quality - Determination of hydrocarbon oil index - Part 2:

Method using solvent extraction and gas chromatography.

BSS EN ISO 15680:2004. Water quality - Gas-chromatographic determination of a number of monocyclic aromatic hydrocarbons, naphthalene and several chlorinated compounds using purge-and-trap and thermal desorption.

BSS EN ISO 16703:2011. Soil quality - Determination of content of hydrocarbon in the range C10 to C40 by gas chromatography.

Crummer, H. J. (1964). *Landwirtschaftliche Forschung*, *17*(4). 229.

Dimitrov, D. (1995). Project for a Technology for the Restoration of Contaminated Land after Pollution with Oil Products. *Report under contract with Neftochim EAD*, Burgas.

Directive 2000/60/EC. Water Framework Directive. https://eur-lex.europa.eu/legal-content/BG/TXT/PDF/?uri=CELEX:02000L0060-20141120&from=EN

Directive 2006/118/EC. Directive on the protection of groundwater against pollution and deterioration. https://eur-lex.europa.eu/legal-content/BG/ALL/?uri=celex:32006L0118

Ehrenhauser, Franz S., Avij, Paria, Shu, Xin, Dugas, Victoria, Woodson, Isaiah, Liyana-Arachchi, Thilanga, Zhang, Zenghui, Hung, Francisco R., Valsaraj, Kalliat T. (2014). Bubble bursting as an aerosol generation mechanism during an oil spill in the deep-sea environment: laboratory experimental demonstration of the transport pathway. *Environ. Sci.: Processes Impacts, 16*(1), 65-73, https://doi.org/10.1039/C3EM00390F

Environmental Protection Act (EPA). State Gazette, 91 of 25.09.2002 as amended and supplemented by State Gazette, 84 of 6.10.2023.

Gabbasova, I. M., Abrahamov, R. F., Khabirov, I. K., & Haziev, F. Kh. (1997). Changes in soil properties and composition of groundwater with oil and oilfield source waters in Bashkiria. *Soil Science*, *11*. 1362-1372.

Gaydarova, S., & Royachi, M. et al. (1990). Quality of the Danube River Waters in Connection with Irrigation. – In: *Collection of Proceedings on the Protection of the Cleanliness of the Danube River*. Symposium, October 19-20, 1990, Sofia.

Health Law. State Gazette, 70 of 10 August 2004 as amended and supplemented by SG, 39 of 01 May 2024.

Haziev, F. H., Tishkina, E., Kereeva, N. A., & Kuzyahmetov, G. G. (1987). Influence of oil pollution on some components of agroecosystems. *Agrochemistry*, *2*, 56-61.

Li, R., Palm, B.B., Borbon, A., Graus, M., Warneke, C., Ortega, A.M., Day, D.A., Brune, W.H., Jimenez, J.L., & de Gouw, J.A. (2013). Laboratory studies on secondary organic aerosol formation from crude oil vapours. *Environ Sci Technol*., *47*(21). 12566-74.

Markov, E. (2009). Soil pollution with oil and oil products, diagnostics and methods for their restoration. Review. *Ecology and the Future*, IX, 1. 9-18.

Middlebrook, A. M., Murphy, D. M., Ahmadov, R., Atlas, E. L., Bahreinia, R., Blake, D. R., Brioude, J., de Gouwa, J. A., Fehsenfeld, F. C., Frost, G. J., John, S., Holloway, S., Lack, D. A., Langridgea, J. M., Luebe, R. A., McKeen, S. A., Meaghera, J. F., Meinardid, S., J. Neuman, A., Nowak, J. B., Parrish D. D., Peischl, J., Perringa, A. E., Pollack, I. B., Roberts, J. M., Ryersona, T. B., Schwarza, J. P., J., Spackmana, R., Warnekea, C., & Ravishankara, A. R. (2011). Air quality implications of the Deep-water Horizon oil spill. *Proceedings of the National Academy of Sciences*, *109* (50). 20280-20285.

Molodova, L. P. (1978). Peculiarities of the distribution of soil mesofauna. *Oekologia*. 89-91.

Nance, E., King, D., Wright, B., & Bullard, R. D. (2016). Ambient air concentration succeeded health-based standards for fine particulate matter and benzene during the Deepwater Horizon oil spill. *Journal of the Air & Waste Management Association*, 66(2). 224-236.

Odu, C. J. (1972). *Inst. Pet*., 58. 204.

Regulation No.1 of 10 October 2007 year, for the study, use and protection of groundwater. State Gazette, 87, 2007, last amended and supplemented, State Gazette, 102, 2016.

Regulation No.3 of 1 August 2008 year for on the standards for the permissible content of harmful substances in soils. State Gazette, 71, 2008.

Regulation No.4 on the quality of waters for fish farming and shellfish breeding. State Gazette, 88, 27.10.2000.

Regulation No.5 on water monitoring. State Gazette, 44, 2007.

Regulation No.9 on the quality of water intended for drinking and domestic purposes. State Gazette, 30 of 2001; amended, 87 of 2007, amended and supplemented to 6, 2018.

Regulation No.18 of 27 May 2009 on the quality of water for irrigation of agricultural crops. State Gazette, 43 of 09 June 2009.

Regulation on environmental quality standards for priority substances and certain other pollutants (EQS). PMS No. 256 of 01 November 2010, State Gazette, 88, 09 November 2010, amended and supplemented to State Gazette, 97 of 11 December 2015.

Regulation No.H-4 of 14 September 2012 for surface water characterization. State Gazette, 22 of 05 March 2013 with amendment and addendum to State Gazette, 67 of 04 August 2023.

Sarbatly, R. A. (2016). Review of polymer nanofibers by electrospinning and their application in oil-water separation for cleaning up marine oil spills. *Marine Pollution Bulletin*, *106*. 8-16.

Suleĭmanov, R. A., Safonnikova, S. M., Yakhina, M. R., & Magzhanova, S. A. (1996). Influence of the petrochemical and oil refining industries on the sanitary condition of the soil cover. *Hygiene and sanitation*, *3*. 12-5.

Tidwell, L. G., Allan, S. E., O'Connel, S. G., Hobbie, K. A., Smith, B. W., & Anderson, K. A. (2015). Polycyclic Aromatic Hydrocarbon (PAH) and Oxygenated PAH (OPAH) Air-Water Exchange during the Deep-water Horizon Oil Spill. *Environmental Science & Technology*, *49*(1). 141–149.

Velev, S. (2015). Ecological security. Sofia, BG: Publishing House of the Military Academy "G. St. Rakovski".

Walther, W. I., & Otto, S. N. (2005). *Oil Refining in Ullmann's Encyclopaedia of Industrial Chemistry*, Weinheim, UK: Wiley-VCH.

Water Law. State Gazette, 67 of 27.07.1999 as amended and supplemented. to State Gazette, 41 of 10.05.2024.

Scientific Papers. Series E. Land Reclamation, Earth Observation & Surveying, Environmental Engineering. Vol. XIV, 2025
Print ISSN 2285-6064, CD-ROM ISSN 2285-6072, Online ISSN 2393-5138, ISSN-L 2285-6064

ANALYSIS OF GROUNDWATER RESOURCES IN STARA ZAGORA DISTRICT, BULGARIA: QUALITY AND ENVIRONMENTAL RISKS

Alexander PETROV[1], Svetla STOYKOVA[1], Diyana DERMENDZHIEVA[1], Gergana KOSTADINOVA[1], Milen STOYANOV[2], Georgi PETKOV[1], Stefka BOYANOVA[1], Georgi BEEV[1]

[1]Trakia University, Faculty of Agriculture, 6000, Stara Zagora, Bulgaria
[2]Trakia University, Medical College, 6000, Stara Zagora, Bulgaria

Corresponding author email: svetla.stoykova@trakia-uni.bg

Abstract

Groundwater, a vital resource in Bulgaria, is increasingly at risk of contamination from anthropogenic activities. A study in the Stara Zagora district for a year, situated in an area with strong anthropogenic pressure (urbanization, 4 TPPs, open-pit mining of lignite coal, large military training ground, intensive agriculture) assessed the groundwater quality of 6 wells (Ws) and 6 springs (Ss), based on 48 samples, analyzing 11 physicochemical (colour, taste, odour, pH, EC, TH, Cl^-, SO_4^{2-}, NH_4^+, NO_3^-, and OM) and 3 bacteriological (AMO, E.coli and Enterococci) parameters. The groundwater partly meets the Bulgarian standards as a natural resource (W1, W2 - summer, autumn and winter, W3 - summer and winter, S1, S2, S5 - autumn, and S6) and as a source for drinking (W1 and S2 - except for spring, W2 - except for spring and autumn, S1 and S6 - except for summer, autumn and winter). The deviation from the norms of groundwater as a natural resource results from pollution with NH_4^+, NO_3 and OM, and for drinking purposes: with E. coli, enterococci, AMO, OM, NH_4^+ and NO_3. Agriculture and livestock waste were identified as major pollution sources. Many positive and negative Pearson correlations existed between controlled groundwater parameters. Immediate treatment of contaminated Ws and Ss, and regular monitoring and health risk assessments are essential to mitigate groundwater pollution and ensure safe water for consumption.

Key words*: environmental risk, groundwater, physico-chemical and bacteriological parameters, quality assessment.*

INTRODUCTION

Water equals life. No living thing on the planet can exist without water. Among all living organisms in the world, humans use the most water. That's why water is a critical resource for people's life as it is used for various purposes – human consumption, industrial processes, agriculture, and recreation (Saadatpour et al., 2021; Nadjai et al., 2024). In the last decades, the quality of water has been impacted by contamination with a wide range of pollutants (Adimalla & Qian, 2019; Taloor et al., 2024). In addition, water will become increasingly scarce as a result of population growth, urbani-zation, anthropogenic activities and climate change (Nawaz et al., 2023; Abdessamed et al., 2023). Water scarcity in many parts of the world is a serious problem. Groundwater seems to be the potential natural resource capable to reverse this situation (Taloor et al., 2020). Due to unavailability or inadequate quality of surface water, demand for groundwater resources has increased over the years and in present days constitutes about 20% of the world's supply (Barakat et al., 2018; Jyothilekshmi et al., 2019). In many countries, groundwater is a major source of water for drinking, irrigation and industry, and its quality is very important regarding its safe use for all these purposes (Sharma et al., 2017; Singh et al., 2022; Kumar et al., 2024). The poor quality of potable water is responsible for 80% of water-borne diseases in the world (Malik et al., 2012). Water quality illustrates the physical, chemical and biological condition of water bodies, aiming to identify and address concerns through a comprehensive approach tailored to specific uses (Giri, 2021). Numerous studies revealed different aspects of the groundwater quality used for drinking purposes: physicochemical and microbial status of spring/well water (Giao et al., 2023; Devolli et al., 2024); physicochemical characterization of ground-water in urban areas (Wakode et al.,

2018; Ali et al., 2022; Subba et al., 2024); water quality and pollution sources in areas with mining activities (Mohammadpour et al., 2024), etc.

According to data from the EEA within the European Union (EU), 65% of water for drinking purposes and 25% for agricultural needs is provided by groundwater. At the same time, groundwater pollution and extraction is a serious threat to this resource: 24% of the total groundwater bodies are in poor chemical status and 9% - in poor quantitative status (EEA, 2023). A study of Sentek et al. (2024) shows that groundwater in the EU-27 is under significant pressure from excessive irrigation, industrial overexploitation, and a cocktail of pollutants, so that the resulting water scarcity is serious enough to affect livelihoods and even entire sectors.

Bulgaria has significant groundwater reserves, with a flow rate of about 193 millions m^3/year. In 2023, groundwater was 10.2% of the total amount of the extracted fresh water in the country (5336.1 million m^3), of which 79.3% were used for drinking, 14.2% for industry, 3.5% for agriculture and 2.9% for other purposes (National Statistical Institute, 2024). In the period 2003-2022, a gradual improvement in groundwater quality was observed for most of the analyzed indicators. Despite this positive trend, the main pollutants of groundwater with exceedance of the quality standards were nitrate (at 25% of all Monitoring points /MPs/) and partly sulfate, total Fe, Na and Mg (at 3.6-5% of MPs) (ExEA, 2024).

In some areas of Bulgaria, mainly semi-urban and rural, groundwater are single sources for water supply, especially in private farmyards and animal farms (Kostadinova, 2014). Usually, those sources are outside the National Monitoring System (NMS) and the lack of reliable information about the groundwater quality is a major concern. All the above have motivated conducting this study, aiming to assess the groundwater quality as a natural resource and for drinking purposes by physico-chemical and microbiological parameters from wells and springs out of the NMS in Stara Zagora district, exposed to strong anthropogenic pressure – urbanization, energetics, industry, transport and intensive agriculture.

MATERIALS AND METHODS

Study area

The study was conducted during the period July 2023 - June 2024 in Stara Zagora district, situated in South-Central Bulgaria (5.151 km^2), divided into 11 municipalities with 11 towns and 195 villages and population of 307,140 inhabitants (86 people/km^2). About 72% of the population lives in the cities, of which about 80% lives in the two largest cities – Stara Zagora (142,000) and Kazanlak (64,000) (National Statistical Institute, 2025). The region is characterized by a moderately continental climate (average annual maximum/minimum temperature +17.9°C and +8.0°C, respectively, average annual rainfall 598 mm), diverse and fertile soils, relatively good water resources and flat, hilly and low mountainous relief. Stara Zagora district is under strong anthropogenic pressure: the industry - the largest energy complex in the country Maritsa-Iztok (4 coal-fired Thermal Power Plants, 3400 MW, and open-pit mining of lignite coal) operates here as well as many other enterprises; transport - the region is an important road and railway center, connecting the eastern and western, northern and southern parts of Bulgaria; agriculture, characterized by intensive crop (mainly grain) and animal (milk, eggs and meat) production; in addition a large military training ground is also situated here (District administration - Stara Zagora, 2025). The region is rich in groundwater sources, with a significant portion of the population relying on groundwater for their daily needs. The depth of the aquifers varies from 30 to 200 m. Boreholes wells are a cost-effective and sustainable solution for accessing groundwater resources. They provide a reliable source of water for domestic, agricultural and industrial use (ExEA, 2024).

Monitoring Points

For the purpose of the study, 12 monitoring points (MPs), outside the National Monitoring System, covering 12 groundwater sources used for drinking purposes were selected: six open wells (Ws) and six springs (Ss), situated on the territory of Stara Zagora district (Table 1, Figure 1).

Table 1. Type, location and coordinates of underground water sources

No	Water source's location	Coordinates		a.s.l. (m)
		Latitude	Longitude	
A	*Wells (Ws)*			
1	W1	42.632	25.794	278
2	W2	42.382	25.432	349
3	W3	42.574	25.555	324
4	W4	42.299	25.937	111
5	W5	42.389	25.722	168
6	W6	42.401	25.652	174
B	*Springs (Ss)*			
1	S1	42.667	25.394	450
2	S2	42.671	25.787	354
3	S3	42.543	25.569	309
4	S4	42.489	25.689	334
5	S5	42.433	25.544	322
6	S6	42.381	25.540	280

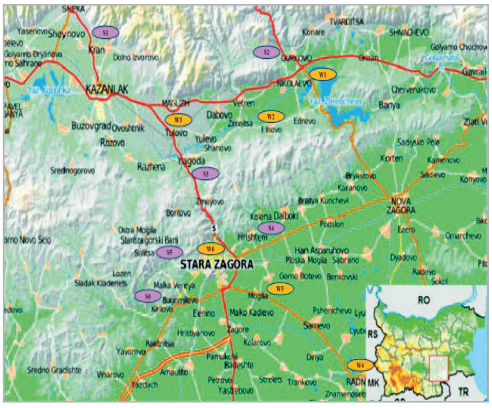


Figure 1. Map with monitoring points in Stara Zagora district, Bulgaria

Sampling and sample preparation

During the one-year monitoring period, groundwater samples were collected once in a season (March, June, September and December) from each MP, a total of 48 samples, including 24 samples from the wells and 24 samples from the springs. For water sampling and sample preparation for analyses, international references (ISO 5667-5, 11) were used. The samples for physicochemical analysis were collected in chemically clean polypropylene containers (1L) and for the microbiological analysis - in sterile glass containers (0.5L), transported in a cooler bag (2-5ºC), and processed for analysis within 2 hours after collection in the laboratories of the Environmental Center at Trakia University.

Physico-chemical parameters and analysis

All analyses were performed in triplicate. In the study, the following 11 physicochemical parameters were determined: colour, taste and odour (visual, organoleptic observation), pH and electrical conductivity (EC) - *in situ*, with portable Multi-340i/SET meter; the other parameters were analyzed in the laboratory: total hardness (TH) - titrimetrically, using standard EDTA, chloride (Cl^-) - by standard $AgNO_3$ titration (ISO 9297), sulfate (SO_4^{2-}) - by Bulgarian State Standard (BDS) 3588, ammonia (NH_4^+) - by BDS 3587 and nitrate (NO_3^-) - by BDS 3758, using UV-VIS Spectrophotometer JENWAY 6705, and oxidizability (organic matter, OM) - by titration method with $KMnO_4$.

Microbiological parameters and analysis

The bacteriological analyses included three microbiological parameters: total aerobic mesophilic bacteria (AMO) at 22°C - by ISO 6222, *Escherichia coli* - by ISO 9308-1 and enterococci - by ISO 7899-2. The total germs were counted after filtering the water using 0.45 µm pore size membranes, incorporated on selective chromogenic medium sheets (Rida® Count, R-Biopharm AG, Germany), and incubated at 22°C for 24 to 48 hours. The results are expressed in colony forming units (cfu/ml).

Assessment of groundwater quality

The assessment of groundwater quality from the monitored water bodies was conducted in two aspects:

a) the groundwater as a natural resource: the evaluation was based on eight physicochemical parameters (pH, EC, TH, Cl^-, SO_4^{2-}, NH_4^+, NO_3^-, and OM) as stipulated in Ordinance No. 1/2007. The chemical status of each groundwater body was classified as "good" if the parameter values were below the permissible limits, and "poor" if the values exceeded these limits. The overall ecological status of each water body was then determined by the lowest status recorded among the individual parameters assessed;

b) the groundwater as a source for drinking and domestic purposes by 14 parameters - 3 organoleptic (colour, taste and odour), 8 physicochemical (similar as in "a") and 3 microbiological (AMO, *E. coli* and Enterococci), according to Ordinance No. 9/2001.

Statistical analysis

All data ware analyzed by statistical software and data analysis tool XLSTAT, Version 2016.02, Addinsoft.

RESULTS AND DISCUSSIONS

Assessment of groundwater quality as a natural resource

The assessment was conducted using eight physicochemical parameters (Tables 2 and 3).

Among these, **pH**, which indicates the acidity or alkalinity of water, is a key parameter in groundwater quality assessment, as it influences the chemical and biological properties of groundwater. The pH values ranged between 6.89 and 8.22 and confirmed the results from previous studies that groundwater from wells/spring has natural or light alkalinity: 6.3-8.5 (Barakat et al., 2018, Ali et al., 2022, Abdessamed et al., 2023, Kumar et al., 2024). The coefficient of variation shows that pH is a conservative parameter with low variability - Cv = 2.41-3.47%. The same variation was reported by Nadjai et al. (2024), Cv = 2-5%.

Electrical Conductivity (EC) is an indicator of the total dissolved solids and salinity of the water. High salinity can affect the taste, sight, and smell of drinking water, and can worsen its quality. The EC values ranged between 382 and 5470 µS/cm for Ws, average 1487 µS/cm (Table 2), and within a much narrower range 298-910 µS/cm, average 627.4 µS/cm for Ss (Table 3). The coefficient of variation reflected those differences and demonstrated higher variability at Ws (Cv=88.8%) than at Ss (Cv=31.6%). The high EC values for Ws, except for W4 indicated high salinity and mineral content in groundwater with low runoff and high intensity of infiltration (Ravikumar & Somashekar, 2017).

Table 2. Physico-chemical and microbiological parameters of the wells (Ws) groundwater (n = 3)

MP*	Season	pH	EC, µS/cm	TH, mgeqv/l	Cl^-, mg/l	SO_4^{2-}, mg/l	NH_4^+, mg/l	NO_3^-, mg/l	OM, mg/l	AMO**, cfu/ml	*E.coli*, cfu/ml	*Ent.****, cfu/ml
W1	*Spring*	7.22	474	5.62	13.1	8.62	0.31	12.5	2.49	80	1	< 0.1
	Summer	7.46	718	5.11	14.2	8.20	0.08	13.1	2.30	< 0.1	< 0.1	< 0.1
	Autumn	7.91	478	2.49	11.7	8.36	0.06	11.3	3.31	2	< 0.1	< 0.1
	Winter	7.42	486	2.25	12.6	7.75	0.06	12.6	1.83	56	< 0.1	< 0.1
W2	*Spring*	7.19	1283	9.41	31.8	29.5	0.85	40.9	2.21	26	< 0.1	90
	Summer	7.21	1116	10.4	27.4	19.3	0.21	23.4	2.53	3	< 0.1	< 0.1
	Autumn	7.56	928	2.08	19.6	26.6	0.18	38.5	1.13	17	< 0.1	8
	Winter	7.27	1055	3.62	25.3	26.7	0.06	18.8	1.90	< 0.1	< 0.1	< 0.1
W3	*Spring*	7.40	388	5.88	11.6	7.84	1.33	42.4	1.28	210	5	45
	Summer	7.56	386	3.73	7.82	5.25	0.09	13.1	3.71	< 0.1	7	< 0.1
	Autumn	7.82	382	2.79	6.38	8.28	0.55	13.8	2.85	< 0.1	< 0.1	< 0.1
	Winter	7.63	392	1.83	10.4	8.42	0.37	28.4	3.93	90	< 0.1	192
W4	*Spring*	7.37	5470	38.0	398.5	394.2	1.85	96.1	2.31	267	< 0.1	50
	Summer	7.55	5180	27.3	269.6	385.5	3.82	511.8	7.35	100	103	208
	Autumn	8.18	4577	27.6	274.3	392.8	2.87	409.5	5.29	160	< 0.1	80
	Winter	7.47	3800	16.2	253.7	256.7	1.80	72.6	6.68	81	< 0.1	100
W5	*Spring*	7.59	513	3.75	10.6	15.7	0.92	48.8	2.31	5	1	3
	Summer	7.11	780	3.45	14.5	25.8	3.27	80.8	2.28	770	6	72
	Autumn	7.62	1243	2.66	43.0	28.5	1.03	43.3	0.81	4	< 0.1	2
	Winter	7.47	514	3.30	8.89	15.7	0.92	48.9	1.87	3	< 0.1	2
W6	*Spring*	7.41	1208	11.9	7.23	46.7	0.90	43.6	2.13	13	< 0.1	< 0.1
	Summer	7.17	1451	3.69	7.55	68.1	0.99	65.8	2.49	14	3	58
	Autumn	7.77	1406	2.67	7.37	59.6	0.92	48.7	2.06	30	< 0.1	2
	Winter	7.44	1452	3.09	7.73	64.9	0.70	45.5	1.48	76	1	4
Average (n=24) *Cv, %*		7.46± 0.18 *2.41*	1487± 1320 *88.8*	8.20± 8.28 *101.0*	62.3± 104.0 *167.0*	80.0± 112.1 *140.1*	1.00± 0.71 *71.0*	74.3± 48.1 *64.7*	2.77± 1.26 *45.8*	83.9± 90.9 *108.3*	5.41± 9.81 *181.3*	38.4± 50.5 *131.5*
***** Standards		6.5-9.5	2000	12	250	250	0.50	50	5.0	100/ml 22°C	0/100 ml	0/100 ml
			Meets the standard				*Deviation from the standard*					

*MP - Monitoring point; **AMO - Aerobic mesophilic microorganisms; ****Ent.* - Enterococci;
*****Ordinance No. 9/16.03.2001 (for drinking water - includes all tested parameters) and Ordinance No. 1/10.10.2007 (for groundwater as natural resource - includes only physicochemical parameters).

Table 3. Physico-chemical and microbiological parameters of the springs (Ss) groundwater (n = 3)

MP*	Season	pH	EC, µS/cm	TH, mgeqv/l	Cl^-, mg/l	SO_4^{2-}, mg/l	NH_4^+, mg/l	NO_3^-, mg/l	OM, mg/l	AMO**, cfu/ml	*E.coli*, cfu/ml	*Ent.****, cfu/ml
S1	*Spring*	7.15	304	4.56	10.6	12.7	0.17	8.98	1.75	< 0.1	< 0.1	< 0.1
	Summer	7.45	298	3.08	5.00	11.9	0.06	5.99	2.33	< 0.1	< 0.1	< 0.1
	Autumn	7.72	300	2.43	10.7	11.0	0.07	7.34	2.84	13	< 0.1	< 0.1
	Winter	7.31	306	3.06	11.9	9.64	0.12	5.52	2.14	< 0.1	< 0.1	< 0.1
S2	*Spring*	7.28	655	7.32	11.6	5.93	0.34	30.5	2.59	70	9	< 0.1
	Summer	7.26	645	5.11	6.33	5.25	0.16	24.9	2.87	1	< 0.1	< 0.1
	Autumn	7.91	421	1.86	3.97	3.38	0.23	33.5	2.90	13	< 0.1	< 0.1
	Winter	7.43	652	2.75	10.4	6.21	0.16	27.4	1.97	21	< 0.1	3
S3	*Spring*	7.63	844	3.34	47.0	26.8	0.55	19.7	2.52	< 0.1	< 0.1	< 0.1
	Summer	7.31	825	3.13	19.9	27.4	0.18	13.2	7.51	< 0.1	7	< 0.1
	Autumn	7.88	852	3.60	76.7	26.9	0.31	17.3	7.63	< 0.1	< 0.1	5
	Winter	7.72	849	2.91	35.4	27.5	0.14	18.6	5.67	< 0.1	< 0.1	< 0.1
S4	*Spring*	7.14	910	8.87	11.9	68.8	0.62	13.8	2.72	7	< 0.1	< 0.1
	Summer	6.89	768	2.76	16.6	52.1	1.48	18.5	6.37	< 0.1	< 0.1	< 0.1
	Autumn	7.99	452	3.54	8.23	53.2	1.13	33.6	3.41	60	50	118
	Winter	7.53	905	3.98	11.8	66.4	0.53	11.9	3.25	< 0.1	< 0.1	< 0.1
S5	*Spring*	7.28	693	5.70	25.1	49.1	0.50	49.9	1.81	67	6	100
	Summer	7.69	513	6.40	23.9	30.7	0.78	49.6	23.1	56	61	218
	Autumn	7.42	669	5.94	32.7	41.4	0.18	4.45	1.98	102	< 0.1	4
	Winter	7.43	693	5.36	25.8	46.5	0.50	48.1	1.85	109	< 0.1	52
S6	*Spring*	7.35	609	8.88	25.2	41.5	0.49	34.5	1.47	16	< 0.1	< 0.1
	Summer	7.34	762	7.60	3.99	51.2	0.33	36.4	2.58	8	< 0.1	4
	Autumn	8.22	366	2.39	8.63	56.3	0.32	41.0	4.23	26	< 0.1	3
	Winter	7.20	764	1.70	11.7	50.1	0.27	36.4	1.77	25	< 0.1	1
*****	Standards	6.5-9.5	2000	12	250	250	0.50	50	5.0	100/ml 22°C	0/100 ml	0/100 ml
			Meets the standard				*Deviation of the standard*					

*MP - Monitoring point; **AMO - Aerobic mesophilic microorganisms; ****Ent.* - Enterococci;
*****Ordinance No. 9/16.03.2001 (for drinking water - includes all tested parameters) and Ordinance No. 1/10.10.2007 (for groundwater as natural resource - includes only physicochemical parameters).

The low values for Ss could be related to high-elevation topography, high runoff, low infiltration, and recharge water type with low salt enrichment (Rao et al., 2012).

Previous studies also reported significant variation of that parameter: 220-8250 µs/cm, Cv = 35-51% (Barakat et al., 2018; Abdessamed et al., 2023; Kumar et al., 2024; Nadjai et al., 2024). The results obtained classified the ecological status of all tested groundwater as "good"; the exemption was W4, whose water's ecological status was determined as "bad".

TH in groundwater is computed as the total sum of Ca and Mg ion concentrations. The range of TH values in our study was between 1.83 and 38.0 mg/l, average 8.20 mg/l, Cv = 101.0% for Ws (Table 2), and between 1.83 and 8.88 mg/l, average 4.43 mg/l, Cv = 37.9% for Ss (Table 3). All concentrations were under the permissible level (<12 mg/l) according to the standard and classified the ecological status groundwater as "good"; the only exception was the W4, where concentrations were over the norm and determined the "bad" ecological status of water. In comparison to our results, other authors found higher levels of TH in groundwater: 90-940 mg/l (Barakat et al., 2018, Ali et al., 2022, Kumar et al., 2024), which is logical as the conditions of the studies were different than those in our study. **Chloride** is found in almost all-natural groundwater resources due to its high stability. The main sources of Cl^- include anthro-pogenic activities as well as leaching and weathering of different minerals. The chloride content imparts a salty taste to groundwater (Nag, 2009). The chloride concentration ranged from 6.38 to 398.5 mg/l for Ws (Table 2) and from 3.97 to 76.7 mg/l for Ss (Table 3). The coefficient of variation revealed a high variability of that parameter - Cv = 62.0-167.0% and indicated its sensibility to environmental factors.

The results obtained determine groundwater of all monitored water bodies as water in "good" ecological status (<250 mg/l) with one exception - W4, where Cl^- exceeded the norm in spring, summer, autumn and winter. Data from

previous studies also reveal a large variation in the groundwater chloride concentration from differ-rent sources: 9-2400 mg/l, Cv = 63-74% (Ali et al., 2022, Kumar et al., 2024; Subba et al., 2024; Nadjai et al., 2024).

Sulfate ions are a natural component of groundwater, as they are the result of diverse processes - dissolution and precipitation of minerals, wastewater penetration from diffuse sources, deposition from the atmosphere (SO_2, H_2SO_4, and sulfate), others; the main source of SO_4^{2-} in groundwater are metallic sulfides (Tiwari et al., 2016). The indicator values varied from 5.25 to 394.2 mg/l, average 80.0 mg/l, Cv = 140.1% for Ws, and from 3.8 to 68.8 mg/l, average 32.6 mg/l, Cv = 64.4% for Ss. All SO_4^{2-} concentrations from Ss, and those from W1, W2, W3, W5, and W6 met the requirements of the standard for "good" ecological status, while the W4 groundwater was determined in "bad" ecological status. Some authors reported SO_4^{2-} concentrations in ranges close to ours: 7-421 mg/l, Cv = 76-81% (Ali et al., 2022; Panneerselvam et al., 2023; Kumar et al., 2024; Subba et al., 2024).

The **ammonium** is a common contaminant in groundwater, in many cases as result of human activities, mostly from the application of fertilizers, disposal of manure, discharge of sewage and leakage from landfills. That's why the traceability of ammonium in groundwater is of great importance (Liang et al., 2022; Liu et al., 2023). The range of NH_4^+ in groundwater of both water source types was 0.06 to 3.82 mg/l. Under the permissible level, determining "good" ecological status of the water body were the NH_4^+ concentrations for W1, W2 (summer, autumn and winter), W3 (summer and winter), S1, S2, S3 (summer, autumn and winter), S5 (autumn) and S6; in all other cases groundwater status was "bad". Devolli et al. (2024) found lower concentrations of NH_4^+ in spring and well water than in our study - 0.03-0.48 mg/l.

Nitrates are a major groundwater pollutant, especially in areas with high levels of industrialization, agricultural activities, and urbanization. Nitrate fertilizers, which are water-soluble (e.g., urea, ammonium sulfate), easily leach into the groundwater system, leading to serious NO_3^- pollution (Adimalla & Qian, 2019); septic tanks and leaks from wastewater pipes are other anthropogenic sources of nitrate in groundwater (Pawar & Shaikh, 1995). The NO_3^- concentration in the study area ranged from 11.3 to 511.8 mg/l, average 74.3 mg/l, Cv = 64.7% for Ws and from 5.52 to 49.9 mg/l, average 24.7 mg/l, Cv = 58.7% for Ss. The measured levels determine a "good" ecological status for groundwater from all monitored water bodies; the exceptions were W4 and W5 (summer) which fell in the "bad" ecological status category. Comparable to our results were data reported by Barakat et al. (2018), Panneerselvam et al. (2023), Subba et al. (2024), and Nadjai et al. (2024), (0.12-280 mg/l, Cv = 92-167%).

OM is an indicator characterizing the groundwater quality. Dissolved OM in groundwater is generally low compared to inland surface waters, but even traces of OM can lead to insipid taste of water and promote bacterial growth (Prasad et al., 2023). The ecological impact of OM inputs does not solely depend on its quantity but also by form of the constituents - dissolved or bound (Harjung et al., 2923). OM levels were between 0.81 and 23.1 mg/l and classified groundwater from all water bodies in the "good" ecological status category; exceptions were W4 and S3 (summer, autumn, winter), and S4 and S5 (summer) where the ecological status of groundwater was "bad".

Based on the assessments of the different physicochemical parameters, the final assessment determined W1, W2 (summer, autumn and winter), W3 (summer and winter), S1, S2, S5 (autumn) and S6 in "good" ecological status, meeting the Bulgarian standard quality requirements for a natural resource (Ordinance No. 1/2007). In all other cases, the water bodies were classified as the "bad" ecological status category. The status of W4 was particularly worrying, as throughout the entire monitoring period the levels of the analyzed physico-chemical parameters (except for pH) exceeded the permissible levels (Table 2). The poor state of the groundwater can be explained with the water body location, characterized with many anthropogenic activities: close vicinity to a TPP (908 MW), lignite coalmine and slag heap; in addition, intensive agriculture, involving fertilization and irrigation, is practiced in the area. Obviously, those activities influence the groundwater quality and determine the *bad* ecological status of that natural resource. It is

necessary to conduct systematic monitoring of groundwater resources in order to identify the sources of pollution with a view to taking measures to improve the groundwater quality in the region.

Assessment of groundwater quality as a source for drinking purposes

The assessment was made by 14 physico-chemical and microbiological parameters as follows (Tables 2 and 3):

Physico-chemical parameters: The first group of those parameters included 3 organoleptic parameters - colour, taste and odour. By those parameters, all groundwater samples collected (total 48) met the requirements of the standard (Ordinance No. 9/2001), as they were "acceptable for users and without significant fluctuations from the usual for the indicator". The second group covered 8 parameters (pH, EC, TH, Cl^-, SO_4^{2-}, NH_4^+, NO_3^-, and OM), with permissible levels equal for both standards - for drinking water (Ordinance No. 9/2001), and for groundwater as a natural resource (Ordinance No. 1/2007). That's why, the assessments of the Ws and Ss as natural resources are also valid as sources of drinking water. Therefore, the groundwater resources in good ecological status can be used for drinking and conversely, the groundwater from water bodies in poor ecological status are not suitable for potable purposes (Tables 2 and 3).

Microbiological parameters: Microbes influence and often control geochemical processes and hence, are important to the quality of the natural water, they determine when the wells' clogging is a problem, and often whether anthropogenic chemicals (contaminants) disappear or persist in groundwater or not (Ferris, 2021). The quality assessment of the tested groundwater, made by three groups sanitary indicator microorganisms - Aerobic mesophilic microorganisms (AMO), *E. coli* and Enterococci, showed that the counts of all bacterial groups ranged within large limits: AMO - <0.1-770 cfu/ml, Cv = 108.3% for Ws, and <0.1-109 cfu/ml, Cv = 113.6% for Ss; *E. coli* - <0.1-103 cfu/ml, Cv = 181.3% for Ws, and <0.1-61 cfu/ml, Cv = 97.7% for Ss; enterococci - <0.1-208 cfu/ml, Cv = 131.5% for Ws, and <0.1 - 218 cfu/ml, Cv = 218.2% for Ss (Tables 2 and 3). Colony counts at 22ºC or AMO, provide a general idea of how contaminated the water is. Their presence in natural water can raise concerns regarding water quality and safety. *E. coli* and Enterococci indicate a fecal contamination of groundwater and the possible presence of disease-causing bacteria, viruses, and protozoa (Ateba & Maribeng, 2011; Tropea et al., 2021; Naily et al., 2023). Barakat et al. (2018) reported higher upper borders for *E. coli* (1-650 cfu/100 ml) and Enterococci (0-750 cfu/100 ml) for water from 8 springs in Morocco, while much lower variation for *E. coli* was established by Nawaz et al. (2023), 0-5 cfu/100 ml in groundwater from 10 different sites of Panjab city, Pakistan, and Devolli et al. (2024), 0-3 cfu/100 ml in groundwater form 7 wells in Albania. The established bacterial counts meet the requirements of the standard as follows: for AMO at W1, W2, W3 (except for spring), W4 (except for summer, autumn and winter), W6, S1, S2, S3, S4, S5 (except for autumn and winter), and S6; for *E. coli* at W1 and S2 (except for spring), W2, W3, W5 and S5 (except for spring and summer), W4, S3 and S4 (except for summer), W6 (except for summer and winter), S1 and S6, and for Enterococci at W1, W2 (except for spring and autumn), W3 (except for spring and winter), W4 (except for summer), W6 and S6 (except for summer, autumn and winter), S1, S2 (except for spring), S3 and S4 (except for autumn); in the other cases the quality of ground-water deviated from the norms for drinking water.

Considering that the final assessment of groundwater of the relevant water body is made based on the lower quality assessment for the tested physicochemical and microbiological parameters, it can be concluded that only groundwaters from W1 and S2 (except for spring), W2 (except for spring and autumn), S1 and S6 (except for summer, autumn and winter) meet the standard. In all other cases the groundwaters were not suitable for drinking. The most aggravating factor is the presence of *E. coli* and Enterococci and partly of AMO, OM, NH_4^+ and NO_3^- above the permissible limits. All these pollutants contribute to organic sources of pollution, most likely with wastewater from settlements and livestock farms, including farmyards in the villages. It is necessary to continue monitoring groundwater sources used for drinking purposes, aiming to develop

measures to eliminate or reduce organic/microbial contamination within the limits set by the standard.

Correlation analysis

The correlation matrices, calculated using Pearson correlation coefficients, revealed strong and moderate relationships (both positive and negative) among the investigated parameters for both types of groundwater sources (Tables 4 and 5).

In **wells**, significant correlations were identified between EC and TH, Cl^-, SO_4^{2-}, NH_4^+, NO_3^-, *E. coli*, and Enterococci; between TH and Cl^-, SO_4^{2-}, NH_4^+, NO_3^-, *E. coli*, and Enterococci; and between Cl^- and SO_4^{2-}, NH_4^+, NO_3^-, and Enterococci. Additional correlations were observed between SO_4^{2-} and NH_4^+, NO_3^-, *E. coli*, and Enterococci; between NH_4^+ and NO_3^-, AMO, *E. coli*, and Enterococci; as well as between NO_3^- and *E. coli* and Enterococci, and between *E. coli* and Enterococci, with correlation coefficients ranging from r = 0.40 to 0.99.

In **springs**, notable correlations included those between season and TH (r = -0.58); EC and Cl^- and SO_4^{2-}; SO_4^{2-} and NH_4^+; NH_4^+ and *E. coli* and Enterococci; NO_3^- and AMO, *E. coli*, and Enterococci; OM and *E. coli* and Enterococci; AMO and Enterococci; and *E. coli* and Enterococci, with correlation coefficients ranging from r = 0.44 to 0.90.

Table 4. Pearson correlation matrix for the open well's groundwater quality parameters

	Season	Ph	EC	TH	Cl^-	SO_4^{2-}	NH_4^+	NO_3^-	OM	AMO	*E.coli*	*Ent.*
Season	1.00											
pH	0.33	1.00										
EC	-0.07	0.18	1.00									
TH	-0.29	0.13	0.93	1.00								
Cl^-	-0.08	0.20	0.96	0.95	1.00							
SO_4^{2+}	-0.07	0.20	0.99	0.93	0.97	1.00						
NH_4^+	-0.18	0.07	0.70	0.63	0.64	0.72	1.00					
NO_3^-	-0.04	0.37	0.75	0.68	0.66	0.77	0.81	1.00				
OM	-0.17	-0.08	0.11	0.10	0.08	0.07	0.04	0.04	1.00			
AMO	-0.18	-0.27	0.18	0.21	0.22	0.20	0.63	0.20	-0.10	1.00		
E.coli	-0.13	0.02	0.48	0.40	0.37	0.52	0.60	0.75	0.09	0.07	1.00	
Ent.	0.03	0.03	0.51	0.44	0.48	0.54	0.62	0.61	0.30	0.29	0.60	1.00

Table 5. Pearson correlation matrix for the spring fountains groundwater quality parameters

	Season	pH	EC	TH	Cl^-	SO_4^{2-}	NH_4^+	NO_3^-	OM	AMO	*E.coli*	*Ent.*
Season	1.00											
pH	0.34	1.00										
EC	-0.03	-0.28	1.00									
TH	-0.58	-0.35	0.25	1.00								
Cl^-	-0.01	0.20	0.45	0.02	1.00							
SO_4^{2+}	0.02	-0.03	0.47	0.28	0.05	1.00						
NH_4^+	-0.20	-0.11	0.24	0.14	0.04	0.56	1.00					
NO_3^-	-0.05	0.21	0.06	0.22	-0.06	0.26	0.30	1.00				
OM	-0.04	0.21	0.03	0.05	0.24	0.01	0.30	0.26	1.00			
AMO	0.07	0.07	-0.04	0.31	0.05	0.20	0.16	0.48	0.04	1.00		
E.coli	-0.08	0.30	-0.18	0.13	-0.04	0.10	0.47	0.40	0.70	0.34	1.00	
Ent.	0.08	0.23	-0.14	0.19	0.05	0.18	0.44	0.58	0.70	0.48	0.90	1.00

There was overlap in certain correlations observed in both types of water bodies; for example, correlations were found between EC and Cl^- and SO_4^{2-}, as well as between NH_4^+ and NO_3^-, *E. coli*, and Enterococci, and between *E. coli* and Enterococci. However, notable differences were also identified. Some correlations observed in wells were not present in springs (e.g., TH with Cl^- and SO_4^{2-}; Cl^- with SO_4^{2-}; NH_4^+ with NO_3^-), while certain correlations present in springs were absent in wells (e.g., OM with *E. coli* and Enterococci; NO_3^- with AMO, *E. coli*, and Enterococci; AMO with Enterococci). Previous studies have also reported significant correlations among several monitored parameters, consistent with the findings of our study. For example, correlations between TH and NO_3^- and Cl^- have been reported by Ali et al. (2022); between EC and TH and SO_4^{2-}, and between TH and Cl^- and SO_4^{2-} by Abdessamed et al. (2023); and between EC and Cl^-, NH_4^+, and NO_3^-, as well as between

TH and Cl^-, NH_4^+, and NO_3^-, by Shrestha et al. (2023). Additionally, Giao et al. (2023) observed a correlation between NO_3^- and TH.

Several of the correlations identified in our study are logical and causally linked. For example, the correlations between EC and TH, Cl^-, and SO_4^{2-} can be attributed to the fact that higher EC reflects higher levels of dissolved salts in water, which correspond to increased concentrations of Ca^{2+}, Mg^{2+}, chloride, and sulfate (Schubert et al., 2024). Similarly, correlations between NH_4^+ and NO_3^- and AMO, *E. coli*, and Enterococci are expected, as nitrogen is an essential element for microbial growth, and higher nitrogen concentrations can support increased microbial populations (Mattoo & Suman, 2023). The correlation between NH_4^+ and NO_3^- is consistent with the nitrification process, in which ammonium is oxidized to nitrite and subsequently to nitrate, leading to higher NO_3^- concentrations in the presence of elevated NH_4^+ levels (Mattoo & Suman, 2023). Additionally, correlations between OM and *E. coli* and Enterococci are expected, as higher organic matter concentrations provide a substrate for microbial growth, resulting in increased microbial counts (Harjung et al., 2023). The correlation between *E. coli* and Enterococci is also logical, as both bacteria are indicators of fecal contamination, and their concentrations typically correspond in contaminated water sources (Wang et al., 2013). However, some observed correlations, such as those between TH and Cl^- and SO_4^{2-}, Cl^- and SO_4^{2-}, NH_4^+, NO_3^-, and Enterococci, EC and Cl^- and SO_4^{2-}, and SO_4^{2-} and NH_4^+, are more difficult to interpret. Further targeted research is needed to confirm or clarify the underlying mechanisms of these associations.

CONCLUSIONS

This study assessed the quality of groundwater from six wells (Ws) and six springs (Ss) in the Stara Zagora region, an area characterized by strong anthropogenic pressure, including high levels of urbanization, four thermal power plants (3400 MW), a large lignite coal mine, a military training ground, and intensive agriculture. The evaluation was conducted using 11 physicochemical parameters (colour, taste, odour, pH, EC, TH, Cl^-, SO_4^{2-}, NH_4^+, NO_3^-, and OM) and three microbiological parameters (AMO, *E. coli*, and Enterococci), considering groundwater both as a natural resource and as a source for drinking water.

The findings indicate that:

(i) Groundwater met the Bulgarian standards for ecological status (as a natural resource) based on pH, EC, TH, Cl^-, SO_4^{2-}, NH_4^+, NO_3^-, and OM in W1, W2 (summer, autumn, and winter), W3 (summer and winter), and in S1, S2, S5 (autumn), and S6. In all other cases, groundwater exhibited poor ecological status, with NH_4^+ identified as the main pollutant, followed by NO_3^- and OM.

(ii) Groundwater met the Bulgarian standards for drinking water for all tested parameters in W1 and S2 (except in spring), in W2 (except in spring and autumn), and in S1 and S6 (except in summer, autumn, and winter). Deviations from the standards in other cases were primarily due to contamination with *E. coli* and Enterococci, and to a lesser extent with AMO, OM, NH_4^+, and NO_3^-.

(iii) Numerous significant positive and negative Pearson correlations were identified among the monitored groundwater parameters, with 28 correlations observed in wells and 13 in springs.

AKNOWLEDGEMENTS

This paper was supported by the National Program of the Ministry of Education and Science “Young Scientists and Postdoctoral Students-2”.

REFERENCES

Abdessamed, D., Jodar-Abellan, A., Ghoneim, S.M.S., Almaliki, A., Hussein, E.E., & Pardo, M.A. (2023). Groundwater quality assessment for sustainable human consumption in arid areas based on GIS and water quality index in the watershed of Ain Sefra (SW of Algeria). *Environmental Earth Sciences*, 82, 510.

Adimalla, N., & Qian, H. (2019). Groundwater quality evaluation using water quality index (WQI) for drinking purposes and human health risk (HHR) assessment in an agricultural region of Nanganur, South India. *Ecotoxicol. Environ. Saf.*, 176, 153-61.

Ali, S., Deolia, R.K., Singh, S., Ali, H., Akhtar, M., & Islam R. (2022). Physico-chemical characterization of ground-water in terms of Water Quality Index (WQI) for urban areas of Agra, North India. *Applied Ecology and Environmental Sciences*, 10(6), 409-416.

Ateba, C.N., & Maribeng, M.D. (2011). Detection of Ente-rococcus species in groundwater from some rural

commu-nities in the Mmabatho area, South Africa: A risk analysis. *African J. of Microbiol. and Research.*, 5(23), 3930-3935.

Barakat, A., Redouane Meddah, R., Afdali, M., & Touhami, F. (2018). Physicochemical and microbial assessment of spring water quality for drinking supply in Piedmont of Béni-Mellal Atlas (Morocco). *Physics and Chemistry of the Earth*, 104, 39-46.

Devolli, A., Shahinasi, E., Sallaku, E., Osmani, M., Hoxha, B., & Dara, F., (2024). Assessment of physicochemical and bacteriological quality of well water used for drinking and domestic purposes in an industrial area of Elbasan district, Albania. Scientific Papers. Series E. *Land Reclamation, Earth Observation & Surveying, Environmental Engineering*, 13.

District administration - Stara Zagora, (2025). Available online: https://www.sz.government.bg/district-stara-zagora

Executive Environment Agency (ExEA), Bulgaria, (2024). National report on the state and protection of the environment in the Republic of Bulgaria - 2024 (in Bulgarian). Available online: https://eea.government.bg/bg/dokladi/Greenbook_2024.pdf

European Environment Agency (EEA), (2023). Europe's groundwater - a key resource under pressure. Published 22 Mar 2022, Last modified 19 Jul 2023. Available online: https://www.eea.europa.eu/publications/europes-groundwater

Ferris, F.G., Szponar, N., & Edwards, B.A., (2021). Ground-water Microbiology. *The Groundwater Project*, Guelph, Ontario, Canada, 66.

Giao, N.T., Nhien, H.T.H., Anh, P.K., & Thuptimdang, P., (2023). Groundwater quality assessment for drinking purposes: a case study in the Mekong Delta, Vietnam. *Scientific Reports*, 13, 4380.

Giri, S., (2021). Water quality prospective in Twenty First Century: Status of water quality in in major river basins, contemporary strategies and impediments: A review. *Environ. Pollut*., 271, 116332.

Harjung, A., Schweichhart, J., Rasch, G., & Griebler, C., (2023). Large-scale study on groundwater dissolved organic matter reveals a strong heterogeneity and a complex microbial footprint. *Science of the Total Environment*, 854, 158542.

Jyothilekshmi, S., Sajan, S., Anjali, P., Yadhu Krishnan, R., Kumar, A., Sudhakaran, R., Franklin, N., & Chandran, R.P. (2019). Physicochemical and microbio-logical analysis of well water samples collected from North of Punnapra village, Alappuzha district, Kerala state, India. *Int. J. Adv. Res. Biol. Sci*., 6(6), 104-113.

Kostadinova, G. (2014). Assessment of underground water quality from wells used for irrigation and livestock. *Journal of Balkan Ecology*, 17(2), 181-194.

Kumar, R., Sharma, S., & Prashant, M., (2024). Assessment of groundwater quality for drinking, irrigation and industrial purposes in Aik Watershed, Jammu and Kashmir, India. *Discover Geoscience*, 2, 58.

Liang, Y., Ma, R., Nghiem, A., Xu, J., Tang, L., Wei, W., Prommer, H., & Gan, Y. (2022). Sources of ammonium enriched in groundwater in the central Yangtze River Basin: Anthropogenic or geogenic? *Environmental Pollution*, 306, 119463.

Liu J., Yuan J., Yilong Zhang Y., Zhang, H., Luo, Y., & Su, Y. (2023). Identification of ammonium source for groundwater in the piedmont zone with strong runoff of the Hohhot Basin based on nitrogen isotope. *Science of the Total Environment*, 882, 163650.

Malik, A., Yasar, A., Tabinda, A.B., & Abubakar, M., (2012). Water-borne diseases, cost of illness and willingness to pay for diseases interventions in rural communities of developing countries, *Iran. J. Public Health*, 41, 39-49.

Mohammadpour, A., Gharehchahi, E., Gharehchahi, M.A., Shahsavani, E., Golaki, M., Berndtsson, R., Mousavi Khaneghah, A., Hashemi, H., & Abolfathi, S. (2024). Assessment of drinking water quality and identifying pollution sources in a chromite mining region. *J. of Hazardous Materials* 480, 136050.

Mattoo, R., Suman, B.M., (2023). Microbial roles in the terrestrial and aquatic nitrogen cycle-implications in climate change. *FEMS Microbiology Letters*, 370, 1-10.

Nadjai, S., Bouderbala, A., Khammar, H., Nabed, A.N., & Benaabidate, L. (2024). Assessment of groundwater suitability for drinking and irrigation purposes in the middle Cheliff Aquifer, Algeria. *Desalination and Water Treatment*, 319, 100528.

Nag, S.K., (2009). Quality of groundwater in parts of ARSA block, Purulia District. *West Bengal Bhu-Jal*., 4(1), 58-64.

Naily, W., Sunardi, S., Asdak, C., Dida, E.N., Hendarmawan, H., (2023). Distribution of *Escherichia coli* and coliform in groundwater at Leuwigajah and Pasirkoja Areas, West Java, Indonesia. *IOP Conf. Ser.: Earth Environ. Sci*., 1201, 012105.

National Statistical Institute (NSI), (2024). Water statistics (in Bulgarian). Available online: https://www.nsi.bg/bg/content/2602/

National Statistical Institute (NSI), (2025). Population by districts, municipalities, place of residence and gender (in Bulgarian). Available online: https://www.nsi.bg/bg

Nawaz, R., Nasim, I., Irfan, A., Islam, A., Naeem, A., Ghani, N., Irshad, M.A., Latif, M., Un Nisa, B., Ullah, R., (2023). Water quality index and human health risk assessment of drinking wa-ter in selected urban areas of a mega city. *Toxics*, 11, 577.

Ordinance No. 9/16.03.2001 for water quality, intended for drinking and household purposes. Official Gazette (OG) No. 30/28.03.2001, last amendment OG No. 43/16.05.2023 (in Bulgarian). Available online: https://lex.bg/laws/ldoc/-549175806

Ordinance No. 1/10.10.2007 on the research, use and protection of groundwater. OG No. 87/30.10.2007, last amendment OG No. 102/23.12.2016 (in Bulgarian). Available online: https://lex.bg/laws/ldoc/2135569070

Panneerselvam, B., Ravichandran, N., Kaliyappan, Karuppannan, S., & Bidorn, B. (2023). Quality and health risk assessment of ground-water for drinking

and irrigation purpose in semi-arid region of India using entropy water quality and statistical techniques. *Water*, 15, 601.

Pawar, N.A., & Shaikh, I.J., (1995). Nitrate pollution of ground waters from shallow basaltic aquifers, Deccan Trap Hydrologic Province, India. *Environ. Geol*., 25(3), 197-204.

Prasad, G., Ramesh, M.V., Siddik, A.M., Ramesh, T., & Thomas, G.M. (2023). Changing profile of natural organic matter in groundwater of a Ramsar site in Kerala implications for sustainability. *Case Studies in Chemical and Environmental Engineering*, 8, 100390.

Rao, S.N., Rao, S.P., Reddy, V.G., Nagamani, M., Vidyasagar, G., & Satyanarayana, N.L.V.V. (2012). Chemical characteristics of groundwater and assessment of groundwater quality in Varaha river basin, Visakhapatnam District, Andhra Pradesh, India. *Environ. Monit. Assess*., 184, 5189-214.

Ravikumar, P., & Somashekar, R.K., (2017). Principal component analysis and hydrochemical facies characterrization to evaluate groundwater quality in Varahi River basin, Karnataka state, India. *Appl. Water Sci*., 7(2), 745–55.

Saadatpour, M., Javaheri, S., Afshar, A., & Solis, S.S., (2021). Optimization of selective withdrawal systems in hydropower reservoir considering water quality and quantity aspects. *Expert Syst. Appl*., 184, 115474.

Schubert, L., Harrison, J., Kent-Buchanan, L., Bonds, V., McElmurry, S.P., & Love, N.G. (2024). A point-of-use drinking water quality dataset from feldwork in Detroit, Michigan. *Scientific Data*, 11, 443.

Sentek, Z., Jelena Prtorić, J., & Sarah Pilz, S., (2024). Unred the surface – The hidden crisis in Eurppe's groundwater. EEA, 15 May 2024.

Sharma, D.A., Rishi, M.S., & Keesari, T., (2017). Evaluation of groundwater quality and suitability for irrigation and drinking purposes in southwest Punjab, India using hydro-chemical approach. *Appl. Water Sci.*, 7, 3137-3150.

Shrestha, S., Bista, S., Byanjankar, N., Joshi, D.R., & Joshi, P.T. (2023). Groundwater quality evaluation for drinking purpose using water quality index in Kathmandu Valley, Nepal. *Water Science*, 37, 1, 239-250.

Singh, S., Gautam, P.K., Sarkar, T., & Taloor, A.K. (2022). Characterization of the groundwater quality in Udham Singh Nagar of Kumaun Himalaya, Uttarakhand. *Environ. Earth Sci.*, 81, 468.

Subba, R.N., Das, R., Sahoo, H.K., & Gugulothu, S., (2024). Hdrochemical characterization and water quality perspectives for groundwater management for urban development. *Groundwater for Sustainable Development*, 24, 101071.

Taloor, A.K., Pir, R.A., Adimalla, N., Ali, S., Manhas, D.S., Roy, S., & Singh, A.K. (2020). Spring water quality and discharge assessment in the Basantar watershed of Jammu Himalaya using geographic information system (GIS) and water quality Index (WQI), *Groundwater for Sustainable Development*, 10, 100364.

Taloor, A.K., Sharma, S., Suryakiran, S., Sharma, R., Sharma, M., (2024). Groundwater contamination and health risk assessment in Indian subcontinent: A geospatial approach. *Current Opinion in Environmental Science & Health*, 39, 100555.

Tiwari, A.K., Singh, P.K., & Mahato, M.K., (2016). Hydro-geochemical investigation and qualitative assessment of surface water resources in West Bokarocoalfield, India. *J. Geol. Soc. India*, 87, 85–96.

Tropea, E., Hynds, P., McDermott, K., Brown, R.S., & Majury A. (2021). Environmental adaptation of *E. coli* within private groundwater sources in southeastern Ontario: Implications for groundwater quality monitoring and human health. *Environmental Pollution*, 285, 117263.

Wakode, H.B., Baier, K., Jha, R., & Azzam, R. (2018). Impact of urbanization on groundwater recharge and urban water balance for the city of Hyderabad, India. *Intern. Soil and Water Conservation Research*, 6, 51-62.

Wang, D., Farnleitner, A.H., Field, K.G., Field, K.G., Green, H.C., Shanks, O.C., & Boehm, A.B. (2013). *Enterococcus* and *Escherichia coli* fecal source apportionment with microbial source tracking genetic markers – Is it feasible? *Water Research*, 47, 18, 6849-6861.

Scientific Papers. Series E. Land Reclamation, Earth Observation & Surveying, Environmental Engineering. Vol. XIV, 2025
Print ISSN 2285-6064, CD-ROM ISSN 2285-6072, Online ISSN 2393-5138, ISSN-L 2285-6064

ASSESSMENT OF SOIL CONTAMINATION BY POLYCYCLIC AROMATIC HYDROCARBONS (PAHs) IN BUCHAREST: SOURCES AND DISTRIBUTION

Mihaela PREDA, Veronica TĂNASE, Nicoleta Olimpia VRÎNCEANU, Florența JAFRI, Mihaela COSTEA, Bogdan-Ștefan OPREA

Research and Development Institute for Soil Science, Agrochemistry and Environmental, 61 Mărăşti Blvd, District 1, Bucharest, Romania

Corresponding author email: cosmihaela96@gmail.com

Abstract

Polycyclic aromatic hydrocarbons (PAHs) are organic pollutants composed of two or more aromatic rings of carbon and hydrogen atoms. PAHs are characterized by low water solubility, low vapor pressure, high melting and boiling points. As the molecular mass increases, the lipophilic character increases, making them more persistent in the environment. Incomplete combustion is the main source of PAHs. This study evaluates PAHs contamination in soil samples collected from 30 locations in Bucharest, focusing on potential pollution sources such as industrial activities, vehicular emissions, and domestic sources. Industrial zones and high-traffic areas recorded the highest total PAH concentrations at 1.06 mg/kg and 1.01 mg/kg, respectively. Diagnostic ratios analysis suggests combustion as the predominant source of PAHs.

Key words*: diagnostic ratios, PAHs, soil pollution, urban contamination.*

INTRODUCTION

Polycyclic aromatic hydrocarbons (PAHs) are widespread environmental pollutants consisting of two or more benzene rings arranged in linear, clustered, or angular formations (Arey & Atkinson, 2003). They have low solubility in water, low vapor pressure, and high melting and boiling points. As their molecular weight increases, their lipophilic nature intensifies, making them more resistant to degradation (Lee & Vu, 2010).

PAHs are found in terrestrial, aquatic, and atmospheric environments (Adeniji et al., 2019). In soils and sediments, PAHs accumulate due to their lipophilic properties, binding strongly to soil particles, which serve as reservoirs for these compounds (Kuppusamy et al., 2017).

Many PAHs are mutagenic, carcinogenic, teratogenic, immunotoxic for living organisms, including microorganisms, mammals and humans (Bolden et al., 2017). Benzo(a)pyrene is considered one of the most carcinogenic PAHs and generally used as an exposure marker for risk assessments (Lee & Vu, 2010).

In 1983, the US Environmental Protection Agency (USEPA) designated 16 polycyclic aromatic hydrocarbons (PAHs) as priority pollutants, due to their high environmental concentrations, their recalcitrant nature and toxicity (Deziel et al., 2014). PAHs can be divided into two groups according to their properties and molecular weights: low molecular weight (LMW-PAHs) which have two or three aromatic rings and high molecular weight (HMW-PAHs) with four to six aromatic rings (Jia et al., 2021).

LMW-PAHs typically form during incomplete combustion of organic matter, such as in vehicle exhaust, industrial emissions, and biomass burning. Their appearance is linked to low temperatures.

HMW-PAHs tend to form in more complex combustion conditions, at high temperature as in coal or oil burning, and they are found in higher concentrations in soot (Wang et al., 2013).

Sources of PAHs are classified as either anthropogenic or natural. Some PAHs are produced by natural processes such as volcanic eruptions, vegetation fires or pyrolysis of organic matter in geological processes.

While natural sources contribute minimally to overall PAH emissions, anthropogenic sources dominate. So, anthropogenic sources are considered the main cause of pollution with these compounds and can be divided into

industrial, vehicular, domestic and agricultural activities (Ravindra et al., 2008).

The most common anthropogenic sources are:

- Industrial sources when incomplete combustion, the main source of PAHs pollution can appear:
  - waste incineration,
  - iron and steel production, aluminum production, cement production, tar, asphalt, rubber production;
  - coke oven emissions, and petroleum refining (Mojiri et al., 2019);
  - paint and pigment production;
  - insecticide and fungicide production;
  - energy production (Srogi, 2007).
- Vehicular sources represented by gases from aircraft, boats, trains, vehicles (Ravindra et al., 2008)
- Domestic sources: household activities such as burning waste, burning wood or coal for heating (Gupte et al., 2016).
- Agricultural sources: burning of plant residues left after harvesting (Ravindra et al., 2008).

The aim of this study is to assess PAHs contamination in Bucharest soils, identify major pollution sources, and analyse the impact of different environmental factors on PAH distribution.

MATERIALS AND METHODS

Soil sampling

A total of sixty topsoil samples were collected from depths of 0-10 cm and 10-20 cm across 30 locations in Bucharest and its surrounding areas, including Chitila, Jilava, and Popești-Leordeni. These sites were selected to target various pollution sources, such as industrial zones, high-traffic areas, and residential neighborhoods.

The industrial sites, represented by sampling points S1, S2, S10, S12-S19, S21, S23, S24, S26 and S27, cover a range of facilities including paint factories, concrete factories, incinerators, rubber manufacturing units, a power station, pharmaceutical plants, an emulsion station, as well as the IMGB and Faur-Laminorului industrial platforms.

High traffic areas are covered by sampling points S4, S5, S6, S8, S9, S11, S25 and S28, where vehicle emissions are a significant source of pollution. In addition, the Ruteni and Vidra landfill sites are designated as sampling points S3 and S22, respectively. Residential areas and urban green spaces were also considered, with sampling points S20 and S7 representing these environments.

All sampling sites were georeferenced using GPS for accurate spatial analysis (Figure 1).

Samples were collected in March when air temperatures averaged 15°C.

Each sample was a composite of five subsamples taken from the four corners and the centre of a 5 × 5 m² plot.

The samples were placed in glass containers, shielded from light, and stored under refrigeration until analysis. In proximity to potential pollution sources (e.g., the Green Global Chitila waste dump, S1), additional samples were taken at distances of 200 m and 400 m from the source.

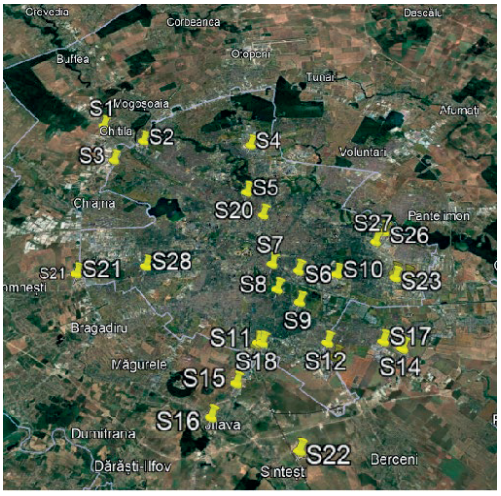


Figure 1. Map of the sampling points

Soil physicochemical properties

Soil properties were analysed using standard methods:

- pH: potentiometric method (SR-7184-13);
- Organic carbon (C, %): wet oxidation method (Walkley-Black, STAS 7184/21-82);
- Mobile Phosphorus (PAL, mg/kg): Egner-Riehm-Domingo method (STAS 7184/19-82);
- Electrical Conductivity (EC, µS/cm): aqueous extract and conductometric method (STAS 7184/7-87);

- Nitrate (N-NO_3, mg/kg): potentiometric method (ICPA methodology);
- Particle size distribution: wet/dry sieving and sedimentation (STAS 7184/7-87).

The soils studied are classified into the following textural classes: sand, sandy loam and loam (Table 1). The chemical properties of the studied soils are summarised in Table 2.

Table 1. Textural classes of the soil analysed in the study

Textural classes	Number of collection points
Sand	10
Sandy Loam	22
Loam	28

Table 2. Chemical properties of the analysed soil samples

Chemical properties of the analysed soil sample (N = 60)	Range
pH	4.98-8.56
C (%)	0.86-6.19
N (%)	0.09-0.499
EC (µS/cm)	23.3-1521
N-NO_3 (mg/kg)	2.68-65
P (mg/kg)	16.34-271.2

The analysed soils exhibit a broad spectrum of chemical properties, which is typical for urban soils (Preda et al., 2010). The pH varied from slightly acidic to alkaline, organic carbon levels ranged from extremely low to high, as did electrical conductivity (EC). Nitrate levels fluctuated between low and high, while phosphorus and nitrogen availability ranged from low to very high, respectively from low to high.

PAHs extraction from soil and analysis

PAHs are analysed from soil according to the standards set forth in the European Standards (SR EN 17503:2022). To extract these compounds from soil, an automated Soxhlet extractor and a mixture of hexane and acetone (in a 1:1 ratio) were employed. The extract is washed with water for chromatography to remove acetone and it is passed through anhydrous sodium sulphate. If necessary to remove the sulphur, copper powder can be used. The determination of PAHs was performed on a Knauer ultrahigh pressure liquid chromatograph (UHPLC) with UV-VIS detection, at 254 nm. The concentration for each compound were quantitatively determined by comparison the peak area of the standard with that of the samples.

In accordance with Order 756/1997, the following priority PAHs are to be quantified: anthracene, benzo(a)anthracene, benzo[b]fluoranthene, benzo[k]fluoranthene, benzo[a]pyrene, benzo[ghi]perylene, chrysene, fluoranthene, indeno(1,2,3)pyrene, naphthalene, and phenanthrene, as well as pyrene. The pair consisting of benzo[*ghi*]perylene and indeno(1,2,3)pyrene cannot be determined with UV-VIS detector. The separation of the other compounds was performed with a C18 column (2.1 mm x 100 mm x 1.8 µm) operated at 40°C. The mobile phase is composed of water and acetonitrile and the gradient of this mobile phase is presented in Table 3.

Table 3. Flow and gradient of the mobile phase

Time (minute)	Flow (ml/min)	Acetonitrile (%)	Water (%)
0	0.4	50	50
1.6	0.4	55	45
2.9	0.4	60	40
3.7	0.4	70	30
8.5	0.4	85	15
13	0.4	50	50
13	0.4	50	50

Quality assurance/Quality control

To ensure the accuracy and reliability of the results, quality control and quality assurance procedures included duplicate samples, blank samples, and certified reference materials. The limit of quantification for PAHs ranged from 0.02 mg/kg to 0.05 mg/kg. Reagents are of chromatographic grade. To minimize the contamination, all the glassware is rinsed with hexane, acetonitrile and acetone.

RESULTS AND DISCUSSIONS

PAHs concentrations and patterns in the analysed soil samples

The total concentration of the PAH compounds in soil ranged between 0.047 mg/kg and 1.060 mg/kg, with an average value of 0.212 mg/kg (Figure 2). According to Order 756/1997, 33.3% from analysed soil samples have normal concentration (<0.1 mg/kg), 66.7% have concentrations ten times higher than normal

values. The highest PAHs concentrations were observed at S4 (Ficusului Blvd), a high-traffic area, and at S12 and S13 (IMGB), a well-known industrialized zone in Bucharest (Figure 2). Similar studies in other European cities have reported comparable PAHs concentrations, suggesting common urban pollution patterns. For example, the total PAHs content was reported to range from 0.148 mg/kg to 3.410 mg/kg in Torino, from 0.218 mg/kg to 4.490 mg/kg in Ljubljana (Morillo et al., 2007), and from 0.450 mg/kg to 5.650 mg/kg in the soil of the River Seine basin in Paris (Motelay-Massei et al., 2004). These results are significantly lower compared to those found in soils with specific pollution sources. For instance, near a tar works in the UK, the total concentration of PAHs ranged from 6.6 mg/kg to 872 mg/kg (Lorenzi et al., 2010). This suggests that the study data presented represents diffuse pollution sources.

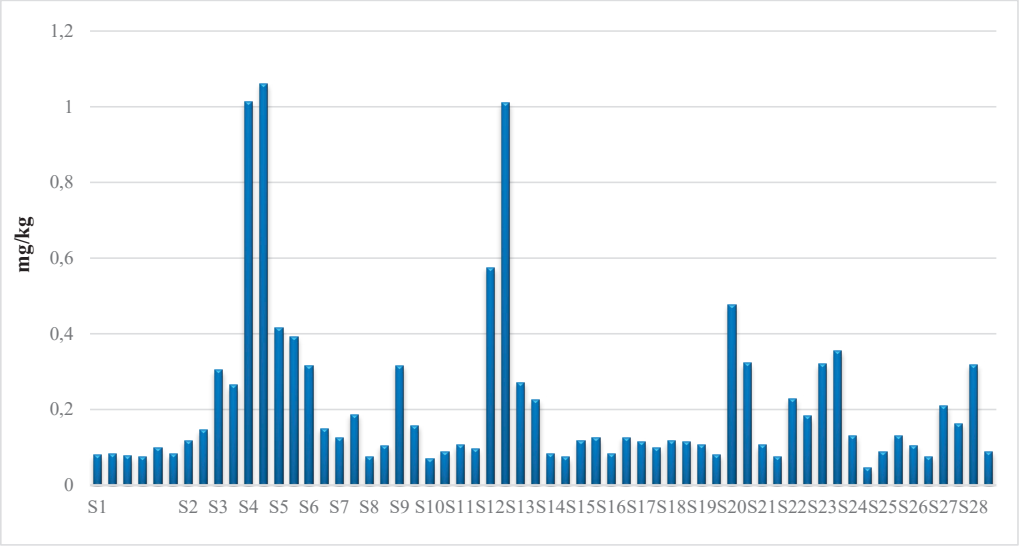


Figure 2. Total PAHs concentration in soil samples collected from Bucharest

The mean concentration of the individual PAH compounds increases in order: benzo(a)pyrene, benzo(k)fluoranthene, naphthalene, anthracene, phenanthrene, pyren, benzo(b)fluoranthen, benzo(a)anthracene, fluoranthen (Figure 3).

The highest concentrations were reported for fluoranthene, benzo(a)antracene and benzo(b)fluoranthene. Similar results were obtained by Wang (2013) in a study regarding the soil contamination with PAHs in Beijing.

The range of the concentration for the individual PAHs are presented in Table 4. The PAH distribution in Bucharest soils shows a minor contribution from LMW-PAHs (2-3 rings), such as naphthalene, phenanthrene, and anthracene. Instead, 4-ring polynuclear aromatic hydrocarbons (fluoranthene, pyrene, chrysene, and benzo(a)anthracene) are dominant (Figure 4). Among this group, fluoranthene and benzo(a)anthracene has the highest concentration.

Regarding 5-ring PAHs, benzo(b)fluoranthene has the highest contribution to the total PAH content.

Naphthalene is one of the most volatile PAHs, meaning it can evaporate relatively quickly from the soil surface. Naphthalene contaminates 46.7% from the analysed soil sample. The highest concentration was recorded in the soil sample collected from the S3 (Ruteni landfill). Naphthalene can be found in landfills due to its presence in various waste materials, including plastics, coal tar, petroleum products, and mothballs. Jia & Batterman (2010) also reported the presence of naphthalene in a landfill site.

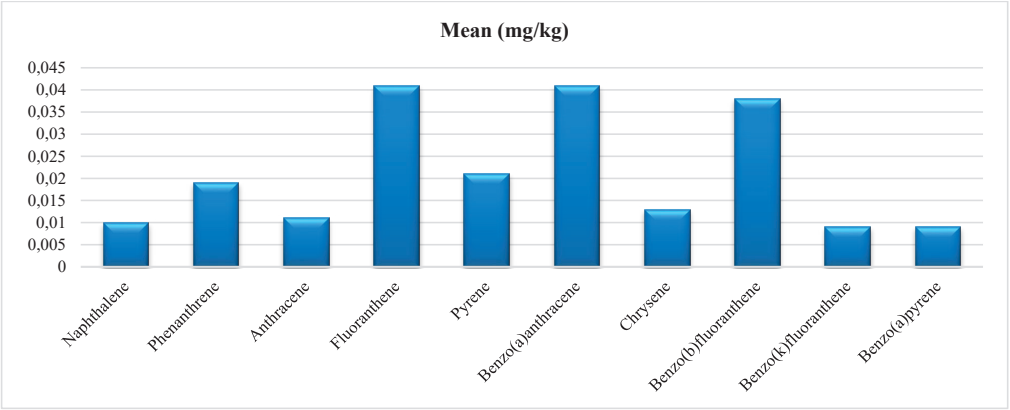


Figure 3. Concentration of the individual PAH compounds in the soil samples collected from Bucharest

Table 4. Range and mean value of concentration of the individual PAHs in studied soil samples

PAH compounds	Type of PAH	Range (mg/kg)		Mean (mg/kg)
		Min.	Max.	
Naphthalene	LMW	ND	0.104	0.010
Phenanthrene	LMW	0.004	0.072	0.019
Anthracene	LMW	ND	0.089	0.011
Fluoranthene	HMW	0.012	0.280	0.041
Pyren	HMW	ND	0.128	0.021
Benzo(a)anthracene	HMW	0.004	0.632	0.041
Chrysen	HMW	ND	0.054	0.013
Benzo(b)fluoranthene	HMW	ND	0.525	0.038
Benzo(k)fluoranthene	HMW	ND	0.054	0.009
Benzo(a)pyrene	HMW	ND	0.032	0.009

LMW = Low molecular weight
HMW = High molecular weight
ND = Not detection

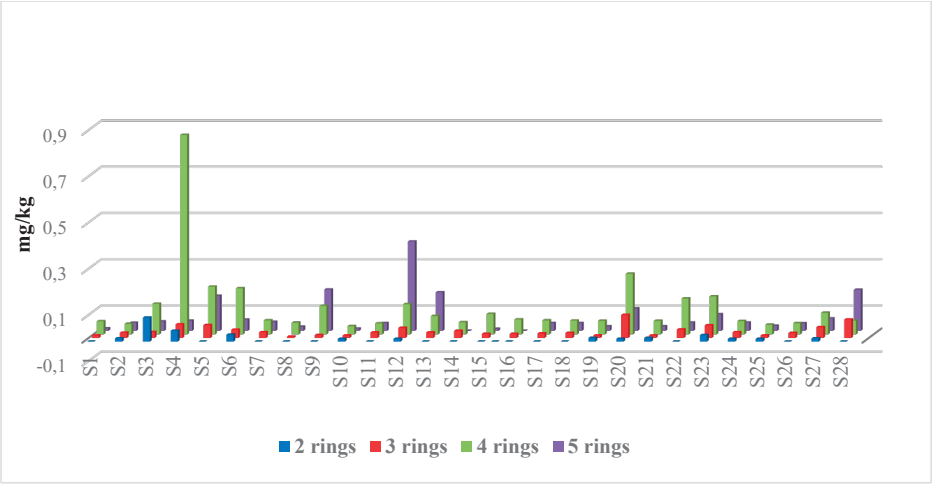


Figure 4. Profiles of the PAHs in the soil samples by number of rings

Phenanthrene is the most thermodynamically stable of the 3-ringed PAHs. This can be the reason it contaminates all the soil samples, even at small concentrations that slightly exceed the

upper limit of the normal threshold (<0.05 mg/kg). Similar results were reported by Vane et al. (2014). The highest concentrations were identified in a boulevard with heavy traffic congestion, S28 (Prelungirea Ghencea).

In contrast, there is a major presence of HMW-PAHs (4-5 rings), including fluoranthene, pyrene, benzo[a]anthracene, chrysene, and particularly benzo[b]fluoranthene (Figure 4). This suggests a dominance of HMW-PAHs, likely indicating sources such as combustion processes rather than petrogenic inputs (McCready et al., 2000).

Fluoranthene, a 4 rings PAH contaminates all the soil samples. 80% from collected samples have concentrations that exceed the upper threshold of normal values (<0.02 mg/kg). Fluoranthene is relatively stable in soil, it strongly binds to soil particles, especially in organic-rich soils (Abdel-Shafy & Mansour, 2016). The highest concentration of fluoranthene was recorded in S4, once again in an area with heavy car traffic.

70% from soil samples are contaminated with pyrene, another 4 rings PAH. The highest concentration (0.128 mg/kg), which is considered a normal value according to Order 756/1997 (<0.5 mg/kg), was recorded in the IMGB industrial area. Pyrene is not the most toxic PAH, but it can act as a precursor to more harmful compounds like benzo[a]pyrene, which is carcinogenic (Gabriele et al., 2021).

Chrysene contaminates almost all soil samples, with 60% of them having normal concentrations (<0.02 mg/kg). The highest concentration (0.054 mg/kg) was recorded in S5 (Kiseleff Boulevard).

Benzo(a)anthracene has also 4 aromatic rings in the molecule and it can persist in soil for long periods due to its low volatility and stability. It can adhere strongly to soil particles, making it resistant to degradation. It is considered a possible human carcinogen (Group 2B by the International Agency for Research on Cancer, IARC) (Abdel-Shafy & Mansour, 2016). Long-term exposure can increase the risk of cancers, especially if the compound enters the human body through ingestion or inhalation. 63% from the studied soil samples have concentrations that exceed the upper threshold of normal values (<0.02 mg/kg). The highest concentrations (0.632 mg/kg) were obtained in sample collected from S4 (Ficusului Boulevard). This value exceeds the normal upper threshold (<0.02 mg/kg) but remains below the alert threshold (2 mg/kg).

From the 5-ring PAHs, benzo(b)fluoranthene, benzo(k)fluoranthene and benzo(a)pyrene were evaluated. The compound with a major contribution to the total content of PAH is benzo(b)fluoranthene. It is relatively persistent in the environment. It does not readily degrade in the presence of sunlight, air, or water, and can remain in soil or sediments for a long time. The highest concentration (0.535 mg/kg) was obtained in the sample collected from the IMGB area. This value exceeds the normal upper threshold (<0.02 mg/kg) but remains below the alert threshold (2 mg/kg).

The highest concentrations of benzo(k)fluoranthene and benzo(a)pyrene (0.054 mg/kg, respectively 0.032 mg/kg) were recorded in S5 (Kiseleff Boulevard). These concentrations slightly exceed the normal value (<0.02 mg/kg) according with Order 756/1997.

Effect of soil properties on the total PAHs concentration

PAHs are hydrophobic and have a high affinity for organic matter. Soils rich in organic matter tend to adsorb and retain PAHs more effectively, reducing their mobility and bioavailability (Yang et al., 2010). Higher organic carbon content is often correlated with higher PAH concentrations due to stronger sorption (Du et al., 2022). No correlation found in this study between the total content of PAHs in soil and organic carbon. A lack of a correlation is not an uncommon finding for soils (Ribes et al., 2003; Bucheli et al., 2004; Heywood et al., 2006) and has been attributed to a state of non-equilibrium. Low molecular weight PAHs (2-3 rings) associated with soot tend to partition and equilibrate more easily between the vapor phase and the soil organic matter, whereas high molecular weight PAHs (4-6 rings) remain more strongly bound to particles (Bucheli et al., 2004).

The influence of pH on PAHs content in soil is indirect, as PAHs are nonpolar compounds and do not ionize in response to pH changes. However, pH affects PAHs behaviour by influencing microbial degradation and their interactions with metal ions or organic matter.

Pawar (2015) was observed that soil with pH 7.5 was most suitable for the degradation of phenanthrene, anthracene, fluoranthene, and pyrene. Thus, on Theodor Pallady Boulevard, the pH is 7.54, the phenanthrene content is 0.011 mg/kg, anthracene is below the limit of quantification, and fluoranthene has the lowest concentration: 0.012 mg/kg.

Soils with high EC can adsorb more PAHs due to electrostatic interactions with organic matter. Studies show a positive correlation between PAH content in soil and conductivity, instead nitrate, which acts as an electron acceptor, has played a significant role in the oxidation of PAHs (Du et al., 2022).

In soil samples collected from Bucharest, no correlation can be established between PAHs and EC or nitrate, likely because the total concentration of PAHs is more influenced by pollution sources, which are highly diverse in Bucharest.

Identifying PAHs sources using isomer ratios

Diagnostic ratios are used to distinguish between pyrogenic (fire-related) and petrogenic (oil or fossil fuel-related) sources of polycyclic aromatic hydrocarbons.

The key point mentioned is that while these diagnostic ratios are useful, their application can be limited because there may be overlap in the ratios from both pyrogenic and petrogenic sources.

This overlap can make it challenging to pinpoint specific types of pyrogenic or petrogenic sources using these ratios alone. (Stout et al., 2004; Galarneau, 2008). In the real world, PAHs often originate from multiple sources, making it difficult to pinpoint one specific source. For instance, both vehicular emissions and industrial activities might contribute to contamination in the same area. This mixing complicates the identification and assessment of specific sources. Despite this, ratios are widely used and applied in various environments for source apportionment estimations of PAHs (Dickhut et al., 2000; Yunker et al., 2002; Tobiszewski & Namieśnik, 2012).

The following diagnostic ratios were used to indicate possible sources (Davis et al., 2019):

- ∑LMW/∑HMW PAHs;
- Anthracene/ (Anthracene + Phenanthrene);
- Fluoranthene/ (Fluoranthene + Pyrene);
- Benzo[*a*]anthracene/(Benzo[*a*]anthracene + Chrysene).

The ratio of LMW to HMW PAHs aims to distinguish between petrogenic and pyrogenic sources. Values < 1 suggest pyrogenic sources, while a value > 1 suggests petrogenic sources (Zhang et al., 2008). In this study the ratio ranged from 0.03 to 0.91, suggesting the pyrogenic sources may be most impactful in soil collected (Figure 5).

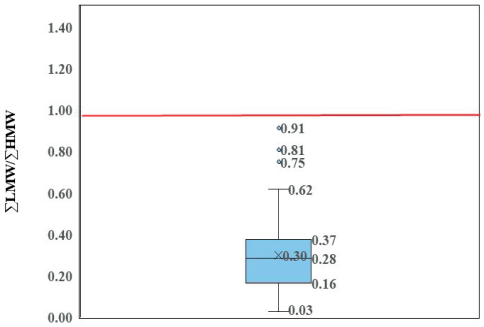


Figure 5. PAH diagnostic ratio plot of ∑LMW/∑HMW

The Anthracene/(Anthracene + Phenanthrene) ratio distinguishes between petrogenic and combustion sources, as values <0.1 indicate petrogenic and those > 0.1 indicate combustion (Yunker et al., 2002). Values obtained for this ratio ranged between 0.1 and 0.62. The value 0.1 is obtained in sample collected from S 28, Prelungirea Ghencea (Figure 6).

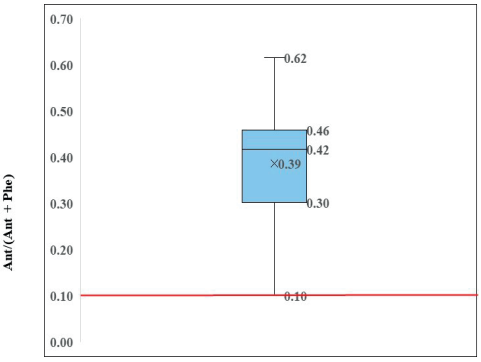


Figure 6. PAH diagnostic ratio plot of Ant/(Ant+Phe)

The Fluoranthene/(Fluoranthene + Pyrene) ratio provides valuable insight into distinguishing between petroleum sources, petroleum combustion, and other combustion processes. Ratio values < 0.4 indicate petrogenic sourcing, values between 0.4 and 0.5 are indicative of petroleum combustion, while values > 0.5 suggest wood, grass, and/or coal combustion (Yunker et al., 2002). This ratio is greater than 0.5 for all the soil samples collected from Bucharest (Figure 7).

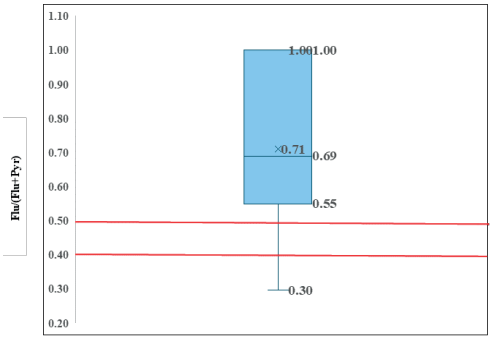


Figure 7. PAH diagnostic ratio plot of Flu/(Flu+Pyr)

The Benzo[*a*]anthracene/(Benzo[*a*]anthracene + Chrysene) ratio distinguishes between petrogenic and combustion (pyrogenic) sources, with a range indicating mixed sourcing. Values below 0.2 suggest petrogenic sources, values between 0.2 and 0.35 indicate mixed sources, while values above 0.35 point to combustion sources (Yunker et al., 2002). According to Figure 8, the same theory is confirmed once again, indicating that the source of PAH compounds is combustion.

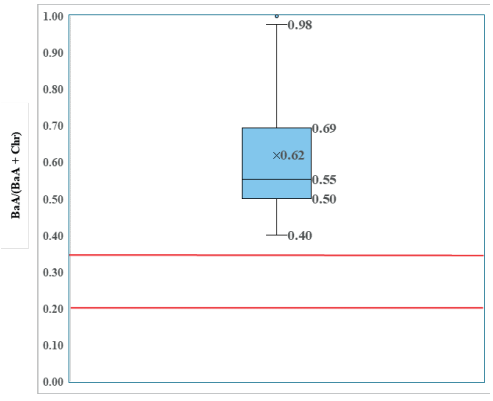


Figure 8. PAH diagnostic ratio plot of BaA/(BaA+Chr)

CONCLUSIONS

33.3% from analysed soil samples have normal concentration (<0.1 mg/kg), 66.7% have concentrations ten times higher than normal values.

The highest values of PAHs concentration were observed in S4 (Ficusului Blvd.) a very crowded boulevard and S12, S13 (IMGB), a well-known industrialized area from Bucharest.

The PAH distribution in Bucharest soils shows a minor contribution from LMW- PAHs (2–3 rings). Of these, phenanthrene is the contaminant present in all the analysed samples, even at low concentrations.

In contrast, there is a major presence of HMW-PAHs (4-5 rings), including fluoranthene, pyrene, benzo[a]anthracene, chrysene, and particularly benzo[b]fluoranthene.

The application of the three types of diagnostic ratios led to the same conclusion, namely that the source of PAHs pollution of the studied soil samples could be the combustion process as: vehicle exhaust (gasoline and diesel engines), residential heating (coal, wood, oil burning), industrial processes.

ACKNOWLEDGEMENTS

This research work was financed with the support of the Project PN 23 29 01 01- "Research on the soil emissions inventory of some persistent organic pollutants - an important stage of the national implementation of EU Regulation 1021/2019".

REFERENCES

Abdel-Shafy, H.I., & Mansour, M.S.M. (2016). A review on polycyclic aromatic hydrocarbons: Source, environmental impact, effect on human health and remediation. *Egyptian Journal of Petroleum*, 25(1). https://doi.org/10.1016/j.ejpe.2015.03.011

Arey, J., & Atkinson, R. (2003). Photochemical reactions of PAH in the atmosphere. In P. E. T. Douben (Ed.), *PAHs: An ecotoxicological perspective* (pp. 47–63). John Wiley & Sons Ltd. https://doi.org/10.1002/0470867132.ch4

Adeniji, A., Okoh, O., & Okoh, A. (2019). Levels of polycyclic aromatic hydrocarbons in the water and sediment of Buffalo River Estuary, South Africa and their health risk assessment. *Archives of Environmental Contamination and Toxicology,* 76(4), 657–669.

https://link.springer.com/article/10.1007/s00244-019-00617-w

Bolden, A.L., Rochester, J.R., Schultz, K., & Kwiatkowski, C. F. (2017). Polycyclic aromatic hydrocarbons and female reproductive health: a scoping review. *Reproductive Toxicology*, 73, 61–74. https://doi.org/10.1016/j.reprotox.2017.07.012

Bucheli, T.D., Blum, F., Desaules, A., & Gustafsson, O. (2004). Polycyclic aromatic hydrocarbons, black carbon, and molecular markers in soils of Switzerland. *Chemosphere*, 56(11): 1061–1076. https://doi.org/10.1016/j.chemosphere.2004.06.002

Deziel, N.C., Rull, R.P., Colt, J.S., Reynolds, P., Whitehead, T.P., Gunier, R.B., Month, S.R., Taggart, D.R., Buffler, D., Ward, M.H., & Metayer, C. (2014). Polycyclic aromatic hydrocarbons in residential dust and risk of childhood acute lymphoblastic leukemia. *Environmental Research*, 133, 388-395. https://doi.org/10.1016/j.envres.2014.04.033

Dickhut, R.M., Canuel, E.A., Gustafson, K.E., Liu, K., Arzayus, K.M., Walker, S.E., Edgecombe, G., Gaylor, M.O., & MacDonald, E.H. (2000). Automotive Sources of Carcinogenic Polycyclic Aromatic Hydrocarbons Associated with Particulate Matter in the Chesapeake Bay Region. *Environmental Science & Technology,* 34(22), 4635–4640. http://dx.doi.org/10.1021/es000971e

Du, J., Liu, J., Jia, T., & Chai, B. (2022). The relationships between soil physicochemical properties, bacterial communities and polycyclic aromatic hydrocarbon concentrations in soils proximal to coking plants. *Environmental Pollution*, 298, 118823. https://doi.org/10.1016/j.envpol.2022.118823

Galarneau, E. (2008). Source specificity and atmospheric processing of airborne PAHs: Implications for source apportionment. *Atmospheric Environment*, 42(35), 8139–8149. https://doi.org/10.1016/j.atmosenv.2008.07.025

Gabriele, I., Race, M., Papirio, S., & Esposito, G. (2021). Phytoremediation of pyrene-contaminated soils: A critical review of the key factors affecting the fate of pyrene. *Journal of Environmental Management*, 293, 112805. https://doi.org/10.1016/j.jenvman.2021.112805

Gupte, A., Tripathi, A., Patel, H., Rudakiya, D., & Gupte, S. (2016). Bioremediation of polycyclic aromatic hydrocarbon (PAHs): A perspective. *Open Biotechnology Journal,* 10, 363–378 https://doi.org/10.2174/1874070701610010363

Heywood, E., Wright, J., Wienburg, C.L., Black, H.I., Long, S.M., Osborn, D., & Spurgeon, D.J. (2006). Factors influencing the national distribution of polycyclic aromatic hydrocarbons and polychlorinated biphenyls in British soils. *Environmental Science & Technology,* 40, 7629–7635. https://doi.org/10.1021/es061296x

Jia, C., & Batterman, S. (2010). A Critical Review of Naphthalene Sources and Exposures Relevant to Indoor and Outdoor Air. *International Journal of Environmental Research and Public Health*, 7, 2903–2939. https://doi:10.3390/ijerph7072903

Jia, T., Guo, W., Xing, Y., Lei, R., Wu, X., Sun, S., He, Y., & Liu, W. (2021). Spatial distributions and sources of PAHs in soil in chemical industry parks in the Yangtze River Delta, China. *Environmental Pollution,* 283, 11712. https://doi.org/10.3389/fenvs.2024.1363297

Kuppusamy, S., Thavamani, P., Venkateswarlu, K., Lee, Y. B., Naidu, R., & Megharaj, M. (2017). Remediation approaches for polycyclic aromatic hydrocarbons (PAHs) contaminated soils: technological constraints, emerging trends and future directions. *Chemosphere,* 168, 944–968. https://doi.org/10.1016/j.chemosphere.2016.10.115

Lee, B.K., & Vu, V.T. (2010). Sources, distribution, and toxicity of polyaromatic hydrocarbons (PAHs) in particulate matter. *Air Pollution*, 99–122. IntechOpen http://dx.doi.org/10.5772/10045

Lorenzi, D., Cave, M.R., & Dean, J.R. (2010). An investigation into the occurrence and distribution of polycyclic aromatic hydrocarbons in two soil size fractions at a former industrial site in NE England, UK using in situ PFE-GC-MS. *Environmental Geochemistry and Health*, 32(6), 553–565 http://dx.doi.org/10.1007/s10653-010-9316-8

McCready, S., Slee, D.J., Birch, G.F., & Taylor, S.E. (2000). The distribution of polycyclic aromatic hydrocarbons in surficial sediments of Sydney harbour, Australia. *Marine Pollution. Bull*etin, 40 (11), 999–1006. https://doi.org/10.1016/S0025-326X(00)00044-8

Mojiri, A., Zhou, J.L., Ohashi, A., Ozaki, N., & Kindaichi, T. (2019). Comprehensive review of polycyclic aromatic hydrocarbons in water sources, their effects and treatments. *Science of The Total Environment,* 133971. https://doi.org/10.1016/j.scitotenv.2019

Morillo, E., Romero, A.S., Maqueda, C., Madrid, L., Ajmone-Marsan, F., Grcman, H., Davidson, C.M., Hursthousee A.S., & Villaverde, J. (2007). Soil pollution by PAHs in urban soils: a comparison of three European cities, *Journal of Environmental Monitoring*, 9, 1001–1008. http://dx.doi.org/10.1039/b705955h

Motelay-Massei, A., Ollivon, D., Garban, B., Teil, M., Blanchard, M., & Chevreuil, M. (2004). Distribution and spatial trends of PAHs and PCBs in soils in the Seine River basin, France, *Chemosphere*, 55, 555–565. https://doi.org/10.1016/j.chemosphere.2003.11.054

Pawar, M.R. (2015). The Effect of Soil pH on Bioremediation of Polycyclic Aromatic Hydrocarbons (PAHs). *Journal of Bioremediation & Biodegradation*, 6(3) 1000291 http://dx.doi.org/10.4172/2155-6199.1000291

Preda, M., Dumitru, M., Lăcătuşu, R., Motelică, D.M. (2010). *Poluanți organici persistenți în solurile urbane*, București, Editura Estfalia.

Ravindra, K., Sokhi, R., & Van Grieken, R. (2008). Atmospheric polycyclic aromatic hydrocarbons: source attribution, emission factors and regulation. *Atmospheric Environment* 42(14), 2895–2921 https://doi.org/10.1016/j.atmosenv.2008.02.001

Ribes, S., Van Drooge, B., Dachs, J., Gustafsson, O., & Grimalt, J.O. (2003). Influence of soot carbon on the soil-air partitioning of polycyclic aromatic hydrocarbons*. Environmental Science & Technology*,

37(12), 2675–2680 http://dx.doi.org/10.1021/es0307118

Srogi, K., (2007). Monitoring of environmental exposure to polycyclic aromatic hydrocarbons: A review. *Environmental Chemistry Lett*ers 5(4), 169–195. https://doi.org/10.1007/s10311-007-0095-0

Stout, S.A., Uhler, A.D., & Emsbo-Mattingly, S.D. (2004). Comparative evaluation of background anthropogenic hydrocarbons in surficial sediments from nine urban waterways. *Environmental Science & Technol*ogy, 38 (11), 2987–2994. https://doi.org/10.1021/es040327q

Tobiszewski, M., & Namiesnik, J. (2012). PAH diagnostic ratios for the identification of pollution emission sources. *Environmental Pollution*, 62, 110-119. http://dx.doi.org/10.1016/j.envpol.2011.10.025

Vane, C.H., Kim, A.W., Beriro, D.J., Cave, M.R., Knights, K., Moss-Hayes, V. & Nathanail, P.C. (2014). Polycyclic aromatic hydrocarbons (PAH) and polychlorinated biphenyls (PCB) in urban soils of Greater London, UK. *Applied Geochemistry*, 51, 303–314. https://doi.org/10.1016/j.apgeochem.2014.09.013

Wang, D.G., Yang, M., Jia, H.L., Zhou, L., Li, Y.F. (2009). Polycyclic Aromatic Hydrocarbons in Urban Street Dust and Surface Soil: Comparisons of Concentration, Profile, and Source. *Archives of Environmental Contamination and Toxicology* 56:173–180. http://dx.doi.org/10.1007/s00244-008-9182-x

Wang, X., Miao, Y., Zhang, Y., Li, Y., Wu, M., & Yu, G. (2013). Polycyclic aromatic hydrocarbons (PAHs) in urban soils of the megacity Shanghai: occurrence, source apportionment and potential human health risk. *Science of the Total Environment,* 447, 80–89. https://doi.org/10.1016/j.scitotenv.2012.12.086

Yang, Y., Zhang, N., Xue, M., & Tao, S. (2010). Impact of soil organic matter on the distribution of polycyclic aromatic hydrocarbons (PAHs) in soils. *Environmental Pollution*, 158(6), 2170-2174. https://doi.org/10.1016/j.envpol.2010.02.019

Yunker, M.B., Macdonald, R.W., Vingarzan, R., Reginald R.H., Goyette, D., & Sylvestre, S. (2002). PAHs in the Fraser River basin: a critical appraisal of PAH ratios as indicators of PAH source and composition. *Organic Geochemistry*, 33(4), 489–515. http://dx.doi.org/10.1016/ S0146-6380(02)00002-5

Zhang, W., Zhang, S., Wan, C., Yue, D., Ye, Y., & Wang, X. (2008). Source diagnostics of polycyclic aromatic hydrocarbons in urban road runoff, dust, rain and canopy throughfall. *Environmental Pollution,* 153(3), 594–601. https://doi.org/10.1016/j.envpol.2007.09.004

Scientific Papers. Series E. Land Reclamation, Earth Observation & Surveying, Environmental Engineering. Vol. XIV, 2025
Print ISSN 2285-6064, CD-ROM ISSN 2285-6072, Online ISSN 2393-5138, ISSN-L 2285-6064

THE EFFECTS OF AIR POLLUTION WITH PARTICULATE MATTER ON HUMAN HEALTH

Elena-Denisa PREDESCU, Carmen Otilia RUSĂNESCU, Irina Aura ISTRATE, Roxana-Elena FRÎNCU, Sabrina Maria BĂLĂNESCU

National University of Science and Technology Politehnica Bucharest,
Faculty of Biotechnical Systems Engineering, Department of Biotechnical Systems,
313 Splaiul Independenţei, District 6, 060042, Bucharest, Romania

Corresponding authors emails: denisa.predescu23@yahoo.com, rusanescuotilia@gmail.com, ia_istrate@yahoo.com

Abstract

This review examines the literature on particulate matter (PM), covering studies published between 2019 and 2024. Articles were selected based on their relevance to PM sources, chemical composition, atmospheric behaviour, and health impacts, prioritizing the studies in English. The review synthethizes findings on PM origin, including traffic, industrial emissions, constructing activities, and natural processes such as wildfires and volcanic eruptions. It also highlights the relationship between particle size and chemical composition, as well as the health-related effects of PM exposure, including respiratory and cardiovascular outcomes. The results underline the urgency of implementing measures to reduce PM emissions and protect public health.

Key words*: particulate matter; air; pollution; chemical composition, health impacts.*

INTRODUCTION

Air pollution represents a major issue affecting both the environment and human health. Particulate matter (PM) is one of the most damaging components found in air pollution. PM originates from a wide variety of sources, both natural and anthropogenic.

Due to its small size, PM can be inhaled easily, and its effects on human health can be severe, posing a significant risk. Numerous studies have been conducted to identify the wide range of effects caused by long-term exposure to PM, many of which have been linked to respiratory and cardiovascular diseases (Šarkan et al., 2023). Moreover, recent literature suggests potential links between PM exposure and metabolic disorders, including diabetes and obesity (Mahiyuddin et al., 2023).

Advanced wastewater treatment processes, such as the anaerobic-anoxic-aerobic (A_2O) (configuration studied by Marin et al., 2023) are pivotal in reducing environmental pollutants. By effectively removing nutrients like phosphorus from urban wastewater, these systems prevent eutrophication in aquatic ecosystems, which can lead to increased biological activity and the subsequent release of volatile compounds into the atmosphere. These compounds can act as precursors to secondary particulate matter formation, thereby contributing to air pollution. Thus, efficient wastewater treatment not only safeguards water quality but also plays an indirect role in mitigating airborne particulate matter levels, highlighting the interconnectedness of water and air pollution control strategies (Marin et al., 2023).

This review explores the origins, composition, and health impacts of PM, highlighting the significance of regulatory measures in protecting public health.

MATERIALS AND METHODS

Articles for this review were identified through searches in Scopus, Web of Science, DOAJ, and MDPI.

This review is based on the analysis of 13 articles published between 2019 and 2024, as listed in the bibliography. All included articles were directly selected for their relevance to particulate matter (PM), including its sources, chemical composition, atmospheric behaviour, and health impacts.

Inclusion criteria were articles addressing PM origin, particle size, chemical composition, or human health effects.
Exclusion criteria were studies not related to PM or human health.
The selected articles provide the data and figures presented in this review.

RESULTS AND DISCUSSIONS

This section provides a synthesis of the findings from various studies regarding the sources and health impacts of particulate matter (PM). The results are organised into several key themes, including the primary sources of PM, the health effects associated with exposure, and the long-term consequences for both individuals and populations.

Sources of Particulate Matter (PM)

Particulate matter (PM) consists of primary and secondary particles. Primary particles, especially ultrafine particles (≤0.1μm), are directly emitted from combustion processes, including transport, industry, power generation and heating. Secondary particles (2.5-10 μm) form through atmospheric chemical reactions. PM also contains dust, biological particles, and gaseous pollutants. Ultrafine particles can originate from gaseous precursors such as sulphur dioxide and nitrogen oxides. Natural sources include volcanic eruptions, forest fires, sea spray, pollen, and fungal spores (Chauhan et al., 2024).
Figure 1 illustrates the sources of PM pollutants and their atmospheric transport. Through chemical reactions, these particles interact with water and liquid molecules, leading to their accumulation in clouds. Wind currents then facilitate their upward movement (Amnuaylojaroen & Parasin, 2024).
Particulate matter (PM) is a major contributor to atmospheric pollution. In modern settings, residential heating and vehicular emissions are the primary sources, with higher concentrations in urban areas with dense traffic. Non-exhaust emissions result from resuspension of deposited particles, road abrasion, and tire or brake wear. Overall, PM pollution is largely driven by fossil fuel combustion.
(Šarkan et al., 2023).

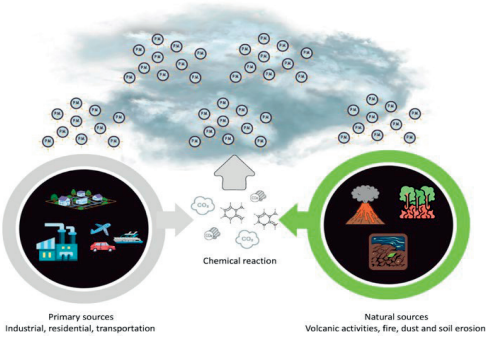


Figure 1. Emission sources of PM pollutants (Amnuaylojaroen T., & Parasin, N., 2024)

Table 1 provides a classification of ultra fine particles according to their types, subcategories, and particle diameters, facilitating a better understanding of their characteristics (Chauhan et al., 2024).

Table 1. Categories of Ultra fine Particles based on their type and size (Chauhan et al., 2024)

Type		PM Diameter(μm)
Particulate contaminants	Soot	0.01-0.8
	Smog	0.01-1
	Tobacco smoke	0.01-1
	Fly ash	1-100
	Cement dust	8-100
Biological contaminants	Viruses	0.01-1
	Bacteria and Bacterial spores	0.7-10
	Fungi and moulds	2-12
	Allergens (dogs, cats, pollen, household, dust)	0.1-100
Types of dust	Atmospheric dust	0.01-1
	Settling dust	1-100
	Heavy dust	100-1000
	Different gaseous contaminants	0.0001-0.01

Figure 2 shows that ultra fine particles (UFPs) come from both natural and anthropogenic sources. On the left are natural sources of PM, and on the right are human-made sources. In the middle, UFPs are shown as resulting from both types, underlining their mixed origin (Chauhan et al., 2024).

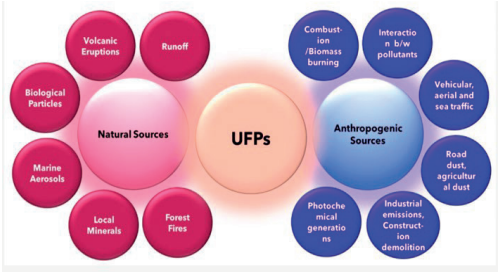


Figure 2. The main sources regarding the particulate matters (Chauhan, B.V.S. et al., 2024)

Health effects of PM exposure

Particle size is a key factor in PM toxicity. Smaller particles pose greater health risks as PM2.5 can reach the lower respiratory tract and settle in the bronchi, while particles larger than PM10 are mostly filtered by the nasal cavity. The chemical composition of PM further influences its effects. Poor air quality is a major global health threat, reducing life expectancy and surpassing even the risks of cigarette smoking (Šarkan et al., 2023).

Air pollution affects not only the respiratory system but also the cardiovascular system. PM exposure is linked to systemic inflammation, oxidative stress, endothelial dysfunction, and altered blood pressure, which can contribute to stroke and other cardiovascular conditions. The health impact of PM depends on particle size and composition. PM10 particles mostly deposit in the trachea and bronchi, while PM2.5 and ultrafine particles can reach alveoli and enter the bloodstream, spreading to other organs. PM may contain carbon monoxide, nitrates, sulphates, ozone, volatile organic compounds, heavy metals, and polycyclic aromatic hydrocarbons. Chronic PM exposure can trigger cellular stress, apoptosis, ferroptosis, pyroptosis, as well as DNA damage, epigenetic changes, and homeostatic disruption, increasing the risk of multiple disease (Lim & Kim, 2024).

The skin serves as a barrier against chemicals, pathogens, air pollutants, and UV radiation, while maintaining proper moisture levels. Keratinocytes, which make up 90% of the epidermis, respond to antigens by releasing cytokines and chemokines that regulate immune and inflammatory responses. Dysregulation of keratinocyte function can lead to excessive inflammation, contributing to skin aging and related disorders.

Figure 3 illustrates the relationship between particle size and their site of deposition in the human respiratory system. At the top, various particles such as molecules, viruses, bacteria, and pollen are shown according to their diameter, with reference to PM0.1, PM2.5, and PM10 size ranges. The bottom part of the figure illustrates how particles of various sizes accumulate in the respiratory tract. Particles between 10 and 30 µm are trapped in the oropharyngeal region; those between 2 and 10 µm reach the conducting airways; while ultrafine particles smaller than 2 µm can penetrate deep into the respiratory zone, including the alveolar ducts and sacs (Lim & Kim, 2024).

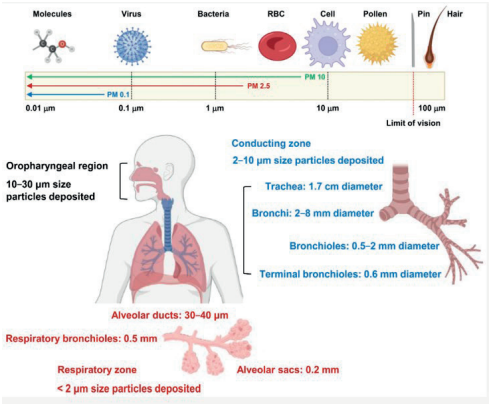


Figure 3. PM classification by aerodynamic particle size (Lim & Kim, 2024)

Constant exposure to particulate matter emissions provokes alveolar inflammation, induces disorders of the metabolic system and sets off the risk of cardiovascular diseases. In comparison, people with a history of chronic cardiovascular and respiratory diseases are much more vulnerable than others. They are significantly more susceptible to infections caused by PM exposure. Each of the two types of PM exposure, long or short term, has been associated with a high risk of cardiovascular and respiratory disease, along with the mortality rates. These associations were clearly demonstrated in earlier research, highlighting $PM_{2.5}$ as a significant contributor to non-accidental mortality (Mahiyuddin et al., 2023).

Figure 4 illustrates the human body with organs affected by particulate matter (PM) exposure, showing the brain impacted by cognitive

impairment and neuroinflammation, the neck with inflammation leading to irritation, the lungs affected by respiratory issues, the liver showing signs of hepatic damage, the skin with irritation and dermatitis, the vascular system inflamed and the heart at increased risk of damage or dysfunction (Lim & Kim, 2024).

The evaluation of exposure to pollution includes two divisions of health risk: non-carcinogenic and carcinogenic risks. The heavy metals Hg, Cu, Pb, Zn, Cr, Cd, and Ni are associated with chronic non-carcinogenic health effects. Additionally, Cd, Cr, and Ni pose a carcinogenic health risk, through dust inhalation.

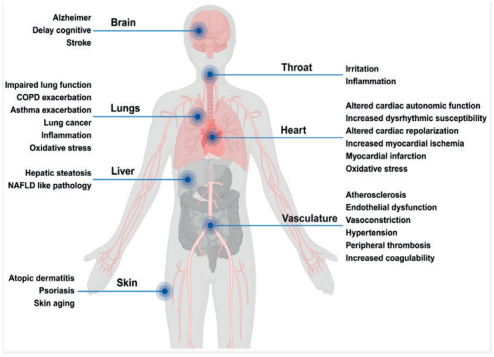


Figure 4. major affected organs by long exposure to PM (Lim & Kim, 2024)

The main routes of exposure to PM are ingestion, inhalation, and dermal absorption. The health risk assessment model is defined as follows:

$$ADD_{ing} = c*(IngR*CF*EF*ED)/(BW*AT) \quad (1)$$

$$ADD_{inh} = c*(InhR*EF*ED)/(PEF*BW*AT) \quad (2)$$

$$ADD_{derm} = c*(SA*CF*SL*ABS*EF*ED)/(BW*AT) \quad (3)$$

where:

ADD_{ing} = Daily contaminant intake via ingestion (mg/kg/day);

ADD_{inh} = Daily contaminant exposure via inhalation (mg/kg/day);

ADD_{derm} = Daily contaminant absorption through the skin (mg/kg/day);

c = contaminant concentration in the medium (e.g., soil, air, water);

IngR = Ingestion rate (amount ingested per day);

CF = Conversion factor (to ensure unit consistency);

EF = Exposure frequency (days per year of exposure);

ED = Exposure duration (total years of exposure);

BW = Body weight (kg);

AT = Averaging time (for non-carcinogens: ED × 365 days, for carcinogens: 70 years × 365 days);

InhR = Inhalation rate (volume of air inhaled per day);

PEF = Particulate emission factor (used for inhalation exposure modelling);

SA = Exposed skin surface area (cm^2);

SL = Skin adherence factor (mg/cm^2);

ABS = Dermal absorption factor (fraction of the contaminant absorbed through the skin) (Dunea, 2019).

Meteorological factors play a crucial role in disease occurrence due to PM exposure. Cold stress during winter is linked to a higher incidence of influenza and respiratory infections, which may contribute to cardiovascular complications. The accumulation of PM_{10} and its inverse correlation can be attributed to the low cloud cover and frequent fog events (Bodor et al., 2024).

Whereas the effect of air pollution on metabolic conditions has been extensively studied, its impact during pregnancy remains poorly evaluated. Pregnant women experience unique physiological changes, including increased energy intake, an accelerated basal metabolic rate, and natural insulin resistance, which may heighten their vulnerability to air pollutants. However, findings on this association remain inconclusive due to the limited number of studies focused on pregnant populations. Additional studies are needed to clearly understand the long-term exposure to PM on glucose metabolism during pregnancy and its potential effects on maternal and fetal health (Wu et al., 2024).

Long-Term Impact of PM on human health

PM pollution is higher in winter. Wind speed affects pollutant dispersion: higher speeds dilute pollutants, while lower speeds allow accumulation and prolong secondary chemical transformations (Fu et al., 2019).

Long-term exposure to PM10 (over than two years) increases non-accidental and cardiovascular mortality, particularly in individuals aged 40 and above. Older adults are more vulnerable, especially on hazy days, with higher risks of cardiovascular and respiratory diseases (Hu et al., 2023). Chronic PM2.5 exposure is linked to elevated blood pressure, thrombosis, insulin resistance, and oxidative stress in the lungs. Meta-analyses also indicate a higher risk of cardiorespiratory diseases even shortly after exposure to PM2.5 (Urbanowicz et al., 2024).

Extended observational studies over six years show that PM exposure worsens pre-existing lung conditions such as idiopathic pulmonary fibrosis (IPF) and other respiratory diseases. Fine particles can accelerate lung function deterioration and increase the risk of complications, highlighting the importance of reducing exposure for individuals with lung issues (Mariscal et al., 2024).

Certain populations are more susceptible to the harmful effects of PM. Children have developing lungs and immune systems, making them more prone to respiratory issues (Amnuaylojaroen & Parasin, 2024). Elderly individuals face higher risks of cardiovascular diseases due to prolonged exposure to PM2.5 and PM10 (Hu et al., 2023; Mahiyuddin et al., 2023). Pregnant women may experience adverse effects on fetal development from particulate exposure (Amnuaylojaroen T. & Parasin N., 2024).

To mitigate these risks, it is recommended that authorities implement air quality monitoring, stricter emission controls, and public awareness campaigns (Lim & Kim, 2024; Mariscal Aguilar et al., 2024). Sensitive groups should limit exposure to high pollution days, for example by staying indoors or using air purifiers (Mahiyuddin et al., 2023). Future research should focus on long-term health impacts in these vulnerable populations and evaluate the effectiveness of intervention strategies (Wu et al., 2024).

CONCLUSIONS

This research analyses the provenance, the composition, and the health impact of the pm on human condition after the pollution exposure.

PM derives from both natural and Anthropogenic sources, and it is classified into primary, secondary, and ultra fine particles. It results from various activities, including fossil fuel combustion, atmospheric chemical reactions, heating emissions, transportation, industrial processes, power generation, volcanic eruptions, and biological activity.

PM contains a wide range of contaminants such as dust, biological particles, gaseous pollutants, tire wear particles, carbon monoxide, nitrates, sulphates, volatile organic compounds, and heavy metals.

Health effects are mainly influenced by the size and chemical composition of PM.

Smaller particles are more hazardous upon inhalation, penetrating deeper into the body and affecting organs such as the brain, lungs, throat, heart, liver, vasculature, and skin.

Air pollution is linked not only to respiratory health issues but also to cardiovascular and cerebrovascular diseases. Moreover, prolonged exposure to PM induces systemic inflammation and DNA damage. Individuals with pre-existing chronic illnesses are particularly vulnerable to PM exposure.

Although PM exposure has also been studied in pregnant women, findings remain inconclusive due to the limited number of studies focused on this population.

Meteorological factors significantly influence the health risks associated with PM.

During winter, increased risk is observed due to cloudy days, low temperatures, and minimal wind speed, which allow pollutants to accumulate and suffer chemical transformations.

In comparison to short-term contact, long-term exposure has a deeper influence on human condition along with its outcomes linked to the age and medical history of the individual.

REFERENCES

Amnuaylojaroen, T., & Parasin, N. (2024). Environmental Epigenomes, Pathogenesis of $PM_{2.5}$-Related Disorders in Different Age Groups: Children, Adults, and the Elderly. *Journal of Environmental Epigenomes*, *8*(2), 13

Bodor K., Micheu, M.M., Keresztesi, Á., Birsan, M.-V., Nita, I.-A., Bodor, Z., Petres, S., Korodi, A. & Szép, R. (2024). Effects of PM_{10} and Weather on Respiratory and Cardiovascular Diseases in the Ciuc Basin (Romanian Carpathians). *Atmosphere*, *12*(2), 289

Chauhan, B.V.S., Corada, K., Young, C., Smallbone, K.L. & Wyche, K.P. (2024). Review on Sampling Methods and Health Impacts of Fine ($PM_{2.5}$, ≤ 2.5 μm) and Ultrafine (UFP, $PM_{0.1}$, ≤ 0.1 μm) Particles. *Atmosphere*, *15*(5), 572

Dunea, D. (2019). Effects of Airborne Particulate Matter on Human Health in Urban Environments. *Atmosphere*, *10*(11), 656

Fu, S., Xie, C., Zhuang, P., Tian, X., Zhang, Z., Wang, B., & Liu, D. (2019). Atmospheric Applications of Lidar, Study of Persistent Foggy-Hazy Composite Pollution in Winter over Huainan Through Ground-Based and Satellite Measurements. *Atmosphere*, *10*(11), 656

Hu, J., Yu, L., Yang, Z., Qiu, J., Li, J., Shen, P., Lin, H., Shui, L., Tang, M., Jin, M., Chen, K. & Wang, J. (2023). Long-Term Exposure to $PM_{2.5}$ and Mortality: A Cohort Study in China. *Toxics*, *11*(9), 727

Lim, E.Y., & Kim, G.-D. (2024). *Particulate Matter*-Induced Emerging Health Effects Associated with Oxidative Stress and Inflammation. *Antioxidants*, *13*(10), 1256

Mahiyuddin, W.R.W., Ismail, R., Mohammad Sham, N., Ahmad, N.I., & Nik Hassan, N.M.N. (2023). Air Pollution and Respiratory Health, Cardiovascular and Respiratory Health Effects of Fine Particulate Matters ($PM_{2.5}$): A Review on Time Series Studies. *Atmosphere*, *14*(5), 856

Marin Rusănescu E., Paraschiv C.O., G., Ciuca C.V. (2023). Research on wastewater treatment using activated sludge technology in the anaerobic-anoxic-aerobic configuration. *U.P.B. Scientific Bulletin, Series B: Chemistry and Materials Science, 85*(4).

Mariscal Aguilar, P., Gomez Carrera, L., Bonilla, G., Carpio, C., Zamaron, E., Fernandez-Velilla, M., Diaz-Almiron, M., Gaya, F., Villamanan, E., Prados, C., & Alvarez Sala, R. (2024). Air Pollution Exposure and Health Impact Assessment (2nd Edition), Impact of Air Pollution on the Long-Term Decline of Non-Idiopathic Pulmonary Fibrosis Interstitial Lung Disease. *Atmosphere*, *15*(12), 1405

Šarkan, B., Gnap, J., Loman, M. & Harantová, V. (2023). Examining the Amount of Particulate Matter (PM) Emissions in Urban Areas. *Applied Sciences*, *13*(3), 1845

Urbanowicz, T., Skotak, K., Olasinska-Wisniewska, A., Filipik, K.J., Bratkowski, J., Wyrwa, M., Sikora, J., Tyburski, P., Krasinska, B., Krasinski, Z., Tykarski, A., & Jemielity, M. (2024). Composition Analysis and Health Effects of Atmospheric Particulate Matter, Long-Term Exposure to PM_{10} Air Pollution Exaggerates Progression of Coronary Artery Disease. *Atmosphere*, *15*(2), 216

Wu, T., Lan, Y., Li, G., Wang, K., You, Y., Zhu, J., Ren, L., & Wu, S. (2024). The Effect of Airborne Contaminants Exposure on Early Health Damage Biomarkers: 2nd Edition, Association Between Long-Term Exposure to Ambient Air Pollution and Fasting Blood Glucose: A Systematic Review and Meta-Analysis. *Toxics*, *12*(11), 792

Scientific Papers. Series E. Land Reclamation, Earth Observation & Surveying, Environmental Engineering. Vol. XIV, 2025
Print ISSN 2285-6064, CD-ROM ISSN 2285-6072, Online ISSN 2393-5138, ISSN-L 2285-6064

ASSESSMENT OF SUSPENDED SEDIMENT CONCENTRATION AND GRANULOMETRY USING AQUASCAT 1000S ON THE SULINA BRANCH OF THE DANUBE RIVER

Adrian ROȘU[1, 3], Mădălin CRISTEA[1], Bogdan ROȘU[3], Maxim ARSENI[1, 3], Mihai Ștefan PETREA[2], Cătălina ITICESCU[1, 3], Puiu-Lucian GEORGESCU[1, 3], Silvia DRĂGAN[4]

[1]"Dunărea de Jos" University of Galaţi, Faculty of Sciences and Environment, 111 Domnească Street, 800201, Galaţi, Romania
[2]"Dunărea de Jos" University of Galaţi, Faculty of Food Science and Engineering, 111 Domnească Street, 800201, Galaţi, Romania
[3]"Dunărea de Jos" University of Galaţi, REXDAN Research Centre, 98 George Coşbuc Blvd, 800223, Galaţi, Romania
[4]EnviroEcoSmart S.R.L., 189 Tecuci Street, 800276, Galaţi Romania

Corresponding author email: adrian.rosu@ugal.ro

Abstract

This study presents an analysis of suspended sediment concentration and granulometric distribution along the Sulina branch of the Danube River, based on data collected using the AQUASCAT 1000S acoustic backscatter system. Measurements were conducted at six monitoring stations near or between the localities of Sulina, Gorgova, Crişan, Maliuc, Partizani, and an intermediate station between Sulina and Crişan. The AQUASCAT 1000S was employed to gather high-resolution acoustic data using its four frequency channels, ranging from kilohertz to megahertz, allowing for simultaneous observation of both fine and coarse sediment fractions. Data processing involved comparative analyses using different combinations of acoustic channels to evaluate their effectiveness in characterizing sediment concentration and size distribution across diverse hydrological and morphological conditions along the branch. Results reveal spatial variability in suspended sediment characteristics, influenced by local hydrodynamics and proximity to tributaries, human settlements, and natural channels. The study highlights the advantages and limitations of multi-frequency acoustic techniques in riverine sediment monitoring and contributes to the development of improved methodologies for sediment characterization in deltaic environments.

Key words*: AQUASCAT 1000S, Danube River, granulometry, multi-frequency analysis, Sulina branch, suspended sediment concentration.*

INTRODUCTION

The transport of suspended particulate matter (SPM) is a major problem for the aquatic environment, modifying the morphology of the seabed, marine habitats and the water quality index (WQI). In addition, there are also problems related to the health of aquatic flora and fauna because in the water, in addition to sand and silt, microplastics, heavy metals and even nuclear waste can be found as suspended matter, which can be consumed by fish and accumulate in their bodies.(Hunter et al., 2010; 2011; Iticescu et al., 2016; Popa et al., 2018; Arseni et al., 2020; Hussain et al., 2020; Călmuc et al., 2022; Lazăr et al., 2024). If people spend too much time in contact with such waters where the amounts of SPM are high or consume fish from these areas, the negative effects of these suspended matter can have negative effects on the human body (Falciola et al., 2022). In general, this toxic pollution is strictly anthropogenic, resulting from discharges of pollutants into waters and even naval transport. For such determinations related to the amount of SPM in water and sediment transport, modern acoustic technologies are becoming increasingly important in the assessment and monitoring of the aquatic environment, and equipment based on Acoustic Backscatter (ABS) technology, such as the AQUAscat 1000S, are essential for obtaining accurate data on SPM.(Smerdon & Thorne, 2008; Foote et al., 2010; Martini et al.,

2010; Hunter et al., 2012a; 2012b; Bux et al., 2015; Divinsky & Kosyan, 2019; Fromant et al., 2017; 2021; Van Dijk et al., 2024; Zhu et al., 2024). This equipment uses high-frequency sound waves to evaluate the intensity of the signal reflected by suspended particles such as fine sediments, organic materials or microorganisms. The instrument measures the sound reflected by sediments or other materials suspended in water at precise intervals, which can be set between 2.5 mm and 4 cm. For depth measurements, this interval can be several tens of centimeters, and for monitoring suspended sediments, the typical distance is about 1-2 meters. In the case of dredging slab estimation, measurements can reach up to 10 meters (Bux, 2016; www.Aquatecsubsea.com). This study aims to highlight the advantages and limitations of multi-frequency acoustic techniques in river sediment monitoring and contribute to the development of improved methodologies for sediment characterization in deltaic environments.

MATERIALS AND METHODS

Study area and localization

The field measurements, made on 23 August 2023, targeted the Sulina branch of the Danube River located in Danube Delta, Romania. Monitoring stations were strategically positioned along this channel to capture spatial variability in hydrological and sedimentological conditions. Each station was named based on the nearest locality.

The geographic coordinates of the Aquascat measurement sites are:

- Partizani sampling station (Partizani): 45.19330° N, 28.95869° E
- Maliuc sampling station (Maliuc): 45.17459° N, 29.11427° E;
- Gorgova sampling station (Gorgova): 45.18153° N, 29.17888° E;
- Crisan sampling station (Crisan): 45.17358° N, 29.42541° E;
- Interim Sulina sampling station (near Sulina): 45.18125° N, 29.51804° E;
- Sulina sampling station (Sulina): 45.16208° N, 29.68527° E.

A map of the measurement sites where Aquascat observations were carried out is presented in Figure 1. The map was made using a Geographic Information System (GIS) providing spatial reference relative to key settlements and hydrological features of the Danube Delta.

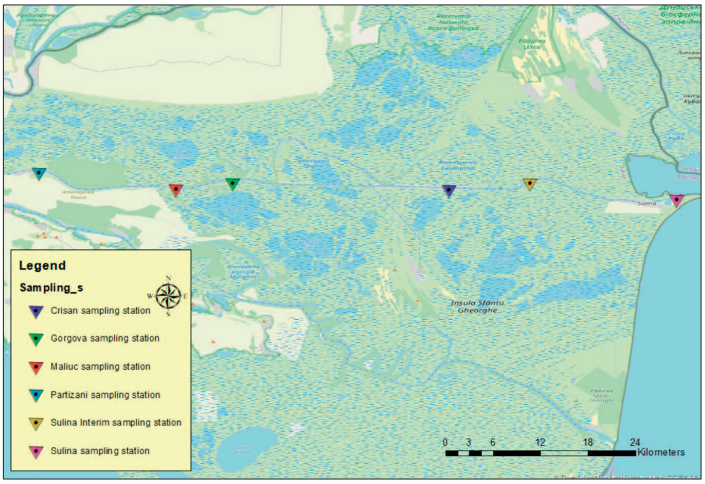


Figure 1. Location of the six sampling stations on Sulina branch located in Danube Delta

Equipment and data used

The AQUAscat 1000S is an advanced acoustic backscatter system designed for high-precision monitoring of suspended sediment concentrations (SSC) and particle dynamics in aquatic environments such as rivers, lakes,

estuaries, and coastal waters. It operates by transmitting sound pulses at multiple frequencies (typically between 300 kHz and 5 MHz) into the water and recording the intensity of the backscattered signals. Unlike light, sound propagates more slowly and is less attenuated in water, enabling the AQUAscat to generate continuous backscatter profiles rather than discrete point measurements.

SSC estimation relies on the frequency-dependent scattering properties of suspended particles. By analyzing the backscatter from multiple transmitted frequencies, the system differentiates particle sizes within a sensitivity range of 20–500 µm (radius), enabling the derivation of both particle size distribution and sediment concentration along the profiling range.

Designed to meet the demand for enhanced accuracy and efficiency, the AQUAscat 1000S significantly improves understanding of sediment dynamics, which are critical for assessing ecological processes and potential impacts on water quality and human health. Built with marine-grade materials, the AQUAscat 1000S is suitable for deployment in harsh environments and supports flexible installation (e.g., moorings, frames, or vessels). For this study, a vessel-mounted configuration was used, with the instrument secured to maintain vertical orientation and prevent transducer obstruction it can be seen in Figure 2. In this study, the AQUAscat 1000S was deployed at six monitoring stations along the Sulina branch (Partizani, Maliuc, Gorgova, Crișan, Interim Sulina, and Sulina), as illustrated in Figure 2. The main specifications of the device are detailed in Table 1.

The AQUAscat 1000S frequency range enables detection of a broad spectrum of particle sizes, from fine silt to coarse sand. High frequencies enhance sensitivity to small particles, while lower frequencies penetrate denser sediment clouds, allowing effective differentiation of particle sizes and analysis of sediment composition and transport.

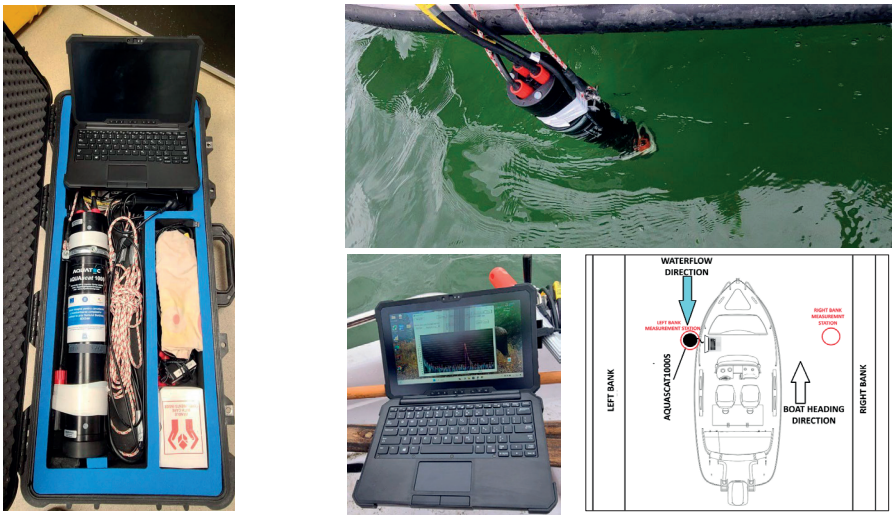
Using time-gated signal processing, the instrument divides the water column into depth bins to generate high-resolution vertical profiles of suspended sediment concentration (SSC) and particle size. Depth range and resolution are configurable to suit specific research needs.

Data analysis using AquaTalk toolkit software

Real-time data acquisition is supported through the AQUAscatTalk interface (Figure 3), which visualizes backscatter intensity per frequency. Post-processing, including calibration and application of acoustic scattering models, converts raw backscatter into SSC and particle size values.

Table 1. AQUAscat 1000S specifications (adapted after www.aquatecsubsea.com)

Specification	Description and ranges
Sediment range	Sensitive to a wide range of grain sizes Size inversion typically feasible for 20 µm to 500 µm radius Typically 0.01 g/l to 20 g/l over 1 m, or more over shorter range
Frequencies	4 frequencies - 500 kHz, 1 MHz, 2 MHz, 4 MHz
Transducers	Ø10-25mm ceramic discs (beam width according to frequency) 4 fixed transducers
Gain	Software controlled transmitter and receiver gain adjustment
Range	150 cm (typical), up to 10 m at frequencies below 2 MHz depending on options
Transmission rate	128 Hz max pulse rate for each frequency (i.e. 512 pulses per second for four), subject to acoustic range limits. Minimum rate 1 Hz for calibration
Range cells	256 cells. 2.5 mm, 5 mm, 10 mm, 20 mm and 40 mm at 1500 m/s speed of sound. Start/end range set by software
Burst duration and interval	Defined by number of profiles requested. The duration is internally generated from once every minute to once every 255 minutes, user definable start time of first burst
Trigger output	A digital output allows triggering of external instruments
Additional sensors	Built-in turbidity sensor
Data comms	RS232 up to 115 kbaud; USB 1.1 typically 2-3 Mbaud
Housing options	1000m rated aluminium alloy housing.
Software	AQUAtalk ® for AQUAscat ® for logger interaction AQUAscat ® toolkit for data processing



a) b)

Figure 2. AQUASCAT1000S: a) AQASCAT1000S equipament with all accesories and PC used for in field measurements; b) AQASCAT1000S equipment, PC and procedure (used for data recording) during deployment in measurement campaign on Sulina branch

The AQUAscatToolkit (Figures 3 and 4) is a MATLAB-based interface for processing and visualizing suspended sediment data from AQUAscat instruments.

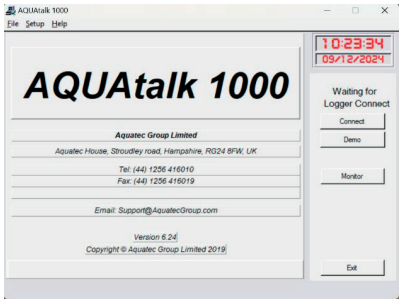


Figure 3. Software used for in-situ data measurement AQUAtalk 1000

It supports .aqa file handling, signal preprocessing, and SSC estimation.

Figure 3 shows first step of processing the raw data from the Partizani station, measured over a 10 m depth range during a 3-minute deployment. One-minute averaged profiles were generated by combining ~600 measurements per acoustic channel. Each channel targets specific sediment size ranges, enabling grain size distribution and concentration analysis. Final SSC values are computed by inverting backscatter data in the Calculated Suspended Sediment panel, providing an integrated sediment profile. Raw acoustic data from each 3-minute deployment was processed using the AQUAscatToolkit, with one-minute averaging and a 40 cm depth bin (Figure 5).

This initial preprocessing yields absolute backscatter (ABS) profiles, providing a first estimate of sediment distribution.

Suspended sediment data processing involved two main phases: (1) preprocessing, where backscatter profiles were averaged into one-minute intervals (~600 profiles per bin) to define vertical particle distribution from 40 to 1024 cm depth; and (2) post-processing, which included extensive averaging using ancillary data (temperature, pressure, salinity) to refine ABS profiles, followed by computational post-processing of raw data to derive high-resolution SSC and grain size profiles across the full 10.24 m water column.

Results were derived using the Calculated Suspended Sediment Profiles (SSCP) module, producing modeled grain size (μm) and concentration (g/L) for each 40 cm depth interval over a 10.24 m water column.

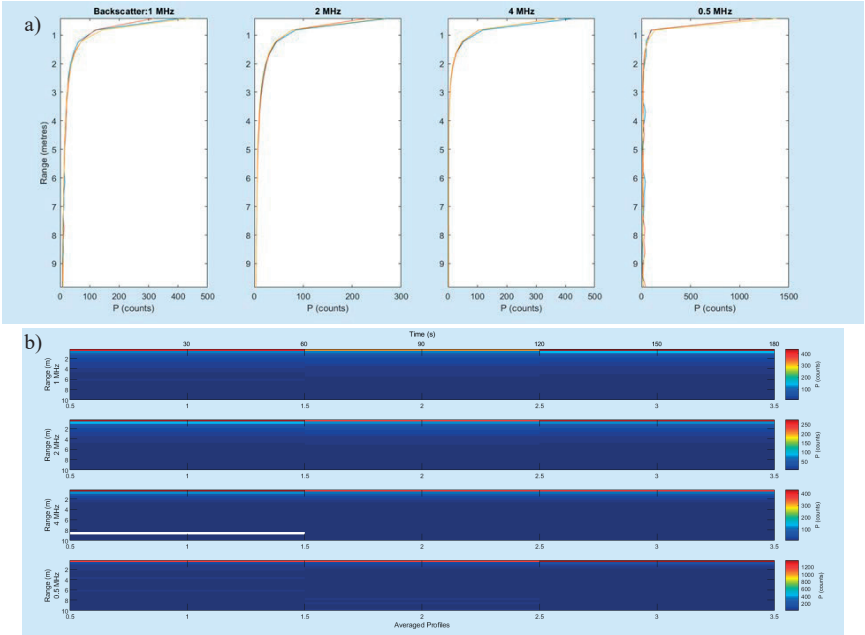


Figure 4. Measurement preprocessed results: a) Profiles of each channel recorded during monitoring campanin on 23 August 2023 at Partizani station, b) Backscater of each channel recorded during monitoring campanin on 23 August 2023 at Partizani station

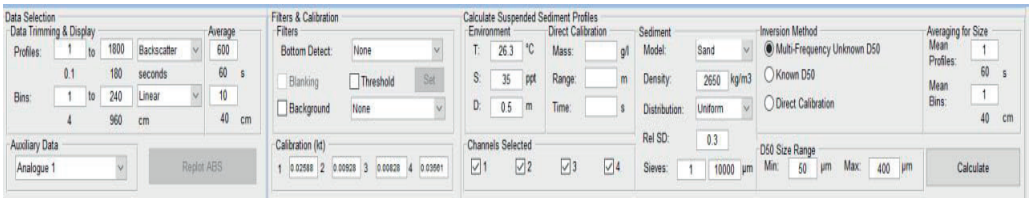


Figure 5 Settings used in AQUASCATToolkit for determining the average 1 minute grain size and concentrations

RESULTS AND DISCUSSIONS

The results obtained from AQUAscat1000S measurements at each of the six of the measurement stations on Sulina branch presented provide detailed insight into the vertical and temporal distribution of suspended sediment concentration (SSC) and particle size within the water column. The data reflects both the intensity of sediment transport processes and the stratification of grain sizes under varying hydrodynamic conditions.

Figure 6 displays the SSC and means grain radius profiles (top panels), as well as their corresponding time-series distributions (bottom panels). The vertical SSC profile shows a marked increase in concentration with depth, reaching values over 200 g/L between approximately 8.1 m and 9.5 m, indicating significant near-bed sediment presence. In contrast, concentrations decrease sharply above 6 m, with surface values below 50 g/L, likely due to strong surface flows inhibiting particle settling. The mean grain radius profile reveals coarser sediments near the surface, with values between 150-200 µm in the 0.5-4.5 m depth range. Grain size gradually decreases below this zone, reaching a minimum of around 50 µm between 6.7 m and 9 m. Notably, a secondary increase in grain size, again nearing 200 µm, is observed below 9.5 m, suggesting active sediment resuspension or bedload interaction at the channel bottom.

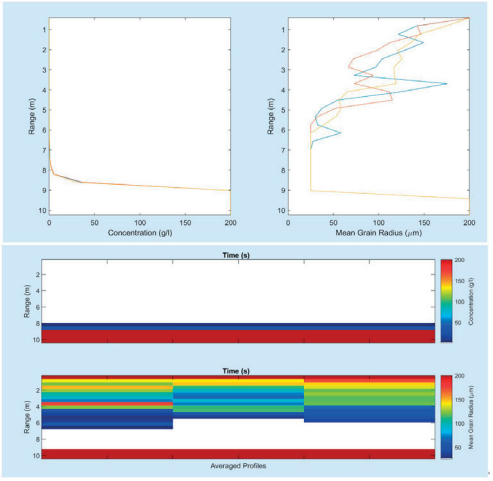


Figure 6. Profiles and time series of SSC grain size and concentration for Partizani station on 23.08.2023

These findings highlight a vertically stratified sediment structure, with finer particles suspended at mid-depths and coarse materials concentrated near the surface and bed. The distribution patterns reflect the interplay between flow velocity, sediment input, and depth-dependent turbulence, providing a representative snapshot of sediment dynamics in the Sulina branch at the time of measurement.

The measurements conducted at Maliuc station on 23 August 2024 reveal clear vertical stratification in both suspended sediment concentration (SSC) and particle size. As shown in Figure 7, SSC peaks near the channel bed, reaching values up to 200 g/L between 8.4 m and 10.2 m, while concentrations remain low (below 50 g/L) in the upper 8 m of the water column, consistent with enhanced surface flow limiting particle settling.

The grain size profile indicates coarser material near the surface, with mean grain radii reaching 200 μm in the top 0.5-2.5 m, followed by a mid-depth layer (2.5-5.7 m) of finer particles ranging from 50-120 μm. Below 5.7 m, grain sizes decrease significantly, dropping below 50 μm until approximately 9.2 m, where a second band of coarse particles (~200 μm) reappears near the bed (9.2-10.2 m), likely due to sediment resuspension or bedload interaction. These patterns show a typical two-layer structure, with coarse particles transported at the surface and near the bed, and finer sediments suspended in the mid-column, driven by local hydrodynamic conditions.

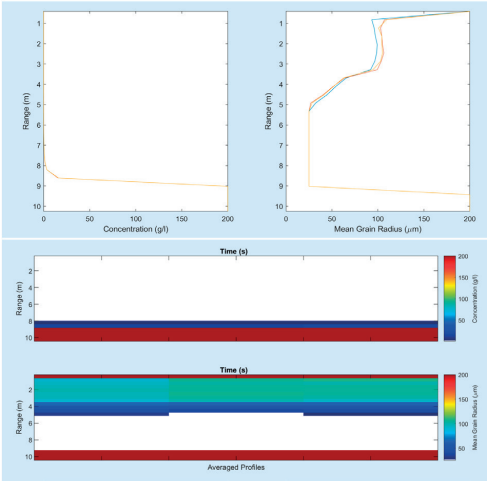


Figure 7. Profiles and timeseries of SSC grain size and concentration for Maliuc station on 23.08.2023

The vertical profiles and time-series recorded at Gorgova station (Figure 8) reveal a clear stratification of suspended sediment concentration (SSC) and grain size.

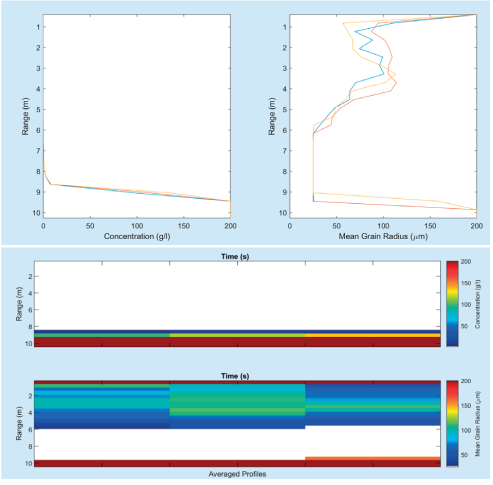


Figure 8. Profiles and timeseries of SSC grain size and concentration for Gorgova station on 23.08.2023

As shown in Figure 8, SSC values increase with depth, with concentrations of approximately 50 g/L observed between 8.5 m and 8.7 m, followed by a layer with concentrations

between 100-130 g/L from 8.7 m to 9 m. The highest SSC, exceeding 200 g/L, is concentrated near the channel bed (below 9 m), indicating active sediment resuspension or accumulation. Grain size profiles show coarse particles at the surface, with values near 200 µm in the upper 0.5-2 m, transitioning to a mid-depth band (2-6 m) where particle radii range between 50-120 µm.

Below 6 m, particle sizes decrease further, falling below 50 µm until 9.4 m. A distinct increase in grain size, again nearing 200 µm, is evident in the bottom layer (9.4-10.2 m), consistent with bedload material or localized turbulence effects. The SSC and grain size profiles recorded at Crișan station during the late summer survey indicate a clear vertical structure in sediment transport (Figure 9).

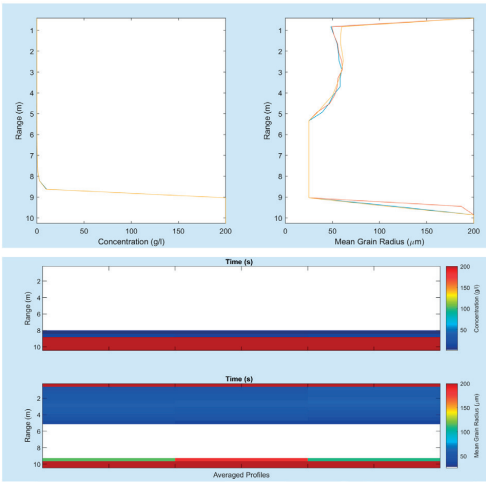


Figure 9. Profiles and timeseries of SSC grain size and concentration for Crișan station on 23.08.2023

SSC values begin to increase at depth, reaching ~50 g/L between 8.0 m and 8.7 m, with the highest concentrations exceeding 200 g/L near the channel bed (below 9 m). Near-surface concentrations remain low (below 50 g/L), likely due to higher surface flow velocities inhibiting particle settling. The anisys of calculated grain size profiles show the coarsest particles (~200 µm) at the surface in the 0-0.4 m depth bin, followed by a band of smaller particles (50-70 µm) between 0.4 m and 5.8 m. Below this, grain sizes decrease further, dropping below 50 µm between 5.8 m and 9 m, indicating a mid-column zone dominated by fine suspended sediments. A secondary increase in grain size is observed below 9 m, with values between 100-150 µm and peaking above 200 µm near the bed (9.0-9.8 m), suggesting active bedload transport or sediment resuspension in this deeper layer.

The profiles and time-series recorded at the Intermediary Crișan-Sulina station reveal pronounced vertical gradients in both suspended sediment concentration (SSC) and particle size (Figure 10).

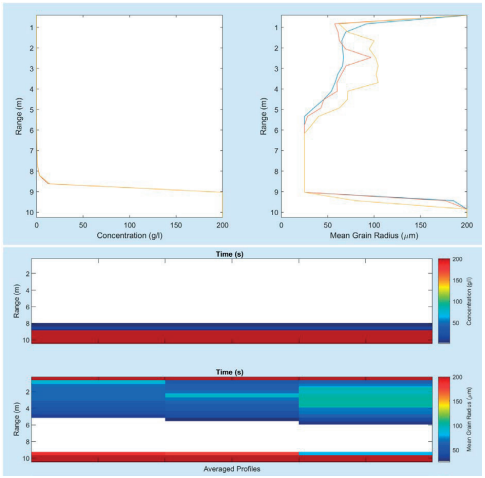


Figure 10. Profiles and time series of SSC grain size and concentration for Interim Sulina station on 23.08.2023

SSC values reach approximately 50 g/L between 8.7 m and 8.9 m, increasing to over 200 g/L near the channel bed (below 9 m), indicating significant sediment accumulation or resuspension in deeper layers. Surface concentrations remain low, under 50 g/L, likely due to enhanced turbulent mixing and flow velocity in the upper water column. Analysis on grain size distribution shows the coarsest material (~200 µm) at the surface within the 0-0.4 m bin. This is followed by a mid-layer (0.4-5.3 m) containing particles between 50-110 µm, and a further decrease below 5.7 m, where grain sizes drop below 50 µm, marking a zone dominated by fine sediments. At depths greater than 9 m, grain sizes increase again to 70-180 µm, with the bed layer exhibiting coarse material close to 200 µm, consistent with bedload transport dynamics.

At Sulina station, the suspended sediment concentration (SSC) and particle size profiles exhibit well-defined vertical patterns (Figure 11).

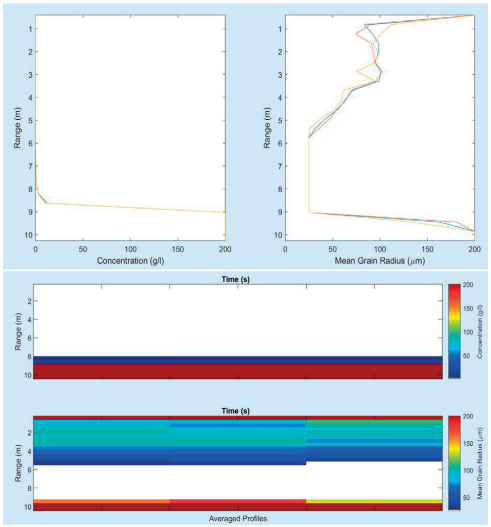


Figure 11. Profiles and time series of SSC grain size and concentration for Sulina station on 23.08.2023

SSC values begin to rise at depth, reaching approximately 50 g/L between 8.7 m and 9.0 m, and peak above 200 g/L near the channel bed (below 9 m), suggesting sediment accumulation in the deeper zone. In contrast, surface concentrations remain very low, under 50 g/L, likely due to stronger surface currents maintaining sediment in suspension or transporting it downstream. The grain size distribution reveals coarse particles (~200 μm) at the water surface within the 0-0.4 m layer, followed by a band of 50-110 μm particles in the 0.4-5.7 m depth range. Below this, grain sizes drop below 50 μm, indicating the dominance of fine sediment between 5.7 m and 9 m. At depths greater than 9 m, particle size increases again to 140-180 μm, with the bed layer (~10 m) showing grain sizes of ~200 μm, indicative of bedload transport or deposition.

These results confirm a vertically stratified sediment structure at Sulina, with coarse sediment layers at both the surface and bed, and a mid-column zone dominated by finer particles, shaped by local hydrodynamic conditions and channel morphology.

Statistical analysis of the sediment profile and transport dynamics

The Sulina branch, the only fully regulated and navigable channel of the Danube River in the Danube Delta, plays a key role in sediment transport and hydrodynamics. To assess sediment behavior along this branch, acoustic backscatter data from six stations were analyzed using Python. The analysis included vertical profiling of particle size and suspended sediment concentration (SSC), inter-station statistical comparisons, grain-size-based sediment classification (clay, silt, sand), and transport indicators such as cumulative mass and near-bed concentration, collectively offering insights into sediment distribution, flow intensity, and transport dynamics shaped by both natural and engineered conditions. Figure 12 presents overlaid line plots representing the vertical variation in particle size (μm) and suspended sediment concentration (g/l) for all six stations.

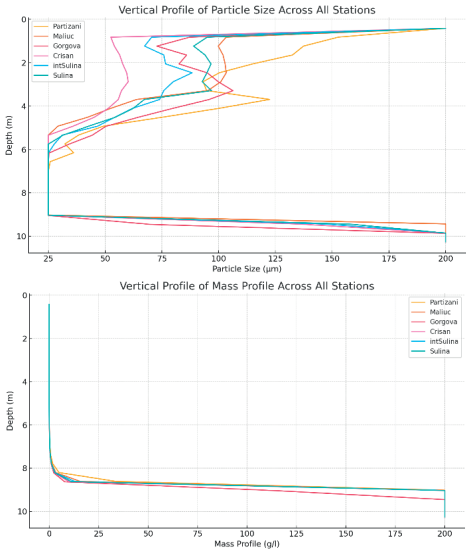


Figure 12. Vertical profiles of (a) particle size and (b) suspended sediment concentration (mass profile) across all six stations along the Sulina branch of the Danube River

Depth profiles are shown from surface to near-bed, revealing structural layering of sediment. Particle size tends to be coarser near the surface and bed, while SSC peaks at greater depths, especially below 8 m, where near-bed

resuspension is evident. The vertical separation between size and concentration layers reflects complex sediment transport regimes influenced by both turbulence and flow regulation. Partizani and Crișan show the most pronounced layering, suggesting localized energy gradients or bedload interactions.

To evaluate sediment variability along the Sulina branch, descriptive and inferential statistics were computed for each station, including measures of central tendency, dispersion, and depth correlations for both particle size and suspended sediment concentration (SSC). This statistical assessment offers insight into sediment heterogeneity, vertical structuring, and transport intensity under regulated flow conditions.

The results presented in Table 2 reveal that mean particle sizes ranged from approximately 63 to 90 μm, with highest variability observed at Partizani and Maliuc, suggesting greater sediment heterogeneity upstream. Suspended sediment concentrations (MP) exhibited large standard deviations and maximum values of 200 g/L at all stations, indicating the presence of high-density near-bed sediment layers.

Correlation analysis shows strong positive relationships between SSC and depth at all stations ($r \approx 0.64$-0.66, $p < 0.001$), consistent with typical stratified sediment profiles in energetic fluvial systems. In contrast, particle size-depth correlations were weaker and less consistent, reflecting more complex sediment sorting influenced by flow velocity gradients and local morphology. These statistical indicators support the presence of depth-dependent sediment stratification and highlight upstream-to-downstream shifts in sediment composition and concentration patterns along the Sulina branch. Classifying suspended sediments by grain size in our dataset allowed us to evaluate flow energy conditions, dominant sediment transport modes, and potential depositional environments along the Sulina branch.

Table 2. Statistical summary of suspended sediment parameters by station

Station	Mean Size (μm)	Std Size (μm)	Min Size (μm)	Max Size (μm)	Mean MP (g/l)	Std MP (g/l)	Min MP (g/l)	Max MP (g/l)	r(S,D)*	p(S,D)*	r(MP,D)*	p(MP,D)*
Partizani	90.23	64.08	25.00	200.00	33.67	74.39	0.0004	200.00	-0.224	0.2818	0.6637	0.0003
Maliuc	77.82	63.21	25.00	200.00	32.86	74.52	0.0002	200.00	-0.079	0.7074	0.6504	0.0004
Gorgova	74.71	55.15	25.00	200.00	29.10	68.37	0.0007	200.00	-0.173	0.4095	0.6398	0.0006
Crișan	62.90	56.93	25.00	200.00	32.59	74.60	0.0015	200.00	0.104	0.6224	0.6457	0.0005
Int. Sulina	71.09	56.86	25.00	200.00	32.74	74.55	0.0006	200.00	-0.006	0.9784	0.6483	0.0005

*D - Water column depth or depth; MP - mass profile or concentration sediment particles; S - Size of the sediment particles.

Given the high-energy, regulated nature of this channel, we used standard granulometric thresholds - clay (<4 μm), silt (4-63 μm), and sand (>63 μm) - to distinguish between suspended, wash load, and bedload transport regimes.

Based on the measured particle size values at each depth, we categorized sediment samples into these three classes. For each station, we calculated the percentage contribution of clay, silt, and sand within the water column, enabling a clear assessment of the dominant sediment fractions and their vertical distribution across the branch. The results can be seen in Table 3.

The results confirm that sand-sized particles dominate the suspended load at all stations (>89%), indicative of a high-energy, turbulent regime capable of mobilizing and suspending coarse material. The low clay and silt content further suggests that fine sediments are either scoured or flushed downstream, consistent with the artificially regulated and navigable nature of the Sulina branch.

Table 3. Sediment classification by grain size

Station	Clay (%)	Silt (%)	Sand (%)
Partizani	1.52	4.55	93.94
Maliuc	1.52	4.55	93.94
Gorgova	1.52	7.58	90.91
Crișan	1.52	9.09	89.39
Int. Sulina	1.52	7.58	90.91

Slightly higher silt content at downstream stations may signal reduced turbulence or

localized deposition zones, but these remain minor. To assess sediment mobility and deposition potential along the Sulina branch, we calculated three key indicators based on our data: cumulative sediment mass (g/l) as a proxy for total load, near-bed average suspended sediment concentration (SSC) to identify potential resuspension zones, and the correlation between particle size and SSC to evaluate the relationship between sediment coarseness and concentration. These metrics enabled comparative analysis between stations, highlighting differences in transport energy, vertical sediment structure, and the contribution of coarser particles to the suspended load (Tabel 4).

Table 4. Sediment transport indicators

Station	Cumulative Mass (g/l)	Near-Bed Avg MP (g/l)	Size-MP Correlation
Partizani	841.86	166.74	0.438
Maliuc	821.48	163.14	0.545
Gorgova	727.59	144.64	0.473
Crișan	814.66	161.98	0.604
Int. Sulina	818.41	162.61	0.558

The upstream stations Partizani and Maliuc register the highest cumulative sediment loads, likely due to greater sediment input or upstream scouring. Near-bed concentrations exceeding 160 g/l across all stations confirm the presence of dense sediment layers at depth, characteristic of bedload interaction or resuspension zones. Moreover, the moderate-to-strong positive correlations ($r = 0.44$-0.60) between particle size and SSC suggest that coarser particles are frequently suspended when concentrations are high, pointing to intense turbulent mixing and localized energy peaks within the flow.

CONCLUSIONS

This study provided a detailed assessment of suspended sediment dynamics along the Sulina branch, the only fully regulated and navigable distributary of the Danube River. Using high-resolution acoustic backscatter data from six monitoring stations, we analyzed vertical profiles of suspended sediment concentration (SSC) and particle size, supported by statistical classification and transport indicators.

The results revealed a clear vertical stratification of sediments, with SSC peaking near the riverbed (often exceeding 160 g/l) and particle sizes ranging from fine silts to coarse sands. Statistical analysis showed strong positive correlations between SSC and depth, confirming concentrated sediment layers at depth across all stations. In contrast, particle size showed more variable vertical patterns, suggesting localized flow effects.

Sediment classification based on grain size demonstrated a clear dominance of sand (>63 μm) at all stations, consistent with the high-energy, engineered channel environment. Fine sediment fractions (clay and silt) were minimal, indicating efficient downstream flushing and limited deposition zones.

Transport indicators further supported these findings, with upstream stations exhibiting higher cumulative sediment loads, and moderate to strong correlations between particle size and SSC indicating the frequent suspension of coarse material under energetic flow conditions.

Together, these analyses confirm that the Sulina branch functions as a high-capacity sediment transport corridor, where flow regulation enhances both sediment throughput and vertical stratification. The findings have important implications for navigation management, dredging operations, and understanding sedimentary processes in modified deltaic systems.

ACKNOWLEDGEMENTS

The authors acknowledge the support of the project "HORIZON-MISS-2021-OCEAN-02, DANUBE REGION WATER LIGHTHOUSE ACTION," Project No. 101094070 — DALIA, funded by the European Union's Horizon Europe programme. The equipment used for this study is part of the REXDAN Research Infrastructure (REXDAN RI).

REFERENCES

Arseni, M., Rosu, A., Calmuc, M., Calmuc, V. A., Iticescu, C., & Georgescu, L. P. (2020). Development of flood risk and hazard maps for the lower course of

the Siret River, Romania. *Sustainability, 12*(16), 6588. https://doi.org/10.3390/su12166588

Bux, J., Peakall, J., & Biggs, S. (2015). *In situ* characterisation of a concentrated colloidal titanium dioxide settling suspension and associated bed development. *Powder Technology.* https://www.sciencedirect.com/science/article/pii/S0032591015005604

Bux, J. (2016). *Novel characterisation of concentrated dispersions by in situ acoustic backscatter systems* [Doctoral thesis, University of Leeds]. White Rose eTheses Online. https://etheses.whiterose.ac.uk/id/eprint/14306/

Călmuc, M., Călmuc, V. A., Arseni, M., Simionov, I. A., Antache, A., Apetrei, C., & Georgescu, P. L. (2022). Identification and characterization of plastic particles found in the Lower Danube River. *Scientific Papers. Series E. Land Reclamation.* https://landreclamationjournal.usamv.ro/pdf/2022/Art40.pdf

Divinsky, B. V., & Kosyan, R. D. (2019). Bottom sediment suspension under irregular surface wave conditions. *Oceanology, 59*(4), 482–490. https://doi.org/10.1134/S0001437019040039

Falciola, L., Ancona, V., Zlati, M. L., Georgescu, L. P., Iticescu, C., Ionescu, R. V., & Antohi, V. M. (2022). New approach to modelling the impact of heavy metals on the European Union's water resources. *International Journal of Environmental Research and Public Health, 20*(1), 45. https://doi.org/10.3390/ijerph20010045

Foote, K., & Martini, M. A. (2010). Standard-target calibration of an acoustic backscatter system. In *OCEANS 2010 MTS/IEEE Seattle*. IEEE. https://ieeexplore.ieee.org/abstract/document/5664362/

Fromant, G., Le Dantec, N., & Perrot, Y. (2021). Suspended sediment concentration field quantified from a calibrated MultiBeam EchoSounder. *Applied Acoustics.* https://www.sciencedirect.com/science/article/pii/S0003682X21002000

Fromant, G., Floc'h, F., Lebourges-Dhaussy, A., Jourdin, F., Perrot, Y., Le Dantec, N., & Delacourt, C. (2017). In situ quantification of the suspended load of estuarine aggregates from multifrequency acoustic inversions. *Journal of Atmospheric and Oceanic Technology, 34*(8), 1703–1717. https://journals.ametsoc.org/view/journals/atot/34/8/jtech-d-16-0079.1.xml

Hunter, T., Biggs, S., & Peakall, J. (2010). An acoustic backscatter system (ABS) for the characterisation of legacy waste dispersions. In *DIAMOND Annual Conference*. https://www.researchgate.net/publication/267684290

Hunter, T., Biggs, S., Young, J., Fairweather, M., & Peakall, J. (2011). Ultrasonic techniques for the in situ characterization of nuclear waste sludges. In *WM Symposia*. https://archivedproceedings.econference.io/wmsym/2011/papers/11275.pdf

Hunter, T., Darlison, L., Peakall, J., & Biggs, S. (2012a). Using a multi-frequency acoustic backscatter system as an in situ high concentration dispersion monitor. *Chemical Engineering Science.* https://www.sciencedirect.com/science/article/pii/S0009250912003946

Hunter, T., Peakall, J., & Biggs, S. (2012b). An acoustic backscatter system for in situ concentration profiling of settling flocculated dispersions. *Minerals Engineering.* https://www.sciencedirect.com/science/article/pii/S0892687511004298

Hussain, S. T., Hunter, T. N., Peakall, J., & Barnes, M. (2020). Utilisation of underwater acoustic backscatter systems to characterise nuclear waste suspensions remotely. *Proceedings of Meetings on Acoustics, 40*(1), 070005. https://doi.org/10.1121/2.0001303

Iticescu, C., Murariu, G., Georgescu, L. P., Burada, A., & Topa, C. M. (2016). Seasonal variation of the physico-chemical parameters and Water Quality Index (WQI) of Danube water in the transborder Lower Danube area. *Revista de Chimie, 67*(9), 1772–1779. http://bch.ro/pdfRC/ITICESCU%20C%209%2016.pdf

Lazăr, N. N., Simionov, I. A., Petrea, Ș. M., Iticescu, C., Georgescu, P. L., Dima, F., & Antache, A. (2024). The influence of climate changes on heavy metals accumulation in *Alosa immaculata* from the Danube River Basin. *Marine Pollution Bulletin, 200,* 116145. https://doi.org/10.1016/j.marpolbul.2024.116145

Martini, M. A., & Foote, K. G. (2010). Measurements of echo stability of an acoustic backscatter system. In *OCEANS 2010 MTS/IEEE Seattle*. IEEE. https://ieeexplore.ieee.org/abstract/document/5664356/

Popa, P., Murariu, G., Timofti, M., & Georgescu, L. P. (2018). Multivariate statistical analyses of water quality of Danube River at Galati, Romania. *Environmental Engineering and Management Journal.* https://www.researchgate.net/publication/307955477

Smerdon, A. M., & Thorne, P. D. (2008). A coastal deployment of a commercial multiple frequency acoustic backscatter sediment profiler. https://nora.nerc.ac.uk/id/eprint/6491/

Van Dijk, T. A. G. P., Roche, M., Lurton, X., Fezzani, R., Simmons, S. M., Gastauer, S., Mesdag, C., Berger, L., Klein Breteler, M., & Parsons, D. R. (2024). Bottom and suspended sediment backscatter measurements in a flume—Towards quantitative bed and water column properties. *Journal of Marine Science and Engineering, 12*(4), 609. https://doi.org/10.3390/jmse12040609

Zhu, Q., Xing, F., Wang, Y. P., Syvitski, J., Overeem, I., Guo, J., Li, Y., Tang, J., Yu, Q., Gao, J., & Gao, S. (2024). Hidden delta degradation due to fluvial sediment decline and intensified marine storms. *Science Advances, 10*(18), eADK1698. https://doi.org/10.1126/sciadv.adk1698

Scientific Papers. Series E. Land Reclamation, Earth Observation & Surveying, Environmental Engineering. Vol. XIV, 2025
Print ISSN 2285-6064, CD-ROM ISSN 2285-6072, Online ISSN 2393-5138, ISSN-L 2285-6064

ADVANCING URBAN AIR POLLUTION MONITORING WITH REMOTE SENSING AND LOW-COST SENSOR TECHNOLOGIES

Adrian ROȘU[1, 2], Daniel-Eduard CONSTANTIN[1, 2], Maxim ARSENI[1, 2], Mirela VOICULESCU[1, 2], Cătălina ITICESCU[1, 2], Puiu-Lucian GEORGESCU[1, 2], Ionuț Cornel BEJAN[1, 3], Sorin FRĂSINĂ[1], Silvia DRĂGAN[4], Mădălin CRISTEA[1]

[1]"Dunărea de Jos" University of Galați, Faculty of Sciences and Environment, Department of Chemistry, Physics and Environment, 111 Domnească Street, Galați, Romania
[2]"Dunărea de Jos" University of Galați, REXDAN Research Infrastructure, 98 George Coşbuc Blvd, Galați, Romania
[3]Environmental Guard Galați, 24 Logofăt Tăutu Street, Galați, Romania
[4]EnviroEcoSmart S.R.L., 189 Tecuci Street, Galați, Romania

Corresponding author emails: rosu_adrian_90@yahoo.ro, adrian.rosu@ugal.ro

Abstract

Urban air pollution poses a critical challenge due to rapid urbanization, increasing vehicular emissions, industrial activities, and infrastructure expansion. Accurately assessing pollution levels and pinpointing emission sources is essential for effective environmental management. This study integrates advanced remote sensing techniques with cost-effective sensor technologies to monitor air quality in an urban setting. Mobile measurements were conducted on April 18, 2024, using the UGAL MDOAS system and the Sniffer 4D sensor, both mounted on a vehicle. The UGAL MDOAS system employs Differential Optical Absorption Spectroscopy (DOAS) to detect atmospheric trace gases, while the Sniffer 4D utilizes electrochemical sensors to quantify pollutant concentrations. This study focuses on measuring and comparing NO_2, O_3, SO_2, O4 and PM levels from both instruments. The findings contribute to enhancing urban air pollution monitoring by demonstrating the effectiveness of hybrid measurement approaches in identifying pollution hotspots and improving air quality assessments.

Key words*: air pollution, urban monitoring, remote sensing, low-cost sensors, DOAS, air quality assessment.*

INTRODUCTION

In recent years, the increase in air pollution in urban areas has become a significant problem. The development and expansion of rural areas comes at the same time as increasing pollution and decreasing the quality of the environment in which we live. It affects the health of residents, causing everything from respiratory discomfort to chronic lung and even heart diseases (Adebayo-Ojo et al., 2022.; Bernstein et al., 2004; Brunekreef et al., 2022; Zhang et al., 2014). Among these dangerous pollutants are NO_2, O_3, SO_2 and particulate matter (PM) (Adebayo-Ojo et al., 2022; Al-Janabi et al., 2021). In addition to negative effects on human health in their primary state, these pollutants can transform, with the help of other substances in the air or ultraviolet radiation, into other much more dangerous pollutants such as photochemical smog, which has represented and represents a major problem in heavily industrialized rural areas with increased traffic (Rani et al., 2011; Tiao et al., 1975; Carlos Meier et al., 2017; D. Constantin et al., 2013; Constantin et al., 2020).

The main sources of these pollutants are industrialization, infrastructure development and expansion of urban areas as well as the increased number of vehicles, but there can also be natural sources such as fires, lightning or volcanic eruptions and even biological sources like microbial activity in soil. Advancing technology offers us increasingly advanced possibilities for monitoring air quality, including techniques and devices such as UGAL MDOAS and Sniffer4D v2.

This analysis aims to determine whether emission sources are identified by mobile monitoring. Also, the study aims to compare if the data from both equipment's are suited to identify emissions sources of know pollutants such as: NO_2, SO_2, O_3 and PM. Another direction is to compare the recorded data from both instruments to show how emissions are dispersed on altitudes depending on emission

source such as industry or car traffic (Constantin et al., 2017; Roșu et al., 2017; Roșu et al., 2020).

MATERIALS AND METHODS

Study area and measurement system configuration

The study aims to measure air pollution levels and identify emission sources in the city of Galati by using the measurements made on April 18, 2024, along the city's main street. The measurement route is presented in Figure 1 along with general wind speed and direction during measurement, also some with the local air quality stations (AQS). Unfortunately, that day all the were on maintenance routine and no data for comparison with our measurements was possible.

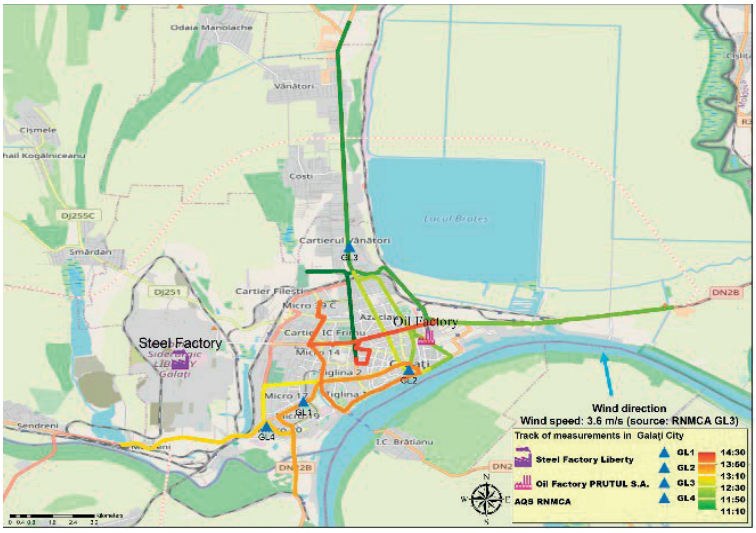


Figure 1. The route on which the measurements were taken correlated with the time interval

This study presents the results of mobile air quality measurements conducted in one of the largest cities in Romania using a remote sensing system developed by the Faculty of Science and Environment, University "Dunărea de Jos" of Galați called UGAL MDOAS, along with a multisensory system, Sniffer 4D. Both instruments were mounted on the same vehicle, allowing simultaneous data collection and facilitating direct comparison between the two systems. (Figure 2).

The UGAL MDOAS system uses differential optical absorption spectroscopy (DOAS) techniques to determine gas densities in the atmosphere with capabilities of measurement of the pollutants located in troposphere as molecules/cm^2, while Sniffer 4D uses electrochemical sensors to quantify pollutant concentrations in the air around the car where the system is mounted. These two complementary measurement techniques provide a more comprehensive understanding of air pollution dynamics by combining remote sensing with direct low cost *in situ* monitoring methods.

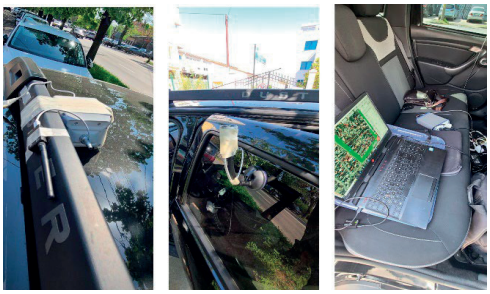


Figure 2. Mobile system setup for Sniffer4Dv2 and MDOAS UGAL

Equipment and data used

The equipment Sniffer4D V2 is an advanced gas detection and mapping system, designed to simultaneously measure up to 9 types of gases and particles at a time, providing real-time 2D

and 3D maps of their distribution. The system can monitor parameters such as: $PM_{2.5}$, PM_{10}, O_3, NO_2, CO, SO_2, VOCs, Odor (OU), CH_4, Cl_2, H_2S, H_2, HF, PH_3, Gas sampling, wind and speed direction and other customised parameters. Our system configuration has only the sensors for: PM_{10}, $PM_{2.5}$, O_3 NO_2 and SO_2. Other features that Sniffer4D V2 has are presented in Table 1.

The system is composed of multi-gas detection hardware and powerful analytical software, that can easily be integrated onto drones or ground vehicles for efficient inspections in various environments. (Godfrey et al., 2022; h*ttps://Enterprise.Dji.Com/Ecosystem/Sniffer-V2*; Jiang et al., 2024; Kulakova et al., 2024; Liu et al., 2024; Prisacariu et al., 2022; Yu et al., 2022).

In addition, by assessing spatial variations in pollutant concentrations, the study analyses the evaluation of stationary monitoring networks in capturing hotspots of transient emission events that would otherwise be overlooked.

Table 1. Specifications and capabilities of Sniffer4D V2 equipment (https://Enterprise.Dji.Com/Ecosystem/Sniffer-V2)

Category	Specification/Feature
Dimensions	157 × 103 × 87 mm
Weight	< 500 g
Ingress Protection	IPX2 (protection against vertically dripping water)
Explosion Proof	Yes (Ex-proof rated)
Casing	Aluminium alloy with anti-EMI shielding
Mounting	Internal suspension mechanism for shock and vibration isolation
Air Intake	Active air intake system
Connectivity	Supports GSM/cellular network connectivity
Data Management	- Automatic data backup to SD card (if installed) - Built-in data retrieval algorithm
Mobility Potential	Compact and lightweight design suitable for mounting on drones or mobile platforms

The DOAS technique, in particular the differential oblique column density (DSCD) retrieval method for measuring trace gases in upper atmosphere (troposphere). The system used, called UGAL MDOAS (employs Differential Optical Absorption Spectroscopy), was at "Dunărea de Jos" University of Galați, Faculty of Science and Environment (D. Constantin et al., 2013; D.E. Constantin et al., 2017; Roșu et al., 2017; Roșu et al., 2020). Configuration of the UGAL MDOAS system can be found below in Table 2 for main components and Table 3 for the details on the main component (spectrometer) of the UGAL DOAS instrument.

Table 2. The main components of the UGAL MDOAS

Component	Description
UV–Vis spectrometer	Avantes AvaSpec-ULS2048, one channel Black baffle: internal diameter: 9 mm, length: 2 cm
Telescope (baffle+lens)	Black baffle: internal diameter: 9 mm, length: 2 cm Avantes collimating lens; confocal length: 8.7 mm Telescope's field of view: 2.56°
Optical fiber	Avantes 600 µm chrome plated brass optical fiber, 1 or 10 m length
GPS	Mouse GPS for positioning of recorded data
PC	Laptop with win 10 or 11

Table 3. The main characteristics of the Avantes UV-Vis spectrometer

Specification	Description
Optical Bench	symmetrical Czerny-Turner, 75 mm focal length
Wavelength range	200-550 nm
Resolution	0.7 nm
Sensitivity	250,000 counts/µW per ms int. time
Detector	Back-thinned CCD [1] image sensor 2048 × 16 pixels, non-cooled
Signal/Noise	450:1
Integration time	1.82 ms–60 s
Interface	USB 2.0 high speed, 480 Mbps RS-232, 115,200 bps
Data transfer speed	1.82 ms/scan (USB2.0 [2])
Power supply	Default USB power, or with SPU2 external 12 V DC
Dimensions; weight	175 × 110 × 44 mm (1 channel), 855 g

RESULTS AND DISCUSSIONS

Using the data collected by both devices and using a GIS software we have made a series of maps that highlight spatial comparison of the recorded values for each parameter such as: NO_2, SO_2, O_3, O_4 and $PM_{2.5}$. The entire measurement timeline for the track analyzed on April 18, 2024, is represented using a color gradient, with measurements taken after 11:00 displayed in green and those after 14:00 shown in red, as illustrated in Figure 1. Spatial analysis of the data using maps enables a detailed evaluation of parameter variations and provides

a clearer understanding of their distribution in the troposphere and their dynamics near the surface.

These observations are essential for identifying and quantifying factors that influence air quality, such as industrial activity within the city, as well as the effects of other variables, including wind direction and the influence of urban topography on the positioning of emission plumes.

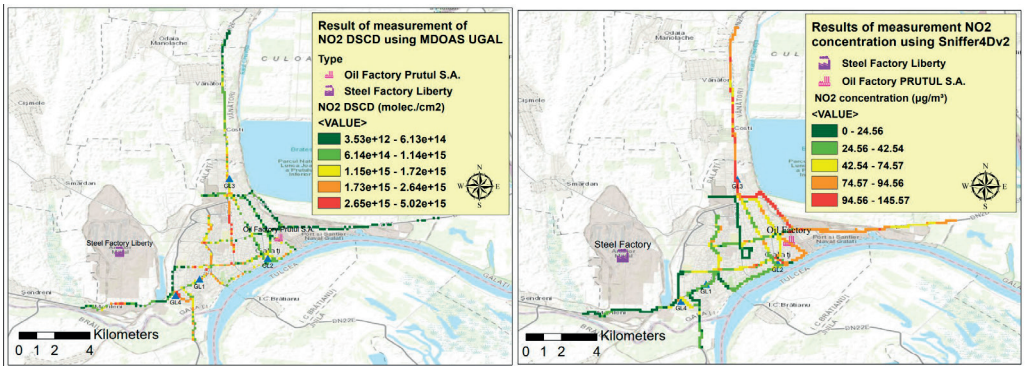


Figure 3. Spatial comparisons of NO_2 measured by the mobile system Sniffer 4Dv2 and MDOAS UGAL

As shown in Figure 3, the measurement units differ between the two instruments. This is because the Sniffer4Dv2 detects NO_2 concentrations at ground level, reporting values in µg/m³, whereas the MDOAS UGAL (UM) measures the vertical column density of NO_2 molecules over a 1 cm² cross-sectional area, expressed in molecules/cm².

Due to these differing units and sensing approaches, comparisons between the two instruments rely on colour-coded ranges. At the beginning of the measurement route, the MDOAS UGAL registers relatively low NO_2 values, with the first segments mostly falling into the green to light green range (3.53×10^{12} to 1.14×10^{15} molecules/cm²). In contrast, the Sniffer4Dv2 shows moderate to high concentrations for the same segments, predominantly within the orange to red classes (74.57 – 145.57 µg/m³), particularly in the northern and eastern parts of the city.

This discrepancy suggests that, during the measurement period, NO_2 was more concentrated near the surface, likely due to localized emissions such as road traffic and industrial activities. The MDOAS UGAL, measuring total column density, might underrepresent surface-level pollution when vertical mixing is limited or when pollutants are trapped in the lower atmospheric layers.

In the southern and central parts of Galați, especially after 12:40 (as inferred from route direction and segment labels), the MDOAS UGAL data reveal greater spatial variability. While most areas, including the zone near the Steel Factory Liberty, show low to moderate NO_2 columns (dark green to yellow), a localized hotspot (red) south of the industrial area indicates a significant vertical NO_2 presence, possibly from a point source or stack emissions. Meanwhile, the Sniffer4Dv2 continues to show elevated ground-level concentrations in these areas, especially near the oil factory, the steel plant, and key urban intersections, indicating intense surface-level NO_2 due to industrial and vehicular emissions. Some segments in the south and near the lake show improved air quality (green), suggesting either fewer emissions or better pollutant dispersion.

These contrasting observations highlight the different sensitivities and spatial resolutions of the instruments. The MDOAS UGAL is influenced by the vertical distribution of NO_2, while the Sniffer4Dv2 reflects surface concentrations, where human exposure is most relevant. The data suggest that during the measurement period, NO_2 pollution was largely confined to the lower atmosphere, emphasizing the dominant influence of ground-level sources such as traffic and localized industrial activity.

A spatial comparison of SO_2 measurements from both devices is presented in Figure 4.

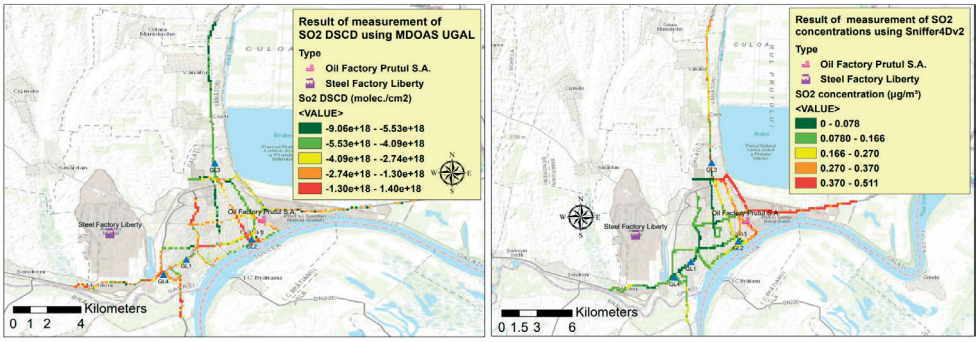


Figure 4. Spatial comparisons of SO_2 measured by the mobile sistems Sniffer 4Dv2 and MDOAS UGAL

Figure 4 presents a comparison of SO_2 concentrations measured by the MDOAS UGAL system (top) and the Sniffer4Dv2 (bottom). The MDOAS UGAL device measures SO_2 vertical column densities, which are especially sensitive to elevated emission sources such as those from industrial chimneys. Accordingly, it detects higher values of SO_2 (up to 1.30×10^{18} molecules/cm²) around industrial areas, particularly near the Steel Factory Liberty and the Oil Factory Prutul S.A., indicating the influence of high-altitude emissions. In contrast, lower values (as low as 4.86×10^{15} molecules/cm²) are observed on the road exiting the city to the north and in less industrialized zones during the first half hour of monitoring, suggesting cleaner atmospheric columns in those areas.

Meanwhile, the Sniffer4Dv2, which measures ground-level SO_2 concentrations, records significantly higher values (up to 0.511 µg/m³) in the eastern and north-eastern parts of the city, where emissions are likely trapped near the surface due to low wind speeds or limited vertical mixing. However, in the southwestern industrial area, Sniffer4Dv2 shows lower concentrations (mostly below 0.166 µg/m³), even though MDOAS UGAL reports high column densities in the same area. This contrast supports the conclusion that the industrial SO_2 emissions there are released at higher altitudes - above the sensitive range of the Sniffer4Dv2 but well captured by the DOAS system.

It is important to note that the Sniffer4Dv2, being a compact and portable sensor, is primarily designed for ground-level monitoring. However, its capability to be mounted on unmanned aerial vehicles (UAVs) such as drones offers the potential to detect elevated industrial plumes in future studies. This application will be further explored to assess vertical emission structures more comprehensively.

This comparison underscores the complementary nature of the two instruments: while the MDOAS UGAL is effective in detecting elevated plumes from point sources such as stacks, the Sniffer4Dv2 provides detailed information about ground-level exposure relevant for human health assessments, and potentially, in future configurations, about elevated sources as well.

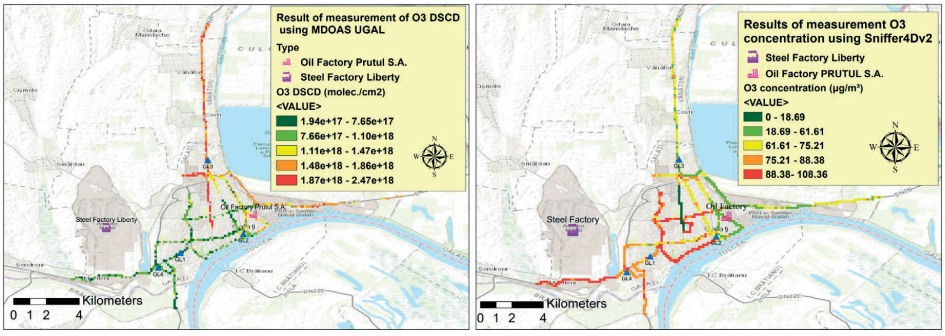


Figure 5. Spatial comparisons of O_3 measured by the mobile sistems Sniffer 4Dv2 and MDOAS UGAL

Figure 5 presents the spatial distribution of ozone (O_3) concentrations measured by MDOAS UGAL (top panel) and Sniffer4Dv2 (bottom panel). The results show a notable inversion in the spatial trends between the two instruments.

In the northern and eastern sections of the city, before 12:50, the MDOAS UGAL recorded higher ozone column densities, with values predominantly in the range of 1.46×10^{18} to 2.04×10^{18} molecules/cm², indicating elevated ozone presence in the vertical atmospheric column. In contrast, the Sniffer4Dv2 recorded lower ground-level ozone concentrations in the same areas, generally between 16.01 and 58.31 µg/m³, suggesting better air quality at the surface in those regions. After 12:50, the situation reverses: the MDOAS UGAL measurements show reduced column densities, mostly in the range of 7.66×10^{17} to 1.18×10^{18} molecules/cm², with only isolated moderate values at traffic intersections. However, the Sniffer4Dv2 records increased ground-level concentrations, with values reaching the highest range of 78.31–103.56 µg/m³, particularly in the central and southwestern parts of the route. These are indicators of poor air quality likely driven by surface-level ozone formation from traffic-related precursors and sunlight-driven photochemical activity.

This comparison emphasizes the different vertical sensitivities of the two instruments. MDOAS UGAL detects total atmospheric column densities, making it sensitive to ozone aloft, while Sniffer4Dv2 provides data directly relevant to human exposure at ground level.

The O_4 (oxygen dimer) is formed when two O_2 molecules interact and briefly bind together, typically under high-pressure conditions. Although O_4 is not stable as a separate pollutant, its absorption features are useful for atmospheric remote sensing, as its concentration is proportional to air density and can provide information about the vertical distribution of pollutants (Wagner et al., 2004). It also plays a role in radiative transfer and can indicate regions with higher aerosol presence (Wagner et al., 2004).

On the other hand, $PM_{2.5}$ is a particulate matter with a diameter less than 2.5 micrometres, which is comparable to O4, is a major air pollutant that may cause serious health risks. Due to their small size, $PM_{2.5}$ particles can penetrate deep into the respiratory system, reaching the alveoli and even entering the bloodstream. Long-term exposure is associated with respiratory and cardiovascular diseases, including asthma, bronchitis, heart attacks, and increased mortality (Pope and Dockery, 2006).

While O_4 is measured by the MDOAS UGAL instrument as a tracer of air mass density and potential aerosol interaction in the atmospheric column (Wagner et al., 2004), $PM_{2.5}$ is measured directly at ground level by the Sniffer4Dv2. When interpreted together, these parameters can help infer the vertical and horizontal distribution of particulate pollution: elevated O_4 may indicate dense air layers or aerosol-rich zones, which could be linked to high surface $PM_{2.5}$ concentrations under stagnant or stratified atmospheric conditions.

In our study, we also addressed this research direction by leveraging the unique capabilities of the MDOAS UGAL to retrieve O_4 column densities and the Sniffer4Dv2 to measure $PM_{2.5}$ concentrations, providing a more comprehensive perspective on atmospheric composition and air quality dynamics, as shown in Figure 6.

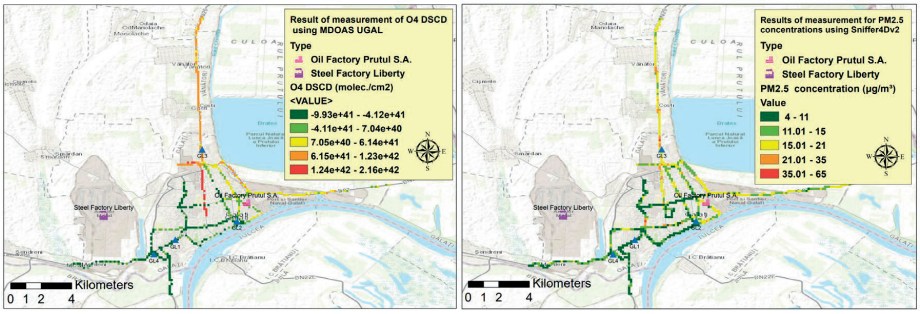


Figure 6. Spatial distribution of O_4 and $PM_{2.5}$ measured by MDOAS UGAL respectively Sniffer4Dv2

Figure 6 illustrates the spatial and temporal behaviour of two distinct atmospheric parameters: O_4 (oxygen dimer) measured by the MDOAS UGAL system (top panel), and $PM_{2.5}$ (particulate matter < 2.5 μm) measured at ground level by Sniffer4Dv2 (bottom panel).

The upper map shows a clear decreasing trend in O_4 differential slant column densities throughout the measurement period. Initially, the O_4 values are highest, exceeding 1.62×10^{42} molec./cm², but progressively decline, reaching the lowest range (4.85×10^{41} to 1.02×10^{42} molec./cm²) toward the end of the route. This pattern is likely influenced by increasing solar radiation and temperature, both of which can affect the stability of O_4. The oxygen dimer is transient and weakly bound, and under elevated temperature and strong UV radiation, it can dissociate more rapidly, leading to lower detected column densities as the day progresses. In contrast, the $PM_{2.5}$ ground-level concentrations measured by Sniffer4Dv2 show a more consistent spatial-temporal distribution. Higher values (15-35 μg/m³) are recorded at the beginning of the measurement period, with concentrations gradually decreasing to values below 15 μg/m³, predominantly within the 4-11 μg/m³ range by the second half of the route. This trend reflects the settling or dispersion of fine particulate matter, possibly aided by morning turbulence or changing traffic patterns.

A significant factor contributing to the observed differences between the instruments lies in their measurement geometry and altitude sensitivity. The MDOAS UGAL captures slant column densities through the atmosphere, with sensitivity up to approximately 2 km altitude. Therefore, it can detect pollution plumes situated aloft, which may not be captured by ground-based systems such as Sniffer4Dv2. Conversely, Sniffer4Dv2 records near-surface concentrations, reflecting immediate human exposure but missing elevated layers of pollution.

When Sniffer4Dv2 reports lower values than MDOAS UGAL, it may indicate that the pollution plume is located at higher altitudes - a condition potentially linked to emissions from tall industrial stacks. In particular, areas near factories may exhibit these discrepancies due to elevated release points of SO_2 and PM precursors.

Additionally, wind shear and vertical wind profiles can lead to significant variability in pollutant distribution. Wind direction and speed often vary with altitude and time of day. These variations may explain temporal shifts in the measured pollution and the spatial differences between zones with similar sources. For example, plumes emitted during the early morning might drift at higher altitudes due to thermal uplift, while later in the day, ground-level dispersion may dominate. Our future studies will include the research direction where we will incorporate meteorological data such as wind speed, wind direction, and temperature profiles to more accurately characterize the spatial distribution and intensity of emission plumes, as well as to identify their likely sources.

CONCLUSIONS

This study presented a comparative analysis of trace gases and particulate matter ($PM_{2.5}$) using two complementary mobile measurement systems: the MDOAS UGAL (based on Differential Optical Absorption Spectroscopy) and the Sniffer4Dv2 (a compact air quality system with electrochemical sensors). Despite differences in measurement principles and vertical sensitivity, both instruments consistently identified key pollution hotspots, particularly at major intersections and industrial areas, where emissions from traffic congestion and heavy-duty vehicles were clearly detected.

From the results, NO_2, SO_2, and O_3 measurements showed converging spatial patterns between the two instruments in high-traffic zones, confirming the influence of urban infrastructure and transportation on localized air pollution. The findings presented from the coupling between O_4 and $PM_{2.5}$ in which O_4 was analyzed from MDOAS UGAL data and $PM_{2.5}$ from Sniffer4Dv2, further highlighted how these systems offer complementary insights. The O_4 column densities decreased gradually over time, likely due to increasing solar radiation and atmospheric instability, while $PM_{2.5}$ showed a more stable distribution, initially peaking at 15-35 μg/m³ and declining below 15 μg/m³ toward the end of the route.

Discrepancies observed between the instruments - such as elevated O_4 or NO_2 column

densities where $PM_{2.5}$ or NO_2 ground concentrations remained low - can be explained by their distinct vertical sensitivities. MDOAS UGAL, which integrates slant column densities across atmospheric layers, is sensitive to elevated plumes from point sources such as industrial stacks, whereas the Sniffer4Dv2, positioned at ground level, detects near-surface pollutants more directly linked to human exposure. In cases where MDOAS recorded high values, but Sniffer4Dv2 did not, pollution was likely present at higher altitudes, potentially transported by wind or emitted from tall chimneys. Conversely, elevated surface concentrations with lower column values suggest that pollution remained confined near ground level.

To reduce such discrepancies and enable a more integrated vertical interpretation, future work will focus on converting Differential Slant Column Densities (DSCDs) into true vertical columns using satellite-derived stratospheric corrections (e.g., from OMI or TROPOMI data collected on the same day). Additionally, Air Mass Factor (AMF) simulations using radiative transfer modeling (RTM) will be employed to estimate near-surface pollutant concentrations from DOAS measurements with greater accuracy.

Moreover, integrating high-resolution meteorological parameters such as wind speed, wind direction, temperature, and atmospheric pressure will enhance pollutant transport modeling and source attribution. This multi-parameter framework will provide improved insight into both vertical and horizontal pollution dynamics.

Importantly, this study's dual-system approach has broader implications for urban environmental monitoring and policy development. By combining mobile, high-resolution surface-level data with atmospheric column measurements, the methodology enables a more comprehensive and scalable assessment of air quality. This is particularly valuable in urban areas with complex emission profiles or limited fixed monitoring infrastructure. The approach can support evidence-based urban planning and regulatory strategies, such as optimizing the placement of air quality stations, identifying priority areas for emission reduction, and informing traffic and industrial zoning decisions.

In summary, the integration of complementary remote sensing and low-cost sensor technologies offers a robust and flexible monitoring framework. It strengthens both scientific understanding and policy-making capacity, paving the way for more adaptive and informed air quality management in rapidly urbanizing environments.

ACKNOWLEDGEMENTS

The authors acknowledge the support of the project "Support for the operation of Romania's facilities within the ACTRIS ERIC research infrastructure", MySMIS code 309113, funding contract No. 309010/19.12.2024. The autors acknowledge that equipement used for this study are part of REXDAN Research Infrastructure (REXDAN RI) and European Center of Environmental Excellence (ECEE) from Faculty of Science and Environment, "Dunărea de Jos" University of Galați.

REFERENCES

Adebayo-Ojo, T. C., Wichmann, J., Arowosegbe, O. O., Probst-Hensch, N., Schindler, C., & Künzli, N. (2022). Short-term effects of PM_{10}, NO_2, SO_2 and O_3 on cardio-respiratory mortality in Cape Town, South Africa, 2006–2015. *International Journal of Environmental Research and Public Health, 19*(13), 8078. https://doi.org/10.3390/ijerph19138078

Al-Janabi, S., Alkaim, A., Al-Janabi, E., Aljeboree, A., & Mustafa, M. (2021). Intelligent forecaster of concentrations ($PM_{2.5}$, PM_{10}, NO_2, CO, O_3, SO_2) caused air pollution (IFCsAP). *Neural Computing and Applications, 33*(21), 14199–14229. https://doi.org/10.1007/s00521-021-05937-7

Bernstein, J. A., Alexis, N., Barnes, C., Bernstein, I. L., Nel, A., Peden, D., & Williams, P. B. (2004). Health effects of air pollution. *Journal of Allergy and Clinical Immunology, 114*(5), 1116–1123. https://doi.org/10.1016/j.jaci.2004.08.030

Brunekreef, B., & Holgate, S. T. (2002). Air pollution and health. *The Lancet, 360*(9341), 1233–1242. https://doi.org/10.1016/S0140-6736(02)11274-8

Carn, S. A., Clarisse, L., & Prata, A. J. (2016). Multi-decadal satellite measurements of global volcanic degassing. *Journal of Volcanology and Geothermal Research, 311*, 99–134. https://doi.org/10.1016/j.jvolgeores.2016.01.002

Constantin, D. E., Merlaud, A., Voiculescu, M., Van Roozendael, M., Arseni, M., Roșu, A., & Georgescu, L. (2017). NO_2 and SO_2 observations in southeast Europe using mobile DOAS observations. *Royal Belgian Institute for Space Aeronomy*. https://orfeo.belnet.be/handle/internal/5240

Constantin, D. E., Bocăneala, C., Voiculescu, M., Roșu, A., Merlaud, A., Van Roozendael, M., & Georgescu, P. L. (2020). Evolution of SO_2 and NO_x emissions from several large combustion plants in Europe during 2005–2015. *International Journal of Environmental Research and Public Health, 17*(10), 3630. https://doi.org/10.3390/ijerph17103630

Constantin, D. E., Merlaud, A., Van Roozendael, M., Voiculescu, M., Fayt, C., Hendrick, F., & Georgescu, L. (2013). Measurements of tropospheric NO_2 in Romania using a zenith-sky mobile DOAS system and comparisons with satellite observations. *Sensors, 13*(3), 3922–3940. https://doi.org/10.3390/s130303922

Constantin, D. E., Voiculescu, M., & Georgescu, L. (2013). Satellite observations of NO_2 trend over Romania. *The Scientific World Journal, 2013*, Article 261634. https://doi.org/10.1155/2013/261634

DJI Enterprise. (*Sniffer4D V2 payload overview*. https://enterprise.dji.com/ecosystem/sniffer-v2 (accessed on 02 February 2025)

Flemming, J., Stern, R., & Yamartino, R. J. (2005). A new air quality regime classification scheme for O_3, NO_2, SO_2 and PM_{10} observation sites. *Atmospheric Environment, 39*(33), 6121–6129. https://doi.org/10.1016/j.atmosenv.2005.06.045

Godfrey, I., Avard, G., Brenes, J. P. S., Cruz, M. M., & Meghraoui, K. (2023). Using Sniffer4D and SnifferV portable gas detectors for UAS monitoring of degassing at the Turrialba Volcano, Costa Rica. *Advanced UAV, 3*(1), 54–90.

Godfrey, I., Avard, G., Sibaja, J., Martínez Cruz, M., & Meghraoui, K. (2023). Using UAS for monitoring the summit of the Arenal Volcano, Costa Rica, *Advanced UAV, 2023, 3(2), 100-135*. http://hdl.handle.net/11056/28101

Godfrey, I., Sibaja, J., Martínez Cruz, M., & Meghraoui, K. (2022). Using UAS with Sniffer4D payload to document volcanic gas emissions for volcanic surveillance, *Advanced UAV, 2022, 2(2), 86-99*. http://hdl.handle.net/11056/26193

Jiang, S., Wang, Y., Huang, X., Liu, B., Nie, D., Ge, Y., & Ye, J. (2024). Characteristics of nocturnal boundary layer over a subtropical forest: Implications for the dispersion and fate of atmospheric species. *Environmental Science & Technology, 58*(52), 23075–23087. https://doi.org/10.1021/acs.est.4c05051

Kulakova, E. A., & Muravyova, E. S. (2024). Technical information system for determining the sources of greenhouse gases in the territory of human habitation near petrochemical enterprises. *Ecological Systems and Devices, 2024*(4). https://doi.org/10.62972/1726-4685.2024.4.1027

Liu, Y., Miao, C., Cui, A., & Wang, D. (2024). Spatial distribution of air pollutants in different urban functional zones based on mobile monitoring and CFD simulation. *International Journal of Environmental Science and Technology*, 1–14. https://doi.org/10.1007/s13762-024-06057-x

Meier, A. C., Schönhardt, A., Bösch, T., Richter, A., Seyler, A., Ruhtz, T., Constantin, D.-E., Shaiganfar, R., Wagner, T., Merlaud, A., Van Roozendael, M., Belegante, L., Nicolae, D., Georgescu, L., & Burrows, J. P. (2017). High-resolution airborne imaging DOAS measurements of NO_2 above Bucharest during AROMAT. *Atmospheric Measurement Techniques, 10*, 1831–1857. https://doi.org/10.5194/amt-10-1831-2017

Ott, L. E., Pickering, K. E., Stenchikov, G. L., Allen, D. J., & DeCaria, A. J. (2007). Production of lightning NOx and its vertical distribution calculated from three-dimensional cloud-scale chemical transport model simulations. *Journal of Geophysical Research: Atmospheres, 112*(D4). https://doi.org/10.1029/2006JD007365

Pilegaard, K. (2013). Processes regulating nitric oxide emissions from soils. *Philosophical Transactions of the Royal Society B: Biological Sciences, 368*(1621), 20130126. https://doi.org/10.1098/rstb.2013.0126

Pope, C. A., & Dockery, D. W. (2006). Health effects of fine particulate air pollution: Lines that connect. *Journal of the Air & Waste Management Association, 56*(6), 709–742. https://doi.org/10.1080/10473289.2006.10464485

Prisacariu, V., Piticar, A., & Stoiculete, A. (2022). Aspects regarding environmental and atmospheric monitoring with unmanned aerial vehicles. *Scientific Bulletin "Mircea cel Bătrân" Naval Academy, 25*(2), 1–12.

Rani, B., S. U., C. A. K., S. D., & M. R. (2011). Photochemical smog pollution and its mitigation measures. *Journal of Advanced Scientific Research, 2*(4), 28–33. https://www.sciensage.info/index.php/JASR/article/view/56

Roșu, A., Constantin, D.-E., Voiculescu, M., Arseni, M., Merlaud, A., Van Roozendael, M., & Georgescu, P. L. (2020). Observations of atmospheric NO_2 using a new low-cost MAX-DOAS system. *Atmosphere, 11*(2), 129. https://doi.org/10.3390/atmos11020129

Roșu, A., Roșu, B., Arseni, M., Constantin, D. E., Voiculescu, M., Georgescu, L. P., & Van Roozendael, M. (2017). Tropospheric nitrogen dioxide measurements in South-East Romania using zenith-sky mobile DOAS observations. *New Technologies, Products and Machines Manufacturing Technologies, 44*, 189–194.

Tiao, G. C., & Box, G. E. P. (1975). Analysis of Los Angeles photochemical smog data: A statistical overview. *Journal of the Air Pollution Control Association, 25*(3), 260–268. https://doi.org/10.1080/00022470.1975.10470082

Wagner, T., Beirle, S., & Deutschmann, T. (2004). MAX-DOAS O_4 measurements: A new technique to derive information on atmospheric aerosols - Principles and information content. *Journal of Geophysical Research: Atmospheres, 109*(D22). https://doi.org/10.1029/2004JD004904

Yu, B., Fan, S., Cui, W., Xia, K., & Wang, L. (2024). A multi-UAV cooperative mission planning method based on SA-WOA algorithm for three-dimensional space atmospheric environment detection. *Robotica, 42*(7), 2243–2280.

Zhang, X., Li, F., Zhang, L., Zhao, Z., & Norbäck, D. (2014). A longitudinal study of sick building syndrome (SBS) among pupils in relation to SO_2, NO_2, O_3 and PM_{10} in schools in China. *PLOS ONE, 9*(11), e112933. https://doi.org/10.1371/journal.pone.0112933

Scientific Papers. Series E. Land Reclamation, Earth Observation & Surveying, Environmental Engineering. Vol. XIV, 2025
Print ISSN 2285-6064, CD-ROM ISSN 2285-6072, Online ISSN 2393-5138, ISSN-L 2285-6064

HYDROTHERMAL ASSESSMENT OF MAIN AGRICULTURAL AREAS IN SOUTHERN ROMANIA AND NORTHERN BULGARIA

Nadezhda SHOPOVA[1], Desislava SLAVCHEVA-SIRAKOVA[2]

[1]Climate, Atmosphere and Water Research Institute at Bulgarian Academy of Sciences (CAWRI-BAS), 66, Tzarigradsko Chaussee Blvd, 1784, Sofia, Bulgaria
[2]Agricultural University - Plovdiv, 12 Mendeleev Blvd, 4000, Plovdiv, Bulgaria

Corresponding author email: nadashopova@gmail.com

Abstract

In these papers, the bioclimatic index de Martonne was used to assess the hydrothermal conditions in some agricultural areas in Southern Romania and Northern Bulgaria during the period 1961-2020. The conditions from October to June were analyzed in view of the cultivation of winter cereals, as well as those from April to October, marking the time for growing spring crops. Additionally, indices were selected during some critical periods for both types of crops. The evaluation of the indices with the Mann-Kendall test and the Sen slope shows a significant (0.01) negative trend or an increase in the degree of unfavorability for growing winter crops in the Danube Plain. The indices during the period for growing rain fed spring crops 1961-2020 also show a negative, but insignificant trend.

Key words*: de Martonne index, Southern Romania, Northern Bulgaria, spring crops, cereal, trends.*

INTRODUCTION

Climate change and especially extreme droughts pose risks to agriculture, and spring crops grown under rainfed conditions are the most vulnerable. Also, due to the nature of its cultivation, winter cereals are not grown with supplemental irrigation and rely on rainfall alone. Dry periods and insufficient rainfall, especially during water-critical phases of crop development, lead to low yields. The relationship between temperature and rainfall, expressed as indices, often gives a good general idea of the hydrothermal conditions of individual regions; of the conditions of favourability as well as of the precise use of irrigation water. In the other hand, indices are mathematically verified indicators directly correlated with biophysical processes (Poggio et al., 2018). In this sense, many different indices and parameters are the subject of scientific interest, including in the regions of Northwestern Bulgaria and Southern Romania where large part of the areas are not irrigated. Studies on droughts show an expansion by the end of the 21st century in the Mediterranean region, and in particular in areas of Southeastern Europe such as Romania and Bulgaria (Charalampopoulos et al., 2023; Gao & Giorgi, 2008). Central Europe has good precipitation in all seasons and a maximum in July, while Eastern Europe has less precipitation distributed throughout the year than Northwestern Europe, but summer amounts are mostly higher (Mikolaskova, 2009). The same author reports that continentality in terms of precipitation increases to the east. A correct quantitative assessment of humidity conditions can be obtained by calculating various meteorological, hydrological and biometeorological indices. Therefore, they are the subject of scientific interest of many researchers studying the climate in different regions of Europe (Koleva & Alexandrov, 2008; Vlăduţ et al., 2017; Prăvălie et al., 2017; Mitkov & Topliyski, 2018; 2019; Radeva et al., 2018; Passarella et al., 2020; Chmist-Sikorska et al., 2022; Shopova et al., 2022. A study for Bulgaria for the period 1979–2023 found that the precipitation-evaporation difference is relatively stable and no increase in the water deficit in Bulgaria is observed on an annual basis (Nojarov, 2024).

Other authors (Drenovski, 2024) pay attention to the continental index during the warm and cold half-year, comparing several climatic periods: 1931-1985, 1995-2010 and 1990-

2023. The author found very slight fluctuations in the stations with transitional and Mediterranean type of precipitation. A decrease of about 0.1-0.2 on average is observed in the values of the continentality coefficient of precipitation (Cc) for the regions with temperate continental precipitation regime (Pleven). However, the weakening of the continental influence is not defined as a significant change in the precipitation regime during the two half-years. One of the main results of climate change, directly related to the cultivation of agricultural crops, is the occurrence of prolonged periods of meteorological and hydrological droughts and a decrease in soil moisture. The southern, southeastern and eastern parts of Romania are most vulnerable to drought. In very dry years, average yields of various crops barely reach 35-60% of potential yields (Ionita et al., 2016). Changes in Romania and Bulgaria after 1989 have a similar nature and bring many risks and challenges to agriculture and irrigation opportunities (Dumitrașcu et al., 2018; Kolcheva, 2024; Seymenov & Kolcheva, 2025). The anthropogenic factor responsible for the condition of irrigation systems can significantly affect yields through planning and provision of irrigation water. This publication aims to complement the hydrothermal assessment of some agricultural regions of Northwestern Bulgaria and Southern Romania using the de Martonne bioclimatic index during the main and critical periods of crop development. The study period is 1961-2020.

MATERIALS AND METHODS

Research area: The stations Turnu Severin, Craiova, Pitesti and Bucharest for the territory of Romania and Vidin, Montana, Vratsa and Pleven in Northern Bulgaria were analyzed (Figure 1). The climate of the studied agricultural regions is characterized by relatively cold winters and humid and hot summers. The regime of precipitation has a spring-summer maximum and the highest total amounts between April and July. The average summer air temperatures are higher than 22°C, and the precipitation is between 150 mm and >200 mm. The territories near the mountain ranges such as Pitesti and Turnu Severin have higher rainfall and shorter and cooler summers. Both orchards and vineyards are grown there, as well as spring and winter cereals.



Figure 1. The study area

Data used and study period: Average monthly air temperature °C; Monthly Σ precipitation in mm; Study period: 1961-2020. The data are derived from the ERA5 reanalysis (here used at a resolution of 0.5º x 0.5º). Climatological averages and trends should be considered in relation to inter annual variability (https://climateknowledgeportal.worldbank.org).

Methods: The bioclimatic index of De Martonne (De Martonne, 1926) was used, which describes the studied areas quite well (Croitoru et al., 2013). This index is considered of great relevance not only for environmental or climatological applications but also for agriculture and land resources management (Passarella et al., 2020). The equation was modified according to the coefficients proposed by the same authors (Croitoru et al., 2013):

$$IdM = 1{,}714 * \frac{\Sigma R}{T(GSS) + 10}$$

$$IdM = 1{,}333 * \frac{\Sigma R}{T(GSW) + 10}$$

$$IdM = 6 * \frac{\Sigma R}{T(IV + V) + 10}$$

$$IdM = 4 * \frac{\Sigma R}{T(SS) + 10}$$

where:

- T (GSS) represents average air temperature (ºC) during the growing season of spring crops;

- T (GSW) represents average air temperature (ºC) during the growing season of winter wheat;
- T (SS) represents average air temperature (ºC) during the summer season;
- ΣR represents precipitation in mm.

The climate classification of the regions is made according to Passarella et al., 2001, Baltas, 2007, Deniz et al., 2011, Rahimi et al., 2013, Zareiee, 2014, Nistor, 2016 (Table 1).

Table 1. De Martonne climate classification

Climate	Index range	Description
Arid or dry	IDM≤10	Needs continuous irrigation
Semi-arid	10 ≤IDM<20	Needs irrigation
Mediterranean	20 ≤IDM<24	Need supplementary irrigation
Semi-humid	24 ≤IDM<28	Need supplementary irrigation
Humid	28 ≤IDM<35	Need occasional irrigation
Very humid	35 ≤IDM≤55	Need infrequent irrigation
Extremely humid	IDM>55	Water self-sufficient

Statistical assessment of trends: The Excel template MAKESENS of the Finnish Meteorological Institute (Salmi et al., 2002) was applied for data processing. The bioclimatic indices were checked for direction and statistical significance of trends using the non-parametric Mann-Kendall test. The template tests for the presence of a monotonic increase or decrease using the non-parametric Mann-Kendall test and calculates the slope of a linear trend estimated using the non-parametric Sen method (Gilbert, 1987) at statistical significance levels of 0.001***, 0.01**, 0.05* and 0.1^{+}. The Z value indicates whether the trend is positive or negative, as well as whether it is statistically significant, and Q is a characteristic of the slope.

RESULTS AND DISCUSSIONS

In the regions of Northern Bulgaria and Southern Romania, main spring and winter cereal crops are grown. The development of winter wheat from sowing through dormancy to ripening and harvesting takes place during the period from October to June. In October, precipitation provides moisture for the germination and initial development of winter wheat (Croitoru et al., 2012). This month is considered the beginning of the moisture accumulation process, which ends with the resumption of active vegetation in the spring. The months of April and May are critical in terms of moisture conditions, because the reproductive period of crop development takes place in the same month - the processes of flowering, fertilization and milk maturity (Hershkovich, 1984; Georgieva, 2013). The same authors indicate insufficient moisture in May as the main yield-limiting factor. The hydrothermal conditions during the development period of cereals, expressed by the De Martonne dryness index for GSW, are shown in the Figures 2 to 5.

The index values classify the region as humid and very humid, with the best conditions for the development of winter wheat crops being observed in the stations of Pitesti, Montana and Turnu Severin. The period was wetter before 1980, with the most unfavorable conditions for Bulgaria between 1982 and 1994, and for Romania from 1991 to 2002.

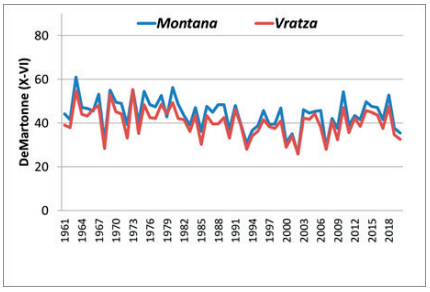


Figure 2. The distribution of the De Martonne index (GSW) Craiova and Bucharest

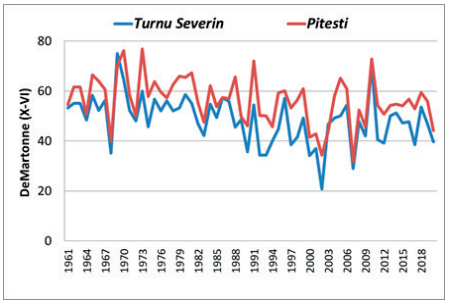


Figure 3. The distribution of the De Martonne aridity index (GSW) Turnu Severin and Pitesti

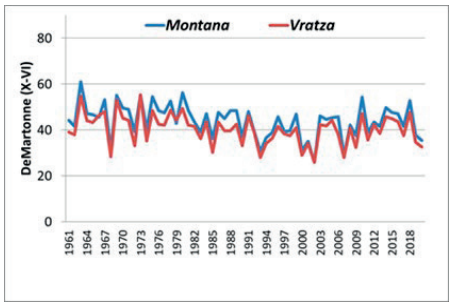


Figure 4. The distribution of the de Martonne aridity index (GSW) 1961-2020 Montana and Vratza

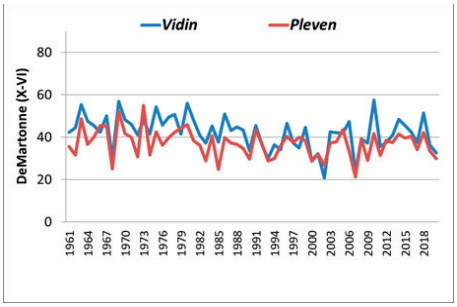


Figure 5. The distribution of the De Martonne aridity index (GSW) 1961-2020 Vidin and Pleven

Table 2. Statistical assessment of the trend (GSW)

Mann-Kendal trend	*Sen's slope estimate*		
De Martonne (IX-VI)	**Test Z**	**Signific.**	**Q**
Turnu Severin	-3.4	***	-0.2
Craiova	-3.0	**	-0.2
Pitesti	-2.7	**	-0,2
Bucharest	-1.2		-0.2

Table 3. Statistical assessment of the trend (GSW)

Mann-Kendal trend	*Sen's slope estimate*		
De Martonne (IX-VI)	**Test Z**	**Signific.**	**Q**
Vratza	-2.2	*	-0.1
Vidin	-2.9	**	-0.2
Montana	-2.5	*	-0,1
Pleven	-1.6		0.0

When growing winter wheat, hydrothermal conditions during the critical periods of flowering and milk maturity are of great importance for biological and total yields. Lower temperatures and the good rainfall are a prerequisite for high yields. Therefore, the index values in this critical period have a pronounced impact on the final yield (Figures 6 and 7).

In the stations of northern Bulgaria, two peaks are observed in the periods around 1979 and 2014. The variations and contrast values are no exception and are characteristic of the periods before and after 2000.

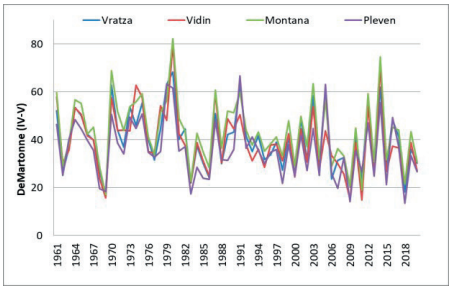


Figure 6. The distribution of the De Martonne aridity index April-May

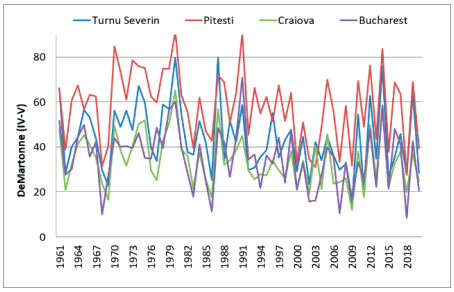


Figure 7. The distribution of the De Martonne aridity index April-May

The period 1991-2000 is the driest. The results show that during this period winter wheat crops develop in conditions ranging from semi-arid to semi-humid, with the most vulnerable being the regions of Craiova and Pleven. Based on some modeling studies (Constantin et al., 2025), in other agricultural regions of northern Romania, irrigation of winter wheat is recommended precisely during the critical months of April to May. Several extreme high values are observed in 1972, 1991 and 2005, with the lowest values in 1962, 1977, 1993, 2000 and 2011. In Southern Romania, the two wettest years were before 1990. The average values of the index define the region as Humid with the exclusion of Pitesti. The assessment of the index trends during the period April-May is similar to that of the index during the period September-June (Table 4).

Except for Vratza, Pleven and Pitesti stations, the trends for the study period are negative and significant at the 0.05 level.
The development of spring crops in the region of study occurs during the period from April to October (Hershkovich, 1984). The De Martonne index for this period is shown in Figures 8 to 11.

Table 4. Statistical assessment of the trend April-May

Mann-Kendal trend	*Sen's slope estimate*		
De Martonne (IV-V)	**Test Z**	**Signific.**	**Q**
Turnu Severin	-2.1	*	-0.2
Pitesti	-1.8	+	-0.2
Craiova	-2.1	*	-0.2
Bucharest	-2.0	*	-0.2
Vratza	-1.9	+	-0.2
Vidin	-2.6	**	-0.3
Montana	-2.1	*	-0.2
Pleven	-1.8	+	-0.2

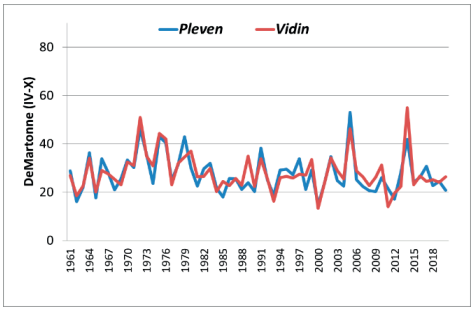


Figure 8. The distribution of the De Martonne aridity index CSS

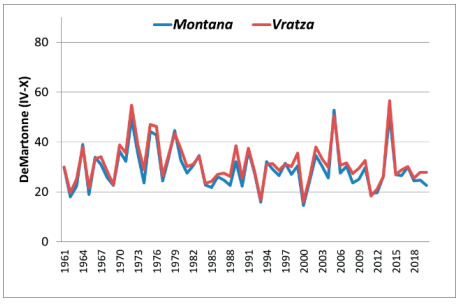


Figure 9. The distribution of the De Martonne aridity index GSS

During the period of growing spring crops, the driest was 2000. The prevailing years were years in which the conditions were Mediterranean and humid and which required irrigation. The exception is the Pitesti station, in which the conditions were very humid. For the period of maize growing before 2010, data series reveal mostly positive slopes, but few of them are statistically significant for the period 1961-2007 (Croitoru et al., 2013).

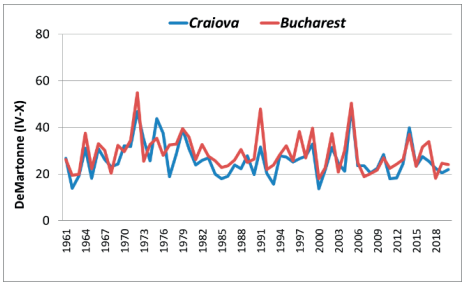


Figure 10. The distribution of the De Martonne aridity index (GSS) Craiova and Bucharest

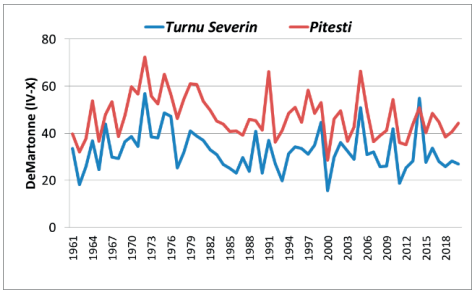


Figure 11. The distribution of the De Martonne aridity index (GSS) Turnu Severin and Pitesti

According to the data (Table 5), the trend reverses in a negative direction, with the slope remaining without statistical significance. The probable reason is the extreme values observed in recent decades.

Table 5. Statistical assessment of the trend (GSS)

Mann-Kendal trend	*Sen's slope estimate*		
De Martonne (IV-V)	**Test Z**	**Signific.**	**Q**
Turnu Severin	-1.6		-0.1
Pitesti	-1.9	+	-0.1
Craiova	-1.3		-0.1
Bucharest	-1.5		-0.1
Vratza	-1.5		-0.1
Vidin	-1.2		-0.1
Montana	-1.2		-0.1
Pleven	-1.4		-0.1

The assessment of the trend slope during the summer season (Table 6) corresponds to that

during the vegetation period of spring crops. At stations Pitesti and Bucharest, the negative trend has a significance level of 0.1. According to the index values during the studied period, the climate is classified from semi-arid to humid apart from station Pitesti where the conditions are predominantly humid to very humid (Figures 12 and 13). Two peaks are observed around 1976 and in 2005, better shown in the stations from Northern Bulgaria.

Table 6. Statistical assessment of the trend of the De Martonne aridity index (SS)

Mann-Kendal trend	*Sen's slope estimate*		
De Martonne (IV-V)	**Test Z**	**Signific.**	**Q**
Turnu Severin	-1.2		-0.1
Pitesti	-1.8	+	-0.1
Craiova	-1.4		-0.1
Bucharest	-1.8	+	-0.1
Vratza	-1.5		-0.1
Vidin	-1.1		-0.1
Montana	-1.6		-0.1
Pleven	-1.6		-0.1

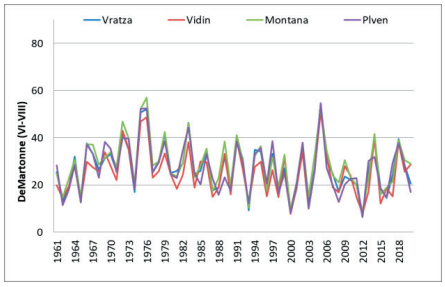


Figure 12. The distribution of the De Martonne aridity index June-August

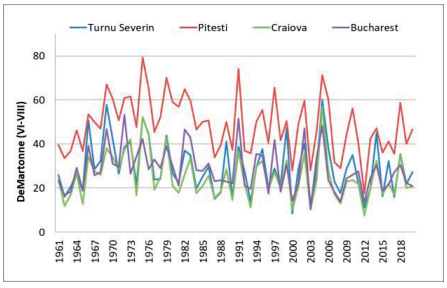


Figure 13. The distribution of the De Martonne aridity index June-August

Additional information related to plant security is provided by the number of cases with different types of climates during the study period (Figures 14 to 17). During the growing season of winter wheat, the conditions are predominantly extremely humid and very humid (Figure 14). In the stations Bucharest and Craiova, in about 40% of the cases the climate is semi-humid, and in the second station a number of years with an index below 20 and semi-arid climate conditions are also recorded. However, the second critical period in terms of humidity shows that even values below 10 - arid or dry conditions (Bucharest) are observed during the period (Figure 15).

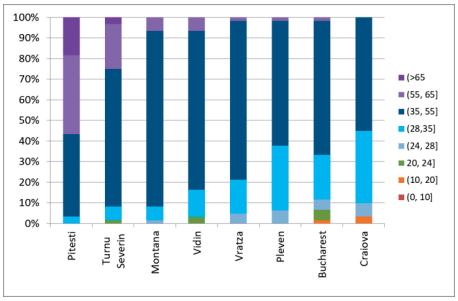


Figure 14. Distribution of climate types 1961-2020 according to De Martonne aridity index September-June

The best conditions are shown by Pitesti, Turnu Severin and Montana, and the most unfavorable years are found in Craiova and Pleven.

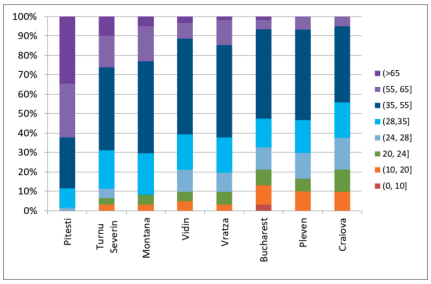


Figure 15. Distribution of climate types 1961-2020 according to the De Martonne aridity index April-May

The results show that the humidity conditions during the growing season are risky in rainy conditions (Figure 16).

Apart from Pitesti, where the climate is humid and very humid, irrigation is necessary in all other stations. Turnu Severin and Montana have predominantly semi-humid to humid conditions and a low need for irrigation. The most unfavorable conditions during the

growing season are observed in the stations Craiova and Pleven, where in over 80% of the years the climate is Mediterranean and semi-arid and the need for irrigation for the spring crops is mandatory.

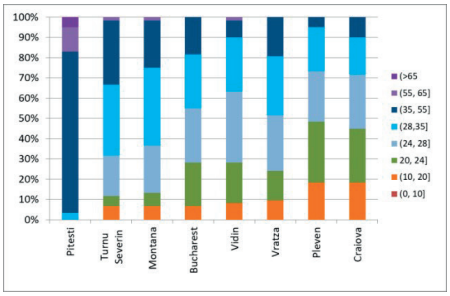


Figure 16. Distribution of climate types1961-2020, according to the De Martonne aridity index April-October

During the summer period, the stations with the most unfavorable conditions, years with an index below 10 and arid or dry conditions are Pleven, Craiova Vidin and Vratza (Figure 17).
In the region of Southern Bulgaria, the best conditions during the studied period are observed at Montana station. Conditions range from humid to extremely humid in the Pitești region.

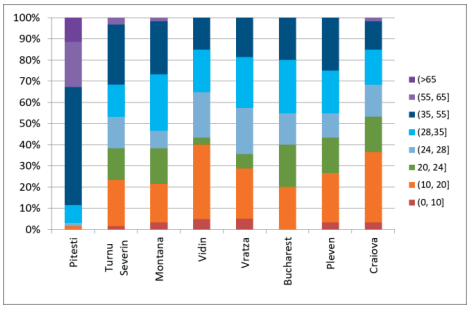


Figure 17. Distribution of climate types 1961-2020 according to the de Martonne aridity index June-August

CONCLUSIONS

An assessment of the hydrothermal conditions in the main agricultural regions of Southern Romania and Northern Bulgaria was made. The results show that the humidification conditions do not ensure the development of spring crops during their growing season and during the summer period. With the exception of Pitesti, where the climate is humid and very humid, irrigation is necessary for all other stations. Turnu Severin and Montana have prevailing semi-humid to humid conditions and a low need for irrigation. The most unfavourable conditions are during the potential growing season in the stations Craiova and Pleven, where in over 80% of the years the climate is Mediterranean and semi-arid and the need for irrigation for the spring crops is mandatory. The assessment of the trends shows a significant decrease in the index during the entire wheat growing period, as well as during the critical stages of earing and flowering in May and June. The observed negative trends during the growth and development of spring crops are not statistically significant. The same is observed during the summer period when only the regions closer to the mountain ranges such as Pitesti and Bucharest tend to be at statistical significance levels of 0.1. Despite the proven high temperatures, the distribution of the summer precipitation manages to maintain a negative insignificant trend for the entire period 1961-2020, most likely due to the higher extreme values in recent decades.

ACKNOWLEDGEMENTS

This research work was carried out with the support of „Danube Wetlands and flood plains Restoration through systemic, community engaged and sustainable innovative actions “.

REFERENCES

Baltas, E. (2007). Spatial distribution of climatic indices in northern Greece. *Meteorol. Appl. 14*(1), 69–78.

Charalampopoulos, I., Droulia, F., & Tsiros, I. X. (2023). Projecting Bioclimatic Change over the South-Eastern European Agricultural and Natural Areas via Ultrahigh-Resolution Analysis of the de Martonne Index. *Atmosphere, 14*(5), 858.

Chmist-Sikorska, J., Kępińska Kasprzak, M., & Struzik, P. (2022). Agricultural drought assessment on the base of Hydro-thermal Coefficient of Selyaninov in Poland. *Italian Journal of Agrometeorology, 1*, 3-12.

Croitoru, A.E., Holobaca, I.H., Lazar, C., Moldovan, F., & Imbroane, A. (2012) Air temperature trend and the impact on winter wheat phenology in Romania. *Clim Chang, 111*(2), 393–410.

Croitoru, A.E., Piticar, A., Imbroane, A.M., & Burada D.C. (2013). Spatiotemporal distribution of aridity indices based on temperature and precipitation in the

extra-Carpathian regions of Romania. *Theor Appl Climatol., 112*, 597–607.

Constantin, D. M., Mincu, F. I., Diaconu, D. C., Burada, C. D., & Bălțățeanu, E. (2025). Water Management in Wheat Farming in Romania: Simulating the Irrigation Requirements with the CROPWAT Model. *Agronomy, 15*(1), 61.

Deniz, A., Toros, H., & Incecik, S. (2011). Spatial variations of climate indices in Turkey. *Int. J. Climatol, 31*(3), 394–403.

De Martonne, E. (1926). Une nouvelle fonction climatologique. L'indice d'aridité. – In: *La Météorologie*, *2*, 449–458.

Drenovski, I**.** (2024). Changes in the continentality index (coefficient) of precipitation in Bulgaria. Proceedings of 6-th International Conference "Global Warming's Imprints on the Elements of the Climatic System", 24-28 September 2024, Hisarya, 52–56.

Dumitrașcu, M., Mocanu, I., Mitrică, B., Dragotă, C., Grigorescu, I., & Dumitrică C. (2018). The assessment of socio-economic vulnerability to drought in Southern Romania (Oltenia Plain), *International Journal of Disaster Risk Reduction*, *27*, 142-154.

Ionita, M., Scholz, P. & Chelcea, S. (2016). Assessment of droughts in Romania using the Standardized Precipitation Index. *Nat Hazards, 81*, 1483–1498.

Gao, X., & Giorgi, F. (2008). Increased aridity in the Mediterranean region under greenhouse gas forcing estimated from high resolution simulations with a regional climate model, *Global and Planetary Change*, *62*(3–4), 195-209.

Georgieva, V. (2013). Conditions of natural soil moisture of main soil types in relation to growing winter wheat in Bulgaria. PhD theses.

Gilbert, R.O. (1987) Statistical Methods for Environmental Pollution Monitoring. John Wiley and Sons, New York, ISBN 0-442-23050-8.

Hershkovich, E. (1984). Agoclimatic resources of Bulgaria, Publisher, BAS, pp. 115 (in Bulgarian)

Kolcheva, K. (2024). Irrigation changes in the Maritsa river basin. A case study from the Plovdiv region. *Scientific Papers. Series E. Land Reclamation, Earth Observation & Surveying, Environmental Engineering., 13,* 2285 - 6064.

Koleva, E., & Alexandrov, V. (2008). Drought in the Bulgarian low regions during the 20th century. *Theor Appl. Climatol., 92*, 113–120.

Mikolaskova, K. (2009). Continental and oceanic precipitation regime in Europe. *Cent. Eur. J. Geosci*, *1*(2), 176-182.

Mitkov, S., & Topliyski D. (2018). Climate change in Bulgaria presented by complete indices. *Annual of Sofia University "St. Kliment Ohridski" Faculti de geologie et geographie Livre 2* – Geographie, *110*, 25-38.

Mitkov, S., & Topliyski D. (2019). Climate classification in Bulgaria according to de Martonne and Thornthwaite indices. *Annual of Sofia University "St. Kliment Ohridski" Faculti de geologie et geographie Livre 2* – Geographie, *112*, 54–67.

Nistor, M.M. (2016). Spatial distribution of climate indices in the Emilia-Romagna region. *Meteorol Appl., 23*(2), 304–313.

Nojarov, P. (2024) Evaporation and the difference between precipitation and evaporation in Bulgaria. Journal of the Bulgarian. *Geographical Society, 51*, 131–149.

Passarella, G., Vurro, M., Giuliano, G., & D'Agostino, V. (2001). Il rischio spazio-temporale di contaminazion da Nitrati delle acque sotterranee usando il kriging disgiuntivo. In: Russo, E., Zavatti, A. (Eds.), Prevenzione dell'inquinamento dei sistemi idrogeologici. ARPA Emilia Romagna, Bologna, pp. 179–190.

Passarella, G., Bruno, D., Lay-Ekuakille, A., Maggi, S., Masciale, R., & Zaccaria, D. (2020). Spatial and temporal classification of coastal regions using bioclimatic indices in a Mediterranean environment. *Sci Total Environ, 700*, 134415.

Poggio, L., Simonetti, E., Gimona, A., Jun. (2018). Enhancing the WorldClim data set for national and regional applications. *Sci. Total Environ., 625*, 1628–1643.

Prăvălie, R., Bandoc, G., Patriche, C. Tomescu M. (2017). Spatio-temporal trends of mean air temperature during 1961–2009 and impacts on crop (maize) yields in the most important agricultural region of Romania. *Stoch Environ Res Risk Assess, 31*, 1923–1939.

Radeva, K., Nikolova N., Gera, M. (2018). Assessment of hydro-meteorological drought in the Danube Plain, Bulgaria. *Hrvatski geografski glasnik*, *80*(1), 7-25.

Rahimi, J., Ebrahimpour, M., & Khalili, A. (2013). Spatial changes of Extended De Martonne climatic zones affected by climate change in Iran. *Theor. Appl. Climatol*., *112*(3-4), 409–418.

Salmi, T., Maatta, A., Anttila, P., Ruoho-Airola, T., & Amnell, T. (2002). Detecting trends of annual values of atmospheric pollutants by the Mann-Kendall test and Sen's slope estimates – The excel template application Makesens. Federal Meteorological Institute Publications on Air Quality, 31. Helsinki, Finland.

Shopova, N., Alexandrov, V., & Tsaikin, N. (2022). Hydrothermal conditions in the agricultural areas of Bulgaria expressed by the indices of Ped and De Martonne. "Climate, atmosphere and water resources in the face of climate change", Sofia, 2022, 4, 85-92

Seymenov, K., & Kolcheva, K. (2025). Trends in the Use of Water Resources in Bulgaria. In: Dobrinkova, N., Fidanova, S. (eds) Environmental Protection and Disaster Risks (EnviroRisks 2024). EnviroRISKs 2024. Lecture Notes in Networks and Systems, vol 883, 92–97. Springer, Cham.

Vlăduț, A., Nikolova N., & Licurici M. (2017). Aridity assessment within southern Romania and northern Bulgaria. *Hrvatski geografski glasnik*/*Croatian Geographical Bulletin, 79*(2), 5–26.

Zareiee, A.R. (2014). Evaluation of changes in different climates of Iran, using De Martonne index and Mann-Kendall trend test. *Nat. Hazards Earth Syst. Sci. Discuss., 2*, 2245–2261.

Scientific Papers. Series E. Land Reclamation, Earth Observation & Surveying, Environmental Engineering. Vol. XIV, 2025
Print ISSN 2285-6064, CD-ROM ISSN 2285-6072, Online ISSN 2393-5138, ISSN-L 2285-6064

FIRE SAFETY OF ETICS BASED ON EPS TYPE POLYSTYRENE

Adrian SIMION[1], Claudiu-Sorin DRAGOMIR[1, 2]

[1]National Institute for Building Research, Town Planning and Sustainable Territorial Development - URBAN-INCERC, 266 Pantelimon Road, District 2, Bucharest, Romania
[2]University of Agronomic Sciences and Veterinary Medicine of Bucharest, 59 Mărăşti Blvd, District 1, Bucharest, Romania

Corresponding author email: simion_i_adrian@yahoo.com

Abstract

Due to the requirements to reduce energy consumption, the thermal rehabilitation of existing buildings has gained momentum in recent years, both in Romania and at the European level (Petcu et. al., 2023). The most accessible and used technical solution for the thermal rehabilitation of residential buildings, is represented by the external cladding systems with polystyrene thermal insulation. For this type of buildings thermal insulation system, the most unfavourable and most common external actions are represented by compartment fires. The researchers of the Fires Research Laboratory within the INCERC Bucharest Branch, have carried out a series of experimental studies on a natural scale, in order to develop a method of testing ETICS systems for fires generated from fire compartments. Through these studies and experimental research, conclusive results were obtained regarding the development of compartment fires, the evolution of temperatures inside the combustion chamber and the propagation of fire on the combustible facades of buildings.

Key words*: experimental research, fire resistance, fire behavior, ETICS.*

INTRODUCTION

Internationally, there are a number of full-scale or intermediate-scale testing methods for assessing the fire performance of external thermal insulation composite systems (ETICS) based on EPS type polystyrene (Lalu et al., 2017). All these methods define fire exposure scenarios inside buildings, which are characterized by different thermal loads that generate flames that propagate on building facades (Yoshioka, 2011). In Romania, full-scale tests are not yet accepted through which to test the fire resistance of ETICS (Simion et. al., 2019). In this context, it is necessary that a full-scale testing method for ETICS be adopted in our country, so as to demonstrate the fulfilment of fire safety requirements in accordance with the harmonized testing standards at European level. To meet this objective, the Fires Research Laboratory within the INCERC Bucharest carried out, for the first time in our country, a series of theoretical studies and experimental tests within a research project funded by the Ministry of Research, Innovation and Digitalization, which reproduced as closely as possible to reality, the propagation phases of compartment fires on building facades. Through this testing method, conclusive experimental results were obtained regarding the development of the compartment fire and the evolution of temperatures on the combustible facade of a building. The general purpose of the project was to conduct experimental research on the fire safety of the built environment: concepts and methods of fire resistance testing, new materials and solutions, including fire-built environment interaction (Ovadiuc et al., 2024).

The objectives of the project were the following: construction of a full-scale test stand for fire resistance of ETICS; adoption of a full-scale test method similar to one of the most commonly used test methods internationally; justification of the choice of the test model for conducting the experimental test; conducting an experiment on the newly built test stand in order to evaluate the mode of compartment fire propagation on the combustible facade of a multi-storey building; provision of protection measures against compartment fires that can be adopted when putting into operation the exterior cladding systems of buildings;

proposals for the extension of the experimental study.

MATERIALS AND METHODS

The fire resistance test stand for ETICS was designed by the engineering team from the INCERC Fires Research Laboratory based on the provisions of the British test method standard BS 8414 and was built at the facade tower of the laboratory in several stages. The research test stand for testing the fire resistance of exterior cladding systems of buildings, was designed by the team of researchers after an analysis of the fire testing concepts of ETICS at European and even worldwide level. Thus, a stand was put into operation with characteristics similar to the stand regulated in BS 8414, with one difference (BS 8414-1, 2002). This difference lies in the fact that in the continuation of the side wing and 2 m opposite the combustion chamber, a reinforced concrete diaphragm is additionally placed over the entire height of the stand (8.5 m), which has the role of both accentuating the chimney effect during the experiment and protecting the combustion phenomenon from possible wind from the North (Figure 1).

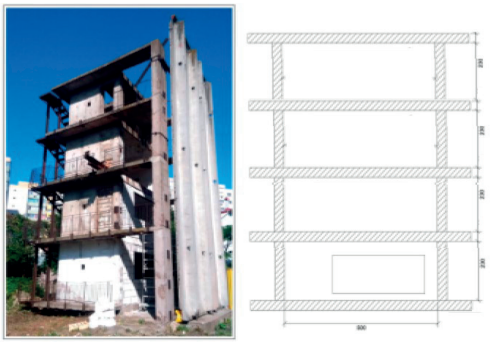


Figure 1. The construction used for the test stand

The ETICS installed on the two wings of the stand was made of 10 cm thick expanded EPS polystyrene (is a minimum thickness taken into account in current energy calculations that are made before thermal insulation of buildings), glued with adhesive and fixed with dowels to the BCA support layer (Michalak, 2021). The polystyrene was fireproof type EPS 80 – AF 80 with a density of 14.5 kg/m³ and was classified for reaction to fire according to SR EN 13501-1, class B-s2, d0. Over the EPS, a reinforcement layer consisting of an exterior fiberglass mesh (145 g/m²) embedded in adhesive mortar for plastering was installed with a crowbar. After the plastering mass had dried, a primer and a layer of structured decorative plaster type 2R were applied to it (Figure 2).

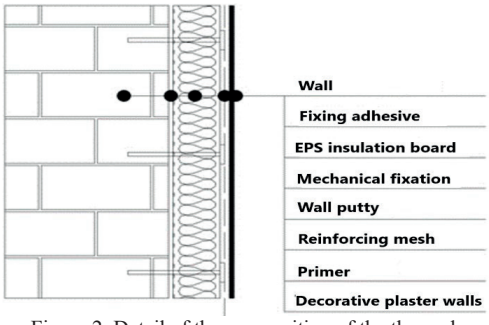


Figure 2. Detail of the composition of the thermal insulation system tested for fire resistance

The ETICS performed on the building for fire resistance testing was installed without non-combustible barriers between floors. Also, the polystyrene boards were installed in the worst case, namely on mortar beads, as is often done in current construction practice on site (Figure 3).



Figure 3. Test stand with ETICS prepared for fire resistance testing generated from the fire compartment

The ceiling of the combustion chamber was lined with 10 cm thick ceramic wool and the walls with 5 cm thick wool. The ceramic wool was fixed with high temperature resistant

refractory anchors. A 1.0 cm thick ceramic board was placed on the floor of the combustion chamber. In the test stand, researchers from the INCERC Bucharest conducted an experimental test to determine the compartment fire behaviour of an ETICS mounted on the facade of a building. During the fire resistance test experiment of the ETICS, a series of qualitative parameters were measured in order to evaluate the response of the construction materials from which the system was made up, to the propagation of fire in height. These parameters are: the moment of ignition of the system, the variation of temperatures in the fire compartment and in height, the variation of the mass of the thermal load, the height of the flames, detachment of elements from the system, losses of local stability and the amount of smoke released. The thermal load consisted of a softwood stack measuring 1.5 m (L) × 1.0 m (W) × 1 m (H) (Figure 4).



Figure 4. Wood stack

The wood was conditioned before combustion to reach a moisture content between 13 and 17% (Figure 5).



Figure 5. Wood conditioner

From the records presented above, the evolution of temperatures during the experiment results. The temperatures recorded under the specific conditions of the test (composition of the ETICS, choice of thermal load, geometric conformation of the stand as well as environmental conditions), highlight and provide data on the mode of propagation of fire in the combustion chamber, starting with the moment of initiation of the fire and ending with its regression (Figure 6).



Figure 6. Fire ignition

During the test, the variation in time of the following parameters was recorded:
- The temperature of the outer surface of the thermal insulation at 2.5 and 5 m above the combustion chamber (of the fire compartment);
- The temperature inside the thermal insulation at 5 m above the combustion chamber;
- The temperature inside the combustion chamber.

Also, during the test, the moment of ignition of the ETICS, the development of the fire on the facade and the moment of flash-over, the maximum height of the flames, the detachment of burning elements from the ETICS, the regression and extinguishing of the fire were monitored (Malgorzata et al., 2022).

The height of the flames in the fire compartment varied during the experiment and it was found that their maximum height was reached approximately in the 15th minute, when the flames propagated above the combustion chamber to a height of approximately 2.5 m (Figure 7).

During the experiment, an increasing evolution of the temperatures along the height of the

tested system under the action of the fire is observed.



Figure 7. The beginning of the fire propagation on the height of the ETICS on the front wall

It is also found that the propagation of the fire along the height and especially after the polystyrene thermal insulation began to burn generalized, influenced the increase in temperatures both on the external surface of the ETICS and from inside it (Figure 8).



Figure 8. The beginning of the fire propagation on the height of the ETICS on the side wall

During the test, component elements of the system were detached and burning particles fell from the system. Following the action of the fire on the thermal system, the expanded polystyrene thermal insulation layer did not withstand in terms of mechanical resistance and fire tightness over the entire height of the test stand (Figures 9, 10).

The amount of smoke released into the atmosphere was relatively constant, increasing slightly around the flash-over moment (Figure 11).



Figure 9. Complete combustion of the ETICS on the side wall to the fire compartment



Figure 10. Burning particles detached from the thermal system



Figure 11. Smoke plume stock

RESULTS AND DISCUSSIONS

Following the correlation of the temperature recording times presented in the tables above, with the photo-video recordings corresponding to the time points of the most important stages of the experiment, it results that a series of conclusions can be drawn regarding the behaviour of ETICS in the event of compartment fires, which can contribute to increasing the degree of fire safety of the built environment.

Following the action of the fire on the ETICS, it was found that the thermal insulation layer made of EPS polystyrene was burned and melted down to the support structure, in the area of direct action of the fire.

After the thermal insulation ignited, a significant amount of black and gray smoke was released. The tested system favoured the propagation of the fire both vertically and laterally. During the duration of the fire, burning detachments of the thermal insulation system were found.

The maximum temperatures were recorded in the combustion chamber was over 920°C. The maximum temperatures recorded 2.5 m above the combustion chamber was over 740°C (Figure 12).

Timp / Termocuplu	TF7	TF8	TF9	TF0	T 1	T 2	T 3	T 4	T 5	T 6	T 7	T 8
Minute / °C	°C	°C	°C	°C	°C	°C	°C	°C	°C	°C	°C	°C
0	12	16	16	16	17	17	17	17	17	17	17	17
13.30	37	798	783	196	77	234	430	152	202	189	78	32
20.30	29	634	595	283	276	413	746	598	184	175	82	52
25.06	25	367	362	55	76	115	163	113	115	104	45	23
29	36	772	770	219	82	227	476	157	189	184	82	35
32	28	717	605	394	150	305	410	327	244	202	261	95
36	29	720	616	430	212	347	318	228	222	238	452	149
38.40	29	777	693	487	214	337	287	194	246	275	288	161
44.50	29	770	547	396	105	163	228	215	210	205	258	188
48.30	26	927	576	360	109	191	204	149	181	171	193	109
51.20	22	495	315	221	72	110	153	126	125	126	151	83
57.20	18	233	178	145	43	69	64	57	78	80	94	60
59.10	17	193	135	101	36	55	60	67	76	79	89	61

Figure 12. Temperatures recorded in the combustion chamber and 2.5 m above the combustion chamber

The maximum temperatures recorded 5.0 m above the combustion chamber was over 820°C (Figure 13).

The temperatures measured at the height of the thermally insulated facade with ETICS during the experimental test indicate that around 20 minute by ignite the fire, the fire became generalized and encompassed the entire ETICS above the combustion chamber, resulting an additional heat input compared to the heat released following the combustion of the wood stack

Timp / Termo-cuplu	2 1	2 2	2 3	2 4	2 5	2 6	2 7	2 8	2 9	2 10	2 11	2 12	2 13	2 14	2 15	2 16
Minute / °C	°C	°C	°C	°C	°C	°C	°C	°C	°C	°C	°C	°C	°C	°C	°C	°C
0	17	17	18	17	17	13	17	17	15	14	15	15	13	17	13	14
13.30	80	137	156	107	115	24	72	44	320	199	399	43	31	118	17	16
20.30	759	821	747	622	614	83	113	72	786	816	731	614	596	250	31	33
25.06	375	437	393	325	324	261	270	77	382	454	455	325	330	268	249	74
29	389	402	357	316	292	290	277	278	392	405	366	317	296	294	270	282
32	252	267	289	283	266	259	274	245	254	266	287	286	269	271	256	230
36	287	277	276	276	281	278	369	371	285	276	274	275	283	296	409	358
38.40	258	249	250	234	227	226	261	249	258	248	250	237	230	230	251	250
44.50	159	165	170	171	173	171	188	195	160	164	172	171	172	176	192	205
48.30	146	152	165	147	129	125	154	158	147	153	168	152	130	128	158	172
51.20	109	116	119	115	108	102	130	133	110	116	121	118	107	102	133	144
57.20	65	66	64	60	65	61	89	89	65	67	66	62	64	59	91	95
59.10	63	62	61	58	69	65	85	84	63	62	62	60	67	63	87	90

Figure 13. Temperatures recorded 5.0 m above the combustion chamber

It is also noted that in a relatively short period of time (10 min) the entire thermal insulation facade located above the combustion chamber was destroyed by the fire.

Specialists draw attention to the results obtained, that in the case of installing ETICS on high-rise buildings, without installing non-combustible barriers between floors, there is a very high risk that combustible facades will burn along their entire height when exposed to compartment fires (Lalu, 2016).

CONCLUSIONS

Based on the experimental research carried out, unique results were obtained in Romania regarding the development of a fire on the combustible facade of a building, with results that can be transposed to a normative level and with applicability from the design phases of the buildings. Also, a unique stand was created in Romania for carrying out experimental research testing the compartment fire action of ETICS, open to both the academic and the economic environment.

In this way, INCERC Bucharest contributes to the development of a database that will support the establishment of criteria and performance levels for ETICS used to enclose residential

buildings, so that they can ensure a high degree of fire safety.

ACKNOWLEDGEMENTS

This research work was carried out with the support of the Ministry of Research, Innovation and Digitalization and was financed from Project PN 19 33 02 01.

REFERENCES

British Standards Institution (2005). *BS 8414-1: Fire performance of external cladding systems applied to the face of the building* (pp. 4–6). London: BSI.Yoshioka, H., Yang, H.-C., Tamura, M., Yoshida, M., Noguchi, T., Kanematsu, M., Koura, K., & Ozaki, Y. (2011). Study of test method for evaluation of fire propagation along façade wall with exterior thermal insulation. *Fire Science and Technology, 30*(1), 27–44.

Lalu, O. (2016). *Cercetări privind elaborarea unor soluții durabile de reabilitare termică a anvelopei clădirilor. Comportamentul la acțiunea focului, soluții de securitate la incendiu* [Doctoral thesis, Universitatea Tehnică de Construcții București].

Lalu, O., & Bubulete, L. (2017). Termosistem pentru placări exterioare utilizat pentru anveloparea construcțiilor. Răspuns la acțiunea focului. *Revista Construcțiilor, 133*, 8.

Malgorzata, N., Wieczorek, M., & Borkowicz, K. (2022). Fire safety of external thermal insulation systems (ETICS) in the aspect of sustainable use of natural resources. *Sustainability, 14*(3). https://doi.org/10.3390/su14031224.

Michalak, J. (2021). External Thermal Insulation Composite Systems (ETICS) from Industry and Academia Perspective. *Sustainability*, *13*(24), 13705. https://doi.org/10.3390/su132413705

Ovadiuc, E. P., Calotă, R., Năstase, I., & Bode, F. (2024). Integration of phase-change materials in ventilated façades: A review regarding fire safety and future challenges. *Sustainability, 7*(7), 244. https://doi.org/10.3390/fire7070244.

Petcu, C., Hegyi, A., Stoian, V., Dragomir, C. S., Ciobanu, A. A., Lăzărescu, A. V., & Florean, C. (2023). Research on thermal insulation performance and impact on indoor air quality of cellulose-based thermal insulation materials. *Sustainability, 16*(15), 5458. https://doi.org/10.3390/ma16155458.

Simion, A., Anghel, I., Dragne, H., & Stoica, D. (2019). Contributions on the fire performance assessment of ETICS systems. *IOP Conference Series: Materials Science and Engineering, 572*, 012112.

Scientific Papers. Series E. Land Reclamation, Earth Observation & Surveying, Environmental Engineering. Vol. XIV, 2025
Print ISSN 2285-6064, CD-ROM ISSN 2285-6072, Online ISSN 2393-5138, ISSN-L 2285-6064

DEVELOPMENT AND APPLICATION OF AN OPTIMIZED TD-GC/MS METHOD FOR MONITORING VOLATILE ORGANIC COMPOUNDS (VOCs) IN AMBIENT AIR

Alexandru-Florin SIMION, Angela-Nicoleta GĂMAN, Sorin SIMION, Marius KOVACS

National Institute for Research and Development in Mine Safety and Protection to Explosion - INSEMEX, 32 General Vasile Milea Street, 332047, Petroșani, Romania

Corresponding author email: alexandru.simion@insemex.ro

Abstract

Volatile Organic Compounds (VOCs) are organic chemicals with high vapor pressure, originating from natural and anthropogenic sources, and are major contributors to environmental issues like photochemical smog and atmospheric pollution. This study introduces an optimized TD-GC-MS method for detecting and quantifying VOCs in ambient air, employing internal standards and certified reference materials to ensure analytical accuracy and traceability. The method is designed to deliver exceptional sensitivity, precision, and reproducibility, suitable for diverse environmental conditions. Key improvements include optimized thermal desorption, fine-tuned chromatographic separation, and calibrated mass spectrometric detection. Aligned with Eurachem guidelines, the integration of internal standards mitigates instrumental variability, while certified reference materials ensure traceable calibration, enhancing result reliability. The research demonstrates the method`s applicability to air quality monitoring, environmental assessments, and public health research. The findings validate TD-GC-MS as a robust, reliable solution for continuous VOC monitoring and routine environmental applications, providing critical insights into pollution sources and impacts, particularly in urban and industrial contexts. This research addresses the needs of scientists, policymakers, and environmental professionals seeking effective tools to combat air pollution.

Key words*: air quality monitoring, environmental pollution, GC-MS, thermal desorption, Volatile Organic Compounds.*

INTRODUCTION

Volatile Organic Compounds (VOCs) are produced from both natural and anthropogenic sources (Piccot et al., 1992). Natural sources include microbial activity, marine phytoplankton, volcanic and geothermal emissions, as well as wildfires (Ling & Guo, 2014). Anthropogenic sources comprise petroleum extraction and refining, vehicle emissions, the production and application of solvents on different surfaces, incomplete combustion of fossil fuels or biomass, and the fugitive emissions of VOCs from plastic materials during regular use (Atkinson & Arey, 2003). In the atmosphere, non-methane volatile organic compounds (VOCs) react with nitrogen oxides (NOx) in the presence of UV radiation, leading to the formation of ground-level ozone (O_3), a key component of photochemical smog. This reaction significantly contributes to air pollution and has detrimental effects on human health, both aquatic and terrestrial ecosystems, and plays a crucial role in climate change (Li et al., 2018). Elevated ground-level ozone concentrations can deteriorate air quality and lead to severe health problems, including respiratory conditions, heart disease, and cancer (Alford & Kumar, 2021). Prolonged exposure to VOCs has also been linked to neurological disorders, liver and kidney damage, and developmental issues, particularly in vulnerable groups like children and the elderly (Agency for Toxic Substances and Disease Registry, 2007).
The health impacts of VOC exposure depend on the specific compound, its concentration, and the duration of exposure. Brief exposure to high levels of VOCs, including benzene, toluene, and formaldehyde, can cause symptoms like irritation of the eyes and throat, headaches, dizziness, and nausea (Alford & Kumar, 2021). Long-term exposure, especially in urban and industrial zones, is associated with more severe health consequences, such as diminished lung function, weakened immune response, and reproductive issues. Some studies suggest a link between chronic VOC exposure and neurodegenerative diseases, underscoring the

need for stricter air quality regulations (Mølhave, 1991; Li et al., 2018).

In this regard, accurate monitoring of VOCs is essential for pollution control, regulatory compliance, and public health studies. In Romania, VOCs in ambient air are regulated by Law 104/2011 regarding air quality, which establishes a threshold value for the hazardous compound benzene, while other compounds such as toluene, ethylbenzene, and xylene (BTEX) are subject to general European regulations. According to the same law, benzene, in particular, is required to be monitored in major urban areas, given its significant concentration from human activities like traffic and industrial operations (Law No. 104, 2011). Other VOCs of concern include dichloroethene, dibromochloromethane, carbon tetrachloride trichloroethene, ethylbenzene, chlorobenzene, styrene, naphthalene et. all. These compounds contribute to atmospheric pollution and must be carefully monitored to assess their environmental impact and ensure regulatory compliance (Maceira et al., 2017).

Nowadays, several methods are available to detect VOCs in ambient air, including portable sensors such as the Photoionization Detector (PID) and Flame Ionization Detector (FID), as well as analysers utilizing Fourier Transform Infrared Spectroscopy (FTIR) and Ultraviolet (UV) fluorescence (Qualley et al., 2019; Epping & Koch, 2023; Elia et al., 2024). Each method has different advantages, such as real-time monitoring, simultaneous measurement of multiple compounds, and not requiring complex sample preparation. However, they also have disadvantages, such as poor selectivity, sensitivity and reduced precision. On the other hand, Thermal Desorption Gas Chromatography coupled with Mass Spectrometry (TD-GC-MS) offers increased selectivity (in multiple reaction monitoring mode) and specificity (Jia et al., 2006). Additionally, the method is quite robust, reproducible, and traceable, which facilitates compliance with regulatory standards and enhances our understanding of air pollution dynamics. Moreover, it is crucial to monitor non-methane VOCs (NMVOCs) as defined in Law No. 104/2011, including aliphatic hydrocarbons (such as ethane, propane, and butane), aromatic hydrocarbons (such as benzene, toluene, and xylene), oxygenated compounds (such as ethanol and acetone), and halogenated compounds (such as CFCs and halons). These VOCs contribute significantly to the formation of tropospheric ozone, a harmful pollutant that can adversely affect human health, especially in regions with high levels of emissions (Zhou et al., 2023).

MATERIALS AND METHODS

The analysis of VOCs in ambient air using Gas Chromatography-Mass Spectrometry (GC-MS) requires calibration across multiple concentration levels, achieved through serial dilution of certified standard solutions. (Rodríguez-Navas et al., 2012; Cai et al., 2015; Chung et al., 2019). Thus, the following reference mixtures were used for calibration:

502.2 Calibration mix 30043, Batch A0189182;
502.2 Calibration mix 30044, Batch A0180278;
502.2 Calibration mix 30045, Batch A0181037;
502.2 Calibration mix 30046, Batch A0175597;
502.2 Calibration mix 30047, Batch A0189197.

The reference mixtures, manufactured by RESTEK, were diluted with Methanol SupraSolv 1.00837.1000, using Eppendorf Xplorer plus micropipettes 0.5-10 µL and Eppendorf Xplorer plus 0.2-5 mL pipettes.

TD glass tubes filled with deactivated glass wool (Restek, Deactivated wool 24324, Batch 365237-1) were used for the introduction of substances, and the calibration solutions were introduced by dispensing 1 µL of each solution using a Shimadzu 10 µL syringe (10F-S-0.63, Batch 51W-074109M).

Analytical analysis of Thermal Desorption (TD) Tubes was performed using the Shimadzu Thermal Desorption System TD 30R, with a temperature program of 10 minutes at 280°C and 70 ml/min, followed by trap cooling to -20°C (Brown & Crump, 1998). The analyses were carried out using the Shimadzu Gas Chromatograph Mass Spectrometer - TQ8050NX, coupled with an SH-5Sil MS chromatographic column for effective separation of VOCs. The mass spectrometer was operated in both SCAN mode, where a broad range from 50 m/z to 350 m/z was rapidly scanned to capture a full spectrum of ions in order to identify the retention time for each VOC compound, and Selected Ion Monitoring (SIM) mode, where the mass spectrometer focused on

specific ions of VOC compounds within this range to enhance sensitivity and selectively detect VOC compounds (Pleil et al., 1991). The gas chromatograph temperature program for VOCs separation is presented in Figure 1.

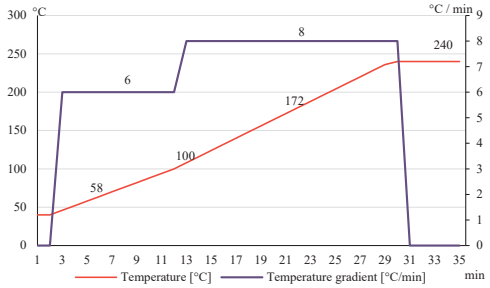


Figure 1. GC temperature profile for VOCs separation

Sampling of VOCs in ambient air was performed on TD tubes, Tenax 60/80 mesh, O.D x L ¼ in x 3 ½ in glass and Tenax TA/Carboxen1018, O.D x L ¼ in x 3 ½ in glass from Markes International (Figure 2), using the Acti-VOC Low Pump from Markes International (SN: 20220201001). The pump flow rate was calibrated for the desorption tubes using the 7000 Flowmeter from Ellutia (SN: 200235).



Figure 2. Tenax TA/Carboxen1018 and Tenax TA tubes

Additionally, helium 6.0 was used as the carrier gas, deuterated toluene as the internal standard from Linde Gaz Romania, also 4 mL glass vials and racks from Shimadzu were employed for sample storage.

RESULTS AND DISCUSSIONS

The optimalization of the chromatographic method was conducted to ensure its robustness, precision, and reliability. In this context, key performance parameters were evaluated according to established international standards (Eurachem/CITAC Guide; 2012; Eurachem, 2025; SR EN ISO 17025, 2018), along with the analytical conditions of the mass spectrometer used for detection. Linearity was assessed by evaluating the correlation coefficient (R^2), confirming the proportional relationship between analyte concentration and detector response within the defined range. Similarly, the limit of detection (LOD) and limit of quantitation (LOQ) were determined by analyzing the signal-to-noise ratios and the regression line intercept, which reflect the method's sensitivity in detecting and quantifying low analyte concentrations. The precision of the method was assessed by examining intra- and inter-day reproducibility, with the relative standard deviation (RSD) being used to evaluate variability across various concentration levels. Accuracy was confirmed through recovery studies, where theoretical concentrations were compared with measured values. In addition, specificity was evaluated to ensure the method's ability to effectively separate the analyte from potential matrix interferences.

In addition, the analytical conditions of the mass spectrometer, including ionization source parameters, collision energy, and mass resolution, were optimized and validated to ensure accurate and reproducible measurements. These conditions were carefully adjusted to achieve maximum sensitivity and specificity for the target analyte.

Development of solutions at multiple concentration levels

Multiple concentration levels were carried out starting from a stock solution of 2000 µg/mL, using the following calibration mixtures from Method 502.2: Calibration mix 30043 (Batch A0189182), Calibration mix 30044 (Batch A0180278), Calibration mix 30045 (Batch A0181037), Calibration mix 30046 (Batch A0175597), and Calibration mix 30047 (Batch A0189197). These mixtures were dissolved in methanol to create eight concentration levels: 0, 1.6, 3.5, 5, 8, 10, 19, and 32 ng, ensuring a comprehensive calibration range for the analyte. The VOCs (volatile organic compounds) were quantified across these levels to evaluate the

method's effectiveness in detecting and measuring these compounds.

Mass spectrometer tuning and optimization

The United States Environmental Protection Agency (US EPA) methods for VOC analysis in ambient air recommend adjusting the tuning conditions by modifying the perfluorotri-butylamine (PFTBA) target abundances to ensure that subsequent 1-Bromo-4-fluorobenzene (BFB) analysis meets the established relative abundance criteria (U.S. Environmental Protection Agency, 1999; 2003). Thus, the research supports the recommended BFB tune conditions using m/z 69 as the target mass and mass pattern adjustment, as presented in Table 1.

Table 1. 1-Bromo-4-fluorobenzene tuning conditions

Mass (m/z)	Intensity Ratio %
69	100
219	50
502	1.5
131	42
414	2.5
614	0.4

The tuning process was performed on the Shimadzu GCMS-TQ8050NX using an automated tuning procedure prior to sample analysis. The optimized conditions ensure stable instrument performance, enhancing sensitivity and accuracy in VOC quantification (U.S. Environmental Protection Agency, 2025). Regular tuning verification, following United States Environmental Protection Agency (US EPA) protocols, maintains compliance with analytical standards and ensures reproducible results throughout the study.

Studies have shown that these conditions produce a tune that meets the strict BFB relative abundance criteria for all VOC methods across multiple instruments and remains stable over an evaluation period of approximately three months (Shimadzu, 2023). Additionally, the tune file obtained was applied to the Thermal Desorption-Gas-chromatography-Mass spectrometry (TD-GC-MS) method, ensuring optimal ionization efficiency and accurate mass detection for VOC analysis.

The stability of the tuning parameters was maintained throughout the thermal desorption process, ensuring reliable quantification of target compounds.

Selectivity and specificity

The method's selectivity was achieved through the SH-5Sil (0.25 mm x 0.25 µm x 30 m) chromatographic column, renowned for its high efficiency and low bleed characteristics. The column facilitated the precise separation of complex VOC mixtures present in different matrices (ambient air), with distinct retention times (Table 2) for each compound (Figure 3). The effective resolution of individual VOC peaks within the chromatogram was crucial in preventing peak overlap and enhancing the method's sensitivity. This superior selectivity ensured the accurate identification and quantification of each VOC in the challenging environmental matrix.

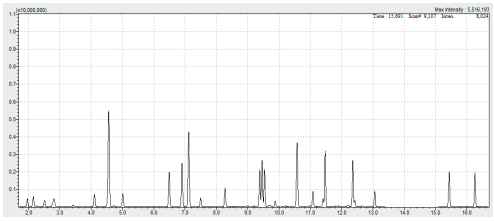


Figure 3. Separation of VOCs in ambient air

To further enhance the specificity and sensitivity of the analysis, the mass spectrometer was operated in Selective Ion Monitoring (SIM) mode. In this configuration, three ions were meticulously selected for each compound: one quantifier ion (e.g., 78 m/z for benzene) and two qualifier ions (e.g., 77 m/z, 51 m/z) to confirm compound identity (Figure 4), following the guidelines established by the TO-14, TO-15, and TO-17 methods for VOC analysis.

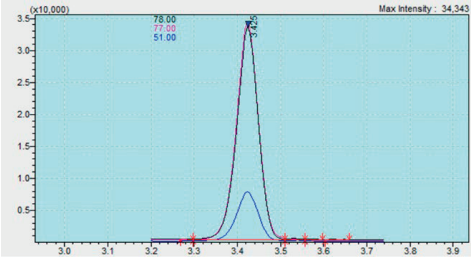


Figure 4. Benzene quantifier and qualifier ions (m/z)

This dual-ion approach ensures the integrity of the analysis by enabling compound-specific verification. The SIM mode provided substantial improvements in sensitivity, reducing background noise and minimizing potential interferences from non-target compounds. Through this integration of selectivity, chromatographic resolution, and ion-specific detection, the method achieved a high degree of specificity and reliability, making it suitable for the precise.

Linearity Assessment and Calibration Curve Validation for VOC Quantification

The linearity of the method was assessed by constructing a calibration curve through the injection of a series of calibration standards onto the thermal desorption tube at distinct concentration levels (0, 1.6, 3.5, 5, 8, 10, 19, and 32 ng), as detailed in the experimental procedure. The ambient air matrix was spiked with precisely known concentrations (theoretical concentrations) of target VOCs, while the internal standard method utilizing deuterated toluene was implemented to ensure robust and accurate quantification. The data obtained were then employed to generate calibration curves for each analyte (Table 2), ensuring that a comprehensive range of concentrations was thoroughly represented.

Table 2. Correlation Coefficient (R), Coefficient of Determination (R^2), and Retention Times for VOC Calibration Curves

Compound name	Retention time (min)	R Coefficient	R^2 Coefficient
Dichloroethene	1.950	0.99961	0.99923
Cis - 1,2 dichlorethene	2.157	0.99982	0.99965
1,1 - Dichloroethane	2.250	0.99817	0.99963
Bromochloromethane	2.500	0.99972	0.99972
Chloroform	2.505	0.99864	0.99973
1,1,1 - Trichloroethane	2.801	0.99987	0.99974
1,2 - Dichloroethane	2.802	0.99992	0.99985
Carbon tetrachloride	3.000	0.99985	0.99969
Benzene	3.434	0.99988	0.99976
Dibromomethane	3.450	0.99976	0.99952
1,2 - Dichloropropane	3.425	0.99983	0.99966
Trichloroethene	3.425	0.99956	0.99912
Bromodichlorometh.	3.587	0.99985	0.99971
cis13-Dichloropropene	4.101	0.99988	0.99975
tra13-dichloropropene	4.602	0.99977	0.99955
Toluene	4.620	0.99980	0.99961
1,1,2 - trichloroethane	4.720	0.99979	0.99957
1,3 – Dichloropropane	5.000	0.99970	0.99985
Dibromochlorometh.	5.250	0.99977	0.99954
1,2-Dibromoethane	5.498	0.99987	0.99975
Tetrachloroethene	5.590	0.99975	0.99950
Chlorobenzene	6.500	0.99982	0.99965
1,1,1,2-Tetrachloroeth.	6.600	0.99981	0.99962
Ethylbenzene	6.980	0.99984	0.99968
mp-Xylene	7.188	0.99978	0.99957
Bromoform	7.500	0.99942	0.99884
Styrene	7.684	0.99987	0.99974
o-Xylene	7.756	0.99936	0.98729
1,1,2,2-Tetrachloroeth.	8.300	0.99929	0.99858
1,2,3Trichloropropane	8.501	0.99980	0.99960
Isopropilbenzene	8.651	0.99982	0.99963
Bromobenzene	8.800	0.99984	0.99968
o-Chlorotoluene	9.382	0.99925	0.99849
n-Propylbenzene	9.491	0.99479	0.98961
4-Chlorotoluene	9.555	0.99978	0.99957
1,3,5-Trimethylbenz.	9.850	0.99982	0.99636
S-butylbenzene	11.101	0.99980	0.99960
1,4-Dichlorobenzene	11.103	0.99978	0.99956
p-Cymene	11.510	0.99968	0.99936
1,2-Dichlorbenzene	11.770	0.99981	0.99961
n-Butylbenzene	12.360	0.99864	0.99728
1,2,4-Trichlorobenz.	15.451	0.99974	0.99948
Naphthalene	15.625	0.99986	0.99973
1,2,3-Trichlorobenz.	16.241	0.99966	0.99932
Hexachlorobutadiene	16.528	0.99968	0.99935

Each calibration point for the VOCs was determined based on the quantifier ion (e.g., 78 m/z for benzene), which was selected to ensure precise and consistent quantification (Figure 5).

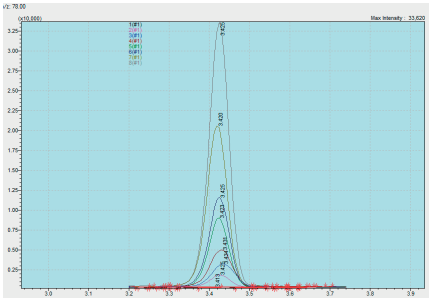


Figure 5. Peak identification quantifier ion 78 m/z

This methodological approach facilitated a comprehensive evaluation of the system's capacity to generate a consistent and linear response across the defined concentration spectrum, which is critical for the accurate and reliable quantification of VOCs in complex environmental matrices. The calibration curves were meticulously constructed by plotting the peak area of each analyte against its corresponding concentration (Figure 6), ensuring a broad concentration range was covered.

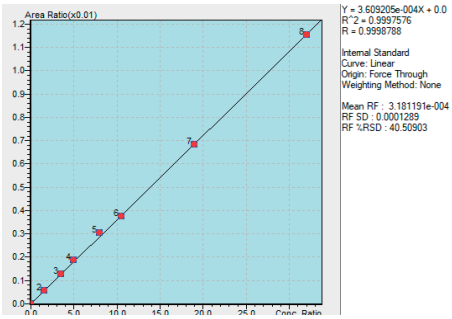


Figure 6. Calibration curve for benzene quantification

Additionally, the internal standard response was strategically employed to correct for potential variations, such as instrumental fluctuations or matrix interferences, thereby ensuring the precision of the quantification process.

The calibration data obtained were used to rigorously evaluate the linearity of the method across the specified concentration range, thereby affirming the precision and robustness of the analytical technique. The calibration curve, along with the comprehensive table displaying the correlation coefficients (R and R^2) for each analyte, was utilized to provide a detailed representation of the method's consistency for quantification of VOCs in ambient air.

Poor correlation coefficients were observed for 1,2-Dibromo-3-Chloropropane, tert-Butylbenzene, 1,2,4-Trimethylbenzene, and 1,3-Dichlorobenzene, and their signal intensities increased significantly, causing interference with the detector. This interference, likely caused by the injection of deuterated toluene (d8), compromised the accuracy and reliability of their quantification. For both technical and economic considerations, these compounds were excluded from the analysis to maintain the integrity and efficiency of the method.

Analytical Performance Parameters: Repeatability, Limit of Detection, Limit of Quantification, and Recovery

Ensuring the reliability and accuracy of an analytical method is essential in environmental monitoring, particularly when using Gas Chromatography-Mass Spectrometry (GC-MS) for the determination of volatile organic compounds (VOCs) in ambient air. The validation process involves assessing key performance parameters that define the method's precision, sensitivity, and accuracy. Among these, repeatability, limit of detection (LOD), limit of quantification (LOQ), and recovery are crucial for determining its suitability for air quality assessment and regulatory compliance (Eurachem, 2025).

Repeatability refers to the method's ability to produce consistent results when the same air sample is analyzed multiple times under identical conditions. It is a key aspect of precision and is expressed as the relative standard deviation (RSD) of repeated measurements. Repeatability is assessed both within the same day (*intra-day precision*) and across multiple days (*inter-day precision*) to ensure robustness. The results of these evaluations are summarized in Table 3, which presents the intra-day and inter-day repeatability data for VOCs in ambient air.

Limit of Detection (LOD) represents the lowest concentration of a VOC that can be detected but not necessarily quantified with confidence (Eurachem, 2025). It is a crucial parameter for evaluating the sensitivity of an analytical method, particularly when analyzing trace-level VOCs in urban and industrial environments. LOD is often determined using statistical approaches based on the signal-to-noise ratio or the standard deviation of the baseline noise.

Limit of Quantification (LOQ) is the lowest concentration of a VOC that can be quantitatively measured with acceptable accuracy and precision (Wang & Austin, 2006; Eurachem, 2025).

While the LOD merely indicates the presence of an analyte, the LOQ ensures that the VOC concentration can be determined with statistical confidence. Typically, LOQ is defined as a multiple (e.g., 10 times) of the standard deviation of the baseline noise or the calibration curve residuals.

Recovery measures the accuracy of the method by assessing how efficiently VOCs can be collected, desorbed, and quantified from air samples (Gallego et al., 2011; Eurachem, 2025). This is determined by spiking known amounts of VOCs onto sorbent tubes or into air sampling canisters, followed by analysis and comparison with the expected values. High recovery values indicate minimal losses during sampling, desorption, and analysis, ensuring reliable

quantitative results. Together, these parameters form the foundation of method validation, ensuring that the analytical technique employed for VOC analysis in ambient air is robust, sensitive, and precise.

By systematically evaluating repeatability, LOD, LOQ, and recovery, researchers can establish the credibility of their GC-MS method, making it suitable for air quality monitoring, exposure assessment, and regulatory reporting.

Table 3. Method validation for the analysis of Volatile Organic Compounds in ambient air

Compound name	Repeatability								LOD (ng)	LOQ (ng)	Recovery (%)
	Intra-day 1.6 ng	RSD (%) n = 6	Inter-day 1.6 ng	RSD (%) n = 6	Intra-day 10 ng	RSD (%) n = 6	Inter-day 10 ng	RSD (%) n = 6			
Dichloroethene	1.56	3.11	1.65	4.27	9.98	2.67	10.09	3.48	0.15	0.38	94
Cis - 1,2 dichlorethene	1.64	3.68	1.69	4.84	9.86	2.94	9.74	3.52	0.18	0.42	87
1,1 - Dichloroethane	1.57	3.21	1.66	3.84	9.62	2.47	10.41	3.80	0.12	0.85	93
Bromochloromethane	1.57	3.15	1.66	3.39	9.86	2.94	9.60	3.50	0.11	0.88	82
Chloroform	1.62	3.99	1.61	4.80	9.95	2.57	9.52	3.69	0.11	0.82	105
1,1,1 - Trichloroethane	1.63	4.09	1.54	4.16	9.98	2.67	10.30	3.98	0.13	0.72	98
1,2 - Dichloroethane	1.58	3.17	1.58	4.67	9.73	2.41	9.51	3.93	0.18	0.79	121
Carbon tetrachloride	1.63	2.70	1.62	3.84	10.03	2.28	9.74	4.31	0.13	0.75	91
Benzene	1.64	3.65	1.66	4.58	9.65	2.29	9.75	3.45	0.08	0.70	88
Dibromomethane	1.63	4.48	1.56	4.06	10.26	2.85	9.47	3.51	0.16	0.47	108
1,2 - Dichloropropane	1.58	4.01	1.55	5.00	9.97	2.15	9.61	3.42	0.14	0.73	117
Trichloroethene	1.64	4.47	1.67	3.22	9.74	2.56	9.76	3.59	0.12	0.60	93
Bromodichlorometh.	1.59	3.94	1.52	4.33	9.89	2.12	10.38	3.20	0.09	0.27	95
cis13-Dichloropropene	1.60	3.44	1.60	3.76	9.83	2.43	10.27	4.40	0.10	0.80	84
tra13-dichloropropene	1.63	4.04	1.67	4.22	10.04	2.17	10.47	3.70	0.14	0.88	118
Toluene	1.62	3.29	1.53	4.04	10.24	2.53	9.94	3.50	0.10	0.30	105
1,1,2 - trichloroethane	1.63	3.90	1.67	3.77	10.27	2.64	10.49	4.10	0.17	0.54	110
1,3 – Dichloropropane	1.58	3.89	1.57	3.89	9.69	2.45	9.53	3.22	0.09	0.36	101
Dibromochlorometh.	1.56	3.29	1.63	4.70	9.80	2.70	10.47	4.41	0.11	0.39	108
1,2-Dibromoethane	1.62	4.21	1.65	4.08	9.99	2.70	9.84	3.15	0.12	0.50	116
Tetrachloroethene	1.63	3.31	1.68	3.38	10.15	2.51	9.49	4.35	0.10	0.52	98
Chlorobenzene	1.58	2.62	1.58	5.08	9.69	2.63	9.48	4.06	0.09	0.56	102
1,1,1,2-Tetrachloroeth.	1.56	3.62	1.57	3.77	9.88	2.95	10.09	4.02	0.17	0.65	88
Ethylbenzene	1.61	4.41	1.63	3.31	9.90	2.18	9.44	3.26	0.09	0.30	105
mp-Xylene	1.58	2.73	1.51	4.35	10.27	3.12	9.96	4.12	0.10	0.63	121
Bromoform	1.56	3.18	1.53	5.05	9.65	2.48	9.62	4.36	0.15	0.80	94
Styrene	1.60	3.78	1.54	3.95	10.13	3.09	9.47	3.53	0.14	0.63	98
o-Xylene	1.57	2.52	1.67	3.87	9.99	2.74	10.02	3.21	0.15	0.57	124
1,1,2,2-Tetrachloroeth.	1.57	4.31	1.63	3.76	10.22	2.32	9.76	3.97	0.09	0.89	86
1,2,3Trichloropropane	1.64	3.92	1.59	3.91	10.12	2.35	9.50	3.17	0.16	0.72	79
Isopropilbenzene	1.56	4.29	1.65	4.12	9.81	2.73	10.01	4.24	0.16	0.44	105
Bromobenzene	1.61	3.38	1.56	4.90	10.28	2.77	9.65	3.14	0.15	0.75	119
o-Chlorotoluene	1.64	3.23	1.68	4.87	9.81	3.14	10.55	4.14	0.09	0.25	116
n-Propylbenzene	1.56	4.24	1.67	4.38	10.19	2.40	9.72	3.51	0.09	0.56	118
4-Chlorotoluene	1.57	3.04	1.58	4.83	10.04	3.03	9.87	3.95	0.11	0.27	101
1,3,5-Trimethylbenz.	1.58	2.63	1.54	3.92	9.70	2.44	9.63	3.68	0.12	0.58	94
S-butylbenzene	1.57	3.43	1.66	4.59	9.79	2.23	9.74	3.32	0.13	0.56	98
1,4-Dichlorobenzene	1.63	3.88	1.59	5.01	10.18	2.33	10.12	4.21	0.10	0.37	110
p-Cymene	1.63	4.49	1.64	3.65	10.09	2.21	9.66	4.03	0.16	0.68	79
1,2-Dichlorbenzene	1.57	2.64	1.53	3.92	10.25	2.63	9.61	3.92	0.10	0.37	89
n-Butylbenzene	1.58	3.06	1.67	4.01	9.72	2.97	10.52	3.70	0.14	0.52	116
1,2,4-Trichlorobenz.	1.57	4.47	1.56	4.55	9.96	2.57	9.85	3.38	0.13	0.29	105
Naphthalene	1.62	3.39	1.66	3.74	10.25	2.72	9.57	4.54	0.13	0.69	87
1,2,3-Trichlorobenz.	1.59	3.22	1.53	3.50	10.25	2.61	9.74	3.92	0.14	0.35	101
Hexachlorobutadiene	1.56	3.44	1.59	3.21	10.08	2.93	9.94	3.65	0.08	0.82	92

The validation of the analytical method used for the determination of volatile organic compounds (VOCs) in ambient air has demonstrated high performance in terms of precision, repeatability, and sensitivity. The obtained values for the limits of detection (LOD) and limits of quantification (LOQ) indicate an adequate capability to identify and quantify compounds at

low concentrations, which is essential for ambient air monitoring (Demeestere et al., 2008; Kim & Park, 2020;). Furthermore, the achieved recovery rates, falling within an optimal range, confirm the accuracy of the method and the reliability of the results (Wang et al., 2018). Intra and inter-day repeatability, expressed through the relative standard deviation (RSD), has shown the stability of the method under various analytical conditions, further demonstrating its robustness. These aspects are crucial for applying the method in long-term monitoring studies aimed at assessing population exposure to VOCs and their impact on air quality and human health.

In conclusion, the validated TD-GC-MS method exhibits analytical characteristics that comply with international standards for VOC analysis in ambient air. Its high sensitivity and precision make it a reliable tool for monitoring volatile organic compounds in urban and industrial environments, providing essential data for the development of air pollution mitigation strategies and the protection of public health (Chung et al., 2019; Zou & Yang, 2022).

Field Monitoring of Volatile Organic Compounds (VOCs)

Field monitoring of volatile organic compounds (VOCs) is essential for assessing air quality and understanding the spatial and temporal distribution of these pollutants in different environments. The selection of monitoring sites, sampling techniques, and analytical methods plays a crucial role in obtaining representative and reliable data.

Preparation of Tenax Tubes: Calibration and Verification

The Acti-VOC pump was calibrated to a flow rate of 200 mL/min using the 7000 Ellutia electronic flowmeter to ensure accuracy and consistency in sample collection. Prior to conditioning, each Tenax tube was individually inspected to verify proper airflow and sorbent integrity (Figure 7).

The recorded parameters were systematically analysed, and the data distribution, along with the potential variability for the Tenax tubes, was evaluated and presented in Figure 8 to ensure reliability and reproducibility in the adsorption process.



Figure 7. Flow Rate adjustment and flow monitoring

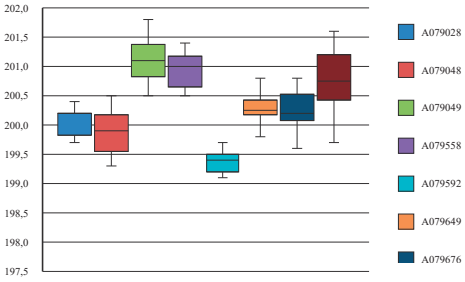


Figure 8. Flow assessment for Tenax TA tubes

To ensure consistency and verify the results, the same experiment was conducted on tubes containing both Tenax and Carboxen 1018, following the same procedure as for the tubes containing only Tenax. The data for the Tenax/ Carboxen 1018 tubes are presented in Figure 9, where the distribution and variability of the recorded parameters are analysed.

The flow rate measurements for the Tenax-only tubes and the combined Tenax and Carboxen tubes showed consistent performance throughout the experiments. While the Tenax-only tubes exhibited stable flow characteristics within the expected range, the inclusion of Carboxen did not significantly affect the flow dynamics.

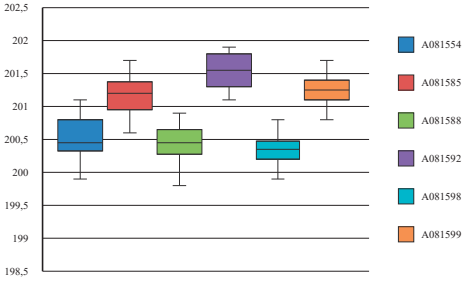


Figure 9. Flow assessment for TA Tubes/Carboxen1018

Both configurations demonstrated reliable flow rates, making them suitable for the collection of volatile organic compounds (VOC) from ambient air. These results confirm that both types of tubes are appropriate for accurate VOC sampling from ambient air, with minimal impact on the flow rate.

Conditioning of Tenax and Tenax/Carboxen Tubes for VOC Analysis

Tenax and Tenax/Carboxen tubes were conditioned using a Shimadzu Thermodesorber 30R. Desorption was performed at a temperature of 280°C and a flow rate of 70 mL/min for 20 minutes (Maria, 1996; SR EN 14662-4, 2005). The conditioning process was carried out in the reverse direction of the sampling flow to ensure complete desorption of any retained compounds and to prepare the tubes for subsequent analysis (SR EN 14662-5, 2005). According to the performed experiments, this method effectively removed any potential contaminants and ensured the integrity of the tubes prior to their use in VOCs sampling.

System checks and quality control

In order to ensure the reliability and accuracy of TD-GC-MS measurements, routine system checks, and quality control procedures were performed daily or after every 20 thermal desorption tubes analysed. These procedures included instrument warm-up, carrier gas flow verification, vacuum pressure monitoring, and mass spectrometer performance assessment. BFB (4-bromofluorobenzene) tuning check (30026; Batch A0189204) was conducted in full scan mode according to the requirements of EPA Method TO-17, to verify mass calibration, resolution, and detector sensitivity. Ion abundance criteria, as outlined in Table 4, were applied to specific fragment ions and the tune was accepted only when all values fell within the predefined range.

Moreover, using the system performance mix (30075; Batch A0189066), retention times, peak heights and area were verified for the following compounds: Bromoform, Chlorobenzene, 1,1-Dichloroethane and 1,1,2,2-Tetrachloroethane. These parameters were evaluated to ensure consistency and accuracy of the system performance and analytical method in detecting analytes. Both BFB tuning and system performance checks were performed at 10 ng to ensure the precision and sensitivity of the system during analysis of target compounds in the environmental samples.

Table 4. Ion abundance criteria for 4-bromofluorobenzene

m/z	Spectrum check criteria
50	15 to 40 % of 95 mass 95
75	30 to 60 % of mass 95
95	Base peak, 100% relative abundance
96	5 to 9 % of mass 95
173	< 2% of mass 174
174	> 50% of mass 95
175	5 to 9 % of mass 174
176	95 to 101 % of mass 174
177	5 to 9% of mass 176

Monitoring Sites and Sampling Techniques for VOC Assessment

The placement of monitoring stations for volatile organic compounds (VOCs) is a critical step in assessing air quality. In this study, VOC samples were collected in two distinct locations within the Jiu Valley region: the industrial area near the Lonea mine and the urban/pedestrian area of the Petroșani city center. The sampling points were selected to evaluate VOC concentrations in both an industrial environment and an urban area with high pedestrian traffic.

At each of these points, multiple sequential samples were collected using both Tenax and Tenax/Carboxen tubes. For each location, a blank sample was also collected using one of the tubes to assess potential contamination during the sampling process. The active sampling was conducted with the Acti-VOC pump at a flow rate of 200 mL/min, and each sample was collected for a 15-minute period. After the sampling process, the tubes were analysed using Thermal Desorption Gas Chromatography-Mass Spectrometry (TD-GC-MS) to quantify and identify the VOCs present in the ambient air. This approach ensured that a comprehensive analysis of VOC levels was conducted at both the industrial and urban/pedestrian sites, providing valuable insights into the air quality in these different environments. The results of these analyses, including VOC concentrations at the respective sites, are presented in Figure 10.

Together, these parameters form the foundation of method validation, ensuring that the analytical technique employed for VOC analysis

in ambient air is robust, sensitive, and precise. By systematically evaluating repeatability, LOD, LOQ, and recovery, researchers can establish the credibility of their GC-MS method, making it suitable for air quality monitoring, exposure assessment, and regulatory reporting.

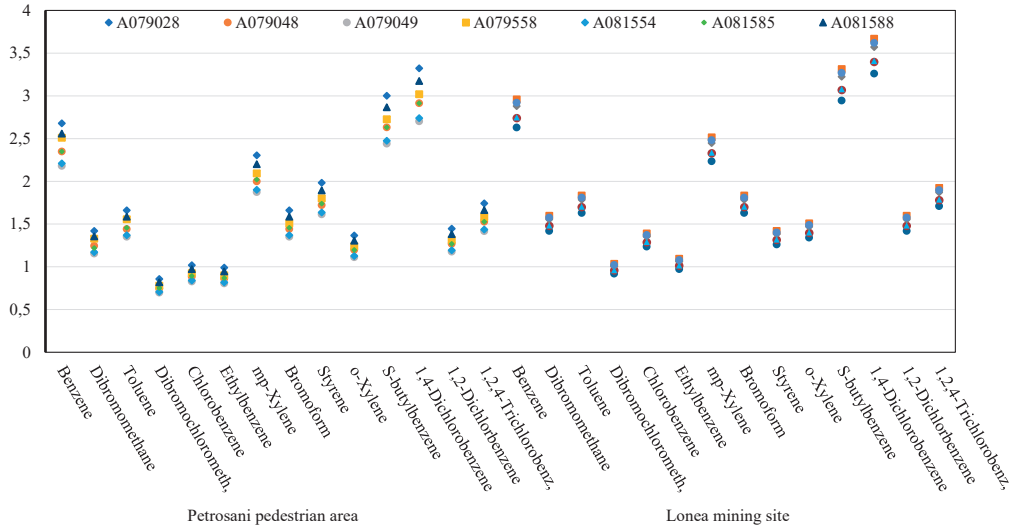


Figure 10. Analysis of Volatile Organic Compounds in ambient air on Petrosani and Lonea mining site

The measured concentrations of the investigated VOCs reveal discernible differences between the Petroșani pedestrian area (left cluster) and the Lonea mining site (right cluster). Each compound is represented by multiple data points (A079028, A079048, A079049, A079558, A081554, A081585, and A081588), thereby illustrating both inter-sample variability and site-specific emission characteristics.

Certain aromatic hydrocarbons (e.g., p-xylene, ethylbenzene, and benzene) appear more pronounced in the urban/pedestrian environment, potentially reflecting the influence of vehicular traffic, commercial activities, and population density. Conversely, the mining area exhibits elevated or comparable concentrations of halogenated compounds, such as 1,2-dichloroethane, suggesting contributions from industrial or mining-related processes. The overall range of values, extending from roughly 1.0 to 3.5 $\mu g/m^3$ underscores the necessity for robust sampling strategies and precise analytical methods to capture the nuances of VOC distribution.

Moreover, the fluctuations in measured concentrations highlight the impact of temporal factors (e.g., time of day, operational cycles) and microclimatic conditions (e.g., temperature, wind speed) on ambient VOC levels. This dataset thus reinforces the importance of employing comprehensive monitoring protocols, encompassing both spatial and temporal dimensions, to inform targeted mitigation measures and support evidence-based policymaking in air quality management.

CONCLUSIONS

This research aimed to develop and validate an optimized TD-GC-MS method for monitoring VOCs in ambient air. The applied methodology, which combined thermal desorption with gas chromatography-mass spectrometry and incorporated the use of internal standards and certified reference materials, ensured high analytical accuracy and traceability in calibration. The optimized method demonstrated excellent sensitivity - evident in its low detection and quantification limits - allowing for the reliable identification of VOCs at trace levels, as well as high precision and repeatability, with minimal variability observed in both short and long-term analyses. Additionally, the recovery rates obtained during

the method validation fell within optimal ranges, further confirming the accuracy and reliability of the analytical procedure. These performance characteristics comply with international standards in the field, which underscores the robustness of the method and its suitability for continuous air quality monitoring.

Key findings and contributions of this study include the provision of a robust, validated analytical solution for the systematic monitoring of VOCs in urban and industrial environments, thereby generating critical data for air pollution assessments. The field application of the optimized TD-GC-MS method confirmed its utility in obtaining detailed information on the spatial and temporal distribution of organic pollutants, which is essential for identifying emission sources and population exposure levels. Such information is highly relevant to public health, as more precise and reliable VOC monitoring contributes to a better understanding of the relationships between pollutant exposure and adverse health effects (e.g., respiratory, cardiovascular, or neurological issues), thereby supporting the development of risk mitigation strategies. Moreover, this study has significant implications for environmental regulations. The proposed method, which aligns with international guidelines (e.g., Eurachem), can be employed by regulatory bodies and laboratories to ensure compliance with air quality standards and to inform environmental policy. Overall, the successful validation of this optimized TD-GC-MS method represents a significant advancement in atmospheric pollution monitoring, offering a dependable tool for protecting both the environment and public health. The method proves to be highly effective and reliable for VOC monitoring in ambient air, providing exceptional sensitivity and precision, even at trace concentrations. Given its robustness, it is strongly recommended for continuous air quality assessments, particularly in urban and industrial environments, where accurate tracking of volatile organic compounds is crucial for public health protection and compliance with environmental regulations.

ACKNOWLEDGEMENTS

The current paper was carried out through the Nucleu Program within the National Research Development and Innovation Plan 2022-2027, carried out with the support of MCID, project no. PN 23 32 01 01, IOSIN PCDIEX

REFERENCES

Agency for Toxic Substances and Disease Registry. (2007). Toxicological Profile for Benzene. U.S. Department of Health and Human Services, Public Health Service. Retrieved from https://www.atsdr.cdc.gov/toxprofiles/tp3.pdf

Alford, K.L., & Kumar, N. (2021). Pulmonary Health Effects of Indoor Volatile Organic Compounds-A Meta-Analysis. *International Journal of Environ Research and Public Health, 18*(4), 1578.

Atkinson, R., & Arey, J. (2003). Atmospheric degradation of volatile organic compounds. *Chemical Reviews, 103*(12), 4605–4638.

Brown, V. M., & Crump, D. R. (1998). Diffusive sampling of volatile organic compounds in ambient air.*Environmental Monitoring and Assessment*, *52*, 43-55.

Cai, X. M., Xu, X. X., Bian, L., Luo, Z. X., & Chen, Z. M. (2015). Measurement of volatile plant compounds in field ambient air by thermal desorption–gas chromatography–mass spectrometry.*Analytical and bioanalytical chemistry*, *407*(30), 9105-9114.

Chung, H., Lee, S., & Kim, D. (2019). Method Development and Validation of TD-GC-MS for Analysis of Volatile Organic Compounds in Urban Air. *Analytical Methods*, *11*(7), 1234–1242.

Demeestere, K., Dewulf, J., De Roo, K., De Wispelaere, P., & Van Langenhove, H. (2008). Quality control in quantification of volatile organic compounds analysed by thermal desorption–gas chromatography–mass spectrometry. *Journal of Chromatography A, 1186*(1-2), 348-357.

Epping, R., & Koch, M. (2023) On-Site Detection of Volatile Organic Compounds (VOCs). *Molecules, 28*(4), 1598.

Elia, E. A., Stylianou, M., & Agapiou, A. (2024). Investigation on the source of VOCs emission from indoor construction materials using electronic sensors and TD-GC-MS. *Environmental Pollution*, *348*, 123765.

Eurachem. (2025). *The Fitness for Purpose of Analytical Methods. A Laboratory Guide to Method Validation and Related Topics (3nd ed.)*. Retrieved from https://www.eurachem.org/images/stories/Guides/pdf/MV_guide_3rd_ed_V1_EN.pdf.

Eurachem/CITAC Guide (2012). *Quantifying Uncertainty in Analytical Measurement (3nd ed.)*. Retrieved from https://www.eurachem.org/images/stories/Guides/pdf/QUAM2012_P1.pdf.

Gallego, E., Roca, F. J., Perales, J. F., & Guardino, X. (2011). Evaluation of the effect of different sampling time periods and ambient air pollutant concentrations on the performance of the Radiello® diffusive sampler for the analysis of VOCs by TD-GC/MS. *Journal of Environmental Monitoring*, *13*(9), 2612-2622.

Jia, C., Batterman, S., & Chernyak, S. (2006). Development and comparison of methods using MS scan and selective ion monitoring modes for a wide

range of airborne VOCs. *Journal of environmental monitoring*, *8*(10), 1029-1042.

Kim, J., & Park, S. (2020). Application of Thermal Desorption GC-MS for VOC Analysis in Urban Environments. *Environmental Science and Pollution Research*, *27*(15), 18890–18898.

Law No. 104/2011 on Air Quality. (2011). *Official Monitor, Part I, No. 689, 23 July 2011*. Retrieved from http://www.monitoruloficial.ro.

Li, X., Zhang, Y., & Wang, H. (2018). Assessment of BTEX Exposure and Its Impact on Human Health in Urban Areas. *Environmental Science & Technology*, *52*(7), 3751–3759.

Ling, Z. H., & Guo, H. (2014). Contribution of VOC sources to photochemical ozone formation and its control policy implication in Hong Kong. *Environmental Science & Policy, 38*, 180-191.

Maceira, A., Vallecillos, L., Borrull, F., Marce, R.M. (2017). New approach to resolve the humidity problem in VOC determination in outdoor air samples using solid adsorbent tubes followed by TD-GC–MS. *Science of The Total Environment*, *599–600*, 1718-1727.

Maria, P. (1996). Evaluation of Anasorb CMS and comparison with Tenax TA for the sampling of volatile organic compounds in indoor and outdoor air by breakthrough measurements. *Analyst*, *121*(3), 303-307.

Mølhave, L. (1991). Volatile Organic Compounds, Indoor Air Quality and Health. *Indoor Air*, *1*(4), 357-376.

Piccot, S. D., Watson, J.J., & Jones, J.W. (1992). A global inventory of volatile organic compound emissions from anthropogenic sources. *Journal of Geophysical Research: Atmospheres, 97*(D9), 9897-9912.

Pleil, J. D., Vossler, T. L., McClenny, W. A., & Oliver, K. D. (1991). Optimizing sensitivity of SIM mode of GC/MS analysis for EPA's TO-14 air toxics method. *Journal of the air & waste management association*, *41*(3), 287-293.

Qualley, A., Hughes, G. T., & Rubenstein, M. H. (2019). Data quality improvement for field-portable gas chromatography-mass spectrometry through the use of isotopic analogues for in-situ calibration. *Environmental Chemistry*, *17*(1), 28-38.

Rodríguez-Navas, C., Forteza, R., & Cerdà, V. (2012). Use of thermal desorption–gas chromatography–mass spectrometry (TD–GC–MS) on identification of odorant emission focus by volatile organic compounds characterisation. *Chemosphere*, *89*(11), 1426-1436.

Shimadzu Corporation. (2023). Operating manual for the TQ8050NX gas chromatograph-mass spectrometer, https://www.shimadzu.com/an/sites/shimadzu.com.an/files/pim/pim_document_file/manuals/11177/225-39105.pdf.

SR EN 14662-4. (2005). *Air Quality – Ambient air quality. Standard method for measurement of benzene concentrations Diffusive sampling followed by thermal desorption and gas chromatography*. Bucharest, Romania: Romanian Standards Association.

SR EN 14662-5. (2005). *Air Quality – Ambient air quality - Standard method for measurement of benzene concentrations - Part 5: Diffusive sampling followed by solvent desorption and gas chromatography.* Bucharest, Romania: Romanian Standards Association.

SR EN ISO 17025. (2018). *Testing and calibration laboratories.* Bucharest, Romania: Romanian Standards Association.

U.S. Environmental Protection Agency. (1999). *Method TO-17: Determination of volatile organic compounds in ambient air using active sampling onto sorbent tubes and analysis by gas chromatography/mass spectrometry* (EPA-600/R-99-043). Washington, DC: U.S. EPA.

U.S. Environmental Protection Agency. (2003). Method TO-15: Determination of volatile organic compounds in ambient air using active sampling onto Summa canisters and analysis by gas chromatography/mass spectrometry (EPA-600/R-15-006). Washington, DC: U.S. EPA.

U.S. Environmental Protection Agency. (2025). *Volatile Organic Compounds (VOCs): Basic Information*. Retrieved March 9, from https://www.epa.gov/voc.

Wang, D. K. W., & Austin, C. C. (2006). Determination of complex mixtures of volatile organic compounds in ambient air: an overview. *Analytical and bioanalytical chemistry*, *386*(4), 1089-1098.

Wang, M., Li, X., & Chen, H. (2018). Comprehensive Analysis of VOCs in Ambient Air Using Advanced TD-GC-MS Techniques. *Journal of Environmental Monitoring*, *20*(4), 456–464.

Zhou, X., Zhou, X., Wang, C., & Zhou, H. (2023). Environmental and human health impacts of volatile organic compounds: A perspective review. *Chemosphere*, 313, 137489.

Zou, Z., & Yang, X. (2022). Volatile organic compound emissions from the human body: Decoupling and comparison between whole-body skin and breath emissions. *Building and Environment*, *226*, 109713.

Scientific Papers. Series E. Land Reclamation, Earth Observation & Surveying, Environmental Engineering. Vol. XIV, 2025
Print ISSN 2285-6064, CD-ROM ISSN 2285-6072, Online ISSN 2393-5138, ISSN-L 2285-6064

NUMERICAL STUDY OF THE CYLINDRICAL SHAFT'S BEHAVIOUR USING 3D FINITE ELEMENT METHOD

Elena-Mihaela STAN, Horațiu POPA, Daniel MANOLI

Technical University of Civil Engineering of Bucharest,
122-124 Lacul Tei Blvd, District 2, Bucharest, Romania

Corresponding author email: elena-mihaela.stan@phd.utcb.ro

Abstract

The numerical modelling of the cylindrical shafts can be done using finite element method in axisymmetric or three-dimensional conditions. For this study, the 3D finite element method has been used to analysed the cylindrical shaft's behaviour regarding the earth pressure distribution, the vertical displacements of the soil and the horizontal displacements of the diaphragm wall. Thus, a parametric study has been carried out in which the cylindrical shafts radius, the length of the diaphragm wall and the excavation depth have been varied. For all the numerical models, the cohesive and cohesionless soil has been used. The results show the influence of all these parameters on the retaining walls' behaviour. Also, the influence of the soil type is explained.

Key words*: 3D finite element method, cylindrical shafts, lateral displacements, excavation.*

INTRODUCTION

Cylindrical shafts are used for specific constructions like pumping stations, tunnel access, underground parkings, launch points for the TBM, tunnel ventilation systems. Due to these specific functionalities and their shape, there is limited information regarding the cylindrical shaft's calculation methods and their behaviour. It is necessary to determine the earth pressure acting on the retaining wall and its lateral displacements. The classical earth pressure theories can be successfully used under plane strain conditions, but, in the case of cylindrical shafts, due to the arching effect developed around the retaining wall, these theories have to be updated.

The first studies regarding the earth's pressure distribution on cylindrical shafts were performed by (Westergaard, 1940) and later on improved by (Terzaghi, 1943). They have shown that the lateral earth pressure increases with depth and reaches a constant value. (Prater, 1977) consider that the lateral earth pressure is increasing up to a maximum value and then is decreasing until reaching a zero value at a depth equal to 8.5 of the excavation's radius.

There is a solid correlation between the lateral earth pressure distribution determined using physical modelling of cylindrical shafts and the one calculated using Terzaghi's theory (Tobar & Meguid, 2011). Also, the results obtained using finite element method are in good agreement with the one determined using physical modelling. The lateral displacements of the retaining wall increase with depth up to a maximum value which is located above the final excavation surface (Tangjarusrutaratorn et al., 2022).

Based on the measured vertical and horizontal displacements obtained from the centrifuge tests and in situ works, equations that can be used to calculate the vertical and horizontal displacements have been developed (New & Bowers, 1994; Le et al., 2019). Generally, these equations do not take into account the shaft diameter and the soil parameters and use empirical coefficients. Schwamb and Soga, (2015), made a comparison between multiple field measurements of the ground settlement and the equation propose by (New & Bowers, 1994). They have shown that the measured ground settlements are smaller than those calculated using the proposed equation and that the results are influenced by the shaft diameter. Schwamb and Soga, (2015), also performed a series of numerical back-analysis carried out using the finite element method in 2D axisymmetric conditions. They analysed the influence of different parameters such as diaphragm wall

thickness, wall stiffness and anisotropy, soil models or the diaphragm wall installation type. The results shown that the thickness of the diaphragm wall has a slightly effect on the wall deflections. The field data are in good agreement with the results of the analysis of an isotropic wall, while the analysis of an anisotropic wall overestimated the wall deflections indicating that the diaphragm wall behaved isotropically despite the joints between the diaphragm wall's panels. Assuming a wished-in-place wall is a reasonable simplification compared to modelling the diaphragm wall installation.

The finite element method (FEM) is a common calculation method used in geotechnical engineering which allows the soil-structure interaction modelling and requires to use complex constitutive models for describing the soil behaviour. One of these complex constitutive models is hardening soil model (HSM), which is used for this paper purpose also.

The circular shafts can be modelled using the finite element method in 2D axisymmetric or 3D conditions. This paper presents the results of a parametric study which has been conducted using the 3D finite element method.

MATERIALS AND METHODS

For this study, the 3D finite element method has been used to analyse the cylindrical shaft behaviour in terms of lateral earth pressure, displacements of the soil and of the retaining wall. The design software used for numerical modelling was Plaxis 3D.

A parametric study has been carried out in which the cylindrical shafts radius (r), the excavation depth (H) and the length of the diaphragm wall (L) have been varied. The excavation depth has values between 10 and 50 m and the length of the diaphragm wall was given values ranging from the excavation depth plus one meter to double of the excavation depth. Generally, the shafts radius has values between 10 and 500 m. For the 10 m deep excavation and the 20 m long diaphragm wall, the excavation radius ranges between 10 and 1000 m.

Generally, the soil parameters must be chosen based on the geotechnical study carried out on the analysed site. There are multiple methods of computing the characteristic values of the soil parameters, including the shearing resistance parameters (Olinic, 2014).

For the purpose of this study, the soil parameters have been chosen based on previous experience for two common soil types. Thus, for all the numerical models, the cohesive and cohesionless soil have been used.

The parameters for the two types of soil are shown in Table 1. For this study, the hardening soil model has been used. Totally, a number of 1392 numerical models have been carried out. Due to the large number of numerical models, Python 3.11.5 was employed to facilitate their calculus.

Table 1. Soil parameters used in the numerical analysis

Soil type	γ	γ_{sat}	E_{50}^{ref}	E_{oed}^{ref}	E_{ur}^{ref}	ν_{ur}	m	c'	ϕ'	R_{inter}
	[kN/m^3]	[kN/m^3]	[kPa]	[kPa]	[kPa]	[-]	[-]	[kPa]	[kPa]	[-]
Cohesionless	19.5	20.50	25000	25000	75000	0.30	0.5	5	30	0.67
Cohesive	19.5	20.50	15000	15000	45000	0.35	0.6	40	15	0.67

γ - unit weight; γ_{sat} - saturated unit weight; E_{50}^{ref} - secant stiffness in standard drained triaxial test; E_{oed}^{ref} - tangent stiffness for primary oedometer loading; E_{ur}^{ref} - unloading/reloading stiffness; ν_{ur} - Poisson's ratio for unloading-reloading; m - power for stress-level dependency of stiffness; c' - effective cohesion; ϕ' - Effective angle of internal friction; R_{inter} - strength reduction factor.

The diaphragm wall is modelled as a plate and the capping beam is defined as a beam element. For both, the linear elastic constitutive model has been used. The material properties are shown in Tables 2 and 3.

The dimensions of the numerical model are chosen according to the excavation depth: the model is extended to 5 times the excavation depth upstream of the retaining wall and 3 times below the excavation surface (Figure 1).

Table 2. Material properties of the diaphragm wall

Material	γ	E_1	ν_{12}	d
	[kN/m^3]	[kPa]	[-]	[m]
Concrete	25	3.10e7	0.2	0.45

Table 3. Material properties of the capping beam

Material	γ	E	height	width
	[kN/m^3]	[kPa]	[m]	[m]
Concrete	25	3.10e7	0.60	0.45

Regarding the model boundaries, the bottom boundary is fixed in all directions and the vertical boundaries are fixed on horizontal directions and free on vertical direction.

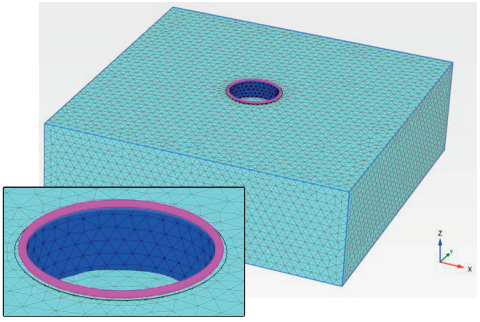


Figure 1. Numerical model – mesh generation

In order to perform finite element calculations, the numerical model has to be divided into finite elements. The relative element size of 0.02 has been chosen.

RESULTS AND DISCUSSIONS

The lateral earth pressure

Figure 2 show the lateral earth pressure diagrams acting on the retaining wall of a 10 m depth circular excavation (H), with 20 m wall length and 0.45 m wall thickness, in cohesionless soil. The excavation radius ranges between 10 and 100 m. Also, the active (γHk_a) and at rest (γHk_0) earth pressure diagrams are plotted.

The at-rest earth pressure coefficient has been calculated using the Jaky empirical relationship, $k_0 = 1 - \sin(\varphi)$, the same relationship used by Plaxis 3D, for both types of soil. Figure 3 shows the lateral earth pressure diagrams acting on the retaining structure with the same geometric parameters as in the Figure 2, but in the case of the cohesive soil.

The results obtained using FEM do not correspond to the ones obtained using the analytical solutions presented in the first section of this paper. Generally, the lateral earth pressure has values between the active and at rest earth pressure. Also, the lateral earth pressure varies approximatively linearly with depth.

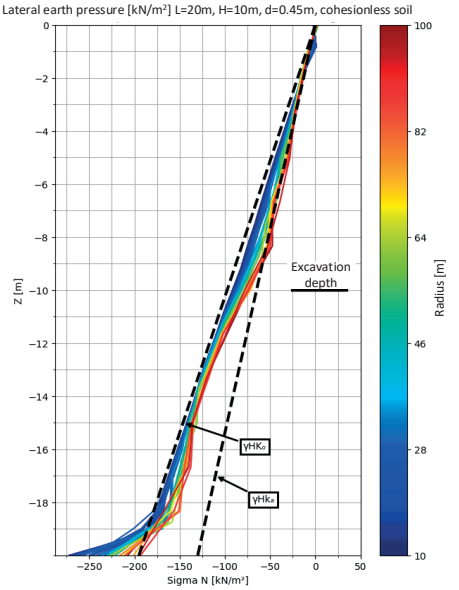


Figure 2. The lateral earth pressure diagrams for a circular excavation with H = 10 m, L = 20 m and r = 10÷100 m, cohesionless soil

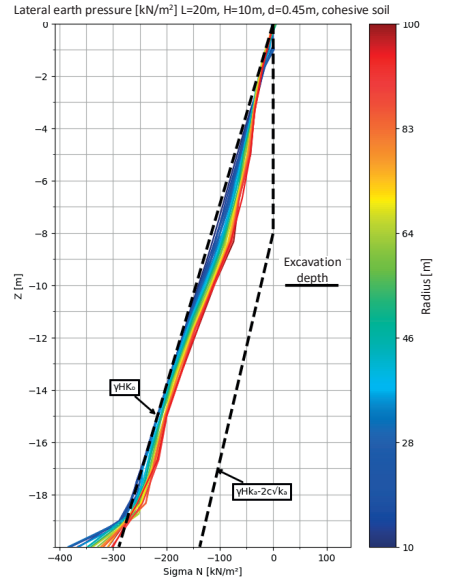


Figure 3. The lateral earth pressure diagrams for a circular excavation with H = 10 m, L = 20 m and r = 10÷100 m, cohesive soil

In the case of the cohesionless soil, for small values of the radius, the lateral earth pressure has values close to those of the at rest earth pressure. For larger values of the radius, the lateral earth pressure diagrams no longer vary linearly with depth. Also, at the final excavation depth, the values of the lateral earth pressure decrease to values lower than that of the active earth pressure. In the case of cohesive soil (Figure 3), the earth pressure variation with increasing radius is smaller and its values are close to those of the at rest earth pressure.

Horizontal displacements of the retaining structure

Figure 4 and Figure 5 show the lateral displacements diagram of the retaining wall of a 10m depth circular excavation (H), with 20 m wall length and 0.45 m wall thickness, in cohesionless soil. The excavation radius varies between 10 and 250 m (Figure 4) and between 10 and 1000 m (Figure 5).

Figure 5 shows also the lateral displacements diagram for a plane strain calculus of an excavation with the same characteristics.

For cylindrical shafts, the maximum value of the horizontal displacement of the retaining wall is located above the final excavation depth, due to the arching effect.

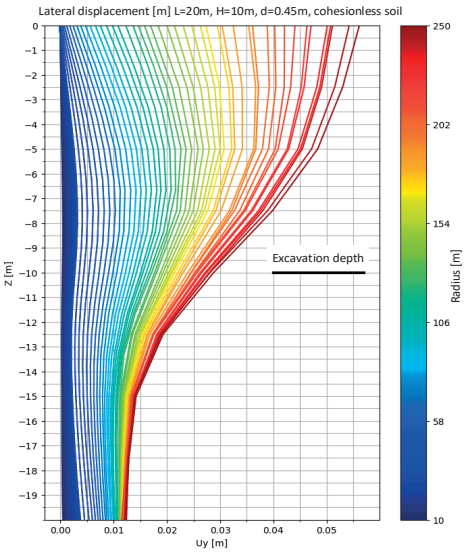


Figure 4. The lateral displacement diagram of the retaining wall, for a circular excavation with H = 10 m, L = 20 m and r = 10÷250 m, cohesionless soil

For a radius greater than 200 m, the shape of the lateral displacement diagram changes, the maximum value being located at the upper part of the retaining wall. This behaviour is specific to the plane strain conditions.

However, even for large radii up to 1000 m, the maximum value of the horizontal displacement is smaller than that obtained from the plane strain calculus, further indicating the presence of the arching effect.

The maximum horizontal displacement increases with increasing radius and excavation depth. For the same excavation depth, the variation of the maximum horizontal displacement with the radius is showing a trend.

Figure 6 and Figure 7 show the variation of the maximum horizontal displacement normalized with the excavation depth with the radius, for cohesionless and cohesive soil, for radius smaller than 100 m.

For each type of soil and each excavation depth, these variations show a similar trend and the differences between them are slight.

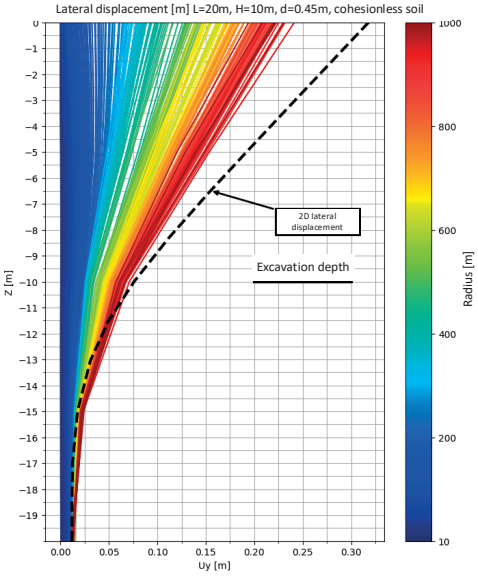


Figure 5. The lateral displacement of the retaining wall's diagram, for a circular excavation with H = 10 m, L = 20 m and r = 10÷1000 m, cohesionless soil

In order to found a function that can be used to approximate the maximum horizontal displacement depending on the excavation depth, on the type of soil and on the radius, for

each graph, the median values of the maximum horizontal displacements have been calculated and plotted on the graph.

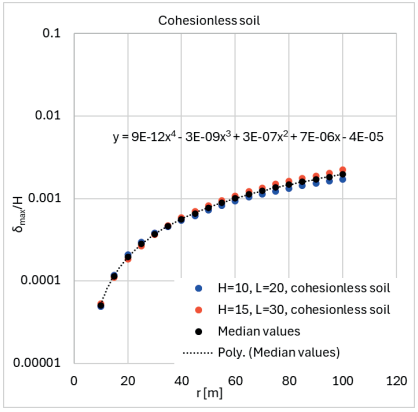


Figure 6. Variation of the maximum horizontal displacement normalized with the excavation depth, with the radius, r≤100 m, cohesionless soil

For these median values, a fourth-degree polynomial function has been determined. The resulted functions for each type of soil are presented below.

For cohesionless soil, the radii between 10 and 100 m and excavation depths between 10 and 15 m, the maximum horizontal displacement can be approximated with the following function:

$$\frac{\delta_{max}}{H} = 8.84E-12 \cdot r^4 - 2.54E-9 \cdot r^3 + 2.89E-7 \cdot r^2 + 6.70E-6 \cdot r - 4.26E-5$$

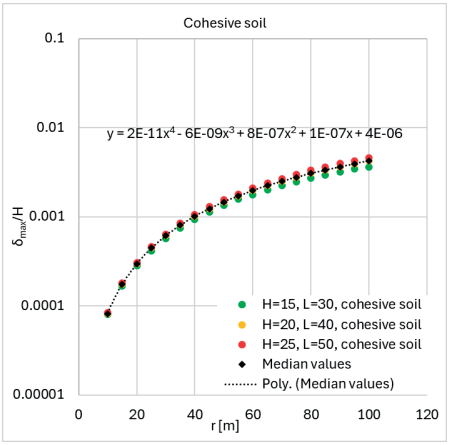


Figure 7. Variation of the maximum horizontal displacement normalized with the excavation depth, with the radius, r≤100 m, cohesive soil

For cohesive soil, the radii between 10 and 100 m and excavation depths between 15 and 25 m, the maximum horizontal displacement can pe approximate with the following function:

$$\frac{\delta_{max}}{H} = 1.81E-11 \cdot r^4 - 5.96E-9 \cdot r^3 + 8.39E-7 \cdot r^2 + 1.19E-7 \cdot r - 3.97E-6$$

The differences between the calculated and the approximated horizontal displacements are, generally, smaller than 10% and maximum 16% for radii greater than 60 m.

The maximum value of the horizontal displacement of the retaining wall is located above the final excavation level (Figure 8). For the same excavation depth, the maximum horizontal displacements occur at the same depth for both cohesive and cohesionless soil types.

For excavation depths smaller than 20 m, the maximum horizontal displacement with respect to the final excavation depth, is encountered for a ratio $z/H = (0.66 \div 0.86)$.

For excavation depths greater than 25 m, the maximum horizontal displacement with respect to the final excavation depth, is encountered for a ratio $z/H = (0.75 \div 0.93)$.

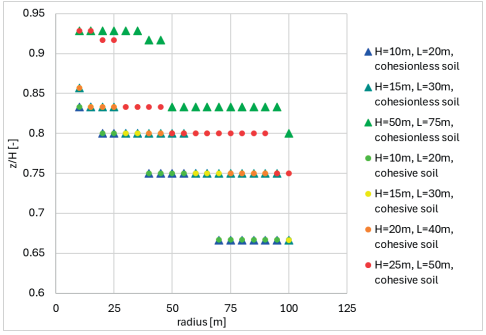


Figure 8. Depth at which the maximum horizontal displacement (z) occurs, normalized with the final excavation depth (H), depending on the radius, excavation depth and soil type

As the radius increases, the depth at which the maximum horizontal displacement occurs decreases but cannot be expressed as a function.

Vertical displacements of the ground behind the retaining structure

Considering the shape of the horizontal displacement diagram and its values at the top of

the wall, it is expected that the vertical displacement of the ground behind the retaining structure will swell in its immediate vicinity and then will start to settle at a certain distance away from the retaining wall. This behaviour is highlighted in Figures 9 and 10.

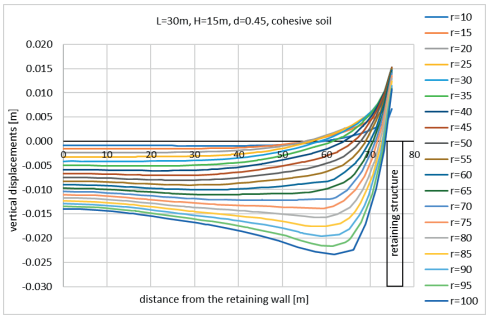


Figure 9. The vertical displacements of the ground behind the retaining wall, for a circular excavation with H = 15 m, L = 30 m and r = 10÷100 m, cohesive soil

The maximum vertical displacements for cylindrical shafts modelled in cohesive soil are greater than those obtained for circular excavation executed in cohesionless soil.

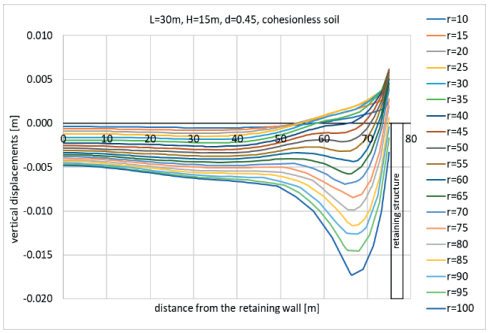


Figure 10. The vertical displacements of the ground behind the retaining wall, for a circular excavation with H = 15 m, L = 30 m and r = 10÷100 m, cohesionless soil

Depending on the type of soil and the radius, the maximum values of the vertical displacement of the soil occurs at different distance from the retaining wall. For small values of the circular excavation radius, the maximum vertical displacement occurs at a large distance from the retaining wall, between $(2 \div 5)H$, the ratio increasing with the excavation depth.

For large values of the circular excavation radius, the maximum vertical displacement occurs at a smaller distance from the retaining wall, between $(0.45 \div 1.40)H$, the ratio increasing with the excavation depth (Figure 11).

Figure 12 shows the relationship between the maximum vertical displacements (s_{max}) and the maximum horizontal displacements (δ_{max}), normalized with the excavation depth (H), for different excavation depths and circular excavation radii.

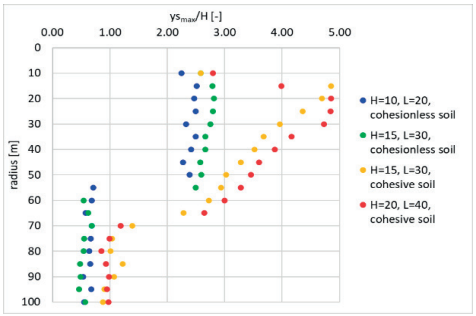


Figure 11. The distance at which the maximum vertical displacements occur from the retaining wall, normalized by the excavation depth (ys_{max}/H), for different excavation depths, depending on the circular excavation radius

The maximum vertical displacements are not equal to the maximum horizontal displacements, but there is the following relationship between them:

$$s_{max} = \frac{\delta_{max}}{2} \div \frac{\delta_{max}}{4}$$

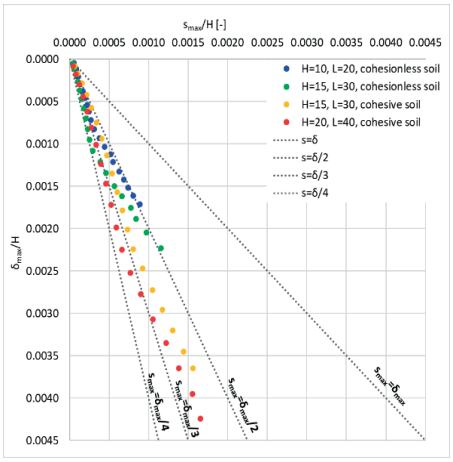


Figure 12. The dependence between the maximum vertical displacements (s_{max}) and maximum horizontal displacements (δ_{max}), normalized by the excavation depth (H), for different excavation depth and excavation radius

CONCLUSIONS

This paper presents a parametric study regarding the cylindrical shaft behaviour, in which the radius, the length of the diaphragm wall and the excavation depth have been varied. Also, two types of soil have been used: cohesionless and cohesive.

For this parametric study, the finite element method has been used to perform the numerical modelling and calculus.

The results show the lateral earth pressure acting on the retaining wall and its comparison with the at-rest and active earth pressure diagrams. Thus, for common shafts radii smaller than 100 m, the lateral earth pressure acting on the retaining wall varies approximatively linearly with depth and has values close to those of the at rest earth pressure.

For each type of soil, relationships that can be used to approximate the maximum horizontal displacement depending on the excavation depth, on the type of soil and on the radius were proposed.

However, these relationships are limited for a small interval of excavation depths and cannot be applied to a mixed stratigraphy.

Generally, in the immediate vicinity of the retaining structure, the vertical displacements of the ground swell. For small values of the shaft radius, the maximum vertical displacement occurs at a large distance from the retaining wall.

For large values of the circular excavation radius, the maximum vertical displacement occurs at a smaller distance from the retaining wall.

The ratio between the maximum vertical and horizontal displacements is not equal to one, as proposed in the technical literature.

REFERENCES

Le, B.T., Goodey, R.J., & Divall, S. (2019). Subsurface ground movements due to circular shaft construction. *Soils and Foundations, 59,* 1160-1171.

New, B.M., & Bowers, K.H. (1994). Ground movement model validation at the Heathrow Express trial tunnel. *Tunelling'94,* 301-329.

Olinic, E. (2014). The influence of geotechnical investigations magnitude on characteristic values of soils parameters. *International Multidisciplinary Scientific GeoConference: SGEM: Surveying Geology & Mining Ecology Management, 2,* 915-920.

Prater, E.G. (1977). An examination of some theories of earth pressure on shaft linings. *Canadian Geotechnical Journal*, *14*(1), 91–106.

Schwamb, T. & Soga, K. (2015). Numerical modelling of a deep circular excavation at Abbey Mills in London. *Geotechnique, 65*(7), 604-619.

Tangjarusrutaratorn, T., Miyazaki, Y., Sawamura, Y., Kishida, K., & Kimura, M. (2022). Numerical investigation on arching effect surrounding deep cylindrical shaft during excavation process. *Underground space, 7*(5), 944–965.

Terzaghi, K. (1943). *Theoretical Soil Mechanics*. New York: John Wiley and Sons.

Tobar, T., & Meguid, M.A. (2011). Experimental Study of the Earth Pressure Distribution on Cylindrical Shafts. *Journal of geotechnical and geoenvironmental engineering, 137*(11), 1121-1125.

Westergaard, H.M. (1940). Plastic state of stress around a deep well. *Journal of the Boston Society of Civil Engineers*, *27*(1), 387–391.

Scientific Papers. Series E. Land Reclamation, Earth Observation & Surveying, Environmental Engineering. Vol. XIV, 2025
Print ISSN 2285-6064, CD-ROM ISSN 2285-6072, Online ISSN 2393-5138, ISSN-L 2285-6064

AMBIENT AIR POLLUTION: A GLOBAL HEALTH CRISIS

Svetla STOYKOVA[1], Diyana DERMENDZHIEVA[1], Gergana KOSTADINOVA[1], Miroslava IVANOVA[2], Milen STOYANOV[3], Georgi PETKOV[1], Lilko DOSPATLIEV[4], Georgi BEEV[1]

[1]Trakia University, Faculty of Agriculture, 6000, Stara Zagora, Bulgaria
[2]Trakia University, Faculty of Economics, 6000, Stara Zagora, Bulgaria
[3]Trakia University, Medical College, 9 Armeiska Street, 6000, Stara Zagora, Bulgaria
[4]Trakia University, Faculty of Veterinary Medicine, Studentski Grad, 6000, Stara Zagora, Bulgaria

Corresponding author email: svetla.stoykova@trakia-uni.bg

Abstract

Air pollution is a significant environmental and public health threat, contributing to approximately 7 million deaths annually, as reported by the World Health Organization (WHO). Major pollutants such as particulate matter (PM10 and PM2.5), carbon monoxide (CO), ozone (O3), nitrogen dioxide (NO2), and sulfur dioxide (SO2) are linked to severe health conditions such as cardiovascular diseases, strokes, respiratory illnesses, chronic obstructive pulmonary disease (COPD), and cancer. Vulnerable populations - the elderly, children, pregnant women, and individuals with pre-existing conditions - face the highest risks. Long-term exposure to air pollution has been associated with a tenfold increase in health complications compared to short term exposure. While research has clarified many of the biological pathways through which pollutants affect human health, ongoing studies continue to explore the full extent of these effects. This study provides a comprehensive analysis of the latest data on the health effects of ambient air pollution, with a particular focus on Bulgaria. It identifies key trends, examines policy gaps, and evaluates the effectiveness of existing air quality regulations. By incorporating a comparative analysis of WHO, EU, and Bulgarian air quality standards, this research underscores the pressing need for stricter regulatory measures and enhanced mitigation strategies to curb pollution-related morbidity and mortality. The findings highlight the urgency of aligning national air quality policies with WHO guidelines to safeguard public health and drive sustainable environmental initiatives.

Key words*: ambient air pollution, air pollutants, air quality, diseases, health impacts, regulatory policies, WHO guidelines.*

INTRODUCTION

Air pollution is a major environmental factor that affects every individual and is a leading cause of numerous diseases worldwide. Globally, the main sources of air pollution are industry (large enterprises, TPPs, steel plants, petroleum refineries, cement factories), transport (road, air, maritime), households and agriculture. According to the WHO, each year 7 million deaths including 600,000 children are caused by polluted air (4.2 million from outdoor air pollution, and 3.8 million from indoor air pollution). Nine out of 10 people around the world live in regions where air pollution exceeds the WHO guidelines. More than 89% of deaths caused by air pollution occur in low- and middle- income countries (WHO, 2024a; Le et al., 2024). Some scientists believe that this number is even bigger estimating at least 9 million people to die every year from the air they breathe (UNEP, 2021; Vohra et al., 2021). Air pollution has also considerable economic impacts, reducing life expectancy, increasing medical costs and reducing productivity through working days lost across various economic sectors (EEA, 2020). The World Bank estimated global air pollution cost at $8.1 trillion in 2019, equivalent to 6.1% of global GDP. In individual countries, the economic burden of pollution associated with premature mortality and morbidity is significant, equivalent to 5-14% of countries' GDPs (WB, 2023). The Organisation for Economic Co-operation and Development (OECD) reported "that a 1 μg/m^3 decrease in annual mean $PM_{2.5}$ concentration would increase Europe's GDP by 0.8%, representing around €200 per capita per year as result of increases in output per worker, through lower absenteeism at work or increased labour productivity, due to lower air pollution" (EEA, 2020).

Pollutants with the strongest evidence for public health concern include particulate matter (PM), carbon monoxide (CO), ozone (O_3), nitrogen dioxide (NO_2) and sulfur dioxide (SO_2). Health problems can occur after both short- and long-term exposure to these various pollutants (Cesaroni et al., 2014; Schwartz et al., 2017; Burnett et al., 2018; Kermani et al., 2018; Zheng et al., 2021; Dass et al., 2021; Popa et al., 2021; Babu et al., 2022). For some pollutants (VOCs, PAHs, O_3), there are no thresholds below which adverse effects do not occur (Papadogeorgou et al., 2019; Manisalidis et al., 2020). Air pollution usually has a greater impact on people living in urban rather than in rural areas. The bigger air polluting sources (industry, traffic, household burning, etc.) and higher population density in the cities lead to high concentration and retention of the atmospheric pollutants (Olstrup et al., 2021; Kozlov et al., 2022; Carozzi & Roth, 2023; Akomolafe et al., 2024; Kar et al., 2024).
Numerous studies reveal the link between polluted air and human health. Air pollution is associated with many diseases affecting different human body systems and functions - respiratory system (Sierra-Vargas & Teran, 2012; Thurston et al., 2017; Heger et al., 2019; Popa et al., 2021; Lee et al., 2021; Kienzler et al., 2022; Lan et al., 2024), cardiovascular system (Shahrbaf et al., 2021; D'Acquisto et al., 2023; Bhatt, 2024; Sadeghi & Sadeghi, 2024), immune system (Dobreva et al., 2015; Ivanov et al., 2016; Glencross et al., 2020), reproductive system (Popa et al., 2020; Shetty et al., 2023), endocrine system (Saleem et al., 2024), nervous system (Solaimani et al., 2017; Thurston et al., 2017), cognitive functions (Meo et al., 2024), mental health (Keswani et al., 2022; Bai et al., 2024) as well as with increased mortality of the affected people (Turner et al., 2020; WHO, 2024b). Vandyck et al. (2022) point out that health considerations form a strong argument in favor of policy action to concurrently mitigate climate change and control air pollution.
EU's policy and legislation on reducing the emissions of harmful substances through the years give positive results; today the air is cleaner than it was two decades ago. Nevertheless, human health is still threatened by various air pollutants (EEA, 2022, 2023a, 2023b). In 2021, premature deaths attributed to exposure to fine PM decreased by 41%, compared to 2005 (EEA, 2023b). The Zero Pollution Action Plan aims to decrease premature deaths caused by exposure to fine particulate matter (PM) by 55% by 2030, compared to 2005 levels. However, despite continued emission reductions, a significant portion of the EU's urban population remained exposed to harmful concentrations of key air pollutants - $PM_{2.5}$, PM_{10}, O_3, NO_2, Benzo[a]pyrene (BaP), and SO_2 - in 2022 (EEA, 2024). In 2021 in the EU-27, total of 327,000 deaths were attributable to exposure to $PM_{2.5}$ (77.4% of all deaths), NO_2 (15.9% of all deaths) and O_3 (6.7% of all deaths) concentrations above 2021 WHO's guideline levels (EEA, 2023b). In 2020, the EC initiated a revision of the ambient air quality directives, aiming to align the air quality standards more closely with the WHO recommendations. As a result, a new Directive (EU) 2024/2881 of 23 October 2024 on ambient air quality and cleaner air for Europe was accepted. Further efforts will be needed to meet the zero-pollution vision for 2050 of reducing air pollution to levels no longer considered harmful to health.
Following the EU policy and legislation referring to the air quality improvement, Bulgaria reported a significant reduction of the air pollution in the last decades. Positive trends in air quality are attributed to active policies and measures at all levels, including legislative harmonization with European standards. The amendments made in the Air Purity Act (1996) emphasize municipal responsibility for air quality improvement, strengthen central government oversight, and the effective implementation of municipal programs (Zheleva, 2024). In 2022, the emissions of $PM_{2.5}$, SO_2, NO_x and NMVOCs have decreased by 30, 94, 53 and 26%, respectively compared to 2005. However, pollution with PM and partly with BaP continues to be a major problem for the ambient air quality in many settlements in the country. The main causes of excessive particulate pollution are solid fuel heating during the winter season and emissions from road and public transport (ExEA, 2024).
The brief review shows that addressing air pollution, which is the second highest risk factor for non-communicable diseases, is key to protecting public health. Despite the progress made, the problem with air pollution has not yet

been solved. The tools for achieving this goal include well-motivated policies, adequate legislation, effective practices (monitoring, control, etc.) and reliable and sustainable results. It turns out that there are differences at global (WHO), regional (EU) and local (individual countries) level, both in the regulation of air pollutant levels and interim targets for a gradual shift from high to lower concentrations and their associated health benefits. This gave us the basis to define the scope of our review: the paper first explores the key air ambient pollutants, then assesses their health impacts, partly in Bulgaria, make a comparative analysis of WHO, EU and Bulgarian standards, and concludes with policy recommendations for air quality improvement.

MATERIALS AND METHODS

This review summarizes and analyses the primary information from databases like Google Scholar, PubMed, ResearchGate, and Science Direct. The keywords used were air pollution, particulate matter, gaseous pollutants, human health risks, morbidity, mortality, and air quality standards. We have reviewed 245 studies, including journal articles, conference papers, WHO, EEA, USEPA and Word Bank reports, and country-specific reports, focusing on ambient air pollution and its impact on human health, respectively morbidity and mortality. After the selection, 104 literature sources (mainly from the recent years), including 88 scientific articles published in a peer-reviewed journals and 16 reports and data from different institutions were used.

RESULTS AND DISCUSSIONS

Classic air pollutants

Since 1987, WHO has periodically issued health-based air quality guidelines (AQGs) to assist governments and civil society in reducing air pollution and its adverse effects on human. Those guidelines are not legally binding standards but are a science-based tool that countries around the world can use to improve their policy and legislation aimed at air quality improvement. The new WHO guidelines, published in 2021 (WHO-AQG, 2021), recommend specific air quality levels regarding six pollutants ($PM_{2.5}$ and PM_{10}, NO_2, SO_2, CO and O_3) with the highest evidence for a negative impact on people's health. The WHO determines those pollutants as "classic" pollutants; briefly, they are characterized as follows:

Particulate matter (PM): PM is a complex mixture of solids and aerosols (organic, inorganic) composed of small droplets of liquid, dry solid fragments, and solid cores with liquid coatings. Particles vary widely in terms of size, shape and chemical composition (Estuardo-Moreno et al., 2022). PM may be either directly emitted from sources (primary particles) – natural (ground surface dust, volcanic activity, salts, etc.) and anthropogenic (industry, transport, energetics, household heating, etc.), or may be formed in the atmosphere through chemical reactions of gases (secondary particles) such as SO_2, NO_x, NH_3 and VOCs. According to their size, PM may be divided in 5 groups – supercoarse PM ($d_{pa} > 10$ μm; d_{pa} – aerodynamic particle diameter), coarse PM ($2.5 < d_{pa} \leq 10$ μm), fine PM ($0.1 < d_{pa} \leq 2.5$ μm), ultra-fine PM ($d_{pa} \leq 0.1$ μm) and nanoparticles (NPs) ($1 < d_{pa} \leq 100$ nm). PMs consist mainly of sulfates, nitrates, ammonia, sodium chloride, black carbon (BC), mineral dust and water (Sierra-Vargas & Teran, 2012; Khan et al., 2019; Manisalidis et al., 2020; Kumari & Sarkar, 2021; WHO, 2024a).

Nitrogen dioxide (NO_2): NO_2 is a reddish-brown, highly reactive water-soluble gas, and a strong oxidant. It results from both anthropogenic and natural processes; the main anthropogenic activity leading to NO_2 emissions being the combustion of fossil fuels from industrial sources (coal, gas and oil), vehicles and power plants (Mesas-Carrascosa et al., 2020; Babu et al., 2022).

Sulfur dioxide (SO_2): SO_2 is a toxic colourless gas with a sharp odour; it mainly originates from burning of fossil fuels that contain sulfur (coal, crude oil) in power stations and refineries. The volcanos and oceans are the main natural source of SO_2; it causes health problems in humans, animals and plants (Babu et al., 2022; WHO, 2024a).

Carbon monoxide (CO): CO is a colourless, odourless and tasteless toxic gas produced by incorrect combustion processes (transport, thermal power plants, combustion installations etc. (Babu et al., 2022; WHO, 2024a).

Ozone (O_3) – tropospheric: O_3 is formed through chemical reactions between hydrocarbons, CH_4 and NO_x under the influence of ultraviolet light; it is a strong oxidant and one of the major constituents of photochemical smog (Popa et al., 2020; Babu et al., 2022).

It is important to note that the new WHO AQGs do not include recommendations about pollutant mixtures as well as the combined effects of pollutant exposures, which is a serious omission as usually the people are exposed to a mixture of air pollutants that varies in space and time. Nevertheless, the achievement of the WHO AQGs permissible levels for all these pollutants is necessary to minimize the health risk for humans.

Impact of air pollution on health

In present days, the air pollution is one of the most serious ecological problems with significant impacts on the human health everywhere in the world, particularly in the urban areas. Some population groups are more affected by air pollution than others, because they are more exposed (lower socio-economic groups) or susceptible (older people, children and those with pre-existing health conditions) to environmental hazards (EEA, 2022). The degree of effect on the body depends on the pollutant composition, source and dose, level and duration of exposure to polluted air (Le et al., 2024). To solve the problem, two aspects must be considered - on one hand, to know how the individual air pollutants influence human health and on the other - how the mixtures of pollutants do that.

Air pollutants – human body effects

PM_{10}, $PM_{2.5}$, SO_2, NO_2, CO, and O_3 are the air pollutants considered most harmful to humans (Manisalidis et al., 2020; Ruwali et al., 2024; Saleem et al., 2024). There is suggestive evidence linking the individual air pollutants with human health status, which could be summarized as follows:

(PM): Exposure to fine particle outdoor air pollution is the largest environmental risk factor for premature death globally. In 2022, 96% of the urban population was exposed to concentrations of fine PM above the health-based guideline level set by the WHO (EEA, 2024). In the same year, around 4.7 million people died from exposure to fine particulate outdoor air pollution (28% of all deaths) and the average global life expectancy was reduced by approximately one year and eight months (UNEP, 2021). New research reveals some of the mechanisms behind PM's harmful effects on human health. Li et al. (2024) analyzed the long-term oxidative potential (OP) of water-soluble $PM_{2.5}$ and found that dust, gaseous pollutants (NO_2 and SO_2), black carbon and biomass combustion are the main sources of the OP of $PM_{2.5}$. It is well documented that short-term and long-term exposure to $PM_{2.5}$, PM_{10} and NPs have a significant influence on the human body. Exposure has been linked to a wide range of adverse health effects, including neurological disorders, exacerbation of asthma, and chronic obstructive pulmonary disease (COPD). It also contributes to reduced lung function, lung cancer, silicosis, and tuberculosis. Furthermore, it impacts the reproductive system and increases the risk of cardiovascular conditions such as cardiac arrhythmias, nonfatal heart attacks, and myocardial infarction. Additional effects include irritation of the eyes, throat, and nose, impairment of mucociliary and macrophage activity, neurodegenerative diseases, cerebrovascular conditions, cognitive decline, dementia, and disruptions in children's brain development (Solaimani et al., 2017; Zaheer et al., 2018; Kermani et al., 2018; Silva et al., 2020; Popa et al., 2021; USEPA, 2024). Hofmann et al. (2015) established a relationship between fine dust exposure and the incidence of stroke. Short, mid-, and long-term pre-exposure can significantly exacerbate small-airway inflammation, particularly in males, children, smokers, and individuals with pre-existing respiratory conditions (Lei et al., 2024). Prolonged exposure to PM10 and PM2.5 has been linked to a higher incidence of acute coronary events, even at concentrations below the EU regulatory limits (Cesaroni et al., 2014), as well as an increased risk of premature mortality (Vohra et al., 2021; Isaifan, 2023). Not only long-term exposure, but also acute increases in PM_{10}/$PM_{2.5}$ concentration (up to 10 $\mu g/m^3$) are associated with cardiovascular hospitalization or death with an increase of 1.63% per PM_{10} and 2.12% for $PM_{2.5}$, the most prominent on the day of exposure (Shah et al., 2013). Heger et al. (2019) suggested that the

concentration of PM_{10} in the air was an important predictor of the respiratory diseases. The proportion of deaths attributed to outdoor fine particulate air pollution varied by disease, with chronic obstructive pulmonary disease (COPD) accounting for 48%, lower respiratory infections for 30%, ischemic heart disease for 28%, and stroke for 27%. Additionally, 19% of deaths were linked to tracheal, bronchus, and lung cancer, 18% to type 2 diabetes, and 14% to neonatal disorders (UNEP, 2021).

(SO_2): That toxic gas affects susceptible people with lung disease, old people, and children, who present a higher risk of damage. Exposure to high concentrations of SO_2 in the air is associated with headache, anxiety, respiratory problems (facilitates bronchoconstriction, cough, affects the mucous membranes of the throat, nose and eyes) and cardiovascular diseases (Manisalidis et al., 2020; Popa et al., 2020; USEPA, 2024).

(NO_2): NO_2 creates respiratory problems as affects the mucous membranes of the nose, eyes and throat; increases bronchial reactivity and susceptibility to infections; provokes bronchitis, allergic rhinitis, chronic lung disease and even pulmonary edema and tuberculosis; affects some organs (liver, spleen) and the circulatory system (Lin et al., 2019; Manisalidis et al., 2020; Babu et al., 2022).

(CO): CO in the air penetrates very easily through the alveoli of the lung into the human circulatory system, has effects on hemoglobin by blocking oxygen transport (the affinity of CO to hemoglobin is about 250 times greater than that of oxygen). The result is hypoxia, ischemia and cardiovascular disease, effects on the fetus, headaches, nausea, vomiting, dizziness, weakness, vomiting, tuberculosis and eventually loss of consciousness; also, working with CO may result in fatal poisoning (Lin et al., 2019; To et al., 2020; USEPA, 2024).

(O_3): As a strong oxidant, O_3 affects predominantly the respiratory system, which is manifested with inflammation of the mucous membranes of the respiratory tract, causes coughing, chest discomfort, obstruction of the airways, damage to the epithelium lining the airways. It can also cause cardiovascular diseases (Popa et al., 2020; USEPA, 2024). The European research project APHEA2 found out a correlation between daily fatalities and ozone levels; a short-term rise in ozone concentration was connected to an increase in daily fatalities (0.33%), respiratory deaths (1.1%), and cardiovascular deaths (1.1%), (Babu et al., 2022).

Diseases associated with exposure to air pollution

Air pollution typically consists of a complex mixture of multiple pollutants, which together have a more pronounced impact on human health than individual pollutants alone. To evaluate these effects, two key indicators - mortality and morbidity - are commonly used (Thacker et al., 2006). A widely applied metric for assessing the combined burden of both mortality and morbidity is Disability-Adjusted Life Years (DALY), which quantifies the total number of years lost due to disease, injury, or exposure to harmful risk factors. One DALY represents the loss of one year of healthy life (EEA, 2023b) (Figure 1).

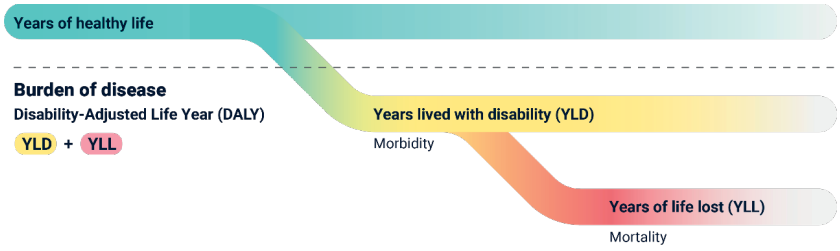


Figure 1. Burden of disease (DALY) as sum of years lived with disability (YLD) and years of life lost (YLL) (Source: EEA, 2023b)

Mortality: This indicator represents the number of deaths resulting from a specific disease or a group of diseases. In scientific studies, reports, and analyses, mortality is commonly expressed as premature deaths (PD) or years of life lost (YLL) to quantify the impact of early mortality.

Schwartz et al. (2017) established a causal association of local air pollution with daily deaths at concentrations below USEPA standards; the increase of the $PM_{2.5}$ and black carbon concentrations was associated with a 0.90% increase in daily deaths; a weaker association was observed for NO_2. In 2021, air pollution led to a significant number of premature deaths in Europe (excluding Türkiye): exposure to concentrations of fine PM above the 2021 WHO guideline level (5 $\mu g/m^3$) resulted in 293,000 premature deaths; exposure to NO_2 above the respective guideline level (10 $\mu g/m^3$) led to 69,000 premature deaths; acute exposure to O_3 (70 $\mu g/m^3$) caused 28,000 premature deaths (EEA, 2023b).

Morbidity: This is a very precise indicator to assess the public health deviation. Morbidity is generally divided in two categories - outpatient care and inpatient care (hospitalization). The morbidity is affected by changes in atmospheric pollutant concentrations (Thacker et al., 2006; Platikanova & Penkova-Radicheva, 2016). Numerous studies have established a strong link between air pollution exposure and morbidity. Platikanova et al. (2018) developed a mathematical model to predict morbidity rates in different residential areas based on correlations between air pollutants (PM10, SO_2, NO_2, and Pb-aerosol) and health outcomes. Short-term exposure to air pollutants and smog is strongly associated with conditions such as COPD, coughing, shortness of breath, wheezing, asthma, respiratory diseases, and increased hospitalization rates. Meanwhile, long-term exposure has been linked to chronic asthma, pulmonary insufficiency, cardiovascular diseases, cardiovascular mortality, and reproductive system impairments in both males and females (Manisalidis et al., 2020; Tran et al., 2023; Saleem et al., 2024). Recently, some researchers suggested that air pollution, especially with $PM_{2.5}$, may be associated with cardiac arrhythmias due to the oxidative stress, autonomic dysfunction, coagulation dysfunc-tion, and inflammation (Shahrbaf et al., 2021). Air pollution (O_3, NO_2, SO_2, and PM) may exacerbate asthmatic symptoms, to increase the morbidity and mortality and risk of hospi-talization associated with respiratory diseases (Lee et al. 2021; Yuan et al., 2024). Data, based on the ETC/HE report (Kienzler et al., 2022), showed that in 2020 in Europe, COPD associated with exposure to $PM_{2.5}$ was on the average 51.6 years lived with disability (YLDs) per 100,000 inhabitants ≥25 years (lowest value 1.2 Iceland - highest value 89.5 Serbia, Bulgaria 70.4); for NO_2 the highest morbidity burden resulted from diabetes mellitus with 54.6 YLDs per 100,000 inhabitants ≥35 years (lowest value 3.7 Estonia - highest value 145.5 Türkiye, Bulgaria 49.0), and for short-term O_3 exposure hospital admissions due to respiratory diseases were estimated at 18 cases per 100,000 inhabitants ≥65 years (lowest value 4 Iceland - highest value 29 Austria). For each specific air pollution-related disease, the relative contribution to poor health (the burden of disease) from mortality and morbidity can vary significantly. For instance, mortality is by far the dominant contributor for ischemic heart disease and lung cancer, while for asthma it is morbidity (EEA, 2023b).

Air quality and human health: a focus on Bulgaria

Bulgaria (111,000 km^2, population 6,440,000) is divided into six regions for atmospheric air quality (AQ) assessment and management: the agglomerations of Sofia (capital, 1,224,000 residents), Plovdiv (325,000 residents), and Varna (314,000 residents), and the North Danube, South-West, and South-East regions. The Bulgarian National Environmental Monitoring System assesses air quality (AQ) across these regions by 12 air pollutants according to the national and EU legislation, as follows: PM_{10}, $PM_{2.5}$, O_3, NO_2, SO_2, CO, benzo(a)pyrene (BaP), heavy metals (Pb, Cd, Ni), As, and benzene /C_6H_6/ as well as population exposure (ExEA, 2024).

In the last decades Bulgaria has constantly reduced the levels of air pollutants. Bulgaria's commitments under Directive (EU) 2016/2284 and the amended Gothenburg Protocol to the Convention on Long-Range Transboundary Air Pollution (LRTP) for emission levels of SO_2, NO_x, NMVOCs and $PM_{2.5}$ for 2022 have been fulfilled. Unfortunately, these changes occur slowly and despite improvements, pollutant levels still have significant adverse impacts on human health and the environment. The effects of air pollution are felt most strongly in urban

areas, where lives 73.3% of the population and the people experience significant health problems (ExEA, 2024; Zheleva, 2024). Large anthropogenic sources of air pollution are electricity and heat production, industry, domestic heating, road transport and agriculture. Thermal power plants (TPPs), including refineries, are the largest sources of SO_2 - 66% of the total amount emitted in the country; the main sources of NO_x are road transport - 38%, TPPs - 25%, agriculture - 18%, combustion processes in industry – 6%, and other transport - 4%; domestic heating is a major source of PM (47% of the total PM_{10} and 69% of total $PM_{2.5}$ emissions), other sources are the agriculture and road transport (ExEA, 2024).

Nowadays, PM air pollution continues to be a major problem for the air quality at the national level (Naydenova et al., 2018; Georgieva et al., 2021; Zheleva, 2024), especially during the winter months in the big cities– Sofia (Dimitrova & Velizarova, 2021), Plovdiv (Ivanov et al., 2023), Ruse (Takuchev et al., 2018; Nikolova et al., 2023), Stara Zagora (Stoykova et al., 2023; Ivanova et al., 2023), Pernik (Ivanov, 2016), and Vidin (Minkova et al., 2023; Kostova-Ivanova, 2024). In 2020, fine particle pollution caused the death of 71 per 100,000 people, a rate higher than that in Slovenia - 16, Croatia - 38 and Romania - 46, and lower than that in Serbia - 79 and North Macedonia - 120 (UNEP, 2021). In 2022, the population share exposed to excessive PM_{10} levels was substantially higher than the EU countries average (10-19% for 2015-2020), reaching 41% (2,640 million people). About 60% of the population in Bulgaria lives in areas with pollution levels above the target norm for benzo(a)pyrene (in EU countries it is 15-17% of the population for the period 2017-2021), and about 0.5% of the population lives in the areas with above-average annual NO_x levels (for EU it is between 0.8-8.0% of the population for the period 2015-2021). The others key pollutants - $PM_{2,5}$, O_3 and SO_2 did not exceed the relevant norm, while in EU up to 8.0% of the population was exposed to O_3 levels above the norm for the period 2015-2021. Notably, individuals in rural areas are exposed to higher levels of O_3 compared to urban residents. In cities, ozone levels are lower due to its depletion through the oxidation of NO to NO_2, which reduces its concentration (ExEA, 2024). Exposure to outdoor air pollution is associated with a broad spectrum of acute and chronic health effects ranging from irritant effects to death. Ivanov et al. (2016) observed an increase of the respiratory diseases, reduced immune defense and activation of the cardiovascular diseases among the population of Pernik town (81,700 residents) in the period 1980-2010, when the levels of PM and SO_2 in the air were over the standard. Platikanova and Penkova-Radicheva (2016) reported that the air pollution (PM, SO_2, NO_2, H_2S and Pb) of Stara Zagora (142,000 residents), one of the industrial centers in the country, located near the Maritsa-Iztok energy complex (4 TPPs), affects human health directly through pathological changes in the human organism. Epidemiological studies of Dobreva et al. (2015) demonstrated that the exposure to different air pollutants, including PM_{10} and $PM_{2.5}$ has been related to adverse effects on the immune system (modulate cytokine production and change the balance between pro-inflammatory TNF-α and anti-inflammatory IL-10 production) of adolescents, living in the cities of Stara Zagora, Kazanlak, and Chirpan. Takuchev et al. (2018) established statistically significant positive correlations between the concentrations of the investigated air pollutants (PM_{10}, $PM_{2.5}$, NO_2, SO_2, O_3, CO, CH_4, benzene and BC) in the town of Ruse and the health status of the patients in 73 of the 125 clinical pathways; the pollutant with the greatest impact on the health was the CH_4, often in combination with benzene and fine PM. Georgiev et al. (2025) found a general increase in hospital admissions for respiratory diseases, ischemic heart disease and cerebral infarction associated with higher pollution levels ($PM_{2.5}$, PM_{10}, NO_2, SO_2, O_3, and CO) in the cities Sofia, Plovdiv and Vidin during 2009-2018.

According to data of the European Environment Agency (EEA), in 2021 the estimated number of attributable deaths in Bulgaria resulting from $PM_{2.5}$ pollution (15.1 $\mu g/m^3$ annual mean value) was 10,800; resulting from NO_2 pollution (17.5 $\mu g/m^3$ annual mean value) - 2,200 and resulting from O_3 pollution (2,668 annual sum of daily maximum running 8-h average concentrations over 70 $\mu g/m^3$) was 460. The values for the absolute number of the attributable deaths resulting from $PM_{2.5}$, NO_2 and O_3 pollution are

calculated based on the number of the population of the different countries and because of that, they could not be compared. Logically, countries with larger populations (Poland, Italy and Germany) had a higher number of deaths than countries with smaller populations (Estonia, Finland and Sweden). A suitable indicator for between-countries comparison of deaths resulting from air pollution is years of life lost (YLL). In 2021 in Bulgaria, the YLL per 100,000 inhabitants attributable to exposure to $PM_{2.5}$ was 1,443, to NO_2 - 294 and to and to O_3 - 63. Those data were higher than the average values for EU-27 - by 2.47 times for $PM_{2.5}$, by 2.45 times for NO_2 and by 1.19 times for O_3. Referring to the neighboring countries, similar data were reported for Romania (1,111, 275 and 60, respectively) and higher for Serbia (1,938, 212 and 99, respectively) and North Macedonia (2,115, 169 and 88, respectively), (EEA, 2023). The comparison of the new WHO guidelines (2021) with the standards applicable in Bulgaria (Regulation No.12/2010) and with the new EU Directive (Directive /EU/ 2024/2881) revealed that the WHO AQGs are more stringent than the standards in Bulgaria and EU (Table 1).

Table 1. Comparison of WHO, Bulgarian and EU standards regarding air quality

Pollutant	Unit	WHO AQG, 2021		Bulgarian standard[a]	EU AQS, 2024[b]	
		Reference period	Recommendation		Target by 11.12.2026	Target by 01.01.2030
$PM_{2.5}$	$\mu g/m^3$	24-hour[c]	15	-	-	25[k]
		calendar year	5	20	25	10
PM_{10}	$\mu g/m^3$	24-hour[c]	45	50[e] (20%)[l]	50[e]	45[k]
		calendar year	15	40 (50%)[l]	40	20
O_3	$\mu g/m^3$	peak season[d]	60	-	-	-
		8-hour[c]	100	120[f]	120[f]	120[f]
NO_2	$\mu g/m^3$	24-hour[c]	25	-	-	50[k]
		calendar year	10	40	40	20
SO_2	$\mu g/m^3$	24-hour[c]	40	125[j]	125[j]	50[k]
		calendar year	-	-	-	20
CO	mg/m^3	8-hour	-	10[i] (60%)[l]	10	10
		24-hour[c]	4	-	-	4[k]

Notes: a - Bulgarian standard, Regulation No.12/15.07.2010; b - EU Air Quality Standard (AQS), Directive (EU) 2024/2881; c - 99th quantile range (e.g., exceeding 3-4 days/calendar year); d - the highest average O_3 concentration over 8 hours daily for 6 consecutive months; e - not to be exceeded on more than 35 days per calendar year; f - not to be exceeded on more than 25 days/calendar year, averaged over 3 years; j - not to be exceeded on more than 3 days per calendar year; i - maximum 8-hour average value within 24 hours; k - not to be exceeded more than 18 times per calendar year; l - permissible deviation (%).

The permissible annual levels for $PM_{2.5}$, PM_{10} and NO_2, and for O_3 (8-hour exposure) in the Bulgarian standard, in force since 2010, are higher than those in the 2021 WHO AQGs by 4.0, 2.67, 4.0 and 1.2 times, respectively; for the 24-hour norms – by 1.11 times for PM_{10} and by 3.12 times for SO_2. In fact, a similar picture can be observed in other EU countries, as the EU legislation is mandatory for all member-states. For example, Góra (2024) made the same conclusion when comparing WHO AQGs with the Polish standard. The norms of the classic air pollutants in the new EU standard (2024) are also higher than those in the 2021 WHO recommendations: for 2026 (the first target) the EU annual permissible levels exceed the WHO norms by 5.0 times for $PM_{2.5}$, by 2.67 times for PM_{10} and by 4.0 times for NO_2 (for a calendar year), and by 1.2 times for O_3 (for 8-hour exposure); for the 24-hour norms – by 1.11 times for PM_{10} and by 3.12 times for SO_2. The EU norms of the pollutants that must be reached in 2030 (the second target) are closer to those of the 2021 WHO recommendations, but remain higher: for the annual norms – by 2.00 times for $PM_{2.5}$ and NO_2, by 1.33 times for PM_{10}, and by 1.20 times for O_3 (8-hour exposure); for the 24-hour norms – by 1.67 times for $PM_{2.5}$, by 2.0 times for NO_2 and by 1.25 times for SO_2. Only the PM_{10} 24-hour norm is equal to the WHO standard (45 $\mu g/m^3$). In the EU 2026-first target/Bulgarian standard there neither average daily norms for $PM_{2.5}$, NO_2 and CO, nor average annual norms for SO_2 and O_3 (peak season). In the EU standard for 2030-second target, norms are included for all reference periods with one exception, there is no standard for O_3 (peak season). However, the new EU Directive makes

a serious progress in gradually reducing the permissible levels of classic air pollutants, comparable to the levels proposed by the WHO. According to the EU Zero Pollution Action Plan, the first goal must be reached until 11.12.2026, the second – until 01.01.2030, and the last one – until 2050 ("zero pollution"), when air pollution must be reduced to levels safe to human health and ecosystems (EEA, 2024).

Policy recommendations

There are many examples of successful policies that reduce air pollution (WHO, 2024a). Below, we present some well-addressed, specific and feasable solutions to improve the air quality and reduce the health risk to people.

For citizens: It all depends on the people, that's why, the civil society play a key role in achieving better air quality as it can pose a constant pressure on the authorities to improve the environment, respectively, the quality of life. To be able to carry out this activity, the people must be well informed about the air quality in the regions where they live, work or travel. Along with the traditional sources of information - TV, radio, internet, etc., a very reliable source is the European Air Quality Index (EAQI), available online in the internet. It reflects the potential impact of air quality on health, based on the lowest safety concentrations for five key pollutants - PM_{10}, $PM_{2.5}$, O_3, NO_2 and SO_2. The EAQI indicates the short-term air quality situation; it does not reflect the long-term (annual) air quality state, which may differ significantly (EEA, 2025).

For the industry: implementation of cleaner technology that reduce industrial smokestack emissions; stricter rules and control of the industrial emissions (Mahala, 2024).

For power generation: the promotion of clean energy use; increase the use of low-emissions fuels and renewable combustion-free power sources (solar, wind or hydropower); co-generation of heat and power.

For urban planning: improving the energy efficiency of buildings and making cities greener and more compact, thus energy-efficient; improving the management of urban and agricultural waste, including capture of methane gas emitted from waste sites as an alternative to incineration (for use as biogas); street sweeping and washing as methods for urban PM control - those practices are very effective for reducing the near-ground levels of fine PM and related pollutants (Bogacki et al., 2018; Lin et al., 2023; Das & Wiseman, 2024).

For the transport*:* promotion of the use of electric vehicles; prioritizing rapid urban transit, walking and cycling networks in cities; shifting to cleaner heavy-duty vehicles with low emissions and fuels with reduced sulphur content.

For the households*:* ensuring access to affordable clean household energy solutions for cooking, heating and lighting (electricity or gas instead of briquettes, pellets, etc.).

For health-care activities: putting health services on a low-carbon development path, which leads to a decrease in environmental health risks for patients, health workers and the community.

For future research directions: the use of artificial intelligence (AI) for air quality monitoring and prediction (Li et al., 2022; Awasthi et al., 2024; Rautela & Goyal, 2024; Olawade et al., 2024) as well as for the long-term impact of climate change on pollution patterns (Kaur & Pandey, 2021; Pinho-Gomes et al., 2023; Afifa et al., 2024; Ofremu et al., 2024; Stanisci et al., 2024; Ayyamperumal et al., 2024) is very promising and should be encouraged. Having in mind that air pollution is a pervasive public health issue with major economic consequences; it should remain a key target for global, regional and national health policy and standards.

CONCLUSIONS

In this review, we presented a detailed overview about the main ("classic") ambient air pollutants ($PM_{2.5}$, PM_{10}, SO_2, NO_2, and O_3,) and their influence (individually and in combination/ mixtures) on human health, expressed by two keys indicators - morbidity and mortality. Despite the reduction of the harmful emissions and improving the air quality in EU countries, including Bulgaria, the concentrations of some air pollutants (PM_{10}, $PM_{2.5}$, BaP) remain over the standard levels. In 2022, 96% of the urban population was exposed to concentrations of fine particulate matter ($PM_{2.5}$) above the 2021 WHO annual guideline of 5 $\mu g/m^3$. To meet the WHO goals, the annual reduction of the levels of the individual air pollutants must be between 1.2 times for O_3 to 5.0 times for $PM_{2.5}$ up to 2026

- the first target of 2024 EU standard and between 1.2 times for O_3 to 2.0 times for $PM_{2.5}$ and NO_2 up to 2030 - the second target of 2024 EU standard. For Bulgaria, the respective figures range from 1.11 times for PM_{10} to 4.00 times for $PM_{2.5}$ and NO_2. To curb the harmful effect of the air pollutants and to improve the health status of people, the policy, legislation and standards of air quality must follow the WHO guidelines. In this sense, the efforts of monitoring and decreasing the industrial/urban pollution in Europe and in the world must be continued, the European Green Deal must be joined, as initiatives and policies on reducing pollution and reaching environmental sustainability must facilitate the transition to sustainable, low-carbon economy. Some of the successful policies that can reduce air pollution, and consequently improve the health status of humans, refer to stricter rules and emission control; implementation of cleaner technology; promotion of clean energy (solar, wind or hydropower); expansion of the urban green spaces; street sweeping and washing; more extensive use of electric vehicles.

ACKNOWLEDGEMENTS

This paper was realized within the project 7AF/23 “Application of mathematical modeling for analysis and assessment of ambient air quality”, Trakia University, and co-financed by the National Program of the Ministry of Education and Science “Young Scientists and Postdoctoral Students-2”.

REFERENCES

Afifa, Arshad K., Hussain, N., Ashraf, M.H., & Saleem, M.Z. (2024). Air pollution and climate change as grand challenges to sustainability. *Science of the Total Environment*, *928*, 172370. https://doi.org/10.1016/j.scitotenv.2024.172370.

Air Purity Act, 1996. Ministry of Environment and Water, Official Gazette (OG), No 41/28.05.1996; Last amended OG No 41/10.05.2024 (in Bulgarian), Available online: https://lex.bg/laws/ldoc/2133875712

Akomolafe, O.O., Olorunsogo, T., Anyanwu, E.C., Osasona, F., Ogugua, J.O., & Daraojimba, O.H. (2024). Air quality and public health: a review of urban pollution sources and mitigation measures. *Engineering Science & Technology Journal*, *5*(2), 259-271. doi: 10.51594/ estj/v5i2.751.

Awasthi, A., Pattanayak, K.C., Dhiman, G., & Tiwari, P.R. (Eds.) (2024). *Artificial Intelligence for Air Quality Monitoring and Prediction*. 1st edition, CRC Press, 3-246. https://doi.org/10.1201/9781032683805.

Ayyamperumal, R., Banerjee, A., Zhang, Z., Nazir, N., Li, F., Zhang, C., & Huang, X. (2024). Quantifying climate variation and associated regional air pollution in southern India using Google Earth Engine. *Science of the Total Environment, 909*, 168470. https://doi.org/10.1016/j.scitotenv.2023.168470.

Babu, B., Nallasivam, J.D., & Natrayan, M. (2022). Air pollution's environmental and health effects: a review. *YMER*, *21*(12), 948-960. https://www.researchgate.net/ publication/ 366542755.

Bai, L., Jiang, Y., Wang, K., Xie, C., Yan, H., You, Y., Liu, H., Chen, J., Wang, J., Wei, C., Li, Y., Lei, J., Su, H., Sun, S., Deng, F., Guo, X., & Wu, S. (2024). Ambient air pollution and hospitalizations for schizophrenia in China. *JAMA Netw Open*., *7*(10), e 2436915. doi: 10.1001/jamanetworkopen.2024.36915

Bhatt, B.P. (2024). Air pollution and cardiovascular diseases. *World Journal of Advanced Research and Reviews*, *21*, 1742-1751. https://doi.org/10.30574/wjarr.2024.21.1.2010.

Bogacki, M., Oleniacz, R., Rzeszutek, M., Szulecka, A., & Mazur, M. (2018). The impact of street cleaning on particulate matter air concentrations: a case study of a street canyon in Krakow (Poland). *E3S Web of Conferences 45, 00009, INFRAEKO 2018*, 1-8. https://doi.org/10.1051/e3sconf/20184500009.

Burnett, R., Chen, H., Szyszkowicz, M., Fann, N., Hubbell, B., Pope, C.A. 3rd, e*t al*. (2018). Global estimates of mortality associated with long-term exposure to outdoor fine particulate matter. *Proc. Natl. Acad. Sci. USA*, *115*(38), 9592-9597. doi: 10.1073/pnas.1803222115.

Carozzi, F., & Roth, S., 2023. Dirty density: Air quality and the density of American cities. *Journal of Environmental Economics and Management*, *118*, 102767. https://doi.org/10.1016/j.jeem.2022.102767.

Cesaroni, G., Forastiere, F., Stafoggia, M., & Andersen, Z.J., *et al*. (2014). Long-term exposure to ambient air pollution and incidence of acute coronary events: prospective cohort study and meta-analysis in 11 European cohorts from the ESCAPE Project. *BMJ*, 348, f7412. https://www.bmj.com/content/348/bmj.f7412.full.

D’Acquisto, M.P., Krause, D., Klaassen-Mielke, R., Trampisch, M., Trampisch, H.J., Trampisch, U., & Rudolf, H. (2023). Does residential exposure to air pollutants influ-ence mortality and cardiovascular morbidity of older people from primary care? *BMC Public Health*, *23*, 1281. https://doi.org/10.1186/s12889-023-16166-w.

Das, S., & Wiseman, C.L.S. (2024). Examining the effectiveness of municipal street sweeping in removing road-deposited particles and metal(loid)s of respiratory health concern. *Environment International*, *187*, 108697. https://doi.org/10.1016/j.envint.2024.108697.

Dass, A., Srivastava, S., & Chaudhary, G. (2021). Air pollution: A review and analysis using fuzzy techniques in Indian scenario. *Environ. Technol. & Innovation*, *22*, 101441. https://doi.org/10.1016/j.eti.2021.101441.

Dimitrova, R. & Velizarova, M. (2021). Assessment of the Contribution of Different Particulate Matter Sources on Pollution in Sofia City. *Atmosphere*, *12*, 423. https://doi.org/10.3390/atmos12040423.

Directive (EU) 2024/2881 of the European Parliament and of the Council of 23 October 2024 on ambient air quality and cleaner air for Europe (recast). OJ EU, 20.11.2024. Available online: https://eur-lex.europa.eu/eli/dir/2024/2881/oj/eng.

Dobreva, Z.G., Kostadinova, G.S., Popov, B.N., Petkov, G.S., & Stanilova, S.A. (2015). Proinflammatory and anti-inflammatory cytokines in adolescents from Southeast Bulgarian cities with different levels of air pollution. *Toxicology and Industrial Health*, *31*(12), 1210-1217. doi:10.1177/0748233713491812.

Estuardo-Moreno, H., Gomez-Alvarez, A., Lucero-Acuña, J.A., Almendariz-Tapia, F.J., Esparza-Ponce, H.E., & Ramirez-Leal, R. (2022). Physical and chemical morphology of organic compounds at PM10 by TEM-EDS and GC-SM. *Microscopy and Microanalysis*, *28*(1), 3218-3219. doi:10.1017/S1431927622011977.

European Environment Agency (EEA), 2020. Air quality in Europe - 2020 report, No 09/2020. Available online: https://www.eea.europa.eu/en/analysis/publications/air-quality-in-europe-2020-report (accessed December 18, 2024).

European Environment Agency (EEA), 2022. Air quality in Europe – 2022: Health impacts of air pollution in Europe, 2022. Published 24 Nov 2022. Last modified 20 Nov 2023. Available online: https://www.eea.europa.eu/publications/air-quality-in-europe-2022/health-impacts-of-air-pollution (accessed December 10, 2024).

European Environment Agency (EEA), 2023a. Europe's air quality status 2023. Published 24 Apr 2023. Last modified 05 Nov 2024. Available online: https://www.eea. europa.eu/publications/europes-air-quality-status-2023 (accessed December 12, 2024).

European Environment Agency (EEA), 2023b. Harm to human health from air pollution in Europe: burden of disease 2023. Published 24 Nov 2023. Last modified 12 Nov 2024. Available online: https://www.eea.europa.eu/publications/harm-to-human-health-from-air-pollution (accessed December 12, 2024).

European Environment Agency (EEA), 2024. Europe's air quality status 2024. Published 06 Jun 2024. Last modified 30 Jul 2024. Available online: https://www.eea.europa.eu/publications/europes-air-quality-status-2024 (accessed January 22, 2025).

European Environment Agency (EEA), 2025. The European Air Quality Index (EAQI). Available online: https://airindex.eea.europa.eu/AQI/index.html (accessed January 20, 2025).

Executive Environment Agency (ExEA), 2024. National report on the state and protection of the environment in the Republic of Bulgaria 2024 (in Bulgarian). Available online: ttps://eea.government.bg/bg/dokladih/Greenbook_2024.pdf (accessed February 05, 2024).

Georgiev, S.S., Dzhambov, A.M., & Dimitrova, R.N. (2025). Study of short-term effects of air pollution on hospital admissions in Bulgarian cities Sofia, Plovdiv and Varna. In: N. Dobrinkova, & S. Fidanova (Eds.), Environmental Protection and Disaster Risks (Enviro Risks 2024) - *Proceeding of the 3rd International Conference on Environmental Protection and Disaster Risks and 12th Annual CMDR COE Conference on Crisis Management and Disaster Response*, pp. 70-84. https://doi.org/10.1007/978-3-031-74707-6_9.

Georgieva E., Syrakov D., Atanassov D., Spassova T., Dimitrova M., Prodanova M., Veleva B., Kirova H., Neykova N., Neykova R., Hristova E., & Petrov A., 2021. Use of satellite data for air pollution modeling in Bulgaria. *Earth, 2*, 586-604. https://doi.org/10.3390/earth2030034.

Glencross, D.A., Ho, T-R., Camiña, N., Hawrylowicz, C.M., & Pfeffer, P.E. (2020). Air pollution and its effects on the immune system. *Free Radical Biology and Medicine*, *151*, 56-68. https://doi.org/10.1016/j.freeradbiomed.2020.01.179.

Góra, D. (2024). Review of selected air pollutants in Bielsko-Biała in 2018-2022. *Health Problems of Civilization*, *18*(2), 194-202. https://doi.org/10.5114/hpc.2023.133680.

Heger, M., Zens, G., & Meisner, C. (2019). Particulate matter, ambient air pollution, and respiratory disease in Egypt. The World Bank, Washington DC, USA. Available online: https://openknowledge.worldbank.org/server/api/core/bitstreams/023788cd-c17d-522e-aea8-132424b2d815/content.

Hofmann, B., Weinmayr, G., Hennig, F., Fuks, K., Moebus, S., Weimar, C., Dragano, N., Hermann, D.M., Kälsch, H., Mahabadi, A.A., Erbel, R., & Jöckel, K-H. (2015). Air quality, stroke, and coronary events: results of the Heinz Nixdorf Recall Study from the Ruhr Region. *Dtsch Arztebl Int*., *112*(12), 195-201. doi: 10.3238/arztebl.2015.0195.

Isaifan, R.J. (2023). Air pollution burden of disease over highly populated states in the Middle East. *Front. Public Health*, *10*, 1002707. doi: 10.3389/fpubh.2022.1002707.

Ivanov, K. (2016). Health effects from air pollution in the city of Pernik. *Annual of Sofia University "St. Kliment Ohridski", Faculty of Geology and Geography, Book 2 - Geography*, *109*, 55-61 (in Bulgarian). Available online: https://www.researchgate.net/publication/324953281.

Ivanov, A.V., Gocheva-Ilieva, S.G., & Stoimenova-Minova, M.P. (2023). Temporal-causal modeling of air pollution in the city of Plovdiv, Bulgaria: a case study. *Journal of Physics*, *Conference Series, 2675*, 012002. doi:10.1088/1742-6596/2675/1/012002.

Ivanova, M., Stoykova, S., Dermendzhieva, D., Dospatliev, L., Kostadinova, G., & Petkov, G. (2023). Time series forecasting using ARIMA model and Kalman filter algorithm: a comparative study to air pollutants data (PM_{10}, SO_2 and NO_2) in Bulgaria. *Journal of Environmental Protection and Ecology*,

24(6), 1837-1856. Available online: https://www.scopus.com/record/display. uri? eid=2-s2.0-85178408666&origin=recordpage.

Kar, S., Chowdhury, S., Gupta, T., Hati, D., De, A., Ghatak, Z., Tinab, T., Rahman, I.T., Chatterjee, S., & RoyChowdhury, A. (2024). A study on the impact of air pollution on health status of traffic police personnel in Kolkata, India. *Air*, *2*, 1-23. https://doi.org/10.3390/air2010001.

Kaur, R. & Pandey, P. (2021). Air pollution, climate change, and human health in Indian cities: A Brief Review. *Front. Sustain. Cities*, *3*, 705131. doi: 10.3389/frsc.2021.705131.

Kermani, M., Goudarzi, G., Shahsavani, A., Dowlati, M., Asl, F.B., Karimzadeh, S., Jokandan, S.F., Aghaei, M., Kakavandi, B., Rastegarimehr, B., Ghorbani-Kalkhajeh, S., & Tabibi, R. (2018). Estimation of short-term mortality and morbidity attributed to fine particulate matter in the ambient air of eight Iranian cities. *Ann Glob Health*, *84*(3), 408-418. doi: 10.29024/aogh.2308.

Keswani, A., Akselrod, H., & Anenberg, S.C. (2022). Health and clinical impacts of air pollution and linkages with climate change. *NEJM Evid*, *1*(7). doi: 10.1056/EVIDra2200068.

Khan, I., Saeed, K., & Khan, I. (2019). Nanoparticles: Proper-ties, applications and toxicities. *Arabian Journal of Chemistry*, *12*(7), 908-931. https://doi.org/10.1016/j.arabjc.2017.05.011.

Kienzler, S., Soares, J., Ortiz, A.G., & Plass, D. (2022). Estimating the morbidity related environmental burden of disease due to exposure to $PM_{2.5}$, NO_2 and O_3 in outdoor ambient air. *Eionet Report - EEA*, *ETC HE Report 2022/11*. Available online: file:///C:/Users/

Kostova-Ivanova, D. (2024). Analysis of GHG emissions by sectors in city of Vidin. *Scientific Papers. Series E. Land Reclamation, Earth Observation & Surveying, Environ. Engin.*, *13*, 115-124. https://landreclamationjournal.usamv.ro/pdf/2024/Art14.pdf.

Kozlov, A., Gura, D., Repeva, A., & Lushkov, R. (2022). Assessing Air pollution and determining the composition of airborne dust in urbanized areas: Granulometric characteristics. *Atmosphere*, *13*, 1802. https://doi.org/10.3390/atmos13111802.

Kumari, S. & Sarkar L. (2021). A Review on Nanoparticles: Structure, Classification, Synthesis & Applications. *Journal of Scientific Research of the Banaras Hindu University*, *65*(8), 42-46. doi: 10.37398/JSR.2021.650809.

Lan, D., Fermoyle, C.C., Troy, L.K., Knibbs, L.D., & Corte, T.J. (2024). The impact of air pollution on interstitial lung disease: a systematic review and meta-analysis. *Front. Med*., *10*, 1321038. https://doi.org/10.3389/fmed.2023.1321038.

Le, L-T., Quang, K-B.V., Vo, T-V., Nguyen, T-M.T., Dao, T-V-H., & Bui, X-T. (2024). Environmental and health impacts of air pollution: A mini-review. *Environ-mental Sciences*, *66*(1), 120-128. https://doi.org/10.31276/VJSTE.66(1).120-128.

Lee Y.-G., Lee P.-H., Choi S.-M., An M.-H., & Jang A.-S., 2021. Effects of air pollutants on airway diseases. *Int. J. Environ. Res. Public Health*, 18, 9905. https://doi.org/10.3390/ijerph18189905.

Lei, J., Liu, C., Meng, X., Sun, Y., Huang, S., Zhu, Y., Gao, Y., Shi, S., Zhou, L., Luo, H., Kan, H., & Chen, R. (2024). Associations between fine particulate air pollution with small-airway inflammation: A nationwide analysis in 122 Chinese cities. *Environmental Pollution*, *344*, 123330. https://doi.org/10.1016/j.envpol.2024.123330.

Li, Y., Guo, J-e, Sun, S., Li, J., Wang, S., & Zhang, C. (2022). Air quality forecasting with artificial intelligence techniques: A scientometric and content analysis. *Environmental Modelling & Software*, *149*, 105329. https://doi.org/10.1016/j.envsoft.2022.105329.

Li, J., Hua, C., Ma, L., Chen, K., Zheng, F., Chen, Q., Bao, X., Sun, J., Xie, R., Bianchi, F., Kerminen, V-M., Petäjä, T., Kulmala, M., & Liu, Y. (2024). Key drivers of the oxidative potential of $PM_{2.5}$ in Beijing in the context of air quality improvement from 2018 to 2022. *Environment International*, *187*, 108724. https://doi.org/10.1016/j.envint.2024.108724.

Lin, Y.J., Lin, H.C., Yang, Y.F., Chen, C.Y., Ling, M.P., Chen, S.C., Chen, W.Y., You, S.H., Lu, T.H., & Liao, C.M. (2019). Association between ambient air pollution and elevated risk of tuberculosis development, *Infect Drug Resist*, *12*, 3835-3847. doi: 10.2147/IDR.S227823.

Lin, S-L., Deng, Y., Lin, M-Y, & Huang, S-W. (2023). Do the street sweeping and washing work for reducing the near-ground levels of fine particulate matter and related pollutants? *Aerosol and Air Quality Research*, *23*, 220338. https://doi.org/10.4209/aaqr.220338.

Mahala, K.R. (2024). The impact of air pollution on living things and Environment: A review of the current evidence. *World Journal of Advanced Research and Reviews*, *24*(03), 3207-3217. https://doi.org/10.30574/wjarr.2024.24.3.3929.

Manisalidis, I., Stavropoulou, E., Stavropoulos, & A., Bezirtzoglou, E. (2020). Environmental and Health Impacts of Air Pollution: A Review. *Frontiers in Public Health*, *8*, 14. doi.org/10.3389/fpubh.2020.00014.

Meo, S.A., Salih, M.A., Al-Hussain, F., Alkhalifah, J.M., Meo, A.S., & Akram, A. (2024). Environmental pollutants $PM_{2.5}$, PM_{10}, carbon monoxide (CO), nitrogen dioxide (NO_2), sulfur dioxide (SO_2), and ozone (O_3) impair human cognitive functions. *European Review for Medical and Pharmacological Sciences*, *28*, 789-796. doi: 10.26355/eurrev_202401_35079.

Mesas-Carrascosa, F.J., Porras, F.P., Triviño-Tarradas, P., García-Ferrer, A., & Meroño-Larriva, J.E. (2020). Effect of lockdown measures on atmospheric nitrogen dioxide during SARS-CoV-2 in Spain. *Remote Sensing*, *12*, 2210. doi: 10.3390/rs12142210.

Minkova, I., Zheleva, I., & Filipova, M. (2023). Statistic study of particulate matter air contamination in the city of Vidin, Bulgaria. *Journal of Physics, Conference Series 2675*, 012005. doi:10.1088/1742-6596/2675/1/012005

Naydenova, I., Petrova, Ts., Velichkova, R., & Simova, I. (2018). PM_{10} Exceedance in Bulgaria. *CBU*

International Conference on Innovations in Science and Education, March 21-23, 2018, Prague, Czech Republic, 1129-1138. http://dx.doi.org/10.12955/cbup.v6.1305.

Nikolova, M., Filipova, M., & Zheleva, I. (2023). Statistic study of gaseous air contamination in the city of Ruse, Bulgaria. *AIP Conference Proceedings*, 2953, 040010. https://doi.org/10.1063/5.0177811.

Ofremu, G.O., Raimi, B.Y., Yusuf, S.O., Dziwornu, B.A., Nnabuife, S.G., Eze, A.M., & Nnajiofor, C.A. (2024). Exploring the relationship between climate change, air pollutants and human health: Impacts, adaptation, and mitigation strategies. *Green Energy and Resources*, 100074. https:// doi.org/10.1016/j.gerr.2024.100074.

Olawade, D.B., Wada, O.Z., Ige, A.O., Egbewole, B.I., Olojo, A., & Oladapo, B.I. (2024). Artificial intelligence in environmental monitoring: Advancements, challenges, and future directions. *Hygiene and Environmental Health Advances*, *12*, 100114. https://doi.org/10.1016/j.heha.2024.100114.

Olstrup, H., Johansson, C., Forsberg, B., Åström, C., & Orru, H. (2021). Seasonal variations in the daily mortality associated with exposure to particles, nitrogen dioxide, and ozone in Stockholm, Sweden, from 2000 to 2016. *Atmosphere*, *12*, 1481. https://doi.org/10.3390/atmos12111481.

Papadogeorgou, G., Kioumourtzoglou, M.A., Braun, D., & Zanobetti, A. (2019). Low levels of air pollution and health: Effect estimates, methodological challenges, and future directions. *Current Environmental Health Reports*, *6*(3), 105-115. https://doi.org/10.1007/s40572-019- 00235-7.

Pinho-Gomes, A-C., Eleanor Roaf, E., Fuller, G., Fowler, D., Lewis, A., ApSimon, H., Noakes, C., Johnstone, P., Stephen & Holgate, S. (2023). Air pollution and climate change. *The Lancet Planetary Health*, *7*(9), e727-e728. https://www.thelancet.com/journals/lanplh/article/PIIS2542-5196(23)00189-4/fulltext.

Platikanova, M., & Penkova-Radicheva, M. (2016). Obser-vable effects of atmospheric pollution on outpatient and inpatient morbidity in Bulgaria. *Iran J Public Health*, *45*(4), 515-22. https://pmc.ncbi.nlm.nih.gov/articles/PMC4888179/pdf/IJPH-45-515.pdf.

Platikanova, M., Hristova, P., & Milcheva, H. (2018). Mathe-matical model for forecasting the influence of atmospheric pollution on population morbidity in Stara Zagora Municipality (Bulgaria). *Macedonian Journal of Medical Sciences*, *6*(5), 934-939. https://doi.org/10.3889/oamjms.2018.205.

Popa, C.R., Balint, R., Mocanu, A., & Tomoaia-Cotisel, M. (2020). Cardiovascular diseases induced by air pollution. *Academy of Romanian Scientists Annals - Series on Biological Sciences*, *9*(2), 133-170. https://www.aos.ro/wp-ontent/anale/BVol9Nr2Art.12.pdf.

Popa, C.R., Tomoaia, G., Paltinean, G.A., Mocanu, A., Cojocaru, I., & Tomoaia-Cotisel, M. (2021). Atmospheric pollution and the impact on the respiratory tract and lungs. *Academy of Romanian Scientists Annals - Series on Biological Sciences*, *10*(1), 60-89. https://www.aos. ro/wp-content/anale/BVol10Nr1Art.7.pdf.

Rautela, K.S., & Goyal, M.K. (2024). Transforming air pollution management in India with AI and machine learning technologies. *Sci. Rep.*, *14*, 20412. https://doi.org/10.1038/s41598-024-71269-7.

Regulation No. 12/15.07. 2010 on standards for sulfur dioxide, nitrogen dioxide, particulate metter), lead, benzene, carbon monoxide and ozone in ambient air. Official Gazette (OG) No 58/30.07.2010, Last amendment OG, No 79/08.10.2019 (In Bulgarian). Available online: https://lex.bg/laws/ldoc/2135691821

Ruwali, S., Talebi, S., Fernando, A., Wijeratne, L.O.H., Waczak, J., *et al*. (2024). Quantifying inhaled concentrations of particulate matter, carbon dioxide, nitrogen dioxide, and nitric oxide using observed biometric responses with machine learning. *Bio Med Informatics*, *4*, 1019-1046. https://doi.org/10.3390/biomedinformatics4020057.

Sadeghi, H.A. & Sadeghi, R. (2024). Temporal analysis of air pollution effects on cardiovascular diseases and mortality in Ahvaz, Iran. *International Journal of Population*, *1*(2), 71-85. https://doi.org/10.36312/ijpi.v1i2.1828.

Saleem, A., Awan, T., & Akhtar, M.F. (2024). A comprehend-sive review on endocrine toxicity of gaseous components and particulate matter in smog. *Frontiers in Endocrinology*, *15*, 1294205. https://doi.org/10.3389/fendo.2024.1294205.

Schwartz, J., & Bind, M.A., Koutrakis, P. (2017). Estimating causal effects of local air pollution on daily deaths: effect of low levels. *Environmental Health Perspectives*, *125*(1), 23-29. http://dx.doi.org/10.1289/EHP232.

Shah, A.S., Langrish, J.P., Nair, H., McAllister, D.A., Hunter, A.L., Donaldson, K., Newby, D.E., & Mills, N.L. (2013). Global association of air pollution and heart failure: a systematic review and meta-analysis. *Lancet*., *382*(9897), 1039-48. doi: 10.1016/S0140-6736(13) 60898-3

Shahrbaf, M.A., Akbarzadeh, M.A., Tabary, M, & Khaheshi, I. (2021). Air pollution and cardiac arrhythmias: A comprehensive review. *Current Problems in Cardiology*, *46*(3), 100649. doi: 10.1016/j.cpcardiol.2020.100649.

Shetty, S.S., Deepthi, D., Harshitha, S., Sonkusare, S., Naik, P.B., Kumari, N. S., & Madhyastha, H. (2023). Environmental pollutants and their effects on human health. *Heliyon*, *9*, e19496. https://doi.org/10.1016/j.heliyon.2023.e19496.

Sierra-Vargas, M.P., & Teran L.M. (2012). Air pollution: Impact and prevention. *Respirology*, *17*, 1031-1038. doi: 10.1111/j.1440-1843.2012.02213.x.

Silva, L.F.O., Milanes, C., Pinto, D., Ramirez, O., & Lima, B.D. (2020.) Multiple hazardous elements in nano-particulate matter from a Caribbean industrialized atmosphere. *Chemosphere*, *239*, 124776. https://doi.org/10.1016/j.chemosphere.2019.124776.

Solaimani, P., Saffari, A., Sioutas, C., Bondy, S.C., & Campbell, A. (2017). Exposure to ambient ultrafine particulate matter alters the expression of genes in

primary human neurons. *Neuro Toxicology*, *58*, 50-57. doi: 10.1016/j.neuro.2016.11.001.

Stanisci, I., Sarno, G., Curzio, O., Maio, S., Angino, A.A., Silvi, P., Cori, L., Viegi, G., & Baldacci, S. (2024). Air pollution and climate change: A pilot study to investigate citizens'perception. *Environments*, *11*, 190. https://doi.org/10.3390/ environments1109019.

Stoykova, S., Ivanova, M., Dermendzhieva, D., Varbanov, M., Dospatliev, L., Kostadinova, G., & Petkov, G. (2023). Assessment of air pollution in Stara Zagora region, Bulgaria, based on PM_{10} and $PM_{2.5}$ concentrations and content of Mn, Cu, Pb, Fe, Zn, Ni, Cd in PM_{10}. *J. of Environmental Protection and Ecology*, *24*(3), 717-728. Available online: https://www.scopus.com/record/display.uri?eid=2-s2.0-85163184380&origin= recordpage.

Takuchev, N., Kostadinova, P., Naydenova, G.I. & Stoilova, I. (2018). Combined ground level and satellite monitoring of urban air pollution, estimation of the number of patients treated in hospitals due to air pollution and the cost of their treatment - case study of Ruse, Bulgaria. *Trakia Journal of Sciences*, *16*, Suppl. 1, 158-168. doi:10.15547/tjs.2018.s.01.033.

Thacker, S.B., Stroup, D.F., Carande-Kulis, V., Marks, J.S., Roy, K., & Gerberding, J.L. (2006). Measuring the Public's Health. *Public Health Reports*, *121*(1), 14-22. doi: 10.1177/003335490612100107.

Thurston, G.D., Kipen, H., Annesi-Maesano, I., *et al.* (2017). A joint ERS/ATS policy statement: what constitutes an adverse health effect of air pollution? An analytical framework. *European Respiratory Journal*, *49*(1), 160 0419. https://doi.org/10.1183/13993003.00419-2016

To, T., Zhu, J., Stieb, D., Gray, N., Fong, I., Pinault, L., *et al*. (2020). Early life exposure to air pollution and incidence of childhood asthma, allergic rhinitis and eczema, *Eur. Respir. J.*, *55*(2), 1900913. doi: 10.1183/13993003.00913-2019.

Tran, H.M., Tsai, F.J., Lee, Y.L., Chang, J.H., Chang, L.Te, Chang, T.Y., Chung, K.F., Kuo, H.P., Lee, K.Y., Chuang, K.J., & Chuang, H.C. (2023). The impact of air pollution on respiratory diseases in an era of climate change: A review of the current evidence. *Science of the Total Environment*, *898*, 166340. doi:10.1016/j.scitotenv.2023.166340.

Turner, M.C., Andersen, Z.J., Baccarelli A., *et al*. (2020). Outdoor air pollution and cancer: An overview of the current evidence and public health recommendations. *CA Cancer Journal for Clinicians*, *70*, 460-479. doi: 10.3322/caac.21632.

United Nation Environmental Program (UNEP), 2021. Pollution Action Note – Data you need to know. Published 7 Sept 2021, Updated 6 Sept 2023. Available online: https://www.unep.org/interactives/air-pollution-note (accessed December 5, 2024).

United Stated Environmental Protection Agency (USEPA), 2024. Health and environmental effects of particulate matter (PM). Last updated on July 16, 2024. Available online: https://www.epa.gov/pm-pollution/health-and-environmental-effects-particulate-matter-pm.

Vandyck, T., Ebi, K.L., Green, D., Cai, W., Sotiris, Vardoulakis, S. (2022). Climate change, air pollution and human health. *Environmental Research Letters*, *17*, 100402. https://doi.org/10.1088/1748-9326/ac948e.

Vohra, K., Vodonos, A., Schwartz, J., Marais, E.A., Sulprizio, M.P., Mickley, L.J. (2021). Global mortality from outdoor fine particle pollution generated by fossil fuel combustion: Results from GEOS-Chem. *Environmental Research*, *195*, 110754. https://doi.org/10.1016/j.envres.2021.110754.

WHO global air quality guidelines (WHO-AQGs), 2021. Particulate matter ($PM_{2.5}$ and PM_{10}), ozone, nitrogen dioxide, sulfur dioxide and carbon monoxide. Available online: https://iris.who.int/bitstream/handle/10665/345334/9789240034433-eng.pdf (accessed December 10, 2024).

World Bank (WB), 2023. Pollution. Last Updated Sep. 19, 2023. Available online: https://www.worldbank.org/en/topic/pollution (accessed December 5, 2024).

World Health Organization (WHO), 2024a. Ambient (outdoor) air pollution. Available online: https://www.who.int/news-room/fact-sheets/detail/ambient-(outdoor)-air-quality-and-health (accessed November 20, 2024).

World Health Organization (WHO), 2024b. Sustainable Development Goal Indicator 3.9.1 mortality attributed to air pollution. Available online: https://iris.who.int/bitstream/handle/10665/379020/9789240099142-eng.pdf?sequence=1 (accessed November 22, 2024).

Yuan, K., Zhang, Y., Lv, X., Cao, W., Zhang, Z., Wu, L., & Sun, S. (2024). Exposure to hourly ambient air pollutants and risk of emergency department visits for asthma: A multicenter time-stratified case-crossover analysis. *Atmospheric Environment*, *319*, 120307. https://doi.org/10.1016/j.atmosenv.2023.120307.

Zaheer, J., Jeon, J., Seung-Bok Lee, S-B., Kim, J.S. (2018). Effect of particulate matter on human health, prevention, and imaging using PET or SPECT. *Progress in Medical Physics*, *29*(3), 82-91. https://doi.org/10.14316/pmp.2018.29.3.81.

Zheleva, I. (2024). Air quality in Bulgaria-Monitoring data, perspectives, scientific research. *Pollution Study*, *5*(1), 2798. https://doi.org/10.54517/ps.v5i1.2798.

Zheng, X-Y., Orellano, P., Lin, H-l., Jiang, M., Guan, W-J. (2021). Short-term exposure to ozone, nitrogen dioxide, and sulphur dioxide and emergency department visits and hospital admissions due to asthma: A systematic review and meta-analysis. *Environment International*, *150*, 106435. doi: 10.1016/j.envint.2021.106435.

Scientific Papers. Series E. Land Reclamation, Earth Observation & Surveying, Environmental Engineering. Vol. XIV, 2025
Print ISSN 2285-6064, CD-ROM ISSN 2285-6072, Online ISSN 2393-5138, ISSN-L 2285-6064

STUDY ON THE DYNAMICS OF CEREALS CULTIVATED IN TULCEA COUNTY IN THE CONTEXT OF CLIMATE CHANGE

Traian Ciprian STROE[1, 2], Oana MIHAI-FLOREA[1], Liliana MIRON[2]

[1]University of Agronomic Sciences and Veterinary Medicine of Bucharest,
59 Mărăști Blvd, District 1, 011464, Bucharest, Romania
[2]"Ovidius" University of Constanța, University Alley, Campus Building B,
900470, Constanța, Romania

Corresponding author email: str_ciprian@yahoo.com

Abstract

Climate change in recent decades has had a significant impact on Romanian agriculture. In this context, Tulcea County, located in the south-eastern part of the country, has experienced a trend of increasing average annual temperatures, an increase in the number of days with temperatures above 30°C and a decrease in total annual precipitation. The study analyzed meteorological data, the evolution of crop structure, cultivated area, and yield trends over a 20-year period (1994-2023). The results showed an increase in average annual temperature from 12.39°C in 1994 to 13.8°C in 2023. Precipitation was low and showed significant variability, ranging from 215.8 mm in 2022 to 732 mm in 1997, with uneven distribution during the crop growing season. The area planted with cereals for grain varied considerably, influenced by both the predicted climatic conditions and the extent of irrigated land. Statistical analysis was performed using the Python software package, applying Pearson correlation tests to examine the relationship between climatic variables and agricultural yields. Linear regression methods were also used to identify long-term trends. The statistical tests showed that both increasing temperatures and decreasing precipitation were correlated with declining maize and wheat yields, highlighting the vulnerability of agriculture to climate change. Maize production ranged from a minimum of 323 kg/ha in 2003 to a maximum of 8,820 kg/ha in 2018. The overall trend indicates a slight decrease in average production ($R^2 = 0.41$, $p < 0.05$), correlated with increasing temperatures. Wheat showed a more stable yield, reaching a maximum of 4,738 kg/ha in 2021. The production trend was positive in periods with moderate rainfall ($R^2 = 0.63$, $p < 0.01$).

Key words*: climate change, cereals, precipitation trends, heat stress, crop yields.*

INTRODUCTION

Tulcea County, located in the eastern part of Romania, represents a region characterized by an arid climate and an agriculture that has devolved significantly throughout history. With an agricultural area of approximately 303.2 thousand hectares, the region faces challenges related to climate change, such as rising temperatures, decreasing precipitation, and the increasing frequency of extreme weather events.

Agricultural activity in the region has been documented since prehistoric times, with evidence coming from both historical records and archaeological sites. The Greek historian Apollonius of Rhodes, in the *Argonautica*, describes how Jason's sailors, while navigating the Danube Delta via the "Beautiful Arm" - probably the present-day Sfântu Gheorghe Arm - encountered flocks of sheep and shepherds, indicating early pastoral activity in the area (Filipescu, 1928; Lup, 2003). In addition, archaeological excavations in the ancient settlement of Hamangia (modern Baia, Tulcea County) provide tangible evidence of the Hamangia culture, a Neolithic civilization that flourished between the 4th and 2nd millennia BC, demonstrating an early reliance on agriculture and animal husbandry (Hasotti, 1997). These historical and archaeological findings underscore the deep-rooted agricultural traditions of the region, providing context for its long-standing adaptation to environmental and climatic changes (Lup, 2012).

Extensive international research highlights the profound impact of climate change on agriculture, particularly in arid and semi-arid regions (IPCC, 2021). The presence of water is inextricably linked to crop production in agricultural systems (Dușa & Stan, 2022).

Rising temperatures and declining water availability have been linked to reduced agricultural productivity and shifts in crop composition (Lal et al., 2007; Rosenzweig et al., 2001; Horoiaş et al., 2013; Ciocan et al., 2024). However, while these studies provide valuable insights at a global and regional scale, they often lack localized assessments that account for specific crop responses and tailored adaptation strategies at the county level. Tulcea County, characterized by significant climatic variability, remains underrepresented in such analyses despite its agricultural importance.

This study aims to address this gap by evaluating long-term climate trends and their direct impact on cereal yields (wheat, maize, and barley). By providing a data-driven, localized perspective, the research contributes to a deeper understanding of climate-induced shifts in cereal production and informs the development of adaptive strategies for sustainable agriculture in vulnerable regions.

To achieve these objectives, this study integrates Pearson correlation analysis and linear regression modeling to quantify the relationships between temperature, precipitation, and crop productivity. The findings indicate a significant correlation between rising temperatures and declining maize yields, while wheat production shows a more stable trend, benefiting from moderate precipitation levels. By highlighting these climate-yield interactions, the study provides valuable insights for policymakers and farmers in developing targeted adaptation measures and sustainable agricultural strategies in response to ongoing climate variability.

MATERIALS AND METHODS

To analyze the impact of climate change on the dynamics of cultivated cereals, data from multiple official sources were utilized. Meteorological data for the period 1994-2023, including annual average temperatures, total annual precipitation, and the number of days with temperatures exceeding 30°C, were obtained from National Institute of Statistics (INS, 2023b). Agricultural data, covering cultivated areas and average cereal yields per hectare, were extracted from the Statistical Yearbooks of Romania and the archives of the Tulcea County Directorate of Statistics (INS, 1990; 2023a). Additionally, information regarding land use and irrigation infrastructure was sourced from the National Agency for Land Improvements.

Statistical analysis was conducted using the Python software package, applying Pearson correlation tests to examine the relationship between climate variables and agricultural yields. Linear regression methods were also used to identify long-term trends.

RESULTS AND DISCUSSIONS

The climate of Tulcea County is characterized by a warm and dry climate, specific to areas with the most generous thermal resources but also the lowest precipitation levels compared to other regions of the country. A 30-year climatic analysis shows the following: the annual average temperature is 12.03°C, the average annual precipitation is 488.79 mm, and the average number of days with temperatures exceeding 30°C is 42.4 days per year.

During the 1994-2003 period, statistical analysis highlighted significant fluctuations in annual average temperatures, as illustrated in Figure 1. The year 1994 was characterized by a high annual average temperature of 12.39°C, marked by favorable climatic conditions. However, the 1995-1997 period experienced a notable decline in annual average temperature, from 11.27°C (1995) to 10.49°C (1997), the lowest recorded value in the analyzed period. These values were influenced by negative temperatures in January and December. Between 1998 and 2002, a progressive increase in temperature was observed, from 11.51°C (1998) to 12.27°C (2002), followed by slight variations between 11.68°C and 11.73°C in 2000-2001. In contrast, the year 2003 was notable for a drop in the annual average temperature to 10.78°C, driven by the low temperatures recorded in January (-1°C) and February (-4.5°C).

Between 2004 and 2023, statistical analysis identified the following trends: the years 2004-2006 and 2011 had annual average temperatures varying between 11.18°C (2011) and 11.59°C (2004), marking lower values compared to the subsequent period. The 2007-2013 period saw a significant increase in

temperatures, ranging from 12.03°C (2007) to 12.43°C (2013). Similarly, the years 2014-2023 recorded annual average temperatures consistently above 12°C, reaching a peak of 13.80°C in 2023. During this period, 2019-2023 had the highest temperatures, all exceeding 13°C.

Data analyzed from 1994 to 2023, using linear regression tests, indicate a significant upward trend in annual average temperatures (R^2 = 0.84, $p < 0.01$), increasing from an average of 11.27°C in 1995 to 13.8°C in 2023. This increase has been associated with a rise in the number of heatwave days, reaching 65 days in the years 2012 and 2022.

Moreover, the length of the growing season for key cereal crops, such as wheat, corn, barley, sunflower, and peas, has been affected by these changes, leading to earlier planting and harvesting periods.

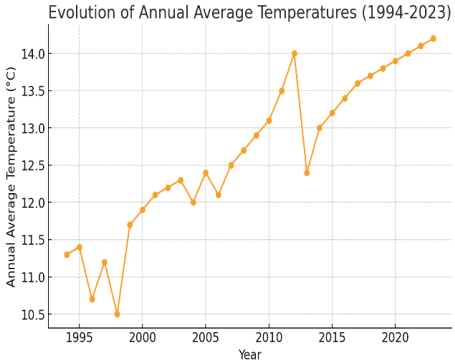


Figure 1. Evolution of annual average temperatures between 1994 and 2023

The period analyzed showed a decreasing trend in precipitation, as illustrated in Figure 2. Notably, between 1994 and 2003, annual precipitation varied from a minimum of 298.1 mm in 2003 to a maximum of 732 mm in 1997. In addition to temperature variations, the precipitation regime has also undergone significant changes. The analysis of rainfall data between 1994 and 2023 indicates a gradual decrease in annual precipitation from 480 mm in 1994 to 430 mm in 2023. This downward trend has contributed to an increased risk of drought and a reduction in soil moisture levels, impacting agricultural productivity. Years of drought, including 2003, 2004, 2009, 2011, and 2012, experienced total annual precipitation below 300 mm. Additionally, from 2014 to 2020, annual precipitation remained below 400 mm, impacting cereal crop yields and prompting the adoption of adaptive irrigation systems. The correlation with agricultural yields indicated that insufficient precipitation during drought years significantly reduced crop productivity. From 2004 to 2023, the declining trend persisted, with annual average values remaining below 488.79 mm. Notably, in 2022, precipitation dropped to just 215.8 mm. Linear regression analysis showed a moderate but significant decrease in precipitation (R^2 = 0.59, $p < 0.05$), declining from an average of 488.79 mm per year to values below 300 mm in drought years, such as 2022.

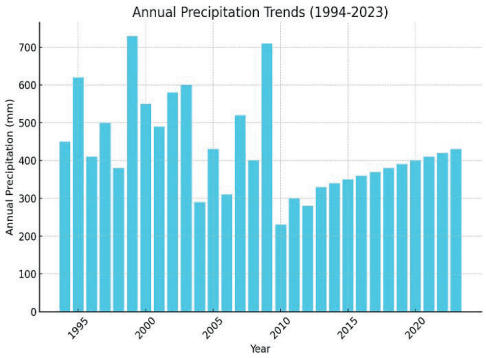


Figure 2. Evolution of average annual precipitation between 1994 and 2023

Along with high temperatures and low precipitation, the frequency of days with temperatures exceeding 30°C also contributes to the arid climate of Tulcea County. Notable instances were recorded in 1995, 1997, 2004, and 2005, with 25 days in 1995, 10 days in 1997, 13 days in 2004, and 24 days in 2005. During the rest of the analyzed period, the number of such days ranged between 30 and 65, including 60 days in 2016 and 2018, 62 days in 2019, and 65 days in both 2012 and 2022 (Table 1). In years with a high frequency of extremely hot days, these events were primarily concentrated between June and September.

The increase in the number of extreme weather events, including heatwaves, storms, and prolonged dry spells had led to higher

evapotranspiration rates, negatively impacting plant growth cycles and increasing the demand for soil conservation techniques, such as no-tillage farming and mulching.

Table 1. Number of days with temperatures exceeding 30°C in Tulcea County (1994-2023)

Year	No. of days	Year	No. of days	Year	No. of days
1994	34	2004	13	2014	40
1995	25	2005	24	2015	51
1996	31	2006	27	2016	60
1997	10	2007	57	2017	46
1998	31	2008	44	2018	60
1999	43	2009	39	2019	62
2000	36	2010	50	2020	57
2001	48	2011	43	2021	45
2002	43	2012	65	2022	65
2003	37	2013	42	2023	43

To evaluate the impact of climate conditions on agricultural yields, Pearson correlation tests were applied between annual average temperatures, annual precipitation, and the average yields of the main agricultural crops in Tulcea County. Additionally, linear regression analyses were conducted to identify long-term trends. These characteristics highlight the challenges associated with managing agriculture in this region, where high temperatures and precipitation deficits significantly affect crop production.

Statistical tests showed that both rising temperatures and decreasing precipitation levels are correlated with declining maize and wheat yields, emphasizing the vulnerability of agriculture to climate change.

Cultivated cereal areas have varied significantly, influenced by climate conditions. The areas cultivated with grain cereals showed notable variations depending on the evolution and forecast of climatic conditions. Available data indicates a direct correlation between fluctuations in annual average temperatures, precipitation levels, and the dynamics of cultivated areas.

Favorable annual average temperatures, ranging between 10.49°C (1997) and 12.18°C (1999), combined with precipitation levels between 454.3 mm (1995) and 640.9 mm (1999), supported the stability of cultivated areas. Thus, in 2000, the total area cultivated with grain cereals reached 162,310 ha, increasing further to 181,463 ha in 2001.

The year 2001 was marked by low precipitation (419.3 mm) and an annual average temperature of 11.73°C, as well as an increase in the number of days with temperatures above 30°C (48 days, compared to 10-36 days in previous years). These climate conditions led to a reduction in cultivated areas in 2002 to 166,001 ha.

The decline in precipitation and the rise in annual average temperatures continued to influence cultivated areas, reaching a minimum of 118,948 ha in 2007, a year characterized by average temperatures above 12°C and below-average precipitation levels.

Favorable precipitation and stable annual temperatures, ranging from 12.03°C to 12.30°C, led to a slight increase in cultivated area between 2008 and 2009, reaching values of 151,772-154,447 ha. During 2012-2013, cultivated areas increased significantly, reaching 181,757 ha in 2012 and 179,691 ha in 2013, due to a rise in precipitation from 537.9 mm in 2012 to 671.1 mm in 2017.

Between 2014 and 2023, annual average temperatures consistently exceeded 12°C, peaking at 13.8°C in 2023. Although cultivated areas temporarily increased from 151,986 ha in 2014 to 158,164 ha in 2018, severe drought and irregular precipitation patterns caused a decline to 131,884 ha by 2022 (Table 2).

An analysis of the crop structure indicates that wheat consistently ranked first in cultivated areas, primarily due to its greater drought resistance compared to maize. The area dedicated to wheat cultivation varied from 43,023 ha in 2004 to 92,120 ha in 2023. During periods of low precipitation, wheat occupied larger areas due to its ability to withstand drought conditions. The correlation between wheat cultivated area and annual temperatures was positive ($\rho = 0.52$, $p < 0.05$).

Maize was more sensitive to climatic conditions, with cultivated areas fluctuating between 29,458 ha (2010) and 90,487 ha (2004), depending on water availability forecasts. Due to maize's greater sensitivity to climatic conditions, its cultivated areas showed significant variations, with a strong correlation

between cultivated area and annual precipitation ($\rho = 0.76$, $p < 0.01$).

Due to the arid climate, rye found a place in this region, although the cultivated areas remained small, ranging between 15 ha (2000) and 200 ha (2023).

Barley and spring barley, being short-cycle crops with good resistance to high temperatures, heat waves, and drought, were cultivated on fluctuating areas between 2000 and 2023. However, the ratio between barley and spring barley changed over time based on economic demands.

Table 2. Structure of source cultivated areas with Grain Cereals in the period 2000-2023 (hectares)

Year	CROP									
	Total cereals	Common wheat	Durum wheat	Rye	Barley	Spring barley	Oats	Maize grain	Triticale	Sorghum
2000	162310	60644	-	15	7914	6580	5190	81967	-	-
2001	181463	81582	311	25	12258	5930	3445	77912	-	-
2002	166001	76389	-	17	9079	8868	6271	65377	-	-
2003	134619	46855	30	24	1815	7614	5620	74476	-	-
2004	145300	43023	-	40	-	9188	4562	90487	-	-
2005	140752	60901	-	80	5741	13959	4873	55198	-	-
2006	118104	46348	17	110	2616	10229	3952	54832	-	-
2007	118984	56968	233	20	4125	12529	2089	43020	-	-
2008	151772	84199	538	50	6681	10352	3898	45454	-	-
2009	154447	76272	811	150	12165	20548	3952	40549	-	-
2010	143757	72619	2087	97	15299	19282	4570	29458	-	-
2011	144799	62530	344	169	12910	8083	3948	56815	-	-
2012	181757	90180	1225	107	15014	8098	6219	60914	-	-
2013	179691	87536	1123	113	15169	8843	6200	60707	-	-
2014	151986	80875	177	81	14856	5524	2353	48120	-	-
2015	152653	78869	425	107	16084	4073	1869	51226	-	-
2016	165614	84719	3632	117	20636	4363	1787	50360	-	-
2017	152624	83957	22	115	16777	6441	1998	43314	-	-
2018	158164	83984	575	92	18518	4567	1670	48758	-	-
2019	165660	85717	2865	121	19785	4119	1988	51065	-	-
2020	158547	84694	1194	117	17631	4538	1274	46256	2694	149
2021	136153	76533	199	269	18811	1741	274	36977	1200	150
2022	131884	76525	194	152	14493	2697	336	36197	800	490
2023	174770	92120	-	200	26000	3400	700	50500	1300	550

Source: National Institute of Statistics, Romania. County Directorate for Agriculture – Tulcea. *Statistical Data (1994-2023).*

Since 2020, a new cereal, triticale, known for its drought and heat resistance, was introduced, with cultivation areas of 2,694 ha (2020), 1,200 ha (2021), 1,300 ha (2023), and only 800 ha (2022). The cultivated areas for triticale varied between 800 ha and 2,694 ha, while sorghum cultivation increased to 550 ha in 2023. The introduction of sorghum and triticale starting from 2020 reflects farmers' adaptation to arid conditions, as these crops are more drought resistant.

The average grain cereal yields in the period 2000-2023 were strongly influenced by climatic conditions, experiencing significant fluctuations. The lowest yields per hectare were recorded in 2003 and 2007, primarily due to high spring temperatures, which led to early drought onset. During May and June, tropical temperatures were reported, combined with very low precipitation levels.

Rye recorded a minimum yield of 958 kg/ha in 2003, while barley had a yield of 977 kg/ha in 2007, marking the lowest production levels for these crops during the analyzed period.

The increase in annual average temperatures and decrease in precipitation levels prompted the introduction and expansion of drought resistant crops, such as sorghum and triticale. These crops have demonstrated superior adaptability to thermal and hydric stress.

In 2018, the average maize yield reached a peak of 8,820 kg/ha, due to favorable climatic conditions, with moderate temperatures and adequate precipitation during the growing season. Maize yields fluctuated from a

minimum of 323 kg/ha in 2003 to a maximum of 8,820 kg/ha in 2018.

The overall trend indicates a slight decline in average yield ($R^2 = 0.41$, $p < 0.05$), correlated with rising temperatures. Wheat showed more stable yields, reaching a maximum of 4,738 kg/ha in 2021. The yield trend showed a positive correlation during periods of moderate precipitation ($R^2 = 0.63$, $p < 0.01$) (Figure 3).

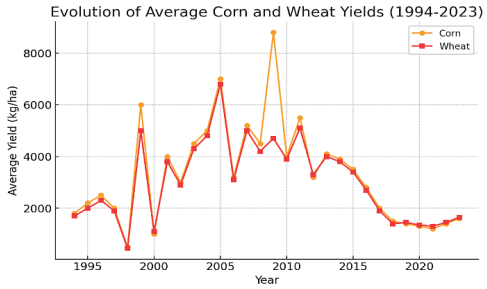


Figure 3. Evolution of average yield per hectare for corn and wheat crops between 1994-2023

The maximum wheat yield, of 4,738 kg/ha, was recorded in 2021, a year that also saw high yields for other crops: barley: 4,121 kg/ha, oats: 2,454 kg/ha, rye: 3,948 kg/ha, triticale: 3,925 kg/ha, and sorghum: 3,800 kg/ha (Table 3).

The agricultural yields in Tulcea County reflect the direct impact of climatic conditions on cereal crops. Drought years, characterized by high temperatures and insufficient precipitation, have significantly reduced yields, particularly for maize.

Adapting to climate change through the expansion of drought-resistant crops, the use of irrigation technologies, and the selection of high-performance varieties remains an essential strategy for ensuring the sustainability of agriculture in the region.

A strong negative correlation was found between annual average temperatures and average cereal production. This analysis suggests that annual average temperatures differently influence the production of corn and wheat, which is relevant for agricultural strategies and adaptation to climate change. Key observations: corn is negatively affected by temperature increases above 12°C, with a significant negative correlation ($\rho = -0.20$, $p < 0.01$). This can be explained by its high sensitivity to drought and heat stress, which can reduce yield. Wheat adapts better to rising temperatures, showing a moderate positive correlation ($\rho = 0.48$, $p < 0.05$). In the case of corn, there is a negative correlation ($\rho = -0,20$, $p < 0.05$), as can be seen in Figure 4, suggesting that very high temperatures have an adverse effect on corn production. This may indicate that, under moderate aridity conditions, wheat benefits from higher temperatures, either through a longer growing season or by optimizing physiological processes. Precipitation also plays a crucial role in cereal production. Reduced rainfall can exacerbate the negative impact of elevated temperatures on corn, making drought-resistant hybrids essential. For wheat, moderate water stress may still be manageable, but prolonged droughts could limit its yield potential despite its higher adaptability to temperature variations.

Future agricultural planning should consider both temperature and precipitation patterns to develop sustainable crop management techniques, such as improved irrigation systems, drought-resistant crop varieties, and optimized sowing periods.

Drought events during key growth stages, such as flowering and grain filling, significantly hinder production, as illustrated in Figure 5. This outcome is anticipated, as corn has high moisture demands, and inadequate precipitation during the growing season can cause severe water stress, ultimately reducing yields. Beyond the total rainfall amount, its distribution throughout the growing season is also crucial, as shown in Figure 6. The strong positive correlation between annual precipitation and corn yields ($\rho = 0.57$, $p < 0.01$) underscores the crop's reliance on adequate water availability, as illustrated in Figure 7.

The impact of high temperatures is particularly severe for corn, which is highly sensitive to thermal stress, especially in the absence of irrigation. Similarly, barley and winter barley followed a pattern akin to wheat, displaying a higher tolerance to adverse climatic conditions and demonstrating their adaptability to heat extremes (Figure 8).

For wheat, the correlation was lower ($\rho = 0.06$, $p < 0.05$) but still significant, indicating a lower sensitivity to water deficit compared to corn.

This suggests that wheat is more resilient to variations in precipitation, likely due to its growth cycle and ability to utilize soil moisture more efficiently. However, prolonged drought conditions or extreme weather events could still impact its yield, albeit to a lesser extent than corn. The number of heatwave days exhibited a strong and significant negative correlation with corn production ($\rho = -0.77$, $p < 0.01$) as can be seen in Figure 9, highlighting the crops vulnerability to extreme temperatures. In contrast, wheat showed a negative but statistically insignificant correlation ($\rho = -0.32$, $p > 0.05$), suggesting greater resilience to heat stress.

Table 3. Average yields of grain cereals recorded in the period 2000-2023 (kilograms per hectare)

Year	CROP						
	Wheat	Maize	Barley	Oats	Rye	Triticale	Sorghum
2000	1327	1645	959	611	1875	-	-
2001	1918	1547	1875	1843	1000	-	-
2002	2119	2512	2196	1210	1352	-	-
2003	487	323	587	723	958	-	-
2004	3086	5853	-	1896	1500	-	-
2005	2654	3748	1985	1348	537	-	-
2006	2605	2803	2085	1236	1436	-	-
2007	859	727	977	268	700	-	-
2008	3030	3087	1842	1329	4900	-	-
2009	1350	3247	2108	1019	1026	-	-
2010	2428	3549	2820	1210	1484	-	-
2011	3404	4057	3497	1708	2153	-	-
2012	1226	1319	1084	970	1102	-	-
2013	2987	4430	2893	1390	1761	-	-
2014	3658	4689	3552	1844	2209	-	-
2015	3719	3067	3378	1666	3112	3435	-
2016	4065	3232	3617	2001	2410	3625	-
2017	4706	6345	4231	2130	2904	3270	-
2018	4588	8820	3975	2163	5365	2734	-
2019	4090	3573	3409	2074	3041	1559	-
2020	1581	1296	1585	1009	2202	791	340
2021	4738	4120	4121	2454	3948	3925	3800
2022	3213	2782	3076	2230	1358	2323	1200
2023	2988	2083	2680	1528	2409	1445	1100

Source: National Institute of Statistics, Romania. County Directorate for Agriculture – Tulcea (2023). *Statistical Data (1994–2023).*

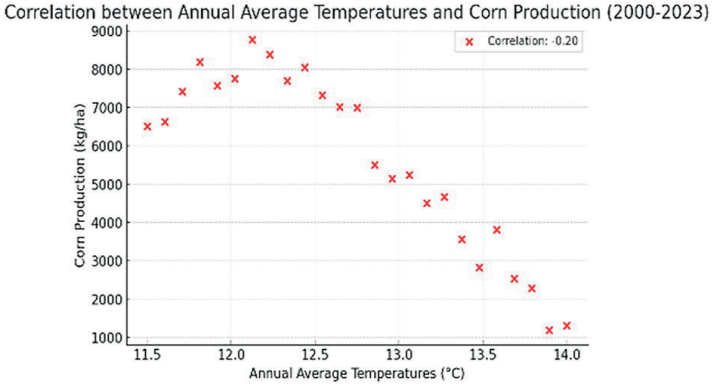


Figure 4. Correlation between annual average temperatures and corn yields from 2000 to 2023

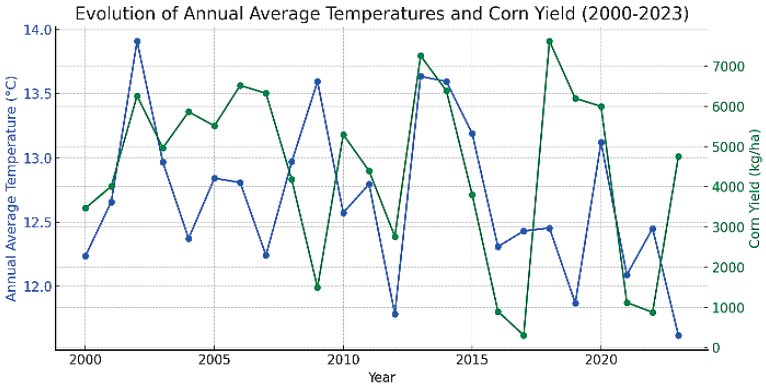


Figure 5. Evolution of annual average temperatures and corn yield from 2000 to 2023

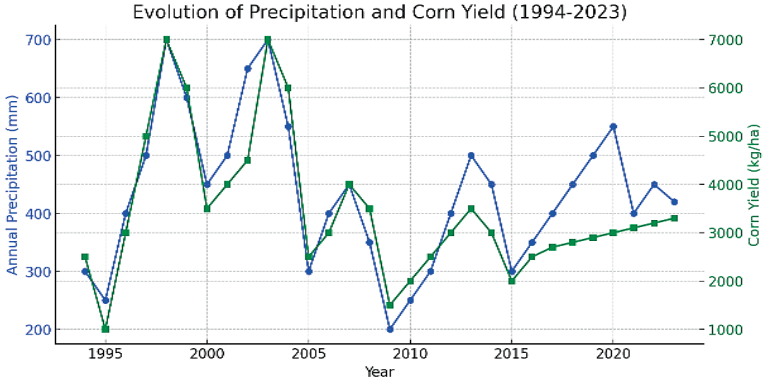


Figure 6. Evolution of average annual precipitation and corn production between 1994-2023

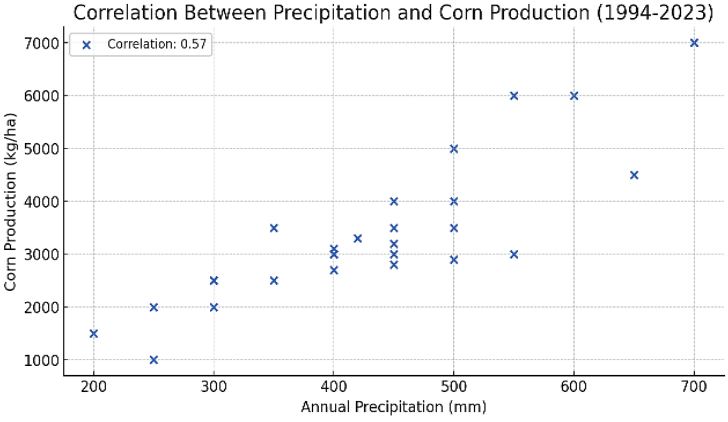


Figure 7. Correlation between average annual precipitation and corn production between 1994-2023

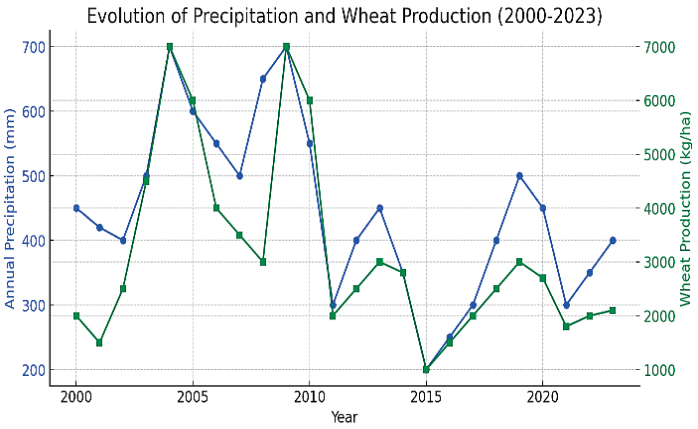


Figure 8. Evolution of average annual precipitation and wheat production Between 2000-2023

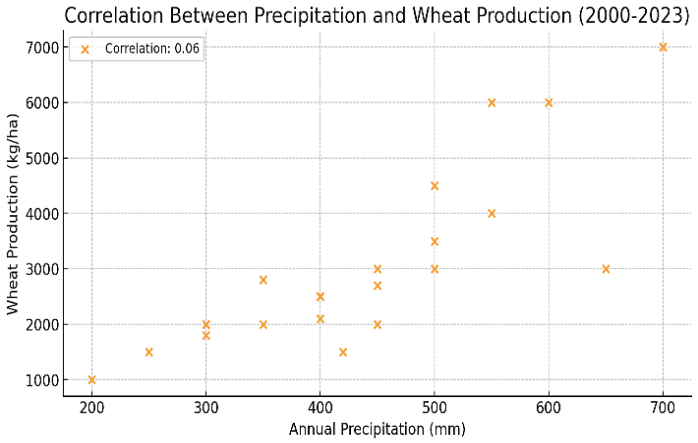


Figure 9. Corelation between average annual precipitation and wheat production between 2000-2023

CONCLUSIONS

The analysis of climate and agricultural data from 1994 to 2023 highlights a significant increase in average annual temperatures and a decline in precipitation, confirming global climate change trends. Average annual temperatures rose from approximately 10.49°C in the 1990s to 13.8°C in 2023**,** leading to intensified drought conditions and heat stress for crops. Annual precipitation dropped below the multiannual average of 488.79 mm, with considerable fluctuations from year to year. This uneven distribution of precipitation has negatively impacted crop development, particularly corn**,** which is highly sensitive to water deficits.

The area cultivated with grain cereals has been significantly influenced by climate conditions. In drought years with high temperatures, cultivated areas declined considerably**,** reaching a minimum of 118,948 ha in 2007. Due to its greater drought resistance, wheat occupied larger areas than corn during years with challenging climate conditions.

Agricultural yields reflect a partial adaptation to climate conditions, with significant fluctuations in productivity. Favorable years, such as 2018**,** allowed for maximum production levels (corn: 8,820 kg/ha, wheat: 4,738 kg/ha). In contrast, years with high temperatures and insufficient rainfall, such as 2003 and 2007, resulted in the lowest yields**,** emphasizing the vulnerability of crops to climate change.

The introduction of sorghum and triticale**,** crops more resistant to heat and water stress, represents a positive adaptation to the new climate conditions. However, their expansion remains limited, requiring greater promotion and support.

The findings suggest a complex relationship between climate variables and agricultural performance. Rising temperatures and decreasing precipitation pose major challenges for agriculture, leading to reduced productivity and changes in crop structure. Recent adaptations, such as the expansion of drought-resistant crops (sorghum, triticale), are essential strategies to ensure the sustainability of agriculture in Tulcea County.

The study highlights the necessity of implementing agricultural policies focused on expanding irrigation systems and modernizing existing infrastructure to mitigate water shortages during drought periods.

Key recommendations involve promoting efficient irrigation technologies, such as drip irrigation, to enhance water efficiency and strengthen agricultural resilience. Investing in research to develop wheat, corn, and other cereal varieties with increased tolerance to climatic stress.

Encouraging farmers to adopt alternative crops, such as sorghum and triticale, to reduce risks associated with extreme weather conditions.

Reducing dependence on monocultures by introducing a diversified range of crops, capable of buffering the impact of climate variability.

Organizing training programs for farmers on sustainable agricultural practices, efficient resource management, and adaptation to changing climate conditions.

Integrating climate adaptation strategies into national and regional agricultural development policies to ensure long-term resilience.

These conclusions and recommendations emphasize the importance of climate adaptation in securing the sustainability of agricultural production in Tulcea County. By implementing these measures, the vulnerability of local agriculture can be reduced, fostering the conditions for sustainable agricultural development.

REFERENCES

Ciocan (Nuncă), E., Dobre, Ș.C., Marin D.I. (2024). Research on wheat seed germination as a function of temperature, under the influence of treatment with biostimulators and at different levels of fertilization. *Scientific Papers. Series A. Agronomy, Vol. LXVII, No. 2*, (Accessed on 09.01.2025).

Dușa, E. M. & Stan V. (2022). Effects of climatic conditions, organic amendments and plant cultivation system on soil water content. *Scientific Papers. Series A. Agronomy, Vol. LXV, No. 2* (Accessed on 11.01.2025).

Filipescu, I. (1928). *Fifty Years of Romanian Life (1878–1928).* National Culture Printing, Bucharest. *pp. 230.*

Hasotti, P. (1997). *The Neolithic Era in Dobrogea.* Ex Ponto Publishing House, Constanța*. pp. 164.*

Horoiaș, R., Berca, M., Cristea, S. (2013). Researches on the main field crops yields variation in the burnas plain between the dry years 2000 and 2012*. Scientific Papers. Series A. Agonomy., Vol. LVI*, ISSN 2285-5785, 270-275. (Accessed on 13.010.2025).

IPCC-Intergovernmental Panel on Climate Change (2021). *Climate Change 2021: Impacts, Adaptation, and Vulnerability.* Special Report, Geneva. Retrieved from https://www.ipcc.ch/ (Accessed on 10.12.2024).

Lal, R., Reicosky, D.C., & Hansen, D.O. (2007). Soil carbon sequestration for climate change mitigation and food security. *Journal of Environmental Quality, 36*(6), 1420-1432. DOI: 10.2134/jeq2007.0123

Lup, A. (2003). *Agricultural Dobrogea, from legend to globalization (Dobrogea agricolă, de la legendă la globalizare).* Ex Ponto Publishing House, Constanța*. pp.928.*

Lup, A. (2012). *40 Years of Socialist Agriculture in Dobrogea (1949–1989) (40 de ani de agricultură socialistă în. România).* Ex Ponto Publishing House, Constanța. pp.460.

Rosenzweig, C., Iglesias, A., Yang, X. B., Epstein, P. R., & Chivian, E. (2001). Climate Change and Extreme Weather Events: Implications for Food Production, Plant Diseases, and Pests. *Nasa Publications, 24.* Retrieved from pubs.giss.nasa.gov (Accessed on 22.12.2024)

***INS - National Institute of Statistics, Bucharest. *Romanian Statistical Yearbooks 1960–1990,* (1990). Retrieved from insse.ro (Accessed on 22.11.2024).

***INS - National Institute of Statistics, Romania. County Directorate for Agriculture – Tulcea (2023a). *Statistical Data (1994–2023).* Retrieved from insse.ro (Accessed on 27.12.2024).

***INS - National Institute of Statistics, Romania. County Directorate of Statistics – Tulcea (2023b). *Climate and Agricultural Reports (1994–2023).* Retrieved from insse.ro. (Accessed on 14.01.2025).

***National Agency for Land Improvement – Territorial Branch for Land Improvement – Tulcea. *Annual Report (various editions).* Retrieved from www.anif.ro (Accessed on 20.11.2024)

.

Scientific Papers. Series E. Land Reclamation, Earth Observation & Surveying, Environmental Engineering. Vol. XIV, 2025
Print ISSN 2285-6064, CD-ROM ISSN 2285-6072, Online ISSN 2393-5138, ISSN-L 2285-6064

STUDIES AND MEASUREMENTS FOR THE IDENTIFICATION OF NOISE AND VIBRATION LEVELS IN A SITE IN BUCHAREST - CASE STUDY

Marta Cristina ZAHARIA[1, 2], Daniela DOBRE[1, 3], Claudiu-Sorin DRAGOMIR[1, 2]

[1]National Institute for Research and Development in Construction, Urban Planning and Sustainable Spatial Development – URBAN-INCERC, 266 Pantelimon Road, District 2, 021652, Bucharest, Romania
[2]University of Agronomic Sciences and Veterinary Medicine of Bucharest, 59 Mărăşti Blvd, District 1, 011464, Bucharest, Romania
[3]Technical University of Civil Engineering of Bucharest, 122-124 Lacul Tei Blvd, District 2, 020396, Bucharest, Romania

Corresponding author email: marta_cristina_zaharia@yahoo.co.uk

Abstract

Specific studies and research are necessary to find out the existing noise and vibrations coming from various zonal sources, in an urban area where a new building will be placed. Depending on the activity that will be carried out in the new building, it is necessary to obtain certain maximum values of the noise and vibration levels, inside the building, so that the psychoacoustic comfort of the inhabitants can be achieved during the period of use of the building. As part of a research contract, carried out by INCD URBAN INCERC, INCERC Bucharest Branch, for a client who wanted to build a new residential building for his family, on-site experiments were carried out at the client`s land located in Bucharest. The results of the acoustic measurements, the values of the noise levels, are presented in the article numerical and in graphic forms in the frequency range 12.5...20000 Hz. For vibrations the recordings are presented in the form of time-histories for accelerations and velocities, as well as Fourier spectra and response spectra.

Key words*: acoustics, vibrations, civil buildings, urban polluting sources.*

INTRODUCTION

The placement of a new building in an urban area requires specific studies and investigations to assess the existing levels of noise and vibrations at the site, originating from various local pollution sources (Zaharia, 2020). Depending on the intended use of the building, certain maximum permissible levels of noise and vibration must be established to ensure the psychoacoustic comfort of occupants throughout the building's operational lifespan (C125:2013).

The assessment of noise and vibration levels generated by metro networks at surface locations (or at specific elevations above ground) is a relevant issue in urban environments, where the propagation and potential attenuation or amplification of such disturbances may influence both the structural integrity of buildings and the acoustic comfort of their occupants (Mouzakis et al., 2019; Bratu et al., 2023; 2024).

To assess this impact, acoustic and vibration measurements were conducted during a preliminary phase of a real estate development project involving the construction of a G+2F residential building without a basement, situated within the metro's minimum safety zone.

The research aimed to determine the noise levels generated by two categories of noise and vibration sources:

1) surface-level sources, including street traffic and human activity;
2) underground sources, specifically metro traffic, with the tunnel running beneath the measurement site.

The location of the land on which the measurements were conducted is shown in Figure 1. At the time of the measurements, the site was devoid of any constructions. The surrounding urban area predominantly comprises civil buildings, including both residential and office structures. Directly opposite the site, across the street, there is a building designated as a kindergarten.

Consequently, during the acoustic measurements, the sources of ambient noise included street-level human activities; road traffic from both nearby and more distant streets; air traffic, with noise levels enhanced by reflection from the cloud cover; bird songs from the trees adjacent to the site; and activities from a construction site located within the area, at an approximate distance of 50-70 m from the measurement location.



Figure 1. Land positioning in the urban area and positioning of measurement points P1 and P2

The acoustic measurements were conducted simultaneously at two distinct points, positioned as illustrated in Figures 2a and 2b, as follows:

a) the first measurement point, P1, to determine the noise level coming from underground noise sources – the metro, was placed in a pit with approximate dimensions of: length L=1.60 m, width l=1.10 m and depth H=1.35 m, at a height of 0.15 m from the bottom of the pit (microphone 1 placed at Measurement Point 1); this positioning of the microphone was done in order to simulate the position of the microphone at the base of the foundation of the future building and to be able to select the noise produced by the metro traffic at this level as relevant as possible.

b) the second measurement point, P2, to determine the noise level from surface noise sources, was located above ground level, at a height of h=1.30 m, (microphone 2 located at P2); this positioning of the microphone was done in order to simulate the microphone position two meters from the main facade of the future building and to be able to select the most relevant noise produced by surface sources at this level.

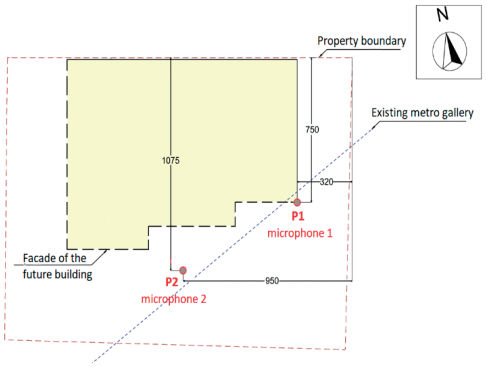


Figure 2a. Positioning of the measurement points, P1 and P2, on the site located in District 1 - Bucharest



Figure 2b. Positioning of the measurement point P1

To determine vibration levels, non-seismic sequential measurements were performed using four GMSPlus multichannel stations (GeoSIG), each comprising three data channels and internal triaxial transducers (model AC73i).

Vibration monitoring was carried out in distinct stages and at various locations, both during daytime and nighttime, under a range of conditions - from low-background noise environments to periods of active metro traffic - with time intervals of 10, 5, and 3 minutes between successive train passings. Stations ST02, ST03, and ST04 were installed at ground level, whereas station ST01M was positioned within an excavated pit at a depth of 1.35 m, as shown in Figure 3.

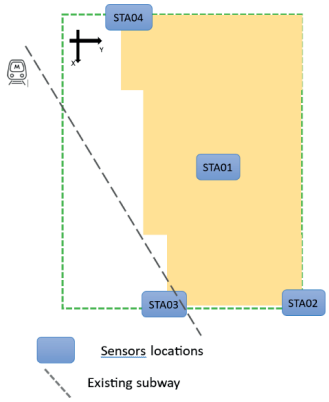


Figure 3. Location of GMSPlus digital stations/accelerometers (longitudinal direction - OY axis; transverse direction - OX axis)

MATERIALS AND METHODS

The in-situ acoustic measurement method used was provided for in the laboratory's acoustic procedure and in the legislation in force at the time the measurements were made, namely PTE– AC/03.02 and the measurement standards SR 6161-3:1982, SR 6161-1:2008, SR 6161-1/C91:2009 correlated with SR ISO 1996-2:2018 and with STAS 6156-86.

The following parameters were determined:

- L_{Aeq} - equivalent noise level (weighted average of noise levels recorded in a given time interval), recorded at the measurement point, in dB(A);
- L_{AF90} - background noise level, (exceeded in 90% of the measurement time), in dB(A);
- L_{AF10} - peak noise level, (exceeded in 10% of the measurement time), in dB(A).

"L_{Aeq}" corresponds to the notation "L_{ech}" in SR 6161-1:2008 and to the notation "L_{eqT}" in SR ISO 1996-2:2018; "L_{AF90}" and "L_{AF10}" correspond to the notation "$L_{N,T}$" in SR ISO 1996-2:2018.

The measurement situations were established in agreement with the future owner of the house and were determined in a such way as to be useful for the acoustic design of the future residential building.

For the noise measurements, two measurement points were established, to carry out effective acoustic measurements that could determine both the noise level coming from surface noise sources and the noise level coming from underground noise sources, namely the metro.

The determination of the equivalent noise level was carried out simultaneously at the two measurement points, P1 and P2.

The first measurement point, P1, was located on the ground in the area where the future building would be located with the facade and the corner of the building that could be most affected by the noise produced by the metro; In P1, the microphone was placed in a pit, with approximate dimensions of: length L=1.50 m, width l=1.50 m and depth H=1.35 m, at a height of 0.15 m from the bottom of the pit (microphone 1 placed at Measurement Point 1), arranged according to Figure 1, Figure 2a, Figure 2b and Figure 4. This positioning of the microphone was done to simulate the position of the microphone at the base of the foundation of the future building and to be able to detect the noise produced by the metro traffic at this level as relevant as possible.



Figure 4a. Positioning of measurement points P1 and P2

The second measurement point, P2, was placed on the ground above ground level, at a height of h=1.30 m, (microphone 2 placed at Measurement Point 2), arranged according to Figures 4a and 4b; this positioning of the microphone was done to simulate the microphone position two meters from the main facade of the future building and to be able to select the noise produced by surface sources at this level as relevant as possible.

The *in situ* acoustic measurements, implicitly the recordings of the equivalent noise level "L_{Aeq}", in dB(A), were carried out at night and during the day, on one day in April 2019, as follows: starting with the night time period (23:00-07:00) in the time interval 04:51-07:00, continuing in the day time period (07:00- 23:00)

in the time interval 07:00-08:35, according to the technical regulations in force at that date, respectively: STAS 6161-3:1982 "Acoustics in constructions. Measurement of noise levels in urban localities. Measurement methods", SR 6161-1:2008 "Acoustics in constructions. Measurement of noise levels in civil constructions. Measurement methods", SR 6161-1/C91:2009) and SR ISO 1996-2:2018 "Acoustics. Description, measurement and evaluation of ambient noise. Part 2: Determination of ambient noise levels", correlated with STAS 6156-86 "Acoustics in buildings. Protection against noise in civil and socio-cultural buildings. Admissible limits and acoustic insulation parameters".



Figure 4b. Positioning of measurement point P2

Considering the above, the sampling of the measurement intervals was done by choosing time periods of max. approx. 20, 15, 10, 5 and 1 minutes, depending on the measurement situation. It is mentioned that the measurement time intervals, specific for P1 and those for P2, do not overlap 100%, due to the slightly different stop-start times of the two sound level meters used for the recordings.

The following devices were used to measure and record the equivalent noise level:

- Sound calibrator Bruel & Kjaer type 4231 - 94 dB (+/- 0.2 dB), series 2671272;
- Real-time noise level analyzer, (Sound level meter), Bruel & Kjaer type 2250, series: 2559226;
- Real-time noise level analyzer, (Sound level meter), Bruel & Kjaer type 2250, series: 3010381;
- Thermo hygro barometer TESTO 622, series 39515263.

During the recording of noise levels, the outdoor temperature was between 9.9 and 10.3°C and the humidity between 83 and 87%. In this regard, it is mentioned that the day of the measurements was a cloudy day, with a compact cloud ceiling and with temporary light drizzle conditions.

During the acoustic measurements and recordings, a plywood was installed over the space in the pit where the measurement point P1 was positioned, as shown in Figure 5 and Figure 6, to create an *acoustic shadow* against the noise coming from surface sources.



Figure 5. Position of a plywood which was installed over the space measurement point P1, in day time



Figure 6. Position of a plywood which was installed over the space measurement point P1, in night time

For the microphone location at measurement point P2, mounted on a tripod, the microphone height from the ground was 1.30 m, as shown in Figure 7a and Figure 7b The microphone was protected with a windscreen.



Figure 7a. Position of microphone in measurement point P2, in night time



Figure 7b. Position of microphone in measurement point P2, in night time

On the other hand, the methodology for data acquisition and processing involves the following steps (Dragomir et al., 2019):

- Establish the locations of the seismic stations based on the objectives;
- Develop layout schemes for the sensors;
- Effectively position the seismic stations according to the pre-established schemes;
- Connect the stations to the equipment and laptop;
- Start the multichannel recording stations and the laptop, and launch the communication application with the equipment;
- Conduct recordings, verification, and calibration tests following the procedures specified by the equipment supplier;
- Trigger recordings to capture ambient vibrations, ensuring that at least five sets of recordings (two minutes each) are made at the same location;
- Verify each recording upon completion using the available monitoring tools;
- Process the data to generate graphical representations of the time histories of accelerations, velocities, and displacements;
- For each time history, specify the maximum amplitude obtained in that recording.

This structured approach will ensure accurate data collection and processing for seismic analysis (Dragomir et al., 2021; Dobre et al., 2015).

Regarding the values of the maximum regulated noise limits (valid in 2019 year), correlated with the residential function of the rooms in the future residential building, for specific periods (daytime and nighttime), for this studied case, the principal admissible limits are presented according to the regulations in force, respectively from C125 - 2013 "Normative regarding Acoustics in Constructions and Urban Areas" as follows:

1) "In cases where the background noise (in the absence of external noise sources) is less than 30 dB(A), the equivalent indoor noise level due to all noise sources external to the functional unit must not exceed the background noise level by more than 5 units".
2) Parameter 2: Noise level outside residential buildings, located in quiet residential areas in an agglomeration with a population of more than 100,000 inhabitants, measured at 2.00 m from the building facade (according to SR 6161-1 and SR 6161-1/C91):

$$L_{ech} = 50 \text{ dB(A)}$$

3) Parameter 4: The noise level outside residential buildings, measured at 2.00 m from the building facade (according to SR 6161-1 and SR 6161-1/C91), in the case of buildings located in areas where the background noise level, L_{AF90}, is less than 50 dB(A), will be chosen as the minimum value between the value of 50dB(A) and L_{ech} calculated with the relationship below:

$$L_{ech} = L_{AF90} + 5 \text{ dB(A)}$$

4) Parameter 5: In the case of the design of new buildings, the noise level outside residential buildings, measured at 2.00 m from the building facade (according to SR 6161-1 and SR 6161-1/C91):

$$L_{ech} = 50 \text{ dB(A)}$$

5) For Apartments in Residential Buildings, the permissible limit of the equivalent indoor noise level is 35 dB(A) (Cz 30).

According to the provisions of the standard SR 10009:2017 "Acoustics. Admissible limits of the ambient noise level", the admissible limit of the external noise level at the facade of the

residential building that is most exposed to the sound action of a noise source external to the building, respectively the equivalent continuous A-weighted acoustic pressure level, L_{AeqT}, is 50dB(A), for any type of residential building or similar to it, considering that the most exposed facade of the building is understood as that facade of the building that is closest to an external noise source.

"If the value of the background noise level L_{AF90T} is less than 45 dB, then the admissible limit is calculated with the relationship:

$$L_{AeqT}\ [dB] = L_{AF90T} + 5\ dB".$$

In addition, there is another Romanian legal act applicable to the residential buildings (Order of the Ministry of Health, no. 119 of February 4, 2014, for the approval of the Hygiene and Public Health Norms regarding the population's living environment, published in the Official Gazette of Romania, no. 127 of February 21, 2014, which states the following:

- "For the purposes of these norms, the following terms are defined as follows: a) living room: rooms with living room and bedroom functions".
- "The sizing of sanitary protection zones will be done in a such way that in the protected territories the limit values of the noise indicators will be ensured and respected, as follows: a) during the day, the A-weighted equivalent continuous acoustic pressure level (L_{AeqT}), measured outside the dwelling according to the SR ISO 1996/2-2018 standard, at 1.5 m height from the ground, shall not exceed 55 dB and the noise curve Cz 50; b) during the night, between hours 23:00 and 7:00, the equivalent continuous A-weighted sound pressure level (L_{AeqT}), measured outside the dwelling according to the SR ISO 1996/2-2018 standard, at 1.5 m above the ground, shall not exceed 45 dB and, respectively, the noise curve Cz 40".
- "For dwellings, the equivalent continuous A-weighted sound pressure level (L_{AeqT}), measured during the day, inside the room with the windows closed, shall not exceed 35 dB(A) and, respectively, the noise curve Cz 30. During the night (hours 23:00- 7:00), the L_{AeqT} noise level shall not exceed 30 dB and, respectively, the Cz curve 25".

One important criterion for evaluating the impact of vibrations on buildings is the velocity criterion (Dragomir et al., 2023; Bratu et al., 2024). Velocity is significant in this assessment because it provides a reliable indication across different vibration frequencies, and there is a strong statistical correlation with data related to structural degradation (Rybak, 2016). The allowable vibration levels are detailed in Table 1, according to DIN 4150-3/1999 regarding vibrations in buildings, and in Table 2, according to the norm on acoustics in buildings and urban areas (C 125/4-2013).

Table 1. Permissible vibration level (DIN 4150-3/1999)

Structure type	Frequency at foundation level			Combined frequency (at ground floor/upper floor level)
	<10 Hz	10...50 Hz	50...100 Hz	
Commercial, industrial buildings	20 mm/s	20...40 mm/s	40...50 mm/s	40 mm/s
Residential buildings	5 mm/s	5...15 mm/s	15...20 mm/s	15 mm/s
Buildings other than those in 1 and 2	3 mm/s	3...8 mm/s	8...10 mm/s	8 mm/s

Table 2. Permissible vibration level, Parameter 9 (C 125/4-2013)

Historical monuments		Any building (except monuments)
1-50 Hz	50-90 Hz	1-100 Hz
<8mm/s	8-12 mm/s	<12-20mm/s

RESULTS AND DISCUSSIONS

The results of the acoustic measurements, the values of the noise levels, are presented in numerical and in graphic forms in the frequency range 12.5...20000 Hz, and for vibrations the recordings are presented in the form of time-histories for accelerations and velocities, as well as Fourier spectra and response spectra.

This chapter presents the results of the acoustic measurements carried out, for each of the specific measurement situations considered, in number of 19, each corresponding to one of the two sound level meters, (Project 1, …. Project 10, for measurement point 1, P1, and Project 1, …. Project 9, for measurement point 2, P2), with the recorded values.

The results of the acoustic measurements were studied, considering the specificity of human acoustic perception, namely the spectrally recorded noise levels weighted in frequency with A-weighting specific to human hearing perception, L_{Aeq}, expressed in decibels (dB(A)),

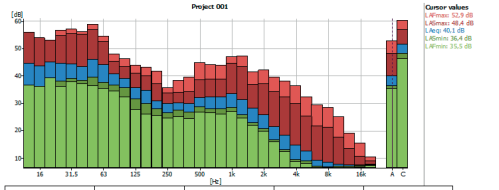
specified in the legislation and technical regulations in force, as well as time-weighted noise levels.

Acoustic recordings were made for the central frequencies of the 1/3 octave band, respectively the nominal frequency range: 6.3 Hz, 8.0 Hz, 10 Hz, 12.5 Hz, 16 Hz, 20 Hz, 25 Hz, 31.5 Hz, 40 Hz, 50 Hz, 63 Hz, 80 Hz, 100 Hz, 125 Hz, 160 Hz, 200 Hz, 250 Hz, 315 Hz, 400 Hz, 500 Hz, 630 Hz, 800 Hz, 1000 Hz, 1250 Hz, 1600 Hz, 2000 Hz, 2500 Hz, 3150 Hz, 4000 Hz, 5000 Hz, 6300 Hz, 8000 Hz, 1000 Hz, 125 Hz, 16000 Hz, 20000 Hz.

Determining the number of metros that circulated during the hourly intervals of acoustic measurement and recording, for the specific number of metros on the two underground metro lines (round trip), the hourly intervals were correlated with the determination of the vibration level coming from the metro, received at the study site, were used.

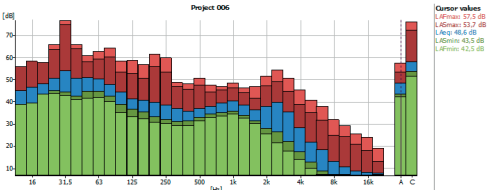
Next, also for acoustic analysis reasons, considering *human psychoacoustic perception*, correlated with the human audibility range and time weighting, the time-weighted noise levels F and S, $L_{xy}(t)$, where x is A for A weighting, and y is F for Fast weighting, L_{AFmax} , L_{AFmin} , or S for Slow weighting, L_{ASmax} , L_{ASmin}, which take into account the exponential time constants and averaging times, expressed in seconds or milliseconds, corresponding to the equipment (sound level meters) used to perform acoustic measurements. The time-weighted acoustic level is a continuous function of time and is expressed in decibels (dB). For these reasons, in Figure 8 … Figure 15, which presents a part of the results of the acoustic measurements carried out, both the recorded values for the equivalent noise level, L_{ech} , in dB(A) are given, in order to be able to compare them with the values of the admissible limits specified in the technical regulations in force, and, additionally, the values of the other types of time-weighted levels, respectively L_{AFmax} , L_{AFmin} , and L_{ASmax} , L_{ASmin}. It can be estimated that L_{ASmin} is approx. equivalent to the minimum noise level, L_{AF95}, and L_{ASmax} is approx. equivalent to the peak noise level, L_{AF05}; also, L_{AFmin} is approx. equivalent to the minimum peak noise level, L_{AF99}, and L_{AFmax} is approx. equivalent to the maximum peak noise level, L_{AF01}. The noise levels recorded at measurement point P1, were between minimum L_{Aeq} = 30.3 dB(A) (in Project 1, in the early morning, hours 04:55) when the metro train was not running, and maximum L_{Aeq} = 41.9 dB(A) (in Project 10, in the morning, hours 08:35) when the metro train is running and also with specific street noise. The noise levels recorded at measurement point P2, were between minimum L_{Aeq} = 40.1 dB(A) (in Project 1, in the early morning, hours 04:55) when the metro train was not running, and maximum L_{Aeq} = 52.0 dB(A) (in Project 09, in the morning, hours 08:35) when the metro train is running and also from specific street noise. The noise levels recorded at measurement point P2, related to some of the 9 projects in the sound level meter whose microphone was placed in P2, are exemplary presented graphically, with the corresponding values tabulated, according to the sound level meter data, in Figures 8-10.

Additionally, analyses of each type of recorded noise levels were also performed (L_{Aeq}, L_{AF90}, L_{AF10}, L_{AFmax}, L_{AFmin}, and L_{ASmax}, L_{Asmin}) and represented on the same graph, for the same type of noise level, of its values recorded in the two measurement points, P1 and P2, for all 19 projects in the two sound level meters, (Project 1, … Project 10, for measurement point 1, P1, and Project 1, … Project 9, for measurement point 2, P2). These graphs are presented below, in Figure 11 to Figure 15.



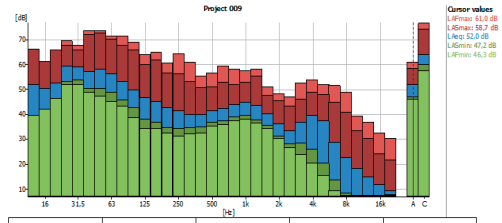
LAF_{max} (dB)	LAS_{max} (dB)	**LA_{eq} (dB)**	LAS_{min} (dB)	LAF_{min} (dB)
52.9	48.4	**40.1**	36.4	35.5

Figure 8. Graphic and values of Project 1



LAF_{max} (dB)	LAS_{max} (dB)	**LA_{eq} (dB)**	LAS_{min} (dB)	LAF_{min} (dB)
57.5	53.7	**48.6**	43.5	42.5

Figure 9. Graphic and values of Project 6



LAF_{max} (dB)	LAS_{max} (dB)	**LA_{eq} (dB)**	LAS_{min} (dB)	LAF_{min} (dB)
61.0	58.7	**52.0**	47.2	46.3

Figure 10. Graphic and values of Project 9

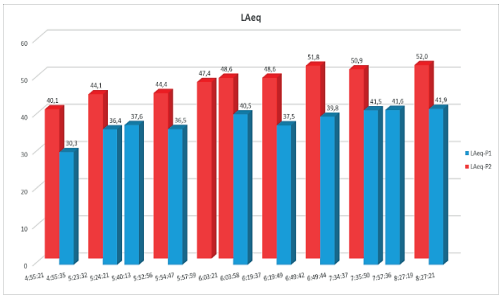


Figure 11. Values of L_{Aeq} in measurement point P1 and measurement point P2

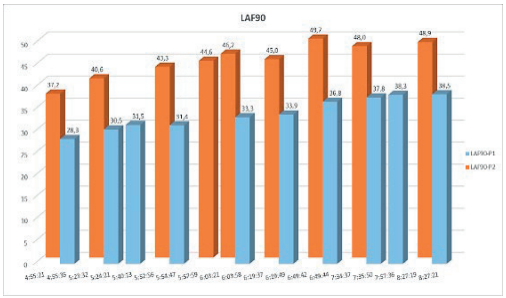


Figure 12. Values of L_{AF90} in measurement point P1 and measurement point P2

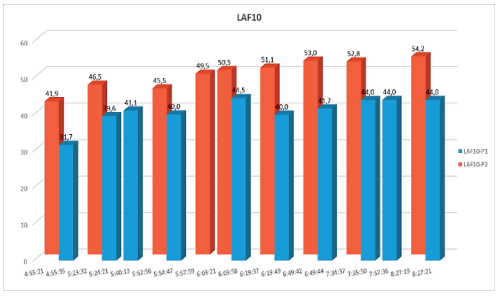


Figure 13. Values of L_{AF10} in measurement point P1 and measurement point P2

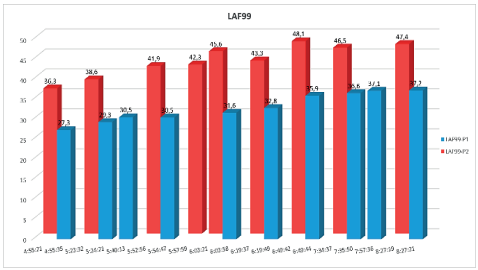


Figure 14. Values of L_{AF99} (L_{AFmin}) in measurement point P1 and measurement point P2

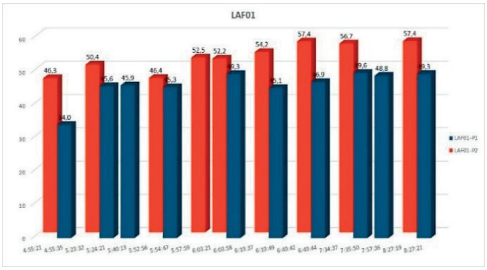


Figure 15. Values of L_{AF01} (L_{AFmax}) in measurement point P1 and measurement point P2

From the analysis and comparison of the results obtained from the acoustic research and measurements carried out, corroborated with the values of the maximum noise limits regulated by the legislation in force and correlated with the living function of the rooms in the future residential building that is intended to be built, the following observations emerge:

a) Regarding the measurements carried out at measurement point P1, for underground noise sources, mainly coming from metro traffic and with somewhat significant influences also from the noise produced simultaneously aboveground (depending on the type of surface noise sources, coming from human street activities, road traffic, air traffic noise - an airplane, birdsong, etc.), the noise level produced by metro traffic will not influence the noise level inside the rooms of the future residential building that is intended to be built on the studied site; a judicious acoustic design, combined with vibration protection of all construction elements of the future residential building, will be able to meet the requirements regarding the maximum admissible noise levels inside the rooms of this building. It is mentioned that certain peak noise levels recorded were due to isolated actions (in the context of the entire

reference period, for which the admissible level is established), for example: birds chirping, sirens in street traffic, slamming car doors, noise from the construction site, etc.

b) Regarding the measurements carried out at measurement point P2 for the surface noise sources, coming from human street activities, street road traffic, air traffic noise (an airplane), birdsong, etc., the analysis of these values shows that the noise level outside residential buildings, $L_{ech} = L_{AF90} + 5$ dB(A), measured at 2.00 m from the building facade, will be able to be met according to the recommendations of the legislation in force, for the future residential building that is intended to be built on the studied site. It is mentioned that the noise produced by the metro will not significantly influence the noise level outside the future residential building, measured at 2.00 m from its facade. Also, through a judicious acoustic design of the closing construction elements and the facades of the future residential building, the requirements regarding the maximum permissible noise level inside the rooms of this building will be met. All noise levels presented in the previous chapters, levels existing in the technical regulations and legislation in force, will have to be met through a judicious acoustic design of the future residential building G+2F, without basement, which is intended to be located on the studied land in District 1 - Bucharest.

Regarding the part of the study dedicated to vibrations, the measurements made in the 20 files recorded in the two stages - quiet and metro/zonal traffic - led to time domains of accelerations, velocities and displacements, with response spectra in the range 0.016 - 100 Hz. By analysing the results obtained, it will be ascertained whether the vibration level falls within the admissible limits recommended by the technical regulations in force.

During the quiet phase, the highest velocity was noted in the z direction at STO1M (from the response spectrum), while the maximum values in the x and y directions were recorded at ST03 and ST02, respectively. In the metro/zonal traffic (noise) phase, the situation is presented comparatively in Figure 16.

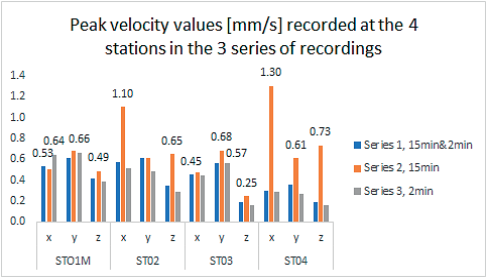


Figure 16. Variation of velocities in recordings

The analysis of the velocity time histories and the Fourier spectra revealed the following findings:

- the maximum velocity recorded in the excavated pit was 0.67 mm/s, while at the ground surface, in the center of the area, the recorded velocity was 1.27 mm/s;
- the Fourier spectra identified ranges for amplifications at 10 Hz, 30 Hz, and between 40 and 90 Hz.

The vibration propagation mode is highlighted. There is a trendline indicating a correlation between the maximum velocities recorded by the STO1M and STO3 sensors. The STO1M sensor measures velocities from a depth point, while the STO3 sensor measures them from a surface point. This trendline has a correlation coefficient of 0.84 (Figure 17).

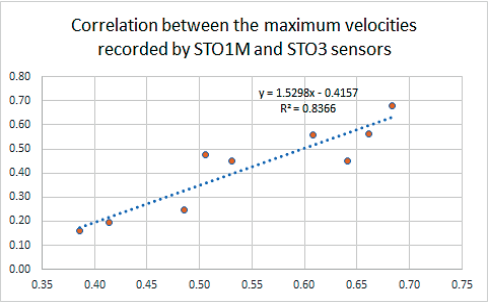


Figure 17. Propagation of vibrations between two points (STO1M and STO3 sensors)

Additionally, there is a trendline for the maximum velocities recorded by STO2 and STO4, both of which are situated at surface points along a diagonal of the study area. This trendline has a correlation coefficient of 0.88.

CONCLUSIONS

An acoustic characterization, as efficient as possible, of the studied area, namely the identification of the noise and vibration level in the study site in Bucharest, was achieved by performing acoustic measurements of the noise level coming from both surface noise sources and underground noise sources, namely the metro. The measurement situations were determined in a such way as to be useful for the design of a future residential building. The results of acoustic measurements show that the noise level produced by metro traffic will not influence the noise level inside the rooms of the future residential building that is intended to be built on the studied site in Sector 1 – Bucharest, because a judicious acoustic design, combined with vibration protection, of all construction elements of the future residential building, will be able to meet the requirements regarding the maximum admissible noise levels inside the rooms of the future building.

Although the recorded velocity values do not exceed the permissible limits (they are below 3 mm/sec), special attention is required in the design to avoid possible overlaps of vibration frequencies (from the soil-structure interaction).

ACKNOWLEDGMENTS

This research work was done within the "Nucleu" Programme in PNCDI 2022-2027, with the support of MCDI, Project PN 23 35 and Contract no. 10804 / 06.02.2019.

REFERENCES

Bratu, P., Dobrescu, C.F., Nitu, & M.C. (2023). Dynamic response control of linear viscoelastic materials as resonant composite rheological models. *Romanian Journal of Acoustics and Vibration*, *20*(1), 73–77.

Bratu, P., Murzea, P., Tonciu, O., Dragan, N., & Dobrescu, C.F. (2024). Evaluation of the dynamic parameters under seismic conditions for a Maxwell rheological base isolation system. *Buildings, 14*(12), 4075. https://doi.org/10.3390/buildings14124075.

Dobre, D., Dragomir, C.-S., Georgescu, E.-S. (2015). Pounding effects during an earthquake, with and without consideration of soil-structure interaction. *Constructii*, *16*(1), ID2015160106_Dobre.pdf.

Dragomir, C.S., & Dobre, D. (2019). Processing data from vibration recordings. *IOP Conf. Ser.: Mater. Sci. Eng.*, *471*, 052089. Doi 10.1088/1757-899X/471/5/052089.

Dragomir, C.S., & Dobre, D. (2021). From seismic instrumentation towards disaster prevention and mitigation. *IOP Conf. Ser.: Mater. Sci. Eng*., *1203*, 032090. Doi: 10.1088/1757-899X/1203/3/ 032090.

Dragomir, C.S., & Dobre, D. (2023). Monitoring sensor techniques for an integrated and digitalized database. *AIP Conference Proceedings, 2928*, 170001. https://doi.org/10.1063/5.0171161.

Mouzakis, C., Konstantinos Vogiatzis, K., Zafiropoulou, V. (2019). Assessing subway network ground borne noise and vibration using transfer function from tunnel wall to soil surface measured by muck train operation. *Science of The Total Environment*, *650*(2), 2888-2896, https://doi.org/10.1016/j.scitotenv.2018.10.039.

Rybak, J. (2016). Calibration of Ground Improvement Technology on the Basis of Vibration Control. *Proceedings of 2nd International Conference on Engineering Sciences and Technologies*, High Tatras Mountains, Slovak Republic.

Zaharia, M.C. (2020). The influence of the coefficient of acoustic absorption of the facades of the buildings from the street profiles on the noise level from the urban road traffic. *ATINER's Conference Paper Proceedings Series No. CIV2020-0197 of the 10th Annual International Conference on Civil Engineering*, Greece: https://www.atiner.gr/presentations/CIV2020-0197.pdf. ISSN: 2529-167X.

DIN 4150-3:1999-02, Vibration in buildings - Part 3: Effects on structures.

ISO 2631-1:2001, Mechanical vibration and shock - Evaluation of human exposure to whole-body vibration, Part 1: General requirements.

Normative regarding acoustics in constructions and urban areas, C125 – 2013 (in Romanian).

Order of the Ministry of Health, no. 119 of 4 February 2014, for the approval of the Norms of hygiene and public health regarding the living environment of the population.

Procedure Determination of noise levels in situ, code PTE – AC/03.02.

STAS 6156-86 "Building Acoustics. Protection against noise in dwellings and public buildings. Admissible limits and sound insulation values" (in Romanian).

STAS 6161/3-82 "Building acoustics. Determination of noise levels in urban areas. Determination method" (in Romanian).

SR 6161-1:2008 "Building acoustics. Determination of noise level in civil buildings. Measurement methods" (in Romanian).

SR 6161-1/C91:2009 "Building acoustics. Determination of noise level in civil buildings. Measurement methods." (in Romanian).

SR 10009:2017 "Acoustics. Permissible limits of environmental noise level" (in Romanian).

SR ISO 1996-2:2018 "Acoustics - Description, and assessment of environmental noise - Part 2: Determination of sound pressure" (in Romanian).

Scientific Papers. Series E. Land Reclamation, Earth Observation & Surveying, Environmental Engineering. Vol. XIV, 2025
Print ISSN 2285-6064, CD-ROM ISSN 2285-6072, Online ISSN 2393-5138, ISSN-L 2285-6064

INCREASING THE SAFETY LEVEL CONSIDERING SOIL-STRUCTURE INTERACTION IN HIGH SEISMIC HAZARD-PRONE AREAS

Stefan Florin BALAN, Bogdan Felix APOSTOL

National Institute for Research and Development for Earth Physics,
12 Călugăreni Street, Măgurele, 077125, Ilfov, Romania

Corresponding author email: sbalan@infp.ro

Abstract

The work describes assessments and public policies that would account for safety increase and duration in the exploitation of structures. The level at which the soil-structure interaction is approached in actual normative/codes is highlighted. Proposals for approaching different ways to rise the protection level of structures to be in seismic zones were examined, starting from their location and design; this implies the knowledge of the site seismicity, earthquakes-related parameters prediction, the importance of (extended) geotechnical studies, etc. The interaction wave-structure is studied by using the model of harmonic oscillator coupled to an elastic medium. This analysis is meant to be relevant for the effects of seismic motion upon localized structure. Also, the model of an elastic structural element embedded at one end is envisaged and the normal modes and the eigenfrequencies of this independent module are highlighted. The response to oscillating shocks is computed for various ground excitations applied to its base. The response of two coupled modules, viewed as simplified structures thereby harmonic oscillators as well, to an oscillating shock is calculated, and amplification factors are highlighted.

Key words*: soil-structure interaction, wave-oscillator coupling, localized structures, risk evaluation, public policies.*

INTRODUCTION

The buildings behaviour is influenced by the site characteristics and the way it acts under strong seismic shaking. For certain geophysical characteristics, such as deep sedimentary basins, soft layered soils, amplification, inhomogeneities, or non-linearities presence, the level of hazard is increased. Therefore, the assessment of the seismic risk level is a challenging task. For Bucharest city, the old buildings and various types of design add to this state of things. The employed analyses, proposed actions to be taken, provisions and public policies are meant to lead to safety increasing and exploitation duration for the objective of interest. Thus, the soil-structure interaction (SSI) was considered in the project for the normative act "Seismic design code - part I - Design provisions for buildings Indicator P 100-1/2025" (P100-1/2025) developed by the Technical University of Construction Bucharest in 2024 (currently being in the consultation stages); therein this issue was approached explicitly for the first time in a Romanian design code. The present work can also be taken as a guide for the general contractor to be aware of what elements to look for when making the choice for the location of a future building or an urban or industrial complex. In this sense, compliance with the legislation/norms in force must be taken with the obligation/recommendation to add a thorough assessment of the following elements:

1) Local hazard, seismicity maps (peak values for recorded parameters, estimated intensities, etc.), microzoning (if any);
2) Possible prediction of future earthquakes (characteristics, ground shake level, amplifications) at the chosen location;
3) Geotechnical engineering studies, standard (required by the laws/codes/norms in force) or more complex according to the future requirements of the objectives to be built on the chosen area;
4) History of landslides and the risk of future ones on the chosen site, and measures to prevent them (if applicable);
5) Checking the area where the future site was chosen for the potential of liquefaction and if this phenomenon exists, what measures should be taken to reduce/exclude the risk of liquefaction in the event of a strong earthquake;

6) Measures to improve the bearing capacity of the soil if the respective site does not meet the conditions required in the project;
7) In the case of future objectives enrolled in Class I (Buildings with essential functions for which the preservation of integrity during earthquakes is vital for civil protection), detailed knowledge of the geological stratification of the soil deposit from the bedrock to the surface, especially for areas known to be soft soils is of uttermost importance. This should be done because of the potential of the soil layers to amplify the local seismic input at the site, which in some cases can lead to significant structural damage.
The site-structures interaction systems performance is assessed and thereby applied as a contribution to the safety level improvement for the structures located in the seismic areas or characterised by a high hazard level. Some features of both seismological and earthquake engineering interest are discussed that account for the vulnerability mitigation of the constructed medium since its design stage. The research studies that are carried out in the work refer to needs that involve the development of advanced methods for foreseeing interaction effects, the development of practical computational methods for estimating and incorporating these effects into the building design.

MATERIALS AND METHODS

Reference to soil - structure interaction in current codes/norms

The following section outlines how soil-structure interaction is addressed in Romanian legislation and selected international standards.
In the national normative "Seismic design code – part I – design provisions for buildings, indicative P 100-1/2013" there is no explicit treatment of the soil-foundation-structure interaction phenomenon (P100-1/2013).
In the draft "Seismic Design Code – Part I – Design Provisions for Buildings, Indicative P 100-1/2025" developed by the Technical University of Construction Bucharest in 2024, (P100-1/2025) (currently in the consultation stages at various professional levels) the notion of soil-structure interaction appears in several paragraphs as an additional calculation method in certain design situations.
Some examples of how this type of interaction was addressed in several international design codes are given below.
In Eurocode 8 (EUR 25204 EN – 2012), Seismic Design of Buildings soil-structure interaction appears in Chapter 4, "Introduction to the RC building example. Modelling and analysis of the design example"; 4.9. "Soil Structure Interaction". This subchapter presents qualitative/introductory elements about the phenomenon. Throughout Chapter 4, reference is also made to the soil-structure interaction phenomenon, and it is recommended that it be considered in certain practical situations.
National Institute of Standards and Technology (NIST, USA) has published guidelines on soil-structure interaction for building structures (Gcr, N. 2012; Stewart et al., 2012).
Techniques for simulating SSI phenomena in engineering practice are described. The recommendations are specifically addressed to the modelling of the effect of seismic soil-structure interaction on buildings. Realistic building examples are used to illustrate and test these recommendations.
One of the codes in Japan that specifically addresses soil-structure interaction is ISO 23469 (ISO 23469/2005). It provides guidelines for seismic actions in the design, including various types of structures that interact with the soil. This standard recognizes the importance of considering the effects of soil-structure interaction in seismic engineering. It complements ISO 3010, which focuses on seismic actions for superstructures of buildings and bridges. Designers use ISO 23469 to evaluate seismic loads on geotechnical works, considering factors such as soil displacement and the dynamic behaviour of buried structures.

Tasks to be accomplished for safety level increase

The features that need to be assessed within the oversight process of the soil-structure interaction are described; they may support the increase of the protection level of the buildings located in seismically dangerous areas.
1. Seismicity of the area. Studying the seismicity of the future site by complying with

the legislation/norms in force is essential, and if the objective is of particular importance, additional local/regional seismic hazard studies will be carried out (Welsh-Huggins & Liel, 2018; Joyner & Sasani, 2020).

2. Prediction of the earthquake's parameters. Predicting strong ground motion for future earthquakes is currently accomplished primarily by applying attenuation laws or parametric scaling relationship (Manea et al., 2022; Manea et al., 2025; Ardeleanu et al., 2005). These relationships related parameters describing the seismic source, such as the magnitude, to the location of a site relative to that source, to ground motion datasets (for example maximum (damped) spectral acceleration and the corresponding oscillation period). The current lack of recorded data, for some sites, at shorter or longer distances from the epicentres of strong earthquakes means that there is not enough hazard data to represent the presumed hazard of the most dangerous events. Dedicated computing programs and computational simulation, using various methods, offer a way to fill this data gap, for which structural engineers need histories of future ground motion.

3. Importance of Geotechnical Engineering Studies. The properties of the soil at a construction site substantially affect the performance of the construction and its associated facilities during earthquakes. However, these materials (soils) are usually the most variable in properties, the least investigated, and the least controlled of all materials in the built environment.

Knowledge of soil behaviour is key for a high-level structural design. Constructions and associated facilities (of all kinds) built in seismic regions on saturated sands, reclaimed land, and deep deposits of soft clays are vulnerable to damage from strong earthquakes. (Basu et al., 2014). Soils of the aforementioned types are common in marine environments and alluvial deposits, where large cities are often founded. For example, Mexico City is located on deep alluvial land (Beresnev et al., 1998). The Los Angeles Basin, consisting of unconsolidated sediments (Rukos, 1988) and Kobe city also are among these areas. The latter, comprises few not too deep different layers, was experienced liquefaction phenomenon occurred during strong Hyogoken-Nanbu earthquake (Ishihara et al., 1996). Damage to structures is worsened by soil liquefaction which causes the loss of foundation support and contributes to dramatic settlement of large buildings. Bucharest is crossed by 2 rivers (Dâmbovița with a length of 22 km and Colentina) and has several lakes on its territory, being located on an alluvial plain, formed by thick layers of sediments (sands, loess, etc.), with a preponderance of soft soils. Deep deposits of soft clays are particularly prone to amplifying the amplitude of seismic movement and decreasing the frequency content in the event of a strong earthquake, a situation that often leads to major damage to a structure, especially if resonance occurs between the soil and the structure.

4. Ground motion amplification. In addition to their tendency to cause structural damage, poor soil conditions are often associated with damage due to their tendency to amplify ground motions and/or to resonance with above infrastructure during strong earthquakes.

A spectacular example of ground motion amplification occurred during the 1985 Mexico City earthquake (M_W = 8.0, depth =20 km). The earthquake epicentre was over 400 km from the city, and the shaking amplitude at bedrock level in Mexico City was almost negligible (Anderson et al., 1986; Stone et al., 1987). However, since much of the city is built on soft soils that extend to considerable depths, these generated a seismic response that led to ground motion amplifications at frequencies close to those built structures. The structures display a strong resonance and were subjected to movements well above their design loads. Significant damage occurred, followed by the collapse of buildings, producing over 8,000 victims, and leaving over 50,000 people homeless. The significant increase in the potential for damage due to soft soil requires a better understanding of how local soil conditions modify seismic action and how these conditions can be identified, designed, and/or modified.

5. Considerations upon buildings. The 1994 Northridge (M_W = 6.7, depth = 18.2 km) (Mahin et al., 1998; Arboleda-Monsalve, 2020), 1995 Kobe (M_W = 6.9, depth = 21.9 km)

(Scawthorn et al., 1995; Aguirre & Irikura, 1997), and numerous other major earthquakes around the world illustrate that, despite advances in seismic design over the past decades, we need to develop a better understanding of the behaviour of built systems to ensure that new buildings are designed and old buildings are retrofitted to reduce their vulnerability to excessive damage and large economic losses during earthquakes.

5.1. ***Predicting the seismic capacity and performance of existing and new buildings***. Certain types of buildings are particularly vulnerable to major earthquakes: unreinforced masonry buildings, concrete frame buildings, precast concrete buildings etc. and many structures built before 1977 (the case of Romania) (Balan et al., 1982). Depending on their age, storage tanks, buried and above ground pipelines, and bridges may also be vulnerable.

Therefore, it is imperative to develop tools to identify buildings in this category, the facilities and supply lines (electricity, water etc.) that are vulnerable to cost-effective rehabilitation. Historic buildings present a particular challenge for seismic rehabilitation due to the limitations imposed on physical modification of the structure and the difficulty of structurally testing equivalent systems and components.

5.2. ***Assessment of non-structural building systems***. Most direct economic losses in buildings result from damage to non-structural systems, as opposed to structural systems (Balan et al., 1982). Even in earthquakes with minimal structural damage, non-structural damage can be substantial. The behaviour of non-structural components, such as architectural cladding, interior walls, and utility distribution systems, and their interactions with buildings, during earthquakes are complex phenomena. To adequately and better understand these interactions, they should be modelled (with accurate representation of both the structure and the non-structural components), at natural or smaller scale. Actions taken to protect non-structural elements from degradation during an earthquake must also consider a detailed cost-benefit analysis.

6. Performance of soil-foundation-structure interaction systems. Soil-foundation-structure interaction can have a significant effect on the seismic performance of building structures during strong earthquakes. Testing should be performed on representative structures and foundation systems to adequately represent the interaction on both the building and the foundation.

Currently, data on the response of soil-foundation-structure systems are quite scarce, and research needs include the development of advanced methods for predicting the effects of interaction, performing large-scale shake table tests and, where required, centrifuge testing of interaction mechanisms, developing practical computational methods for estimating the effects of interaction, and incorporating these effects into building design.

This issue will be particularly addressed in the next section.

7. Determining the performance of innovative materials and structures. Innovative materials and structures will include new intelligent uses and configurations of conventional materials and new "smart" developments of materials and structures. The use of smart materials and structures is an emerging concept in mechanical, aeronautical, and civil engineering.

Smart structures ("self-adaptive" or "intelligent") have the ability to respond to internal and/or external stimuli by varying their shape or mechanical properties. Smart materials can be used in sensors or actuators.

Examples of "smart" sensing materials include: optical fibre, piezoelectric ceramics, magnetorheological, electrorheological fluids and microelectromechanical systems (MEMS). The integration of these materials with sensing-actuating capabilities into conventional materials or structural systems will lead to smart structural systems. Research into "smart" materials has been conducted for many years, but few companies are putting these results into practice.

Cost-benefit analyses are needed to fully illustrate the relative benefits of these new technologies and materials and to systematically evaluate their innovative performance.

8. Risk assessment. The challenge in risk assessment is to provide decision-makers with accurate and understandable information about

risk exposure and alternative risk mitigation with the tools that will enable them to make prudent decisions based on this information.

More specifically, it is necessary to do the following:

• Develop risk assessment methods that are comprehensive, based on sound scientific and engineering principles, and usable by a variety of stakeholders.

• Development of the base of decision-making tools that leads to its reduction.

• Formulating a framework for risk mitigation and mitigation policies that can be implemented by the public and private sector.

Although strong earthquakes are rare events, their consequences can be devastating. Decision-makers are often complacent about earthquake hazard because a major earthquake may not have occurred in their lifetime or where they live.

Risk assessment requires knowledge of the following types of issues:

• The probability of earthquakes occurrence, their magnitude and location, the characteristics of the terrain in the area, the probability that they will cause tsunamis.

• Physical damage, with its direct consequences in terms of death, injury, loss of operational functionality and destruction of property.

• The social and economic consequences of direct physical damage, including losses due to damage to buildings, supply lines and other critical elements.

9. Public Policy. A major challenge for communities exposed to major earthquakes is the need to have risk reduction placed on the public, municipal, and legislative agendas.

Although research findings will advance over time, changes will only be achieved through policy development and implementation. Adopting policy measures, supported by cutting-edge technology, will significantly increase the capacity to prevent major disasters and thus reduce the devastating economic impact and social consequences.

One of the major difficulties in reducing the economic and social consequences of earthquakes is that disaster mitigation policies and preparedness are generally inadequate to meet the challenge of disasters for a community. The many directions that need to be addressed on the path to disaster policy formulation and implementation include: the appropriateness of relevant policy; educating decision-makers; educating stakeholders to gain support for the introduction of legislation; identifying appropriate alternatives that are consistent with the risk, exposure, and capacity of a community to implement these policies; and developing strategies for implementing legislation.

Proposals for public policies that can help promote an increasing safety policy are presented below:

• Setting the agenda. After any disaster, there is a reset of the agenda for those directly involved. It is necessary to be prepared and to take advantage of these moments. A community must understand its risks to determine how to mitigate them and how it can respond to emergencies. The technical basis comes from integrating all geological, structural, and sociological data and simulations that would provide a rational reason and an understandable basis for public and private policy decisions on preparing/mitigating shocks to large earthquakes:

• Policy justification. In formulating public policies, it is often necessary to undertake a cost-benefit analysis of the proposed policy or regulation;

• Defining alternatives. Policy decisions on earthquake mitigation must be based on sound and up-to-date technical knowledge;

• Educating the public. Most often, public policies are developed in response to public demand. The public can make and influence political decisions, but only if people are sufficiently well informed about the underlying problems and the solutions and their implications.

10. Landslide study. Evaluating geotechnical hazards is a crucial responsibility in the field of geotechnical engineering. This involves assessing the potential impacts of natural events, such as earthquakes and landslides, on construction projects. Hence the history of landslides and the risk of future ones on the chosen site, and measures to prevent them (if applicable) is useful to be known.

11. Liquefaction. Is important to check the area where the future site was chosen for the potential for liquefaction and if this

phenomenon exists, what measures should be taken to reduce/exclude the risk of liquefaction in the event of a strong earthquake. The prevention of liquefaction phenomena requires a combination of geotechnical measures and appropriate planning when building structures in areas susceptible to soil liquefaction. Finally, structures built in areas prone to liquefaction must be designed to withstand the forces and settling induced by this phenomenon. Special design techniques, such as deep piles, reinforced foundations or retaining walls, may be required to ensure the stability of structures (Youd at al., 2001; Ishihara et al., 1996).

12. Soil improvement measures. Measures to improve the bearing capacity of the soil if the respective site does not meet the conditions required in the project must be taken. Besides conducting geotechnical assessments, additional measures can be considered, such as soil drainage and reinforcement through the incorporation of granular materials or chemical binders to enhance its properties. Alternatively, soil compaction can be employed to increase its density

13. Utility supply lines. Best practices from utilities that have used mitigation measures to address the earthquake threat are needed to be known. To protect the utility will need to assess the potential damage to buildings and key assets. Utilities include water, wastewater, fuel, electricity, gas, and telecommunications systems. The basic components of utilities include supply and storage equipment, transmission lines, and the connections between these components. Underground utility pipelines and connections are often too weak or inflexible to withstand earthquake ground movements and differential settlements, causing them to crack or fail. Materials that are too flexible, however, also cannot handle additional displacements from earthquake forces. From ground shaking, pipes often crack at brittle joints or are crushed at the bell or pipe barrel. From liquefaction or lateral spreading, pipes often break or separate at the joints (Deelstra & Bristow, 2022).

Performance of soil- foundation-structure interaction systems

The effects of seismic waves on structures on the Earth's surface are studied by considering features of major interest in the assessment of seismic risk. The input generated by the phenomena that affect the structures can be appreciated in terms of physical and mathematical problems related to shocks, oscillations, and vibrations (Apostol, 2025a). In these circumstances the advanced study of the response of elastic elements to external mechanical excitations is pursued. Overall, the characteristics of the interest site (site to be chosen for the construction) directly influence the structures and construction materials behaviour, innovative assembles and utility supply lines included. Therefore, the necessity was inferred for taking into consideration the complex phenomenon of site-foundation-structure interaction and particularly the structural behaviour to seismic input or vibrations.

The protection of the buildings erected at the Earth’s surface is a continuous preoccupation in earthquake engineering for countering the destructive action of the earthquakes. The buildings are represented by vibrating units (or simply bars), which, under the seismic action may resonate; also, sub-surface inhomogeneities may behave as resonating embedded elements (Apostol, 2025a). In both cases we get local amplification factors, for displacement, velocity, and acceleration, which are evaluated in resonance conditions and may attain large values. The amplification factors are given by a combination of the shock duration, the height of the bar above the ground surface and the velocity of the elastic waves in the beam; they arise because of the excitation of the normal modes in the structure (Apostol, 2025a).

A distinct instance is devoted to the interaction of a harmonic oscillator model with an elastic wave, the associated amplification factors, and particularly the coupling of structure-site, viewed as localized harmonic oscillator coupled with the elastic medium.

The problem of selecting the type of seismic excitation is examined considering the possible expected damages. This innovative method is distinguished by its precise and high-quality outcomes. The approach utilizes and applies mathematical physics equations pertaining to oscillating beams, coupled oscillations, and medium-structure interactions. The significance

of this method lies in its ability to deliver valuable insights that can be used in the design and construction of buildings.

We consider as an appropriate model for investigating the response of a building to ground vibrations a simple structure assimilated to an embedded bar at one end. The input can be considered as various ground oscillations such harmonic oscillations and oscillating shocks characterized by a sharp wave front. This special case is the most interesting excitation, since it is deemed that such a shock may correspond to the seismic main shock with its long tail.

The model of the embedded beam provides a way of understanding the well-known amplification site effects of the earthquakes, as arising from the excitation of the normal modes in local inhomogeneities (Apostol, 2025a).

For the seismic excitations which have a general aspect of shocks, i.e. they are concentrated in at the initial moment of time, we assume first a shock-like ground motion:

$$u_0(t) = u_0 T\,\delta(t),\ u_0(\omega) = u_0 T,$$

where T is a measure for the duration of the shock. We get:

$$u(z,t) = \frac{1}{2}u_0 T[\delta(t - z/c) + \delta(t + z/c)] + \\ + u_0 \frac{cT}{l}\sum_n sin\omega_n t \cdot sin\omega_n z/c \qquad (1)$$

for the displacement along the bar, where $\omega_n = (2n + 1)\pi c/2l$, and n is any integer. Vibrations given by the normal modes with the eigenfrequencies ω_n are excited in the bar.

The summation over n in equation (1) gives a pulse going forth and back along the bar. The amplitude of the pulse is of the order u_0, while the amplitude of the normal modes is of the order $u_0 cT/l$.

For computing the amplification factors we introduce the parameter $g = \frac{cT}{l}$ and denote by $u_n(t, z)$ the contribution to the displacement of the n-th normal mode.

For modelling the seismic main shock with its long tail an oscillating shock with a sharp wavefront, attenuated in time with the rate α is employed; a ground motion given by $u_0(t) = u_0\theta(t)e^{-\alpha t}cos\omega_0 t$, is assumed, where $\theta(t) = 1$ for $t > 0$, $\theta(t) = 0$ for $t < 0$ is the step function and $0 < \alpha \ll \omega_0$. The solution is now:

$$u(z,t) \cong u_0 e^{-\alpha t}cos\omega_0 t \cdot \frac{tan\omega_0 l}{c}\cdot\frac{sin\omega_0 z}{c} - \\ - \frac{c}{2l}u_0\sum_n\left[\frac{(\omega_n-\omega_0)cos\omega_n t-\alpha sin\omega_n t}{(\omega_n-\omega_0)^2+\alpha^2} + \right. \\ \left. + \frac{(\omega_n+\omega_0)cos\omega_n t-\alpha sin\omega_n t}{(\omega_n+\omega_0)^2+\alpha^2}\right] sin\omega_n z/c \qquad (2)$$

for ω_0 different from all ω_n , and in which are included contributions from the poles $\pm\omega_0 - i\alpha$ of the shock and contributions from the normal modes with eigenfrequencies ω_n (the poles of $tan\kappa l$).

For $\omega_0 = \omega_n$ (resonance):

$$u(z,t) = u_0\frac{c}{l}\frac{1-e^{-\alpha t}}{\alpha}\cdot sin\omega_0 t\frac{sin\omega_0 z}{c}, \qquad (3)$$

from which can see that the displacement amplitudes at resonance are $\frac{c}{l\alpha}u_0$, i.e. in the amplification factor $g = cT/l$ the duration T is replaced by $1/\alpha$, as expected. We note that for $\omega_0 = 0$ the amplitude is reduced to $\left(\frac{c}{l\omega_n}\right)u_0$. Similarly, the response velocity and acceleration include factors $u_0\omega_0$ and $u_0\omega_0^2$, respectively, which now can be viewed as corresponding to the ground velocity and acceleration; the amplification factor for these quantities is $g = c/l\alpha$, as for the displacement.

Let us assume a bar with length l fixed at $z = 0$ to another long bar with length l_0; we denote the former bar by 1 and the latter bar by 2; The model of two coupled bars is employed as follows: bar 1 with length l fixed (at $z = 0$) extends above the ground surface, while bar 2 with length l_0 is buried in the ground.

The equations of elastic motion in the two bars are:

$$\ddot{u}_1 - c_1^2 u_1'' = 0, \ddot{u}_2 - c_2^2 u_2'' = 0 \qquad (4)$$

where $u_{1,2}$ is the displacement in the two bars; after imposing the appropriate boundary conditions, we get, for a force, for a shear displacement applied at the lower end $z = -l_0$:

$$u_1(z,\omega) = u_0(\omega)\frac{cos\kappa_1(z-l)}{cos\kappa_1 l cos\kappa_2 l_0 - \frac{\mu_1\kappa_1}{\mu_2\kappa_2}sin\kappa_1 l sin\kappa_2 l_0} \qquad (5)$$

$$u_2(z,\omega) = \\ = u_0(\omega)\frac{cos\kappa_1 l cos\kappa_2 z + \frac{\mu_1\kappa_1}{\mu_2\kappa_2}sin\kappa_1 l sin\kappa_2 z}{cos\kappa_1 l cos\kappa_2 l_0 - \frac{\mu_1\kappa_1}{\mu_2\kappa_2}sin\kappa_1 l sin\kappa_2 l_0}$$

The eigenfrequencies are given now by

$$\frac{tan\omega_n l}{c_1}\cdot\frac{tan\omega_n l_0}{c_2} = \frac{\mu_2\kappa_2}{\mu_1\kappa_1} = \sqrt{\frac{\rho_2\mu_2}{\rho\mu_1}} \qquad (6)$$

and amplification factors appear, similarly with a single bar. If bar 2 is much "softer" than bar 1 ($\mu_2/\rho_2 \ll \mu_1/\rho_1$) the (lowest) eigenfrequencies are given by $\omega_n = (c_2/l_0)\alpha_n$, where α_n are the roots of the equation $\alpha_n \tan\alpha_n = \rho_2 l_0/\rho_1 l$. If bar 1 is "softer", the eigenfrequencies are $\omega_n = (c_1/l)\beta_n$, where $\beta_n \tan\beta_n = \mu_2 l/\mu_1 l_0$.

We can see that the eigenfrequencies are controlled by the elastic properties of the "softer" bar. This result gives an indication regarding the vibration properties of bars with a composite structure (e.g., including voids).

In studies of seismic risk and hazard it is important to assess the effects of the seismic motion upon localized structures, either natural or man-made. Such structures are viewed herein as localized harmonic oscillators, with corresponding eigenfrequencies (characteristic frequencies). It is assumed that the seismic motion acts as an external force upon such oscillators and the resonant regime is highlighted.

For a realistic use of the coupled-oscillator model we consider two oscillators as corresponding to a building (oscillator 2) and its foundation (oscillator 1). For a stiff foundation, such that $\omega_1 > \omega_2$ the eigenfrequencies of the building are reduced to an appreciable extent (down to zero), while the eigenfrequencies of the foundation are increased by the coupling. For a soft foundation ($\omega_1 < \omega_2$) the situation is reversed, the eigenfrequencies of the building are raised by the coupling and those of the foundation are reduced. Let us assume that the foundation (oscillator 1) is subject to a force $\theta(t) f_0 e^{-\alpha t} cos\omega_0 t, \alpha \ll \omega_0$, arising from the ground motion. The full solution is obtained as:

$$u_1 = A_1 e^{i\Omega_1 t} - \frac{\omega_2^2}{k_2} B_2 e^{i\Omega_2 t} + f\frac{\omega_2^2 - \varpi_0^2}{\Delta} e^{i\varpi_0 t},$$
$$u_2 = \frac{\omega_2^2}{k_1} A_1 e^{i\Omega_1 t} + B_2 e^{i\Omega_2 t} - f\frac{k_2}{\Delta} e^{i\varpi_0 t} \quad (7)$$

with the notations $\Delta = (\varpi_0^2 - \Omega_1^2)(\varpi_0^2 - \Omega_2^2)$; $\varpi_0 = \omega_0 + i\alpha$, where $1/\alpha$ is the attenuation factor.

The constants A_1, and B_2 are determined from the initial conditions:

$x_{s,b}(t=0) = 0;\ \dot{x}_{s,b}(t=0) = 0.$

We focus on the resonance of the building, where $\omega_0 = \Omega_2 (\alpha \ll \Omega_2)$ and $\Delta \cong \alpha\Omega_1^2(\alpha - 2i\Omega_2)$; the initial conditions give $A_1 \cong 0$ and $B_2 \cong \frac{fk_2}{4\Omega_1^2\Omega_2^2}\left(1 + i\frac{\Omega_2}{\alpha}\right)$; hence we get the displacements:

$$u_1 = \frac{-f\omega_2^2}{4\Omega_1^2\Omega_2^2}\left(cos\Omega_2 t - \frac{\Omega_2}{\alpha} sin\Omega_2 t\right)(1 - e^{-\alpha t}) + +O(\alpha)$$

$$u_2 = \frac{fk_2}{4\Omega_1^2\Omega_2^2}\left(cos\Omega_2 t - \frac{\Omega_2}{\alpha} sin\Omega_2 t\right) \cdot \cdot (1 - e^{-\alpha t}) + O(\alpha) \quad (8)$$

We can see that the original damped excitation is lost in time and for a long time both the building and the foundation oscillate with the resonance frequency Ω_2 of the building; the amplitudes of the oscillations are enhanced by the attenuation factor $1/\alpha$, as expected; the oscillation amplitude of the foundation is controlled by the exciting force, while the amplitude of the building is controlled by the coupling constant. We note that we have considered the above oscillations without a damping factor; a damping factor affects the contribution of the normal modes and add to the attenuation factor of the excitation.

At resonance the coupled oscillators exhibit amplification factors, like the vibrating bar. The coupling lowers the low frequency of the system and raises the upper frequency (Apostol, 2025b).

With a direct reference to the subject addressed herein, and perhaps a more realistic assessment of the site-structure interaction we examine the approach involving the motion of a localized point harmonic oscillator coupled to a homogeneous elastic medium. Two new elements are introduced, one regarding the reaction of the oscillator upon the medium and another concerning a coupling function. It is shown that the reaction of the oscillator modifies its inertia, which in turn leads to a change in the oscillator's eigenfrequency; this change is controlled by the coupling function. The present treatment opens the way of introducing new, more realistic features in analysing the effect of the seismic motion upon localized structures, in particular the non-linear features of the coupling of the structure with its local site's motion (Apostol, 2025b).

Equation of motion for harmonic oscillator is considered as:

$$m\ddot{v} + m\Omega^2 v = gS(F\Delta u)_{r=r_0}; \quad (9)$$

where v is the oscillator's displacement from its equilibrium position, $(F\Delta u)_{r=r_0}$ is superficial force density the medium acts upon oscillator; S is the area of the contact surface between oscillator and medium, and the force $S(F\Delta u)_{r=r_0}$ that acts upon oscillator; g is the coupling function hence the force is written as $gS(F\Delta u)_{r=r_0}$. Of course, the area S must be much smaller than constructed surface and any other relevant wave lengths.

One must mention that coupling function *g* may achieve a complex structure; it may depend on the oscillator eigenmodes (frequency Ω), on the oscillator amplitude, on the local amplitude **u** of the waves and even on the time *t*. For simplicity, herein we consider a constant *g*; obviously g ≤ 1.

The elastic waves propagating on the surface exhibit a (two-dimensional) movement with the displacement vector **u**; while *F* stands for (generic) elasticity modulus, hence the wave velocity is $c^2 = \frac{F}{\rho}$, where ρ is the superficial mass density. The symbol delta (Δ) in the above equation is the laplacian.

Similarly, the oscillator reacts back upon the elastic medium through its inertia force $-gm\ddot{v}S\delta(r - r_0)$, localized at $\mathbf{r}_0$ and depending on the coupling function; hence we have a wave equation:

$$\rho\ddot{u} - F \cdot \Delta u = -gm\ddot{v}\delta(r - r_0) \quad (10)$$

The solution for the oscillator displacement is:

$$v(\omega) = \frac{-\omega_0^2}{\Omega^2 - \omega^2(1-g^2)} \times \frac{gS\rho}{m}\pi A\left[\delta(\omega - \right.$$
$$\left. -\omega_0)e^{\frac{i\omega_0 x_0}{c}} + \delta(\omega + \omega_0)e^{\frac{-i\omega_0 x_0}{c}}\right] \quad (11)$$

where the Fourier transforms were taken and the modulus of the wave vector $k = \omega/c$ introduced.

Hence one can see the change of the oscillator resonant eigenfrequency $\Omega \to \Omega/\sqrt{1-g^2}$ because of its interaction with the elastic medium (gets "renormalized"). By taking the inverse Fourier transform is obtained

$$v(t) = \frac{-\omega_0^2}{\Omega^2 - \omega_0^2(1-g^2)}\frac{gS\rho}{m}A\cos\omega_0(t - x_0/c) \quad (12)$$

Considering the contribution of the poles $\omega = \pm\Omega/\sqrt{1-g^2}$ we get the solution corresponding to the free oscillation at resonance; it occurs now at the modified eigenfrequency. One may specify that for a perfect coupling, $g = 1$, there is no resonance anymore.

RESULTS AND DISCUTIONS

In this paper certain site's features are analysed, that influence the behaviour of built structures, building materials, innovative structures, including utility supply lines, vital to communities. These analyses, measures and public policies are meant to contribute to increasing the safety and operational life of the objective in question.

The evaluation of the complex soil-foundation-structure interaction phenomenon must specifically consider the influence of the site characteristics themselves and especially under strong seismic movement. Thus, the proposals for approaching the different stages of the design-construction activity are examined to increase the safety and the operational duration of the objective in question.

The method and procedures for monitoring the soil-foundation-structure interaction are described, considering both the design elements and for the purpose of analysing the behaviour in operation.

It is well known that the effects of seismic waves on structures located at the Earth's surface represent a major interest in seismic risk assessment. These effects are herein evaluated considering typical excitation input upon simple (representative) structural models.

The contribution generated by the phenomena affecting the structures can be appreciated in terms of physical and mathematical problems related to shocks, oscillations, and vibrations, so the work proposes the advanced study of the response of elastic elements to external mechanical excitations.

In such a simplified picture introduced herein the reaction of the structure back on the elastic medium is particularly considered and the coupling of the structure to the elastic medium. Ways is shown of introducing these two elements in the analysis and describe the consequences, some surprising, of including these two more realistic features. The most important is the modification of the oscillator frequency with which the structure is

assimilated, due the coupling constant (which remains undetermined).
It is desirable of course, to avoid the resonance, i.e. the structure's characteristic frequencies must be different from the main frequencies of the seismic motion at the site of the structure (local seismic motion).
The normal/natural eigenmodes and the eigenfrequencies of the simplified model of an embedded elastic structure (embedded bar) are highlighted and the response to oscillating shocks is computed for several typical shock configurations. Special attention is devoted to the oscillating shock with a sharp wave front, deemed as a suitable model for the seismic main shock with its long tail. It is shown that in all cases the response of the bar is governed by an amplification factor, which includes cumulative information about the shock duration, height of the bar above the ground surface and the velocity of the elastic waves in the bar. The amplification of the response is due to the excitation of the normal modes (eigenmodes). The effect is much enhanced at resonance, for oscillating shocks which contain eigenfrequencies of the bar.
The model of coupled harmonic oscillators was formulated to investigate its response to an oscillating shock. It is shown that the lower frequency of the system is lowered by the coupling, while the higher frequency is raised. At resonance the coupled oscillators exhibit amplification factors, similar with the vibrating bar.
The results achieved in this paper concern urban seismology and specific analyses of earthquake engineering, constituting a starting point for the implementation of complex analysis methods of soil-structure interaction.
The present work can also be considered as a guide for the general contractor to know what elements to consider for when choosing the location of a future building or an urban or industrial complex.
This material can represent a methodology to be followed with the aim of increasing the degree of safety of structures located in seismic zones. It also considers important elements that could represent a potential danger to the safety of constructions, from the phase of site selection to the exploitation phase.

CONCLUSIONS

The points discussed herein refer to implementing the methods of complex analysis of the soil-structures interaction including the evaluation of dynamic structural characteristics and building monitoring.
The pursued targets, which consider the laws and regulations in force, give coherence to the approach from the point of view of the seismic analysis of the entire path from the location to the exploitation of the considered (structural) objective.
The treatment of the interaction phenomenon was considered within the project for the normative act "Seismic design code - part I - Design provisions for the present works Indicator P 100-1/2025" developed by the Technical University of Construction Bucharest in the year 2024; respectively, the phenomenon being treated explicitly for the first time in a Romanian project code.
One shall develop a good knowledge for the construction systems behaviour to assure an enhanced level of resilience for the new buildings. As regard the old buildings, they must be rehabilitated to mitigate their vulnerability at future strong earthquakes.
Research priorities in seismic engineering include: prediction of seismic capacity of buildings, performance of existing and new buildings, evaluation of non-structural systems, soil – foundation - structure interaction performance and determining the performance of future innovative materials and structures. It is important to ensure the protection of built objectives and maintain the safety of community utility supply lines and the risks that arise from not giving them special attention.
Within the study the importance of materials used in construction is emphasized and cost-benefit analyses are considered, regarding new technologies and materials. It is also proposed a manner of assessing the risks to which the built objectives are exposed and how they should be approached.
The present work brings into discussion a less known and used element, but which we consider equally important for the ways of increasing the degree of safety of structures located in seismic zones: public policies. These

must represent ways of raising awareness among communities, local/county councils, and politicians of the importance of funding future earthquake-safe works and of giving greater importance to building rehabilitation works, thus avoiding the risk of major damage to a future strong earthquake.

ACKNOWLEDGEMENTS

This paper was carried out within Program Nucleu SOL4RISC, contract number 24N/03.01.2023, supported by Ministry of Research, Innovation and Digitization, project no. PN23360202.

REFERENCES

Aguirre, J., Irikura, K. (1997). Nonlinearity, liquefaction, and velocity variation of soft soil layers in Port Island, Kobe, during the Hyogo-ken Nanbu earthquake. *Bulletin of the Seismological Society of America*. 87(5), 1244-1258.

Anderson, J. G., Bodin, P., Brunbe, J. N., Prince, J., Singh, S. K., Quaas, R., Onate, M. (1986). Strong ground motion from the Michoacan, Mexico earthquake. *Science*. 33(4768), 1043-1049; doi: 10.1126/science.233.4768.1043.

Apostol, B. F. (2017). A resonant coupling of a localized harmonic oscillator to an elastic medium. *Romanian Reports in Physic,* 69, 116.

Apostol, B. F., Balan, S. F., Ionescu, C. (2017). Realistic features in analysing the effect of the seismic motion upon localized structures considering aseismic devices influence on their dynamic behaviour, *IOP Conf. Series: Earth and Environmental Science,* 95, 032017 doi:10.1088/1755-1315/95/3/032017.

Apostol, B. F. (2025). Isolating layer in foundation-structure dynamic behaviour, accepted *Romanian Journal of Physics*.

Apostol, B. F. (2025). Modal analysis of elementary structural models subjected to local perturbation, submitted *Romanian Journal of Physics.*

Arboleda-Monsalve, L. G., Mercado, J. A., Terzic, V., Mackie, K. R. (2020). Soil–Structure Interaction Effects on Seismic Performance and Earthquake-Induced Losses in Tall Buildings. *J. Geotech. Geoenviron. Eng,.* 146(5), 04020028.

Ardeleanu, L., Leydecker, G., Bonjer, K.-P., Busche, H., Kaiser, D., and Schmitt, T. (2005). Probabilistic seismic hazard map for Romania as a basis for a new building code. *Nat. Hazards Earth Syst. Sci,.* 5, 679–684; doi: 10.5194/nhess-5-679-2005.

Balan, S., Cristescu, V., Cornea, I. (Eds) (1982). *March 4, 1977, Earthquake*. Bucharest RO: Romanian Academy Printing House (in Romanian).

Basu, D., Misra, A., Puppala, A. D. (2014). Sustainability and geotechnical engineering: perspectives and review. *Can. Geotech. J.* 52: 96–113; dx.doi.org/10.1139/cgj-2013-0120.

Beresnev, I., Field, E., Abeele, K.V., Johnson, P. (1998). Magnitude of Nonlinear Sediment Response in Los Angeles Basin during the 1994 Northridge, California, Earthquake. *Bulletin of the Seismological Society of America*, 88(4), 1079-1084.

Deelstra, A., Bristow, D. N. (2022). Assessing the effectiveness of disaster risk reduction strategies on the regional recovery of critical infrastructure systems. *Resilient Cities and Structures*, 2(3), 41-52.

EUR 25204 EN - 2012 *Eurocode 8: Seismic Design of Buildings Worked examples*, presented at the Workshop EC 8: Seismic Design of Buildings, Lisbon, 10-11 Feb. 2011. Support to the implementation, harmonization and further development of the Eurocodes, P. Bisch, E. Carvalho, H. Degee, P. Fajfar, M. Fardis, P. Franchin, M. Kreslin, A. Pecker, P. Pinto, A. Plumier, H. Somja, G. Tsionis Cornejo,J. Raoul, G. Sedlacek, G. Tsionis; Editors B. Acun, A. Athanasopoulou, A. Pinto E. Carvalho, M. Fardis Cornejo,J. Raoul, G. Sedlacek, G. Tsionis.

Gcr, N. (2012). Soil-structure interaction for building structures. *National Institute of Standards and Technology (NEHRP)*.

Ishihara, K., Yasuda, S., and Nagase, H. (1996). Liquefaction induced ground settlement in reclaimed areas during the 1995 Hyogoken-Nanbu earthquake. *Soils and Found*., 36(1),135-147.

ISO 23469:2005, *Bases for design of structures — Seismic actions for designing geotechnical works*. This publication was last reviewed and confirmed in 2022. Technical Committee ISO/TC 98, *Bases for design of structures*, Subcommittee SC 3, *Loads, forces, and other actions* in collaboration with ISSMGE/TC4 and CEN/TC205/SC8.

Joyner, M.D. & Sasani, M. (2020). Building performance for earthquake resilience. *Engineering Structures*, 210(2), 110371.

Mahin, S.A. (1998). Lessons from Steel Buildings Damaged by the Northridge Earthquake. National Information Service for Earthquake Engineering, University of California, Berkeley. Available online at http://nisee.berkeley.edu/northridge/mahin.html

Manea, E.F., Cioflan, C.O., Danciu, L. (2022). Ground-motion models for Vrancea intermediate-depth earthquakes. *Earthquake Spectra*., 38(1), 407-431. doi:10.1177/87552930211032985

Manea, E. F., Danciu, L., Cioflan, C. O., Toma-Danila, D., Gerstenberger, M. C. (2025). Testing the 2020 European Seismic Hazard Model (ESHM20) against observations from Romania. *Nat. Hazards Earth Syst. Sci.*, 25, 1–12, https://doi.org/10.5194/nhess-25-1-2025.

P 100-1/2013, *Seismic Design Code - Part I: Earthquake Resistant Design of buildings*, (2013), Ministry of Regional Development and Public Administration (M.D.R.A.P.); Bucharest, Romania (in Romanian).

Rukos, E. A. (1988). The Mexico Earthquake of September 19, 1985 - Earthquake Behavior of Soft Sites in Mexico City. *Earthquake Spectra*., 4(4), 771-786.

Scawthorn, C., et al. (1995). The January 17, 1995, Kobe Earthquake. An EQE Summary Report. Available online at http://www.eqe.com/publications/kobe/kobe.htm.

Stewart, J., Crouse, C., Hutchinson, T., Lizundia, B., Naeim, F., Ostadan, F. (2012). Soil-Structure Interaction for Building Structures, Grant/Contract Reports (NISTGCR), National Institute of Standards and Technology, Gaithersburg, MD [online], https://tsapps.nist.gov/publication/get_pdf.cfm?pub_id=915495 (Accessed December 18, 2024).

Stone, W., Yokel, F., Celebi, M., Hanks, T., Leyendecker, E. (1987). Engineering Aspects of the September 19, 1985. Mexico Earthquake (NBS BSS 165). *Building Science Series*, National Institute of Standards and Technology, Gaithersburg, MD, [online], https://doi.org/10.6028/NBS.BSS.165 (Accessed December 24, 2024).

Welsh-Huggins, S.J., Liel, A.B. (2018). Evaluating multiobjective outcomes for hazard resilience and sustainability from enhanced building seismic design decisions. *J. Struct. Eng*., 1449(8), DOI: 10.1061/(ASCE)ST.1943-541X.0002001

Youd, T.L., Idriss, I.M., Andrus, R., Arango, I., Castro, G., Christian, J., Dobry, R., Finn, L., Harder Jr., L., Hynes, H.M., Ishihara, K., Koester, J., Liao, S.S., Marcuson, W.F., Martin, G., Mitchell, J.K., Moriwaki, Y., Power, M.S., Robertson, P.K., Seed, R.B., and Stokoe II. (2001). K.H. Liquefaction Resistance of Soils: Summary Report from the 1996 NCEER and 1998 NCEER/NSF Workshops on Evaluation of Liquefaction Resistance of Soils. *Journal of Geotechnical and Geoenvironmental Engineering*, ASCE, 127(GT10), pp. 817-833.

Scientific Papers. Series E. Land Reclamation, Earth Observation & Surveying, Environmental Engineering. Vol. XIV, 2025
Print ISSN 2285-6064, CD-ROM ISSN 2285-6072, Online ISSN 2393-5138, ISSN-L 2285-6064

DURABILITY AND SUSTAINABILITY OF MOUNTAIN FARMS IN ROMANIA WITH A FOCUS ON AGRICULTURAL DIVERSIFICATION

Daniela-Mihaiela BOCA[1], Tudor Panfil TOADER[2], Andreea HEGYI[2], Marius VLADU[3]

[1]University of Agronomic Sciences and Veterinary Medicine of Bucharest,
59 Mărăști Blvd, District 1, 011464, Bucharest, Romania
[2]National Institute for Research and Development in Construction, Urban Planning and Sustainable Spatial Development – URBAN-INCERC,
266 Pantelimon Road, District 2, 021652, Bucharest, Romania
[3]University of Craiova, Faculty of Agronomy, 19 Libertăţii Street, 200583, Craiova, Romania

Corresponding author emails: toader.tudor@yahoo.com, mihaiela_boca@yahoo.com

Abstract

This study highlights the durability and sustainability of mountain farms, focusing on agricultural diversification as a method of adaptation and development. Mountain regions in Romania face significant challenges, such as climate change, population migration, and declining agricultural incomes. Diversifying agricultural products proves to be an effective solution for increasing the resilience of these farms, enhancing both food security and economic stability. The article examines development strategies, public policies for mountain areas, and support initiatives, including a case study on their implementation. Through an integrated approach, this study emphasizes the necessity of combining agricultural traditions with innovation to ensure a sustainable future for mountain farms. In conclusion, agricultural diversification is not just a survival strategy but also an opportunity for sustainable development in mountain communities.

Key words*: agricultural diversification, durability, mountain farms, resilience, sustainability.*

INTRODUCTION

The mountainous regions in Romania are covering approximately 30% of the country's territory. However, these regions face significant challenges due to steep slopes, poor soil fertility, fragmented land ownership and harsh climatic conditions that limit the agricultural potential of these areas (Popescu et al., 2022; Oros, 2022). These areas face natural disadvantages (high altitude, harsh climate, poor soil fertility) and structural disadvantages (population migration, poorly developed infrastructure leading to reduced accessibility, very limited access to markets / poor access to markets).

The lack of a unified definition of mountain areas makes it difficult to develop coherent development strategies (Popescu et al., 2010). We can say that these regions are ecologically fragile and economically disadvantaged, resulting in higher costs of agricultural activity and limited economic opportunities (INS, 2019). More, demographic issues like the migration of young people to urban areas and the aging population have exacerbated socioeconomic difficulties in mountain communities (Academia Română, 2008). As mentioned by Antonescu (2022), depopulation in the mountain rural areas is related to the limited infrastructure, wich reduce access to quality education, healthcare, and the most important the absence of long-term public investment in community development.

At this time, agriculture remains the most important economic activity in the mountain regions of Romania, with 19.7% of the total utilized agricultural area while employing 18.5% of the economically active population (MADR, 2018). More than 65% of the farms are classified as small or very small, with less than 2 hectares of farmland. These farms are traditionally oriented to the production of cattle and dairy for meat and milk. It is important to understand that reduced access to agricultural resources (e.g., wool and dairy products), as well as low productivity, lead to a consistent reduction in the number of animals and low profitability for small farmers (MADR, 2020).

The mountain ecosystems in Romania are very important and are crucial for protecting

biodiversity, protecting water resources, and supporting rural economies. Around 50% of freshwater resources are found in these areas, as well as a variety of plant and animal life (RNDR, 2015).

The ecological importance of mountain areas is highlighted in the Carpathian Convention through a series of fundamental principles, which focus on the conservation and sustainable use of biodiversity and landscape, sustainable rural development, integrated management of natural resources, as well as transboundary cooperation and active public involvement. These principles reflect the commitment of the Carpathian states to protect and enhance the natural heritage of the region, thus ensuring that economic and social activities do not negatively affect mountain ecosystems (Carpathian Convention, 2025). Protected areas in mountain regions play an essential role in biodiversity conservation, but their effectiveness is influenced by numerous challenges, such as accessibility issues, demographic factors and economic difficulties, despite the fact that they have a high tourism potential. These conclusions are supported by GIS-based studies Geographic Information Systems (GIS). These aspects clearly limit the effective implementation of biodiversity protection measures and thus impose the urgent need for strategic interventions to ensure a balance between conservation and development. In this sense, policymakers must adopt that allow the protection of fragile ecosystems and, simultaneously, the sustainable use of natural resources through ecotourism and sustainable initiatives. By increasing awareness and using solutions based on accurate data, it will be possible to maintain the biodiversity of these valuable mountain regions as well as offering new opportunities for the development of local communities (Petrișor, 2009).

Much like in other parts of the world, these regions in Romania are at a greater risk of natural resource depletion owing to climate change, soil erosion, deforestation, and overgrazing. Economic factors coupled with rural depopulation contribute to agricultural land abandonment which poses a greater risk to these fragile ecosystems as well and amplifies these vulnerabilities (Oancea, 2003). A longitudinal study covering the period 1968-2018 shows how reduced human presence and farm activity in high-altitude areas directly accelerates soil erosion, biodiversity decline, and broader ecosystem dysfunction, increasing ecological fragility (Săvulescu et al., 2019).

The Common Agricultural Policy (CAP) of the European Union has made it possible to tackle these issues through cash prizes and assistance to long-term development. The National Rural Development Program (NRDP) 2014-2020 has assigned significant resources to mountain regions, concentrating on investments in infrastructure, young farmers, and small agricultural businesses (AFIR, 2022). Encouraging young entrepreneurs through successful implementation of sub-measure sM 6.1, referred to as referred to as “Support for Young Farmers” and entrepreneurs with positive activity sM 6.3 named as “Support for Small Farms” have greatly increased farm resilience (PNDR, 2015).

The diversification of agriculture has turned out to be one of the most viable means of making mountain farms more productive.

This strategy integrates traditional agricultural practices with innovative approaches, such as organic agriculture, agro-tourism, and value-added activities. In addition to increasing farm profits, diversification also aids in achieving food security, protecting the environment, and safeguarding culture (Gavrilescu, 2000; Oros, 2022).

In addition, it promotes global sustainability by reducing dependence on monocultures and increasing resilience to environmental and economic changes.

Despite the above-mentioned challenges, there are several obstacles such as: lack of access to markets, insufficient infrastructure, ambiguous and incomplete administrative procedures, which most often stand in the way of correct implementation. In addition, rural depopulation and population aging contribute to the reduction of the labor force, thus agricultural development is delayed (INS, 2019). It is clear that only through an integrated approach to policy support, through local community involvement and through innovative agricultural methods, these challenges can be overcome.

This paper studies the role of agricultural diversification in promoting the sustainability and resilience of mountain farms in Romania.

The paper attempts to identify some good practices and the potential for improvement, achieved by synthesizing the adoption and implications of a set of pioneering PNDR sub-measures.

The research contributes to a better understanding of sustainable rural development and has knowledge transfer implications for decision-makers and stakeholders involved in supporting mountain societies.

MATERIALS AND METHODS

This research uses a multidisciplinary framework to examine the resilience and sustainability of Romanian mountain agricultural systems, with a focus on the relevance of diversification in agriculture. Primary and secondary data were collected to establish an in-depth understanding of the financial, physical and socio-economic effects of diversification measures under the National Rural Development Programme (NRDP) 2014-2020.

Primary data are obtained from the Ministry of Agriculture and Rural Development (MADR), the Agency for Rural Investment Financing (AFIR) and the National Institute of Statistics (INS) (MADR, 2019; AFIR, 2022; INS, 2019). Secondary data were also obtained from academic sources, official reports and statistical reports (Oros, 2022; Gavrilescu, 2000; Oancea, 2003).

The research focused on key sub-measures of the NRDP, i.e., sM 4.1 (Investments in Agricultural Holdings), sM 6.1 (Support for Young Farmers), sM 6.3 (Support for Small Farms), and sM 7.2 (Investments in Basic Infrastructure).

The selection of these sub-measures is because they contribute significantly to the economic viability and long-term sustainability of the mountain farming business. In a bid to understand the effectiveness of these initiatives, several financial and physical performance metrics were analyzed, such as utilization levels of funds, project completion rates, and regional distribution of projects.

Quantitative data were analyzed through descriptive statistics in the form of means, percentages, and time trends to assess the implementation of the project and fund use. Table 1 shows the description of the main performance indicators of the sub-measures under investigation. Time-series analysis was conducted to emphasize the trend in approvals of projects and the use of funds during the implementation. Figure 1 shows the trends in annual approvals of projects with a clear spike in submissions for sM 6.3 and sM 6.1.

Table 1. Key Performance indicators for NRDP sub-measures

Indicator	Definition	Example sub-measure
Fund Utilization Rate (%)	Percentage of allocated funds utilized	sM 6.1, sM 6.3
Project Success Rate (%)	Approved projects / Total applications	sM 7.2
Regional Distribution (%)	Percentage of projects by region	sM 4.1, sM 4.2

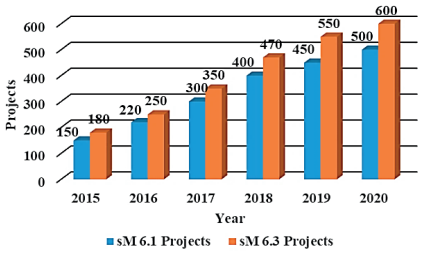


Figure 1. Yearly trends in project approvals for sM 6.1 and sM 6.3.

The geographical scope of the study are Romania's mountain areas, as delineated by the MADR's criteria, e.g., those with altitudes above 500 meters, slopes more than 15%, or other biophysical constraints. The study covered 948 administrative units (UATs) that were classified as mountain areas. Table 2 shows the spatial distribution of the UATs, and Figure 2 is a graphical representation of the percentage allocation by regions.

Table 2. Geographical distribution of mountain areas by region

Region	Total UATs	Percentage of total UATs (%)
Central	230	24.3
Northwest	198	20.9
Other Regions	520	54.8

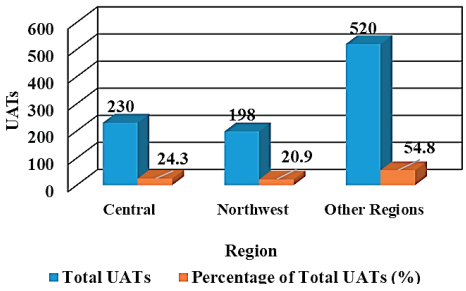


Figure 2. Regional breakdown of mountain UATs

To complement the quantitative analysis, qualitative information was collected through semi-structured interviews of 30 stakeholders, including farmers, local authorities, and agricultural association representatives. The interview themes were diversification barriers, socio-economic impacts of funding, and infrastructure issues. Table 3 presents the most significant issues brought up during the interviews, while Figure 3 shows the most prevalent barriers cited, including delayed funding, limited market access, and inadequate infrastructure (RNDR, 2015; MADR, 2020).

Table 3. Interview topics and stakeholder groups

Topic	Stakeholder group
Barriers to diversification	Farmers, local authorities
Impact of funding on livelihoods	Farmers, associations
Infrastructure challenges	Local authorities

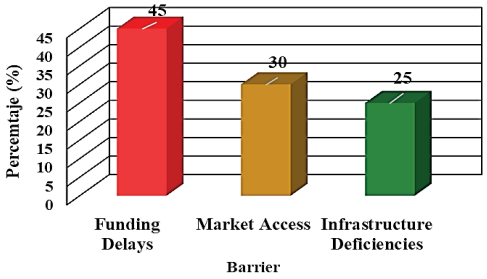


Figure 3. Common barriers identified during interviews

In addition, the analysis includes efficiency analysis by sub-measures, i.e., approval rates, fund utilization, and average project size. A comparative analysis of these efficiency measures is presented in Table 4, whereas Figure 4 presents the performance of each sub-measure relative to fund utilization.

Table 4. Performance of sub-measures in terms of efficiency

Sub-measure	Approval rate (%)	Utilization rate (%)	Average project size (€)
sM 4.1	52.9	63.6	140,712
sM 6.1	71.4	84.5	95,020
sM 6.3	68.6	77.9	57,764

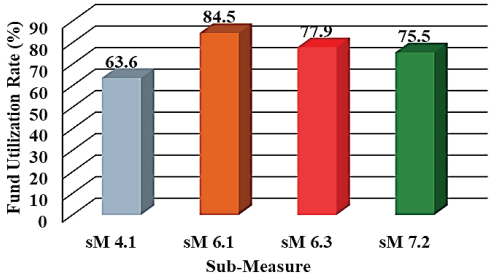


Figure 4. Performance of sub-measures in terms of fund utilization

RESULTS AND DISCUSSIONS

This chapter provides an examination of the application of agricultural diversification actions in Romania's mountain regions in the 2014–2020 programming period. The results are organized into three sections: financial and physical performance of the sub-measures of the NRDP, geographical distribution of the projects, and socio-economic effects of agricultural diversification.

Innovation in technologies, such as the production of enhanced agricultural construction material infrastructure, plays a critical role in driving sustainability (Cherecheș et al., 2021). The use of industrial wastes to add to clay-composite material provides a feasible way of promoting sustainable construction agriculture (Hegyi et al., 2023).

Results from this mixed-methods design give a comprehensive picture of the effects and challenges of farming diversification in mountain regions. Visualization instruments like bar graphs, pie graphs, and line graphs were utilized to facilitate interpretation of the results. Figure 5 illustrates project categorization with noteworthy financial input into infrastructure and small-scale farms, while Table 5 delineates the respective finance allocations.

Table 5. Funding distribution across project categories

Category	Total funding (€)	Percentage (%)
Infrastructure	300,000,000	40
Young Farmers	150,000,000	20
Small Farms	200,000,000	30
Cultural Heritage	50,000,000	10

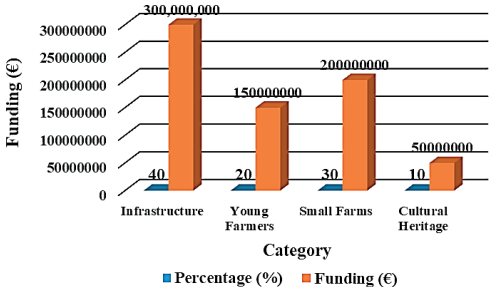


Figure 5. Funding distribution by category

This study, though buttressed with ample data gathering and analysis, is not free of limitations. Its dependence on government data can potentially lead to the exclusion of unofficial or unrecorded activities, and variations in data availability by region may impinge on the cross-region comparability of results. Still, the integration of qualitative and quantitative approaches provides ample probing into agricultural diversification in Romania's mountains.

Financial and physical performance of sub-measures

Implementation of NRDP sub-measures differed greatly in their financial and performance success, with significant disparity between various sub-measures and regions. As can be seen from Table 6, the fund utilization rates ranged from 63.66% for sM 4.1 to 84.50% for sM 6.1, indicating that schemes for the support of young farmers were realized more effectively than schemes for the support of bigger agricultural holdings.

Table 6. Financial and physical performance of sub-measures in mountain areas (2014-2020) (Source: AFIR, 2022)

Sub-measure	Financial allocation (€)	Projects submitted	Projects approved	Projects funded	Fund utilization (%)
sM 4.1	251,979,586	336	178	167	63.66
sM 6.1	100,362,967	3,579	2,557	2,268	84.50
sM 6.3	63,854,499	6,861	4,705	3,855	77.88
sM 7.2	148,355,461	121	90	84	75.50

The high performance of sM 6.1 ("Support for Young Farmers") is attributed to easier application processes and the availability of expert advisory services. Young farmers were able to get funding for diversification activities, e.g., agrotourism, organic production, and value-added production, which raised their competitiveness and income levels significantly. Figure 1 shows the increasing trend of approvals for sM 6.1 projects during the programming phase, which indicates higher awareness and demand for the project. Conversely, sM 4.1 ("Investments in Agricultural Holdings") was faced with complexity challenges in funding needs, which discouraged smallholder farmers from accessing assistance. Stakeholder consultations revealed that co-financing requirements and complicated paperwork were significant hindrances to small-sized agricultural businesses, particularly where administrative capacity is weak. Consequently, only 63.66% of financial resources were absorbed under this program, reflecting the need for process simplification (AFIR, 2022).

The performance of sM 6.3 ("Support for Small Farms") was remarkable, with a fund use rate of 77.88%. Through this scheme, small-scale farmers were able to modernize, purchase equipment, and diversify farm activities. The beneficiaries of the sM 6.3 experienced an average 25% income increase, as confirmed by qualitative interviews and financial data analysis. These findings emphasize the imperative function of targeted programs in strengthening the resilience of smallholder farmers (Oros, 2022).

Sub-measure sM 7.2 ("Investments in Basic Infrastructure") was used at a level of 75.50%, with emphasis placed on the development of rural roads, water supply, and other basic infrastructure. Although these investments are important for long-term rural development, their direct impact on agricultural productivity was lower than that of measures targeting farms directly. Stakeholders said that infrastructure development indirectly improved access to markets and lowered transport costs, which are major drivers of economic growth in mountains. The contrast between annual trends (Figure 6) highlights the diversity in the performance of the sub-measures. The consistent rise in project approvals for sM 6.1 and sM 6.3 reflects the

effectiveness of support schemes aimed at young and small farmers, which are tailored to the socio-economic realities of mountain regions. The relatively stable trend for sM 4.1, on the other hand, suggests ongoing challenges to access financing for relatively larger farm investments.

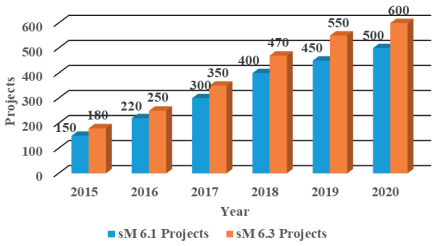


Figure 6. Yearly trends in project approvals for sM 6.1 and sM 6.3.

These findings point to the necessity for targeted policy measures to surmount regional disparities and administrative hurdles. Future editions of rural development programmes ought to consider the simplification of financing prerequisites, the expansion of advisory services, and the prioritisation of measures having direct applicability to the interests of young and small farmers.

Regional distribution of projects

The regional implementation of NRDP sub-measures showed notable disparities across mountain areas. Figure 7 illustrates the distribution of approved projects by region, highlighting the dominance of the Central and Northwest regions in terms of project approvals. These two regions accounted for the majority of approved projects, with significant contributions from sub-measures sM 6.1 and sM 6.3.

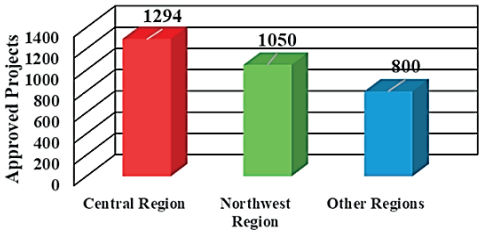


Figure 7. Distribution of approved projects by region (2014-2020)

This distribution is due to various reasons such as greater awareness levels, improved infrastructure, and increased access to avenues of funds in the Northwest and Central regions. In these regions, the local governments and agricultural associations were also actively engaged in assisting applicants by providing training workshops and consultancy services, thus boosting the success rate of applications (MADR, 2019). The agrarian potential of the areas was taken into consideration, as both sites are characterized by a high number of small-sized farms and young farmers, who are the primary target group for sM 6.1 and sM 6.3. For a better insight into the financial situation in relation to the project implementation, Table 7 gives a breakdown of the total funding allocated to different regions between the programming periods 2014-2020.

Table 7. Regional funding allocation for mountain areas (2014-2020) (Source: AFIR, 2022)

Region	Total funding (€)	Percentage of total allocation (%)
Central	98,563,215	32.1
Northwest	86,427,892	28.1
Other Regions	121,735,406	39.8

The Central region received the highest allocation of funds (32.1%), a reflection of its extensive participation in diversification and infrastructure investments.

This comes after the outstanding performance of the region in approving projects under sM 6.1, where young farmers reaped the most benefits.

Similarly, the Northwest region, which received 28.1% of the overall funding, had massive success in small farm modernization projects, which were implemented under sM 6.3.

While the bulk of the mountain UATs belonged to the "Other Regions" category (54.8%), they were assigned only 39.8% of the overall funding. This imbalance is proof of lingering problems such as lack of awareness of the available funding opportunities, poor advisory services, and infrastructural weaknesses that beset accessibility in these areas. The stakeholders in these areas were more likely to state difficulties in managing the complex application process and co-financing requirements, and this indirectly translated into lower approval rates for projects.

The skewed distribution of projects and finance identifies the need to decrease regional disparities. The Central and Northwest regions have benefited from their closeness to urban areas, which improved their market and logistical resource endowments. The regions also boast a history of structured farming operations and highly established farmer association networks, which played a crucial role in disseminating information about NRDP activities and providing technical assistance. On the other hand, "Other Regions" faced ingrained issues such as poorly developed infrastructure and advisory services' limited availability. Farmers from these regions indicated difficulties in product transportation to markets, expensive operations, and insufficient local facilitation in dealing with administrative demands.

In the interests of fostering equal access to finance and project opportunities for all mountain regions, policymakers can look to consolidate advisory services by sending regional advisors into rural areas to offer on-the-ground assistance to farmers. Investments in basic infrastructure such as roads, water pipes, and warehouses are key to reducing market access barriers and operating costs. In addition, increasing the frequency and coverage of informational campaigns in poorly performing districts will inform all eligible farmers about NRDP opportunities.

By tackling these imbalances, NRDP funding can achieve a more even effect on all mountain regions, promoting sustainable development and enhancing the well-being of farmers in less favored areas.

Socio-economic impact of agricultural diversification

Agricultural diversification has presently been introduced as a game-changing strategy to enhance the socioeconomic resilience of mountain farms in Romania. Incorporation of value-added practices such as organic farming, agrotourism, and processing of agricultural products has had a positively significant impact on farmers' incomes and created much greater opportunities for employment and the general economy. According to Figure 8, diversified farms, over a five-year period, reported an average income increase of 30% when compared with non-diversified farms.

Aside from financial advantages, diversification has acted as a stimulus for creating job opportunities in mountain areas. Small farms working in dairy processing, organic honey production, or agrotourism events have propped up local economies by creating demand for ancillary services. Farms benefiting from sM.63 ("Support for Small Farms") reported on average a 40% job increase, summarized in Table 8.

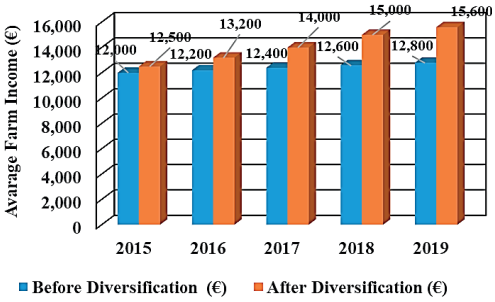


Figure 8. Changes in average farm income before and after diversification (2015-2019)

Table 8. Socio-Economic Benefits of Agricultural Diversification (Source: RNDR, 2015)

Indicator	Before diversification	After diversification	Change (%)
Average Farm Income (€)	12,000	15,600	+30
Employment Opportunities	3,000 jobs	4,200 jobs	+40
Market Access (Producers)	35%	60%	+25

A very recent development in this regard was particularly seen to create a positive impact in terms of access to markets. Farmers using strategies involving direct sales to consumers - either through farmers' markets or within the digital sphere - reported a 25% increase in the number of customers they reach. This is also another contribution to individual farm revenues and will enhance regional food security through an increase in the promotion of locally grown high-quality agricultural products (Oros, 2022).

Another critical benefit of agricultural diversification is that it can continue helping organizations engage in cultural heritage practices and techniques. For instance, program sM 7.6, which is involved in the investments of cultural heritage, led farmers to leave traditional

modes of production and integrate them into the modern to be effective. Some examples of this tend to indicate that artisanal cheeses, as well as the cultivation of varieties of crops deemed to have a historical context, allow for communities in mountainous areas to be economically viable. Yet, challenges continue. Farmers face barriers to diversification, such as financial limitations (45%), lack of adequate market infrastructure (30%), and limited technical assistance (25%), which underline the need for targeted policy measures to maximize socio-economic impact diversification, as shown in Figure 9.

In addition, climate change presents another growing challenge for mountain farming, as increasing variability in weather is affecting yields and profitability.

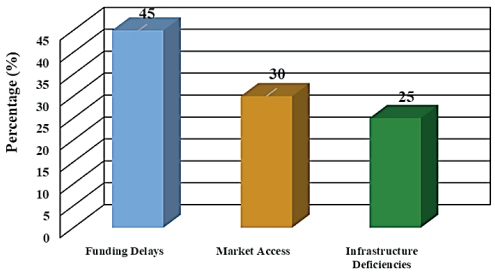


Figure 9. Proportion of projects affected by key issues

Diversified farms showed more resilience to these impacts, as their income streams were less reliant on a single crop or activity. For example, farms combining crop cultivation with agrotourism managed to survive droughts or floods better than others, with tourist income bolstering agricultural losses.

Moreover, diversification brings a more vibrant social dimension to the lives of rural people, whereby strengthening ties through collaboration among farmers, local authorities, and the organizations of regions. Cooperative marketing initiatives and collaborative knowledge-sharing platforms enhanced not only the economic outcomes but also advanced the social fabric of rural communities. The concerted efforts of the collective benefit regional diversification, spreading the whole gamut of advantages from individual farms to the region for inclusive and sustainable development.

For example, in the mountain regions of Sweden, traditional agriculture is threatened by the implementation of modern practices, leading to conflicts between biodiversity conservation and agricultural development. Society's expectations of farmers, such as providing recreational opportunities and maintaining cultural landscapes, create additional pressures. In addition, new support systems and regulations encourage the intensification of summer farms for modern meat production, which can lead to changes in the landscape and dissatisfaction among farmers (Rytkönen et al., 2016).

In rural areas, implementing biodiversity conservation measures can constrain agricultural development, generating environmental conflicts. These measures can limit agricultural land use and impose restrictions on traditional agricultural practices, thus affecting farmers' incomes and the sustainability of rural communities. To mitigate these conflicts, it is essential to develop policies that balance conservation objectives with agricultural development needs, promoting sustainable agricultural practices that protect biodiversity without compromising agricultural productivity (Barnaud & Couix, 2020).

CONCLUSIONS

This study pinpoints agrarian diversification as the very heart of promoting sustainability and building resilience for the mountain farms in Romania. This has been made possible by identifying contributions made and persisting challenges faced in the implementation and outcomes of NRDP sub-measures during the 2014-2020 programming period. The findings point to the benefits of diversification efforts in bolstering the socio-economic stability of the mountain communities. The farms that opened themselves to diversification strategies such as organic, agrotourism, and value-added production have raised their incomes to 30 percent. New job opportunities have also increased by 40% in the case of diversified farms, thus strengthening the local economy and reducing poverty in rural areas.

Despite those successes, the disparities in regional implementation are still evident. Central and Northwest areas accounted for most of the approved projects and funding allocations owing to better infrastructure, institutional

support, and higher awareness among farmers. In contrast, "Other Regions," which account for over half of mountain UATs, faced barriers like limited market access, poor infrastructure as well as administrative constraints, which resulted in much lower participation in NRDP programs. Addressing these inequalities is crucial to ensure equal funding and opportunity access across all mountain areas.

By diversifying these measures, a series of benefits for the environment and culture naturally appear. Through various Programs that support various aspects of traditional agricultural practices and investments in cultural heritage, the identity and uniqueness of mountain areas are maintained and at the same time new sources of income due to rural tourism and niche products specific to the respective areas are allowed to emerge. These programs highlight the dual role of diversification in promoting economic growth and sustainability. However, unfortunately, there will always be challenges such as financing delays, complex and cumbersome administrative processes and inadequate market infrastructure that always hinder the benefits of diversification. For example, farmers living in more remote areas have immense difficulties in accessing these resources and completing applications to feasibly apply diversification strategies.

Another important challenge is the impact of climate change, which exacerbates the already existing vulnerabilities of mountain agriculture. The most resilient farms are diversified farms, where income is spread across multiple activities and which are thus a buffer against environmental inequities. A good example is farms that combine agritourism with crop production and have spread the losses resulting from extreme weather events, thus suggesting crop diversification as a viable adaptation strategy. Maximizing agricultural diversification requires that, in future rural development programmes, the focus be on simplifying the administrative burdens associated with access to advisory services and investments in rural infrastructure. It is also necessary to expand training programmes and regional equity in the direction of focusing interventions on the needs of underperforming areas, and thus play equally important roles. The promotion of innovation in modern technology and techniques should generally be encouraged to increase productivity and competitiveness.

In conclusion, agricultural diversity is not simply a survival strategy, but clearly a transition towards sustainable development in all mountain regions.

Integrating traditional practices with modern innovations makes it possible for mountain communities to strengthen economic resilience, foster environmental conservation, and preserve cultural heritage. Lessons from the previous programming period of NRDP of 2014-2020 shall serve as fertile ground for future policies addressing the unique challenges mountain areas encounter. With continued support and collaboration, Romanian mountain farms can become a model in sustainable rural development at national and international levels.

REFERENCES

Academia Română (2008). *Rural Development and Mountain Regions in Romania*. București: Academia Română.

AFIR (2022). *Results and Indicators of NRDP Implementation (2014–2020)*. Agenția pentru Finanțarea Investițiilor Rurale. Retrieved from www.afir.info.

Antonescu, M. (2022). Challenges and opportunities for the sustainable development of mountain rural areas in Romania. *Grassroots Journal of Natural Resources*, 6(1), 54–73. Available at: https://grassrootsjournals.org/gjnr/nr-06-01-04-antonescu-m00327.pdf

Barnaud, C. & Couix, N. (2020). The multifunctionality of mountain farming: Social constructions and local negotiations behind an apparent consensus. *Journal of Rural Studies, 73*, 34–45.

Carpathian Convention (2025). About the Carpathian Convention. Retrieved at: http://www.carpathianconvention.org/ (accessed: 5 March 2025).

Cherecheș, M. L., Cherecheș, N. C., Ciobanu, A. A., Hudișteanu, S. V., Țurcanu, E. F., Bradu, A., & Popovici, C. G. (2021). Experimental Study on Airflow and Temperature Predicting in a Double Skin Façade in Hot and Cold Seasons in Romania. *Applied Sciences, 11*(24), 12139. https://doi.org/10.3390/app112412139

Gavrilescu, D. (2000). Dairy farming in small subsistence households. *Tribuna Economica*, *1*(5), 5–7.

Hegyi, A., Petcu, C., Ciobanu, A. A., Calatan, G., & Bradu, A. (2023). Development of Clay-Composite Plasters Integrating Industrial Waste. *Materials, 16*(14), 4903. https://doi.org/10.3390/ma16144903.

INS (2019). *Statistical Yearbook of Romania*. National Institute of Statistics.

MADR (2019). *Mountain area development strategies*. Ministry of Agriculture and Rural Development.

MADR (2020). *Rural Development Needs in Romanian Mountain Areas*. Ministry of Agriculture and Rural Development.

Petrișor, A.I. (2009). GIS assessment of landform diversity covered by natural protected areas in Romania. *Studia Universitatis Vasile Goldiș, Life Sciences Series*, *19*(2), 359-363.

Popescu, O.C. & Petrișor, A.I. (2010). GIS analysis of an area representative for the Romanian hardly accessible mountain regions with a complex and high-valued touristic potential. *Carpathian Journal of Earth and Environmental Sciences, 5*(2), 203-210.

Popescu, A., Dinu, T. A., Stoian, E., Șerban, V., & Ciocan, H. N. (2022). Romania's mountain areas – Present and future in their way to a sustainable development. *Scientific Papers. Series "Management, Economic Engineering in Agriculture and Rural Development"*, *22*(4), 549–564.

Oancea, M. (2003). *Modern management of agricultural holdings*. Bucharest, RO: Ceres Publishing House.

.

Oros, A. (2022). Mountain regions in Romania: Challenges and opportunities. *Journal of Rural Studies*, *35*(2), 125–138.

RNDR (2015). *National Rural Development Report 2014–2020*. Retrieved from www.rndr.ro.

Rytkönen, P., Bonow, M., & Dinnétz, P. (2016). Mountain agriculture at the crossroads: Biodiversity, culture, and modernization - Conflicting and interacting interests. In *11th European IFSA Symposium, Berlin, 1–4 April 2014* (pp. 893–904). Leibniz-Zentrum für Agrarlandschaftsforschung (ZALF).

Săvulescu, I., Mihai, B.-A., Vîrghileanu, M., Nistor, C. & Olariu, B. (2019). Mountain Arable Land Abandonment (1968-2018) in the Romanian Carpathians: Environmental Conflicts and Sustainability Issues. *Sustainability, 11*(23), article 6679. DOI: 10.3390/su11236679, https://www.mdpi.com/2071-1050/11/23/6679

Scientific Papers. Series E. Land Reclamation, Earth Observation & Surveying, Environmental Engineering. Vol. XIV, 2025
Print ISSN 2285-6064, CD-ROM ISSN 2285-6072, Online ISSN 2393-5138, ISSN-L 2285-6064

INTEGRATING VEGETABLE WASTE IN CLAY COMPOSITIONS: A SUSTAINABLE PATH FOR ECO CONSTRUCTION

Aurelia BRADU[1], Alexandrina-Elena ANDON[1], Alexandra-Marina BARBU[1], Claudiu-Sorin DRAGOMIR[1, 2]

[1]National Institute for Research and Development in Construction, Urban Planning and Sustainable Spatial Development – URBAN-INCERC, 266 Pantelimon Road, District 2, 021652, Bucharest, Romania
[2]University of Agronomic Sciences and Veterinary Medicine of Bucharest, 59 Mărăști Blvd, District 1, 011464, Bucharest, Romania

Corresponding author email: aurelia.bradu@incd.ro

Abstract

Since the dawn of industrialization, technological advancements have progressed rapidly, outpacing the planet`s natural resources` ability to sustain them. In the face of global warming, habitat destruction the imperative to invest in sustainable development practices has become increasingly evident. Clay-based construction materials are gaining traction at the national level, with their benefits recognized for the technical advantages and their contribution to the long-term durability of construction elements. The issue of vegetable waste is a large-scale, multifaceted challenge that continues to grow in urgency alongside rising consumption. Integrating vegetable waste into clay compositions exemplifies how traditional materials can be innovatively adapted to meet contemporary challenges. By combining ancient building techniques with modern knowledge and technology, clay composites can pave the way for a greener construction industry. This sustainable solution not only addresses pressing environmental concerns but also fosters a circular economy where waste becomes a resource. Through such practices, the construction industry can evolve into a model of resilience and sustainability for other sectors to follow.

Key words*: clay composite, sustainable development, vegetable waste.*

INTRODUCTION

Since the beginnings of industrialization, technological advances have progressed rapidly, exceeding the planet's natural resource capacity to sustain them. If modern society, in its industrial phase, was a production-based society, today, on a global scale, we live in a consumer society. The late 1970s marked the start of the hyper-consumption era, associated with the significant development of capitalist economies, which operate in an economy driven by the continuous and aggressive stimulation of demand, the constant creation of new and often unjustified needs, and the excessive consumption of goods and services. This has led to multiple social and environmental problems (Popescu et al., 2010).

In this context, an essential condition for the sustainable development of modern human society is the need to promote and develop sustainable production and consumption, adapted to the requirements of ecological resource management and environmental preservation (Geissdoerfer et al., 2017).

According to data published by the National Institute of Statistics, agriculture accounted for approximately 5% of Romania's GDP in 2022, generating over 60% of the total municipal waste in the form of plant waste (Hegyi et al., 2023). The issue of waste, seen in its entirety, is complex and large-scale, becoming increasingly strident as consumption continues to rise. These biodegradable wastes contribute, through their decomposition, to the emission of greenhouse gases, such as methane, further exacerbating climate change (Lachheb et al., 2023). The reuse of these materials in construction can significantly reduce their environmental impact (Cobzaru et al., 2017).

MATERIALS AND METHODS

In the presented study are described five types of recipes, based on matrices of clay, lime, sand, and cement, with plant-based materials (such as

straw) incorporated into each. These formulations were designed to create composite materials with improved properties by utilizing sustainable, locally sourced resources. The specific compositions of the clay, lime, sand, and cement matrices used in each formulation are presented in Table 1.

Table 1. The composition of the clay, lime, sand, and cement matrices

Materials	Indicative	R1	R2	R3	R4	R5
Clay	A	10 kg	7 kg	4 kg	13 kg	16 kg
Lime	V	20 kg	26 kg	32 kg	14 kg	8 kg
Sand	N	5 kg	3.5 kg	2 kg	6.5 kg	8 kg
cement	CI	5 kg	3.5 kg	2 kg	6.5 kg	2 kg
Straw	P	2 kg	2 kg	2 kg	2 kg	2 kg
Water	A	8l	8l	8l	8l	8l

The compositions of the different recipes are as follows:

- *Recipe R1* contains 50% lime and 50% of a mixture of clay, sand, and cement;
- *Recipe R2* contains 65% lime and 35% of a mixture of clay, sand, and cement;
- *Recipe R3* contains 80% lime and 20% of a mixture of clay, sand, and cement;
- *Recipe R4* contains 35% lime and 65% of a mixture of clay, sand, and cement;
- *Recipe R5* contains 20% lime and 80% of a mixture of clay, sand, and cement.

These formulations were designed to balance the mechanical properties of the materials with sustainable practices by incorporating agricultural residues such as straw, thereby reducing environmental impact while enhancing the thermal and structural performance of construction materials. Each of the recipes varied in terms of the lime-to-clay ratio, which influences the material's strength and thermal conductivity.

Straw, generated in significant quantities from wheat production (with Romania ranking 4th in the EU in this regard), represents an available resource, with millions of tons produced annually. Straw-light clay is a mixture of straw and clay with a density of less than 1200 kg/m^3, (Azzolino et al., 2020). This density is considered optimal for light clay with straw, providing a good balance between thermal insulation and material strength. The mixture allows for efficient insulation and adequate compressive strength, preventing deformation and loss of thermal properties (Petcu et al, 2023). If the density exceeds 1200 kg/m^3, it is referred to as clay with straw. The resulting material is denser, stronger, with reduced insulating properties, and becomes heavier and harder to handle during construction.

Elements with densities under 600 kg/m^3 are not recommended because the resulting material would be too fragile and prone to sedimentation and rot of the straw due to moisture infiltration. In this case, the straw is more vulnerable to microbial attacks and pests (such as wood lice), which can affect durability (Tavakoli, 2015).

Although studies have been conducted on selecting the appropriate types of straw, more important than the type of straw is the structure of the nodes (Figure 1).



Figure 1. The structure of the nodes in wheat straw

Straws with rigid nodes are preferred to increase thermal insulation because they do not deform easily and keep the air trapped inside, prevent excessive compaction of the clay-straw mixture, as these do not easily deform under the weight of the clay (Barone et al., 2011). This improves the durability and thermal insulation properties of the material. They also contain cellulose and lignin, which reinforce the plant stem's structure. These components are resistant and help protect against rot and degradation under the influence of moisture. At the same time, lignin provides resistance and structural durability. As the plant matures, the lignin in the nodes becomes more concentrated, further strengthening the node structure and giving an advantage to older straws, which are better suited for construction.

The length of the straw should not exceed the thickness of the elements. The straw can be cut by various mechanical methods (with specialized machines or shredders) or manually (with scissors or other tools).

Adding straw to the mixture can significantly reduce the shrinkage of the clay. Since the fibers increase the bonding strength of the mixture, cracks are minimized. To avoid the internal rotting of the straw, fungal growth, and to reduce shrinkage, clay elements with straw additions are recommended to have a thickness of less than 25 cm (Minke, 2000).

The workability of the clay composite can be improved by additives. The shrinkage process is influenced by the amount of sand or other large aggregates, the water content, the types and amounts of clay minerals, the distribution of the granulation of the aggregates (Calatan et al., 2020). The analysis of the clay's composition can be performed through a series of field tests (Carraro et al., 2021), such as water content test, sedimentation test, and ball throwing test, as well as laboratory conditions: Atterberg plasticity test, Proctor compaction test, and drying shrinkage test.

The addition of chopped straw contributes to increasing the bonding strength of the mixture, reducing the appearance of cracks (Figure 2 and Figure 3).



Figure 2. The introduction of straw into the composition

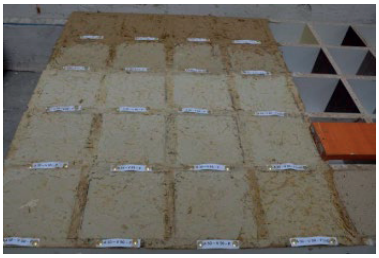


Figure 3. Casting of the samples

To enhance stability, straw is incorporated into the composition using a mechanical mixing process. The stabilizers coat the clay minerals, preventing water infiltration and minimizing volumetric changes.

Water resistance can be increased by altering the distribution of the earth and sand granulation. The straw bale technology (Minke, 2000) involves placing straw bales on the foundation and covering them with a layer of clay. This protects the straw from moisture and helps improve thermal insulation. The technology is fast and efficient, and the straw bales provide a stable frame and good protection against extreme temperatures.

The "Clay-Straw" technology (Goodhew & Griffiths, 2005) involves mixing straw with clay to produce a composite mass used for manufacturing tiles or panels. These elements are dried and subsequently installed on-site. This technology enables the rapid construction of walls while providing a user-friendly material with good thermal performance.

The "Tuf with Straw" technology combines tuff with straw to produce a lightweight yet strong construction material (Belayachi et al., 2016). The tuff helps stabilize the structure, and the straw improves flexibility and insulation. The structured elements are then assembled on-site and protected with a layer of clay or other materials to make them more durable.

The "Rammed Earth with Fibers" technology involves combining raw clay with fibers such as straw or hemp, which are then compacted within a mold to construct solid walls (Tesoro et al., 2021). Although traditional rammed earth technology uses earth without fibers, adding fibers increases flexibility and crack resistance. The clay is mixed with sand and fibers to create a more durable and elastic material. Water is added to help form the mixture. The clay-fiber mixture is placed into a mold and compacted with a hammer or a mechanical device to ensure density. The wall is built layer by layer, with each layer being compacted to increase its density and strength. Controlled drying helps achieve solid and durable walls.

The "Adobe" technology involves mixing unbaked clay blocks with fibers to improve cohesion and strength (Illampas et al., 2009). The blocks are poured into moulds and left to dry in the sun, then used to build self-supporting

walls. This is a traditional and cost-effective construction method, with reduced costs. Adobe blocks have excellent insulation properties and are resistant to extreme temperatures. The cement addition aims increase the compressive strength, improve mechanical performance and durability of the traditional material without compromising thermal insulation properties. Cement reduces porosity and improves water resistance, making the material less susceptible to cracking and deformation under load while providing protection against environmental factors such as moisture and temperature fluctuations. The use of cement in unburned clay with straw elements must be well calculated so as not to decrease the thermal performance of the material (Mircea et al., 2021). Too much cement quantity can reduce the insulating capacity of the straw, which could negatively affect the energy efficiency of the construction. The ideal is to find an optimal balance between straw, clay, and cement to achieve a strong and durable material with good thermal properties.

RESULTS AND DISCUSSIONS

The behaviour of composite thermal insulation materials based on plant fibers in a clay-lime matrix has been studied by performing the following measurements at the material level, in accordance with the laboratory procedures and relevant standards (Bailly et al., 2024; Zhao et al., 2021).

The linear dimensions were determined using a caliper with an accuracy of 0.01 mm, densities of samples dried at 80°C were measured using the gravimetric method, mass was determined using a balance, thermal conductivity, and thermal resistance of samples dried at 80°C were evaluated using the thermofluxmetric method.

Finally, the compressive strength was measured by applying a uniformly distributed load to the samples, which was gradually increased until rupture (Table 2, Figure 4 and Figure 5).

All these procedures allow for a comprehensive characterization of materials and a detailed understanding of their mechanical and thermal performance.

Together, these detailed measurements allow for a complete picture of the physical-mechanical characteristics of the material to be obtained for determining its suitable applications in sustainable and energy-efficient constructions. They are also suitable and for selecting the optimal material for the specific conditions of the project and ensuring a balance between mechanical performance and thermal efficiency.

Table 2. Maximum load at failure and compressive strength

Recipe	Length (mm)	Width (mm)	Thickness (mm)	Area (mm^2)	F (kN)	f_b (N/mm^2)
R1	145.6	146.36	146.35	21,308	18.1	0.85
R2	146.64	145.47	147.33	21,332	13.7	0.64
R3	145.29	148.3	143.73	21,548	13.3	0.62
R4	145.32	147.27	146.88	21,401	14.8	0.69
R5	146.88	145.96	146.6	21,581	16.1	0.75



Figure 4. Testing of R2 samples

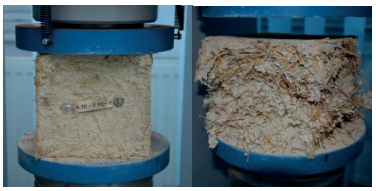


Figure 5. Testing of R3 samples

The data from Table 2 shows that the maximum load at failure (F) and compressive strength (f_b) vary depending on the recipe, with compressive strength values ranging between 0.62 and 0.85 N/mm^2, indicating differences in the structure and mechanical behaviour of the tested materials. These differences can be attributed to the variability of the ingredients in the composition of each recipe, which directly influences the material's structure, mechanical behaviour, and stability against environmental factors.

Recipe with 50% lime and 50% of clay, sand and cement mixture shows the best compressive strength, indicating superior mechanical performance, while recipe with 80% lime and 20% of clay, sand and cement mixture has the lowest strength, which could impact its use in demanding structural applications.

Data from Table 3 highlight significant variations in thermal conductivity (0.1332-0.2306 W/mK) and thermal resistance (0.27-

0.46 m²K/W), suggesting that certain recipes are more efficient in thermal insulation than others. Recipe with 80% lime and 20% clay, sand, and cement mixture shows the best performance as a thermal insulator, while recipe with 20% lime and 80% clay, sand, and cement mixture is the least efficient in this regard.

Table 3. Thermal conductivity and thermal resistance

Recipe	Thickness (m)	Thermal conductivity (W/mK)		Thermal resistance (m^2K/W)	
R1	0.0625	0.1577	0.1535	0.40	0.41
R2	0.0636	0.1492	0.1453	0.43	0.44
R3	0.0610	0.1369	0.1332	0.45	0.46
R4	0.0615	0.1742	0.1696	0.35	0.36
R5	0.0623	0.2368	0.2306	0.26	0.27

Recipes with lower conductivity have higher thermal resistance, making them more suitable for applications where thermal insulation is important.

The results suggest that higher lime content enhances thermal resistance, while higher cement content improves mechanical strength. The key takeaway is that a moderate use of lime and cement allows for a balance between durability and environmental sustainability.

The studied recipes may represent an excellent option for sustainable and eco-friendly construction, with improvements in both mechanical and thermal performance. However, using this mixture requires a balance between ecological advantages and technical requirements, with particular attention to the materials used and their environmental impact. A moderate use of cement and lime can help achieve a balance between durability, performance, and ecology.

CONCLUSIONS

The mixture containing 50% lime and 50% clay, sand, and cement demonstrated the best mechanical performance, while the mixture with 80% lime and 20% clay, sand, and cement provided the best thermal insulation. The selection of the appropriate material depends on the intended application: for high mechanical strength, the 50% lime and 50% clay, sand, and cement mixture is the optimal choice, whereas for enhanced thermal insulation, the 80% lime and 20% clay, sand, and cement mixture is preferable.

To enable the creation of new domestic products and methodologies, with lower costs compared to imports, targeting the balance between accessibility, cost, performance, durability, and optimizing insulating materials composed of renewable raw material resources, further experimental research is needed, either in the laboratory or on-site, to provide new insights regarding the maintenance of thermal, mechanical, and hygroscopic characteristics over time.

ACKNOWLEDGEMENTS

This paper was supported by the Program Advanced research on the development of eco-innovative solutions, composite materials, technologies and services, in the concept of a circular economy and increased quality of life, for a sustainable digitized infrastructure in a built and urban environment resilient to climate change and disasters, "ECODIGICONS", Program code: PN 23 35 03 01: "Integrated system of development and scientific research of constructions and vital infrastructures exposed to extreme seismic and climatic environmental actions and the exploitation of sustainable resources of materials and energy", financed by the Romanian Government.

REFERENCES

Azzolino, C., Macrì, M., & Mancuso, S. (2020). Straw Buildings: A Good Compromise between Environmental Sustainability and Energy-Economic Savings. *Applied Sciences, 10*(12), 4361-4378.

Bailly, G. C., El Mendili, Y., Konin, A., Khoury, & E. (2024). Advancing Earth-Based Construction: A Comprehensive Revw of Stabilization and Reinforcement Techniques for Adobe and Compressed Earth Blocks. *Engineering, 5*(2), 750-783.

Barone, J., & Kuehling, R. (2011). *Building with Straw Bales: A Handbook for Designers and Builders.* Earthscan, 50-70.

Belayachi, N., Bederina, M., Makhloufi, Z., Dheilly, R. M., Montrelay, N., & Queneudec, M. (2016). Contribution to the development of a sand concrete lightened by the addition of barley straws. *Construction and Building Materials, 113*, 513-522.

Calatan, G., Hegyi, A., Dico, C., & Szilagyi, H. (2020). Opportunities regarding the use of adobe-bricks within

contemporary architecture. *Procedia Manufacturing*, *46*, 150-157

Carraro, A., Fauchille, A., Di Filippo, E., Kotronis, P., & Sciarra, G. (2021). A Review of Sand-Clay Mixture and Soil-Structure Interface. *Geotechnics, 1*(1), 12-34.

Cobzaru, A., Cherecheș, M., & Ciobanu, A. (2017). *Cercetări experimentale pentru creșterea performanței materialelor de construcții: 2010-2017.* Editura INCD - URBAN-INCERC.

Geissdoerfer, M., Savaget, P., Bocken, N. M. P., & Hultink, E. J. (2017). The Circular Economy - A new sustainability paradigm. *Journal of Cleaner Production*, *143*, 757-768.

Goodhew, S., & Griffiths, R. (2005). Sustainable earth walls to meet the building regulations. *Energy and Buildings, 37*, 451-459.

Hegyi, A., Petcu, C., Ciobanu, A. A., Calatan, G., & Bradu, A. (2023). Development of Clay-Composite Plasters Integrating Industrial Waste. *Materials*, *16*(14), 4903

Illampas, R., Ioannou, I., & Charmpis, D. C. (2009). Adobe: An Environmentally Friendly Construction Material. *WIT Transactions on Ecology and the Environment*, 120, 245-256.

Lachheb, H., Bencheikh, A., & Bouhicha, M. (2023). Sustainable construction with unburnt clay bricks reinforced with agricultural residues. *Civil and Environmental Engineering Journal*, 1-12.

Minke, G. (2000). *Building with Earth: A Handbook,* Birkhäuser Verlag, 120-150.

Mircea, C., Toader, T.-P., Hegyi, A., Ionescu, B.-A., & Mircea, A. (2021). Early Age Sealing Capacity of Structural Mortar with Integral Crystalline. *Materials, 14*(2), 348-358.

Petcu, C., Dobrescu, C. F., Dragomir, C. S., Ciobanu, A. A., Lăzărescu, A. V., & Hegyi, A. (2023). Thermophysical Characteristics of Clay for Efficient Rammed Earth Wall Construction. *Materials*, *16*(17), 6015.

Popescu, C., Popescu S.-F., & Stroe C. (2010), Consumul din perspectiva împlinirii vieții umane, *Amfiteatrul Economic*, *vol. XII*, nr. 28, 529-544

Tavakoli, H. (2015). Straw Bale Construction: A Practical Guide for the UK. *The Crowood Press*, 45-95.

Tesoro, M., Falcicchio, C., & Foti, D. (2021). Rammed Earth with Straw Fibers and Earth Mortar: Mix Design and Mechanical Characteristics Determination. *Fibers*, *9*(5), 30.

Zhao, L., Li, J., & Zhang, S. (2021). Effect of fiber addition on the mechanical properties of unfired clay bricks. *Journal of Building Materials*, *23*(7), 1234-1245.

Scientific Papers. Series E. Land Reclamation, Earth Observation & Surveying, Environmental Engineering. Vol. XIV, 2025
Print ISSN 2285-6064, CD-ROM ISSN 2285-6072, Online ISSN 2393-5138, ISSN-L 2285-6064

THE IMPACT OF EXTREME WEATHER PHENOMENA ON THE MANAGEMENT OF CONIFEROUS STANDS

Ghiţă Cristian CRAINIC

University of Oradea, Faculty of Environmental Protection,
26 General Magheru Street, 410048, Oradea, Romania

Corresponding author email: gccrainic@yahoo.com

Abstract

Coniferous stands are relatively vulnerable to the impact of extreme weather events, often being affected by windfalls, because the spruce species (Picea abies L.) has a trailing root system. As a result, high-intensity winds cause windfalls on compact surfaces and the breaking of tree crowns and trunks. Windfalls in spruce stands also affect the forest soil, on considerable surfaces. The case study was carried out in spruce stands in the Horea Apuseni Forest District, Alba County, which were affected by windfalls and breakages. The objectives of the case study refer to the impact of the extreme weather events of 2011-2017 on spruce stands, forest soil and implicitly on the management of the affected forest unit. The wood affected by these extreme phenomena was valued at a price specific to the assortments and quality of accidental wood products, registering considerable financial losses. Also, a microrelief specific to wind fellings was formed, with a extremely negative impact on the ecological rehabilitation process of the affected spruce stands. The regeneration process of these stands was carried out over a relatively long period, 10-12 years, with very large financial efforts

Key words*: extreme weather events, spruce stands, forest soil, accidental wood products, ecological rehabilitation.*

INTRODUCTION

Spruce-dominated coniferous stands in mountainous areas are highly susceptible to windthrows and windbreaks caused by extreme weather events.

In recent years, the frequency of extreme weather events has increased, and as a result/ thus, their effects have significantly influenced the stability of spruces. As a result, spruce stands in the stages of youth and maturity, which are characterized by relatively high thickness and density, are relatively vulnerable to windthrows and windbreaks.

The increasingly evident emphasis of climate change exerts a direct influence on the frequencies and intensities of extreme weather events in areas covered with forest vegetation in Europe. As a result, major issues have been reported in spruce (*Picea abies* L. Karst) stands.

Although they are considered some of the most important forest formations in Northern Europe, in terms of ecological and economic importance, they present a high vulnerability to the action of strong dominated winds (Krišans et al., 2020). Because the spruce species has a trailing root system, uprooting and felling caused by potentially destabilizing environmental factors, such as strong winds, high-intensity storms, heavy rainfall, and especially combinations thereof, are frequently reported (Figure 1) (Cristea, 2004).



Figure 1. Root system of a windthrown spruce tree (Crainic, G. C., 25.07.2011, plot 80A, Production Unit I Vadul Moţilor, Horea Apuseni Forest District, Alba County)

The image in Figure 1 indicates that the windthrown spruce specimen has a superficial root system, with roots developed horizontally and without a distinct central taproot.

As a result, the cause of the low degree of ecosystem stability of spruce stands to the destabilizing action of high-intensity winds is due to the architecture of the spruce roots, which is essential for their anchoring in the soil and their stability. In well-drained and deep soils, spruce roots develop optimally, and the volume of the root system, consisting of roots and soil, is large, ensuring high anchoring and stability. Consequently, on shallower soils, with rock relatively to the surface, the volume of tree root systems is reduced, and the anchoring and stability of trees is considerably reduced (Krišans et al., 2020).



Figure 2. Spruce stand in plot 83A, affected by windthrow and windbreak (Crainic, G. C., July 25, 2011, Production Unit I Vadul Moţilor, Horea Apuseni Forest District, Alba County)

Climate change is recognized as one of the biggest problems the world is facing nowadays, representing a potential threat to the environment (Psistaki et al., 2024). These favor and trigger a series of extreme weather phenomena, which represent major stress and destabilization factors for forest ecosystems, causing both immediate and long-term effects (Barbagallo et al., 2024).

Windthrows and windbreaks, as direct effects of extreme weather events, cause major changes in the growth, development and evolution of coniferous stands. In this context, both isolated trees and compact stands are affected, with a particularly strong ecological, social and economic impact.

In Romania, in recent years, a series of windthrows and windbreaks have been reported in spruce stands. These events impacted large areas of spruce forests in the Apuseni Carpathians during July 2011 (Figure 2) and September 2017, affecting stands at multiple developmental stages (Crainic et al., 2024).

Exploitable stands were also affected, on various areas in the Curvature Carpathians (a transitional zone between the Eastern and Southern Carpathians of Romania) in February 2020, such as the upper basin of the Bâsca River where large-scale windfalls were recorded in 1995 (Ciocirlan & Câmpu, 2024).

Recent research conducted in the Curvature Carpathians, mainly pure spruce stands, located on land with a slope between 16 and 30°, highlights the fact that the impact of extreme weather phenomena had a maximum intensity when the wind came from the north - northeast direction, and reached a maximum speed of 32 m/s (Ciocîrlan & Câmpu, 2024).

In recent decades, windthrows and windbreaks, followed by bark beetle infestations, represented by the species *Ips typographus* L. in softwood stands, have caused widespread disturbances in forest ecosystems. As a result, the Earth's carbon balance has been significantly affected, modifying soil respiration, with direct implications for the decrease in gross primary productivity in the affected stands (Bozzini et al., 2023; Tomes et al., 2024).

Dead wood from trees affected by extreme weather events influences the increase in soil heterogeneity, due to the formation of a specific microrelief due to windfalls (Geambaşu, 1984; Kikeeva et al., 2024). A series of soil properties are also determined by the physical and chemical characteristics of wood during its decomposition, under the direct influence of environmental conditions and

microorganisms in forest ecosystems (Sicoe et al., 2023; Kikeeva et al., 2024).

Recent studies confirm that fallen spruce logs, in moderate and advanced stages of degradation, have a direct influence on the horizontal distribution and heterogeneity of the soil cover with herbaceous and shrub species, in the area bordering them. Consequently, dead spruce wood influences the coverage of the bordering areas with acidophilic and slightly acidophilic species. It was also found that the impact of wood in different stages of decomposition on soil heterogeneity parameters can be traced up to 20 cm from the tree (Kikeeva et al., 2024). Storms in recent years have also affected the stands of conifers of the *Pinus halepensis* and *Pinus sylvestris* species in the Mediterranean forest area. Their effects on soil characteristics were evident, as a result of which the percentage of clay increased in the gaps where the trees were felled, and the value of the concentrations of the elements K and Mg decreased. As a consequence, especially the soil surfaces that were affected by the destruction of the *Pinus halepensis* stands became less fertile, being dominated by species of bacteria specific to the new conditions created (Camarero et al., 2021).

Studies conducted in balsam fir - *Abies balsamea* (L.) Mill stands, which grow over large areas in Quebec and are very vulnerable to the impact of strong winds, highlight their differentiated stability, depending on the growing season, season and the specific climatic elements, especially precipitation. As a result, the moment of recovery from bending of balsam fir trees (*Abies balsamea)* is relatively greater in winter than in summer (during the growing season) for the same characteristics of the dominant wind (Duperat et al., 2020).

Although harsh winter conditions, with low temperatures and heavy snow, are considered to pose an additional risk to the stability of trees and, implicitly, of the branches, the increase in the resistance and rigidity of the stem and root system during freezing temperatures and the change in wind flow through the forest, due to snow on the canopy and on the ground during this period, is evident (Duperat et al., 2020).

There are cases where windthrows and windbreaks can significantly interfere with management practices applied in some forest ecosystems. In situations where the impact of extreme weather events is frequently reported, without any human intervention, management and regeneration cutting of stands carried out without adequate management for the respective seasonal conditions, can lead to an increase in the ecosystem instability of the respective stands (Ruel, 2020). As a result, a series of concerns are currently being reported for promoting a management of forest ecosystems using natural disturbances related to their stability (Ruel, 2020). It is obvious to promote an adaptive management for this particular situations which are in many cases even extreme (Pomara & Lee, 2021).

Adopting a management approach, that has as its main objective the minimization of damage induced by strong wind storms in various forest ecosystems, can be based on the knowledge and results obtained from the vast research and studies carried out to date in this field. Consequently, the use of complex management templates, obtained based on the simulation of the conditions for facilitating and achieving fellings and ruptures caused by strong prevailing winds, can be successfully exploited for the design of optimal strategies for sustainable management of forest resources (Ruel, 2020).

The use of wind damage prediction and simulation models, such as ForestGALES_BC, for a series of boreal stands in North America, for both normal and extreme wind speeds, has made it possible to create the premises for adopting optimal decisions and strategies regarding risk management and planning for competitive forest management (Anyomi et al., 2017). The results of the simulations in the studied stands present the following three scenarios:

- at a wind speed of 5 m/s, the estimated amount of felling varied from 0 to 20% of the area;
- for winds with a speed of 20 m/s, the damage increased to 2 to 90% of the area;
- for winds of 40 m/s, the damage varied from 10 to 100% of the area (Anyomi et al., 2017).

The area affected by windthrows, and respectively their intensity, varied depending on the type of stands. As a result, the stands that present high ecosystem stability are those

represented by deciduous, hard-core species (Anyomi et al., 2017).

The genetic diversity of tree populations is one of the most important factors determining the stability and sustainability of forest ecosystems. The results of recent studies on the possible changes in the genetic diversity of naturally regenerating populations of spruce and Scots pine in various habitats indicate that a pronounced genetic diversity in regenerating populations provides a basis for the formation of stands capable of adapting to constantly changing climatic conditions (Verbylaite et al., 2017).

Naturally regenerated spruce and Scots pine seedlings, which were randomly analyzed from a spatial point of view, presented the same genetic diversity as the presumed maternal populations. Therefore, the genetic differentiation between trees from maternal populations and the naturally regenerated seedlings from them was low for the two species. More than this, information about the genetic dynamics of natural populations of Scots pine and spruce species that were studied may be important for the analysis and assessment of possible changes in genetic diversity at a local scale, which were induced by the disturbance of ecosystem stability and the interruption of the climax state and, respectively, by the modification of vegetation conditions in the new habitats related to the stands on which they were established (Verbylaite et al., 2017).

The variability in site conditions, genetic diversity of coniferous stands, and the forest management strategies employed are key factors in enhancing stand resilience to extreme weather events.

The solutions proposed by current forest strategies, to protect and promote ecosystem services and biodiversity, require a deep understanding of how global climate change will affect the dynamics and processes in forest ecosystems (Girona et al., 2023).

MATERIALS AND METHODS

This case study was conducted in nine coniferous stands within Production Unit I Vadul Moților, managed by the Horea Apuseni R.A. Forest District in Alba County (Figure 3), which were severely impacted by windthrows and breakages resulting from the extreme weather event of July 20, 2011.

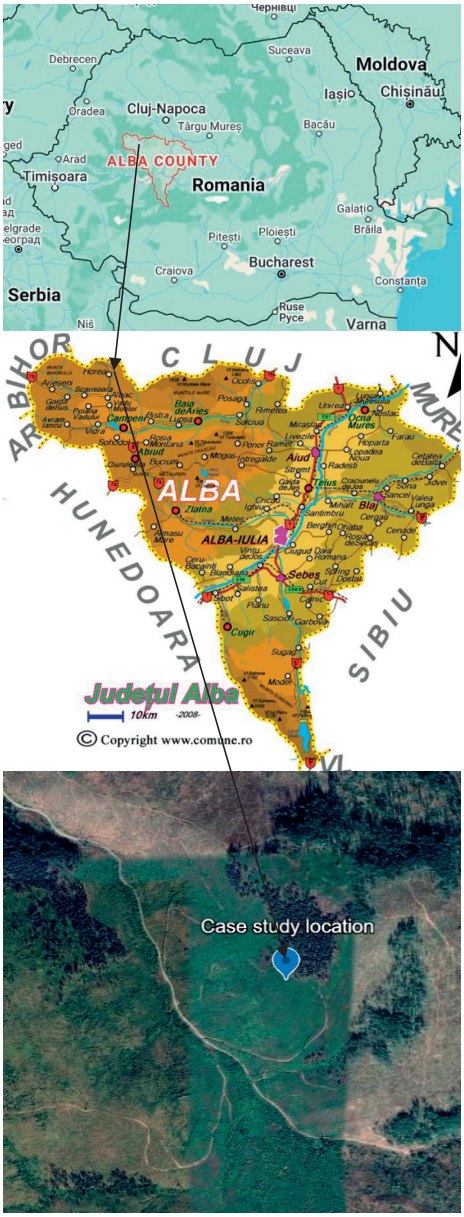


Figure 3. Case study location (https://www.google.com/search...; https://www.comune.ro/?/judet/ijud1/.; https://earth.google.com/web/search/Cabana...)

The objective of this study is to analyze the impact of the July 20, 2011 extreme weather

event on the management of coniferous stands severely affected by windthrows and windbreaks.

Field surveys were conducted to identify the affected stands, followed by stationary observations to determine the specific interventions required for their rehabilitation.

The experiment involved a complete inventory of the affected trees and the implementation of ecological rehabilitation measures.

Since the studied stands were entirely affected by windthrow and windbreak, for the quantitative-and implicitly, economic-assessment of the damaged timber, the technical regulations in force within the forestry sector and the Forest Code require a complete inventory of these areas.

All trees affected by the extreme weather event of July 20, 2011, were inventoried, and their volumes were calculated using the SUMAL 1.0 software. The economic value of the assessed timber was determined in accordance with the legal regulations in force at that time.

To study the factors and conditions that contributed to the occurrence of windbreak and windthrow events, elements of the forest site were analyzed, specifically the vegetation conditions and the characteristics of the forest vegetation. For the studied stands, the corresponding forest management plan was analyzed in detail, in parallel with field observations.

Rehabilitation efforts included the removal of harvesting residues, completion of regeneration through planting, and the management of mixed stands until they reached a closed-canopy (massif) condition. Materials used for the study included the project and management map of Production Unit I Vadul Moţilor (Horea Apuseni Forest District, Alba County), accounting records, forestry work contracts, relevant technical regulations, and specialized software for the quantitative and economic evaluation of the damaged timber.

RESULTS AND DISCUSSIONS

Analysis of the seasonal and vegetation conditions of the affected stands, summarized in Table 2, revealed that all plots shared similar stand types, soils, and forest classifications. The average elevation ranged from 1,300 to 1,475 meters, while slope gradients varied between 12 and 23. According to Figure 4, 34% of the plots faced east, 33% north, 22% southwest, and 11% northeast, indicating two predominant and two intermediate exposure types (Table 2). Most affected plots were located on undulating slopes in a proportion of 89% and the undulating upper slope in a proportion of 11% (Table 6).

Regarding the composition of the affected stands, 45% are almost pure, 44% are mixed and 10% are pure (Figure 7 and Table 2).

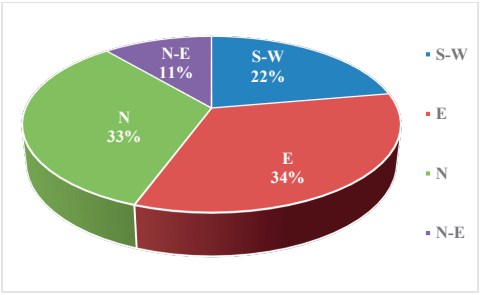


Figure 4. Distribution of affected plots according to exposure

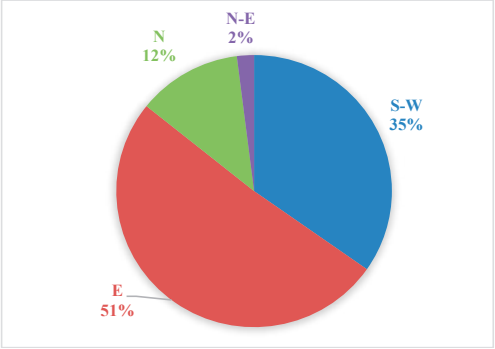


Figure 5. Volume distribution of affected trees by stands exposure

According to the results shown in the diagrams in Figures 4 and 5, the NE exposure accounts for 11% of the surface area of the affected stands, while the volume of affected trees in stands with this exposure represents 2% of the total volume.

Based on field observations, the direction in which the trees were windthrown is NE-in areas shaped like parallel strips. Consequently, the wind that caused the damage blew with high intensity from this direction.

Recent studies on spruce stands in two management units within the Curvature Carpathians - located opposite to the prevailing wind direction and situated at elevations between 1,300 and 1,500 meters on cambisols and spodosols - have yielded differing results. The same environmental factors were found to influence the intensity of windthrows and breakages inconsistently, with some factors proving statistically insignificant or relevant to only a small portion of the observed variation (Ciocîrlan & Câmpu, 2024).

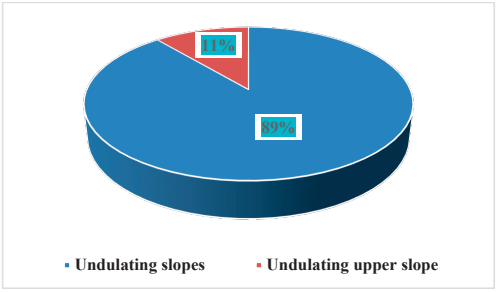


Figure 6. Distribution of affected plots according to landform

Consequently, based on current research and considering recent climate change trends, it remains challenging to accurately determine the relative contribution of predisposing factors and immediate triggers to wind-induced fellings and breakages across the studied stands.

As a consequence, it is relatively difficult to accurately determine the proportion of predisposing and triggering factors responsible for windthrow and windbreak in the studied areas based on the analysis of research conducted in stands affected by extreme weather events - both coniferous and broadleaved - within Production Unit (P.U.) VII Văratec, Sudrigiu Forest District, Bihor Forest Directorate, from 2017 to the present (Research contract no. 9, 19.07.2019), and considering the trend of climate changes in recent years.

Following the analysis of the affected stands and the complete inventory of windthrown and broken trees, the presence of accidental wood products was confirmed.

Given that the age of these stands exceeded half of their exploitable rotation age, the resulting timber was classified as 'Accidental I' products (Figure 8).

In accordance with current forestry regulations, such products are assimilated to the main wood harvest and are therefore deducted from the allowable cut volume established in the existing forest management plan (Paluš et al., 2020; Law 331/2024 Forestry Code, 2025).

After processing the field data, the values related to the volumes for each plot were obtained. The total volume of trees inventoried and considered as accidental products I, in the nine affected stands, is 28,466 m^3, on an area of 147.30 ha (Table 1). The market price was primarily influenced by wood quality, which declined significantly due to damage from windthrows and windbreaks (Figure 9a).

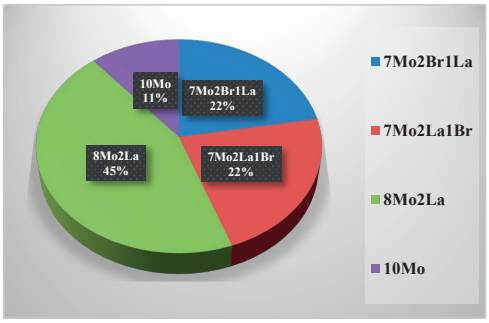


Figure 7. Distribution of affected plots according to the target composition of the stands

Table 1. Volume of trees felled and broken by the wind, in the affected stands

Forest plot	Surface (ha)		Affected volume (m^3)		Percentage of damage (%)
	The total	Affect	Total	per hectare	
63A	27.90	27.90	7,202	258.136	100
64A	19.70	19.70	2,687	136.396	100
80A	38.50	38.50	9,092	236.156	100
81A	17.00	17.00	492	28.941	100
83B	17.30	17.30	4,933	285.145	100
84B	1.90	1.90	571	300.526	100
85A%	35.60	3.40	335	98.529	9.55
85B	11.50	11.50	2,417	210.174	100
86B	10.10	10.10	737	72.970	100
Total	**179.50**	**147.30**	**28,466**	**193.252**	**82.06**

Ecological rehabilitation of the affected stands involved a range of targeted interventions (Govedar et al., 2018; Research contract no. 9 19 07 2019). The use of tree species for the regeneration of wind-damaged stands must ensure increased ecosystem stability. As a result, the compositions used must be made up

of tree species with ecological behavior adapted to environmental conditions in areas vulnerable to the effects of extreme weather phenomena, in order to ensure consolidated ecosystem stability (Ikonen et al., 2020; Konôpka et al., 2021).

Priority was given to promoting biogroups of naturally regenerated spruce, established effectively through wind-assisted seed dispersal (Figure 8). As a result, natural regeneration was successfully achieved on a total area of 57.10 hectares (Table 4), in the upper part of the slopes, bordering the unaffected stands, which produced abundant fruit during the period 2011-2014. In areas where natural regeneration did not occur, reforestation was implemented through staged artificial planting, using species-specific approaches tailored to site conditions.

Table 2. Seasonal and vegetation conditions in affected stands

Forest plot	S (ha)	Foret site	Type forest	Soil	Relief	Exposition	Declivity	Altitude	Flora indicators	Stand	
										Structure	Composition
63A	27.90	2312*	1121**	4101***	undulated slope	S-W	20	1300	*Hylocomium splendens*	even-aged stand	7Mo2Br1La
64A	19.70	2312	1121	4101	undulated slope	S-W	18	1350	*Hylocomium splendens*	even-aged stand	7Mo2La1Br
80A	38.50	2312	1121	4101	undulated slope	E	15	1375	*Hylocomium splendens*	even-aged stand	7Mo2Br1La
81A	17.00	2312	1121	4101	upper side slope	E	12	1475	*Hylocomium splendens*	even-aged stand	7Mo2La1Br
83B	17.30	2312	1121	4101	undulated slope	E	22	1325	*Hylocomium splendens*	even-aged stand	8Mo2La
84B	1.90	2312	1121	4101	undulated slope	N-E	23	1300	*Hylocomium splendens*	even-aged stand	8Mo2La
85A%	35.60	2312	1121	4101	undulated slope	N	18	1325	*Hylocomium splendens*	relativ even-aged stand	10Mo
85B	11.50	2312	1121	4101	undulated slope	N	18	1325	*Hylocomium splendens*	even-aged stand	8Mo2La
86B	10.10	2312	1121	4101	undulated slope	N	18	1350	*Hylocomium splendens*	even-aged stand	8Mo2La

*2312 - The phytoclimatic layer of Mountain spruce forests, of medium quality, with brown podzolic-brown podzol soil, with medium - submedium edaphic volume, with *Hylocomium splendens*; **1121 - Spruce forest type, with green mosses - *Hylocomium splendens*, of medium productivity; ***4101 - Typical brown alluvial soil; Mo - spruce species, Br - fir species, La - larch species, S-W -South-West, E – East, N-E -North East, N-North.



Figure 8. Trees broken and felled following extreme weather events, in the stand of plot 63 A (G. C. Crainic, July 25, 2011, Production Unit I Vadul Moţilor, Horea Apuseni Forest District, Alba County)

The artificial regeneration process involved a series of specific forestry operations, including the following technical works:

- C1IIIb - clearing land in preparation for afforestation;
- C21.a+b1 - developing or redeveloping storage glaciers for seedlings;
- C20IIb3 - excavating trenches for seedling storage;
- C23Ic12 - transporting seedlings by manual carrying;
- C24Ia1 + C24IIa - storing seedlings in trenches and preserving them in glaciers;
- C70Ic - planting seedlings in planting spots on unprepared land designated for reforestation;
- C70Ic - planting seedlings in hearths in unprepared land, in lands intended for reforestation.

In areas where incidental wood products had been harvested and natural regeneration did not occur; it was necessary to mitigate the negative impacts of logging.

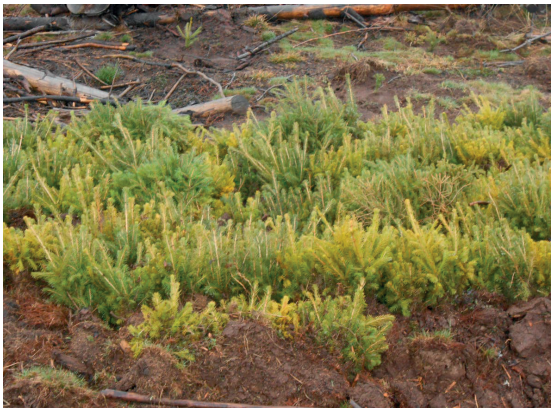
To ensure optimal conditions for artificial reforestation, logging residues and abandoned wood - primarily from broken trees - were collected and deposited in uprooting cavities and small clearings (Figure 9a). Stages of carrying out regeneration and maintenance works on areas where accidental products have been harvested are suggestively illustrated in the images in Figure 9.



a) Wood material to be removed from natural regeneration biogroups of spruce species, in plot 85B (G.C. Crainic, 03.04.2014, Production Unit I Vadul Moţilor)



b) Successful definitive mixed regeneration of spruce, in plot 63A (G.C. Crainic, April 11, 2025, Production Unit I Vadul Moţilor)



c) Bare-rooted seedlings of spruce, fir and larch species, kept in the trench, on the day they were planted, in plot 64A (G.C. Crainic, 05.04.2014, Production Unit I Vadul Moţilor)



d) Removal of overwhelming shrub and herbaceous vegetation, mechanized, from coniferous sapling biogroups, in plot 85B (G.C. Crainic, 05.11.2014, Production Unit I Vadul Moţilor)

Figure 9. Stages of establishing and managing (maintaining) natural and mixed regenerations in the affected stands of Production Unit I Vadul Moţilor

Table 3. The market value of wood assessed in the affected plots, in 2011

Forest plot	Average selling price		Total amount	
	RON/m^3	EURO/m^3	RON	EURO
63A	180	42.00	1296360	302484,00
64A	180	42.00	483660	112854,00
80A	180	42.00	1636560	381864,00
81A	105	24.50	51660	12054,00
83B	180	42.00	887940	207186,00
84B	180	42.00	102780	23982,00
85A%	105	24.50	35175	8207,50
85B	105	24.50	253785	59216,50
86B	105	24.50	77385	18056,50
Total	**Average price**		**4825305**	**1125904,50**
	169.51	**39.55**		

Much of the wood, particularly from visibly damaged or weakened trees, was left in various parts of the impacted plots. As a result, this aspect affected the health of the neighboring stands and, respectively, of the future mixed regenerations that were established between 2012 and 2024.

Consequently, in the spring of 2015, an attack of the spruce sapling borer - *Hylobius abietis* L. on spruce saplings, artificially regenerated (Figure 10).



Figure 10. Attack of the species *Hylobius abietis* L. on spruce seedlings, in artificial regenerations in the affected plots (G.C. Crainic, 03.04.2014, plot 84B, Production Unit I Vadul Moţilor)

To prevent these pests, poisoned baits were used, made from fresh spruce bark that had been treated with insecticide (Figure 11). As a result, the effects of the attack were limited to an area of 2.00 hectares, on which the regeneration of the spruce species was completely compromised.

Another consequence of maintaining considerable quantities of wood in the affected plots was the reduction of the area on which it was necessary to establish forest vegetation in the following decade.

Bare-rooted seedlings of spruce, fir and larch species were planted on an area of 90.20 hectares (Table 4). The number of seedlings planted per hectare was 5000, which were arranged in a rectangular arrangement (in the corners of a rectangle), at 1 m per row and 2 m between rows.

The saplings used for the afforestation works were purchased by the owner of the forest fund, respecting their area of origin.



Figure 11. Combating the attack of the *Hylobius abietis* L. species with poisoned baits, made from fresh spruce bark, which has been treated with insecticides (G.C. Crainic, 03.04 .2014, plot 84B, Production Unit I Vadul Moţilor)

Table 4. Evidence of areas that have been naturally and artificially regenerated in the affected plots

Forest plot			
Number	Regenerated surface (ha)		Species used
	Natural	Artificial	
63A	11.40	16.50	spruce, fir and larch
64A	5.90	13.80	
80A	27.00	11.50	
81A	0.00	17.00	
83B	0.00	17.30	spruce and larch
84B	0.00	1.90	
85A%	2.50	0.90	spruce
85B	5.40	6.10	spruce and larch
86B	4.90	5.20	
Total	**57.10**	**90.20**	-

Until they were transported to the plantation site, the saplings were kept on the ice, in optimal conditions, in accordance with the technical regulations in force. On the day they were planted, they were transported and stored in the ditch, in the afforestation site, with the

roots covered with soil to protect them from degradation (Figure 9c).
Biogroups of larch seedlings were placed on the areas exposed to the wind (Figure 12), fir seedlings were planted in the wetter, relatively shaded portions, and spruce seedlings were planted on the surface difference (Figure 13).
The works necessary for the management of natural and artificial regenerations until the achievement of the under-canopy stage were represented by:
- completion of regeneration through plantations of bare-root seedlings of spruce, fir and larch species;
- C58Ib-clearing of forest species of grassy, shrub and woody species over the entire surface;
- C58IIb3-clearing of forest species of grassy, shrub and woody species around the seedlings;
- C46c-review of natural regenerations and plantations.



Figure 12. Larch seedlings planted in an area exposed to the wind, in plot 86B (G.C. Crainic, 03.04 .2014, Production Unit I Vadul Moților)

The work to complete the natural and artificial regeneration was carried out by planting bare-root saplings on the areas where it is missing on an area greater than 9 m^2 (Figure 14). The working technique is similar to that of integral plantations. Consequently, completions were carried out with saplings of the three previously mentioned coniferous species.
The excessive grassy, shrubby, and woody vegetation around the spruce sapling groups, which were established naturally and artificially, was removed was carried out manually and mechanized with power tools with cutting discs (Figure 9d), as appropriate.
These works were carried out towards the end of the vegetation season, starting on September 15, for reasons that depend on the evolution of the climate in the mountainous areas, but equally on local experience.



Figure 13. Spruce seedlings planted in an area without natural regeneration, in plot 85B (G.C. Crainic, 03.04.2014, Production Unit I Vadul Moților)

The works to review the natural and artificial regeneration aimed to remove the remains of grassy, shrubby and woody vegetation from the saplings, after the snow melted, and bring them to a vertical position. During these works, all the surfaces undergoing regeneration were covered, and these were effectively carried out only in the areas where the saplings were affected.
The achievement of the under-canopy state for natural and artificial regeneration on the surface of the affected plots was carried out in successive stages, during the period 2014-2024, due to the climatic conditions in this interval.
In accordance with Order no. 2537 of September 28, 2022, the under-canopy state for natural regeneration of coniferous trees is considered achieved when the height of the

seedlings is 1.00-1.20 m, and in artificial regenerations the height of the seedlings varies between 1.20-1.40 m (Figure 9b).
Consequently, work was necessary to complete the regeneration in considerable areas, due to high temperatures and lack of precipitation during the vegetation season. These climatic elements were the main limiting factors that conditioned the final success of the established silvicultural crops.



Figure 14. Spruce saplings, planted during the regeneration completion works, to protect a stump (G.C. Crainic, 03.04 .2014, Production Unit I Vadul Moţilor)

All works carried out between 2012 and 2024 were considered investment works and were financed from the conservation fund, which was set up in the amount of 25% of the total value of the incidental wood products I, considered as main products, from the affected plots. Therefore, the conservation fund corresponding to the volume of wood recovered is 1,206,326.25 ron, the equivalent of 281,476.13 euro.
The recovery of spruce wood from the affected plots at an average price of 169.51 lei/m^3, or the equivalent of 39.55 euros/m^3, was carried out under extreme conditions, given its quality (Figure 8). If the price of the softwood wood is considered, obtained from main products, it is found that it has at least double the value compared to that of accidental products I. It is also found that the wood from the affected plots was recovered at a lower price, thus registering a consistent economic loss.
Recent studies conducted in Italy have also highlighted that following the storm in 2018, in the Upper Valtellina area, during the period 2019-2020, losses due to wood destruction were recorded, amounting to 5.10 million euros for the Valdisotto location, 0.32 million euros for Valfurva and 0.43 million euros for Sondalo, respectively. These losses were also added to those caused by the lack of carbon sequestration on the affected areas (Barbagallo et al., 2024).
Although the high diversity of tree species cannot necessarily cushion the economic consequences due to extreme weather phenomena (Fuchs et al., 2024), it nevertheless constitutes a factor of stability in spruce stands in the mountain area.
To promote an adaptive forest management, it is necessary to consider the concept of expected loss. This is an appropriate measure for integrating risk when establishing tree species and determining the optimal period of the production cycle (Möllmann & Möhring, 2017).
An alternative (differentiated) forest management can provide a specific value of resilience to storm adaptations. As a result, the specific goals of the cultivation and management of the stands and their structure, respectively, aim to maximize tree growth and resistance to various stresses and disturbances, rather than optimizing their productivity (Hahn et al., 2021).
To reduce the risk of future windthrows in the spruce stands, it is recommended to improve young plantation composition by introducing 30-40% beech species (Govedar et al., 2018).
The efficiency of the establishment works of forest vegetation on the surface of the affected plots could be achieved if there were conditions for direct sowing, with certified seeds of spruce, fir, larch and beech species.
It is also necessary to analyze the post-disturbance time period and the intensity of the disturbance (Camarero et al., 2021), in order to evaluate the growth and development dynamics and respectively the resistance of future stands, in a spatio-temporal approach.
Currently, it is necessary to promote forestry policies and strategies that ensure the reduction of investment risks for forest owners, in order to promote stable forests, with a diversified

structure, that provide multiple ecosystem services (Fuchs et al., 2024), under optimal conditions of administration and management.
The efficient implementation management of ecological restoration projects in the case of the forests affected by the devastating effect of climate change must be oriented towards both nature and the market. Consequently, ecological and economic objectives will be harmonized at a regional scale, in order to promote sustainable development in the region with high functional efficiency (Zhao et al., 2025).

CONCLUSIONS

The direction of the wind that caused the damage in the studied stands was from the NE exposure, which, according to the compartment descriptions in the forest management plan, accounts for 11% of their surface area.
In the context of global climate change, accurately determining the predisposing and triggering factors of windthrow and windbreak in spruce stands in the mountain zone is relatively difficult for various geographical areas.
The implementation of ecological rehabilitation works in spruce stands affected by extreme weather events presents a series of specific challenges related to the vegetation conditions and the morphological and ecological characteristics of these species.
Natural regeneration has been highly effective in 38.80% of the affected area, particularly in the upper part of the slopes, at distances of 300-400 meters from the unaffected spruce stands, which produced abundant seed during the period 2011-2014.
Although the Forest Code stipulates that the conservation and regeneration fund for forests should represent between 10-25% of the value of harvested wood, including main and accidental products I, for the ecological rehabilitation of the affected stands studied, this percentage is insufficient.
For optimal ecological rehabilitation of spruce stands that have been completely affected by various calamities, the conservation and regeneration fund must cover the cost of all necessary works, as established by the projects and execution estimates prepared for this purpose.
Given the current climate instability, the specific strategies for forest management of coniferous stands vulnerable to destabilizing factors must be integrated into adaptive forest management.
In extreme and exceptional situations, the conservation and regeneration fund for forests can be represented by the total value obtained from the sale of accidental products I, regardless of the owner or the administrator of the forest fund. This aspect must be urgently implemented in the Forest Code.
The consolidation of the ecosystem stability of spruce stands in the mountain zone, affected by various calamities, must be carried out as quickly as possible by introducing beech species through direct sowing under the canopy, and by expanding existing mixtures of spruce, fir, and beech species.

ACKNOWLEDGEMENTS

The studies and research were carried out with the agreement and collaboration of the management of the Horea Apuseni R.A. Forest District, Alba County, and the field staff of the Vadul Moţilor Production Unit I.
We also thank the representatives of the economic operator specialized in forestry works S.C. ECOPROD FOREST S.R.L., headquartered in Bihor County, who carried out all the forestry works in 2014 and 2015 in the case study location, based on service contracts and related additional documents, for their help and collaboration.

REFERENCES

Anyomi, K. A., Mitchell, S. J., Perera A. H., & Ruel, J. C. (2017). Windthrow Dynamics in Boreal Ontario: A Simulation of the Vulnerability of Several Stand Types across a Range of Wind Speeds. *Forests*, *8*, 233. doi:10.3390/f8070233. www.mdpi.com/journal/forests.

Barbagallo, B., Rocca, N., Cresi, L., Diolaiuti, G.A., & Senese, A. (2024). Enhanced Impacts of Extreme Weather Events on Forest: The Upper Valtellina (Italy) Case Study. *Remote Sens., 16*(19), 3692. https://doi.org/10.3390/rs16193692.

Bozzini, A., Francini, S., Chirici, G., Battisti, A., & Faccoli, M. (2023). Spruce Bark Beetle Outbreak Prediction through Automatic Classification of

Sentinel-2 Imagery. *Forests, 14*, 1116. https://doi.org/10.3390/f14061116.

Camarero, J.J., Colangelo, M., Gazol, A., Pizarro, M., Valeriano, C., & Igual, J.M. (2021). Effects of Windthrows on Forest Cover, Tree Growth and Soil Characteristics in Drought-Prone Pine Plantations. *Forests, 12*, 817. https://doi.org/10.3390/f12070817.

Ciocirlan, M., & Câmpu, V.R. (2024). Characteristics of Forest Windthrow Produced in Eastern Carpathians in February 2020. *Forests, 15*, 176. https://doi.org/10.3390/f15010176.

Crainic, G. C., Irimie, F., Cioflan, F. M., Dorog, S. L., Iovan, C. I., & Șerban, E. (2024). Influence of extreme weather phenomena on the management of deciduous forests. *Scientific Papers. Series E. Land Reclamation, Earth Observation & Surveying, Environmental Engineering*, *13,* Print ISSN 2285-6064, CD-ROM ISSN 2285-6072, Online ISSN 2393-5138, ISSN-L 2285-6064.

Cristea, M. (2004). *Climatic risks in the Crişurilor hydrographic basin).* Oradea, RO: Abaddaba Publishing House.

Duperat, M., Gardiner, B. & Ruel, J. C. (2020). Wind and Snow Loading of Balsam Fir during a Canadian Winter: A Pioneer Study. *Forests*, *11*, 1089; doi:10.3390/f11101089. www.mdpi.com/journal/forests.

Fuchs, J. M., Husmann, K., Schick, J., Albert, M., Lintunen, J., & Paul, C. (2024). Severe and frequent extreme weather events undermine economic adaptation gains of tree-species diversification. *Sci Rep*, *14*, 2140. https://doi.org/10.1038/s41598-024-52290-2.

Geambaşu, N.M. (1984). Research on the soils and forestry stations in the Rarău Massif in order to optimally exploit their silvoproductive potential - Doctoral thesis. University of Braşov, Faculty of Forestry and Forestry Exploitations.

Girona, M. M., Aakala, T., Aquilué, N., Bélisle, A. C., Chaste, E., Danneyrolles, V., Díaz-Yáñez, O., D'Orangeville, L., Grosbois, G., Hester, A., Kim, S., Kulha, N., Martin, M., Moussaoui, L., Pappas, C., Portier, J., Teitelbaum, S., Tremblay, J. P., Svensson, J., Versluijs, M., Wallgren, M., Wang, J. & Gauthier S. (2023). Challenges for the Sustainable Management of the Boreal Forest Under Climate Change. *Advances in Global Change Research, 74. Springer, Cham*. https://doi.org/10.1007/978-3-031-15988-6_31. https://link.springer.com/chapter/10.1007/978-3-031-15988-6_31#citeas.

Govedar, Z., Krstic, M., Keren, S., Violeta Babic, V., Zlokapa, B., & Kanjevac, B. (2018). Actual and Balanced Stand Structure: Examples from Beech-Fir-Spruce Old-Growth Forests in the Area of the Dinarides in Bosnia and Herzegovina. *Sustainability*, *10*(2), 540. https://doi.org/10.3390/su10020540.

Hahn T., Eggers, J., Subramanian, N., Caicoyad, A. T., Uhld, E., & Snäll, T. (2021). Specified resilience value of alternative forest management adaptations to storms. *Scandinavian Journal of Forest Research*, *36,* Nos. 7-8, 585-597. https://doi.org/10.1080/02827581.2021.1988140.

Ikonen, V. P., Kilpeläinen, A., Strandman, H., Asikainen, A., Venäläinen, A., & Peltola, H. (2020). Efects of using certain tree species in forest regeneration on regional wind damage risks in Finnish boreal forests under diferent CMIP5 projections. *European Journal of Forest Research*, *139,* 685-707. https://link.springer.com/article/10.1007/s10342-020-01276-6.

Kikeeva, A.V., Romashkin, I.V., Nukolova, A.Y., Fomina, E.V., & Kryshen, A.M. (2024). Influence of Picea Abies Logs on the Distribution of Vascular Plants in Old-Growth Spruce Forests. *Forests*, *15*, 884. https://doi.org/10.3390/f15050884.

Konôpka, B., Šeben, V., & Merganicová, K. (2021). Forest Regeneration Patterns Differ Considerably between Sites with and without Windthrow Wood Logging in the High Tatra Mountains. *Forests, 12,* 1349. https://doi.org/10.3390/f12101349.

Krišans, O., Samariks, V., Donis, J., & Jansons, A. (2020). Structural Root-Plate Characteristics of Wind-Thrown Norway Spruce in Hemiboreal Forests of Latvia. *Forests, 11*, 1143. doi:10.3390/f11111143, www.mdpi.com/journal/forests.

Möllmann, T. B., & Möhring, B. (2017). A practical way to integrate risk in forest management decisions. *Annals of Forest Science 74,* 75. https://doi.org/10.1007/s13595-017-0670-x. https://hal.science/hal-02976564/document.

Paluš, H., Parobek, J., Moravčík, M., Kovalčík, M., Dzian, M., & Murgaš, V. (2020). Projecting Climate Change Potential of Harvested Wood Products under Different Scenarios of Wood Production and Utilization: Study of Slovakia. *Sustainability*, *12*(6), 2510. https://doi.org/10.3390/su12062510.

Psistaki, K., Tsantopoulos, G., & Paschalidou, A.K. (2024). An Overview of the Role of Forests in Climate Change Mitigation. *Sustainability, 16*(14), 6089. https://doi.org/10.3390/su16146089.

Pomara, L. Y., & Lee, D. C. (2021). The Role of Regional Ecological Assessment in Quantifying Ecosystem Services for Forest Management, *Land*, 10(7), 725. https://doi.org/10.3390/land10070725.

Ruel J. C. (2020). Ecosystem Management of Eastern Canadian Boreal Forests: Potential Impacts on Wind Damage. *Forests, 11*, 578. doi:10.3390/f11050578. www.mdpi.com/journal/forests.

Sicoe, S.I., Crainic, G.C., Samuel, A.D., Bodog, M.F., Iovan, C.I., Curilă, S., Hâruța, I.O., Șerban, E., Dorog, L.S., & Sabău, N.C. (2023). Analysis of the Effects of Windthrows on the Microbiological Properties of the Forest Soils and Their Natural Regeneration. *Forests*, *14*. 1200. https://doi.org/10.3390/f14061200.

Tomes, J., Fleischer, P., Jr., Kubov, M., & Fleischer, P. (2024). Soil Respiration after Bark Beetle Infestation along a Vertical Transect in Mountain Spruce Forest. *Forests, 15,* 611. https://doi.org/10.3390/f15040611.

Verbylaite, R., Pliura, A., Lygis, V., Suchockas, V., Jankauskien, J., & Labokas, J. (2017). Genetic

Diversity and Its Spatial Distribution in Self-Regenerating Norway Spruce and Scots Pine Stands. *Forests*, 8, 470. doi: 10.3390/f8120470. ww.mdpi.com/journal/fores

Zhao, H., Wei, W., & He, M. (2025). Sustainable Implementation Strategies for Market-Oriented Ecological Restoration: Insights from Chinese Forests. *Forests, 16,* 1083. https://doi.org/10.3390/f16071083.

***Ecological rehabilitation of the stands affected by the storm of 17.09.2017 within the Sudrigiu Forest District, Bihor County Forest Administration, Research contract with the socio-economic environment no. 9 19 07 2019, University of Oradea. https://protmed.uoradea.ro/facultate/cercetare/proiecte_nationale_files/web0009/index.html.

***_Forest management of Production Unit (P.U.) I Vadul Moţilor, Horea Apuseni Forest District R.A., Alba County_ (2011).

***_Forestry map of of Production Unit (P.U.) I Vadul Moţilor, Horea Apuseni Forest District R.A., Alba County_ (2011).

***Law on the Forestry Code - 331/2024, Official Gazette of Romania, Part I, No. 7/9 I, 2025.

***Order no. 2,537 of September 28, 2022, for the approval of the Technical Norms on forest regeneration and the annual control of regenerations and the Guide to good practices on forest regeneration and the annual control of regenerations. Ministry of Environment, Waters and Forests, Official Gazette no. 995 of October 13, 2022.

***https://www.google.com/search?q=harta+judet+alba&rlz=1C1GCEA_enRO900RO900&oq=&gs_lcrp=EgZjaHJvbWUqCQgDECMYJxjqAjIJCAAQIxgnGOoCMgkIARAjGCcY6gIyCQgCECMYJxjqAjIJCAMQIxgnGOoCMgkIBBAjGCcY6gIyDwgFEC4YJx

***https://www.comune.ro/?/judet/ijud1/.

***https://earth.google.com/web/search/Cabana+Bl%c4%83joaia,+Dealu+L%c4%83m%c4%83%c8%99oi/@46.54832534,23.09041778,1333.49947918a,4328.82423534d,30.00035283y,0h,0t,0r/data=CiwiJgokCWz5f84vSUdAEQD9tX70QkdAGa-EiCvPJjdAIaLUqw6kADdAQgIIATIpCicKJQohMWFzVExvN0dJM19wLVJNT3EwenZYNF9XMWYxRm8zQWlpIAE6AwoBMEICCABKCAjV3KbZBhAB.

***https://lege5.ro/Gratuit/ge3dcmbqgu4tk/codul-silvic-din-2025.

Scientific Papers. Series E. Land Reclamation, Earth Observation & Surveying, Environmental Engineering. Vol. XIV, 2025
Print ISSN 2285-6064, CD-ROM ISSN 2285-6072, Online ISSN 2393-5138, ISSN-L 2285-6064

UPGRADING THE TRADITIONAL DATABASE THROUGH BIM-BASED SHM VISION

Daniela DOBRE[1, 2], Claudiu-Sorin DRAGOMIR[1, 3], Iolanda-Gabriela CRAIFALEANU[1, 2], Cornelia-Florentina DOBRESCU[1, 4], Emil-Sever GEORGESCU[1]

[1]National Institute for Research and Development in Construction,
Urban Planning and Sustainable Spatial Development – URBAN-INCERC,
266 Pantelimon Road, District 2, 021652, Bucharest, Romania
[2]Technical University of Civil Engineering of Bucharest,
122-124 Lacul Tei Blvd, District 2, 020396, Bucharest, Romania
[3]University of Agronomic Sciences and Veterinary Medicine of Bucharest,
59 Mărăști Blvd, District 1, 011464, Bucharest, Romania
[4]"Dunărea de Jos" University of Galaţi, 47 Domnească Street, 800008, Galați, Romania

Corresponding author email: dobred@hotmail.com

Abstract

Structural Health Monitoring (SHM) is a technology and methodology designed to assess the condition of structural systems by evaluating potential damage that may occur after an earthquake. Building Information Modeling (BIM) tools provide storage and visualization capabilities for digitally representing a building, incorporating raw data such as photographs, measurements, point clouds, and damage information. This paper presents a framework aimed at enhancing traditional databases. It integrates data collected from various sensors installed within a structure, employing post-processing techniques like finite element analysis to evaluate the health of both structural and non-structural elements. Additionally, the soil conditions are taken into account during these assessments. The collected information is then incorporated into a BIM environment featuring an improved interface that enhances connectivity between the two system architectures. This integration utilizes standardized file formats as defined by ISO standards. Developing scientific and experimental databases for building structures is an emerging trend in global research and a key component of the Romanian National Strategy for Seismic Risk Reduction. Digital building information models facilitate real-time updates and improve coordination among intervention teams following significant earthquakes.

Key words*: monitoring, digital data, damage, earthquake.*

INTRODUCTION

Structural health monitoring (SHM) is a non-destructive in-situ methodology and technology designed to assess the condition of structural systems by evaluating potential damage that may occur before or after an earthquake. It features a modular architecture that includes components related to sensors, data acquisition and transmission, data processing and control, data management, evaluation and maintenance, among others (Georgescu et al., 2010; Dragomir et al., 2019; Arif & Craifaleanu, 2023; Chacon et al., 2023; Sun et al., 2025). Any discrete or progressive changes in the structural parameters are considered potential condition indicators for damage identification.
Nowadays, at URBAN-INCERC, SHM is conducted by using the ARTeMIS Modal Pro software, which is currently in the process of implementation within an experimental project for real-time damage detection in instrumented and monitored buildings (Dragomir et al., 2019; Dragomir & Dobre, 2023). The analysis of modal and deflection shapes, along with damage detection through the identification of changes in the dynamic characteristics of a structure - using data from ambient vibrations or seismic motions - includes several important features.
These features consist of notifications when a specified control value is exceeded and warnings about potential damage to the structure, as highlighted in Figure 1. Incorporating the phenomenon of soil-structure interaction into structural analysis, either through analytical methods or real-time monitoring using sensors positioned in the free-

field (near the building or in boreholes), can provide valuable insights into the structural response during an earthquake (Craifaleanu & Borcia, 2011; 2012; Craifaleanu, 2013; Craifaleanu, 2025; Dobre, 2006; Dobre et al., 2015).

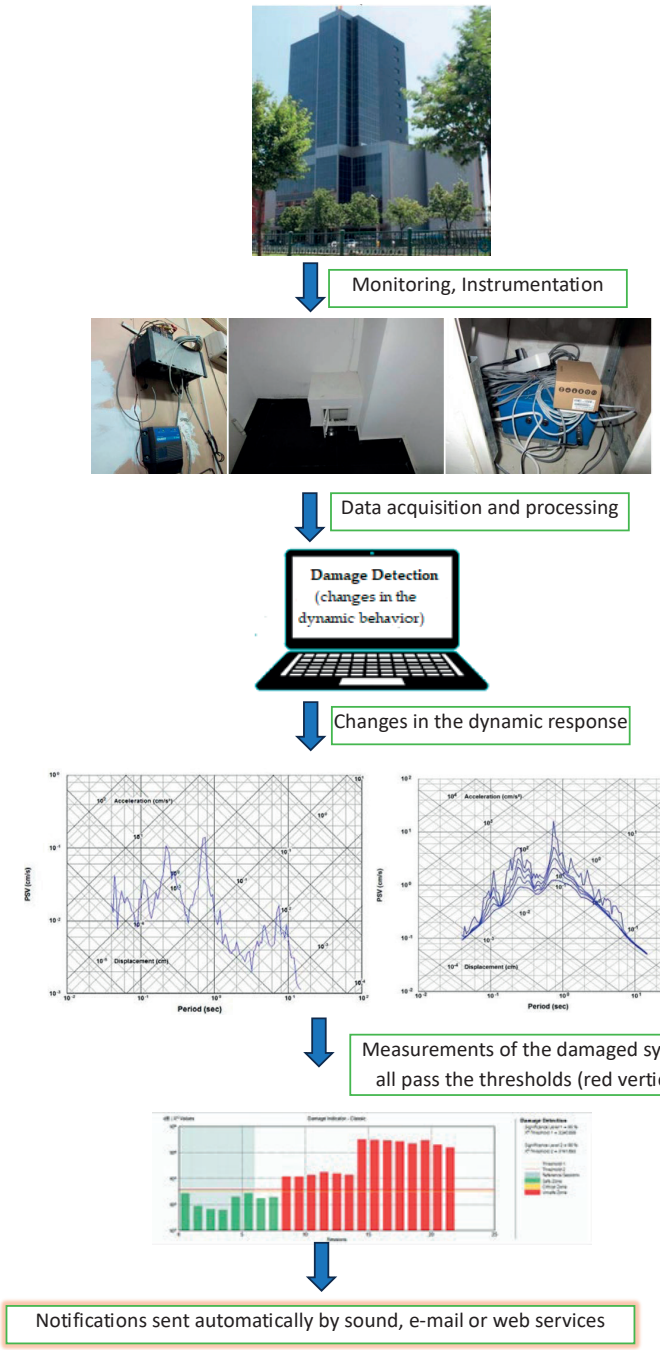


Figure 1. Implementing a remote access earthquake damage detection system within SHM for a high-rise building

The use of the finite element method in developing even simplified models of structural systems strengthens the connection between SHM and BIM by determining dynamic characteristics that evolve over time (Dragomir & Dobre, 2023). Another important factor to consider in this context is the seismic response of structures with active tuned mass dampers or any control dissipation system (Bratu et al., 2024; Paulet-Crainiceanu et al., 2024). However, the interpretation of long-term data collected from continuous monitoring SHM can be overwhelming due to the processing of an enormous amount of data. On the other hand, Building Information Modelling (BIM) tools provide storage and visualisation capabilities for digitally representing a 3D building, including lifecycle management information, with the possibility for a structural analysis and damage detection visualised in the model by assimilating the sensor data within the BIM model, that can aid the stakeholders and infrastructure owners in monitoring in real-time the state of any construction (An et al., 2015; Colucci et al., 2020; Hamdan & Scherer, 2018; Theiler et al., 2018; Singh & Sadhu, 2019; Castelli et al., 2023; Xu et al., 2023; Gragnaniello et al., 2024; Riggio & Nasir, 2024). BIM uses a static data source to assess the structure, and the sensor data can extend the application of BIM model from static to dynamic model to get the current performance of the structure (Chen et al., 2014). Within the framework established by SHM and BIM approaches, various theoretical, technical, syntactic, and semantic elements (connections between concepts and objects) aim to enhance reports generated after a major earthquake. The research directions involved in SHM with BIM and monitoring networks (seismic, but not only) show a strong correlation between key terms such as BIM, SHM, technology, damage detection, response, modal identification etc., as can be seen in Figure 2.

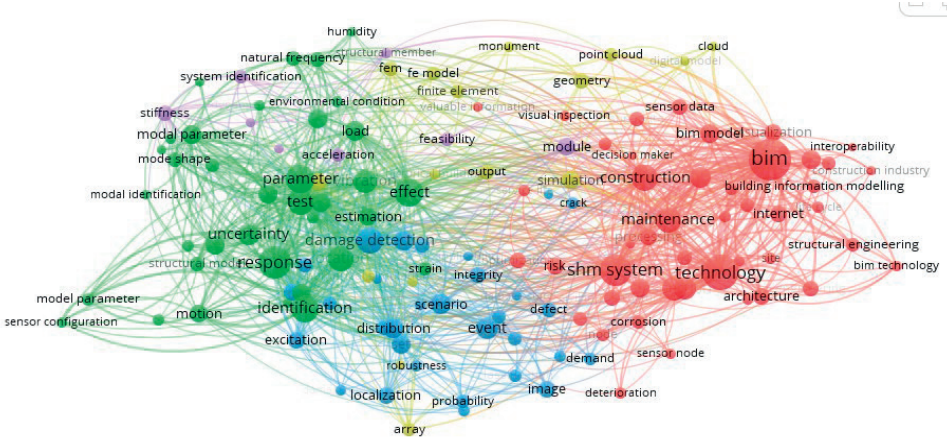


Figure 2. Frequency keywords clustering

MATERIALS AND METHODS

Elements of SHM and BIM as they relate to seismic monitoring

The integrated concept BIM-based SHM, i.e. to insert real-time data into the BIM model, is possible by standardizing the formats of the two approaches (formulate a standard data model to include and visualize SHM data directly to BIM models, including damage sensitive features in the object properties, data to sensor representations within the BIM model). Specific aspects of SHM and BIM are presented below, along with their technical compatibility - objectives, components, format standards, software, damage assessment.

a. Objectives:

- SHM: extracting information from structural response data collected by sensors attached to buildings;
- BIM: conventional building information (geometry, material, costs), communication,

feedback and user-input, sharing of asset data, damage visualization;

- SHM-BIM: modelling and integrating SHM-related algorithms into IFC-based Building Information Models (IFC monitoring-related information).

b. Components:

- SHM: sensors, data acquisition system, wired/wireless connection (data transmission), communication system, data processing and storage, data analysis, damage detection, data interpretation;
- BIM: physical geometry of the building, management of vast amounts of data associated with the building, Common Data Environment (CDE) platform (all project information is stored, managed and shared).

c. Format standards

- SHM: sensor-related information - Sensor Model Language (SensorML), Semantic Sensor Network (SSN) Ontology, Systems Modeling Language (SysML), Web Ontology Language (OWL);
- BIM: Proprietary file formats (RVT, NWD, DWG), Non-Proprietary file formats (Construction operation building information exchange (COBie); Industry Foundation Classes (IFC));
- SHM-BIM: IFC Monitor to describe SHM (semantic compositions of SHM systems, network topologies, and semantic relationships between components of SHM systems and components of structural systems to be monitored), Exporting Revit SHM model to IFC, Information delivery specification (IDS) based on specific Level of Information Need (LoIN).

d. Software:

Revit and Robot Structural Analysis, REVIT and MATLAB, Excel, Autodesk, Dynamo, GIS.

e. Damage assessment:

- SHM: without any particular physical model, only data-driven approaches, but analytical models (identify the characteristics of damage progress and predict the future state); physics-based approaches, with a physical damage model and with measured data (An et al., 2015);
- BIM: plug-in for BIM environments to study the preservation of any structural element (Fernández-Mora et al., 2025; Ionita & Stoian, 2024); BIM through the Revit add-ins able to store and manage real-time data (Chen et al., 2014), developed using Revit's NET API (Application Programming Interface);
- SHM-BIM: identify and visualize the damage status of the structural and non-structural elements following a seismic event, from direct measurements by sensors installed on the building; The information processed therefore it can be inserted into fragility curves relating the performance of the element as a function of an engineering demand parameter such as the absolute acceleration or the inter-story drift ratio; information imported into modelling software working on a BIM architecture through a specific code. The procedure provides both a clear and immediate visualization of the building's health status, and its real-time sharing in the cloud (Castelli et al., 2023).

Figure 3 shows the already multidimensional relationship based on all aspects presented above between SHM and BIM.

RESULTS AND DISCUSSIONS

How could the traditional database be upgraded?

The main objective of enhancing the relationship between Structural Health Monitoring (SHM) and Building Information Modeling (BIM) is to evaluate how a structure performs and to detect potential damage. This is accomplished by analyzing changes in its dynamic characteristics, which include natural frequencies, damping ratios, mode shapes, inter-story drift ratios, and the modal assurance criterion.

Keeping in mind the classic components of SHM (Figure 1) and the possible multidimensional relationship between SHM-BIM (Figure 3), for a correct upgrade of the existing database, with several buildings already instrumented and/or seismically monitored, it is necessary to initially evaluate the current situation of all data formats acquired in fields such as urban planning, cadastre, design, research, signal processing, or multidisciplinary ones.

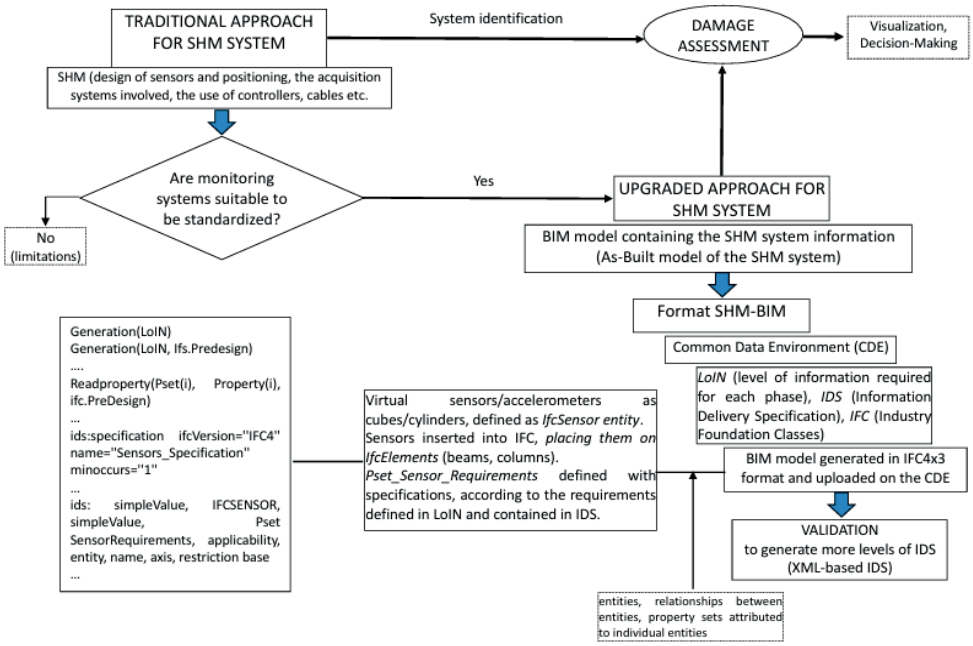


Figure 3. A multidimensional relationship SHM-BIM

The text describes the integration of Structural Health Monitoring (SHM) and Building Information Modelling (BIM) to enhance the management of building data. It emphasizes that providing accurate geospatial information and attributes about the condition of buildings is essential. By leveraging the strengths of both SHM and BIM, it is crucial to ensure compatibility of the data formats used, as this is a key factor in achieving effective real-time monitoring and modelling. Then, the compatibility of these formats with the corresponding structural software for linear and nonlinear static and dynamic analyses is considered. In the next stage, a data management system for storage, retrieval and sharing of extremely large measurement data sets constantly acquired from SHM systems and the creation of web interfaces are required. The options for a database are relational (MySQL)/non-relational (NoSQL), with adaptability, high traffic capacity and open-source.

An integrative concept for the digital analysis of seismic monitoring data is currently being developed at INCD URBAN-INCERC. This initiative aims to cover a large area of the national territory and its built environment, facilitating the rapid identification of the destructive potential of earthquakes. The effectiveness of this concept is evident in its ability to characterize seismic motion and evaluate the structural system of the monitored building. This includes real-time visualization, processing, and analysis of seismic recordings using SeisComP software, as well as the graphical representation of shake maps that incorporate attenuation laws. SeisComP has its own data storage and archiving system, compatible with SeedLink (an international standard in the field). Data archiving is done through SDS (SeisComP Data Structure), in which the archiving format is compatible with SeedLink. The seismic data storage structure follows pre-established hierarchical levels, adapted to specific needs. Certain essential BIM elements are currently absent, which limits the provision of crucial technical information related to buildings, utility networks, ground conditions, acoustic parameters, energy consumption, various costs, and solutions for data access, storage, archiving, data security, software updates, AI and machine learning integration, as well as backup and recovery tools. As part of an experimental program focused on seismic

monitoring of buildings, data is generated in a standardized format for several purposes. This includes finite element modelling, static and dynamic load testing, enhancement of existing structural health monitoring (SHM) systems, building information modelling (BIM), and supporting both national and international advancements in this field (Guide on the management and monitoring of information generated in the BIM system; EN ISO 19650).

CONCLUSIONS

The behaviour of structural systems of buildings under dynamic actions and the detection of damage shortly after their occurrence represent important technical aspects and are, to a certain extent, obtained rapidly through monitoring, non-destructive testing. The SHM-BIM approach offers a significant advantage by enabling the definition and modelling of the pre-earthquake structural system in a compatible digital format. This aligns with established regulations for structural analysis and allows for results to be presented in the same format. Additionally, it facilitates real-time damage assessment, utilizing fragility curves as indicators of probabilistic damage or real-time identification methods based on frequency analysis for damage detection. It is also beneficial to incorporate elements related to the architecture and acoustics of buildings and installations (Zaharia, 2010; Zaharia & Voloaca, 2023), or integrating information from requirements of 3D-printing applications for the field of constructions, current technologies, the advantages of 3D printed buildings/houses with seismic/ambient vibration monitoring possibilities (Vitalie et al., 2020).

The conceptual methods and data gathered through seismic monitoring are essential for a database directly associated with seismic vulnerability. The development of scientific and experimental databases for building stock is an emerging approach in current global research and serves as a fundamental component of the Romanian National Strategy for Seismic Risk Reduction. Digital building information models enable real-time updates and enhance coordination among intervention teams after significant earthquakes.

ACKNOWLEDGMENTS

This research work was done within the "Nucleu" Programme in PNCDI 2022-2027, with the support of MCDI, Project PN 2335 (incd.ro/national projects).

REFERENCES

An, D., Kim, N. H., Choi, J.H. (2015). Practical options for selecting data-driven or physics-based prognostics algorithms with reviews. *Reliability Engineering & System Safety*, *133*, 223-236, ISSN 0951-8320. Doi.org/10.1016/j.ress.2014.09.014.

Arif, W., Craifaleanu, I.G. (2023). Assessment of the Seismic Vulnerability of a Multi-storey RC Structure with Plan Irregularity: A Case Study. *IOP Conf. Ser.: Earth Environ. Sci.,* 1185, 012021. Doi: 10.1088/1755-1315/1185/1/012021.

Bratu, P., Dobre, D., Vasile, O.; Dobrescu, C.F. (2024). The seismic behavior of a base-isolated building with simultaneous translational and rotational motions during an earthquake. *Buildings, 14, 3099.* https://doi.org/10.3390/ buildings14103099.

Castelli, S., Belleri, A., Graziosi, L.R., Locatelli, L., Zirpoli, A., Svaluto, G. (2023). Integrated BIM-SHM techniques for the assessment of seismic damage. The XIX ANIDIS Conference, Seismic Engineering in Italy. *Procedia Structural Integrity, 44*, 846–853. Doi: 10.1016/j.prostr.2023.01.110.

Chacón, R., Casas, J. R., Ramonell, C., Posada, H., Stipanovic, I., Škarić, S. (2023). Requirements and challenges for infusion of SHM systems within Digital Twin platforms. *Structure and Infrastructure Engineering*, 1–17. Doi.org/10.1080/ 15732479. 2023.2225486.

Chen, J., Bulbul, T., Taylor, J. E., & Olgun, G. (2014). A Case Study of Embedding Real-time Infrastructure Sensor Data to BIM. *Construction Research Congress*. Doi:10.1061/9780784413517.028.

Colucci, E., De Ruvo, V., Lingua, A., Matrone, F., Rizzo, G. (2020). HBIM-GIS Integration: From IFC to CityGML Standard for Damaged Cultural Heritage in a Multiscale 3D GIS. *Appl. Sci., 10*, 1356. Doi.org/10.3390/app10041356.

Craifaleanu, I.-G., Borcia, I.S. (2011). Instrumental Intensity as a Tool for Post-Earthquake Damage Assessment: Validation for the Strong Vrancea Earthquakes of August 1986 and May 1990. *Constructii Journal, 11.* Doi 10.48550/arXiv.1210.3745.

Craifaleanu, I.-G., Borcia, I. S. (2012). Damage Index vs. Instrumental Intensity: A Comparison of Two Different Approaches in Seismic Damage Assessment. *Proceedings of 15th Earthquake Engineering*. ISBN 9781634396516.

Craifaleanu, I.-G. (2013). Standardized Multiapartment Blocks Built in Romania Before 1990: Seismic Design Levels Vs. Earthquake Performance. *Structural Engineering International, 23*(4), 519–527.

https://doi.org/10.2749/101686613X1376834839959 3.

Craifaleanu, I.-G. (2025) An in-depth investigation of ground jerk characteristics for the four strongest Vrancea (Romania) earthquakes in the past half-century. *Front. Built Environ*., *11*, 1569201. Doi: 10.3389/fbuil.2025.1569201

Dobre, D. (2006). An application of substructure method. *U.P.B. Sci. Bull., Series A-Applied Mathematics and Physics*, *68*(1).

Dobre, D., Dragomir, C.-S., Georgescu, E.-S. (2015). Pounding effects during an earthquake, with and without consideration of soil-structure interaction. *Constructii*, *16*(1), ID2015160106_Dobre.pdf.

Dragomir, C.S., Craifaleanu, I.-G., Dobre, D., Georgescu, E.S. (2019). Prospective studies for the implementation of a remote access earthquake damage detection system for high-rise buildings in Romania. *IOP Conference Series: Earth and Environmental Science*, *221*, 012036. Doi: 10.1088/1755-1315/221/1/012036.

Dragomir, C.S., Dobre, D. (2023). Monitoring sensor techniques for an integrated and digitalized database. *AIP Conf. Proc., 2928*, 170001. Doi.org/ 10.1063/ 5.0171161.

Fernández-Mora, V., Navarro, I.J., Yepes, V. (2025). Structural damage index evaluation in BIM environments. *Structures, 74*, 108544. Doi.org/10.1016/j.istruc.2025.108544.

Georgescu, E.S., Praun, I.C., Borcia, I.S. (2010). Earthquake instrumental monitoring of buildings [in Romanian]. *Urbanism. Architecture. Constructions*, *1*(2). ISSN 2069-6469. https://uac.incd.ro/Art/ v1n2a13.pdf

Gragnaniello, C., Mariniello, G., Pastore, T., Asprone, D. (2024). BIM-based design and setup of structural health monitoring systems. *Automation in Construction*, *158*, 105245, ISSN 0926-5805, Doi.org/10.1016/j.autcon.2023.105245.

Hamdan, A.H., Scherer, R. (2018). A Generic Model for the Digitalization of Structural Damage. *Life Cycle Analysis and Assessment in Civil Engineering: Towards an Integrated Vision*, CRC Press, eBook ISBN 9781315228914.

Ionita, A., Stoian, M. (2024). Analysis on the integration of BIM in construction economy. Proceedings of the INCD URBAN-INCERC Research Conference on Constructions, Economy of Buildings, Architecture, Urban and Territorial Development, XXVI Edition, Vol. 26.

Paulet-Crainiceanu, F., Florea, V., Luca, S.G., Pastia, C., Rosca, O.V. (2024). Analysis of Practical Application Aspects for an Active Control Strategy to Civil Engineering Structures. Awrejcewicz, J. (eds) Perspectives in Dynamical Systems II — Numerical and Analytical Approaches. DSTA 2021. *Springer Proceedings in Mathematics & Statistics*, *454*. Doi.org/10.1007/978-3-031-56496-3_26.

Riggio, M., Nasir, V. (2024). Digital Twins in Structural Health Assessment and Monitoring: Applications in Historical Timber Buildings. *International Journal of Architectural Heritage*. Doi: 10.1080/15583058. 2024.2437618

Singh, P., Sadhu, A. (2020). System Identification-Enhanced Visualization Tool for Infrastructure Monitoring and Maintenance. *Front. Built Environ*., *6*, 76. Doi: 10.3389/fbuil.2020.00076.

Sun, Z., Jayasinghe, S., Sidiq, A., Shahrivar, F., Mahmoodian, M., Setunge, S. (2025). Approach Towards the Development of Digital Twin for Structural Health Monitoring of Civil Infrastructure: A Comprehensive Review. *Sensors*, *25*, 59. Doi.org/10.3390/ s25010059.

Theiler, M., Dragos, K., Smarsly, K. (2018). Semantic description of structural health monitoring algorithms using building information modelling. *Advanced Computing Strategies for Engineering, 10864.* Springer. Doi.org/10.1007/978-3-319-91638-5_8.

Vitalie, F., Paulet-Crainiceanu, F., Septimiu, L., Pastia, C. (2020). 3D Printing of Buildings. Limits, Design, Advantages and Disadvantages. Could This Technique Contribute to Sustainability of Future Buildings? *Critical Thinking in the Sustainable Rehabilitation and Risk Management of the Built Environment, CRIT-RE-BUILT. Proceedings of the International Conference*, Iași, Romania, pp. 298-308. Doi 10.1007/978-3-030-61118-7_26.

Xu, J., Shu, X., Qiao, P., Li, S. (2023). Developing a digital twin model for monitoring building structural health by combining a building information model and a real-scene 3D model. *Measurement, 217*. Doi.org/10.1016/j.measurement. 2023.112955.

***Guide on the management and monitoring of information generated in the BIM system, RTC 8-2022 (in Romanian). Ministry of Development, Public Works, and Administration.

***EN ISO 19650-Part 1, 2:2018, Parts 3, 4, 5:2020, Part 6:2025.

***https://incd.ro/proiecte-nationale/

Scientific Papers. Series E. Land Reclamation, Earth Observation & Surveying, Environmental Engineering. Vol. XIV, 2025
Print ISSN 2285-6064, CD-ROM ISSN 2285-6072, Online ISSN 2393-5138, ISSN-L 2285-6064

RISK OF WINDTHROWS STANDS WITH VARIOUS STRUCTURES USING VERTICAL DIFFERENTIATION INDEX

Lucian Sorin DOROG

University of Oradea, Faculty of Environmental Protection,
26 General Magheru Street, 410087, Oradea, Romania

Corresponding author email: Lucian Sorin Dorog_dorogsorin@gmail.com

Abstract

This study investigates how different stand structures influence vulnerability to windthrows, using the vertical differentiation index as an analytical tool. Measurements were conducted in three forest districts containing stands with varying structures: even-aged, relatively even-aged, relatively uneven-aged, and uneven-aged. Findings indicate that the vertical differentiation index has subunit values close to zero in even-aged stands and approaches one in uneven-aged stands. A significant inverse correlation was observed between this index and the percentage of wood affected by windthrows. These results underscore the importance of diversifying stand structures in Romanian forest management to mitigate ecological and economic losses.

Key words*: stand structure, windthrows, vertical differentiation index, correlation.*

INTRODUCTION

Due to ongoing climate change, forest stands' increasing vulnerability to extreme weather events, particularly windthrows, is a significant concern. Historically, pure even-aged spruce stands were considered highly susceptible, primarily due to shallow rooting systems (Barbu & Barbu, 1993). However, recent evidence suggests that stand structure and management practices also play a crucial role in determining susceptibility to windthrows (Gardiner & Quine, 2000).

The susceptibility of forest stands can be further increased by soil characteristics and land orography, significantly raising the likelihood and severity of these phenomena, particularly in areas where multiple contributing factors interact simultaneously (Negron-Juarez et al., 2023). Additionally, water retention from precipitation in the tree canopy and soil can amplify the impact of windthrows while also causing rapid fluctuations in stream flow over short periods in mountainous regions (Iovan et al., 2024). The vertical differentiation index serves as a valuable tool for assessing the vulnerability of forest stands to various disturbance factors. By providing insights into stand stability, it aids in the development of resilient forests capable of withstanding extreme climatic events in the future (Valinger & Fridman, 2011).

Windthrows, caused by strong winds, can be categorized based on their intensity and impact into endemic and catastrophic windthrows. Catastrophic windthrows result from extreme weather conditions, involving high-intensity winds that devastate large areas, often affecting thousands of cubic meters of wood. In contrast, endemic windthrows occur more frequently - almost annually - due to moderate-intensity winds and are influenced by a combination of site-specific, meteorological, and stand structure factors. Addressing endemic windthrows is a pressing challenge for forestry management, as their cumulative effects can disrupt forest ecosystems, degrade wood quality, and cause economic and ecological disturbances over time. Without proper intervention, these disturbances may ultimately lead to the fragmentation and deterioration of forest stands. Given the increasing frequency and intensity of windthrows, it is crucial to implement adaptive forestry strategies that enhance stand resilience and promote sustainable forest management (Popa, 2005).

The decline of natural forest structures, coupled with environmental degradation and the growing impact of climate change, has intensified extreme weather events, even in

forested areas that were previously considered stable 15-20 years ago - excluding pure spruce stands, which have historically been more vulnerable (Duduman, 2011). Large-scale windthrows were predominantly observed in artificially regenerated spruce stands, highlighting the structural weaknesses of such forests in the face of climatic stressors.

To address these challenges, rational forestry practices grounded in ecological principles must be prioritized.

Sustainable forestry should focus on conservation, protection, and the development of structurally diverse and resilient forest ecosystems that align with contemporary environmental realities (Ichim, 1990).

Over the past few decades, forest management has largely promoted uniform stand structures, minimizing horizontal and vertical differentiation. However, these homogeneous stands have exhibited declining self-protection capacity as they age, making them increasingly vulnerable to external stressors and complicating the implementation of effective management plans. In the forests of Trentino, Italy, researchers have identified key stand structure indices that serve as the foundation for modern management strategies, emphasizing the importance of diversified forest structures (Pastorella & Paletto, 2013).

The size and spatial distribution of trees within a stand significantly influences its overall complexity and ability to fulfill eco-protective functions. Greater structural diversity enhances forest stability and resilience, underscoring the need for management strategies that prioritize stand complexity and adaptability to environmental changes (Peck et al., 2014).

This study aims to analyze the relationship between vertical differentiation index values and windthrow vulnerability to inform sustainable forest management practices. To support this analysis, three locations encompassing various types of stand structures were examined. Data were collected and analyzed, vertical differentiation indices were determined, and the occurrence of disruptive phenomena was assessed probabilistically. The results section presents the findings, which served as the basis for formulating the conclusions.

MATERIALS AND METHODS

Study area

Field data were collected from three forest districts:

- U.P. II Valea Seaca, O.S. Gârda, D.S. Alba - this area consists of pure beech stands and mixed stands of beech, fir, and spruce, with little to no silvicultural interventions. These forests are characterized by complex natural structures that have adapted to the local site conditions. Field observations indicate that windthrows in these stands occur sporadically over small areas. Notably, the gaps created by these windthrows provide ideal conditions for natural regeneration, allowing the forest to recover and evolve without human intervention
- U.P.I Sâniob, O.S. Săcuieni, D.S. Bihor - this area consists of pure and mixed Quercus cerris stands, predominantly even-aged, with a few exceptions. While forestry measures have been consistently applied, the stands exhibit limited structural diversity both horizontally and vertically. According to the analyses conducted in this study, these structurally simplified stands are potentially more vulnerable to disturbance factors.
- U.P. VII Văratec, O.S. Sudrigiu D.S. Bihor - included stands affected by severe windthrows in 2017, characterized by high densities and instability due to insufficient silvicultural interventions (Crainic et al., 2024). Field observations indicate that stands with simplified horizontal and vertical structures are prone to both isolated and large-scale windthrows, which can occur frequently due to the combined influence of various disturbance factors. To enhance the resilience of these stands against such disturbances, future management strategies should focus on increasing structural diversity.

Data collection and analysis

In the analyzed stands, a minimum of 30 trees were measured, with their closest neighboring trees identified. For each measured tree, the heights of both the tallest and shortest trees within its group were recorded. The vertical differentiation index for each analyzed stand was determined using the equation provided by Ciubotaru & Păun (2014) and Keren et al. (2020):

$$DHn = \frac{1}{N} * \sum \left[\sum \frac{1}{n} \left(1 - \frac{Xijmin}{Xijmax} \right) \right]$$

where:

- DHn is vertical differentiation index;
- N - number of measured trees;
- n - number of neighboring trees;
- Xijmin - minimum tree height in the group;
- Xijmax - maximum tree height in the group.

The relationship between the vertical differentiation index and the percentage of volume affected by disturbance factors was analyzed. Special attention was given to stands with even-aged and relatively even-aged structures, as distinguishing between these two categories in the field can sometimes be challenging. Some stands contain areas that could be classified into either category, despite the management plan specifying only one structure type. For consistency, relatively uneven-aged and uneven-aged stands were analyzed separately using the same approach.

To estimate the risk of windthrows over the duration of the management plan with sufficient accuracy, a probabilistic model was developed, based on the approach proposed by Popa I. (2005). The probabilistic model utilized in this study is expressed as follows:

$$V_{dob} = p_{dec} \cdot pdv_{dec} \cdot V_{ha}$$

where:

- V_{dob} is probable decadal volume of windthrows (m^3/ha/decade);
- p_{dec} - decadal probability of occurrence of windthrows;
- pdv_{dec} - decadal intensity of the windthrows caused by the wind (% of the volume per hectare);
- V_{ha} -volume per hectare.

This model provides an estimation of windthrow risk by quantifying the probable volume of wood affected by wind over a ten-year period.

RESULTS AND DISCUSSIONS

The analysis of the four types of stand structures in relation to their stability against disturbance factors, assessed using the vertical differentiation index, provides valuable insights for both theoretical and practical forest management. Understanding these relationships allows for the development of strategies that minimize stand vulnerability to windthrows. The following section explores how different structural types influence the likelihood of windthrow occurrence.

Windthrows result in significant economic and ecological losses. From an economic perspective, they lead to wood depreciation, increased costs for evaluation and extraction, and difficulties in adhering to forest management plans. Ecologically, they can cause a partial or complete disruption of forest functions, with long-term effects that may take decades to fully manifest. While economic losses can be quantified relatively easily during timber assessment and harvesting, ecological impacts - such as biodiversity reduction, habitat disruption, and changes in microclimatic conditions - are more challenging to measure.

Statistical analyses reveal a strong and consistent correlation between windthrow probability and key stand parameters, including production class, average tree diameter, and height. However, the most influential factor appears to be standing age. Research conducted in the Suceava Forestry District indicates that the highest windthrow susceptibility occurs in stands aged between 60 and 80 years (Popa, 2005).

To estimate the volume of wood likely to be affected, an average value was calculated based on the minimum and maximum values within specific probability intervals. The classification of windthrow intensities is as follows:

- 20-40% probability (Table 1): windthrows at this level are generally low-intensity and occur sporadically across the landscape. These events, often classified as endemic windthrows, are particularly beneficial in uneven-aged and relatively uneven-aged stands, as they promote continuous natural regeneration.
- 40-60% probability (Table 1): windthrow intensity increases slightly, but the events remain localized and do not immediately threaten the overall stability of the stand. These can still be considered endemic windthrows, albeit with slightly higher intensities.
- 60-80% probability (Table 1): windthrows become more concentrated over large areas, indicating structural instability

within the stand. This level of impact highlights the need for urgent management interventions to reduce the volume of affected wood and prevent further stand degradation. Such stands require targeted silvicultural measures to restore their resilience and shift them into structural categories where windthrows remain isolated rather than widespread disturbances.

By integrating these findings into forest management planning, strategies can be refined to enhance stability, reduce economic losses, and ensure long-term ecological sustainability.

The probable volume of wood affected by windthrows follows an increasing trend as the probability class rises. Specifically:

- at the 20-40% probability level, the affected wood volume ranges between 8-10%.
- for the 40-60% probability level, this increases to 13-16%.
- at the 60-80% probability level, the percentage of affected wood reaches 18-22% (Table 1).

Table 1. Probably affected volume per hectare based on probability classes

Average volume per hectare (m^3)	Probability classes (%)		
	20-40%	40-60%	60-80%
	Probable volume affected per hectare (m^3)		
300	24	41	60
400	31	56	79
500	49	80	105
600	60	96	112
700	70	112	154

The similarity between the percentage of wood affected across different probability classes and the harvesting indices at the stand level suggests that regular and well-executed silvicultural interventions reduce the likelihood of windthrows. Field observations reinforce this conclusion, as it stands that systematic and properly executed management practices are significantly less affected by destabilizing factors compared to those with irregular or poorly implemented interventions.

Figure 1 illustrates the relationship between the percentage of wood affected by windthrows and the vertical differentiation index for even-aged and relatively even-aged stands. The data indicate that when the vertical differentiation index is low (0-0.1), windthrow damage is substantial, ranging from 60-80%. However, as vertical differentiation increases, the percentage of affected wood declines sharply. This trend is clearly demonstrated by the regression equation, which has a coefficient of determination (R^2) of 0.63, indicating a strong negative correlation.

For even-aged and relatively even-aged stands, improving vertical differentiation through consistent silvicultural practices can significantly enhance stand stability. The correlation coefficient of -0.55 further supports this relationship, highlighting the crucial role of structural diversity in mitigating windthrow susceptibility (Figure 1).

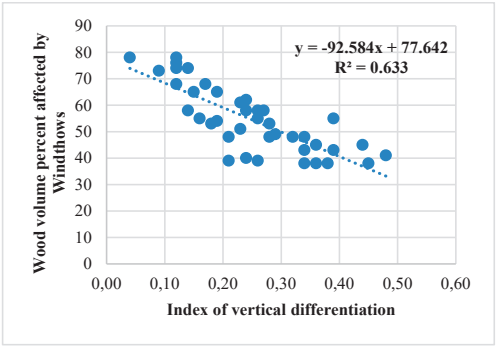


Figure 1. Wood volume percent affected by windthrows in correlation with vertical differentiation index in even-aged and relative even-aged stands

Figure 2 illustrates the relationship between the percentage of wood affected by windthrows and the vertical differentiation index for uneven-aged and relatively uneven-aged stands. The data indicate that these stands experience significantly lower windthrow impact compared to even-aged stands.

A clear downward trend in the regression equation confirms that as the vertical differentiation index increases, windthrow susceptibility decreases. However, in contrast to even-aged stands, the affected wood volume generally remains below 50%, with only a few exceptions.

The coefficient of determination (R^2 = 0.65) closely aligns with the findings for even-aged stands, reinforcing the consistency of this relationship.

For uneven-aged stands, stability can be further enhanced through silvicultural interventions where applicable. However, in cases where

management constraints prevent interventions, maintaining a high vertical differentiation index through continuous natural regeneration proves to be the most effective strategy for reducing windthrow susceptibility.

The correlation coefficient of -0.81 between the percentage of volume affected by windthrows and the vertical differentiation index further supports the strong inverse relationship between these variables, demonstrating that greater structural complexity significantly enhances stand resilience (Figure 2).

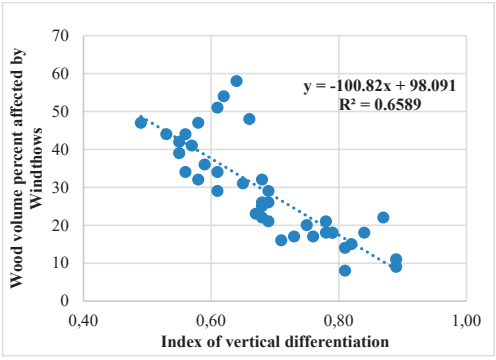


Figure 2. Wood volume percent affected by windthrows in correlation with vertical differentiation index in uneven-aged and relative uneven-aged stands

The percentage of wood likely to be affected by windthrows starts at approximately 10% for windthrow intensities in the 20-40% range. This percentage increases to around 15% for intensities between 40-60% and further rises to an average of 20% for windthrow intensities in the 60-80% range (Figure 3).

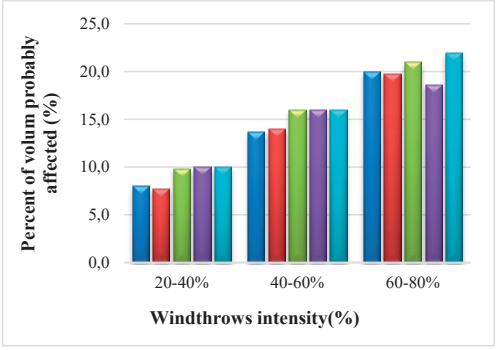


Figure 3. The percentage of volume probably affected in correlation with windthrows intensity

The vertical differentiation index serves as a reliable indicator of stand stability in the face of various disturbance factors. Higher index values, approaching 1, indicate structurally complex and resilient stands where only isolated windthrows occur, often benefiting natural regeneration. Conversely, index values close to zero suggest highly vulnerable stands, where the likelihood of extensive windthrows is significantly increased.

Windthrow probability is also influenced by site conditions, which can either amplify or mitigate the effects of these disturbances. Previous studies have identified three primary factors contributing to windthrows: stand structure, site conditions, and extreme weather events (Popa, 2005).

In the medium to long term, forestry practices must focus on developing uneven-aged stands with high structural diversity, ensuring greater stability against disturbances. The vertical differentiation index not only assesses stand resilience but also provides insights into long-term sustainability. Stands with higher differentiation indices demonstrate strong resistance to disturbances, whereas those with lower values remain highly susceptible (Dorog, 2021).

The impact of climate change is becoming increasingly evident in forests, with more frequent extreme events such as prolonged droughts, heavy rainfall over short periods, and large-scale windthrows affecting entire ecosystems. Findings from this study confirm that stands with both vertical and horizontal structural diversity are significantly less vulnerable to such disturbances. This reinforces the urgent need for Romanian forestry to prioritize diversified stand structures, ensuring they can perform multiple ecological functions effectively.

To address these evolving challenges, forestry regulations and technical norms must be revised to incorporate strategies that reduce damage and enhance stand resilience. The eco-protective role of forests should be evaluated not only in terms of their ecosystem functions but also their structural stability against extreme events.

Future silvicultural interventions must be adapted to align with the new realities brought by intensifying climatic events. In addition to achieving traditional management goals, these

interventions should prioritize enhancing stand complexity. Forestry operations should be conducted at low intensities (6-10%), with a maximum threshold of moderate intensities (10-16%), ensuring that no large gaps are created, as these can become weak points for future windthrows.

A localized approach is also essential-forest management strategies should be tailored to specific site conditions, considering regional variations and unique environmental challenges. Implementing adaptive solutions at the local level will be key to increasing stand stability and resilience to combined disturbance factors.

This study serves as a foundation for future research, focusing both on identifying factors that negatively impact forest stability and on developing effective, science-based solutions to mitigate the risks associated with climate-induced disturbances.

CONCLUSIONS

The vertical differentiation index serves as a key indicator of stand structure complexity and stability. In diversified stands (uneven-aged and relatively uneven-aged), the index exhibits subunit values, with figures approaching 1 reflecting a highly organized and resilient forest ecosystem. Conversely, in simplified stands (even-aged and relatively even-aged), the index also takes subunit values, but as it approaches zero, it signifies a simplified and structurally vulnerable forest ecosystem.

A strong negative correlation is observed between the vertical differentiation index and the percentage of wood volume affected by windthrows. In areas where windthrows have severely impacted more than 60% of the stand volume, the vertical differentiation index is typically low (0–0.2). In contrast, in areas experiencing localized or point windthrows, the index tends to be significantly higher (0.7–0.9).

Field observations confirm that stands most affected by disturbance factors are those with simplified structures. These stands, with only minor exceptions, are highly susceptible to windthrows, leading to the loss of significant wood volumes over time. To reduce the long-term risk of stand collapse, forest management should prioritize structural diversification as a preventative measure.

For diversified stands, it is recommended to maintain and further enhance structural complexity to mitigate risks. Notably, these stands experience localized windthrows, which are beneficial as they facilitate continuous natural regeneration and help sustain or even increase structural diversity over time.

In areas with low windthrow probability, the affected volumes remain minimal, aligning with the concept of point windthrows, which naturally support ongoing regeneration and structural maintenance.

In areas with moderate windthrow probability, a higher proportion of stands are affected, leading to progressive structural degradation and increased vulnerability.

In areas with high windthrow probability, the impact is often irreversible, requiring the complete extraction of affected wood, which disrupts the forest's ecological functions and jeopardizes long-term sustainability.

Both ecological and economic losses are significant in simplified stands, reinforcing the urgent need for structural diversification as a core forest management strategy. The structure of a stand directly influences its stability, and therefore, forest management must prioritize the promotion of diverse, resilient stand structures. Naturally regenerated stands demonstrate higher stability against disturbances compared to artificially regenerated stands, which often lack the necessary structural complexity.

To enhance the stability of artificially regenerated stands, it is recommended to use genetically selected planting material that aligns with both current and future stand stability requirements.

Moreover, an analysis of harvesting indices in various forestry interventions reveals that stands systematically managed through appropriate silvicultural practices are significantly less vulnerable to disturbances. In contrast, stands with above-normal density and high slenderness coefficients - where interventions are irregular or absent - are at a greater risk of windthrows.

Moving forward, Romanian forestry must adopt complex and adaptive management solutions aimed at diversifying stand structures to minimize ecological and economic damage while ensuring the long-term sustainability of forest ecosystems.

REFERENCES

Barbu, I. & Barbu, V. (1993). Norway spruce (*Picea abies L. Karst*) in Romanian literature (1890-1990). *Bucovina Forestieră, 1*(1-2), 46-52.

Ciubotaru, A. & Păun, M. (2014). *The structure of the stands*. Transilvania University Publishing House Brașov, pp. 169.

Crainic, Gh.C., Irimie, Fl., Cioflan, Fl.M., Dorog, L.S., Iovan, C.I., Șerban, E. (2024). The influence of extrem weather phenomena on the management of hardwood trees. *Land Reclamation, Earth Observation & Surveying, Environmental Engineering. Series E., 13*, 397-407.

Duduman, G. (2011). A forest management planning tool to create highlydiverse uneven-aged stands. *Forestry: An International Journal of Forest Research, 84*(3), 301–314, https://doi.org/10.1093/forestry/cpr014

Gardiner, B.A. & Quine, C.P. (2000). Management of forests to reduce the risk of abiotic damage – a review with particular reference to the effects of strong winds. *Forest Ecology and Management*, *1-3*, 261-277, https://doi.org/10.1016/S0378-1127(00)00285-1

Ichim, R. (1990). *Gospodărirea rațională pe baze ecologice a pădurilor de molid*. Ceres Publishing House, pp. 194.

Iovan, C.I., Sabău, N.C., Dorog, L.S., Covaci, F., Iovan, A.R., Crainic, Gh.C. (2024). Analysis of some parameters of the hydrographic basins in the forest fund. *Scientific Papers*. *Land Reclamation, Earth Observation & Surveying, Environmental Engineering. Series E., 13,* 564-571.

Keren, S., Svoboda, M., Janda, P., Nagel, T.A. (2020). Relationships between Structural Indices and Conventional Stand Attributes in an Old-Growth Forest in Southeast Europe. *Forests, 11*(1), 4. https://doi.org/10.3390/f11010004

Negron-Juarez, R., Magnabosco-Marra., D., Feng, Y., Urquiza-Muñoz, J, D., Riley, W. J., Chambers, J. Q., (2023). Windthrow characteristics and their regional association with rainfall, soil, and surface elevation in the Amazon. Published by IOP Publishing Ltd. *Environmental Research Letters, 18*, https://doi.org/10.1088/1748-9326/acaf10

Pastorella, F. & Paletto, A. (2013). Stand structure indices as tools to support forest management: An application in Trentino forests (Italy). *J. For. Sci., 59*(4), 159-168. doi: 10.17221/75/2012-JFS.

Peck, J.E., Zenner, E.K., Brang, P., Zingg, A. (2014). Tree size distribution and abundance explain structural complexity differentially within stands of even-aged and uneven-aged structure types. *European Journal of Forest Research*, *133*(2), 335-346, https://doi.org/10.1007/s10342-013-0765-3

Popa, I. (2005). Windthrow – Risk factor in mountainous forest. *Analele ICAS, 48*, 3-28.

Valinger, E., Fridman, E. (2011). Factors affecting the probability of windthrow at stand level as a result of Gudrun winter storm in southern Sweden. *Forest Ecology and Management 262*(3), 398-403, https://doi.org/10.1016/j.foreco.2011.04.004

Scientific Papers. Series E. Land Reclamation, Earth Observation & Surveying, Environmental Engineering. Vol. XIV, 2025
Print ISSN 2285-6064, CD-ROM ISSN 2285-6072, Online ISSN 2393-5138, ISSN-L 2285-6064

InSAR TECHNOLOGY FOR RISK MANAGEMENT AND NATURAL DISASTER IMPACT ASSESSMENT IN BUCHAREST

Ana-Maria GLOD-LENDVAI[1], Iuliana ARMAŞ[2], Razvan TEODORESCU[3], Aurora DIACONEASA[1], Virgil MOISE[1], Daniel DUNEA[1]

[1]Valahia University of Târgoviște, 13 Aleea Sinaia, 130004, Târgoviște, Romania
[2]University of Bucharest, 1 Nicolae Bălcescu Blvd, District 1, 010041, Bucharest, Romania
[3]University of Agronomic Sciences and Veterinary Medicine of Bucharest,
59 Mărăşti Blvd, District 1, 011464, Bucharest, Romania

Corresponding author email: dan.dunea@valahia.ro

Abstract

The study analyzes the use of InSAR technology and validated data for risk management and natural disaster impact assessment, focusing on the subsidence in Bucharest, associated with underground works and activities, and earthquakes. The TerraSAR-X and TanDEM-X satellites provide crucial information for rapid mapping, spatial analysis, and thematic mapping, supporting effective responses to earthquakes, floods, and other hazards. The analysis identifies ground changes based on radar data using techniques such as Persistent Scatterers (PS) and Small Baseline Subset (SBAS). The study integrates decision analysis into the ILWIS software, using the multi-criteria method (SMCE) to assess vulnerabilities along the M5 Metro Line. The methodology involves structuring problems, evaluating alternatives, and prioritizing solutions, demonstrating the applicability of innovative tools in reducing urban risks. The results highlight the importance of advanced technologies in risk prevention and management, providing recommendations for reducing the impact of subsidence and improving urban planning. There is a clear need for integrated, rapid, and accurate approaches to respond to the more frequent and complex challenges in contemporary society based on validated data and modern technologies.

Key words*: remote sensing, interferometry, subsidence, risk management, urban planning.*

INTRODUCTION

With rapid population growth and urban expansion, urban risk management has become a global priority (Oprea et al., 2015; Sabău et al., 2023; Sanda et al., 2023). Bucharest, a city with an intense pace of development, faces major challenges related to subsidence, seismic vulnerability, and the impact of anthropogenic activities on soil and buildings. Previous studies have shown that Bucharest is one of the most vulnerable cities to earthquakes, with a historical rate of 2-3 major earthquakes per century (Armaș et al., 2017). Research conducted after the earthquake from 1977 highlighted the influence of the surface geological layer on seismic movements, and the damage reported to tall buildings is closely related to the subsurface sedimentology and the seismic amplification effects due to the Vrancea earthquakes (Radulian et al., 2007). More recently, to improve the understanding of seismic risks, a 3D geological model of the city was developed, based on hundreds of boreholes made for the metro and a digital terrain model (DEM), using GIS kriging interpolation, thus highlighting the Quaternary layers and the influence of hydrogeology on seismic micro-zonation (Bala et al., 2023).

The first decision-making analyses on urban vulnerability were conducted for the Historic Center of Bucharest by Gheorghe and Armaș (2015), identifying buildings that can serve as shelters in case of disaster.

In addition to seismic risk, subsidence is an aggravating factor of urban vulnerability and is caused by both natural phenomena and anthropogenic activities (Huang et al., 2016). New constructions, including taller buildings, deep foundations, expansion of the metro network, and aboveground transportation infrastructure, can have a significant impact on soil stability (Poncos et al., 2014). In this context, monitoring land surface deformations is one of the most reliable methods for assessing and managing geological hazards.

In Bucharest, using Sentinel-1 data and the PSI technique, a map of vertical displacements was produced for the period 2014-2018, identifying several subsidence areas, one of which contains a thick layer of debris from urban constructions, analyzed in detail in correlation with the local geological model and the urban hydrogeological system (Radutu et al., 2020).
Also, a combined *in situ* monitoring and remote sensing study investigated the effects of metro tunneling and groundwater pumping, demonstrating that interferometric remote sensing is a viable alternative to *in situ* measurements (Boukhemacha et al., 2021).
Long-term monitoring of urban subsidence and its correlation with metro infrastructure development and local hydrogeological characteristics are essential for risk prevention and optimization of urban planning (Bala et al., 2023). International studies have shown that subsidence is more pronounced in cities with intense economic activity and extensive urban infrastructure (Wang et al., 2024). Cities such as Mexico City and Istanbul have implemented effective risk reduction strategies, demonstrating that adopting proactive measures can significantly contribute to the protection of infrastructure and population (Glod-Lendvai, 2019). In this context, Bucharest must adapt its monitoring and prevention strategies to face the challenges related to subsidence and seismic risk in a continuously expanding urban environment.
The present study explores the use of InSAR (Interferometric Synthetic Aperture Radar) technology for monitoring and assessing urban subsidence, providing a solid scientific basis for the reliable management of urban planning and associated risk reduction.

MATERIALS AND METHODS

Subsidence monitoring was carried out using advanced Persistent Scatterers (PS) and Small Baseline Subset (SBAS) techniques, applied to a set of 24 TRS-X (downslope) and 27 TRS-X (upslope) scenes, covering the period 2011-2014. Analysis of radar data provided by the TerraSAR-X and TanDEM-X satellites provided a detailed picture of ground changes, and their correlation with field measurements allowed the identification of areas with the highest risk of instability.
An essential component of the study was the application of the Spatial Multi-Criteria Evaluation (SMCE) method in the ILWIS software, to classify vulnerable areas based on critical factors, such as geological composition, infrastructure density, and the impact of anthropogenic activities.
By using InSAR technology and advanced analysis methods, the study provides a detailed perspective on soil dynamics, contributing to a better understanding of geotechnical risks and the substantiation of decisions regarding sustainable urban development. The vulnerability of buildings was analyzed through an analytical method based on the correlation of information about buildings, obtained from the Digital Terrain Model (DTM) and the Digital Surface Model (DSM). In parallel, the vulnerability of the population was determined through the analytical method.
The validation of the results was achieved by correlating radar images provided by the TerraSAR-X and TanDEM-X satellites with field measurements. This integrated approach provided a detailed perspective on the evolution of subsidence and the risks associated with it, contributing to a better understanding of the phenomenon and the substantiation of decisions regarding urban infrastructure.
The decision-making analysis carried out for the M5 Metro line from Drumul Taberei was carried out using the multicriteria method, using a spatial decision-making assistance system through the SMCE (Spatial Multicriteria Evaluation) module of the ILWIS software. The study aimed to identify the most vulnerable sectors along the M5 Metro Line, considering the impact of subsidence caused by underground works, in the seismic context specific to the city of Bucharest.
The analyzed area includes a 400-meter-wide corridor, located along the M5 metro line (Figure 1). The route starts from the Dâmbovița meadow and crosses the Drumul Taberei neighborhood to the west, passing through a complex urban environment, with different types of constructions and varied geotechnical conditions.

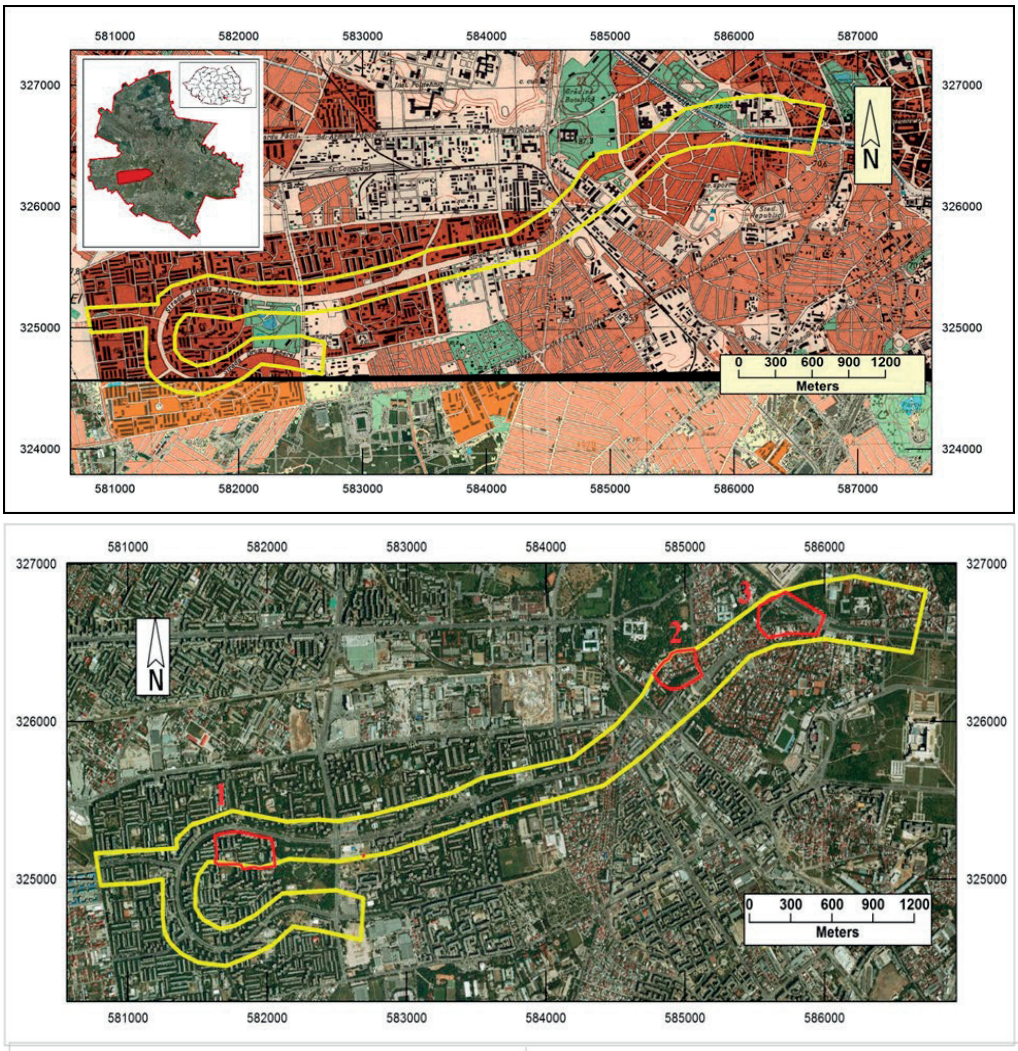


Figure 1. Study area in Bucharest, Romania

The incident at Eroilor station raised essential questions regarding the safety of buildings located above the metro tunnels.

The main concerns focused on their vulnerability in the event of an earthquake and on the influence that underground works may have on the stability of the buildings. Also, the trends of vertical movements captured by satellite interferometry were studied, to determine to what extent these phenomena are the result of anthropogenic interventions.

The analysis followed a clear methodology, structured in several stages. In the first phase, the problem was defined and organized by developing a decision tree using the ILWIS-SMCE module. In the next stage, relevant InSAR points were selected for the assessment of subsidence, using the PS (Persistent Scatterer) and SBAS (Small Baseline Subset) techniques (Figure 2). The obtained data were statistically analyzed to determine the speed of land movement over one year, highlighting the areas with the highest subsidence (Figure 3).

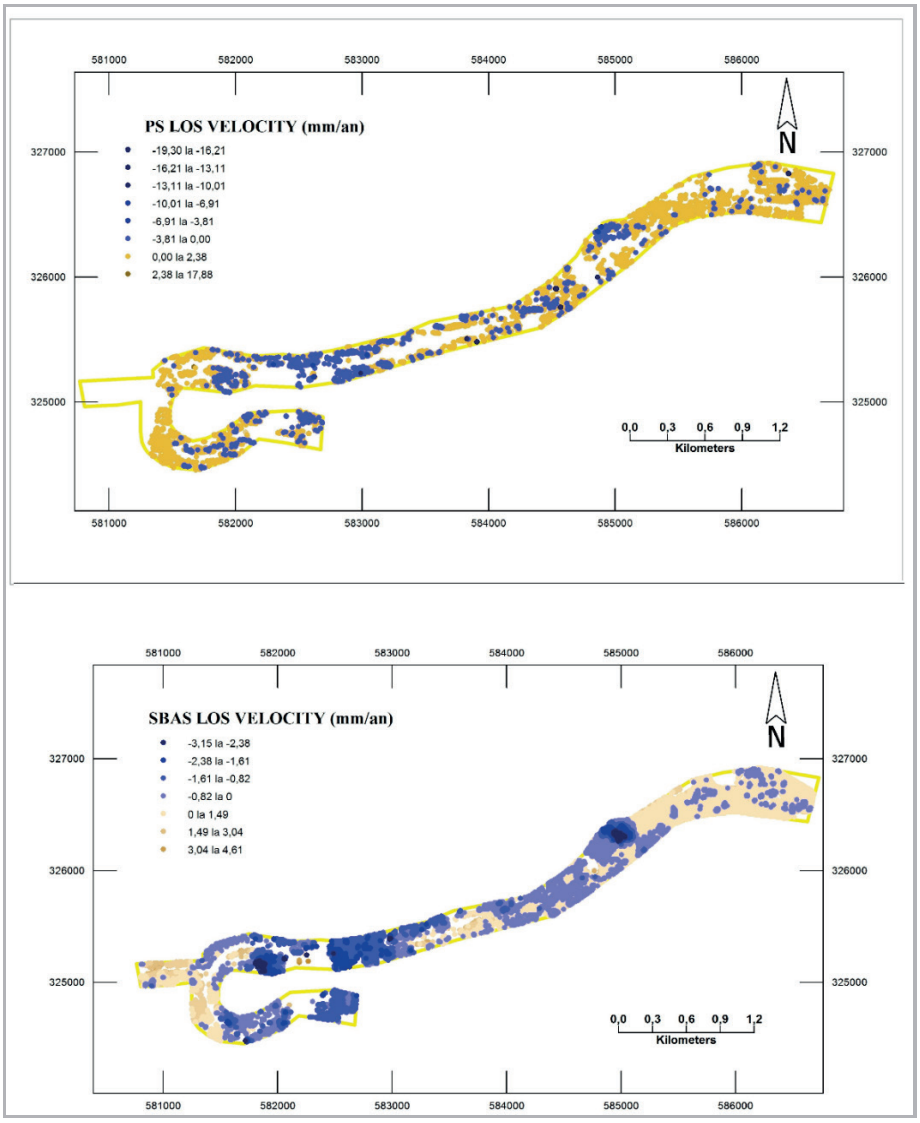


Figure 2. Deformation rates in the M5 metro line area

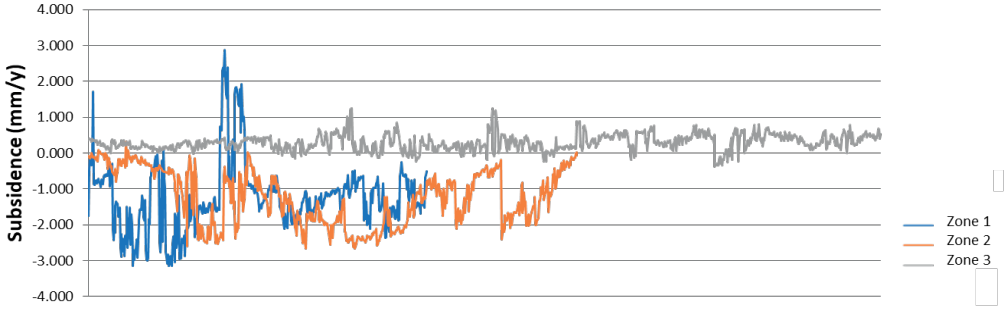
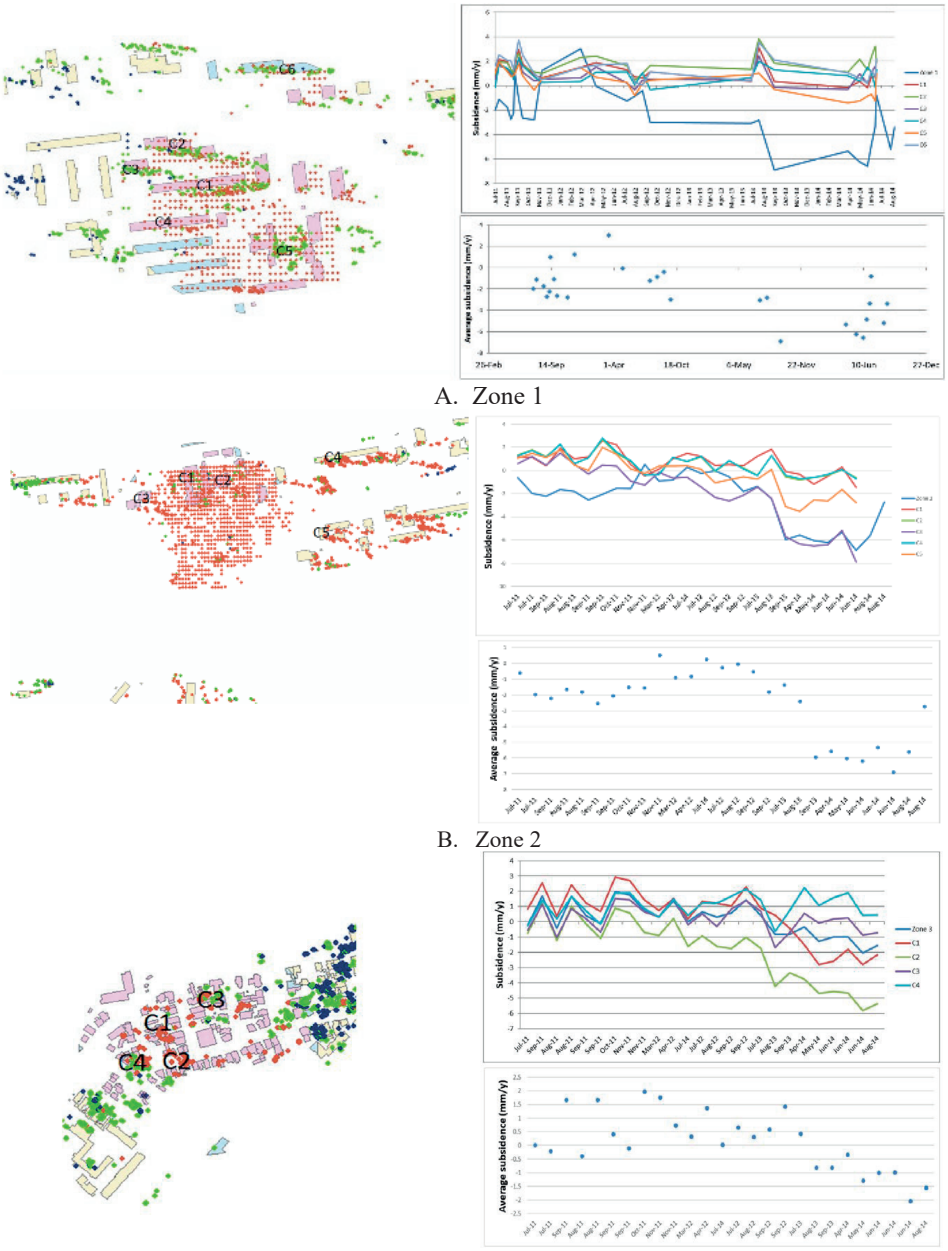


Figure 3. Vertical displacements from SBAS points in time

RESULTS AND DISCUSSIONS

The results showed that the most pronounced subsidence was found in two main areas, located in sectors where infrastructure works were carried out between 2011 and 2020. The Eroilor area was also identified as the most affected, given the major incident that occurred during the execution of the metro line (Figure 4).



A. Zone 1

B. Zone 2

C. Zone 3

Figure 4. Estimation of subsidence at the level of buildings in all three zones between 2011 and 2014

To understand the impact of these phenomena on buildings, the InSAR analysis was extended to buildings in the most affected areas. The results indicated that, in general, most buildings are stable, and the observed subsidence movements did not exceed the critical threshold of 25 mm mentioned in the specialized literature. The highest values were recorded in the Eroilor area, where settlements reached a peak of 21 mm during the incident.

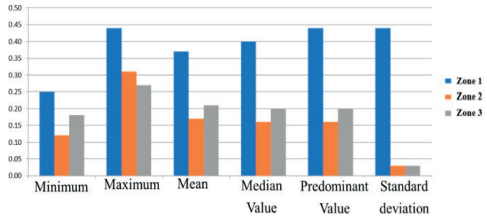
The study highlighted significant differences between the construction typologies in the three analyzed areas. The buildings in the first area are reinforced concrete structures, with a high height regime, built between 1977 and 1985 according to the construction norms of that period. In contrast, most buildings in areas two and three are masonry constructions, with rigid or flexible ceilings, built before the earthquakes of 1977 and even 1940, which makes them more vulnerable to seismic risks and subsidence phenomena.

For a correct assessment of vulnerability, the data were subjected to a normalization process. The interval procedure was used to highlight and differentiate even the smallest variations in the datasets. Regarding the seismic vulnerability of buildings, the maximum procedure was applied, thus avoiding any intervention that could alter the initial distribution of the data. Also, the distance from the RATB stations was considered an important factor, being evaluated in inverse proportion to the vulnerability of the area, with short distances being perceived as an advantage.

To rank the risk factors and calculate the specific scores, the SMCE module of ILWIS was used. After selecting the indicators, normalizing them, and defining the weights, the analysis led to the generation of vulnerability maps.

The final results indicated a variable vulnerability index depending on the area analyzed. The lowest values of this index, i.e., 0.12, were recorded in zone two, while zone one presented the highest level of vulnerability, with a maximum index of 0.44. The detailed analysis of each indicator and sub-objective confirmed that zone one is the most vulnerable of the entire investigated sector (Figure 5). By applying a rigorous multi-criteria assessment method, this decision-making analysis allowed the identification of the sectors with the highest degree of vulnerability and provided a solid basis for making informed decisions regarding the necessary protection and consolidation measures along the M5 Metro Line.

The results of the study showed that the vulnerability index varied between 0.12 and 0.44, with the highest values being recorded in the area delimited by Drumul Taberei (north), Târgu Neamț Street (east), Pașcani Alley (south), and Cetății Street (west). In this region, the analysis indicated a higher predisposition to soil instability and possible negative effects on buildings.



Zone	Minimum	Maximum	Mean	Median Value	Predominant Value	Standard deviation
Zone 1	0.25	0.44	0.37	0.40	0.44	0.44
Zone 2	0.12	0..31	0.17	0.16	0.16	0.03
Zone 3	0.18	0.27	0.21	0.20	0.20	0.03

Figure 5. Statistical analysis for the three studied areas

A consistent uplift pattern was identified in the interfluve area between the Dâmbovița and Colentina rivers, suggesting an active process of land deformation. In addition, subsidence phenomena were evident in the northwestern and southeastern outskirts of Bucharest, highlighting the need for prevention and intervention measures to reduce the risks associated with these areas.

CONCLUSIONS

The analysis of urban vulnerability and subsidence in Bucharest highlighted the need to implement advanced risk monitoring and management strategies. The use of modern technologies, such as InSAR, together with advanced analytical methods, provides a solid basis for informed decision-making, contributing to the protection of infrastructure and population against natural and anthropogenic hazards.

The application of these methods allows for an efficient management of urban risks, demonstrating that validated data can be used to reduce the impact of subsidence, optimize urban planning, and prevent disasters. By integrating advanced technologies, such as InSAR and multi-criteria analysis, it is possible to identify and classify vulnerable areas, providing support for evidence-based urban policies.

These conclusions confirm that an integrated approach, based on long-term state-of-the-art monitoring technologies, is an essential tool in securing the urban environment and adapting the city to geodynamic risks. Implementing proactive strategies can significantly contribute to reducing infrastructure vulnerability and creating a safer and more sustainable urban environment.

ACKNOWLEDGEMENTS

We thank Dr. Mihaela Gheorghe for the support in processing the InSAR data. The publishing of this research work received support from the Valahia University of Târgovişte research fund.

REFERENCES

Armaş, I., Cretu R.Z, Ionescu R. (2017). Self-efficacy, stress, and locus of control: The psychology of earthquake risk perception in Bucharest, Romania. *International Journal of Disaster Risk Reduction 22*, 71-76, https://doi.org/10.1016/j.ijdrr.2017.02.018.

Bala, A., Toma-Danila, D., Ciugudean-Toma, V. (2023). 3D geological model and geotechnical data for Bucharest: necessary input for assessing local seismic hazard of a densely populated area. *Acta Geod Geophys 58*, 175–196. https://doi.org/10.1007/s40328-023-00412-z

Boukhemacha, M. A., Teleaga, D., Serbulea, M. S., Poncos, V., Serpescu, I., Manoli, D. M., Haagmans, R. (2021). Combined in-situ and Persistent Scatterers Interferometry Synthetic Aperture Radar (PSInSAR) monitoring of land surface deformation in urban environments - case study: tunnelling works in Bucharest (Romania). *International Journal of Remote Sensing, 42*(7), 2641–2662. https://doi.org/10.1080/01431161.2020.1857876

Glod-Lendvai, A.M. (2019). Comparative analysis of disaster risk management practices in Bucharest, Ciudad de Mexico and Istanbul. *GeoPatterns*, *4*, 16–25, https://doi.org/10.5719/GeoP.4/2

Huang, J., Khan, S. D., Ghulam, A., Crupa, W., Abir, I. A., Khan, A. S., Kakar, D. M., Kasi, A., Kakar, N. (2016). Study of Subsidence and Earthquake Swarms in the Western Pakistan. *Remote Sensing, 8*(11), 956. https://doi.org/10.3390/rs8110956

Lendvai (Glod-Lendvai) Ana-Maria (2019). Current subsets of Bucharest Municipality with case studies in seismic risk management, *Ph.D. thesis*, University of Bucharest, available on https://rei.gov.ro/

Oprea, M., Ianache, C., Mihalache, S.F., Dragomir, E.G., Dunea, D., Iordache, S., Savu, T. (2015). On the development of an intelligent system for particulate matter air pollution monitoring, analysis and forecasting in urban regions. 19th International Conference on System Theory, Control and Computing (ICSTCC), 711–716. https://doi.org/10.1109/ICSTCC.2015.7321377

Poncos V., Teleaga D., Boukhemacha M.A., Toma S.A., Serban F. (2014). Study of urban instability phenomena in Bucharest city based on PS-InSAR, *International Geoscience and Remote Sensing Symposium* (IGARSS). 10.1109/IGARSS.2014.6946450.

Popovici, D., Armas, I. (2015). GIS based decision support system support system for seismic risk in Bucharest. Case study– the historical centre. *Journal of Engineering Studies and Research, 21*, 35–42. https://doi.org/10.29081/jesr.v21i3.141.

Radulian, M., Grecu, B., Mandrescu, N. (2007). Source and site effects implications on Bucharest (Romania) microzonation. *American Geophysical Union*, Spring Meeting, abstract #S33B-10.

Radutu, A., Venvik, G., Ghibus, T., Gogu, C.R. (2020). Sentinel-1 Data for Underground Processes Recognition in Bucharest City, Romania. *Remote Sensing 12*(24), 4054. https://doi.org/10.3390/rs12244054

Sabău, D.A., Şerban, G., Breţcan, P., Dunea, D., Petrea, D., Rus, I., Tanislav, D. (2023). Combining radar quantitative precipitation estimates (QPEs) with distributed hydrological model for controlling transit of flash-flood upstream of crowded human habitats in Romania. *Nat Hazards 116*, 1209–1238. https://doi.org/10.1007/s11069-022-05718-9

Sanda, M., Dunea, D., Iordache, S., Pohoata, A., Glod-Lendvai A.M., Onutu, I (2023). A three-year analysis of toxic benzene levels and associated Impact in Ploieşti City, Romania, *Toxics 11*(9), 748. https://doi.org/10.3390/toxics11090748

Wang, S., Chen, Z., Zhang, G., Xu, Z., Liu, Y., Yuan, Y. (2024). Overview and Analysis of Ground Subsidence along China's Urban Subway Network Based on Synthetic Aperture Radar Interferometry. *Remote Sensing 16*(9), 1548. https://doi.org/10.3390/rs16091548

Scientific Papers. Series E. Land Reclamation, Earth Observation & Surveying, Environmental Engineering. Vol. XIV, 2025
Print ISSN 2285-6064, CD-ROM ISSN 2285-6072, Online ISSN 2393-5138, ISSN-L 2285-6064

FLOOD IMPACT ASSESSMENT ON RAILWAY INFRASTRUCTURE USING NUMERICAL MODELLING: CASE STUDY OF NĂDAB, ROMANIA

**Dorian HAUSLER COZMA, Teodor Eugen MAN,
Robert Florin BEILICCI, Erika BEILICCI**

Politehnica University of Timișoara,
1A Splaiul Spiru Haret, 300022, Timișoara, Romania

Corresponding author email: robert.beilicci@upt.ro

Abstract

Railway infrastructure is constantly undergoing processes of change and development, it is becoming an important means of transportation. At European level, railways are going through a period of transformations aimed at increasing the transportation capacity for both goods and passengers, as well as increasing travel speeds. Railway infrastructure is constantly exposed to the action of rainwater, groundwater or extreme weather events such as floods. The problem arises when the water is not quickly drained, it remains for a longer period in the embankments leading to wetting or even saturation of the ground. Soil saturation leads to a decrease in bearing capacity and contributes to soil degradation, compromising infrastructure stability. This paper presents advanced numerical modelling with MIKE11 software of real flood situations in the Nădab area, as well as to assess mitigation scenarios through works on railway infrastructure and land improvement

Key words*: flooding, hazard maps, MIKE11, railway infrastructure, soil saturation.*

INTRODUCTION

Floods are among the most frequent and destructive natural phenomena globally, with significant impacts on the environment, population, and critical infrastructure. In recent decades, Central and Eastern Europe have experienced an increase in both the frequency and intensity of flood events, a trend amplified by climate change. These climatic changes directly affect infrastructure vulnerability, particularly in the transport sector, such as railway networks.

Floods rank among the most widespread natural disasters and are third in terms of global impact. These disasters impact both the natural environment, where they take place, and the socio-economic sphere, causing loss of human lives, damage to transportation infrastructure, destruction of agricultural land, the spread of diseases, and interruptions in drinking water supply systems, among other consequences.

Climate change is one of the greatest challenges of the 21st century, having a significant impact on both natural and human systems. In particular, hydro-geomorphological risk events, such as floods, landslides, and erosion, have become more frequent and more intense as a result of climate changes. Floods, in particular, are complex events with significant impact at both global and regional levels, driven by a combination of natural and anthropogenic mechanisms. Their geographical distribution is influenced by climatic, topographic, and hydrological factors specific to each region. Modern risk assessments increasingly rely on geomatic tools and hydrological modeling to better predict and manage these events.

In Romania, the Crișul Alb River Basin, located in the western part of the country, is an area exposed to flood risks due to both geomorphological conditions and extreme weather events. In this context, railway infrastructure in the region is becoming increasingly vulnerable, frequently affected by flash floods and terrain erosion.

The Crișul Alb Basin (Figure 1) largely overlaps with Arad County, and in the southeastern part, with Hunedoara County; in the east, it extends slightly into Alba County, and in the north, it also partially overlaps with a small area of Bihor County.

The hydrographic basin features varied climate, influenced by differences in altitude and the shape of the terrain through which it flows. It covers several geographical units, such as the

Bihor Mountains, the Metaliferi Mountains, the Codru-Moma Mountains, the Zărand Mountains, and the associated hills and plains. The distribution of precipitation in the Crișul Alb Basin varies significantly from east to west (Figure 2).

The mountainous areas in the east are characterized by the highest amounts of precipitation, while in the western area, the amounts are lower. The diversity of soil types (Figure 3) reflects the geological, geomorphological, and climatic variability of the region. Fertile soils such as chernozems and alluvial soils predominate in the plains, while less fertile soils or those with special characteristics (such as lithosols and dystric cambisols) are found in the mountainous areas (NARW, 2024).

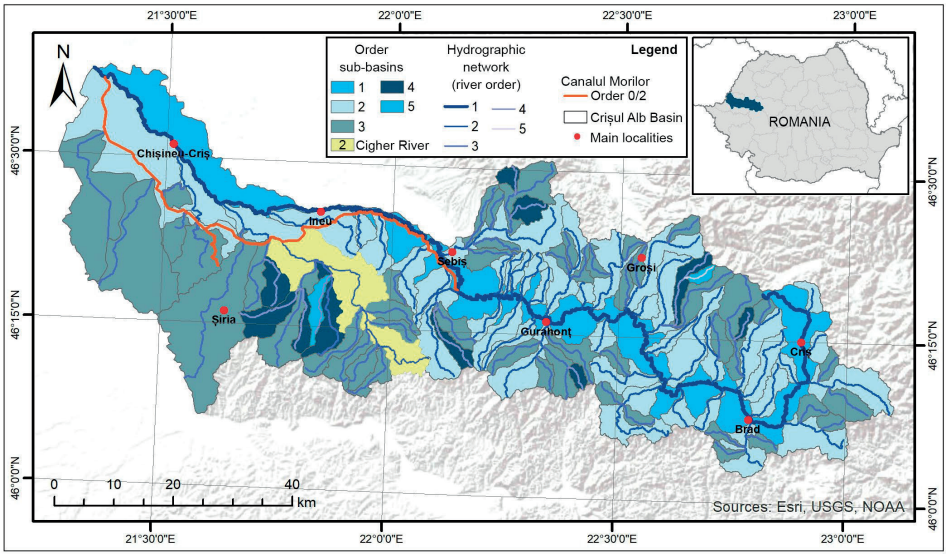


Figure 1. Overview map of the Crișul Alb River Basin, showing administrative boundaries and main hydrographic features

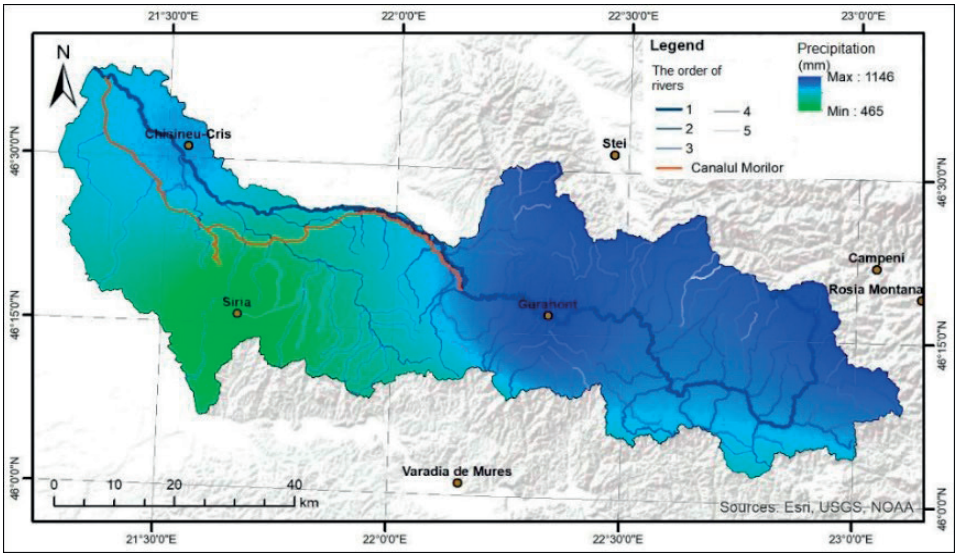


Figure 2. Annual precipitation distribution in the Crișul Alb Basin (mm/year), highlighting east-west variation

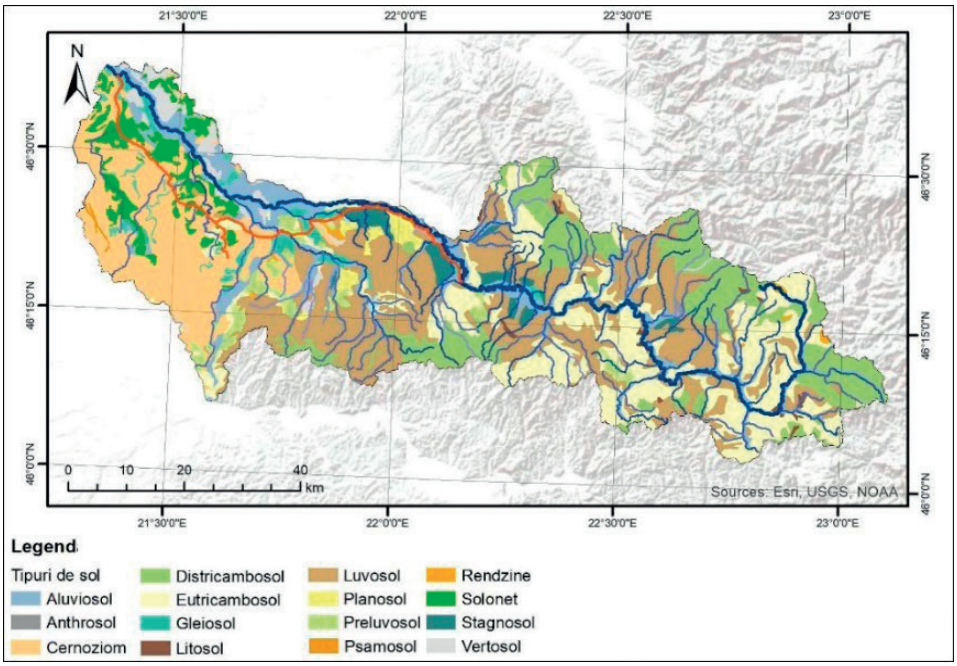


Figure 3. Spatial distribution of soil types in the study area, based on NARW classification

The Crișul Alb River originates in the Apuseni Mountains, in the northern area of the Bihor Mountains, at an altitude of approximately 1,250 meters. It flows through the counties of Hunedoara, Arad, and Bihor, covering a distance of about 234 km before discharging into the Tisza River on the territory of Hungary. In the Crișul Alb Basin, the hydrographic network is composed of 103 rivers, with a total length of 1,667 km.

The Crișuri hydrographic area has a complex system of hydraulic works for the quantitative management of water resources, containing several water diversion structures that transfer water volumes from one river course to another. To supply water for various uses (drinking water, irrigation, fish farming), as well as for collecting high waters from interfluves, 27 water intakes and diversions have been constructed.

The existing flood protection works in the Crișuri hydrographic area include river regulation, embankments, bank reinforcements, as well as permanent and temporary reservoirs or polders.

This study aims to assess the impact of floods on railway infrastructure using numerical modelling, with a case study focused on the locality of Nădab. The main objective is to gain understand hydraulic behaviour in critical flood-prone areas and to propose solutions to reduce risks to railway transport.

MATERIALS AND METHODS

The analyzed area is located in the western part of Romania, in the Crișul Alb River Basin, with a focus on the sector corresponding to the locality of Nădab. This region is characterized by a predominantly low-plain relief and the presence of critical infrastructure, including the Arad-Oradea railway line, which is vulnerable to recurrent flooding.

In the last two decades, Europe has experienced over 100 major floods, resulting in more than 700 casualties, displacing over half a million people, and causing damages exceeding 25 billion EUR.

The extreme hydrological phenomena occurring in recent decades, both globally and in Romania, highlight the fact that society is affected not only by slow floods, caused by rivers with medium and large catchment areas, but also, to the same extent, by fast floods, typical of small basins, generally less than 200-300 km^2. There is a

growing trend in the frequency of severe flash floods, which have caused significant material damage and, in many cases, loss of human lives (Biali et al., 2022).

Global practice has shown that the occurrence of floods cannot be avoided, but they can be managed their effects on the social, economic, environmental, and cultural heritage sectors can be reduced through a process involving complex analyses and targeted prevention and mitigation measures at the local, regional, and national levels, designed to contribute to reducing the risk associated with these phenomena (Hausler et al., 2020).

The National Flood Risk Management Strategy for the medium and long term encourages the construction of communication routes (roads, railways) with embankments reinforced to appropriate levels whitch serve as flood localization lines, and must include properly dimensioned bridges.

Additionally, it encourages the construction embankments for national roads and railways in such a way that they can serve as flood protection lines in areas identified with a high flood risk particularly where geographic conditions require such measures to be the only viable option for protecting settlements. These specific cases will be included in the River Basin Master Plan and, later, in the Flood Risk Management Plan, and will be carried out in accordance with the approved budgets.

The history of risk phenomena in the Crișul Alb basin highlights the need for proactive management of hydrographic resources and flood protection measures. Repeated flooding and landslide events underscore the region's vulnerability and the importance of risk prevention and management interventions.

Floods are natural phenomena, and of the 20 types of hazards considered natural disasters, they are ranked highest terms of geographic spread, number of events, and number of people affected.

In determining areas at risk of flooding, both river overflow floods (medium/large basins) and flash floods (small catchments) are considered.

Flash floods are floods that occur in a short period of time and are characterized by sudden increases in water levels and flow rates. The main characteristic of flash floods is that they have a maximum growth time of 4 to 6 hours, occurring in small catchment areas ranging from a few to several hundred km². The main cause of these flash floods is torrential rainfall, with exceptionally high intensities. However, there are also other physical and geographical factors that contribute to or trigger flash flood events, factors that will be detailed in the section dedicated to hazard analysis.

Historical flood events with significant impacts on health, the environment, cultural heritage, and economic activity were included in the assessment, including those that could occur in areas with hydraulic infrastructure, such as embanked zones. (Gabor et al., 2019).

To carry out hydraulic simulations and assess the potential impact of floods on railway infrastructure, the MIKE21 and MIKE FLOOD applications developed by DHI were used.

MIKE 11 is a software developed by DHI (Danish Hydraulic Institute) and is designed to perform one-dimensional hydraulic and hydrodynamic calculations, with integrated storage zones to represent networks of natural and engineered channels (Armas et al., 2016).

In essence, the calculation procedure is based on a numerical solution of the one-dimensional energy and mass conservation equations (the Barre-de-Saint-Venant system of equations). Energy losses are primarily evaluated through friction (Manning's equation) and contraction/expansion (via a dynamic head loss coefficient) (Marossy et al., 2016).

The hydraulic modeling of river sections identified as potentially flood-prone, using specialized software, consisted of one-dimensional (1D) and two-dimensional (2D) simulations of flow on the analyzed river courses. For 1D hydraulic modeling, the dependence of water level on flow rate was determined using the MIKE 11 (DHI) application, while for areas requiring more detailed analysis, the MIKE 21 (DHI) application was used. The 1D and 2D hydrodynamic modeling was applied with calibration and verification for significant historical floods (DHI, 2021).

MIKE21 allows for the two-dimensional modeling of surface runoff, which is useful for assessing the spatial extent of water in flood-prone areas.

MIKE FLOOD integrates 1D and 2D models, enabling complex analysis of the interaction

between watercourses and surrounding land, including transport infrastructure.

Flood hazard maps were obtained using the MIKE Flood (DHI) mathematical model, a model that allowed the coupling of 2D and 1D models into a single calculation system. These maps indicate, for different analyzed scenarios (Qp%), the extent of flooded areas and water depth.

The model was fed with data obtained from multiple sources:

- Topography: High-resolution digital terrain model (DTM) obtained using LiDAR technology;
- Hydrographic Network: Cross-sections and hydraulic parameters of the Crișul Alb River;
- Climatic and Hydrological Data: Historical records of precipitation and discharge, obtained from ANAR;
- Railway Infrastructure: Positioning and physical characteristics of the Nădab railway line, including embankment levels and existing flood defense works.

The railway infrastructure is constantly exposed to the action of water.

Types of water that affect railway infrastructure:

- Surface water comes from atmospheric precipitation that falls directly on the railway embankment or on the adjacent land (berms, slopes);
- Groundwater is found in aquifer layers located beneath the ground level;
- Extreme weather events: Floods result from flash floods, heavy rains, storms, or river flooding. Although the railway infrastructure is not designed within riverbeds, there are situations where high waters affect the embankments. The embankments serve as dikes against high waters, which leads to soil erosion and landslides, consequently damaging the railway infrastructure (Vara et al., 2024).

The problem arises when water is not quickly evacuated, remaining for a longer period of time in the embankments, which leads to the dampening or even saturation of the soil. (Kellermann et al., 2016). Dampening or saturation of the soil with water leads to a decrease in load-bearing capacity and soil degradation (Hausler et al., 2020). The MIKE11 program was used for numerical modeling. At the beginning, the existing situation of the Crișul Alb River was modeled. The model plan is shown in Figure 4.

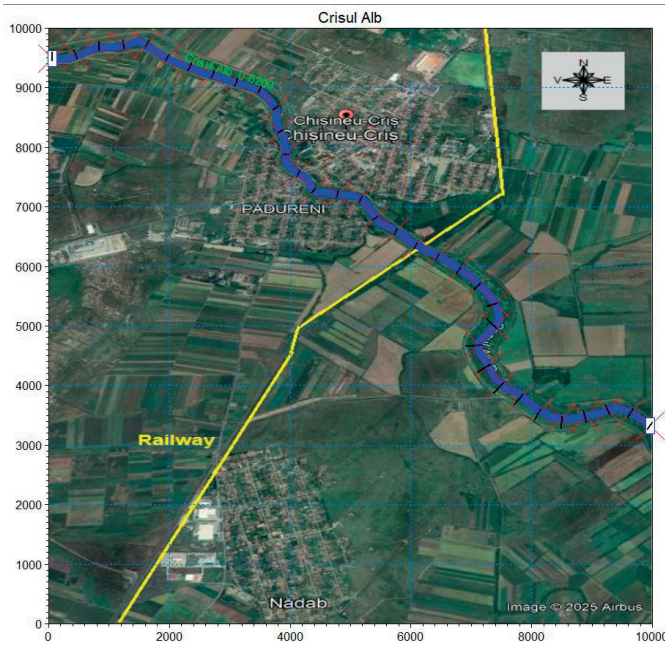


Figure 4. MIKE11 model plan view for the Crișul Alb River, showing simulation domain in the Nădab sector

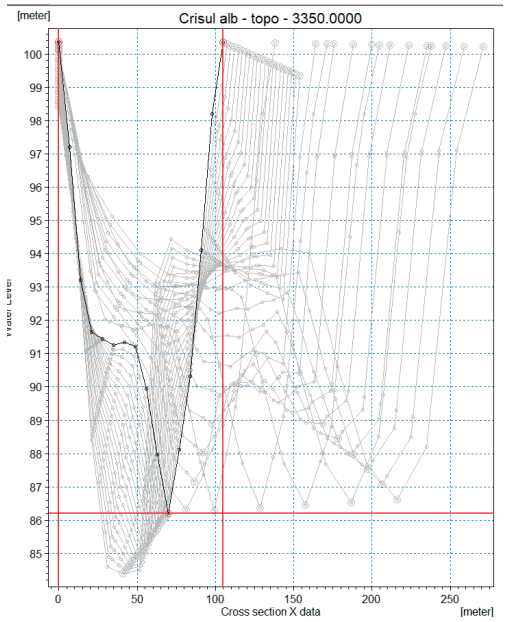


Figure 5. Topographic cross-sections of the canal used in MIKE11 hydraulic modeling

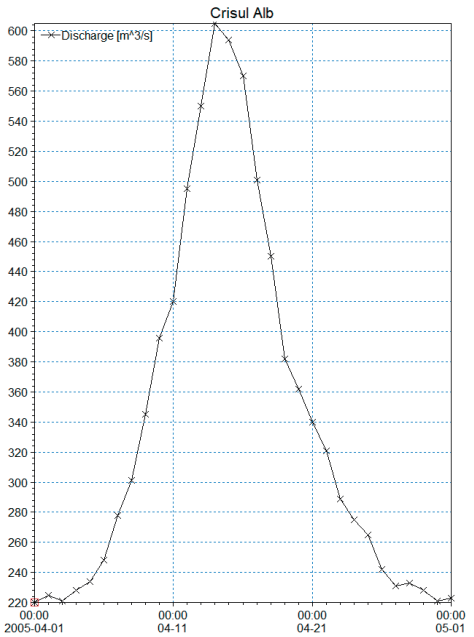


Figure 6. Inflow hydrograph (m³/s) used as upstream boundary condition for the 2005 flood event simulation

Cross-sections obtained from topographic surveys are shown in Figure 5.

Boundary conditions included an upstream flood hydrograph at chainage 0+000 and a downstream rating curve at chainage 8+200 (Damian et al., 2022).

The flow hydrograph is shown in Figure 6.

RESULTS AND DISCUSSIONS

The model was configured to simulate flood scenarios with different occurrence probabilities (1%, 2%, 10%). Hydraulic parameters, such as Manning's roughness and loss coefficients, were adapted based on local characteristics. Built-up areas and agricultural lands were treated differently to improve the accuracy of flow distribution.

The model was calibrated using data from historical events (the floods of 2000 and 2006) by adjusting hydraulic parameters the simulated values closely matched observed water extents and recorded levels. Validation was performed on a separate data set to ensure the robustness and applicability of the model for future scenarios.

The water levels from the initial results were compared with measured levels in several sections. Roughness coefficients were adjusted in specific sections until the simulated levels aligned with observed data.

By carrying out the MIKE11 program, a longitudinal profile of the canal was obtained showing water levels over the simulation period (Figure 7).

From Figures 7, it follows that for the hydrograph of the inflows introduced in 2005 on the Crisul Alb River, the maximum water transport capacity of the canal was exceeded, with the flood risk occurring for flows greater than those considered. Flood hazard maps generated with the MIKE Flood model show the spatial extent and depth of inundation under each flood scenario (Figure 8).

The results included detailed maps of the water extent and longitudinal profiles of the affected railway line, as well as estimates of water depth and flow velocity along sections of the railway line.

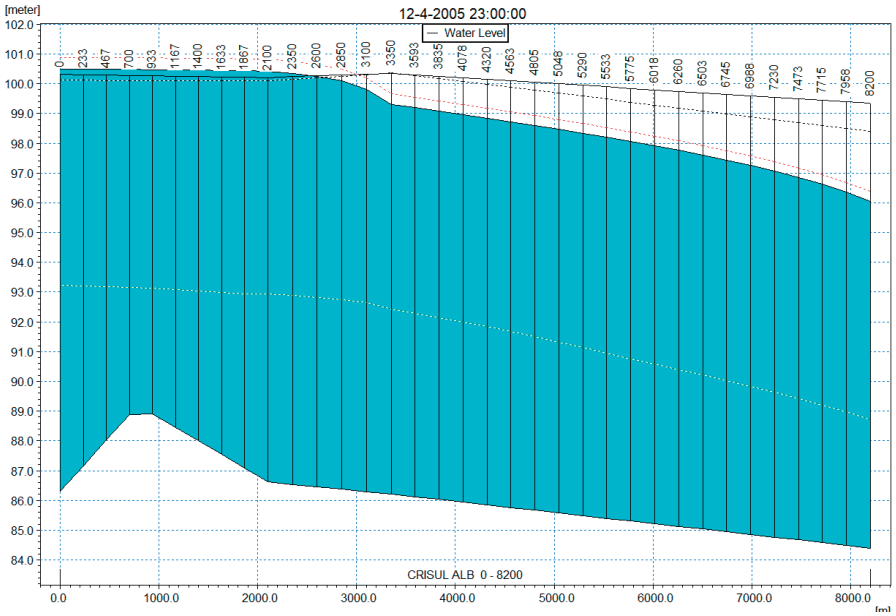


Figure 7. Longitudinal profile of the Crișul Alb Canal, showing simulated water levels during peak flow

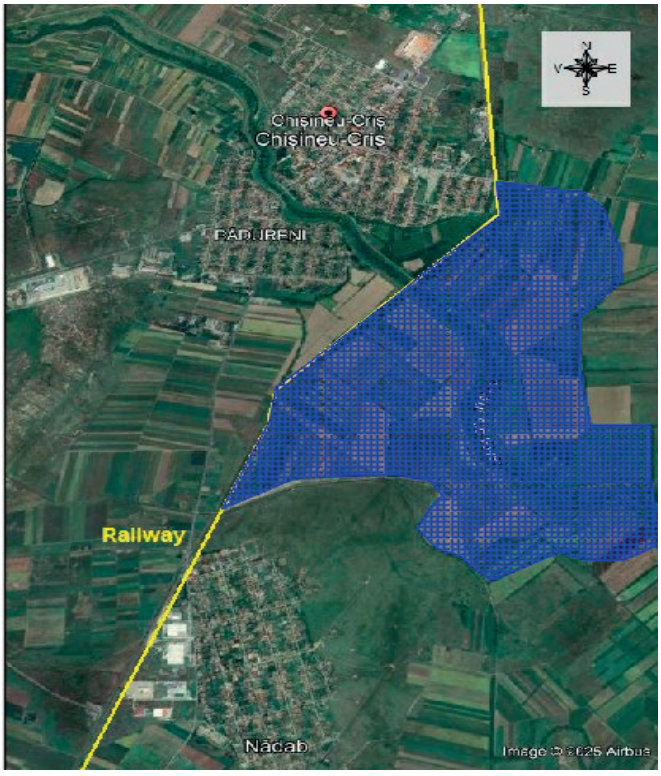


Figure 8. Flood hazard map of the Nădab area for the 1% probability scenario (Q100), showing extent and depth of inundation

In the specific context of the Nădab locality, the results suggest the need for additional protective measures, such as raising the railway embankments or constructing protective barriers to prevent flooding of the railway line during extreme events. Additionally, interventions to improve drainage systems in the area should be considered to reduce the risk of railway infrastructure blockage due to heavy precipitation.

On a broader scale, the results of this model help to improve understanding of the impact of flooding on critical infrastructure, especially in areas vulnerable to extreme weather events. This information may inform urban and infrastructure planning, considering climate change and the increased risks of flooding in the future. Furthermore, it can assist authorities in developing prevention strategies and rapid-response plans for natural disasters.

Comparisons with existing studies suggest that the vulnerability of railway infrastructure to flooding is a well-documented issue, especially in regions with low-lying terrain and nearby watercourses. While previous research has indicated similar protective measures (e.g., raising embankments and improving drainage systems), the current study highlights the specificity of the Nădab area, with its unique topographic and hydrological characteristics.

Among the limitations of the study are the simplified assumptions of the hydraulic model and the limited availability of historical flood data, which could have improved the model's calibration. In the future, it would be useful to expand studies to include long-term flood scenarios, considering climate forecasts and potential changes in the region's hydrological regime. Additionally, innovative solutions, such as green infrastructure (e.g., water retention zones), could be explored to enhance the flood resilience of railway infrastructure.

CONCLUSIONS

The study showed that the Nădab railway sector is vulnerable to flooding, especially in low-probability scenarios (1%), where water levels can exceed the capacity of the embankments. The results of the hydraulic simulations indicate significant water extent along the railway line during flood conditions, which poses a major risk infrastructure stability and operational safety.

The railway infrastructure in the Nădab area is vulnerable to recurring floods, particularly under he influence of climate change, which is expected to increase both the frequency and intensity of extreme weather events.

The greatest threat is the overload of local drainage capacity and subsequent flooding of the railway corridor, which can lead to major disruptions in train circulation and material damage.

Hydraulic modeling and hazard maps provide a clear picture of flood risks and help identify critical areas that require protective measures. These tools are essential for assessing potential impacts and supporting well-informed infrastructure protection strategies, particularly in flood risk planning and management.

Protective actions such as embankment elevation and the installation of barriers should be urgently considered to prevent flooding of the railway. Moreover, authorities are encouraged to prioritize drainage system upgrades and to invest in long-term infrastructure resilience strategies in light of future flood risk escalation.

Looking ahead, it is important to continue monitoring flood risks and improving hydraulic models by incorporating reliable climate projections.

Additionally, innovative green infrastructure solutions, such as water retention areas and the use of permeable materials, should be explored to enhance the resilience of railway infrastructure and help mitigate the effects of a changing climate.

The growing recognition of climate-related risks has brought the issue of water-related impacts on railway infrastructure to the forefront of discussions at the European level.

ACKNOWLEDGEMENTS

Thanks to the project: Development of knowledge centers for lifelong learning through the involvement of specialists and decision-makers in flood risk management, this activity can be possible using advanced hydroinformatics tools, AGREEMENT NO. LLP-LdV-ToI-2011-RO-002/2011- 1-RO1-LEO05-5329, was funded with the help of the European Commission.

REFERENCES

Armas, A., Beilicci, R., Beilicci, E. (2017). Numerical limitations of 1D hydraulic models using MIKE11 or HEC-RAS software - Case study on the Baraolt River, Romania, *IOP Conference Series: Materials Science and Engineering*, *245*, DOI10.1088/1757-899X/245/7/072010.

Biali, G., Cojocaru, P. (2022), GIS Hydrological modeling in an agricultural river basin with high potential for water erosion, *Scientific Papers-Series E-Land Reclamation Earth Observation & Surveying Environmental Engineering*, *11*, 418-425, WOS:000931961700050.

Damian, G., Pricop, C., Statescu, F. (2022), The study of hydrological regime modeling using HEC-RAS model. case study river basin Bahluet, *Scientific Papers-Series E-Land Reclamation Earth Observation & Surveying Environmental Engineering*, *11*, 338-343, WOS:000931961700039.

DHI - Danish Institute of Applied Hydraulics, 2021, MIKE 11 user manual - *A modeling system for rivers and channels, Short introduction and tutorial*, DHI, Horsholm, Denmark

Gabor, E., Beilicci, E., Beilicci, R. (2019), Advanced Hydroinformatic Tools for Modelling of Reservoirs Operation", *IOP Conference Series: Materials Science and Engineering*, *471*, DOI10.1088/1757-899X/471/4/042002.

Hausler, P.C.D., Beilicci, E., Beilicci, R (2020), Modelling of Privalul Tinoasa channel, in irrigation system Borcea 2-Danube Romania, *IOP Conference Series: Materials Science and Engineering*, Volume 960, DOI10.1088/1757-899X/960/2/022023.

Kellermann, P., Schönberger, C., Thieken, A.H., (2016), Large-scale application of the flood damage model RAilway Infrastructure Loss (RAIL). *Natural hazards and earth system sciences*, *16*(11), DOI10.5194/nhess-16-2357-2016.

Marossy, Z., Beilicci, R., Beilicci, E, Visescu, M. (2016), Advanced hydraulic modeling of the Cp3 irrigation channel, in the Teba - Timiş irrigation system, Romania, Timiş County, SGEM *Water, Resources, Forest, Marine And Ocean Ecosystems Conference Proceedings, I*, 39-46, WOS:000391653400006.

NARW - National Administration "Romanian Waters", Crişuri (2024), *Flood Risk Management Plan*, 005-049.

Varra, G., Morte, R.D., Tartaglia, M., Fiduccia, A., Zammuto, A., Agostino, I., Booth, C.A., Quinn, N., Lamond, J.E., Cozzolino, L (2024), Flood Susceptibility Assessment for Improving the Resilience Capacity of Railway Infrastructure Networks, *Water, 16(18), 2592.* https://doi.org/10.3390/w16182592

Scientific Papers. Series E. Land Reclamation, Earth Observation & Surveying, Environmental Engineering. Vol. XIV, 2025
Print ISSN 2285-6064, CD-ROM ISSN 2285-6072, Online ISSN 2393-5138, ISSN-L 2285-6064

NATURE-BASED SOLUTIONS FOR THE SUSTAINABLE DEVELOPMENT OF GREEN AND BLUE INFRASTRUCTURE IN ROMANIA

Andreea Catalina POPA[1], Teodora UNGUREANU[1], Claudiu-Sorin DRAGOMIR[1, 2], Antonio-Valentin TACHE[1]

[1]National Institute for Research and Development in Construction, Urban Planning and Sustainable Spatial Development – URBAN-INCERC, 266 Pantelimon Road, 021652, District 2, Bucharest, Romania
[2]University of Agronomic Sciences and Veterinary Medicine of Bucharest, 59 Mărăşti Blvd, 011464, District 1, Bucharest, Romania

Corresponding author email: andreeacatalina.popa@incd.ro

Abstract

Romania faces challenges related to climate change, such as rising temperatures, floods, and droughts, while urban areas struggle with air and water pollution. The growing public awareness of sustainability and environmental protection creates a favorable context for the large-scale implementation of such infrastructure across the country. This research provides a detailed classification of green and blue infrastructure types, highlighting their diversity and the specific functions each fulfills in improving urban life. Green and blue areas are essential for improving urban life quality and protecting the environment. The growing significance of green and blue infrastructure is reflected in Romania's urban laws and policies, highlighting a shift towards sustainable development and city resilience. However, implementing this is difficult due to the lack of a single legal definition, causing inconsistent use and confusion. Additionally, there is no cohesive national strategy, and legal frameworks addressing different aspects are uncoordinated. Local authorities also need clearer guidelines and better methods for planning, designing, and managing these infrastructures effectively.

Key words*: climate change, environmental quality, sustainability.*

INTRODUCTION

Currently, over half of the global population (55%) resides in urban areas, and this percentage is projected to rise in the coming years (United Nations, 2019). Cities are increasingly confronting various risks, with escalating heat stress driven by rising temperatures being one of the most pressing challenges (Sari Kovats & Hajat, 2007). As urban areas grow, the heat island effect amplifies heat stress, reducing quality of life and increasing heat-related mortality, particularly among vulnerable groups like the elderly, children, and those with health conditions (Oleson et al., 2015; Argüeso et al., 2015). These factors make it necessary for cities to implement effective adaptation strategies to mitigate the health risks associated with extreme heat, including nature-based solutions by integrating green and blue infrastructure.

Nature-based solutions (NBS) and green-blue infrastructure (GBI) are key components of sustainable urban development and environmental policies. By integrating green spaces and water bodies into the urban landscape, GBI helps cities address today's challenges, providing practical solutions to mitigate the impact of climate change, biodiversity loss, and the rapid expansion of urban areas. Nature-based solutions and the responsible management of natural resources are acknowledged as fundamental elements of sustainable development (Martin et al., 2020).

Our studies have found that many documents and research investigations, including reports by the European Commission and studies by environmental organizations, feature nature-based solutions as a cross-cutting topic, proposing the use of natural processes to address urban challenges such as climate change, pollution reduction, or increasing the resilience of cities. European documents establish the general framework for integrating nature-based solutions and green-blue infrastructure into environmental, urban planning, and economic development policies (European Parliament, 1998; 2015; 2018). At the national level, Romania's legislation details how these

principles are implemented, with specific laws like Law no. 24/2007 for the regulation and administration of green spaces, Emergency Ordinance no. 114/2007 for flood risk management, and the National Strategy for Sustainable Development of Romania 2030 for urban regeneration (The Government of Romania, 2007). At the European level, the general direction regarding green and blue infrastructure focuses on integrating nature-based solutions into environmental, urban planning, and economic development policies. The European Union promotes a holistic approach that emphasises biodiversity protection through initiatives like the Natura 2000 network, climate change adaptation by implementing emissions reduction targets, and the creation of more resilient and sustainable cities through funding programs for green infrastructure projects. European programs and strategies like the European Green Deal and the 2030 Agenda for Sustainable Development highlight coordinated efforts to enhance quality of life, decrease pollution, and manage natural resources efficiently.

We have observed that NBS has different definitions that vary based on cultural and regional contexts, but the overall goal remains consistent: to harness the power of nature to address environmental challenges. Thus, our research uses the encompassing definition provided by the European Commission's Report on NBS as those actions that enhance existing natural processes and develop innovative approaches that leverage nature's ability to store carbon and regulate water, contributing to disaster risk reduction, well-being, and green growth. The European Commission recognises that the concept aligns with ecosystem-based approaches and emphasises sustainable alternatives inspired by ecological principles (European Commission, 2015).

Romanian legislation has adopted European principles regarding the protection of green spaces, flood risk management, and urban regeneration by adopting and transposing European Union directives and strategies into its national regulatory framework (Ungureanu et al., 2024). In the context of current global challenges such as climate change, biodiversity loss, and rapid urbanization, nature-based solutions and sustainable management of natural resources are recognized as an integral part of sustainable development at both the European and national levels.

MATERIALS AND METHODS

NBS and GBI have become integral to environmental policy and urban planning at the European and national levels. The world's climate change, biodiversity loss, and urbanization challenges have made it imperative for governments to prioritize nature-based solutions and green infrastructure in order to create more sustainable and resilient cities.

The documents selected for this study cover various regulations and strategies that support environmental protection, sustainable development, and urban regeneration. They underscore the critical importance of incorporating NBS and GBI into local and national policy frameworks.

Our analysis examined legislative and strategic documents, offering a comprehensive view of the regulations and policies related to green and blue infrastructure at the European and national levels. These documents cover a wide array of issues, from environmental protection and sustainable resource management to biodiversity conservation, water quality, natural disaster risk reduction, urban regeneration, and sustainable development.

Romania's national legislation outlines the implementation of these principles, focusing on the protection and management of green spaces, flood risk reduction, and urban regeneration efforts.

RESULTS AND DISCUSSIONS

A total of 18 legislative and strategic documents were carefully analysed in the reviewed studies. Among these, 13 were European Union (EU) documents, comprising strategies, directives, and conventions that outline the general framework for green and blue infrastructure and nature-based solutions. Five national documents from Romania were analysed, including laws, emergency ordinances, and national strategies that incorporate European principles into the Romanian framework. One national bill proposal has been examined (Draft Law, 2024).

European Legislation regarding NBS

The European Union places significant emphasis on integrating nature-based solutions into its environmental, urban planning, and economic development policies. This holistic approach aims at biodiversity protection, adaptation to climate change, and the creation of more resilient and sustainable cities. We have identified a series of documents and strategies that support and promote the use of nature-based solutions in the urban environment:

- ***The Green Infrastructure Strategy, 2013*** aims to promote investments in ecological solutions and avoid costly gray solutions. This encourages the use of green infrastructure to protect ecosystems and reduce costs through natural and sustainable solutions (European Commission, 2013). It offers recommendations for using nature-based solutions to replace or complement grey infrastructure, emphasizing that green infrastructure is a planned network of natural and semi-natural areas that contribute to increased resilience and significant savings.
- ***Strategic Research and Innovation Agenda Biodiversa*** supports research in biodiversity and natural solutions to address ecological, climate, and social crises, promoting innovation (Eggermont et al., 2021).
- ***The amendments adopted on October 5, 2023, regarding wastewater treatment*** propose measures to reduce emissions from wastewater treatment and encourage the use of nature-based solutions for water management (European Parliament and the Council, 2015).
- ***The review of progress regarding the implementation of the EU strategy for green infrastructure (2019)*** highlights that green infrastructure is an important tool for ensuring ecosystem services, reducing costs, and supporting biodiversity. It also provides guidance for integrating green infrastructure into spatial planning and sustainable development (European Commission, 2019).
- Major European strategies, such as the ***European Green Deal*** and ***The 2030 Agenda for Sustainable Development***, emphasize the need for concerted actions to improve quality of life, reduce pollution, and use natural resources efficiently (European Commission, 2020; UN, 2015).

Romanian Legislation regarding NBS

Romania has made progress in implementing European principles on green space protection, flood risk management and urban regeneration through the adoption of specific legislation and national strategies, although the implementation and mainstreaming of concepts such as green-blue infrastructure still requires coordinated efforts and a unified approach at local and national level.

Regarding the protection of green spaces, Romania has adopted a legal framework that reflects European concerns for biodiversity conservation and the improvement of quality of life in urban areas. Law no. 24/2007 regarding the regulation and administration of green spaces within urban areas establishes the legal framework for the protection and management of these spaces, including regulations for administration, protection, and penalties for deterioration (Parliament of Romania, 2007). This law was amended and supplemented by Emergency Ordinance no. 114/2007 and Law no. 47/2012, with the aim of the continuous protection of green spaces and the prohibition of changing the destination of green lands (The Government of Romania, 2007; Parliament of Romania, 2012). Moreover, the Technical Norms for the Development of the Local Register of Green Spaces provide guidelines for the inventory, management, and expansion of urban green spaces, establishing criteria for their monitoring (Ministry of Regional Development and Tourism, 2010). These initiatives are in line with European strategies that emphasize the role of expanding green and blue networks to support ecosystems and create connections between natural and urban areas.

In the field of flood risk management, Romania has implemented relevant European directives, such as the Water Framework Directive 2000/60/EC and the Floods Directive (2018/2019). These directives require member states to assess and manage flood risks, encouraging the implementation of ecosystem-based measures and green infrastructure. The Water Framework Directive regulates the protection of water resources, setting standards

for the quality and quantity of water for sustainable uses. The Directive on the assessment and management of flood risks improves cooperation between member states in the assessment and management of flood risks, with an emphasis on green infrastructure.

For urban regeneration, Romania has adopted legislative and strategic measures that align with European objectives for sustainable development and improving the quality of life in urban and rural communities. Emergency Ordinance no. 183/2022 regarding the establishment of measures for the financing of urban regeneration projects regulates the financing of these projects from non-reimbursable funds and establishes the eligibility criteria (The Government of Romania, 2022). This ordinance emphasizes the necessity of conserving and expanding green spaces within urban areas as an integral part of urban policies. The National Strategy for Sustainable Development of Romania 2030 represents the strategic framework for the implementation of the 2030 Agenda in Romania and highlights the need for a transition towards more responsible economic and social practices, aligned with global and European objectives (The Government of Romania, 2018). This includes objectives related to sustainable urban development and the integration of sustainability principles into public policies (Parliament of Romania, 2022).

Nature based solutions as tools for sustainable urban developments

By examining the key documents at both the European and Romanian levels, we have identified the legislative and strategic frameworks that guide the implementation of Nature-Based Solutions (NBS). These policies define the integration of green and blue infrastructure within urban regeneration initiatives, water management systems, and overarching sustainability strategies. The findings underscore the advancements achieved and the obstacles that persist in integrating NBS into policy frameworks, providing insights on how cities can more effectively utilise nature to tackle current urban and environmental issues (Bockarjova et al., 2017).

Green and blue spaces are vital in sustainable urban development, significantly affecting the environment, public health, and residents' quality of life. Integrating them into urban infrastructure offers numerous advantages: better biodiversity, reduced urban heat island effects, and improved stormwater management. Additionally, their contributions help conserve aquatic ecosystems, creating healthier, more enjoyable community environments. Green and blue infrastructure are crucial for building sustainable, climate-resilient cities. These spaces provide numerous environmental and social benefits, enhancing ecological balance and residents' well-being (Semeraro et al., 2021).

Bockarjova et al. (2017) developed a key tool for understanding and quantifying the financial and economic benefits of nature-based solutions in urban contexts. The tool relies on a transdisciplinary classification framework and data from previous research. Based on this research, we utilised and extended this classification, integrating the previously examined local documents, as shown in Table 1. This study presents a detailed classification of green and blue infrastructure and its contributions to better urban living.

Table 1. Nature based solutions as tools for sustainable urban developments throughout types of Green and Blue Urban Infrastructures

Nature based solutions as tools for sustainable urban developments	
Green Infrastructure	**Blue Infrastructure**
Urban park or forest • have many benefits for the city's quality of life: environmental benefits, economic benefits, social and psychological benefits, and planning and design (Sadeghian & Vardanyan, 2013).	**Lake/pond** • the shores can be developed into recreational spaces, becoming areas for relaxation, recreational activities, and ecological education platforms.
Pocket park • neighborhood green spaces, including pocket parks of less than 5000 m², contribute to the health and well-being of residents (Baur &Tynon, 2010; Peschardt et al., 2012; Kerishnan & Maruthaveeran, 2021).	**River/ Estuary** • flowing water bodies with freshwater aquatic communities (or, in the case of estuaries, both freshwater and saltwater).
Botanical garden • showcase plant species from different regions, providing a rich diversity of	**Sea coast** • area of contact between the sea and land, with diverse characteristics (e.g., sandy

Nature based solutions as tools for sustainable urban developments	
Green Infrastructure	**Blue Infrastructure**
flora (Primack & Miller-Rushing, 2009).	beaches, cliffs, dunes).
Green parking lots ● can be considered small heat islands and sources of pollutants from vehicles (Hahn & Pfeifer, 1994; Onishi et al., 2010). ● can lead to lower temperatures, improved water management, and better air quality.	**Delta** ● as a complex aquatic ecosystem, the delta is vital in conserving biodiversity and providing shelter for numerous plant and animal species (Bănăduc et al., 2016).
Community garden ● is established in urban, suburban, or rural areas and is close to schools, hospitals, or residential areas (American Community Gardening Association, 2014);	**Wetland** ● is essential for water purification and flow regulation, filtering pollutants, preventing floods by controlling water levels, and reducing soil erosion (Erwin, 2009).
Green corridor ● network that provides the community ecological, recreational, and cultural benefits (Ndubisi et al., 1995).	**Swale** ● is relatively inexpensive to construct and maintain (Dillaha et al., 1986, cited by Delgado et al., 1995). Their primary purpose is to reduce water pollution by capturing and filtering heavy metals and chemicals.
Green roof ● is classified into four categories: intensive, semi-intensive, single-layer extensive, and multi-layer extensive (Shafique et al., 2018).	**Rain garden** ● is recommended as an effective solution for managing stormwater runoff and enhancing biodiversity in urban environments (Ishimatsu et al., 2017).
Green wall and facade ● the „greening" of building facades represents one of the most effective solutions for energy savings in buildings and reducing the urban heat island effect (Perez et al., 2017).	**Permeable pavements** ● are ideal for a range of applications, including residential, commercial, and industrial settings (Scholz &Grabowiecki, 2007).
Institutional green space ● improve urban aesthetics by creating a pleasant contrast between vegetation and the architecture of the buildings.	**Rainwater harvesting** ● in urban areas, rainwater harvesting involves capturing, collecting, storing, and treating rainwater from rooftops, terraces, courtyards, and other impervious surfaces for on-site use (Campisano et al., 2017)
Riverbank green ● a river with a width of 35 m can lead to a temperature decrease of approximately 1–1.5°C, and this decrease can be more pronounced if	**Green roofs with water retention** ● help manage water flow to reduce flood risks and address drought conditions effectively (Graceson et al.,

Nature based solutions as tools for sustainable urban developments	
Green Infrastructure	**Blue Infrastructure**
there are green spaces on both banks of the river (Heggem et al., 2000).	2013).
Green balcony ● it refers to plants on balconies and terraces, primarily planted in pots.	**Daylighting streams** ● uncovering buried urban streams and restoring them to a natural state (e.g., Cheonggyecheon Stream in Seoul) (Hwang, 2004).
Street trees ● streets with tree alignments can be up to 10 degrees cooler in the summer, and a mature, healthy tree has a cooling effect equivalent to two air conditioning units running 20 hours a day (Voinescu, 2020).	**Riverbank stabilization with vegetation** ● using plants to prevent erosion instead of concrete embankments.
Green playground/ school ground ● the conversion of paved schoolyards by adding green spaces brings children closer to nature, stimulates daily physical activity, and supports social well-being (Raney et al., 2019).	**Canal** ● help manage water flow to reduce flood risks and address drought conditions effectively.
House garden ● include areas around private homes, mainly cultivated for ornamental purposes or non-commercial food production.	**Mangroves** ● protect coastlines from erosion and provide nursery habitats for marine species.
Vertical greeneries (walls, ceilings) ● plant selection must consider climate, building design, and context (Manso & Castro-Gomez, 2015).	**Eco-friendly seawall** ● are designed to minimize environmental impact and enhance habitat potential compared to traditional designs (Fish Habitat Network, 2019).

CONCLUSIONS

The analysis of the documents reveals the importance of nature-based solutions for the sustainable development of green and blue infrastructure in Romania. The analyzed legislative and strategic documents provide a comprehensive overview of the regulations and policies related to green and blue infrastructure, highlighting the importance of integrating it into local and national policies. This is recognised as a central element in environmental and urban planning policies at both the European and national levels in the context of global

challenges such as climate change and biodiversity loss.

The documents emphasise the role of green and blue infrastructure in protecting biodiversity, reducing natural risks, and improving quality of life. European strategies and national legislation promote the integration of these solutions into territorial planning and urban development. Even though not all local strategies explicitly mention the terms nature-based solutions, green infrastructure, or blue infrastructure, the concern for environmental issues and the sustainable use of natural resources is evident.

For a sustainable and resilient future in Romania, it is imperative to embrace and expand a variety of green and blue infrastructure types such as urban parks, wetlands, and green roofs. These solutions effectively manage water, enhance biodiversity, and contribute to sustainable urban development.

Therefore, it is necessary to emphasize the need for an integrated and multidimensional approach to urban development, which prioritises the protection of natural resources and the extensive implementation of nature-based solutions, thus coherently promoting green and blue infrastructure. The efficient integration of NBS in the urban environment brings significant ecological benefits, contributing to biodiversity conservation, sustainable water management, pollution reduction, and climate change mitigation. From an economic perspective, NBS and GBI can stimulate investments in ecological solutions, reduce costs through natural alternatives for grey infrastructure, and support the development of sustainable tourism. Last but not least, the social benefits should be considered in Romanian cities, including the improvement of quality of life through the creation of green spaces for recreation, the promotion of public health, and the increase of urban community resilience. Adopting a holistic perspective that combines environmental protection with economic and social considerations is fundamental to ensuring a sustainable and prosperous urban future in Romania.

ACKNOWLEDGEMENTS

This work was supported by the PN 23 35: "*Advanced research on the development of eco-innovative solutions, composite materials, technologies and services, in the concept of circular economy and quality of life enhancement, for a sustainable digital infrastructure in a built and urban environment resilient to climate change and disasters*" Acronym: ECODIGICONS, PN 23.35.06.01. project with the title "*Integrated IT-urban planning system for the evaluation of blue-green infrastructure at the level of municipalities and cities in Romania with a view to implementation in urban development plans. Case study: Râmnicu Vâlcea Municipality*", financed by the Ministry of Education and Research of Romania.

REFERENCES

American Community Gardening Association (2014). Community Garden Management Toolkit. https://www.communitygarden.org/resources/e32345c2-b0c2-4b86-89fc-489c629e630b

Argüeso, D., Evans, J. P., Pitman, A. J., & Di Luca, A. (2015). Effects of City Expansion on Heat Stress under Climate Change Conditions. *PLoS ONE, 10*(2), e0117066. https://doi.org/10.1371/journal.pone.0117066

Baur, J. W., & Tynon, J. F. (2010). Small-scale urban nature parks: Why should we care? *Leisure Sciences, 32*(2), 195-200.

Bănăduc, D., Rey, S., Trichkova, T., Lenhardt, M., & Curtean-Bănăduc, A. (2016). The Lower Danube River - Danube Delta – North-West Black Sea: A pivotal area of major interest for the past, present and future of its fish fauna - A short review. *Science of the Total Environment, 545*, 137-151.

Bockarjova, M., Botzen, W. W. J., & Koetse, M. (2017). Briefing Note Financial and Economic Values Database. https://naturvation.eu/sites/default/files/result/files/briefing_note_financial_and_economic_values_database.pdf#page=3.00

Campisano, A., Butler, D., Ward, S., Burns, M. J., Friedler, E., DeBusk, K., Fisher-Jeffes, L. N., Ghisi, E., Rahman, A., Furumai, H., & Han, M. (2017). Urban rainwater harvesting systems: Research, implementation and future perspectives. *Water research, 115*, 195-209.

Delgado, A. N., Periago, E. L., & Viqueira, F. D. F. (1995). Vegetated filter strips for wastewater purification: A review. *Bioresource Technology, 51*(1), 13-22. https://doi.org/10.1016/0960-8524(94)00113-f

Dillaha, T. A., Sherrard, J. H., Lee, D., Shanholtz, V. O., Mostaghimi, S., & Magette, W. L. (1986). Use of vegetative filter strips to minimize sediment and phosphorus losses from feedlots. Phase 1, *Experimental plot studies.*

Draft Law (2024). Law on the regime of urban protected natural areas and urban biodiversity conservation. https://www.cdep.ro/proiecte/2020/100/90/3/se295.pdf

Eggermont H., Le Roux, X., Tannerfeldt, M., Enfedaque, J., Zaunberger, K. & Biodiversa+ partners (2021). Strategic Research & Innovation Agenda. Biodiversa+, 108 pp.

Erwin, K. L. (2009). Wetlands and global climate change: the role of wetland restoration in a changing world. *Wetlands Ecology and management, 17*(1), 71-84.

European Commission (2020). The European Green Deal. Brussels: Commission European Commission.

European Commission (2019). Review of progress on implementation EU green infrastructure strategy. Brussels: European Commission.

European Commission (2015). Towards an EU Research and Innovation Policy Agenda for Nature- Based Solutions & Re-Naturing Cities - Final Report of the Horizon 2020 Expert Group on Nature Based Solutions and Re-Naturing Cities. Publications Oce.

European Commission (2013). Green Infrastructure (GI)-Enhancing Europe's Natural Capital. Brussels: European Commission.

European Parliament (2018). Directive on the assessment and management of flood risks. Brussels: European Parliament.

European Parliament (1998). Directive 98/83/EC on the quality of water intended for human consumption. Brussels: European Parliament.

European Parliament and the Council (2015). Water Framework Directive and Floods Directive: Actions for achieving good water status and reducing flood risks. Brussels: European Parliament.

Fish Habitat Network (2019). Environmentally friendly erosion protection: seawalls (Fish Friendly Marine Infrastructure). https://www.fishhabitatnetwork.com.au/environmentally-friendly-erosion-protection-seawalls-fish-friendly-marine-infrastructure

Gómez Martín, E., Girdano, R., Pagano, A., van der Keuer, P., & Costa, M. M. (2020). Using a system thinking approach to assess the contribution of nature based solutions to Sustainable Development Goals, *Science of The Total Environment, 738*, 139693. https://doi.org/10.1016/j.scitotenv.2020.139693.

Graceson, A., Hare, M., Monaghan, J., & Hall, N. (2013). The water retention capabilities of growing media for green roofs. *Ecological Engineering*, *61*, 328-334.

Hahn, H. H., & Pfeifer, R. (1994). The contribution of parked vehicle emissions to the pollution of urban run-off. *Science of the total environment, 146*, 525-533.

Heggem, D. T., Edmonds, C. M., Neale, A. C., Bice, L., & Jones, K. B. (2000). A landscape ecology assessment of the Tensas River Basin. In Monitoring Ecological Condition in the Western United States: Proceedings of the Fourth Symposium on the Environmental Monitoring and Assessment Program (EMAP), San Franciso, CA, April 6-8, 1999 (pp. 41-54). Springer Netherlands.

Hwang, K. Y. (2004). Restoring Cheonggyecheon stream in the downtown Seoul. Seoul: Seoul Development Institute, 3.

Ishimatsu, K., Ito, K., Mitani, Y., Tanaka, Y., Sugahara, T., & Naka, Y. (2017). Use of rain gardens for stormwater management in urban design and planning. *Landscape and Ecological Engineering*, *13*, 205-212.

Kerishnan, P. B., & Maruthaveeran, S. (2021). Factors contributing to the usage of pocket parks - A review of the evidence. *Urban Forestry & Urban Greening*, *58*, 126985.

Manso, M., & Castro-Gomes, J. (2015). Green wall systems: A review of their characteristics. *Renewable and Sustainable Energy Reviews, 41*, 863–871. https://doi.org/10.1016/j.rser.2014.07.203.

Martín, E. G., Costa, M. M., & Máñez, K. S. (2019). An operationalized classification of Nature Based Solutions for water-related hazards: From theory to practice. *Ecological Economics*, *167*, 106460. https://doi.org/10.1016/j.ecolecon.2019.106460.

Ministry of Regional Development and Tourism. (2010). Technical standards for the development of the Local Register of Green Spaces. The Official Monitor of Romania.

Ndubisi, F., DeMeo, T., & Ditto, N. D. (1995). Environmentally sensitive areas: a template for developing greenway corridors. *Landscape and Urban Planning, 33*(1-3), 159-177.

Oleson, K. W., Monaghan, A., Wilhelmi, O., Barlage, M., Brunsell, N., Feddema, J., Hu, L., & Steinhoff, D. F. (2015). Interactions between urbanization, heat stress, and climate change. *Climatic Change, 129*, 525–541. https://doi.org/10.1007/s10584-013-0936-8

Onishi, A., Cao, X., Ito, T., Shi, F., Imura, H. (2010). Evaluating the potential for urban heat - island mitigation by greening parking lots. *Urban forestry & Urban greening, 9*(4), 323-332.

Parliament of Romania (2022). Law no. 246/2022 regarding metropolitan areas and the amendment of certain normative acts. The Official Monitor of Romania

Parliament of Romania (2012). Law no. 47/2012 on the amendment and completion of Law no. 24/2007 on the regulation and administration of green spaces within the urban areas of localities. The Official Monitor of Romania.

Parliament of Romania (2007). Law no. 24/2007 on the regulation and administration of green spaces within the urban areas of localities. The Official Monitor of Romania.

Pérez, G., Coma, J., Sol, S., & Cabeza, L. F. (2017). Green facade for energy savings in buildings: The influence of leaf area index and facade orientation on the shadow effect. *Applied energy*, *187*, 424-437.

Peschardt, K. K., Schipperijn, J., & Stigsdotter, U. K. (2012). Use of Small Public Urban Green Spaces (SPUGS). *Urban Forestry & Urban Greening, 11*(3), 235–244. https://doi.org/10.1016/j.ufug.2012.04.002

Primack, R. B., & Miller-Rushing, A. J. (2009). The role of botanical gardens in climate change research. *New Phytologist, 182*(2), 303-313.

Raney, M. A., Hendry, C. F., & Yee, S. A. (2019). Physical activity and social behaviors of urban children in green playgrounds. *American journal of preventive medicine, 56*(4), 522-529.

Sadeghian, M. M., & Vardanyan, Z. (2013). The benefits of urban parks, a review of urban research. *Journal of Novel Applied Sciences*, *2*(8), 231-237.

Sari Kovats, R., & Hajat, S. (2007). Heat Stress and Public Health: A Critical Review, *Annual Review of Public Health, 29*, 41-55. https://doi.org/10.1146/annurev.publhealth.29.020907.090843

Semeraro, T., Scarano, A., Buccolieri, R., Santino, A., & Aarrevaara, E. (2021). Planning of Urban Green Spaces: An Ecological Perspective on Human Benefits. *Land, 10*(2), 105. https://doi.org/10.3390/land10020105

Scholz, M., & Grabowiecki, P. (2007). Review of permeable pavement systems. *Building and environment, 42*(11), 3830-3836.

Shafique, M., Kim, R., & Rafiq, M. (2018). Green roof benefits, opportunities and challenges – A review. *Renewable and Sustainable Energy Reviews, 90*, https://doi.org/10.1016/j.rser.2018.04.006.

The Government of Romania (2022). Emergency Ordinance no. 183 of December 28, 2022, regarding the establishment of measures for the financing of urban regeneration projects. The Official Monitor of Romania.

The Government of Romania (2018). The National Strategy for Sustainable Development of Romania 2030. Bucharest: Government of Romania.

The Government of Romania (2007). Emergency Ordinance no. 114 of October 17, 2007, for the amendment and completion of the Government Emergency Ordinance no. 195/2005 regarding environmental protection. The Official Monitor of Romania

Ungureanu, T., Popa, A.-C., Tache, A.-V., & Simion, A. (2024). Integration of nature and city: A strategic approach to green-blue infrastructure in Râmnicu Vâlcea. *Lucrările conferinţei de cercetare în construcţii, economia construcţiilor, urbanism şi amenajarea teritoriului, 26*, 57-62.

United Nations (2015). 2030 agenda for sustainable development. New York: Organization United Nations.

United Nations, Department of Economic and Social Affairs, Population Division (2019). World Urbanization Prospects: The 2018 Revision (ST/ESA/SER.A/420). New York: United Nations.

Voinescu, C. (2020). Alegerea arborilor pentru plantarea în spaţiul urban, https://www.brasovcity.ro/stiri-wp/wp-content/uploads/2021/05/Alegerea-arborilor-pentru-plantare-in-spatiul-urban.pdf.

Scientific Papers. Series E. Land Reclamation, Earth Observation & Surveying, Environmental Engineering. Vol. XIV, 2025
Print ISSN 2285-6064, CD-ROM ISSN 2285-6072, Online ISSN 2393-5138, ISSN-L 2285-6064

COMPATIBILITY BETWEEN NATURAL AGRO-INDUSTRIAL BY-PRODUCTS AND SYNTHETIC MATERIALS, A BASIC ELEMENT IN OBTAINING BIOCOMPOSITE MATERIALS WITH POTENTIAL FOR USE IN CONSTRUCTION

Irina POPA, Vasilica VASILE, Alexandrina MUREȘANU

National Institute for Research and Development in Construction, Urban Planning and Sustainable Spatial Development – URBAN-INCERC, 266 Pantelimon Road, 021652, District 2, Bucharest, Romania

Corresponding author email: irinapopa2006@yahoo.com

Abstract

Agriculture is one of the main sources generating significant quantities of natural agro-industrial by-products, such as stalks, fibrous residues, husks and cobs, etc. Based on the principles of the circular economy, such natural materials can have numerous possibilities for superior valorization, often as biocomposite materials, in various fields, not least in construction. Starting from the recognized potential for valorization of natural agro-industrial by-products in this sector, the paper presents aspects regarding the importance of compatibility and interaction between two natural materials, namely rice husks and industrial hemp fibers, and a synthetic resin as their binder. The implications of the compatibility and interactions between such types of materials and how this can influence the evolution over time of some characteristics of the biocomposite material expected to be used in the construction field as coatings are also presented.

Key words*: adhesion, coatings, hemp, pre-reaction time, rice husks.*

INTRODUCTION

It is currently known that organic raw materials can be used in a sustainable way, with increased efficiency and lower processing costs. The reducing waste, reusing and maximizing the value of resources can generate valuable products, promoting sustainable development and maximizing ecological and socio-economic benefits (Coelho Vianna et al., 2024).

The agricultural sector is one of the main sectors generating impressive amounts of waste (Ufitikirezi et al., 2024; Capanoglu et al., 2022; Pradhan et al., 2024), which has led to concern among public opinion and the scientific community.

Data published by the Food and Agriculture Organization (FAO) shows that agriculture produces over 140 billion tons of biomass each year, with over 2 tons per day in some rural areas (Ufitikirezi et al., 2024). It is also recognized that, by valorizing agricultural waste, farmers and agricultural industries can contribute through sustainable practices to resource efficiency and the development of the circular economy (Ufitikirezi et al., 2024).

Agricultural wastes, such as straw, stalks, fibrous residues, husks and cobs, constitute a significant part of the waste that can be recovered through various techniques, being able to be transformed into fuels and value-added materials (Ufitikirezi et al., 2024; Capanoglu et al., 2022; Wazed Ali et al., 2022). Through such an approach, the circular economy aims to minimize the quantities of waste generated, by optimizing their superior use, through viable processes, in order to increase their value and establish circular practices in the agri-food sector.

At the same time, it promotes the conservation and economic value of products, trying to extend the maximum lifespan of their components and obtain the highest possible added value (Coelho Vianna et al., 2024).

In the spirit of the principles of the circular economy, within the experimental research presented in this paper, the aim is to obtain innovative construction materials in the form of covering products. In order to achieve higher added value, will be integrated two natural local agro-industrial by-products, namely rice husks - plant material resulting from the food industry,

and industrial hemp - in the form of yarn, resulting from the use of seeds in the food sector, in the textile industry, etc.

Rice, one of the staple foods for almost half of the world's population, is cultivated on all continents, in over 100 countries (Pradhan et al., 2024), resulting in one of the abundant natural resources, namely rice husks.

However, this natural by-product is usually abandoned in a post-harvest area, resulting in an average of 2 million tons accumulated per year (Raki-in et al., 2021), a quantity that, if stored uncontrolled, seriously affects the environment (Raki-in et al., 2021; Milawarni et al., 2023; Pradhan et al., 2024).

The construction industry can promote sustainable development and minimize this type of natural agro-industrial by-product considered as waste, by incorporating rice husks into various construction products.

For example, embedded into bricks and blocks as a lightweight aggregate, rice husks lead to improved thermal properties and reduced overall weight (Selvaranjan et al., 2021).

Also, using this natural material as a filler or binder in the production of insulation materials, such as panels, boards or filler insulation, improves the thermal and acoustic insulation properties of the resulting products (Muthuraj et al., 2019; Sembiring et al., 2016; Aravind et al., 2020).

In other cases, combining rice husks with other lignocellulosic materials and binders has resulted in particleboards and fiberboards, which can be used in various construction applications, such as flooring, wall panels and furniture components (Manatura et al., 2023). Moreover, the integrating of these husks into a matrix of natural or synthetic polymers, as a reinforcing material, results in biocomposites that can be used in a number of other construction applications, such as decking, cladding and interior finishes (Faruk et al., 2012; Wang et al., 2020).

As for hemp, especially in the form of hemp pulp, it is currently being exploited through integration into numerous types of building materials, with the recognized role of improving both the thermal insulation properties and acoustic performance of the resulting building product, as well as the humidity and durability of the environment with which it comes into contact.

Among the numerous hemp-containing materials, for example, a few products recognized as being used/usable in construction are mentioned, namely: Hempcrete, a lightweight material obtained by mixing hemp powder with a thermally insulating lime-based binder, the resulting mixture being able to be used as a non-load-bearing filling material in walls, floors and roofs, with very good thermal and acoustic insulation and the ability to regulate humidity levels (Arrigoni et al., 2017; Demir et al., 2020; Piot et al., 2017; Yadav et. al, 2022); insulation materials in the form of panels, sticks or filling insulation (Abdellatef et al., 2020), with good thermal and acoustic insulation properties; boards usable as floors, wall panels and even furniture components, made by mixing hemp pulp with other lignocellulosic materials and binders; floors, cladding elements and interior finishes, practically biocomposite materials resulting from combining hemp pulp with a matrix of synthetic or natural polymers (Cigasova et al., 2015; Dhakal et al., 2015; Requile et al., 2019); hemp concrete which, although it does not have high strength or portability characteristics, has low thermal conductivity, high water vapor permeability, fire resistance, biodegradation, good acoustic properties and therefore can be used for walls, roofs and floors, for insulating walls on their outer side (Gołębiewski, 2017).

All these examples regarding the creation of biocomposite products usable/used in the construction field and the study of their characteristics clearly demonstrate, at an international level, the interest of researchers in obtaining, studying and promoting for use new construction materials that contain natural agro-industrial by-products, with properties comparable to those of traditional materials, made on a synthetic basis.

MATERIALS AND METHODS

In this work, rice husks (Figure 1) and hemp threads (Figure 2) were used, natural agro-industrial by-products provided by local producers.



Figure 1. Rice husks



Figure 2. Hemp fiber

The experimental research aimed at the superior valorization of these natural materials by obtaining innovative materials with ecological characteristics/coating products, with potential for use in the construction field.

Two series of innovative products were obtained and studied, namely: Series 1 - products with added rice husk content and Series 2 - products with mixed content of rice husk and hemp fibers.

In Series 1, two innovative basic products were first obtained, by embedding rice husks in an acrylic binder.

From a compositional point of view, these biocomposite materials were designed in such a way as to mainly study the influence of the constituent elements - the synthetic binder and the vegetable component. Two variants of acrylic resins were used as binder, denoted by R1 - acrylic base for interior/exterior coatings, respectively R2 - silicone acrylic base for interior/exterior coatings, the mass ratio of mixing rice husks: binder being 1:10, resulting in the first stage the products SP1RI, SP1R2.

In addition to the influence that compositional factors have on the main characteristics of the products, it was also aimed to study the influence that the method of preparing the plant material before application would have in this regard. For this purpose, a pre-reaction time was introduced, during which the binder and natural components were maintained in contact, before the application of the biocomposite.

The notion of pre-reaction time, specific to two-component anti-corrosion epoxy protections, is the time in which, before being put into operation, the two components are mixed, homogenized and left to interact, the lack or non-compliance with this time affecting the characteristics and performance of the anti-corrosion protection. Starting from this principle, in the case of coatings made from innovative products that integrated the rice husk, a pre-reaction time of 30 minutes was established for the rice husk-binder mixture. Thus, starting from the initial products, SP1R1 and SP1R2, without pre-reaction time, the corresponding products, SP1R1/30, SP1R2/30, were made, for which the pre-reaction time of 30 minutes was considered.

In order to determine the influence that the nature of the embedded agro-industrial by-products has on the characteristics of the resulting bilayer coatings, additional biocomposites with mixed plant content were made and tested.

Series 2 of innovative materials was made respecting, in principle, the same approach as in the case of the products in the Series 1.

This time, four basic innovative products with mixed plant content were initially obtained from rice husks and hemp threads of an average length of approx. 1 cm, embedded in the same types of binders, namely resin R1 and R2, respectively. The length at which the hemp threads were cut, and the content of this natural component were conditioned by obtaining a homogeneous biocomposite material, with good workability when applied to a concrete substrate. The mixing ratios of the hemp:rice husks:binder components were 1:2.5:40, resulting in the products marked SP1R1T and SP1R2T, and 1:3:40, respectively, for the products marked SP2R1T and SP2R2T.

As in the case of the innovative products in Series 1, for the products in Series 2, the influence of the 30-minute pre-reaction time between the synthetic binder and the mixture of

the two natural agro-industrial by-products was studied. This resulted in four other new recipes of biocomposite materials, denoted as follows: SP1R1T/30, SP1R2T/30, SP2R1T/30 and SP2R2T/30.

It is worth emphasizing that, from the beginning, for each product obtained in the two series, there was compatibility between the synthetic and vegetable components, resulting in homogeneous materials with good workability. As a result, each of the twelve biocomposites was applied to concrete support surfaces, in two layers, with an interval of 24 hours between them, the coatings being applied and subsequently maintained under standard laboratory atmospheric conditions, namely at a temperature of 23 ± 2°C and a relative air humidity of 50 ± 5%.

At this stage of the experimental research, the innovative products obtained were characterized by determining the average total thickness, and adhesion to concrete, a first evaluation of the resulting coatings, from the point of view of the potential for use in construction. Considering the organic, acrylic nature of the R1 and R2 binders used, as well as the average values of the thicknesses of the resulting bilayer coatings, ranging between 3.26 and 6.43 mm, without taking into account at this stage the influence of the pre-reaction time on the total thickness of the coating, the determinations were carried out referring to the condition specified in the technical specification SR EN 15824 - "Specifications for external renders and internal plasters based on organic binders", and the test conditions were those provided for in SR EN 1542 - "Products and systems for the protection and repair of concrete structures. Test methods. Measurement of bond strength by pull-off".

Referring to these documentations, the resulting coatings being atypical in terms of component materials, it was considered appropriate to monitor the evolution of the adhesion values to concrete for 56 days, establishing the measurements to be carried out at 7, 28 and 56 days after application. Since for each series of products obtained, the appearance of the bilayer coatings is very similar, regardless of the resin used, the absence or presence of pre-reaction time, in the following, exemplary images of the samples made will be presented.

Thus, for the products in the Series 1, the appearance of the SP1R2/30 coating is presented as an example, with the addition of rice husks and pre-reaction time, as well as the way the coating breaks when performing adhesion by pulling, after 7 days from the application (Figure 3), respectively after 28 days from the application (Figure 4).

For the coatings in Series 1, without analyzing for the moment the influence of the pre-reaction time, the average thickness values varied between 3.26 mm and 6.43 mm, and the average adhesion values to the concrete substrate, over the 56 days, between 0.22 MPa and 0.36 MPa (Figure 5).



Figure 3. Appearance of the SP1R2/30 coating containing rice husks and the way it breaks when pulled off, for determining adhesion at 7 days



Figure 4. Appearance of the SP1R2/30 coating containing rice husks and the way it breaks when pulled off, for determining adhesion at 28 days

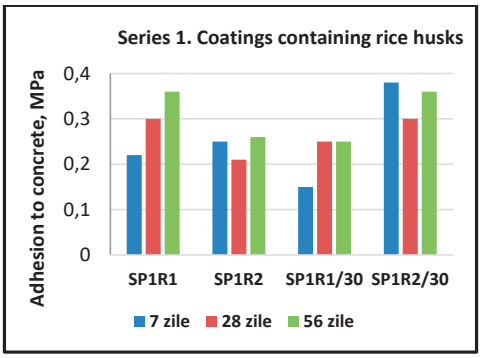


Figure 5. Variation of the adhesion to concrete for the two-layer coatings of Series 1

Given the diversity of materials used to obtain products from the Series 2 and, as a result, the possibility of particular manifestations of these coatings over time, adhesion to the substrate was monitored at shorter time intervals compared to previous cases, namely at 7, 28, 42 and 56 days after the application of the two-layer coatings on concrete substrate surfaces. Also in Series 2, regardless of the resin used, the absence or presence of pre-reaction time, the coatings obtained had a very similar external appearance. As a result, the appearance of the SP1R1T coating, having the hemp: rice husks: binder ratio of 1: 2.5: 40 (Figure 6), respectively of the SP2R1T/30 coating, characterized by the hemp: rice husks: binder ratio of 1:2.5:40 (Figure 7), are presented below as examples, as well as the way the coatings break when performing adhesion by pulling, 28 days after application.



Figure 6. Appearance of the SP1R1T coating, containing rice husks and hemp fibers, and the way it breaks when pulled off, for determining adhesion at 28 days



Figure 7. Appearance of the SP2R1T/30 coating, containing rice husks and hemp fibers, and the way it breaks when pulled off, for determining adhesion at 28 days

For the coatings in Series 2, without analyzing at this time the influence of the pre-reaction time, the average values of the thickness of the bilayer coatings containing rice husks and hemp fibers varied between 3.81 mm and 5.09 mm, and the average values of the adhesions to the concrete support, during the 56 days, between 0.35 MPa and 0.39 MPa (Figure 8).

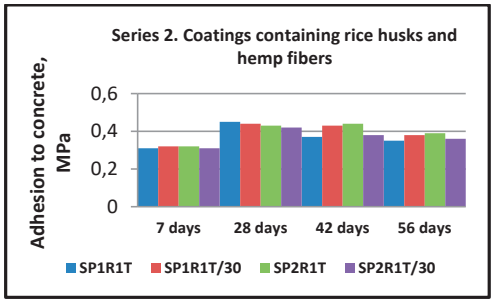


Figure 8. Variation of the adhesion to concrete for the two-layer coatings of Series 2

RESULTS AND DISCUSSIONS

In the experimental research presented in this paper, was mainly studied the possibility of obtaining biocomposite materials, by integrating, in acrylic binders, rice husks or/and mixtures in variable proportions of rice husks and hemp fibers, from the perspective of material compatibility.

At the same time, the evaluation of the potential for use in construction of the obtained materials, in the form of plaster-type coatings, was pursued. The extent to which the adhesion of the resulting coatings to concrete was influenced by

the type and content of the two natural materials, by their application conditions, meaning by the pre-reaction time between the main components, was also studied.

A first response considered favorable under the mentioned aspects was the existence of compatibility between the specified natural and synthetic materials, resulting in biocomposites containing rice husks (SP1R1, SP1R2, SP1R1/30 and SP1R2/30), respectively in those with mixed rice husks and hemp threads (SP1R1T, SP2R1T, SP1R1T/30 and SP2R1T/30). The establishment of the usability of the eight innovative product variants was achieved by analyzing and correlating the experimental results obtained after determining the average total thickness and the adhesion to concrete of each bilayer coating.

Thus, a further positive outcome was the formation of two-layer, rustic-style plaster coatings after applying both categories of biocomposites onto concrete surfaces. The coatings containing rice husks achieved average total thicknesses ranging from 3.26 mm to 6.43 mm, while those with mixed plant content exhibited thicknesses between 3.81 mm and 5.09 mm.

The third favorable aspect was that regarding the potential for use in construction of this category of innovative plaster-type coatings, given the good adhesion to the concrete support surface. This statement is supported by the fact that, at the end of the monitoring period of the coatings, after 56 days from application, the condition specified in the technical specification SR EN 15824 was met, according to which the adhesion of a plaster with an organic binder must be greater than or at least equal to 0.3 MPa.

In this context, from the point of view of adhesion to the support, we consider that six of the eight variants of the innovative coatings obtained have a potential for use in construction, however, additional research is necessary to achieve an experimentally substantiated, detailed and multidisciplinary characterization of the respective coatings. This potential for use as a multidisciplinary coating is suggested by the specific characteristics that each of the two integrated natural agro-industrial by-products has, implicitly by the properties that they are likely to confer on the products, respectively the plasters in which they are included.

All these favorable and encouraging aspects being specified, it is interesting and useful to highlight a series of specific aspects observed regarding the effects of integrating hemp fibers into the composition of such innovative materials.

Reference is made to a series of findings, resulting from the comparison of biocomposites/coatings containing only rice husks vs. those with mixed content, of rice husks and hemp threads.

The first finding is the existence of a good interaction between plant materials and the synthetic binder, with the obtaining of biocomposites with good workability. This allowed their application in two layers on concrete support surfaces. The resulting average adhesion values, at 28 days after application, generally had an upward trend in all eight coatings, those with mixed plant content having higher adhesion than those of coatings containing only rice husks. All the favorable aspects were highlighted during the determination of the adhesion by pulling, in most cases, through an adhesive rupture mode, between the coating and the concrete, which indicated a cohesive character of the coating, with a potential for continued increase in adhesion to the substrate over time.

However, by the end of the monitoring of the adhesion to the substrate for the two series of coatings, 56 days after their application, a slow but clearly different evolution of this characteristic was observed. Namely, if in the case of the coatings in Series 1, containing exclusively rice husks, the adhesions had an upward trend until the end of the analyzed period, in the case of the coatings in Series 2, in which hemp threads were also introduced, the trend was slightly downward, for all four coatings.

Even in this context, the final values of the average adhesions to concrete were higher for coatings with mixed vegetal content, values that even though in a decreasing trend, were above the limit value of 0.3 MPa.

We consider that such an evolution of the adhesion values was generated by the synergistic effect of two aspects: firstly, by the compositional difference, by the addition of hemp threads, and secondly, by the introduction of the pre-reaction time. Comparing the

experimental results obtained on the coatings from the two series, it is found that the effects of the second factor were highlighted both by the increase in the average thickness values of the coatings, and by the average values of the adhesions to the support, during the 56 days. We consider it also useful to point out that the cumulative effect of the two mentioned factors was more pronounced in the case of coatings containing hemp, which underlines the importance of this type of agro-industrial by-product in ensuring compatibility and maintaining good interaction between the natural and synthetic components of this type of innovative coating.

CONCLUSIONS

The paper presents experimental research that had as its main purpose the study of the possibility of obtaining biocomposite materials, by integrating, in a synthetic binder, two local natural agro-industrial by-products, namely rice husks or/and hemp fibres, from the perspective of their compatibility and interaction, as well as the possibility of using the obtained materials in construction.

Eight innovative products were obtained and studied: four products with rice husk content, and four products with mixed content of rice husk and hemp fibers.

In addition to the influence that compositional factors have on the main characteristics of the coatings, it was also aimed to study the influence that the method of preparing the plant material before application would have in this regard. For this purpose, a pre-reaction time of 30 minutes was introduced, during which the binder and natural components were maintained in contact, before application of the resulting biocomposites.

From the point of view of adhesion to the concrete support, we consider that six of the eight variants of the innovative coatings obtained have a potential for use in construction. However, additional research is necessary to achieve an experimentally detailed and multidisciplinary characterization of the respective coatings. After applying each biocomposite–on concrete surfaces, two-layer plaster-type coatings with a rustic appearance were obtained.

At the end of monitoring the adhesion of the coatings to the concrete substrate, it was observed that in the case of those containing exclusively rice husks, the adhesions had an upward trend, and in the case of those in which hemp fibers were also introduced, the trend was slightly downward. Even so, the values fell within the adhesion limits provided by the specifications for classic organic plasters for concrete. Referring to the compatibility and interaction between the synthetic binder and the two natural materials, mainly the hemp fibers, that this research pointed out, we consider that additional research are necessary to establish the long-term evolution of these aspects.

ACKNOWLEDGEMENTS

The research paper was carried out within Project PN 23 35 02 01, financed by the Ministry of Education and Research.

REFERENCES

Abdellatef, Y., Khan, M. A., Khan, A., Alam, M. I., &Kavgic, M. (2020). Mechanical, thermal, and moisture buffering properties of novel insulating hemp-lime composite building materials. *Materials, 13*(21), 5000.

Aravind, N. R., Sathyan, D., & Mini, K. M. (2020). Rice husk incorporated foam concrete wall panels as a thermal insulating material in buildings. *Indoor and built environment, 29*(5), 721–729.

Arrigoni, A., Pelosato, R., Melià, P., Ruggieri, G., Sabbadini, S., &Dotelli, G. (2017), Life cycle assessment of natural building materials: the role of carbonation, mixture components and transport in the environmental impacts of hempcrete blocks. *Journal of Cleaner Production, 149*, 1051–1061.

Capanoglu, E., Nemli, E., Tomas-Barberan, F. (2022), Novel Approaches in the Valorization of Agricultural Wastes and Their Applications. *J. Agric. Food Chem., 70*, 6787–6804.

Cigasova, J., Stevulova, N., Schwarzova, I., Sicakova, A., Junak, J. (2015). Application of hemp hurds in the preparation of biocomposites. In *IOP Conference Series: Materials Science and Engineering, Vol. 96*, No. 1, p. 012023. IOP Publishing.

Coelho Vianna, L.M., de Oliveira, L., Mühl, D. D. (2024). Waste valorization in agribusiness value chains. *Waste Management Bulletin, 1*, 195–204.

Demir, İ., & Doğan, C. (2020). Physical and mechanical properties of hempcrete. *The Open Waste Management Journal, 13*(1).

Dhakal, H. N., & Zhang, Z. (2015). The use of hemp fibres as reinforcements in composites. *Biofiber Reinforcements in Composite Materials*, 86–103.

Faruk, O., Bledzki, A. K., Fink, H. P., & Sain, M. (2012). Biocomposites reinforced with natural fibers: 2000-2010. *Progress in polymer science, 37*(11), 1552–1596.

Gołębiewski, M. (2017). Hemp-Lime Composites in Architectural Design. *KNUV, 4*(54), 162–171.

Manatura, K., Chalermsinsuwan, B., Kaewtrakulchai, N., Chao, Y. C., & Li, Y. H. (2023). Co-torrefaction of rice straw and waste medium density fiberboard: A process optimization study using response surface methodology. *Results in Engineering*, 101139.

Milawarni, M., Sri Aprilia, Nasrullah Idris, Elfiana, E., Yassir, Y., Yasir Asnawi, Suryati, S., Novi Quintena R, Jenne Syarif, Nawawi Juhan (2023), Analysis of Physical and Mechanical Properties of Rice Husk-based Particle Board. *Journal of Advanced Research in Applied Sciences and Engineering Technology, 31*(3), 40–46.

Muthuraj, R., Lacoste, C., Lacroix, P., & Bergeret, A. (2019). Sustainable thermal insulation biocomposites from rice husk, wheat husk, wood fibers and textile waste fibers: Elaboration and performances evaluation. *Industrial Crops and Products, 135*, 238–245.

Piot, A., Béjat, T., Jay, A., Bessette, L., Wurtz, E., Barnes-Davin, L. (2017). Study of a hempcrete wall exposed to outdoor climate: Effects of the coating. *Construction and Building Materials, 139*, 540-550.

Pradhan, S., Entsminger, E., Mohammadabadi, M., Seale, D., Ragon, K. (2024). Evaluation of rice husk composite boards prepared using different adhesives and processing methods. *BioResources, 19*(1), 595–604.

Raki-in, J. M. et al. (2021), Fabrication of a Wall-Panel Board Using Rice Husk and Red Clay-Based Geopolymer, Mindanao. *Journal of Science and Technology, 19*(1), 250–268.

Requile, S., Le Duigou, A., Bourmaud, A., Baley, C. (2019). Hygroscopic and Mechanical Properties of Hemp Fibre Reinforced Biocomposites. Revue des Composites et des Matériaux. *Avancés-Journal of Composite and Advanced Materials, 29*(4), 253–260.

Revelo-Cuarán., E.A. Nieves-Pimiento., N. y Toledo-Bueno., C.A. (2022). Homogenization Analysis in Particle Boards with Rice Husk. *Reinforcement, Tecnura, 26*(71), 59–79.

Selvaranjan, K., Navaratnam, S., Gamage, J. C. P. H., Thamboo, J., Siddique, R., Zhang, J., & Zhang, G. (2021). Thermal and environmental impact analysis of rice husk ash-based mortar as insulating wall plaster. *Construction and Building Materials, 283*, 122744.

Sembiring, S., Simanjuntak, W., Situmeang, R., Riyanto, A., &Sebayang, K. (2016). Preparation of refractory cordierite using amorphous rice husk silica for thermal insulation purposes. *Ceramics International, 42*(7), 8431–8437.

SR EN 15824 - "Specifications for exterior and interior renders based on organic binders", and the test conditions were those provided for in SR EN 1542 - "Products and systems for the protection and repair of concrete structures. Test methods. Measurement of bond strength by pull-off".

Ufitikirezi, J.d.D.M.; Filip, M.; Ghorbani, M.; Zoubek, T.; Olšan, P.; Bumbálek, R.; Strob, M.; Bartoš, P.; Umurungi, S.N.; Murindangabo, Y.T.; et al. (2024), Agricultural Waste Valorization: Exploring Environmentally Friendly Approaches to Bioenergy Conversion. *Sustainability, 16*, 3617.

Wang, S., Li, H., Zou, S., & Zhang, G. (2020). Experimental research on a feasible rice husk/geopolymer foam building insulation material. *Energy and Buildings, 226*, 110358.

Wazed Ali, S, Bairagi, S., Bhattacharyya, D. (2022). Valorization of Agricultural Wastes: An Approach to Impart Environmental Friendliness, in: Shahid-ul-Islam, Aabid Hussain Shalla and Salman Ahmad Khan (eds.) Handbook of Biomass Valorization for Industrial Applications, pp. 369–394, Scrivener Publishing LLC.

Yadav, Madhura, and Ayushi Saini (2022). Opportunities & challenges of hempcrete as a building material for construction: An overview. *Materials Today: Proceedings, 65*, 2021–2028, https://doi.org/10.1016/j.matpr.2022.05.576.

Scientific Papers. Series E. Land Reclamation, Earth Observation & Surveying, Environmental Engineering. Vol. XIV, 2025
Print ISSN 2285-6064, CD-ROM ISSN 2285-6072, Online ISSN 2393-5138, ISSN-L 2285-6064

THE INTEGRATION OF CERAMIC WASTE AS A PARTIAL SUBSTITUTE OF NATURAL AGGREGATES IN EXPERIMENTAL CONCRETE RECIPES

Mircea SĂLCUDEAN[1], Maria POPA[2]

[1]Lucian Blaga University of Sibiu, Faculty of Engineering, Doctoral School,
10 Victoriei Blvd, 550024, Sibiu, Romania
[2]"1 Decembrie 1918" University of Alba Iulia, Faculty of Economic Sciences,
15-17 Unirii Street, 510009, Alba Iulia, Romania

Corresponding author email: salcudean.mircea@uab.ro

Abstract

The work aimed to show that it is feasible to integrate ceramic waste from the construction industry and demolitions into the content of concrete recipes, as a partial replacement for natural aggregates in standard concrete recipes. The integration of these wastes into the composition of concrete is of particular importance because, on the one hand, we reduce the amount of waste resulting from the construction industry, and on the other hand, we achieve savings of raw materials used in the manufacture of concrete, coming from exhaustible natural resources. Compared to the standard C16/20 concrete recipe used as the control sample in the experimental recipe, the natural aggregates of size 4-8 mm were partially replaced by 50% ceramic waste. Various physical-mechanical tests were performed, such as determining the density of fresh concrete, determining the compressive strength of concrete containing ceramic waste compared to a standard concrete recipe containing natural aggregate. Following tests on experimental recipes, very good results were obtained in determining the compressive strength, which were similar to the test results on standard concrete recipes.

Key words*: ceramic waste, natural aggregates, concrete.*

INTRODUCTION

Concrete, which due to its qualities, strength, durability, versatility and the fact that it can be cast into almost any shape and reproducing any surface texture, is the most used construction material in the world (Shelton et al., 1982). Concrete is a mixture of materials composed of 60-75% sand and gravel, 15-20% water and 10-15% binders, which is the basic ingredient that binds the composition. The Romans used a volcanic ash as a binder in the composition of concrete but currently, the binder used is called Portland cement (Gagg, 2014). Given that aggregates occupy from 60 to 75% of the volume of concrete, this influences its physical-mechanical properties. The strength of normal concrete is affected by the size of the aggregates, therefore optimal dosage is very important to obtain the best results (Albarwary et al., 2017). Very rapid urbanization, coupled with population growth, has led to an increasing consumption of building materials (Kamali et al., 2019). The increase in global consumption of construction materials has inevitably led to high pollutant emissions and an increasing generation of waste. The production of cement, steel and concrete has the heaviest environmental burden during their manufacture (Huang et al., 2020). The construction industry is the largest consumer of material resources (40-60% of the total raw material extractions), water, and energy (40% of energy consumption) (Spence & Mulligan, 1995). Intensive activities in the construction industry are considered to be the main responsible for the scarcity of natural resources (Ghisellini et al., 2018), including water, crushed aggregates , increased pollution and demands for materials (Eray et al., 2019).
Construction waste is primarily caused by demolition activities ,equivalent to 40% of total waste (de Castro & de Brito, 2013) almost half of the total waste generated worldwide (Nasir et al., 2017), causing both noise and pollution (Çimen, 2021). The construction industry is the main generator of waste, accounting for up to 40% of urban solid waste (Chen et al., 2019). Due to the high consumption of natural aggregates, the use of recycled aggregates from construction and demolition waste in concrete is becoming increasingly widespread these days, with concrete made with recycled aggregates

potentially becoming the most widely used material in the coming years (Chitra, 2018).

The use of construction and demolition waste in concrete manufacturing, especially as raw materials replacing natural aggregates, is one of the most efficient ways to utilize these wastes (M. Ramesh & Kumaravel, 2014). Ceramic aggregate is resistant to abrasion. Ceramic products also have high strength, wear resistance over time, etc (Ray et al., 2021). Therefore, the use of these industrial wastes in concrete as a replacement for aggregates can be an effective solution in the recycling process of waste from construction and demolition (Ay & Ünal, 2000).

Aggregates from ceramic waste have similar properties to those from natural rocks (Halicka et al., 2013).

Unlike glass and rubber waste, ceramic waste has a porous structure that allows binder penetration, improving compressive strength in concrete (Sabbrojjaman et al., 2024).

Few studies have explored using ceramic waste as an aggregate substitute in concrete. Given that ceramic waste accounts for about 30% of daily tile production, or roughly 22 billion tons annually worldwide (Ahmad et al., 2023; Alyousef et al., 2021), its incorporation into concrete could help conserve natural resources and benefit the environment (Meena et al., 2022).

The rising cement production over the years, as shown in Figure 1, and the corresponding increase in concrete production, underscore the need to incorporate greater amounts of recycled aggregates in concrete (Production Volume of Cement Worldwide from 1995 to 2023, n.d.).

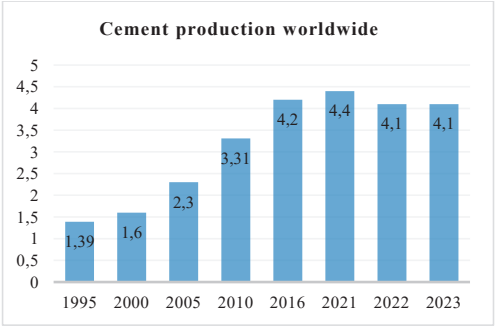


Figure 1.Cement production worldwide from 1995 to 2023 (Billion metric tons)

MATERIALS AND METHODS

According to a study published by Eurostat in 2018, an estimated amount of construction and demolition waste is generated in the European Union at over 850 million tons (Chapter 36:Production and Management - The Problem, n.d.) .This figure represents approximately 25-30% of all waste generated in the EU in 2020, reaching approximately 37.5% of total waste (Villoria Sáez & Osmani, 2019). Waste management is essential because the construction industry generates huge amounts of waste (Can & Taş, 2022). As the construction industry has a major influence on other industries, waste reuse can make a significant contribution to the circular economy (Aboginije et al., 2021). A medium and long-term estimate shows that almost 80% of the construction and demolition waste generated is recyclable and usable (Begum et al., 2010; Huang et al., 2020).

To practically demonstrate the usefulness of various wastes from the construction industry and from demolitions, it is necessary to manufacture some experimental recipes containing waste and then to compare various parameters of these recipes with the parameters of standard concrete recipes.

To do this, scraps of ceramic products (plates and tiles) from construction and demolition waste, 4-8 mm in size, shown in Figure 2, were used.

The samples will be tested for compression resistance and their density will be calculated.

The device for testing compressive strength is the Matest C058-05N automatic concrete press with a maximum capacity of 2000KN, which is shown in Figure 3.



Figure 2. Aggregates from ceramic waste size 4-8 mm



Figure 3. Matest 2000KN concrete press

RESULTS AND DISCUSSIONS

To verify and test the experimental recipes with ceramic waste content from construction and demolition, as a control, a sample prepared according to the standard recipe of concrete C16/20 is used.

C16/20 concrete, also called B250 in the past, is the most popular class of concrete used in constructions in Romania. Mainly used in the structures of houses and in the foundations of low-rise buildings, concrete class C16/20 (B250), is a common concrete preferred in general for civil constructions and various related construction elements.

C16/20 (B250) concrete is used for the construction of foundations, beams, columns, belts, sidewalks and other elements (C16/20(B250) concrete n.d.). The components of the standard recipe for concrete C16/20 in Table 1 are according to the recipe from the concrete station belonging to S.C. ELIS PAVAJE S.A Petrești, the quantities being presented in cubic meters (m^3) but also in percentage of 0.5% of this quantity, being used in the preparation of experimental recipes.

Table 1. Concrete recipe C16/20

Component	kg/m^3	0.5% (kg)
Cement 42.5 R	295	1.475
Aggregate 0-4 mm 43%	789	3.945
Aggregate 4-8 mm 20%	367	1.835
Aggregate 8-16 mm 37%	679	3.395
Water	170	0.85

Figure 4 shows photos of the grades and the cement used in the preparation of the standard C16/20 concrete recipe as well as in the composition of the experimental recipes with the addition of ceramic waste and polystyrene.

Aggregates in concrete recipes can be:

- Natural aggregates from ballast pits - material excavated from pits or riverbeds consists of a mixture of sand and gravel;
- Natural aggregates from quarries - the rock (raw material) is crushed with a crusher and sorted by size using a sorting station.

The aggregates used in these recipes are ballast aggregates.



Figure 4. Components of concrete recipes

In order to prepare these experimental recipes, waste ceramic products from construction and demolition were used (sandstones and earthenware), as a partial substitute for some aggregates. Figure 5 shows the process of crushing ceramic waste manually using a Hammer.



Figure 5. The grinding process of ceramic waste

To sort the crushed ceramic remains, an electric sieving device was used to determine the granularity, as shown in Figure 6. Following this size separation process, the required quantity was obtained to replace the standard 4-8 mm aggregate fraction in the experimental recipe.



Figure 6. Size sorting of shredded ceramic waste

The Figure 7 shows how to prepare the experimental recipes manually by incorporating the waste prepared in the previous stage. These wastes used replaced the 4-8 mm grade with 50% ceramic waste in the experimental recipe.



Figure 7. Preparation of experimental recipes

Figure 8 shows the manual homogenization of the experimental recipe components with the help of a trowel and Table 2 presents the experimental recipe components.

Table 2. Experimental concrete recipe

Component	Quantity (kg)
Cement	1.475
0-4 mm river aggregate	3.945
4-8 mm river aggregate	0.9175
4-8 mm ceramic aggregate	0.9175
8-16 mm river aggregate	3.395
Water	0.85



Figure 8. Homogenization of experimental recipe components

Figure 9 shows the concrete samples resulting from the preparation of the experimental recipes, poured into standard models (3 samples to be tested at 7 days and 3 samples to be tested at 28 days), then it is kept for 24 hours in these patterns, after which it is removed and placed in the sample storage basin for 28 days at a constant temperature of 20 degrees Celsius, according to NE 012/2-2010.

Or performed compressive strength measurement tests 7 days and 28 days after their manufacture according to SR EN 12390-3:2002 Test on hardened concrete. Part 3: Compressive strength of specimens.

The tests were done for the standard recipe as well as for the experimental recipes. Our determinations of the fresh and hardened concrete densities of these samples were also made. Figure 10 shows the tests to determine the compressive strength carried out.



Figure 9. Concrete samples immersed in the storage basin

Following the tests performed regarding the compressive strength at 7 days and at 28 days, as well as the density, the results presented in Table 3 were obtained.

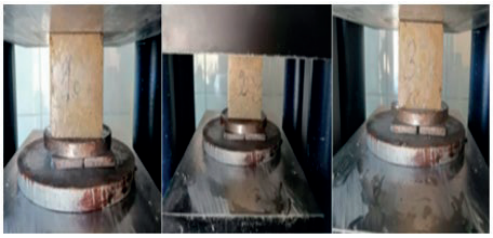


Figure 10. Performing compressive strength tests

Table 3. The results of the tests performed

Concrete type	Sample density (kg/m^3)	Compressive strength 7 days (MPA)	Compressive strength 28 days (MPa)
C16/20	2310	11.850	17.410
C16/20+ ceramic	2274	13.486	19.456

Compared to other research on the use of ceramic waste as a partial substitute for natural aggregates in concrete composition in terms of compressive strength, the basic trend is not significantly different from conventional concrete retention with natural aggregates.
Table 4 presents previous results of researchers who have addressed the topic of partial replacement of natural aggregates with ceramic waste, using different concrete recipes.

Table 4. Results of tests conducted by other researchers

Contains ceramic waste	Results	Authors
For 0% replacement	32.29 MPa	(Bommisetty et al., 2019)
For 25% replacement	33.48 MPa	(Bommisetty et al., 2019)
For 0% replacement	39 MPa	(Siddique et al., 2018)
For 40% replacement	45.16 MPa	(Siddique et al., 2018)
For 0% replacement	52.9 MPa	(Nepomuceno et al., 2018)
For 50% replacement	48.1 MPa	(Nepomuceno et al., 2018)
For 0% replacement	23 MPa	(Awoyera et al., 2018)
For 50% replacement	25 MPa	(Awoyera et al., 2018)
For 0% replacement	46.2 MPa	(Anderson et al., 2016)
For 50% replacement	45.2 MPa	(Anderson et al., 2016)

CONCLUSIONS

Preliminary tests using recipes incorporating construction industry waste were conducted, providing reference quantities for developing subsequent experimental formulations.
The use of construction and demolition of waste offers several benefits:

- Reduction of waste generated by industry;
- Conservation of non-renewable natural resources;
- Decreased demand for storage space.

Recommend and support the idea of using waste in the construction industry in the concrete manufacturing process and the search for the new experimental recipe with the highest possible content of waste.
The results of the tests performed on these experimental concrete recipes confirm that the partial replacement of waste with waste (the natural aggregates of size 4-8 mm were partially replaced by 50% with ceramic waste) is viable and can successfully replace these components in the composition of the concrete. In future experiments, it is intended to integrate as much waste from construction and demolition into the composition of concrete to use them and to get results as close to standard recipes.
The compressive strength of experimental concrete containing ceramic waste increased by up to 12% compared to standard concrete.
The results obtained show that research can be continued by progressively integrating increasing amounts of ceramic waste as a substitute for natural aggregates in the concrete structure. Once this research is continued and practically demonstrated, new paragraphs can be drawn up in construction standards so that ceramic waste can become a more common choice among recycled aggregates.
Future studies should evaluate the long-term behavior of ceramic waste concrete, including freeze-thaw resistance, shrinkage, water absorption, and sulfate attack resistance to ensure its practical application in various environmental conditions.

ACKNOWLEDGEMENTS

This research activity was carried out with the support of SC ELIS PAVAJE SRL, a company

whose object of activity is the manufacture of paving stones and various communication paths, which uses various waste from CDW in their manufacturing process, and which shows a great interest in using as much waste as possible in their products.

REFERENCES

Aboginije, A., Aigbavboa, C., & Thwala, W. (2021). A Holistic Assessment of Construction and Demolition Waste Management in the Nigerian Construction Projects. *Sustainability*, *13*(11), 6241. https://doi.org/10.3390/su13116241

Ahmad, J., Alattyih, W., Jebur, Y. M., Alqurashi, M., & Garcia-Troncoso, N. (2023). A review on ceramic waste-based concrete: A step toward sustainable concrete. *Reviews on advanced materials science*, *62*(1). https://doi.org/10.1515/rams-2023-0346

Albarwary, I. H. M., Aldoski, Z. N. S., & Askar, L. K. (2017). Effect of Aggregate Maximum Size upon Compressive Strength of Concrete. *The Journal of The University of Duhok*, *20*(1), 790–797. https://doi.org/10.26682/sjuod.2017.20.1.67

Alyousef, R., Ahmad, W., Ahmad, A., Aslam, F., Joyklad, P., & Alabduljabbar, H. (2021). Potential use of recycled plastic and rubber aggregate in cementitious materials for sustainable construction: A review. *Journal of Cleaner Production*, *329*, 129736. https://doi.org/10.1016/j.jclepro.2021.129736

Anderson, D. J., Smith, S. T., & Au, F. T. K. (2016). Mechanical properties of concrete utilising waste ceramic as coarse aggregate. *Construction and Building Materials*, *117*, 20–28. https://doi.org/10.1016/j.conbuildmat.2016.04.153

Awoyera, P. O., Ndambuki, J. M., Akinmusuru, J. O., & Omole, D. O. (2018). Characterization of ceramic waste aggregate concrete. *HBRC Journal*, *14*(3), 282–287. https://doi.org/10.1016/j.hbrcj.2016.11.003

Ay, N., & Ünal, M. (2000). The use of waste ceramic tile in cement production. *Cement and Concrete Research*, *30*(3), 497–499. https://doi.org/10.1016/S0008-8846(00)00202-7

Begum, R. A., Satari, S. K., & Pereira, J. J. (2010). Waste Generation and Recycling: Comparison of Conventional and Industrialized Building Systems. *American Journal of Environmental Sciences*, *6*(4), 383–388. https://doi.org/10.3844/ajessp.2010.383.388

Bommisetty, J., Keertan, T. S., Ravitheja, A., & Mahendra, K. (2019). Effect of waste ceramic tiles as a partial replacement of aggregates in concrete. *Materials Today: Proceedings*, *19*, 875–877. https://doi.org/10.1016/j.matpr.2019.08.230

Can, G., & Taş, E. F. (2022). Classification of Construction Waste. *In Proceedings of 6th International Project and Construction Management Conference*, 143–150.

Chapter 36:production and management - The problem. (n.d.). https://www.eea.europa.eu/publications/92-826-5409-5/page036new.html#:~:text=It is estimated that Europe,at around 3 per cent.

Chen, W., Jin, R., Xu, Y., Wanatowski, D., Li, B., Yan, L., Pan, Z., & Yang, Y. (2019). Adopting recycled aggregates as sustainable construction materials: A review of the scientific literature. *Construction and Building Materials, 2018,* 483-496, https://doi.org/10.1016/j.conbuildmat.2019.05.130

Chitra, K. R. (2018). Concrete Using Recycled Aggregates. *International Journal of Civil Engineering and Technology*, *8*(9), 413–419. http://www.iaeme.com/IJCIET/issues.asp?JType=IJCIET&VType=8&IType=9

Çimen, Ö. (2021). Construction and built environment in circular economy: A comprehensive literature review. *Journal of Cleaner Production*, *305*, 127180. https://doi.org/10.1016/j.jclepro.2021.127180

de Castro, S., & de Brito, J. (2013). Evaluation of the durability of concrete made with crushed glass aggregates. *Journal of Cleaner Production*, *41*, 7–14. https://doi.org/10.1016/j.jclepro.2012.09.021

Eray, E., Sanchez, B., & Haas, C. (2019). Usage of Interface Management System in Adaptive Reuse of Buildings. *Buildings*, *9*(5), 105. https://doi.org/10.3390/buildings9050105

Gagg, C. R. (2014). Cement and concrete as an engineering material: An historic appraisal and case study analysis. *Engineering Failure Analysis*, *40*, 114–140. https://doi.org/10.1016/j.engfailanal.2014.02.004

Ghisellini, P., Ripa, M., & Ulgiati, S. (2018). Exploring environmental and economic costs and benefits of a circular economy approach to the construction and demolition sector. A literature review. *Journal of Cleaner Production*, *178*, 618–643. https://doi.org/10.1016/j.jclepro.2017.11.207

Halicka, A., Ogrodnik, P., & Zegardlo, B. (2013). Using ceramic sanitary ware waste as concrete aggregate. *Construction and Building Materials*, *48*, 295–305. https://doi.org/10.1016/j.conbuildmat.2013.06.063

Huang, B., Gao, X., Xu, X., Song, J., Geng, Y., Sarkis, J., Fishman, T., Kua, H., & Nakatani, J. (2020). A Life Cycle Thinking Framework to Mitigate the Environmental Impact of Building Materials. *One Earth*, *3*(5), 564–573. https://doi.org/10.1016/j.oneear.2020.10.010

Kamali, M., Hewage, K., & Sadiq, R. (2019). Conventional versus modular construction methods: A comparative cradle-to-gate LCA for residential buildings. *Energy and Buildings*, *204*, 109479. https://doi.org/10.1016/j.enbuild.2019.109479

M. Ramesh, K. S. K., & Kumaravel, T. K. and A. (2014). Construction Materials From Industrial Wastes-A Review of Current Practices. *International Journal of Environmental Research and Development*, *4*(4), 317–324. https://d1wqtxts1xzle7.cloudfront.net/40835473/ijerdv4n4spl_08-libre.pdf?1450720294=&response-content-disposition=inline%3B+filename%3DIjerdv4n4spl_08.pdf&Expires=1739277693&Signature=euHL1jzyV

zPd~fVRm~Mn07LoscmDU0jNUavkenLkU1qcWi9m3H3m6oVGgfQvOWSIwho-RY5

Meena, R. V., Jain, J. K., Chouhan, H. S., & Beniwal, A. S. (2022). Use of waste ceramics to produce sustainable concrete: A review. *Cleaner Materials*, *4*, 100085. https://doi.org/10.1016/j.clema.2022.100085

Nasir, M. H. A., Genovese, A., Acquaye, A. A., Koh, S. C. L., & Yamoah, F. (2017). Comparing linear and circular supply chains: A case study from the construction industry. *International Journal of Production Economics*, *183*, 443–457. https://doi.org/10.1016/j.ijpe.2016.06.008

Nepomuceno, M. C. S., Isidoro, R. A. S., & Catarino, J. P. G. (2018). Mechanical performance evaluation of concrete made with recycled ceramic coarse aggregates from industrial brick waste. *Construction and Building Materials*, *165*, 284–294. https://doi.org/10.1016/j.conbuildmat.2018.01.052

Production volume of cement worldwide from 1995 to 2023. (n.d.). https://www.statista.com/statistics/1087115/global-cement-production-volume/

Ray, S., Haque, M., Sakib, M. N., Mita, A. F., Rahman, M. D. M., & Tanmoy, B. B. (2021). Use of ceramic wastes as aggregates in concrete production: A review. *Journal of Building Engineering*, *43*, 102567. https://doi.org/10.1016/j.jobe.2021.102567

Sabbrojjaman, M., Liu, Y., & Tafsirojjaman, T. (2024). A comparative review on the utilisation of recycled waste glass, ceramic and rubber as fine aggregate on high performance concrete: Mechanical and durability properties. *Developments in the Built Environment*, *17*, 100371. https://doi.org/10.1016/j.dibe.2024.100371

Shelton, David P. and Harper, J. M. (1982). G82-623 An Overview of Concrete as a Building Material. *Historical Materials □mUniversity of Nebraska-Lincoln Extension*, *603*. https://www.researchgate.net/publication/266468220_G82-623_An_Overview_of_Concrete_as_a_Building_Material

Siddique, S., Shrivastava, S., Chaudhary, S., & Gupta, T. (2018). Strength and impact resistance properties of concrete containing fine bone china ceramic aggregate. *Construction and Building Materials*, *169*, 289–298. https://doi.org/10.1016/j.conbuildmat.2018.02.21

Spence, R., & Mulligan, H. (1995). Sustainable development and the construction industry. *Habitat International*, *19*(3), 279–292. https://doi.org/10.1016/0197-3975(94)00071-9

Villoria Sáez, P., & Osmani, M. (2019). A diagnosis of construction and demolition waste generation and recovery practice in the European Union. *Journal of Cleaner Production*, *241*, 118400. https://doi.org/10.1016/j.jclepro.2019.118400

Scientific Papers. Series E. Land Reclamation, Earth Observation & Surveying, Environmental Engineering. Vol. XIV, 2025
Print ISSN 2285-6064, CD-ROM ISSN 2285-6072, Online ISSN 2393-5138, ISSN-L 2285-6064

IMPACT OF FLOOD DISCHARGE ON WATER QUALITY IN DANUBE RIVER BIFURCATIONS AND SELECTED LAKES (GORGOVA-UZLINA HYDROGRAPHIC UNIT)

Irina CATIANIS, Dumitru GROSU, Laura DUTU, Albert SCRIECIU, Andrei TOMA, Ana Bianca PAVEL, Ovidiu BORZAN, Gabriel IORDACHE

National Institute of Marine Geology and Geoecology - GeoEcoMar, Bucharest,
23-25 Dimitrie Onciul Street, 024053, District 2, Bucharest, Romania

Corresponding author email: irina.catianis@geoecomar.ro

Abstract

Significant progress in water conservation and environmental preservation has been made through efforts by worldwide authorities in ecological water management. However, unexpected water pollution events continue to threaten water quality and biodiversity. Monitoring pollution levels in surface waters is essential for supporting aquatic ecosystem services and sustainability. This study aimed to quantify heavy metal pollution in several sampling sites to assess water quality and its impact on biodiversity. Elements like As, Cd, Co, Cr, Cu, Fe, Mn, Ni, Pb, and Zn were analyzed using ICP-OES from samples collected during low-water (September 2024) and high-water (October 2024) conditions due to an upstream flood event. Results were compared to Romanian water quality standards. During low-water conditions, heavy metal concentrations were mostly below the limit for Quality Class I, except for Cd, which exceeded this limit. After the flood event, concentrations of most metals were within the Quality Class I limit. Still, Cd, Fe, and Pb showed varied results, with Ni levels ranging from very good to inferior water quality. Continuous monitoring is needed to prevent further degradation of delta ecosystems.

Key words*: concentration, flood event, heavy metal pollution, quality standard, surface water.*

INTRODUCTION

Fluvial-dominated delta ecosystems are vulnerable to the impacts of climate change induced by exogenous terrestrial pressures (droughts, river floods, intense storms, sediment starvation) and/or exogenous marine influences (erosion, sea-level rise, coastal flooding, saltwater intrusion) (Syvitski et al., 2009). Moreover, anthropogenic stressors represented by industrialization, urbanization, intensified agricultural practices and human intervention in catchment and delta plain land use contributed to significant environmental concerns, including water pollution (Nicholls et al., 2008). These ecosystems accumulate inorganic and organic compounds, heavy metals, nutrients, waste, plastic, pathogens, sediments, and other pollutants that heavily impact water quality (De Jonge, 2002). All these contaminants have harmful consequences on aquatic life, impeding vulnerable ecosystems and threatening biodiversity. Among chemical compounds, special attention must be paid to the toxic heavy metals from water and sediments, that can manifest bioaccumulation and biomagnification processing (Kumar et al., 2017) through the food web, compromising wildlife and ultimately affecting human health (Tovar-Sánchez et al., 2018). In addition to human-related activities, poor water quality may be endangered by flow rate fluctuations, precipitation, intense drought, weathering, soil erosion, etc. Thereby, successfully monitoring and assessing water quality and ecological status involves a multi-faceted approach that covers a wide range of physical and bio-geo-chemical variables and biotics of water in space and time (Chapman & Sullivan, 2022). In this context of concerns about the impacts of climate change on the fate of contaminants through unpredictable weather events, the subject of this scientific paper is included. The Danube River is the second-largest river basin in Europe, after the Volga River (Russia), emptying into the Danube Delta before reaching the Black Sea (Panin et al., 2016). The Danube River runs for a length of 2857 km, drains an area of roughly 801463 km^2, and traverses through or bordering ten European countries. Due to its pan-European character in

socio-economic and cultural aspects (Padło et al., 2021) had attracted administrative authorities and technical governmental departments from several involved countries, supporting and expressing sustain for the environmental policies related to good environmental quality of natural resources. On its lower course (on the Romanian territory), the Danube has three branches: Chilia, Sulina, and Sf. Gheorghe. Chilia, the northern branch, has a length of 104 km, transporting 60% of the river's water and silt. Sulina, the middle arm, with a length of 71 km and carrying 18% of the Danube's flow, is considered the only navigable arm of the Danube, where large ships can enter. The southern branch, namely, Sf. Gheorghe Arm has a length of 112 km carrying 22% of the Danube's alluvial input. In the last few years, acute hydrological events have become more prevalent in the Danube River Basin, due to precipitation in the watershed, and/or a prolonged dry season. For example, the lower course of the Danube River recorded both historical high-flows (*i.e.,* 1970, 1991, 1998, 2002, 2005, 2010, 2013, 2014, 2018, 2019, 2024) and low-flows (*i.e.,* 1921, 2003, 2007, 2010, 2011,2012, 2015, 2017, 2018, 2019, 2020, 2021, 2022, 2023, 2024) than the multi-year average. It is well known that the adaptive capacity and resilience of rivers are attributable to their dynamic characteristic and self-purification potential (Bennett & Rathbun, 1971). However, the acute effects of the Danube River flow fluctuations should not be overlooked, since they may have further ecological repercussions in the stable state of the Danube Delta shallow freshwater lakes assignable to extreme weather and climate events. Data on the flow of the Danube River in Romania are monitored by the National Authority for Romanian Waters and various meteorological and hydrological institutions. The river flow usually varies depending on the season and climatic conditions, and the values can be influenced by factors such as precipitation, snowmelt, the river regime in the upstream surrounding basins etc. The Danube Delta's surface area is roughly 4180 km^2, of which 3510 km^2 stands on Romanian territory. The delta evolved mainly from alternating layers of silt and sand, delivered by the Danube River over the past 10 to 12 thousand years, creating the complex network of channels, islands, and wetlands we see today. Its evolution is closely linked to river dynamics, sediment transport, and changes in sea levels (Gâștescu & Știucă, 2008). The delta is in a state of continuous change, shaped by both natural influences and human activity. It continues to grow and evolve as sediment accumulates, making it one of the most dynamic and recent landforms. The process of its formation is ongoing, with new islands and channels forming, while others may erode, resulting in a landscape that is both young and active. The present study aims to investigate seasonal changes in water quality and decipher the upstream flood event contribution of the lower Danube River to the spatial distribution of heavy metals in the water quality of several sampling sites investigated at the river bifurcations, including several Danube Delta lakes. Accordingly, the contents of ten (As, Cd, Co, Cr, Cu, Fe, Mn, Ni, Pb, and Zn) technophile elements (Ptitsyn, 2018) were analyzed. Consequently, systematic monitoring and assessment of the water quality's status is mandatory in deltaic aquatic environments of inestimable value from an ecological and unique biodiversity point of view.

MATERIALS AND METHODS

Study area

This investigation was performed at the Danube River bifurcations within its delta, specifically, at the *Ceatal Izmail* and the *Ceatal Sf. Gheorghe*, including several lakes attributed to the *Rusca-Gorgova-Uzlina* Hydrographic Unit, Danube Delta Romania. The selected sampling sites for this study illustrate a relevant example of the potential environmental impact of climate change (such as extreme weather events, including drought and flooding, wildfires, heavy rainfall, sea-level rise etc.). The Danube's bifurcations play an important role in the hydrological connectivity between the river's distributary branches and inter-distributary channels, streams, and lakes of the entire Danube Delta edifice. The *Rusca-Gorgova-Uzlina* Hydrographic Unit is situated in the western floodplain area, between the Sulina (north) and the Sf. Gheorghe (south) branches, and east of the Letea-Caraorman Spit (Panin et al., 2016) and is mainly characterized by a

relatively dynamic hydrographic network influenced by the two above-mentioned branches, including, the *Litcov Canal* and the *Perivolovca Stream*.

Field sampling and data analysis

Field measurements and sample collection, preservation, preparation, and storage before any laboratory analyses were accomplished at the R/V "Istros" owed by the National Institute for Research and Development of Marine Geology and Geoecology-GeoEcoMar, Romania. In this study, several spot water samples were considered in two distinct hydrological periods of the Danube River's flow: low-water level (September 2024) and high-water level (October 2024) (Figure 1). During the low-water period (September), the Danube River's flow was at its lowest level, while a maximum amplitude was reached at the peak high-water stage (October), after an upstream flood event.

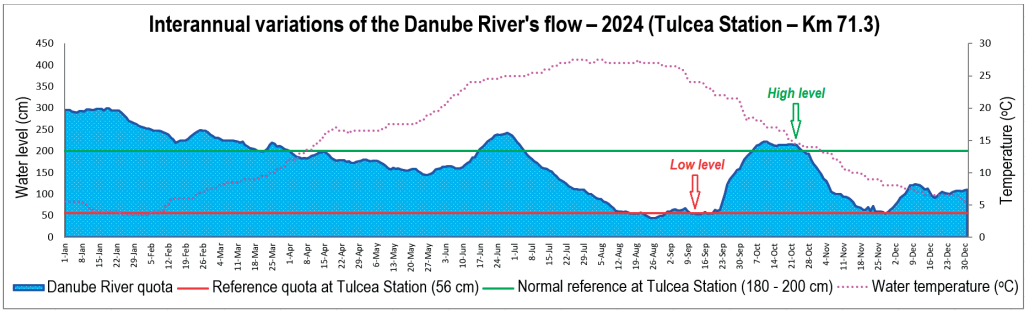


Figure. 1. Interannual variations of the Danube River's flow (Source Data: https://www.afdj.ro/ro/cotele-dunarii)

During the low-water period, the sampling sites were considered: *Ceatal Izmail, Ceatal Sf. Gheorghe*, including lakes such as *Uzlina, Isacova, Durnoliatca, Bleziuc-Pojarnia* and *Pojarnia* (Figure 2). Due to their proximity to the Sf. Gheorghe Branch alluvial input, these lakes are constantly filled, receiving appreciable amounts of water and silts. During the high-water period, the succeeding perimeters were investigated: *Ceatal Izmail*, *Ceatal Sf. Gheorghe*, *Cuzminţul Mare L., Rotund L., Rădăcinos L., Gorgova L., Gorgovăţ L., Potcoava de Sud L.*, *Litcov Canal* and *Old Danube River Meander* (Figure 2). The hydrological connection within these lakes varies mainly seasonally, alternating between relatively consistent connectivity with at least the *Old Danube River Meander via Litcov Canal*, and recurrent water deficiency (insufficient supply from rivers and streams), especially between lakes during the dry periods. The analysis to assess the environmental risk of heavy metals in freshwater deltaic environments was carried out using their spatial distribution, their content, and the possible origin of several investigated heavy metals. The sampling sites were chosen to determine the longitudinal distribution (along the upstream-downstream gradient of the Danube River bifurcations), including the horizontal distribution (along investigated lakes) of some specific heavy metals. For each site, 1-liter surface water samples for the chemical analyses were collected using sterile glass bottles at the sub-surface level (0-0.5 m) and close to the lake bottom. Nitric acid preservation of samples was performed in the field. Then, samples were filtered through a 0.45 µm membrane filter at the R/V "Istros" laboratory. After filtering, the bottle samples were plastic-bagged and iced quickly. Sample bottles were shipped to the analytical laboratory. Water samples were analyzed at a special and accredited (SR EN ISO/IEC 17025:2018) water testing laboratory ("The Pollution Control Department - Laboratory for water, soil, waste control"), from the National Research-Development Institute for Industrial Ecology - ECOIND, Bucharest, Romania. Ten selected heavy metals, namely As, Cd, Co, Cr, Cu, Fe, Mn, Ni, Pb, and Zn, commonly present in surface waters due to anthropogenic sources were determined by inductively coupled plasma atomic emission spectroscopy (ICP-EOS). The method for the

quantification of heavy metals levels in surface waters was performed according to the SR EN ISO 11885:2009 standard. Evaluation of the heavy metals content in the investigated water samples and their potential risk assessment was done in comparison with the Romanian water quality standards (Order 161/2006).

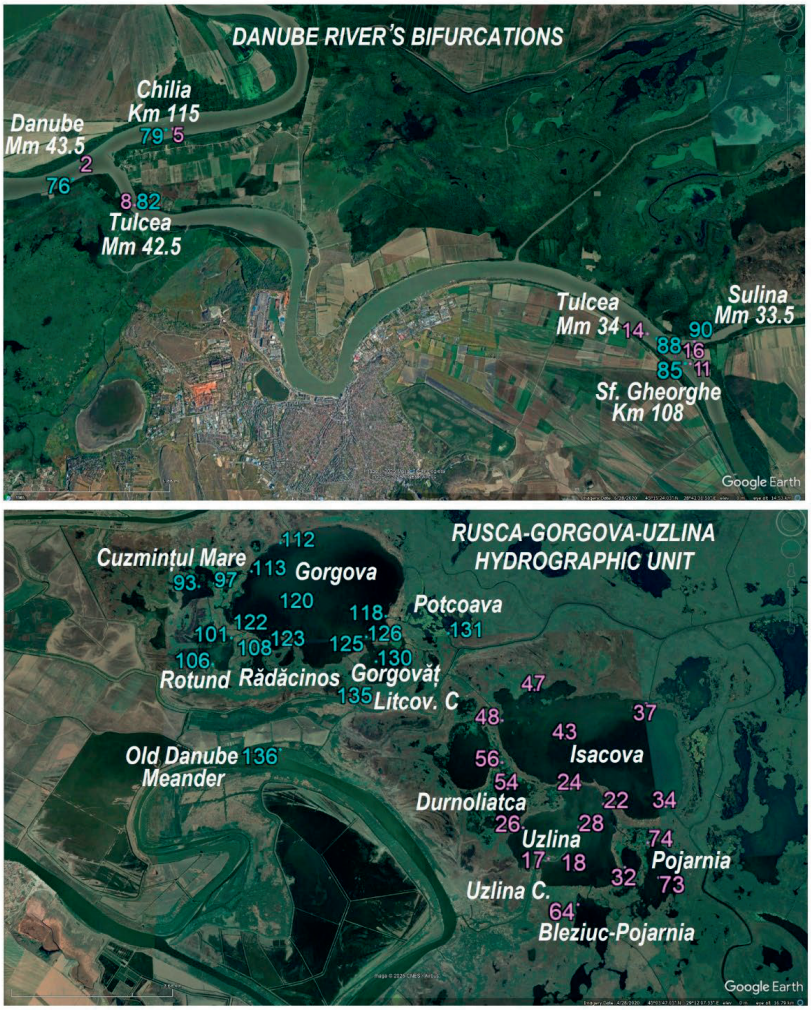


Figure 2. Location of the investigated perimeters. Pink dots mark the sampling sites during the low-water periods; Blue dots mark the sampling sites during the high-water periods (Base Map Source: https://www.google.com/maps/)

RESULTS AND DISCUSSIONS

Water quality and sustainable ecological ecosystems are fundamental to the proper functioning of the Danube River Delta region. The important benefits of healthy ecosystems contribute to maintaining good conditions for the wetlands and aquatic ecosystems of the Danube Delta which are of international ecological importance, being recognized worldwide as UNESCO World Heritage Sites, Biosphere Reserve, and Ramsar Site (Ramsar Convention, 1987). Correspondingly, water quality impairment may impact the ecosystem services provided by the Danube Delta (*i.e.,* unique and fascinating natural landscapes, habitats for flora and fauna species, reed resources, flood control, water supply,

agricultural uses, recreational activities, tourism, fishing activities, etc.) (Cazacu & Adamescu, 2017). The Danube Delta ecosystems are vulnerable to the water quality of the Danube River, which could be contaminated by numerous pollutants such as toxic heavy metals and organic contaminants from upstream and local sources. All these contaminants may often end up in the Danube River and subsequently, the coastal area of the Black Sea. Generally, the Danube River water quality status is mainly correlated to anthropogenic activities (industrial use, wastewater discharges, agricultural practices) (Chitescu et al., 2021), past hydro-technical projects on the river that restrict the flow of water and sediment discharge downstream (Panin & Jipa, 1998), and to some extent to climate change and hydroclimatic extremes (such as floods and rainstorms, droughts and heatwaves etc.) (Leščešen et al., 2024). Consequently, various natural and anthropogenic stressors could be responsible for water quality degradation, water biodiversity loss, and affected ecosystem services (Belacurencu, 2007). In this study, the contents of heavy metals *i.e.,* As, Cd, Co, Cr, Cu, Fe, Mn, Ni, Pb, and Zn, in water samples collected from several sampling locations of the Danube Delta area, were determined by Inductively Coupled Plasma-Optical Emission Spectrometry (ICP-EOS). The reference values were used to determine and evaluate the heavy metals' water quality status and spatial distribution in investigated freshwater samples. The Romanian current legislation imposed the reference values (Order 161/2006 - Normative regarding the classification of surface water quality to establish the ecological status of water bodies). The reference values represent the maximum permissible values of pollutant concentration corresponding to the five-surface water quality standard classes: Class I (Very Good), Class II (Good), Class III (Moderate), Class IV (Poor), and Class V (Bad).

Heavy metals' distribution during the low-water period investigation

During the low-water period (September 2024), at the *Ceatal Izmail* bifurcation area, the *Danube* carried a flow of approximately 2851 $m^3 \cdot s^{-1}$ at the entrance to the delta. This was unequally distributed between the *Tulcea* - 1701 $m^3 \cdot s^{-1}$ and *Chilia* - 1168 $m^3 \cdot s^{-1}$ branches, in favor of the *Tulcea* branch. The average velocities on the profiles were between 0.34 and 0.4 $m \cdot s^{-1}$. The riverbed was symmetrical in the *Ceatal Ismail* bifurcation area, with velocities homogeneously distributed on the cross sections. At the entrance to the second hydrographic node at the *Ceatal Sf. Gheorghe* bifurcation area, the flow of the *Tulcea* branch was at the time of measurements approximately 1572 $m^3 \cdot s^{-1}$. The flow was unequally distributed between the *Sulina* - 643 $m^3 \cdot s^{-1}$ and *Sf. Gheorghe* branches - 955 $m^3 \cdot s^{-1}$. The average velocities on the profiles were between the values of 0.39 and 0.5 $m \cdot s^{-1}$, with higher values on the *Sulina Canal*. The riverbed of the three branches was asymmetric in the bifurcation area at the *Ceatal Sf. Gheorghe*, with velocities homogeneously distributed on the cross sections. The chemical analyses were performed for 24 spot water samples collected from *Ceatal Izmail* (at the *Danube - Mm 43.5, Chilia Arm - Km 115, Tulcea Arm - Mm 43.5*), *Ceatal Sf.* Gheorghe (at the *Tulcea Arm - Mm 43, Sulina Arm - Mm 33.5, Sf. Gheorghe Arm - Km 108*), including lakes such as *Uzlina, Isacova, Durnoliatca, Bleziuc-Pojarnia* and *Pojarnia* (Figure 3). During the low-water period, the values of the investigated heavy metals pointed to an insignificant variability related to the heavy metals' distribution between the collection points, in both investigated Danube River bifurcations, as well as deltaic lakes. The results are illustrated in Table 1. Following the results obtained for samples taken under hydrodynamic conditions of low-water levels of the Danube, it can be observed that the investigated heavy metals such as: As, Co, Cr, Cu, Fe, Mn, Ni, Pb, and Zn recorded low concentrations, close to those corresponding to quality class I (very good condition), while, for the Cd element, the concentrations varied from one sampling station to another, incidentally exceeding the limit of class II (good condition). The dynamics of the investigated heavy metal concentrations during the low-water period will be presented further on.

Arsenic. The As concentration (µg/L) identified in the water samples presented a series of insignificant variations. Most of the obtained values were low, below the detection limit (< 2 µg/L), implicitly, below the limit corresponding to quality class I (10 µg/L).

Cadmium. The Cd concentration (µg/L) determined in the investigated water samples presented a series of interesting variations. Generally, most of the values were below the limit set for water quality Class I. However, values that slightly reached or exceeded the first two quality classes (Class I - 0.5 µg/L, Class II - 1 µg/L) were encountered in different samples taken from the investigated locations. For example, several sampling sites showed results that overpassed the limit set for water quality Class I (Figure 3): the *Sf. Gheorghe Arm - Km 108* (*DD24-11*), *Sulina Arm - Mm 33.5* (*DD24-16*), *Uzlina C.* (*DD24-17*), *Uzlina L.* (*DD24-26*) (situated close to the mouth of the connection canal with *Durnoliatca L.*), *Isacova L.* (*DD24-34*) (located in the south-eastern part of the lake, close to the mouth of the connection canal with *Perivolovca C.*), *Durnoliatca L.* (*DD24-49*) (located in the south-eastern part of the lake, close to the mouth of the connection canal with *Uzlina L.*) and *DD24-56* (situated in the northern part of the lake, close to the mouth of the connection canal with *Isăcel L.*). Alternatively, the concentration of Cd tested in water samples taken from *Tulcea Arm - Mm 42.5* (*DD24-08*) and *Uzlina L.* (*DD24-24*) (situated in the northern part of the lake, close to the mouth of a connection canal with *Isacova L.*) exceeded the limit set for water quality Class II.

Cobalt. The Co concentration (µg/L) tested in all collected water samples showed no significant variations. The majority of the results were below the limit set for water quality Class I (10 µg/L).

Chromium. The Cr concentration (µg/L) identified in the water samples collected during the low-water period showed no significant variations.

All the obtained values were low, below the limit set for water quality Class I (25 µg/L).

Table 1. Results of the heavy metal analysis in the investigated control sections (point samples) (Danube branches, canals, lakes, etc.) (low-water hydrodynamic conditions)

No. crt.	Location	Sample's indicative	As µg/L	Cd µg/L	Co µg/L	Cr_{tot} µg/L	Cu µg/L	Fe_{tot} mg/L	Mn mg/L	Ni µg/L	Pb µg/L	Zn µg/L
1	Danube Mm 43.5	DD24-02	<2.0	0.4	< 0.6	<2.0	2.7	0.024	0.002	<2.0	<2.0	5.8
2	Chilia Km 115	DD24-05	<2.0	<0.4	< 0.6	<2.0	<2.0	0.065	0.003	<2.0	<2.0	<5.0
3	Tulcea Mm 42.5	DD24-08	<2.0	1.1	< 0.6	<2.0	2.3	0.027	0.002	<2.0	<2.0	<5.0
4	Sf. Gheorghe km 108	DD24-11	<2.0	0.6	< 0.6	<2.0	6.2	0.025	0.005	<2.0	<2.0	<5.0
5	Tulcea Mm 34	DD24-14	<2.0	0.4	< 0.6	<2.0	2.5	0.028	0.003	<2.0	<2.0	10.8
6	Sulina Mm 33.5	DD24-16	<2.0	0.8	< 0.6	<2.0	<2.0	0.018	0.003	<2.0	<2.0	<0.5
7	Uzlina C.	DD24-17	<2.0	0.6	< 0.6	<2.0	2	0.056	0.009	<2.0	<2.0	<0.5
8	Uzlina L.	DD24-18	<2.0	<0.4	< 0.6	<2.0	2.3	0.039	0.005	<2.0	<2.0	6.8
9	Uzlina L.	DD24-22	<2.0	<0.4	< 0.6	<2.0	<2.0	0.028	0.004	<2.0	<2.0	<5.0
10	Uzlina L.	DD24-24	<2.0	1.6	< 0.6	<2.0	<2.0	0.018	0.008	<2.0	<2.0	<5.0
11	Uzlina L.	DD24-26	<2.0	0.6	< 0.6	<2.0	<2.0	0.021	0.003	<2.0	<2.0	<5.0
12	Uzlina L.	DD24-28	<2.0	<0.4	< 0.6	<2.0	<2.0	0.020	0.003	<2.0	<2.0	<5.0
13	Isacova L.	DD24-32	<2.0	<0.4	< 0.6	<2.0	<2.0	0.011	0.003	<2.0	2.3	<5.0
14	Isacova L.	DD24-34	<2.0	0.6	< 0.6	<2.0	2.1	0.012	0.005	2.1	<2.0	<5.0
15	Isacova L.	DD24-37	<2.0	0.5	< 0.6	<2.0	<2.0	0.026	0.012	2.2	2.9	<5.0
16	Isacova L.	DD24-43	<2.0	<0.4	< 0.6	<2.0	<2.0	0.026	0.022	2.9	<2.0	<5.0
17	Isacova L.	DD24-47	<2.0	0.4	< 0.6	<2.0	<2.0	0.022	0.010	2.6	<2.0	<5.0
18	Isacova L.	DD24-48	<2.0	<0.4	< 0.6	<2.0	<2.0	0.028	0.005	3.6	<2.0	<5.0
19	Durnoliatca L.	DD24-49	<2.0	0.7	< 0.6	<2.0	<2.0	0.025	0.006	2.8	<2.0	<5.0
20	Durnoliatca L.	DD24-54	<2.0	<0.4	< 0.6	<2.0	<2.0	0.007	0.021	2.6	<2.0	<5.0
21	Durnoliatca L.	DD24-56	<2.0	0.6	< 0.6	<2.0	<2.0	0.006	0.004	3.2	<2.0	<5.0
22	Bleziuc L.	DD24-64	<2.0	<0.4	< 0.6	<2.0	<2.0	0.020	0.002	3.6	<2.0	<5.0
23	Pojarnia L.	DD24-73	<2.0	<0.4	1	<2.0	<2.0	0.054	0.012	<2.0	<2.0	<5.0
24	Pojarnia L.	DD24-74	<2.0	<0.4	< 0.6	<2.0	<2.0	0.009	0.008	<2.0	2.9	<5.0

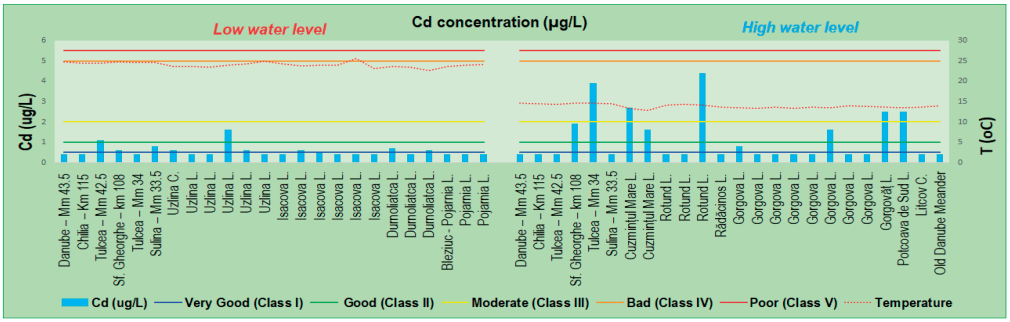


Figure 3. Cd (µg/L) concentration in investigated freshwater samples

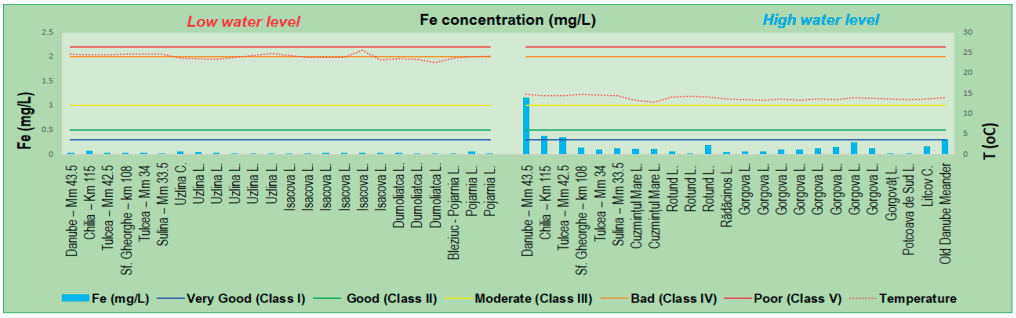


Figure 4. Fe (mg/L) concentration in investigated freshwater samples

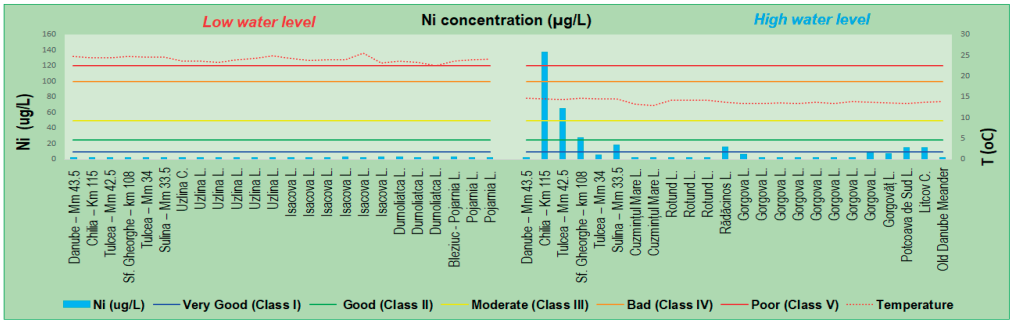


Figure 5. Ni (µg/L) concentration on investigated freshwater samples

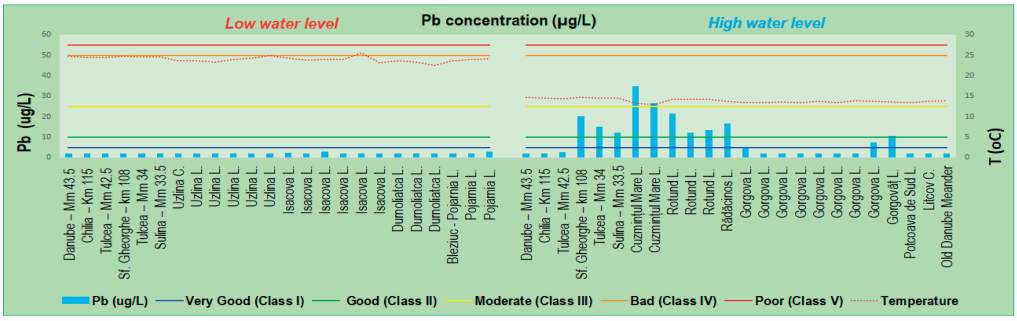


Figure 6. Pb (µg/L) concentration in investigated freshwater samples

Copper. The Cu concentration (µg/L) measured in the water samples collected during the low-water period, showed no significant variations. All the values obtained were low, below the limit set for water quality Class I (20 µg/L).

Iron. During the low-water period, the Fe concentration (mg/L) defined in the water samples collected from all sampling points, showed no significant variations. All the obtained values were low, below the limit set for water quality Class I (0.3 mg/L) (Figure 4).

Manganese. The results showed an inconsiderable Mn concentration (mg/L) detected in the water samples collected from all sampling points. All the values were low, below the limit set for water quality Class I (0.05 mg/L).

Nickel. The Ni concentration (µg/L) spotted in the water samples collected during the low-water period showed no significant variations. All the value obtained were low, below the limit set for water quality Class I (10 µg/L) (Figure 5).

Lead. The Pb concentration (µg/L) observed in the water samples collected during the low-water period showed no significant variations. All the obtained values were low, below the limit set for water quality Class I (5 µg/L) (Figure 6).

Zinc. The Zn concentration (µg/L) noticed in the water samples collected during the low-water period showed no significant variations. All the obtained values were low, below the limit set for water quality Class I (100 µg/L)

Heavy metals' distribution during the high-water period investigation

The field expedition occurred when an impetuous increase in Danube water levels was expected due to a flood wave owing to storms and heavy rainfall coming from upstream countries. Consequently, during the high-water period (October 2024), at the *Ceatal Izmail* bifurcation area, the *Danube* carried a flow of approximately 6970 $m^3 \cdot s^{-1}$ at the entrance to the delta. This was unequally distributed between the *Tulcea* - 3896 $m^3 \cdot s^{-1}$ and *Chilia* - 3032 $m^3 \cdot s^{-1}$ branches. The average velocities on the profiles were between 0.72 and 0.93 $m \cdot s^{-1}$.

Table 2. Results of the heavy metal analysis in the investigated control sections (point samples) (Danube branches, canals, lakes, etc.) (high-water hydrodynamic conditions)

No. crt.	Location	Sample's indicative	As µg/L	Cd µg/L	Co µg/L	Cr_{tot} µg/L	Cu µg/L	Fe_{tot} mg/L	Mn mg/L	Ni µg/L	Pb µg/L	Zn µg/L
1	Danube Mm 43.5	DD24-76	<2.0	<0.4	<0.6	<2.0	<2.0	1.160	0.005	<2.0	<2.0	67.6
2	Chilia Km 115	DD24-79	<2.0	<0.4	<0.6	<2.0	<2.0	0.379	0.004	138	<2.0	57.2
3	Tulcea Mm 42.5	DD24-82	<2.0	<0.4	<0.6	<2.0	<2.0	0.348	0.001	65.2	2.5	60.2
4	Sf. Gheorghe Km 108	DD24-85	<2.0	1.9	7.8	<2.0	<2.0	0.130	0.000	28.2	20	40
5	Tulcea Mm 34	DD24-88	<2.0	<0.4	7.6	<2.0	<2.0	0.092	0.000	5.5	14.8	59.6
6	Sulina Mm 33.5	DD24-90	<2.0	<0.4	<0.6	<2.0	<2.0	0.125	0.000	18.1	12.2	33.3
7	Cuzmințul Mare L.	DD24-93	<2.0	2.7	<0.6	<2.0	<2.0	0.111	0.003	<2.0	34.6	30.4
8	Cuzmințul Mare L.	DD24-97	<2.0	1.6	1.5	<2.0	<2.0	0.109	0.005	<2.0	26.4	35.7
9	Rotund L.	DD24-101	<2.0	<0.4	<0.6	<2.0	<2.0	0.052	0.000	<2.0	21.2	48.5
10	Rotund L.	DD24-102	<2.0	<0.4	<0.6	<2.0	<2.0	0.016	0.001	<2.0	12	25.4
11	Rotund L.	DD24-106	<2.0	4.4	4.7	<2.0	<2.0	0.188	0.024	<2.0	13.2	25.1
12	Rădăcinos L.	DD24-108	<2.0	<0.4	3.3	<2.0	<2.0	0.042	0.003	15.8	16.4	9.7
13	Gorgova L.	DD24-112	<2.0	0.8	<0.6	<2.0	<2.0	0.059	0.001	6.7	4.7	49.4
14	Gorgova L.	DD24-113	<2.0	<0.4	<0.6	<2.0	<2.0	0.056	0.003	<2.0	<2.0	30.8
15	Gorgova L.	DD24-118	<2.0	<0.4	<0.6	<2.0	<2.0	0.094	0.003	<2.0	<2.0	61.7
16	Gorgova L.	DD24-120	<2.0	<0.4	1.2	<2.0	<2.0	0.097	0.010	<2.0	<2.0	34
17	Gorgova L.	DD24-122	<2.0	<0.4	<0.6	<2.0	<2.0	0.123	0.008	<2.0	<2.0	<5.0
18	Gorgova L.	DD24-123	<2.0	1.6	2.1	2.3	<2.0	0.154	0.003	<2.0	<2.0	44.6
19	Gorgova L.	DD24-125	<2.0	<0.4	<0.6	2.2	<2.0	0.246	0.023	<2.0	<2.0	47.3
20	Gorgova L.	DD24-126	<2.0	<0.4	1.8	<2.0	<2.0	0.124	0.002	8.1	7.4	12.9
21	Gorgovăț L.	DD24-130	<2.0	2.5	<0.6	5.7	<2.0	0.003	0.006	7.7	10.6	37.8
22	Potcoava de Sud L.	DD24-131	<2.0	2.5	<0.6	6.3	<2.0	0.006	0.003	15.5	<2.0	10
23	Litcov C.	DD24-135	<2.0	<0.4	<0.6	<2.0	<2.0	0.167	0.010	14.9	<2.0	<5.0
24	Old Meander	DD24-136	<2.0	<0.4	1.3	<2.0	<2.0	0.306	0.009	<2.0	<2.0	30.6

At the entrance to the second hydrographic node at the *Ceatal Sf. Gheorghe* bifurcation area, the flow of the *Tulcea* branch was at the time of measurements approximately 3738 $m^3 \cdot s^{-1}$. The

flow was unequally distributed between the *Sulina* - 1377 $m^3 \cdot s^{-1}$ and *Sf. Gheorghe* branch - 2328 $m^3 \cdot s^{-1}$. The average velocities on the profiles were between 0.76 and 0.95 $m \cdot s^{-1}$, with higher values on the *Sulina* Canal. The chemical analyses were fulfilled for 24 spot water samples collected from *Ceatal Izmail* (at the *Danube - Mm 43.5, Chilia Arm - Km 115, Tulcea Arm - Mm 43.5*), *Ceatal Sf. Gheorghe* (at the *Tulcea Arm - Mm 43, Sulina Arm - Mm 33.5, Sf. Gheorghe Arm - Km 108*), including *Cuzmințul Mare L., Rotund L., Rădăcinos L., Gorgova L., Gorgovăț L., Potcoava de Sud L.*, *Litcov Canal* and *Old Danube River Meander* (Figure 2). During the high-water period, the values of the investigated heavy metals showed a higher variability associated with the heavy metals' distribution between the collection points, in both investigated Danube River bifurcations, as well as in deltaic lakes. The results are shown in Table 2. In general, the content values of certain heavy metals (Cd, Fe, Ni and Pb) acquired within hydrodynamic conditions of high-water levels of the Danube (October 2024) were higher than the values obtained within the low-water level period (September 2024). Regarding the other investigated heavy metals (As, Co, Cr, Cu, Mn and Zn), they maintained a similar trend so that no significant exceedances were registered between the two seasons (September 2024 and October 2024). The distribution trend of these heavy metals had a pattern with low values, close to those corresponding to quality class I (very good condition), registered in all investigated sampling stations. The dynamics and changes in the concentrations of ten investigated heavy metals (As, Cd, Co, Cr, Cu, Fe, Mn, Ni, Pb, and Zn) during the high-water period will be shown below.

Arsenic. The As concentration (µg/L) identified in the water samples presented a series of insignificant variations. Most of the obtained values were low, below the detection limit (< 2 µg/L), implicitly, below the limit corresponding to quality class I (10 µg/L).

Cadmium. The Cd concentration (µg/L) determined in the investigated water samples presented a series of interesting variations. A part of the values was below the limit set for water quality Class I, but also were observed values that slightly reached or exceeded the first three quality classes (Class I - 0.5 µg/L, Class II - 1 µg/L, Class III - 2 µg/L) (Figure 3). The water sample that exceeded class I was encountered in the *Gorgova L.* (*DD24-112*) (situated in the northwestern part of the lake, close to the mouth of the connection canal with *Sulina Arm*). Then, the sampling sites with values higher than class II are represented by: *Sf. Gheorghe Arm - Km 108* (*DD24-85*), *Cuzmințul Mare L.* (*DD24-97*) (situated in the northeastern part of the lake, close to the mouth of a connection canal) and *Gorgova L.* (*DD24-123*) (located in the west southern part of the lake, close to the mouth of a connection canal with *Rădăcinos L.*). The water samples that overpassed the limit set for water quality Class III were noticed in: the *Tulcea Arm - Mm 34* (*DD24-88*), *Cuzmințul Mare L.* (*DD24-93*) (situated in the middle part of the lake), *Rotund L.* (*DD24-106*) (located in the southern part of the lake, close to the mouth of a connection canal with *Litcov C.), Gorgovăț L. (DD24-130)* (located in the middle of the lake) and *Potcoava de Sud L.* (*DD24-131*) (situated in the southern part of the lake, close to the mouth of a connection canal with *Litcov C.*).

Cobalt. The Co concentration (µg/L) identified in all collected water samples showed no significant variations. Most of the results were low values, below the limit set for water quality Class I (10 µg/L).

Chromium. The Cr concentration (µg/L) tested in the water samples collected during the high-water period showed no significant variations. All the value obtained was low, below the limit set for water quality Class I (25 µg/L).

Copper. The Cu concentration (µg/L) noted in the water samples collected during the high-water period showed no significant variations. All the values obtained were low, below the limit set for water quality Class I (20 µg/L).

Iron. During the high-water period, the Fe concentration (mg/L) identified in most of the water samples showed no significant variations, with low values, below the limit set for water quality Class I (0.3 mg/L). For all that, three samples slightly reached or exceeded the first quality class (Figure 4), namely: the *Chilia Arm - km 115* (*DD24-79*), the *Tulcea Arm - Mm 42.5* (*DD24-82*) and the *Old Danube Meander* (*DD24-136*). In addition, it was also noticed one sample overpassed the limit set for water quality

Class III (1.0 mg/L), specifically, the *Danube - Mm 43.5* (*DD24-76*).

Manganese. The results showed an insignificant Mn concentration (mg/L) detected in the water samples collected from all sampling points. All the values were low, below the limit set for water quality Class I (0.05 mg/L).

Nickel. Overall, the Ni concentration (µg/L) spotted in several water samples collected during the high-water period showed no significant variations, with low values, below the limit set for water quality Class I (10 µg/L). Even so, four water samples exceeded the first quality class, namely: the *Sulina Arm - Mm 33.5* (*DD24-90*), *Rădăcinos L.* (*DD24-108*) (situated in the northern part of the lake), *Potcoava de Sud L.* (*DD24-131*) (situated in the southern part of (situated close to the mouth of the connection canal with *Durnoliatca L.*), (situated close to the mouth of the connection canal with *Durnoliatca L.*), *135)*. The other two samples overpassed the limit set for water quality Class II (25 µg/L), namely, *Sf. Gheorghe Arm - Km 108* (*DD24-85*), and respectively, Class III (50 µg/L) at the *Tulcea Arm - Mm 42.5* (*DD24-82*). Finally, at the *Chilia Arm - Km 115* (*DD24-79*) was depicted a Ni concentration overpassed the limit set for water quality Class V (>100 µg/L) (Figure 5).

Lead. Almost half of the water samples investigated showed lower Pb concentration (µg/L), with values below the limit settled for water quality Class I (5 µg/L). Instead, the other half of the samples showed values that exceeded the first three quality classes (Class I - 5 µg/L, Class II - 10 µg/L, Class III - 25 µg/L). So, the following sampling sites revealed Pb concentration (µg/L) higher than Class I: *Gorgova L.* (*DD24-126*) (located in the south-eastern part of the lake, close to the mouth of a connection canal with *Gorgovăț L.*) and *Gorgovăț L.* (*DD24-130*) (located in the middle part of the lake). Then, the upcoming water samples were included in the quality class II: *Sf. Gheorghe Arm - km 108* (*DD24-85*), *Tulcea Arm - Mm 34 (DD24-88)*, *Sulina Arm - Mm 33.5* (*DD24-90*), *Rotund L.* (*DD24-101*) (located in the eastern part of the lake, close to the mouth of a connection canal with *Gorgova L.*), *Rotund L.* (*DD24-102*) (located in the northern part of the lake, close to the mouth of a connection canal with *Cuzmințul Mare L.*), *Rotund L.* (*DD24-106*) (located in the southern part of the lake, close to the mouth of a connection canal with *Litcov C.*), and *Rădăcinos L.* (*DD24-108*) (located in the northern part of the lake, close to the mouth of a connection canal with *Gorgova L.*). Relatively, higher values of Pb concentration corresponding to the quality class III were identified in: *Cuzmințul Mare L.* (*DD24-93*) (located in the middle part of the lake) and *Cuzmințul Mare L.* (*DD24-97*) (located in the eastern part of the lake, close to the mouth of a connection canal) (Figure 6).

Zinc. The Zn concentration (µg/L) determined in the water samples collected during the high-water period, showed no significant variations. All the obtained values were low, below the limit set for water quality Class I (100 µg/L).

The heavy metals investigated in the surface water samples collected under distinct hydrodynamic conditions (low and high water levels of the Danube River in 2024) show a varying degree of distribution, ranging from very low values below the detection limit, implicitly below the limit corresponding to Class I quality (very good status) to relatively higher values (in certain stations) that exceed the maximum allowed limit, corresponding to Class II (good status), Class III (moderate status), Class IV (poor status), and Class V (bad status). To some extent, the results obtained in this study are similar to those of previous research conducted on the Danube Delta ecosystems (Vignati, 2013; Vasiliu, 2021; Catianis, 2022). It is assumed that the increased concentrations of particular heavy metals (*i.e.,* Cd, Fe, Ni and Pb) observed during the high-water period may be due to the flood wave. When the flow of a river increases (*e.g.,* due to heavy rains, snowmelt, etc.), it can transport pollutants from the upstream areas of the watercourse. These pollutants may include chemicals, heavy metals, waste, and even pathogens. Increased flow can lift pollutants from upstream soil, sediments, and waters, transporting them downstream and affecting water quality. Particularly, during flooding, contaminants can be carried in much greater quantities than under normal flow conditions. Generally, even areas located far from the potential pollution sources can suffer from the transport of these pollutants, which may reach sensitive ecosystems or even drinking water sources. Higher concentrations of Cd, Fe,

Ni and Pb in the investigated freshwater samples can be attributed to several natural and anthropogenic factors. Among the most relevant factors that could contribute to the increase in Cd, Fe, Ni, and Pb concentrations are industrial activities, mining, transportation, agricultural waste and fertilization practices, upstream contamination, atmospheric particle deposition, urban and industrial waste, illegal or uncontrolled discharges, soil erosion, sediment input, in-lake processes, etc. However, it should be noted that in the Danube Delta, there are sediments that may contain nickel in higher concentrations due to the natural geochemical background. Additionally, soil and rock erosion in the upstream areas of the delta may release nickel into the water. More than that, the combination of natural sedimentation, erosion, flood-induced transport, anthropogenic pollution, and geochemical factors leads to the higher concentration of heavy metals near the mouths of connecting channels with lakes. These areas may act as collection points for pollutants, both from upstream sources and from local environmental processes.

The impact of heavy metals on the aquatic environment. Higher concentrations of Cd, Fe, Ni and Pb in the Danube and the lakes of the Danube Delta represent a complex phenomenon, generated by both natural sources and anthropogenic influences, which requires constant monitoring. Their impact on the ecosystems of the Danube Delta depends not only on the concentrations of these metals but also on their interactions with other biological and physical-chemical factors in the area. Higher concentrations of Cd, Fe, Ni and Pb can lead to water pollution, affecting the health of aquatic ecosystems either through direct toxicity or by modifying the physical-chemical characteristics of the water. This can also disrupt biodiversity and the normal functioning of the ecosystem. Therefore, monitoring and managing this type of pollution are essential for protecting the environment of the Danube Delta.

Tracking heavy metal contamination in water and sediments is important for developing targeted management strategies to mitigate their impact on deltaic ecosystems. Heavy metal pollution disrupts ecosystem functions, such as nutrient cycling and water purification, leading to habitat degradation. It also threatens biodiversity by accumulating in aquatic organisms and affecting the food chain. Human health risks arise from contaminated fish and water, while economic impacts include reduced fish stocks, harmed agriculture, and decreased eco-tourism. To ensure long-term sustainability, advanced remediation, stronger policies, ecosystem restoration, and community involvement are essential to mitigate the effects of heavy metal contamination in the Danube River-Danube Delta-Black Sea system, which is important for both the surrounding regions and Europe.

CONCLUSIONS

The natural and anthropogenic factors leave their mark on the water quality of the Danube Delta ecosystems. The most evident impact of anthropogenic stressors is the influence of climate change (i.e., floods, droughts, geological factors, sediment matrix, etc.). The effects of climate change, particularly extreme weather events, have the potential to abruptly modify the physical-chemical, biological, and heavy metal characteristics of the Danube Delta ecosystems. Instantly, the contaminant load and soil processes may make the water more vulnerable to pollution, consequently affecting its ecological functions.

The water quality status within the Danube Delta region is primarily linked to seasonal fluctuations and, to a lesser extent, spatial variations in the hydrological regime of the Danube River. This study highlighted the influence of the Danube River during the high-water period, which showed a considerable increase in some heavy metal concentrations at certain sampling stations, compared to the low-water period when most of the values were negligible. Although the results were not alarming, being recorded only at specific stations, this study provided evidence that systematic monitoring and assessment of the water quality's status is essential in such deltaic aquatic environments, which are of inestimable ecological and biodiversity value.

ACKNOWLEDGEMENTS

This research work was carried out through the support of the Romanian Ministry of Research, Innovation and Digitalization of the Research Core Program, within the National Plan for Research, Development and Innovation 2022-2026, implemented with the support of MCID, Project – PN 23 30 03 02 and PN 23 30 03 04.

REFERENCES

Belacurencu, T. (2007). Implementation of Ecological Policies in Danube Delta Area. *Theoretical and Applied Economics*, 9-24.

Bennett, J. P., Rathbun, R. E. (1971). Reaeration in Open-Channel Flow, 737, US Department of the Interior, Geological Survey, Fort Collins, CO, 75.

Catianis, I., Tiron Duțu, L., Grosu, D. (2022). Heavy metals occurrence in lakes of the Danube Delta, Romania. *Geo-Eco-Marina*, *28*, 49-63, ISSN 1224-6808.

Cazacu, C., Adamescu, M.C. (2017). Ecosystem services provided by the bio-physical structure of natural capital in the Danube Delta Biosphere Reserve Romania, *Conference Volume of 6th Symposium for Research in Protected Areas*, 2 to 3 November 2017, Salzburg, 97-102.

Chapman, D. V., Sullivan, T. (2022). The role of water quality monitoring in the sustainable use of ambient waters. *One Earth*, *5(2)*, 132-137.

Chitescu, C.L., Ene, A., Geana, E.-I., Vasile, A.M., Ciucure, C.T. (2021). Emerging and Persistent Pollutants in the Aquatic Ecosystems of the Lower Danube Basin and North West Black Sea Region-A Review, *Appl. Sci.*, *11*, 9721. https://doi.org/10.3390/app11209721

De Jonge, V.N., Elliott, M., Orive, E. (2002). *Causes, Historical Development, Effects and Future Challenges of a Common Environmental Problem: Eutrophication*. In Nutrients and Eutrophication in Estuaries and Coastal Waters, Springer, Dordrecht, 1-19. https://doi.org/10.1007/978-94-017-2464-7_1

Gâștescu, P., Știucă, R. (2008). *The Danube Delta - A Biosphere Reserve*. CD Press Publishing House, Bucharest [in Romanian, with Contents and Introduction in English], 400 p.

Kumar, S.B., Padhi, R.K., Mohanty, A.K., Satpathy, K.K. (2017). Elemental distribution and trace metal contamination in the surface sediment of south east coast of India, *Marine Pollution Bulletin*, *114 (2)*, 1164-1170, ISSN 0025-326X, https://doi.org/10.1016/j.marpolbul.2016.10.038. (https://www.sciencedirect.com/science/article/pii/S0025326X16308530)

Leščešen, I., Basarin, B., Pavić, D., Mudelsee, M., Pekárová, P., Mesaroš, M. (2024). Are extreme floods on the Danube River becoming more frequent? A case study of Bratislava station. *Journal of Water and Climate Change, 15(3)*, 1300-1312. DOI: 10.2166/wcc.2024.587.

Nicholls, R. J., Wong, P. P., Burkett, V., Woodroffe, C. D., Hay, J. (2008). Climate change and coastal vulnerability assessment: scenarios for integrated assessment. *Sustain. Sci*., *3*, 89-102.

Order no. 161/2006 - Normative concerning the classification of surface water quality to establish the ecological status of water bodies (Romanian Order MEWM no. 161/2006), Annex C-Elements and physico-chemical quality standards in water, published in *Romanian Official Monitor*, part I, no. 511 bis, from 13th of June, 2006.

Padło, T, Struś, P, Gil, A. (2021). Danube as a symbol of Europe. Perception of the river from varied geographical perspectives. *PLoS One*. 2021 Dec 2; *16(12)*: e0260848. doi: 10.1371/journal.pone.0260848. PMID: 34855880; PMCID: PMC8638847.

Panin, N., Jipa, D. (1998). Danube River Sediment Input and its Interaction with the North-Western Black Sea, *Estuarine, Coastal and Shelf Science*, *54(2)*, 551-562.

Panin, N., Tiron Duțu, L., Duțu, F. (2016). The Danube Delta: An overview of its Holocene evolution. *Méditerranée*, *126*, 37-54.

Ptitsyn, A. B. (2018). *Lectures in Geochemistry* (1st ed.), CRC Press, 2018, ISBN 0429833938, 9780429833939, doi. org/10.1201/9780429450518, 89.

Ramsar Convention (1987). Convention on Wetlands of International Importance especially as Waterfowl Habitat. Ramsar (Iran), 2 February 1971, UN Treaty Series No. 14583, As amended by the Paris Protocol, 3 December 1982, and Regina Amendments, 28 May 1987, Ramsar Convention on Wetlands, Gland, Switzerland.

Syvitski, J.P.M., Kettner, A.J., Overeem, I., Hutton, E.W.H., Hannon, M.T., Brakenridge, G.R., Day, J., Vorosmarty, C., Saito, Y., Giosan, L., Nicholls, R.J. (2009). Sinking deltas due to human activities. *Nature Geosci.*, *2*, 681-686, https://doi.org/10.1038/ngeo629

Tovar-Sánchez, E., Hernández-Plata, I., Martínez, M. S., Valencia-Cuevas, L., Galante, P. M. (2018). *Heavy Metal Pollution as a Biodiversity Threat*. In Hosam Saleh & Refaat Fekry Eid Sayed Aglan (ed.), Heavy Metals, IntechOpen, https://doi.org/10.5772/intechopen.74052, 412.

Vasiliu, D., Tiron Duțu, L., Bucșe, A., Lupașcu, N., Duțu, F. (2021). Geochemical characteristics of riverbed sediments in the Danube Delta, Romania. *Scientific Papers. Series E. Land Reclamation, Earth Observation & Surveying, Environmental Engineering*, *X*, 258-264.

Vignati, D. A., Secrieru, D., Bogatova, Y. I., Dominik, J., Céréghino, R., Berlinsky, N. A., Oaie, G., Szobotka, S., Stănică, A. (2013). Trace element contamination in the arms of the Danube Delta (Romania/Ukraine): current state of knowledge and future needs. *Journal of Environmental Management, 125*,169-178.

Scientific Papers. Series E. Land Reclamation, Earth Observation & Surveying, Environmental Engineering. Vol. XIV, 2025
Print ISSN 2285-6064, CD-ROM ISSN 2285-6072, Online ISSN 2393-5138, ISSN-L 2285-6064

SPATIAL DISTRIBUTION OF TOTAL ORGANIC MATTER IN RECENT SEDIMENTS OF DANUBE DELTA LAKES (GORGOVA-UZLINA HYDROGRAPHIC UNIT)

Irina CATIANIS, Ion STANESCU, Dumitru GROSU, Ana Bianca PAVEL, Albert SCRIECIU, Ovidiu BORZAN, Andrei TOMA, Florin DUTU, Gabriel IORDACHE

National Institute of Marine Geology and Geoecology - GeoEcoMar, Bucharest,
23-25 Dimitrie Onciul Street, 024053, District 2, Bucharest, Romania

Corresponding author email: irina.catianis@geoecomar.ro

Abstract

Organic matter plays a crucial role in maintaining lake health and trophic balance. It mainly originates from autochthonous sources like phytoplankton, microorganisms, and macrophytes, as well as allochthonous inputs from the surrounding terrestrial ecosystem. Understanding the origin of organic matter is important for assessing ecosystem quality and trends in lake evolution. This study uses the Loss of Ignition method to estimate the distribution, sources, and quantity of total organic matter (TOM %) in lakes of the Gorgova-Uzlina hydrographic unit in the Danube Delta, Romania. Results indicate that TOM concentrations (15-30%) in surface sediments primarily originate from in-situ lacustrine production, with minor contributions from upstream terrestrial inputs. Accomplished analysis revealed recent organo-sedimentary accumulations based on lithological components (TOM %, carbonates - CAR %, and minerogenic fraction - SIL %). The organic matter in these sediments may reflect both natural processes and anthropogenic impacts, emphasizing the need for monitoring to understand the dynamics and vulnerability of the delta ecosystem and perform conservation efforts.

Key words*: areal distribution, lacustrine ecosystems, LOI method, surface sediments, total organic matter.*

INTRODUCTION

Delta shallow lakes, which are formed at the mouths of rivers, are vital ecosystems that support a rich diversity of flora and fauna while also providing significant key ecosystem services (Verpoorter et al., 2014; Laignel et al., 2023). These lakes are highly dynamic systems, shaped by sediment deposition, hydrological flow, and anthropogenic influences. However, one of the critical issues facing delta lakes is the phenomenon of clogging or siltation, wherein excessive sediment accumulation results in a reduction of water quality, decreased oxygen levels, and altered habitat conditions for aquatic species (Walton et al., 2024; How et al., 2024; Wang et al., 2024). The process of siltation in delta lakes is primarily driven by the deposition of fine sediments, such as silt and clay, which can accumulate at the lakebed due to changes in flow velocity, river damming, land-use changes, and climate variability (Zhang et al., 2022; Wang et al., 2024). Siltation not only affects the sedimentary structure of the lakebed but also contributes to the loss of biodiversity and can significantly alter the hydrodynamics of the lake (Ho & Goethals, 2019; Tammeorg et al., 2024). Additionally, autochthonous aquatic vegetation contributes to the clogging of deltaic lakes. Aquatic vegetation plays a vital role in the ecological health of wetlands (Sun et al., 2023), providing habitat for various aquatic animal species and contributing to water quality by stabilizing sediments. However, excessive growth of aquatic vegetation can lead to challenges (Tan et al., 2020), particularly, dealing with clogging water channels and reducing flow, ultimately accumulating organic matter and sediments. Studies have shown that several plant species may exacerbate these issues by rapidly colonizing large areas of delta lakes, forming dense mats that could restrict water movement or create other impediments to the overall health of aquatic ecosystems (Oteman et al., 2021; Schneider et al., 2024). The overabundance of these plants is often a result of nutrient-rich conditions in the water, frequently fueled by agricultural runoffs and industrial discharges. The Danube Delta, one of Europe's largest and most biodiverse wetlands,

plays a key role in regulating water quality, supporting wildlife, and providing livelihoods for local communities. The delta, which spans across Romania and Ukraine, consists of a complex network of lakes, channels, and marshes (Gâștescu & Știucă, 2008). However, over the past several decades, deltaic aquatic ecosystems have been increasingly susceptible to being impacted by the phenomenon of clogging or siltation (Tiron Duțu et al., 2022). Siltation refers to the accumulation of fine sediments, such as silt and clay, that degrade water quality and ecosystem health and obstruct various connecting channels or other deltaic aquatic systems (Constantinescu et al., 2023). This process is primarily driven by changes in riverine sediment load, hydrological modifications, and anthropogenic activities, including damming the Danube River upstream. The Danube Delta's lakes are particularly vulnerable to siltation due to the reduced sediment transport caused by upstream river regulation via the construction of dams or diversions and altered flow patterns (Panin & Jipa, 2002; Duțu et al., 2022). As sediments accumulate, they can clog channels, reducing water flow, oxygen levels, and habitat quality for aquatic species such as fish, birds, and invertebrates (Năstase et al., 2022). This study intends to investigate the responses of several selected middle Danube Delta floodplain lakes to natural siltation or clogging by studying the main lithological components dissemination in lakebed sediment samples. The selected lakes with relatively different hydrological conditions, situated in the same catchment area *(i.e., Rusca-Gorgova-Uzlina* Hydrographic Unit), include hydrologically connected lakes such as *Uzlina, Isacova, Durnoliatca, Bleziuc-Pojarnia* and *Pojarnia*, as well as relatively hydrologically isolated lakes, namely *Cuzmințul Mare, Cuzmințul Lat, Rotund, Rădăcinos, Gorgova, Gorgovăț* and *Potcoava de Sud*. Even though the natural processes of siltation and organic deposit accumulations are characteristic of the Danube Delta aquatic ecosystems, the intensification of processes from the last periods demands special attention. Given the importance of these lakes for biodiversity and human activities, understanding the processes and consequences of siltation/clogging is essential for effectively conserving and managing Danube Delta's aquatic ecosystems.

MATERIALS AND METHODS

Study area

This investigation was realized at the *Rusca-Gorgova-Uzlina* Hydrographic Unit (Figure 1), the Danube Delta, Romania. The unit is included in the fluvial western area of the Danube Delta, being delimited by the *Sulina* (north) and the *Sf. Gheorghe* (south) branches, and east of the *Letea-Caraorman* Spit (Panin et al., 2016). In the southern part, this hydrographic unit is represented by lakes such as *Uzlina, Isacova, Durnoliatca, Isăcel, Pojarnia, Bleziuc-Pojarnia* etc. Then, the northern part consists of the *Gorgova* lake and other satellite lakes such as *Gorgovăț, Cuzmințul Mare, Cuzmințul Lat, Rotund, Rădăcinos, Potcoava de Sud*. The southern part is separated from the northern part by the *Litcov Canal*. The freshwater input in the southern part of the *Rusca-Gorgova-Uzlina* Hydrographic Unit is assured mainly by the *Sf. Gheorghe* Branch via *Uzlina Canal*, including several connecting channels between lakes and streams (*i.e.*, *Perivolovca Stream*). Contrarily, the northern part has an inconstant water supply, through the *Old Danube River Meander via Litcov Canal* and other connecting channels between lakes. The chosen sampling sites for this study portray a notable example of the potential environmental impact of both mineral and/or organic recent sediment accumulations yielded by the allochthonous sources from the Danube River flowing alluvial input and streams, or due to the local autochthonous sources.

Field sampling and data analysis

The lakebed sediment samples, and field data collection (including field observations and measurements) were performed at the R/V "Istros" belonging to the National Institute for Research and Development of Marine Geology and Geoecology-GeoEcoMar, Romania. The field surveys were carried out during two distinct hydrological periods of the Danube River's flow: *low-water level* (06-13 September 2024) and *high-water level* (21-28 October 2024). In the low-water period, the Danube River's water level height (cm) registered at the

Tulcea hydrometric station was the lowest level, *i.e.,* 70.25 cm *versus* 180-200 cm normal reference quota, whilst the maximum value was measured in October 2024, *i.e.,* 205.12 cm versus the above-mentioned reference quota. Sediment samples were collected at a depth of ~25 cm using a Van Veen grab sampler. The macroscopic description of the sedimentary material was made *in situ*, such as the structure, texture, main litho-clastic elements (clay, mud, silt, sand, gravel etc.), and bioclastic components (detritus, shells, other organic fragments), color, odor etc. Then, the samples were transferred to sterile plastic recipients maintained at a constant temperature (4°C) and shipped to the specific laboratory for analysis.

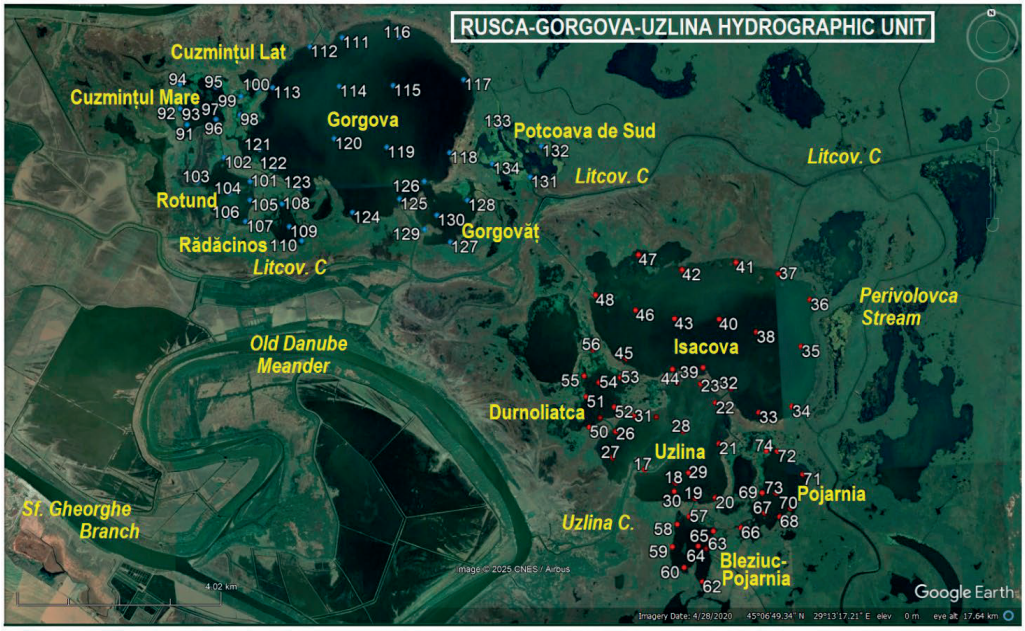


Figure 1. Location of the perimeters investigated. Red dots mark the sampling sites during the low-water periods; Blue dots mark the sampling sites during the high-water periods
(Base Map Source: https://www.google.com/maps)

A percentage quantitative analysis standard technique for the review of the main lithological components was used. In the preparatory phase, the sediments were probed for their moisture content (%) by the Loss On Drying (LOD) method, using a laboratory heater (Universal Memmert Oven) at 105°C temperature (Smith & Mullins, 2000; ASTM-D221). Subsequently, the percentage proportion of the main lithological components was performed in line with the LOI (Loss of Ignition) method. The sediment samples were subjected to sequential heating to distinguish the organic matter (TOM %), carbonates (CAR %), and siliciclastic fraction (SIL %) constituents. The loss in mass by combustion at 550°C was attributed to total organic matter content (Dean, 1974; Bengtsson & Enell, 1986). The total organic matter content was related to a standard classification (Perrin, 1974; Tate, 1987; Van der Veer, 2006), that allows the grouping of *organic matter-rich sediments (≥ 15-30% organic matter)* and *mineral-rich sediments (≤ 15-30% organic matter)*. The loss in mass by calcination at 950-1000ºC was related to the total carbonate content (Digerfeldt et al., 2000; www.geog.cam.ac.uk). The total carbonate content was correlated with the well-known sedimentary systematization (Emelyanov & Shimkus, 1986), presenting: *non-carbonated sediments ($CaCO_3 \leq 10\%$)*, *low calcareous sediments ($10\% < CaCO_3 \leq 30\%$)* and *calcareous sediments ($30\% < CaCO_3 \leq 50\%$)*. Finally, the remaining residual sediment mass after calcination was associated with the siliciclastic fraction content. The obtained

results were assessed as percentages of the TOM %, CAR % and SIL % content from the total sample mass by weight loss procedure. The spatial distribution of the data points has been plotted by the Surfer software package (Golden Software Inc., 2010, Golden, CO, USA) using the kriging method of gridding.

RESULTS AND DISCUSSIONS

The sites represent a good example of environmental exposure to different types of recent sedimentary depositional environments of allochthonous or autochthonous origins. The extent to which the allochthonous or autochthonous source may have a potential impact on the sedimentary depositional environment is mainly determined by the alluvial input contribution brought by the Danube River, and subsequently, is given by the processes that take place in the catchment area *i.e.,* small and shallow reservoirs, the fluvial-dynamic conditions, and the hydrogeochemical background susceptibility to siltation/clogging. In the present study, the main lithological components (*i.e.,* TOM %, CAR %, SIL %) were used as proxy indicators to reflect changes in sediment composition resulting from allochthonous or autochthonous sources. Generally, the freshwater/marine sediments, (porous, soft, or lithified) are composed of three main components, *i.e.,* organic matter, carbonate, and siliciclastics, representing their solid fraction (Ricken, 1993). The lithological analysis of the aquatic sediments in the Danube Delta is important for several reasons, as these data help to gain insight into the processes of formation and evolution of the Danube Delta, as well as to manage natural resources and protect the environment. Among the main reasons for which lithological analysis (*e.g.,* organic matter, carbonates and siliciclastic fraction) is important, the following are specified:

• ***Understanding sedimentary processes***: the lithological analysis facilitates the identification of the sources of sediments and deciphering how they are transported and deposited in the Danube Delta. The composition of the sediments (*e.g.,* organic matter content, carbonates and siliciclastic fraction) can provide information about the environment of transport and deposition of sedimentary particles (the sedimentary environment of the fluvial zone, the marine zone and the transition zone between them).

• ***Study of the evolution of the Danube Delta***: the Danube Delta is a dynamic system being in a constantly changing status. Lithological analysis of sediments allows the reconstruction of the history of geological processes and the geomorphological evolution of the delta, helping to gain an overview of the formation of various habitat types (lakes surrounded by dense reed beds, adjacent channels, reeds formations etc.) and how they have evolved;

• ***Biodiversity and habitat assessment***: Danube Delta sediments, especially those containing organic matter (e.g., plant and animal remnants), are fundamental for supporting biodiversity in the Danube Delta ecosystems. Organic matter in sediments influences substrate fertility and nutrient availability, which affects aquatic and terrestrial ecosystems. Knowledge of the distribution of organic matter in sediments can help assess the state of ecosystems in the Danube Delta;

• ***Impact of climate change***: the lithological analysis can provide information on the impact of climate change on the delta. For example, changes in the ratio of siliciclastic to carbonate fractions may indicate changes in the hydrological regime or water level, which are consequently influenced by climatic factors.

• ***Natural resource management***: the Danube Delta is an important area for fishing, tourism, and agriculture, and sediment analysis can help assess the natural resources of the region. For example, carbonate sedimentation can be an indicator of the potential for the formation of fertile soils, while the analysis of siliciclastic material can contribute to the identification and assessment of natural resources, which represent both ecological and economic value.

• ***Pollution and conservation studies***: sediment analysis can identify contaminants in the Danube Delta ecosystems, such as heavy metals or toxic substances from industrial or agricultural activities. Therefore, lithological analysis may contribute to the assessment of pollution risks and the development of strategies for the conservation of the delta and the protection of biodiversity.

• ***Water management and wetland protection***: the Danube Delta is an important wetland

ecosystem with multiple ecological functions. Lithological analysis may contribute to understanding the interaction between sediments, water and vegetation, essential for the efficient management of water resources and the protection of sensitive habitats. In this study, the percentage concentration of the main lithological components (TOM %, CAR %, SIL %) noticeably ranged between the investigated sampling sites based on their geographical position and lithological content.
The study case situations will be presented below.

The lithological components areal distribution during the low-water period investigation

During the low-water period (September 2024), several lakes in the southern part of the Rusca-Gorgova-Uzlina depression were investigated. Accordingly, lakes such as *Uzlina, Isacova, Durnoliatca, Bleziuc-Pojarnia* and *Pojarnia* (Figure 1) illustrated different patterns of the main lithological components' horizontal distribution. The results are shown in Table 1.

Total organic matter fraction (TOM %). The organic matter of lake sediments is subjected to various sources. Generally, allochthonous sources (terrestrial material) may enter the lake's receiving basin along with plant fragments, eroded sediments, wastewaters, sewages, organic contaminants, and long-range transport associated with the potentially contaminated water of the Danube River. Autochthonous sources are mainly attributed to the primary production of lakes, such as algae, macrophytes, zooplankton, and a mixture of decomposed vegetal and animal organisms. An overall assessment of the investigated sediment samples indicated that the TOM (%) content fractions dominate in most samples, presenting values included in a wide range of variations ($34.31\% < TOM \leq 90.24\%$), of the total weight of the dry residue (Table 1). This distribution trend is evident in most of the lakes investigated. However, the highest values were found in very small, shallow lakes such as *Durnoliatca* (90.24% TOM), *Bleziuc-Pojarnia* (87.66% TOM) and *Pojarnia* (87.65% TOM). These lakes have plenty of underwater vegetation, are characterized by slower hydrodynamic conditions and are less disturbed by the bottom water currents. Regarding the *Uzlina* and *Isacova*, it was noticed that the inlet/outlet parts of the investigated lakes are characterized by relatively decreased TOM % values in the sediments compared to other sectors of the lakes (Figure 2).

Table 1. Results expressed as the percentage concentration (%) of the main lithological components

Location	Tested samples	TOM (%)			CAR (%)			SIL (%)		
		Min.	Max.	Ave-rage	Min.	Max.	Ave-rage	Min.	Max.	Ave-rage
Uzlina	(n=15)	49.40	72.57	65.02	6.51	20.05	12.10	14.53	44.09	22.89
Isacova	(n=16)	34.31	78.37	69.57	1.35	18.16	12.23	8.37	56.00	18.19
Durnoliatca	(n=8)	80.20	90.24	84.66	2.25	11.28	7.06	5.60	11.80	8.29
Bleziuc-Pojarnia	(n=9)	77.94	87.66	83.28	2.99	11.30	6.42	5.91	15.60	10.30
Pojarnia	(n=9)	80.13	87.65	84.02	2.96	12.96	8.69	5.83	10.38	7.29

Total carbonates fraction (CAR %). The presence of carbonates in aquatic environments could be both biogenic (*e.g.,* tests of benthic and pelagic organisms, skeletal parts, shells, and shell debris) and inorganic (*e.g.,* calcite, aragonite) in origin.
The contents of the carbonate fractions identified in the set of tested samples showed a notable surface area variation along the investigated lakes (Table 1). Generally, the range of variation for the CAR % content was relatively lower ($2.25\% < CAR \leq 12.96\%$) in lakes such as *Durnoliatca*, *Bleziuc-Pojarnia* and *Pojarnia*. The other investigated lakes revealed relatively higher ranges of variations, *i.e., Uzlina* ($6.51\% < CAR \leq 20.05\%$) and *Isacova* ($1.35\% < CAR \leq 18.16\%$). The maximum values of the CAR% contents encountered in certain sediment samples (Figure 2) are about to the extent of local or short-range differences in data points, due to the incorporation of shells and shell debris abundance within the sediment matrices.

Siliciclastic fraction (SIL %). The content of siliciclastic fractions in the bottom sediments may be owed to upstream allochthonous fluvial

sediment supply (*e.g.,* siliciclastic material, like quartz-rich sand, gravel, and silt, from the surrounding weathered rock, soils, and other materials) or autochthonous sediment supply (*e.g.,* siliciclastic materials such as sand, silt, and clay that are generated or derived locally, within the lake's drainage basin or directly from the surrounding environment by weathering of lake shoreline materials, river inputs from nearby watersheds, suspension and settlement of fine silts and clay, erosion). Broadly, the investigated lakes illustrated lower contents of the siliciclastic fractions (SIL %) (Table 1). The smallest ranges of variation were found in lakes such as *Durnoliatca* (5.60% < SIL ≤ 11.80%), *Bleziuc-Pojarnia* (5.91% < SIL ≤ 15.60%) and *Pojarnia* (5.83% < SIL ≤ 10.38%). Next, *Uzlina* (14.53% < SIL ≤ 44.09%) and *Isacova* (8.37% < SIL ≤ 56%) exposed relatively higher ranges of SIL% variations, especially near the inlets/outlets or connecting channels between the lakes (Figure 2). Generally, a significant inverse correlation was found between the SIL% and TOM% variables.

Conclusively, according to the organic matter (TOM%) and the siliciclastic (SIL%) fraction (calculated from the total dry sediment weight), the following types of mixed sediments were differentiated in the investigated sediment samples from *Uzlina, Isacova, Durnoliatca, Bleziuc-Pojarnia* and *Pojarnia* (Figure 3):

- *the organic-rich sediments*, subsequently followed by the *silica-rich sediments*;
- *organic-rich sediments* (> 15-30% TOM). From the total number of 57 analyzed samples, 12 samples are included in the range of variations with values between 30 and 70% TOM, and the rest of the 45 samples had increased values, more than 70% TOM;
- *silica-rich sediments* (> 15-30% SIL). From the total number of 57 analyzed samples, 52 samples are included in the range of variations with values between 0 and 30% SIL, and the rest of the 5 samples had increased values, between 30 and 70% SIL.

Subsequently, based on the total carbonate content (CAR%) the following types were spotted:

- *non-carbonated sediment* (CAR ≤ 10%). In this regard, from the total number of 57 analyzed sediment samples, 34 samples had lower values of ≤ 10%;
- *slightly carbonated sediments* (10% < CAR ≤ 30%). From this perspective, from the total number of 57 analyzed sediment samples, 23 samples had values included in the 10% < CAR ≤ 30% range interval.

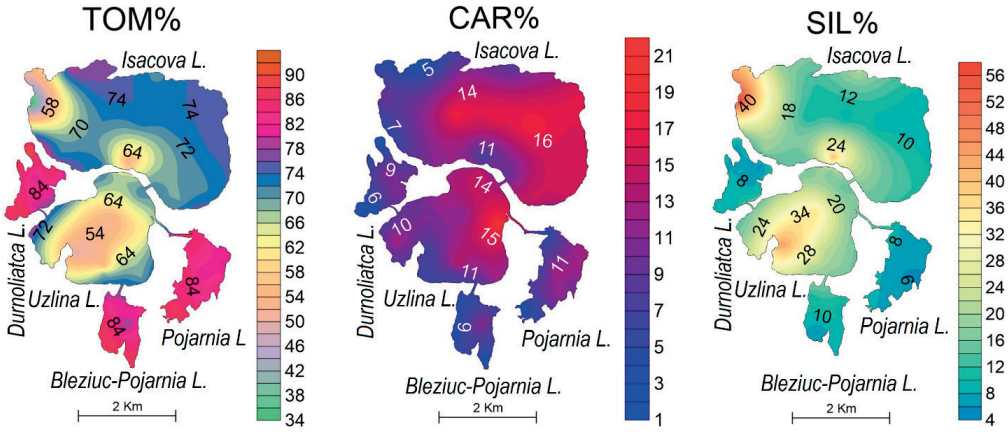


Figure 2. Spatial distribution of TOM, CAR and SIL (%) fractions according to their spatial distribution in the lake sediments of *Uzlina, Isacova, Durnoliatca, Bleziuc-Pojarnia* and *Pojarnia*

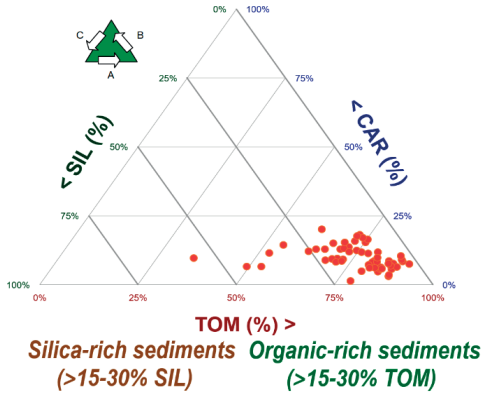


Figure 3. Ternary diagrams showing the percentage distribution (%) of the lithological parameters in the lake sediments of *Uzlina, Isacova, Durnoliatca, Bleziuc-Pojarnia* and *Pojarnia*

The lithological components areal distribution during the high-water period investigation

Within the high-water period (October 2024), several lakes in the northern part of the Rusca-Gorgova-Uzlina depression were surveyed. Therefore, lakes such as *Cuzmințul Mare, Cuzmințul Lat, Rotund, Rădăcinos, Gorgova, Gorgovăț* and *Potcoava de Sud* (Figure 1) displayed different patterns of the main lithological components' horizontal distribution. The results are shown in Table 2.

Total organic matter fraction (TOM %). Generally, the sediment samples taken from *Cuzmințul Mare, Cuzmințul Lat, Rotund, Rădăcinos, Gorgova, Gorgovăț* and *Potcoava de Sud* are characterized by a relatively higher organic matter content (TOM %), with values included in a wide range of variations (28.18% < TOM ≤ 89.99%), of the total weight of the dry residue (Table 2). The highest values of TOM% were found in the superficial sediments of the shallow plant-dominated lakes as *Cuzmințul Mare* (89.23% TOM), *Cuzmințul Lat* (85.03% TOM), *Rădăcinos* (89.99% TOM) and *Gorgovăț* (71.11% TOM), but also in certain sectors of the lakes like *Rotund* (85.80% TOM), *Gorgova* (81.93% TOM) and *Potcoava de Sud* (87.90% TOM) (Figure 4). In shallow plant-dominated lakes, the organic matter content is typically higher than larger, deeper lakes due to a combination of factors such as higher biological productivity, better light penetration, greater interaction with surrounding land, and specific physical characteristics that favor organic matter accumulation.

Table 2. Results expressed as the percentage concentration (%) of the main lithological components

Location	Tested samples	TOM (%)			CAR (%)			SIL (%)		
		Min.	Max.	Ave-rage	Min.	Max.	Ave-rage	Min.	Max.	Ave-rage
Cuzmințul Mare	(n=7)	76.50	89.23	84.43	1.46	9.11	4.25	7.61	19.32	11.32
Cuzmințul Lat	(n=3)	71.81	85.03	77.82	4.36	11.61	6.78	10.61	23.80	15.40
Rotund	(n=7)	35.30	85.80	63.02	2.22	14.79	8.69	11.97	56.03	28.29
Rădăcinos	(n=3)	81.76	89.99	84.76	0.89	8.61	5.84	9.12	9.63	9.41
Gorgova	(n=16)	30.89	81.93	62.23	5.60	34.78	12.29	10.48	56.33	25.48
Gorgovăț	(n=4)	52.34	71.11	63.55	6.77	17.42	11.33	19.13	40.90	25.12
Potcoava de Sud	(n=4)	28.18	87.90	70.02	2.26	12.57	7.28	9.05	59.26	22.70

Total carbonates fraction (CAR %). In general, the contents of the carbonate fractions spotted in the investigated sediment samples did not show a significant surface area variation along the investigated lakes (Table 2), excepting some sectors of the *Gorgova* and *Gorgovăț* lakes. The range of variation for the CAR% content was relatively lower (0.89% < CAR ≤ 14.79%) in lakes such as *Cuzmințul Mare* (1.46% < CAR ≤ 9.11%), *Cuzmințul Lat* (4.36% < CAR ≤ 11.61%), *Rotund* (2.22% < CAR ≤ 14.79%), *Rădăcinos* (0.89% < CAR ≤ 8.61%) and *Potcoava de Sud* (2.26% < CAR ≤ 12.57%). The other investigated lakes revealed relatively higher ranges of variations, *i.e., Gorgova* (5.60% < CAR ≤ 34.78%) and *Gorgovăț* (6.77% < CAR ≤ 17.42%) (Figure 4). The maximum values of the CAR % contents identified in some samples are owed to shells and shell debris abundance within the sediment matrices. The provenance of the carbonate content in delta lake sediments comes from a combination of biogenic processes (such as the precipitation of calcium carbonate by aquatic organisms),

detrital input (weathering of carbonate rocks in the catchment area), chemical precipitation (from lake water under certain conditions). Each of these sources contributes to the overall carbonate content found in the sediment of delta lakes.

Siliciclastic fraction (SIL %). Mostly, the investigated lakes displayed lower contents of the siliciclastic fractions (SIL %) (Table 2). The smallest ranges of variation were found in lakes such as *Cuzminţul Mare* (7.61% < SIL ≤ 19.32%), *Cuzminţul Lat* (10.61% < SIL ≤ 23.80%) and *Rădăcinos* (9.12% < SIL ≤ 9.63%). Further, lakes as *Rotund* (11.97% < SIL ≤ 56.03%), *Gorgova* (10.48% < SIL ≤ 56.33%), *Gorgovăţ* (19.13% < SIL ≤ 40.90%), and *Potcoava de Sud* (9.05% < SIL ≤ 59.26%) disclosed relatively higher ranges of SIL % variations, especially near the mouth of the connection canals with lakes (Figure 4).

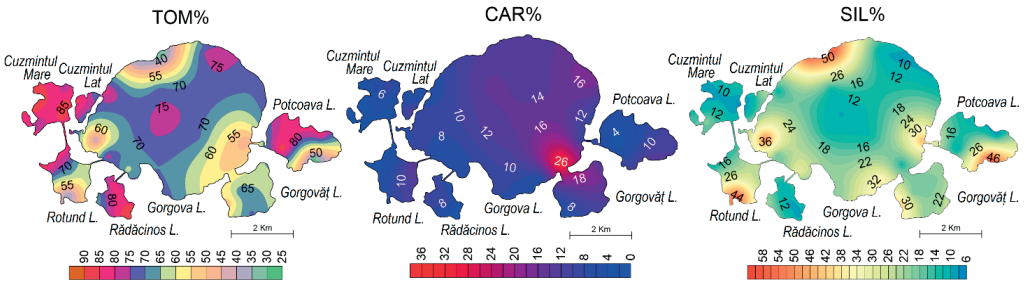


Figure 4. Spatial distribution of TOM, CAR and SIL (%) fractions according to their spatial distribution in the lake sediments of *Cuzminţul Mare, Cuzminţul Lat, Rotund, Rădăcinos, Gorgova, Gorgovăţ* and *Potcoava de Sud*

Near the mouth of the connection canals with delta lakes, there is more siliciclastic fraction content because of the higher energy environment, which allows for the deposition of coarser materials, such as sand and gravel. In contrast, inside the lakes, where water flow is slower, the energy is lower, the finer sediments (such as clay and silt) dominate the sediment composition. The hydrodynamic conditions of the currents near the canal mouth and slower currents inside the lake, largely, determine the grain size distribution and sediment composition in these areas.

Based on the organic matter (TOM %) and the siliciclastic (SIL %) fraction (calculated from the total dry sediment weight), the following types of mixed sediments were differentiated in the investigated sediment samples from *Cuzminţul Mare, Cuzminţul Lat, Rotund, Rădăcinos, Gorgova, Gorgovăţ* and *Potcoava de Sud* (Figure 5):

- *the organic-rich sediments*, subsequently followed by the *silica-rich sediments*;
- *organic-rich sediments* (> 15-30% TOM). From the total number of 45 analyzed samples, 2 samples had values less than 30% TOM, 15 samples were included in the range of variations with values between 30 and 70% TOM, and the rest of the 28 samples had increased values, more than 70% TOM.
- *silica-rich sediments* (> 15-30% SIL). From the total number of 45 analyzed samples, 34 samples are included in the range of variations with values between 0 and 30% SIL, 10 samples had increased values between 30 and 70% SIL, and 1 sample had values more than 70% SIL.

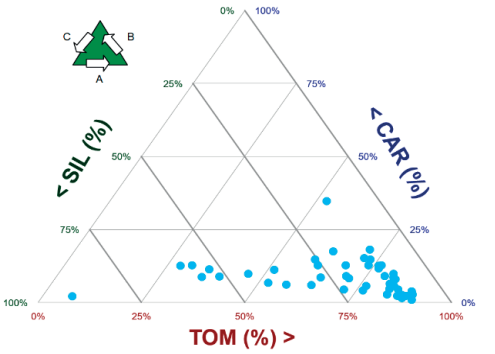


Figure 5. Ternary diagrams showing the percentage distribution (%) of the lithological parameters in the lake sediments of *Cuzminţul Mare, Cuzminţul Lat, Rotund, Rădăcinos, Gorgova, Gorgovăţ* and *Potcoava de Sud*

Subsequently, based on the total carbonate content (CAR %) the following types were spotted:
- *non-carbonated sediment* (CAR ≤ 10%). Accordingly, from the total number of 45 analyzed sediment samples, 29 samples had lower values ≤ 10%;
- *slightly carbonated sediments* (10% < CAR ≤ 30%). Considering this, from the total number of 45 analyzed sediment samples, 15 samples had values included in the 10% < CAR ≤ 30% range interval;
- *carbonated sediments* (30% < $CaCO_3$ ≤ 50%). Consequently, from the total number of 45 analyzed sediment samples, 1 sample had values included in the 30% < CAR ≤ 50% range interval.

CONCLUSIONS

The present study was performed in a transitional depositional environment in several lacustrine ecosystems, belonging to the Danube Delta, Romania. No significant seasonal variation (September vs. October 2024) was observed in the distribution of lithological components. Generally, the investigated lakes showed favorable conditions for accumulating the organic matter-rich sediments due to the inputs of autochthonous organic matter derived mainly from the underwater herbaceous plants and local specific arboreal vegetation. The accumulation of autochthonous organic matter in these shallow plant-dominated lakes may facilitate detrimental long-term challenges both in the size distribution of lakes and in the vertical sediment profiles, promoting shifts in shallow lake water levels, and ultimately causing the installation of the clogging phenomenon. The results obtained within this study are conducive to a better understanding of the total organic matter content and its horizontal distribution in deltaic aquatic environments, especially shallow-plant-dominated lakes, that are prevalent in the Danube Delta region. While these changes are part of the natural evolution of aquatic environments, long-term monitoring is essential to manage the impact of aquatic vegetation clogging in delta lakes. The ecological consequences of these physical changes considerably differ in function of the lake location, the lake depth and size, mixing regime and trophic status.

ACKNOWLEDGEMENTS

This research work was carried out through the support of the Romanian Ministry of Research, Innovation and Digitalization of the Research Core Program, within the National Plan for Research, Development and Innovation 2022-2026, implemented with the support of MCID, Project - PN 23 30 03 02, PN 23 30 03 04 and PN 23 30 01 03.

REFERENCES

ASTM-D2216 (2010). *Standard test method for laboratory determination of water (moisture) content of soil and rock by mass*, Standard D2216-10, ASTM International, West Conshohocken, PA.

Bengtsson, L., Enell, M. (1986). *Chemical analysis*. In B.E. Berglund (Ed): Handbook of Holocene Palaeoecology and Palaeohydrology, Wiley, Chichester, 423-445.

Constantinescu, A., M., Tyler, A., N., Stanica, A., Spyrakos, E., Hunter, P., D., Catianis, I., Panin, N. (2023) A century of human interventions on sediment flux variations in the Danube-Black Sea transition zone. *Front. Mar. Sci*. 10:1068065. doi: 10.3389/fmars.2023.1068065

Dean, W. E., Jr. (1974). Determination of carbonate and organic matter in calcareous sediments and sedimentary rocks by loss on ignition: Comparison with other methods, *J. Sediment. Petrol*., *44*(1), 242-248.

Digerfeldt, G., Olsson, S., Sandgren, P. (2000). Reconstruction of lake-level changes in Lake Xinias, central Greece, during the last 40 000 years, *Palaeogeography, Palaeoclimatology, Palaeoecology*, *158*, 65-82.

Duţu, F., Duţu, L., T., Catianis, I., Ispas, B.-A. (2022). Sediment dynamics and hydrodynamical processes in the Danube delta (Romania): A response to hydrotechnical works. *Z. für Geomorphologie, 64,* 365–378. doi: 10.1127/zfg/2021/0707

Emelyanov, E.M., Shimkus, K.M. (1986). *Geochemistry and Sedimentology of the Mediterranean Sea*, D. Reidel Publishing Company, Dordrecht, Holland, 567 pp.

Gâștescu, P., Ştiucă, R. (2008). *The Danube Delta - A Biosphere Reserve*. CD Press Publishing House, Bucharest [in Romanian, with Contents and Introduction in English], 400 pp.

Golden Software, SURFER Version 10, 2010. Reference Manual, Golden Software, Inc., Golden, Colorado, U.S.A.

Ho, L. T., Goethals, P. L. M. (2019). Opportunities and Challenges for the Sustainability of Lakes and Reservoirs in Relation to the Sustainable Development

Goals (SDGs). *Water*, *11*(7), 1462. https://doi.org/10.3390/w11071462

Hou, W., Liang, S., Sun, Z., Ma, Q., Hu, X., Zhang, R. (2024). Depositional dynamics and vegetation succession in self-organizing processes of deltaic marshes. *Sci Total Environ., 912*, 169402. DOI: 10.1016/j.scitotenv.2023.169402. PMID: 38114033.

Laignel, B., Vignudelli, S., Almar, R., Becker, M., Bentamy, A., Benveniste, J., Birol, F., Frappart, F., Idier, D., Salameh, E., Passaro, M., Menende, M., Simard, M., Turki, E.I., Verpoorter C. (2023). Observation of the Coastal Areas, Estuaries and Deltas from Space. *Surv Geophys, 44,* 1309–1356, https://doi.org/10.1007/s10712-022-09757-6

Năstase, A., Honț, Ș., Iani, M., Paraschiv, M., Cernișencu, I., Năvodaru, I. (2022). Ecological status of fish fauna from Razim Lake and the adjacent area, the Danube Delta Biosphere Reserve, Romania. *Acta Ichthyologica et Piscatoria*, *52*(1), 43–52. https://doi.org/10.3897/aiep.52.79646

Oteman, B., Scrieciu, A., Bouma, T. J., Stanica, A., Van der Wal, D. (2021). Indicators of Expansion and Retreat of Phragmites Based on Optical and Radar Satellite Remote Sensing: A Case Study on the Danube Delta. *Wetlands*, *41*(6), 1-15, https://doi.org/10.1007/s13157-021-01466-x

Panin, N., Jipa, D. (2002). Danube River sediment input and its interaction with the north-western black Sea. *Estuarine Coast. Shelf Sci. 54*, 551–562, doi: 10.1006/ecss.2000.0664

Panin, N., Tiron Duțu, L., Duțu, F. (2016). The Danube Delta: An overview of its Holocene evolution. *Méditerranée*, *126*, 37-54.

Perrin, J. (1974). Classification des sols organiques, *Bulletin De Liaison Des Laboratoires Des Ponts Et Chaussées* [in French], 36-47.

Ricken, W. (1993). *Sedimentation as a Three-Component System. Organic Carbon, Carbonate, Noncarbonate*, Lecture Notes in Earth Sciences Series, XII, Berlin, Heidelberg, New York, London, Paris, Tokyo, Hong Kong: Springer-Verlag, 51, 211 pp.

Schneider, S.C., Coetzee, J.A., Galvanese, E.F., Harpenslager, S.F., Hilt, S., Immerzeel, B., Köhler, J., Misteli, B., Motitsoe, S.N., Padial, A.A., Petruzzella, A., Schechner, A., Thiebaut, G., Thiemer, K., Vermaat, J. E. (2024). Causes of macrophyte mass development and management recommendations. *Sci. Total Environ.*, *931*, 172960.

Smith, K.A. & Mullins, C.E. (2000). *Soil and Environmental Analysis: Physical Methods.* Revised and Expanded, New York, NY, USA: Marcel Dekker, Inc. Soil Survey Division Staff (1993). Soil Survey Manual. Washington, DC, USA: United States Department of Agriculture, 651 pp.

Sun, Y., Wu, G., Mao, M., Duan, X., Hu, J., Zhang, Y., Xie, Y., Qiu, X., Gong, W., Liu, T., and Liu Tiedong. (2023). Remote sensing and environmental assessment of wetland ecological degradation in the Small Sanjiang Plain, Northeast China. *Front. Ecol. Evol.*, *11*, 1125775.

Tammeorg, O., Chorus, I., Spears, B., Nõges, P., Nürnberg, G. K., Tammeorg, P., Søndergaard, M., Jeppesen, E., Paerl, H., Huser, B., Horppila, J., Jilbert, T., Budzyńska, A., Dondajewska-Pielka, R., Gołdyn, R., Haasler, S., Hellsten, S., Härkönen, L. H., Kiani, M., Kotamäki, A.K., Kowalczewska-Madura, K., Newell, S., Nurminen, L., Nõges, T., Reitzel, K., Rosińska, J., Ruuhijärvi, J., Silvonen, S., Skov, C., Važić, T., Ventelä, A.M., Waajen,G., Lürling, M. (2024). Sustainable lake restoration: From challenges to solutions. *Wiley Interdisciplinary Reviews: Water*, *11*(2), https://doi.org/10.1002/wat2.1689

Tan, L., Ge, Z., Zhou, X., Li, S., Li, X., Tang, J. (2020). Conversion of coastal wetlands, riparian wetlands, and peatlands increases greenhouse gas emissions: A global metaanalysis. *Global change biology*, *26*(3), 1638-1653.

Tate, R.L. (1987). *Soil organic matter. Biological and Ecological Effects*. John Wiley and Sons, New York, 291 pp.

Tiron Duțu, L., Panin, N., Duțu, F., Popa, A., Iordache, G., Pojar, I., Catianis, I. (2022). *The Danube Delta environment changes generated by human activities*. In: Negm, A.M., Diaconu, D.C. (eds) The Danube River Delta. Earth and Environmental Sciences Library. Springer, Cham., 403 pp., https://doi.org/10.1007/978-3-031-03983-6_1

Van der Veer, G. (2006). *Geochemical soil survey of The Netherlands. Atlas of major and trace elements in topsoil and parent material; Assessment of natural and anthropogenic enrichment factors*, Ph.D thesis, Utrecht University, the Netherlands/Netherlands Geographical Studies, *347*, 1-245.

Verpoorter, C., Kutser T., Seekell, D. A., Tranvik L. J. (2014). A global inventory of lakes based on high-resolution satellite imagery, *Geophys. Res. Lett., 41*, 6396-6402, doi:10.1002/2014GL060641.

Walton, R. E., Moorhouse, H. L., Roberts, L. R., Salgado, J., Ladd, C. J., Do, N. T., Panizzo, V. N., Van, P. D. T., Downes, N. K., Trinh, D. A., McGowan, S., Taylor, S., Henderson, A. C. (2024). Using lake sediments to assess the long-term impacts of anthropogenic activity in tropical river deltas. *The Anthropocene Review*, *11*(2), 442-462.

Wang, Z., Zeng, L., Wang H., Long X., Jia P., Chen X. (2024). Different effects of natural siltation, damming and pollution on two adjacent lakes of Dongting Lake Wetland: Evidence from paleolimnology. *Journal of Hydrology*, *638*, 131499.

Wang, H., Wang, Z., Wang, Y., Tang, H., Zhang, X., Luo, X., Mai, Y., Huang, X., Zheng, Y., Yin, P., Lai, Z. (2024). Preliminary study on the depositional model in the wave-dominated delta evolution during the Anthropocene: a case study of the Hanjiang River Delta in China[J]. *Acta Oceanologica Sinica*, *43*(11), 45-56.

Zhang, X., Fang, C., Wang, Y., Lou, X., Su, Y., Huang D. (2022). Review of effects of dam construction on the ecosystems of river estuary and nearby marine areas. *Sustainability, 14*(10), 5974, doi: 10.3390/su14105974

www.geog.cam.ac.uk

www.google.com/maps

Scientific Papers. Series E. Land Reclamation, Earth Observation & Surveying, Environmental Engineering. Vol. XIV, 2025
Print ISSN 2285-6064, CD-ROM ISSN 2285-6072, Online ISSN 2393-5138, ISSN-L 2285-6064

ADAPTING ROMANIA'S IRRIGATION INFRASTRUCTURE TO CLIMATE CHANGE: OPPORTUNITIES AND CHALLENGES

Mihai Teopent CORCHEȘ

"1 Decembrie 1918" University of Alba Iulia, 5 Gabriel Bethlen Street, 510009, Alba Iulia, Romania

Corresponding author email: mihai.corches@uab.ro

Abstract

In the context of climate change, where Romania faces increasingly frequent droughts, significantly impacting water availability in several regions, the issue of efficient water resource management is becoming more pressing. The phenomenon of drought is having a growing impact on agriculture, necessitating the development of new irrigation systems and the modernization of existing ones, which may need to be more efficient in water use, such as drip irrigation, subsurface irrigation, or sprinkler irrigation, which can also be equipped with smart irrigation technologies (soil moisture sensors, automatic control, remote monitoring and management, aerial surveillance of agricultural crops, etc.). This study analyzes the opportunities for adapting irrigation infrastructure in the current context, focusing on the possibility of implementing best practices and modern technologies used worldwide in Romania. It also critically examines the challenges Romania faces in the development of irrigation systems, as well as the solutions adopted by other countries to overcome these challenges.

Key words*: climate change, irrigation, water management.*

INTRODUCTION

Climate change represents one of the most complex and pressing challenges of the 21st century, having a profound impact on the dynamics of extreme meteorological phenomena. The increasing frequency and intensity of floods, because of climate change, put pressure on existing infrastructure and risk management capacity (IPCC, 2021). Global climate changes and the intensification of climate risk events, such as changes in precipitation patterns and intensity, combined with modifications in land use practices and improper management of agricultural lands, have a significant impact on soil (Sestras et al, 2023). This reality necessitates not only the modernization and expansion of irrigation systems but also their integration into a unified water management strategy, including effective flood prevention measures. Such a holistic approach is essential for reducing risks associated with extreme climatic events and minimizing damages caused by sudden variations in the hydrological regime. In this regard, a fundamental shift in planning and implementing adaptation strategies is necessary so that irrigation infrastructure and flood prevention works are designed in correlation with future climate risks, based on scenario analyses and advanced predictive models. At present, there are a number of climate models, some of which are global, such as CMIP6 (Coupled Model Intercomparison Project, Phase Six) and HadGEM3 (Hadley Centre Global Environment Model version 3), which are used to simulate long-term climate change. There are also regional climate models, such as REMO (The Regional Climate Model REMO) developed at the Max Planck Institute for Meteorology, currently managed and further developed by the Climate Service Center Germany (GERICS) in Hamburg, Germany; the CNRM-ALADIN model (Aire Limitée Adaptation dynamique Développement InterNational), developed at the National Centre for Meteorological Research in France; or the COSMO-CLM model (Consortium for Small-scale Modeling – Climate Limited-area Model), managed by the European Consortium COSMO. At the European Union level, data can be accessed through the European Climate Adaptation Platform Climate-ADAPT, which was created through a partnership between the European Commission and the European Environment Agency (EEA), with the aim of

supporting Europe's adaptation to climate change.

In this context, adapting irrigation infrastructure to new climatic realities becomes an urgent necessity. This involves not only modernizing existing systems but also adopting innovative strategies that consider uncertainties and future risks (Jongman et al., 2012). Thus, the modernization of irrigation infrastructure in Romania represents not only a complex challenge but also a significant opportunity to strengthen the resilience of the agricultural sector to climate change. The implementation of appropriate policies and the efficient use of available financial resources are essential for establishing a sustainable irrigation system that meets both current and future agricultural needs. In light of intensifying climate change, reducing the national water footprint has become imperative for all countries, including Romania (Sandu & Vîrsta, 2021).

MATERIALS AND METHODS

This study analyzes the current state of irrigation infrastructure in Romania, highlighting both the main deficiencies and limitations, as well as the existing opportunities for attracting investments and developing sustainable solutions. In this regard, aspects related to available funding sources are addressed, both at the national level through government funds and at the European level through support mechanisms offered by the European Union, such as the National Strategic Plan 2023-2027, which was approved by the European Commission through Commission Implementing Decision C(2022) 8783 of December 7, 2022, under which Romanian farmers can benefit from up to €15.83 billion to improve outcomes and enhance the performance of Romanian agriculture. Additionally, major challenges that may arise in the implementation process of irrigation projects, such as soil and biodiversity impact, are identified.

The study is based on an analysis of recent research in the specialized literature that highlights these aspects. Furthermore, certain considerations such as the energy efficiency of pumping systems, the use of modern irrigation technologies to reduce water losses, and the necessity of an integrated water resource management approach are also discussed.

For the creation of maps, the open-source software QGIS was used, along with publicly available vector datasets from the website https://geo-spatial.org/vechi/download/romania-seturi-vectoriale.

RESULTS AND DISCUSSIONS

Water Resources of Romania

According to data presented by the National Institute of Statistics (INS, 2025), Romania possesses considerable water resources; however, their distribution shows significant regional variability. As shown in the figure below, Romania's water resources are unevenly distributed across the country, being more abundant in the northern half, while the southern regions face a significantly lower level of water availability. This variation directly affects irrigation needs, as the southern areas - being more water-scarce - require more extensive and efficient irrigation systems to support agricultural activities and cope with frequent drought conditions. Moreover, the southern part of Romania is characterized by larger expanses of arable land compared to the north, making it a key agricultural zone. This combination of extensive farmland and limited water resources further intensifies the pressure on irrigation infrastructure, highlighting the need for targeted investments and climate-resilient water management strategies in the region.

In 2023, the total volume of available water resources, based on the level of infrastructure development, was estimated at 50,150 million m³/year. The volume of water for each hydrographic basin, according to the source, was graphically represented in Figure 1.

Surface waters contributed approximately 37,644 million m³/year, while groundwater sources provided 12,506 million m³/year. The distribution analysis reveals that the southern and eastern regions are more vulnerable to drought, primarily due to low precipitation levels and high water demand for irrigation and industry.

These regional discrepancies highlight the necessity of implementing efficient water resource management strategies, including optimizing storage and distribution infrastructure and promoting sustainable water use practices in key economic sectors.

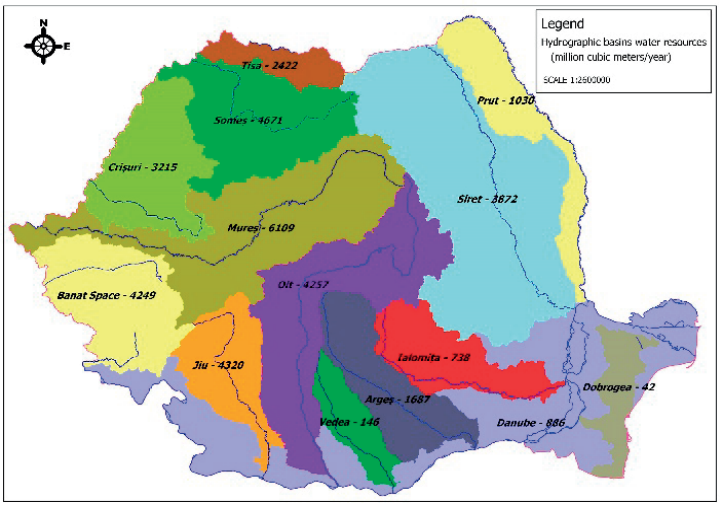


Figure 1. Water resources ensured, according to the development level, in 2023 (original)

Irrigation Network in Romania

The irrigation network in Romania is a complex system, primarily developed during the communist period (1960-1989) to support agriculture by ensuring water availability for crops during drought periods. This infrastructure was built in key agricultural areas of the country, such as the Romanian Plain, the Banat Plain, the Crișuri Plain, and other regions in southern and eastern Romania. Currently, the irrigation network is undergoing rehabilitation and modernization, with support from European funds, to address climate challenges and increase agricultural productivity. During the communist period, Romania invested heavily in irrigation infrastructure, constructing a network covering over 3 million hectares. These systems included canals, pipelines, pumping stations, reservoirs, and dams, designed to capture, store, and distribute water from natural sources such as rivers and lakes. The primary goal was to ensure food self-sufficiency and support intensive agriculture. After the 1989 Revolution, many of these systems were neglected or abandoned due to a lack of funding and changing economic priorities. Currently, the area prepared for irrigation is approximately 1,606,847.97 hectares, according to data published on the ANIF website. Of these, the contracted irrigation area is 1,047,301.55 hectares, and the filled irrigation canals total 2,827.33 km, serving an area of 827,404.19 hectares (ANIF, 2024).

According to ANIF data, the total area designated for irrigation in Romania is 2,989,390 hectares, and the primary irrigation infrastructure includes (ANIF, 2024):

- 10,422 km of adduction and distribution canals;
- 24,547 km of buried pipeline networks;
- 2,568 pumping stations, both floating and fixed.

Adapting irrigation infrastructure to climate change

Adapting irrigation infrastructure to climate change is a complex process requiring significant investments, strategic planning, and cooperation at all levels. This adaptation is essential for ensuring agricultural sustainability and food security. To achieve this objective, the following steps are necessary:

1. ***Assessing vulnerability and climate risks***

The first step in ensuring the resilience of irrigation infrastructure in the face of climate change is assessing the vulnerability of existing systems. This involves conducting detailed studies to identify agricultural areas most exposed to extreme climatic events, such as droughts or floods. Current climate models indicate that many regions will experience more intense and frequent precipitation, which may exceed the design capacity of existing infrastructure (Kundzewicz et al., 2014). Vulnerability assessment allows for the

prioritization of investments and adaptation measures. It is necessary to develop detailed climate forecasts for all regions of the country to support decision-making.

2. ***Modernization and optimization of existing infrastructure**:*

A crucial first step is conducting a detailed inventory of the existing infrastructure using GIS spatial analysis to determine the condition and design capacity of the systems. The use of advanced satellite imagery is essential for monitoring climate change and managing water resources, minimizing uncertainty, and helping to establish optimal mitigation measures (Burghila D., et al 2015). Understanding this information enables the proper design of irrigation works, considering the agricultural areas that require irrigation and the available water resources. Additionally, a quantitative assessment of losses in existing systems is essential to establish a plan for their reduction.

The design of rehabilitation and expansion works for irrigation systems should be based on studies and hydrological simulations to estimate the climate impact on water sources. Rehabilitation should include measures to optimize water consumption, such as:

- using buried pipes or covered channels to reduce evaporation losses;
- implementing drip irrigation;
- utilizing IoT sensors and artificial intelligence to monitor water flow, soil moisture, and optimize water consumption.

3. ***Diversification of water sources for irrigation**:*

Climate change and the increasing frequency of drought periods require the diversification of water sources for irrigation to enhance agricultural resilience.

Currently, irrigation in Romania relies primarily on water from rivers and reservoirs but exploring efficient and sustainable alternatives is necessary. Exploring and utilizing alternative water sources, such as constructing rainwater collection basins or reusing treated wastewater, can reduce dependence on traditional sources and ensure a stable water supply for irrigation. However, these water collection systems are suitable mainly for small land areas and using wastewater for irrigation - although beneficial for recycling nutrients and improving soil fertility - requires modern treatment plants, advanced purification technologies, and continuous water quality monitoring to prevent potential health risks if not treated properly.

4. ***Implementation of sustainable agricultural practices**:*

Sustainable agricultural practices play a crucial role in conserving water resources, ensuring the long-term viability of agriculture, and protecting the environment. Implementing efficient water management methods not only improves productivity but also reduces negative impacts on aquatic ecosystems. Promoting soil water conservation techniques, such as conservation agriculture - which focuses on minimizing soil disturbance and mulching (Bojariu et al., 2021) and crop rotation can reduce irrigation needs and enhance crop resilience to variable climate conditions.

5. ***Strengthening institutional capacity and legislative framework**:*

Better cooperation between central authorities, local authorities, farmers, and other water users is necessary to efficiently manage available water resources and ensure a more coherent and effective approach. The development of centralized irrigation infrastructure reduces the burden on farmers to secure their own irrigation water resources and can lead to more efficient water use and conservation.

Developing policies and regulations that support climate change adaptation, including financial incentives for farmers adopting sustainable practices and efficient irrigation technologies, is essential. Promoting financing programs or subsidies for the implementation of efficient irrigation systems could encourage farmers to adopt solutions that reduce water consumption.

Adapting these steps to the specific context of each region can lead to a more resilient and efficient irrigation infrastructure, capable of addressing the challenges posed by climate change. Educating farmers and engaging local communities are essential for the success of adaptation measures. Farmers must be aware of the risks posed by climate change and be prepared to take preventive measures.

Opportunities for the rehabilitation and construction of irrigation infrastructure in Romania

Funding for irrigation infrastructure is crucial for modernizing and expanding existing systems, particularly in the context of climate change and the need to support sustainable agriculture.

Available funding sources for irrigation projects include the National Strategic Plan 2023-2027, which allocated €400 million for the 2024 funding session under the DR-25 intervention: "Modernization of Irrigation Infrastructure". The public support was 100% non-reimbursable for eligible costs. This plan also includes an additional €1.5 billion for modernizing the primary irrigation infrastructure, managed by the National Agency for Land Improvements.

Challenges in the rehabilitation and construction of irrigation infrastructure in Romania

Developing irrigation infrastructure can impact biodiversity, bringing both benefits and risks to ecosystems. The Natura 2000 network in Romania (Figure 2), covering approximately 23% of the country's territory, is an extensive system of protected areas aimed at conserving biodiversity and protecting natural habitats, as well as significant flora and fauna species at the European level.

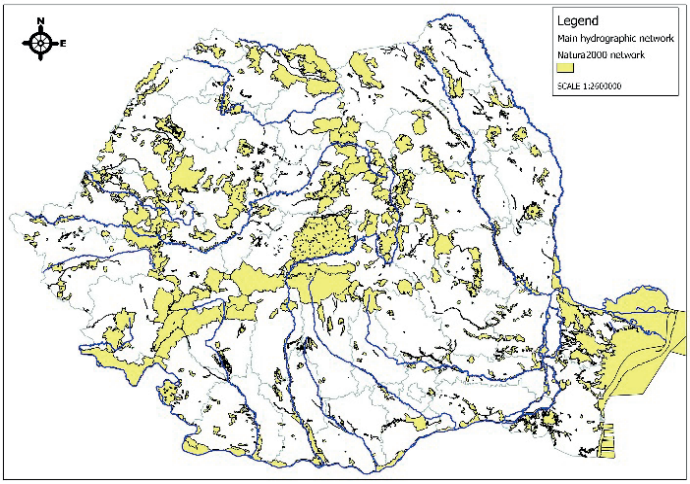


Figure 2. The Natura 2000 network in Romania (original)

Some areas, such as the Danube Delta, are globally recognized for their biodiversity and are also included in other protection programs, such as the Ramsar Convention (on wetlands).

To ensure effective conservation, conservation objectives have been established for all sites, and for some of them, management plans have been developed, outlining conservation measures for the habitats and species present in these sites.

A significant portion of these sites, designated for the protection of aquatic and water-dependent habitats and species, overlaps with watercourses and other wetlands. Therefore, the implementation of irrigation projects should consider the measures set in the conservation objectives and management plans. Carrying out such projects in these areas could significantly impact the conservation status of habitats and species of community interest, as well as the ecological condition of watercourses, which is a key parameter for the preservation of these habitats and species.

1. ***The positive impact of irrigation on biodiversity***

Irrigation can support biodiversity in arid or semi-arid areas by providing the water necessary for plant and animal survival and improving soil fertility. Recent studies show that drip irrigation significantly impacts soil properties, both on the surface and deeper within the profile,

influencing soil conditions and plant development (Tsurkan O. et al., 2021). As demonstrated by Olinic et al. (2024), the development of plant root systems plays a crucial role in improving soil structure and enhancing its water retention capacity, especially when integrated with geosynthetic materials for erosion control.

2. ***The negative impact of irrigation on biodiversity***

Irrigation infrastructure can have significant adverse effects, including:

Dams and irrigation channels can disrupt natural water flow, affecting aquatic ecosystems. A study examining the ecological impact of dam construction on river environments, using intertidal nematode communities as bioindicators, found that interrupting longitudinal connectivity and accumulating contaminants upstream altered nematode structures, affecting abundance, diversity, dominant genera, and community compositions (Tran et al., 2022).

A recent study (Cabodevilla et al., 2022) highlights a significant impact of irrigation systems and associated land-use changes on bird communities in an arid Mediterranean ecosystem. The study found that 55% of bird species responded negatively to irrigation (with a reduced probability of occurrence), while only 11% showed a positive response. These changes led to a 24% overall decline in species richness at the site level. The impact was particularly pronounced in ground-nesting bird species, followed by those associated with shrubs and forests, suggesting that the effects of irrigation on biodiversity may be more extensive and complex than initially assumed. The implementation of irrigation, combined with landscape transformations, changes in agricultural practices (such as monoculture), and the intensive use of agrochemical products, can induce substantial modifications in the composition and dynamics of local bird communities. Another study (Poff et al., 2010) indicates that alterations in river flow regimes can lead to the loss of aquatic habitats and the decline of species.

Excessive irrigation can cause soil salinization, reduce fertility and harm native plant species (Qadir et al., 2014).

A crucial aspect to consider when designing irrigation systems is energy efficiency, as these systems can significantly increase operating costs.

CONCLUSIONS

In the context of increasingly evident climate change in recent years in Romania, adapting irrigation infrastructure to new climate realities is a strategic priority for ensuring food security and agricultural sustainability. One of the most cited global examples of irrigation and technological reform comes from Israel, a country with limited water resources and uneven water distribution, which has become a world leader in efficient irrigation systems. In the 1960s, the Israeli company Netafim pioneered drip irrigation. The use of this irrigation method on over 75% of agricultural crops, combined with the reuse of treated wastewater for irrigation at over 86%, rainwater harvesting, seawater desalination, the construction of numerous reservoirs for storing irrigation water, controlling the consumption behavior of the population through media and online campaigns, and the use of IT solutions, has made Israel a global example to follow (Kaplan, 2022). The increasing frequency of extreme weather events, such as prolonged droughts or intense rainfall, necessitates urgent and effective measures to modernize and expand irrigation systems, optimize water resource use, and reduce the agricultural sector's vulnerability.

REFERENCES

ANIF – National Agency for Land Improvements. (2024). *Despre noi*. Retrieved March 7, 2025, from https://www.anif.ro/despre-noi/

ANIF – National Agency for Land Improvements. (2024). *Irigatii*. Retrieved March 7, 2025, from https://www.anif.ro/irigatii/

Bojariu, R., Nedealcov, M., Boincean, B., Bejan, I., Rurac, M., Pîntea, M., Caisin, L., Cerempei, V., Hurmuzachi, I., Baltag, G., & Zaharia, N. (2021). *Ghid de bune practici întru adaptarea la schimbările climatice și implementarea măsurilor de atenuare a schimbărilor climatice în sectorul agricol*. Chișinău: S.n. Retrieved March 7, 2025, from https://www.researchgate.net/publication/357649368_Ghid_de_bune_practici...

Burghila, D., Bordun, C. E., Doru, M., Sarbu, N., Badea, A., & Cimpeanu, S. M. (2015). Climate change effects – where to next? *Agriculture and Agricultural Science*

Procedia, 6, 405–412. https://www.sciencedirect.com/science/article/pii/S2210784315002405

Cabodevilla, X., Wright, A. D., Villanua, D., Arroyo, B., & Zipkin, E. F. (2022). The implementation of irrigation leads to declines in farmland birds. *Agriculture, Ecosystems & Environment, 323*. https://www.sciencedirect.com/science/article/pii/S0167880921004059

INS – National Institute of Statistics. (2025). *Romanian Statistical Yearbook* (ISSN 1220-3246). Retrieved March 5, 2025, from https://insse.ro/cms/sites/default/files/field/publicatii/anuarul_statistic_al_romaniei_carte_ed_2024_en.pdf

IPCC. (2021). *Climate Change 2021: The Physical Science Basis*. In V. Masson-Delmotte et al. (Eds.), *Contribution of Working Group I to the Sixth Assessment Report of the Intergovernmental Panel on Climate Change* (2391 pp). Cambridge University Press. https://www.ipcc.ch/report/ar6/wg1/downloads/report/IPCC_AR6_WGI_FullReport.pdf

Jongman, B., Warda, P. J., & Aerts, J. C. J. H. (2012). Global exposure to river and coastal flooding: Long-term trends and changes. *Global Environmental Change, 22*, 820–835. https://www.researchgate.net/publication/329415777_Global_exposure...

Kaplan-Zantopp, M. (2022). How Israel used innovation to beat its water crisis. Retrieved April 11, 2025, from https://www.israel21c.org/how-israel-used-innovation-to-beat-its-water-crisis/

Kundzewicz, Z. W., Kanae, S., Seneviratne, S. I., Handmer, J., Nicholls, N., Peduzzi, P., Mechler, R., Bouwer, L. M., Arnell, N., Mach, K., Muir-Wood, R., Brakenridge, G. R., Kron, W., Benito, G., Honda, Y., Takahashi, K., & Sherstyukov, B. (2014). Flood risk and climate change: Global and regional perspectives. *Hydrological Sciences Journal, 59*(1), 1–28. https://www.tandfonline.com/doi/full/10.1080/02626667.2013.857411

Olinic, T., Olinic, E. D., & Butcaru, A. C. (2024). Integrating geosynthetics and vegetation for sustainable erosion control applications. *Sustainability, 16*(23), 10621. https://doi.org/10.3390/su162310621

Poff, N. L., & Zimmerman, J. K. H. (2010). Ecological responses to altered flow regimes: A literature review to inform the science and management of environmental flows. *Freshwater Biology, 55*, 194–205. https://pofflab.colostate.edu/wp-content/uploads/2019/08/Poff_2010_LitreviewtoEflows.pdf

Sandu, A. M., & Vîrsta, A. (2021). The water footprint in context of circular economy. *AgroLife Scientific Journal, 10*(2), 170–177. https://agrolifejournal.usamv.ro/index.php/agrolife/article/view/318/317

Sănduleac, P., Sevastel, M., Roșca, S., Bilașco, S., Sălăgean, S., Dragomir, L. O., Herbei, M. V., Bruma, S., Sabou, C., Marković, R., & Kader, S. (2023). GIS-based soil erosion assessment using the USLE model for efficient land management: A case study in an area with diverse pedo-geomorphological and bioclimatic characteristics. *Notulae Botanicae Horti Agrobotanici Cluj-Napoca, 51*(3), Article 13263. https://www.notulaebotanicae.ro/index.php/nbha/article/view/13263

Tran, T. T., Nguyen, M. Y., Quang, N. X., Hoai, P. N., & Veettil, B. K. (2022). Ecological impact assessment of irrigation dam in the Mekong Delta using intertidal nematode communities as bioindicators. *Environmental Science and Pollution Research, 29*, 90752–90767. https://link.springer.com/article/10.1007/s11356-022-22135-4

Tsurkan, O., Burykina, S., & Leah, T. (2012). Methodological approaches for assessing the drip irrigation impact on the pedo-ecological state of irrigated soils. *Scientific Papers. Series A. Agronomy, LXIV*(2), 81–86. https://agronomyjournal.usamv.ro/pdf/2021/issue_2/Art11.pdf

Qadir, M., Quillérou, E., Nangia, V., Murtaza, G., Singh, M., Thomas, R. J., Drechsel, P., & Noble, A. D. (2014). Economics of salt-induced land degradation and restoration. *Natural Resources Forum, 38*, 282–295. https://www.researchgate.net/publication/267571092_Economics_of_salt-induced_land_degradation_and_restoration

Scientific Papers. Series E. Land Reclamation, Earth Observation & Surveying, Environmental Engineering. Vol. XIV, 2025
Print ISSN 2285-6064, CD-ROM ISSN 2285-6072, Online ISSN 2393-5138, ISSN-L 2285-6064

DRIP IRRIGATION'S INFLUENCE ON CHERNOZEM SOIL: ELECTROPHYSICAL AND SALINITY DYNAMICS

Yurii DEHTIAROV, Zinaida DEHTIAROVA

State Biotechnological University, 44 Alchevskyh Street, 61002, Kharkiv, Ukraine

Corresponding author email: degt7@ukr.net

Abstract

The study of the influence of drip irrigation on electrophysical parameters and water-soluble salt content in soil and strawberry plants (petioles and fruits) under different fertilization systems is presented. The mineralization and pH of the water used to irrigate the strawberries were measured. The increased content of water-soluble sodium cation salts in irrigation water leads to soil salinization (typical chernozem) and an increase in its amount in the thickness of 0-50 cm during the study period. At the same time, the electrical conductivity of the soil-water suspension decreases. Water pH and salt pH tend to change to an alkaline reaction. The highest amount of calcium, sodium and potassium cations is found in the plants of the control variant, the lowest - in the mineral and organic-mineral variants, and the intermediate amount - in the organic system of fertilization with drip irrigation. Adjusting and regularly monitoring the salinity and pH of irrigation water will help grow healthy and beautiful plants, and plant sap analysis complements soil solution analysis.

Key words*: chernozem, drip irrigation, pH, soil conductivity, water-soluble salts.*

INTRODUCTION

Soil is the most key component of agricultural biocenoses. The condition and nature of the soil cover, its water, air, salinity, nutrient, thermal and microbiological regimes and its bioproductivity have a critical impact on crop yields.

Irrigation is the most powerful factor of human intervention in the natural environment and a strong factor in the transformation of chernozem soils. Irrigation, by increasing water inputs into the landscape, can significantly alter soil characteristics. These alterations include changes in soil morphology, such as the formation of dense soil layers or the breakdown of aggregates, as well as shifts in soil composition, such as the accumulation of salts or the loss of organic matter (Zeng et al., 2013).

In contemporary agriculture, drip irrigation technology is rapidly gaining popularity due to its numerous benefits. Drip irrigation ensures optimal moisture conditions for plant roots over extended periods. This fosters both robust physiological activity and enhanced crop development (Yan et al., 2022). In this context, local irrigation methods ensure minimal environmental impact on the landscape and soils, while maintaining optimal crop productivity, and are the most appropriate and promising in terms of conserving soil and land resources with naturally insufficient and unstable atmospheric moisture (Brovarets, 2017; Neilsen et al., 2004).

Salinization, a major consequence of irrigation, refers to the accumulation of easily soluble salts such as sodium carbonate, chlorides, and sulfates in the soil. Primary or residual salinization occurs when salts build up in the soil column due to natural processes or the intrusion of saline groundwater and surface water. For instance, in arid and semi-arid regions, high evaporation rates can draw salts from deeper soil layers to the surface, leading to primary salinization. Similarly, the use of saline irrigation water can contribute to the accumulation of salts in the soil over time. This accumulation of salts negatively affects soil health by hindering water and nutrient uptake by plants, ultimately reducing crop yields and potentially leading to land degradation. Soils are considered saline if they contain more than 0.1% by weight of salts toxic to plants or more than 0.25% of salts in the dense residue. The main mechanism of this process is the introduction of salts in dissolved form with irrigation water and the precipitation of salts in the soil column from mineralized groundwater. Large areas of irrigated land become unsuitable for cultivation

due to the accumulation of large amounts of salts in the soil.

The accumulation of salts in the soil is activated in the first years of irrigation and decreases 3-5 years after the start of irrigation (Neilsen et al., 2004). Over time, the soil salinity regime reaches a dynamic equilibrium.

The process of sodium sorption in irrigated soils starts with active absorption in the first 2-3 years of irrigation, then slows down and reaches a quasi-stationary state in 3-5 years (Gamkalo, 2009). The duration of irrigation also affects the progression of salinity and salinization processes deeper in the soil profile.

The soil parameters most affected by drip irrigation are primarily the amount and composition of water-soluble salts and carbonate content. According to scientific sources, drip irrigation with water of different content and quality in Ukraine shows trends in the accumulation of water-soluble salts in the soil, changes in the composition of their absorption complex, i.e. the development of salination and salinization processes.

The underestimation of the possible negative impact of drip irrigation on soil properties due to the low irrigation rates compared to traditional methods and the local character of soil moisture makes research on this issue irrelevant. However, the localized nature of the wetting and the much larger specific volumes of water applied to the wetted part of the soil surface are associated with the potential risk of negative soil effects from drip irrigation.

So far, the technical and technological aspects of using this method of supplying moisture to plants have been well studied. At the same time, various aspects of the impact of drip irrigation on the dynamics and direction of processes in soils during long-term use of this irrigation method, and differences in their direction both in the wetting zones and beyond, remain insufficiently studied.

To improve soil fertility and obtain high and stable crop yields, it is necessary to create favourable chemical, physico-chemical and physical properties of irrigated chernozems based on the study of the nature and direction of their changes (Dehtiar'ov et al., 2021; Zhernova et al., 2022).

The aim of the study is to investigate the effect of drip irrigation on soil electrophysical parameters and water-soluble salt content under different fertilization systems, as well as to determine the degree of water mineralization and pH.

MATERIALS AND METHODS

For the fourth consecutive year, garden strawberries (*Fragaria ananassa*) have been cultivated at the "Dokuchaevske Experimental Field" Educational, Research and Production Center (ERPC) of the State Biotechnological University, located in the forest steppe zone of Ukraine (49.899434, 36.452007). This research employed both field and laboratory methods to investigate the effects of drip irrigation and fertilizer application on strawberry growth and yield (Figure 1).



Figure 1. Location of the study area

The "Dokuchaevske Experimental Field" ERPC was selected for this study due to its representative soil and climatic conditions typical of the forest steppe zone. By conducting research at this location, the findings can be applied to a wider range of strawberry cultivation areas in similar environments. Strawberry plants are highly susceptible to salt damage. While all irrigation water contains dissolved mineral salts, the concentration and composition of these salts can differ significantly. Higher salt concentrations in irrigation water led to increased salinity problems in the root zone. Factors influencing root zone salinity include water quality, fertilizer application rates, and irrigation depth.

It is important to note that it is not only drought in the soil that affects strawberry yields, but also drought in the atmosphere. When the air temperature is between 28-30ºC, additional watering should be done in addition to the main watering.

The "Roxanne" strawberries were irrigated using a drip irrigation system (Figure 2). The strawberries were cultivated on raised ridges covered with black PVC sheeting to suppress weeds and conserve soil moisture. A drip irrigation hose was positioned in the center of each ridge beneath the sheeting to deliver water directly to the plant roots. The strawberry plants were arranged in two rows per ridge, spaced 25 cm apart, with a 25 cm gap between the rows.



Figure 2. General view of a strawberry field

Drip irrigation keeps the topsoil constantly moist at the capillary moisture capacity level, but keeps the space between the rows dry, which helps to reduce weeds. The advantages of drip irrigation are water savings, i.e. minimal evaporation from the free surface, no soil crust and preservation of the soil structure.

The experimental design incorporated the following drip-irrigated variants:

Control: strawberries grown without any fertilizer application. This variant serves as a baseline to assess the effects of fertilization.

Mineral System: nitroammophoska (N16P16K16) applied at a rate of 400 kg/ha. This variant evaluates the impact of mineral fertilizer on strawberry growth and yield.

Organic-Mineral System: a combination of mineral fertilizer (nitroammophoska (N16P16K16) at 400 kg/ha) and organic fertilizer (semi-rotted manure at 50 t/ha). This variant investigates the potential synergistic effects of combining mineral and organic fertilizers.

Organic System: semi-rotted manure applied at a rate of 50 t/ha. This variant assesses the effects of organic fertilization on strawberry growth and yield.

The experimental field is characterized by typical chernozem, a fertile black soil rich in organic matter known for its excellent water-holding capacity and nutrient content.

During 2018-2020, analytical studies were conducted on soil, irrigation water, and strawberry plants (petioles and fruits) using portable equipment to assess various parameters:

- electrical conductivity, total dissolved solids, salinity, and pH were measured using the EZODO 8200M conductometer (Figure 3).
- the content of calcium, sodium, and potassium cations in the soil, petioles, fruits, and irrigation water was determined using HORIBA LAQUAtwin ionometers: Na-11 (Na^+); K-11 (K^+), and Ca-11 (Ca^{2+}) (Figure 4).



Figure 3. EZODO 8200M



Figure 4. HORIBA LAQUAtwin ionometers

The results were summarized in 2024 within the project "Development of measures to ensure sustainable productivity of agrophytocenoses under the influence of abiotic and biotic stress factors" (state registration number 0124U000457).

RESULTS AND DISCUSSIONS

Dynamics of changes in soil electrophysical parameters

A modern soil monitoring system on agricultural land includes a system for monitoring, collecting, processing, transmitting, storing and analyzing information on changes in soil quality and fertility, and for developing practical and scientifically based recommendations for decision-making on the prevention and elimination of various types of negative processes.

High agricultural productivity is only possible with comprehensive soil management and prevention of soil degradation. This is done through ongoing research into the use of agrochemicals on farmland, based on monitoring the condition of the soil cover and developing proposals for the effective and environmentally friendly use of agrochemicals.

Comprehensive soil analysis, including determination of basic and additional agrochemical parameters (soil pH, organic matter, content of available forms of nitrogen, phosphorus, potassium, trace elements, sulphur, electrical conductivity, and soil texture) to determine soil potential and optimize mineral nutrition for plants (Yatsuk et al., 2019).

The research conducted from 2018 to 2020 examined the changes in electrophysical parameters in soil where garden strawberries were cultivated (Figures 5, 6 and 7). Electrophysical parameters, such as electrical conductivity, offer insights into the soil's ability to retain and transport water and nutrients, crucial factors for plant growth. Focusing on the control variant which represents the typical cultivation practices without any experimental treatments we observed fluctuations in these parameters across different soil depths and years. In 2020, the highest values were recorded at depths of 30-40 cm and 40-50 cm, reaching 249 and 302 µs/cm, respectively. This suggests potentially higher salt concentrations or compaction at these depths. Interestingly, the ridge part of the field showed the highest value in 2018, measuring 268 µs/cm (Figure 5).

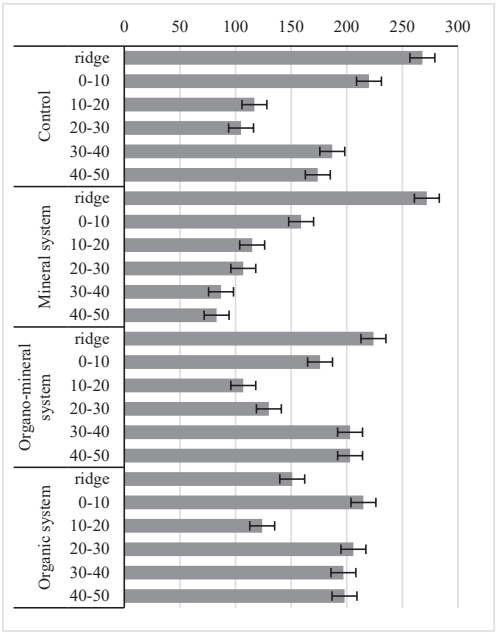


Figure 5. Change in electrical conductivity of typical chernozem in 2018, µs/cm

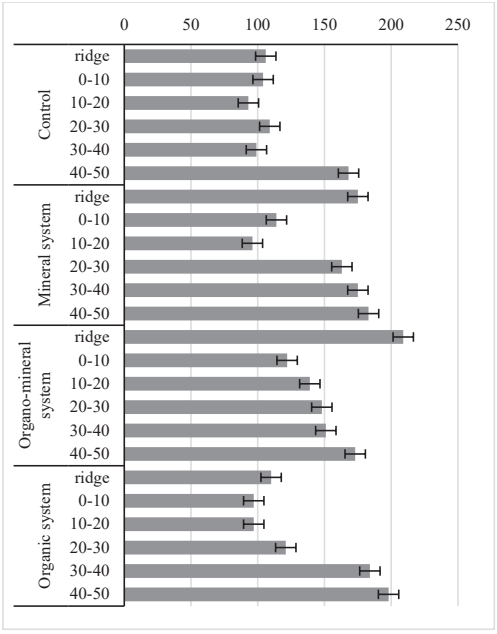


Figure 6. Change in electrical conductivity of typical chernozem in 2019, µs/cm

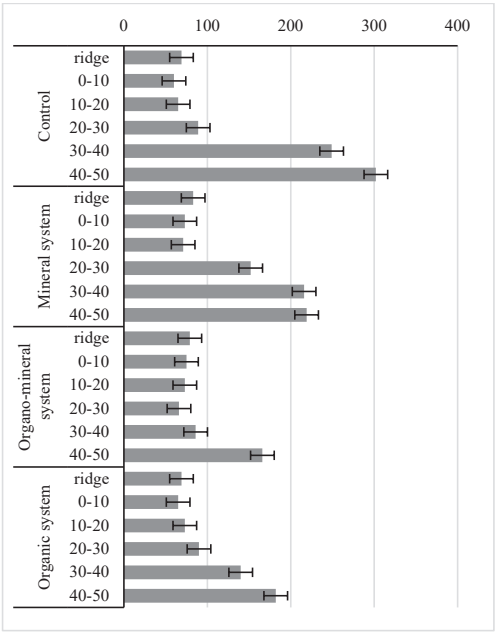


Figure 7. Change in electrical conductivity of typical chernozem in 2020, µs/cm

Conversely, the lower soil layers exhibited average electrophysical parameter values in 2018 and 2019. The lowest values were consistently found in the middle layer in 2018 and the upper layer in 2019 and 2020, ranging from 60 to 106 µs/cm. These variations highlight the dynamic nature of soil properties and their potential influence on strawberry growth (Figure 5 and 7).

The dynamics of the maximum values of the variant with mineral fertilizers shows the highest values in the ridge part in 2018 with 272 µs/cm and the lowest in 2020 with 219 µs/cm. The average electrical conductivity of most of the samples analyzed in 2019 is 163-183 µs/cm (Figure 6).

The lowest values in the soil thickness from 10 to 50 cm in 2018 were 83-115 µs/cm and in the upper part up to 20 cm in 2020 were 71-83 µs/cm.

In 2018, the highest electrical conductivity of soil-water suspensions was observed in the organic-mineral fertilizer variant in the upper and lower parts of the depth studied. In most cases, electrical conductivity averaged 122-151 µs/cm in 2019 and low 66-86 µs/cm in 2020.

The organic fertilizer variant displayed a distinct pattern in electrophysical parameters. In 2018, this variant showed the highest electrical conductivity values, ranging from 197 to 215 µs/cm in certain soil layers, with an overall average conductivity of 124-151 µs/cm. This suggests that organic fertilizers may have initially increased the soil's electrical conductivity. However, in 2019 and 2020, the lowest values were observed in the upper soil layers (20-30 cm), decreasing to 97-110 µs/cm and 65-90 µs/cm, respectively. Conversely, the deeper soil layers (30-50 cm) exhibited the highest conductivity, reaching 182-198 µs/cm. This shift in conductivity over time and depth may indicate changes in the soil's properties due to the continuous application of organic fertilizers (Figure 6 and 7).

Thus, in most cases, the electrical conductivity of soil-water suspensions decreased in 2020 compared to 2019 and 2018. The largest changes occurred in the control variant in the ridge part, where values decreased from 268 µs/cm in 2018 to 69 µs/cm in 2020, the mineral system variant (decrease of 189 µs/cm) and the organo-mineral variant (decrease of 146 µs/cm). On the contrary, there was an increase in electrical conductivity in 2020 compared to previous years in the lower investigated layer of the control and mineral fertilizer system. The 30-40- and 40-50-centimetre thicknesses of the organic fertilizer variant have been almost constant for three years.

Total dissolved solids and salinity indicators show a similar trend in the dynamics of change, but with slightly different numerical values.

Dynamics of the content of water-soluble salts of sodium, calcium, and potassium cations in soil

The soil parameters most affected by drip irrigation are primarily the amount and content of water-soluble salts and carbonates. According to scientific sources, drip irrigation with water of different composition and quality in Ukraine shows trends in the accumulation of water-soluble salts in the soil, changes in the composition of their absorption complex, i.e. the development of salination and salinization processes. The speed and direction of these processes depend on quantitative and qualitative indicators of irrigation water, irrigation regime, amount and type of autumn and winter rainfall (Balyuk et al., 2009).

For example, in 2018, the highest water-soluble sodium salts were observed in the control 360 ppm and mineral 300 ppm systems in the ridge. In 2019, these values decreased slightly but were also the highest in the control 172 ppm, organo-mineral 200 ppm and organic 166 ppm systems in the ridge. In 2020, in the control and organic systems, the highest values were recorded in the lower part of the profile, up to 200-220 ppm. In the first two years, the lowest values were observed in the 30-40 cm and 40-50 cm depths in the soil of all fertilization systems studied, while in the third year, the lowest values were observed in the top layer (ridge).

Conversely, the highest levels of water-soluble calcium salts were found in the 30-40 cm and 40-50 cm thickness sections of all the variants studied over the three years. In the same period, the lowest calcium salt content was found in the ridge part and up to the limit of 10-20 cm of the control variant of the experiment 88-106 ppm.

The content of water-soluble potassium salts was not detected in any of the samples analyzed, with the exception of two. For example, the lowest potassium content in the first year of the study was found in the control and organic-mineral fertilized plots, at 8-10 ppm in the samples taken from the ridge.

The reason for the increased content of water-soluble salts in the soil is therefore the irrigation with mineralized water, which was confirmed by the analysis of the content of soluble salts (electrical conductivity, total dissolved solids, salinity as well as calcium, sodium and potassium) in the irrigation water.

Dynamics of soil pH

The chemical properties of the aqueous soil solution are determined by the acidity or alkalinity of the soil (soil pH); the salinity or total salt content of the soil; the content of inorganic trace elements, such as most alkaline earth metals, transition metals and heavy metals; and the content of organic trace elements.

According to the Food and Agriculture Organization of the United Nations (FAO), only 1/10 of the world's soils have favourable acid-base conditions for growing major crops. At the same time, more than a third of the world's soils are characterized by various forms of 'acid stress' associated with changes in the actual and exchangeable acids present in natural soils.

Acidification of the pedosphere is a global environmental problem. However, most scientists tend to believe that it is of natural rather than anthropogenic origin. Even small changes in natural biogeochemical cycles have a much greater effect on the acid-base balance of soils and surface waters than acid precipitation.

In recent years, however, the rate of acidification of the pedosphere and the biosphere in general has increased. As a reliable relationship between precipitation acidity and changes in the pH of different environmental components can rarely be established, it is advisable to compare the acid-base properties of soils under different anthropogenic pressures.

Plants are the main source of hydrogen ions that cause the acidification of the environment. During their vital activity, they exchange them for equivalent amounts of biophilic ions: Ca^{2+} for $2H^+$, K^+ for H^+, etc. This is what cationic plant nutrition looks like. It is characteristic of most trees. In contrast, herbal plants are characterized by a mixed - cationic-anionic - type of nutrition. In addition to H^+, they actively release OH^- and HCO_3^- into the environment. This mechanism is based on the need to maintain a certain electrical potential across the membranes of root cells to protect them from electrical damage (Gamkalo, 2009). The phenomenon described is called 'trophic acidification' - a shift in the acid-base balance of the soil towards an acid reaction - and is a criterion for an integrated assessment of soil health. Therefore, quantitative assessment of active (water extract pH) and exchangeable (salt extract pH) soil acidity is a prerequisite for determining the edible comfort and ecological quality of the soil in general.

In control, there is a general tendency towards acidification in the lower soil layers. For example, at depths of 30-40 cm and 40-50 cm, the water pH decreased significantly from 8.81 and 8.70 to 7.55 and 7.42. Up to a depth of 20-30 cm there is no increase in pH. The indicator ranges from 7.32 to 7.94.

The mineral system shows a general increase in alkalinity at most depths, apart from 30-50 cm where a slight acidification is observed. The maximum increase in alkalinity is observed at a depth of 20-30 cm from 7.81 to 8.45.

The organo-mineral system shows a general increase in alkalinity at all depths over the years

of investigation. The maximum values were recorded at a depth of 30-40 cm, where the water pH increased from 7.21 to 8.20, and 40-50 cm - the reaction changed from 7.33 to 8.47.

In the organic system we have a significant increase in alkalinity at all depths. In contrast to the other variants, the maximum increase in water pH is observed in the crestal part, from 7.24 to 8.45.

In the control, there is a general tendency towards acidification at most depths, except at 20-30 cm, where the salt pH increases from 5.66 to 5.92. This is particularly noticeable at depths of 30-40 cm and 40-50 cm, where the salt pH has decreased significantly from 7.79 to 6.68 and from 7.64 to 6.52 respectively.

The mineral system shows a general increase in alkalinity at most depths. The soil reaction changes from slightly acidic to slightly alkaline from the surface down to 20-30 cm. A slight acidification of 0.15-0.17 units is observed at depths of 30-50 cm.

The organic-mineral system shows a general increase in alkalinity at all depths. Over the years of research, the salt pH increased from 5.97 to 6.35 in the crestal part and from 6.12 to 6.34 in the 0-10 cm part. There is also an increase in alkalinity of more than one unit from 6.71 to 7.75 at a depth of 40-50 cm.

The organic fertilizer system demonstrated a notable increase in soil pH across all depths, indicating a shift toward alkalinity. Over the research period, an average increase of 0.50 to 1.00 pH units was observed. This change moved the soil reaction from slightly acidic to nearly neutral. So, in most cases, over the years of research, we have seen a change in the pH water and pH salt towards an alkaline reaction.

Electrical Conductivity (EC), Total Dissolved Solids (TDS), Salinity (Salt) and water suitability for irrigation

In drip irrigation systems, where watering is frequent, the electrical conductivity (EC) of the irrigation water can be considered a reliable indicator of the soil solution's EC. This is because the frequent application of water closely maintains the equilibrium between the two. Crops have established thresholds for EC, beyond which their growth is inhibited. To estimate potential yield loss due to salinity, measuring the EC of the irrigation water provides a practical alternative to measuring the EC of the soil (Bedernichek et al., 2009; Hamkalo et al., 2012).

By comparing the water's EC with the established limits for soil EC, one can assess the risk of salinity-induced yield reduction. If the water's EC is lower than the threshold value, yield reduction due to salinity is unlikely. However, if the water's EC exceeds the limit, it indicates potential salinity stress, which can hinder water and nutrient uptake by the plants, ultimately leading to reduced yields.

Electrical conductivity was measured in microSiemens (µs/cm). The unit of mineralization is usually milligrams per liter (mg/l). Salinity can also be expressed in parts per million of water particles (ppm). The ratio between mg/l and ppm is almost the same - 1 mg/l = 1 ppm.

During the electrophysical analysis of the water, it was found that the electrical conductivity is 1047 µs/cm, the total amount of all salts dissolved in the water is 708 mg/l (ppm) and its salinity reaches 540 mg/l (ppm).

The maximum value of water conductivity when strawberries are grown on loamy soils (such as the typical chernozems of the experimental field) is 900 µs/cm. In our case, the value is 147 µs/cm higher. For further cultivation, it is therefore necessary to normalize the level of electrical conductivity of the irrigation water according to the stage of development and variety of garden strawberries.

In addition, water can be classified as medium saline based on the number of dissolved salts (electrical conductivity in the range of 650-1300 µs/cm).

Therefore, determining the actual salinity of the irrigation water through its electrical conductivity becomes crucial for making informed decisions about crop suitability. If salinity exceeds the tolerance of the desired crop, alternative salt-tolerant crops, such as barley or cotton, could be considered to maintain yields. This proactive assessment helps ensure sustainable agricultural practices and optimizes crop production in varying salinity conditions.

The water mineralization rate for strawberry plants is 1260-1540 mg/l (ppm). This means that the salinity of the water is 1.6-2.0 times lower than optimal.

Plants need not only constantly access to minerals, but also the conditions in which they

can be well absorbed. The most important parameter in determining the availability of nutrients to the plant is the pH of the water. The optimum pH of the aqueous solution is different for each type of plant; for some crops it is around 6.8-7.5, for others around 5.5-6.8.

The optimum pH for strawberries is around 6.00. According to the measurement results, the pH of the irrigation water is 6.78, which is 0.78 units higher than the optimum value.

Different chemicals can be used to adjust the pH of the water. For example, you can lower the pH by adding phosphoric, nitric or citric acid to the water. To raise the pH, add baking soda, carbonate or potassium hydroxide.

Using the electrical conductivity indicator, you can quickly determine the suitability of water for irrigating the proposed crop with a known soil particle size distribution, assess a yield reduction or select an alternative crop.

Calcium, sodium, and potassium content of irrigation water

The total content of water-soluble salts, or salinity, indicates the toxicity of water irrigation to agricultural crops and the risk of soil salinization. Prolonged irrigation with high salinity water contributes to the accumulation of salts in the upper layers of the soil, which disrupts the stability of agroecosystems and reduces the yield and quality of crop production. Excessive salt content in irrigation water reduces the osmotic activity of plants and prevents normal soil aeration. The concentration of water-soluble salts in irrigation water, which can be used without restriction, should not exceed 450 mg/l. Water with a concentration of water-soluble salts up to 2000 mg/l is considered to be of limited use for irrigation. The use of water with a salt content of more than 2000 mg/l is risky and strictly limited. The salinity of irrigation water is not strictly regulated by state standards in Ukraine, but for drip irrigation the optimum salinity of water is up to 1000 mg/l (Hamkalo, 2000).

The content and ratio of cations and anions in irrigation water is of great importance in assessing its effect on the soil-plant system. Thus, an excessive content of monovalent sodium and potassium cations compared to divalent calcium and magnesium cations indicates a risk of disruption of soil permeability, soil structure, development of peptization processes, transition of soil colloids to an unnatural ash state, etc. In addition, the increased content of hydrocarbonates, against a background of high concentrations of monovalent sodium and potassium cations in irrigation water, contributes to a more pronounced deterioration of soil permeability.

In turn, changes in soil conditions affect plants: their growth and development deteriorate (sometimes to the point of complete failure), yields decrease, and the quality of the crop deteriorates significantly. The effect and interaction of monovalent and divalent cations in irrigation water is assessed by the sodium adsorption ratio. This considers the electrical conductivity of the irrigation water (EC_W), which is a proxy for the salinity of the water, and the absorption capacity of the soil.

Elevated levels of hydrocarbonate, sulphate and chloride anions in irrigation water indicate potentially high mineralization and the presence of toxic salts. Even tiny amounts of these salts can be harmful to plants. The complete absence of these elements is detrimental to crops, but their levels should not exceed the maximum allowable concentration. The content of non-toxic salts (calcium sulphate, calcium bicarbonate, etc.) up to 1 g/l is safe for plants (Hamkalo et al., 2012; Shum et al., 2013). Thus, the water used for irrigation contains a small amount of water-soluble potassium salts - 6 mg/l (ppm); much more water-soluble calcium salts - 93 mg/l (ppm); and most of all water-soluble sodium salts - 190 mg/l (ppm) (Table 1).

Table 1. Cation content in irrigation water, mg/l (ppm)

Cation content	Na	Ca	K
	190	93	6

The calcium (Ca^{2+}) content of irrigation water affects the hardness of the water. Excessive amounts of calcium salts can cause damage to irrigation systems, particularly by depositing on the nozzles of sprinklers or other irrigation equipment. Using such water to prepare fertilizer solutions, particularly sulphate fertilizers, can lead to the formation of calcium sulphate and affect the pH of the soil.

High sodium (Na^{+}) in irrigation water displaces calcium and magnesium from the soil colloidal absorption complex and increases the sodium

content. If such water is used over a long period, salinization of the soil can occur.

The potassium (K^+) content of irrigation water is usually low, and its infiltration into the soil increases the supply of this element. However, too much potassium together with sodium cations in relation to the total cations can lead to salinity.

At the same time, the ratio of calcium, magnesium, sodium and potassium cations in the water makes it possible to predict their effect on the soil and consequently on the plant.

In our studies, the ratio of water-soluble calcium salts to sodium (Ca:Na) in water is 1:2, and Ca:Na:K is 1:2:0.06. Thus, we can say that the increased content of water-soluble sodium salts in irrigation water leads to soil salinization and an increase in their amount in the studied soil thickness during the research period.

Calcium, sodium and potassium content of strawberry plants

Regular monitoring of essential nutrients like nitrate nitrate (NO_3^-), potassium (K^+) and calcium (Ca^{2+}) in various components of the strawberry production system plant stems, soil solution, irrigation water, and wastewater offers multiple benefits. It not only contributes to achieving optimal yields and fruit quality but also helps reduce fertilizer costs and minimize environmental impact.

Strawberry plants require adequate root space and a balanced supply of nutrients for optimal growth, fruit quality, and yield. Soil pH plays a crucial role in nutrient availability. For instance, nitrate (NO_3^-) influences fruit size, potassium (K^+) affects flavor, and Ca^{2+} contributes to firmness. Maintaining the correct soil pH ensures that these nutrients are readily available to the plants in the right proportions, preventing competition or incorrect assimilation. In addition to pH, careful and frequent monitoring of electrical conductivity is vital, as strawberry plants are sensitive to high salinity levels. By managing both soil pH and electrical conductivity, growers can optimize nutrient availability and create a favorable environment for strawberry production.

Plant sap analysis is a valuable tool for growers to actively manage nutrient levels and refine their fertilizer strategies. By providing a snapshot of the nutrients currently available to the plant for growth and development, this method can quickly identify nutrient deficiencies or excesses. However, to gain a more complete understanding of the plant's nutritional status, it's essential to consider the soil environment as well.

Soil analysis offers crucial information about the overall nutrient levels and salinity within the soil. It also helps assess the potential for nutrient leaching outside the root zone. Analyzing the soil solution, the water held in the soil that carries dissolved nutrients absorbed by the roots provides further insights into the actual nutrients accessible to the plants.

Combining plant sap analysis with soil and soil solution analysis empowers growers with a comprehensive picture of nutrient dynamics. This integrated approach enables more informed decisions about fertilizer application, ensuring that plants receive the necessary nutrients at the right time and at the right amounts.

To assess the nutritional status of strawberry plants, sap analysis was conducted using a calibrated LAQUAtwin pocket meter. This meter measures the ion concentrations in the sap, providing insights into nutrient availability. Before conducting the analysis, the meter was calibrated according to the manufacturer's instructions to ensure accurate readings.

A consistent sampling protocol is crucial for obtaining reliable results. The last mature trifoliate leaf was selected for analysis because it serves as the best indicator of essential nutrients like phosphorus (P), potassium (K), and calcium (Ca). The petiole of this leaf is specifically used to determine the levels of nitrate-nitrogen (NO_3-N). For optimal sampling, the plant's temperature should be between 20-25°C. This standardized approach ensures consistent and comparable results across different measurements.

The examination of the content of cations in the stems should be carried out in accordance with the following scheme:

1. Sample collection: gather the two most recently mature trifoliate leaves, along with their petioles, from 20 different strawberry plants. This ensures a representative sample of the plant population. Tear the petioles from the plant near the crown to avoid damaging the main stem.
2. Sample preparation: separate the petioles from the leaves and cut them into small pieces to increase the surface area for sap extraction.

3. Sap extraction: place the petiole pieces in a garlic press or hydraulic press and apply pressure to extract the sap.
4. Measurement: place a drop of the extracted sap directly onto the corresponding sensors of the LAQUAtwin pocket meter. The meter will provide readings for the different cations present in the sap.
5. Analysis: compare the obtained results with the reference values provided in Table 2. This comparison helps assess the current nutritional status of the plants.
6. Cleaning: rinse the sensors thoroughly with clean water before testing another sample or storing the device. This prevents cross-contamination and ensures accurate reading for future measurements.

Table 2. Reference nutrient levels for petiole sap in strawberry cultivation (Cadahía et al., 2008)

Days after sowing	NO_3-N	P	K
	ppm		
30	500-700	150-350	4000-5000
60	550-750	150-350	4000-5000
90	400-600	150-350	4000-5000
120	500-300	150-350	4000-5000

In addition to plant sap analysis, monitoring the soil solution provides valuable information for optimizing irrigation programs and nutrient management strategies. While soil solution analysis may not reflect the overall nutrient reserves in the soil, it offers insights into the nutrients readily available to plants at a given time. Specifically, soil solution analysis helps growers fine-tune their fertilizer applications and irrigation practices. For example, by tracking nitrate levels in the soil solution, growers can identify potential issues with nitrogen management. Excessive nitrate accumulation in the root zone can lead to nutrient imbalances and environmental concerns due to leaching.
Soil solution analysis allows for timely adjustments to fertilizer application rates, ensuring that nitrogen is supplied in the right amounts at the right time. Furthermore, monitoring salinity levels in the soil solution helps prevent the adverse effects of high salt concentrations on strawberry growth. By tracking these key parameters, growers can make informed decisions to maintain a balanced and productive growing environment.
While potassium and calcium are predominantly bound to soil particles, making their levels in the soil solution less indicative of their overall availability to plants, regular monitoring of these nutrients in the soil, irrigation water, and wastewater remain crucial. This comprehensive assessment provides a broader understanding of their presence and potential movement within the growing system.
Monitoring salinity levels in the soil solution allows for proactive management of potential salinity issues. By detecting rising salinity levels early on, growers can take corrective actions, such as adjusting irrigation practices, before they negatively impact plant health, yield, or fruit quality. This preventive approach helps maintain optimal growing conditions and ensures consistent production.
Excessive irrigation leading to waterlogging can also be detrimental. It washes essential nutrients, including fertilizers, out of the root zone, reducing their availability to plants. Moreover, this leaching process poses environmental risks, such as groundwater pollution. Analyzing the soil solution throughout the growing season helps identify potential nutrient deficiencies or excesses, enabling timely adjustments to irrigation and fertilization practices.
Regarding the calcium content in strawberry petioles, the organic fertilization variant exhibited the highest levels, reaching up to 104 mg/l (ppm) (Figure 8). In contrast, the mineral fertilization variant showed the lowest calcium content, averaging 79 mg/l (ppm). The control variant and the organic-mineral system variant had slightly higher calcium levels, measuring 82 mg/l (ppm) and 84 mg/l (ppm), respectively. These variations suggest that different fertilization regimes can influence calcium uptake and accumulation in strawberry plants. Further investigation is needed to understand the underlying mechanisms and implications of these differences.
Compared to the highest calcium content, the sodium content of strawberry plants in the organic system variant is 60 mg/l (ppm) (Figure 9). The value is even lower, at 56 mg/l (ppm), in the variant with simultaneous application of organic and mineral fertilizers. A slight increase in the indicator is observed in the variant with

mineral fertilization - 69 mg/l (ppm). The highest amount of sodium in petioles was found in the control variant of the experiment - 87 mg/l (ppm).

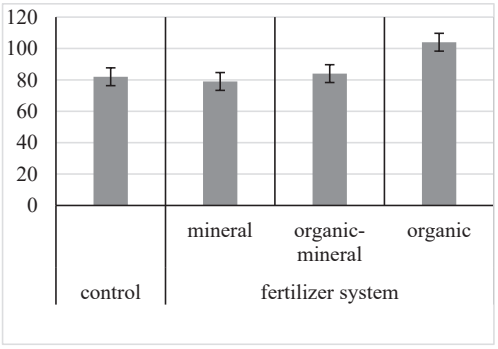


Figure 8. Calcium content in strawberry petioles, mg/l (ppm)

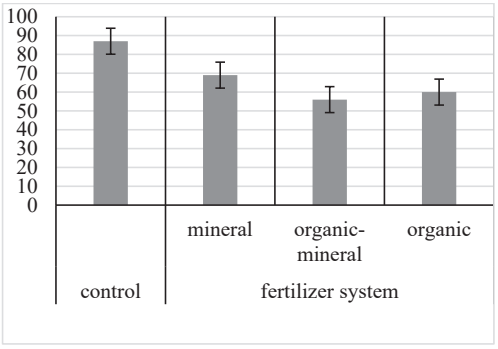


Figure 9. Sodium content in strawberry petioles, mg/l (ppm)

The potassium content of strawberry petioles is at least 20 times higher than that of calcium and sodium (Figure 10). The highest amount of potassium was found in the plants of the control variant - 2600 mg/l (ppm), and the lowest - 2167 on average - in the variant with the organic-mineral system. Average values of 2300 mg/l (ppm) were obtained for two variants with mineral and organic fertilizer application systems.

Based on the data presented in Figure 10, we can say that at least the amount of potassium in the petioles of garden strawberry plants is almost 2 times less than the optimum value.

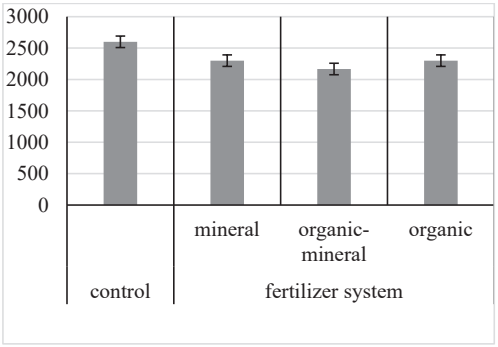


Figure 10. Potassium content in strawberry petioles, mg/l (ppm)

While the analysis of cations in strawberry fruits follows a similar procedure to petiole analysis, with no significant deviations, the specific steps involved are as follows:

1. Sample collection: gather fruit from various strawberry plants to ensure a representative sample.
2. Sap extraction: place small pieces of the fruit in a garlic press or hydraulic press and apply pressure to extract the sap.
3. Measurement: place a drop of the extracted sap directly onto the corresponding sensors of the LAQUAtwin pocket meter.
4. Cleaning: rinse the sensors thoroughly with clean water before testing another sample or storing the device. This prevents cross-contamination and ensures accurate reading for future measurements.

The highest level of calcium in garden strawberry fruit was found in the control variant of the study at 24 mg/l (ppm). The level is slightly lower, at 5 mg/l (ppm), in the variant with the mineral fertilizer system. The lowest level of calcium in the sap analysis was found in the variant with simultaneous application of organic and mineral fertilizers - 13 mg/l (ppm). The calcium content in the fruit is about 20 mg/l (ppm) when an organic fertilizer system is used (Figure 11).

The sodium content is 3.75 times higher than the calcium content in strawberries from the control variant of the study. The element content was also almost three times lower in the mineral and organo-mineral fertilizer variants - 27 mg/l (ppm). In the samples of fruit from the organic fertilization system, we have 39 mg/l (ppm) of

sodium, which is two times less than in the control variant (Figure 12).

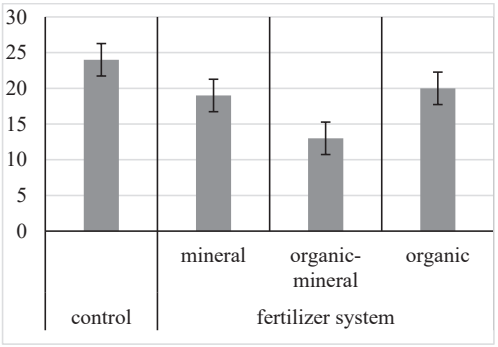


Figure 11. Calcium content in strawberry fruit, mg/l (ppm)

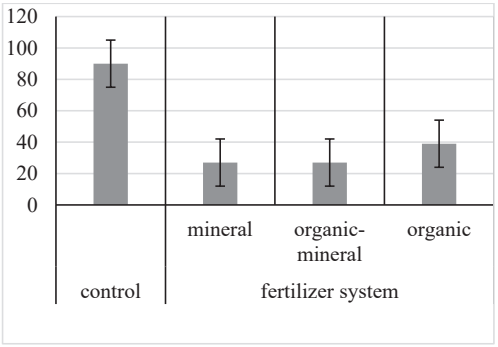


Figure 12. Sodium content of strawberry fruit, mg/l (ppm)

In contrast to the low potassium levels observed in the petioles, the strawberry fruits exhibited significantly higher potassium concentrations (Figure 13). The potassium content in the fruits ranged from 900 mg/l (ppm) to 1300 mg/l (ppm), demonstrating a substantial accumulation of this nutrient in the fruits. Among the different fertilization variants, the control variant showed the highest potassium content, averaging 1267 mg/l (ppm). The mineral fertilizer variant had the lowest potassium content, measuring 330 mg/l (ppm). The variants with organo-mineral and organic fertilization systems exhibited similar potassium levels, averaging 1107 and 1167 mg/l (ppm), respectively. These findings suggest that fertilization practices can significantly influence potassium uptake and distribution in strawberry plants. While the control variant showed the highest potassium content in fruits, the organic and organo-mineral systems also resulted in substantial potassium accumulation. The lower potassium levels in the mineral fertilizer variant may indicate a need for adjustments in fertilizer composition or application rates to optimize potassium availability for fruit development.

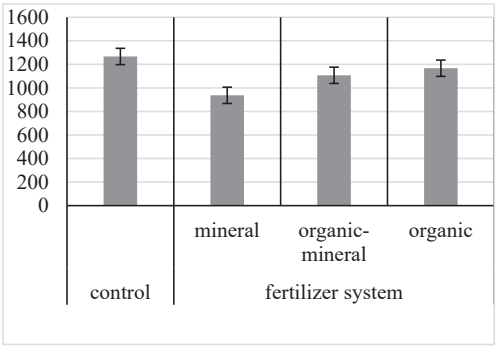


Figure 13. Potassium content of strawberry fruit, mg/l (ppm)

The analysis of strawberry fruits revealed distinct variations in cation content across the different fertilization variants. The control variant exhibited the highest concentration, followed by the organic system. The mineral and organic-mineral variants showed the lowest cation content. These differences highlight the influence of fertilization practices on nutrient uptake and accumulation in strawberry fruits, potentially affecting fruit quality and nutritional value.

CONCLUSIONS

This study revealed several key trends in the electrical conductivity of soil-water suspensions. Notably, most variants showed a decrease in electrical conductivity in 2020 compared to 2019 and 2018. This decline was particularly pronounced in the control variant's ridge part, where values dropped from 268 µs/cm in 2018 to 69 µs/cm in 2020. Similar reductions were observed in the mineral system variant (189 µs/cm decrease) and the organo-mineral variant (146 µs/cm decrease). Conversely, the lower soil layers of the control and mineral system variants exhibited an increase in electrical conductivity in 2020 compared to previous years. This contrasting trend suggests potential differences in soil

properties or nutrient dynamics at varying depths. Interestingly, the 30-40 cm and 40-50 cm depths of the organic fertilizer variant maintained relatively constant electrical conductivity throughout the three-year study period. This stability may indicate a more balanced nutrient distribution and reduced leaching under organic fertilization. These findings highlight the dynamic nature of soil electrical conductivity and its response to different fertilization regimes. Further investigation is needed to elucidate the underlying mechanisms and their implications for optimizing nutrient management practices in strawberry cultivation.

According to preliminary research results, we can state that the increased content of water-soluble sodium salts in irrigation water leads to a slight salinization of soils and an increase in its amount in the studied soil layer during the research period (2018-2020).

Water pH and salt pH tend to change the reaction of the soil environment towards alkaline.

The water used for irrigation has the following electrophysical characteristics: electrical conductivity - 1047 µs/cm; total dissolved solids - 708 mg/l (ppm); salinity - 540 mg/l (ppm); pH - 6.78, which is characterized as water with an average level of dissolved salts.

The water used for irrigation has a small amount of water-soluble potassium - 6 mg/l (ppm); much more water-soluble calcium - 93 mg/l (ppm); and the highest amount of water-soluble sodium - 190 mg/l (ppm).

The potassium content of strawberry petioles is at least twenty times higher than that of calcium and sodium. In the control variant of the research, the cation content in the fruits of garden strawberries is the highest. The lowest levels of calcium and sodium are found in the fruit of plants from the organic-mineral fertilizer system and the mineral fertilizer system. The average calcium, sodium and potassium content of the organic fertilizer system among the variants studied.

Plant sap analysis offers real-time insights into the nutritional status of plants, enabling growers to fine-tune nutrient applications, optimize yield and quality, and potentially extend the fruiting season. By complementing soil solution analysis, plant sap analysis provides a comprehensive picture of nutrient dynamics, facilitating informed decisions about fertilizer management.

Maintaining optimal salinity and pH levels in irrigation water is crucial for cultivating healthy and productive plants. Regular monitoring and adjustments of these parameters ensure a favorable environment for nutrient uptake and overall plant growth.

REFERENCES

Balyuk, S.A., Romashchenko, M.I., Stashuk, V.A. (2009). *Scientific basis for protection and rational use of irrigated lands in Ukraine.* Kyiv: Agrarian science (in Ukrainian).

Bedernichek, T., Kopij, S., Partyka, T., Hamkalo, Z. (2009). Electrical conductivity as express indicator of ion activity of forest ecosystems soils. *Biological systems, 1*(1), 85–89 (in Ukrainian).

Bedernichek, T., Partyka, T., Hamkalo, Z. (2009). Soil organoprofile and ion activity quantitive changes in consequence of subedificator cutting. *Scientific Bulletin of NLTU of Ukraine: a collection of scientific and technical papers* (19.9), 28–36 (in Ukrainian).

Brovarets, A. (2017). Information and technical system for monitoring the state of the soil environment by Alexander Brovarets. *Bulletin of Lviv National Agrarian University. Series: Agroengineering research, (21),* 9–29 (in Ukrainian).

Cadahía, C., Frutos, I., Neymar, E. (2008). La savia como índice de fertilización: cultivos agroenergéticos, hortícolas, ornamentales y frutales. Madrid: *Mundi Prensa*. ISBN: 9788484763567.

Zeng, C., Wang, Q., Zhang, F., Zhang, J. (2013). Temporal changes in soil hydraulic conductivity with different soil types and irrigation methods. *Geoderma, 193-194,* 290–299. https://doi.org/10.1016/j.geoderma.2012.10.013

Dehtiar'ov, Y., Havva, D., Kovalzhy, N., Rieznik, S. (2021). Transformation of Physical Indicators of Soil Fertility in Typical Chernozem of the Eastern Forest-Steppe of Ukraine. In: Dmytruk, Y., Dent, D. (eds) *Soils Under Stress.* Springer, Cham. https://doi.org/10.1007/978-3-030-68394-8_11.

Gamkalo, Z. (2009). *Ecological soil quality.* Lviv: Ivan Franko LIGU Publishing Centre.

Hamkalo, Z. (2000). Electrical conductivity as a criterion for assessing the ionic activity of pasture soil under different mineral fertilisation of grasslands. *Bulletin of the Ivan Franko National University of Lviv, (27),* 147–151 (in Ukrainian).

Hamkalo, Z., Bedernichek, T., Partyka, T., Partem, Y. (2012). Specific electrical conductivity of aqueous soil suspensions as a express criterion for soil diagnostics. *Biological systems, 4*(1), 16–19 (in Ukrainian).

Neilsen, G.H., Herbert, L.C., Hogue, E.J. (2004). Response of apple to fertigation of N and K under conditions susceptible to the development of K deficiency. *Journal of the American Society for*

Horticultural Science, 129(1), 26–31, https://doi.org/10.21273/JASHS.129.1.0026

Ryabkov, S.V. (2009). Assessment of the impact of drip irrigation on agrophysical properties, salt composition and salinity of soils. *Agrochemistry and soil science*, 138-141, ISSN 0587-2596, e-ISSN 2616-6852 (in Ukrainian).

Shum, I.V., Bedernichek, T.Yu. (2013). Soil environmental quality: criteria of evaluation. *Scientific Bulletin of NLTU of Ukraine: a collection of scientific and technical papers* (23.18), 72–80 (in Ukrainian).

Yan, S., Wu, Y., Fan, J., Zhang, F., Guo, J., Zheng, J., Wu, L. (2022). Quantifying grain yield, protein, nutrient uptake and utilization of winter wheat under various drip fertigation regimes. *Agricultural Water Management*, 261, 107380, https://doi.org/10.1016/j.agwat.2021.107380

Yatsuk, I.P., Balyuk, S.A. (2019). *Methodology for agrochemical certification of agricultural lands (guiding regulatory document)*. Kyiv, 108 (in Ukrainian).

Zhernova, O., Dehtiarov, Yu., Kuts, O. (2022). Soil-saving technologies and their influence on agrophysical and colloid-chemical parameters of chernozem. *Scientific papers Series A. Agronomy, LXVI*(1), 157–166.

Scientific Papers. Series E. Land Reclamation, Earth Observation & Surveying, Environmental Engineering. Vol. XIV, 2025
Print ISSN 2285-6064, CD-ROM ISSN 2285-6072, Online ISSN 2393-5138, ISSN-L 2285-6064

WATER RESOURCE MANAGEMENT IN FRUIT AND VEGETABLE PRODUCTION USING ALTERNATIVE MULCHES

Gary L. HAWKINS

University of Georgia, 1420 Experiment Station Road, Watkinsville, GA 30677, USA

Corresponding author email: ghawkins@uga.edu

Abstract

Water management and conservation tillage practices can be important when producing fruit and vegetable crops in areas of limited water resources. This study evaluated six alternative mulching materials - compost, biofilm plastic, newspaper, craft paper, compost with glycerin, and a no-mulch control - against standard low-density polyethylene (LDPE) plastic in a bedded watermelon production system. Three replications of each treatment (mulches) were randomly placed in sections of watermelon rows. Weed density, soil moisture, and temperature were monitored to assess the performance of each mulch. Results showed that all treatments, except for the control and compost, provided effective weed suppression comparable to LDPE. Soil temperature and moisture levels varied across treatments, with compost producing the highest and lowest recorded temperatures. These findings suggest that several alternative mulches, when used in combination with conservation tillage, offer viable, sustainable options for small-scale fruit and vegetable production.

Key words*: sustainability, alternative mulches, water, conservation practices.*

INTRODUCTION

Farmers produce a wide variety of crops that supply the food and fiber essential to our daily lives. In the cultivation of many of these crops - particularly fruits and vegetables - plastic mulches have been used since the 1950s to conserve soil moisture, suppress weeds, stabilize soil temperature, reduce insect pressure, and enhance crop yield (Goldberger et al., 2013; Ibarra-Jimenez et al., 2006; Anderson et al., 1995; Diaz-Perez, 2023; David & Kumar, 2023; Kasirajan & Ngouajio, 2012). These mulches are typically made from low-density polyethylene (LDPE) (Beriot et al., 2023; Kasirajan & Ngouajio, 2012) and are usually removed after one or more production cycles. However, during removal or repeated use, LDPE fragments often remain in the soil, where they do not degrade, or they may be carried to marine environments via runoff (Serrano-Ruiz et al., 2021). When left in the field over multiple seasons, these fragments can form concave pockets that trap water and nutrients, potentially limiting root penetration and affecting plant health (David & Kumar, 2023; Beriot et al., 2023).

A conceptual illustration of these issues is provided in Figure 1.

While recycling may appear to be a potential solution, the processes of removing, cleaning, and repurposing LDPE are complex and largely impractical for most producers (Kasirajan & Ngouajio, 2012). This raises an important question: what are the viable alternatives?

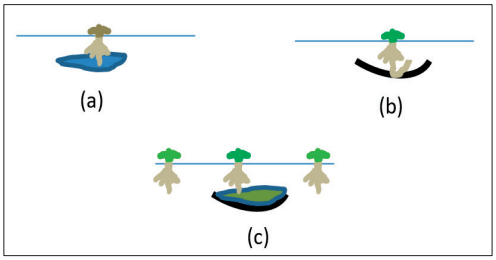


Figure 1. Conceptual illustration of the potential negative effects of residual plastic mulch in the soil: (a) Plastic traps water, leading to root rot and plant death; (b) Plastic impedes downward root growth; (c) Plastic creates isolated zones of water and nutrients, preventing their uptake by surrounding plants (Illustration by G. Hawkins)

Farmers are generally recognized as responsible stewards of the land they manage for food and fiber production (Carmichael et al., 2023; Sherval et al., 2018). While the use of plastic mulch is common and not inherently problematic, many producers seek alternative

approaches that allow them to maintain soil moisture, suppress insect pressure, and, in some cases, protect crops from wind. These approaches often involve the use of alternative mulches in fruit and vegetable production systems (Anderson et al., 1995; David & Kumar, 2023; Kasirajan & Ngouajio, 2012). The farmer collaborating on this project employs conservation tillage practices, incorporating cover crops to enhance soil organic matter, reduce erosion, support soil biota, and provide wind protection for young watermelon plants. He currently uses LDPE plastic mulch to achieve many of these agronomic benefits. However, he has expressed concerns about the long-term accumulation of LDPE in the soil, particularly the potential for creating perched water tables or obstructing root penetration - issues illustrated in Figure 1b. As a result, the objective of this study was to evaluate practical alternatives to LDPE mulch, particularly those that may be better suited for adoption on small farms or in conservation-oriented production systems.

MATERIALS AND METHODS

The project was conducted in the watermelon-growing region near Cordele, Georgia, USA. The collaborating farmer employs conservation tillage practices and plants a cover crops each fall following the harvest of his commercial crop. He also practices crop rotation. In late winter or early spring, he terminates strips of the cover crop in preparation for bedding and planting watermelon. Once the cover crop has fully died back, he prepares the watermelon beds by tilling, forming raised beds, and laying plastic mulch over the planting rows (Figure 2). The plastic is applied using a custom-built plastic layer designed to form beds with a width of 0.45 meters (18 inches), as shown in Figure 2b.

After the plastic mulch was laid, the author cut 8.8-meter (29-foot) sections to install three randomized, replicated treatments: (1) control (no alternative cover), and contractor-grade or brown craft paper. Due to limited availability, treatments using compost and compost mixed with glycerin (a byproduct of biodiesel production) were restricted to shorter sections measuring 2.7 meters (9 feet) in length. A portion of the installed treatments is shown in Figure 3, along with the dataloggers used to monitor soil temperature and moisture.

As shown in Figure 3a and 3b, various sensors were installed during the treatment setup to monitor environmental conditions. Soil moisture sensors (Decagon Devices 10HS Capacitance Sensors; see NOTE), temperature sensors (Decagon Devices), a rain gauge (Decagon Devices ECRN-50), and a datalogger (Decagon Devices EM-50) were used to collect data on soil moisture and temperature at 15-minute intervals. Soil moisture sensors were installed vertically to monitor the top 15 cm (6 inches) of the soil profile, while temperature sensors were placed directly on the soil surface beneath each mulch treatment.



(a)



(b)

Figure 2. (a) Bed preparation by tilling a narrow 0.6 m (24-inch) strip through the cover crop and installing biodegradable plastic or four layers of newspaper; (b) Formation of a 0.5 m (20-inch) finished bed with plastic mulch laid over the tilled area between standing cover crop rows
(Images by G. Hawkins)



(a)



(b)



(c)

Figure 3. Alternative mulch treatments installed in a watermelon field, along with dataloggers used to monitor soil temperature and moisture. (a) Multiple treatment rows with various mulch types; (b) Newspaper mulch with planted watermelon seedlings; (c) Craft paper mulch with planted watermelon seedlings (Images by G. Hawkins)

Throughout the growing season, weed density was also monitored. Weeds were counted, averaged by treatment, and normalized to a per-acre basis to enable comparison.
All collected data were stored, analyzed, and graphed using Microsoft Excel.
After sensor installation and treatment setup, the farmer mechanically planted the watermelon crop

RESULTS AND DISCUSSIONS

The findings from this study are presented in the following figures and categorized by key parameters: weed count, temperature, and soil moisture.

Weed Count

As shown in Figure 4, the standard LDPE plastic mulch resulted in minimal weed emergence, with yellow nutsedge being the only species able to penetrate the mulch, averaging fewer than 444 plants per acre across five weekly sampling events (Webster, 2005). Similarly, biodegradable plastic, newspaper, craft paper, and compost with glycerin treatments also exhibited low weed pressure, with the newspaper treatment recording the highest among them - averaging 900 plants per acre.
Microbial activity trends corresponding to these treatments are summarized in Table 1, which presents colony counts over a five-week period. Compost treatment showed a steady increase in microbial populations, peaking at 47,329 CFU by May 17. In contrast, the control treatment had the highest microbial counts overall, while treatments like biofilm, newspaper, and craft paper exhibited moderate microbial activity. Compost with glycerin showed minimal microbial growth until the final sampling date, when a notable increase was observed.
In contrast, significantly higher weed densities were observed in the compost and no-mulch (control) treatments. The compost treatment averaged over 20,000 weeds per acre, while the control plot had the highest count, averaging over 48,000 plants per acre across the sampling period.

Tabel 1. Temporal dynamics of microbial populations under different organic amendments and controls

Sampling Date	Control	Biofilm	Newspaper	Craft Paper	Compost Gly	Compost
4/19/2010	18000	0	0	0	0	4303
4/26/2010	32333	0	0	333	0	6454
05/03/2010	48000	1000	667	333	0	15059
05/10/2010	63333	1500	1333	1000	0	31194
5/17/2010	78667	500	2667	0	2151	47329

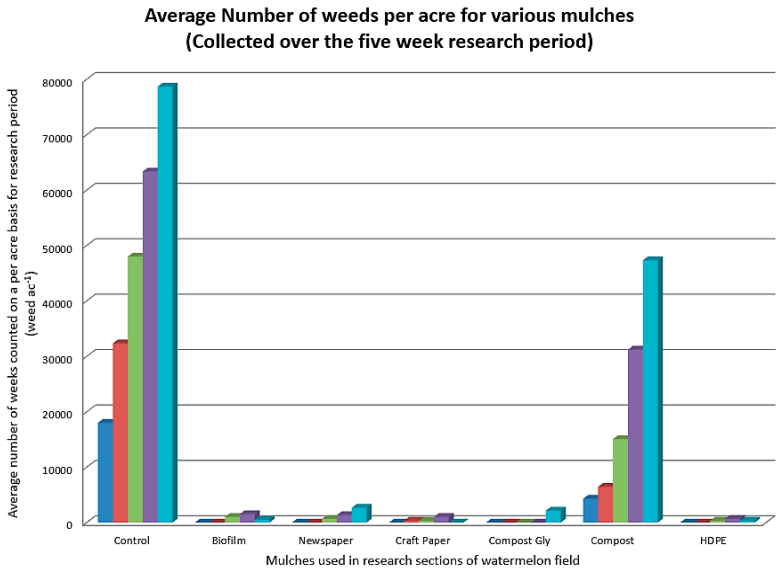


Figure 4. Graph and associated table showing the number of weeds collected from each mulch type during the five-week research period as indicated standardized to a per acre basis

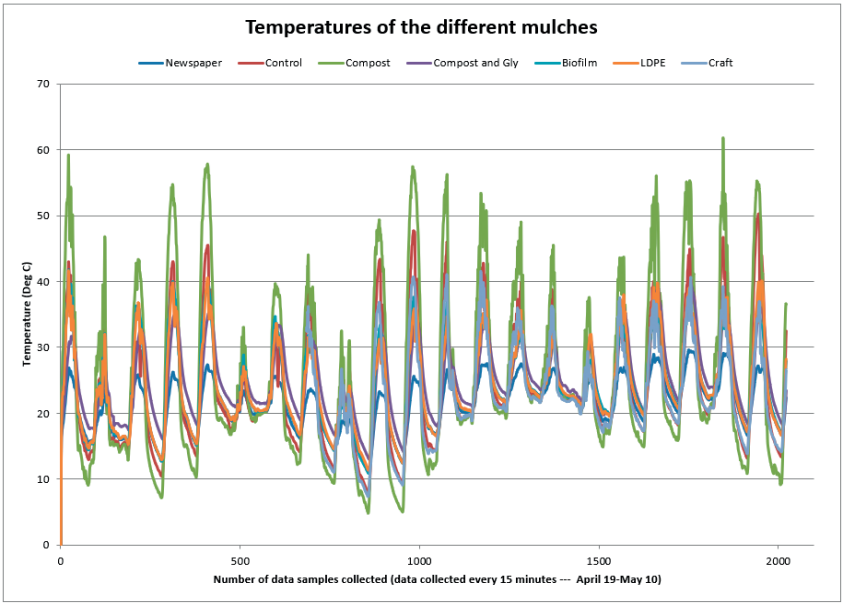


Figure 5. Temperatures as measured for the different treatments

Soil Moisture

Figure 6 illustrates the soil moisture dynamics under each mulch treatment throughout the study period. Soil moisture was measured to evaluate how different mulches influenced water retention in response to precipitation, which in this case included both natural rainfall and supplemental irrigation via a center pivot system.

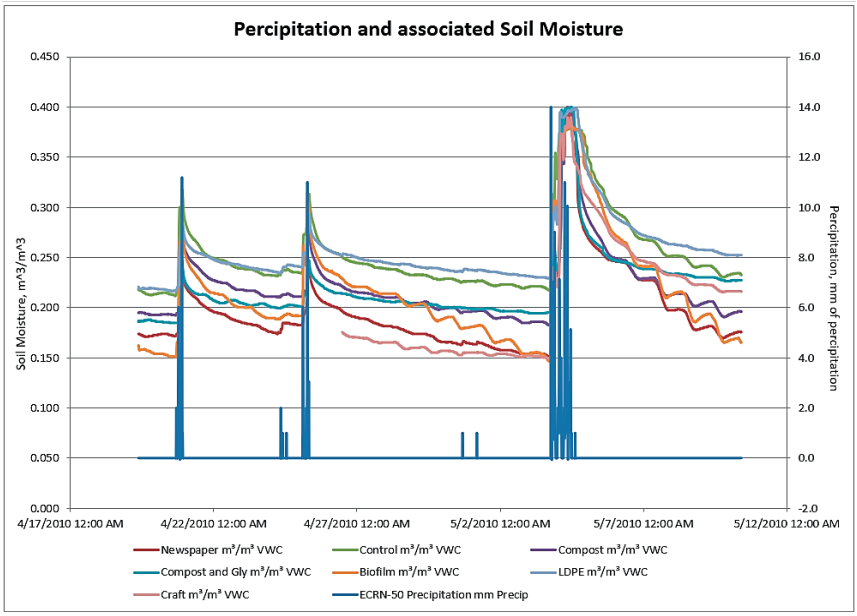


Figure 6. Precipitation and associated soil moisture under each mulch as measured in the top vertical 15 cm (6 inches) of soil

Soil moisture levels under the LDPE and control treatments were generally the highest, ranging from 0.22 to 0.40 $m^3 m^{-3}$. In contrast, the craft paper and newspaper treatments exhibited lower soil moisture levels, ranging from 0.15 to 0.40 $m^3 m^{-3}$. These differences suggest that denser or less permeable mulches like LDPE are more effective at conserving soil moisture.

Moisture loss patterns also varied based on precipitation intensity. Following small rainfall events (e.g., 10 mm), water infiltration and retention were relatively steady across treatments. However, during larger precipitation events (e.g., around May 4, which included multiple days with up to 14 mm of rainfall), the rate of moisture loss increased -likely due to higher soil saturation and increased evapotranspiration from expanding watermelon vines.

Overall, the soil moisture under all treatments was reasonably well maintained, aided by the irrigation system. For smaller-scale farms, drip or solid-set irrigation systems could offer similar benefits. Despite differences in volumetric water content across treatments, the rate of soil moisture decline remained consistent, highlighting the importance of mulch type in managing soil water retention.

CONCLUSIONS

This project demonstrated that several alternative mulches can be viable options for fruit and vegetable production, particularly for farmers seeking more sustainable practices. All tested mulches, except for compost, were effective in suppressing weeds and maintaining soil moisture levels comparable to those under standard LDPE plastic.

However, soil temperature responses varied among treatments, and some materials - such as compost - produced extreme temperature fluctuations that could pose risks depending on the crop. Additionally, practical considerations such as ease of deployment remain important. While all alternative mulches in this study were hand-laid, scaling their use for larger operations may present logistical challenges without specialized equipment.

Overall, with appropriate selection based on crop needs and farm scale, alternative mulches offer promising potential to support sustainable and conservation-oriented production systems.

ACKNOWLEDGEMENTS

This research was conducted under a grant from the Southern SARE located in Griffin, Georgia. The author would also like to thank his technician for all his help with the project.

NOTE

Mention of specific company names does not imply recommendation by the author, or the University of Georgia, USA and other products may provide the same data. Decagon Devices were used in this study, but the company has been purchased by METER Group since the date of this research, but the current sensors are the same capacitance sensors as used in the research.

REFERENCES

Anderson, D. F., Garisto, M-A, Bourrut, J-C, Schonbeck, M. W., Jaye, R., Wurzberger, A., DeGregoria, R. (1995). Evaluation of a Paper Mulch Made from Recycled Materials as an Alternative to Plastic Film Mulch for Vegetables. *Journal of Sustainable Agriculture*, 7(1), 39-61. https://doi.org/10.1300/J064v07n01_05

Beriot, N., Zornoza, R., Lwanga, E. H., Zomer, P., van Schothorst, B., Ozbolat, O., Lloret, E., Ortega, R., Miralles, I., Harkes, P., van Steenbrugge, J., Geissen, V. (2023). Intensive Vegetable Production under Plastic Mulch: A Field Study on Soil Plastic and Pesticide Residues and Their Effects on the Soil Microbiome. *Science of the Total Environment.* 900. DOI: 10.1016/j.scitotenv.2023.165179

Carmichael J, Cran A, Hrvatin F, Matthews, J. (2023). We are stewards and caretakers of the land, not exploiters of resources": A qualitative study exploring Canadian farmers' perceptions of environmental sustainability in agriculture. *PLoS ONE* 18(8): e0290114. https://doi.org/10.1371/journal.pone.0290114.

Diaz-Perez, J. C. (2023) Plant Growth and fruit yield of watermelon as influenced by colored plastic film mulch. *International Journal of Vegetable Science*, 29(1), 84-92. DOI: 10.1080/19315260.2022.2117756

Goldberger, J. R., Jones, R. E., Miles, C. A., Wallace, R. W., Ingilis, D.A. (2013) Barriers and bridges to the adoption of biodegradeable plastic mulches for US specialty crop production. *Renewable Agriculture and Food Systems*, 30(2), 143-153. DOI: 10.1017/S1742170513000276

Ibarra-Jimenez, L., Quezada-Martin, R., Cedeno-Rubalcava, B., Lozano-del Rio, A. J., de la Rosa-Ibarra, M. (2006). Watermelon response to plastic mulch and row covers. *Eur. J. Hortic. Sci*. 71:262–266. DOI: 10.17660/eJHS.2006/173691

Kasirajan, S., Ngouajio, M. (2012). Polyethylene and biodegradable mulches for agricultural applications: A review. *Agron. Sustain. Dev* 32(2):501–529. doi: 10.1007/s13593-011-0068-3.

Manidurai Manoharan David, P., Kumar, G. (2023). Poly-Coated brown wrapping paper sheet as an alternative to black plastic film mulch in Bhendi. *Journal of Madras Agriculture*, https://doi.org/10.29321/MAJ.10.000726

Serrano-Ruiz, H., Martin-Closas, L., Pelacho, A. M. (2021). Biodegradable plastic mulches: Impact on the agricultural biotic environment. *Science of the Total Environment*, 750 (2021) 141228. https://doi.org/10.1016/jscitotenv.2020.141228.

Sherval, M., Askland, H. H., Askew, M., Hanley, J., Farrugia, D., Threadgold, S., Coffey, J. (2018) Farmers as modern-day stewards and the rise of new rural citizenship in battle over land use. *Local Environment*, 23(1), 100-116. https://doi.org/10.1080/13549839.2017.1389868.

Webster, T. (2005). Mulch type affects growth and tuber production of yellow nutsedge (*Cyperus esculentus*) and purple nutsedge (*Cyperus rotundus*). *Weed Science*, 53, 834-838. doi:10.1614/WS-05-029R.1.

Scientific Papers. Series E. Land Reclamation, Earth Observation & Surveying, Environmental Engineering. Vol. XIV, 2025
Print ISSN 2285-6064, CD-ROM ISSN 2285-6072, Online ISSN 2393-5138, ISSN-L 2285-6064

ASSESSMENT OF GROUNDWATER QUALITY AND POLLUTION RISKS NEAR A HYDROCARBON POWER PLANT

Ramona-Carmen HĂRȚĂU[1, 2, 3], Simona GAVRILAȘ[2], Claudiu-Ștefan URSACHI[2], Simona PERȚA-CRIȘAN[2], Florentina-Daniela MUNTEANU[1, 2]

[1]"Aurel Vlaicu" University of Arad, Interdisciplinary School of Doctoral Studies, 2-4 Elena Drăgoi Street, Arad, Romania
[2]"Aurel Vlaicu" University of Arad, Faculty of Food Engineering, Tourism and Environmental Protection, 2-4 Elena Drăgoi Street, Arad, Romania
[3]S.C. CET Hidrocarburi S.A., 65-71 Iuliu Maniu Blvd, Arad, Romania

Corresponding author email: florentina.munteanu@uav.ro

Abstract

This study assesses the groundwater quality at the CET HIDROCARBURI ARAD site using a Global Pollution Index (I^*_{GP}) methodology that integrates multiple water quality indicators concerning legal thresholds. Water samples from three monitoring wells were collected annually over 11 years (2010-2020) and analyzed for pH, total suspended solids, fixed residue at 105°C, and chemical oxygen demand. The findings reveal that 93.94% of the samples exceeded acceptable limits based on 2008 regulatory references, with pollution levels surpassing ecological thresholds, particularly in Control Well No. 3, indicating persistent ecological stress. Despite this, long-term trends suggest overall groundwater stability, with 78.79% of historical data (2008-2017) falling within permissible ranges. Statistical analysis highlighted variations in pH and COD, suggesting localized impacts from nearby facilities such as a reagent store. The study recommends implementing a sustainable, site-specific water management plan supported by real-time monitoring and targeted assessments of emerging contaminants to enhance environmental protection and risk mitigation.

Key words*: groundwater quality, global pollution index, hydrocarbon power plant, environmental risk, statistical analysis.*

INTRODUCTION

Water is a fundamental resource essential for human development and ecological stability. It plays a critical role in agriculture, industry, and domestic use; however, only a tiny fraction of the Earth's water is readily accessible and of acceptable quality.

One critical concern is the degradation of groundwater due to industrial activities. Modern industrialization and population growth have amplified pollutant loads in surface and subsurface waters, surpassing nature's regenerative limits. This imbalance threatens aquatic ecosystems and poses risks to human health (Ahmed et al., 2022; Bashir et al., 2020).

Water quality, therefore, is not only an immediate environmental issue but a strategic national priority. It intersects local, regional, and global geospheres, which is key in maintaining Earth's ecological balance (Ullah et al., 2024). Protecting water resources requires the integration of comprehensive environmental policies into urban planning, especially in densely populated areas where contamination risks are highest (Guan et al., 2024).

Groundwater, a vital resource for drinking and irrigation, is increasingly vulnerable to pollution from surface-level industrial and technological activities (Ahmed et al., 2022; Al-Awah et al., 2023; Jayaswal et al., 2018; Zaharia, 2012; Zaharia et al., 2009). Such activities often discharge hazardous substances that pose immediate and long-term threats to environmental and public health (Biswas et al., 2014; Jalali et al., 2024; Krenkel, 2012; Sutadian et al., 2016; Ullah et al., 2024; Zainudin et al., 2024).

Among industrial sources, district heating plants present a significant risk to groundwater safety. Ageing infrastructure, corroded pipes, and fuel storage failures can lead to the release of heavy metals, hydrocarbons, salts, and industrial chemicals into soils and aquifers (Xiao et al., 2020; Liu et al., 2019). Understanding the migration of these contaminants through hydrogeological modeling enables early risk

identification, remediation planning, and legal compliance.

Pollutants associated with heating plants vary by fuel type and may include heavy metals (Bashir et al., 2020; Deshmukh et al., 2021; Hu & Shan, 2020a), nutrients like phosphates and nitrates (Isiuku & Enyoh, 2020), salts (Al-Aboodi et al., 2018), hydrocarbons (Jiang et al., 2022), and even radioactive substances in the case of nuclear facilities (Aly et al., 2020). Their monitoring is essential to maintaining water safety (Mokarram et al., 2023).

Pollution indices are widely used, cost-effective tools for evaluating water quality and informing environmental policy, especially in resource-limited settings (Berhanu et al., 2024; de Rosemond et al., 2009; Ravindiran et al., 2024; Thirumoorthy et al., 2024; Zaharia, 2012; Kumar et al., 2024). When combined with hydrogeological data, these indices offer a practical framework for understanding and managing contamination risks near industrial sites.

In line with EU regulations, including Directive 2000/60/EC and Directive 2006/118/EC, continuous groundwater monitoring is required to prevent and detect anthropogenic pollution, particularly where groundwater is a primary drinking water source. Romanian legislation reinforces these directives through national acts such as Water Law no. 107/1996 and Government Decision no. 188/2002, although explicit pollutant thresholds are sometimes lacking.

At CET H Arad, groundwater monitoring follows these legal frameworks, with four key indicators - pH, total suspended solids, fixed residue at 105°C, and COD-Cr - specified in the water management permit. These values are benchmarked against a 2008 reference sample (Analysis Bulletin, 14.11.2008). Any exceedance triggers immediate response to limit environmental harm.

To evaluate groundwater quality from 2010 to 2020, this study applied the Global Pollution Index (I_{GP}^{*}), integrating multiple parameters into a single, comprehensive score. Measurements at three monitoring wells revealed spatiotemporal variations in pollution levels linked to plant operations and well proximity, particularly in downstream locations.

These findings support the development of a robust, site-specific water management strategy and provide a replicable methodology for similar industrial environments. By coupling long-term data with integrated assessment tools, this research advances interdisciplinary knowledge at the intersection of environmental monitoring, regulatory policy, and industrial ecology.

MATERIALS AND METHODS

The municipality of Arad is situated in western Romania, bridging the southern Crisana and northern Banat regions within the expansive Tisza River plain. Geographically, it lies in the alluvial Arad Plain - part of the Western Plain - at 46°11′N latitude and 21°19′E longitude. The city spans 252.85 km² and is located at an altitude of 107 meters above sea level, alongside the Mureș River near the Deva-Lipova corridor. CET H Arad is located in the eastern central area of the municipality, approximately 1 km from the Arad railway station. Positioned on both sides of the Mureșel Canal - a branch of the Mureș River and a discharge route for treated wastewater – the plant occupies 3.62 hectares. It is not part of any protected area.

Commissioned in 1897 as Arad's first electricity source, the plant began with steam-driven generators and transitioned through various fuels: coal dust (1897-1953), fuel oil (1953-1963), a fuel oil-natural gas mix (1963 onward), and exclusively natural gas since 2009. It has long served the region’s thermal and industrial energy needs via combined heat and power systems.

No other major external pollution sources are identified in the study area. However, a sewage reservoir located roughly 15 meters from Control Well No. 1, belonging to a neighboring facility, may pose a potential risk. Similarly, a reagent store near Control Well No. 3 handles substances used for chemical water treatment, representing another possible contamination source.

Historically, CET H Arad operated four large combustion facilities, totaling over 50 MW of thermal output, regulated under EU industrial emission directives. These included two steam generators, a TA1 turbogenerator, and two hot water boilers, with a combined 362 MWt thermal and 12 MWe electric capacity. Electricity production ceased in 2008, and the facility is currently undergoing modernization, with older units scheduled for decommissioning.

Two medium combustion units remain in operation, providing 99 MWt of thermal energy. Groundwater quality at the site is monitored through three boreholes designated as control wells. Positioned in relation to the plant, Well No. 1 lies upstream, while Wells No. 2 and No. 3 are located downstream (Figure 1 and Table 1).



Figure 1. Geographic location of the study area: City of Arad, Romania, Europe. The map highlights the regional context and includes a satellite image of the CET Hidrocarburi power plant site (https://earth.google.com/web/search/europa+românia/)

Table 1. STEREO 70 coordinated of the sampling sites (https://www.cetharad.ro/mediu/)

Authorized sampling point	STEREO 70 Coordinates	
	Coordinate X	Coordinate Y
Control well No. 1	217188.26	526720.76
Control well No. 2	217343.56	526687.81
Control well No. 3	217182.34	526835.62

Methodology

Groundwater samples were analyzed for four key parameters: pH, Total Suspended Solids (TSS), Fixed Residue at 105°C, and Chemical Oxygen Demand (COD-Cr). Sampling was conducted annually over an 11-year period (2010–2020), following national standards and regulatory frameworks, including the Water Law no. 107/1996, Government Decision no. 188/2002, and the Ministry of Environment's Monitoring Plan (Romanian Parliament, 1996; Romanian Government, 2002; MMGA, 2006). A minimum of four duplicate samples were collected and analyzed each year, in accordance with officially approved methods outlined in Romanian legislation (MMGA, 2006). The measured values were compared against multiple reference points:

- Authorized baseline values from CET H Arad's 2008 test report.
- Historical groundwater quality levels (2008-2017).
- National standards for drinking water (STAS 1342/91; Romanian Standards Institute, 1991).
- Legal thresholds for wastewater discharged into the aquatic environment.

Sampling was limited to the three existing control wells on-site, as mandated by the

operational permits, which stipulate annual testing per well. The results, including the calculated Global Pollution Index ((I^*_{GP}), were graphically represented for each sampling location to visualize trends and deviations.

Reference data, including authorized and historical limits, are detailed in Table 2, while national drinking water standards used for comparative analysis are presented in Table 3.

To evaluate groundwater pollution, the study employed the methodology developed by Zaharia (Zaharia, 2012; Zaharia & Murarasu, 2009), which is particularly well-suited for regulatory assessments focused on legal compliance. This approach offers a practical and straightforward means of aggregating multiple pollutant measurements into a single standardized index. Its simplicity, combined with its ability to track trends and facilitate comparisons, makes it an effective tool for communicating findings to policymakers, regulators, and other stakeholders.

The first step involves calculating a quality index (EQ_i) for each parameter using the following formula:

$$EQ_i = \frac{C_{i,measured}}{MACi} \quad (1)$$

where:

- EQ_i is the quality index for parameter I;
- C_i is the measured concentration of parameter I;
- MAC_i is the maximum allowable concentration according to applicable standards.

Following the calculation of the quality index (EQ_i), each parameter was assigned an Evaluation Score (ES_i) based on the scale provided in Table 4.

Table 2. Reference levels for groundwater at CET H ARAD
(Water Management Authorization, 2018*Aut. G. Water; Integrated Environmental Authorization *AIM CET H Arad, 2018; Dumescu, 2018)

Sampling point	Legal reference level *Test control_ Year 2008 cf. *Aut. G. Water CET H and *AIM				Historical reference level CET H cf.			
Location CET H Arad	Quality indicators (i) Maximum Allowable Values (MACi)				Location CET H Arad			
Authorized zone	pH	TSS	Fix residue at 105°C	COD-Cr	pH	TSS	Fix residue at 105°C	COD-Cr
	[pH units]	[mg/l]	[mg/l]	[mg/l]	[pH units]	[mg/l]	[mg/l]	[mg/l]
Control well No. 1	7.00	3.00	401.0	8.40	7.00-7.50	17.40-19.00	303.00-411.60	5.70-8.40
Control well No. 2	7.50	2.10	503.00	5.60	7.00-7.50	8.20-14.00	264.00-417.20	2.40-5.80
Control well No. 3	7.00	1.60	458.20	4.90	7.00-7.50	9.40-13.00	192.00-421.60	4.90-5.50

Table 3. The admissible values according to STAS 1342/91 - drinking water
("Romanian Standards Institute, STAS 1342-91, Drink Water" 1991) for the quality indicators considered in the study

STAS 1342-91-DRINKING WATER Quality indicators (i)							
Allowed values (A)				Exceptionally allowed values (EA)			
pH	TSS	Fix residue at 105°C	COD-Cr	pH	TSS	Fix residue at 105°C	COD-Cr
[pH units]	[mg/l]	[mg/l]	[mg/l]	[pH units]	[mg/l]	[mg/l]	[mg/l]
6.50 -7.40	-	100.00-800.00	3.00	max. 8.50	-	30.00-1200.00	5.00

Both the Specific Quality Index and corresponding Evaluation Score were computed for each monitored parameter in the groundwater samples. These calculations referenced four benchmarks:

- Legal thresholds defined in the water management and integrated environmental authorizations;
- Historical groundwater data from CET H Arad (2008-2017);
- National drinking water standards (STAS 1342/91);
- Regulatory limits for wastewater discharge into aquatic environments.

Subsequently, the groundwater pollution status at each sampling location was evaluated using

the Global Pollution Index (I^*_{GP}), integrating all reference cases.

The overall Global Pollution Index for each sample was calculated using the following equation (Zaharia, 2012; Zaharia & Murarasu, 2009):

$$I^*_{GP} = (100 * n)/(ES_1 * ES_n + \sum_{i=1}^{n-1} ES_i * ES_{i+1}) \quad (2)$$

where:

- I^*_{GP} is the Global Pollution Index,
- n is the number of parameters,
- ES refers to the assigned Evaluation Score for each parameter.

The final pollution classification for each sampling point was determined using the interpretation scale provided in Table 5.

Table 4. Correlation scale between Quality Index (EQi), Evaluation Score (ESi), and environmental impact on the pollution level for the sampling points monitored on the CET H Arad sit (Zaharia, 2012)

Quality Index (EQ_i)	Evaluation Score (ES_i)	Environmental Impact
$EQ_i = 0$	10	Water bodies are unaffected by industrial activity.
$0.00 < EQ_i \leq 0.20$	9	Industrial influence is present but not quantifiable.
$0.20 < EQ_i \leq 0.70$	8	Impact detected, but below first alert threshold. Alert level: Possible consequences.
$0.70 < EQ_i \leq 1.00$	7	Impact within second-level permissible limits. Intervention level: Potential outcomes expected.
$1.00 < EQ_i \leq 2.00$	6	Pollution exceeds the first legal limit. Effect: Noticeably strong impact.
$2.00 < EQ_i \leq 4.00$	5	Pollution surpasses the second limit. Effect: Environmentally detrimental.
$4.00 < EQ_i \leq 8.00$	4	Third limit exceeded. Effect: Clear negative consequences.
$8.00 < EQ_i \leq 12.00$	3	Severe degradation – Level 1. Impact: Fatal effects over average exposure duration.
$12.00 < EQ_i \leq 20.0$	2	Severe degradation – Level 2. Impact: Rapid onset of fatal effects.
$EQ_i > 20.00$	1	Environment rendered unsuitable for life.

Table 5. Correlation of Global Pollution Index, I^*_{GP}, with effects in the water body (Zaharia, 2012)

Values I^*_{GP}	Consequences in the body of water
1	Water body unaffected by human activity.
$1 \leq I^*_{GP} < 2$	Minor anthropogenic influence; human activity is within acceptable environmental bounds.
$2 \leq I^*_{GP} < 3$	Noticeable stress on aquatic life is caused by human activity.
$3 \leq I^*_{GP} < 4$	Significant disruption of biological processes due to pollution.
$4 \leq I^*_{GP} < 6$	Serious ecological damage; aquatic life is endangered.
$I^*_{GP} > 6$	degraded body of water unfit for all living forms

To evaluate whether the monitored parameters varied significantly across the control wells, the F-test (ANOVA: Single Factor) was applied. This statistical approach was essential in determining whether differences in parameter values could be attributed to the wells' positions relative to the potential pollution source.

The analysis involved hypothesis testing as a structured method to assess statistical significance using the variables detailed in Table 6. The null and alternative hypotheses were defined as follows:

- H_0 (Null Hypothesis): The parameter values across the wells do not significantly differ; any observed variations are random, indicating that the well's location does not influence the results.
- H_1 (Alternative Hypothesis): The parameter values differ significantly, suggesting that variations are influenced by the sampling well's proximity to the potential source of contamination.

This framework provided the basis for interpreting spatial trends and assessing localized impacts on groundwater quality.

Table 6. Variables considered in the statistical analysis of groundwater quality at CET H Arad

Independent variable	Dependent variable	Constant elements
Control well No. 1	pH, COD-Cr, Total Suspended Solids (TSS), Fixed Residue	Well position relative to the pollution source
Control well No. 2		Temperature periodicity
Control well No. 3		Precipitation regime periodicity

RESULTS AND DISCUSSIONS

Evaluation of the power plant activity on the quality of groundwater based on global pollution index

To assess the impact of CET H Arad's operations on groundwater quality, multiple evaluation scenarios were considered. Maximum permissible values for the monitored parameters - pH, TSS, fixed residue at 105°C, and COD-Cr - were derived from the site's Water Management Authorization and Integrated Environmental Authorization.

After calculating the Global Pollution Index, the results were illustrated in Figure 1. These indicate a general deterioration of groundwater quality, with pollution levels causing discomfort to aquatic life - except in 2016, when I^*_{GP}, values remained within allowable limits (Figure 2).

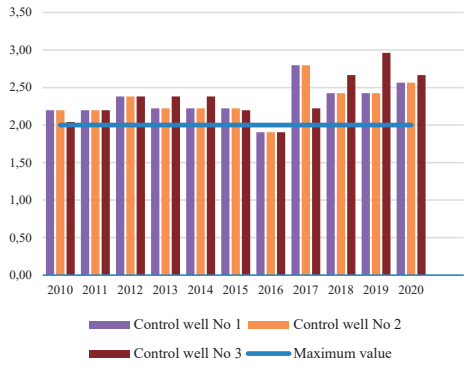


Figure 2. Results of groundwater quality assessment based on the referential values from the Water Management Authorization and Integrated Environmental Authorization for CET H Arad

A second scenario involved benchmarking results against the site's historical baseline values. As illustrated in Figure 3, groundwater quality generally remained within acceptable historical limits. However, notable exceptions were observed:

- Control Well No. 1 in 2017 and 2020;
- Control Well No. 2 in 2018, 2019, and 2020;
- Control Well No. 3 in 2019 and 2020.

In these cases, the I^*_{GP}, values exceeded thresholds, signaling environmental stress and potential ecological discomfort.

While many values did not surpass regulatory limits, a concerning upward trend in I^*_{GP}, values over the last three years suggest emerging risks. This trend warrants closer investigation into potential operational changes or external factors influencing groundwater quality during that period.

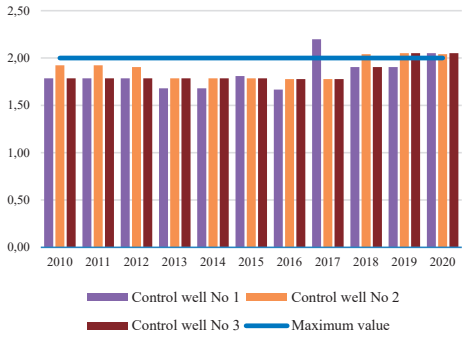


Figure 3. Groundwater quality results based on historical annual mean values (2008-2017) for CET H Arad

The analysis also included a comparison of groundwater quality results against standardized drinking water values: the Accepted (A) limits shown in Figure 4, and the Exceptionally Accepted (AE) limits presented in Figure 5.

These reference values were sourced from national standards for drinking water quality (Romanian Standards Institute, STAS 1342-91, 1991).

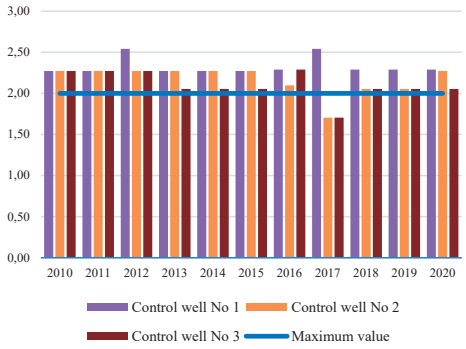


Figure 4. Results obtained according to STAS 1342-91 - Drinking water - Permissible values (A)

Although this comparison does not imply that groundwater from the CET H Arad site is intended or suitable for human consumption, it serves as a meaningful benchmark for evaluating the aquifer's environmental condition. This approach strengthens the broader purpose of the study, which is to understand, monitor, and manage groundwater quality in proximity to hydrocarbon power plant operations.

Assessing the site's groundwater status was a central objective of this investigation. It provides critical insights into the environmental impact of CET H Arad's activity and supports the formulation of preventive strategies to mitigate pollution and maintain groundwater quality.

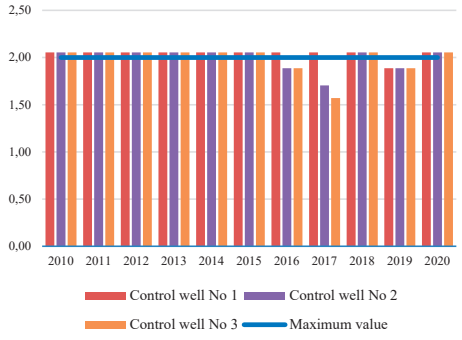


Figure 5. Results obtained in accordance with STAS 1342-91 drinking water - Exceptionally permissible values (EA)

When compared to the accepted drinking water standards (A), the I^*_{GP} values generally indicate discomfort to life forms throughout the study period, except for Control Wells 1 and 3 in 2017, where values fell within acceptable limits (Figure 4). Similarly, when assessed against the exceptionally accepted values (AE), discomfort was still observed in most years, except for Control Well No. 1 in 2019, and Control Wells No. 2 and 3 in 2016, 2017, and 2019, which showed groundwater quality within acceptable bounds (Figure 5).

Despite these occasional acceptable readings, groundwater from the CET H Arad site is not suitable for drinking, as contaminants from hydrocarbon-related processes pose potential health risks if leaked into the aquifer.

Further analysis was performed using Romanian regulatory standards for wastewater discharged into aquatic environments ("Romanian Government, Decision No. 188/2002"). When comparing I^*_{GP} values against these permissible limits, groundwater quality was again generally poor, with discomfort levels indicated across most years. Exceptions were noted in:

- Control Well No. 1 in 2019,
- Control Well No. 2 in 2016 and 2019,
- Control Well No. 3 in 2016, 2017, and 2019 (Figure 6).

These findings reinforce the need for continued monitoring and risk management at the site, especially considering localized pollution trends.

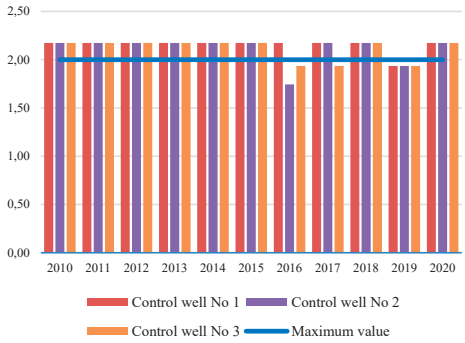


Figure 6. Groundwater quality assessment results compared to the permissible values for technological wastewater discharged into the aquatic environment, as specified by *Government Decision No. 188/2002* (HG 188/2002)

Across the 2010-2020 study period, various referential benchmarks were used to calculate the Global Pollution Index (I^*_{GP}) for groundwater at the CET H Arad site. The results consistently indicate a state of environmental discomfort for life forms in most cases, except for comparisons to historical site-specific values from 2008-2017. When evaluated against this Historical Level, 78.79% of the samples remained within permissible limits.

In contrast:

- Using the Water Management Authorization and Integrated Environmental Authorization thresholds, 93.94% of values exceeded acceptable levels, with only 6.06% falling within legal limits.
- The same proportion (93.94%) was observed when compared to standardized drinking water values (A).
- For exceptionally accepted values (AE) for drinking water, 78.79% of samples were categorized as causing discomfort, while 21.21% were within limits.

- A similar distribution was found when comparing I^*_{GP} results against the permissible values for technological wastewater discharge, mirroring the percentages associated with AE.

These findings emphasize the groundwater body's vulnerability to industrial impact, highlighting the need for continuous monitoring and targeted mitigation strategies.

Evaluation Based on Statistical Analysis

In addition to index-based evaluation, the study incorporated statistical analysis of four key groundwater parameters - pH, COD-Cr, TSS, and fixed residue - monitored at the three control wells from 2010 to 2020. Given the nature of hydrocarbon power plant operations, impacts may arise from combustion byproducts, chemical treatments (acids or alkalis), or accidental spills.

A Fisher F-test (ANOVA: Single Factor) was used to determine whether variations in these parameters were statistically significant across the wells. The analysis was grounded in the previously defined null (H_0) and alternative (H_1) hypotheses regarding spatial variation due to the plant's location.

As an example, pH variation is shown in Figure 7. Between 2010 and 2015, pH levels in Control Well No. 2 (downstream) were consistently higher than those in Well No. 3 (also downstream). Interestingly, the pH values for Well No. 1 (upstream) closely resembled those of Well No. 2 during this period, suggesting minimal or no influence from plant operations on this parameter.

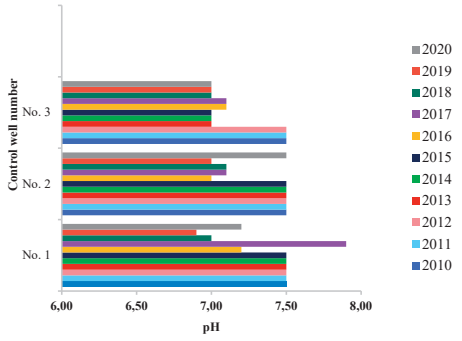


Figure 7. Variation in pH levels across the three control wells (Wells 1, 2, and 3) at CET H Arad during the 2010–2020 monitoring period

To visualize potential trends and deviations, the average pH values across the wells were plotted (Figure 8). This graph highlights long-term fluctuations and can be used to assess whether pH variations fall within standardized limits, potentially revealing early signs of deviation or pollution influence.

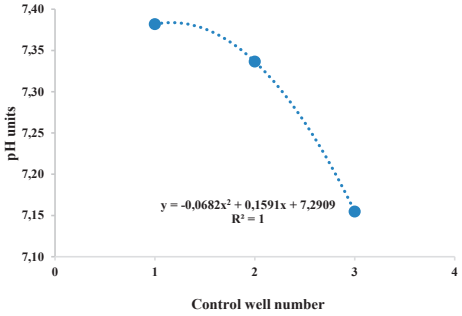


Figure 8. The function for calculating the pH variation in the three sampling points

A distinct pattern emerged when analyzing the variance in Chemical Oxygen Demand (COD-Cr) across the wells. Statistically significant differences were identified between Control Wells 1 and 2 and Wells 1 and 3, indicating that well location relative to the power plant (upstream vs. downstream) may influence COD-Cr concentrations.

This conclusion is further supported by the lack of significant variation between Wells 2 and 3, both situated downstream of the CET H Arad facility. These findings validate hypothesis H_1 (the location affects parameter variation), rejecting H_0 (no significant difference). Specifically:

- For Wells 1 and 2, $P = 0.045 < 0.05$ and $F = 4.57 > F_{crit} = 4.35$.
- For Wells 1 and 3, the variation is even more pronounced, with $P = 0.013$ and $F = 7.51 > F_{crit} = 4.35$.

Average COD-Cr values exhibited a descending trend from Well 1 to Wells 2 and 3, indicating a reduction in oxidizable substances and oxygen demand. This may be explained by a sewage collection reservoir located approximately 15 meters from Well 1, which likely contributes to higher concentrations of organic compounds upstream. As groundwater flows downstream, these substances appear to dilute, improving aerobic conditions for aquatic life.

In recent years, Well 1 consistently recorded higher COD-Cr values, especially from 2016

onward, except for 2017. That year, Wells 2 and 3 showed a nearly 80% drop in COD-Cr levels compared to the previous year (Figure 9). This anomaly may correlate with significant rainfall and elevated Mureș River discharge in 2017, leading to increased groundwater recharge and dilution of pollutants in the aquifer. The trend of COD-Cr over time is best represented by a second-degree polynomial function, reflecting the non-linear pattern of concentration changes (Figure 10).

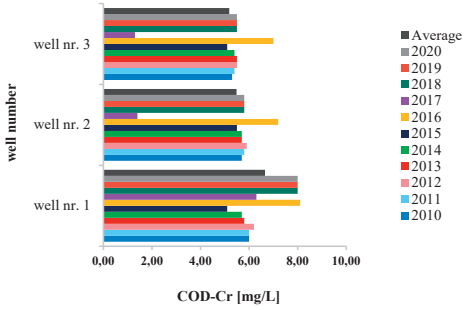


Figure 9. Variation in Chemical Oxygen Demand (COD-Cr) across the three control wells at CET H Arad during the 2010–2020 monitoring period

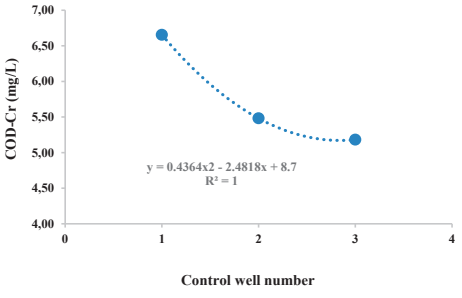


Figure 10. The function for calculating the COD-Cr variation in the three sampling points

A consistent pattern was observed across all control wells for Total Suspended Solids (TSS) (Figure 11). From 2010 to 2016, TSS concentrations remained relatively stable, averaging around 2 mg/L. However, a sharp increase was noted during 2017–2019, with average values rising by approximately eightfold. In 2020, TSS levels declined by about 30% compared to the peak period, suggesting a potential link with annual rainfall volume and temperature fluctuations.

Unlike other parameters, TSS exhibited a linear variation across the three wells (Figure 12), indicating a consistent spatial distribution pattern unaffected by well location.

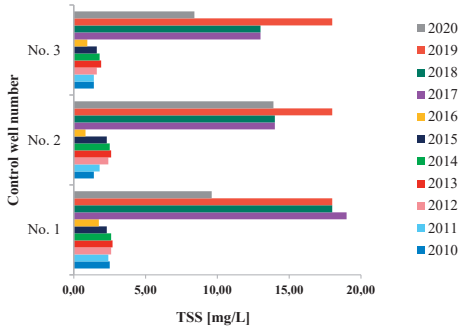


Figure 11. TSS variation in the three wells during the studied period

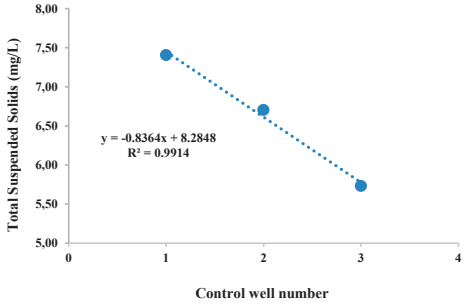


Figure 12. The function for calculating the TSS variation in the three sampling points

As expected, Fixed Residue followed a similar trend to TSS over the study period (Figure 13), given that suspended particles significantly contribute to the residual solids in water samples.

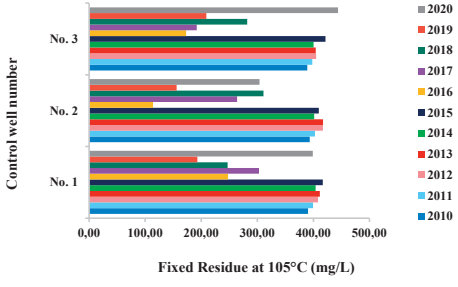


Figure 13. Fixed residue variation in the three wells during the studied period

The inter-well variation in Fixed Residue (Figure 14) showed a second-degree polynomial trend, comparable to the observed pattern in pH variations, highlighting non-linear distribution influenced by both suspended load and water chemistry dynamics.

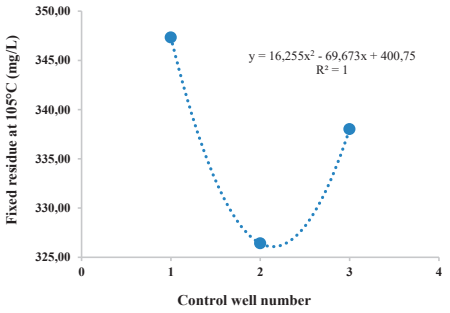


Figure 14. The function for calculating the fixed residue variation in the three sampling points

As shown in Table 7, the statistical comparison of pH values between control wells revealed no significant differences among most pairings.

For Wells 1 and 2, the *P-value = 0.683 > 0.05* and $F = 0.172 < F_{crit} = 4.351$, indicating that variations are likely due to random factors rather than spatial influences. A similar outcome was observed between Wells 2 and 3, where $P = 0.082 > 0.05$ and $F = 3.521 < F_{crit} = 4.351$. These results suggest that pH levels remained relatively stable across the sampling points and were not significantly influenced by the wells' positions in relation to the power plant.

The results summarized in Table 7 support the acceptance of the null hypothesis (H_0) in the comparisons of pH values between Wells 1 and 2, and Wells 2 and 3, where no statistically significant differences were found. These variations appear to result from arbitrary or random factors rather than systematic spatial influences.

Table 7. The ANOVA F and P parameters resulted after the comparison of the measured groundwater quality parameters for the control wells

Comparison Between Wells	Parameter	F Value	F Critical	p Value	Significant Difference*
Well No. 1 vs Well No. 2	pH	0.172	4.351	0.683	No
	COD-Cr	4.571	4.351	0.045	Yes
	TSS	1.11	4.351	0.314	No
	Fixed Residue at 105°C	0.793	4.351	0.388	No
Well No. 1 vs Well No. 3	pH	4.358	4.351	0.05	Slight (borderline)
	COD-Cr	7.511	4.351	0.013	Yes
	TSS	2.136	4.351	0.181	No
	Fixed Residue at 105°C	3.14	4.351	0.103	No
Well No. 2 vs Well No. 3	pH	3.521	4.351	0.082	No
	COD-Cr	2.401	4.351	0.145	No
	TSS	1.893	4.351	0.203	No
	Fixed Residue at 105°C	0.922	4.351	0.356	No

This pattern extends to Total Suspended Solids (TSS) and Fixed Residue, where all inter-well comparisons, including Wells 2 and 3 for COD-Cr, showed no significant differences. As with pH, the lack of significance suggests that these parameters were largely unaffected by well positioning or hydrocarbon plant activity during the evaluated period.

However, in contrast, a slight but statistically significant difference in pH was detected between Wells 1 and 3 ($P = 0.0498 < 0.05$; $F = 4.358 > F_{crit} = 4.351$), implying potential localized influence. More pronounced effects were observed for COD-Cr:

- Between Wells 1 and 2: $P = 0.0451 < 0.05$; $F = 4.5708 > 4.351$.
- Between Wells 1 and 3: $P = 0.0126 < 0.05$; $F = 7.511 > 4.351$.

These findings partially reject H_0 and weakly support H_1, suggesting that well positioning relative to the power plant may influence groundwater chemistry - particularly for parameters like pH and COD-Cr.

On average (2010-2020):

- pH at Well 3 was approximately 3% lower than at Well 1.
- COD-Cr was 28% higher at Well 3, and 21% higher at Well 2, compared to Well 1.

This may reflect the effects of chemical reagent use and disposal near downstream wells, potentially linked to the hydrocarbon plant's daily operations. While the differences are not

universally significant, the results warrant further investigation and highlight the need for a targeted environmental management strategy to monitor and mitigate potential impacts.

CONCLUSIONS

This study applied the Global Pollution Index (I^*_{GP}) to evaluate the groundwater quality at the CET H Arad hydrocarbon power plant site. Annual water quality data collected over an 11-year period (2010-2020) from three control wells formed the basis for assessing key environmental indicators.

The findings reveal that, in 93.94% of cases - when measured against legal thresholds outlined in the Water Management Authorization and Integrated Environmental Authorization - pollution levels were high enough to cause discomfort to aquatic life. This conclusion is based on comparisons with a 2008 baseline sample defined as legal reference.

Control Well No. 3, located downstream of the plant, emerged as the most impacted, consistently exhibiting I^*_{GP}values indicative of ecological stress. Nonetheless, the overall groundwater system appeared stable during the studied period. When compared to the site's historical quality baseline (2008-2017), 78.79% of the readings fell within permissible limits, suggesting no significant long-term degradation. Statistical analysis further confirmed that Control Well No. 3 is most affected, especially in terms of pH and COD-Cr levels. These differences are likely linked to the well's proximity to potential pollutant sources, supporting the idea of localized environmental influence from plant activities.

Given the high proportion of samples exceeding authorized values and the aquifer's connection to the ROMU20 and ROMU22 groundwater bodies, which serve as sources for drinking water downstream, the potential risk to human health and ecosystems is significant. This underscores the urgent need for a sustainable and adaptive groundwater management plan.

Although the Global Pollution Index and statistical tools provide valuable insight, their effectiveness is limited by their reliance on historical or annual data, which may fail to capture temporal fluctuations or short-term pollution events. Thus, a more robust monitoring strategy is recommended, incorporating:

- Quarterly or monthly sampling to improve data resolution;
- Expanded monitoring networks with additional wells positioned at varying distances from the plant;
- Real-time data collection systems and assessment of emerging contaminants,
- Consideration of pedological and hydrogeological variability that may affect pollutant migration and sample integrity.

Further, it is advised to:

- Establish protective perimeters around existing wells to minimize external contamination;
- Investigate the chemical status of the deeper ROMU22 aquifer supplying the CET H Arad area;
- Develop protocols for new well placements, especially considering planned new plant infrastructure on the same site.

Ultimately, long-term protection of groundwater resources in industrial settings like CET H Arad depends on an integrated strategy - combining science-based monitoring, stricter regulatory enforcement, and proactive infrastructure planning.

ACKNOWLEDGEMENTS

This research was partially funded by Ministry of Research, Innovation and Digitalization, project POC/448/1/1/128019 BioEcoES project No. 356/390032/2021.

REFERENCES

Ahmed, F., Ali, I., Kousar, S., & Ahmed, S. (2022). The environmental impact of industrialization and foreign direct investment: Empirical evidence from Asia-Pacific region. *Environmental Science and Pollution Research*, *29*, 29778–29792.

Al-Aboodi, A. H., Abbas, S. A., & Ibrahim, H. T. (2018). Effect of Hartha and Najibia power plants on water quality indices of Shatt Al-Arab River, south of Iraq. *Applied Water Science*, *8*, 64.

Al-Awah, H., Redwan, M., & Rizk, S. (2023). Groundwater hydrogeochemistry impacted by industrial activities in Ain Sukhna Industrial Area, north-western part of the Gulf of Suez, Egypt. *Sustainability*, *15*.

Aly, A. I. M., Hussien, R. A., & Nassar, N. (2020). Radioactive dispersion in groundwater resulting from postulated accident at a proposed nuclear power plant,

northwestern coast of Egypt. *Groundwater for Sustainable Development*, *10*, 100326.

Bashir, I., Lone, F. A., Bhat, R. A., Mir, S. A., Dar, Z. A., & Dar, S. A. (2020). Concerns and threats of contamination on aquatic ecosystems. In *Bioremediation and Biotechnology*, 1-26 pp.

Berhanu, K. G., Lohani, T. K., & Hatiye, S. D. (2024). Spatial and seasonal groundwater quality assessment for drinking suitability using index and machine learning approach. *Heliyon*, *10*, e30362.

Biswas, A. K., Tortajada, C., & Izquierdo, R. (2014). Water quality management: Present situations, challenges and future perspectives. In *Routledge Special Issues on Water Policy and Governance*. Routledge.

Chaudhari, M. P., George, A., Sanyal, M., & Shrivastav, P. S. (2024). Hydrochemistry and groundwater quality assessment of Gujarat, India: A compendious review. *Physics and Chemistry of the Earth, Parts A/B/C*, *135*.

De Rosemond, S., Duro, D. C., & Dubé, M. (2009). Comparative analysis of regional water quality in Canada using the Water Quality Index. *Environmental Monitoring and Assessment*, *156*, 223–240.

Deshmukh, V. U., Panaskar, D. B., Pujari, P. R., & Pawar, R. S. (2021). Groundwater quality assessment in and around thermal power plants in central India. In P. M. Pawar et al. (Eds.), *Techno-Societal 2020* (pp. 963–969). Springer.

Hu, Z., & Shan, W. (2020b). Analysis of the groundwater resource pollution of coal-fired power plants and its impact on geotechnical engineering properties by numerical simulation technology. *IOP Conference Series: Earth and Environmental Science*, *450*.

Isiuku, B. O., & Enyoh, C. E. (2020). Pollution and health risks assessment of nitrate and phosphate concentrations in water bodies in South Eastern, Nigeria. *Environmental Advances*, *2*, 100018.

Jalali, M., Jalali, M., & Morrison, L. (2024). Groundwater hydrogeochemical processes, water quality index, and probabilistic health risk assessment in an arid and semi-arid environment (Hamedan, Iran). *Groundwater for Sustainable Development*, *26*.

Jayaswal, K., Sahu, V., & Gurjar, B. R. (2018). Water pollution, human health and remediation. In S. Bhattacharya, A. B. Gupta, A. Gupta, & A. Pandey (Eds.), *Water Remediation* (Springer Singapore).

Jeong, H., Bhattarai, R., Adamowski, J., & Yu, D. J. (2020). Insights from socio-hydrological modeling to design sustainable wastewater reuse strategies for agriculture at the watershed scale. *Agricultural Water Management*, *231*, 105983.

Jiang, C., Zhao, D., Chen, X., Zheng, L., Li, C., & Ren, M. (2022). Distribution, source and ecological risk assessment of polycyclic aromatic hydrocarbons in groundwater in a coal mining area, China. *Ecological Indicators*, *136*.

Krenkel, P. (2012). *Water quality management*. Elsevier Science.

Kumar, D., Kumar, R., Sharma, M., Awasthi, A., & Kumar, M. (2024). Global water quality indices: Development, implications, and limitations. *Total Environment Advances*, *9*.

Lamari, H., Mesbah, M., & Cherchali, M. E. H. (2024). Groundwater chemistry origin and quality assessment of the Sahel−Soummam aquifer, in northeast Algeria: A combined hydrochemical and isotopic approach. *Groundwater for Sustainable Development*, *26*.

Liu, F., Yi, S. A., Ma, H., Huang, J., Tang, Y., Qin, J., & Zhou, W. H. (2019). Risk assessment of groundwater environmental contamination: A case study of a karst site for the construction of a fossil power plant. *Environmental Science and Pollution Research*, *26*, 30561–30574.

Ministry of Environment and Water Management. (2006). *Plan of monitoring: Guide for the modernization and development of integrated water monitoring system in Romania*.

Mokarram, M., Mokarram, M. J., & Najafi, A. (2023). Thermal power plants pollution assessment based on deep neural networks, remote sensing, and GIS: A real case study in Iran. *Marine Pollution Bulletin*, *192*, 115069.

Mu'azu, N. D., Abubakar, I. R., & Blaisi, N. I. (2020). Public acceptability of treated wastewater reuse in Saudi Arabia: Implications for water management policy. *Science of The Total Environment*, *721*, 137659.

Muscarella, S. M., Alduina, R., Badalucco, L., Capri, F. C., Di Leto, Y., Gallo, G., Laudicina, V. A., Paliaga, S., & Mannina, G. (2024). Water reuse of treated domestic wastewater in agriculture: Effects on tomato plants, soil nutrient availability and microbial community structure. *Science of The Total Environment*, *928*, 172259.

Penserini, L., Moretti, A., Mainardis, M., Cantoni, B., & Antonelli, M. (2024). Tackling climate change through wastewater reuse in agriculture: A prioritization methodology. *Science of The Total Environment*, *914*, 169862.

Ravindiran, G., Janardhan, G., Rajamanickam, S., Sivarethinamohan, S., Murali, V., & Hayder, G. (2024). Study on hydrogeochemical assessment, groundwater quality index for drinking, seawater mixing index and human health risk assessment of nitrate and fluoride. *Groundwater for Sustainable Development*, *25*.

Romanian Government. (2002). *Decision No. 188 of February 28, 2002 for the approval of some rules on the conditions of discharge of wastewater into the aquatic environment*.

Romanian Parliament. (1996). *Water Law no. 107/1996*.

Romanian Standards Institute. (1991). *STAS 1342-91, Drink Water*.

Romanian National Waters' Administration, Târgu Mureș City's Basin Administration. (2018). *Water Management Authorization - S.C. CET HIDROCARBURI S.A. ARAD, no. 148 / 02.05.2018*.

Saliba, R., Callieris, R., D'Agostino, D., Roma, R., & Scardigno, A. (2018). Stakeholders' attitude towards the reuse of treated wastewater for irrigation in

Mediterranean agriculture. *Agricultural Water Management*, *204*, 60–68.

Sutadian, A. D., Muttil, N., Yilmaz, A. G., & Perera, B. J. C. (2016). Development of river water quality indices - A review. *Environmental Monitoring and Assessment*, *188*, 58.

Thirumoorthy, P., Murugasamy, M. V., Dhanasekaran, J., Sasikumar, K., Periyasamy, M., & Selvam, J. (2024). Assessment of groundwater quality in Perundurai region of south India using water quality index and statistical modelling. *Groundwater for Sustainable Development*, *25*.

Ullah, A., Hussain, S., Wang, Y., Awais, M., Sajjad, M. M., Ejaz, N., Javed, U., Waqas, M., Zhe, X., & Iqbal, J. (2024). Integrated assessment of groundwater quality dynamics and land use/land cover changes in rapidly urbanizing semi-arid region. *Environmental Research*, *260*, 119622.

Xiao, Y., Zhu, L., Wu, Y., Zhao, X., Xi, J., & Chen, S. (2020). Analysis of groundwater environment evaluation and prediction. *IOP Conference Series: Earth and Environmental Science*, *571*.

Zaharia, C. (2012). Evaluation of environmental impact produced by different economic activities with the global pollution index. *Environmental Science and Pollution Research*, *19*, 2448–2455.

Zaharia, C., & Murarasu, I. (2009). Environmental impact assessment induced by an industrial unit of basic chemical organic compounds synthesis using the alternative method of global pollution index. *Environmental Engineering and Management Journal*, *8*, 107–112.

Zainudin, A. M., Isa, N. M., Husin, N. H., Looi, L. J., Aris, A. Z., Sefie, A., & Idris, A. N. (2024). Groundwater potability assessment through integration of pollution index of groundwater (PIG) and groundwater quality index (GWQI) in Linggi River Basin, Negeri Sembilan, Malaysia. *Groundwater for Sustainable Development*, *26*.

Scientific Papers. Series E. Land Reclamation, Earth Observation & Surveying, Environmental Engineering. Vol. XIV, 2025
Print ISSN 2285-6064, CD-ROM ISSN 2285-6072, Online ISSN 2393-5138, ISSN-L 2285-6064

METAL CONTAMINATION IN THE SYSTEM WATER - SEDIMENTS – *PERCA FLUVIATILIS* LINNAEUS, 1758 AND *EUSTRONGYLIDES EXCISUS* JÄGERSKIÖLD, 1909 LARVAE

Nikolina ILIEVA[1], Diana KIRIN[1, 2]

[1]Agricultural University - Plovdiv, 12 Mendeleev Blvd, 4000, Plovdiv, Bulgaria
[2]National Institute of Geophysics, Geodesy and Geography (NIGGG),
Hydrology and Water Management Research Center, Bulgarian Academy
of Sciences, 3 Acad. G. Bonchev Street, 1113, Sofia, Bulgaria

Corresponding author email: ilieva.nikolina@gmail.com

Abstract

The study presents the first data on the accumulation circulation of Al, Ba and Cd in the samples of skin, muscles and liver of the European perch (Perca fluviatilis Linnaeus, 1758), its dominant parasite species Eustrongylides excises Jägerskiöld, 1909 larvae, water and sediments from the freshwater ecosystem of the anthropogenically affected protected area Mandra-Poda, Black Sea Basin, Bulgaria. The potential of European perch and E. Excises for bioaccumulation towards the studied elements has been studied. The bioindicator significance of P. fluviatilis and E. Excises for assessing the pollution of the freshwater ecosystem with Al, Ba, and Cd has been revealed. The risk to human health and living organisms has been evaluated. Measures for the protection of the ecosystem have been indicated.

Key words*: aluminium, barium, cadmium, bioindication, European perch.*

INTRODUCTION

The Mandra-Poda Complex is located south of the industrial zone of Burgas, along the sea coast. It is part of the Burgas Wetlands, within the Black Sea Basin Region and Ecoregion 12: Pontic Province, Sub-Ecoregion 12-2: Black Sea, in southeastern Bulgaria. The Mandra-Poda Complex is recognized as a wetland of international importance under the Ramsar Convention on Wetlands (1971). The site is also protected under the Habitats Directive (Directive 92/43/EEC) and the Birds Directive (Directive 79/409/EEC). Additionally, it is designated as a Corine Biotope (Corine, 1985) and classified as an Important Bird Area by BirdLife International. According to national legislation (Law on Protected Areas, 1989), three protected areas have been designated within the territory of the Mandra-Poda Complex: "Poda" (State Gazette No. 37/1989), "Ustie na reka Izvorska" (State Gazette No. 18/1990), and "Uzungeren" (State Gazette No. 102/2005). These areas were established for the conservation of habitats supporting endangered and rare bird species. The Complex lies along the "Via Pontica" migration route. Four rivers - Izvorska, Fakiyska, Sredetska, and Rusokastrenska - flow into the Complex.

Despite its international and national significance for habitat protection and exceptional biodiversity, the Mandra-Poda Complex is under significant anthropogenic pressure. Nearby, the Lukoil Neftochim Burgas oil refinery utilizes water from the Complex for industrial purposes.

Serious threats to the protection of biodiversity and water resources are the great anthropogenic pressure from the construction around the wetland, associated with the destruction of natural habitats (wet meadows and others), eutrophication of the wetland, pollution with industrial wastewater, household waste, overfishing, poaching, disturbance of birds and other organisms. Studies on parasites and parasite communities of freshwater fish from the Complex Mandra-Poda are scarce (Margaritov, 1959; Ilieva & Kirin, 2024). There were established single scientific studies on the chemical indicators of water pollution and the content of pollutants in the muscles of freshwater fish species (Georgieva et al., 2015; Peycheva et al., 2022), as well as on the contamination of Se in organs and tissues of

European perch and its parasite *Eustrongylides excisus*, in waters and sediments (Ilieva & Kirin, 2024).

The study aims to present ecohelminthological and monitoring results for contamination with aluminium (Al), barium (Ba), and cadmium (Cd) in tissues and organs of *Perca fluviatilis* Linnaeus, 1758 its dominant helminth species *Eustrongylides excises* Jägerskiöld, 1909 larvae, waters and sediments, as well as an assessment of their bioindicator significance for the condition of the Complex Mandra-Poda.

MATERIALS AND METHODS

The helminthological and environmental monitoring study was conducted on thirty specimens of *Perca fluviatilis* collected from the Mandra-Poda Complex. The perch samples were obtained using multi-mesh gillnets in accordance with BSS EN 14757:2015 - *Water quality: Sampling of fish with multi-mesh gillnets*. Sampling was performed with permission from the Executive Agency for Fisheries and Aquaculture, under the Ministry of Agriculture of Bulgaria.

The scientific names of the studied fish species were verified using the FishBase database (Froese & Pauly, 2024).

Sampling was carried out at three sites located in the eastern (Poda), northern (Meden Rudnik), and western (Konstantinovo) areas of the Mandra-Poda Complex (42°24′12.31″N, 27°19′18.05″E; 309 m; Figure 1).

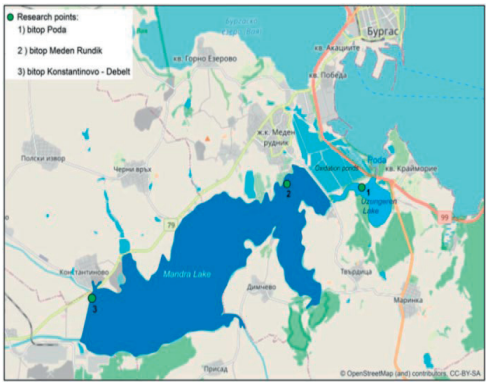


Figure 1. Studied biotopes from the Complex Mandra-Poda

The helminthological examination of *Perca fluviatilis* was conducted following the methodologies outlined by Zashev and Margaritov (1966), Bauer (Ed.) (1987), and Moravec (2013). Collected helminth specimens were preserved in 70% ethyl alcohol. Dominant nematode specimens were identified using temporary slides, in accordance with Moravec (2013). The predominant species, *Eustrongylides excisus* (Jägerskiöld, 1909), was selected as a model helminth for subsequent monitoring studies.

Tissue samples (skin, muscle, and liver) from *P. fluviatilis*, along with *E. excisus* larvae, were prepared to assess aluminium (Al), barium (Ba), and cadmium (Cd) concentrations, following the protocol of Nachev et al. (2013). Pre-weighed and thawed samples of fish tissues (up to 300 mg wet weight) and helminths (up to 100 mg wet weight) were subjected to acid digestion using aqua regia and microwave heating (Method B: Microwave heating with temperature control at 175 ± 5 °C). Approximately 2 g of each sample were digested in closed vessels under pressure with 6.0 mL HCl and 2.0 mL HNO_3. Elemental concentrations were determined using inductively coupled plasma optical emission spectrometry (ICP-OES), in accordance with EN ISO 16170:2016.

In addition, concentrations of Al, Ba, and Cd in surface water and sediment samples were measured using EN ISO 11885:2009 (*Water quality - Determination of selected elements by ICP-OES*) and ISO 22036:2024 (*Environmental solid matrices - Determination of elements by ICP-OES*).

The Bioconcentration Factors for determining the capacity for accumulation of Al, Ba, and Cd in the muscles, skin, and liver of European perch and *E. excisus* from freshwater environments (Bioconcentration Factor, $BCF=C_{Al,Ba,Cd_Skin}/C_{Al,Ba,Cd_Liver}/C_{Al,Ba,Cd_Muscle}/C_{Al,Ba,Cd_E.excisus}/C_{Al,Ba,Cd_Water}/C_{Al,Ba,Cd_Sediments}$) (Sures et al., 1999), as well as the Bioaccumulation Factor for determining the capacity for accumulation of Al, Ba, and Cd in *E. excisus* from organs and tissues of European perch (Bioaccumulation Factor, $BAF=C_{Al,Ba,Cd_E.excisus}/C_{Al,Ba,Cd_fish_tissues_organs}$) (Sorensen, 1991; Zaharieva, 2022a) are presented. Spearman's rank correlation coefficient (rs) values were determined to

establish the relationship between the concentrations of Al, Ba and Cd in environmental samples (water, sediments), in samples of liver, muscle and skin of host fish and in samples of the nematode *E. excisus* (Sokal & Rohlf, 1981). The coefficient of determination (r_s^2) was presented to determine what percentage of the factor variable would cause changes in the output variable. The Friedman test (Friedman's ANOVA test) was calculated to assess the significance of the differences between the contents of Al, Ba and Cd in the studied tissues and organs of fish and *E. excisus* (Sokal & Rohlf, 1981). The results are statistically processed using Statistic 10 (Stat Soft Inc., 2011) and MS Excel (Microsoft 2010).

RESULTS AND DISCUSSIONS

Characteristics of the studied fish species

European perch, *Perca fluviatilis* Linnaeus, 1758 (Percidae), was chosen as a model freshwater fish species due to its dominant behavior in the samples and as a predatory species. *P. fluviatilis* is also a demersal and brackish fish species. The perch feeds mainly on zooplankton, zoobenthos and small fish. *Perca fluviatilis* is in the category of Least Concern species according to the International Union for Conservation of Nature Red List (LC; IUCN) (Kottelat & Freyhof, 2007; Froese, & Pauly 2024). The species are not protected in the territory of Bulgaria (Karapetkova & Zhivkov, 2006). The perch inhabits various water bodies in the country and is widely distributed. *P. fluviatilis* is mainly targeted by recreational fishing. Each specimen's maximum length (TL, cm) and weight (B, g) were measured. The maximum length of the studied specimens ranged from 12-22.50 cm (17.77±3.06), and the weight from 21-227 g (75.77±57.09).

Characteristics of the studied endohelminth species

The ecohelminthological study of 30 specimens of European perch, *Perca fluviatilis* Linnaeus, 1758 from the Complex Mandra-Poda shows a clear dominance of the nematode *Eustrongylus excisus* (Jägerskiöld, 1909) (P%=90). The definitive hosts of *Eustrongylus excisus* (Jägerskiöld, 1909) are cormorants (*Phalacrocorax carbo* (Linnaeus, 1758), *Ph. pygmaeus* (Pallas, 1773)). The adult nematodes are localized in the glandular stomach of the host. The life cycle of *E. excisus* occurs with the participation of two intermediate hosts: the first intermediate hosts are aquatic oligochaetes (*Lumbricus variegatus* (Müller, 1774), *Tubifex tubifex* (Müller, 1774), *Limnodrilus* sp.). The first stage of larvae development is localized in the intestine and then in the body cavity. The second stage larva is localized in the abdominal blood vessel, and the third stage larva with the bloodstream passes to the head and tail of the host. Benthic fish species are the second intermediate host (*Ponticola kessleri* (Günther, 1861), *Neogobius melanostomus* (Pallas, 1814), *Rutilus rutilus* (Linnaeus, 1758)). The intermediate hosts and the final host are infected by feeding. In the body of the second intermediate host, the fish and the third-stage larvae are localized in the body cavity or coiled in a circle under the serous coating on the surface of the internal organs. After another moult, they migrate into the muscles of the fish. The fourth stage larva is invasive, coiled and encapsulated. *P. fluviatilis* is a reservoir host of *E. excisus*. Other species, reservoir hosts of *E. excisus* are: *Leuciscus aspius* (Linnaeus, 1758), *Silurus glanis* Linnaeus, 1758, *E. lucius*, *Sander lucioperca* (Linnaeus, 1758), *Sander volgensis* (Gmelin, 1789), *G. cernua*, *Alburnus chalcoides* (Güldenstädt, 1772), *Bentophilus macrocephalus* (Pallas,1787), *Huso huso* (Linnaeus, 1758), *Acipenser ruthenus* Linnaeus, 1758, *A. gueldenstaedtii* Brandt & Ratzeburg, 1833, *Leuciscus idus* (Linnaeus, 1758), *Luciobarbus brachycephalus* (Kessler, 1872). Accidental hosts can also be amphibians (frogs, *Pelophylax ridibundus* (Pallas, 1771)), reptiles (*Natrix tessellata* (Laurenti, 1768), turtles and others), mammals (rabbits, rats, seals, even humans) (Bauer, 1987; Kakacheva-Avramova, 1983; Honcharov et al., 2022). *E. excisus* has been reported in Bulgaria for *P. fluviatilis* from Lake Srebarna (Shukerova, 2010; Shukerova et al., 2010; Hristov, 2013; Kirin et al., 2013a); from the Arda River (Kirin et al., 2013b); from the Danube River (Atanasov, 2012; Kirin et al., 2013a; Zaharieva, 2022b). *E. excisus* has been reported for the Mandra-Poda complex from *S. lucioperca* as a reservoir host and from *Gobius* sp. as an intermediate host (Margaritov, 1959); from

P. fluviatilis (Ilieva & Kirin, 2024 and in the present study).

Concentration of aluminium (Al), barium (Ba) and cadmium (Cd) in the system Water - Sediments - *P. fluviatilis* – *E. excisus*

Chemical analyses were performed to determine the Al, Ba, and Cd content in the skin, muscle, and liver of *P. fluviatilis*, in samples of *E. excisus*, water, and sediments (Table 1).

Table 1. Contamination with aluminium (Al), barium (Ba), and cadmium (Cd) in tissues and organs of *P. fluviatilis*, its nematode species *E. excisus*, waters and sediments [mg/kg]

Samples	**Min.-Max. Mean±SD**	**Min.-Max. Mean±SD**	**Min.-Max. Mean±SD**
Wet weight	**Al**	**Ba**	**Cd**
Skin	3.38 – 86.16	1.18- 4.07	0.00-0.00
P. fluviatilis	58.69±7.54	2.62±0.32	0.00±0.00
Muscle	81.52-133.28	0.53-0.93	0.00-0.00
P. fluviatilis	107.40±12.94	0.73±0.10	0.00±0.00
Liver	10.49-18.07	0.06-0.26	0.09-0.15
P. fluviatilis	14.28±1.89	0.16±0.05	0.124±0.01
E. excisus	28.51-53.13	0.05-0.33	0.05-0.08
	40.82±6.16	0.19±0.07	0.07±0.008
Dry weight	**Al**	**Ba**	**Cd**
Skin	87.04-147.16	3.94-6.54	0.00-0.00
P. fluviatilis	117.1±15.03	5.23±0.65	0.00±0.00
Muscle	155.78-258.02	1.01-1.83	0.00-0.00
P. fluviatilis	207.9±25.06	1.42±0.21	0.00±0.00
Liver	41.75-71.87	0.26-1.04	0.38-0.60
P. fluviatilis	56.81±7.53	0.65±0.19	0.49±0.05
E. excisus	83.92-156.44	0.15-1.01	0.16-0.24
	120.18±18.13	0.68±0.21	0.19±0.02
Water	0.01-0.02	0.02 – 0.03	0.03 – 0.04
	0.013±0.003	0.03±0.005	0.03±0.008
Sediments	2.65 – 39.97	7.08 – 140.1	0.23 – 2.75
	25.68±20.14	77.97±66.94	1.85±1.41
Maximum permissible concentration (MPC)			
Reg. 31/2004	30	-	0.05
FAO/ WHO	7	0.3	0.5
MAFF			0.2

Cd is a major toxic metal until Ba is a minor toxic metal (Mostafa et al., 2022). Human exposure to aluminium can and will result in toxicity (Exley, 2016). Cd causes toxic effects at very low concentrations (Sorensen, 1991; Peycheva et al., 2014). The maximum permissible concentration (MPC) for Cd, according Regulation No. 31/2004), is 0.05 mg/kg fish; according to FAO, it is 0.5 mg/kg, and according to MAFF, it is 0.2 mg/kg. Sources of pollution are industrial wastewater (Yablanski, Petkov (eds.), 2011). In nature, sources of Ba are fossil fuels, igneous rocks, feldspar and mica deposits. The entry of soluble $BaCl_2$, $Ba(NO_3)_2$, or $Ba(OH)_2$ is important for aquatic ecosystems. Ba is quickly released and binds to naturally occurring sulfates or carbonates, forming less soluble compounds - $BaSO_4$ and $BaCO_3$, most found in soils and waters (Verbruggen et al., 2020). Therefore, the toxicity of Ba is closely related to the hardness of the water and the amount of sulfates/carbonates. As the pH decreases, the solubility of Ba increases. This explains the higher concentrations of Ba in sediments (precipitation of poorly soluble barium compounds). A dissolved Ba value of 0.022 $mg \cdot L^{-1}$ has been adopted for human health (Verbruggen et al., 2020).

The highest concentrations of Ba and Cd were found in sediments. The lowest contamination was in water samples for the three elements. The results of the studied tissues and organs of the perch and its parasites showed the highest value of Al in the muscles, followed by those in the skin. The lowest values of Al were found in the liver. The Al content in *E. excisus* was 2.63 times lower than in the muscles. Therefore, the Al content decreased in the order muscles - skin - *E. excisus* - liver - sediments - water. The Al content in the muscles was 7.54 times higher than in the liver and in the parasite - 2.85 times higher than in the liver of the European perch. The highest concentrations of Ba were found in the skin of *P. fluviatilis*. The Ba content decreased in the order sediments - skin - muscles - *E. excisus* - liver - water. The Ba content in the skin was 16.37 times higher than in the liver samples, and the parasite – 1.18 times higher than in the liver samples. No Cd was detected in the skin and muscle samples. The Cd content decreased in the order sediments - liver - *E. excisus* - water. The cadmium (Cd) concentration detected in the liver samples of *Perca fluviatilis* was 1.85 times higher than that found in *Eustrongylides excisus* (Table 1).

According to Regulation No. 31/2004, the MPC for Al in freshwater fish is 30 mg/kg wet weight. Exceedance of the norm was not found only in liver samples. The Al content in muscle samples is 3.58 times higher than the approved MPC, in the skin - 1.95 times, and in the parasite - 1.36 times. According to the same regulation, the MPC for Cd is 0.05 mg/kg wet weight. The exceedances are respectively 2.48 times in the liver and 1.32 times in the nematode. The Al content in water samples is within the norm and has been approved according to Regulation No. H-4/2012. No exceedances of the Cd content

were found according to the approved norms by FAO and WHO for food (FAO/WHO (1998)) (0.2 and 20 mg/kg wet weight, respectively), according to Regulation No. 3/2008 on the standards for permitted content of Harmful Substances in soil, and Regulation on environmental quality standards for priority substances and certain other pollutants. Exceedances of these norms were found in liver and *E. excisus* samples.

The obtained results show excesses in the content of Al in skin (1.96 times), in muscles (3.58 times), and in *E. excisus* (1.36 times) according to the national legislation (Regulation No. 31/2004) for the content of Al in freshwater fish species (MPC 30 mg/kg); excesses in water samples (0.005 $mg.l^{-1}$ norm according to Regulation No. 18/2002) when using surface waters for irrigation. The content of Ba was exceeded in skin samples (119.09 times) and muscles (33.18 times). Cd concentrations were exceeded in liver samples (1.8 times) and *E. excisus* (1.4 times), according Regulation No. 31/2004. Cd concentrations were exceeded in water samples (3000 times, Regulation No. 18/2002). Cd concentrations were exceeded in sediment samples on average 2.31 times (Regulation No. 18/2002) (Table 1).

The bioconcentration factors (BCF) and bioaccumulation factors (BAF) are presented. The highest BCF and BAF were obtained for Al and the lowest for Cd (Table 2).

Very high correlations (r_s) were found between all the results obtained for Al, Ba and Cd content in water, sediments, skin, muscles and liver of *P. fluviatilis* and the dominant parasite species *E. excisus* (Table 2).

Significant differences were found between contaminations with Al and Ba in *E. excisus* and the samples of skin, muscles, liver of European perch, waters and sediments, as well as between contaminations with Cd in *E. excisus* and in the samples of liver (Friedman's ANOVA, $p<0.05$). The coefficient of determination (r_s^2) in all cases is 100%. This gives reason to believe that all changes in the concentrations with Al, Ba, and Cd in the waters and sediments of the Complex Mandra-Poda and the specific habitats of *P. fluviatilis* will lead to changes in the concentrations of these elements in the skin, muscles, and liver of the fish and the dominant nematode *E. excisus* in them.

Table 2. Bioconcentration factor (BCF), Bioaccumulation factor (BAF), and Spearman correlation coefficient (r_s) between the content of Al, Ba, and Cd in water, sediments, *P. fluviatilis* and *E. excisus*

Fish - Parasite - Water (wet weight)	**Al BCF**	**Ba BCF**	**Cd BCF**
Skin - Water	4514.62****	109.17****	0.00
Muscle - Water	8261.54****	30.42****	0.00
Liver - Water	1098.46****	6.67****	4.14****
E. excisus - Water	3140.00****	7.92****	2.20****
Fish - Parasite - Sediments (dry weight)	**Al BCF**	**Ba BCF**	**Cd BCF**
Skin - Sediments	4.56****	0.07****	0.00
Muscle - Sediments	36.60****	0.02****	0.00
Liver - Sediments	2.21****	0.008****	0.26****
E. excisus - Sediments	4.68****	0.009****	0.10****
***E. excisus* - Fish** (wet weight)	**Al BAF**	**Ba BAF**	**Cd BAF**
E. excisus- Skin	0.69****	0.07****	0.00
E. excisus - Muscle	0.38****	0.26****	0.00
E. excisus - Liver	2.85****	1.19****	0.53****
***E. excisus* - Fish** (dry weight)	**Al BAF**	**Ba BAF**	**Cd BAF**
E. excisus - Skin	1.03****	0.13****	0.00
E. excisus - Muscle	0.58****	0.47****	0.00
E. excisus - Liver	2.12****	1.05****	0.38****

r_s **** - very significant correlation, $p = 0.001$.

In this study, the liver accumulated higher concentrations of Cd than the parasite. Similar results have been obtained by other authors regarding the content of the studied elements (Al, Ba and Cd) in the liver of freshwater fish species, followed by that in the intestine and muscle (Leite et al., 2019; Mostafa et al., 2022). This is explained by Cd's affinity for proteins rich in the liver (Dallinger et al., 1987). In contrast to these results for Ba in the liver, the skin accumulated the highest concentrations of Ba in this study. According to other studies (Mazhar et al., 2014), Al is one of the few metals that accumulate in the highest concentrations in the muscles, which was also revealed by the present study. The highest content of Al was found in the samples from *E. excisus*, followed by that of Ba and Cd. The L4 larvae (fourth-stage larvae) were studied, localized in the body cavity, where they feed on blood and tissues before being encapsulated, which is associated with higher levels of Al (Nachev et al., 2013; Honcharov, 2022). Al, Ba and Cd contents are much higher in sediment samples than in water samples. This has also been found in other studies and is explained by the fact that metals attach to suspended particles or are adsorbed to

organic matter and thus precipitate and accumulate at the bottom of reservoirs (Mostafa et al., 2022). Only about 1% dissolves in water during the hydrological cycle (Salomons & Stigliani, 1995).
According to the results obtained in this study, it could be assumed that the main source of Al, Ba and Cd for *P. fluviatilis* is food and, to a lesser extent, water.

CONCLUSIONS

As a result of the study it was found that the highest concentrations of Al accumulate in the muscles, the highest concentrations of Ba in the skin, and the highest concentrations of Cd in the liver. The main sources of Al, Ba and Cd for *P. fluviatilis* are food and to a lesser extent water. *E. excisus* can be used as a sensitive bioindicator for Al pollution of freshwater ecosystems. Sediment samples contain much higher concentrations of Al, Ba and Cd than water samples. Very significant correlations were found between the content of the observed metals (Al, Ba and Cd) and their amounts in water, sediments, organs and tissues of *P. fluviatilis* and its dominant nematode species *E. excisus*.

ACKNOWLEDGEMENTS

This research was carried out with the financial support of Agricultural University - Plovdiv, Bulgaria and VANG EOOD, Bulgaria.

REFERENCES

Anonymous (1991). *Empfehlungen für die Nährstoffzufuhr*. Deutsche Gesellschaft für Ernährung, Germany, 72-75.

Atanasov, G. (2012). Fauna, morphology and biology on the endohelminths of fish from Bulgarian part of the Danube River. *PhD these, Sofia.*

Bauer, O. N. (1987). *Key to the Parasites of Freshwater Fishes of the USSR*. Leningrad, RU: Nauka (in Russian).

BSS EN 14757:2015 Water quality. Sampling of fish with multi-mesh gillnets.

Dallinger, R., Prosi, F., Segner, H., & Back, H. (1987). Contaminated food and uptake of heavy metals by fish: a review and a proposal for further research. *Oecologia*, *73*, 91-98.

Directive 79/409/EC of 2 April 1979 on the conservation of the wild birds. http://www.central.eu

Directive 92/43/EEC on the Conservation of natural habitats and of wild fauna and flora. http://ec.europa.eu

EN ISO 11885:2009 Water quality - Determination of selected elements by inductively coupled plasma optical emission spectrometry (ICP-OES)

EN ISO 16170:2016 In situ test methods for high efficiency filter systems in industrial facilities

FAO (Food and Agriculture Organization) (1983). FAO Fishery Circular No. 464,5-10. Food and Agriculture. The results obtained for toxic and trace elements in analyzed fish. Organization of the United Nations, Rome.

FAO/WHO (1998) *Preparation and use of food-based dietary guidelines.* Report of a joint FAO/WHO consultation. Geneva, World Health Organization (WHO Technical Report Series, No. 880).

Exley, C. (2016). The toxicity of aluminium in humans. *Morphologie*, *100*(329), 51-55.

Froese, R. and D. Pauly. Editors. 2024. FishBase.
World Wide Web electronic publication. www.fishbase.org, (10/2024)

Georgieva, G., Stancheva, M., Makedonski, L. (2015). Persistent Organochlorine Compouds (PcBs, DDTs, HCB &HBDE) in Wils Fishfrom the Lake Burgasand the Lake Mandra, Bulgaria. *Ecology & Safety*, 9, 515-523.

Honcharov, S. L., Soroka, N. M., Galat, M. V., Zhurenko, O. V., Dubovyi, A. I., & Dzhmil, V. I. (2022). Eustrongylides (Nematoda: Dioctophymatidae): epizootology and special characteristics of the development biology. *Helminthologia*, *59*(2), 127.

Hristov, S. (2010). Circulation of some heavy metals in the freshwater ecosystem of the Srebarna Biosphere Reserve. *Journal of Ecology&Safety*, *4*(2), 204-213.
https://lex.bg/laws/ldoc/2134445060

Ilieva, N., & Kirin, D. (2024). Helminth biodiversity and heavy metal contamination of *Perca fluviatilis* (Linnaeus, 1758) and *Eustrongylides excisus* (Jägerskiöld, 1909) larvae from the wetland Mandra-Poda. *Scientific Papers. Series D. Animal Science*, *67*(2)

ISO 22036:2024 Environmental solid matrices — Determination of elements using inductively coupled plasma optical emission spectrometry (ICP-OES).

IUCN. 2022. *The IUCN Red List of Threatened Species. Version 2022-2*. https://www.iucnredlist.org

Kakacheva-Avramova, D. (1983). *Helminths of freshwater fishes in Bulgaria*. Sofia, Bulgarian Academy of Sciences.

Karapetkova, M., Zhivkov, M. (2006). *Fishes in Bulgaria*. Publ. house Gea-Libris, Sofia (in Bulgarian).

Kirin, D., Hanzelová, V., Shukerova S., Hristov S., Turčeková, L., Spakulova, M., Barciová T.(2013a). Biodiversity and ecological appraisal of the freshwater ecosystem of the Arda River, Bulgaria. *Scientific Papers. Series D. Animal Science. LVI,* 341-348.

Kirin, D., Hanzelová, V., Shukerova S., Hristov S., Turčeková, L., Spakulova, M. (2013b). Helminth communities of Fishes from the River Danube and Lake Srebarna, Bulgaria. *Scientific Papers. Series D. Animal Science, LVI*, 333-340.

Kottelat, M. &Freyhof, J. (2007). Handbook of European freshwater fishes. *Publications Kottelat, Cornol and Freyhof, Berlin*. 646.

Law for the Protected Areas. State Gazette, issue 133 of November 11, 1998.

Leite, L.A., Januário, F.F., Padilha, P.M., do Livramento, E.T., de Azevedo, R.K., Abdallah, V.D. (2019) Heavy Metal Accumulation in the Intestinal Tapeworm *Proteocephalus macrophallus* Infecting the Butterfly Peacock Bass (*Cichlao cellaris*), from South-eastern Brazil. *Bulletin of Environmental Contamination and Toxicology* 103, 670– 675.

MAFF (1995). Monitoring and surveillance of non-radioactive contaminants in the aquatic environment and activities regulating the disposal of wastes at sea, 1993. *Aquatic Environment Monitoring. Report No. 44. Direcorate of Fisheries Research, Lowestoft*

Margaritov, N. (1959). *Parasites of some fresh water fishes.* Varna, BG: Publishing House NIRRP (in Bulgarian).

Mazhar, R., Shazili, N. A., & Harrison, F. S. (2014). Comparative study of the metal accumulation in *Hysterothalycium reliquens* (nematode) and *Paraphilometroides nemipteri* (nematode) as compared with their doubly infected host, *Nemipterus peronii* (Notched threadfin bream). *Parasitology Research*, *113*, 3737-3743.

Moravec, F. (2013). Parasitic nematodes of freshwater fishes of Europe. *Academia, Prague.* 601 pp.

Mostafa, O., Hanfi, T., Abd-eltwab, D., Al-Shehri M., Moustafa M., Al-Emam A., Alhamdi, H., Nigm, A. (2022). Fish Parasites as Biological Indicators of Metals Pollution in the Aquatic Environments. *Research Square*, 1-17.

Nachev, M., Schertzinger, G., Sures, B. (2013). Comparison of the metal accumulation capacity between the acanthocephalan *Pomphorhynchus laevis* and larval nematodes of the genus *Eustrongylides* sp. infected barbel (*Barbus barbus*). *Parasites & Vectors*, *6*(21), 1-8.

Peycheva, K., Panayotova, V., Makedonski, M., Stancheva, R. (2014). Toxic and essential concentration of freshwater fishes from *Pyasachnik* Dam, Bulgaria. *Agricultural Science and Technology*, 6(3), 364-369.

Peycheva, K., Panayotova, V., Stancheva, R., Makedonski, L., Merdzhanova, A., Parrino, V., Nava, V., Cicero, N., Fazio, F. (2022). Risk Assessment of Essential and Toxic Elements in Freshwater Fish Species from Lakes near Black Sea, Bulgaria. *Toxics*, *10*(11), 675.

Ramsar Convention of Wetlands (1971). www.ramsar.org

Regulation No. 18 of 27.05.2009 on the quality of water for irrigation of agricultural crops Issued by the Minister of Environment and Water and the Minister of Agriculture and Food. *State Gazette*, 43 of 09.06.2009.

Regulation no. 3 of August 1, 2008 on the standards for permitted content of Harmful Substances in soils. *State Gazette*, 71 of 12.08.2008.

Regulation No. 31 of 29 July 2004 on the Maximum Permitted Quantities of contaminants in foodstuffs. *State Gazette*, 88 of 08.10.2004.

Regulation No. H-4 of September 14, 2012 on characterization of Surface Waters. *State Gazette*, 22 of 05.03.2013.

Regulation on environmental quality standards for priority substances and certain other pollutants. *State Gazette*, 88 of 09.11.2010.

Salomons W, Stigliani W (1995) Biogeodynamics of Pollutants in Soils and Sediments. *Springer Verlag, Heidelberg*, pp. 352

Shukerova, S. (2010). Helminths and helminth communities of fishes from Biosphere Reserve Srebarna. *PhD thesis*

Shukerova, S., Kirin, D., Hanzelova V. (2010). Endohelminth communities of the perch, *Perca fluviatilis* (Perciformes, Percidae) from Srebarna Biosphere Reserve, Bulgaria. *Helminthologia, 47*(2), 99-104.

Sokal, R. R. (85). RohlfFJ (1981) Biometry. The principles and practice of statistics in biological research. *WR Freeman and Company, New York*, 429-450.

Sorensen, E.M.B. (1991) Metal Poisoning in Fish. *CRC Press, Boca Raton.*

State Newspaper 102, 2005. Order No. РД-1152 of 23.11.2005. Protected area Uzungeren.

State Newspaper 18, 1990. Order No. 170 of 16.02.1990. Protected area "Ustie na reka Izvorska".

State Newspaper 37, 1989. Order No. 443 of 20.04.1989. Protected area Poda.

Statsoft Inc. (2011) (n.d.). STATISTICA, version 10. Retrieved from www.statsoft.com.

Sures, B., Siddall, R., & Taraschewski, H. (1999). Parasites as accumulation indicators of heavy metal pollution. *Parasitology Today*, *15*(1), 16-21.

Verbruggen, E.M.J., Smit, C.E., Vlaardinger, P.L.A. (2020). Environmental quality standards for barium in surface water. *Published by: National Institute for Public Health and the Environment, Ministry of Health, Welfare and Sport, RIVM,* The Netherlands.

Yablanski, Z., Perkov, G. (Eds.), 2011. Manual Book of Applied Ecology. Alfamarket, Stara Zagora.

Zaharieva, P. (2022a). Content of heavy metals in Fishes and their Parasites from the Danube River - Ecology and Bioindication. *PhD thesis,* Plovdiv (in Bulgarian).

Zaharieva, R. (2022b). Parasites and Parasite Communities on Fishes from the Danube River - Ecology and Biodiversity. *PhD thesis,* Plovdiv (in Bulgarian).

Zashev, G., Margaritov, N. (1966). *Diseases of fish.* Sofia, BG: Naukaiizkustvo (in Bulgarian).

Scientific Papers. Series E. Land Reclamation, Earth Observation & Surveying, Environmental Engineering. Vol. XIV, 2025
Print ISSN 2285-6064, CD-ROM ISSN 2285-6072, Online ISSN 2393-5138, ISSN-L 2285-6064

CONTAMINATION OF POLLUTANTS IN *ABRAMIS BRAMA* (LINNAEUS, 1758), BIOINDICATION AND ECOLOGICAL RISK ASSESSMENT OF THE WETLAND MANDRA-PODA, BULGARIA

Nikolina ILIEVA[1], Diana KIRIN[1, 2]

[1]Agricultural University - Plovdiv, 12 Mendeleev Blvd, 4000, Plovdiv, Bulgaria
[2]National Institute of Geophysics, Geodesy and Geography (NIGGG),
Hydrology and Water Management Research Center, Bulgarian Academy of Sciences,
3 Acad. G. Bonchev Street, 1113, Sofia, Bulgaria

Corresponding author email: ilieva.nikolina@gmail.com

Abstract

The study presents the data on the contamination of Cd, Cu, Hg, Ni, and Pb in the samples of skin, muscles, and liver of freshwater bream (Abramis brama (Linnaeus, 1758)), as well as in water and sediments samples from the studied ecosystem of the protected wetland Mandra-Poda, Black Sea Region, Bulgaria. Basic ecological indices have been determined. New data for the bioindicator significance of freshwater bream for the accumulation of trace elements in skin, muscles, and liver has been reported. Basic correlation dependencies have been indicated. Discussions on the use of freshwater bream as a food resource have been attached. The risk of pollution to human health and the environment has been assessed.

Key words*: bioindication, chemical status, ecological state, freshwater bream, risk assessment.*

INTRODUCTION

Wetlands play a crucial role in regulating water regimes and supporting unique habitats for diverse plant and animal communities. One such ecologically significant site in Bulgaria is the Mandra-Poda Complex, recognized for its national and international importance. It forms part of the Burgas Wetlands, situated in the Black Sea Basin Region—Ecoregion 12: Pontic Province, Sub-Ecoregion 12-2: Black Sea, in southeastern Bulgaria. The complex is located south of the industrial zone of Burgas, adjacent to the Black Sea coast. The Mandra-Poda Complex is designated as a wetland of international importance under the Ramsar Convention (1971) and is protected by the Habitats Directive (92/43/EEC), the Birds Directive (79/409/EEC), as well as through its status as a Corine Biotope and an Ornithologically Important Site. In accordance with Bulgaria's Law for the Protected Areas (1989), three protected zones have been established within the Complex: "Poda," "Ustie na reka Izvorska," and "Uzungeren," aimed at preserving habitats for endangered and rare bird species. Despite these protections and its recognized ecological value, the area remains under significant anthropogenic pressure. The Lukoil Neftochim Burgas oil refinery uses waters from the Complex Mandra-Poda for industrial needs. Intense anthropogenic pressure from construction activities around the wetland - leading to the destruction of natural habitats (such as wet meadows), eutrophication, pollution from industrial wastewater and household waste, overfishing, poaching, and disturbance of birds and other organisms - poses significant threats to the biodiversity and water resources of the area. Scientific studies examining water pollution indicators and the accumulation of pollutants in freshwater fish species remain limited (Georgieva et al., 2015; Peycheva et al., 2022; Ilieva & Kirin, 2024). The present study aims to provide ecological monitoring data on contamination levels of cadmium (Cd), copper (Cu), mercury (Hg), nickel (Ni), and lead (Pb) in the skin, muscle, and liver of *Abramis brama* (Linnaeus, 1758), as well as in water and sediment samples. The findings are intended to support an assessment of the species' potential as a bioindicator of environmental conditions in the Mandra-Poda Complex.

The freshwater bream, *Abramis brama* (Linnaeus, 1758) (family Cyprinidae), was selected as a model species for this study due to its ecological role as a benthopelagic, brackish-water predator. This species feeds primarily on zooplankton, insects, crustaceans, mollusks, aquatic plants, and small fish. According to the International Union for Conservation of Nature (IUCN) Red List, *A. brama* is classified as a species of Least Concern (LC) (Kottelat & Freyhof, 2007; Froese & Pauly, 2024). In Bulgaria, the species is not legally protected (Karapetkova & Zhivkov, 2006). *A. brama* is widely distributed across the country's aquatic ecosystems and is an important species for both sport and commercial fisheries.

MATERIALS AND METHODS

The study was conducted on ten specimens of freshwater bream (*Abramis brama* Linnaeus, 1758) collected from the Mandra-Poda Complex. Sampling was carried out using multi-mesh gillnets in accordance with BSS EN 14757:2015 (*Water quality – Sampling of fish with multi-mesh gillnets*), following approval from the Executive Agency for Fisheries and Aquaculture, Ministry of Agriculture, Bulgaria. The scientific name of the species was verified using the FishBase database (Froese & Pauly, 2020). Specimens were obtained from three locations within the complex: the eastern site (Poda), the northern site (Meden Rudnik), and the western site (Konstantinovo), situated at coordinates 42°24'12.31″N, 27°19'18.05″E, at an altitude of 309 meters (Figure 1).

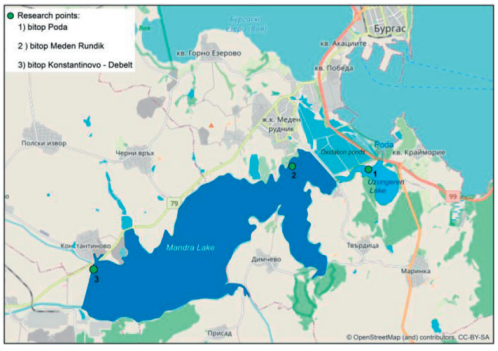


Figure 1. Studied biotopes from the Complex Mandra–Poda

Maximum length (TL, cm) and weight (W, g) were measured for each specimen. Samples of skin, muscle, and liver of A. brama were prepared for determination of Cadmium (Cd), Copper (Cu), Mercury (Hg), Nickel (Ni), and Lead (Pb) content. The pre-weighed and thawed samples of liver, muscle and skin of *A. brama* (to 300 mg wet weight) were subjected to acid digestion with aqua regia and microwave heating - Method B: “Microwave heating with temperature control at 175±5°C”. Samples of 2 g were used in closed vessels under pressure with 6.0 ml HCl and 2.0 ml HNO_3, and the element was determined using ICP-OES, according to EN ISO 16170:2016. In surface water and sediment samples, concentrations of Cd, Cu, Hg, Ni, and Pb were determined according to EN ISO 11885:2009 Water quality - Determination of selected elements by inductively coupled plasma optical emission spectrometry (ICP-OES) and EN ISO 22036:2024 Environmental solid matrices - Determination of elements using inductively coupled plasma optical emission spectrometry (ICP-OES). The Bioconcentration Factors are presented for determining the capacity for accumulation of Cd, Cu, Hg, Ni, and Pb in the muscles, skin, and liver of European perch, waters and sediments from freshwater ecosystem Mandra-Poda (Bioconcentration Factor, $BCF=C_{Cd,Cu,Hg,Ni,Pb_Skin}/C_{Cd,Cu,Hg,Ni,PbLiver}/C_{Cd,Cu,Hg,Ni,Pb_Muscle}/C_{Cd,Cu,Hg,Ni,Pb_Water}/C_{Cd,Cu,Hg,Ni,Pb\ Sediments}$) (Sorensen, 1991; Zaharieva, 2022). Spearman's rank correlation coefficient (r_s) values are determined to establish the relationship between the concentrations of Cd, Cu, Hg, Ni, and Pb in environmental samples (water, sediments), in samples of liver, muscle and skin of fish. The coefficient of determination (r_s^2) was presented to determine what percentage of the factor variable would cause changes in the output variable. The Friedman test (Friedman's ANOVA test) was calculated to assess the significance of the differences between the contents of Cd, Cu, Hg, Ni, and Pb in the studied tissues and organs of fish (Sokal and Rohlf, 1981). The results are statistically processed using Statistica 10 (StatSoft Inc., 2011) and MS Excel (Microsoft 2010).

RESULTS AND DISCUSSIONS

Characteristics of the studied fish species

The maximum length of the studied specimens ranged from 8.5-21.0 cm (12.27±3.49), and the weight from 11-203 g (37.27±59.39).

Concentration of Cadmium (Cd), Copper (Cu), Mercury (Hg), Nickel (Ni), and Lead (Pb) in the system Water – Sediments - *A. brama*

Chemical analyses were performed to determine the concentrations of Cd, Cu, Hg, Ni, and Pb in the skin, muscle, and liver of *A. brama*, water, and sediments (Table 1).

Cd is toxic in very low concentrations (Sorensen, 1991; Peycheva et al., 2014), and a non-degradable cumulative pollutant (Ghosh, 2021). The MPC for Cd, according to the Bulgarian Food Codex (Regulation № H-4/2012), is 0.05 $mg.kg^{-1}$ fish; according to FAO, it is 0.5 $mg.kg^{-1}$. Sources of pollution are industrial wastewater. Sources of Cd in the environment are plant protection products, fertilizers, pesticides, wastewater, and mining activities (Yablanski, Petkov (eds.), 2011). Biomagnification of Cd is observed when the concentration of the element increases from one level to higher levels of the food chain (Ghosh, 2021). Sources of Cu are the mining and ore processing industries. It is contained in insignificant quantities in natural waters. According to national legislation, the norm for Cu content in freshwater fish is 10 $mg.kg^{-1}$ (Regulation № 31/2004). According to FAO, it is 30 $mg.kg^{-1}$, and according to WHO regulations, it is 20 $mg.kg^{-1}$. Sources of Hg contamination are organic mercury compounds. Entry into freshwater fish occurs through contaminated food (Ghosh, 2021). According to the Bulgarian Food Authority (Regulation 31/2004), the maximum level permitted of Hg is 0.5 $mg.kg^{-1}$, and according to FAO/WHO, the permissible weekly intake is 0.3 $mg.kg^{-1}$ for humans (FAO/WHO, 1998; Regulation № 31/2004). Sources of Ni pollution for aquatic organisms are Ni-laden water and food from mining. It is necessary for living organisms as a microelement, but high concentrations are toxic to organisms. According to Regulation № 31/2004 provisions, the norm for Ni content in freshwater fish species is 0.5 $mg.kg^{-1}$. Sources of Pb are lead ore deposits and industrial wastewater. Pb is a highly toxic element for living organisms, especially aquatic ones. Pb is one of the most persistent toxic elements. The transfer to aquatic organisms occurs with food (Yablanski & Petkov (eds.), 2011; Peycheva et al., 2014; Ghosh, 2021). According to Regulation № 31/2004, the norm for Pb in freshwater fish is 0.2 $mg.kg^{-1}$.

Table 1. Contamination of Cadmium (Cd), Copper (Cu), Mercury (Hg), Nickel (Ni), and Lead (Pb) in tissues and organs of *A. brama* [$mg.kg^{-1}$], waters [$mg.l^{-1}$], and sediments [$mg.kg^{-1}$]

Samples	Min.-Max. Mean±SD	Min.-Max. Mean±SD	Min.-Max. Mean±SD	Min.-Max. Mean±SD	Min.-Max. Mean±SD
Wet weight	**Cd**	**Cu**	**Hg**	**Ni**	**Pb**
Skin (wet weight) *P. fluviatilis*	0.00-0.00 0.00±0.00	2.115-3.663 2.889±0.387	00.00-0.00 0.00±0.00	0.065-0.257 0.161±0.048	0.00-0.00 0.00±0.00
Muscle (wet weight) *P. fluviatilis*	0.00-0.00 0.00±0.00	5.150-8.302 6.726±0.788	0.00-0.00 0.00±0.00	0.29-0.45 0.37±0.042	0.085-0.137 0.111±0.013
Liver (wet weight) *P. fluviatilis*	0.18-0.28 0.232±0.026	12.61-20.34 16.48±1.932	5.466-9.018 7.242±0.888	0.885-1.761 1.323±0.219	0.595-1.123 0.859±0.132
Dry weight	**Cd**	**Cu**	**Hg**	**Ni**	**Pb**
Skin (dry weight) *P. fluviatilis*	0.00-0.00 0.00±0.00	4.146-7.178 5.662±0.758	0.00-0.00 0.00±0.00	0.125-0.505 0.315±0.095	0.00-0.00 0.00±0.00
Muscle (dry weight) *P. fluviatilis*	0.00-0.00 0.00±0.00	9.826-15.834 12.83±1.502	0.00-0.00 0.00±0.00	0.544-0.865 0.705±0.08	0.163-0.259 0.211±0.024
Liver (dry weight) *P. fluviatilis*	0.817-1.293 1.055±0.119	57.35-92.48 74.913±8.782	24.85-40.99 32.92±4.036	4.022-8.006 6.014±0.996	2.706-5.102 3.904±0.599
Water	0.025-0.040 0.031±0.007	0.002-0.004 0.003±0.001	0.016-0.004 0.013±0.008	0.001-0.005 0.003±0.002	0.400-0.467 0.436±0.034
Sediments	0.228-2.755 1.85±1.41	53.94-172.2 99.10±63.88	0.044-0.143 0.079±0.055	4.343-33.66 29.117±22.844	2.592-69.61 0.257±35.004

The standards for the content of Cd, Cu, Hg, Ni, and Pb in water samples are respectively MPC of 0.015 $mg.l^{-1}$ Cd (Regulation № H-4/2012), 0.02 $mg.l^{-1}$ Cu AAC EQS (Average Annual value, Environmental Quality Standarts, Regulation № H-4/2012) and 2 $mg.l^{-}$

[1] according to WHO, 0.07 $mg.l^{-1}$ Hg (Regulation № H-4/2012), MPC 0.034 $mg.l^{-1}$ Ni (Regulation № H-4/2012), AAC EQS 0.012 $mg.l^{-1}$ and MPC 0.014 $mg.l^{-1}$ Pb and according to WHO 0.01 $mg.l^{-1}$. The standards for Cd, Cu, Hg, Ni, and Pb content in sediment samples are 3 $mg.kg^{-1}$, 150 $mg.kg^{-1}$, 1.5 $mg.kg^{-1}$, 110 $mg.kg^{-1}$, 100 $mg.kg^{-1}$. The liver samples found the highest concentrations for the five studied elements. The average values in the bream liver show excesses compared to Regulation № 31/2004 norms for the samples from the three studied biotopes. The most considerable excess compared to the norms in Regulation № 31/2004 was registered in terms of the content of Hg (14.44 times), followed by that of Cu and Pb (4.64 and 4.29 times, respectively), of Ni (2.65 times), of Cu (1.65 times). Regarding the samples from the three biotopes, the excesses in the concentrations of Cd compared to the norm under the same regulation are 3.6-5.6 times; of Cu – from 0.98-1.58 times; of Hg – from 49.7-81.98 times; of 8.04-16.01 times; of Pb – from 13.53-25.51 times. The highest exceedances of Cd, Hg and Pb are recorded in the "Konstantinovo" Biotope and the lowest in the "Poda" biotope. The highest excesses of Cu were recorded in the biotope "Meden Rudnik", followed by the biotope Konstantinovo and Poda. According to the FAO norm (0.2 $mg.kg^{-1}$ Cd in food), the excess in the liver is, on average, 1.16 times for the three biotopes and 1.4 times for the biotope "Konstantinovo". According to the WHO human health norm (20 mg Cu/kg fresh weight), the excess in the liver samples is, on average, 1.65 times for the three biotopes and 0.04 times for the biotope "Meden Rudnik". Muscles accumulate more significant amounts of Cu and Ni than the skin (on average, 2.33 and 2.3 times, respectively). Compared to the liver samples, the content in Cu, Ni, and Pb muscle was 2.45, 3.57, and 7.74 times lower, respectively. No excesses of Cu and Ni were detected in skin and muscle samples, and no excesses of Pb were detected in muscle samples. No Cd, Hd, and Pb were detected in skin samples of *A. brama*, and no Cd, Hg were detected in muscle samples (Table 1). In the water samples, exceedances of the MPC for Cd (0.015 $mg.l^{-1}$) were found, respectively 1.67 times, 1.87 times and 2.67 times in the Poda, Meden Rudnik and Konstantinovo biotopes; of the MIC for Pb (0.014 $mg.l^{-1}$) - 28.57 times in the Poda biotope, 33.36 times in the Meden Rudnik biotope, 31.5 times in the Konstantinovo biotope or on average for the three biotopes - 31.14 times, regulated in the Regulation on Environmental Quality Standards for Priority Substances and Certain Other Pollutants/2010 under national legislation (Table 1). The analyses of sediment samples show excesses in the Cd content in the Poda biotopes (2.567 $mg.kg^{-1}$ dry matter – 1.28 times) and Meden Rudnik (2.755 $mg.kg^{-1}$ dry matter – 1.39 times), as well as in the Cu content in the Poda biotope (172.2 $mg.kg^{-1}$ dry matter – 1.15 times) compared to the norms regulated in Regulation No. 3/2008 of the national legislation. According to the Effects Range-Low (ERL), developed by the US Environmental Protection Agency (US ERA) to assess the ecological significance of concentrations in sediments, the excesses of Cd concentrations (norm 1.2 $mg.kg^{-1}$ dry weight) are 2.14 times in the Poda biotope, 2.3 times in the Meden Rudnik biotope or an average of 1.54 times for the studied freshwater ecosystem; excesses of Cd are not reported only for the Konstantinovo biotope. According to the same document, the excesses of Cu concentrations (norm 34 $mg.kg^{-1}$ dry weight) were obtained for all three studied biotopes – 5.07 times, 23.73 times, 1.59 times, respectively. Regarding the content of Ni (ERL=21 $mg.kg^{-1}$ dry weight) in the sediments, excesses were found in the biotopes Poda and Meden Rudnik (1.60 and 2.35 times, respectively), as well as about Pb (ERL=47 $mg.kg^{-1}$ dry weight) for both biotopes (1.48 times and 0.40 times, respectively). Exceedances of the norms for Ni and Pb were not found in the samples from the biotope Konstantinovo. Adverse effects on organisms are expected at values of the elements below the ERL (Assessment criteria for contaminants in sediment) (Table 1). Therefore, Cd concentrations decrease in the order sediments – liver – waters – skin – muscles; of Cu and Ni: sediments – liver – muscles – skin – waters; of Hg: liver – sediments – waters – skin – muscles; of Pb: liver – sediments – waters – muscles – skin. The bioconcentration factors (BCF) and bioaccumulation factors (BAF) are presented. The highest BCF were obtained for

Cu in liver and the samples of water and the lowest for Pb in muscles, as well as highest BCF for Hg in liver and lowest for Ni in skin and in the samples of sediments. Very significant positive correlations were established between contamination of Cd in liver and water; of Cu in skin, muscle, liver and in waters and sediments; of Hg in liver and sediments; of Ni in skin, muscle, liver and waters and sediments; of Pb in muscle, liver and water and sediments. A significant but negative correlation ($-r_s$) was determined only between contamination of Hg in the liver and in water samples (Table 2).

Table 2. Bioconcentration factor (BCF), and Spearman correlation coefficient (r_s) between the content of Cd, Cu, Hg, Ni, and Pb in water, sediments, *Abramis brama*

Fish – Water (wet weight)	**Cd BCF**	**Cu BCF**	**Hg BCF**	**Ni BCF**	**Pb BCF**
Skin – Water	0.00	963.00****	0.00	53.67****	0.00
Muscle – Water	0.00	2242.00****	0.00	123.34****	0.25****
Liver – Water	7.48****	5494.00****	557.00****	441.00****	1.97****
Fish – Sediments (dry weight)	**Cd BCF**	**Cu BCF**	**Hg BCF**	**Ni BCF**	**Pb BCF**
Skin – Sediments	0.00	0.057****	0.00	0.01****	0.00
Muscle – Sediments	0.00	0.129****	0.00	0.02****	0.82****
Liver – Sediments	0.125****	0.756****	416.71****	0.21****	15.19****

r_s **** - very significant correlation, p=0,001.

Significant differences were found between contaminations of Cu and Ni in the samples of skin, muscles, and liver of Freshwater bream, waters and sediments, between contaminations of Cd and Hg in water and sediments and the samples of liver, as well as between contaminations of Pb in water and sediments and in the samples of muscles and liver (Friedman's ANOVA, $p<0.05$). The coefficient of determination (r_s^2) in all cases is 100%. This gives reason to believe that all changes in the concentrations of Cd, Cu, Hg, Ni, and Pb in the waters and sediments of the Complex Mandra-Poda and the specific habitats of *A. brama* will lead to changes in the concentrations of these elements in the skin, muscles, and liver of the fish. The content of heavy metals in *A. brama* from the Mandra-Poda complex has been studied only by Peycheva et al., 2022. The authors studied the content of As, Cd, Cr, Cu, Fe, Mn, Ni, Pb, and Zn in muscle samples. They found much lower values for Cu (0.12 and 6.73 $mg.kg^{-1}$ fresh weight, respectively) and Ni (0.06 and 0.37 $mg.kg^{-1}$ fresh weight, respectively) than in this study and slightly higher values for Pb content (0.15 and 0.11 $mg.kg^{-1}$ fresh weight, respectively).

Cd, Hg, Ni, and Pb are major toxic metals, and Cu is in the group of essential metals with potentially toxic effects (Yablanski & Petkov, 2011; Mostafa et al., 2022). According to Peycheva et al. (2014a), even at low concentrations, Hg is a very toxic element in metabolically active tissues and is associated with an ecological risk for aquatic organisms. They point out that Hg concentrations increase towards higher levels in the food chain, which is why predatory fish species can be suitable bioindicators. Conversely, for Cd, no such increase was found along the food chain (Peycheva et al., 2014b). According to studies by several authors, the liver accumulates Cd, Cu, Hg, Ni, and Pb in much higher concentrations than other tissues and organs of fish, which was also found in this study (Leite et al., 2017; Mostafa et al., 2022).

The content of the studied elements is higher in sediments than in water samples, as also obtained in other studies, which is explained by the fact that they are adsorbed by organic particles and precipitate and accumulate at the bottom, with only 1% of the pollutants participating in the hydrological cycle (Salomons & Stigliani, 1995; Mostafa et al., 2022).

CONCLUSIONS

As a result of the ecological monitoring study of liver, skin and muscle samples of *A. brama* from the Mandra-Poda complex, the highest content of heavy metals was found in the liver samples. The liver of the Freshwater bream appears as a sensitive bioindicator for the Cd, Cu, Hg, Ni, and Pb content.

ACKNOWLEDGEMENTS

This research was carried out with the financial support of Agricultural University – Plovdiv, Bulgaria and VANG EOOD, Bulgaria.

REFERENCES

Assessment criteria for contaminants in sediment. Effects Range-Low (ERL). https://dome.ices.dk/OHAT/trDocuments/2019/help_ac_sediment_metals.html

BSS EN 14757:2015 Water quality. Sampling of fish with multi-mesh gillnets.

Directive 92/43/EEC on the Conservation of natural habitats and of wild fauna and flora. http://ec.europa.eu

Directive 79/409/EC of 2 April 1979 on the conservation of the wild birds. http://www.central.eu

EN ISO 11885:2009 Water quality – Determination of selected elements by inductively coupled plazma optical emission spectrometry (ICP-OES).

EN ISO 22036:2024 Environmental solid matrices – Determination of elements using inductively coupled plasma optical emission spectrometry (ICP-OES).

FAO (Food and Agriculture Organization) (1983). FAOFisheryCircularNo. 464,5-10. Food andAgriculture. The results obtained for toxicand trace elements in analyzed fish. Organization of the United Nations, Rome.

FAO/WHO (1998) *Preparation and use of food-based dietary guidelines.* Report of a joint FAO/WHO consultation. Geneva, World Health Organization (WHO Technical Report Series, No. 880).

FishBase Database (2024). http://www.fishbase.org.

Fröse, R., Pauly, D. (2024). *Fish Base.World Wide Web electronic publication.* Retrieved October 10, 2024, fromwww.fishbase.org.

Georgieva, G., Stancheva, M., Makedonski, L. (2015). Persistent Organochlorine Compouds (PcBs, DDTs, HCB &HBDE) in Wils Fishfrom the Lake Burgas and the Lake Mandra, Bulgaria. *Ecology & Safety*, 9, 515-523.

Ghosh, D. (2021). Impact of Heavy Metal Pollution on Freshwater Fish Species. *ZENITH International Journal of Multidisciplinary Research*, 11(8), 42-53.

Ilieva, N., Kirin, D. (2024). Helminth biodiversity and heavy metal contamination of *Perca fluviatilis* (Linnaeus, 1758) and *Eustrongylides excisus* (Jägerskiöld, 1909), larvae. Scientific Papers. Series D. Animal Science, LXVII, 2, 574-581.

IUCN Red List Status (n.d.). Retrieved fromhttps://www.iucnredlist.org.

Karapetkova, M. Zhivkov, M. (2006). *Fishes in Bulgaria*. Sofia, BG: GeaLibris (in Bulgarian).

Kottelat, M. & Freyhof, J. (2007). Handbook of European freshwater fishes. *Publications Kottelat, Cornol and Freyhof, Berlin*. 646.

Law for the Protected Areas.State Gazette, issue 133 of November 11, 1998. https://lex.bg/laws/ldoc/2134445060

Leite, L. A., Januário, F. F., Padilha, P. M., do Livramento, E. T., de Azevedo, R. K., Abdallah, V. D. (2019). Heavy Metal Accumulation in the Intestinal Tapeworm *Proteocephalus macrophallus* Infecting the Butterfly Peacock Bass (Cichlaocellaris), from Southeastern Brazil. *Bulletin of Environmental Contamination and Toxicology* 103, 670– 675.

Mostafa, O., Hanfi, T., Abd-eltwab, D., Al-Shehri M., Moustafa M., Al-Emam A., Alhamdi, H., Nigm, A. (2022). Fish Parasites as Biological Indicators of Metals Pollution in the Aquatic Environments. *Research Square*, 1-17.

Peycheva, K., Panayotova, V., Makedonski, L., Stancheva, R. (2014a). Toxic and essential concentration of freshwater fishes from Pyasachnik Dam, *Bulgaria. Agricultural Science and Technology*, 6(3), 364-369.

Peycheva, K., Makedonski, L., Merdzhanova, A., Stancheva M. (2014b). Evaluation of toxic metal levels in edible tissues of three wild captured freshwater fishes. *Ovidius University Annals of Chemistry*, 25(1), 53-58.

Peycheva, K., Panayotova, V., Stancheva, R., Makedonski, L., Merdzhanova, A.,Parrino, V., Nava, V., Cicero, N., Fazio, F. (2022). Risk Assessment of Essential and Toxic Elements in Freshwater Fish Species from Lakes near Black Sea, Bulgaria.*Toxics*, 10, 675.

Regulation No. 31 of 29 July 2004 on the Maximum Permitted Quantities of contaminants in foodstuffs. *State Gazette*, 88 of 08.10.2004.

Regulation H-4 of September 14, 2012 on characterization of Surface Waters. *State Gazette*, 22 of 05.03.2013.

Salomons, W., & Stigliani, W. (1995) Biogeodynamics of Pollutants in Soils and Sediments. SpringerVerlag, Heidelberg, p 352.

Sokal, R., & Rohlf, J. (1981). *Biometry. The Principles and practice of statistics in biological research*. Second Edition. New York, US: W. H. Freeman and Co.

Sorensen, E.M. (1991). *Metal Poisoningin Fish. VI. Cadmium*. CRC Lenhardt, M., Jarić, I., Višnjić-Jeftić, Ž., Skorić, S., Gačić, Z., Pucar, M. Press: Boca Raton, FL.

Statsoft Inc. (2011) (n.d.). STATISTICA, version 10. Retrieved from www.statsoft.com.

Yablanski, Z., Perkov, G. (Eds.), 2011. *Manual Book of Applied Ecology*. Alfamarket, Stara Zagora.

Zaharieva, P. (2022). Content of heavy metals in Fishes and their Parasites from the Danube River - Ecology and Bioindication. PhD Thesis, Plovdiv (in Bulgarian).

Scientific Papers. Series E. Land Reclamation, Earth Observation & Surveying, Environmental Engineering. Vol. XIV, 2025
Print ISSN 2285-6064, CD-ROM ISSN 2285-6072, Online ISSN 2393-5138, ISSN-L 2285-6064

SEDIMENT TRANSPORT MODELING WITH ADVANCE HYDRAULICS SOFTWARE

Dorina Gabriela IONESCU, Robert Florin BEILICCI, Erika Beata Maria BEILICCI, Mihai NEGURA, Mirela Laura IEREMCIUC

Politehnica University of Timisoara, 1A Splaiul Spiru Haret, 300022, Timișoara, Romania

Corresponding author email: robert.beilicci@upt.ro

Abstract

This study investigates sediment transport dynamics in the Dognecea River, located in Caraș Severin County using MIKE 11. Numerical simulations were conducted to analyze sediment deposition, erosion patterns, and structural interactions. The sediment transport model considers multiple factors, including riverbed sediment characteristics, hydrodynamic conditions, and structural modifications. The sediment transport model has several applications, with variations in parameters such as study objectives, allocated resources, time scale, space, context of the study team, required accuracy, etc. The characteristics of the sediments in the riverbed are a necessary component to know for modeling sediment transport. It is proposed to collect additional sediment samples from the sediments of the layer. The samples obtained will be analyzed according to the size of the particles in the bed. To address sediment transport issues in the Dognecea River, advanced water flow modeling programs are used. Numerical modeling was performed using the MIKE11 software, incorporating hydraulic flow simulations to analyze sediment transport dynamics. Transport models can be used in the case of small alluvium, such as mud or clay, to non-cohesive deposited alluvium, such as boulders, small ballast and sand, but also mixed sediments. MIKE 11 provides several options for modeling the movement over time of alluvial transport, as well as structural changes in the riverbed. The results provide insights into alluvial transport behavior and offer solutions for mitigating sediment-related challenges such as riverbed clogging and erosion control. The findings demonstrate the effectiveness of MIKE11 in modeling hydraulic and sediment transport processes, making it a valuable tool for water resource management and flood risk mitigation.

Key words*: bed roughness, hydraulic modelling, sediment transport.*

INTRODUCTION

The Dognecea River, located in Caraș Severin County is affected by significant sediment transport processes. These issues impact infrastructure, water quality and flow parameters, necessitating advanced modeling techniques for effective management.

The Dognecea River originates in the Dognecea Mountains and flows through valleys and hilly areas, carrying alluvial materials, including loess deposits.

The upstream section is the built-up area, where the process of riverbed erosion manifests itself, this erosion threatens the stability of the county road, houses, as well as in the lower region of the village, where new households appeared in the area and the riverbed was completely clogged, which led to the overflow of the stream and the riverbeds.

Near the dam, built in 1750 to supply industrial water to the furnaces in Dognecea, sediment deposition occurs along the entire stretch from upstream to downstream, even starting from upstream to downstream, the sediments are deposited by transporting water to a depth of 265 m that causes erosion up to the rock, the banks being eroded, thus washing away the existing works, and the area presents phenomena of unconsolidated erosion. As a result of the floods, the existing works on the downstream section of the dam as well as the town hall are damaged. The masonry constructions have also been affected; the stone walls have been washed and the bridges destroyed.

Downstream, due to the low slopes and lack of excessive banks, the materials released from upstream are deposited downstream of the village. This leads to the accumulation of fine sediments that cause clogging and flooding of roads and households (Figure 1) (ANIF, 2024).

To mitigate flood-related damage, erosion protection measures have been implemented along the Dognecea River, aiming to stabilize the banks and safeguard the surrounding settlements. At the confluence with the Calina

River, upstream, the hydrograph of the Dognecea River has the following characteristics: route length 18 km, basin area 61 km, upstream altitude 420 mdM, downstream altitude 151 mdM, average altitude 388 mdM, average slope of 15%, convolution coefficient 1.27, forest area 4741 ha. In order to verify the capacity of the natural riverbed, transition calculations of the probability of exceeding Q5% flow were performed for determining the appropriate section sizing.

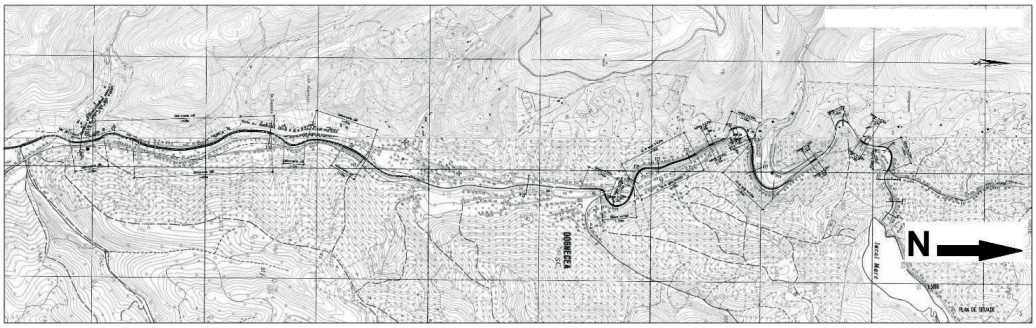


Figure 1. Plan view of Dognecea River

As a result, a remodeled, the remodeled section of the Dognecea stream was established between two predetermined trapezoidal points, which have a slope of 1:1.5 and 8 m wide at the base and a length of 2000 m.

Following the excavations, the resulting embankment material will be used for filing or lateral reinforcement, ensuring profile compensation across sections.

The weight of the stone retaining wall, L = 1000 m is applied in the major riverbed of the Dognecea stream (causing erosion and soil overload). Reinforcement bench with gabion boxes along a length of 1165 m with a section of 1.0×1.0×3.0 m, 1.0×1.5×3.0 m made of OB37 concrete steel frames, with a diameter of 16mm located at a distance of 1.00 m and OB37, with a diameter of 10 mm internally welded at a distance of 0.5 m, galvanized mesh with a size of 40×40 mm.

The foundation will be made on a bed of fascines 0.3 m thick and 3.0 m in length, and the boxes are filled with ballast of different sizes. The stone elements will be arranged similarly to plasterboard layers for enhanced load distribution. The cassettes are connected from all directions with OB steel (6 mm diameter), with a 2 mm gap (NARW, 2024).

The boxes are mounted on both banks of the stream to protect riparian roads, stabilize the riverbanks, and prevent sediment entrainment. These structures will also help reinforce existing constructions along the river. To mitigate bank erosion, gabion boxes will be applied on the fascines and a layer of earth on the calculation slope h = 2.0 m total length L = 2130 m. The studied section features a box gabion structure with the following dimensions of 1.0×1.0×3.0 m, the section is based on an elastic mattress with a thickness of 0.3 m and a free length of 1.0 m.

To achieve the required height, the transit flow measurements of the embankment were ensured by tilting the embroidery by 1.00 m from 0.30 m of broken stone for the drainage of aggregates to 0.15 m. Box gabions shall be at least 1.0 m thick. The installation of gabion boxes will help achieve the following objectives the reduction of drainage tariffs, the reduction of the longitudinal slope and the stabilization of the riverbed.

This study aims to model sediment transport dynamics using MIKE 11 software to assess potential mitigation measures and improve flood risk management.

MATERIALS AND METHODS

The MIKE 11 program is a hydraulic modeling software designed to simulates water flow and level, water quality, sediment transport in rivers, canals, estuaries, sewage systems and different types of water systems. The MIKE 11 model was used to simulate unsteady flow and sediment transport, following methodologies

similar to those applied in previous studies (Ivanescu et al., 2014), where MIKE 11-UHM and MIKE 11-HD were used for hydrodynamic modeling and runoff simulations. Connecting MIKE 11 can be integrated with GIS and ArcGIS enabling them to extract cross-sections, watershed contouring and which assist in risk assessment and mitigation. Flax to achieve these objectives or to be used as a forecasting tool. Hydrotechnical structures such as: spillways, canals/galleries, ridges, staves, pumps or control and regulation structures; or even the breaking of dams and dams (Huai et al., 2021).

Because of accumulation, we get a modeling dynamic that:

- Consider accumulation volume available in the canals and in the adjacent major riverbeds;
- Flood mitigation by delaying the peak of the flood, it allows a slow accumulation in the riverbeds Major;
- Allows water to retreat into riverbeds as flooding subsides.

Within the MIKE 11 software package, the MIKE Zero interface provides access to a range of modeling options.

Once in the actual numerical modeling phase, a program will be created. simulation (Simulation Editor - .sim11) that will be always kept open (valid for any type of work in MIKE 11), this is the main control center in MIKE 11. Access all the files necessary for running the program and their intercommunication.

The simulation editor also specifies the type of models that will be used and the simulation mode (permanent/non-permanent). The files used in the simulation will be added, depending on the type. The simulation we want to create. These will be:

- Network configuration;
- Cross sections data;
- Boundary conditions;
- Precipitation and runoff parameters;
- Hydrodynamic parameters;
- Advection/dispersion parameters;
- ECOLab parameters for water quality modeling;
- Time series data;
- Frost related parameters, etc.

The "Simulation" table within the simulation editor contains the initial conditions, the time step taken into account and aditional details regarding the simulation.

The period can also be calculated from here maximum simulation, based on the data entered the system; Time step can be entered as fixed, tabular or adaptive. Also, the time step can be set from seconds to days depending on the scale and precision required for the simulation. The difference between the start and end times of the simulation is proportional to the selected time step and the total duration of the model run.

In the "Start" section of the Simulation Editor, the system validates whether all input files are correctly set up. If any file is not marked in green, it is considered invalid, preventing the simulation from running. Once all files are validated (green indicators), the simulation can proceed, generating a text file ("Simulation") that can be edited in any text editor.

The Network Editor (.nwk11) defines the plan view, river network, and hydrotechnical structures. Users can upload graphical visualizations of the network, import saved files (e.g., JPEG, ASCII), and modify dimensions as needed. The interface also allows integration with MIKE 21 (DFS2) files, enabling overlaying and adjusting data layers (Hausler et al., 2019).

The hydrological network data can be modified within the network options settings, allowing users to select or deselect connected components dynamically. The river network is displayed graphically, enabling adjustments to nodes, river arms, and structures, while maintaining a record of all applied settings.

The tabular module provides a list of all digitized points in the model, which can be edited via the "Overview" or "Data Entry Panel". Users can import/export data from Excel tables for efficient data handling. In the Network Editor, the "Network" option facilitates watercourse discretization and node spacing, while the "Structures" option lists all hydrotechnical works, categorized by structure type and model settings.

Upon completing the simulation, a "Network" text file is generated, which can be edited in any text editor.

The Section Editor (.xns11) operates on a binary database, allowing multiple sections to be registered. Each section is identified by the river name (tributary), Topo identifier (Topo ID), and

route number (increasing downstream). Sections include:

- Raw data (X, Z coordinates, roughness markers);
- Processed data (hydraulic radius, storage area, width, and flow mode).

Users can modify node positions, rename sections, interpolate multiple sections, or adjust tabular data. The editor supports five common graphical markers affecting data calculations:

- Left bank pier;
- Low flow on the left bank;
- Left coordinate;
- Minimum riverbed height;
- Reduced flow on the right bank;
- Right coordinate.

Embankment markers define the active simulation area, and global modifications can be applied to both raw and processed data. Before running the simulation, a pre-check is recommended to ensure all sections are precalculated.

The Edge Conditions Editor (.bnd11) allows the inclusion of advection-dispersion and multilayer flow conditions, providing a structured panel for managing boundary conditions and simulation parameters.

The overview panel includes a description box (open, global, structures, closed), one for the type of condition (supply, levels, Q-h curves, bed level), one for for user identification and 3 for location (rich name, start (km), end (km). The specification panel contains a box for the type of download; one for the type temporal step (fixed, tabular, adaptive); one for values (used for editing time series) and one for information about the passage of time.

The conditions file, once created, can be modified with a text editor. The Time File Editor (.dfs0) is an editor and database for time series and communicates directly with the edge condition editor.

It can be viewed both tabular and graphically. Selected points in the view are drawn. The visualization is done only in the Time Series (TS) file.

You can also change or add/delete the type and units of time from here.

In the "Tools" menu, you can select the subset or the entire period of interest.

You can zoom in on the area of interest (zoom) or move the area (pan).

Files of type * DFS0 (TS) can be created from a blank document or from a ASCII document.

You can also create hydrograph files for projects in the Time Series editor Developed.

The HD Parameter Editor (.hd11) contains the initial conditions and resistance data.

The table of initial conditions includes the local conditions superimposed on the global ones, the values specified globally, local values (strings), etc. The initial conditions will set the water level to the first step of time.

The lateral resistance factor in the section applies to the overall values or locally. If lateral resistance is specified as the value, then the file in question will be ignored. The resistance of the bed results from the overwriting of local values over the global value, along the course.

The local approximation can be solved for an entire sector or only for a part of it. Kinematic or diffusive waves can be associated with fast channels without shaking. In this editor, additional results will be given to the default constants in the simulation (which will create an additional editable file with the name from "Simulation" and the extension "HDAdd"). All other panels in the editor can be used for more advanced use of MIKE 11 (DHI, 2021).

These are the interconnection editors, required by MIKE 11 for the creation of all numerical modeling projects. The MIKE 11 program is created by DHI Water•Environment•Health, Denmark, to solve the Saint-Venant equations, the basic component of the model was used in the simulation, i.e. the hydrodynamic module (HD), which contains a 6-point Abbott-Ionescu default scheme with finite differences (Lagos et al., 2024).

MIKE 11 was created to make detailed modeling of gate and dam openings, special treatment of floodplains, road overflows, bridges, rivers.

The program has the ability to use vertically integrated, diffusive, kinematic, or fully dynamic momentum and mass equations. Types of limits include Q-h relationship, water level, resistance factor, flow rate, wind field, dam failure. The limit of the Q-h relation can only be applied to the downstream limit. The water level limit applies to the model either downstream or upstream. The flow limit applies in the same way as the water level limit, either downstream or upstream, and can also be used at the lateral

tributary flow (flow). To describe the leakage, lateral flow is applied.

MIKE 11 is a well-known program since the beginning of its use, that could be operated through an efficient interactive menu, menu sequencing and systematic layouts.

The latest generation of the "classic" MIKE 11 has been developed - version 3.20, which usefully uses the experiences and features of the "classic" era with the Windows-based user interface, including calculation speed and graphical editing.

In many applications around the world it has been used over time, among its main areas of application being flood mitigation analysis and design, dam failure analysis, flood forecasting today, improvement of channel and reservoir sources, sediment transport and morphological studies, ecological estimates of water in rivers and wetlands, saline intrusion into estuaries and rivers (Merz et al., 2021).

The MIKE 11 program has a variety of options for modeling morphological changes and sediment transport dynamics in the riverbed (Lee et al., 2021).

RESULTS AND DISCUSSIONS

Numerical flow modeling was performed using MIKE 11, which proved effective for unsteady flow simulation with MIKE 11-HD. Figure 2 shows the model layout, and Figure 3 presents the channel cross-section profiles based on topographic surveys.

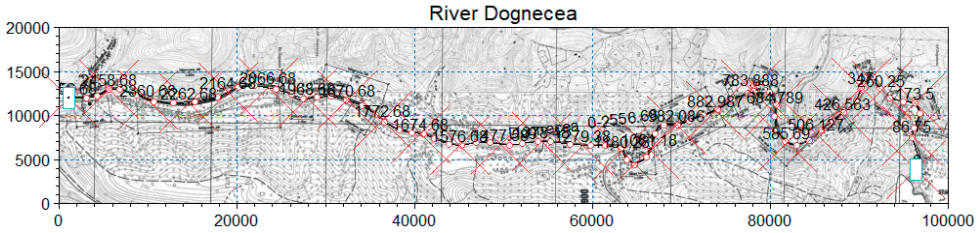


Figure 2. Plan view with the network model

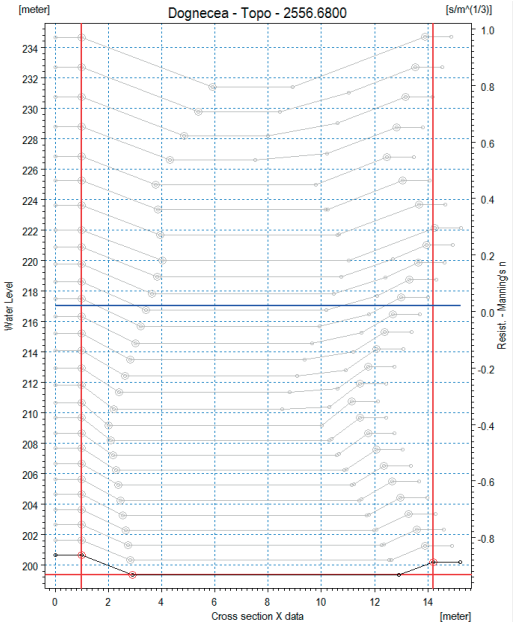


Figure 3. Cross sections

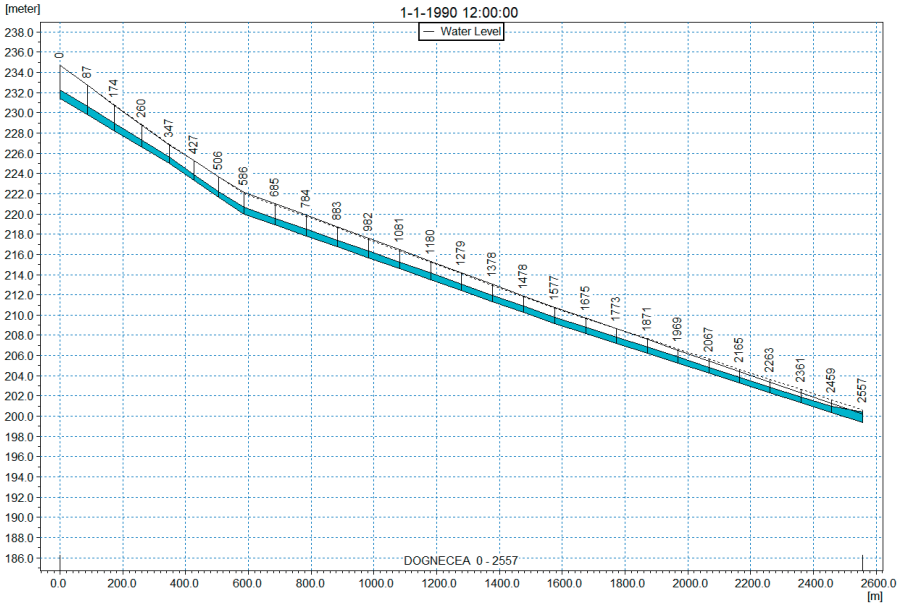


Figure 4. Water Level in longitudinal profile

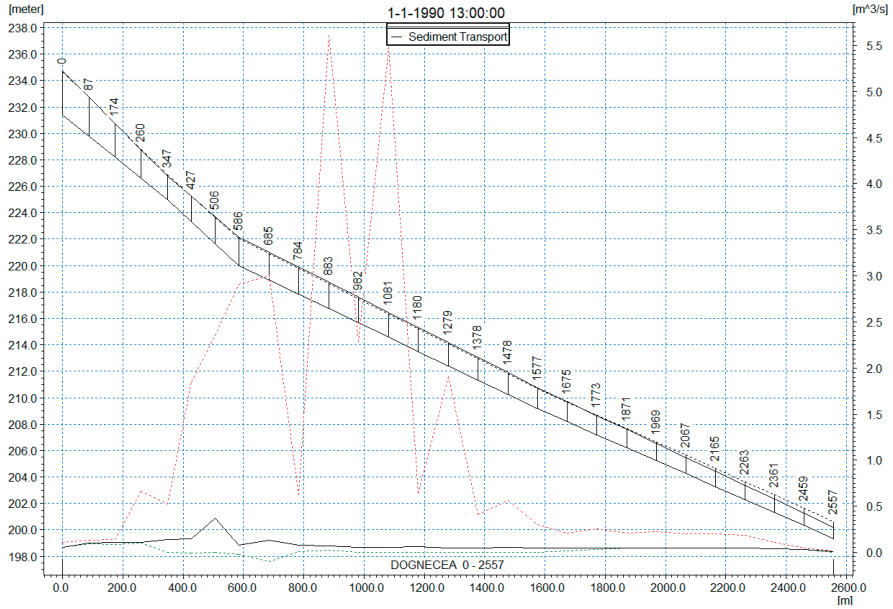


Figure 5. Sediment transport in longitudinal profile

According to the introduction of the data or the limit conditions formulated, the upstream flow at chain 0 is constant Q 19.9 mc/s the downstream flow at chain 2556, the key to the curve of the downstream river sector (Biali et al., 2022). Following modeling with the MIKE11 program, the longitudinal profile of the existing canal was obtained (Figure 4).

The downstream boundary condition is important in terms of alluvial flow in a morphological and dynamic model between sediment transport, bed level, hydrodynamics

and plane shape changes, and another condition is the simulation time which should be as long as possible. (Damian et al, 2022).

The following boundary conditions are required: the boundaries of the sediment beds in the riverbed and the level of displacement of the alluvial at the limit. The first applies when it is considered with a certain precision that the riverbed remains at the same level as the upstream limit. The second applies if it is accurately known for alluvium transport (e.g. zero transport) (Grozav et al, 2018).

According to the formulated boundary conditions or data, the sediment flow upstream to chain 0 and downstream to chain 2556 is 0.

The MIKE 11 ST module simulated sediment transport dynamics along the canal, showing variations in transport rates over time. The longitudinal profile (Figure 5) highlights areas of significant sediment accumulation and erosion, which are critical for understanding flood risks and designing mitigation strategies.

The results from the sediment transport model show the variation over time across the entire river section of erosion and deposition, which aligns with the expected results (Najafi et al., 2021).

There are areas with higher erosion in zones where the river slope changes, while higher deposition occurs in areas with a lower slope.

Over time, if the deposited sediments are not removed, they will reduce certain river sections, decreasing the river's water discharge capacity, ultimately leading to an increase in water levels, which will negatively impact flood control.

The water levels from the initial results were compared with measured levels in several sections. To correct the differences, the roughness values were adjusted in certain river sections until values close to the measured ones were obtained. After validating the model regarding water movement, the sediment transport model was then run.

The calculation of the transport capacity of non-cohesive sediments, the morphological changes and the transformation of the alluvial resistance in relation to a water system can be done with the MIKE 11 program.

The input data for the properties of non-cohesive sediments are:

- Diameter of sediment grains;
- Data for graded ST;
- Transport model;
- Calibration factors;
- Bed level without cleanliness;
- Passive branches;
- Predetermined distribution of sediments in nodes.

CONCLUSIONS

This study applied a one-dimensional hydraulic model to simulate unsteady flow using the MIKE 11 software.

The MIKE 11 model demonstrated several advantages easy to view and extract results analyses, short simulation time, accurate hydraulic description in flowing waters/channels of hydrotechnical structures.

The MIKE 11 program presents a complex and efficient modeling and design system in various engineering applications, water sources, water quality management and planning, extraordinary flexibility, speed, as well as a very easy use of the program.

The core of the MIKE 11 modeling system, the hydrodynamic module (HD) forms the basis for almost all modules, including water quality, flood forecasting, advection spread, as well as alluvial displacement modules of various sizes and non-cohesive.

The MIKE 11 model successfully simulated sediment transport, identifying key areas of erosion and deposition. These insights are valuable for improving flood risk assessment and designing effective river management strategies.

However, one-dimensional models have limitations, particularly in capturing complex flow interactions in floodplains. Future research should consider integrating 2D or 3D hydraulic models to improve accuracy in predicting morphological changes and extreme flood events.

ACKNOWLEDGEMENTS

This paper can be possible thanks to project: Development of knowledge centers for life-long learning by involving specialists and decision makers in flood risk management using advanced hydroinformatic tools, Agreement no LLP-LdV-ToI-2011-RO-002/2011-1-RO1-LEO05-5329. This project has been funded with

support from the European Commission. This publication [communication] reflects the views of the author, and the Commission cannot be held responsible for any use which may be made of the information contained therein.

REFERENCES

ANIF – National Agency for Land Reclamation Archive (2024). *Data from various documents and studies*.

Biali, G., & Cojocaru, P. (2022). GIS hydrological modeling in an agricultural river basin with high potential for water erosion. *Scientific Papers. Series E. Land Reclamation, Earth Observation & Surveying, Environmental Engineering, 11*, 418–425.

Damian, G., Pricop, C., & Stătescu, F. (2022). The study of hydrological regime modeling using HEC-RAS model: Case study – River basin Bahlueț. *Scientific Papers. Series E. Land Reclamation, Earth Observation & Surveying, Environmental Engineering, 11*, 338–343.

DHI – Danish Institute of Applied Hydraulics (2021). *MIKE 11 user manual – A modeling system for rivers and channels: Short introduction and tutorial*. DHI.

Huai, WX (Huai, Wen-xin) Li, SL Li, Shuolin Katul, GG Katul, Gabriel G. Liu, MEU Liu, Meng-yangYang, ZH Yang, Zhong-hua (2021). Flow dynamics and sediment transport in vegetated rivers: A review. *Journal of hydrodynamics, 33*(3), 400–420, DOI10.1007/s42241-021-0043-7

Lagos, MSLagos, Magdalena SofiaMuñoz, JFMunoz, Jose FranciscoSuárez, FISuarez, Francisco IgnacioFuenzalida, MJFuenzalida, Maria JoseYáñez-Morroni, GYanez-Morroni, GonzaloSanzana, PSanzana, Pedro (2024). Investigating the effects of channelization in the Silala River: A review of the implementation of a coupled MIKE-11 and MIKE-SHE modeling system. *Wiley interdisciplinary reviews-water, 11,* Issue 1, Special Issue SI, DOI10.1002/wat2.1673.

Lee, SLee, SanghyunChu, MLChu, Maria L.Guzman, JAGuzman, Jorge A.Botero-Acosta, ABotero-Acosta, Alejandra (2021). A comprehensive modeling framework to evaluate soil erosion by water and tillage. *Journal of environmental management, 279*, DOI10.1016/j.jenvman.2020.111631.

Ivănescu, V., Mocanu, P., & Sandu, M.-A. (2014). Application of a hydrodynamic MIKE 11 model for Argeșel River. In *Proceedings of the 14th SGEM GeoConference on Water Resources, Forest, Marine and Ocean Ecosystems* (Vol. 1, pp. 65–72). SGEM2014 Conference Proceedings. https://doi.org/10.5593/SGEM2014/B31/S12.009

Merz, BMerz, BrunoBlösch, GBloesch, GuenterVorogushyn, SVorogushyn, SergiyDottori, FDottori, FrancescoAerts, JCJHAerts, Jeroen C. J. H.Bates, PBates, PaulBertola, MBertola, MiriamKemter, MKemter, MatthiasKreibich, HKreibich, HeidiLall, ULall, UpmanuMacdonald, EMacdonald, Elena (2021). Causes, impacts and patterns of disastrous river floods. *Nature reviews earth & environment, 2*(9), 592–609, DOI10.1038/s43017-021-00195-3.

Najafi, SNajafi, SaeedDragovich, DDragovich, DeirdreHeckmann, THeckmann, TobiasSadeghi, SHSadeghi, Seyed Hamidreza (2021). Sediment connectivity concepts and approaches. *CATENA, 196,* DOI10.1016/j.catena.2020.104880.

NARW – National Administration "Romanian Waters", Banat (1987-2024). *Data from various documents and studies*.

Scientific Papers. Series E. Land Reclamation, Earth Observation & Surveying, Environmental Engineering. Vol. XIV, 2025
Print ISSN 2285-6064, CD-ROM ISSN 2285-6072, Online ISSN 2393-5138, ISSN-L 2285-6064

ECOLOGICAL MONITORING OF THE PARVENETSKA RIVER, PART OF THE MARITSA RIVER WATERSHED

Diana KIRIN[1, 2], Radoslava ZAHARIEVA[1, 2], Petya ZAHARIEVA[1, 2], Marian VARBANOV[1], Georgi PATRONOV[3], Gergana METODIEVA[1]

[1]National Institute of Geophysics, Geodesy and Geography (NIGGG),
Hydrology and Water Management Research Center, Bulgarian Academy
of Sciences, 3 Acad. G. Bonchev Street, 1113, Sofia, Bulgaria
[2]Agricultural University - Plovdiv, Department of Chemistry, Phytopharmacy and Ecology,
and Environmental Protection, 12 Mendeleev Blvd, 4000, Plovdiv, Bulgaria
[3]University of Plovdiv "Paissii Hilendarski", Department of Chemical Technology,
24 Tsar Assen Street, Plovdiv, 4000, Bulgaria

Corresponding author email: dianaatanasovakirin@gmail.com

Abstract

This study aims to carry out ecological monitoring of the surface water of the Parvenetska River (Eastern Aegean Sea region, Southern Bulgaria). For the study, samples of macrozoobenthos were collected in the spring of 2024 – a basic biological quality element according to the Water Framework Directive. The taxonomic affiliation of macroinvertebrates was determined, and 26 taxa were ident3ified. The number of EPT taxa, % (Oligochaeta & Diptera), % Filtering feeders, % EPT taxa, German trophic index, and species diversity indices were calculated. As a result of the study, it was established that in the studied biotope, macroinvertebrate taxa of sensitivity group C (relatively tolerant forms) dominate, followed by taxa of group B (less sensitive forms).

Key words*: chemical status, ecological state, indices, metrics, river ecosystem.*

INTRODUCTION

The Parvenetska River (Tamrashka River; Dermendere River) rises from the Modar Peak in the Chernatitsa Ridge, Western Rhodopes, at 1 816 m above sea level.

The river flows in a north-northeast direction, and at the village of Parvenets, it leaves the Rhodopes and enters the Upper Thracian Lowland (Pazardzhik-Plovdiv Plain), passes through the city of Plovdiv and flows from the right into the Maritsa River at 164 m above sea level. The riverbed in the river's lower reaches (after the village of Parvenets) has been corrected with dikes. The length of the Parvenetska River is 37 km. The river passes through the lands of the villages of Hrabrino, Parvenets and the city of Plovdiv. The river's waters are used for irrigation, electricity generation and water supply to industry. The river is at its highest point in April-May (Kiradzhiev, 2013; Integrated Development Plan of Municipality of Plovdiv, 2021-2027; Integrated Development Plan of Municipality of Rhodope, 2021-2027). According to the typology of rivers in Bulgaria, the Parvenetska River is of type R3 "Mountain Rivers" (Tamrashka River to the village of Hrabrino and tributaries - Dormushevska and Pepelasha Rivers) and of type R5 "Semi-Mountain Rivers" (Parvenetska River from the confluence of the Pepelasha River to the mouth) in Ecoregion 7 (East Aegean River Basin Directorate, 2018).

The Water Framework Directive aims to achieve good water state in Europe and reduce harmful impacts on them. The qualitative elements for assessing the ecological state of rivers are biological, hydromorphological and physico-chemical elements. The latter two elements support the biological elements. The main biological quality elements are macroinvertebrates (Directive 2000/60/EU). At present, no studies have been established on the ecological state of the water of the Parvenetska River in the area of the village of Parvenets based on biological elements (macrozoobenthos) and physicochemical quality elements. Such studies have been conducted for other rivers in the

Maritsa River basin, for example the Luda Yana River (Vidinova et al., 2008; Georgieva et al., 2014; Gartsiyanova et al., 2020; Gartsiyanova et al., 2021; Gartsiyanova et al., 2022; Zaharieva et al., 2024), the Topolnitsa River (Gartsiyanova et al., 2020; Irikov & Atanasova, 2008; Kancheva, 2016; Park et al., 2022; Varadinova et al., 2022), Sazliyka River (Vidinova et al., 2008; Park et al., 2022; Varadinova et al., 2022), Chepelarska River (Kirin, 2002; Vidinova et al., 2008; Boyanov et al., 2011a; 2011b; Park et al., 2022; Patronov & Kirin, 2024; Zaharieva et al., 2024). Data on macroinvertebrates of Ephemeroptera, Plecoptera, and Trichoptera from water bodies in the Plovdiv city region, including Parvenetska River, were given by Vidinova et al. (2018).

This study aims to conduct ecological monitoring of the surface water of the Parvenetska River, part of the Maritsa River basin in Southern Bulgaria.

MATERIALS AND METHODS

The macroinvertebrate samples were collected in the spring of 2024 from the Parvenetska River, on the outskirts of the village of Parvenets (designated as Parvenets biotope; 42°04'53.1"N 24°39'41.1" E), Plovdiv district. The village is located at 454 m above sea level. The selected biotope is located northwest of the village and is characterized by a fast current and a rocky bottom (Figures 1 and 2).

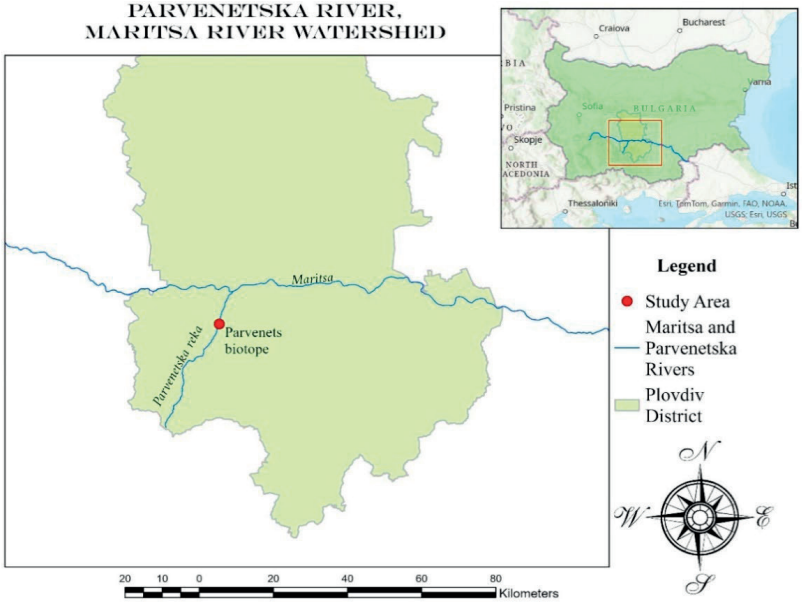


Figure 1. Researched section of the Parvenetska River



Figure 2. View from the Parvenets biotope

The studied section of the river belongs to type R5, "Semi-mountainous rivers". Macroinvertebrate sampling was carried out by national standards (Cheshmedjiev et al., 2011; EN ISO 10870:2012; EN 16150:2012; Regulation No. H-4 of 14.09.2012; Belkinova et al., 2013).

Macroinvertebrate samples were taxonomically defined and counted. The main metrics were determined: total number of taxa, number of Ephemeroptera, Plecoptera and Trichoptera (EPT) taxa, % (Oligochaeta & Diptera), % Filtering feeders; % EPT taxa; German trophic index RETI and species diversity indices according to Cheshmedjiev et al. (2011) and Belkinova et al. (2013).

RESULTS AND DISCUSSIONS

During the ecological monitoring of the Parvenetska River (Parvenetska biotope), 26 taxa (*Haliplus lineolatus* Mannerheim, 1844; *Oulimnius tuberculatus* (Müller, 1806); *Lumbricus rubellus* Hoffmeister, 1843; *Atherix ibis* (Fabricius, 1798), larva; Ceratopogonidae; *Chironomus plumosus* (Linnaeus, 1758), larva; *Tipula* sp., larva; *Baetis* sp., nymph; *Caenis horaria* (Linnaeus, 1758), nymph; *Ecdyonurus* sp., nymph; *Oligoneuriella rhenana* (Imhoff, 1852), nymph; *Serratella ignita* (Poda, 1761), nymph (*Ephemerella ignita* (Poda, 1761)); *Gerris* sp., nymph; *Nepa cinerea* Linnaeus, 1758, nymph; *Plea minutissima* Leach, 1818, nymph; *Physella acuta* (Draparnaud, 1805); *Bithynia tentaculata* (Linnaeus, 1758); *Aeshna* sp. larva; *Enallagma cyathigerum* (Charpentier, 1840), larva; *Gomphus* sp., larva; *Hydropsyche* sp., larva; *Hydropsyche ornatula* McLachlan, 1878, larva; *Hydroptila* sp., larva; *Limnephilus rhombicus* (Linnaeus, 1758), larvae; *Oligotricha striata* (Linnaeus, 1758) (syn. Phryganea striata L.); *Sericostoma personatum* (Kirby & Spence, 1826), larva) with 316 specimens of macroinvertebrates belonging to 9 orders were found.

The largest number of taxa and specimens are the macroinvertebrates belongs to the order Trichoptera (Figure 3). Due to the high number of taxa, the ecological state of the Parvenetska River in the studied biotope is very good.

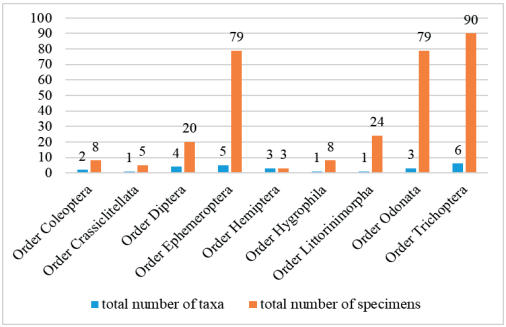


Figure 3. Total number of taxa and specimens of macroinvertebrate organisms from the Parvenetska River

Eleven EPT taxa with a total of 169 specimens of macroinvertebrates were identified in the Parvenetska biotope. Of these, 5 and 6 taxa (79 and 90 specimens) are from Ephemeroptera and Trichoptera, respectively. The ecological state of the river in the studied biotope based on the number of EPT taxa is very good. In previous studies (Vidinova et al., 2018), 9 EPT taxa were reported for the Parvenetska River (five from Ephemeroptera and four from Trichoptera). Of these, two taxa - *S. ignita* (Ephemeroptera) and *Hydropsyche* sp. (Trichoptera) were also found in the Parvenets biotope of the present study.

One taxon, Oligochaeta, and four taxa, Diptera, were found, represented by 5 and 20 specimens, respectively, which represent 7.91% of the total abundance. Two taxa (with five specimens) from the ecological group of filtering feeders were found. Therefore, the filtering feeders group represents 1.58% of the total abundance. The percentage of EPT taxa is high - 53.48% of the total abundance.

According to the mode of feeding, macroinvertebrate organisms in the Parvenets biotope are distributed as follows: "scrapers (SC)" - 91 specimens (7 taxa); "collectors (CL)" - 52 specimens (2 taxa); "shredders (SH)" and "deposit feeders (DF)" - 38 specimens (4 and 3 taxa, respectively); "filtering feeders (FL)" - 5 specimens (2 taxa). The studied biotope is dominated by scrapers and collectors, typical of mountain areas without anthropogenic load. Based on the distribution of macroinvertebrates from the Parvenetska River by trophic groups, the German Trophic Index (RETI) was calculated.

The index value was 0.58, indicating that the river's ecological state in the studied biotope is good.

The Shannon-Weaver species diversity index (H') is 2.62 and indicates β-mesosaprobic conditions for the studied section of the Parvenetska River. The Pielou's evenness index (E) is high, and the Simpson's dominance index (C) is low, indicating good environmental conditions (Table 1).

Table 1. Species diversity indices

Indices	Parvenets biotope
Species richness index of Margalef (Dmg)	4.34
Shannon-Weaver species diversity index (H')	2.62
Pielou's evenness index (E)	0.805
Simpson's dominance index (C)	0.102

Of the 26 macroinvertebrate taxa identified, 23 belong to 9 saprobity groups. By number of taxa, macroinvertebrates dominate for 0-β-mesosaprobic conditions (7 taxa), and by number of specimens - for β-mesosaprobic conditions (91 specimens) (Figure 4).

The results obtained for the value of the saprobic index (SPUB = 1.97) indicate a good state of the water of the Parvenetska River at the Parvenets biotope.

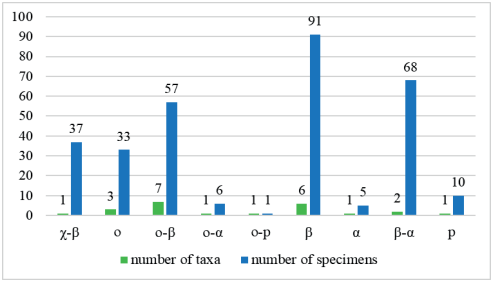


Figure 4. Number of macroinvertebrates from the Parvenetska River by saprobity groups

The bioindicator macroinvertebrate organisms from the Parvenetska River include 23 taxa belonging to the five sensitivity groups - Group A (sensitive forms), Group B (less sensitive forms), Group C (relatively tolerant forms), Group D (tolerant forms), Group E (the most tolerant forms). Group C is distinguished by the largest number of taxa and specimens and groups A and E by the smallest (Figure 5).

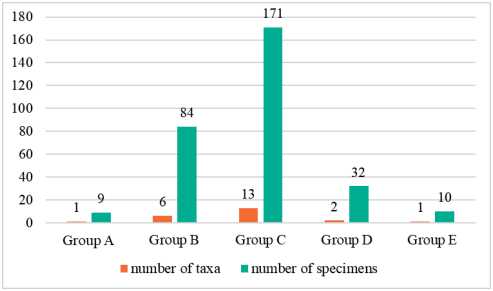


Figure 5. Number of macroinvertebrates from the Parvenetska River by sensitivity groups

The ecological state of the Parvenetska River in the studied biotope has a biotic index of 3 (nEQR=0.6) (moderate ecological state).

According to a report from the East Aegean River Basin Directorate (EARBD), by 2023, the ecological state of the section of the Tamrashka River to the village of Hrabrino and tributaries - the Dormushevska and Pepelasha rivers is good. The ecological state is moderate in the section of the Parvenetska River from the confluence of the Pepelasha River to the mouth (Table 2).

According to the EARBD database, in the period March-June 2024, only in April was pollution with dissolved aluminium (32 µg/l) recorded at a maximum permissible concentration -environmental quality standards (MPC-EQSs) of 25 µg/l, in the section of the Parvenetska River from the confluence of the Pepelashka River to the mouth, where the studied biotope is located. In 2024, based on the study conducted, we established a deterioration of the ecological state from good (2022-2023) to moderate (2024).

Table 2. Comprehensive ecological assessment for the period 2020-2023 (EARBD) (ES - ecological state; EP - ecological potential; BQEs - biological quality elements; PQEs - physicochemical quality elements)

	Overall assessment of the ES/EP on the BQEs	Overall assessment of the ES on the PQEs	Overall assessment of the ES/EP	Chemical state
Tamrashka River to the village of Hrabrino and tributaries - Dormushevska and Pepelasha Rivers - R3				
2023	good	good ES	good	good
2022			good	good
2021	good	good	good	good
2020	very good	good	good	good
	Overall assessment of the ES/EP on the BQEs	**Overall assessment of the ES on the PQEs**	**Overall assessment of the ES/EP**	**Chemical state**
Parvenetska River from the confluence of the Pepelasha River to the mouth - R5				
2023	good ЕП	good ES	good EP	good
2022			good EP	unknown
2021	good	moderate	moderate	good
2020	good	moderate	moderate	good

CONCLUSIONS

During the ecological monitoring of the Parvenetska River (Parvenets biotope), 26 taxa of bioindicator macrozoobenthos were identified. Based on the determined ecological indices, the biotic index with the lowest indicators indicates a moderate ecological state.

ACKNOWLEDGEMENTS

The results of this study have been published with the financial support of the Centre of Research, Technology Transfer and Protection of Intellectual Property Rights at the Agricultural University-Plovdiv under project No. 17-12 in the direction of “Support for publication activities”.

REFERENCES

Belkinova, D., Gecheva, G., Cheshmedzhiev, S., Dimitrova-Dyulgerova, I., Mladenov, R., Marinov, M., Teneva, I., Stoyanov, P., Ivanov, P., Mihov, S., Pehlivanov, L., Varadinova, E., Karagyozova, Ts., Vassilev, M., Apostolu, A., Velkov, B., & Pavlova, M. (2013). *Biological analysis and ecological assessment of surface water types in Bulgaria*. Plovdiv, BG: Univ “P. Hilendarskii” Publishing House (in Bulgarian).

Boyanov, B., Kirin, D., & Manolova I. (2011a). Ecological appraisal for the condition of the Chepelarska River, Bulgaria. *International Conference on the Biogeochemistry of Trace Elements in Florence*, Italy, July 3-7, 2011.

Boyanov, B., Kirin, D., & Manolova I. (2011b). Physicochemical and Hydrobiological Monitoring of the Chepelarska River, Bulgaria. *Sixth Symposium on Recycling Technologies and Sustainable Development*, Serbia, 2011, 353–359.

Cheshmedjiev, S., Soufi, R., Vidinova, Y., Tyufekchieva, V., Yaneva, I., Uzunov, Y., & Varadinova, E. (2011). Multi-habitat sampling method for benthic macroinvertebrate communities in different river types in Bulgaria. *Water Research and Management, 1*(3), 55–58.

Directive 2000/60/EU of the European Parliament and of the Council, 2000. Luxembourg, 23.

East Aegean River Basin Directorate (2018). https://earbd.bg/ (in Bulgarian).

EN ISO 10870:2012 Water quality - Guidelines for the selection of sampling methods and devices for benthic macroinvertebrates in fresh waters (ISO 10870:2012)

EN 16150:2012 Water quality - Guidance on pro-rata Multi-Habitat sampling of benthic macroinvertebrates from wadeable rivers

Gartsiyanova, K., Varbanov, M., Kitev, A., Genchev, S., & Georgieva, S. (2020). Territorial features and dynamics in the water quality change in the Topolnitsa and Luda Yana rivers. *Journal of the Bulgarian Geographical Society*, *43*. 9–15.

Gartsiyanova, K., Varbanov, M., Kitev, A., & Genchev, S. (2021). Water quality analysis of the rivers Topolnitsa and Luda Yana, Bulgaria using different indices. *Journal of Physics: Conference Series, 1960*(1), p. 012018.

Gartsiyanova, K., Kitev, A., Varbanov, M., Georgieva, S., & Genchev, S. (2022). Water quality assessment and conservation of the river water in regions with various anthropogenic activities in Bulgaria: A case study of the catchments of Topolnitsa and Luda Yana rivers. *International Journal of Conservation Science*, *13*(2), 733–742.

Georgieva, G., Uzunova, E., Hubenova, T., & Uzunov, Y. (2014). Ecological assessment of the rivers Luda Yana and Banska Luda Yana as Based on Selected Biological Parameters. *Ecologia Balkanica*, *5*. 89–94.

Integrated Development Plan of Municipality of Plovdiv, 2021-2027. https://www.plovdiv.bg/piro/piro-plan/ (in Bulgarian).

Integrated Development Plan of Municipality of Rhodope, 2021-2027. https://rodopi.bg/wp-content/uploads/2021/02/PIRO_2021-2027.pdf (in Bulgarian).

Irikov, A., & Atanasova, V. (2008). Ecological evaluation of river ecosystems in the east Aegean Sea region in Bulgaria. In: Il. Velcheva & A. Tsekov (Eds.), *Proceedings of the anniversary scientific conference of ecology*, (pp. 326–370) (in Bulgarian).

Kancheva, V. (2016). The ecological state of the Topolnitsa River basin and waters. In: M. Teoharov & B. Hristov (Eds.), *Geochemical and agroecological problems of the Zlatishko-Pirdopskoto field and its surroundings*. Sofia, BG: Bulgarian Soil Society Publishing House (in Bulgarian).

Kiradzhiev, S. (2013). *Encyclopedic Geographical Dictionary of Bulgaria*. Sofia, BG: Iztok-zapad Publishing house (in Bulgarian).

Kirin, D. (2002). Ecological study of the intestinal helminth communities of *Leuciscus cephalus* (L., 1758) and appraisal of the conditions of the studied freshwater ecosystems from the Chepelarska River, Bulgaria. *Acta zoologica bulgarica*, *54*(2), 73–85.

Park, J., Sakelarieva, L., & Varadinova, E. (2022). Comparative analysis of the water policies and the systems for ecological status assessment of the running waters in Bulgaria and South Korea: Case study on Maritsa River and Han River. *Ecologia Balkanica*, *14*(2), 171–189.

Patronov, G., & Kirin, D. (2024). Biodiversity and ecological assessment of the Chepelarska River, Bulgaria. Scientific Papers. *Series E. Land Reclamation, Earth Observation & Surveying, Environmental Engineering*, *XIII*, 592–599.

Regulation No. H-4 of 14.09.2012 on the characterization of surface waters. Promulgated in the Official Gazette, No. 22 of 5.03.2013, amended and supplemented, No. 67 of 04.08.2023.

Varadinova, E., Sakelarieva, L., Park, J., Ivanov, M., & Tyufekchieva, V. (2022). Characterization of Macroinvertebrate Communities in Maritsa River (South Bulgaria) - Relation to Different Environmental Factors and Ecological Status Assessment. *Diversity*, *14*. 833.

Vidinova, Y.N., Botev, I.S., Tyufekchieva, V.G., Nedyalkova, T.V., Yaneva, I.Y., Zadneprovski, B.E., & Varadinova, E.D. (2008). Results of rapid hydrobiological monitoring of watersheds from the East-and West Aegean Sea River basin districts in Bulgaria. *Acta zoologica bulgarica*, 233–242.

Vidinova Y.N., Evtimova V.V. & Tyufekchieva V.G. (2018). Ephemeroptera, Plecoptera and Trichoptera (Insecta) from water bodies in the region of Plovdiv city. Faunistic diversity of the city of Plovdiv (Bulgaria), Vol.1 – Invertebrates. *Bulletin of the Natural History Museum – Plovdiv*, *Supplement, 1*. 69–79.

Zaharieva, P., Kirin, D., & Zaharieva, R. (2024). Hydrobiological monitoring of two rivers from the Maritsa River basin based on a biological quality element macrozoobenthos. *Scientific Papers. Series D. Animal Science*, *LXVII* (2), 660–667.

Scientific Papers. Series E. Land Reclamation, Earth Observation & Surveying, Environmental Engineering. Vol. XIV, 2025
Print ISSN 2285-6064, CD-ROM ISSN 2285-6072, Online ISSN 2393-5138, ISSN-L 2285-6064

ECOLOGICAL ASSESSMENT OF THE BOROVITSA RIVER, EAST AEGEAN SEA BASIN

Diana KIRIN[1, 2], Petya ZAHARIEVA[1, 2], Radoslava ZAHARIEVA[1, 2], Georgi PATRONOV[3], Marian VARBANOV[1], Gergana METODIEVA[1], Dimitrinka KUZMANOVA[2]

[1]National Institute of Geophysics, Geodesy and Geography (NIGGG),
Hydrology and Water Management Research Center, Bulgarian Academy
of Sciences, 3 Acad. G. Bonchev Street, 1113, Sofia, Bulgaria
[2]Agricultural University-Plovdiv, Department of Chemistry, Phytopharmacy and Ecology,
and Environmental Protection, 12 Mendeleev Blvd., Plovdiv, 4000, Bulgaria
[3]University of Plovdiv "Paissii Hilendarski", Department of Chemical Technology,
24 Tsar Assen Street, Plovdiv, 4000, Bulgaria

Corresponding author email: dianaatanasovakirin@gmail.com

Abstract

This study assesses the ecological state of the Borovitsa River, a tributary of the Arda River sub-basin, and the Maritsa River basin using a methodology approved for the European Union and Bulgaria. For the purpose of the study, in the spring of 2024, macroinvertebrates samples were collected from the Borovitsa River near the village of Nenkovo (in the section between Borovitsa Reservoir and Kardzhali Reservoir, according to Bulgarian river typology, this section is classified as R14:"Sub-Mediterranean small and medium-sized rivers" according to the typology of rivers in Bulgaria. The collected macrozoobenthos were taxonomically identified. Fourteen taxa were identified, based on which key ecological metrics were calculated - EPT taxa, Margalef species richness index (Dmg), Shannon-Weaver species diversity index (H'), Pielou's evenness index (E), Simpson's dominance index (C) and biotic index (BI). The findings provide valuable insights into the biodiversity and ecological status of the Borovitsa River, contributing to regional water quality assessments and conservation efforts.

Key words*: biotic index, chemical status, ecological state, macrozoobenthos, Maritsa River basin.*

INTRODUCTION

The Arda River originates from the northeastern foothills of Ardin Peak, located in the Western Rhodopes, and flows for 241 km before reachingthe Bulgarian-Greek border. It then joins the Maritsa River in Turkey. The Arda River is one of the largest tributaries of the Maritsa River. Major tributaries of the Arda River include the Varbitsa River (98.1 km), Krumovitsa River (58.5 km), Cherna River (48.1 km), Perperek River (44 km), and Borovitsa River (42.1 km). Its highest water levels occur between December and April. The Borovitsa River originates in the Rhodopes and flows into the Arda River, eventually draining into the Kardzhali Reservoir. The Borovitsa River catchment area is 301 km^2 (Kiradzhiev, 2013; East Aegean River Basin Directorate, 2018). The Borovitsa Reservoir supplies drinking and domestic water. The surrounding area is lightly inhabited (Kiradzhiev, 2013; Integrated Development Plan of Municipality of Kardzhali, 2021-2027). The European Water Framework Directive (Directive 2000/60/EU) mandates that all surface waters achieve a "good ecological status".

The Borovitsa River falls into Ecoregion 7 and belongs to type R14 "Sub-Mediterranean small and medium-sized rivers" (Belkinova et al., 2013). A key role in the assessment of the ecological state of surface water is played by biological quality elements (BQEs) includingphytoplankton, macrophytes, phytobenthos, macrozoobenthos and fish. Additionally, physicochemical and hydromorphological parameters contribute to the evaluation. The final assessment of the ecological state is determined on the principle of "one out – all out" (Cheshmedjiev & Marinov, 2008; Belkinova et al., 2013). Despite extensive research on the Arda River and its sub-basin, no previous studies have assessed the Borovitsa River's ecological state using macrozoobenthos

as a BQE. Such studies exist for the Arda River (Kirin et al., 2002; Kuzmanov et al., 2002; Kirin et al., 2003; Kirin, 2006) and for the Arda River sub-basin - from the Borovitsa Reservoir (Varadinova et al., 2019). Vidinova (2006) studied mayflies (Ephemeroptera, Insecta) from the Rhodopes Mountains, including from the Arda River, the Malka Arda River, the Varbitsa River, the Krumovitsa River, the Borovitsa River and others. Vidinova et al. (2016) presented a taxonomic list of macroinvertebrates from various standing water bodies in Bulgaria, including the Borovitsa Reservoir.

This study aims to evaluate the ecological state of the Borovitsa River, a tributary of the Arda River sub-basin and the Maritsa River basin, using macrozoobenthos - based bioindicators. The results contribute to regional water quality assessments and environmental management strategies.

MATERIALS AND METHODS

Macrozoobenthos samples were collected from the Borovitsa River in the spring of 2024. The selected biotope (designated as the Nenkovo biotope) is located between the Borovitsa Reservoir and Kardzhali Reservoir, next to the Roman Bridge (41°43'59.8"N 25°13'11.7" E) (Figures 1-2), south of the village of Nenkovo, at an altitude of 420 m. In this section, the river bed is represented by stones and sand.



Figure 1. Borovitsa River, Arda River sub-basin, Maritsa River basin



Figure 2. Views from the Borovitsa River, Nenkovo biotope

Macroinvertebrate sampling followed EU and Bulgarian legislative requirements and standards (Cheshmedjiev et al., 2011; EN ISO 10870:2012; EN 16150:2012; Regulation No. H-4 of 14.09.2012; Belkinova et al., 2013). The taxonomic identification and abundance assessment of the collected macroinvertebrates were conducted under laboratory conditions using a stereo zoom microscope, KERN OZL 464T24. According to Regulation No. H-4 of 14.09.2012 and Belkinova et al. (2013), the following metrics were calculated: - total number of taxa; - number of Ephemeroptera, Plecoptera and Trichoptera (EPT) taxa; - Trichoptera taxa was the dominant group.

Additionally, the following indices were calculated: 1) Margalef species richness index (Dmg) (Margaleff, 1958); 2) Shannon-Weaver species diversity index (H') (Shannon & Weaver, 1963); 3) Pielou's evenness index (E); 4) Simpson's dominance index (C) (Magurran, 1988); 5) Saprobic index (SPUB) and 6) Biotic index (BI) based on Flanagan & Toner (1972), modified by Clabby (1979), Clabby (1982).

The indices were calculated using the following formulas:

1) $\mathbf{Dmg} = \frac{(\mathbf{S-1})}{\mathbf{\log_2 N}}$,

where:

S - number of species in the sample;

N - total number of organisms in the sample.

2) $\mathbf{H'} = (\mathbf{P})(\mathbf{\log P})$,

where:

H' - index of individual species diversity;

P - the proportion of the taxon (amount of the taxon divided by the total number of organisms in the sample).

3) $\mathbf{E} = \frac{\mathbf{H'}}{\mathbf{\log_2 N}}$,

where:

H' - index of individual species diversity;

N - number of specimens.

4) $\mathbf{C} = \sum \left(\frac{\mathbf{n_i}}{\mathbf{N}}\right)^{\mathbf{2}}$,

where:

n_i - number of specimens of each i-species;

N - number of specimens of all species (total abundance)

5) $\mathbf{SPUB} = \sum(\mathbf{s_i h_i I_i}) / \sum(\mathbf{h_i I_i})$,

where:

s_i - saprobic importance of species/taxon i;

h_i - relative abundance of species/taxon i;

I_i - indicator weight of species/taxon i.

RESULTS AND DISCUSSIONS

In the study of macrozoobenthos from the Borovitsa River, Nenkovo biotope, 14 taxa with 219 specimens belonging to 6 orders were identified. Trichoptera taxa were the most dominant group. The most abundant taxon was *Schmidtea polychroa* (Schmidt, 1861) (order Tricladida; 79 specimens) (Table 1). The number of identified taxa suggests a very good ecological state of the water of the Borovitsa River in the studied biotope.

More than half of the macroinvertebrate taxa in the Nenkovo biotope belong to the EPT taxa (8 taxa). Taxa from these orders are sensitive to anthropogenic pressure, and their presence indicates a good ecological status for the river in the selected biotope. A previous study (Vidinova, 2006) reported four taxa of Ephemeroptera for the Borovitsa River - *Electrogena lateralis* (Curtis, 1834), *Electrogena macedonica* (Ikonomov, 1954), *Electrogena quadrilineata* (Landa, 1970) and *Choroterpes picteti* (Eaton, 1871), but these species were absent in the Nenkovo biotope.

In the Borovitsa Reservoir a total of 14 macrozoobenthos taxa were recorded, including:

- 1 taxon Oligochaeta (*Limnodrilus* sp. juv.),
- 1 taxon Ephemeroptera (*Caenis macrura* Stephenes, 1835),
- 1 taxon Odonata (*Gomphus vulgatissimus* (Linnaeus, 1758)),
- 2 taxa Trichoptera (*Ecnomus tenellus* (Rambur, 1842), *Holocentropus stagnalis* (Albarda, 1874)) and
- 9 Diptera taxa (*Chironomus* gr. *riparius* Meigen, 1804, *Chironomus* sp., *Cricotopus* sp., *Cryptochironomus* gr. *defectus* Kieffer, 1913, *Dicrotendipes* sp., *Eukiefferiella* sp., *Tanytarsus* gr. *gregarius* Kieffer, 1909, *Tvetenia* sp., Chironomidae, gen. sp.) (Vidinova et al., 2016). None of these taxa were recorded in the present study for the Nenkovo biotope of the Borovitsa River.

The abundance of macroinvertebrate fauna is represented by the metrics: % (Oligochaeta & Diptera), % Filtering feeders and % EPT taxa. In the present study, no representatives of Oligochaeta were found. Two Diptera taxa were found (with 33 specimens). Only one taxon (9 specimens) belongs to the filtering feeders

group. EPT taxa contributed the highest proportion of macrozoobenthos (Table 2).
The Margalef species richness index (Dmg) is low. The Shannon-Weaver species diversity index (H') is also low, indicating α-mesosaprobic conditions. However, the Pielou's evenness index (E) is high, the Simpson's dominance index (C) is low, which indicates favourable environmental conditions (Table 3).

Table 1. Taxonomic composition and abundance of bioindicator macroinvertebrate organisms from the Borovitsa River, Nenkovo biotope

No.	Taxa	Number of specimens	Genus	Family	Order
1	*Limnephilus rhombicus* (Linnaeus, 1758), larva	36	*Limnephilus* Leach, 1815	Limnephilidae	Trichoptera
2	*Hydropsyche* sp., larva	2	*Hydropsyche* Pictet, 1834	Hydropsychidae	Trichoptera
3	*Hydropsyche ornatula* McLachlan 1878, larva	40	*Hydropsyche* Pictet, 1834	Hydropsychidae	Trichoptera
4	*Psychomyia pusilla* (Fabricius, 1781), larva	1	*Psychomyia* Latreille, 1829	Psychomyiidae	Trichoptera
5	*Chironomus plumosus* (Linnaeus, 1758), larva	24	*Chironomus* Meigen, 1803	Chironomidae	Diptera
6	*Hydroptila* sp., larva	5	*Hydroptila* Dalman, 1819	Hydroptilidae	Trichoptera
7	*Simulium* sp., larva	9	*Simulium* Latreille, 1802	Simuliidae	Diptera
8	*Baetis* sp., nymph	3	*Baetis* Leach, 1815	Baetidae	Ephemeroptera
9	*Schmidtea polychroa* (Schmidt, 1861)	79	*Schmidtea* Ball, 1974	Dugesiidae	Tricladida
10	*Gomphus* sp., nymph	10	*Gomphus* Leach, 1815	Gomphidae	Odonata
11	*Enallagma cyathigerum* (Charpentier, 1840), larva	2	*Enallagma* Charpentier, 1840	Coenagrionidae	Odonata
12	*Platambus maculatus* (Linnaeus, 1758)	1	*Platambus* Thomson, 1859	Dytiscidae	Coleoptera
13	*Oligotricha striata* (Linnaeus, 1758) (syn. *Phryganea striata* L.), larva	3	*Oligotricha* Rambur, 1842	Phryganeidae	Trichoptera
14	*Ecdyonurus* sp., nymph	4	*Ecdyonurus* Eaton, 1868	Heptageniidae	Ephemeroptera

Table 2. Abundance of macroinvertebrate organisms from the Borovitsa River, Nenkovo biotope

Metrix	% (Oligochaeta & Diptera)	% Filtering feeders	% EPT taxa
14 taxa (219 specimens)	15.07%	4.11%	42.92%

A total of five macrozoobenthos taxa were associated with 0-β-mesosaprobic conditions; three taxa corresponded to β-α-mesosaprobic conditions, three to β-mesosaprobic conditions and one taxon each - χ-0 saprobic; χ-β-mesosaprobic and p saprobic conditions. The study reports a saprobic index SPUB of 2.38, indicating a moderate ecological state of the Borovitsa River.

Table 3. Biotic indices of the bioindicator macrozoobenthos from the Borovitsa River, Nenkovo biotope

Indices	Margalef species richness index (Dmg)	Shannon-Weaver species diversity index (H')	Pielou's evenness index (E)	Simpson's dominance index (C)
14 taxa (219 specimens)	2.41	1.9	0.721	0.208

The macroinvertebrate organisms discovered in this study belong to four sensitivity groups. The largest number of taxa and specimens (9 taxa with 99 specimens) were classified as relatively tolerant forms (group C), followed by the group of less sensitive ones (group B) - 3 taxa with 92 specimens. With one taxon each (4 and 24 specimens), the groups of sensitive (group A) and the most tolerant forms (group E) are represented, respectively. Notably, no taxa belonged to the tolerant group (Group D). The determined biotic index (BI (nEQR) = 3 (0.6)) indicates a moderate ecological state.

According to a report from the East Aegean River Basin Directorate (EARBD) covering the period 2020-2023, the ecological state of the Borovitsa River varies along different sections. The section from the river's source to the Borovitsa Reservoir is classified as good, while the section from the Borovitsa River and tributaries from the Borovitsa Reservoir to the confluence with the Kardzhali Reservoir is categorized as having a moderate ecological state (Table 4). In the spring (March-June) of 2024, there were no exceedances of key physicochemical parameters, specific pollutants, or priority substances in the Borovitsa River's freshwater ecosystem (East Aegean River Basin Directorate, 2018).

Table 4. Comprehensive ecological assessment for the period 2020-2023 (EARBD) (ES - ecological state; EP - ecological potential; BQEs - biological quality elements; PQEs - physicochemical quality elements)

	Overall assessment of the ES/EP on the BQEs	Overall assessment of the ES on the PQEs	Overall assessment of the ES/EP	Chemical state
Source of the Borovitsa River to the Borovitsa Reservoir - R14				
2023	good	good ES	good	good
2022			good	good
2021	good		good	unknown
2020	good		good	unknown
Borovitsa River and tributaries from Borovitsa Reservoir to the confluence with Kardzhali Reservoir - R14				
2023	moderate	good ES	moderate	Good
2022			moderate	Good
2021	good		good	Unknown
2020	good		good	Unknown

The findings of this study confirms preserving the ecological state from 2022-2023 - moderate ecological state.

CONCLUSIONS

This study assessed the ecological state of the Borovitsa River, focusing on macrozoobenthos as a biological quality element.

The identification of 14 macroinvertebrate taxa comprising 219 specimens confirmed that the Borovitsa River exhibits a moderate ecological state.

The relatively high proportion of EPT taxa (Ephemeroptera, Plecoptera, Trichoptera) indicates good ecological integrity, although the absence of certain previously recorded species suggests potential environmental pressures. It is hypothesized that this moderate classification is primarily influenced by reduced water levels, potentially leading to habitat degradation and adverse effects on macroinvertebrate communities.

Although no physicochemical exceedances were detected during the study period, long-term monitoring is required to evaluate potential

impacts from seasonal variations, climate change, and anthropogenic activities on water quality.

ACKNOWLEDGEMENTS

The results of this study have been published with the financial support of the Agricultural University-Plovdiv.

REFERENCES

Belkinova, D., Gecheva, G., Cheshmedzhiev, S., Dimitrova-Dyulgerova, I., Mladenov, R., Marinov, M., Teneva, I., Stoyanov, P., Ivanov, P., Mihov, S., Pehlivanov, L., Varadinova, E., Karagyozova, Ts., Vassilev, M., Apostolu, A., Velkov, B., & Pavlova, M. (2013). *Biological analysis and ecological assessment of surface water types in Bulgaria*. Plovdiv, BG: Univ "P. Hilendarskii" Publishing House (in Bulgarian).

Cheshmedjiev, S., & Marinov, M. (2008). *Typology of aquatic ecosystems in Bulgaria (implementation of the Water Framework Directive 2000/60/EU).* In: Il. Velcheva & A. Tsekov (Eds.), Proceedings of the anniversary scientific conference of ecology (pp. 371–383) (in Bulgarian).

Cheshmedjiev, S., Soufi, R., Vidinova, Y., Tyufekchieva, V., Yaneva, I., Uzunov, Y., & Varadinova, E. (2011). Multi-habitat sampling method for benthic macroinvertebrate communities in different river types in Bulgaria. *Water Research and Management*, 1(3), 55–58.

Clabby, K.J., & Bowman, J.J. (1979). *Report of Irish Participants*. In: Ghetti P.F. (Ed.): Third Technical Seminar on Biological Water Assessment Methods, Parma, 1978. Vol. 1. Commission of the European Communities.

Clabby, K.J. (1982). The National Survey of Irish Rivers: River Quality Investigations--biological Results of the 1980 & 1981 Investigations: Summary Report. Environmental Research Unit.

Directive 2000/60/EU of the European Parliament and of the Council, 2000. Luxembourg, 23.

East Aegean River Basin Directorate (2018). https://earbd.bg/ (in Bulgarian).

EN ISO 10870:2012 Water quality - Guidelines for the selection of sampling methods and devices for benthic macroinvertebrates in fresh waters (ISO 10870:2012)

EN 16150:2012 Water quality - Guidance on pro-rata Multi-Habitat sampling of benthic macroinvertebrates from wadeable rivers

Flanagan, P.J. Toner, P.F. (1972). Notes on the chemical and biological analysis of Irish River waters. An FORAS Forbartha.

Integrated Development Plan of Municipality of Kardzhali, 2021-2027. https://www.kardjali.bg/docs/PIRO/Proekt-nalitichna-Strategicheska_chast-PIRO-022022.pdf (in Bulgarian).

Kiradzhiev, S. (2013). Encyclopedic Geographical Dictionary of Bulgaria. Sofia, BG: Iztok-zapad Publishing house (in Bulgarian).

Kirin, D., Buchvarov, G., & Kuzmanov, N. (2002). Biological diversity and ecological evaluation of the fresh water ecosystems of the Arda River. *Journal of Environmental Protection and Ecology*, 3(2), 449–456.

Kirin, D., Buchvarov, G., Kuzmanov, N., & Koev, K. (2003). Biological diversity and ecological evaluation of the fresh water ecosystems from the Arda River. *Journal of Environmental Protection and Ecology*, 4(3), 550–556.

Kirin, D. (2006). *Biological diversity and ecological evaluation of the fresh water ecosystems from the Arda River, Bulgaria.* National Scientific Conference with International Participation under the heading "20 Years Union of Scientists in Bulgaria - Branch Smolyan", October, 20th–21st, Smolyan, Bulgaria, 1099–1110.

Kuzmanov, N., Kirin, D., & Buchvarov, G. (2002). Ecological evaluation of the waters of the Arda River after the reservoir "Studen kladenets". *Journal of Environmental Protection and Ecology*, 3(2), 457–463.

Magurran, A., 1988. Ecological diversity and its measurement. Princeton, USA: Princeton University Press.

Margaleff R. (1958). *Temporal succession and spatial heterogeneity in Phytoplankton*. In: A.A. Buzzati-Traverso (Ed.), Perspectives in Marine Biology (pp. 323–347). Berkeley, USA: University of California Press.

Regulation No. H-4 of 14.09.2012 on the characterization of surface waters. Promulgated in the Official Gazette, No. 22 of 5.03.2013, amended and supplemented, No. 67 of 04.08.2023.

Shannon C.E. & Weaver, W. (1963). The Mathematical Theory of Communication. Urbana. USA: Univ. of Illinois Press.

Varadinova, E.D., Kerakova, M.Y., Ihtimanska, M. K., & Soufi, R.A. (2019). Trophic structure of macrozoobenthos and assessment of ecological status of lakes and reservoirs in Bulgaria. *Acta zoologica bulgarica*, 71(1), 113–120.

Vidinova Y. (2006). Mayflies (Ephemeroptera, Insecta) from the Rhodopes Mountains (Bulgaria and Greece). - In: Beron P. (Ed.), Biodiversity of Bulgaria. 3. Biodiversity of Western Rhodopes (Bulgaria and Greece) (pp. 269–281). Sofia, Bulgaria: I. Pensoft & Nat. Mus. Natur. Hist.

Vidinova, Y., Tyufekchieva, V., Varadinova, E., Stoichev, S., Kenderov, L., Dedov, I., & Uzunov, Y. (2016). Taxonomic list of benthic macroinvertebrate communities of inland standing water bodies in Bulgaria. *Acta zoologica bulgarica*, 68(2), 147–158.

Scientific Papers. Series E. Land Reclamation, Earth Observation & Surveying, Environmental Engineering. Vol. XIV, 2025
Print ISSN 2285-6064, CD-ROM ISSN 2285-6072, Online ISSN 2393-5138, ISSN-L 2285-6064

ADVANCED HYDRAULIC MODELING OF IRRIGATION CHANNEL

Mihai NEGURA, Robert Florin BEILICCI, Erika Beata Maria BEILICCI, Mirela Laura IEREMCIUC, Dorina Gabriela IONESCU

Politehnica University of Timisoara, 1A Splaiul Spiru Haret, 300022, Timişoara, Romania

Corresponding author email: robert.beilicci@upt.ro

Abstract

The Sânnicolau Mare-Saravale Canal covers an area of 20,060 ha, with land rehabilitation works accounting for 19,998 ha. Sânnicolau Mare is located in the western part of Romania, in Timiș County. The MIKE11 program was used for numerical modelling. MIKE 11 has flow calculation modules that include hydraulic structures, and ways to describe the operation of the structure. With the MIKE 11 model, they draw up flood risk maps. The keywords are productivity, reliability, quality and versatility for professional engineers who use the MIKE 11 program. The MIKE 11 model has been shown to be highly reliable for generating flood risk maps.

Key words*: advanced modelling, flood maps irrigation channel.*

INTRODUCTION

The objective of this paper is to model the movement of water in the Aranca channel in the area of Sânnicolau Mare, with the aim of determining water levels and flow rates along the channel.

This allows for the anticipation of situations that may arise under different inflow conditions in extreme precipitation or drought scenarios. The numerical modelling was carried out using the MIKE11 program.

Sânnicolau Mare drainage system - in the northern part of Timiș county there are Saravale and the Tisa - Mureș basin; subsection II Aranca being delimited as follows:

- North Mureș sewerage system and left Mureș dam km 32+000 - 43+400;
- South Basin, subsection III Aranca Galatca;
- To the west, subsection IV Aranca;
- East under the Aranca I compartment - the limit of Arad County;

Sânnicolau Mare System - The rehabilitation works of the lands belonging to Saravale occupied 19,998 ha of the total area of 20,060 ha (Figure 1).

The excess moisture in the drainage system manifests itself differently on different surfaces in local orographic, solar and hydrogeological conditions, created as a result of rainfall in the area of the drainage system and the Mureș River that produce an abundant supply of groundwater in the area.



Figure 1. Map of Timiș County, Romania

The land has a natural slope from east to west 0.02-0.05%.

The emissary is generally the Mureș River. The depression of the main collector Aranca, the regularized discharges made at Mureș being carried out through a system of dams near the Silvia Canal and SP Cenad at Aranca have reached the border restrictions, the rest is done through the periods of flow of the Aranca canal over the border with Yugoslavia through the discharge of the Tisza canal or the canal into the DTD.

The main collector system for all departments is the Aranca Canal, which conducts the inland waters generally collected across the Yugoslav Roman border to the height of 77.60 m recorded share the miraculous smiles - the confluence of the Tisza when the Yugoslav border dam closes on the Aranca.

At that time, the gates of Sections IV and II (Aranca km 40+250) and Compartments II and

I (Aranca km 77+940) are closed, and the appropriate distribution of the collected domestic wastewater and drainage subunits is carried out.

Existing natural conditions - partitioning perimeter imposed by Sânnicolau Mare - Saravale drainage system, four independent functional units as follows:

1. UD Sânnicolau Mare - Tomnatic an area of 6,390 ha located on the left bank of the Aranca between 40+250 - 53+300 km forming the northern limit, Dc27 Simpetru-Lovrin the eastern limit of the drainage system compartment III Aranca and Section IV the southern limit of the southern limit.
2. Simpetru Lovrin UD, area of 3,885 ha located on the left bank of the canal, also Aranca, between 53+300 - 59+700 km, northern limit, bordered to the northeast and south, Periam UD, compartment III (Galatca), to the west, is limited to the DU. Sânnicolau Mare-Tomnatic.
3. Saravale UD - the Igris area of 3,690 ha on the right bank of the Aranca canal (km 40+250 - 59+700) and Silvia (km 0+000 - 0+300) limited to the northern Mureșan and left Mureș dam system (km 31+000 - 35+000) and to the east by the Periam UD dam system.
4. The Periam UD area, 6,033 ha, is located in the upstream compartment II, Aranca (km 59+700 - 77+940) to the left with the dam north of the Mures river (35+000 - 43+500 km) to the east the Aranca subdivision dam with section. I, the southern limit of the Checea - Jimbolia Aranca drainage system compartment III and UD Lovrin Simpetru - and west - Lovrin Simpetru UD and UD Saravale - Igriș.

The Aranca originates from the Felnac Mureș Valley - where dam construction began in 1816 - and flows into the Tisza River. It passes through the center of Sânnicolau Mare, having been channelized in 1888 following severe spring floods. The Aranca hydraulic system was developed between 1887 and 1894 (Figure 2). The crossing of the Aranca Sânnicolau Mare canal was aimed at draining the flooded lands, being widened and deepened in 1959 and 1960. The canal has a total length of 10.532 km, a depth ranging from 1 to 3 meters, and a width between 6 and 16 meters. It has a slope of 0.1 to 0.15 per km, with a difference in elevation between the entry points and the exit points outside the city. The maximum flow occurs in spring, reaching 2.5 m³/s, while the minimum flow is observed in summer (Biali et al., 2022).

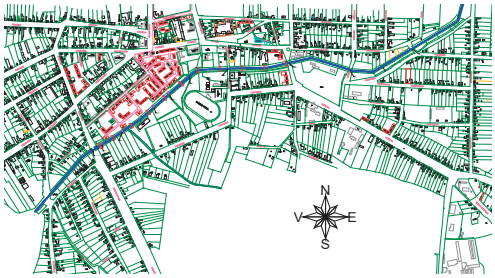


Figure 2. Map of the Aranca Canal, Timiș county

MATERIALS AND METHODS

The movement of water is free on watercourses, rivers, canals and pipes.

"Level-free, straight, and prismatic channels exhibit uniform flow. In straight, artificial, and prismatic channels, uniform flow occurs under free surface conditions (gutters, canals, galleries, ditches, etc.). Hydraulic calculation formulas are the Chezy-type analytical solutions that are obtained by the Manning relation.

$$Q = \frac{1}{n} \frac{S^{\frac{5}{3}}}{P^{\frac{2}{3}}} \sqrt{i} \quad (1)$$

For the trapezoidal section we have:

$$Q = \frac{1}{n} \frac{(\beta+m)^{1.5+y}}{(\beta+m')^{1.5+y}} h^{2.5+y} \sqrt{i} \quad (2)$$

where:

- $m' = 2\sqrt{1+m^2}$ (David, 1984).

Given the complexity of water movements in surface courses, it is an analytical calculation that considers the natural conditions of the land. Modeling the water flow and displacement in the Aranca Canal requires numerical simulation using the MIKE 11 program.

Description of MIKE 11 modules (input data, results)

Input data HD:
- Longitudinal profile;
- cross-sections;
- boundary conditions: hydrograph of flows, levels and boundary key.

Input data ST:
- data on sediments.

Input data RR:
- precipitation, temperature, evapotranspiration;

- data on the hydrographic basin (area, average slope and uses).
Input data ECO-LAB:
- water quality measurements.
Output Data HD:
- hydrograph of flows and levels in each cross-section (flow and level);
- the variation of the water level in longitudinal profile.
Output Data ST:
- Dragged suspended solid flow;
- modification of the levels of the bottom of the riverbed (small erosions, deposits).
Output Data RR:
- hydrograph of flows in the outlet section of the hydrographic basin.
Output Data ECO-LAB:
- the variation of the water quality parameters in the longitudinal profile (Paudel et al., 2022).
MIKE 11 is a widely used tool for simulating flow, water quality, and sediment transport in irrigation canals, rivers, estuaries, and other surface water bodies.
It provides a wide range of solutions, from basic flow routing to complex dynamic modeling, while remaining efficient and user-friendly. The efficient, fast, and robust hydrodynamic simulation engine is the computing core of this program-MIKE 11.
Every aspect of watercourse modeling is a combination of modules and extensions.
The calculation of unsteady flows in rivers and estuaries is performed using a default finite difference scheme of the MIKE 11 hydrodynamic module.
Depending on the local flow conditions, (in space and time) the module can describe both subcritical and supercritical flow conditions through a numerical relationship.
Calculation modules are included for the operation of the hydraulic structure and flow description. On floodplains of flow (Lagos et al., 2024) quasi-two-dimensional formulations and simulations of loop networks can be applied.
From river flows to tidally influenced estuaries, calculation schemes for homogeneous vertical flow conditions are applied (Nannawo et al., 2022). This System is used worldwide for engineering studies
For river management, hydraulic models are applied. For flood warning or planning the operation of reservoirs in forecasting systems, certain flood mitigation potential analysis applications are used (Kumar et al., 2021).
The models provide descriptions of the variations in flow and water level at certain points along, which are then interpreted by the user of the model regarding the consequences it may have on the population and properties in the vicinity of the river (Pareta et al., 2023).
The calibration of the model was performed for fixed inflow discharges measured upstream, which corresponded to water levels measured downstream by National Agency for Land Reclamation (ANIF). After calibration, by adjusting the roughness coefficients, validation was carried out for other measured values, resulting in an accuracy of approximately 96%.

RESULTS AND DISCUSSIONS

The results of the topographic studies for the Aranca Canal are: width at the bottom b = 3.0 m, slope inclination m = 2, slope i = 0.0002, roughness n = 0.02.
For the existing channel curve Q = Q (h) is presented in Figure 4.
The MIKE11 program was used for numerical modeling. Initially, the existing conditions of the Aranca Canal were modeled. Figure 3 shows the location of the canal, and in Table 1 nods coordinates for the model.
The cross-sections through the canal in the form of topographic studies in Figure 6 and raw data in Figure 7 respectively de processed data in Figure 8.
The input of the data according to the formulated boundary conditions, of the upstream flow to the 35+600 chainage are the flood evacuation hydrograph and downstream to the 34+600 chainage the graph of the key curve of the downstream section presented in Figure 5 (Damian et al., 2022).
The flow hydrograph is shown in Figure 9 and the discharges in all periods are presented in Table 2.

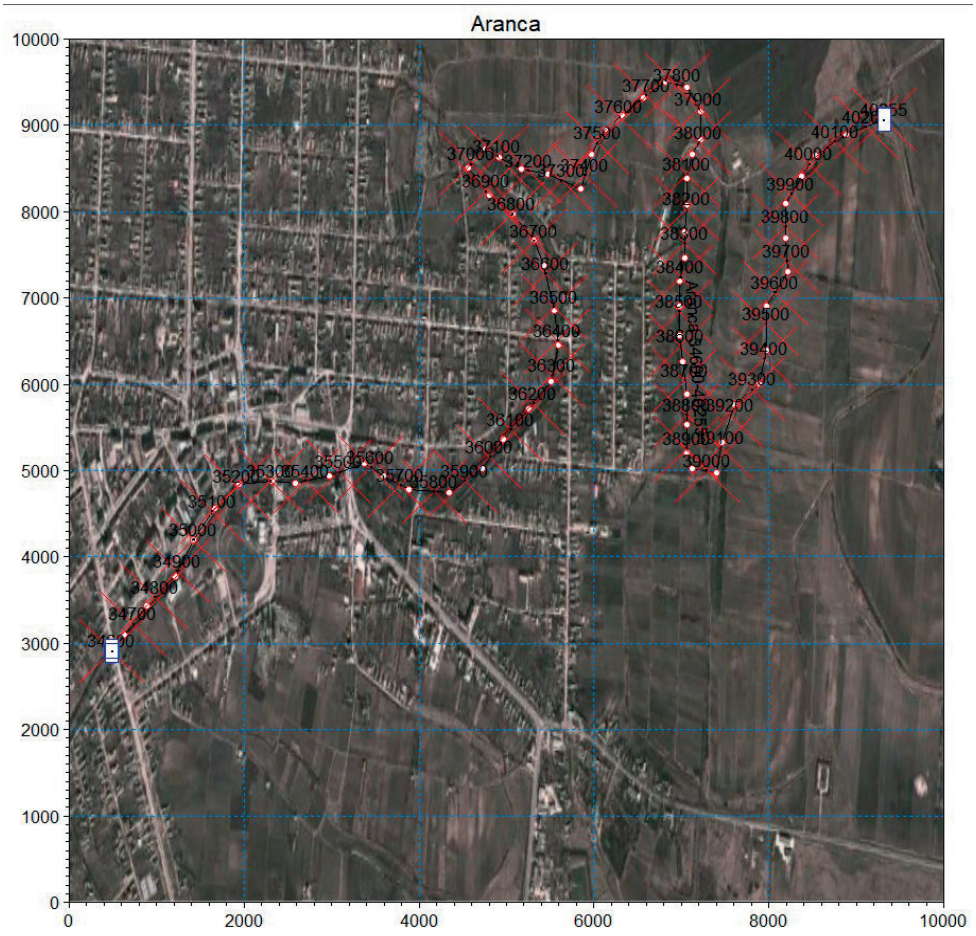


Figure 3. Plan view with grid pattern

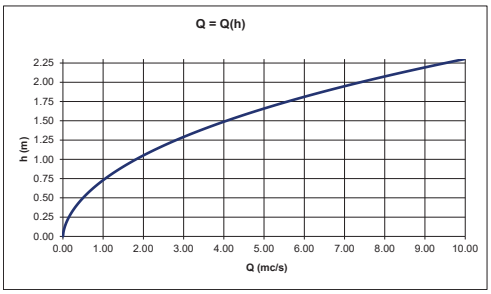


Figure 4. Curve Q = Q (h) for the upstream Aranca Canal

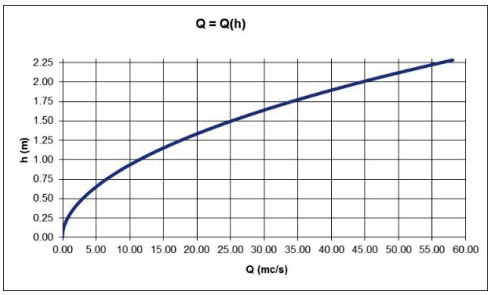


Figure 5. Key curve of the downstream section

Table 1. Nods coordinate for the model

X	Y	River	Chainage
490	2910	Aranca	34600
630	3090	Aranca	34657.1
890	3430	Aranca	34764.3
1210	3780	Aranca	34883
1420	4200	Aranca	35000.6
1660	4560	Aranca	35109
1940	4840	Aranca	35208.1
2320	4880	Aranca	35303.8
2590	4860	Aranca	35371.6
2970	4940	Aranca	35468.8
3370	5090	Aranca	35575.8
3590	4940	Aranca	35642.5
3880	4780	Aranca	35725.4
4340	4740	Aranca	35841
4720	5030	Aranca	35960.7
4960	5370	Aranca	36065
5250	5710	Aranca	36176.9
5510	6030	Aranca	36280.1
5590	6460	Aranca	36389.6
5550	6860	Aranca	36490.3
5430	7380	Aranca	36623.9
5310	7670	Aranca	36702.5
5070	7970	Aranca	36798.7
4800	8190	Aranca	36885.9
4560	8510	Aranca	36986.1
4760	8730	Aranca	37060.5
4920	8630	Aranca	37107.8
5170	8490	Aranca	37179.5
5470	8430	Aranca	37256.2
5850	8270	Aranca	37359.4
5970	8670	Aranca	37464
6130	8960	Aranca	37546.9
6320	9120	Aranca	37609.1
6560	9320	Aranca	37687.3
6820	9500	Aranca	37766.5
7060	9440	Aranca	37828.5
7220	9160	Aranca	37909.2
7220	8840	Aranca	37989.4
7120	8670	Aranca	38038.7
7060	8390	Aranca	38110.4
7060	8070	Aranca	38190.6
7040	7770	Aranca	38265.9
7040	7460	Aranca	38343.5
6980	7200	Aranca	38410.3
6980	6900	Aranca	38485.4
6980	6560	Aranca	38570.6
7020	6260	Aranca	38646.4
7060	5890	Aranca	38739.6
7060	5530	Aranca	38829.7
7060	5210	Aranca	38909.8
7120	5030	Aranca	38957.3
7400	4980	Aranca	39028.6
7460	5330	Aranca	39117.5
7610	5770	Aranca	39233.9
7890	6010	Aranca	39326.2
7970	6400	Aranca	39425.9
7970	6900	Aranca	39551.1
8210	7300	Aranca	39667.9
8190	7690	Aranca	39765.7
8190	8090	Aranca	39865.9
8370	8410	Aranca	39957.8
8530	8650	Aranca	40030.1
8880	8900	Aranca	40137.8
9320	9060	Aranca	40255

Table 2. Discharges in all periods in the upstream section

No	Time	Q	No	Time	Q
1	21 Jul 2008 06:00:00	0.92	66	25 Jul 2008 23:45:00	5.17
2	21 Jul 2008 18:00:00	0.92	67	25 Jul 2008 23:55:00	5.24
3	22 Jul 2008 06:00:00	0.92	68	26 Jul 2008 00:40:00	5.35
4	22 Jul 2008 18:00:00	1.11	69	26 Jul 2008 01:00:00	5.36
5	22 Jul 2008 23:00:00	1.37	70	26 Jul 2008 01:30:00	5.39
6	23 Jul 2008 01:00:00	1.74	71	26 Jul 2008 02:00:00	5.35
7	23 Jul 2008 02:00:00	1.02	72	26 Jul 2008 03:00:00	5.10
8	23 Jul 2008 04:00:00	1.26	73	26 Jul 2008 04:00:00	4.83
9	23 Jul 2008 06:00:00	1.24	74	26 Jul 2008 04:15:00	4.72
10	23 Jul 2008 07:00:00	1.20	75	26 Jul 2008 05:00:00	4.43
11	23 Jul 2008 09:00:00	1.38	76	26 Jul 2008 05:30:00	4.28
12	23 Jul 2008 10:00:00	1.70	77	26 Jul 2008 06:00:00	4.07
13	23 Jul 2008 11:00:00	2.24	78	26 Jul 2008 07:00:00	3.88
14	23 Jul 2008 11:30:00	2.61	79	26 Jul 2008 08:00:00	3.73
15	23 Jul 2008 11:50:00	2.76	80	26 Jul 2008 09:00:00	3.73
16	23 Jul 2008 12:00:00	2.85	81	26 Jul 2008 10:00:00	3.73
17	23 Jul 2008 12:45:00	3.46	82	26 Jul 2008 11:00:00	3.68
18	23 Jul 2008 14:00:00	4.32	83	26 Jul 2008 12:00:00	3.63
19	23 Jul 2008 14:15:00	4.51	84	26 Jul 2008 13:00:00	3.54
20	23 Jul 2008 14:45:00	4.78	85	26 Jul 2008 14:00:00	3.43
21	23 Jul 2008 15:15:00	4.97	86	26 Jul 2008 15:00:00	3.34
22	23 Jul 2008 16:00:00	5.32	87	26 Jul 2008 16:00:00	3.24
23	23 Jul 2008 16:45:00	5.78	88	26 Jul 2008 17:00:00	3.17
24	23 Jul 2008 17:15:00	5.84	89	26 Jul 2008 18:00:00	3.12
25	23 Jul 2008 18:00:00	5.97	90	26 Jul 2008 19:00:00	3.06
26	23 Jul 2008 18:30:00	6.00	91	26 Jul 2008 20:00:00	3.02
27	23 Jul 2008 19:00:00	6.00	92	26 Jul 2008 21:00:00	3.00
28	23 Jul 2008 20:00:00	5.97	93	26 Jul 2008 23:55:00	3.03
29	23 Jul 2008 21:00:00	5.90	94	27 Jul 2008 01:00:00	3.10
30	23 Jul 2008 22:00:00	5.77	95	27 Jul 2008 02:00:00	3.13
31	23 Jul 2008 23:00:00	5.57	96	27 Jul 2008 03:00:00	3.18
32	23 Jul 2008 23:55:00	5.29	97	27 Jul 2008 04:00:00	3.22
33	24 Jul 2008 01:00:00	4.94	98	27 Jul 2008 05:00:00	3.28
34	24 Jul 2008 02:00:00	4.68	99	27 Jul 2008 06:00:00	3.24
35	24 Jul 2008 03:00:00	4.34	100	27 Jul 2008 07:00:00	3.19
36	24 Jul 2008 04:00:00	4.07	101	27 Jul 2008 09:00:00	2.82
37	24 Jul 2008 05:00:00	3.83	102	27 Jul 2008 18:00:00	2.27
38	24 Jul 2008 06:00:00	3.63	103	28 Jul 2008 06:00:00	2.24
39	24 Jul 2008 07:00:00	3.49	104	28 Jul 2008 18:00:00	1.57
40	24 Jul 2008 07:20:00	3.43	105	29 Jul 2008 06:00:00	1.80
41	24 Jul 2008 09:30:00	3.31	106	29 Jul 2008 10:40:00	1.64
42	24 Jul 2008 10:00:00	3.29	107	29 Jul 2008 11:10:00	1.61
43	24 Jul 2008 11:00:00	3.22	108	29 Jul 2008 18:00:00	1.44
44	24 Jul 2008 13:00:00	2.97	109	30 Jul 2008 06:00:00	1.18
45	24 Jul 2008 14:00:00	2.95	110	30 Jul 2008 18:00:00	1.14
46	24 Jul 2008 15:00:00	2.82	111	31 Jul 2008 06:00:00	1.09
47	24 Jul 2008 18:00:00	2.67	112	31 Jul 2008 18:00:00	1.07
48	24 Jul 2008 20:00:00	2.48	113	1 Aug 2008 06:00:00	1.06
49	25 Jul 2008 06:00:00	2.19	114	1 Aug 2008 18:00:00	0.96
50	25 Jul 2008 13:00:00	1.87	115	2 Aug 2008 06:00:00	0.94
51	25 Jul 2008 17:00:00	2.00	116	2 Aug 2008 18:00:00	0.93
52	25 Jul 2008 17:45:00	2.48	117	3 Aug 2008 06:00:00	0.92
53	25 Jul 2008 18:00:00	2.55	118	3 Aug 2008 18:00:00	0.92
54	25 Jul 2008 18:45:00	2.63	119	4 Aug 2008 06:00:00	0.91
55	25 Jul 2008 19:30:00	2.95	120	4 Aug 2008 18:00:00	0.91
56	25 Jul 2008 20:10:00	3.28	121	5 Aug 2008 06:00:00	0.91
57	25 Jul 2008 20:20:00	3.46	122	5 Aug 2008 18:00:00	0.91
58	25 Jul 2008 21:00:00	3.89	123	6 Aug 2008 06:00:00	0.91
59	25 Jul 2008 21:30:00	4.14	124	6 Aug 2008 18:00:00	0.90
60	25 Jul 2008 22:00:00	4.34	125	7 Aug 2008 06:00:00	0.90
61	25 Jul 2008 22:10:00	4.55	126	7 Aug 2008 18:00:00	0.90
62	25 Jul 2008 22:25:00	4.70	127	8 Aug 2008 06:00:00	0.90
63	25 Jul 2008 22:35:00	4.75	128	8 Aug 2008 09:30:00	0.89
64	25 Jul 2008 23:00:00	4.78	129	8 Aug 2008 10:00:00	0.89
65	25 Jul 2008 23:20:00	5.05	130	8 Aug 2008 18:00:00	0.89

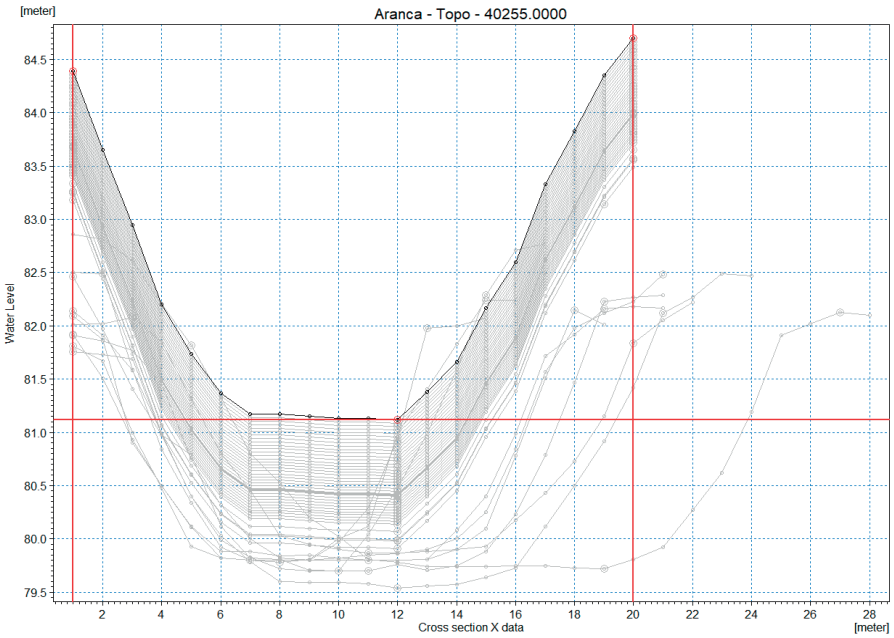


Figure 6. Cross-section for the Aranca Canal

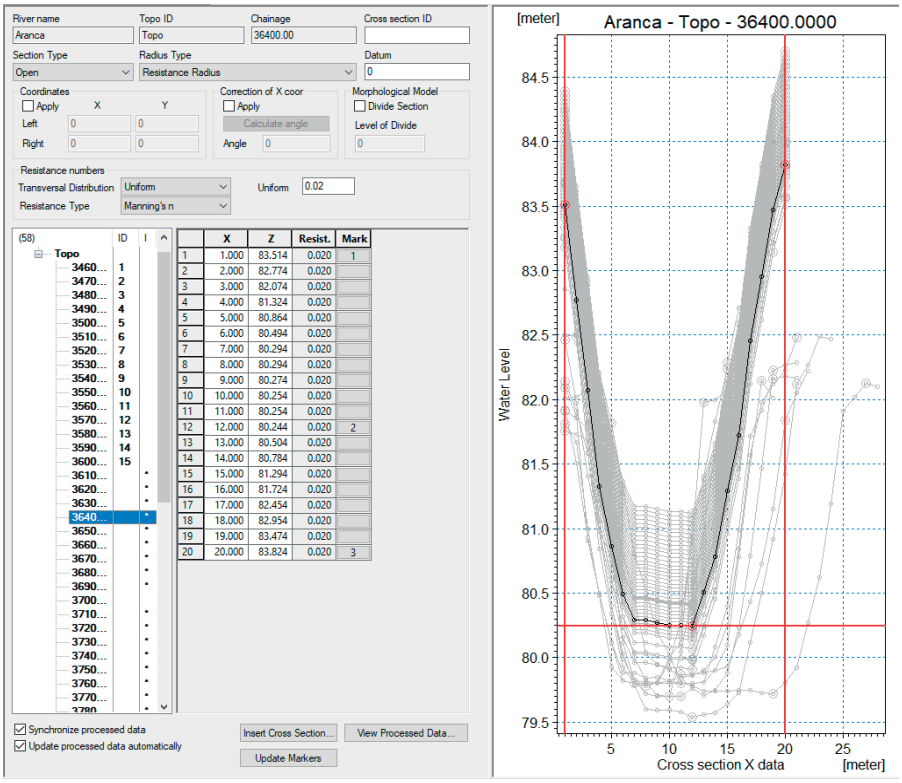


Figure 7. Raw data in Cross-sections

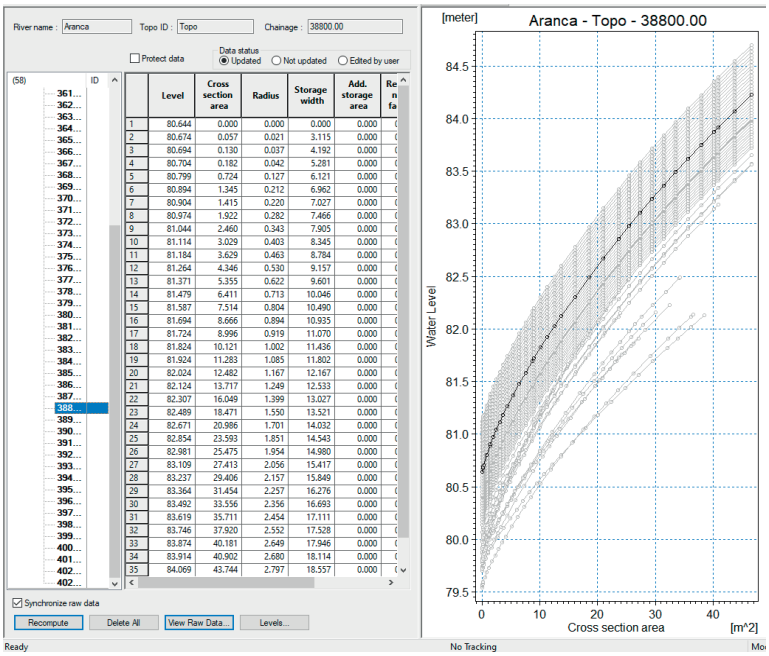


Figure 8. Processed data in Cross-sections

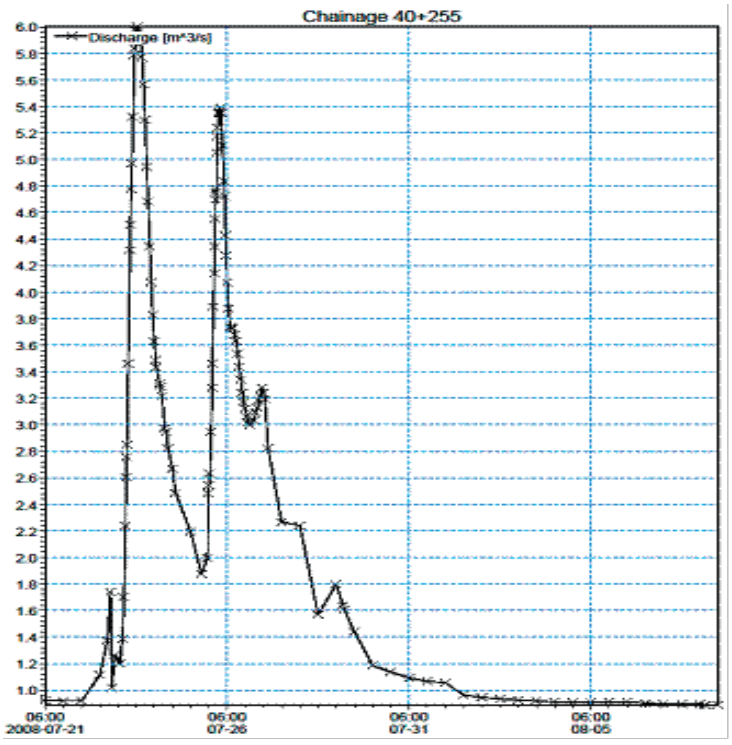


Figure 9. Flood evacuation hydrograph

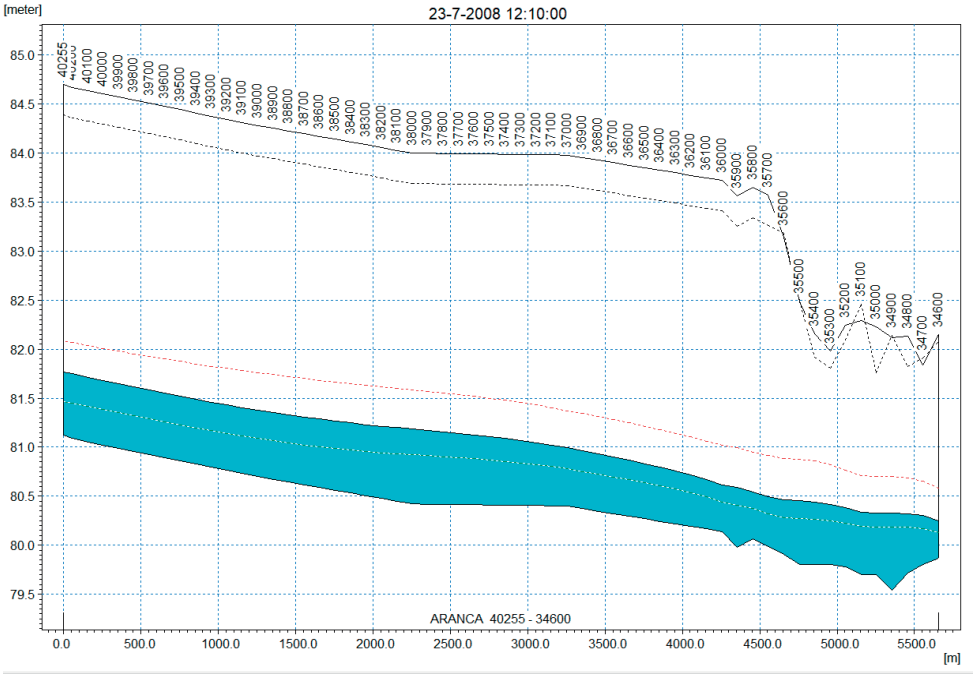


Figure 10. Longitudinal profile whit water level

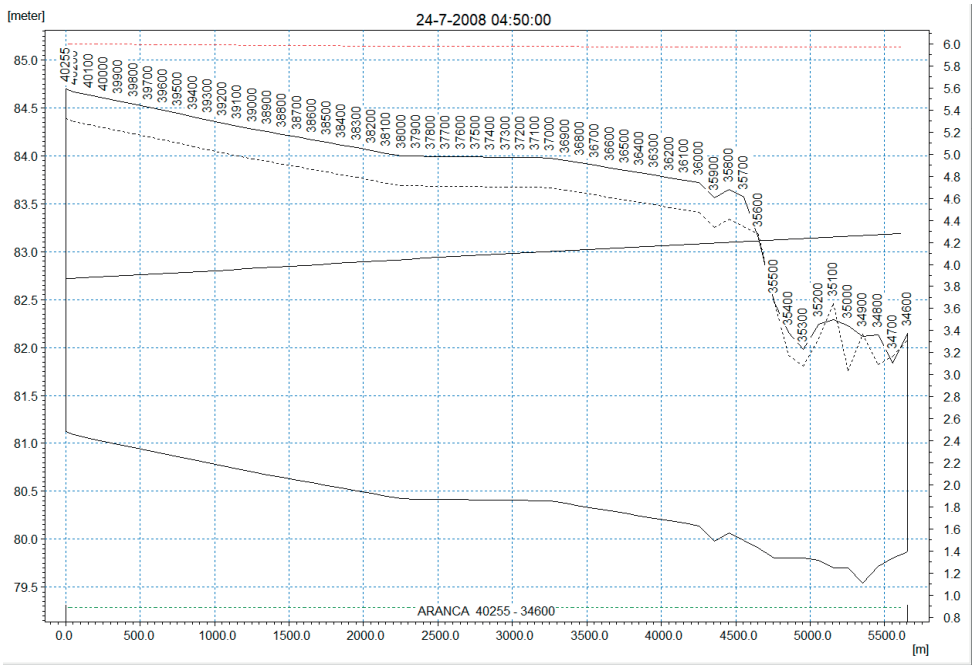


Figure 11. Longitudinal profile with discharge

By carrying out the MIKE11 program, a longitudinal profile of the canal was obtained with the water level for the entire period. (Figure 10) respectively with the discharge for the entire period (Figure 11). From Figures 10 and 11, it follows that for the hydrograph of the inflows introduced in 2008 on the Aranca Canal, the maximum water transport capacity of the canal was not exceeded, with the flood risk occurring for flows greater than those considered.

CONCLUSIONS

The model simulation using the MIKE 11 program showed that the Aranca Canal can manage a maximum flow of 58 m³/s, at which the town of Sânnicolau Mare does not experience flooding. This indicates that under current hydrological conditions, the canal is adequately designed to handle major flood events. However, changes in climate patterns or land use may alter these conditions, requiring periodic reassessment.

The model can provide real-time data or predict water levels and flow rates along the canal for any measured or hypothetical inflows from future flood events. Authorities can manage defense or prediction methods for any high-water events real-time flood forecasting, and optimization of irrigation water distribution. By leveraging MIKE 11's predictive capabilities, stakeholders can enhance proactive flood mitigation strategies and ensure efficient water resource management in the region.There are usually constraints in the modeling process due to the availability of data regarding the roughness of the canal bed along the entire studied section.

Future studies should compare MIKE 11 results with real flood events observed in the past to validate the model's accuracy. The Danish Institute of Hydraulics (DHI) simulates the flow in rivers with the MIKE 11 program and creates models.

ACKNOWLEDGEMENTS

Thanks to the project: Development of knowledge centers for lifelong learning through the involvement of specialists and decision-makers in flood risk management, this activity can be possible using advanced hydroinformatics tools, AGREEMENT NO. LLP-LdV-ToI-2011-RO-002/2011- 1-RO1-LEO05-5329, was funded with the help of the European Commission.

REFERENCES

Biali, G., & Cojocaru, P. (2022). GIS hydrological modeling in an agricultural river basin with high potential for water erosion. *Scientific Papers – Series E: Land Reclamation, Earth Observation & Surveying, Environmental Engineering, 11*, 418–425.

Damian, G., Pricop, C., & Stătescu, F. (2022). The study of hydrological regime modeling using HECRAS model: Case study river basin Bahlueț. *Scientific Papers – Series E: Land Reclamation, Earth Observation & Surveying, Environmental Engineering, 11*, 338–343.

David, I. (1984). *Hidraulics* [In Romanian] (Vol. 2, pp. 42–73). Institutul Politehnic Traian Vuia, Timișoara.

Kumar, PKumar, PrashantDebele, SEDebele, Sisay E.Sahani, JSahani, JeetendraRawat, NRawat, NidhiMarti-Cardona, BMarti-Cardona, BelenAlfieri, SMAlfieri, Silvia MariaBasu, BBasu, BidrohaBasu, ASBasu, Arunima SarkarBowyer, PBowyer, PaulCharizopoulos, NCharizopoulos, NikosGallotti, GGallotti, (2021). Nature-based solutions efficiency evaluation against natural hazards: Modelling methods, advantages and limitations. *Science of the total environment, 784,* DOI10.1016/j.scitotenv.2021.147058.

Lagos, MS; Muñoz, JF; Suárez, FI; Fuenzalida, MJ; Yáñez-Morroni, G; Sanzana, P (2024). Investigating the effects of channelization in the Silala River: A review of the implementation of a coupled MIKE-11 and MIKE-SHE modeling system. *Wiley interdisciplinary reviews-water, 11*(1), Special Issue SI, DOI10.1002/wat2.1673.

Nannawo, ASNannawo, Abera ShiguteLohani, TKLohani, Tarun KumarEshete, AAEshete, Abunu AtlabachewAyana, MTAyana, Melkamu Teshome (2022). Evaluating the dynamics of hydroclimate and streamflow for data-scarce areas using MIKE11-NAM model in Bilate river basin, Ethiopia. *Modeling earth systems and environment, 8*(4), 4563-4578, DOI10.1007/s40808-022-01455-x.

Pareta, KPareta, Kuldeep (2023). Hydrological modelling of largest braided river of India using MIKE Hydro River software with rainfall runoff, hydrodynamic and snowmelt modules. *Journal of water and climate change, 14*(4), Page1314-1338, DOI10.2166/wcc.2023.484.

Paudel, SPaudel, SabinBenjankar, RBenjankar, Rohan (2022). Integrated Hydrological Modeling to Analyze the Effects of Precipitation on Surface Water and Groundwater Hydrologic Processes in a SmallWatershed. *Hydrology, 9(*2), DOI10.3390/hydrology9020037.

Scientific Papers. Series E. Land Reclamation, Earth Observation & Surveying, Environmental Engineering. Vol. XIV, 2025
Print ISSN 2285-6064, CD-ROM ISSN 2285-6072, Online ISSN 2393-5138, ISSN-L 2285-6064

WATER USE EFFICIENCY IN IRRIGATED AGRICULTURE IN ROMANIA: OPTIMIZATION STRATEGIES IN THE CONTEXT OF CLIMATE CHANGE

Oana Alina NIȚU[1], Ionuț Ovidiu JERCA[1], Mihaela BĂLAN[2], Elena Ştefania IVAN[1]

[1]University of Agronomic Sciences and Veterinary Medicine of Bucharest,
59 Mărăști Blvd, District 1, 011464, Bucharest, Romania
[2]University of Craiova, Faculty of Agronomy, 19 Libertății Street, 200583, Craiova, Romania

Corresponding author email: mihaela_balan_if@yahoo.com

Abstract

Climate change significantly impacts agriculture, especially in Romania's semi-arid and sub-humid regions, such as Dobrogea, Southern Moldova, and Muntenia. This study analyzes water use efficiency in irrigated agriculture, considering the increase in average annual temperatures and its effect on water consumption. The three irrigation methods – drip, sprinkler, and furrow irrigation – were compared to identify the most efficient strategies. The results indicate that drip irrigation is the most efficient, with minimal water losses and optimized consumption, although high initial costs may pose a disadvantage. Sprinkler irrigation demonstrates moderate efficiency but is influenced by weather conditions, while furrow irrigation has high water losses and low efficiency. In scenarios where temperatures increase by 2°C and 5°C, water consumption for major crops – maize, sunflower, soybean, and sugar beet – increases by up to 25%. The study emphasizes the need to modernize irrigation infrastructure and adopt sustainable technologies to address climate challenges. Financial support for implementing drip irrigation and educational programs for farmers is strongly recommended.

Key words*: adaptation, climate change, evapotranspiration modeling, irrigation efficiency.*

INTRODUCTION

This study aims to test the hypothesis that climate-induced evapotranspiration changes significantly affect irrigation efficiency in southeastern Romania, and that drip irrigation provides superior water use efficiency under these conditions.

Globally, drought and desertification affect approximately 47% of arid lands, manifesting in varying degrees of aridity. In recent years, drought-affected areas have progressively expanded across most regions of Romania, accompanied by a decline in water resources available for irrigation (Humă, 2004). Climate variability impacts all sectors of the economy, but agriculture remains the most vulnerable, with its effects becoming increasingly severe as climate change intensifies (Chitu et al., 2015). In Romania, the effects of climate change are already evident and are expected to manifest through rising temperatures, altered rainfall patterns, melting ice and snow, and rising sea levels. The impact on ecosystems, economic sectors, public health, and regional vulnerability varies across the country (Daniel et al., 2019).

Without appropriate mitigation and adaptation measures, climate change is projected to significantly reduce agricultural productivity. Plant breeders play a crucial role in developing varieties and hybrids with low evapotranspiration requirements, thereby supporting agricultural adaptation to changing climatic conditions (IPCC Press Release, 2018). Increasing temperatures and intensifying aridification are expected to lead to higher evapotranspiration rates and greater water deficits, severely impacting crop yields. Adapting to these conditions requires the development of efficient water management strategies and the implementation of optimized irrigation systems. Adapting to these climatic conditions requires the development of efficient water management strategies and the use of optimized irrigation systems. A crucial role belongs to breeders, who must create drought-resistant genotypes capable of maintaining productivity under water stress conditions (Nițu

et al., 2023). Choosing an appropriate irrigation scheduling strategy is essential to optimize plant physiological processes, thus enhancing crop yields (Kumar Jha et al., 2018). Moreover, a well-designed irrigation plan significantly reduces water and energy use. Conversely, improper irrigation practices-such as excessive or insufficient water application-generally result in lower grain yields, reduced irrigation water productivity, and environmental problems including land flooding, soil salinization, and rising groundwater levels (Yohannes et al., 2019; Almeida et al., 2022; Quiloango-Chimarro et al., 2022). The impact of climate change on the yields of major agricultural crops worldwide is expected to be negative (Roudier et al., 2011), while the exact effect remains highly uncertain when high temperatures, increased atmospheric CO2 concentrations, and changes in precipitation patterns occur simultaneously (Roudier et al., 2011). In Romania, the effects of climate change are being felt through rising temperatures, altered precipitation patterns, melting glaciers and snow, and rising sea levels. Extreme weather events, which cause negative environmental impacts (floods and droughts), are expected to become more frequent and intense in many regions (Rummukainen, 2012).The effects of water stress resulting from various sowing dates and irrigation rates is not yet fully understood. In the absence of weeds, diseases, nutritional deficiencies, or other limiting factors, the reduction in yield caused by water shortage depends on the phenological stage of the plant. Research has shown that soybeans exhibit varying sensitivity to water stress at different developmental stages, such as the vegetative phase, flowering, pod formation, and seed filling (Brevedan & Egli, 2003). Studies suggest that supplementary or deficit irrigation applied during specific periods of the growing season can significantly improve water use efficiency and positively influence soybean yield (Giménez et al., 2017; Jha et al., 2018). Drip irrigation, an advanced and water-efficient method, ensures the maintenance of plant roots in optimal moisture conditions for extended periods, thus promoting both physiological activity and crop development (Yan et al., 2022).

MATERIALS AND METHODS

The study was conducted using climatic data from five meteorological stations located in southeastern Romania: Constanța, Tulcea, Galați, Brăila, and Călărași. These regions are representative for irrigated agriculture and are frequently exposed to water stress caused by increased temperatures and rainfall variability.

The selected crops - corn, soybean, and wheat - are among the most important in Romanian agriculture, each with specific sensitivities to water deficits. The decision to evaluate these crops was based on their widespread cultivation and different growing periods and evapotranspiration demands.

Climatic data, including, the annual average temperature and precipitation data used in the study were obtained from the Romanian National Meteorological Administration (ANM), corresponding to the year 2024. To calculate the reference evapotranspiration (ET_0), the Penman-Monteith FAO-56 equation was used, which incorporates air temperature, solar radiation, wind speed (3.2 m/s), and relative humidity (65%). A constant average net radiation of 15.5 MJ/m²/day was used for the southeastern region.

The specific crop evapotranspiration (ETc) was calculated by applying crop coefficients (Kc) for each growth stage-initial, development, and maturity-following FAO guidelines. The crop growth stages were defined as follows:

- Corn: 30–50–40 days
- Soybean: 25–55–35 days
- Wheat: 30–60–45 days

The calculations were carried out using Microsoft Excel and Python to ensure accuracy in the estimation of evapotranspiration and for the structured presentation of results.

Soil conditions were considered in three standard texture scenarios-sandy, loamy, and clayey-because soil water retention capacity significantly affects irrigation efficiency.

In 2024, southeastern Romania was severely affected by extreme climate events, with high temperatures and heavy rainfall during certain periods. The summer was dominated by an exceptionally intense and prolonged heatwave, considered the most severe in the country's recent history. Between May 31 and July 31, heatwave conditions persisted for 46 out of 62

days, accounting for 75% of this period. The average summer temperature was 0.69°C higher than the 1991-2020 reference period, surpassing the previous record set in 2023. At the end of summer, on august 30 and 31, a quasi-stationary extratropical cyclone over the Black Sea brought heavy rainfall, causing floods in several coastal towns. In just 24 hours, precipitation exceeded 100 mm in numerous areas, with maximum recorded values of 225.9 mm in Mangalia, 145 mm in Agigea, and 118 mm in Tuzla (Tabel 1).

Table 1. Climatic data for Southeastern Romania - 2024

Weather station	Annual average temperature (°C)	Annual precipitation (mm)
Constanța	14.8	450
Tulcea	14.5	420
Galați	14.2	480
Brăila	14.3	460
Călărași	14.6	440

To calculate the total evapotranspiration (ETc) for corn, soybean, and wheat at each weather station in southeastern Romania, the Penman-Monteith FAO 56 equation was used to determine the reference evapotranspiration (ET_0), and then the values were adjusted for each crop using crop coefficients (Kc).

$$ETo = \frac{0{,}408\ x\ \Delta\ x(Rn-G)+\gamma\ x\frac{900}{T+273}\ x\ u\ 2(es-ea)}{\Delta+J\ x(\ 1+0{,}34\ x\ u\ 2)} \quad (1)$$

where:

- ET_0 - reference evapotranspiration (mm/day);
- R_n - net radiation at the crop surface (MJ/m²/day) - the average value used for southeastern Romania: 15.5 MJ/m²/day;
- G - soil heat flux - considered 0 for long periods;
- T - average air temperature (°C), obtained for each weather station;
- u_2 - wind speed at 2 m (m/s) – the average value used for southeastern Romania: 3.2 m/s;
- e_s - saturation vapor pressure (kPa);
- e_a - actual vapor pressure (kPa);
- Δ - slope of the vapor pressure curve (kPa/°C);
- γ - psychrometric coefficient (kPa/°C).

These values were calculated for each weather station (Constanța, Tulcea, Galați, Brăila, Călărași) using the annual average temperature specific to each location.

After calculating ET_0 for each weather station, crop coefficients (Kc) were applied to obtain the specific evapotranspiration for each crop.

$$ETe = ETo \times Kc \quad (2)$$

where:

- ETe - specific evapotranspiration for each crop;
- ETo - reference evapotranspiration (mm/day);
- Kc - crop coefficients.

For each crop, the Kc coefficients vary depending on the growth stage (Tabel 2).

Table 2. Coefficients vary depending on the growth stage (Kc)

Crop	Initial stage	Development stage	Maturity stage
Corn	0.3	1.2	0.6
Soybean	0.4	1.15	0.5
Wheat	0.4	1.1	0.5

The duration of each phase (in days) is presented in Table 3.

Table 3. The duration of each phase, in days

Crop	Initial stage (days)	Development stage (days)	Maturity stage (days)
Corn	30	50	40
Soybean	25	55	35
Wheat	30	60	45

For each crop and weather station, the total evapotranspiration was calculated as follows:

$$ETc\ total = (ET_0 \times Kc_0 \times number\ of\ days) + (ET_0 \times Kc_1 \times number\ of\ days) + (ET_0 \times Kc_2 \times number\ of\ days) \quad (3)$$

The formula (3) was applied for corn, soybean, and wheat at each of the five weather stations.

RESULTS AND DISCUSSIONS

The total evapotranspiration for each crop was calculated for each station, with the highest values observed in Constanța and Călărași. For example, wheat reached a seasonal ETc of 437.03 mm in Constanța and 434.09 mm in Călărași, followed by corn and soybean.

In Galați and Brăila, where temperatures were slightly lower and precipitation somewhat higher, ETc values were reduced by up to 10%, suggesting a lower irrigation requirement. This confirms that regional climatic differences significantly affect irrigation planning.

Among irrigation methods, drip irrigation - due to its localized application and minimal evaporative losses - proved to be the most efficient system for meeting crop water demands. Sprinkler irrigation performed well in loamy soils, while furrow (surface) irrigation showed the lowest efficiency, particularly in sandy soils.

Figure 1 illustrates the variation in total crop evapotranspiration (ETc) across the five weather stations for corn, soybean, and wheat.

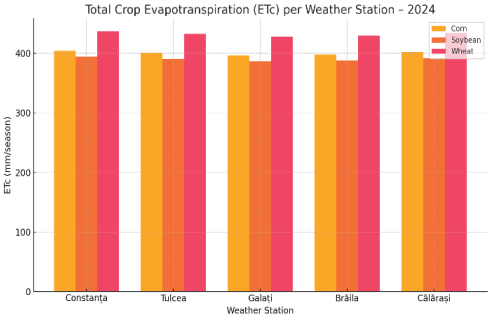


Figure 1. Seasonal crop evapotranspiration (ETc) by weather station - 2024

The graphical comparison highlights the higher ETc values observed for wheat across all stations, especially in Constanța and Călărași, and confirms the lower water requirements of soybean. This visual representation supports the numerical findings and emphasizes the impact of regional climatic differences on crop water needs.

Climate projections indicate that an increase of 2°C in average temperature could lead to a 6-10% increase in evapotranspiration, while a 5°C rise may result in a 15-20% increase, especially in already water-stressed regions such as Dobrogea. These estimations highlight the urgency of adapting irrigation strategies to cope with climate variability.

The results are consistent with previous studies (Chitu et al., 2015), confirming that crop water requirements in southern and southeastern Romania are increasing in response to climate trends. This underscores the need for investment in modern irrigation systems and support programs for farmers.

After performing all calculations, the total seasonal evapotranspiration was obtained for each crop and each weather station. These values represent the total amount of water required to ensure optimal plant growth under irrigation conditions (Tabel 4).

Tabel 4. Total seasonal evapotranspiration for each crop and each weather station

Weather station	Crop	Total Evapotranspiration (mm/season)
Constanța	Corn	404.41
Constanța	Soybean	394.63
Constanța	Wheat	437.03
Tulcea	Corn	400.34
Tulcea	Soybean	390.66
Tulcea	Wheat	432.63
Galați	Corn	396.28
Galați	Soybean	386.69
Galați	Wheat	428.24
Brăila	Corn	397.63
Brăila	Soybean	388.01
Brăila	Wheat	429.7
Călărași	Corn	401.7
Călărași	Soybean	391.98
Călărași	Wheat	434.09

The total evapotranspiration varies slightly between weather stations, being influenced by the annual average temperature and the specific precipitation levels of each area.

Călărași and Constanța record higher evapotranspiration values for all crops, indicating a greater need for irrigation, probably due to higher temperatures and lower precipitation compared to other stations. Galați and Brăila show lower total evapotranspiration values, suggesting a reduced water demand for crops, possibly due to higher precipitation levels or slightly lower temperatures.

Wheat requires the highest amount of water for the growing season across all weather stations (values ranging from 428.24 mm in Galați to 437.03 mm in Constanța). This is explained by its longer vegetative cycle and constant moisture requirements, especially during the stem elongation and grain filling stages.

Corn has a moderate water requirement, ranging from 396.28 mm in Galați to 404.41 mm in Constanța, which confirms the high water demands of this crop during the vegetative growth and flowering stages.

Soybean requires the least amount of water, with values ranging from 386.69 mm in Galați to 394.63 mm in Constanța, as it is a drought-adapted crop with a root system that efficiently absorbs water from the soil.

Constanța and Călărași counties have the highest total evapotranspiration values for all analyzed crops. This is due to higher temperatures and lower precipitation levels, which increase the risk of water stress. Under these conditions, implementing efficient irrigation systems is essential to maintain high agricultural yields.

Solutions for optimizing irrigation in Constanța and Călărași:

- Drip irrigation - ensures efficient water use by applying precise amounts directly to the plant roots, reducing evaporation losses.
- Sprinkler irrigation - an effective method for uniform water distribution, especially in areas with well-drained soils.
- Controlled deficit irrigation - adjusting the volume and frequency of irrigation according to the crop development stage and water availability.

In these regions, it is also essential to apply soil water conservation techniques, such as mulching, minimum tillage, and crop rotation, to reduce evapotranspiration and optimize water use.

Galați and Brăila counties have lower total evapotranspiration values, indicating a reduced need for irrigation compared to Constanța and Călărași. This may be due to more frequent precipitation or slightly lower average temperatures.

Optimizing water use in Galați and Brăila:

- Supplemental irrigation - can be applied only during critical periods, such as flowering and grain formation in wheat, soybean, or corn.
- Soil moisture monitoring - using moisture sensors to adjust irrigation frequency and volume based on the actual water needs of plants.
- Rainwater harvesting and storage – implementing rainwater collection systems to reduce dependency on irrigation.

These measures can help reduce water consumption and increase the efficiency of available resource utilization.

CONCLUSIONS

Climate change, characterized by rising temperatures and altered precipitation patterns, directly affects water use efficiency in agriculture, especially in the southeastern regions of Romania. The results obtained show that total evapotranspiration varies depending on geographic location, crop type, and local climatic conditions, with the highest values recorded in Constanța and Călărași counties.

Among the analyzed irrigation methods, drip irrigation proved to be the most efficient in terms of water consumption, offering minimal losses and precise control over applied volumes. Sprinkler irrigation is a viable alternative in areas with well-drained soils, while furrow irrigation is less efficient due to significant water losses.

To address current and future climate challenges, it is essential to modernize irrigation infrastructure, implement soil water conservation practices, and adapt irrigation strategies to the specific conditions of each region.

Financial support for the implementation of modern technologies, along with training programs for farmers, is recommended to improve water use efficiency and ensure the sustainability of agricultural production.

Promoting drip irrigation in regions affected by water scarcity or high temperatures is essential for efficient resource management. It is necessary to subsidize efficient irrigation systems to support farmers in transitioning to modern methods. Irrigation technologies must be adapted according to soil type, with particular attention to avoiding furrow irrigation in sandy soils. Additionally, investments in agricultural research are needed to evaluate the performance of different irrigation methods under various

climatic conditions. Last but not least, farmer education and training on best water management practices represent a key pillar for the success of these measures.

REFERENCES

Brevedan, R. E., & Egli, D. B. (2003). Short periods of water stress during seed filling, leaf senescence, and yield of soybean. *Crop Science*, *43*(6), 2083–2088. https://doi.org/10.2135/cropsci2003.2083

Chitu, E., Giosanu, D., & Mateescu, E. (2015). The variability of seasonal and annual extreme temperature trends of the latest three decades in Romania. *Agriculture and Agricultural Science Procedia*, *6*, 429–437. https://doi.org/10.1016/j.aaspro.2015.08.082

Daniel, A., Mateescu, E., Tudor, R., & Leonard, I. (2019). Analysis of agroclimatic resources in Romania in the current and foreseeable climate change – Concept and methodology of approaching. *Agronomy Series of Scientific Research*, *61*, 221–229.

de Almeida, A. M., Coelho, R. D., da Silva Barros, T. H., de Oliveira Costa, J., Quiloango-Chimarro, C. A., Moreno-Pizani, M. A., & Farias-Ramírez, A. J. (2022). Water productivity and canopy thermal response of pearl millet subjected to different irrigation levels. *Agricultural Water Management*, *272*, 107829. https://doi.org/10.1016/j.agwat.2022.107829

Giménez, L., Paredes, P., & Pereira, L. S. (2017). Water use and yield of soybean under various irrigation regimes and severe water stress: Application of AquaCrop and SIMDualKc models. *Water*, *9*(6), 393. https://doi.org/10.3390/w9060393

Humă, C. (2004). Aspecte globale privind fenomenele de secetă, aridizare și deșertificare. *Calitatea Vieții*, *15*(1–2), 113–121.

IPCC. (2018). *Summary for policymakers of IPCC special report on global warming of 1.5ºC approved by governments* [Press release]. Intergovernmental Panel on Climate Change. https://www.ipcc.ch/sr15/

Jha, P. K., Kumar, S. N., & Ines, A. V. (2018). Responses of soybean to water stress and supplemental irrigation in upper Indo-Gangetic plain: Field experiment and modeling approach. *Field Crops Research*, *219*, 76–86. https://doi.org/10.1016/j.fcr.2018.01.028

Niţu, O. A., Ivan, E. S., & Niţu, D. S. (2023). Climate change and its impact on water consumption in the main agricultural crops of the Romanian plain and Dobrogea. *Scientific Papers. Series A. Agronomy*, *66*(1).

Quiloango-Chimarro, C. A., Coelho, R. D., Heinemann, A. B., Arrieta, R. G., da Silva Gundim, A., & França, A. C. F. (2022). Physiology, yield, and water use efficiency of drip-irrigated upland rice cultivars subjected to water stress at and after flowering. *Experimental Agriculture*, *58*, e15. https://doi.org/10.1017/S0014479721000242

Roudier, F., Ahmed, I., Bérard, C., Sarazin, A., Mary-Huard, T., Cortijo, S., ... & Colot, V. (2011). Integrative epigenomic mapping defines four main chromatin states in Arabidopsis. *The EMBO journal*, *30*(10), 1928-1938.

Rummukainen, M. (2012). Changes in climate and weather extremes in the 21st century. Wiley Interdisciplinary Reviews: Climate Change, 3(2), 115– 129

Yan, S., Wu, Y., Fan, J., Zhang, F., Guo, J., Zheng, J., & Wu, L. (2022). Quantifying grain yield, protein, nutrient uptake and utilization of winter wheat under various drip fertigation regimes. Agricultural Water Management, 261, 107380

Yohannes, D. F., Ritsema, C. J., Eyasu, Y., Solomon, H., Van Dam, J. C., Froebrich, J., & Meressa, A. (2019). A participatory and practical irrigation scheduling in semiarid areas: The case of Gumselassa irrigation scheme in Northern Ethiopia. *Agricultural Water Management*, *218*, 102–114. https://doi.org/10.1016/j.agwat.2019.03.014

Scientific Papers. Series E. Land Reclamation, Earth Observation & Surveying, Environmental Engineering. Vol. XIV, 2025
Print ISSN 2285-6064, CD-ROM ISSN 2285-6072, Online ISSN 2393-5138, ISSN-L 2285-6064

ASSESSMENT OF SURFACE WATER QUALITY IN THE SFÂNTU GHEORGHE BRANCH OF THE DANUBE DELTA

Ana Bianca PAVEL, Laura DUTU, Florin DUTU, Irina CATIANIS, Gabriel IORDACHE, Catalina GAVRILA

National Institute for Research and Development on Marine Geology and Geoecology – GeoEcoMar, 23-25 Dimitrie Onciul Street, 024053, District 2, Bucharest, Romania

Corresponding author email: biancapavel@geoecomar.ro

Abstract

The aquatic ecosystems of the Danube Delta are highly vulnerable to ecological pressures caused by natural and anthropogenic factors. This study investigates the surface water quality along the Sfântu Gheorghe Branch, (km 85-km 15), including control sections such as Mahmudia Meander, Uzlina Lake, Isac Lake, Dunavăț Meander, Dranov Meander, and Ivancea Meander. Surface water samples were collected from 58 locations during spring and autumn (May and September 2024). Physico-chemical parameters were measured in situ using the multiparameter EXO2 probe. Key indicators assessed included water temperature, pH, dissolved oxygen, chlorophyll "a", conductivity, total dissolved solids, salinity, turbidity, and redox potential (ORP). The results revealed generally stable seasonal and spatial trends, with most parameters falling within Class I and II water quality categories, as defined by Romanian Order 161/2006. Noteworthy findings include well-oxygenated waters (>5 mg/L DO), low chlorophyll "a", concentrations (<25 µg/L), and stable pH values, all indicative of good to very good ecological status. Variations in turbidity and ORP were primarily localized and attributed to sediment resuspension or flow dynamics. Overall, the findings suggest that the monitored sections of the Sfântu Gheorghe Branch maintain resilient freshwater conditions, with limited signs of ecological degradation.

Key words*: chlorophyll a, Danube Delta, ecological status, nutrient input, physico-chemical indicators, seasonal variation, Sfântu Gheorghe Branch, surface water quality.*

INTRODUCTION

Aquatic ecosystems are characterized by remarkable diversity, shaped by both the concentration of dissolved salts (freshwater vs. brackish water) and the dynamic movement of water masses (Chapman, 1996). In the predeltaic region of the Black Sea, brackish waters cover approximately 100,000 hectares, supplemented by the expansive Razelm-Sinoe lagoon complex, which spans 1,015 km². This system falls into the oligo-mixohaline category, with salinity levels ranging between 0.50 and 6.00 g/L (Coteț, 1960; Almazov et al., 1963; Bondar & Panin, 2000; Cazacu & Adamescu, 2017). Despite this, freshwater ecosystems are predominant within the Danube Delta's aquatic environment (Chiriac & Udrescu, 1965; Kirschner et al., 2009).

The rheophilic ecosystems of the Danube Delta encompass the river's main branches and a secondary network of channels. These watercourses vary in flow permanence and intensity - from channels with a continuous, column-wide current to shallow gullies where flow is weak and generally restricted to near-bottom layers, becoming more pronounced during floods (Driga, 2004; Gâștescu & Știucă, 2008). Compared to the main river channel, the Danube branches exhibit distinct ecological characteristics due to biotopic variations such as reduced depth and current velocity, greater isolation from adjacent land, consolidated alluvial banks, and differences in nutrient concentrations and turbidity levels (Gâștescu, 2009).

At the apex of the deltaic triangle, the Danube splits into two main branches: the Chilia to the north and the Tulcea to the east. Seventeen kilometers downstream from Izmail Ceatal, the Tulcea Branch divides again at Sfântu Gheorghe Ceatal into the Sulina Branch (continuing eastward) and the Sfântu Gheorghe Branch (turning southward) (Panin & Jipa, 2002; Romanescu, 2013). Each branch has unique morphological and hydrological features. Water discharge is unevenly distributed: 58% flows through the Chilia

Branch, 22% through the Sulina, and 20% through the Sf. Gheorghe (Panin, 2003; Driga, 2004; Sommerwerk et al., 2022). Sediment transport also varies significantly, with the Chilia Arm carrying about 66% of the annual alluvium load (80,000-300,000 tons), followed by the Sulina (14%) and Sfântu Gheorghe (20%) Arms, with considerable interannual variability (Tiron Duțu, 2014; Syeed et al., 2023).

The Sfântu Gheorghe Arm, due to its substantial solid discharge, experiences significant sediment accumulation, resulting in higher banks compared to the other branches. Unlike the Chilia Arm, neither the Sulina nor the Sf. Gheorghe Arms form internal deltas, though they feature sinuous courses with multiple meanders. This is particularly true for the Sf. Gheorghe Arm, which originally extended 109 km with a high meandering coefficient (2.35). Before discharging into the Black Sea, it forms a secondary delta (Sfântu Gheorghe Secondary Delta II). Rectification efforts carried out between 1985 and 1990 eliminated six meanders, reducing the arm's length to approximately 70 km. While these modifications improved navigability, they significantly impacted flow distribution among the Danube's branches (Habersack, 2016; Oaie, 2015; Madhav et al., 2020; Duțu, 2023).

This study aims to evaluate the overall surface water quality along the Sf. Gheorghe Arm by analysing the spatial distribution and variability of key environmental indicators across several control sections. Specifically, the research investigates water quality along a longitudinal gradient from upstream (km 85) to downstream (km 15) on the Sf. Gheorghe Arm.

Relevance and impact of the study

This research provides a comprehensive assessment of water quality using advanced analytical techniques, enabling immediate and accurate measurement of multiple physicochemical parameters. Such an approach offers valuable insights into the spatial variability of essential water quality indicators.

The findings significantly enhance our understanding of both anthropogenic influences and natural dynamics affecting aquatic ecosystems within the Danube Delta. The study holds substantial environmental relevance by supplying critical data for ecosystem monitoring, resource management, and policy decision-making. Ultimately, it not only advances scientific knowledge but also supports practical, sustainable strategies for the conservation and management of one of Europe's most important wetland ecosystems.

MATERIALS AND METHODS

Study area

The study was conducted in the Danube Delta, a vast wetland system covering approximately 5,600 km², which serves as the primary source of freshwater and sediment input to the Black Sea via its three main distributary branches: Chilia, Sulina, and Sfântu Gheorghe (Botnariuc, 1985). The Sfântu Gheorghe Branch, the southernmost of these, originates at the Ceatal Sfântu Gheorghe bifurcation and flows approximately 108 km before discharging into the Black Sea. This branch conveys about 23-24% of the Danube's total water discharge and approximately 21% of the suspended sediment load (Bondar & Panin, 2000; 2001). It is characterized by a pronounced morphological dynamic, having a sinuous course with active, migratory meanders (Popa, 1997; Jugaru et al., 2006; Tiron, 2010; Tiron Duțu et al., 2014), as well as a rapid evolution of the mouth, manifested by the progradation of the deltaic lobe and significant displacements of the Sakhalin barrier island throughout the 20th century (Panin, 2003). The width of the Sf. Gheorghe arm varies between 150 and 550 m, and the water depth is between 3 and 27 m compared to the local low water level (Bondar & Panin, 2000). The banks of this arm are covered by dense and continuous vegetation, consisting of poplars, trees and reed communities. During the period 1984-1988, significant anthropogenic interventions were carried out to facilitate navigation. Six natural meanders were artificially cut, reducing the total length of the arm from 108 km to approximately 70 km. The newly created navigable channels were initially 7-8 m deep and 75-100 m wide (Popa, 1997). These hydrotechnical works caused substantial changes in the local dynamics of water and sediments, increasing water flows and sediment flux through the Sf. Gheorghe arm and

influencing sedimentary processes at the level of the entire deltaic system (Ichim & Rădoane, 1986; Popa, 1997; Panin & Jipa, 2002; Panin, 2003; Tiron, 2010). During the same period, earthen dams, with heights of approximately 2-3 m, were built along the banks.

Methodology

To evaluate the overall condition of surface water quality, the study investigated the longitudinal distribution of key environmental indicators along a gradient from upstream to downstream. Sampling was conducted at multiple control points located across the Sfântu Gheorghe Branch, including rectified meanders, natural channels, and adjacent lakes, covering the river stretch between kilometer 85 and kilometer 15.

Notable locations included Mahmudia Meander, Uzlina Lake, Isacova Lake, Dunavăț Meander, Dranov Meander, and Ivancea Meander. Surface water samples were collected at 58 sites during two separate field campaigns in May and September 2024, as shown in Figure 1, which maps the spatial distribution of sampling points. Several sampling points were strategically positioned in zones where water and sediment are redistributed from the main branch to the secondary network of channels, smaller distributaries, and adjacent floodplain depressions (such as lakes and temporary shallow ponds).

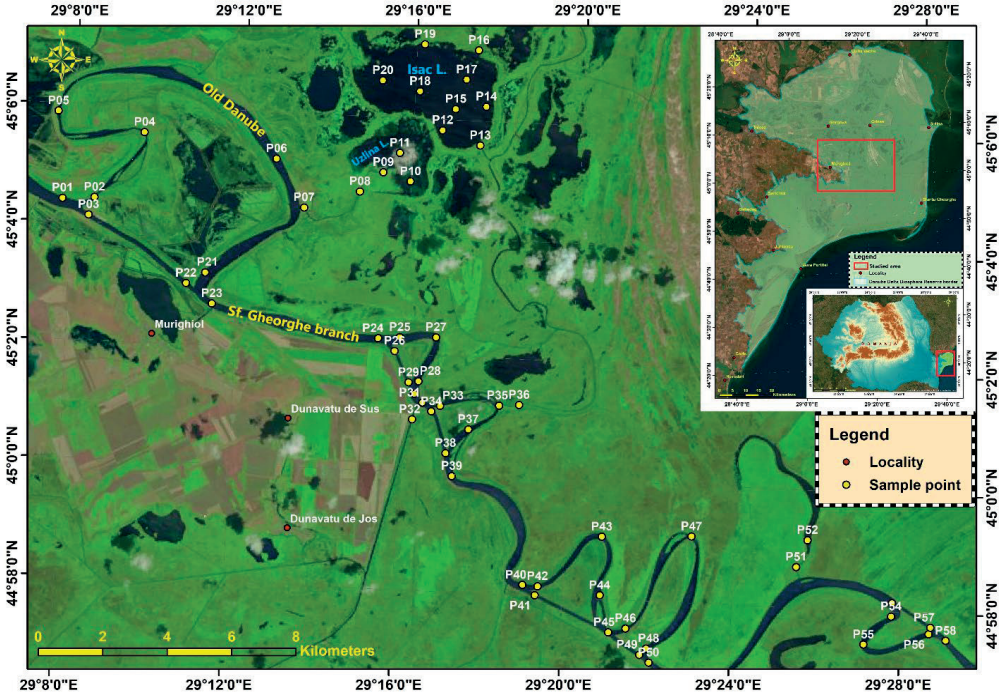


Figure 1. Sampling stations from the Sf. Gheorghe Arm

The general characterization of surface water quality was conducted through *in situ* measurements of various physico-chemical parameters using the EXO2 multiparameter probe (YSI, USA) (Figure 2).

This device is equipped with advanced sensors that utilize physical, optical, and electrochemical detection methods to measure a wide range of water quality indicators (Lipps et al., 2023).



Figure 2. Multiparameter probe, model EX02

The recorded parameters include: temperature (°C), pH (pH units), turbidity (FNU), total dissolved solids (TDS, mg/L), conductivity (µS/cm), dissolved oxygen (ODO, mg/L), oxygen saturation (ODO, %), oxidation-reduction potential (ORP, mV), salinity (PSU), nitrate (NitraLED, mg/L), chlorophyll-a (RFU), and total algal content (TAL–PC, RFU).

Water quality classification was primarily based on the criteria set out in Order No. 161/2006, which defines five quality classes: Class I (very good), Class II (good), Class III (moderate), Class IV (poor), and Class V (bad). For a more comprehensive evaluation, both national standards (Order No. 161/2006 regarding reference objectives for surface water quality classification) and international standards, particularly the European Water Framework Directive (WFD 2000/60/EC), were applied. The WFD provides a unified framework for the qualitative and quantitative management of water resources and the preservation of aquatic ecosystem health across member states.

All physicochemical analyses followed internationally recognized methodologies and standard procedures. These included: SR EN ISO 5667-1:2023 for water sampling; SR EN ISO 10523:2012 for pH determination; and SR EN ISO 5814:2013 for measuring dissolved oxygen concentrations.

Statistical analysis

Statistical analyses were conducted using xlSTAT version 7.5.2 software (Addinsoft, 2020) and PAST version 4 (https://past.en.lo4d.com/download). To examine the relationships between physicochemical parameters, Pearson correlation analysis was applied. This method was chosen to identify the strength and direction of linear associations among the measured variables.

All analyses were performed on data sets obtained from the two sampling campaigns (May and September 2024), with significance levels set at $p < 0.05$ unless otherwise specified.

RESULTS AND DISCUSSIONS

The lotic ecosystems formed by the Danube and its deltaic network fall within the Pontic Ecoregion (Ecoregion 12), as defined in Annex XI of the European Union Water Framework Directive (EU-WFD, 2000).

According to the Synthesis of the Draft Management Plans for River Basin Districts (2022), a total of 19 natural watercourse types has been identified within the Danube and Danube Delta regions. The areas investigated in this study fall within the classification RO15 – Danube River (Isaccea) to Danube Delta.

The results presented in this study provide valuable input for enhancing current water quality databases and contribute to fulfilling the data requirements outlined in the EU-WFD. By integrating multiple data sources and conducting high-resolution, in situ analyses, this study enables a more detailed and spatially explicit assessment of water quality conditions across the Sfântu Gheorghe Branch. In line with the objectives of the EU-WFD, which mandates all member states to ensure that rivers, lakes, groundwater, estuaries, and coastal waters reach at least "good" ecological status by 2027, this research offers insight into the current state of surface water in a critical section of the Danube Delta.

Physico-chemical parameters of surface water

Table 1 summarizes the physicochemical properties of surface water - minimum, maximum, and mean values (± standard deviation) - recorded at control points during the May and September 2024 campaigns. Measurements along the Sfântu Gheorghe Branch (km 85 to km 15) showed typical seasonal and spatial variations, with no major anomalies, though some local deviations were noted.

Water temperature (°C). Water temperature followed seasonal trends and was strongly influenced by air temperature fluctuations typical of the spring and early autumn periods (AccuWeather, 2024). In May, values ranged from 16.31 to 20.30°C with a mean of 18.50 ± 0.70°C, remaining within the expected seasonal variation for the region. The lowest temperature was recorded at station P36 (Gârla Perivolovca), while the highest occurred at station P19 (Isacova Lake). In September, temperatures increased notably, ranging from 23.82 to 29.98°C with an average of 25.90 ± 0.98°C. The coolest site was station P20, while the warmest was station P27 (Figure 3).

Table 1. A synopsis of the physico-chemical parameters of water surface samples from Sf. Gheorghe Arm in May and September 2024

May			
Parameter	**Min.**	**Max.**	**Mean ± SD**
Temperature (°C)	16.31	20.30	18.50±0.70
pH	8.06	9.42	8.58±0.21
Turbidity (FNU)	0.18	57.55	10.91±10.27
Total Dissolved Solids (TDS mg/L)	182.36	290.38	246.02±17.49
Conductivity (µS/cm)	254.11	382.14	331.19±19.75
Dissolved Oxygen (ODO mg/L)	6.82	14.81	10.67±1.20
Oxygen Saturation (ODO % sat)	69.66	163.92	114.09±14.29
Oxidation-Reduction Potential (ORP mV)	1.74	100.96	41.04±20.79
Salinity (PSU)	0.13	0.22	0.18±0.01
Nitrate (NitraLED mg/L)	0.01	16.28	1.49±2.24
Chlorophyll (RFU)	0.26	8.57	3.93±2.06
Total Algal Content (TAL - PC RFU)	0.05	1.83	0.70±0.41

September			
Parameter	**Min.**	**Max.**	**Mean ± SD**
Temperature (°C)	23.82	29.98	25.90±0.98
pH	7.88	8.83	8.19±0.24
Turbidity (FNU)	2.58	53.86	10.17±9.34
Total Dissolved Solids (TDS mg/L)	228.91	277.73	242.13±6.54
Conductivity (µS/cm)	354.47	419.31	378.83±11.97
Dissolved Oxygen (ODO mg/L)	3.44	14.57	7.84±2.05
Oxygen Saturation (ODO % sat)	40.97	178.84	96.55±25.15
Oxidation-Reduction Potential (ORP mV)	14.60	66.09	48.70±12.18
Salinity (PSU)	0.17	0.21	0.18±0.01
Nitrate (NitraLED mg/L)	0.04	9.34	1.70±1.87
Chlorophyll (RFU)	0.27	12.65	2.55±3.78
Total Algal Content (TAL - PC RFU)	0.01	14.62	2.13±3.85

Water pH (pH units). pH levels across the study area generally conformed to acceptable limits for freshwater ecosystems (6.5-8.5 pH units, Order 161/2006), although slight alkalinity was observed at several stations. In May, pH ranged between 8.06 and 9.42 (mean 8.58 ± 0.21), with values exceeding the upper guideline limit at station P16 (Isacova Lake). The lowest value was recorded at P36 (Gârla Perivolovca). In September, pH ranged from 7.88 to 8.83 (mean 8.19 ± 0.24), remaining mostly within the regulatory threshold. Elevated values were observed at P12, while P35 showed the lowest pH (Figure 4).

Turbidity (NTU). The turbidity values measured in the water samples from the control sections showed variations within the normal limits for surface waters (1-1000 NTU) (Chapman, 1996). In May, turbidity values varied widely between 0.18 and 61.61 NTU, with an average of 11.42 NTU. In September, turbidity varied between 2.58 and 53.86 NTU, with an average of 10.17 NTU. The lowest turbidity in May was recorded at station P20 (Isacova Lake), while in September, the lowest was at station P22. The highest turbidity in May occurred at station P42 (M. Dranov – bifurcation – rectified mead), while in September, the highest was measured at station P24. Remarkably, some samples showed higher turbidity levels compared to the values provided by SR ISO 5667-5:2017 (5 NTU – permitted, 10 NTU – exceptionally permitted), indicating a localized deterioration of water quality. In general, increased turbidity is due to Danube River inflows, which carry dissolved and suspended organic and inorganic materials through secondary necks and internal channels (Figure 5).

Total dissolved solids (TDS, mg/L). TDS concentrations, representing the sum of dissolved organic and inorganic substances, were well within freshwater standards (<1000 mg/L) (Lehr, 1980; De Zuane, 1997). In May, values ranged from 182.36 to 290.38 mg/L (mean: 246.02 ± 17.49 mg/L), and in

September from 228.91 to 277.73 mg/L (mean: 242.13 ± 6.54 mg/L). The lowest concentrations were recorded at P16 (May) and P14 (September), while the highest occurred at P52 (Erenciuc Lake) in May and P36 in September (Figure 6).

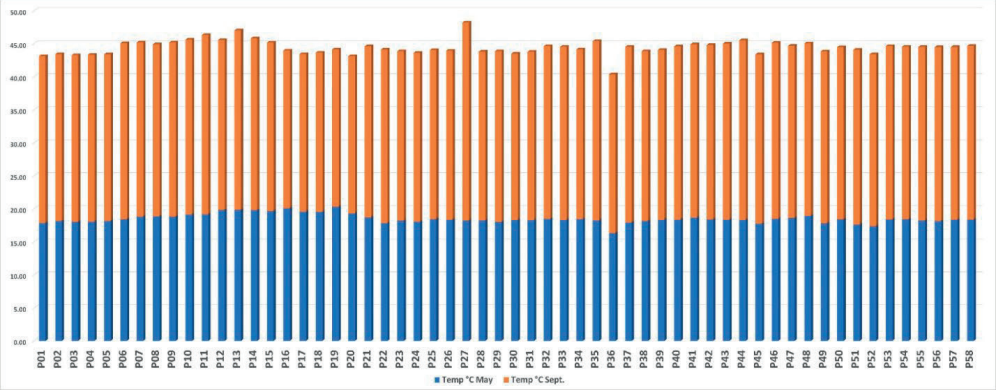


Figure 3. Evolution of the Temperature indicator in the investigated surface water samples

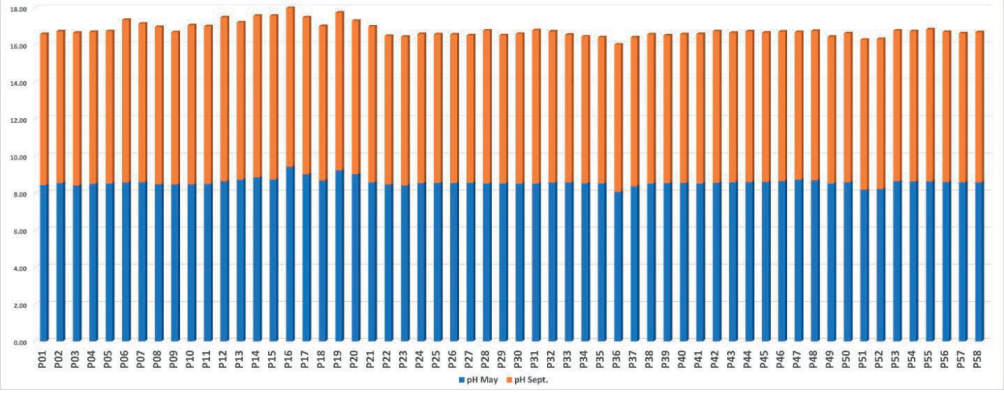


Figure 4. Evolution of the pH indicator in the investigated surface water samples

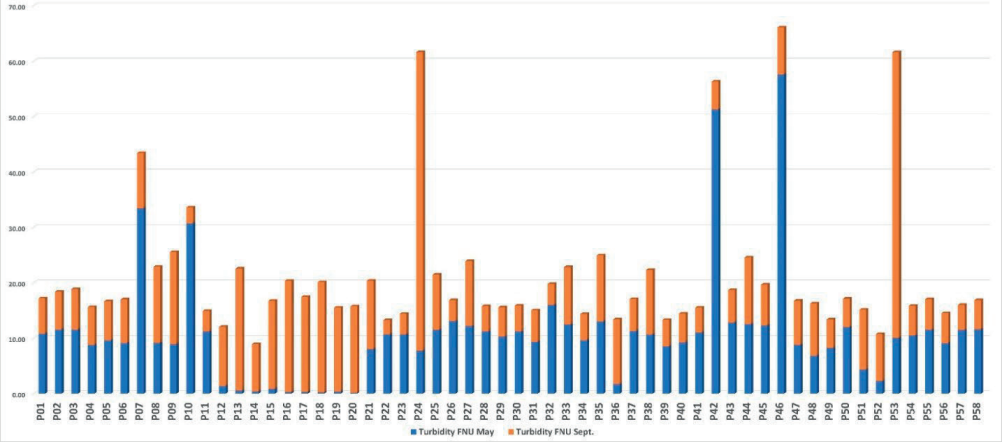


Figure 5. Evolution of the Turbidity FNU indicator in the investigated surface water

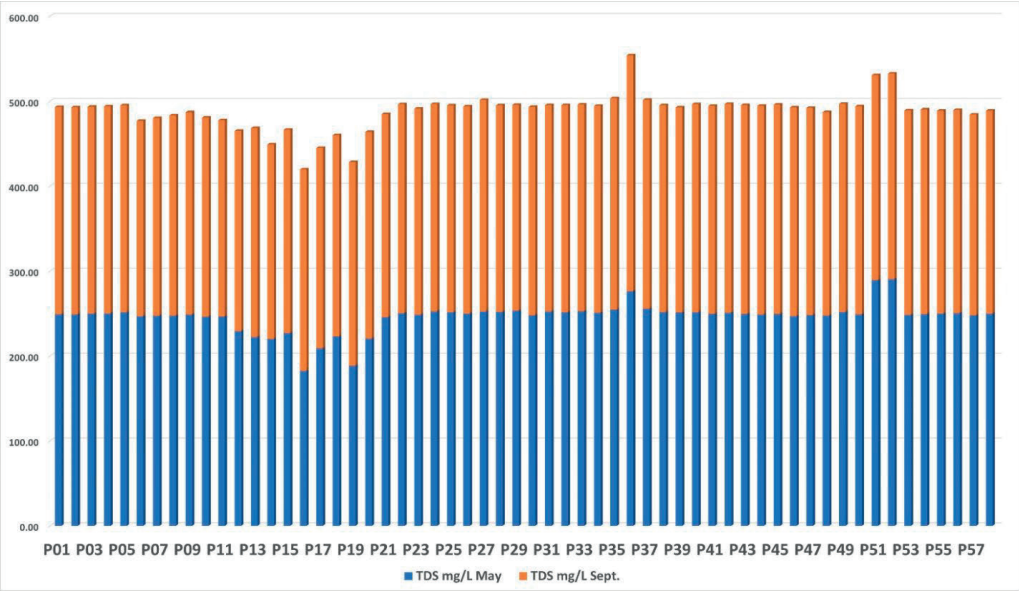


Figure 6. Evolution of the TDS mg/L indicator in the investigated surface water samples

Electrical conductivity (µS/cm). All measured conductivity values classified the water samples in quality class I (≤500 µS/cm, Order 161/2006). In May, conductivity values ranged from 254.11 to 382.14 µS/cm (mean: 331.19 ± 19.75 µS/cm), increasing slightly in September, with values between 354.47 and 419.30 µS/cm (mean: 378.83 ± 11.97 µS/cm). The highest readings were recorded at P51 (May) and P36 (September) (Figure 7).

Dissolved Oxygen (mg/L). Dissolved oxygen concentrations indicate that all water samples tested fall into the well-oxygenated surface water category (quality class I, ≥9 mg/L, Order 161/2006), with all values exceeding the recommended minimum level of 5 mg/L required to support aquatic life (www.niwa.co.nz). Dissolved oxygen varied significantly in May, from 6.82 to 14.81 mg/L, with an average of 10.67 mg/L. In September, values ranged from 3.44 to 14.57 mg/L, with an average of 7.84 mg/L. The lowest values in both May and September were recorded at station P36 (Gârla Perivolovca), while the highest concentrations were observed at station P19 (Isacova Lake) in May and at station P12 in September (Figure 8).

Oxidation-Reduction Potential (ORP, mV). ORP values serve as an indicator of the oxidation state of the water body and its potential to support aerobic processes. In both sampling periods, values fell within the typical range for natural waters (–500 to +700 mV) (Chapman, 1996; Sigg, 2000), suggesting stable redox conditions. In May, ORP values ranged from 1.74 to 100.96 mV (mean: 41.04 ± 20.79 mV), while in September, values ranged from 14.60 to 66.09 mV (mean: 48.70 ± 12.18 mV). The lowest ORP was observed at P19 (Isacova Lake) in May and at P55 in September. The highest values were recorded at P58 (Ivancea Meander – confluence) in May and P35 in September (Figure 9).

Salinity (‰). Salinity levels remained low and consistent throughout the monitoring period, reflecting the freshwater character of the Danube Delta system. All values were well below the 0.5 PSU threshold commonly used to define freshwater ecosystems (Montagna et al., 2013). In May, salinity ranged from 0.13 to 0.22 PSU (mean: 0.18 ± 0.01 PSU), and in September, from 0.17 to 0.21 PSU (mean: 0.18 ± 0.01 PSU), confirming minimal marine influence and dominance of fluvial inputs.

Distribution of nitrate concentrations. Nitrate concentrations (NitraLED, mg/L) showed significant spatial variability between measurement stations. In May, values ranged from 0.01 to 16.28 mg/L (mean: 1.49 ± 2.24 mg/L), with the highest value at P42

(Dranov – bifurcation) and the lowest at P54. In September, concentrations ranged from 0.04 to 9.34 mg/L (mean: 1.70 ± 1.87 mg/L), peaking at P24 and reaching a minimum at P12 (Figure 10). While most values remained within acceptable ecological thresholds, elevated readings at isolated sites may indicate localized nutrient enrichment.

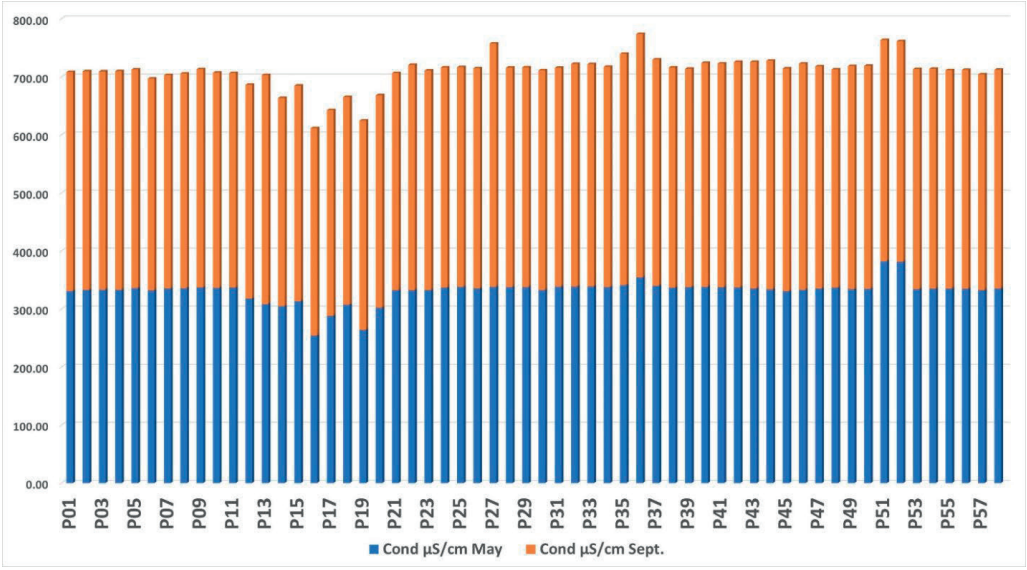


Figure 7. Evolution of the Cond µS/cm indicator in the investigated surface water samples

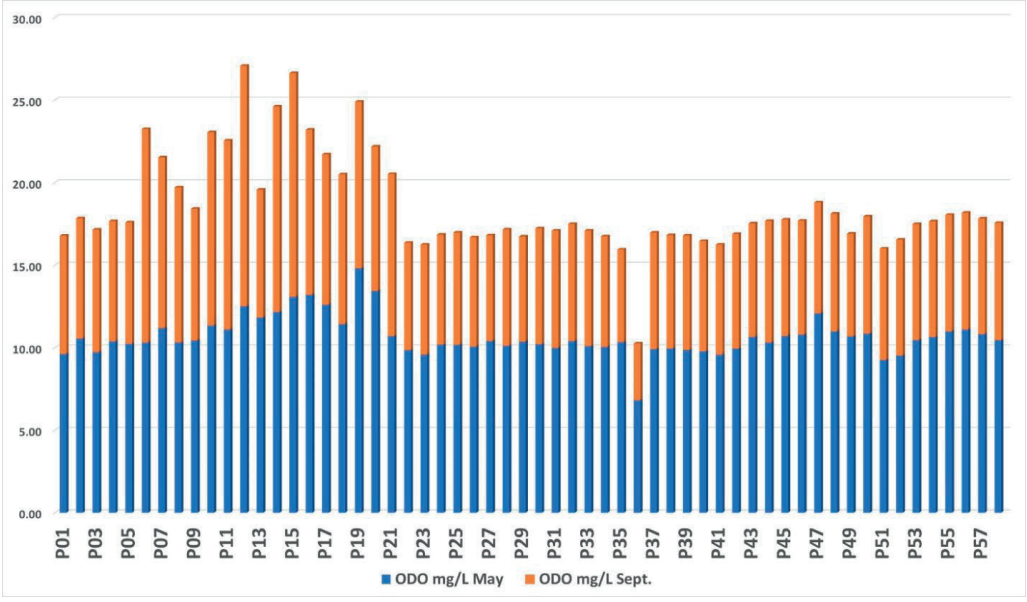


Figure 8. Evolution of the ODO mg/L indicator in the investigated surface water samples

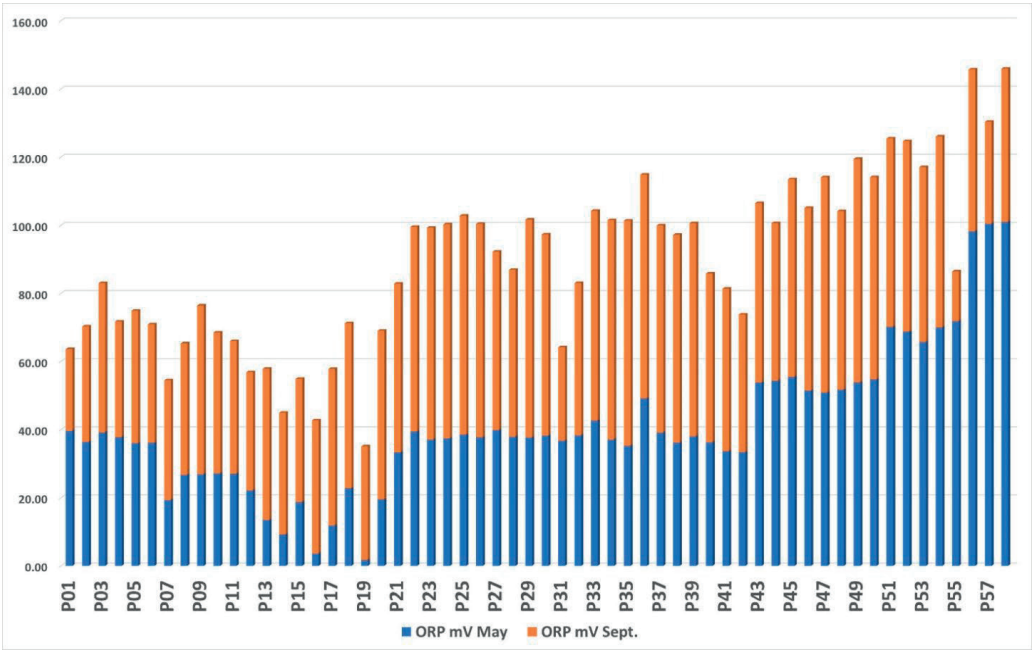


Figure 9. Evolution of the ORP mV indicator in the investigated surface water samples

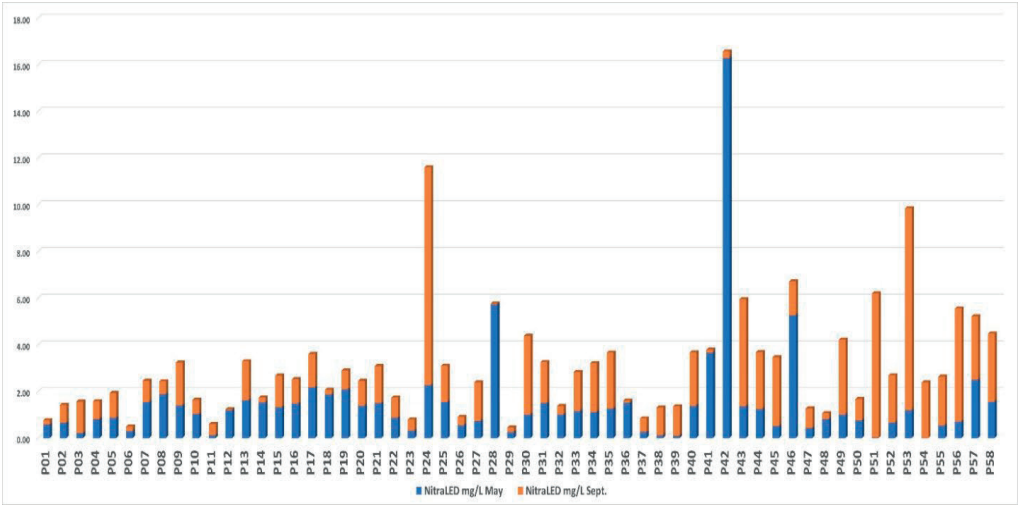


Figure 10. Evolution of the NitraLED mg/L indicator in the investigated surface water samples

Chlorophyll a (µg/L). The concentrations of chlorophyll *a* in the water samples from the investigated sections showed considerable variability. In May, values ranged from 0.26 to 8.57 µg/L (mean: 3.93 ± 2.06 µg/L), while in September, they varied more widely—from 0.27 to 12.65 µg/L (mean: 2.55 ± 3.78 µg/L). Lowest concentrations were found at P20 (May) and P22 (September), while the highest were measured at P46 (May) and P19 (September). All recorded values remained below the class I threshold of 25 µg/L (Order 161/2006), indicating low-to-moderate algal productivity and absence of eutrophic conditions (Figure 11).

Total Algae Content (TAL - PC RFU). TAL values, indicative of overall algal abundance (including cyanobacteria), showed greater variability in September compared to May. In May, TAL ranged from 0.05 to 1.83 RFU (mean: 0.70 ± 0.41 RFU), while in September, values spanned from 0.01 to 14.62 RFU (mean: 2.13 ± 3.85 RFU). Minimal algal content was recorded at P20 (May) and P27 (September), while peak values were observed at P30 (May) and P17 (September) (Figure 12). The overall range suggests a localized increase in algal activity toward the end of the warm season, potentially linked to temperature and nutrient availability

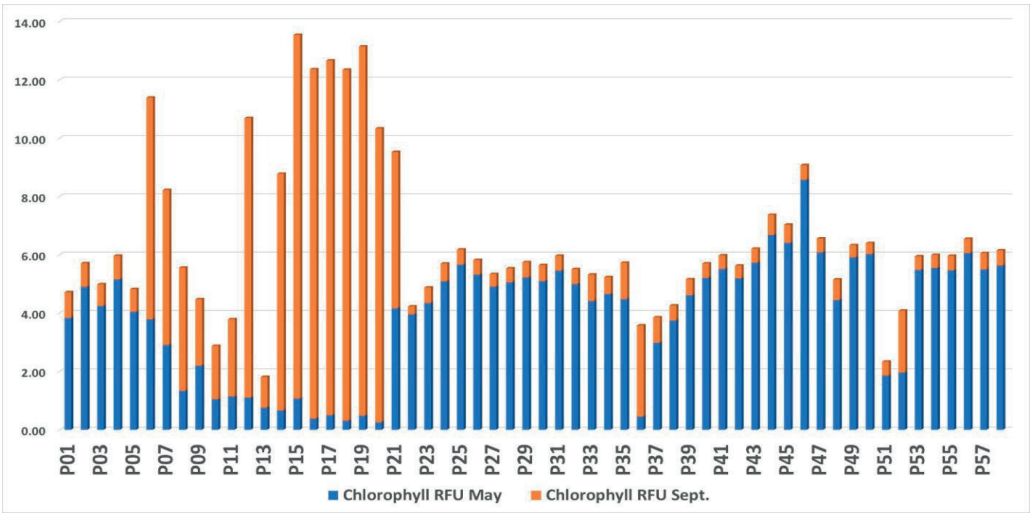


Figure 11. Evolution of the chlorophyll *a* RFU indicator in the investigated surface water samples

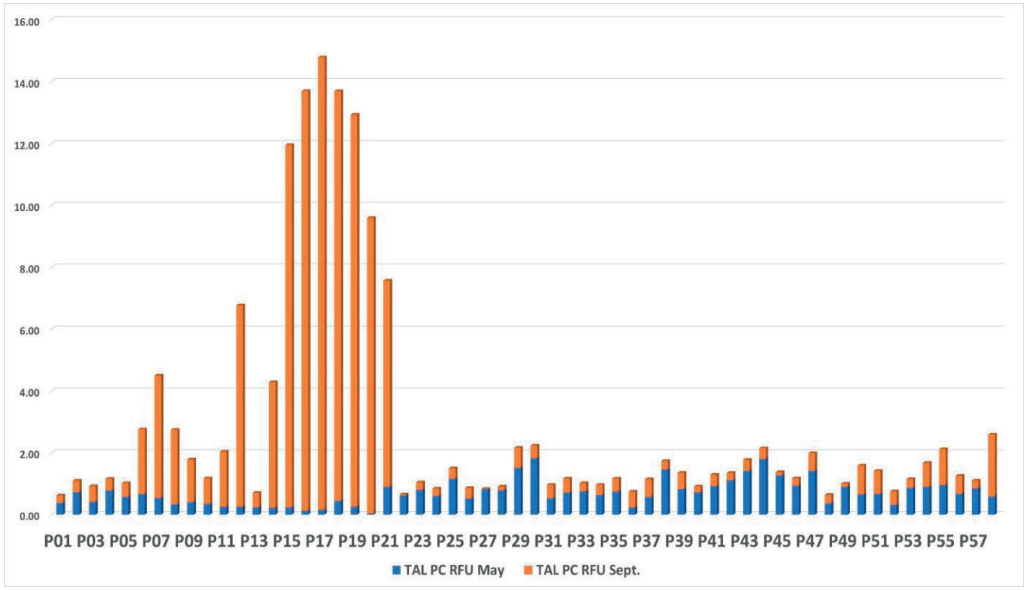


Figure 12. Evolution of the Total Algal Content (TAL - PC RFU) indicator in the investigated surface water samples

Interpretation of seasonal and spatial variability

The seasonal increase in Temperature in September is expected due to higher solar radiation and air temperatures in late summer. Water temperature plays a crucial role in biochemical reactions, dissolved oxygen levels, and biological activity. Higher temperatures generally correlate with lower dissolved oxygen concentrations, as observed in September. Localized differences in temperature values may indicate areas of variable flow dynamics, depth variations, or thermal influences from adjacent land areas. The relatively stable range suggests that there have been no extreme temperature fluctuations that would otherwise indicate thermal pollution or abrupt environmental changes.

Slightly *alkaline conditions*, particularly in stations such as Isacova Lake, indicate biological influences, notably the photosynthetic activity of aquatic plants and phytoplankton. In May, elevated pH levels may result from increased photosynthesis, which reduces CO_2 concentrations and shifts water chemistry toward alkalinity. In contrast, the slight decline in *pH* observed in September could be linked to enhanced respiration and decomposition of organic matter, which releases CO_2 into the water. Nonetheless, all values remained within the acceptable range for freshwater ecosystems, suggesting no immediate risk of acidification or excessive alkalinity.

Turbidity is influenced by sediment transport, organic matter and the presence of phytoplankton. Recent studies, such as Sandu et al. (2023), have reinforced this perspective by demonstrating how elevated turbidity levels in freshwater systems can be linked to nutrient input, sediment resuspension, and decreased water transparency, particularly in areas affected by anthropogenic influence. Higher values at certain stations suggest localized resuspension of sediments or particle growth due to water flow dynamics, bank erosion or anthropogenic influences. The slight decrease in mean turbidity from May to September suggests potential settling of suspended particles as the water flow stabilizes. The high turbidity values at P42 (May) and P24 (September) could be related to increased sediment input from channels or main arm, algal blooms or stormwater runoff. Excessively high values could have a negative impact on submerged vegetation and aquatic organisms by reducing photosynthetic efficiency. Comparisons with standard limits (SR ISO 5667-5:2017: 5 NTU permitted, 10 NTU exceptionally permitted) indicate that some samples exceed these thresholds, indicating localized deterioration of water quality.

Total Dissolved Solids (TDS) values remained within the normal range for freshwater systems (0-1000 mg/L, Lehr, 1980; De Zuane, 1997), indicating good water quality. Seasonal variations were minimal, suggesting that the system maintains stable ion concentrations, without significant dilution or concentration effects. The higher TDS values at P52 (May) and P36 (September) could be due to localized groundwater influence, mineral dissolution, or reduced flushing rates.

Electrical conductivity, closely linked to TDS, increased slightly from May to September, likely due to ion accumulation driven by reduced flow rates and evaporation during late summer. Spatial variation suggests that areas such as the Erenciuc Canal may experience greater mineralization, potentially due to limited water exchange or specific geochemical conditions.

Dissolved oxygen levels were sufficient to support aquatic life during both campaigns, although a noticeable decline from May to September points to temperature-driven oxygen depletion and increased organic matter decomposition. The lowest DO values at P36 may reflect slow circulation, organic accumulation, or microbial respiration. Despite this, most values exceeded the 5 mg/L threshold required for aquatic fauna (NIWA, 2024), indicating overall good oxygenation.

Oxidation-Reduction Potential (ORP) values suggest that the water body remains well oxygenated and capable of supporting aerobic biochemical processes. The slight variations in ORP values between May and September could be attributed to fluctuations in microbial activity, decomposition of organic matter and seasonal variations in dissolved oxygen levels. The highest ORP values at the confluence points probably indicate higher oxygenation due to increased water mixing.

Salinity remained low across all stations, reinforcing the freshwater character of the Sfântu Gheorghe Branch. Minor variations between May and September can be attributed to precipitation, evaporation, and localized mineral input. The consistently low salinity values indicate hydrological stability with minimal marine influence.

Nitrate levels in freshwater systems are influenced by agricultural runoff, wastewater discharge and natural biological processes. The increase in the average nitrate concentration from May to September suggests a seasonal accumulation of nutrients, potentially due to lower dilution rates, organic matter decomposition or anthropogenic inputs. The high values at P42 and P24 warrant closer monitoring as they could indicate localized pollution sources or increased nitrogen inputs from surrounding land use activities.

Chlorophyll a serves as an indicator of phytoplankton biomass and primary productivity. The results suggest a moderate algal growth, with some seasonal and spatial variation. The decrease in mean values from May to September could reflect nutritional limitations or grazing pressures from zooplankton. However, localized peaks (e.g. at P46 and P19) may indicate areas of higher nutrient availability or reduced water flow, favouring phytoplankton accumulation.

The increase in *Total Algal Content (TAL)* values from May to September suggests that phytoplankton biomass was higher in late summer, possibly due to increased water residence time, higher temperatures, and nutrient availability. The peaks observed at P30 and P17 may indicate localized eutrophic conditions where algal growth is enhanced. Further investigation is needed to determine whether these fluctuations are natural seasonal trends or signs of nutrient enrichment from external sources.

Correlation analysis and interpretation - Pearson Correlation – May 2024

Based on the Pearson correlation matrix for May (Table 2, Figure 13), several strong and statistically significant relationships were identified ($\alpha = 0.05$)

1. *Strong positive correlations (directly proportional)*

- ODO % sat and ODO mg/L (r = 0.998): a near-perfect correlation, indicating the expected interdependence between oxygen concentration and its saturation in water.
- Conductivity, TDS, and Salinity: very strong positive correlations were found among Conductivity (µS/cm) and TDS (mg/L) (r = 0.990), Conductivity and Salinity (r = 0.960), and Salinity and TDS (r = 0.978), confirming their shared dependence on dissolved ion concentrations.
- pH and DO (r ≈ 0.881-0.877): higher pH is positively associated with higher dissolved oxygen and percent saturation.
- Temperature and DO (r ≈ 0.895-0.869): increasing temperature is strongly positively associated with higher dissolved oxygen levels.
- Chlorophyll and TAL (r = 0.713): increased chlorophyll concentration (an indicator of primary productivity) is positively correlated with TAL PC RFU, suggesting a link between chlorophyll and other fluorescent particles or phytoplankton.
- Turbidity and Nitrate (r = 0.589): suggests that higher nitrate concentrations are associated with increased turbidity, potentially due to suspended organic material or nutrient-rich runoff.

2. *Strong negative correlations (inversely proportional)*

- pH vs Conductivity, Salinity, TDS (r ≈ -0.914 to -0.923): lower pH is associated with increased values of conductivity, salinity and total dissolved substances, which indicates acidification in more mineralized waters.
- Temperature vs Conductivity, Salinity, TDS (r ≈ -0.783 to -0.870): higher temperatures are associated with lower conductivity and lower salinity, suggesting dilution or the influence of other processes that reduce ion concentration with warming.
- Conductivity vs DO (r ≈ -0.809 to -0.794): higher conductivity correlates negatively with dissolved oxygen, suggesting that waters with more dissolved substances have lower dissolved oxygen levels.
- Chlorophyll (May) vs Chlorophyll (September): a previously observed strong negative correlation (r = -0.732) highlights significant seasonal variability in primary productivity.

Table 2. Correlation matrix (Pearson), in May 2024

Variables	Chla RFU May	Cond µS/cm May	ODO % sat May	ODO mg/L May	ORP mV May	Sal psu May	TAL PC RFU May	TDS mg/L May	Turbidity FNU May	pH May	Temp °C May	NitraLED mg/L May
Chla RFU May	**1**	**0.404**	**-0.417**	**-0.384**	**0.588**	**0.402**	**0.713**	**0.426**	**0.470**	-0.254	**-0.496**	0.112
Cond µS/cm May	**0.404**	**1**	**-0.809**	**-0.794**	**0.567**	**0.960**	**0.319**	**0.990**	0.248	**-0.914**	**-0.783**	-0.059
ODO% sat May	**-0.417**	**-0.809**	**1**	**0.998**	**-0.442**	**-0.858**	**-0.323**	**-0.858**	-0.213	**0.881**	**0.895**	-0.009
ODO mg/L May	**-0.384**	**-0.794**	**0.998**	**1**	**-0.409**	**-0.840**	**-0.298**	**-0.840**	-0.204	**0.877**	**0.869**	-0.017
ORP mV May	**0.588**	**0.567**	**-0.442**	**-0.409**	**1**	**0.523**	**0.359**	**0.591**	0.124	**-0.419**	**-0.586**	-0.097
Sal psu May	**0.402**	**0.960**	**-0.858**	**-0.840**	**0.523**	**1**	**0.332**	**0.978**	0.209	**-0.902**	**-0.870**	-0.032
TAL PC RFU May	**0.713**	**0.319**	**-0.323**	**-0.298**	**0.359**	**0.332**	**1**	**0.336**	**0.309**	-0.215	**-0.383**	0.084
TDS mg/L May	**0.426**	**0.990**	**-0.858**	**-0.840**	**0.591**	**0.978**	**0.336**	**1**	0.232	**-0.923**	**-0.861**	-0.066
Turbidity FNU May	**0.470**	0.248	-0.213	-0.204	0.124	0.209	**0.309**	0.232	**1**	-0.181	-0.171	**0.589**
pH May	-0.254	**-0.914**	**0.881**	**0.877**	**-0.419**	**-0.902**	-0.215	**-0.923**	-0.181	**1**	**0.798**	0.078
Temp°C May	**-0.496**	**-0.783**	**0.895**	**0.869**	**-0.586**	**-0.870**	**-0.383**	**-0.861**	-0.171	**0.798**	**1**	0.076
NitraLED mg/L May	0.112	-0.059	-0.009	-0.017	-0.097	-0.032	0.084	-0.066	**0.589**	0.078	0.076	**1**

Values in bold are different from 0 with a significance level alpha=0.05

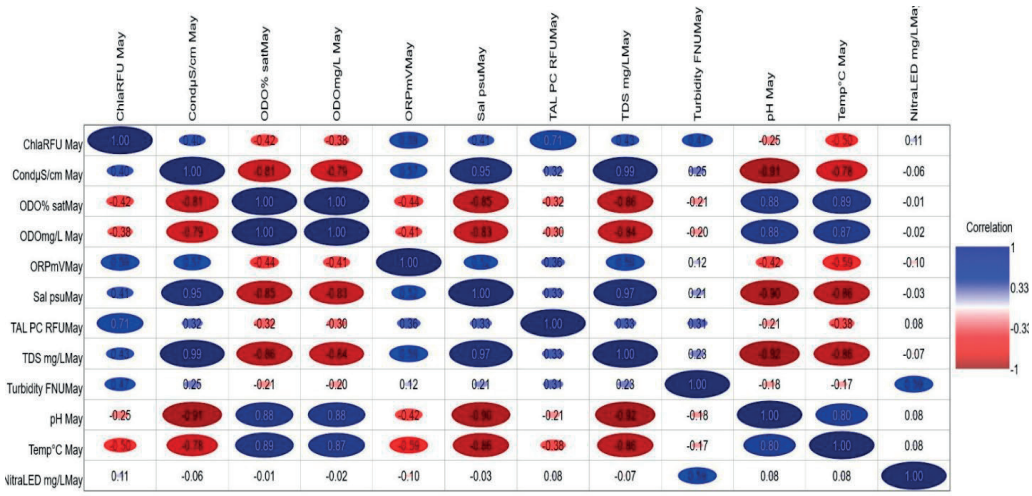


Figure 13. Correlation matrix (Pearson), in May 2024

Pearson Correlation – September 2024

In September (Table 3, Figure 14), the correlation matrix also revealed several statistically significant relationships

1. *Significant positive correlations (directly proportional):*

- ODO % sat and ODO mg/L (r = 0.998). Strongly positive and almost perfect relationship, demonstrating that oxygen saturation and its concentration are directly related and interdependent.
- Chlorophyll and TAL (r = 0.950): An extremely strong correlation indicating that the presence of chlorophyll (an indicator of algal activity) is directly related to the fluorescence of other organic or biological substances.
- Salinity and TDS (r = 0.928): Reflects the direct relationship between salinity and total dissolved solids, being indicators that vary simultaneously.
- pH and ODO mg/L (r = 0.932), ODO % sat (r = 0.923), Chlorophyll (r = 0.739). High pH is associated with increased dissolved oxygen levels and increased chlorophyll concentrations, suggesting high photosynthetic activity, which generates oxygen and raises the pH of the water.
- Turbidity and NitraLED (r = 0.633): Indicates that higher nitrates are related to

increased turbidity, possibly due to organic loading or nutrient input.

- TDS and Conductivity (r = 0.807): Increased conductivity indicates increased ions and dissolved substances, explaining the positive relationship with TDS.

2. *Significant negative correlations (inversely proportional):*

- Conductivity and Chlorophyll (r = -0.612): Suggests that high conductivity is associated with lower chlorophyll values, possibly indicating the negative influence of high salinity on algae growth.
- DO vs TDS (r = -0.711) and Conductivity (r = -0.653): High dissolved solids and high conductivity are negatively associated with dissolved oxygen, indicating that waters with high salt and other substances are poorer in dissolved oxygen.
- pH vs ORP (r = -0.639) and Conductivity (r = -0.618): Higher pH (basic) is associated with lower ORP and conductivity values, suggesting that alkaline water has a lower redox potential and lower mineralization.
- Temperature vs Chlorophyll (r = -0.517) and TAL (r = -0.568): Higher temperatures are associated with decreases in chlorophyll concentration and fluorescence of other organic substances, possibly due to thermal stress on photosynthetic organisms.

General observations on specific parameters

Chlorophyll (May) have moderate positive relationships with Turbidity, ORP, and TAL, suggesting the influence of biological activity (algae and phytoplankton) on physicochemical parameters.

Nitrates (NitraLED) did not show strong correlations with most variables, except Turbidity, possibly indicating its association with suspended particles or runoff rather than in situ biological processes.

Table 3. Correlation matrix (Pearson) in September 2024

Variables	Chla RFU Sept.	Cond µS/cm Sept.	ODO % sat Sept.	ODO mg/L Sept.	ORP mV Sept.	Sal psu Sept.	TAL PC RFU Sept.	TDS mg/L Sept.	Turbidity FNU Sept.	pH Sept.	Temp °C Sept.	NitraLED mg/L Sept.
Chla RFU Sept.	**1**	**-0.612**	**0.675**	**0.712**	**-0.334**	**-0.370**	**0.950**	**-0.363**	0.239	**0.739**	**-0.517**	-0.255
Cond µS/cm Sept.	**-0.612**	**1**	**-0.616**	**-0.653**	**0.438**	**0.721**	**-0.615**	**0.807**	-0.086	**-0.618**	**0.539**	0.117
ODO % sat Sept.	**0.675**	**-0.616**	**1**	**0.998**	**-0.513**	**-0.667**	**0.531**	**-0.714**	0.049	**0.923**	-0.014	-0.247
ODO mg/L Sept.	**0.712**	**-0.653**	**0.998**	**1**	**-0.518**	**-0.662**	**0.575**	**-0.711**	0.060	**0.932**	-0.082	-0.254
ORP mV Sept.	**-0.334**	**0.438**	**-0.513**	**-0.518**	**1**	**0.497**	**-0.283**	**0.464**	0.068	**-0.639**	0.077	0.211
Sal psu Sept.	**-0.370**	**0.721**	**-0.667**	**-0.662**	**0.497**	**1**	**-0.368**	**0.928**	0.003	**-0.568**	-0.102	0.066
TAL PC RFU Sept.	**0.950**	**-0.615**	**0.531**	**0.575**	**-0.283**	**-0.368**	**1**	**-0.335**	0.252	**0.610**	**-0.568**	-0.186
TDS mg/L Sept.	**-0.363**	**0.807**	**-0.714**	**-0.711**	**0.464**	**0.928**	**-0.335**	**1**	-0.015	**-0.596**	-0.062	0.034
Turbidity FNU Sept.	0.239	-0.086	0.049	0.060	0.068	0.003	0.252	-0.015	**1**	0.127	-0.126	**0.633**
pH Sept.	**0.739**	**-0.618**	**0.923**	**0.932**	**-0.639**	**-0.568**	**0.610**	**-0.596**	0.127	**1**	-0.188	**-0.275**
Temp°C Sept.	**-0.517**	**0.539**	-0.014	-0.082	0.077	-0.102	**-0.568**	-0.062	-0.126	-0.188	**1**	0.148
NitraLED mg/L Sept.	-0.255	0.117	-0.247	-0.254	0.211	0.066	-0.186	0.034	**0.633**	**-0.275**	0.148	**1**

Values in bold are different from 0 with a significance level alpha=0.05

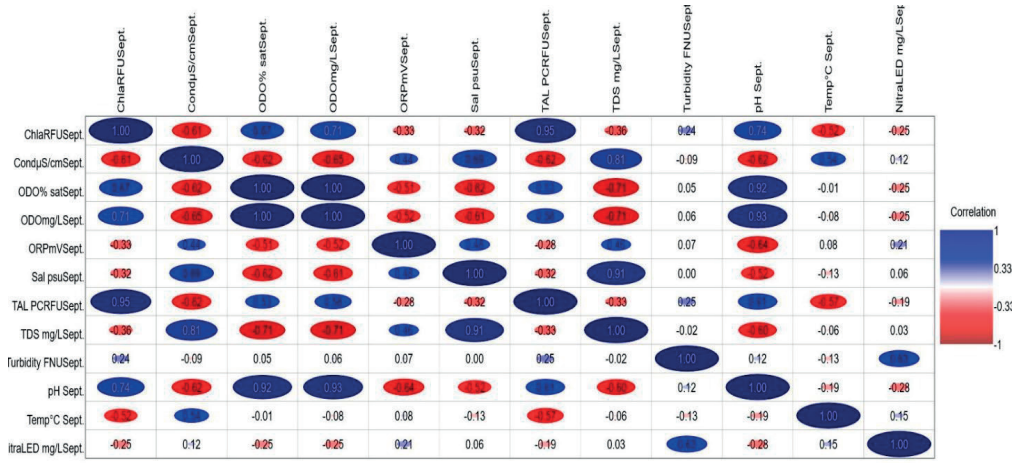


Figure 14. Correlation matrix (Pearson), in September 2024

Practical significance of the results

Conductivity and salinity are inversely related to oxygen availability and pH, emphasizing the impact of mineralization on water quality.

Temperature plays a pivotal role in modulating *DO, pH,* and *ion concentration*, reinforcing its importance in ecosystem metabolism and management.

Chlorophyll correlates with biological productivity and responds to both physicochemical conditions and seasonal shifts.

The *strong link between nitrates and turbidity* suggests external nutrient inputs that may degrade water transparency and stimulate eutrophication.

Comparison with previous studies

The results of this study are consistent with previous findings reported for the Danube Delta and lower Danube River, including those by Calmuc et al. (2021), Catianis et al. (2024), Isvoranu (1979), Iticescu et al. (2014), Najamuddin et al. (2016), Bashir et al. 2020, Teodorof et al. (2021), Ene et al. (2024), and Podlasek et al. 2024.

These studies also highlighted the influence of seasonal dynamics, hydrological variation, and anthropogenic factors such as sediment input and nutrient loading.

The current findings support these trends and contribute additional spatial and seasonal resolution to the understanding of ecological variability in the Danube Delta.

CONCLUSIONS

This study highlights the influence of *seasonal dynamics* - particularly temperature, hydrological conditions, and biological activity - on the water quality of the Sfântu Gheorghe Arm. Observed variations in *temperature, dissolved oxygen,* and *oxidation-reduction potential (ORP)* are consistent with expected physicochemical responses to seasonal change, especially the inverse relationship between temperature and dissolved oxygen driven by thermal stratification and increased biological oxygen demand in late summer.

Turbidity and *nitrate* concentrations exhibited localized fluctuations, likely influenced by sediment resuspension, surface runoff, and biological productivity. Although certain stations (e.g., P42, P24, and P53) recorded nitrate peaks exceeding recommended thresholds, the overall water quality remained within acceptable ranges for freshwater ecosystems. These sites may be subject to nutrient enrichment, warranting further investigation into potential agricultural or wastewater inputs.

The stability of *pH, salinity,* and *TDS* across the sampling campaigns indicates a well-buffered system with consistent hydrological conditions and no significant signs of acidification or salinity stress.

Meanwhile, moderate values of *Chlorophyll a* and *total algal content (TAL-PC)* suggest ongoing primary production, with spatial

variation likely influenced by nutrient levels and local hydrodynamic conditions.

RECOMMENDATIONS

Regular Monitoring
Continuous assessment of turbidity, nitrate concentrations and dissolved oxygen levels is essential to detect potential changes in water quality.
Nutrient Management
High nitrate concentrations at P42, P24 and P53 may indicate agricultural runoff or wastewater inputs; further analysis is needed to identify sources and mitigate impacts.
Erosion and Sediment Control
Elevated turbidity values suggest possible sediment transport issues; implementing land use management and erosion control measures could reduce sediment input.
Ecological Risk Assessment
The decrease in dissolved oxygen in September indicates a risk of hypoxic conditions, which should be further examined to assess potential effects on aquatic life.
Hydrodynamic Investigation
Investigation of flow dynamics and mixing processes could provide insights into localized variations in water quality and help optimize water management strategies.
By integrating these findings with long-term monitoring and cross-seasonal studies, a more comprehensive understanding of the ecological functioning of the Sfântu Gheorghe Arm can be achieved. This knowledge is crucial for the development of effective conservation, restoration, and sustainable water resource management practices in the Danube Delta.

ACKNOWLEDGEMENTS

The research leading to their results was financed by the Ministry of Research and Innovation - “Program Nucleu” - PN 23.30.03.04, PN 23.30.03.02, PN 23.30.03.01 and HORIZON-MISS-2021-OCEAN-02-02, DANUBE4all - Restoration of the Danube River Basin Waters for Ecosystem and People from Mountains to Coast.

REFERENCES

AccuWeather (2024). *Tulcea Weather Forecast*. Retrieved March 10, 2025, from https://www.accuweather.com/ro/ro/tulcea/

Addinsoft. (2020). *XLSTAT statistical and data analysis solution*. Addinsoft. https://www.xlstat.com

Almazov, A. A., Bondar, C., Diaconu, C., Ghederim, V., Mihailov, A. N., Mita, P., Nichiforov, I. D., Rai, I. A., Rodionov, N. A., Stănescu, S., Stănescu, V., & Vaghin, N. F. (1963). *Zona de vărsare a Dunării. Monografie hidrologică* (p. 396). Editura Tehnică [in Romanian].

Bashir, I., Lone, F. A., Bhat, R. A., Mir, S. A., Dar, Z. A., & Dar, S. A. (2020). Concerns and threats of contamination on aquatic ecosystems. In I. Bashir, F. A. Lone, R. A. Bhat, S. A. Mir, Z. A. Dar, & S. A. Dar (Eds.), *Bioremediation and biotechnology* (pp. 1–26). Springer. https://doi.org/10.1007/978-3-030-35691-0_1

Bondar, C., & Panin, N. (2000). The Danube Delta hydrologic database and modeling. *Geo-Eco-Marina*, 5–6, 5–53.

Bondar, C., & Panin, N. (2001). The Danube Delta hydrologic database and modelling. *Geo-Eco-Marina*, 5–6, 5–52.

Botnariuc, N. (1985). Fluxul de energie din ghiolurile Puiu, Roşu, Porcu şi potenţialul lor bioproductiv. *Studii şi Comunicări Ecologie Delta Dunării*, 1, 9–14. [in Romanian]

Calmuc, V. A., Calmuc, M., Arseni, M., Topa, C. M., Timofti, M., Burada, A., Iticescu, C., & Georgescu, L. P. (2021). Assessment of heavy metal pollution levels in sediments and of ecological risk by quality indices, applying a case study: The Lower Danube River, Romania. *Water, 13*(13), 1801. https://doi.org/10.3390/w13131801

Catianis, I., Constantinescu, A. M., Grosu, D., Iordache, G., Duțu, F., & Pavel, A.-B. (2024). Assessment of the surface water quality data collected seasonally at the Danube River bifurcations (Ceatal Izmail and Ceatal Sf. Gheorghe). *Scientific Papers. Series E. Land Reclamation, Earth Observation & Surveying, Environmental Engineering, 13*, 503–514.

Cazacu, C., & Adamescu, M. C. (2017). Ecosystem services provided by the bio-physical structure of natural capital in the Danube Delta Biosphere Reserve Romania. In *Conference volume of 6th symposium for research in protected areas* (pp. 97–102).

Călmuc, M., Călmuc, V. A., Dragu, M. D., Roșu, A., Munteanu, D., Roşu, B., & Murariu, G. (2018). Comparative study of descriptive statistics on physico-chemical parameters describing water quality. Case study—the Danube River in the Galati area. *Annals of the University Dunarea de Jos of Galati: Fascicle II, Mathematics, Physics, Theoretical Mechanics, 41*.

Chapman, D. (1996). *Water quality assessments: A guide to use of biota, sediments and water in environmental monitoring* (2nd ed.). Cambridge University Press.

Chiriac, E., & Udrescu, M. (1965). *Ghidul naturalistului în lumea apelor dulci*. Editura Științifică. [in Romanian]

Coteț, P. (1960). *Evoluția morfohidrografică a Deltei Dunării (O sinteză a studiilor existente și o nouă interpretare)*. Probl. de Geogr., Vol. VII. Editura Academiei R.P. România. [in Romanian]

De Zuane, J. (1997). *Handbook of Drinking Water Quality* (2nd ed.). John Wiley and Sons.

Driga, B.V. (2004). *Delta Dunării – Sistemul de Circulație Apei*. Editura Casa Cărții de Știință, Cluj Napoca. [in Romanian]

Duțu, F., Tiron Duțu, L., & Catianis, I. (2023). Dramatic reduction of the water and sediment fluxes in a human modified meandering ecosystem from the Danube Delta, Romania. *Scientific Papers. Series E. Land Reclamation, Earth Observation & Surveying, Environmental Engineering, 12*, 267–274.

European Union. (2013). Directive 2013/39/EC of the European Parliament and of the Council of 12 August 2013 amending Directives 2000/60/EC and 2008/105/EC as regards priority substances in the field of water policy. *Official Journal of the European Union, L226*, 1–17.

Ene, A., Moraru, D. I., Pintilie, V., Iticescu, C., & Georgescu, P. L. (2024). Metals and natural radioactivity investigation of Danube River water in the lower sector. *Romanian Journal of Physics, 69*(3–4), 702. https://doi.org/10.59277/RomJPhys.2024.69.802

Gâștescu, P. (2009). The Danube Delta biosphere reserve: Geography, biodiversity, protection, management. *Revue Roumaine de Géographie, 53*(2), 139–152.

Gâștescu, P., & Știucă, R. (2008). *The Danube Delta – A biosphere reserve*. CD Press Publishing House [in Romanian, with contents and introduction in English].

Habersack, H., Hein, T., Stănică, A., Liska, I., Mair, R., Jager, E., Hauer, C., & Bradley, C. (2016). Challenges of river basin management: Current status of, and prospects for, the River Danube from a river engineering perspective. *Science of the Total Environment, 543*, 828–845. https://doi.org/10.1016/j.scitotenv.2015.12.123

Ichim, I., & Rădoane, M. (1986). *Efectele barajelor în dinamica reliefului. Abordare geomorfologică*. Editura Academiei [in Romanian].

Isvoranu, V. (1979). *Raport de cercetare: Sinteza Roșu – Puiu – Porcu (1976-1979)* [in Romanian].

Iticescu, C., Georgescu, L. P., Popa, C., & Murariu, G. (2014). Water pollution monitoring: The Danube water quality near the Galati city. *Journal of Environmental Protection and Ecology, 15*(1), 30–38.

Jugaru, L., Provansal, M., Panin, N., & Dussouillez, P. (2006). Apports des systèmes d'information géographiques à la perception des changements morphodynamiques (1970-2000) dans le delta du Danube. Le cas du bras de Saint-George. *Geo-Eco-Marina, 12*, 29–42.

Kirschner, A. K. T., Kavka, G. G., Velimirov, B., Mach, R. L., Sommer, R., & Farnleitner, A. H. (2009). Microbiological water quality along the Danube River: Integrating data from two whole-river surveys and a transnational monitoring network. *Water Research, 43*(15), 3673–3684. https://doi.org/10.1016/j.watres.2009.05.028

Lehr, J. H., Gass, T. E., Pettyjohn, W. A., & DeMarre, J. (1980). *Domestic water treatment*. McGraw-Hill Book Company.

Lipps, W. C., Braun-Howland, E. B., & Baxter, T. E. (Eds.). (2023). *Standard methods for the examination of water and wastewater* (24th ed.). American Public Health Association, American Water Works Association, Water Environment Federation.

Madhav, S., Ahamad, A., Singh, A. K., Kushawaha, J., Chauhan, J. S., Sharma, S., & Singh, P. (2020). Water pollutants: Sources and impact on the environment and human health. In D. Pooja, P. Kumar, P. Singh, & S. Patil (Eds.), *Sensors in water pollutants monitoring: Role of material* (pp. 43–62). Springer. https://doi.org/10.1007/978-981-15-0671-0_4

Montagna, P., Palmer, P., & Pollack, J. (2013). *Hydrological changes and estuarine dynamics* (Vol. 8). Springer. https://doi.org/10.1007/978-1-4614-5833-3

Najamuddin, Prartono, T., Harpasis, S., Sanusi, I., & Nurjaya, W. (2016). Seasonal distribution and geochemical fractionation of heavy metals from surface sediment in a tropical estuary of Jeneberang River, Indonesia. *Marine Pollution Bulletin, 111*(1–2), 456–462. https://doi.org/10.1016/j.marpolbul.2016.06.098

NIWA. (n.d.). *Dissolved oxygen thresholds for aquatic ecosystems*. Retrieved January 2025, from https://www.niwa.co.nz

Oaie, G., Secrieru, D., Bondar, C., Szobotka, S., Duțu, L., Stănescu, I., Opreanu, G., Duțu, F., Pojar, I., & Manta, T. (2015). Lower Danube River: Characterization of sediments and pollutants. *Geo-Eco-Marina, 21*, 19–34.

Order no. 161/2006. (2006). *Normative concerning the classification of surface water quality to establish the ecological status of water bodies* (Romanian Order MEWM no. 161/2006). Romanian Official Monitor, Part I, No. 511 bis.

Panin, N. (2003). The Danube Delta: Geomorphology and Holocene evolution – A synthesis. *Géomorphologie: Relief, Processus, Environnement, 4*, 247–262.

Panin, N., & Jipa, D. (2002). Danube River sediment input and its interaction with the north-western Black Sea. *Estuarine, Coastal and Shelf Science, 54*(2), 551–562. https://doi.org/10.1006/ecss.2000.0660

Podlasek, A., Koda, E., & Kwas, A. (2024). Anthropogenic and natural impacts on surface water quality: The consequences and challenges at the nexus of waste management facilities, industrial zones, and protected areas. *Water Resources Management, 38*, 1123–1142. https://doi.org/10.1007/s11269-024-04041-1

Popa, A. (1997). Environmental changes in the Danube Delta caused by the hydrotechnical works on the St. George branch. *Geo-Eco-Marina, 2*, 135–147.

Romanescu, G. (2013). Alluvial transport processes and the impact of anthropogenic intervention on the Romanian littoral of the Danube Delta. *Ocean & Coastal Management, 73*, 31–43. https://doi.org/10.1016/j.ocecoaman.2012.12.002

Sandu, M. A., Vîrsta, A., Scăețeanu, G. V., Iliescu, A.-I., Ivan, I., Nicolae, C. G., Stoian, M., & Madjar, R. M. (2023). Water quality monitoring of Moara Domnească Pond, Ilfov County, using UAV-based RGB imaging. *AgroLife Scientific Journal, 12*(1), 191–201.

Sigg, L. (2000). Redox potential measurements in natural waters: Significance, concepts and problems. In J. Schüring, H. D. Schulz, W. R. Fischer, J. Böttcher, & W. H. M. Duijnisveld (Eds.), *Redox* (pp. 1–12). Springer. https://doi.org/10.1007/978-3-662-04080-5_1

Sommerwerk, N., Bloesch, J., Baumgartner, C., Bittl, T., Čerba, D., Csányi, B., Davideanu, G., Dokulil, M., Frank, G., Grecu, I., Hein, T., Kováč, V., Nichersu, I., Mikuska, T., Pall, K., Paunović, M., Postolache, C., Raković, M., Sandu, C., … Tockner, K. (2022). The Danube River Basin. In K. Tockner, C. Zarfl, & C. T. Robinson (Eds.), *Rivers of Europe* (2nd ed., pp. 81–180). Elsevier. https://doi.org/10.1016/B978-0-08-102612-0.00003-1

SR EN ISO 10523:2012. (2012). *Water quality – Determination of pH*. ASRO.

SR EN ISO 5667-1:2023. (2023). *Water quality – Sampling – Part 1: Guidance on the establishment of sampling programmes and techniques*. ASRO.

SR EN ISO 5814:2013. (2013). *Water quality – Determination of dissolved oxygen content – Electrochemical probe method*. ASRO.

SR ISO 5667-5:2017. (2017). *Water quality – Sampling – Part 5: Guidance for the sampling of drinking water from treatment plants and distribution networks*. ASRO.

Statistical analysis app for Windows. (n.d.). Retrieved from https://past.en.lo4d.com/download

Syeed, M. M., Hossain, M. S., Karim, M. R., Uddin, M. F., Hasan, M., & Khan, R. H. (2023). Surface water quality profiling using the water quality index, pollution index and statistical methods: A critical review. *Environmental and Sustainability Indicators, 18*, 100247. https://doi.org/10.1016/j.indic.2023.100247

Teodorof, L., Ene, A., Burada, A., Despina, C., Seceleanu-Odor, D., Trifanov, C., Ibram, O., Bratfanof, E., Tudor, M.-I., Tudor, M., Cernisencu, I., Georgescu, L. P., & Iticescu, C. (2021). Integrated assessment of surface water quality in Danube River Chilia Branch. *Applied Sciences, 11*(19), 9172. https://doi.org/10.3390/app11199172

Tiron Duțu, L., Provansal, M., Le Coz, J., & Duțu, F. (2014). Contrasted sediment processes and morphological adjustments in three successive cutoff meanders of the Danube Delta. *Geomorphology, 204*, 154–164. https://doi.org/10.1016/j.geomorph.2013.08.024

Tiron, L. (2010). Delta du Danube – Bras de St. George. Mobilité morphologique et dynamique hydro-sédimentaire depuis 150 ans. *Geo-Eco-Marina Special Publication, 4*, 1–280.

Tiron, L., & Provansal, M. (2010). Dynamique sédimentaire dans un milieu deltaïque – Le Bras de St. George dans le delta du Danube. *Zeitschrift für Geomorphologie, 54*(4), 417–441.

Scientific Papers. Series E. Land Reclamation, Earth Observation & Surveying, Environmental Engineering. Vol. XIV, 2025
Print ISSN 2285-6064, CD-ROM ISSN 2285-6072, Online ISSN 2393-5138, ISSN-L 2285-6064

PHYSICO-CHEMICAL CHARACTERISTICS OF SURFACE WATER SAMPLES FROM THE GORGOVA-UZLINA DEPRESSION AND THE IZMAIL AND SF. GHEORGHE CONFLUENCES (SEPTEMBER–OCTOBER 2024)

Ana Bianca PAVEL, Irina CATIANIS, Laura DUTU, Gabriel IORDACHE, Catalina GAVRILA

National Institute for Research and Development on Marine Geology and Geoecology – GeoEcoMar, 23-25 Dimitrie Onciul Street, 024053, District 2, Bucharest, Romania

Corresponding author email: biancapavel@geoecomar.ro

Abstract

The Danube Delta's ecosystems, encompassing riverine branches, lakes, and wetlands, face ecological pressures driven by natural and anthropogenic factors. This study evaluates the physico-chemical characteristics of surface water samples collected in September and October 2024 from 25 locations in the Gorgova-Uzlina Depression and 32 sites near the Izmail and Sf. Gheorghe confluences. Measurements were performed in situ using the EXO2 multiparameter probe (YSI, USA), which recorded parameters including temperature, pH, dissolved oxygen, chlorophyll "a," turbidity, electrical conductivity, and oxidation-reduction potential. Results indicate that most water samples fall within Class I and II of the Romanian water quality classification (Order 161/2006), reflecting good ecological status. Local variations in dissolved oxygen, turbidity, and chlorophyll "a" suggest potential ecological vulnerabilities, particularly in areas with elevated sediment loads. Conductivity and salinity values confirm the freshwater nature of the investigated sites. The findings highlight the importance of continuous monitoring to assess seasonal and anthropogenic influences on water quality and maintain the ecological integrity of the Danube Delta's aquatic ecosystems.

Key words: *Danube Delta; surface water quality; physico-chemical parameters.*

INTRODUCTION

The Danube Delta, located in the southeastern part of Romania, is one of the most important ecosystems globally, hosting over 3500 plant species and approximately 1800 animal species (Gâștescu, 2009). With an area of approximately 5640 km², it represents a distinct geomorphological unit within the Danube-Danube Delta-Black Sea geosystem, acting as an ecological interface between the Danube River and the Black Sea basin. This strategic position allows the delta to function as a natural filter, influencing sedimentation processes by retaining solid materials and chemical substances transported by the river, either dissolved or associated with suspended particles (Cotet, 1960; Almazov et al., 1963; Oaie et al., 2015).

The complex hydrographic network of the delta includes natural and artificial channels, interconnected lakes and wetlands (Chiriac & Udrescu, 1965), significantly influencing sediment transport, nutrient dynamics, pollutant distribution and general water quality. These processes are determined by both natural factors and extensive anthropogenic interventions, which have substantially modified the hydrological and sedimentological dynamics within the delta (Isvoranu, 1979; Bondar & Panin, 2000; Panin, 2003; Romanescu, 2013). Anthropogenic activities, such as dam construction, hydrotechnical works (grooves, embankments, dikes, meander cuts) and canalization have a significant impact on sediment transport and deposition processes. Specifically, the construction of the Iron Gates I (1973) and Iron Gates II (1984) dams dramatically reduced downstream sediment discharge by approximately 25–30%, consequently affecting environmental conditions (Panin & Jipa, 2002; Habersack et al., 2016; Tiron Duțu et al. 2014; 2019; Kanownik et al., 2019).

Numerous studies have highlighted the importance of analysing water flow regimes, sediment transport, pollutant dynamics, flood impacts, trophic gradients, and nutrient cycling

within the delta, given their profound effects on biodiversity, ecosystem health, navigation, and fishing activities (Calmuc et al., 2021a, 2021b). Accurate hydrochemical analyses require precise topographic data to characterize channel cross-sections and underwater terrain. Modern topographic equipment facilitates the collection of reliable data essential for studying these complex interactions. In addition, geochemical analyses play a crucial role in determining sediment provenance, weathering processes, diagenesis, anthropogenic impacts, and environmental risks (Wu et al., 2013; Najamuddin et al., 2016; Zhang et al., 2017; Bucșe et al., 2020; Teaca et al., 2020).

This study aims to analyse the physicochemical characteristics of surface waters in representative areas such as the Gorgova-Uzlina Depression and the confluence of Izmail and Sfântu Gheorghe during September and October 2024. The research will provide essential insights into the variability of hydrochemical parameters, identifying the influences of both natural factors and human activities on water quality and ecosystem dynamics in the Danube Delta.

The findings of this research have significant relevance for environmental management, conservation efforts, and policy formulation regarding the use and protection of water resources in the Danube Delta. By examining the physicochemical variability of surface waters and the specific impacts of anthropogenic activities, the study contributes crucial data for understanding and mitigating ecological risks (József et al., 2023; Kirschner et al., 2024). These insights can guide targeted interventions and inform sustainable management strategies aimed at conserving biodiversity, maintaining ecosystem functionality, and supporting socio-economic activities such as fishing, navigation, and tourism in this sensitive and internationally recognized region (Frîncu et al., 2021).

MATERIALS AND METHODS

Study area

The Gorgova-Uzlina Depression is located between the Sulina and Sfântu Gheorghe Arms, being influenced by the hydrographic system formed by the Litcov Canal, the Gârla Perivolovca and the Gorgova, Isacova and Uzlina Lakes. This region is characterized by variations in the hydrological regime, determined by morphological and hydrotechnical changes, which influence water circulation, sediment transport and water chemical quality. The closure and reopening of some channels (e.g. Gârla Filatului, Uzlina Canal) have modified the water and sediment supply over time, affecting the ecological balance of the lakes (Antipa, 1937; Driga, 2004). The confluences at Izmail and Sfântu Gheorghe are critical points for assessing water quality, being areas of mixing between river and lake waters, with intense sedimentation processes and changes in physico-chemical parameters (Poonam et al., 2013; Paun et al., 2017). These interactions are relevant for understanding the impact of the Danube on deltaic and coastal ecosystems (Gastescu & Stiuca, 2008; Dutu et al., 2023).

Methodology

The assessment of surface water quality in the Gorgova-Uzlina lake complex was carried out through in situ measurements of key physicochemical parameters at 25 stations in lakes Uzlina, Isacova, Durnoliatca, Isaccel, Gorgova, Potcoava, Gorgovăț, Rădăcinoș and Rotund and in 32 stations from Ceatal Izmail bifurcation (Danube-Mm 43.5, Chilia-Km 115, Tulcea-Mm 42.5) and Ceatal Sf. Gheorghe bifurcation (Tulcea-Mm 34, Sulina-Mm 33, Sf. Gheorghe-Km 108) in September and October 2024 (Figures 1 and 2).

Field analyses were performed using the multiparameter probe EXO 2 (YSI – USA) (Figure 3), equipped with sensors that collect water quality data through physical, optical and electrochemical detection methods (STAS 6323).

The determined parameters included:

Temperature (°C), pH (pH units), Turbidity (FNU), Total Dissolved Solids (TDS) (mg/L), Conductivity (µS/cm), Dissolved Oxygen (ODO mg/L), Oxygen Saturation (ODO%), Oxidation-Reduction Potential (ORP, mV), Salinity (PSU), Nitrate (NitraLED mg/L), Chlorophyll (RFU), Total Algal Content (TAL) – PC RFU.

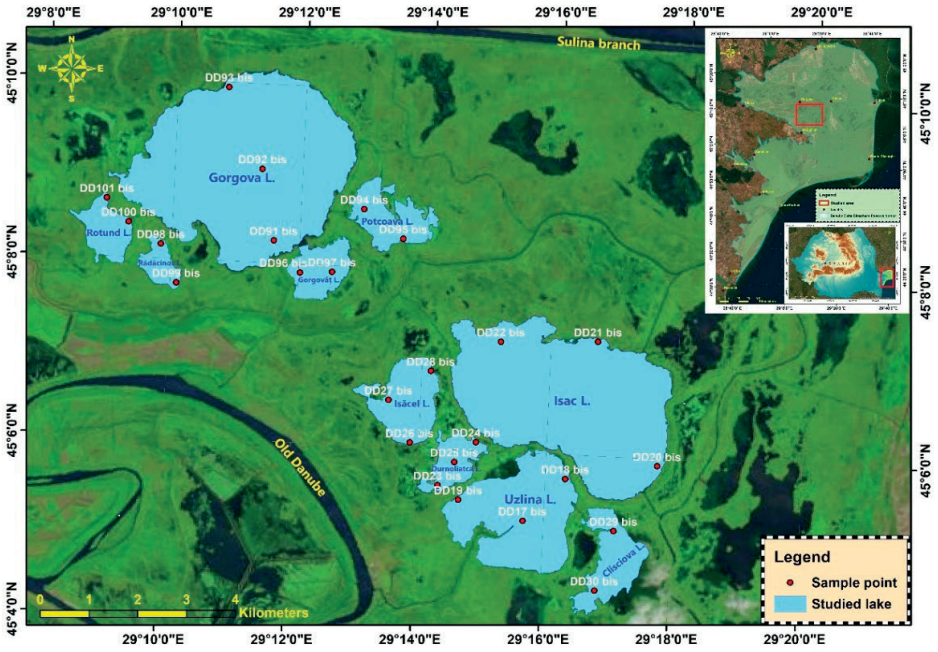


Figure 1. Sampling stations from Gorgova – Uzlina Complex

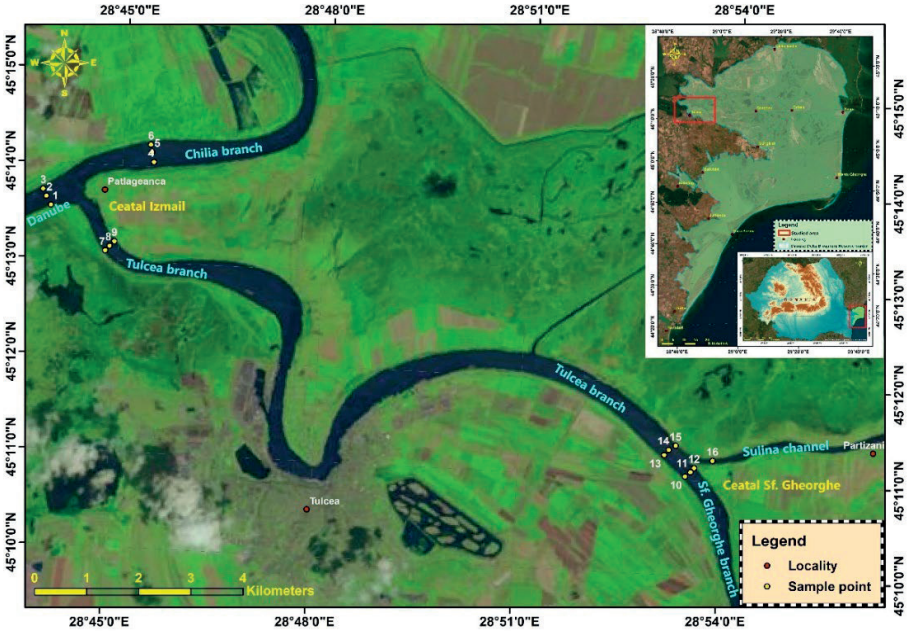


Figure 2. Sampling stations from the Ceatal Izmail and Ceatal Sf. Gheorghe

The water quality assessment was performed based on the classification provided by Order 161/2006, which defines five quality classes:

- Class I – Very good;
- Class II – Good;
- Class III – Moderate;
- Class IV – Poor;
- Class V – Bad.

In addition, reference standards from both national and international regulatory frameworks were considered to ensure a comprehensive assessment of water quality.



Figure 3. Multiparameter probe, model EX02

For a detailed analysis, both national and international water quality standards were applied. The assessment followed the European Union Water Framework Directive (WFD, 2000/60/EC), which sets requirements for managing aquatic resources to ensure a 'good' water quality status. In Romania, the evaluation was based on Regulation no. 161/2006 (Official Monitor of Romania, Part I, no. 511 bis), which outlines criteria for classifying surface water quality and ecological status, using parameters such as total dissolved solids (TDS) and turbidity (ISO 5667-5:2017). Physicochemical analyses were conducted in accordance with international standards, including SR EN ISO 5667-1:2023, SR EN ISO 10523:2012 (pH determination), and SR EN ISO 5814:2013 (dissolved oxygen measurement).

Statistical analysis

All statistical analyses were conducted using xlSTAT 7.5.2 software (Addinsoft, 2020) and Past 4 (https://past.en.lo4d.com/download). Pearson correlation was used to examine relationships between parameters.

RESULTS AND DISCUSSIONS

The ecosystems of the Danube Delta – including the branches of the Danube River, channels, lakes, ponds and coastal ecosystems – are subject to ecological pressures resulting from natural factors such as hydrological fluctuations, sedimentation processes and climate variability, as well as anthropogenic activities, including agriculture, navigation, water pollution, fishing and infrastructure development (Cazacu & Adamescu, 2017; Chapter 10 Nutrients, 2025).

According to Annex XI of the WFD, the complexes of lotic ecosystems, represented by the Danube River and the Danube Delta, are part of the Pontic Ecoregion (12).

Based on to the updated Management Plan for the Danube River, the Danube Delta, the Dobrogea River Basin and Coastal Waters (2021), in conjunction with the details provided in sub-chapter 6.3, a total of 112 surface water bodies have been identified and classified into:

- 92 natural water bodies, including 20 rivers, 68 lakes, 2 transitional water bodies and 2 coastal water bodies;
- 15 heavily modified water bodies, comprising 3 rivers, 4 reservoirs, 6 heavily modified natural lakes and 2 coastal water bodies;
- 5 artificial water bodies (mainly river-type channels).

Of these 112 surface water bodies, 2 (approximately 1.78%) are classified as non-permanent, both belonging to the river category. The specific area of this study falls within the category RO15 (Danube – Isaccea – Danube Delta). Within the current management plan, natural water bodies have been identified for types RO15, RO19, RO06* and RO08*, while types RO13 and RO14 consist exclusively of heavily modified water bodies:

- RO06*: Lowland streams naturally devoid of fish fauna, usually characterised by intermittent flows, shallow depths and limited ecological complexity.
- RO08*: Similar to RO06*, these are also lowland streams without naturally occurring fish populations, frequently subject to dry periods and minimum water flow.
- RO13 (Danube River - Cazane - Călărași): A heavily modified river sector, significantly influenced by human activities such as navigation, river training and infrastructure development.
- RO14 (Danube River - Călărași - Isaccea): Another extensively modified section

of the Danube River, shaped by navigation channels, hydraulic engineering works and associated anthropogenic pressures.

- RO15 (Danube River - Isaccea - Danube Delta): Represents the lower section of the Danube, characterized by complex hydrological dynamics, high ecological diversity, significant sediment transport and natural interactions between fluvial and deltaic ecosystems.
- RO19: Non-permanent lowland streams, characterized by seasonal or intermittent flow regimes, which usually dry up periodically.

The values of the physicochemical parameters generally varied within the limits set by environmental standards, in particular national standards set by Romanian legislation (such as Order 161/2006), international guidelines and the criteria highlighted by the European Union Water Framework Directive (EU-WFD, 2000). The results obtained in this study contribute to improving the existing database on water quality by providing relevant and detailed information, aligned with the EU-WFD guidelines. The integration of data from multiple authorized sources, including national monitoring programmes, scientific studies and regulatory frameworks, ensures a complete and robust assessment of water quality. According to the EU-WFD provisions, European Union Member States must ensure that rivers, lakes, groundwater, estuaries and coastal waters achieve at least a "good" ecological status by 2027 at the latest. The results of the physicochemical determinations obtained at the sampling points are presented in Tables 1 and 2, indicating the minimum, maximum and average values (±standard deviation) for each analysed parameter.

Table 1. A synopsis of the physico-chemical parameters of water surface samples from Izmail and Sf. Gheorghe confluences

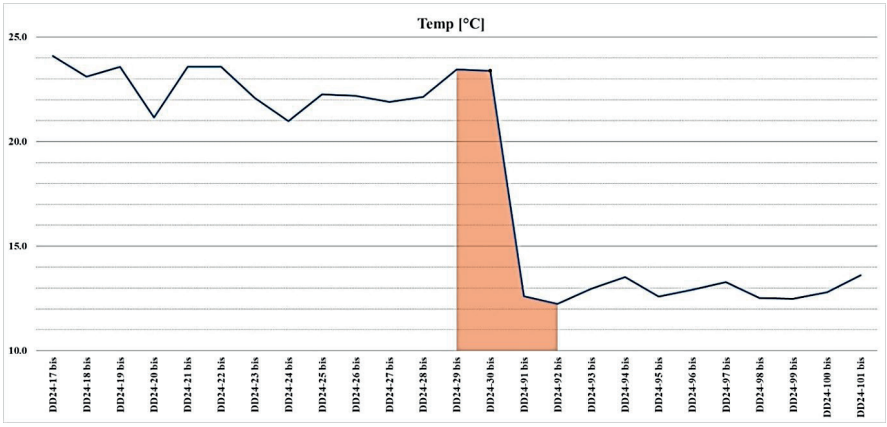
Parameter	**Min.**	**Max.**	**Mean ± SD**
Temperature (°C)	14.46	25.11	19.60±5.04
pH	8.05	8.33	8.16±0.07
Turbidity (FNU)	2.46	58.26	9.96±9.73
Total Dissolved Solids (TDS mg/L)	228.14	256.00	250.56±5.19
Conductivity (µS/cm)	300.82	385.10	345.38±34.89
Dissolved Oxygen (ODO mg/L)	7.14	9.93	8.54±0.94
Oxygen Saturation (ODO % sat)	85.73	97.41	92.34±2.85
Oxidation-Reduction Potential (ORP mV)	49.93	107.14	84.00±20.97
Salinity (PSU)	0.17	0.19	0.18±0.01
Nitrate (NitraLED mg/L)	0.11	18.36	5.78±4.73
Chlorophyll (RFU)	0.34	0.78	0.52±0.11
Total Algal Content (TAL - PC RFU)	0.10	1.37	0.64±0.41

Table 2. A synopsis of the physico-chemical parameters of water surface samples for Gorgova-Uzlina Complex

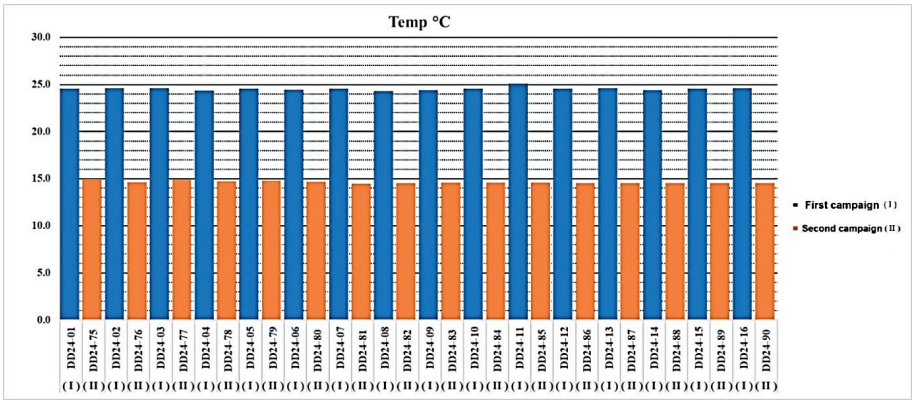
Parameter	**Min.**	**Max.**	**Mean ± SD**
Temperature (°C)	12.24	24.09	18.36±5.03
pH	7.77	8.98	8.20±0.30
Turbidity (FNU)	1.14	91.60	14.59±18.78
Total Dissolved Solids (TDS mg/L)	212.05	273.74	251.33±12.45
Conductivity (µS/cm)	292.84	399.04	336.99±35.20
Dissolved Oxygen (ODO mg/L)	4.67	14.13	9.14±1.92
Oxygen Saturation (ODO % sat)	53.47	166.61	96.82±22.07
Oxidation-Reduction Potential (ORP mV)	-22.37	254.70	75.25±58.65
Salinity (PSU)	0.16	0.20	0.19±0.01
Nitrate (NitraLED mg/L)	0.10	10.46	4.64±3.35
Chlorophyll (RFU)	0.51	22.48	4.89±4.79
Total Algal Content (TAL - PC RFU)	0.44	12.47	2.78±3.17

Water temperature (°C). Water temperature generally follows the trend of autumn air temperatures (https://www.accuweather.com). Recorded values fell within the natural variability of the study areas. In the Gorgova-Uzlina Complex, temperatures ranged from 12.24 to 24.09 °C (average 18.36 °C), while in Ceatal Izmail and Sf. Gheorghe, they ranged from 14.46 to 25.11 °C (average 19.60 °C). The lowest temperature was recorded at station DD24-92 bis (Gorgova Lake), and the highest at station DD24-11 (Ceatal Izmail) (Figure 4a, b). These results reflect typical seasonal fluctuations, with temperature variation mainly influenced by air temperature dynamics during the sampling period.

Water pH (pH units). The values of the results obtained place the tested water from most of the investigated samples within the pH range of normal values (6.5-8.5 pH units), which is considered optimal for aquatic life. The range of variation of the values was relatively narrow (7.77-8.98, average = 8.20) for Gorgova-Uzlina Complex and for Ceatal Izmail and Sf. Gheorghe, the values varied between 8.05-8.33, average 8.16, so that the lowest value was found in station DD24-26 bis (Lake Isaccel), and the highest value was measured in station DD24-21 bis (Lake Isacova) (Figure 5 a, b). These pH values indicate that the water quality at the sampled sites is generally within a range favourable for the sustainability of aquatic ecosystems.

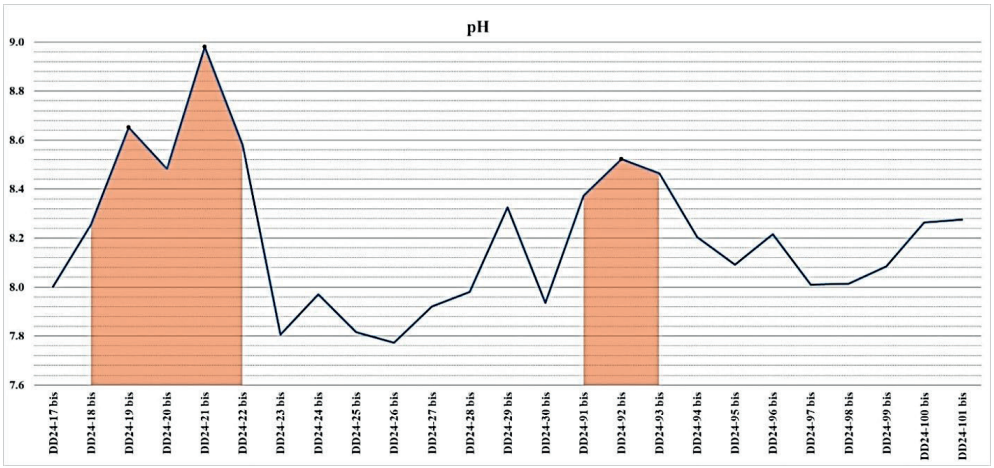


a

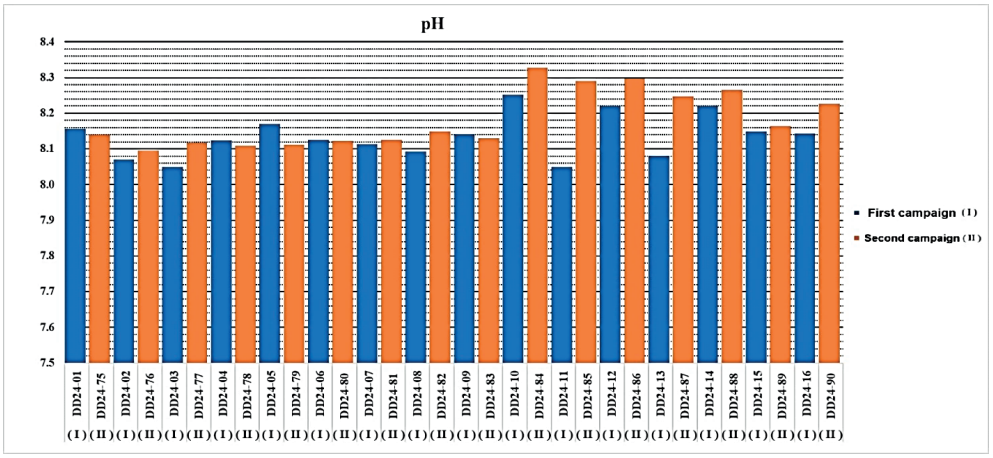


b

Figure 4 a) Evolution of the Temperature indicator in the investigated surface water samples for Gorgova-Uzlina Complex; b) Evolution of the Temperature indicator in the investigated surface water samples for Izmail and Sf. Gheorghe Confluences



a



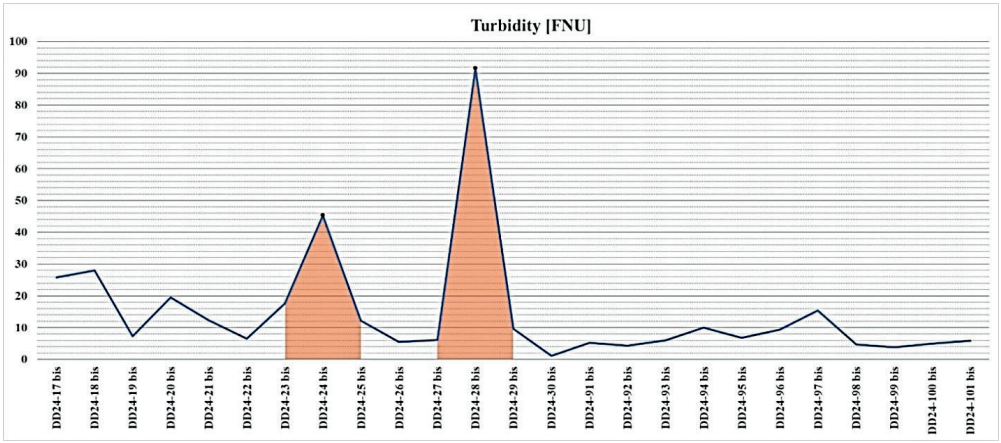
b

Figure 5 a) Evolution of the pH indicator in the investigated surface water samples for Gorgova-Uzlina Complex; b) Evolution of the pH indicator in the investigated surface water samples for Izmail and Sf. Gheorghe Confluences

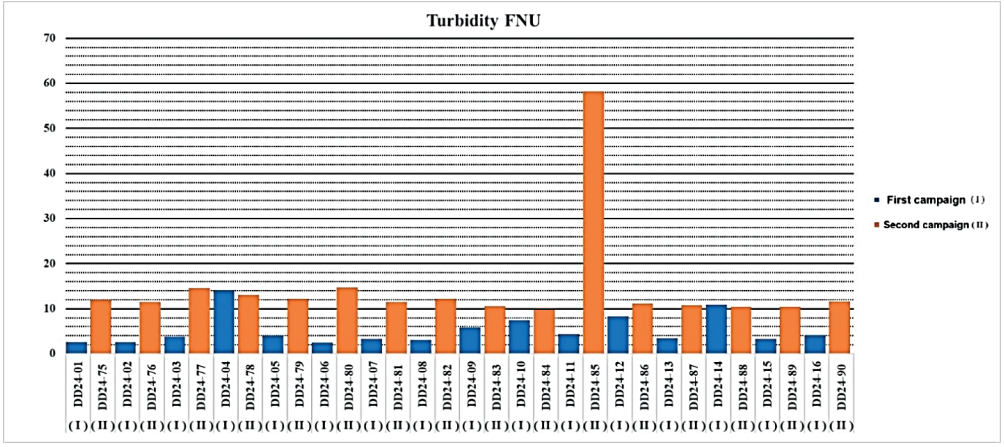
Turbidity (NTU). The turbidity values measured in the water samples taken from the study lakes show a series of variations that fall within the normal range of surface waters (1-1000 NTU) (Chapman, 1996). The range of values was relatively wide (1.14-91.60, average = 14.59) for Gorgova-Uzlina Complex and for Ceatal Izmail and Sf. Gheorghe, the values varied between 2.46-58.26, average 9.96, so that the lowest value was recorded in station DD24-30 bis, Clisciova Lake, and the highest value was measured in station DD24-28 bis, Isaccel Lake (Figure 6 a, b). several samples exhibited relatively high turbidity values compared to the limits stipulated in SR ISO 5667-5:2017, which sets 5 NTU as the allowed value and 10 NTU as the exceptionally allowed value~~), indicating a deterioration in water quality. In general, increased turbidity levels can be attributed to the Danube's fluvial input, which carries water and sediments loaded with dissolved or suspended organic/inorganic substances.

The TDS concentration (total dissolved organic and inorganic substances) places the tested water in a good condition (values corresponding to fresh waters = 0 – 1000 mg/L TDS), (Lehr, 1980; De Zuane, 1997). The range of variation of the values was relatively narrow (212.05-273.74; average = 251.33) for Gorgova-Uzlina Complex and for Ceatal Izmail and Sf. Gheorghe, the values varied between 228.14-256.00, average – 250.56, so that the lowest

value was found in station DD24-19 bis, Lake Uzlina, and the highest value was measured in station DD24-25 bis, Lake Durnoliatca (Figure 7 a, b). These results indicate that the investigated lakes are in good condition in terms of the concentration of dissolved inorganic and organic substances and that the water is not excessively influenced by external sources of pollution.



a



b

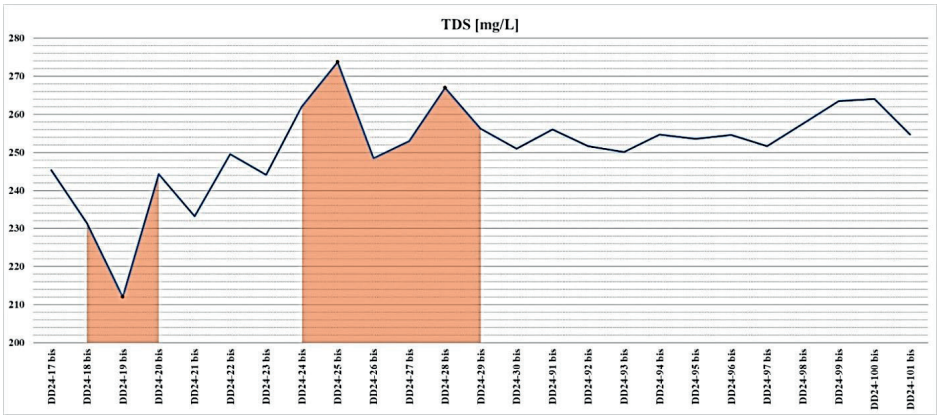
Figure 6 a) Evolution of the Turbidity FNU indicator in the investigated surface water samples for Gorgova-Uzlina Complex; b) Evolution of the Turbidity FNU indicator in the investigated surface water samples for Izmail and Sf. Gheorghe Confluences

The level of electrical conductivity places the tested water from all investigated samples in the category of quality class I (500 µS/cm) (Order 161/2006). The range of variation of the values was relatively narrow (292.84-399.04, average = 336.99) for Gorgova-Uzlina Complex and for Ceatal Izmail and Sf. Gheorghe, the values varied between 300.82-385.10, average = 345.38, so that the lowest value was found in station DD24-92 bis, Lake Gorgova, and the highest value was measured in station DD24-25 bis, Lake Durnoliatca (Figure 8 a, b). These values are typical of freshwaters with low mineralization, which is characteristic of the studied lakes, indicating that the water chemistry is consistent with a good ecological status.

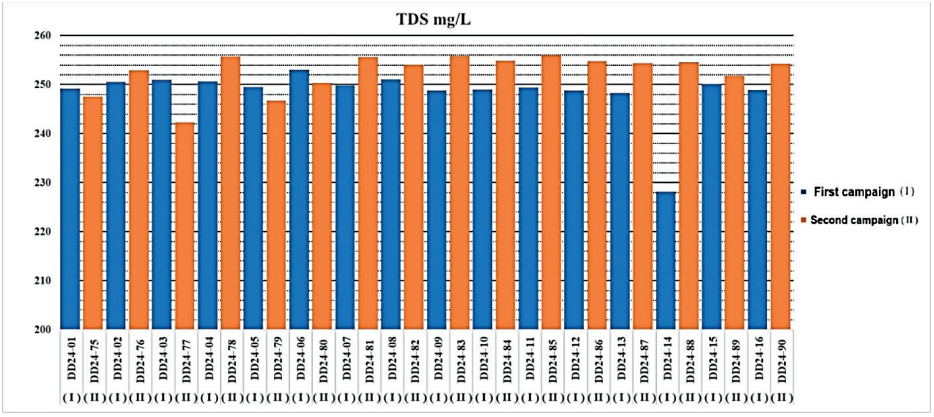
The dissolved oxygen regime (mg/l) ranged from quality class I - 9 mg/L to quality class IV - 4 mg/L (Order 161/2006). The dissolved oxygen

concentrations (measured in all evaluated water samples) were also below the value of 5 mg/L. A minimum concentration of 5 mg/L dissolved oxygen is recommended to adequately support aquatic life (www.niwa.co.nz). The range of values includes a relatively wide gap (4.67-14.13, average = 9.14) for Gorgova-Uzlina Complex and for Ceatal Izmail and Sf. Gheorghe, the values varied between 7.14 and 9.93, average = 8.54, so that the lowest value was found in station DD24-23 bis, Durnoliatca Lake, and the highest value was measured in station DD24-21 bis, Isacova Lake (Figure 9 a, b). These variations suggest that oxygen levels in water are influenced by a variety of factors, including water temperature, biological activity and hydrodynamic conditions.

The oxidation-reduction potential (ORP) (mV) places the tested water in a good condition. The values obtained for the tested water samples fall within the ORP range of natural waters (with values in the range -500 to + 700 mV) (Chapman, 1996; Sigg, 2000). The range of variation was included in both the positive and negative spectrum (-22.37-254.70; average = 75.25) for Gorgova-Uzlina Complex and for Ceatal Izmail and Sf. Gheorghe, the values varied between 49.93-107.14, average 84.00, so that the lowest value was found in station DD24-17 bis, Uzlina Lake, and the highest value was measured in station DD24-27 bis, Isaccel Lake (Figure 10 a, b). These results suggest that water quality is generally good and that the investigated lakes maintain a healthy balance of redox reactions.

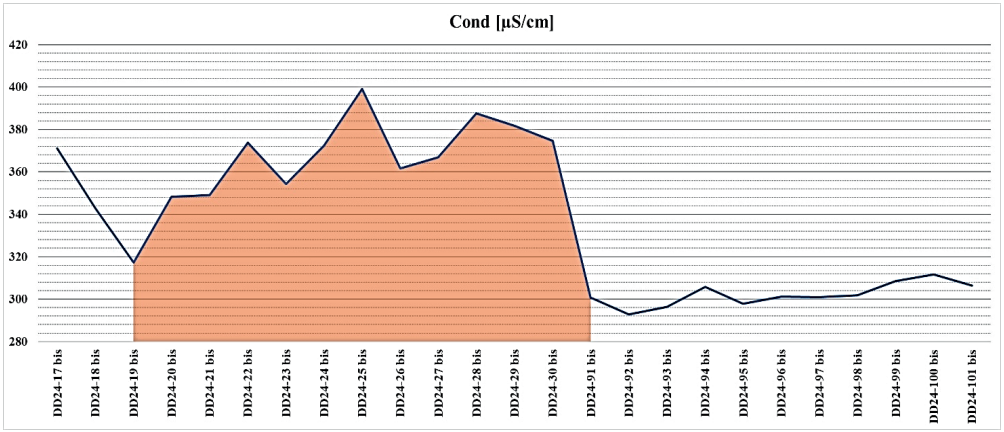


a

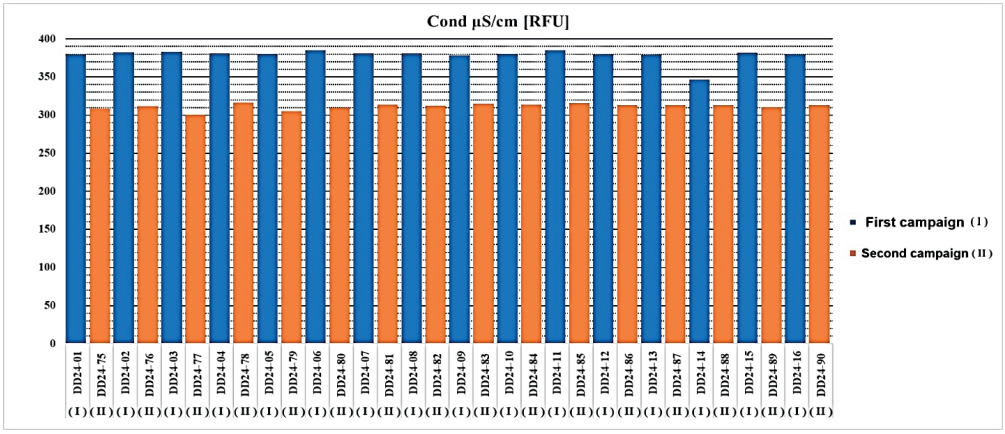


b

Figure 7 a) Evolution of the TDS mg/L indicator in the investigated surface water samples for Gorgova-Uzlina Complex; b) Evolution of the TDS mg/L indicator in the investigated surface water samples for Izmail and Sf. Gheorghe Confluences



a



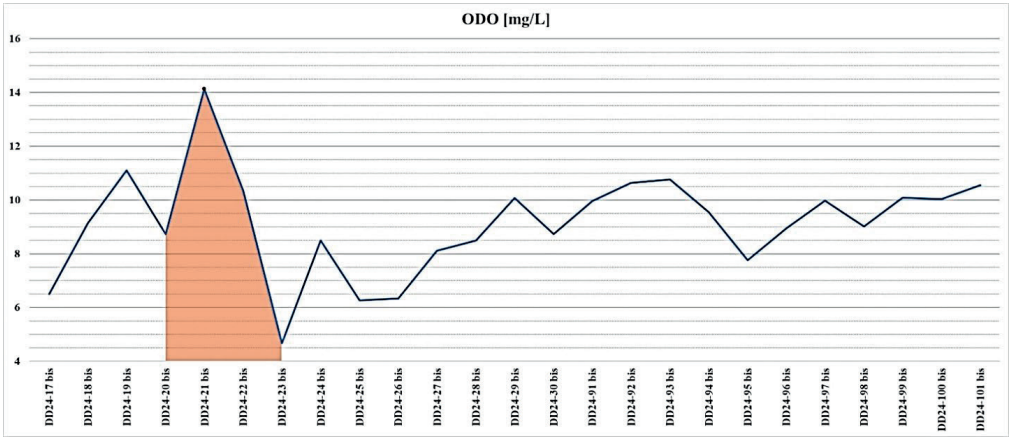
b

Figure 8 a) Evolution of the Cond µS/cm indicator in the investigated surface water samples for Gorgova-Uzlina Complex; b) Evolution of the Cond µS/cm indicator in the investigated surface water samples for Izmail and Sf. Gheorghe Confluences

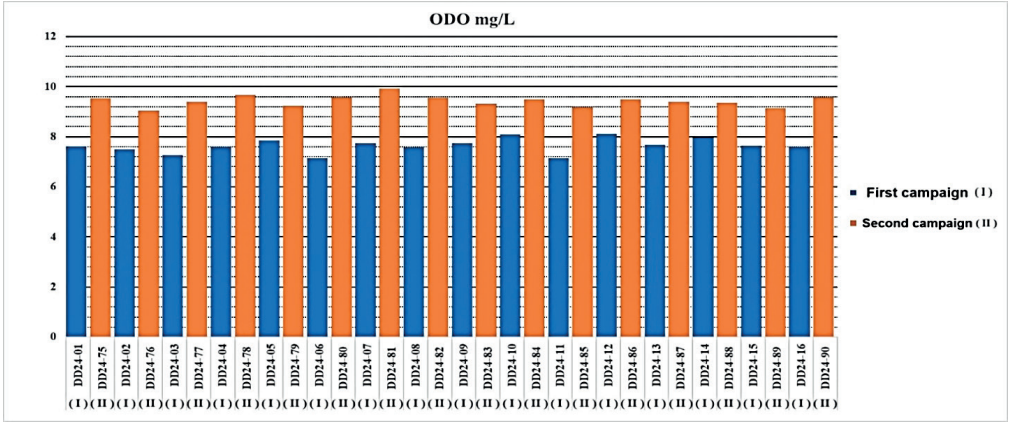
Salinity level (‰). The investigated water samples showed salinity values ranging between 0.16-0.20‰ (average = 0.19) for Gorgova-Uzlina Complex and for Ceatal Izmail and Sf. Gheorghe, the values varied between 0.17-0.19, average = 0.18. These values indicate fresh surface waters, with low salinity (salinity below 0.5‰) (Montagna et al., 2013) characteristic of the fluvial and lacustrine domain.

These low salinity values confirm that the lakes are characteristic of freshwater environments, typically found in fluvial and lacustrine settings, and are minimally influenced by marine waters.

Distribution of nitrate concentrations. Measurements made with the NitraLED sensor indicated significant variations in nitrate concentration (mg/L) at different sampling stations. The recorded values range from 0.10 mg/L to 10.46 mg/L, for Gorgova-Uzlina Complex and for Ceatal Izmail and Sf. Gheorghe, the values varied between 0.11-18.36, average = 5.78, suggesting notable differences in the chemical composition of the water depending on location (Figure 11 a, b).

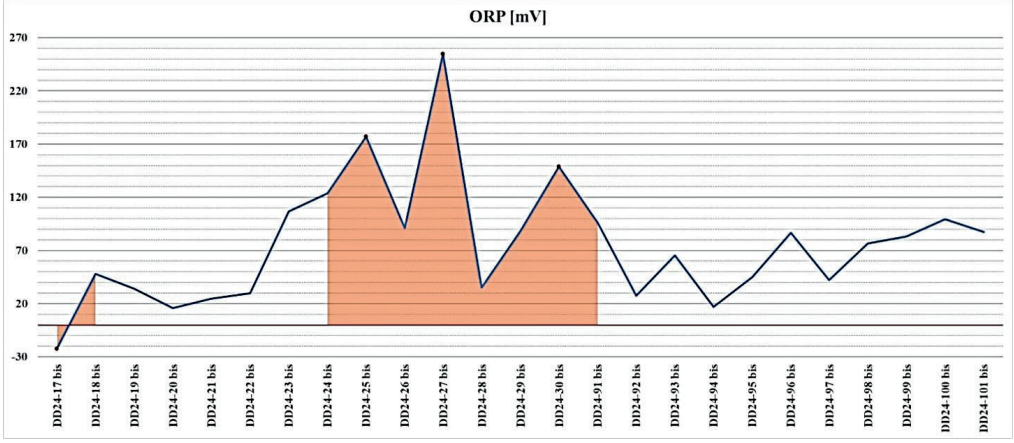


a

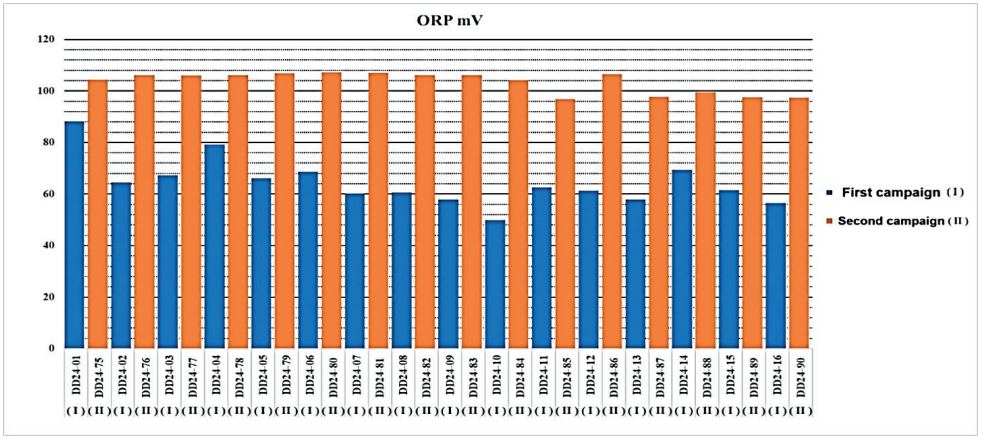


b

Figure 9 a) Evolution of the ODO mg/L indicator in the investigated surface water samples for Gorgova-Uzlina Complex; b) Evolution of the ODO mg/L indicator in the investigated surface water samples for Izmail and Sf. Gheorghe Confluences

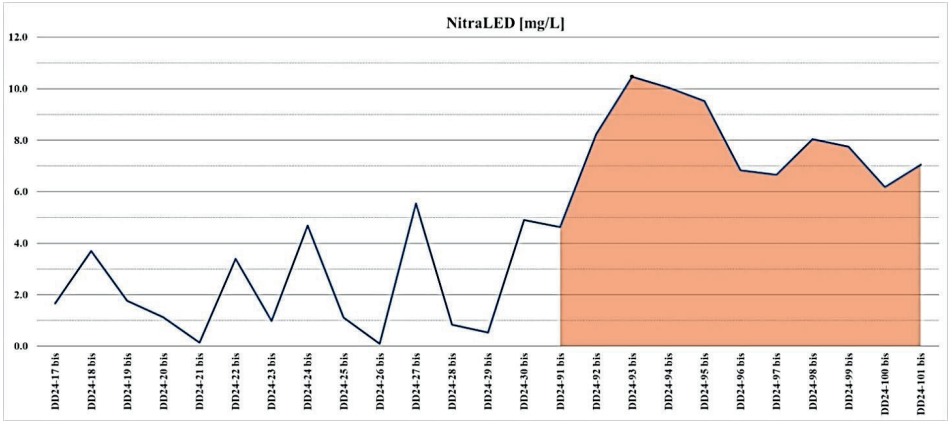


a

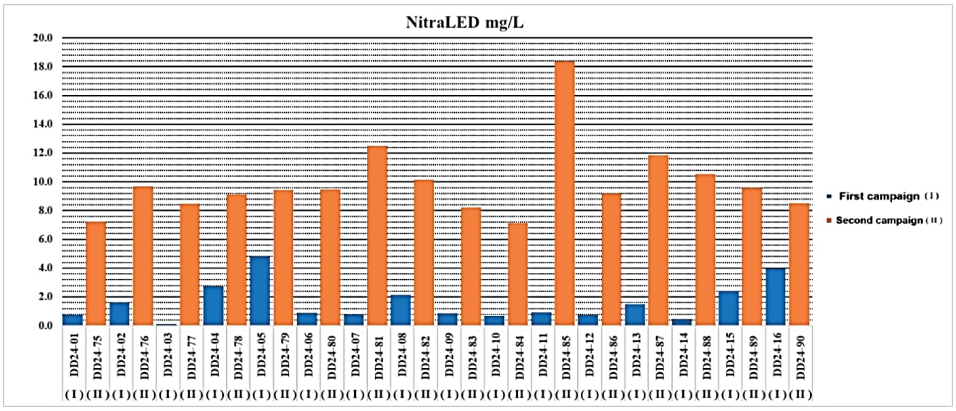


b

Figure 10 a) Evolution of the ORP mV indicator in the investigated surface water samples for Gorgova-Uzlina Complex; b) Evolution of the ORP mV indicator in the investigated surface water samples for Izmail and Sf. Gheorghe Confluences



a



b

Figure 11 a) Evolution of the NitraLED mg/L indicator in the investigated surface water samples for Gorgova-Uzlina Complex; b) Evolution of the NitraLED mg/L indicator in the investigated surface water samples for Izmail and Sf. Gheorghe Confluences

Grouping of stations by nitrate concentration

- *Low concentrations (≤1 mg/L)*

Stations such as DD24-03 – Ceatal Izmail (0.1108 mg/L), DD24-26 bis – Isaccel lake (0.095 mg/L) and DD24-21 bis – Isacova lake (0.144 mg/L) indicate very low nitrate presence. These values may reflect areas with low anthropogenic impact or geochemical conditions that limit nitrate accumulation.

- *Moderate concentrations (1 – 5 mg/L)*

This range includes most of the stations in the first sets of measurements (e.g. DD24-02, DD24-04, DD24-15) – Ceatal Izmail and Ceatal Sf. Gheorghe in September, and the stations (e.g. DD24-17 bis, DD24-19 bis, DD24-22 bis) – Uzlina and Isacova Lakes.

Moderate values may indicate a natural influence or a limited source of pollution.

- *High concentrations (>5 mg/L)*

The highest values occur at stations DD24-75, DD24-76, DD24-81, DD24-85 – Ceatal Izmail in October, with a maximum concentration of 18.362 mg/L.

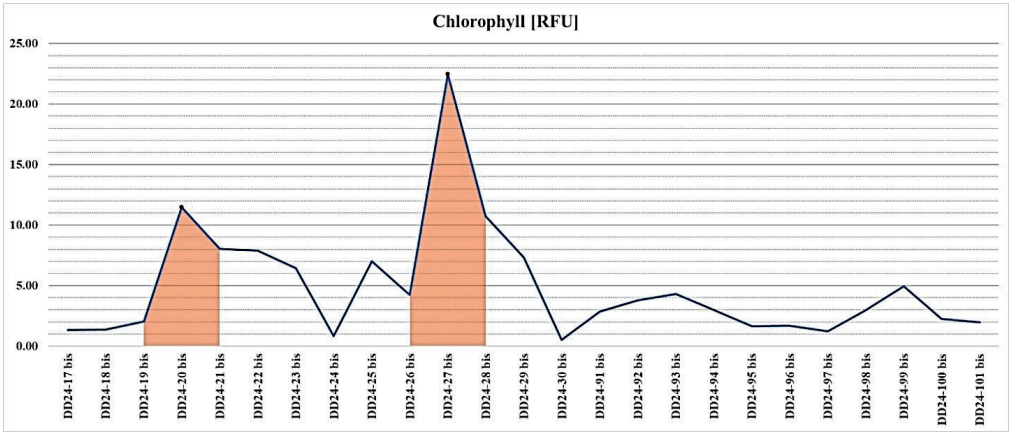
These concentrations are significantly higher and may indicate either a point source of contamination (e.g. anthropogenic activities, domestic effluents, agricultural inputs, industrial waste) or specific geological and hydrological factors, in the upstream urban section of the Danube River.

The concentration of chlorophyll a RFU concentration measured in the samples from the investigated lakes showed significant variability. Specifically, the values ranged broadly from 0.51 to 22.48 (mean = 4.89) in the Gorgova-Uzlina Complex and from 0.34 to 0.78 (mean = 0.52) in the Ceatal Izmail and Sf. Gheorghe areas. The lowest concentration was recorded at station DD24-81 (Ceatal Izmail), while the highest was observed at station DD24-27 bis (Isaccel Lake) (Figure 12 a, b).

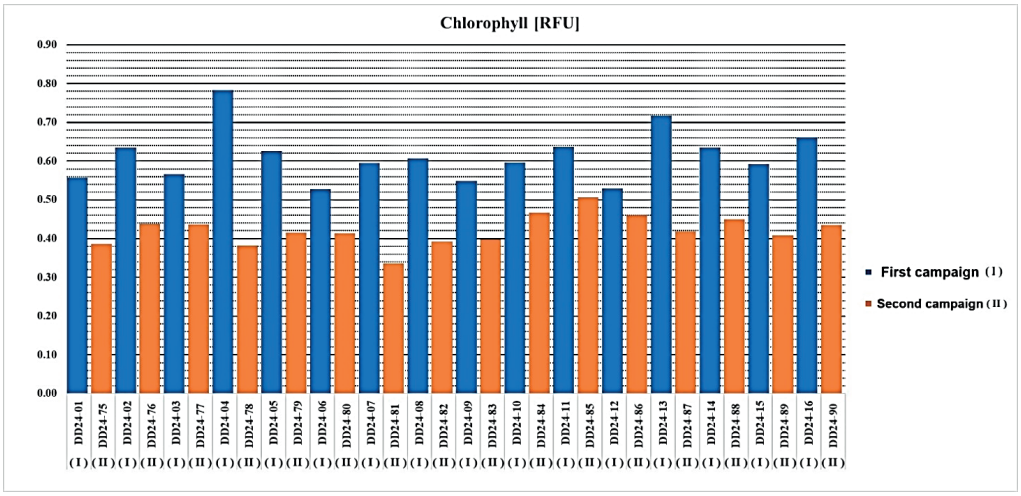
Several factors contribute to this variability:

- *Nutrient availability*: the main cause of variations in chlorophyll "a" concentration is the differences in nutrient availability (especially nitrogen and phosphorus) between lakes. High nutrient levels can stimulate algal growth, leading to increased chlorophyll concentrations.
- *Hydrological conditions*: Lakes differ in water renewal rates, connectivity to major channels, and water residence time. Lakes with slower water exchange rates or limited flushing often accumulate nutrients, promoting higher algal productivity.
- *Biological activity*: Differences in algal community composition and the presence or absence of macrophytes or other aquatic vegetation can significantly influence chlorophyll levels. Lakes with abundant aquatic vegetation may have lower chlorophyll concentrations due to competition for nutrients.
- *Anthropogenic influence*: Human activities, such as agricultural runoff, wastewater discharge, or fish farming operations, can lead to increased nutrient inputs, stimulating algal growth and chlorophyll concentration.
- *Physical factors*: Light availability, temperature variations and mixing conditions in lakes can also affect algal growth rates and therefore chlorophyll concentrations.

Most samples showed chlorophyll values below the threshold of 25 µg/l established for water quality class I (very good status) according to Order 161/2006, suggesting that the lakes generally have a good ecological status in terms of primary productivity. However, the wide range of chlorophyll values clearly indicates variability driven by the interaction between nutrient dynamics, hydrological conditions, biological communities, anthropogenic pressures and physical environmental factors.



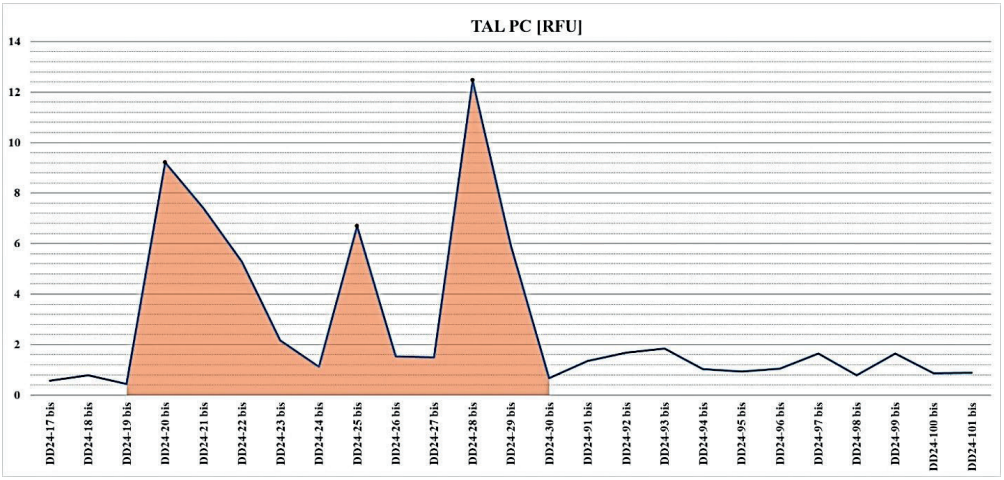
a



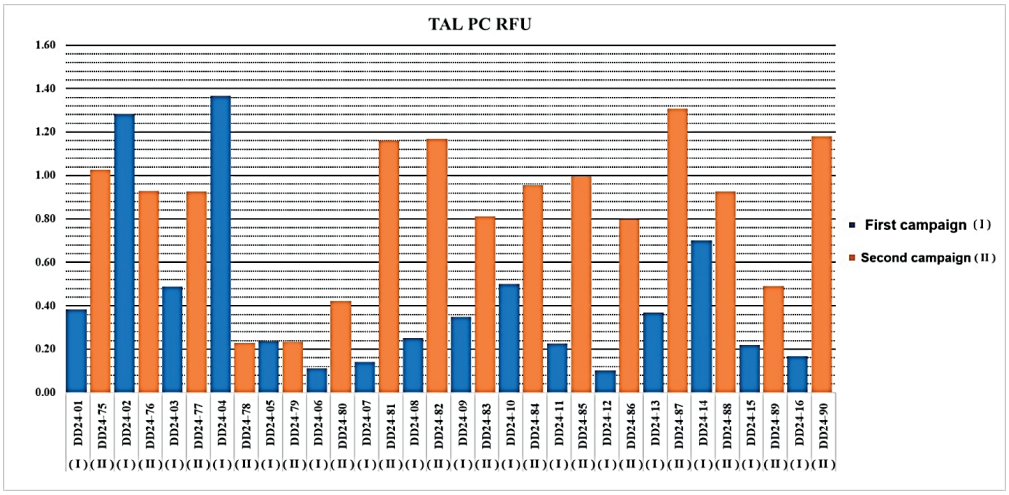
b

Figure 12 a) Evolution of the chlorophyll a RFU indicator in the investigated surface water samples for Gorgova-Uzlina Complex; b) Evolution of the chlorophyll a RFU indicator in the investigated surface water samples for Izmail and Sf. Gheorghe Confluences

Total Algal Content (TAL - PC RFU). The TAL PC values show significant variations between stations, ranging from a minimum of 0.44 µg/L to a maximum of 12.47 µg/L, average = 2.78, for Gorgova-Uzlina Complex and for Ceatal Izmail and Sf. Gheorghe, the values varied between 0.10-1.37, average = 0.64 (Figure 13, a b). The lowest concentration values (below 0.5 µg/L) occur at stations DD24-78, DD24-79 and DD24-80, indicating reduced contamination or better water quality conditions at these points. In contrast, the highest concentrations (above 1.5 µg/L) are observed at stations DD24-92 bis, DD24-93 bis, DD24-97 bis and DD24-99 bis, suggesting possible local sources of pollution or increased accumulation of the analysed compounds. Most values are around the range of 0.8-1.2 µg/L, indicating a moderate concentration, possibly reflecting a relatively balanced state of the waters at most of the investigated points. The distribution of the data may suggest differences in the intensity of anthropogenic or natural factors influencing each sampling point, reflecting specific local impacts.



a



b

Figure 13 a) Evolution of the Total Algal Content (TAL - PC RFU) indicator in the investigated surface water samples for Gorgova-Uzlina Complex; b) Evolution of the Total Algal Content (TAL - PC RFU) indicator in the investigated surface water samples for Izmail and Sf. Gheorghe Confluences

Based on Pearson correlation for all the samples, a strong positive correlation was found between (Table 3, Figure 14):

Strong positive correlations:

- ODO % sat and ODO mg/L (0.803): As expected, the percentage of dissolved oxygen saturation and its concentration measured in mg/L are strongly correlated. This is because both measure oxygen, but in different units, influenced by temperature and pressure.
- Salinity and TDS (0.937): Total dissolved solids (TDS) concentration is closely related to salinity, as dissolved salts contribute significantly to TDS.
- Conductivity and temperature (0.936): As temperature increases, the conductivity of water increases significantly, as ions in the water become more mobile.

Strong negative correlations:

- Temperature and TAL PC ug/L (-0.892): As temperature increases, the concentration of algal pigments decreases significantly, suggesting a decrease in phytoplankton biomass under warmer conditions.

- Temperature and NitraLED mg/L (-0.838): Higher temperatures are associated with lower nitrate levels, likely due to increased biological consumption in the ecosystem.
- Temperature and ODO mg/L (-0.498): While there is a negative relationship between temperature and dissolved oxygen, the correlation is moderate. In general, warmer water holds less oxygen.

Moderate correlations:

- pH and ODO % sat (0.811): higher pH is correlated with higher oxygen saturation, likely due to photosynthetic activity.
- pH and ORP (-0.420): There are a moderately negative relationship between pH and redox potential (ORP), suggesting that at higher pH, the environment becomes more reductive.
- TAL PC ug/L vs. NitraLED mg/L (0.748) → The number of algal pigments is correlated with the concentration of nitrates, suggesting that nitrates are an important source of nutrients for phytoplankton.

Weak correlations:

- Chlorophyll RFU and turbidity (0.191): The relationship between chlorophyll levels measured by fluorescence and turbidity is weak. Therefore, algae growth does not fully explain water turbidity.
- Chlorophyll ug/L and temperature (-0.676): Chlorophyll measured as actual concentration is negatively influenced by temperature, but to a moderate to strong extent.

Table 3. Proximity matrix (Pearson correlation coef.)

	Chlorophyll RFU	Chlorophyll ug/L	Cond µS/cm	ODO % sat	ODO mg/L	ORP mV	Sal psu	TAL PC RFU	TAL PC ug/L	TDS mg/L	Turbidity FNU	pH	Temp °C	NitraLED mg/L
Chlorophyll RFU	**1.000**	0.040	0.172	0.170	0.060	0.244	0.159	0.637	-0.162	0.091	0.191	0.052	0.129	-0.217
Chlorophyll ug/L	0.040	**1.000**	-0.622	-0.027	0.399	-0.099	0.433	-0.083	0.754	0.284	-0.164	0.181	-0.676	0.426
Cond µS/cm	0.172	-0.622	**1.000**	-0.036	-0.589	-0.072	-0.234	0.203	-0.843	-0.004	0.043	-0.273	0.936	-0.787
ODO % sat	0.170	-0.027	-0.036	**1.000**	0.803	-0.249	-0.366	0.314	-0.054	-0.410	-0.001	0.811	0.114	-0.091
ODO mg/L	0.060	0.399	-0.589	0.803	**1.000**	-0.101	0.011	0.183	0.499	-0.141	0.004	0.765	-0.498	0.419
ORP mV	0.244	-0.099	-0.072	-0.249	-0.101	**1.000**	0.421	-0.147	0.064	0.369	-0.085	-0.420	-0.200	0.276
Sal psu	0.159	0.433	-0.234	-0.366	0.011	0.421	**1.000**	0.192	0.468	0.937	0.208	-0.328	-0.547	0.435
TAL PC RFU	0.637	-0.083	0.203	0.314	0.183	-0.147	0.192	**1.000**	-0.148	0.179	0.525	0.214	0.127	-0.262
TAL PC ug/L	-0.162	0.754	-0.843	-0.054	0.499	0.064	0.468	-0.148	**1.000**	0.297	-0.057	0.182	-0.892	0.748
TDS mg/L	0.091	0.284	-0.004	-0.410	-0.141	0.369	0.937	0.179	0.297	**1.000**	0.182	-0.426	-0.354	0.283
Turbidity FNU	0.191	-0.164	0.043	-0.001	0.004	-0.085	0.208	0.525	-0.057	0.182	**1.000**	-0.099	-0.024	0.123
pH	0.052	0.181	-0.273	0.811	0.765	-0.420	-0.328	0.214	0.182	-0.426	-0.099	**1.000**	-0.103	0.073
Temp °C	0.129	-0.676	0.936	0.114	-0.498	-0.200	-0.547	0.127	-0.892	-0.354	-0.024	-0.103	**1.000**	-0.838
NitraLED mg/L	-0.217	0.426	-0.787	-0.091	0.419	0.276	0.435	-0.262	0.748	0.283	0.123	0.073	-0.838	**1.000**

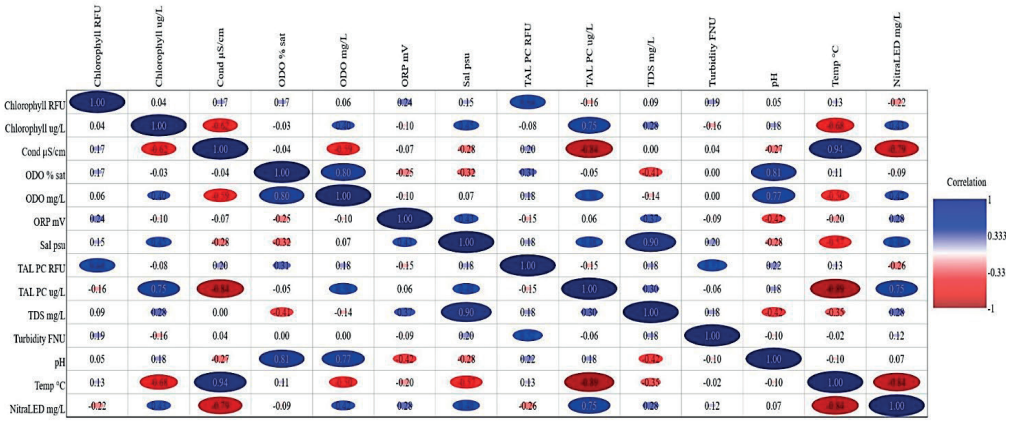


Figure 14. Pearson correlation

The physico-chemical parameters measured in this study varied within ranges compatible with natural seasonal fluctuations and environmental standards. Water temperature closely followed air temperature trends, reflecting typical autumn conditions. pH values consistently indicated optimal conditions for aquatic life, demonstrating stability in the ecosystem. Turbidity levels showed a wide range, with some stations showing high values, probably influenced by sediment inputs from the Danube River. Electrical conductivity and total dissolved solids (TDS) values demonstrated typical freshwater conditions with low mineralization, indicating minimal impacts of external pollution. Similarly, low salinity values confirmed the predominantly freshwater nature of the lakes.

Dissolved oxygen levels showed significant variability, with some sites recording concentrations below the recommended minimum of 5 mg/L, potentially influenced by biological activity and hydrodynamic conditions. Oxidation-reduction potential (ORP) values fell within natural limits, indicating healthy redox conditions in the water bodies. Nitrate concentrations varied significantly, highlighting areas with potential anthropogenic impact. Chlorophyll "a" concentration generally indicated very good ecological conditions, although some sites displayed higher values, suggesting localized variations in nutrient availability and primary productivity. In addition, the total algal content (TAL - PC RFU) reflects variations in primary productivity and algal biomass between sampling points, highlighting potential eutrophication patterns. The observed variability in TAL PC values could thus be related to differences in nutrient availability, water circulation or local anthropogenic inputs influencing algal growth.

The results obtained in this study on the physicochemical parameters of the Danube Delta waters closely align with the findings of previous research conducted in the same region and in similar environments. Studies focused on areas such as the Gorgova-Uzlina Depression, the Somova-Parches area and the Matita-Merhei Complex have similarly reported good overall ecosystem conditions (Botnariuc, 1985). Furthermore, the measured values are consistent with those documented in other recent water quality assessments for the Sfântu Gheorghe and Chilia branches (Sener et al., 2016; Oz et al., 2019; Teodorof et al., 2021) and the predeltaic area near Galați (Iticescu et al., 2014). Collectively, these studies suggest a medium-term stability of the hydrochemical characteristics in the Danube Delta region (Karabulut et al., 2014).

Pearson correlation analysis revealed strong relationships between parameters such as dissolved oxygen and oxygen saturation, salinity and TDS, as well as conductivity and temperature. These correlations indicate interdependencies between physicochemical factors and underline the importance of integrated monitoring approaches for managing the ecological health of the Danube Delta.

CONCLUSIONS

To determine the water quality status of the studied areas of the Izmail and Sf. Gheorghe Rivers and the Danube Delta, several physicochemical parameters were evaluated, including temperature, pH, turbidity, total dissolved solids (TDS), conductivity, dissolved oxygen, oxygen saturation, oxidation-reduction potential (ORP), salinity, nitrate concentration, chlorophyll and total algae content (RFU-PC). The measurements and interpretations followed the established reference standards and methods.

• *Water quality in the investigated ecosystems of the confluence areas and lakes of the Gorgova Uzlina Lake Complex*.

According to the analysed parameters, most of the water samples from the studied lakes and canals fell predominantly into quality classes I and II according to Order 161/2006, indicating a generally good ecological status. However, localized variations were identified, reflecting specific environmental conditions or pressures.

• *Ecological vulnerabilities and anthropogenic pressures*

Ecosystems remain vulnerable to fluvial inputs of organic and inorganic substances, influencing turbidity and dissolved substance concentrations. Elevated turbidity values recorded in certain locations, such as Lake Isaccel, highlight potential negative impacts on aquatic organisms and overall water quality, requiring continuous monitoring.

• *Physico-chemical water parameters*

Temperature (°C): the values recorded were characteristic of the autumn season, showing minimal variability and remaining within natural limits.

pH (pH units): most samples indicated values within the normal range (6.5–8.5), suggesting a chemically stable aquatic environment.

Turbidity (FNU): localised increased turbidity was observed, indicating variations due to sediment influx or anthropogenic impact, which may negatively affect aquatic life.

Total Dissolved Solids (TDS) (mg/L): values were consistent with freshwater systems, reflecting limited dissolved salt content.

Conductivity (µS/cm): all measurements are aligned with quality class I, confirming the minimal presence of dissolved salts and indicating low contamination.

Dissolved Oxygen (ODO mg/L) and Oxygen Saturation (ODO%): although generally reflecting good ecological status, certain locations (e.g. Durnoliatca Lake) showed lower dissolved oxygen values (below 5 mg/L), posing risks to aquatic biota.

Oxidation-Reduction Potential (ORP, mV): ORP values indicate favourable oxidative conditions in most locations, leading to a balanced ecological environment.

Salinity (PSU): the recorded values affirmed the freshwater nature of the studied aquatic environments, with no significant saline influence.

Nitrate (NitraLED mg/L): concentrations were within acceptable limits, with no significant indication of nutrient pollution in the studied areas.

Chlorophyll (RFU): Chlorophyll values remained generally low, suggesting minimal risks of eutrophication and reduction of algal biomass.

Total Algal Content (TAL-PC RFU): significant variations were identified between stations, reflecting differences in nutrient availability or localized anthropogenic influences affecting algal biomass.

• *Risk factors and recommendations*

Sediment and organic matter inputs from the Danube significantly influence water quality. Continuous monitoring is essential to detect and mitigate potential deterioration, especially in areas with high turbidity and low dissolved oxygen levels.

Future monitoring efforts should correlate physicochemical data with meteorological and hydrological conditions of the Danube – Danube Delta lakes, improving the understanding of seasonal and anthropogenic impacts on these sensitive ecosystems.

ACKNOWLEDGEMENTS

The authors thank to Cioroiu Catalin for helping to improve the paper. The research leading to their results was financed by the Ministry of Research and Innovation - “Program Nucleu” - PN 23.30.03.04, PN 23.30.03.02, PN 23.30.03.01 and HORIZON-MISS-2021-OCEAN-02-02, DANUBE4all - Restoration of the Danube River Basin Waters for Ecosystem and People from Mountains to Coast.

REFERENCES

AccuWeather (2024). Tulcea Weather Forecast. Retrieved March 10, 2025, from https://www.accuweather.com/ro/ro/tulcea/

Addinsoft. (2020). XLSTAT Statistical and Data Analysis Solution; Addinsoft: New York, NY, USA, Available online: https://www.xlstat.com.

Almazov, A.A., Bondar, C., Diaconu, C., Ghederim, V., Mihailov, A.N., Mita, P., Nichiforov, I.D., Rai, I.A., Rodionov, N.A., Stanescu, S., Stanescu, V., Vaghin, N.F. (1963). *Zona de vărsare a Dunării. Monografie hidrologică*. pp. 396, Ed. Tehnică, Bucureşti. [in Romanian]

Antipa, Gr. (1937). *Les Bonifications Biologiques des Deltas, Ciesm*. Raport Et Proces-Verbaux Des Reunions, 10 Paris, pp. 99-120.

Bondar, C., Panin, N. (2000). The Danube Delta Hydrologic Database and Modeling. *Geo-Eco-Marina*, 5-6, 5-53

Botnariuc, N. (1985). *Fluxul de energie din ghiolurile Puiu, Roşu, Porcu şi potenţialul lor bioproductiv*. St. Com. Ecol. Delta Dunării, 1, Tulcea, 9-14; [in Romanian].

Bucse, A., Vasiliu, D., Balan, S., Parvulescu, O.C, Dobre T. (2020). Heavy Metalspatial Distribution and Pollution Assessment in the Surface Sediments of the North-Western Black Sea Shelf. *Revista de Chim*ie, *71*(4), 155-170.

Calmuc, V. A., Calmuc, M., Arseni, M., Topa, C. M., Timofti, M., Burada, A., Iticescu, C., & Georgescu, L. P. (2021a). Assessment of heavy metal pollution levels in sediments and of ecological risk by quality indices, applying a case study: The Lower Danube River,Romania. *Water, 13*(13), 1801.

Calmuc, V. A., Calmuc, M., Arseni, M., Topa, C. M., Timofti, M., Burada, A., Iticescu, C., & Georgescu, L. P. (2021b). Assessment of Heavy Metal Pollution Levels in Sediments and of Ecological Risk by Quality Indices, Applying a Case Study: The Lower Danube River, Romania. *Water, 13*(13), 1801. https://doi.org/10.3390/w13131801

Chapter 10 Nutrients—Nitrogen and phosphorus from Volunteer Estuary Monitoring Manual, a Methods Manual, Second Edition, EPA-842-B-06-003. 2006. Available online: http://wwwepagov/owow/estuaries/monitor (accessed on 10 january 2025)

Cazacu, C., Adamescu, M.C. (2017). *Ecosystem services provided by the bio-physical structure of natural capital in the Danube Delta Biosphere Reserve Romania*. Conference Volume of 6th Symposium for Research in Protected Areas, 2 to 3 November 2017, Salzburg, 97-102.

Călmuc, M., Călmuc, V. A., Dragu, M. D., Rosu, A., Munteanu, D., Rosu, B., & Murariu, G. (2018). Comparative study of descriptive statistics on physico-chemical parameters describing water quality. Case study-the Danube River in the Galati area. Annals of the University Dunarea de Jos of Galati: Fascicle II, *Mathematics, Physics, Theoretical Mechanics*, 41.

Chapman, D. (1996). *Water quality assessments. a guide to use of biota, sediments and water in environmental monitoring* - Second Edition, Published on behalf of UNESCO, WHO, UNEP. E /FNSPON. London. Great Britain, University Press, Cambridge, 626

Chiriac, E. & Udrescu, M. (1965). *Ghidul naturalistului în lumea apelor dulci*, Editura Științifică București. [in Romanian]

Coteț, P., (1960). *Evoluția morfohidrografică Deltei Dunării (O sinteză a studiilor existente și o nouă interpretare*), Probl. De Geogr., Vol. VII, Ed. Acad. R.P.România, București. [in Romanian].

De Zuane, J. (1997). *Handbook of Drinking Water Quality* (2nd ed.), John Wiley and Sons, 592 p., ISBN 0-471-28789-X.

Driga, B.V., (2004). *Delta Dunării – Sistemul De Circulație Apei*, Editura Casa Cărții De Știință, Cluj Napoca, pp. 256 [in Romanian].

Dutu, F., Tiron Dutu, L., Catianis, I. (2023). Dramatic reduction of the water and sediment fluxes in a human modified meandering ecosystem from the Danube Delta, Romania. *Scientific Papers-Series E-Land Reclamation Earth Observation & Surveying Environmental Engineering, 12*, 267-274, ISSN 2285-6064, Online ISSN 2393-5138.

Frîncu, R.-M. (2021). Long-term trends in water quality indices in the Lower Danube and tributaries in Romania (1996–2017). *International Journal of Environmental Research and Public Health, 18*(4), 1665. https://doi.org/10.3390/ijerph18041665

Gâștescu, P. & Știucă, R. (2008). *The Danube Delta - A biosphere reserve.* CD Press Publishing House, Bucharest, 400. [in Romanian, with Contents and Introduction in English]

Gâștescu, P. (2009). The Danube Delta biosphere reserve. Geography, biodiversity, protection, management. *Rev. Roum. Géogr., 53*(2), 139–52

Habersack, H., Hein, T., Stanica, A., Liska, I., Mair, R., Jager, E., Hauer, C., Bradley, C. (2016). Challenges of river basin management: Current status of, and prospects for, the Riber Danube from a river engeneering perspective. *Science of the Total Environnement, 543*, 828-845.

Isvoranu, V. (1979). Raport de cercetare: Sinteza Roșu – Puiu – Porcu (1976-1979). [in Romanian].

Iticescu, C., Georgescu, L. P., Popa, C., & Murariu, G. (2014). Water pollution monitoring the Danube water quality near the Galati city. *Journal of Environmental Protection and Ecology, 15*(1), 30–38.

József, T., Kiss, S. R., Muzslay, F., Máté, O., Stromájer, G. P., & Stromájer-Rácz, T. (2023). Detection and quantification of pharmaceutical residues in the Pest County section of the River Danube. *Water, 15*(10), 1755. https://doi.org/10.3390/w15101755

Kachroud, M., Trolard, F., Kefi, M., Jebari, S., & Bourrié, G. (2019). Water quality indices: Challenges and application limits in the literature. *Water, 11*(2), 361. https://doi.org/10.3390/w11020361

Kanownik, W., Policht-Latawiec, A., & Fudała, W. (2019). Nutrient pollutants in surface water—Assessing trends in drinking water resource quality for a regional city in Central Europe. *Sustainability, 11*(7), 1988. https://doi.org/10.3390/su11071988

Karabulut, A., Bouraoui, F., Grizetti, B., Bidoglio, G., & Pistochi, A. (2014). Managing nitrogen and phosphorus loads to water bodies: Characterisation and solutions. In *Towards macro-regional integrated nutrient management* (Report EUR 26822 EN, pp. 1–73). Joint Research Centre, JRC-Ispra; Publications Office of the European Union. https://doi.org/10.2788/17023

Kirschner, A. K., Schachner-Groehs, I., Kavka, G., Hoedl, E., Kovacs, A., & Farnleitner, A. H. (2024). Long-term impact of basin-wide wastewater management on faecal pollution levels along the entire Danube River. *Environmental Science and Pollution Research, 31*, 45697–45710. https://doi.org/10.1007/s11356-023-30478-

Lehr, J. H., Gass, T. E., Pettyjohn, W. A., DeMarre, J. (1980). *Domestic Water Treatment*, New York, NY: McGraw-Hill Book Company, pp. 264.

Montagna, P., Palmer, P., Pollack, J. (2013). Hydrological Changes and Estuarine Dynamics. Springer briefs in Environmental Science Volume 8. 94 pp. DOI: DOI 10.1007/978-1-4614-5833-3, © The Author(s) 2013. https://www.springer.com/life+sciences/ecology/book/978-1-4614-5832-6

Najamuddin, Tri Prartono, Harpasis S., Sanusi, I., Wayan Nurjaya. (2016). Seasonal distribution and geochemical fractionation of heavy metals from surface sediment in a tropical estuary of Jeneberang River, Indonesia. *Marine Pollution Bulletin, 111*, 1, 456-462.

NIWA. (n.d.). Dissolved oxygen thresholds for aquatic ecosystems. Retrieved [January 2025], from https://www.niwa.co.nz.

Oaie, Gh., Secrieru, D., Bondar, C., Szobotka, S., Duțu, L., Stănescu, I., Opreanu, G., Duțu, F., Pojar, I., Manta, T. (2015). Lower Danube River:

characterization of sediments and pollutants. *Geo-Eco-Marina, 21*, 19-34.

Order no. 161/2006. (2006). Normative concerning the classification of surface water quality to establish the ecological status of water bodies (Romanian Order MEWM no. 161/2006), Annex C-Elements and physico-chemical quality standards in water, published in Romanian Official Monitor, part I, no. 511 bis, from 13th of June 2006

Oz, N., Topal, B., & Uzun, H. (2019). Prediction of water quality in Riva River watershed. *Ecological Chemistry and Engineering S, 26*(4), 727–742. https://doi.org/10.1515/eces-2019-0051

Panin, N. & Jipa, D. (2002). Danube River Sediment Input and its Interaction with the North-western Black Sea. Estuarine, Coastal and Shelf Science, 54, 2, 551-562.

Panin, N. (2003). The Danube Delta. Geomorphology and Holocene evolution: a Synthesis. *Geomorphologie: relief, processus, environnement, 4*, 247-262.

Paun, I., Chiriac, F. L., Marin, N. M., Cruceru, L. V., Pascu, L. F., Lehr, C. B., & Ene, C. (2017). Water quality index, a useful tool for evaluation of Danube River raw water. *Revista de Chimie, 68*(8), 1732–1739.

Poonam, T., Tanushree, B., & Sukalyan, C. (2013). Water quality indices - Important tools for water quality assessment: A review. *International Journal of Advanced Chemistry, 1*(1), 15–28.

Romanescu, Gh. (2013). Alluvial transport processes and the impact of Anthropogenic intervention on the Romanian littoral of the Danube Delta. *Ocean & Coastal Management, 73*, 31-43.

Sener, S., Sener, E., & Davraz, A. (2017). Evaluation of water quality using water quality index (WQI) method and GIS in Aksu River (SW-Turkey). *Science of the Total Environment, 584–585*, 131–144. https://doi.org/10.1016/j.scitotenv.2017.01.102

Sigg, L. (2000). Redox Potential Measurements in Natural Waters: Significance, Concepts and Problems, 1-12, In: Schüring, J., Schulz, H.D., Fischer, W.R., Böttcher, J., Duijnisveld, W.H.M. (eds) Redox. Springer, Berlin, Heidelberg, Germany, https://doi.org/10.1007/978-3-662-04080-5_1

SR EN ISO 10523:2012, Water quality. Determination of pH. [January 2025], from [https://magazin.asro.ro/ro/standard/248767].

SR EN ISO 5667-1:2023, Water quality. Sampling. Part 1: Guidance on the establishment of sampling programmes and techniques. [January 2025], from [https://magazin.asro.ro/ro/standard/248767].

SR EN ISO 5814:2013, Water quality. Determination of dissolved oxygen content. Electrochemical method with probe. [January 2025], from [https://magazin.asro.ro/ro/standard/248767].

SR ISO 5667-5:2017, Water quality. Sampling. Part 5: Guidance for the sampling of drinking water from treatment plants and distribution networks Retrieved [January 2025], from [https://magazin.asro.ro/ro/standard/248767].

Statistical analysis app for Windows, https://past.en.lo4d.com/download

Teaca, A., Muresan, M., Menabit, S., Bucse, A., Begun, T. (2020). Assessment of romanian circalittoral soft bottom benthic habitats under Danube River influence. *Regional Studies in Marine Science, 40*, 1-15.

Tiron Duţu, L., Duţu, F., Secrieru, D., Opreanu, G. (2019). Sediments grain size and geo-chemical interpretation of three successive cutoff meanders of the Danube Delta, Romania. *Geochemistry, 79*, 399-407.

Teodorof, L., Ene, A., Burada, A., Despina, C., Seceleanu-Odor, D., Trifanov, C., Ibram, O., Bratfanof, E., Tudor, M.-I., Tudor, M., Cernisencu, I., Georgescu, L. P., & Iticescu, C. (2021). Integrated assessment of surface water quality in Danube River Chilia Branch. *Applied Sciences, 11*(19), 9172. https://doi.org/10.3390/app11199172

Tiron Duţu, L., Provansal, M., Le Coz, J., Duţu, F. (2014). Contrasted sediment processes and morphological adjustments in three successive cutoff meanders of the Danube Delta. *Geomorphology, 204*, 154-164.

Wu, W., Zheng, H., Xu, S., Yang, J., Liu, W. (2013). Trace element geochemistry of riverbed and suspended sediments in the upper Yangtze River. *Journal of geochemical exploration, 124*, 67-78.

Zhang, G., Bai, J., Xiao, R., Zhao, Q., Jia, J., Cui, B., Liu, X. (2017). Heavy metal fractions and ecological risk assessment in sediments from urban, rural and reclamation-affected rivers of the Pearl River estuary, China. *Chemosphere, 184*, 278-288.

Scientific Papers. Series E. Land Reclamation, Earth Observation & Surveying, Environmental Engineering. Vol. XIV, 2025
Print ISSN 2285-6064, CD-ROM ISSN 2285-6072, Online ISSN 2393-5138, ISSN-L 2285-6064

ASSESSMENT OF SURFACE WATER QUALITY ACROSS SELECTED DANUBE RIVER SECTORS BASED ON PHYSICO-CHEMICAL PARAMETERS AND HYDROCARBON LEVELS

Ana Bianca PAVEL, Andrei TOMA, Albert SCRIECIU, Catalina GAVRILA, Irina CATIANIS

National Institute for Research and Development on Marine Geology and Geoecology – GeoEcoMar, 23-25 Dimitrie Onciul Street, 024053, District 2, Bucharest, Romania

Corresponding author email: biancapavel@geoecomar.ro

Abstract

This study evaluated the surface water quality of selected Danube River sectors (km 549-990) in the RO13 Cazane-Călărași area using direct field measurements. A multiparameter EXO 2 probe (YSI, USA) was used to analyze key physico-chemical parameters, while hydrocarbon concentrations (Oil in Water and HC micro-g/L) were assessed using PAH probes. Results indicate that most water quality parameters remain within environmental standards, classifying the waters as either "Very Good" or "Good." Temperature (15.03-24.40°C) and pH (7.92-8.36) remained stable, while dissolved oxygen levels (7.01-9.43 mg/L) and chlorophyll concentrations (0.27–1.49 RFU) suggested low risk of eutrophication. Conductivity (262.53-411.56 µS/cm), TDS (207.56-280.80 mg/L), and salinity (0.15-0.21 psu) confirmed freshwater conditions. Turbidity values (2.44-28.75 FNU) and oxidation-reduction potential (-26.59 to 238.79 mV) indicated relatively stable conditions. Hydrocarbon levels (0.03-1.46 mg/L) were within acceptable environmental limits, though localized variations suggested potential pollution sources. These findings emphasize the need for long-term monitoring and transboundary collaboration to address localized pollution concerns and ensure sustainable water management in the Danube Basin.

Key words*: Danube River, surface water quality, hydrocarbon pollution, ecosystem monitoring, environmental assessment.*

INTRODUCTION

The Danube, the second longest river in Europe, crosses ten countries and plays a key role in the economy, biodiversity and hydrological dynamics of the region (Banu, 1967; Panin, 2003). The lower Danube, between Drobeta-Turnu Severin and the Black Sea, is characterized by a complex hydrographic network, fed by tributaries such as the Siret, Olt, Prut and Jiu. In this area, hydromorphological diversity determines significant variations in the flow regime, sediment transport and distribution of aquatic habitats (Călinescu & Iana, 1967; Bușniță et al., 1970; Cioboiu & Brezeanu, 2017; Nike et al., 2022). Assessing water quality in this sector is essential for monitoring the impact of anthropogenic pressures and climate change on the river ecosystem (Calmuc et al., 2020; Radu et al., 2022). The main threats to water quality include pollution with nutrients, hazardous substances, hydromorphological changes and organic pollution (Gasparotti, 2014). These problems are aggravated by industrial, agricultural and urban activities in the Danube basin, which influence the physico-chemical parameters of the water and, implicitly, the ecological status of the river (Rico et al., 2016).
This research aims to answer the question: How do natural and anthropogenic factors influence water quality in the Lower Danube? To address this, the study assesses spatial and temporal variations in key physicochemical water parameters, including temperature, pH, dissolved oxygen (DO), chlorophyll, turbidity, salinity, total dissolved solids (TDS), oxidation-reduction potential (ORP), and hydrocarbon contamination.
By identifying potential pollution sources and assessing deviations from reference standards, this research provides insights into both natural variability and human-induced impacts on Danube water quality. The findings contribute to ongoing monitoring efforts and serve as a reference for future water management and conservation strategies in the region.

Relevance and impact of the study

By analyzing water quality and hydromorphological pressures in detail, this research contributes to sustainable management strategies and the implementation of the Water Framework Directive (WFD). The results will support the development of effective measures to reduce pollution, protect aquatic biodiversity and improve navigation, providing a solid scientific basis for conservation policies and sustainable use of Danube River resources.

According to Annex XI of the Water Framework Directive (WFD), the Danube is classified within the Pontic Ecoregion. Based on the hydromorphological and physico-chemical characteristics outlined in the River Basin Management Plans, 19 distinct natural river types have been identified for the Danube and its delta. These classifications play a crucial role in assessing water quality, monitoring ecosystem health, and guiding conservation strategies.

MATERIALS AND METHODS

Study sectors

The selection and delimitation of key monitoring sectors in the Lower Danube were based on hydromorphological characteristics and anthropogenic pressures.

The primary investigated sectors included Calnovat (km 604-616; D2_24_01 - D2_24_39), Corabia (km 626-631), Bechet (km 674-678; D2_24_40 - D2_24_54), Pisculet Desa (km 760-631; D2_24_26_; D2_24_72), and Bogdan Seclan (km 781-786; D2_24_73 - D2_24_90). These locations were chosen based on their hydromorphological diversity and potential exposure to anthropogenic influences.

In addition to these core sectors, supplementary sampling points were distributed in key areas to capture a comprehensive picture of spatial variations in water quality. These included sites downstream (km 594) and upstream (km 599) of Zimnicea, upstream of the Iskar River (km 638), as well as both downstream (km 689) and upstream (km 696) of the Jiu River. Further sampling was carried out upstream of Kozloduy (km 705 and 407), at the Lom River, upstream of Vidin/downstream of Calafat (km 794), upstream of Calafat (km 798) and near the Timok River, both downstream (km 844) and upstream (km 847). Additional sites were surveyed around the Iron Gates II Dam (km 860-878), a critical hydropower infrastructure that influences the hydrodynamics of the Danube.

Further upstream, monitoring was conducted at strategic locations, including downstream (km 882) and upstream (km 885) of Brza Palanka, downstream (km 925) and upstream (km 934) of Drobeta-Turnu Severin, and several locations in the Orșova region. These included downstream (km 951), Orșova Bay (km 954), and upstream of Orșova (km 954). Additional sites were examined in Eșelnița (km 963), downstream (km 968) and upstream (km 971) of Dubova, as well as downstream (km 986) and upstream (km 990) of the Poreka River.

These study sites are part of the RO13 Danube – Cazane - Călărași sector, ensuring a comprehensive assessment of hydromorphological conditions, pollution sources and ecosystem health in the lower Danube (Figure 1).

Methodology for analyzing physico-chemical parameters of water

The assessment of surface water quality in selected Danube sectors was conducted through in situ measurements of key physico-chemical parameters across 201 monitoring stations.

Field analyses were performed using the EXO 2 multiparameter probe (YSI - USA) (Figure 2), which utilizes physical, optical, and electrochemical detection methods to collect water quality data through a variety of sensors.

Measured parameters: Temperature (°C), pH (pH units), Turbidity (FNU), Total Dissolved Solids (TDS) (mg/L), Conductivity (µS/cm), Dissolved Oxygen (ODO mg/L), Oxygen Saturation (ODO%), Oxidation-Reduction Potential (ORP, mV), Salinity (PSU), Nitrate (NitraLED mg/L), Chlorophyll (RFU), Total Algal Content (TAL) - PC RFU.

Additionally, Polycyclic Aromatic Hydrocarbon (PAH) levels were monitored using PAH probes (microFlu oil sensors) for real-time hydrocarbon detection in water (Figure 2).

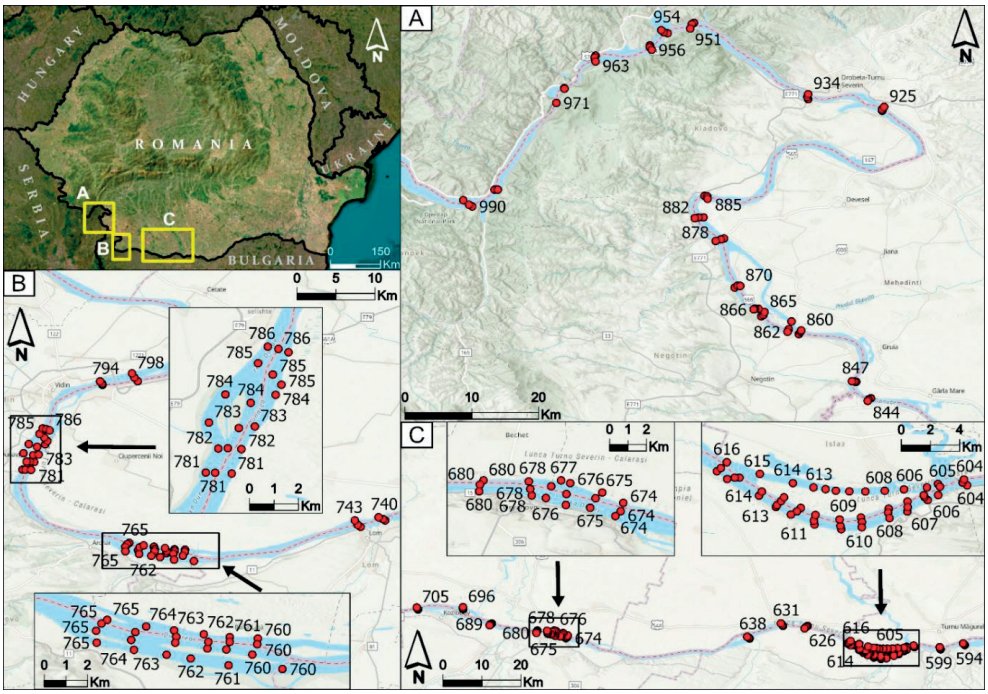


Figure 1. Sampling stations on the Danube River

The water quality assessment was carried out mainly based on the classification provided for in Order 161/2006, which defines five quality classes:

- Class I – Very good;
- Class II – Good;
- Class III – Moderate;
- Class IV – Poor;
- Class V – Bad.

For comprehensive analysis, both national and international standards regulating water quality were taken into account. The EU Water Framework Directive (WFD, 2000/60/EC) requires qualitative and quantitative management of water resources, with the objective of maintaining healthy aquatic ecosystems and achieving "good status" of water quality. In this regard, the assessment of surface water quality was carried out in accordance with the Romanian National Environmental Standards, in particular Regulation no. 161/2006 (on the approval of reference objectives for the classification of surface water quality, Official Gazette of Romania, Part I, no. 511 bis). This regulation establishes the criteria for the classification of surface waters and the assessment of ecological status, using environmental parameters such as total dissolved solids (TDS) and turbidity (ISO 5667-5:2017).

The physicochemical determinations were carried out in accordance with applicable international standards, including SR ISO 5667/2007 (General Guide for the Establishment of Sampling Programs and Techniques), SR EN ISO 10523:2012 for the determination of pH and SR ISO 5814:1984 for the measurement of dissolved oxygen (DO). The data obtained for the physicochemical parameters of water at the sampling points are presented in Table 1, highlighting the minimum, maximum and average values (± standard deviation) for each parameter.

Methodology for hydrodynamic measurements (velocities, currents, and water discharges)

Hydrodynamic measurements, including current velocity, flow rate and direction, are essential for understanding the distribution and transport of pollutants in the aquatic environment. They influence both chemical dispersion and oxygenation and sedimentation processes,

having a direct impact on water quality (Kern et al., 2014; Teodorof et al., 2015; Iticescu et al., 2016; Catianis et al., 2024).
To determine the hydrodynamic parameters, a high-precision system based on the Doppler effect was used - Acoustic Doppler Current Profiler (ADCP), model River Ray 600 kHz, produced by Teledyne RD Instruments. The measurements were carried out exclusively in the sectors Calnovat, Corabia, Bechet, Pisculet Desa and Bogdan Seclan (Figure 2).

Statistical analysis
All statistical analyses were performed using xlSTAT 7.5.2 software (Addinsoft, 2020) and Past 4 (https://past.en.lo4d.com/download). Correlation between parameters were analysed using the Pearson correlation.



Figure 2. Multiparameter probe, model EX02 and the PAH probes, microFlu from Aquams and ADCP River Ray 600 kHz

RESULTS AND DISCUSSIONS

Water is a central element in the integration of various environmental concerns and strategies, playing an essential role in multiple human activities, such as agriculture, economy, transport, energy, industry and environmental protection (Podlasek et al., 2024). It is a determining factor in development, being indispensable both for maintaining the balance of aquatic ecosystems and for human health and well-being, ensuring fundamental needs such as food, hygiene, comfort and health (Gasparotti, 2014). Water quality is significantly influenced by industrial and agricultural activities, energy production and domestic activities (Banaduc et al., 2016). In the context of climate change, a resilient and integrated approach to water resources management is required (Poff et al., 2002; Capon et al., 2013).

Water quality parameters analysis
The values of the physicochemical parameters generally varied within the limits established by environmental standards (Table 1).
Rapid and persistent increases in global temperatures are expected in the coming decades (Diop et al., 2018). Global warming does not only affect the atmosphere, but also significantly influences aquatic environments (Hannesson, 2007). This phenomenon has led to an increase in the global average temperature of between 1.8 and 4.0°C, changes in climatic and hydrodynamic patterns, and rising sea levels (Madeira et al., 2016; Simionov et al. 2020).
Water temperature is closely linked to seasonal air temperature variations, particularly in autumn (https://www.accuweather.com). The recorded values ranged from 15.03°C to 24.40°C (mean 18.55°C), aligning with natural seasonal fluctuations. The lowest temperature was measured at km 968 (left bank), while the highest was recorded at km 631 (center). These variations can influence biological activity, affecting metabolic rates of aquatic organisms and oxygen solubility (Figure 3).
Water pH (pH units). The measured pH values ranged from 7.92 to 8.36 (mean 8.10), staying within the expected range for freshwater systems (6.5-8.5). These stable conditions indicate no significant acidification or alkalization events. The lowest pH was observed

at km 860 center, while the highest was recorded at km 605 right bank. The slight alkalinity corresponds to the buffering capacity of the Danube, primarily influenced by the carbonate-bicarbonate balance (Figure 4).

Turbidity (NTU). The turbidity values measured in the investigated water samples exhibited variations within the normal range for surface waters (1-1000 NTU) (Chapman, 1996). Turbidity ranged from 2.44 to 28.75 FNU, with a mean of 11.02 FNU, the highest value recorded at km 762 right bank, and the lowest at km 611 bis left bank. Although turbidity fluctuated widely, several values exceeded the 10 NTU limit specified in ISO 5667-5:2017. Increased turbidity at km 762 right bank was likely caused by sediment resuspension or an increased particle load from the upstream fluvial inlet. In contrast, the lowest turbidity recorded at km 611 Bis left bank may be attributed to reduced sediment influx or localized settling processes that contributed to water clarification. Overall, turbidity variations were primarily influenced by the Danube's fluvial input, which transports water and sediments loaded with dissolved and suspended organic/inorganic substances (Figure 5).

The *TDS concentration (*representing total dissolved organic and inorganic substances) indicates that the tested water is in good condition, with values consistent with freshwater standards (0-1000 mg/L TDS) (Lehr, 1980; De Zuane, 1997). The TDS concentration ranged from 207.56 to 280.80 mg/L, with a mean of 249.47 mg/L, the lowest value recorded at km 762 Bis right bank, and the highest at km 740 (right bank). These values suggest limited influence of dissolved salts or pollutants from upstream sources (Figure 6).

The *electrical conductivity* values ranged from 262.53 to 411.56 µS/cm, with a mean of 337.56 µS/cm (Figure 7). Electrical conductivity and TDS values confirm the freshwater characteristics of the investigated sectors, with no significant deviations that would indicate excessive mineralization or contamination.

Table 1. Synopsis of physico-chemical parameters in surface water samples

Parameter	Min.	Max.	Mean ± SD
Temperature (°C)	15.03	24.40	18.55 ± 2.65
pH	7.92	8.36	8.10 ± 0.07
Turbidity (FNU)	2.44	28.75	11.02 ± 4.72
Total Dissolved Solids (TDS mg/L)	207.56	280.80	249.47 ± 19.02
Conductivity (µS/cm)	262.53	411.56	337.56±41.75
Dissolved Oxygen (ODO mg/L)	7.01	9.43	8.06 ± 0.55
Oxygen Saturation (ODO % sat)	78.94	94.91	85.93 ± 3.09
Oxidation-Reduction Potential (ORP mV)	-26.59	238.79	122.69 ± 59.28
Salinity (PSU)	0.15	0.21	0.18 ± 0.01
Nitrate (NitraLED mg/L)	2.67	101.82	12.80 ± 12.71
Chlorophyll (RFU)	0.27	1.49	0.48 ± 0.16
Total Algal Content (TAL - PC RFU)	0.01	1.91	0.69 ± 0.41
Total Flow Rate (m^3/s)	1368.31	7750.719	6196.83 ± 1339.17

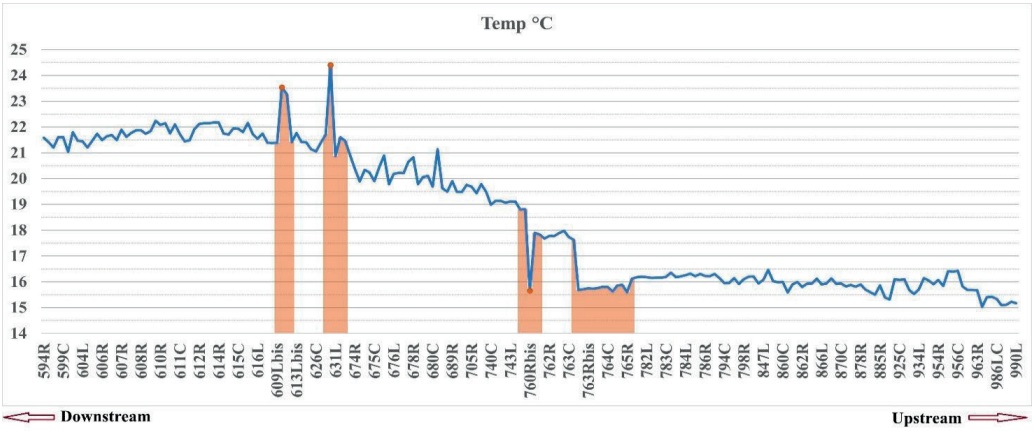


Figure 3. Evolution of the Temperature (°C) indicator in investigated surface water samples

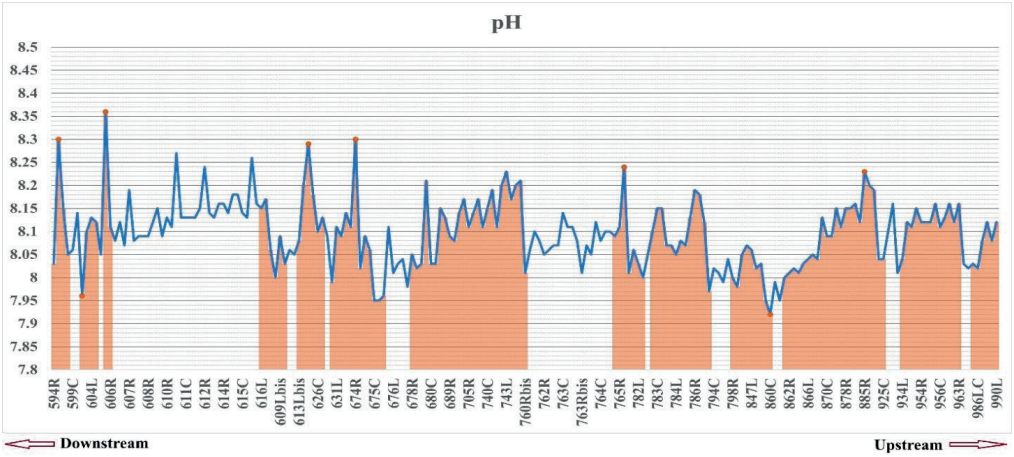


Figure 4. Evolution of the pH indicator in the investigated surface water samples

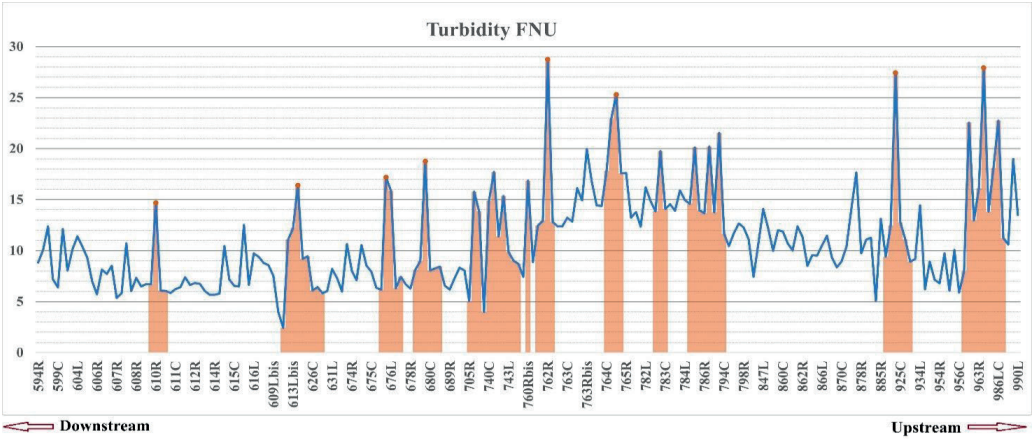


Figure 5. Evolution of the Turbidity (FNU) indicator in the investigated surface water samples

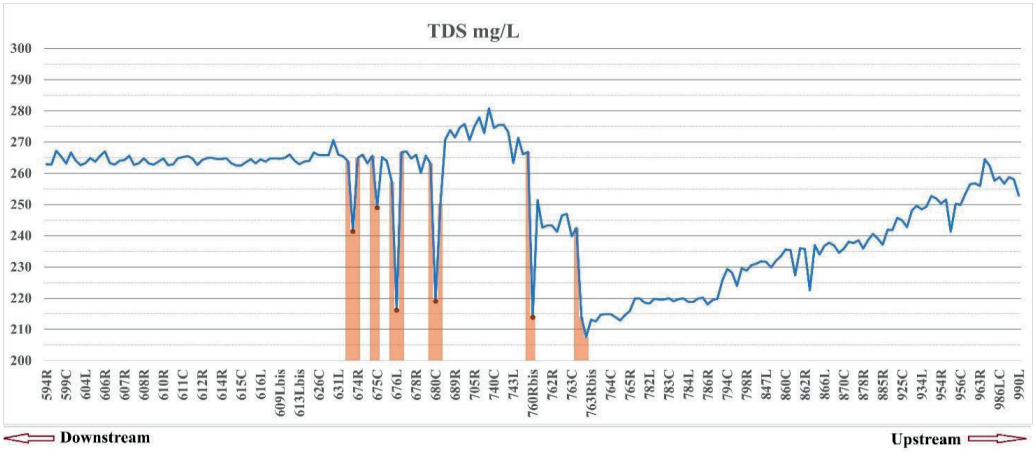


Figure 6. Evolution of the TDS (mg/L) indicator in the surface water samples investigated

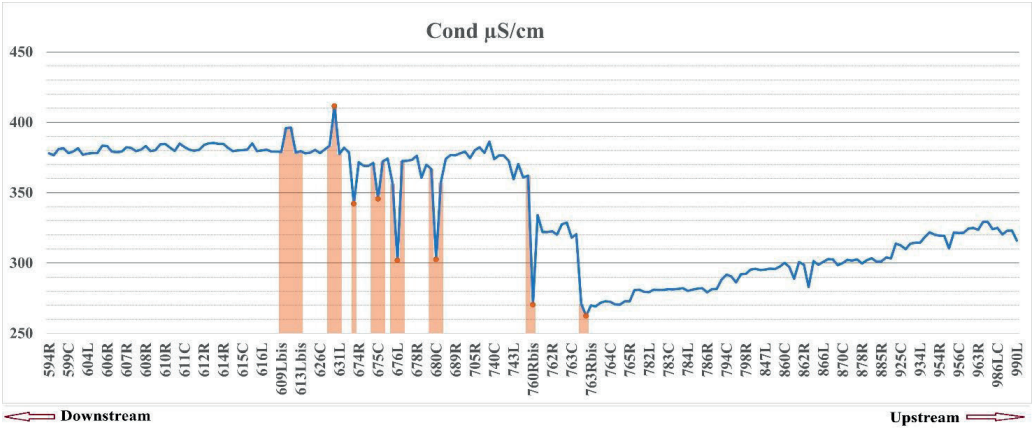


Figure 7. Evolution of the Conductivity (µS/cm) indicator in the investigated surface water samples

The dissolved oxygen regime (mg/l). The dissolved oxygen (DO) concentrations confirmed that the investigated waters belong to the well-oxygenated surface water category (quality class I, ≥9 mg/L), as defined by Order 161/2006. All measured values were above the 5 mg/L threshold, which is the minimum recommended concentration to support aquatic life (www.niwa.co.nz). Measured DO concentrations ranged from 7.01 to 9.43 mg/L, with an average of 8.06 mg/L. The lowest concentration was recorded at km 610 Bis left bank, while the highest was observed at km 762 Bis right bank. Oxygen saturation levels ranged from 78.94% to 94.91%, confirming good aeration and the absence of significant hypoxic conditions (Figure 8). These findings highlight stable oxygen levels, ensuring adequate conditions for aquatic ecosystems.

The *oxidation-reduction potential* (ORP) values indicate that the tested water is in good condition, falling within the typical range for natural waters (-500 to +700 mV) (Chapman, 1996; Sigg, 2000). The oxidation-reduction potential (ORP) ranged from -26.59 to 238.79 mV, with a mean of 122.69 mV, the lowest value recorded at km 674 center, and the highest at km 763 center. The presence of both positive and negative values suggests dynamic redox conditions influenced by organic matter decomposition, microbial activity, and oxygen availability. These variations reflect localized environmental factors that regulate oxidation-

reduction processes in the Danube's aquatic system (Figure 9).

Salinity values (0.15-0.21 PSU, mean 0.18) confirm the freshwater nature of the Danube, in agreement with previous studies. Low salinity levels reflect limited seawater intrusion or evaporative concentration effects. These values indicate fresh surface waters, with low salinity (salinity below 0.5‰), (Montagna et al., 2013) characteristic of the fluvial and lacustrine domain.

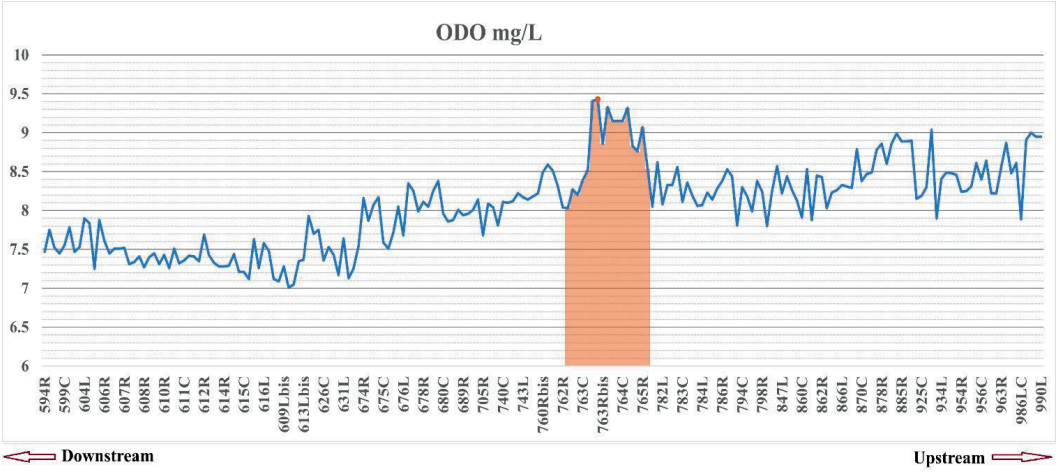


Figure 8. Evolution of the ODO (mg/L) indicator in the investigated surface water samples

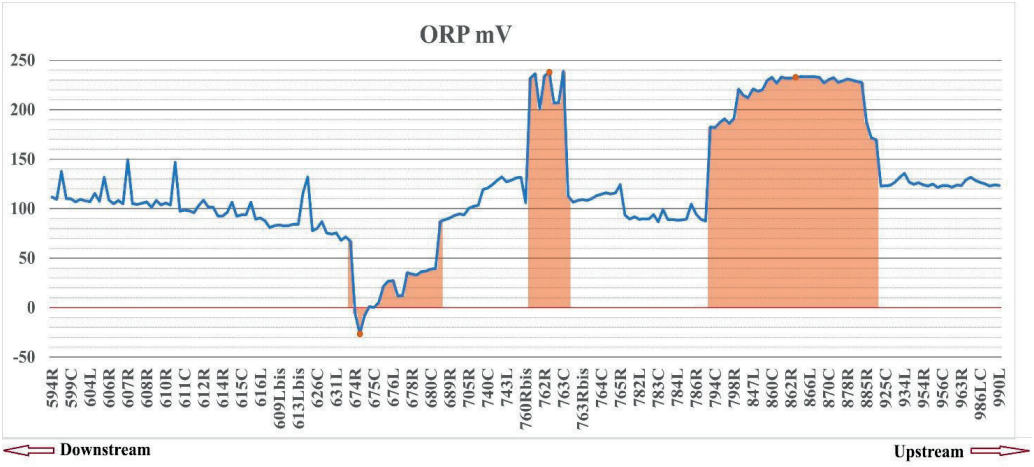


Figure 9. Evolution of the ORP (mV) indicator in the investigated surface water samples

The *NitraLED (mg/L)* values indicate significant variations in nitrate concentrations at different measurement points. The Nitrate concentrations (mg/L) ranged from 2.67 to 101.82 mg/L, with a mean of 12.80 mg/L. The highest value recorded was 101.82 mg/L at km 956 right bank, followed by 92.56 mg/L at km 925 central and 80.45 mg/L at km 677 right bank. These levels are significantly higher than the rest of the measurements and may indicate local sources of nitrate pollution. Other significantly elevated values include 74.19 mg/L (km 866 left bank), 53.69 mg/L (km 608 left bank), and 52.73 mg/L (km 638 central).

Most measurements range between 10 and 20 mg/L, which is relatively common for surface waters affected by anthropogenic activities. For example, at km 594, concentrations are relatively constant between 14.8 and 15.54 mg/L, suggesting a stable source of nitrates in this area. The lowest concentrations are found in the range of 4 to 7 mg/L, such as km 844 central (4.29 mg/L), km 798 right bank (4.07 mg/L) and km 794 central (4.32 mg/L). These values may indicate areas less affected by agricultural activities or industrial discharges (Figure 10).

High nitrate levels may be associated with agricultural discharges (fertilizers), wastewater or natural sources (organic remineralization).

Sudden increases in certain locations (e.g. km 956 md) suggest localized contamination.

Chlorophyll RFU values ranged from 0.27 to 1.49 (mean 0.48), remaining well below the 25 µg/L threshold for quality class I, which indicates low phytoplankton biomass and minimal risk of eutrophication. The lowest value was recorded at km 762 left bis. The highest value was observed at km 638 (left bank). These results suggest stable trophic conditions, with no significant algal blooms detected, supporting a balanced aquatic ecosystem (Figure 11).

Total Algal Content (TAL - PC RFU) values ranged from 0.01 to 1.91 (mean 0.69). High values (RFU > 1.0) were recorded in the Calnovat areas (km 604-616): km 609 center (1.46), km 609 right bank (1.33); Corabia (km 631 left bank): 1.58 (strong local input from the grain port); Bogdan Seclan (km 781-786): km 783 center (1.91); Drobeta Turnu-Severin (km 925-934): km 934 left bank (1.39), km 935 center (1.37); Orșova and surroundings (km 951-954): km 951 center (1.37), km 954 left bank (1.54); Iron Gates II area (km 860-878): km 878 center (1.5); Eșelnița–Dubova: km 971 center (1.1) (Figure 12). These values suggest intense anthropogenic influences, particularly related to port, industrial, urban and tourist activities.

Medium values (RFU between 0.3 and 1.0) were recorded in the areas such as Zimnicea (km 594): 0.58 (moderate urban impact); Bechet (km 674-678): 0.13-0.55 (low to moderate impact); Pisculet Desa (km 760 center): 0.97 (significant local variation, local moderate influences);

Bogdan Seclan (km 781-786): most values between 0.3 and 0.9, reflecting local moderate to high impact. Instead, low values (RFU < 0.3) were recorded at Zimnicea (km 599 upstream): 0.08-0.13 (low anthropogenic influence); Corabia (km 626-631 centru/right bank): 0.01-0.06 (clean, uncontaminated areas); Pisculet Desa (km 760 left bank): 0.1 (minimal local impact). These values indicate relatively clean areas, with little or no anthropogenic impact.

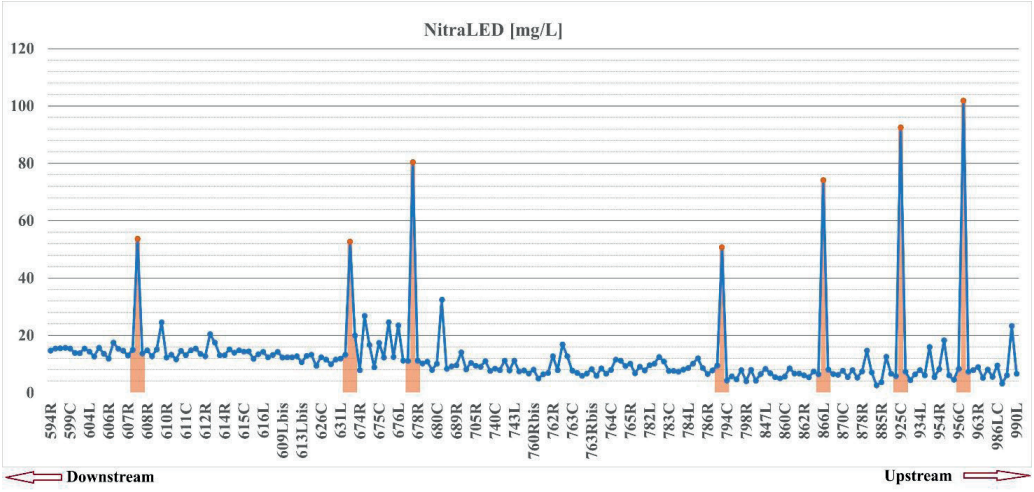


Figure 10. Evolution of the NitraLED (mg/L) indicator in the investigated surface water samples

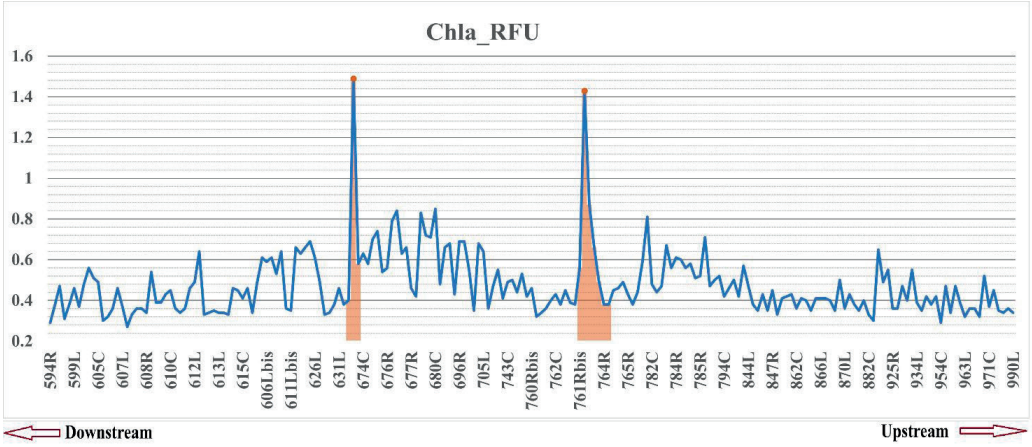


Figure 11. Evolution of the Chlorophyll RFU indicator in the investigated surface water samples

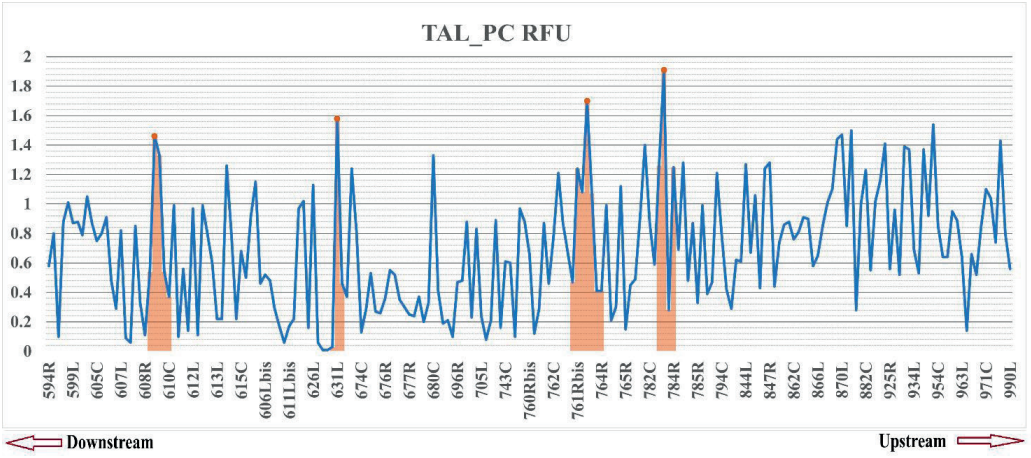


Figure 12. Evolution of the TAL_PC RFU indicator in the investigated surface water samples

Hydrocarbon contamination levels remained relatively low, with oil-in-water concentrations ranging from 0.03 to 1.46 mg/L (mean 0.44 mg/L) and hydrocarbon (HC) concentrations between 0.89 and 48.70 µg/L (mean 14.74 µg/L). The highest hydrocarbon levels were detected at km 675 (right bank) in the Bechet Sector, suggesting possible localized sources of pollution. However, despite these findings, overall concentrations remained below critical thresholds for significant environmental risk, indicating no immediate threat to water quality (Table 2, Figures 13 and 14).

Table 2. Hydrocarbon concentrations of water surface samples

Parameter	Oil in Water (mg/L)	Hydrocarbons (HC) (µg/L)	Custom#3 (mg/L)
Minimum	0.03	0.89	0.41
Maximum	1.46	48.70	48.70
Mean ± SD	0.44 ± 0.17	14.74 ± 5.67	14.27 ± 6.14

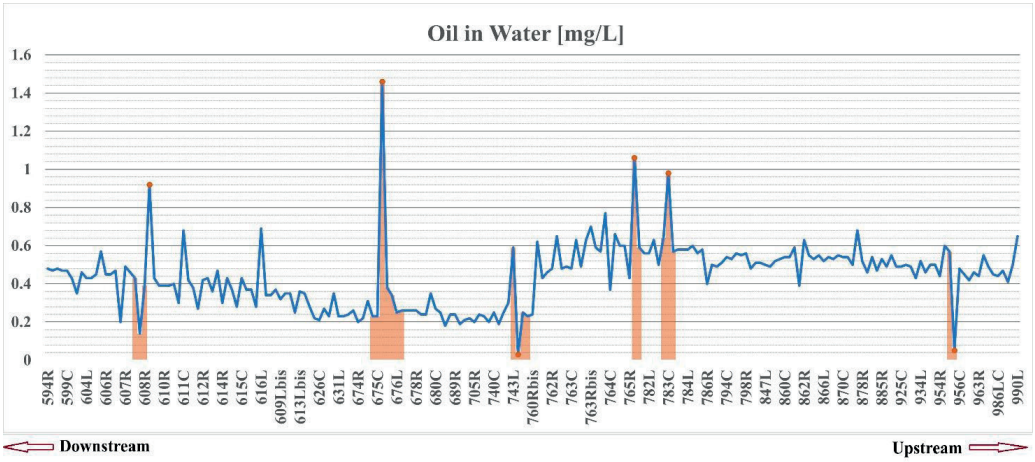


Figure 13. Evolution of the Oil in water (mg/l) indicator in the investigated surface water samples

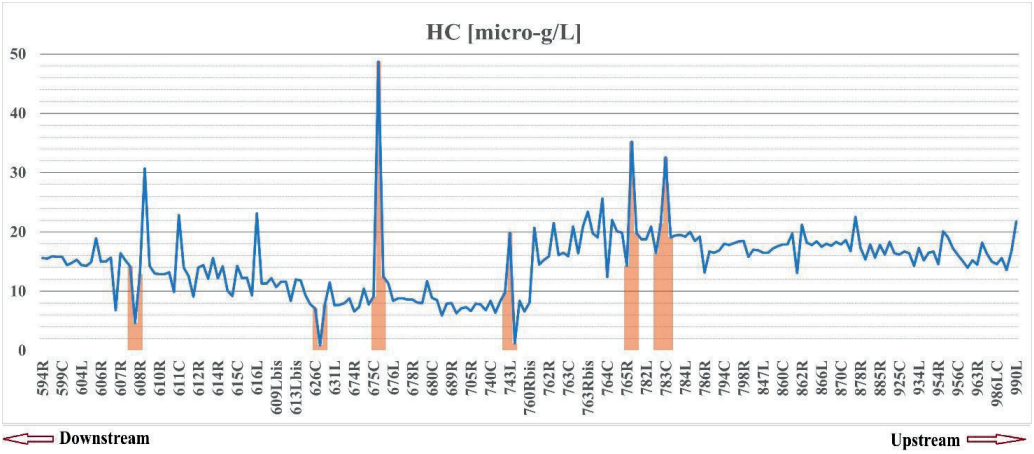


Figure 14. Evolution of the HC (micro-g/l) indicator in the investigated surface water samples

The values of the monitored physicochemical parameters were generally within the limits allowed by environmental standards, reflecting a good state of water quality in the analyzed sectors of the Danube (Pavlović et al., 2016; Calmuc et al., 2018; Radu et al., 2022).

The *water temperature* varied between 15.03°C (km 968, left bank) and 24.40°C (km 631, center), with an overall average of 18.55°C, reflecting natural seasonal influences specific to autumn. These variations can influence biological activity, metabolism of aquatic organisms and solubility of dissolved oxygen in water.

pH values ranging from 7.92 (km 860 center) to 8.36 (km 605 right bank), with an average of 8.10, indicate a slightly alkaline state of the water, characteristic of aquatic systems with high buffer capacity, due to the carbonate-bicarbonate balance present in the Danube River. No significant acidification or alkalization events were identified.

Water turbidity showed significant variations, with values between 2.44 FNU (Km 610, left bank, Calnovăț sector) and 28.75 FNU (km 762 right bank Pisculet-Desa Sector), with an average of 11.02 FNU. Values exceeding the standard limit of 10 NTU (ISO 5667-5:2017) indicate increased local sediment input or intense resuspension processes, especially at km 762 right bank, while low turbidity (km 610 left bank) reflects areas with increased

sedimentation or reduced suspended sediment flux.

TDS concentration values ranged between 207.56 mg/L (km 762 right bank) and 280.80 mg/L (km 740, right bank), with an average of 249.47 mg/L. These values reflect a moderate influence of dissolved salts, indicating good quality water, without significant contamination from upstream.

The *water conductivity* had values between 262.53 µS/cm and 411.56 µS/cm (km 631 center), with an average of 337.56 µS/cm. The higher conductivity in the km 631 - Upstream Corabia/Downstream River Isker, area suggests local influences, possibly geological or anthropogenic, but generally confirms the typical characteristics of freshwaters, with moderate mineralization.

Dissolved oxygen concentration ranged from 7.01 mg/L (km 610 bis left bank) to 9.43 mg/L (km 762 right bank), with an overall average of 8.06 mg/L, above the recommended minimum limit (5 mg/L) for aquatic life support. However, some points with lower values suggest intense biological activity or localized organic matter input.

Oxygen saturation levels ranged from 78.94% to 94.91%, indicating good overall water aeration and the absence of extensive hypoxic conditions. Lower values may indicate point sources of organic pollution or active local microbial processes.

The measured *ORP values* ranged from -26.59 mV (km 674 center) to 238.79 mV (km 763 center), with an average of 122.69 mV. The presence of both positive and negative values suggests complex dynamics of the redox environment, influenced by organic matter decomposition, microbial activity and oxygen availability. The negative values observed in the Bechet sector (km 674 right bank to km 674 left bank) indicate possible local anoxic conditions, related to organic matter decomposition or reducing groundwater inputs.

The *water salinity* remained low (between 0.15 and 0.21 PSU, average 0.18 PSU), confirming the freshwater characteristics of the Danube and indicating the lack of significant influences from seawater or intense evaporative processes.

Nitrate concentrations varied significantly (between 2.67 and 101.82 mg/L), with an average of 12.80 mg/L. Very high values were identified at km 956 (101.82 mg/L), km 925 center (92.56 mg/L) and Km 677, Bechet Sector (80.45 mg/L), indicating possible local sources of contamination (agricultural runoff, urban wastewater). Most of the average values (10-20 mg/L) suggest moderate anthropogenic influences, while low values (4-7 mg/L) indicate areas with low impact.

Chlorophyll values were low (0.27-1.49 RFU, mean 0.48 RFU), reflecting a low phytoplankton biomass and minimal risk of eutrophication. Moderate peaks (km 638, left bank, (Upstream of Isker River) suggest local algal blooms caused by nutrient inputs.

Total Algae Content (TAL-PC RFU). Algal indicators showed significant variations (between 0.01-1.91 RFU, average 0.69 RFU). High values (>1.0 RFU) indicate significant anthropogenic influences in the areas of Calnovăț, Corabia, Bogdan Seclan, Drobeta-Turnu Severin, Orșova and the area of Iron Gate Dam II. Medium values (0.3-1.0 RFU) reflect moderate impacts in other urban and port areas, and low values (<0.3 RFU) suggest clean areas, without notable anthropogenic influences.

Polycyclic aromatic hydrocarbons and total hydrocarbons. The level of hydrocarbons (0.89-48.70 µg/L HC and 0.03-1.46 mg/L Oil in Water) was relatively low, with moderate peaks in the Bechet sector (km 675). Although indicating the presence of local sources of contamination, the values are below the critical thresholds, suggesting the absence of an immediate ecological risk.

Data analysis using the Pearson correlation matrix indicates statistically significant relationships at a significant level of $\alpha = 0.05$, as shown in Table 3 and Figure 15.

Positive correlations:

- Electrical conductivity (Cond µS/cm) and total dissolved solids (TDS mg/L): Strong positive correlation (r=0.943), confirming that TDS directly depends on the ionic concentration of water, reflected by conductivity.
- Hydrocarbons (HC µg/L) and oil concentration in water (Oil in Water mg/L): Very strong positive correlation (r=0.974), suggesting that hydrocarbons contribute significantly to the total oil concentration in water, indicating common sources, possibly local oil pollution.
- Conductivity and Salinity (Sal psu): Significant positive correlation (r=0.911),

indicating a clear link between the total dissolved salt concentration and water conductivity.

- Conductivity and Water Temperature: Positive correlation (r=0.694), which may indicate that temperature variations significantly influence ionic concentrations and implicitly water conductivity.
- Oxygen Saturation (ODO % sat and ODO mg/L): Moderate to high positive correlation (r=0.632), signaling the consistency of these measurements in reflecting the concentration of dissolved oxygen in water.

Negative correlations:

- Temperature and Dissolved Oxygen (ODO mg/L): Strong negative correlation (r=-0.847), indicating that higher temperatures lead to lower concentrations of dissolved oxygen, a common fact in aquatic systems.
- Temperature and Redox Potential (ORP mV): Significant negative correlation (r=-0.517), with higher temperatures being associated with reduced redox conditions, reflecting a change in chemical conditions due to temperature.
- Electrical Conductivity and Dissolved Oxygen (ODO mg/L): Strong negative correlation (r=-0.764), indicating that waters with high conductivity (possibly with inputs of inorganic pollutants or salts) have low dissolved oxygen concentrations.

Based on the Euclidian similarity index (Figure 16), it can be observed that as the total flow rate increases, the percentage of oxygen saturation tends to decrease moderately, while the concentration of dissolved oxygen in mg/L is almost unaffected. In stations km 761 bis right bank and km 762 bis right bank, where a very low flow was recorded, due to their location after the ostrov, in an area with weaker currents and reduced depth, high dissolved oxygen concentrations, low TDS values and lower water temperatures were recorded.

Table 3. Correlation matrix (Pearson)

Variables	Chlorophyll RFU	Cond µS/cm	ODO % sat	ODO mg/L	ORP mV	Sal psu	TAL PC RFU	TDS mg/L	Turbidity FNU	pH	Temp °C	NitraLED mg/L	HC micro-g/L	Oil in water mg/L
Chlorophyll RFU	**1**	-0.071	**0.168**	0.048	**-0.390**	**-0.161**	0.105	**-0.151**	0.134	-0.049	0.043	-0.039	-0.121	-0.118
Cond µS/cm	-0.071	**1**	-0.092	**-0.764**	**-0.452**	**0.911**	**-0.368**	**0.943**	**-0.563**	**0.292**	**0.913**	**0.167**	**-0.530**	**-0.519**
ODO % sat	**0.168**	-0.092	**1**	**0.632**	-0.119	-0.014	0.012	-0.055	**0.167**	**0.333**	-0.126	-0.110	-0.045	-0.058
ODO mg/L	0.048	**-0.764**	**0.632**	**1**	**0.345**	**-0.554**	**0.289**	**-0.601**	**0.518**	-0.006	**-0.847**	**-0.194**	**0.341**	**0.322**
ORP mV	**-0.390**	**-0.452**	-0.119	**0.345**	**1**	**-0.331**	**0.276**	**-0.343**	**0.162**	-0.098	**-0.517**	**-0.164**	**0.312**	**0.312**
Sal psu	**-0.161**	**0.911**	-0.014	**-0.554**	**-0.331**	**1**	**-0.339**	**0.973**	**-0.499**	**0.296**	**0.694**	**0.158**	**-0.505**	**-0.505**
TAL PC RFU	0.105	**-0.368**	0.012	**0.289**	**0.276**	**-0.339**	**1**	**-0.325**	**0.193**	0.024	**-0.360**	-0.038	**0.266**	**0.258**
TDS mg/L	**-0.151**	**0.943**	-0.055	**-0.601**	**-0.343**	**0.973**	**-0.325**	**1**	**-0.500**	**0.298**	**0.726**	**0.144**	**-0.525**	**-0.519**
Turbidity FNU	0.134	**-0.563**	**0.167**	**0.518**	**0.162**	**-0.499**	**0.193**	**-0.500**	**1**	-0.100	**-0.552**	-0.113	**0.277**	**0.276**
pH	-0.049	**0.292**	**0.333**	-0.006	-0.098	**0.296**	0.024	**0.298**	-0.100	**1**	**0.236**	-0.086	**-0.145**	**-0.144**
Temp °C	0.043	**0.913**	-0.126	**-0.847**	**-0.517**	**0.694**	**-0.360**	**0.726**	**-0.552**	**0.236**	**1**	**0.173**	**-0.455**	**-0.439**
NitraLED mg/L	-0.039	**0.167**	-0.110	**-0.194**	**-0.164**	**0.158**	-0.038	**0.144**	-0.113	-0.086	**0.173**	**1**	-0.113	-0.105
HC_micro-g/L	-0.121	**-0.530**	-0.045	**0.341**	**0.312**	**-0.505**	**0.266**	**-0.525**	**0.277**	**-0.145**	**-0.455**	-0.113	**1**	**0.974**
Oil in water mg/L	-0.118	**-0.519**	-0.058	**0.322**	**0.312**	**-0.505**	**0.258**	**-0.519**	**0.276**	**-0.144**	**-0.439**	-0.105	**0.974**	**1**

Values in bold are different from 0 with a significance level alpha=0.05

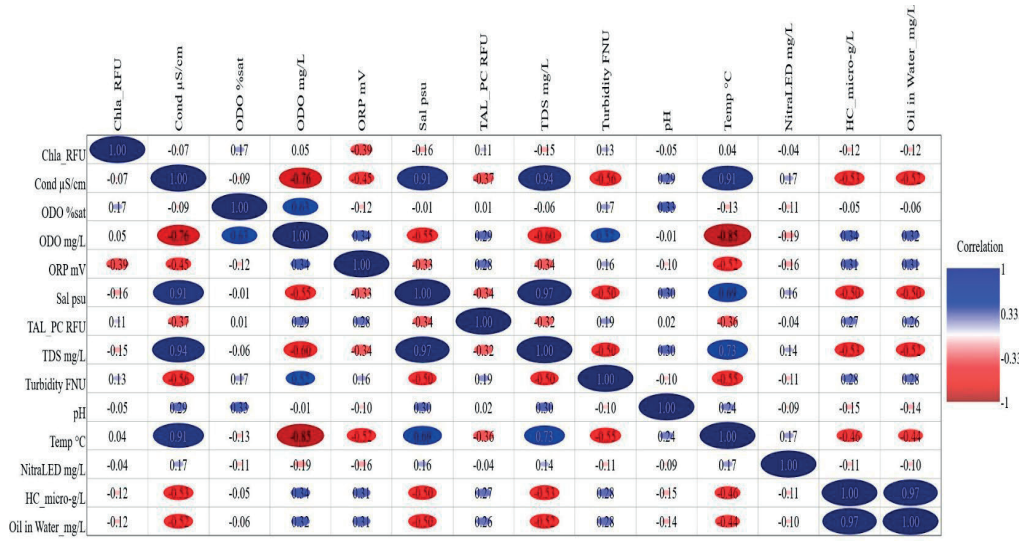


Figure 15. Correlation matrix (Pearson)

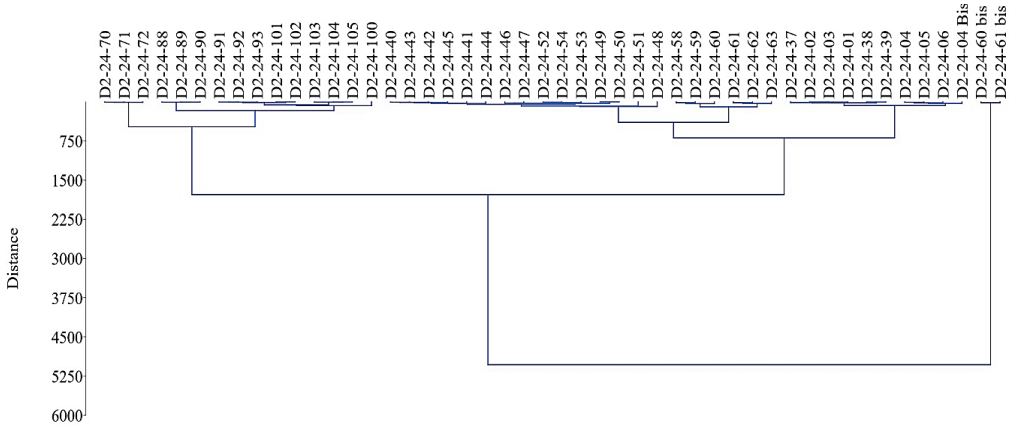


Figure 16. Similarity index based on Euclidian transformed data

Possible causes and ecological implications

Agricultural runoff: high nitrate and turbidity levels suggest significant inputs of fertilizers or animal manure.

Urban/industrial pollution: atypical values of conductivity, TDS and ORP may indicate anthropogenic influences, such as wastewater discharges.

Geological factors: variability of TDS, conductivity and ORP could be influenced by inputs of mineralized groundwater.

The results indicate that the investigated Danube River sectors generally maintain good water quality, parameters that fall within regulatory standards. However, localized variations in turbidity, dissolved oxygen and hydrocarbon levels highlight the importance of continuous monitoring to detect potential environmental stressors and anthropogenic impacts (Chitescu et al., 2021; Halder et al., 2022).

In order to determine the water quality status of the investigated control sections, a series of physicochemical parameters were taken into account (water temperature, pH, dissolved oxygen chlorophyll *a*, electrical conductivity, total dissolved solids, salinity, turbidity and oxidation-reduction potential).

The determination and interpretation of the results obtained was carried out using the methods provided in the reference standards.
In general, no significant increases/decreases were recorded, except for some specific cases, which can be attributed mainly to the local conditions of the fluvial environment.
Overall, the results obtained are within the limits provided for the first quality classes (Very good status and good status).

CONCLUSIONS

Comprehensive analysis of water quality parameters - temperature, pH, turbidity, total dissolved solids (TDS), conductivity, dissolved oxygen (ODO), oxygen saturation, oxidation-reduction potential (ORP), salinity, nitrates, chlorophyll levels, total algal content and hydrocarbons - indicates generally favorable conditions in the investigated areas of the lower Danube, though localized areas of concern have been identified.
These localized problems, such as high nitrate concentrations, increased turbidity, occasional anoxic conditions and high algal fluorescence, highlight critical anthropogenic pressures mainly related to agricultural runoff, urban wastewater discharges, port operations and other local sources. Although current concentrations remain largely below critical ecological thresholds, persistent anthropogenic pressures may compromise water quality and ecosystem stability if not managed.
Therefore, these findings highlight the need for targeted monitoring and mitigation actions, especially around urban centers, the port and agricultural areas, to prevent long-term deterioration of water quality. Ensuring consistent and high-quality water in the Danube basin is vital for supporting biodiversity, preserving ecological balance and supporting the socioeconomic well-being of riparian communities dependent on river resources. These insights highlight the need for proactive environmental management strategies, targeted pollution control and continuous monitoring to protect the health of the Danube ecosystem and its resilience against future anthropogenic pressures.

ACKNOWLEDGEMENTS

The authors thank Cioroiu Catalin for helping to improve the paper. The research leading to their results was financed by the Ministry of Research and Innovation - “Program Nucleu” - PN 23.30.03.03, PN 23.30.03.01, PN 23.30.03.02 and HORIZON-MISS-2021-OCEAN-02-02, DANUBE4all - Restoration of the Danube River Basin Waters for Ecosystem and People from Mountains to Coast

REFERENCES

Addinsoft. XLSTAT Statistical and Data Analysis Solution; Addinsoft: New York, NY, USA, 2020; Available online: https://www.xlstat.com.

Annex 6.1.1.C. (n.d.). Ecological status – Biological element - Benthic macroinvertebrates - Natural rivers. Retrieved [January 2025], from https://www.mmediu.ro/app/webroot/uploads/files/Proiect-Plan-National-de-Management-Actualizat-2021-Volum-2.pdf

Banu, C. (1967). *Limnology of the Romanian sector of the Danube*. Ed. Acad Romane.

Bănăduc, D., Rey, S., Trichkova, T., Lenhardt, M., & Curtean-Bănăduc, A. (2016). The Lower Danube River - Danube Delta - North West Black Sea: A pivotal area of major interest for the past, present and future of its fish fauna - A short review. *Science of the Total Environment, 545,* 137–151.

Bondar, C. (2008). *Morphological balance on the Danube in the system of retention lakes Porţile De Fier 1 and 2 for the intervals 1971-2005, respectively 1985-2005*. Earth Sciences. Knowledge and Environment. Geoecomarina 14/2008-Supplement No.1, pp. 32-37, Bucharest.

Brezeanu, G., Nicolescu, N., Zinevici, V., & Petcu, M. (1974). *Studiul evoluţiei biocenozelor lacului de baraj de la Porţile de Fier în perioada 1970 – 1974* [Manuscript]. Universitatea din Bucureşti.

Bușniță, T., Brezeanu, G., Oltean, M., Popescu Marinescu, V., & Prunescu Arion, E. (1970). *Monograph of the Iron Gates area*. Publishing House of the Academy of the Socialist Republic of Romania.

Calmuc ,M., Calmuc, V., Arseni, M., Topa, C., Timofti, M., Georgescu, L.P., Iticescu, C. (2020). A Comparative Approach to a Series of Physico-Chemical Quality Indices Used in Assessing Water Quality in the Lower Danube. *Water, 12*, 3239; doi:10.3390/w12113239.

Calmuc, M., Calmuc, V.A., Topa, M.C., Timofti, M., Iticescu, C., Georgescu, L.P. (2018). Review on water quality assessment in the Danube River Basin. *Annals Of “Dunarea De Jos” University Of Galati Mathematics, Physics, Theoretical Mechanics Fascicle II*, Year X (XLI), 2, https://doi.org/10.35219/ann-ugal-math-phys-mec.2018.2.11

Catianis, I., Constantinescu, A.M., Grosu, D., Iordache, G., Duțu, F., & Pavel, A.-B. (2024). Assessment of the surface water quality data collected seasonally at the Danube river bifurcations (Ceatal Izmail and Ceatal Sf. Gheorghe). *Scientific Papers. Series E. Land Reclamation, Earth Observation & Surveying, Environmental Engineering*, *13.* Print ISSN 2285-6064.

Capon, S.J., Chambers, L.E., Mac Nally, R., Naiman, R.J., Davies, P., Marshall, N., Pittcock, J., Reid, M. et al. (2013). Riparian ecosystems in the 21st century: Hotspots for global change adaptation. *Ecosystems, 16*, 359–381.

Călinescu, R., & Iana, S. (1967). *The Danube Gorge of the Iron Gates, Biogeographical Characterization*. In *Geography of the Romanian Danube Valley,* Annals of the University of Bucharest, Geology-Geography Series, Bucharest, XIII, l, 151-168. (in Romanian)

Chapman, D. (1996). *Water quality assessments: A guide to use of biota, sediments and water in environmental monitoring* (2nd ed.). University Press, Cambridge.

Chitescu, C. L., Ene, A., Geana, E.-I., Vasile, A. M., & Ciucure, C. T. (2021). Emerging and persistent pollutants in the aquatic ecosystems of the Lower Danube Basin and North West Black Sea region - A review. *Applied Sciences, 11*(21), 9721.

Cioboiu, O., & Brezeanu, G. (2017). Iron Gate I reservoir – ecological evolution, Romania. *International Journal of Ecosystems and Ecology Sciences (IJEES)*, 7(2), 199-206.

De Zuane, J. (1997). *Handbook of drinking water quality* (2nd ed.). John Wiley and Sons. pp. 592, ISBN 0-471-28789-X.

Diaconu, S. (1997). On the ecological implications of hydrotechnical works for the development of watercourses. *Hidrotehnica*, *42*(6), pp. 155-160.

Diop, B., Sanz, N., Duplan, I. J. J., Guene, E. H. M., Blanchard F., Pereau J.C., Doyen L. (2018). Maximum Economic Yield Fishery Management in the Face of Global Warming. *Ecological Economics, 154*, 52-61.

Gasparotti, C. (2014). The main factors of water pollution in Danube river basin. *Euro. Econ. 33*, 91–106.

Halder, J., Vystavn, Y., & Wassenaar, L. I. (2022). Nitrate sources and mixing in the Danube watershed: Implications for transboundary river basin monitoring and management. *Scientific Reports, 12*, 2150.

Hannesson, R. (2007). Geographical distribution of fish catches and temperature variations in the northeast Atlantic since 1945. *Marine Policy, 31*, 32-39.

Iticescu, C., Murariu, G., Georgescu, L. P., Burada, A., & Topa, C. M. (2016). Seasonal variation of the physico-chemical parameters and Water Quality Index (WQI) of Danube water in the transborder Lower Danube area. *Revista de Chimie*, 67, 1843–1849.

Kern, K. (2014). New standards for the chemical quality of water in Europe under the new Directive 2013/39/EU. *Journal of European Environmental & Planning Law*, 11, 31–48.

Lehr, J. H., Gass, T. E., Pettyjohn, W. A., & DeMarre, J. (1980). *Domestic water treatment*. McGraw-Hill. pp. 264.

Madeira, D., Araujo, J.E., Vitorino, R., Capelo, J.L., Vinagre, C., Diniz, M.S. (2016). Ocean warming alters cellular metabolism and induces mortality in fish early life stages: A proteomic approach. Environmental Research, 148, 164-176.

Manea, G. (2003). *The impact of the Iron Gates hydropower development on the biodiversity of terrestrial and aquatic ecosystems*. University of Bucharest Publishing House.

Montagna, P., Palmer, P., Pollack, J. (2013). Hydrological Changes and Estuarine Dynamics. *Springer briefs in Environmental Science*, 8, 94. https://doi.org/10.1007/978-1-4614-5833-3

Nike, S., Bloesch, J., Baumgartner, C., Bittl, T., Čerba, D., Csányi, B., Davideanu, G., Dokulil, M., Frank, G., Grecu, I., et al. (2022). The Danube River Basin. In K. Tockner, C. Zarfl, & C. T. Robinson (Eds.), *Rivers of Europe* (2nd ed., pp. 81–180). Elsevier. ISBN 9780081026120.

Order no. 161/2006. (2006). *Regulation on the classification of surface water quality for the purpose of establishing the ecological status of water bodies* (Official Gazette of Romania, Part I, No. 511bis/13.VI.2006). Retrieved [January 2025], from [https://legislatie.just.ro/Public/DetaliiDocument/74255].

Panin, N. (2003). *The Danube Delta. Geomorphology And Holocene Evolution: A Synthesis* / Le Delta Du Danube. Géomorphologie Et Évolution Holocène: Une Synthèse, Géomorphologie Publishing House: Relief, Processus, Environnement, 9(4), 247-262.

Pavlović, P., Mitrović, M., Đorđević, D., Sakan, S., Slobodnik, J., Liška, I., Csanyi, B., Jarić, S., Kostić, O., Pavlović, D., Marinković, N., Tubić, B., & Paunović, M. (2016). Assessment of the contamination of riparian soil and vegetation by trace metals - A Danube River case study. *Science of The Total Environment, 540*, 396–409.

Podlasek, A., Koda, E., Kwas, A., Vaverková, M. D., & Jakimiuk, A. (2024). Anthropogenic and natural impacts on surface water quality: The consequences and challenges at the nexus of waste management facilities, industrial zones, and protected areas. *Water Resources Management, 39*(6), 1697–1718.

Poff, N.L., M.A. Brinson, M.A., Day, J.W. (2002). *Aquatic ecosystems and global climate change: potential impacts on inland freshwater and coastal wetland ecosystems in the United States.* Report of PEW Center on Global Climate Change, Arlington, Virginia, VA: 44.

Radu, C.; Manoiu, V.-M.;Kubiak-Wójcicka, K.; Avram, E.; Beteringhe, A.; Craciun, A.-I. Romanian Danube River Hydrocarbon Pollution in 2011–2021. (2022). *Water, 14*, 3156. https://doi.org/10.3390/w14193156.

Rico, A., Van den Brink, P. J., Leitner, P., Graf, W., & Focks, A. (2016). Relative influence of chemical and non-chemical stressors on invertebrate communities: A case study in the Danube River. *Science of The Total Environment, 571,* 1370–1382.

Sigg, L. (2000). *Redox potential measurements in natural waters: Significance, concepts, and problems*. In J. Schüring, H. D. Schulz, W. R. Fischer, J. Böttcher, & W. H. M. Duijnisveld (Eds.), *Redox Processes in*

Natural Waters (pp. 1-12). Springer. https://doi.org/10.1007/978-3-662-04080-5_1.

Simionov, I.-A. Petrea, S.-M., Mogodan, A., Nica, A., Cristea, D., Neculita, M. (2020). Effect Of Changes In The Romanian Lower Sector Danube River Hydrological And Hydrothermal Regime On Fish Diversity. *Scientific Papers. Series E. Land Reclamation, Earth Observation & Surveying, Environmental Engineering*, *9,* 106-111, Print ISSN 2285-6064.

SR ISO 5667-5:2017, Water quality. Sampling. Part 5: Guidance for the sampling of drinking water from treatment plants and distribution networks Retrieved [January 2025], from [https://magazin.asro.ro/ro/standard/248767].

Teodorof, L., Despina, C., Burada, A., Seceleanu-Odor, D., & Anuti, I. (2015). Methods for monitoring physical-chemical indicators in aquatic ecosystems of the Danube Delta. In I. M. Tudor (Ed.), *Methodological guide for monitoring hydromorphological, chemical and biological factors for surface waters in the Danube Delta Biosphere Reserve* (ISBN 978-606-93721-8-0). Danube Delta Technological Information Center.

AccuWeather. (2024). *Tulcea Weather Forecast*. Retrieved March 10, 2025, from https://www.accuweather.com/ro/ro/tulcea/

NIWA. (n.d.). *Dissolved oxygen thresholds for aquatic ecosystems*. Retrieved [January 2025], from https://www.niwa.co.nz.

Statistical analysis app for Windows, https://past.en.lo4d.com/download

Scientific Papers. Series E. Land Reclamation, Earth Observation & Surveying, Environmental Engineering. Vol. XIV, 2025
Print ISSN 2285-6064, CD-ROM ISSN 2285-6072, Online ISSN 2393-5138, ISSN-L 2285-6064

EVALUATION OF THE DEGREE OF MICROBIOLOGICAL CONTAMINATION OF GROUNDWATER IN GORJ COUNTY

Emil Cătălin ȘCHIOPU[1], Roxana Gabriela POPA[1], Irina Ramona PECINGINĂ[1], Ramona Violeta CAZALBAȘU[1], Marinela Florica BODOG[2]

[1]"Constantin Brâncuşi" University of Târgu Jiu, 30 Geneva Street, Târgu Jiu, Gorj, Romania
[2]University of Oradea, 26 General Magheru Blvd, 410013, Oradea, Bihor, Romania

Corresponding author email: marinelabodog@gmail.com

Abstract

Gorj County is located in the south-west of Romania with a predominantly mountainous relief, and the main economic activities are specific to the exploitation of natural resources, agriculture and tourism. As a result of the lack of sewerage systems in most of the villages in Gorj County and the uncontrolled storage of manure resulting from animal husbandry activities, the groundwater has suffered significant microbiological contamination. This paper describes the investigations carried out to determine the degree of microbiological contamination of groundwater in the northern part of Gorj County, in one of the most attractive tourist localities. The investigations consisted of taking 45 water samples from public and private wells in the villages of Gureni and Frâncești, in the commune of Peștișani. The most important microbiological indicators for determining water quality were determined from samples: the number of bacterial colonies, the number of coliform bacteria, the number of Escherichia coli and the number of intestinal enterococci.

Key words*: Evaluation, groundwater, contamination, microbiologic, bacteria.*

INTRODUCTION

Romania, situated in South-Eastern Europe at the crossroads of Central Europe and the Balkans, covers about 238,397 km², ranking as the 12th largest country in Europe. Its landscape features diverse relief - mountains, hills, and plains - and a rich hydrographic network of rivers, lakes, and groundwater.

Gorj County, in southwestern Romania, is known for its mountainous landscapes and cultural heritage. Traversed by the Southern Carpathians and near Retezat National Park, its capital, Târgu Jiu, hosts the iconic works of sculptor Constantin Brâncuși. Rich in forests and minerals, Gorj is a key energy hub, with an economy driven by industry, agriculture, and tourism.

Peștișani commune, located in Gorj County, is a picturesque locality near the city of Târgu Jiu, which stands out for its mountain landscapes and folk traditions. The commune is known for its agricultural activities and local crafts, and among the attractions are the old churches and specific customs, which reflect the culture of the area. The commune of Peștișani is associated with the life and activity of the artist Constantin Brâncuși, having links with the cultural heritage of the county and offering opportunities for rural tourism and nature exploration. The villages that make up the commune of Peştişani are: Boroşteni, Brădiceni, Frâncești, Gureni, Hobiţa, Peştişani and Seuca (Puianu, 2019)

The main source of water in Peștișani commune is groundwater from public and private wells, because not all the inhabitants of the commune have access to the public drinking water network. Given the characteristics of groundwater, it is a very convenient source of drinking water, provided that the reserves are large enough and the quality indicators regulated by the legislation in force are respected. Groundwater composition can be significantly altered by human activities such as improper fertilizer use, household waste disposal, and the infiltration of wastewater or fuels (Begea et al., 2024)

Due to the multiple possibilities of pollution of water sources, it is necessary to establish the sanitary conditions that drinking water must meet. The drinking conditions of the water are the organoleptic characteristics (taste, smell, color), as well as the physical, chemical and biological indicators within the maximum allowed limits and the normal values provided in the national and international legislation in force. The relationship of water with infectious diseases has led to the development of bacteriological

conditions for drinking water. The first bacterial conditions appeared in 1904 and are due to Christiaan Eijkman, being perfected later.

The drinking conditions of the water are divided into four groups:

- organoleptic (taste, smell, coloured);
- (temperature, pH, turbidity, conductivity, radioactivity);
- chemical (fluorine, heavy metals, nitrites, nitrates, ammonia nitrogen);
- microbiological (mesophilic germs, coliform germs, enterococci) (Masciopinto et al., 2021; Cirtină & Căpățână 2017).

The most important bacteriological condition of potability is the total lack of pathogenic germs in the water:

- **Mesophilic germs** bacteria that grow at 37°C, typically originating from humans and warm-blooded animals; higher counts indicate a greater presence of potentially pathogenic microorganisms.
- **Coliform germs** (relatively heterogeneous group, found in large numbers in the feces of humans and warm-blooded animals)
- **Enteric virus** (germs that are found in feces, but in smaller numbers than coliforms, which makes them more difficult to determine; they are more resistant in water than fecal coliforms and do not suffer from the phenomenon of microbial variability; they have types characteristic for humans and animals, which allows differentiation of the type of water pollution) (Cheong et al., 2009)

The presence and intensity of fecal pollution is an important factor in assessing water quality and the infectious risk posed to human health. Examination of water samples for the presence of *Escherichia coli*, which normally populates the intestines of humans and other warm-blooded animals, provides an indication of water pollution (Kampouris et al., 2022).

Analyzing the latest statistical information provided by the National Institute of Statistics in 2022, the population connected to the public water supply system was 14,277,262 people, representing 74.9% of Romania's resident population. At the level of the development regions, the lowest degree of connection to the public water supply system was recorded in the North-East region (50.7%), followed by the South-West Oltenia region (63.4%), a region to which Gorj county, the area taken in the study belongs (Figure 1).

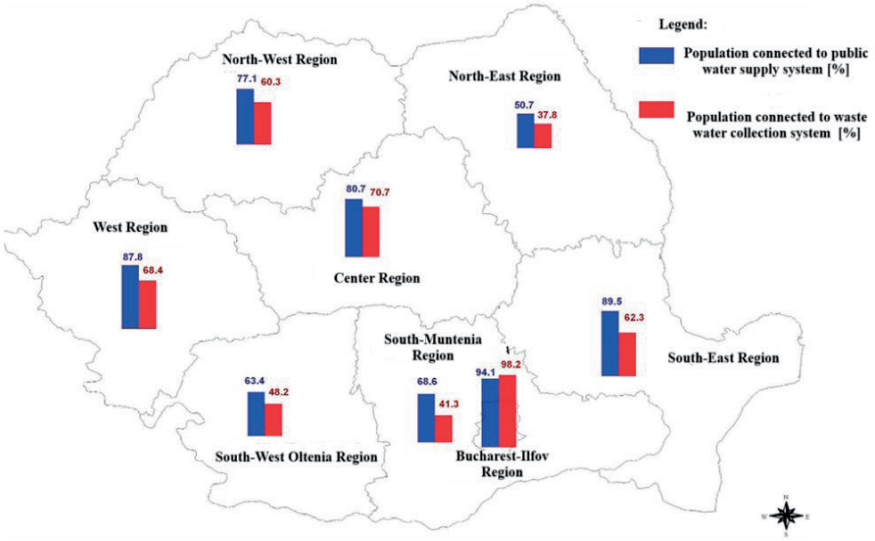


Figure 1. Romania's population connected to the public drinking water supply and sanitation system, by development regions, in 2022 (National Institute of Statistics of Romania, 2022)

Regarding wastewater treatment, 11,062,432 people - 58.1% of Romania's resident population - were connected to sewerage systems with treatment plants. The lowest

connection rates were in the North-East (37.8%), South-Muntenia (41.3%), and South-West Oltenia (48.2%) regions.

MATERIALS AND METHODS

To assess groundwater microbiological contamination in Gorj County, a case study was conducted in the Gureni and Frâncești villages of Peștișani commune.

A total of 45 water samples were collected from public and private wells - 19 from Gureni village and 26 from Frâncești village - as shown in Figure 2.



Figure 2. Distribution of the sampling points of the 45 water samples in the area of Gureni and Frâncești villages

The microbiological quality indicators determined from the collected groundwater samples, as well as the methods of analysis were:

- *The number of colonies at 22^{0}C*, by counting the cultures formed in a nutrient agar culture medium, after incubation in aerobiosis at a temperature of 22^{0}C, in accordance with the international technical provisions referred to in SR EN ISO 6222:2004.
- *Number of colonies at 37^{0}C*, by counting cultures formed in a nutrient agar culture medium, after incubation in aerobiosis at a temperature of 37 ^{0}C, in accordance with the international technical provisions referred to in SR EN ISO 6222:2004.
- *Coliform bacteria*, by filtering the analysis water sample through the membrane, followed by chromogenic agar culture and counting the coliform bacteria in the sample, in accordance with the international technical provisions mentioned in SR EN ISO 9308:2015.
- *Escherichia coli,* by filtering the analysis water sample through the membrane, followed by chromogenic agar culture and counting the coliform bacteria in the sample, in accordance with the international technical provisions referred to in SR EN ISO 9308:2015.
- *Intestinal enterococci,* by filtering the analysis water sample through the membrane, followed by chromogenic agar culture and counting the coliform bacteria in the sample, in accordance with the international technical provisions mentioned in SR EN ISO 9308:2015.

The permissible limits for microbiological indicators in groundwater taken from wells are regulated by Ordinance no. 7/2023 on the quality of water intended for human consumption, which transposes Directive (EU) 2020/2.184 of the European Parliament and of the Council of 16 December 2020 on the quality of water intended for human consumption, published in the Official Journal of the European Union, series L, no. 435 of 23 December 2020 and which provides that for the indicators: number of colonies at 22 ^{0}C, Number of colonies at 37^{0}C, coliform bacteria, *Escherichia coli* and intestinal *Enterococci,* the permissible value is 0 Cfu/ml.

Thus, for the evaluation of the level of microbiological pollution, the values obtained

were compared with the allowed value 0 Cfu/ml and graphically represented. (Popa et al., 2022)

RESULTS AND DISCUSSIONS

The evolution of colony counts at 22°C for water samples from Gureni and Frâncești villages is presented in Figures 3 and 4.

According to Figure 3, 17 out of 19 water samples from Gureni village exceeded the permitted limit, representing 89.47%. Similarly, Figure 4 shows that 19 out of 26 samples from Frâncești village were above the allowed limit, accounting for 73.07% (Șchiopu, 2023). The evolution of colony counts at 37°C for samples from both villages is shown in Figures 5 and 6.

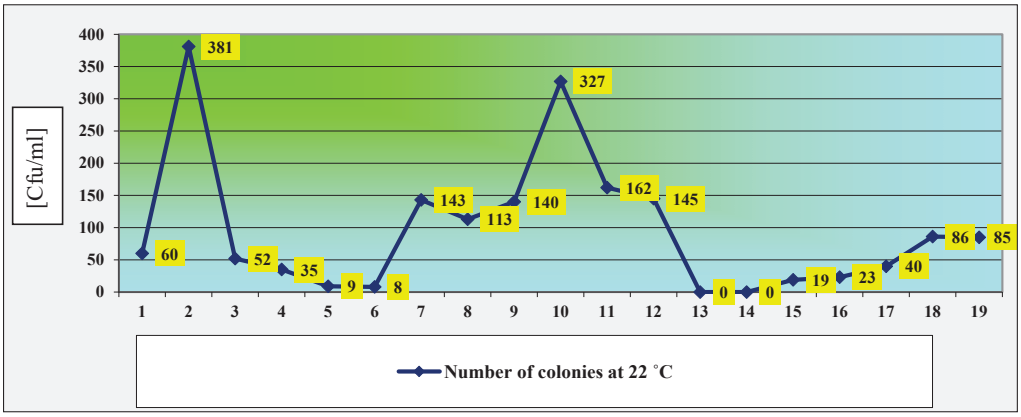


Figure 3. Number of colonies at 22^{0}C from groundwater samples taken on 22.02.2023 from Gureni village, Gorj county, South-West region Romania

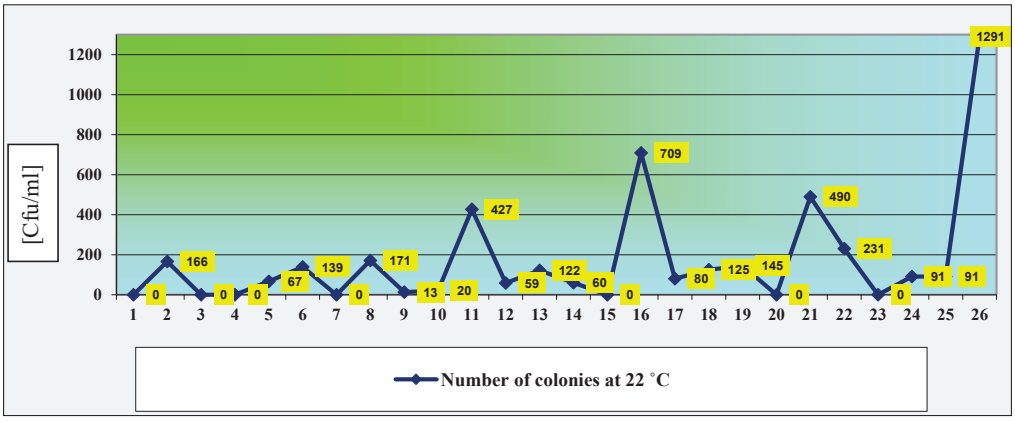


Figure 4. Number of colonies at 22^{0}C from groundwater samples taken on 22.02.2023 from Frâncești village, Gorj County, South-West region Romania

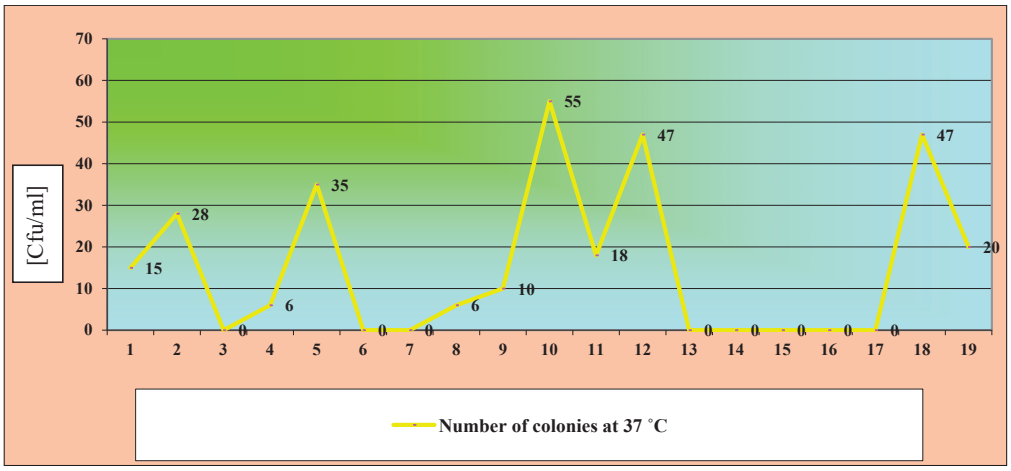


Figure 5. Number of colonies at 37^{0}C in groundwater samples taken on 22.02.2023 from Gureni village, Gorj County, South-West region Romania

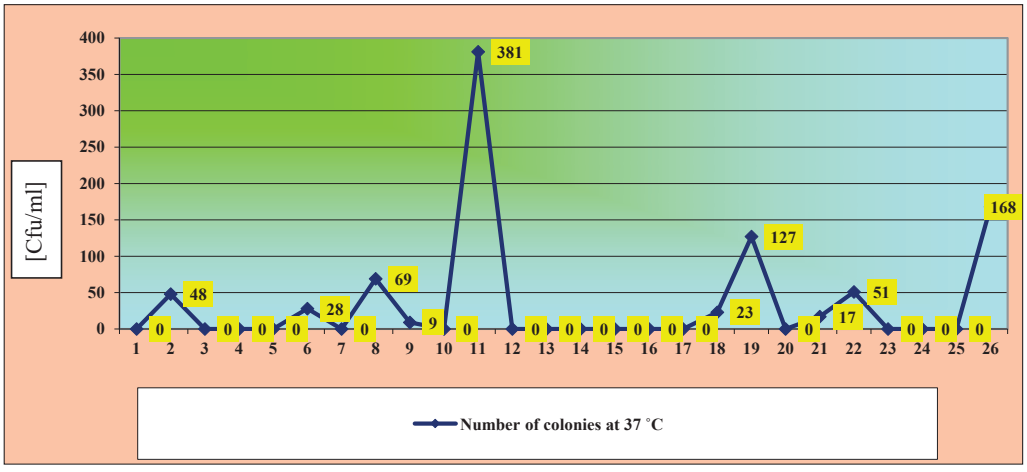


Figure 6. Number of colonies at 37^{0}C from groundwater samples taken on 22.02.2023 from Frâncești village, Gorj County, South-West region Romania

Figure 5 shows that 11 of the 19 water samples from Gureni village exceeded the maximum limit, representing 57.89%. In Figures 6-10 of the 26 samples from Frâncești village also surpassed the limit, accounting for 38.46%. The evolution of coliform bacteria in samples from Gureni and Frâncești villages is illustrated in Figures 7 and 8, respectively.

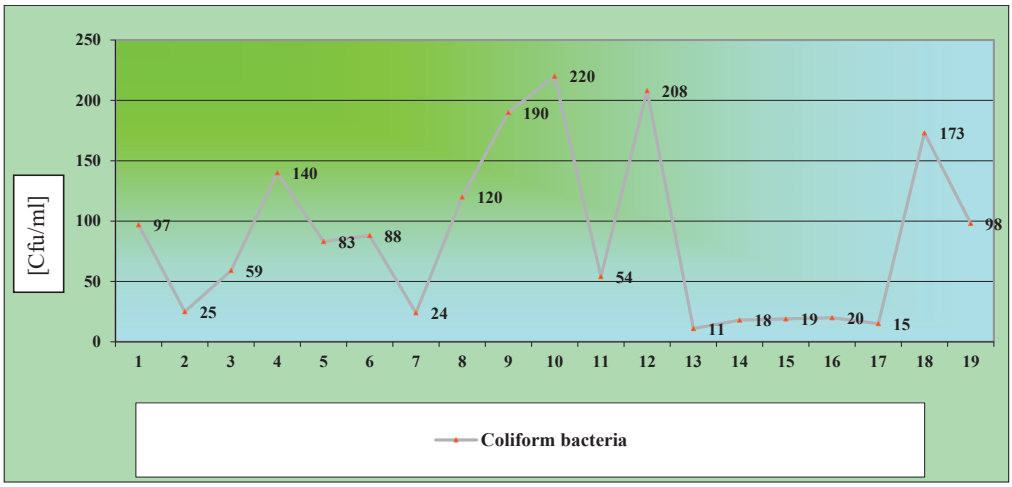


Figure 7. Concentration of coliform bacteria in groundwater samples taken on 22.02.2023 from Gureni village, Gorj County, South-West region Romania

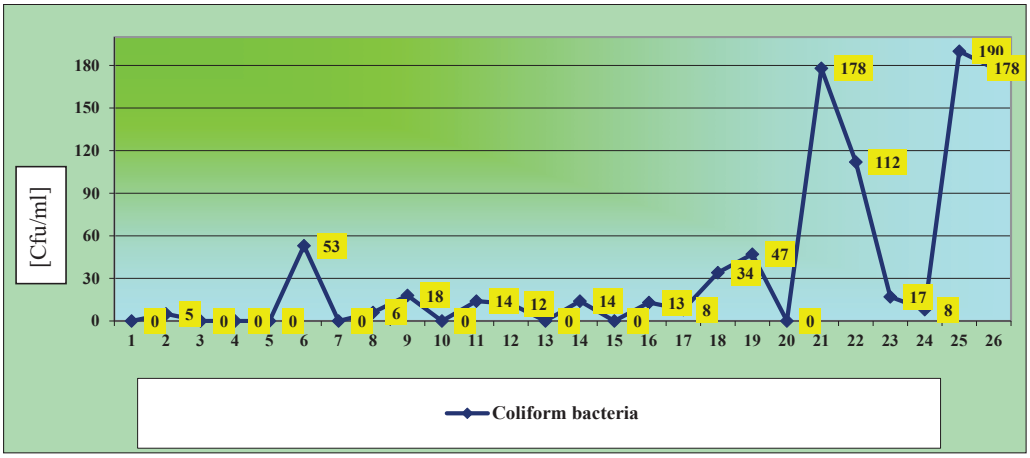


Figure 8. Concentration of coliform bacteria in groundwater samples taken on 22.02.2023 from Gureni village, Gorj County, South-West region Romania

As shown in Figure 7, all water samples from Gureni village exceeded the maximum limit for coliform bacteria, representing 100%. Figure 8 indicates that 17 of the 26 samples from Frâncești village also surpassed the limit, accounting for 65.38%. Figures 9 and 10 present the evolution of *Escherichia coli* levels in water samples from Gureni and Frâncești villages, respectively.

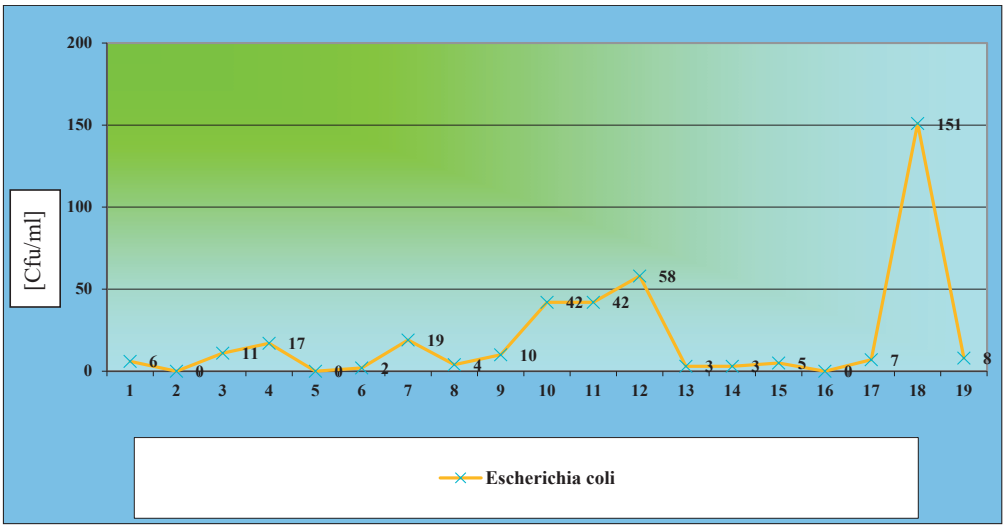


Figure 9. The number of *Escherichia coli* in groundwater samples taken on 22.02.2023 from Gureni village, Gorj County, South-West region Romania

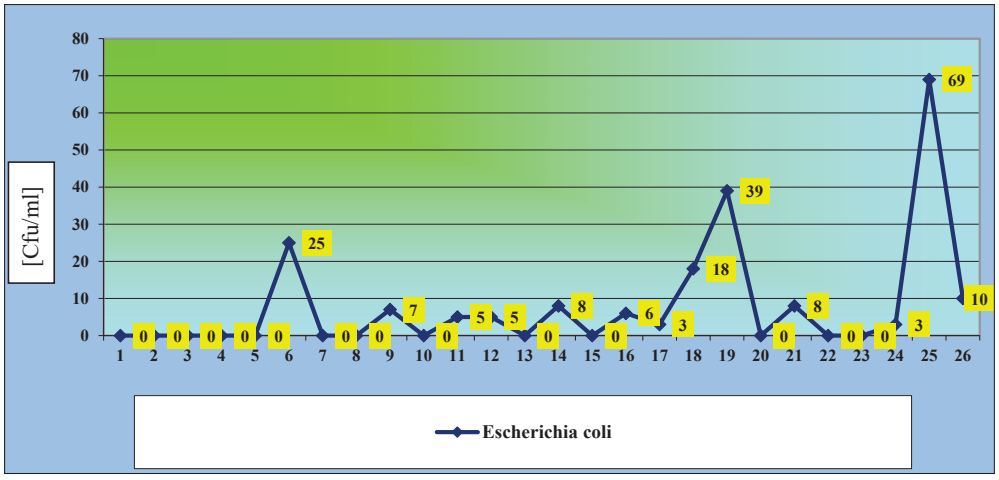


Figure 10. The number of *Escherichia coli* in groundwater samples taken on 22.02.2023 from Frâncești village, Gorj County, South-West region Romania

Figure 9 shows that 16 of the 19 water samples from Gureni village exceeded the maximum limit for *Escherichia coli*, representing 84.21%. According to Figure 10, 13 of the 26 samples from Frâncești village also exceeded the limit, accounting for 50%.

Figures 11 and 12 illustrate the evolution of intestinal Enterococci levels in water samples from Gureni and Frâncești villages, respectively.

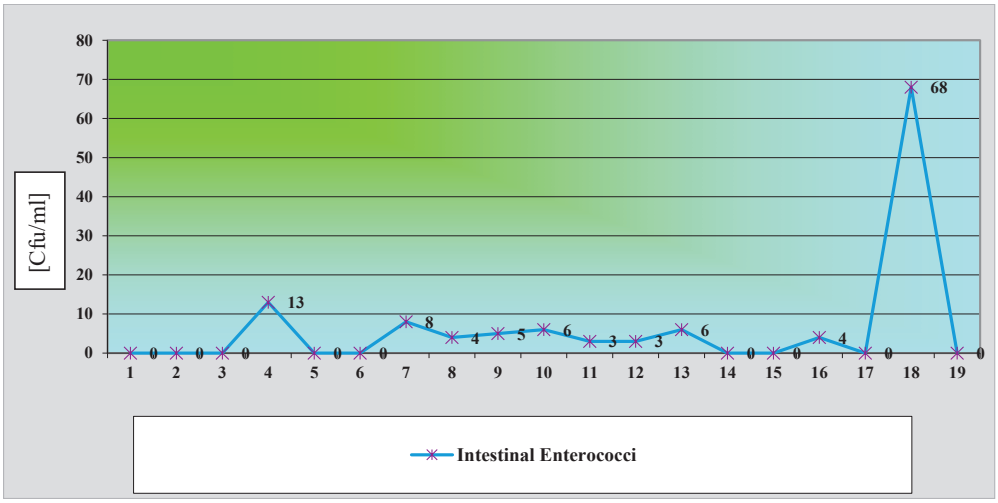


Figure 11. The number of intestinal *Enterococci* in groundwater samples taken on 22.02.2023 from Gureni village, Gorj County, South-West region Romania

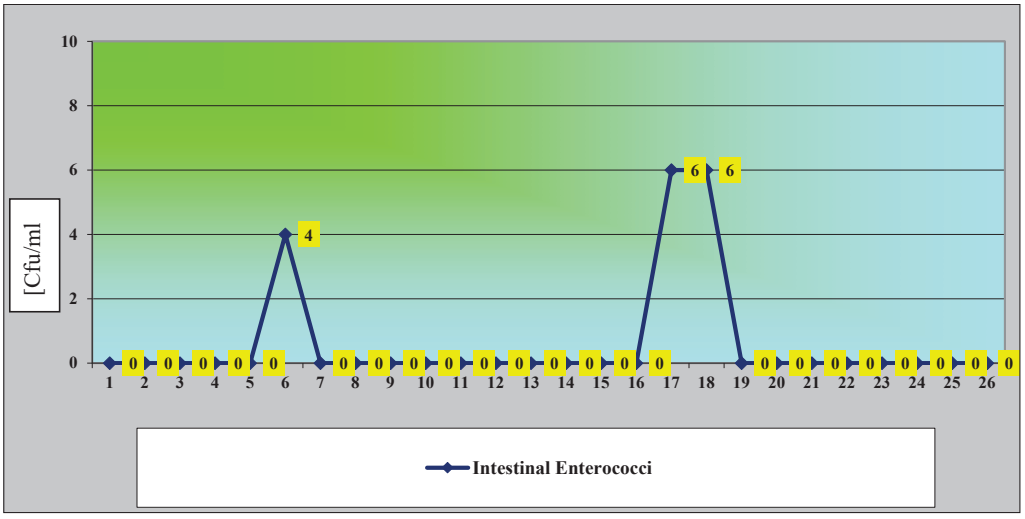


Figure 12. The number of intestinal *Enterococci* in groundwater samples taken on 22.02.2023 from Gureni village, Gorj County, South-West region Romania

Figure 11 shows that 10 of the 19 water samples from Gureni village exceeded the maximum limit for intestinal Enterococci, representing 52.63%. In Figure 12, only 3 of the 26 samples from Frâncești exceeded the limit, accounting for 11.53%.

Overall, analysis of all microbiological indicators confirmed that all 19 samples from public and private wells in Gureni exceeded at least one microbiological parameter, rendering them unfit for human consumption. Specifically, 7 samples exceeded the limit for all five indicators, 3 samples for four indicators, 8 for three indicators, and 1 sample for two indicators. The primary cause of contamination is the proximity of animal shelters and manure storage areas to the wells.

The sample with exceedances for only two of the five indicators came from a public well located at a relatively greater distance from known pollution sources. In Frâncești village, 6 of the 26 analyzed wells (codes: 1, 3, 4, 7, 15, and 20)

were free of exceedances for all five microbiological indicators and are considered safe for drinking. These samples were collected from public wells near roads or institutions (e.g., schools, cultural centers, and stores) where no animal waste was stored and septic tanks are regularly emptied.

Among the remaining 20 samples, 3 exceeded all five indicators, 5 exceeded four, 8 exceeded three, and 4 exceeded only one. The primary cause of microbiological contamination in both villages is the absence of a sewerage system and the uncontrolled storage of animal manure.

For consumption, contaminated water from wells must be applied by one of the following methods:

1. Treatment with chlorine solution, going through the steps mentioned in Order 119/2014 for the approval of Rules of hygiene and public health regarding the living environment of the population, applicable on the territory of Romania, namely:

Calculating the volume of water in the well:

$$V = 3.14r\ x\ rH$$

where:

V = volume of water (m^3);

r = 1/2 of the diameter of the well (m);

H = the height of the water column in the well (m);

Choosing a substance with a chlorine concentration of 15 – 25%;

Calculation of the quantity of chlorine substance according to the concentration of free residual chlorine to be obtained, according to the following example:

0.5 mg Residual Cl ..... 1 l water

X mg Residual Cl ..... 1,000 l water

X = 0.5 g residual chlorine/m^3 water

100 g chlorine ..... 25 g active chlorine

X ..... 0.5 g active chlorine

X = 2 g chlorine/m^3 water

For a water column height of 7 m and a well tube diameter of 1 m, the volume of water is determined as follows:

$$V = 3.14 \cdot 0.5\ x\ 0.5 \cdot 7$$

$$V = 11.02\ m^3 \text{ water}$$

The amount of chlorine required to disinfect the volume of water is calculated as follows:

2 g chlorine/m^3 water x 11.02 m^3 = 22.04 g chlorine of concentration 25%

2. Boil water before consumption for at least 1-3 minutes, to destroy pathogenic microorganisms.

CONCLUSIONS

Human activities, such as: uncontrolled and improper use of fertilizers, disposal of household waste, infiltration of wastewater or fuels, carried out in the South-West area of Romania, Gorj County, Peștișani commune are sources of groundwater pollution, and it is necessary to establish the sanitary conditions that must meet the drinking water.

The bacteriological condition of potability of the water in the wells is the total absence of pathogenic germs (mesophils, coliforms and enterococci). In this regard, this study provided for the collection of groundwater samples and microbiological analysis, according to international standards, of five microbiological indicators of drinking water quality (Number of colonies at 22^0C, Number of colonies at 37^0C, coliform bacteria, *Escherichia coli* and intestinal *Enterococci).*

Following the analysis of the 45 water samples collected from public and private wells and the comparison of the results obtained with the admitted value 0 Cf/ml, it was shown that for most of them there were exceedances of the analyzed microbiological indicators, the main cause being the lack of a centralized sewerage system and the uncontrolled storage of animal manure.

It is recommended that drinking water extracted from wells be treated with chlorine solution or boiled.

REFERENCES

Cheong, S., Lee, C. C. H., Song, S. W., Choi ,W. C., Lee, C. C. H., Kim, S. J. (2009). Enteric viruses in raw vegetables and groundwater used for irrigation in South Korea. *Appl Environ Microbiol, 75*(24), 7745–51. https://doi.org/10.1128/AEM.01629-09

Cirtină, D., & Căpățână, C. (2017). Preliminary study on assessment of mineralization degree and nutrient content of groundwater bodies in Gorj County. *Journal of Chemistry, 68*(2), 221–225.

Directive (EU) 2020/2184 of the European Parliament and of the Council of 16 December 2020 on the quality of water intended for human consumption. *Official Journal of the European Union*, L 435, 23 December 2020.

Government of Romania. (2014). *Order no. 119/2014 for the approval of the hygiene and public health norms regarding the living environment of the population*.

Government of Romania. (2023). *Ordinance no. 7/2023 on the quality of water intended for human consumption*.

Kampouris, I., Alygizakis, N., Klumper, U., Agrawal, S., Lackner, S., Cacace, D., Kunze, S., Thomaidis, N., Slobdonik, J., Berndonk, T. (2022). Elevated levels of antibiotic resistance in groundwater during treated wastewater irrigation associated with infiltration and accumulation of antibiotic residues. *Journal of Hazardous Materials, 423*, 127155, 1-10, *https://doi.org/10.1016/j.jhazmat.2021.127155*

Masciopinto, C., Passarella, G., Caputo, M., Masciale, R., De Carlo, L. (2021). Hydrogeological Models of Water Flow and Pollutant Transport in Karstic and Fractured Reservoirs. *AGU Advencing Earth and Space Science, Water Resurces Resarch, 57*(8), 1-17, 10.1029/2021WR029969

National Institute of Statistics of Romania (2022). *Statistical information – Environmental statistics series*.

Popa, M., Glevitzky, I., Dumitrel, G. A., Popa, D., Vîrsta, A., & Glevitzky, M. (2022). Qualitative analysis and statistical models between spring water quality indicators in Alba County, Romania. *Scientific Papers. Series E: Land Reclamation, Earth Observation and Topography, Environmental Engineering, 11*, 358–366.

Puianu, M. (2019). *Gorj County Monograph*. La Fontaine Publishing House.

S.C. Artoprod S.R.L. (2023, March 22). *Reports no. 116–160 on the microbiology test of groundwater samples*.

Șchiopu, E. C. (2023). *Study of the evaluation of the quality of water in the wells and public network of Peștișani commune* [Expert report funded by the Valea Bistriței Foundation].

SR EN ISO 6222:2004. *Water quality – Counting of culture microorganisms – Colony counting by seeding in nutrient agar culture medium*.

SR EN ISO 9308-1:2015/A1:2017. *Water quality – Counting Escherichia coli and coliform bacteria – Part 1: Membrane filtration method for low-bacterial waters*.

Scientific Papers. Series E. Land Reclamation, Earth Observation & Surveying, Environmental Engineering. Vol. XIV, 2025
Print ISSN 2285-6064, CD-ROM ISSN 2285-6072, Online ISSN 2393-5138, ISSN-L 2285-6064

ECOLOGICAL STATUS ASSESSMENT OF MECHKA RIVER WATER (MARITSA RIVER BASIN)

Petya ZAHARIEVA[1, 2], Radoslava ZAHARIEVA[1, 2], Diana KIRIN[1, 2]

[1]National Institute of Geophysics, Geodesy and Geography (NIGGG),
Hydrology and Water Management Research Center, Bulgarian Academy of Sciences,
3 Acad. G. Bonchev Street, 1113, Sofia, Bulgaria
[2]Agricultural University - Plovdiv, 12 Mendeleev Blvd, 4000, Plovdiv, Bulgaria

Corresponding author email: petya.zaharieva3@gmail.com

Abstract

This study assesses the ecological state of the surface water of the Mechka River from the Maritsa River Basin usingthe biological quality element macrozoobenthos. Four sampling sites (biotopes) were investigated in autumn 2024 along the Mechka River - 1) near the village of Lenovo; 2) near the village of Poroyna; 3) between the town of Parvomay and the village of Poroyna and 4) before the town of Parvomay. A total of 772 specimens of macrozoobenthos from 36 taxa were identified. The highest number of macroinvertebrate taxa was identified in the second biotope (21 taxa) and the lowest - in the first (14 taxa). The study shows that in three of the four biotopes, macroinvertebrates of Group C (relatively tolerant forms) dominate, whereas in Biotope 3) Mechka River between the town of Parvomay and the village of Poroyna, Group D (tolerant forms) dominates. Basic indices and metrics were calculated according to an established methodology.

Key words*: biological monitoring, ecological status, macrozoobenthos, Mechka River, water quality.*

INTRODUCTION

The Maritsa River originates in the Rila Mountains, Mancho Peak, at 2,378 m above sea level. The river's catchment area on Bulgarian territory is 21,084 km^2. The Maritsa River flows into the Aegean Sea. The catchment area of the Maritsa River falls into Ecoregion 7: Eastern Balkans. It includes numerous tributaries, the largest of which are the Topolnitsa River, the Luda Yana River, the Stryama River, the Sazliyka River, the Tundzha River, the Arda River and others (Belkinova et al., 2013; Kiradzhiev, 2013).

The Mechka River (43 km) is a right tributary of the Maritsa River. The river originates in the Western Rhodopes, entering the Upper Thracian Lowland in the village of Poroyna and flowing into the Maritsa River near the town of Parvomay. The river's waters are used for irrigation (Kiradzhiev, 2013). A significant part of the country's territory is occupied by agricultural lands, of which approximately 30% is irrigated (Metodieva et al., 2024; Kilifarska et al., 2025).

According to the typology of rivers in Bulgaria, the Mechka River is of type R5 "Semi-mountainous rivers" (East Aegean River Basin Directorate, 2018). The largest tributary of the river is the Chinardere River (left tributary; 31 km) (Kiradzhiev, 2013).

According to the Water Framework Directive (Directive 2000/60/EU), in the assessment of the state of surface water, biological elements (listed in Annex V) play a leading role, while physicochemical and hydromorphological elements have a complementary role.

Studies concerning the assessment of the ecological state of the water of the Maritsa River have been conducted by Vidinova et al. (2008), Park et al. (2022a), Varadinova et al. (2022). At present, no studies have been established on the ecological state of the water of the Mechka River based on the biological quality element macrozoobenthos. Park et al. (2022b) and Park et al. (2023) provide data on the taxonomic composition and structure of the macrozoobenthos from the Maritsa River. Georgiev (2012) studied the freshwater malacofauna of rivers from the Upper Thracian Lowland, including the Mechka River.

The present study aims to assess the ecological state of the surface water of the Mechka River from the Maritsa River basin based on the

biological quality element (BQE) macrozoobenthos.

MATERIALS AND METHODS

Macrozoobenthos sampling was carried out in the autumn of 2024 from four locations (biotopes) along the Mechka River - 1) near the village of Lenovo (41°57'05.7"N 25°05'48.1"E); 2) near the village of Poroyna (42°02'19.9"N 25°08'42.8"E); 3) between the town of Parvomay and the village of Poroyna (42°03'11.7"N 25°09'08.3"E) and 4) before the town of Parvomay, Debar district (42°04'27.7"N 25°11'49.1"E) (Figure 1).

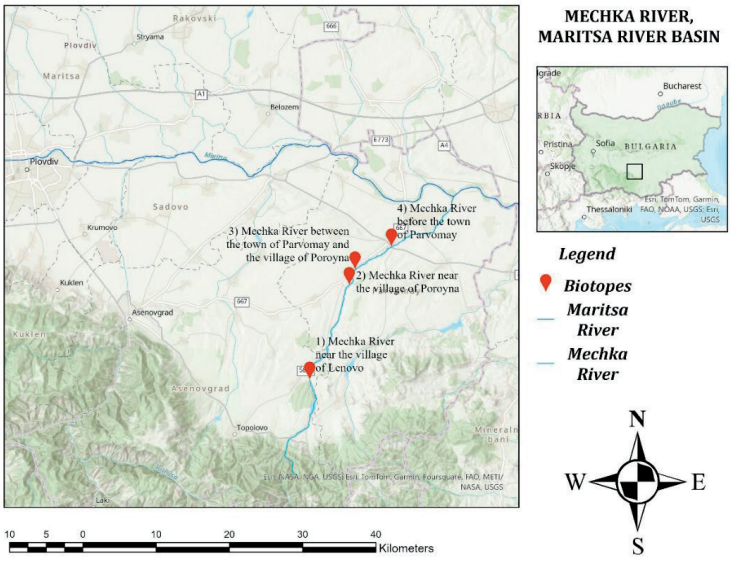


Figure 1. Map of the studied biotopes of the Mechka River

Biotope 1 is located along the Mechka River, northwest of the village of Lenovo (300 m above sea level), downstream of the Mechka Dam. The current is moderate to fast. Biotope 2 is located along the Mechka River, west of the village of Poroyna (215 m above sea level), upstream of the confluence with the Chinardere River. The current is moderate to fast. Biotope 3 is located along the Mechka River, between the village of Poroyna and the town of Parvomay (202 m above sea level), downstream of the confluence of the Chinardere River. The current is slow. Biotope 4 is located along the Mechka River, west of the Debar district, in the town of Parvomay (185 m above sea level). The current is moderate to fast. The river bed in all studied biotopes is sandy and rocky (Figure 2).

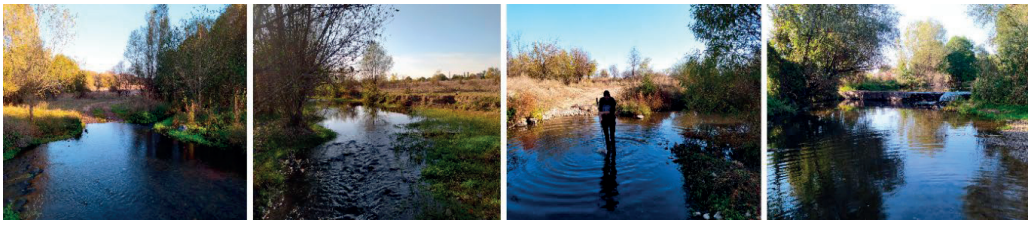


Figure 2. Views of the studied biotopes from the Mechka River (from left to right: 1) near the village of Lenovo; 2) near the village of Poroyna; 3) between the town of Parvomay and the village of Poroyna and 4) before the town of Parvomay)

Macrozoobenthos samples were collected in accordance with European and national water legislation and established methodologies (Cheshmedjiev et al., 2011; EN ISO 10870:2012; EN 16150:2012; Regulation No. H-4 of 14.09.2012; Belkinova et al., 2013). The taxonomic composition and abundance of macrozoobenthos from all biotopes were determined.

The ecological state of the Mechka River was assessed based on the following metrics: total number of taxa; number of Ephemeroptera, Plecoptera and Trichoptera (EPT) taxa; metrics for abundance of benthic macroinvertebrate fauna; Margalef species richness index (Dmg); Shannon-Weaver species diversity index (H'); Pielou's evenness index (E); Simpson's dominance index (C); saprobic index (SPUB); trophic index (RETI) and biotic index (BI) according to Flanagan & Toner (1972), modified by Clabby & Bowman (1979), Clabby (1982) (Belkinova et al., 2013).

RESULTS AND DISCUSSIONS

In this study, 772 specimens of macrozoobenthos belonging to 36 taxa and 15 orders (Allogastropoda, Amphipoda, Arhynchobdellida, Coleoptera, Diptera, Ephemeroptera, Hemiptera, Hygrophila, Isopoda, Odonata, Plecoptera, Sphaeriida, Trichoptera, Tricladida, Tubificida) were identified.

In the study of the macroinvertebrate fauna from the four biotopes along the Mechka River, the largest number of taxa was found in Biotope 2 (21 taxa) and the smallest – in Biotope 1 (14 taxa). The highest number of specimens was recordedin Biotope 3 (273 specimens) and the lowest – in Biotope 4 (Figure 3).

In the four biotopes, different macroinvertebrate taxa dominated: *Simulium* sp., larva (221 specimens; order Diptera) in Biotope 1; *Baetis* sp., nymph (64 specimens; order Ephemeroptera) in Biotope 2; *Asellus* (*Asellus*) *aquaticus* (Linnaeus, 1758) (128 specimens; order Isopoda) in Biotope 3; *Gammarus pulex* (Linnaeus, 1758) (11 specimens; order Amphipoda) in Biotope 4.

Only in Biotope 2 is the ecological state of the river according to the metric "total number of taxa" assessed as very good. In contrast, it is assessed as good in the other three biotopes.

Georgiev (2012) studied the freshwater malacofauna of the Mechka River (at the bridge of Parvomay town) and reported the species *Planorbis planorbis* (Linnaeus 1758) and *Anodonta cygnaea* (Linnaeus 1758). These two species were not found in any of the studied biotopes in the present study.

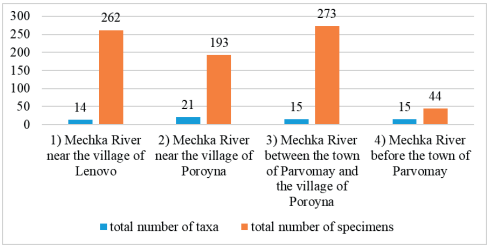


Figure 3. Taxonomic composition and abundance of macrozoobenthos in the studied biotopes

The highest number of EPT taxa was found in Biotope 2 (6 taxa with 105 specimens), followed by Biotope 1 (5 taxa with 20 specimens). An equal number of EPT taxa were found in biotope 3 (4 taxa with 53 specimens) and Biotope 4 (4 taxa with eight specimens) (Figure 4). Taxa from the orders Ephemeroptera, Plecoptera and Trichoptera are known to be sensitive to pollution. Therefore, their higher abundance in the Mechka River, Biotope 2, indicates a better ecological state of the water in this section. According to this metric, the Mechka River's ecological state ranges from good in Biotope 2 to moderate in the remaining three biotopes.

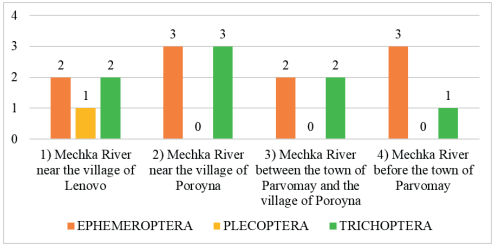


Figure 4. Number of EPT taxa in the studied biotopes

The obtained values for the Margalef species richness index (Dmg) indicate conditions that are suboptimal in all biotopes. The Shannon-Weaver species diversity index (H') indicates

better conditions in Biotopes 2 and 4 (β-mesosaprobic) compared to Biotope 1 (p-saprobic conditions) and Biotope 3 (α-mesosaprobic conditions). The Pielou's evenness index (E) and Simpson dominance index (C) indicate the most favourable conditions in Biotopes 2 and 4 and the most unfavourable in Biotope 1 (Table 1).

The highest percentage of Oligochaeta and Diptera, as well as the highest percentage of filtering feeders in total abundance was found for Biotope 1, where the percentage of EPT taxa was also the lowest. In Biotope 1, two Diptera taxa (*Simulium* sp., larva and *Chironomus plumosus* (Linnaeus, 1758), larva) represented by 234 specimens, and two filtering feeders taxa (*Simulium* sp., larva and *Pisidium* sp.) represented by 222 specimens were identified. The highest percentage of EPT taxa was recorded in Biotope 2 (Table 2).

Table 1. Species diversity indices

	Species richness index of Margalef (Dmg)	**Shannon-Weaver species diversity index (H')**	**Pielou's evenness index (E)**	**Simpson's dominance index (C)**
1) Mechka River near the village of Lenovo	2.33	0.763	0.289	0.716
2) Mechka River near the village of Poroyna	3.8	2.17	0.714	0.174
3) Mechka River between the town of Parvomay and the village of Poroyna	2.5	1.8	0.665	0.266
4) Mechka River before the town of Parvomay	3.46	2.34	0.888	0.124

Table 2. Abundance of macroinvertebrate fauna from the studied biotopes of the Mechka River

	% (Oligochaeta & Diptera)	**% Filtering feeders**	**% EPT taxa**
1) Mechka River near the village of Lenovo	89.31 %	84.73 %	7.63 %
2) Mechka River near the village of Poroyna	23.32 %	18.65 %	54.40 %
3) Mechka River between the town of Parvomay and the village of Poroyna	9.52 %	1.1 %	19.41 %
4) Mechka River before the town of Parvomay	15.91 %	4.55 %	18.18 %

To assess the ecological state of the Mechka River, the German trophic index RETI was calculated, which reflects varying levels of trophic impact across the studied sites. The index has the lowest value in biotope 1 ($RETI_{Biotope1}$ = 0.08), indicating a significant imbalance in the river ecosystem at this site. According to this index, the ecological state of the Mechka River varies from very bad in Biotope 1 to very good in Biotope 3 ($RETI_{Biotope3}$ = 0.8). The ecological state is good in the remaining two studied biotopes ($RETI_{Biotope2}$ = 0.74; $RETI_{Biotope4}$ = 0.59).

In Biotope 1, macrozoobenthos typical of 0-β-mesosaprobic conditions predominate (4 taxa). In Biotope 2, taxa indicative of β-mesosaprobic conditions predominate (4 taxa). In Biotopes 3 and 4, macroinvertebrates characteristic for β to β-α-mesosaprobic (3 taxa each) and 0-β to β-mesosaprobic conditions (3 taxa each), respectively, dominate (Figure 5).

The saprobic index (SPUB) was calculated based on the bioindicator potential of the macrozoobenthos from each biotope. A moderate ecological state was established in Biotope 3 ($SPUB_{Biotope3}$ = 2.43); good in Biotope 4 ($SPUB_{Biotope4}$ = 2.09) and very good ecological state in the remaining two biotopes ($SPUB_{Biotope1}$ = 1.68; $SPUB_{Biotope2}$ = 1.9).

The macroinvertebrate organisms found in this study belong to four groups of sensitivity: Group B (less sensitive forms), Group C (relatively tolerant forms), Group D (tolerant forms) and Group E (the most tolerant forms).

In three of the studied biotopes, the highest number of taxa and specimens belong to Group C. Only in Biotope 3 did the highest number of taxa belong to Group C, while the highest number of specimens belonged to Group D (Figure 6).

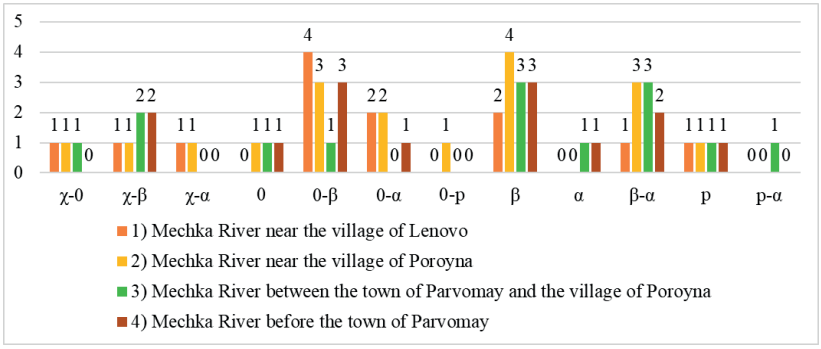


Figure 5. Distribution of macroinvertebrate taxa from the studied biotopes of the Mechka River by saprobity groups

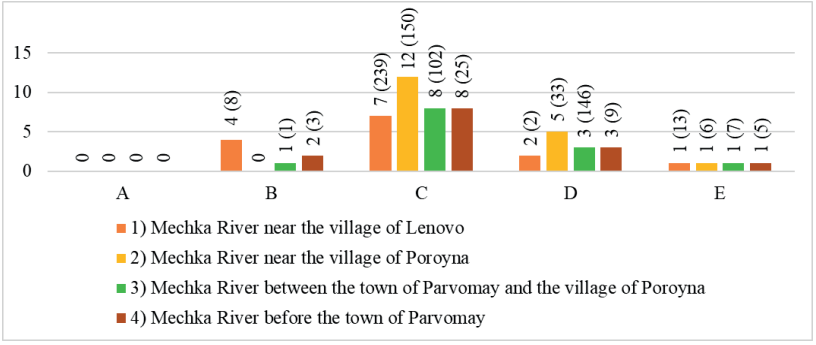


Figure 6. Distribution of macroinvertebrate taxa from the studied biotopes of the Mechka River by sensitivity groups

To determine the ecological state of the river, the biotic index (BI) was calculated, indicating a moderate ecological state in Biotopes 1 and 2 (BI (nEQR) = 2.5 (0.5)) and a bad ecological state in Biotopes 3 and 4 (BI (nEQR) = 2 (0.4)). During the period of this study, according to data from the East Aegean River Basin Directorate (2018) on deviations in the quality of surface water of the Mechka River, an exceedance of total nitrogen (2.5 mg/l at environmental quality standards (EQSs) set at 1.5 mg/l) was recorded on 12.11.2024 in the area of the town of Parvomay, Lyubenovo district. From September to November 2024, no other excesses of basic physicochemical elements and specific substances were established in the water of the Mechka River. According to the 2023 Report on the State of Water in the East Aegean Region, the ecological state of the upper section of the Mechka River (up to the confluence of Chinardere River), based on biological quality elements (BQEs), is unknown, while the ecological status of the lower reaches and tributary sections is assessed as moderate (East Aegean River Basin Directorate, 2018).

CONCLUSIONS

In the present study, 772 specimens of macrozoobenthos belonging to 36 taxa were identified. The highest number of taxa was identified in Biotope 2 near the village of Poroyna (21 taxa), and the lowest in Biotope 1) near the village of Lenovo (14 taxa). Based on the calculated metrics, the ecological state of the Mechka River is assessed as very bad in Biotope 1) near the village of Lenovo; bad in Biotopes 3 (between the town of Parvomay and the village of Poroyna), and 4 (before the town

of Parvomay, Debar district); and moderate in Biotope 2 near the village of Poroyna.

These findings indicate varying levels of ecological degradation along the river, with Biotope 1 showing the most critical conditions. We recommend that Biotope 1 be prioritized for inclusion in long-term monitoring programs to support targeted river management and conservation efforts.

ACKNOWLEDGEMENTS

This research is supported by the Bulgarian Ministry of Education and Science under the national Program "Young Scientists and Postdoctoral Students-2". The research results were published with the financial support of the Centre of Research, Technology Transfer and Protection of Intellectual Property Rights at the Agricultural University-Plovdiv under project No. 17-12, "Support for publication activities".

REFERENCES

Belkinova, D., Gecheva, G., Cheshmedzhiev, S., Dimitrova-Dyulgerova, I., Mladenov, R., Marinov, M., Teneva, I., Stoyanov, P., Ivanov, P., Mihov, S., Pehlivanov, L., Varadinova, E., Karagyozova, Ts., Vassilev, M., Apostolu, A., Velkov, B., & Pavlova, M. (2013). *Biological analysis and ecological assessment of surface water types in Bulgaria*. Plovdiv, BG: Univ "P. Hilendarskii" Publishing House (in Bulgarian).

Cheshmedjiev, S., Soufi, R., Vidinova, Y., Tyufekchieva, V., Yaneva, I., Uzunov, Y., & Varadinova, E. (2011). Multi-habitat sampling method for benthic macroinvertebrate communities in different river types in Bulgaria. *Water Research and Management, 1*(3), 55–58.

Clabby, K.J., & Bowman, J.J. (1979). *Report of Irish Participants.* In: Ghetti P.F. (Ed.): Third Technical Seminar on Biological Water Assessment Methods, Parma, 1978. Vol. 1. Commission of the European Communities.

Clabby, K.J. (1982). *The National Survey of Irish Rivers: River Quality Investigations--biological Results of the 1980 & 1981 Investigations: Summary Report*. Environmental Research Unit.

Directive 2000/60/EU of the European Parliament and of the Council, 2000. Luxembourg, 23.

East Aegean River Basin Directorate (2018). https://earbd.bg/ (in Bulgarian).

EN ISO 10870:2012 Water quality - Guidelines for the selection of sampling methods and devices for benthic macroinvertebrates in fresh waters (ISO 10870:2012)

EN 16150:2012 Water quality - Guidance on pro-rata Multi-Habitat sampling of benthic macroinvertebrates from wadeable rivers

Flanagan, P.J. Toner, P.F. (1972). *Notes on the chemical and biological analysis of Irish River waters*. An FORAS Forbartha.

Georgiev, D. (2012). Freshwater malacofauna of Upper Thracian Lowland (Southern Bulgaria). *Acta zoologica bulgarica, 64*. 413–420.

Kilifarska, N.A., Metodieva, G.I., & Mokreva, A.C. (2025). Detection and Attribution of a Spatial Heterogeneity in the Temporal Evolution of Bulgarian River Discharge. *Geosciences, 15*. 12.

Kiradzhiev, S. (2013). *Encyclopedic Geographical Dictionary of Bulgaria*. Sofia, BG: Iztok-zapad Publishing house (in Bulgarian).

Metodieva, G., Mokreva, A., & Kilifarska, N. (2024). Parametric and non-parametric estimations of Bulgarian rivers' outflow trends. *Sixth International Conference, CAWRI-BAS "Global Warming's Imprints on the Elements of the Climatic System", Hisarya, 24–28 September 2024*, 109–116.

Park, J., Sakelarieva, L., & Varadinova, E. (2022a). Comparative Analysis of the Water Policies and the Systems for Ecological Status Assessment of the Running Waters in Bulgaria and South Korea: Case study on Maritsa River and Han River. *Ecologia Balkanica, 14*(2), 171–189.

Park, J., Sakelarieva L., Varadinova E., Evtimova E., Evtimova V., Vidinova Y., Tyufekchieva V., Georgieva G., Ihtimanska M., & Todorov M. (2022b). Taxonomic Composition and Dominant Structure of the Macrozoobenthos in the Maritsa River and Some Tributaries, South Bulgaria. *Acta zoologica bulgarica, Supplement, 16*. 61–74.

Park, J., Sakelarieva, L.G., & Varadinova, E.D. (2023). Comparative Analysis of the Structure of Benthic Macroinvertebrate Communities in Maritsa River (Bulgaria) and Han River (South Korea). *Ecologia Balkanica, 15*(2).

Regulation No. H-4 of 14.09.2012 on the characterization of surface waters. Promulgated in the Official Gazette, No. 22 of 5.03.2013, amended and supplemented, No. 67 of 04.08.2023.

Varadinova, E., Sakelarieva, L., Park, J., Ivanov, M., Tyufekchieva, V. (2022). Characterization of Macroinvertebrate Communities in Maritsa River (South Bulgaria) - Relation to Different Environmental Factors and Ecological Status Assessment. *Diversity, 14*. 833.

Vidinova, Y.N., Botev, I S., Tyufekchieva, V.G., Nedyalkova, T.V., Yaneva, I.Y., Zadneprovski, B.E., & Varadinova, E.D. (2008). Results of rapid hydrobiological monitoring of watersheds from the East-and West Aegean Sea River basin districts in Bulgaria. *Acta zoologica bulgarica, Supplement, 2*. 233–242.

Scientific Papers. Series E. Land Reclamation, Earth Observation & Surveying, Environmental Engineering. Vol. XIV, 2025
Print ISSN 2285-6064, CD-ROM ISSN 2285-6072, Online ISSN 2393-5138, ISSN-L 2285-6064

ECOLOGICAL ASSESSMENT OF THE KAYALIIKA RIVER WITHIN THE MARITSA RIVER WATERSHED USING MACROZOOBENTHOS AS A BIOINDICATOR

Radoslava ZAHARIEVA[1, 2], Petya ZAHARIEVA[1, 2], Diana KIRIN[1, 2]

[1]National Institute of Geophysics, Geodesy and Geography (NIGGG), Hydrology and Water Management Research Center, Bulgarian Academy of Sciences, 3 Acad. G. Bonchev Street, 1113, Sofia, Bulgaria
[2]Agricultural University - Plovdiv, 12 Mendeleev Blvd, 4000, Plovdiv, Bulgaria

Corresponding author email: radoslava.zaharieva7@gmail.com

Abstract

The study aims to conduct hydrobiological monitoring of the Kayaliika River (Maritsa River watershed) based on the biological quality element macrozoobenthos. The monitoring was performed following methodologies approved by the European Union and Bulgaria. Macrozoobenthos samples were collected in the autumn of 2024 from four locations (biotopes) along the Kayaliika River near the village of Ezerovo, Bodrovo, Varbitsa and Skobelevo. The number and taxonomic composition of the macrozoobenthos were determined, with the highest number of taxa found in the Kayaliika River biotope near the village of Skobelevo – 28 taxa, and the lowest – in the Kayaliika River biotope near the village of Varbitsa – 12 taxa. Basic indices for species diversity and abundance were calculated. The number of macrozoobenthos taxa by saprobity groups and sensitivity groups from the four biotopes of the studied river ecosystem was presented and compared. The results provide valuable insights into the ecological status of the Kayaliika River and contribute to regional water quality assessments.

Key words*: biological quality elements (BQE), ecological assessment, Kayaliika River, macrozoobenthos, water quality.*

INTRODUCTION

The territory of Bulgaria covers an area of 110,994 km^2 (Metodieva et al., 2024; Kilifarska et al., 2025), characterized by a complex hydrogeographic network (Belkinova et al., 2013). The countryis divided into four river basin management regions: Danube, Black Sea, East Aegean and West Aegean (Cheshmedjiev et al., 2010). The East Aegean region covers 31% of Bulgaria's territory and encompasses the catchments of four rivers (Maritsa, Tundzha, Arda and Byala). The Maritsa River is the largest river on the Balkan Peninsula and has over 100 tributaries (Belkinova et al., 2013), one of which is the Kayaliika River.

The Kayaliika River originatesin the Rhodope Mountains near the village of Zhalt Kamak. It flows for 39 km, passing through the villages of Iskra, Bregovo, Dragoynovo, Ezerovo, Bodrovo, Varbitsa and the village of Skobelevo, before discharging into the Maritsa River (Kiradzhiev, 2013). According to the East Aegean River Basin Directorate (2018), the Kayaliika River is classified as type R5 ("Semi-mountainous river").

Water is a valuable natural resource. River waters are used for irrigation and domestic and industrial needs. However, various anthropogenic activities contribute to water pollution (Gartsiyanova et al., 2022; Gartsiyanova et al., 2024). Benthic macroinvertebrates a key component of aquatic ecosystems, are widely used as bioindicators due to their low mobility, long life cycles, and sensitivity to pollution. Their abundance and diversity depend on the physicochemical properties of the water and substrate. Any environmental changes directly influence macrozoobenthos communities, making them essential for biological monitoring (Rashid & Pandit, 2014). According to the Water Framework Directive (Directive 2000/60/EU), the leading role in assessing the ecological state of surface water is played by the biological quality elements (BQEs) (algae, macrophytes, benthic macroinvertebrates, fish) listed in Annex V of the Directive. Physicochemical and

hydromorphological quality elements have a complementary role and provide information about the causes that led to the deterioration of the ecological state. The final ecological state assessment is determined according to the "one out – all out" rule (Belkinova et al., 2013). Despite extensive hydrobiological studies in Bulgaria, no prior research has assessed the ecological state of the Kayaliika River using biological quality elements.

This study aims conduct hydrobiological monitoring of the Kayaliika River using macrozoobenthos as a biological quality element, contributing to regional water quality assessments and ecological status evaluation.

MATERIALS AND METHODS

Hydrobiological monitoring of the Kayaliika River was carried out in the autumn of 2024. Four biotopes located along the Kayaliika River were selected and surveyed: the Ezerovo biotope (42°00'49.0"N 25°17'24.2"E); the Bodrovo biotope (42°01'41.6"N 25°18'54.6"E); the Varbitsa biotope (42°03'07.8"N 25°20'40.2"E) and the Skobelovo biotope (42°05'35.4"N 25°22'33.8"E) (Figures 1-2; Table 1).

Macrozoobenthos samples were collected using standardized methods (Cheshmedjiev et al. 2011; EN ISO 10870:2012; EN 16150:2012; Regulation No. H-4 of 14.09.2012; Belkinova et al., 2013). Sampling was conducted using a kick net sampler. The collected material was preserved in 70% ethyl alcohol until subsequent laboratory processing. In laboratory conditions, the taxonomic affiliation of the macrozoobenthos was determined using a Micros Austria MZ 1240 stereomicroscope. The following metrics were calculated:

- The total number of taxa;
- The number of taxa from the orders Ephemeroptera, Plecoptera and Trichoptera (EPT);
- Margalef species richness index (Dmg);
- Shannon-Weaver species diversity index (H');
- Pielou's evenness index (E);
- Simpson's dominance index (C);
- Abundance metrics (% (Oligochaeta & Diptera), % Filtering feeders, % EPT taxa);
- Saprobic index (SPUB), trophic index (RETI) and
- Adapted Biotic Index (BI) according to Regulation No. H-4 of 14.09.2012 and Belkinova et al. (2013).

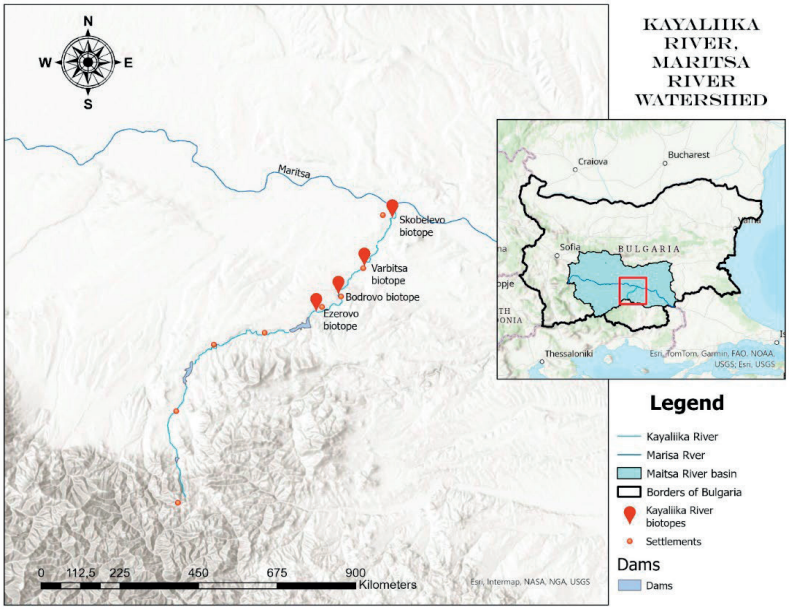


Figure 1. Researched biotopes along the Kayaliika River, Maritsa River watershed



Figure 2. Views of the studied biotopes from the Kayaliika River (from left to right: 1) near the village of Ezerovo; 2) near the village of Bodrovo; 3) near the village of Varbitsa and 4) near the village of Skobelevo)

Table 1. Characteristics of the studied biotopes from the Kayaliika River

Biotopes	Altitude	Location	Bottom substrate and current speed
Ezerovo	197 м	Along the Kayaliika River, southwest of the village of Ezerovo, after the Ezerovo Dam	Sandy/muddy bottom and slow current
Bodrovo	180 м	Along the Kayaliika River, northwest of the village of Bodrovo	Sandy/muddy bottom and slow current
Varbitsa	173 м	Along the Kayaliika River, within the borders of the village of Varbitsa	Sandy/rocky bottom and slow current
Skobelevo	148 м	Along the Kayaliika River, east of the village of Skobelevo, before flowing into the Maritsa River	Sandy/rocky bottom and slow current

RESULTS AND DISCUSSIONS

During the hydrobiological monitoring of the Kayaliika River, a total of 970 specimens of 42 taxa were identified. These taxa included: (*Asellus (Asellus) aquaticus* (Linnaeus, 1758); *Anodonta cygnea* (Linnaeus, 1758); *Atherix ibis* (Fabricius, 1798), larva; *Baetis* sp., nymph; *Bithynia tentaculata* (Linnaeus, 1758); *Caenis horaria* (Linnaeus, 1758), nymph; Ceratopogonidae; Chironomidae, larva and pupa; *Chironomus plumosus* (Linnaeus, 1758), larva; *Cloeon* sp., nymph; *Corixa* sp., nymph; *Culex* sp., larva; *Dytiscus* sp., larva; *Enallagma cyathigerum* (Charpentier, 1840), larva; *Gammarus pulex* (Linnaeus, 1758); *Gerris* sp., nymph; *Glossiphonia* sp.; *Gomphus* sp., larva; *Gyraulus (Gyraulus) albus* (O.F.Müller, 1774); *Gyrinus substriatus* Stephens, 1829; *Haemopis sanguisuga* (Linnaeus, 1758); *Hydropsyche ornatula* McLachlan, 1878, larva; *Hydroporus* sp.; *Hydroptila* sp., larva; *Hyphydrus ovatus* (Linnaeus, 1761); *Ilyocoris cimicoides* (Linnaeus, 1758), nymph; *Lethocerus patruelis* (Stål, 1854); *Limnodrilus hoffmeisteri* Claparède, 1862; *Lumbricus rubellus* Hoffmeister, 1843; *Notonecta* sp., nymph; *Peregriana peregra* (O.F.Müller, 1774) (syn. *Radix peregra*); *Physella acuta* (Draparnaud, 1805); *Platambus maculatus* (Linnaeus, 1758); *Plea minutissima* Leach, 1818; *Radix (Radix) auricularia* (Linnaeus, 1758); *Rhantus frontalis* (Marsham, 1802); *Schmidtea polychroa* (Schmidt, 1861); *Sialis lutaria* (Linnaeus, 1758); *Simulium* sp., larva; *Sphaerium (Sphaerium) corneum* (Linnaeus, 1758); *Tipula* sp., larva; *Valvata (Cincinna) piscinalis* (O.F.Müller, 1774)). These taxa belonged to 18 orders and were found in the four studied biotopes, including: Amphipoda, Arhynchobdellida, Coleoptera, Crassiclitellata, Diptera, Ephemeroptera, Gastropoda, Hemiptera, Isopoda, Littorinimorpha, Megaloptera, Odonata, Rhynchobdellida, Sphaeriida, Trichoptera, Tricladida, Tubificida, Unionida. Insects in the order Hemiptera do not undergo a larval and pupal stage; instead, they develop through several nymph stages or "instars". The highestnumber of macrozoobenthos taxa was found in the Skobelevo biotope, and the lowest– in the Varbitsa biotope (Figure 3). The dominant macrozoobenthos taxon in the Ezerovo and Varbitsa biotopes is *En. cyathigerum*, larva (order Odonata), with 103 and 40 specimens, respectively. Dominant in the Bodrovo biotope

is *G. pulex* (order Amphipoda) with 40 specimens, and in the Skobelevo biotope – *Cloeon* sp., nymph (order Ephemeroptera) with 141 specimens. According to the total number of taxa metric, the ecological state of the Kayaliika River was classified as very good in three of the studied biotopes and good in the Varbitsa biotope.

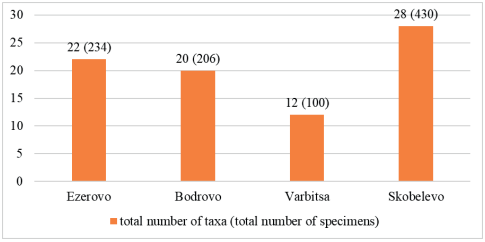


Figure 3. Total number of macrozoobenthos taxa by biotope

In general, acrossall four studied biotopes, there were few representatives of the Ephemeroptera and Trichoptera. Plecoptera taxa were absent, which contribute to the classification of a moderate ecological state for Ezerovo, Bodrovo and Skobelevo biotopes and a bad ecological state for the Varbitsa biotope (Figure 4).

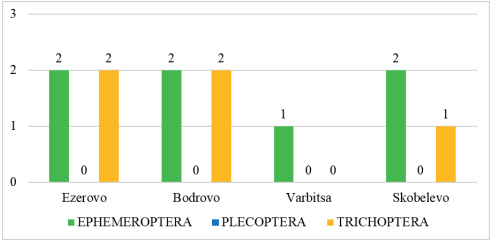


Figure 4. Number of taxa from the orders Ephemeroptera, Plecoptera and Trichoptera by biotope

The percentage of Oligochaeta and Diptera, as well as the percentage of Filtering feeders, is lowest in the Ezerovo biotope, while the percentage of EPT taxa is relatively high, indicating a weakly influenced river ecosystem. In contrast, the Varbitsa biotope shows the highest percentage of Oligochaeta and Diptera and the lowest percentage of EPT taxa, suggesting anthropogenic pressure on the aquatic environment in this section of the river (Figure 5).

The value of the German trophic index RETI increases downstream along the Kayaliika River, with the highest value observed in the Skobelevo biotope ($RETI_{Skobelevo}$ = 0.79), indicating a stable and undisturbed river ecosystem in this biotope. According to the RETI index, the ecological state of the Kayaliika River is classified as good across all four biotopes ($RETI_{Ezerovo}$ = 0.51; $RETI_{Bodrovo}$ = 0.62; $RETI_{Varbitsa}$ = 0.67).

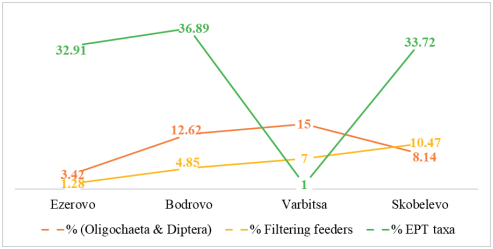


Figure 5. Macrozoobenthos abundance metrics by biotopes

The macrozoobenthos identified in this study belong to 4 sensitivity groups –: Group B (less sensitive forms), Group C (relatively tolerant forms), Group D (tolerant forms) and Group E (the most tolerant forms). No taxa were identified from Group A (sensitive forms). In three of the studied biotopes (Ezerovo, Bodrovo and Skobelevo), the majority ofmacrozoobenthos taxa belonged to Group C. In the Varbitsa biotope, an equal number of taxa for Groups C and D were identified (Figure 6).

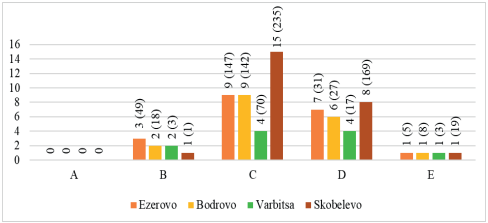


Figure 6. Distribution of macrozoobenthos taxa by sensitivity groups

In the Ezerovo biotope, indicator macrozoobenthos for β and β-α-mesosaprobic conditions prevails (6 taxa each). In the Bodrovo biotope, taxa indicating β-mesosaprobic conditions were dominant (6 taxa), while in the Varbitsa biotope taxa

indicating for 0-β and β-α-mesosaprobic conditions (3 taxa each). In the Skobelevo biotope taxa characteristic of 0-β and β-mesosaprobic conditions dominated (6 taxa each) (Figure 7).

According to the obtained values of the saprobic index (SPUB), the ecological state of the Ezerovo, Bodrovo and Varbitsa biotopes was classified as very good ($SPUB_{Ezerovo}$ = 1.89; $SPUB_{Bodrovo}$ = 1.69; $SPUB_{Varbitsa}$ = 1.80), while in the Skobelevo biotope the ecological state was assessed as good ($SPUB_{Skobelevo}$ = 2.07).

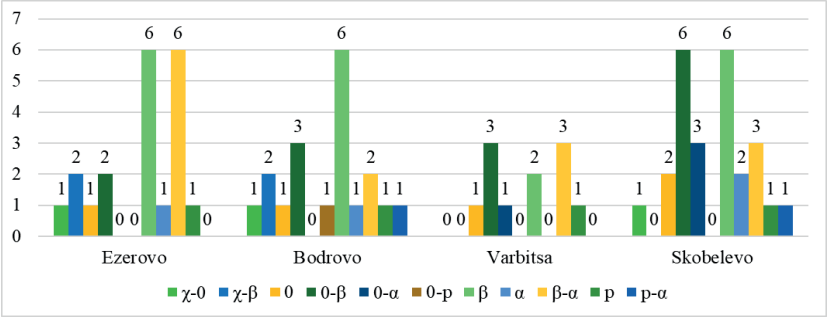


Figure 7. Distribution of macrozoobenthos taxa by saprobity groups

The Margalef species richness index (Dmg) in all studied biotopes was below 8, indicating that the environmental conditions in the studied river ecosystem are not optimal. The Shannon-Weaver species diversity index (H') indicated β-mesosaprobic conditions in three of the studied biotopes (Ezerovo, Bodrovo and Skobelevo) and α-mesosaprobic conditions in the Varbitsa biotope. The calculated Pielou's evenness index (E) and Simpson's dominance index (C) showed the most favorable conditions in the Bodrovo biotope (E = 0.845; C = 0.106) (Figure 8).

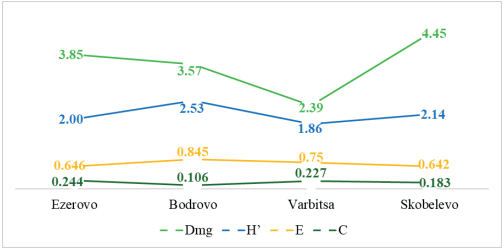


Figure 8. Species diversity indices (Margalef species richness index (Dmg), Shannon-Weaver species diversity index (H'), Pielou's evenness index (E), Simpson's dominance index (C)) by biotope

The biotic index (BI) indicates a bad ecological state in the Varbitsa biotope – BI (nEQR) = 2 (0.4) and a moderate state in the other three biotopes – BI (nEQR) = 2.5 (0.5).

CONCLUSIONS

During the hydrobiological monitoring of the Kayaliika River, a total of 42 taxa of macroinvertebrate organisms were identified, represented by 970 specimens, from the four studied biotopes. The highest number of macrozoobenthos taxa was recorded in the Skobelevo biotope (28 taxa), while the lowest number was observed in the Varbitsa biotope (12 taxa). Based on the assessment of biological quality elements (BQE), particularly macrozoobenthos, the ecological state of the river was classified as moderate in the Ezerovo, Bodrovo, and Skobelevo biotopes, and bad in the Varbitsa biotope, reflecting potential anthropogenic pressures.

These findings underscore the importance of regular biological monitoring to detect early signs of ecological degradation and guide targeted conservation measures. Further research integrating physicochemical parameters and land-use impacts is recommended to support comprehensive water management strategies for the Kayaliika River.

ACKNOWLEDGEMENTS

This research is supported by the Bulgarian Ministry of Education and Science under the national Program "Young Scientists and

Postdoctoral Students-2". The study results have been published with financial support (project No. 17-12) of the Centre of Research, Technology Transfer and Protection of Intellectual Property Rights at the Agricultural University-Plovdiv.

REFERENCES

Belkinova, D., Gecheva, G., Cheshmedzhiev, S., Dimitrova-Dyulgerova, I., Mladenov, R., Marinov, M., Teneva, I., Stoyanov, P., Ivanov, P., Mihov, S., Pehlivanov, L., Varadinova, E., Karagyozova, Ts., Vassilev, M., Apostolu, A., Velkov, B., & Pavlova, M. (2013). *Biological analysis and ecological assessment of surface water types in Bulgaria.* Plovdiv, BG: Univ "P. Hilendarskii" Publishing House (in Bulgarian).

Cheshmedjiev, S.D., Karagiozova, T.L., Michailov, M.A., & Valev, V.P. (2010). Revision of river & lake typology in Bulgaria within Ecoregion 12 (Pontic Province) and Ecoregion 7 (Eastern Balkans) According to the Water Framework Directive. *Ecologia Balkanica, 2*. 75–96.

Cheshmedjiev, S., Soufi, R., Vidinova, Y., Tyufekchieva, V., Yaneva, I., Uzunov, Y., & Varadinova, E. (2011). Multi-habitat sampling method for benthic macroinvertebrate communities in different river types in Bulgaria. *Water Research and Management, 1*(3), 55–58.

Directive 2000/60/EU of the European Parliament and of the Council (2000). *Establishing a framework for Community action in the field of water policy*. Luxembourg, 23.

East Aegean River Basin Directorate (2018). https://earbd.bg/ (in Bulgarian).

EN ISO 10870:2012 *Water quality - Guidelines for the selection of sampling methods and devices for benthic macroinvertebrates in fresh waters (ISO 10870:2012)*

EN 16150:2012 *Water quality - Guidance on pro-rata Multi-Habitat sampling of benthic macroinvertebrates from wadeable rivers*

Gartsiyanova, K., Kitev, A., Varbanov, M., Georgieva, S., & Genchev, S. (2022). Water quality assessment and conservation of the river water in regions with various anthropogenic activities in Bulgaria: A case study of the catchments of Topolnitsa and Luda Yana rivers. *International Journal of Conservation Science, 13*(2), 733–742.

Gartsiyanova, K., Genchev, S., & Kitev, A. (2024). Assessment of water quality as a key component in the water–energy–food nexus. *Hydrology, 11*(3), 36.

Kilifarska, N.A., Metodieva, G.I., & Mokreva, A.C. (2025). Detection and Attribution of a Spatial Heterogeneity in the Temporal Evolution of Bulgarian River Discharge. *Geosciences, 15*. 12.

Kiradzhiev, S. (2013). *Encyclopedic Geographical Dictionary of Bulgaria.* Sofia, BG: Iztok-zapad Publishing house (in Bulgarian).

Metodieva, G., Mokreva, A., & Kilifarska, N. (2024). Parametric and non-parametric estimations of Bulgarian rivers' outflow trends. *Sixth International Conference, CAWRI-BAS "Global Warming's Imprints on the Elements of the Climatic System", Hisarya, 24-28 September 2024,* 109–116.

Rashid, R., & Pandit, A.K. (2014). Macroinvertebrates (oligochaetes) as indicators of pollution: A review. *Journal of Ecology and the Natural Environment, 6*(4), 140–144.

Regulation No. H-4 of 14.09.2012 on the characterization of surface waters. *Promulgated in the Official Gazette, No. 22 of 5.03.2013, amended and supplemented, No. 67 of 04.08.2023.*

Scientific Papers. Series E. Land Reclamation, Earth Observation & Surveying, Environmental Engineering. Vol. XIV, 2025
Print ISSN 2285-6064, CD-ROM ISSN 2285-6072, Online ISSN 2393-5138, ISSN-L 2285-6064

THE EFFECTS OF APPLYING THE LAW IN CADASTRE ACTIVITY – A COMPARATIVE STUDY OF THE RESOLUTIONS THAT CAN BE ADOPTED FOR THE REGISTRATION OF REAL ESTATE PROPERTIES IN THE LAND REGISTRY

Andreea BEGOV-UNGUR[1], Ioana Aurica BERINDEIE[2], Levente DIMEN[1]

[1]"1 Decembrie 1918" University of Alba Iulia,
13 Gabriel Bethlen Street, 510009, Alba Iulia, Romania
[2]Total Business Land SRL, 5 Bucovinei Street, 510217, Alba Iulia, Romania

Corresponding author email: ioana_berindeie@yahoo.com

Abstract

Starting from the statement "A good cadastre of the parcels will be the complement of my civil code," the fundamental importance of the cadastre in the management of land and real estate properties becomes evident. It provides a detailed and up-to-date record of land parcels, including their owners, describing the boundaries and characteristics of each property. Through this, the cadastre facilitates the implementation and adherence to legal norms regarding property rights and their transfer. In the context of societal development and evolution, a well-maintained cadastre becomes an essential tool for urban planning, natural resource management, and infrastructure project implementation. Furthermore, a modern cadastre system can help prevent legal disputes related to property and serve as a crucial instrument in urbanization and economic development processes. An efficient cadastre is not only a technical necessity but also a fundamental element for the functioning of a coherent legal system and for responsible real estate management, contributing to the establishment and maintenance of a cohesive societal structure.

Key words*: property rights, legislative changes, real estate, collectivization, possession.*

INTRODUCTION

The study of the effects of applying the law in cadastre activity, through a comparative analysis of the resolutions adopted for the registration of real estate properties in the land registry, represents a research endeavor that warrants the attention and careful analysis of the academic community and decision-makers. This complex and current topic is essential for the preservation and efficiency of land and real estate management systems.

The evolution of legislation in the field of cadastre and real estate is inevitable in a continuously changing society. In this context, the current law regulating the cadastre and real estate publicity in Romania, Law no. 7/1996, represents a crucial pillar in defining the legal framework for land and property management (Badea & Badea, 2015 a).

The year 2023 brought significant legislative changes, highlighted by the modification of Order 700/2014 into the new reception and registration order 600/2023. This legislative change was subsequently adjusted by Decision no. 6 of 13.04.2021 regarding Minute no. 16893/2753 of 13.04.2021 of the Director of the Real Estate Publicity Directorate and Decision 1255 of 17 July 2023, reflecting the necessary adaptations to the continuously changing societal requirements. Through these changes, the legislation aims to streamline cadastral processes, provide a clear and updated framework for owners, and facilitate the implementation of new technologies within cadastre and real estate publicity activities. It is essential to evaluate and understand these legislative changes to appreciate how they might influence research and practice in the field of cadastre.

A well-defined and clear legal framework regarding the cadastre offers owners confidence in the management system of their properties. By adopting effective resolutions, property rights can be protected, and real estate transactions facilitated, contributing to the stimulation of the real estate market and economic growth.

MATERIALS AND METHODS

Technical and cadastral documentation is prepared based on Law 7/1996 on cadastre and real estate publicity and Order of the General Director no. 600/2023 with subsequent amendments and completions. The technical documentation for initial registration is categorized into the following main types (Badea & Badea, 2015 b; Pădure et al., 2006):

- Initial registration in the integrated cadastre and land registry system; This involves preparing technical documentation for initial registration in the integrated cadastre and land registry system, with the allocation of a cadastral number for:

1. The registration of property rights acquired under property laws:

Law 18/1991	Law 123/2023	Law 15/1990	Law 1/2000	Law 247/2005
Land Fund	For the amendment and completion of Law 18/1991	Regarding the reorganization of state economic units as autonomous regies and commercial companies	Reconstitution of property rights over agricultural and forest lands	Regarding the reform in property and justice domains, as well as some adjacent measures

2. Technical documentation for initial registration – possession notation (Art. 41, para. (8) of Law no. 7/1996 on Cadastre and Real Estate Publicity, Art. 119 ODG 600/2023, for which no registrations have been made in the last 30 years prior to the coming into force of Law 287/2009 regarding the Civil Code). For preparing the documentation, after measurements are completed, land registry identification will be necessary (required both if the property is located within and outside the built-up area of a locality).

3. Technical documentation for initial registration based on a civil judgment; Given that the judgment noted in the land registry, it must be final, irrevocable, and enforceable.

4. Technical documentation for initial registration – identification of the property located in a different administrative territorial unit (UAT) than the one recorded in the land registry (Art. 120-122 of ODG 600/2023). In fact, this is an update of the old land registry with current attributes and the registration of the correct UAT. The particularity of this documentation is represented by the "report of finding and cancellation of cadastral number, prepared by the cadastral inspector and approved by the chief engineer, which is registered ex officio in the General Entry Register, based on which the old land registry is terminated".

5. Consolidation of properties registered in the land registry opened according to Decree-Law no. 115/1938, which were not the subject of registration in the land registry by allocating a cadastral number with the appearance of Law 7/1996 on Cadastre and Real Estate Publicity, but have always been part of the same property body; If only part of the property registered in a land registry based on Decree-Law no. 115/1938 was the subject of one of the aforementioned normative acts, it is necessary to detach that part by forming a new property for which a new land registry will be prepared. This procedure will be mentioned in the existing land registry. The unaffected part will be re-registered in favor of the old owners from the old land registry, while the detached part will have a new land registry created. The existing land registry will mention the cadastral number and the land registry number in which the property has been transcribed. Regarding the opening of the new land registry, if the property is assigned a cadastral number, the area and categories of use will be assimilated according to the cadastral documentation, and for the second and third parts of the land registry, the information will be taken. Thus, a land registry decision will be generated, which will be communicated to all interested parts.

Registration in a new land registry is carried out by preparing initial cadastral documentation for the actual measured area of the property, based on the provisions of Art. 41 of Law 7/1996 on Cadastre and Real Estate Publicity and Art. 72, para. (1) of ODG 600/2023.

When referring to the area where the property is located, we will consider the built-up area and outside built-up area of the administrative territorial unit within which it is classified. Thus, concerning these areas, both in terms of address and the choice of suitable and correct documentation type, we will refer.

This refers to the initial registration in the integrated cadastre and land registry system of a property located in the built-up area, where the area determined from measurements may be up to 15% larger and in the outside built-up area up to 5%, otherwise, registration is not permitted.
Regarding the categories and subcategories of land use, these are determined based on observations made in the field and the documents proving the legality of the changes made.
In other words, for registration, we distinguish the following cases:

Urban land	Rural land	
	Cooperativism area	**Uncooperative area**
The categories of use will be entered according to the actual use (of the cadastral documentation). The deviation from the rule is made in the case of vineyards with an area greater than 200 sq m, which will not be able to be modified. Equally, the categories of use will be those in the sentence, if it exists.	The categories of use of the property do not change unless it is removed from agricultural use.	The categories of use will be recorded according to the cadastral documentation (with the updated fiscal attestation certificate according to the location and delimitation plan) or based on a civil sentence, where applicable.

- Registration in the cadastral plan of real estate located in the land registry regions subject to Decree-Law 115/1938.

This type of documentation applies if the real estate has not been the subject of registration in the land registry by allocating a cadastral number since the advent of Law 7/1996 on the cadastre and real estate advertising, but it was registered based on Decree-Law 115/1938, in other words in the situation where the land has never been the subject of cadastral documentation. This case should not be confused with the situation in which the real estate comes from the same old land registry, being registered under the title of reconstitution by tabulation of some plots of a property title, in which case correction of the error by conversion is requested.
This will result in a single land registry which will subsequently be subject to the cadastral data update offer.

RESULTS AND DISCUSSIONS

This study refers to the Land Registry of identifying a property, with records dating before 1st of October 1981. It is important to note that the registered owner in the document is not in the direct line of descent of the benefiting family. According to the documentation, the nominal area of the property is 462 m², while actual measurements indicate an area of 528 m². In fact, the property is owned by Mr. Nicolae Popescu, who is also the seller in the transaction that constitutes the subject of this study. It is noted that the real estate transaction will occur between the father and his son, Marcu Popescu.
Since the property is located in a cooperative area, as certified by the Cugir City Hall, the following resolutions can be adopted for the property under study:

- Technical and Cadastral Documentation for Issuance of the Property Title Based on the Provisions of Law No. 18/1991 on the Land Fund and Law No. 1/2000 for the Restoration of Property Rights on Agricultural and Forest Land. The property title will be issued in favor of Mr. Nicolae Popescu, who is registered in the agricultural register for which a tax certificate can be issued. The technical documentation will be delivered in 3 copies (one copy for the beneficiary, one copy for the municipality, and one copy for the Local Land Fund Commission, which will be forwarded to the Cadastre and Real Estate Publicity Office for verification and approval). Following the issuance of the property title, it will be registered in the land register as the first entry based on the property title. Subsequently, based on the land registry extract and the sale-purchase contract, the notary will submit the registration request to the Cadastre and Real Estate Publicity Office for registration in favor of the new owner.
- Technical Documentation for the First Registration Based on Article 41 (10) of Law No. 7/1996, Republished with Subsequent Amendments and Additions. In this case, the atypical document required is the certificate according to Annex 1.51/1 of Order No. 3442/2019, which demonstrates that the owner was a cooperative member, thus enabling him to obtain registration in his favor. For this property, until April 13, 2021, possession could have been noted in favor of the actual possessor. However,

according to Decision No. 6/April 16, 2021, and Minute No. 16983/2753 dated April 13, 2021, attached to it, point b) states that possession "is not possible for properties located in former cooperative zones, regardless of whether property titles have been issued under Law No. 18/1991 on the Land Fund".

➢ Extra-Tabulary Adverse Possession: First Registration Based on a Civil Judgment. Extratabular adverse possession is defined as the situation where the adverse possessor is not registered as the owner in the land register (even though the property has a land register) or the property does not even have a land register. The adverse possessor can claim adverse possession as an exception if sued by the rightful owner or can file a request with the court to definitively consolidate his ownership right. The conditions that must be met by the beneficiary of our work are as follows:

1. Possession of 10 Years: This period can be interrupted due to defects in possession; however, these defects only suspend the process of adverse possession (if they occur). Overall, the possessor must hold the property as a true owner for a period of 10 years. It is possible to combine (junction) possessions when multiple possessors use the property successively. To prove this union or accumulation of possessions, especially regarding the peaceful transfer of possession from one possessor to another, appropriate evidence is needed. The 10-year period refers to the possession of the property, not to the possessors themselves. During these 10 years, there can be 2-3-4 possessors, and the last possessor who completes the legal 10-year period can benefit from adverse possession if he can demonstrate the connection between his possession and previous possessions.

2. A useful Possession: The possession must be unblemished, public/non-secretive, and peaceful.

3. No Land Register or Deceased/Removed Registered Owner: The property must not have a land register, or if there is one, the registered owner in the land register has died or is no longer alive (being removed/dissolved in the case of legal entities), or he has submitted a declaration of renunciation of ownership in the land register. In the case of death or removal/dissolution of the registered owner, the 10-year term begins at the earliest from the date of death/removal/dissolution, even if the possession began before this event. In the case of a declaration of renunciation of ownership, the 10-year term begins at the earliest from the date of registration of that declaration in the land register.

Once the above conditions are met, based on the technical judicial expertise report prepared by an authorized physical/legal person, a definitive, irrevocable, and enforceable civil judgment will be issued, which will grant ownership that will subsequently be registered.

➢ First Registration Based on the Property Title + Other Successive Documents of the Property. This possibility is viable based on successive documents issued up to January 1, 2005. The explanation for this is that, until this date, extratabulary sales and transfers of rights were conducted. Since then, any authentic transaction (carried out through a notary), except for inheritance, could no longer be performed. However, a transaction can be carried out through a handwritten document, regardless of the number of transactions. The documents are registered and recorded in chronological order, and their history is detailed in section B of the land register, which contains information regarding owners and documents.

The accelerated digital transformation of cadastral operations, spurred by the integration of GIS technologies, poses notable adaptation challenges for professionals, particularly in terms of aligning with continuously evolving procedural and legislative frameworks (Tereşneu & Tereşneu, 2023).

From an engineering perspective, the imperative to translate conceptual work into tangible, measurable outcomes is a defining professional attribute. In this sense, for easier evidence of cadastral documentation and resolutions that can be adopted we propose an interactive cadastral WEB Page.

This WEB page is designed as an interface between the contractor and beneficiaries and could provide support for all those interested in cadastral operations in the field of cadastre and land registry (employees of cadastral companies, beneficiaries of works, as well as other interested parts from related fields, students, etc.).

The graphical interface of the WEB Page is presented in Figure 1.



Figure 1. Graphical interface of the WEB Page

The WEB Page presented in Figure 1 has the following structure:
- Theoretical concepts;
- Types of documentation;
- Property location;
- Equipment and working methods;
- Resolutions that can be adopted.

The developed WEB Page includes all types of cadastral documentation that can be elaborated according to Order 600/2023 (Figure 2).



Figure 2. The Cadastral Documentation Menu of the WEB page

By selecting a certain type of cadastral documentation from Cadastral Documentation Menu, is shown a list with all cadastral documentation, of that type, elaborated within the company.

By selecting one type of cadastral documentations from the list, the cadastral documentation is displayed as well as all the information regarding that documentation (Figure 3).



Figure 3. Information regarding cadastral documentation

Property location menu - provides information about property localization and help users to locate their properties using cadastral maps and geographic tools.

Also, for each cadastral documentation elaborated, the WEB Page provides information about the topographic equipment used for measurements, the working methods, the solutions adopted and about the resolution that can be adopted.

The WEB Page incorporates current legislation and explains relevant laws, regulations and procedures related to property registration into the Land Registry.

It includes contact forms, chat support or FAQs for user assistance, which allow users to request or submit cadastral documents online and check the status of their cadastral documentation.

CONCLUSIONS

In the context of globalization, adapting to international standards becomes a priority. Comparative studies provide relevant information regarding the need or advantages of complying with these standards, which can contribute to increasing competitiveness at the national or even international level.

Moreover, the results of such a study can serve as a significant contribution to discussions on the legislative reforms needed in the field of cadastre and real estate publicity. This can guide legislative decisions towards optimizing and improving existing processes, ensuring that the legislation reflects current needs and challenges.

In conclusion, the examination of the effects of applying the law in cadastre activities is not just

an academic concern but a vital step for ensuring effective and transparent management of real estate properties. It not only reflects but actively contributes to the evolution and efficiency of the legal and administrative system in the field.

REFERENCES

Badea G. & Badea A.C. (2015 a). A study about new cadastral legislative provisions in Romania correlated with Cadastre 2034, *15th International Multidisciplinary Scientific GeoConference SGEM 2015*, *2*(2), 21-26.

Badea G. & Badea A.C. (2015 b). From Cadastral Background of Romania to the Present. *FIG Working Week 2015*, 1-14.

Pădure, I., Koncsag, E., & Ungur, A. (2006). *General cadastre – Practical work guide*. Cluj-Napoca: Risoprint.

Tereşneu C.C. & Tereşneu C.S. (2023). GIS facilities for the automation of cadastral documentations. *Scientific Papers. Series E. Land Reclamation, Earth Observation & Surveying, Environmental Engineering*, *12,* 371-376.

Agenția Națională de Cadastru și Publicitate Imobiliară. (2023). *Ordinul directorului general nr. 600/2023*. Retrieved from https://www.ancpi.ro/wp-content/uploads/2023/02/ODG-600_2023.pdf

Ministerul Justiției. (n.d.). *Legea fondului funciar nr. 18/1991*. Retrieved from https://legislatie.just.ro/Public/DetaliiDocumentAfis/25

Parlamentul României (1996). *Legea cadastrului și a publicității imobiliare nr. 7/1996*. Retrieved from https://lege5.ro/gratuit/gm2dmobtgy/legea-cadastrului-si-a-publicitatii-imobiliare-nr-7-1996

Parlamentul României (2000). *Legea nr. 1/2000 pentru reconstituirea dreptului de proprietate asupra terenurilor agricole și celor forestiere*. Retrieved from https://lege5.ro/Gratuit/gi3domzz/legea-nr-1-2000

Scientific Papers. Series E. Land Reclamation, Earth Observation & Surveying, Environmental Engineering. Vol. XIV, 2025
Print ISSN 2285-6064, CD-ROM ISSN 2285-6072, Online ISSN 2393-5138, ISSN-L 2285-6064

THE APPLICABILITY OF GIS TECHNOLOGY IN THE STUDY OF RIVERBED DYNAMICS AND MORPHOLOGY

Gabriela BIALI[1], Maria Catalina PASTIA[1], Paula COJOCARU[1], Carmen Elena MAFTEI[2]

[1]Gheorghe Asachi Technical University of Iași,
63-65 Prof. Dr. Docent Dimitrie Mangeron Blvd, 700050, Iași, Romania
[2]Transilvania University of Brașov, 5 Turnului Street, 500152, Brașov, Romania

Corresponding author email: mariapastia@yahoo.com

Abstract

This study examines the geomorphological conditions of representative gravel extraction sites along the Moldova River and assesses the impact of riverbed material extraction on the stability of the riverbed and the sediment regeneration rate. The analyzed sector spans approximately 26 km, encompassing the stretch of the Moldova River between Păltinoasa and Cornu Luncii in Suceava County, with a particular focus on the Capu Câmpului extraction site. The intensity of gravel extraction activities is reflected in the variations of suspended sediment hydrographs, which exhibit an increasing trend over time in the Moldova River, contrasting with the general decreasing trend observed in other rivers of the Siret Basin. Utilizing GIS techniques, including orthophotoplans and ArcGIS 9.2 software (via Digital Elevation Model creation), calculations were made for the volumes of mineral aggregates potentially extractable between 2017 and 2021. Previous studies have demonstrated that riverbed material extraction can lead to significant modifications in river morphology, including channel erosion and changes in hydraulic regimes, with effects on aquatic biodiversity and water quality. In conclusion, the research underscores the importance of detailed evaluation of the impact of riverbed material extraction on the geomorphological and ecological stability of the Moldova River, to support the development of sustainable management practices for fluvial resources.

Key words*: GIS techniques, riverbed, extraction.*

INTRODUCTION

Before 1990, Romania's construction materials industry faced a significant annual demand of approximately 80 million cubic meters of sorted sands and gravels (Călinoiu et al., 1988). These natural resources were regularly extracted from riverbeds and surrounding lands, playing a crucial role in supporting infrastructure development. However, ballast extraction was insufficiently regulated, leading to considerable environmental impacts, especially concerning alterations to watercourses and degradation of adjacent soils.
Following a period of economic decline, the demand for ballast increased again, reflecting a revitalization of the construction industry and, implicitly, greater pressure on natural resources. Currently, the requirements are much higher, placing considerable strain on riverbeds and the lands of major riverbeds, which are used for extracting sand and gravel. Romanescu (2009) observed this trend and emphasized that despite increased demand, there is a lack of detailed assessments of these activities' effects on riverbeds.
One of the main constraints regarding sand and gravel extraction is the imposition of quality conditions and strict environmental regulations. Consequently, the extraction area has significantly narrowed, and extraction activities are mainly concentrated in the middle and lower sectors of the minor riverbeds of major rivers, where there is greater resource availability and more flexibility in managing environmental impact. Thus, in the case of the Siret River, for example, approximately 230 gravel pits operate, with an annual production of about 2 million cubic meters of ballast, representing a considerable potential for transforming minor riverbeds (Călinoiu et al., 1988). This constitutes an important resource but poses a significant challenge for the sustainable management of river ecosystems (Gâștescu 2014). Despite this high ballast extraction potential, studies on the ecological impact of gravel pits on riverbeds are relatively limited. Romanescu (2009) observes that

comprehensive or detailed evaluations of how these gravel pits contribute to modifying riverbeds or changing river landscapes are lacking. Instead, most research focuses on isolated observations and case studies of individual rivers, limiting the general understanding of the phenomenon. This highlights the critical need for comprehensive research to systematically evaluate the effects of ballast extraction on river morphology and adjacent ecosystems. Such studies are essential for developing informed and sustainable resource management strategies. Additionally, it's important to note that changes in riverbeds resulting from ballast extraction activities can have profound effects on their biodiversity and ecological stability (Bătucă et al., 1992). For example, the disappearance of natural habitats for aquatic species and soil erosion can lead to a significant decline in biological diversity. Therefore, ballast extraction must be conducted within a regulated framework that minimizes environmental harm.

In conclusion, extracting sand and gravel from riverbeds represents a vital resource for the construction industry, but also poses major challenges for environmental conservation.

GIS technology enables the integration of various data sources, such as satellite imagery, aerial photographs, topographic maps, and remote sensing data, to provide a detailed and updated view of riverbed changes. This spatial data integration is essential for long-term monitoring, helping to document erosion, sedimentation, and channel migration processes.

Thorne et al. (2012) demonstrated that remote sensing and GIS technologies facilitate the rapid detection of river morphology changes, including erosion and channel shifts, which are often challenging to observe using conventional methods. Similarly, Goss et al. (2004) showed that GIS-based analysis of multi-temporal georeferenced data enables the monitoring of sequential riverbed changes following human interventions, such as dam construction or water diversion, revealing trends in channel migration and their ecological impacts.A relevant example highlighting the effectiveness of these tools is the study by Zhang et al. (2017), which applied GIS to assess channel changes in the Yangtze River, successfully identifying areas prone to erosion and flooding. Such spatial analyses are essential for flood disaster prevention and infrastructure protection in vulnerable regions (Vlad, 2017; Moldovan et al., 2023).

This study aims to enhance our understanding of the long-term effects of gravel pit operations on riverbeds and aquatic ecosystems (Cercel, 2019). The findings highlight the necessity for comprehensive research to systematically evaluate the impact of ballast extraction on river morphology and surrounding ecosystems. Such studies are essential for developing and implementing more effective resource management strategies that balance development with environmental conservation.

MATERIALS AND METHODS

This study employs ArcGIS 9.2 technology, encompassing: (i) the development of a Digital Elevation Model (DEM) through triangulation techniques and delineation of the study area's boundaries; and (ii) the computation of aggregate volumes resulting from both extraction and alluvial transport processes, as illustrated in Figure 1.

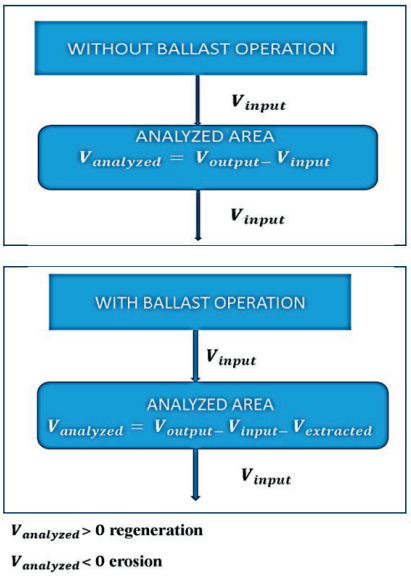


Figure 1. Calculation of aggregate volume

This methodology is applied to the profiles situated on the middle course of the Moldova

River, between Păltinoasa and Cornu Luncii localities. The research is conducted for the period 2017-2021.

Study Area

The study area is situated on the Moldova River, which is located in the northeastern part of the Eastern Carpathians and the northwestern part of the Moldavian Plateau (Figure 2).

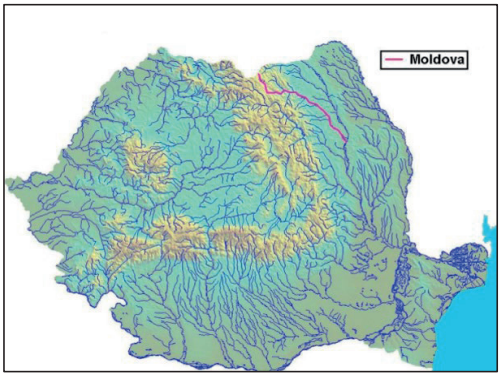


Figure 2. Location of the Moldova River on the hydrographic map of Romania (source: Wikipedia)

The Moldova Valley forms a depression between the Subcarpathians of Moldova and the Suceava Plateau, shaped by the Moldova River. Originating in the Obcina Feredeu Mountains (Suceava County), the river flows through Suceava and Neamț counties before joining the Siret River near Roman. As a right tributary of the Siret, the Moldova River features a broad and low floodplain up to Ciumulești, with its widest floodplain and terrace development observed at Baia, where the landscape adopts a depression-like character (Bartha et al., 2014; Bălan et al., 2016). The floodplain hosts a single, highly productive aquifer (yielding over 10 l/s), representing a key high-quality water reserve for eastern Romania (Cercel, 2018). The alluvial plain of the Moldova River, characterized by a grain size distribution well-suited for construction aggregates, represents one of the most significant exploitable sources in the Moldova region (Amăriucăi, 2000; Marcoie et al., 2023). This renewable resource is continuously replenished due to the river's mountainous hydrological regime, which alternates with plateau influences, and notably due to the absence of hydroelectric infrastructure in the Moldova River basin (Ichim et al., 1989). The analyzed extraction sites are located along the middle course of the Moldova River, between Păltinoasa and Cornu Luncii, entirely within the Subcarpathian sector of the Moldavian Plateau. This region is defined by hilly terrain with altitudes ranging from 400 to 600 meters, gradually decreasing from north to south.

According to detailed geomorphological mapping by Rădoane (2007), the middle sector of the Moldova River in Suceava County, between Păltinoasa and Cornu Luncii, features a well-developed alluvial plain with alluvial terraces rising 4-5 meters above the current riverbed. Key extraction perimeters within this area include Pod Izvor, Capu Câmpului, and Cornu Luncii (Figure 3).

The Capu Câmpului extraction site is located outside the built-up area (extravilan) of Capu Câmpului village, Suceava County, along the riverbed of the Moldova River, just downstream of the confluence with the Isachia stream. The operational perimeter lies between cadastral markers C.S.A. 116 and C.S.A. 117 (Figure 4).



Figure 3. Plan with the location of the three exploitation perimeters. Source: Google maps



Figure 4. Plan with the location of the Capu Câmpului exploitation perimeters. Source: Google maps

The following data sets were used in this study: updated situation plans with contour lines at a scale of 1:5000 and orthophotoplans. The contour lines were vectorized and together with the measured points on the situation plans allowed the creation of a Digital Elevation Model (Biali, 2013). The interpolation method chosen was TIN (Triangulated Irregular Network). TIN interpolation is another popular tool in GIS. A common TIN algorithm is called Delaunay triangulation.

The updated situation plans and orthophotoplans used to represent the study sectors are documents provided and authorized by ANCPI Suceava. Over these orthophotoplans, the Modova riverbed was vectorized and the positions of the transversal profiles were drawn. These profiles tracking the riverbed that frames the exploitation perimeter were maintained in the same place year after year (by means of field markers) so that the measurement results are correct and consistent in accordance with the initiated study.

RESULTS AND DISCUSSIONS

The study commenced in 2017 with field measurements conducted across five cross-sections (P1-P5). Figure 5 shows the 2017 boundary of the mineral aggregate extraction perimeter (points 1–2–3–4) along the Moldova River bed.

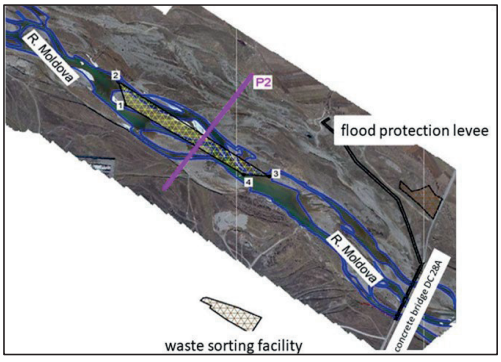
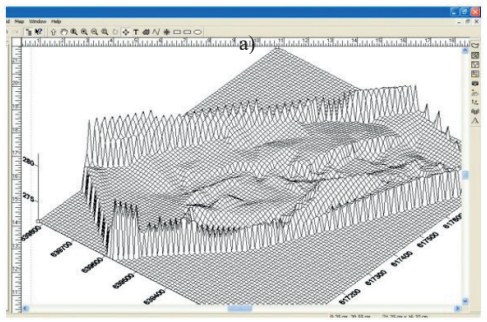


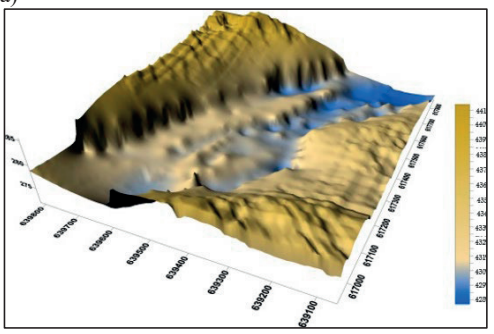
Figure 5. Orthophotomap of the Capu Câmpului perimeter from 2017

The Numerical Terrain Model in Figure 6 represents the studied Capu Câmpului sector. The hypsometry is in the range of 428 (thalweg) 441 m (left slope).

The Numerical Terrain Model served as the foundation for calculating the volumes of mineral aggregates present within the riverbed.



a)



b)

Figure 6. 3D representation of the Numerical Terrain Model for the studied perimeter (a. wireframe; b. grid fill)

This study employs two complementary research methods: profile-based approaches and Digital Terrain Model (DTM)-based analyses. Transversal profile measurements, conducted annually within the same cross-section, yield direct and reliable results. These measurements are processed using ArcGIS 9.2 software to model the riverbed of the Moldova River. The DTM results are utilized for both aggregate volume calculations and monitoring the morphological evolution of the riverbed over time. Field measurements were performed using the Trimble® R780 GNSS receiver, an advanced geospatial instrument. The R780 features a 9 GB internal memory and operates with Trimble Access software. It incorporates Trimble Inertial Platform™ (TIP) technology, providing tilt compensation based on an Inertial Measurement Unit (IMU), ensuring resistance to magnetic interference. This system is designed to withstand harsh environmental

conditions, offering high precision and reliability for geospatial data collection.

Tables 1 and 2 show the calculation of the volumes of mineral aggregates potentially exploitable in the Capu Câmpului perimeter for the year 2017 and year 2018 (without lowering below the current riverbed thalweg elevation).

Table 1. Estimated volumes of mineral aggregates exploitable in the Capu Câmpului perimeter (2017), without lowering below the current thalweg elevation

Profile	Surface	Average surface area	Partial distance	Partial volume	Total volume
P1	17.243	8.622	0.000	0.000	0.000
P2	66,628	41.936	164.548	6,900.365	6,900.365
P3	28.504	47.566	175.540	8,349.746	15,250.111
P4	13.688	21.096	112.957	2,382.950	17,633.061
P5	0.000	6.844	141.931	971.374	18,604.435
Total			**595**		**18,604.435**

The total length of the exploitation perimeter is approximately 595 meters, with a maximum extractable volume (V_{max}) of 18,600 m³. Based on the 2017 volume calculations, the sand and gravel reserve within the analyzed section - spanning approximately 595 meters of the riverbed - was estimated at V_i = 18,600 m³ per gravel bar. Figure 7 shows the 2019 boundary of the mineral aggregate extraction perimeter along the Moldova River bed.

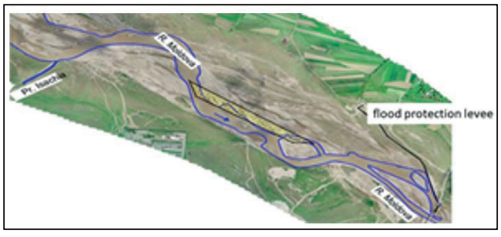


Figure 7. Orthophotomap of the Capu Câmpului perimeter from 2019

The 2019 volume calculations, based on a current measured riverbed length of 460 meters, indicate an updated reserve of V_{actual} = 20,387 m³ per gravel bar. Furthermore, a volume of V_e = 15,000 m³ of gravel was extracted from the analyzed section between 2017 and 2019, according to data reported by the operating extraction company. Based on these figures, the following resource balance equation can be established to quantify the reserve dynamics over the evaluation period:

$$V_{actual} = V_i + V_e + V_{regeneration} \quad (1)$$

The regeneration volume $V_{regeneration}$ is calculated as:

$$V_{regeneration} = V_{actual} - V_i + V_e \quad (2)$$

Applying the provided data, the regeneration volume is:

$V_{regeneration}$ = 20,387 - 18,600 + 15,000 = 16,787 mc/year.

Considering the current reserve volume of V_{actual} = 1,787,486 mc, the percentage variation in reserve volume is:

$$P_{regeneration} = 100 \cdot (V_{regeneration} / V_{actual}) \quad (3)$$

$P_{regeneration}$ = 82.34%

Note: Volume calculations can be performed using either the cross-sectional profile method or by creating a Digital Terrain Model (DTM), with the latter providing greater precision.

Table 2. Volumes of mineral aggregates potentially exploitable in the Capu Câmpului perimeter in 2019, without lowering below the existing riverbed thalweg elevation

Profile	Surface	Average surface area	Partial distance	Partial volume	Total volume
P1	0.000	0.000	0.000	0.000	0.000
P2	47.632	23.816	172.641	4,111.584	4,111.584
P3	53.561	50.597	174.732	8,840.811	12,952.395
P4	78.634	66.098	112.484	7,434.910	20,387.305
P5	0.000	39.317	0.000	0.000	20,387.305
Total			460		20,387.305

The total length of the exploitation perimeter is 460 meters, with a maximum extractable volume (V_{max}) of 20,387 m³.

Figure 8 shows the 2021 boundary of the mineral aggregate extraction perimeter (points 1–2–3–4) along the Moldova River bed.

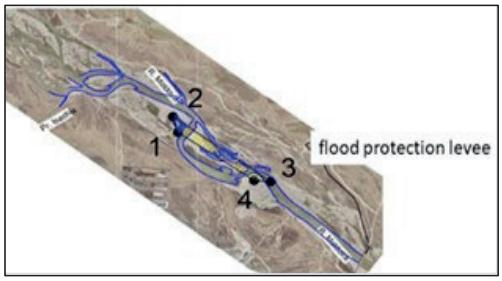


Figure 8. Orthophotomap of the Capu Câmpului perimeter from 2021

Table 3. Estimated volumes of mineral aggregates exploitable in the Capu Câmpului perimeter (2021), without lowering below the current thalweg elevation

Profile	Surface (m²)	Average Surface Area (m²)	Partial Distance (m)	Partial Volume (m³)	Total Volume (m³)
P1	3.912	1.956	0.000	0.000	0.000
P2	83.535	43.724	0.000	0.000	0.000
P3	30.655	57.095	174.636	9,970.823	9,970.823
P4	32.222	31.439	113.304	3,562.129	13,532.952
P5	0.000	16.111	140.379	2,261.643	15,794.595
Total			428		15,795.000

The total length of the exploitation perimeter is 428 meters, with a maximum extractable volume (V_{max}) of 15,795 m³.

According to the volume calculations performed in 2019, the reserve of sand and gravel within the approved exploitation perimeter - spanning approximately 460 meters of riverbed - was estimated at V_i = 20,387 m³ of ballast. Updated measurements in 2021 for the same perimeter, adjusted to a current riverbed length of 428 meters, indicate a revised reserve of V_{actual} = 15,795 m³. Additionally, the volume extracted from the area between 2019 and 2021 was reported as V_e = 15,000 m³, based on operator records.

Using the resource balance equation:

$V_{regeneration} = V_{actual} - V_i + V_e$,

we obtain:

$V_{regeneration}$ = 15,795 – 20,387 + 15,000 = 10,408 m³,

representing the net accumulation or loss in the riverbed over the period.

The regeneration percentage is calculated as:

$P_{regeneration} = 100 \times (V_{regeneration} / V_{actual})$ = 65.89%

Interpretation:

- $V_{regeneration} > 0$: indicates an aggradation process (material accumulation);
- $V_{regeneration} < 0$: indicates a degradation process (erosion or material loss).

An analysis of overlapping cross-sections from the years 2017, 2019, and 2021 reveals a relatively stable riverbed, with elevation fluctuations ranging from +0.12 m to –0.29 m (Figure 9). These variations are within acceptable limits and do not necessitate additional stabilization measures for the riverbed at this time.

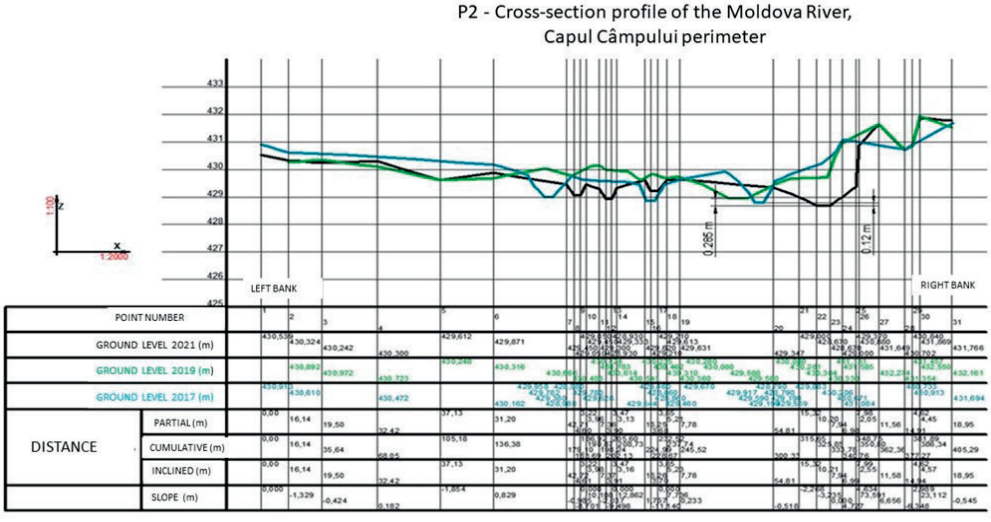


Figure 9. Cross-section of the Moldova River in the Capu Câmpului extraction perimeter area

CONCLUSIONS

Our analysis reveals that the Moldova River channel undergoes ongoing horizontal shifts, with lateral erosion occurring at an average rate of 4-5 meters per year. These processes are mainly confined to the active river corridor, which ranges in width from 500 to 800 meters.

Before 2010, approximately 15 extraction perimeters were active along the analyzed river

section. Currently, this number has significantly decreased, indicating a corresponding reduction in the volume of extracted mineral aggregates. The intensity of gravel mining activities is further evidenced by variations in suspended sediment hydrographs, which, in the case of the Moldova River, show an increasing trend over time. This contrasts with other rivers in the Siret Basin, where the general tendency is a reduction in sediment load. One plausible explanation for this divergence is the mobilization of sediments resulting from gravel extraction, a process that increases water turbidity.

The mobile riverbed depth along this section of the Moldova River has been measured at 2-3 meters, increasing to over 4 meters near the confluence with the Siret River, close to the Roman city. Cross-sectional analyses and measurements reveal a significant deepening of the riverbed in the Pod Izvor area. Long-term monitoring confirms the Moldova River's high sensitivity to two main categories of controlling factors: the natural variability of hydrological flow and anthropogenic influences. While natural factors were predominant before 1978, post-1978 observations indicate a marked dominance of human activities, particularly through an accelerated trend of riverbed incision.

In light of these findings, the following hydrotechnical interventions are proposed:

- *Channel development* through localized excavation, reprofiling of consolidated banks, and desilting, without altering the channel's width or depth.
- *Bank stabilization* in areas affected by active erosion poses risks to nearby infrastructure, using gabion walls or riprap with stone revetments.
- *Flood protection measures,* including embankments made from local materials, concrete parapets, elevation of riverbanks through reinforcement works, or the raising of existing access roads.
- *Longitudinal stabilization* through the construction of grade control structures using raw stone or gabions.

Recalibration of the channel is recommended in areas where sediment deposits or islands have formed, in order to improve flow capacity during medium and high discharge events and to restore the riverbed to dimensions derived from hydraulic modeling.

As demonstrated in this study - and supported by other research such as that conducted by Hooke (2004) - the use of GIS for monitoring land and land-use changes provides critical insights into the impact of human activities on river morphology, particularly in the context of land-use transformations.

In conclusion, GIS technology proves to be an indispensable tool for the monitoring and management of riverbed dynamics. It offers a robust and efficient methodology for spatial data collection and analysis. The application of GIS enables a comprehensive understanding of both natural and anthropogenic processes influencing river systems and facilitates the development of effective strategies for environmental protection, water resource management, and disaster risk reduction. The present study, alongside existing literature, reinforces the importance of GIS in fluvial geomorphology research and highlights its relevance in environmental policy and climate change adaptation.

REFERENCES

Amăriucăi, M. (2000). *Sesul Moldovei extracarpatice între Păltinoasa şi Roman*. Editura Corson.

Bartha, I., Vlad, L. M., Toma, D., Toacă, D., & Cotiușcă-Zaucă, D. (2014). Rehabilitation and extension of wetlands within floodplains of embanked rivers. *Environmental Engineering and Management Journal*, *13*(12), 3143–3152.

Bălan, A., Luca, M., & Toma, D. (2016). Research of morphological processes into the Moldova riverbed using periodic topographic measurements. *Scientific Papers. Series E. Land Reclamation, Earth Observation & Surveying, Environmental Engineering*, *5*. University of Agronomic Sciences and Veterinary Medicine of Bucharest.

Bătucă, D., & Mocanu, P. (1992). Efectele balastierelor asupra albiilor de râu. In *Lucrările celui de-al IV-lea Simpozion PEA*, Piatra Neamț.

Biali, G. (2013). *Inițiere în GIS: Sisteme informaționale geografice* (237 pp.). Editura Performantica.

Călinoiu, M., Paraschivescu, G., & Ungureanu, C. (1988). Influența factorilor antropici asupra formării şi valorificării acumulărilor de nisipuri şi pietrişuri în R.S. România. In *Lucrările celui de-al II-lea Simpozion "Proveniența şi Efluența Aluviunilor"*, Piatra Neamț.

Cercel, P., & Vorovei, C. (2019). Rehabilitation of hydrotechnical structures in the actual conditions of climate and anthropic changes. *Environmental*

Engineering and Management Journal, *18*(7), 1609–1620.

Cercel, P., & Cercel, M. (2018). Considerations for ensuring the safe operation of a hydrotechnical arrangement located in the upper part of a river basin in the context of climate change. In *Proceedings of the 17th International Technical-Scientific Conference on Modern Technologies for the 3rd Millennium* (pp. 215–220). Oradea.

Gâștescu, P. (2014). Water resources in the Romanian Carpathians: Genesis, territorial distribution, management. In V. Sorocovschi (Ed.), *Riscuri și catastrofe* (Vol. 14, No. 1). Casa Cărții de Știință.

Goss, M., Smith, B., & Johnson, L. (2004). Using GIS and remote sensing to monitor channel change: A case study on the Colorado River. *Geomorphology*, *63*(3), 111–122.

Hooke, J. M. (2004). River channel adjustments: A GIS approach to river modification and erosion. *Journal of River Research*, *45*(2), 138–149.

Ichim, I., Bătucă, D., Rădoane, M., & Duma, D. (1989). *Morfologia și dinamica albiilor de râu*. Editura Tehnică.

Marcoie, N., Toma, D., Boboc, V., Hraniciuc, T. A., & Bălan, C. D. (2023). Hydroinformatics tools used to quantify the impact of urban expansion on water bodies in the context of the intensification of extreme phenomena (Bacău urbanization case study). *IOP Conference Series: Earth and Environmental Science*, *1136*, 012015. https://doi.org/10.1088/1755-1315/1136/1/012015

Moldovan, A. C., Hraniciuc, T. A., Micle, V., & Marcoie, N. (2023). Research on the sustainable development of the Bistrița Ardeleană River in order to stop the erosion of the riverbanks and the thalweg. *Sustainability*, *15*, 7431. https://doi.org/10.3390/su15097431

Rădoane, M., & Rădoane, N. (2007). *Geomorfologie aplicată*. Editura Universității Suceava.

Romanescu, G. (2009). *Evaluarea riscurilor hidrologice*. Editura Terra Nostra.

Thorne, C. R., Russell, A., & O'Donnell, G. (2012). Remote sensing and GIS for river morphology monitoring. *Journal of Hydraulic Engineering*, *138*(3), 267–279.

Vlad, L., & Toma, D. (2017). Restoring wetlands and natural floodplain along the lower Başeu River in Romania. *Environmental Engineering and Management Journal*, *16*(10), 2337–2346.

Zhang, Y., Wang, J., Liu, X., & Zhao, L. (2017). GIS-based analysis of river channel change and flood risk: A case study of the Yangtze River. *Environmental Management*, *60*(5), 919–930.

Scientific Papers. Series E. Land Reclamation, Earth Observation & Surveying, Environmental Engineering. Vol. XIV, 2025
Print ISSN 2285-6064, CD-ROM ISSN 2285-6072, Online ISSN 2393-5138, ISSN-L 2285-6064

CASE STUDY ON THE USE OF SCANNING EQUIPMENT UAV IN ORDER TO DRAW UP A MULTIFUNCTIONAL DATABASE, IN CÂRȚIȘOARA LOCALITY, SIBIU COUNTY

Jenica CĂLINA, Aurel CĂLINA, Marius MILUȚ

University of Craiova, Faculty of Agronomy, 19 Libertății Street, Craiova, Romania

Corresponding author emails: aurelcalina@yahoo.com, milutmarius@yahoo.com

Abstract

The paper presents a case study in which the application of a modern aerial scanning technology with the help of drones is carried out through a specific method, for the creation of a multifunctional database, with a wide applicability in several fields of economic activity and production specific to rural areas, as well as in cadastre real estate advertising works and rural tourism. The choice of the study topic is justified by actuality and necessity, as it contributes significantly to increasing the degree of predictability of the management as a result of the real-time collection of a very large number of data and information, the processing in a short time in order to identify vulnerabilities and their quick and efficient solution, as a result of the increase in knowledge, respectively of minimizing situations of risk and uncertainty. The use of aerial scanning equipment in cadastral works, agriculture, forestry, rural tourism and other important areas for rural development is an activity of great interest and allows to obtain in a short time a large volume of data used for the sustainable development of the community.

Key words*: aerial scanning, drone, multifunctional database, tourism promotion*

INTRODUCTION

The development of unmanned aircraft systems is a certainty of the present in which society shows increased interest. If at the time of their appearance they were intended and used in various military applications, we have gradually witnessed their adoption by civil society where there is a rapid increase in interest in their use in various civilian applications. They target multiple services that have as a common point the technique of terrestrial measurements using emerging technologies. The use of aerial scanning equipment with the help of drones is based on photogrammetry and remote sensing. The high capacity to collect data and information naturally leads to the design, development, and implementation of a geographic information system, a tool that allows for easy analysis of the collected data (Călina et al., 2022).

Unmanned aircraft systems comprise different components (unmanned aerial vehicle, launch and recovery station, data network, technical support systems, control station, human interface, etc.) whose complexity configures different classes among which the mini UAS is considered the fastest growing class (Iagăru et al., 2022). The growth is due to recognized characteristics such as: low costs, implementability directly from the field, accessibility of technologies (Iagăru et al., 2021), flexibility, etc., which give it advantages and ensure a dominant presence in civil applications in all fields of activity (Aswini et al., 2018; Barbedo, 2019; Călina et al., 2020; Wang et al., 2015; Borra-Serrano et al., 2022; Parraga-Alava et al., 2021).

The first uses of drones in civil applications were made by Yamaha Motor Company (Japan, 1987) through the RMAX-R50 concept dedicated to spraying pesticides on rice crops. Cisneros (2013) proposed the low-cost concept for use in emerging countries in South America (especially Peru). Later, Glen (2015) anticipated the downsizing effect and showed a possible market entry of medium and small UAV robotic systems that take advantage of the size reduction of specific multispectral sensor systems (Iagăru et al., 2022). Regarding drones for precision agriculture/horticulture (aircraft or multicopter type), there are very few bibliographic references (Krishna, 2016). In this case, the elements of interest (performance, flight qualities, specific transport aspects) refer to semi-autonomous flight

capabilities, initial acquisition cost, level of complexity of possible missions, maintenance costs (including periodic corrections specific to small drones).

Information collection takes place using sensors mounted on mini UAV. There are four types of sensors that cover almost all research applications in UAV remote sensing in precision agriculture: RGB, multispectral, hyperspectral and thermal sensors (Kovanič et al., 2023). The first three categories contribute to the creation of georeferenced reflectance maps, and the last category to the creation of temperature maps (Maes & Steppe, 2019).

The choice of the study topic is justified by its topicality and necessity, as it significantly contributes to increasing the degree of predictability of management based on the real-time collection of a very large number of data and information, processing in a short time in order to identify vulnerabilities and their rapid and efficient resolution, as a result of increasing the degree of knowledge, respectively minimizing risk and uncertainty situations.

The use of aerial scanning equipment in cadastral works and agriculture for rural development is an area of interest and allows obtaining in a short time a large volume of data that, when properly processed, provides a realistic overview, which leads to the development of relevant strategic options for sustainable community development (Călina et al., 2020).

The concretization of aerial monitoring takes place by carrying out flight missions at certain heights (for example, 100 m), according to a flight plan made by selecting a land area on a Google Earth or Map support. Approvals from the Aeronautical Authority and the Ministry of National Defense for flying over a land area at this height with the specification of take-off and landing points follow; creating the flight plan, aiming first of all to cover the area of interest, then generating the flight paths that the drone must cover, so that the photos taken have an overlap of 70% and the flight times are supported by the battery power (about 25 min for one battery); preparing for the drone take off (favorable weather conditions - clear sky and wind below 7 m/s, telephone network coverage necessary for data transmissions, adequate GPS signal); carefully following the trajectories travelled (Sălăgean et al., 2016).

The images obtained during aerial monitoring of ecosystems are processed with the help of dedicated software leading to the early detection of diseases and pests in the crop; precise mapping of weeds; precision in forecasting; precise application and reduced volume of pesticide solution; optimization of nutrient management; monitoring plant growth (Achtilik, 2015; Zhang et al., 2014). Mini UAVs for disease and pest control manage to maintain their control in identified areas, by applying variable doses of pesticides (Filho et al., 2020).

MATERIALS AND METHODS

The purpose of the work is represented by the study of aerial scanning equipment and UAV systems, respectively by its use in the data collection process in order to create a multifunctional database corresponding to the current requirements for sustainable development of the territory.

The achievement of the purpose is mediated by the establishment of objectives that represent stages in its achievement. These are:

- geographical and socio-economic characterization of the Cârțișoara locality,
- knowledge of aerial scanning equipment and traffic vectors;
- presentation of the research methodology;
- carrying out a study on the scanning of the Cârțișoara locality in order to create a GIS database.

The research methodology employed is the case study approach, as it allows for a comprehensive examination of the rural economy within the natural environment of Cârțișoara commune, viewed from various perspectives.

This study represents a detailed analysis method applied to complex scenarios and provides an in-depth view of the phenomenon being analysed “in a real-life context and using multiple sources of information (interviews, questionnaires, testimonies, evidence, documents, direct observation, participant observation)” (Glen, B., 2015). In particular, the research methodology utilized both quantitative and qualitative methods in parallel

and complementary ways (Upadhyaya et al., 2022), including secondary analysis of specialized literature and documentation from the Cârțișoara city hall to identify the object of interest, as well as from the Cadastre and Real Estate Advertising Office in Sibiu.

To achieve the established objectives, the research was structured and carried out in four stages, as shown in Figure 1. In stage 1, data and information were collected in accordance with the research purpose using the questionnaire applied at the level of administrative-territorial unit (ATU), secondary analysis of statistical data and relevant specialized literature, and observation for qualitative improvement of information. As a result, an accurate representation was achieved, highlighting critical factors and identifying best practices.

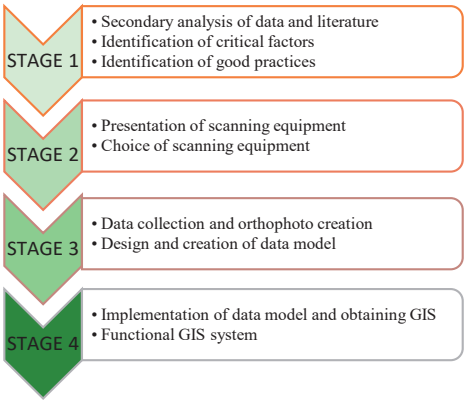


Figure 1. Schematic structure of the research

Case study

The study was conducted in the locality of Cârțișoara, Sibiu County, located at coordinates 45°43′34″N and 24°34′28″E. The primary objective of this research is to examine aerial scanning equipment and UAV systems and their application in the data collection process. The collected data will be used to design and develop a database aligned with current requirements for the sustainable development of the territory.

Cârțișoara commune is situated in the southeastern part of Sibiu County, in the central region of Țara Oltului, at the base of the Arpășel, Bâlea, Valea Doamnei, and Laița Mountains. To the east, it borders the village of Arpașul de Sus (part of Arpașu de Jos commune); to the west, it is adjacent to Scorei village (belonging to Porumbacu de Jos commune); to the south, it borders Argeș County; and to the north, it neighbors the commune of Cârța.

Documentarily, the commune is attested since the 13th century (yearbook of the Institute of History of Cluj-Napoca, volume VII-1964, page 317). The total area of the commune is 8.576 hectares. The commune of Cârțișoara presents a number of 4 main relief elements with their own specificity in terms of geomorphology. Geology, hydrology, climatology, lora and fauna, as follows: a) the Bâlii plain area; b) the hilly area; c) the pre-alpine area; d) the alpine area.

Stages of the research

To ensure the successful achievement of the project objectives, the research activities - both fieldwork and office-based - were structured into specific stages, as outlined in Table 1.

Table 1. Stages of carrying out activities

Activity type	Activity type	Activity type
Office	Establishing the work stages and inventorying the resources to be used (equipment, software products, documents, data, human resources, etc.)	01.08.2023 – 30.09.2023
Field	Obtaining raw data through aerial photography	01.10.2023– 15.10.2023
Field	Carrying out the analysis stage to identify the needs, requirements, and methods for obtaining the data of interest.	16.10.2023 – 30.10.2023
Office	Validating the raw data collected and performing photogrammetric processing in order to obtain an orthophoto map.	01.11.2023 – 15.11.2023
Office	Designing, testing, validating, and implementing a specific data model (database).	16.11.2023 - 30.11.2023
Office	Writing the technical specifications to be used for the administration and operation of the database.	01.12.2023 – 15.01.2024

Raw data collection by aerial photography

The data collection required the following activities:

• marking (materializing) on the ground of known coordinate points that will be used to georeference the obtained orthophoto map;

• using a GNSS receiver to determine the coordinates of the ground control points (GCP);
• planning and conducting the flight to acquire the photogrammetric data, from which the necessary orthophoto map will be generated.
• marking the ground points using FENO topographic markers.

For easy recognition on the photograms of the points marked on the ground, 50x50 cm marking panels were made and used (by positioning centered on the ground markings) painted in two colors (white/red). At the same time, for the areas that allowed, the marking was done directly on the ground, by applying a layer of paint (white, red).

The GCP coordinates were determined in the Stereo 70 reference system, by using GNSS equipment using the RTK method. Considering that the goal is to achieve a pixel size of 3 cm/pixel, we deemed the use of the RTK measurement method sufficient, as it ensures the required accuracy.

The coordinates were determined for 18 points marked or identified on the ground and which ensure visibility on the acquired photograms. In Table 2 are presented coordinates for 12 marked points.

Table 2.GPS coordinates inventory

Point no.	X	Y	Z
1	467013.193	470317.381	494.870
2	466953.872	469902.502	494.900
3	466731.680	469672.695	494.950
4	466914.265	469494.041	495.101
5	466768.974	469154.739	495.205
6	467204.136	469931.276	494.400
7	467338.487	469895.056	494.381
8	467525.948	470182.443	495.501
9	467744.810	470118.427	495.602
10	467515.69	469716.783	495.750
11	467593.025	469534.312	495.859
12	467661.940	469164.808	496.050

Planning and execution of the flight

The proposed goal of the graphic data acquisition flight was to obtain data that met certain minimum requirements from a technical and functional (content) point of view, such as:

- ensuring an orthophoto resolution of approximately 3cm/pixel;
- respecting the degree of lateral and longitudinal overlap (60°/85°);
- ensuring ground visibility.

The Matrice 300 RTK UAV was used for aerial scanning and DJI Zenmuse P1 (35 mm) sensor. The construction parameters of the DJI Zenmuse P1 (35 mm) are shown in Figure 2.



Figure 2. DJI Zenmuse P1 (35 mm) parameters

For flight planning, UgCS Drone flight planning software was used. This software includes background maps on which the area for the photogrammetric flight was identified and marked. Then, the other necessary flight planning parameters were entered: the type and model of the drone used, the specifications of the camera used, pixel size, flight speed, lateral and longitudinal overlap, etc. (Figure 3 and 4, Table 3).

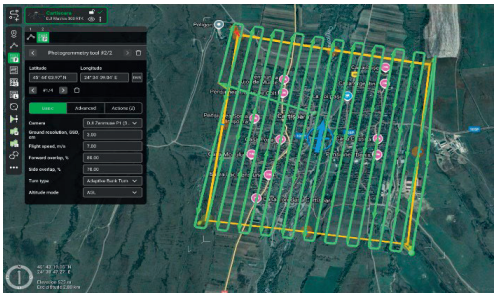


Figure 3. Flight planning and flight parameters



Figure 4. Elevation profile and flight details (area, size of footprint, no. of waypoints, camera triggering details)

Table 3. Presentation of the field book - photogram acquisition

# Label	X/East	Y/North	Z/Altitude
DJI_0114.JPG	23.785530	44.318153	222.074000
DJI_0115.JPG	23.785585	44.318210	222.074000
DJI_0116.JPG	23.785715	44.318330	221.974000
DJI_0117.JPG	23.785829	44.318433	221.874000
DJI_0118.JPG	23.785963	44.318555	221.874000
DJI_0119.JPG	23.786064	44.318644	221.874000
DJI_0120.JPG	23.786181	44.318745	221.874000
DJI_0121.JPG	23.786275	44.318828	221.974000
DJI_0122.JPG	23.786376	44.318917	221.874000
DJI_0123.JPG	23.786468	44.319000	221.874000
Due to volume considerations, only 10 positions from the field notebook are presented for illustration purposes.			

Processing raw data and obtaining an orthophoto map

The raw data collected was processed to produce a high-resolution orthophoto map (Table 4). The following activities were conducted during this stage:

- processing the raw data acquired in the field (1,172 photograms);
- generating the primary output: a digital 2D orthophoto map;
- producing secondary outputs, including: Digital Elevation Model (DEM); 3D Digital Surface Model; Point cloud; KMZ map format compatible with Google Earth.

Table 4. Resources required and used for processing raw data (photograms)

Resource type	Name	Features
Hardware	Workstation Fujitsu Siemens Celsius R570-2	Processor: 2 x Intel Xeon Six Core X5650, 2.66 GHz, 12M Cache, 6.40 GT/s Intel QPI, 12 Cores, 24 Logical processors Video card: NVIDIA Quadro FX1700, 512 MB GDDR2 128-Bit, 2 x DVI Network: integrated 10/100/1000 Mbps Chipset: Intel 5520 RAM: 48 GB DDR3 ECC Storage: HDD 2 x 320 GB 7200 rpm (RAID 1 - mirror) SSD 1 x 500 GB Samsung 850 EVO Optical drive: DVD-RW Operating system: Windows 8.1 Pro 64-bit Monitor: LCD Acer B243HL, 24 inch, 1920 x 1080, VGA, DVI Keyboard, Mouse
Software	ZwCAD Professional	ZwCAD offers performance in CAD design and significantly increased work speed, works with files up to DWG 2018 inclusive, includes 3D editing mode. It has efficient functions for 2D drafting and 3D modeling, ZwCAD offers perfect DWG compatibility
Software	Agisoft Metashape Professional	Agisoft Metashape Professional is a software product for advanced image processing and generation of 3D models based on static images. This software product is based on 3D reconstruction technology and can process images both under certain predefined conditions and in an unconstrained environment.
Software	ArcGIS Desktop	ArcGIS is a software product used for managing various datasets (both geographic and descriptive) and facilitating their manipulation. It allows working with maps and geospatial information and is mainly used for: creating and using maps, analyzing recorded data, sharing information, organizing and managing geographic information within databases, etc. During this stage of the project, ArcGIS was used to georeference the previously obtained orthophoto map.

The main steps involved in raw data processing using Agisoft Metashape Professional are illustrated in Figure 5. Following the completion of the data processing workflow, a 2D orthophoto map was generated (Figure 6), already georeferenced in the Stereo70 coordinate system.

Point cloud generation was the next step, during which a dense point cloud was created and visualized (Figure 7). This was achieved by aligning the photograms using the estimated camera positions recorded at the time of image capture. The resulting point cloud can be further refined or exported for additional use.

Subsequently, a 3D polygonal model was constructed using processed data and pre-defined parameters.

As shown in Figure 8, ground control points (GCPs) were identified, marked, and integrated into the processing workflow to enhance spatial accuracy.

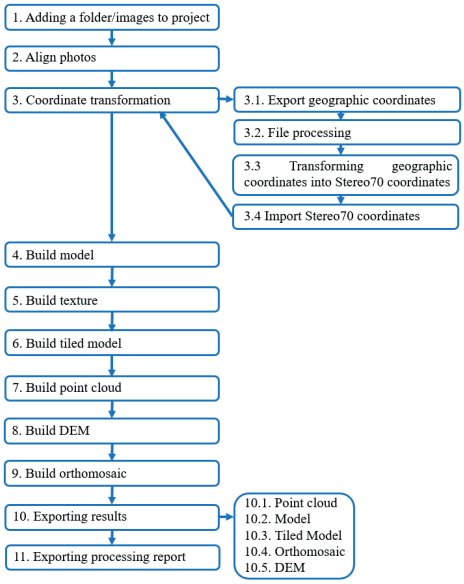


Figure 5. Workflow and results

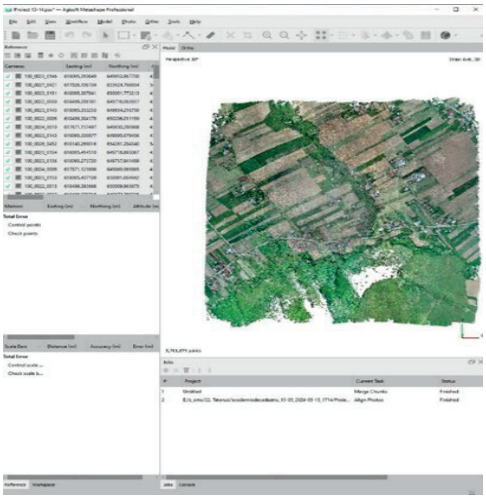


Figure 6. Orthophoto map

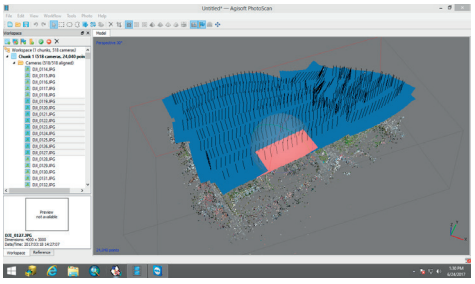


Figure 7. Point cloud generation

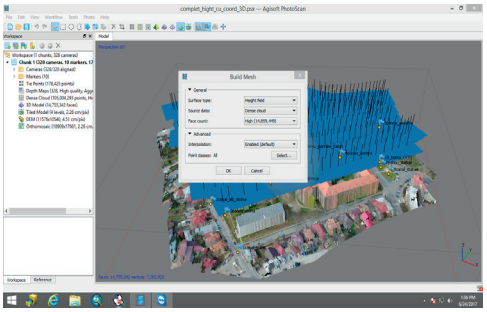


Figure 8. Parameters for generating 3D polygon model

• Surface type: height field – is the specific setting for wide planes (especially in the case of aerial photography);
• Source data: dense cloud – the dense point cloud was utilized as the source, as the goal is to generate a high-resolution orthophoto map;
• Face count: high – specifies the maximum number of facets of the generated model;
• Interpolation: enabled – this allows areas not covered by photograms to be generated through interpolation, based on data from surrounding areas; it is possible that uncovered areas will still remain.

Structure generation – proper structure generation determines the manner and quality of subsequent visualization of the generated model.

Therefore, the structure generation was carried out with the proper configuration of the generation parameters:
• The adaptive orthophoto mode was selected for mapping mode, so objects are segmented into flat/smooth areas and vertical parts. This ensures processing quality for both smooth areas and vertical surfaces (such as buildings, walls, etc.);
• Blending mode: defines how pixels with different values (from various photograms) will be merged in the final structure; According to the user manual, the mosaic value was used for the blending mode.
• Enable color correction: true - a helpful option when there are significant brightness variations (though it can be time-consuming and resource-intensive).

After processing, a ground resolution of 2,256 cm/pixel is obtained.

DEM creation - the DEM will be generated based on the processing parameters selected:
• reference system: Stereo 70;

• DEM is build using the existing dense point cloud;
• Interpolation mode: active.
After processing, the obtained DEM resolution is 4.51 cm/pixel. All the obtained results can be saved/exported. Thus, it is possible to export both the main result sought (orthophoto map) and other obtained products such as: point cloud, DEM, etc. (Figure 9).

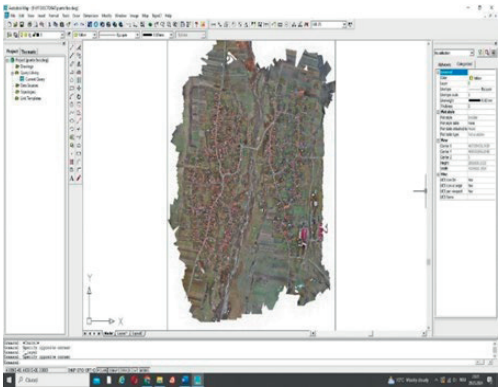


Figure 9. Export results

Design of the data model (database)
In general terms, a database is a collection of information that can be accessed and used as needed. Databases, as organized data structures, are present in all fields of activity. If we consider the users of the data and the need to organize it, the concept can be defined more broadly as follows: a database represents a structured collection of logically interconnected information, which can be shared and includes both the relationships between the data and their descriptions. The database design is carried out in such a way as to meet the specific requirements of the users it serves.
Any database must fulfil the basic functions, which are: storing and organizing data, ensuring data accuracy, easy exploitation, non-redundant data recording, ensuring data retrieval and extraction, and updating through CRUD operations (create, read, update, delete).
Database design is a complex process that includes several working phases, from planning the process to maintenance during operation. The main stages of database architecture design are shown in Figure 10.

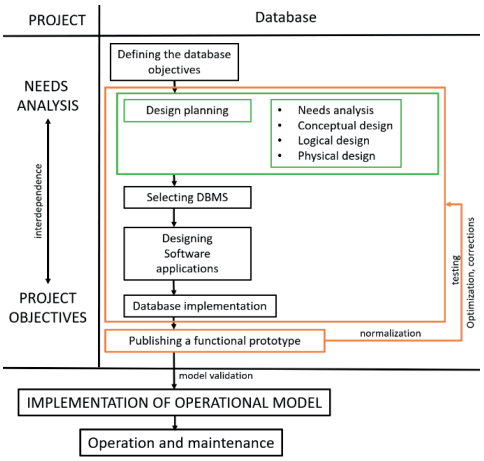


Figure 10. The logical flow for designing a database. Source: Own elaboration, adapted from (Vangu et al., 2023)

GIS systems use spatial databases, which ensure their scalability, allowing them to be used at local, regional, national, or global levels. From an IT perspective, the process of designing, developing, and implementing the database is the same, but the structure and content of the database must be adapted and aligned with the requirements of each project.
The database designing, testing, validating, and implementing is mainly based on the results of the analysis stage. Starting from these results, a structuring and filtering of the data of interest was carried out.

RESULTS AND DISCUSSIONS

As a result of the case study, the orthophoto map obtained through the application of photogrammetric techniques has multiple uses and can provide valuable data for various applications. Below are the main ways to exploit it.

Mapping and updating maps: the orthophoto map can be used to update the digital maps of the area, providing a detailed and up-to-date image of the terrain (Vangu et al., 2025).
Urban planning and rural development: local authorities can use the orthophoto map to analyze existing infrastructure, plan expansions, and identify areas for development.

Tourism promotion: the orthophoto map can be used to create interactive maps and tourist guides based on real images, enhancing the tourist experience (Chen et al., 2017).

Land use analysis: it can be used to assess land use (built-up areas, agricultural land, forests, watercourses) (Budiharto et al., 2021).

Environmental monitoring: the orthophoto map allows the analysis of the impact of human activities on the environment and the identification of potential issues (deforestation, erosion, pollution).

Based on the orthophoto map, information can be extracted regarding: the exact boundaries of land and properties, with direct benefits in real estate management; infrastructure and transport networks; the typology of buildings and their use (guesthouses, traditional houses, tourist attractions, etc. can be classified and analyzed); vegetation and natural resources studies; 3D modeling and topographic and spatial analyses (Sedano-Cibrian et al., 2023).

Considering the touristic nature of the Cârțișoara commune, we focused on the possibilities of exploiting the orthophoto map for tourism purposes.

As mentioned before, the most important stage in database design is the needs analysis, which is the stage where a detailed analysis of the requirements and expectations of the end users is carried out. Any aspect overlooked during this stage can compromise the final results.

As a result of the needs analysis stage (through consulting specialized literature and discussions with local authorities and tourism operators), we found that a well-structured local tourism development plan should contain both information about attractions and infrastructure, as well as promotion strategies, services offered, and statistical data about tourists. By using the orthophoto map, we can create interactive maps, optimize routes, and plan sustainable tourism development.

An orthophoto map of a rural tourist locality can significantly contribute to the development and promotion of tourism by providing accurate and up-to-date. Below are the main ways it can be used for promoting and developing local tourism.

Creating interactive tourist maps: the orthophoto map can be used to develop interactive digital maps integrated into mobile apps or web platforms; based on it, tourist attractions such as historical monuments, old churches, hiking trails, guesthouses, traditional restaurants, etc., can be marked (Quamar et al., 2023). Tourists can explore the locality virtually before visiting, with access to detailed information about the attractions in the area.

Planning tourist routes: the orthophoto map helps in identifying and optimizing tourist routes, whether for hiking, cycling, or car tours. Trails through forests, access roads to lesser-known attractions, or scenic routes for spectacular photos can be marked. Rural tourism organizers can create thematic routes, such as gastronomic, eco-tourism, or historical routes (Hognogi et al., 2021).

Promoting guesthouses and other accommodation units: guesthouse and agro-tourism owners can use the orthophoto map to showcase the exact location of their units along with the surrounding landscapes. Maps based on the orthophoto map can help tourists visualize the distances between accommodation locations and main attractions, highlighting nearby facilities like local restaurants, shops, or cultural points of interest.

Monitoring and developing tourism infrastructure: local authorities and tourism entrepreneurs can analyze the existing infrastructure and plan the development of new facilities, such as parking lots, camping areas, or viewpoints. Areas with untapped tourism potential can be identified, where recreational activities (e.g., equestrian centers, off-road trails, water sports) can be developed. Issues related to accessibility, such as deteriorated roads or the lack of tourist signs, can be highlighted.

Analyzing the impact of tourism on the environment: by comparing orthophoto maps made at different time intervals, the impact of tourism on the environment can be monitored. Areas affected by deforestation, erosion, waste accumulation, or other issues requiring intervention can be identified. This helps promote sustainable tourism by establishing nature protection rules and conserving ecologically valuable areas.

Creating virtual tours and online promotion: using the orthophoto map together with high-resolution aerial images, virtual tours can be created for promoting the locality. These can be

integrated into tourism websites, online booking platforms, or tourism apps. Tourists can have an immersive experience, exploring the area before deciding to visit.

Support for tour guides and travel agencies: Tour guides can use maps derived from the orthophoto map to provide detailed explanations about the relief and history of the locality. Travel agencies can use this data to personalize tourism experiences, offering routes and activities tailored to each visitor type. The orthophoto map can also help organize local events, such as festivals, traditional fairs, or sports competitions.

Therefore, the orthophoto map provides a valuable tool for planning, promoting, and managing local tourism. From creating interactive maps and optimizing tourist routes to developing infrastructure and protecting the environment, this type of data contributes to increasing the attractiveness of a destination and improving visitors' experiences.

Specifically, the orthophoto map can be integrated into GIS, websites, or various tourist applications where a multitude of tourist information can be marked and published, and which can be structured as shown in Table 5.

Table 5. Structuring of the main information that can be included in databases specific to tourist areas.

Type	Category	Details
General information about the locality	Geographical location	coordinates, county, distance from major cities
	Type of tourism practiced	rural tourism, ecotourism, cultural tourism, agrotourism, etc
	Climate and seasonality	optimal periods for visiting
	Accessibility	access routes: roads, public transport, nearby airports
Tourist infrastructure	Accommodation units	Guesthouses, agrotourism guesthouses, hotels, cabins Accommodation capacity (number of rooms, room types) Facilities (restaurant, swimming pool, accessibility, WiFi, parking) Classification and average prices
	Restaurants and local cuisine	Restaurants, inns, traditional wineries Specific regional menus (traditional dishes, local products) Local culinary events (gastronomy festivals)
	Tourist routes and trails	Hiking trails, cycling, equestrian routes Difficulty and estimated duration Viewpoints and rest areas Accessibility (for families, athletes, elderly tourists)
	Other tourist facilities	Tourist information centers Equipment rentals (bicycles, ATVs, horses, boats) Local transport (taxis, buses, transfers)
Tourist and cultural attractions	Natural landmarks	Mountains, lakes, rivers, forests Nature reserves and protected areas Wildlife and flora observation points
	Cultural and historical landmarks	Old churches, monasteries, castles Museums and memorial houses Historical monuments and archaeological sites
	Traditions and crafts	Pottery workshops, weaving, wood carving Cultural events and traditional fairs Folk music and dances
Tourist services and local experiences	Recreational and adventure activities	Guided tours (cultural, gastronomic, ecotourism) Sports activities (mountaineering, skiing, fishing, hunting) Nature-guided excursions Workshops (traditional cooking, basket weaving, cheese making)
	Other services	Spa and wellness centers Camping and glamping sites Tour guide services and equipment rentals
Statistical data and tourism demand analysis	Annual number of tourists and seasonality Tourist typology (families, adventurers, weekend tourists) Tourist preferences (preferred activities, average budget, length of stay) Assessment of the impact of tourism on the community (economic, social, environmental)	
Tourism promotion strategies	Digital marketing platforms (websites, social media, Google Maps, TripAdvisor) Events and fairs (tourism exhibitions, themed festivals) Collaborations with travel agencies and industry influencers Sustainable tourism (environmental protection strategies, local community involvement)	

Both the previously mentioned datasets and other relevant information can be structured into relational or non-relational data models (databases), as determined by database design

specialists. Relational databases operate with lower hardware resource consumption but may be more challenging to use for inexperienced personnel. Non-relational models require higher hardware resources but can be much easier to use for basic operations.

Figure 11 illustrates a partial relational model of a database in the tourism domain, which structures and organizes information regarding the types of tourism available in the area, accommodation units and their capacities, types of facilities and their locations, tourist attractions, and transportation capacities to these attractions. The presented model can be completed and extended to include additional relevant information, depending on the beneficiaries (tourists, tourism operators, local authorities, etc.).

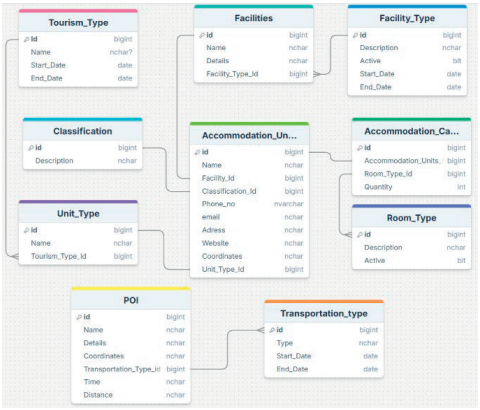


Figure 11. Basic database model for tourism

UAV systems contain a series of emerging technologies that have different levels of evolution and progress, bringing an accelerating role of innovation in a complex mechanism in which those who adopt this innovation early can influence the processes of evolution of technological capacity, with an impact on investments in subsequent stages. The adoption rate of innovation is known to be 20-30%, but taking into account the specific particularities and conditions in Romania, it was found that there is a particularly uneven distribution by age, but it is based on trust in young people who adapt much more easily to new technologies. The proposed topic also has the role of creating a unique integrated framework for analyzing the opportunities, expectations and restrictions of the scalable implementation of UAV systems in the context of the fruition of innovations specific to this emerging field, in the context of the area. The possibility of analyzing different paths of progress at different stages was also pursued, which is why it is valid to apply a quantitative and qualitative analysis to present the opportunities and restrictions of UAV implementation and relevant factors that contribute to or inhibit the technological diffusion specific to UAV missions in the different fields. From the work with students, specialists in the field of terrestrial measurements and farmers, it was observed that in terms of innovation, the use of UAVs is at an early stage because, despite the technological progress at the level of UAV system components, the development of batteries does not yet allow increases in maximum take-off weight, with implications on the maximum payload, specifically affecting active work in precision missions in the different fields of activity. However, there are future expectations of increased performance of propulsion systems and batteries, with an impact on payloads. This aspect is, however, compensated by the advantage of increasing the accuracy of UAV drones and data quality. Innovation is at a level that allows for further growth.

Difficulties in applying this technology also arise due to some operational bottlenecks at the institutional and legislative levels, where transformations are still needed. This leads us to discuss the emergence of signs of scepticism or disappointment given the existence of restrictions on use and safety issues. Legitimizing the use of UAVs is essential in a rather confusing legislative context, but the benefits of previous work by specialists on other sets of UAV applications and missions are relevant. The implementation of UAV systems in specific technology in different fields is also restricted by the level of specialized education, entrepreneurial education and the reduced capacity to create partnerships for the joint use of aerial monitoring platforms and the analysis and interpretation of results. All these problems lead to the emergence of skepticism regarding the interest in this technology, especially

among many older people. However, the ambition of those who understood the usefulness of technology for creating sustainable and intelligent ecosystems and their success in implementing UAV systems, was materialized by early detection of vulnerabilities, intervention focused exclusively on them, reducing resource consumption, highlighting the true potential and offering efficient solutions. Agricultural producers and foresters in the future will adopt UAVs in their business portfolios and will better understand the progress they offer in the context of sustainability. Although there are still a number of uncertainties and risks, significant cost reductions and increased performance will favor the recovery phase that will extend sustainably. Users, despite not having specialized education, are surprisingly becoming more sophisticated and demanding superior performance without deeply understanding the aspects of technological leaps.

This study has certain limitations and constraints that should be taken into account in future research. These are related to the following: the goal of offering a comprehensive understanding of the specific processes of innovation transfer in a field characterized by unknown evolutionary dynamics and the lack of relevant data on aerial scanning and precision applications; understanding the capacity of reliability aspects, digital footprint and the influence of innovation dynamics in the field on the performance of aerial scanning and precision applications in the different domains. The motivation to continue this research is also determined by the fact that the proposed systems work very well from a technical point of view and have the advantage of being easy to use by inexperienced end users. Also, the challenges related to the digital footprint will be further addressed to increase competitiveness in the different fields of activity, where it is very well suited.

The development of a territory/zone/area represents the capitalization under superior conditions of endogenous resources that give it specificity, and the creation of a geographic information system at the UAT level is defining. Rural areas have a relevant heritage of resources that give it specificity and lead to the development of a specific economic structure in accordance with the diversity of endogenous resources that, when digitized, accelerate this process.

CONCLUSIONS

The commune of Cîrțișoara has many resources that can act as a generator of local development, by outlining a vision of sustainable development, for which a multifunctional base provides faster, more detailed necessary data that underpins the strategic planning process.

The research methodology adopted is the case study because it involves the in-depth study of the rural economy, in the natural setting of the commune of Cârțișoara, from several perspectives.

The development of unmanned aircraft systems is a certainty of the present towards which society shows increased interest, including in collecting data for the creation of a geographic information system.

The design and implementation of a multifunctional database requires:

- the existence of a team of specialists in various fields (cartography, photogrammetry, informatics, etc.);
- the development of a data model (database structure);
- the existence of a graphic support (raster type);

The stages of acquiring raw data through aerial photography and their graphic processing are resource-intensive (financial, time, technical);

The stage of vectorizing the elements of interest and recording the related attributes is time-consuming;

The success of implementing a multifunctional database depends on the team's ability to collect the necessary data;

The structure and content of a geographic information system can be updated at any time (with greater or lesser efforts and, of course, with awareness of all subsequent implications);

The built multifunctional database system allows:

- displaying and extracting results in various forms: images, graphs, tables, maps, etc.;
- ensures flexibility in the analysis of data of interest.

The integration of UAV-based data acquisition, database development, and GIS systems constitutes a synergistic process that generates significant added value. Each piece of equipment and each technological procedure serves a well-defined purpose, contributing to the achievement of broader spatial planning and development objectives.

The methodology proposed in this study was validated through a case study, during which all the designed stages were implemented and the targeted objectives were successfully met.

The generation of an orthophoto map and its integration into an information system designed to support local development represent a multi-stage and complex workflow, where technical operations and data modeling are coherently combined. The first essential stage involves the execution of a photogrammetric flight using an UAV, with the main objective of acquiring primary data in the form of overlapping aerial images (photograms) at a spatial resolution tailored to the project requirements. The flight planning process - including the determination of flight altitude, image overlap, and flight path - plays a decisive role in ensuring the quality and accuracy of the subsequent photogrammetric products.

Following data acquisition, a rigorous photogrammetric processing workflow is applied using specialized software. This involves the alignment of photograms, generation of a dense point cloud, construction of a digital terrain model (DTM), and ultimately, the creation of the orthophoto map. The resulting orthophoto map, which is both georeferenced and highly accurate, serves as a fundamental spatial dataset for thematic data extraction and the development of derived cartographic products.

In parallel with these technical activities, an analysis of user requirements is conducted to design a database tailored to the specific needs of the local community or the field of application. In the present study, considering the predominantly rural tourism profile of the investigated area, the proposed data model was specifically developed to meet the requirements of the tourism sector. Accordingly, the conceptual database schema incorporates relevant entities such as accommodation facilities, tourist trails, cultural landmarks, protected areas, infrastructure networks, and tourist amenities. Performing this analysis concurrently with the orthophoto map generation facilitated the optimization of the subsequent data integration stages.

Although the case study focused on supporting tourism-related activities, the validated methodology is adaptable and transferable to a variety of domains, including environmental protection, territorial planning, urban and rural development, the updating of local cartographic products, and utility and infrastructure management.

Once both the orthophoto map and the database structure were finalized, the database population stage was initiated, with the orthophoto map serving as the primary support for the identification, digitization, and recording of spatial features. The collected data were then integrated into a Geographic Information System, enabling efficient spatial analysis, visualization, and data exploitation.

The final outcome of this workflow is a geospatial database integrated within a GIS environment, with direct applicability for local and central authorities, economic operators - particularly those in the tourism sector - and for the general public, facilitating access to relevant spatial information. The integrated use of these data provides a robust foundation for the development of sustainable development strategies, territorial planning, and the promotion of the region's touristic potential.

The study undertaken is oriented towards the use of modern methods, means and tools of analysis carried out within the framework of the case study methodology and represents a contribution to the management of strategic orientation activities of sustainable development in the Cârțișoara ATU model, by using modern aerial scanning techniques, creating a GIS database and integrating information for the development of relevant strategic options for sustainable development.

Further research will refer to the establishment of partnerships, entrepreneurial education and specialized education. These, together with the innovative management framework adopted at the level of agricultural and non-agricultural enterprises, are capable of accelerating the implementation and future development of UAV systems.

REFERENCES

Achtilik, M. (2015). UAV Inspection and Survey of Germany's Highest Dam. Ascending Technologies. pp 1–3. Anderson, K., & Gaston, K. J. (2013). Lightweight unmanned aerial vehicles will revolutionize spatial ecology. *Frontiers in Ecology and the Environment*, *11*(3), 138-146.

Aswini, N., Krishna, E.K. and Uma, S.V. (2018). UAV and obstacle sensing techniques – a perspective. *International Journal of Intelligent Unmanned Systems*, *1*(3), 256-275.

Barbedo, J.G.A. (2019). A review on the use of unmanned aerial vehicles and imaging sensors for monitoring and assessing plant stresses. *Drones*, 3(2), 40.

Borra-Serrano, I., Van Laere, K., Lootens, P., & Leus, L. (2022). Breeding and Selection of Nursery Plants Assisted by High-Throughput Field Phenotyping Using UAV Imagery: Case Studies with Sweet Box (Sarcococca) and Garden Rose (Rosa). *Horticulturae, 8*(12), 1186.

Budiharto, W., Irwansyah, E., Suroso, J.S., Chowanda, A., Ngarianto, H., & Gunawan, A.A.S. (2021). Mapping and 3D modelling using quadrotor drone and GIS software. *J Big Data, 8*, 48. https://doi.org/10.1186/s40537-021-00436-8

Călina, J., Călina, A., Iancu, T. and Vangu, G.M. (2022). Research on the Use of Aerial Scanning and Gis in the Design of Sustainable Agricultural Production Extension Works in an Agritourist Farm in Romania. *Sustainability*, *14*(21), 14219.

Călina, J., Călina, A., Miluț, M., Croitoru, A., Stan, I., Buzatu, C. (2020). Use of drones in cadastral works and precision works in silviculture and agriculture. *Romanian Agricultural Research*, *37*, 273-284.

Chen, L., Thapa, B., Kim, J., & Yi, L. (2017). Landscape Optimization in a Highly Urbanized Tourism Destination: An Integrated Approach in Nanjing, China. *Sustainability*, *9*(12), 2364. https://doi.org/10.3390/su9122364

Cisneros, L. J. In Peru, Drones Used for Agriculture, Archaeology. AFP News. 2013, pp 1–4. http://phys.org/news/2013-08-peru-drones-agriculture-archaeology.html (accessed June 18, 2024).

Filho, I. H., Heldens, W. B., Kong, Z., & de Lange, E. S. (2020). Drones: innovative technology for use in precision pest management. *Journal of economic entomology*, *113*(1), 1-25.

Glen, B. (2015). Rise of the Field Drones. Precision Agriculture of the Future Employs Robots to Work Fields and it's Here Now. The Western Producer, pp 1–12.

Hognogi, G.-G., Pop, A.-M., Marian-Potra, A.-C., & Someşfălean, T. (2021). The Role of UAS–GIS in Digital Era Governance. A Systematic Literature Review. *Sustainability*, *13*(19), 11097. https://doi.org/10.3390/su131911097

Iagăru, P., Pavel, P., Iagăru, R., & Șipoș, A. (2021). Using drone technology for preserving the economic sustainability of the agricultural holdings. *International Journal of Advanced Statistics and IT&C for Economics and Life Sciences*, *11*(1), 85-90.

Iagăru, P., Pavel, P., Iagăru, R., & Șipoș, A. (2022). Aerial Monitorization - A Vector for Ensuring the Agroecosystems Sustainability. *Sustainability*, *14*(10), 6011.

Kovanič, Ľ., Topitzer, B., Peťovský, P., Blišťan, P., Gergeľová, M.B., & Blišťanová, M. (2023). Review of Photogrammetric and Lidar Applications of UAV. *Applied Sciences*, *13*(11), 6732. https://doi.org/10.3390/app13116732

Krishna, K. R. (2016). Push Button Agriculture: Robotics Drones and Satellite Guided Soil and Crop Management; *Apple Academic Press Inc.: Waretown, New Jersey*, *405*.

Maes, W. H., & Steppe, K. (2019). Perspectives for remote sensing with unmanned aerial vehicles in precision agriculture. *Trends in plant science*, *24*(2), 152-164.

Parraga-Alava, J., Alcivar-Cevallos, R., Morales Carrillo, J., Castro, M., Avellán, S., Loor, A. and Mendoza, F. (2021). LeLePhid: an image dataset for aphid detection and infestation severity on lemon.

Quamar, M. M., Al-Ramadan, B., Khan, K., Shafiullah, M., & El Ferik, S. (2023). Advancements and Applications of Drone-Integrated Geographic Information System Technology - A Review. *Remote Sensing*, *15*(20), 5039. https://doi.org/10.3390/rs15205039

Sălăgean, T., Rusu T., Poruţiu, A., Jutka, D.E.A.K., Manea, R., Virsta, A. and Călin, M. (2016). Aspects regarding the achieving of a geographic information system specific for real estate domain. *AgroLife Scientific Journal*, *5*(2).

Sedano-Cibrián, J., de Luis-Ruiz, J.M., Pérez-Álvarez, R., Pereda-García, R., & Tapia-Espinoza, J.D. (2023). 4D Models Generated with UAV Photogrammetry for Landfill Monitoring Thermal Control of Municipal Solid Waste (MSW) Landfills. *Applied Sciences*, *13*(24), 13164. https://doi.org/10.3390/app132413164

Upadhyaya, A., Jeet, P., Sundaram, P.K., Singh, A.K., Saurabh, K. and Deo, M. (2022). Efficacy of drone technology in agriculture: A review: Drone technology in agriculture. *Journal of AgriSearch*, *9*(3), 189-195.

Vangu, G.M., Croitoru, A., Mitrache, M. and Dima, N. (2023). Design of a GIS Database for Surface Mining. *Journal of Applied Engineering Sciences*, *13*(2), 289-296. https://doi.org/10.2478/jaes-2023-0037

Vangu, G.M., Miluț, M., & Croitoru, A.C. (2025). Use of Modern Technologies Such as UAV, Photogrammetry, 3D Modeling, and GIS for Urban Planning. *Journal of Applied Engineering Sciences*, *15*(1), 165-174. https://doi.org/10.2478/jaes-2025-0020

Wang D-C, Zhang G-L, Zhao M-S, Pan X-Z, Zhao Y-G, Li D-C, et al. (2015). Retrieval and Mapping of Soil Texture Based on Land Surface Diurnal Temperature Range Data from MODIS. *PLoS ONE, 10*(6), e0129977. https://doi.org/10.1371/journal.pone.0129977.

Yamaha. *RMAX-History*. 2014, pp 1–4.

Zhang, C., Walters, D., & Kovacs, J. M. (2014). Applications of low altitude remote sensing in agriculture upon farmers' requests–a case study in northeastern Ontario, Canada. *PloS one*, *9*(11), e112894.

Scientific Papers. Series E. Land Reclamation, Earth Observation & Surveying, Environmental Engineering. Vol. XIV, 2025
Print ISSN 2285-6064, CD-ROM ISSN 2285-6072, Online ISSN 2393-5138, ISSN-L 2285-6064

STUDY ON THE IMPACT OF THE APPLICATION OF INFORMATION SYSTEMS ON THE EFFICIENCY AND PRECISION OF TOPO-CADASTRAL WORKS IN THE PREPARATION OF DOCUMENTATION FOR A ROAD IN DOLJ COUNTY

Jenica CĂLINA, Aurel CĂLINA, Alin CROITORU

University of Craiova, Faculty of Agronomy, 19 Libertății Street, Craiova, Romania

Corresponding author emails: aurelcalina@yahoo.com, croitorualinc@yahoo.com

Abstract

The work was carried out based on the experience of over 30 years of study of the authors' team in the field of land measurements, during which, throughout the specific activities of topography and cadastre, they worked with both classic equipment and high-performance, modern equipment. Based on this, we thought of presenting in this short work, the essence of the experience, which aims to target the impact of modern information systems on all aspects related to topo-cadastral works. A case study was presented for the technical documentation necessary for the tabulation of a road in a locality in Dolj County. As a result, all the advantages and novelties related to the application in topo-cadastral works of the complex information system, consisting of high-performance modern equipment used to collect data from the field, combined with automatic data processing, with a high-performance specialized program, with wide applicability in several fields in Romania. The results were very relevant and significant in terms of their impact on the efficiency, cost-effectiveness and accuracy of the terrestrial measurement work carried out in the presented case study.

Key words*: information systems, topographic measurements, documentation, AutoCAD, road registration, geospatial accuracy*

INTRODUCTION

It is widely recognized that for an organization to succeed and remain competitive in a dynamic economic environment, managers must identify optimal solutions and drive radical innovations despite uncertainty. To support this, organizations need to invest in information systems that add value to business processes. These systems are primarily designed to automate information processing, which serves as the foundation for informed decision-making (Furby & Akhavian, 2024).

Information systems play a crucial role in enhancing the flow of information between tools, equipment, and work methods. This integration leads to the automation of processes and improved efficiency in topo-cadastral measurement activities (Călina et al., 2018; https://gisgeography.com/trilateration-triangulation-gps).

Studies show that, in order to complete tasks on time and make accurate decisions, professionals in the field must rely on high-performance information systems that align with the core requirements of their activities. All data and information collected from the field and processed through various activities or procedures can be easily accessed by users of information systems, while also offering a unified and integrated perspective. These systems provide a range of advantages for their users, facilitating not only the sharing and transfer of data and information but also supporting the optimization and automation of work processes (Sestras et al., 2022). Efficient data exchange can accelerate the achievement of objectives and reduce the time required to complete specific tasks. The implementation of such systems often results in improved data quality, reduced working time, enhanced communication between operators, more accurate decision-making, and significantly increased productivity (Doneus & Neubauer, 2005; https://rompos.ro/index.php/informatii-tehnice/sisteme-gnss). In the domain of land surveying, automation has substantially improved the quality of topo-cadastral data, particularly through enhanced positional accuracy and resolution. These systems integrate a wide range of technical tools with varying levels of automation, with the electronic

computer at the core. Minimizing manual operations reduces the risk of errors. The integration of real-time position determination using global positioning systems (GPS) and automated data processing contributes to increased accuracy and uniformity across all digital and analog products (Păunescu et al., 2020).

New knowledge in the field of land surveying is already being applied to address both local and global challenges. However, specific issues often arise with certain techniques and technologies - likely due to the absence of well-defined methodologies for designing and utilizing information systems (Stöcker et al., 2020). Numerous studies highlight the growing need for practical geospatial solutions to address social, environmental, and economic problems. One of the most pressing challenges today is balancing the exploitation of natural resources with the preservation of ecological systems. This tension calls for a reevaluation of development strategies at local, regional, and global levels. Information systems will undoubtedly play a critical role in supporting these new directions by providing essential data and tools for managing, analyzing, visualizing, and applying geospatial knowledge (Mihai et al., 2015).

The current development of integrated information systems is characterized by substantial transformations, both in terms of procedures for collecting and processing data and information, and in terms of defining and creating final products, thus analyzing the data collected both as sources and as products. With the launch of the first artificial earth satellites and spacecraft, a new era in the development of topo-cadastral measurements from all points of view opened. Satellite systems have been differentiated from the beginning into: reconnaissance systems; meteorological systems; systems for the study of terrestrial resources; commercial satellite systems. In this field, there have been significant developments in recent decades, which have targeted both theoretical foundations and cartographic technologies, means of representation and equipment for collecting, processing, organizing, storing, retrieving and using topo-cadastral data and information (Longley et al., 2011; https://gisgeography.com/trilateration-triangulationgps).

Among these are: what is the nature of geocoded data (X,Y,Z) at different scales and after different transformations; how does data quality behave at different transformations; how to manage the large volume of data resulting from raster or vector digitization or imported from photogrammetric and remote sensing systems; how to generalize and reduce this amount of data to optimize storage; the criteria to be followed to choose the necessary archives to keep; how to generate missing data, either for the "lost" ones or from those previously compacted; how to choose a national or international standard for data exchange or to collaborate on the creation of maps with continental or global changes (Herbei & Sala, 2020).

In the context of cadastral works, the use of modern technologies plays a crucial role in ensuring the accuracy and efficiency of measurement and recording processes. Among these technologies are GPS systems, modern measurement equipment (total stations), CAD systems, and GIS technology. Each of these tools contributes to the creation of an accurate cadastral framework and proper documentation of land ownership (Dragomir et al., 2025). The technologies serve as tools for primary data collection and processing, while GIS represents an advanced solution that enables the collection, storage, analysis, and visualization of spatial data (Nițu & Tomoioagă, 2015; Roșca et al., 2020).

In cadastral work, GIS proves essential for the integration and efficient management of geographic data. Through GIS, information regarding property boundaries, roads, and existing infrastructure is centralized in a digital system that can be easily accessed and updated. This system allows for precise analysis of land development and changes, which is vital for legal and administrative purposes, including the registration of a road sector in the land registry (Sestras et al., 2025).

One of the key advantages of GIS over other technologies is its ability to manipulate and analyze data within a geographical context. GIS can integrate data from multiple sources (GPS, digital maps, satellite imagery), making it extremely useful for creating a detailed and accurate cadastral framework. Additionally,

through GIS, spatial analyses can be performed to determine risk areas, evaluate the impact of new constructions on existing networks, or optimize land use.

Moreover, it is important to understand the main similarities and differences between CAD products (such as AutoCAD) and GIS products. Both CAD and GIS are essential tools in the field of cadastral work, but each focus on different aspects of the mapping process. AutoCAD is a software primarily dedicated to drafting and creating detailed technical plans, including contours, lines, and geometric shapes. It is frequently used in the design of infrastructure and construction works, and files generated in AutoCAD are often used for cadastral documentation (Akinci et al., 2010).

On the other hand, GIS focuses on managing and analyzing geospatial data. While AutoCAD is geared towards creation and drawing, GIS is concerned with manipulating and interpreting location- and land-related data. GIS allows for advanced analyses such as generating thematic maps, calculating distances, or assessing the impact of various changes on land.

In a complementary manner, AutoCAD can be used to create detailed drawings of an area, which can then be integrated into a GIS system for more detailed geographical analysis and visualization. Data related to a road sector can be created in AutoCAD and then transferred into a GIS to study its impact on the road network in a larger area, considering factors such as topography, land use, or existing infrastructure.

In this study, the use of the AutoCAD work system integrated with field equipment such as total stations and GPS was analyzed. This method was used because AutoCAD represents a standard for design in the fields of mechanics, architecture and geodetic engineering, being very useful for both designers and draftsmen (Becker et al., 2011).

At the same time, this was also due to the advantages obtained by using the AutoCAD program, such as:

- creating 3D (three-dimensional) constructions;
- obtaining virtual images of the designed objects;
- avoiding any routine work, by using the commands that create the required graphic element;
- obtaining drawings of exceptional clarity, due to the fact that the drawing, once created, is printed, and the changes made during the work do not appear on paper;
- perfect quality of the drawing created on the computer;
- its accuracy;
- reduced execution of modification time;
- easy transfer of information (CDs, DVDs, USB Sticks).

This paper aims to evaluate the efficiency and precision of topo-cadastral documentation using modern integrated information systems in a real-world case study.

MATERIALS AND METHODS

Reducing efforts and costs is essential for improving the competitiveness and long-term sustainability of any company. Geodetic engineering activities involve complex processes that require significant time and labor resources, and optimizing these processes can bring major benefits. Automation and digitalization are key solutions for minimizing manual intervention, eliminating errors, and enhancing the precision and speed of operations. Implementing advanced software solutions can significantly reduce the time needed for processing documentation and fieldwork, thus contributing to lower operational costs (Carrera-Hernández et al., 2020).

The applied methodology is presented in Figure 1, with the stages of the applied case study being presented and detailed further.

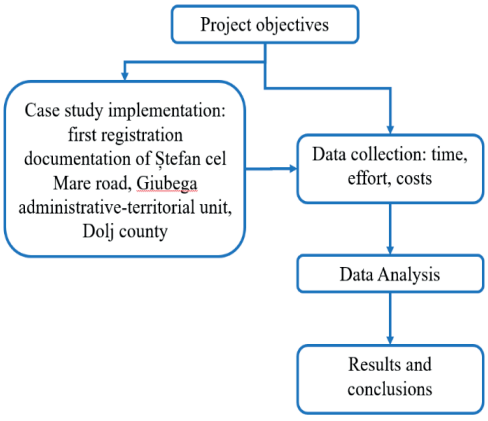


Figure 1. Applied methodology

To analyze efficiency and identify potential areas for improvement, we have conductes a detailed case study. This includes collecting and analyzing data on the time spent, efforts made, and costs involved in carrying out various cadastral activities. The aim of this study is to better understand workflows and discover optimization opportunities. The results obtained will be used to identify solutions that reduce the resources needed to complete projects, thus contributing to the streamlining of the cadastral firm's activities and increasing its profitability.

The case study presents a first registration documentation of the Ștefan cel Mare Street, ATU Giubega, Dolj County.

The process of preparing the cadastral documentation for the first registration of a road sector in the Land Register involves a series of methodical and sequential operations, carried out in accordance with national legislation and technical norms in force. The methodology adopted in this study ensures the acquisition of accurate spatial data, the legal identification of the land parcel, and the formalization of the necessary cadastral documents for submission to the competent cadastral and land registration office.

Field measurements were performed using high-precision GNSS equipment in RTK (Real Time Kinematic) mode, specifically a GPS Hi-Target V200 GNSS receiver and iHand55 controller, with RTK correction through the ROMPOS network, using the Stereo 70 projection system. Coordinates were exported in CSV format and processed in AutoCAD using the TopoLT plugin. To complement the geodetic data, a total station Leica TCA 1205 was used for areas with limited satellite signal reception or for detailing specific construction elements (e.g., curbs, culverts, or road infrastructure boundaries). For data processing, the AutoCAD Civil 3D platform (and TopoLT plugin) was employed for drafting the technical plans, while the geospatial database was managed and analyzed using QGIS 3.28. The final cadastral documentation was structured according to the requirements of the National Agency for Cadastre and Land Registration (ANCPI), using the specialized software e-Terra.

Figure 2 illustrates the main working stages, as well as their logical sequence within the framework of the present project. As shown, the entire workflow is illustrated, starting from equipment preparation and document analysis, all the way to final processing, printing, and exporting the cadastral plan for the measured road sector.

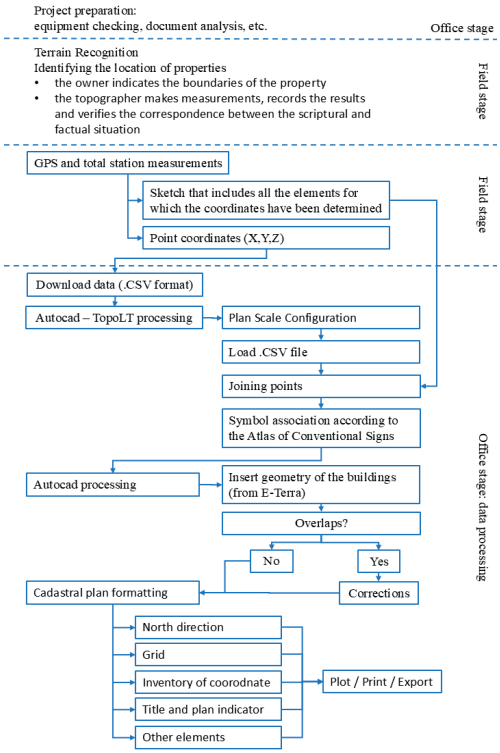


Figure 2. Workflow for measurements and data processing

The cadastral works were executed by a multidisciplinary team consisting of: a certified geodetic engineer (responsible for field measurements and technical verification), a legal consultant (responsible for verifying property rights, administrative boundaries, and legal acts), and a technician (responsible for assisting in field operations and document preparation).

Measurements for the Ștefan cel Mare Road were taken over a distance of about 430 meters and an area of about 6050 sqm. The field data were collected in a single day, in September 2023.

In this case study, a complex work system was used in which modern and high-performance equipment was used for field work, such as

global positioning systems (GPS) for collecting the main data, and total stations with high precision were used to complete the details. After collecting the data with high precision and high efficiency, they were processed with an older specialized program but widely used in several fields of activity in Romania, namely AutoCAD.

Working with this integrated computer system allows the total replacement of the pencil, the drawing board, the ruler, the square, the compass and the eraser. However, this program does not eliminate the need to pay increased attention to details, to thoroughly analyze the project. Emphasis must be placed on accuracy in drawing, as these drawings often go directly to numerically controlled machining machines (Pop et al., 2019).

Considering that the purpose of this article is to study the effectiveness of applying modern data acquisition and processing techniques, in addition to the technical data collected, details regarding execution time, efforts, and costs required to achieve the expected results were also recorded.

RESULTS AND DISCUSSIONS

The case study presents a First Registration Documentation of the Ștefan cel Mare Road, ATU Giubega, Dolj County. For the first registration documentation, the cadastral work was carried out based on field measurements, using the data processing method using the Auto-CAD program and drawing up the plan of this work.

The preparation of cadastral documentation involves the following stages (Sălăgean et al., 2016; Călina et al., 2022):

- identification of the location of the property and technical documentation;
- execution of field and office work;
- preparation of documentation.

This approach was chosen because it was concluded that it is very important and interesting how Auto-CAD has become an essential tool in cadastral works, offering the possibility of creating detailed plans of real estate. By using this complex information system GPS-Total Stations - Auto-CAD, it is possible to create and manage all the information regarding the lands registered in the cadastre, thus facilitating the process of recording and monitoring them. This system ensures precision and efficiency in the creation of cadastral plans, representing a crucial component in cadastral activity.

As is known, the owner is responsible for knowing, indicating the boundaries of the property and preserving them, as well as for making available to the authorized person all the acts/documents he holds regarding the property. The authorized person is responsible for measuring the property indicated by the owner, for the correctness of the documentation and its correspondence with the reality on the ground and with the documents proving the ownership right made available by the owner. In the case of tracings, the authorized person is responsible for materializing the boundaries of the property in accordance with the up-to-date geometry of the property in the database of the territorial office.

The road subject to modernization is located in the village of Giubega, a village located in the immediate vicinity of the city of Băilești. The Ștefan cel Mare Road is a road of national interest connecting the European road DN 56 and the city of Calafat. With the completion of the project for the modernization of the road, traffic in the area will increase, leading to the development and economic growth of the commune.

Before starting the measurement, the team moves into the field to reconnoiter the terrain. In this process, the area to be measured, the length of the route and the fixed elements are checked. Depending on the complexity of the details, the scale at which the documentation will be drawn up is established.

As shown in Figure 3, the survey team used a GPS receiver connected to ROMPOS for real-time measurements and a Leica TCA 1205 total station in the Giubega area.



Figure 3. Taking field measurements

The field trip was carried out with representatives of the Giubega Commune City Hall, who identify the neighborhoods of the building. A person who is part of the measurement team draws up a sketch of the building, respecting the numbering of the points in the GPS and representing all the measured elements.

As a result of the case study, the following concrete outcomes were obtained for Ștefan cel Mare Street, which has a length of approximately 430 meters and a surface area of 6,055 square meters:

- a coordinate inventory consisting of 104 points, for which coordinates were determined in the Stereo 70 reference system, as presented in Table 1;
- the cadastral documentation required for the first registration of this road sector in the land register;
- the site location map at a 1:2000 scale, as shown in Figure 4;
- used resources, as presented in Table 2.

Table 1 presents the inventory of coordinates for the surveyed points, and the publication of this table contributes to the methodological transparency of the study, providing a verifiable and useful database for researchers, professionals in engineering and surveying, as well as cadastral authorities. Thus, the obtained coordinates can serve as a concrete example of the application of advanced geodetic techniques in road infrastructure projects and in the process of updating cadastral data. At the same time, they are essential for the correct integration of the rehabilitated road section into the land registry, a process that guarantees the legal validity of the work.

Including these coordination points in this article not only supports the scientific validity of the research but also adds practical value, contributing to the improvement of precision standards in infrastructure projects and cadastral data management.

Table 1. Inventory of road coordinates for Ștefan cel Mare Street, Giubega, Dolj county

Point no.	X [m]	Y [m]	Point no.	X [m]	Y [m]	Point no.	X [m]	Y [m]
1	373031.405	293299.467	36	372942.966	293313.618	71	373234.649	293188.745
2	373027.910	293301.139	37	372961.875	293307.499	72	373250.633	293181.744
3	373025.650	293302.040	38	372965.594	293306.295	73	373274.911	293171.727
4	373020.493	293304.056	39	372984.714	293300.108	74	373282.102	293168.695
5	373007.259	293309.164	40	372988.265	293298.923	75	373287.293	293181.286
6	373005.719	293309.623	41	373003.589	293293.766	76	373273.794	293186.911
7	372998.818	293312.475	42	373021.302	293287.805	77	373262.180	293191.714
8	372986.210	293316.486	43	373029.009	293284.462	78	373254.655	293194.313
9	372968.615	293322.450	44	373048.373	293276.217	79	373244.484	293199.130
10	372963.801	293323.416	45	373053.878	293273.305	80	373240.910	293201.017
11	372954.017	293326.152	46	373064.956	293268.475	81	373234.289	293203.895
12	372950.478	293327.043	47	373080.983	293260.970	82	373231.553	293205.024
13	372939.208	293330.413	48	373095.493	293254.629	83	373223.596	293208.290
14	372927.691	293333.619	49	373109.521	293247.270	84	373199.108	293218.547
15	372922.822	293335.439	50	373123.063	293240.654	85	373189.392	293222.830
16	372921.708	293335.814	51	373127.459	293238.183	86	373187.057	293223.582
17	372909.671	293340.034	52	373130.319	293236.755	87	373176.619	293228.289
18	372901.063	293343.305	53	373132.494	293235.665	88	373164.576	293233.719
19	372894.108	293345.948	54	373140.467	293231.669	89	373157.284	293238.541
20	372893.612	293344.160	55	373140.578	293231.613	90	373153.638	293240.630
21	372891.487	293337.706	56	373144.770	293229.495	91	373147.529	293243.748
22	372888.381	293329.141	57	373156.902	293223.566	92	373134.976	293249.932
23	372889.218	293328.838	58	373158.082	293222.886	93	373126.402	293254.274
24	372890.937	293329.868	59	373158.653	293222.557	94	373120.013	293257.407
25	372902.362	293326.255	60	373159.465	293222.201	95	373114.085	293260.243
26	372907.173	293324.734	61	373167.783	293218.551	96	373100.169	293266.989
27	372909.658	293323.977	62	373171.884	293216.752	97	373094.662	293269.819
28	372918.366	293321.074	63	373175.584	293215.106	98	373087.326	293273.776
29	372921.827	293319.839	64	373189.604	293208.870	99	373074.715	293279.946
30	372931.071	293316.834	65	373193.861	293206.977	100	373057.536	293287.037
31	372933.014	293316.174	66	373209.027	293200.188	101	373048.174	293290.099
32	372934.712	293315.212	67	373216.905	293196.661	102	373037.436	293296.648
33	372937.488	293314.694	68	373216.876	293196.608	103	373032.345	293299.017
34	372937.864	293314.856	69	373230.162	293190.711	104	373031.405	293299.467
35	372942.825	293313.910	70	373230.318	293190.642			

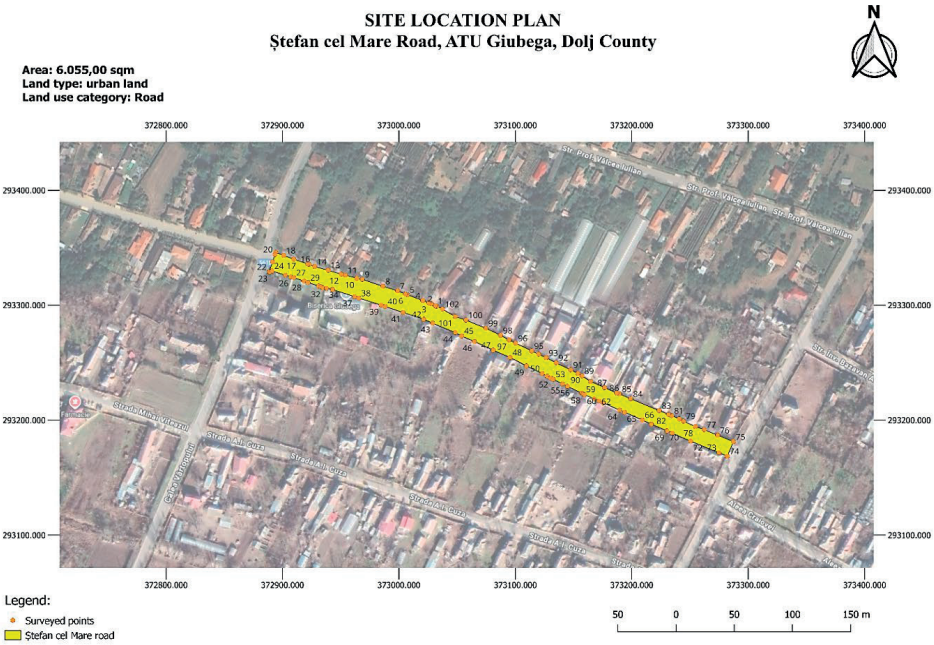


Figure 4. Site location plan

Table 2. Resources used in the case study implementation

No.	Type	Resource	Measuring units	Quantity
1	Personnel	Geodetic engineer	Minutes	530
2	Personnel	Legal consultant	Minutes	45
3	Personnel	Technician	Minutes	305
4	Material	Hi-Target V200 GNSS receiver	Units	1
5	Material	Leica TCA 1205 total station	Units	1
6	Software	AutoCAD, TopoLT plugin	Units	1
7	Software	QGIS v.3.28	Units	1
8	Other	Consumable materials		
9	Other	Transportation expenses		
10	Other	Indirect costs		

In any company, efficient cost management is essential to ensuring profitability and maintaining competitiveness in the market.

A company's efficiency cannot be measured solely by the volume of activities carried out, but also by the ratio between the costs incurred and the results achieved. A company can only be considered efficient when it manages to intelligently reduce costs without compromising the quality of the services or products offered, while simultaneously increasing profitability. This objective can be achieved by adopting modern technological solutions which, although requiring initial investments, bring considerable long-term savings (Šafář et al., 2021).

Therefore, only through constant cost analysis and the identification of optimization opportunities can a company ensure its financial stability and remain relevant in an increasingly competitive economic environment. Cost reduction should not be seen as a crisis measure, but as a strategic practice, integrated into the organizational culture, focused on performance and sustainable development.

It is important to note that the cost structure of a company differs from the cost structure associated with a project. Thus, in order to identify opportunities for reducing efforts and costs, and for optimizing activity, cost analysis must be conducted from at least three

perspectives: the type of expenses, the elements that generate them, and the stage at which they occur. Table 3 presents the main cost structure associated with a project and assesses the impact that each type of cost may have on the total cost of the project.

Table 3. Project cost structure and its impact

Expense type	Generated by:	Details	Impact on the project	Can be optimized	Remarks
Direct	Involved personnel	Primarily includes personnel costs associated with the project.	High	Yes	The personnel can work more accurately and efficiently. The personnel can use optimal solutions to achieve objectives, depending on the field conditions.
	Material consumption	Includes the consumption of materials within the project: survey markers, spray paint, etc.	Low	No	Modifying these cannot have a significant impact.
	Transport expenses	Includes transport expenses within the project.	Low	No	
	Other expenses	Other unforeseen expenses initially not anticipated.	Low	No	
Indirect	Uninvolved personnel	Includes the costs associated with administrative personnel and the costs for the professional training of the staff.	Low	No	
	Equipment	Includes the costs for the depreciation and insurance of the equipment.	High	Yes	They can vary by acquiring more efficient equipment that reduces execution times.
	Licenses	Includes the costs for licensing the software products used.	High	Yes	They can vary by licensing more efficient solutions that reduce processing times.
Administrative	General costs	Includes costs for rent, utilities, etc.	Low	No	

Therefore, it can be observed that the elements with the greatest impact on a project's costs are: the personnel directly involved, the equipment, and the software solutions used. At the same time, these are also the main elements that can be optimized within the context of a project.

The directly involved personnel can contribute to cost reduction through continuous professional development, which enables them to work more efficiently and accurately. Additionally, they can help lower expenses and increase efficiency by using appropriate technologies (best suited to field conditions) and software products that automate data processing. The “high” impact attributed to the equipment and software solutions used does not refer to their depreciation or insurance costs, but to the benefits that can be generated by using optimal equipment and software in the context of a project.

For example, in the case study carried out, measurements could have been performed using either a total station or a GNSS receiver. However, the surveyor chose to use the GNSS receiver because field conditions were favorable, and the execution time was significantly shorter than when using the total station.

Moreover, during the office phase, the surveyor used both TopoLT and AutoCAD to process the data, which reduced the time needed for processing and preparing the required documentation. Table 4 presents the possibilities

for optimizing activities and reducing costs depending on the project phase.

Table 4. Optimization opportunities according to project phase

	Personnel	Equipment	Software
Project preparation	No	No	No
Terrain recognition	No	No	No
Measurements	Yes	Yes	Yes
Data processing	Yes	No	Yes
Cadastral plan formatting and export	Yes	No	Yes

Considering the aspects mentioned above, the equipment and software solutions used, as well as the measurement methods applied, we can conclude that the case study was carried out under optimal conditions. This assessment is based on the following considerations:

- The personnel had access to all necessary resources (equipment, software licenses);
- The participants were properly trained and used the best methods and techniques suited to the field conditions;
- During the office phase, the personnel used all available software solutions (including the TopoLT plugin) to automate data processing;
- Field conditions (absence of interference and good visibility) allowed the use of a GNSS receiver for determining point coordinates. The surveyor also had access to a total station, but its use would have required more time for measurements;
- Data recorded by the GNSS receiver is easier to process compared to data collected by total stations;
- The use of the TopoLT plugin facilitated data processing;
- Predefined templates were used in AutoCAD, which reduced the time required for preparing the necessary documentation.

CONCLUSIONS

From the beginning, great importance was given to the accuracy of the data and products of the complex information system. A good treatment of this problem allowed the choice of the best data sources, the choice of the most correct methods of data collection and the choice of the most correct procedures for processing and creating the final products. Considering the various types of data and procedures for collection, validation and processing, it can be shown that:

- data have different measures and methods of assessing accuracy;
- the required level of accuracy specific to different types of applications varies greatly;
- data accuracy is strictly related to the collection methods, the equipment used, the data sources, the processing procedures, etc.;
- as a result of the above, data accuracy also depends on the costs of the information systems and vice versa.

By strictly respecting all the requirements listed above, the study team achieved much greater precision through this modern method of combining data collection with modern equipment and their automated processing with specialized programs, compared to the classic methods used over time in cadastral works. The classic equipment had a very low precision by construction, little or no possibility of collecting and storing data and a cumbersome maneuverability, aspects that led to the recording of very large total errors, which ultimately resulted in low precisions, which were difficult to achieve within the tolerance limits allowed in the case of such works and especially in the case of engineering works such as those presented in this case study. It was also found that technological and scientific progress led in the field of terrestrial measurements to the emergence of new methods and techniques necessary for the proper conduct of the activity, the computer offering greater precision compared to traditional drawing and design methods. Precision, accuracy, flexibility, ease of manipulation and modification are attributes of graphic representations created with specialized programs.

With the help of computer systems, which have a friendly, easy-to-use interface, the tedious tasks of drawing and detailing are greatly simplified by using geometric construction tools, such as: grid, snap, auto-quotation senders. The dimensions and technical notes are always legible on the drawings made, and the paper drawings produced by these systems are of a much higher quality than drawings made by hand. These performances obtained are

undoubtedly related to the qualities of the programs, but they depend mainly on the way in which their capabilities are exploited. A detailed knowledge of these modern computer capabilities and tools represents the basic premise of a high-performance activity, being at the same time powerful tools that can help, but cannot replace, the experience and knowledge of the specialist or user in a certain field.

In terms of the efficiency and profitability of specific land surveying and cadastral works, these have increased considerably, as modern computer systems represent essential tools, which offer the possibility of creating detailed, faithful and highly accurate plans of real estate properties, in a much shorter time and with a much-reduced volume of personnel and material expenses. By using these new systems, it is possible to create and manage all the information relating to real estate registered in the cadastre, thus facilitating the process of recording and monitoring properties, while they also become an essential component in the cadastre and real estate advertising activity.

REFERENCES

Akinci, B., Karimi, H., Pradhan, A., Wu, C.C., Fichtl, G. (2010). CAD and GIS Interoperability through Semantic Web Services. *Electronic Journal of Information Technology in Construction*, *13*. DOI: 10.1201/9781420068061-c9.

Becker, T., Nagel, C., Kolbe, T.H. (2011). Integrated 3D Modeling of Multi-utility Networks and Their Interdependencies for Critical Infrastructure Analysis. In: Kolbe, T., König, G., Nagel, C. (eds) Advances in 3D Geo-Information Sciences. *Lecture Notes in Geoinformation and Cartography*. Springer, Berlin, Heidelberg. https://doi.org/10.1007/978-3- 642-12670-3_1.

Carrera-Hernández, J. J., Levresse, G., & Lacan, P. (2020). Is UAV-SfM surveying ready to replace traditional surveying techniques? *International Journal of Remote Sensing*, *41*(12), 4820–4837. https://doi.org/10.1080/01431161.2020.1727049

Călina, J., Călina, A., Bădescu, G., Vangu, G.M., Ionică, C.E. (2018). Research on the use of aerial scanning for completing a GIS database. *AgroLife Scientific Journal*, *7*(1), 25-32.

Călina, J., Călina, A., Iancu, T. and Vangu, G.M. (2022). Research on the Use of Aerial Scanning and Gis in the Design of Sustainable Agricultural Production Extension Works in an Agritourist Farm in Romania. *Sustainability*, *14*(21), 14219.

Doneus, M. & Neubauer, W. (2005). 3D Laser Scanners on Archaeological Excavations. In Proceedings of CIPA 2005 XX *International Symposium, Torino*, Vol. 34(5/C34/1), 226- 231.

Dragomir, L.O., Popescu, C.A., Herbei, M.V., Popescu, G., Herbei, R.C., Salagean, T., Bruma, S., Sabou, C., & Sestras, P. (2025). Enhancing Conventional Land Surveying for Cadastral Documentation in Romania with UAV Photogrammetry and SLAM. *Remote Sensing*, *17*(13), 2113. https://doi.org/10.3390/rs17132113

Furby, B., & Akhavian, R. (2024). A Comprehensive Comparison of Photogrammetric and RTK-GPS Methods for General Order Land Surveying. *Buildings*, *14*(6), 1863. https://doi.org/10.3390/buildings14061863

Herbei, M.V. & Sala, F. (2020). Evaluation of urban areas by remote sensing methods in relation to climatic conditions: Case study City of Timisoara. Carpathian *Journal of Earth and Environmental Sciences*, *15*(2), 327-337.

Longley, P.A., Goodchild, M.F., Maguire, D.J., Rhind, D.W. (2011). Geographic Information Systems and Science, 3rd ed, Wiley, New York, 46-89.

Mihai, D., Teodorescu, R.I., Burghilă, D., Mudura, R. (2015). A modern approach in data updating for a vineyard agro-system modernization. *15th International Multidisciplinary Scientific GeoConference, SGEM*, 651-656.

Nițu, C. & Tomoioagă T. (2015). *Sisteme Informatice Geografice în cartografie și cadastru*, Editura Universitară, București. ISBN 978-606-28-0185-4.

Păunescu, R.D., Simon, M., Șmuleac, L., Pașcalău, R., Smuleac, A. (2020). Topo-cadastral works regarding the realization of the gas distribution network in the locality of Constantin Daicoviciu. *Research Journal of Agricultural Science*, *52*(3), 145-152.

Pop, N., Pop, S., Ortelecan, M., Luca, L.C. (2019). Verification of a triangulation network in Cluj-Napoca for future topographic surveys. *Agricultura*, *111*(3-4), 368-373.

Rosca, A., Juca, I., Timbota, O., Belin, V., Bertici, R., Herbei, M. (2020). Methods for digitalizing information from analogic support and creating GIS databases. *Research Journal of Agricultural Science*, *52*(4), 104-112.

Šafář, V., Potůčková, M., Karas, J., Tlustý, J., Štefanová, E., Jančovič, M., & Cígler Žofková, D. (2021). The Use of UAV in Cadastral Mapping of the Czech Republic. *ISPRS International Journal of Geo-Information*, *10*(6), 380. https://doi.org/10.3390/ijgi10060380

Sălăgean, T., Rusu T., Poruțiu, A., Jutka, D.E.A.K., Manea, R., Virsta, A. and Călin, M. (2016). Aspects regarding the achieving of a geographic information system specific for real estate domain. *AgroLife Scientific Journal*, *5*(2).

Sestras, P., Bilașco, Ș., Roșca, S., Veres, I., Ilies, N., Hysa, A., Spalević, V., & Cîmpeanu, S. M. (2022). Multi-Instrumental Approach to Slope Failure Monitoring in a Landslide Susceptible Newly Built-Up Area: Topo-Geodetic Survey, UAV 3D Modelling and Ground-Penetrating Radar. *Remote Sensing*, *14*(22), 5822. https://doi.org/10.3390/rs14225822

Sestras, P., Badea, G., Badea, A.C., Sălăgean, T., Roșca, S., Kader, S., & Remondino, F. (2025). Land surveying with UAV photogrammetry and LiDAR for optimal building planning. *Automation in Construction,* 173, 106092. https://doi.org/10.1016/j.autcon.2025.106092

Stöcker, C., Nex, F., Koeva, M., & Gerke, M. (2020). High-Quality UAV-Based Orthophotos for Cadastral Mapping: Guidance for Optimal Flight Configurations. *Remote Sensing*, *12*(21), 3625. https://doi.org/10.3390/rs12213625

***GIS Geography (2021). How GPS Receivers Work - Trilateration vs Triangulation. https://gisgeography.com/trilateration-triangulationgps/, accesed 10.09.2024.

***ROMPOS, Sisteme GNSS. https://rompos.ro/index.php/informatii-tehnice/ sisteme-gnss, accesed 06.09.2024

Scientific Papers. Series E. Land Reclamation, Earth Observation & Surveying, Environmental Engineering. Vol. XIV, 2025
Print ISSN 2285-6064, CD-ROM ISSN 2285-6072, Online ISSN 2393-5138, ISSN-L 2285-6064

TECHNICAL METHODOLOGIES FOR CADASTRAL PLAN DEVELOPMENT USING GNSS AND UAV TECHNOLOGIES: A CASE STUDY IN PIETROASA, ROMANIA

Flavia Mălina CIOFLAN[1], Flavius IRIMIE[2], Nicu Cornel SABĂU[1]

[1]University of Oradea, 1 University Street, 410087, Oradea, Bihor, Romania
[2]"Ștefan cel Mare" University of Suceava, 13 University Street, 720229, Suceava, Romania

Corresponding author email: irimieflavia@gmail.com

Abstract

The realization of the cadastral plan for administrative territorial units, involves as field activities, the identification of owners and neighbors, the identification and spatial positioning of plots, and the verification of the category of use. The case study was carried out within the administrative territorial unit Pietroasa, Bihor County, and aims to analyze the technical aspects related to the realization of the cadastral plan of cadastral sector 31. For the identification of the cadastral sector and the plots, a drone flight was carried out, thus obtaining an orthophotogram of the respective location. The spatial positioning of the detailed topographic points related to the plots was carried out with GNSS technology, GPS system, using the RTK method, based on the GNSS station Beiuș. The reporting of the coordinates of the characteristic points of detail, and the preparation of the cadastral plan in digital format was done with the program MapSys 9.0. In the end, a total of 652 plots were reported in cadastral sector 31. By using the above-mentioned logistics and working methods, a high degree of automation and superior positioning accuracy was achieved.

Key words: *cadastral plan, cadastral sector, GNSS technology, GPS system,* plots*, land use categories.*

INTRODUCTION

In Romania, the general cadastre is established by Law No. 7/1996 on Real Estate Cadastre and Advertising. It represents a unified, mandatory system for the systematic registration and inventory of real estate assets nationwide, addressing their legal, quantitative, and qualitative aspects (Mihăilă et al., 1995).

The International Federation of Geodesy (FIG) defines cadastre as "an updated land information system based on cadastral parcels and records of land interests" (Ercan, 2023). Cadastre can also be defined as a creation of man, namely "the effect of his relationship with the land" (Comparetti & Raimondi, 2019).

The cadastre plays a fundamental role in identifying, documenting, and graphically representing properties in official registers and cadastral maps, serving as legal proof of ownership (Boș & Iacobescu, 2009; Nistor et al., 2012).

In the European Union (EU), there are currently two original models of cadastral system, related to land registration systems. As a result, there is the central model, in which the cadastre appears as a graphic basis (map) of land registration (land registry), so that physical changes must be reflected in the cadastre, and legal changes in the land registry, by maintaining a perfect parallelism, and respectively a Latin model, in which it appears only as a taxation instrument, useful for collecting land taxes. Knowledge of the cadastral models related to the EU Member States is a fundamental condition for the harmonisation of the land cadastre at EU level, as an inventory for environmental, social, economic, legal and fiscal purposes (Comparetti & Raimondi, 2019).

The National Agency for Cadastre and Real Estate Advertising (A.N.C.P.I.) is responsible for updating the national land fund records. This includes registering real estate transactions, creating new properties, modifying existing ones, and updating cadastral data in collaboration with local authorities, licensed service providers, public notaries, and survey professionals (https://lege5.ro/Gratuit/g44dcmjsge/...).

Accurate records support territorial planning, urban and r ural development, environmental protection, and sustainable natural resource management, while also enhancing land tenure security and investment stability (Boș & Iacobescu, 2009).

Systematic registration of property rights and cadastre in Romania is free of charge for property owners. The financing is full and comes from three different sources: from ANCPI's own revenues worth approximately 900 million euros, non-reimbursable funds from the European Union, worth approximately 312 million euros, and respectively from allocations from the budget of the administrative-territorial units, through co-financing (Bancioiu & Kovacs, 2022).

Systematic registration relies on field measurements using established surveying methods to generate parcel and cadastral plans. These activities are carried out ex officio, free of charge, and apply to both public and private property, irrespective of legal ownership status, as per Article 918 of the Civil Code. All measurements conform to applicable technical norms and legal requirements (https://lege5.ro/Gratuit/g44dcmjsge/...).

As of January 31, 2025, systematic registration had been completed in 298 administrative-territorial units (U.A.T.s), while in 1,773 U.A.T.s - approximately 64% of the national total-work was still underway (https://www.ancpi.ro/pnccf/documente/H3.).

Key elements of the cadastre include (Badea, 2005; Grecea, 2007, Novac, 2006):

- Cadastral sector: a subdivision of a commune or city, encompassing multiple plots, typically 50-200 ha in plains and 20-100 ha in hilly areas;
- Building: one or more adjacent parcels, with or without constructions, under single ownership;
- Parcel: A land area with a single use category;
- Land register: the official document recording ownership, use rights, area, encumbrances, and other legal attributes;
- Agricultural register: contains data on the ownership and use of agricultural lands, supporting land-use planning and agricultural policy;
- Basic cadastral plan: derived from the topographic plan and enhanced with cadastral attributes, showing location, surface, and boundaries of properties;
- Parcel plan: graphical representation of properties within a cadastral sector, verified by the County Cadastre Office and integrated into the cadastral plan (https://topogalati.ro/ce-este-planul-parcelar/).
- Land use category: a coded cadastral attribute used to determine property taxation.

The systematic registration of properties in Romania, within the framework of the National Cadastre and Real Estate Advertising Program, successfully requires the unitary integration of legal, institutional and geospatial components, for the optimal achievement of transparent and responsible land governance, efficient management of all resources and sustainable rural development (Gherheș et al., 2025).

Although a legal and technical framework exists, the lack of standardized software and methods for creating digital cadastral plans has caused inconsistencies in data handling across counties. National norms offer guidance, but their varied implementation reveals a need for unified standards. At present, research on standardizing digital cadastral plans and systematic registration at the ATU level is scarce, highlighting the need for further studies to improve and align cadastral processes nationally.

Registration in the Land Book through the Systematic Cadastre of real estate, although some difficulties have been reported in some areas, represents an efficient solution and an alternative to the Sporadic Cadastre, which was carried out in the past at the national level. Consequently, field work and working time will be optimized, and the determination of the areas of plots in the cadastral sectors will be achieved with high accuracy (Pop et al., 2021).

MATERIALS AND METHODS

Study location

The case study was carried out within the Pietroasa territorial administrative unit (UAT), Bihor County (Figure 1).

The town of Pietroasa is situated in the meadow zone at the point where the Crișul Pietros River emerges between the surrounding hills, partially extending to the base of the slope along the Bălătrucului Valley.

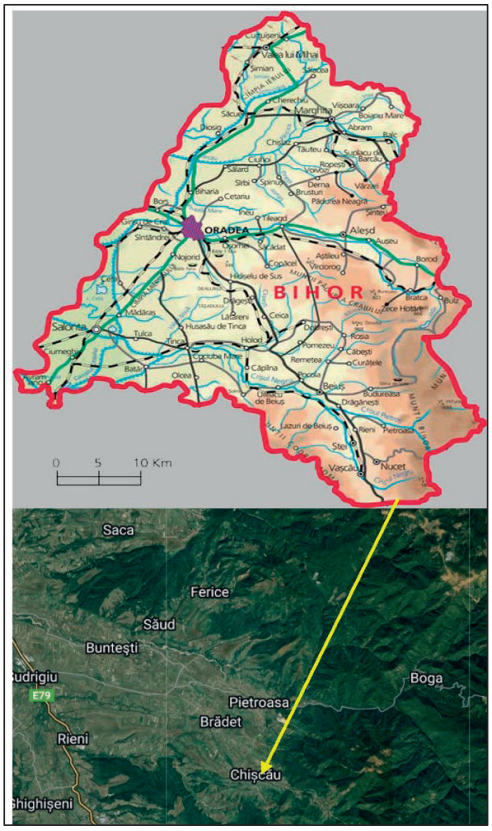


Figure 1. Location of research (https://provinciacrisana.wordpress.com/2017/10/06/scurta-descriere-a-judetului-bihor-provincia-crisana/; http://www.searchromania.net/harta_harti/bihor/pietr./)

The Crișul Pietros flows through the town from east to west, receiving three left-side tributaries - Lazului Valley, Bălătrucului Valley, and Mare Valley. On the right side, within the built-up area, it is joined by the Bălăcel Valley and a smaller, unnamed tributary (General Urban Plan, 2008).

The primary objectives of this case study are to investigate and analyze the specific characteristics and procedural aspects of creating the parcel plan and, subsequently, the cadastral plan for cadastral sector 31 in UAT Pietroasa, Bihor County. This is examined within the broader framework of systematic property registration in the integrated cadastre and land registry system, particularly within the built-up area and non-collectivized zones.

According to data as of January 31, 2025, the process of systematic registration in Bihor County had been completed in six administrative-territorial units (UATs), was ongoing in 49, and had not yet commenced in 46 (Figure 2) (https://www.ancpi.ro/pnccf/documente/H3_Lucrari). This distribution underscores the relevance of the current research in capturing the unique dynamics, implementation challenges, and progression of cadastral registration in the selected study area.

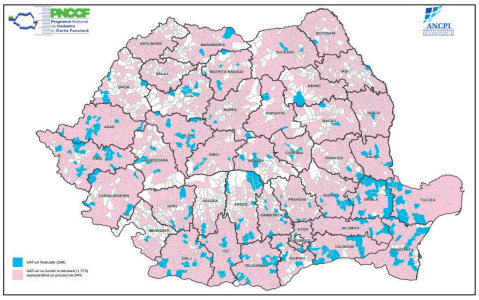


Figure 2. Status of systematic registration works of real estate at the ATU level as of 31 01 2025 (https://www.ancpi.ro/pnccf/documente/H3_Lucrari...)

The research employed a combination of methods, including bibliographic documentation, route and stationary observation, experimentation, simulation, comparison, and analytical techniques.

The bibliographic documentation involved a thorough review of specialized sources such as university courses, technical standards, scientific publications, technical projects in land surveying and cadastre, the General Urban Plan (PUG), and the agricultural register relevant to the case study area.

Field data recording

The experiment consisted of generating GNSS recordings for the spatial positioning of characteristic detail points that define the boundaries of plots and buildings (Crainic, 2024; Pica et al., 2021). This process included data processing, calculation of final coordinates within the national reference system, and the subsequent creation of both the parcel plan and the cadastral plan for cadastral sector 31, located within the Pietroasa administrative-territorial unit (A.T.U.).

To accurately identify the cadastral sector, buildings, and plots included in the plans, reference was made to the General Urban Plan

(PUG) and the coordinate inventory for the boundary points of cadastral sector 31, as provided by the Bihor County Office for Cadastre and Real Estate Advertising (OCPI).



Figure 3. Rebel FAE1718FW drone used for the work (https://fae-drones.com/2023/08/18/drona-fae-1718-fixed-wing-rebel/)

Currently, for the implementation of the National Cadastre and Land Registry Program, for the systematic registration of real estate properties, the recording and processing of the necessary data can be achieved under optimal conditions, through the successful integration of intelligent technologies, namely the Global Navigation Satellite System (GNSS) and Unmanned Aerial Vehicles (UAV) or drones (Ghergar et al., 2023).

To effectively capture, record, and analyze the attributes, features, and specific characteristics of land across different use categories, advanced techniques from geomatics - such as digital photogrammetry and satellite remote sensing - can be employed with high efficiency (Popescu et al., 2024, Tereșneu, & Tereșneu, 2023). Accordingly, an aerial survey was conducted using the Rebel FAE1718FW drone model (Figure 3), resulting in the production of an up-to-date orthophoto map of the targeted area (Figure 4).

The spatial positioning of the characteristic detail points related to the plots was carried out with GNSS technology, the GPS system, with the RTK method, using the Beiuș GNSS station as a base, and the ROMPOS system, respectively. As a result, used as rover GNSS receiver STONEX S900A IMU.



Figure 4. Orthophoto of the work area

Processing of recorded data. Programs used

Real-time data processing was carried out using the STONEX CUBE application, and the transformation of ellipsoidal coordinates into the national reference system STEREO-1970 was carried out using the TransDatRO4.01 application (Bodog et al., 2024; Crainic, 2024).

For reporting the coordinates of the detailed characteristic points, and for drawing up the parcel plan and subsequently the cadastral plan in digital format, the MapSys 10.0 program was used (Marton, 2007).

The simulation was used to obtain the final graphic products in digital format, for all the properties that were positioned and described.

The comparison was carried out at the stage of establishing the attributes of the positioned plots, having the results of the experiment and the records from the property deeds related to them.

The analysis was carried out upon completion of the experiment and the preparation of the plot plan, depending on the specifics and particularities of its elements and those from the property deeds, presented in accordance with the

legislation in force (Law on Cadastre and Real Estate Advertising no. 7/1996 updated in 2025). The case study was carried out according to the steps presented in Figure 5.

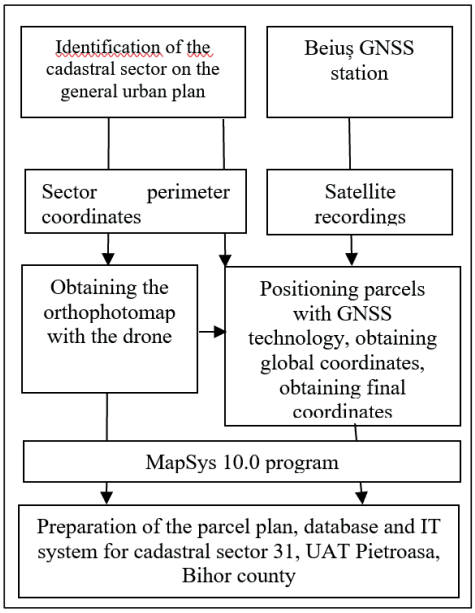


Figure 5. Sequence of stages for carrying out the case study

RESULTS AND DISCUSSIONS

In order to create the parcel plan and implicitly for the systematic registration of real estate at the level of cadastral sector 31, UAT Pietroasa, a number of 658 parcels were identified and verified on the current orthophoto map.

As a result, the use of UAV (Unmanned Aerial Vehicle) technology, by performing multiple flights, optimizes the process of preparing a topographic plan, reducing the time for recording field data and providing various details necessary for architectural planning, both in the studied area and in neighboring areas, compared to other methods, which require more time and provide fewer details, with similar precision (Naș et al., 2023).

As a result, the coordinates for a total of 5404 characteristic topographic points, necessary for the delimitation and positioning of the identified plots, were positioned with GNSS technology and determined in the national reference system STEREO-1970 (in 2D space).

The coordinates of the points are characterized by high precision, since the transformation into the national reference system was performed with the updated transformation parameters for the work area.

The inventory of the coordinates of the detailed characteristic topographic points is presented in a file with the extension txt., configured with four columns, namely the point number, the X coordinate, the Y coordinate and the layer into which it will be imported into the MapSys 10.0 program (Table 1). To obtain the parcel plan and subsequently the cadastral plan, the coordinates of the topographic points were graphically reported with the MapSys 10.0 program.

The way to work with this program is presented suggestively in Figure 6.

Table 1. Extract from the inventory of the coordinates of the detailed topographic points, in the national reference system

No. crt.	X(m)	Y(m)	Layer
1	568496.138	310959.577	1
2	568502.816	310944.096	1
3	568505.244	310939.163	1
4	568521.033	310927.350	1
5	568514.632	310890.788	1
6	568532.234	310862.699	1
7	568542.175	310857.842	1
8	568569.975	310853.287	1
9	568594.639	310864.433	1
10	568643.367	310879.990	1
11	568666.170	310838.515	1
12	568667.722	310824.888	1
13	568674.932	310821.094	1
14	568692.386	310829.368	1
15	568696.655	310827.755	1
16	568699.975	310818.269	1

Analysis of the data presented in Figure 6 reveals that the workflow for generating the cadastral plan using the MapSys 10.0 software follows a logical and well-structured sequence, dictated by the program's internal algorithms and marked by a high degree of automation.

At the initiation of a new project (work-job), the working parameters and necessary metadata were defined to support the specific requirements of the cadastral task. Consequently, the datum elements corresponding to the national land fund were integrated into the system (Figure 7).

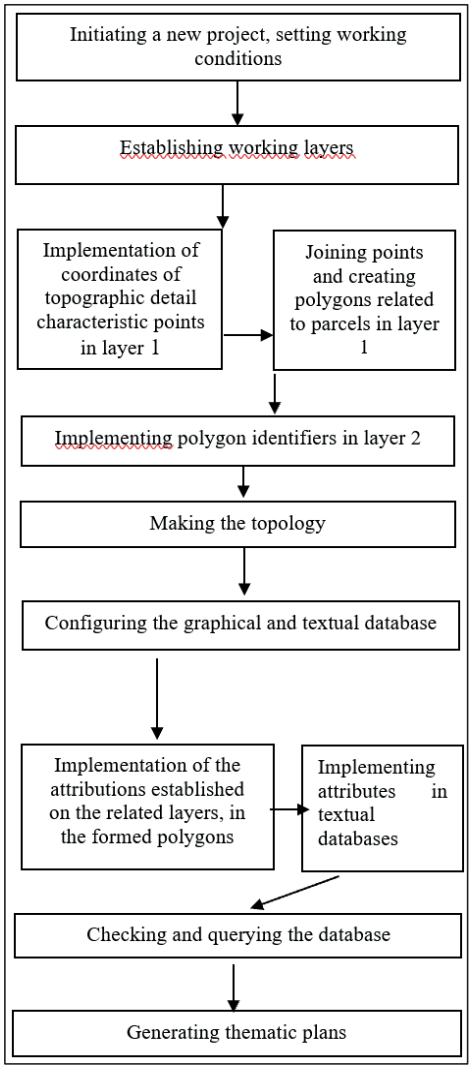


Figure 6. Working steps with the MapSys 10.0 program, to obtain the cadastral plan

The creation and organization of working layers were structured hierarchically, aligned with the operational algorithms of the MapSys software and the logical sequence of inputting collected spatial and attribute data. This hierarchical arrangement ensured consistency in data processing and efficient integration of graphical and textual components.

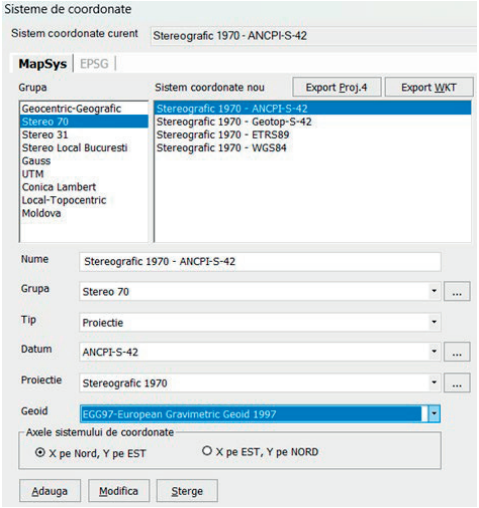


Figure 7. Implementation of the elements of the datum related to the national land fund

The layers were organized as follows:
- Layer 1 - coordinates of detailed topographic points and subsequent creation of plot (real estate) polygons.
- Layer 2 - cadastral identifiers, linking graphical data with the textual database, supporting topology generation and configuration of the primary textual dataset.
- Layer 3 - characteristic points marking the boundaries of cadastral sector 31.
- Layer 4 - text annotation indicating the cadastral sector number under investigation.
- Layer 5 - planimetric coordinates of electric poles located within the plots.
- Layer 6 - textual attributes referencing property deeds and existing topographic numbers associated with positioned plots.
- Layer 7 - records of possession minutes and corresponding property titles.
- Layer 8 - documents confirming possession and actual land use by property holders.
- Layer 9 - land registry extract data available at the time of the study.
- Layer 10 - existing data on newly assigned cadastral numbers as of the study date.
- Layer 11 - data regarding cadastral numbers established by final court decisions.

- Layer 12 - surface discrepancies, where applicable.
- Layer 13 - information on plots with unidentified owners.
- Layer 14 - data concerning areas designated as land reserves.
- Layer 15 - land use categories attributed to the studied plots.
- Layer 16 - coordinates of localities adjacent to cadastral sector 31 in U.A.T. Pietroasa, Bihor County.

The initial stage of the workflow involved importing the planimetric coordinates of the detailed characteristic points corresponding to the parcels within cadastral sector 31 into Layer 1 (Figure 8). Subsequently, within the same layer, a total of 5,404 characteristic topographic points were connected, resulting in the generation of 658 parcel polygons representing the spatial configuration of the positioned plots (Figure 9).

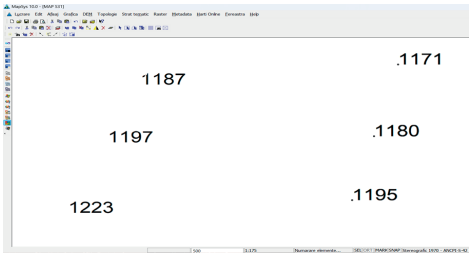


Figure 8. Implementation of feature points

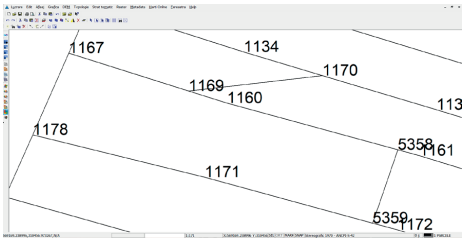


Figure 9. Obtaining polygons

The overlay of the generated parcel polygons onto the newly created orthophotomap enabled optimal verification of the accuracy and precision of the digital graphic representations (Figure 10).

A critical stage in the development of both the parcel plan and the subsequent cadastral plan involved the implementation of cadastral identifiers and the marking of individual parcels. This process commenced in the northwestern part of the locality and progressed toward the southwest, following a systematic spatial logic.

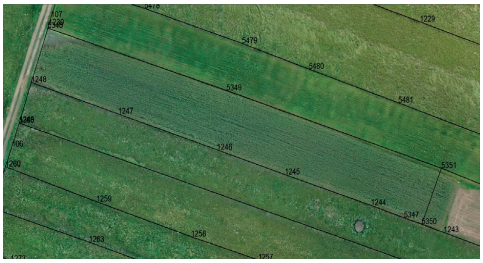


Figure 10. Overlaying polygons on the orthophoto plane

This step was carried out using the cadastral number creation/digitization function, which involved assigning a unique identifier to each polygon (Figure 11). These identifiers establish a direct and exclusive link between each polygon in the graphical database and its corresponding entry in the textual database, ensuring data consistency and integration (Marton, 2007).

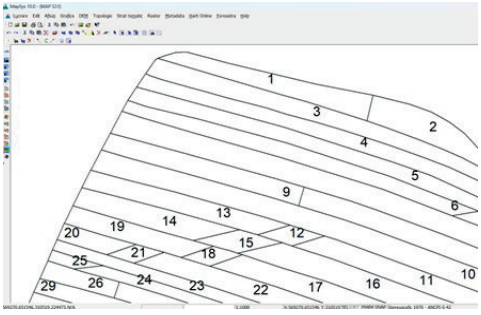


Figure 11. Implementation of cadastral identifiers for each polygon obtained

Verification of non-closure errors in the polygons representing the positioned parcels, the generation of the primary Geographic Information System (GIS) database, and the execution of operations on spatially referenced objects were performed using the Topology menu within the software.

Analysis of the data presented in Figure 12 confirms the absence of non-closure errors in the polygons generated. Additionally, it verifies that the total number of areas computed using the analytical method matches the total number of polygons. The cumulative area of cadastral

sector 31 was determined to be 984,546.153 m², equivalent to 98.45 hectares.

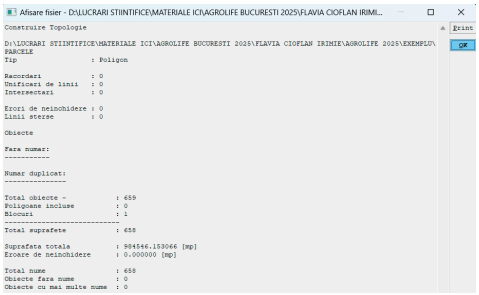


Figure 12. Topology creation

Upon completion of the topology creation process, the primary database (databank) was automatically generated for the polygons (plots) that had been graphically represented in Layer 1 (Figure 13).

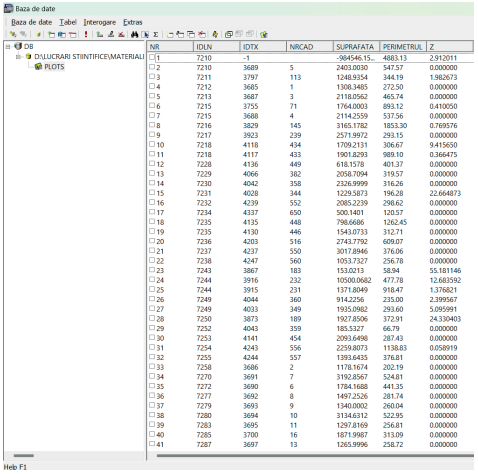


Figure 13. Generation of the primary database related to the polygons (parcels) that were graphically reported in layer 1

To gather all attributes required for the development of the parcel plan and, subsequently, the cadastral plan, the database was modified and configured accordingly (Figure 14). The necessary columns were implemented in alignment with the layer structure defined during the initial project configuration.

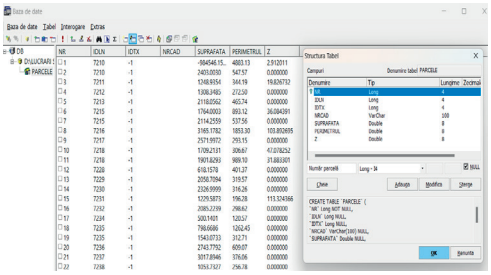


Figure 14. Primary database configuration, depending on the way the layers are organized and the implementation of the established attributes related to the starts

The implemented attributes were assigned to specific layers as follows:
- Layer 3: boundary of the cadastral sector;
- Layer 4: cadastral sector number;
- Layer 5: locations of concrete electric poles;
- Layer 6: property deeds with associated topographic numbers;
- Layer 7: minutes of taking possession, with ownership titles pending issuance as of the study date;
- Layer 8: certificates of actual land use, issued by Pietroasa City Hall based on entries in the agricultural register;
- Layer 9: land register extracts available at the time of the study, confirming property rights based on deeds or converted old registry sheets;
- Layer 10: newly assigned cadastral numbers;
- Layer 11: cadastral numbers granted through final court decisions.

The various documents used to establish ownership or possession rights, which formed the basis for the creation of the parcel plan, are summarized in Figure 15 as percentage distributions. These documents include:
- 254 certificates of actual land use;
- 237 property deeds with topographic numbers;
- 119 land register extracts;
- 30 minutes of taking possession;
- 11 new cadastral numbers.

As illustrated in Figure 15, the largest proportion of documentation consists of certificates of actual use (39%), followed by property deeds with topographic numbers (36%), existing land register extracts (18%), minutes of possession (5%), and new cadastral numbers (2%).

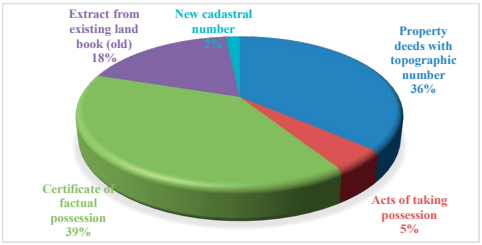


Figure 15. Percentage of documents attesting to the ownership right over the positioned and studied plots

Another important stage was represented by the verification of the areas of the polygons related to the plots, with those in the documents certifying ownership, or with the areas in the official records, respectively with the uses.
Currently, there is a possibility that the changes that are necessary to correct errors in parcels (real estate) can be made efficiently by preparing digital vector parcel plans, only for the respective area, based on accurate measurements, with modern geospatial technologies. As a result, in such situations, it will not be necessary to redo the entire parcel plan and subsequently the cadastral plan, for the entire respective sector (Kyseľ & Hudecová, 2022).
As a result, in layer 12, a number of 13 corrections were implemented for the area of 13 plots, for which it was necessary to reposition the boundaries, due to the differences between the area of the identified and positioned plots and the area in the property documents, respectively.
Also, in layer 13, a number of 6 observations were implemented for 6 plots, with a total area of 6851 m^2, for which the owners were not identified. Finally, in layer 14, a number of 3 plots were implemented, with a total area of 1007 m^2, which were considered as a reserve.
Resolving inconsistencies between the cadastral map in analog format and the cadastral register can be solved by obtaining new parcel plans and cadastral plans, respectively, through vectorization. Consequently, computer processing does not guarantee quality if it is not carried out professionally and conscientiously, and the inadequate maintenance of cadastral maps has facilitated the constant presence of inconsistencies between the two entities mentioned (Roić et al., 2021).
After clarifying the situation of the plots' areas reported graphically, the land use category for the studied buildings was implemented in layer 15. According to the results presented in Figure 16, 651 plots have the arable land use category (A), and 4 plots have the exploitation road use category (Er).

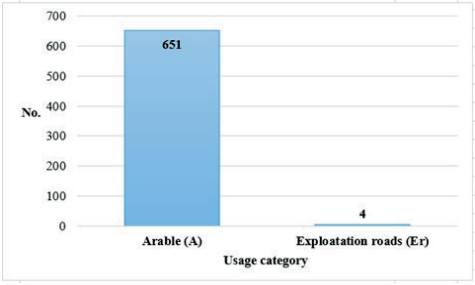


Figure 16. Representation of the number of land use categories for cadastral sector 31 Pietroasa

The land use categories were identified based on ownership documents and official records, with the following distribution:
- 651 parcels classified as arable land (A);
- 4 parcels identified as exploitation roads (Er).

Attributes corresponding to Layers 3 through 16 were incorporated into the database using the Attribute Collection menu. Through this process, the values extracted from text elements located within the topological objects of the active layer were systematically loaded into the respective database fields of the current topological layer.
The updated database containing all necessary attributes for the creation of the parcel plan and, subsequently, the cadastral plan, can be efficiently accessed and managed as needed. A representative extract from the parcel plan and the associated database is presented in Figure 17.

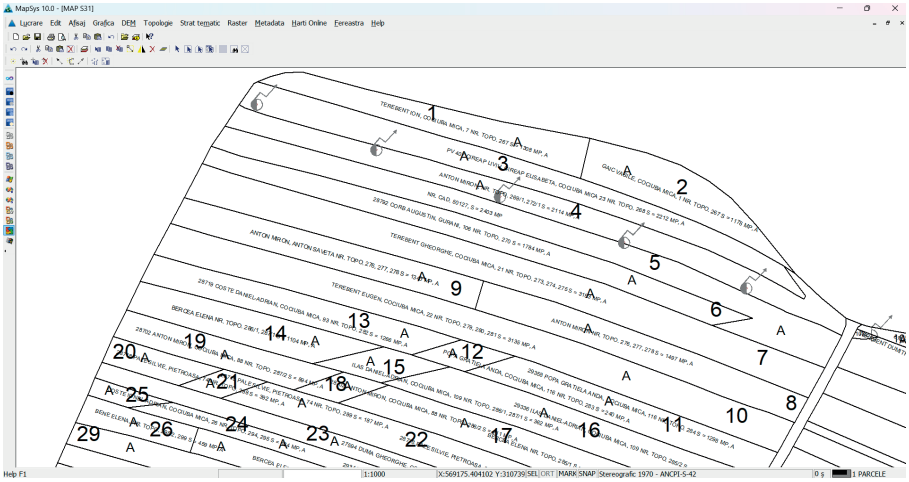


Figure 17. Extract from the parcel plan for cadastral sector 31, UAT Pietroasa, Bihor County with all attributes activated

The MapSys 10.0 software enabled efficient graphical input of contour point coordinates and supported the creation of both the parcel plan and its associated database. The platform allows for direct adjustments based on verified ownership documents. In cases where discrepancies existed between calculated parcel areas and legal records, boundaries were corrected within the software. Revised coordinates were exported as .txt files and transferred to a dual-frequency GNSS receiver for precise field repositioning.

The finalized parcel plan and database were submitted in digital format to the Bihor County Office for Cadastre and Real Estate Advertising (OCPI) for cadastral number assignment and integration into the national land registry system.

The work of registering real estate in the Systematic Cadastre in Romania, performed by the private sector, is perceived as qualitative or predominantly qualitative, based on the verifications carried out by the county Cadastre and Real Estate Advertising Offices (OCPI). Consequently, three elements of the quality of the work carried out by the private sector were highlighted, which need to be optimized, namely credibility, reliability of the service and the level of competence of the human resource (Păunescu et al., 2023).

Field positioning of parcel boundaries is a crucial step requiring the involvement of landowners to ensure spatial and legal accuracy. Recent studies have shown that the success factors in establishing the cadastral boundaries of parcels are the surveyor and the land owner, while paradoxically, land data (cadastral data) is the least important factor (Golob & Lisec, 2022). Consequently, the experienced and well-intentioned surveyor can effectively manage the issues related to cadastral boundaries, especially for lands with unidentified boundaries, which are frequently the subject of possible litigation, which can have a negative impact on cadastral recording activities.

Surveying activities included GNSS-based positioning of characteristic points, enhanced through RTK (Real-Time Kinematic) positioning with data from the Beiuș GNSS permanent station via the ROMPOS service, ensuring high precision.

Final coordinates referenced to the national geodetic system enhanced the accuracy of the digital parcel plan. Legal documents were used to resolve discrepancies between measured and recorded areas.

The cadastral database for Sector 31 was configured under optimal conditions, adapted to the specific requirements of systematic registration. Overall, the use of MapSys 10.0 proved effective in producing high-quality digital outputs - parcel plans, cadastral plans, integrated databases, and thematic maps - critical tools for modern cadastral operations.

From the synthetic analysis of the implementation of the National Systematic Land

Cadastre Program in Romania, by some specialists, it was concluded that it was not designed as an approach fit for purpose. Consequently, there are a number of suggestions that the transition to such a system would optimize the systematic registration process. Also, high standards of precision without flexibility, the use of large-scale field measurements or the lack of provisions for improving and updating the system, are considered factors that significantly delay this process (Păunescu et al., 2022).

Currently, cadastral systems that manage the people-land relationship have evolved into a multifunctional form, supporting various land activities. As a result, it has become necessary to modernize traditional land administration systems and cadastral systems in order to effectively manage the people-land relationship. Consequently, the interest in promoting 3D cadastre is increased, while the cadastre of public right restrictions and the disaster-responsive cadastre are the least promoted (Uşak et al., 2024).

Current research on the possibilities of implementing 3D cadastre shows that the registration of objects for its implementation involves the use of data from various sources, namely laser scanning measurements and technical documentation (Grzelka et al., 2024), as well as other additional data, as appropriate.

CONCLUSIONS

This study highlights the effectiveness of integrating GNSS and UAV technologies with specialized GIS software (MapSys 10.0) in the systematic development of cadastral plans, using Cadastral Sector 31 in Pietroasa, Romania, as a case study. The approach demonstrated high precision in spatial data acquisition and efficient data processing, providing a model for similar cadastral operations in non-collectivized, rural settings.

Key insights include the operational benefits of combining RTK positioning with orthophotomap overlays for boundary verification, and the flexibility of digital workflows in updating parcel attributes based on legal documents. The involvement of landowners verifying plot boundaries was identified as a critical factor for accurate cadastral representation.

Limitations of the study include the reliance on the completeness and accuracy of historical land documents, and challenges in identifying owners for certain plots. Additionally, software-specific constraints in data structuring may affect standardization across regions if not uniformly implemented.

Practical applications of this workflow extend to national cadastral programs, especially in areas undergoing systematic registration. The integration of UAV, GNSS, and GIS technologies offers a scalable, cost-effective solution that can accelerate cadastral mapping efforts and enhance land administration services.

ACKNOWLEDGEMENTS

The research and study were carried out in collaboration with the Local Council of Pietroasa City Hall, Bihor County.

We would like to thank S.C. TOPOGEOTERM S.R.L. Salonta, Bihor County for their logistical support and help in carrying out the experiment related to the case study.

REFERENCES

Badea, G. (2005). *General Cadastre*. Conspress Publishing House Bucharest, Romania.

Bancioiu, R., & Kovacs, L. (2022). The Systematic Registration of Property Law and Cadastre on the Territory in Romania: Discussing a Case Study. *Nova Geod. 2*(2), 28. https://doi.org/10.55779/ng2228.

Bodog, M. F., Șchiopu, E. C., Crainic, G. C., & Lazăr, A. N. (2024). Assessment of contamination degree of oil residues on a former agricultural site. *Journal of Agricultural Science and Technology A, 14*, 67–82. https://doi.org/10.17265/2161-6256/2024.02.003.

Boș, N., & Iacobescu, O. (2009). *Cadastre and land registry*. C.H. Beck Publishing House.

Comparetti, A., & Raimondi, S. (2019). Cadastral models in EU member states. *EQA - International Journal of Environmental Qualit,y 33*, 55-78. https://doi.org/10.6092/issn.2281-4485/8558.

Crainic, G. C., (2024). Issues related to the implementation of geomatic applications in the national forestry fund. *Scientific Papers. Series E. Land Reclamation, Earth Observation & Surveying, Environmental Engineering, 13*, 794-804.

Ercan, O. (2023). Evolution of the cadastre renewal understanding in Türkiye: A fit-for-purpose renewal model proposal. *Land Use Policy, 131*. https://doi.org/10.1016/j.landusepol.2023.106755.

Ghergar, A., Madăra, R., Popescu, G., & Dragomir, L. (2023). Aplication of Modern Measurement Technologies in the Process of Sistematic Registration of Real Estate. *Res. J. Agric. Sci.*, *55*(3). ISSN: 2668-926X.

Gherheș, V., Grecea C Vilceanu., C.-B., Herban S., & Coman, C. (2025). Challenges in Systematic Property Registration in Romania: An Analytical Overview. *Land*, *14*(5), 1118. https://doi.org/10.3390/land14051118.

Golob, P., & Lisec, A. (2022). Success factors in cadastral boundary settlements based on land surveyor's opinions. *Land Use Policy, 114*, 105990. https://doi.org/10.1016/j.landusepol.2022.105990.

Grzelka, K., Pargieła, K., Jasińska, A., Warchoł, A., & Bydłosz, J. (2024). Registration of Objects for 3D Cadastre: An Integrated Approach. *Land*, *13*(12), 2070. https://doi.org/10.3390/land13122070.

Grecea, C. (2007). Cadastral system: New trends and experiences. *Journal of Geodesy and Cadastre, 7*.

Kysel, P., & Hudecová, L. (2022). Testing of a new way of cadastral maps renewal in Slovakia. *Geodetski Vestnik, 66*(4), 521-535. DOI: https://doi.org/10.15292/geodetski-vestnik.2022.04.521-535.

Marton, H. (2007). *MapSys, TopoSys - User manual*. Odorheiu Secuiesc, Romania.

Mihăilă, M., Corcodel, Gh., & Chirilov, I. (1995). *General Cadastre and Real Estate Advertising – The Basics and Component Works*. Ceres Publishing House, Bucharest, Romania.

Naș, S.M., Bondrea, M.V., Rădulescu, V.M., Gâlgău, R., Vereș, I.S., Bondrea, R., & Rădulescu, A.T. (2023). The Use of UAVs for Land Use Planning of Brownfield Regeneration Projects-Case Study: Former Brick Factory, Cluj Napoca, Romania. *Land*, *12*(2), 315. https://doi.org/10.3390/land12020315.

Nistor, Gh., Georgescu, D., & Nica, D. C. (2012). Aspects concerning the achievement of the digital cadastral plan of a road. *Buletinul Institutului Politehnic din Iași, LVIII (LXII)*(1-2), *Hidrotehnică*.

Novac, Gh. (2006). *Specialized cadastres*. Solness Publishing House, Timișoara, Romania.

Păunescu, V., Iliescu, A. I., Călin, M. C., Sălăgean, T., Kohli, D., Nap, M. E., & Șuba, E. E. (2023). A Quality Assessment of the Romanian National Program of Systematic Land Registration the Point of View of Local Cadastral Offices Directors. *Survey Review*, *56*(396), 284–299. https://doi.org/10.1080/00396265.2023.2233825.

Păunescu, V., Kohli, D., Iliescu, A. I, Nap, M. E., Șuba, E. E., & Sălăgean, T. (2022). An Evaluation of the National Program of Systematic Land Registration in Romania Using the Fit for Purpose Spatial Framework Principles. *Land*, *11*(9), 1502. https://doi.org/10.3390/land11091502.

Pop, S.B., Pop N., Miluț M., & Bădescu G. (2021). Research on how to Implement the Systematic Cadastre within Medias Municipality, Sibiu County. *Bulletin Of University of Agricultural Sciences and Veterinary Medicine Cluj-Napoca. Horticulture*, *78*(2). DOI:15835/buasvmcn-hort:2021.0008.

Popescu, G., Popescu, C. A., Dragomir, L. O., Herbei, M. V., Horablaga, A., Țenche Constantinescu, A. M., Sălăgean, T., Bruma, S., Dinu-Roman Szabo, M., Colișar, A., Ceuca, V., Kader, S., & Sestraș, P. (2024). Utilizing UAV technology and GIS analysis for ecological restoration: A case study on *Robinia pseudoacacia* L. in a mine waste dump landscape rehabilitation. *Notulae Botanicae Horti Agrobotanici Cluj-Napoca, 52*(4), Article 13937. https://doi.org/10.15835/nbha52413937.

Roić, M., Križanović, J., & Pivac, D. (2021). An Approach to Resolve Inconsistencies of Data in the Cadastre. *Land*, *10*(1), 70. https://doi.org/10.3390/land10010070.

Tămăioagă, G., & Tămăioagă, D. (2007). *Automation of cadastre works*. Matrix Rom Publishing House.

Tereșneu, C. C., & Tereșneu, C. S. (2023). GIS facilities for the automation of cadastral documentations. *Scientific Papers. Series E. Land Reclamation, Earth Observation & Surveying, Environmental Engineering, 12*, 371-376.

***Agenția Națională de Cadastru și Publicitate Imobiliară (ANCPI). (n.d.). *Lucrări de înregistrare sistematică a imobilelor la nivel de UAT*. https://www.ancpi.ro/pnccf/documente/H3_Lucrari%20de%20inregistrare%20sistematica%20a%20imobilelor%20la%20nivel%20de%20UAT.pdf.

***Cadastral plan for cadastral sector 31, U.A.T. Pietroasa, Bihor County*.

***FAE Drones. (2023, August 18). *Drona FAE 1718 fixed wing Rebel*. https://fae-drones.com/2023/08/18/drona-fae-1718-fixed-wing-rebel/.

***Law on Cadastre and Real Estate Advertising No. 7/1996, updated 2025.

***Lege5. (n.d.). *Organizarea lucrărilor sistematice de cadastru în vederea înscrierii în cartea funciară – Legea 7/1996*. https://lege5.ro/Gratuit/g44dcmjsge/organizarea-lucrarilor-sistematice-de-cadastru-in-vederea-inscrierii-in-cartea-funciara-lege-7-1996?dp=hazdsmjygu2dc.

***Provincia Crișana. (2017, October 6). *Scurtă descriere a județului Bihor – Provincia Crișana*. https://provinciacrisana.wordpress.com/2017/10/06/scurta-descriere-a-judetului-bihor-provincia-crisana/.

***Search Romania. (n.d.). *Harta Pietroasa, județul Bihor*. http://www.searchromania.net/harta_harti/bihor/pietroasa/.

Scientific Papers. Series E. Land Reclamation, Earth Observation & Surveying, Environmental Engineering. Vol. XIV, 2025
Print ISSN 2285-6064, CD-ROM ISSN 2285-6072, Online ISSN 2393-5138, ISSN-L 2285-6064

ASSESSMENT OF LAND USE CHANGES IN NON-COLLECTIVIZED AREAS USING GEOMATIC APPLICATIONS: A CASE STUDY IN VÎRFURILE, ROMANIA

Flavia Mălina CIOFLAN

University of Oradea, 1 University Street, 410087, Oradea, Bihor, Romania

Corresponding author email: irimieflavia@gmail.com

Abstract

After 1990, land use categories in non-collectivized hilly and mountainous areas experienced distinct changes, influenced by various socio-economic and environmental factors. This study focuses on cadastral sector 15 within the administrative territorial unit of Vîrfurile, Arad County - an area that was not subjected to collectivization. The objective is to analyze the current state of land use categories using geomatic applications. Plot localization was achieved using orthophotoplans, while spatial positioning was conducted via GNSS technology employing the Real-Time Kinematic (RTK) method, with data transmission between receivers facilitated by internal radio. Base point coordinates were determined using data from the GNSS station in Gurahonț. The coordinates of the characteristic detail points were processed with the MapSys10 software and overlaid onto the orthophotoplan. Analysis of the results reveals that several plots formerly designated for agricultural use are now partially covered by arboreal forest vegetation, indicating a significant process of natural succession and land use transformation.

Key words: *geomatic applications, land use categories, non-collectivized areas, spatial positioning, GNSS technology.*

INTRODUCTION

Land can be classified based on its use and economic designation - criteria that are essential to both general and specialized cadastre activities (Novac, 2007). The land use category serves as the primary basis for this classification and constitutes one of the cadastral attributes of a land parcel. It is codified in accordance with applicable legislation and technical regulations. This classification may reflect natural conditions or result from human intervention (anthropogenic activity). It is documented in the technical component of the general cadastre, primarily to establish tax liabilities associated with real estate (Novac, 2007).

The land use category is a subset of a broader group of uses and can be further divided into subcategories. However, in general cadastre practices, these subcategories are not individually recorded; they are only identified and registered within specialized cadastres (Novac, 2007). Land use monitoring and analysis are effective tools for identifying the most important developments with positive and negative effects on their use categories. Consequently, the need for the immediate implementation of the national general cadastre system, appropriate policies and legislative provisions, with direct implications for optimal management practices of the national land fund, is highlighted (Călina et al., 2025).

The built-up area refers to the densely constructed portion of the territory - essentially the settlement itself. These areas include buildings, yards, roads, socio-cultural facilities, parks, forests, water bodies, and other land uses within the established boundaries of urban or rural localities. They are regulated by specific legal provisions related to construction permits and urban planning (Novac, 2007; Table 1).

Table 1. Land fund of Romania on 1.01.2004 (statistical data, Novac, 2007)

Land use category	**Area (ha)**	**%**
Arable	9,414,341	38.35
Grassland	3,354,970	14.07
Rough	1,490,384	6.25
Vineyards	230,527	0.97
Orchards	227,204	0.95
Agricultural total	**14,717,426**	**61.74**
Private property	14,155,954	59.38
Forestry	6,751,645	28.32
Water	843,710	3.54
Other lands	1,526,290	6.40
Total non-agricultural	**9,121,645**	**38.26**
Total land fund	**23,839,071**	**100.00**

The extra-urban area refers to the territory located between a locality's administrative boundary and the outer limit of its built-up zone. This area encompasses land designated for various uses, including agriculture, forestry, transportation infrastructure (roads and railways), water bodies, yard-buildings, and non-productive functions. In accordance with current legislation, these lands are systematically subdivided into cadastral sectors, fields, plots, and subplots, following specific cadastral rules. The agricultural use group comprises lands utilized for agricultural purposes and includes the following use categories: arable land, pastures, hayfields, vineyards, and orchards (Figure 1).

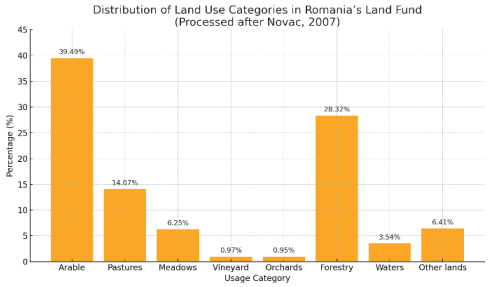


Figure 1. The share of use categories in the agricultural and non-agricultural use group in Romania's land fund (processing after Novac, 2007)

The non-agricultural use group comprises lands not designated for farming, including forests and areas with forest vegetation, water bodies and wetlands (including reed-covered areas), transport infrastructure (roads and railways), lands used for courtyards and other specific purposes, as well as unproductive lands (Novac, 2007; Tămăioagă & Tămăioagă D., 2005).

The credibility of cadastral data on land use and the methodology for their verification and updating. Information on the category of land use is of particular importance in all countries, constituting the basis for taxation and urban planning, directly influencing real estate values and land management procedures. Modern geospatial technologies can facilitate the regular verification of data and information on land use, ensuring future economic benefits for territorial administrative units. As a result, the results of research conducted using unmanned aerial vehicles (UAVs) resulted in obtaining high-resolution orthophotomaps (with a GSD of 3 cm), which provide precise data on the specificity and dynamics of land use at the time of photogrammetric registration (Cienciała et al., 2021).

In conclusion, land use categories are fundamental attributes within the cadastre and real estate registration systems. They play a key role in property classification, taxation, and land management processes.

Land use change has been a major concern for many countries around the world over the years. The main reasons for this situation are: rapid population growth, population migration, the transformation of rural areas into urban areas, changing political systems, and the effect of climate change (Nedd et al., 2021).

Since 1989, uncultivated, hilly, and mountainous regions in Romania have experienced notable shifts in land use categories due to socio-political changes. The declining interest in traditional agricultural activities has led to the abandonment of several arable land subcategories, rendering some parcels unsuitable for conventional crop production.

Currently, obtaining high-precision land use classification can be achieved from high-resolution remote sensing images, using models that can be used as automatic tools for precise land classification and mapping (Kang et al., 2022).

A Western method for recording land use categories, used in Switzerland, is based on two inputs, namely information provided by base topographic maps at a scale of 1:25,000 and national land use statistics, which were obtained from high-precision aerial photointerpretation, performed on a rectangular grid with a side of 100 m. Consequently, the method combines a simple spatial weighting of the inverse distance of information about 36 nearest neighbors and an expert system of correspondence between land use categories on base maps, as input data, and possible land use types obtained by photointerpretation, as output data. This method can be used with high efficiency to transform and use different types of geographic information at scale (Giuliani, 2022).

Additionally, many administrative territorial units (ATUs) in these regions have not updated their agricultural registers, often due to a lack of initiative from landowners. Consequently, the

real land use categories recorded during the systematic property registration and cadastral plan development were based on outdated documents and registry information, rather than on-site verification.

To address these discrepancies, it is essential to conduct field identification, observation, and analysis of plots to accurately determine the productive capacities of the land. In many cases, prolonged abandonment has allowed for the growth of subshrub, shrub, and woody vegetation, obstructing access and complicating evaluation.

Modern geomatic technologies offer effective solutions for analyzing and updating land use categories. These include spatial positioning of cadastral features, data processing, and generation of accurate coordinates through integrated methods. For defining the boundaries of cadastral sectors and individual parcels, tools such as the Global Navigation Satellite System (GNSS), total stations, and other integrated surveying technologies are commonly employed.

Collectively referred to as geomatics, these advanced geospatial technologies ensure accurate acquisition, verification, and processing of spatial data, all referenced to the national coordinate system (Crainic, 2024; Boș, 2003). Their application greatly enhances the efficiency and precision of cadastre-related activities, supporting identification, positioning, area measurement, and classification of land uses across Romania's national land fund.

Geomatics applications are particularly effective for analyzing agricultural land use. They enable the creation of thematic maps that classify agricultural areas by category and subcategory, offering valuable insights into land suitability for various crop types. Furthermore, geomatics tools facilitate spatial analysis and classification of lands for fruit tree cultivation, enhancing land management strategies in agriculture (Roşca et al., 2015).

As a result, space technologies and related applications in the land survey sector support the integrity and record of land, with direct implications for climate change monitoring, disaster risk reduction, land tenure security, land governance, geospatial information management, sustainable land administration and management, spatial planning and land valuation (Upadhyaya, 2024).

MATERIALS AND METHODS

This study was conducted in cadastral sector 15 within the administrative territorial unit (ATU) Vârfurile, located in Arad County, Romania. The region is a rural, non-collectivized area situated at the intersection of Arad, Bihor, and Alba counties, at the foot of the Bihor and Codru-Moma Mountains, within the northwestern part of the Hălmagiu Depression along the Crișul Alb River.

The dominant landforms in the study area are represented by hills, with good accessibility, which in the past were cultivated with potatoes, wheat, oats and corn. There were also lands on which fruit tree orchards were installed, of the apple, plum, pear and cherry species. After 1989, the activities related to the agricultural sector in this location reduced their intensity, because currently they are found only sporadically, due to the lack of adequate equipment and the recent climate changes.

The objectives of the research refer to the study and analysis of the current situation of the categories and subcategories of land use, in cadastral sector 15, which belongs to the territorial administrative unit (UAT) Vârfurile, using geomatic applications. These are necessary due to the current situation of the lands in the mentioned location, in order to establish the necessary strategies for their inclusion in a productive circuit, in correlation with their real use and agricultural production capacity.

This study is conducted as part of a doctoral research program and benefits from the completion of systematic registration works for buildings located outside the built-up area within the targeted cadastral sector. As a result, a parcel plan has been developed and is available in both digital and analog formats (Figure 2).

The primary objective of this research was to analyze the current state of land use categories using geomatic applications. The study benefits from the recent completion of systematic land registration in this area, which resulted in the creation of both digital and analog parcel plans. The research is part of ongoing doctoral studies

and employed a combination of the following methodologies:
- bibliographic analysis of cadastre-related literature, technical norms, cadastral records, agricultural registers, and monographs;
- field observations, both in motion and stationery, for identifying and mapping topographic features;
- experimental measurements using GNSS-based techniques;
- comparative analysis of historical and current land use data;
- simulation and interpretation of land use category transformations.

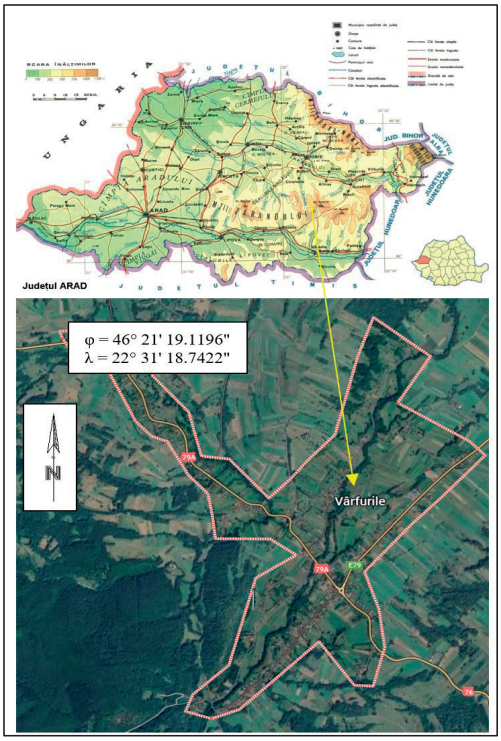


Figure 2. Location of the case study (https://pe harta.ro/judete/Arad.jpg;ttps://www.google.com/maps/place/317390+V%C3%A2rfurile)

To identify and map the characteristic topographic points defining parcel boundaries and land use separations, GNSS positioning was performed. These characteristic detail points delineate the contours of the land plots and subcategories of use.

During the field campaign, GNSS data were collected using the Trimble R8 receiver (with 4W external radio) as the base and the Trimble R10 (with 2W internal radio) as the rover. Positioning was executed using the RTK (Real-Time Kinematic) method. Additionally, remote RTK corrections from the ROMPOS system, using satellite recordings from the Deva GNSS permanent station in Hunedoara County, were integrated to enhance positional accuracy. Five base points were positioned and used as GPS references. The Trimble Access software was employed for field data acquisition and processing, while coordinate transformations into the national reference system were performed using TransDatRO 4.01. Eighteen plots with known use classifications from 1990 were initially surveyed. Subsequently, field validation and digital analysis were expanded to 50 plots, leveraging access to current data from the agricultural register of Vârfurile City Hall and the newly established parcel plan (Figure 3). The recorded coordinates of characteristic point were graphically reported using MapSys 10 software (Marton, 2007).
Digital transformation is vital for modernizing Land Administration Systems (LAS), ensuring efficient, transparent and secure land services. This suggests the implementation of digital workflows, automation services and collaboration with the land survey sector (Chehrehbargh et al., 2024).
Identified subcategories of land use were then compared with historical data from the agricultural register to detect changes and transformations over time.
To further support the interpretation, representative images of selected plots were analyzed, focusing on notable land cover transitions relevant to the case study objectives. These visual and spatial data formed the basis for simulating the evolution of land use subcategories in the studied area.
Also, satellite recordings from the permanent GNSS station Deva, Hunedoara County, were used, with the remote RTK method, using the ROMPOS system. As a result, 18 plots were positioned, where access was allowed and information was held about the categories of use in 1990. After carrying out the systematic registration works of the buildings outside the built-up area and drawing up the plot plan in

digital format, the use categories were analyzed on this plan, superimposed on the orthophoto plan, in parallel with field observations, for a number of 50 plots, where access to the field and to the necessary information was also facilitated.



Figure 3. Location of Cadastral Sector 15, Vârfurile ATU, Arad County

To collect satellite data, the TRIMBLE R8 GNSS receiver with an external 4w radio was used for the base and the TRIMBLE R10 receiver, with an internal 2w radio, as the rover. The Trimble Access program was used to record and process the satellite data. Consequently, rigorously compensated ellipsoidal coordinates were obtained, which were transformed into final coordinates in the national reference system. The coordinates were transformed with the TransDatRO4.01 program, using the updated transformation parameters for Arad County.

This program can be found on the website of the National Agency for Cadastre and Real Estate Advertising (ANCPI) and is used free of charge. As a result, the precision of the coordinates thus obtained is high.

For the graphic reporting of the final coordinates obtained and obtaining the contour of the positioned buildings, the MapSys 10 program was used.

The use subcategories that were identified based on the observations made and the results obtained, for the studied plots, were analyzed and compared with those recorded in the

agricultural register in digital format, related to UAT Vârfurile, Arad County.
Based on the analysis and comparison of the results obtained, a simulation of the current use categories and subcategories was carried out, with the related particularities and occupied areas.

RESULTS AND DISCUSSIONS

The final coordinates of the 307 characteristic points defining the plot boundaries were determined using GNSS technology and are presented in Tables 2 and 3. These coordinates were referenced to the national coordinate system and represent the spatial framework for analyzing current land use categories.
Figure 4 specifically highlights arable land that has undergone natural succession, now being partially or fully covered by forest vegetation, particularly native oak species such as *Quercus cerris* and *Quercus robur*. This transition is indicative of land abandonment and the ongoing ecological succession in previously cultivated areas.
Analysis of field data and imagery (Figures 4 and 5) reveals that portions of the arable plots have undergone natural succession, leading to the establishment of forest vegetation. This transition is characterized by the emergence of biogroups composed of native oak species (*Quercus cerris* and *Quercus robur*) as shown in Figure 4 and pioneer species such *Betula pendula* and *Populus tremula* in Figure 5. These species exhibit clear tendencies toward biological independence and are progressing toward the massif stage of forest development.
A comparative assessment of 50 plots included in the digital parcel plan was conducted, contrasting current land use subcategories (as of 2024) with those recorded in 1989. The synthesized data, grouped by area and category, are presented in Table 2.
Figures 6 and 7 illustrate the spatial positioning of these plots on the orthophoto map of the study area. The positioning method, utilizing base and rover units, allowed for high-precision delineation of parcel boundaries. These boundaries align closely with the current land use categories, as visualized on the orthophoto map.
Proper management of images obtained through remote sensing technologies can facilitate the interpretation and efficient use of spatiotemporal information, which can be used for land use classification. As a result, mapping land use categories, and their changes using, for example, Landsat 5, 7 and 8 images, ensures an optimal investigation of their impact on the environment and implicitly on society (Amini, 2022).
Findings reveal that in 1989, land ownership in the Vârfurile ATU was fragmented, with each plot typically assigned a single use category due to the lack of collectivization.
Today, many plots contain multiple land use subcategories, reflecting shifts in land use driven by reduced agricultural activity - especially potato farming - and widespread abandonment, which has enabled natural ecological succession.
Agricultural land is a basic resource, representative of territorial resilience. In many situations, fertile and relatively accessible soils are subject to pressure caused by urbanization processes, abandonment, the establishment of non-agricultural uses, and due to an agriculture, that is not well adapted to territorial resources. Consequently, the analysis of agricultural land use categories, for the planning of their use, can be carried out according to the properties of the soil and the requirements of society, respectively demographic pressure. Recent studies in the Madrid metropolitan area identified three land use strategies based on suitability: introducing crops in priority zones, designating agricultural protection areas, and promoting ecological regeneration (Morán-Alonso et al., 2025). Declining agricultural activity has led to ecological succession, with spontaneous tree and shrub growth now covering large areas. In addition, climate change - particularly in western Romania - has further contributed to the expansion of areas dominated by native oak species, including holm oak (*Quercus cerris*) and pedunculate oak (*Quercus robur*). These species have regenerated naturally from seed, colonizing many of the abandoned plots
This trend is consistent with findings reported in recent ecological studies. Figure 8 provides a visual summary of the current distribution of land use subcategories across the analyzed plots.

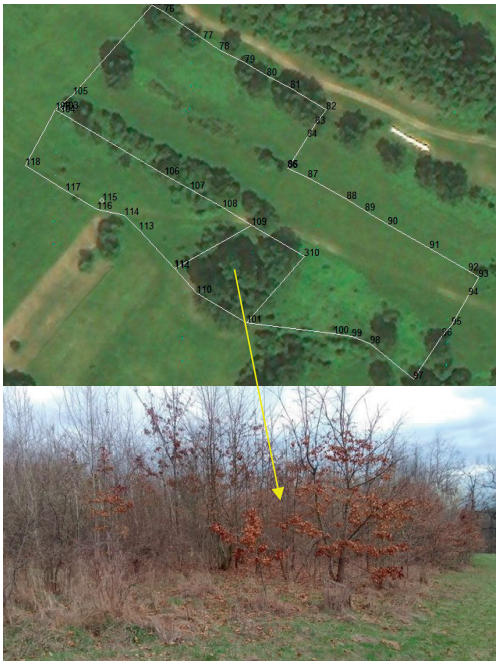


Figure 4. Land areas in the arable use category, on which forest vegetation has been established, native oak species, *Quercus cerris* and *Quercus robur*

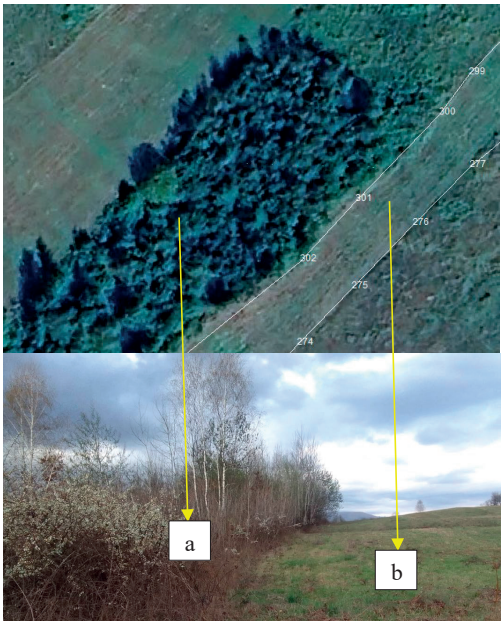


Figure 5. Land areas in the arable use category, on which pioneer forest vegetation has been established (a) and which have been transformed into hayfields (b), due to their improper management

Table 2. Inventory of coordinates of characteristic points related to the analyzed plots

Nr. pct.	X (m)	Y (m)	Z (m)	Nr. pct.	X (m)	Y (m)	Z (m)	Nr. pct.	X (m)	Y (m)	Z (m)
1	538272.727	307751.215	282.088	80	538146.476	307925.075	273.802	151	538202.427	307432.717	262.429
10	538286.930	307741.747	282.681	81	538141.430	307934.378	273.873	152	538208.704	307449.117	263.032
11	538290.370	307743.809	282.791	82	538132.684	307948.609	273.649	153	538.221.184	307.492.569	261.896
12	538295.585	307746.958	283.099	83	538126.966	307944.397	271.103	154	538.223.805	307.514.293	261.243
13	538289.447	307762.806	282.782	84	538121.494	307941.259	268.559	155	538.172.211	307.549.862	252.118
14	538278.606	307789.459	281.686	85	538109.257	307933.463	265.301	156	538.169.227	307.534.707	252.886
15	538262.44	307825.819	280.047	86	538109.024	307933.262	265.247	157	538.167.522	307.512.184	253.036
16	538253.762	307846.404	279.119	87	538105.082	307941.427	264.559	158	538.165.067	307.489.725	254.429
17	538252.177	307849.609	279.062	88	538096.261	307956.850	264.456	159	538.162.914	307.475.563	255.484
18	538249.235	307856.066	278.543	89	538091.576	307964.340	264.354	160	538.158.534	307.459.492	256.278
19	538246.669	307860.822	278.174	90	538086.191	307973.324	264.395	161	538154.020	307442.110	253.989
20	538240.796	307871.47	277.092	91	538076.335	307990.113	264.041	162	538141.460	307.446.524	251.880
21	538235.491	307880.654	275.910	92	538067.429	308005.434	263.276	163	538.130.131	307454.460	249.819
22	538231.013	307887.994	274.731	93	538064.819	308009.759	263.087	164	538.145.202	307.465.217	252.868
23	538230.981	307887.64	274.866	94	538057.384	308005.602	262.920	165	538.146.333	307.476.944	252.138
24	538227.262	307893.682	273.886	95	538045.350	307998.874	260.720	166	538.151.295	307.499.437	251.448
25	538221.752	307901.004	273.124	96	538041.118	307994.864	260.425	167	538.153.354	307.517.298	251.385
26	538218.181	307906.459	272.608	97	538023.408	307983.464	252.790	168	538.158.479	307.550.503	250.382
27	538213.835	307913.17	271.909	98	538037.758	307966.398	254.138	169	538.157.929	307550.600	250.321
28	538211.699	307916.817	271.720	99	538040.699	307959.118	254.320	170	538.147.715	307.553.624	248.744
29	538207.720	307922.572	271.128	100	538041.885	307951.543	254.516	171	538.143.013	307.554.639	248.153
30	538201.165	307932.811	270.225	101	538046.188	307916.929	256.506	172	538.136.482	307.506.472	249.292
31	538191.867	307948.452	269.508	102	538132.625	307840.314	261.802	173	538.132.699	307.478.238	249.303
32	538208.154	307889.491	276.291	103	538132.972	307843.554	262.243	174	538.115.599	307.507.471	249.094
33	538196.548	307902.105	274.628	104	538131.565	307842.386	261.597	175	538.095.516	307.508.148	251.534
34	538194.510	307904.627	274.525	105	538138.85	307847.484	264.045	176	538.082.406	307.509.327	253.732
35	538186.192	307915.564	274.129	106	538106.467	307884.141	260.233	177	538.076.599	307.509.527	253.487
36	538174.391	307938.664	274.279	107	538100.446	307894.260	259.673	178	538.065.195	307.509.139	251.073
37	538195.754	307942.409	269.772	108	538093.071	307907.091	259.852	179	538.067.057	307.517.567	251.425
38	538177.334	307933.692	274.123	109	538085.834	307918.789	259.931	180	538.063.561	307.519.389	250.649
39	538208.899	307888.804	276.391	110	538058.183	307896.984	257.061	181	538.063.763	307.534.223	250.352
40	538207.173	307889.811	276.318	111	538068.420	307888.225	257.892	182	538.072.335	307535.46	251.641
41	538222.564	307868.182	278.176	112	538068.723	307887.796	257.936	183	538.072.384	307.535.504	251.626

Table 3. Inventory of coordinates of characteristic points related to the analyzed plots (continued)

Nr. pct.	X (m)	Y (m)	Z (m)	Nr. pct.	X (m)	Y (m)	Z (m)	Nr. pct.	X (m)	Y (m)	Z (m)
42	538232.754	307851.770	278.815	113	538084.166	307873.654	258.654	184	538.082.948	307.536.021	252.535
43	538244.107	307833.343	279.560	114	538089.803	307867.975	259.098	185	538.084.535	307.518.025	253.239
44	538248.198	307826.812	279.678	115	538095.841	307859.221	259.669	186	538.091.938	307.518.041	251.35
45	538256.029	307813.526	280.247	116	538092.296	307857.057	259.411	187	538.115.476	307.517.373	248.644
46	538263.246	307798.137	280.962	117	538099.997	307844.339	259.536	188	538.113.148	307.537.303	248.498
47	538271.651	307778.792	281.837	118	538110.181	307828.326	259.835	189	538116.550	307.537.222	248.173
48	538275.570	307768.692	282.212	119	538181.871	307685.093	259.191	190	538.081.021	307.492.428	254.566
49	538282.424	307751.181	282.563	120	538168.264	307680.153	257.678	191	538.071.805	307469.500	255.273
50	538286.438	307741.204	282.619	121	538181.362	307648.443	258.315	192	538.051.081	307.472.286	251.776
51	538278.100	307736.984	282.191	122	538188.584	307628.054	259.576	193	538.071.926	307.469.403	255.282
52	538280.504	307733.920	282.036	123	538208.062	307577.166	259.927	194	538.075.256	307.468.738	255.572
53	538283.200	307730.032	281.948	124	538221.345	307542.646	259.223	195	538090.390	307.465.935	255.758
54	538288.233	307721.691	281.598	125	538.215.049	307611.001	261.595	196	538101.920	307.462.039	254.516
55	538293.236	307713.595	281.116	126	538225.948	307585.440	262.102	197	538.114.594	307.458.148	252.758
56	538297.695	307706.286	280.584	127	538237.582	307555.174	261.310	198	538.114.709	307.482.532	250.979
57	538302.909	307698.123	279.925	128	538259.510	307563.160	265.894	199	538.304.637	307.372.146	279.234
58	538308.956	307687.577	278.839	129	538266.992	307536.188	267.254	200	538.300.835	307.377.686	278.591
59	538314.649	307676.597	277.968	130	538271.500	307520.973	268.165	201	538.296.131	307.389.494	278.168
60	538321.253	307664.438	276.840	131	538272.949	307504.617	268.593	202	538.287.173	307.401.685	277.099
61	538326.561	307654.417	276.104	132	538273.389	307493.285	269.016	203	538280.240	307410.740	277.653
62	538332.024	307643.175	275.276	133	538265.299	307491.561	268.100	204	538275.480	307.416.257	275.484
63	538334.851	307636.555	274.915	134	538270.751	307465.212	273.130	205	538269.090	307.420.633	274.688
64	538339.551	307626.223	274.718	135	538268.507	307452.288	275.341	206	538.287.713	307445.140	274.083
65	538344.969	307611.087	275.116	136	538267.840	307431.847	273.914	207	538.335.681	307.389.272	281.115
66	538331.603	307604.636	274.123	137	538260.058	307418.405	274.041	208	538.028.705	307.022.064	271.954
67	538325.331	307618.941	273.798	138	538253.267	307410.437	273.242	209	538.006.721	307.024.786	279.351
68	538317.828	307635.255	274.088	139	538247.899	307415.961	271.887	210	538.006.717	307.024.804	279.330
69	538308.222	307652.854	273.914	140	538247.799	307415.980	271.852	211	537.998.757	307.026.456	280.152
70	538297.241	307671.895	274.881	141	538253.547	307425.640	272.595	212	537.956.196	307.006.218	285.672
71	538287.493	307687.328	276.289	142	538263.810	307443.859	272.336	213	537.947.622	307.005.818	286.005
72	538279.410	307701.427	278.124	143	538265.642	307459.992	283.517	214	537.949.397	307.011.019	285.474
73	538269.165	307717.593	278.741	144	538241.138	307481.678	263.170	215	537972.130	307.004.151	285.595
74	538261.384	307728.645	278.638	145	538234.324	307457.776	264.550	216	538.030.671	307.003.574	278.328
75	538175.28	307878.903	275.567	146	538219.091	307401.040	263.605	217	538.029.956	306.996.126	278.686
76	538172.141	307884.013	275.733	147	538219.120	307400.161	263.665	218	538.028.829	306.981.575	279.048
77	538161.261	307899.513	275.400	148	538227.599	307406.750	265.697	219	538.029.043	306.983.245	279.026
78	538156.949	307905.969	275.121	149	538206.649	307406.614	261.193	220	537.873.384	308.282.923	244.207
79	538151.615	307916.146	274.637	150	538195.544	307413.333	260.118	221	537.867.488	308.279.819	244.011
222	537857.992	308275.388	243909	251	537836.019	308297.410	241313	280	536295.006	310484.474	293.031
223	537845.326	308269.244	243.943	252	537840.860	308282.503	242.797	281	536305.88	310495.575	293.530
224	537845.103	308269.198	243.885	253	537844.259	308272.064	243.604	282	536322.203	310511.979	293.364
225	537878.112	308285.077	244.317	254	537845.030	308269.931	243.787	283	536335.433	310525.694	293.173
226	537886.276	308289.609	244.461	255	537845.016	308269.882	243.753	284	536347.667	310536.968	293.100
227	537875.081	308303.462	243.365	256	537841.589	308280.047	242.998	285	536363.612	310551.485	294.198
228	537864.885	308317.928	242.095	257	537974.347	308479.104	241.681	286	536373.264	310560.801	294.864
229	537857.749	308327.891	241.357	258	537.987.495	308483.803	241.444	287	536385.474	310571.807	295.905
230	537846.870	308340.283	240.342	259	538001.230	308488.406	241.142	288	536393.851	310579.457	296.363
231	537845.410	308341.705	240.158	260	538012.186	308492.841	240.981	289	536402.552	310570.480	295.057
232	537837.906	308350.649	239.438	261	538026.288	308498.893	240.479	290	536394.076	310562.631	293.880
233	537829.796	308360.410	238.724	262	538021.762	308504.451	239.659	291	536364.445	310531.671	291.213
234	537817.345	308374.553	237.269	263	538015.373	308511.827	238.162	292	536354.906	310522.169	291.244
235	537810.661	308383.896	236.335	264	538013.931	308513.332	237.854	293	536348.434	310516.285	291.304
236	537801.655	308397.707	234.918	265	538004.518	308511.686	237.780	294	536343.170	310511.006	291.328
237	537789.269	308417.307	233.137	266	537991.022	308509.854	238.395	295	536333.504	310502.239	291.496
238	537781.481	308430.283	231.919	267	537978.974	308508.347	238.668	296	536318.573	310485.745	291.995
239	537779.678	308433.795	231.664	268	537957.830	308505.213	239.413	297	536302.277	310468.734	291.028
240	537774.403	308441.842	230.783	269	536180.558	310377.956	284.636	298	536283.879	310452.580	290.083
241	537773.803	308431.955	231.029	270	536176.002	310376.201	283.538	299	536275.307	310444.628	289.744
242	537774.311	308418.835	234.531	271	536189.914	310384.330	285.304	300	536266.828	310438.508	289.371
243	537781.605	308401.295	232.593	272	536200.724	310393.823	286.516	301	536248.527	310421.006	288.857
244	537792.237	308385.777	234.130	273	536207.859	310399.783	286.424	302	536235.853	310409.266	287.939
245	537801.809	308370.031	235.187	274	536218.175	310408.687	288.304	303	536214.554	310383.360	285.784
246	537809.841	308355.666	236.980	275	536230.041	310420.072	289.653	304	536185.722	310355.955	281.686
247	537819.967	308339.963	238.210	276	536243.435	310432.846	290.607	305	536185.713	310355.895	281.679
248	537823.787	308330.278	238.767	277	536255.749	310444.891	290.682	306	536183.512	310359.650	282.004
249	537830.186	308313.456	239.696	278	536264.295	310454.975	291.267	307	536180.337	310364.972	282.456
250	537836.003	308297.397	241.307	279	536278.544	310468.304	291.764	-	-	-	-



Figure 6. Positioning of plots occupied by forest vegetation using the RTK method, with radio modules



Figure 7. Positioning of characteristic points of parcels by RTK method with internal radio - external radio modules

Analysis of the diagram in Figure 9 shows that 75% of the analyzed plots are currently classified as meadows, while the remaining 25% are categorized as forested meadows.

The tree species identified on the studied plots include a diverse range of native and naturalized species (Stănescu, Șofletea, & Popescu, 1997). These are: *Quercus cerris* L., *Quercus robur* L. (Figure 10), *Carpinus betulus* L., *Tilia tomentosa* Moench., *Robinia pseudoacacia* L., *Populus tremula* L. (Figure 11), *Betula pendula* Roth (Figure 11)., *Fagus sylvatica* L., *Quercus petraea* Matt., *Prunus avium* L., *Salix caprea* L., *Ulmus minor* Mill., *Ulmus laevis*, *Pinus sylvestris* L., *Alnus glutinosa* L., and *Fraxinus excelsior* L.

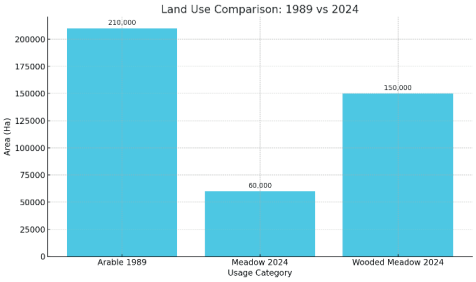


Figure 8. Comparative presentation of use categories for the years 1989 and 2024

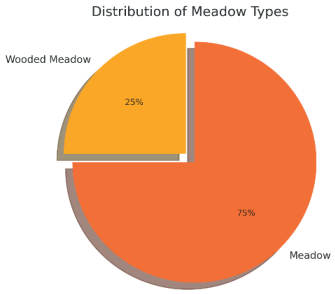


Figure 9. Percentage of subcategories of use, 75% meadow, 25% wooded meadow

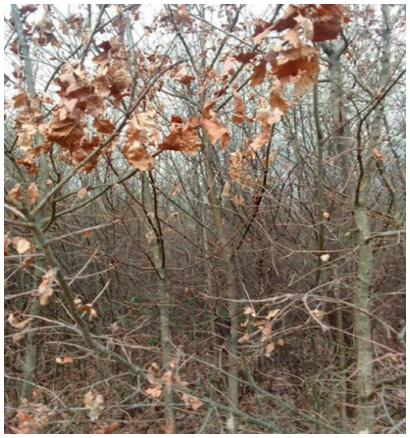


Figure 10. Naturally regenerated forest vegetation of *Quercus robur* (pedunculate oak) established on formerly arable land in Cadastral Sector 15, Vârfurile ATU

Shrub and bush species observed include *Prunus spinosa* L., *Malus sylvestris* Mill., *Pyrus pyraster* L., and *Prunus cerasifera* Ehrh. (Stănescu, Şofletea, & Popescu, 1997).

It is important to note that the maintenance of some plots in good agricultural condition has been supported by financial incentives provided through the Payments and Interventions Agency for Agriculture (PIAA), which encourage landowners to manage and preserve their land use categories effectively.

The changes in land use reported in recent decades are determined by various economic activities carried out in agricultural ecosystems, which have profound implications for society, while also having a major impact on agriculture, the environment, and in the assessment of the sustainability of food and organic products (Barbara et al., 2023).



Figure 11. Biogroups of *Betula Pendula* and *Populus tremula* established through natural succession on former arable land in Cadastral Sector 15, Vârfurile ATU, illustrating the early stages of forest regeneration following land abandonment

CONCLUSIONS

The application of geomatics technologies provides a modern and effective approach for analyzing land use categories and subcategories, particularly in non-collectivized, hilly regions. The integration of GNSS positioning, specifically using RTK methods with dual-frequency receivers and internal/external radio modules, enabled the collection of high-precision spatial data while significantly optimizing fieldwork efforts.

The completion of systematic cadastral registration in Cadastral Sector 15 and the development of parcel plans in both digital and analog formats facilitated a detailed analysis of land use through the MapSys 10 digital cartography program. The overlay of parcel plans onto orthophoto imagery, combined with field observations, allowed for the accurate identification of current land use categories and their spatial distribution.

A comparative analysis revealed that the current land use classifications differ significantly from those recorded in 1990. This shift reflects broader socio-economic changes, particularly the decline in interest in traditional crop cultivation (e.g., potatoes) and the drastic reduction in livestock farming, which has led to widespread abandonment of hayfields and pastures. Consequently, natural ecological succession has occurred, resulting in the

expansion of arboreal and shrub vegetation on previously arable lands. Native deciduous species, especially pedunculate oak (*Quercus robur*) and Turkey oak (*Quercus cerris*), have naturally regenerated and established themselves in biogroups and strips across these abandoned areas. These changes have been further accelerated by evolving climatic conditions in the region.

The land classified under forested and shrub-dominated categories has increased considerably since 1990, often at the expense of arable land and hayfields. Conversely, orchard areas have expanded, supported by the establishment of new plantations financed through European structural funds or private investment.

The continued preservation and productive use of arable land, pastures, and hayfields are largely sustained by financial support provided through the Agricultural Payments and Interventions Agency (APIA). Access to non-reimbursable European development funds has also played a key role in maintaining the viability of traditional land use categories under optimal conditions.

This study highlights significant land use transformations in non-collectivized rural areas, driven by agricultural decline and supported by natural ecological processes. Using modern geomatic tools and precise spatial data, it was found that arable land has increasingly transitioned into meadows and forested areas, reflecting both human inactivity and climate-driven regeneration. Targeted funding - particularly through APIA and European programs - has played a vital role in maintaining productive land use where possible. These insights can inform future land management strategies, support sustainable rural development, and guide the efficient allocation of financial resources.

ACKNOWLEDGEMENTS

The authors would like to express their gratitude to the Local Council of Vârfurile City Hall (Arad County) and the Arad Cadastre and Real Estate Advertising Office for their valuable support in conducting this research. Special thanks are extended to the landowners in Cadastral Sector 15, UAT Vârfurile, for their cooperation and access to relevant data.

The GNSS equipment and software used for spatial positioning and graphical data processing were kindly provided by S.C. TOPO SISTEM S.R.L. (Oradea, Bihor County) and S.C. ECOPROD FOREST S.R.L. (Paleu, Bihor County).

REFERENCES

Amini, S., Saber, M., Rabiei-Dastjerdi, H., & Homayouni, S. (2022). Urban land use and land cover change analysis using random forest classification of Landsat time series. *Remote Sensing, 14*(11), 2654. https://doi.org/10.3390/rs14112654

Bodog, M. F., Șchiopu, E. C., Crainic, G. C., & Lazăr, A. N. (2024). Assessment of contamination degree of oil residues on a former agricultural site. *Journal of Agricultural Science and Technology, A, 14*, 67–82. https://doi.org/10.17265/2161-6256/2024.02.003

Boș, N. (2003). *Cadastru general*. ALL BECK Publishing House.

Călina, J., Călina, A., Vangu, G. M., Croitoru, A. C., Miluț, M., Băbucă, N. I., & Stan, I. (2025). A study on the management and evolution of land use and land cover in Romania during the period 1990–2022 in the context of political and environmental changes. *Agriculture, 15*(5), 463. https://doi.org/10.3390/agriculture15050463

Cienciała, A., Sobolewska-Mikulska, K., & Sobura, S. (2021). Credibility of the cadastral data on land use and the methodology for their verification and update. *Land Use Policy, 102*, 105204. https://doi.org/10.1016/j.landusepol.2020.105204

Chehrehbargh, J. F., Rajabifard, A., Atazadeh, B., & Steudler, D. (2024). Current challenges and strategic directions for land administration system modernisation in Indonesia. *Journal of Spatial Science, 69*(4), 1097–1129. https://doi.org/10.1080/14498596.2024.2360531

Chezan, M., Petanec, D., Popescu, C., & Fazakas, P. (2006). *Sisteme Informatice Geografice*. Eurobit Publishing House.

Crainic, G. C. (2024). Issues related to the implementation of geomatic applications in the national forestry fund. *Scientific Papers. Series E. Land Reclamation, Earth Observation & Surveying, Environmental Engineering, 13*, 794–804.

Giuliani, G., Rodila, D., Külling, N., Maggini, R., & Lehmann, A. (2022). Downscaling Switzerland land use/land cover data using nearest neighbors and an expert system. *Land, 11*, 615. https://doi.org/10.3390/land11050615

Kalisz, B., Żuk-Gołaszewska, K., Radawiec, W., & Gołaszewski, J. (2023). Land use indicators in the context of land use efficiency. *Sustainability, 15*(2), 1106. https://doi.org/10.3390/su15021106

Marton, H. (2007). *MapSys, TopoSys - User manual*. Odorheiu Secuiesc.

Morán-Alonso, N., Viedma-Guiard, A., Simón-Rojo, M., & Córdoba-Hernández, R. (2025). Agricultural land suitability analysis for land use planning: The case of the Madrid region. *Land, 14*(1), 134. https://doi.org/10.3390/land14010134

Nedd, R., Light, K., Owens, M., James, N., Johnson, E., & Anandhi, A. (2021). A synthesis of land use/land cover studies: Definitions, classification systems, meta-studies, challenges and knowledge gaps on a global landscape. *Land, 10*(9), 994. https://doi.org/10.3390/land10090994

Novac, G. (2007). *Cadastre*. Mirton Publishing House.

Popescu, G., Popescu, C. A., Dragomir, L. O., Herbei, M. V., Horablaga, A., Țenche Constantinescu, A. M., Sălăgean, T., Brumă, S., Dinu-Roman Szabo, M., Colișar, A., Ceuca, V., Kader, S., & Sestraș, P. (2024). Utilizing UAV technology and GIS analysis for ecological restoration: A case study on *Robinia pseudoacacia* L. in a mine waste dump landscape rehabilitation. *Notulae Botanicae Horti Agrobotanici Cluj-Napoca, 52*(4). https://doi.org/10.15835/nbha52413937

Popescu, A. C. (2007). *Remote sensing and geographic information systems in agriculture*. Eurobit Timișoara.

Roșca, S., Bilașco, Ș., Păcurar, I., Oncu, M., Negrușier, C., & Petrea, D. (2015). Land capability classification for crop and fruit product assessment using GIS technology: Case study: The Niraj River Basin (Transylvania Depression, Romania). *Notulae Botanicae Horti Agrobotanici Cluj-Napoca, 43*(1), 235–242. https://doi.org/10.15835/nbha4319860

Sabău, N. C. (2010). *Terrestrial measurements*. Publishing House of the University of Oradea.

Stănescu, V., Șofletea, N., & Popescu, O. (1997). *The woody forest flora of Romania*. Ceres Publishing House.

Tămăioagă, G., & Tămăioagă, D. (2005). *General and specialized land registers*. MATRIX ROM Publishing House.

Upadhyaya, S., Gyawali, P., Shrestha, S., Bhandari, S., & Shanker, K. C. (2024). The fundamental role of GNSS in modern surveying and mapping to support climate responsive land governance and to enhance disaster resilience. *FIG Regional Conference 2024 - Nepal: Climate Responsive Land Governance and Disaster Resilience*. https://www.fig.net/resources/proceedings/fig_proceedings/nepal/papers/ts03b/TS03B_upadhyaya_gyawali_et_al_12890.pdf

Zheng, K., Wang, H., Qin, F., & Han, Z. (2022). A land use classification model based on conditional random fields and attention mechanism convolutional networks. *Remote Sensing, 14*(11), 2688. https://doi.org/10.3390/rs14112688

***Google. (n.d.). *Vârfurile, România – Google Maps*. https://www.google.com/maps/place/317390+V%C3%A2rfurile,+Rom%C3%A2nia/@46.317759,22.4906651,8093m/data=!3m1!1e3!4m6!3m5!1s0x474f30614b6843c7:0xf9735b4e3536ebda!8m2!3d46.3112927!4d22.5274424!16s%2Fg%2F1ptwx6qmh?hl=ro&entry=ttu

***Guvernul României. (1991). *Legea nr. 18/1991 privind fondul funciar*. https://www.emitent.ro/resurse/legi/legea18_1991.pdf

***Ministerul Justiției. (n.d.). *Legea fondului funciar nr. 18/1991 (republicată)*. https://legislatie.just.ro/Public/DetaliiDocument/11269

***Pe-Harta.ro. (n.d.). *Harta județului Arad*. https://pe-harta.ro/judete/Arad.jpg

***Primăria Comunei Vârfurile. (n.d.). *Plan cadastral pentru sectorul 15, U.A.T. Vârfurile, județul Arad*.

***Turism-Zone.ro. (n.d.). *Harta Vârfurile, județul Arad, România*. https://harti.turism-zone.ro/harta_varfurile_arad_romania_1452.html

Scientific Papers. Series E. Land Reclamation, Earth Observation & Surveying, Environmental Engineering. Vol. XIV, 2025
Print ISSN 2285-6064, CD-ROM ISSN 2285-6072, Online ISSN 2393-5138, ISSN-L 2285-6064

ACCURACY IN VERTICAL ASSESSMENT OF TELECOMMUNICATIONS TOWERS THROUGH 3D SCANNING

Andreea Diana CLEPE, Sorin HERBAN, Clara-Beatrice VÎLCEANU, George CRISTIAN

Politehnica University of Timișoara, 1 Ioan Curea Street, 300224, Timișoara, Romania

Corresponding author email: sorin.herban@.upt.ro

Abstract

Telecommunications towers are essential infrastructures that serve various functions, including telecommunications, meteorological data collection, and surveillance. Maintaining their structural integrity and accurate vertical alignment is crucial for ensuring operational efficiency, safety, and long-term durability. However, evaluating the verticality of tall structures presents significant challenges, necessitating the use of modern and precise methods. Traditional techniques, such as manual surveys using level instrument, are often limited by human error, environmental factors, and the complexity of the structures involved. This study investigates the use of LiDAR (Light Detection and Ranging) technology as a modern method for assessing verticality. By employing advanced LiDAR scanning techniques, the research establishes a thorough framework for accurate and efficient structural monitoring. The paper highlights how LiDAR technology outperforms traditional methods in accuracy, speed, and flexibility, providing a safer and more dependable solution for managing the vertical alignment of observation towers.

Key words*: 3D scanning, vertical assessment, point cloud, surveying accuracy, LiDAR.*

INTRODUCTION

The rapid expansion of telecommunications infrastructure has necessitated precise and reliable methods for assessing verticality and structural integrity in telecommunication towers. Given the increasing demand for high-speed connectivity and the expansion of cellular networks, ensuring the stability and accuracy of tower installations is essential to maintaining service quality, structural safety, and compliance with regulatory standards. The resistance criteria for these kinds of towers are defined based on the current applicable technical standards and within the framework of the conditions specified in the beneficiary's project requirements (Sîrbu et al., 2023).

Recent advancements in three-dimensional scanning technologies (Kantaros et al., 2023) have revolutionized structural assessment by enabling high-resolution, non-contact measurements with enhanced accuracy and efficiency. 3D laser scanning, photogrammetry, and LiDAR (Light Detection and Ranging) have emerged as powerful tools for capturing detailed spatial data of telecommunications towers. These technologies facilitate the generation of precise digital replica, which allow for comprehensive structural analysis, deformation monitoring, and early detection of anomalies (Kaartinen et al., 2022).

This paper focuses on the use of 3D scanning technologies for the vertical assessment of observation towers, aiming to analyse their stability over time. Observation towers, with their large dimensions and complex structures, require precise measurements to ensure their integrity and safety in the long term. The main goal of this paper is to demonstrate the effectiveness of 3D scanning technologies, especially LiDAR systems and laser scanners, in performing accurate vertical assessments that contribute to monitoring the structural condition of the towers.

Traditional methods of vertical assessment, such as manual plumb-line measurements, total station surveys, and inclinometer readings, often suffer from limitations in precision, efficiency, and accessibility. Compared to traditional surveying methods, 3D scanning provides superior data density, automated processing, and enhanced reproducibility, making it a compelling alternative for vertical assessment in telecommunication infrastructure (El-Tokhey et al., 2019).

In the context of observation towers, maintaining verticality is essential for their structural stability, as significant deviation from verticality can lead to safety risks or deterioration. Thus, by using 3D scanning technologies, extremely high precision can be achieved in measuring angles and tower height, allowing the detection of any deformations or changes that may affect its stability. 3D laser scanners are among the most effective tools for three-dimensional monitoring of various types of constructions, including observation towers, as they provide detailed data such as shape, intensity, and colour, which can be used to study crack growth and detect possible structural weaknesses (Mihai et al., 2014).

A recent study by Wang et al. (2024) introduced an automated 3D reconstruction framework for communication towers using TLS point clouds. Their model-driven approach achieved an average root-mean-square error (RMSE) of 1.3 cm in antenna reconstruction and 1.2 cm in tower body reconstruction, demonstrating high accuracy in capturing complex geometries. This high-precision methodology enables improved structural assessment and facilitates better decision-making in maintenance and design processes.

Figure 1 illustrates the scanned object, a tall telecommunication tower, which has been examined using 3D scanning technology.



Figure 1. The study area

The tower features a cylindrical structure with alternating red and white segments; a typical design used for visibility and aviation safety compliance. It stands on a concrete base, which is slightly elevated from the surrounding ground level. The tower is equipped with antennas and transmission equipment at the top, indicating its function in communication and signal transmission.

The height of the tower necessitates multiple elevation perspectives to accurately capture the structural details. Furthermore, consideration must be given to potential obstacles and reflections from metallic surfaces at the top, as these factors may influence the quality of the scanning process.

MATERIALS AND METHODS

The study utilized the Leica BLK360 G2 laser scanner, a high-precision LiDAR system capable of capturing detailed 3D point clouds with a range accuracy of ±4 mm at 10 meters (ArcTron, n.d.). This scanner operates using a combination of infrared scanning and photogrammetry to generate dense and precise spatial data (ArcTron, n.d.). The determination of control points was carried out using a fully robotic total station to establish 12 ground control points (GCPs) at strategic locations surrounding the telecommunications tower. These GCPs were crucial in georeferencing and validating the accuracy of the scan data (Liu et al., 2022). The total station captured accurate spatial data, ensuring alignment between the scan data and real-world references.

The total station used belongs to the class of high-precision total stations, providing angular accuracy of up to 1” (one second) and distance measurement accuracy of 2 mm + 2 ppm (Stonex, n.d.). The angular measurement system includes a dual-axis compensator, offering stability and an angular accuracy of 1” or 2” with a resolution of 0.1” (Stonex, n.d.). Distance measurements in prism mode reach up to 5000 m with an accuracy of 2 mm + 2 ppm, while reflectorless measurements can extend up to 1000 m with an accuracy of 3 mm + 2 ppm, depending on surface reflectivity (Stonex, n.d.). Initially, the total station was set up at a known reference point or a strategically chosen temporary setup point, with its exact position

pre-established using high-precision GNSS (Global Navigation Satellite System) collected survey data. At the location of the control point, a prism or reflector was positioned to serve as the target for the total station's measurements. The total station employed electromagnetic distance measurement (EDM) technology to precisely calculate the slant distance between the total station and the prism, while simultaneously recording the horizontal and vertical angles to the target. The total station's integration with an Android-based software interface further enhanced this process, enabling real-time data collection, immediate calculations, and seamless display of results either on the instrument itself or through connected devices (Stonex, n.d.). Data processing and analysis were conducted using AutoCAD CIVIL 3D for technical drawing and structural modelling, while CloudCompare was used for point cloud processing, alignment, and accuracy assessment.

Data acquisition involved scanning the telecommunications tower using the Leica BLK360 G2 at 17 scan stations, ensuring full coverage from multiple vantage points. Between these positions, 77 connections were established, each representing an overlap between data acquired from two different perspectives, contributing to the overall coherence of the point cloud. For a detailed evaluation of the coverage and measurement consistency, a data presence matrix was generated (Figure 2).

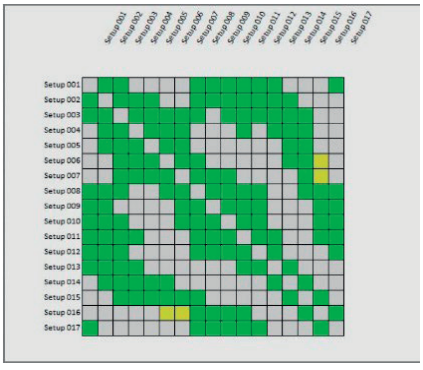


Figure 2. Distribution of overlaps between scanning stations - 3D scan coverage matrix

This matrix indicates the degree of connectivity between scanning stations and helps identify areas where the measurements can be considered reliable for verticality analysis. Cells that are filled indicate the presence of valid data and useful overlaps, while empty or unevenly marked cells point to potential gaps in data capture or regions where accuracy is reduced due to blind spots or obstacles.

The scanning process included pre-scan calibration to ensure measurement precision, positioning the scanner at pre-determined points for optimal visibility of the tower's vertical structure, capturing 3D point clouds using a full panoramic scan, and utilizing the scanner's built-in camera to supplement the LiDAR data with high-resolution images.

Ground control and georeferencing were established by placing GCP markers at fixed, stable locations around the base of the tower, measuring their coordinates using the total station with centimetre-level accuracy, and integrating the GCPs into the point cloud during post-processing to align the scan data with real-world coordinates (Figure 3).

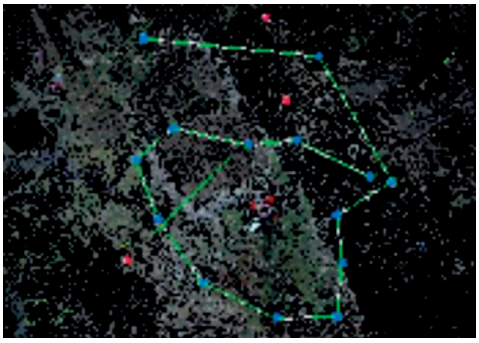


Figure 3. Ground Control and Georeferencing Using GCP Markers

Point cloud processing began with preliminary data cleaning in CloudCompare (Figure 4), where noise reduction and outlier removal were performed to eliminate erroneous data points.

Multi-scan registration was conducted using iterative closest point (ICP) algorithms to align the multiple scan stations into a unified 3D dataset. The total station-derived GCPs were used to refine the spatial accuracy of the point cloud through georeferencing. To determine the vertical accuracy of the telecommunications tower, the central vertical axis of the tower was extracted from the point cloud by identifying key structural elements, followed by a vertical

deviation analysis that compared the actual scanned position of the tower elements with their expected theoretical positions based on the AutoCAD structural model. Statistical assessment was conducted using CloudCompare's cloud-to-cloud distance measurement tool to quantify vertical misalignments.

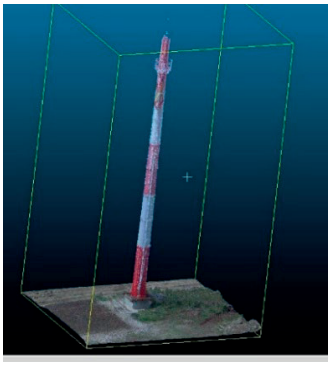
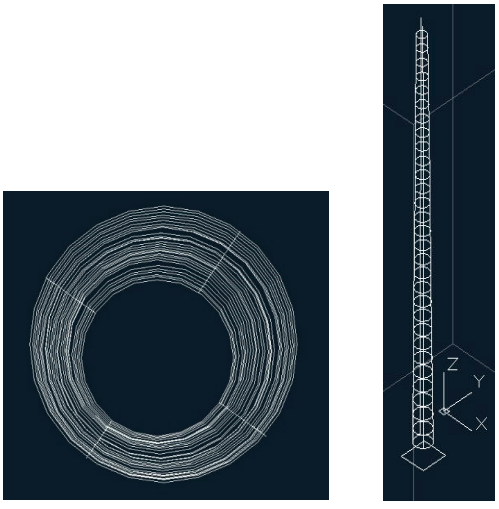


Figure 4. Point Cloud Cleaning and Noise Reduction using CloudCompare

Cross-sections were generated at regular intervals along the height of the tower, providing detailed sectional views that allowed for precise assessment of deviations and misalignments (Figure 5).



a) b)

Figure 5. a) Top-view cross-section b) 3D-view cross-section of the telecommunication tower

These cross-sections were analysed to compare the actual tower profile with its designed specifications. Measurements were taken at multiple points along each section to identify any lateral displacements or distortions in the structure. Additionally, vertical alignment was assessed by projecting reference lines along the tower's intended axis and calculating the deviations at different heights (Figure 6).

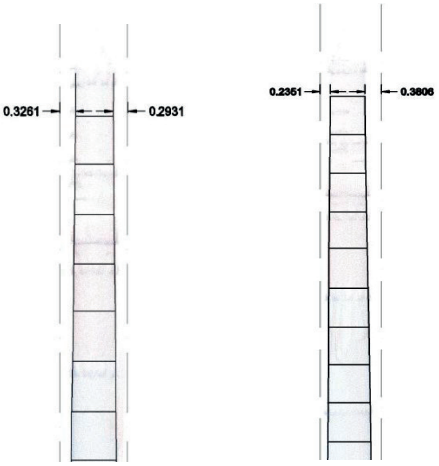


Figure 6. Vertical Alignment Assessment Using Reference Lines

Upon completion of the analysis, final data outputs were generated providing a comprehensive visualization of structural integrity and alignment. Although the overall coverage was 48% and the coherence of the connections between positions was 25%, these values proved sufficient for measuring verticality. The accuracy of the data was confirmed by the very low global errors reported in the technical registration analysis, as follows in Table 1.

Table 1. Summary of mean error values

Type of Error	**Mean Value (m)**
Global bundle adjustment error	0.004
Bundle error	0.006
Cloud-to-cloud error	0.008
Target registration error	0.004

RESULTS AND DISCUSSIONS

The assessment of vertical accuracy in telecommunications towers through 3D scanning provided detailed insights into structural alignment, deviations, and potential deformations. The use of terrestrial laser scanning (TLS) and point cloud analysis allowed for a precise evaluation of the tower's verticality by identifying misalignments and detecting subtle structural shifts that could impact long-term stability. The findings of this study are categorized into different aspects of analysis, including point cloud processing, vertical alignment evaluation, deformation analysis, and implications for structural integrity.

In terms of point cloud processing, advanced computational techniques were employed to generate an accurate 3D representation of the tower. The data was carefully filtered and processed to eliminate noise and ensure precise modelling. This step was crucial in providing a reliable reference for further analysis, particularly in assessing deviations from the ideal structural alignment. However, at the top of the tower, the point cloud was not as dense due to the increased distance from the scanner to the top. Despite the scanner's capability to collect information up to 35 meters, the data density decreased with height, leading to reduced detail in the uppermost sections.

Regarding vertical alignment evaluation, a series of precise measurements were conducted and compared against an ideal perfectly vertical tower. The results indicate that the actual inclination of the structure deviates by approximately ±0.3 meters from the theoretical vertical alignment (Figure 7). This minor deviation is considered negligible in practical terms, as it falls well within acceptable construction tolerances and does not pose any structural or functional risks to the stability of the tower.

Deformation analysis was conducted to identify any structural deformations beyond simple inclinations. The results reveal that while minor deformations exist, they are primarily localized and do not compromise overall structural integrity. Potential causes for these deformations include environmental factors such as wind loads, thermal expansion, and material aging. The findings suggest that these minor deformations are within acceptable engineering limits and do not warrant immediate corrective action. Additionally, the local axis misalignment (Figure 8, Figure 9) was verified, and it was concluded that there are no fabrication or installation irregularities.

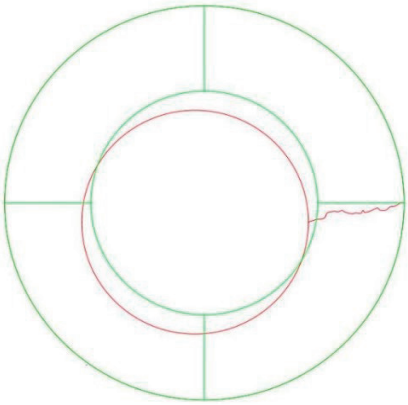


Figure 7. Comparison of Actual (red) and Theoretical (green) Tower Inclination

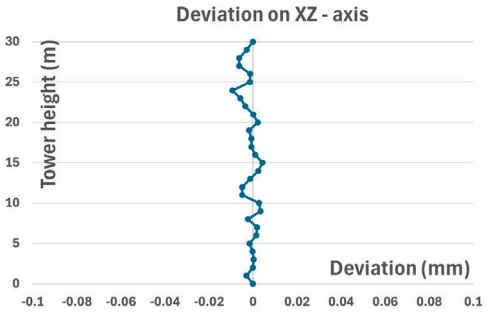


Figure 8. Deviation on XZ axis

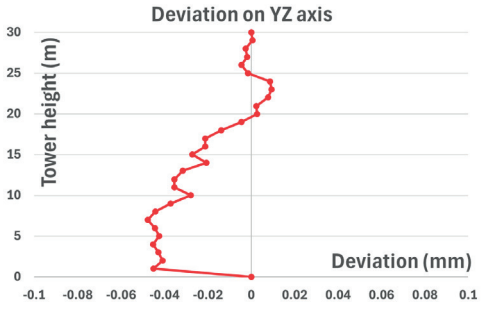


Figure 9. Deviation on YZ axis

Furthermore, deformations might influence long-term stability. The results confirm that the tower maintains a high level of structural reliability and that its slight inclination does not impact on its overall performance or safety. However, the observed deviation may be attributed to minor settlement effects, material deformations, or external environmental influences, all of which remain within industry-accepted limits. These results reinforce the reliability of the construction techniques used and confirm that the tower's alignment remains well within the anticipated engineering standards.

CONCLUSIONS

The assessment of vertical accuracy in telecommunications towers through 3D scanning has proven to be a significant advancement in structural evaluation and maintenance. This study has demonstrated that 3D scanning technology, particularly LiDAR, provides highly precise and reliable data for measuring tower verticality, structural integrity, and component alignment.

A key observation from this research is the detection of slight local axis misalignments that, while measurable, fall within acceptable tolerance limits and are not attributed to fabrication errors. These minor misalignments are typically the result of external factors, such as foundation settlement, small environmental forces or slight variations in installation, which are common in large structures. The environmental factors identified, while seemingly minor at first, have the potential to significantly impact the structural stability of the telecommunication tower over time through cumulative effects, particularly if not consistently and properly monitored. Uneven foundation settlement can lead to a progressive tilting of the structure and the development of additional stresses in load-bearing elements, while repeated environmental actions, such as wind or temperature fluctuations, can induce material ware. Furthermore, even slight deviations in the tower's axis can cause uneven load redistribution, generating unwanted moments and eccentric forces that place extra stress on the structure. In addition, the natural aging of materials, if not countered by proper maintenance, contributes to the decline in overall durability and resistance. Therefore, given that a residential neighbourhood and a public park are planned to be developed in the immediate proximity of the tower, it is essential that comprehensive geodetic measurements and structural evaluations be conducted at intervals of no more than four years, in order to ensure both the integrity of the structure and the safety of the surrounding community. The precision of 3D scanning allows for the identification of these deviations, which, although present, do not pose any immediate structural risk and are well within the industry standards for alignment tolerance.

The ability to quantify such minor misalignments is crucial, as it helps engineers confirm that the tower's alignment remains structurally sound, even when there are small deviations from the ideal vertical. This finding suggests that such misalignments are not a result of poor fabrication or manufacturing defects but rather natural, expected variations that occur during the installation and aging process of the tower.

In conclusion, 3D scanning provides a reliable method for assessing vertical alignment, ensuring that any misalignments are accurately identified, even when they are small and within acceptable limits. This technology allows for proactive monitoring without the need for immediate intervention, promoting the long-term health and operational efficiency of telecommunications towers. As scanning technology continues to improve, future research could focus on further refining the detection of misalignments that could influence tower stability over time, particularly in dynamic environmental conditions.

REFERENCES

ArcTron (n.d.). *Leica BLK360 laser scanner*. Retrieved from https://www.arctron.de/products/leica-blk360-laser-scanner/

El-Tokhey, M., Mogahed, Y., & Abd-elmaaboud, A. (2019). Comparative assessment of terrestrial laser scanner against traditional surveying methods. *nternational Journal of Engineering and Applied Sciences 6*(4), (IJEAS), ISSN: 2394-3661, ISSN: 2394-3661.

Kaartinen, E., Dunphy, K., & Sadhu, A. (2022). LiDAR-based structural health monitoring: Applications in

civil infrastructure systems. *Sensors*, *22*(12), 4610. https://doi.org/10.3390/s22124610

Kantaros, A., Ganetsos, T., & Petrescu, F. I. T. (2023). Three-dimensional printing and 3D scanning: Emerging technologies exhibiting high potential in the field of cultural heritage. *Applied Sciences*, *13*(8), 4777. https://doi.org/10.3390/app13084777

Liu, X., Lian, X., Yang, W., Wang, F., Han, Y., & Zhang, Y. (2022). Accuracy assessment of a UAV direct georeferencing method and impact of the configuration of ground control points. *Drones*, *6*(2), 30. https://doi.org/10.3390/drones6020030

Mihai, D., & Marinescu, C. C. (2014). Creating the solid 3D model of a building using laser scanning technology. *Scientific Papers. Series E. Land Reclamation, Earth Observation & Surveying, Environmental Engineering*, *3*, 111–114.

Sîrbu, O., Vîlceanu, C.-B., Herban, S., Chendeș, R., & Pescari, S. (2023). 3D modeling for the spatial positioning and verticality of a cell tower. In *Proceedings of ICNAAM 2023. (Conference location and publisher can be added if known.)*

Stonex (n.d.). *Total stations*. Retrieved from https://www.stonex.it/total-stations/

Wang, Y., Li, J., Chen, P., & Zhang, X. (2024). Model-driven 3D reconstruction of communication towers using TLS point clouds. *International Journal of Digital Earth*, *17*(2), 236–251. https://doi.org/10.1080/17538947.2024.2366431

Scientific Papers. Series E. Land Reclamation, Earth Observation & Surveying, Environmental Engineering. Vol. XIV, 2025
Print ISSN 2285-6064, CD-ROM ISSN 2285-6072, Online ISSN 2393-5138, ISSN-L 2285-6064

FLOOD SUSCEPTIBILITY ASSESSMENT IN THE NERA RIVER BASIN USING GIS: IMPACTS ON LAND USE AND LAND COVER

Loredana COPĂCEAN[1], Luminiţa COJOCARIU[1, 2]

[1]University of Life Sciences "King Mihai I" from Timişoara,
119 Calea Aradului Street, 300645, Timişoara, Romania
[2]Agricultural Research and Development Station Lovrin,
200 Principala Street, 307250, Lovrin, Romania

Corresponding author email: luminita_cojocariu@usvt.ro

Abstract

Floods, rapid and destructive phenomena, significantly impact the environment, including agricultural lands. Geospatial methods for analysis, mapping, and monitoring have been developed over time to identify vulnerable areas. In this context, the present study applies a complex GIS model based on geospatial data, remote sensing data and the Analytic Hierarchy Process (AHP) to determine flood susceptibility in the Nera river basin, located in the southwest of Romania (Caraş-Severin County). The analysis includes nine factors: precipitation, drainage density, elevation, slope, distance to rivers, soils, topography, land use and land cover (LULC) and distance to roads. The results are synthesized into a susceptibility map, classified by risk levels and correlated with LULC to evaluate the impact on agriculture. Theoretically and practically, such models are essential for preventing and managing the effects of floods and for implementing optimal measures in line with sustainable development principles

Key words*: GIS models, flood susceptibility, watershed, impact, agricultural land.*

INTRODUCTION

Floods, destructive events with rapid occurrence, are among the most damaging hydro-geomorphological phenomena (Khosh et al., 2022). They result from the complex interaction of natural and anthropogenic factors, affecting the hydrological regime of river basins in various ways and proportions (Papaioannou et al., 2018; Syarifudin et al., 2022). These phenomena have significant effects on both the environment and society, causing loss of human lives, infrastructure damage, and public health issues, including the contamination of drinking water sources (Peker et al., 2024).

The impact of floods on agricultural land manifests through complex abiotic stress, affecting light availability, soil oxygenation, and nutrient cycling (Wang et al., 2022; Barneze et al., 2023). These changes alter soil properties and reduce fertility (Arabameri et al., 2020), negatively impacting plant growth and crop productivity (Bharadwaj et al., 2023).

To better understand and manage the impact of floods on agricultural land, the use of advanced hydrological risk modeling methods is essential. These methods have continuously evolved, enabling more precise identification of flood-prone areas.

Being dynamic and complex phenomena (Swain et al., 2020), floods are most effectively analyzed and mapped using geomatic techniques (Cai et al., 2021; Hagos et al., 2022; Covaci et al., 2023; Copăcean et al., 2025). Methods used for susceptibility assessment include Multi-Criteria Decision Analysis (MCDA) (Souissi et al., 2019) and the Analytic Hierarchy Process (AHP) (Chen et al., 2015), applied globally, including in river basins in Romania (Costache & Zaharia, 2017; Dragomir et al., 2020; Popescu & Bărbulescu, 2023). These methods contribute to identifying vulnerable areas and implementing measures to mitigate the effects on soil and agricultural crops.

In this context, the present study applies a complex spatial analysis model in a GIS environment, based on Multi-Criteria Decision Analysis (MCDA) and the Analytic Hierarchy Process (AHP), to identify flood-prone areas in the Nera River basin and assess their potential impact on agricultural land.

The main objectives include: (1) analyzing the physical-geographical conditions; (2) selecting

and evaluating relevant factors in flood occurrence; (3) creating thematic maps of the involved factors; (4) classifying the basin territory according to flood susceptibility, and (5) analyzing the impact of floods on agricultural land.

MATERIALS AND METHODS

Study area

The Nera River basin, covering 138,084 hectares, is located in southwestern Romania along the Serbian border (Figure 1)

It is bordered by the hydrographic basins of the Caraș, Cerna, and Danube rivers. The hydrographic network is well-defined, with the Nera river having numerous tributaries, whose sources are in the adjacent mountainous area.

The relief varies considerably, with altitudes ranging between 62 m and 1430 m (Figure 1), an aspect that is reflected in the geographical and hydrographic characteristics of the region (Simon et al., 2022) and, further, in hydrogeomorphological phenomena, water resource management strategies, and territorial planning (Posea & Badea, 1984; Rusu, 2007).

The shape of the Nera basin and the varied relief, with significant altitude differences, favor the rapid water concentration downstream, increasing the risk of floods, torrential erosion, and landslides, especially in areas with steep slopes and impermeable soils..

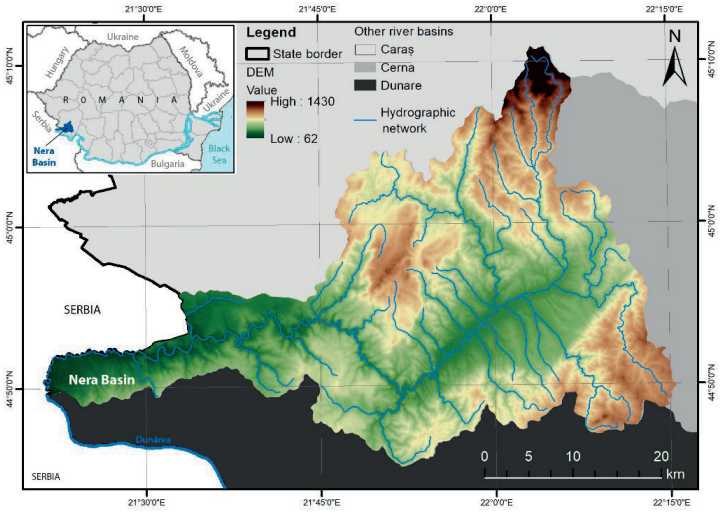


Figure 1. Study area location and Digital Elevation Model (DEM) (processing after EEA-DEM, 2016; Geospatial, 2021)

The working methodology

The methodology for assessing flood susceptibility in the Nera basin was adapted from the MCDA and AHP models applied through GIS, following the research conducted by Hammami et al. (2019), Swain et al. (2020), GIS and RS Solution and Copăcean et al. (2024). The analysis considered nine main factors in triggering and developing floods:

- ***Elevation Factor*** highlights the terrain relief and indicates the altitude and position of the land relative to the water level (Kumar et al., 2023). The Elevation factor map was derived from a Digital Elevation Model (DEM) with a spatial resolution of 25 m (EEA, 2016);

- ***Distance from River Factor*** shows that flood risk is high near rivers and decreases as their distance increases (Vegad et al., 2018). The river distance map was generated in ArcGIS using the Euclidean Distance tool applied to the vector hydrographic network (Geospatial, 2021);

- ***Topographic Wetness Index (TWI) Factor*** estimates soil moisture levels and areas of water accumulation (Kumar et al., 2023). TWI parameters were derived from DEM, and the TWI map was obtained by applying the relation $TWI = \ln(\alpha/\tan\beta)$ (Swain et al., 2020), where α represents the cumulative drainage area per unit contour length, and $\tan\beta$ is the slope at the contact point;

- ***Precipitation Factor***, essential in flood formation (Osman & Das, 2023), influences the susceptibility of the territory by increasing water input and potential runoff (Eriyagama et al., 2017; Kumar et al., 2023). The precipitation factor map was generated based on the amount of rainfall (mm) recorded at meteorological stations near the study area in 2022, a year that experienced significantly higher precipitation than the regional average (Climatic Databases, 2024). Data was integrated into GIS and geostatistically interpolated using the IDW (Inverse Distance Weighting) method;
- ***Slope Factor*** influences water runoff; on steep slopes, water drains quickly, reducing accumulation, whereas on flat or low-slope terrain, runoff is slower, favoring accumulation (Tehrany & Kumar, 2018). The slope map was generated from DEM and expressed in degrees;
- ***Drainage Density Factor*** indicates the development of the hydrographic network and is calculated as the ratio between its length and the drained area (Dube, 2018). Higher density implies a higher flood risk (Mitra & Das, 2022). In this study, the drainage density map (km/km²) was created using the Line Density tool in ArcGIS, based on the vector hydrographic network;
- ***Soil Type Factor*** influences water runoff and infiltration through its structure and texture. Clayey soils retain water on the surface, promoting accumulation, while sandy soils allow its infiltration (Anni et al., 2020). The map for this factor was created based on vector soil types (Geospatial, 2021), classified according to flood susceptibility and converted into raster format for analysis;
- ***Land Use/Land Cover (LULC) Factor*** affects water infiltration, runoff, and flood dynamics (Osman & Das, 2023). In the study area, the LULC map is based on Corine Land Cover 2018 (CLC, 2025) data, classified according to flood susceptibility. Forest areas have the lowest risk, while arable land has the highest. After reclassifying the vector data, the map was rasterized for cumulative analysis;
- ***Distance from Road Factor*** influences infiltration, as land near roads has reduced permeability, favoring water accumulation (Osman & Das, 2023). For the study area, the road distance map (m) was generated in ArcGIS using the Euclidean Distance tool applied to the vector road network (Geospatial, 2021).

The nine factors analyzed for assessing the flood susceptibility of the Nera basin were represented as raster maps with a resolution of 25 m, in the WGS 1984 system. Based on the specific values of the study area, they were reclassified into five susceptibility classes (Swain et al., 2020): very low, low, moderate, high, and very high.

To determine the value classes, the Natural Break method in ArcGIS was used, and the weight of each factor was determined using the AHP method (GIS and RS Solution, 2025). The final flood susceptibility map was obtained using the Weighted Overlay tool in ArcGIS, following specific workflow algorithms (ArcGIS Desktop Documentation, 2022). In the final analysis, the factors were weighted as follows: Elevation (m): 14%; Distance from River (m): 14%; TWI (dimensionless): 14%; Precipitation (mm/year): 13%; Slope (degrees): 12%; Drainage density (km/km²): 11%; Soil type: 8%; LULC: 8% and Distance from Road (m): 6%.

RESULTS AND DISCUSSIONS

A comprehensive assessment of flood susceptibility in the Nera Basin was conducted by analyzing nine key factors that influence hydrological risk. By examining these factors, it is possible to identify vulnerable areas and understand the mechanisms that determine the extent and intensity of floods.

The altitude factor influences the position of the terrain relative to the water level (Kumar et al., 2023), determining the direction of runoff and water accumulation, with low-lying areas, such as plains, being the most vulnerable to flooding (Hammami et al., 2019).

In terms of altitude, low-lying areas (61 - 335 m) along rivers in the Nera Basin (Figure 2) are the most susceptible to flooding, presenting the highest risk. Intermediate altitudes (336 - 550 m) remain vulnerable but with a lower risk, while transition zones (551-781 m) exhibit moderate susceptibility. In contrast, high-altitude regions (782-1430 m) have minimal risk due to rapid water runoff. An inverse relationship is observed between altitude and flood susceptibility, with low-lying terrains being the most exposed.

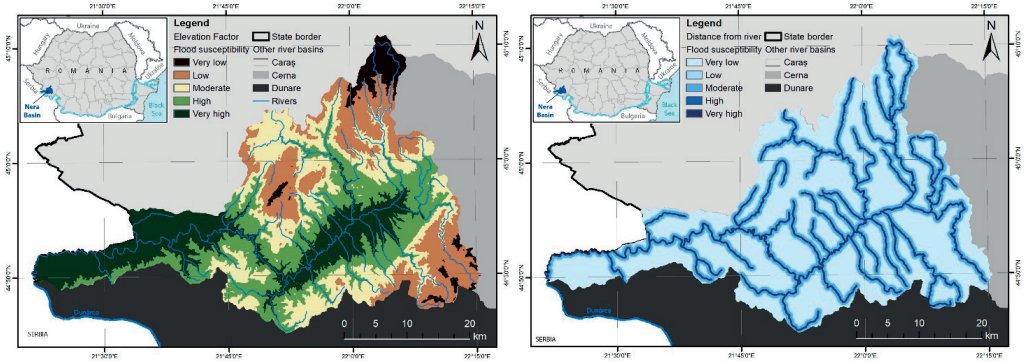


Figure 2. Susceptibility to flooding in the Nera basin based on the Elevation factor - m (left) and the Distance from rivers factor - m (right)

The distance from rivers factor (Figure 2) highlights a direct correlation between proximity to watercourses and flood risk (Vegad et al., 2018). Areas located within 0 - 100 m of rivers exhibit very high susceptibility, frequently experiencing flooding during rainy periods. Regions situated 101 - 150 m away have a high risk, those between 151 - 500 m face a moderate risk, while areas at 501 - 700 m show low susceptibility. Zones beyond 701 m are the least exposed to flooding.

The TWI (Topographic Wetness Index) factor reflects the terrain's tendency to accumulate and retain water (Kumar et al., 2023). In the analyzed area, areas with very high susceptibility (TWI 14.68-28.09) are found in valleys and depressions, where water naturally accumulates, presenting the highest flood risk. High susceptibility (TWI 10.21- 14.67) characterizes low-lying areas near rivers. Moderate susceptibility regions (TWI 7.32-10.20) are located in transitional zones, with partial water accumulation. Low and very low susceptibility (TWI 2.64-7.31) is specific to slopes and higher areas, where natural drainage reduces the flood risk (Figure 3).

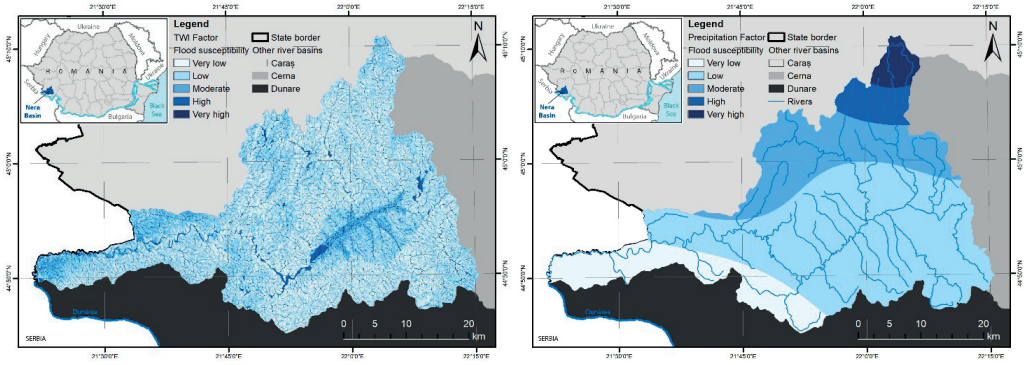


Figure 3. Susceptibility to flooding in the Nera basin based on the TWI factor (left) and the Precipitation factor - mm/year (right)

The precipitation factor plays a crucial role in triggering floods, influencing the land's susceptibility through increased water input and intensified surface runoff (Osman & Das, 2023). In the Nera basin, the distribution of flood risk varies depending on the amount of precipitation (Figure 3). Areas with very high susceptibility (1876-2261 mm) are located in the north, where precipitation is most abundant, significantly increasing flood risk, especially during rainy periods. High susceptibility regions (1562-1875 mm) extend toward the center, indicating a considerable risk. Moderate susceptibility areas (1353-1561 mm) are centrally located, where

precipitation levels are lower, reducing the probability of flooding. In the southern part of the basin, where precipitation is lower, areas with low susceptibility (1221-1352 mm) and very low susceptibility (1098-1220 mm) can be found.

The relationship between **terrain slope** and flood risk is inverse: areas with gentle slopes facilitate water accumulation and present a higher flood risk, whereas regions with steep slopes allow rapid water drainage, reducing vulnerability (Tehrany & Kumar, 2018).

In the Nera basin (Figure 4), areas with very high susceptibility (0-6.50°) are found in river floodplains and depressions, where water drains slowly and can stagnate, favoring floods. High susceptibility (6.51-12.76°) characterizes transitional areas, where the risk remains significant. Moderate susceptibility (12.77- 19.26°) is typical for steeper terrains, where water runoff is more efficient. Areas with low and very low susceptibility (19.27-64.05°) are located in hilly and mountainous regions, where water is rapidly evacuated, reducing the flood risk.

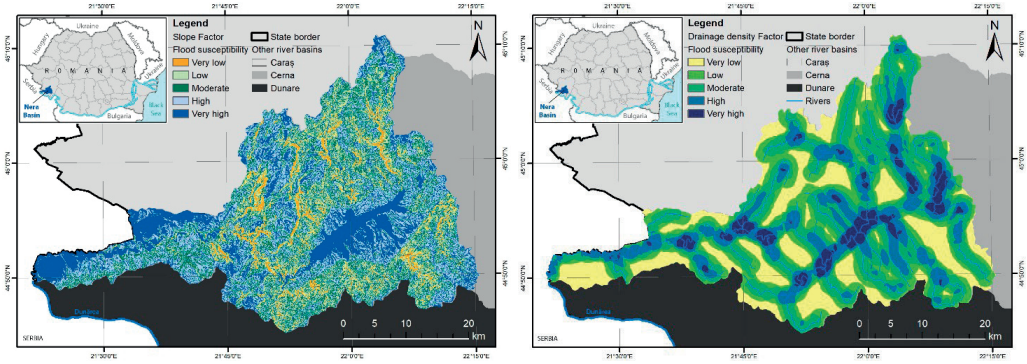


Figure 4. Susceptibility to flooding in the Nera basin based on the Slope factor - degrees (left) and the Drainage density factor - km/km² (right)

The drainage density reflects the degree of fragmentation of the hydrographic network and influences the land's capacity to evacuate water (Mitra & Das, 2022). Areas with high drainage density are more exposed to flooding as they collect and transport a large volume of water. Areas with very high susceptibility (0.78-1.22 km/km²) are located near major rivers and dense secondary watercourses, where water accumulation is frequent. High susceptibility (0.54-0.77 km/km²) extends along watercourses, indicating a significant but lower flood risk. Regions with moderate susceptibility (0.35-0.53 km/km²) are farther from rivers, with a lower risk of water accumulation.

Areas with low susceptibility (0.15-0.34 km/km²) and very low susceptibility (0-0.14 km/km²) are situated in regions with poorly developed drainage, where the probability of flooding is minimal (Figure 4).

The type of soil influences the degree of water infiltration and runoff, determining the flood risk level (Anni et al., 2020). Areas with very high susceptibility correspond to clay soils (Figure 5). These have very low permeability, favoring water accumulation and increasing the flood risk. Such soils are predominant in lowland areas and near rivers.

Regions with moderate susceptibility are associated with medium-textured soils. These allow partial water infiltration, reducing the flood risk compared to clay soils but still having limited drainage capacity. Areas with low susceptibility consist of sandy soils, which have high permeability, allowing rapid water infiltration and thus reducing the flood risk. These regions are less exposed to surface water accumulation.

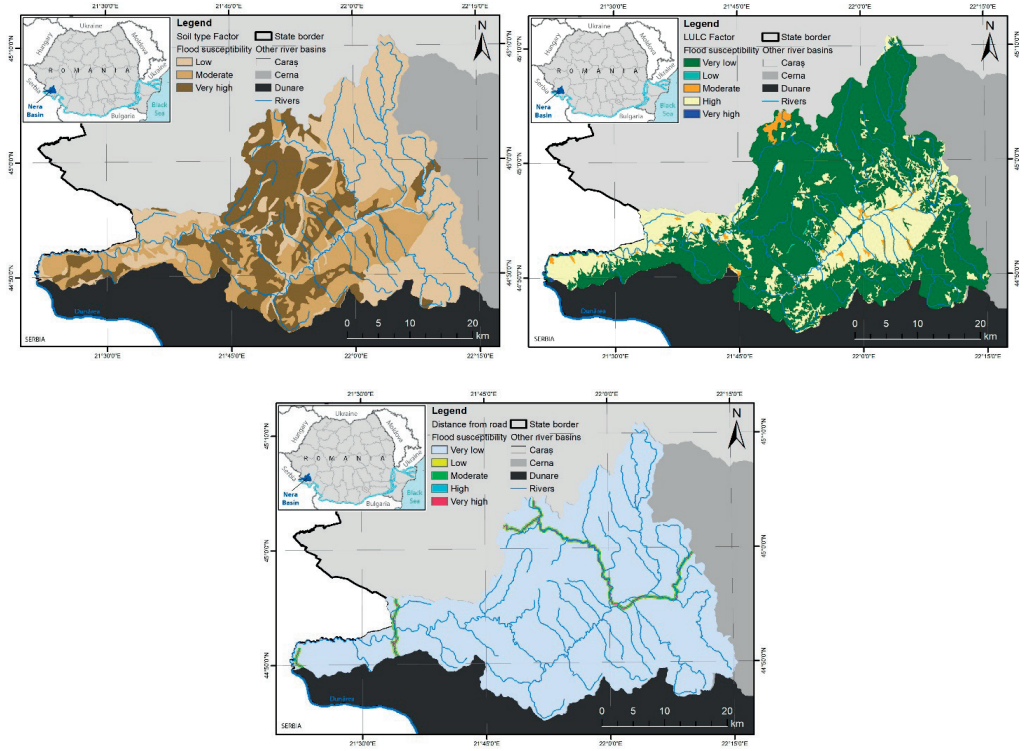


Figure 5. Susceptibility to flooding in the Nera basin based on the Soil Types factor (left), the Land Use/Land Cover factor (right), and the Distance to Roads factor - m (center)

LULC influence the water infiltration capacity, determining the degree of flood vulnerability (Osman & Das, 2023). Areas with very high susceptibility are those covered by water, where accumulation is permanent, presenting the highest flood risk (Figure 5). Agricultural lands, with low permeability, have high susceptibility, being exposed to flooding during periods of heavy rainfall. Built-up areas exhibit moderate susceptibility, as they reduce water infiltration and promote accumulation in the absence of adequate drainage. In contrast, areas covered by dense vegetation, especially forests, have very low susceptibility.

The Distance from Road (m) factor influences the water infiltration and accumulation capacity (Osman & Das, 2023). Areas with very high susceptibility (0-50 m) are located to the near roads (Figure 5). In these areas, the flood risk is at its maximum due to insufficient drainage or obstruction of natural runoff. Regions with high susceptibility (51-100 m) are also near roads, where the effect of water accumulation is significant but slightly less intense. Areas with moderate susceptibility (101-200 m) are situated at greater distances from roads and have a lower flood risk. Regions with low susceptibility (201-300 m) and very low susceptibility (>301 m) are located far from roads, where the terrain allows for better water infiltration and dispersion, reducing flood risk.

Based on the nine factors analyzed previously, a flood susceptibility map was generated, and by applying the Weighted Overlay Analysis (WOA) method, the final distribution of areas with different degrees of vulnerability was obtained (Figure 6).

The area with very low susceptibility represents only 441 ha, equivalent to 0.32% of the basin, indicating a minimal flood risk in these territories. The low susceptibility zone occupies the largest area of the basin, covering 72,356 ha, representing 52.4% of the total. This zone is predominantly located in regions less exposed to water accumulation. The moderate susceptibility zone covers 59,498 ha, or 43.1% of the basin. These regions lie in the transition between lowland and highland areas, presenting

a considerable flood risk. The high susceptibility zone extends over 5,784 ha (4.2%), being concentrated near watercourses, where water accumulation is frequent.

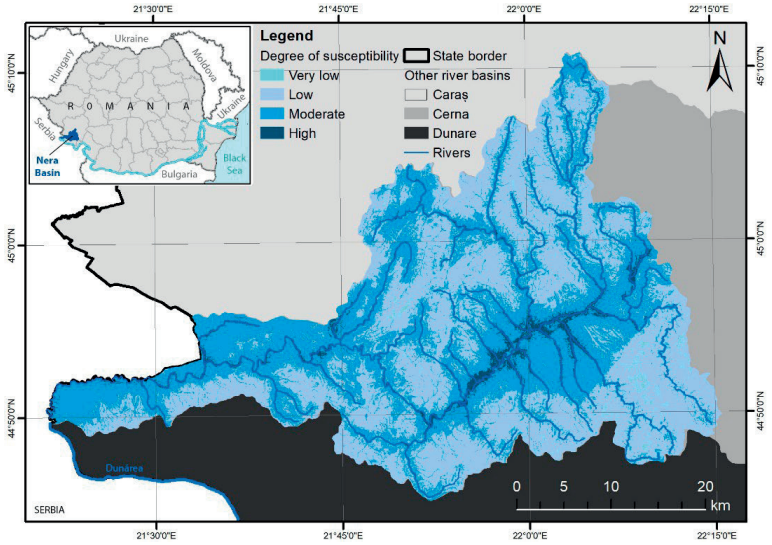


Figure 6. Flood susceptibility map in the Nera basin

The map in Figure 6 indicates a prevalence of low and moderate susceptibility classes, suggesting that most of the basin is not highly exposed to flooding. However, areas located near rivers require special preventive measures. The flood susceptibility analysis in the Nera basin provides a clear picture of the distribution of areas at hydrological risk (Figure 6). However, for a more detailed assessment of the effects of these phenomena, it is essential to examine and analyze the impact of floods, with varying intensities, on different types of LULC. Floods affect soil properties, agricultural fertility, and ecosystem functioning, with a significant impact on land use (Furtak & Wolińska, 2023; Rupngam & Messiga, 2024).

In the analyzed area, forests represent the most extensive type of land cover (Table 1), occupying 97,322 ha. Among these, 30,233 ha (31%) are exposed to moderate risk, while only 794 ha (0.8%) fall into the high-risk category, confirming the role of forests in reducing the impact of floods. Artificial areas (settlements, infrastructure) total 2,213 ha, with 1,954 ha (88.3%) classified under moderate and high susceptibility categories, indicating a significant vulnerability of urban infrastructure to flooding. Bare soils cover a very small area (86 ha) and are mainly affected by low or moderate susceptibility floods.

Table 1 The impact of floods on different types of LULC in the Nera River basin

LULC classes	Flood susceptibility degree (ha)				
	Very low	Low	Moderate	High	Total (ha)
Artificial surfaces	0	293	1543	411	2213
Forest areas	467	65828	30233	794	97322
Agricultural land	1	6087	27704	4635	38426
Bare soil	1	82	2	0	86
Total (ha)	469	72290	59485	5840	138084

Agricultural lands cover a total of 38,426 hectares, of which 32,339 hectares (84.2%) are classified as moderate or high susceptibility to flooding. Only 6,087 hectares (15.8%) are located in a low-risk area, indicating a limited percentage of agricultural land protected from

floods. Following flood events, arable lands are the most vulnerable, as nutrient losses and the accumulation of toxic metabolites reduce crop yields (Rupngam & Messiga, 2024). In the case of grasslands, flooding induces physiological stress on plants, which can lead to biodiversity loss (Căluşeru et al., 2013; Pedersen & Colmer, 2013). Additionally, soils may undergo structural changes, reducing drainage capacity and long-term fertility, which impacts vegetation regeneration and the use of land for agricultural or pastoral activities (Copăcean et al., 2020; Barneze et al., 2023).

CONCLUSIONS

The analysis of factors influencing flood susceptibility in the Nera basin has highlighted that elevation, distance from rivers, Topographic Wetness Index (TWI), precipitation, slope, drainage density, soil type, land use/land cover, and distance from roads play a crucial role in determining vulnerable areas. Factors related to terrain positioning and hydrological characteristics directly influence water accumulation and drainage. Low-lying areas close to watercourses with poorly permeable soils are the most exposed to flood risks.

The flood susceptibility map of the Nera basin, classified based on susceptibility levels, shows that most of the analyzed area falls into low and moderate susceptibility categories, covering over 95% of the total surface. However, approximately 4% of the territory is at high risk, concentrated in lowland areas along rivers where water accumulation is frequent. This underscores the importance of implementing prevention and risk management measures, particularly in regions vulnerable to flooding.

The impact of floods on LULC classes is significant, with agricultural lands being the most affected. Over 84% of these areas are in moderate and high susceptibility zones, making them vulnerable to nutrient loss, decreased productivity, and soil degradation.

Geomatic models, through the integration and analysis of spatial data, have proven to be essential tools in flood susceptibility assessment. These models enable detailed risk mapping and the identification of vulnerable areas, providing scientific support for decision-making regarding territorial planning and prevention measures. The application of GIS techniques and the Weighted Overlay Analysis method demonstrates the importance of multidisciplinary approaches in managing natural hazards, contributing to the development of effective strategies for reducing flood impact.

REFERENCES

Anni, A.H., Cohen, S., & Praskievicz, S. (2020). Sensitivity of urban flood simulations to stormwater infrastructure and soil in-filtration. *J Hydrol*, 588, https://doi.org/10.1016/j.jhydrol.2020.125028

Arabameri, A., Saha, S., Chen, W., Roy, J., Pradhan, B., & Bui, D.T. (2020). Flash flood susceptibility modelling using functional tree and hybrid ensemble techniques. *J. Hydrol*., 587, 125007. https://doi.org/10.1016/j.jhydrol.2020.125007

ArcGIS Desktop Documentation. (2022). ArcMap (Including ArcCatalog, ArcScene, ArcGlobe), https://desktop.arcgis.com/en/documentation/ (accessed on 15 June 2022)

Barneze, A.S., van Groenigen, J.W., Philippot, L., Bru, D., Abalos, D., & De Deyn, G.B. (2023). Plant communities can attenuate flooding induced N2O fluxes by altering nitrogen cycling microbial communities and plant nitrogen uptake. *Soil Biol. Biochem*., 185, 109142. https://doi.org/10.1016/j.soilbio.2023.109142

Bharadwaj, B., Mishegyan, A., Nagalingam, S., Guenther, A., Joshee, N., Sherman, S.H., & Basu, C. (2023). Physiological and genetic responses of lentil (*Lens culinaris*) under flood stress. *Plant Stress*, 7, 100130. https://doi.org/10.1016/j.stress.2023.100130

Cai, S., Fan, J., & Yang, W. (2021). Flooding Risk Assessment and Analysis Based on GIS and the TFN-AHP Method: A Case Study of Chongqing, China. *Atmosphere*, 12(5), 623. https://doi.org/10.3390/atmos12050623

Căluşeru, A.L., Cojocariu, L., Horablaga, M.N., Bordean, D-M., Horablaga, A., Cojocariu, A., Borozan A.B., & Iancu, T. (2013). Romanian National Strategy for the conservation of biodiversity 2013 – 2020 – integration of european environmental policies. *SGEM Conf Proceedings*, 2, 723-728. https://doi.org/10.5593/SGEM2013/BE5.V2/S23.013

Chen, J., Zhang, Y., Chen, Z., & Nie, Z. (2015). Improving assessment of groundwater sustainability with analytic hierarchy process and information entropy method: A case study of the Hohhot Plain, China. *Environ Earth Sci*, 73, 2353–2363. https://doi.org/10.1007/s12665-014-3583-0

Climatic Database. (2024). https://rp5.ru/Weather_in_Romania (accessed on 15.11.2024)

Copăcean, L., Cojocariu, L., Simon, M., Zisu, I., & Popescu, C. (2020). Geomatic techniques applied for remote determination of the hay quantity in agrosilvopastoral systems. *Present Environ. Sustain.*

Dev., 14, 89–101. https://doi.org/10.15551/pesd2020142006

Copăcean, L., Man, E.T., Herban, S., Popescu, C.A., & Cojocariu, L. (2024). Estimating flood susceptibility based on GIS and remote sensing. Case study: Hydrographic Basin of Crisul Alb river. *Present Environ. Sustain. Dev*., 18(1), 121-140. https://doi.org/10.47743/pesd2024181009

Copăcean, L., Man, E.T., Cojocariu, L.L., Popescu, C.A., Vîlceanu, C.-B., Beilicci, R., Creţan, A., Herbei, M.V., Cuzic, O.Ş., & Herban, S. (2025). GIS-Based Flood Assessment Using Hydraulic Modeling and Open Source Data: An Example of Application. *Appl. Sci*., 15, 2520. https://doi.org/10.3390/app15052520

Corine Land Cover - CLC (2025). Copernicus Land Monitoring Service. Available online: https://land.copernicus.eu/pan-european/corine-land-cover (accessed on 10.02 2025)

Costache, R., & Zaharia, L. (2017). Flash-flood potential assessment and mapping by integrating the weights-of-evidence and frequency ratio statistical methods in GIS environment - Case study: Bâsca Chiojdului River catchment (Romania). *J Earth Syst Sci*, 126, 59. https://doi.org/10.1007/s12040-017-0828-9

Covaci, O., Gazda, M.R., Niga, B.I., Enea, A., Iosub, M., & Tirnovan, A. (2023). Automation of the Rational Formula using GIS infrastructure - Case study Siret River Basin - Romania. *Present Environ. Sustain. Dev*, 17(2), 31-44. https://doi.org/10.47743/pesd2023172003

Dragomir, A., Tudorache, A-V., & Costache, R-D. (2020). Assessment of flash-flood susceptibility in small river basins. *Present Environ. Sustain. Dev*, 14(1), 119-130. https://doi.org/10.15551/pesd2020141010

Dube, M. (2018). Bihar Floods: A Report on Bihar Floods 2016; Bihar Disaster Management Authority, Government of Bihar: Patna, India; p. 36

Eriyagama, N., Thilakarathne, M., Tharuka, P., Munaweera, T., Muthuwatta, L., Smakhtin, V., Premachandra, W.W., Pindeniya, D., Wijayarathne, N.S., & Udamulla, L. (2017). Actual and perceived causes of flood risk: Climate versus anthropogenic effects in a wet zone catchment in Sri Lanka. *Water Int*, 42, 874–892, https://doi.org/10.1080/02508060.2017.1373321

European Environment Agency (EEA). (2016). Digital Elevation Model (DEM), https://www.eea.europa.eu/data-and-maps/data/copernicus-land-monitoring-service-eu-dem (accessed on 13.12.2016)

Furtak, K., & Wolińska, A. (2023). The impact of extreme weather events as a consequence of climate change on the soil moisture and on the quality of the soil environment and agriculture - A review. *Catena*, 231, 107378. https://doi.org/10.1016/j.catena.2023.107378

Geospatial. (2021). România: seturi de date vectoriale generale – http://geo-spatial.org/vechi/download/romania-seturi-vectoriale (accessed on 10.01.2021)

GIS & RS Solution. (2025). Flood Susceptibility Mapping using GIS-AHP Multi-criteria Analysis. Available online: https://www.youtube.com/watch?v=Lbbyi1YV2Hc&list=RDCMUCs1fLqqz84QbQ89DnRmMEVQ&index=1 (accessed on 10.02.2025)

Hagos, Y.G., Andualem, T.G., & Yibeltal, M. et al. (2022). Flood hazard assessment and mapping using GIS integrated with multi-criteria decision analysis in upper Awash River basin, Ethiopia. *Appl Water Sci*, 12, 148. https://doi.org/10.1007/s13201-022-01674-8

Hammami, S., Zouhri, L., & Souissi, D. et al. (2019). Application of the GIS based multi-criteria decision analysis and analytical hierarchy process (AHP) in the flood susceptibility mapping (Tunisia). *Arab J Geosci*, 12, 653. https://doi.org/10.1007/s12517-019-4754-9

Khosh Bin Ghomash, S., Bachmann, D., Caviedes-Voullième, D., & Hinz, C. (2022). Impact of Rainfall Movement on Flash Flood Response: A Synthetic Study of a Semi-Arid Mountainous Catchment. *Water*, 14, 1844. https://doi.org/10.3390/w14121844

Kumar, R., Kumar, M., Tiwari, A., Majid, S.I., Bhadwal, S., Sahu, N., & Avtar, R. (2023). Assessment and Mapping of Riverine Flood Susceptibility (RFS) in India through Coupled Multicriteria Decision Making Models and Geospatial Techniques. *Water*, 15, 3918. https://doi.org/10.3390/w15223918

Mitra, R., & Das, J. (2022). A comparative assessment of flood susceptibility modelling of GIS-based TOPSIS, VIKOR, and EDAS techniques in the sub-himalayan foothills region of Eastern India. *Environ Sci Pollut Res*, 30, 16036–16067. https://doi.org/10.1007/s11356-022-23168-5

Osman, S.A., & Das, J. (2023). GIS-based flood risk assessment using multi-criteria decision analysis of Shebelle River Basin in southern Somalia. SN *Appl Sci*, 5, 134. https://doi.org/10.1007/s42452-023-05360-5

Papaioannou, G., Efstratiadis, A., Vasiliades, L., Loukas, A., Papalexiou, S.M., Koukouvinos, A., Tsoukalas, I., & Kossieris, P. (2018). An operational method for flood directive implementation in ungauged urban areas. *Hydrology*, 5, 24. https://doi.org/10.3390/hydrology5020024

Pedersen, O., & Colmer, T.D., (2013). Sand-Jensen, K. Underwater photosynthesis of submerged plants - recent advances and methods. Front. *Plant Sci*., 4, 140. https://doi.org/10.3389/fpls.2013.00140

Peker, İ.B., Gülbaz, S., Demir, V., Orhan, O., & Beden, N. (2024). Integration of HEC-RAS and HEC-HMS with GIS in Flood Modeling and Flood Hazard Mapping. *Sustainability*, 16, 1226. https://doi.org/10.3390/su16031226

Popescu, N.C., & Bărbulescu, A. (2023). Flood Hazard Evaluation Using a Flood Potential Index. *Water,* 15, 3533. https://doi.org/10.3390/w15203533

Posea, G., & Badea, L. (1984). România. *Unităţile de relief (Regionarea geomorfologică),* Ed. Ştiinţifică şi Enciclopedică, Bucureşti

Rupngam, T., & Messiga, A.J. (2024). Unraveling the Interactions between Flooding Dynamics and Agricultural Productivity in a Changing Climate. *Sustainability*, 16, 6141. https://doi.org/10.3390/su16146141

Rusu, R. (2007). *Organizarea spaţiului geografic în Banat*, Ed. Mirton, Timişoara.

Simon, M., Copăcean, L., & Cojocariu, L. (2022). Techniques for identification, mapping and analysis of grasslands. Case study: Arad county. *PESD, 16*(2), 39-49. https://doi.org/10.47743/pesd2022162004

Souissi, D., Zouhri, L., Hammami, S., Msaddek, M.H., Zghibi, A., & Dlala, M. (2019). GIS-based MCDM-AHP modeling for flood susceptibility mapping of arid areas, southeastern Tunisia. *Geocarto Int*, 35, 991–1017. https://doi.org/10.1080/10106049.2019.1566405

Swain, K.C., Singha, C., & Nayak, L. (2020). Flood Susceptibility Mapping through the GIS-AHP Technique Using the Cloud. *ISPRS Int J Geo-Inf*, 9, 720. https://doi.org/10.3390/ijgi9120720

Syarifudin, A., Satyanaga, A., & Destania, H.R. (2022). Application of the HEC-RAS Program in the Simulation of the Streamflow Hydrograph for Air Lakitan Watershed. *Water*, 14, 4094. https://doi.org/10.3390/w14244094

Tehrany, M.S., & Kumar, L. (2018). The application of a Dempster–Shafer-based evidential belief function in flood susceptibility mapping and comparison with frequency ratio and logistic regression methods. *Environ Earth Sci*, 77, 490. https://doi.org/10.1007/s12665-018-7667-0

Vegad, U., Pokhrel, Y., Mishra, V., Ghosh, A., & Kar, S.K. (2018). Application of analytical hierarchy process (AHP) for flood risk assessment: A case study in Malda district of West Bengal, India. *Hydrol. Earth Syst Sci Discuss*, 94, 349–368. https://doi.org/10.1007/s11069-018-3392-y

Wang, X., Liu, Z., & Chen, H. (2022). Investigating Flood Impact on Crop Production under a Comprehensive and Spatially Explicit Risk Evaluation Framework. *Agriculture,* 12, 484. https://doi.org/10.3390/agriculture12040484

Scientific Papers. Series E. Land Reclamation, Earth Observation & Surveying, Environmental Engineering. Vol. XIV, 2025
Print ISSN 2285-6064, CD-ROM ISSN 2285-6072, Online ISSN 2393-5138, ISSN-L 2285-6064

ADVANCING CADASTRAL UPDATES AND GIS SPATIAL ANALYSIS FOR FORESTED AREAS

Iulia COROIAN[1], Silvia CHIOREAN[1], Rodica SOBOLU[1], Diana FICIOR[1], Paul SESTRAS[1, 2], Luca-Pavel RUS[1], Catalin-Stefanel SABOU[1], Luisa ANDRONIE[1]

[1]University of Agricultural Sciences and Veterinary Medicine Cluj-Napoca, 3-5 Calea Mănăștur Street, 400372, Cluj-Napoca, Romania
[2]Academy of Romanian Scientists, 3 Ilfov Street, District 5, 060044, Bucharest, Romania

Corresponding author emails: silvia.chiorean@usamvcluj.ro, diana.ficior@usamvcluj.ro

Abstract

This article explores innovative approaches to improving cadastral systems and utilizing Geographic Information System (GIS) tools for forest management. It emphasizes the importance of accurate and up-to-date cadastral records to support sustainable forest management, land ownership clarity, and environmental preservation. The study outlines methodologies for integrating cadastral updates with advanced GIS spatial analysis techniques, enabling the efficient mapping and monitoring of forested areas. Key applications include assessing land use changes, detecting illegal activities, and planning conservation efforts. The research highlights how GIS tools enhance spatial data visualization, offering insights into forest density, composition, and land-use dynamics. By analysing case studies from forested regions, the article demonstrates practical implementations and benefits, including improved decision-making for policymakers, forest managers and environmental stakeholders. The integration of cadastral updates and GIS-based analysis represents a significant step toward ensuring the sustainable management of forested areas, balancing ecological protection with economic and social considerations.

Key words*: forested area, GIS, cadastral updates.*

INTRODUCTION

Given the rapid growth of the global population, land emerges as a critical resource requiring strategic management. In this context, ensuring legal assessment, clear definition, and accurate registration of real estate is essential - especially when advancing cadastral updates and GIS spatial analysis for forested areas, where precise land delineation supports sustainable planning and resource protection (Chiorean et al., 2024). The Geographic Information System (GIS) is a contemporary tool widely applied across various domains for managing both attribute and spatial data, including demographic information, playing a vital role in advancing cadastral updates and spatial analysis for forested areas by enabling precise mapping, monitoring, and informed decision-making.

The primary objective of this study is to develop updated cadastral documentation for a land parcel within the Administrative-Territorial Unit (ATU) Telciu and to conduct a spatial analysis within a Geographic Information System (GIS) framework. The spatial and raster analyses focus on evaluating the forested area and timber volume, encompassing a precise assessment of forest extent, species composition, and available timber resources. To achieve this, an accurate delineation of property and forest boundaries was performed using advanced measurement techniques and high-precision GPS equipment, ensuring a clear and reliable definition of land contours. Additionally, a photogrammetric flight was conducted to obtain high-resolution imagery of the terrain. The data acquired through photogrammetric processing in Agisoft Metashape has been integrated into ArcGIS Pro for in-depth spatial analysis. The results are to be disseminated via ArcGIS Online, enabling interactive visualization and efficient data sharing with both stakeholders and the broader public. This approach enhances the accessibility and interpretability of geospatial information. Ultimately, the study is set to result in the development of accurate and up-to-date cadastral documentation, incorporating all

analyzed and processed data. This documentation comprises detailed cadastral maps and technical reports, prepared in accordance with current regulations and standards, thereby ensuring precise property registration and long-term availability of data for land management and administrative purposes.

The inherent nature of agricultural activities means that risks and uncertainties are a constant presence in agricultural value chains. Therefore, it is crucial for decision support models in farming to incorporate risk management metrics and strategies. This becomes particularly relevant in the context of advancing cadastral updates and GIS spatial analysis for forested areas, where accurate spatial data and land parcel information can significantly enhance risk assessment and support more resilient decision-making in forest-related agricultural systems.

MATERIALS AND METHODS

Telciu is located in Bistrița-Năsăud County, in the Transylvania region of Romania. The locality is situated at coordinates 47°24'N 24°53'E and covers an area of 291.42 km². It is traversed by two rivers, Sălăuța and Telcișor, which originate from the Rodna and Țibleș Mountains. The commune of Telciu consists of the villages of Telciu, Fiad, Telcișor, and Bichigiu. It borders the localities of Romuli, Dragomirești (Maramureș), Rebra, Rebrișoara, Coșbuc, Runcu Salvei (Salva), Suplai, and Zagra (Figure 1).

The initial phase of the study involved defining the study area, with a specific focus on the targeted forest (Figure 2).

Data processing was conducted using ArcGIS Pro and ArcGIS Online, ensuring the integration and standardization of all raster and vector datasets. These datasets were harmonized in terms of spatial resolution, coordinate reference system (Stereographic 1970, Romania's national projection system), and the extent of the study area. The Digital Elevation Model (DEM) and Digital Surface Model (DSM) were utilized to generate thematic maps representing slope, aspect, curvature, and hill shade, which provided a detailed understanding of the terrain characteristics. The results were synthesized through spatial analysis, facilitating the classification of the study area, forest structure assessment, and the evaluation of tree volume and height.

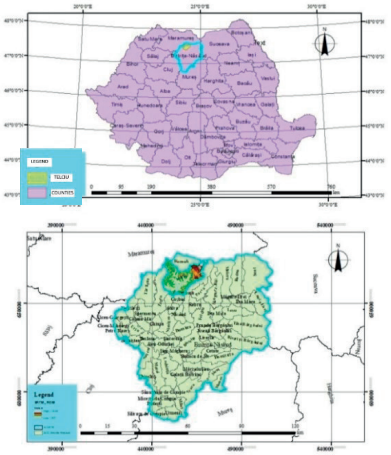


Figure 1. Macrolocalization of Bistrița-Năsăud County

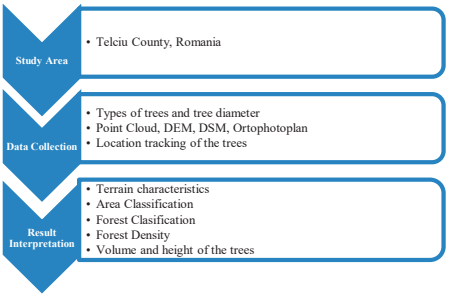


Figure 2. Research methodology

For the study of the proposed objective, the following equipment and instruments were used to conduct field measurements, delineate and map the forest, and inventory the trees: GPS V200, DJI MAVIC 3M drone, forestry calliper, and forestry measuring tape. Additionally, various specialized software tools were employed to ensure the collection, processing, and analysis of the data required for forest evaluation. For effective forest management, ArcGIS Online was utilized: a secure cloud-based platform for mapping and spatial analysis, provided as a software-as-a-service solution. This platform enables organizations to leverage geospatial insights through its scalable and resilient technology, supporting the collection, management, and analysis of geospatial data. By facilitating data-driven decision-making,

ArcGIS Online allows for seamless sharing of maps and applications. With a configurable sharing model and a wide range of integrated applications and analytical tools, the platform enhances collaboration and efficiency among users.

RESULTS AND DISCUSSIONS

As part of the cadastral documentation preparation, a property data update file was compiled, encompassing operations such as boundary and area modifications, land use category updates, and corrections to other critical property information. These procedures require the submission of specific supporting documents and may involve multiple types of technical updates simultaneously. The resolution of such requests is conducted while preserving the area determined through measurements as recorded in the land registers, thereby ensuring the accuracy and currency of cadastral data. The reception and registration request form is intended to facilitate the update of cadastral information, including revisions to land use classifications and parcel identifiers. The approved updates are subsequently integrated into the national cadastral and land registration system. The property is not subject to litigation/is subject to litigation with the property ID [property ID], case number [case number], court [name of the court], subject [subject of the dispute].

After updating the land use categories, the property located in the outskirts of Telciu, Bistrița-Năsăud County, is described as follows: it consists of three distinct parcels. Parcel 1 has an area of 4,944 sqm and is classified as PD (forest). Parcel 2 has an area of 8,027 sqm and is classified as F (hayfield). Parcel 3 has an area of 2,522 sqm and is also classified as PD (forest). Following the update process, the total measured area of the property remains 15,495 square meters, as illustrated in Figure 3. In the absence of leaves, flowers, and fruits, species identification relies primarily on the morphological characteristics of bark and branches. During the winter season, features such as bark texture, color, and pattern serve as key diagnostic traits for differentiating between species (Figure 4; Mikita et al., 2016).

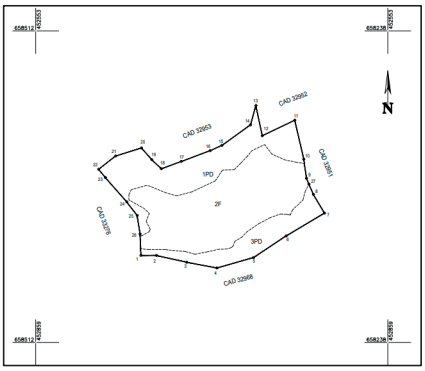


Figure 3. Delimitation Plan after Update



Figure 4. Types of trees



Figure 5. Determination of tree diameter

Figure 5 presents the methodology and equipment utilized for measuring tree diameter, employing the traditional approach. This method involves the use of a specialized forestry instrument, the caliper, to obtain precise diameter measurements. In the context of tree height measurement, the described method utilizing a forestry tape requires ascending the tallest tree to obtain a direct measurement, which serves as a reference for estimating the height of other trees. While this approach can provide practical and accurate results, it presents considerable safety risks due to the necessity of climbing tall trees. To enhance both accuracy and safety, tree height was determined using

data derived from photogrammetric processing (Figure 6) (Meng et al., 2019).

To conduct the planned study, a photogrammetric flight was performed using the DJI Phantom 4 RTK drone. This drone is widely utilized for photogrammetric applications due to its high-resolution camera and integrated sensors, which collectively ensure superior imaging performance. The advanced technology incorporated in this drone enables data acquisition with centimetre-level accuracy, eliminating the necessity for additional ground control points. Equipped with an integrated RTK module, the drone provides real-time positioning data, ensuring absolute geo-tagging of the captured images. Additionally, to optimize flight safety and enhance data precision, the DJI Phantom 4 RTK records satellite observation data, which can be post-processed (PPK) (Risna et al., 2023). The photogrammetric data was processed using Agisoft Metashape software, involving the reconstruction of previously acquired images to generate a dense point cloud (Soubry et al. 2021).

Figure 6 illustrates the resulting 3D model/point cloud, which consists of a set of data points within a three-dimensional coordinate system (X, Y, Z axes). Each point corresponds to a precise spatial measurement on the surface of the object (Coroian et al., 2021).

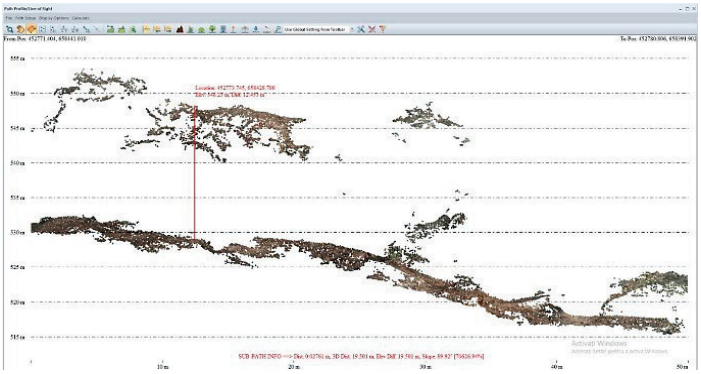


Figure 6. Point Cloud of the terrain

In contrast, Figure 7 illustrates a more efficient and safer approach for measuring tree height by utilizing Point Cloud technology. This method leverages photogrammetrically acquired data to generate an accurate three-dimensional model of the studied area, enabling precise height measurements (Zlinszky et al., 2015).

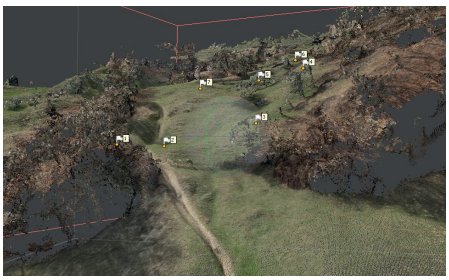


Figure 7. Point Cloud

Figure 8 presents the orthophoto map, an aerial image that has been geometrically corrected to remove distortions caused by aircraft tilt during image acquisition, variations in photogrammetric scale, and topographic relief differences (Qiu et al., 2018).



Figure 8. Ortophotomap

For the forest monitoring system, a technology was employed that enables real-time tree localization and tracking using ArcGis Online (Figure 9) (Boroushaki et al., 2010).
Utilizing a mobile device, the precise position of each tree is determined with centimetre-level accuracy through integrated GPS technology. During field data collection, trees are documented through photographs and videos captured with the mobile device's camera, ensuring a comprehensive visual record for identification and assessment (Brovelli et al., 2016). Additionally, a digital field notebook is used to record essential attributes for each tree, including species, diameter, height, and volume (Li et al., 2011).

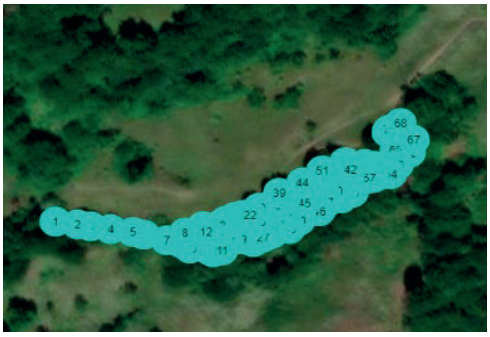


Figure 9. Real-time location tracking

Table 1 presents the classification of the study area, which has been categorized into three distinct land types: Upper Forest, Lower Forest, and Meadow (Figure 10). The Upper Forest covers 4,944.47 square meters, making up 32% of the total land area. The Lower Forest occupies 2,522.89 square meters, which constitutes 16% of the total. The Meadow extends over 8,027.37 square meters, accounting for the remaining 52%. Altogether, these areas sum to a total of 15,495 square meters.

Table 1. The classification of the area

Land use category	**Area**
The Upper Forest	4944 (32%)
The Lower Forest	2523 (16%)
Meadow	8027 (52%)
Total Area	15495



Figure 10. Thematic Map for area classification

Using the data presented in the Tables 2 and 3, a direct comparison can be made between the upper and lower forest in terms of species diversity and tree abundance. The upper forest comprises four tree species beech, hornbeam, maple, and willow while the lower forest contains only three species: beech, maple, and willow. Additionally, differences are observed in the number of trees per species. The upper forest consists of 48 beech trees, 39 hornbeams, 12 maples, and 2 willows, amounting to a total of 101 trees (Table 2). In contrast, the lower forest contains 45 beech trees, 16 maples, and 11 willows, summing up to 72 trees (Table 3) (Cammerino et al., 2023).

Table 2. The Upper Forest Classification

The Upper Forest	**Area**
Beech	48 (48%)
Hornbeam	39 (39%)
Maple	12 (12%)
Willow	2 (2%)
Total	101

Table 3. The Lower Forest Classification

The Lower Forest	**Area**
Beech	45 (63%)
Maple	16 (22%)
Willow	11 (15%)
Total	72

Figure 11 presents the forest classification, in which four tree species have been identified: beech, hornbeam, willow, and maple.

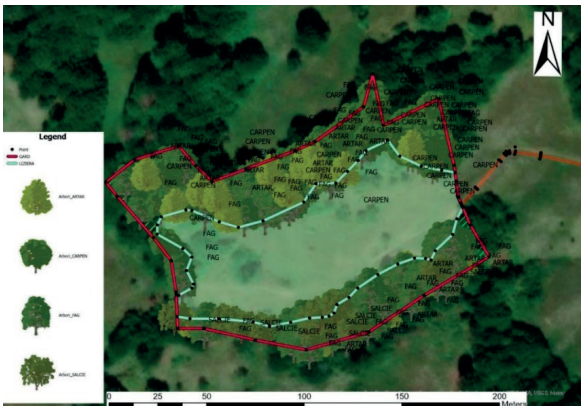


Figure 11. Thematic Map for forest classification

In assessing forest density, the analysis was conducted based on the volume of each tree species. Figure 12 visually represents forest density using a color-coded classification, as indicated in the legend. Areas with high tree density, where trees are closely spaced and create a shaded environment, are depicted in yellow. Conversely, regions with low tree density, characterized by widely spaced trees and a more open landscape, are represented in gray blue. This colour differentiation facilitates a rapid and clear interpretation of the spatial distribution of tree density within the forest. Identifying areas of higher density enables the planning of thinning operations to promote the optimal growth and diameter expansion of the remaining trees (Chakhar et al., 2008).

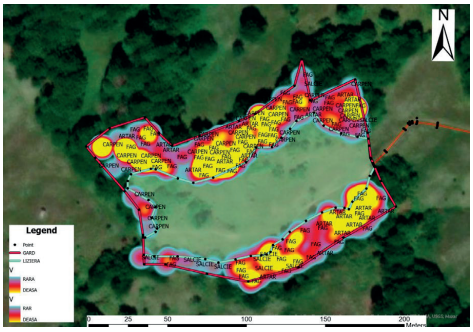


Figure 12. Thematic Map for forest density classification

Using the graphs presented in Figure 13 and Figure 14, a comparative analysis of the timber volume between the Upper Forest and the Lower Forest was conducted. The volume was calculated based on Huber's Theory, allowing for an objective assessment of the differences in timber mass between the two forest areas.

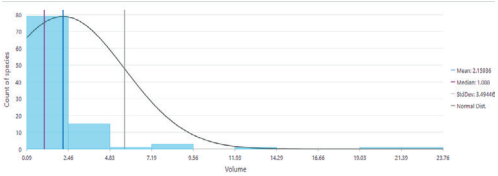


Figure 13. Volume of Upper Forest

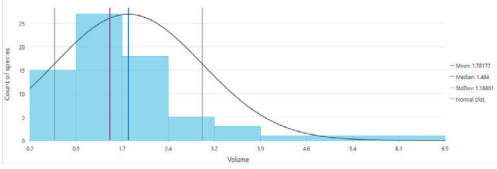


Figure 14. Volume of Lower Forest

In the Upper Forest, the predominant timber volume ranges from 0.09 m³ to 2.46 m³, encompassing most tree species, with a total of 79 trees within this range. Conversely, in the Lower Forest, the dominant volume falls between 1.1 m³ and 1.5 m³, with 19 trees recorded in this interval.

Additional comparisons, displayed on the right side of each graph, include the mean and standard deviation. These statistical indicators provide further insights into the distribution of timber volumes, highlighting differences in variability and central tendencies between the two forest areas.

Figure 15 represents the tree heights in both the upper and lower forests. As shown in the legend, the heights are categorized into five distinct

ranges, each represented by a specific colour: white for trees ranging from 10 to 14 meters, green for those between 15 and 18 meters, light blue for trees between 19 and 21 meters, blue for heights between 22 and 26 meters, and dark blue for towering trees measuring between 26 and 30 meters. This color-coded classification offers a clear and visually informative representation of the variation in tree heights across the two forests (Sestras et al., 2019).



Figure 15. Thematic Map for tree height classification

Using the graphs provided below (Figure 16 and Figure 17), a direct comparison can be made between the Upper Forest and the Lower Forest with respect to tree heights, categorized into five distinct classes.

Further comparisons are provided through the mean values and standard deviations, offering additional insights into the distribution of tree heights in both forests and emphasizing the differences in variability and central tendencies between the Upper Forest and the Lower Forest (Felicisimo et al., 2002). Figure 18 illustrates the tree diameters in both the Upper and Lower Forests. According to the legend: in the Upper Forest, tree diameters range from 0.10 meters to 1.1 meters, with a gradual colour transition from white to dark green and in the Lower Forest, tree diameters range from 0.16 meters to 0.58 meters, following a similar colour progression from white to dark green. This color-coded representation emphasizes the variation in three sizes across both forests, offering a clear and visually informative view of their structural composition (Curovic et al., 2020).

Using the graphs from Figure 19 and Figure 20, a direct comparison can be made between the central tendencies of diameter distributions in the Upper and Lower Forests. In the Upper Forest, the most common diameter range is between 0.1 meters and 0.3 meters, encompassing 69 trees. In contrast, in the Lower Forest, the predominant diameter range is between 0.24 meters and 0.33 meters, with 31 trees within this range. Additional comparisons, including mean values and standard deviations, offer further insights into the distribution of tree diameters in both forests.

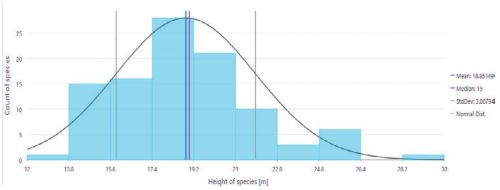


Figure 16. Tree Height in the Upper Forest

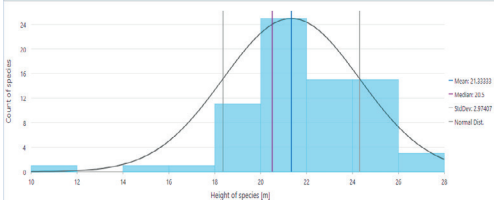


Figure 17. Tree Height in the Lower Forest



Figure 18. Thematic Map for Tree Diameter Classification

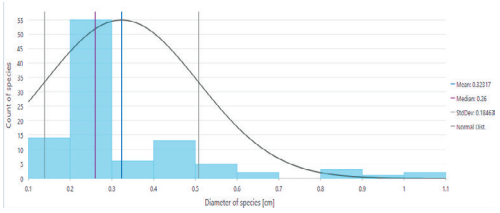


Figure 19. Diameter of the Upper Forest

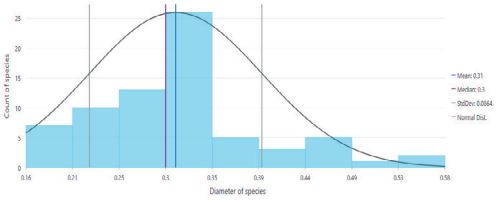


Figure 20. Diameter of the Lower Forest

Figure 21 presents the Digital Elevation Model (DEM), which offers detailed information exclusively about the terrain. This DEM is critical for understanding the area's topography. According to the legend, the elevation difference spans 255 meters, from the lowest to the highest point. This substantial variation in elevation is fundamental for various geospatial analyses and can impact a range of applications, from infrastructure planning to natural resource management.

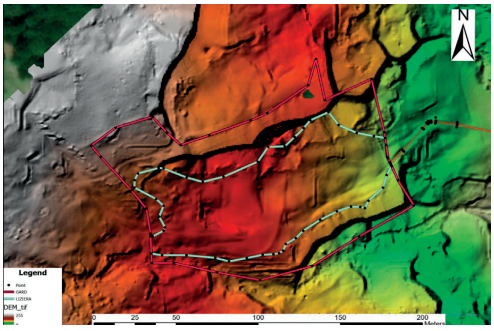


Figure 21. DEM - Digital Elevation Model

Figure 22 presents the Digital Surface Model (DSM), which depicts the elevations of all surface features within the terrain. Unlike the Digital Elevation Model (DEM), the DSM incorporates not only the ground level but also the heights of structures such as buildings, trees, and other forms of vegetation.

The DSM essentially captures all surface elements, providing a comprehensive and detailed representation of the topography and all objects located above the ground.

It offers valuable insights into the canopy structure, including its height and density. These models are particularly useful for monitoring temporal changes, such as deforestation, reforestation, and forest health.

Figure 23 illustrates the aspect, which indicates the orientation of slope exposure. This information is essential for planning future afforestation efforts, as it influences microclimatic conditions, soil moisture distribution, and species selection (Pasqualini et al., 2011).

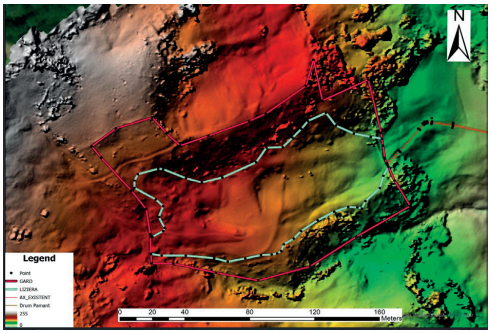


Figure 22. DSM - Digital Surface Model

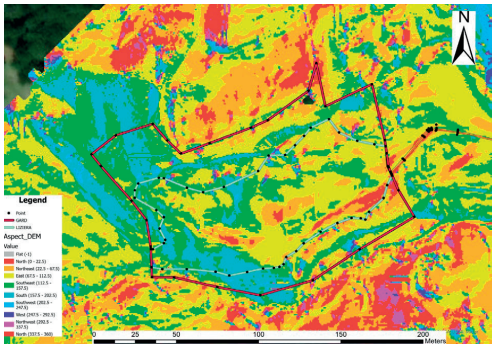


Figure 23. Aspect

Figure 24 presents the Curvature tool, which facilitates the analysis of landforms and geological processes. This tool is instrumental in land use planning, natural resource management, and environmental studies. By utilizing curvature analysis, a detailed assessment of terrain morphology can be conducted, providing essential data for various geological and environmental applications.

Figure 25 presents the HillShade tool, which generates a shaded relief raster from a surface raster by simulating the effects of a light source and shadow formation. This tool assumes a distant light source to create a realistic terrain representation. The resulting raster contains integer values ranging from 0 to 255, indicating the intensity of light and shadow distribution across the terrain, enhancing the visualization of topographic features.

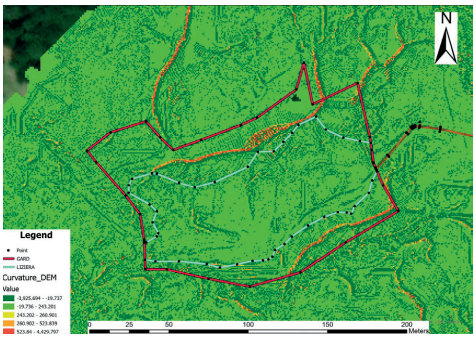


Figure 24. Curvature

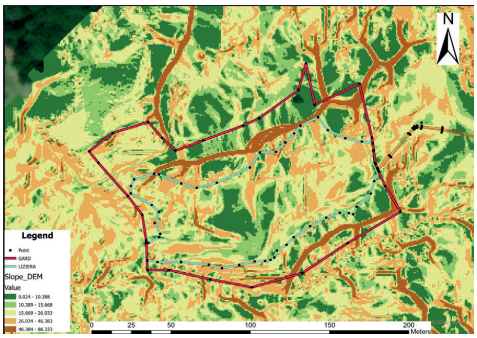


Figure 26. The terrain slope

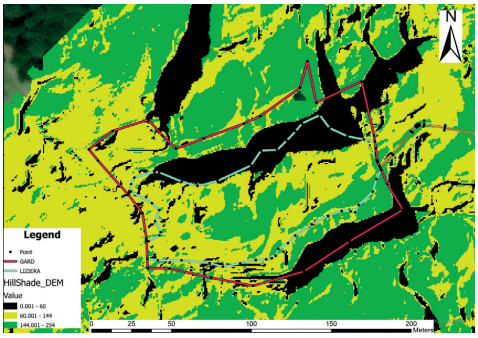


Figure 25. HillShade

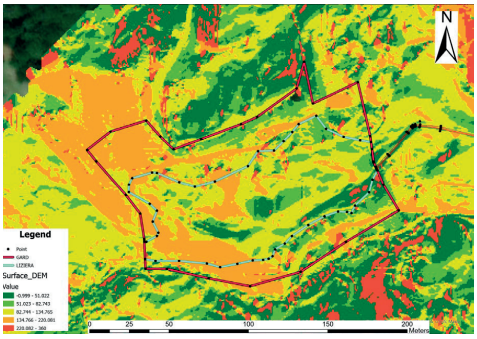


Figure 27. Surface parameters aspect

Figure 26 illustrates the terrain slope. According to the legend, the slope is categorized into five classes based on degrees of inclination. The green range represents slopes between 0 and 11 degrees, while the brown range corresponds to slopes between 47 and 87 degrees.

The Surface Parameters tool in ArcGIS Pro is a key resource for analyzing raster surface characteristics, including aspect, slope, and curvature. These parameters provide crucial information about terrain orientation and inclination across different locations. For example, the aspect defines the direction of the terrain slope and is classified into five categories, expressed in degrees, as indicated in the Surface result legend.

Figure 27 illustrates the natural risk assessment, which supports informed decision-making and strategy development. Areas highlighted in red represent risk zones located outside the studied terrain but requiring stabilization measures, such as planting deep-rooted trees to enhance slope stability.

CONCLUSIONS

The integration of advanced software tools, GPS technology, and traditional forestry methods enabled precise delineation of property and forest boundaries, ensuring accurate measurements and mapping. Modern inventory technologies, including mobile applications, specialized forestry tools, and Point Cloud technology, facilitated an efficient and secure assessment of forest resources.

By utilizing ArcGIS Online and smartphone-based geolocation, a detailed forest inventory was created, documenting essential attributes such as species, diameter, height, and volume. Photogrammetric flights and subsequent data processing yielded high-precision results, contributing to effective land and forest management. Geospatial analyses provided key topographic insights: the Digital Elevation Model (DEM) revealed a 255-meter elevation difference between the lowest and highest points, the Digital Surface Model (DSM) captured terrain objects such as buildings and vegetation, aiding in monitoring deforestation,

reforestation, and forest health, aspect analysis provided slope exposure data, supporting afforestation and land management planning, contour lines illustrated terrain relief, while curvature analysis enhanced the understanding of landforms and geological processes, slope classification divided the terrain into five categories based on incline, aiding in landscape and the Surface Parameters tool in ArcGIS Pro enabled the evaluation of aspect, slope, and curvature, offering essential data for environmental and resource management applications.

These comprehensive assessments support sustainable forestry practices, informed decision-making, and effective land use planning.

ACKNOWLEDGEMENTS

This research was carried out with the support of the Ministry of Education and was financed through the CNFIS-FDI-2024-F-0195 project, funded by the National Council for Financing Higher Education (CNFIS).

REFERENCES

Boroushaki, S., & Malczewski, J. (2010). A WebGIS-based collaborative multicriteria decision analysis. *Journal of the Urban and Regional Information Systems Association, 22*(1), 23–32.

Brovelli, M. A., Minghini, M., & Zamboni, G. (2016). Public participation in GIS via mobile applications. *ISPRS Journal of Photogrammetry and Remote Sensing, 114*, 306–315. https://doi.org/10.1016/j.isprsjprs.2015.06.008

Cammerino, A. R. B., Ingaramo, M., Piacquadio, L., & Monteleone, M. (2023). Assessing and mapping forest functions through a GIS-based, multi-criteria approach as a participative planning tool: An application analysis. *Forests, 14*(1), Article 1. https://doi.org/10.3390/f14010001

Chakhar, S., & Mousseau, V. (2008). GIS-based multicriteria spatial modelling generic framework. *International Journal of Geographical Information Science, 22*(11–12), 1159–1196. https://doi.org/10.1080/13658810701739099

Chiorean, S., Coroian, I., Sălăgean, T., Nap, M. E., Deak, J., & Lupuț, I. (2024). Global trends on research towards the valuation process of agricultural land. *Scientific Papers Series Management, Economic Engineering in Agriculture & Rural Development, 24*(2), [page numbers].

Coroian, I., Nap, M. E., Pop, I., Matei, F., Sălăgean, T., Deak, J., Chiorean, S., Suba, E. E., Luput, I., & Ficior, D. (2021). Using GIS analysis to assess urban green space in terms of real estate development. *Bulletin of University of Agricultural Sciences and Veterinary Medicine Cluj-Napoca. Horticulture, 78*(1), [page numbers].

Curovic, M., Spalevic, V., Sestras, P., Motta, R., Dan, C., Garbarino, M., ... & Urbinati, C. (2020). Structural and ecological characteristics of mixed broadleaved old-growth forest (Biogradska Gora-Montenegro). *Turkish Journal of Agriculture and Forestry, 44*(4), 428–438. https://doi.org/10.3906/tar-1912-62

Felicísimo, Á. M., Francés, E., Fernández, J. M., González-Díez, A., & Varas, J. (2002). Modeling the potential distribution of forests with a GIS. *Photogrammetric Engineering & Remote Sensing, 68*(5), 455–461.

Li, C., & Jiang, Y. (2011). Development of mobile GIS system for forest resources second-class inventory. *Journal of Forestry Research, 22*, 263–268. https://doi.org/10.1007/s11676-011-0169-z

Meng, Y., Cao, B., Dong, C., & Dong, X. (2019). Mount Taishan forest ecosystem health assessment based on forest inventory data. *Forests, 10*(8), Article 685. https://doi.org/10.3390/f10080685

Mikita, T., Janata, P., & Surový, P. (2016). Forest stand inventory based on combined aerial and terrestrial close-range photogrammetry. *Forests, 7*(3), Article 40. https://doi.org/10.3390/f7030040

Pasqualini, V., Oberti, P., & Vigetta, S. (2011). A GIS-based multicriteria evaluation for aiding risk management in *Pinus pinaster* Ait. forests: A case study in Corsican Island, western Mediterranean region. *Environmental Management, 48*, 38–56. https://doi.org/10.1007/s00267-011-9655-y

Qiu, Z., Feng, Z., Jiang, J., Lin, Y., & Xue, S. (2018). Application of a continuous terrestrial photogrammetric measurement system for plot monitoring in the Beijing Songshan National Nature Reserve. *Remote Sensing, 10*(4), Article 562. https://doi.org/10.3390/rs10040562

Risna, R. A., Prasetyo, L. B., Lughadha, E. N., Aidi, M. N., Buchori, D., & Latifah, D. (2023). Forest resilience research using remote sensing and GIS – A systematic literature review. *IOP Conference Series: Earth and Environmental Science, 1266*, [page/article number]. https://doi.org/10.1088/1755-1315/1266/1/012001

Sestraș, P., Sălăgean, T., Bilașco, S., Bondrea, M. V., Naș, S., Fountas, S., & Cîmpeanu, S. M. (2019). Prospect of a GIS-based digitization and 3D model for better management and land use in a specific micro-areal for crop trees. *Environmental Engineering and Management Journal, 18*(6), 1269–1277.

Soubry, I., Doan, T., Chu, T., & Guo, X. (2021). A systematic review on the integration of remote sensing and GIS to forest and grassland ecosystem health attributes, indicators, and measures. *Remote Sensing, 13*(7), https://doi.org/10.3390/rs13071271

Zlinszky, A., Heilmeier, H., Balzter, H., Czúcz, B., & Pfeifer, N. (2015). Remote sensing and GIS for habitat quality monitoring: New approaches and future research. *Remote Sensing, 7*, 7987–7994. https://doi.org/10.3390/rs70607987

Scientific Papers. Series E. Land Reclamation, Earth Observation & Surveying, Environmental Engineering. Vol. XIV, 2025
Print ISSN 2285-6064, CD-ROM ISSN 2285-6072, Online ISSN 2393-5138, ISSN-L 2285-6064

INTEGRATING UAS, LiDAR, AND GROUND-BASED SURVEYING FOR PRECISE DEMOLITION VOLUME ASSESSMENT: A CASE STUDY OF THE DOLJ CHIM INDUSTRIAL COMPLEX

George CRISTIAN, Sorin HERBAN, Carmen GRECEA, Clara-Beatrice VÎLCEANU, Andreea Diana CLEPE

Politehnica University of Timișoara, 2 Traian Lalescu Street, 300223, Timișoara, Romania

Corresponding author email: beatrice.vilceanu@upt.ro

Abstract

This study presents a case analysis of an integrated surveying and mapping initiative conducted at the Dolj Chim industrial complex in Romania, with the primary objective of determining material volumes expected from impending demolition activities. Employing a multi-faceted approach, the research combined data acquisition using a handheld LiDAR system for the interior and data acquired through a UAS equipped with high-resolution imaging sensors for the exterior. These complementary datasets were georeferenced using ground control points collected via Global Positioning System (GPS) receivers and Total Station measurements, ensuring a consistently accurate and spatially coherent representation of the site. This integrated approach streamlines data management and enhances the utility of subsequent analyses. The results emphasize the significance of selecting and integrating appropriate surveying technologies tailored to the complexities of industrial environments. By leveraging the strengths of various methods, high-density interior scanning and external imaging, reinforced by reliable ground-based control, the study achieves an enriched and precise dataset conducive to informed decision-making in demolition planning. Beyond its immediate relevance, this approach demonstrates broader applicability in complex geospatial contexts, illuminating best practices for harmonizing sensor technologies and conventional surveying techniques. Consequently, the research contributes insights into optimizing data quality, operational efficiency, and overall methodological rigor in contemporary geospatial applications.

Key words*: LiDAR, photogrammetry, industrial survey, demolition planning, 3D modelling, Romania.*

INTRODUCTION

This paper explores the crucial role that surveying and mapping plays in various engineering and geospatial applications and the implementation of integrated surveying techniques in the context of the Dolj Chim industrial complex demolition project.

The main objective of the study is to quantify the volumes of various construction materials (e.g. concrete, iron, wood, glass etc.) that will result from the demolition process, by harnessing the synergetic potential LiDAR scanning for interior spaces and UAS based photogrammetry for the roof of the buildings and surrounding area. In the case of industrial demolition, precise 3D modelling is essential to ensure cost-effective waste management while complying with environmental and work safety regulations, as underscored by (Nikmehr et al., 2021).

While traditional surveying methods can be time-consuming and challenging in degraded industrial environments (Zhan et al. 2020), this study aims to demonstrate the efficiency of integrating LiDAR, UAS photogrammetry and ground-based control points to achieve an accurate and comprehensive 3D model for demolition planning.

This project presented challenges that are common in old industrial complexes throughout Romania due to their advanced state of degradation, including water damage, overgrown vegetation and hazardous conditions such as shattered glass and unstable structures (Matsimbe et al., 2022).

The aim of this study is to highlight how modern surveying technologies complement traditional methods, leading to improved data acquisition and processing efficiency in complex industrial areas, offering a template for best practices in the field.

MATERIALS AND METHODS

In modern surveying, SLAM and UAS both enable spatial data acquisition. SLAM's real-time 3D mapping suits complex indoor environments, ensuring mobility. Meanwhile,

UAS excels at broad aerial surveys. The optimal choice depends on specific project needs, environment, and data requirements. A GeoSLAM Zeb Horizon RT LiDAR scanner (Figure 1) was used to scan the interior of the buildings and the ground level of the entire complex. The technical specifications of the GeoSLAM Zeb Horizon, which was used in the data acquisition process, are presented in Table 1.



Figure 1. GeoSLAM Zeb Horizon RT

Table 1. GeoSLAM Zeb Horizon technical specifications

Scanner	
Type	VLP-16
Acquisition	300.000 pts/sec
Channels	16
Range	100 m
Class	Class 1 eye safe laser
Wavelength	903 nm
Angular resolution	2°
Angular resolution	0.1-0.4°
Weight	1.3 kg
Raw data file size	100-200 MB a minute
Rotation	10 Hz
Datalogger	
Battery	PAG L90 SLIM, 90 Wh, 14.8V, 6.1 Ah
Operational time	3.5 hours
Storage	120 GB
Operational temp	0 – 50°
Weight	2.4 kg
System	
Protection Class	IP54
Processing	Post
Accuracy	1-3 cm
Protection Class	IP54

This device captures high density point clouds in near real-time at a rate of 300.000 points per second and has a range of up to 100 meters. It utilizes an inertial measurement unit (IMU) and Simultaneous Localization and Mapping (SLAM) algorithms to achieve a relative accuracy of up to 6 millimeters, depending on the environment which made it the ideal equipment for this project.

For the exterior and for the roofs of the buildings a DJI Mavic 3 Enterprise (Figure 2), equipped with a high-resolution imaging sensor, was deployed, enabling wide-scale coverage at various altitudes and oblique angles resulting in aerial imagery for photogrammetric processing. The technical specifications of the DJI Mavic 3 Enterprise, employed for aerial data collection, are detailed in Table 2.



Figure 2. DJI Mavic 3 Enterprise

Table 2. DJI Mavic 3 Enterprise technical specifications

Aircraft	
Weight	915 g
Max take-off weight	1050 g
Max flight speed	15 m/s (Normal Mode)
Max wind speed resistance	12 m/s
Max flight time (no wind)	45 mins
GNSS	GPS+Galileo+BeiDou+GLONASS (GLONASS is supported only when the RTK module is enabled)
Operating temperature range	-10° to 40°C
Max Pitch Angle	30° (Normal Mode) 35° (Sport Mode)
Max Angular Velocity	200°/s
Wide Camera	
Sensor	4/3 CMOS, Effective pixels: 20 MP
Lens	FOV: 84° Format Equivalent: 24 mm Aperture: f/2.8-f/11 Focus: 1 m to ∞
ISO Range	100-6400
Shutter Speed	Electronic Shutter: 8-1/8000 s Mechanical Shutter: 8-1/2000 s
Max Image Size	5280×3956
Ghimbal	
Stabilization	3-axis (tilt, roll, pan)
Mechanical Range	Tilt: -135° to 100° Roll: -45° to 45° Pan: -27° to 27°
Controllable Range	Tilt: -90° to 35° Pan: Not controllable
Max Control Speed	100°/s
Angular Vibration Range	±0.007°

To ensure proper georeferencing and alignment of data sets, ground control points were placed throughout the area of interest. The distribution of these points was influenced by existing vegetation, accessibility constraints, varying floor elevations and isolated structures.

A total of 50 ground control points were surveyed using a Trimble R10 GNSS receiver and a Trimble Geodimeter 5000 Series Total

Station in places where GPS signal was obstructed and on the facade of the buildings (Figure 3). This approach is in line with similar studies that emphasize the necessity of combining ground-based control methods with aerial and LiDAR data to ensure spatial coherence (Son et al., 2020).



Figure 3. Distribution of ground control points

The ground control points used for georeferencing the spatial data are listed in Table 3.

Table 3. Ground control points used for georeferencing

ID	X [m]	Y [m]	Z [m]
1C	397983.415	320330.852	97.22
2C	398026.357	320271.036	97.23
3C	397987.333	320325.041	86.31
4C	397999.317	320300.834	90.34
5C	398003.089	320295.676	90.41
6C	398021.967	320276.478	86.40
7C	398067.865	320391.053	97.34
8C	398074.750	320395.231	94.55
9C	398110.599	320331.028	97.19
10C	398236.541	320322.801	97.29
11C	398188.794	320388.529	97.67
12C	398208.191	320372.677	101.14
13C	398232.677	320338.422	101.15
14C	398285.683	320368.307	97.56
15C	398287.387	320387.713	99.18
16C	398262.451	320422.548	99.12
17C	398281.931	320373.321	101.06
18C	398257.741	320407.651	101.16
19C	398243.615	320427.338	97.61
20C	398202.071	320485.712	100.06
21C	398215.934	320479.656	98.90
22C	398212.722	320470.714	106.41
23C	398223.587	320455.645	106.44
24C	398240.667	320445.206	98.80
25C	398234.269	320440.692	99.97
26C	398147.486	320446.756	100.06
27C	398158.116	320431.829	106.45
28C	398168.994	320416.626	106.45

A subset of these control points was not used in the georeferencing process, instead they served as verification markers to assess the accuracy of the final merged data set. Verification points are used to provide an independent check on alignment errors and is recommended in large scale surveying projects (Salzano et al., 2024). The ground control points utilized for the verification of spatial accuracy are presented in Table 4.

Table 4. Ground control points used for verification

ID	X [m]	Y [m]	Z [m]
30V	397991.781	320319.529	95.75
31V	397997.310	320311.693	95.81
32V	398012.675	320290.222	95.75
33V	398016.155	320285.396	95.61
34V	398047.468	320286.101	95.66
35V	398094.811	320319.848	95.67
36V	398101.300	320357.350	89.28
37V	398100.105	320359.088	89.33
38V	398193.174	320382.344	90.55
39V	398195.124	320379.612	90.55
40V	398224.435	320338.345	90.62
41V	398226.432	320335.641	90.57
42V	398222.296	320352.961	101.19
43V	398218.775	320358.001	101.21
44V	398281.792	320395.517	97.59
45V	398273.270	320407.371	97.54
46V	398217.892	320476.944	97.68
47V	398238.669	320447.953	97.65
48V	398161.659	320426.547	103.75
49V	398165.165	320421.694	103.70
30V	397991.781	320319.529	95.75
31V	397997.310	320311.693	95.81
32V	398012.675	320290.222	95.75
33V	398016.155	320285.396	95.61
34V	398047.468	320286.101	95.66
35V	398094.811	320319.848	95.67
36V	398101.300	320357.350	89.28
37V	398100.105	320359.088	89.33
38V	398193.174	320382.344	90.55

Data processing consisted in converting the raw LiDAR scans into georeferenced point clouds through the manufacturer's proprietary software, which facilitates simultaneous localization and mapping (SLAM) algorithms. Initial denoising operations entailed statistical outlier detection and removal, aimed particularly at mitigating irregularities caused by reflective surfaces, shattered glass and metal debris. These operations aligned with protocols noted in earlier research, where industrial sites frequently produce erroneous reflections in laser-based recordings (Zakaria et al., 2025).

The aerial imagery was processed using Agisoft Metashape 2.0, generating an independent three-dimensional point cloud. The software automatically identified tie points through feature matching followed by a bundle adjustment procedure to optimize camera orientations and intrinsic parameters.

Georeferencing was completed by incorporating the ground control points.

The point cloud was generated using the depth maps computed for each image by stereo-

matching algorithms. The resulting point cloud was then filtered by removing redundant points, outliers and noise. The filtering was done using iterative statistical filtering and confidence-based filtering, as recommended by (Zakaria et al., 2025), to eliminate the noise derived from unstructured debris piles and partial obstructions, therefor consolidating a more homogeneous and trustworthy dataset.

After generating and filtering the LiDAR and photogrammetric point clouds, the datasets were imported into Trimble Business Center for co-registration. Tie points were first manually identified in overlapping areas to ensure rough alignment, followed by refinement using the iterative closest point algorithm, as applied in similar complex survey environments (Abreu et al., 2023).To quantify the quality of the merged data, a series of verification points (Table 4), distinct from the control points used for georeferencing (Table 3), were surveyed on-site using the Total Station and then compared to their corresponding positions in the unified point cloud. Figure 4 illustrates the verification points used to assess the accuracy of the merged dataset.

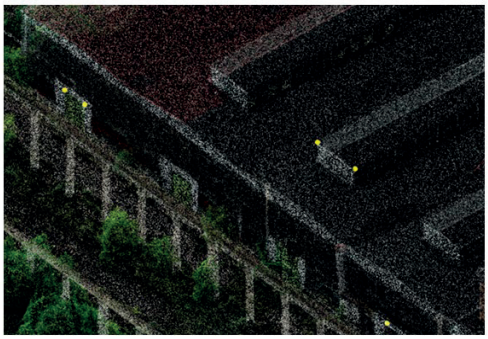


Figure 4. Verification points

The root means square errors and the probable error along the X, Y and Z axes were computed to characterize horizontal and vertical deviations as shown in (Table 5).

Once the point clouds had been successfully fused, they served as the foundation for constructing a three-dimensional model of the industrial complex. In the initial stage of this modeling process, three horizontal cross-sections were extracted from the point cloud at the ground level, as well as the first and second floors (Figure 5). These cross-sections provided the reference data necessary to generate accurate floor plans for each building within the complex. Subsequently, vertical sections were derived along each principal building axis (Figure 6), and the combined use of horizontal and vertical cross-sections enabled precise modeling of all structural elements.

Each modeled component was then classified according to its constituent material (e.g., concrete, metal, wood, or glass).

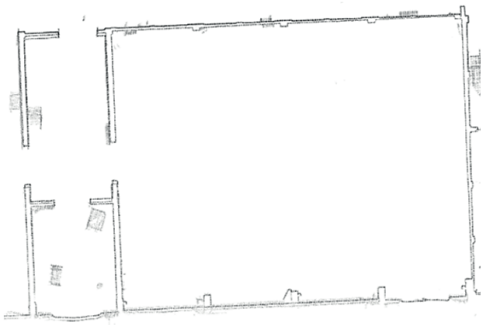


Figure 5. Horizontal section of the point cloud

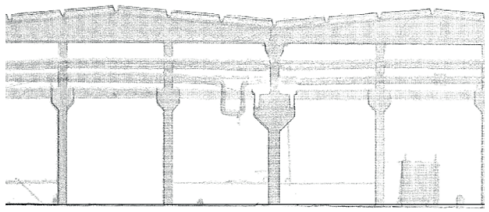


Figure 6. Vertical section of the point cloud

Studies focusing on point cloud–to–CAD workflows in complex industrial environments highlight the recurring challenges posed by irregular geometries, occlusions, and noise (Abreu et al., 2023).

Table 5. Precision estimate

Point code	Field survey			Points in the point cloud			Δ		
	X1 [m]	Y1 [m]	Z1 [m]	X2 [m]	Y2 [m]	Z2 [m]	ΔX [m]	ΔY [m]	ΔZ [m]
30V	397991.781	320319.529	95.75	397991.708	320319.461	95.74	0.073	0.068	0.01
31V	397997.310	320311.693	95.81	397997.304	320311.661	95.72	0.006	0.032	0.09
32V	398012.675	320290.222	95.75	398012.658	320290.257	95.69	0.017	-0.034	0.06
33V	398016.155	320285.396	95.61	398016.112	320285.441	95.68	0.043	-0.044	-0.07
34V	398047.468	320286.101	95.66	398047.411	320286.063	95.64	0.057	0.038	0.02
35V	398094.811	320319.848	95.67	398094.886	320319.817	95.63	-0.075	0.031	0.04
36V	398101.300	320357.350	89.28	398101.321	320357.351	89.30	-0.020	-0.001	-0.02
37V	398100.105	320359.088	89.33	398100.188	320359.097	89.40	-0.083	-0.008	-0.06
38V	398193.174	320382.344	90.55	398193.161	320382.32	90.54	0.013	0.024	0.01
39V	398195.124	320379.612	90.55	398195.093	320379.634	90.54	0.031	-0.021	0.01
40V	398224.435	320338.345	90.62	398224.419	320338.328	90.58	0.016	0.017	0.03
41V	398226.432	320335.641	90.57	398226.402	320335.637	90.55	0.030	0.005	0.02
42V	398222.296	320352.961	101.19	398222.333	320353.021	101.19	-0.036	-0.059	-0.01
43V	398218.775	320358.001	101.21	398218.838	320358.050	101.20	-0.062	-0.048	0.01
44V	398281.792	320395.517	97.59	398281.738	320395.611	97.54	0.054	-0.093	0.04
45V	398273.270	320407.371	97.54	398273.325	320407.358	97.58	-0.054	0.013	-0.03
46V	398217.892	320476.944	97.68	398217.817	320476.938	97.64	0.075	0.006	0.03
47V	398238.669	320447.953	97.65	398238.598	320447.893	97.64	0.071	0.060	0.01
48V	398161.659	320426.547	103.75	398161.647	320426.533	103.76	0.012	0.015	-0.01
49V	398165.165	320421.694	103.70	398165.159	320421.689	103.77	0.006	0.005	-0.06
Root mean square Error: $e_m=\pm\frac{m}{\sqrt{n}}$, where $m=\pm\sqrt{\frac{[vv]}{n-1}}$							**±0.048**	**±0.039**	**±0.039**
Probable error: $e_p=\pm\frac{2}{3}e_m$							**±0.032**	**±0.026**	**±0.026**

In the Dolj Chim project, structural complexity was addressed through the use of repetitive, prefabricated elements - particularly standardized concrete beams - a strategy aligned with approaches used in projects involving repetitive architectural components (Abreu et al., 2023). The merged point cloud facilitated the extraction and visualization of key structural elements within the industrial complex. As shown in Figure 7, the resulting 3D model accurately represents the spatial and architectural configuration of the site, forming a reliable basis for further spatial analyses, documentation, and integration into planning or monitoring processes.

To assess surface material accumulation, Figure 8 illustrates the debris volume derived from the processed point cloud. This sheet displays the spatial distribution and elevation variation of debris, enabling quantitative evaluation necessary for planning site clearance, estimating transport needs, and assessing environmental impact.



Figure 7. 3D elements of the industrial complex

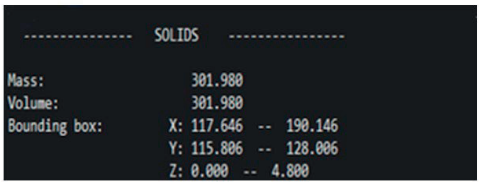


Figure 8. Debris volume sheet

Following the completion of the full 3D model (Figure 10), it was possible to estimate the total volume of debris projected from demolition

activities. Calculations were conducted separately for each material class. The results were compiled into dedicated volume sheets that specify debris quantities by material type, allowing for more accurate planning and resource allocation. The final material-specific volume estimates are presented in Figure 9.

For more complex structural components, such as reinforced concrete, it was necessary to estimate the internal steel content. To this end, standardized material ratios were applied, and the corresponding values used for these calculations are presented in Table 6.

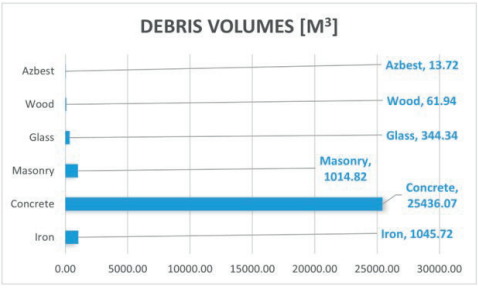


Figure 9. Bar chart representing debris values

Table 6. Amount of iron in complex structures

Element	Iron [kg/m³]
Foundation structure	40
Structural framework	100
Concrete wall structure	80
Floor slab	80
Roof slab	60

The final stage of the workflow involved the preparation of a comprehensive bill of quantities, detailing the demolition costs for each individual structure alongside associated expenses for logistics, environmental remediation, and labor. This cost assessment highlights the critical value of integrating detailed 3D modeling with economic and environmental parameters - an approach that is increasingly acknowledged as best practice in modern industrial demolition planning.

RESULTS AND DISCUSSIONS

The circular economy and the recycling of construction materials are essential strategies for reducing the negative impact on the environment. In this context, accurately determining the value of construction waste resulting from demolition is a critical element for the conservation of natural resources and the development of a more sustainable and economically efficient construction sector (Oliveira, Schreiber & Jahno, 2024).

The final integrated point cloud provided a comprehensive depiction of the Dolj Chim industrial complex, encompassing both interior and exterior elements in a single, unified coordinate system. The RMSE and probable error values underscored the high fidelity of the merged dataset and align with benchmarks reported in comparable industrial scanning endeavours (Gibson & Alderson, 2019; Zhan et al., 2020).

The final dataset achieved high georeferencing accuracy, with a mean square error (MSE) of ±0.048 meters in the X-axis, ±0.039 meters in the Y-axis, and ±0.039 meters in the Z-axis. The probable error values were ±0.032 meters in the X-axis, ±0.026 meters in the Y-axis, and ±0.026 meters in the Z-axis (Table 5). These values indicate a high level of precision, ensuring that the resulting point cloud was reliable for demolition volume estimation.

Notably, the LiDAR system achieved superior results in capturing enclosed spaces devoid of strong ambient illumination, whereas the UAS-derived photogrammetry excelled in mapping extensive exterior surfaces and rooftops. These findings reaffirm established conclusions from parallel studies, which highlight the complementary nature of LiDAR and photogrammetry in scenarios that demand both detailed internal scans and large-scale external mapping (Zakaria et al., 2025; Son et al., 2020).

The differences between the LiDAR and UAS-based point clouds were evident due to the nature of the data collection methods. The UAS-generated point cloud, being a product of photogrammetric processing, exhibited a more uniform structure resembling a "sheet" draped over the buildings. In contrast, the LiDAR-derived dataset was denser and contained more irregularities, capturing finer details of the structures. Although these datasets did not align perfectly due to their inherent differences, the integration of control points allowed for an acceptable level of matching that met project requirements.

The efficiency gains achieved through this integrated approach were significant. The entire data collection phase was completed within

three days, a fraction of the time required for traditional methods, which could have taken weeks. Traditional surveying would have been especially challenging in this case due to the lack of sufficient lighting inside the buildings, making it nearly impossible to obtain detailed measurements without advanced scanning technology. Additionally, the availability of drone imagery and LiDAR data significantly reduced human error, as surveyors had comprehensive datasets to reference instead of relying solely on manually collected points and field notes.

In conjunction with precise 3D reconstruction, attention was directed toward the potential integration of Building Information Modeling (BIM) in demolition planning. Although BIM has historically been employed for new construction, its application in demolition contexts (Salzano et al., 2024) has grown in recent years owing to increased awareness of sustainability and resource management issues (Nikmehr et al., 2021). The detailed as-built data generated in this study can serve as a basis for a retrospective BIM, thus offering significant advantages in managing the dismantling of complex industrial structures. Empirical studies suggest that a robust BIM framework can reduce construction and demolition waste by optimizing the quantity and reusability of extracted materials (Nikmehr et al., 2021). While the Dolj Chim complex predates widespread BIM adoption, the dataset assembled here can streamline sustainable demolition procedures by enabling precise volume calculations, safety assessments, and resource allocation (Sestras et al., 2025).

Furthermore, a comparative analysis of the Dolj Chim survey with similar multi-sensor projects revealed numerous shared benefits and recurring obstacles. One frequently encountered challenge in industrial environments is the presence of heavy clutter or debris, which can generate considerable levels of noise in raw point clouds (Zakaria et al., 2025). The Dolj Chim dataset exemplified this issue but benefited from repeated structural designs and standard prefabricated elements, thereby alleviating some of the modeling difficulties. This finding is consistent with research indicating that templated modeling and semi-automated segmentation can reduce the manual labor required for point cloud processing in repetitive architectural environments (Abreu et al., 2023; Gibson & Alderson, 2019). Nonetheless, further work is required to optimize these processing pipelines, especially when such workflows must contend with expansive, congested, or partially collapsed structures.

One of the key improvements noted from this project was the realization that excessive data collection could be a challenge. In this case, the slow pace of LiDAR scanning resulted in a very large dataset, which increased processing time. To optimize future projects, a higher walking speed was adopted in subsequent surveys, reducing unnecessary data density while maintaining accuracy. Additionally, future projects included a greater number of control points inside buildings where conditions allowed, further improving georeferencing quality.

Overall, this study demonstrated that integrating LiDAR and UAS-based photogrammetry provides a robust and efficient method for industrial demolition planning. The approach is adaptable to various environments, though urban applications may require special permissions for UAS flights.

CONCLUSIONS

The integrated LiDAR and photogrammetric methodology employed in this study proved highly effective for generating an accurate and comprehensive 3D model of the Dolj Chim industrial complex (Figure 10).

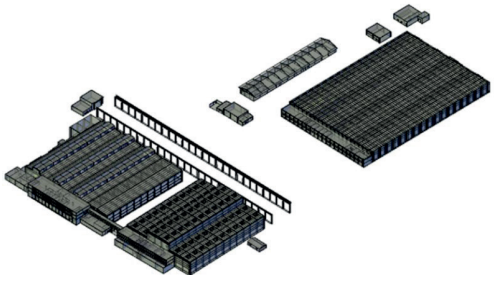


Figure 10. 3D model of Dolj Chim industrial complex

By leveraging the respective strengths of high-density interior scanning and wide-area exterior imaging, this approach yielded precise data for volume estimation, despite the presence of degraded, cluttered, and poorly illuminated

structures. The resultant root means square errors aligned well with benchmarks reported in comparable industrial surveys, thereby confirming that a multi-sensor data fusion framework is vital in contexts demanding a thorough understanding of both internal and external site conditions (Son et al., 2020).

In addition, this study reinforces the growing importance of integrating as-built 3D data into BIM-driven workflows. Although the Dolj Chim facility was not originally modeled in BIM, the accurate digital data obtained here can facilitate subsequent retrospective modeling, an approach that promises to improve demolition planning and waste management (Nikmehr et al. 2021). Future efforts should examine ways to refine data processing routines, particularly with respect to advanced feature recognition and template-based modeling, as these techniques could further accelerate the extraction of 2D and 3D deliverables (Abreu et al. 2023). Enhanced scanning speeds, improved dynamic SLAM capabilities, and expanded use of indoor GCPs stand as promising directions for achieving still greater accuracy and operational efficiency.

The methodological insights gained through this project appear highly transferable to similar industrial or urban settings, with the principal constraint being regulatory limitations on drone operation and on-site safety considerations. Consequently, this study contributes practical and theoretical knowledge that can inform subsequent surveys and research. By bridging multiple data sources and adopting rigorous registration processes, scholars and practitioners alike can develop robust, data-rich models that foster safer, more sustainable, and more cost-effective demolition projects.

ACKNOWLEDGEMENTS

This research work was carried out and financed with the support of GAUSS S.R.L. The authors wish to acknowledge the invaluable assistance of the site management team and all colleagues who contributed to the data collection and processing stages.

REFERENCES

Abreu, N., Pinto, A., Matos, A., & Pires, M. (2023). Procedural point cloud modelling in scan-to-BIM and scan-vs-BIM applications: A review. *ISPRS International Journal of Geo-Information, 12*(7), 260. https://doi.org/10.3390/ijgi12070260

DJI (2022). *Mavic 3 Enterprise Series - Product Specifications*. https://www.dji.com

GeoSLAM. (2022). *Zeb Horizon RT LiDAR Scanner - Technical Datasheet*. https://geoslam.com

Matsimbe, J., Mdolo, W., Kapachika, C., Musonda, I., & Dinka, M. (2022). Comparative utilization of drone technology vs. traditional methods in open pit stockpile volumetric computation: A case of Njuli quarry, Malawi. *Frontiers in Built Environment, 8*, 1037487. https://doi.org/10.3389/fbuil.2022.1037487

Nikmehr, B., Hosseini, M. R., Wang, J., Chileshe, N., & Rameezdeen, R. (2021). BIM-based tools for managing construction and demolition waste (CDW): A scoping review. *Sustainability, 13*(15), 8427. https://doi.org/10.3390/su13158427

Oliveira, J. de, Schreiber, D., & Jahno, V. D. (2024). Circular economy and buildings as material banks in mitigation of environmental impacts from construction and demolition waste. *Sustainability, 16*(12), 5022. https://doi.org/10.3390/su16125022

Son, S. W., Kim, D. W., Sung, W. G., & Yu, J. J. (2020). Integrating UAV and TLS approaches for environmental management: A case study of a waste stockpile area. *Remote Sensing, 12*(10), 1615. https://doi.org/10.3390/rs12101615

Trimble (2019). *Trimble Geodimeter 5000 Series - Technical Specifications*. https://www.trimble.com

Trimble (2021). *Trimble R10 GNSS Receiver - User Guide*. https://www.trimble.com

Zakaria, M. H., Fawzy, H., El-Beshbeshy, M., & Farhan, M. (2025). A comparative study of terrestrial laser scanning and photogrammetry: Accuracy and applications. *Civil Engineering Journal, 11*(3), 1196–1216. https://doi.org/10.28991/CEJ-2025-011-03-021

Nikmehr, B., Hosseini, M. R., Wang, J., Chileshe, N., & Rameezdeen, R. (2021). BIM-Based Tools for Managing Construction and Demolition Waste (CDW): A Scoping Review. *Sustainability, 13*(15), 8427. https://doi.org/10.3390/su13158427

Salzano, A., Cascone, S., Zitiello, E. P., & Nicolella, M. (2024). Construction Safety and Efficiency: Integrating Building Information Modeling into Risk Management and Project Execution. *Sustainability, 16 (10), 4094.* https://doi.org/10.3390/su16104094

Sestras, P., Badea, G., Badea, A. C., Salagean, T., Roșca, S., Kader, S., & Remondino, F. (2025). Land surveying with UAV photogrammetry and LiDAR for optimal building planning. *Automation in Construction, 173, 106092.* https://doi.org/10.1016/j.autcon.2025.106092

Scientific Papers. Series E. Land Reclamation, Earth Observation & Surveying, Environmental Engineering. Vol. XIV, 2025
Print ISSN 2285-6064, CD-ROM ISSN 2285-6072, Online ISSN 2393-5138, ISSN-L 2285-6064

THE USE OF THE GIS TECHNIQUE IN HIGHLIGHTING THE HUMAN PRESSURE ON THE ENVIRONMENT IN OLTEȚ PIEDMONT (SOUTHERN ROMANIA)

Raluca Lucia DINCULOIU[1], Daniel SIMULESCU[2], Carmen Otilia RUSĂNESCU[1], Irina Aura ISTRATE[1], Gabriel Alexandru CONSTANTIN[1], Mihaela BEGEA[1], Edmond MAICAN[1], Gheorghe VOICU[1], Maria CIOBANU[1]

[1]National University of Science and Technology Politehnica Bucharest, Faculty of Biotechnical Systems Engineering, 313 Splaiul Independenţei, 060042, District 6, Bucharest, Romania
[2]University of Craiova, Faculty of Sciences, Department of Geography, 13 A. I. Cuza Street, Craiova, Romania

Corresponding authors emails: daniel.simulescu@edu.ucv.ro, rusanescuotilia@gmail.com

Abstract

This study represents an assessment of the spatio-temporal dynamics of anthropic pressure in the Olteț Piedmont (a subdivision of the Getic Piedmont), located in the southern part of Romania. With the help of ArcGIS 10.5 software, we managed to process the statistical data provided by Dolj, Olt, Gorj and Vâlcea County Statistics Offices (for 2004 and 2014) by creating a vector database and calculating the following environmental indicators: population density, human pressure through arable land use (0.68 ha/inh. - 2014), landscape naturality (0.29 ha/ha - 2014), environmental change (12.91 ha/ha - 2014) and landscape artificialization (0.053 ha/ha - 2014). By comparing the results, for the two reference years (2004 and 2014), we managed to identify some areas were the anthropogenic impact on the environment of the Olteț Piedmont is significantly. Thus, the southern part of the piedmont is the most affected especially by the expansion of rural areas around the major urban areas (such as Craiova, Filiaşi, Balş, Piatra-Olt, and Drăgăşani cities); built-up area increased from 17,110 hectares to 17,248 hectares. The central and northern part of the piedmont, widely forested, is very little affected by the impact of human activities.

Key words*: human pressure; environmental change; naturality index; Olteț Piedmont, Romania.*

INTRODUCTION

In Romania, the excessive fragmentation of croplands remains prevalent even in areas with high agricultural potential. This persistence is the result of a combination of factors related to both land governance and farm-level characteristics (Dogaru et al., 2024).
Land cover and land use changes play a critical role in the sustainable development of local communities, as well as in shaping natural systems (Hooke et al., 2012; Marin et al., 2023). The expansion of cropland has been one of the primary drivers behind the widespread transformation of natural landscapes into anthropogenic ones. The intensification of anthropogenic impact, beginning in the late 19th and early 20th centuries, led to a significant imbalance in the natural environment. This was largely due to extensive deforestation aimed at converting land for agricultural purposes - such as crop cultivation, orchards, vineyards, pastures, and hayfields - as well as for the expansion of rural and urban settlements (Bălteanu et al., 2011)
Human activities have significantly influenced the environment and landscape, contributing to increased land vulnerability and ecological imbalances (Mi et al., 2016). Vegetation, as both an indicator and regulator of human impact, plays a crucial role in modulating carbon, water, and energy cycles (Huryna et al., 2014). It also influences climate by sequestering greenhouse gases and affecting the distribution of solar energy (Huryna & Pokorný, 2016). However, vegetation is increasingly sensitive to climate change, largely due to ongoing anthropogenic pressures.
Following the fall of the communist regime in Romania in December 1989, the country experienced profound transformations across all sectors, particularly in agriculture. One of the major consequences of Law no. 18/1991

was the excessive fragmentation of agricultural land and the shift in ownership from the state to private individuals. This led to the emergence of small-scale subsistence farms characterized by inadequate agricultural practices, including poor fertilization, unregulated use of fertilizers and pesticides, and limited mechanization. As a result, the land use system became more vulnerable to extreme environmental disturbances - marked by notable land use/land cover changes - and less resilient to both climatic and anthropogenic pressures (Grigorescu et al., 2012).

MATERIALS AND METHODS

The use of GIS software has proven its usefulness and functionality in various studies, with diverse themes such as: assessing green urban infrastructure (Wu et al., 2025), road infrastructure assessment and traffic dynamics (Freulda et al., 2025), risk assessment in the transportation of dangerous goods (Tomasoni et al., 2025), enhancing spatial interpretability of fluoride in groundwater (Singh et al., 2025), illegal abandoned waste sites (Ragazzo et al, 2025) and also the assessement of human pressure on the environment (Filimon et al., 2024; Fan et al., 2017; Sencovici & Pehoiu, 2016; Ekim et al., 2021; Mammides, 2020).

Study area

The Olteț Piedmont, a subdivision of the Getic Piedmont (Figure 1), with a surface of approximately 3771 km^2, whose altitudes decrease from north to south, from the contact with the Getic Subcarpathians towards the contact with the Oltenia Plain.

It's an intensely populated area (93 administrative-territorial units from four counties - Gorj, Vâlcea, Dolj and Olt, overlap over the piedmont) with an attractive natural and economic potential, that led to a steady population growth and expansion of the settlement network (Bălteanu et al., 2003). Human activities have a major impact on the environment, due to land cover/use changes, which amplify the degradation of the land through geomorphological processes (gullying, rilling, sheet wash, surface erosion and sometimes landslides). Activities like deforestation, excess grazing, plowing along the slope line etc. are an important factor in the development of gullying (Popovici et al., 2010).

Beside land cover and land use changes, among the activities with negative impact on the biodiversity (conservation status of protected habitats and species of plants and animals) are: the construction of mineral aggregate sorting stations, extraction of gravel, sand, clay, kaolin, uncontrolled expansion of accommodation units (hotels, guesthouses), the removal from the forest fund of some terrains intended for construction, expansion of mineral aggregate mining quarries, the expansion of the urban areas.

In this study, we aim to evaluate the spatio-temporal dynamics of human pressure in the Olteț Piedmont - a subdivision of the Getic Piedmont - located in the southern Romania. Using GIS techniques, we processed the statistical data provided by the County Statistics Offices of Dolj Olt, Gorj and Vâlcea for the years 2004 and 2014.

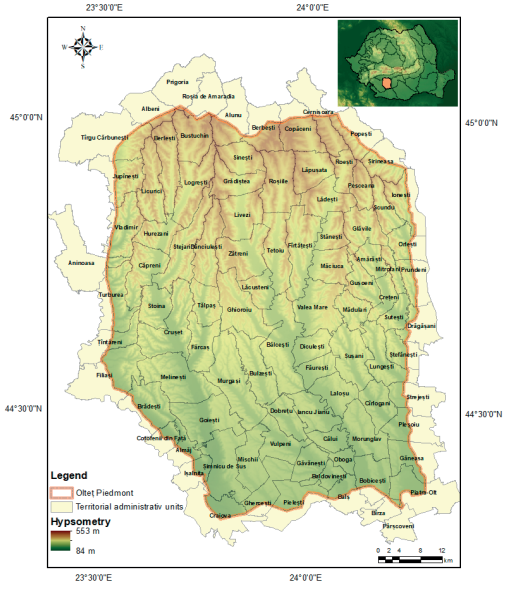


Figure 1. Study area - Olteț Piedmont (Romania)

The evaluation was conducted using a set of environmental indicators, including population density, human pressure through arable land, the landscape naturality index, the environmental change indicator and the landscape artificialization indicator.

With the help of ArcToolbox feature Extract, we managed to identify and draw out all the 93

administrative-territorial units that overlap our study area. In the newly created layer, we added multiple fields and inserted the statistical data collected from the four County Statistics Offices for 2004 and 2014. In addition, in the Attribute Table of this layer we used the Field Calculator function to insert the equation for each environmental indicator and calculate the values for each parameter for every administrative-territorial unit. The results were displayed in cartographic materials, for a better a better view of the areas that are most vulnerable to human activities.

For our study we chose the datas from 2004 and 2014. Prior to 2004, some of the settlements that overlap the study area were part of different administrative territorial units (ATU). In that year, the Law No. 84/2004 led to the administrative reorganization of several communes throughout Romania and the emergence of new administrative territorial units, whose limits have not changed until now. In 2014, The National Cadastre and Real Estate Advertising Agency started.

The national cadastre and land register program in order to intabulate all the terrains from Romania, and because of that, until the ending of this program no newer data available regarding land cover/use at administrative territorial unit level. Therefore, because of these two restrictions we couldn't expand our study and focused only on the 2004-2014 period.

In order to give an overview of the impact of human activities on the environment in the Olteț Piedmont, for each of the two statistical years we calculated human pressure on the environment indicators like:

- *population density* (P_d = *No. inhabitants/ Total area);*
- *indicator of human pressure through arable use of land* (P_a = Arable area/No. inh.);
- *naturality index* (N_i = *Forest area/Total area);*
- *environmental change index* (E_{ch} = Forest+pasture+hayfield area/Built-up area);
- *landscape arficialization index* (Ai = Built-up+industry+communication roads/Total area).

Several Romanian researchers have published studies (Bălteanu et al., 2010; Pătroescu et al., 2010; Ionuș et al., 2011; Zarea et al., 2012; Popovici, 2010; Petrișor & Petrișor, 2021) in which they successfully employed human pressure indicators to assess the impact of anthropogenic activities on the environment across various regions of Romania. These regions include the Getic Piedmont, the Romanian Plain, the Oltenia Plain or the Bâsca Chiojdului River basin.

Whether applied to smaller or larger territorial units, these studies have demonstrated the effectiveness of such indicators in improving our understanding of the ways in which human activities influence the natural environment.

RESULTS AND DISCUSSIONS

Population density

Population density is the first indicator that was determined and represents the number of inhabitants that live in an area of 1 ha (Figure 2).

The total number of inhabitants living in the 93 administrative territorial units is 618113 persons (2014), with the highest number of 308114 inhabitants in Craiova Municipality and the lowest number of 940 inhabitants in Mitrofani commune.

The average population density of the study area is 1.08 inhabitants/hectar, the lowest value is 0.21 inh./ha in Ghioroiu commune and the highest value is 37.85 inh./ha in Craiova Municipality.

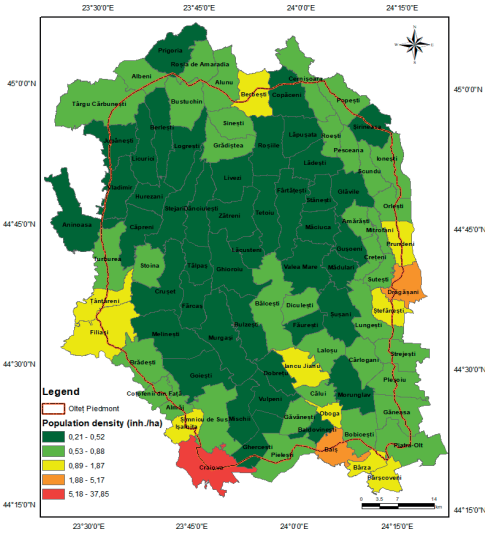


Figure 2. Population density in the Olteț Piedmont (2014)

Higher values are registered in towns like Balș (5.17 inh./ha), Drăgășani (4.43 inh./ha), Filiași (1.87 inh./ha) and Berbești (1.04 inh./ha).

The lowest values of the population density are registered in communes: Ghioroiu (0.21 inh./ha), Bulzești (0.23 inh./ha) and Murgași (0.25 inh./ha).

Human pressure through arable use of the land

This indicator represents the intensity of anthropic activities on the environment through arable use of the land. The main use of the lands in the study area is agricultural use. The total arable surface in the study area in 2004 is 180306 ha and 178447 ha in 2014.

In 2004 the mean value of this indicator was 0.66 ha/inh., with the highest values recorded in the communes of Ghercești (2.52 ha/inh.), Mischii (2.21 ha/inh.), Bulzești (1.72 ha/inh.), Baldovinești (1.68 ha/inh.), Dobrețu (1.68 ha/inh.) and the lowest values in Craiova (0.01 ha/inh.), Drăgășani (0.11 ha/inh.), Balș (0.12 ha/inh.), Berbești (0.22 ha/inh.) towns (Figure 3).

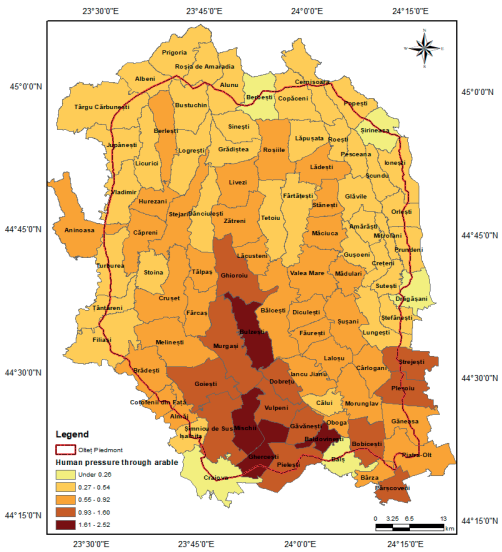


Figure 3. Human pressure through arable use of the land (2004)

The biggest changes of the values for this indicator (from 2004 to 2014) were recored in the administrative territorial units of Orlești (from 0.35 to 0.40), Fârtățești (from 0.46 to 0.50), Lungești (from 0.49 to 0.53), Tetoiu (from 0.52 to 0.56), Vladimir (from 0.51 to 0.57), Glăvile (from 0.53 to 0.60), Dănciulești (from 0.54 to 0.66), Stănești (from 0.55 to 0.66), Stejari (from 0.60 to 0.71), Morunglav (from 0.64 to 0.78), Lăcusteni (from 0.57 to 0.83), Vulpeni (from 1.13 to 1.44), Bulzești (from 1.72 to 1.92).

In 2014 the mean value was 0.68 ha/inh. A decrease of the values of this indicator can be seen in Baldovinești, Oboga, Pârșcoveni and an increase of the values in Găneasa, Vladimir, Dănciulești, Tetoiu and Găvile (Figure 4).

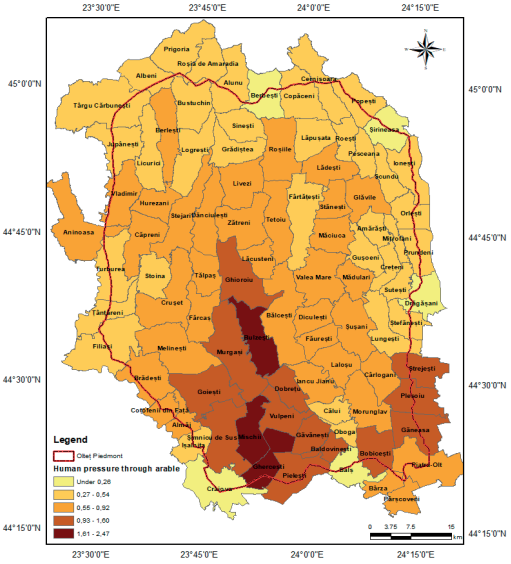


Figure 4. Human pressure through arable use of the land (2014)

Landscape naturality indicator

The landscape naturality indicator represents the ratio between the forest area and the total area (thus determining the degree of afforestation), being calculated at the level of administrative-territorial unit.

The total surface of the forests increased from 147186 ha in 2004 to 147361 ha in 2014. The mean value of this indicator, for both reference years was 0.29 ha/ha.

Because the values didn't change very much, in both years, the highest value was recorded in Jupânești (0.62 ha/ha), Șirineasa (0.61 ha/ha), Morunglav (0.59 ha/ha), Călui (0.58 ha/ha) and the lowest values in Drăgășani (0.01 ha/ha), Mischii (0.02 ha/ha), Ghercești (0.02 ha/ha), Pielești (0.02 ha/ha).

Some changes of the values for this indicator were recorded in Vulpeni (from 0.15 to 0.2), Găneasa (from 0.18 to 0.16), Diculești (from 0.30 to 0.28), Sinești (from 0.43 to 0.38).

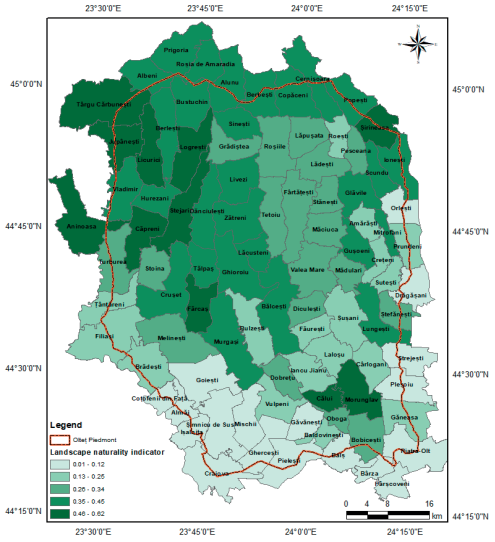


Figure 5. Landscape naturality indicator (2004)

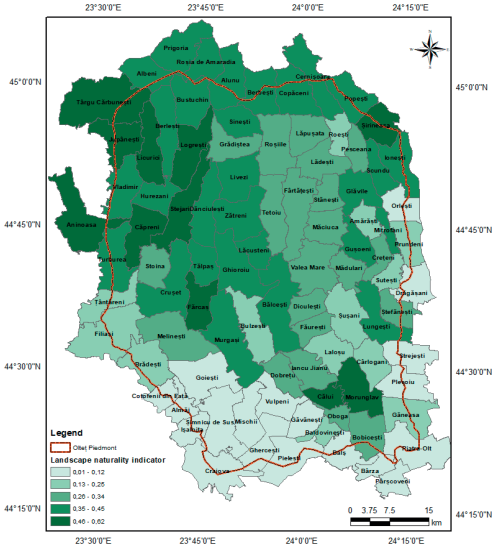


Figure 6. Landscape naturality indicator (2014)

The territorial administrative units with values of the landscape naturality indicator unde 0.10 are considered to have a landscape with very strong affected ecological balance, and those with the values of the indicator between 0.45-0.60 to have a landscape with relatively stable ecological balance (Figure 5, Figure 6).

Environmental change indicator

The environmental change indicator was calculated as the ratio between the natural and the anthropic surfaces.

In 2004 the mean value of this indicator was 12.83 ha/ha with the highest values recored in Ghioroiu (35.49 ha/ha), Copăceni (33.59 ha/ha), Berlești (27.32 ha/ha), Aninoasa (25.15 ha/ha) and the lowest values in Craiova (0.34 ha/ha), Işalnița (0.93 ha/ha), Drăgășani (1.13 ha/ha) and Pleșoiu (1.69 ha/ha) (Figure 7).

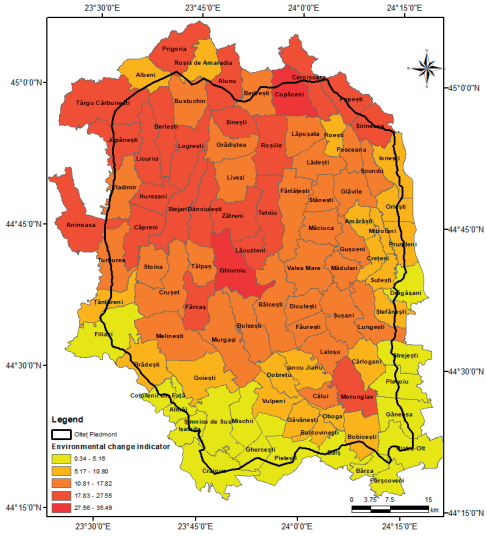


Figure 7. Environmental change indicator (2004)

In 2014 the mean value was 12.91 ha/ha with the highest values in Ghioroiu (36.41 ha/ha), Copăceni (33.59 ha/ha), Berlești (27.55 ha/ha), Aninoasa (25.15 ha/ha) and the lowest values in Craiova (0.34 ha/ha), Işalnița (0.93 ha/ha), Drăgășani (1.13 ha/ha) and Pleșoiu (1.45 ha/ha) (Figure 8).

Important changes of the values of this indicator were recorded in Almăj (from 3.67 to 2.67), Vulpeni (from 6.48 to 4.64), Bobicești (from 7.38 to 5.16), Lăcusteni (from 22.72 to 17.82) and Sinești (from 20.53 to 19.01).

The territorial administrative units with a high value of the environmental change indicator are located mainly in the northern and north-

western part of the Olteț Piedmont and have the least affected landscape.

In the eastern, southern and south-western part of the piedmont, the territorial administrative units have a lower value of this indicator; they are located near big cities like Craiova, Filiași, Balș, Piatra-Olt, Drăgășani and therefore subjected to the influence of the development of these urban areas.

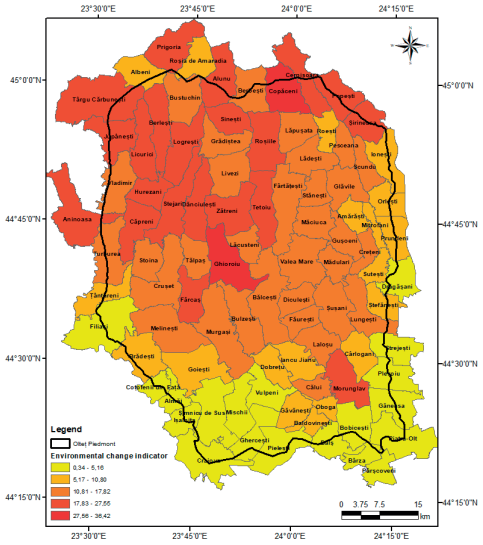


Figure 8. Environmental change indicator (2014)

Landscape artificialization indicator

The landscape artificialization indicator represents the ratio between the built-up areas and the total area of the administrative-territorial unit and is often used to complete the landscape naturality indicator.

The mean value of the landscape artificialization indicator in 2004 was 0.052 ha/ha with the highest values recorded in Craiova (0.47 ha/ha), Işanița (0.17 ha/ha), Drăgășani (0.15 ha/ha), Balș (0.12 ha/ha) and the lowest values in Ghioroiu (0.02 ha/ha), Copăceni (0.02 ha/ha), Pârșcoveni (0.03 ha/ha), Morunglav (0.03 ha/ha).

In 2014 the mean value of the indicator increased to 0.053 ha/ha with the highest values in Craiova (0.48 ha/ha), Işalnița (0.17 ha/ha), Drăgășani (0.15 ha/ha), Balș (0.13 ha/ha) and the lowest values in Ghioroiu (0.02 ha/ha), Copăceni (0.02 ha/ha), Morunglav (0.03 ha/ha), Berlești (0.03 ha/ha).

Small changes in the values of this indicator were recorded in Pârșcoveni (from 0.3 to 0.4), Turburea (from 0.4 to 0.5), Bobicești (from 0.4 to 0.6), Balș (from 0.12 to 0.13).

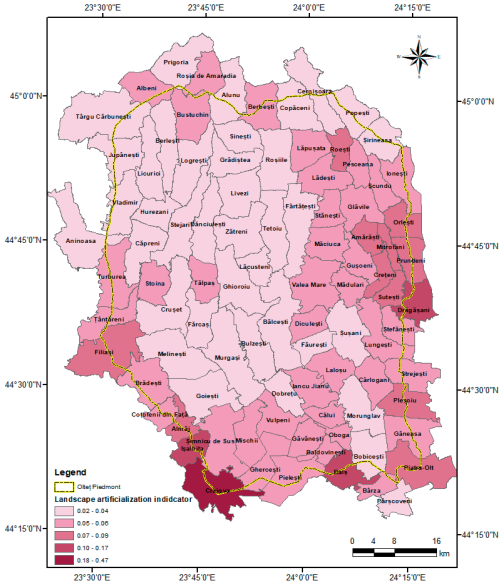


Figure 9. Landscape artificialization indicator (2004

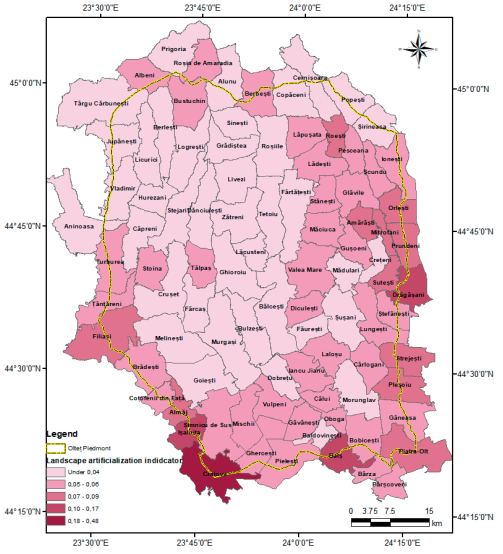


Figure 10. Landscape artificialization indicator (2014)

An analysis of Figures 9 and 10 reveals that the areas with the highest degree of landscape artificialization are located in the eastern, southern, and southwestern parts of the Olteț

Piedmont. This pattern is primarily influenced by the expansion of urban centers such as Craiova, Filiași, Balș, Piatra-Olt, and Drăgășani.

Between 2004 and 2014, the built-up area increased from 17,110 hectares to 17,248 hectares, while the area occupied by road infrastructure expanded from 8,701 hectares in 2004 to 8,904 hectares in 2014. This growth is largely attributable to residents of these cities seeking to escape urban congestion by relocating to nearby rural communes, where they constructed vacation or secondary residences.

CONCLUSIONS

In order to assess the impact of human activities on the environment, as well as to follow the evolution over time of the phenomenon of environmental degradation, there is a need to use a global assessment method of the state of health or environmental pollution at a given moment.

Anthropic activities exert pressure on the environment, which differs from one type of space to another and from one society to another.

Our study highlights the predominance of agicultural activities in the southern part of the Olteț Piedmont and built-up areas around urban areas, like Craiova, Balș, Piatra-Olt and Filiași cities, to be the main anthropic activities that exert a pressure on the enivronment. The constant expansion of these cities and of their periuban areas (many people have built a second home in the communes near the urban communities) define how the landscape is transformed every day.

Because we only managed to assess the changes between 2004 and 2014, we consider that a future study (when newer data will be available, having as a target the year 2024) is needed to determine a trend of the impact of human activities on the environment of the Olteț Piedmont. Also, new research regarding the land use/land cover changes in the study area, for a period of 20 years, is needed in order to have a better understanding of how human activities have transformed and will impact on the environment.

REFERENCES

Ávila Ragazzo, A. V., Mei, A., Mattei, S., Fontinovo, G., & Grosso, M. (2025). Illegal abandoned waste sites (IAWSs): A multi-parametric GIS-based workflow for waste management planning and cost analysis assessment. *Earth, 6*(2), 33. https://doi.org/10.3390/earth6020033

Bălteanu, D., Costache, A., & Tanislav, D. (2003). Modificările mediului şi vulnerabilitatea aşezărilor umane. Exemplificări din Subcarpaţii şi Piemontul Getic. *Analele Universităţii Valahia din Târgovişte, Seria Geografie*, *3*, 183–187.

Bălteanu, D., Dogaru, D. (2011). Geographical perspectives on human-environment relationships and anthropic pressure indicators. *Revue Roumaine de Géographie/Romanian Journal of Geography*, *55*(2), 69–80.

Bălteanu, D., & Popovici, E. A. (2010). Land use changes and land degradation in post-socialist Romania. *Romanian Journal of Geography*, *54*(2), 95–107.

Dogaru, D., Petrișor, A. I., Angearu, C. V., Lupu, L., & Bălteanu, D. (2024). Land governance and fragmentation patterns of agricultural land use in Southern Romania during 1990-2020. *Land, 13*, 1084. https://doi.org/10.3390/land13091084

Ekim, B., Dong, Z., Rashkovetsky, D., & Schmitt, M. (2021). The naturalness index for the identification of natural areas on regional scale. *International Journal of Applied Earth Observation and Geoinformation, 105*, 102622. https://doi.org/10.1016/j.jag.2021.102622

Fan, X., Dai, X., Yang, G., Jia, Z., Liu, L., & Sun, N. (2017). Detecting artificialization process and corresponding state changes of estuarine ecosystems based on naturalness assessment. *Ocean & Coastal Management, 146*, 178–186. https://doi.org/10.1016/j.ocecoaman.2017.07.007

Filimon, C., Herman, G. V., Filimon, L., Nistor, S., Herman, L. M., & Bucur, L. (2024). The human pressure in the Apuseni Natural Park. *Revista Română de Geografie Politică*, *26*(2), 140–152. https://doi.org/10.30892/rrgp.262107-383

Fruelda, M. J., Fampulme, S. L., Fontamillas, F., Lilang, J., & III, A. F. (2025). Road infrastructure assessment and traffic dynamics using GIS: A case study in the Philippines. *Revue Internationale de Géomatique, 34*(1), 187–207. https://doi.org/10.32604/rig.2025.063247

Grigorescu, I., Mitrică, B., Kucsicsa, G., Popovici, E. A., Dumitrașcu, M., & Cuculici, R. (2012). Post-communist land use changes related to urban sprawl in the Romanian metropolitan areas. *Human Geographies - Journal of Studies and Research in Human Geography, 6*(1), 35–46.

Hooke, R. L., Martín Duque, J. F., & Pedraza, J. (2012). Land transformation by humans: A review. *GSA Today, 22*(12), 4–10.

Huryna, H., Brom, J., & Pokorný, J. (2014). The importance of wetlands in the energy balance of an agricultural landscape. *Wetlands Ecology and Management, 22*, 363–381.

Huryna, H., & Pokorný, J. (2016). The role of water and vegetation in the distribution of solar energy and local climate: A review. *Folia Geobotanica, 51*, 191–208. https://doi.org/10.1007/s12224-016-9261-0

Ionuș, O., Licurici, M., Boengiu, S., & Simulescu, D. (2011). Indicators of the human pressure on the environment in the Bălăciţa Piedmont. *Forum Geografic. Studii și cercetări de geografie și protecţia mediului, 10*(2), 287–294. https://doi.org/10.5775/fg.2067-4635.2011.013

Marin, E., Rusănescu, C. O., Paraschiv, G., & Ciuca, C. V. (2023). Research on wastewater treatment using activated sludge technology in the anaerobic-anoxic-aerobic configuration. *U.P.B. Scientific Bulletin, Series B: Chemistry and Materials Science, 85*(4).

Mammides, C. (2020). A global assessment of the human pressure on the world's lakes. *Global Environmental Change, 63*, 102084. https://doi.org/10.1016/j.gloenvcha.2020.102084

Mi, L., Xiao, H., Zhang, J., Yin, Z., & Shen, Y. (2016). Evolution of the groundwater system under the impacts of human activities in middle reaches of Heihe River Basin (Northwest China) from 1985 to 2013. *Hydrogeology Journal, 24*(4), 971–986. https://doi.org/10.1007/s10040-015-1346-y

Pătroescu, M., Toma, S., Rozylowicz, L., & Cenac-Mehedinți, M. (2000). Ierarhizarea peisajelor rurale din Câmpia Română în funcție de vulnerabilitatea la degradare și suportabilitatea presiunii umane. *Geographica Timisiensis, VIII–IX*, 235–245.

Petrișor, A. I., & Petrișor, E. (2021). Recent land cover and use in Romania: A conservation perspective. *Present Environment and Sustainable Development, 15*(1), 81–92.

Popovici, E. A. (2010). *Cotmeana Piedmont. Land use dynamics and environmental quality*. București, RO: Editura Academiei Române.

Popovici, E. A., Bălteanu, D., Dumitrașcu, M., & Sima, M. (2010). Land use and human pressure in the Getic Piedmont. In *Proceedings of BALWOIS, Conference on Water Observation and Information Systems for Decision Support*, Ohrid, Macedonia.

Sencovici, M., & Pehoiu, G. (2016). The anthropic pressure on the landscapes of the Subcarpathian and Piedmont Basin of Dâmbovița River (Romania). *InTech*. https://doi.org/10.5772/63722

Singh, R., Tripathy, S., Gupta, A. K., et al. (2025). Enhancing spatial interpretability of fluoride in groundwater using an integrated GIS and machine learning approach. *Earth Systems and Environment*. https://doi.org/10.1007/s41748-025-00657-4

Tomasoni, A. M., Soussi, A., Zero, E., & Sacile, R. (2025). A GIS-based safe system approach for risk assessment in the transportation of dangerous goods: A case study in Italian regions. *Systems, 13*(7), 580. https://doi.org/10.3390/systems13070580

Wu, X., Liu, J., & Hou, Y. (2025). Data and methods for assessing urban green infrastructure using GIS: A systematic review. *PLOS ONE, 20*(6), e0324906. https://doi.org/10.1371/journal.pone.0324906

Zarea, R., & Ionuș, O. (2012). Land use changes in the Bâsca Chiojdului river basin and the assessment of their environmental impact. *Forum Geografic. Studii și cercetări de geografie și protecţia mediului, 11*(1), 36–44. https://doi.org/10.5775/fg.2067-35.2012.023.i

Scientific Papers. Series E. Land Reclamation, Earth Observation & Surveying, Environmental Engineering. Vol. XIV, 2025
Print ISSN 2285-6064, CD-ROM ISSN 2285-6072, Online ISSN 2393-5138, ISSN-L 2285-6064

ASPECTS RELATING TO THE POSITIONING BY THE SEMI-KINEMATIC METHOD (STOP AND GO) OF DETAIL CHARACTERISTIC POINTS, NECESSARY FOR THE DESIGN OF COMMUNICATION WAYS

Călin Ioan IOVAN, Tudor Andrei FLORIŞ, Georgiana Denisa BOJINCĂ

University of Oradea, 1 Universității Street, 410087, Oradea, Bihor, Romania

Corresponding author email: calin_iovann@yahoo.com

Abstract

The case study was carried out with the help of satellite technologies for the spatial positioning of the various characteristic points of detail in the town of Suiug, Bihor county, and has as its objective the spatial positioning of the points of detail with the GPS system, through the post-processing kinematic method (pseudokinematics) Stop and Go, for the realization of the topographic plans in digital format, and respectively, of the digital models of the land, necessary for the rehabilitation and expansion of the roads in the locality. Trimble R3 receivers were used as base, and Trimble R4 as rover. When recording data from the field, we worked with the Trimble Digital Fieldbook and Trimble Access programs, and the processing with the Trimble Total Control (TTC) program. The coordinates of the base and initialization points of the rover were determined with the Trimble R4 receiver, with information acquired from the Oradea GNSS station, within the ROMPOS system. Mapsys 10.0 and Surfer programs were used to obtain the plan and land model in digital format.

Key words*: characteristic points of detail, Stop and go method, digital terrain model.*

INTRODUCTION

Modern Global Navigation Satellite System (GNSS) technologies provide highly accurate spatial positioning for topographic features, with the selection of a specific method being influenced by both logistical considerations and terrain conditions (Crainic, 2024). GNSS-based satellite positioning systems enable the automation and efficiency of data acquisition across diverse geographic areas, ensuring precise planimetric coordinates vital for applications such as cartography, navigation, transport infrastructure, and emergency response services (Mohanty & Gao, 2024; Kunisada & Premachandra, 2022).

In standard Stop & Go workflows, a static receiver is installed at a known geodetic control point, while a mobile receiver initiates the positioning process, which is influenced by both the equipment's technical capabilities and the field environment. The initialization consists of resolving the ambiguities linked to the carrier phase measurements, which involves determining the integer number of wavelengths of the received signal (Adam et al., 2006).

Technological advances have made it possible to perform this process "on-the-fly" (OTF), allowing real-time initialization while moving, thereby eliminating downtime. Once initialized, the mobile receiver (rover) sequentially occupies each target point, maintaining uninterrupted contact with satellites throughout movement. As a result, the rover must follow clear-signal paths within the work area to avoid satellite signal loss, which would otherwise require reinitialization (Adam et al., 2004; Hofmann-Wellenhof et al., 1997).

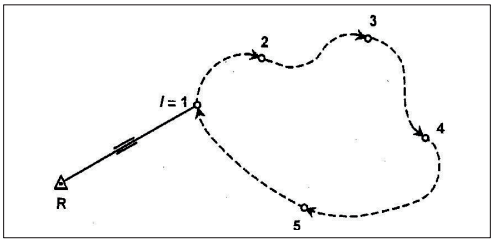


Figure 1. Stop & Go measurement scheme (from Adam et al., 2004)

For short distances between points along the predefined route, the operator typically moves on foot, carrying the mobile receiver mounted on a fixed-length support known as a bipod. This setup allows for quick stationing with high accuracy and operational efficiency. When the

target points are situated farther apart or at significant distances from the base station, the rover can be transported by vehicle, if satellite signal continuity is maintained and the connection to at least five satellites is ensured. This condition also applies to pedestrian movement over open terrain. Although not mandatory for on-the-fly (OTF) initialization, maintaining such signal stability can significantly reduce the required data acquisition time and help avoid signal disturbances (Hofmann-Wellenhof et al., 1997).
At the base station - positioned at a known reference coordinate - the fixed receiver and antenna are mounted on a tripod via a dedicated base featuring an optical centering mechanism. The mobile receiver and its antenna are secured on the bipod, approximately 2 meters in height, equipped with a spherical leveling device to ensure precise vertical and horizontal alignment. Because the antenna height remains constant throughout the process, it only needs to be entered once in the measurement project.
Initial setup involves placing the fixed receiver on the tripod and the bipod-mounted rover at the initial known point, followed by configuring the working parameters in the control unit (U.C.), which interfaces directly with both the receiver and the antenna. If satellite signal is lost, the operator must either return to a previously recorded point (if the system allows reinitialization from that location) or repeat the initialization process entirely (Adam et al., 2004).
As the rover moves from point to point, data collection is optimized by briefly pausing (typically 1-2 minutes) at each new station to ensure accurate data recording, depending on the length of the data collection epochs (Păunescu et al., 2006; Neuner, 2000). Consequently, only those positions where the mobile receiver was properly stationed and data were actively recorded are retained in the final dataset (Adam et al., 2004).
For enhanced efficiency in Post-Processed Kinematic (PPK) surveying, a single fixed receiver may be used to simultaneously support multiple mobile rovers, provided that the appropriate logistics are available.
In single-base PPK configurations, each newly determined point relies on a single position vector. When using two fixed receivers as reference bases, positioning is achieved using two independent vectors for increased redundancy and accuracy (Adam et al., 2004). Optimal conditions for implementing PPK satellite positioning depend on several factors, including:

- the availability of geodetic or GNSS network points within the survey area, with at least two single-frequency GNSS receivers (Zuliani, 2022);
- or one dual-frequency and one single-frequency receiver, along with access to data from a permanent GNSS station.

Under these conditions, several working approaches can be adopted:

- positioning known reference points along the survey route;
- returning to the initialization point to close a measurement loop;
- finalizing at another known point;
- or static positioning at the last station with subsequent post-processing.

Alternatively, when starting from the final surveyed point, software equipped with advanced algorithms can compute the positions of intermediate points where satellite signals were captured (Basso et al., 2021). This flexibility ensures that brief signal interruptions do not invalidate all previous recordings, if the processing model accounts for such gaps.
The method is particularly effective for detailed positioning tasks within a 5-6 km radius from the base station. On smaller areas, it offers a cost-efficient alternative. Recent studies highlight that for short GNSS baselines, PPK performance surpasses that of RTK, although over longer distances, a slight reduction in accuracy is noted. To meet accuracy standards, recording durations should exceed one hour, and the baseline distance must fall within the manufacturer's recommended range (Jemai et al., 2023).
PPK offers several advantages:

- data recording is faster since a continuous base-rover link is not needed, allowing for extended operational distances;
- fewer base stations are required compared to total station surveys;
- it provides high positional accuracy;
- and it can operate with minimal equipment - sometimes even a single dual-frequency receiver - if access to permanent

GNSS stations is available within 30-50 km (Zavate, 2008; Adam et al., 2004).

Despite the requirement of maintaining visibility to at least five satellites between consecutive points (Adam et al., 2004), the horizontal accuracy typically ranges from 1-3 cm, and vertical accuracy between 1-10 cm (Pirti, 2021). The method has proven efficient and reliable in cadastral surveys within both urban and rural contexts (Tang et al., 2017; Sicoe et al., 2023), as well as in environmental assessments and real-time or post-processed GNSS applications (Bodog et al., 2024; Jaskowski et al., 2022).

Moreover, research demonstrates that PPK solutions anchored by high-precision ground control points yield more accurate results than those derived from low-precision observations, particularly in drone-based photogrammetric workflows. Thus, the number, spatial arrangement of control points, and baseline length to the GNSS station are critical factors for achieving optimal results (Tamimi & Toth, 2023).

In the civil engineering sector (Costinaș et al., 2024), the success of infrastructure projects relies heavily on accurate site plans derived from GNSS data, alongside effective logistical planning (Costinaș et al., 2024; Sabău, 2010; Coşarcă, 2003). For the planning and construction of roads in rural or urban settings and for improving forest accessibility, detailed coordinate inventories and cartographic materials - both analog and digital - are indispensable (Călina & Călina, 2022; Călina et al., 2020; Coşarcă, 2003). The geometric layout of transportation routes must follow the terrain configuration and the precise spatial coordinates of topographic elements to accurately reflect the real-world situation (Belc, 1999).

Thus, field surveys must capture the transverse and longitudinal profile elements in the national reference system to support the development of execution projects.

MATERIALS AND METHODS

The case study was carried out in the village of Șuiug, part of Abram Commune, Bihor County, Romania (Figure 2). The main goal of the research was to evaluate the applicability and efficiency of GNSS technology - specifically the Stop & Go method using Post-Processed Kinematic (PPK) positioning - for determining the spatial coordinates of topographic detail necessary in the planning and rehabilitation of rural transport infrastructure.

The Stop & Go technique is particularly suitable when rapid, yet highly accurate point positioning is required, with minimal time spent at each location. This method relies on post-processing of satellite data, hence the term Post-Processed Kinematic (PPK) (Chiţea et al., 2009; Neuner, 2000).

Accurate positioning is ensured by employing at least two GNSS receivers: one serves as the fixed base station, while the other(s), referred to as rovers, operate as mobile units to measure the detail points.

Methodological Approach

The study employed a combination of the following research methods:

- *Bibliographic review:* analysis of specialized literature, standards, and previously completed contracts involving similar GNSS-based topographic work.
- *Field observation*: including route inspection and on-site evaluation of positioning conditions.
- *Experimental work:* application of GNSS positioning methods under real terrain conditions.
- *Comparison and analysis:* assessment of technical performance and outcome reliability.

Figure 2 presents the geographical location of the study area.

GNSS equipment and data collection

The experiment involved the spatial positioning of detailed topographic points using GNSS technology and the Post-Processed Kinematic (PPK) method, conducted along three separate routes, tailored to field conditions. To carry out the measurements, two Trimble R3 GNSS receivers paired with A3 antennas and one Trimble R4 dual-frequency receiver were employed. One Trimble R3 unit, equipped with an A3 antenna, was mounted on a tripod to serve as a base station, while the second R3 receiver, installed on a 2.04-meter bipod, was used as a rover for positioning characteristic detail points along the routes.



Figure 2. Location of the case study: Şuiug village, Abram commune, Bihor County (https://ro.wikipedia.org/wiki/Suiug,_Bihor)

In addition, satellite recordings from the permanent GNSS station in Oradea were accessed via the ROMPOS service to enhance positioning accuracy through the RTK method. The Trimble R4 receiver, also mounted on a 2.00-meter bipod, was used as a rover for data acquisition on Routes 1 and 2.

Field data were collected using Trimble Digital Fieldbook (for the R3 receiver) and Trimble Access (for the R4 receiver), both licensed programs provided with the equipment. A critical step during the fieldwork involved defining specific layers for recording each positioned point and assigning corresponding attribute codes. These codes were applied during stationing with the rover and are essential for the organized import of final coordinates into mapping software. This structured approach ensures efficient graphical representation and accurate generation of digital plans.

Data processing and graphical reporting

The graphic representation of the final coordinates of the characteristic detail points, referenced to the national coordinate systems STEREO-1970 and MN-1975, as well as the generation of the detailed digital plan, was performed using the Mapsys 10.0 software (Marton, 2007). The experiment followed a structured sequence of steps, including field data collection, data transfer, validation and processing, computation of ellipsoidal coordinates, transformation into the national reference system, and the preparation of the final coordinate inventory. These stages, along with the graphical reporting process and detailed plan generation, are summarized in the schematic diagram shown in Figure 3.

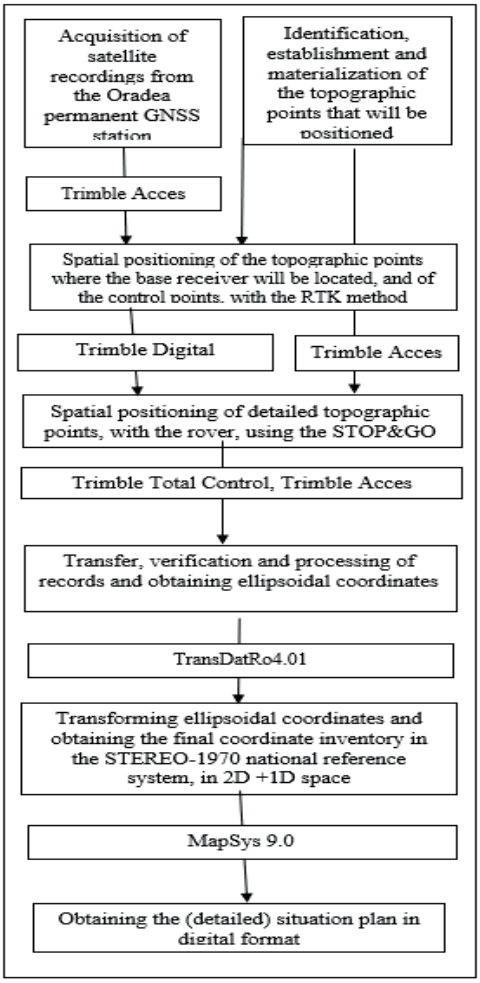


Figure 3. Summary presentation of the stages of carrying out the case study

The case study was further evaluated by comparing the technical implementation and

results with similar projects conducted under both comparable and varying field conditions. Based on this comparative analysis, several insightful conclusions were drawn.

RESULTS AND DISCUSSIONS

The processing of satellite recordings was performed using specialized computational models (Borko & Even-Tzur, 2021; Amiri-Simkooei et al., 2016). The data were processed differently depending on the type of receiver used. Specifically, the Trimble Access software was employed to process data recorded with the Trimble R4 receiver, as well as data obtained from the permanent GNSS station in Oradea using the RTK method, in order to determine the coordinates of the base and control points along the three routes. Additionally, Trimble Access was used to process recordings collected via the PPK method with the same receiver type.

Data recorded with Trimble R3 receivers were processed using Trimble Total Control (TTC) software. The ellipsoidal coordinates obtained from both programs were then converted into the national reference system using the TransDatRo4.01 software (Păunescu et al., 2010).

After completing these work stages, the final coordinates were inventoried by activating the corresponding layers within the mapping software.

The analysis of the plan with the reported details can be done in digital format, or after printing in analog format. In digital format, the details that need to be materialized on the plan will be activating all the layers that contain attributes, depending on the corresponding codes.

The graphical reporting of the measured detail points was conducted using orthophoto imagery for visual verification and planimetry purposes. The spatial distribution and positioning accuracy of the detailed points collected using the PPK method are illustrated in Figures 4, 5, and 6, which correspond to the three surveyed routes. These visual outputs demonstrate the precision and completeness of the data acquisition process across different sectors of the study area, facilitating the generation of the final site plan.

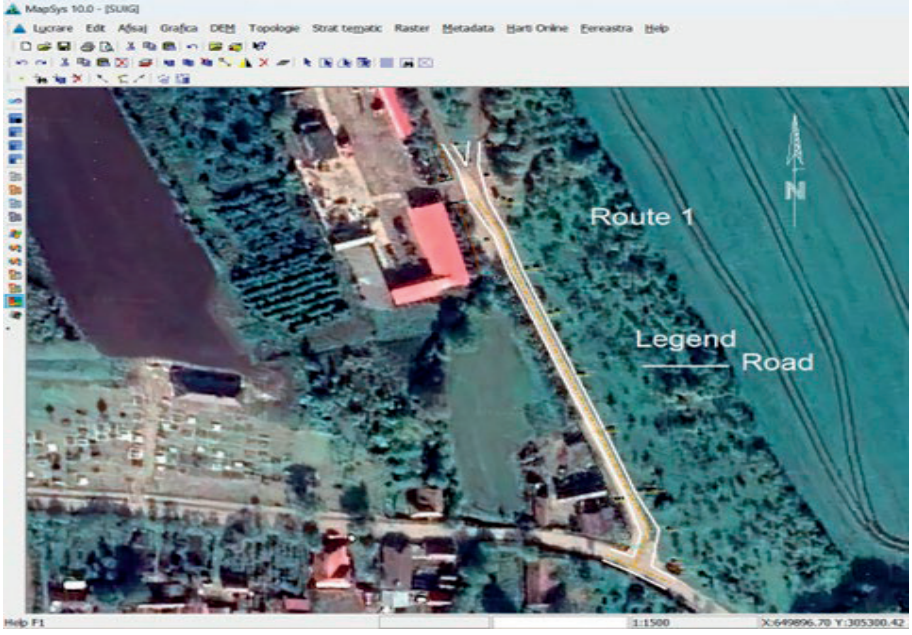


Figure 4. Reporting on the orthophoto plane of the routes on which the positioning of the detailed points carried out, using the PPK method (Route 1)

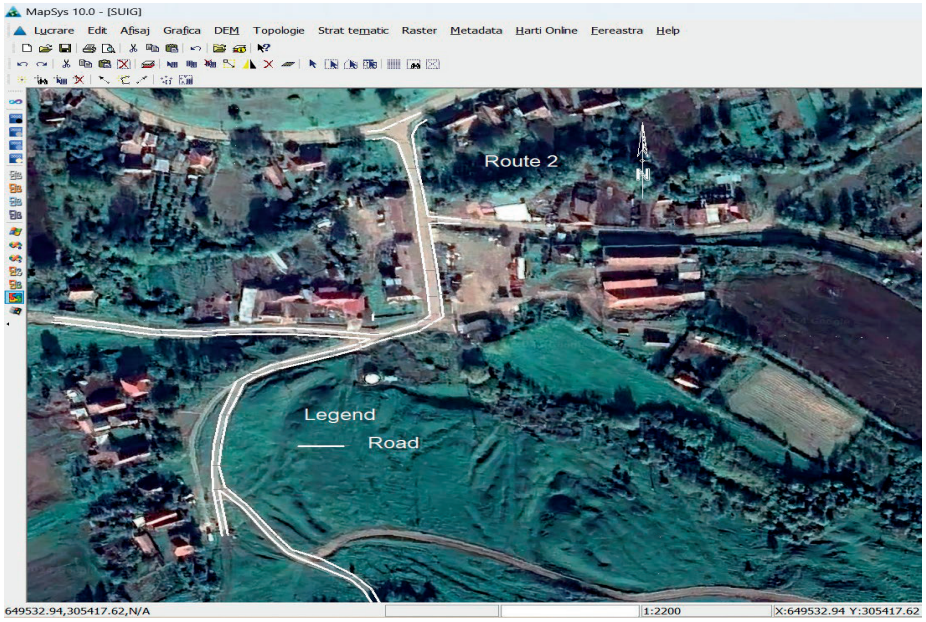


Figure 5. Reporting on the orthophoto plane of the routes on which the positioning of the detailed points were carried out, using the PPK method (Route 2)

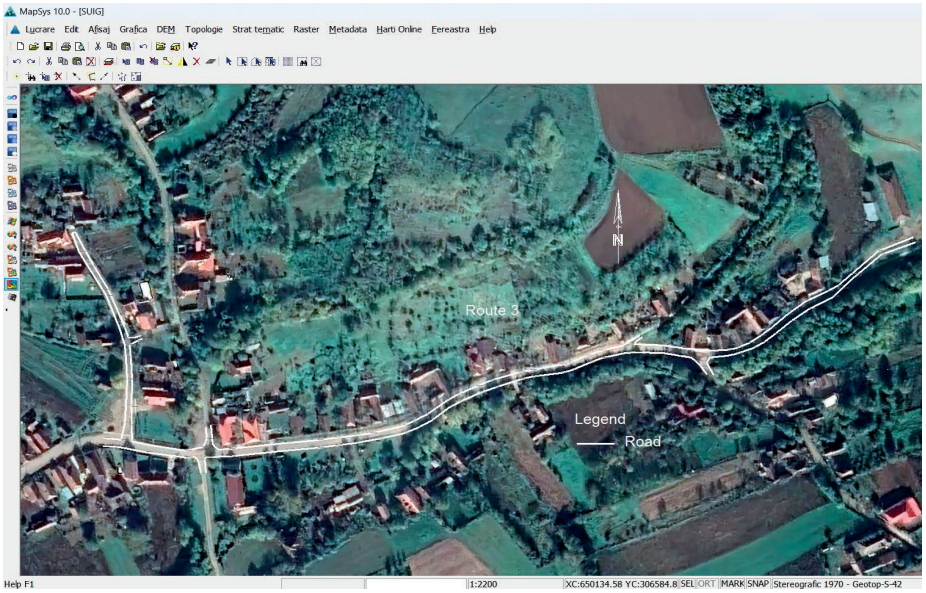


Figure 6. Reporting on the orthophoto plane of the routes on which the positioning of the detailed points were carried out, using the PPK method (Route 3)

The reporting of the final coordinates of the characteristic points was carried out with the found that a number of 1048 detail characteristic points, 292 lines, 680 symbols and 724 text attributes were graphically reported for the creation of the situation plan.

A representative extract from this inventory of coordinates is presented in Table 1. As a result,

1048 detail points were positioned on the three routes traveled.

Table 1. Extract from the inventory of coordinates of detailed topographic points, in the national reference system

No. point	X (m)	Y (m)	Z (m)	Cod
500	649930.48	305156.50	157.26	3
501	649930.28	305160.00	157.15	3
502	649930.01	305163.32	157.29	8
503	649929.43	305152.63	156.11	8
504	649929.54	305151.22	155.48	3
505	649929.26	305147.91	155.33	3
506	649928.90	305146.85	155.38	45
507	649927.87	305141.76	155.03	10
508	649927.56	305144.35	153.63	6
509	649918.64	305152.76	155.09	3
510	649919.77	305155.67	155.35	3
511	649919.82	305159.82	155.66	3
512	649915.73	305162.54	155.59	8
513	649914.09	305151.49	154.87	9
514	649912.69	305146.59	154.93	10
515	649913.22	305147.28	154.71	45
516	649913.85	305148.98	153.51	6
517	649910.60	305144.81	154.46	10
518	649904.83	305146.71	154.26	10
519	649903.43	305149.69	154.47	9
520	649903.26	305151.29	153.48	6
521	649903.89	305153.18	154.56	9
522	649904.25	305156.58	154.62	3
523	649904.54	305159.60	154.91	23
524	649904.81	305163.02	154.96	3
525	649905.59	305167.73	155.13	8
526	649904.77	305170.13	156.98	8
527	649891.29	305168.99	154.33	3
528	649890.41	305167.42	154.32	23
529	649888.97	305164.78	154.32	3
530	649887.70	305162.44	154.10	8
531	649886.41	305157.72	154.04	45
532	649886.61	305156.69	153.05	6
533	649871.86	305160.21	153.06	45
534	649872.27	305159.48	152.06	6
535	649869.78	305161.42	150.86	10

From the analysis of the data presented in Table 2, it was found that topographic detail points represent the largest share of elements included in the situation plan (38%), followed by text attributes (26%), symbols (25%), and lines (11%). These proportions are visually illustrated in Figure 7, offering a synthetic overview of the spatial features graphically reported using the MapSys 10.0 software.

Extracts from the situation plans, illustrating the reported topographic details, are presented in Figures 8, 9, and 10.

The results of comparative research indicate that the PPK-GPS method is clearly superior to classical topographic positioning methods, which have as their main objective the preparation of contour topographic maps, on very large surfaces. Consequently, it was found that by applying this method the estimated time of the works was reduced by approximately 70% (El Shouny et al., 2017).

Table 2. Synthetic evidence of the details that were graphically reported with the MapSys 10.0 program

Layer	Item name	Point	Line	Symbol	Attribute Text	Total
3	Building	0	0	0	0	**120**
4	Road	135	26	0	0	**161**
6	Groove	90	33	0	0	**123**
7	Zero altitude	6	0	0	0	**6**
8	Altitudes	114	0	0	0	**114**
9	Bridge < 5 m	94	49	0	0	**143**
10	Fence	86	48	0	0	**134**
11	Building	10	4	0	0	**14**
16	Concrete electric pole	29	0	0	0	**29**
17	Gate access	0	0	1	0	**1**
19	Retaining wall	2	1	6	0	**9**
21	Indication	0	0	1	0	**1**
23	Road axis lin	105	15	0	0	**120**
24	Bridge tube	4	1	0	0	**5**
26	Text attributes	0	0	12	47	**59**
27	Shrubby vegetation	0	0	1	0	**1**
28	Concrete fence	2	1	0	0	**3**
29	Trinity	0	0	1	0	**1**
32	Attribute Text for Zero altitude	0	0	6	7	**13**
33	Altitude text	0	0	1	659	**660**
34	Symbols	0	0	651	0	**651**
38	Alleys	56	11	0	0	**67**
39	Hydrant	4	0	0	0	**4**
45	Trench edge	149	79	0	0	**228**
50	Building w. elevation	6	6	0	0	**12**
56	Limit without altitude	36	18	0	0	**54**
78	Route text	0	0	0	11	**11**
Total		**1048**	**292**	**680**	**724**	**2744**

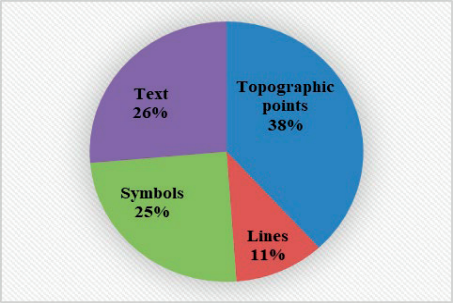


Figure 7. Graphical distribution of the elements included in the detail plan for the three surveyed routes

The application of RTK/PPK GNSS methods, for carrying out drone flights, which aim to map inaccessible forest areas, led to obtaining slight standard deviations in the plane of 0.026 m on the OX axis and 0.035 m on the OY axis, and on the OZ axis of 0.082 m. Consequently, RTK/PPK technology in combination with drones, constitutes a feasible and sufficiently precise solution for mapping areas covered with forest vegetation, and characterized by reduced accessibility (Tomaštík et al., 2019).

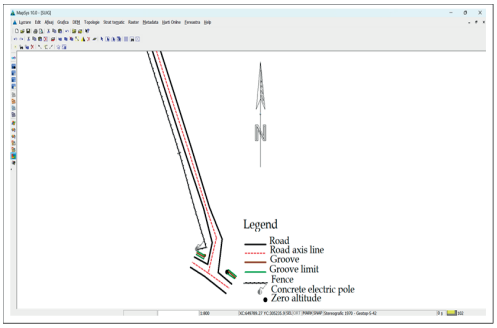


Figure 8. Extract from the detailed plan for route 1

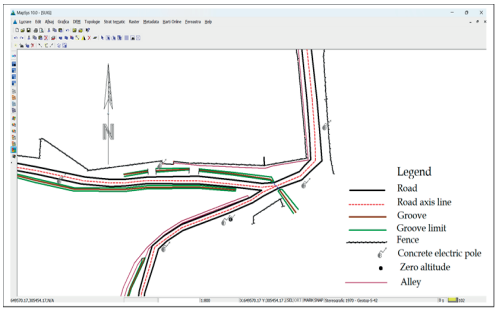


Figure 9. Extract from the detailed plan for route 2

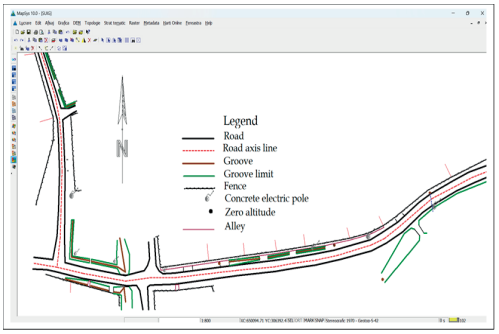


Figure 10. Extract from the detailed plan for route 3

CONCLUSIONS

The spatial positioning of the detailed characteristic points necessary for the design and rehabilitation of transport routes in rural areas can be achieved under optimal conditions with GNSS technology, through the Stop and Go method, if at least two GNSS receivers with single and dual frequency are available.

The optimal length of the routes on which positioning is performed with the PPK method, from the base to the end of the route, should not exceed 4-5 km.

Obtaining superior precision for the coordinates of the positioned points and substantially reducing working time is conditioned by the continuous recording of the signal by the base and rover receivers used, along the travel routes.

The use for base and control points of the coordinates of points in the geodetic network or those determined by the RTK method, with the use of recordings from permanent GNSS stations, through the ROMPOS system, ensures the PPK positioning method has extensive applicability.

The use of control points, with known coordinates, along the route and at the completion of the recordings, optimizes the positioning process within the PPK method, contributing to increasing the accuracy of determining the coordinates of new points.

To optimize the positioning process with the Stop and Go method, especially to reduce working time, multiple single-frequency GNSS receivers can be used as a rover, and the base will be located approximately in the middle of the route, depending on the field working conditions.

If two receivers are used as rovers on a single route, it is optimal for them to move from the base point towards the ends of the route, and the base is optimal for it to be located halfway along the route.

For two or more positioning routes with the PPK method, it is optimal to place the base at approximately equal distances from them, and to perform positioning with a rover for each route.

If the routes are located at large distances from each other, the base will be conveniently located in terms of distance and access to satellite recordings, for each separate route.

In the variant where multiple single-frequency GNSS receivers are available, for example four, the necessary base and control points can be positioned later using the traditional static method, and the recordings are post-processed. Also, the coordinates of the base and control points can be determined at the completion of the route positioning, by the RTK method, with a dual-frequency receiver, using the records from the nearest permanent GNSS station. They can also be determined with the total station, by a framed polygonometric survey, or by the free station method, if there are points from the support network in the work area.

ACKNOWLEDGEMENTS

The research was carried out with the support of S.C. TOPOSISTEM and S.C. ECOPROD FOREST SRL, which provided the logistical base and facilitated access to the case study location and participation in the case study. We also thank the Local Council of Abram Commune, Bihor County, for their collaboration.

REFERENCES

Ádám, J., Bányai, L., Borza, T., Busics, G., Kenyeres, A., Krauter, A., & Takács, B. (2004). *Satellite positioning*. University Publishing House.

Amiri-Simkooei, A.R.., Jazaeri, S., Zangeneh-Nejad, F. & Asgari, J. (2016). Role of stochastic model on GPS integer ambiguity resolution success rate. *GPS Solut. 20*, 51–61.

Basso, M., Martinelli, A., Morosi, S., Sera, F. (2021). A Real-Time GNSS/PDR Navigation System for Mobile Devices. *Remote Sens., 13*, 1567. https://doi.org/10.3390/rs13081567.

Belc, F. (1999). *Land communication routes - Design elements*. Timișoara, Romania: Orizonturi Universitare Publishing House.

Bodog, M.F., Șchiopu, E.C., Crainic, G.C., & Lazăr, A.N. (2024). Assessment of contamination degree of oil residues on a former agricultural site. *Journal of Agricultural Science and Technology, A 14*, doi: 10.17265/2161-6256/2024.02.003, 67-82.

Borko, A., Even-Tzur, G. (2021). Stochastic model reliability in GNSS baseline solution. *J. Geod.*, *95*, 20.

Călina, A. & Călina, J. (2022). Study on the preparation of technical documentation necessary for the rehabilitation and modernization of road infrastructure in the agritouristic area, Giubega-Băilești. *Annals of the University of Craiova - Agriculture, Montanology, Cadastre Series*, *52*(2), 204-214.

Călina J., Călina A., Milut M., Vangu M., Dinucă C. (2020). Study regarding the preparation of technical documentation necessary to modernize the road that crosses the Bucovat-Leamna, Dolj agroturistic area. *Annals of the University of Craiova - Agriculture, Montanology, Cadastre Series, I*, 253-262. https://anale.agrocraiova.ro/index.php/aamc/article/view/1119/1051

Costinaș A. M. G., Șmuleac L.I., Șmuleac A. (2024). The use of modern technologies for the execution of civil and industrial construction works. *Research Journal of Agricultural Science, 56*(3), 67-75.

Coșarcă, C. (2003). *Engineering topography*. Bucharest, Romania: Matrix Rom Publishing House.

Crainic, G. C. (2024). Issues related to the implementation of geomatic applications in the national forestry fund. *Scientific Papers. Series E. Land Reclamation, Earth Observation & Surveying, Environmental Engineering, 13*, 794-804. https://landreclamationjournal.usamv.ro/pdf/2024/Art97.pdf

Chițea, G., Iordache, E., & Chițea, C.G. (2009). *Space Geodetic Technologies, Part I, Global Positioning Systems (GPS)*, Brașov,RO: Lux Libris Publishing House.

El Shouny, A., Yakoub, N., Hosny, M. (2017). Evaluating the Performance of Using PPK-GPS Technique in Producing Topographic Contour Map. *Marine Geodesy, 40*(11), 224-238. DOI: 10.1080/01490419.2017.1321594

Hofmann-Wellenhof B., Lichtenegger H. & Collins J. (1997). *Global Positioning System, Theory and Practice*, Springer Wien New York, AUT.

Jaskowski, P., Tomczuk, P. & Chrzanowicz, M. (2022). Construction of a Measurement System with GPS RTK for Operational Control of Street Lighting. *Energies, 15*, 9106. https://doi.org/10.3390/en15239106

Jemai, M., Loghmari, M. A., Naceur, M. S. (2023). A Height Accuracy Study Based on RTK and PPK Methods Outside the Standard Working Range. *(IJACSA) International Journal of Advanced Computer Science and Applications, 14*(5). https://thesai.org/Downloads/Volume14No5/Paper_20A_Height_Accuracy_Study_based_on_RTK_and_PPK_Methods.pdf

Kunisada, Y., Premachandra, C. (2022). High Precision Location Estimation in Mountainous Areas Using GPS. *Sensors, 22*, 1149. https://doi.org/10.3390/s22031149

Marton, H. (2007). *MapSys, TopoSys - User manual*. Odorheiu Secuiesc, Romania.

Mohanty, A. & Gao, G. (2024). A survey of machine learning techniques for improving Global Navigation Satellite Systems. *EURASIP Journal on Advances in Signal Processing*, *273*. https://doi.org/10.1186/s13634-024-01167-7.

Neuner, J., (2000). *Global positioning systems.* Bucharest,RO: Matrix-Rom Publishing House.

Păunescu, C., Necula, D., Smadu, M., Păunescu, V. (2010). Study on coordinates transformations from the three-dimensional system on WGS-84 ellipsoid in the stereographic 1970 plan system (Elipsoid Krasovski), *Annals of the University of Oradea, Fascicle*

Constructions and Hydro-Edilitial Installations, XII(2), 235-244.

Păunescu, C., Mocanu, V., & Dimitriu, S.G. (2006). *Global positioning system G.P.S.,* Bucharest, RO: University Publishing House.

Pirti, A. (2021). Evaluating the accuracy of post-processed kinematic (PPK) positioning technique. *Geodesy and Cartography, 47*(2), 66-70. https://doi.org/10.3846/gac.2021.12269.

Sabău, N.C. (2010). *Terrestrial measurements*, Oradea,RO: University Publishing House.

Sicoe, S. I., Crainic, G. C., Samuel, A. D., Bodog, M., Iovan, C. I., Curilă, S., Hâruța, I. O., Șerban, E., Dorog, L. S., & Sabău, N. C. (2023). Analysis of the effects of windthrows on the microbiological properties of the forest soils and their natural regeneration, *Forests*, *14*(6), 1200. https://doi.org/10.3390/f14061200.

Rus, T. (2004). *Satellite Geodesy, Course Notes*, Bucharest, RO: Technical University of Construction.

Tamimi, R., Toth, C. (2023). Assessing the Viability of PPK Techniques for Accurate Mapping with UAS. *The International Archives of the Photogrammetry, Remote Sensing and Spatial Information Sciences,* XLVIII-1/W1-*12th International Symposium on Mobile Mapping Technology (MMT 2023)*, Padua, Italy.https://isprs-archives.copernicus.org/articles/XLVIII-1-W1-2023/479/2023/isprs-archives-XLVIII-1-W1-2023-479-2023.pdf.

Tang, X., Roberts, G., Li, X. & Hancock, C. (2017). Real-time kinematic PPP GPS for structure monitoring applied on the Severn Suspension Bridge, UK. *Adv. Space Res*, *60*, 925-937.

Tomaštík J., Mokroš M., Surový P., Grznárová A., Merganic J. (2019). UAV RTK/PPK Method-An Optimal Solution for Mapping Inaccessible Forested Areas? *Remote Sens., 11*(6), 721. https://doi.org/10.3390/rs11060721.

Zavate F. L. (2008). Current status in the field of national spatial data infrastructures and GPS differential correction services. *Journal of Geodesy, Cartography and Cadastre, 17*(1, 2), 70-78.

Zuliani, D., Tunini, L., Di Traglia, F., Chersich, M. & Curone, D. (2022). Cost-Effective, Single-Frequency GPS Network as a Tool for Landslide Monitoring. *Sensors, 22,* 3526, https://doi.org/10.3390/s22093526.

***https://ro.wikipedia.org/wiki/Suiug,_Bihor.

Scientific Papers. Series E. Land Reclamation, Earth Observation & Surveying, Environmental Engineering. Vol. XIV, 2025
Print ISSN 2285-6064, CD-ROM ISSN 2285-6072, Online ISSN 2393-5138, ISSN-L 2285-6064

SPATIAL POSITIONING OF TOPOGRAPHIC DETAILS WITH INTEGRATED MODERN TECHNOLOGIES, IN AREAS WITH FOREST VEGETATION

Călin Ioan IOVAN, Tudor Andrei FLORIȘ, Georgiana Denisa BOJINCĂ, Călin Gheorghe PĂȘCUȚ

University of Oradea, 1 Universității Street, 410087, Oradea, Bihor, Romania

Corresponding author email: calin_iovann@yahoo.com

Abstract

In order to achieve the various objectives related to the sector of terrestrial measurements in areas occupied by forest vegetation, high-performance satellite technologies are currently used. The case study was carried out within the radius of Câmpani, Bihor County, having the objective of analyzing the possibilities of positioning the topographical details, with integrated modern technologies, in areas with forest vegetation. The GNSS receivers Trimble R8, Trimble R10, Trimble R12I, the Trimble S6 total station, as well as real-time data collection and processing software - Trimble Access, were used. The rover-based real-time kinematics (RTK) method was used, with data transmission between receivers via external radio, and framed polygonal journeys. To determine the spatial position of the base points, the data recorded from the permanent GNSS station Beiuș, were used. The data collected were processed in the 2D+1D space, and the results obtained were characterized by superior precision.

Key words*: spatial positioning, GNSS technology, total station, integrated technologies, digital topographical plan.*

INTRODUCTION

The implementation of urban development projects in rural areas, situated across diverse geographic regions, necessitates adequate infrastructure. Consequently, the provision of essential utilities for various sectors requires the establishment of access routes and a minimum level of comfort for the population within the targeted administrative-territorial units. In hilly and mountainous regions, forest vegetation constitutes a significant proportion, comprising approximately 92% of the national forested area (Florescu & Nicolescu, 1996). As a result, the establishment of infrastructure to support the spatial positioning of topographic elements in these forested terrains presents distinct technical and operational challenges, requiring tailored methodologies and equipment adapted to the environmental context (Rus, 2004). Currently, the determination of planimetric and altimetric coordinates for various characteristic topographic points within the national reference system can be efficiently performed using Global Navigation Satellite Systems (GNSS), total stations, drone-based photogrammetric recordings, or integrated combinations of these methods (Păunescu et al., 2006; Neuner, 2000). Therefore, the selection of appropriate spatial positioning technologies and corresponding working methods requires a comprehensive analysis of the site-specific working conditions, the technical requirements established by the project beneficiary, as well as the available logistics and existing infrastructure relevant to terrestrial surveying activities (Crainic, 2024; Chiţea et al., 2009).

When conditions allow for GNSS-based positioning of detail points, the most widely used method is Real-Time Kinematic (RTK) positioning. This technique employs a dual-frequency GNSS setup, consisting of a fixed receiver (base station) and a mobile receiver (rover), which work together to ensure high spatial accuracy (Adam et al., 2004).

The fixed receiver (reference station) is stationed at a point of known coordinates, and is equipped with a transmitter, and the mobile receiver - the rover (Figure 1) is equipped with a receiving device. A real-time radio link is established between the two receivers (Figure 2) (Adam et al., 2004).

The components of the reference station are represented by: GPS antenna (1), controller (3), GPS receiver (4), tripod (4), radio antenna (5) and radio modem (6) (Adam et al., 2004).

The mobile receiver is made up of the following components: GPS antenna (1), antenna support rod (2), GPS receiver (2), controller (3), radio modem (5) and radio antenna (6) (Adam et al., 2004).

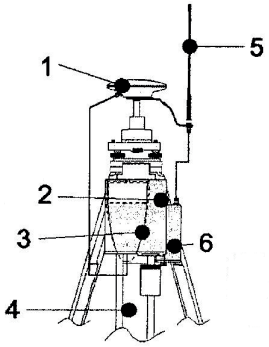


Figure 1. Elements of the reference station (Adam et al., 2004)

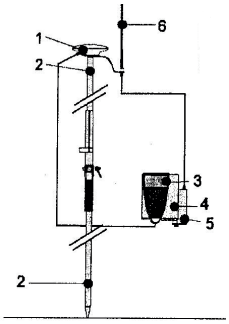


Figure 2. Mobile receiver éléments (Adam et al., 2004)

Once the receivers are mounted and the positioning method and recording parameters are configured, the initialization process - resolving carrier-phase ambiguities - is performed. With modern receivers, this process typically takes only 1-2 minutes (Adam et al., 2004).

The fixed receiver, positioned at a reference point with known coordinates, acts as a radio station that captures satellite signals and relays them, unprocessed and without delay, to the mobile receiver located at a new point. The mobile receiver then interprets this radio signal to determine its position relative to the stationary point. The position is computed by combining the components of the vector between the base station and the rover with the WGS84 coordinates of the reference station, thus obtaining the coordinates of the new point in the WGS84 system (Adam et al., 2004). These coordinates are subsequently converted into the national reference system using established transformation parameters, providing real-time final positioning data (Crainic, 2024; Teunissen & Khodabandeh, 2015).

This workflow is illustrated in Figure 3, which presents the RTK positioning method used in this study.

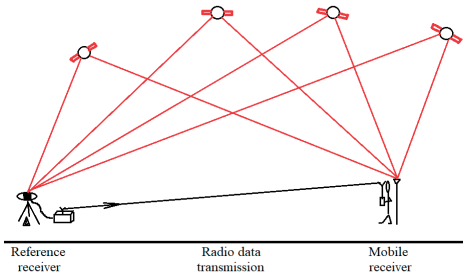


Figure 3. RTK positioning method (processing after Adam J. et al., 2004)

RTK-based spatial positioning can achieve high accuracy, efficiency, and reliability when at least five satellites are available and properly configured. The widespread adoption of this method is largely due to advancements in the rapid transmission of satellite data between receivers - now achieved within fractions of a second (Xingxing et al., 2019; Adam, 2004) - as well as the continuous refinement of computational models that enhance data processing (Odijk et al., 2016).

The accuracy obtained using this GPS measurement method is ± 1-3 cm. This GPS measurement method is recommended for tracing construction elements, positioning details in cadastral works, extension and rehabilitation of communication routes, extension and rehabilitation of water supply and sewage networks, in the agricultural and forestry sectors (Sicoe et al., 2023; Pica et al., 2022), etc. Although in specialized treatises it is not recommended for determining the coordinates of support or thickening network points, currently, due to the existence of an appropriate infrastructure in the terrestrial measurement sector and efficient logistics, geodetic network thickening works can also be carried out, with optimal precision (Adam et al., 2004).

The RTK positioning method appeared in the first half of the 1990s, using single-frequency receivers. In this case, the distance between the fixed and mobile receivers did not exceed a few km, due to the technical possibilities of performing initialization over long distances and transmitting records at an increased distance from the base (Adam et al., 2004; Hofmann-Wellenhof et al., 1997). With the rapid development of satellite positioning technology, and the existence of permanent GNSS stations, at optimal distances in each county, the remote RTK method emerged (Zavate, 2008). In this variant, the distance between the reference receiver, which can be represented by the permanent GNSS station (or a virtual station, as the case may be), and the mobile one, can reach even 30-40 km, in which case dual-frequency receivers will be used (Adam et al., 2004).

Modern programs can perform the initialization again in case of signal loss, even while moving - on-the-fly (OTF) technique, recordings made with the second frequency also play an important role (Adam et al., 2004). Currently, increasing the distance between the reference receiver and the rover is only required by the possibility of transmitting recordings in record time, continuously, using a modern infrastructure, appropriate for these applications and respectively high-performance computational models (Basso et al., 2021; Haojun et al., 2018). Variations in atmospheric conditions can negatively influence the atmospheric error modeling process, resulting in significant atmospheric errors that affect the coordinate determination accuracy, initialization speed, and efficiency of network RTK positioning. Consequently, there is now the possibility of using a fast and reliable network RTK positioning method that uses sequential ambiguity resolution (SAR) of combined multi-frequency observations (Liu et al., 2024).

Also, current research has highlighted the fact that there is currently the possibility of integrating conventional RTK-GNSS methods with a new working technique that capitalizes on recordings from surplus satellites, namely those that were not initially used for positioning, to more efficiently identify incorrect fixation solutions. Consequently, this positioning variant improves positioning accuracy, characterized by high reliability (Fredeluces et al., 2024).

In some situations, working conditions determined by the terrain configuration and respectively the presence of forest vegetation become unsuitable for the use of established positioning methods with GNSS technology. As a result, in these situations, the total station (T.S.) can be used to determine the coordinates of the detail points, using established working methods, such as: polygonometric tracking framed with erasures, polygonometric tracking closed on the starting point, with views to known points and the free station.

Consequently, to streamline the positioning process of detailed topographic points, integrated working methods can be used, related to satellite technology and total station technology, respectively. An opportunity for integrated use of positioning technologies is represented by the presence of permanent GNSS stations, at optimal distances in each county (Rus, 2004). In this context, the existence of an appropriate infrastructure and, respectively, of a high-performance equipment, ensures the obtaining of coordinates with high precision and accuracy (Tang et al., 2017).

MATERIALS AND METHODS

The case study was conducted in Cîmpani Commune, Bihor County (Figure 4).

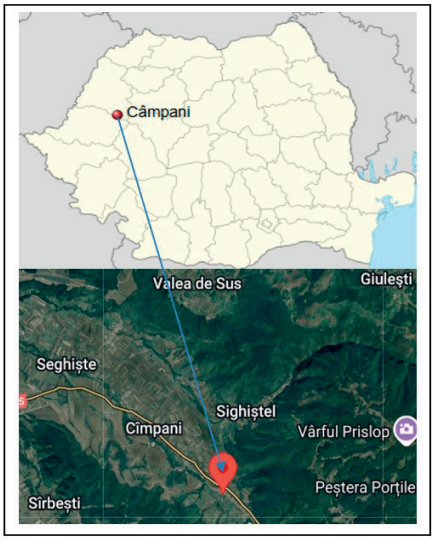


Figure 4. Case study location
(https://ro.wikipedia.org/wiki/C%C3%A2mpani,_Bihor; https://comuna.info/harta-campani-bh/)

The objectives of this case study focus on the research and analysis of spatial positioning methods for topographic detail points required in the design and implementation of water supply and sewage network expansion and rehabilitation projects in the forested areas of Câmpani commune, Bihor County, Romania. Additionally, the study explores the specific aspects of generating detailed plans in both digital and analog formats for the case study site.
The research methodology employed includes bibliographic review, on-site and in-station observations, experimentation, simulation, comparison, and analysis.
The bibliographic documentation covered spatial positioning techniques for topographic details in forested environments, based on specialized literature, technical reports, and related project documentation.
Observations conducted in the field and at control stations aimed to identify and mark detail points, define the positioning technologies, and establish the field routes.
The experiment involved the practical spatial positioning of the detailed points required for infrastructure development.
Simulation was used to generate final products based on experimental data.
All methods, outcomes, and observed particularities were critically analyzed and compared, leading to the formulation of conclusions.
The equipment and software used included:

- GNSS receivers with internal and external radio transmission, accompanied by data logging and processing programs;
- recordings from the Beiuș permanent GNSS station;
- a total station with corresponding software;
- digital cartography software for reporting the coordinates and producing graphical outputs in both digital and print formats.

Although low-cost single- and dual-frequency GNSS receivers (SF-LC and DF-LC) can perform comparably to geodetic-class receivers in open-sky conditions, geodetic receivers are preferred for large-area surveys requiring high precision (Hamza et al., 2025).
Satellite data acquisition was conducted using high-performance GNSS receivers from the Trimble range: R8, R10, and R12I. RTK-GNSS and UAV-based multispectral photogrammetry both offer high-precision mapping. A comparative study showed minimal geometric discrepancies between maps derived from the two methods - only −0.26% in perimeter and −0.23% in area (Dlamini & Ouma, 2025). Therefore, in forested yet accessible areas, RTK-GNSS remains the preferred solution.
Studies have demonstrated that geodetic positioning using network RTK, even with GNSS baselines up to 40 km, does not significantly affect coordinate accuracy (Gökdaş & Özlüdemir, 2020). When nearby permanent stations are inaccessible, a Virtual Reference Station (VRS) may be used, generating correction data from surrounding GNSS stations without extra hardware. This approach provides horizontal accuracy of 1- 2 cm and vertical accuracy of 2-5 cm, even in forested areas (Kurtulgu & Pirti, 2025).
The spatial positioning method applied was the real-time kinematic (RTK) base-rover configuration. In the first stage, ten base points were established for detail point measurements. This process occurred in three phases using data from the Beiuș permanent GNSS station.
In the second stage, topographic detail points were positioned using RTK-GNSS receivers wherever satellite signal reception was optimal. Routes and point attributes were predefined for consistency.

- At base points 1 through 8, the Trimble R8 (4W external radio) functioned as the base, while R10 and R12I units (2W internal radios) served as rovers.
- For base points 9 and 10, the R10 (2W external radio) was used as the base and the R12I as the rover.

In areas with suboptimal GNSS signal due to forest cover, a Trimble S6 total station was used. Surveying was performed via framed polygonal traverses or closed traverses connected to known points. These methods were applied on portions of the routes connected to GNSS base points 1, 2, 7, 8, and 10.
As a result, integrated positioning methods were adopted, tailored to site-specific conditions - an approach previously validated in similar research (Crainic, 2024).
Data collection, processing, and conversion were performed using:

- Trimble Access – for recording and processing GNSS and total station data;

- TransDatRo4.01 – for transforming ellipsoidal coordinates into the national reference system;
- MapSys 11.0 – for graphical reporting of positioned points (Marton, 2007).

The stages of the experimental process are summarized in Figure 5, which was developed following extensive field inspections and consultations with project beneficiaries.

The case study involved a high volume of fieldwork, primarily due to terrain configuration and challenges related to spatial positioning in densely vegetated areas.

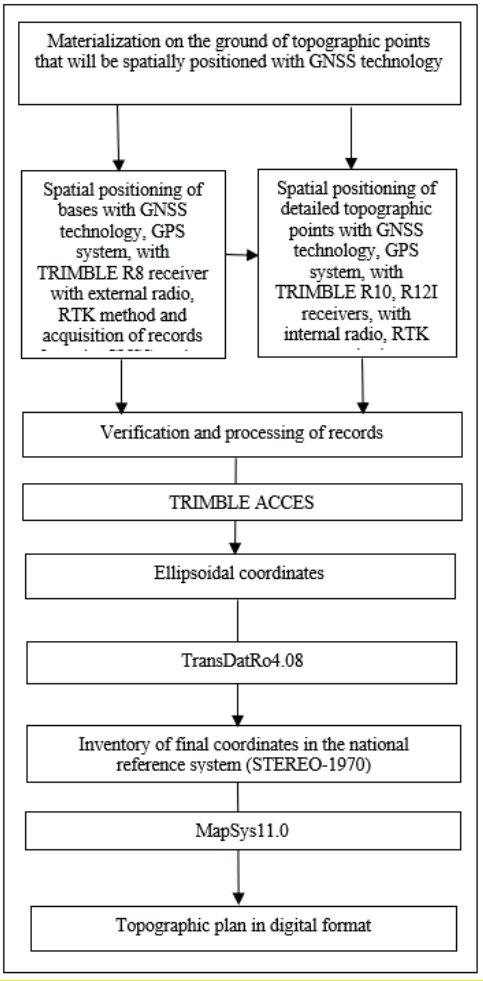


Figure 5. The sequence of steps for carrying out the case study

RESULTS AND DISCUSSIONS

The GNSS-based positioning results were obtained in two stages. First, the coordinates of ten densification base points were determined via the RTK-distance method using data from the Beiuș GNSS station (Table 1). Second, coordinates for the detail points positioned from these bases using RTK and total station measurements were recorded, with a representative sample shown in Table 2.

Table 1. Inventory of coordinates of topographic points for the support network density, in the national reference system STEREO-1970, MN-1975

No. point	X (m)	Y (m)	Z (m)	Code
1	558161.822	313687.201	480.774	1
2	558189.851	313283.842	427.653	1
3	558197.790	313247.390	425.990	1
4	558029.432	312190.031	377.281	1
5	558118.550	312494.411	396.370	1
6	559983.221	310006.410	324.461	1
7	561449.041	312888.373	387.982	1
8	563843.210	311435.491	307.411	1
9	561350.431	308104.100	304.390	1
10	560646.620	311262.131	337.382	1

Table 2. Extract of coordinate inventory for detailed topographic points in the national reference system

No. point	X (m)	Y (m)	Z (m)	Code
2000	558699.750	311654.233	359.123	8
2001	558699.761	311654.231	359.159	8
2002	558699.765	311654.225	359.139	8
2003	558699.751	311654.211	359.128	8
2004	558700.057	311654.252	359.142	8
20005	558700.049	311654.247	359.167	8
20006	558699.733	311654.057	359.117	8
20007	558699.736	311654.058	359.109	8
20008	558699.732	311654.054	359.124	6
20009	558650.975	311618.299	357.702	10
20010	558647.208	311619.045	357.970	16
20011	558645.940	311617.726	357.749	4
20012	558640.476	311622.345	357.891	4
20013	558643.866	311624.572	357.902	3
20014	558636.674	311630.409	358.192	3
20015	558634.739	311632.161	358.239	17
20016	558633.450	311633.239	358.236	28
20017	558632.932	311629.894	358.189	20
20018	558634.333	311629.659	358.094	8
20019	558629.894	311632.099	358.236	4
20020	558624.162	311637.450	358.448	4
20021	558623.258	311642.443	358.692	28
20022	558622.084	311643.597	358.730	10
20023	558619.047	311644.945	358.853	16
20024	558614.824	311646.680	358.801	4
20025	558615.370	311650.340	359.044	10
20026	558613.984	311648.645	358.877	8
20027	558612.612	311650.768	358.893	20
20028	558613.652	311652.786	359.059	10
20029	558614.321	311655.261	359.285	10
…	…	…	…	…
22590	558988.527	311309.790	349.843	38
22591	558991.803	311306.062	349.829	38
22592	558992.446	311306.525	349.396	6
22593	558988.461	311311.027	349.427	6
22594	558984.196	311314.825	350.151	38

The identified detail points are essential for implementing the water supply and sewage network expansion and rehabilitation project in the case study area. To ensure efficient data integration, each point was assigned a code corresponding to a specific layer, depending on the type of detail it represents. The relationship between point codes and their respective layers is summarized in Table 3.

To streamline the use of the final coordinates in accordance with the project's technical requirements, the data was organized into a .txt file. This was subsequently imported and graphically rendered using the MapSys 11 software, resulting in a digital topographic plan containing all the positioned detail points. Overlaying the topographic plan onto the orthophoto map of the project area provides a comprehensive visual representation of the spatially positioned features (Figure 6). Representative excerpts from the graphic outputs are shown in Figures 7 and 8. The digital plan enables versatile usage - either in digital or printed analog format (Figure 9).

Printing of the detail plan was carried out after the layout, sheet coverage, and sequencing were established (Figure 10). In addition, a printed version of the coordinates inventory was prepared for delivery to the project beneficiary.

Based on the analysis of the results obtained during the case study, the total surveyed area was S = 399,550 m², with a cumulative measured route length of L = 32,000 m.

Table 3. Characteristics of the detailed points spatially positioned and graphically represented using the MapSys 11 program

Layer	Name	Point	Line	ArcDeC	Curve	Symbol
1	Street limit	11	0	0	0	11
3	Construction	2940	1084	0	4	4028
4	Roadside	6483	442	0	3	6928
5	Forest vegetation	496	0	0	0	496
6	Groove	4251	1071	0	0	5322
8	Altitudes	6303	0	0	0	6303
9	Bridge (h<5)	1113	433	0	0	1546
10	Fence	2570	750	0	0	3320
14	Duct	1196	0	0	0	1196
15	Wooden telephone pole	162	0	0	0	162
16	Concrete electric pole	365	0	0	0	365
17	Gate access	1109	0	0	0	1109
18	Tap	1	0	0	1	2
19	Retaining wall	590	176	0	0	766
20	Sewerage house	1196	0	0	0	1196
21	Traffic signs	84	0	0	0	84
23	Road axis line	2858	223	0	0	3081
24	Bridge tube	243	95	0	0	338
26	Text	0	0	0	626	626
27	Shrubby vegetation	106	0	0	0	106
28	Concrete fence	874	415	0	1	1290
29	Trinity	18	0	0	0	18
35	Kilometer milestone	6	0	0	4	10
37	Telephone home	3	0	0	0	3
38	Alley	2809	868	0	44	3721
39	Hydrant	20	0	0	0	20
40	Hectometric milestone	40	0	0	17	57
42	Gas pipeline	12	0	0	0	12
43	Fountain	2	0	0	1	3
45	Trench edge	3255	606	0	0	3861
47	Gabions	182	44	0	5	231
48	Lighting pole	26	0	0	0	26
49	Battlement	5	0	0	0	5
50	Construction without elevation	1	0	0	0	1
52	Ditch without elevation	1	0	0	0	1
53	Gate symbol	0	0	1081	0	1081
68	Street fountain	4	0	0	0	4
69	Border	124	54	0	3	181
Total		**38566**	**6368**	**1081**	**716**	**46731**

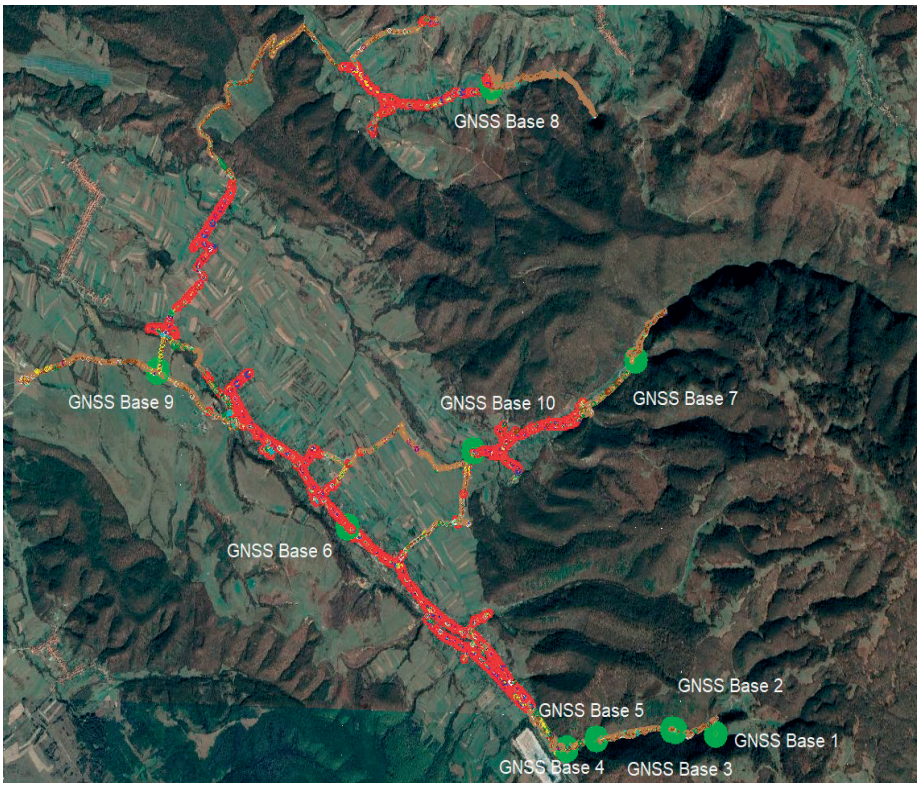


Figure 6. The location of the ten GNSS bases on the orthophoto plane, which were positioned in stage I, and were used as density points for the following stages of work

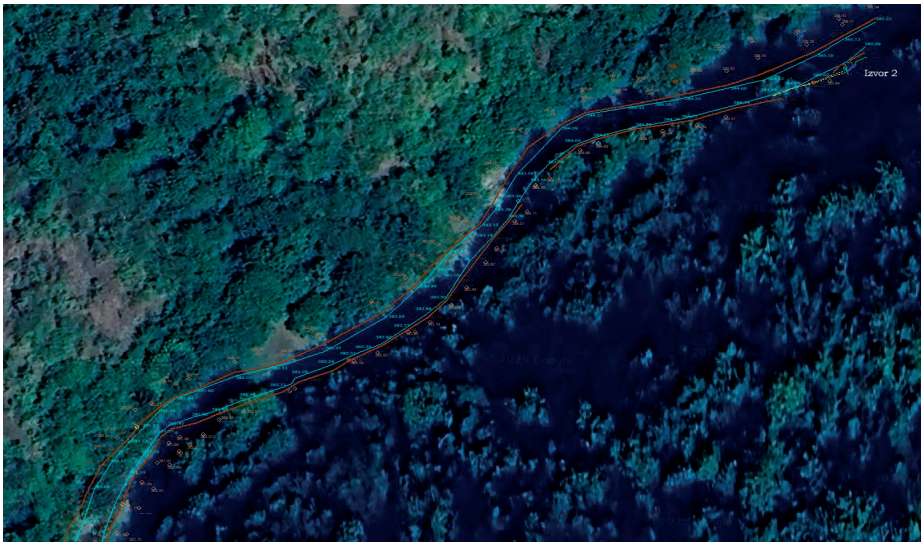


Figure 7. Overlay of the detailed plan of the water supply network on the orthophoto plane, in the spring 2 area



Figure 8. Detailed plan of the water supply and sewage network, superimposed on the orthophoto plane

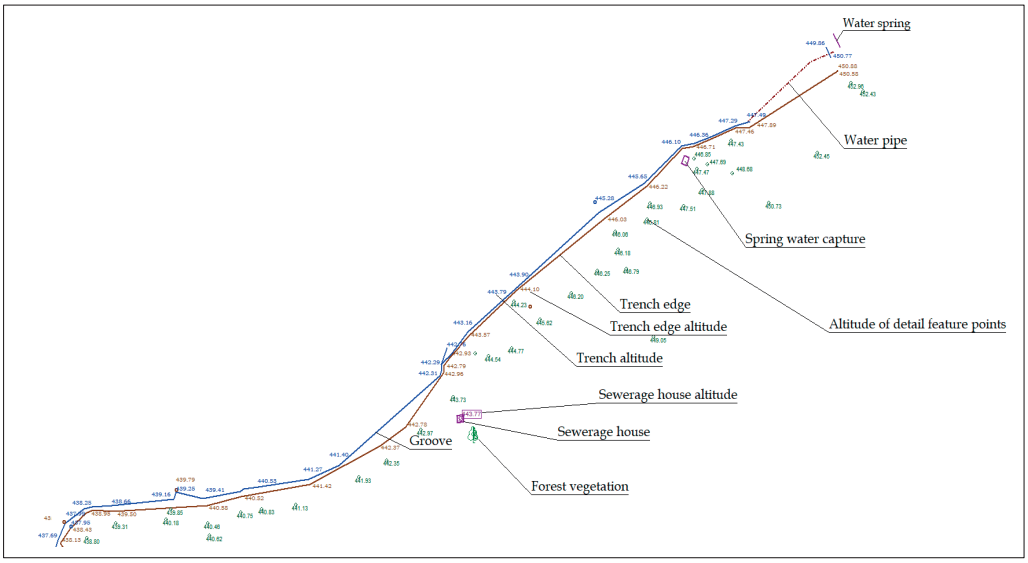


Figure 9. Extract from the detailed plan, related to the water supply network (spring collection)

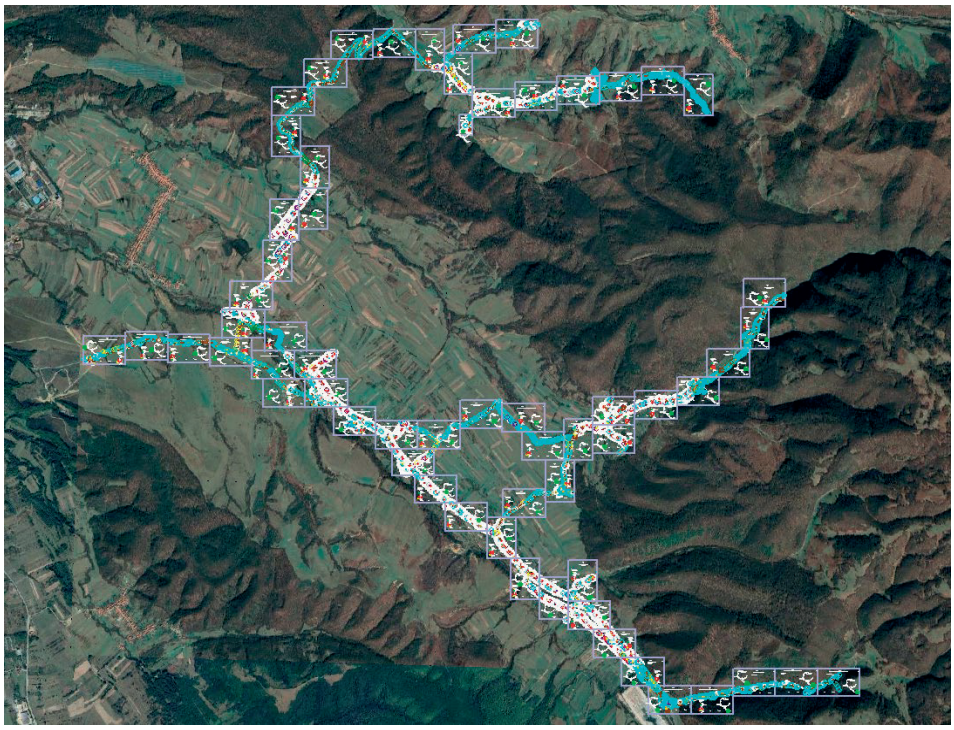


Figure 10. Layout, coverage and sequence of the sheets related to the situation plan

CONCLUSIONS

Given the topographic and vegetation characteristics of the analyzed area, appropriate spatial positioning methods were selected to ensure the successful completion of the case study. The use of GNSS receivers with radio communication between base and rover units - within the RTK framework - proved to be a technically efficient solution under challenging field conditions, particularly those imposed by rugged terrain and forested areas.

Data transmission from the base station was performed using a 4W external radio module, while data reception at the rover was handled by a 2W internal radio, both operating with high efficiency. Under optimal conditions, this configuration enables transmission over distances of up to 20-25 km. In contrast, when both transmission and reception are managed by 2W modules, the effective communication range varies from 5-6 km in suboptimal conditions to a maximum of approximately 11 km under ideal conditions.

The selection of base points was made with strict consideration for uninterrupted satellite signal reception throughout each observation session, accounting for the presence of forest canopy or other local obstructions. The integration of recordings from the Beiuș permanent GNSS station - located within a reasonable range of the study area - further optimized the RTK method's application. Additionally, the use of a total station in zones where satellite positioning was impeded proved to be a suitable alternative, enabling continued detail acquisition. This dual approach - merging GNSS-based satellite positioning (for densification points) with total station surveying methods - resulted in a cohesive, integrated spatial positioning strategy. Finally, the use of the MapSys 11 digital cartography program allowed us to produce comprehensive graphical outputs, facilitating multi-format usage of the final deliverables (alphanumeric, digital, and analog). Moreover, derivative products such as databases and GIS components specific to the surveyed site and associated activities were generated under optimal conditions.

ACKNOWLEDGEMENTS

The research and studies were carried out with the collaboration and logistical support of S.C. TOPOSISTEM S.R.L. from Oradea, within the project "Priority works for the expansion and rehabilitation of water supply and sewage networks in the Commune of Câmpani - Bihor County", carried out in 2024.
We also thank the Local Council of the Commune of Câmpani, Bihor County, for their collaboration.

REFERENCES

Ádám, J., Bányai, L., Borza, T., Busics, G., Kenyeres, A., Krauter, A., & Takács, B. (2004). *Satellite positioning*. University Publishing House.

Basso, M., Martinelli, A., Morosi, S., & Sera, F. (2021). A real-time GNSS/PDR navigation system for mobile devices. *Remote Sensing, 13*(8), 1567. https://doi.org/10.3390/rs13081567

Bodog, M. F., Șchiopu, E. C., Crainic, G. C., & Lazăr, A. N. (2024). Assessment of contamination degree of oil residues on a former agricultural site. *Journal of Agricultural Science and Technology A, 14*(2), 67–82. https://doi.org/10.17265/2161-6256/2024.02.003

Chițea, G., Iordache, E., & Chițea, C. G. (2009). *Space geodetic technologies. Part I: Global positioning systems (GPS)*. Lux Libris.

Crainic, G. C. (2024). Issues related to the implementation of geomatic applications in the national forestry fund. *Scientific Papers. Series E. Land Reclamation, Earth Observation & Surveying, Environmental Engineering, 13*, 794–804.

Dlamini, S. M., & Ouma, Y. O. (2025). Large-scale topographic mapping using RTK-GNSS and multispectral UAV drone photogrammetric surveys: Comparative evaluation of experimental results. *Geomatics, 5*(2), 25. https://doi.org/10.3390/geomatics5020025

Florescu, I. I., & Nicolescu, N. V. (1996). *Silviculture. Vol. I: Forest study*. Lux-Librix.

Fredeluces, E., Tomohiro, O., Kubo, N., & El-Mowafy, A. (2024). Modified RTK-GNSS for challenging environments. *Sensors, 24*(9), 2712. https://doi.org/10.3390/s24092712

Gökdaş, Ö., & Özlüdemir, M. T. (2020). A variance model in NRTK-based geodetic positioning as a function of baseline length. *Geosciences, 10*(7), 262. https://doi.org/10.3390/geosciences10070262

Hamza, V., Stopar, B., Sterle, O., & Pavlovčič Prešeren, P. (2025). Recent advances and applications of low-cost GNSS receivers: A review. *GPS Solutions, 29*, 56. https://doi.org/10.1007/s10291-025-01815-x

Haojun, L., Jingxin, X., Shoujian, Z., Jin, Z., & Jiexian, W. (2018). Introduction of the double-differenced ambiguity resolution into precise point positioning. *Remote Sensing, 10*(11), 1779. https://doi.org/10.3390/rs10111779

Hofmann-Wellenhof, B., Lichtenegger, H., & Collins, J. (1997). *Global positioning system: Theory and practice* (4th ed.). Springer.

Kurtulgu, Z., & Pirti, A. (2025). Evaluating accuracy and performance of CORS-VRS in forested area. *Bosque, 46*(1), 77–85. https://doi.org/10.4067/S0717-92002025000100077

Liu, H., Zhang, Z., Sheng, C., Yu, B., Gao, W., & Meng, X. (2024). Fast and reliable network RTK positioning based on multi-frequency sequential ambiguity resolution under significant atmospheric biases. *Remote Sensing, 16*(13), 2320. https://doi.org/10.3390/rs16132320

Marton, H. (2007). *MapSys, TopoSys - User manual*. Odorheiu Secuiesc.

Neuner, J. (2000). *Global positioning systems*. Matrix-Rom.

Odijk, D., Zhang, B., Khodabandeh, A., Odolinsk, R., & Teunissen, P. J. G. (2016). On the estimability of parameters in undifferenced, uncombined GNSS network and PPP-RTK user models by means of S-system theory. *Journal of Geodesy, 90*(1), 15–44. https://doi.org/10.1007/s00190-015-0854-y

Păunescu, C., Mocanu, V., & Dimitriu, S. G. (2006). *Global positioning system G.P.S.* University Publishing House.

Pica, A., Boja, F., Fora, C., Moatar, M., & Boja, N. (2022). Advantages of using GNSS technology and QGIS software in inventory stands exploiters. *Scientific Papers. Series E. Land Reclamation, Earth Observation & Surveying, Environmental Engineering, 11*, 434–443.

Rus, T. (2004). *Satellite geodesy: Course notes*. Technical University of Civil Engineering.

Sicoe, S. I., Crainic, G. C., Samuel, A. D., Bodog, M., Iovan, C. I., Curilă, S., Hârțuța, I. O., Șerban, E., Dorog, L. S., & Sabău, N. C. (2023). Analysis of the effects of windthrows on the microbiological properties of forest soils and their natural regeneration. *Forests, 14*(6), 1200. https://doi.org/10.3390/f14061200

Tang, X., Roberts, G., Li, X., & Hancock, C. (2017). Real-time kinematic PPP GPS for structure monitoring applied on the Severn Suspension Bridge, UK. *Advances in Space Research, 60*(5), 925–937.

Teunissen, P. J. G., & Khodabandeh, A. (2015). An analytical study of PPP-RTK corrections: Precision, correlation and user-impact. *Journal of Geodesy, 89*(11), 1109–1132.

Zavate, F. L. (2008). Current status in the field of national spatial data infrastructures and GPS differential correction services. *Journal of Geodesy, Cartography and Cadastre, 17*(1-2), 70–78.

Xingxing, L., Hongbo, L., Fujian, M., Xin, L., Jinghui, L., & Zihao, J. (2019). GNSS RTK positioning augmented with large LEO constellation. *Remote Sensing, 11*(3), 228. https://doi.org/10.3390/rs11030228

Wikipedia (n.d.). *Câmpani, Bihor*. https://ro.wikipedia.org/wiki/C%C3%A2mpani,_Bihor

Comuna.info. (n.d.). *Harta Câmpani*. https://comuna.info/harta-campani-bh/

Scientific Papers. Series E. Land Reclamation, Earth Observation & Surveying, Environmental Engineering. Vol. XIV, 2025
Print ISSN 2285-6064, CD-ROM ISSN 2285-6072, Online ISSN 2393-5138, ISSN-L 2285-6064

SPATIAL POSITIONING WITH COMBINED METHODS OF TOPOGRAPHIC POINTS NECESSARY FOR ACCESSIBILITY OF FORESTS IN MOUNTAIN AREA

Flavius IRIMIE

"Ștefan cel Mare" University of Suceava, Faculty of Forestry, Doctoral School of Applied Sciences and Engineering, 13 University Street, 720229, Suceava, Romania

Corresponding author email: flaviusirimie1975@gmail.com

Abstract

Since in the mountain area the area occupied by forest is over 60% of the area of the national forest fund, making forests accessible is an obvious necessity for the sustainable management of various forest resources. The research was carried out within the III Galbena production unit, Sudrigiu Forest District, within the scope of the Bihor Forestry Directorate, with the objectives of applying combined methods of spatial positioning of topographical details, necessary for the design and construction of transport facilities, in the perspective of making 15 inaccessible stands accessible, on an area of 174.48 ha. For the positioning of the topographical details, GNSS technology, GPS system and total station were used, and the working methods used are represented by real-time kinematic positioning (RTK), combined with polygonometric mapping framed with erasures, carried out with the total station. The use of modern combined methods for positioning topographic details in the inaccessible forest fund in the mountain area ensures the obtaining of products in alphanumeric and digital format with superior precision, necessary for the design and construction of transport installations in optimal technical conditions.

Key words: *combined technologies, contour lines, digital terrain model, forest accessibility, GNSS technology, spatial positioning.*

INTRODUCTION

The implementation of forestry strategies established by forest management plans relies on the existence of appropriate infrastructure to ensure effective access to the forest fund. In Romania, current infrastructure allows access to approximately 4.1 million hectares of forest - around 65% of the total 6.3 million hectares - within a maximum collection distance of 2.0 km. The remaining 2.2 million hectares (35%) remain inaccessible (Ciubotaru, 2007).

Internal accessibility works enable the creation of access networks within forest stands to support silvicultural operations, starting from the thicket stage, and the application of specific treatments (Order no. 2,534 of September 28, 2022). Improving accessibility aims to:

- enable operations across the entire stand under safe and efficient working conditions;
- prevent damage to retained trees;
- facilitate timber collection and reduce skidding distances;
- lower operational costs and increase recoverable wood volume.

Developing and maintaining a functional forest road network serves not only silvicultural, technical, and economic purposes but also:

- supports the rational exploitation and utilization of timber and forest products (Săndoiu, 2010; FAO, 2016);
- assists in forest fire prevention and control (Iordache et al., 2016);
- protects hunting species and biodiversity (Iordache et al., 2016);
- connects forest stands to primary transport networks;
- promotes sustainable forest management (Florescu & Nicolescu, 2000);
- enables recreation and tourism (Dumitru, 2014);
- contributes to local economic development.

Prior to establishing access infrastructure, a comprehensive field survey must be conducted to collect data on existing access routes (such as roads, paths, and parcel lines), their condition and dimensions, local hydrography, slope and terrain morphology, the structural and compositional characteristics of the stands (including density, age, and previous

interventions), as well as the optimal directions for timber extraction.
This information helps determine the feasibility and urgency of access works, define road network layouts, estimate costs, and produce a sketch of existing and proposed routes.
Technical, ecological, and economic criteria for designing tractor roads include:

- Avoiding areas with natural regeneration;
- Operating during dry or cold weather to prevent road damage;
- Protecting edge trees using guards;
- Minimizing costs and route lengths;
- Avoiding marshy areas;
- Ensuring a transverse slope of 4–6% and terrain-specific longitudinal slopes;
- Designing a 3-4 m wide platform (OM 1540/2011);
- Incorporating safety features like curbs in dangerous bends;
- Installing temporary wooden bridges over streams;
- Ensuring proper gradient: 25% empty/10% loaded for universal tractors, 40% empty/18% loaded for forestry tractors;
- Mechanized, low-cost construction with daily maintenance using local materials;
- Fixing road alignments by a certified technician or engineer.

According to the updated OM 1540/2011, the maximum width of the tractor road is 4 meters. A standard example of its transverse profile is illustrated in Figure 1 (Ciubotaru, 1996).

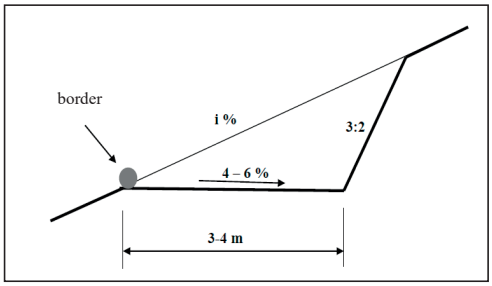


Figure 1. Transverse profile of the tractor road (Ciubotaru, 1996)

This study aims to analyze the spatial positioning methods used for detailed topographic points necessary for designing transport infrastructure in mountainous forest stands with extremely low accessibility. These detail points will be positioned using suitable technologies and surveying methods tailored to the site conditions.

MATERIALS AND METHODS

The research was conducted in inaccessible deciduous and coniferous stands located in a mountainous area, within Production Unit (P.U.) III Galbena, managed by the Sudrigiu Forestry District under the authority of the Bihor Forestry Directorate. The study was carried out in the context of doctoral research.
The targeted stands are located in plots 43B, 44A, 44D, 44C, 45A, 45B, 46A, 46B, 47A, 47B, 47C, 47D, 48A, 48B, 48C, and 49A, covering a total area of 174.48 ha in a highly inaccessible mountainous region (Figures 2 and 3).
The research methodology included bibliographic review, direct observation of trees and access routes, experimentation, simulation, comparative analysis, and image recording on digital media.
The bibliographic documentation phase provided a thorough understanding of the need to improve accessibility in the studied forest areas and its implications for forestry operations. For this purpose, the forest management plan, the associated management map, and the applicable technical regulations were examined.
In addition, documentation regarding available technologies and equipment for high-precision spatial positioning in mountainous deciduous and coniferous stands was also required.



Figure 2. Case study location (https://www.google.com/maps/d/viewer?mid)

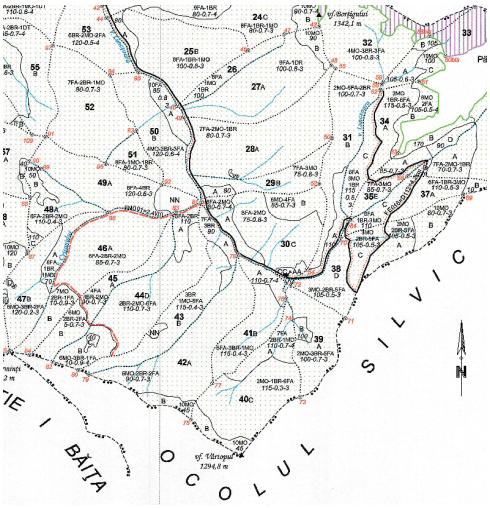


Figure 3. Positioning of the researched and studied stands (according to the Management Map of U.P. III Galbena, 2014)

The positioning of topographic detail points was carried out in the inaccessible stands, including those located in plot 43B, characterized by steep slopes, dense forest vegetation, and limited access infrastructure. Figure 4 illustrates the specific field conditions encountered during the positioning work in this plot.



Figure 4. The inaccessible grove in plot 43B where the positioning of the topographic detail points was carried out (original photograph)

Field observations were conducted by thoroughly surveying the designated stands, during which the proposed routes for forest road construction were identified. Characteristic topographic detail points were also marked and spatially positioned to determine their planimetric coordinates and elevations within the national reference system.

The experiment involved positioning these detail points, determining their coordinates, graphically representing them, and proposing accessibility solutions for the study area. GNSS technology, specifically the NAVSTAR GPS system, as well as total station measurements, were employed for this purpose.

Previous and recent studies have shown that satellite-based positioning in forested areas is significantly influenced by the structural and functional characteristics of the stands. These factors can lead to statistically significant variations in spatial coordinates. Variables such as DOP values affect the precision - though not the accuracy - of the topographic point coordinates (Căteanu & Moroianu, 2024).

One viable method for positioning forest detail points under specific working conditions using GNSS technology is the static method - applied in traditional, rapid, or GPS tracking variants (Ádám et al., 2004). This approach involves placing a GNSS receiver at the point of interest for a variable period, while three additional receivers are stationed at control points with known coordinates. The duration of each stationing depends on technical and environmental conditions, as well as the spatial configuration of the known reference points, either from legacy geodetic networks or the passive GNSS network.

Final coordinates are obtained through post-processing of the satellite data, with results varying depending on the software and computational algorithms used. Despite offering high precision and accuracy, this method is time-intensive and requires well-trained personnel, which limits its current widespread use (Crainic, 2011).

Recent comparative studies using four GNSS receivers - both GIS - and geodetic-grade - revealed notable differences in performance. The GIS-grade receiver yielded an accuracy of 1.38 m and a precision of 1.29 m, whereas the geodetic-grade receiver achieved 0.74 m in

accuracy and 0.91 m in precision. These discrepancies, despite identical data collection conditions, are primarily attributed to the distinct operational principles and processing algorithms of each device type, alongside forest-specific challenges such as cycle slips and the multipath effect (Brach, 2022).

The real-time kinematic (RTK) method is widely used today for positioning various topographic features, due to its high precision, operational efficiency, and accessibility when appropriate logistics and infrastructure are available. In forestry, spatial accuracy is critical for numerous applications, and GNSS-based technologies provide effective solutions for acquiring geolocation data (Căteanu & Moroianu, 2024).

RTK delivers results almost instantaneously - within fractions of a second - after data acquisition and transformation into the national reference system. The method can be applied in two configurations: short-range and long-range (Ádám et al., 2004). The applicability of the long-range variant was significantly expanded following the introduction of the ROMPOS service in August 2008, which enabled high-accuracy transformation parameters across regional and geographical zones. In this configuration, the base station is a permanent GNSS reference point, allowing real-time positioning of detail points using a rover at distances of 30-70 km (Figure 5).

Drones equipped with high-precision GNSS receivers offer another alternative for field measurements, significantly reducing time on site while ensuring high data accuracy. However, recent studies indicate that the RTK method yields superior accuracy, particularly in elevation data for forest road longitudinal profiles. For instance, using drone-based GNSS data resulted in over 22.64% higher calculated embankment volumes compared to RTK-based point positioning, highlighting substantial discrepancies (Lepoglavec, 2023).

The short-range application of the real-time kinematic (RTK) method involves the use of two dual-frequency GNSS receivers: one is stationed at a spatially determined base point, while the other (rover) is used to record data at target points, with short occupation times. To ensure real-time positioning, both receivers must be equipped with radio modules for transmitting and receiving satellite data and differential corrections (Crainic, 2011; Pica, 2022).

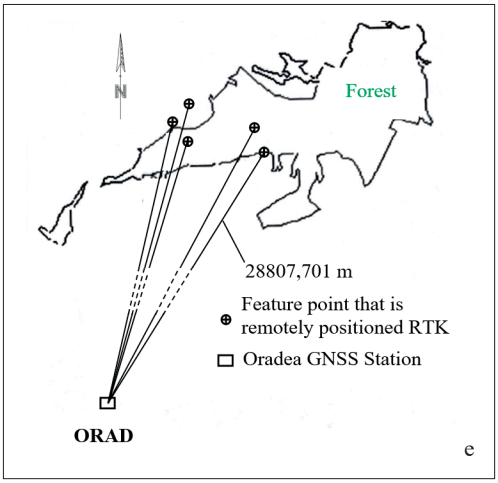


Figure 5. The method of positioning topographic points in the forest fund using the RTK method at long distance (adapted from Crainic, 2011)

This approach is effective even in forested environments, particularly when the base receiver uses a 4W internal radio and the rover a minimum 2W radio. Under these conditions, the connection between the devices is reliably maintained up to 10-12 km, and data transmission can reach distances of 22-25 km, regardless of terrain complexity.

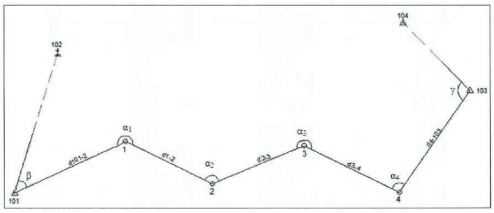
Recent studies demonstrate that individual tree selection for extraction can now be conducted using digitally acquired data from forest inventories. Consequently, tree locations can be identified in real time using RTK-GNSS with dual-frequency receivers and short-range radio communication. When operating within 1 km of the base station, the horizontal positioning error (RMSE) was found to be 0.26 m in *Larix kaempferi* stands and 0.48 m in *Pinus koraiensis* stands, confirming the method's reliability for detailed forest applications (Cho et al., 2024).

With the introduction of additional satellite systems such as BEIDOU, GALILEO, and QZSS - alongside GPS and GLONASS - the broader concept of Multi-GNSS has emerged. This integration increases satellite availability, enhancing performance under challenging conditions like dense canopy cover. Studies in forest environments with 40–90% tree cover

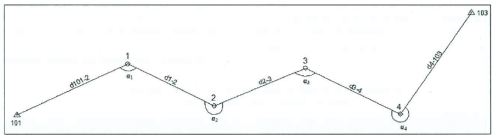
confirm that RTK positioning using Multi-GNSS systems provides superior coordinate accuracy compared to traditional GNSS RTK, even in areas with highly restricted satellite visibility (Andreas, 2019).

For accuracy assessment of GNSS-based coordinates in forested areas, reference values are typically obtained using high-precision total stations via polygonometric traverses, supported by orientation marks. These measurements are processed with specialized software using rigorous adjustment models (Feng et al., 2021).

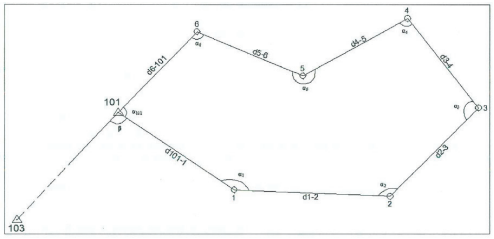
When satellite positioning is impractical due to forest canopy or rugged terrain, several polygonometric surveying methods may be employed to determine new point coordinates: (i) framed (supported) traverses on spatially defined points with orientation marks (Figure 6.a), (ii) unsupported traverses without orientation marks (Figure 6.b), and (iii) closed traverses with orientation marks (Figure 6.c). These methods are carried out using advanced total stations, with robotic models offering the highest efficiency (Sabău, 2010).



a. Main traverse supported (framed) with orientation visas



b. Main traverse supported without orientation visas



c. Main traverse closed with orientation visas

Figure 6. Principle of creating polygonometric roads (Cranic, 2011)

This method is frequently used in the preparation of forest maps, when carrying out the forest management plan.

Considering the particular conditions of spatial positioning of topographic points on surfaces covered with forest vegetation, efficient combinations of modern geospatial technologies can also be used. Consequently, their positioning principles will be integrated, ensuring obtaining coordinates characterized by superior accuracy and precision.

The positioning of various topographic details in the forestry sector and the preparation of related graphic representations can currently be achieved using combined working technologies such as GNSS systems and total stations. Consequently, alphanumeric and graphic final products of high accuracy and precision are obtained, directly correlated with the logistics used and the working methods used (Călina et al., 2020).

In extreme working conditions, determined by the lack of points in the classical geodetic network or the passive GNSS, the free station method can also be applied at the limit. In this case, a total station and at least two accessible points of known coordinates are required, which have usually been positioned with satellite recordings. As a result, an intersection will be made at the limit, and the point where the total station will be stationed can be determined with high precision through post-processing, if specialized calculation programs are used, with rigorous compensation, for example TERRAMODEL, MATLAB (Crainic, 2011; Nero, 2023). In this situation, a major inconvenience arises regarding logistics and, respectively, working time.

The logistics used to carry out the case study are relatively varied.

Currently, the use of low-cost multi-constellation and multi-frequency receivers for obtaining high-precision coordinates in various stands of deciduous and coniferous trees is facilitated by the use of high-performance software for data recording and processing. For example, the Google Pixel 5 smartphone model and the u-Blox ZED F9P standalone receiver are two variants of low-cost receivers that can be used to position details under the tree canopy. Obtaining accurate results with these receivers was facilitated by using the latest version of the

Demo5 fork of the RTKLIB software. Consequently, the use of low-cost receivers can be effective in the variant of using high-performance software, but also with hardware improvements, especially of the antenna, which is an absolute priority (Tomaštík & Everett, 2023).

Although there is currently a wide range of GNSS receivers and various satellite constellations, the spatial positioning accuracy in trees depends on the class of the receiver, and obviously on the working methods. As a result, geodetic-class GNSS receivers ensure superior accuracy, even in the case of autonomous solutions, compared to modern dual-frequency Smartphones. The obvious differences in accuracy between the various types of satellite receivers are mainly determined by their composition and the software used to record and process satellite information. Consequently, geodetic-class receivers ensure the determination of highly accurate coordinates, in the centimetric-decimetric range, and modern Smartphone-type receivers determine coordinates with GIS accuracy, in the metric-decametric range (Purfürst, 2022).

The logistics used for spatial positioning were provided by S.C. TOPOCONSULT S.R.L. from Oradea, Bihor County, Romania, and were represented by:

- two dual-frequency GNSS receivers, one TRIMBLE R10 with internal 4W radio for the base, and the other TRIMBLE R12I with external 2W radio, as rover;
- TRIMBLE S8 robot total station with all related accessories;
- recordings from the Beiuş GNSS station, using the ROMPOS service;
- TRIMBLE ACCESS program for collecting and processing field data.

The MapSys10.0 program for graphical reporting of positioned points, creating the database and obtaining the related graphic products in digital format was used within the topography laboratory.

The forest management plan (management plan) for Production Unit (P.U.) III Galbena and the forest map at a scale of 1:20000 in digital format, for the area of Production Unit (P.U.) III Galbena, were provided by the Sudrigiu Forest District, Bihor Forestry Directorate.

The experiment related to the case study (research) was carried out in several integrated stages, depending on the working methods used and the working conditions in the field.

In the first stage, the point that was used as a GPS base was established. It was located at an appropriate altitude, in order to receive and record satellite data in optimal conditions.

In the second stage, in order to carry out measurements with the total station, the routes on which the supported polygonometric roads were carried out were established. These were designed through the plots that are to be covered with silvotechnical interventions, and implicitly to be accessible. Consequently, the station points were established and materialized on the ground, where the device will be stationed.

In the next stage, the points that were positioned with GNSS technology, as points for thickening the support network, and which were used to support the polygonometric roads, were established and materialized.

These were located in areas where there were optimal conditions for receiving the satellite signal, without obstructions. These were mostly represented by the open meshes for the installation of natural regeneration, in the stands engaged in the exploitation-regeneration process, and in those caused by felling and wind breakage, as a result of extreme weather phenomena. It was also necessary that they could be observed and targeted from the nearest polygonometric survey station points, in order to comply with the rigorous data processing and compensation algorithm.

All the projected points that were positioned were materialized on the ground by wooden posts with a square section, 5x5 cm, and the mathematical center of their cross-section was marked with a nail, at the intersection of the diagonals.

In the next stage, the base point was positioned with the remote RTK method and the ROMPOS service, the records from the Beiuş GNSS station being also used. Also, the density points were positioned with the RTK method, at a shorter distance, thus using radio modules, in areas where working conditions did not allow the recording of satellite data in optimal conditions.

The last field stage was represented by the completion of the polygonometric journey,

which involved stopping at each station point, performing direct and reciprocal sightings, and sighting the points determined from the stations with visibility.

Currently, hierarchical models are being designed for collecting and sharing forest and natural resource management data, which are based on the accuracy and variety of different spatial positioning and location hierarchy methods in the forestry sector. As a result, data with diverse spatial and temporal complexity are transmitted and processed incrementally at lower levels of organization, then merged, synthesized and transmitted to higher levels of management for sustainable forest and natural resource management (Keefe et al., 2019).

The data processing stage and obtaining the final coordinates in the national reference system was carried out differently, depending on the positioning technologies and methods used.

The sequence of the work stages described above is presented synthetically in Figure 7.

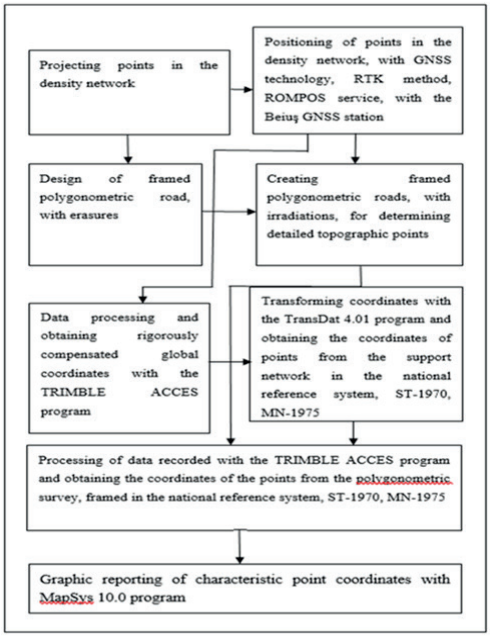


Figure 7. Work steps

After reporting the coordinates of the characteristic points, the obtained travel routes and the optimal accessibility options were simulated, compared and analyzed.

RESULTS AND DISCUSSIONS

The satellite recordings were processed in real time, with the TRIMBLE ACCESS program, obtaining the ellipsoidal coordinates. These were transformed with the TransDatRO4.01 program, using the national transformation parameters recommended for the work area, thus resulting in the final coordinates, in the national reference system (Table 1).

From the analysis of the results of studies conducted in accessible stands of deciduous and coniferous trees, the accuracy of single-frequency GNSS receivers does not depend so much on forest conditions, while the performance of the tested dual-frequency geodetic receiver is very sensitive to satellite visibility. Consequently, in the variant of calculating coordinates with post-processing, especially in combination with data obtained with an IMU inertial system, the improvement of the accuracy of the dual-frequency receiver was significant. As a result, the accuracy of the planimetric coordinates determined with the dual-frequency receiver in real time was 0.7 m, and for the single-frequency receiver, the accuracy ranged between 4.2-9.3 m. The final conclusions resulted from comparing the results obtained with single and dual frequency GNSS receivers, in motion, with those obtained with the total station and a dual frequency GNSS receiver, using the RTK method, for the positions of 224 trees, on the studied route (Kaartinen, 2015).

The data that were recorded during the supported polygonometric surveys were also processed with the TRIMBLE ACCESS program, obtaining directly the final coordinates, in the national reference system (Table 2).

In the case of this case study, the precision of determining the coordinates in the horizontal plane is 3-4 cm and in elevation, 5 cm, an aspect that is also conditioned by the performance of the transformation parameters in the national reference system, for the analyzed location.

All the final coordinates were transferred to a file with the extension txt., configured in five columns, respectively: point number, X (m), Y (m), Z (m) and the code - which represents the layer into which each point will be imported. The points were graphically reported with the

MapSys program 10.0 (Marton, 2007), thus materializing their planimetric position, in the layer corresponding to the code established since the positioning. By joining the station bridges, the routes of the polygonometric roads materialized (Figure 8).

Additionally, sightings to the reference points with known coordinates materialized and used for the precise adjustment of the polygonometric trails. An analysis of the images presented in Figure 8 reveals that the sides of these trails exhibit considerable variability in length. Additionally, sightings to the reference points with known coordinates materialized and used for the precise adjustment of the polygonometric trails.

Table 1. Inventory of coordinates in the national reference system, related to topographic points that were positioned using the RTK remote method

Point No.	X (m)	Y (m)	Z (m)	Code	Point No.	X (m)	Y (m)	Z (m)	Code
1	561004.742	322025.555	1200.828	6	110	562489.607	321574.075	1074.115	6
100	560879.530	321851.244	1236.724	6	111	562399.153	321725.809	1060.914	6
101	560953.860	560953.860	1243.117	6	112	562318.575	322022.644	1024.108	6
102	561437.915	322641.031	1239.886	6	113	562285.771	322118.263	1004.991	6
103	561479.926	322729.207	1009.112	6	114	562422.511	321401.689	1046.621	6
104	561578.910	321397.537	1168.185	6	115	562380.634	321451.243	1044.822	6
105	561706.634	321354.264	1162.224	6	116	562253.608	321637.594	1013.201	6
106	562127.977	321324.216	1087.116	6	117	562320.780	322664.116	873.125	6
107	562651.561	321397.707	1105.991	6	118	562261.863	322675.991	864.212	6
108	562569.315	321444.056	1086.285	6	119	562186.328	322727.992	845.250	6
109	562571.015	321555.389	1104.115	6	-	-	-	-	-

Table 2. Inventory of coordinates in the national reference system, related to topographic points that were positioned by the method of polygonometric mapping

Point No.	X (m)	Y (m)	Z (m)	Code	Point No.	X (m)	Y (m)	Z (m)	Code
11	560965,458	321908,829	1213,268	7	54	562221,139	321264,182	1071,314	7
12	561003,845	321914,341	1208,556	7	55	562162,511	321253,015	1084,322	7
14	561170,524	321985,211	1142,460	7	56	562069,775	321249,589	1114,382	7
15	561281,444	322007,952	1140,224	7	57	562033,482	321320,500	1117,328	7
16	561415,182	322022,118	1107,524	7	58	561986,884	321369,045	1121,369	7
17	561560,658	322045,867	1075,334	7	59	562032,924	321441,664	1188,754	7
18	561643,557	322025,844	1065,614	7	60	562087,084	321516,484	1057,232	7
19	561727,310	322027,240	1060,228	7	61	562122,111	321549,639	1043,875	7
20	561814,962	322039,725	1047,284	7	62	562147,412	321595,005	1030,422	7
21	561975,561	322163,689	986,436	7	63	562172,713	321646,479	1016,638	7
22	562117,076	322342,265	938,624	7	64	562188,067	321770,190	996,658	7
23	562179,084	322471,309	918,317	7	65	562190,161	321835,797	988,458	7
24	562210,471	322569,782	898,116	7	66	562190,738	321892,296	984,841	7
25	562252,596	322642,811	876,232	7	67	562225,128	321939,612	986,448	7
26	561061,177	322002,359	1175,300	7	68	562224,037	322025,765	974,339	7
27	561138,351	322058,343	1142,446	7	69	562204,407	322111,918	965,766	7
28	561211,416	322110,558	1138,140	7	70	562170,601	322204,614	954,724	7
29	561306,511	322171,628	1112,334	7	71	563153,152	322286,405	985,065	7
30	561407,713	322226,592	1077,424	7	72	562162,182	322357,141	937,382	7
31	561502,532	322290,445	1048,742	7	73	562751,684	321394,057	1126,482	7
32	561526,388	322167,759	1047,845	7	74	562708,062	321344,982	1115,937	7
33	561635,473	322383,303	1023,642	7	75	562624,908	321331,351	1085,164	7
34	561717,264	322454,188	1007,649	7	76	562550,752	321352,071	1065,142	7
35	561812,473	322462,452	978,684	7	77	562509,699	321401,640	1063,113	7
36	561893,246	322475,357	968,846	7	78	562472,708	321435,839	1057,224	7
37	561969,043	322488,897	952,167	7	79	562432,925	321490,279	1045,228	7
38	562069,773	322502,921	933,748	7	80	562394,683	321537,044	1040,932	7
39	562137,932	322554,041	921,116	7	81	562359,305	321605,745	1031,854	7
40	561522,798	322758,517	1010,115	7	82	562317,138	321656,846	1022,428	7
41	561592,661	322729,550	1025,889	7	83	562274,971	321692,580	1014,932	7
42	561693,195	322724,438	1038,869	7	84	562251,029	321761,549	1004,992	7
43	561774,986	322669,911	1003,892	7	85	562224,585	321819,082	994,912	7
44	561836,329	322593,232	992,348	7	86	562687,887	321472,031	1024,938	7
45	561878,394	322546,826	978,214	7	87	562640,176	321511,563	1117,624	7
46	561552,545	321438,734	1169,224	7	88	562591,456	321645,804	1125,005	7
47	561612,341	321455,807	1143,229	7	89	562556,734	321743,342	1129,995	7
48	561634,305	321510,022	1130,985	7	90	562460,412	321880,450	1106,311	7
49	561661,976	321562,812	1121,314	7	91	562403,977	321986,506	1076,261	7
50	561676,385	321633,867	1118,117	7	92	562335,272	322101,012	1036,227	7
51	561696,095	321712,651	1110,119	7	93	562279,655	322172,988	1002,639	7
52	561735,515	321807,907	1097,318	7	94	562215,313	322241,692	968,227	7
53	561762,595	321921,602	1088,618	7					

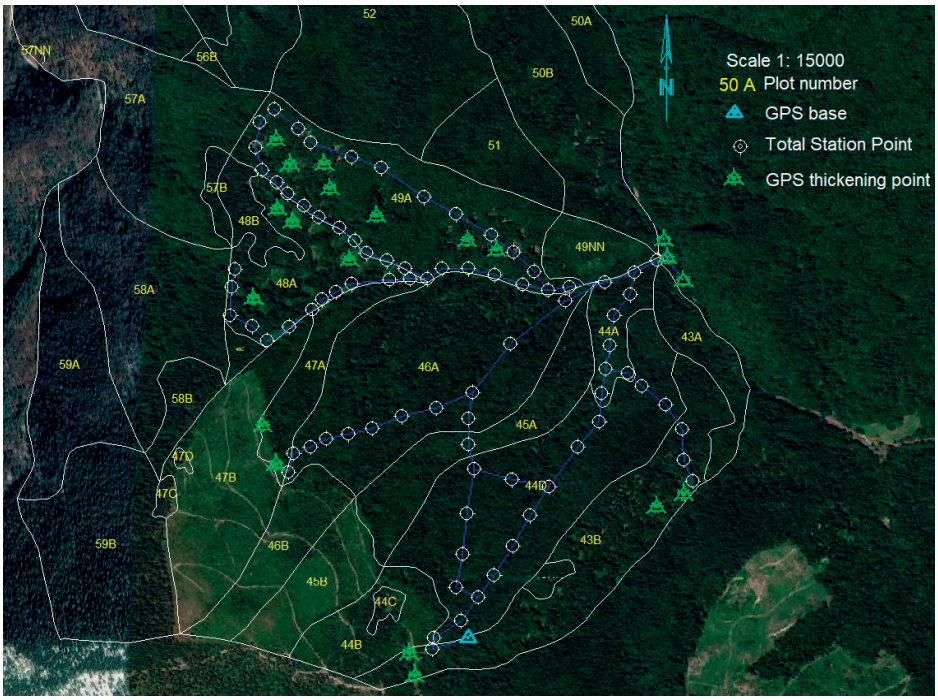


Figure 8. Establishing the GPS base point and total station points
(image capture from MapSys10 program)

An analysis of the images presented in Figure 8 reveals that the sides of these trails exhibit considerable variability in length. This variation is primarily due to limited visibility between station points, caused by the presence of standing trees and natural seedling biogroups within the forest stands. As a result, side lengths range from 34.450 meters to 227.850 meters.

Similarly, the lengths of the sightings to known coordinate points vary depending on their spatial distribution and the presence of visual obstructions such as forest vegetation. The established trails crossed plots undergoing natural regeneration processes, where timber harvesting is currently in progress. In plot 49A, a closed road was constructed and marked with orientation signs to support the efficient planning of transport infrastructure, given the favorable positioning of the area. This newly created road also supports the route along the southern and southwestern boundary of plot 48A.

Closed roads equipped with orientation signs were also constructed in plots 44A, 44D, 45A, and 46A. In contrast, plots 43B and 46 were traversed by supported roads, given their specific positioning and topographical context. The design and implementation of transport infrastructure to improve accessibility in the studied areas will be carried out in stages, in accordance with the current forest management plan and the strategic guidelines established at the forestry district level.

Considering both the provisions of the forest management plan and the dynamics of natural regeneration, priority will be given to the design and construction of transport facilities in plots 43B and 49A (Irimie & Timofte, 2023). Subsequent interventions will focus on improving accessibility in the other plots undergoing natural regeneration - namely 44A, 44D, 45A, 46A, and 48A - based on the condition of the forest stands and the urgency of regeneration and timber harvesting operations.

As a result, roads have also been constructed in stands where maintenance works for natural and mixed regeneration are planned, as well as in those targeted for tending and management cuttings in young and mature stands, depending on their developmental stage.

Regardless of the segment, the spatial coordinates of key topographical detail points will be determined using the total station method, integrated along the full length of each route. The proposed transport infrastructure solutions must ensure full accessibility for all forest stands subject to silvicultural interventions, in compliance with the current forest management plan and applicable technical standards.
Finally, the prioritization of routes and accessibility options for the studied stands will be established through simulations evaluating the realistic potential for timber valorization over the designated management period.

CONCLUSIONS

Making the forest fund accessible is an essential condition for sustainable management
of forests and respectively for the optimal valorization of their wood and non-wood products.
In order to design and build an infrastructure corresponding to the transport facilities in inaccessible mountain areas occupied by deciduous trees mixed with softwoods, and mixtures of softwoods, it is necessary to spatially position the characteristic detail points with high precision.
The use of G.N.S.S. technology, of the G.P.S. system, with TRIMBLE R10 and TRIMBLE R12I dual-frequency receivers, for the positioning of GNSS bases (topographic points of the support network density) in the forest fund, by the remote RTK method, using the records from the Beiuş GNSS station, represents an optimal technical solution.
The positioning of the points necessary for carrying out the supported polygonometric surveys, with the total station, from the GNSS bases, was carried out in optimal conditions using a GNSS receiver with two frequencies with an external 4W radio module for the base, and one with an internal 2W radio module for the rover.
The use of the TRIMBLE S6 robot total station for carrying out the supported polygonometric surveys with radii facilitated the spatial positioning in optimal conditions of the characteristic detail points related to the accessibility variants studied and analyzed.
The variants of transport installations studied and analyzed must ensure the accessibility of all the stands that will be traversed with various silvotechnical interventions, in accordance with the forestry management in force, and respecting the technical norms in force.
The ranking of the routes and accessibility variants of the studied stands will be carried out after simulating the real possibilities of valorization of the wood that will be exploited from them, for the established period of time.

ACKNOWLEDGEMENTS

We would like to thank SC TOPOCONSULT SRL from Oradea for the logistical support and help provided in the process of designing and positioning the GNSS bases and the characteristic detail points, necessary for establishing the accessibility options for the studied stands.
Thanks to the collective of the Sudrigiu Forestry District, Bihor County Forestry Directorate, for their collaboration and support given during the field stage of this research.

REFERENCES

Ádám, J., Bányai, L., Borza, T., Busics, G., Kenyeres, A., Krauter, A., & Takács, B. (2004). *Satellite positioning*. University Publishing House.

Andreas, H., Abidin, H. Z., Sarsito, D. A., & Pradipta, D. (2019). Study the capabilities of RTK Multi GNSS under forest canopy in regions of Indonesia. *E3S Web of Conferences, 94*, 01021. https://doi.org/10.1051/e3sconf/20199401021

Brach, M. (2022). Rapid static positioning using a four system GNSS receiver in the forest environment. *Forests, 13*(1), 45. https://doi.org/10.3390/f13010045

Călina, A., Călina, J., Miluț, M., Stan, I., Buzatu, C., Croitoru, A., Băbucă, N., & Dinucă, C. (2020). The study on the use of the topographic method combined GPS-total station in the works of forestry cadastre. *Scientific Papers. Series A. Agronomy, 63*(1), 71–78. https://www.cabidigitallibrary.org/doi/pdf/10.5555/20219969693

Căteanu, M., & Moroianu, M. A. (2024). Performance evaluation of real-time kinematic global navigation satellite system with survey-grade receivers and short observation times in forested areas. *Sensors, 24*(19), 6404. https://doi.org/10.3390/s24196404

Cho, H. M., Park, J. W., Lee, J. S., & Han, S. K. (2024). Assessment of the GNSS-RTK for application in precision forest operations. *Remote Sensing, 16*(1), 148. https://doi.org/10.3390/rs16010148

Ciubotaru, A. (1996). *Elements of design and organization of forest exploitation* (2nd ed.). Lux Libris Publishing House.

Ciubotaru, A. (2007). *Forestry*. Transilvania University of Brașov, Faculty of Forestry and Hunting.

Crainic, G. C. (2011). *Research on the modernization of topographical works in the forestry sector* [Doctoral dissertation, Transilvania University of Brașov].

Dumitru, M. (2014). Sustainable forest management and forestry infrastructure in Romania. *Annals of Forest Research, 57*(2), 89–100.

Feng, T., Chen, S., Feng, Z., Shen, C., & Tian, Y. (2021). Effects of canopy and multi-epoch observations on single-point positioning errors of a GNSS in coniferous and broadleaved forests. *Remote Sensing, 13*, 2325. https://doi.org/10.3390/rs13122325

Florescu, I., & Nicolescu, V. N. (2000). *General forestry*. Romanian Academy Publishing House.

Iordache, E. (2016). The impact of forest roads on forest ecosystems in Romania. *Journal of Forestry and Hunting, 21*(1), 35–48.

Irimie, F., & Timofte, A. I. (2023). The study of wood collection options and the need for accessibility of the forest in Crișanului Valley from Production Unit III Galbena, Sudrigiu Forest District, Bihor Forest Administration. *Annals of the University of Oradea, Environmental Protection Section - Forestry*.

Kaartinen, H., Hyyppä, J., Vastaranta, M., Kukko, A., Jaakkola, A., Yu, X., Pyörälä, J., Liang, X., Liu, J., Wang, Y., Kaijaluoto, R., Melkas, T., Holopainen, M., & Hyyppä, H. (2015). Accuracy of kinematic positioning using global satellite navigation systems under forest canopies. *Forests, 6*(9), 3218–3236. https://doi.org/10.3390/f6093218

Keefe, R. F., Wempe, A. M., Becker, R. M., Zimbelman, E. G., Nagler, E. S., Gilbert, S. L., & Caudill, C. C. (2019). Positioning methods and the use of location and activity data in forests. *Forests, 10*(5), 458. https://doi.org/10.3390/f10050458

Lepoglavec, K., Šušnjar, M., Pandur, Z., Bacic, M., Kopseak, H., & Nevecerel, H. (2023). Correct calculation of the existing longitudinal profile of a forest/skid road using GNSS and a UAV device. *Forests, 14*(4), 751. https://doi.org/10.3390/f14040751

Marton, H. (2007). *MapSys, TopoSys - User manual*. Odorheiu Secuiesc, Romania.

Niculescu, V. (2003). *Forest roads: Design, construction, maintenance*. Silvica Publishing House.

Nero, M. A., Alves, J. L. F. G., da Silva, D. J. N., Gonçalves, M. de L. A., & Elmiro, M. A. T. (2023). Teaching methodology for topography: Didactic proposal for the free station survey method. *Bulletin of University of Agricultural Sciences and Veterinary Medicine Cluj-Napoca. Horticulture, 80*(1). https://doi.org/10.15835/buasvmcn-hort:14603

Pica, A., Boja, F., Fora, C., Moatar, M., & Boja, N. (2022). Advantages of using GNSS technology and QGIS software in inventory stands exploiters. *Series E. Land Reclamation, Earth Observation & Surveying, Environmental Engineering, 11*, 434–443.

Purfürst, T. (2022). Evaluation of static autonomous GNSS positioning accuracy using single-, dual-, and tri-frequency smartphones in forest canopy environments. *Sensors, 22*(3), 1289. https://doi.org/10.3390/s22031289

Sabău, N. C. (2010). *Terrestrial measurements*. Oradea University Publishing House.

Săndoiu, I. (2010). *Silviculture: Principles and practices of sustainable forest management*. Ceres Publishing House.

Tomaštík, J., & Everett, T. (2023). Static positioning under tree canopy using low-cost GNSS receivers and adapted RTKLIB software. *Sensors, 23*(6), 3136. https://doi.org/10.3390/s23063136

Order No. 2,534 of September 28, 2022. For the approval of the Technical Norms on the care and management of arboretums and the Guide to good practices on the care and management of arboretums. *Official Gazette*, No. 989, October 12, 2022.

Order No. 1540/2011. Instructions regarding the deadlines, methods and periods for the collection, removal and transport of wood material (updated).

FAO. (2016). *Roads and forest management: Guidelines for forest roads planning and construction*. FAO Forestry Paper, No. 87.

Ministry of Environment, Waters and Forests. (2021). *National Forest Strategy 2021–2030*.

Forest Management of U.P. III Galbena, Sudrigiu Forest District, Bihor Forestry Directorate, National Forestry Administration – ROMSILVA. (2014). *Institute of Forest Research and Management*.

Forestry Map of U.P. III Galbena, Sudrigiu Forest District, Bihor Forestry Directorate, National Forestry Administration – ROMSILVA. (2014). *Institute of Forest Research and Management*.

Scientific Papers. Series E. Land Reclamation, Earth Observation & Surveying, Environmental Engineering. Vol. XIV, 2025
Print ISSN 2285-6064, CD-ROM ISSN 2285-6072, Online ISSN 2393-5138, ISSN-L 2285-6064

APPLICATION OF HIGH-RESOLUTION SATELLITE IMAGERY FOR EVAPOTRANSPIRATION ESTIMATION - A SCIENTIFIC REVIEW

Vanya IVANOVA, Zhulieta ARNAUDOVA, Rossitza MERANZOVA

Agricultural University of Plovdiv, 12 Mendeleev Blvd, 4000, Plovdiv, Bulgaria

Corresponding author email: vanyast_ivanova@abv.bg

Abstract

The use of remote sensing technology can facilitate the acquisition of data pertaining to crop evapotranspiration, which can in turn inform precision irrigation practices. This is achieved through the analysis of satellite image data. The acquisition of accurate information regarding the utilisation of water is of significant importance within the domain of agricultural water management and crop production, particularly at the scale of human impact on the natural water cycle, in the context of global climate change and the increased prevalence of droughts. The objective of this study is to investigate and provide a summary of the potential for using satellite imagery and in situ measurements for meteorological factors, crop vegetation and soil water content, with a special focus on the assessment of evapotranspiration. The studies conducted are of significant value in predicting the potential water requirements of plants, the capabilities of irrigation systems and the efficient utilisation of irrigation water in agriculture through the implementation of adaptive irrigation regimes.

Key words*: evapotranspiration, irrigation, satellite imagery, vegetation indices.*

INTRODUCTION

Evapotranspiration is a critical component of the water system, playing a pivotal role in the hydrologic cycle. Evapotranspiration, in conjunction with precipitation and runoff, exerts a profound influence on the availability and distribution of water on the land surface. This dynamic process plays a critical role in crop growth and water demand, making it a pivotal factor in hydrological processes and environmental dynamics.

The accessibility of accurate estimations of evapotranspiration is of critical importance for a multitude of applications within diverse scientific disciplines. These include, but are not limited to, climatology, meteorology and agricultural science (Guzinski et al., 2020; Douglas et al., 2009).

Evapotranspiration (ET) is crucial for determining irrigation requirements, optimizing water use, and improving crop yield in agriculture. Understanding ET helps farmers and irrigation planners balance water supply and demand, ensuring efficient water resource management (FAO, 1998). It is imperative to meticulously monitor soil conditions throughout the growing season to optimise production efficiency. As the crop matures, there is a concomitant change in transpiration and altered water requirements. For example, as a key indicator of crop growth, ET has been identified by scientists as a key indicator of crop growth. The calculation of the amount of water utilised by crops has been demonstrated to show the enormous potential in growing crops under irrigated conditions (Allen et al., 1998a; 1998b). The development of digital technology has led to an increase in techniques for calculating and modelling evapotranspiration based on advanced remote sensing techniques. These advancements have been developed to manage water resources more efficiently and facilitate a deeper understanding of the relationship between plant development and water demand, including climate feedback (Teuling et al., 2009; Vazifedoust et al., 2009; Hollmann et al., 2013; Wagle et al., 2017; Allam et al., 2021).

The most widely used and accessible methods for determining ET on a large scale are those carried out by means of Earth observation and satellite imagery, as well as spectral indices of vegetation. To optimize their effectiveness, images for evaluation of ET must have a spatial resolution that aligns with terrain characteristics and field size (Anderson et al., 2004; Guzinski et al., 2019)

To achieve this objective, it is imperative to undertake a comparative analysis of field measurements of ET with those obtained from remote sensing methodologies.

The comparison of field measurements of ET with those obtained from remote sensing has two principal purposes: to determine the accuracy of remote sensing of ET and to validate the remote sensing algorithms used for ETo estimation (Anderson et al., 2004; Mcabe et al., 2006; Kustas et al., 2018; Mokhtari et al., 2019). To evaluate ET data obtained from satellite imagery or other remote sensing methods and determine whether their scatter in determination is appropriate for crop irrigation, it is critical that they be confirmed with field measurements of ET. (Anderson et al., 2004; Guzinski et al., 2019). The spatial resolution can range from 10 m per pixel to 300 m, depending on the temporal resolution of the acquisition (Allen et al., 2007). Reliable estimates of actual ETo and crop water requirements are best achieved using satellite observations in the visible/near-infrared and thermal infrared electromagnetic spectrum (Anderson et al., 2012; Hoffmann et al., 2016).

The objective of this study is to investigate and provide a summary of the potential for using satellite imagery and *in situ* measurements for meteorological factors, crop vegetation and soil water content, with a special focus on the assessment of evapotranspiration.

MATERIALS AND METHODS

SYNTHESIS OF EXISTING LITERATURE

Description for evapotranspiration and Data Collection

The framework of the study is to integrate in situ and spatial measurements to determine ET during crop vegetation, such as traditional in field measurements with modern remote sensing data.

Evapotranspiration (ET) is the combined process by which water transfers from the land surface to the atmosphere both by evaporation from soil and plant surfaces and by transpiration through plant stomata. It represents the actual water loss under given field conditions (mm/day or mm).

Reference Evapotranspiration (ET_0)

The rate of evapotranspiration from an idealized reference surface - typically a well-watered, actively growing grass of uniform height - under prevailing climatic conditions. ET_0 provides a standard baseline (mm/day) that is independent of crop type or management; it is used to compare atmospheric demand for water across locations and times.

Crop Evapotranspiration (ETc)

The evapotranspiration rate of a specific crop under standard field conditions. It is calculated by adjusting reference evapotranspiration (ET_0) with a crop coefficient (Kc):

$$ETc=Kc\times ET_0$$

where:

- Kc accounts for crop characteristics (e.g. canopy cover, growth stage), climate and soil evaporation;
- ETc represents the crop's water use requirement (mm/day).

Traditional ETo Estimation Methods

ET can be quantified using two primary methodologies:

Direct Measurement Methods:

Climatic Parameters: continuous recordings of air temperature, relative humidity, solar radiation, wind speed, and precipitation levels are used to calculate baseline ETo estimates.

*Crop Characteristics***:** detailed information on crop type, variety, growth stage, and morphological features (such as plant height and density) is collected. These factors are critical since they influence the rate of transpiration and, consequently, the overall ET.

Soil and Agrotechnical Conditions: variations in soil properties, moisture content, and cultivation practices (including tillage and irrigation methods) are monitored. These conditions modify the microclimate around the crop canopy, impacting both soil evaporation and plant transpiration.

Lysimeters: instruments that directly measure changes in soil moisture, thereby estimating the amount of water lost through ET. Although highly accurate, lysimeters are typically expensive and labour-intensive.

Field Moisture Sensors: devices that monitor the water content in the soil, offering real-time data on moisture variations within the root zone.

The only factors affecting ETo are climatic parameters. Consequently, ETo is a climatic parameter and can be computed from weather data.

The methods for calculating evapotranspiration from meteorological data require various climatological and physical parameters. Some of the data are measured directly in weather stations. Other parameters are related to commonly measured data and can be derived with the help of a direct or empirical relationship. (FAO,1998).

To facilitate the management of water resources, it is imperative to make estimates of evapotranspiration ET. This is particularly crucial in the context of climate change, as ET estimates are necessary to predict potential changes at both global and regional scales (Allen et al., 2005; Teuling et al., 2009).

Evapotranspiration is not easy to measure. Determining evapotranspiration requires specialized equipment and accurate measurements of various physical parameters or soil water balance in lysimeters. The methods are often expensive and demanding in terms of accuracy. Although these methods are not suitable for routine measurements, they remain important for evaluating ET estimates obtained by more indirect methods.

***Indirect Estimation Methods**:*

A variety of empirical and physically based models have been developed to estimate crop or reference-crop evapotranspiration (ET_c and ET_0) from readily available meteorological data, yet each is valid only under climatic and field conditions. The FAO-56 Penman-Monteith equation combines radiation, temperature, humidity and wind speed to yield a robust reference ET (ET_0) applicable across humid, arid and temperate zones when comprehensive data are available (Allen et al., 1998).

By contrast, Shaumyan's temperature-based model (ET = k (T + a)) relies solely on mean monthly air temperature (T) and regionally calibrated coefficients (k and a), making it useful where only thermal records exist but requiring local calibration (Shaumyan, 1960).

Turk's semi-empirical formula, ET = 0.013 (T/(T+15)) (23.885R_s+50), incorporates solar radiation (R_s) and temperature (T), performing well in humid climates but underestimating ET under arid conditions (Turc, 1961).

Finally, the Blaney-Criddle method, ETc = p (0.46T+8), uses temperature and daylight fraction (p) to estimate crop ET in temperate to semi-arid regions, though it omits humidity, wind and detailed radiation terms and thus loses accuracy in tropical or highly variable climates (Blaney & Criddle 1950).

The following conclusions and implications can be deducted from the practical applications of evapotranspiration determination.

- The FAO Penman-Monteith method has been approved as the standard method for the determination and calculation of reference evapotranspiration (ETo).

$$ET_0 = \frac{0.408\Delta(R_n - G) + \gamma\frac{900}{T+273}u_2\,(e_s - e_a)}{\Delta + \gamma(1 + 0.34u_2)}$$

where:

- ETo reference evapotranspiration (mm day^{-1});
- R_n net radiation at the crop surface (MJ m^{-2} day^{-1});
- G soil heat flux density (MJ m^{-2} day^{-1});
- T mean daily air temperature at 2 m height (°C);
- u_2 wind speed at 2 m height (m s^{-1});
- e_s saturation vapour pressure (kPa);
- e_a actual vapour pressure (kPa);
- e_s - e_a saturation vapour pressure deficit (kPa);
- Δ slope vapour pressure curve (kPa/ $°C^{-1}$);
- γ psychrometric constant (kPa/$°C^{-1}$) (Allen R. G. et al., 1998).

The crop surface evapotranspiration and crop-specific coefficient (Kc) are determined, thus relating the crop evapotranspiration to reference (Glen et al., 2010). The estimation of ET and soil moisture content is fundamental to the management of water resources, the provision of drinking water and irrigation, and the intensification of the water deficit crisis (Anderson et al., 2007; Mokhtari et al., 2019). Soil moisture content is directly related to the ET process, as it is contained in the soil surface and plant needs (Norman et al., 1995; FAO, 1998).

Empirical models derive ET estimates from relationships between climatic variables and crop characteristics. Single-factor models and multi-factor approaches (including the Penman-Monteith equation, Shaumyan's, Turk's, and Blaney-Criddle methods) are commonly used.

Remote Sensing Models

These methods utilize satellite data to estimate ET. Two prominent approaches include:

Spectral Vegetation Indices (SVI): these indices are derived from reflectance values in the visible and near-infrared spectra. They provide insight into crop vigour and canopy density, which are directly related to water use.

Energy Balance Models: these incorporate both optical and thermal data to assess the energy exchange at the land surface. Models such as Surface Energy Balance Algorithm for Land (**SEBAL**), Mapping Evapotranspiration with Internalized Calibration (**METRIC**), and the Surface Energy Balance System (**SEBS**) use thermal imagery to derive sensible and latent heat fluxes, thereby estimating ET.

Applications and case studies

Sensor Resolution Impact:

McCabe investigated the use of multiple satellite sensors to estimate evapotranspiration (ET) across different spatial scales. The focus is on understanding how satellite sensor resolution affects the accuracy of ET measurements, particularly in agricultural regions. The importance of ET in hydrological and agricultural systems is emphasized as it controls water availability, and there's a strong interest in improving its estimation for water resource management (McCabe et al., 2006).

The utility of satellite imagery is limited by temporal resolution. For practical purposes (i.e. irrigation scheduling/water allocation), the bi-monthly temporal observations offered by high-resolution platforms are insufficient. For estimating the average daily evapotranspiration of a watershed, MODIS provides an extremely valuable data source for assessing the current condition of the land and vegetation - useful for weather forecasting, flood forecasting, and other areas of water resource management.

The authors present different energy balance models that differ in their ability to characterize surface flux at specific model scales, the results presented can serve to predict evaporation flux at different scales regardless of the model used.

Data Fusion Techniques:

Researchers have examined the potential of Sentinel-2 and Sentinel-3 satellites to estimate high-resolution evapotranspiration (ETo), a process vital for agricultural and water resource management. Sentinel satellites have various spatial and spectral resolutions. They lack high-resolution thermal sensors, crucial for precise ET monitoring. The research uses machine learning algorithms to enhance Sentinel-3's low-resolution thermal data with Sentinel-2's high-resolution optical data. The enhanced data is then integrated into a land-surface energy balance model, facilitating more precise ET estimations (Guzinski et al., 2019).

Cloud Cover Mitigation:

Chintala focuses on modeling high-resolution actual evapotranspiration (ETa) using data from the Sentinel satellites, specifically addressing challenges like cloud cover during the monsoon season. The study uses the Sen-ET plugin, combining Sentinel-1, Sentinel-2, and Sentinel-3 data, to improve ETa flux estimations (Chintala et al., 2022)

Crop-Specific Models:

Rozenstein (2018) conducted a study to validate evapotranspiration for cotton water consumption using Sentinel-2 imagery and ground measurements. The research examined the relationships between the crop coefficient and various vegetation indices. The obtained results aim to support the development of irrigation models for cotton crops.

Singh and others researches explored a novel approach to estimate daily evapotranspiration (ET) using a fusion of Landsat 8 and Sentinel-2 data. ET is a critical component for hydrology, agriculture, and climate models, but field measurements are costly and impractical over large areas. While Landsat provides medium-resolution thermal data (30 m, 16-day revisit), Sentinel-2 offers higher spatial resolution (10–20 m, 5-day revisit) but lacks thermal bands. This study bridges these gaps by combining data from both satellites to enhance spatio-temporal resolution for ET estimation. (Singh et al., 2020)

Irrigation Detection:

Chakhar et al. (2024) investigated time series from Sentinel-1 and Sentinel-2, along with biophysical coefficients, to improve irrigation in orchards. The authors utilized meteorological data, specifically rainfall data from SAR (Synthetic Aperture Radar). To obtain time series of derived indices from the Sentinel-1 and Sentinel-2 satellite missions, Python scripts were used during development to retrieve processed NDVI.

Both remote sensing datasets have a spatial resolution of 10 m and are configured to have a temporal resolution of 7 days. In terms of temporal resolutions, the goal was to acquire

weekly information from both remote sensing sources and to use this information in an integrated manner. It should be noted that the normal coverage (temporal resolution) of Sentinel-2 in the study area is typically 3-4 days, while for Sentinel-1 it is 6 days.
(https://servicio.mapa.gob.es/websiar/ accessed on March 27, 2023), provided by the Spanish Ministry of Agriculture, Fisheries, Food, and Environment.

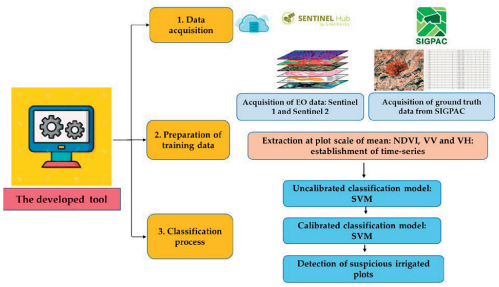


Figure 1 General workflow (Chakhar et al., 2024)

In conclusion, the authors found that integrating in situ measurements with multispectral sensors and radar imagery yields the highest accuracy and efficiency. The proposed method estimates crop water consumption through image classification and time series analysis. As a key outcome of the study, they optimized the Support Vector Machine (SVM) model for detecting irrigated plots, enhancing its performance and reliability. (Chakhar et al., 2024)

RESULTS AND DISCUSSIONS

Comparative insights between traditional and remote sensing approaches

Field measurements of evapotranspiration (ET) are accompanied by methods that are difficult to conduct with the requisite degree of accuracy in situ. Most methodologies rely on the estimation of ET from meteorological data. In contrast, Earth observation has been a powerful and advanced tool for estimating ET over large areas. Satellite imagery is utilized to analyze ET in spatial and time series that cannot be achieved by in situ measurements. The utilization of satellite imagery to estimate ET can be systematized into two primary approaches: spectral vegetation indices (SVI) and energy balance methods.

Evaluation of spatial and temporal resolution needs

Satellite imagery provides the ability to analyze ET in spatial and time series that cannot be achieved by in situ measurements. Research of the spectral vegetation indices time series, such as the normalized difference vegetation index (NDVI) and the soil adjusted vegetation index (SAVI), are evaluated to estimate crop coefficients for cotton and sugarbeet. (González-Dugo et al., 2008) This helps to estimate crop evapotranspiration in irrigated areas by multiplying reference evapotranspiration values by appropriate crop coefficients.

Cost-effectiveness and feasibility of field vs. satellite methods

Accurately measuring evapotranspiration (ET) in the field is often both challenging and expensive. In contrast, remote sensing has become a more practical and cost-effective alternative for estimating ET across large areas. This approach relies on satellite sensors that operate in the electromagnetic spectrum, particularly optical multispectral and thermal bands. One well-established model, the Surface Energy Balance Algorithm for Land (SEBAL), utilizes data from sources such as Landsat 7 and has been extensively calibrated and validated to assess spatial variations in crop yield, ET, and water productivity (Bastiaanssen et al., 1998).
The Surface Energy Balance System (SEBS), introduced by Su (2002), is a remote sensing-based model designed to estimate surface energy balance components. It offers a more detailed representation of the atmospheric boundary layer and surface roughness. SEBS is recognized for its reliability across various climatic conditions and has been successfully applied in a wide range of environments. An advancement of the SEBAL model, known as METRIC, was developed by Allen et al. (2007). This model enhances accuracy through additional calibration steps that incorporate ground-based reference evapotranspiration (ET) data.

Accuracy and limitations of current satellite-based ET Models

The two primary approaches for estimating ET using satellite imagery - spectral vegetation

indices (SVI) and energy balance methods - have been extensively validated using lysimeters. Studies and analyses derived from the energy balance method exhibit a greater degree of similarity to the actual changes in crop condition. However, there are limitations to current satellite-based ET models, including the need for accurate calibration and validation to ensure the reliability of the estimates.

Knowledge gaps and future directions

Satellite base models for estimating crop evapotranspiration have their advantages and continue to develop and improve, despite some limitations.

Advantages:

- High spatial and temporal resolution: energy balance methods can provide detailed ET estimates over large areas and at frequent intervals, which is not feasible with traditional field methods.
- Validation and calibration: these methods have been extensively validated using ground-based measurements like lysimeters, ensuring their reliability.

Limitations:

- Data Requirements: accurate estimation requires high-quality input data, including surface temperature, radiation, and meteorological data.
- Complexity: the models can be complex to implement and require expertise in remote sensing and energy balance principles
- Need for standardization in remote sensing algorithms across climate zones
- Gaps in high-resolution thermal data for ET estimation
- Challenges in integrating multi-source satellite data

To improve the effectiveness of the models and their applicability in practice, it is necessary to make synchronous observations of the ground according to the specific soil, vegetation and climatic conditions. This is necessary due to the lack of sufficient data to validate the models themselves, which still work with wide range values and large scale area.

CONCLUSIONS

The variability in evapotranspiration is governed by a complex interplay of climatic conditions, crop development, and soil management practices. Satellite imagery emerges as a powerful tool for assessing these dynamics over vast areas with diverse landscape features. The integration of high-resolution optical, radar and thermal data, especially when enhanced through data fusion techniques, significantly improves the precision of ET estimates. These advancements support the development of adaptive irrigation regimes and contribute to the sustainable management of water resources in agriculture. The development of sustainable models for precise irrigation management is dependent upon the validation of current spatial observations of vegetation cover according to the specific soil and climatic conditions of a given crop. Future research should continue to refine these remote sensing methodologies to further reduce uncertainties and enhance their applicability across different environmental conditions.

ACKNOWLEDGEMENTS

This research was carried out with the support of the National Program of the Ministry of Education, Science and Technology, and the publication was funded under the Research Project "Young Scientists and Postdoctoral Fellows - 2" - second stage 2024/2025

REFERENCES

Allam, M., Mhawej, M., Meng, Q., Faour, G., Abunnasr, Y., Fadel, A., & Xinli, H. (2021). Monthly 10-m evapotranspiration rates retrieved by SEBALI with Sentinel-2 and MODIS LST data. *Agricultural Water Management*, *243*, 106432.

Allen, R. G., Clemmens, A. J., & Willardson, L. S. (2005). Agro-hydrology and irrigation efficiency. *ICID Working Group Water and Crops*.

Allen, R. G., Irmak, A., Trezza, R., Hendrickx, J. M. H., Bastiaanssen, W. and Kjaersgaard, J. (2011), Satellite-based ET estimation in agriculture using SEBAL and METRIC, *Hydrology Processing*., *25*, 4011–4027, doi:10.1002/hyp.8408

Allen, R. G., Pereira, L. S., Raes, D., & Smith, M. (1998). Crop evapotranspiration - Guidelines for computing crop water requirements. FAO Irrigation and Drainage Paper 56. Food and Agriculture Organization of the United Nations

Allen, R. G., Tasumi, M., Morse, A., Trezza, R., Wright, J. L., Bastiaanssen, W., Kramber, W., Lorite, I., and Robison, C. W. (2007) Satellite-Based Energy Balance for Mapping Evapotranspiration with

Internalized Calibration (METRIC) – *Applications, J. Irrigation Drainage Engineering*., 133, 395–406.

Anderson, M. C., Kustas, W. P., Alfieri, J. G., Gao, F., Hain, C., Prueger, J. H. & Chávez, J. L. (2012). Mapping daily evapotranspiration at Landsat spatial scales during the BEAREX'08 field campaign. *Advances in Water Resources*, *50*, 162–177.

Anderson, M. C., Norman, J. M., Mecikalski, J. R., Otkin, J. A., & Kustas, W. P. (2007). A climatological study of evapotranspiration and moisture stress across the continental United States based on thermal remote sensing: 1. Model formulation. *Journal of Geophysical Research: Atmospheres*, *112*(D10).

Anderson, M. C., Norman, J. M., Mecikalski, J. R., Torn, R. D., Kustas, W. P., & Basara, J. B. (2004). A multiscale remote sensing model for disaggregating regional fluxes to micrometeorological scales. *Journal of Hydrometeorology, 5*(2), 343–363.

Anderson, R. G., Y. Jin, and M. L. Goulden. (2012). Assessing Regional Evapotranspiration and Water Balance across a Mediterranean Montane Climate Gradient. *Agricultural and Forest* Meteorology166–167: 10–22. doi: 10.1016/j.agrformet.2012.07.004.

Barker, J. B., Heeren, D. M., Neale, C. M., & Rudnick, D. R. (2018). Evaluation of variable rate irrigation using a remote-sensing-based model. *Agricultural Water Management*, *203*, 63–74.

Bastiaanssen, W. G., Pelgrum, H., Wang, J., Ma, Y., Moreno, J. F., Roerink, G. J., & Van der Wal, T. (1998). A remote sensing surface energy balance algorithm for land (SEBAL).: Part 2: Validation. *Journal of hydrology*, *212*, 213–229.

Bhattarai, R. P., Ojha, B. R., Thapa, D. B., Kharel, R., Ojha, A., & Sapkota, M. (2017). Evaluation of elite spring wheat (Triticum aestivum L.) genotypes for yield and yield attributing traits under irrigated condition. *International journal of applied sciences and biotechnology*, *5*(2), 194–202.

Blaney, H. F., & Criddle, W. D. (1950). Determining water requirements in irrigation practices. *USDA Soil Conservation Service Technical Paper*, 96, 48.

Chakhar, A., Hernández-López, D., Ballesteros, R., & Moreno, M. A. (2024). Irrigation detection using Sentinel-1 and Sentinel-2 time series on fruit tree orchards. *Remote Sensing*, *16*(3), 458.

Chintala, S., Harmya, T. S., Kambhammettu, B. V. N. P., Moharana, S., & Duvvuri, S. (2022). Modelling high-resolution Evapotranspiration in fragmented croplands from the constellation of Sentinels. *Remote Sensing Applications: Society and Environment*, *26*, 100704.

Dennison, P. E., Nagler, P. L., Hultine, K. R., Glenn, E. P., & Ehleringer, J. R. (2009). Remote monitoring of tamarisk defoliation and evapotranspiration following saltcedar leaf beetle attack. *Remote Sensing of Environment*, *113*(7), 1462–1472.

Douglas, E. M., Jacobs, J. M., Sumner, D. M., & Ray, R. L. (2009). A comparison of models for estimating potential evapotranspiration for Florida land cover types. *Journal of Hydrology*, *373*(3-4), 366–376.

FAO (1998)**:** *Crop Evapotranspiration – Guidelines for Computing Crop Water Requirements (FAO-56)*.

Garatuza-Payan, J., & Watts, C. J. (2005). The use of remote sensing for estimating ET of irrigated wheat and cotton in Northwest Mexico. *Irrigation and Drainage Systems*, *19*, 301–320.

Glenn, E. P., Nagler, P. L., & Huete, A. R. (2010). Vegetation index methods for estimating evapotranspiration by remote sensing. *Surveys in Geophysics*, *31*, 531–555.

González-Dugo, M. P., & Mateos, L. (2008). Spectral vegetation indices for benchmarking water productivity of irrigated cotton and sugar beet crops. *Agricultural water management*, *95*(1), 48–58.

Groeneveld, D. P., Baugh, W. M., Sanderson, J. S., & Cooper, D. J. (2007). Annual groundwater evapotranspiration mapped from single satellite scenes. *Journal of Hydrology*, *344*(1-2), 146–156.

Guerschman, J. P., Van Dijk, A. I., Mattersdorf, G., Beringer, J., Hutley, L. B., Leuning, R., Sherman, B. S. (2009). Scaling of potential evapotranspiration with MODIS data reproduces flux observations and catchment water balance observations across Australia. *Journal of hydrology*, *369*(1-2), 107–119.

Guzinski, R., Nieto, H. (2019), Evaluating the feasibility of using Sentinel-2 and Sentinel-3 satellites for high-resolution evapotranspiration estimations. *Remote Sensing Environment* 221, 157–172. https://doi.org/10.1016/j.rse.2018.11.019

Guzinski, R., Nieto, H., Sandholt, I., Karamitilios, G., (2020). Modelling high-resolution actual evapotranspiration through Sentinel-2 and Sentinel-3 data fusion. *Remote Sensing, 12*(9) https://doi.org/10.3390/RS12091433.

Hoffmann, H., Jensen, R., Thomsen, A., Nieto, H., Rasmussen, J., & Friborg, T. (2016). Crop water stress maps for an entire growing season from visible and thermal UAV imagery. *Biogeosciences*, *13*(24), 6545–6563.

Hollmann, R., Merchant, C. J., Saunders, R., Downy, C., Buchwitz, M., Cazenave, A., ... & Wagner, W. (2013). The ESA climate change initiative: Satellite data records for essential climate variables. *Bulletin of the American Meteorological Society*, *94*(10), 1541–1552.

https://servicio.mapa.gob.es/websiar/ accessed on 27 March 2023)

Hunsaker, D. J., Fitzgerald, G. J., French, A. N., Clarke, T. R., Ottman, M. J., & Pinter Jr, P. J. (2007). Wheat irrigation management using multispectral crop coefficients: I. Crop evapotranspiration prediction. *Transactions of the ASABE*, *50*(6), 2017–2033.

Kamble, B., Kilic, A., & Hubbard, K. (2013). Estimating crop coefficients using remote sensing-based vegetation index. *Remote sensing*, *5*(4), 1588–1602.

Kustas, W. P., Anderson, M. C., Alfieri, J. G., Knipper, K., Torres-Rua, A., Parry, C. K., ... & Hain, C. (2018). The grape remote sensing atmospheric profile and evapotranspiration experiment. *Bulletin of the American meteorological society*, *99*(9), 1791–1812.

Kustas, W., Anderson, M. (2009). Advances in thermal infrared remote sensing for land surface modeling. *Agriculture. For Meteorology. 149*(12), 2071–2081. https://doi.org/10.1016/j.agrformet.2009.05.016.

Leuning, R., Zhang, Y. Q., Rajaud, A., Cleugh, H., & Tu, K. (2008). A simple surface conductance model to estimate regional evaporation using MODIS leaf area

index and the Penman-Monteith equation. *Water Resources Research*, *44*(10).

McCabe, M. F., & Wood, E. F. (2006). Scale influences on the remote estimation of evapotranspiration using multiple satellite sensors. *Remote Sensing of Environment*, *105*(4), 271–285.

MODIS LST data. Agric. Water Manag. 243 (July 2020), 106432. ttps://doi.org/10.1016/j.agwat.2020.106432.

Mokhtari, A., Noory, H., Pourshakouri, F., Haghighatmehr, P., Afrasiabian, Y., Razavi, M., ... & Naeni, A. S. (2019). Calculating potential evapotranspiration and single crop coefficient based on energy balance equation using Landsat 8 and Sentinel-2. *ISPRS Journal of Photogrammetry and Remote Sensing*, *154*, 231–245.

Mokhtari, A., Noory, H., Vazifedoust, M., & Bahrami, M. (2018). Estimating net irrigation requirement of winter wheat using model-and satellite-based single and basal crop coefficients. *Agricultural water management*, *208*, 95–106.

Norman, J. M., Kustas, W. P., & Humes, K. S. (1995). Source approach for estimating soil and vegetation energy fluxes in observations of directional radiometric surface temperature. *Agricultural and Forest Meteorology*, *77*(3-4), 263–293.

Peddinti, S. R., & Kambhammettu, B. P. (2019). Dynamics of crop coefficients for citrus orchards of central India using water balance and eddy covariance flux partition techniques. *Agricultural Water Management,* 212, 68–77.

Reyes-González, A., Kjaersgaard, J., Trooien, T., Hay, C., & Ahiablame, L. (2018). Estimation of Crop Evapotranspiration Using Satellite Remote Sensing-Based Vegetation Index. *Advances in Meteorology*, *2018*(1), 4525021.

Reyes-González, A., Kjaersgaard, J., Trooien, T., Reta-Sánchez, D. G., Sánchez-Duarte, J. I., Preciado-Rangel, P., & Fortis-Hernández, M. (2019). Comparison of leaf area index, surface temperature, and actual evapotranspiration estimated using the METRIC model and in situ measurements. *Sensors*, *19*(8), 1857.

Rozenstein, O., Haymann, N., Kaplan, G., & Tanny, J. (2018). Estimating cotton water consumption using a time series of Sentinel-2 imagery. *Agricultural water managemen*t, 207, 44–52.

Shaumyan, A. S. (1960). On the estimation of evapotranspiration from meteorological data. *Proceedings of the Hydrometeorological Centre*, 12, 45–57 (in Russian).

Singh, R. K., Khand, K., Kagone, S., Schauer, M., Senay, G. B., & Wu, Z. (2020). A novel approach for next generation water-use mapping using Landsat and Sentinel-2 satellite data. *Hydrological Sciences Journal*, *65*(14), 2508–2519.

Su, Z. (2002). The Surface Energy Balance System (SEBS) for estimation of turbulent heat fluxes. *Hydrology and earth system sciences*, *6*(1), 85–100.

Teuling, A. J., Hirschi, M., Ohmura, A., Wild, M., Reichstein, M., Ciais, P., ... & Seneviratne, S. I. (2009). A regional perspective on trends in continental evaporation. *Geophysical Research Letters*, *36*(2).

Turc, L. (1961). Estimation of evapotranspiration from climate data. *Journal of Hydrology*, 12(3), 349–367.

Vazifedoust, M., Van Dam, J. C., Bastiaanssen, W. G. M., & Feddes, R. A. (2009). Assimilation of satellite data into agro hydrological models to improve crop yield forecasts. *International Journal of Remote Sensing*, *30*(10), 2523–2545.

Wagle, P., Bhattarai, N., Gowda, P. H., & Kakani, V. G. (2017). Performance of five surface energy balance models for estimating daily evapotranspiration in high biomass sorghum. *ISPRS Journal of Photogrammetry and Remote Sensing*, *128*, 192–203.

Scientific Papers. Series E. Land Reclamation, Earth Observation & Surveying, Environmental Engineering. Vol. XIV, 2025
Print ISSN 2285-6064, CD-ROM ISSN 2285-6072, Online ISSN 2393-5138, ISSN-L 2285-6064

ANALYZING THE INFLUENCE OF TEMPERATURE ON NDVI FOR A POTATO CROP IN BRAŞOV AREA

Mihai IVANOVICI[1], Maria ŞTEFAN[2], Angel CAŢARON[1], Adrian GHINEA[2], Gheorghe OLTEANU[1]

[1]Transilvania University of Braşov, 29 Eroilor Blvd, Braşov, Romania
[2]National Institute of Research and Development for Potato and Sugar Beet, 2 Fundăturii Street, Braşov, Romania

Corresponding author email: mihai.ivanovici@unitbv.ro

Abstract

It is known that meteorological parameters, among others, are highly determinant for the growth of the agricultural crops. On the other hand, vegetation indices computed on remote sensing data are widely-used for crop monitoring. In this paper we focus on temperature, one of the determinant meteorological parameters, and the Normalized Difference Vegetation Index (NDVI), the most used vegetation index. We use temperature and NDVI time series, the latter one computed based on Copernicus data. Based on the hypothesis that effect accumulations of temperature in time determine the plant age and growth and, implicitly, its vegetation status, we study the influence of temperature on NDVI and attempt to model it. We present a use case for the monitoring of two potato crops during the 2023 and 2024 seasons in Braşov area, Romania and formulate the conclusions.

Key words*: temperature, NDVI, time series, Copernicus data, potato crop.*

INTRODUCTION

It is currently estimated that the world population will increase from 7.5 to 9.7 billion by 2050 (Gu et al., 2021), resulting in a high demand of agricultural products and a high pressure on natural resources. Despite the fact that agriculture is still the major activity in many countries, we face a global decrease in both production and employment in agriculture. The solutions to boost productivity are agricultural investments and technological innovations (Godfray et al., 2010).

In the context of Agriculture 5.0 (Ivanovici et al., 2024), Earth Observation (EO) data is widely used for the monitoring of agricultural crops. Nowadays remote sensing technologies provide support for precise agricultural operations at the scale of farmers' fields, as well as to the management and strategic planning of agricultural production both at regional and national levels (Guo et al., 2017). EU Copernicus programme provides free EO data which can be used for various applications in smart agriculture (EU, 2014).

We focused our research in an area situated in Brasov County, in the central part of Romania. The area is part of the region used to be called *Potato Country* in Romania, being renowned for its large areas cultivated with potatoes. However, in the last decade, due to climate change, the area cultivated with potatoes has dropped to approx. 25%. The potato (*Solanum tuberosum* L.) thrives in moderate temperatures, typically between 14°C and 22°C, and is sensitive to environmental changes during storage (Teper-Bamnolker, 2010). The suitable relative soil moisture content for potato growth and development is 55% to 85%, and the suitable temperature is 15°C to 25°C. The growth and development of potato plants under drought and high-temperature stress conditions are inhibited, and plant morphology is altered, which affects the process of potato stolon formation, tuberization and expansion, ultimately leading to a significant reduction in potato tuber yields and a remarkable degradation of the market grade of tubers, the specific gravity of tubers, and the processing quality of tubers (Fang et al., 2024). According to (Sánchez-Correa, 2024), optimal potato development occurs at temperatures between 15°C and 20°C, with yields ranging from 12 to 60 tons of tubers per hectare. However, observations show a decline in yield when the ambient temperature exceeds 24°C. This is due

to a combination of independent morphological, physiological and developmental issues. According to (Timlin, 2006), the optimum temperature for canopy photosynthesis is 24°C (but this decreases with the plant age) and the total biomass was highest at 20°C. However, the ideal temperature for potato crop may vary with plant growth stages (Singh, 2019).

In this paper we use temperature and NDVI time series for the analysis of their relationship for two potato crops in Brasov area, Romania, in 2023 and 2024. We build our model based on the hypothesis that the accumulations in time of temperature effects determines the plant age and growth and has impact on vegetation status, as observed through vegetation indices such as NDVI. The temperature impacts the entire potato plant (Lazarević et al., 2022). Based on the proposed model, we study the influence of temperature to the vegetation status indicated by NDVI computed on Copernicus data. We present the materials and methods, then we show experimental results, as well as a discussion, and conclude the paper.

MATERIALS AND METHODS

For the current study, we used Sentinel-2 data, more specifically, the satellite images were freely downloaded from the Copernicus browser (https://browser.dataspace.copernicus.eu/). In particular, we were interested in monitoring the evolution of potato crops belonging to the National Institute of Research and Development for Potato and Sugar Beet (NIRDPSB), Braşov, Romania (see Figure 1).

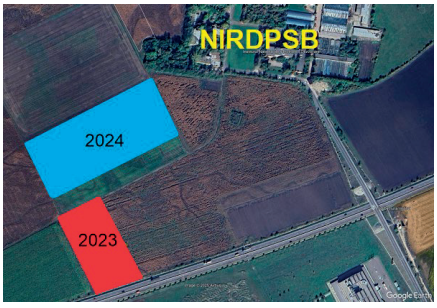


Figure 1. NIRDPSB and the two potato crops of interest, Braşov area, Romania (source: Google Earth)

With more than 60 years of experience, NIRDPSB plays an important role in the preservation of the potato heritage at the national level (Chiru et al, 2017). Through its activities, NIRDPSB promotes both fundamental and applicative research in the domain of potato and sugar beet cultivation. In Figure 1 we show a satellite view with the under-study potato crops for 2023 and 2024 highlighted with red and blue, respectively, with respect to the location of NIRDPSB, for easy identification. For the two potato crops of interest, the time period of interest was from 1st May to 31st of August (122 days), both for 2023 and 2024.

In Figure 2 one can see the evolution of average daily temperature for 2023 and 2024, with a minimum of approximately 10ºC (both in 2023 and 2024) and a maximum of 28ºC in 2023 and 30ºC in 2024. The temperature readings were provided by the NMA Braşov-Ghimbav Station, located at approx. 3 km from the potato crops.

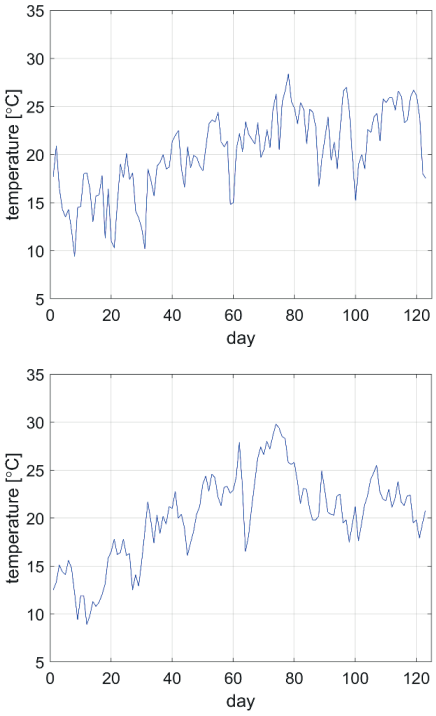


Figure 2. The average daily temperature for 2023 (top) and 2024 (bottom) for the potato crops of interest

From the Copernicus data we downloaded the NDVI product for the two corresponding potato crops, for 2023 and 2024, respectively. The two

original NDVI time series are depicted with black in Figure 3. One can notice that for some dates the NDVI values are erroneous, i.e. they exhibit very low values. These erroneous values were filtered out by using a morphological filter in order to produce a smoother variation of the NDVI – depicted with green. The filtering was applied both for the 2023 and 2024 time series.

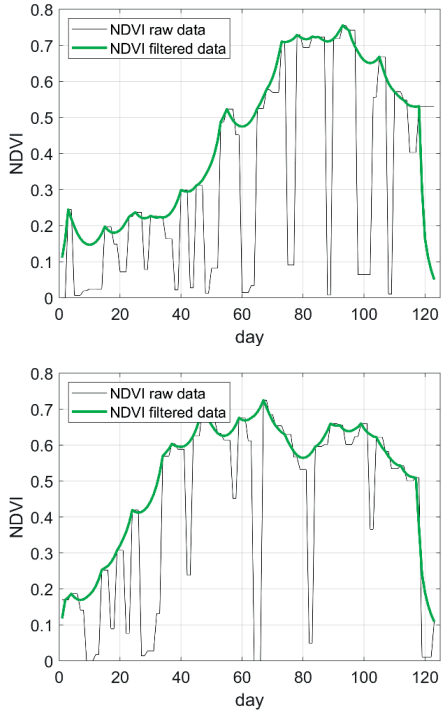


Figure 3. The NDVI time series for 2023 (top) and 2024 (bottom) for the potato crops of interest

In order to build our model, we considered the following observations. Potato develops best at approximately 20°C (Rykaczewska, 2015). An increase with 5°C above this optimum temperature causes a reduction in the photosynthetic rate with 25%, which ultimately affects biomass accumulation and, later, the sink activity (Obiero et al., 2019). Transitory or constant high temperatures cause an array of morpho-anatomical, physiological and biochemical changes in plants, which affect plant growth and development and may lead to a drastic reduction in economic yield (Wahid et al. 2007; Lal et al., 2022). These inhibitory effects occurred at all developmental stages (Van Harsselaar et al., 2021), including growth inhibition at the seedling stage (Daim and Zhangzz, 2018), decreased number of stolons and hindered tuber expansion, which resulted in lower yields, abnormal tuber morphology and fewer salable tubers (Liu et al., 2025).

Based on these observations, we propose the following approach to perform the analysis of temperature influence on NDVI (see the block diagrams in Figure 4). The first block maps the daily temperature to the degree of influence of temperature to the overall vegetation status and, implicitly, NDVI, assuming a purely Gaussian model (in blue), similar to the ones seen in the literature. Alternatively, we propose the usage a piecewise linear model (in red), better matching the observations made above. The second block cumulates the degrees of influence over a specified period of time, significant for the process of plant growth. The resulting cumulated degree of influence is then correlated with the NDVI time series, resulting in the Pearson correlation coefficient ρ.

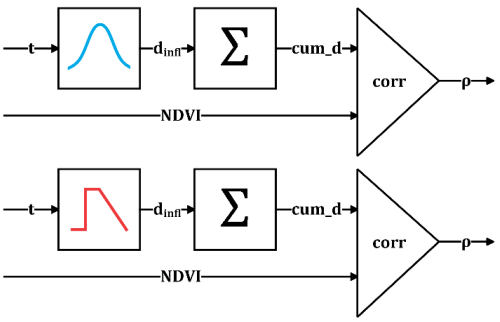


Figure 4. The block diagram of the proposed approach – based on the Gaussian (top) and piecewise linear (bottom) model for the temperature degree of influence

There exist several attempts to model the influence of the temperature for the development of the roots of plants. We make the assumption that such a model can be designed for the degree of influence of temperature to the overall vegetation status of the plants. Consequently, we assume a direct relationship between the degree of influence of temperature and the measured NDVI (as it is measured by means of remote sensing). For the degree of influence of temperature to NDVI, we considered a generic, symmetric Gaussian model, as the one depicted in Figure 5. This

choice was inspired by the existing models for other crops (Walne, 2022). We assume a symmetrical mapping of the range of temperatures from 0ºC to 40ºC to the [0,1] interval. The maximum degree of influence corresponds to a temperature of 20ºC. This particular choice was merely to have a starting base for experiments, the shape can be later on determined by experiments or by inverting the model. In red, we propose a piecewise linear model that better suits the observations made in the literature.

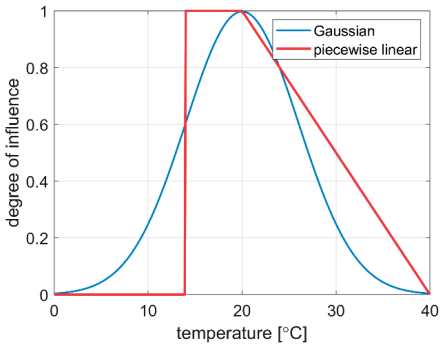


Figure 5. The chosen Gaussian model for mapping the temperature to the degree of influence

After mapping the daily temperature to the degree of influence, we further cumulate the degrees of influence over a time period significant to the plant development process. Basically, we compute a moving sum over N samples, as described in eq. (1):

$$cum_d_{infl}(i) = \sum_{k=0}^{N-1} d_{infl}(i-k) \qquad (1)$$

The summation corresponds to the accumulation effects (e.g. of biomass) in the plant, as a direct consequence of the temperature to the plant's growth processes.

RESULTS AND DISCUSSIONS

In Figure 6 we present the daily degree of influence of temperature d_{infl} computed for 2023, with thin blue line, which shows values from 0.2 to 1 (for the Gaussian model) and from 0 to 1 (for the piecewise linear model). The thick blue line corresponds to the averaged degree of influence over a period of 13 days, which roughly corresponds to two weeks. The noticeable difference is for the beginning of the season, when lower temperatures are impacting in different ways the plant's growth. In Figure 7 we show the same comparison for the year 2024.

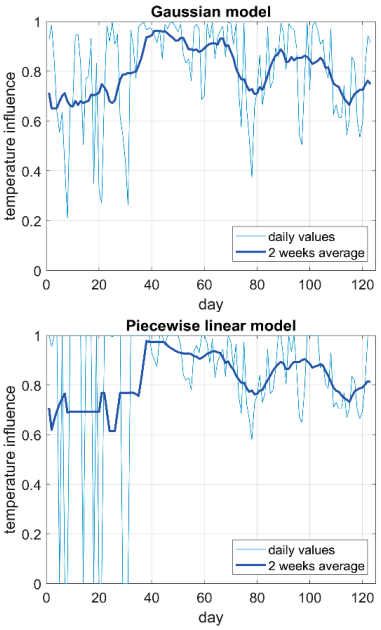


Figure 6. The degree of influence of temperature d_{infl} and for 2023. Gaussian (top) vs. linear (bottom)

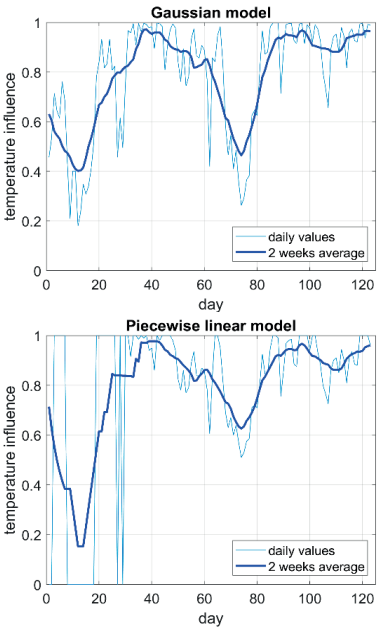


Figure 7. The degree of influence of temperature d_{infl} and for 2024. Gaussian (top) vs. linear (bottom)

In Figure 8 we show, for a qualitative comparison, the normalized filtered NDVI time series (in blue) and the normalized cumulated degree of influence of temperature *cum_d*$_{infl}$ (in green), when the Gaussian model is applied, the latter one being computed over three summation intervals corresponding to 1, 2 and 3 weeks. One can notice a good resemblance between the NDVI time series and the cumulated degree of influence. However, differences may be due to the fact that influence of other parameters (such as solar radiation, precipitations, or soil-related parameters, as well as the occurrence of diseases that may affect the plants) was disregarded in this study.

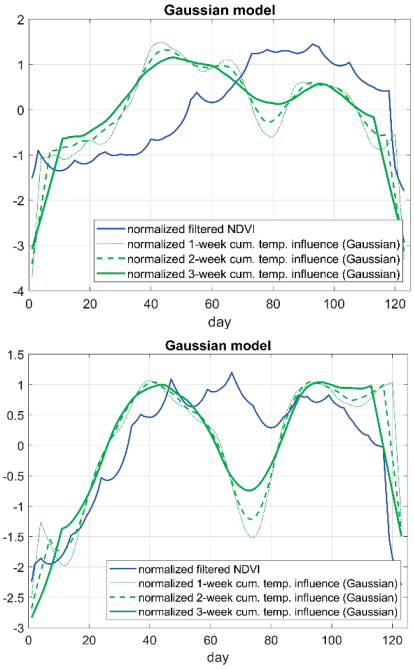


Figure 8. The normalized filtered NDVI time series (in blue) and the normalized cumulated degree of influence of temperature *cum_d*$_{infl}$ (in green), Gaussian case, for 3 summation intervals, for 2023 (top) and 2024 (bottom)

One may notice that the choice of the size of the summation interval has some considerable impact on the shape of the curve. The analysis results for both 2023 and 2024 are shown. The resemblance of the curves is higher for 2024.
The same comparison is presented in Figure 9 for the case when the linear model is used, for both 2023 and 2024. Again, the choice of the size of the summation interval has a relatively small impact on the shape of the curve and the similarity of the curves is, again, higher for 2024.

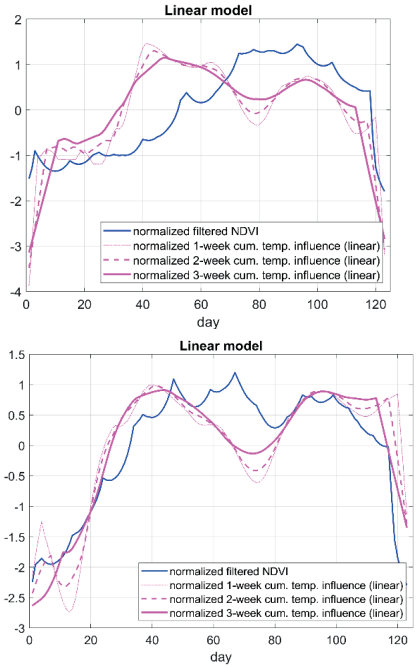


Figure 9. The normalized filtered NDVI time series (in blue) and the normalized cumulated degree of influence of temperature *cum_d*$_{infl}$ (in green), linear case, for 3 summation intervals, for 2023 (top) and 2024 (bottom)

Furthermore, we performed a comparison between the two models for the degree of influence of temperature (Gaussian versus piecewise linear). From a quantitative perspective, in Table 1 we show the values of the Pearson correlation coefficient ρ as a function of the choice of the length of the summation interval (N = 5, 7, 13 and 21 days) for the analysis performed for the 2023 crop, for the two cases – the Gaussian and the linear model. One can notice that the correlation coefficient increases with the increase of the summation interval, however the length of the interval should be chosen or determined to be pertinent to the plants' growth processes. The values, however, indicate a relatively weak correlation for the Gaussian model and slightly larger for the linear model. In Table 2 we show the same comparison for the analysis performed

on the 2024 potato crop. We see higher values of the correlation coefficient for the analysis of the 2024 potato crop, indicating a stronger correlation between NDVI and the temperature influence. Both for 2023 and 2024, the proposed piecewise linear model led to higher correlation. Figure 10 compares normalized NDVI (blue) with normalized cumulative temperature influence over three weeks, showing both the Gaussian (green) and linear (magenta) cases for 2023 and 2024.

Table 1. The Pearson correlation coefficient ρ as a function of the number of samples N (the length of the summation interval) for the crop in 2023

Cumulative sum over N =	5 days	7 days	13 days	21 days
Pearson correlation coeff. (Gaussian model)	0.3669	0.3907	0.4384	0.4573
Pearson correlation coeff. (Piecewise Linear model)	0.4770	0.4994	0.5416	0.5529

Table 2. The Pearson correlation coefficient ρ as a function of the number of samples N (the length of the summation interval) for the crop in 2024

Cumulative sum over N =	5 days	7 days	13 days	21 days
Pearson correlation coeff. (Gaussian model)	0.5613	0.5977	0.6934	0.7701
Pearson correlation coeff. (Piecewise Linear model)	0.7022	0.7357	0.8204	0.8745

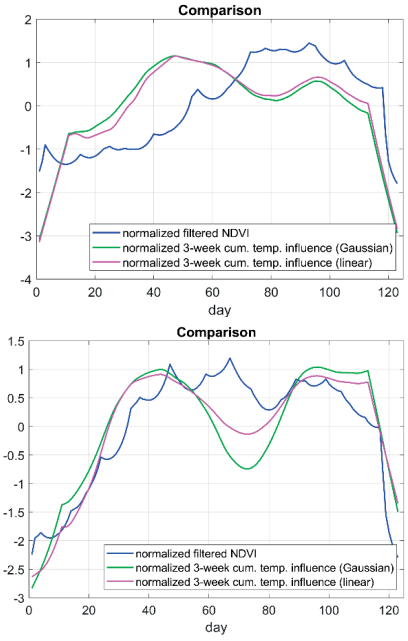


Figure 10. Normalized NDVI (in blue) and cumulated temperature influence over 3 weeks, for the Gaussian case (in green) and the linear case (in magenta), for 2023 (top) and 2024 (bottom)

One may notice that the difference between the Gaussian and the proposed piecewise linear models is better emphasized for the analysis performed on the 2024 data.

CONCLUSIONS

In this study we propose a model for the influence of temperature to the measured NDVI, as temperature is one determinant parameter for the plant growth processes. The proposed model is based on the hypothesis that the temperature has a certain degree of influence to the plant growth and that degree has, eventually, a cumulative effect on NDVI. We model the degree of influence of the temperature both as a Gaussian and a piecewise linear model. The proposed piecewise linear model better matches the observations made in the literature about the influence of temperature on the potato plant growth and vegetation status.

We show experimental results for a potato crop in Brasov area, Romania, in 2023 and 2024. The cumulated degree of influence curve showed good resemblance to the NDVI curve and the computed Pearson correlation coefficient between the two showed that there is significant correlation between the two times series. Differences, however, may be due to the fact that we did not consider in our study the influence of other parameters which have also an important role in the development of plants. The proposed piecewise linear model showed better performance compared with the Gaussian. As future work, we consider including in our study other parameters such as soil moisture, solar radiation, precipitations etc. In addition, given the correlation between NDVI and the proposed cumulative degree of influence, we consider assessing the causality between temperature and NDVI time series.

ACKNOWLEDGEMENTS

This research work was carried out with the support of the European Union's Horizon Europe research and innovation program, as it was financed from the AI4AGRI project entitled "Romanian Excellence Center on Artificial Intelligence on Earth Observation Data for Agriculture" under grant agreement no. 101079136.

Funded by the European Union

REFERENCES

Chiru, S., Donescu, V., Bărăscu, N., Olteanu, G., Gherman, I., Chiru, N., Bădărău, C., Ștefan, M., Donescu, D., Hermeziu, M., Hermeziu, R., & Vulcu, N. (2017). *50 years of activity at the National Institute of Research and Development for Potato and Sugar Beet Braşov*. In S. Chiru, G. Olteanu, & V. Donescu (Eds.), *Lucrări Ştiinţifice, Anale, INCDCSZ Braşov, Volum Jubiliar, 50 de ani de activitate în cercetarea agricolă românească* (pp. 9–37). https://potato.ro/wp-content/uploads/2022/06/Anale-50.pdf

Daim, K., & Zhangzz, L. (2018). Effects of high temperature stress on growth and some physiological indices of potato seedlings. *Journal of Agriculture*, *8*(9), 9–14.

European Union. (2014). *EU Regulation No. 377/2014 of the European Parliament and of the Council establishing the Copernicus Programme and repealing Regulation (EU) No. 911/2010*.

Fang, G., Yang, S., Ruan, B., Ye, G., He, M., Su, W., Zhou, Y., Wang, J., & Yang, S. (2024). Research progress on physiological, biochemical, and molecular mechanisms of potato in response to drought and high temperature. *Horticulturae*, *10*(8), 827. https://doi.org/10.3390/horticulturae10080827

Godfray, H. C. J., Beddington, J. R., Crute, I. R., Haddad, L., Lawrence, D., Muir, J. F., Pretty, J., Robinson, S., Thomas, S. M., & Toulmin, C. (2010). Food security: The challenge of feeding 9 billion people. *Science*, *327*(5967), 812–818. https://doi.org/10.1126/science.1185383

Gu, D., Andreev, K., & Dupre, M. E. (2021). Major trends in population growth around the world. *China CDC Weekly*, *3*(28), 604–613. https://doi.org/10.46234/ccdcw2021.160

Guo, H., Liu, Z., Jiang, H., Wang, C., Liu, J., & Liang, D. (2017). Big Earth data: A new challenge and opportunity for Digital Earth's development. *International Journal of Digital Earth*, *10*(1), 1–12. https://doi.org/10.1080/17538947.2016.1264490

Ivanovici, M., Olteanu, G., Florea, C., Coliban, R. M., Ștefan, M., & Marandskiy, K. (2024). Digital transformation in agriculture. In L. Ivașcu, L. I. Cioca, D. Boja, & F. G. Filip (Eds.), *Digital Transformation* (Vol. 257). Springer. https://doi.org/10.1007/978-3-031-63337-9_9

Lal, M. K., Tiwari, R. K., Kumar, A., Dey, A., Kumar, R., Kumar, D., Jaiswal, A., Changan, S. S., Raigond, P., Dutt, S., Luthra, S. K., Mandal, S., Singh, M. P., Paul, V., & Singh, B. (2022). Mechanistic concept of physiological, biochemical, and molecular responses of the potato crop to heat and drought stress. *Plants*, *11*(21), 2857. https://doi.org/10.3390/plants11212857

Lazarević, B., Carović-Stanko, K., Safner, T., & Poljak, M. (2022). Study of high-temperature-induced morphological and physiological changes in potato using nondestructive plant phenotyping. *Plants*, *11*(24), 3534. https://doi.org/10.3390/plants11243534

Liu, C., Li, Y., Liu, Y., Kear, P., Feng, Y., Wang, L., Wang, D., Luo, M., & Li, J. (2025). Effect of elevated temperature and CO_2 on growth of two early-maturing potato (*Solanum tuberosum* L.) varieties. *Climate Smart Agriculture*, *2*(1). https://doi.org/10.1016/j.csag.2024.100034

Obiero, C. O., Milroy, S. P., & Bell, R. W. (2019). Importance of whole plant dry matter dynamics for potato (Solanum tuberosum L.) tuber yield response to an episode of high temperature. *Environmental and Experimental Botany*, *162*, 560–571. https://doi.org/10.1016/j.envexpbot.2019.04.001

Rykaczewska, K. (2015). The effect of high temperature occurring in subsequent stages of plant development on potato yield and tuber physiological defects. *American Journal of Potato Research*, *92*(3), 339–349. https://doi.org/10.1007/s12230-015-9436-x

Sánchez-Correa, M. del S., Reyero-Saavedra, M. del R., Jiménez-Nopala, G. E., Piña, M. M., & Ortiz-Montiel, J. G. (2024). High temperature effect on plant development and tuber induction and filling in potato (*Solanum tuberosum* L.). In M. Hasanuzzaman & K. Nahar (Eds.), *Abiotic Stress in Crop Plants – Ecophysiological Responses and Molecular Approaches*. IntechOpen. https://doi.org/10.5772/intechopen.114336

Singh, B., Kukreja, S., & Goutam, U. (2019). Impact of heat stress on potato (*Solanum tuberosum* L.): Present scenario and future opportunities. *The Journal of Horticultural Science and Biotechnology*. https://doi.org/10.1080/14620316.2019.1700173

Van Harsselaar, J. K., Claußen, J., Lübeck, J., Wörlein, N., Uhlmann, N., Sonnewald, U., & Gerth, S. (2021). X-ray CT phenotyping reveals bi-phasic growth phases of potato tubers exposed to combined abiotic stress. *Frontiers in Plant Science*, *12*, 613108. https://doi.org/10.3389/fpls.2021.613108

Wahid, A., Gelani, S., Ashraf, M., & Foolad, M. R. (2007). Heat tolerance in plants: An overview. *Environmental and Experimental Botany*, 61(2), 199–223. https://doi.org/10.1016/j.envexpbot.2007.05.011

Walne, C. H., & Reddy, K. R. (2022). Temperature effects on the shoot and root growth, development, and biomass accumulation of corn (*Zea mays* L.). *Agriculture*, *12*(4), 443. https://doi.org/10.3390/agriculture12040443

Scientific Papers. Series E. Land Reclamation, Earth Observation & Surveying, Environmental Engineering. Vol. XIV, 2025
Print ISSN 2285-6064, CD-ROM ISSN 2285-6072, Online ISSN 2393-5138, ISSN-L 2285-6064

ENGINEERING AN INTERACTIVE MAP OF STATUES AND MONUMENTS FROM CLUJ-NAPOCA

Florica MATEI[1], Tudor SĂLĂGEAN[1, 2, 3], Ioana POP[1], Elemer-Emanuel ŞUBA[1], Mircea-Emil NAP[1], Silvia CHIOREAN[1], Paul SESTRAŞ[1, 2], Simion BRUMĂ[1, 2], Ştefan BORCAN-CONȚEVICI[1], Cristian MĂLINAŞ[1], Lucia-Adina TRUȚĂ[1]

[1]University of Agricultural Sciences and Veterinary Medicine Cluj-Napoca,
Faculty of Forestry and Cadastre, 3-5 Calea Mănăştur Street, 400372, Cluj-Napoca, Romania
[2]Technical University of Civil Engineering of Bucharest, Doctoral School,
122-124 Lacul Tei Blvd, District 2, 020396, Bucharest, Romania
[3]Technical Sciences Academy of Romania, 26 Dacia Blvd, District 2, 030167, Bucharest, Romania

Corresponding author email: lucia-adina.truta@usamvcluj.ro

Abstract

While the technology in Earth observation and Surveying fields advances, it's possible to learn more information in less time. This research aimed to design a web application that provides useful information about the public monuments from Cluj-Napoca near the user's location. Users can fix their position on the map, define the range of interest, and identify the monuments on the web map. Also, they can find the best route to the touristic objectives, pictures of the monuments, and their history. To achieve these, we first retrieved the coordinates of the statues and monuments using the Mobile Topographer application. We included these coordinates and information about the studied objectives' history and type in a geodatabase. Secondly, we used ArcGIS Pro to obtain information based on the collected data, and a map was created. We created customized scalable icons for each studied monument type. Once data was analysed, it was uploaded into ArcGIS Online as a hosted feature layer based on which a web application was built. This application will be publicly accessible, without conditional on software licenses or the device used.

Key words*: ArcGIS, monuments, Satellite Geodesy, web application.*

INTRODUCTION

Romania has more than 50 historic towns (Bucurescu, 2018). Cluj-Napoca is one of the most notable Romanian historic towns due to its rich cultural heritage and architectural significance (Popescu et al., 2018). Its foundation can be traced back to the Napoca village from the Roman province, Dacia, which was elevated to the rank of municipality 1,900 years ago by the Roman emperor Hadrian (Pascu et al., 1974; Ropa & Ropa, 2017). In time, Cluj-Napoca was adapted to different ages and needs, and due to its distinctive structural and functional features, it became a very refined monumental cultural landscape with a strong identity and a space rich in cultural significance (Maroşi et al., 2019). The Ministry of Culture 2015 records listed 1,791 historical monuments in Cluj county (Romania's Ministry of Culture). Part of the cultural heritage, the statues and monuments, generically called in this paper 'monuments', are symbols of cultural identity, power, and remembrance, helping us understand who we are (UNESCO). Understanding the meaning of a place may improve the public perception of the authenticity of urban heritage (Garcia-Esparza & Altaba Tena, 2020).

Europe's economic growth is interconnected with culture and tourism (Dulau & Coros, 2005). Cultural tourism in urban areas represents the most dynamic aspect (Bucurescu, 2015). While in 2015 the tourist inflow to Romania was negligible compared to this country's significant number of UNESCO-listed heritage sites (Lupu C. et al., 2015), an increase in the number of visitors was reported in 2023 compared to 2019 (WTTC, 2024). In 2016, the tourism density recorded for Cluj-Napoca was almost two times higher than at the country level (Popescu et al., 2018). Prior research found that the presence of educational material enhances the experience of visiting a historic site and that the more easily accessible a location is, the more enjoyable it is to see a historical monument or statue (Cameron & Gatewood, 2000). One challenge associated

with this issue is that, while some locations are strongly linked to a specific historical event or period, others may lack such associations or be tied to multiple, overlapping narratives (Ries & Schwan, 2023). Furthermore, to foster public awareness and ensure the preservation of cultural heritage, it is essential to systematically document and visually present relevant information (Horbinski & Smaczynski, 2023). This highlights the growing need to assist potential visitors of Cluj-Napoca in connecting a monument's visual representation with its detailed description and precise geographic location through an interactive map. Recently, the expansion of information technology, especially mobile applications, and web platforms has enhanced tourist experiences by facilitating access to data needed by tourists to know the locations, distance to, and description of the monuments (Markhasi Rupilu et al., 2018). Digital documentation has transformed visitor interaction with heritage sites, enhancing education and surpassing user expectations (Comes et al., 2020). However, even if there exist some web applications for monuments in Romania, including Cluj-Napoca (e.g., Attractive Romania, Cluj Tourism App, Explore Romania - Official App, Monuments Romania, Cluj Now), the problem is that the list of monuments is very brief, hard to find, or no longer contains up-to-date information. Consequently, people who want to find information about the historical, cultural, and religious monuments in Cluj-Napoca will encounter great difficulties.

Monuments mirror Cluj-Napoca's historical evolution, offering visitors an emotional and enjoyable connection to the past (Ries & Schwan, 2023). Yet, without awareness of their historical significance, the psychological impact on visitors remains minimal (Ries & Schwan, 2023). To address the above-mentioned issues, needs, and problems, we aimed to design an interactive map with updated, detailed information about the monuments in public places of the Cluj-Napoca municipality, a map shareable as a web application and usable as a guide or information resource for all potential users. This agrees with the aim of cultural heritage organizations joining efforts to preserve and share information about our common heritage (Vilceanu et al., 2022).

The importance of our work in environmental engineering is emphasized by: the sustainable integration of cultural heritage in the urban landscape, using interactive mapping as a tool for informed spatial planning; awareness of the built environment like monuments, and improving tourism in Cluj-Napoca.

Some of the unique features that our web application offers to users are:

- precision and accuracy in mapping, by including the rectangular coordinates in our app, hence providing high-precision geographic information to users who need exact geospatial data, whether for academic, governmental, or navigational purposes;
- localized and in-depth focus on Cluj-Napoca, offering more detailed and accurate information about its public monuments;
- customizable user experience. The interactive map with dynamic search and navigation, enables the users i) to visualize monuments within a selectable area, which adds a dynamic, real-time mapping; ii) to choose their starting location, and the application automatically generates a route to the monument they selected; iii) to search a monument by its name;
- historical and contextual information about monuments, providing users with a richer educational experience that might help them learn about the cultural significance of each monument;
- friendly, with no special accounts required, making it more accessible and convenient for the users.

These features generate certain benefits of our web application, for example:

- serves tourists who want to navigate the city and learn about its historical context;
- facilitates public cultural awareness, giving users the possibility to understand the significance of the monuments in their urban environment and contributing to a sense of pride and deeper connection to local heritage;
- offers potential for future expansion, as the structure we created could turn into a scalable model for other places;
- it is free and open to the public, so tourists, locals, and anyone interested can access it without worrying about hidden costs, subscriptions, premium features, or login requirements.

The unique features and benefits emphasize the novel contributions of our web application compared to the existing solutions in the field.

MATERIALS AND METHODS

The list of monuments per county, issued in 2015 encompasses 33 historical monuments in the Cluj-Napoca municipality (Romania's Ministry of Culture). However, our study is based on the most comprehensive source relevant to this topic, which describes over 150 monuments (Ciorca, 2020). A study from 2015 indicated that 75% of existing monuments in Cluj-Napoca are concentrated in its historic centre, particularly in the Fortress of Cluj (Orban & Puiu, 2015). Monument selection followed the criteria in Figure 1, and the methodology involved six steps, as shown in Figure 2.

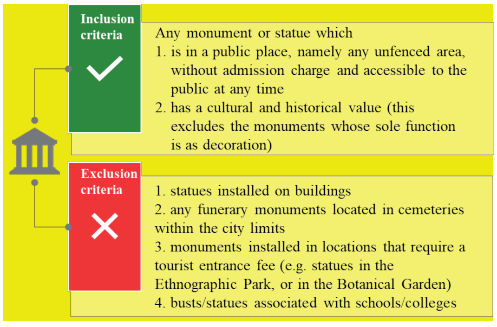


Figure 1. Monuments' selection criteria



Figure 2. Flow of the study steps
(Icons used in this diagram were freely downloadable from Freepik.com)

1. Collecting data on the monuments. These data fall into two categories: data on the location and data on the significance of the monuments. We obtained the data on the position of monuments using the procedures detailed in the next sub-section. The information on the monuments' significance was gathered from the main source document (Ciorca, 2020) and was entered into the database. The information conceptualization consisted of identifying information that could be represented as a map. Data on the monuments' chronology were also collected. For many of them, the information on the monument installation was incomplete, and often, only the year of origin was identified.

2. Determining the position of monuments. Given that monuments are located in urban environments, in areas with constant vehicular or pedestrian traffic, the conditions for determining rectangular coordinates by the resection method are not favorable, as often the sights from the station to the monument may be blocked by buildings, cars, or pedestrians. Thus, we decided to use satellite geodetics, specifically GPS determination of point coordinates using the Mobile Topographer application, running version 9.3.2., from a Samsung smartphone, model Galaxy A54 5G. In this application, we selected the Projection System Stereo 70 from the settings. Coordinate determination was performed by connecting to GPS constellations, Glonass, Beidou and Galileo, with access to an average of 25 satellites for each measurement. We stationed as close as possible to each monument for approximately 5 minutes to increase the accuracy of the measurements. The position determination procedure was repeated for each monument, on different days, due to weather and time factors. The coordinates were recorded in a database and organized in a Microsoft Excel file to facilitate the project's next steps.

3. Designing the icons. The icons we created represent in a very suggestive, visual way the type of monuments to which they correspond in the interactive maps and web application. We chose to generate these icons in the Inkscape software version 1.3.2. because the outcome is vector images, which maintain their resolution at different zooming levels. In the case of the icon for the monuments, the Carolina Obelisk was taken as a model. For the group of statues

icon, the Transylvanian School group of statues was taken as a model. The icons were drawn in such a way as to be recognizable and distinct from any distance. The created icons have a minimalist style so that their meaning is immediately apparent to any user without the need for written information.

4. Creating the monuments map in ArcGIS Pro. The geographic information system (GIS) was implemented using ArcGIS Pro version 3.3.0., projection system Pulkovo 1942 Adj 1958 Stereo 70. The Excel file with the monument's coordinates was added in the ArcGIS Pro, and using the XY table to point function, the points representing the monuments were materialized on the map. We then performed a visual classification by unique values and used the created icons to show each monument's location on the map and its type, symbolized by these icons. Due to the project's complexity, we used ArcGIS Pro to build the map layers that will constitute the hosted feature layer in the web map.

5. Creating the web map. We created a web map, using ArcGIS Online and based on the designed GIS. First, we exported the map layers from the project created in ArcGIS Pro. These map layers contain coordinate data for monuments. Exporting these layers as shape files greatly shortened the work that had to be done in the ArcGIS Online platform. Shapefiles exported from ArcGIS Pro were imported into ArcGIS Online as hosted feature layers. This web map and the project in ArcGIS Pro are intended for geodesy and cartography specialists.

6. Creating and publishing the web application. The web map created in ArcGIS Online platform was used to develop the web application, based on pre-established templates that can be accessed by selecting the 'create web app' option when inspecting a map. We illustrated the nearby function, generated a route to a monument, and searched a monument by its name. This last step of the process will use all the previous operations, with the final goal of creating a map that will serve as a guide for the monuments found in public places in Cluj-Napoca. The web application is for any user, regardless of the level of expertise or software available, and will run on any device without requiring an ArcGIS account or license.

RESULTS AND DISCUSSIONS

Based on the inclusion and exclusion criteria, 76 monuments were included in our study. Of these, 53 monuments (70%) were considered of great interest to future users of the interactive map and the web application, therefore, these were called 'main monuments', while the other 23 monuments were called 'secondary monuments'.

After performing the survey, the determined rectangular coordinates were organized in tabular form to facilitate input into ArcGIS Pro, along with other details like the location, the classification by type of monument, the date when it was installed, and the monument's author.

Table 1 summarizes the main monuments included in the study, with the related available details.

Table 1. Main monuments database

ID	Monument	X coordinate	Y coordinate	Location	Type	Installation date	Authors
1	Lupa Capitolina	586524.993	392629.182	on Eroilor Blvd, vis-a-vis of Greek Catholic Cathedral	M	29.11.2008	Ettore Ferrari
2	Statue of Cardinal Iuliu Hossu	586539.517	392652.688	on Eroilor Blvd, at crossing with Bolyai Janos street	RS	30.11.2018	Ilarion Voinea
3	Memorandists Monument	586492.936	392534.342	on Eroilor Blvd, near Unirii Square	M	1994	Eugen Paul
4	Matthias Corvinus Statuary Group	586500.951	392439.574	on Unirii Square, near the Saint Michael's Church	SG	12.10.1902	Fadrusz Janos, Pakey Lajos
5	Shot Pillars Monument	586428.226	392410.92	at the crossing between Unirii Square and Napoca street	M	10.2003	Liviu Mocan
6	Statue of Bishop Marton Aron	586563.964	392366.061	Garden of Saint Michael's Church	RS	03.2009	Bocskay Vincze
7	Monument of glory of the Romanian Soldier	586813.542	392917.373	behind the Orthodox Metropolitan Cathedral	M	1996	Radu Aftene
8	Statue of Bishop Nicolae Ivan	586736.827	392955.374	in front of the steps of the Orthodox Cathedral	RS	30.11.2018	Alexandru Păsat

ID	Monument	X coordinate	Y coordinate	Location	Type	Installation date	Authors
9	Statue of the Mitropolitul Bartolomeu Anania	586730.25	392944.015	in front of the steps of the Orthodox Cathedral	RS	30.11.2018	Septimiu Jugrestan
10	Statue of Avram Iancu	586688.742	392968.99	in Avram Iancu Square, between the Orthodox Cathedral and the National Theatre	S	1993	Ilie Berindei
11	Statue of Lucian Blaga	586629.843	393010.028	in front of National Theatre	S	1986	Romul Ladea
12	Statue of Mihai Eminescu	586620.47	392989.221	in front of National Theatre	S	1976	Ovidiu Maitec
13	Bust of Alexandru Vaida Voevod	586579.082	392979.331	on West side of National Theatre	B	16.03.2012	Ilarion Voinea
14	Statue of Iuliu Maniu	586382.839	393016.956	in front of the wall of Tailor's Bastion	S	8.02.2019	Ioan Marchiș
15	Statue of Baba Novac	586325.309	393021.148	in front of Tailors' Bastion	S	1975	Virgil Fulicea
16	Statue of Andrei Mureșan	586247.98	393209.714	at the crossing between Andrei Mureșan str. with Ciparius Square	S	2019	Ilarion Voinea
17	Statue of St. George (the Dragon Slayer)	586340.742	392840.777	Mihail Kogălniceanu str., in front of Calvinist Reformed Church	RS	1960	Rona Jozsef, Kalman Lux
18	Statuary group the Ardelean School	586300.011	392608.623	close to the main entrance of Babeș-Bolyai University	SG	30.06.1973	Romulus Ladea
19	Statue of the Virgin Mary	586270.014	392472.095	in front of Piarists' Church	RS	11.2023	Anton Schuchbauer
20	Bust of Octavian Goga (Students' Culture House)	586237.649	392156.759	in front of Students' Culture House	B	1988	Info not available
21	Bust of George Coșbuc (Students' Culture House)	586232.154	392135.787	in front of Students' Culture House	B	1988	Info not available
22	Bustul lui Lucian Blaga	586240.039	392090.04	in front of Central Universitary Library	B	1970	Eugen Gogan
23	Statue of Francisc David	586761.946	392606.419	On 21 Decembrie Boulevard, near the Unitarian Cathedral	RS	08.2019	
24	Carolina Obelisk	586759.919	392237.872	in Museum Square, in front of Mikes Palace	M	1831	Mihaly și Antal Schindler, Anton Csuros, Samuel Nagy, Josef Klieber
25	Statue of Constantin Daicoviciu	586750.028	392202.931	in Museum Square, in front of the National History Museum of Transylvania	S	NA	NA
26	Monument to anti-communist resistance	586747.307	392012.929	at crossing between Iuliu Hossu and George Barițiu streets	M	12.06.2006	Virgil Salvanu
27	Statue of Antonin Ciolan	586704.3	391824.764	in the Central Park	S	NA	NA
28	Statue of Nicolae Bretan	586697.91	391746.925	in the Central Park	S	2013	Ana Rus
29	Bust of Sigismund Toduță	586655.82	391758.898	in the Central Park	B	NA	NA
30	Bust of George Coșbuc	586632.156	391715.782	in the Central Park	B	NA	Vetro Artur
31	Bust of Octavian Goga	586580.211	391544.008	in the Central Park	B	NA	NA
32	Statue of Liviu Rebreanu	586564.944	391499.166	in the Central Park	S	NA	NA
33	In memoriam 1956 (Hungarian revolution monument)	586677.175	391710.431	in the Central Park	M	2009	NA
34	Statue of Mircea Luca	586398.124	390979.666	behind Cluj Arena Stadium	S	NA	NA
35	Statuary group Horea, Cloșca and Crișan	586769.785	391463.852	near Napoca Hotel	SG	1974	Ion Vasiliu
36	The Monument to the Salvation of the Nation	587001.165	391915.552	on the Citadel (Cetățuie) Hill	M	01.12.1997	Virgil Salvanu
37	Statue of Mihai Viteazul	587047.343	392410.101	Mihai Viteazul Square	S	1976	Marius Butonoiu
38	The eternal flame	587005.512	392341.481	Mihai Viteazul Square	M	23.04.2003	Paul Eugen
39	Bust of Alexandru Ioan Cuza	586869.267	392827.959	vis-a-vis of Prefect's Palace in front of CEC Bank	B	NA	Marcel Voinea
40	Bust of Emil Racoviță	586323.519	392764.12	Mihail Kogălniceanu str., in front of National College Emil Racoviță	B	NA	NA
41	Bronze model of the old town	586936.076	392529.621	on top of the former Fire Tower	M		NA
42	Statue of Saint George (Regele Ferdinand str.)	586701.415	392457.505	Regele Ferdinand str., no. 1	RS	1941	Kende Ferenc, Rahman Maria

ID	Monument	X coordinate	Y coordinate	Location	Type	Installation date	Authors
43	Bust of Woodrow Wilson	585730.461	391981.403	Louis Pasteur str., no. 4	B	2002	NA
44	Bust of Florian Ştefănescu Goangă	585817.667	392340.48	in front of Psychology Institute	B	NA	David Şandor
45	Bust of Ion Chiricuţă	585835.672	392278.313	in front of the Oncologic Institute 'Ion Chiricuţă'	B	2008	Alexandru Lupu
46	Bust of Alexandru Lapedatu	585834.755	393331.799	Dimitrie Bolintineanu str., no. 16, at the street corner	B	NA	NA
47	Bust of Ion Agârbiceanu	585888.921	393393.103	at the crossing of Andrei Muresan and Brasov streets	B	NA	Romul Ladea
48	Statue of Gheorghe D. Mărdărescu	586911.563	394883.525	in front of Faculty of Economics and Business Administration	S	08.2019	Valentin Tănase
49	Troiţa (Mărăşti)	587509.23	394364.209	at the crossing of Fabricii and Aurel Vlaicu streets	M	1990	NA
50	Column from Expo Transilvania	587778.062	395536.276	near Expo Transilvania	M	1974	Virgil Salvanu
51	Whistlers at Expo Transilvania	587770.719	395506.434	near Expo Transilvania	M	1974	Târnovan Vid
52	Bust of General Nicolae I. Dăscălescu	586457.724	393133.71	in front of the Infantry Division	B	NA	Anton Tănase
53	Bust of General Gheorghe V. Avramescu	586486.637	393122.765	in front of the Infantry Division	B	NA	Anton Tănase

M = monument; RS = religious statue; SG = statuary group; B = bust; S = statue; NA = information not available.

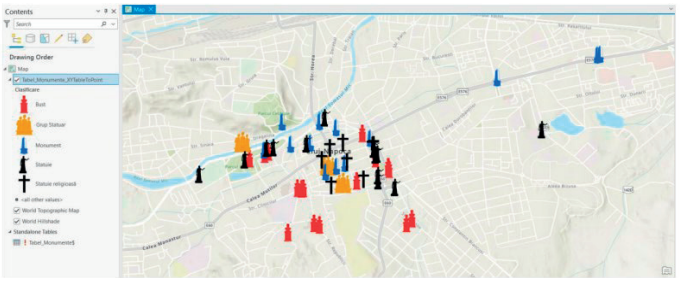


Figure 3. The map with the monuments' classification by type, symbolized by the icons we designed

After including the monuments' coordinates, we classified the monuments based on their types and added their visual symbols. The unique values representation mode from the Symbology section was used to create the point layer. Unique values were designated based on the Classification field in the Attribute Table, which had five values: bust, statue, statuary group, monument, and religious statue.

Figure 3 illustrates the map created in ArcGIS Pro and monuments classified by type, and visually represented by the icons we created in Inkscape. Monuments' classification by type was done according to the criteria specified in Table 2, which also shows the corresponding icon we created for each monument type. Once created, the icons were introduced into the project folder, where they could be accessed from the properties page of the Symbology tab.

Table 2. Monuments' classification criteria and the icons created for each monument type

Type	Classification criteria	Icon
Bust	any monumental installation depicting only the shoulders and head of the personality represented	
Statue	any monumental installation that reproduces in whole or in part, the body of the person represented	
Statuary group	any monumental installation representing several distinct personalities	
Monument	any monumental installation not representing any personality	
Religious statue	any monumental installation representing an ecclesiastical personality or Saints	

The purpose of these icons is to visually and concisely communicate the monument's type while enhancing the map's appearance.
After visual classification by unique values, the created layer was saved as a layer file in the Share ribbon.
Following the classification by unique values, we made a chart with the number and proportion of each monument type (Figure 4).

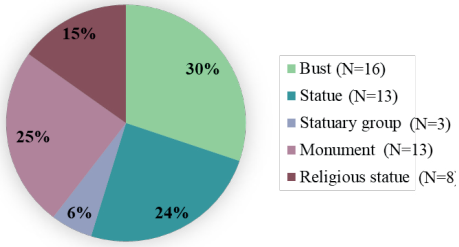


Figure 4. The proportions of various types of monuments out of the overall number of main monuments (N = 53)

The age of the monuments or the installation date, for some of the monuments in our study, is unknown. Since the analyses we performed required such information, we assigned a date, in the following way:

- for monuments with missing information about the day, but with data about the month and year of installation, we indicated the last day of the installation month;
- for monuments with data only on the year of installation, the day and month used in subsequent analyses is the 31st of December;
- for the monuments with no precise information on the installation or building date, we considered them to have been installed within the last three decades because of the available data suggesting this period. Consequently, they were not considered for the following analyses.

Two criteria were taken into account for this determination, i.e., the date of monument installation on its original site and the actual age of the monument, meaning from the day it was built until the present.
Based on the criteria considered, we concluded that the Carolina Obelisk (Figure 5), installed in Museum's Square in 1898, is the oldest monument in Cluj-Napoca. This monument honours the stay of the royal couple Emperor Francis I and Caroline Augusta in Cluj, in 1817. It was built south of the city's Central Square in 1831.
The monument classified as the newest one based on the same criteria, is the Statue of the Virgin Mary (Figure 6), in front of the Piarists' Church. This monument was considered the newest because the present statue is new, created in response to the excessive deterioration of the old statue, which is no longer displayed in public places, but is preserved in museum conditions, together with the original angels. The old statue, erected in 1774 as a sign of gratitude for the protection given to Cluj during the last great plague epidemic between 1738 and 1742, was also named the "Plague Column". The new statue, a faithful copy of the old statue, was installed in 2023, in front of the Piarists' Church, in the place formerly occupied by the old statue.

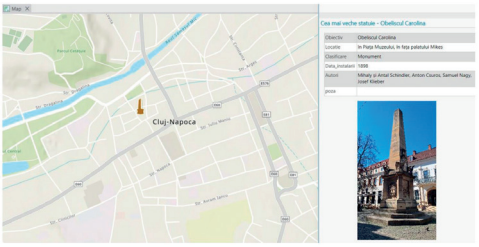


Figure 5. The oldest monument in Cluj-Napoca

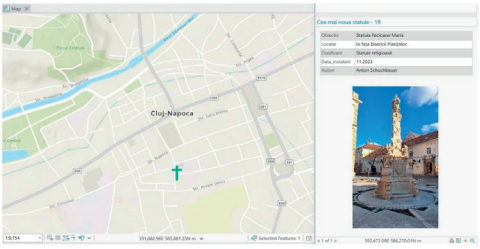
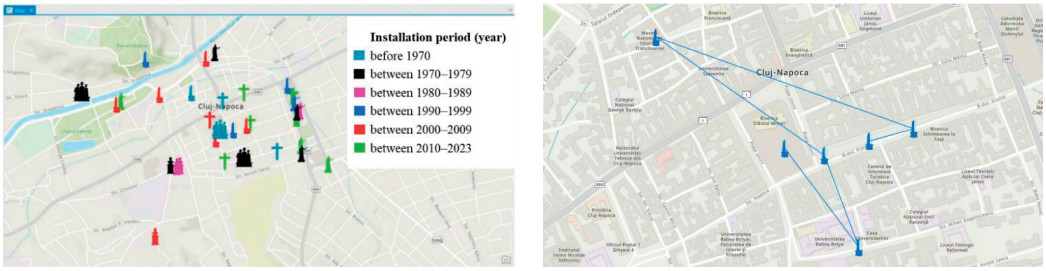


Figure 6. The newest monument in Cluj-Napoca

Another interesting analysis was on the number of monuments installed in the last decades and, of course, visualizing them on the interactive map. Monuments were grouped into ten-year periods according to the date of installation, with two exceptions: i) monuments installed before 1970 were grouped in the same category, because the quantity of these monuments is small and the periods between their installation are too long to justify creating separate categories; ii) monuments after 2010, which also includes statues installed until now. In Figure

7A we have overlaid the layers containing monuments from each defined period. The monuments in each layer have been colored according to the period in which they were installed.

Another analysis performed on the location of the monuments consisted in representing on the map the previous locations for the monuments if it was relocated over time. In Cluj-Napoca, infrastructure changes or construction and renovation of various buildings or parks occur frequently. These works may require moving monuments to facilitate the access of workers and machinery. Depending on the nature and form of the works, the site previously occupied by the monument may become unavailable and as such, it will be allocated a new site. In the case of very old monuments, the reason for their relocation may be war protection. Of the statues and monuments included in this paper, four have been relocated from their original installation site. These are the Statue of the Virgin Mary, Lupa Capitolina, the Carolina Obelisk and the statue of Saint George. Although previous analysis has revealed statues that have been relocated from their original installation site, the exact coordinates of previous monuments' locations are lacking. The only existing information verbally describes the previous locations, but this is not sufficient to represent the previous locations correctly on the map. As a compromise, the monuments' previous locations were marked manually, by placing nodes, which approximate the locations described verbally. The route of the monument's relocations was also marked on the map (Figure 7B).



A B

Figure 7. A. Analysis based on the time in which monuments were installed; B. Illustration of viewing on the interactive map the route of previous locations for the Lupa Capitolina monument

The web map development is an important step towards the project's aim, i.e., to create the web application.

With the shapefiles imported from ArcGIS Pro a map was created, containing two layers named 'Main Monuments' and 'Secondary Monuments'. The 'Main Monuments' layer (Figure 8) contains the monuments considered of major interest to future users.

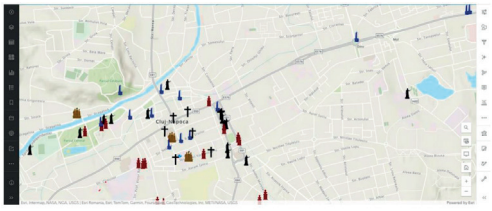


Figure 8. The layer with the main monuments

Monuments in the map layer called 'Secondary Monuments' are monuments that have a lower cultural and historical value. The criterion for classifying monuments as secondary was that their location was within the premises of higher education institutions. The secondary monuments' classification was done by creating a new field in the Attribute Table of the map layer. This field combined the values from the classification and membership fields to facilitate the use of unique value styles to represent them. Based on the unique values, the monuments were symbolized using the icons previously created and colored according to the institution they belong to. For example, in Figure 9, green is for the University of Agricultural Sciences and Veterinary Medicine, red for the University of Medicine and Pharmacy, and blue for Babes-Bolyai University. The web map is then ready to be transformed into a web application. In this

form, the map can be distributed and accessed by anyone wishing to enrich their knowledge of the monuments of Cluj-Napoca.

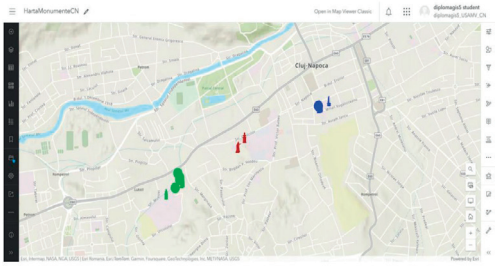


Figure 9. The layer with secondary monuments

Using the models made available through the Instant Apps function of the ArcGIS Online platform, a nearby application was created (Figure 10). This application allows the user to select his/her position on the map by tapping the screen or with a click, and the application will highlight all targets within a selectable radius. The nearby model was chosen because it fits with one of the project's aims, namely to help users discover statues they did not know about. After selecting the application type, we used the express configuration mode.

We set the minimum (100 m) and maximum (2 km) values of the selection area, designated the search sources (Main Monuments and Secondary Monuments layers in the web map), and left the theme-related settings as in the original configuration. We then added the legend and share button because, after configuration, the web application can be published and shared.

The first function of the application, conferred by the template used, is to highlight the monuments located in the selected area (Figure 10). We selected the maximum radius of the coverage area to cover several statues regardless of the point selected by the user.

Another useful feature of the created application is the ability to suggest a navigation route to a monument of interest (Figure 11).

To generate a route, the user chooses a starting position on the map surface. Then, the destination monument is chosen from the list and the route will be generated automatically. At this point, one can choose the traveling method and see an estimate of the time needed to cover the route (Figure 11).

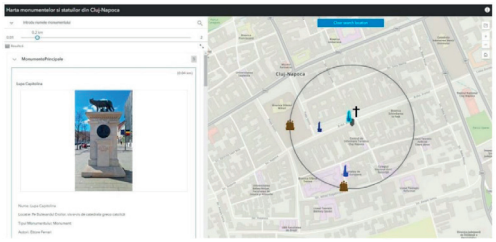


Figure 10. Illustration of the 'nearby' function in the web application

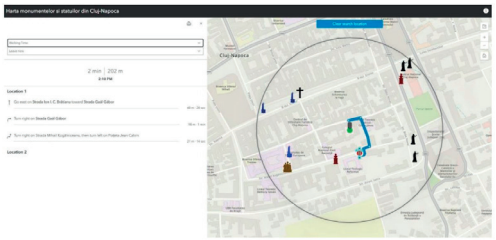


Figure 11. Example of a navigation route generated in the web application

There is also the possibility to search for a specific monument by its name. To do this, one should use the search box, which will present autocompleting suggestions for the name of the monument (Figure 12).



Figure 12. Illustration of the function that searches by monument's name

Selecting a monument on the map will display a list of the monuments in the selection area, where one can see the pop-up windows on the web map. These windows contain the monument's photo, location, type of monument, and information about its significance. The pop-up information has been selected according to its relevance to potential users (Figure 12).

For each monument in the defined proximity area, one can determine the route according to the traveling mode, by using the options included in the pop-up (Figure 13).

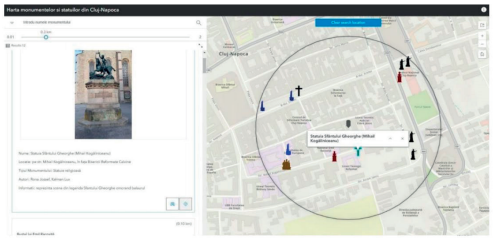


Figure 13. Example of a pop-up list, with information on the monuments

This application can be shared as a link, namely https://usamv-cn.maps.arcgis.com/apps/instant/nearby/index.html?appid=2db1f35fda164895bc87a534b321f9ab&center=23.6815;46.7911&level=13&hiddenLayers=1903b181a0a-layer-4

CONCLUSIONS

The monuments of Cluj-Napoca are numerous and indicate an abundant history, but most are unknown. We classified (as completely as possible) the monuments found in public spaces in Cluj-Napoca, more precisely, their location, type, history, and significance. Using our web application, it is possible to visualize the monuments within a selected area (with a selectable radius of the coverage area, ranging between 100 m and 2 km). In addition, users could also search for a monument by its name, and it is also possible to select the destination monument from the list, choose a starting position on the map surface, and the route will be generated automatically.

Gathering and integrating this data into a web application facilitated the dissemination of information about the monuments. The methods used in our study were effective. Determining the coordinates of the monuments by GPS with the Mobile Topographer application considerably shortened the measurement time. The ArcGIS software ecosystem also proved to be a powerful tool in processing the data needed to create the web application that may be a guide to the Cluj-Napoca statues and monuments.

The personalized route generation is a standout feature of our web app, particularly useful for visitors or those exploring the city.

Our interactive map (and the related web app) is similar to other web applications in that it provides non-experts without extensive training in GIS applications (Kydonakis et al., 2012). It represents a basic toolset to add value to the cultural heritage record and supplies topographic and cartographic information to show the monument's precise location and address (Kydonakis et al., 2012) being the most localized, user-centric, and comprehensive tool for exploring the historical monuments of Cluj-Napoca. Moreover, the costs implied to develop it are incomparably lower than for advanced measurement techniques and processing of the measurement data (e.g., laser scanning technology and low-altitude photogrammetry) (Horbinski & Smaczynski, 2023). Compared to the more general or broader apps available, our web app focuses on the city, interactive map features, ease of access, and detailed historical information. It is particularly valuable for anyone looking to navigate Cluj-Napoca's rich history, whether visiting or exploring their hometown in more depth, to enjoy the diversified offer of historical and cultural patrimony (Popescu et al., 2018).

In summary, we provide a tool that may educate and make the city more accessible and engaging for a wider audience, from history enthusiasts to casual explorers. By leveraging advanced mapping technology with comprehensive cultural insights, our study's results advance tourists' interaction with Romania's monuments, enriching the travel experience and contributing to the appreciation of Romania's vast heritage.

REFERENCES

Bucurescu, I. (2015) Managing tourism and cultural heritage in historic towns: examples from Romania. *Journal of Heritage Tourism, 10*(3), 248–262.

Comes, R., Neamțu, C., Buna, Z., Bodi, S., Popescu, D., Tompa, V., Ghinea, R., & Mateescu-Suciu, L. D. (2020). Enhancing accessibility to cultural heritage through digital content and virtual reality: a case study of the Sarmizegetusa Regia UNESCO site. *Journal of Ancient History and Archaeology*, *7*(3), 124–139.

Ciorca, I. (2020). *Monumente si statui clujene*. Cluj-Napoca, RO: Casa Cărții de Știință.

Dulău, A. V., & Coroș, M. M. (2009). Investigating Cultural Tourism Development and Attractiveness in Transylvania, Romania. A Focus on the Counties of Cluj and Sibiu. Conference Paper. DOI: 10.13140/2.1.1443.3606. Retrieved from https://www.researchgate.net/publication/271442875_Investigating_Cultural_Tourism_Development_and_Attractiveness_in_Transylvania_Romania_A_Focus_on_the_Counties_of_Cluj_and_Sibiu

Garcia-Esparza, J. A. & Altaba Tena, P. (2020). A GIS-based methodology for the appraisal of historical, architectural, and social values in historic urban cores. *Frontiers of Architectural Research*, *9*(4), 900–913.

Horbinski, T. & Smaczynski, M. (2023). Interactive thematic map as a means of documenting and visualizing information about cultural heritage objects. *ISPRS International Journal of Geo-Information, 12*(17), 257.

Kydonakis, A., Chliaoutakis, A., & Sarris, A. (2012). A GIS based application for the management of monuments and antiquities of Cyprus. *In 32nd EARSeL Annual Symposium "Advances in Geosciences", Mykonos, Greece*.

Lupu, C., Padhi, S. S, Pati, R. K., & Stoleriu, O. M. (2021). Tourist choice of heritage sites in Romania: a conjoint choice model of site attributes and variety seeking behavior. *Journal of Heritage Tourism, 16(*6), 646–668.

Maroşi, Z., Adorean, E.-C., Ilovan, O.-R., Gligor, V., Voicu, C.-G., Nicula, A.-S., & Dulamă M. E. (2019). Living the urban cultural landscapes in the city centre of Cluj-Napoca / Kolozsvár / Klausenburg, Romania. *Annals of the Austrian Geographical Society*, *161*, 117–160.

Orban, M., & Puiu, V. (2015). Studies and research on cultural built heritage in Cluj-Napoca fortress and its tourist valorification. *Studii şi cercetări, Geology-Geography, 20*, 109–117. Museum of Bistriţa-Năsăud, RO: Ecou Transilvan Publishing House.

Pascu, Ş., Marica, V., Ţoca, M., & Wagner, R. (1974). *1850 Clujul istorico-artistic*. Cluj-Napoca, RO: Consiliul Popular al Municipiului Cluj.

Popescu, A, Grigoras, M. A., & Pleşoianu, D. (2018). The city of Cluj-Napoca and the Cluj county, important tourist attractions in Romania. *Scientific Papers Series Management, Economic Engineering in Agriculture and Rural Development*, *18*(1), 401–416.

Ries, M., & Schwan, S. (2023). Experiencing places of historical significance: A psychological framework and empirical overview. *Journal of Environmental Psychology*, *92*, 102179.

Romania's Ministry of Culture (2024). List of historical monuments by county, 2015. Retrieved February 8, 2025, from https://www.cultura.ro/lista-monumentelor-istorice

Ropa, L., & Ropa, M. (2017). Schimbarea denumirii oraşelor Cluj şi Turnu Severin (1974): o manifestare a megalomaniei protocronist-naţionaliste. *Annals of Oradea University. Fasciola History-Archaeology, 27*, 171.

UNESCO, https://www.unesco.org/en/cultural-heritage-7-successes-unes https://www.unesco.org/en/cultural-heritage-7-successes-unescos-preservation-work cos-preservation-work

Vilceanu, C. B., Herban, S., Pescari, S., & Budău, L. I. (2022). Comparative study of 3D modeling by short-range photogrammetry. *Scientific Bulletin of Politehnica University Timisoara*, 67(1), 45–49.

WTTC. (2024). Tourism Satellite accounting: *Romania Travel & Tourism Economic Impact Factsheet 2024*. London: World Travel and Tourism Council. Retrieved February 6, 2025, from https://researchhub.wttc.org/factsheets/romania

Scientific Papers. Series E. Land Reclamation, Earth Observation & Surveying, Environmental Engineering. Vol. XIV, 2025
Print ISSN 2285-6064, CD-ROM ISSN 2285-6072, Online ISSN 2393-5138, ISSN-L 2285-6064

HYBRID MODELLING APPROACHES FOR LAND USE/LAND COVER CHANGE PREDICTION AND CARBON DYNAMICS IN MAROWIJNE, SURINAME

Tamara MYSLYVA[1, 2], Christiaan Max HUISDEN[2], Marek MROZ[3], Nataliia TSUMAN[4], Yurii BILYAVSKYI[4]

[1]Ministry of Spatial Planning and Environment of Suriname,
22 Prins Hendrikstraat, Paramaribo, Republic of Suriname
[2]Anton de Kom University of Suriname, 86 Leysweg, Paramaribo, Republic of Suriname
[3]University of Warmia and Mazury in Olsztyn,
Michała Oczapowskiego, 1 Street, 10-719, Olsztyn, Poland
[4]Zhytomyr Agricultural Technical Professional College,
96 Pokrovska Street, 10008, Zhytomyr, Ukraine

Corresponding author email: byrty41@yahoo.com

Abstract

Land use changes monitoring and predicting, as well as assessing their impact on carbon storage dynamics, play a pivotal role in addressing environmental challenges and ensuring effective land use management. This study aims to identify land use changes and their impact on carbon storage in the Marowijne district of Suriname from 2017 to 2024 and predict changes for 2034. Sentinel-2 images were used to analyze land change patterns and predict future trends. A hybrid approach combining Markov chain analysis, cellular automata, multilayer perceptron, support vector machines, and logistic regression was used to forecast future land use dynamics, while InVEST and YASSO models were utilized for carbon storage and sequestration predictions. The support vector machine-Markov chain hybrid model achieved an impressive accuracy of over 97%, outperforming other hybrid models. This model is recommended for generating land use change prediction maps, providing a crucial baseline for sustainable land use management. During the subsequent decade (2024-2034), the net loss of high-carbon areas is expected to intensify, affecting 15-20% of the district's territory. The identified spatiotemporal distribution of carbon storage provides valuable insights that will play a key role in achieving the objectives of Suriname's national green development strategy.

Key words: *land cover change dynamics, hybrid prediction models, carbon storage dynamics.*

INTRODUCTION

With significant impact on ecosystems and human lives, land use change is one of the major forces behind environmental and socioeconomic transformations. Analysing spatiotemporal patterns of land use and land cover (LULC) changes provides essential insights for sustainable land management and environmental conservation (van Ommeren-Myslyva et al., 2024; Devi & Shimrah, 2023; Girma et al., 2022). Understanding and managing land assets, natural resources, and environmental dynamics requires creating reliable LULC change predictive models (Song et al., 2020; Kafy et al., 2021). By providing valuable data on land potential and degradation risks, these models offer relevant and useful information on land suitability for various types of use or exploitation (Lambin & Meyfroidt, 2019; Aloqaili et al., 2021). Additionally, LULC modelling contributes to climate change mitigation by improving our understanding of carbon sequestration potential across different land cover types (Deng et al., 2020; Luo et al., 2021). Predicting land use change requires advanced methodologies that analyze historical data and observed trends to project future land cover patterns (van Ommeren-Myslyva et al., 2024). Several modelling approaches are commonly used, including statistical methods (Yeh & Liaw, 2021), Cellular Automata (CA) models (Muhammad et al., 2021), Markov Chain (MC) models (Mohamed & Worku, 2020), hybrid models (Asif et al., 2023), and multi-agent-based models (Robinson et al., 2021). Among these, hybrid models, which combine multiple predictive techniques to

leverage their respective strengths, have shown greater accuracy in forecasting future LULC changes. Suriname's forest ecosystems play a crucial role in global carbon dynamics, acting both as a major carbon reservoir and a significant net carbon sink. Between 2001 and 2023, these forests sequestered approximately 28.3 $MtCO_2e$ per year while emitting an average of 8.38 $MtCO_2e$ annually, resulting in a net carbon sink of -19.9 $MtCO_2e$ per year (Global Forest Watch, 2024). Land use and land cover are fundamental to carbon regulation, as changes in LULC deeply affect the capacity of ecosystems to store and sequester carbon (Sarathchandra et al., 2021). Suriname's ranking among the top three countries for High Forest Cover and Low Deforestation (HFLD) underscores its pivotal role in mitigating climate change. However, the ability of its forest ecosystems to store and sequester carbon is at risk due to changes in forest cover, whether from land conversion, land consumption, deforestation, or other land use and land cover alterations. To understand how these changes affect carbon storage, it is essential to evaluate carbon dynamics and predict the potential impacts on carbon budgets. This information is essential for creating land management plans that safeguard Suriname's forests and strengthen their ability to combat climate change. Marowijne – a district in Suriname – is facing increasing pressure on its land due to factors like urban growth, infrastructure development, and natural challenges such as a changing coastline and the impacts of climate change. To ensure the region's long-term sustainability and protect its natural environment, it's crucial to better understand these ongoing changes. Despite the clear occurrence of land use changes in Marowijne, there is a significant gap in studies that focus on detecting current trends, predicting future land use and land cover dynamics, and assessing the impact of land use changes on carbon storage and sequestration.

This study aims to achieve four interconnected objectives: (1) to collect and process geospatial data on land use and land cover; (2) to evaluate the accuracy and reliability of hybrid predictive models combining Markov chains with cellular automata (CA), multilayer perceptron (MLP), support vector machines (SVM), and logistic regression (LR) in predicting future land use changes within the Marowijne district of Suriname; (3) to develop a robust hybrid simulation model for forecasting LULC changes over the next 10 years; and (4) to project the spatial distribution of carbon storage and sequestration.

MATERIALS AND METHODS

Study area

The area of interest is Marowijne, a district of Suriname covering a total area of 4803 km^2, situated in the north-eastern part of the country. Geographically, Marowijne is located to the north between 4.0° and 5.95° N and to the west between 54.0° and 54.80° W mostly within the Young and Old Coastal Plains (only the southern and south-eastern parts are situated within the Savanna Belt and Interior Uplands), ranging from 35 below to 572 m above MSL. The district is divided into six administrative units (resorts), namely Galibi, Moengo, Moengo Tapoe, Wanhatti, Albina and Patamacca.

Figure 1 depicts the research area's location. The climate of the study area is tropical-equatorial (Af) according to the Köppen-Geiger climate classification. The soil cover is represented by Umbric Gleysols, Albic Plinthosols and Albic Arenosols according to the international soil classification system (WRB, 2014).

Datasets used. This study used three satellite image sets to analyze LULC change dynamics and build a predictive model (Table 1).

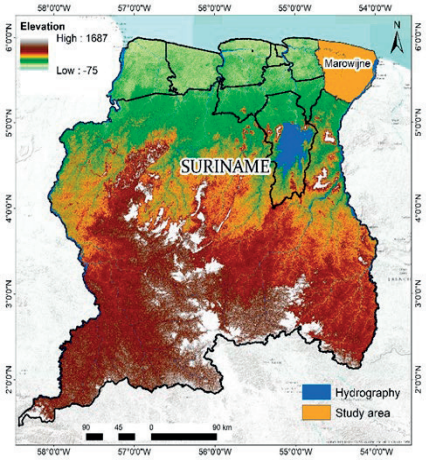


Figure1. Location of the study area

Table 1. Characteristics of data collected

Data	Source	Acquisition year	Scale/ Resolution
Multispectral satellite imagery	Esri Land Cover: https://livingatlas.arcgis.com/ladcover/	2017 2020	10 m
	Google Earth Engine Data Catalogue: https://developers.google.com/earth-engine/datasets/catalog/	2024	
Digital Elevation Model (DEM)	30-Meter SRTM Tile Downloader: https://dwtkns.com/srtm30m/	2018	1-arcsecond (3601x 3601 pixels)
Shape-file with locations of gold mining activity	National Environmental Authority: https://nimos.org/en/about-us/	2018	–
Shapefile with locations of deforestation areas	National Land Monitoring System of Suriname GONINI https://www.gonini.org/	2023	–

Slope, distance from water bodies (rivers and creeks), distance from roads, distance from gold mining and deforestation areas, distance from key settlements (growth poles), and population density datasets were developed individually in 2024 with a spatial resolution of 10 m. These datasets were processed in QGIS 3.34 and ArcGIS 10.8. The Euclidean distance function was employed to generate distance maps from roads, rivers, gold mining areas, and growth poles using vector data of the features (Kafy et al., 2021; Gharaibeh et al., 2020). The DEM was processed in ArcGIS Spatial Analyst tools to create elevation and slope maps.

Image classification. Sentinel imageries for the year 2024 were classified using the Random Forest (RF) classifier and Google Earth Engine (GEE) capabilities.

Random Forest is a non-parametric, multivariate technique known for its ability to handle high-dimensional data and multicollinearity effectively. It is also robust against overfitting and tolerant of suboptimal training data quality (Hemmerling et al., 2021).To evaluate classification accuracy, a random sample comprising 30% of the reference data for 2024 was used. The error matrix, generated in Google Earth Engine (GEE), included key metrics such as overall accuracy and the kappa coefficient (Congalton & Green, 1999; Lu & Weng, 2007). These metrics are widely recognized for measuring the agreement between the classification results and the validation dataset (Mhanna et al., 2023).

The bands 4–3–2 combination (true colour combination), bands 8–4–3 combination (false colour combination) and bands 12–11–4 combination were utilised to perform Sentinel-2 image classification.

A total of 5000 LULC reference data points representing various land use categories, including water, forest-covered and flooded areas, agricultural land, bare ground, built-up areas, and rangelands, were collected within the Marowijne district (Table 2).

Table 2. Major land use land cover types used and their descriptions

LULC class	Class description
Water bodies	Areas covered by rivers, streams, canals and reservoirs
Forest covered area	Landcover with primary trees, palm, and bamboo with a minimum crown tree cover of 30% with the potential to reach a canopy height of a minimum of 5 m and a minimum area of 1.0 hectares
Flooded area	Areas of any type of vegetation with obvious intermixing of water throughout a majority of the year; seasonally flooded area that is a mix of grass/shrub/trees/bare ground
Agricultural land	Includes areas used for perennial and annual crop production, irrigated areas, commercial farms
Bare ground	Includes land areas of exposed soil, bare soil and open areas consisting of sand, rocks and loam
Built-up area	Includes commercial areas, urban, residential, and rural settlements, industrial areas
Rangeland	Open areas covered in homogenous grasses with little to no taller vegetation; wild grasses with no obvious human plotting (i.e., not a plotted field)

Adopted from Karra et al., 2021. Retrieved from https://www.arcgis.com/

This data was derived from field surveys, expert knowledge, and high-resolution imagery from Google Earth Pro (https://earth.google.com/web). The dataset was then randomly split into two groups: 70% for training and 30% for validation (Aryal et al., 2023; Amindin et al., 2024). The training data were used to perform supervised classification, while the validation data were used to evaluate the accuracy of the resulting map (Sawant et al. 2023).

The classification performance was assessed by calculating key metrics, including overall accuracy, user accuracy, producer accuracy, and the kappa coefficient, based on the confusion matrix. The overall accuracy and kappa coefficient for the classified LULC map of 2024 were 90% and 84%. This indicates a reliable and accurate classification of image for analysing land use/land cover change. Figure 2 shows the statistical distribution of LULC classes for 2017, 2020, and 2024 within the area of interest.

Driving variables. Driving variables, also known as driving factors or drivers, represent various biophysical, socioeconomic, and infrastructural elements that influence land use patterns and the processes of land transformation over time.

Recognizing the need to incorporate the potential influence of independent variables in simulating LULC changes (Gharaibeh et al., 2020), this study considered eight key driving variables (Figures 3 to 6).

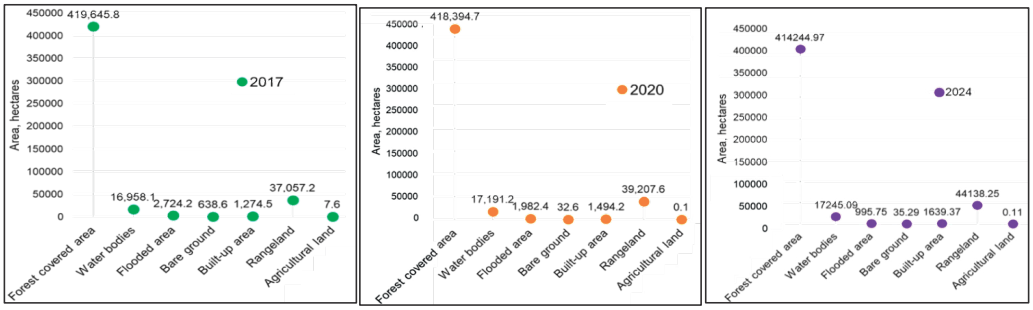


Figure 2. Area of LULC classes in Marowijne district for the years 2017, 2020, and 2024

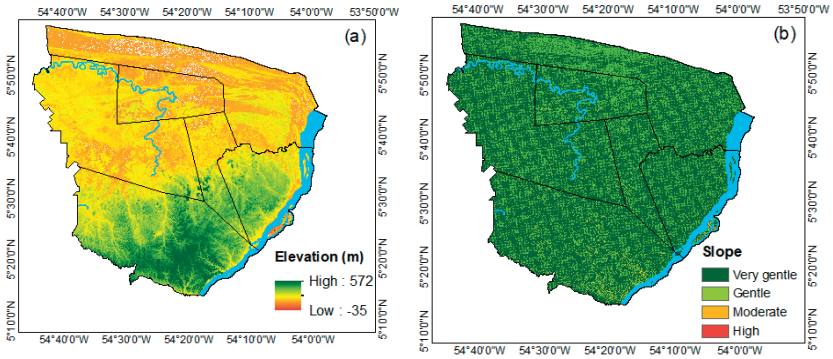


Figure 3. Biophysical driving variables: elevation (a) and slope (b)

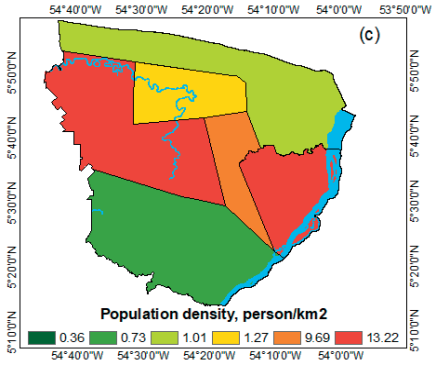


Figure 4. Socioeconomic driving variables: population density (c)

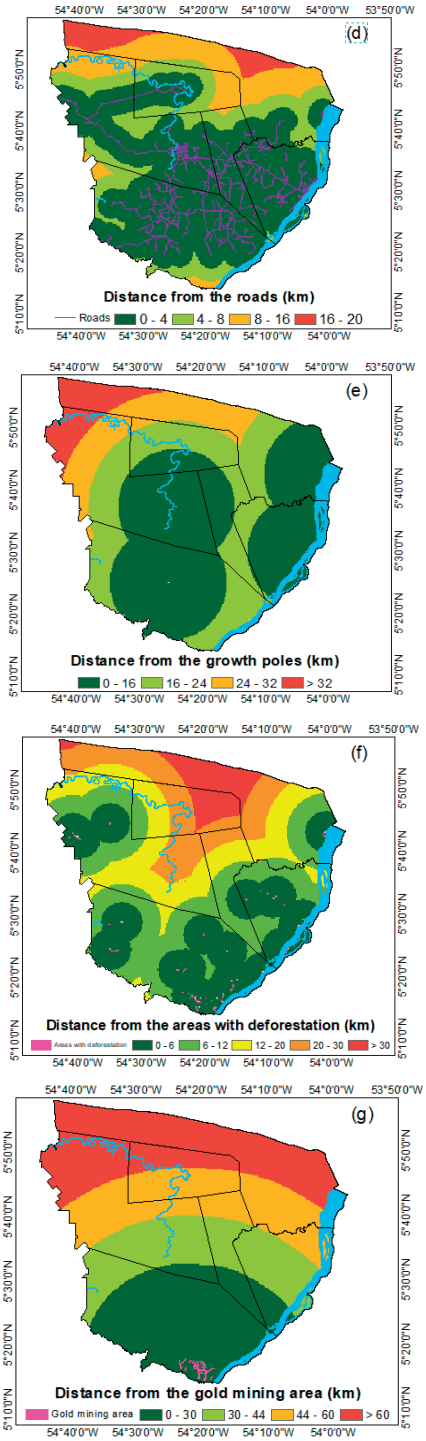


Figure 5. Proximity driving variables: distance from roads (d), growth poles (e), areas with deforestation (f) and gold mining area (g)

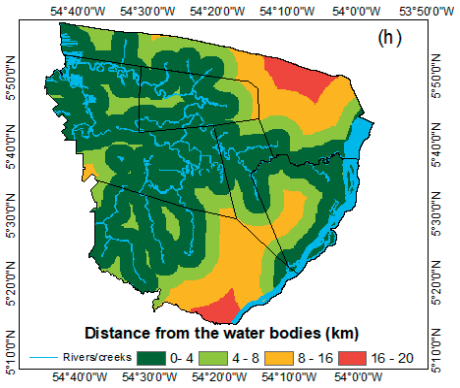


Figure 6. Proximity to water bodies (h)

InVEST model. The InVEST carbon pools model was used to calculate carbon storage and sequestrate potential of landscapes. The carbon storage module of the InVEST model assesses carbon storage using land use types as the units of measurement for the land surface. It can effectively evaluate the quantity and value of ecosystem services. The total carbon storage in the study area was estimated by multiplying the total area of different land types by their corresponding average carbon densities.

The InVEST model was utilized to analyze carbon storage and predict its spatial distribution based on simulated LULC in the area by 2034. The equations are as follows:

$$Ci = Ci_{above} + Ci_{below} + Ci_{soil} + Ci_{dead} \quad (1)$$

$$C_{total} = \sum_{i=1}^{n} Ci \times Si \quad (2)$$

where:

- i is the i-th land use type;
- Ci is the total carbon density of land use type i (Mg·hm^{-2});
- Ci_{above}, Ci_{below}, Ci_{soil} and Ci_{dead} are the aboveground, underground, soil, and dead organic average carbon density of land use type i (Mg·hm^{-2}), respectively;
- C_{total} is the total carbon storage (Mg); Si is the area of land use type i (hm^2);
- n is the number of land use types, with a value of 7 in this study (Maanan et al., 2019; Natural Capital Project, 2023; Li et al., 2023).

The carbon density values of the four carbon pools corresponding to different land use types are shown in Table 3.

YASSO Model. Due to the lack of local data about soil organic matter content the YASSO model (Yasso20) was utilized to assess the soil carbon pool within the study area. This model is a dynamic soil carbon model used to simulate carbon dynamics both in litter and soil organic matter.

Table 3. Biophysical data used in the InVEST carbon storage and sequestration model (unit: Mg/hm^2)

LULC class name	Above ground carbon pool	Below ground carbon pool	Soil carbon pool	Dead wood carbon pool	Data sources
Forest cover	155.34	35.91	27.5*	4.54	Eggleston et al., 2006; SBB; CELOS; CATIE; NZCS, 2017
Flooded area	44.41	10.66	26.55	2.9	
Rangeland	72.63	8.96	26.55	1.94	
Water bodies	0	0	0	0	CELOS; CATIE; NZCS, 2017; Zhang et al., 2019
Bare ground	0	0	0	0	
Built-up area	4.11	0.98	13.5	1.94	
Agricultural land	4.11	0.98	13.5	1.94	Dida et al., 2021; Natural Capital Project, 2023

* – value was estimated with YASSO model.

It predicts the decomposition of organic materials (like plant litter) and the resulting carbon storage and release over time. The model uses climate data (temperature and precipitation) and litter input data to estimate carbon fluxes and long-term soil carbon storage (Viskari et al., 2022).

LULC change detection and simulation. The Land Change Modeler (LCM) within the TerrSet software was applied to analyze and project future LULC changes in the study area. This data-driven, step-by-step approach included change detection, modelling transition potentials, and forecasting changes based on historical data from 2017 to 2020. A Markov probability matrix was employed to estimate the likelihood of transitions between LULC classes over time. Transition potential maps, representing the probability of land use transitions, were generated using a multi-layer perceptron neural network (MLP), support vector machine (SVM), cellular automata (CA), and logistic regression (LR).

Validation of model outputs. The validation process was conducted using the Validate module in the TerrSet software. This module calculated kappa statistics to assess the agreement between the hard prediction and reference map. The computed metrics included kappa for no information (K_{no}), kappa for grid cell-level location ($K_{location}$), kappa for stratum-level location ($K_{locationStrata}$), and kappa standard ($K_{standard}$) (Girma et al., 2022; Mishra et al., 2018). Generally, a strong and acceptable kappa value is considered to be around 80% or higher (Girma et al., 2022; Gharaibeh et al., 2020). For forecasting, the LULC maps from 2017 and 2020 were used as input variables to predict the 2034 LULC distribution. The LULC maps from 2024 and 2034 were utilized as input variables for the InVEST model to predict the 2034 carbon storage and sequestration. Figure 7 illustrates the modelling and validation processes employed in this study.

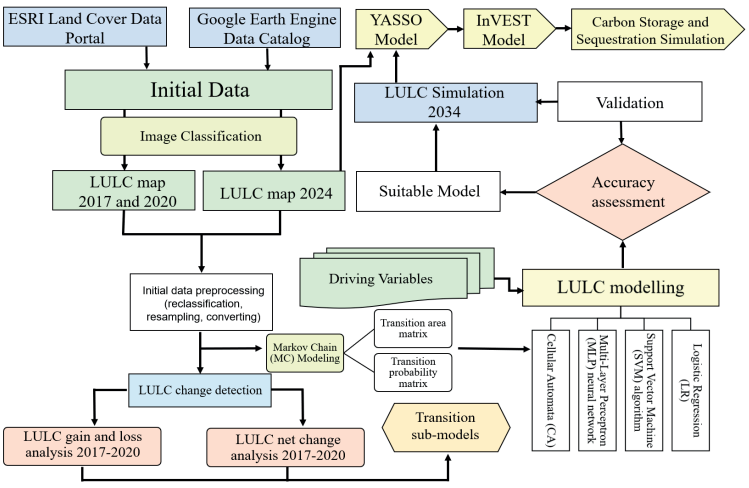


Figure 7. Research design flowchart

RESULTS AND DISCUSSIONS

To accurately predict future LULC trends over the next 10 years, it is pivotal to identify and comprehend past trends in land use and land cover changes (Girma et al., 2022; Regasa et al., 2021). The study area underwent notable landscape transformations and shifts in land use between 2017 and 2020, as shown in Figures 8 and 9.

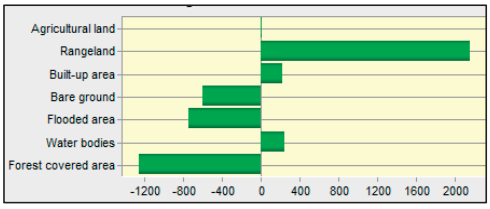


Figure 8. Net changes in LULC within the limits of Marowijne district between 2017 and 2020, hectares

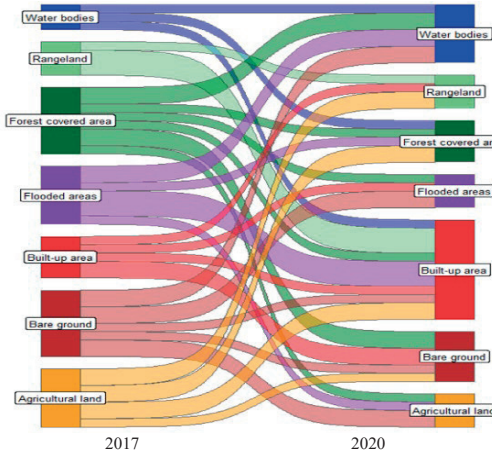


Figure 9. Sankey diagram of LULC classes mutual conversion from 2017 to 2020

A significant conversion of forest-covered areas into rangeland indicates ongoing forest loss, which may negatively impact biodiversity and carbon storage. Considering that over 86% of the district's territory is forested, logging and land clearing for commercial or subsistence farming have been the primary drivers of deforestation from 2017 to 2020.

A decrease in flooded areas suggests the drying or degradation of wetlands, which adversely affects water resources and ecosystem services. These changes are driven by altered hydrological cycles due to climate change, poor water management, and deforestation. The notable net increase in rangeland is primarily attributed to the reduction in forest cover and bare ground. Although built-up areas constitute only 0.3% of the total land in the Marowijne district, they have expanded significantly during the observed period, signaling the intensification of urbanization, particularly within established urban growth poles. The net change in water bodies is mainly influenced by shifts in forest cover and bare ground. The outcomes of the LULC change analysis serve as the foundation for constructing transition sub-models (Table 4). Based on these results, considering the most significant gains and losses for each land use class, seven sub-transition models were identified, the best of which was incorporated into the final predictive model.

This study employed biophysical, socioeconomic, and proximity-related driving variables to predict LULC changes. Before incorporating these drivers into the predictive model, their explanatory power was evaluated. Cramer's V was used to assess the strength of association, while p-values were applied to determine statistical significance (Table 5).

Table 4. Transition sub-models and their descriptors

Transition sub-model	Land cover transition	Description
Forest covered areas losses (FLO)	Forest-covered areas to rangeland, water bodies and built-up area	FLO sub-model describes the process of deforestation where forest areas are replaced by other land-use types such as rangeland, water bodies, or urban development
Forest covered areas gains (FGA)	Bare ground and flooded areas to forest covered areas	Represents reforestation or afforestation where non-forested areas like bare ground or flooded areas are transformed into forest-covered areas
Water bodies transformation (WAT)	Forest-covered areas, flooded areas, bare ground, built-up area and rangeland to water bodies	This refers to the conversion of land types such as forests, flooded areas, bare ground, rangeland, and urban areas into water bodies, often due to flooding or human interventions like dam creation

Transition sub-model	**Land cover transition**	**Description**
Flooded areas transformation (FAT)	Flooded areas to forest covered areas, rangeland and water bodies	Involves the draining or reclamation of flooded areas for conversion into forest, rangeland, possibly for agriculture or urban development
Bare ground transformation (BAT)	Bare ground to forest covered areas, flooded areas, water bodies, built-up areas and rangeland	Bare land transitions into various types, including forest cover, urban areas, or agricultural rangelands, driven by natural ecological succession or deliberate land-use planning
Urban expansion (UEX)	Forest-covered areas, flooded areas, bare ground and rangeland to built-up areas	Describes urban expansion, where natural landscapes like forests and rangelands are converted into residential, industrial, or commercial areas to meet the demands of a growing population within the key settlements
Rangeland transformation (RAT)	Rangeland to forest covered areas, flooded areas and bare ground	Involves the transformation of rangelands into forests or bare land, often resulting from land reclamation initiatives, degradation processes, or targeted reforestation efforts.

Table 5. Cramer's V and p-value for each of the explanatory variables

Driver variables	Cramer's V	p-value
Distance from deforestation	0.2363	<0.0001
Slope	0.2847	<0.0001
Elevation	0.3888	<0.0001
Distance from water bodies	0.3705	<0.0001
Distance from roads	0.3779	<0.0001
Distance from growth poles	0.4012	<0.0001
Distance from gold mining area	0.4026	<0.0001
Population density	0.4600	<0.0001

According to Eastman (2016), Cramer's V values above 0.15 are considered "useful," and values over 0.4 are seen as "good." In this study, population density stands out with the highest Cramer's V of 0.4600, making it the most important factor in explaining changes in land use. The distance from gold mining areas (0.4026) and from growth poles (0.4012) also show strong connections, suggesting that mining and urbanization play major roles in shaping land-use patterns. The proximity to roads (0.3779) and water bodies (0.3705) are somewhat important, reflecting how accessibility and water resources influence land changes. Elevation (0.3888) and slope (0.2847) show a moderate to strong link, emphasizing the role of terrain features in determining land use. While distance from areas of deforestation (0.2363) has the weakest association, it is still statistically significant. All variables are found to be significant predictors of land-use change (p-value <0.0001), with population density, proximity to gold mining, and growth poles having the strongest associations. On the other hand, elevation and slope appear to have the least impact. This analysis underscores the significant role of human-driven factors in land-use changes within the Marowijne district.

To find the most suitable transition sub-model, accuracy rates were calculated for each hybrid model and its respective sub-models. The performance of the LR-MC hybrid model was assessed using the ROC method (Myslyva et al., 2023). A summary of the accuracy assessment for various transition sub-models is provided in Table 6.

Table 6: Hybrid modelling approaches and their accuracy

Transition sub-model	Modelling approach accuracy rate (%)		
	MLP-MC	SVM-MC	LR-MC
FLO	78.95	85.33	72.50
FGA	81.34	91.49	75.20
WAT	64.63	71.50	59.80
FAT	63.97	78.36	57.45
BAT	69.77	73.64	65.30
UEX	92.66	97.14	87.50
RAT	79.45	88.66	73.80

The suitability assessment for various transition sub-models was not conducted for the CA-MC predictive model, as it relied on a transition areas file generated through Markov Chain analysis, which accounted for all-to-all transitions. However, due to the limited availability of historical data on LULC dynamics (covering the period from 2017 to 2020), this model was still selected to predict LULC changes. A model accuracy of 80% or higher is generally considered acceptable to validate training results (Gharaibeh et al., 2020; Silva et al., 2020). As a result, only the LR-MC hybrid model with the UEX transition sub-model, the MLP-MC hybrid models with the FGA and UEX transition sub-models, and the SVM-MC hybrid models with the FLO, RAT, FGA, and UEX transition sub-models met the suitability criteria for LULC

change prediction. However, the overall agreement between the actual LULC map and the CA-MC model-simulated map did not reach the satisfactory range. While previous studies report higher accuracy rates for MLP (Girma et al., 2022; Leta et al., 2021; Gharaibeh et al., 2020; Gibson et al., 2018), this study demonstrated that SVM is a more effective machine learning approach, offering a robust and flexible solution for LULC change prediction. SVM excels at handling complex, non-linear relationships between land cover and its driving factors, resulting in high accuracy. The superior performance of SVM can also be attributed to its ability to work effectively with smaller datasets (Myslyva et al., 2024), such as the limited four-year dataset used in this study. This higher accuracy is reflected in the SVM-MC model, as shown by the parameters in Table 7.

Table 7. Model parameters and accuracy

Parameter	Value
Modelling approach	SVM learning algorithm
Sub-model	Urban expansion (UEX)
Kernel type	Radial Basis Function
Epsilon (ε)	0.0100
Class number	8
Total cross-validation number	272
Total sample number	2272
Overall cross-validation accuracy	0.9714
Overall out-of-sample accuracy	0.9751
Overall skill measure	0.9503

To validate the model, the Kappa statistic (k- index) for quantity and location was computed by comparing the hard simulation with the reference map of 2024 (Table 8).

Table 8. The k-index values of the simulated LULC map of 2024

Index	Value
K_{no}	0.9824
$K_{location}$	0.9848
$K_{locationStrata}$	0.9848
$K_{standard}$	0.9723

The statistics reveal that all kappa index values surpass the satisfactory range (≥ 80%). The overall disagreement between the reference and predictive maps is generally low, primarily attributed to allocation errors (0.0083) rather than quantity errors (0.0071). Despite the presence of allocation errors, the overall agreement between the actual and simulated maps is high, reaching 98.47%.

The developed model was then used to predict future land use changes during next 10 years under the business-as-usual scenario. Figure 10 illustrates the LULC predictive map for the year 2034 and Figures 11 and 12 depicts the transformations in LULC classes between 2024 and 2034.

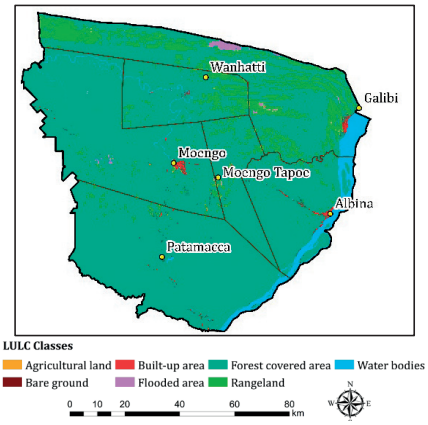


Figure 10. Projected LULC map for the territory of the Marowijne district for 2034

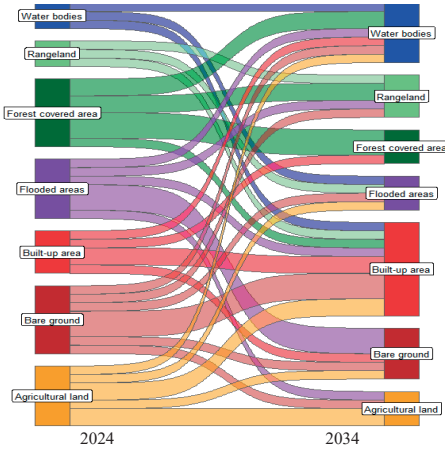


Figure 11. Sankey diagram of LULC classes mutual conversion from 2024 to 2034

The prediction of LULC changes over the next decade offers key insights into how carbon storage and sequestration might be impacted within the area of interest. Between 2024 and 2034, forest-covered areas, essential for storing carbon, are expected to increase slightly by 3,332.39 ha, which could contribute modestly to carbon sequestration. On the other hand, the

significant decrease in rangeland (about 5300 ha) could reduce its ability to act as a carbon sink, especially if these areas are converted to built-up spaces.

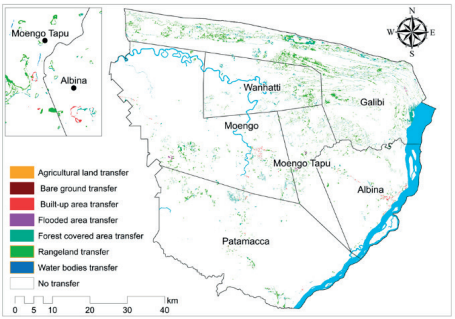


Figure 12. Areas where land use types will change from 2024 to 2034

Urbanization, with built-up areas expanding by about of 1000 ha, will likely lower the carbon sequestration potential as vegetation gives way to impervious surfaces. The rise in flooded areas (also about 1000 ha) could also affect carbon dynamics, as wetlands can either store carbon or release methane, depending on the type of flooding and vegetation. The small reduction in bare ground (-4.64 ha) and minimal changes in agricultural land and water bodies are unlikely to significantly impact carbon storage. Overall, these shifts highlight the complex relationships between land use changes and carbon balance.

The modelling results revealed the spatial and temporal dynamics of carbon storage and sequestration in the Marowijne district from 2017 to 2034 (Figures 13 and 14).

In 2017, areas with high carbon storage (1.8–2.23 MgC/pixel) made up around 40–50% of the district, while those with moderate storage (1.35-1.79 MgC/pixel) covered about 30–40%. Low-storage areas were relatively rare. By 2024, the high-carbon storage areas had decreased to roughly 30-35%, and the moderate storage areas expanded to 40-50%. At the same time, low-carbon storage areas (0.46-0.89 MgC/pixel) will began to spread, covering around 15-20% of the district. Looking ahead to 2034, the high-carbon storage areas are expected to shrink further to 20-25%, while both low and moderate storage areas will likely cover about 25-30% and 50-55%, respectively.

Between 2017 and 2024, reductions in carbon storage affected about 20-25% of the district, primarily in coastal zones and areas around Albina and Moengo. Increases in carbon storage were limited to less than 5%, reflecting localized improvements likely due to afforestation. During the subsequent decade (2024–2034), reductions in carbon storage are expected to intensify and spread to broader areas, particularly in central and coastal zones, affecting 15-20% of the district and focusing on already degraded areas. Only a few areas (under 3%) are projected to exhibit increases, further highlighting a net decline in carbon sequestration potential within the limits of the study area.

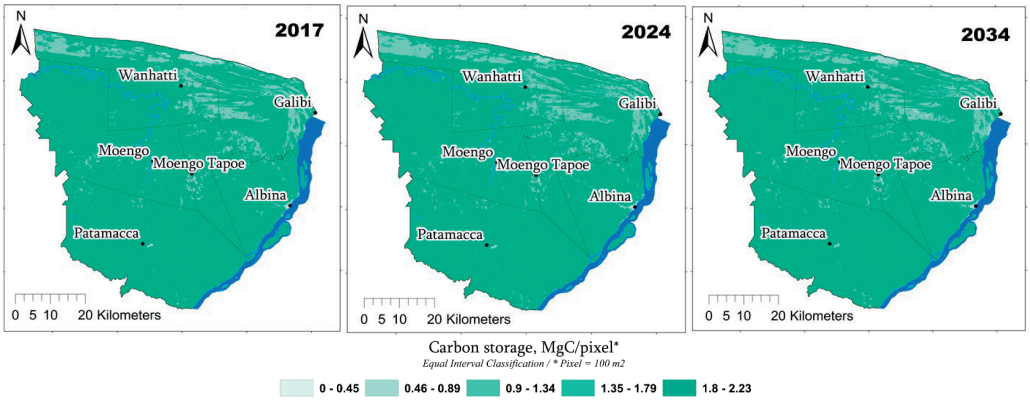


Figure 13. Dynamic of carbon storage and sequestration in Marowijne district

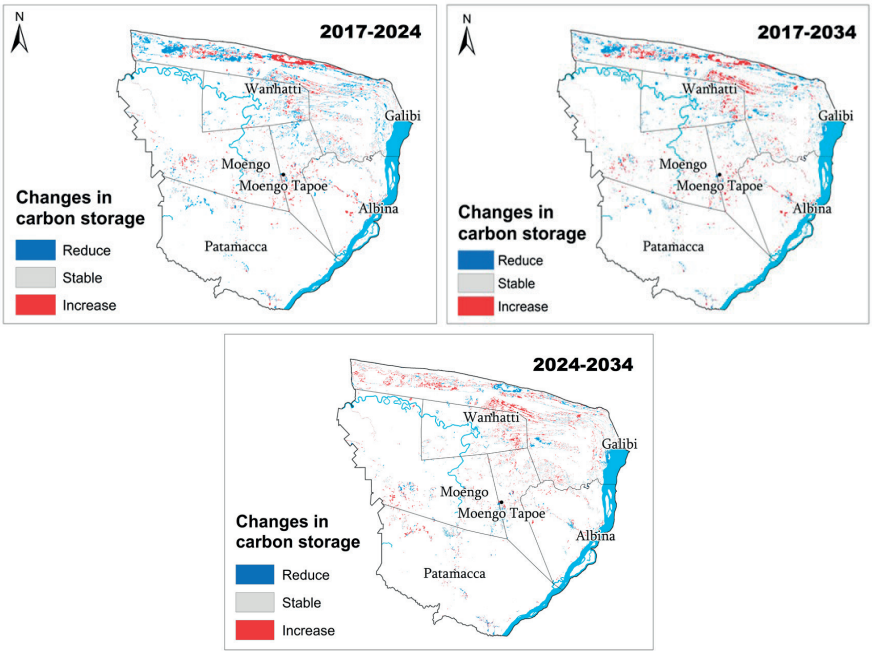


Figure 14. Change areas of carbon storage and sequestration in Marowijne district

Coastal and settlement areas, such as Albina and Moengo, are expected to experience the most significant losses in carbon storage, with reductions impacting 30–35% of the district by 2034. The net loss of high-carbon areas (~15–25%) between 2017 and 2034 reflects intensifying anthropogenic pressures and underscores the urgent need for effective land-use management strategies.

CONCLUSIONS

The transformation of land use and land cover (LULC) in the Marowijne district of Suriname from 2024 to 2034 was simulated using four hybrid predictive models: Markov chain analysis with cellular automata (CA-MC), multilayer perceptron (MLP-MC), support vector machines (SVM-MC), and logistic regression (LR-MC). This research utilized a combination of dependent (driver) and independent spatial datasets, analyzed through both statistical and graphical methods. Eight biophysical, socioeconomic, and proximity variables were identified as the primary drivers of LULC change. Based on the land use change analysis and the most significant gains and losses for each land use class, seven sub-transition models were developed. Among these, the urban-expansion model was selected as the most appropriate for inclusion in the final predictive model.

Accuracy assessments revealed that the SVM-based model, which incorporated the UEX transition sub-model for transitions such as the conversion of forest-covered areas, flooded areas, bare ground, and rangeland to built-up areas, achieved an overall accuracy of 97.14%. While previous studies indicated higher accuracy for MLP models, the SVM model proved superior in this study due to its robustness with small datasets and its ability to effectively handle high-dimensional data. The reliability of the SVM model was further confirmed by a Kappa statistic of 98.47% for predictions in 2024.

Using the business-as-usual scenario, future LULC changes for 2034 were forecasted. The model predicts a slight increase in forest-covered areas, a significant reduction in rangelands, expansion of built-up areas, and an increase in flooded areas. These trends underscore the intricate interplay between human activities and environmental factors,

highlighting the urgent need for sustainable land management practices.

The expected decline in carbon storage suggests a decrease in carbon sequestration, which could have negative effects on both climate regulation and the overall stability of ecosystems. To counteract this loss, it's crucial to implement strategies like reforestation and more stringent land-use policies.

Given the unique characteristics of different resorts in Marowijne, future research should aim to create more specific predictive models that take into account the particular driving factors of each separate resort. This would improve the accuracy of LULC predictions and support more focused, effective land management practices.

REFERENCES

Aloqaili, H., Alomar, S., Elgazzar, R., & Mahmoud, S. (2021). Assessing land suitability and management strategies through LULC models. *Journal of Land Use Science*, *16*(2), 121-139. 8.

Amindin, A., Siamian, N., Kariminejad, N., Clague, J. J., Reza Pourghasemi, H. (2024). An integrated GEE and machine learning framework for detecting ecological stability under land use/land cover changes. *Global Ecology and Conservation*, *53*, e03010.

Aryal, J., Sitaula, C., Frery, A. C. (2023). Land use and land cover (LULC) performance modeling using machine learning algorithms: a case study of the city of Melbourne, Australia. *Scientific Reports, 13*(1), 13510.

Asif, M., Kazmi, J., Tariq, A., Zhao, N., Guluzade, R., Soufan, W., Almutairi, Kh., El Sabagh, A., & Aslam, M., (2023), Modelling of land use and land cover changes and prediction using CA-Markov and Random Forest, *Geocarto International*, *38*(1).

Congalton, R. G., & Green, K. (1999). Assessing the accuracy of remotely sensed data: Principles and practices. Boca Raton, FL: Lewis Publishers.

Deng, X., Liu, H., Li, W., & Zhou, X. (2020). The role of land use/land cover change in carbon sequestration. *Environmental Research Letters*, *15*(6), 064010.

Devi, A. R., Shimrah, T. (2023). Modelling LULC using Multi-Layer Perceptron Markov change (MLP-MC) and identifying local drivers of LULC in the hilly district of Manipur, India. *Environmental Science and Pollution Research International*, *30*(26), 68450–68466.

Dida, J. J., Tiburan, C., Tsutsumida, N., Saizen, I. (2021). Carbon stock Estimation of Selected Watersheds in Laguna, Philippines Using InVEST. *Philippine Journal of Science*, *150*(2), 501–513.

Eastman, J. R. (2016). TerrSet Manual, Geospatial Monitoring and Modeling System. Clark University, Worcester, USA. Clark University, Worcester, USA.

Eggleston, H. S., Buendia, L., Miwa, K., Ngara, T., Tanabe, K. (2006). *IPCC guidelines for national greenhouse gas inventories*. Institute for Global Environmental Strategies, Hayama, Japan, 2, 48–56.

Gharaibeh, A., Shaamala, A., Obeidat, R., Al-Kofahi, S. (2020). Improving land-use change modelling by integrating ANN with cellular automata-Markov chain model. *Heliyon*, *6*.

Gibson, L., Munch, Z., Palmer, A., Mantel, S. (2018). Future land cover change scenarios in South African grasslands – implications of altered biophysical drivers on land management. *Heliyon*, *4*(7).

Girma, R., Fürst C., Moges A. (2022). Land use land cover change modelling by integrating the artificial neural network with cellular Automata-Markov chain model in Gidabo river basin, main Ethiopian rift. *Environmental Challenges, 6*, 100419.

Global Forest Watch. (n.d.). Suriname. Retrieved January 2, 2025, from https://www.globalforestwatch.org.

Hemmerling, J., Pflugmacher, D., Hostert, P. (2021). Mapping temperate forest tree species using dense Sentinel-2 time series. *Remote Sensing of Environment, 267*, 12743.

Kafy, A.-A., Naim, M. d. N. H., Subramanyam, G., Faisal, A.-A., Ahmed, N. U., al Rakib, A., Kona, M. A., Sattar, G. S. (2021). Cellular Automata approach in dynamic modelling of land cover changes using RapidEye images in Dhaka, Bangladesh. *Environmental Challenges*, *4*, 100084.

Karra, K., Kontgis, C., Statman-Weil, Z., Mazzariello, J. C., Mathis, Brumby, M. S. P. (2021). Global land use / land cover with Sentinel 2 and deep learning. 2021 IEEE International Geoscience and Remote Sensing Symposium IGARSS, Brussels, Belgium, 2021, 4704–4707.

Lambin, E. F., & Meyfroidt, P. (2019). Global land use change, economic globalization, and the looming land scarcity. *Proceedings of the National Academy of Sciences*, *116*(15), 7350-7357.

Leta, M. K., Demissie, T. A., Tränckner, J. (2021). Modelling and prediction of land use land cover change dynamics based on land change modeller (LCM) in Nashe watershed, upper Blue Nile basin, Ethiopia. *Sustainability*, *13*.

Li, P., Chen, J., Li, Y., Wu, W. (2023). Using the InVEST-PLUS model to predict and analyze the pattern of ecosystem carbon storage in Liaoning Province, China. *Remote Sensing*, *15*, 4050.

Lu, D., Weng, Q. (2007). A survey of image classification methods and techniques for improving classification performance. *International Journal of Remote Sensing, 28*(5), 823–870.

Luo, Y., Sun, J., Li, Z., & Hu, X. (2021). Evaluating carbon sequestration potential in different land cover types. *Global Change Biology*, *27*(8), 1647-1660.

Maanan, M., Karim, M., Kacem, H., Soukaina, A., Rueff, H., Snoussi, M., Rhinane, H. (2019). Modelling the potential impacts of land use/cover change on terrestrial carbon stocks in north-west Morocco. *International Journal of Sustainable Development & World Ecology*, *26*.

Mhanna, S., Halloran, L. J. S., Zwahlen, F., Haj Asaad, A., Brunner, Ph. (2023). Using machine learning and remote sensing to track land use/land cover changes

due to armed conflict. *Science of The Total Environment*, 898, 165600.

Mishra, V. N., Rai, P. K., Prasad, R., Punia, M., Nistor, M.–M. (2018). Prediction of spatiotemporal land use/land cover dynamics in rapidly developing Varanasi district of Uttar Pradesh, India, using geospatial approach: a comparison of hybrid models. *Applied Geomatics*, *10*(3), 257–276.

Mohamed, A., Worku, H. (2020). Simulating urban land use and cover dynamics using cellular automata and Markov chain approach in Addis Ababa and the surroundings. *Urban Climate*, *31*, 100545.

Muhammad, R., Zhang, W., Abbas, Z., Guo, F., Gwiazdzinski L. (2021). Spatiotemporal change analysis and prediction of future land use and land cover changes using QGIS MOLUSCE plugin and remote sensing big data: A case study of Linyi, China. *Land*, *11*(3), 419.

Myslyva, T., Dasai, M., Huisden, C. M., Nadtochiy, P., Bilyavskyi, Y. (2024). Application of machine learning approaches for land use change modelling in Suriname. *Scientific Papers. Series E. Land Reclamation, Earth Observation and Surveying, Environmental Engineering, 13*, 830–840.

Myslyva, T., Nadtochiy, P., Bilyavskyi, Y., Trofymenko, P. (2023). Intra-field spatial heterogeneity prediction for the purposes of precision farming: Comparison of frequency ratio and Shannon's entropy models. *Scientific Papers. Series A. Agronomy, 66*(1).

Natural Capital Project. (2023). InVEST (Integrated Valuation of Ecosystem Services and Tradeoffs) Version 3.14.2. Stanford University, University of Minnesota, The Nature Conservancy, and World Wildlife Fund.

Regasa, M. S., Nones, M., Adeba, D. (2021). A review on land use and land cover change in Ethiopian basins. *Land*, *10*(10), 585.

Robinson, D.T., (2021), Towards a spatially explicit agent-based model of land use change and ecosystem service provisioning in semi-arid rural regions. *Environmental Modelling and Software*, *139*, 104990

Sarathchandra, C., Abebe, Y. A., Worthy, F. R., Wijerathne, I. L., Ma, H., Yingfeng, B., Jiayu, G., Chen, H., Yan, Q., Geng, Y., Weragoda, D. S., Li, L.-L., Fengchun, Y., Wickramasinghe, S., & Xu, J. (2021). Impact of land use and land cover changes on carbon storage in rubber-dominated tropical Xishuangbanna, South West China. *Ecosystem Health and Sustainability*, *7*(1), 1915183.

Sawant, S., Garg, R. D., Meshram, V., Mistry, S. (2023). Sen-2 LULC: Land use land cover dataset for deep learning approaches. *Data in Brief*, *51*, 109724.

SBB; CELOS; CATIE; NZCS. 2017. State-of-the-art study: Best estimates for emission factors and carbon stocks for Suriname. SBB. Paramaribo, Suriname.

Silva, L. P. E., Xavier, A. P. C., da Silva, R. M., Santos, C. A. G. (2020). Modeling land cover change based on an artificial neural network for a semiarid river basin in northeastern Brazil. *Global Ecology Conservation*, *21*.

Song, C., Xu, B., Caylor, K. K. (2020). Impact of deforestation and urbanization on ecosystem services. *Ecosystem Services*, *42*, 101114.

van Ommeren-Myslyva, T., Satnarain, U., Wesenhagen, F. (2024). Hybrid modelling approach for land use change prediction and land management in the Coronie district of Suriname. *South Asian Journal of Management Research*, *14*(4), 388–406.

van Ommeren-Myslyva, T., Wesenhagen, F., Kadirbaks R., Abdoelrahman F. (2024). Application of machine learning approaches for land use change modelling in Commewijne district of Suriname. *Science and Innovation*, *3*, 13–29.

Viskari, T., Pusa, J., Fer, I., Repo, A., Vira, J., Liski, J. (2022). Calibrating the soil organic carbon model Yasso20 with multiple datasets. *Geoscientific Model Development*, *15*, 1735–1752.

Yeh, C.-K., Liaw, S.-C. (2021). Applying spatial autocorrelation and logistic regression to analyze land cover change trajectory in a forested watershed. *Terrestrial, Atmospheric and Oceanic Sciences*, *32*, 35–52.

Zhang, Y., Kong, D., Gan, R., Chiew, F. H. S., McVicar, T. R., Zhang, Q., Yang, Y. (2019). Coupled estimation of 500 m and 8-day resolution global evapotranspiration and gross primary production in 2002–2017. *Remote Sensing of Environment*, *222*, 165–182.

Scientific Papers. Series E. Land Reclamation, Earth Observation & Surveying, Environmental Engineering. Vol. XIV, 2025
Print ISSN 2285-6064, CD-ROM ISSN 2285-6072, Online ISSN 2393-5138, ISSN-L 2285-6064

DETERMINATION OF LAND VALUATION FACTORS FOR THE PROCESS OF LAND CONSOLIDATION - A CASE STUDY IN SASCHIZ ADMINISTRATIVE UNIT IN ROMANIA

Vlad PAUNESCU[1], Divyani KOHLI[2], Raluca MANEA[1], Mariana (CALIN) CIOLACU[1], Alexandru Iulian ILIESCU[1]

[1]University of Agronomic Sciences and Veterinary Medicine of Bucharest, 59 Mărăști Blvd, District 1, Bucharest, Romania
[2]ITC - Faculty of Geo-Information and Science & Earth Observation, 8 Hallenweg, 7522 NH Enschede, Netherlands

Corresponding author email: vlad.paunescu@topoexim.ro

Abstract

Land fragmentation is a phenomenon that affected Western Europe in the past and, starting from 1989, the countries of Eastern Europe. One of the ways in which the effect of land fragmentation can be diminished is the process of land consolidation. Through land consolidation, owner can get better shaped parcels that can help increase agricultural productivity. Using the existent literature in the field of land consolidation, this exploratory study proposes a series of factors for land evaluation for the land consolidation process. These factors are applied in Saschiz administrative unit in Romania using different type of data to calculate the score for each factor. The result shows how this framework functions in real conditions.

Key words*: systematic land registration, cadastre, operations, processes, cadastre.*

INTRODUCTION

Climate change and the growth of world population are challenges that have pushed decision makers around the globe to look for policies for a more efficient use of land and its soil. This must be done in a sustainable way to improve the use of its resources and systems (Mihailescu & Cîmpeanu, 2019; Coman et al., 2016). Subsistence agriculture cannot anymore feed the growing population of the world. There is a need for extending the arable land areas, sustainable land use and increase of farm yield (Nsabimana et al., 2023; Moteva, 2016).
Attaining food security by increasing agricultural productivity can make possible the achievement of the 17 Sustainable Development Goals and its 169 associated targets as defined by the United Nations. One of the ways in which land professionals can contribute to goals like: gender equality, increasing agriculture productivity or sustainable use of freshwater is by using the process of land consolidation that can reduce land fragmentation and increase agricultural output (Veršinskas et al., 2020; Hartvigsen, 2015).
Land fragmentation is a problem that increases production costs in agriculture, inefficiency and land abandonment (Di Falco et al., 2010; Latruffe & Piet, 2014). Eastern Europe has had the problem of land fragmentation after the anti-communist revolutions from 1989 when property started to return from state ownership to private ownership (Șuba et al., 2019; Sabates-Wheeler, 2002; Van Dijk, 2003). However, not in all these countries land reforms conducted in the 90s had the same effects. Baltic countries, Slovakia or the Czech Republic have a much less fragmented ownership than Romania or Bulgaria (Van Dijk, 2005; Van Holst et al., 2018), due to different ways in which the land was given back to the owners.
Romania is the country that has been affected the most by land fragmentation. According to (Eurostat, 2022) one third of the farms in existence in the EU are in Romania, more than twice than in Poland that is the next country in the classification. The problem does not only consist in the number of farms in existence, but also in the size of the farms. Over 90% of them have sizes that are less than 5 hectares

(Eurostat, 2022). This fragmentation is mainly caused by the land reforms conducted in the 90s. Through successive inheritances the land was split between the heirs, in accordance with the existent rural traditions (Rusu et al., 2002).

To counteract the effects of land fragmentation, most countries have implemented land consolidation projects (Hartvigsen, 2014). In this landscape, Romania is an exception. There have been few attempts to implement land consolidation projects in the country. None of these projects ended with a redistribution of parcels. The problems that have been signalled by different authors refer to lack of specialized institutions, legislation and the fact that land registration in Romania hasn't been finalized (Blenesi-Dima, 2010; Ciobanu, 2021; Dima et al., 2007; Păunescu et al., 2024).

This paper aims to provide a framework for evaluating land in the process of land consolidation for projects that may be developed in Romania in the future. The factors for evaluation of land in the land consolidation process will be taken from the existent literature regarding the subject and adapted to the specificities of the country. The land evaluation factors will be tested by applying them in a study area containing 766 parcels, in the Saschiz administrative unit from county Mures, Romania.

In the first section of this research, the literature concerning land fragmentation, land consolidation and land evaluation for land consolidation processes is analysed. In the second section, the methodology of the study is described in detail. In the third section, the factors for evaluation are determined from the existent literature and are applied in the study area. The fourth section of the study contains the conclusion of the research.

1. Land fragmentation

Land fragmentation is a sign of an underdeveloped agricultural system (Teshome et al., 2016). The effect of land fragmentation is less income for farmers and waste resources in agricultural production (Mert et al., 2023; Rashidpour & Azar, 2016). For (Ntihinyurwa et al., 2019) land fragmentation can be considered when: "more than 10 users are in 10 hectares, the average parcel is less than 1 ha, more than 50% of the owners have more than 2 parcels with irregular forms located in more than two different places more than 500 meters from home with more than two uses, land is fragmentated because of inheritance laws, land sharing or land redistribution". On the other hand, several authors have underlined some advantages that land fragmentation can provide in some instances. Having different parcels in different areas with different land use can constitute a form of protection against environmental changes and increase food security (Chigbu & Kalashyan, 2015; Van Hung et al., 2007). Regular shape parcels may not be appropriate where there are natural limits. Moreover, (Delgado, 1998; Bezus & Samofal, 2019) affirm that in some cases family farms can be more productive than large scale agricultural exploitations. However, contradicting these affirmations (Agarwal, 2010) and (Ruben & Lerman, 2005) show that group farms can mobilize more resources in a more efficient way, while (Sabates-Wheeler, 2005) talk about the increase agricultural output that group farms have.

2. Land consolidation

Land consolidation has been a tool implemented in many countries in Europe and Africa for a more efficient land management and sustainable development of rural areas (Demetriou, 2016). The result of the reallocation of land is parcels with better dimensions and shapes (Sklenicka, 2006).

Land consolidation represents an efficient instrument for agricultural development helping farmers to have less, bigger, better shaped parcels and proposes measures to adjust terrain parcel configuration (Akdemir et al., 2024). Land consolidation is designed to counteract the effect of land fragmentation, but its purpose goes further, involving complex social and economic reforms (FAO, 2007). Land consolidation is applied in the case of disparate parcels and represents a repositioning of the spatial location of the private ownership in order to form new land ownership that contain one or as less parcels possible with the same or higher value than the initial ones (FAO, 2007). In this process no owner should lose (Oldenburg, 1990). In a European context, land consolidation consists in "rearrangement and/or putting together of different, distributed

plots; removal of terraces and defiles; construction of rural roads; restructuring of local streams; and soil improvement" (Bronstert et al., 1995). However, in many countries, land consolidation has remained oriented to agriculture. This can be seen mostly in countries in Eastern Europe and East Asia where land consolidation is more concerned with the agricultural aspects of the process than with land improvements (Gorgan & Bavorova, 2022).

For (Louwsma et al., 2022) there are four types of land consolidation:

- Voluntary land exchange. It is the simplest type of land consolidation and implies voluntary exchanges of parcels between owners. The size and shape of parcels hardly change.
- Voluntary land consolidation. It is also based on the voluntary participation of the people but has a more systematic approach and it is coordinated by the authority. Improvements may be done on a small scale.
- Majority based land consolidation. It is based on the consent of the majority of the landowners and is done in a systematic way. Medium to large scale improvements is possible.
- Mandatory land consolidation. Land consolidation is decided by a public authority. Besides the redistribution of parcels there are a lot of improvements that are implemented.

In short, the process of land consolidation consists of the following steps (FAO, 2003; FAO, 2007):

- Initiation of the land consolidation project.
- Design of the project or the feasibility study in which the cost-benefit analysis is conducted, and the area is chosen.
- Inventory of the existing situation in which the legal rights for every parcel must be determined and an evaluation of land is conducted.
- Elaboration of the land consolidation plan in which the preferences of the owners are considered, and the parcels are relocated and reallocated in accordance with the evaluation conditions.
- Implementation of the land consolidation plan.
- Concluding phase in which the cadastral map is actualized with the new formed parcels, the owners are compensated for eventual loses and the new legal situation is established.

For the process of land consolidation to be applied with success, the cadastral situation of all land in the area must be clear. Information in the land administration system is diverse and can contain data concerning: the ownership, the location of parcels, the legal status of the parcels, land use and other data (Constantin et al., 2015). Without it, it is very difficult to apply the land consolidation process.

3. Evaluation of parcels in the land consolidation process

The process of land consolidation needs to have a type of land evaluation. There are two types of land evaluation that can be applied (Demetriou, 2016):

- Evaluation that reflects land productivity and soil quality that can be expressed in a form of a score for every parcel.
- Land market evaluation that is done to find out the monetary value of every parcel according to the traditional evaluation standardized methods.

In land consolidation, market-based valuation is often less relevant, as farmers tend to prioritize agricultural productivity over potential sale value. Consequently, Van Dijk (2003) considers agricultural output and soil quality as the key evaluation factors. However, Demetriou (2014) notes that these criteria are applicable mainly in extra-urban areas where construction is prohibited. Several factors are considered when assessing agricultural productivity for land consolidation, each assigned a specific weight. The weighted scores are summed to determine the overall value of each parcel. For Wyatt (1996) factors can be of four types: physical, legal, locational and economic. Branković et al. (2015) indicate that land evaluation in Serbian land consolidation projects considers soil fertility, climate conditions, and economic factors, while Tezcan et al. (2018) propose a broader approach with at least 14 evaluation factors (Table 1).

Table 1. Factors of land evaluation proposed by several authors

Demetriou, 2018	Tezcan et al., 2020	Ertunç & Uyan, 2022	Asiama et al., 2018	Ertunç et al., 2021	Wyatt, 1996
Factors of evaluation	Factors of evaluation	Factors of evaluation	Factors of evaluation	Factors of evaluation	Factors of evaluation
Size of the parcel	Parcel area	Area of parcel	Land tenure	Size of parcels	Size of the parcel
Shape of the parcel	Parcel share situation	Shape of the parcel	Proximity to town square	Soil fertility	Shape of the parcel
Slope of the parcel	Parcels adjacent to agricultural areas	Share statue of parcel	Road access	Slope	Slope
Elevation	Existing land use	Soil fertility of the parcel	Soil quality	Market value of the parcel	Elevation
Aspect	Fixed facility	Distance of the parcel from the village centre	Parcel shape	Distance to village centre	Land tenure
Stream	Zoning situation of agricultural area	Distance of the parcel to the road	Proximity to main road	Distance to water source	Soil type
Soil type	Distance to the district centre	Distance of the parcel to the water source	Slope	Distance to main road	Soil quality
Access (through different kind of roads)	Distance to a highway	Economic value of the parcel	Land use	Accessibility to main road	Distance to main road
Distance from the main road to the motorway	Availability of agricultural drainage system	-	Soil type	Parcels near the river edge	Distance to town square
Land use	Distance to natural resources	-	Elevation	-	Access to national/regional road
Irrigation	Availability of electrical power	-	-	-	Access feeder roads
Sea view	Proximity to forest	-	-	-	Access to other roads
Distance from residential zone	Presence of historical resources	-	-	-	Land use
	Status of state support	-	-	-	-

Each evaluation factor is assigned a score, and the sum of these scores determines the parcel's overall value in the land consolidation process. These scores are typically weighted based on the relative importance of each factor, with weights ranging from 0 to 1 or 0 to 10. While some researchers, like Zhou et al. (2017), emphasize soil quality, others prioritize factors such as area or shape. Alternatively, Asiama et al. (2018) suggest that equal weights can be used or adjusted based on landowners' preferences.

MATERIALS AND METHODS

1. Paradigm of research

Researchers generally operate within two main paradigms. The **positivist paradigm** views reality as objective and measurable through scientific methods (Park et al., 2020; Kaboub, 2008), aiming for objectivity and broad generalization (Firestone, 1987). In contrast, the **constructivist paradigm** sees reality as socially constructed, shaped by individuals' experiences, interpretations, and contextual influences (Adom et al., 2016; Alharahsheh & Pius, 2020).

This study, focused on land evaluation in the land consolidation process in the Saschiz administrative unit, adopts a predominantly constructivist approach. While it incorporates statistical methods aligned with positivism, the overall perspective reflects constructivist principles. These paradigms are not mutually exclusive but rather represent ends of a methodological spectrum, allowing researchers to draw from both as needed to explore complex realities (Morgan & Smircich, 1980).

2. Methodology and methods

Given the limited coverage of this research area in Romanian literature, legislation, and practice, the study adopts an exploratory approach, drawing on both positivist and constructivist paradigms. The methodology is predominantly qualitative and is structured as a case study focusing on a real-world context (Yin, 2009; Anderson, 1993). The study analyzes 766 parcels located in the Saschiz administrative unit, Mureș County, Romania. As such, the findings are context-specific and not intended for generalization.

The first method employed was content analysis, which involved a critical review of literature on land evaluation in consolidation processes, recognizing that texts are shaped by their social and contextual background. Content analysis, defined as "a method of analysing written, verbal or visual communication messages" (Cole, 1988), allows for categorizing terms or phrases with shared meanings (Cavanagh, 1997). From this analysis, a framework of evaluation factors relevant to the study area was developed.

In addition, statistical methods were used to assess each land evaluation factor - parcel shape, size, location, road accessibility, slope, flood risk, legal restrictions, irrigation, and soil quality - with results expressed in percentages and scores. Two software tools supported the analysis: "Reparcelare", developed specifically for land consolidation projects, and Global Mapper 18.1, a GIS application. These tools were used to calculate scores for each factor, as detailed in Table 2.

Table 2. The data use for calculating each factor

Factor	Application used	Data used	Explanation
Shape of the parcel	Reparcelare	Secondary data: data existent in the cadastral database	The application "Reparcelare" calculated automatically the score of each parcel based on the number of sides and the preset intervals
Surface of the parcel	Reparcelare	Secondary data: data existent in the cadastral database	The application "Reparcelare" calculated automatically the score of each parcel based on the preset surface intervals
Location of the parcel	Reparcelare	Secondary data: cadastral geodatabase with the location of each parcel	The application "Reparcelare" calculated automatically the distance to every parcel and calculated the score according to preset intervals
Accessibility to roads	Reparcelare	Secondary data: the location of the roads and the parcels from the cadastral geodatabase	"Reparcelare" calculated automatically the surface of road that the parcel has access to
Slope	Global Mapper Reparcelare	Primary data: Digital Terrain Model from aerial pictures. Secondary data: position of the parcel from the cadastral geodatabase	From the DTM, slopes were calculated automatically in Global Mapper for every parcel. The values of slope were introduced in application "Reparcelare" and intervals were preseted. The application calculated the score for every parcel
Legal restrictions	Reparcelare	Secondary data: textual data from the cadastral database	The application "Reparcelare" calculates automatically the score based on the type of restrictions
Irrigation	-	There is no data concerning irrigation in the area	-
Flood risk	Global Mapper Reparcealare	Primary data: DTM from aerial pictures Secondary data: historic data concerning the level of water overflow position of the parcel from the cadastral geodatabase	Based on the DTM an overflow of water was simulated to see the parcels that are affected by flood. Depending on this risk, intervals were preset in the application "Reparcelare" and the score was automatically calculated
Soil quality	Global Mapper Reparcelare	Secondary data: Pedologic map of the area georeferenced in Glaobal Mapper The values representing soil quality were introduced in "Reparcelare" application that calculates the score for each parcel	

3. Limitations

The premise of the study was that this was a voluntary land consolidation process in which all the owners agree with the project proposed and no litigations regarding the use of land exists. In practice, situations of conflict may arise. These situations were not considered for this study.

There are limitations concerning the use of research paradigms. Constructivist's methods and methodologies have a high degree of reliability, but they cannot be generalized. The lack of generalization has led authors like (Liu & Matthews, 2005) to affirm that "where no absolute truth, any truth exists is good as the other". However, the constructivism paradigm compensates with a high degree of reliability because of the small samples used. The findings are restricted only to that case and cannot be generalized.

There is no legislation in Romania concerning land consolidation. In this study, no legal obstacles were considered in the process of land evaluation for the land consolidation process. In the eventuality of such evaluation in practice, the legislation, if existent, must be considered.

RESULTS AND DISCUSSIONS

1. Evaluation factors

Taking into consideration Table 1, it can be observed that there are several features that are common for most authors in designing any process of land evaluation for the land consolidation process. Distance and access to roads are the most common conditions that appear, the transport of agricultural goods being an important factor for farmers. Size or area of the parcel is another important feature appearing in four different instances as well as land use, soil quality, slope, access to water sources or the existence of irrigation systems and the legal situation of the parcel. Another aspect that appears three times in Table 1 is the shape of the parcel. One of the purposes of the land consolidation process is to have better shaped parcels.

Considering the literature studied, the factors considered for land evaluation for the land consolidation process for this study were: shape of the parcel, surface of the parcel, location of the parcel, accessibility to the parcel, slope, irrigation and soil quality. However, the evaluation procedure must consider specificities to the area in which are applied. Romania has been confronted with floods on large surfaces that brought considerable damage to the agricultural sector and loss of life. There are parcels that are in the flood risk areas and that can decrease their value for the land consolidation process. That is why; the flood risk factor is introduced in the list for land evaluation for land consolidation purposes.

Although land tenure is commonly cited by many authors, it was not considered in this study. The research is based on the assumption that land consolidation in the area was voluntary, with all landowners consenting to participate - even in cases of shared ownership. Instead, legal restrictions, like areas that cannot benefit from improvements of are under legal constrains from exchanging or selling the land were considered. Therefore, the factor legal restrictions were introduced for this study.

The weight assigned for each factor can be express in percentages or from values from 0 to 1. There can be different weights, or all factors can have the same weight. For this study the same weight was assigned for each factor (Table 3).

Table 3. Weights assigned for each factor

Factor	Weight %
Shape of the parcel	11.11
Surface of the parcel	11.11
Location of the parcel	11.11
Accessibility to roads	11.11
Slope of the land	11.11
Flood risk	11.11
Legal restrictions	11.11
Irrigation	11.11
Soil quality	11.11

2. Application of land evaluation factors in the study area

The administrative unit of Saschiz, where the case study takes place, is situated in Mures County in Romania. The area chosen for the case study comprises 766 parcels.

Shape. The ideal parcel has four sides. These are the parcels that received the highest score. For every extra side, the score of the parcel was

reduced. In Table 4 it can be observed that under 1% of the parcels have an ideal shape and got the highest score, while most of the parcels have between 5 and 7 sides.

Table 4. Score for the factor shape

Number of sides	Score	Number of parcels	Percentage
4	10	2	0.26
5	9	374	48.82
6	8	149	19.46
7	7	83	10.84
8	6	52	6.79
9	5	30	3.92
10	4	28	3.65
11	3	14	1.83
12	2	15	1.96
13	1	11	1.44
>13	0	8	1.04

Surface. Saschiz administrative unit is situated in a hilly area. The ideal surface for a parcel in this area is between 20 and 50 hectares (Paunescu et al., 2024). However, the average surface that a parcel has in Saschiz is 4063 square meters. Considering this specificity of the area of study, 10 intervals of 5000 square meters was considered. For every 5000 square meters the parcels were awarded 1 score point extra compared to the previous interval. From Table 5 can be observed that large sized parcels are under 1% in the studied area, while small size parcels are the vast majority. This is not a surprise, as land consolidation is applied exactly to counteract land fragmentation and obtain larger, better shaped parcels.

Table 5. Score for the factor surface

Interval (hectares)	Score	Number of parcels	Percentage
>5.18	10	1	0.13
4.67-5.17	9	1	0.13
4.16-4.66	8	0	0
3.65-4.15	7	0	0
3.14-3.64	6	0	0
2.63-3.13	5	0	0
2.12-2.62	4	3	0.39
1.61-2.11	3	14	1.83
1.01-1.6	2	58	7.57
0.5-1	1	162	21.15
0.5 <	0	527	68.80

Location. As it can be seen in Table 6, the distance from the parcel to the village or district centre is well documented. However, more important for agricultural products is the distance to the processing or storage facilities. A point was placed, that represents the point of collection for agricultural products, outside of the study zone (Figure 1). In "Reparcelare" software, the shortest distance was calculated from the point of collection to the closest point of the parcel. The distance is calculated by application by simulating the shortest route on existent roads. The longest calculated distance is 5100.01 meters, while the shortest distance is 1297.23 meters. The shortest distance was deducted from the longest distance and the difference was split into ten intervals as in Table 6. It can be observed that the score of the parcels for this factor is dispersed in a more homogenous manner, in comparison with other factors.



Figure 1. The study area as seen in "Reparcelare" application

Table 6. Score for the factor location

Interval (meters)	Score	Number of parcels	Percentage
380.278<	10	1	0.13
380.278-760.556	9	33	4.31
760.556-1140.834	8	48	6.27
1140.834-1521.112	7	76	9.92
1521.112-1901.31	6	138	18.02
1901.31-2281.668	5	112	14.62
2281.668-2661.946	4	92	12.01
2661.946-3042.224	3	137	17.89
3042.224-3422.502	2	112	14.62
3422.502-3802.78	1	17	2.22
>3802.78	0	0	0

Accessibility. This factor is linked with the access that a parcel has to a road. The highest scores were attributed to the parcels that have the longest distance that overlaps the limit of

the parcel with a road. If the parcel is bordered by more than one road, then the sum of the distances that overlap the parcel was calculated (Table 7).

Table 7. Score for the factor accessibility

Score	Number of parcels	Percentage
10	0	0
9	3	0.39
8	0	0
7	1	0.13
6	4	0.52
5	25	3.26
4	21	2.74
3	19	2.48
2	39	5.09
1	615	80.29
0	39	5.09

Slope. Slope was determined using a digital terrain model obtained from aerial images. To calculate the score, in "Reparcelare" software were introduced the average maximum slope, that is 32.40%, and the average minimum slope which is 1.41%. The difference between the two values was divided into ten intervals. The highest score was awarded to the parcels with the minimum slope. It can be observed from Table 8 that most parcels are in the hilly area with slopes from 0.01 to 6.5 percent.

Table 8. Score for the factor slope

Interval	Score	Number of parcels	Percentage
0	10	0	0
0.01-3.24	9	183	23.89
3.25-6.49	8	231	30.16
6.5-9.74	7	196	25.59
9.75-12.99	6	71	9.27
13-16.24	5	25	3.26
16.25-19.49	4	40	5.22
19.5-22.74	3	18	2.35
22.75-25.99	2	1	0.13
26-29.24	1	1	0.13
29.25-32.40	0	0	0

Flood risk. To assess the risk of flooding for parcels a risk map for the river Scroafa that runs through Saschiz was used. This was done by taking the historic data concerning the level of the water overflow. A simulation was performed in the GIS software Global Mapper in order to see the parcels that can be affected by the overflow (Figure 2).

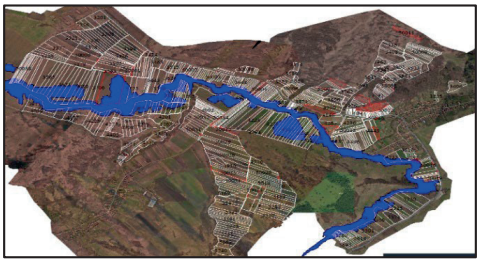


Figure 2. Overflow of the water in the study area as seen in Global Mapper application

The parcels that were least affected received the highest score. Taking into consideration 10 intervals from 0% flood affected parcel and 100% the scores were calculated as in Table 9. It can be observed that most of the parcels are in the safe area.

Table 9. Score for the factor flood risk

Interval (%)	Score	Number of parcels	Percentage (%)
0	10	571	74.54
1-9	9	52	6.79
10-19	8	50	6.53
20-29	7	27	3.52
30-39	6	20	2.61
40.-49	5	22	2.87
50-59	4	5	0.65
60-69	3	5	0.65
70-79	2	10	1.31
80-89	1	3	0.39
90-100	0	1	0.13

Legal restrictions. The legal restrictions considered were the legal impossibility to improve tha land, exchange or sell it. There were no legal restrictions in the study area of such, so all the parcels received the highest score.

Irrigation. There were no irrigation improvements in the area of study. That is why all the parcels received no points for this factor.

Soil quality. The soil quality is assessed using a system of points that takes into consideration a coefficient based on 17 indicators (Musat, 2014). These coefficients are written on pedologic maps. For this study the map for the study area was used. The map was georeferenced in the Global Mapper GIS application and a layer containing the geometry of the parcels was placed above (Figure 3).

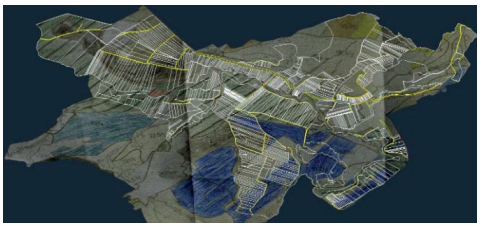


Figure 3. Parcels in the study area overlap on the pedologic map as seen in Global Mapper application

The highest soil quality score is 71.9, while the lowest soil quality score is 14.1. The difference was divided in 10 equal intervals and the score for soil quality was awarded as in Table 10.

Table 10. Score for the factor soil quality

Interval	Score	Number of parcels	Percentage
>72.68	10	50	6.53
66.18-72.68	9	27	3.52
59.67-66.17	8	2	0.26
53.16-59.66	7	2	0.26
46.65-53.15	6	20	2.61
40.14-46.64	5	13	1.70
33.63-40.13	4	16	2.09
27.12-33.62	3	151	19.71
20.61-27.11	2	148	19.32
14.1-20.6	1	335	43.73
<14.1	0	2	0.26

Based on all these factors, by applying the weights, the application "Reparcelare" calculates the score of every parcel that can be seen in the right corner of Figure 4.

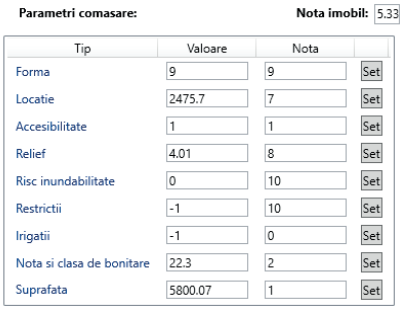


Figure 4. Example of score for one parcel as seen in "Reparcelare" application

Parcels are ranked from highest to lowest based on their total scores. Each owner's cumulative score, calculated by summing the values of all their parcels, determines their position in the reallocation and relocation phase of the land consolidation process (Figure 5).

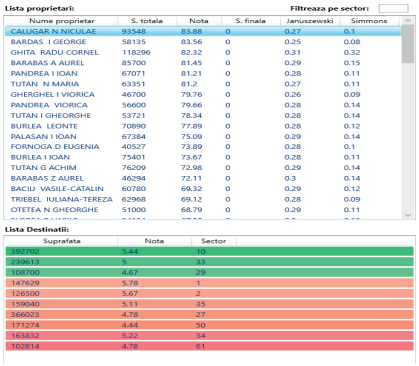


Figure 5. Classification of owners based on the added score of their parcels as seen in "Reparcelare" application

CONCLUSIONS

This research studies the existent literature concerning land evaluation for land consolidation processes. Based on conditions for evaluation determined by other researchers, this study proposes a series of factor for land evaluation that can be applied for a land consolidation project in Romania. These factors are adapted to the specificities of Romania and tested, with real data, in Saschiz administrative unit in Romania.

The factors that are used for land evaluation are: shape of the parcel, surface of the parcel, location of the parcel, accessibility to the roads, slope, legal restrictions, irrigations, flood risk, soil quality. The score is weighted with the same percentage and a score for each parcel is obtained. The results show that these factors can be applied to the study area, and, with the use of software applications and real data, the parcels can be evaluated for land consolidation purposes.

This study complements the studies conducted by (Demetriou, 2018; Tezcan et al., 2020; Ertunç & Uyan, 2022; Asiama et al., 2018; Ertunç, et al., 2021; Wyatt, 1996) and introduces two new factors that are specific to the study area: legal restrictions and flood risk.

The findings in this research can help Romanian researchers and policy makers to:

- Have a framework for land evaluation for land consolidation purposes;

- Design legislation for land consolidation;
- Complement these factors with other, more specific to the country in which land consolidation is applied.

These factors for land evaluation have taken into consideration the area studied and specificities of it and of the country. However, land consolidation is a multidisciplinary process in which are involved: land surveyors, agronomists, infrastructure engineers, landscapers or legal professional. All these professions can contribute to develop more appropriate factors that can be use in practice.

Future research can concentrate on applying these factors in more study cases and reevaluate these factors. Legislation design for land consolidation purposes is needed. Future research can also cover the topic of designing and testing of land consolidation application software that not just evaluate land but also help in the process of reallocating and relocating land parcels for land consolidation.

REFERENCES

Adom, D., Yeboah, A., & Ankrah, A. K. (2016). Constructivism philosophical paradigm: Implication for research, teaching and learning. *Global Journal of Arts, Humanities and Social Sciences*, *4*(10), 1–9.

Agarwal, B. (2010). Rethinking agricultural production collectivities. *Economic and Political Weekly*, *45*(50), 64–78.

Akdemir, Ş., Gultekin, U., Tuna, K. E., & Ismailla, I. S. (2024). Effects of land consolidation on agricultural enterprises in Cihanbeyli District, Türkiye: An evaluation from the producer perspective. *Scientific Papers Series Management, Economic Engineering in Agriculture & Rural Development*, *24*(2), 51–62.

Alharahsheh, H. H., & Pius, A. (2020). A review of key paradigms: Positivism vs. interpretivism. *Global Academic Journal of Humanities and Social Sciences*, *2*(3), 39–43.

Anderson, G. (1993). *Fundamentals of educational research*. Falmer Press.

Asiama, K. O., Bennett, R., Zevenbergen, J., & Asiama, S. O. (2018). Land valuation in support of responsible land consolidation on Ghana's rural customary lands. *Survey Review*, *50*(361), 288–300.

Bezus, R., & Samofal, O. (2019). Challenges of small-scale farming in Ukraine. *AgroLife Scientific Journal*, *8*(1), 35–42.

Blenesi-Dima, A. (2010). Some aspects regarding the necessity of implementing the agricultural land consolidation projects in Romania. *Research Journal of Agricultural Science*, *42*(3), 432–437.

Branković, S., Parezanović, L., & Simović, D. (2015). Land consolidation appraisal of agricultural land in the GIS environment. *Geodetski Vestnik*, *59*(2), 260–273.

Bronstert, A., Vollmer, S., & Ihringer, J. (1995). A review of the impact of land consolidation on runoff production and flooding in Germany. *Physics and Chemistry of the Earth*, *20*(3-4), 321–329.

Cavanagh, S. (1997). Content analysis: Concepts, methods and applications. *Nurse Researcher*, *4*(3), 5–16.

Chigbu, U. E., & Kalashyan, V. (2015). Land-use planning and public administration in Bavaria, Germany: Towards a public administration approach to land-use planning. *Geomatics, Landmanagement and Landscape*, *2*(1), 27–36.

Ciobanu, L. (2021). An overview of the efforts and initiatives towards land consolidation in Romanian agriculture. *Annals of "Constantin Brancusi" University of Targu-Jiu, Economy Series*, *6*, 30–36.

Cole, F. L. (1988). Content analysis: Process and application. *Clinical Nurse Specialist*, *2*(1), 53–57.

Coman, M., Cioruta, B., & Pop, R. (2016). Regarding the evolution of soils polluted with oil products in Săcel oilfield, Romania. *AgroLife Scientific Journal*, *5*(2), 44–49.

Constantin, M. C., Beatrice, V. C., & Maria, M. A. (2015). Systematic registration of properties - a new challenge for Romanian cadastral system. *Journal of Geodesy, Cartography and Cadaster*, *1*(1), 15–20.

Delgado, C. L. (1998). Sources of growth in smallholder agriculture in Sub-Saharan Africa: The role of vertical integration of smallholders with processors and marketers of high value-added items. *Agrekon*, *38* (Special Issue), 165–189.

Demetriou, D. (2014). *The development of an integrated planning and decision support system (IPDSS) for land consolidation*. Springer.

Demetriou, D. (2016, June). GIS-based automated valuation models (AVMs) for land consolidation schemes. In *6th International Conference on Cartography and GIS* (pp. 13–20). Albena, Bulgaria.

Demetriou, D. (2016). The assessment of land valuation in land consolidation schemes: The need for a new land valuation framework. *Land Use Policy*, *54*, 487–498.

Demetriou, D. (2018). Automating the land valuation process carried out in land consolidation schemes. *Land Use Policy*, *75*, 21–32.

Di Falco, S., Penov, I., Aleksiev, A., & Van Rensburg, T. M. (2010). Agrobiodiversity, farm profits and land fragmentation: Evidence from Bulgaria. *Land Use Policy*, *27*(3), 763–771. https://doi.org/10.1016/j.landusepol.2009.10.007

Dima, A. B., Magureanu, I., & Zaharia, V. (2007). *Romania: Country report*. Food and Agriculture Organization of the United Nations. https://www.fao.org/fileadmin/user_upload/reu/europe/documents/LANDNET/2007/Romania.pdf

Ertunç, E., Karkınlı, A. E., & Bozdağ, A. (2021). A clustering-based approach to land valuation in land consolidation projects. *Land Use Policy*, *111*, 105739. https://doi.org/10.1016/j.landusepol.2021.105739

Ertunç, E., & Uyan, M. (2022). Land valuation with Best Worst Method in land consolidation projects. *Land*

Use Policy, *122*, 106360. https://doi.org/10.1016/j.landusepol.2022.106360

Eurostat. (2022). *Farms and farmland in the European Union – statistics*. https://ec.europa.eu/eurostat/statistics-explained/index.php?title=Farms_and_farmland_in_the_European_Union_-_statistics#Farms_in_2020

FAO (2003). *FAO land tenure studies: The design of land consolidation pilot projects in Central and Eastern Europe*. Food and Agriculture Organization of the United Nations.

FAO (2007). *Operations manual for land consolidation pilot projects in Central and Eastern Europe*. Food and Agriculture Organization of the United Nations.

Firestone, W. A. (1987). Meaning in method: The rhetoric of quantitative and qualitative research. *Educational Researcher*, *16*(7), 16–21.

Gorgan, M., & Bavorova, M. (2022). How to increase landowners' participation in land consolidation: Evidence from North Macedonia. *Land Use Policy*, *123*, 106424. https://doi.org/10.1016/j.landusepol.2022.106424

Hartvigsen, M. (2014). Land reform and land fragmentation in Central and Eastern Europe. *Land Use Policy*, *36*, 330–341.

Hartvigsen, M. B. (2015). *Experiences with land consolidation and land banking in Central and Eastern Europe after 1989* (FAO Land Tenure Working Paper No. 26). Food and Agriculture Organization of the United Nations.

Kaboub, F. (2008). Positivist paradigm. In F. T. L. Leong (Ed.), *Encyclopedia of Counseling* (Vol. 2, p. 343). SAGE Publications.

Latruffe, L., & Piet, L. (2014). Does land fragmentation affect farm performance? A case study from Brittany, France. *Agricultural Systems*, *129*, 68–80. https://doi.org/10.1016/j.agsy.2014.05.005

Liu, C. H., & Matthews, R. (2005). Vygotsky's philosophy: Constructivism and its criticisms examined. *International Education Journal*, *6*(3), 386–399.

Louwsma, M., Vries, W., & Hartvigsen, M. (2022). *Land consolidation - The fundamentals to guide practice*. International Federation of Surveyors (FIG).

Mert, A., Akdemir, Ş., & Önen, D. (2023). Evaluation of land consolidation works in terms of legal results: The case of Adana Province, Türkiye. *Scientific Papers Series Management, Economic Engineering in Agriculture & Rural Development*, *23*(2), 471–486.

Mihailescu, D., & Cîmpeanu, S. M. (2019). Multi-temporal analysis of land cover changes in Oltenia Plain, using TerrSet Land Change Modeler. *AgroLife Scientific Journal*, *8*(2), 82–91.

Morgan, G., & Smircich, L. (1980). The case for qualitative research. *Academy of Management Review*, *5*(4), 491–500.

Moteva, M. (2016). Agricultural land-use planning and the role of the state. *AgroLife Scientific Journal*, *5*(1), 144–149.

Mușat, C. (2014). *Cadastru. Note de curs*. Universitatea Politehnica Timișoara.

Nsabimana, A., Adom, P. K., Mukamugema, A., & Ngabitsinze, J. C. (2023). The short and long run effects of land use consolidation programme on farm input uptakes: Evidence from Rwanda. *Land Use Policy*, *132*, 106787. https://doi.org/10.1016/j.landusepol.2023.106787

Ntihinyurwa, P. D., de Vries, W. T., Chigbu, U. E., & Dukwiyimpuhwe, P. A. (2019). The positive impacts of farm land fragmentation in Rwanda. *Land Use Policy*, *81*, 565–581.

Oldenburg, P. (1990). Land consolidation as land reform in India. *World Development*, *18*(2), 183–195.

Park, Y. S., Konge, L., & Artino, A. R., Jr. (2020). The positivism paradigm of research. *Academic Medicine*, *95*(5), 690–694. https://doi.org/10.1097/ACM.0000000000003093

Păunescu, V., Popescu, C., Lupașcu, D., & Popa, D. (2024). Theoretical aspects for designing a land consolidation software. *Bulletin of University of Agricultural Sciences and Veterinary Medicine Cluj-Napoca. Forestry and Cadastre*, *81*(1), 1–7.

Păunescu, V., Popescu, C., Mihalache, E., & Ștefan, M. (2024). An analysis of strategic goals and public procurement strategy regarding the implementation of the National Program for Land Registration in Romania. *Land Use Policy*, *146*, 107334. https://doi.org/10.1016/j.landusepol.2024.107334

Rashidpour, L., & Azar, S. R. (2016). Analysis of the barriers leading to failure of land consolidation of the fields. *Scientific Papers Series Management, Economic Engineering in Agriculture & Rural Development*, *16*(3), 285–292.

Ruben, R., & Lerman, Z. (2005). Why Nicaraguan peasants stay in agricultural production cooperatives. *Revista Europea de Estudios Latinoamericanos y del Caribe / European Review of Latin American and Caribbean Studies*, *(79)*, 31–47.

Rusu, M., Florian, V., Lile, R., & Rusu, C. (2002). Land fragmentation and land consolidation in the agricultural sector. In *International Symposium on Land Fragmentation and Land Consolidation in CEEC: A Gate Towards Sustainable Rural Development in the New Millennium*. Munich, Germany.

Sabates-Wheeler, R. (2002). Consolidation initiatives after land reform: Responses to multiple dimensions of land fragmentation in Eastern European agriculture. *Journal of International Development*, *14*(7), 1005–1018.

Sabates-Wheeler, R. (2005). *Cooperation in the Romanian countryside: An insight into post-soviet agriculture*. Lexington Books.

Sklenicka, P. (2006). Applying evaluation criteria for the land consolidation effect to three contrasting study areas in the Czech Republic. *Land Use Policy*, *23*(4), 502–510. https://doi.org/10.1016/j.landusepol.2005.03.001

Șuba, E. E., Roșca, I., Pușcă, I., & Ștefan, M. (2019). Creating the cartographic database and informatization of the systematic cadastre works process. *Bulletin USAMV Horticulture*, *76*(1), 114–119.

Teshome, A., de Graaff, J., Ritsema, C., & Kassie, M. (2016). Farmers' perceptions about the influence of land quality, land fragmentation and tenure systems

on sustainable land management in the north western Ethiopian highlands. *Land Degradation & Development*, *27*(4), 884–898. https://doi.org/10.1002/ldr.2298

Tezcan, A., Büyüktaş, K., & Aslan, Ş. A. (2018). Determination of parcel value number with detailed method in the land consolidation. *Asian Research Journal of Agriculture*, *9*(2), 1–10. https://doi.org/10.9734/ARJA/2018/40142

Tezcan, A., Büyüktaş, K., & Aslan, Ş. T. A. (2020). A multi-criteria model for land valuation in the land consolidation. *Land Use Policy*, *95*, 104572.

Van Dijk, T. (2003). *Dealing with Central European land fragmentation: A critical assessment on the use of Western European instruments* (Doctoral dissertation). Wageningen University.

Van Dijk, T. (2003). Scenarios of Central European land fragmentation. *Land Use Policy*, *20*(2), 149–158.

Van Dijk, T. (2005). The dangers of transplanting planning instruments: The case of land fragmentation in Central Europe. *European Journal of Spatial Development*, *16*, 1–21.

Van Holst, F., Hartvigsen, M., & Ónega López, F. (2018). Land governance for development in Central and Eastern Europe: Land fragmentation and land consolidation as part of Sustainable Development Goals. In *World Bank Land and Poverty Conference*. Washington, D.C.

Van Hung, P., MacAulay, T. G., & Marsh, S. P. (2007). The economics of land fragmentation in the north of Vietnam. *Australian Journal of Agricultural and Resource Economics*, *51*(2), 195–211.

Veršinskas, T., Sudonienė, V., Hartvigsen, M., & Beinarovičа, A. (2020). *Legal guide on land consolidation: Based on regulatory practices in Europe*. Food and Agriculture Organization of the United Nations.

Wyatt, P. (1996). The development of a property information system for valuation using a geographical information system (GIS). *Journal of Property Research*, *13*(4), 317–336.

Yin, R. K. (2009). *Case study research: Design and methods* (4th ed.). SAGE Publications.

Zhou, J., Qin, X., Liu, L., & Hu, Y. (2017). A potential evaluation model for land consolidation in fragmental regions. *Ecological Indicators*, *74*, 230–240.

Scientific Papers. Series E. Land Reclamation, Earth Observation & Surveying, Environmental Engineering. Vol. XIV, 2025
Print ISSN 2285-6064, CD-ROM ISSN 2285-6072, Online ISSN 2393-5138, ISSN-L 2285-6064

INVESTIGATION BETWEEN VEGETATION INDICES, METEOROLOGICAL DATA AND PHENOLOGY OF WINE GRAPE VARIETIES

Anelia POPOVA, Zhulieta ARNAUDOVA

Agricultural University of Plovdiv, 12 Mendeleev Blvd, 4000, Plovdiv, Bulgaria

Corresponding author email: aneliyapopova@abv.bg

Abstract

The successful cultivation of vines must be aware of the phenological phases during the growing season. However, conventional phenological measurements on the ground are limited due to their spatial coverage. The use of Sentinel-2 imagery has led to an increased interest in its application to viticulture, with the data providing access to global spatial coverage and the potential for high temporal resolution. The present study was conducted during the period 2021-2022 in the experimental vineyard of the Agricultural University of Plovdiv, with the aim of studying the phenological phases of the wine grape varieties Merlot, Mavrud and Chardonnay. The results will enhance the interpretation of the spatiotemporal dynamics between meteorological data, vegetation indices (Normalized Difference Vegetation Index Normalized Difference Vegetation Index - NDVI), and phenological stages in vine cultivation. This study highlights the effectiveness of remote sensing for monitoring vineyard phenology, both retrospectively and in real time, as a valuable tool for maintaining high-quality standards in precision viticulture.

Key words*: Grape varieties, meteorological data, NDVI, phenological stages.*

INTRODUCTION

Climate is a key factor in enabling plants to complete their vegetative and productive cycles, directly influencing the timing and duration of the main phenological stages (Dalla Marta et al., 2010). The influence of air temperature on grapevine development and the timing of growth phases has been well-documented in numerous studies (Chuine et al., 2013; De Cortázar-Atauri et al., 2009; Parker et al., 2011; 2013; 2020). Network analyses of meteorological stations have been used to characterize temperature variability on regional scales (Bois, 2007; Cuccia, 2013; Madelin & Beltrando, 2005). In the context of global climate change, growers must adapt to the spatial variability of temperature and its temporal evolution. There is broad scientific consensus that the climate is changing (IPCC, 2013). The recent rise in temperatures has already impacted grapevine development, particularly by accelerating the timing of phenological phases (Bock et al., 2011; Duchêne et al., 2012; Tomasi et al., 2011; van Leeuwen et al., 2019). According to Cunha et al. (2010), conducting phenological observations in vineyards is essential for improving the ecological adaptability of grape varieties, as well as for effective crop management and modeling. Traditionally, these observations are made on the ground, offering localized insights but limited spatial coverage and temporal frequency. In contrast, time-series satellite imagery provides a fast and objective view of grapevine dynamics, enhancing vineyard management. Integrating ground-based phenology observations with the temporal profiles of the Normalized Difference Vegetation Index (NDVI), as captured by the SPOT VEGETATION sensor, is particularly useful for regional, inter-annual vineyard monitoring. Earth observation data and NDVI are vital tools for assessing vineyard vegetation health (Pastonchi et al., 2020), while also enabling efficient and accurate data collection in remote areas (Krishna, 2017). The use of vegetation indices (VIs) is a practical approach for applying remote sensing in viticulture, relying on spectral information to assess vine development and yield (Hall et al., 2002; Arnaudova & Stalev, 2024). Remote sensing technologies - such as UAVs, airborne sensors, and satellite imagery - are among the most employed methods for vineyard monitoring (Hall et al., 2002; Matese & Di Gennaro,

2015). UAVs equipped with multispectral sensors, along with radar measurements, provide high-resolution imagery that enables the extraction of various types of information about vineyards (Pichon et al., 2019). However, the high cost of this equipment can limit the spatial coverage needed for generating reliable results (Candiago et al., 2015).

Satellites are more time-efficient and cost-effective for monitoring large areas, but they are less adaptable to growers' needs due to limitations in revisit frequency and spatial resolution (Sozzi et al., 2019). In recent years, the availability of free satellite data - such as that provided by the Copernicus program through the European Space Agency (ESA)'s Sentinel-2 mission - has sparked increased interest in its application to viticulture. Studies have demonstrated that Sentinel-2 imagery can support regional vineyard management by extracting agricultural information and quantifying drought impacts (Devaux et al., 2019; Cogato et al., 2019). The use of geographic information systems (GIS) enhances image acquisition and processing for vegetation indices such as the Normalized Difference Vegetation Index (NDVI) and the Green Normalized Difference Vegetation Index (GNDVI). A geoprocessing approach further integrates environmental parameters - such as rainfall, temperature and soil moisture - as key variables (Jesus et al., 2020).

The objective of this study was to explore the relationship between vegetation indices derived from Earth observation and climatic data, and the phenology of wine grape varieties measured in situ.

MATERIALS AND METHODS

Study area

The experiment was conducted on the experimental training field of the Agricultural University, located in the town of Kuklen, Plovdiv District, in Central-Southern Bulgaria (Figure 1).

In situ measurements

The study was conducted in the experimental vineyard of the Agricultural University of Plovdiv, situated near the town of Kuklen, on the border with the village of Brestnik, in Rodopi Municipality. The vineyard is in full fruit-bearing condition. Vines are planted with a spacing of 3.0 meters between rows and 1.0 meter between vines within a row, resulting in a planting density of approximately 333 vines per hectare.

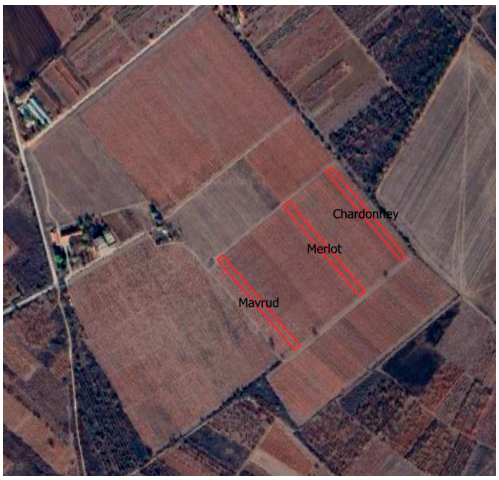


Figure 1. Location of study area
(Google Earth 17.11.2024)
L 42° 3'29.71"N B 24°47'0.18"E

The vineyard rows are oriented northwest–southeast (NW-SE) and are situated on a gentle eastward slope of 3.2% (1.8°), at an average elevation of 194 meters above sea level. Vines are cultivated using a tall-stem training system with a double-sided cordon formation supported by an appropriate trellis structure. The vineyard is managed under non-irrigated (dry-farmed) conditions.

The experimental scheme includes the following variants:

- V_1 - Mavrud variety;
- V_2 - Merlot variety;
- V_3 - Chardonnay variety.

Each variant consists of 60 vines, arranged in four replications of 15 vines each.

A series of in situ observations were made to The phenological development of the main growth stages of vine development during the vegetation period was monitored, including: bud burst, first leaf appearance, mass flowering, "pea"-size berries, veraison, and technological maturity. Observations were conducted on normally developed, fully fruiting vines. For the *Mavrud*, *Merlot*, and

Chardonnay varieties, the phenological stages were recorded as the calendar days when most of the vines (50%) had reached each respective stage. The identification and classification of the phenological phases followed the methodology described by Braykov et al. (2005).

Climatic data for the study period (April to October) in 2021 and 2022 including mean daily air temperature (°C) and daily precipitation (mm) were obtained from the meteorological station located within the university vineyard. According to Del Rio et al. (2024), the following heat indices were calculated from the temperature data:

The Winkler Index (WI) is a viticultural metric used to assess cumulative heat exposure during the grapevine growing season. It is calculated by summing the average daily temperatures that exceed 10°C. Also known as the Winkler Scale or Winkler Regions, this index was developed by Winkler et al. (1974) to classify wine-growing regions based on growing degree-days (GDD). It divides geographical areas into five climatic regions (Regions I to V), with each category corresponding to a range of accumulated heat units (Table 1), thereby guiding the selection of grape varieties suitable for each region.

$$\mathrm{WI} = \sum_{April\ 1}^{Oct31}(T_{mean} - 10^0C)$$

where:

- T_{mean} is the average daily temperature in °C from 1st April to 31 October;
- 10°C is the baseline temperature below which grapevine does not grow.

Table 1. Winkler Index classification (Winkler et al., 1974)

Region	GDD Range (°C)	Climate Type
Region I	< 1,390	Cool
Region II	1,391-1,670	Intermediate
Region III	1,671-1,940	Warm
Region IV	1,941-2,220	Hot
Region V	> 2,220	Very Hot

The Huglin Index (HI) is a bioclimatic heat index developed by Huglin for vineyards. It is a metric used to predict the potential maximum temperature of a given location over a given period (Huglin, 1978). The index is calculated by taking the meaning of the maximum and average daily temperatures recorded from early April to late September (Table 2). The calculated total is slightly adjusted based on the latitude of the area, using the K factor.

$$HI = K\left(\sum_{April\ 1}^{Sept30}\frac{T_{mean}+T_{max}}{2} - 10^0C\right)$$

where:

- T_{mean} is daily mean temperature (°C);
- T_{max} is daily maximum temperature (°C);
- 10°C is the baseline temperature below which grapevines do not grow;
- K is a latitude correction factor (ranges from 1.02 to 1.06).

Table 2. Huglin Index Classification (Huglin, 1978)

HI Range	Climate Classification
≤ 1500	Very Cool
1,500-1,800	Cool
1,800-2,100	Temperate
2,100-2,400	Warm
2,400-2,700	Hot

Growing Season Temperature (GST) - The growing season temperature index is an indicator employed in viticulture to assess the suitability of a particular region for wine production. The GST index is calculated as the mean daily temperature between 1 April and 31 October in the Northern Hemisphere. A positive correlation has been observed between the GST index and the maturity potential of grape varieties (Table 3). Different varieties of wine grapes grow within different GST thresholds (Jones, 2007).

$$\mathrm{GST} = \sum_{April\ 1}^{Oct\ 31}\frac{T_{mean}}{n}$$

where:

- T_{mean} is daily mean temperature (°C);
- n is days from April 1 to October 31.

Table 3. GST Index classification (Jones, 2007)

GST (°C)	Climate Type
< 13°C	Very Cool
13-15°C	Cool
15-17°C	Intermediate
17-19°C	Warm
19-21°C	Hot
> 21°C	Very Hot

Satellite imagery

The Sentinel-2 multispectral images for the NDVI were obtained from the official open-access site of the Copernicus Land Monitoring Service (Copernicus Europe's Eyes on Earth, n.d.). Within this online database, cloud-free images were selected according to their proximity to the dates of the phenological stages.

NDVI was obtained from the Copernicus Land Monitoring Service as a daily update of the NDVI, provided at pan-European level and in near real time. The data were available at 10 m x 10 m spatial resolution from Sentinel-2 HR multispectral satellite imagery (according to Data Viewer - Copernicus Land Monitoring Service).

NDVI defines values from - 1.0 to 1.0, where negative values are mainly formed from clouds, water and snow, and values close to zero are primarily formed from rocks and bare soil.

Very small values (0.1 or less) of the NDVI function correspond to empty areas of rocks, sand or snow.

Moderate values (from 0.2 to 0.3) represent shrubs and meadows, while large values (from 0.6 to 0.8) indicate temperate and tropical forests (Eos Date Analytics, n.d.)

The formula for the NDVI is as follows:

$$\text{NDVI} = \frac{NIR - RED}{NIR + RED}$$

where:

- NIR is near-infrared light;
- RED is red light.

For Sentinel-2:

$$\text{NDVI} = \frac{B_8 - B_4}{B_8 + B_4}$$

where:

- B8 = 842 nm;
- B4 = 665 nm.

The images and sample raster values from NDVI imagery were processed by QGIS 3.34.14.

Time series imageries were downloaded for the main stages of the vine plant in the experimental field and in situ data collection for 2021-2022. The growth stages are calculated in the Days Of the Year (DOY). The correlations between the studied variables were obtained by regression analysis in Excel Microsoft 365 and were valid within the time range studied.

RESULTS AND DISCUSSIONS

The grape varieties included in the study demonstrated varying ripening periods within the Plovdiv region.

Mavrud, a red wine variety, is distinguished by its protracted ripening period, which can extend from late summer to the onset of winter. In 2021, bud burst commenced on 16 April/DOY 116, and technological maturity was achieved on 6 October/DOY 279. The duration of the period from the initial phase to technological maturity is 174 days. In the second experimental year of the study (2022), the onset of budbreak occurred earlier than in the first year, on 9 April/DOY 111. The attainment of technological maturity was observed on 1 October/DOY 274. As presented in Table 4, the duration of the period from the budding growth phase to technological maturity is 176 days.

Merlot is a late-ripening French red wine variety. In 2021, bud burst is initiated on 12 April/ DOY 102, and technological maturity is observed on 13 September/ DOY 256. The duration of the period from the initial growth stage to technological maturity is 155 days. In consequence of the increased temperatures recorded in April 2022, the phenological stage of bud burst occurred earlier than in the first year, on 6 April/ DOY 96, and harvesting took place on 10 September/DOY 256. The duration of the period from bud burst to technological maturity is 158 days.

Chardonnay is a medium ripening French white wine variety. The onset of bud burst is observed on 10 April 2021 (DOY 100), while technological maturity is recorded on 30 August 2021 (DOY 242). The duration of the period from bud burst to technological maturity is 145 days. In 2022, bud burst occurred on 5 April/DOY 95, and technological maturity was attained on 28 August/DOY 240. The vegetation period was therefore 146 days.

The ripening process of the grapes was influenced by the average daily air temperature and the amount of precipitation. During the two experimental years, resulting in changes in the phenological stages during the growing season. At a temperature of 25ºC, the flowering of the

vines was observed to occur at a shorter time. The temperature in July plays a major role in the ripening of the grapes and should be between 28-32ºC for high quality table wines. The highest recorded precipitation (103.8 mm) was in June 2022 (Figure 2 and Figure 3).

Table 4. Phenological stages of Mavrud, Merlot and Chardonnay grape varieties for 2021 and 2022

Phenological Stage	Year	Mavrud	Merlot	Chardonnay
		Date/DOY	Date/DOY	Date/DOY
Bud Burst	2021	16.04.21/116	12.04.21/102	10.04.21/100
	2022	09.04.22/111	06.04.22/96	05.04.22/95
First Leaf Appearance	2021	30.04.21/120	22.04.21/112	19.04.21/109
	2022	24.04.22/114	16.04.22/106	10.04.22/100
Mass Flowering	2021	09.06.21/160	31.05.21/151	27.05.21/147
	2022	03.06.22/153	29.05.22/149	25.06.22/145
"Pea" Size	2021	10.07.21/191	05.07.21/186	30.06.21/181
	2022	06.07.22/187	01.07.22/182	27.06.22/178
Veraison	2021	20.08.21/232	04.08.21/216	29.07.21/210
	2022	16.08.22/228	02.08.22/214	25.07.22/206
Technological Maturity	2021	06.10.21/279	13.09.21/256	30.08.21/242
	2022	01.10.22/274	10.09.22/253	28.08.22/240
Bud Burst - Technological Maturity (Days)	2021	174	155	145
	2022	176	158	146

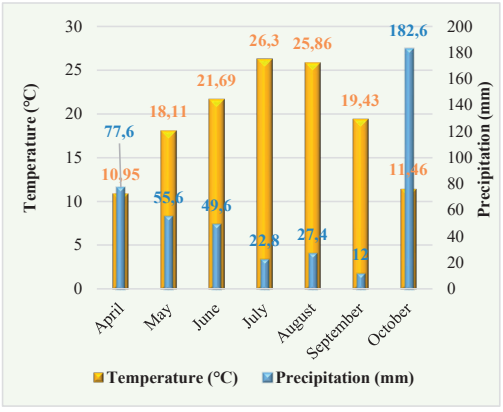


Figure 2. Monthly climate characteristics - mean temperatures and sum of precipitation for 2021

The meteorological data obtained from the station in the vineyard is of great importance for the vines. It enables the monitoring of temperature and precipitation, which influences the growth and development of the vines and plays a decisive role in the quality and yield of the grapes.

An assessment of the microthermal conditions during the grape harvesting period was conducted by determining the Winkler Index, the Huglin Index, and the Growing Season Temperature (GST) Index for the years 2021 and 2022 (Table 5).

The thermal indices allow for the comparison of vineyards with wine-growing areas all over the territory. These indices suggest that the optimal grape varieties are those capable of adapting to both lower and higher temperatures, exhibiting a suitable ripening period, and yielding wines with balanced acidities and flavours.

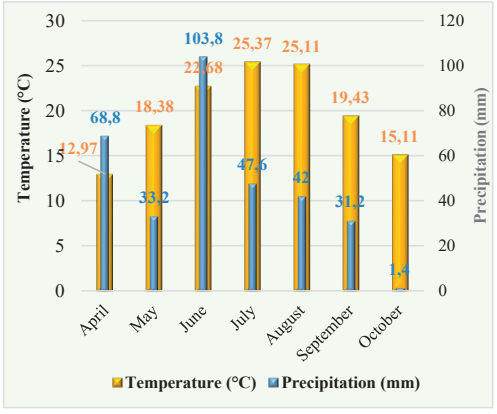


Figure 3 Monthly climate characteristics - mean temperatures and sum of precipitation for 2022

Table 5. Assessment microthermal conditions

	Index	2021Year/ Category	2022 Year/ Category
Meteo station Brestnik village	Winkler (WI)	1990°C Region IV	2132°C Region IV
	Huglin (HI)	2619°C Warm	2689°C Warm
	Growing Season Temperature (GST)	19.4°C Hot	19.8°C Hot

Satellite observations

The dynamics of the NDVI values were traced by the average index values in the plots, obtained from the zonal statistics in QGIS in 2021 and 2022. The index values are for the stages from the first leaf appearance to the technological maturity for the three varieties. Each of the varieties under observation cover an area of 2,500 square meters (Figure 4, Figure 5). The obtained results for the varieties are corresponding to the occurrence of the respective stages in each of the varieties. On the Figure 4 and Figure 5 are presented NDVI images for the growth stages of Mavrud variety in 2021 and 2022.

It is observed that the NDVI values start to increase with the beginning of flowering in May, and reach their maximum at the "pea" size in June. From August, due to the onset of drought and maturity, the leaves turn yellow and the index values decrease. The two years under consideration, 2021 and 2022, differ significantly in terms of climate, particularly with regard to rainfall, which has a direct impact on plant development.

In 2021, July and August rainfall were significantly lower, with values of 22.8 mm and 27.4 mm respectively. This results in a deficiency of moisture in the leaves, consequently leading to reduced NDVI values.

In 2022, the rainfall was almost double that of the previous year, at 47.6 and 42 mm, which is indicative of favourable conditions for the development of the vine crop. Consequently, NDVI values are elevated.

This provides a rationale for the observed delay in the onset of the phenophases, which in 2021 occurred 4-5 days later than in 2022.The phenological development of the varieties was established on the basis of climatic data and in situ observations (Figures 6 and 8).

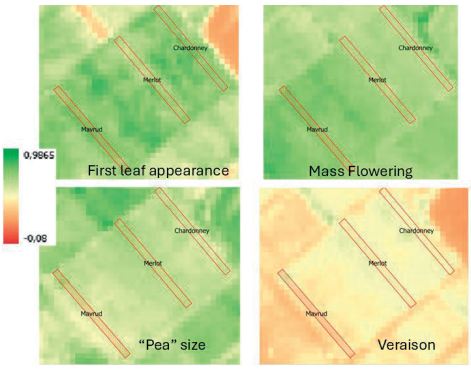


Figure 4. NDVI images for the phenological stages of Mavrud in 2021

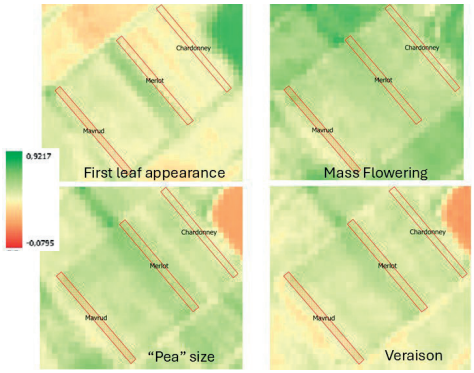


Figure 5. NDVI images for the phenological stages of Mavrud in 2022

There were no significant differences in the index values, but due to the different timing of the phenological phases and the development of the varieties, differences were observed. The analysis indicates a high degree of correlation.

The highest degree of multiple correlation is observed for the red varieties Merlot and Mavrud with R^2=0.99 for 2021 and R^2=0.97 for 2022 and R^2 = 0.90 and R^2=0.94, respectively.

In the case of Chardonnay, the coefficient of possible correlation is lower degree than the others, but also with a very good result. R^2=0.8 for 2021 and R^2=0.73 for 2021.

Figures 7 and 9 illustrate the NDVI from Sentinel-2 images for the verasion growth stage for the three varieties. The phases between the Chardonnay and Mavrud varieties exhibit a 20-day discrepancy, with the Chardonnay variety entering its phase at a more accelerated rate. A clear distinction in the years and index values is evident between the earlier veraison phase in

Chardonnay and the later veraison growth stage in Mavrud.

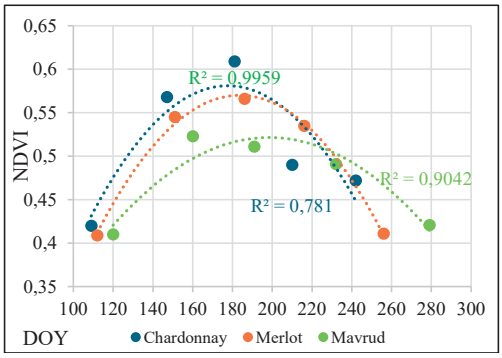


Figure 6. Dynamics of NDVI values for main growth stages for 2021

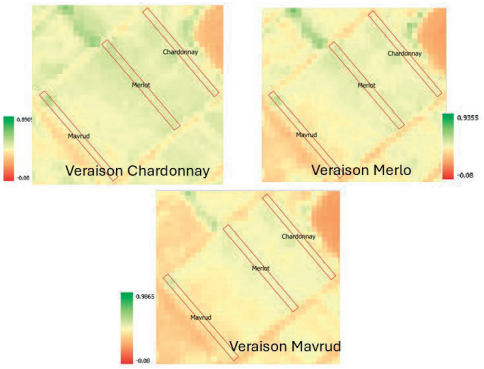


Figure 7. NDVI images for the growth stage Veraison in 2021

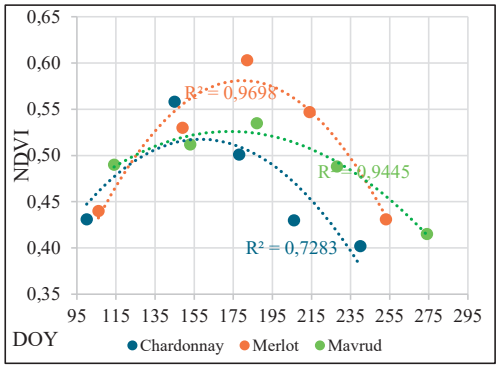


Figure 8. Dynamics of NDVI values for main growth stages for 2022

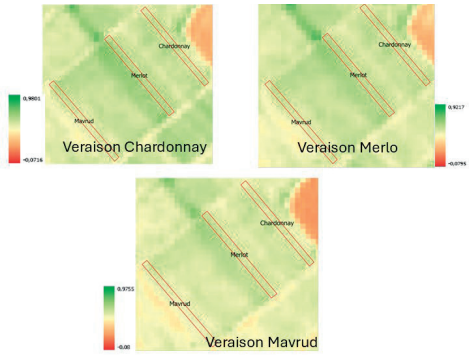


Figure 9. NDVI images for the growth stage Veraison in 2022

CONCLUSIONS

The present study employed regression equations and multiple correlation to evaluate the relationship between NDVI and the phenological phases of cultivars with varying maturation dates and growing season durations. The coefficients' values for R^2 in both years exhibited analogous results. The analysis revealed the highest result for the Merlot and Mavrud varieties. The multiple correlation coefficient for the Merlo variety was found to be $R^2 = 0.99$ and 0.97 for the year 2021 and 2022, respectively.

The NDVI time series has been utilised to monitor vineyard phenological phases, exhibiting a high degree of data validity. The survey is subject to several significant limitations. Firstly, there is a high probability of cloud cover and precipitation during the months of May and June. This may result in a lack of NDVI values during the growth stages of "flowering" and "pea size".

The evaluation of the investigated varieties was conducted by means of thermal indices in the experimental field in which they were cultivated.

The integration of meteorological data, vegetation indices and heat indices has demonstrated its potential in determining the phenological dynamics of diverse grape varieties. The integration process under discussion has been demonstrated to facilitate the identification of the most suitable grape variety for specific regional contexts. This, in turn, has been shown to contribute to the optimisation of viticultural practices.

ACKNOWLEDGEMENTS

This research was carried out with the support of the National Program of the Ministry of Education, Science and Technology, and the publication was funded under the Research Project "Young Scientists and Postdoctoral Fellows - 2" - second stage 2024/2025.

REFERENCES

Arnaudova, Z., & Stalev, B. (2024). Relationships between spectral vegetation indices (SVIS) and growth stages in a table grape vineyard. *Scientific Papers. Series E. Land Reclamation, Earth Observation & Surveying, Environmental Engineering, 13*, 750–755.

Bock, A., Sparks, T., Estrella, N., & Menzel, A. (2011). Changes in the phenology and composition of wine from Franconia, Germany. *Climate Research, 50*, 69–81. https://doi.org/10.3354/cr01048

Bois, B. (2007). *Cartographie agroclimatique à méso-échelle: Méthodologie et application à la variabilité spatiale du climat en Gironde viticole. Conséquences pour le développement de la vigne et la maturation du raisin* (Doctoral dissertation). Université de Bordeaux.

Braykov, D., Pandeliev, S., Masheva, L., Mievska, T., Ivanov, A., Roychev, V., & Botyanski, P. (2005). *Viticulture [Students' guide to viticulture]*. Academic Publishing House of the Agricultural University, Plovdiv.

Candiago, S., Remondino, F., De Giglio, M., Dubbini, M., & Gattelli, M. (2015). Evaluating multispectral images and vegetation indices for precision farming applications from UAV images. *Remote Sensing, 7*(4), 4026–4047.

Chuine, I., de Cortázar-Atauri, I. G., Kramer, K., & Hänninen, H. (2013). Plant development models. In M. D. Schwartz (Ed.), *Phenology: An integrative environmental science* (pp. 275–293). Springer.

Cogato, A., Pagay, V., Marinello, F., Meggio, F., Grace, P., & De Antoni Migliorati, M. (2019). Assessing the feasibility of using Sentinel-2 imagery to quantify the impact of heatwaves on irrigated vineyards. *Remote Sensing, 11*(23), 2869.

Copernicus Europe's Eyes on Earth. (n.d.). *Land monitoring service*. https://land.copernicus.eu/en

Cuccia, C. (2013). *Impacts du changement climatique sur la phénologie du Pinot noir en Bourgogne* (Doctoral dissertation). Université de Bourgogne.

Cunha, M., Marçal, A. R., & Rodrigues, A. (2010). A comparative study of satellite and ground-based vineyard phenology. In *Imagine [e, g] Europe* (pp. 68–77). IOS Press.

Dalla Marta, A., Grifoni, D., Mancini, M., Storchi, P., Zipoli, G., & Orlandini, S. (2010). Analysis of the relationships between climate variability and grapevine phenology in the Nobile di Montepulciano wine production area. *The Journal of Agricultural Science, 148*(6), 657–666.

De Cortázar-Atauri, I. G., Brisson, N., & Gaudillère, J. P. (2009). Performance of several models for predicting budburst date of grapevine (*Vitis vinifera* L.). *International Journal of Biometeorology, 53*, 317–326. https://doi.org/10.1007/s00484-009-0217-4

Del Rio, M. S., Cicuéndez, V., & Yagüe, C. (2024). Characterisation of two vineyards in Mexico based on Sentinel-2 and meteorological data. *Remote Sensing, 16*(14), 2538.

Devaux, N., Crestey, T., Leroux, C., & Tisseyre, B. (2019). Potential of Sentinel-2 satellite images to monitor vine fields grown at a territorial scale. *OENO One, 53*(1).

Duchêne, E., Butterlin, G., Dumas, V., & Merdinoglu, D. (2012). Towards the adaptation of grapevine varieties to climate change: QTLs and candidate genes for developmental stages. *Theoretical and Applied Genetics, 124*, 623–635. https://doi.org/10.1007/s00122-011-1734-1

Eos Data Analytics. (n.d.). *Satellite data analytics for daily Earth insights & decision-making*. https://eos.com

Hall, A., Lamb, D. W., Holzapfel, B., & Louis, J. (2002). Optical remote sensing applications in viticulture: A review. *Australian Journal of Grape and Wine Research, 8*(1), 36–47.

Huglin, M. P. (1978). Nouveau mode d'évaluation des possibilités héliothermiques d'un milieu viticole. *Comptes Rendus des Séances de l'Académie d'Agriculture de France, 64*.

Intergovernmental Panel on Climate Change (IPCC). (2013). *Climate change 2013: The physical science basis*. Cambridge University Press.

Jesus, J., Santos, F., Gomes, A., & Teodoro, A. C. (2020, September). Temporal analysis of the vineyard phenology from remote sensing data using Google Earth Engine. In *Remote Sensing for Agriculture, Ecosystems, and Hydrology, XXII* (Vol. 11528, pp. 39–50). SPIE.

Jones, G. V. (2007, July). Climate change and the global wine industry. In *Proceedings of the 13th Australian Wine Industry Technical Conference* (Vol. 28). Adelaide, Australia.

Krishna, K. R. (2017). *Push button agriculture: Robotics, drones, satellite-guided soil and crop management*. CRC Press.

Madelin, M., & Beltrando, G. (2005). Spatial interpolation-based mapping of the spring frost hazard in the Champagne vineyards. *Meteorological Applications, 12*, 51–56. https://doi.org/10.1017/S1350482705001568

Matese, A., & Di Gennaro, S. F. (2015). Technology in precision viticulture: A state-of-the-art review. *International Journal of Wine Research*, 69–81.

Parker, A. K., De Cortázar-Atauri, I. G., van Leeuwen, C., & Chuine, I. (2011). General phenological model to characterise the timing of flowering and veraison of *Vitis vinifera* L. *Australian Journal of Grape and Wine Research, 17*, 206–216. https://doi.org/10.1111/j.1755-0238.2011.00140.x

Parker, A. K., García de Cortázar-Atauri, I., Gény, L., Spring, J.-L., Destrac, A., et al. (2020). Temperature-based grapevine sugar ripeness modelling for a wide

range of *Vitis vinifera* L. cultivars. *Agricultural and Forest Meteorology, 285–286*, 107902. https://doi.org/10.1016/j.agrformet.2020.107902

Parker, A., de Cortázar-Atauri, I. G., Chuine, I., Barbeau, G., Bois, B., Boursiquot, J.-M., et al. (2013). Classification of varieties for their timing of flowering and veraison using a modelling approach. *Agricultural and Forest Meteorology, 180*, 249–264. https://doi.org/10.1016/j.agrformet.2013.06.005

Pastonchi, L., Di Gennaro, S. F., Toscano, P., & Matese, A. (2020). Comparison between satellite and ground data with UAV-based information to analyse vineyard spatio-temporal variability. *OENO One, 54*(4), 919–934. https://doi.org/10.20870/oeno-one.2020.54.4.4028

Pichon, L., Leroux, C., Macombe, C., Taylor, J., & Tisseyre, B. (2019). What relevant information can be identified by experts on unmanned aerial vehicles' visible images for precision viticulture? *Precision Agriculture, 20*, 278–294.

Sozzi, M., Kayad, A., Giora, D., Sartori, L., & Marinello, F. (2019). Cost-effectiveness and performance of optical satellites constellation for precision agriculture. In *Precision Agriculture, 19*, 501–507. Wageningen Academic.

Tomasi, D., Jones, G. V., Giust, M., Lovat, L., & Gaiotti, F. (2011). Grapevine phenology and climate change: Relationships and trends in the Veneto region of Italy for 1964–2009. *American Journal of Enology and Viticulture, 62*, 329–339. https://doi.org/10.5344/ajev.2011.10108

van Leeuwen, C., Destrac-Irvine, A., Dubernet, M., Duchêne, E., Gowdy, M., Marguerit, E., et al. (2019). An update on the impact of climate change in viticulture and potential adaptations. *Agronomy, 9*, 514. https://doi.org/10.3390/agronomy9090514

Winkler, A. J., Cook, J. A., Kliewer, W. M., & Lider, L. A. (1974). *General viticulture*. University of California Press.

Scientific Papers. Series E. Land Reclamation, Earth Observation & Surveying, Environmental Engineering. Vol. XIV, 2025
Print ISSN 2285-6064, CD-ROM ISSN 2285-6072, Online ISSN 2393-5138, ISSN-L 2285-6064

RIVER CORRIDOR CHANGE DETECTION USING SATELLITE IMAGERY AND LIDAR DATA: A CASE STUDY OF THE SIRET RIVER NEAR CORBU VECHI VILLAGE

Catalin-Stefanel SABOU[1, 2], Simion BRUMA[1, 2], Ioana POP[1], Florica MATEI[1], Paul SESTRAS[1, 4], Jutka DEAK[1], Silvia CHIOREAN[1], Tudor SALAGEAN[1, 2, 3]

[1]University of Agricultural Sciences and Veterinary Medicine Cluj-Napoca,
3-5 Calea Mănăștur Street, 400372, Cluj-Napoca, Romania
[2]Technical University of Civil Engineering of Bucharest, Doctoral School,
122-124 Lacul Tei Blvd, District 2, 020396, Bucharest, Romania
[3]Technical Sciences Academy of Romania,
26 Dacia Blvd, District 2, 030167, Bucharest, Romania
[4]Academy of Romanian Scientists, 3 Ilfov Street, District 5, 050044, Bucharest, Romania

Corresponding author emails: tudor.salagean@usamvcluj.ro, popioana@usamvcluj.ro

Abstract

The evaluation of river course variations, such as bank erosion, sediment deposition, and the influence of nearby human-made structures, is facilitated by the use of remote sensing data and topographic analysis. These changes result from natural events, such as floods, as well as human activities, including the removal of fertile soil, sand extraction, and deforestation. This study highlights the impacts of these changes on river corridor ecosystems, as well as on the infrastructure and properties located along the watercourse. Continuous changes to the Earth`s surface are driven by both natural and artificial factors, which contribute to the erosion, transport, and accumulation of sediments. Among geomorphological agents, flowing water exhibits a particularly high erosive capacity. A primary objective of this study is to identify these changes, with a secondary focus on providing an overview of the current state of river corridors and bank erosion. To achieve this, the research utilizes remote sensing (RS) techniques and geographic information systems (GIS), along topographic data, to effectively monitor and analyze these transformations.

Key words*: remote sensing, change detection, river, GIS.*

INTRODUCTION

The Earth's surface is constantly changing due to a variety of anthropological, morphological, and atmospheric factors. The ground's surface degradation processes, such as weathering and erosion, are responsible for changes in landform (Aher et al., 2012).

Flooding and erosion naturally alter land use and land cover, leading to land loss, which significantly impacts livelihoods (Hazarika et al., 2015). Flood risk is expected to rise due to climate change, increasing flood frequency and magnitude, along with growing populations and assets in vulnerable areas. This intensifies riverbank erosion and river shifts, threatening nearby communities, causing land loss, displacement, and instability (Kundzewicz et al., 2014; Bodoque et al., 2023).

When the forces holding soil particles together are exceeded by the power of wind and water on the soil surface, it results in the natural process of soil erosion (Spalevic et al., 2020). Soil erosion is an environmental problem affecting the entire globe. Changes in land use across all river basins influence sediment dynamics, soil vulnerability to erosion, and hydrological responses (Sestras et al., 2023).

Rainfall activates the erosion process, impacting soil erosion through both the intensity and volume of precipitation, which subsequently affects the physical and chemical properties of the soil. Furthermore, topography significantly influences surface runoff, with steeper slopes and longer distances enhancing the erosion potential of precipitation, thereby increasing the risk of soil erosion (Costea et al., 2022).

To ensure the effectiveness of management and mitigation strategies, it is important to understand and examine the hydrological events (Bammou et al., 2024).

In Romania, water erosion affects approximately 3.5 million hectares of land, with certain regions in the Subcarpathian Curvature area (Vrancea and Buzău counties) experiencing erosion rates of 30-45 tons per hectare per year. This is in clear contrast to the soil's regenerative capacity, which is only about 3-6 tons per hectare per year (Mircea et al., 2010).

The shape and size of a river are primarily influenced by factors such as the steepness of the slope, water volume, water velocity, and nature of the river (Aher et al., 2012).

River channel changes, including bank erosion, down cutting, and bank accretion, are inherent processes in alluvial rivers. Bank erosion occurs when water erodes the riverbanks, while down cutting involves water activity on riverbed deepening due to erosion. Bank accretion refers to the accumulation of sediments on the banks, leading to the creation of new landforms. These processes are driven by factors such as water flow, sediment transport and deposition, and climate changes (Langat et al., 2019; Dabojani et al., 2014; Yao et al., 2013).

The bank shift of river path is a natural process in fluvial systems, caused by both human activities and climatic factors (Langat et al., 2019).

MATERIALS AND METHODS

Study Area

The primary aim of this study is to identify changes in the river corridor. The area of interest is located near Corbu Vechi village, in Brăila County, as shown in Figure 1, where the Siret River has been monitored from 2016 to 2025 using satellite images from Sentinel 2 RS (Remote Sensing) data. These changes are validated through topographical data collected in February 2025 with a LiDAR (Light Detection and Ranging) sensor mounted on an UAS (Unmanned Aerial System). This approach provides valuable insights into the evolution of river ecosystems over the specified period, offering a detailed assessment of the river's dynamics.

The Siret River, originating in the Northern Carpathians in Ukraine, flows through Romania for a distance of 559 km before merging with the Danube. Its upper course begins in Ukraine, while the middle course passes through the Suceava Plateau and the border between the Moldavian Sub-Carpathians and the Bârlad Plateau. The river's drainage network includes 1,013 water courses, covering 15,157 km, which represents 19.2% of Romania's total river network. With a drainage basin of 44,871 km², the Siret has the largest basin in Romania, covering 18.1% of the country's total area. From its source to its mouth, the river experiences an elevation difference of 1,236 meters (Romanescu et al., 2013).



Figure 1. Siret River near Corbu Vechi village

The area of interest lies in the lower Siret Valley, with elevations between 3 and 60 meters. During the 70's, extensive engineering projects were undertaken to manage frequent flooding and bank erosion, particularly in the floodplain. These efforts included regularizing the river's course and reinforcing its banks (Olariu et al., 2015).

However, over time, the efficiency of these interventions has diminished due to natural processes such as sediment buildup and erosion, along with changes in land use. As a result, the Siret River continues to present challenges, requiring new rehabilitation, development, and reinforcement works, as well as the adaptation of flood control measures to account for climate change and growing human influence.

MATERIALS AND METHODS

Remote sensing is a technique that allows data collection without physical contact with the target, using sensors to capture or analyze different forms of energy, including

electromagnetic radiation and acoustic signals, as they are emitted, reflected, or dispersed by the object being studied (Yang et al., 2022; Aher et al., 2012; Campbell et al., 2011).

Change detection is the process of finding and evaluating changes in multispectral images that present spatial or spectral variations. It is commonly described as the analysis of two co-registered images of the same geographic region taken at different time periods to detect and evaluate changes over time (Cheng et al., 2024; Goswami et al., 2022).

The area of interest is analyzed using Sentinel-2 satellite data, which provides multispectral imagery with a resolution suitable for identifying changes in the river corridor. For watercourse extraction, the NDWI (Normalized Difference Water Index) is computed, a remote sensing index specialized in detecting and analyzing water bodies. It is calculated based on reflectance in specific wavelengths of the electromagnetic spectrum, specifically the green and NIR (Near-Infrared) bands, according to Gao (1996), or the NIR and SWIR (Short Wave Infrared) bands, according to K. McFeeters (1996), allowing accurate classification of water areas and their differentiation from other surface types, such as vegetation or dry soil.

By integrating satellite-based remote sensing data, the analysis of the Normalized Difference Water Index (NDWI) provides valuable insights into water trends, which can significantly inform decision-making processes. This method helps identify changes in water bodies over time, enabling more effective management strategies (Ghalehteimouri et al., 2024).

The calculation of NDWI and the extraction of information from the obtained results were carried out using GIS (Geographic Information Systems) software, which allowed the analysis and interpretation of spatial data.

GIS and RS are indispensable tools for monitoring and detecting changes in the physical environment, including river dynamics and bank erosion. By utilizing advanced remote sensing technologies and satellite data, these tools enable the tracking of Earth's surface changes, significantly enhancing environmental assessments. Their combined application has revolutionized the way we detect, analyze, and assess environmental transformations, making them essential for sustainable management and decision-making (Ghalehteimouri et al., 2024; Sestras et al., 2023; Bilasco et al., 2021; Aher et al., 2012; Dabojani et al., 2014). Subsequently, remote sensing results from Sentinel-2 were validated in situ through precise topographic information collected with LiDAR technology.

While remote sensing products are commonly used to assess planform changes (2D), they often neglect vertical changes (3D). However, evaluating both planform and vertical changes is essential for understanding morphological transformations. By incorporating spatio- temporal aerial imagery along with topographic data, remote sensing becomes a valuable tool for assessing changes in rivers morphology, providing a more comprehensive picture of the river system's dynamics (Andualem et al., 2024).

LiDAR sensors represent the next generation of efficient and precise land surveys. Aerial and satellite mapping, such as photogrammetry and airborne LiDAR, have greatly improved land surface elevation sampling. Traditionally, topographic data was gathered through ground surveys using total stations, GPS (Global Positioning System), or other GNSS (Global Navigation Satellite System) tools. However, this method can be time-consuming, particularly in complex topographic areas (Sestras et al., 2025; Ouédraogo et al., 2014).

Data processing and spatial analysis were performed using Romania's national projection system Stereographic 1970. The utilized workflow is presented in Figure 2 and includes several essential applications for data downloading, processing, and analysis.

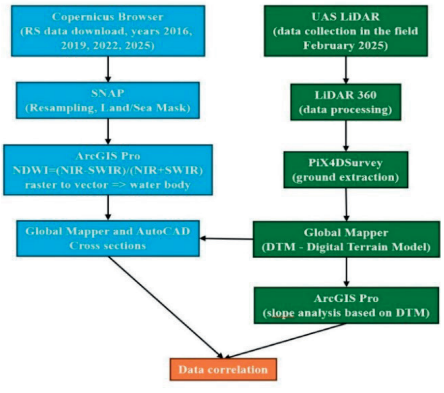


Figure 2. The workflow for satellite imagery and LiDAR data

For downloading satellite RS data, the open-source platform Copernicus Browser was used. Later, for processing the remote sensing data, the applications SNAP and ArcGIS Pro were utilized. After calculating the remote sensing indices, the analysis of the resulting vector data was performed using the applications GlobalMapper and AutoCAD for generating cross-sections. The second part involved collecting 3D data using a system composed of the DJI Matrice M200 PPK drone, equipped with the Topodrone LiDAR 200+ Hesai sensor. Flight processing and the generation of point cloud data were carried out using Topodrone PostProcessing and LiDAR 360. Subsequently, the data was filtered to obtain the necessary ground data for creating the DTM (Digital Terrain Model) using GlobalMapper. Finally, the DTM was used for spatial analysis in ArcGIS Pro.

RESULTS AND DISCUSSIONS

The Siret sector from Movileni to its confluence with the Danube, where the area of interest is situated, faces exceedances of flood protection works, as it is entirely embanked. Rising water levels are sometimes aggravated by a backflow effect from the Danube, which can contribute to an additional rise in water levels in certain sections of the Siret River. In this context, confluence areas, such as those where the Siret meets major tributaries, are exposed to flooding from both the Siret and its tributaries. At the same time, in this sector, the Siret is also affected by phenomena such as bank erosion, as can be observed in Figure 3.



Figure 3. Bank erosion Siret River near Corbu Vechi village - February 2025

To analyze the changes that occurred, Sentinel 2 images for the dates of 4 December 2016, 4 December 2019, 28 December 2022, and 13 february 2025, were downloaded. These images were processed by applying the resampling command in the SNAP software to bring the spatial resolution of all spectral bands to 10 meters. The images were then cropped to focus on the study area, and the NDWI was calculated using ArcGIS Pro. This generated raster images of the index, with values ranging from -1 to 0 indicating areas with bare soil or covered with vegetation without water, while values between 0 and 1 identified water-covered regions.

In Figure 4 and Figure 5, the NDWI index for the years 2016 and 2025 is shown, covering the same area over a span of 9 years. By comparing the two images, changes in the distribution of water and vegetation can be observed.

By comparing the two images, the phenomenon of bank erosion and the process of sediment deposition or accumulation along the river course can be observed, indicating a dynamic evolution of the river during the analyzed period.

The next step involved extracting the water body from each image using the NDWI index calculated for each year. These water bodies were then overlaid to allow the comparison and analysis of changes in the distribution of water over the studied period.

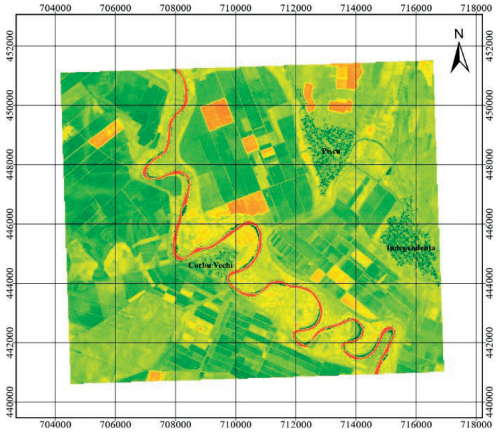


Figure 4. The Normalized Difference Water Index for the year 2016 (red - water bodies, orange and yellow - vegetation and surfaces with moisture content, light and dark green - bare soils and built-up areas)

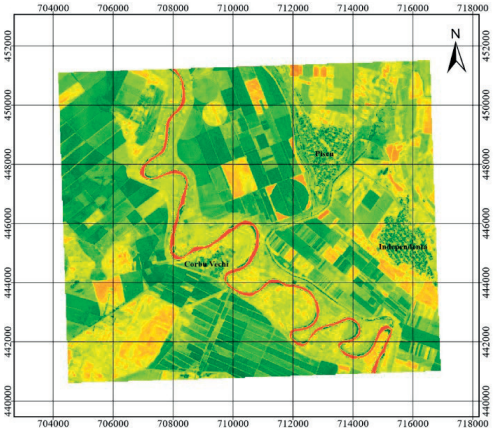


Figure 5. The Normalized Difference Water Index for the year 2025 (red - water bodies, orange and yellow - vegetation and surfaces with moisture content, light and dark green - bare soils and built-up areas)

A closer look reveals the dynamics of the changes that have occurred along the river course, an aspect highlighted in Figure 6. These changes occurring in the water bodies are caused by bank erosion and sediment deposition, which have led to shifts in the river's path.



Figure 6. Spatio-temporal changes in water bodies between 2016-2025 based on NDWI Index

In Figure 7, the evolution of the Siret River between 2016 and 2025 is illustrated using different colors to represent the river's path each year. The river exhibits significant lateral migration over this period, with visible zones of bank erosion and sediment deposition occurring along various segments of its meandering course. These geomorphological processes are primarily governed by the highly sinuous morphology of the Siret River in this sector, where the channel forms pronounced meanders. The observed pattern of bank erosion on the outer curves and sediment deposition on the inner curves is consistent with classical fluvial dynamics described in meandering river systems. In such systems, higher flow velocities on the outer bends lead to increased erosive forces, while lower velocities on the inner bends favor sediment accumulation. This natural mechanism of lateral channel migration contributes to the continuous reshaping of the river corridor over time.



Figure 7. Water bodies dynamics between 2016-2025 based on NDWI Index (orange - 2016, green - 2019, red - 2022 and blue - 2025)

The raster data of water bodies were converted into vector data in polygon format, enabling more accurate analysis and representation. Using Global Mapper and AutoCAD software, 12 cross-sectional profiles were generated along the 27.5 km length of the river course under investigation, as shown in Figure 8.

These cross-sections facilitated the extraction of river width at each specific location. The resulting data, which highlight the variations in the river's morphology along the analyzed stretch, are presented in Table 1.

Based on Table 1 it can be concluded that the studied area exhibits changes in certain profiles. For example, cross-section 2 maintains a relatively consistent width throughout the studied period, with only minor variations. This data can be correlated with Figure 9, where the changes observed in the river's course are influenced by the linear flow of the Siret River and the presence of forest belts along the banks.

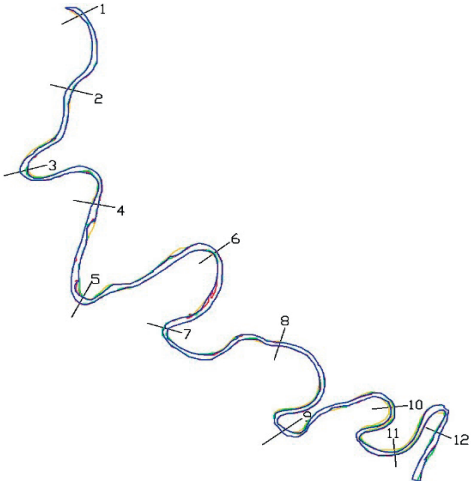


Figure 8. Cross-section of water bodies created in AutoCAD

Table 1. Variation in Siret River width from 2016 to 2025 in the studied area obtained from water bodies cross-sections

Cross section	2016 width (m)	2019 width (m)	2022 width (m)	2025 width (m)
1	112.75	77.17	88.62	89.19
2	107.51	103.23	108.11	105.68
3	151.06	112.44	136.66	144.19
4	116.26	116.32	106.89	106.34
5	150.25	154.56	146.8	138.84
6	95.59	48.88	76.27	78.3
7	91.74	85.75	77.36	69.67
8	86.22	74.86	79.41	74.93
9	92.02	84.87	94.05	88.58
10	71.00	63.95	74.04	73.6
11	98.11	58.27	54.26	56.9
12	107.69	103.24	101.5	92.04



Figure 9. Cross-section 2

The linear flow of the river, characterized by its relatively straight course in this section, contributes to some degree of erosion and sediment deposition. However, its effects are less pronounced compared to areas with more pronounced meanders. The forest belts, on the other hand, provide some stabilization to the riverbanks by acting as a natural barrier against water-induced erosion. While these forest belts can reduce bank erosion to a certain extent, their impact remains limited.

In contrast, cross-section 6 shows major changes, and when correlating the data with Figure 10, it can be concluded that cross section 6 is located on a river meander, where the phenomena of transportation and deposition of alluvial materials occur.



Figure 10. Cross-section 6

Aerial LiDAR data collected was conducted in the areas corresponding to cross-sections 5 and 7. Based on the LiDAR data, the ground was filtered, serving as the basis for vectorizing the necessary elements to create the topographic plan for these areas, as can be seen below in Figure 11.

Topographic observations were requested in these zones due to the execution of bank protection works; however, both upstream and downstream of these riverbank stabilization interventions, the phenomenon of erosion continues to persist. To better understand the effectiveness and impact of the stabilization works, aerial LiDAR data collection was conducted in the areas corresponding to cross-sections 5 and 7. These data were collected by the company BDS Topografie, which

subsequently developed detailed 2D and 3D digital topographic plans. The plans were based on high-resolution LiDAR information gathered on-site, complemented by bathymetric surveys conducted in the same areas.



Figure 11. Topographic plan

The purpose of these data acquisitions was to assess how water interacts with and affects the implemented bank protection measures in these specific zones along the Siret River. The LiDAR-derived point clouds enabled the generation of a high-precision DTM for both areas. This DTM served as foundational tool for analyzing topographic variation and hydrodynamic behavior within the river corridor. In addition, the LiDAR data provided confirmation and refinement of the information obtained through remote sensing analyses, ensuring a multi-source validation of geomorphological changes. All geospatial outputs, including the DTM and topographic plans, were delivered to the project beneficiary to support further assessment and monitoring of the stability and effectiveness of the bank protection works.

Based on the data collected through LiDAR technology and bathymetric surveys, DTM was generated, as shown in Figure 12.

For cross-section 5, which shows a water body width of 138.84 meters according to NWDI, the LiDAR data indicates a width of 152.80 meters. In the case of cross-section 7, where NDWI indicates a width of 69.67 meters, the LiDAR data shows a width of 83.69 meters. The values are close, the data collection periods also being similar, with only a one-week difference between the LiDAR and remote sensing data. However, it should be noted that the remote sensing data have a spatial resolution of 10 meters, which may influence the accuracy of the output.

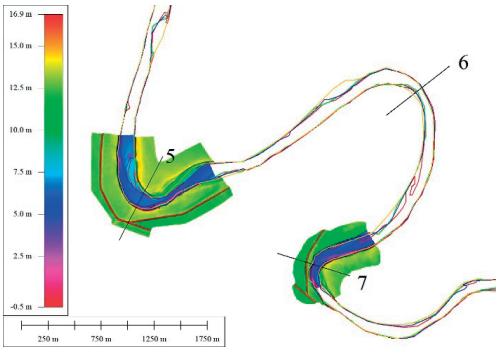


Figure 12. DTM based on LiDAR data

The Digital Terrain Model was imported into ArcGIS Pro for detailed analysis of the slope characteristics within the study area. Through this analysis, regions with higher risk were identified and marked in red as can be observed in Figure 13.

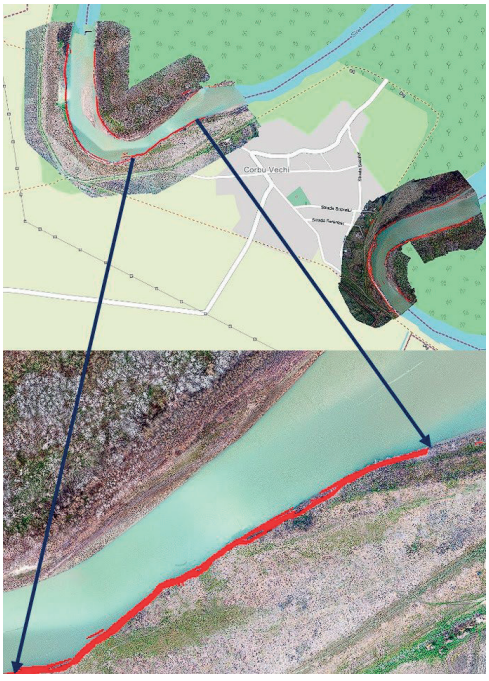


Figure 13. Slopes with an inclination between 30 and 70 degrees - with color red

These areas, where the slope of the riverbank ranges from 30 to 70 degrees, extend over

approximately 2,115 meters on the DTM near the cross-section 5 area and around 1,350 meters in the vicinity of cross-section 7, as determined through slope length calculations performed in ArcGIS Pro. These zones were flagged as particularly vulnerable, specifically, for slopes between 30 and 50 degrees, it is typically recommended to implement bank stabilization measures. These include the installation of protective mesh, as well as the planting of trees, shrubs, and other vegetation to help secure the soil and prevent further erosion. For areas where the slope exceeds 50 degrees, the erosion risk is significantly higher, and more solid engineering solutions are required. In these situations, it is necessary to construct retaining walls, gabion baskets, stone revetments, or even apply concrete to the embankment to stabilize the slope effectively. These engineering measures provide structural support to prevent soil movement and mitigate the long-term risk of erosion, ensuring the durability of the riverbank in the face of continuous environmental pressures.

The slope analysis aligns with the study's main objective outlined in the title and abstract, detecting changes within the Siret River corridor using satellite imagery and LiDAR data. By identifying steep riverbanks ranging from 30 to 70 degrees near cross-sections 5 and 7 based on the DTM, the study highlights areas with elevated erosion risk. These results also support the secondary objective stated in the abstract: providing an overview of the current condition of the river corridor and assessing riverbank stability. Steep slopes significantly influence erosion processes and increase the likelihood of landslides. The use of the Digital Terrain Model enables a detailed spatial assessment of these vulnerabilities, while satellite imagery facilitates the evaluation of changes over time in a spatio-temporal context. These analyses enhance the study's value in detecting changes and evaluating current geomorphological conditions, while also identifying high-risk areas to guide effective mitigation strategies.

CONCLUSIONS

River channels undergo morphological changes due to both human activity and natural processes. Remote sensing and remote sensing indices, particularly the NDWI index applied in this study, provide valuable tools for monitoring and understanding the dynamics of river flows. By using satellite image archives spanning several years or even decades if past satellite missions are considered, these techniques offer a quick and cost-effective means of monitoring changes in water bodies over extended periods.

In the case of the Siret River, the NDWI index was used to track variations in the river's width, which were essential for identifying events like erosion and sediment deposition. With a spatial resolution of 10 meters, the satellite data proved sufficient for this type of study. These satellite data were subsequently verified with topographic information collected using LiDAR technology.

The integration of GIS in processing and analyzing satellite data, combined with LiDAR data, represents an effective approach to extracting and integrating information on the changes occurring in the river course over time. These tools are essential for evaluating risks and identifying vulnerable sections of the riverbanks. For example, in the areas corresponding to cross-sections 5 and 7, detailed topographic observations were carried out. The LiDAR data, collected just one week prior to the satellite data, confirmed and enhanced the initial observations made through remote sensing, providing a comprehensive understanding of the river's dynamics and morphology in these areas. Sustainable management of water resources and safeguarding infrastructure from natural hazards depends on understanding the dynamics of river courses, especially hydrological events such as erosion and sediment deposition. In the case of the Siret River, the combined study of LiDAR data and RS has revealed how the riverbanks have evolved over time.

ACKNOWLEDGEMENTS

This research was carried out with the support of the Ministry of Education and was financed through the CNFIS-FDI-2024-F-0195 project, funded by the National Council for Financing Higher Education (CNFIS).

REFERENCES

Aher, S. P., Bairagi, S. I., Deshmukh, P. P., & Gaikwad, R. D. (2012). River change detection and bank erosion

identification using topographical and remote sensing data. *Int J Appl Inf Syst*, *2*(3), 1-7.

Andualem, T. G., Peters, S., Hewa, G. A., Myers, B. R., Boland, J., & Pezzaniti, D. (2024). Channel morphological change monitoring using high-resolution LiDAR-derived DEM and multi-temporal imageries. *Science of The Total Environment*, *921*, 171104.

Bammou, Y., Benzougagh, B., Igmoullan, B., Ouallali, A., Kader, S., Spalevic, V., ... & Marković, S. B. (2024). Optimizing flood susceptibility assessment in semi-arid regions using ensemble algorithms: a case study of Moroccan High Atlas. *Natural Hazards*, *120*(8), 7787-7816.

Bilașco, Ș., Roșca, S., Vescan, I., Fodorean, I., Dohotar, V., & Sestras, P. (2021). A GIS-based spatial analysis model approach for identification of optimal hydrotechnical solutions for gully erosion stabilization. Case Study. *Applied Sciences*, *11*(11), 4847.

Bodoque, J. M., Aroca-Jiménez, E., Eguibar, M. Á., & García, J. A. (2023). Developing reliable urban flood hazard mapping from LiDAR data. *Journal of Hydrology*, *617*, 128975.

Campbell, J. B., & Wynne, R. H. (2011). *Introduction to remote sensing*. Guilford press.

Cheng, G., Huang, Y., Li, X., Lyu, S., Xu, Z., Zhao, H., ... & Xiang, S. (2024). Change detection methods for remote sensing in the last decade: A comprehensive review. *Remote Sensing*, *16*(13), 2355.

Costea, A., Bilasco, S., Irimus, I. A., Rosca, S., Vescan, I., Fodorean, I., & Sestras, P. (2022). *Evaluation of the risk induced by soil erosion on land use. Case study: Guruslău Depression. Sustainability 14*(2)*: 652*.

Dabojani, D., Mithun, D., & Kanti, K. K. (2014, June). River change detection and bankline erosion recognition using remote sensing and GIS. In *Forum geographic*, *13*(1), 12-17.

Ghalehteimouri, K. J., Ros, F. C., Rambat, S., & Nasr, T. (2024). Spatial and temporal water pattern change detection through the normalized difference water index (NDWI) for initial flood assessment: a case study of Kuala Lumpur 1990 and 2021. *Journal of Advanced Research in Fluid Mechanics and Thermal Sciences*, *114*(1), 178-187.

Goswami, A., Sharma, D., Mathuku, H., Gangadharan, S. M. P., Yadav, C. S., Sahu, S. K., ... & Imran, H. (2022). Change detection in remote sensing image data comparing algebraic and machine learning methods. *Electronics*, *11*(3), 431.

Hazarika, N., Das, A. K., & Borah, S. B. (2015). Assessing land-use changes driven by river dynamics in chronically flood affected Upper Brahmaputra plains, India, using RS-GIS techniques. *The Egyptian Journal of Remote Sensing and Space Science*, *18*(1), 107-118.

Kundzewicz, Z. W., Kanae, S., Seneviratne, S. I., Handmer, J., Nicholls, N., Peduzzi, P., ... & Sherstyukov, B. (2014). Flood risk and climate change: global and regional perspectives. *Hydrological Sciences Journal*, *59*(1), 1-28.

Langat, P. K., Kumar, L., & Koech, R. (2019). Monitoring river channel dynamics using remote sensing and GIS techniques. *Geomorphology*, *325*, 92-102.

Mircea, S., Petrescu, N., Musat, M., Radu, A., & Sarbu, N. (2010). Soil erosion and conservation in Romania–some figures, facts and its impact on environment. *Landslides*, *15*, 105-110.

Olariu, P., Cojoc, G. M., Tirnovan, A., & Obreja, F. (2015). The future of the reservoirs in the Siret River Basin considering the sediment transport of rivers (ROMANIA). *GEOREVIEW: Scientific Annals of Stefan cel Mare University of Suceava. Geography Series*, *24*(1), 65-75.

Ouédraogo, M. M., Degré, A., Debouche, C., & Lisein, J. (2014). The evaluation of unmanned aerial system-based photogrammetry and terrestrial laser scanning to generate DEMs of agricultural watersheds. *Geomorphology, 214*, 339-355.

Romanescu, G., & Stoleriu, C. (2013). Causes and effects of the catastrophic flooding on the Siret River (Romania) in July-August 2008. *Natural hazards*, *69*, 1351-1367.

Sestras, P., Badea, G., Badea, A. C., Salagean, T., Roșca, S., Kader, S., & Remondino, F. (2025). Land surveying with UAV photogrammetry and LiDAR for optimal building planning. *Automation in Construction*, *173*, 106092.

Sestras, P., Mircea, S., Cîmpeanu, S. M., Teodorescu, R., Roșca, S., Bilașco, Ș., ... & Spalević, V. (2023). Soil erosion assessment using the intensity of erosion and outflow model by estimating sediment yield: Case study in river basins with different characteristics from Cluj County, Romania. *Applied Sciences*, *13*(16), 9481.

Sestras, P., Mircea, S., RoȘCA, S., Bilașco, Ș., Sălăgean, T., Dragomir, L. O., ... & Kader, S. (2023). GIS based soil erosion assessment using the USLE model for efficient land management: A case study in an area with diverse pedo-geomorphological and bioclimatic characteristics. *Notulae Botanicae Horti Agrobotanici Cluj-Napoca*, *51*(3), 13263-13263.

Spalevic, V., Barovic, G., Vujacic, D., Curovic, M., Behzadfar, M., Djurovic, N., ... & Billi, P. (2020). The impact of land use changes on soil erosion in the river basin of Miocki Potok, Montenegro. *Water*, *12*(11), 2973.

Yang, H., Kong, J., Hu, H., Du, Y., Gao, M., & Chen, F. (2022). A review of remote sensing for water quality retrieval: Progress and challenges. *Remote Sensing*, *14*(8), 1770.

Yao, Z., Xiao, J., Ta, W., & Jia, X. (2013). Planform channel dynamics along the Ningxia–Inner Mongolia reaches of the Yellow River from 1958 to 2008: analysis using Landsat images and topographic maps. *Environmental earth sciences*, *70*, 97-106.

Scientific Papers. Series E. Land Reclamation, Earth Observation & Surveying, Environmental Engineering. Vol. XIV, 2025
Print ISSN 2285-6064, CD-ROM ISSN 2285-6072, Online ISSN 2393-5138, ISSN-L 2285-6064

A GIS-BASED MULTICRITERIA APPROACH FOR IDENTIFYING OPTIMAL REFUGE LOCATIONS FOR SEVERE STORMS: A CASE STUDY IN CLUJ COUNTY, ROMANIA

Paul SESTRAS[1, 2], Ioana POP[1], Florica MATEI[1], Catalin-Stefanel SABOU[1, 3], Simion BRUMA[1, 3], Silvia CHIOREAN[1], Elemer Emanuel SUBA[1], Mircea NAP[1], Iulia COROIAN[1], Jutka DEAK[1], Tudor SALAGEAN[1, 3, 4]

[1]University of Agricultural Sciences and Veterinary Medicine Cluj-Napoca, 3-5 Calea Mănăștur Street, 400372, Cluj-Napoca, Romania
[2]Academy of Romanian Scientists, 3 Ilfov Street, District 5, 050044, Bucharest, Romania
[3]Technical University of Civil Engineering of Bucharest, Doctoral School, 122-124 Lacul Tei Blvd, District 2, 020396, Bucharest, Romania
[4]Technical Sciences Academy of Romania, 26 Dacia Blvd, District 2, 030167, Bucharest, Romania

Corresponding author emails: popioana@usamvcluj.ro, tudor.salagean@usamvcluj.ro

Abstract

In recent years, Romania has experienced an increasing frequency and intensity of severe storms, driven by climate change and resulting in amplified weather-related risks such as heavy rainfall, windstorms, and flash flooding. To enhance regional preparedness and support risk mitigation, this study proposes a GIS-based multi-criteria decision-making framework using the Analytic Hierarchy Process to identify optimal locations for severe storm refuges in Cluj County, Romania. Seven spatial factors were selected, consisting of elevation, slope, land use/land cover, population density, and proximity to roads, rivers, and healthcare facilities. Each factor was reclassified and weighted based on expert input and AHP pairwise comparisons, followed by a weighted overlay analysis in ArcGIS. The final suitability map categorizes the county into five classes: not suitable, less suitable, moderately suitable, suitable, and highly suitable. Results indicate that 68.67% of the total area (4569.5 km²) is moderately suitable, while only 0.07% (4.3 km²) is classified as highly suitable for refuge development. The most favourable areas are found near Cluj-Napoca, due to optimal elevation, gentle slopes, built-up and vegetated land cover, and high accessibility to infrastructure and services. This spatial approach offers a replicable model for enhancing disaster resilience in storm-affected regions of Eastern Europe.

Key words*: GIS, disaster preparedness, climate change, geospatial data, hierarchy classification.*

INTRODUCTION

In recent decades, high-intensity weather events - including cyclones, windstorms, and severe convective storms - have intensified globally (Hussainzad & Gou, 2024). While tropical cyclones are well-monitored, temperate regions now face more frequent non-cyclonic storms, such as derechos and tornadic supercells. These short-lived, localized events can produce flash floods, infrastructure damage, and fatalities, rivalling the impact of larger systems (Bammou et al., 2024). Between 1970 and 2019, such disasters caused nearly 1.9 million deaths and $1.965 trillion in losses worldwide, with risks amplified by urban sprawl, aging infrastructure, and limited preparedness. To mitigate these threats, monitoring systems and spatial risk assessment are essential (Sbihi et al., 2024). Tools like real-time mapping and geospatial modelling help identify hazard-prone zones and inform emergency planning. The integration of Geographic Information Systems (GIS) with multi-criteria decision analysis (MCDA), particularly the Analytic Hierarchy Process (AHP), has proven effective for vulnerability mapping and storm shelter planning (Mamun et al., 2024), strengthening both response strategies and long-term resilience.

In Romania, convective storms are becoming more frequent and intense, especially in regions like Cluj County. These events bring damaging winds, hail, floods, and tornado-like conditions, with thunderstorm activity reaching 270 to 390 hours annually. Wind gusts exceeding 30 m/s often disrupt infrastructure, and over 760,000 lightning flashes occur each year (Calotescu et al., 2024). Climate change has intensified these

hazards through increased moisture, rising temperatures, and shifting airflows (Oprea, 2009), while thunderstorms have surpassed synoptic winds as the main driver of Romania's extreme wind climate (Cristian et al., 2024).

In this context, GIS has become essential for hazard mapping and shelter site selection (Bilașco et al., 2021). By integrating layers such as terrain, land use, hydrology, infrastructure, and demographics, GIS enables spatial analysis for planning and evacuation (Parajuli et al., 2023). Weighted overlays and remote sensing help classify land into suitability zones, improving infrastructure and emergency coordination (Khalaj et al., 2021).

AHP further supports this by ranking decision criteria through expert-driven pairwise comparisons (Das et al., 2024). It accommodates both physical and socio-economic factors (Swain et al., 2020), and its outputs, like weights and consistency ratios, increase transparency and replicability. Widely applied in shelter and hazard mapping (Hasan et al., 2024), AHP becomes more effective when embedded in GIS.

This study presents a GIS-AHP-based methodology to assess storm refuge suitability in Cluj County, Romania, an increasingly vulnerable region. It integrates environmental and infrastructural variables such as elevation, slope, land cover, proximity to rivers, roads, hospitals, and population density. By combining reclassification, weighted overlay, and spatial validation, it produces a suitability map to aid local planning. The approach enhances climate resilience in Central and Eastern Europe and serves as a replicable model for disaster preparedness in other hazard-prone regions.

MATERIALS AND METHODS

Study Area

Cluj County, situated in the heart of Transylvania, Romania, serves as the focal area for this study (Figure 1). Covering an area of 6,674 square kilometers, it ranks as the 12th largest county in the country, accounting for approximately 2.8% of Romania's total land area. Geographically, Cluj County is positioned between latitudes 46°24' and 47°28' N, and longitudes 23°39' and 24°13' E, encompassing a diverse landscape that includes the Apuseni Mountains, the Someș Plateau, and the Transylvanian Plain.

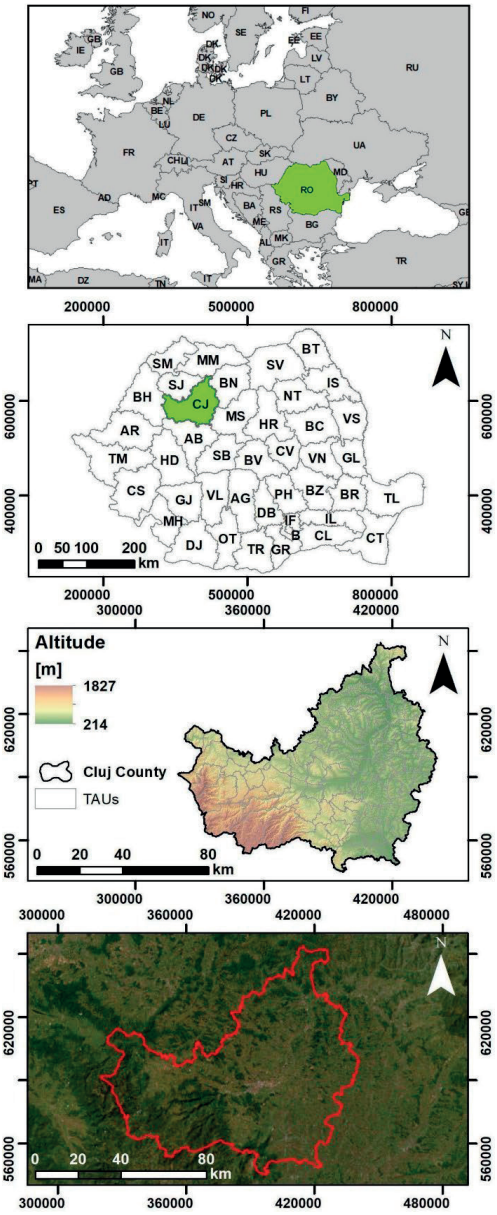


Figure 1. Location and geographic context of Cluj County, Romania. The panels show its position in Europe and within Romania, along with elevation variation and satellite imagery

Cluj-Napoca, the administrative centre of Cluj County and Romania's second-most populous city, is a major cultural and economic hub. The county features a mix of mountainous terrain and plains, creating diverse climate patterns that influence both weather conditions and

infrastructure planning. This varied landscape necessitates tailored hazard mapping and shelter strategies, as local topography directly affects environmental risk and emergency preparedness.

Cluj County was selected due to its increasing exposure to severe convective storms and its strategic role in national disaster planning. Between 2013 and 2022, the county experienced 12 storm-related damage events, including a notable storm on September 17, 2017, with gusts reaching 28.4 m/s. Though historically not a tornado hotspot, Cluj has recorded events like the June 12, 1961, tornado, and rising mesocyclone activity suggests increasing vulnerability (Antonescu & Bell, 2015). Its position along the Carpathian foothills, combined with orographic and climatic factors, leads to frequent summer thunderstorms and high lightning activity (Stan-Sion & Antonescu, 2006). These conditions, especially in the Cluj-Napoca peri-urban zone, highlight the urgency for systematic refuge planning supported by geospatial analysis.

Methodological Approach

This study's methodological framework aims to identify optimal storm refuge locations in Cluj County, Romania, by integrating geospatial data with multicriteria decision-making. The approach includes spatial data collection, preprocessing, AHP-based evaluation, and GIS-weighted overlay analysis. The overall workflow is illustrated in Figure 2. The first step defined the study area within Cluj County, Romania, selected for its rising exposure to severe convective storms and recent documented damage. Geospatial datasets representing seven key variables, elevation, slope, land use/land cover (LULC), population density, and proximity to rivers, roads, and healthcare facilities, were collected from open-access and national sources to ensure spatial consistency for hazard mapping (Nap et al., 2022).

In the preprocessing phase, all data were harmonized in spatial resolution, coordinate system (Stereographic 1970), and study extent. Raster layers were resampled and reclassified into five ordinal suitability classes (1 to 5), enabling comparability and standardized overlay analysis.

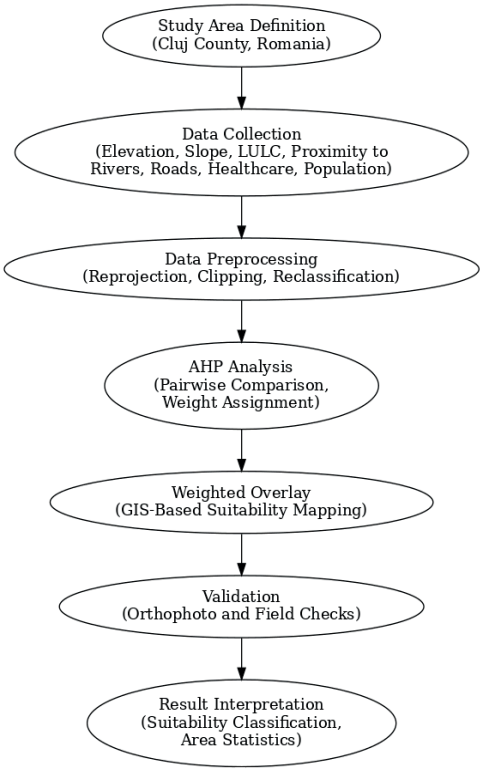


Figure 2. Methodological workflow used for severe storm refuge suitability assessment in Cluj County, Romania, integrating geospatial analysis, AHP-based factor weighting, GIS overlay, and validation steps

To assign importance to each criterion, the Analytic Hierarchy Process (AHP) was applied. Expert-based pairwise comparisons generated weights via the principal eigenvector method, and a consistency ratio (CR < 0.1) validated matrix coherence. This ensured a structured, transparent weighting process.

The core analysis used ArcGIS's weighted overlay tool. Each raster was multiplied by its corresponding AHP weight, and the weighted layers were then summed to generate a final suitability index, which was classified into five categories ranging from 'Not Suitable' to 'Highly Suitable'. Each raster was multiplied by its AHP weight, and the layers summed to produce a final suitability index, classified into five categories: not suitable to highly suitable. The resulting map identified optimal zones for storm shelters or natural refuges.

Model outputs were validated through visual comparisons with 2022 orthophoto imagery and

expert review of known safe zones. "Highly suitable" areas were field-verified for feasibility. Spatial statistics and area metrics summarized storm preparedness potential across Cluj County.

Data Sources and Processing

The methodological strength of this study lies in the integration of geospatial datasets capturing Cluj County's physical, infrastructural, and demographic attributes. These serve as the foundation for the GIS-based multi-criteria analysis aimed at identifying optimal storm refuge sites (Bammou et al., 2024). Seven key thematic layers were selected, elevation, slope, land use/land cover (LULC), population density, and proximity to rivers, roads, and healthcare facilities, due to their relevance in assessing terrain accessibility, environmental risk, and infrastructure connectivity. As in comparable studies, these diverse datasets were converted into standardized raster layers with a uniform spatial resolution and reclassified on a common scale from 1 (not suitable) to 5 (highly suitable). This standardization ensured consistency and enabled integration through weighted overlay analysis. The careful selection and processing of these layers reflect local geographic realities while aligning with international disaster resilience frameworks, thereby enhancing the model's reliability, transferability, and practical relevance.

The geospatial database for this study was meticulously assembled to enable a robust multi-criteria evaluation of storm refuge suitability in Cluj County. Diverse spatial datasets were acquired based on their relevance to storm exposure, accessibility, and demographic vulnerability. Processing was conducted primarily using ArcGIS 10.8, which supported data reprojection, rasterization, reclassification, and spatial analysis (Sestras et al., 2019).

A core input was the 25 m/pixel resolution digital elevation model (DEM) from the Shuttle Radar Topography Mission (SRTM), from which both elevation and slope layers were derived - critical for assessing runoff, flood risk, and structural vulnerability (Sestras et al., 2023).

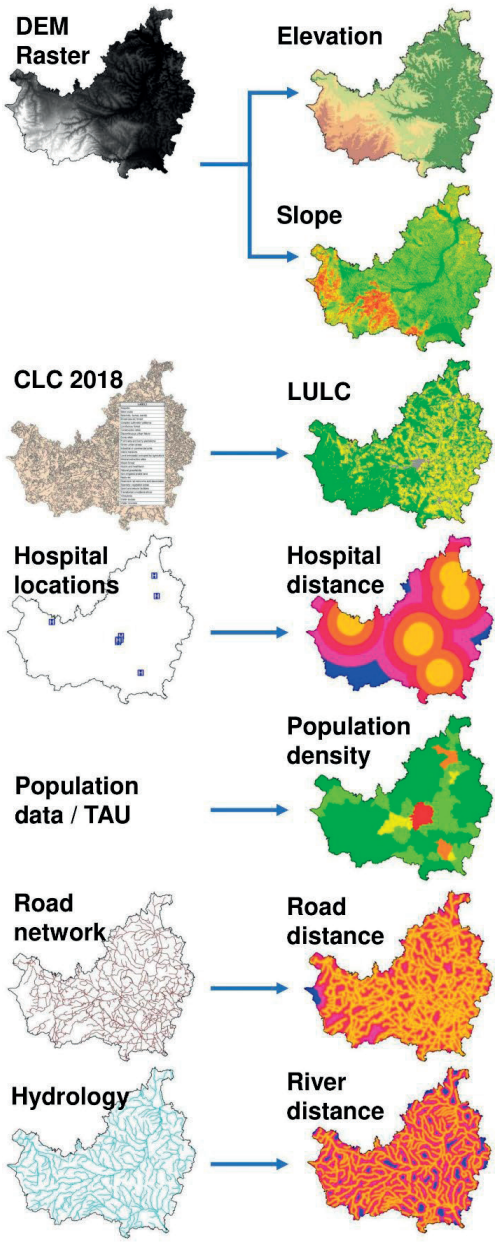


Figure 3. Input geospatial datasets used for storm refuge suitability assessment in Cluj County, including elevation, slope, land use/land cover (CLC 2018), distance to hospitals, population density, road network proximity, and distance to rivers

Land use and land cover were sourced from the Corine Land Cover 2018 (CLC 2018) dataset, developed under the Copernicus program. This standardized European classification system, mapped at 1:100,000, provided surface typologies such as urban, agricultural, and forested areas, each influencing storm impact and shelter feasibility (Popescu et al., 2024). Demographic layers, including population density and hospital proximity, were generated from Romanian government portals, producing rasters of population distribution and healthcare accessibility.

Hydrographic and transportation data were obtained as open-access shapefiles from national and EU platforms, then converted into continuous distance rasters representing proximity to rivers and roads, vital for minimizing flood exposure and ensuring emergency mobility. All raster layers were standardized in resolution, reclassified into five suitability classes, and structured for weighted overlay analysis. This spatial database forms the analytical core of the study, enabling a scientifically sound model for identifying suitable storm refuge zones amid increasing climate-related hazards.

RESULTS AND DISCUSSIONS

Spatial Distribution of Suitability Factors and Final Refuge Suitability Map

Elevation is a key factor in storm refuge planning, influencing both hazard exposure and accessibility. The Elevation Map of Cluj County (Figure 4), derived from 25-meter resolution SRTM data using ArcGIS 10.8, illustrates the county's varied terrain. Elevation was classified into five ranges, from 214 meters (lowest) to 1827 meters (highest), reflecting the topographic gradient from lowland basins and rolling hills in the east and northeast to rugged mountain zones in the south and southwest, notably the Apuseni Mountains.

Lower elevation zones (214-439 m), shown in dark green, are concentrated in the Someșul Mic valley and adjacent plains. These areas typically offer better infrastructure, higher population density, and easier evacuation, making them more suitable for storm refuges. In contrast, zones above 916 meters, marked in brown and orange, are less accessible and prone to hazards such as landslides or snow, making them unsuitable for rapid response or shelter deployment.

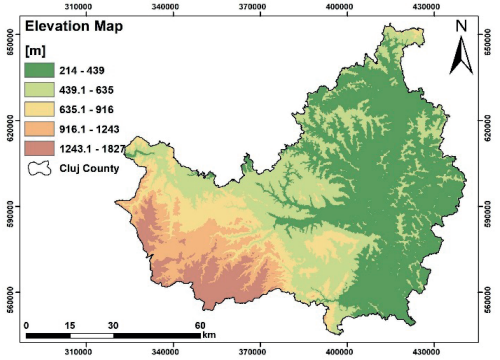


Figure 4. Elevation map of Cluj County derived from SRTM data, reclassified into five elevation ranges to support refuge suitability analysis based on terrain accessibility and storm-related exposure

In cyclone-prone areas, shelters are often built on elevated ground to avoid flooding. While Cluj County doesn't face storm surges, flash floods and heavy rainfall, intensified by climate change, pose serious risks. Thus, elevation must strike a balance: avoiding low-lying flood zones while remaining accessible. The 439-635 meter range was deemed optimal, minimizing flood risk without compromising access for emergency services.

Elevation also influences drainage, infrastructure stability, and emergency logistics. Moderately elevated areas with gentle slopes offer safer, more stable ground. The elevation layer was therefore reclassified to reflect these criteria, increasing the model's relevance for shelter site selection.

By aligning international shelter planning practices (Hasan et al., 2024) with local terrain, the elevation variable strengthens the model's utility for climate-resilient planning in Cluj.

Slope is another critical factor, affecting land use, construction feasibility, and resilience to storms. Derived from the 25-meter SRTM DEM, the slope map (Figure 5) classifies terrain into five categories, from gentle (0-9%) to very steep (49.1-87%). Low-gradient areas in the north and east are ideal for shelter siting due to ease of construction and accessibility, especially for vulnerable groups.

Steeper slopes, concentrated in the southern Apuseni foothills, are unsuitable because of erosion risks, poor access, and construction difficulty (Sestras et al., 2023). Slope also affects runoff, erosion, and infiltration (Costea et al., 2022). Research suggests ideal shelter sites lie on 2-5% slopes, not exceeding 7%, to support safe evacuation and emergency response. Steep areas exceed this threshold, reducing safety and logistics efficiency.

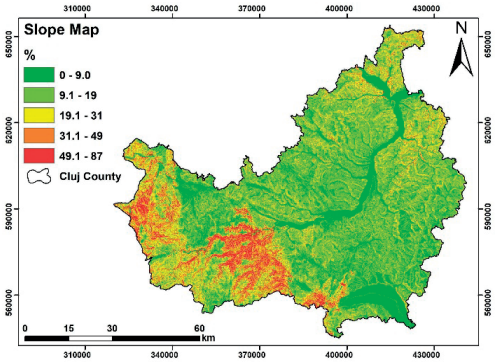


Figure 5. Slope classification map of Cluj County, derived from SRTM data, used to assess terrain suitability for storm refuges based on five slope categories ranging from flat to very steep

In this study, slope is used as a restrictive criterion, assigning higher suitability scores to flatter areas in the AHP model. This approach excludes high-risk or inaccessible terrain, aligning with international best practices, such as those from the IFRC, for emergency shelter siting. Including slope as a core biophysical factor enhances the model's ability to identify stable, accessible refuge zones and supports storm preparedness in diverse topographies.

Land Use and Land Cover (LULC) is another critical spatial variable influencing refuge suitability by affecting environmental stability, functionality, and site accessibility. The LULC map of Cluj County (Figure 6), developed from the Corine Land Cover 2018 dataset using ArcGIS 10.8, reflects five primary land types: agricultural land, vegetation (mainly forests), built-up areas, barren land, and water bodies (Bilașco et al., 2016).

Vegetation-dominated zones, especially in the west and south, overlap with hilly and mountainous terrain. While forests serve as natural buffers during storms and offer protection in rural or peripheral settings, they are generally rated as moderately suitable due to access limitations, rough terrain, and environmental restrictions (Curovic et al., 2020).

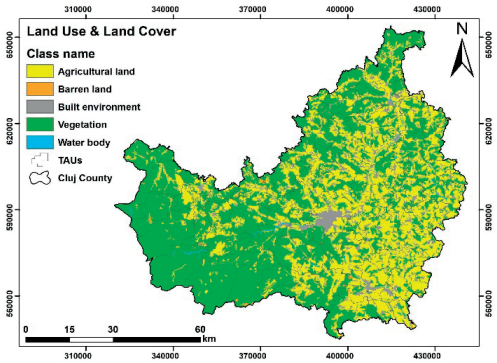


Figure 6. Land Use and Land Cover (LULC) map of Cluj County classified into five categories, supporting the assessment of land suitability for severe storm refuge placement

Agricultural lands, mainly in central and eastern Cluj County, lie on accessible, gently sloped terrain (Chiorean et al., 2024). Though primarily used for farming, they can accommodate storm refuges, especially on less cultivated or public plots. While generally rated as less suitable, with proper land-use planning they can support multipurpose shelter roles.

Built-up areas in cities like Cluj-Napoca, Turda, and Dej include schools and public buildings that are ideal for conversion into storm refuges. Their infrastructure and proximity to dense populations enhance suitability. However, urban congestion and limited space may restrict new shelter construction, reinforcing the need to integrate storm safety into existing urban design.

Barren land, though scarce, is typically open and underused, making it highly suitable for shelter development due to minimal environmental constraints. Conversely, water bodies and floodplains are unsuitable, being prone to flooding, unstable soils, and high exposure during extreme weather.

Including LULC in the multicriteria analysis offers a land-based understanding of site suitability, considering functional roles, adaptability, and environmental priorities (Chiorean et al., 2024). This helps balance refuge placement with ecological and

development needs, supporting a more resilient storm preparedness strategy in Romania.

Population density is another crucial factor, indicating human exposure and emergency logistics needs. The Population Density Map (Figure 8), based on TAU-level data, categorizes values from 702 to 286,598 residents into five classes, from dark green (low) to red (high). This enables targeted refuge planning in high-risk, densely populated zones, where vulnerability and response demands are highest. The Population Density Map (Figure 7), derived from TAU-level data, classifies population values ranging from 702 to 286,598 residents into five categories, from dark green (low density) to red (high density). This classification supports targeted refuge planning in high-risk, densely populated areas where vulnerability and emergency response needs are highest.

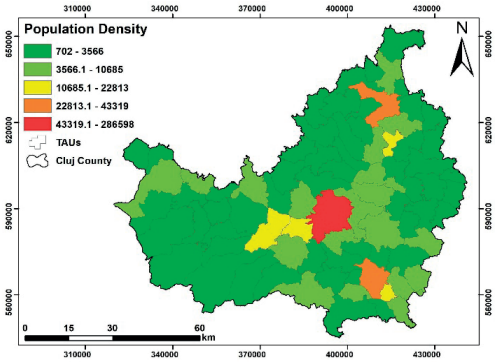


Figure 7. Population density distribution across Cluj County, categorized into five classes, highlighting high-density zones essential for prioritizing storm refuge locations

Cluj-Napoca, marked in red, is the demographic core of Cluj County, with significantly higher population density than surrounding areas. As the administrative and economic hub, it needs a well-distributed shelter network to ensure equitable access. Planning must consider limited space, urban mobility, and integration with existing public buildings, ideally within 1.5 km, following global guidelines for rapid access and minimal evacuation delays.

The orange and yellow zones, representing populations between 10,000 and 43,000 residents, encompass cities such as Turda, Dej, and surrounding peri-urban areas. While these zones are less densely populated, they often lack adequate emergency infrastructure, making them reliant on mobile or temporary shelters. Including these areas in the suitability model ensures that resources are distributed based on both density and spatial coverage.

Rural areas, shown in green, span most of the county but have sparse populations. Despite lower exposure, their isolation, weak healthcare access, and poor transport increase vulnerability. Smaller, strategically placed shelters are essential for timely response.

Population density was weighted in the AHP model to align site prioritization with real-world needs. Dense zones were prioritized for efficiency, while rural communities were considered proportionally to enhance regional resilience. This inclusive, people-centred approach supports equitable storm preparedness.

Access to healthcare is also crucial during and after storms. The Distance from Hospitals Map (Figure 8), created using Euclidean analysis in ArcGIS, divides proximity into five classes from 0 to over 44,000 meters. The most accessible zones, within 9,040 meters, appear in blue to orange and cluster around urban centres like Cluj-Napoca, Turda, Dej, and Huedin. These well-connected areas are ideal for shelters, ensuring rapid medical response during emergencies and improving survival outcomes.

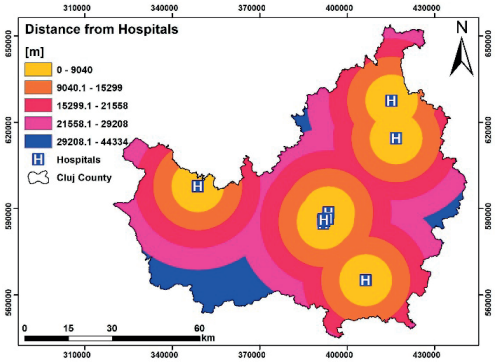


Figure 8. Euclidean distance from hospitals across Cluj County, classified into five distance zones, used to assess healthcare accessibility in emergency refuge site selection

Peripheral and southern rural areas, shown in dark pink and violet, fall into the least accessible zones, often over 29 km from the nearest hospital. These sparsely populated regions face major emergency challenges due to limited

infrastructure. Shelters here risk delayed medical response unless supplemented with mobile clinics or stocked supplies. Thus, hospital proximity is a key constraint in determining site suitability.

Including hospital access in the MCDA framework ensures the model supports human-centred planning, not just physical analysis. Globally, co-locating shelters near medical services is best practice, as immediate access to trauma care, maternal support, and mental health services is vital during disasters. This is echoed in the Sendai Framework, which promotes healthcare resilience and coverage.

In Cluj County, where harsh winters and rural health disparities complicate access, hospital distance is crucial. Including it in the AHP model supports socially responsible storm shelter planning, using realistic travel thresholds to ensure emergency accessibility. Proximity to roads is another essential factor for refuge suitability. The Distance from Roads Map (Figure 9), produced via Euclidean analysis in ArcGIS 10.8, classifies areas within 545 meters of roads as highly suitable, while those beyond 5 km are least suitable. This variable has strong operational relevance. In Cluj's mountainous terrain, evacuation success hinges on road access. Studies show people often delay evacuation, so short, reliable access routes are crucial. Shelters near road networks reduce delays and serve vulnerable populations more effectively. In rugged areas, road proximity often determines whether a refuge is functionally viable.

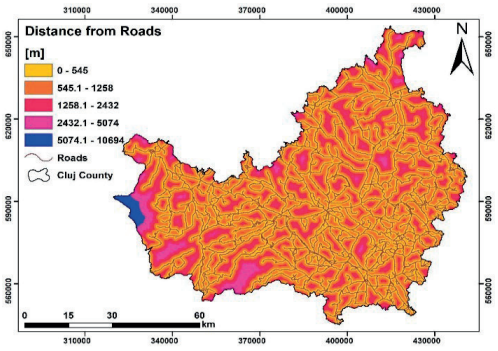


Figure 9. Road distance map of Cluj County showing Euclidean proximity to primary and secondary roads, essential for evaluating emergency accessibility and evacuation efficiency in storm refuge site planning

Most highly accessible zones in Cluj County, shown in yellow and orange, overlap with densely populated, economically active areas, making them ideal for storm refuge placement. In contrast, blue and purple areas in remote and forested regions have limited road access, increasing the risk of evacuation delays, isolation, and restricted emergency response during storms.

Including road proximity in the GIS-based multicriteria model ensures that shelters are not only structurally feasible but also functionally accessible. Prioritizing transport connectivity strengthens an inclusive, resilient shelter network serving both urban and rural communities facing climate-driven storm risks.

Proximity to rivers is equally important in assessing storm refuge suitability, as areas near watercourses are vulnerable to flooding, erosion, and overbank flow during heavy rainfall. Figure 10 shows Euclidean distance from Cluj County's river networks, grouped into five suitability classes, from 0-404 meters (least suitable) to 2073-4480 meters (most suitable). These were derived using hydrological vector data and ArcGIS 10.8 spatial analysis, clearly outlining flood-sensitive zones.

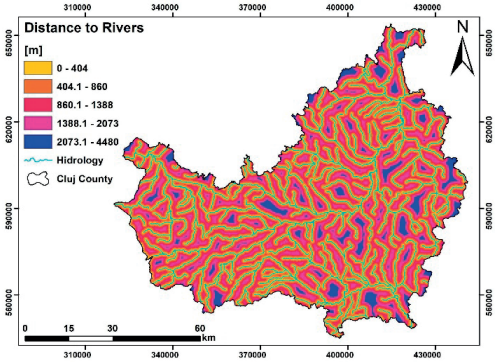


Figure 10. River distance map of Cluj County derived through Euclidean analysis, used to assess flood exposure and prioritize storm refuge sites located at safer distances from hydrological networks

Shelters near rivers face increased risks during storms due to overflow, runoff, and saturated soils. Evacuation delays or structural failures in these areas can threaten safety. Greater distances from rivers often align with higher elevation and slope, reducing flood exposure and improving shelter performance (Yang et al., 2022). This

highlights the need to balance accessibility with environmental resilience.

Standard practice considers locations over 2 km from rivers as highly suitable, minimizing flood risk and supporting evacuation. In Cluj County, these zones, marked in blue, lie on interfluves and plateaus, offering secure and practical options. Areas within 860 meters of rivers (yellow to red) are less suitable and should be avoided.

Incorporating Distance to Rivers into the multicriteria analysis improves the overall resilience of the shelter network. It ensures sites are outside flood zones, helping to safeguard infrastructure, maintain emergency access, and enhance public safety.

The final Severe Storm Refuge Suitability Map for Cluj County (Figure 11) represents the output of a GIS-based multicriteria analysis (MCA) using the Analytic Hierarchy Process (AHP). It combines seven key spatial factors, elevation, slope, land use/land cover, population density, and proximity to rivers, roads, and hospitals, each contributing to the safe and accessible placement of storm refuges.

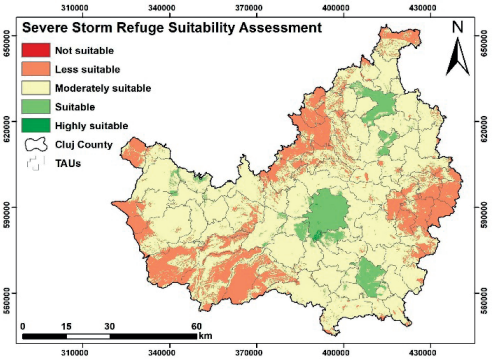


Figure 11. Final storm refuge suitability map for Cluj County, illustrating five suitability classes derived from weighted overlay analysis, integrating elevation, slope, land use, population density, and proximity to infrastructure and rivers

The process began with reclassifying each spatial factor into five standardized suitability classes, followed by a pairwise comparison matrix based on Saaty's (1987) AHP method, informed by expert input and field knowledge. The normalized weights prioritized healthcare proximity (25%) and population density (22%) due to their role in protecting vulnerable, high-density zones. These were followed by proximity to roads (18%) and elevation (16%) for access and hazard mitigation. Slope (7%), LULC (6%), and river distance (6%) had lesser weights due to localized variation.

A weighted overlay in ArcGIS 10.8 then generated a composite map categorizing Cluj County into five refuge suitability levels: Highly Suitable, Suitable, Moderately Suitable, Less Suitable, and Not Suitable. This serves as a clear decision-making tool for emergency planners and local authorities.

The results show that moderately suitable areas dominate the county's central region, with stable terrain and moderate access. Highly suitable zones are located around Cluj-Napoca and peri-urban areas, while mountainous and remote regions, particularly in the southwest and northeast, are largely unsuitable due to steep slopes and limited infrastructure.

Overall, the map offers a reliable, integrated planning tool, combining topographic, infrastructural, and demographic data to support informed storm preparedness and climate resilience strategies.

Interpretation of Suitable Refuge Zones: Spatial Insights and Planning Implications

The final composite figure presents the GIS-based multi-criteria analysis results, showing storm refuge suitability across Cluj County. Generated through an AHP-guided weighted overlay, the map categorizes the area into five classes: not suitable, less suitable, moderately suitable, suitable, and highly suitable. Supporting charts indicate that 68.67% of the region is moderately suitable, while only 0.07% (4.308 km²) qualifies as highly suitable, reflecting the stringent conditions for optimal shelter placement.

A notable highly suitable area is the Făget neighbourhood in southern Cluj-Napoca, characterized by moderate elevation, low slopes (<5%), and a mix of built-up and vegetated land, enhancing accessibility and natural buffering. Its proximity to roads and hospitals and distance from rivers further improve suitability, as assessed through Euclidean distance metrics.

A detailed zoom-in, overlaid with orthophoto imagery, validates the GIS outputs and supports local-scale planning. This visualization serves as

a tool for municipal authorities to prioritize interventions and guide resource distribution.

The study aligns with global emergency planning standards, where factors like elevation, slope, and infrastructure access are central to GIS-AHP approaches. Its successful adaptation to Romania's varied terrain demonstrates the method's versatility. By combining spatial analysis with policy-relevant insights, the study offers a transferable model for disaster preparedness in Eastern Europe and similar regions.

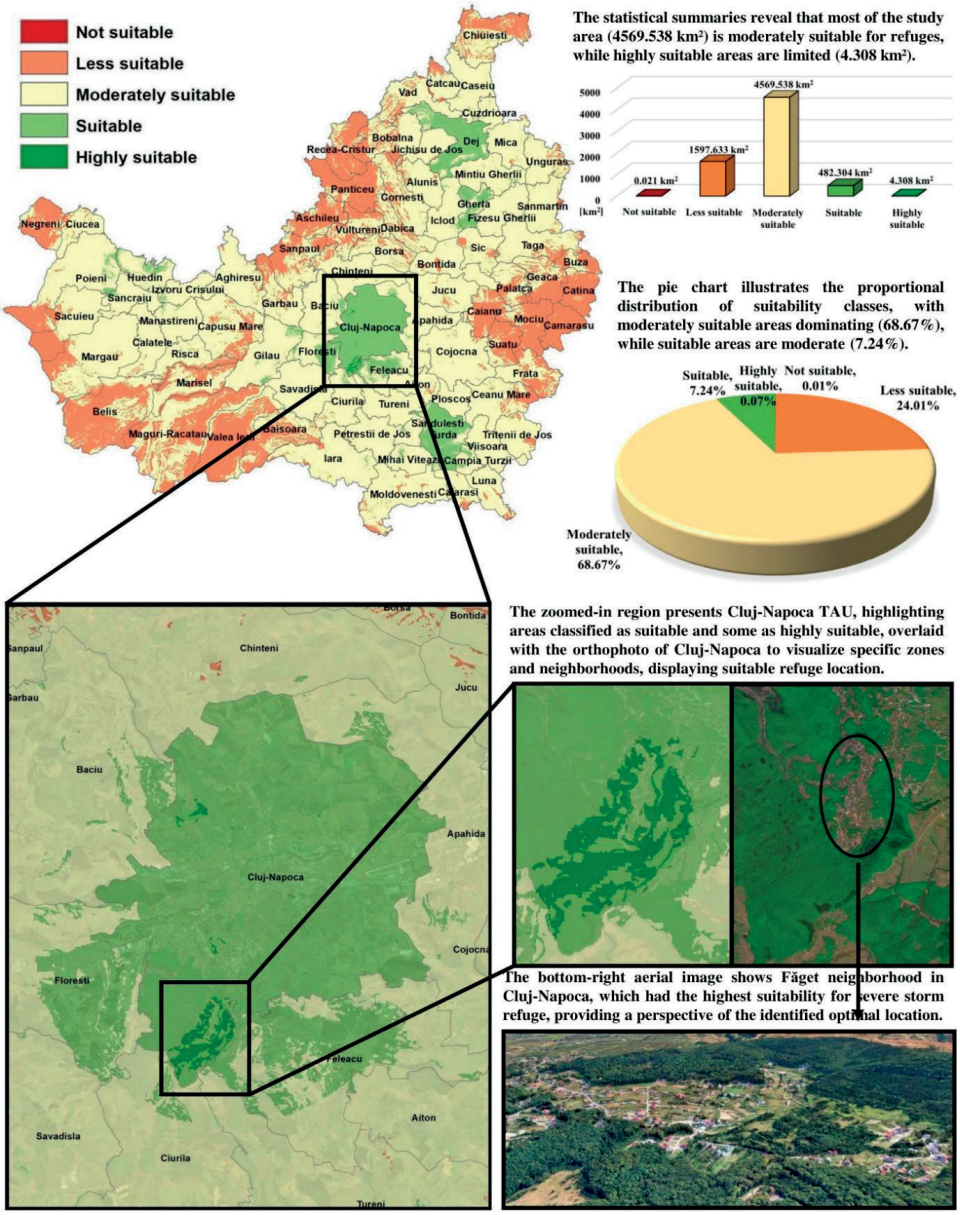


Figure 12. Spatial and statistical synthesis of the final storm refuge suitability analysis in Cluj County, highlighting highly suitable zones around Cluj-Napoca. Includes area statistics, proportional class distribution, orthophoto overlays, and aerial imagery of Făget neighbourhood, identified as the optimal refuge location

CONCLUSIONS

This study employed a GIS-based multicriteria approach to identify optimal storm refuge locations in Cluj County, Romania, an area increasingly exposed to extreme weather due to climate change. Using the Analytic Hierarchy Process, seven critical factors were weighted: elevation, slope, population density, land use/land cover, and proximity to rivers, roads, and healthcare facilities.

The final suitability map, validated through orthophoto overlays and field verification, showed that most of the county (68.67%) is moderately suitable, while only 0.07% is highly suitable. The Făget neighbourhood in Cluj-Napoca stood out as an ideal refuge site due to its balanced elevation, low slopes, strong infrastructure access, and diverse land cover.

These results demonstrate the value of GIS-AHP models for disaster risk reduction and spatial planning. The methodology offers a replicable, objective framework for shelter site selection, providing a model for climate resilience strategies not only in Romania but across other vulnerable regions in Eastern Europe.

ACKNOWLEDGEMENTS

This research was carried out with the support of the Ministry of Education and was financed through the CNFIS-FDI-2024-F-0195 project, funded by the National Council for Financing Higher Education (CNFIS).

REFERENCES

Antonescu, B., & Bell, A. (2015). Tornadoes in Romania. *Monthly Weather Review*, 143(3), 689-701.

Bammou, Y., Benzougagh, B., Igmoullan, B., Kader, S., Ouallali, A., Spalevic, V., ... & Kuriqi, A. (2024). Spatial mapping for multi-hazard land management in sparsely vegetated watersheds using machine learning algorithms. *Environmental Earth Sciences*, 83(15), 447.

Bammou, Y., Benzougagh, B., Igmoullan, B., Ouallali, A., Kader, S., Spalevic, V., ... & Marković, S. B. (2024). Optimizing flood susceptibility assessment in semi-arid regions using ensemble algorithms: a case study of Moroccan High Atlas. *Natural Hazards*, 120(8), 7787-7816.

Bilaşco, Ş., Roşca, S., Păcurar, I., Moldovan, N., Boţ, A., Negruşier, C., ... & Naş, S. (2016). Identification of land suitability for agricultural use by applying morphometric and risk parameters based on GIS spatial analysis. *Notulae Botanicae Horti Agrobotanici Cluj-Napoca*, 44(1), 302-312.

Bilaşco, Ş., Roşca, S., Vescan, I., Fodorean, I., Dohotar, V., & Sestras, P. (2021). A GIS-based spatial analysis model approach for identification of optimal hydrotechnical solutions for gully erosion stabilization. Case Study. *Applied Sciences*, 11(11), 4847.

Calotescu, I., Chitez, A. S., Birsan, M. V., Micu, D., & Dumitrescu, A. (2024). Assessment of thunderstorm-prone areas in Romania based on wind damage occurrence and surface observation data. *Journal of Wind Engineering and Industrial Aerodynamics*, 250, 105765.

Chiorean, S., Arion, I. D., Sălăgean, T., Nap, M. E., Șuba, E. E., & Colișar, A. (2024). The Impact of Market Analysis in Determining the Market Value of Agricultural Land in Romania. *Scientific Papers Series Management, Economic Engineering in Agriculture & Rural Development*, 24(1).

Chiorean, S., Coroian, I., Sălăgean, T., Nap, M. E., Deak, J., & Lupuț, I. (2024). Global Trends on Research Towards the Valuation Process of an Agriculture Land. *Scientific Papers Series Management, Economic Engineering in Agriculture & Rural Development*, 24(2).

Costea, A., Bilasco, S., Irimus, I. A., Rosca, S., Vescan, I., Fodorean, I., & Sestras, P. (2022). Evaluation of the risk induced by soil Erosion on land use. Case study: Guruslău depression. *Sustainability*, 14(2), 652.

Cristian, A., Zuzeac, M., Ciocan, G., Iorga, G., & Antonescu, B. (2024). A Thunderstorm Climatology of Romania (1941–2022). *Romanian Reports in Physics*, 76, 710.

Curovic, M., Spalevic, V., Sestras, P., Motta, R., Dan, C., Garbarino, M., ... & Urbinati, C. (2020). Structural and ecological characteristics of mixed broadleaved old-growth forest (Biogradska Gora-Montenegro). *Turkish journal of Agriculture and Forestry*, 44(4), 428-438.

Das, T., Talukdar, S., Naikoo, M. W., Ahmed, I. A., Rahman, A., Islam, M. K., & Alam, E. (2024). Integration of fuzzy AHP and explainable AI for effective coastal risk management: A micro-scale risk analysis of tropical cyclones. *Progress in Disaster Science*, 23, 100357.

Hasan, I., Faruk, M. O., Katha, Z. T., Goni, M. O., Islam, M. S., Chakraborty, T. R., ... & Hossain, M. S. (2024). Geo-spatial based cyclone shelter suitability assessment using analytical hierarchy process (AHP) in the coastal region of Bangladesh. *Heliyon*, 10(21).

Hussainzad, E. A., & Gou, Z. (2024). Climate Risk and Vulnerability Assessment in Informal Settlements of the Global South: A Critical Review. *Land*, 13(9), 1357.

Khalaj, M. R., Noor, H., & Dastranj, A. (2021). Investigation and simulation of flood inundation hazard in urban areas in Iran. *Geoenvironmental Disasters*, 8, 1-13.

Mamun, M. A. A., Zhang, L., Chen, B., Rahman, Z. U., Mahzabin, T., Zuo, J., ... & Reza, S. A. (2024). Assessment of spatial cyclone surge susceptibility through GIS-based AHP multi-criteria analysis and frequency ratio: a case study from the Bangladesh

coast. *Geomatics, Natural Hazards and Risk*, 15(1), 2368071.

Mourato, S., Fernandez, P., Pereira, L. G., & Moreira, M. (2023). Assessing vulnerability in flood prone areas using analytic hierarchy process - group decision making and geographic information system: a case study in Portugal. Applied Sciences, 13(8), 4915.

Nap, M. E., Ficior, D., Sălăgean, T., Pop, I. D., Matei, F., Coroian, I., ... & Șuba, E. E. (2022). A GIS study about forest management in Strâmbu Baiut. *Bulletin of University of agricultural sciences and veterinary medicine Cluj-Napoca. Horticulture,* 79(1), https://doi.org/10.15835/buasvmcn-hort:2021.0025

Oprea, C. I. (2009). A torrential precipitation event in the eastern part of Romania–a case study. *Romanian reports in physics*, 61(1), 139-150.

Parajuli, G., Neupane, S., Kunwar, S., Adhikari, R., & Acharya, T. D. (2023). A GIS-based evacuation route planning in flood-susceptible area of Siraha municipality, Nepal. *ISPRS International Journal of Geo-Information*, 12(7), 286.

Popescu, G., Popescu, C. A., Dragomir, L. O., Herbei, M. V., Horablaga, A., Țenche-Constantinescu, A. M., ... & Sestras, P. (2024). Utilizing UAV technology and GIS analysis for ecological restoration: A case study on Robinia pseudoacacia L. in a mine waste dump landscape rehabilitation. *Notulae Botanicae Horti Agrobotanici Cluj-Napoca*, 52(4), 13937-13937.

Saaty, R. W. (1987). The analytic hierarchy process - what it is and how it is used. *Mathematical modelling*, 9(3-5), 161-176.

Sbihi, A., Mastere, M., Benzougagh, B., Spalevic, V., Sestras, P., Radovic, M., ... & Kader, S. (2024). Assessing landslide susceptibility in northern Morocco: A geostatistical mapping approach in Al Hoceima-Ajdir. *Journal of African Earth Sciences*, 218, 105361.

Sestras, P., Mircea, S., Cîmpeanu, S. M., Teodorescu, R., Roșca, S., Bilașco, Ș., ... & Spalević, V. (2023). Soil erosion assessment using the intensity of erosion and outflow model by estimating sediment yield: Case study in river basins with different characteristics from Cluj County, Romania. *Applied Sciences*, 13(16), 9481.

Sestras, P., Mircea, S., Roșca, S., Bilașco, Ș., Sălăgean, T., Dragomir, L. O., & Kader, S. (2023). GIS based soil erosion assessment using the USLE model for efficient land management: a case study in an area with diverse pedo-geomorphological and bioclimatic characteristics. *Notulae Botanicae Horti Agrobotanici Cluj-Napoca* 51 (3): 13263-13263.

Sestraș, P., Sălăgean, T., Bilașco, S., Bondrea, M. V., Naș, S., Fountas, S., & Cîmpeanu, S. M. (2019). Prospect of a GIS based digitization and 3D model for a better management and land use in a specific micro-areal for crop trees. *Environmental Engineering and Management Journal*, 18(6), 1269-1277.

Stan-Sion, A., & Antonescu, B. (2006, November). Mesocyclones in Romania–characteristics and environments. In *Preprints of the 23rd Conference on Severe Local Storms. St. Louis, MO*.

Swain, K. C., Singha, C., & Nayak, L. (2020). Flood susceptibility mapping through the GIS-AHP technique using the cloud. *ISPRS International Journal of Geo-Information*, 9(12), 720.

Yang, F., Xiong, S., Ou, J., Zhao, Z., & Lei, T. (2022). Human settlement resilience zoning and optimizing strategies for river-network cities under flood risk management objectives: taking Yueyang City as an example. *Sustainability*, 14(15), 9595.

Scientific Papers. Series E. Land Reclamation, Earth Observation & Surveying, Environmental Engineering. Vol. XIV, 2025
Print ISSN 2285-6064, CD-ROM ISSN 2285-6072, Online ISSN 2393-5138, ISSN-L 2285-6064

MONITORING DIFFERENT GRASS VARIETIES USING MULTISPECTRAL IMAGERY BASED ON DIFFERENT IRRIGATION REGIMES

Elemer-Emanuel SUBA[1], Tudor SALAGEAN[1, 2, 3], Ioana Delia POP[1], Florica MATEI[1], Silvia CHIOREAN[1], Mircea-Emil NAP[1], Paul SESTRAS[1, 2], Simion BRUMA[1, 2], Catalin-Stefanel SABOU[1, 2], Vlad PAUNESCU[4], Valentin-Sebastian DAN[1], Ferencz VAKAR[1]

[1]University of Agricultural Sciences and Veterinary Medicine Cluj-Napoca,
3-5 Calea Mănăștur Street, 400372, Cluj-Napoca, Romania
[2]Technical University of Civil Engineering of Bucharest, Doctoral School,
122-124 Lacul Tei Blvd, District 2, 020396, Bucharest, Romania
[3]Technical Sciences Academy of Romania, 26 Dacia Blvd, District 2, 030167, Bucharest, Romania
[4]University of Agronomic Sciences and Veterinary Medicine of Bucharest,
59 Mărăști Blvd, District 1, 011464, Bucharest, Romania

Corresponding author emails: tudor.salagean@usamvcluj.ro, mircea.nap@usamvcluj.ro

Abstract

This study analyses the physiological response and visual quality of several grass varieties grown on four experimental lots, using multispectral imaging for monitoring. The control lot did not receive irrigation, while the other three experimental lots were subjected to distinct irrigation regimes: rotors (lot 1), sprays (lot 2), and underground drip irrigation (lot 3). Multispectral data allowed the assessment of vegetative parameters, to analyse the differences in vegetative state and water stress levels between the lots and grass varieties. The results showed significant variations between the experimental lots, depending on both the type of irrigation and the grass variety, highlighting the efficiency of different irrigation systems in both water conservation and maintaining an optimal vegetative state. The study offers valuable insights for optimizing irrigation practices and selecting grass varieties suited to both specific site conditions and the implementation of sustainable maintenance strategies.

Key words*: monitoring, multispectral imagery, remote sensing.*

INTRODUCTION

Parks represent an important resource in the sustainable and lasting development of cities and municipalities. The grass within these areas serves numerous roles, besides its aesthetic function, it also contributes to maintaining adequate air quality (Chiesura, 2004). Maintaining green spaces with lawns presents a challenge in terms of irrigation while also ensuring efficient water management (Schebella et al., 2014). The management of water resources, particularly in the context of climate change and the rapid expansion of large cities at the expense of diminishing water supplies, remains a constant concern for specialists (Kenna & Horst, 1993). The use of multispectral imaging to assess the efficiency of irrigation systems and optimize turfgrass mixtures to reduce water consumption is an important focus in the current context of climate change and urban development (Krum et al., 2010). Building on previous studies (Kerry et al., 2024), our research differs by implementing a field experiment differently as other studies (Orta et al., 2023) with four test lots, each subjected to three different irrigation treatments, along with a control lot that received no irrigation. The irrigation treatments delivered the same amount of water to the grass in each respective lot. Additionally, all test lots contained 12 different turfgrass mixtures, allowing us to evaluate their behaviour using multispectral imaging. The study was conducted during autumn, just before the dormancy period, to highlight the resilience of turfgrass based on the accumulated vegetative growth over the season. Furthermore, the research aimed to emphasize the importance of fertilizer application in maintaining turfgrass performance and adaptability.

MATERIALS AND METHODS

This study investigates the influence of different irrigation types on various vegetation indices across multiple lawn mix types. The vegetation indices analysed include the Green Normalized Difference Vegetation Index (GNDVI; Gitelson et al., 1996), Leaf Chlorophyll Index (LCI; Sousa-Souto et al., 2018), Modified Chlorophyll Absorption Ratio Index (MCARI; Daughtry et al., 2000), Normalized Difference Red Edge Index (NDRE; Gitelson et al., 1996), Normalized Difference Vegetation Index (NDVI; Tucker, 1979), and Structure Insensitive Pigment Index (SIPI_2; Peñuelas et al., 1995). The study aims to determine the most effective irrigation method for maintaining optimal plant health and nutrient absorption.

A series of field trials were conducted on multiple lawn mix types under different irrigation treatments. The experimental design of the field and office works are presented (Sestras et al., 2019) in Figure 1.

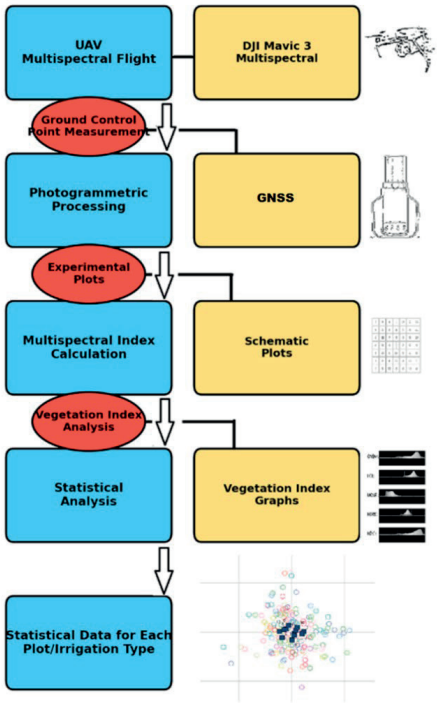


Figure 1. Experimental design

Measurements were taken using remote sensing techniques, and statistical analysis was performed to identify trends among irrigation types and lawn mix performance. For this study, a DJI Mavic 3 Multispectral (3M) drone was utilized, equipped with two advanced cameras that enable high-precision scanning and analysis of various crops. The photogrammetric processing was conducted in Agisoft Photoscan and the Ground Control Points (GCPs) served just as verification points, as the drone was equipped with RTK Module. All the indices were computed in Agisoft metashape, using raster calculator, then exported as raster images. This type of equipment is widely used in agriculture and forestry applications, providing valuable insights into vegetation health and land management. The analyses were preformed using ArGis (Popescu et al., 2024; Bilaşco et al., 2016; Sestras et al., 2018), and IBM SPSS Statistics (SPSS).

The main characteristics of the equipment are presented in Table 1. Because we were able to fly at low altitudes, we obtained a spatial resolution under 1 cm/pixel.

Table 1. Multispectral drone specifications

Component	Specification
Multispectral Camera - Spectral Bands	Green (560 ± 16 nm), Red (650 ± 16 nm), Red Edge (730 ± 16 nm), Near-Infrared (860 ± 26 nm)

These spectral bands offer valuable insights for assessing plant health, identifying stress factors, and enhancing precision agriculture practices. By integrating both RGB and multispectral imaging capabilities, the DJI Mavic 3M drone proves to be a versatile instrument for remote sensing in agriculture, forestry, and environmental monitoring.

In this study, experimental plots featuring twelve distinct lawn types were analyzed, arranged as shown in Figure 2.

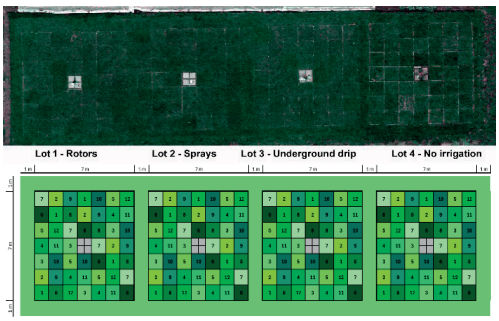


Figure 2. Experimental lots

The twelve lawn mix types are described in the Table 2, with all the mixt numbering correlated with the lots and all the components and the percentage of each lawn used (Hitter et al., 2021). As shown in the experimental design, we conducted a multispectral image acquisition and then applied diverse spectral vegetation indices are presented in Table 3.
The desired quantity of water used for irrigation is presented in Table 4.

Table 2. Lawn Mixes and composition

No.	Mix Name	Composition
1	**BRB Bar Power RPR**	*Lolium perenne* 40%, *L. perenne* 20%, *Festuca rubra commutata* 20%, *F. rubra rubra* 10%, *Poa pratensis* 10%
2	**BRB Rapid**	*Lolium perenne* 30%, *L. perenne* 25%, *L. perenne* 20%, *Festuca rubra* 15%, *Poa pratensis* 10%
3	**BRB Shadow**	*Festuca rubra* 60%, *Lolium perenne* 20%, *Poa pratensis* 20%
4	**BRB SOS - Super Over Seeding**	*Lolium perenne* 50%, *L. perenne* 50%
5	**BRB Speedy Green**	*Lolium perenne* 34%, *L. p.* BARRAGE 31%, *L. perenne* 31%, *L. perenne* 4%
6	**BRB WaterSaver**	*Lolium perenne* 10%, *Festuca arundinacea* 20%, *F. around.* 20%, *F. around.* 40%, *Poa pratensis* 10%
7	**DLF TURFLINE Eco Lawn**	*Lolium perenne* 30%, *Festuca rubra* 40%, *F. rubra litoralis* 20%, *Poa pratensis* 5%, *Trifolium repens* 5%
8	**DLF TURFLINE Sport**	*Lolium perenne* 30%, *Festuca rubra commutata* 30%, *F. rubra litoralis* 15%, *F. ovina* 5%, *Poa pratensis* 20%
9	**DLF TURFLINE Waterless**	*Lolium perenne* 10%, *Festuca arundinacea* 80%, *Poa pratensis* 10%
10	**ICL Landscaper Pro Performance**	*Lolium perenne* 80%, *Festuca rubra rubra* 20%
11	**ICL Landscaper Pro Rapid**	*Lolium perenne* 75%, *Festuca rubra rubra* 15%, *Poa pratensis* 10%
12	**ICL ProSelect Regenerator Plus**	*Lolium perenne* 75%, *Poa pratensis* 25%

Table 3. Spectral Vegetation Indices used

Index	Description	Calculation Formula	Author
NDVI (Normalized Difference Vegetation Index)	Assesses vegetation health and vigour.	(NIR - Red) / (NIR + Red)	Tucker, 1979
GNDVI (Green Normalized Difference Vegetation Index)	Evaluates chlorophyll levels and plant health.	(NIR - Green) / (NIR + Green)	Gitelson, 1996
NDRE (Normalized Difference Red Edge Index)	Measures nitrogen uptake and chlorophyll concentration.	(NIR - RedEdge) / (NIR + RedEdge)	Haboudane, 2004
LCI (Leaf Chlorophyll Index)	Estimates chlorophyll concentration in leaves.	(NIR - RedEdge) / (NIR + RedEdge)	Souto, 2018
MCARI (Modified Chlorophyll Absorption in Reflective Index)	Determines chlorophyll absorption and plant stress levels.	1.2 * (2.5 * (NIR - Red) - 1.3 * (NIR - Green)) / (normalized to reflectance in red, green, and NIR bands)	Daughtry, 2000
SIPI_2 (Structure Insensitive Pigment Index)	Analyses pigment ratios and stress resistance in plants.	(NIR - Blue) / (NIR + Red)	Peñuelas et al., 1995

Table 4. Desired Irrigation quantity

Irrigation Type	Precipitation Rate (mm/h)	Run Time (minutes)	Desired depth of water application (mm/sqm
Spray Irrigation (2)	40	6	4.5
Rotor Irrigation (1)	24	12	4.5
Drip Irrigation (3)	18.37	15	4.5
No Irrigation (0)	0	0	0

RESULTS AND DISCUSSIONS

The photogrammetric survey was made on 7th As shown in the Figure 4 it could be clearly seen that the moisture is decreasing gradually, as there was no irrigation used on this period, having in mind that the lawn was prepared for winter. Also correlating this graph with the weather graph presented in Figure 3 it can be clearly seen that the temperatures were below 0 degrees, so that no irrigation could have been applied.
November 2024, in order to see how the post vegetative stage affects the grass health, and in what percentage the fertilization and the accumulated nutrients help the plants to maintain a healthy aspect. The weather evolution before the photogrammetric survey it is presented Figure 3.

The soil moisture was also recorded on the ground level, at approximately 5cm underground, the main results for soil moisture are presented in Figure 4, as a medium value of three sensors each placed on lot 1, 2 and 3.

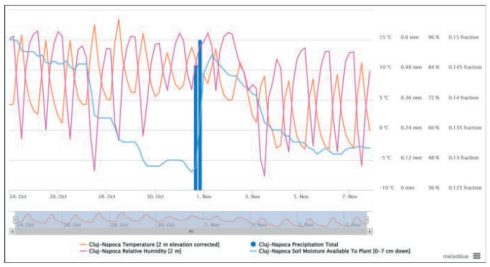


Figure 3. Weather and precipitations before and around the survey (Source Meteoblue)

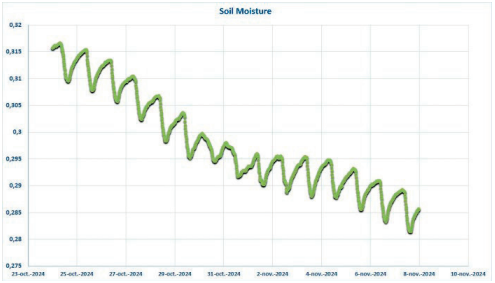


Figure 4. Soil Moisture graph for the period before the survey

The NDVIis a widely used metric for assessing vegetation health and density based on spectral reflectance. It measures the difference between the absorption of red light by chlorophyll and the reflection of near-infrared (NIR) light by plant structures (Herbei& Badaluta-Minda, 2024).
In Figure 5 it can be seen the results obtained for the NDVI index applied on our experimental lots.

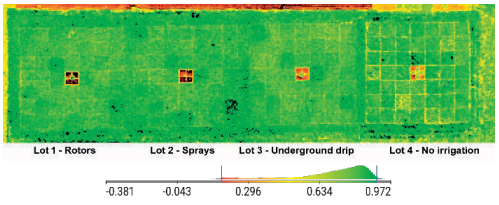


Figure 5. NDVI Index applied on the experimental lot

Range: NDVI values typically vary between -1 and +1, providing insights into vegetation cover and health (Constantinescu et al., 2018).
High NDVI Values (close to +1): represent dense, healthy green vegetation with high chlorophyll content. These areas appear bright green on NDVI maps.
Moderate NDVI Values (around 0): indicate sparse vegetation or grassland areas with lower chlorophyll levels. These zones are often shown in yellow or light green.
Low NDVI Values (close to -1): correspond to barren land, exposed soil, or rock surfaces, where vegetation is absent. Such areas appear in brown or reddish tones.
The Green Normalized Difference Vegetation Index (GNDVI) is a widely used vegetation index that measures the amount of healthy green vegetation within an area. By comparing the reflectance values of specific spectral bands, GNDVI provides a quantitative assessment of vegetation health and vigour. The results for our experimental lots are presented in Figure 6.

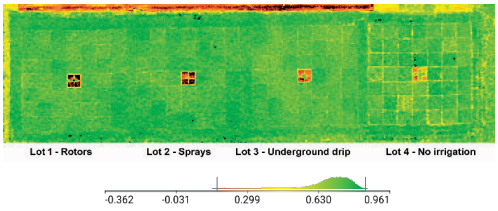


Figure 6. GNDVI Index applied on the experimental lot

GNDVI values range from -1 to +1, with higher values indicating denser and healthier vegetation cover.
High GNDVI values (closer to +1) suggest areas with high chlorophyll content and strong photosynthetic activity, typically associated with lush, healthy vegetation.
Moderate GNDVI values indicate areas with some vegetation, such as grasslands or sparse crops, where plant health varies.
Low GNDVI values (close to 0) are characteristic of bare soil, urban areas, or areas with low vegetation density.
Negative values suggest the presence of water bodies, barren land, or non-vegetated surfaces.
For our studied area, the distribution of GNDVI values shows a peak in the positive range, indicating a predominance of vegetation with healthy chlorophyll levels.
The colour gradient in the legend transitions from grey (-1) to orange (low values), yellow (moderate values), and green (high values),

which visually represents the varying density of vegetation.
The histogram peak in the green region suggests that most of the analysed area consists of healthy and dense vegetation, while smaller portions fall in the yellow and orange ranges, indicating areas with moderate or lower vegetation health.
The Normalized Difference Red Edge Index (NDRE) is a vegetation index closely related to NDVI but incorporates Red Edge light instead of the traditional Red band. The Red Edge wavelength penetrates deeper into the leaf structure, allowing for a more accurate assessment of chlorophyll content and plant stress.
The results for our experimental lots are presented in Figure 7.

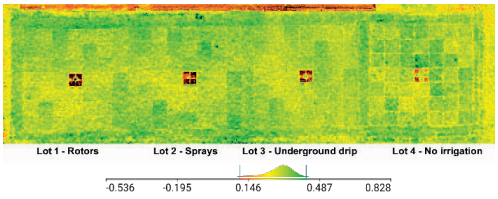


Figure 7. NDRE Index applied on the experimental lot

The representation of NDRE, as shown Figure 7, follows a gradient:
Negative values or values close to zero (grey to dark orange) represent barren land, non-vegetated surfaces, or unhealthy vegetation.
Moderate values (yellow to light green) indicate areas with some vegetation, but with possible stress or lower chlorophyll content.
High values (bright green) are associated with dense, healthy vegetation, indicating strong chlorophyll activity and robust plant health.
The NDRE histogram suggests that most of the measured values are concentrated in the positive range (yellow to green), indicating overall good vegetation health in the analysed area.
A gradual transition from orange to yellow and then to green demonstrates variations in plant vigour, with some areas experiencing stress while others remain healthy.
The use of Red Edge light makes NDRE particularly valuable for detecting subtle variations in vegetation health before visible symptoms appear, making it a powerful tool for precision agriculture and crop monitoring.
The Leaf Chlorophyll Index (LCI) is a vegetation index designed to measure chlorophyll content in leaves, offering valuable insights into plant health and photosynthetic efficiency. LCI utilizes the Near Infrared (NIR) and Red Edge spectral bands, as NIR is sensitive to the internal structure and moisture content of the leaf, while Red Edge strongly correlates with chlorophyll concentration. The results for our experimental lots are presented in Figure 8.

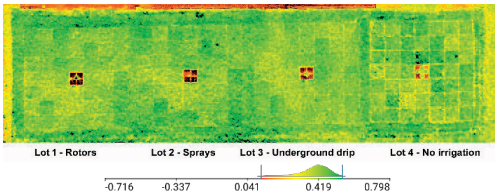


Figure 8. LCI Index applied on the experimental lot

The representation of LCI, as shown in Figure 6 colour scale, follows a gradient:
Low values (grey to dark orange): indicate areas with low chlorophyll content, which could be associated with barren land, non-vegetated surfaces, or vegetation experiencing severe stress.
Moderate values (yellow to light green): represent regions with some vegetation, but with possible deficiencies in chlorophyll due to environmental stress or suboptimal nutrient availability.
High values (bright green): correspond to healthy, thriving vegetation with high chlorophyll concentration, indicating strong photosynthetic activity and robust plant growth.
The LCI histogram suggests that most of the measured values are concentrated in the positive range (yellow to green), indicating overall good vegetation health in the analysed area.
A gradual transition from orange to yellow and then to green illustrates variations in plant vigour, with certain areas experiencing mild to moderate stress while others exhibit optimal growth.
The combination of NIR and Red Edge bands enhances LCI's ability to detect subtle chlorophyll variations, making it particularly useful for monitoring nutrient status, irrigation effectiveness, and early stress detection.
The Modified Chlorophyll Absorption Ratio Index (MCARI) is a vegetation index designed to measure the intensity of chlorophyll absorption in plants. It is highly sensitive to

variations in chlorophyll concentration and the Leaf Area Index (LAI), making it a valuable tool for assessing plant health and stress levels. Unlike some other indices, MCARI is less influenced by lighting conditions, soil background reflectance, and non-photosynthetic materials. The results for our experimental lots are presented in Figure 9.

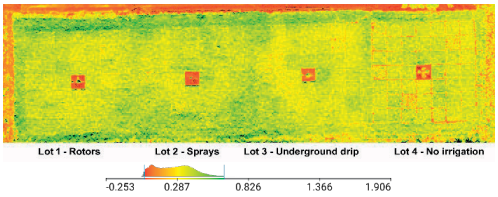


Figure 9. MCARI Index applied on the experimental lot

The MCARI colour scale presented on Figure 9 provides a visual representation of its values:
Low values (dark to light green) indicate a higher chlorophyll content, meaning healthier and more vigorous vegetation.
Moderate values (yellow to orange) represent areas with moderate chlorophyll levels, possibly indicating some plant stress or early signs of nutrient deficiency.
High values (dark orange to red) correspond to regions with low chlorophyll content, which may be associated with plant stress, chlorosis, or reduced photosynthetic activity.
The MCARI histogram shows that most of the analysed area has values in the moderate-to-high range, suggesting a mix of healthy and slightly stressed vegetation.
A strong presence of orange and red areas highlights zones with lower chlorophyll content, possibly indicating stress or poor nutrient absorption.
Since MCARI is primarily used for detecting chlorophyll variations, it is often interpreted in combination with NDVI or LAI to gain a more comprehensive understanding of vegetation health.
The Structure Insensitive Pigment Index (SIPI_2) is a vegetation index that helps assess plant stress and pigment composition, particularly the ratio of carotenoids to chlorophyll. It is widely used to evaluate plant health, stress resilience, and photosynthetic efficiency. Unlike indices that are highly influenced by leaf structure, SIPI_2 minimizes these structural effects, providing a more stable assessment of pigment balance. The results for our experimental lots are presented in Figure 10.

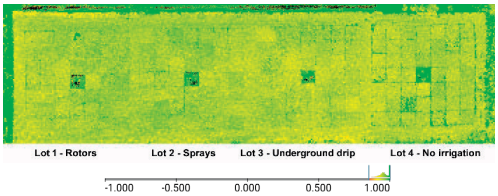


Figure 10. SIPI 2 Index applied on the experimental lot

The SIPI_2 colour scale presented in Figure 10 provides a visual representation of its values:
Low values (dark green to light green) indicate a higher chlorophyll-to-carotenoid ratio, representing healthy, unstressed vegetation with optimal photosynthetic capacity.
Moderate values (yellow to orange) suggest a more balanced ratio, possibly indicating early signs of stress or pigment imbalance.
High values (red to dark orange) correspond to regions with a lower chlorophyll-to-carotenoid ratio, often associated with plant stress, senescence, or nutrient deficiencies. The SIPI_2 histogram shows that most of the analysed area falls within the high-value range (orange to red), suggesting that a significant portion of the vegetation is experiencing some level of stress or chlorophyll degradation.
The limited presence of green areas indicates that only a small portion of the analysed vegetation is in an optimal health state.
A concentration of high SIPI_2 values may be a sign of drought stress, nutrient limitations, or advanced stages of plant aging, which can impact overall biomass production and vigour.
Later, some analyses were conducted on each lot, and we extracted the statistical values for each applied index. The lawn mixes were vectorised, and each one got its own zonal statistic value as a table (Coroian I. et al., 2020).
As could be seen in Figure 11, some statistical analyses were conducted later on. In figure 11 the Clustered boxplot on each Lawn mixt type for the GNDVI index could be seen.

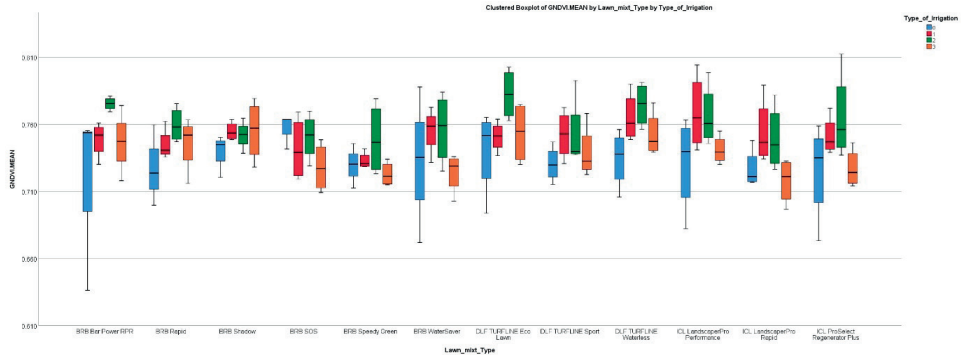


Figure 11. GNDVI index boxplot for each lawn mixt type

This boxplot illustrates the distribution of GNDVI Mean values for various Lawn Mix Types under different irrigation methods. Type 0 (blue) represents No Irrigation, Type 1 (red) represents Rotor Irrigation, Type 2 (green) represents Spray Irrigation, and Type 3 (orange) represents Underground Drip. Since GNDVI (Green Normalized Difference Vegetation Index) reflects plant health, higher values indicate better vegetation quality and water efficiency.

For BRB Bar Power RPR, No Irrigation shows high variability and the lowest median GNDVI, while Spray Irrigation achieves the highest values. BRB Rapid exhibits inconsistent chlorophyll levels under No Irrigation, with Spray performing best. BRB Shadow has a compact distribution across irrigation types, with Rotors and Underground Drip slightly outperforming Spray. BRB SOS performs worst with Underground Drip, while Spray and Rotors yield better results. BRB Speedy Green shows a stable GNDVI distribution, with Spray and Rotors having slightly higher medians. BRB WaterSaver is among the top-performing mixes, with Spray producing the highest chlorophyll content.

DLF TURFLINE Eco Lawn performs better with Rotor and Underground Drip compared to No Irrigation. DLF TURFLINE Sport maintains consistently high GNDVI values, with Spray providing the best results. DLF TURFLINE Waterless shows a large variation across irrigation types, but Spray leads in performance. ICL LandscapePro Performance has a narrow GNDVI spread, with Rotors and Spray performing slightly better than No Irrigation. ICL LandscapePro Rapid achieves high GNDVI values across all irrigation types, with Spray as the top performer. ICL Professional Regeneration Plus exhibits moderate variability, where Spray and Underground Drip perform better than Rotors.

Overall, Spray Irrigation consistently yields the highest GNDVI values, followed by Underground Drip and Rotor, while No Irrigation results in the lowest and most variable GNDVI, indicating water stress.

In Figure 12 the Clustered boxplot on each Lawn mixt type for the LCI index could be seen.

This boxplot illustrates the distribution of LCI Mean (Leaf Chlorophyll Index) values for different Lawn Mix Types under various irrigation methods, including No Irrigation, Rotor Irrigation, Spray Irrigation, and Underground Drip. Since LCI measures chlorophyll content, higher values indicate healthier and more photosynthetically active plants.

For BRB Bar Power RPR, No Irrigation shows high variability and a lower median, indicating inconsistent chlorophyll content and potential water stress. Spray Irrigation and Underground Drip provide more stable distributions and better performance, while Rotor Irrigation performs moderately, with a slightly lower median than Spray and Drip. BRB Rapid has a broad spread and a lower median under No Irrigation, reflecting inconsistent chlorophyll content. Spray Irrigation achieves the highest median, suggesting optimal plant health, while Rotor and Underground Drip show moderate and similar performance. BRB Shadow exhibits similar performance across irrigation types with a moderate spread, with Spray and Underground Drip slightly outperforming No Irrigation.

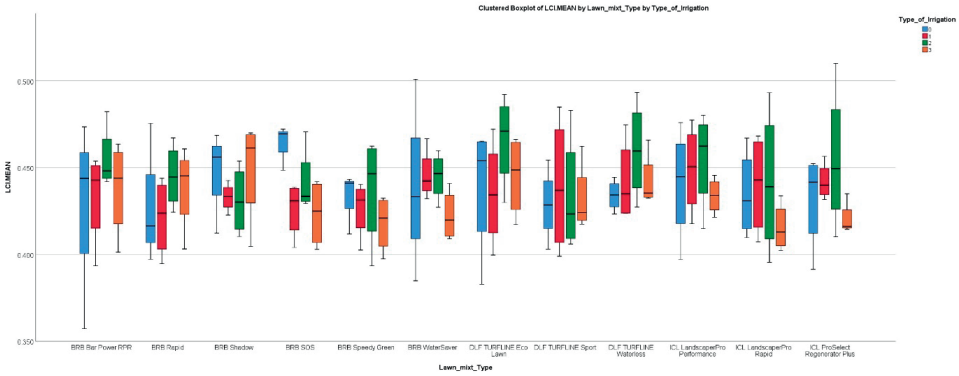


Figure 12. LCI index boxplot for each lawn mixt type

BRB SOS has the lowest median under Underground Drip, suggesting less effectiveness, while No Irrigation, Rotor, and Spray show higher and more stable LCI values. BRB Speedy Green has a compact LCI distribution, indicating consistent performance, with Spray and Rotor Irrigation slightly improving chlorophyll levels. BRB WaterSaver is one of the highest-performing mixes, with Spray Irrigation achieving the highest median, indicating optimal chlorophyll levels, while No Irrigation shows the widest variability and inconsistent performance. DLF TURFLINE Eco Lawn performs slightly better with Rotor and Underground Drip than with No Irrigation, which results in lower LCI values and suggests water stress.

DLF TURFLINE Sport maintains consistently high LCI values across irrigation types, with Spray performing best and No Irrigation showing greater variability and fluctuating chlorophyll levels. DLF TURFLINE Waterless exhibits large variation across irrigation types, with Spray producing the highest median and No Irrigation displaying a widespread, indicating inconsistent plant health. ICL LandscapePro Performance has a narrow LCI spread, reflecting consistent vegetation health, with Rotors and Spray performing slightly better than No Irrigation. ICL LandscapePro Rapid achieves high LCI values across all irrigation types, with Spray producing the highest median and Underground Drip offering stable performance with minimal variation. IL Professional Regeneration Plus shows moderate LCI variability across irrigation types, with Rotor slightly underperforming compared to Spray and Underground Drip.

Overall, Spray Irrigation is the best-performing method, consistently achieving higher LCI values and indicating better chlorophyll levels and plant health. Underground Drip provides stable performance and is often comparable to Rotor Irrigation, though slightly less effective than Spray. Rotor Irrigation shows moderate performance, performing better than No Irrigation but lower than Spray and Drip in most cases. No Irrigation results in moderately variable LCI values, with median levels that are not consistently the lowest across indices - suggesting that while water stress may occur, it does not always lead to the poorest or most inconsistent plant health outcomes

In Figure 13 the Clustered boxplot on each Lawn mixt type for the MCARI index could be seen.

This boxplot illustrates the distribution of MCARI Mean (Modified Chlorophyll Absorption Ratio Index) values for different Lawn Mix Types under various irrigation methods, including No Irrigation, Rotor Irrigation, Spray Irrigation, and Underground Drip. MCARI is an index used to estimate chlorophyll content and stress levels in vegetation, where higher values indicate better chlorophyll retention and lower stress, while lower values may suggest chlorosis, senescence, or water stress.

For BRB Bar Power RPR, No Irrigation shows high variability and the lowest median, suggesting inconsistent chlorophyll content and potential water stress. Spray and Rotor Irrigation have higher median values, indicating better performance, while Underground Drip shows moderate results with a slightly lower median.

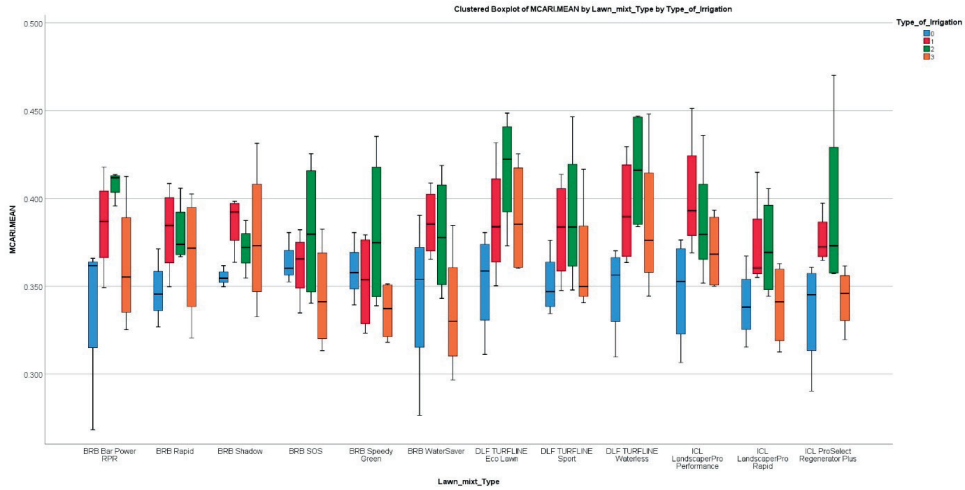


Figure 13. MCARI index boxplot for each lawn mixt type

BRB Rapid has a low median and high variability under No Irrigation, reflecting unstable chlorophyll levels. Spray Irrigation achieves the highest median, suggesting optimal chlorophyll content, while Rotor and Underground Drip demonstrate moderate performance. BRB Shadow exhibits less variability across irrigation types, indicating consistent chlorophyll content, with Spray and Rotor performing slightly better than No Irrigation.

BRB SOS has the lowest median under Underground Drip, suggesting reduced effectiveness, whereas No Irrigation, Rotor, and Spray exhibit higher and more stable MCARI values. BRB Speedy Green maintains a compact MCARI distribution, reflecting consistent chlorophyll levels, with Spray and Rotor achieving higher median values that suggest better chlorophyll retention. BRB WaterSaver is among the highest-performing mixes, with Spray reaching the highest median and indicating optimal chlorophyll content, while No Irrigation presents wide variability and inconsistent plant health. DLF TURFLINE Eco Lawn performs slightly better with Rotor and Underground Drip than with No Irrigation, which results in lower MCARI values and suggests water stress.

DLF TURFLINE Sport consistently maintains high MCARI values across all irrigation types, with Spray performing best, while No Irrigation introduces more variability and fluctuating chlorophyll levels. DLF TURFLINE Waterless exhibits large variations across irrigation types, with Spray achieving the highest median and No Irrigation displaying a widespread, indicating inconsistent plant health. ICL LandscapePro Performance has a narrow MCARI spread, reflecting consistent vegetation health, with Rotors and Spray slightly outperforming No Irrigation. ICL LandscapePro Rapid attains high MCARI values across all irrigation types, with Spray achieving the highest median and Underground Drip providing stable performance with minimal variation. IL Professional Regeneration Plus shows moderate MCARI variability across irrigation types, with Rotor slightly underperforming compared to Spray and Underground Drip.

Overall, Spray Irrigation is the best-performing method, consistently producing higher MCARI values and indicating better chlorophyll retention and lower stress. Underground Drip provides stable performance, often comparable to Rotor Irrigation but slightly less effective than Spray. Rotor Irrigation shows moderate performance, performing better than No Irrigation but lower than Spray and Drip in most cases. No Irrigation produces the lowest and most variable MCARI values, highlighting water stress and inconsistent plant health.

In Figure 14 the Clustered boxplot on each Lawn mixt type for the NDRE index could be seen.

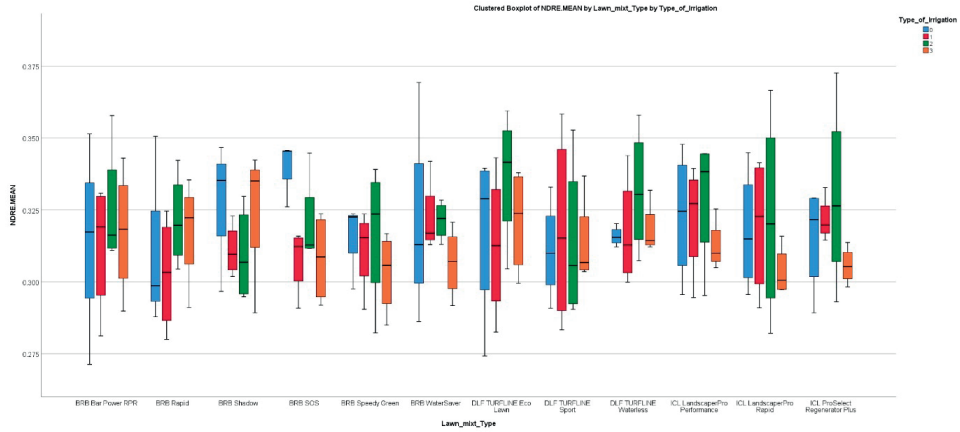


Figure 14. NDRE index boxplot for each lawn mixt type

This boxplot illustrates the distribution of NDRE Mean (Normalized Difference Red Edge Index) values for different Lawn Mix Types under four irrigation types: No Irrigation, Rotor Irrigation, Spray Irrigation, and Underground Drip NDRE is a vegetation index that measures chlorophyll content and nitrogen status in plants. Higher values indicate better plant health, increased nitrogen uptake, and stronger chlorophyll levels, while lower values suggest potential nutrient deficiency or stress.

For BRB Bar Power RPR, No Irrigation presents a moderate spread and a slightly lower median, indicating chlorophyll stress due to water deficiency. Spray Irrigation and Underground Drip show higher medians, suggesting improved nitrogen uptake, while Rotor Irrigation exhibits moderate performance with some variability. BRB Rapid displays a higher spread and lower median under No Irrigation, reflecting unstable chlorophyll levels. Spray Irrigation has the highest median, indicating optimal chlorophyll content, whereas Rotor and Underground Drip demonstrate moderate performance. BRB Shadow maintains similar NDRE values across irrigation types, showing consistent nitrogen uptake, with Spray and Rotor slightly outperforming No Irrigation.

BRB SOS has the lowest median under Underground Drip, suggesting reduced nitrogen uptake efficiency, while Spray, Rotor, and No Irrigation produce higher and more stable NDRE values. BRB Speedy Green shows a compact NDRE distribution, reflecting consistent nitrogen content, with Spray and Rotor achieving higher median values that suggest better nitrogen retention. BRB WaterSaver is among the highest-performing mixes, with Spray reaching the highest median and indicating optimal nitrogen absorption, while No Irrigation presents the widest variability, suggesting inconsistent plant health. DLF TURFLINE Eco Lawn performs slightly better with Rotor and Underground Drip compared to No Irrigation, which results in lower NDRE values and suggests water and nutrient stress.

DLF TURFLINE Sport consistently maintains high NDRE values across all irrigation types, with Spray performing best, while No Irrigation introduces more variability and fluctuating chlorophyll levels. DLF TURFLINE Waterless exhibits large variation across irrigation types, with Spray achieving the highest median and No Irrigation displaying a wide spread, indicating inconsistent plant health. ICL LandscapePro Performance has a narrow NDRE spread, reflecting consistent vegetation health, with Rotors and Spray slightly outperforming No Irrigation. ICL LandscapePro Rapid attains high NDRE values across all irrigation types, with Spray achieving the highest median and Underground Drip providing stable performance with minimal variation. IL Professional Regeneration Plus shows moderate NDRE variability across irrigation types, with Rotor slightly underperforming compared to Spray and Underground Drip.

Overall, Spray Irrigation consistently produces the highest NDRE values, indicating the best nitrogen uptake and plant health. Underground

Drip offers stable performance, often comparable to Rotor Irrigation but slightly less effective than Spray. Rotor Irrigation shows moderate performance, ranking above No Irrigation but below Spray and Underground Drip in most cases. No Irrigation generally shows moderate to high variability in NDRE values, but not consistently the lowest values - indicating that while water and nutrient stress may impact plant health, its effects vary depending on the turfgrass type and conditions.

In Figure 15 the Clustered boxplot on each Lawn mixt type for the NDVI index could be seen.

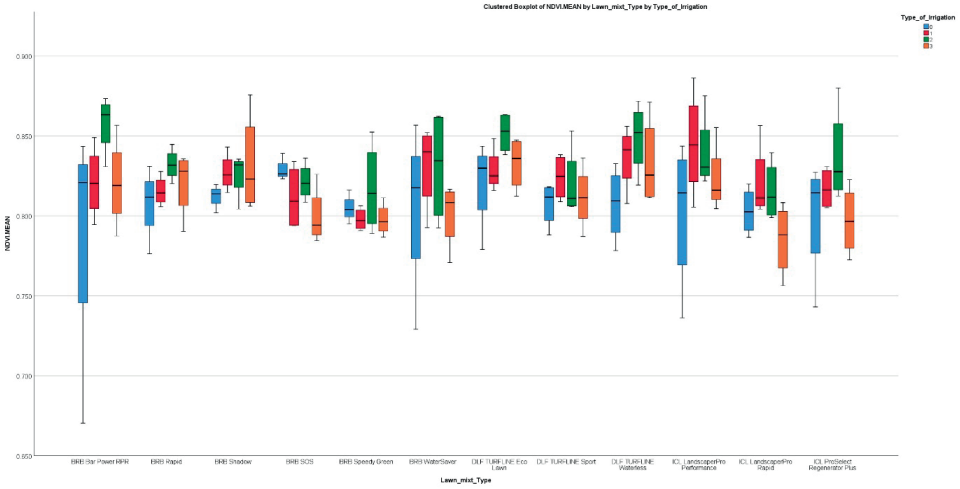


Figure 15. NDVI index boxplot for each lawn mixt type

This boxplot illustrates the distribution of NDVI Mean (Normalized Difference Vegetation Index) values for different Lawn Mix Types under four irrigation methods: No Irrigation, Rotor Irrigation, Spray Irrigation, and Underground Drip. NDVI is a widely used vegetation index that measures plant health, biomass, and chlorophyll levels. Higher NDVI values indicate healthier vegetation with greater chlorophyll content and better water retention, while lower values suggest plant stress due to drought, poor nutrition, or water deficiencies.

For BRB Bar Power RPR, No Irrigation exhibits high variability and the lowest median, indicating inconsistent vegetation health and water stress. Spray and Underground Drip show higher median values, suggesting improved water retention and better plant health, while Rotor Irrigation demonstrates moderate performance with less variability. BRB Rapid has a lower median and high variability under No Irrigation, reflecting fluctuating plant health. Spray Irrigation achieves the highest median, indicating strong chlorophyll levels and water availability, whereas Rotor and Underground Drip display moderate NDVI values. BRB Shadow presents a compact distribution across irrigation types, signifying consistent NDVI performance, with Spray and Rotor achieving slightly higher values than No Irrigation.

BRB SOS has the lowest median under Underground Drip, suggesting less effectiveness in improving NDVI, while Spray, Rotor, and No Irrigation yield higher and more stable values. BRB Speedy Green maintains a compact NDVI distribution, reflecting consistent vegetation health, with Spray and Rotor achieving higher median values, suggesting better chlorophyll retention. BRB WaterSaver is one of the highest-performing mixes, with Spray reaching the highest median and indicating excellent vegetation health, while No Irrigation shows the widest variability, suggesting inconsistent performance. DLF TURFLINE Eco Lawn performs slightly better with Rotor and Underground Drip than with No Irrigation, which results in lower NDVI values and suggests water stress.

DLF TURFLINE Sport consistently maintains high NDVI values across all irrigation types,

with Spray achieving the best performance and the highest median, while No Irrigation introduces more variability and fluctuating chlorophyll levels. DLF TURFLINE Waterless exhibits large variation across irrigation types, with Spray showing the highest median, suggesting better water efficiency and plant health, whereas No Irrigation presents a wide spread, indicating inconsistent performance. ICL LandscapePro Performance has a narrow NDVI spread, reflecting consistent plant health, with Rotors and Spray performing slightly better than No Irrigation. ICL LandscapePro Rapid attains higher NDVI values across all irrigation types, with Spray producing the highest median and Underground Drip providing stable performance with minimal variation. IL Professional Regeneration Plus demonstrates moderate NDVI variability across irrigation types, with Rotor slightly underperforming compared to Spray and Underground Drip.

Overall, Spray Irrigation proves to be the most effective method, consistently producing higher NDVI values and indicating better chlorophyll levels and overall plant health. Underground Drip provides stable performance, often comparable to Rotor Irrigation but slightly less effective than Spray. Rotor Irrigation performs moderately well, ranking above No Irrigation but below Spray and Underground Drip in most cases. No Irrigation results in the lowest and most variable NDVI values, highlighting the effects of water stress on plant health. In Figure 16 the Clustered boxplot on each Lawn mixt type for the SIPI_2 index could be seen.

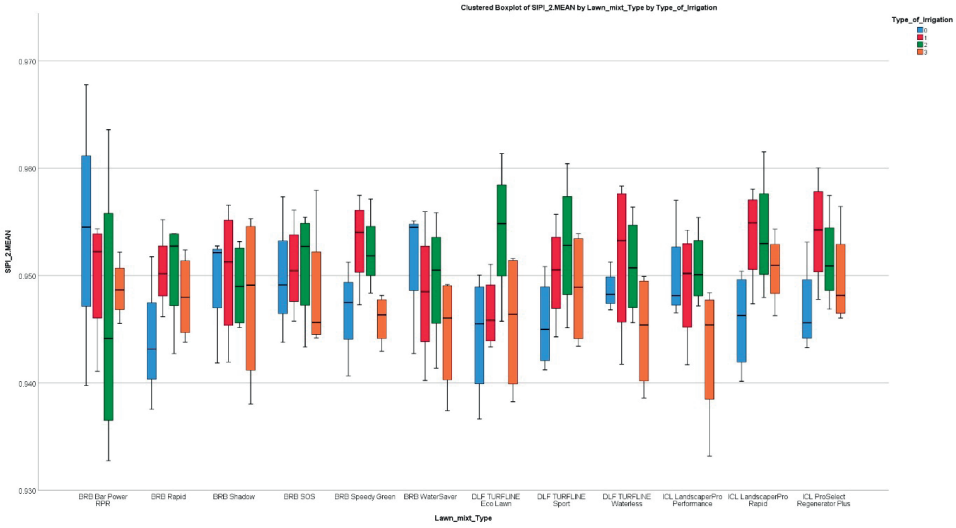


Figure 16. SIPI_2 index boxplot for each lawn mixt type

This boxplot illustrates the distribution of SIPI_2 Mean values across Lawn Mix Types under four irrigation methods: No Irrigation, Rotor, Spray, and Underground Drip. SIPI measures pigment content, where higher values indicate better stress resistance.

Spray consistently achieves the highest SIPI values, reflecting better pigment stability and plant health. Underground Drip provides stable performance, while Rotor performs moderately well. No Irrigation results in the lowest and most variable SIPI values, indicating increased stress and pigment imbalances. Among Lawn Mixes, BRB WaterSaver and DLF TURFLINE Sport show strong pigment retention, while BRB SOS and DLF TURFLINE Waterless exhibit more variability. Efficient irrigation strategies enhance plant resilience and pigment balance.

In order to determine if the multispectral imagery is, or not efficient for lawn monitoring, a canonical discriminant function was applied to the whole data set (Figure 17).

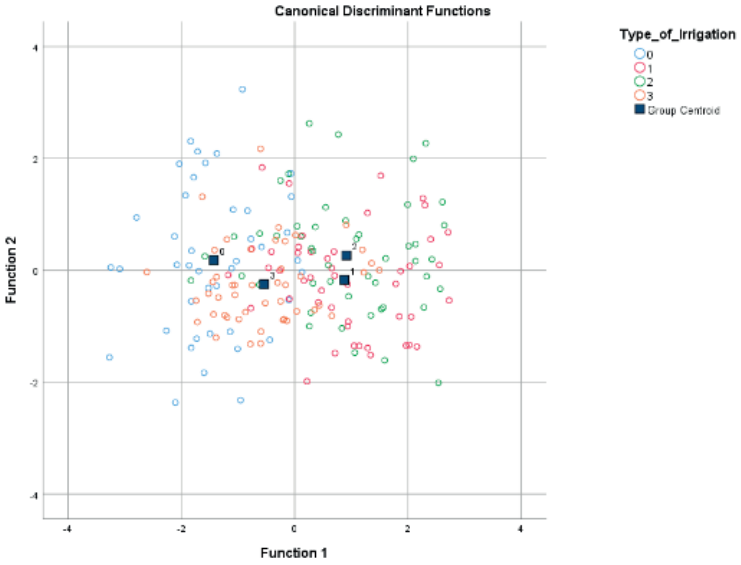


Figure 17. Statistical analysis for the 4 irrigation types – Canonical discriminant function

The Canonical Discriminant Function plot illustrates the distribution of four irrigation types, showing significant overlap, with No Irrigation displaying the greatest separation along Function 1, while Rotor, Spray, and Underground Drip share similar characteristics. However, Underground Drip is closer to No Irrigation due to the lack of applied irrigation and recorded rainfall, which delayed the absorption of granulated fertilizer, further influencing plant response and differentiation.

CONCLUSIONS

The study demonstrates the effectiveness of turf monitoring technology using the multispectral photogrammetric method, highlighting its ability to accurately classify irrigation types and assess their advantages and disadvantages across different lawn mix types.

This study demonstrates that Spray Irrigation (Green) consistently outperforms other irrigation methods across all spectral vegetation indices, making it the most effective for maintaining plant health and optimizing chlorophyll content.

Underground Drip (Orange) provides stable performance, while Rotor Irrigation (Red) is moderately effective. No Irrigation (Blue) results in the lowest values across all indices, indicating significant plant stress and water deficiency.

Best Performing Lawn Mixes: BRB WaterSaver and DLF TURFLINE Sport exhibited the highest resilience and adaptability across multiple irrigation types.

The response to lawn fertilization, in the case of the lot with underground irrigation, had a particularity, most likely due to the fact that, on the one hand, the fertilizer was of the granulated type, with controlled release, and the fact that it did not rain in the period following the fertilizer application prevented the complex of nutrients from reaching the roots.

ACKNOWLEDGEMENTS

This research was carried out with the support of the Ministry of Education and was financed through the CNFIS-FDI-2024-F-0195 project, funded by the National Council for Financing Higher Education (CNFIS).

REFERENCES

Bilaşco, Ş., Roşca, S., Păcurar, I., Moldovan, N., Boţ, A., Negruşier, C., ... & Naş, S. (2016). Identification of land suitability for agricultural use by applying morphometric and risk parameters based on GIS spatial analysis.

Notulae Botanicae Horti Agrobotanici Cluj-Napoca, *44*(1), 302–312.

Chiesura, A. (2004). The role of urban parks for the sustainable city. *Landscape and Urban Planning*, *68*(1), 129–138.

Constantinescu, C., Herbei, M., Rujescu, C., & Sala, F. (2018). Characterization of the interdependency relations between the spectral information, vegetation indices, and the number of classes for the analyzed territory. *AIP Conference Proceedings*, *1978*(1), 390002.

Coroian, I., Nap, M. E., Pop, I. D., Matei, F., Sălăgean, T., Deak, J., Chiorean, S., Șuba, E. E., Lupuț, I., & Ficior, D. (2020). Using GIS analysis to assess urban green space in terms of real estate development. *Bulletin of University of Agricultural Sciences and Veterinary Medicine Cluj-Napoca. Horticulture*, *78*(1), 1–10.

Daughtry, C. S. T., Walthall, C. L., Kim, M. S., de Colstoun, E. B., & McMurtrey, J. E. (2000). Estimating corn leaf chlorophyll concentration from leaf and canopy reflectance. *Remote Sensing of Environment*, *74*(2), 229–239.

Gitelson, A. A., Kaufman, Y. J., & Merzlyak, M. N. (1996). Use of a green channel in remote sensing of global vegetation from EOS-MODIS. *Remote Sensing of Environment*, *58*(3), 289–298.

Herbei, M. V., & Badaluta-Minda, C. (2024). The use of remote sensing techniques in the analysis of the influence of forest ecosystems over the precipitation. *Rocznik Ochrona Środowiska*, *26*, 296–304.

Hitter, T., Buta, E., Cantor, M., Crișan, I. E., Szekely-Varga, Z., & Dan, V. S. (2021). Seed germination rate of different turfgrass mixtures under controlled conditions. *Scientific Papers. Series B, Horticulture*, *65*(1).

Kenna, M. R., & Horst, G. L. (1993). Turfgrass water conservation and quality. *International Turfgrass Society Research Journal*, *7*, 99–113.

Kerry, R., Ingram, B., Sanders, K., Henrie, A., Hammond, K., Hawks, D., Hansen, N., Jensen, R., & Hopkins, B. (2024). Precision turfgrass irrigation: Capturing spatial soil moisture patterns with ECa and drone data. *Agronomy*, *14*(6), 1238.

Krum, J., Carrow, R. N. M., & Karnok, K. (2010). Spatial mapping of complex turfgrass sites: Site-specific management units and protocols. *Crop Science*, *50*, 301–315.

Orta, A. H., Todorovic, M., & Ahi, Y. (2023). Cool- and warm-season turfgrass irrigation with subsurface drip and sprinkler methods using different water management strategies and tools. *Water*, *15*(2), 272.

Peñuelas, J., Baret, F., & Filella, I. (1995). Semi-empirical indices to assess carotenoids/chlorophyll a ratio from leaf spectral reflectance. *Photosynthetica*, *31*(2), 221–230.

Popescu, G., Popescu, C. A., Dragomir, L. O., Herbei, M. V., Horablaga, A., Țenche-Constantinescu, A. M., ... & Sestraș, P. (2024). Utilizing UAV technology and GIS analysis for ecological restoration: A case study on *Robinia pseudoacacia* L. in a mine waste dump landscape rehabilitation. *Notulae Botanicae Horti Agrobotanici Cluj-Napoca*, *52*(4), 13937–13937.

Schebella, M. F., Weber, D., Brown, G., & Hatton MacDonald, D. (2014). The importance of irrigated urban green space: Health and recreational perspectives. *Technical Report*, Goyder Institute for Water Research, Adelaide, Australia.

Sestraș, P., Bondrea, M. V., Cetean, H., Sălăgean, T., Bilașco, Ș., Naș, S., ... & Cîmpeanu, S. M. (2018). Ameliorative, ecological and landscape roles of Făget Forest, Cluj-Napoca, Romania, and possibilities of avoiding risks based on GIS landslide susceptibility map. *Notulae Botanicae Horti Agrobotanici Cluj-Napoca*, *46*(1), 292–300.

Sestraș, P., Sălăgean, T., Bilașco, Ș., Bondrea, M. V., Naș, S., Fountas, S., & Cîmpeanu, S. M. (2019). Prospect of a GIS-based digitization and 3D model for better management and land use in a specific micro-areal for crop trees. *Environmental Engineering and Management Journal*, *18*(6), 1269–1277.

Sousa-Souto, L., Bocchiglieri, A., Dias, D. D. M., & Ferreira, A. (2018). Changes in leaf chlorophyll content associated with flowering and its role in the diversity of phytophagous insects in a tree species from a semiarid Caatinga. *PeerJ*, *6*(2), e5059.

Tucker, C. J. (1979). Red and photographic infrared linear combinations for monitoring vegetation. *Remote Sensing of Environment*, *8*, 127–150.

Scientific Papers. Series E. Land Reclamation, Earth Observation & Surveying, Environmental Engineering. Vol. XIV, 2025
Print ISSN 2285-6064, CD-ROM ISSN 2285-6072, Online ISSN 2393-5138, ISSN-L 2285-6064

GIS-BASED SUITABILITY ANALYSIS FOR SKI RESORT DEVELOPMENT IN THE BRAN–RÂȘNOV AREA, BRAȘOV COUNTY, ROMANIA

Cornel Cristian TEREȘNEU

Transilvania University of Brașov, 25 Eroilor Street, Brașov, Romania

Corresponding author email: cteresneu@unitbv.ro

Abstract

This study assesses the suitability of an area located between the localities of Bran and Râșnov in Brașov County, Romania, for the development of a ski resort. A combination of cartographic resources - including orthophoto maps and topographic-cadastral plans - was initially employed, followed by detailed field measurements using GNSS technology. Climatic variables critical to ski infrastructure planning were evaluated using data from four meteorological stations, with a focus on air temperature, frost days, solid precipitation, and snow cover duration and depth. Geospatial analysis was conducted using GIS tools to examine key orographic parameters such as altitude, slope, aspect, shading, land curvature, and drainage patterns. By integrating climatic and terrain data, the study identifies the area as favorable for ski resort development based on both environmental suitability and technical feasibility.

Key words*: ski resort, GIS, GNSS, terrain suitability, climatic assessment, spatial planning.*

INTRODUCTION

This study explores the potential for developing a ski resort in the northern and northwestern sector of the Bucegi Mountains, specifically in the area situated between the localities of Bran and Râșnov (Figure 1). The region is characterized by favorable topographic and climatic conditions and holds untapped potential for winter tourism infrastructure.

Despite Romania's mountainous geography, existing ski areas remain insufficiently developed. According to recent statistical evaluations, many resorts suffer from poor service quality and high operational costs, leading to a decline in domestic tourism in favor of more established destinations such as Austria. Additionally, numerous ski slopes in Romania have been developed at suboptimal altitudes or on poorly oriented terrain, resulting in limited seasonal usability and low investment returns (Comănescu et al., 2009). These issues are exacerbated by recent climate trends, including reduced winter precipitation and rising temperatures, particularly at lower elevations.

Considering these challenges, the identification of more suitable locations for ski infrastructure - both from a climatic and geomorphological perspective - is essential. This paper aims to evaluate such a location using integrated geospatial and climatic analyses.

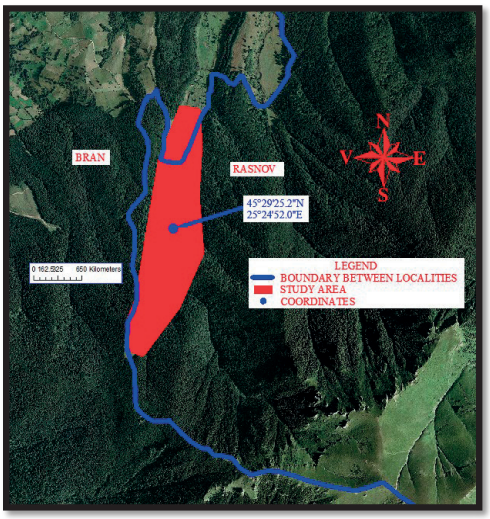


Figure 1. Study area

Both Bran and Râșnov have significant tourism potential, attracting a growing number of visitors during the winter season, including weekend travelers. Although there is an existing sports complex in the area that includes ski slopes, its usability is limited by two major factors: its low elevation and predominantly southern exposure. As a result, snow is either absent for much of the winter or melts rapidly after snowfall. Furthermore, recent years have seen a diversification of winter tourism

activities beyond traditional skiing, increasing the demand for well-situated and versatile winter sports infrastructure.

The proposed ski resort would be located in a forested area, which is beneficial as forest cover positively influences snow retention and microclimatic stability (Nap et al., 2022). However, since the location lies within a protected area, all development plans must adhere to relevant environmental regulations and conservation principles (Olariu, 2019).

It is known that there are a number of constraints regarding the manner of removing an area from the forest fund, but this aspect was also thought beforehand and a suitable area was prepared (at the parity required by the Forest Code) to be introduced into the forest fund. The situation was studied on appropriate plans and maps (Teodor & Dobre, 2015), after which concrete measurements were made in the field. Steps were taken to obtain the appropriate permits.

Another important aspect to be taken into account in such investments is the possibility of snow avalanches (Jamieson & Johnson, 1998; Voiculescu & Popescu, 2011; Voiculescu & Ardelean, 2012).

The site is also favorable from a geomorphological perspective, with advantageous terrain curvature that minimizes excessive slope deformation during tight ski turns (Yoneyama et al., 2010).

To guide the development of the proposed ski area, several fundamental planning principles were applied (Cernaianu & Sobry, 2021):

Environmental integration: planning must ensure the preservation of natural resources - both ecological and visual - by aligning slope design with climate conditions, land use constraints, and natural hazard risks (Mihai et al., 2008, Wegler & Kuenzer, 2024). Understanding local environmental characteristics enhances the return on investment and promotes sustainable development (Ielenicz et al., 2010).

- *Customer-oriented planning:* this includes considerations of accessibility, market size and proximity, resort accessibility, and demographic and socioeconomic characteristics of the target clientele. Easy access is crucial for attracting tourists and investors alike (Lesenciuc et al., 2013). Estimating the proportions of day tourists versus overnight guests is essential for aligning slope capacity with lodging infrastructure. Lifestyle trends, age, income, and education level also influence demand (Gingulescu, 2010).

- *Operational and economic efficiency:* this involves optimizing slope capacity, estimating infrastructure and capital costs, human resource needs, revenue streams, and pricing strategies. These parameters are critical for assessing project feasibility and profitability (Ilieș, 2007).

- *Urban planning and legal compliance:* finally, all development must align with existing general urban plans (PUGs) and be supported by detailed zonal urban plans (PUZs) for both Bran and Râșnov (Ionescu, 2004).

MATERIALS AND METHODS

This study employed a combination of cartographic materials, remote sensing tools, GNSS-based field measurements, and geospatial analysis software to evaluate the suitability of the study area for ski resort development.

Materials

The following datasets and equipment were utilized:

- Orthophoto maps (2020 edition, scale 1:5,000; 2023 edition, scale 1:1,000);
- Topo-cadastral plans L-35-87-B-d-3-IV and L-35-87-D-b-1-II (scale 1:5,000);
- Forest management maps (scale 1:20,000);
- G7 South GNSS receiver with H6 data collectors, providing a horizontal accuracy of 25mm + 1 ppm RMS and a vertical accuracy of 15 mm + 1 ppm RMS;
- Dell Latitude 5411 laptop with Intel® Core™ i7-10850H CPU @ 2.70 GHz and 16 GB RAM;
- ArcMap GIS software;
- AutoCAD Civil 3D software;
- A topographic survey comprising over 4,500 georeferenced points.

Methods

The research methodology integrated the following techniques:

- *Direct geodetic measurements:* coordinates of key points within the study area were determined using GNSS equipment for high-precision spatial positioning.

- *GIS-based spatial analysis:* cadastral plans were georeferenced and vectorized. Custom analyses were conducted using VBA programming within the GIS environment to assess terrain parameters (e.g., slope, aspect, shading, curvature, drainage).

This multi-source approach enabled both the validation of field measurements and the derivation of relevant terrain and climatic indicators to support the site suitability assessment.

RESULTS AND DISCUSSIONS

Initial terrain analysis was conducted using topographic-cadastral plans L-35-87-B-d-3-IV and L-35-87-D-b-1-II, at a scale of 1:5,000. A preliminary evaluation of the study area revealed the following characteristics:

- An elevation difference of approximately 450 meters (the minimum altitude is 955m and the maximum is 1410m);
- Terrain gradients suitable for ski slopes across all skill levels, ranging from slopes of less than 20% (for beginners) to over 45% (for advanced skiers);
- A maximum slope length exceeding 3.2 kilometers.

Following the terrain assessment, climatic conditions relevant to snow retention and winter sports were analyzed. The study considered several key meteorological variables: average air temperature, number of frost days, monthly and seasonal solid precipitation, frequency of snow events, and snow cover duration and depth.

Climatic data were sourced from four meteorological stations in the region: Predeal (altitude 1096 m), Vf. Omu (altitude 2505 m), Sinaia 1500 (altitude 1510 m), Fundata (altitude 1376 m). Notably, two of these stations (Sinaia 1500 and Fundata) are located at altitudes similar to the target development site, providing a relevant climatic reference. The data spans the period 2014–2023, focusing on the core winter months: December through April. All data were collected from the National Meteorological Administration's network stations.

Table 1 presents the multiannual average air temperatures recorded during this period across the four stations.

Table 1. Multiannual average air temperature (°C) for the period 2014-2023

Station	December (XII)	January (I)	February (II)	March (III)	April (IV)
Predeal	-3.2	-4.3	-4.1	-0.2	4.8
Vf. Omu	-8.7	-10.5	-10.7	-8.2	-4.0
Sinaia-1500	-3.3	-4.8	-5.0	-1.5	3.3
Fundata	-3.2	-4.5	-4.5	-0.6	4.5

In terms of the number of frost days - defined as days with minimum temperatures below 0 °C - the observed data from the four meteorological stations over the 2014–2023 period is presented in Table 2.

Table 2. Average number of frost days per month (2014-2023)

Station	December (XII)	January (I)	February (II)	March (III)	April (IV)
Predeal	28.5	29.3	27.2	26.3	13.4
Vf. Omu	31.0	30.9	28.3	31.0	29.7
Sinaia-1500	26.6	29.3	26.8	25.7	13.6
Fundata	25.8	28.0	25.4	24.3	10.3

The next climatic factor considered in the analysis was precipitation, with a focus on parameters relevant to snow availability and sustainability in winter sports environments. The evaluation included the following aspects:

a. *Average monthly solid precipitation:* these values, presented in Table 3, reflect the total amount of monthly precipitation in solid form (e.g., snow, sleet). It is noted that the lowest values typically occur in February. However, this may be due to strong wind activity during that period, which can result in snow being redistributed or blown away, rather than reflecting actual precipitation scarcity.

b. *Average number of days with solid precipitation:* Table 4 summarizes the monthly averages of days featuring solid-phase precipitation, including snowfall, snow showers, sleet, soft drizzle, and fine snow.

c. *Snow cover characteristics:* observations are based on standardized 08:00 a.m. daily measurements recorded by meteorological stations across Romania. Two key parameters were analyzed:

- i. Average monthly snow depth, shown in Table 5;
- ii. Average annual duration of snow cover, presented in Table 6.

Table 3. Average monthly amounts of solid precipitation (mm), 2014-2023

Station	December (XII)	January (I)	February (II)	March (III)	April (IV)
Predeal	48.9	56.7	45.4	65.9	76.2
Vf. Omu	57.8	60.4	54.0	63.7	64.5
Sinaia-1500	73.0	62.7	62.2	58.2	73.5
Fundata	53.6	48.1	43.3	61.8	71.8

Table 4. Average monthly number of days with solid precipitation, 2014-2023

Station	December (XII)	January (I)	February (II)	March (III)	April (IV)
Predeal	11.4	12.3	12.9	12.1	3.6
Vf. Omu	13.0	12.9	13.5	16.6	16.2
Sinaia-1500	9.5	10.9	12.2	10.3	5.5
Fundata	11.0	12.7	13.9	12.7	5.5

Table 5. Average monthly snow depth (cm), 2014-2023

Station	December (XII)	January (I)	February (II)	March (III)	April (IV)
Predeal	18.8	30.7	44.1	33.0	4.6
Vf. Omu	43.1	63.9	83.8	101.0	104.0
Sinaia-1500	21.4	35.6	54.6	54.7	11.3
Fundata	12.3	22.5	32.8	28.6	2.5

Table 6. Average annual duration of snow cover (days), 2014-2023

Station	Average Duration (days)
Predeal	170
Vf. Omu	266
Sinaia-1500	178
Fundata	192

Following the climatic analysis, a detailed field survey was conducted to assess the orographic characteristics of the study area. The topographic-cadastral plans (L-35-87-B-d-3-IV and L-35-87-D-b-1-II) were georeferenced and overlaid on forest management maps obtained from the Bucegi - Piatra Craiului Private Forestry Office (Tereșneu, 2022). This process revealed that the proposed development area spans six forest management subcompartments. Subsequently, an extensive field campaign was carried out, during which over 4,500 spatial data points were collected using a South G7 GNSS receiver and H6 controller. The coordinates of the boundaries for both the forest subcompartments and the proposed ski slope routes - classified by difficulty level - were precisely recorded. Due to the significant elevation differences and dense forest cover, the terrain presented logistical challenges during data acquisition. As a result, some of the initially mapped slope routes were adjusted based on field conditions.

To construct a detailed 3D topographic model of the area, the GNSS data were integrated with contour lines (with an equidistance of 5m) automatically vectorized using ArcScan (Tereșneu, 2013). In areas where GNSS measurements were not feasible, elevation data were extracted from the cadastral maps. To improve vertical accuracy, a custom algorithm was implemented to adjust the contour line altitudes. This correction accounted for historical modeling errors: 3D terrain models in forested areas were originally generated during 1960s-1970s photogrammetric surveys that captured canopy heights, necessitating corrections based on average stand height.

Studies by Tereșneu and Vasilescu (2019) have shown that stand height in mountainous terrain varies considerably - from taller growth at the base of slopes to shorter vegetation near ridgelines. These insights were incorporated into the correction model using data from forest management plans. Adjustments were applied through VBA-coded routines, ensuring that the contour lines accurately reflected ground elevation rather than canopy height.

Further analysis was conducted to evaluate the key orographic parameters relevant to ski slope planning. Each criterion was derived from a digital elevation model and associated spatial datasets, with results visualized in Figures 2 to 10.

- *Altitudinal analysis* (Figure 2). Due to recent climatic changes, ski slopes are recommended at higher elevations where snow cover persists for more than four months annually. In the study area, elevation ranges from a minimum of 955m m to a maximum of approximately 1400 m (1410 m), which is favorable for maintaining consistent snowpack during the winter season (5m resolution model).
- *Slope* (Figure 3 and 4). Slope gradient is a critical factor in ski slope classification. The terrain was analyzed and raster layers reclassified to generate a Boolean map of slope suitability. Areas with acceptable gradients were assigned a value of 1 (favorable), and steeper or flatter regions a value of 0. This analysis revealed that the area can accommodate slopes for all difficulty levels - from very easy to expert - based on the distribution of gradient classes.
- *Aspect (Exposure)* (Figure 5 and 6). Solar exposure significantly influences snow

quality and duration. Northern and northwestern exposures are preferred for preserving snow, especially at altitudes below 1500 m. The terrain was classified into seven 45° segments (sexagesimal) representing cardinal and intercardinal orientations. Southern-facing slopes (112.5°-247.5°) were excluded by assigning a value of 0, while others were assigned a value of 1. This exposure-based suitability analysis indicated that the majority of the area benefits from favorable orientations for slope development (Vorovencii, 2024).

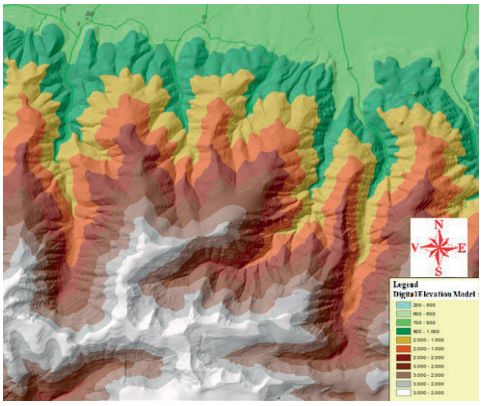


Figure 2. Digital Elevation Model (DEM)

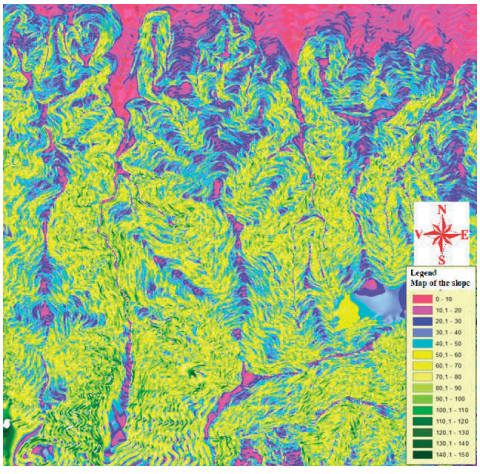


Figure 3. Slope Map of the Study Area

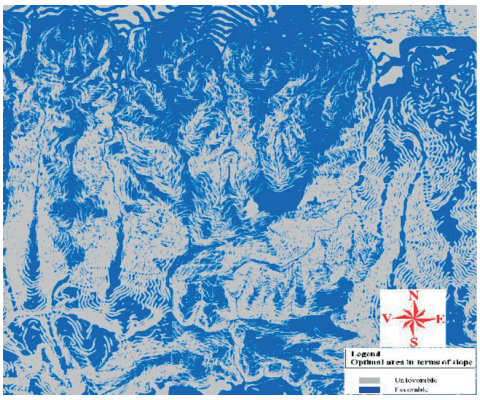


Figure 4. Slope-Based Suitability Map for ski area development

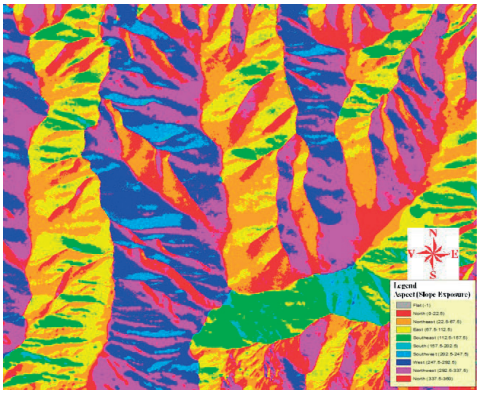


Figure 5. Aspect (Slope Exposure) Map of the Study Area

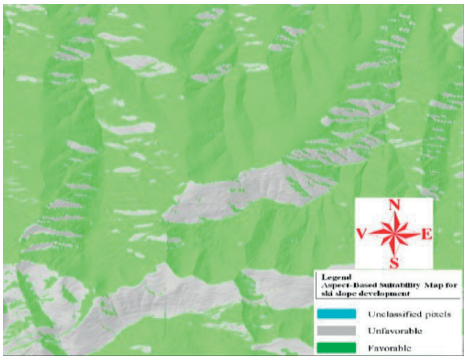


Figure 6. Aspect-Based Suitability Map for ski slope development

- *Shading* (Figures 7 and 8). Shading was analyzed using the Hillshade tool in ArcGIS, which simulates the illumination of the terrain based on specified azimuth and altitude of a hypothetical light source. This technique is not only useful for visual interpretation but also helps identify interpolation artifacts in the DEM. Shading maps were produced for two time points - 10:00 and 15:00 - on February 12 to assess variation in light exposure during typical winter conditions.
- *Land curvature* (Figure 9). Curvature is a morphometric variable that reflects surface convexity or concavity, influencing water runoff behavior and erosion susceptibility. The Curvature tool in ArcGIS was used to compute this parameter as the second derivative of the surface. In the resulting map, red indicates concave surfaces (potential accumulation zones), and yellow indicates convex areas (dispersal zones), which is useful for preliminary landscape stability assessments.
- *Flow Direction* (Figure 10). Hydrological flow paths were calculated using the Flow Direction tool from the Hydrology toolbox in ArcGIS. This analysis determines the direction of water runoff for each raster cell, based on the steepest descent among eight neighboring cells. While flow direction is not a primary determinant in ski slope planning, it is critical for identifying erosion-prone areas and designing sustainable drainage systems. The raster output supports broader environmental risk assessments during both construction and operation phases (Irimuș, 2006; Vorovencii, 2016).

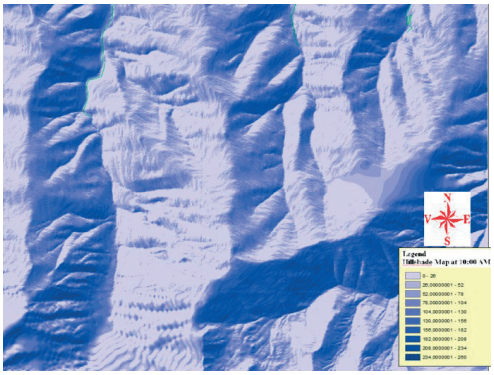


Figure 7. Hillshade Map at 10:00 AM on February 12

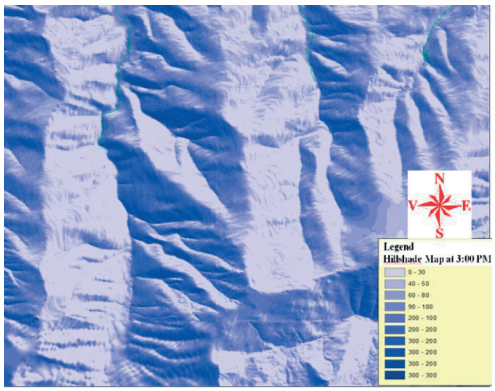


Figure 8. Hillshade Map at 3:00 PM on February 12

The result of the flow direction analysis is a raster in which each pixel's attribute value indicates the direction of surface runoff, calculated relative to its eight neighboring cells by identifying the path of steepest descent (i.e., the "shortest fall"). While flow direction does not directly influence the spatial placement of ski slopes, it is essential for assessing the potential for erosion. Such analyses are particularly relevant in mountainous environments, where natural erosion processes or slope destabilization can be intensified by infrastructure development and intensive slope usage. Understanding drainage patterns is therefore critical for mitigating geomorphological risks throughout both the construction and operational phases of a ski resort (Wang et al., 2024; Irimuș, 2006; Dietenberger et al., 2025; Vorovencii, 2016).

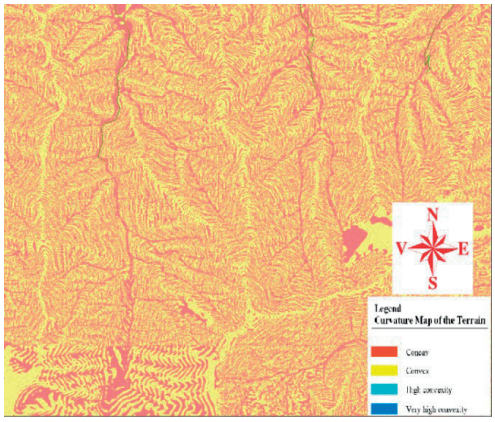


Figure 9. Curvature Map of the Terrain

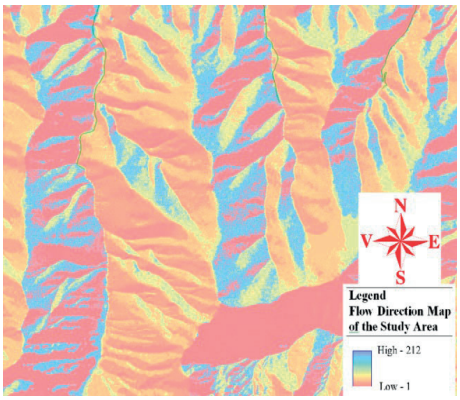


Figure 10. Flow Direction Map of the Study Area

CONCLUSIONS

Based on the integrated analysis of climatic conditions and orographic characteristics, the study area - located between Bran and Râșnov - is deemed suitable for the development of a ski resort. The conclusions are summarized below:

Climatic Factors

- Although recorded air temperatures have increased compared to previous decades (e.g., the 1970s and 1980s), they remain within acceptable ranges for maintaining snow cover, particularly when considered alongside other favorable climatic variables.
- The number of frost days supports the persistence of snow cover into April, extending the operational window of a ski slope.
- Average monthly snow cover, while not exceptionally high, is sufficient to ensure consistent slope usability during the winter season. Artificial snowmaking would be required only occasionally.
- Despite a downward trend, the frequency of days with solid precipitation remains adequate for natural snow accumulation.
- Snow cover characteristics - both in terms of thickness and annual duration - are favorable, confirming the natural viability of the site for winter sports.

Orographic Conditions

- Although the site's elevation (950-1400 m) falls below the ideal threshold of 1500 m, its overall suitability is reinforced through complementary terrain factors.
- The slope configuration accommodates all skier proficiency levels, from beginner to advanced.
- Aspect analysis indicates predominantly northern and northwestern exposures, which help offset limitations related to altitude by enhancing snow retention.
- Shading analysis places the area in a favorable category, particularly at higher elevations, reinforcing snow preservation potential.
- Terrain curvature suggests minimal need for significant grading or earthworks, which is beneficial for sustainable development.
- Flow direction analysis indicates stable drainage patterns and a low risk of landslides, confirming the geomorphological stability of the site.

In summary, the combined climatic and topographical assessment confirms that the studied area is highly suitable for ski resort development. Moreover, its location within an already well-developed tourist region with existing accommodation infrastructure further enhances its potential to attract a substantial number of winter sports visitors.

REFERENCES

Cernaianu, S., & Sobry, C. (2021). The development of ski areas in Romania: What environmental, political, and economic logic? *Sustainability, 13*(1), 274. https://doi.org/10.3390/su13010274

Comănescu, L., Nedelea, A., & Dobre, R. (2009). Inventoring and evaluation of geomorphosites in the Bucegi Mountains. *Geographical Forum – Geographical Studies and Environment Protection Research, 8*, 38–44.

Dietenberger, S.; Mueller, M.M.; Stöcker, B.; Dubois, C.; Arlaud, H.; Adam, M.; Hese, S.; Meyer, H.; Thiel, C. (2025). Accurate Mapping of Downed Deadwood in a Dense Deciduous Forest Using UAV-SfM Data and Deep Learning. *Remote Sens. 17*, 1610. https://doi.org/10.3390/rs17091610

Gingulescu, D. M. (2010). *Potențialul schiabil al României* [Doctoral dissertation, Universitatea Babeș-Bolyai].183 pp.

Ielenicz, M., Comănescu, L., & Nedelea, A. (2010). Romania's touristic potential: The differentiation of the potential units. *South Asian Journal of Tourism and Heritage, 3*(1), 26–38.

Ilieș, M. (2007). *Amenajare turistică*. Editura Casa Cărții de Știință, Cluj-Napoca. 210 pp.

Ionescu, G. (2004). *Predeal. Istoria schiului*. Editura Ecran Magazin, Brașov. 156p.

Irimuș, I. A. (2006). *Hazarde și riscuri asociate proceselor geomorfologice în aria cutelor diapire din Depresiunea Transilvaniei*. Editura Casa Cărții de Știință. Cluj-Napoca. 275 p.

Jamieson, B., & Johnson, D. C. (1998). Snowpack characteristics for skier triggering. *Canadian Avalanche Association, Avalanche News, 85*, 31–39.

Yoneyama, Takeshi, Kitade, Motoki, Osada, Kazutaka. (2010). Investigation on the ski-snow interaction in a carved turn based on the actual measurement. Procedia Engineering. 2. 2901-2906. 10.1016/j.proeng.2010.04.085.

Lesenciuc, D. C., Boengiu, S., & Huşupaşu, M. (2013). The characteristics of the ski domains from the Romanian Carpathians. *Forum Geografic. Studii şi Cercetări de Geografie şi Protecţia Mediului, 12*(1), 89–99.

Mihai, B.-A., Sandric, I., & Chitu, Z. (2008). Some contributions to the drawing of the general geomorphic map using GIS tools. *Revista de Geomorfologie, 10*, 39–50.

National Meteorological Administration. https://www.meteoromania.ro/

Nap, M.-E., Ficior, D., Salagean, T., Pop, I., Matei, F., Coroian, I., Deak, J., Chiorean, S., & Suba, E.-E. (2022). A GIS study about forest management in Strâmbu Băiuţ. *Bulletin of University of Agricultural Sciences and Veterinary Medicine Cluj-Napoca. Horticulture, 79*(1), 18–25.

Olariu, B. (2019). *Analysis methods of mountain environmental quality in protected areas: Case study – Bucegi Natural Park* [Doctoral dissertation, Universitatea din Bucureşti]. 185 pp.

Teodor, M., & Dobre, R. (2015). Relief suitability for developing a macro ski area between Predeal and Azuga Resort. *Revista de Geomorfologie, 17*, 95–106.

Tereşneu, C. C. (2013). Using GIS for the determination of peak discharge in a small forested watershed. *Bulletin of the Transilvania University of Braşov, 6*(55), 69–74.

Tereşneu, C. C. (2022). The use of geographical information systems for issues of forest land retrocessions. *Scientific Papers – Series E – Land Reclamation, Earth Observation & Surveying, Environmental Engineering, 11*, 452–457.

Tereşneu, C. C., & Vasilescu, M. M. (2019). The influence of orographic and tree stand factors on the precision of planimetric coordinates determined using GPS equipment in a forest environment. In *Forest and Sustainable Development*, 177–184.

Voiculescu, M., & Popescu, F. (2011). Management of snow avalanche risk in the ski areas of the Southern Carpathians: Case studies from the Făgăraş and Bucegi Mountains. In *Sustainable Development in Mountain Regions: Southeastern Europe*, 103–121.

Voiculescu, M., & Ardelean, F. (2012). Snow avalanche: Disturbance of high mountain environment – Case study: The Doamnei glacial valley, Făgăraş Massif, Romanian Carpathians. *Carpathian Journal of Earth and Environmental Sciences, 7*, 95–108.

Vorovencii, I. (2016). Soil erosion estimation for Secaşelor Plateau, Romania, using the E30 model and Landsat imagery. *REVCAD, 21*, 187–194.

Vorovencii, I. (2024). Assessing various scenarios of multitemporal Sentinel-2 imagery, topographic data, texture features, and machine learning algorithms for tree species identification. *IEEE Journal of Selected Topics in Applied Earth Observations and Remote Sensing, 17*, 15373–15392.

Wang T, Zhang W, Li J, Liu D, & Zhang L. (2024). Identification of Complex Slope Subsurface Strata Using Ground-Penetrating Radar. *Remote Sensing*. 16(2):415. https://doi.org/10.3390/rs16020415.

Wegler M, & Kuenzer C. (2024). Potential of Earth Observation to Assess the Impact of Climate Change and Extreme Weather Events in Temperate Forests -A Review. *Remote Sensing*. 16(12):2224. https://doi.org/10.3390/rs16122224.

Scientific Papers. Series E. Land Reclamation, Earth Observation & Surveying, Environmental Engineering. Vol. XIV, 2025
Print ISSN 2285-6064, CD-ROM ISSN 2285-6072, Online ISSN 2393-5138, ISSN-L 2285-6064

TRENDS AND INSIGHTS IN MACHINE LEARNING FOR WASTE MANAGEMENT: A DECADE OF BIBLIOMETRIC ANALYSIS

Sneha BASKARAN, Ezhilmaran DEVARASAN

Vellore Institute of Technology, School of Advanced Science, Department of Mathematics, Vellore, 632 014, Tamil Nadu, India

Corresponding author email: ezhil.devarasan@yahoo.com

Abstract

This article investigates the evolving landscape of machine learning and its application in waste management from 2014 to 2024, utilizing data from Scopus and employing the VOSviewer software for bibliometric analysis. The research identified 217 articles related to machine learning in waste management. Our analysis aimed to assess metrics such as yearly publication trends, citation rates, top publishing countries, and the most influential authors in the field. Additionally, we examined the evolution of research on machine learning in waste management, focusing on highly cited articles, leading journals, authors' keywords, co-citation patterns, and co-authorship networks among countries and organizations. This comprehensive review provides a deeper understanding of the growth and collaborative nature of the field. The results indicate a notable rise in machine learning publications in waste management, increasing from 1 in 2016 to 62 in 2024, for a total of 217 publications. China, India, and South Korea led the research output, contributing 19.35%, 15.67%, and 10.60%, respectively. Leading journals such as the Journal of Cleaner Production, Waste Management, and Sustainability Switzerland emerged as critical contributors. A sharp increase in publications was observed post-2020, especially in the Journal of Cleaner Production. One of the most notable findings was the high citation rate of research on machine learning techniques in waste management, underscoring their practical relevance and mathematical significance in optimizing waste handling and reduction. Frequently occurring keywords included "machine learning", "waste management", and "deep learning". The VOSviewer visualizations indicated strong international collaboration networks, highlighting a robust global research framework. Our study emphasizes the growing influence of machine learning in waste management, marked by increasing research activity and international cooperation, and showcases the transformative potential of machine learning driven models in improving global waste management practices.

Key words*: Bibliometric Analysis, Machine Learning, Scopus, VOSviewer Software, Waste Management.*

INTRODUCTION

The rapid pace of urbanization and industrialization in recent years has intensified challenges in waste management (WM), with an increase in waste generation necessitating innovative approaches to ensure sustainable waste handling practices that effectively mitigate environmental impacts. Traditional WM practices generally follow linear processes that include collection, transportation, and disposal, resulting in inefficiencies, higher costs, and low recycling rates. These conventional methods often rely on manual sorting and fixed collection schedules, which limit their ability to effectively manage the complexities of contemporary waste generation. In contrast, Machine learning (ML) has emerged as a transformative tool in response to these pressing challenges, capable of enhancing various facets of waste management. ML techniques have gained substantial attention due to their potential to optimize waste management processes, including waste sorting, predictive modeling, and recycling efficiency. ML has notably enhanced the accuracy of waste generation forecasts across various waste types, such as construction waste (Cha et al., 2021), municipal solid waste (Ayeleru et al., 2021), hospital waste (Golbaz et al., 2019), food industry waste (Garre et al., 2020), and more. By leveraging advanced algorithms, researchers are developing models that facilitate more effective WM. The application of data-driven planning through machine learning not only enhances the efficiency and sustainability of waste management practices but also contributes to the development of smarter, more resilient urban environments (Ahmad et al., 2020).

Moreover, integrating ML with the Internet of Things (IoT) has opened new avenues for efficient WM. Recent explorations into IoT-enabled solutions emphasize the potential of real-time data collection and analysis to promote cleaner, more sustainable urban environments (Rutqvist et al., 2019; Cheah et al., 2022; Patil & Gidde, 2023).

This study performs a bibliometric analysis that focuses on exploring and analyzing the development of ML technologies in WM. This investigation can lead to sophisticated ML models designed to address the complexities associated with WM, such as predicting waste production, sorting automation, and improving collection route efficiency. The bibliometric analysis of ML applications in this field yields important insights into its evolution, identifies major research contributions, and highlights gaps for future investigations. Additionally, it offers an in-depth view of these technologies and the dynamics of international collaborations within this domain over time, showcasing how different organizations and countries contribute to advancing the field. This research utilizes publications and data from Scopus and employs VOSviewer software to create graphical representations that examine keyword co-occurrences, citation patterns, bibliographic links, and co-authorship relationships. These findings can help the researchers with effective strategies and innovations in sustainable WM.

This study is organized as follows: Section 2 reviews the specialized literature on machine learning in waste management, highlighting key advancements and methodologies used in recent research. Section 3 outlines the methodology used for this bibliometric analysis, detailing the criteria for selecting publications and the analytical tools applied. Section 4 presents the findings along with their interpretations, revealing significant trends in the application of machine learning technologies and their impact on WM practices. Drawing on the trends identified in the results section, Section 5 will engage in discussions regarding these trends, addressing the implications for future research directions. Finally, Section 6 will summarize the key conclusions and provide recommendations for further exploration in the field, emphasizing the importance of continuous innovation in sustainable WM practices.

Literature review

Effective WM is essential for environmental sustainability, resource conservation, and public health protection. WM encompasses a range of processes focused on the collection, transportation, treatment, reuse, and disposal of waste materials. As urban populations grow, the volume and complexity of waste generated have increased, creating a need for more efficient and effective WM strategies. ML, a branch of artificial intelligence (AI), focuses on developing algorithms that allow computers to learn from data and make informed predictions. Its application in WM has significant potential to optimize processes, enhance decision-making, and improve sustainability outcomes. A key application of ML in WM is the classification and segregation of waste materials. Traditional sorting methods often rely on manual labor, which can be time-consuming, error-prone, and inefficient. For example, Nnamoko et al. (2022) introduced an optimized five-layer convolutional neural network (CNN) for classifying organic and recyclable waste, which reduces computational demands by using lower-resolution images, ultimately outperforming both higher-resolution models and baseline classifiers. Recent literature (Al Duhayyim et al., 2023; Ali et al., 2024; Nezerka et al., 2024) highlights substantial advancements in WM through machine learning, employing sophisticated algorithms such as custom CNNs, K-nearest neighbors (KNN), and ensemble learning models to achieve greater classification accuracy and efficiency. These studies emphasize ML's transformative role in automating sorting processes, reducing errors, and supporting a more sustainable future. Additionally, studies (Gondal et al., 2021; Carrera et al., 2022; Mohammed et al., 2023; Jin et al., 2023) address various waste types for improved classification and recycling. Techniques include using infrared spectrums for plastic identification, applying artificial neural networks (ANN) to urban waste sorting, deploying hybrid CNN models for real-time metal and non-metal sorting, and enhancing

MobileNetV2 models with attention mechanisms to improve classification accuracy. ML-driven predictive analytics has become an essential tool for anticipating waste generation patterns. By examining historical data, these models can detect trends and forecast future waste production. Namoun et al. (2022) discussed an optimized ensemble learning model for predicting urban household waste generation, which supports more effective waste management in smart cities. In the literature (Cha et al., 2020; Cha et al., 2022; Cha et al., 2022; Cha et al., 2024), advanced machine learning models, including ANN, support vector machines (SVM), and random forests (RF), have been applied to accurately predict construction and demolition waste production. Furthermore, ML models enhance the forecasting of municipal waste production by leveraging socioeconomic data, with optimization techniques improving accuracy. Many researchers (Oguz-Ekim et al., 2021; Yang et al., 2021; Zhang et al., 2022; Munir et al., 2023; Singh et al., 2023) utilize ML algorithms like XGBoost, and RF to predict municipal solid waste (MSW), highlighting population and gross domestic product (GDP) as key indicators.

Huang and Koroteev (2021) analyzed an ML framework to optimize waste and energy management, achieving a 90% reduction in waste processing time, a 40% decrease in landfill dependency, and a 15% reduction in transportation costs by predicting waste volumes and adapting to fluctuations in energy markets. Altarazi F. (2024) explores EcoEfficientNet, an advanced ML tool for sustainable manufacturing that uses deep learning to analyze production data and identify waste reduction opportunities. Through continuous learning, EcoEfficientNet adapts to new data and evolving production conditions, achieving up to a 30% reduction in waste generation. ML models are increasingly essential for enhancing waste-to-energy (WTE) processes by reliably forecasting the energy potential and volume of MSW based on diverse factors. Studies indicate that advanced techniques, including ANNs, SVMs, and ensemble approaches, improve WM efficiency and support the strategic siting of WTE facilities, as shown in the literature (Kaya et al., 2021; Al-Ruzouq et al., 2022; Taki & Rohani, 2022; Yatim et al., 2022).

In references (Mookkaiah et al., 2022; Belsare et al., 2024; Chavhan et al., 2024), artificial intelligence (AI), IoT, and ML have driven innovative solutions, utilizing CNN models like ResNet for precise automated classification of MSW, thereby improving sorting accuracy and promoting sustainable WTE practices. Moreover, numerous scholars (Mudannayake et al., 2022; Zia et al., 2022; AlJamal et al., 2024; Hossen et al., 2024; Mishra et al., 2024) have implemented AI and ML models such as GCDN-Net and DenseNet-121 - SVM to achieve highly accurate automated waste classification, enhancing recycling processes and supporting sustainable WM amid the challenges of urbanization.

Literature (Medina-Mijangos & Seguí-Amórtegui, 2020) offers a comprehensive bibliometric analysis of the economic dimensions of MSW management. This methodology has gained substantial traction across various disciplines, primarily due to its capacity to deliver intricate scientific mappings over specified temporal frameworks. Such analyses illuminate emerging trends that decision-makers can strategically utilize in diverse contexts (Tamala et al., 2022; Oladinrin et al., 2023; Martins et al.,2024). Recent studies (Negrete-Cardoso et al., 2022; Sohail et al., 2023) highlight, through bibliometric analyses, waste management strategies based on multi-criteria decision-making methods and circular economy principles, emphasizing current research trends in the field.

MATERIALS AND METHODS

In this study, data from the Scopus (Elsevier, accessed 17 October 2024). database is utilized. Scopus is a multidisciplinary citation database managed by Elsevier, widely recognized, and commonly used for analyzing research output. The database includes content from various subjects, including science, technology, medicine, and social sciences. Scopus provides detailed statistics and visualizations for assessing data on research areas, document types, countries, authors, institutions, publication timelines, and universities. Additionally, it allows users to export

publication records in formats such as CSV or Excel, which are compatible with data visualization and analysis tools like VOSviewer or Bibliometrix. Besides journal articles, Scopus also indexes conference proceedings, book series, and patents, offering a comprehensive view of the global research landscape.

A key challenge in bibliometric research is defining the boundaries of the specific field being analyzed. To gain a broader perspective on publications related to ML in waste management systems, searches were conducted using the key words: "waste", "management", and "machine", "learning." The search was limited to publications from 2014 to 2024, and the data was collected on 17 October 2024. The objective of this search was to identify articles that explored the application of ML in waste management. A total of 217 results were found. To map and analyze the network, the full records which primarily included the titles, sources, authors, affiliations, abstracts of the research articles, and the cited references were downloaded in CSV format. Figure 1 illustrates the methodology employed for searching, data collection, and information processing.

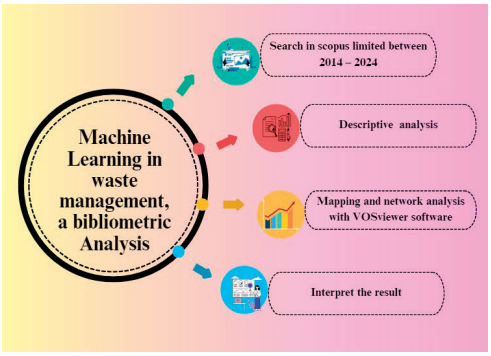


Figure 1. Methodology employed in this study

An exploratory analysis was conducted to examine and highlight the most impactful journals, authors, countries, and articles within the database. In reference (Seguí-Amortegui et al., 2019), the research employed bibliometric measures, including (i) productivity, determined by the total count of publications (Reuters, 2008); (ii) impact, analyzed by the total citation count (Reuters, 2008); (iii) the H-index (Hirsch index), which indicates that N publications have received at least N citations, providing a combined measure of both productivity and impact in a single figure (Reuters, 2008; Hirsch, 2005); and (iv) the impact factor (IF), a metric used to evaluate journals by calculating the average number of citations for articles published within a two-year period (Reuters, 2008).

The research employed VOSviewer software, developed by Leiden University, to map and analyze networks of scientific publications, including journals, institutions, countries, authors, and keywords (Van Eck & Waltman, 2016). Analyzing these networks creates a graphical representation that visualizes the relationships within the data (Ji, 2018). These networks allow for the viewing and exploration of maps by connecting the articles through citations, authorship, co-occurrence, bibliographic links, or co-citation connections (Van Eck & Waltman, 2016).

VOSviewer software represents the interest of items, such as publications, authors, sources, or keywords, using nodes; larger nodes indicate greater weight or significance of the item. A link refers to the connection between two objects, displaying the count of articles where one particular object is found alongside another. The thickest lines exhibit more frequent co-occurrence or higher levels of cooperation (Seguí-Amortegui et al., 2019; Van Eck & Waltman, 2016). The distance between the nodes also reflects their co-occurrence. Elements are grouped by colour to signify their connection to research topics, with elements sharing the same colour referred to as clusters (Van Eck & Waltman, 2016).

RESULTS AND DISCUSSIONS

First, we highlighted key research trends, including annual publication numbers, citation rates per article and field, leading countries in publication output, and the most prominent authors (Seguí-Amortegui et al., 2019). Next, we examined the current state and evolution of research on ML in waste management, analyzing 217 articles. In the second section, we focused on the most cited articles on ML in waste management. The third section examined the leading journals in this area. The fourth

section investigated the overlap of authors' keywords in ML within waste management. The article then analyzed the co-citation patterns of references, sources, and authors related to ML in waste management. Finally, it explored the networks of co-authorship among countries and organizations involved in ML in waste management research.

Significant trends

In 2014 and 2015, no articles were published in Scopus on ML in waste management. However, from 2016 to 2024, the number of publications shows a significant increase, beginning with one publication in 2016 and rising to 62 in 2024. Despite a slight decline in 2024, with the number dropping to around 60, the overall trend indicates a substantial rise in research activity during this period, totalling 217 publications. This growth highlights the growing interest and contributions to the field over the years. Figure 2 illustrates the yearly publication count on ML in waste management as indexed in Scopus.

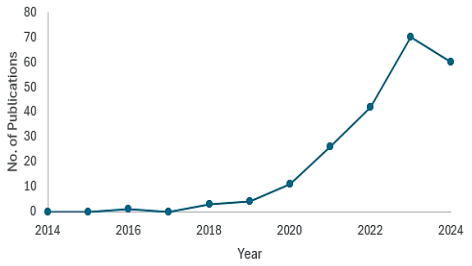


Figure 2. Yearly publication counts on ML in waste management

The bar chart in Figure 3 highlights the countries with the highest number of publications focused on ML in waste management. The x-axis represents the number of publications, ranging from 0 to 45, while the y-axis lists the countries involved. The analysis shows that China leads with 42 articles, followed by India with 34 and South Korea with 23. Iran has the fewest publications among the listed countries. In total, 62 countries have contributed to the production of 217 publications, corresponding to 19.35%, 15.67%, and 10.60% of the total publications on the topic, respectively. This visual representation effectively demonstrates the comparative research contributions of different nations.

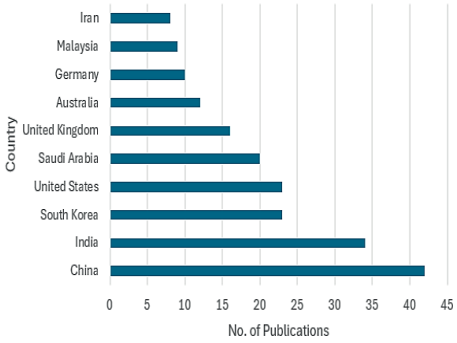


Figure 3. Publications in Scopus on ML in waste management, categorized by country

The horizontal bar chart visually represents the number of publications by different authors in the field. The x-axis indicates the number of publications, ranging from 0 to 8, while the y-axis lists the authors' names. Figure 4 shows that the top authors in ML research in waste management are Cha, G.W. with 8 publications, Kim, Y.C. with 6 publications, and Hong, W.H. with 5 publications. These figures represent 3.69%, 2.76%, and 2.30% of the 217 total publications in this area, respectively.



Figure 4. Publications in Scopus on ML in waste management, categorized by author

Citation counts provide a clear measure of an article's impact. Table 1 provides a detailed breakdown of articles based on their citation count, offering insights into the citation performance of publications related to ML in

waste management. Only 1 article (0.46%) has more than 251 citations, and articles with 151 to 250 citations represent 0.92% of the total. Moderately cited articles (51 to 100 citations) account for 6.45%, while a larger portion has fewer citations: 12.91% (26 to 50 citations) and 17.06% (11 to 25 citations). Notably, 44.23% of the articles have fewer than 11 citations, and 16.12% have not been cited at all, indicating that many publications have relatively low visibility and impact in the academic community. Overall, this highlights a significant opportunity for increased recognition and dissemination of research in this field.

Table 1. Overview of Citation Distribution on ML in waste management

Citation Count	Number of Articles	Accumulated Articles	% Articles	% Accumulated Articles
≥251	1	1	0.46%	0.46%
≥201	0	1	0%	0.46%
≥151	2	3	0.92%	1.38%
≥101	4	7	1.84%	3.22%
≥51	14	21	6.45%	9.66%
≥26	28	49	12.91%	22.61%
≥11	37	86	17.06%	39.63%
<11	96	182	44.23%	83.89%
0	35	217	16.12%	100%

Most-cited publications on ML in waste management

Table 2 provides a ranking of influential articles that apply ML to waste management, detailing important factors such as the reference, year of publication, country of origin, journal source, article title, and the number of citations each work has received. This ranking helps to highlight the most impactful contributions in this research area. At the top of the list is the work by Abbasi & El Hanandeh (2016) from Australia, which has garnered 276 citations. Following closely is the study by Palansooriya et al. (2022) from South Korea, with 195 citations. Another notable contribution comes from Yuan et al. (2021) from South Korea, which has received 173 citations. These top-cited articles illustrate the critical role of ML in addressing global waste management challenges, with each contributing to advancements in predictive modeling and sustainable practices within the field.

Table 2. Most-Cited Articles

Rank	Reference	Country	Journal source	Title	Citations
1	Abbasi & El Hanandeh (2016)	Australia	*Waste Management*	Forecasting municipal solid waste generation using artificial intelligence modelling approaches	276
2	Palansooriya et al. (2022)	South Korea	*Environmental Science and Technology*	Prediction of soil heavy metal immobilization by biochar using machine learning	195
3	Yuan et al. (2021)	South Korea	*Environmental Science and Technology*	Applied machine learning for prediction of CO 2 adsorption on biomass waste-derived porous carbons	173
4	Kumar et al. (2018)	India	*Waste Management*	Estimation of the generation rate of different types of plastic wastes and possible revenue recovery from informal recycling	123
5	Anh Khoa et al. (2020)	Vietnam	*Wireless Communications and Mobile Computing*	Waste management system using iot-based machine learning in university	118
6	Kontokosta et al. (2018)	United States	*Computers, Environment and Urban Systems*	Using machine learning and small area estimation to predict building-level municipal solid waste generation in cities	106

Rank	Reference	Country	Journal source	Title	Citations
7	Yu et al. (2021)	United Kingdom	*Environmental Impact Assessment Review*	Environmental planning based on reduce, reuse, recycle and recover using artificial intelligence	103
8	Nguyen et al. (2021)	Vietnam	*Resources, Conservation and Recycling*	Development of machine learning - based models to forecast solid waste generation in residential areas: a case study from Vietnam	95
9	Vu et al. (2019)	Canada	*Waste Management*	Time-lagged effects of weekly climatic and socio-economic factors on ANN municipal yard waste prediction models	90
10	Lu et al. (2021)	Australia	*Waste Management*	Estimating construction waste generation in the Greater Bay Area, China using machine learning	77

Analysis of the Research Journals in ML in Waste Management

In this bibliometric analysis, Table 3 highlights the top 10 local sources that play a significant role in assessing the influence and relevance of research in the field of ML in waste management. Among these, the *Journal of Cleaner Production* stands out as a particularly impactful source. With an H-index of 9 and a G-index of 14, this journal demonstrates a strong influence in the domain, reflecting that many of its articles have significantly contributed to the research community. Its M-index of 1.5 suggests an average of 1.5 citations per article, further emphasizing its academic value. Since 2019, this journal has published 14 papers on ML in waste management, contributing a total of 302 citations to the field. Next in line is the *Waste Management Journal*, with an H-index of 9 and a G-index of 12. It has been a prominent contributor since 2016, with 12 articles accumulating an impressive 714 total citations, making it a highly referenced source in the field, even though its M-index is slightly lower at 1.

The *Journal of Environmental Management*, active in this area since 2021, also makes a notable contribution with an H-index of 6 and a G-index of 9, featuring an M-index of 1.5. Despite having published only 9 papers, it has garnered 177 citations, indicating that the work published here is also well-regarded in the academic community.

Table 3. Influence of Research Journal

Source	H_index	G_index	M_index	TC	NP	PY_start
Journal of Cleaner Production	9	14	1.5	302	14	2019
Waste Management	9	12	1	714	12	2016
Journal of Environmental Management	6	9	1.5	177	9	2021
Sustainability (Switzerland)	5	6	1.667	48	9	2022
International Journal of Environmental Research and Public Health	4	4	0.8	119	4	2020
Sensors	4	5	1	122	5	2021
Environmental Science and Technology	3	4	0.75	393	4	2021

Keyword analysis

Keywords typically signify the main topics and themes of a research article, highlighting key trends and essential subjects within a particular field (Segui-Amortegui et al., 2019). An analysis of 217 articles on ML in waste management identified 779 unique keywords. Figure 5 illustrates the network map of keywords in ML for waste management. The central node, machine learning (blue), connects to several related terms, such as artificial intelligence (red), deep learning (green), solid waste management (yellow), municipal solid waste (orange), sustainability (purple), and artificial neural network (teal).

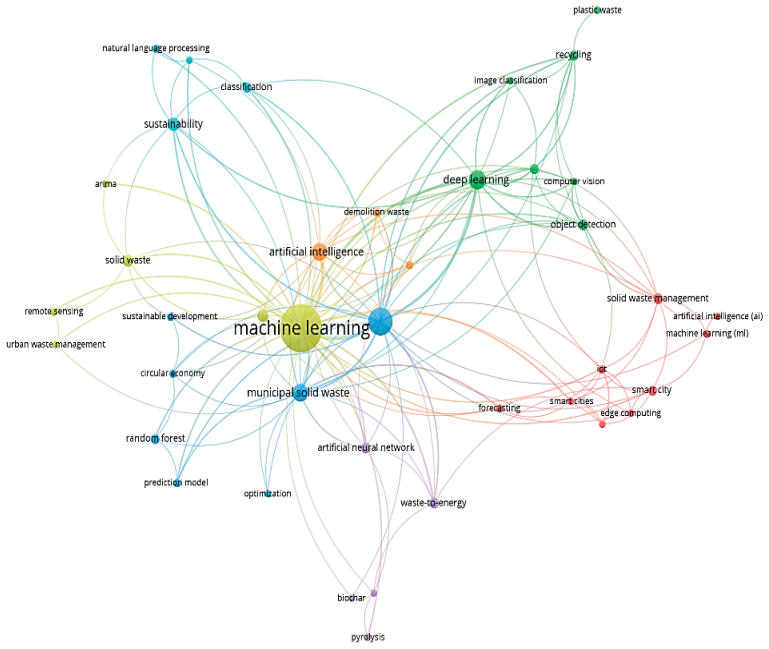


Figure 5. Author keywords network of co-occurrence. The figure showcases the 41 most frequently occurring keywords out of a total of 779 keywords, each meeting a minimum occurrence threshold of 3

The top 10 keywords highlighted in this analysis emphasize the integration of ML within waste management. Keywords such as machine learning, deep learning, and artificial intelligence underscore the role of advanced algorithms in improving waste processing systems. Terms like municipal solid waste and waste classification reflect efforts to optimize waste handling and categorization through technology. Additionally, the inclusion of object detection and recycling highlights the importance of automation in enhancing sorting processes, while sustainability and prediction emphasize the commitment to sustainable practices and the anticipation of waste trends to inform better management strategies.

Table 4 presents the 10 most prominent keywords, along with their occurrences and link strengths.

VOSviewer offers powerful density visualizations, as shown in Figure 4. In the keyword density plot, each node is colored according to the concentration of elements around it, making patterns in the data easily identifiable.

Table 4. The top 10 keywords of the ML in waste management

Rank	Keywords	Occurrences	Link strength
1	Machine learning	109	121
2	Waste management	37	67
3	Deep learning	19	36
4	Municipal solid waste	15	35
5	Artificial intelligence	15	27
6	Object detection	6	15
7	Recycling	5	15
8	Sustainability	9	15
9	Prediction	8	14
10	Waste classification	5	14

In other words, a node's color reflects the number of surrounding objects, with denser areas showing higher concentrations of keywords. Keywords highlighted in red occur more frequently, indicating major areas of focus, while those in yellow are less common and represent peripheral topics. Density visualizations are particularly useful for gaining a quick overview of the distribution of research trends, identifying clusters, and detecting key themes.

As demonstrated in Figure 6, this method provides a clear and intuitive view of the primary research areas in machine learning within WM systems. Keywords such as "machine learning", "waste management", "deep learning", "municipal solid waste", and "artificial intelligence" emerge as significant.

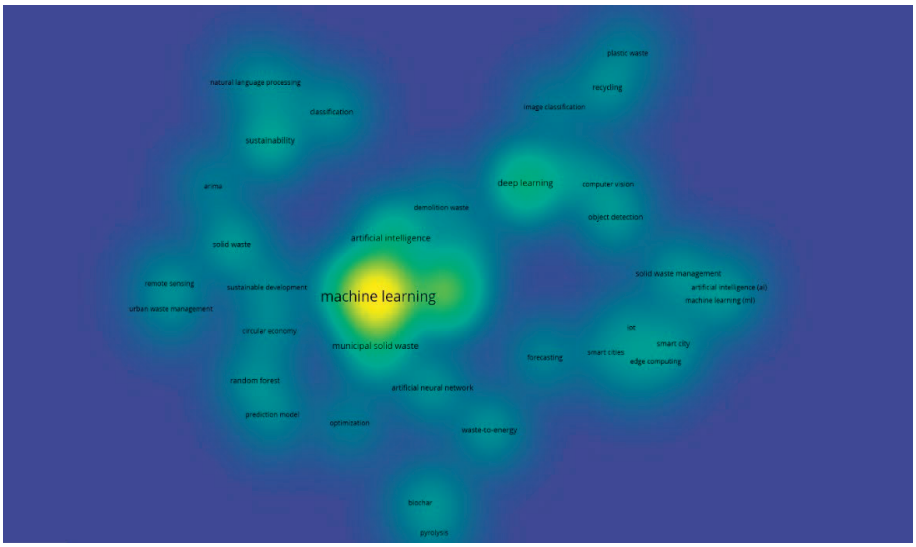


Figure 6. A density map illustrating the keyword distribution in publications related to ML in waste management

Analysis of co-citations for authors, references, and research journals

This section focused on the concept of co-citation among authors, references, and research journals. Co-citation occurs when two documents are cited in tandem by a third source, reflecting how frequently these items (authors, research journals, or references) are jointly referenced, thus forming a co-citation link between them (Small, 1973). A co-citation link connects two elements that are cited within the same document. Here, the proximity between two authors, references, or research journals indicates the strength of their relationship based on shared citation links. Generally, nodes that are closer together indicate a stronger relationship. Connections between nodes are also depicted with lines, highlighting the strongest co-citation (Van Eck & Waltman, 2016).

The initial analysis focused on author co-citation patterns. The network of author co-citations illustrated in Figure 7 identifies three main clusters: a red cluster, which is the largest, containing 70 authors; a green cluster with 46 authors; and a blue cluster with 7 authors. Key authors include Li J., who has 109 citations along with a link strength of 6,425; Wang X., who has 105 citations along with a link strength of 5,622; and Wang Y., who has 102 citations along with a link strength of 4,796.

The network of reference co-citations presented in (Figure 8) reveals three primary clusters: a red cluster, the most extensive, which includes 8 references; a green cluster comprising 7 references; and a blue cluster featuring 3 references. The red cluster may represent the most influential or foundational works in the field, while the green and blue clusters highlight additional areas of research that are interconnected but perhaps less frequently cited. This visualization aids in understanding the relationships between key references and their contributions to the overall scholarly discourse.

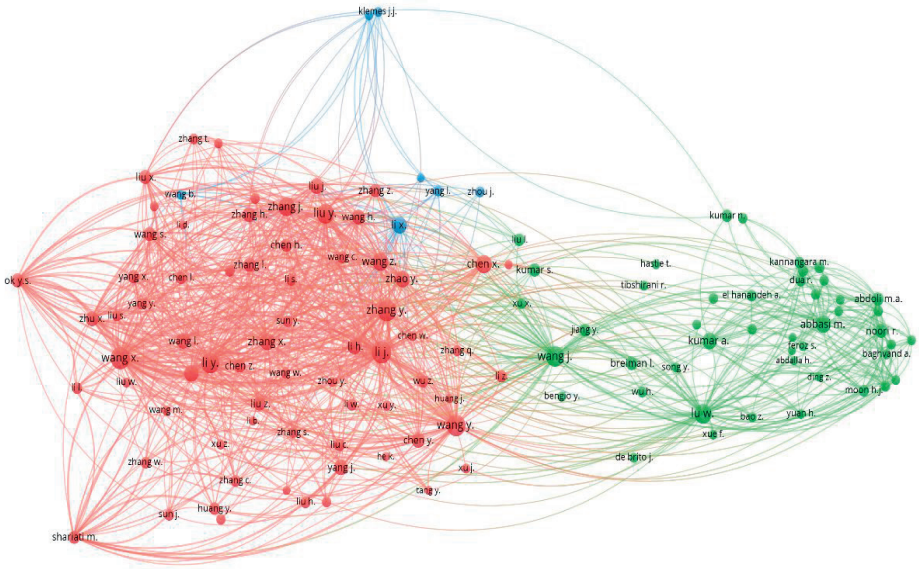


Figure 7. Network of author co-citations, highlighting 123 authors out of 25,398 cited authors who meet the minimum threshold of 20 citations each



Figure 8. Co-citation of references, 19 references from a total of 11,490 that meet the minimum citation threshold of 5

Concerning journal co-citation patterns, the network discussed in Figure 9 identifies seven clusters. The first three clusters are as follows: The red cluster, the largest, includes 10 research journals, with the *Journal of Cleaner Production* as the most prominent source, having 223 citations and a link strength of 5,875. This cluster consists of interdisciplinary journals addressing topics related to environmental sustainability. The second cluster is green, also containing 10 research journals, with *Waste Management* as the leading source, having 181 citations and a link strength of 3,755. This cluster covers journals on various aspects of WM, including generation, features, reduction, gathering, sorting, treatment, and disposal. The third cluster is blue and includes 8 research journals, with *Sustainability* as a key source, showing 104 citations and a link strength of 2,090. This cluster features journals that publish research on sustainability, including topics such as energy production, conversion, and utilization. The remaining clusters include yellow and purple with 7 journals, light blue with 5 journals, and orange with 2 journals.

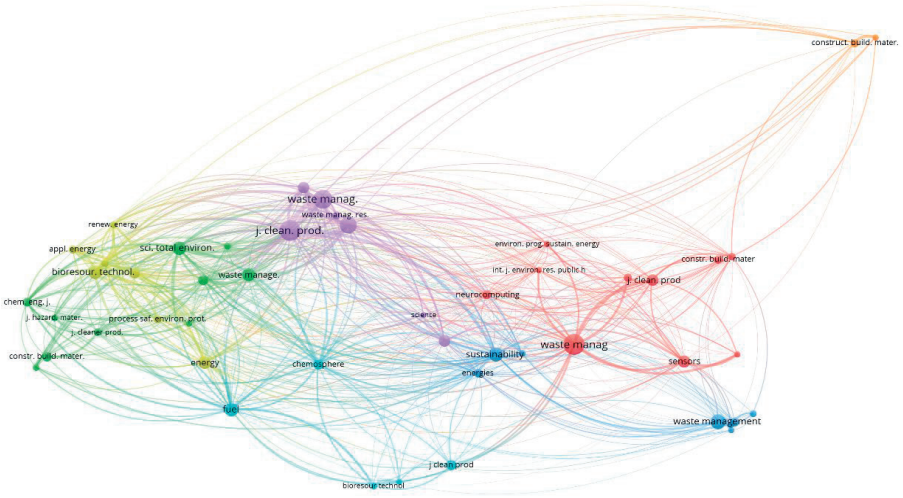


Figure 9. Network of journal co-citations 49 core journals from a total of 5,262 that meet the minimum citation threshold of 20

Authors' bibliographical coupling

The analysis of bibliographic coupling among authors enabled us to determine whether authors A and B reference the works of author C. This means that two authors sharing common citations are more interconnected and likely have comparable research interests (Gazni & Didegah, 2016). The bibliographic coupling of authors (Figure 10) revealed two clusters consisting of 10 authors in total. The primary cluster is red, featuring 6 authors, with the most notable being Cha, Gi-Wook. The green cluster contains 4 authors, with Li, Jie being the most prominent. The authors with the highest number of publications include Cha, Gi-Wook (155 citations), who has 8 publications in Scopus; Kim, Young-Chan (136 citations), who has 6 publications; and Hong, Won-Hwa (72 citations) has 5 publications.

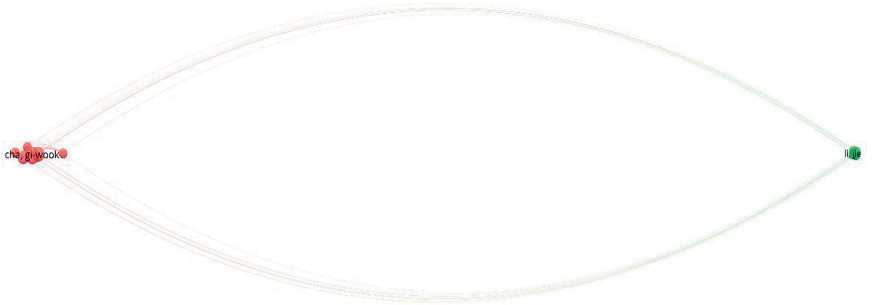


Figure 10. Authors' bibliographical coupling: 10 authors out of 928 meet the minimum threshold of 3 documents per author

Analysis of co-authors by country and institution

Co-authorship among cities and Institution was examined, with node size representing the importance of Institution or countries and the spacing indicates the extent of their collaboration.

Examining the co-authorship connections among countries reveals a network of 20 countries divided into 5 clusters (Figure 11). The cluster of red includes 7 countries, with China as the most prominent (42 documents, 745 citations), followed by Hong Kong (7 documents, 323 citations) and South Korea (23 documents, 842 citations). The cluster of green comprises 4 countries, with Saudi Arabia as the leading country (20 documents, 210 citations), along with Pakistan (8 documents, 135 citations) and Poland (8 documents, 166 citations). In the cluster of blue, which includes 3 countries, the United States is the primary contributor (23 documents, 426 citations), followed by Bangladesh (5 documents, 67 citations) and Canada (6 documents, 121 citations). The cluster of yellow is made up of 3 countries, led by India (35 documents, 516 citations), while the cluster of purple also contains 3 countries, led by the United Kingdom (16 documents, 59 citations). The countries with the highest number of publications and citations are China, Saudi Arabia, and the United Kingdom.

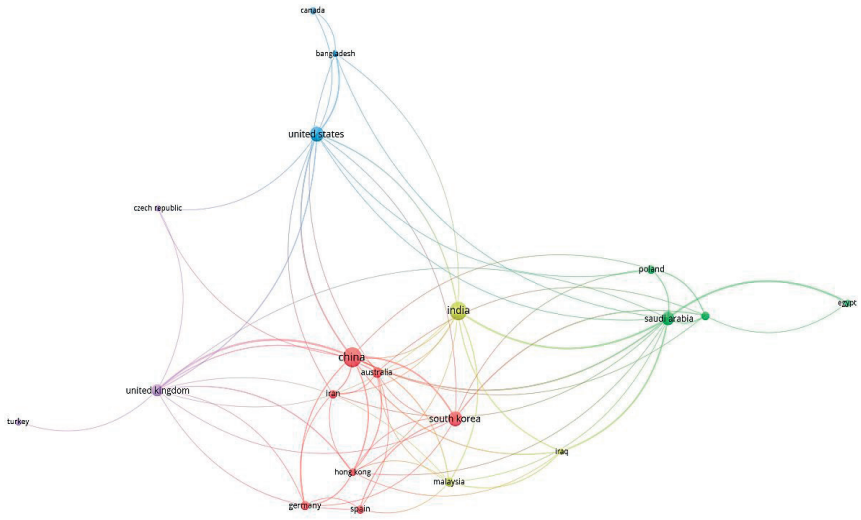


Figure 11. Co-authorship network of countries: 20 countries out of 63 meet the minimum threshold of 5 papers per country

Finally, the co-authorship network of institutions Figure 12 reveals that there is limited collaboration among different organizations that satisfy the threshold of having at least 2 published documents. Out of the 608 universities listed, the largest group comprises only 5, divided into two clusters: the cluster of red consists of 3 organizations, while the cluster of green includes 2 organizations. A notable organization is the School of Science and Technology in Acceleration Engineering at Kyungpook, National University in Daegu, South Korea, which has 4 documents and 27 citations.



Figure 12. Co-authorship network of organizations: 5 organizations out of 608 meet the minimum threshold of 2 documents

This study examined the application of ML in waste management to understand how these advanced algorithms can enhance decision-making processes and improve WM outcomes. The results highlight several critical factors that could advance the field and help scholars make more informed decisions. This paper also explores how ML integration impacts current practices and influences future developments in waste management. China, India, and South Korea lead in the highest number of publications in this area. Keyword analysis indicates a strong focus on specific waste types, including "solid waste", "demolition waste", and "organic waste". Research on these types of waste is essential, as they represent the most generated waste worldwide and pose multiple potential negative impacts (economic, sustainability, and environmental) if not managed properly.

In general, there is a noticeable rise in publications focused on WTE. Recovering energy from waste through incineration plants offers a way to reduce the volume of waste directed to landfills. Moreover, it can aid in decreasing reliance on energy produced from fossil fuels, which are often imported. However, the increase in publications does not align with the waste hierarchy outlined by organizations like the European Parliament. This hierarchy emphasizes the importance of implementing strategies to minimize waste generation, enhance efforts for recycling and reuse, and discourage reliance on landfills and incinerators, which remain common in certain areas of Europe and other parts of the world. Evaluating WM systems (collection and processing) is crucial because they can help minimize waste generation and enhance opportunities for recycling and reuse instead of relying on landfills and incineration.

The present study can help researchers identify various concepts and their interconnections, paving the way for further research opportunities. In this context, the article reveals several trends within the research landscape. The first trend is the growing importance of machine learning in waste management, as demonstrated by the increase of publications in Scopus. Additionally, there is heightened interest in researching WTE technologies. Another significant point is the need for collaboration among various universities across different countries, as limited cooperation has been observed. Such collaboration would facilitate knowledge sharing and the development of improved WM systems. Ultimately, there is a pressing need for increased research in this area on a global scale.

CONCLUSIONS

This bibliometric analysis highlights the application of ML in waste management from 2014 to 2024, covering trends and developments that underscore the growing importance of ML in this field. The significance of this study lies in its being the first bibliometric analysis to examine the role of ML in waste management. The data reveals substantial growth in ML-related studies within waste management, increasing from a single publication in 2016 to 62 in 2024, culminating in 217 publications. China, India, and South Korea have emerged as leading contributors to global research, driving significant advancements in the application of ML to waste management. The recognition of key journals, including the Journal of Cleaner Production and Waste Management, further underscores the academic significance of research in this domain. We also analyzed the evolution of research by examining highly cited papers, top journals, authors' keywords, co-citation patterns, and co-authorship networks among countries and organisation. This analysis highlights the ongoing need for further exploration and application of ML in waste management. VOSviewer visualizations revealed extensive international collaboration, emphasizing a robust research framework. However, the study has limitations. The use of broad keywords like "machine learning in waste management" could be refined to focus more specifically on waste-related topics. Additionally, the reliance on the Scopus database, while favored for its wide coverage and credibility in bibliometric studies, limits the study’s overall scope. Overall, this bibliometric analysis provides a comprehensive overview of the evolving role of ML within waste management, it highlights the field's rapid growth, the strength of international collaborations, and the rising significance of

ML techniques in enhancing waste management processes. In the near future, research could investigate a comparison between conventional bibliometric methods and machine learning-driven bibliometric models in waste management. Expanding this comparison over several decades may reveal trends in the development and effectiveness of these approaches. This approach helps researchers identify various concepts and their connections, paving the way for new research directions.

REFERENCES

Abbasi, M., & El Hanandeh, A. (2016). Forecasting municipal solid waste generation using artificial intelligence modelling approaches. *Waste management*, *56*, 13-22.

Ahmad, S., & Kim, D.H. (2020). Quantum GIS based descriptive and predictive data analysis for effective planning of waste management. *IEEE Access*, *8*, 46193-46205.

Al Duhayyim, M., Alotaibi, S.S., Al-Otaibi, S., Al-Wesabi, F.N., Othman, M., Yaseen, I., & Motwakel, A. (2023). An Intelligent Hazardous Waste Detection and Classification Model Using Ensemble Learning Techniques. *Computers, Materials & Continua*, *74*(2).

Ali, Z., Jamil, Y., Anwar, H., & Sarfraz, R.A. (2024). Classification of e-waste using machine learning-assisted laser-induced breakdown spectroscopy. *Waste Management & Research*, 0734242X241248730.

AlJamal, M., Mughaid, A., Bani-Salameh, H., Alzubi, S., & Abualigah, L. (2024). Optimizing risk mitigation: A simulation-based model for detecting fake IoT clients in smart city environments. *Sustainable Computing: Informatics and Systems*, *43*, 101019.

Al-Ruzouq, R., Abdallah, M., Shanableh, A., Alani, S., Obaid, L., & Gibril, M.B.A. (2022). Waste to energy spatial suitability analysis using hybrid multi-criteria machine learning approach. *Environmental Science and Pollution Research*, *29*, 2613-2628.

Altarazi, F. (2024). Optimizing Waste Reduction in Manufacturing Processes Utilizing IoT Data with Machine Learning Approach for Sustainable Production. *Scalable Computing: Practice and Experience*, *25*(5), 4192-4204.

Anh Khoa, T., Phuc, C. H., Lam, P. D., Nhu, L. M. B., Trong, N. M., Phuong, N. T. H., ... & Duc, D. N. M. (2020). Waste Management System Using IoT-Based Machine Learning in University. *Wireless Communications and Mobile Computing*, *2020*(1), 6138637.

Ayeleru, O.O., Fajimi, L.I., Oboirien, B.O., & Olubambi, P.A. (2021). Forecasting municipal solid waste quantity using artificial neural network and supported vector machine techniques: A case study of Johannesburg, South Africa. *Journal of Cleaner Production*, *289*, 125671.

Belsare, K., Singh, M., Gandam, A., Malik, P.K., Agarwal, R., & Gehlot, A. (2024). An integrated approach of IoT and WSN using wavelet transform and machine learning for the solid waste image classification in smart cities. *Transactions on Emerging Telecommunications Technologies*, *35*(4), e4857.

Carrera, B., Piñol, V.L., Mata, J.B., & Kim, K. (2022). A machine learning based classification models for plastic recycling using different wavelength range spectrums. *Journal of Cleaner Production*, *374*, 133883.

Cha, G. W., Choi, S. H., Hong, W. H., & Park, C. W. (2022). Development of machine learning model for prediction of demolition waste generation rate of buildings in redevelopment areas. *International Journal of Environmental Research and Public Health*, *20*(1), 107.

Cha, G.W., Moon, H.J., & Kim, Y.C. (2021). Comparison of random forest and gradient boosting machine models for predicting demolition waste based on small datasets and categorical variables. *International Journal of Environmental Research and Public Health*, *18*(16), 8530.

Cha, G.W., Moon, H.J., & Kim, Y.C. (2022). A hybrid machine-learning model for predicting the waste generation rate of building demolition projects. *Journal of Cleaner Production*, *375*, 134096.

Cha, G.W., Moon, H.J., Kim, Y.M., Hong, W.H., Hwang, J.H., Park, W.J., & Kim, Y.C. (2020). Development of a prediction model for demolition waste generation using a random forest algorithm based on small datasets. *International Journal of Environmental Research and Public Health*, *17*(19), 6997.

Cha, G.W., Park, C.W., & Kim, Y.C. (2024). Optimal Machine Learning Model to Predict Demolition Waste Generation for a Circular Economy. *Sustainability*, *16*(16), 7064.

Chavhan, P.G., Khedka, V.N., Gupta, M., & Agarwal, K. (2024). Automatic Waste Segregator Based on IoT & ML Using Keras model and Streamlit. *International Journal of Intelligent Systems and Applications in Engineering*, *12*(2), 787-799.

Cheah, C.G., Chia, W.Y., Lai, S.F., Chew, K.W., Chia, S.R., & Show, P.L. (2022). Innovation designs of industry 4.0 based solid waste management: Machinery and digital circular economy. *Environmental Research*, *213*, 113619.

Elsevier Scopus Database. Available online: https://www.elsevier.com/solutions/scopus/content (accessed on 17 October 2024).

Garre, A., Ruiz, M.C., & Hontoria, E. (2020). Application of Machine Learning to support production planning of a food industry in the context of waste generation under uncertainty. *Operations Research Perspectives*, *7*, 100147.

Gazni, A., & Didegah, F. (2016). The relationship between authors' bibliographic coupling and citation exchange: analyzing disciplinary differences. Scientometrics, *107,* 609-626.

Golbaz, S., Nabizadeh, R., & Sajadi, H.S. (2019). Comparative study of predicting hospital solid waste generation using multiple linear regression and artificial intelligence. *Journal of Environmental Health Science and Engineering*, *17*, 41-51.

Gondal, A.U., Sadiq, M.I., Ali, T., Irfan, M., Shaf, A., Aamir, M., & Kantoch, E. (2021). Real time multipurpose smart waste classification model for efficient recycling in smart cities using multilayer convolutional neural network and perceptron. *Sensors, 21*(14), 4916.

Hirsch, J.E. (2005). An index to quantify an individual's scientific research output. *Proceedings of the National academy of Sciences*, *102*(46), 16569-16572.

Hossen, M.M., Ashraf, A., Hasan, M., Majid, M.E., Nashbat, M., Kashem, S.B.A., & Chowdhury, M.E. (2024). GCDN-Net: Garbage classifier deep neural network for recyclable urban waste management. *Waste Management*, *174*, 439-450.

Huang, J., & Koroteev, D.D. (2021). Artificial intelligence for planning of energy and waste management. *Sustainable Energy Technologies and Assessments*, 47, 101426.

Ji, L., Liu, C., Huang, L., & Huang, G. (2018). The evolution of Resources Conservation and Recycling over the past 30 years: A bibliometric overview. *Resources, Conservation and Recycling*, *134*, 34-43.

Jin, S., Yang, Z., Królczykg, G., Liu, X., Gardoni, P., & Li, Z. (2023). Garbage detection and classification using a new deep learning-based machine vision system as a tool for sustainable waste recycling. *Waste Management*, *162*, 123-130.

Kaya, K., Ak, E., Yaslan, Y., & Oktug, SF. (2021). Waste-to-Energy Framework: An intelligent energy recycling management. *Sustainable Computing: Informatics and Systems*, *30*, 100548.

Kontokosta, C.E., Hong, B., Johnson, N.E., & Starobin, D. (2018). Using machine learning and small area estimation to predict building-level municipal solid waste generation in cities. *Computers, Environment and Urban Systems*, *70*, 151-162.

Kumar, A., Samadder, S.R., Kumar, N., & Singh, C. (2018). Estimation of the generation rate of different types of plastic wastes and possible revenue recovery from informal recycling. *Waste Management*, *79*, 781-790.

Lu, W., Lou, J., Webster, C., Xue, F., Bao, Z., & Chi, B. (2021). Estimating construction waste generation in the Greater Bay Area, China using machine learning. *Waste management*, *134*, 78-88.

Martins, J., Gonçalves, R., & Branco, F. (2024). A bibliometric analysis and visualization of e-learning adoption using VOSviewer. *Universal Access in the Information Society*, *23*(3), 1177-1191.

Medina-Mijangos, R., & Seguí-Amórtegui, L. (2020). Research trends in the economic analysis of municipal solid waste management systems: A bibliometric analysis from 1980 to 2019. *Sustainability*, *12*(20), 8509.

Mishra, S., Yaduvanshi, R., Rajpoot, P., Verma, S., Pandey, A.K., & Pandey, D. (2024). An integrated deep-learning model for smart waste classification. *Environmental Monitoring and Assessment*, *196*(3), 279.

Mohammed, M.A., Abdulhasan, M.J., Kumar, N.M., Abdulkareem, K.H., Mostafa, S.A., Maashi, M.S., & Chopra, S.S. (2023). Automated waste-sorting and recycling classification using artificial neural network and features fusion: A digital-enabled circular economy vision for smart cities. *Multimedia tools and applications*, *82*(25), 39617-39632.

Mookkaiah, S.S., Thangavelu, G., Hebbar, R., Haldar, N., & Singh, H. (2022). Design and development of smart Internet of Things–based solid waste management system using computer vision. *Environmental Science and Pollution Research*, *29*(43), 64871-64885.

Mudannayake, O., Rathnayake, D., Herath, J.D., Fernando, D.K., & Fernando, M. (2022). Exploring Machine Learning and Deep Learning Approaches for Multi-Step Forecasting in Municipal Solid Waste Generation. *IEEE Access*, *10*, 122570-122585.

Munir, M.T., Li, B., & Naqvi, M. (2023). Revolutionizing municipal solid waste management (MSWM) with machine learning as a clean resource: Opportunities, challenges and solutions. *Fuel*, *348*, 128548.

Namoun, A., Hussein, B.R., Tufail, A., Alrehaili, A., Syed, T.A., & BenRhouma, O. (2022). An ensemble learning based classification approach for the prediction of household solid waste generation. *Sensors, 22*(9), 3506.

Negrete-Cardoso, M., Rosano-Ortega, G., Álvarez-Aros, E.L., Tavera-Cortés, M.E., Vega-Lebrún, C.A., & Sánchez-Ruíz, F.J. (2022). Circular economy strategy and waste management: a bibliometric analysis in its contribution to sustainable development, toward a post-COVID-19 era. *Environmental Science and Pollution Research*, *29*(41), 61729-61746.

Nežerka, V., Zbíral, T., & Trejbal, J. (2024). Machine-learning-assisted classification of construction and demolition waste fragments using computer vision: convolution versus extraction of selected features. *Expert Systems with Applications*, *238*, 121568.

Nguyen, X.C., Nguyen, T.T.H., La, D.D., Kumar, G., Rene, E.R., Nguyen, D.D., & Nguyen, V.K. (2021). Development of machine learning-based models to forecast solid waste generation in residential areas: A case study from Vietnam. *Resources, Conservation and Recycling*, *167*, 105381.

Nnamoko, N., Barrowclough, J., & Procter, J. (2022). Solid waste image classification using deep convolutional neural network. *Infrastructures*, *7*(4), 47.

Oguz-Ekim, P. (2021). Machine learning approaches for municipal solid waste generation forecasting. *Environmental Engineering Science*, *38*(6), 489-499.

Oladinrin, O.T., Arif, M., Rana, M.Q., & Gyoh, L. (2023). Interrelations between construction ethics and innovation: A bibliometric analysis using VOSviewer. *Construction Innovation*, *23*(3), 505-523.

Palansooriya, K.N., Li, J., Dissanayake, P.D., Suvarna, M., Li, L., Yuan, X., & Ok, Y.S. (2022). Prediction of soil heavy metal immobilization by biochar using

machine learning. *Environmental science & technology*, *56*(7), 4187-4198.

Patil, S.C., & Gidde, M.R. (2023). RFID and IoT Enabled Framework to Make Pune City an Eco-friendly Smart City. *Nature Environment and Pollution Technology*, *22*(2), 553-563.

Reuters, T. (2008). Whitepaper using bibliometrics. *Thomson Reuters*, *12*.

Rutqvist, D., Kleyko, D., & Blomstedt, F. (2019). An automated machine learning approach for smart waste management systems. *IEEE transactions on industrial informatics*, *16*(1), 384-392.

Seguí-Amortegui, L., Clemente-Almendros, J.A., Medina, R., & Grueso Gala, M. (2019). Sustainability and competitiveness in the tourism industry and tourist destinations: A bibliometric study. *Sustainability*, *11*(22), 6351.

Singh, T., & Uppaluri, R.V.S. (2023). Machine learning tool-based prediction and forecasting of municipal solid waste generation rate: a case study in Guwahati, Assam, India. *International Journal of Environmental Science and Technology*, *20*(11), 12207-12230.

Small, H. (1973). Co-citation in the scientific literature: A new measure of the relationship between two documents. *Journal of the American Society for information Science*, *24*(4), 265-269.

Sohail, S.S., Javed, Z., Nadeem, M., Anwer, F., Farhat, F., Hussain, A., & Madsen, D.Ø. (2023). Multi-criteria decision making-based waste management: A bibliometric analysis. *Heliyon*.

Taki, M., & Rohani, A. (2022). Machine learning models for prediction the Higher Heating Value (HHV) of Municipal Solid Waste (MSW) for waste-to-energy evaluation. *Case Studies in Thermal Engineering*, *31*, 101823.

Tamala, J.K., Maramag, E.I., Simeon, K.A., & Ignacio, J.J. (2022). A bibliometric analysis of sustainable oil and gas production research using VOSviewer. *Cleaner Engineering and Technology*, *7*, 100437.

Van Eck, N.J. & Waltman, L. (2016). VOSviewer Manual 1.6.11. Manual, No. Version 1.6.4, 2016, pp. 1–28. Available online: http://www.vosviewer.com/documentation/Manual_VOSviewer_1.5.4.pdf

Vu, H.L., Ng, K.T.W., & Bolingbroke, D. (2019). Time-lagged effects of weekly climatic and socio-economic factors on ANN municipal yard waste prediction models. *Waste Management*, *84*, 129-140.

Yang, L., Zhao, Y., Niu, X., Song, Z., Gao, Q., & Wu, J. (2021). Municipal solid waste forecasting in China based on machine learning models. *Frontiers in Energy Research, 9,* 763977.

Yatim, F.E., Boumanchar, I., Srhir, B., Chhiti, Y., Jama, C., & Alaoui, F.E.M.H. (2022). Waste-to-energy as a tool of circular economy: Prediction of higher heating value of biomass by artificial neural network (ANN) and multivariate linear regression (MLR). *Waste Management, 153,* 293-303.

Yu, K.H., Zhang, Y., Li, D., Montenegro-Marin, C.E., & Kumar, P.M. (2021). Environmental planning based on reduce, reuse, recycle and recover using artificial intelligence. *Environmental Impact Assessment Review*, *86*, 106492.

Yuan, X., Suvarna, M., Low, S., Dissanayake, P.D., Lee, K.B., Li, J., & Ok, Y.S. (2021). Applied machine learning for prediction of CO_2 adsorption on biomass waste-derived porous carbons. *Environmental Science & Technology*, *55*(17), 11925-11936.

Zhang, C., Dong, H., Geng, Y., Liang, H., & Liu, X. (2022). Machine learning based prediction for China's municipal solid waste under the shared socioeconomic pathways. *Journal of Environmental Management*, *312*, 114918.

Zia, H., Jawaid, M.U., Fatima, H.S., Hassan, I.U., Hussain, A., Shahzad, S., & Khurram, M. (2022). Plastic waste management through the development of a low cost and light weight deep learning based reverse vending machine. *Recycling*, *7*(5), 70.

Scientific Papers. Series E. Land Reclamation, Earth Observation & Surveying, Environmental Engineering. Vol. XIV, 2025
Print ISSN 2285-6064, CD-ROM ISSN 2285-6072, Online ISSN 2393-5138, ISSN-L 2285-6064

ANALYSIS OF DIAMETER AND HEIGHT GROWTH OF SCOTS PINE SAPLINGS PLANTED IN 2023 ON THE STERILE DUMPS OF RECEA ȘUNCUIUȘ QUARRY, BIHOR COUNTY

Bogdan BODEA[1], Cristian Mihai ENESCU[2], Ovidiu Ioan HÂRUȚA[3], Camelia Elena MOGA[1], Ruben BUDĂU[3], Adrian Ioan TIMOFTE[1, 3]

[1]"Ștefan cel Mare" University of Suceava,
13 Universității Street,720229, Suceava, Romania
[2]University of Agronomic Sciences and Veterinary Medicine of Bucharest,
59 Mărăști Blvd, District 1, 011464 Bucharest, Romania
[3]University of Oradea, 1 Universității Street, 410087, Oradea, Romania

Corresponding author email: adi_timofte@yahoo.com

Abstract

This study evaluates the success of Scots pine sapling plantings conducted in 2023 on the waste deposits at the Recea Șuncuiuș Quarry in Bihor County. Four experimental plots were established, divided into two slope categories. Half of the saplings received fertilizer, and for all saplings, survival rates were assessed, along with measurements of diameter and height growth. The findings indicate no significant differences in sapling growth between the slopes, and the application of fertilizer did not notably affect their development in the first year after planting. However, in the second year, significant changes were observed. The slope became a negative factor, while fertilization had a significant positive impact on growth in terms of diameter and height, particularly under the harsh conditions of the exceptionally dry and hot summer of 2024.

Key words*: diameter, height, pine, Pinus, survival rate.*

INTRODUCTION

Over the past century, the global population has increased from 2 billion to over 8 billion, placing significant strain on natural resources. Growing demand for products has intensified landscape impacts, particularly through the extraction of underground resources, leading to a considerable expansion of degraded lands in recent years. In this context, restoring ecosystems has become a key responsibility for foresters, with afforestation widely recognized as an essential component of this effort (Huang et al., 2024).

Afforestation offers a practical solution for the ecological restoration of degraded lands, providing a foundation for their sustainable use and development in the medium and long term (Constandache et al., 2020). Additionally, afforestation efforts are widely acknowledged as effective measures for combating climate change by sequestering carbon (Zhiyanski et al., 2016).

One of the most used worldwide tree species for afforestation is the Scots pine (*Pinus sylvestris* L.). It has the largest natural range of any pine species, extending across both Europe and Asia (Przybylski et al., 2015; Bonciu et al., 2023). Latitudinally, it ranges from northern Scandinavia (70°N) to the Sierra Nevada mountains in southern Spain (37°N) (Houston Durrant et al., 2016).

During the twentieth century, Scots pine forests saw significant expansion throughout Europe, currently accounting for over 20 percent of the EU's forest area. Although the initial focus of this expansion was to enhance timber production, recent decades have shifted towards a broader set of management goals (Mason & Alia, 2000). Scots pine exhibits significant morphological and genetic diversity due to its wide distribution (Stoica et al., 2022; Sheller et al., 2023), with several varieties, including *Pinus sylvestris* "Glauca", *Pinus sylvestris* var. *hamata* Stev, and *Pinus sylvestris* var. *mongolica* Litvin (Budău et al., 2024). Scots pine is a pioneer species with a wide range of uses, including in the wood and chemical industries, household applications, decoration, ecological restoration, as well as in medicinal and cosmetic products (Papp et al., 2022; Gurău,

2024; Szanto et al., 2025). Particularly, it is recognized for its resilience to frost and drought, as well as its capacity to grow in nutrient-poor soils, allowing it to inhabit a variety of ecologically diverse environments (Enescu, 2015). It forms a deep root system, allowing it to tap into water from deeper soil layers and stabilize land prone to erosion. Its rapid growth supports the restoration of vegetation in degraded areas. Scots pine can thrive in both lowland and mountainous regions due to its adaptability to diverse climatic conditions and its ability to grow in nutrient-poor soils, making it an important resource for ecosystem restoration and the fight against desertification (Kelly and Conolly, 2000; Doniță et al., 2004; Pietrzykowski et al., 2013). Through the decomposition of its needles, *P. sylvestris* contributes to the formation of raw humus (Traci et al., 1981), thereby enhancing biodiversity in the soil's upper layer (Xue et al., 2022).

In many European countries, Scots pine is one of the primary coniferous species used for afforestation and is often considered the dominant species for forest formation (Oszako et al., 2023; Okon et al., 2024). For example, Scots pine has been successfully planted in the Czech Republic, where it ranks as the second most important tree species for industrial wood production (Brichta et al., 2023), and has been established in various terrains, including post-mining sites (Zeidler et al., 2024). In Latvia, Scots pine has been successfully used for afforestation of abandoned peat extraction sites (Skrastiņa et al., 2021), while in Ukraine, it has been planted to establish forest plantations resilient to environmental factors in the northern steppe region (Gritsan et al., 2019). Positive results have also been reported in Russia (Belan et al., 2024) and Mongolia (Sukhbaatar et al., 2018).

In Romania, Scots pine has been planted in a variety of site conditions, including the sandy soils of the Oltenia region in southwestern Romania (Nuță, 2005), abandoned mining lands in the northwestern part of Transylvania (Buta et al., 2019), and degraded terrains in eastern part of the country (Vlad et al., 2019). In most cases, Scots pine exhibited a rapid growth rate, particularly during the initial years of vegetation (Batsaikhan et al., 2018; Colișar et al., 2024).

This study aimed to evaluate the growth in diameter and height of Scots pine saplings planted in 2023 on sterile dumps at the Recea Șuncuiuș Quarry in Bihor County.

MATERIALS AND METHODS

The experiments were conducted within the 2.89 km² Recea perimeter, situated in the Șuncuiuș refractory clay deposit in the northern part of the Pădurea Craiului Mountains, Bihor County (46°55'11"N, 22°30'34"E), where the first afforestation experiments were made in 2008-2009 (Bodea et al., 2023).

According to Ministerial Order no. 2533/2022 (MMAP, 2022), the landfill site in this case is classified as YD1B (Y - landfill; D - hill region; 1 - for raw waste dumps or terrigenous materials from mining and B - anthropogenic materials composed of small materials such as sand, gravel, loess, and clay). The planting materials were sourced locally, and 4 experimental plots, 50 m^2 each, noted with E, F, G and H, were established (Figure 1).

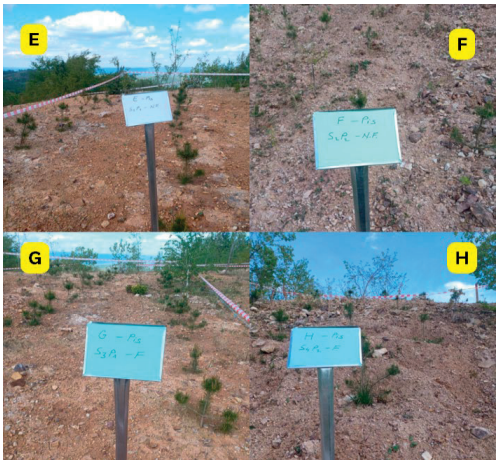


Figure 1. The 4 experimental plots

In the four experimental plots, 3-year-old Scots pine seedlings, averaging 30 cm in height, were planted using a 2x1 m spacing arrangement, with 25 seedlings in each plot. During the spring and autumn of 2023 and 2024, the following characteristics were measured:

- the survival rate after planting in the field, expressed as a percentage;

- the survival rate of seedlings, recorded at the end of the first vegetation period, expressed as a percentage;
- seedling height (cm), measured from ground level to the top of the main stem;
- seedling diameter at the root collar (mm) at the end of the first vegetation year in the field;
- the number of whorls;
- the number of branches per whorl.

The four experimental plots were labelled as follows:

- Variant E, code Pi.s. S_1P_1N: small slope P1≤10°, N - unfertilized substrate;
- Variant F, code Pi.s. S_2P_2N: large slope P2>10°, N - unfertilized substrate;
- Variant G, code Pi.s. S_3P_1F: small slope P1≤10°, F - fertilized substrate;
- Variant D, code Pi.s. S_4P_2F: large slope P2>10°, H - fertilized substrate.

The saplings' height was measured with a height measuring tape (Figure 2a), and the trunk diameter at the base was measured using a digital caliper (Figure 2b).



Figure 2. Measuring the height and the collar diameter of the saplings

Fertilization was applied in experimental plots G and H using a chemical fertilizer specifically formulated for softwood seedlings, containing 14% N, 7% P_2O_5, 17% K_2O, 2% MgO, 9% S, 0.02% B, and 0.01% Zn. The fertilizer was distributed around the seedlings at a rate of 15–20 grams per plant (Figure 3).

For most of the analyzed characteristics (degree of survival after planting, degree of survival after the first year, plant height, diameter at the root collar, number of whorls, and number of branches per whorl), the arithmetic mean was calculated using the standard formula: $x = \sum x/n$.



Figure 3. Applying fertilizers

For the number of branches per first whorl, as each sample contained groups of plants with varying numbers of branches (ranging from 0 to 6 branches per whorl per plant), the weighted arithmetic mean was used, calculated with the following formula:

$$X_{med.pond.} = \frac{\bar{x}_1 n_1 + \bar{x}_2 n_2 + \ldots + \bar{x}_k n_k}{N},$$

where:

$N = n_1 + n_2 + \ldots + n_k$;

$\bar{x}_1 \ldots \bar{x}_k$ = group averages.

To determine the degree of survival after planting in the field, the following formula was used:

$$Gp(\%) = \frac{Pveg}{Pplant}\ 100,$$

where:

- P_{veg} represents seedlings started in vegetation on April 20, 2023;
- P_{plant} accounts for planted seedlings.

To determine the degree of survival after planting in the field, the following formula was used:

$$Gm(\%) = \frac{Pviab}{Pveg}\ 100$$

where:

- Pviab represents viable seedlings at the time of determination;
- Pveg represents the number of seedlings that started growing on April 20, 2023.

The results from the biometric measurements were statistically analyzed using analysis of variance, appropriate for monofactorial experiments conducted in randomized blocks. The significance of differences between the two tested varieties was assessed using the DL test or the multiple comparisons test (DS5%). For certain characteristics, the Student's *t* test was also applied (Ardelean et al., 2005; Ardelean, 2011).

The coefficients of variability (s%) were calculated using data from the series of measurements taken on the 25 individuals in each variant, following the formula described by Ardelean (2011):

$$s\% = \frac{s}{\bar{x}}\ 100,\%$$

where:

- s represents the standard deviation;
- x is the average of the series.

Simple correlation coefficients were calculated using Microsoft Excel, with their significance assessed at the 5% and 1% levels.

RESULTS AND DISCUSSIONS

The data presented in Tables 1 and 2 confirm the uniformity of the planted material, indicating that at the time of planting, there were no significant differences in seedling height or diameter within the parcel.

Tables 3 and 4 present the mean diameters and heights of *P. sylvestris* measured in spring and autumn of 2023 and 2024 across the four experimental plots.

Table 1. Mean collar diameter (mm) in the 4 plots

Var	Initial diameter, mm $\bar{X} \pm s_x$	± d, cm	t	Significance of difference	s%
E	12.66 ± 0.63	-	-	-	21.9
F	10.81 ± 0.44	-1.85	-0.84	n.s.	17.7
G	14.57 ± 0.53	1.91	0.79	n.s.	13.8
H	11.22 ± 0.34	-1.44	-0.70	n.s.	27.9
$t_{calc} < t_{P5\%} = 1.9$					

Table 2. Mean height (cm) in the 4 plots

Var	Initial height, cm $\bar{X} \pm s_x$	± d, cm	t	Significance of difference	s%
E	28.90 ± 1.26	-	-	-	24.9
F	29.54 ± 1.04	0.64	0.07	n.s.	20.1
G	31.58 ± 0.87	2.68	0.30	n.s.	18.1
H	30.48 ± 1.70	1.58	0.10	n.s.	15.3
$t_{calc} < t_{P5\%} = 1.9$					

In terms of survival rate after planting, it was observed that losses were minimal, with only 1% in the first year and an additional 1% (one dried seedling in experimental plot H) in 2024.

Table 3. Mean diameters and heights measured in spring and autumn 2023 for *P. sylvestris* in the 4 experimental plots

Code	Variant	Collar diameter, mm		Diameter growth, mm	Height, cm		Height growth, cm
		03.2023	11.2023		03.2023	11.2023	
Pi.s. - S1P1N	E	12.66	12.95	0.28	28.90	45.60	16.70
Pi.s. - S2P2N	F	10.81	11.10	0.24	29.54	46.50	16.73
Pi.s. - S3P1F	G	14.57	14.99	0.42	31.58	45.70	14.12
Pi.s. - S4P2F	H	11.22	11.71	0.49	30.48	46.10	15.62

Table 4. Mean diameters and heights measured in spring and autumn 2024 for *P. sylvestris* in the 4 experimental plots

Code	Variant	Collar diameter, mm		Diameter growth, mm	Height, cm		Height growth, cm
		03.2024	11.2024		03.2024	11.2024	
Pi.s. - S1P1N	E	12.95	19.85	6.90	45.60	57.53	11.94
Pi.s. - S2P2N	F	11.10	17.34	6.24	46.50	59.94	13.44
Pi.s. - S3P1F	G	14.99	26.75	11.75	45.70	66.79	21.08
Pi.s. - S4P2F	H	11.71	20.36	8.65	46.10	63.94	17.84

An analysis of the 25 seedlings from the first variant (E; no slope, unfertilized) revealed that, at the end of the first year of growth, the seedlings' height ranged from 25 to 67.5 cm, with a variability coefficient of 23.8% (high variability).

The calculation and interpretation of results from the bifactorial experiments involve the following factors:

- Factor A: fertilization method, with two levels: N (unfertilized) and F (fertilized);
- Factor B: slope, with two levels: P1 (0-10°) and P2 (>10°).

The experiment was carried out using a randomized block design with 25 replications (n = b = 25). The total number of experimental variants (v = 4) was determined by the combination of the two factors at two levels each (2 × 2 = 4). Each experimental plot contained 25 seedlings, and the average height growth for each replication area was calculated as the mean of the measurements from all 25 seedlings within the plot. The analysis of variance for the bifactorial experiment (2 × 2), considering slope and fertilization method, is presented in Table 5.

Table 5. Analysis of variance for the bifactorial experiment (2 x 2) with slope and fertilization mode

Source of variation	Sum of squares (SS)	Degrees of freedom (DF)	Mean square (MS)	F-Statistic (F)			
Total	3892.70	99					
blocks	872.0596	24				5%	1%
fertilization	56.7009	1	56.70	1.39	<	3.98	7.01
slope	502.7481204	1	502.75	12.35	>	3.98	7.01
fertilization x slope	-469.80	1	-469.80	-11.54	>	3.98	7.01
Error	2930.99	72	40.708				

According to the data in Table 5, the calculated *F* values for the slope factor exceed the theoretical *F* values at the 5% significance level (P5%), indicating that slope has a significant influence on seedling height growth during the first year after planting.

The significance of differences between variants is assessed below. Given the potential for multiple types of comparisons, the analysis of variance method was used to calculate the standard deviation (sd) and least significant difference (LSD) values for each comparison.

a) In Table 6, the variants are compared to the control variant:

- sd = 1.80 cm
- $LSD_{5\%}$ = 3.59 cm
- $LSD_{1\%}$ = 4.78 cm
- $LSD_{0.1\%}$ = 6.19 cm

Table 6. Summary of the results

Var.	Variant name	hm, cm	h rel, %	±d, cm	Significance of difference
11	NP1 (Control variant)	16.70	100.0	-	-
12	NP2	16.73	100.2	0.0	-
21	FP1	14.12	84.6	-2.6	-
22	FP2	15.62	93.5	-1.1	-
	LSD 5%=	3.59			
	1%=	4.78			
	0.1%=	6.19			

b) The influence of fertilization on height growth was evaluated relative to the unfertilized variant, which served as the control. The error and least significant difference (LSD) values corresponding to the fertilization factor were as follows:

- sd (fertilization) = 11.51 cm;
- $LSD_{5\%}$ = 22.91 cm;
- $LSD_{1\%}$ = 30.51 cm;
- $LSD_{0.1\%}$ = 39.49 cm.

The results are given in Table 7.

Table 7. The influence of fertilization on hm

Variant name	hm, cm	h rel, %	±d, cm	Significance of difference
unfertilized (Mt)	16.4	100.0	-	-
fertilized	14.9	90.8	-1.8	-
LSD 5%=	22.9			
1%=	30.51			
0.1%=	39.49			

It can be observed that regardless of the slope, the applied fertilization does not result in significant growth in the seedlings.

c) The influence of slope on growth height is compared to the variant without slope as a control. The results are given in Table 8. Regardless of the fertilization applied, slope negatively influences seedling growth, but insignificantly.

d) Comparing all variants with each other using the Duncan test (multiple comparisons method). It is applied when the interaction of the 2 factors is significant.

d1) To compare the influence of fertilization on height growth, regardless of slope:

- sx = 0.90 cm
- Degrees of freedom for error = 72

The $DS_{5\%}$ values for different comparison limits between the mean effects of the fertilization factor were calculated as follows:

- Number of variants within the comparison limits: 2
- q5%, (for DF = 72) = 2.82
- sx = 0.90 cm
- $DS_{5\%}$ = 2.54 cm

The $DS_{5\%}$ values for the different comparison limits between variants are presented in Table 9.
d2) The same as variant d1) - All non-significant.

Table 8. The influence of slope on hm

Variant name	hm, cm	h rel, %	±d, cm	Significance of difference
P1 (Mt)	15.41	100	-	-
P2	15.836	102.7644	-0.86	-
LSD 5%=	22.91			
1%=	30.51			
0.1%=	39.49			

Table 9. The $DS_{5\%}$ values for different comparison limits between variants

Variant	hm	1	4	3
2	16.73	0.03	1.11	2.61
1	16.7	-	1.08	2.58
4	15.62		-	1.5
3	14.12			-

All non-significant

d3) To compare the influence of fertilization on the same or different slopes, as well as the effect of slope under the same or different conditions on height growth: sx = 1.28 cm. The DS5% values for the different comparison limits between variants are presented in Table 10. Table 11 presents the seedling height growth (cm) one year after planting, under the influence of two slope categories and two fertilization methods. Differences between two variants followed by the same letter in the table are not statistically significant.
The same procedure was applied for the year 2024. The average increases in collar diameters in the first 2 years in all 4 experimental plots are given in Figure 4. The average increase in height in the first 2 years in all 4 experimental plots are given in Figure 5.

Table 10. The DS5% values for different comparison limits

The number of variants within the comparison limits.	2	3	4
$q_{5\%}$ for DF= 72	2.82	2.97	3.07
s_x in cm	1.28		
$DS_{5\%}$	3.60	3.79	3.92

Table 11. Seedling height growth (cm) one year after planting by slope category and fertilization method. Variants sharing the same letter do not differ significantly

Fertilization \ Slope	P1	P2	Fertilization average
N - Unfertilized	16.7 b	16.7 b	16.7 A
F - Fertilized	14.1 a	15.6 a	14.9 A
Average slope	15.4 M	16.2 M	

$DS_{5\%}$ to compare two averages fertilization =2.5
$DS_{5\%}$ to compare two averages slope =2.5
$DS_{5\%}$ to compare two averages: fertilization x slope =3.6-3.9

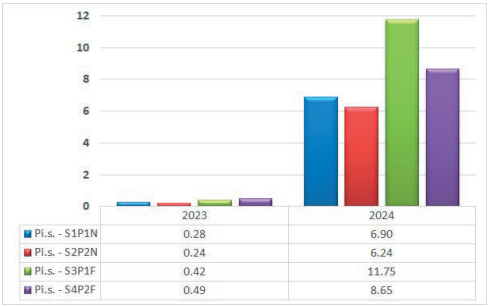


Figure 4. The average increase in collar diameters (mm) in the first 2 years in all 4 experimental plots

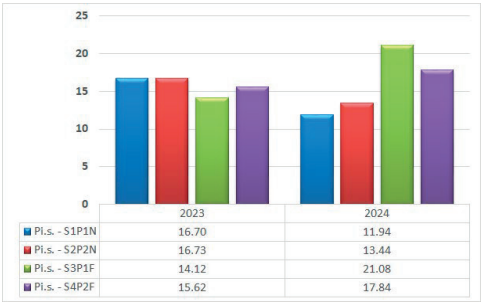


Figure 5. The average increase in height (cm) in the first 2 years in all 4 experimental plots

CONCLUSIONS

Scots pine seedlings of local origin (Șuncuiuș nursery, Bihor County), planted in 2023, demonstrated a high survival rate of 98% during the first two years after planting.
The 3-year-old seedlings, planted in large planting holes (40 × 40 × 40 cm), showed no significant differences in diameter and height growth during the first year, regardless of fertilization, due to prior nursery growth and initial site conditions. However, in the second year, seedlings in plot G, where fertilizers were

applied on a gradual slope, exhibited significantly higher growth, with height increases 70.2% greater than in the unfertilized plot E. On steeper slopes, diameter growth was 26.3% lower compared to flat or gently sloping areas.

In 2024, height growth was lower than in 2023 for unfertilized seedlings. In contrast, fertilized seedlings on gradual slopes achieved height increases 49.2% higher than in the first year and 76.5% higher than unfertilized seedlings on the same slope in the second year. Overall, fertilization significantly enhanced height and diameter growth in 2024 compared to 2023. However, due to exceptional climatic conditions in 2024, including three months of severe drought, growth increments were lower in unfertilized seedlings compared to the previous year.

During the first year after planting, slope had a clear and significant influence on height growth. Scots pine has proven to be a valuable species for afforesting degraded lands due to its exceptional adaptability to challenging conditions. It has demonstrated effectiveness in restoring areas impacted by vegetation removal and excavation, particularly in high clay content soils where other species struggle to establish. With its capacity to stabilize soil and support ecosystem recovery, Scots pine plays a critical role in ecological restoration projects, contributing to vegetation recovery, biodiversity enhancement, and long-term environmental protection.

REFERENCES

Ardelean, M., Sestraș, R., Cordea, M. (2005). *Horticultural experimental technique*. Cluj-Napoca, AcademicPres Publishing House.

Ardelean, M. (2011). *Metodologia elaborării tezelor de doctorat, Ediție revăzută și completată*. Cluj-Napoca, AcademicPres Publishing House.

Batsaikhan, G., Tsogtbaatar, J., Gerelbaatar, S. (2018). The growth trend of planted trees (*Pinus sylvestris* L.) in the early stage of plantation establisment. *Proceedings of the Mongolian Academy of Sciences*, *58*(4), 48-56.

Belan, L., Bogdan, E., Suleymanov, R., Fedorov, N., Shirokikh, P., Suleymanov, A., Vildanov, I., Sayfullin, I., Tuktarova, I., Bakhtiyarova, R., Zaitsev, G., Fayruzov, I., Vitsenko, A. (2024). Carbon sequestration at different stages of succession during pine (*Pinus sylvestris*) Afforestation of abandoned lands. *Forests*, *15*, 2094.

Bodea, B., Budău, R., Timofte, A.I. (2023). Study on the Evolution of the Black Pine Stand (*Pinus nigra*) Artificially Installed on the Site of the Recea Șuncuiuș Quarry, Bihor County. *Analele Universității din Oradea, Fascicula Protecția Mediului*, *XLI*, 63-70.

Bonciu, E., Olaru, A.L., Slusarczyk, J. (2023). The main characteristics of the genetic system in some forest tree species. *Scientific Papers. Series A. Agronomy*, *LXVI*(1), 655-664.

Budău, R., Bodea, B., Racz, K.A., Haiduc, I.N., Pantea, S.D., Stancea, M. (2024). The origin of the woody species of pines cultivated in the Sylva Arboretum in Gurahonț, Romania. *Annals of the University of Oradea, Fascicle: Environmental Protection*, 61-66.

Buta, M., Blaga, Gh., Paulette, L., Păcurar, I., Roșca, S., Borsai, O., Grecu, F., Sînziana, P.E., Negrușier, C. (2019). Soil reclamation of abandoned mine lands by revegetation in northwestern part of Transylvania: A 40-Year Retrospective Study. *Sustainability, 11*, 3393.

Brichta, J., Vacek, S., Vacek, Z., Cukor, J., Mikeska, M., Bilek, L., Simunek, V., Gallo, J., Brabec, P. (2023). Importance and potential of Scots pine (*Pinus sylvestris* L.) in 21st century. *Central European Forestry Journal, 69*, 3-20.

Colișar, A., Dîrja, M., Simonca, V., Sîngeorzan, S.M.M Sfeclă, V., Vlasin, H.D., Negrusier, C., Truța, A.M., Brebean, F.A., Ceuca, V. (2024). Sustainability of some forest species' associations established on degraded lands from the Transylvania Plain, in the context of climate change. *Scientific Papers. Series E. Land Reclamation, Earth Observation & Surveying, Environmental Engineering*, *13*, 937-950.

Constandache, C., Dincă, L., Tudor, C. (2020). The bioproductive potential of fast-growing forest species on degraded lands. *Scientific Papers. Series E. Land Reclamation, Earth Observation & Surveying, Environmental Engineering*, *9*, 87-93.

Doniță, N., Geambașu, T., Brad, R.R. (2004). *Dendrologie*, Vasile Goldiș University Press, Arad.

Enescu, C.M. (2015). Shrub and tree species used for improvement by afforestation of degraded lands in Romania. *Forestry Ideas*, *21*(1), 3-15.

Gritsan, Y.I., Sytnyk, S.A., Lovynska, V.M., Tkalich, I.I. (2019). Climatogenic reaction of *Robinia pseudoacacia* and *Pinus sylvestris* within Northern Steppe of Ukraine. *Biosystems Diversity*, *27*(1), 16-20.

Gurău, M. (2024). Plants from the spontaneous flora of Romania that have decorative value. *Scientific Study & Research. Biology*, *33*(1), 1-24.

Houston Durrant, T., de Rigo, D., Caudullo, G. (2016). *Pinus sylvestris* in Europe: distribution, habitat, usage and threats. In: San-Miguel-Ayanz, J., de Rigo, D., Caudullo, G., Houston Durrant, T., Mauri, A. (Eds.), European Atlas of Forest Tree Species. Publ. Off. EU, Luxembourg, pp. e016b94+.

Huang, K.C., Zhao, W., Li, J.N., Mumin, R., Song, C.G., Wang, H., Sun, Y.F., Cui, B.K. (2024). Afforestation-Induced Shifts in soil bacterial diversity and community structure in the Saihanba Region. *Microorganisms, 12*, 479.

Kelly, D.L., Connolly, A. (2000). A review of the plant communities associated with Scots pine (*Pinus sylvestris* L.) in Europe, and an evaluation of putative

indicator/specialist species. *Invest. Agr.: Sist. Recur. For.: Fuera de Serie*, *1*, 15-39.

Mason, W.L., Alia, R. (2000). Current and future status of Scots pine (*Pinus sylvestris* L.) forests in Europe. *Invest. Agr. Sist. Recur. For. Fuera de Serie*, *1*, 317-335.

Ministerul Mediului, Apelor și Pădurilor (MMAP), (2022). Ordin nr. 2.533 din 28 septembrie 2022 pentru aprobarea Normelor tehnice privind compoziții, scheme și tehnologii de regenerare a pădurilor și de împădurire a terenurilor degradate și a Ghidului de bune practici privind compoziții, scheme și tehnologii de regenerare a pădurilor și de împădurire a terenurilor degradate.

Nuță, S. (2005). Structural and functional features of the protection forest belts in the south of the Oltenia. *Analele I.C.A.S., 48*, 3-11.

Okon, S., Wieruszewski, M., Dynowska, J., Ankudo-Jankowska, A., Adamowicz, K. (2024). Cost of Regeneration of Scots Pine (*Pinus sylvestris* L.) Crops in national forests. *Forests*, *15*, 1218.

Oszako, T., Kukina, O., Dyshko, V., Moser, W.K., Slusarski, S., Okorski, A., Borowik, P. (2023). Afforestation of land abandoned by farmers poses Threat to Forest Sustainability Due to *Heterobasidion* spp. *Forests*, *14*, 954.

Papp, N., Purger, D., Czigle, S., Czegenyi, D., Stranczinger, S., Toth, M., Denes, T., Kocsis, M., Takacsi-Nagy, A., Filep, R. (2022). The importance of Pine species in the ethnomedicine of Transylvania (Romania). *Plants*, *11*, 2331.

Pietrzykowski, M., Wos, B., Haus, N. (2013). Scots pine needles macronutrient (N, P, K, CA, MG, and S) supply at different reclaimed mine soil substrates – as an indicator of the stability of developed forest ecosystems. *Environ. Monit. Assess.*, *185*, 7445-7457.

Przybylski, P., Matras, J., Sulkowska, M. (2015). Genetic variability of Scots pine (*Pinus sylvestris* L.) in maternal regions of provenance. *Folia Forestalia Polonica, Series A*, *57*, 112–119.

Sheller, M., Toth, E.G., Ciocîrlan, E., Mikhaylov, P., Kulakov, S., Kulakova, N., Melnichenko, N., Ibe, A., Sukhikh, T., Curtu, A.L. (2023). Genetic Diversity and Population structure of Scots Pine (*Pinus sylvestris* L.) in Middle Siberia. *Forests*, *14*, 119.

Skrastiņa, E., Straupe, I., Lazdins, A. (2021). Afforestation of abandoned peat extractions sites with Scots pine (*Pinus sylvestris* L.) as a solution of climate change mitigation. *Forestry and Wood Processing*, *36*, 63-69.

Stoica, E., Alexandru, A.M., Mihai, G. (2022). Assessment of genetic variability in Scots pine (Pinus sylvestris L.) provenance trials in Romania. *Revista de Silvicultură și Cinegetică*, *51*, 21-29.

Sukhbaatar, G., Suran, B., Nachin, B., Chultem, D. (2018). Effects of Scots Pine (Pinus sylvestris L.) plantations on plant diversity in Northern Mongolia. *Mongolian J. of Biological Sciences*, *16*(1), 59-70.

Szanto, L.G., Marc, R.A., Mureșan, A.E., Mureșan, C.C., Pusacs, A., Ranga, F., Fetea, F., Moraru, P.I., Filiș, M., Muste, S. (2025). Biofortification of Acacia and Polyflower Honey with *Pine sylvestris* L. Bud Extracts: Exploring antioxidant variation across developmental stages for enhanced nutritional value. *Plant Food for Human Nutrition*, *80*, 47.

Traci, C., Gașpar, R., Munteanu, S.A. (1981). The effect of afforestation of degraded lands and torrent's control in Mușca site from Valea Arieșului. *Silvicultura și Exploatarea Pădurilor*, *2*, 83-87.

Vlad, R., Constandache, C., Dincă, L., Tudose, N.C., Sidor, C.Gh., Popovici, L., Ispravnic, A. (2019). Influence of climatic, site and stand characteristics on some structural parameters of Scots pine (*Pinus sylvestris*) forests situated on degraded lands from east Romania. *Range Management & Agroforestry*, *40*(1), 40-48.

Xue, H., Wang, Q., Mao, K., Liu, Y., Jiang, X., Murray, P.G., Zhang, L., Liu, W. (2022). Positive effects of reforestation on the diversity and abundance of soil fauna in a landscape degraded red soil area in subtropical China. *Forests*, *13*(10), 1596.

Zeidler, A., Boruvka, V., Tomczak, K., Vacek, Z., Cukor, J., Vacek, S., Tomczak, A. (2024). The Potential of non-native pines for timber production – A case study from afforested post-mining sites. *forests*, *15*, 1388.

Zhiyanski, M., Glushkova, M., Ferezliev, A., Menichetti, L., Leifeld, J. (2016). Carbon storage and soil property changes following afforestation in mountain ecosystems of the Western Rhodopes, Bulgaria. *iForest*, *9*, 626-634.

Scientific Papers. Series E. Land Reclamation, Earth Observation & Surveying, Environmental Engineering. Vol. XIV, 2025
Print ISSN 2285-6064, CD-ROM ISSN 2285-6072, Online ISSN 2393-5138, ISSN-L 2285-6064

FIRE CHANGES IN SOIL FERTILITY AND MICROBIAL DYNAMICS IN NORTHWESTERN BULGARIA

Simeon BOGDANOV, Bilyana GRIGOROVA-PESHEVA

University of Forestry, 10 Kliment Ohridski Blvd, 1797 Sofia, Bulgaria

Corresponding author email: b.pesheva@ltu.bg

Abstract

Some sentences are overly long or repetitive. Consider: Forest fires induce significant environmental changes, with long-term impacts on forest ecosystems and soil properties. These changes affect soil temperature, chemical composition, organic matter content, and microbial communities. This study investigates the alterations in silvicultural properties of Gray Forest soils (Gray Luvisols) in Northwestern Bulgaria following forest fires, considering key variables such as fire type and intensity, time since fire, forest type, and stand density. The results show that forest fires generally reduce soil organic matter and total nitrogen content, alter soil acidity, and affect soil microbial abundance. In particular, low-intensity fires may stimulate microbial activity, whereas high-intensity fires tend to suppress it. These findings provide insights into the mechanisms of post-fire soil transformation and offer a scientific basis for afforestation and land reclamation planning in fire-affected forest areas.

Key words*: forest fires, soil fertility, silvicultural properties, soil microflora, Gray Luvisols, soil recovery, post-fire management.*

INTRODUCTION

Forest fires, whether natural or anthropogenic in origin, represent a major ecological disturbance with both immediate and long-term consequences for forest ecosystems. One of the most significant effects is the alteration of soil properties, which play a critical role in supporting vegetation recovery and maintaining ecosystem functions.

Soil characteristics are closely tied to vegetation cover and organic matter inputs both of which are drastically altered by fire. The extent and nature of these changes depend on multiple factors, including the type and intensity of the fire, the amount and distribution of combustible material, fuel moisture content, and prevailing weather conditions. These variables introduce considerable variability, making it challenging to generalize the effects of forest fires across different landscapes (Barnes et al., 1998; Kimmins, 1996; DeBano et al., 1998; Bogdanov, 2023a).

Post-fire changes in soils occur on both short- and long-term timescales. Immediately after a fire, the release of energy alters soil temperature regimes and may lead to the combustion of organic matter, volatilization of nutrients, and disruption of soil structure and microbial habitats (Jiménez Esquilín et al., 2008; Neary et al., 1999). Long-term impacts are often associated with increased solar absorption due to surface darkening and reduced organic matter, which can further influence soil temperature and moisture regimes (Molla et al., 2014).

The increase in the concentration of nutrients after a fire is associated with the increase or recovery of the soil microflora. The initial impact of fires usually leads to a decrease in the total amount of microorganisms in the soil, and this is often followed by their increase, which is beneficially affected by the increase in soil temperature (Bogdanov, 2023b).

Microbial communities in soil are particularly sensitive to fire. Initially, fire often results in a decline in microbial abundance and diversity due to elevated temperatures and loss of organic substrates. However, recovery dynamics vary widely. In some cases, microbial populations rebound quickly, facilitated by increased nutrient availability and warmer soil temperatures (Bogdanov, 2023b). The extent of microbial recovery is influenced by both the physical-chemical properties of the soil and the intensity and duration of the fire (Mataix-Solera et al., 2002; Barreiro & Diaz-Ravina, 2021).

In forest management, fires are classified based on the location of fuel consumption (crown,

surface, or ground fires) and by their spread and severity. These classifications are important for evaluating the degree of ecological damage and planning appropriate restoration strategies (Bogdanov, 2023a). One of the key post-fire challenges in forestry is the restoration of burned stands, which often cannot regenerate naturally and require targeted afforestation efforts. These efforts depend on a thorough understanding of the soil's silvicultural properties - factors such as organic matter content, nutrient status, and microbial health that determine soil fertility for tree growth (Bogdanov, 2023b).

The present study aims to assess the changes in the silvicultural properties of soils affected by forest fires in Northwestern Bulgaria. Specifically, it analyzes how different factors - fire type and intensity, time elapsed since the fire, forest type, and stand density - affect soil properties such as organic matter, total nitrogen, pH, and microbial abundance. By identifying these relationships, the study contributes to improved understanding of post-fire soil dynamics and supports science-based forest restoration planning.

MATERIALS AND METHODS

Study area and soil classification

The study was conducted in Northwestern Bulgaria, within the territory of the Belogradchik State Forestry. According to Bulgaria's forest-vegetation zoning system (Zahariev et al., 1979), the area is situated in the Lower Forest Vegetation Belt (700-2000 m above sea level) of the Misian Forest Zone.

The soils under investigation are classified as Gray Forest soils (Gray Luvisols), based on the classification system of Penkov et al. (1992). These correspond to the Luvisols soil group in the World Reference Base for Soil Resources (WRB) (IUSS, 2022), with dominant qualifiers being Haplic and Albic (Bogdanov, 2024).

Plot design and sampling procedure

To assess the effects of forest fires, nine paired sample plots (100 m² each) were established - each including a burned area and a corresponding unburned control plot. The plots were selected based on fire history, fire characteristics (type and intensity), forest type (deciduous or coniferous), and stand density (Table 1). Table 1 provides an overview of the plot characteristics, including year of fire occurrence, type and strength of fire, altitude, forest type, and stand density.

Soil samples were collected from the 0-5 cm surface layer, which is known to exhibit the most pronounced post-fire changes (Barnes et al., 1998; Bogdanov, 2023a). For microbiological analysis, all soil samples were collected using sterile tools, placed in sterile bags, and processed within 48 hours to preserve microbial integrity.

Table 1. Characteristics of the sample plots

Sample plots (SP)	Year of the fire	Fire type/strength	Area (1000 m^2)	Altitude (m)	Forest group	Stand density
1	2020	Surface/ Middle	8.0	150	D	0.2
2	2020	Surface/ Middle	4.2	180	D	0.5
3	2020	Surface/ Middle	3.2	200	D	0.5
4	2021	Surface/ Middle	4.4	170	D	0.5
5	2021	Surface/ Middle	1.8	180	C	0.6
6	2022	Crown/ Middle	1.6	180	D	0.5
7	2022	Surface/ Middle	6.0	170	D	0.4
8	2022	Surface/ Strong	2.0	200	D	0.5
9	2022	Surface/ Weak	1.5	200	D	0.4

*D - deciduous; C - coniferous

Fire classification

Within the scope of this study, forest fires were classified based on the visible intensity of their impact on vegetation, following the approach of Bogdanov (2023b). This classification distinguishes between crown fires and surface fires, with further categorization into three levels of severity - weak, medium, and strong.

A strong crown fire involves complete combustion of the tree canopy and stems, corresponding to what is commonly referred to as a "total fire," resulting in the complete destruction of the stand. A medium crown fire also affects the tree crowns but typically results

in full stand mortality without complete combustion of all stems. In contrast, a weak crown fire affects the upper canopy more sporadically, causing partial or mosaic mortality within the stand.

Surface fires were characterized by stem scorching at heights ranging from 0.5 to 1.5 meters. A strong surface fire results in significant stem damage and the eventual destruction of the stand. A medium surface fire causes variable mortality within the stand, leading to a mosaic pattern of tree survival. A weak surface fire, while still affecting stem bases within the same height range, does not result in substantial tree mortality.

Laboratory analyses

To analyze the changes in the silvicultural properties of the soil following forest fire events, both primary and supplementary indicators were assessed. The primary indicators included the content of soil organic matter and total nitrogen, which are key determinants of soil fertility. Supplementary indicators - such as soil pH, the carbon-to-nitrogen (C:N) ratio, and the abundance of total soil microflora - were also evaluated, as these parameters are critical to soil biological functioning and are known to undergo significant changes under the influence of fire (Bogdanov, 2023a; Bogdanov, 2023c; Donov, 1976).

Laboratory analyses were conducted using standardized methods. Soil organic matter was determined using the modified Turin method (Filcheva & Tsadilas, 2002). Total nitrogen content was measured using a modified version of the classic Kjeldahl method (ISO 11261:2002). Soil pH was assessed potentiometrically in a water extract. The C:N ratio was calculated based on measured concentrations of carbon and nitrogen, following the method outlined by Bogdanov (2023c). The abundance of total soil microflora was quantified through the method of serial dilutions and inoculation on selective solid nutrient media, followed by incubation (Gousterov et al., 1977). Microbial abundance was expressed in colony-forming units (CFU) per gram of oven-dry soil.

RESULTS AND DISCUSSION

Effects of forest fires on soil organic matter, total Nitrogen, and pH

The analysis of soil samples from burned and corresponding unburned control plots revealed certain changes in the key indicators of soil fertility following forest fires (Table 2).

Table 2. Properties of soils influenced by forest fires

Sample plot (SP)	SOM % M ± SD	Total N % M ± SD	C: N	pH M ± SD
FP 1	2.11 ± 0.02	0.142 ± 0.003	8.6	5.7 ± 0.007
Contro l	2.35 ± 0.04	0.135 ± 0.006	10.1	5.4 ± 0.005
FP 2	2.26 ± 0.05	0.121 ± 0.007	10.8	5.9 ± 0.004
Control	2.77 ± 0.04	0.117 ± 0.007	13.7	5.2 ±0.005
FP 3	1.70 ± 0.04	0.173 ± 0.003	5.7	6.1 ± 0.002
Control	2.04 ± 0.03	0.180 ± 0.005	6.6	5.4 ± 0.002
FP 4	2.17 ± 0.03	0.123 ± 0.003	10.2	6.0 ± 0.007
Control	2.33 ± 0.05	0.135 ± 0.004	10.0	5.2 ± 0.006
FP 5	2.22 ± 0.02	0.131 ± 0.005	9.8	6.3 ± 0.004
Control	2.48 ± 0.06	0.160 ± 0.005	9.0	5.3 ± 0.007
FP 6	2.22 ± 0.04	0.110 ± 0.006	11.7	6.2 ± 0.007
Control	2.41 ± 0.06	0.128 ± 0.003	10.9	5.8 ± 0.007
FP 7	2.21 ± 0.04	0.116 ± 0.004	11.1	6.0 ± 0.004
Control	2.43 ± 0.04	0.120 ± 0.006	11.7	5.5 ± 0.006
FP 8	1.98 ± 0.03	0.097 ± 0.002	11.8	6.4 ± 0.005
Control	2.61 ± 0.05	0.147 ± 0.002	10.3	5.1 ± 0.006
FP 9	2.33 ± 0.05	0.132 ± 0.004	10.2	5.4 ± 0.005
Control	2.47 ± 0.06	0.126 ± 0.005	11.4	5.0 ± 0.007

Note: FP- fire plot, SOM - soil organic matter, M - Mean, SD - Standard Deviation, Amount of soil microflora - 103/g absolutely dry soil

One of the most immediate and pronounced effects observed was the reduction in organic soil matter (SOM). This decline was especially evident in plots affected by moderate to high-intensity fires. The combustion of organic matter during fire events not only reduces humus content but also disrupts soil structure and affects water retention, aeration, and nutrient availability - factors critical to tree growth and regeneration.

Changes in SOM are inherently complex due to the variable composition of organic compounds and the influence of multiple environmental factors, such as topography, microclimate, and vegetation type.

Nevertheless, the consistent decline in SOM across multiple fire-affected plots underscores its vulnerability to fire disturbance and its central role in post-fire soil degradation.

Similarly, total nitrogen content showed a general decrease in the burned plots compared to the control plots. This reduction is attributed to increased soil temperatures during fires, which accelerate volatilization and intensify nitrification processes (Barnes et al., 1998). Furthermore, although microbial populations often recover after fire, the initial microbial decline can lead to immobilization and limited availability of nitrogen in both ammonium and nitrate forms (Bogdanov, 2023a).

The data also indicate an increase in soil pH following fire exposure, suggesting a reduction in acidity. This is commonly observed in post-fire soils and is primarily due to the accumulation of ashes and basic cations such as calcium, magnesium, and potassium. These cations are released during the combustion of organic matter and contribute to an alkaline reaction in the soil solution (Kimmins, 1996). The increase in pH can have both beneficial and detrimental effects depending on the species-specific requirements of the vegetation and microbial communities. High pH levels tend to inhibit the development of micromycetes while favoring the proliferation of non-spore-forming bacteria (Lauber et al., 2009; Ammitzbøll et al., 2022).

These findings clearly demonstrate that forest fires disrupt the balance of key soil properties that are essential for maintaining silvicultural productivity and soil ecological health.

Microbial community responses to fire

The influence of forest fires on soil microbial abundance was assessed by comparing total microbial counts in fire-affected plots and their respective control areas (Figure 1).

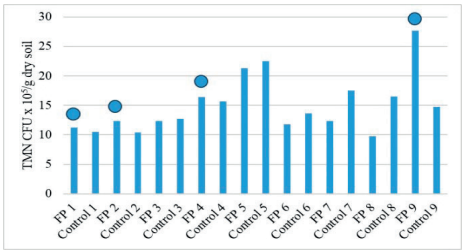


Figure 1. Total microbial number
Samples with increased TMN compared to controls

The results reveal a heterogeneous response, with no uniform trend across all sites. In some plots - specifically FP1, FP2, FP4, and FP9 - the total microbial number (TMN) was higher in the burned soils than in the control soils. This trend was most pronounced in FP9, where microbial abundance nearly doubled following a low-intensity surface fire. These findings suggest that weak surface fires may not significantly disrupt microbial communities and, under certain conditions, may even stimulate microbial activity due to increased nutrient availability and elevated soil temperatures. In contrast, in the remaining plots, microbial abundance was consistently lower in burned areas compared to controls. The most notable reduction occurred in FP8, which experienced a strong surface fire. Here, microbial counts in the control plot were approximately 40% higher than in the corresponding burned area. This pattern indicates that high-intensity fires exert a stronger suppressive effect on microbial communities, likely due to lethal temperatures and the destruction of habitat and organic substrates. On average, across all other sites (excluding FP8), microbial abundance in control plots was approximately 12.5% higher than in the burned plots. A parallel trend was observed in the population of ammonifying bacteria, which play a vital role in nitrogen cycling (Figure 2). As with total microflora, elevated counts of ammonifying bacteria were recorded in FP1, FP2, and FP9. A marginal increase (approximately 4%) was also observed in FP4. This pattern confirms that ammonifying bacteria constitute a substantial proportion of the total microbial community and respond similarly to fire-induced changes in the soil environment.

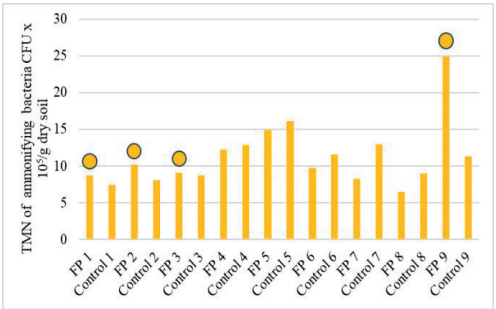


Figure 2. TMN of ammonifying bacteria
Samples with increased TMN of ammonifying bacteria compared to controls

The variability of microbial responses was further analyzed through the standard distribution of microbial abundance across all sample plots (Figure 3).

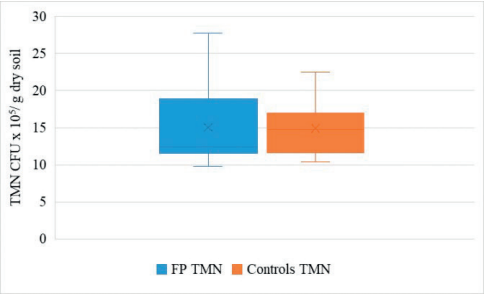


Figure 3. Standard distribution of FPs and Controls

The data show that in the control plots, the mean value closely aligns with the median, indicating a symmetrical distribution of microbial abundance. In contrast, in the burned plots, the mean and median values differ significantly, suggesting a more skewed distribution. In both control and burned areas, the values in the first quartile display a narrow range. However, in the second quartile, the control plots exhibit a wider range (11.5×10^5 to 12.4×10^5 CFU/g of dry soil) compared to the burned plots. This pattern reverses in the third quartile. In the burned plots, 25% of the values fall within a broader range - from 12.4×10^5 to 18.9×10^5 CFU/g - while in the control plots the corresponding range is narrower, from 14.8×10^5 to 17×10^5 CFU/g. A similar trend is observed in the fourth quartile: burned plots exhibit greater variability (18.9×10^5 to 27.8×10^5 CFU/g) than control plots (17×10^5 to 22.5×10^5 CFU/g).

These findings indicate that microbial abundance in burned soils is more variable, reflecting the heterogeneous impact of fire depending on its type and intensity. Such variability underscores the complex influence of fire on soil microbial communities, which play a fundamental role in ecosystem processes in forest environments.

Changes in soil microbial communities resulting from both the direct and indirect effects of forest fires can lead to significant disruptions in ecosystem functions, particularly by slowing the transformation and cycling of nutrients (Mataix-Solera et al., 2009). The impact of fire on soil microbial communities is highly variable and depends on several factors, including fire intensity, duration, and depth of penetration into the soil (Yeager et al., 2005). In some cases, high-intensity fires can lead to near-complete sterilization of the soil, whereas in other instances, fires may have minimal long-term effects on microbial populations (Vázquez et al., 1993).

Zhou et al. (2014) emphasized that the loss of soil microbial life following a fire is not only due to elevated temperatures but also to post-fire conditions that inhibit microbial recovery. In a more recent study, Zhou et al. (2024) further noted that the strength of a fire's impact on microbial communities is influenced by multiple factors, including its intensity, duration, and the depth of soil affected.

The findings of the present study support the idea that, although there is an initial decline in microbial populations after fire, in some cases, microbial abundance may increase beyond control levels in the post-fire environment. This pattern was observed in plots FP1, FP2, FP4, and FP9 (Figure 1). The observed increase in microbial abundance is likely driven by elevated soil temperatures and the enhanced availability of nutrients released during the combustion of organic matter - conditions that can temporarily boost the biogenicity of soils in fire-affected areas (Bogdanov, 2023a; 2023b).

Correlation analysis between microbiological and soil properties

To better understand the relationships between microbial parameters and the physicochemical properties of fire-affected soils, a correlation analysis was conducted. The focus was on examining how total microbial number (TMN) and ammonifying bacteria relate to key soil indicators, including soil organic matter, total nitrogen, and pH. A strong positive correlation was found between the abundance of ammonifying bacteria and the total microbial number in both burned and control plots. However, this relationship was notably stronger in burned areas, where the correlation coefficient reached $r = 0.97$ (Figure 4), compared to $r = 0.87$ in control plots (Figure 5). These results suggest that ammonifying bacteria constitute a substantial proportion of the total microbial community, especially under post-fire conditions. This observation is consistent with previous research indicating that fire-altered environments can

accelerate nitrogen cycling by enhancing the conversion of ammonium to nitrate (Duran et al., 2008; Ball et al., 2010).

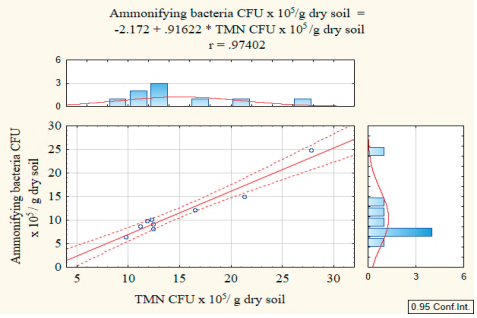


Figure 4. Correlation between TMN and number of ammonifying bacteria in Fire

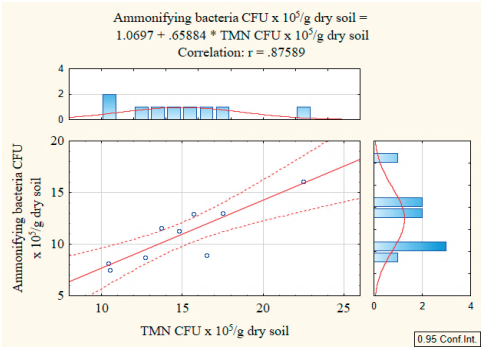


Figure 5. Correlation between TMN and number of ammonifying bacteria in Control Plots

Further analysis explored the relationship between microbial abundance and environmental factors. In unburned control plots, no statistically significant correlations were found between TMN and the soil's organic matter content (r = 0.05), total nitrogen (r = 0.26), or pH (r = –0.09). Similarly, no meaningful correlations were observed between ammonifying bacteria and these soil parameters in the control areas.

In contrast, several noteworthy correlations emerged in burned plots. A moderate positive correlation was identified between TMN and organic matter content (r = 0.48; Figure 6), suggesting that soils with higher residual organic content support a more robust microbial community even after fire. This indicates that partial retention of organic matter can buffer microbial populations against fire-induced decline.

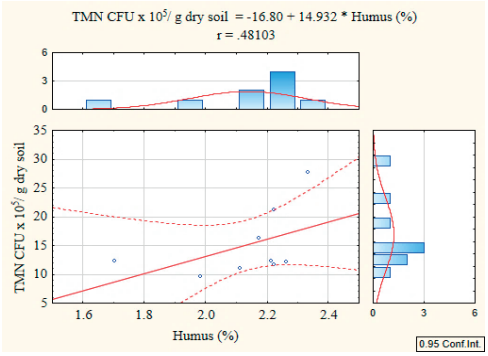


Figure 6. Correlation between total microbial number and humus (%) in fire plots

No significant correlation was found between total nitrogen content and total microbial number (TMN), with a correlation coefficient of r = 0.16, indicating a weak and statistically insignificant relationship. In contrast, the correlation between soil pH and TMN revealed a moderate negative association (r = –0.51, Figure 7), similar to the relationship observed between TMN and soil organic matter.

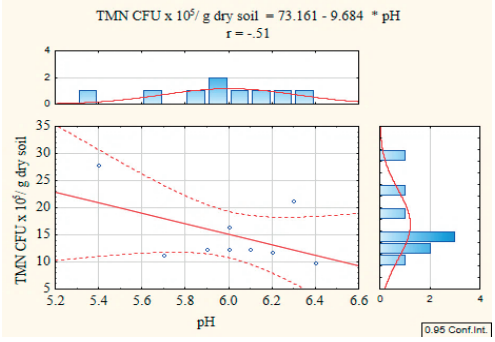


Figure 7. Correlation between total microbial number and pH in fire plots

This inverse correlation suggests that microbial abundance tends to be higher in more acidic soils. This pattern may be attributed to the high sensitivity of soil microbial communities to variations in pH following fire. Even slight deviations from pre-fire acidity levels, when compared to those in control plots, appear to have a positive influence on microbial activity. In such transitional conditions, reduced environmental stress may promote microbial adaptation and facilitate recovery.

These observations highlight the need for more nuanced, multifactorial investigations into the

complex interactions between post-fire soil chemistry and microbial dynamics. Notably, previous studies have identified soil pH as a key determinant in structuring the composition and diversity of microbial communities, especially in ecosystems subjected to disturbance events such as wildfires (Lauber et al., 2009).

The strongest correlation observed was between soil pH and the abundance of ammonifying bacteria, with a correlation coefficient of r = –0.63 (Figure 8).

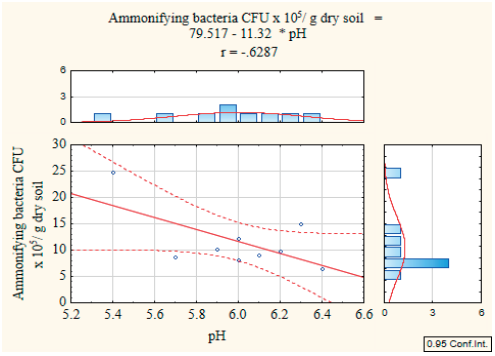


Figure 8. Correlation between number of ammonifying bacteria and pH in fire plots

This significant inverse relationship indicates that the activity of ammonifying bacteria is closely influenced by soil acidity. The findings suggest that microbial communities are particularly responsive to shifts in pH, with greater abundance occurring in soils where acidity levels remain closer to pre-fire conditions.

It is likely that in environments where pH changes are minimal, microbial stress is reduced, allowing for better survival and function of sensitive groups such as ammonifiers. However, to fully understand the thresholds and resilience of microbial communities under more extreme conditions, further research is required, particularly in sites that experience substantial post-fire shifts in soil pH.

Influence of stand density on soil properties after fire

Soil properties are strongly influenced by vegetation cover and the accumulation of organic matter, both of which are significantly altered by fire. The extent of these changes depends largely on the intensity of the fire and the volume of biomass consumed during combustion (Kimmins, 1996). As fire affects vegetation structure and organic inputs, it can lead to substantial modifications in soil chemical and biological characteristics.

In this context, it is particularly important to examine how stand density influences post-fire soil dynamics, as it determines both the amount and spatial distribution of combustible material. In the present study, soils beneath stands of differing densities - 0.2 and 0.5 - were analyzed. Both stands experienced fires of comparable type and intensity, allowing for a focused comparison of density-related effects. The changes in key soil properties, expressed as percentage differences relative to unburned control plots, are illustrated in Figure 9.

Although differences in total nitrogen content remained relatively minor three years after the fire, the stand with higher density exhibited notably higher pH values compared to the unburned control. This increase can be attributed to the combustion of a larger volume of organic matter and the subsequent release of base cations (e.g., Ca^{2+}, Mg^{2+}, K^{+}), which contribute to soil alkalization (Figure 9).

The soil organic matter content in the denser stand was significantly lower, reflecting a higher degree of fire impact due to the increased volume of biomass consumed. This trend was consistent with observed differences in both the C:N ratio and the abundance of total microflora. Following a fire, elevated soil temperatures and enhanced nutrient solubility can stimulate microbial growth in some cases; however, intense fires may lead to the near-complete destruction of microbial communities (Bogdanov, 2023a).

In line with this, the carbon-to-nitrogen (C:N) ratio - an indicator of the rate of organic matter decomposition - was significantly lower in the denser stand. This suggests more rapid mineralization of organic residues, likely driven by post-fire microbial activity and favorable thermal and chemical conditions resulting from a more severe fire impact (Figure 9).

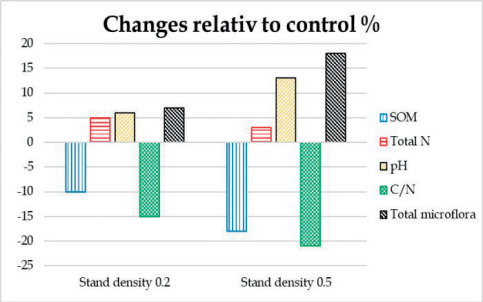


Figure 9. Change in the studied indicators in burned soils compared to control plots depending on the stand density

Influence of forest type on post-fire changes in soil silvicultural properties

To evaluate the influence of forest type on soil response to fire, soil samples were analyzed from both coniferous and deciduous stands affected by moderate-intensity surface fires in 2021, along with samples from their corresponding unburned control plots. The aim was to determine how forest composition affects post-fire changes in silvicultural soil properties. The results indicate that fire-induced changes were more substantial and persistent in soils under coniferous stands. This finding is consistent with previous studies and can be attributed to the higher combustibility of coniferous litter, which results in more intense and longer-lasting fires compared to those in deciduous forests (Bogdanov, 2023b; Velizarova, 2011). The most significant difference was observed in total nitrogen content, where the largest reduction, relative to the control, occurred in the coniferous stand (Figure 10).

Similar trends were observed for organic soil matter, pH, and the C:N ratio. In all cases, greater deviations from the control were recorded under coniferous stands, indicating more intense alteration of soil chemistry. These changes reflect both the severity of the fire and the nature of the organic material present in coniferous ecosystems, which tends to burn more thoroughly and penetrate deeper into the soil profile. In contrast, the total microbial abundance showed an inverse pattern, though within a narrow margin of 5%. In the deciduous stand, microbial numbers slightly increased post-fire, while in the coniferous stand, they slightly decreased. This discrepancy may be explained by the deeper thermal impact under conifers, which likely caused a greater initial decline in microbial populations. In deciduous forests, the fire's effects appear to have been more superficial, allowing microbial communities to recover more quickly or even benefit from short-term post-fire conditions.

These findings underscore the importance of forest composition as a key factor influencing soil resilience and recovery after fire. From a silvicultural perspective, deciduous stands may offer a degree of natural protection against severe soil degradation, supporting more stable post-fire ecosystem recovery.

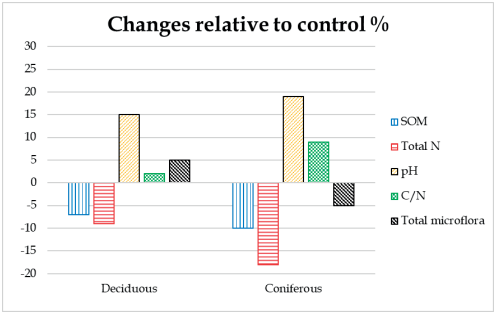


Figure 10. Changes in the studied soil indicators in burned plots compared to control plots, grouped by forest type

Effects of fire type on silvicultural properties of soil

The spatial characteristics of a forest fire - whether it is a surface fire or a crown fire - significantly influence the degree and depth of soil disturbance. These fire types differ in terms of fuel consumption patterns, heat transfer to the soil, and post-fire ecological consequences. In this study, changes in soil properties were analyzed in two forest stands with similar silvicultural characteristics that experienced medium-intensity crown and surface fires in 2022 (SP6 and SP7, respectively), along with their corresponding control plots.

The comparative analysis revealed notable differences in the response of silvicultural soil indicators based on fire type (Figure 11). More pronounced changes were observed in the surface fire-affected plot, particularly in terms of total microflora abundance, total nitrogen content, and the C:N ratio. In this case, microbial populations and nitrogen content decreased more significantly, likely due to more intense

heat transfer into the upper soil layers and increased combustion of surface organic matter. The C:N ratio increased in soils affected by crown fires, while it decreased in those affected by surface fires. This suggests that in the case of crown fires, the decomposition of organic matter slowed down, a finding further supported by the observed reduction in total nitrogen content. In contrast, the soil affected by the surface fire exhibited an accelerated rate of organic matter mineralization, as indicated by the lower C:N ratio - even though total nitrogen levels also declined (Figure 11). These opposing trends reflect the distinct thermal and biological impacts associated with each fire type.

This contrasting pattern can be explained by the differing ecological consequences of the two fire types. Moderate-intensity surface fires typically result in mosaic tree mortality, allowing partial canopy retention and less drastic alteration of microclimatic conditions. In contrast, moderate-intensity crown fires often lead to complete stand mortality, causing more abrupt and extensive changes in light, temperature, and moisture regimes. These environmental shifts have a significant influence on the intensity and direction of organic matter transformation in the soil. These findings suggest that the type of forest fire, determined by the spatial distribution of combustible materials, exerts an indirect yet significant impact on the silvicultural properties of soil - primarily through its influence on the rate and dynamics of organic matter decomposition.

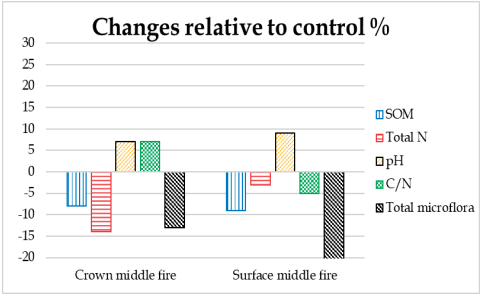


Figure 11. Change of the studied indicators in burnt soils compared to control plots depending on the type of fire

Effects of fire intensity on silvicultural soil properties

The intensity or strength of a forest fire plays a crucial role in determining the extent of its impact on soil properties. To examine this effect, soil samples were analyzed from areas affected by a weak surface fire and a strong surface fire, both occurring in 2022, along with their respective unburned control plots. The results, presented as percentage changes relative to the controls, are summarized in Figure 12.

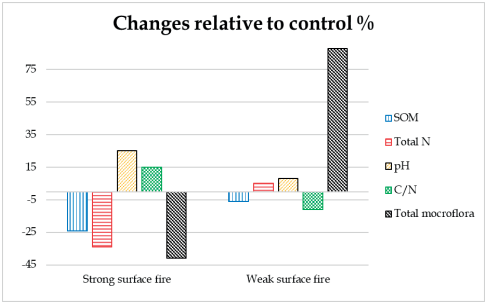


Figure 12. Change of the studied indicators in burnt soils compared to control plots depending on the strength of the fire impact

The analysis revealed that all soil indicators were influenced by fire strength, with the most pronounced changes observed in the strongly burned plots. In areas affected by weak surface fires, the combustion of organic matter was relatively limited, resulting in a slight increase in total nitrogen and minimal changes in pH. In this case, a moderate rise in soil temperature likely stimulated microbial activity, which led to a decrease in the C:N ratio, indicating enhanced decomposition and mineralization of organic material.

Conversely, strong surface fires caused more substantial degradation of silvicultural soil properties. A significant reduction in soil organic matter was observed, accompanied by a decline in total nitrogen content. The more intense combustion released higher quantities of base cations, resulting in elevated soil pH, while simultaneously creating conditions less favorable for microbial recovery. This was reflected in the lower abundance of soil microflora and a higher C:N ratio, suggesting that microbial processes related to organic matter turnover were suppressed.

These findings underscore the fact that fire severity amplifies the disruption of soil fertility, not only by physically consuming organic substrates, but also by altering the chemical and biological environment essential for post-fire

recovery. Understanding these variations is critical for predicting the resilience of forest soils and planning appropriate post-fire management strategies.

Temporal changes in silvicultural soil properties following forest fire

Changes in the silvicultural properties of soil following forest fires were examined as a function of time since the disturbance, based on the analysis of soil samples collected from areas affected by fires of similar characteristics in 2020 and 2022.

The results indicate that all studied soil indicators exhibited more pronounced deviations from control values in the more recently burned plots (2022), while the soils affected by the 2020 fire showed changes of reduced magnitude (Figure 13). This trend suggests a gradual recovery of silvicultural soil properties over time.

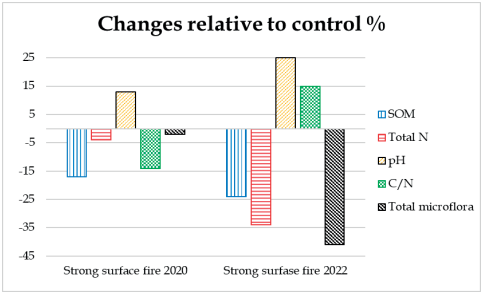


Figure 13. Change of the studied indicators in burnt soils compared to control plots depending on the time after the fire impact

These findings demonstrate that the impact of forest fires on soil silvicultural properties is not necessarily permanent, and that recovery processes can begin within a few years, depending on fire severity and site conditions. However, the rate and completeness of recovery are strongly influenced by factors such as vegetation type, post-fire management, and climatic conditions. This underscores the importance of timing in the implementation of restoration measures, which should consider the post-fire developmental stage of the soil ecosystem to align with periods of optimal nutrient availability and biological activity.

CONCLUSIONS

Forest fires have a pronounced negative impact on the silvicultural properties of soils, primarily through the reduction of soil organic matter and, in most cases, total nitrogen content. Additionally, fires often alter soil pH, creating conditions that may be incompatible with the ecological requirements of dominant tree species.

The response of soil microflora is strongly influenced by fire intensity. While low-intensity fires can stimulate microbial development by increasing soil temperature and releasing readily available nutrients from burned organic matter, high-intensity fires may lead to near-complete microbial destruction and hinder community recovery. In several sampled sites - particularly those affected by weak surface fires - microbial abundance exceeded that of the unburned controls, highlighting the potential for short-term biological enrichment under mild fire conditions. Furthermore, correlations between environmental factors and microbial abundance were observed in burned areas, whereas such relationships were absent in control soils. Notably, microbial suppression was more severe in coniferous stands than in deciduous stands under equivalent fire conditions, likely due to the higher combustibility of coniferous biomass. Stand density was also found to be a critical factor. Higher density forests tend to accumulate more biomass, which, when burned, leads to more severe and longer-lasting impacts on soil properties. Similarly, fires in coniferous forests resulted in more significant and persistent changes than those in deciduous stands, again linked to differences in fuel load and combustibility.

The type of fire - whether surface or crown - was shown to influence soil conditions indirectly, primarily through its effects on the rate and nature of organic matter transformation. In contrast, fire intensity and the time elapsed since the fire had a direct and measurable effect on all assessed soil indicators. These results demonstrate that the changes induced by forest fires are not irreversible; recovery is possible under favorable conditions, especially if supported by appropriate post-fire management.

Restoration efforts in burned areas should be tailored to specific changes in soil composition and fertility, considering the time since the fire and the temporary increase in nutrient availability. Special attention should be given to coniferous plantations in the Lower Forest Vegetation Belt, which are particularly vulnerable to fire. In these areas, afforestation using native deciduous species, along with timely silvicultural interventions, is essential for reducing long-term fire risk and promoting ecological stability.

This study provides a valuable reference for future in-depth investigations on the topic and offers a practical foundation for developing forest restoration and afforestation strategies in fire-affected regions.

REFERENCES

Ammitzbøll, H., Jordan, J., Baker, C., Freeman, J., & Bissett, A. (2022). Contrasting successional responses of soil bacteria and fungi to post-logging burn severity. *Forest Ecology and Management, 508*, 120059. https://doi.org/10.1016/j.foreco.2022.120059

Ball, P., MacKenzie, M., & Holben, W. (2010). Wildfire and charcoal enhance nitrification and ammonium-oxidizing bacterial abundance in dry montane forest soils. *Journal of Environmental Quality, 39*(4), 1243–1253. https://doi.org/10.2134/jeq2009.0082

Barreiro, A., & Díaz-Raviña, M. (2021). Fire impacts on soil microorganisms: Mass, activity, and diversity. *Current Opinion in Environmental Science & Health, 22*, 100264. https://doi.org/10.1016/j.coesh.2021.100264

Barnes, B. V., Zak, D. R., Denton, S. R., Spurr, S. H. (1998). *Fire and the Forest Site*. Forest Ecology. 4th ed. pp. 290-297.

Bogdanov, S. (2023a). *Soil characteristics changes in soils of class Luvisols influenced by forest fires*. Avangard Prima (in Bulgarian).

Bogdanov, S. (2023b). Changes in silvicultural properties of soils influenced by forest fires in Bulgaria. *Ecological Engineering and Environmental Protection, 3–4*(2023), 69–76 (in Bulgarian).

Bogdanov, S. (2023c). *Manual for exercises in forest soil science*. Publishing House at LTU. (in Bulgarian)

Bogdanov, S. (2024). *Forest soil science* (p. 226). LTU Publishing House (in Bulgarian).

Donov, V. (1976). *Assessment of forest soils* (p. 168). Zemizdat (in Bulgarian).

Gousterov, G., Todorov, Z., & Kominkov, K. (1977). *Manual of microbiology* (p. 180). Nauka i Izkustvo (in Bulgarian).

ISO 11261:2002. (2002). *Soil quality - Determination of total nitrogen - Modified Kjeldahl method*. International Organization for Standardization.

IUSS Working Group WRB. (2022). *World reference base for soil resources, 4th edition*. International Union of Soil Sciences (IUSS). https://www3.ls.tum.de/boku/?id=141

Jiménez Esquilín, A. E., Stromberger, M. E., Massman, W. J., Frank, J. M., & Shepperd, W. D. (2008). Microbial community structure and activity in a Colorado Rocky Mountain forest soil scarred by slash pile burning. *Soil Biology and Biochemistry, 40*(9), 2472–2480. https://doi.org/10.1016/j.soilbio.2008.06.005

Kimmins, J. P. (1996). *Forest ecology: A foundation for sustainable management* (2nd ed.). Prentice Hall.

Lauber, C. L., Hamady, M., Knight, R., & Fierer, N. (2009). Pyrosequencing-based assessment of soil pH as a predictor of soil bacterial community structure at the continental scale. *Applied and Environmental Microbiology, 75*(15), 5111–5120. https://doi.org/10.1128/AEM.00335-09

Mataix-Solera, J., Guerrero, C., García-Orenes, F., Bárcenas, G., & Pascual, J. A. (2009). Forest fire effects on soil microbiology. In A. Cerdà & P. R. Robichaud (Eds.), *Fire effects on soils and restoration strategies* (pp. 133–175). Science Publishers.

Molla, I., Ilieva, I., Donov, V., Iliev, N., & Atanassova, V. (2014). Some changes of physical soil properties as a result of forest fire. *Ecologia Balkanica, 6*(1), 71–76.

Neary, D. G., Klopatek, C. C., DeBano, L. F., & Ffolliott, P. F. (1999). Fire effects on belowground sustainability: A review and synthesis. *Forest Ecology and Management, 122*(1–2), 51–71. https://doi.org/10.1016/S0378-1127(99)00032-8

Penkov, M., Yolev, I., Enikova, M., Donov, V., & Blagoeva, R. (1992). *Classification and diagnostics of the soils in Bulgaria*. Zemizdat (in Bulgarian).

Vázquez, F. J., Acea, M. J., & Carballas, T. (1993). Soil microbial populations after wildfire. *FEMS Microbiology Ecology, 13*(2), 93–103. https://doi.org/10.1111/j.1574-6941.1993.tb00040.x

Velizarova, E. (2011). Fire risk in pine plantations in Bulgaria. *Ecological Engineering and Environmental Protection, 2*, 11–17 (in Bulgarian).

Yeager, C. M., Northup, D. E., Grow, C. C., Barns, S. M., & Kuske, C. R. (2005). Changes in nitrogen-fixing and ammonia-oxidizing bacterial communities in soil of a mixed conifer forest after wildfire. *Applied and Environmental Microbiology, 71*(5), 2713–2722. https://doi.org/10.1128/AEM.71.5.2713-2722.2005

Zahariev, B., Donov, V., Petrunov, K., & Masarov, S. (1979). *Forestry-vegetation zoning of the NRB* (p. 197). Zemizdat (in Bulgarian).

Zhou, H., Yang, M., Luo, X., Yang, Z., Wang, L., Liu, S., Zhang, Q., Luo, M., Ou, J., Xiong, S., Qin, Y., & Li, Y. (2024). Short-term impacts of fire and post-fire restoration methods on soil properties and microbial characteristics in Southern China. *Fire, 7*(12), 474. https://doi.org/10.3390/fire7120474

Scientific Papers. Series E. Land Reclamation, Earth Observation & Surveying, Environmental Engineering. Vol. XIV, 2025
Print ISSN 2285-6064, CD-ROM ISSN 2285-6072, Online ISSN 2393-5138, ISSN-L 2285-6064

EUROPEAN UNIVERSITY STUDENTS' ATTITUDES TOWARD THE EUROPEAN GREEN DEAL: A COMPARATIVE STUDY

Mihai Dan CARMIHAI[1], Nicoleta RADU[2, 3], Zina PARASCHIV[2], Francisca BLANQUEZ CANO[4], Oksana MULESA[5], Adrián SILVA[6], Razvan TEODORESCU[2]

[1]National University of Science and Technology Politehnica Bucharest, 313 Splaiul Independenței Street, District 6, 060042, Bucharest, Romania
[2]University of Agronomic Sciences and Veterinary Medicine of Bucharest, 59 Mărăști Blvd, District 1, 011464, Bucharest, Romania
[3]National Institute for Research and Development in Chemistry and Petrochemistry – ICECHIM, 202 Splaiul Independenței, District 6, 060021, Bucharest, Romania
[4]Autonomous University of Barcelona, 08193, Bellaterra (Cerdanyola del Vallès), Barcelona, Spain
[5]Uzhhorod National University, 3 Narodna Square, 88000, Uzhhorod, Ukraine
[6]University of Porto, Praça de Gomes Teixeira, 4099-002, Porto, Portugal

Corresponding author email: nicoleta.radu@biotehnologii.usamv.ro

Abstract

The attitudes of students toward the European Green Deal were assessed through a survey involving master's and doctoral students from four European universities: Universitat Autònoma de Barcelona (Spain), University of Porto (Portugal), University of Agronomic Science and Veterinary Medicine of Bucharest (Romania), and Uzhhorod University (Ukraine). Results revealed strong overall support among students for actions promoting environmental sustainability and reducing carbon footprints. Significant variations were observed across countries, with students from Spain, Portugal, and Romania demonstrating particularly high agreement regarding the importance of balancing economic growth with environmental protection. While respondents generally recognized the long-term benefits of the Green Deal, concerns regarding implementation costs were notably higher among students from Romania and Ukraine. Additionally, a vast majority expressed interest in tools to monitor personal carbon footprints, highlighting growing awareness of individual environmental responsibilities. These findings suggest a positive attitude among European university students toward environmental sustainability initiatives, though addressing concerns about economic implications could enhance broader support.

Key words*: European Green Deal, environmental sustainability, students attitude, higher education, comparative study.*

INTRODUCTION

Anthropogenic climate change is an undeniable reality that requires immediate and coordinated action. In response, the European Union has established ambitious targets to reduce carbon emissions by 55% by 2030 compared to 1990 levels (European Commission, 2019; 2021). Achieving these goals demands broad societal engagement, including the active participation of educational institutions. To support this transition and improve understanding of climate-related challenges, universities across the EU are revising and adapting their curricula. This educational shift aims to equip students with the knowledge and skills essential for effectively addressing environmental concerns.

A growing body of research suggests that higher education plays a significant role in shaping environmental attitudes and policy preferences. For example, survey studies by Harring & Jaegers (2017) demonstrated that university education influences students' support for environmental policies. Their findings highlighted that economics students were more inclined to support market-based environmental policies, illustrating the impact of academic discipline on environmental perspectives. Subsequent studies have expanded on these insights by exploring the roles of education, socioeconomic background, and cultural context. Mónus (2022) examined the effects of environmental education policies and ocioeconomic factors on secondary school

students' attitudes and behaviors. The study concluded that schools with robust environmental education programs more effectively foster pro-environmental behaviors. Similarly, Concina & Frate (2023) analyzed university students' beliefs and attitudes toward sustainability in various countries. Their results showed that while students were generally aware of sustainability issues, this awareness did not always translate into environmentally responsible behaviors.

In alignment with these trends, the present study was designed to assess the attitudes of master's and doctoral students toward the European Green Deal. The research was conducted among students from universities in Spain, Portugal, Romania, and Ukraine - the latter currently a candidate for EU membership. By evaluating students' perceptions and perspectives on this major policy initiative, the study aims to provide valuable insights into how higher education contributes to shaping future leaders' environmental commitments.

MATERIALS AND METHODS

This study assessed the attitudes of master's and doctoral students toward the European Green Deal through a survey-based approach, building on previous research frameworks (Radu et al., 2019; Radu et al., 2020). The participants were selected from four European universities: Universitat Autònoma de Barcelona (Spain), University of Porto (Portugal), University of Agronomic Sciences and Veterinary Medicine of Bucharest (Romania), and Uzhhorod National University (Ukraine).

Participant selection

The target population consisted of students enrolled in engineering sciences at the master's and doctoral levels. This group was selected for several reasons:

1. *Advanced knowledge:* graduate students possess a deeper understanding of complex topics such as environmental policy, sustainability, and European legislative initiatives, allowing them to critically assess the implications of the European Green Deal.

2. *Relevant training:* due to their academic backgrounds and involvement in research related to environmental issues and public policy, these students are capable of providing more informed and nuanced responses.

3. *Future policy influence:* as potential future decision-makers, graduate students often engage more readily in academic research and are motivated by the opportunity to contribute to scientific understanding and policy development.

Participants were recruited via email invitations, and responses were collected anonymously through an online questionnaire. All participants were informed of the study's objectives prior to participation, and their involvement was entirely voluntary. No personally identifiable information - such as names, contact details, or addresses - was collected, ensuring full anonymity and compliance with ethical research standards.

Survey design

The survey consisted of six closed-ended questions designed to evaluate students' attitudes toward the principles and implementation of the European Green Deal. These questions addressed the following core dimensions:

1. *Individual responsibility*: "I believe that my actions can contribute to solving environmental problems."
2. *Willingness to act:* "I am willing to reduce my personal carbon footprint to support the European Green Deal."
3. *Sustainability and growth:* "Economic growth should not occur at the expense of the environment."
4. *Perceived value:* "The cost of implementing the European Green Deal is justified by its long-term benefits."
5. *Self-assessment tools:* "It is appropriate for students to calculate their carbon footprint through their regular daily activities."
6. *Engagement through tools:* "Do you consider that you would pay more attention to your carbon footprint if you had an appropriate tool to quantify it?"

Responses were rated using a 5-point Likert scale, where: 1 = Not Important, 2 = Low Importance, 3 = Medium Importance, 4 = High Importance, and 5 = Very High Importance.

Data collection and analysis

By September 2024, a total of 40 valid responses had been received. The geographic distribution of participants was as follows: 28% from Ukraine, 28% from Romania, 26% from Portugal, and

18% from Spain. Although the sample size is modest, the random selection of participants from each institution helped minimize selection bias and offered a degree of representativeness within the target population.
Given the exploratory nature of the study and the limited sample size, data analysis was primarily descriptive. No inferential statistical tests were applied. The goal was to identify prevailing trends and general patterns in student perceptions of and attitudes toward the European Green Deal and related environmental policies.

RESULTS AND DISCUSSIONS

Regarding the first statement, "I believe that my actions can contribute to solving environmental problems", fewer than 30% of respondents from each university strongly agreed (Figure 1a). Specifically, 29% of respondents from Spain, 27% from Romania, and only 10% each from Portugal and Ukraine expressed strong agreement. However, a higher proportion of respondents expressed high agreement: 70% from Portugal, 50% from Ukraine, 43% from Spain, and 19% from Romania (Figure 1a). Overall, 66% of respondents either highly agreed (44%) or strongly agreed (22%) with this statement, while only 13% considered it of low importance or not important (Figure 1b).

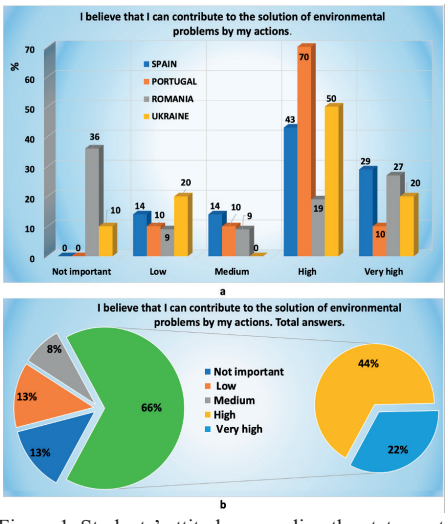


Figure 1. Students' attitudes regarding the statement: *"I believe that I can contribute to solving environmental problems through my actions."*
a) Distribution of responses by country; b) Overall distribution of responses across all participants

In response to the statement, "I am willing to reduce my personal carbon footprint to support the European Green Deal", a high level of strong agreement was observed among students: 60% from Portugal, 64% from Romania, and 57% from Spain (Figure 2a).
In Ukraine, strong agreement was slightly lower at 30%, but a significant proportion expressed high agreement (60%). Overall, 92% of respondents strongly agreed (53%) or highly agreed (39%) with the statement, while only 2% rated it as medium importance, and 3% considered it unimportant (Figure 2b).

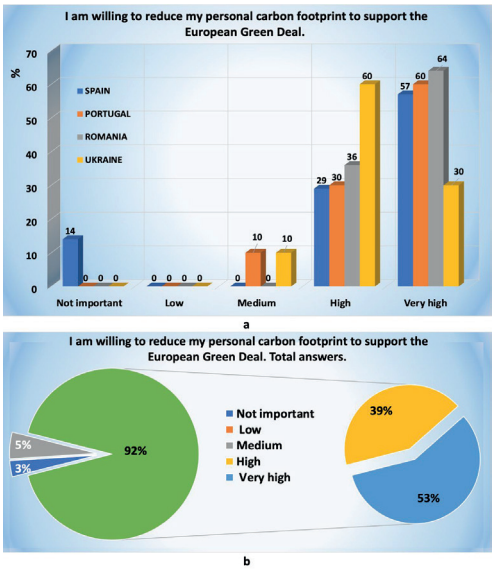


Figure 2. Students' attitudes regarding the statement: *"I am willing to reduce my personal carbon footprint to support the European Green Deal."*
a) Responses categorized by country; b) Overall distribution of responses across all participants

Concerning the statement, "Economic growth should not occur at the expense of the environment," students showed substantial consensus, with 100% from Spain, 82% from Romania, 80% from Portugal, and 60% from Ukraine strongly agreeing (Figure 3a).
Less than 30% from each university expressed high agreement. Overall, 97% of respondents either strongly agreed (79%) or highly agreed (18%), and only 3% viewed this as of low importance (Figure 3b).

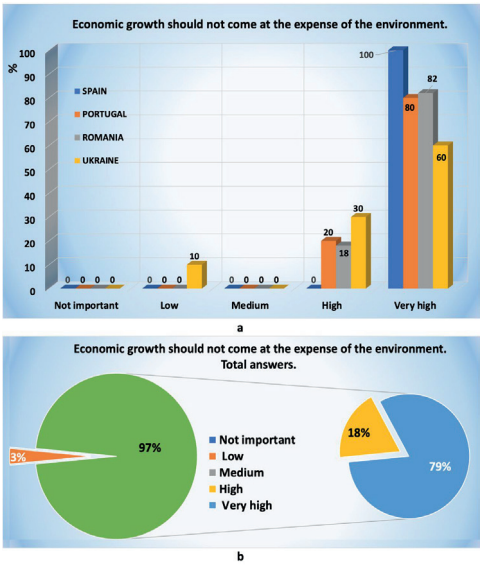


Figure 3. Students' attitudes regarding the statement: *"Economic growth should not come at the expense of the environment."* a) Responses categorized by country; b) Overall distribution of responses across all participants

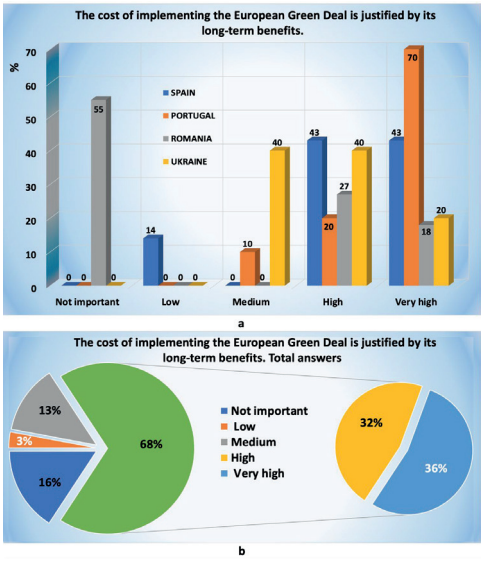


Figure 4. Students' attitudes regarding the statement: *"The cost of implementing the European Green Deal is justified by its long-term benefits."* a) Responses categorized by country; b) Overall distribution of responses across all participants

When evaluating the statement, "The cost of implementing the European Green Deal is justified by its long-term benefits", 70% of respondents from Portugal strongly agreed, followed by 43% from Spain, 20% from Ukraine, and 18% from Romania (Figure 4a). High agreement ranged from 20% to 43% across universities.

Overall, 68% of respondents either strongly agreed (36%) or highly agreed (32%), while 16% considered this statement of no importance, 13% as medium importance, and 3% as low importance (Figure 4b).

Regarding the appropriateness of calculating personal carbon footprints in daily activities, strong agreement was high in Romania (82%) and Spain (57%), while lower in Portugal and Ukraine (20% each) (Figure 5a). High agreement was substantial, especially in Portugal (70%). Overall, 77% of respondents either strongly agreed (45%) or highly agreed (32%), while 13% considered it of medium importance and 10% as low importance (Figure 5b).

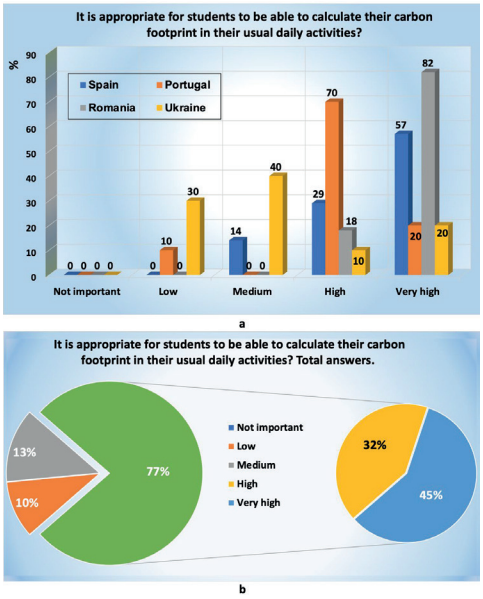


Figure 5. Students' attitudes regarding the statement: *"It is appropriate for students to calculate their carbon footprint in their regular daily activities."* a) Responses categorized by country; b) Overall distribution of responses across all participants

In response to the question about whether using an appropriate tool to quantify carbon footprints would increase personal awareness, 91% of students from Romania, 71% from Spain, 50% from Portugal, and only 10% from Ukraine expressed strong agreement (Figure 6a). High

agreement varied, with notable percentages from Ukraine (50%) and Portugal (40%).
Overall, 87% of respondents strongly agreed (55%) or highly agreed (32%) with this statement, with only 5% rating it as medium importance and 8% as low importance (Figure 6b).

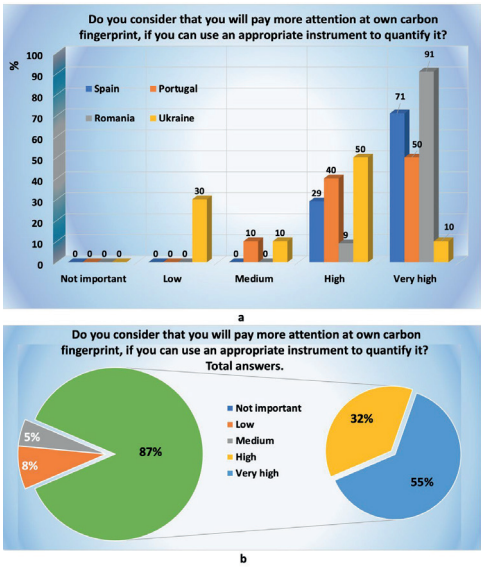


Figure 6. Students' attitudes regarding the statement: *"Do you consider that you will pay more attention to your own carbon footprint if you had an appropriate tool to quantify it?"* a) Responses categorized by country; b) Overall distribution of responses across all participants

Respondents from these European universities generally showed strong support for environmental sustainability, expressing high levels of agreement on the importance of reducing personal carbon footprints, supporting the European Green Deal, and prioritizing environmental protection over economic growth.
While the level of support varies among the different countries, there is a consistent preference for environmentally conscious actions and initiatives. Students expressed significant interest in tools designed to track their carbon footprints, reflecting a growing awareness of their individual environmental impacts. The majority of respondents from the four European universities believe that individual actions can effectively contribute to solving environmental problems. Nevertheless, the strength of agreement varies by country, with students from Portugal and Ukraine more frequently expressing strong agreement compared to those from Spain and Romania. Overall, a substantial proportion of respondents (66%) strongly agree about the importance of individual actions in addressing environmental issues. Additionally, students from all universities indicated high agreement with reducing their personal carbon footprints in support of the European Green Deal, with the highest levels observed in Romania (64%) and Portugal (60%), followed by Spain (57%) and Ukraine (30%). Collectively, 92% of respondents support the Green Deal, demonstrating strong endorsement for this environmental initiative among European students.
The statement "Economic growth should not come at the expense of the environment" received nearly unanimous support, with the highest levels of strong agreement in Spain (100%) and Romania (82%). This suggests that European students strongly prioritize environmental sustainability over economic growth, with 97% of respondents overall agreeing that economic growth should not harm the environment.
Respondents expressed mixed feelings about the cost of implementing the European Green Deal about its long-term benefits. Students from Portugal are the most supportive (70%), while Ukraine and Romania show lower levels of agreement (20% and 18%, respectively). However, a majority (68%) agree that the Green Deal's long-term benefits justify its costs, though a notable portion still considers these costs a problem.
A significant number of respondents believe it is important for students to calculate their carbon footprint. Romania shows the highest agreement (82%), followed by Spain (57%). While a lower percentage of respondents from Portugal and Ukraine agree with this idea, overall, 77% of respondents express the importance of tracking personal carbon footprints, signalling an awareness of individual environmental impact.
There is strong support among students for using tools to calculate and track their carbon footprints. Romania leads again with 91% of respondents very highly agreeing, while Spain (71%) and Portugal (50%) show notable support as well.

Ukraine lags with only 10% agreeing strongly. Nevertheless, 87% of all respondents believe that having the right tools would encourage them to be more conscious of their carbon footprint. The data obtained in this study are in agreement with those reported by other scientific publication.

Economic growth should not come at the expense of the environment," received nearly unanimous support among respondents, with the highest levels of strong agreement observed in Spain (100%) and Romania (82%). This indicates that European students strongly prioritize environmental sustainability over purely economic growth, as 97% of all respondents agreed that economic development should not compromise environmental health.

Respondents expressed mixed opinions regarding whether the long-term benefits of the European Green Deal justify its implementation costs. Students from Portugal showed the strongest agreement (70%), whereas agreement levels were lower among students from Ukraine (20%) and Romania (18%). Nevertheless, the majority (68%) concurred that the Green Deal's long-term advantages justify the associated costs, although a notable proportion remained concerned about the financial implications.

A considerable number of respondents acknowledged the importance of enabling students to calculate their personal carbon footprints. The highest level of strong agreement was recorded in Romania (82%), followed by Spain (57%). Although agreement was lower among respondents from Portugal and Ukraine, overall, 77% recognized the significance of monitoring personal carbon footprints, reflecting increased awareness of individual environmental impacts.

Furthermore, respondents widely supported the use of tools designed to calculate and track carbon footprints. Romanian students again expressed the highest level of strong agreement (91%), followed by students from Spain (71%) and Portugal (50%). Ukrainian students showed less enthusiasm, with only 10% strongly agreeing. Overall, however, 87% of respondents indicated that having appropriate tools available would encourage greater awareness and management of their personal carbon footprints. These findings align well with previous studies reported in the scientific literature.

A survey study conducted by Cernicova-Buca et al. (2023) among Romanian students revealed a high level of interest and readiness to engage in basic sustainable behaviors concerning environmental issues. Similarly, Khanam et al. (2022), in a survey-based analysis conducted across four European countries, found that nations in Central and South-Eastern Europe recorded the highest willingness to reduce their carbon footprints, indicating strong regional support for climate change mitigation.

Bassi (2023) also confirmed that attitudes toward the environment significantly influence ecological behavior, based on research into European consumers' perspectives on climate change.

Predictive studies by Smith et al. (2013), Mielcarek-Bocheńska et al. (2021), and Panchasara et al. (2021) have shown that greenhouse gas emissions are largely produced through agricultural waste and sector-specific processes. Research by Li et al. (2025) emphasized that integrating both nature-based and technological solutions is crucial for sustainable agricultural development. Such integration is essential not only for mitigating climate change but also for ensuring long-term global food security.

CONCLUSIONS

This study reveals that European university students exhibit strong support for the European Green Deal and show high levels of environmental awareness and willingness to adopt sustainable behaviors. The findings highlight that while support for reducing personal carbon footprints is consistently strong across all countries, notable differences emerge regarding economic concerns. Students from Portugal and Romania demonstrate the highest levels of agreement with sustainability goals, whereas respondents from Ukraine show comparatively more apprehension, particularly regarding the financial costs associated with implementing the Green Deal. The results suggest that educational initiatives and policy communication strategies should be tailored to address these national differences. For policymakers, the findings underline the importance of transparent and context-sensitive communication about the costs and long-term

benefits of environmental policies. For educators, integrating practical tools for calculating carbon footprints into university curricula could foster greater personal responsibility and engagement in climate action among students. However, the study is not without limitations. The sample size is relatively small and limited to master's and doctoral students from only four universities, which may not fully represent the broader student population across Europe. Additionally, the survey's reliance on self-reported attitudes introduces the possibility of social desirability bias. Future research should consider expanding the study to include undergraduate students and a more diverse range of universities across different EU regions. Longitudinal studies could also explore how student attitudes evolve over time, particularly in response to policy changes or increased climate-related education. This expanded scope would provide deeper insights into the effectiveness of the European Green Deal's outreach and implementation strategies at the academic level.

ACKNOWLEDGEMENTS

This research was conducted with the support of the project 2023-1-RO01-KA220-HED-000154433, entitled *"Gender, Digitization, Green: Ensuring a Sustainable Future for All in Europe"*, co-funded by the European Union.

REFERENCES

Bassi, F. (2023). European consumers' attitudes towards the environment and sustainable behavior in the market. *Sustainability, 15*(2), 1666.

Cernicova-Buca, M., Dragomir, G.-M., Gherheș, V., & Palea, A. (2023). Students' awareness regarding environment protection in campus life: Evidence from Romania. *Sustainability, 15*(23), 16444.

Concina, E. & Frate, S. (2023). Assessing University Students' Beliefs and Attitudes towards Sustainability and Sustainable Development: A Systematic Review. *Trends High. Educ. 2*, 705-717, https://doi.org/10.3390/higheredu2040041

European Commission. (2019). *The European Green Deal*. https://ec.europa.eu/info/strategy/priorities-2019-2024/european-green-deal_en (Accessed on 15 December, 2023).

European Commission. (2021). *'Fit for 55': Delivering the EU's 2030 climate target on the way to climate neutrality*. Final communication from the Commission to the European Parliament, the Council, the European Economic and Social Committee, and the Committee of the Regions. https://eur-lex.europa.eu/legal (Accessed December 15, 2023).

Harring, N. & Jagers, S. C. (2017). Why do people accept environmental policies? The prospects of higher education and changes in norms, beliefs and policy preferences. *Environmental Education Research*, *24*(6), 791–806. http://dx.doi.org/10.1080/13504622.2017.1343281

Khanam, T., Rahman, A., Xu, X., Mola-Yudego, B., Moula, M. E., & Pelkonen, P. (2022). Assessing the awareness and willingness of European experts to reduce their carbon footprint in everyday consumption. *Environmental Impact Assessment Review, 94*, 106889.

Li, L., Awada, T., Shi, Y., Jin, V. L., & Kaiser, M. (2025). Global greenhouse gas emissions from agriculture: Pathways to sustainable reductions. *Global Change Biology, 31*(1), e70015.

Mielcarek-Bocheńska, P., & Rzeźnik, W. (2021). Greenhouse gas emissions from agriculture in EU countries - State and perspectives. *Atmosphere, 12*(11), 1396.

Mónus, F. (2022). Environmental education policy of schools and socioeconomic background affect environmental attitudes and pro-environmental behavior of secondary school students. *Environmental Education Research*, *28*(2), 169–196. https://doi.org/10.1080/13504622.2021.2023106

Panchasara, H., Samrat, N. H., & Islam, N. (2021). Greenhouse gas emissions trends and mitigation measures in the Australian agriculture sector: A review. *Agriculture, 11*(2), 85.

Radu, N., Chirvase, A. A., Babeanu, Begea, M. (2019). Entrepreneurship in the field of life sciences: the personal skills needed to start an innovative SME. *Scientific Papers Series Management Economic Engineering in Agriculture and Rural Development*, *19*(2), 375-379.

Radu, N., Chirvase, A. A., Babeanu, Begea, M. (2020). Studies regarding personal skills needed in entrepreneurship- case study in France, Lithuania and Romania. *Scientific Papers Series Management Economic Engineering in Agriculture and Rural Development*, *20*(2), 403-408.

Smith, P., Haberl, H., Popp, A., Erb, K.-H., Lauk, C., Harper, R. J., ... & Rose, S. K. (2013). How much land-based greenhouse gas mitigation can be achieved without compromising food security and environmental goals? *Global Change Biology, 19*(8), 2285–2302.

Scientific Papers. Series E. Land Reclamation, Earth Observation & Surveying, Environmental Engineering. Vol. XIV, 2025
Print ISSN 2285-6064, CD-ROM ISSN 2285-6072, Online ISSN 2393-5138, ISSN-L 2285-6064

CHANGES OF PLANKTON COMPOSITION IN WINTER CONDITIONS IN AN URBAN LAKE

Larisa FLORESCU[1], Mirela MOLDOVEANU[1], Ioana ENACHE[2], Rodica CATANA[1]

[1]Institute of Biology Bucharest of Romanian Academy,
296 Splaiul Independentei, District 6, 060031, Bucharest, Romania
[2]University of Bucharest, 91-95 Splaiul Independenței, District 5, 050095, Bucharest, Romania

Corresponding author email: mirela.moldoveanu@ibiol.ro

Abstract

The winter season, characterized by unfavorable conditions for aquatic biota, determined by low temperatures, instigates a series of ecological shifts that intricately shape the phytoplankton and zooplankton communities' structure and function. Our study in Văcărești Lake focuses on the effect of the winter season on plankton communities, highlighting structural and functional changes in these communities. During the winter, environmental parameters significantly changed indicating organic matter decomposition and eutrophic conditions. The winter conditions functioned as ecological stressors on plankton communities. Phytoplankton responded by changing composition, with green algae and diatoms becoming prominent as cyanobacteria declined. Zooplankton, especially Rotifera and Cladocera, showed increased diversity and abundance, while Ciliata and Copepoda decreased. The RDA analysis highlighted phytoplankton's responsiveness to TDS, conductivity, turbidity, pH, and zooplankton's correlation with oxygen and temperature. The Diversity t-test indicated significant changes in both phytoplankton and zooplankton communities in terms of diversity. Zooplankton diversity was higher than phytoplankton, with moderate species composition changes, reflecting cold-tolerant species development and the ecosystem's resilience and adaptability to winter conditions.

Key words: *abundance, cold-season changes, phytoplankton, zooplankton structure, Văcărești Natural Park.*

INTRODUCTION

Winter poses numerous challenges to the biotic components of aquatic ecosystems, particularly the so structurally diverse communities of the zooplankton. The cold season starting with November heralds a multitude of physicochemical transformations determined by temperature and light that shape the dynamics of these vital processes (Molles, 2016). Water temperature undergoes a significant drop, significantly impacting the metabolic activities of plankton. In tandem with temperature, light emerges as another critical factor, its diminishing intensity intricately linked to the seasonal changes in aquatic ecosystems. The reduced light availability during winter precipitates a decline in phytoplankton production, the primary food source for many zooplankton species. The interaction between temperature and light dynamics makes the biotic response of phytoplankton and zooplankton to winter conditions crucial. This scarcity of food resources can influence the composition and abundance of zooplankton communities, as some species may exhibit adaptations to low food availability. In contrast, others may struggle to find sufficient food. Furthermore, changes in winter conditions in temperate zones have significantly impacted the ice and snow regime. During winter, chlorophyll-a content can reach an average of only 43% of its summer level (Negrete-Garcia et al., 2024). Grazing by zooplankton is responsible for phytoplankton losses and changes in community composition. Due to ongoing climate change, warmer winters may also influence the development of overwintering phytoplankton (Hrycik & Stockwell, 2021). Fott et al., 2020 consider that light regime and water temperature significantly positively influence chlorophyll-a concentrations in the cold season. Instead, zooplankton tend to slow down, influencing their growth rates, feeding behaviors, and overall life cycles. Within the diverse structure of zooplankton, many species show pronounced sensitivity to temperature fluctuations, prompting the evolution of adaptive strategies for survival during winter. These strategies manifest through various forms of resistance, allowing certain zooplankton species to endure harsh conditions. According to Litchman et al., 2013,

zooplankton exhibits a high diversity of traits and ecological strategies that impact other trophic levels and the cycles of matter and energy.

Understanding these seasonal shifts provides invaluable insights into the adaptive mechanisms, resilience, and ecological aspects of phytoplankton and zooplankton communities, underscoring the significance of comprehending their responses to the challenges posed by the cold season (Wollschläger et al., 2021; Bramm et al., 2009; Davis & Baird, 2022).

In the seasonal dynamics, the winter period is not only an inactive period of rest but also defines the plankton dynamics of the following year. In temperate eutrophic lakes, there are usually two or more peaks of zooplankton activity during the warm season, typically following the spring and summer/autumn phytoplankton blooms.

Warming climate conditions have led to biodiversity loss, the proliferation of opportunistic and resistant species, and the emergence of invasive species, negatively impacting ecosystems. Ecosystems in temperate zones are particularly affected due to complex seasonal regulation processes and a diminished capacity for resilience (Lenard et al., 2019). However, mild winter temperatures and nutrient availability influence phytoplankton development, demonstrating their temperature sensitivity, which can increase productivity. In urban areas, lakes are exposed to heightened nutrient loading and temperatures, leading to severe phytoplankton blooms. Understanding the role of urbanization and its interaction with climate change in producing these blooms is crucial to preventing negative effects on urban water sources (Li et al., 2023). Consequently, zooplankton peak numbers may vary seasonally and annually, reflecting fluctuations in environmental conditions and food web interactions (Sutton et al., 2021; Jensen, 2019). Our study aimed to identify changes in the structural composition of phyto- and zooplankton, highlighting key species such as *Moina* spp. and *Daphnia* spp., and their potential cascading effects on the overall aquatic food webs. It is known that the winter period directly influences the structure and diversity at the plankton level. Due to the low temperatures, the phytoplankton undergoes significant changes in species composition and density. The changes at this level together with other environmental factors, define the traits of the zooplankton consumers. Our study hypothesizes that winter is a period of decline in plankton communities, characterized by a poor representation of species, even in urban areas, where temperatures are slightly higher as a result of heat islands. We assume that in November, when the cold season starts, we will encounter a higher diversity, with species that have accumulated during the year, while in February both the density and richness of species are much more reduced. This was a pilot study testing the structural changes of the phyto- and zooplankton evaluated at the end of the growing season, late autumn, followed by an evaluation during the cold period of winter and the beginning of the next growing season.

In this aim, we proposed the following (1) to identify the changes in the water physicochemical parameters throughout the cold period, (2) to describe the structure and diversity of phytoplankton and zooplankton communities, (3) to establish the relationships between phyto- and zooplankton and environmental variables and (4) to identify which factors defined the structure of these communities.

MATERIALS AND METHODS

Sample Collection and Laboratory Analyses

The Văcărești Natural Park has its origins in an unfinished hydrological project, initially conceived as a component of the development of the Dâmbovița River. Before 1989, Ceaușescu planned to turn the area into a recreational place with a lake and sports facilities. The project failed, due to the risk of flooding and the lake basin remained unused thus the area became known as "Văcărești Wetlands". Over the previous 20 years, the abandoned area has been transformed into a unique lacustrine ecosystem that appeared in the former Văcărești Pit. The area has become a habitat for various species of birds, reptiles, and mammals. The place attracted the attention of NGOs and the Ministry of the Environment so, in 2016, "Văcărești Wetlands " was declared a Natural Park. The Văcărești Natural Park became Romania's first urban natural park and the only protected area in Bucharest. This initiative has been supported and recognized by international environmental organizations, considering the project as an outstanding

example of cohabitation between urban and wild nature (Atanasiu et al., 2017; Manea et al., 2013). Văcărești Natural Park (Figure 1) has an area of approximately 200 hectares and is located at an altitude of 60-80 meters (Merciu et al., 2017).



Figure 1. The Văcărești Park map with the sampling points (Google Earth app, 2022)

The park is fed primarily by springs from the Dâmbovița River, which support its aquatic ecosystem. This includes lakes, marshes, extensive reed beds, and areas with rich vegetation such as meadows, willows, and various aquatic plants (Danta, 1993).

Bucharest's climate is characterized by hot summers, cold winters, moderate precipitation, and occasional cold snaps. Văcărești experiences typical urban climate effects, including the urban heat island phenomenon. Under these conditions, the wetlands play a crucial role in moderating temperatures, maintaining local humidity, and creating a more favorable microclimate, despite variability caused by urbanization and seasonal changes. These meteorological factors can influence species distribution within the wetland and affect water quality (Legutko-Kobus et al., 2023).

The park is surrounded by residential areas, commercial zones, and busy roads. However, due to the remnants of old communist-era constructions, the wetland remains relatively isolated. Despite its proximity to urban development, Văcărești has become a wildlife sanctuary, supporting over 100 bird species as well as various mammals and reptiles (Manea et al., 2016).

The area is exposed to urban runoff, including contaminants from roads and waste from surrounding areas, which poses a challenge to the park's water quality, noise, and light pollution.

The sampling took place in November 2021 and February 2022 in six stations to cover a representative proportion of the lake in the evaluation of zooplankton communities (Table 1).

Table 1. The GPS coordinates of the sampling points

Sampling points	Latitude	Longitude
S1	44°24'7.82"N	26° 8'18.26"E
S2	44°24'4.19"N	26° 8'20.58"E
S3	44°24'6.48"N	26° 8'13.76"E
S4	44°24'9.99"N	26° 8'13.09"E
S5	44°24'8.38"N	26° 8'11.19"E
S6	4°24'6.58"N	26° 8'9.71"E

Environmental data

The measurements of the water physicochemical factors were done using a Hanna Instruments HI 9829 multiparameter. The device is equipped with sensors for temperature - °C, pH, ORP (Oxidation-reduction potential) - mV, % DO (Dissolved Oxygen Saturation); DO (Dissolved Oxygen) - mg/L; Conductivity - µS/cm; TDS (Total Dissolved Solids) - mg/L, Salinity, and turbidity - NTU. In addition, the Secchi disc was used for Depth and Transparency (m) assessment.

Phytoplankton sampling

The phytoplankton sampling was done on the water column using a Schindler-Patalas device (4 L) and mixed into a 10 L bucket. In 500 mL plastic bottles samples were fixed with formaldehyde (4%) and stored for a period of sedimentation. The taxonomical identification was done using a Zeiss inverted microscope for *Cyanobacteria* (Komárek & Anagnostidis, 1998; Komárek & Anagnostidis, 2005*), Chlorophyceae* (Ettl & Gärtner, 1983; Ettl & Gärtner, 1988), *Bacillariophyceae* (Krammer & Lange-Bertalot, 1986; Krammer & Lange-Bertalot, 1988; Krammer & Lange-Bertalot, 1991a; Krammer & Lange-Bertalot, 1991b) *Dinophyceae* (Huber-Pestalozzi, 1950), and *Xanthophyceae* (Gottfried, 1976) with an additional check on https://www.algaebase.org 2019). Cell densities (cells/L) were determined at the species or genus level using the Utermöhl method (Edler & Elbrächter, 2010). Three aliquots were analyzed microscopically for each sample.

Zooplankton sampling

The samples were taken on a water column, using a Patalas - Schindler plankton trap (4 L) device, and filtered through a standard plankton net (mesh size 50 μm Ø). The filtered samples were collected in 10 ml bottles, preserved in 4% formalin, kept for 2 weeks for sedimentation, and later filtered for the second time to reduce the excess water. Using a Kolkwitz counting chamber, three aliquots (1 mL) from the final sample were analyzed using a Zeiss inverted microscope for taxonomic determination and counting of individuals for abundance as individuals per liter (ind. L^{-1}) estimation according to the Edmonson & Winberg (1971) method. The taxonomic determinations were made using the following taxonomic keys *Ciliata* (Foissner et al., 1991; Foissner et al., 1992; Foissner et al. 1994; Foissner et al., 1995), *Testate Amoeba* or *Testacea* (Bartoš, 1954; Grospietsch, 1972), *Rotifera* (Rudescu, 1960), *Cladocera* (Negrea, 1983). *Copepoda* were identified as the main groups. The juvenile stages were counted together and the adult individuals were classified into *Cyclopida* g. sp.; *Harpacticoida* g. sp. and *Calanoida* g. sp. For both, phytoplankton and zooplankton in the microscopic analyses, three sample aliquots were performed.

Statistical analysis

Descriptive statistics were used to analyze and summarize the data. For this purpose, Minimum (Min), Maximum (Max) Mean, and Standard deviation (n-1) were selected.

The ***IndVal*** measures the strength of the association of a species with period environment conditions, based on abundance and frequency depending on the site and period.

The results include: ***IndVal %*** - is the percentage representation of the IndVal, revealing the relative importance of the species in the ecosystem context. The mathematical formula:

$$IndVal\ \% = \frac{\text{INDVALij}}{\sum \text{INDVAL}} \text{ x } 100$$

IndVal is calculated from the following formula:

$$INDVAL_{ij} = 100 A_{ij} B_{ij}$$

The indicator value of species *i* in group *j*, values range from 0 to 100 (percentage). ***p -*** indicates the statistical significance of the association. A value under $p < 0.05$ suggests a strong significant association, while a higher value indicates no significance. The p-value (statistical significance) of the indicator values is assessed through 9999 permutations of sites across groups.

Specificity (A) - refers to how exclusively a species is found in a particular habitat. The mathematical formula:

$$A_{ij} = N_{ij}/N$$

where:

- Nij - is the mean of individuals of species *i* across sites in group *j*;
- Ni is the sum of the mean numbers of individuals of species *i* over all groups.

A value of 1.00 indicates that the species is only found in that habitat, while lower values indicate broader habitat use.

Fidelity (B) represents the reliability of the species as an indicator of the habitat.

The mathematical formula:

$$B_{ij} = Nsites_i/Nsites_j$$

where:

- $Nsites_{ij}$ - is the number of sites in group j where species *i* is present;
- $Nsites_j$ is the total number of sites in group j. A value of 1.00 indicates the species is consistently found in that habitat when it is present.

The analysis was performed using Past 4.13 software (Hammer & Harper, 2024).

Diversity indices, such as Species richness (SR), Shannon index (H), Evenness (E), and Simpson index (D) are commonly applied measures for biodiversity and are crucial to quantifying the variety and distribution of species within a community. ***Species richness*** refers to the total number of different taxa (species).

Simpson's Dominance Index quantifies how dominant certain species are within a community. A higher value indicates lower diversity and one or a few species dominate the population.

$$D = \sum_i \left(\frac{ni}{n}\right)^2$$

where *ni* is the number of individuals of taxon *i*. The index ranges from 0 (infinite diversity) to 1 (no diversity).

The ***Shannon Index (H)*** measures the uncertainty in predicting the species identity of

a randomly chosen individual from a community. It takes into account both the number of species and their relative abundances:

$$H = -\sum_i \frac{ni}{n} \ln \frac{ni}{n}$$

where:

- ni is the number of individuals of taxon I;
- n is the sum of all ni.

Buzas and Gibson's Evenness Index (E) is a measure of species' evenness derived from the Shannon diversity index. It quantifies how evenly individuals are distributed among the species in a community, providing insights into biodiversity beyond mere species richness.

$$E = \frac{e^H}{S}$$

where:

- e - is Euler's number, approximately equal to 2.71;
- H - is the Shannon index;
- S is the total number of taxa.

The evenness index ranges from 0 to 1, where 0 indicates that all individuals belong to one species (complete dominance) and 1 indicates that all species have equal abundance (maximum evenness).

The ***Diversity t-test (Hutcheson's t-test)*** is based on an adapted variant of the classic t-test, allowing for the comparison of Shannon and Simpson indices values between two samples. This test provides an assessment of the statistical significance of observed differences. The formula used in Hutcheson's t-test is similar to that of the standard t-test but includes adjustments for the variance of the Shannon and Simpson indices (Hammer & Harper, 2006).

Redundancy Analysis (RDA) is a multivariate statistical technique used to evaluate the relationships between plankton groups and physicochemical parameters. Before analysis, data were log-transformed to meet the assumptions of the method. The graphical output of RDA includes quantitative environmental variables represented by lines (vectors) and plankton group variables represented by squares. The first two axes, F1 and F2, explain the data's total variation, providing a robust representation of the explanatory variables. The environmental predictors, shown by red arrows, indicate the magnitude and direction of the parameters. The positioning of the squares (representing plankton groups) and the environmental predictors along the different axes illustrate the strength and direction of the relationships between the variables. This visual representation enables the identification of key environmental factors influencing the distribution and composition of plankton communities. The length and orientation of the arrows in the plot signify the magnitude and direction of the environmental gradients, aiding in interpreting complex ecological interactions (Legendre & Legendre, 2012). XLSTAT pro was used for statistical analysis (XLSTAT pro. 2013; PAST software (Hammer et al., 2001).

RESULTS AND DISCUSSIONS

Abiotic parameters

Environmental parameters showed increasing trends from November to February, except for temperature, oxygen saturation, and ORP. During this period, depth ranged from 1 to 2.35 meters, transparency from 1 to 2 meters, and temperature from 6 to 10.44°C. A redox potential (ORP) variation was also observed, indicating unfavorable ecological conditions. In November, the ORP was positive but low (29.2 mV - 54.3 mV), reflecting organic matter decomposition processes, eutrophic conditions, and high oxygen consumption. By February, the decrease in oxygen content was associated with negative ORP values (Table 2), suggesting ongoing decomposition processes through reducing mechanisms. These conditions can negatively affect both biota and natural nutrient cycling processes.

Table 2. Descriptive statistics, mean, variance, and standard deviation of the measured water environmental parameters

Statistic	Min	Max	Mean	Standard deviation (n-1)
	November			
Depth (m)	1.00	2.00	1.48	0.50
Transparency (m)	1.00	1.70	1.21	0.31
Turbidity (FNU)	0.71	1.93	1.26	0.48
Temperature (°C)	9.45	10.44	9.85	0.36
pH	7.45	9.54	8.37	0.71
O_2 sat %	78.70	110.80	95.18	12.99

Statistic	Min	Max	Mean	Standard deviation (n-1)
DO_2 (ppm)	8.82	12.38	10.60	1.48
Cond. (µS cm^{-1})	797.00	823.00	815.83	9.85
TDS (ppm)	398.00	412.00	407.83	5.23
Salinity	0.39	0.41	0.41	0.01
ORP	29.20	54.30	38.78	9.73
	February			
Depth (m)	1.55	2.35	2.03	0.27
Transparency (m)	1.50	2.00	1.77	0.21
Turbidity (FNU)	1.38	2.38	1.80	0.38
Temperature (°C)	6.00	6.38	6.26	0.13
pH	8.58	9.45	9.21	0.32
O_2 sat %	59.10	122.00	80.52	25.01
DO_2 (ppm)	7.06	15.63	11.01	3.63
Cond. (µS cm^{-1})	864.00	891.00	879.83	9.28
TDS (ppm)	439.00	446.00	441.83	2.64
Salinity	0.43	0.44	0.44	0.01
ORP	-12.40	49.30	20.53	26.21

Phytoplankton community structure

A total of 43 phytoplankton species were recorded, including *Cyanobacteria* (2 species), *Dinophyceae* (1 species), *Xanthophyceae* (1 species), *Bacillariophyceae* (29 species), and *Chlorophyceae* (10 species). While the number of species remained constant during the winter (Table 2), their taxonomic composition and abundance changed. For instance, 2 species of *Cyanobacteria* were present in November (*Chroococcus turgidus* Nägeli, 1849, and *Gomphosphaeria aponina* Kützing, 1836) and no longer found in February. By February, new green algae and diatom species appeared alongside *Dinophyceae* (*Peridinium* sp.) and *Xanthophyceae* (*Tribonema affine* (Kütz.) G.S.West, 1904). The variability in the taxonomic composition and abundance of species like *Chroococcus turgidus* and *Gomphosphaeria aponina* during winter is influenced by several factors. Winter temperatures can reduce the growth of *Cyanobacteria*, which prefer warmer conditions. Reduced daylight limits photosynthesis, impacting phytoplankton. Seasonal nutrient changes and cooler temperatures can favor the growth of species like *Peridinium* and *Tribonema affine*, which appear in February.

In November, the *Cyanobacteria species* reached the algal bloom (1.04×10^7 cells L^{-1}) threshold, followed by diatoms ($9.67Ex10^5$ cells L^{-1}). During the winter, *Bacillariophyceae* and *Chlorophyceae* dominated in species richness and abundance, showing significant increases in density until February (Table 3).

Table 3. The species richness and density of the phytoplankton groups

	Species richness		Density (cells L^{-1})	
	Nov.	Feb.	Nov.	Feb.
Total phytoplankton	27.0	27.0	$1.15 x10^7$	$6.97 x10^6$
Cyanobacteria	2.0	0.0	$1.04 x10^7$	0
Dinophyceae	0.0	1.0	0	$9.10 x10^3$
Xanthophyceae	0.0	1.0	0	$2.19 x10^6$
Bacillariophyceae	19.0	19.0	$9.67 x10^5$	$3.85 x10^6$
Chlorophyceae	6.0	6.0	$1.19 x10^5$	$9.20 x10^5$

Based on IndVal analysis, February generally exhibits a stronger association and higher indicator values for species, suggesting distinct ecological conditions compared to November. In November, *Epithemia zebra* and *Cocconeis placentula* had high IndVal values (72.97 and 70.23, respectively), indicating the species were strongly associated with the period ecological conditions.

In February, a higher number of species presented elevated IndVal values, most of them diatoms thus highlighting the capacity to exhibit several specific adaptations that enable them to thrive in cold periods (Table 4). These adaptations are crucial for their survival and competitive success during winter months when temperatures drop and light conditions change.

Table 4. Significant results of Indicator Species analysis (IndVal) of phytoplankton assemblage

	Group	IndVal%	p
November			
Epithemia zebra (Ehr.) Kütz.	*Bacillariophyceae*	72.97	0.03
Cocconeis placentula Ehrenberg, 1838	*Bacillariophyceae*	70.23	0.04
Gomphosphaeria aponina Kützing 1836	*Cyanobacteria*	66.67	0.03
February			
Synedra ulna (Nitzsch.) Ehrenberg, 1832	*Bacillariophyceae*	100.00	0.00
Gomphonema ventricosum W.Gregory, 1856	*Bacillariophyceae*	96.67	0.00
Fragillaria intermedia (Grunow) Grunow, 1881	*Bacillariophyceae*	89.92	0.00
Synedra affinis Kützing, 1844	*Bacillariophyceae*	83.33	0.01
Mougeotia sp.	*Chlorophyceae*	76.34	0.00
Gomphonema constrictum Ehrenberg, 1832	*Bacillariophyceae*	66.67	0.03
Navicula pupula Kützing, 1844	*Bacillariophyceae*	66.67	0.03
Synedra acus Kützing, 1844	*Bacillariophyceae*	66.67	0.03
Neidium dubium (Ehr.) Cleve, 1894	*Bacillariophyceae*	66.67	0.03
Navicula longirostris Hustedt, 1930	*Bacillariophyceae*	66.67	0.03

Zooplankton community structure

The zooplankton assemblage consisted of 40 taxa, with *Rotifera* (20 species) and *Cladocera* (14 species) being the most representative, both showing an increase from November to February (Table 5).

Ciliata (1 species) and *Testacea* (2 species) were less representative, while *Copepoda* (comprising three groups: *Calanoida*, *Harpacticoida*, and *Cyclopoida*) was present with a high proportion of juvenile stages. In terms of abundance, the zooplankton in November was characterized by few species with high abundance. Total Zooplankton species richness and densities indicate an important increase from November (521.32 ind. L^{-1}) to February (1025.65 ind. L^{-1}), reflecting cold-tolerant species development. *Ciliata* and *Testacea* showed low densities, with *Ciliata* absent in February and *Testacea* exhibited a significant increase during the winter (from 0.10 to 9.97 ind. L^{-1}). *Rotifera* was the dominant group, with an important growth from November (207.20 ind. L^{-1}) to February (764.20 ind. L^{-1}), indicating favorable conditions for their proliferation during this period. *Cladocera* densities increased slightly from November (64.35 ind. L^{-1}) to February (89.17 ind. L^{-1}), while *Copepoda* densities saw a decrease from November (249.43 ind. L^{-1}) to February (162.31 ind. L^{-1}), suggesting varying ecological responses among different taxa (Table 5).

Table 5. Zooplankton composition in Văcărești Natural Park Lake

	Nov.	Feb.	Nov.	Feb.
	Species richness		Density (ind. L^{-1})	
Total zooplankton	23.0	32.0	521.32	1025.65
Ciliata	1.0	0.0	0.25	0.00
Testacea	1.0	2.0	0.10	9.97
Rotifera	10.0	18.0	207.20	764.20
Cladocera	8.0	11.0	64.35	89.17
Copepoda	3.0	1.0	249.43	162.31

Among the species that formed zooplankton assemblages, few exhibited significant specificity ($p < 0.05$) for a particular study period. In November, the highest IndVal index percentages (Table 6) were observed for the cladocerans *Daphnia* sp. and *Moina* sp., as well as the *Calanoida* copepod group. In contrast, only rotifers were found in February. During this month, environmental conditions favored the proliferation of *Synchaeta oblonga* Ehrenberg, 1832, which attained the highest IndVal index percentage (98.90%), followed by *Ascomorpha* sp. (66.67%).

Plankton diversity

The Diversity t-test highlights significant changes in both the phytoplankton and zooplankton communities in terms of diversity during the winter. Of both indices (Shannon and Simpson), t-values and p-values indicate significant differences between the two periods (Table 7).

Table 6. Significant results of Indicator Species analysis (IndVal) of zooplankton assemblage

	Group	IndVal%	p(raw)
November			
Moina spp.	*Cladocera*	62.09	0.03
Calanoida	*Copepoda*	91.18	0.00
Daphnia spp.	*Cladocera*	100.00	0.00
February			
Synchaeta oblonga Ehrenberg, 1832	*Rotifera*	98.90	0.00
Ascomorpha sp.	*Rotifera*	66.67	0.03

Table 7. Diversity t-test ($p < 0.05$) for phytoplankton and zooplankton communities during the study period

	Phytoplankton		Zooplankton	
	Nov.	Feb.	Nov.	Feb.
Shannon index	0.56	1.80	1.69	2.17
Variance	1.81×10^{-7}		0.0023	
t	-1845.30		-7.83	
df	1.53×10^{7}		1142.50	
p	0.00	2.71×10^{-7}	0.00	0.0014
Simpson index	0.82	0.27	0.25	0.18
Variance	2.40×10^{-8}		0.0001	
t	2.83×10^{3}		5.72	
df	1.85×10^{7}		956.32	5.08×10^{-5}
p	0.00	1.35×10^{-8}	0.00	

The phytoplankton Shannon Index showed a significant increase from November (0.56) to February (1.80), indicating a rise in diversity. Conversely, the Simpson Index decreased from November (0.82) to February (0.27), further supporting the observed increase in diversity. On the other hand, the zooplankton showed a higher diversity, compared with phytoplankton, with moderate changes regarding the species composition.

The results of the Diversity t-test indicate that there have been changes in the structure and diversity of the two planktonic components. However, to obtain a complete overview, it is necessary to identify the response of the

communities that form them. Diversity indices, such as Shannon - H; Evenness - E, and Dominance - D are interconnected and provide a robust framework for assessing the health of aquatic ecosystems. These indices not only reflect the state of biological communities but also indicate their trends. Plankton diversity was assessed based on component groups, characterized by various traits related to species richness and abundance.

Shannon index showed that the most diverse were *Bacillariophyceae* (H = 2.26) and *Chlorophyceae* (H = 0.94), while *Cyanobacteria* showed very low diversity (H = 0.01). Until February, all mentioned groups showed a decline (Table 8).

Table 8. Diversity indices Shannon - H; Evenness – E and Dominance – D of phytoplankton and zooplankton groups

	November			February		
	H	E	D	H	E	D
Phytoplankton						
Bacillariophyceae	2.26	0.50	0.15	1.27	0.19	0.54
Chlorophyceae	1.17	0.54	0.44	0.97	0.44	0.43
Cyanobacteria	0.01	0.51	1.00	NA	NA	NA
Dinophyceae	NA	NA	NA	ND	ND	ND
Xanthophyceae	NA	NA	NA	ND	ND	ND
Zooplankton						
Ciliata	ND	ND	ND	NA	NA	NA
Testacea	0.00	1.00	1.00	0.55	0.87	0.64
Rotifera	0.36	0.14	0.88	1.57	0.27	0.29
Cladocera	0.94	0.32	0.61	1.11	0.28	0.44
Copepoda	0.35	0.48	0.83			

NA - Not applicable - no species found; ND - not determined – insufficient data to perform the analysis.

At the zooplankton level, the taxonomic groups were characterized by different traits in diversity. *Protozoa* were poorly represented. Notably, *Testacea* shows an interesting trend where its Shannon value increases from near zero to moderate levels (from H = 0 to H = 0.55), while its dominance decreases significantly from D = 1 to D = 0.64, indicating an increase in diversity. Instead, *Rotifera* demonstrates a development highlighted by the increase of the Shannon Index from November (H = 0.36) to February (H = 1.57), with a corresponding decrease in dominance (from D = 0.88 to D = 0.29). *Cladocera* shows slight improvement in both months but remains relatively low in Evenness and high in Dominance. *Copepoda* indicates a decline during the period (Table 8). The Evenness index varies significantly across categories and periods.

Species groups with low diversity showed high evenness values (Table 8), whereas groups with high Shannon values exhibited low evenness values. This indicates that communities with higher diversity were dominated by one or a few species.

The response of plankton communities to environmental conditions

The environmental conditions during the two periods functioned as ecological stressors on plankton communities. The relationships between environmental variables and plankton communities were established through RDA analysis.

Axes F1 (56.67%) and F2 (21.97%) together explain 78.63% of the total variation in the data. In Redundancy Analysis (RDA), F1 (56.67%) and F2 (21.97%) represent the first two *constrained canonical axes* that capture most of the variation in the biological response variables (species communities) explained by the environmental predictors in the model. Phytoplankton groups, including *Cyanobacteria*, *Chlorophyceae*, *Bacillariophyceae*, and *Xanthophyceae*, exhibited a dispersed distribution in the plot, contrasting with the more cohesive grouping of zooplankton (such as *Cladocera*, *Copepoda*, and *Rotifera*). This difference in dispersion may suggest that phytoplankton and zooplankton employ distinct ecological strategies in response to environmental pressures.

Phytoplankton were more responsive to variations in parameters such as TDS, conductivity, turbidity, and pH, reflecting nutrient availability. Zooplankton (*Cladocera*, *Copepoda*, and *Ciliata*) were closely correlated with oxygen and temperature conditions, indicating a preference for well-oxygenated waters and higher temperatures.

In the RDA biplot, the distribution of physico-chemical parameters highlights an inverse relationship between turbidity and dissolved oxygen (DO%), suggesting that higher turbidity coincides with lower oxygen availability. Conversely, these conditions were unfavorable for *Ciliata*, *Cladocera*, and *Copepoda*. Increases in conductivity, turbidity, and TDS were tolerated by diatoms, green algae, *Dinophyceae* (dino-flagellates), and *Xanthophyceae* (yellow-green

algae). The association of *Rotifera* and *Testacea* (testate amoebae) with these parameters reflects the availability of food resources (phytoplankton and detritus) and a negative response to cyanobacterial blooms. Organisms such as *Cladocera* and *Copepoda* could indicate well-oxygenated and good-quality water, while the presence of *Cyanobacteria* may indicate water quality degradation.

Environmental controlling factors of plankton

Winter conditions significantly affect phytoplankton and zooplankton communities. Seasonal changes, driven by temperature, light, and nutrient fluctuations, also impact water quality parameters. The evaluated physicochemical parameters (Table 2) indicated active organic matter decomposition. Temperature declines during winter significantly alter environmental conditions, affecting biotic components through interconnected chemical processes. In this period, correlations of TDS, conductivity, turbidity, transparency, and depth with plankton reflected nutrient access for primary producers.

Simultaneously, under these conditions, the zooplanktonic components that demonstrated tolerance, such as rotifers and testate amoebae, were observed (Figure 2). On the other hand, the decrease in oxygen saturation showed negative effects on both phytoplankton and zooplankton communities.

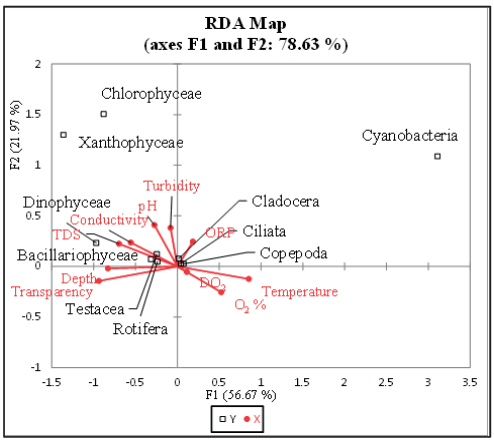


Figure 2. Redundancy analysis (RDA) for the relationship among the phytoplankton and zooplankton groups' abundance and environmental variables in Văcărești Lake

Plankton diversity

The dynamics of plankton communities can exhibit distinct patterns throughout the seasons, often characterized by shifts in species composition and abundance. Previous studies in the Văcărești Natural Park, during the growing warm period, have reported the presence of 80 species in phytoplankton and 89 species in zooplankton structure. Shannon's diversity index for phytoplankton was 1.78 and for zooplankton - 3.48 (Florescu et al., 2022). Thus, our results reveal a decline in diversity; species richness, and abundance of planktonic communities (Table 3; Table 5; Table 7; Table 8) during the winter reflecting the different conditions compared with the vegetation period.

Other studies confirm the critical role of these factors during colder months with a negative impact on both phytoplankton and zooplankton communities, leading to reduced biodiversity and altered community structures (Dokulil & Herzig, 2009). Contrary to expected trends, certain species within the planktonic assemblage exhibited tolerance to winter conditions. As a result, with the shift in community composition during the winter, an increase in diversity was observed (Table 7). The increasing species diversity can be due to the reduction in competition from less tolerant species may allow more resilient species to thrive (Geng et al., 2022).

In urban environments like Văcăresti, anthropogenic pressures have led to eutrophication and algal blooms. Previous studies emphasized that the phytoplankton in Văcăresti Natural Park exhibited seasonal variations with eutrophic and hiper-eutrophic conditions, especially during the autumn The composition of the algal blooms primarily consisted of *Cyanobacteria* and *Chlorophyceae* species (Florescu et al., 2022). The decline of *Cyanobacteria* during the winter period showcased the ecosystem's resilience. This decline could allow other groups like *Dinophyceae* and *Xanthophyceae* to develop, thus maintaining the overall biodiversity and functional stability of the ecosystem. Furthermore, the reduction in cyanobacterial blooms can prevent potential negative effects common during cyanobacteria-dominated periods. The shift in community composition

during the winter underscores the ecosystem's ability to self-regulate and support a diverse range of species, despite the adverse conditions.

The shift of the phytoplankton species during the cold season

Because phytoplankton assemblages play a crucial role in aquatic ecosystems, species that are strongly associated with particular conditions, make them indicators of an ecological state. Identifying key indicator species and their associations with environmental conditions offers a better understanding of ecological dynamics (Sidding et al., 2016). Given these practical applications, the general utility of IndVal for the analysis of phytoplankton assemblages becomes apparent and highly valuable. Conversely, the presence or absence of a particular single species of organism might be used to indicate chemical or physical attributes of the biotope. The data reflects the shifts in phytoplankton assemblages, with different species dominating. The distinction between November and February groups was determined by driven factors such as temperature, light availability, or nutrient dynamics (Figure 2). Thereby, *Epithemia zebra* (IndVal 72.97, p = 0.030), *Cocconeis placentula* preferred, nutrient-rich conditions typical of November (Table 4). The IndVal results of *Gomphosphaeria aponina* (IndVal 66.67, p = 0.03) confirm their role in cyanobacterial blooms from November (Table 4). Instead, species like *Synedra ulna* (IndVal 100.00, p = 0.00) and *Gomphonema ventricosum* (IndVal 96.67, p = 0.00), were highly indicative of February, pointing to the ecological relevance as strong indicators of winter-specific ecological conditions. The higher number of significant species in the IndVal analysis in February compared to November suggests a distinct phytoplankton community that defines the end of the winter.

The dominance of *Bacillariophyceae* in winter is a complex interplay of ecological adaptations, nutrient dynamics, and climatic influences. The group is generally well-adapted to lower temperatures, allowing the species to thrive even in the cold winter months. Diatoms' contribution to the plankton assemblage was also reflected in the highest species diversity in response to environmental changes during the winter season (Table 8). Their ability to develop in cold conditions allowed them to show their ecological importance as most numerous as significant IndVal species in both periods of investigation (Tabel 4) (Zepernick et al., 2024; Zang et al, 2018).

The *Chlorophyceae* was the second group after *Bacillariophyceae* present in phytoplankton during the entire study. Green algae are often abundant in urban lakes during the cold season. This abundance can be attributed to several factors, including reduced competition from other phytoplankton groups, lower grazing rates, and their ability to thrive (Tapolczai et al., 2015). Similar to other studies, the filamentous green algae *Mougeotia* spp. showed a proliferation. *Mougeotia* spp. tends to bloom earlier in the year when conditions are favorable, such as stable water columns and sufficient nutrient availability. The species is adapted to access the light by the water's surface utilizing its buoyant structures. Consequently, its growth can outcompete other phytoplankton species, leading to its dominance in urban lakes during the cold season and impacting the overall plankton community structure (Tapolczai et al., 2015).

During the study, the temperature dropped along with oxygen levels and redox potential (ORP) inhibited cyanobacteria, leading to their decline (Figure 2; Table 3). The cumulative effect of these factors significantly impacts cyanobacterial populations during the winter months, changing the overall composition and dynamics of the aquatic ecosystem. Most cyanobacterial taxa become less active or enter dormancy during winter, producing specialized cells (akinetes) that can survive adverse conditions until warmer temperatures return (Cottingham et al., 2021; Mânica & de Lima Isaac, 2023).

The shift of zooplankton species during the cold season

The changes in structure and composition in the main zooplankton groups depended on the adaptation strategies to the pressures of the winter conditions, their life cycle patterns, and physiological traits. Also, the quality and accessibility of food were important factors (Varpe, 2012). During the study, zooplankton abundance and species richness increased, indicating favorable conditions and

opportunities for some species development. Late warm autumn, without ice cover, has significant hints in aquatic organisms with dormant stages, as temperature stimulates production or release from the overwintering stages. The thermal responses of different species vary and are correlated with their seasonal abundance and distribution. Thus, periods of prolonged warm periods have different effects depending on the thermal tolerance limits and could influence survival and wintering strategies to the advantage of some species and the disadvantages of others (Chen & Folt, 1996).

The structural changes observed in the zooplankton communities in urban lakes during winter, leading to improved diversity, can be attributed to the prevalent environmental conditions. In February, the species richness of *Rotifera* and *Cladocera* showed an increase compared cu November. Thus, this period was opportune for other species to grow and distribute more evenly. This phenomenon underscores the intricate relationship between the ecological factors and zooplankton community dynamics. In addition, the capacity for rapid responses to environmental pressures makes the zooplankton a valuable indicator for evaluating the consequences of anthropogenic impacts (Umi et al., 2024). According to Haberman & Haldna (2017), water temperature in temperate shallow lakes has a significant impact on the abundance and composition of zooplankton. The communities have high dynamics of abundance, with a seasonal trend, such as, in spring with higher values than autumn. In addition, the approximately 10°C water temperature was considered "*a critical time window*" for generating a shift in species composition and abundance.

In the Văcărești Lake, the recorded abundance of rotifers during the winter can be explained by the resilience capacity of these communities to the pressure of unfavorable conditions. Rotifers are versatile organisms characterized by a great diversity of survival strategies, that include tolerance to eutrophication and pollutants, a fast reproductive cycle, and a change in feeding regime depending on the trophic resources. The responses of rotifers can be attributed to various factors (Figure 2) that highlight the species' food availability and cosmopolitan features. Rotifers have shown sensitivity to decreased oxygen saturation and ORP but tolerate fluctuations in water turbidity, pH, conductivity, or depth.

The cladoceran life history strategy is more complex and dependent on selective food availability. Also, cladocerans, are generally more sensitive to lower temperatures (Figure 2). Their metabolic rates slow down, and their reproductive rates decrease in colder conditions, leading to lower overall abundance (May & Wallace, 2019; Jensen, 2019). Also, most copepod species exhibit seasonal diapause in winter to avoid unfavorable conditions. This behavior can contribute to our study's observed decrease in adult copepod abundance. However, water temperature (ranged 6 and 10°C) maintained the presence of juvenile stages in Văcărești. Under these conditions, copepods may exhibit a range of responses to changes in temperature and food availability. Some species might adjust the timing of their life cycle to better align with the new environmental conditions.

The response of copepod assemblages to environmental changes was significantly influenced by temperature. Similar to *Cladocera*, copepods' life-history traits, such as reproductive strategy and generation length, are crucial for understanding how these microcrustaceans adjust their life cycles to align with environmental conditions, including temperature shifts. Research indicates that life-history traits, such as reproductive strategy and generation length, are critical for understanding how copepods adjust their life cycles in response to environmental conditions, including temperature shifts. Studies show that temperature variations and food availability interact to influence copepod life stages, which can contribute to observed changes in adult abundance in specific environments such as urban temperate shallow lakes. These factors differentially affect the naupliar and copepodite stages. For instance, nauplii showed reduced survival at elevated temperatures unless provided with phosphorus-replete food, emphasizing the importance of nutrient quality alongside temperature in shaping copepod life stage dynamics. In our study, after autumn phytoplankton growth, nauplii benefit longer from an abundant food source, favoring high

development. Thus, they were able to develop in the following stages as well. The interaction of these factors may explain the dynamics of the young stages of the copepods in Văcărești Lake. These findings suggest that climate-driven alterations in microplankton communities could affect copepod survival, particularly during periods of food scarcity, thus influencing overall abundance (Banas et al, 2016; Haberman & Haldna, 2017; Mathews et al, 2018; Halsband-Lenk et al., 2002; El-Sherbiny & Al-Aidaroos, 2021).

Regarding the decline of ciliata, low temperatures significantly decreased their growth rates, with effects on their abundance. The development of heterotrophic protists is affected by a decrease in temperature. Numerous studies have claimed that low temperatures have a strong negative impact on herbivorous protozoa; for example, ciliates prefer higher temperatures (20-25°C) (Rose & Caron, 2007). From this point of view, in our study, it was noted that the low representation of ciliates and testate amoeboids may indicate changes in environmental conditions or population dynamics in the ecosystem.

Thereby, the winter compositional patterns in zooplankton were driven by the fitness of rotifers and copepods juveniles to colder temperatures and their ability to exploit available food resources, whereas other communities as cladocerans, adult copepods, and protozoa were less able to cope with the harsh conditions.

The diversity increases were associated with a change in the key species in the ecosystem. Of the species that showed a significant response in abundance during winter (Table 6), some were advantaged by environmental conditions, such as *Ascomorpha* sp. (November – 0; February – 315.44 indv. L^{-1}); *Synchaeta oblonga* (November – 0.42; February – 37.48 indv. L^{-1}); while others such as *Calanoida* adults (November – 29.80; February– 2.88); *Daphnia* spp. (November – 50.25; February – 0.00 indv. L^{-1}) have gone through a decline. The zooplankton the taxonomic composition and diversity traits during the cold period in our study reflected mainly the known responses to a moderate winter. According to these conditions, Goździejewska & Kruk (2023) emphasized a weak interspecific relationship between rotifers, cladocera, and protozoa during moderate winters. Also, the authors mention that *Ascomorpha* spp., and *Synchaeta* spp. were the representatives that outlined the typical features of the period. Stressors such as temperature and phytoplankton availability significantly influence these dynamics. The interplay between the warming effects, nutrient supply, and grazing varies with seasonality and the ecosystems' long-term history. Concerning temperature and grazing, the decrease in temperature is due to modifications in species composition, and the predominance of smaller species (Goździejewska & Kruk, 2023). Also, the research by paleolimnological analyses based on sediment cores indicated a significant negative correlation between *Daphnia* abundance and winter temperature series (Nevalainen et al., 2013). The mild temperatures and the absence of ice on the surface of the lakes during the winter period would be advantageous for some species and allow them to increase.

In Lake Văcărești during winter, limited food sources shape zooplankton structure by quality and quantity. For copepods, size and abundance were linked, with juveniles driving population numbers and adults contributing to biomass despite lower abundance. As part of zooplankton communities, there are taxonomic groups like *Protozoa*, *Rotifera* and *Crustacea* with distinct features that, through their availability through biomass, can decisively influence the feeding behavior of higher consumers. The seasonal succession of the plankton community described by Sommer et al., 1986 as the PEG model, is found in numerous freshwater ecology studies, focused especially on the growth periods, and less on the winter season. Because winter for many species of zooplankton is a period of dormancy, the season was considered less important. Because of the interest in climate change, this period has gained crucial importance for the seasonal dynamics of plankton communities. Thus, is necessary to understand the dynamics of zooplankton under winter conditions (Jensen, 2019).

CONCLUSIONS

Winter conditions led to significant changes in environmental parameters, indicating organic matter decomposition and eutrophic conditions. The phytoplankton responded to the environmental changes: green algae and diatoms became more prominent, while cyanobacteria declined. Zooplankton responded with increased diversity and abundance of *Rotifera* and *Cladocera*, while *Ciliata* and *Copepoda* decreased. Phytoplankton showed responsiveness to TDS, conductivity, turbidity, and pH, while zooplankton correlated with oxygen and temperature. There were significant changes in diversity for both phytoplankton and zooplankton, with zooplankton showing higher diversity and moderate species composition changes. Winter conditions acted as ecological stressors, leading to structural and functional changes in plankton communities.

The development of cold-tolerant species and moderate species composition changes reflected the ecosystem's resilience and adaptability to winter conditions.

The urban lake environment appears to mitigate some of the harsh effects of winter, supporting higher abundance and species richness of zooplankton, while the phytoplankton assemblage showed a decline in abundance but with recovery effects after autumn algal blooms.

These findings underscore the importance of long-term monitoring and comparisons with other urban lakes to gain broader insights into urban aquatic ecosystems.

ACKNOWLEDGEMENTS

This research work was carried out with the support of Institute of Biology Bucharest, Romanian Academy, grant number RO1567-IBB02/2024 and RO1567-IBB08/2024. The authors thank Stela Sofa for the technical assistance received during the development of the study.

REFERENCES

Atanasiu, P., Comănescu, C.P., Nagodă, E., Lițescu, S., Negrean, G. (2017). Nature reclaiming its territory in urban areas. Case study: Văcărești Nature Park, Bucharest, Romania. *Acta Horti Bot Bucuresti, 44*, 71-99.

Bartoš, E. (1954). Rhizopoda Order Testacea, Publisher Slovak Academy of Sciences, Bratislava, Slovakia (in Slovak).

Banas, N.S., Møller, E.F., Nielsen, T.G., & Eisner, L.B. (2016). Copepod life strategy and population viability in response to prey timing and temperature: Testing a new model across latitude, time, and the size spectrum. *Frontiers in Marine Science*, *3*, 225.

Bramm, M.E., Lassen, M.K., Liboriussen, L., Richardson, K., Ventura, M., and Jeppesen, E. (2009). The role of light for fish–zooplankton–phytoplankton interactions during winter in shallow lakes–a climate change perspective. *Freshwater Biol*ogy, *54*(5), 1093-1109.

Chen, C.Y., Folt, C.L. (1996). Consequences of fall warming for zooplankton overwintering success. *Limnology and Oceanography*, *41*(5), 1077-1086.

Cottingham, K.L., Weathers, K.C., Holly, A., Ewing, M.L., Greer, C., Carey, C. (2021). Predicting the effects of climate change on freshwater cyanobacterial blooms requires consideration of the complete cyanobacterial life cycle. *Journal of Plankton Research*, *43*(1), 10–19.

Danta, D. (1993). Ceausescu's Bucharest. Geographical Review, 170-182.

Davidnageli, A.M. & Baird, D.J. (2022). Impact of climate change on aquatic food webs: Light, temperature, and trophic dynamics. *Freshwater Biology*, *67*(3), 443-458.

Dokulil, M.T. & Herzig, A. (2009). An analysis of long-term winter data on phytoplankton and zooplankton in Neusiedler See, a shallow temperate lake, Austria. *Aquatic Ecology*, *43*, 715-725.

Dumont, H.J., Van de Velde, I., Dumont, S. (1975). The dry Weight Estimate of Biomass in a Selection of Cladocera, Copepoda, and Rotifera from the Plankton, Periphyton, and Benthos of Continental Waters. *Oecologia*, *19*, 75-97.

Edmonson, W.T., Winberg, G.G. (1971). A manual on the methods for the assessment of secondary productivity in freshwaters (IPB Handbook 17), Blackwell Scientific Publications, Oxford and Edinburg, 358 pp.

El-Sherbiny, M. M. & Al-Aidaroos, A. (2021). Preliminary Observations of the Effect of Temperature and Food Concentration on the Egg Production Rate and Hatching Success of *Acartia amboinensis* from the Central Red Sea. *Zoological Studies*, 60.

Edler, L., Elbrächter, M. (2010). The Utermöhl method for quantitative phytoplankton analysis. In: Karlson, B., Cusack, C., Bresnan, E. (Eds.), *Microscopic and Molecular Methods for Quantitative Phytoplankton Analysis*, UNESCO, Paris, France, pp. 13–20. Ettl & Gärtner, 1983; Ettl & Gärtner, 1988;

Ettl, H. Chlorophyta I. Süßwasserflora von Mitteleuropa; Spektrum Akademischer Verlag: Berlin/Heidelberg, Germany, 1983.

Ettl, H.; Gärtner, G. Chlorophyta II. Süßwasserflora von Mitteleuropa; Spektrum Akademischer Verlag: Berlin/Heidelberg, Germany, 1988.

Florescu, L.I., Moldoveanu, M.M., Catană, R.D., Păceșilă, I., Dumitrache, A., Gavrilidis, A.A., Iojă, C.I. (2022). Assessing the effects of phytoplankton structure on zooplankton communities in different types of urban lakes. *Diversity*, *14*(3), 231.

Foissner, W., Berger, H., Kohmann, F. (1992). Taxonomical and ecological revision of Ciliata from saprobic systems, Volume II: Peritrichia, Heterotrichida, Odontostomatida, Reports by the Bavarian State Office for Water Management, 5(92), Deggendorf, Germany, (In German).

Foissner, W., Berger, H., Kohmann, F. (1994). Taxonomical and ecological revision of Ciliata from saprobic systems, Volume III: Hymenostomata, Prostomatida, Nassulida, Reports by the Bavarian State Office for Water Management, 1(94), Deggendorf, Germany, (In German).

Foissner, W., Berger, H., Kohmann, F. (1995). Taxonomical and ecological revision of Ciliata from saprobic systems, Volume IV: Gymnostomatea, Loxodes, Suctoria, Reports by the Bavarian State Office for Water Management, 1(95), Deggendorf, Germany, (In German).

Foissner, W., Blatterer, H., Berger, H., Kohmann, F. (1991). Taxonomical and ecological revision of Ciliata from saprobic systems, Volume I: Cyrtophorida, Oligotrichida, Hypotrichia, Colpodea, Reports by the Bavarian State Office for Water Management, 1(91), Deggendorf, Germany (In German).

Fott, J., Nedbalová, L., Brabec, M., Kozáková, R., Řeháková, K., Hejzlar, J., Šorf, M., Vrba, J. (2022). Light as a controlling factor of winter phytoplankton in a monomictic reservoir. *Limnologica*, 95, 125995.

Geng, Y., Li, M., Yu, R., Sun, H., Zhang, L., Sun, L., & Xu, J. (2022). Response of planktonic diversity and stability to environmental drivers in a shallow eutrophic lake. *Ecological Indicators*, *144*, 109560.

Gottfried, H.-P. (1976). Das Phytoplankton des Süßwassers. Systematik und Biologie 2. Teil.2. Hälfte: Chrysophyceen. Farblose Flagellaten, Heterokonten, 1976. 365 Seiten, 443 Abbildungen, 107 Tafeln, 16x24cm, 1300 g Language: Deutsch.

Goździejewska, A.M., Kruk, M. (2023). The response of zooplankton network indicators to winter water warming using shallow artificial reservoirs as model case study. *Scientific Reports, 13*(1), 18002.

Grospietsch, Th. (1972). Rhizopoda, Franckh-Kosmos Verlags-GmbH and Co. KG, Stuttgart, Germany (In German).

Haberman, J., Haldna, M. (2017). How are spring zooplankton and autumn zooplankton influenced by water temperature in a polymictic lake? *Proceedings of the Estonian Academy of Sciences*, *66*(3).

Halsband-Lenk, C., Hirche, H.J., Carlotti, F. (2002). Temperature impact on reproduction and development of congener copepod populations. *Journal of Experimental Marine Biology and Ecology, 271*(2), 121-153.

Hammer, Ø. & Harper, D.A.T. (2024). Paleontological Data Analysis, 2nd ed. Elsevier.

Hammer, O., Harper D.A.T., Ryan P.D. (2001). PAST: Paleontological statistics software package for education and data analysis. *Palaeontologia Electronica*, *4*, 1-9.

Hrycik, A.R., Stockwell, J.D. (2021). Under-ice mesocosms reveal the primacy of light but the importance of zooplankton in winter phytoplankton dynamics. *Limnology and Oceanography*, *66*(2), 481-495.

Huber-Pestalozzi, G. (1950). *Das Phytoplankton des Süßwassers. Systematic und Biologie. Teil 3. Cryptophyceae. Chloromonadinen. Peridineen.* E. Schweizerbart'sche Verlagsbuchhandlung, Stuttgart, Germany.

Jensen, T.C. (2019). Winter decrease of zooplankton abundance and biomass in subalpine oligotrophic Lake Atnsjøen (SE Norway). *Journal of Limnology*, doi:10.4081/jlimnol.2019.1877.

Komárek, J., Anagnostidis, K. Cyanoprokaryota, Teil 1: Chroococcales. Süßwasserflora von Mitteleuropa; Springer: Spektrum, Germany, 1998.

Komárek, J.; Anagnostidis, K. Cyanoprokaryota, Teil 2: Oscillatoriales. Süßwasserflora von Mitteleuropa; Springer: Spektrum, Germany, 2005.

Krammer, K., Lange-Bertalot, H. Bacillariophyceae, Teil 2. Süßwasserflora von Mitteleuropa; Springer: Berlin/Heidelberg, Germany, 1988.

Krammer, K., Lange-Bertalot, H. Bacillariophyceae, Teil 3. Süßwasserflora von Mitteleuropa; Springer: Berlin/Heidelberg, Germany, 1991.

Krammer, K., Lange-Bertalot, H. Bacillariophyceae, Teil 4. Süßwasserflora von Mitteleuropa; Springer: Berlin/Heidelberg, Germany, 1991.

Krammer, K., Lange-Bertalot, H. Naviculaceae I. Süßwasserflora von Mitteleuropa; Springer: Berlin/Heidelberg, Germany, 1986.

Lenard, T., Ejankowski, W., Poniewozik, M. (2019). Responses of phytoplankton communities in selected eutrophic lakes to variable weather conditions. *Water*, *11*(6), 1207.

Legutko-Kobus, P., Nowak, M., Petrisor, A.-I., Bărbulescu, D., Craciun, C., Gârjoabă, A.-I. (2023). Protection of Environmental and Natural Values of Urban Areas against Investment Pressure: A Case Study of Romania and Poland. *Land*, *12*, 245.

Li, Y., Zhu, S., Hang, X., Sun, L., Li, X., Luo, X., Han, X. (2023). Variation of Local Wind Fields under the Background of Climate Change and Its Impact on Algal Blooms in Lake Taihu, China. *Water*, *15*(24), 4258.

Litchman, E., Ohman, M.D., and Kiørboe, T. (2013). Trait-based approaches to zooplankton communities. *Journal of plankton resources, 35*(3), 473-484.

Manea, G., Vijulie, I., Matei, E., Cuculici, R., & Tirlă, L. (2013). Constraints and Challenges in the Creation and Public Use of the Protected Areas within the City. Case Study: Lake Văcărești-Bucharest City. In *5th Symposium for Research in Protected Areas*, Mittersill, pp. 491-495.

May, L., Wallace, R.L. (2019). An examination of long-term ecological studies of rotifers: comparability of methods and results, insights into drivers of change and future research challenges. *Hydrobiologia, 844*(1), 129-147.

Mathews, L., Faithfull, C.L., Lenz, P.H., Nelson, C.E. (2018). The effects of food stoichiometry and temperature on copepods are mediated by ontogeny. Oecologia. 2018 Sep;188(1):75-84. doi: 10.1007/s00442-018-4183-6. Epub 2018 Jun 13. PMID: 29948318; PMCID: PMC6096765.

Mânica, A.N. & de Lima Isaac, R. (2023). Seasonal dynamics and diversity of cyanobacteria in a eutrophic Urban River in Brazil. *Water Supply*, *23*(9), 3868-3880.

Merciu, F.C., Sirodoev, I., Merciu, G., Zamfir, D., Schvab, A., Stoica, I. V., ... & Ianoș, I. (2017). The "Văcărești Lake" Protected Area, a Neverending Debatable Issue? *Carpathian Journal of Earth and Environmental Sciences*, 12(2), 463-472.

Molles, M. C. (2016). *Ecology: Concepts and Applications* (4th ed.). McGraw-Hill Education.

Negrea, Șt. Cladocera, (1983) In: *Romanian Fauna* (in Romanian), Romanian Academy Publishing House, Bucharest, Romania.

Negrete-García, G., Luo, J. Y., Petrik, C. M., Manizza, M., & Barton, A. D. (2024). Changes in Arctic Ocean plankton community structure and trophic dynamics on seasonal to interannual timescales. *Biogeosciences, 21*(4951–4973), 4951–4973. https://doi.org/10.5194/bg-21-4951-2024

Nevalainen, L., Ketola, M., Korosi, J.B., Manca, M., Kurmayer, R., Koinig, K.A., Psenner R., Luoto, T.P. (2013). Zooplankton (Cladocera) species turnover and long-term decline of Daphnia in two high mountain lakes in the Austrian Alps. *Hydrobiologia, 722(*1), 75–91. doi:10.1007/s10750-013-1676-5.

Odermatt, J. (1970). Limnologische Charakterisierung des Lauerzerseesmit besonderen Berücksichtigung des Planktons. Schwerz. Z. *Hydrologie***,** *32*, 1-175.

Rose, J.M., Caron, D.A. (2007). Does low temperature constrain the growth rates of heterotrophic protists Evidence and implications for algal blooms in cold waters. *Limnology and Oceanography*, *52*(2), 886-895.

Rudescu, L. (1960). Rotatoria. The Fauna of Romania. Trochelminthes (in Romanian), Romanian Academy Publishing House, Bucharest, Romania.

Sebestyen, D. (1958a). Quantitative Plankton Studies on Lake Balaton. 5. Biomass Calculations on Open Water Oligotricha, Ciliates, *Annales Biologiques*, *25*, 257-266.

Sebestyén, O. (1958 b). Quantitative Plankton Studies on Lake Balaton. IX. A summary of the biomass studies. *Annales Biologiques, 25*, 281- 292.

Siddig, A.A., Ellison, A.M., Ochs, A., Villar-Leeman, C., & Lau, M. K. (2016). How do ecologists select and use indicator species to monitor ecological change? Insights from 14 years of publication in Ecological Indicators. *Ecological Indicators*, *60*, 223-230.

Sommer, U., Gliwicz, Z.M., Lampert, W., Duncan, A. (1986). The PEG-model of seasonal succession of planktonic events in fresh waters. *Archiv für Hydrobiologie, 106*, 433-471.

Sutton, A.O., Studd, E.K., Fernandes, T., Bates, A.E., Bramburger, A.J., Cooke, S.J., ... and Templer, P.H. (2021). Frozen out: Unanswered questions about winter biology. *Environmental Review, 29*(4), 431-442.

Tapolczai, K., Anneville, O., Padisák, J., Salohary, T., Tadonléké, R.D., Rimet, F. (2015). Occurrence and mass development of *Mougeotia* spp. (Zygnemataceae) in large, deep lakes. *Hydrobiologia*, *745*, 17–29.

Umi, W.A.D., Yusoff, F.M., Balia Yusof, Z.N., Ramli, N.M., Sinev, A.Y., & Toda, T. (2024). Composition, Distribution, and Biodiversity of Zooplanktons in Tropical Lentic Ecosystems with Different Environmental Conditions. *Arthropoda, 2*(1), 33-54.

Varpe, Ø. (2012). Fitness and phenology: annual routines and zooplankton adaptations to seasonal cycles. *Journal of Plankton Resources, 34*(4), 267-276.

Winberg, G. (1971). Methods for the estimation of production of aquatic animals, Academic Press. London, New York.

Wollschläger, J., Neale, P.J., North, R.L., Striebel, M., and Zielinski, O. (2021). Climate change and light in aquatic ecosystems: Variability and ecological consequences. *Frontiers in Marine Science, 8*, 688712.

XLSTAT pro. Data Analysis and Statistical Solutions for Microsoft Excel. Addinsoft, Paris, France, 2013.

Zhang, Y., Peng, C., Wang, Z., Zhang, J., Li, L., Huang, S., Li, D. (2018). The Species-Specific Responses of Freshwater Diatoms to Elevated Temperatures Are Affected by Interspecific Interactions. *Microorganisms*, 7; *6*(3):82. doi: 10.3390/microorganisms6030082.

Zepernick, B.N., Chase, E.E., Denison, E.R., Gilbert, N.E., Truchon, A.R., Frenken, T., Cody, W.R., Martin, R.R., Caffin, J.D., Bullerjahn, G.S., McKay, R.M.L., ... & Wilhelm, S.W. (2024). Declines in ice cover are accompanied by light limitation responses and community change in freshwater diatoms. *The ISME Journal, 18*(1), wrad015.

Scientific Papers. Series E. Land Reclamation, Earth Observation & Surveying, Environmental Engineering. Vol. XIV, 2025
Print ISSN 2285-6064, CD-ROM ISSN 2285-6072, Online ISSN 2393-5138, ISSN-L 2285-6064

EVALUATION OF CURRENT Li-Ion BATTERY RECYCLING TECHNOLOGIES

Roxana-Elena FRÎNCU, Carmen Otilia RUSĂNESCU, Gheorghe VOICU, Gabriel Alexandru CONSTANTIN, Elena-Denisa PREDESCU, Sabrina Maria BĂLĂNESCU

National University of Science and Technology Politehnica Bucharest,
Faculty of Biotechnical Systems Engineering, 313 Splaiul Independentei, District 6,
060042, Bucharest, Romania

Corresponding author emails: roxana_elena.fr@yahoo.com, rusanescuotilia@gmail.com, constantingabrielalex@gmail.com

Abstract

Lithium-ion batteries dominate electrochemical energy storage due to their high charge–discharge efficiency, thermal stability, and safety. With an average lifespan of 3-5 years, their growing end-of-life volume poses environmental and resource management challenges. While recycling efforts have focused on high-value metals, electrolyte recovery remains underdeveloped. This review compares pyrometallurgy, hydrometallurgy, and direct recycling based on literature from 2015–2025, evaluating metal recovery efficiency, energy demand, CO_2 emissions, environmental impact, and technological readiness. Hydrometallurgy emerges as the most viable current method (>90% recovery, ~800 kWh/ton energy use), while pyrometallurgy, though industrially established, has high energy requirements (~2,200 kg CO_2/ton) and poor lithium recovery. Direct recycling shows strong sustainability potential by preserving active material structures yet faces scalability challenges from feedstock variability and process standardization. Advancing sustainable recycling will require innovation in automation, standardized materials, and robust policy frameworks to support a circular economy for critical raw materials.

Key words*: battery, direct recycling, hydrometallurgy, pyrometallurgy.*

INTRODUCTION

In the context of the global transition toward sustainable technologies and electric mobility, lithium-ion batteries (Li-Ion) have become the cornerstone of energy storage for applications such as electric vehicles (EVs), portable electronics, and stationary storage systems. As this sector rapidly expands, the generation of waste from spent Li-Ion batteries has grown exponentially, exerting pressure on both the environment and the supply chains of critical materials such as lithium, cobalt, and nickel.

Recycling Li-Ion batteries is not only an ecological necessity but also a strategic opportunity to reduce dependence on primary resources, enhance the security of critical raw materials, and close the materials loop within a circular economy framework. However, not all recycling methods offer the same level of efficiency, sustainability, or industrial feasibility. Currently, three major technologies are employed or under investigation for battery recycling: pyrometallurgy, hydrometallurgy, and direct recycling. Each of these presents specific advantages and limitations, both from a technical standpoint and in terms of environmental impact and operational costs.

The objective of this study is to provide a comparative evaluation of the three primary recycling technologies, focusing on material recovery efficiency, greenhouse gas emissions (CO_2), energy consumption, and practical applicability within the European and Asian contexts, with particular emphasis on China. This paper offers a critical appraisal of the current landscape of battery-recycling technologies and maps plausible development pathways, emphasizing implications for environmental policy and industrial practice. It addresses three questions: (1) Which recycling method offers the best balance between efficiency, cost, and environmental impact? (2) What are the differences in application between the EU and China? (3) What is the long-term potential of emerging technologies?

The article is structured as follows: Section 2 outlines the methodology used for selecting the

reviewed studies; Section 3 provides a detailed overview of each recycling technology; Section 4 presents the comparative and regional analysis; Section 5 discusses the implications for policy and industry; and Section 6 includes the conclusions and future research directions.

MATERIALS AND METHODS

This review paper was conducted based on a systematic selection of scientific articles from the Scopus, Web of Science, and ScienceDirect databases, covering the period 2015-2025.

The selection criteria included technological relevance, the presence of quantitative data on recovery efficiency, emissions, and technological maturity. Articles without comparable data or those focusing solely on battery reuse were excluded.

The comparative analysis was performed according to five criteria: metal recovery efficiency, energy consumption, CO_2 emissions, environmental impact, and level of industrial maturity.

Li-Ion battery recycling methods

Pyrometallurgical Recycling

Pyrometallurgy represents one of the most established and industrially applied methods for the recycling of spent lithium-ion batteries (LIBs), particularly in the European Union. This technique involves high-temperature processing, typically above 1,200°C, to smelt battery materials and recover valuable metals. The process generally includes thermal pre-treatment (e.g., drying, deactivation), followed by smelting in a furnace where the electrode materials decompose and separate based on their physical and chemical properties.

During smelting, organic components such as electrolytes, binders, and separator materials are combusted, while transition metals like cobalt (Co), nickel (Ni), and copper (Cu) are recovered in a metallic alloy or slag phase. These metals can then be refined through additional hydrometallurgical steps to meet battery-grade purity levels.

One of the primary advantages of pyrometallurgical recycling lies in its process simplicity and robustness, making it suitable for mixed and unclassified battery waste streams. Moreover, the technique ensures relatively high recovery rates for cobalt and nickel, which are among the most economically valuable elements in LIBs.

However, this approach also presents several notable disadvantages. Most importantly, lithium is largely lost during the process, often ending up in the slag and becoming unrecoverable without additional complex treatments. In addition, the high energy demand of the smelting process contributes to significant greenhouse gas emissions, particularly when fossil fuels are used as the energy source. The combustion of electrolyte components can also release toxic gases, such as hydrogen fluoride (HF), which necessitates strict environmental controls and gas scrubbing systems.

Despite these limitations, pyrometallurgy continues to be widely used due to its maturity, scalability, and compatibility with existing metallurgical infrastructure. Nevertheless, in light of increasing environmental regulations and the need to recover lithium and other light elements more efficiently, this method is gradually being complemented or replaced by alternative recycling strategies, such as hydrometallurgy and direct recycling.

We have the following chemical reactions that take place during melting:

Cobalt reduction: $CoO + C \rightarrow Co + CO \uparrow$

Nickel reduction: $NiO + C \rightarrow Ni + CO \uparrow$

Decomposition of $LiPF_6$ from electrolyte:

$LiPF_6 \rightarrow LiF + PF_5 \uparrow$ (at > 60°C).

At high temperatures, PF_5 turns into HF (extremely toxic), and LiF ends up in the slag.

Depending on the chosen pyrometallurgical recycling method, batteries may require a pretreatment stage to extract the active cathode material for subsequent recovery, or they can be directly fed into a furnace, as in smelting processes. Thermal pretreatment techniques used for recovering cathode materials include incineration, calcination, and pyrolysis. The resulting metal-rich fraction is then processed through roasting or smelting. A major technical challenge in these pyrometallurgical processes has been the emission of toxic gases. However, recent advancements in pyrometallurgy have led to the development of integrated gas treatment systems such as the one implemented by Umicore which ensure the complete

removal of volatile organic compounds, effective dust capture, and a significant reduction in gas emissions.

Depending on the chosen pyrometallurgical recycling method, batteries may require a pretreatment stage to extract the active cathode material for subsequent recovery, or they can be directly fed into a furnace, as in smelting processes. Thermal pretreatment techniques used for recovering cathode materials include incineration, calcination, and pyrolysis. The resulting metal-rich fraction is then processed through roasting or smelting.

Regarding pyrometallurgy, its advantages consist of: mature technology that is already used on an industrial scale (e.g. Umicore, Glencore), high tolerance to mixtures where precise sorting of batteries is not necessary, but also efficient recovery of Co, Ni and Cu (over 85-90%).

Analyzing the disadvantages, there are certain limitations such as: lithium losses: Li ends up in the slag and is not economically recovered, high energy consumption: >4,000 kWh/ton processed in some cases, significant CO_2 and HF emissions: high climate impact and need for advanced gas treatment, requires advanced metallurgical infrastructure and large initial investments.

Hydrometallurgical recycling

Hydrometallurgy is an advanced method for recycling lithium-ion batteries that involves the chemical transformation of solid electrode materials into soluble forms, followed by the selective recovery of valuable metals. This process is structured in several stages: leaching (dissolution), separation of metal ions, purification and final recovery of salts or metals in solid form.

Acid leaching stage

The active materials (e.g. $LiCoO_2$, $LiNi_{1-x-y}Mn_xCo_yO_2$) are treated in an acidic solution, usually sulfuric acid (H_2SO_4) or hydrochloric acid (HCl), in the presence of a reducing agent (usually hydrogen peroxide, H_2O_2), which helps to oxidize the transition metals and solubilize them in the form of ions.

Typical dissolution reactions:

- $LiCoO_2 + 2H^+ + H_2O_2 \rightarrow Li^+ + Co^{2+} + O_2 + 2H_2O$
- $LiNiO_2 + 2H^+ + H_2O_2 \rightarrow Li^+ + Ni^{2+} + O_2 + 2H_2O$
- $MnO_2 + 4H^+ + 2e^- \rightarrow Mn^{2+} + 2H_2O$

Li^+ remains dissolved as a soluble ion, without further redox reaction.

The leaching process is generally carried out at temperatures between 60-90°C, for a time of 1–3 hours, in a slightly agitated environment, with a pH < 2.

Metal separation and recovery stage

After complete dissolution, the metal ions (Co^{2+}, Ni^{2+}, Mn^{2+}, Li^+) are separated by sequential techniques such as:

Selective precipitation – e.g. $Co(OH)_2$, CoC_2O_4;

Solvent extraction – D2EHPA, Cyanex 272;

Lithium recovery – e.g. $Li^+ + CO_3^{2-} \rightarrow Li_2CO_3 \downarrow$

The yields are over 90-95% for Co and Ni and between 80-90% for Li, depending on the cathode formulation and process conditions.

The limitations and challenges of this method would be: the generation of liquid waste rich in non-recoverable ions, significant consumption of acidic reagents, the need for rigorous control of process parameters.

The method is applied by companies such as Fortum (Finland), Li-Cycle (Canada), Recupyl (France), all using hydrometallurgical variants adapted for the efficient recovery of strategic metals.

Direct recycling

Direct recycling is an emerging technology with significant potential in the field of circular economy, which aims to recover and directly reuse active materials from used lithium-ion batteries, especially cathode ones, without completely decomposing them into basic chemical elements. Unlike pyrometallurgical and hydrometallurgical methods, which involve the complete destruction of the material structure, direct recycling preserves or regenerates the crystalline structure of transition metal oxides (e.g. $LiCoO_2$, NMC), allowing their direct reuse in the manufacture of new cells.

During charge-discharge cycles, the active material undergoes electrochemical and structural degradation caused by: interstitial lithium loss; phase changes and distortions of the crystal lattice; surface contamination. However, the basic structure of the cathode often remains relatively intact, especially in the

case of post-industrial waste or batteries with a low number of cycles.

Stages of the direct recycling technological process:

1. Battery deactivation and disassembly;
2. Mechanical separation of the active material;
3. Binder and contaminant removal (thermal or chemical);
4. Stoichiometric replenishment with Li_2CO_3 or LiOH;
5. Recrystallization at 700-900°C;
6. Testing and characterization (XRD, SEM, electrochemical cycling).

Representative reaction: $Li_{1-x}MO_2 + xLi_2CO_3 + \Delta T \rightarrow LiMO_2 + xCO_2\uparrow$.

Performance and efficiency:

Material recovery efficiency is up to 95%;

Electrochemical capacity restoration: 85-95%;

Costs: 30–50% lower than in classical methods;

CO_2 emissions: reduced by up to 90%.

Limitations for this method are represented by: the need to sort materials; the lack of a mature industrial infrastructure; sensitivity to contaminants; the need for automation and standardization.

RESULTS AND DISCUSSIONS

Pyrometallurgy is widely adopted due to its simplicity and robustness but suffers from high emissions and energy consumption, with poor lithium recovery. Hydrometallurgy offers a more environmentally friendly alternative with high recovery rates, though it generates liquid waste and involves complex chemical separation. Direct recycling, while still emerging, shows the greatest potential for low-impact, high-efficiency recovery by preserving cathode materials, yet it requires high feedstock purity and standardized battery formats (Table 1).

Table 1. Comparative analysis of Lithium-Ion battery recycling technologies

Criteria	Pyrometallurgy	Hydrometallurgy	Direct Recycling
Recovery Efficiency	~60%	~90%	~95%
Materials Recovered	Co, Ni, Cu (Li, Al lost in slag)	Co, Ni, Li, Mn, Cu	Intact cathode material (e.g., NMC, LFP)
CO_2 Emissions	~2200 kg/ton	~1200 kg/ton	~300 kg/ton
Energy Consumption	~1500 kWh/ton	~800 kWh/ton	~500 kWh/ton
Process Temperature	>1500°C	<100°C	Room temperature to 150°C
Technology Maturity	Industrial	Commercial	Emerging
Feedstock Flexibility	High	Medium	Low
Capital & Operating Costs	High	Medium	Low (with automation)
Environmental Impact	High	Medium	Low
Challenges	Low Li recovery, high CO_2	Chemical waste, separation complexity	Sorting, disassembly, standardization

The European Union and China are the two leading regions implementing large-scale lithium-ion battery recycling programs, each reflecting unique industrial strategies and regulatory frameworks.

In the EU, the recycling landscape is shaped by strong environmental directives such as the EU Battery Regulation (2023), which mandates minimum recycled content and high recovery targets for lithium (35%), cobalt (95%), and nickel (90%) by 2030.

The EU supports direct recycling research through initiatives like the Horizon Europe program, but most commercial plants still use hydrometallurgical techniques, balancing efficiency and sustainability.

China, in contrast, leads the world in both battery production and recycling volume, processing over 600,000 tons of spent LIBs annually. Chinese companies leverage vertical integration and economies of scale, with a strong emphasis on hydrometallurgical recovery.

Recent pilot projects also explore direct recycling, driven by the government's 2021 guideline on battery recycling and reuse, which supports second-life applications and material loop closure. Key differences lie in the policy focus: the EU prioritizes sustainability and traceability, while China emphasizes scale, speed, and economic return. Technologically, both regions are advancing direct recycling, but

with different paces of standardization and investment.

Figure 1 illustrates a comparative assessment between the European Union and China regarding lithium-ion battery recycling, based on key indicators such as recycling volume, recovery efficiency, CO_2 emissions, regulatory strength, and investment in direct recycling technologies.

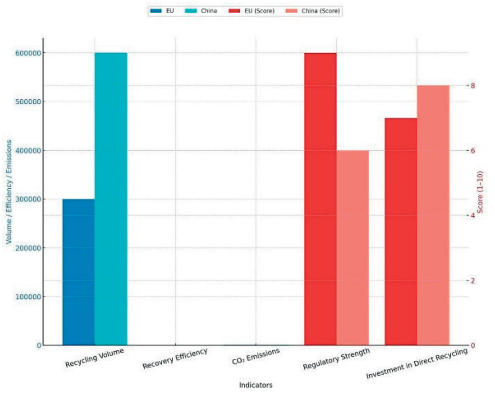


Figure 1. UE vs China in Li-Ion battery recycling (Source: European Commission (2023). Regulation (EU) 2023/1542 of the European Parliament and of the Council on batteries and waste batteries. Official Journal of the European Union. https://eur-lex.europa.eu)

China processes approximately 600,000 tons of lithium-ion batteries annually - about twice the EU's recycling volume of 300,000 tons - reflecting its significant industrial capacity and the high domestic demand for battery reuse and material recovery. In terms of efficiency, the EU achieves an estimated 90%, slightly surpassing China's 85%, a performance advantage attributable to stringent environmental regulations that mandate elevated recovery standards for critical raw materials such as lithium, cobalt, and nickel. From an environmental impact perspective, the EU generates lower carbon emissions, averaging around 800 kg per ton, compared to China's approximately 1,000 kg per ton, largely due to its reliance on cleaner hydrometallurgical processes, while China employs a broader range of technologies, including more carbon-intensive methods. Regarding governance, the EU attains a regulatory strength score of 9/10, underpinned by comprehensive legislative frameworks such as Regulation (EU) 2023/1542, whereas China scores 6/10, with a still-developing and more flexible regulatory environment that prioritizes industrial agility and rapid execution. Finally, in the domain of technological investment, China leads with a score of 8/10, driven by substantial funding for direct recycling initiatives from major industrial actors such as CATL and GEM, while the EU follows with 7/10, primarily through Horizon Europe programs, focusing on scientific validation and regulatory harmonization but progressing more slowly in large-scale commercial deployment.

Table 2 presents a comparative analysis of the three major Li-Ion battery recycling methods: pyrometallurgy, hydrometallurgy and direct recycling, based on energy efficiency, metal recovery yield, environmental impact, costs and technological maturity.

Table 2. Comparative analysis of Li-Ion battery recycling methods

Criterion	Pyrometallurgy	Hydrometallurgy	Direct Recycling
Energy efficiency	Low – requires very high temperatures (>1000°C)	Medium – energy needed for chemical processes and separation	High – low-temperature processes, more efficient
Metal recovery rate	Low–medium – recovers only valuable metals	High – can recover most metals (Li, Co, Ni, Mn)	Very high – preserves the structure of active materials
Environmental impact	High – CO_2 and other toxic gas emissions	Medium – uses acidic chemical substances	Low – fewer emissions and waste
Costs	High – significant energy costs	Medium – chemicals can be reused	Potentially low – but technology is still developing
Technological maturity	Very mature – used at industrial scale	Mature – being optimized for large-scale application	Immature – still under research, limited applications

The comparative analysis of the three primary methods for recycling Li-Ion batteries - pyrometallurgy, hydrometallurgy, and direct recycling indicates that there is no universally optimal solution. Rather, the selection of the recycling method should be guided by specific process objectives, including energy efficiency, cost-effectiveness, environmental sustainability, and scalability. Nevertheless, an integrated assessment of the key criteria yields the following insights:

From the perspective of energy efficiency and environmental impact, direct recycling appears to be the most promising approach. This method enables the preservation of active materials with minimal energy consumption and produces significantly lower amounts of hazardous waste. However, its limited technological maturity and the absence of a well-established industrial infrastructure currently constrain its large-scale deployment.

Direct recycling stands out for its low energy consumption and minimal CO_2 emissions, as it preserves active cathode materials without fully breaking them down. Recovery rates can exceed 90% for certain materials, and the environmental footprint is significantly lower than that of other methods. However, its industrial application is currently limited due to low technological maturity and the lack of a standardized recycling infrastructure.

Hydrometallurgy offers a balanced trade-off between performance and sustainability. It enables high recovery rates - often above 95% - for critical metals such as lithium, cobalt, nickel, and manganese. The energy demand is moderate, and the technology is already being implemented in pilot and commercial-scale facilities. Its adaptability to different battery chemistries makes it the most viable and scalable solution in the medium term.

Pyrometallurgy, while technologically mature and widely industrialized, presents several drawbacks: high energy requirements (often exceeding 5–8 MJ/kg), relatively low lithium recovery (below 50%), and significant CO_2 emissions. These limitations increasingly position it as a transitional or last-resort method, better suited for mixed or contaminated battery waste streams but misaligned with future regulatory and sustainability goals.

The comparative performance chart (Figure 2) clearly illustrates the strengths and limitations of each method across five key criteria: energy efficiency, metal recovery rate, environmental impact, cost-effectiveness, and technological maturity. This multidimensional evaluation supports the discussion and highlights where each method currently stands and what future developments may be needed.

Hydrometallurgy is therefore increasingly favored by researchers and industry stakeholders for integration into large-scale circular economy initiatives.

Although pyrometallurgy is a well-established and industrialized recycling method, it presents significant disadvantages, including high energy consumption, relatively low recovery rates for certain elements (particularly lithium), and major environmental concerns. As a result, pyrometallurgy is increasingly regarded as a transitional or last-resort option, especially in the context of tightening environmental regulations in the European Union and other regions.

In summary, hydrometallurgy currently represents the most efficient and balanced approach for Li-Ion battery recycling, combining high metal recovery rates with proven technical feasibility. However, direct recycling holds substantial long-term potential to become the industry standard, provided that future technological advancements improve its scalability and standardization.

Accelerating the transition toward sustainable battery recycling requires coordinated action from both policymakers and the industry. On the policy side, investments in research, fiscal incentives for emerging technologies, and clear regulations on battery ecodesign (such as standardization of formats and materials) are essential. From an industrial perspective, companies are encouraged to adopt circular business models, develop local recycling infrastructure, and establish strategic partnerships to facilitate the transition from innovation to commercial deployment. International cooperation, particularly between the EU and China, can further support the harmonization of standards and accelerate widespread adoption.

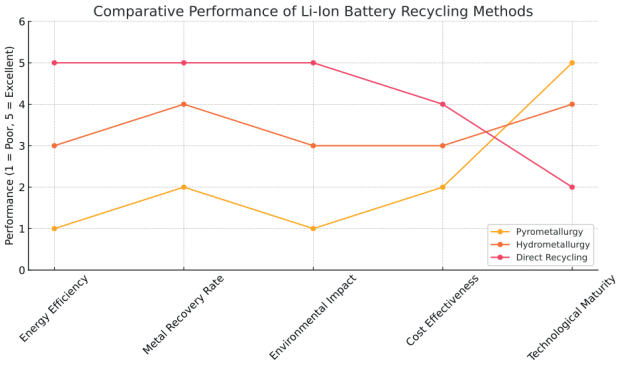


Figure 2. Comparative performance of Li-Ion battery recycling methods
(Source: Data compiled from Gaines, 2018; Xu et al., 2020; Fan et al., 2021; Harper et al., 2019; Zhao et al., 2021; Liu et al., 2021; Cornelio et al., 2024; Makuza et al., 2021)

CONCLUSIONS

As demand for Li-Ion batteries continues to rise - driven by the transition to electric mobility and renewable energy - the development of efficient recycling solutions has become a critical priority. Currently, three main technologies are emerging as viable options for recovering valuable materials from spent batteries: pyrometallurgy, hydrometallurgy, and direct recycling. Each method offers distinct advantages and limitations, and the optimal choice depends on balancing technical performance, environmental impact, and industrial readiness.

Among these, hydrometallurgy stands out as the most balanced and practical option at present. With recovery efficiencies of over 90% for critical metals such as lithium, cobalt, nickel, and manganese, moderate energy consumption (approximately 800 kWh per ton of processed batteries), and proven scalability, this method is already being deployed in commercial facilities. However, the intensive use of chemical reagents and the generation of liquid waste require advanced wastewater treatment solutions to mitigate environmental impact.

Pyrometallurgy, a long-established industrial method used by companies like Umicore and Glencore, offers the advantage of processing entire batteries without prior dismantling. Yet, it performs poorly from an environmental perspective: high CO_2 emissions (~2200 kg/ton), high energy demand (~1500 kWh/ton), and relatively low metal recovery (~60%), with significant lithium losses in the slag.

In contrast, direct recycling is increasingly viewed as the most promising long-term solution. By preserving the chemical structure of active materials - such as $LiCoO_2$ or NMC - it enables their reuse at lower costs and energy requirements. It also delivers excellent performance in key areas: up to 95% recovery efficiency, minimal CO_2 emissions (~300 kg/ton), and low-temperature processing. However, it is still in the early stages of development, facing major challenges such as material variability, the need for precise dismantling and separation processes, and the lack of industrial infrastructure.

To accelerate the advancement of direct recycling, research and innovation efforts should focus on battery standardization, the development of automated dismantling technologies, efficient separation and regeneration methods for cathode materials, and increasing tolerance to the variability of spent batteries. Additionally, integrating direct recycling into existing supply chains through public-private partnerships will be crucial.

From a policy perspective, accelerating the transition toward sustainable battery recycling requires coordinated action between authorities and industry. Key measures include investment in local recycling infrastructure, fiscal incentives for companies adopting emerging technologies, and clear regulations on battery ecodesign - especially regarding material and component standardization. Setting ambitious

material recovery targets and fostering international cooperation - particularly between the European Union and China - could further harmonize technical standards and support the rapid deployment of the most efficient technologies globally.

In conclusion, hydrometallurgy currently offers the best trade-off between environmental responsibility, material recovery, and industrial feasibility, while direct recycling holds strong long-term potential. Unlocking this potential, however, will require a sustained, cross-sectoral effort in research, innovation, and policy development.

REFERENCES

Benchmark Mineral Intelligence. (2022). *Global lithium-ion battery recycling capacity and policy trends.* https://www.benchmarkminerals.com

China Ministry of Industry and Information Technology. (2021). *Guidelines on battery recycling and reuse.* http://www.miit.gov.cn

Cornelio, A., Zhu, H., Wu, J., & Pan, Y. (2024). Recent progress in pyrometallurgy for the recovery of spent lithium-ion batteries: A review of state-of-the-art developments. *Current Opinion in Green and Sustainable Chemistry, 40,* 100859. https://www.sciencedirect.com

Duan, H., Li, J., & Tan, Q. (2021). China's evolving lithium-ion battery recycling market. *Resources, Conservation and Recycling, 174,* 105823. https://www.sciencedirect.com

European Commission. (2023). Regulation (EU) 2023/1542 of the European Parliament and of the Council on batteries and waste batteries. *Official Journal of the European Union.* https://eur-lex.europa.eu

Fan, E., et al. (2021). Sustainable recovery of cathode materials from spent lithium-ion batteries using direct regeneration technologies. *Nature Sustainability, 4,* 938–946. https://www.researchgate.net

Gaines, L. (2018). Lithium-ion battery recycling processes: Research and implications. *Joule, 2*(10), 1923–1933. https://www.sciencedirect.com

Gaines, L. (2020). The future of automotive lithium-ion battery recycling: Charting a sustainable course. *Sustainable Materials and Technologies, 25,* e00155. https://www.sciencedirect.com

Harper, G., Sommerville, R., Kendrick, E., Driscoll, L., Slater, P., Stolkin, R., Walton, A., & Anderson, P. (2019). Recycling lithium-ion batteries from electric vehicles. *Nature, 575*(7781). https://www.sciencedirect.com

International Renewable Energy Agency. (2023). *End-of-life management of lithium-ion batteries: Technical brief.* https://www.irena.org

Li, J., Xu, C., Zhang, Y., & He, W. (2022). A review of the recycling processes for lithium-ion batteries. *Resources, Conservation and Recycling, 180,* 106206. https://www.sciencedirect.com

Liu, Y., Zhang, H., Li, J., & Fan, E. (2021). Direct recycling of spent cathode materials from lithium-ion batteries: Recent advances and future perspectives. *Chemical Engineering Journal, 406,* 127122. https://www.sciencedirect.com

Makuza, B., Tian, Q., Guo, X., Xu, C., & Wang, J. (2021). Pyrometallurgical options for recycling spent lithium-ion batteries: A comprehensive review. *Journal of Power Sources, 491,* 229622. https://www.sciencedirect.com

Ordoñez, J., Gago, E. J., & Girard, A. (2016). Processes and technologies for the recycling and recovery of spent lithium-ion batteries. *Renewable and Sustainable Energy Reviews, 60,* 195–205. https://www.sciencedirect.com

Xu, C., Dai, Q., & Gaines, L. (2020). Recycling of lithium-ion batteries: A review of current processes and technologies. *Joule, 4*(2), 307–340. https://www.sciencedirect.com

Xu, C., Dai, Q., Gaines, L., Hu, M., Tukker, A., & Steubing, B. (2020). Future material demand for automotive lithium-based batteries. *Communications Materials, 1*(1), 99. https://www.nature.com

Zhao, M., Liu, Y., Wang, Z., Zhang, H., & Chen, X. (2021). Pyrometallurgical technology in the recycling of a spent lithium-ion battery: Evolution and the challenge. *ACS ES&T Engineering, 1*(8), 1373–1384. https://pubs.acs.org

Zhao, Y., Zhang, Y., Sun, Z., & Wang, X. (2022). Direct recycling of spent lithium-ion batteries: Current status and future perspectives. *Journal of Power Sources, 520,* 230844. https://www.cell.com/iscience

Scientific Papers. Series E. Land Reclamation, Earth Observation & Surveying, Environmental Engineering. Vol. XIV, 2025
Print ISSN 2285-6064, CD-ROM ISSN 2285-6072, Online ISSN 2393-5138, ISSN-L 2285-6064

STUDY OF MICROBIOLOGICAL STATUS OF SOILS IN BEECH PLANTATIONS

Bilyana GRIGOROVA-PESHEVA, Yordan IVANOV

University of Forestry, 10 Kliment Ohridski Blvd, Sofia, Bulgaria

Corresponding author email: b.pesheva@ltu.bg

Abstract

The main objective of the study is to investigate the microbiological status of soils in beech plantations of the first and second site index. Ten soil profiles were established in ten test areas with beech plantations. The study includes an analysis of the main physico-chemical and microbiological parameters of the ten soil profiles. In each test area, the site index, relative stocking and the average volume (m^3/ha) of the plantation was determined. The studied soils are of the Cambisols, Regosols and Rendzinas type. Soil samples were taken from the A and B (C) horizons. Basic indicators related to soil microorganisms were studied - humus (%), org.C mg/kg^{-1}, pH and mechanical composition. For determination of total microbial number and the amount of individual microbiological groups (bacteria, actinomycetes and fungi), the standard method of serial dilutions and subsequent inoculation was used. The results are reported in Colony-forming unit. A horizon has a greater microbial abundance than the underlying soil horizons, regardless of the considered soil type. There are no clear dynamics in the redistribution of the percentage participation of microbial groups at depth. There is no clear correlation between the microbial abundance and site index of the plantations. The highest microbial abundance was observed at an altitude above 1300 m (TA9 and TA10). Brown forest soils stand out with the highest average biogenicity. It was found that the percentage of microscopic fungi increases in acidic soils, while their amount in Rendzinas decreases below 1.0 × 10^5 CFU/g dry soil.

Key words*: soil, soil microorganism, forest ecosystems, total microbial number.*

INTRODUCTION

Forest ecosystems are of great importance for the Earth's biosphere, covering more than 1/4 of the land (Keenan et al., 2015). When determining the quality (site index) of the plantation, a number of factors are taken into account: the biological characteristics of the tree species, the rank of the tree in the plantation, the rate of growth, soil conditions, soil microorganisms, climatic conditions, growth space - expressed by the density and fullness of the stand, etc. (Callesen et al., 2006; Uroz et al., 2007; Packham et al., 2012; Kirchen et al., 2017). Tree species have specific requirements for environmental conditions and for soils. Growth and productivity of tree species depend on soil fertility, on the activity and abundance of soil microorganisms (Graham et al., 2016). Microorganisms participate in a number of complex processes of organic decomposition and humus synthesis, which determines their important role in the development and stability of forest ecosystems (Paul & Clark, 1989). Without their active participation, the circulation of substances and providing the ecosystem services by the forests is impossible (Strickland et al., 2009). There are studies that highlight the possibility of microorganisms being used as bioindicators for the state of forest ecosystems, given their rapid response to environmental changes. (Turco et al., 1994; Kennedy & Papendick, 1995; Dick, 1997.) Although there are several studies that consider ecosystem services considering the activity and abundance of soil microorganisms (Fonseca, 1990; Staddon et al., 1999; Zhang et al., 2020), there are still no sufficiently in-depth studies on the interrelationships between the condition of the plantation as reflected by its site index and the microbiological status of the soils, as their main characteristic.

The present study represents the pioneering analysis of main characteristics and microbiological status of the soils and the site index of beech plantations from the Vitosha Nature Park region.

MATERIALS AND METHODS

For the study, ten test areas (TA) were laid out on the territory of Vitosha Nature Park, Sofia

region, Bulgaria. The selection of Vitosha Natural Park was prompted by the available information on its background levels of pollution despite its proximity to the capital Sofia, making it a suitable site for studies in an ecologically clean environment (Kadinov, 2019; Kadinov, 2021a; Kadinov, 2021b).

In each test area, the tree stand was surveyed, and its site index, relative stocking (RS) and the average volume (AV) (m^3/ha) were determined was determined. Characterization of the soil type was carried out by making a soil profile. The main microbiological parameters of the soil were studied. The TAs are located at an altitude of 910 to 1445 m.

Soil samples were collected from each of the soil profiles for analysis. The samples were collected from the average depth for each of the investigated horizons. An average sample was formed from five points taken horizontally, at the selected depth of the soil horizon. An approximate amount of 1.5 kg was collected for each sample taken.

The soil analysis includes the study of soil parameters related to the microbiological characteristics of the soil and the assessment of site index of the tree plantations. The following soil parameters were studied: org. C content (kg/mg^{-1}) and humus (%) - according to Turin's method; Mechanical composition - Kaczynski's method; pH - potentiometric.

Microbiological analyzes were performed according to all sterility rules. The microbial abundance of each of the investigated samples was determined by determining the total microbial number (TMN) for all horizons. Microbiological analyzes include determination of the main microbiological groups in the soil related to its biogenicity and to the site index of tree plantations - bacteria, actinomycetes and fungi (micromycetes). Inoculation was carried out on appropriate nutrient media: (Nutrient agar for bacteria, Starch ammonia agar for actinomycetes, Čapek dox agar for fungi). Incubation was carried out at a certain temperature and duration for each of the studied groups (for bacteria 48 hours at 24°C, for actinomycetes 7 days at 35°C and for micromycetes - Czapek-Dox agar for 7 days at 30°C. The number of sprouted colonies was determined. The data are presented in colony forming units (CFUs) per gram of dry soil.

Results were statistically analyzed using the StatSoft Statistica 12 software program at 95% significance thresholds. The program was used to compare and search for correlations between the individual parameters studied, based on direct and inverse correlations.

RESULTS AND DISCUSSIONS

All of the studied tree stands have a 100% participation of *Fagus sylvatica*, with the exception of TA1, in which there is 94% participation of *Fagus sylvatica* and a minimum participation of *Carpinus betulus* - 6%. The stand relative stocking (RS) and the average volume (AV) (m^3/ha) were determined, as follows:

- TA1-1.49 relative stocking; 628 m^3/ha average volume;
- TA2-0.90 relative stocking; 375 m^3/ha average volume;
- TA3-0.99 relative stocking; 493 m^3/ha average volume;
- TA4-1.19 relative stocking; 580 m^3/ha average volume;
- TA5-0.82 relative stocking; 422 m^3/ha average volume;
- TA6-1.07 relative stocking; 619 m^3/ha average volume;
- TA7-1.26 relative stocking; 569 m^3/ha average volume;
- TA8-1.29 relative stocking; 565 m^3/ha average volume;
- TA9-1.11 relative stocking; 472 m^3/ha average volume;
- TA10-1.09 relative stocking;618 m^3/ha average volume.

Table 1 and Table 2 present the results of the conducted research. A total of 10 soil profiles were investigated. Of them, TA7 and TA1 were defined as Regosoli, TA 2 and TA 6 as Rendzini, and TA3, TA4, TA5, TA8, TA9 and TA10 as Cambisols. The main microbiological groups - and the total microbial number was calculated (Table 2).

Data was statistically processed, and the standard deviation is presented. A statistical analysis of the relationship between the TMN of the upper soil horizon and the underlying soil horizon with respect to altitude was performed

without considering soil type (Figure 1 and Figure 2).

Correlation was performed to follow the dynamics of microbial communities in height. Statistical processing of results was also performed to detect potential interrelationships between microbial abundance and environmental factors.

Table 1. Main characteristics of the studied soils and the determined sites index

TA	Altitude(m)	Soil type	Coordinates	Horizon	Humus %	Org. C g.kg^{-1}	Mechanical composition	pH	Site Index
1	910	Regosols	N 42.644786 E 23.241678	A	6.5	37.72	finely dusty	5.4	II
				C1	2.84	16.46	dusty	5.5	
2	1005	Rendzinas	N 42.488373 E 23.195845	A	4.14	23.99	finely dusty	7.2	II
				AC	4.67	27.06	finely dusty	7.3	
3	1092	Cambisols	N 42.552401 E 23.192019	A	6.14	35.62	dusty	6	I
				B	2.85	16.54	dusty	6.2	
4	1153	Cambisols	N 42.604438 E 23.202027	A	4.26	24.69	sandy dusty	4.5	II
				B	1.19	6.93	sandy dusty	5.1	
5	1195	Cambisols	N 42.474051 E 23.258257	A	3.56	20.63	finely dusty	5.2	II
				B	1.14	6.62	clay dusty	5.9	
6	1218	Rendzinas	N 42.468242 E 23.232454	A	3.77	21.86	finely dusty	7.5	I
				AC	1.14	6.60	finely dusty	7.8	
7	1223	Regosols	N 42.46923 E 23.25111	A	4.57	26.52	dusty	4.8	II
				C	0.48	2.25	dusty	4.9	
8	1270	Cambisols	N 42.608444 E 23.298922	A	3.71	21.53	finely dusty	5.8	II
				B	2.8	16.22	finely dusty	5.4	
9	1370	Cambisols	N 42.572043 E 23.205129	A	2.56	15.40	sandy dusty	5.4	II
				B	1.36	7.88	sandy dusty	5.3	
10	1455	Cambisols	N 42.61697 E 23.240181	A	6.5	37.68	sandy dusty	5	I
				B	4.09	23.74	sandy dusty	5	

Table 2. Main microbiological characteristics of the soils

TA	Horizon	TMN	Bacteria	Actinomycetes	Fungi
1	A	17.58 ± 0.34	11.94 ± 0.77	1.61 ± 0.01	4.04 ± 1.12
	C1	2.30 ± 1.22	1.75 ± 0.92	0.31 ± 0.13	0.24 ± 0.17
2	A	19.58 ± 2.48	17.59 ± 5.22	1.01 ± 3.00	0.99 ± 0.26
	AC	2.29 ± 0.58	2.23 ± 0.37	0.05 ± 0.21	0.01 ± 0.07
3	A	18.09 ± 10.74	16.13 ± 10.19	0.60 ± 0.89	1.36 ± 1.89
	Bw	7.01 ± 2.61	5.35 ± 2.95	1.65 ± 0.54	0.02 ± 0.22
4	A	14.24 ± 10.74	8.92 ± 10.19	0.18 ± 0.89	5.14 ± 1.89

	Bw	10.87 ± 2.61	10.81 ± 2.95	0.02 ± 0.54	0.04 ± 0.22
5	A	17.42 ± 10.74	13.55 ± 10.19	1.70 ± 0.89	2.18 ± 1.89
	Bw	4.74 ± 2.61	3.63 ± 2.95	0.65 ± 0.54	0.45 ± 0.22
6	A	16.07 ± 2.48	10.20 ± 5.22	5.25 ± 3.00	0.62 ± 0.26
	AC	3.12 ± 0.58	1.70 ± 0.37	0.34 ± 0.21	0.11 ± 0.07
7	A	18.06 ± 0.34	10.84 ± 0.77	1.59 ± 0.01	5.63 ± 1.12
	C	0.58 ± 1.22	0.44 ± 0.92	0.13 ± 0.13	0.01 ± 0.17
8	A	18.60 ± 10.74	15.75 ± 10.19	1.53 ± 0.89	1.32 ± 1.89
	Bw	4.47 ± 2.61	3.72 ± 2.95	0.59 ± 0.54	0.17 ± 0.22
9	A	39.91 ± 10.74	32.22 ± 10.19	2.62 ± 0.89	5.07 ± 1.89
	Bw	4.53 ± 2.61	3.12 ± 2.95	0.85 ± 0.54	0.56 ± 0.22
10	A	35.02 ± 10.74	33.12 ± 10.19	0.73 ± 0.89	1.17 ± 1.89
	Bw	8.44 ± 2.61	7.24 ± 2.95	1.01 ± 0.54	0.19 ± 0.22

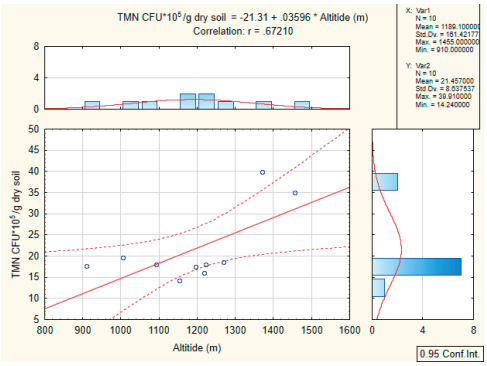


Figure 1. Correlation TMN of A horizon and altitude

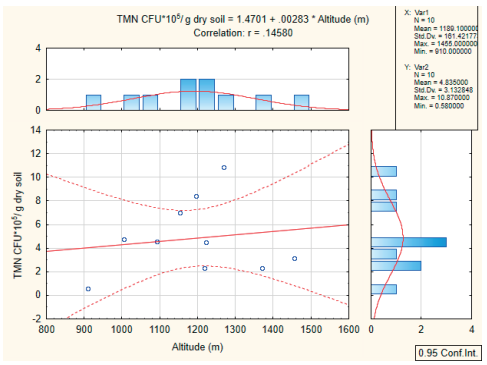


Figure 2. Correlation TMN of B horizon and altitude

Soils from TA1 and TA7 are defined as Regosols. The soil of TA7 is highly acidic, and that of TA1 is moderately acidic. According to the specified levels of Org. C, the considered A horizon of soils of the Regosols type are defined as moderately stocked with organic matter. With an increase in the depth of the soil profile, however, at TA7, a sharp drop in the humus content, respectively, in the amount of org. C and the stock is determined to be very low. In contrast to TA7, in TA1 in the depth of the soil profile, the amount of organic matter does not decrease so sharply, although it falls to class II - low stocking according to the Vanmechelen scale (Vanmechelen et al., 1997). In terms of mechanical composition, both considered profiles have a predominant dust fraction. The soils have a reduced volume of pore spaces and a lack of well-formed aggregates, which leads to a lack of an optimal water-air regime.

Soils from soil profiles TA2 and TA6 are classified as Rendzinas. In these soils, the pH is much higher, and in TA2 soil has a neutral reaction, and in TA6 it has an alkaline reaction. The humus content in the A horizon is lower than the considered Regosols (TA7 and TA1), but in contrast to them, it decreases smoothly in the depth of the soil profile. According to the content of organic carbon, the soils of TA2 are averagely stocked throughout the depth of the soil profile. At TA6, in the humus accumulative horizon, the quantities of organic matter are of class 3 (medium stock), while in depth they pass into class two (low stock). These soils are defined as fine dust. This mechanical composition characterizes the studied Rendzinas, as soils with poor plasticity and stickiness that cannot form stable soil aggregates. In these soils, the pore space is

reduced, leading to a reduction in the air content of the soil.

The remaining soil profiles (TA3, TA4, TA5, TA8, TA9 and TA10) are defined as Cambisols. All soils are defined as acidic, and with increasing altitude there is an increase in acidity due to natural acidification processes. In the overlying humus accumulative horizon, there is an average amount of organic matter for all studied profiles, except for TA9, where the organic matter has a lower content and defines the soil as class two (low amount of organic C) according to Vanmechelen scale. The mechanical composition is diverse. Soil from TA3 is dusty. The soil of TA5 is defined as a fine dusty A horizon and a clayey dusty Bw horizon. The soil of TA8 is defined as fine dust. The soils of TA9 and TA10 are sandy-dusty. The diversity in the mechanical composition of the studied Cambisols shows the influence of the environment and the soil-forming rock on the formation of these soils.

In all soils studied, the microbial abundance decreases in depth of the soil profile. This decrease in total microbial abundance at depth is due to reduced levels of organics as well as altered water–air regimes, as found in the studies of Fierer et al., 2003 and Tripathi et al., 2018. In their study, Taylor et al., 2002 indicates that in the deeper soil horizon there is an absence of microscopic fungi. No such trend was found in the present study. The present study found varying degrees of reduction in microbial abundance in different soil types. Thus, in Regosols and Rendzinas the decrease is much sharper than in Cambisols.

The soils of the Cambisols type stand out as the richest in microorganisms, with an average total microbial number 23 x 10^5. Soils with a sandy-dusty mechanical composition are characterized by greater microbial abundance. No correlation was established between the mechanical composition of the soils and the site index of the stands. There is no clear statistical correlation between humus content and pH. Like the current research, Cho et al., 2016 found that pH, as the only factor considered, did not significantly affect microorganisms' diversity. Furthermore, Lauber et al., 2009 proved that pH is not a sufficient factor to assess the status and diversity of soil microorganisms.

A high correlation coefficient was observed between the increase in total microbial numbers and the increase in altitude ($r = 0.70$), and similar conclusions were generated in the study of Siles & Margesin 2016. In all studied soil profiles, regardless of soil type, the dominant group is bacteria. In highly acidic soils (TA4 and TA7), the percentage participation of the group of fungi increases and reaches over 30% of the total microflora. Looking again at the pH data, the influence of this parameter on the number of microscopic fungi is clearly seen. The neutral and slightly alkaline pH of Rendzinas encourages the development of microscopic fungi, with their levels falling below $1*10^5$. There is no relationship between total microbial number and site index of the stands. No correlation was found between the percentage distribution of microbial groups and the quality site index of the stands.

Further studies of soil parameters are needed to determine which parameters influence the site index of the stands.

CONCLUSIONS

The present study aimed to investigate the microbiological status of soils in beech plantations. There is no clear dynamic between the site index of the stands and the studied soil parameters. No direct correlations were found between stand quality and microbiological characteristics. A decrease in microbial abundance in depth was found in all studied soil profiles. The soils of the Cambisols type stand out as the richest in soil microorganisms. There is no clear correlation between soil characteristics and microbial abundance, regardless of the horizon considered. A positive correlation ($r = 0.70$) was found between increasing total microbial numbers and increasing altitude. Soils above 1,300 meters are characterized by a higher number of microorganisms per gram of soil. The forest and the soil as an element of forest ecosystems are a specific complex, for the understanding and tracking of its functioning, in-depth studies are necessary. We recommend investigating the average content of the total microflora for the entire depth of the soil profile and to look for interrelationships between the microbial abundance and the condition of the stands,

expressed by their site index. We recommend surveying an average sample of the entire stand area, by sampling at least 20-25 points at a depth of 1 m, because soil profiles are likely to reflect the local situation. Microorganisms are a fundamental part of forest ecosystems. Their study and the new information generated can be used to develop strategies and practices for sustainable forest management. Given the important role that soil microorganisms play in the cycling of substances in forest ecosystems, it is necessary to conduct in-depth studies of soil microflora in order to maintain forest massifs in an environmentally friendly manner. Further studies are needed to establish possible interrelationships between environmental factors, soil characteristics, stands site index and soil microbial abundance. The present study can serve as a baseline for future studies.

ACKNOWLEDGEMENTS

This research is supported by the Bulgarian Ministry of Education and Science under the National Program "Young Scientists and Postdoctoral Students - 2".

REFERENCES

Callesen I., K. Raulund-Rasmussen, B. B. Jørgensen, V. Kvist-Johannsen. 2006. Growth of Beech, Oak, and Four Conifer Species Along a Soil Fertility Gradient. *Baltic Forestry, 12* (1), 14–23.

Cho, S., Kim, M. & Lee, Y. (2016). Effect of pH on soil bacterial diversity. *Journal of Ecology and Environment, 40*, Article number: 10.

Dick, R.P. (1994). *Soil enzyme activities as indicators of soil quality.* In J.W. Doran, D.C. Coleman, D.F. Bezdicek and B.A. Stewart (eds.). Defining soil quality for a sustainable environment. pp. 07-124. Soil Science Society of America, Special Publication No. 35. Madison, Wisconsin.

Fierer, N., Schimel, J. & Holden, P. (2003). Variations in microbial community composition through two soil depth profiles. *Soil Biology and Biochemistry, 35*(1), 167-176.

Fonseca, C. (1990). Forest management: impact on soil microarthropods and soil microorganisms. Rev. d'Écol. *Biol. Sol, 27*, 269-283.

Graham, E., Knelman, J., Schindlbacher, A., Siciliano, S., Breulmann, M., Yannarell, A., Beman, J., Abell, G., Philippot, L., Prosser, J., Foulquier, A Yuste,J., Glanville, H., Jones, D., Angel, R., Salminen, J., Newton, R., Bürgmann, H., Ingram, L., Hamer, U., Siljanen, H., Peltoniemi, K. Potthast, K., Bañeras, L., Hartmann, S. Banerjee, S., Yu, R., Nogaro, G., Richter, A., Koranda, M., Casrle, S., Goberna, M., Song, B., Chatterjee, A., Nunes, O., Lopes, A., Cao, Y., Kaisemann, A., Hallin, S., Strickland, M., Garcia-Pausas, J. Barba, J., Kang, H., Isobe, K., Papaspyrou, S., Pastorelli, R.,Lagomarsino, A., Lindström, E., Basiliko, N., Nemergut, D. (2016). Microbes as engines of ecosystem function: when does community structure enhance predictions of ecosystem processes? *Front. Microbiol., 7*, 1-10.

Kadinov, G. (2019). Quantitive Assessment of the Importance of the Atmospheric Environment on Air Pollutant Concentrations at Regional and Local Scales in Sofia. *Ecologia Balcanica, Special Edition, 2*, 63–70.

Kadinov, G. (2021a). Comparative Assessment of Tropospheric Ozone Loads of Two Fagus sylvatica Sites. *Journal of Balkan Ecology, 24*(2), 157– 172.

Kadinov, G. (2021b). Dynamics of Dust Concentration in Atmosphere above Sofia for Last 10 Years. *Journal of Balkan Ecology, 24*(3), 285–305).

Keenan, R., Reams, G., Achard, F., Freitas, J., Grainer, A., Linquist, E. (2015). Dynamics of global forest area: results from the FAO Global Forest Resources Assessment. *Forest Ecol Manage., 352*, 9-20.

Kennedy, A.C. and R.I. Papendick. 1995. Microbial characteristics of soil quality. J. *Soil Water Conserv. 50*, 243-248.

Kirchen G., C. Calvaruso, A. Granier, P.O. Redon, G. Van der Heijden, N. Bréda, M.-P. Turpault. (2017). Local soil type variability controls the water budget and stand productivity in a beech forest. *Forest Ecology and Management, 390*, 89–10.

Lauber, C., Hamady, M., Knight, R. & Fierer, N. (2009). Pyrosequencing-Based Assessment of Soil pH as a Predictor of Soil Bacterial Community Structure at the Continental Scale. *Applied and Environmental Microbiology, 75*(15), 5111-5120.

Packham, J., P. Thomas, M. Atkinson, T. Degen. (2012). Biological Flora of the British Isles: Fagus sylvatica. *Journal of Ecology, 100* (6), 1557–1608.

Paul, E.A. and F.E. Clark. (1989*). Soil Microbiology and Biochemistry*. Academic Press, Toronto. pp. 275.

Siles, J. & Margesin, R. (2016). Abundance and Diversity of Bacterial, Archaeal, and Fungal Communities Along an Altitudinal Gradient in Alpine Forest Soils: What Are the Driving Factors? *Microbial Ecology, 72*, 207–220.

Staddon, W., Duchesne, L., Trevors, J. (1999). The role of microbial indicators of soil quality in ecological forest management. *The Forestry Chronicle, 75*(1), 81-86

Strickland, M., Lauber, C., Fierer, N., Bradford, M. (2009). Testing the functional significance of microbial community composition. *Ecology, 90*, 441-451.

Taylor, J., Wilson, B., Mills, M.S., Burns, R.G. (2002). Comparison of microbial numbers and enzymatic activities in surface soils and subsoils using various techniques. *Soil Biology & Biochemistry, 34*, 387–401.

Tripathi, B., Kim, M., Kim, Y., Byun, E., Yang, J., Ahn, J. & Lee, Y. (2018). Variations in bacterial and archaeal communities along depth profiles of Alaskan soil cores. *Scientific Reports, 8*(1), 504.

Turco, RF., A.C. Kennedy and M.D. Jawson. (1994). *Microbial indicators of soil quality.* In J.W. Doran, D.C. Coleman, D.F. Bezdicek, and B.A. Stewart (eds.). Defining Soil Quality for a Sustainable Environment. pp. 73-90. Soil Science Society of America Special Publication No. 35. Madison Wisconsin.

Uroz, S., C. Calvaruso, M.-P. Turpault, J.C. Pierrat. (2007). Effect of the mycorrhizosphere on the genotypic and metabolic diversity of the bacterial communities involved in mineral weathering in a forest soil. *Appl. Environ. Microbiol., 73*, 3019–3027.

Vanmechelen, L., Groenemans, R. & Van Ranst, E. (1997). Forest Soil Condition in Europe. — Forest Soil Coordinating Centre, International Cooperative Programme on Assessment and Monitoring of Air Pollution on Forest, UN-ECE. pp. 61.

Zhang, J., Yang, X., Song, Y., Liu, H., Wang, G., Xue, Sh., Liu, G., Ritsema, C., Geissen, V. (2020). Revealing the nutrient limitation and cycling for microbes under forest management practices in the Loess Plateau– ecological stoichiometry. *Geoderma 361*, 114108.

Scientific Papers. Series E. Land Reclamation, Earth Observation & Surveying, Environmental Engineering. Vol. XIV, 2025
Print ISSN 2285-6064, CD-ROM ISSN 2285-6072, Online ISSN 2393-5138, ISSN-L 2285-6064

H_2S GAS LEAK EMERGENCY PREPAREDNESS AND COMMUNITY RESPONSE: A CRITICAL REVIEW OF BEHAVIORAL FACTORS AND GAPS

Saeed KARIMI, Ehsan TALEBI, Saeed GIVEHCHI

University of Tehran, Faculty of Environment,
15, corner of Dr. Abdul Hossein Zarinkob Alley, Qods Street, Elginal Street, Tehran, Iran

Corresponding author emails: karimis@ut.ac.ir, karimi.saeed1979@gmail.com

Abstract

Hydrogen Sulfide (H2S) gas leaks are a serious threat to communities near industrial sites, endangering health and the environment. While safety technology has improved, a community's ability to respond effectively depends on how well-prepared people are. This review dives into what shapes community behavior during H2S emergencies, drawing from global research and a study in Assaluyeh and Nakhl Taghi, Iran. We found that understanding risks, trusting local authorities, and clear communication are key to safe responses. Our data shows notable differences in safety behaviors, especially tied to where people live, revealing gaps in awareness and training. We call for community-focused plans with better education, open communication, and practical training to empower people, reduce risks, and build stronger, safer communities worldwide.

Key words: *H_2S gas leak, emergency preparedness, community safety, behavioral factors, risk communication.*

INTRODUCTION

The pervasive threat of H_2S in industrialized regions

Hydrogen sulfide (H_2S) is a colorless, toxic, and flammable gas recognized as one of the most significant industrial pollutants and environmental health hazards (Talebi, 2020). At low concentrations, it produces a distinct "rotten egg" odor that serves as a simple warning; however, at higher and more dangerous concentrations, olfactory fatigue occurs rapidly, making H_2S a true "silent killer" (Beauchamp et al., 2020; Public Services and Procurement Canada, 2023).

H_2S is primarily produced through the anaerobic decomposition of organic matter and is commonly present in industries such as crude oil and natural gas extraction and refining, wastewater treatment, and geothermal energy production (OSHA, 2015; Talebi, 2020).

Accidental or chronic releases of H_2S pose serious health risks, ranging from acute respiratory and neurological symptoms to rapid death at high concentrations (Beauchamp et al., 2020; Ng et al., 2019).

Beyond its direct health impacts, H_2S also contributes to environmental acidification and the deterioration of infrastructure and ecosystems (WHO, 2003). The global expansion of carbon-based energy industries and infrastructure, particularly in resource-rich regions, has further increased community exposure risks, underscoring the urgent need for robust emergency preparedness and effective community-based response strategies (Brahmia & Mannai, 2025).

The indispensable role of community preparedness in disaster mitigation

Although advanced engineering controls and strict industrial safety practices are the primary strategies for mitigating H_2S risks, the readiness and resilience of local communities ultimately determine the success of disaster management efforts (Batterman et al., 2023). Contemporary approaches to disaster management increasingly draw on sociotechnical systems theory, which emphasizes that human behaviors, attitudes, and interactions within a system are as critical as technological safety measures (Legator et al., 2001; Leveson, 2012). Community preparedness is a proactive, multilayered process that includes understanding risk and vulnerability factors, interpreting complex warning systems, identifying safe evacuation sites, and acquiring basic first aid and self-protection knowledge

(Lacher, 2024). Rapid and effective behavioral responses to alarms during an H_2S release are crucial and can significantly reduce exposure, injuries, and fatalities (Woodcock & Au, 2013). This paper emphasizes that community safety behaviors are not passive outcomes but active, dynamic components of industrial disaster resilience, requiring targeted interventions and continuous engagement with human factors (Siegrist, 2000; Wyche Etheridge et al., 2022).

Aim and scope of this critical review

This review aims to synthesize recent, comprehensive insights into community safety behavior in the context of H_2S gas leak emergencies. It focuses on the multifaceted determinants that shape how individuals and communities perceive, anticipate, and respond to such hazardous incidents. The review systematically integrates evidence from the broader scientific literature, including industrial safety, environmental health, behavioral psychology, human factors engineering, and disaster management. Additionally, it is enriched by empirical evidence from a study examining safety behavior in the local populations of Nakhl Taghi and Assaluyeh counties in Bushehr Province, Iran, regions characterized by extensive oil and gas industry activities and associated H_2S risks (Talebi, 2020). By identifying common challenges, evaluating effective practices, and highlighting persistent gaps in preparedness and response systems, this article seeks to provide practical recommendations to enhance public health safety and strengthen emergency response capacities in industrial environments vulnerable to H_2S hazards worldwide.

MATERIALS AND METHODS

Study Design and Scope

This critical review employed a dual-method approach to synthesize evidence on community behavioral responses to H_2S gas leaks:

1. A systematic literature analysis of peer-reviewed studies (2000–2025) focusing on H_2S preparedness, risk perception, and community behavior.
2. Empirical validation using region-specific survey data from high-risk industrial zones in Assaluyeh and Nakhl Taghi counties, Iran.

Literature searches were conducted using Scopus, Web of Science, PubMed, and Google Scholar with the keywords: "H_2S leak," "emergency preparedness," "community behavior," "risk perception," and "industrial disasters" (Table 1). Inclusion criteria prioritized studies examining human behavioral factors, sociodemographic influences, and the effectiveness of communication in H_2S emergency contexts.

Table 1. Literature search keywords and strategy

Database	Keywords	Search fields	Filters applied	Results retrieved
Scopus	"H_2S leak" OR "hydrogen sulfide leak" AND "emergency preparedness"	Title, Abstract, Keywords	Peer-reviewed articles, English language, 2000-2025	142
Web of Science	("hydrogen sulfide" OR H2S) AND ("community behavior" OR "risk perception")	Topic (Title, Abstract, Keywords)	Articles, Reviews, English language, 2000-2025	98
PubMed	("H2S" OR "hydrogen sulfide") AND ("industrial disasters" OR "disaster management")	Title, Abstract	Human studies, English language, 2000-2025	76
Google Scholar	"H2S gas leak" AND ("community preparedness" OR "behavioral factors")	All fields	Exclude patents, citations; English language, 2000-2025	96

Notes:

- Search was conducted in January 2025.
- Boolean operators (AND, OR) were used to combine terms for precision and recall.
- Inclusion criteria: Studies focusing on H2S-related emergencies, community behavior, risk perception, or disaster management.
- Exclusion criteria: Non-peer-reviewed sources, studies unrelated to H2S or community response, pre-2000 publications.
- Total unique records after duplication: 412, with 127 meeting inclusion criteria after screening.

Data Collection and Sources

Literature Review

- **Screening**: a total of 412 records were identified, with 127 studies meeting the inclusion criteria after deduplication and relevance assessment (Figure 1).
- **Quality appraisal**: The included studies were evaluated for methodological rigor, risk of bias, and applicability using the Critical Appraisal Skills Programme (CASP) checklists (CASP, 2023).

Empirical Study

- **Survey instrument**: A validated questionnaire assessed safety behavior determinants, including:
  - Risk perception (5-point Likert scale; adapted from Siegrist & Zingg, 2014).
  - Trust in authorities (items derived from Siegrist, 2000).
  - Preparedness actions (e.g., evacuation plans, kit availability; Perry & Lindell, 2003).
  - Sociodemographic variables (age, education, occupation, health status).
- **Sampling**: Stratified random sampling of 680 residents in Assaluyeh (n=350) and Nakhl Taghi (n=330), ensuring proportional representation by distance from industrial sites (<5 km, 5-10 km, >10 km).
- **Ethics**: Approved by University of Tehran IRB (Ref: UT/ENV/2020-87). Written informed consent was obtained.

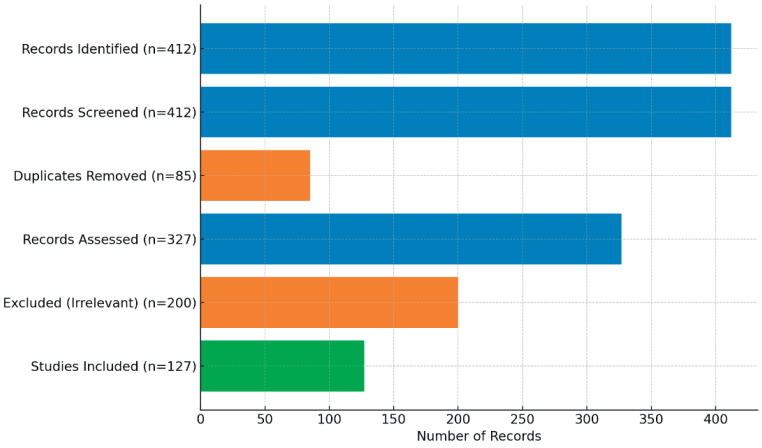


Figure 1. PRISMA flow diagram for literature screening

Data Analysis

- **Quantitative analysis**: survey data were analyzed using multiple linear regression to identify predictors of safety behavior (SPSS v28). The key model was specified as in eq. 1. Covariates included age, education, occupation, and health status. Multicollinearity was assessed using variance inflation factors (VIF), with all values below 2.5 indicating acceptable levels.

$$\text{Safety Behavior} = \beta_0 + \beta_1(\text{City}) + \beta_2(\text{Distance}) + \beta_3(\text{Risk Perception}) + \cdots + \epsilon \quad (1)$$

- **Qualitative synthesis**: a thematic analysis of the literature was conducted using NVivo 12 to identify recurring gaps, including training deficits and communication barriers, within the context of community preparedness and H_2S emergency response.

Integration Framework

Findings from literature and empirical data were triangulated using a **sociotechnical systems lens** (Sasou et al., 1996), evaluating interactions between:

1. *Technical factors* (warning systems, monitoring tools).

2. *Human factors* (risk perception, trust, demographics).
3. *Organizational factors* (policy, community engagement).

Limitations and Mitigation

- **Cross-sectional design** limits causal inference; future work should adopt longitudinal tracking (Barnett et al., 2023).
- **Geographical specificity**: Findings from Assaluyeh/Nakhl Taghi may not generalize globally; contextual factors were explicitly discussed (Keshmiri et al., 2018).
- **Self-reported data**: Potential recall bias was mitigated via pilot-testing instruments and anchoring responses to recent drills.

RESULTS AND DISCUSSIONS

1. Understanding H_2S Exposure and Its Multifaceted Health Impacts

1.1. Characteristics, exposure pathways, and mechanisms of toxicity on H_2S

Characteristics: hydrogen sulfide (H_2S) is a colorless, flammable, and toxic gas that emits a distinct "rotten egg" odor at low concentrations. At higher concentrations (>100 ppm), olfactory fatigue occurs rapidly, leading to an inability to detect its odor, which is why H_2S is often referred to as a "silent killer" (Beauchamp et al., 2020; Public Services and Procurement Canada, 2023).

Physical properties: H_2S is denser than air, allowing it to accumulate in low-lying areas and enclosed spaces, such as trenches and industrial environments, thereby increasing the risk of exposure (Public Services and Procurement Canada, 2023).

Exposure pathway: the primary route of exposure is inhalation, through which H_2S is rapidly absorbed across alveolar membranes into the bloodstream (Beauchamp et al., 2020).

Toxicity mechanism: once absorbed, H_2S inhibits cytochrome c oxidase (Complex IV) in the mitochondrial respiratory chain, disrupting cellular respiration and leading to cellular hypoxia. This mechanism causes rapid systemic effects, particularly in organs with high oxygen demands, such as the brain, heart, and lungs, potentially resulting in critical organ failure (Batterman et al., 2023; Ng et al., 2019; Lewis & Copley, 2015).

Long-Term effects: prolonged or sub-lethal exposure to H_2S can induce oxidative stress, inflammation, and cell death, which may contribute to long-term adverse health outcomes (Rumbeiha et al., 2016).

1.2. Health risks, dose-response relationships, and vulnerable populations

Exposure to H_2S has detrimental health effects that correlate directly with the concentration and duration of exposure (Ng et al., 2019).

- *Low-level chronic exposure* (as low as 0.3 parts per billion) has been associated with mild neurological and respiratory symptoms, including headaches, nausea, and eye and nasal irritation (Legator et al., 2001).
- *Acute moderate exposure* (50-100 ppm) can rapidly induce chest pain, coughing, shortness of breath, conjunctivitis, and keratitis (Beauchamp et al., 2020; Santana Maldonado et al., 2023).
- *High-level exposure* (>500 ppm) may cause severe central nervous system depression, convulsions, unconsciousness, and respiratory arrest, potentially resulting in death (Beauchamp et al., 2020; Lewis & Copley, 2015; Ng et al., 2019).

Certain demographic groups and individuals with pre-existing conditions are particularly vulnerable to H_2S exposure and require targeted protective measures (Talebi, 2020):

- *Children* are more susceptible due to smaller lung capacities, higher metabolic rates, and proportionally larger alveolar surface areas (Talebi, 2020).
- *Elderly people* often have neurological, cardiovascular, or respiratory comorbidities that can be exacerbated by H_2S exposure (ATSDR, 2016; Legator et al., 2001).
- *Individuals with pre-existing conditions*, such as cardiovascular disease, asthma, or chronic obstructive pulmonary disease (COPD), may experience more severe symptoms even at lower exposure levels, as highlighted in studies from Assaluyeh and Nakhl Taghi (Talebi, 2020).
- *Occupational groups* working in high-risk industries with potential H_2S exposure are particularly vulnerable, and their workplace experiences can influence overall community safety practices and perceptions (OSHA, 2005). Developing accurate emergency alerts and preventative measures that are inclusive and

successful across various community segments requires an understanding of these particular vulnerabilities (Ogie et al., 2018).

2. Factors Influencing Community Safety Behavior in Emergencies

Effective community safety behavior in response to H_2S leaks results from a complex interplay of individual cognitive processes, social dynamics, and environmental factors. The empirical study conducted in Assaluyeh and Nakhl Taghi offered valuable real-world insights by systematically examining various demographic and situational factors that influence safety behavior in high-risk industrial contexts (Talebi, 2020).

2.1. Risk perceptions and knowledge

Accurate knowledge of hazards and the subjective estimation of associated risks are central drivers of safety behavior (Siegrist & Zingg, 2014). In the context of H_2S, this includes understanding its odorless nature at hazardous concentrations, its specific health effects, the limitations of odor detection due to olfactory fatigue, and awareness of appropriate first-line protective actions (e.g., moving upwind or uphill, seeking shelter indoors and sealing openings, and activating personal warning systems) (Morgan et al., 2001).

Empirical findings from Nakhl Taghi and Assaluyeh indicate varying levels of knowledge among residents regarding H_2S properties and emergency response strategies (Talebi, 2020). Notably, the significant correlation between “city of residence” and safety behavior suggests variability in risk perception and knowledge distribution, potentially influenced by proximity to industrial areas, prior exposure to industrial incidents, and differing historical exposure levels between the two districts (Talebi, 2020). Groups with a clearer and more precise understanding of specific hazards are more likely to exhibit appropriate and anticipatory safety behaviors during emergencies (Santoro et al., 2023; Siegrist & Zingg, 2014). However, over-reliance on the “rotten egg” odor as an indicator of danger can lead to fatal complacency, highlighting a critical knowledge gap regarding the limitations of sensory detection of H_2S at dangerous concentrations (Public Services and Procurement Canada, 2023).

2.2. Emergency communication and warning systems

Clear, prompt, consistent, and credible communication is the key to effective emergency response (Ogie et al., 2022). Warning systems must be robust, stable, and accessible to all population groups, including vulnerable populations (Karimiziarani & Moradkhani, 2023). Effective strategies necessitate multi-channel communication techniques (e.g., sirens, SMS, local radio/TV, social media, door-to-door warning, community alarm systems) to ensure message penetration and redundancy (Ogie et al., 2022; Tzioutzios et al., 2024). The coherence, specificity, and concision of messages, conveying clear-cut instructions on "what to do", "where to go", and "who to contact", are crucial for triggering appropriate action (Hinsberg & Lamanna, 2024; Woodcock & Au, 2013). Risk communication must also be recognized as an iterative, integrative process throughout the entire risk management stages - preparedness, response, and recovery - calling for openness, participation, and two-way communication to enable informed decision-making and adaptive capacity building (Hinsberg & Lamanna, 2024; Pidgeon & O'Leary, 2000). The variable safety behavior present in the thesis between the two cities could have implicitly shown differences in communication effectiveness or public acceptance of warnings in the two cities (Talebi, 2020).

2.3. Trust in authorities and industry

The baseline level of the community's trust in the government agencies and the nearby industrial sector is an understated but profound determinant of safety behaviour (Siegrist, 2000). High levels of such trust in the community make them much more likely to respond to official warnings, quickly obey evacuation orders, and take voluntary courses in preparedness (Frewer et al., 1996; Siegrist, 2000). Contributing to the development and sustenance of trust are open communication of information, perceived expertise and responsiveness of emergency departments, sustained interaction with the population, and established accountability for past errors or

incidents (Health and Safety Executive (HSE), 2013; Siegrist, 2000). Conversely, prior experience with unresolved problems, expectation of privacy, lack of transparency, or inadequate response to prior incidents can destroy trust, leading to cynicism, delayed responses, or self-imposed non-compliance in a real emergency (Renn & Levine, 1991; Siegrist, 2000). The diversified safety behavior in Assaluyeh and Nakhl Taghi indirectly represents the differences in community-industry/government relations and trust levels in those regions, which reinforce the important role of social capital in crisis management (Behera, 2023; Talebi, 2020).

2.4. Preparedness actions and evacuation behavior

Personal and family preparedness actions are at the heart of community resilience (Lacher, 2024). This includes emergency kit preparations, having family communication plans, establishing safe meeting points, and being familiar with prearranged evacuation routes (Perry & Lindell, 2003). Evacuation decisions are decided by a multidimensional array of factors, including perceived threat severity and proximity, clarity and credibility of directions to evacuate, presence and influence of social networks, and personal resources (Lewis & and Copley, 2015; Shrivastava, 2005). These are barriers to evacuation success and include the absence of transport, caregiving responsibilities (e.g., children or elderly), physical disability, socioeconomic constraints, as well as psychological aspects such as "normalcy bias," where the affected person underestimates the threat and is certain that all would go back to normal (Lewis & and Copley, 2015; Rumbeiha et al., 2016). The thesis, in its general "safety behavior" indicator, indirectly encompasses the dimensions of preparedness behaviors and mentions the role of demographic variables like "number of dependents" and "age" in one's ability or willingness to prepare and evacuate. For instance, individuals with a greater number of dependents will find it more challenging to quickly evacuate, and elderly people will have different mobility problems, which indicates the necessity of inclusive disaster planning (Akama et al., 2014; Talebi, 2020).

2.5. Socioeconomic and demographic factors

Socioeconomic and demographic factors significantly influence individual and collective safety behavior by conditioning access to information, resources, and social networks (Cutter et al., 2003; Legator et al., 2001). Your thesis particularly tested the influence of several such factors, adding empirical validation from the regional context (Talebi, 2020):

- *Gender and age:* both emerged as variables influencing safety behavior, with implications for age- and gender-sensitive communication and training programs (Talebi, 2020).
- *Education level:* a significant influence, with higher levels of education generally linked to better risk understanding, heightened critical thinking, and adherence to safety protocols and emergency instructions (Becker, 2009; Legator et al., 2001).
- *Health status (smoking, chronic illness, medication use):* such health conditions can have direct impacts on one's physical capacity and psychological ability to act effectively in an emergency and demand special planning measures (Ogie et al., 2018; Talebi, 2020).
- *Occupation type, work experience, shift work, second job:* these work-related variables suggest an exploration of whether occupational exposure or experience would translate into general safety awareness and behavior in the broader community. Individuals who work in hazardous industries might have a higher perception of risk or suitable safety awareness that would influence their household's preparedness (Occupational Safety and Health Administration (OSHA), 2005; Talebi, 2020).
- *City of residence (Nakhl Taghi vs. Assaluyeh):* this was the variable most strongly associated with safety behavior (Talebi, 2020). This robust finding highlights that immediate geographical proximity to the industrial complex, coupled with special local policies, community outreach activities, historical exposure to incidents, and socio-economic status within each city, has a dominant and highly localized impact on safety behavior. This highlights the context-dependent nature of preparedness.

3. H_2S Emergency Preparedness and Response Gaps and Challenges

Despite ongoing advancements in industrial safety and emergency management, there are still ongoing and pertinent gaps in fully preparing and enabling communities to respond most effectively to H2S gas releases and other chemical threats.

3.1. Absence of standardized training and drills

The majority of communities residing near chemical hazard sites are seriously short of exposure to routine, standardized, and realistic emergency training exercises specifically targeting chemical releases like H_2S (Santana Maldonado et al., 2023; United Nations Office for Disaster Risk Reduction (UNDRR), 2015). Bystander disaster preparedness training is typically not satisfactory in meeting the unique features of H_2S (e.g., odorlessness in high concentrations, quick onset of bad symptoms, specific ventilation requirements) (Santana Maldonado et al., 2023). Further, the absence of proper public training on H_2S hazards and related protective precautions also increases extensive knowledge gaps, directly hurting proper safety performance (Mileti, 1999). Drills should include escape procedures, shelter-in-place drills, and realistic scenarios in order to create muscle memory and self-assurance (Centers for Disease Control and Prevention (U.S). Center for Preparedness and Response, 2018).

3.2. Inadequate use of local knowledge and participatory approaches

Traditional top-down emergency planning tends to overlook or insufficiently incorporate valuable local knowledge, accessible community social networks, and unique vulnerabilities and assets of affected groups (Atlanta (GA): Agency for Toxic Substances and Disease Registry (US), 2016). This can lead to technically competent but operationally worthless, culturally insensitive, and even unimplementable state plans on the ground (Perry et al., 2001). Effective preparedness demands genuinely participatory approaches where active involvement of community members is made in the risk identification, collaborative plan development, dissemination of information, and feedback so that strategies are feasible to implement, culturally appropriate, and sensitive (Atlanta (GA): Agency for Toxic Substances and Disease Registry (US), 2016; Paton & Johnston, 2006). Disregard of local knowledge can also enhance psychosocial risks among communities who reside in toxic pollution (Couch & Coles, 2011).

3.3. Technological limitations in detection and distribution systems

Although sophisticated H_2S detection systems exist, challenges persist in creating real-time, widespread, and detailed localized monitoring, especially across vast industrial and adjacent residential areas (Morgan et al., 2001; WHO, 2003). Also, providing real-time and focused warning to all at risk, taking into account multiple communication barriers (e.g., language, illiteracy, digital divide, disability), is a significant challenge (Comfort & Haase, 2006; Karimiziarani & Moradkhani, 2023). Obscure warning systems, overreliance on a single mode of communication, or lack of harmonization with smart city systems may lead to vulnerable groups being uninformed or misinformed at moments of high demand (Comfort & Haase, 2006; Elvas et al., 2021).

3.4. Persevering psychological and behavioral barriers

Even with proper knowledge and timely notification, basic human psychological responses can interfere with best safety practice (Rumbeiha et al., 2016). "Normalcy bias" (denial or minimizing of threat), "optimism bias" (sensing personal probability of being harmed as low), "bystander effect," or "panic" (while actual panic is rare, improper conduct can occur) can lead to response delay, maladaptive conduct, or non-compliance (Rumbeiha et al., 2016; Shrivastava, 2005). Neutralizing such widespread behavioral barriers involves not just provision of information but also realistic practice under stress, psychological preparation techniques, and training that aims at the likely exposure to emotional and mental responses to an unexpected, unseen, and lethal threat (Perry & Quarantelli, 2005).

3.5. Policy and regulatory framework gaps

Although industrial emissions, workplace safety, and general disaster management are regulated by law in most nations, policy frameworks specifically addressing general

community emergency preparedness for H_2S and other chemical hazards can have significant gaps (Santana Maldonado et al., 2023; UNEP, 2025). These include the absence of clear mandates for industries to get actively engaged and make financial contributions towards community preparedness activities, defined roles and responsibilities for inter-agency coordination (e.g., between industrial operators, local government, emergency services, and public health agencies), and enforceable standards for risk communication and public education (Santana Maldonado et al., 2023; Tierney, 2025). Moreover, there is sparse scientific monitoring and assessment of environmental and health impacts in communities around long-established industrial facilities, reflecting significant knowledge and policy gaps at national and regional levels (Willis et al., 2018). Inadequate land-use planning around dangerous industrial factories can also exacerbate community vulnerability (Walker, 1991).

4. Future Perspectives and Conclusion

4.1. Towards integrated, community-centric preparedness paradigms

Future effective emergency preparedness for H2S will demand a paradigm shift to synergistic, genuinely community-oriented solutions. This demands integrated synergism of robust technical solutions (e.g., advanced, comprehensive H_2S monitoring networks, hybrid early warning systems), sophisticated human factors analysis (e.g., cognitive ergonomics of signals, behavior-based training on psychological principles), and sophisticated socio-ecological knowledge (e.g., linking to community networks, interpreting cultural matters, reducing social vulnerability) (Legator et al., 2001; Leveson, 2012; Siegrist & Zingg, 2014). Multi-stakeholder collaboration, comprising industry, government departments, emergency services, academia, and not least of all the local communities themselves, is required in a bid to establish common responsibility for resilience and safety (Paton & Johnston, 2006; Siegrist, 2000). Pre-emergent activities like joint drills, scenario planning in unison, and unfettered information sharing can build needed trust and significantly enhance collective response capacities, thus overall preparedness and adaptive capacity of a community (Pidgeon & O'Leary, 2000).

4.2. Leveraging emerging digital technologies for enhanced response

Emerging digital technologies offer game-changing possibilities for transforming H_2S emergency preparedness and response:

- *Predictive analytics & real-time monitoring:* IoT sensors deployed for widespread H_2S sensing, combined with advanced atmospheric dispersion modeling and AI for predictive analytics, have the potential to provide real-time, highly localized risk assessment and hazard mapping (Morgan et al., 2001; Prasad et al., 2024).
- *Customized alerts & communication:* Mobile applications and geo-fencing technologies enable rapid, hyper-targeted alerts to individuals in affected areas, with customized directions based on their precise real-time location and known vulnerabilities (Morgan et al., 2001; Mota et al., 2023).
- *Immersive training & simulation:* Virtual Reality (VR) and Augmented Reality (AR) technologies can offer realistic, safe, and repeatable environments for community members to practice complex emergency response behaviors, e.g., evacuation and shelter-in-place. This addresses the limitations of traditional drills via immersive experiential learning (Perry & Quarantelli, 2005; Srinivasan et al., 2022).
- *Social media & crowdsourcing for situational awareness*: While unofficial, social media can also offer valuable sources of real-time information, citizen reporting, and community sentiment during an emergency. Advanced data analytics can allow emergency managers to rapidly identify emerging needs, identify gaps in resource deployment, and refute misinformation (Elvas et al., 2021; Ogie et al., 2022).

4.3. Imperative research priorities for future advancement

Future research efforts in this critical field should be directed towards:

- *Longitudinal studies:* Investigating the long-term psychosocial and physical health consequences of H2S exposure on residents and the sustainability of safety behavior changes following various interventions (Couch & Coles, 2011; Legator et al., 2001).

- *Culturally sensitive communication:* Developing and rigorously testing communication strategies and warning systems that are not only technologically advanced but also culturally sensitive, linguistically appropriate, and actually resonate with multicultural community segments in H2S-risk zones (Ogie et al., 2018; Tzioutzios et al., 2024).
- *Behavioral economics in safety:* Applying findings from behavioral economics and nudge theory to better comprehend and actively influence pro-safety behaviors and compliance with emergency procedures in high-risk environments (Perry & Quarantelli, 2005).
- *In-depth resilience measurement:* Exhaustively measuring the performance of comprehensive community resilience-building initiatives that are specific to industrial chemical threats, extending beyond preparedness actions (Brahmia & Mannai, 2025; Gisela van et al., 2025).
- *Chronic threat psychological effect:* In-depth exploration of the psychosocial stress and mental health consequences for communities under constant threat of H2S exposure, and the development of community-level coping mechanisms and support systems (Couch & Coles, 2011; Galea et al., 2002).
- *Cost-Benefit analysis of preparedness:* Quantifying the economic and social benefits of robust community preparedness programs versus the cost of inaction in industrial disaster scenarios (Botzen et al., 2019).

CONCLUSIONS

Empirical evidence, supported by findings from Assaluyeh and Nakhl Taghi, demonstrates that adaptive and conscious community safety behavior is a critical pillar for effective emergency response to H_2S gas leaks. The observed variations in safety behavior, particularly influenced by the city of residence, underscore the highly localized, context-dependent, and complex nature of preparedness challenges.

Addressing existing gaps in knowledge, trust, communication, and training requires coordinated, multidisciplinary, and multi-stakeholder efforts. By embracing integrated planning, leveraging advanced digital technologies, and fostering genuine community participation and empowerment, it is possible to create environments where communities near H_2S sources are not only safeguarded by industrial systems but are also equipped to respond promptly and effectively during emergencies.

The overarching goal is to build resilient communities capable of mitigating the human, environmental, and economic impacts of H_2S incidents, thereby ensuring public health safety and promoting sustainable industrial development in high-risk regions globally.

ACKNOWLEDGEMENTS

This research work was carried out with the support of Ministry of Agriculture and Rural Development, Department of Statistics and was financed from Project PN II Partnership No. 2365/2007.

REFERENCES

Akama, Y., Chaplin, S., & Fairbrother, P. (2014). Role of social networks in community preparedness for bushfire. *International Journal of Disaster Resilience in the Built Environment*, *5*(3), 277-291. https://doi.org/10.1108/IJDRBE-01-2014-0010

Atlanta (GA): Agency for Toxic Substances and Disease Registry (US). (2016). *Toxicological profile for hydrogen sulfide and carbonyl sulfide*.

Barnett, T. A., Koushik, A., & Schuster, T. (2023). Invited Commentary: Cross-Sectional Studies and Causal Inference—It's Complicated. *American Journal of Epidemiology*, *192*(4), 517-519. https://doi.org/10.1093/aje/kwad026

Batterman, S., Amelia, G.-A., & and Seo, S.-H. (2023). Low level exposure to hydrogen sulfide: a review of emissions, community exposure, health effects, and exposure guidelines. *Critical Reviews in Toxicology*, *53*(4), 244-295. https://doi.org/10.1080/10408444.2023.2229925

Beauchamp, J., Davis, C., & Pleil, J. (2020). *Breathborne Biomarkers and the Human Volatilome*. Elsevier.

Becker, G. S. (2009). *Human Capital: A Theoretical and Empirical Analysis, with Special Reference to Education*. University of Chicago Press.

Behera, J. K. (2023). Role of social capital in disaster risk management: a theoretical perspective in special reference to Odisha, India. *Int J Environ Sci Technol (Tehran)*, *20*(3), 3385-3394. https://doi.org/10.1007/s13762-021-03735-y

Botzen, W. J. W., Deschenes, O., & Sanders, M. (2019). The Economic Impacts of Natural Disasters: A Review of Models and Empirical Studies. *Review of*

Environmental Economics and Policy, *13*(2), 167-188. https://doi.org/10.1093/reep/rez004

Brahmia, S. Y., & Mannai, S. (2025). Environmental Degradation in Gulf Cooperation Council: Role of ICT Development, Trade, FDI, and Energy Use. *Sustainability*, *17*(1), 54.

Centers for Disease Control and Prevention (U.S). Center for Preparedness and Response. (2018). *Public health emergency preparedness and response capabilities : national standards for state, local, tribal, and territorial public health.* .

Comfort, L. K., & Haase, T. W. (2006). Communication, Coherence, and Collective Action:The Impact of Hurricane Katrina on Communications Infrastructure. *Public Works Management & Policy*, *10*(4), 328-343. https://doi.org/10.1177/1087724x06289052

Couch, S. R., & Coles, C. J. (2011). Community stress, psychosocial hazards, and EPA decision-making in communities impacted by chronic technological disasters. *Am J Public Health*, *101 Suppl 1*(Suppl 1), S140-148. https://doi.org/10.2105/ajph.2010.300039

Critical Appraisal Skills Programme (CASP). (2023). *CASP Checklists*. https://casp-uk.net/casp-tools-checklists/

Cutter, S. L., Boruff, B. J., & Shirley, W. L. (2003). Social Vulnerability to Environmental Hazards. *Social Science Quarterly*, *84*(2), 242-261. https://doi.org/https://doi.org/10.1111/1540-6237.8402002

Elvas, L. B., Mataloto, B. M., Martins, A. L., & Ferreira, J. C. (2021). Disaster Management in Smart Cities. *Smart Cities*, *4*(2), 819-839.

Frewer, L. J., Howard, C., Hedderley, D., & Shepherd, R. (1996). What Determines Trust in Information About Food-Related Risks? Underlying Psychological Constructs. *Risk Analysis*, *16*(4), 473-486. https://doi.org/https://doi.org/10.1111/j.1539-6924.1996.tb01094.x

Galea, S., Ahern, J., Resnick, H., Kilpatrick, D., Bucuvalas, M., Gold, J., & Vlahov, D. (2002). Psychological sequelae of the September 11 terrorist attacks in New York City. *N Engl J Med*, *346*(13), 982-987. https://doi.org/10.1056/NEJMsa013404

Gisela van, K., Steve, M., Janine, D., Daniel, H. d. V., Hayley, M., Sharon, A.,…Nina, G. (2025). Community resilience to health emergencies: a scoping review. *BMJ Global Health*, *10*(4), e016963. https://doi.org/10.1136/bmjgh-2024-016963

Health and Safety Executive (HSE). (2013). Leading health and safety at work. In *Actions for directors, board members, business owners and organisations of all sizes*

Hinsberg, K. L., & Lamanna, A. J. (2024). Crisis communication in construction: Organizational strategies for worksite fatalities. *Journal of Safety Research*, *88*, 145-160. https://doi.org/https://doi.org/10.1016/j.jsr.2023.11.002

Karimiziarani, M., & Moradkhani, H. (2023). Social response and Disaster management: Insights from twitter data Assimilation on Hurricane Ian. *International Journal of Disaster Risk Reduction*, *95*, 103865. https://doi.org/https://doi.org/10.1016/j.ijdrr.2023.103865

Keshmiri, S., Pordel, S., Raeesi, A., Nabipour, I., Darabi, H., Jamali, S.,…Farrokhi, S. (2018). Environmental Pollution Caused by Gas and Petrochemical Industries and Its Effects on the Health of Residents of Assaluyeh Region, Irani-an Energy Capital: A Review Study [Review]. *Iranian South Medical Journal*, *21*(2), 162-185. https://doi.org/10.29252/ismj.21.2.162

Lacher, S. (2024). Exploring disaster preparedness: a scoping review of adult and continuing education approaches in international civil protection research. *Journal of Risk Research*, *27*(10), 1273-1289. https://doi.org/10.1080/13669877.2024.2447252

Legator, M. S., Singleton, C. R., Morris, D. L., & Philips, D. L. (2001). Health effects from chronic low-level exposure to hydrogen sulfide. *Arch Environ Health*, *56*(2), 123-131. https://doi.org/10.1080/00039890109604063

Leveson, N. G. (2012). *Engineering a Safer World: Systems Thinking Applied to Safety*. The MIT Press. https://doi.org/10.7551/mitpress/8179.001.0001

Lewis, R. J., & and Copley, G. B. (2015). Chronic low-level hydrogen sulfide exposure and potential effects on human health: A review of the epidemiological evidence. *Critical Reviews in Toxicology*, *45*(2), 93-123. https://doi.org/10.3109/10408444.2014.971943

Mileti, D. (1999). *Disasters by Design: A Reassessment of Natural Hazards in the United States*. The National Academies Press. https://doi.org/doi:10.17226/5782

Morgan, M. G., Fischhoff, B., Bostrom, A., & Atman, C. J. (2001). *Risk Communication: A Mental Models Approach*. Cambridge University Press. https://doi.org/DOI: 10.1017/CBO9780511814679

Mota, G. d. A., Santos, R. C., dos Santos, J. A., Lovatto, J., Geisenhoff, L. O., Machado, C. A. C.,…de Carvalho, M. M. A. J. (2023). Smart sensors and Internet of Things (IoT) for sustainable environmental and agricultural management. *Caderno Pedagógico*, *20*(7), 2692-2714. https://doi.org/10.54033/cadpedv20n7-014

Ng, P. C., Hendry-Hofer, T. B., Witeof, A. E., Brenner, M., Mahon, S. B., Boss, G. R.,…Bebarta, V. S. (2019). Hydrogen Sulfide Toxicity: Mechanism of Action, Clinical Presentation, and Countermeasure Development. *Journal of Medical Toxicology*, *15*(4), 287-294. https://doi.org/10.1007/s13181-019-00710-5

Occupational Safety and Health Administration (OSHA). (2005). *Hydrogen Sulfide (H_2S) Safety Fact Sheet*.

Occupational Safety and Health Administration (OSHA). (2015). *Fire Service Features of Buildings and Fire Protection Systems*.

Ogie, R., Rho, J. C., Clarke, R. J., & Moore, A. (2018). Disaster Risk Communication in Culturally and Linguistically Diverse Communities: The Role of Technology. *Proceedings*, *2*(19), 1256.

Ogie, R. I., James, S., Moore, A., Dilworth, T., Amirghasemi, M., & Whittaker, J. (2022). Social media use in disaster recovery: A systematic literature review. *International Journal of Disaster*

Risk Reduction, *70*, 102783.https://doi.org/https://doi.org/10.1016/j.ijdrr.2022.102783

Paton, D., & Johnston, D. M. (2006). *Disaster Resilience: An Integrated Approach*. Charles C Thomas.

Perry, R. W., & Lindell, M. K. (2003). Preparedness for Emergency Response: Guidelines for the Emergency Planning Process. *Disasters*, *27*(4), 336-350. https://doi.org/https://doi.org/10.1111/j.0361-3666.2003.00237.x

Perry, R. W., Lindell, M. K., & Tierney, K. J. (2001). *Facing the Unexpected: Disaster Preparedness and Response in the United States*. National Academies Press.

Perry, R. W., & Quarantelli, E. L. (2005). *What is a disaster? new answers to old questions*. International Research Committee on Disasters.

Pidgeon, N., & O'Leary, M. (2000). Man-made disasters: why technology and organizations (sometimes) fail. *Safety Science*, *34*(1), 15-30. https://doi.org/https://doi.org/10.1016/S0925-7535(00)00004-7

Prasad, S., Sharma, K., Karwasra, A., Raj, D., & Gupta, S. (2024). A Review: IOT Based Environmental Monitoring System. *International journal of creative research thoughts - IJCRT (IJCRT.ORG)*, *12*(5).

Public Services and Procurement Canada. (2023, September 21). *Screening Assessment: Hydrogen Sulfide. Government of Canada*. https://www.canada.ca/en/health-canada/services/environmental-workplace-health/reports-publications/risk-assessments/hydrogen-sulfide.html

Renn, O., & Levine, D. (1991). Credibility and trust in risk communication. In R. E. Kasperson & P. J. M. Stallen (Eds.), *Communicating Risks to the Public: International Perspectives* (pp. 175-217). Springer Netherlands. https://doi.org/10.1007/978-94-009-1952-5_10

Rumbeiha, W., Whitley, E., Anantharam, P., Kim, D.-S., & Kanthasamy, A. (2016). Acute hydrogen sulfide–induced neuropathology and neurological sequelae: challenges for translational neuroprotective research. *Annals of the New York Academy of Sciences*, *1378*(1), 5-16. https://doi.org/https://doi.org/10.1111/nyas.13148

Santana Maldonado, C., Abigail, W., & and Rumbeiha, W. K. (2023). A comprehensive review of treatments for hydrogen sulfide poisoning: past, present, and future. *Toxicology Mechanisms and Methods*, *33*(3), 183-196. https://doi.org/10.1080/15376516.2022.2121192

Santoro, S., Lovreglio, R., Totaro, V., Camarda, D., Iacobellis, V., & Fratino, U. (2023). Community risk perception for flood management: A structural equation modelling approach. *International Journal of Disaster Risk Reduction*, *97*, 104012. https://doi.org/https://doi.org/10.1016/j.ijdrr.2023.104012

Sasou, K., Takano, K. i., & Yoshimura, S. (1996). Modeling of a team's decision-making process. *Safety Science*, *24*(1), 13-33. https://doi.org/https://doi.org/10.1016/S0925-7535(96)00029-X

Shrivastava, P. (2005). Managing Risks in the Age of Terror. *Risk Management*, *7*(1), 63-70. https://doi.org/10.1057/palgrave.rm.8240205

Siegrist, M. (2000). The Influence of Trust and Perceptions of Risks and Benefits on the Acceptance of Gene Technology. *Risk Analysis*, *20*(2), 195-204. https://doi.org/https://doi.org/10.1111/0272-4332.202020

Siegrist, M., & Zingg, A. (2014). The role of public trust during pandemics: Implications for crisis communication. *European Psychologist*, *19*(1), 23-32. https://doi.org/10.1027/1016-9040/a000169

Srinivasan, B., Iqbal, M. U., Shahab, M. A., & Srinivasan, R. (2022). Review of Virtual Reality (VR) Applications To Enhance Chemical Safety: From Students to Plant Operators. *ACS Chemical Health & Safety*, *29*(3), 246-262. https://doi.org/10.1021/acs.chas.2c00006

Talebi, E. (2020). ارزیابی رفتار ایمنی جوامع محلی در شهرستانهای عسلویه و نخل تقی در استان بوشهر در مواجهه با شرایط اضطراری نشت گاز H_2S *(Assessment of Safety Behavior of Local Communities in Assaluyeh and Nakhl Taghi Counties, Bushehr Province, in Facing H2S Gas Leak Emergency Conditions)* [Master's Thesis, University of Tehran, Faculty of Environment].

Tierney, K. (2025). *Disasters: A Sociological Approach*. Polity Press.

Tzioutzios, D., Suarez-Paba, M. C., Luo, X., & Cruz, A. M. (2024). Natech Risk Communication. In: Oxford University Press.

UNEP. (2025). *Awareness and preparedness for emergencies at local level (APELL)*. https://www.unep.org/topics/disasters-and-conflicts/response-and-recovery/awareness-and-preparedness-emergencies-local#:~:text=The%20APELL%20Methodology,-The%20APELL%20Process&text=This%20is%20achieved%20by%20assisting,life%2C%20property%20or%20the%20environment.

United Nations Office for Disaster Risk Reduction (UNDRR). (2015). *Sendai Framework for Disaster Risk Reduction 2015-2030*. https://www.undrr.org/publication/sendai-framework-disaster-risk-reduction-2015-2030

Walker, G. P. (1991). Land use planning and industrial hazards: A role for the European community. *Land Use Policy*, *8*(3), 227-240. https://doi.org/https://doi.org/10.1016/0264-8377(91)90036-I

WHO. (2003). *Hydrogen sulfide: Air quality guidelines for Europe*. https://apps.who.int/iris/handle/10665/107381

Willis, M. D., Jusko, T. A., Halterman, J. S., & Hill, E. L. (2018). Unconventional natural gas development and pediatric asthma hospitalizations in Pennsylvania. *Environmental Research*, *166*, 402-408. https://doi.org/https://doi.org/10.1016/j.envres.2018.06.022

Woodcock, B., & Au, Z. (2013). Human factors issues in the management of emergency response at high hazard installations. *Journal of Loss Prevention in the Process Industries*, *26*(3), 547-557. https://doi.org/https://doi.org/10.1016/j.jlp.2012.07.002

Wyche Etheridge, K., Justice, A. D., Lewis, M., & Plescia, M. (2022). Strategies to Operationalize Health Equity in State and Territorial Health Departments. *Journal of Public Health Management and Practice*, *28*(4).

Scientific Papers. Series E. Land Reclamation, Earth Observation & Surveying, Environmental Engineering. Vol. XIV, 2025
Print ISSN 2285-6064, CD-ROM ISSN 2285-6072, Online ISSN 2393-5138, ISSN-L 2285-6064

RESTORATION ACTIVITIES AND BIODIVERSITY SURVEY OF WEST STUPINI MIRE IN THE BÂRSA DEPRESSION: BASELINE FOR NATURA 2000 CONSERVATION

Anca MANOLE[1], Ana-Maria MOROȘANU[1], Attila MÁTIS[2], Anna SZABÓ[2], Georgiana-Roxana NICOARĂ[1], Florența-Elena HELEPCIUC[1], Mihnea VLADIMIRESCU[1], Ioana Cătălina PAICA[1], Mihaela CIOBOTĂ[1], Daniela Elena MOGÎLDEA[1], Constantin-Ciprian BÎRSAN[1], Constanța-Mihaela ION[1], Tiberiu SAHLEAN[1], Sorin ȘTEFĂNUȚ[1]

[1]Institute of Biology Bucharest of the Romanian Academy,
296 Splaiul Independenței, District 6, 060031, Bucharest, Romania
[2]Babeș-Bolyai University, Faculty of Biology and Geology,
5-7 Clinicilor Street, 400006, Cluj-Napoca, Romania

Corresponding author email: anamaria.morosanu@ibiol.ro

Abstract

The Stupini mire, proposed as a new Natura 2000 site, is a wetland located in Romania's Bârsa Depression. The site hosts a diverse range of habitats, including alkaline fens (7230), calcareous fens (7210), Molinia meadows (6410), hygrophilous tall herb communities (6430), and alluvial forests (91E0*). This study highlights the ecological importance of the mire and evaluates the impact of recent restoration efforts. Vegetation surveys conducted between 2022 and 2024 confirmed the presence of rare and protected species, such as Swertia perennis and Primula farinose as well as the glacial relict Ligularia sibirica, a species protected under European legislation. However, the rare orchid Liparis loeselii was not detected, raising concerns about its possible local extinction due to drought and habitat degradation. To counteract these threats, restoration efforts focused on reestablishing the hydrological balance and removing invasive species. These measures resulted in a notable increase in the water table, with levels rising by up to 10 cm. The findings underscore the urgency of continued conservation efforts and formal designation of the site under Natura 2000 to prevent further biodiversity loss.*

Key words*: anthropic pressure, climate change, invasive species, rare species, biodiversity conservation.*

INTRODUCTION

At the United Nations Climate Change Conference held in Paris (COP21) the Intergovernmental Panel on Climate Change (IPCC) concluded the need for carbon neutrality by 2050, in order to prevent the rise of global temperatures beyond 2°C. In this respect, several nature-based solutions for climate change mitigation have been proposed, such as sustainable use of forest lands, croplands, wetlands, and grasslands to enhance their potential to store carbon (IPCC, 2021). The proposed solutions align with Aichi Target 15 from Convention on Biological Diversity, committed to restore at least 15% of degraded ecosystems by 2020 (CBD, 2013). They also correspond with the most recent Kunming-Montreal Global Biodiversity, Framework Target 2, which focuses on the restoration of degraded land to enhance biodiversity and ecosystem functions and services (CBD Secretariat, 2022). According to Bossio et al. (2020), soil carbon represents 25% of the potential of natural climate solutions (total potential, 23.8 Gt of CO_2-equivalent per year) and comprises 72% of the mitigation potential of wetlands. As part of the wetland category, peatlands cover only 3% of the global land area but store more carbon than that contained in the world's tropical rainforest biomass (Page & Baird, 2016). Unfortunately, through degradation, peatland carbon sinks are turned into carbon sources (Erkens et al., 2016).

During the past 150 years extensive peatland areas in the temperate and boreal zones have been drained mainly for agriculture. Over 70% of peatlands in Europe have been lost due to agricultural expansion, forestry, and urban development (Raeymaekers et al., 2000). It is

estimated that peatland drainage contributes to 10% of global annual anthropogenic greenhouse gas emissions (Page & Baird, 2016). Thus, a reliable nature-based solution for climate change mitigation is the restoration of natural carbon sinks, such as degraded peatlands. Peatlands are strategic areas for climate change mitigation as their restoration results in safeguarding existing soil carbon stocks (Günther et al., 2020). Apart from their role in carbon storage and sequestration, peatlands deliver a range of ecosystem services, including water regulation, biodiversity protection, natural risk mitigation, food and fuel, and recreation opportunities (Page & Baird, 2016). Only 17% of peatlands are protected worldwide, according to Austin et al. (2025), which is much less than the percentage for many other high-value ecosystems. Thus, we consider it a pressing need to enhance the efforts made for this purpose, in Romania as well.

In order to restore peatland ecosystems services, the Institute of Biology Bucharest of Romanian Academy implemented a range of projects starting in 2015 (with *PeatRo* acronym), financed through the EEA Grants (https://www.ibiol.ro/). Within one of these projects entitled *Degraded mires and peatlands restoration of North-East 1 region of Romania (PeatRO2)* a series of restoration activities were performed in Stupini mire.

Currently, peatlands in Romania lack biodiversity assessment, habitat restoration strategies and a legal framework to protect these sensitive ecosystems. The present study aims to address these gaps for the Stupini mire. Assessment of the reference state of the site, showed an unfavorable conservation status, resulting from a significant decline in the water table, alterations of the characteristic vegetation with the presence of invasive species, and other anthropic pressures. As a result, a comprehensive restoration plan addressing all these factors was made.

In order to preserve in time and space the results of restoration activities, the Stupini mire was proposed as a Special Area of Conservation (SAC) under Natura 2000 Network. The current work first describes the study site and methods, then presents preliminary results on biodiversity and hydrological restoration and provides perspectives to strengthen conservation efforts of the site by including it in the Natura 2000 Network.

MATERIALS AND METHODS

Study site

The mire is situated in the Bârsa Depression, between the Bârsa and Ghimbășel valleys (45º42′3.04″N, 25º32′37.49″E), at an altitude of 560 m a.s.l. with a slight inclination to the north (Figure 1).

The site extends over 9.257 ha and hosts a meso-eutrophic marsh, being a complex formed by meso-eutrophic marshes, reedbeds and sedge communities, alluvial forests and wet meadows.

Vegetation monitoring and data collection

Between 2022 and 2024, botanical surveys were conducted in order to identify plant species, characterize the vegetation, and evaluate the site's conservation potential. For a comprehensive assessment of the site's ecological integrity and long-term vegetation trends, multiple field investigations were carried out throughout the vegetation seasons, providing complementary data on floristic composition and habitat conditions. Transects were made to capture the variability of all habitat types, with at least one transect established for each habitat type. The number and length of transects varied depending on the size and distribution of each habitat within the site.

In April 2022 we surveyed the springs in the floodplain and primarily the aestival aspect of vegetation, taking GPS coordinates and photo documentation at the springs and traces of previous drainage or other anthropic impact. In addition, we listed the flowering species. In July, homogeneous vegetation patches were delineated based on a preliminary map, which allowed us to determine the size of the habitat patches. We also completed the list of plant species.

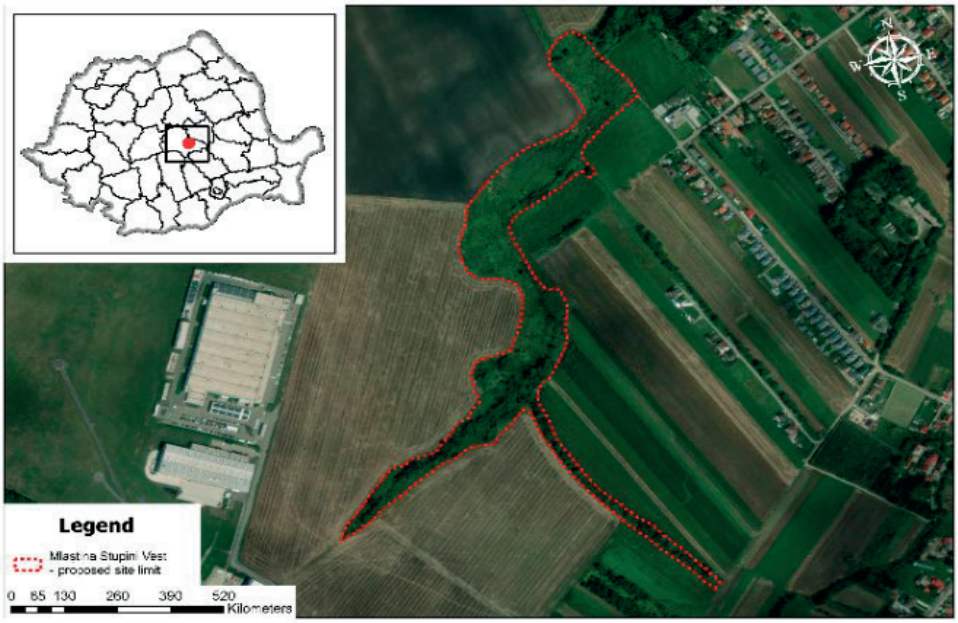


Figure 1. Satellite image of the proposed Stupini mire SAC

In July 2023 and April 2024, further field surveys were carried out to confirm the previously identified species.

Nomenclature for cormophyte taxa follows the Plants of the World Online (POWO) online database published by the Royal Botanic Gardens, Kew, while habitat types and plant associations are given according to Gafta and Mountford (2008).

Restoration Activities

The primary cause of degradation at Stupini mire is water loss due to artificial drainage, which has led to significant habitat alteration. To mitigate this, restoration activities focused on two main objectives: (1) reestablishing water balance and (2) controlling invasive species.

Hydrological restoration

In April 2024, a dam was constructed over the main drainage channel to reduce water loss and restore natural hydrological conditions (Figure 2). The channel, originally straightened and deepened for land drainage, significantly lowered groundwater levels. The dam was designed using a combination of wooden beams, soil, and plant material to mimic natural hydrological barriers. It measured 130 cm in length, 60 cm in width, and 50 cm in depth.



Figure 2. Dam over the main water drainage channel from Stupini mire
(photo by Ana-Maria Moroșanu, 08.04.2024)

Invasive species control

A secondary but equally critical restoration measure involved the removal of invasive species, particularly *Solidago canadensis*, which poses a major threat to native

biodiversity. Invasive plants were manually uprooted along with their root systems to prevent recolonization.

In order to lay the groundwork for creating a legislative framework for the conservation and protection of the Stupini mire, the restoration efforts aimed to improve the site's hydric characteristics. Identification of important species and a continued and improved monitoring strategy will be essential for assessing the stability and effectiveness of long-term restoration initiatives.

Monitoring activities

To assess the effect of restoration activities special devices were placed on site, as follows:

- two Data Loggers (EasyLog EL-USB 2 type), to monitor temperature, relative humidity, and dew point, measured every 30 minutes;
- 5 piezometers (one central and 4 in peripheral position), measured in July 2023 and April 2024.

One of the two data loggers was lost, likely due to its proximity to an urban area, where increased human activity and recreational use make monitoring instruments more susceptible to disturbance. This contrasts with our Norwegian project partner's experience in remote regions of Norway, where such interference with peatland restoration and monitoring is significantly less.

RESULTS AND DISCUSSIONS

Site quality and importance

A vestigial part of the vast marshy areas that covered the Bârsa depression in the past (Pop, 1960), the Stupini mire, although occupying a small area, represents one of the few remaining areas that shelter plant communities of particular scientific importance.

Vegetation surveys revealed that the site hosts several habitats of community importance, included in Annex I of the Habitat Directive, and require special conservation area designation. These habitats are:

- 7230 Alkaline fens, with the plant associations *Orchido-Schoenetum nigricantis,* Oberdorfer 1957, *Caricetum davallianae,* Dutoit 1924 and *Seslerietum uliginosae* (Palongy 1915) Soó 1941 (Figure 3) with an area of 1.2 ha. Their ecological importance lies in their role in sustaining wetland hydrology and providing habitat for rare and specialized plant species and communities, adapted to nutrient-poor, base-rich wetland conditions and dependent upon a constant hydrological regime. These fens act as refuges for numerous orchids, sedges, and bryophytes, contributing to overall ecosystem stability and resilience (Šefferová et al., 2008).
- 7210* Calcareous fens with *Cladium mariscus* (L.) Pohl and species of *Caricion davallianae* Klika 1934 (Figure 4), present on an area of 0.2 ha, forming a rare wetland habitat that depends on stable groundwater levels (Frink et al., 2013).
- 6410 *Molinia* meadows on calcareous, peaty or clayey soils, with the *Molinietum coeruleae* Koch 1926 plant association, with an area of 1.5 ha. *Molinia* meadows are species-rich semi-natural grasslands that support a high diversity of plants; their conservation depends on traditional management, such as mowing or light grazing, to prevent shrub encroachment and maintain their biodiversity value (Ziaja, 2017).
- 6430 Hydrophilous tall herb fringe communities of plains and of the montane to alpine levels with an area of 1.5 ha. This habitat is a species-rich, tall herb community that acts as a biodiversity hotspot along water bodies and offers essential resources for pollinators and wetland species (Joint Nature Conservation Committee, 2013).
- 91E0* Alluvial forests of *Alnus glutinosa* (L.) Gaertn. and *Fraxinus excelsior* L. (*Alno-Padion* ex Medwecka-Kornaś in W. Matuszkiewicz et Borowik 1957*, Alnion incanae,* Pawłowski et al. 1928, *Salicion albae* Soó 1951) with an area of 2 ha. This priority floodplain forest dominated by *Alnus glutinosa* plays a key role in flood regulation and soil stabilisation, and functions as an ecological corridor that supports habitat connectivity within riparian ecosystems (Danci, 2015).

The Stupini site is rich in rare and/or relict plant species such as felwort (*Swertia perennis* L.), the bird's eye primrose (*Primula farinosa* L.), several species of sedge (*Carex davalliana* Sm., *Carex paniculata* L., *Carex lepidocarpa* Tausch, *Carex panicea* J.Carey, and *Carex hostiana* DC.), the black bog-rush (*Schoenus*

nigricans Hoppe), and the brown bog-rush (*Schoenus ferrugineus* Huds.). Also, several species of orchids can be admired in June-July, such as the early marsh-orchid (*Dactylorhiza incarnata* (L.) Soó) (Figure 5), the marsh helleborine (*Epipactis palustris* (L.) Crantz) (Figure 6), and the marsh fragrant-orchid (*Gymnadenia densiflora* (Wahlenb.) A. Dietr.) (Figure 7).

Another important plant species identified in site is *Ligularia sibirica* (L.) Cass., a glacial relict protected under the Habitats Directive, Annex II (Figure 8).

The identified population is relatively small and consists of 15-20 well developed individuals, all in the flowering stage at the end of July. The presence of this glacial relict confirms that Stupini mire functions as a glacial refugia. Fed by cold springs, the site has created conditions for the perpetuation of glacial relict plant species.

During the period 11-14.07.2022, the rare and declining species *Liparis loeselii* (L.) Rich. (fen orchid or yellow widelip orchid, Natura 2000 species code: 1903 was reassessed). The species of community interest was previously identified by one of us at Stupini mire, in 2013 with a population of at least 15 flowering specimens.



Figure 4. Habitat **7210*** with the characteristic swamp sawgrass (*Cladium mariscus*), a priority conservation habitat that persists on only 0.2 ha, making it highly vulnerable to groundwater decline, which threatens its long-term stability and biodiversity
(photo by Attila Mátis, 22.06.2022)



Figure 3. Alkaline fen habitat (**7230**) in summer, showcasing characteristic species and hydrological conditions
(photo by Anna Szabó, 22.06.2022)



Figure 5. *Dactylorhiza incarnata*, a moisture-dependent orchid, now restricted to the few remaining wet areas as the fen habitat continues to degrade
(photo by Attila Mátis, 14.07.2022)



Figure 6. *Epipactis palustris*, a wetland orchid species that endures in isolated refuges where groundwater flow is still high, but where it faces increasing pressure due to drying habitat
(photo by Attila Mátis, 14.07.2022)



Figure 7. *Gymnadenia densiflora*, an orchid species that persists in the last patches where the groundwater level remains high, threatened by habitat desiccation. It occurs in the habitat 7230 Alkaline fens, within the plant association *Orchido-Schoenetum nigricantis*
(photo by Attila Mátis, 14.07.2022)



Figure 8. *Ligularia sibirica*
(photo by Anca Manole, 25.07.2023)

Unfortunately, not a single specimen of *Liparis loeselii* could be detected in any of the three small fragments of habitat 7230, represented mainly by the plant association *Orchido-Schoenetum nigricantis* Oberdorfer 1957. The absence of the species may be due to the exceptional drought of the year 2022, but there is a bleak possibility that the species completely disappeared because of the continuous drainage activities, and because of water capture from the Lauterbach tributary upstream of the mire.

Unfortunately, because of habitat degradation other rare plant species that require humidity, such as: *Drosera anglica* Huds.*, Pinguicula vulgaris* L.*, Menyanthes trifoliata* L. and *Saxifraga mutata* L. could not be reconfirmed in site.

During the survey, an expansion of the eutrophic species *Carex acutiformis* Brot. was observed consequently with a regression of the *Carex* species characteristic of type 7230 habitat. Thus, only a few bushes of *Carex davalliana* Sm. and *Carex paniculata* L. were detected. In alkaline marshes, the species *Carex lepidocarpa* Tausch and *Carex hostiana* DC. are often abundant, but in this area, they were suppressed by a hybrid between the two mentioned species, *Carex* x *leutzii* Kneuck., a

taxon that has not been reported so far from the Romanian flora (Attila Mátis, Anna Szabó - personal communication, 22 June 2022). This sterile hybrid has pronounced vegetative reproduction, becoming the dominant sedge in the *Orchido-Schoenetum nigricantis* plant association.

Habitats of type 7230 and 7210* are also threatened by the expansion of reed (*Phragmites australis* (Cav.) Trin. ex Steud.), which, facilitated by the lowering of the water table, invades and shrinks habitats characterized by sedge species (Figure 9).

Drought, due to climate change, accentuates the negative impact of drainage channels, water captured from the Lauterbach tributary upstream of the Stupini mire, and the presence of invasive species. These are the main causes of lowering the water level in the substratum and ongoing habitat degradation. As a result, rare species that depend on a high water level in the substratum, such as *Liparis loeselii*, *Drosera anglica*, *Pinguicula vulgaris*, *Menyanthes trifoliata*, and *Saxifraga mutata*, are disappearing.



Figure 9. Habitat 7230 invaded by reed
(photo by Attila Mátis, 22.06.2022)

Although no extensive faunistic inventory was carried out, the house snake (*Natrix natrix* L.) was identified on site and should also be considered for conservation because the species was recently reclassified, according to the study carried out by Kindler et al. (2017). Thus, the range of the house snakes has suffered a significant reduction, and the impact of this change on the conservation of the species has not been assessed.

Preliminary effects of restoration activities

Even though the period between measurements was relatively short (between 20.09.2023, and 08.04.2024), the data from all five piezometers showed that the water table raised 1.5, 3.5, 4.5, 7.5, and 10 cm, respectively. Within the same interval, the maximum temperature value (31ºC) was recorded on 23.09.2023, and the minimum value (-17ºC) on 10.01.2024, with an average of 6.1ºC, during the measurement period. The air humidity recorded a maximum of 97% on 11.08.2023, and a minimum of 25%, on 21.07.2023, with an average of 75.8%. The dew point recorded a maximum of 18.4ºC on 1.08.2023, and a minimum of -18.8ºC, on 10.12.2023, with an average of 1.7ºC (Figure 10).

With implications for comprehending the impact of climatic conditions on water table oscillations and general ecosystem function, these data offer insightful information about the site's environmental dynamics. A warmer climate and altered precipitation patterns are driving changes in peatlands` vegetation, resulting in an increase in vascular plant cover, a decrease in peat moss abundance and an earlier onset of the growing season (Antala et al., 2022). Moreover, shifts in plant phenology result from climate change and can serve as indicators of environmental transformation and species adaptation to evolving conditions (Parmesan & Yohe, 2003; Visser and Both, 2005).

Restoring flooding is the first step in maintaining and conserving specific marsh species that depend on water levels. The importance of water levels is highlighted by Lou et al. (2020). In their survey, they found that over 40 years, water levels decreased, leading to a substantial decline in the abundance of species with higher optimal water levels.

The need for improved monitoring strategies is just as pressing even though Romania's peatlands cover a significantly smaller area compared to those in Norway, for example, which have utilized more complex monitoring methodology. According to Kyrkjeeide et al. (2024), current monitoring efforts in Norway

are limited in geographical and hydro morphological diversity hampering a thorough knowledge of restoration outcomes.

In a comparative study of eight national initiatives, Nordbeck & Hogl (2024) indicates that these strategies are making significant progress in raising awareness and building capacity. However, integrating policies across different sectors remains the main obstacle to effective implementation. The experiences of trailblazing nations provide important insights and a solid basis for developing their own effective, integrated approaches to peatland management and restoration for nations that have not yet established a national peatland policy.

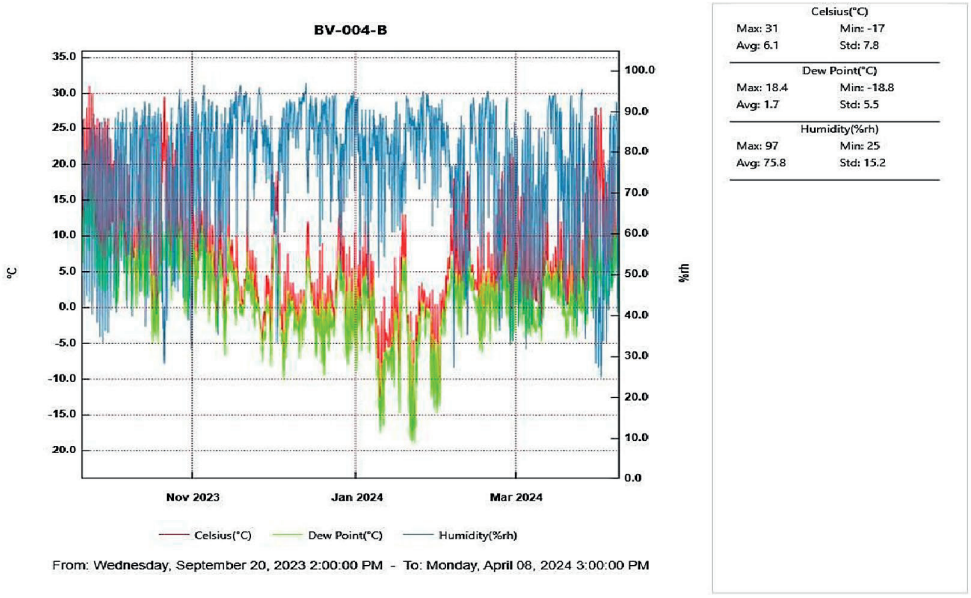


Figure 10. Abiotic parameters of the air recorded in Stupini mire. Most temperatures fall between 0.5°C (25th percentile) and 11.0°C (75th percentile), indicating a predominance of cooler conditions. Humidity values range from 25% to 97%, suggesting significant variation, though most values are above 67.5%. The interquartile range is -1.55°C to 5.3°C, showing that dew points are mostly positive but can drop significantly

CONCLUSIONS

The restoration measures undertaken have contributed to an increase of water table levels, but in order to preserve this result, the Stupini mire must be subjected to additional protection. Assessing the long-term success of the restoration process through continued monitoring of the water table, along with further vegetation surveys, will be essential. The success of future peatland conservation activities will be aided by developing a more comprehensive and varied monitoring strategy, which will guarantee more accurate data and allow future restoration projects to be conducted in an efficient manner.

Considering the species richness of the site, Stupini mire could be considered a biodiversity sink that requires specific conservation measures.

The Natura 2000 Network, composed of SACs designated under the Habitats Directive and the SPAs classified under the Birds Directive, is the central pillar of the Union's conservation policy. Because of their rarity and continuing decline, 13 mire habitat types are included in Annex I of the Habitats Directive. From these, 5 types of habitats were identified on Stupini mire. Also, the presence in Stupini mire of two plant species protected under EU Habitats Directive (*Liparis loeselii* and *Ligularia sibirica*) along with other rare species of the Romanian flora, gives the opportunity to designate this site as SAC under Natura 2000 Network, in order to assure complete legal protection.

ACKNOWLEDGEMENTS

This research work was carried out with the support of the Institute of Biology Bucharest of Romanian Academy and was financed from the Projects: PeatRO2 - EEA grant (RO-ENVIRONMENT-0004), RO1567-IBB06/2024 and RO1567-IBB03/2024.

REFERENCES

Antala M., Juszczak R., van der Tol C., Rastogi A. (2022). Impact of climate change-induced alterations in peatland vegetation phenology and composition on carbon balance, *Science of The Total Environment, 827,* 154294, ISSN 0048-9697. https://doi.org/10.1016/j.scitotenv.2022.154294.

Austin, K. G., Elsen, P. R., Coronado, E. N. H., DeGemmis, A., Gallego-Sala, A. V., Harris, L., Kretser, H. E., Melton, J. R., Murdiyarso, D., Sasmito, S. D., Swails, E., Wijaya, A., Winton, R. S. Zarin, D. (2025), Mismatch Between Global Importance of Peatlands and the Extent of Their Protection. *Conservation Letters, 18*, e13080. https://doi.org/10.1111/conl.13080

Bossio, D. A., Cook-Patton, S. C., Ellis, P. V., Fargione, J., Sanderman, J., Smith, P., Wood, S., Zomer, R. J., von Unger, M., Emmer, I. M., Griscom, B. W. (2020). The role of soil carbon in natural climate solutions. *Nature Sustainability*, *3*(5), 391–398. https://doi.org/10.1038/s41893-020-0491-z

CBD (2013). Quick guides to the Aichi Biodiversity Targets. Version 2 – February 2013. https://www.cbd.int/doc/strategic-plan/targets/compilation-quick-guide-en.pdf (Accessed on 05.02.2025)

CBD Secretariat (2022). Kunming-Montreal global biodiversity framework. 221222-CBD-PressRelease-COP15-Final.pdf (Accessed on 05.02.2025)

Danci, O. (2015). Management of alluvial forests included in Natura 2000 91E0* habitat type in Maramureş Nature Park. *Transylvanian Review of Systematical and Ecological Research, 17*(1), 163-176. https://doi.org/10.1515/trser-2015-0057

Erkens, G., Van Der Meulen, M. J., Middelkoop, H. (2016). Double trouble: subsidence and CO2 respiration due to 1,000 years of Dutch coastal peatlands cultivation. *Hydrogeology Journal*, 24, 551–568. https://doi.org/10.1007/s10040-016-1380-4

EUNIS, European Nature Information System https://eunis.eea.europa.eu/references/2324/habitats (Accessed on 07.03.2025)

Frink, J. P., Szabó, A., Attila, M. (2013). *Metodologiile de evaluare şi monitorizare a habitatelor de interes comunitar (tufărişuri, turbării şi mlaştini, stâncării şi grohotişuri, păduri) prezente în România*. Turbării şi mlaştini In: Institutul Naţional de Cercetare-Dezvoltare pentru Protecţia Mediului, Ghidul sintetic de monitorizare pentru habitatele de interes comunitar: tufărişuri, turbării şi mlaştini, stâncării, păduri. Universitas.

Gafta, D., Mountford, J.-O., eds. (2008). *Manual de interpretare a habitatelor Natura 2000 din România [Romanian Manual for Interpretation of EU Habitats].* 111, Cluj-Napoca: Risoprint

Günther, A., Barthelmes, A., Huth, V., Joosten, H., Jurasinski, G., Koebsch, F., Couwenberg, J. (2020). Prompt rewetting of drained peatlands reduces climate warming despite methane emissions. – *Nature Communications, 11,* 1644. https://doi.org/10.1038/s41467-020-15499-z

IPCC (2021). Annex VII: Glossary. In J. B. R. Matthews, V. Möller, R.van Diemen, J. S. Fuglestvedt, V. Masson-Delmotte, C. Méndez, S. Semenov, A. Reisinger (Eds.), In climate change 2021: The physical science basis. Contribution of working group I to the sixth assessment report of the intergovernmental panel on climate change, pp. 2215–2256, Cambridge University Press.

Joint Nature Conservation Committee. Habitat: H6430: Hydrophilous tall herb fringe communities of plains and of the montane to alpine levels. Peterborough, UK: JNCC. https://sac.jncc.gov.uk/habitat/H6430/

Kindler, C., Chèvre, M., Ursenbacher, S., Böhme, W., Hille, A., Jablonski, D., Vamberger, M., Fritz, U., (2017). Hybridization patterns in two contact zones of grass snakes reveal a new Central European snake species. *Scientific Reports, 7*, 7378. https://doi.org/10.1038/s41598-017-07847-9

Kyrkjeeide, M. O., Jokerud, M., Mehlhoop A. C., Linn Lunde, M. F., Fandrem M., Lyngstad A. (2024). Peatland restoration in Norway – evaluation of ongoing monitoring and identification of plant indicators of restoration success. *Nordic Journal of Botany, 4*, e03988. https://doi.org/10.1111/njb.03988

Lou, Y., Kapfer, J., Smith, P., Liu, Y., Jiang, M., Lu, X., & Ashcroft, M. (2020). Abundance changes of marsh plant species over 40 years are better explained by niche position water level than functional traits. *Ecological Indicators, 117*, 106639. https://doi.org/10.1016/j.ecolind.2020.106639

Nordbeck, R., Hogl, K. (2024). National peatland strategies in Europe: current status, key themes, and challenges. Regional Environmental Change, 24, 5. https://doi.org/10.1007/s10113-023-02166-4

Page, S. E., Baird, A. J. (2016). Peatlands and Global Change: Response and Resilience. *Annual Review of Environment and Resources*, 41, 35–57. https://doi.org/10.1146/annurev-environ-110615-085520

Parmesan, C., Yohe, G. (2003). A globally coherent fingerprint of climate change impacts across natural systems. *Nature, 421*, 37–42. https://doi.org/10.1038/nature01286

Plants of the World Online (POWO) online database published by the Royal Botanic Gardens, Kew. https://powo.science.kew.org/ (Accessed on 05.02.2025)

Pop, E. (1960). *Mlaştinile de turbă din Republica Populară Română* [In Romanian]. Bucureşti, RO: Editura Academiei.

Raeymaekers, G., Sundseth, K., Gazenbeek, A. (2000). *Conserving Mires in the European Union.* Office for

official publications of the European communities. Bernan Associates [U.S. distributor].

Šefferová, S. V., Šeffer, J., Janák, M. (2008). Management of Natura 2000 habitats. 7230 Alkaline fens. DAPHNE-Institute of Applied Ecology, Slovakia.

Visser, M. E., Both C. (2005). Shifts in phenology due to global climate change: the need for a yardstick. Proceedings of the Royal Society B. *Biological Sciences, 272*, 2561–2569. https://doi.org/10.1098/rspb.2005.3356.

Ziaja, M., Wójcik, T., Wrzesień, M. (2017). Conservation status and trends in the transformation of Molinia meadows in the Laki w Komborni Natura 2000 site, SE Poland. *Acta Agrobotanica, 70*(3). 1718. https://doi.org/10.5586/aa.1718

Scientific Papers. Series E. Land Reclamation, Earth Observation & Surveying, Environmental Engineering. Vol. XIV, 2025
Print ISSN 2285-6064, CD-ROM ISSN 2285-6072, Online ISSN 2393-5138, ISSN-L 2285-6064

THE DEGREE OF THE ROOTING AND ADAPTABILITY OF CORMOFLORA ON THE WASTE DUMPS OF THE BAIA NOUĂ QUARRY (MEHEDINȚI COUNTY)

Mariana NICULESCU, Florina GRECU

University of Craiova, 19 Libertății Street, 200583, Craiova, Romania

Corresponding author email: florina.grecu@edu.ucv.ro

Abstract

The studied area includes the former Baia Nouă quarry mining, which belongs to the Dubova locality, Mehedinți County, an integral part of the Banat Mountains. As part of this work, we tried to carry out an ecological rehabilitation study of the area where all mining operations have been closed for a very long time, the Baia Nouă quarry mining is a ruin, here you can find waste and garbage resulting from the abandonment and degradation of the administrative buildings in the quarry. In order to achieve a good rehabilitation of this area, we took into account the type of native vegetation, existing here and in the immediate vicinity, in order to avoid fragmentation of habitats, as well as the existence of an obvious "desire" of some species to establish themselves and conquer new territories in this area.

Key words*: Baia Nouă, quarry, waste dumps, adaptability, cormoflora.*

INTRODUCTION

Mining activity was known and practised worldwide since ancient times. Human impact exerted in a mining career on biodiversity is smaller or greater and it depends on many factors (Niculescu, 2019). Mining environment issues require a systematic approach and sustainable environmental management techniques must be applied correctly in the mining areas around the world. It is very important to establish principles and strategic elements to ensure sustainable development in a mining quarry. For good ecological rehabilitation in a mining quarry, we must first know the biodiversity existing in that area in all its complexity, including the substrate on which it grows (Niculescu, 2019).

Following mining operations, the so-called mining dumps are formed, consisting of the waste material brought to the surface from underground galleries, which over time require the restoration of the land to useful destinations from an ecological, economic and social point of view through a process of improving the natural capital in the mining pits (Niculescu, 2015).

The ecological rehabilitation of degraded lands and the establishment of a vegetal carpet on waste dumps also play an important role in stabilizing and "greening" these dumps, consolidating the resulting coarse deposits, and restoring the natural landscapes of a mining area.

The restoration of biodiversity from a mining quarry, on the dumps left after exploitation, is indispensable, regardless of where it is located.

The studied area includes the former Baia Nouă mine, which belongs to the commune of Dubova, Mehedinți County, an integral part of the Banat Mountains. This area is particularly important from a geographical, floristic and faunal, landscape, cultural and economic point of view, as the "Portile de Fier" Natural Park is located in this area. As part of this work, I tried to carry out an ecological rehabilitation study of the area where all mining operations have been closed for a very long time, the Baia Nouă mine is a ruin, here you can find waste and garbage resulting from the abandonment and degradation of the administrative buildings in the quarry (Figures 1 and 2).

As a result of mining activity in the perimeter of the former Baia Nouă mining pit, an important area has resulted in which the entire biodiversity has suffered. At the same time, there are still waste dumps made up of course materials (gravel, sand), in the form of mounds on which a pioneer vegetation has settled in a continuous expansion and adapted to the current eco-pedo-climatic conditions, as well as with a favourable coenotic and syndamic

evolution for the restoration of the ecological, bio-conservative balance in the studied area.
The study and knowledge of the degree of restoration and regeneration of the cormoflora and implicitly of the entire biodiversity within the perimeter of the former Baia Nouă mining quarry, where they have undergone profound changes due to anthropo-zoogenic factors resulting both during exploitation and after the quarry's closure, in an area of bioconservative interest, responds to a need of great interest.



Figure 1. The remains of an abandoned building in the Quarry (photo: M. Niculescu)



Figure 2. Aspects of the former constructions of the Baia Nouă Mining Quarry (photo: M. Niculescu)

MATERIALS AND METHODS

Study area

As mentioned, the studied territory is located within the perimeter of the former Baia Nouă mining quarry in the village of the same name belonging to Dubova locality, Mehedinți County, Romania. During the period 2021-2024, studies were carried out in this area that falls between the following geographical coordinates: 44°56′73,4″N-22°11′59,4″E and 44°56′73,1″N -22°11′58,8″E, the altitude being between 523-517 m (using Geo Tracker – GPS traker application).
Geographically, the former mining quarry is located in the Banat Mountains, in a narrow valley of the Tisovița River, bordered by forest vegetation often installed on quite steep slopes, which extends to the mines exploited in Baia Nouă. The Baia Nouă village is located approximately 10 km from the Danube basin, namely the Porțile de Fier Gorge, being an integral part, as we mentioned, of the "Porțile de Fier" Natural Park (Figure 3).

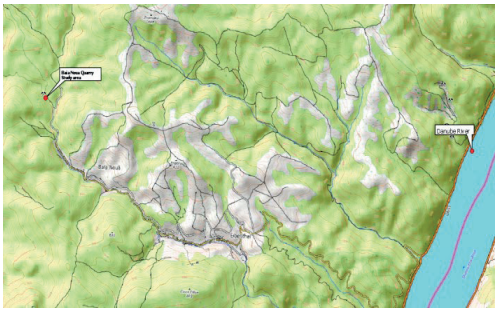


Figure 3. Map of the studied territory - Baia Nouă mining quarry (Mehedinți County)

Floristic and phytosociological analysis

The identification of taxa was based on Illustrated Flora of Romania: *Pteridophyta* and *Spermatophyta* (Ciocârlan, 2000), Romanian Flora (Săvulescu, coord., 1952-1976) and Flora Europaea (Tutin et al., 1964-1980).
For the coenotaxonomic study we used synthesis studies of the following authors Coldea (1991, 1997), Sanda et al. (1997), as well as Oberdorfer (1992), Mucina et al. (1997, 2016), Rodwell (2002).

RESULTS AND DISCUSSIONS

To ensure effective rehabilitation of the area, we considered the native vegetation present locally and in the surrounding vicinity to avoid habitat fragmentation. We also observed the clear tendency of certain species to establish and expand into new territories within the quarry. Field research across the quarry, particularly on the remaining waste heaps, revealed that some plant species exhibited a high degree of rooting ability and adaptability, enabling them to rapidly colonize new areas.

Given these observations, we deemed it essential to conduct a study focusing on these species with high colonization capacity. We classified the identified species based on their rooting ability and adaptability within the former quarry, assigning each species a score from 1 to 10 according to the number of individuals, species ecology, and, most importantly, their rooting, regeneration, and adaptation capacities, as well as the land area occupied (Table 1). These species demonstrated excellent development and vitality on the waste dumps, showing robust growth and successful fruiting without issues. This confirms the area's strong potential for ecological rehabilitation using native species, with natural regeneration holding significant promise. However, realizing this potential requires implementing a green management plan, particularly now that anthropogenic pressures and pollution have decreased following the quarry's closure.

Overall, the conditions within the former quarry are favorable for restoring natural habitats, which can contribute to reducing pollution levels with minimal intervention.

Among the species with notable rooting and regeneration capacities, three are particularly important: *Scleranthus perennis*, *Calamagrostis epigeios*, and *Elymus repens* (syn. *Agropyron repens*).

Scleranthus perennis is a pioneer species that has readily established itself in the area, thriving on skeletal soils.

Calamagrostis epigeios is a perennial species that prefers sandy soils and areas that have experienced disturbance, establishing easily at the base of the dumps or on flat lands surrounding the former constructions of the Baia Nouă mining quarry.

Elymus repens (syn. *Agropyron repens)* is characterized by a broad ecological tolerance, readily colonizing disturbed land surfaces.

A vine species, *Clematis vitalba,* is frequently found within the quarry perimeter, where it is locally dominant as a pioneer species (Figure 4). It primarily establishes on the upper parts of the remaining tailings dumps, occupying significant areas within the study site (Figure 5).

Invasive species have also established within the quarry, with frequent occurrences of *Ambrosia artemisiifolia, Erigeron annuus* (Figure 6), *Galinsoga ciliata,* and *Ailanthus altissima.*



Figure 4. *Clematis vitalba* in the former Baia Nouă mining quarry (photo: M. Niculescu)



Figure 5. *Clematis vitalba* on a waste dump in the former Baia Noua mining quarry (photo: M. Niculescu)

These species demonstrated excellent development and vitality on both soil types, successfully flowering and fruiting without issues. This further confirms the area's strong potential for ecological rehabilitation using native species, with natural regeneration showing great promise. Additionally, anthropogenic pressures and pollution have decreased in intensity within the site.

From a syndynamic perspective, studies indicate that the vegetation on the remaining quarry dumps is progressing towards the establishment of the following plant communities: *Medicagini lupulinae-Agropyretum repentis* Popescu et al. 1980 (Figure 7) and *Medicagini-Festucetum valesiacae* Wagner 1941 (Figure 8).



Figure 6. *Erigeron annuus* in the former Baia Noua mining quarry (photo: M. Niculescu)

The first plant community began to settle in the southern part of the quarry at the base of the dumps, here several phytocoenoses ranging between 10-100 m^2 were observed. The second plant community has settled in the quarry on smaller surfaces, *Medicago minima* as an edifying species frequently occurring alongside *Festuca valesiaca* on stony soils, alongside a well-defined core of species characteristic of this plant community, frequently found in the Tisovița Valley.



Figure 7. *Medicagini lupulinae-Agropyretum repenti s*Popescu et al. 1980 plant community in the former Baia Nouă mining quarry (photo: M. Niculescu)



Figure 8. *Medicagini-Festucetum valesiacae* Wagner 1941 plant community in the former Baia Noua mining quarry (photo: M. Niculescu)

Some species settle at the edge of the forest, next to abandoned buildings in ruins, or within meadow communities with a secondary character, in the floristic structure of ruderal communities, settling on skeletal, on more or less oligotrophic soils, among which we can mention *Teucrium chamaedrys* (Figure 9), *Lysimachia punctata* (Figure 10), *Hypericum perforatum*.



Figure 9. *Teucrium chamaedrys* in the former Baia Nouă mining quarry (photo: M. Niculescu)



Figure 10. *Lysimachia punctata* in the former Baia Nouă mining quarry (photo: M. Niculescu)

Table 1. The degree of the striking root (grip) and adaptability of cormoflora in the Baia-Nouă Quarry

No.	Species	Family	Biologic forms	Phyto-geographic elements	Ecologic gropup: U, T, R (after Zolyomi, 1954)	The degree of the striking root (grip) and adaptability (scal 1-10)
1	*Clematis vitalba* L.	Ranunculaceae	N-E	Ec(Med.)	U3T3R3	10
2	*Calamagrostis epigeios* (L.) Roth.	Poaceae	H (G)	Eua(Med.)	U2T3R0	10
3.	*Scleranthus perennis* L.	Caryphyllaceae	(H) Ch	Eua	U3T0R3	10
4.	*Elymus repens* (L.) Gould (*Agropyron repens* (L.) Beauv.)	Poaceae	G	Cosm	U0T0R0	9
5.	*Medicago lupulina* L.	Fabaceae	TH(H)	Eua	U2,5T3R4	9
6.	*Medicago minima* L.	Fabaceae	Th	Eua(Med.)	U1,5T4R4	8
7.	*Hieracium pilosella L.*	Asteraceae	H	E(Med.)	U2T0R2	8
8.	*Echium vulgare* L.	Boraginaceae	TH	Eua	U2T3R4	7
9.	*Festuca valesiaca* Schleicher ex Gaudin.	Poaceae	H	Eua(Cont.)	U1T5R4	7
10.	*Teucrium chamaedrys* L.	Lamiaceae	Ch	Ec-Med	U2T4R4	7
11.	*Thymus comosus* Heuffel	Lamiaceae	Ch	Carp(End)	U2T3,5R4,5	7
12.	*Potentilla argentea* Borkh.	Rosaceae	H	Eua	U2T4R2	7
13.	*Erigeron annuus* (L.) Pers.	Asteraceae	H	Carp(End)	U4T2R3	7
14.	*Galinsogaciliata* (Rafin.) Blake	Asteraceae	Th	Adv	U2,5T4R3	6
15.	*Melilotus albus* Medik.	Fabaceae	Th-TH	Eua	U2,5T3R0	6
16.	*Tussilago farfara* L.	Asteraceae	G-H	Eua	U3,5T0R4,5	6
17.	*Scabiosa columbaria* L.	Dipsacaceae	H	E (Med.)	U2,5T3R4,5	5
18.	*Salvia nemorosa* L.	Lamiaceae	H	Ec	U2,5T4R5	5
19.	*Artemisia absinthium* L.	Asteraceae	Ch-H	Eua(Med.)	U2T3,5R0	5
20.	*Rubus fruticosus L.* (*R. plicatus* Weihe et Nees)	Rosaceae	N	Atl.-Ec.	U3,5T3,5R2	5
21.	*Dactylis glomerata* L.	Poaceae	H	Eua	U3T0R4	5
22.	*Achillea millefolium* L.	Poaceae	H	Eua	U3T0R0	5
23.	*Robinia pseudoaccacia* L.	Fabaceae	MPh	Adv	U2,5T4R0	5
24.	*Sambucus ebulus* L.	Caprifoliaceae	H	Eua(Med)	U3T3R4,5	5
25.	*Galium verum* L.	Rubiaceae	H	Eua	U2,5T2,5R0	4
26.	*Hypericum perforatum* L.	Hypericaceae	H	Eua	U3T3R0	4
27.	*Ambrosia artemisiifolia* L.	Asteraceae	Th	Adv	U2T0R0	4
28.	*Melica ciliate* L.	Poaceae	H	Ec-Balc	U1,5T4R4	4
29.	*Helianthemum numularia* (L.) Mill.	Cistaceae	Ch-H	Ec(Med)	U2T3R4	3
30.	*Mentha arvensis* L.	Lamiaceae	H-G	Cosm	U3T3R0	3
31.	*Plantago media* L.	Plantaginaceae	H	Eua	U2,5T0R4,5	3
32.	*Plantago lanceolata* L.	Plantaginaceae	H	Eua	U0T0R0	3
33.	*Linaria vulgaris* Mill.	Scrophulariaceae	H (TH)	Eua	U2T3R4	3
34.	*Lotus corniculatus* L.	Fabaceae	H	Eua	U2,5T0R0	2
35.	*Rosa canina* L.	Rosaceae	N	E	U2T3R3	2
36.	*Cichorium intybus* L.	Asteraceae	H-TH	Eua	U2,5T3,5R4,5	2
37.	*Arabis hirsuta* (L.) Scop.	Brassicaceae	TH(H)	Eua (Med.)	U1,5T3R4	2
38.	*Ranunculus repens* L.	Ranunculaceae	H	Eua (Med.)	U4,5T3R0	2
39.	*Trifolium pratense* L.	Fabaceae	H-TH	Eua	U3T0R0	2
40.	*Verbascum nigrum* L.	Scrophulariaceae	TH-H	Eua	U2T3R4	1
41.	*Salvia nemorosa* L.	Lamiaceae	H	Ec	U2,5T4R3	1
42.	*Artemisia vulgaris* L.	Asteraceae	H(Ch)	Cosm	U2,5T3R4	1
43.	*Urtica dioica* L.	Urticaceae	H (G)	Cosm	U3T3R4	1
44.	*Phytolacca americana* L.	Pthytolaccaceae	H	Adv	U2,5T3R4	1
45.	*Chelidonium majus* L.	Papaveraceae	H	Eua	U3T3R4	1
46.	*Papaver rhoeas* L.	Papaveraceae	Th	Cosm	U3T3,5R4	1
47.	*Veronica austriaca* L.	Scrophulariaceae	H	Pont.-Med.-Ec	U2T4R5	1
48.	*Cardaria draba* (L.) Desv.	Brassicaceae	H	Eua (Med)	U2T4R4	1
49.	*Ailanthus altissima* (Miller) Swingle	Simaroubaceae	MPh	Adv.	U0T0R0	1

In Tabel 1 the following abbreviations were used:

- Bioforms: Ch – chamaephytes; MPh – megaphanerophytes; H – hemicryptophytes; N – lianas; Th – annual therophytes; TH – biennial therophytes; Hh – helophytes; G – geophytes.
- Floristic elements: Cosm – cosmopolitan; Adv – adventive; Eua – Eurasian; E – European; Ec – Central European; Atl – Atlantic; Med – Mediterranean; Cont – continental; Pont – Pontic; Pan – Pannonian; End – endemic; Balc – Balkan; Carp – Carpathian.
- Ecological indices: U – humidity; T – temperature; R – soil reaction.

CONCLUSIONS

Mining operations result in the formation of mining dumps, composed of waste material brought to the surface from underground galleries. Over time, these areas require restoration to ecologically, economically, and socially beneficial uses through the improvement of natural capital within mining pits.

The perimeter of the former Baia Nouă mining quarry is characterized by significant Anthropogenic impacts, including waste, abandoned structures, and tailings dumps. However, studies on the bio-ecological rehabilitation of this area have shown that it has gradually undergone natural restoration over several years.

Ruderal vegetation and native plant communities have established on the waste dumps, demonstrating good dynamics and progression. Surveys identified 49 cormophyte species with high capacity and affinity for colonizing and stabilizing these disturbed areas. Among these, several species can form primary or secondary plant communities within the mining landscape.

Two meadow-specific plant communities have developed a well-defined coenotic structure and strong synanthropic relationships, allowing them to expand into larger areas. Given that the study area is part of the "Iron Gates" Natural Park, the restoration of the plant communities *Medicagini-Festucetum valesiacae* Wagner 1941 and *Medicagini lupulinae-Agropyretum repentis* Popescu et al. 1980 holds particular importance for the recovery of natural meadow habitats and the conservation of biodiversity in this region.

REFERENCES

Ciocârlan, V. (2000). *Flora ilustrată a României: Pteridophyta et Cormophyta*. Editura Ceres.

Coldea, G. (1991). Prodrome des associations végétales des Carpates du Sud-Est (Carpates Roumaines). *Documents Phytosociologiques, Nouvelle Série, 13*, 317–539.

Coldea, Gh. (1997). *Les associations végétales de Roumanie*. Presses Universitaires de Cluj.

Mucina, L. (1997). Conspectus of classes of European vegetation. *Folia Geobotanica et Phytotaxonomica, 32*, 117–172. https://doi.org/10.1007/BF02803738

Mucina, L., Bültmann, H., Dierßen, K., Theurillat, J.-P., Raus, T., Čarni, A., Šumberová, K., Willner, W., Dengler, J., Gavilán García, R., Chytrý, M., Hájek, M., Di Pietro, R., Iakushenko, D., Pallas, J., Daniëls, F. J. A., Bergmeier, E., Santos Guerra, T., Ermakov, N., Valachovič, M., Schaminée, J. H. J., Lysenko, T., Didukh, Y. P., Pignatti, S., Zólyomi, J. S., Capelo, J., Weber, H. E., Solomeshch, A. I., Dimopoulos, P., Aguiar, C., Hennekens, S. M., & Tichý, L. (2016). Vegetation of Europe: Hierarchical floristic classification system of vascular plant, bryophyte, lichen, and algal communities. *Applied Vegetation Science, 19* (Suppl. 1), 3–264. https://doi.org/10.1111/avsc.12257

Niculescu, M., &Nuță, I. S. (2019). *Cariera minieră Bicaz-Chei – biodiversitate, reabilitare ecologică*. Editura Sittech.

Niculescu, M., Făgăraș, M., & Niculescu, L. (2015). Environmental rehabilitation and preservation measures in Baita-Craciunesti quarry. In *15th International Multidisciplinary Scientific Geo Conference SGEM 2015* (pp. [page numbers if available]).

Oberdorfer, E. (1992). *Süddeutsche Pflanzen gesellschaften, Teil IV: Wälder und Gebüsche* (2nd ed.). Gustav Fischer Verlag.

Rodwell, J. S., et al. (2002). The diversity of European vegetation. *Rapport EC-LNV*, No. 2002/054, Wageningen.

Sanda, V., Popescu, A., &Barabaș, N. (1997). Cenotaxonomia și caracterizarea grupărilor vegetale din România. *Studii și Comunicări, Muzeul de Științele Naturii Bacău, 14*, 5–366.

Săvulescu, T. (Ed.). (1952-1976). *Flora R.P. Române – R. S. România* (Vols. 1–13). Editura Academiei R.P. Române.

Tutin, T. G., Heywood, V. H., Burges, N. A., Valentine, D. H., Walters, S. M., & Webb, D. A. (Eds.). (1964–1980 & 1993). *Flora Europaea* (Vols. 1–5; Vol. 1, 2nd ed.). Cambridge University Press.

Zólyomi, B. (1954). Phytocénologie et la sylviculture en Hongrie. *Acta Botanica Academiae Scientiarum Hungaricae, 1*.

Scientific Papers. Series E. Land Reclamation, Earth Observation & Surveying, Environmental Engineering. Vol. XIV, 2025
Print ISSN 2285-6064, CD-ROM ISSN 2285-6072, Online ISSN 2393-5138, ISSN-L 2285-6064

FIBONACCI'S SEQUENCE IN NATURE, SCIENCE AND ARTS. THE GOLDEN RATIO

Cosmin-Constantin NIȚU, Anca ROTMAN

University of Agronomic Sciences and Veterinary Medicine of Bucharest,
59 Mărăști Blvd, District 1, 011464 Bucharest, Romania

Corresponding author email: a.rotman@yahoo.com

Abstract

Leonardo Fibonacci (c. 1170 - c. 1240-1250), an Italian mathematician often regarded as the most gifted European mathematician of the Middle Ages, played a crucial role in introducing the Hindu–Arabic numeral system to Europe. His seminal work, Liber Abaci (1202), not only promoted this numerical framework but also featured the now-famous Fibonacci sequence - an integer series with deep mathematical properties and widespread applications. This paper explores the mathematical foundations of the Fibonacci sequence, including its recurrence relations, algebraic and matrix representations, and connections to continuous fractions. Furthermore, it examines the relationship between the sequence and the golden ratio (φ), an irrational number often referred to as the "divine proportion". The golden ratio is linked to aesthetically pleasing proportions and appears in various domains such as art, architecture, music, biology, and cosmology. Through historical analysis and illustrative examples, this work highlights the enduring influence of Fibonacci's legacy and the remarkable intersection between mathematical theory and patterns observed in the natural and cultural world.

Key words*: Fibonacci sequence, Fibonacci numbers, golden ratio, irrational numbers, recursive functions, mathematical modelling, patterns in nature, mathematical aesthetics, interdisciplinary applications.*

"Everything that is correct thinking is either mathematics or susceptible to mathematization"
Grigore Moisil

INTRODUCTION

Mathematics, logic, philosophy, astronomy, and cosmology form the foundation of many of the principles, calculations, and models used in contemporary science and daily life. These disciplines have shaped humanity's understanding of the world and continue to provide tools for discovery and innovation.

Among the great contributors to mathematical thought, names such as Pythagoras, Archimedes, Euler, and Fibonacci stand out. Their works laid the groundwork for theories and methods that remain relevant today. One particularly influential figure is Leonardo Fibonacci (c. 1170 - c. 1240-1250), also known as Leonardo of Pisa, a mathematician widely regarded as the most talented of the Western Middle Ages.

Fibonacci was the son of Guglielmo, an Italian merchant and customs official stationed in Bugia (modern-day Béjaïa, Algeria). Accompanying his father on commercial journeys throughout the Mediterranean, Fibonacci was exposed to diverse mathematical practices. It was in Bugia that he encountered the Hindu-Arabic numeral system - a revolutionary system far superior to the Roman numerals then used in Europe.

The name "Fibonacci" is derived from the Latin *filius Bonacci*, meaning "son of Bonacci". The word "Bonacci" likely comes from the Latin *bonus*, meaning "good," suggesting "fortunate son". This name would eventually become synonymous with one of the most elegant numerical sequences in mathematics.

This paper provides an overview of Fibonacci's mathematical legacy, focusing on his introduction of the Hindu–Arabic numeral system to Europe and the presentation of the Fibonacci sequence in his seminal work *Liber Abaci*. It also explores the mathematical properties of this sequence and its connection to the golden ratio - a number that has fascinated mathematicians, artists, and scientists for centuries due to its unique properties and surprising appearances in both natural and

human-made structures (Livio, 2003; Wang & Johnson, 2008; Choi et al., 2023).

FIBONACCI'S MATHEMATICAL HERITAGE

A pivotal milestone in Fibonacci's mathematical legacy was his role in introducing and promoting the Hindu–Arabic numeral system in Europe. This achievement was primarily realized through the publication of his influential work, *Liber Abaci* (The Book of Calculation), in the early 13th century (Beebe, 2009).

It is important to emphasize that Fibonacci's contributions were made in an era without modern computational tools such as calculators or computers. The introduction of an efficient numerical system was therefore revolutionary, facilitating arithmetic operations that were previously cumbersome under the Roman numeral system.

Among the many examples in *Liber Abaci*, Fibonacci included a now-famous problem involving the growth of a rabbit population. This example led to the popularization of the integer sequence that would later bear his name—the Fibonacci sequence. Although Fibonacci did not invent the sequence, his use of it in this context significantly contributed to its recognition and enduring legacy in mathematical literature.

Liber Abacci

Fibonacci employed a unique fractional notation in *Liber Abaci*, using composite fractions in which a sequence of numerators and denominators was written beneath a single fraction bar. A notable example is found in a manuscript preserved at the National Central Library, where Fibonacci lists the numbers 1, 2, 3, 5, 8, 13, 21, 34, 55, 89, 144, 233, and 377—forming the well-known Fibonacci sequence (Boyer, 1968).

This page, shown in Figure 1, also illustrates how certain digits - particularly 2, 8, and 9 - bear a stronger resemblance to modern Arabic numerals than to their Eastern Arabic or Indian counterparts. While these early numbers are simple to compute or recall, the Fibonacci sequence extends far beyond its initial terms, revealing complex and profound mathematical properties (Sigler, 2002).

Liber Abaci - Latin for "The Book of Calculation" - was published in 1202 and remains one of the most influential arithmetic texts of the medieval period (Devlin, 2012). Although the original edition no longer survives, a revised version was completed in 1227 and dedicated to the scholar Michael Scot. At least nineteen manuscripts containing portions of this work still exist, including three complete versions from the 13th and 14th centuries and nine known incomplete copies dating from the 13th to 15th centuries (Mollin, 2002).

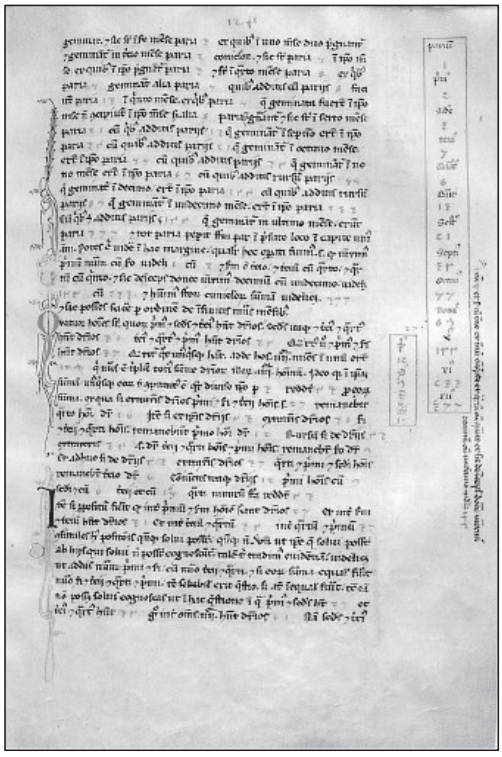


Figure 1. A page from *Liber Abaci*, displaying early use of the Fibonacci sequence and Arabic numeral forms (Pisano & Bussotti, 2015)

The first printed edition of *Liber Abaci* appeared in 1857, translated into Italian by Boncompagni. A complete English translation did not appear until the early 21st century, highlighting the enduring interest in Fibonacci's contributions.

This work is particularly renowned for introducing the base-10 positional system and Arabic numeral symbols to Europe, replacing the cumbersome Roman system. Fibonacci

emphasized the practical superiority of this approach throughout the text.

Beyond arithmetic, *Liber Abaci* demonstrated the widespread presence of Fibonacci numbers in nature. These numbers appear in spiraling arrangements of plant growth, such as sunflower seed patterns, pinecones, and other botanical structures. Similar spirals are observed in non-living systems such as hurricanes, water vortices, and galaxies. Additionally, biological structures like snail shells, nautilus spirals, the cochlea of the inner ear, and even goat horns often follow logarithmic spiral patterns aligned with the Fibonacci sequence.

Significantly, *Liber Abaci* was the first Western book to introduce and promote the Hindu–Arabic numeral system, including symbols resembling modern digits. The work made a compelling case for adopting this new system, explaining its advantages for both theoretical and practical calculations.

Although the title is sometimes mistranslated as *The Book of the Abacus*, Sigler (2002) clarifies that the term *abacus* during Fibonacci's time referred to "calculation" in general, not specifically to the counting device. In fact, in medieval Italy, the spelling *abbacus* (with two "b"s) denoted computations using Hindu–Arabic numerals, thus avoiding confusion.

Liber Abaci outlined techniques for performing arithmetic without relying on the traditional abacus. Ore (1948) noted a long-standing rivalry that persisted after the book's publication—between *algorists*, who promoted the new numerical system, and *abacists*, who remained loyal to the Roman numeral-based counting board.

Mathematics historian Carl Boyer emphasized that *Liber Abaci*, while not a treatise on the abacus itself, is "a very thorough treatise on algebraic methods and problems in which the use of the Hindu–Arabic numerals is strongly advocated" (Boyer, 1968).

The book is organized into four main sections:

- Section I introduces the Hindu–Arabic numeral system, arithmetic operations, and methods for converting between numerical representations. It also includes the earliest known use of trial division for identifying and factoring composite numbers.
- Section II applies arithmetic to commercial problems, including currency conversion, measurements, and interest calculations.
- Section III explores more advanced mathematical topics, such as the Chinese Remainder Theorem, perfect numbers, Mersenne primes, arithmetic series, and square pyramidal numbers. This section also presents the famous rabbit problem, which popularized the Fibonacci sequence.
- Section IV discusses numerical and geometric approximations of irrational numbers, such as square roots.

Notably, *Liber Abaci* contains several Euclidean geometric proofs, revealing Fibonacci's familiarity with classical Greek mathematics. Furthermore, his algebraic problem-solving methods suggest influence from earlier scholars such as the 10th-century Egyptian mathematician Abū Kāmil Shujāʿ ibn Aslam (Mollin, 2002).

Fibonacci's notation for fractions (Moyon et al., 2015)

In reading *Liber Abaci*, it is essential to understand Fibonacci's unique notation for rational numbers. His system represents a transitional form between ancient Egyptian fractions - commonly used up to that time - and the modern fractional notation still in use today. Fibonacci's approach differs from contemporary notation in several keyways:

1. *Order of mixed numbers:* modern notation typically places the fractional part to the right of the whole number (e.g., $2\frac{1}{5}$ for $\frac{11}{5}$). In contrast, Fibonacci wrote the fraction first, followed by the whole number: for instance, he would write "$\frac{1}{5}2$" to represent $2\frac{1}{5}$

2. *Composite fractions:* Fibonacci used a form of composite fraction notation in which a single fraction bar encompassed multiple numerators and denominators. Each term represented a separate fraction, where the numerator was divided by the product of all denominators to its right. For example:

$$\frac{b\ a}{d\ c} = \frac{a}{c} + \frac{b}{cd}, \text{ and } \frac{c\ b\ a}{f\ e\ d} = \frac{a}{d} + \frac{b}{de} + \frac{c}{def}.$$

As a specific example, the fraction, $\frac{27}{30}$ could be represented as $\frac{1\ 1\ 4}{2\ 3\ 5}$, which translates to:

$$\frac{4}{5} + \frac{1}{3{\cdot}5} + \frac{1}{2{\cdot}3{\cdot}5}.$$

This form of mixed radix notation was particularly useful for handling weights, measures, and currencies. Unlike traditional mixed-radix systems that often-omitted denominators, Fibonacci's notation explicitly included them, allowing more precision and adaptability for various practical contexts.

3. *Additive notation:* Fibonacci occasionally wrote multiple simple fractions side by side to indicate their sum. For example, since $\frac{1}{2}+\frac{1}{3}=\frac{5}{6}$, so a notation like $\frac{1}{2}\ \frac{1}{3}\ 4$ would represent the mixed number $4\frac{5}{6}$, or simply the ordinary fraction $\frac{29}{6}$.

This form of notation can be distinguished from composite fractions by a visual break in the fraction bar. Moreover, when all numerators are 1 and the denominators are distinct, the result corresponds to an *Egyptian fraction* - a sum of distinct unit fractions.

Fibonacci sometimes combined additive and composite notations to represent numbers more flexibly. His system allowed for multiple representations of the same value, and *Liber Abaci* includes several methods for converting between these forms.

Notably, Chapter II.7 of *Liber Abaci* features a collection of techniques for expressing improper fractions as sums of unit fractions. Among these is the *greedy algorithm* - a method later referred to as the *Fibonacci–Sylvester expansion* - which selects the largest possible unit fraction at each step to construct the sum (O'Connor et al., n.d.).

Modus Indorum – The Method of the Indians

In *Liber Abaci*, Fibonacci introduces the concept of the *Modus Indorum* - Latin for "method of the Indians" - which refers to what is now known as the Hindu–Arabic numeral system or base-10 positional notation. This system, developed in India and transmitted to the Islamic world, was recognized by Fibonacci for its superior efficiency in calculation and record-keeping.

The text includes a presentation of the nine Indian numerals: 1, 2, 3, 4, 5, 6, 7, 8, 9 and introduces the symbol 0, referred to by the Arabs as *zephyrum* (from the Arabic *ṣifr*), meaning "empty" or "zero". Using these ten symbols, any number can be written through positional value - a concept that was revolutionary in contrast to the Roman numeral system then prevalent in Europe.

Thus, *Liber Abaci* offers not only a practical guide to arithmetic but also a comprehensive introduction to the use of digits 0 through 9, along with the principles of place value, which lie at the core of modern number systems.

Prior to the adoption of this system, Europe relied on Roman numerals, which lacked a symbol of zero and made complex arithmetic operations - such as multiplication, division, and algebraic problem-solving - extremely difficult, if not impossible. As a result, the methods of modern mathematics could not fully develop.

Fibonacci's endorsement of the Hindu–Arabic system marked a turning point in European mathematics. Although *Liber Abaci* was instrumental in initiating this transition, the widespread adoption of the system was gradual and extended over several centuries. As Ore (1948) notes, the process was "long-drawn-out", and it was not until the end of the 16th century that the Hindu–Arabic numeral system became widely accepted across Europe.

Some Mathematical Properties of Fibonacci Numbers

The Fibonacci sequence is a sequence of natural numbers defined by the recurrence relation (Vorobiev et al., 2002):

$$F_1 = 1,\ F_2 = 1$$

$$F_n = F_{n-1} + F_{n-2}, \qquad n \geq 3$$

The recurrence relation has a characteristic equation:

$$r^2 = r + 1$$

Solving this quadratic yields the roots:

$$r_1 = \frac{1+\sqrt{5}}{2} \qquad \text{and} \qquad r_2 = \frac{1-\sqrt{5}}{2}$$

Remark, the first root,

$$\varphi = r_1 = \frac{1+\sqrt{5}}{2}$$

is known as the **Golden Ratio**.

Using these roots, the general term of the Fibonacci sequence can be expressed as:

$$F_n = c_1\left(\frac{1+\sqrt{5}}{2}\right)^n + c_2\left(\frac{1-\sqrt{5}}{2}\right)^n$$

where $c_1, c_2 \in \mathbb{R}$ are the constants.

Applying the initial conditions

$$F_1 = 1, \qquad F_2 = 1,$$

we find:

$c_1 = \frac{1}{\sqrt{5}}$ and $c_2 = -\frac{1}{\sqrt{5}}$,

so, the *general therm* of Fibonacci's sequence is:

$$F_n = \frac{1}{\sqrt{5}}\left(\frac{1+\sqrt{5}}{2}\right)^n - \frac{1}{\sqrt{5}}\left(\frac{1-\sqrt{5}}{2}\right)^n$$

Matrix form

The Fibonacci sequence can also be expressed in matrix form:

$$\begin{pmatrix} F_{n+2} \\ F_{n+1} \end{pmatrix} = \begin{pmatrix} 1 & 1 \\ 0 & 1 \end{pmatrix}\begin{pmatrix} F_{n+1} \\ F_n \end{pmatrix}$$

If we denote:

$$A = \begin{pmatrix} 1 & 1 \\ 1 & 0 \end{pmatrix},$$

we obtain

$$\begin{pmatrix} F_{n+2} \\ F_{n+1} \end{pmatrix} = A^n \begin{pmatrix} F_2 \\ F_1 \end{pmatrix}, n \geq 1.$$

then:

$$A^n = \begin{pmatrix} F_{n+1} & F_n \\ F_n & F_{n-1} \end{pmatrix}$$

Continuous fractions

The golden ratio can be represented as an infinite continued fraction:

$$\varphi = 1 + \frac{1}{\varphi} = \cdots$$

$$= 1 + \frac{1}{1 + \frac{1}{1 + \frac{1}{1+\cdots}}}$$

Selected identities and properties

1. Relation between φ and Fibonacci numbers:

$$\varphi^n = F_n\varphi + F_{n-1}, \qquad n \geq 1$$

Proof: by induction.

For *n = 2* the equality becomes:

$$\varphi^2 = F_2\varphi + F_1 \Leftrightarrow \varphi^2 = \varphi + 1 \text{ (true).}$$

$n \to n+1$

$$\varphi^n = F_n\varphi + F_{n-1} | \cdot \varphi \Longrightarrow$$

$$\varphi^{n+1} = F_n\varphi^2 + F_{n-1}\varphi =$$

$$F_n(\varphi + 1) + F_{n-1}\varphi = (F_n + F_{n-1})\varphi + F_n$$

$$= F_{n+1}\varphi + F_n$$

Inductive step follows by multiplying both sides by φ and simplifying.

2. Cassini's identity:

$$F_{n+1} \cdot F_{n-1} - F_n^2 = (-1)^n$$

Proof. We consider *m = 1* in the equality from below. A more elegant proof is via matrices.

We consider the matrix $A = \begin{pmatrix} 1 & 1 \\ 1 & 0 \end{pmatrix}$ which characterizes Fibonacci's sequence and knowing $\det A = -1$ we obtain this identity.

$$A^n = \begin{pmatrix} F_{n+1} & F_n \\ F_n & F_{n-1} \end{pmatrix}$$

3. Catalan's Identity (Generalization of Cassini's):

$$F_{n+m} \cdot F_{n-m} - F_n^2 = (-1)^{n-m+1}F_m^2$$

Proof. By induction, we leave this to the reader.

4. Addition identity:

$$F_mF_{n+1} + F_{m-1}F_n = F_{m+n}$$

Proof. By induction on m,

Example cases:

- m = 2

$$F_2F_{n+1} + F_1F_n = F_{n+2} \Leftrightarrow F_{n+1} + F_n = F_{n+2}$$
(true)

- m = 3

$$F_3F_{n+1} + F_2F_n = 2F_{n+1} + F_n = F_{n+1} + F_{n+2} = F_{n+3} \text{ (true)}$$

$m - 1, m \to m + 1$

Adding the relations:

$$F_{m-1}F_{n+1} + F_{m-2}F_n = F_{m+n-1} \text{ and } F_mF_{n+1} + F_{m-1}F_n = F_{m+n}$$

we obtain:

$$(F_{m-1} + F_m)F_{n+1} + (F_{m-2} + F_{m-1})F_n = F_{m+n-1} + F_{m+n}$$

which gives:

$$F_{m+1}F_{n+1} + F_mF_n = F_{m+1+n}$$

5. Sum identity:

$$\sum_{k=1}^{n} F_k = F_{n+2} - 1$$

Proof. By induction.

For $n = 1$ the equality becomes $F_1 = F_2 = 1$ (true).
$n \to n+1$

$$\sum_{k=1}^{n+1} F_k = \sum_{k=1}^{n} F_k + F_{n+1} = F_{n+2} + F_{n+1} - 1$$
$$= F_{n+3} - 1$$

6. Pythagorean identity:
Every second term in the Fibonacci sequence starting from F_5 forms the hypotenuse of a right triangle:

$$(F_n F_{n+3})^2 + (2F_{n+1}F_{n+2})^2 = F_{2n+3}^2$$

Proof left to the reader.
7. Odd-Index Sum Identity:

$$\sum_{k=0}^{n-1} F_{2k+1} = F_{2n}$$

Proof. By induction. For n=1 the equality becomes $F_1 = F_2 = 1$ (true).
$n \to n+1$

$$\sum_{k=0}^{n} F_{2k+1} = \sum_{k=0}^{n-1} F_{2k+1} + F_{2n+1} = F_{2n} + F_{2n+1}$$
$$= F_{2n+2}$$

8.

$$\sum_{k=1}^{n} F_k^2 = F_n F_{n+1}$$

Proof. By induction. For $n = 1$ the equality becomes $F_1^2 = F_1 F_2 = 1$ (true).
$n \to n+1$

$$\sum_{k=0}^{n+1} F_k^2 = \sum_{k=0}^{n} F_k^2 + F_{n+1}^2 = F_n F_{n+1} + F_{n+1}^2$$
$$= F_{n+1}(F_n + F_{n+1}) = F_{n+1}F_{n+2}$$

EXAMPLES OF THE GOLDEN RATIO IN ARTS AND NATURE

Golden ratio

The *golden ratio* is a special irrational number, denoted by φ, and is defined by the division of a line into two parts (Figure 2), a and b, such that:

$$\frac{a}{b} = \frac{a+b}{a}$$

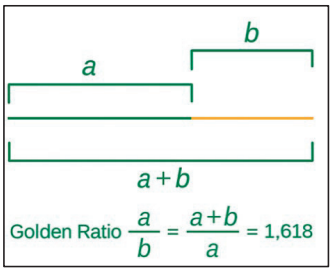


Figure 2. Golden Ratio

Golden Rectangle

A *Golden Rectangle* is a rectangle whose side lengths are in the golden ratio (Figure 3). That is, the ratio of the longer side to the shorter side equals φ.
This geometric figure is known for its aesthetic harmony and has been widely used in art, design, and architecture since antiquity.

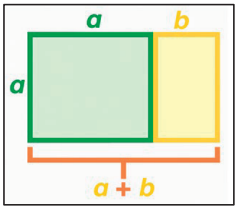


Figure 3. Golden Rectangle

Golden angle

In geometry, the *golden angle* arises when a circle is divided according to the golden ratio (Figure 4). Specifically, it is the smaller of the two angles formed when the circumference is split such that the ratio of the arc lengths is the golden ratio.
Its exact value is:

$$360^o\left(1 - \frac{1}{\varphi}\right) = (3 - \sqrt{5})180^o \approx 137{,}5^o$$
$$= 2\pi(3 - \sqrt{5})\, rad$$

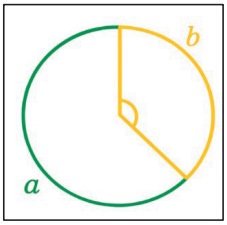


Figure 4. Golden Angle

Golden spiral

A *golden spiral* is a type of logarithmic spiral whose growth factor is equal to the golden ratio φ. Golden spirals are self-similar, meaning their shape remains unchanged under magnification (Figure 5).

The polar equation of a golden spiral is:

$$r = \varphi^{\frac{2\theta}{\pi}}$$

where:

- r is the radius;
- θ is the angle in radians;
- φ is the golden ratio.

More generally, a logarithmic spiral with growth factor B can be written as:

$$r = A\varphi^{B\theta}$$

which can be rewritten:

$$\theta = \frac{1}{B}\log\left(\frac{r}{A}\right)$$

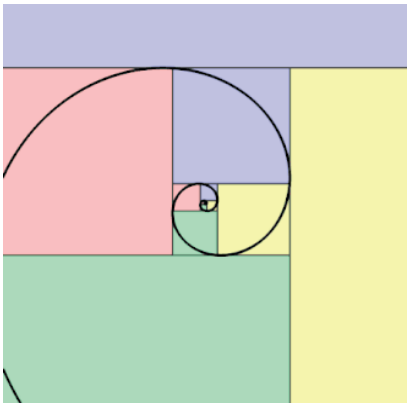


Figure 5. Golden Spiral
(https://en.wikipedia.org/wiki/Golden_spiral)

GOLDEN RATIO IN ARTS

Painting

The golden ratio has played a notable role in the composition of some of the most iconic works of art throughout history. Its presence is believed to enhance visual harmony, balance, and aesthetic appeal, contributing to the emotional and perceptual impact of a painting. Several masterpieces are often cited for their use of this proportion, including: "The Last Supper" and "The Mona Lisa" by Leonardo da Vinci (Figure 6), “The creation of Adam” by Michelangelo, "The Birth of Venus" by Botticelli, "The Starry Night" by Van Gogh, "The Persistence of Memory" by Salvador Dali. In these works, the golden ratio is thought to have guided the spatial arrangement of subjects and background elements, producing a visual equilibrium that resonates with the human sense of proportion and beauty. Artists throughout centuries have adopted the golden ratio, whether consciously or intuitively, as a compositional tool to create visual narratives that are pleasing and memorable. Alongside perspective, symmetry, and contrast, it remains one of the key elements used to achieve artistic coherence.

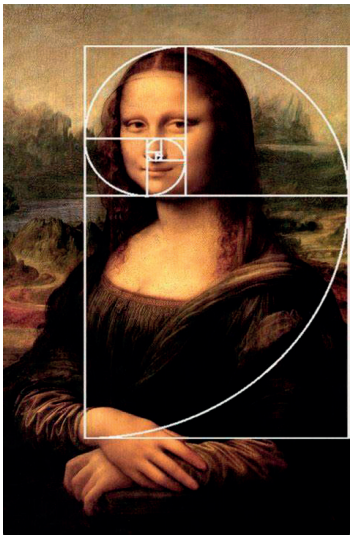


Figure 6. Mona Lisa - a painting frequently associated with golden ratio-based composition
(https://www.bing.com/images/)

Architecture

The golden ratio is also prevalent in architecture, appearing in both ancient monuments and contemporary structures. Long before Fibonacci’s time, this proportion was intuitively employed in designs that were considered naturally harmonious and aesthetically pleasing. Examples of structures often associated with the golden ratio include: The "Pantheon" in Rome (Figure 7), The "Great Pyramids" of Giza (Figure 8).

Architects and builders may have used the golden ratio not just for its beauty but also for structural balance and proportion. In modern times, it continues to inform architectural design

in buildings, bridges, and even furniture, reflecting humanity's enduring appreciation for mathematical harmony in physical space.



Figure 7. Pantheon - a classical Roman example often associated with golden proportions (https://www.bing.com/images/)

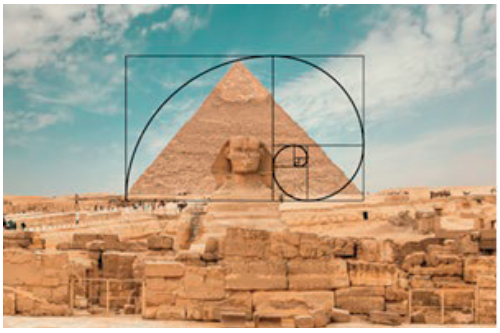


Figure 8. Pyramids - widely analyzed for golden ratio correlations in their dimensions (https://www.bing.com/images/)

Music

The golden ratio has also been observed in the structure and timing of musical compositions. Renowned composers such as Wolfgang Amadeus Mozart, Ludwig van Beethoven, and Claude Debussy are believed to have employed this proportion - either deliberately or intuitively - to shape the form and flow of their works.

For example, in Beethoven's Fifth Symphony, researchers have found structural divisions that align closely with the golden ratio, particularly in the placement of key climactic moments and thematic transitions (Figure 9).

Additionally, the golden ratio has been linked to the design of Stradivarius violins (Figure 10). Studies suggest that certain dimensional proportions in these famous instruments reflect golden ratio principles, potentially contributing to their visual elegance and acoustic excellence.

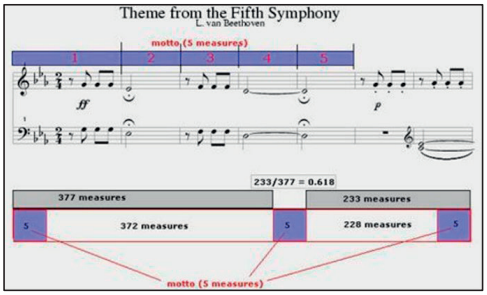


Figure 9. Beethoven's Fifth Symphony - noted for structural divisions consistent with the golden (https://www.bing.com/images/)

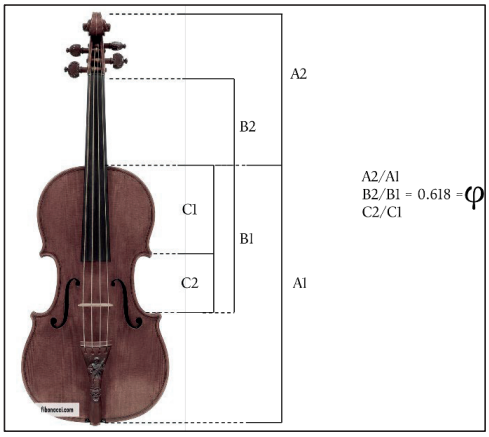


Figure 10. Stradivarius violine - exhibits golden proportions in design (https://www.bing.com/images/)

GOLDEN RATIO IN NATURE

Sunflower seeds

In sunflowers, the seeds located at the center are arranged in spiral patterns that follow Fibonacci numbers (Figure 11). These patterns allow for optimal packing and efficient use of space, maximizing the number of seeds that can fit in each area.

Pinecones

Pinecones frequently exhibit spirals in Fibonacci-related pairs, such as 3 and 5, 5 and 8, or 8 and 13. This form of natural arrangement is part of a broader phenomenon called phyllotaxis - the spiral pattern by which leaves, or other botanical elements are organized around a stem (Figure 12). Similar spiraling patterns are found in the outer petals of artichokes, succulents, and various flower buds.

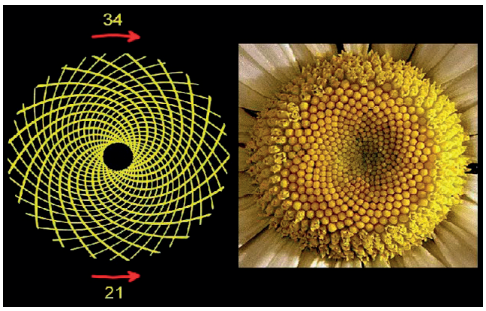


Figure 11. Sunflowers seeds - arranged in spirals that correspond to Fibonacci numbers (https://www.mathnasium.com/blog/golden-ratio-in-nature\)

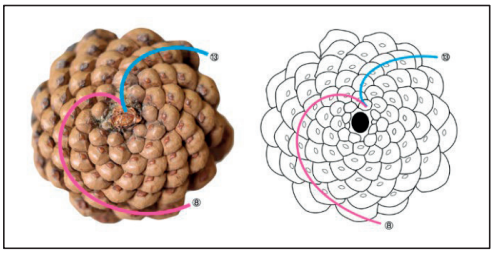


Figure 12. Pinecone with 8/13 configuration (https://craftofcoding.wordpress.com/2022/05/11/fibonacci-and-pinecones/)

Plant leaves

The golden ratio also manifests in the arrangement and structure of plant leaves. To maximize exposure to sunlight, many plants grow their leaves in spiral patterns, minimizing the shadow cast on lower leaves. This spiral spacing often aligns with the golden angle, which helps to optimize photosynthetic efficiency (Figure 13).

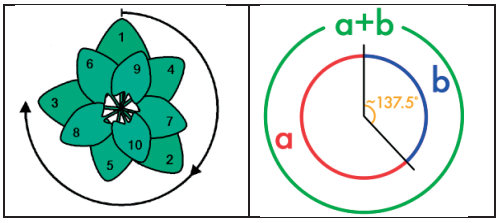


Figure 13. Leaves arrangement - successive leaves are separated by the golden angle (https://www.projectrhea.org/rhea/index.php/MA279Fall2018Topic1_Leaves)

Additionally, internal leaf structures show golden proportions. For instance, the vein spacing in some species approximates the golden ratio, and leaves of the Ginkgo tree often grow with dimensions reflecting this proportion (Figure 14).

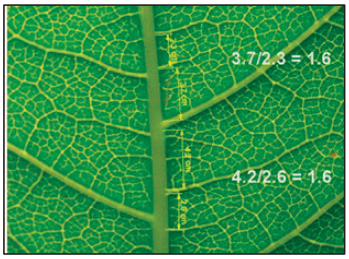


Figure 14. Venation of a leaf - illustrating golden ratio spacing (https://www.projectrhea.org/rhea/index.php/MA279Fall2018Topic1_Leaves)

Nautilus Shells

Nautilus shells are often cited as natural illustrations of the golden spiral, a logarithmic spiral whose growth factor is the golden ratio. As the shell grows, it maintains a consistent spiral shape, exemplifying self-similarity - a key characteristic of golden spirals (Figure 15).

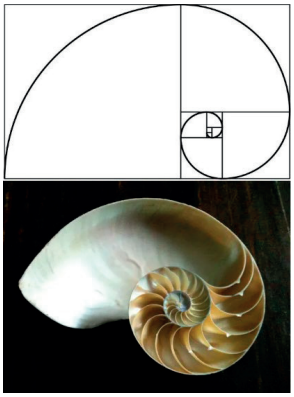


Figure 15. Nautilus shells - a classic example of the golden spiral in nature (https://www.mathnasium.com/blog/golden-ratio-in-nature\)

DNA

The golden ratio appears even at the molecular level. In the structure of DNA, relationships between its geometric features - including the length of a full turn of the helix and the width of the molecule - are often approximated by the golden ratio (Figure 16), suggesting an underlying harmony in the genetic blueprint of life.

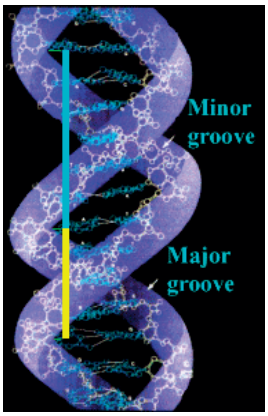


Figure 16. DNA - illustrating proportions that reflect the golden ratio
(https://www.goldennumber.net/dna/)

Fibonacci numbers in tornados, vortices or galaxies?

While many spiral shapes in nature arise from purely physical, non-biological processes - such as whirlpools, vortices in bodies of water, or the swirling formations of hurricane clouds and clear lanes - these spirals do not consistently follow Fibonacci-like patterns in their mathematical structure over time (Figure 17).

It may be possible to capture a snapshot where certain features temporarily exhibit ratios resembling those found in the Fibonacci sequence, but these patterns are neither sustained nor inherent to the structures themselves. In fact, the Fibonacci-like spirals observed in galaxies are more a result of human perception than a fundamental truth of the universe!

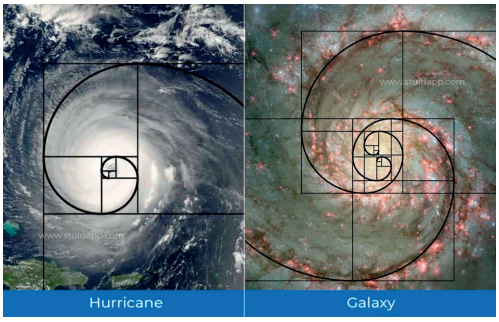


Figure 17. Hurricane and spiral galaxy – natural forms that appear Fibonacci-like, though not mathematically exact
(https://www.bing.com/images/)

CONCLUSIONS

The Fibonacci sequence and the associated golden ratio have long captivated mathematicians, scientists, and artists alike due to their mathematical elegance and their intriguing appearance in a wide range of natural and human-made phenomena.

While their mathematical foundations are firmly rooted in number theory and recurrence relations, their significance extends well beyond abstract theory. In fields such as biology, art, architecture, and music, these concepts often appear - sometimes as a matter of natural optimization, sometimes as a tool for achieving aesthetic harmony.

In nature, the Fibonacci sequence is often observed in plant growth patterns, leaf arrangements, pinecones, and flower petals, where the underlying spiral forms offer practical advantages such as sunlight exposure and space efficiency. The golden spiral appears in natural objects like nautilus shells and hurricanes, though its presence in large-scale phenomena like galaxies is often more interpretive than mathematically precise.

In art and architecture, the golden ratio has been consciously applied to design works that are balanced and pleasing to the eye, from Renaissance masterpieces to ancient monuments and modern constructions. Similarly, in music, some compositions reveal structural proportions aligning with the golden ratio, contributing to their rhythmic and thematic cohesion.

However, it is important to distinguish between intentional use and retrospective attribution. The golden ratio and Fibonacci numbers do not universally govern natural or artistic forms, and their presence is not always exact. In many cases, their appearance is approximate or coincidental and should be appreciated as part of a broader interplay between mathematics and the natural world - not as a universal design code.

In conclusion, the enduring fascination with Fibonacci numbers and the golden ratio lies in their ability to bridge pure mathematics with observable reality. Whether in a sunflower, a symphony, or a spiral staircase, they offer a compelling reminder of mathematical patterns that often underline beauty, function, and structure in both nature and human creativity.

REFERENCES

Beebe, N. H. F. (2009, December 13). *Fibonacci's Liber Abaci (Book of Calculation)*. University of Utah. Retrieved February 27, 2025, from https://www.math.utah.edu/pub/tex/bib/fibonacci.html

Boyer, C. B. (1968). *A history of mathematics*. John Wiley & Sons. pp. 280

Choi, J., Atena, A., and Tekalign, W. (2023). The Most Irrational Number that Shows up Ev-erywhere: The Golden Ratio. *Journal of Applied Mathematics and Physics, 11*, 1185–1193. https://doi.org/10.4236/jamp.2023.114077

Devlin, K. (2012). *The man of numbers: Fibonacci's arithmetic revolution*. Walker Books. ISBN 978-0802779083.

Devlin, K. (2019). *Finding Fibonacci: The quest to rediscover the forgotten mathematical genius who changed the world*. Princeton University Press. pp. 92–93 (quoted on), ISBN 9780691192307, OCLC 975288613.

Livio, M. (2003). *The Golden Ratio: The Story of Phi, The World's Most Astonishing Number*, Broadway Books: New York, NY, USA.

Mollin, R. A. (2002). A brief history of factoring and primality testing B.C. (before computers). *Mathematics Magazine, 75*(1), 18–29. https://doi.org/10.2307/3219180

Moyon, M., & Spiesser, M. (2015). L'arithmétique des fractions dans l'œuvre de Fibonacci: Fondements & usages. *Archive for History of Exact Sciences, 69*(4), 391–427. https://doi.org/10.1007/s00407-015-0155-y

Nițu, C.-C. (2022). P-adic numbers and applications in and outside mathematics – An overview. *Scientific Papers. Series E. Land Reclamation, Earth Observation & Surveying, Environmental Engineering, XI*, 505–510.

O'Connor, J. J., & Robertson, E. F. (n.d.). *Abu Ja'far Muhammad ibn Musa Al-Khwarizmi*. MacTutor History of Mathematics Archive. University of St Andrews. Retrieved from http://www-history.mcs.st-andrews.ac.uk/Biographies/Al-Khwarizmi.html

Ore, Ø. (1948). *Number theory and its history*. McGraw Hill. (Reprinted by Dover Publications, 1988). ISBN 978-0-486-65620-5

Pisano, R., & Bussotti, P. (2015). Fibonacci and the abacus schools in Italy. *Almagest: International Journal for the History of Scientific Ideas, 6*(2), 126–164. https://doi.org/10.1484/J.ALMAGEST.5.109664

Rotman, A.-L. (2015). Global warming between reality, approach and acceptance. *Scientific Papers. Series E. Land Reclamation, Earth Observation & Surveying, Environmental Engineering, IV*, 19–24.

Sigler, L. E. (Trans.). (2002). *Fibonacci's Liber Abaci: A translation into modern English of Leonardo Pisano's Book of Calculation*. Springer-Verlag, ISBN 0-387-95419-8

Vorobiev, N. N., & Martin, M. (2002). *Fibonacci numbers*. Birkhäuser, ISBN 978-3-7643-6135-8

Wang, Q. & Johnson, C. R. (2008). Golden ratio in solid state structures, *Proceedings of the National Academy of Sciences, 105*, 39, 15098–15103, National Academy of Science.s

https://www.mathnasium.com/blog/golden-ratio-in-nature

https://en.wikipedia.org/wiki/Golden_spiral

https://www.projectrhea.org/rhea/index.php/MA279Fall2018Topic1_Leaves

https://www.goldennumber.net/dna/

https://craftofcoding.wordpress.com/2022/05/11/fibonacci-and-pinecones/

Scientific Papers. Series E. Land Reclamation, Earth Observation & Surveying, Environmental Engineering. Vol. XIV, 2025
Print ISSN 2285-6064, CD-ROM ISSN 2285-6072, Online ISSN 2393-5138, ISSN-L 2285-6064

DIMENSIONING OF UNDERGROUND PIPE NETWORKS OF IRRIGATION PLOTS. CASE STUDY - FÂNTÂNELE-SAGU IRRIGATION PLOT, ARAD COUNTY

Antonia Mariana PASC, Teodor Eugen MAN, Robert Florin BEILICCI, Erika BEILICCI, Mircea VISESCU

Politehnica University of Timișoara, 1A Splaiul Spiru Haret, 300022, Timișoara, Romania

Corresponding author email: erika.beilicci@upt.ro

Abstract

To ensure the realization and efficient technical and economic operation of an irrigation system, it is important that, from the design, a correct dimensioning of the network of underground sprinkler irrigation pipes and, respectively, of the pressure station to ensure the necessary flow and pressure on all sections of the network, starting from the calculation of the irrigation regime, is ensured. The paper presents a calculation model for the correct dimensioning of the network of underground pipes within an irrigation plot, applied to the case study of the Fântânele - Sagu plot, Arad County, which takes into account the determination of the diameter of the main, secondary pipes and the antennas in such a way as to ensure the transport of the necessary water flow in each point of the plot and respectively to ensure the pressure necessary for the operation of the mobile watering equipment at all existing hydrants on this network. In the case study, the project for the modernization and retechnology of the secondary irrigation infrastructure is presented of the SPP Fântânele - Sagu plot.

Key words*: antennas, hydrants, irrigation, pipe network.*

INTRODUCTION

Droughts, floods and other climate change-related threats have a significant impact on the stability of agricultural production and food security, and the lack of adequate infrastructure contributes to limiting opportunities for economic development despite the existence of potential in agriculture.

In order to adapt to the effects of climate change, for environmental protection and for reasons of competitiveness, it is necessary to modernize irrigation plots, which ensure the efficient use of water, through the correct technical and economic sizing of underground pipe networks, pressure pumping stations, by using new technologies that lead to a reduction in water and energy consumption at the level of investment.

This is proposed to be carried out within the National Strategic Program 2023-2027 - a program funded by the European Union and the Government of Romania through measures DR-25 (addressed to the OUAI for the rehabilitation and modernization of existing irrigation plots) and DR-26 (addressed to farmers for the realization of new local irrigation arrangements) - Modernization of irrigation infrastructure (AFIR, 2024).

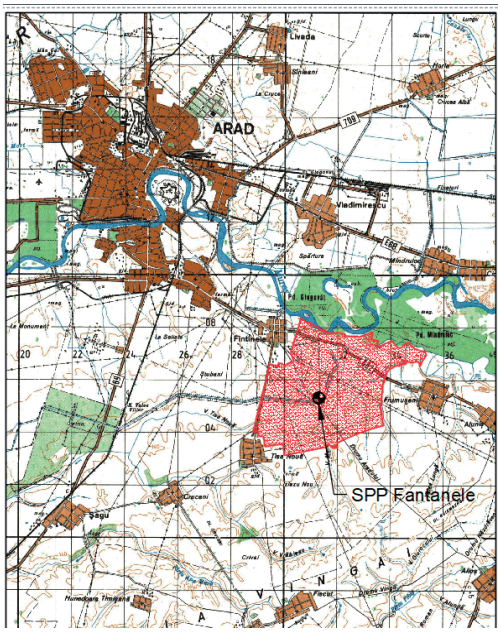


Figure 1. Map of SPP Fântânele, Arad County, Romania

In the process of carrying out these works, it is currently necessary to propose solutions for achieving intelligent irrigation using modern mobile irrigation equipment, as far as possible with automated operation and remote control (from the computer or even from the phone) (Cetin et al., 2023).

Currently worldwide (Biali et al., 2022) there are numerous pieces of equipment that, implemented in projects for the realization of new irrigation arrangements both by sprinkling and by dripping, or for the rehabilitation/ modernization of old arrangements degraded over time, lead to important benefits of labor, water and energy saving. The studied location is located on the administrative territory of Fântânele, Arad County (Figure 1). The plot of SPP Fântânele Sagu is part of the Irrigation Arrangement Sagu Fântânele Arad (Figure 2).

The design of the irrigation system was carried out between 1966 and 1968 on an area of 7154 ha, the entire area being connected to the unique hydrotechnical scheme for this system, with the connection to the Mureș river and served by the adduction channel. The irrigated area is served by means of a floating pumping station, SP floating, located on the left bank of the Mureș River, upstream from Fântânele (ANIF, 2024).

Fântânele pumping station (SPP Fântânele) is located at the downstream end of the Aducțiune I with a length of 2,984 m. It has an installed flow Q=1.45 mc/s and a head of H=70 m with water, necessary for the water supply of the SPP Fântânele plot arranged in the area of 1,914 ha.

Through the technical expertise carried out, it is necessary to replace the pump + drive motors assemblies and the electrical components for control, protection and automation, which present great wear, both physical and moral, due to the more than 50 years from the date of commissioning and non-operation of the irrigation system.

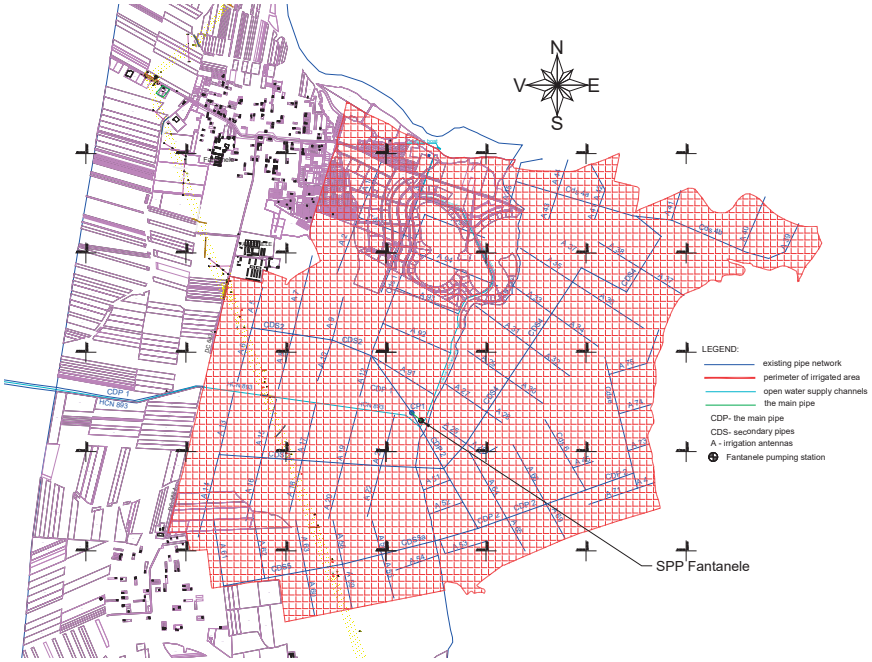


Figure 2. Map of existing irrigation system SPP Fântânele

MATERIALS AND METHODS

The elements of the irrigation regime include: Watering norm (m); Irrigation norm (Ni); Interval between waterings (T); Watering scheme; Irrigation hydromodule and uncoordinated and coordinated watering schedule chart. With these elements, the flow required for irrigation or the flow to be provided by the SPP (necessary to establish the time and number of pumping units) is calculated (Damian

et al., 2022). The calculation relationships of these elements are:

- Irrigation norm is calculated using:

$$m = \frac{N}{\sum n} \quad \left(m^3 / ha\right)$$

where:
N - irrigation norm in (m^3/ha);
n - number of waterings.

- Interval between waterings (or time to recover $T_{i,j}$) is determined using:

$$T_{i,j} = \frac{m}{Epz(luna)} \quad \left(m^3 / ha / day\right)$$

Epz - daily potential evapotranspiration (average water consumption of crops)

- Calculus of watering scheme requires external humidity values W_{min} and W_{max}

$$W_{\min} = 100 \cdot \gamma_v \cdot H \cdot P_{\min}$$
$$W_{\max} = 100 \cdot \gamma_v \cdot H \cdot C_c$$

where:
γ - volumetric weight of soil;
C_c - field capacity (m^3/ha);
P_{min} - minimum humidity ceiling;
H - depth of the active soil layer (m).

- The hydromodulus of irrigation for a rotation is determined with:

$$q_0 = \frac{n_i \cdot m_i}{3.6 \cdot T \cdot t} \ (l / s \times ha)$$

where:
n_i, m_i - the number of waterings, respectively the watering norm for the month of maximum consumption of the crop irrigation season (crop rotation) on the entire surface area (S_{pl});
T - 30 days the duration of surface watering the entire area with the maximum monthly irrigation norm;
T - 20 hours.
The required water flow rate is calculated with the ratio:

$$Q_i = q_i \times S_i \ \left(l / s\right)$$

where:
q_i - irrigation hydromodule (l/s/ha);
m_i - watering norm required by i crop;
T (8-10 days) - total watering time of crop;
t - 20 hours daily watering time;
S_i - i crop occupied area.

- Calculation ratio of the volume of water (V) required for each watering is given by:

$$V = \frac{m \cdot S}{1000 \cdot \eta} \quad \left(\text{k m}^3\right)$$

where:
m - watering norm (m^3/ha);
S - irrigated surface (ha);
η - (watering yield in the field) = (0.85 - 0.90).
The determination of the sizing flow rate of underground pipe networks is based on the theoretical calculation of pressure drops, where in general, Chezy's formulas are used:

$$V = C\sqrt{Ri}$$

Associating the continuity equation is obtained for the flow rate:

$$Q = VS = SC\sqrt{Ri}$$

The hydraulic radius is explained by $R = \frac{S}{P}$ and we obtain:

$$Q = SC\sqrt{\frac{S}{P}i} = \frac{S^{\frac{3}{2}}}{P}C\sqrt{i}$$

Associating the Chezy formula we obtain the flow rate:

$$Q=\text{SC}\sqrt{Ri} = S\frac{1}{n}R^y\sqrt{Ri} = S\frac{1}{n}R^{y+\frac{1}{2}}\sqrt{i} =$$

$$= S\frac{1}{n}\frac{S^{y+\frac{1}{2}}}{P^{y+\frac{1}{2}}}\sqrt{i} = \frac{1}{n}\frac{S^{y+\frac{3}{2}}}{P^{y+\frac{1}{2}}}\sqrt{i}$$

in other words:

$$Q = \frac{1}{n}\frac{S^{1,5+y}}{P^{0,5+y}}\sqrt{i}$$

by substituting with the Manning relation, we obtain:

$$Q = \frac{1}{n}\frac{S^{\frac{5}{3}}}{P^{\frac{2}{3}}}\sqrt{i}$$

For circular pipes we have:

$$Q=\frac{1}{n}\frac{\left(\frac{\pi D^2}{4}\right)^{\frac{5}{3}}}{(\pi D)^{\frac{2}{3}}}\sqrt{i}=\frac{\pi D^{\frac{8}{3}}}{n4^{\frac{5}{3}}}\sqrt{i}$$

flow module is noted:

$$\text{K}=\frac{\pi}{n}\frac{D^{\frac{8}{3}}}{4^{\frac{5}{3}}}$$

hydraulic resistance:

$$\text{M}=\frac{l}{K^2}$$

hence head loss is:

$$\text{h}_r=MQ^2$$

The study method is based on the use of Mike Urban software for hydraulic modeling of the underground irrigation pipeline network and the use of new / modern sprinkler irrigation equipment (DHI, 2024).

RESULTS AND DISCUSSIONS

The solution involves the rehabilitation of the pumping station building, with the replacement of the old pumping equipment with new ones with superior functional parameters, the rehabilitation of the underground network of transmission and distribution pipes with new HDPE pipes. The metering of consumption will be done entirely at the level of the pumping station, fencing (Figure 3)

Irrigation regime - was calculated for corn and wheat crop rotation. In Table 1 we find the calculation of the flow rate and the volume of water needed for sprinkler irrigation of 1857 ha during the vegetation period of one year (dry year). The entire area being cultivated with corn crop.

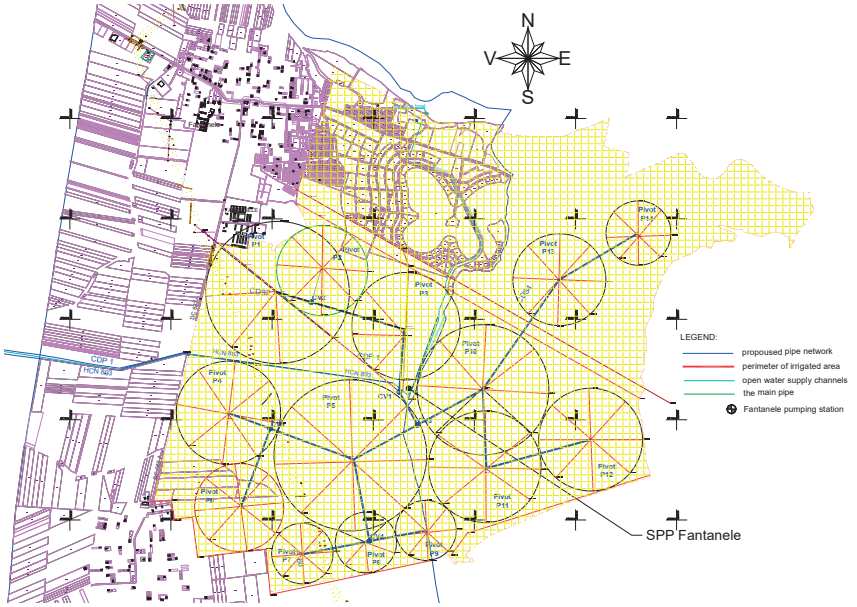


Figure 3. Map of proposed irrigation system SPP Fântânele

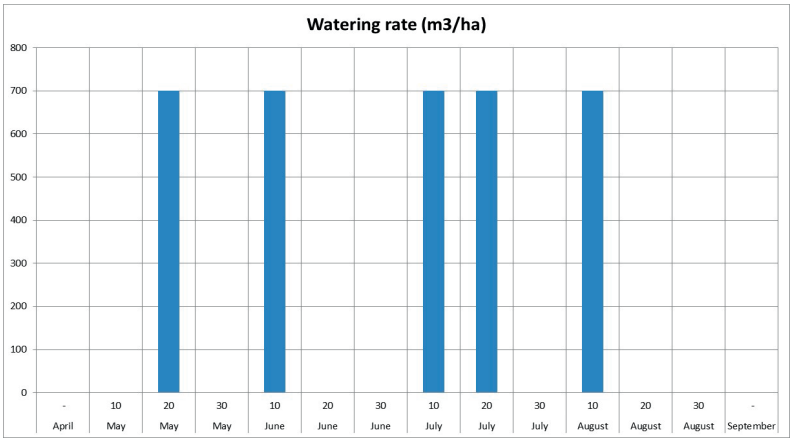


Figure 4. The annual and decadal watering charts

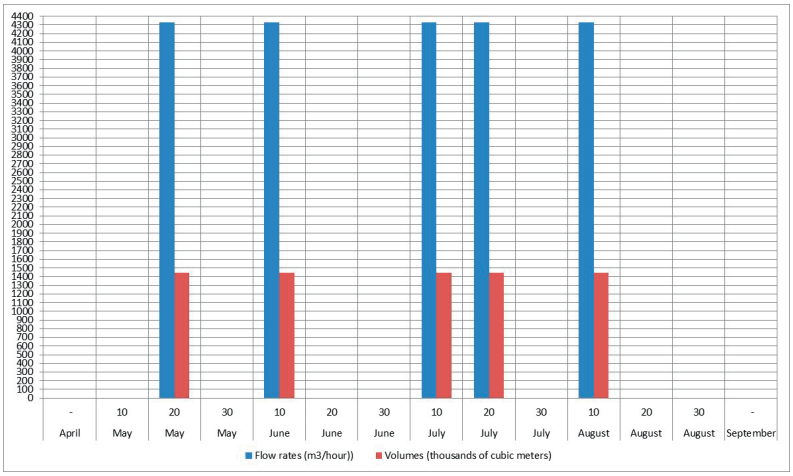


Figure 5. Uncoordinated watering schedule for a dry year

Figure 5 shows the water needs (flows and volumes) for decades, months and, the reference period (V-VIII) that the beneficiary must have a reference for watering.

To perform the modeling, the simulation model was developed by inputting coordinates in the Stereo 70 system, defining network nodes, and inserting pipe segments with specified materials and diameters. This process resulted in the layout plan illustrated in Figure 6. The SP Fântânele pumping station, which is supplied from the ANIF channel and has an installed flow capacity of 3991.9 m³/h, was integrated into the system. After calibrating and running the model, we obtained data on flow (Figure 7), velocity (Figure 8), headloss (Figure 9), and pressure (Figure 10) across all pipes and nodes, which were represented in corresponding diagrams.

Consequently, we were able to generate diagrams showing pressure, velocity, and headloss across all sections, specifically in the directions SP – A01 and SPP15 – P14, as shown in Figures 10 and 11.

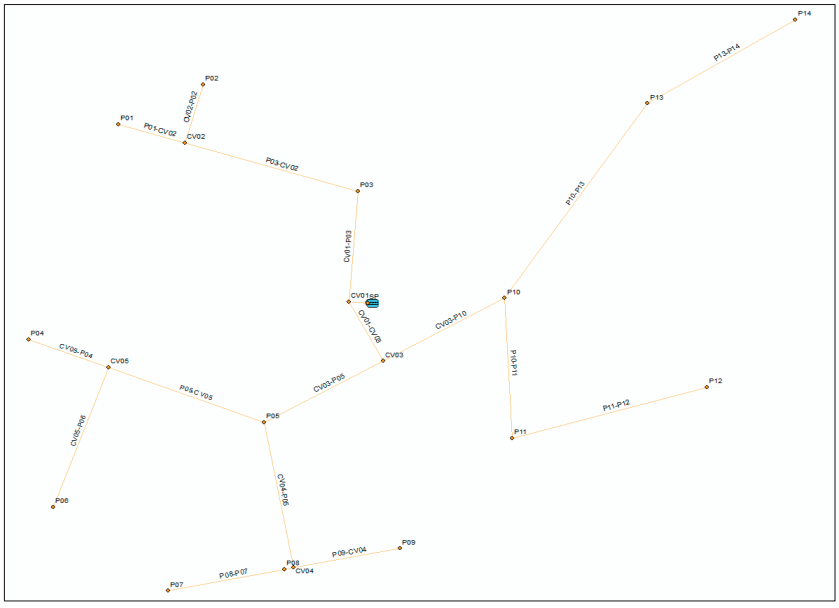


Figure 6. Plan view model

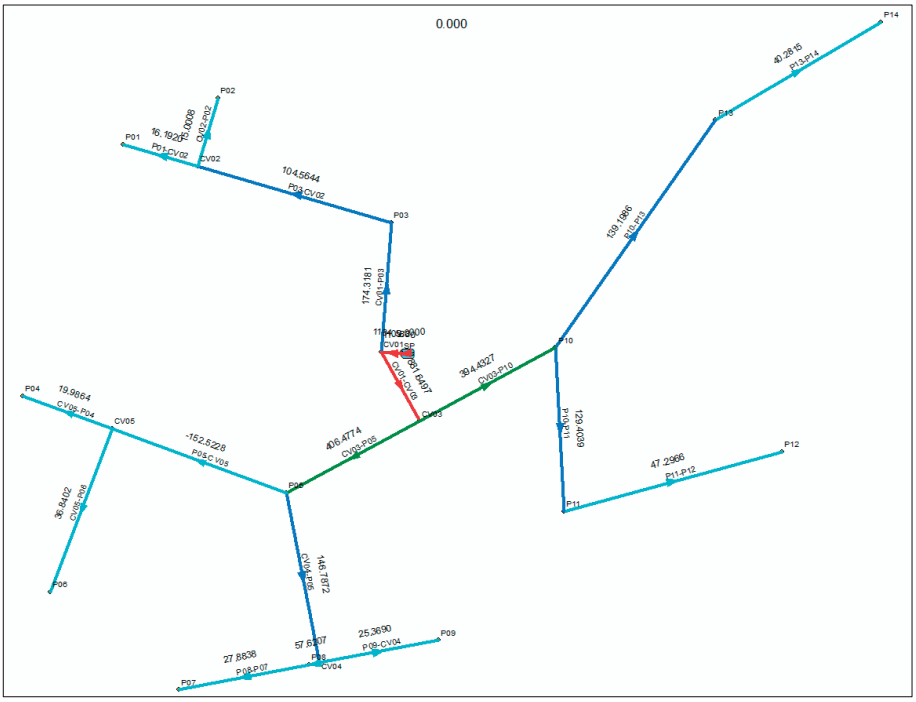


Figure 7. Pipe flows (l/s)

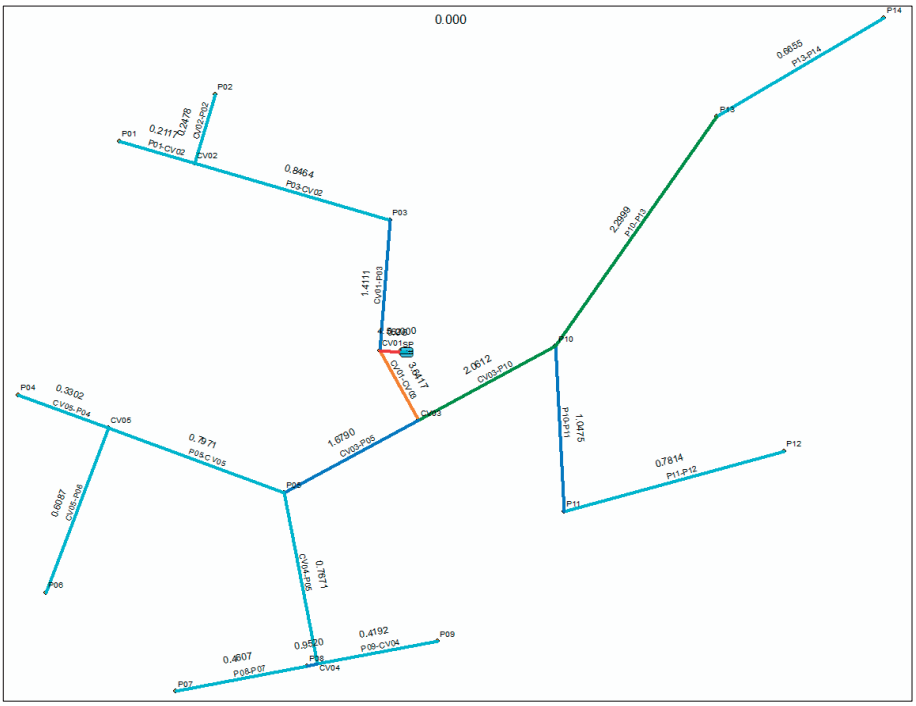


Figure 8. Pipe velocity (m/s)

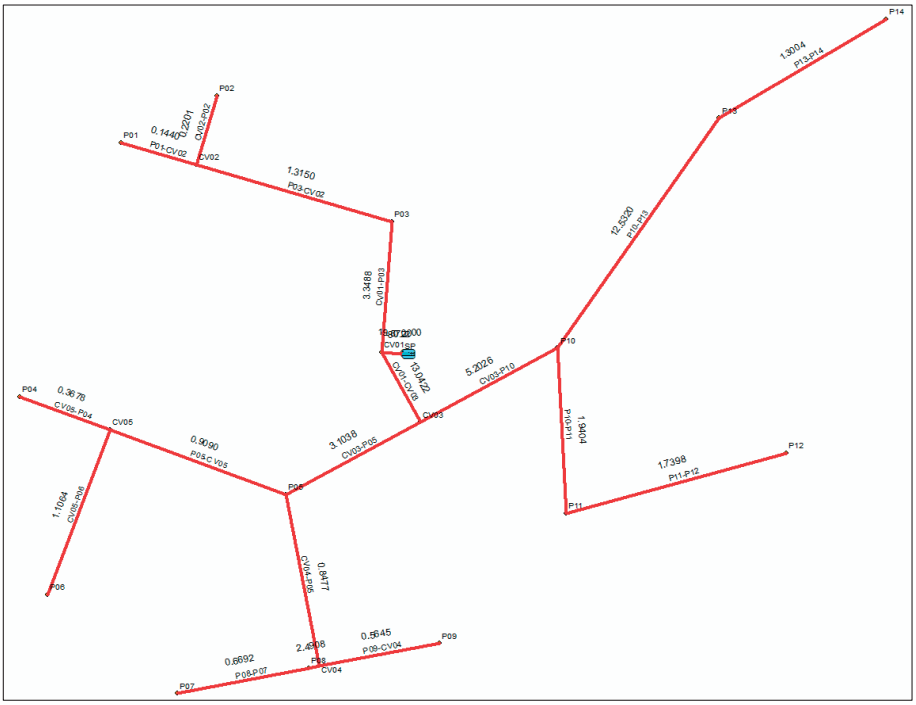


Figure 9. Pipe head-loss (m/km)

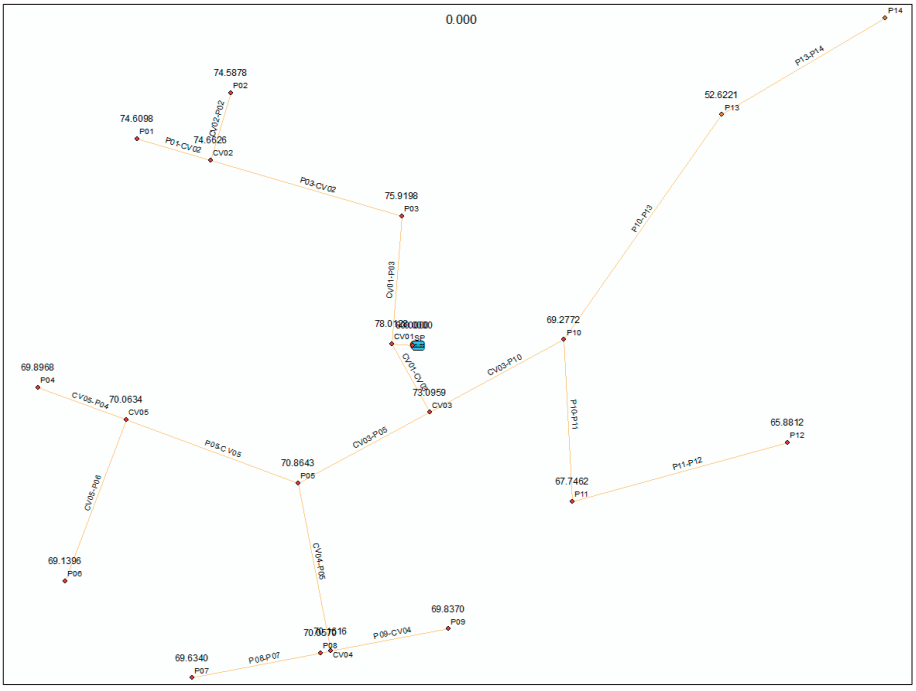


Figure 10. Node pressure (m)

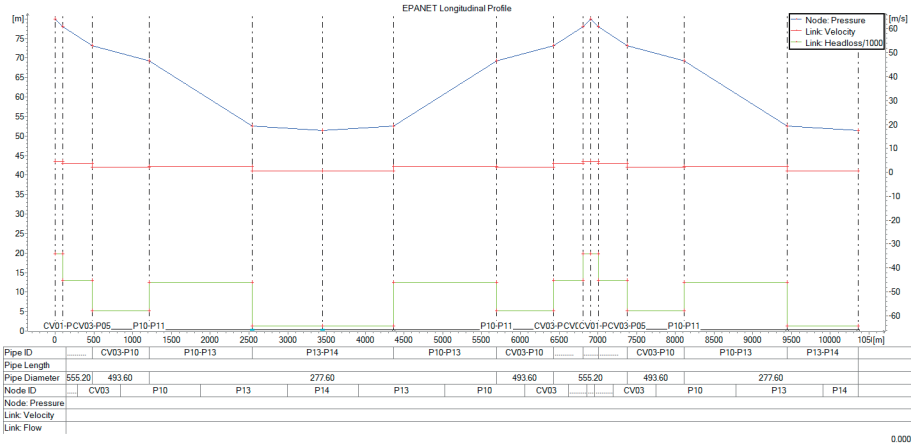


Figure 11. Section pressure diagram SP – P14

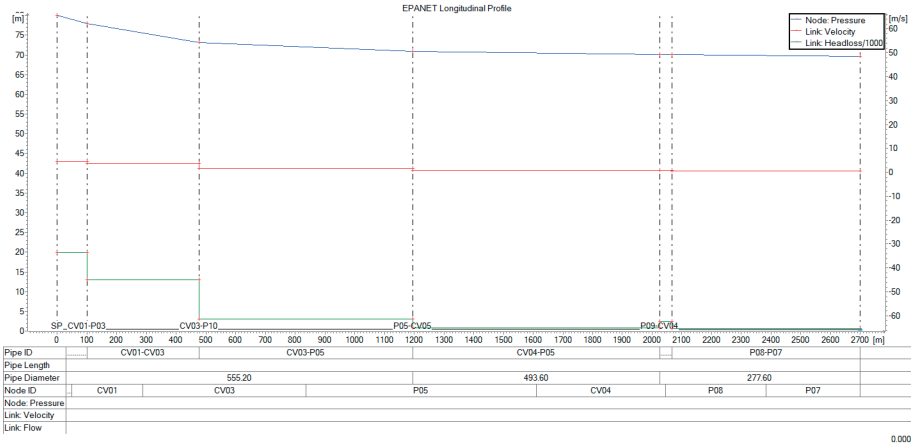


Figure 12. Section pressure diagram SP – P07

Without Project Scenario

Starting from the plant water requirement of 1600 m³/ha for 1198 ha, the total required volume is 1,916,800 m³. Assuming a field irrigation efficiency of 75%, the required volume at the hydrant is: 2,555,734 m³. To achieve this, with a pipeline network efficiency of 85%, the volume to be transported through the buried pipeline network must be 3,006,746 m³. Given the pump efficiency at the pressurization station is 65%, the volume to be extracted from the source (canal) is 4,625,763 m³.

Therefore, the water loss in the scenario WITHOUT the project is 2,708,963 m³.

With Project Scenario

Starting from the same plant water requirement of 1600 m³/ha for 1198 ha, the total needed volume remains 1,916,800 m³.

Assuming a field irrigation efficiency of 85% (due to new irrigation equipment acquired by the OUAI members), the required volume at the hydrant is 2,255,059 m³. To deliver this volume, with a modernized pipeline network efficiency of 95%, the volume to be transported is 2,373,746 m³.

With upgraded pumping units having an efficiency of 80%, the required intake from the source (canal) is 2,967,183 m³. Therefore, the water loss in the scenario WITH the project is 1,050,383 m³.

Water Loss Reduction

The reduction in water losses is calculated as the percentage difference between the losses in the "without project" and "with project" scenarios 61.22% Thus, the project implementation results in a 61.22% reduction in water losses.

The proposed technical solution ensures the functional safety of the entire irrigated area within the current irrigation system, starting from the distribution pipeline network required for water transport to the proper operation of the irrigation installations up to their terminal end.
The initial parameters of flow rate and discharge pressure are maintained to accommodate any crop plan with varying irrigation water requirements.
The new water distribution network, made of PE100 SDR17 PN10 polyethylene pipes, will lead to significant water savings.
Water losses in a pipeline network made of asbestos cement and pre-stressed concrete pipes older than 40 years, operating under a pressure regime of 6 bar, amount to approximately 25% of the volume of water pumped through the system. By replacing the old pipes with new HDPE (High-Density Polyethylene) pipes, these 25% losses can be eliminated.
In the case of the old hydrants, losses in the buried pipeline network are around 5% of the pumped water volume. Replacing the hydrants will eliminate this 5% loss as well.
For furrow and sprinkler irrigation methods, as originally designed for the buried pipeline system, the efficiency of this dual irrigation method is 0.8. By using new irrigation equipment such as boom and reel-type systems, irrigation efficiency increases to 0.9, thereby reducing water losses by approximately 10%.
Considering all three factors that influence water loss - replacement of the buried pipeline network with HDPE pipes, replacement of hydrants, and use of high-performance irrigation equipment - total water losses will be reduced by approximately 40%. Additionally, replacing the pumping units results in a further reduction of losses by around 15%, due to an increase in pump efficiency from 65% (old pumps) to 80% (new pumps).

CONCLUSIONS

The use of hydraulic modeling resulted in the pressure diagrams shown in Figures 11 and 12, which are essential for properly dimensioning the underground pipeline network used for irrigation. These diagrams ensure that both the pressure and flow rates are adequate for the efficient operation of sprinkler irrigation systems.
The proposed modernization scenarios focus primarily on optimizing the performance of the SP Fântânele pressure pumping station and the associated irrigation pipeline network responsible for delivering water to irrigated agricultural areas.
Installing new equipment to measure both water flow and volume distributed for irrigation will support transparent, contract-based operations between the water provider - ANIF Territorial Branch for Land Improvements Arad - and the beneficiary, OUAI Fântânele. This upgrade aims to prevent potential disputes arising from the absence of monitoring systems.
Additionally, the implementation of advanced automation technology is recommended to minimize staffing requirements at the pumping station during the system's operation period, thereby increasing operational efficiency.

REFERENCES

Biali, G., Cojocaru, P. (2022). GIS Hydrological modeling in an agricultural river basin with high potential for water erosion. *Scientific Papers-Series E-Land Reclamation Earth Observation & Surveying Environmental Engineering*, *11*, 418-425. Print ISSN 2285-6064.

Damian, G. Pricop, C., Statescu, F. (2022), The study of hydrological regime modeling using HEC-RAS model. case study river basin Bahluet, *Scientific Papers-Series E-Land Reclamation Earth Observation & Surveying Environmental Engineering*, *11*, 338-343.

DHI (2024). Mike Urban. Training guide.

***Agentia Nationala de Imbunatatiri Funciare (ANIF), Technical Archive - Territorial Branch of Land Improvements Arad, Available online: https://www.anif.ro

***Agentia pentru Finantarea Investitiilor Rurale (AFIR), DR-25 - Modernization of irrigation infrastructure (2024). Available online: www.afir.ro

***DALI (2023). Documentation for approval of intervention works – "Modernization and refurbishment of OUAI Fantanele Arad County ", S.C. Roxad Cioclov, SRL.

Scientific Papers. Series E. Land Reclamation, Earth Observation & Surveying, Environmental Engineering. Vol. XIV, 2025
Print ISSN 2285-6064, CD-ROM ISSN 2285-6072, Online ISSN 2393-5138, ISSN-L 2285-6064

ATTITUDES OF EUROPEAN GRADUATE STUDENTS REGARDING THE ROLE OF ADVANCED TECHNOLOGIES IN ENERGY AND INDUSTRY FOR A GREEN ENVIRONMENT IN THE CONTEXT OF CLIMATE CHANGE AND THE EUROPEAN GREEN DEAL

Nicoleta RADU[1, 2], Mihai Dan CARAMIHAI[3], Francisca BLANQUEZ CANO[4], Oksana MULESA[5], Adrian SILVA[6], Razvan TEODORESCU[1]

[1]University of Agronomic Sciences and Veterinary Medicine of Bucharest,
59 Mărăști Blvd., District 1, 011464, Bucharest, Romania
[2]National Institute for Research and Development in Chemistry and Petrochemistry – ICECHIM,
202 Splaiul Independenței, District 6, 060021, Bucharest, Romania
[3]National University of Science and Technology Politehnica Bucharest,
313 Splaiul Independenței, District 6, 060042, Bucharest, Romania
[4]Autonomous University of Barcelona, 08193 Bellaterra (Cerdanyola del Vallès), Barcelona, Spain
[5]Uzhhorod National University, 3 Narodna Square, 88000, Uzhhorod, Ukraine
[6]University of Porto, Praça de Gomes Teixeira, 4099-002 Porto, Portugal

Corresponding author email: nicoleta.radu@biotehnologii.usamv.ro

Abstract

This study explores the attitudes of European students towards the role of advanced technologies in energy and industry in fostering a green environment, particularly in the context of climate change and the European Green Deal. Survey results highlight a strong recognition of the importance of sustainability-related knowledge, including topics such as Green Agriculture, Zero Pollution, Circular Economy, and Green Sustainable Energy. The findings suggest that while students across Europe acknowledge the transformative potential of advanced technologies in achieving environmental goals, national contexts and current events, such as the ongoing conflict in Ukraine, influence perceptions of climate-related education and policy priorities. The survey results underscore the importance of incorporating green technologies into academic curricula to support the objectives of the European Green Deal.

Key words*: green technology, zero pollution, European Green Deal (EDG), sustainability education.*

INTRODUCTION

The European Green Deal (EGD) is a strategic policy framework aimed at achieving sustainability, economic modernisation, and climate neutrality by 2050, focusing on the circular economy, biodiversity, and sustainable agriculture. Key initiatives - including the Bio-Based Industries Consortium and the integration of digital technologies, green innovation, and renewable energy - are central to achieving these objectives. However, existing studies reveal disparities in progress across EU nations, underscoring the need for a systemic approach combining policy, research, and technological innovation (Stefanidis et al., 2024). The transformation of the energy system is crucial for long-term sustainability, with industrial decarbonisation relying on strategies such as fuel substitution, carbon capture, and circular economy practices (Fernández Gómez, 2022). Other studies explore the EGD's impact on sustainable agriculture, noting that large farms are better positioned to maintain income levels, while small farms may face reduced production and income. This disparity calls for further research on farm incomes, subsidies, and food security across the EU (Pawłowski & Sołtysiak, 2024). Another approach suggests that to attain climate neutrality, the industrialised Member States are the most prepared, Southern/Eastern states have moderate capacity, and Central/Eastern states require targeted investment (Ciot, 2022). In this regard, three European universities (USAMV Bucharest, Romania; Politehnica Bucharest, Romania; UAB Barcelona, Spain; Porto, Porto, Portugal; Uzhhorod University, Uzhhorod,

Ukraine) have developed, since 2023, a study regarding graduates' opinions on the role of advanced technologies in energy and industry for a green environment in the context of climate change and the EGD.

MATERIALS AND METHODS

The study was conducted using a Survey Questionnaire sent online (Radu et al., 2018; Radu et al., 2019; Radu et al., 2020) to graduate students of five European universities involved in the study. A maximum of ten completed survey questionnaires were received from graduate students from each university. A maximum of ten completed Survey Questionnaires were received from graduate students at each university. As of the beginning of 2025, the distribution of respondents (graduate students) from the five universities was as follows: Romania 15%, Spain 27%, and Ukraine 42%.

In a specific questionnaire template distributed online, graduate students were asked to assign scores ranging from 1 to 5 to certain questions, which were interpreted in terms of relevance as follows: Score 1: Not important; Score 2: Low relevance; Score 3: Medium relevance; Score 4: High relevance; Score 5: Very high relevance. In this survey, the responses to six specific questions were chosen and analysed, as follows: 1. Do you appreciate as being important for you as a graduated student to have knowledge regarding Zero Pollution?

2. Do you consider that basic knowledge of climate change will impact your overall activity?

3. Do you consider that basic knowledge on Biodiversity will have a positive impact on your upcoming activity?

4. Do you agree that the understanding of the main issues of Green Agriculture will be fruitful for your future activity?

5. Do you consider it will be effective the graduate students can be able to use knowledge regarding Industrial Strategy for Circular Economy?

6. Do you agree you must be able to use and apply the principles of Green Sustainable Energy? The graduate students were previously informed about the aims of this study. Participation in the survey was voluntary. The Survey Questionnaires distributed and received did not contain personal information such as name, address, phone number, or email address.

Data collection and analysis

Until September 2024, a total of 40 valid responses had been received. The geographic distribution of participants was as follows: 28% from Ukraine, 28% from Romania, 26% from Portugal, and 18% from Spain. Although the sample size is modest, the random selection of participants from each institution helped minimize selection bias and offered a degree of representativeness within the target population.

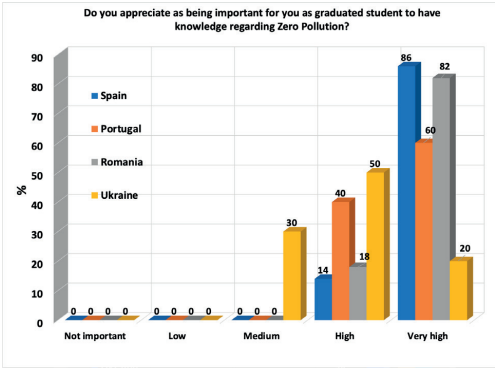
Given the exploratory nature of the study and the limited sample size, data analysis was primarily descriptive. No inferential statistical tests were applied. The goal was to identify prevailing trends and general patterns in student perceptions of and attitudes toward the role of advanced technologies in energy and industry for a green environment in the context of climate change and the European Green Deal.

RESULTS AND DISCUSSIONS

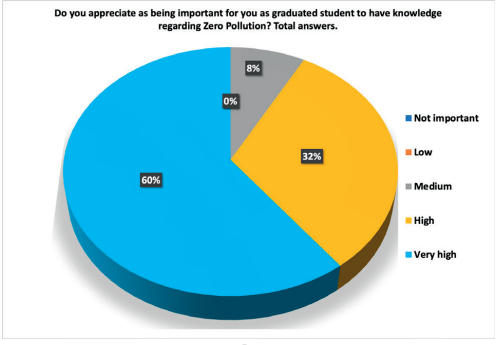
Regarding the statement, "Do you consider it important as a graduate student to have knowledge about Zero Pollution?" the majority of respondents from European countries gave the maximum score (Figure 1a), i.e., 86% of respondents from Spain, 82% from Romania, and 60% from Portugal. In contrast, only 20% of respondents from Ukraine gave the maximum score. Overall, 60% of all respondents considered it strongly important to know about Zero Pollution and assigned the highest score to this question. Additionally, 32% of respondents rated this statement as highly important, while only 8% provided an average rating (Figure 1b).

For the statement "Do you consider that basic knowledge of climate change will impact your entire activity?", 91% of Romanian respondents and 60% of Portuguese respondents stated that basic knowledge of climate change would have a very high impact on their overall activity (Fig. 2a). In contrast, only 29% of Spanish respondents considered this statement to have a very strong impact, as did 20% of Portuguese

respondents. Meanwhile, 43% of Spanish respondents believed that knowledge of climate change would have a high impact (Figure 2a).
Among Ukrainian respondents, 20% stated that basic knowledge of climate change would have a very strong impact on their entire activity, while 30% believed it would have a high impact. Responses indicating medium, low, or no importance did not exceed 15% in any country.
Overall, 53% of all respondents considered this statement to have a very strong impact (Figure 2b), while 24% believed it would have a high impact. Additionally, 18% of respondents rated the importance of this statement as medium, and only 5% considered it of low importance (Figure 2b).



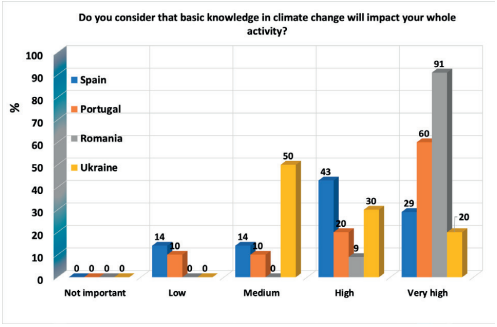
a



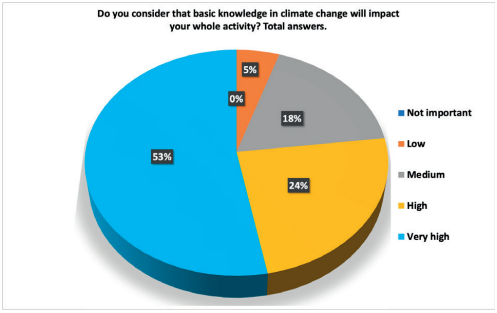
b

Figure 1. Distribution of responses to the question: "*Do you appreciate as being important for you as graduated student to have knowledge regarding Zero Pollution*?"
a) Answer distribution by country; b) Overall answer distribution across all respondents

Regarding the response to the statement: "Do you consider that basic knowledge of biodiversity will have a positive impact on your upcoming activity?", the respondents from Romania strongly agree with this statement in proportion 82% (Figure 3a).



a



b

Figure 2. Distribution of responses to the question: "*Do you consider that basic knowledge of climate change will impact your overall activity?*"
a) Answer distribution by country; b) Overall answer distribution across all respondents

The respondents from Spain and Portugal strongly agree with the statement in proportions of 43% and 40%, respectively, and highly agree in proportions of 43% and 50%, respectively. The respondents from Ukraine moderately agree with this statement in a proportion of 50% (Figure 3a). Overall, 53% of all respondents strongly agree with this statement, while 24% highly agree (Figure 3b).
For the statement "Do you agree that understanding the main issues of Green Agriculture will be beneficial for your future activity?" 100% of Romanian respondents are very high agree that understanding the main issues of Green Agriculture will be beneficial for their future activities. Similarly, 57% of Spanish respondents and 40% of Portuguese respondents very highly agree with this statement (Figure 4a). Only 10% of

respondents from Ukraine very highly agree with this statement, while 40% highly agree, as do the Portuguese respondents (Figure 4a). The percentage of respondents who rated this aspect as low or not important does not exceed 10% for students from each country involved in this study. Overall, 53% of all respondents considered this statement to have a strong impact (Figure 4b), 24% considered that this statement had a high impact, 18% gave an average rating, and only 5% of all respondents considered that this statement had a low importance (Figure 4b).

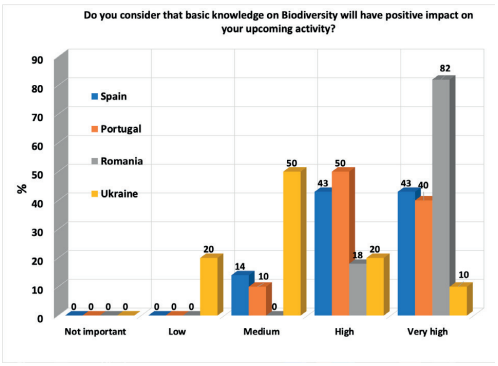


Figure 3. Distribution of responses to the question: "*Do you consider that basic knowledge on Biodiversity will have positive impact on your upcoming activity?*"
a) Answer distribution by country; b) Overall answer distribution across all respondents

In contrast, only 20% of Ukrainian respondents considered this statement to have a very strong impact. Additionally, 43% of Spanish respondents believed that this statement would have a high impact (Figure 5a). A per cent of 40% of Ukrainian respondents and 30% of Portuguese respondents considered it effective for graduates to be able to apply knowledge regarding the Industrial Strategy for the Circular Economy. Responses indicating medium, low, or no importance scores for this statement did not exceed 14% in any country (Figure 5a). Overall, 54% of all respondents considered this statement to have a very strong impact (Figure 5b), while 32% believed it would have a high impact. Additionally, 11% of respondents rated this statement as of medium importance, and only 3% considered it of low importance (Figure 5b).

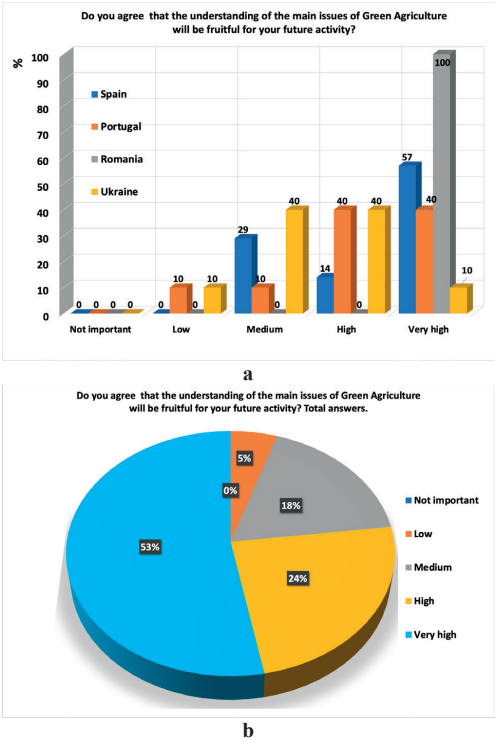
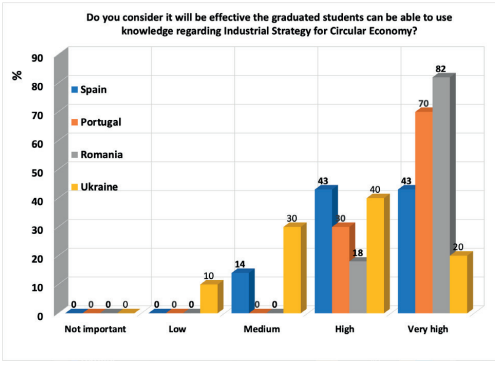


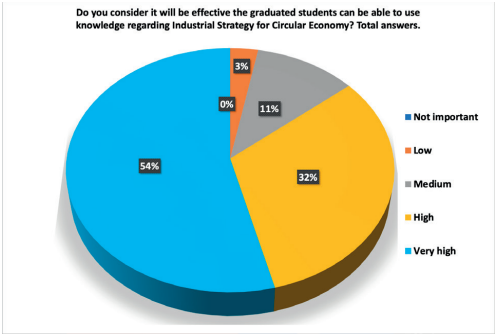
Figure 4. Distribution of responses to the question: "*Do you agree that the understanding of the main issues of Green Agriculture will be fruitful for your future activity?*" a) Answer distribution by country; b) Overall answer distribution across all respondents

Regarding the statement "Do you agree that you must be able to use and apply the principles of Green Sustainable Energy?", 82% of Romanian respondents, 28% of Spanish respondents, and 40% of Portuguese respondents strongly agreed with this statement (Figure 6a). In contrast, only 20% of Ukrainian respondents strongly agreed. Additionally, 71%

of Spanish respondents and 50% of Portuguese respondents highly agreed with this statement (Figure 6a), along with 40% of Ukrainian respondents and 18% of Romanian respondents. Responses indicating medium, low, or no importance for this statement did not exceed 10% in any country (Figure 6a). Overall, 50% of all respondents very strongly agreed with this statement (Figure 6b), while 39% highly agreed. Only 11% of respondents rated this statement as of medium importance (Figure 6b).



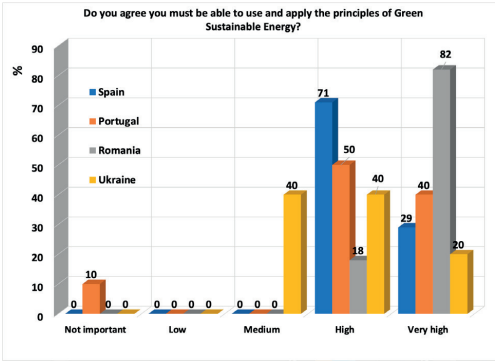
a



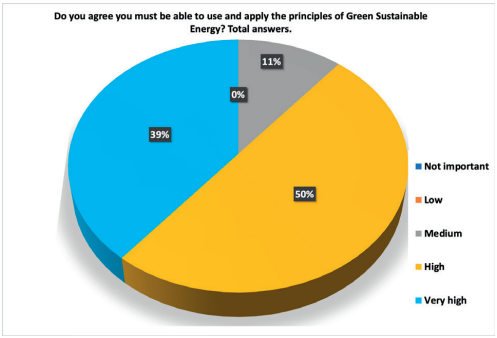
b

Figure 5. Distribution of responses to the question: "*Do you consider it will be effective for graduate students to apply knowledge regarding Industrial Strategy for Circular Economy?*" a) Answer distribution by country; b) Overall answer distribution across all respondents

The survey analysis reveals significant regional differences in graduate students' views on environmental knowledge. Respondents from Romania showed the strongest support for environmental topics, with the highest ratings for Zero Pollution awareness, Green Agriculture, and Green Energy. Spanish and Portuguese respondents also expressed considerable interest, though with less intensity, while Ukrainian responses were notably lower, likely due to the ongoing conflict. Overall, there was strong consensus on the importance of climate change, biodiversity, and sustainability in shaping future careers, highlighting the need for increased emphasis on environmental education across Europe



a



b

Figure 6. Distribution of responses to the question: "*Do you agree you must be able to use and apply the principles of Green Sustainable Energy?*" a) Answer distribution by country; b) Overall answer distribution across all respondents

Yang et al. (2023) highlight that while the Circular Economy (CE) model offers significant environmental benefits by repurposing waste, its success requires a comprehensive approach, integrating economic and social factors alongside environmental considerations. Industrial eco-parks, offer a promising model for enhancing waste recovery, resource utilisation, and energy efficiency (Nyangchak, 2022; Yang et al., 2023; Glockow et al., 2024).

Other experts emphasise the need for stronger links between the bioeconomy and circular economy in the context of the Sustainable Development Goals (SDGs) (Shobande et al., 2024). The systematic review identifies significant gaps in the literature, including a lack of standardised methodologies, geographic imbalance with a focus on Europe and Asia, and insufficient attention to social dimensions like poverty and food security (Ferrez & Pyka, 2023; Niwalkar et al., 2023). The studies performed by Kumar et al. (2023) stress the critical role of Circular Economy (CE) and green energy in advancing environmental sustainability. Moreover, it underscores the importance of investing in renewable energy to reduce CO_2 emissions. By integrating CE with green energy, businesses can develop innovative models, create cross-industry value chains, and seize sustainable commercial opportunities. The adoption of a closed-loop system focused on waste reduction and resource efficiency fosters technological advancements, further contributing to ecological sustainability (Santeramo, 2022; Kumar et al., 2023; Paleari, 2024).

CONCLUSIONS

Based on the survey responses, the following key conclusions can be drawn regarding graduate students' perceptions of environmental and sustainability topics in the context of the European Green Deal. A high degree of awareness regarding Zero Pollution was observed, particularly in Spain, Romania, and Portugal. However, Ukrainian respondents showed less enthusiasm, likely due to the impact of the ongoing war. Overall, 60% of respondents viewed Zero Pollution as extremely important, signaling its relevance to future academic and professional pursuits. Climate change knowledge was seen as impactful by the majority of respondents, especially from Romania and Portugal, where 91% and 60%, respectively, viewed it as a critical factor for their future endeavours. While fewer Spanish respondents shared this view (29%), Ukrainian responses reflected a broader range of opinions, with 50% perceiving it as highly impactful. In total, 53% of respondents recognized the strong influence of climate change knowledge. Knowledge about biodiversity was especially valued by Romanian students, with 82% strongly agreeing that it would positively affect their careers. Spanish and Portuguese respondents demonstrated substantial support, with 43% and 40%, respectively. Across all respondents, 53% strongly agreed, showing consensus on the importance of biodiversity in shaping future professional paths. The importance of Green Agriculture was universally acknowledged in Romania (100%), with substantial support in Spain (57%) and Portugal (40%). On average, 53% of all respondents saw Green Agriculture as a crucial factor in shaping sustainable practices. Knowledge about the Circular Economy Industrial Strategy was viewed as important, particularly by Romanian and Spanish respondents (82% and 43%, respectively). Overall, 54% of all respondents considered it essential for sustainable industrial practices. Green Sustainable Energy knowledge was most strongly endorsed by Romanian respondents (82%), with somewhat less support from Spanish (28%) and Portuguese (40%) students. Nevertheless, 50% of respondents across Europe placed a high value on this knowledge.

ACKNOWLEDGEMENTS

This work was carried out with the support of Project 2023-1-RO01-KA220-HED-000154433 entitled "Gender, Digitization, Green: Ensuring a Sustainable Future for All in Europe" co-funded by the European Union.

REFERENCES

Ciot, M.G. (2022). Implementation Perspectives for the European Green Deal in Central and Eastern Europe. *Sustainability*, *14*(7), 3947. https://doi.org/10.3390/su14073947.

Fernández Gómez, J. (2022). El Pacto Verde Europeo y la transición energética: retos y oportunidades para las empresas industriales.*Boletín De Estudios Económicos*, *76*(232), 191-211. https://orcid.org/0000-0003-3357-8338.

Glockow, T., Kaster, A. K., Rabe, K. S., & Niemeyer, C. M. (2024). Sustainable agriculture: leveraging microorganisms for a circular economy. Applied microbiology and biotechnology, *108*(1), 452. DOI: 10.1007/s00253-024-13294-0.

Kumar, S., Darshna, A., & Ranjan, D. (2023). A review of literature on the integration of green energy and

circular economy. *Heliyon*, *9*(11), e21091. https://doi.org/10.1016/j.heliyon.2023.e21091

Niwalkar, A., Indorkar, T., Gupta, A., Anshul, A., Bherwani, H., Biniwale, R., & Kumar, R. (2023). Circular economy-based approach for green energy transitions and climate change benefits. *Proceedings of the Indian National Science Academy. Part A, Physical Sciences*, *89*(1), 37–50. PMCID: PMC9707248.

Nyangchak, N. (2022). Emerging green industry toward net-zero economy: A systematic review. *Journal of Cleaner Production, 378*, 134622. https://doi.org/10.1016/j.jclepro.2022.134622.

Paleari, S. (2024). The EU policy on climate change, biodiversity and circular economy: Moving towards a Nexus approach, *Environmental Science & Policy*, *151*, 103603. https://doi.org/10.1016/j.envsci.2023.103603.

Pawłowski, K. P., & Sołtysiak, G. (2024). The Potential Impact of the European Green Deal on Farm Production in Poland. *Sustainability*, *16*(24), 11080. https://doi.org/10.3390/su162411080.

Radu, N., Chirvase, A. A., Babeanu, Begea, M. (2019). Entrepreneurship in the field of life sciences: the personal skills needed to start an innovative SME. *Scientific Papers Series Management Economic Engineering in Agriculture and Rural Development*, *19*(2) 375-379.

Radu, N., Chirvase, A. A., Babeanu, Begea, M. (2020). Studies regarding personal skills needed in entrepreneurship- case study in France, Lithuania and Romania. *Scientific Papers Series Management Economic Engineering in Agriculture and Rural Development*, *20*(2), 403-408.

Radu, N., Chirvase, A. A., Babeanu, N., Popa,O. et al. (2018). Education management in the field of life sciences- skills needed to start and develop an innovative SME. *Scientific Papers, Series Management, Economic Engineering in Agriculture and Rural Developmen*t, *18*(2), 375-381.

Shobande, O.A., Tiwari, A.K., Ogbeifun, L. Nader Trabelsi, N. (2024). Demystifying circular economy and inclusive green growth for promoting energy transition and carbon neutrality in Europe. *Structural Change and Economic Dynamics*, *70*, 666-681. DOI: 10.1016/j.strueco.2024.05.016.

Stefanis, C., Stavropoulos, A., Stavropoulou, E., Tsigalou, C., Constantinidis, T. C., & Bezirtzoglou, E. (2024). A Spotlight on Environmental Sustainability in View of the European Green Deal. *Sustainability*, *16*(11), 4654. https://doi.org/10.3390/su16114654.

Yang, M., Chen, L., Wang, J.*et al (2023).*Circular economy strategies for combating climate change and other environmental issues. *Environ Chem Lett, 21*, 55–80. https://doi.org/10.1007/s10311-022-01499-6.

Scientific Papers. Series E. Land Reclamation, Earth Observation & Surveying, Environmental Engineering. Vol. XIV, 2025
Print ISSN 2285-6064, CD-ROM ISSN 2285-6072, Online ISSN 2393-5138, ISSN-L 2285-6064

EXPERT PERCEPTIONS ON DIGITAL EDUCATION TOOLS AND ASSESSMENT STRATEGIES UNDER THE EUROPEAN GREEN DEAL FRAMEWORK

Nicoleta RADU[1, 2], Mihai Dan CARAMIHAI[3], Francisca BLANQUEZ CANO[4], Montserrat Sarrà ADROGUER[4], Oksana MULESA[5], Adrian SILVA[6], Razvan TEODORESCU[1]

[1]University of Agronomic Sciences and Veterinary Medicine of Bucharest, 59 Mărăști Blvd, District 1, 011464, Bucharest, Romania
[2]National Institute for Research and Development in Chemistry and Petrochemistry – ICECHIM, 202 Splaiul Independenței, District 6, 060021, Bucharest, Romania
[3]National University of Science and Technology Politehnica Bucharest, 313 Splaiul Independenței, District 6, 060042, Bucharest, Romania
[4]Autonomous University of Barcelona, 08193 Bellaterra (Cerdanyola del Vallès), Barcelona, Spain
[5]Uzhhorod National University, 3 Narodna Square, 88000, Uzhhorod, Ukraine
[6]University of Porto, Praça de Gomes Teixeira, 4099-002 Porto, Portugal

Corresponding author email: nicoleta.radu@biotehnologii.usamv.ro

Abstract

This study investigates expert opinions from five universities across Romania, Spain, Portugal, and Ukraine regarding the use of digital learning, gamification, and artificial intelligence (AI) in enhancing education aligned with the European Green Deal (EGD). Based on structured survey responses from academic professionals, the findings reveal that 65% of participants view online learning as a potential contributor to social isolation, highlighting the value of blended learning approaches. Gamification received broad support, with over 70% of experts agreeing it improves student engagement and comprehension, although concerns about cost and implementation persist. AI was acknowledged as a valuable tool for academic integrity and assessment, though its effectiveness in providing real-time personalized feedback remains inconclusive. These results suggest that a balanced integration of digital tools can support improved educational outcomes and better understanding of sustainability-related content.

Key words*: gamification, artificial intelligence, European Green Deal.*

INTRODUCTION

The integration of digital education and assessment techniques within the framework of the European Green Deal (EGD) presents both challenges and opportunities in reshaping higher education. The EGD, a strategic initiative by the European Union (EU), aims to achieve climate neutrality by 2050, requiring the transformation of multiple sectors - including education. Digital tools such as Moodle, Coursera, and other e-learning platforms contribute to this shift by facilitating access to educational content and promoting sustainable practices like cloud-based infrastructure and reduced material consumption (Aparisi-Torrijo et al., 2024; Oliveira et al., 2022; Torrez-Ruiz & Moreno Ibarra, 2019). These platforms are increasingly used to equip students with the knowledge and skills necessary to address climate change and sustainability challenges. Notable digital techniques include:

1) *Blended learning* – combining in-person teaching with digital platforms to enhance flexibility and inclusiveness.
2) *Gamification* – incorporating game-based elements into educational content to simulate real-world sustainability scenarios, making EGD-related topics more engaging.
3) *Collaborative learning* – leveraging online tools to support international teamwork on environmental and climate-related challenges (Elfert & Rubenson, 2022; Misra, 2012).

Assessment in digital education has also evolved to include:
1) *AI-Based Personalization* – tailoring learning and evaluation processes to individual student needs through adaptive technologies.
2) *Virtual simulations* – allowing students to interact with sustainability scenarios in realistic, consequence-driven environments.
3) *Digital assessment tools* – including online quizzes, virtual labs, and project-based evaluations (Frazão Santos et al., 2024; Reimers, 2021).
In this context, since 2023, five universities from four European countries and Ukraine have collaborated on a study examining expert perspectives on the most effective digital tools and teaching strategies for fostering a deeper understanding of EGD principles among Master's and Doctoral students. This paper presents the findings of that study, offering insights into current perceptions, regional differences, and key challenges in digital education for sustainability.

MATERIALS AND METHODS

Between 2023 and 2025, a consortium of five universities conducted a structured survey aimed at evaluating expert opinions on digital education methodologies suitable for enhancing students' understanding of the European Green Deal. The study aimed to evaluate preferred learning and assessment strategies aligned with sustainability goals in higher education.
The survey analysis consisted of 20-30 questions, grouped into thematic sections, regarding learning and assessment techniques most appropriate for a digital learning approach. Pilot testing was conducted with a small number of experts from each university or country involved in the study (a maximum of 10 experts per university). Representatives from each participating university selected individuals with specialised knowledge in areas such as environmental policy, digital education, sustainability in education, and European policy development. The selection criteria for experts involved in this study were as follows: a minimum of 15 years of experience; involvement in EU-funded education or green projects; academic publications in relevant areas; and participation in working groups or policymaking bodies related to the European Green Deal or digital education. The experts selected were teachers, researchers, or policymakers in higher education. The participating institutions included: Universitat Autònoma de Barcelona (Spain), University of Porto (Portugal), University of Agronomic Sciences and Veterinary Medicine of Bucharest (Romania), National University of Sciences and Technologies Politehnica of Bucharest (Romania), Uzhhorod National University (Ukraine). The study targeted academic experts involved in Master's and Doctoral education, focusing on identifying the most effective digital learning and assessment strategies aligned with sustainability principles. The survey employed a structured questionnaire developed based on methodologies established in previous educational research by Radu et al. (2018; 2019; 2020). These earlier studies served as the foundation for question framing, relevance scoring, and data analysis. Respondents were drawn from the five partner universities, with the following country-level distribution recorded by early 2025:

- Romania (combined responses from two universities): 15%;
- Spain: 27%;
- Portugal: 15%;
- Ukraine: 42%.

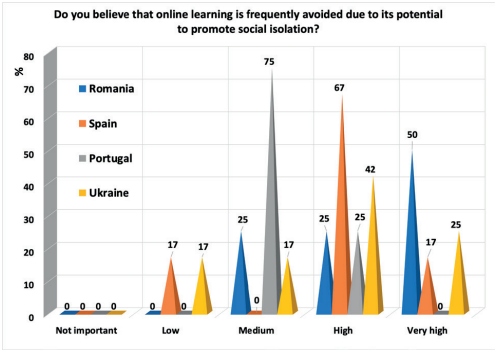
Each question was rated by respondents on a five-point Likert-type scale, with scores interpreted as follows: Score 1 - Not important; Score 2 - Low; Score 3 - Medium; Score 4 - High; Score 5 - Very High.

RESULTS AND DISCUSSIONS

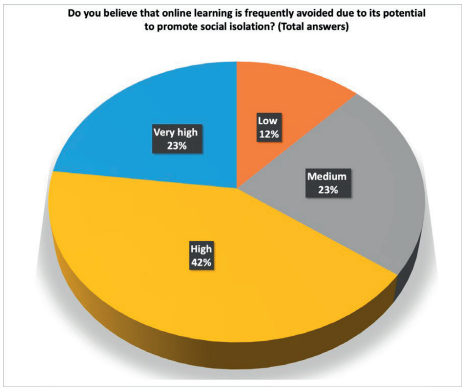
1. Online learning and social isolation

A key concern identified in the survey was the potential of online learning to contribute to social isolation among students. Experts were asked: *"Do you believe that online learning is frequently avoided due to its potential to promote social isolation?"*
The responses varied across countries. In Romania, 50% of experts rated this concern as *Very Important*. In Spain, 67% considered it *Important*, while in Portugal, the responses were more moderate, with most participants selecting *Medium* importance. In Ukraine, 42% of respondents rated it as *Very Important*, and an

additional 25% regarded it as *Important*. These results indicate that, apart from Portugal, most respondents viewed social isolation as a significant barrier to online education (Figure 1a). The overall distribution of responses confirms this pattern, with 42% of participants rating the issue as *Important* and 23% as *Very Important* (Figure 1b). This finding reinforces the value of blended learning models, which combine digital tools with face-to-face interaction to mitigate isolation while leveraging online flexibility.



a



b

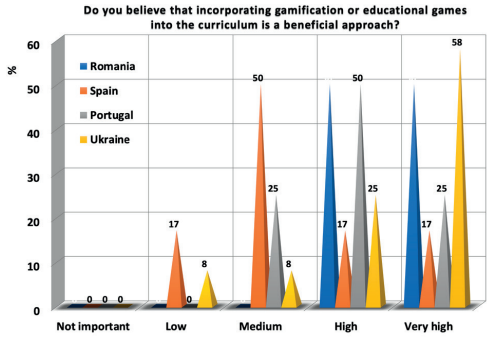
Figure 1. Expert perceptions of social isolation caused by online learning across four European countries:
a) Country-level breakdown;
b) Combined overall results

2. Gamification in digital education

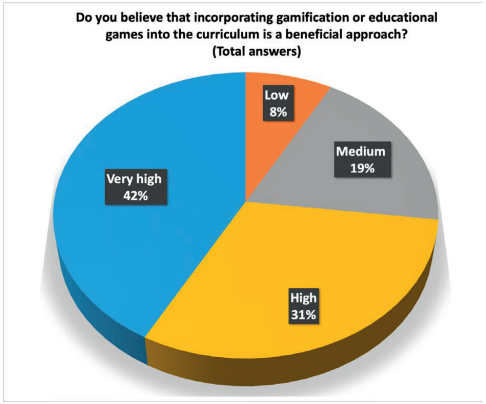
The effectiveness of gamification in supporting the understanding of EGD principles was explored through three distinct survey questions.

a) Perceived benefit of gamification

Responses to the question, *"Do you believe that incorporating gamification or educational games into the curriculum is a beneficial approach?"* indicated that experts from Ukraine and Romania rated this approach as *Very Important* in 58% and 50% of cases, respectively, while those from Portugal and Spain predominantly considered it *Important* (Figure 2a). The overall distribution showed 42% of respondents selected *Very Important*, and 31% selected *Important* (Figure 2b), indicating strong support for gamification as an engaging teaching method.



a



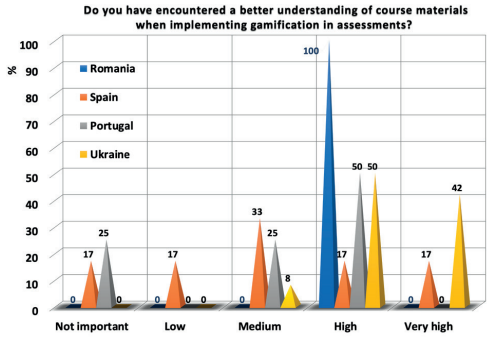
b

Figure 2. Expert perspectives on the educational value of gamification in the curriculum across four European countries: a) Responses by country; b) Overall response trends

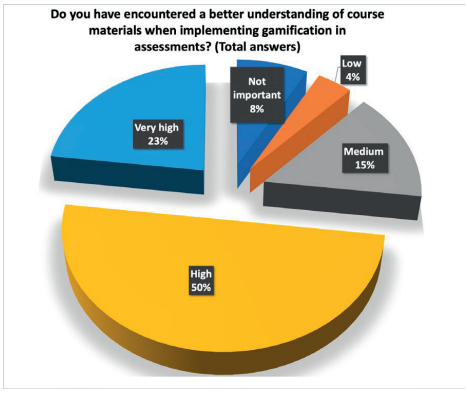
b) Effectiveness in enhancing understanding

The answers to the question: "*Have you observed a better understanding of course materials when implementing gamification in assessments?*" are more nuanced, likely due to practical limitations such as development cost and the need for technical expertise. As a result, 42% of experts from Ukraine rated this aspect as

Very Important. Meanwhile, all respondents from Romania and Portugal considered it *Important*, as did 50% of respondents from Ukraine. In contrast, experts from Spain provided more varied responses, generally leaning toward *Medium Importance* (Figure 3a). Overall, 50% considered gamification *Important*, and 23% *Very Important* (Figure 3b). This indicates a generally positive view, tempered by concerns about implementation feasibility.



a

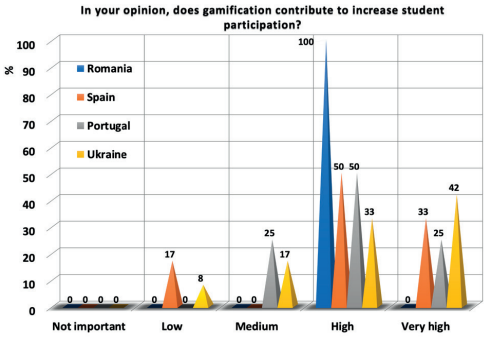


b

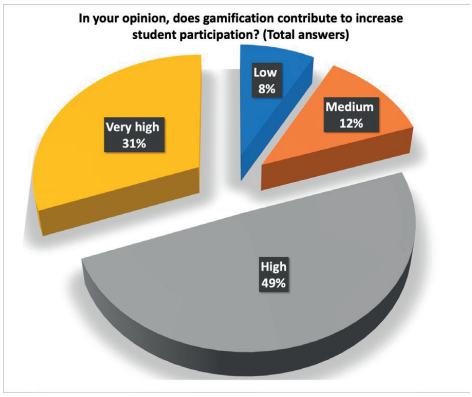
Figure 3. Expert opinions on whether gamification enhances student understanding of course materials: a) By country; b) Overall distribution

c) Impact on student participation

To gauge engagement, experts were asked: "*In your opinion, does gamification contribute to increased student participation?*" Experts from Romania, Spain, and Portugal rated this *Important* in 100% and 50% of responses, respectively. Ukraine: 42% rated it *Very Important* (Figure 4a). In total, 49% rated gamification as *Important* for increasing participation, and 31% as *Very Important* (Figure 4b), confirming its motivational potential.



a



b

Figure 4. Expert views on whether gamification contributes to increased student participation, based on responses: a) Country-specific distribution; b) Overall response distribution

3. Artificial Intelligence (AI) in assessment and feedback

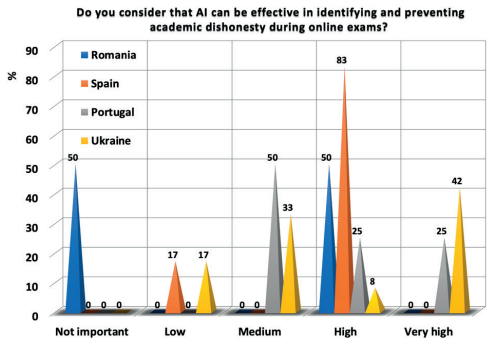
The survey also evaluated expert perspectives on the use of artificial intelligence in academic evaluation, particularly in two key areas: ensuring academic integrity and delivering real-time, personalized feedback.

a) AI for preventing academic dishonesty

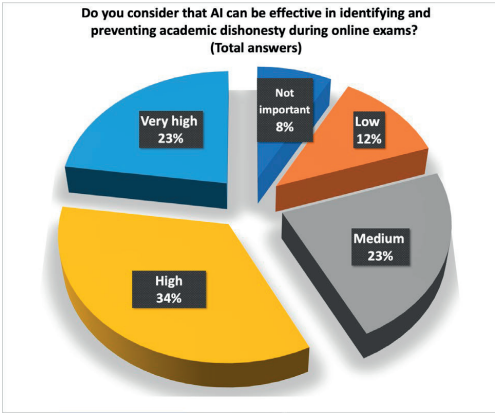
In response to the question: "*Do you consider that AI can be effective in identifying and preventing academic dishonesty during online exams?*", expert opinions reflected moderate to strong support. In Ukraine, 42% of respondents rated this aspect as *Very Important*. In Portugal, 25% of experts considered it either *Important* or *Very Important*. Meanwhile, the majority of respondents in Romania and Spain rated it as

Important, accounting for 50% and 83% of responses, respectively (Figure 5a). Overall, 34% of respondents considered the use of AI for detecting academic dishonesty as *Important*, while 23% rated it as *Very Important* or of *Medium* relevance (Figure 5b).

This indicates a generally positive outlook, though the level of support varied across countries.



a

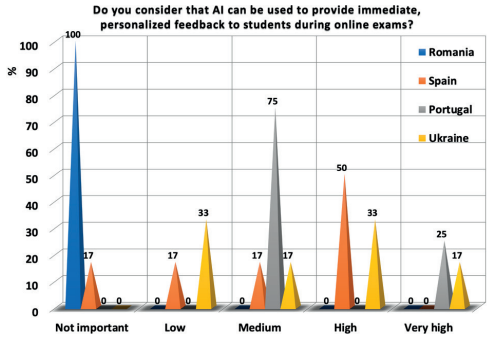


b

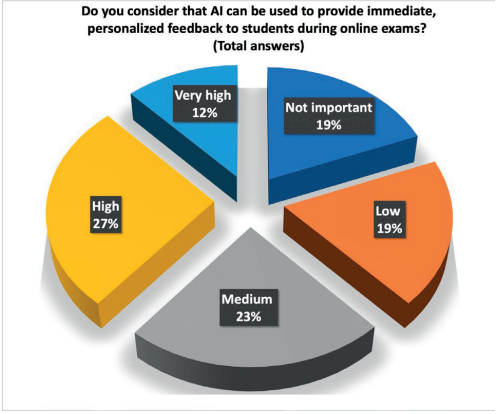
Figure 5. Distribution of expert responses to the question: *"Do you consider that AI can be effective in identifying and preventing academic dishonesty during online exams?"*: a) Responses by country; b) Overall response distribution

b) AI for providing personalized feedback

When asked, "*Do you consider that AI can be used to provide immediate, personalized feedback to students during online exams?*", responses were generally more reserved. In Spain, 50% of respondents rated this aspect as *Important*, while in Ukraine, 33% expressed a similar view. In Portugal, most responses leaned toward *Medium* importance. In contrast, all respondents from Romania considered this functionality *Not Important* (Figure 6a). Overall, only 27% of experts considered AI-based real-time feedback as Important, while 12% rated it as Very Important. A significant portion of the sample rated this function as Moderately Important or Unimportant, reflecting uncertainty about its practical value (Figure 6b).



a



b

Figure 6. Expert perspectives on the effectiveness of AI in providing immediate, personalized feedback to students during online exams: a) Distribution of responses by country; b) Overall response distribution

The survey identified a significant concern associated with fully online learning: the risk of social isolation. This issue was acknowledged by 65% of respondents, who rated it as either *important* or *very important*. In contrast, responses related to game-based learning experiences were largely positive. A substantial proportion of experts viewed gamification as a beneficial approach, highlighting its potential to enhance student engagement and improve the

overall learning experience. More than 70% of respondents agreed that incorporating game-based experiences into the curriculum is a beneficial approach that can enhance the understanding of scientific information. While respondents were in favour of using AI for knowledge assessment in EGD, it remained unclear whether its implementation in online exams could lead to immediate, personalised feedback. The survey results are consistent with recent studies. For instance, Khoshnoodifar et al. (2023) found that gamified learning improved medical students' attitudes toward statistics, making learning more engaging and efficient. Li and al. (2023) highlighted significant effects of gamification, particularly in science disciplines. Lampropoulos & Sidiropoulos (2024) confirmed gamification's superiority over traditional methods in higher education, with improvements in success rates and retention. Ortiz-Rojas et al. (2025) showed that leaderboards boosted learning performance but did not significantly affect self-efficacy. Effective implementation of gamification in education requires a tailored approach that addresses the diverse learning needs of students, particularly within STEM disciplines - science, technology, engineering, and mathematics (Ortiz-Rojas et al., 2025; Qudsi, 2024). Another study concludes that gamification represents a fundamental shift in pedagogical practice, emphasizing its potential to foster deeper learning and highlighting the need for further research to refine and assess its long-term effects (Li et al., 2023; McHenry & Makarius, 2023). According to Wulan et al. (2024), gamification offers several key advantages in the learning process. First, it *enhances student engagement and motivation* by making learning experiences more interactive and enjoyable. Second, it *promotes active learning*, encouraging deeper understanding through direct participation. Third, gamification helps *develop problem-solving and critical thinking skills* by fostering strategic thinking and informed decision-making. Fourth, it *encourages collaboration*, often through multiplayer or team-based activities that promote communication and cooperation. Finally, gamification can *personalize the learning experience,* adapting content and pace to meet the unique needs of individual learners.

CONCLUSIONS

The survey highlighted concerns and views on digital learning, gamification, and AI across four European countries. About 65% agreed that online learning can cause social isolation, seen as important by most experts except in Portugal. Over 70% supported game-based learning for improving understanding and engagement. AI was viewed as useful for reducing cheating and assessing knowledge, though opinions differed between countries. The use of AI for instant, personalised feedback was not supported, with all Romanian respondents finding it irrelevant. Future studies should examine how gamification preferences differ across disciplines and student groups. Differences in views on digital education tools among universities in Spain, Portugal, Ukraine, and Romania may stem from cultural, institutional, and technological factors unique to each country.

Cultural context: in some countries, the adoption of digital education tools is shaped by the local cultural approach to learning and technology. Countries with a strong tradition of face-to-face learning may be slower to adopt fully digital platforms, while others may be more open to innovation and remote learning.

Institutional digital readiness: different countries have varying levels of digital infrastructure and readiness. Spain and Portugal, as EU member states with substantial investment in digital education, may have more advanced systems in place compared to Ukraine and Romania, which may face challenges related to digital infrastructure or government support. These disparities may lead to differing opinions on the effectiveness and feasibility of certain digital education tools.

The digital readiness levels in these countries significantly influence the opinions of stakeholders (teachers, researchers, and policymakers). Countries with higher levels of digital readiness (such as Spain or Portugal) may be more confident in adopting advanced tools like AI-driven platforms or immersive technologies, while countries with lower digital infrastructure (such as Ukraine or Romania) may be more cautious or focused on basic digital tools and platforms. Limitations of this study are due to two factors:

- The maximum number of respondents, limited to 10 experts per country or university, is relatively small. This limits the ability to generalise the findings to the broader population of educators, policymakers, or researchers.
- The study included a maximum of two universities per country, which further restricts the diversity of perspectives. Different institutions may have different levels of digital readiness, and focusing on just a few may not fully reflect the variations that exist within each country's educational landscape,

ACKNOWLEDGEMENTS

This work was carried out with the support of Project 2023-1-RO01-KA220-HED-000154433 entitled "Gender, Digitization, Green: Ensuring a Sustainable Future for all in Europe" co-funded by the European Union.

REFERENCES

Aparisi-Torrijo, S., García-Hurtado, D., & Botella-Carrubi, D. (2024). Towards digitalization in higher education: Conceptual and bibliometric paradigm. *ESIC Market, 55*(2), e349.

Elfert, M., & Rubenson, K. (2022). Lifelong learning: Researching a contested concept in the twenty-first century. In K. Evans, W. O. Lee, J. Markowitsch, & M. Zukas (Eds.), *Third International Handbook of Lifelong Learning* (pp. 22). Springer Netherlands.

Frazão Santos, C., Agardy, T., Crowder, L. B., et al. (2024). Key components of sustainable climate-smart ocean planning. *npj Ocean Sustainability, 3*, 10. https://doi.org/10.1038/s44183-024-00045-x.

Khoshnoodifar, M., Ashouri, A., & Taheri, M. (2023). Effectiveness of Gamification in Enhancing Learning and Attitudes: A Study of Statistics Education for Health School Students. *Journal of advances in medical education & professionalism*, *11*(4), 230–239. doi: 10.30476/JAMP.2023.98953.1817.

Lampropoulos, G., & Sidiropoulos, A. (2024). Impact of Gamification on Students' Learning Outcomes and Academic Performance: A Longitudinal Study Comparing Online, Traditional, and Gamified Learning. *Education Sciences*, *14*(4), 367. https://doi.org/10.3390/educsci14040367.

Li, M, Ma, S. & Shi, Y. (2023). Examining the effectiveness of gamification as a tool promoting teaching and learning in educational settings: a meta-analysis. *Front. Psychol*. 14, https://doi.org/10.3389/fpsyg.2023.1253549

McHenry, W. K. & Makarius, E.E. (2023). Understanding gamification experiences with the benefits dependency network lens. *Computers and Education Open*, 4, https://doi.org/10.1016/j.caeo.2023.100123

Misra, M. (2012). Sustainability Education: Perspectives and Practice Across Higher Education. *International Journal of Environmental Studies*, *69*(5), 838–840. https://api.semanticscholar.org/CorpusID:94923222

Oliveira, K. K. D. S., & De Souza, R. A. (2022). Digital transformation towards education 4.0. *Informatics in Education*, *21*(2), 283-309. Vilnius University, ETH Zürich, DOI: 10.15388/infedu.2022.13

Ortiz-Rojas, M., Chiluiza, K., Valcke, M. et al. (2025). How gamification boosts learning in STEM higher education: a mixed methods study. *IJ STEM Ed., 12*, 1. https://doi.org/10.1186/s40594-024-00521-3

Qudsi, H. (2024). Gamification in education: boosting student engagement and learning outcomes. *ShodhKosh: Journal of visual and performing arts*, *5*(4), 686–693. https://doi.org/10.29121/shodhkosh.v5.i4.2024.2542

Radu, N., Chirvase, A. A., Babeanu, Begea, M. (2019). Entrepreneurship in the field of life sciences: the personal skills needed to start an innovative SME. *Scientific Papers Series Management economic engineering in agriculture and rural development*, *19*(2) 375-379.

Radu, N., Chirvase, A. A., Babeanu, M. (2020). Studies regarding personal skills needed in entrepreneurship-case study in France, Lithuania and Romania. *Scientific Papers Series Management economic engineering in agriculture and rural development*, *20*(2), 403-408.

Radu, N., Chirvase, A. A., Babeanu, N., & Popa, O. (2018). Education management in the field of life sciences-skills needed to start and develop an innovative SME. *Scientific Papers, Series Management, economic engineering in agriculture and rural developmen*t, *18*(2), 375-381.

Reimers, F.M. (2021). Can Universities Help "Build Back Better" in Education? The Socially Embedded University Responds to the Covid-19 Pandemic. *Front. Sustain.* 2, 636769, https://doi.org/10.3389/frsus.2021.636769.

Torres-Ruiz, M. & Moreno-Ibarra, M. (2019). Challenges and Opportunities in the Digital Transformation of the Higher Education Institutions: The Case of Mexico. In book: *Management and Administration of Higher Education Institutions at Times of Change* (pp.137-149). DOI:10.1108/978-1-78973-627-420191012.

Wulan, D. R., Nainggolan, D. M., Hidayat, Y., Rohman, T., & Fiyul, A. Y. (2024). Exploring the Benefits and Challenges of Gamification in Enhancing Student Learning Outcomes. *Global international journal of innovative research*, *2*(7), 1657–1674. https://doi.org/10.59613/global.v2i7.238

Scientific Papers. Series E. Land Reclamation, Earth Observation & Surveying, Environmental Engineering. Vol. XIV, 2025
Print ISSN 2285-6064, CD-ROM ISSN 2285-6072, Online ISSN 2393-5138, ISSN-L 2285-6064

ROLE OF GRASSLANDS IN CARBON SEQUESTRATION: A HYPOTHETICAL RESEARCH APPROACH

Ioan ROTAR[1], Florin PĂCURAR[1], Marcel DÎRJA[2], Anca PLEȘA[1], Alina ȘUTEU[3], Ioana GHEȚE[1], Ferencz VAKAR[2]

[1]University of Agricultural Sciences and Veterinary Medicine Cluj-Napoca, Faculty of Agriculture, Department of Plant Culture, 3-5 Calea Mănăștur, 400372, Cluj-Napoca, Romania
[2]University of Agricultural Sciences and Veterinary Medicine Cluj-Napoca, Faculty of Horticulture, Department of Horticulture and Landscaping, 3-5 Calea Mănăștur, 400372, Cluj-Napoca, Romania
[3]University of Oradea, Faculty of Environmental Protection, 26 General Magheru Street, 410048, Oradea, Bihor, Romania

Corresponding author emails: ferencz.vakar@usamvcluj.ro, anca.plesa@usamvcluj.ro

Abstract

Grasslands are among the most widespread terrestrial ecosystems, covering over one-third of the Earth's surface. They play a pivotal role in carbon sequestration and the accumulation of soil organic matter (SOM), processes essential for soil fertility, biodiversity conservation, and climate regulation. The degradation and conversion of grasslands into croplands have historically contributed to significant soil organic carbon (SOC) losses, intensifying global warming. This hypothetical research paper proposes a comparative analysis of SOM dynamics between grasslands and arable lands worldwide. A standardized experimental design is outlined, involving soil sampling at two depths (0-20 cm and 20-40 cm), across three land-use types (natural grassland, degraded grassland, and arable land). Hypothetical results, based on existing literature, indicate that grassland soils retain 30-50% more SOM than arable soils, particularly in the upper soil layers. Findings emphasize the necessity of protecting grasslands through sustainable management practices such as controlled grazing, overseeding, and restoration programs. Global policies must prioritize grassland conservation to achieve soil health, food security, and climate change mitigation objectives.

Key words*: arable lands, biodiversity, carbon sequestration, grassland, soil organic matter.*

INTRODUCTION

Soil organic matter (SOM) is important for terrestrial ecosystem productivity, regulating essential functions such as nutrient cycling, water, soil structure stability and biodiversity support (Hussain et al., 2023). Globally, soils contain more than three times the amount of carbon stored in the atmosphere, and grasslands alone are estimated to store around 343 billion tons of carbon in the first meter of soil, surpassing forest ecosystems in terms of soil carbon stocks (FAO, 2015). Despite this, grasslands are among the most threatened ecosystems due to land-use conversion, overgrazing, and climate change (Bai et al., 2008; IPCC, 2021).

In recent decades, the expansion of arable land has occurred at the expense of grassland areas, confirming the ongoing trend of their transformation into cropland (FAO, 2015).

Over the past century, approximately 20% of natural grasslands have been converted to agricultural land (Ramankutty et al., 2008), leading to SOM losses of up to 60% (Paustian et al., 1997). This decline not only reduces soil fertility but also exacerbates atmospheric CO_2 concentrations. Understanding and quantifying the contribution of grasslands to SOM accumulation is therefore crucial for sustainable land management and climate change mitigation strategies (Paustian et al., 1997).

Globally, policies promoting grassland conservation are unequal. In Europe, agri-environmental schemes have provided incentives for sustainable grazing, while in developing regions, overgrazing and conversion continue to dominate (Elliott et al., 2023). Future research must focus on quantifying regional variations in SOM accumulation and integrating socio-economic

factors to ensure effective implementation of grassland management strategies.

In Romania, grasslands cover approximately 4.8 million hectares, representing nearly one third of the country's agricultural area (MADR, 2022). These ecosystems are highly diverse, ranging from alpine pastures in the Carpathians to lowland meadows in the Danube Plain, and they constitute a major reservoir of biodiversity and soil organic matter (SOM). However, their ecological and productive potential is often underutilized due to management challenges such as overgrazing, insufficient fertilization, and in some regions, land abandonment. Abandonment of pastures has become an increasingly widespread phenomenon, with negative consequences on biodiversity and the productive value of ecosystems. Studies conducted in the Apuseni Mountains show that grasslands go through distinct successional stages, in which floristic diversity decreases rapidly after the cessation of traditional use (Păcurar et al., 2015; Malinas et al., 2020).

Beyond their agronomic and ecological importance, Romanian grasslands also represent a basic principle for the transition to sustainable agriculture and the green economy. Natural grasslands and perennial crops are agricultural systems that are favourable for increasing the amount of organic matter in the soil. In the following paper, we will refer to natural grasslands in terms of their management to increase the amount of organic matter in the soil.

This study presents bibliographical research framework aimed at comparing the accumulation of soil accumulation in natural grasslands, degraded grasslands, and arable lands. The central hypothesis is that grasslands, due to their perennial root systems and reduced soil disturbance, accumulate and retain considerably more SOM than cultivated croplands.

MATERIALS AND METHODS

The bibliographical experimental design assumes a global comparative study after Guo and Gifford, 2002, involving three land-use types: (i) natural grasslands, (ii) degraded grasslands, and (iii) arable lands. Soil sampling is conducted at two standard depths: 0-20 cm (topsoil) and 20-40 cm (subsoil), with three replicates per site. Sites are assumed to represent diverse climatic zones, including temperate, tropical, and semi-arid regions, to capture the global variability of grassland ecosystems.

Soil organic matter is measured using the Walkley-Black method for organic carbon determination, with values converted to SOM by applying a factor of 1.724. Additional soil parameters include pH (measured in a 1:2.5 soil-to-water ratio), texture (hydrometer method), and bulk density (core method). Hypothetical values are derived from the synthesis of published literature (Guo & Gifford, 2002).

RESULTS AND DISCUSSIONS

The hypothetical results of Guo and Gifford, 2002 demonstrate clear differences in SOM content between land-use types and soil depths. Natural grasslands consistently show the highest SOM concentrations, followed by degraded grasslands, with arable lands having the lowest values. SOM content decreases with depth across all land uses (Figure 1).

The simulated results strongly support the hypothesis that grasslands serve as more effective carbon sinks compared to arable lands. The 30-50% higher SOM content observed in grasslands aligns with global meta-analyses (Guo & Gifford, 2002; Conant et al., 2017). Perennial grasses contribute continuous organic inputs through litterfall and extensive root systems, which penetrate deeper soil layers and enhance soil aggregation. Reduced soil disturbance in grasslands also minimizes carbon losses compared to frequently tilled croplands.

The comparative analysis between land-use types highlights not only quantitative differences in soil organic matter (SOM) levels, but also qualitative differences in the stability and turnover of organic fractions. These emphasize the role of grasslands in global climate strategies, reflecting the recommendations of the IPCC (2021) regarding nature-based solutions for carbon sequestration. In natural grasslands, the continuous input of root exudates and litter promotes the accumulation of stable humic substances,

whereas in arable systems, frequent tillage accelerates the decomposition of labile organic matter (Rotar & Pacurar, 2010). Thus, the vegetation specific to well-established steppe grasslands produces annually 10-20 t/ha of plant residues consisting of roots, stems, leaves, etc. It is worth noting that the majority is represented by roots that accumulate within the soil over a thickness greater than 100 cm with a higher concentration in the first 40-50 cm (Blaga et al., 2005). On the other hand, SOM in croplands is more dynamic and vulnerable to losses under climatic conditions.

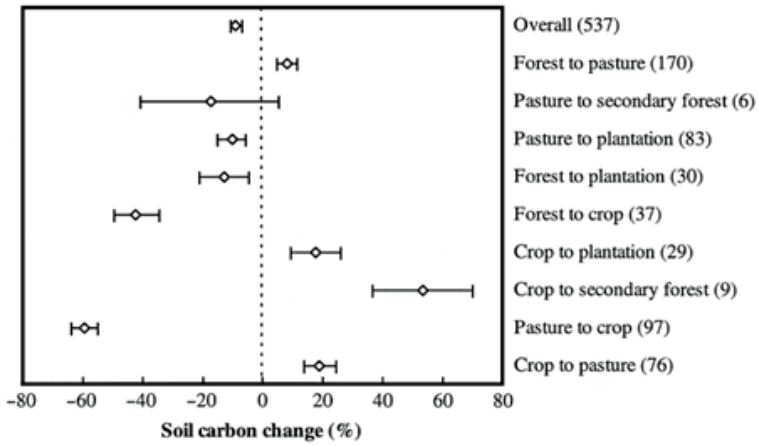


Figure 1. The presence of carbon in soil after different crop modification methods (after Guo & Gifford, 2002)

Recently, European strategies, such as the Biodiversity Strategy for 2030 and the Farm to Fork Strategy, emphasize the need to integrate semi-natural grasslands into more extensive sustainability objectives. In Romania, for example, these ecosystems contribute directly to the provision of public goods: clean water, pollination services, landscape preservation and important in preservation cultural heritage (Dragomir et al, 2023). Semi-natural pastures, many of which are Natura 2000 sites, host rare plant and animal species that cannot survive in intensive agricultural systems, that is the reason why from an economic point of view, grasslands offer opportunities for diversification, through the production of traditional dairy and meat products with high added value, as well as through the development of eco-tourism, species conservation and medicinal raw material. Certified products originating from extensive grassland systems can benefit from European quality schemes (e.g., Protected Designation of Origin-PDO, Protected Geographical Indication-PGI), linking environmental conservation with rural development (European Commission, 2023).

Nevertheless, challenges remain significant: land fragmentation, grassland's abandon and the effects of climate change (droughts, extreme weather) threaten the long-term sustainability of these natural ecosystems. Adaptive management, the integration of traditional practices with technological innovations, and the strengthening of farmer cooperatives are necessary measures to increase grassland resilience.

In this context, Romanian grasslands stand at the interface between tradition and innovation, offering both ecological stability and economic potential. By embedding them into national and European sustainability policies, they can play a decisive role in the transition towards a climate-neutral and resource-efficient agriculture.

Recent studies in Transylvania and the Subcarpathian hills highlight that permanent grasslands managed extensively (mowing and moderate grazing) store between 30-45% more SOM compared to adjacent arable lands (Blaga et al., 2005; Popovici & Ciubotariu, 1992). In contrast, grasslands subjected to frequent ploughing and reseeding exhibit accelerated organic matter mineralization, with losses

comparable to those observed in degraded pastures. The role of microbial communities in the stability and functionality of grassland ecosystems is increasingly recognized, and recent research highlights the link between long-term fertilizer application and changes in the soil microbiome (Stoian et al., 2022; Vidican et al., 2023).

Similar experiments conducted on high-natural value grasslands in the Apuseni Mountains have shown that long-term fertilization modifies colonization strategies at the root level of dominant species, with implications for microbial and plant biodiversity (Corcoz et al., 2022).

The Romanian case provides additional insights. Measurements from the Apuseni Mountains and Subcarpathian areas (Popovici & Ciubotariu, 1992; Blaga et al., 2005) confirm that permanent grasslands managed extensively contain significantly higher organic carbon stocks in the upper 40 cm of soil compared to adjacent arable fields.

At the same time, results suggest that the depth distribution of SOM is critical. In natural grasslands, up to 60% of the total SOM stock is concentrated in the first 20 cm of soil, largely due to dense root mats. However, the deeper layers (20-40 cm) also retain significant amounts, ensuring long-term stability (Lisec et al., 2025). This contrasts with arable systems, where SOM is predominantly surface-bound and more easily lost through erosion or oxidation. The role of deep root systems in perennial grasses is thus central to the long-term sequestration of carbon.

Climate change introduces new dynamics in SOM accumulation. Drying climate, droughts, increasingly frequent even in Romania, may affect plant production, but evidence suggests that root allocation increases under water stress, potentially enhancing belowground carbon inputs (Vörös et al., 2025).

Another important aspect revealed by the simulated results of Guo and Gifford, 2002 is the resilience of degraded grasslands. Although their SOM content is reduced compared to natural grasslands, they still maintain higher levels than arable lands. This indicates that even partially degraded systems retain a carbon sequestration potential that could be restored through interventions such as overseeding with legumes, controlled grazing, or organic fertilization. Case studies from Brașov and Cluj counties show that, after 5-7 years of improved management, SOM levels in degraded grasslands increased by 15-20%, approaching those of semi-natural systems (Dumitrescu et al., 1987).

Sustainable management practices are essential to maintain and enhance SOM in Romanian grasslands. Controlled grazing systems, periodic overseeding with legumes and valuable grasses, as well as organic fertilization with manure or compost have shown positive effects on soil structure and carbon sequestration (Dumitrescu et al., 1987). Moreover, agri-environmental measures supported under the Common Agricultural Policy (CAP) encourage farmers to preserve semi-natural grasslands, recognizing their role in climate change mitigation.

Measures to improve grasslands that contribute to increasing green mass yields and the quantity of roots in the soil are important, like harrowing and overseeding. The success of the work depends mainly on the quality of execution and the era, and in case of success it has a favourable effect on the properties of the soil.

Routine maintenance work (weed control, removal of woody vegetation, area modelling, weed control, etc.) has a favourable effect on soil properties, which has a positive impact on the harvest. Partial mobilization works considerably reduce soil erosion, favourably influence the water balance and protect the soil structure to a greater extent.

Favourable effects on production appear starting from the second year after sowing (Dumitrescu et al., 1987).

Total soil mobilization works on grasslands have a considerable influence on the decomposition and accumulation of organic matter in the soil and, through this, on the soil structure.

Soil organic matter plays an important role in healthy soil functions. Major soil functions such as primary production, water purification and regulation, carbon sequestration and regulation, biodiversity, and nutrient cycling depend largely on soil organic matter. Soil organic matter is made up of approximately 58% carbon, which has largely been taken up

from the atmosphere by plant photosynthesis (Grand & Michel, 2020).

Tillage works lead to rapid decomposition of the mobile fraction of the soil's organic matter, which thereby adversely influences the soil structure (the proportion of stable water aggregate decreases), processes is very rapid, occurring over a few years (Figure 2). Tillage has the opposite effect, leading to the accumulation of organic matter and, at the same time, to the improvement of soil structure. The process is very slow, with the balance between the amount of organic matter accumulated and the amount decomposed being achieved over decades (Dermatti, 1972).

At the opposite pole, increasing soil aeration through ploughing and stimulating the factors that determine its decline, especially in intensive agricultural systems, and over time exposes the soil to a series of degradation processes, sometimes irreversible.

The mineralization of organic matter in the soils of cleared meadows occurs at an accelerated rate in approximately 6 years, reaching the level of that in arable lands.

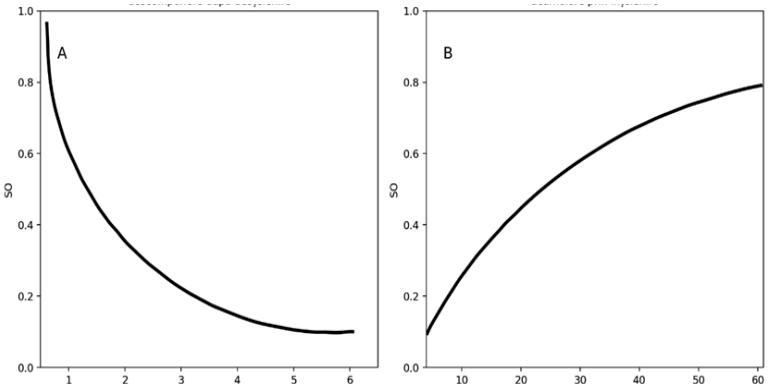


Figure 2. Scheme of the dynamics of organic matter (SO) in a grassland soil, after Dermatti, 1972 (A - the rate of decomposition of organic matter after tillage; mobile SO decomposes, for the most part, within a few years. B - the rate of accumulation of organic matter through tillage; the balance between accumulated SO and decomposed SO is achieved within a few decades

CONCLUSIONS

This bibliographical research emphasizes the role of grasslands in soil organic matter accumulation and carbon sequestration.

Grasslands contain 30-50% more SOM than arable lands, especially in the top 20 cm of soil.

Proper management of natural grasslands to increase harvest also implies an increase in the number of roots in the soil, making considerable progress in the accumulation of organic matter.

Sustainable management practices such as rotational grazing, overseeding, and reduced soil disturbance are essential to maintain SOM stocks.

Global policies must prioritize grassland conservation and restoration in soil health and climate change mitigation even if further research is needed to validate these.

REFERENCES

Bai, Z. G., Dent, D. L., Olsson, L., & Schaepman, M. E. (2008). *Global assessment of land degradation and improvement. Identification by remote sensing* (Report 2008/01). ISRIC – World Soil Information.

Blaga, G., Filipov, F., Udrescu, S., Rusu, I., & Vasile, D. (2005). *Pedology.* AcademicPres Publishing House. ISBN 973-744-004-8

Conant, R. T., Cerri, C. E. P., Osborne, B. B., & Paustian, K. (2017). Grassland management impacts on soil carbon stocks: A new synthesis. *Ecological Applications, 27*(2), 662–668. https://doi.org/10.1002/eap.1473

Corcoz, L., Păcurar, F., Pop-Moldovan, V., Vaida, I., Pleșa, A., Stoian, V., & Vidican, R. (2022). Long-term fertilization alters mycorrhizal colonization strategy in the roots of *Agrostis capillaris*. *Agriculture, 12*(6), 847. https://doi.org/10.3390/agriculture12060847

Dermatti, W. (1972). Effects of crops and grass on soil structure. In D. S. Kimber (Ed.), *Forage in the arable farm* (Occasional Symposium No. 7). British Grassland Society.

Dragomir, N., Mocanu, V., & Dragomir, N. (2023). Multifunctionality of grasslands – Permanent way of sustainable utilization of regional resources in Romania. *Journal of Energy and Natural Resources, 12*(4), 38–46. https://doi.org/10.11648/j.jenr.20231204.11

Dumitrescu, N., Silistru, D., & Calian, D. (1987). Regeneration of grasslands affected by surface erosion. *Scientific Papers of SCPCP Măgurele Brașov, 12*, 83–92.

Elliott, J., Tindale, S., Outhwaite, S., Nicholson, F., Newell-Price, P., Sari, N. H., Hunter, E., Sánchez-Zamora, P., Jin, S., Gallardo-Cobos, R., et al. (2024). European permanent grasslands: A systematic review of economic drivers of change, including a detailed analysis of the Czech Republic, Spain, Sweden, and UK. *Land, 13*(1), 116. https://doi.org/10.3390/land13010116

European Commission. (2023). *CAP strategic plan for Romania 2023–2027.* DG Agriculture and Rural Development.

FAO. (2015). *FAO STAT statistical database 2015.* Food and Agriculture Organization of the United Nations.

Grand, A., & Vincent, M. (2020). *Soil organic matter.* Landwirtschaft Grand & Agroscope. https://www.best4soil.eu/videos/18/ro

Guo, L. B., & Gifford, R. M. (2002). Soil carbon stocks and land use change: A meta-analysis. *Global Change Biology, 8*(4), 345–360. https://doi.org/10.1046/j.1354-1013.2002.00486.x

Hussain, A., Bashir, H., Zafar, S. A., Rehman, R. S., Khalid, M. N., Awais, M., Sadiq, M. T., & Amjad, I. (2023). The importance of soil organic matter (SOM) on soil productivity and plant growth. *Biological and Agricultural Sciences Research Journal, 2*(11).

IPCC. (2021). *Climate change 2021: The physical science basis. Contribution of Working Group I to the Sixth Assessment Report of the Intergovernmental Panel on Climate Change.* Cambridge University Press. https://doi.org/10.1017/9781009157896

Lisec, U., Prevolnik Povše, M., Podvršnik, M., & Kramberger, B. (2025). Impact of grassland management system intensity on composition of functional groups and soil chemical properties in semi-natural grasslands. *Plants, 14*(15), 2274. https://doi.org/10.3390/plants14152274

Mălinas, A., Rotar, I., Vidican, R., Iuga, V., Păcurar, F., Mălinas, C., & Moldovan, C. (2020). Designing a sustainable temporary grassland system by monitoring nitrogen use efficiency. *Agronomy, 10*(1), 149. https://doi.org/10.3390/agronomy10010149

Ministerul Agriculturii și Dezvoltării Rurale (MADR). (2022). *Raport privind suprafețele de pajiști permanente din România.* București, România.

Paustian, K., Collins, H. P., & Paul, E. A. (1997). Management controls on soil carbon. In E. A. Paul, K. Paustian, E. T. Elliott, & C. V. Cole (Eds.), *Soil organic matter in temperate agroecosystems* (pp. 15–49). CRC Press.

Popovici, D., & Ciubotariu, C. (1992). Research on long-term fertilization with different forms of nitrogen fertilizer on *Agrostis tenuis* and *Festuca rubra* meadows. *Scientific Papers of SCPCP Măgurele Brașov, 15*, 9–25.

Ramankutty, N., Evan, A. T., Monfreda, C., & Foley, J. A. (2008). Farming the planet: Geographic distribution of global agricultural lands in the year 2000. *Global Biogeochemical Cycles, 22*(1), GB1003. https://doi.org/10.1029/2007GB002952

Rotar, I., & Păcurar, F. (2010). Grassland management in Transylvania (Romania): Case studies and perspectives. *Romanian Journal of Grassland and Forage Crops, 1*, 35–48.

Stoian, V., Vidican, R., Florin, P., Corcoz, L., Pop-Moldovan, V., Vaida, I., Vâtcă, S.-D., Stoian, V. A., & Pleșa, A. (2022). Exploration of soil functional microbiomes - A concept proposal for long-term fertilized grasslands. *Plants, 11*(9), 1253. https://doi.org/10.3390/plants11091253

Vidican, R., Mihăiescu, T., Pleșa, A., Mălinaș, A., & Pop, B.-A. (2023). Investigations concerning heavy metals dynamics in *Reynoutria japonica* Houtt – soil interactions. *Toxics, 11*(4), 323. https://doi.org/10.3390/toxics11040323

Vörös, A. F., Mojzes, A., Cseresnyés, I., Kalapos, T., Kertész, M., Könnyű, B., Ónodi, G., & Kröel-Dulay, G. (2025). The effects of an initial extreme drought and chronic change in precipitation on plant biomass allocation in a temperate grassland. *Ecology and Evolution, 15*(9), e71625. https://doi.org/10.1002/ece3.71625

Walkley, A., & Black, I. A. (1934). An examination of Degtjareff method for determining soil organic matter and a proposed modification of the chromic acid titration method. *Soil Science, 37*(1), 29–37.

Scientific Papers. Series E. Land Reclamation, Earth Observation & Surveying, Environmental Engineering. Vol. XIV, 2025
Print ISSN 2285-6064, CD-ROM ISSN 2285-6072, Online ISSN 2393-5138, ISSN-L 2285-6064

AN ARDUINO-PYTHON INTEGRATED PREDICTIVE DATA ACQUISITION SYSTEM FOR ENVIRONMENTAL MONITORING

Georgian ROTARU, Gabriel PREDUȘCĂ,
Liana Denisa CÎRCIUMĂRESCU, Emil DIACONU

Valahia University of Targoviste, 13 Sinaia Alley Street, Targoviste, Romania

Corresponding author email: gabriel.predusca@valahia.ro

Abstract

This study presents a predictive data acquisition system that integrates the Arduino Leonardo development platform with the Python programming language for automated environmental monitoring. The system employs a suite of sensors - DHT22 for temperature and humidity, BMP180 for atmospheric pressure, and MQ-7 for gas concentration - to collect real-time data. These measurements are transmitted to a Python-based processing environment, where time-series forecasting algorithms, including ARIMA, are applied to analyze trends and predict environmental variations. The system offers a cost-effective and adaptable solution for air quality assessment, meteorological research, and environmental data analysis, facilitating timely interventions and enhanced resource management.

Key words*: Arduino Leonardo, BMP180, DHT22, MQ3, Python, environmental prediction.*

INTRODUCTION

The automated acquisition of data from sensors deployed in remote or challenging environments is essential for ensuring accuracy and efficiency in environmental monitoring. Automation reduces human error, improves data reliability, and streamlines the information-gathering process - especially in conditions where manual data collection is impractical.

Data acquisition systems (DAQ) play a crucial role in scientific research and engineering, providing solutions for testing, automation, and advanced analysis. These systems utilize various sensors and transducers to convert physical phenomena into measurable signals. Core functions of a DAQ system include signal conditioning, analog-to-digital conversion, and data processing, all of which contribute to a comprehensive understanding of environmental variables and support evidence-based decision-making (Maurizio, 2013).

Two critical components in the data acquisition process are data analysis and prediction. Data analysis enables the identification of patterns, correlations, and statistical relationships within collected datasets, forming the basis for reliable interpretation and trend recognition. Techniques such as descriptive statistics, correlation analysis, and probability distributions are applied to extract actionable insights.

Prediction, in contrast, focuses on estimating future values based on historical data. This is achieved through statistical and machine learning methods, which are used to construct models capable of anticipating environmental changes. These predictive techniques are instrumental in transforming raw data into practical forecasting tools.

Machine learning algorithms form a critical component of this predictive framework. They can be broadly categorized as follows:

- Regression – for forecasting continuous variables such as temperature or pressure.
- Classification – for categorizing environmental conditions (clear, cloudy, rainy).
- Unsupervised Learning – utilized to identify patterns and relationships in data without predefined labels.
- Semi-Supervised Learning – combining labeled and unlabeled data for improved prediction accuracy.

Recent advances in machine learning have significantly enhanced environmental monitoring by enabling automated analysis of complex datasets. In addition to machine learning, statistical methods are essential for predictive modeling, offering a solid theoretical basis for analyzing data relationships. Key statistical approaches include:

- Regression Analysis – used to estimate the relationships between variables, enabling the

prediction of one variable based on the behavior of others.

- Time Series Analysis – focuses on detecting patterns within temporally ordered data, making it especially effective for identifying trends and forecasting future values.
- Bayesian Methods – utilize probabilistic reasoning and prior knowledge to update predictions as new data becomes available, allowing for dynamic and adaptive forecasting (Siahaan et al., 2023).

Given the wide range of signals and parameters that can be sampled and stored, DAQ involves numerous techniques and skills. A DAQ system consists of various components, including sensors, communication links, signal processors, computers, databases, and data acquisition software. These components must function cohesively to ensure the system's reliability and effectiveness (Potter et al., 2012; Singh et al., 2009; Fisher et al., 2012; Sarma et al., 2018).

This study presents the design and evaluation of a predictive DAQ system built on the Arduino Leonardo platform and integrated with Python. The system incorporates key environmental sensors and leverages statistical forecasting methods to facilitate real-time environmental monitoring and predictive analytics. Applications include air quality assessment, meteorological research, and smart environmental management systems.

MATERIALS AND METHODS

Hardware component

Arduino is a popular open-source platform for rapid prototyping and data acquisition. This study uses the Arduino Leonardo, featuring the ATmega32u4 microcontroller with built-in USB communication for efficient data transfer (Arduino Leonardo, 2025; Monk, 2022).

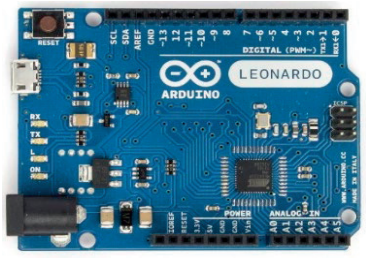


Figure 1. Arduino Leonardo development platform (Arduino Leonardo, 2025)

The Arduino Leonardo board includes 19 digital and 12 analog input/output ports, facilitating compatibility with a wide array of sensors and external modules. This versatility makes it particularly well-suited for customizable applications, such as predictive environmental monitoring.

The board operates at a nominal voltage of 5V, with each I/O pin capable of sourcing or sinking up to 40 mA of current. It features an internal pull-up resistor (disabled by default), which provides enhanced control during circuit design. Additionally, it includes 32KB of flash memory, 2.5KB of SRAM, and runs at a clock speed of 16 MHz.

In the developed system, the ATmega32u4 microcontroller functions as the central unit, responsible for sensor data acquisition and transmission. Its ability to handle multiple I/O operations and communicate via USB makes it an ideal solution for integration with the Python-based processing environment.

Sensor specifications

The proposed system integrates three types of sensors to monitor key environmental parameters – temperature and humidity, atmospheric pressure, and gas concentration.

The **DHT22** sensor (Figure 2, Table 1) provides accurate digital measurements of temperature and relative humidity. It employs proprietary signal acquisition and humidity sensing technology, ensuring both high precision and long-term operational stability. The sensor outputs data into a calibrated digital format, simplifying its integration with microcontroller-based systems.



Figure 2. DHT22 sensor module used for temperature and humidity measurement (DHT22, 2025)

The **BMP180** sensor (Figure 3, Table 1) adds atmospheric pressure monitoring capability to the data acquisition system. It combines a high-resolution barometric pressure sensor with a

temperature sensor, making it suitable for weather-related applications.
As the successor to BMP085, the BMP180 is optimized for accuracy and energy efficiency, and is commonly used in consumer-grade environmental monitoring devices.

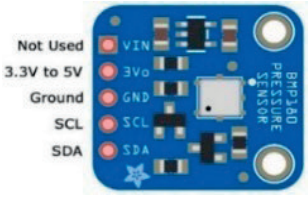


Figure 3. BMP180 sensor module used for atmospheric pressure measurement (BMP180, 2025)

The **MQ-7** sensor (Figure 4, Table 1) is employed for detecting gas concentrations, particularly carbon monoxide (CO) and hydrogen (H_2). It plays a critical role in evaluating air quality, contributing valuable data to the system's predictive analytics. However, it is sensitive to environmental noise and requires a preheating phase to stabilize reading.



Figure 4. MQ-7 sensor module used for gas concentration monitoring (MQ7, 2025)

Table 1. Technical characteristics of sensors

Sensor	DHT22	BMP180	MQ7
Measured parameters	Temperature, humidity	Atmospheric pressure	Gas concentration (CO, H_2)
Accuracy	±0.50°C ±2% RH	±0.12 hPa	Varies by gas
Communication interface	Digital (single wire)	I2C	Analog via ADC
Operating voltage	3.3-6V	1.62-3.6V	5V
Additional notes	Calibrated output, 2s reading interval	Include EEPROM for calibration; temperature compensation	Requires preheating; sensitive to environmenttal noise

Software tools and programming

The Arduino Leonardo microcontroller is programmed using the Arduino language via the Arduino Integrated Development Environment (IDE). This platform allows for the development of custom scripts to control sensor operations, manage collected data, and transmit information to a Python-based environment for further analysis.
Python serves as the core platform for data processing in this study, selected for its readability, versatility, and robust ecosystem of libraries. Its object-oriented structure and extensive community support make it well-suited for implementing complex data analysis and predictive modeling tasks (Fuentes, 2018).

Data processing and prediction pipeline

Figure 5 illustrates the end-to-end data processing workflow of the developed system.
Environmental data from DHT22, BMP180, and MQ-7 sensors is first displayed on the Arduino IDE Serial Monitor. Using Python's serial communication libraries, the data is captured and organized into a Pandas DataFrame for efficient handling. The processed data is then exported to Excel for storage and traceability.

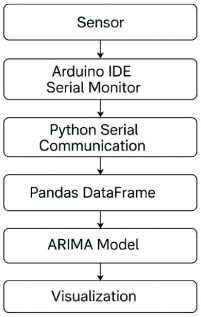


Figure 5. Data processing flow for DAQ system

For predictive analysis, the system applies an ARIMA (AutoRegressive Integrated Moving Average) model to the time-series data, enabling the forecasting of future environmental conditions. Results are visualized through Python-based plotting libraries, providing insights into data trends and supporting real-time, informed decision-making.

RESULTS AND DISCUSSIONS

System implementations

The proposed system utilizes the Arduino Leonardo platform (Figure 6) to acquire data

from three environmental sensors: the BMP180 (atmospheric pressure), the DHT22 (temperature and humidity), and the MQ-2 (gas concentration). Sensor readings are initially displayed on the Arduino IDE Serial Monitor, enabling real-time data visualization.

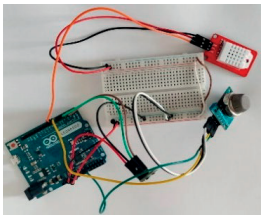


Figure 6. System implementation using Arduino and environmental sensors

Data Collection and Visualization

Sensor data is retrieved via Python using serial communication, structured into data frames, and stored in Excel files for traceability and further analysis. Figures 7 to 10 present graphical outputs generated using the Arduino Plotter, providing a visual overview of temperature, humidity, gas levels, and atmospheric pressure as measured in real time.

This data forms the basis for analyzing environmental conditions and identifying trends over time - supporting applications in air quality monitoring, precision agriculture, and meteorological research.

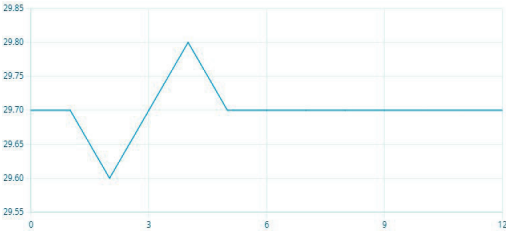


Figure 7. Temperature readings from DHT22 in Arduino Plotter

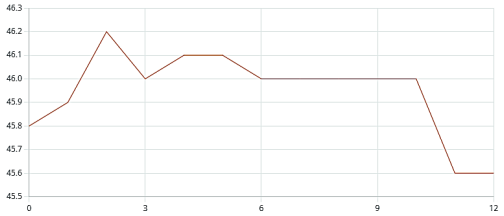


Figure 8. Humidity readings from DHT22 in Arduino Plotter

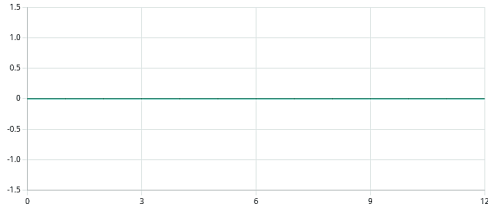


Figure 9. Gas concentration readings from MQ-7 in Arduino Plotter

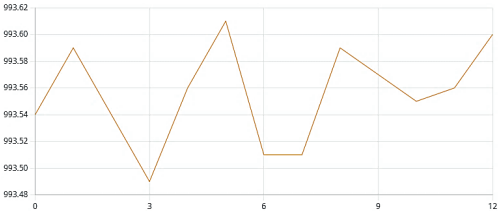


Figure 10. Atmospheric pressure readings from BMP180 in Arduino Plotter

Python's extensive ecosystem enhances the system's data processing and modeling capabilities. Key libraries include:

- Pandas – efficient for managing tabular data, offering tools for filtering, aggregation, and transformation.
- Matplotlib and Seaborn – visualization libraries that support the creation of insightful and interpretable charts.
- Scikit-learn – a machine learning toolkit providing access to models such as linear regression, decision trees, and more.

These tools collectively empower the system to bridge environmental sensing and predictive analytics. To support this, two Python programs were developed - one for data acquisition and formatting, and another for predictive modeling - each playing a vital role in the end-to-end analysis pipeline.

Predictive Modeling with ARIMA

To enable predictive analysis, two Python programs were developed - each with a distinct role in the data acquisition and forecasting pipeline.

In the first program, Python libraries such as serial and pandas were employed to manage communication between the Arduino and the host computer. The serial library facilitated data extraction from the Arduino sensors, while pandas enabled efficient organization, manipulation, and export of the data to Excel format.

This framework ensured clean, structured datasets for further processing.

The second program focused on time-series forecasting using the ARIMA (AutoRegressive Integrated Moving Average) model.

Libraries used included pandas for data handling, statsmodels.tsa.ARIMA.model for implementing the ARIMA algorithm, matplotlib.pyplot for visualization, and NumPy for numerical operations.

ARIMA, a well-established statistical technique, leverages past observations to model and predict future values in a time series - an approach particularly useful in environmental monitoring. An ARIMA model is defined by three parameters:

- p: the autoregressive order (number of lagged observations),
- d: the degree of difference (used to make the data stationary),
- q: the moving average order (size of the error window used for smoothing).

Fine-tuning these parameters allows for the creation of an optimized forecasting model tailored to the nature of the dataset (Wicaksana et al., 2022; Herrera-Gonzalez et al., 2024; Ganghetty et al., 2021; Spyrou et al., 2022; Kulkarni, et al., 2023).

ARIMA models can be adapted into simpler forms - such as AR (AutoRegressive), MA (Moving Average), or ARMA - by setting one or more parameters to zero. While ARIMA assumes that past values influence future trends, it is important to recognize its limitations, particularly in cases where external, non-recurring factors influence environmental conditions (Tibshirani, 2023). To assess the model's predictive accuracy, we evaluated three commonly used performance metrics:

- RMSE (Root Mean Square Error)
- MAE (Mean Absolute Error)
- MAPE (Mean Absolute Percentage Error)

For example, in forecasting humidity using the ARIMA(5,1,0) configuration, the results showed a marked improvement when data was sampled more frequently:

- Case 1 (one reading/day): RMSE = 1.34, MAE = 1.09, MAPE = 2.06%
- Case 2 (three readings/day): RMSE = 0.92, MAE = 0.71, MAPE = 1.28%

These results demonstrate that increasing the sampling frequency significantly enhances forecasting accuracy. The findings underscore the importance of data resolution in predictive modeling, particularly in dynamic environmental contexts.

Table 2. Values for the once-per-day reading frequency

Day	DHT22H (%)	DHT22T (°C)	MQ-7 (ppm)	BMP180 (hPa)
1	59.5	9.4	21	987.41
2	49.6	7.9	0	989.76
3	48.5	9.8	0	988.34
4	52.3	10.1	0	987.98
5	54.3	10.4	3	988.85
6	50.4	10.6	0	987.43
7	52.8	11.2	0	989.32
8	51.5	11.3	0	988.32
9	49.7	11.8	2	988.54
10	53.7	11.9	0	989.53
11	52.4	11.4	0	987.98
12	51.8	12.1	0	988.93
13	50.4	12.3	0	987.78
14	53.2	12.4	0	985.32

Comparative Analysis - Case 1

Table 2 presents the sensor data collected with a sampling frequency of one reading per day.

Notably, the MQ-7 sensor - designed to detect flammable gases such as carbon monoxide (CO) and hydrogen (H_2) - is also sensitive to other environmental variables. This high sensitivity may result in considerable fluctuations in the recorded values, as observed in the dataset.

These unexpected variations in reading highlight the need for careful analysis and interpretation to accurately assess the system's performance and

the environmental conditions affecting the MQ-7 sensor. The corresponding analysis results are illustrated in Figures 11 to 14.

Eight ARIMA model configurations were tested by varying the parameters p and d, as shown in Table 3. Among these, the model with parameters ARIMA (scaled_data, order = (5,1,0)) yielded the best results, producing predicted values that closely matched the actual sensor readings presented in Table 2.

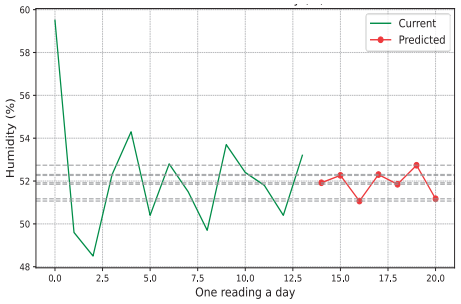


Figure 11. The graph and humidity prediction using DHT22

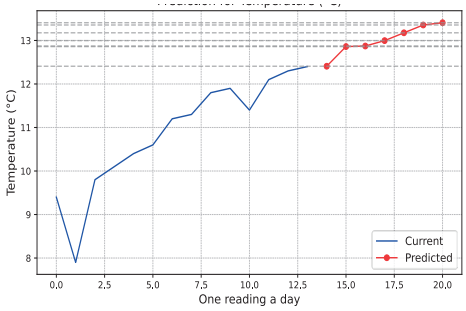


Figure 12. The graph and temperature prediction using DHT22

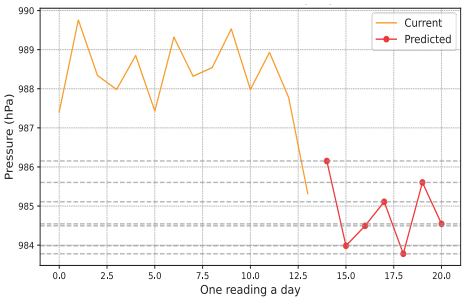


Figure 13. The graph and atmospheric pressure prediction using BMP180

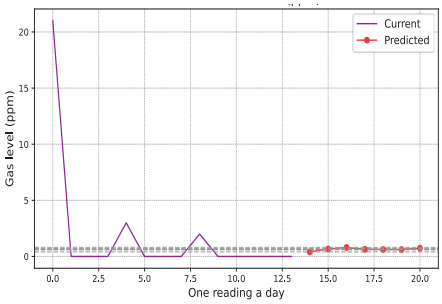


Figure 14. The graph and gas level prediction in the atmosphere using MQ-7

The comparative analysis indicates that the MQ-7 sensor is highly sensitive to environmental changes. This is reflected in its output, which often fluctuates from baseline values (typically zero) to peaks between 2 and 21 ppm in the measured data (Table 2), and from 0.13 to 6.96 ppm in the predicted data (Table 3). Such sensitivity underscores the need for precise calibration and controlled measurement conditions to ensure reliable predictions.

Table 3. Testing the ARIMA model for data acquisition once a day for 7 days

Cases	Sensor	Day						
		1	2	3	4	5	6	7
(3,2,0)	DHT22H	52.05	51.16	51.66	51.69	51.60	51.39	52.13
	DHT22T	12.63	13.07	13.05	13.42	13.66	13.86	14.07
	BMP180	985.01	982.01	980.93	979.33	975.95	975.59	972.25
	MQ7	0	0	0	0	0	0	0
(4,2,0)	DHT22H	52.79	51.30	51.85	53.09	52.55	51.79	52.50
	DHT22T	12.46	12.94	12.98	13.17	13.42	13.65	13.77
	BMP180	985.35	982.15	981.29	980.06	977.22	977.26	974.51
	MQ7	0.73	1.74	3	3.97	4.96	5.83	6.96
(5,2,0)	DHT22H	52.24	52.29	51.22	52.66	52.24	52.71	51.68
	DHT22T	12.48	12.77	12.88	13.17	13.23	13.47	13.64
	BMP180	985.32	982.15	981.18	979.83	976.83	976.66	973.76
	MQ7	0.21	0.71	1.35	1.98	2.53	3.06	3.69
(6,2,0)	DHT22H	52.29	52.03	52.19	51.64	52.36	52.87	52.79
	DHT22T	12.49	12.59	12.69	12.79	12.89	12.99	13.09
	BMP180	982.86	980.40	977.94	975.48	973.02	970.56	968.10
	MQ7	0.003	0.006	0.008	0.011	0.014	0.017	0.020

(3,1,0)	DHT22H	52.15	51.01	51.68	52.85	51.57	51.24	52.29
	DHT22T	12.72	12.69	12.86	12.90	12.93	13.01	13.00
	BMP180	987.11	984.43	984.66	985.06	982.86	984.43	983.14
	MQ7	0	0	0	0	0	0	0
(4,1,0)	DHT22H	52.82	50.69	51.71	52.99	52.04	51.10	52.11
	DHT22T	12.53	12.95	12.87	13.12	13.27	13.40	13.46
	BMP180	986.33	984.02	984.58	985.28	984.01	986.12	985.18
	MQ7	0	0	0	0	0	0	0
(5,1,0)	**DHT22H**	51.92	52.26	51.06	52.30	51.84	52.73	51.17
	DHT22T	12.40	12.86	12.87	12.99	13.17	13.35	13.40
	BMP180	986.15	983.98	984.49	985.10	983.77	985.60	984.54
	MQ7	0.40	0.66	0.80	0.65	0.62	0.61	0.73
(6,1,0)	DHT22H	51.49	52.33	52.02	51.33	51.44	52.03	52.30
	DHT22T	12.44	12.72	12.80	13.06	13.08	13.28	13.40
	BMP180	986.16	984.121	984.54	985.17	983.90	985.75	984.89
	MQ7	0	0.13	0.27	0.41	0.30	0.30	0.26

Comparative Analysis - Case 2

Table 4 shows sensor data collected at a higher frequency - three readings per day. Compared to Case 1, the values display greater variability, especially for the MQ-7 sensor.

Table 4. Data acquisition with a reading frequency of three times a day

Day	DHT22H (%)	DHT22T (°C)	MQ-7 (ppm)	BMP180 (hPa)
1	59.5	9.3	18	987.43
	65.5	8.6	3	987.47
	48.9	8	0	989.75
2	49.5	7.9	0	988.67
	54.9	6.2	0	989.95
	51.4	7.5	0	989.89
3	49.7	9.8	0	988.54
	53.5	9.9	0	988.12
	54.6	10	2	989.68
4	57.2	10.1	1	989.26
	54.3	10.3	0	987.93
	59	10.5	0	988.77
5	50.1	10.4	0	989.11
	59.1	10.5	2	987.85
	52.7	10.6	0	988.29
6	56.1	10.8	0	987.77
	55.7	10.9	0	989.39
	58.1	11	0	989.02
7	49.4	11.1	0	989.53
	52.4	11.2	0	988.64
	59.5	11.3	0	987.7
8	52.9	11.5	2	987.42
	57.5	11.4	3	988.86
	50.9	11.5	0	987.67
9	58.4	11.6	0	988.06
	52.3	11.7	0	989.82
	50.8	11.8	0	989.7
10	59.4	11.9	0	989.16
	56.7	12	0	989.84
	53.7	12.1	0	987.54
11	51.9	12.2	1	989.35
	50.3	12.3	0	987.64
	52.2	12.4	0	989.57
12	59.4	12.5	0	988.49
	51.4	12.6	0	987.98
	54	12.7	3	988.43
13	49.9	12.8	0	989.88
	59.2	12.9	0	988.74
	55.3	13	0	989.04
14	58.8	13.1	0	988.21
	54.7	13.2	0	989.24
	56.3	13.3	0	988.45

Predicted trends for humidity, temperature, gas concentration, and pressure are shown in Figures 15 to 18, demonstrating improved accuracy with increased sampling.

The most accurate results were obtained using the ARIMA model with the configuration ARIMA(scaled_data, order = (4,2,0)), based on multiple test iterations.

The outcomes of these tests are summarized in Table 5.

The results shown in Figures 11–14 and Tables 2-3 correspond to Case 1 (one reading per day), while Figures 15-18 and Tables 4-5 represent Case 2 (three readings per day).

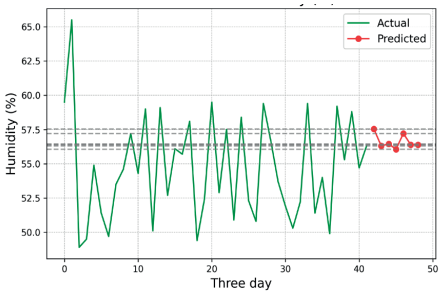


Figure 15. The graph and humidity prediction using DHT22

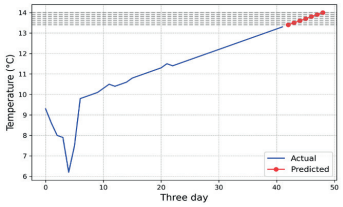


Figure 16. The graph and temperature using DHT22

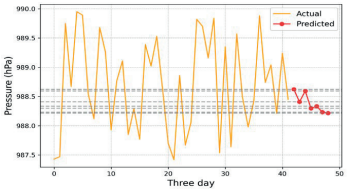


Figure 17. The graph and atmospheric pressure prediction using BMP180

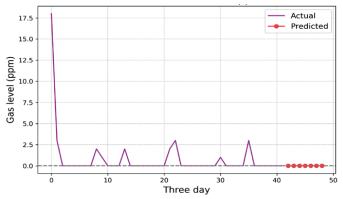


Figure 18. The graph and gas level prediction in the atmosphere using MQ-7

Table 5. Testing the Arima model for data acquisition three times a day

Cases	Days	DHT22H	DHT22 T	BMP 180	MQ7
(3,2,0)	1	52.05	12.63	985.01	0
	2	51.16	13.07	982.01	0
	3	51.66	13.05	980.93	0
	4	51.69	13.42	979.33	0
	5	51.60	13.66	975.95	0
	6	51.39	13.86	975.59	0
	7	52.13	14.07	972.25	0
(4,2,0)	1	52.79	12.46	985.35	0.73
	2	51.30	12.94	982.15	1.74
	3	51.85	12.98	981.29	3
	4	53.09	13.17	980.06	3.97
	5	52.55	13.42	977.22	4.96
	6	51.79	13.65	977.26	5.83
	7	52.50	13.77	974.51	6.96
(5,2,0)	1	52.24	12.48	985.32	0.21
	2	52.29	12.77	982.15	0.71
	3	51.22	12.88	981.18	1.35
	4	52.66	13.17	979.83	1.98
	5	52.24	13.23	976.83	2.53
	6	52.71	13.47	976.66	3.06
	7	51.68	13.64	973.76	3.69
(6,2,0)	1	52.29	12.49	982.86	0.003
	2	52.03	12.59	980.40	0.006
	3	52.19	12.69	977.94	0.008
	4	51.64	12.79	975.48	0.011
	5	52.36	12.89	973.02	0.014
	6	52.87	12.99	970.56	0.017
	7	52.79	13.09	968.10	0.020

(3,1,0)	1	52.15	12.72	987.11	0
	2	51.01	12.69	984.43	0
	3	51.68	12.86	984.66	0
	4	52.85	12.90	985.06	0
	5	51.57	12.93	982.86	0
	6	51.24	13.01	984.43	0
	7	52.29	13.00	983.14	0
(4,1,0)	1	52.82	12.53	986.33	0
	2	50.69	12.95	984.02	0
	3	51.71	12.87	984.58	0
	4	52.99	13.12	985.28	0
	5	52.04	13.27	984.01	0
	6	51.10	13.40	986.12	0
	7	52.11	13.46	985.18	0
(5,1,0)	1	51.92	12.40	986.15	0.40
	2	52.26	12.86	983.98	0.66
	3	51.06	12.87	984.49	0.80
	4	52.30	12.99	985.10	0.65
	5	51.84	13.17	983.77	0.62
	6	52.73	13.35	985.60	0.61
	7	51.17	13.40	984.54	0.73
(6,1,0)	1	51.49	12.44	986.16	0
	2	52.33	12.72	984.121	0.13
	3	52.02	12.80	984.54	0.27
	4	51.33	13.06	985.17	0.41
	5	51.44	13.08	983.90	0.30
	6	52.03	13.28	985.75	0.30
	7	52.30	13.40	984.89	0.26

To illustrate why Case 2 yields better performance, we compare measured and predicted values for each sensor.

For the DHT22H sensor (humidity):

- Case 1: Measured values ranged from 48.5% to 59.5% (Table 2), with predicted values between 51.06% and 52.73% (Figure 11, Table 3).
- Case 2: Measured values ranged from 48.9% to 65.5% (Table 4), while predictions ranged from 56.06% to 57.54% (Figure 15, Table 5).

In both cases, predictions tend to cluster around the mean, underestimating peak values. However, Case 2 shows better alignment with the actual trend, thanks to the increased sampling frequency.

Table 6 summarizes the average measured and predicted humidity values for both cases.

For the DHT22T sensor (air temperature):

- In Case 1, measured values ranged from 7.9°C to 12.4°C (Table 2), while predicted values ranged from 12.4°C to 13.4°C (Figure 12, Table 3).
- In Case 2, measured temperatures varied from 6.2°C to 13.3°C (Table 4), with predictions between 13.4°C and 14.0°C (Figure 16, Table 5).

In both cases, the predicted values exceed the actual measurements, indicating a consistent overestimation. This effect is more pronounced in Case 1, where predictions are centered around a higher average. While Case 2 shows improved responsiveness due to more frequent sampling, the predicted values still reflect a bias toward higher temperatures. The maximum measured temperature in Case 2 was 13.3°C, compared to a predicted peak of 14.0°C.

Table 7 provides a comparison of average measured and predicted temperature values for both cases.

For the MQ-7 sensor (gas concentration):

- In Case 1, measured values ranged from 0 to 21 ppm (Table 2), while predicted values remained between 0.4 and 0.8 ppm (Figure 13, Table 3).
- In Case 2, measured values ranged from 0 to 18 ppm (Table 4), whereas predicted values remained fixed at 0 ppm (Figure 17, Table 5).

In Case 1, although the predicted values generally follow the average trend, they fail to capture peak variations, indicating a degree of underfitting. In Case 2, despite the increased sampling frequency, the model consistently predicts 0 ppm, failing to reflect actual fluctuations. This persistent underestimation may result from sensor calibration issues or excessive environmental noise sensitivity.

Table 8 compares the average measured and predicted gas concentrations for both cases.

Table 6. Comparison of results for DHT22H sensor (air humidity)

Cases	Measured value			Predicted value		
	Min	max	average	min	max	average
1	48.5	59.5	52.15	51	52.7	51.89
2	48.9	65.5	54.69	56	57.5	56.62

Table 7. Comparison of results For DHT22T sensor (air temperature)

Cases	Measured value			Predicted value		
	Min	max	average	min	max	average
Case 1	7.9	12.4	10.9	12.4	13.4	13
Case 2	6.2	13.3	11.05	13.4	14	13.7

Table 8. Comparison of results for MQ-7 sensor (gas level in the atmosphere)

Cases	Measured value			Predicted value		
	Min	max	average	min	max	average
Case 1	0	21	1.87	0.4	0.8	0.63
Case 2	0	18	0.83	0	0	0

For the BMP180 sensor (atmospheric pressure):

- In Case 1, measured values ranged from 985.32 to 989.76 hPa (Table 2), while predicted values ranged from 983.77 to 986.15 hPa (Figure 14, Table 3).
- In Case 2, measured values ranged from 987.42 to 989.95 hPa (Table 4), with predicted values between 988.22 and 988.62 hPa (Figure 18, Table 5).

In Case 1, predicted values were relatively close to actual measurements but tended to underestimate the pressure, clustering around a lower average. In Case 2, with more frequent sampling, the predicted values showed improved alignment, though the model still slightly underpredicted the peak pressure (988.62 hPa vs. the actual 989.95 hPa).

A comparison of prediction performance between the two sampling intervals reveals notable improvements:

- Humidity (DHT22): RMSE reduced by ~23%
- Pressure (BMP180): RMSE reduced by ~19%

These reductions highlight the benefits of increased measurement frequency for enhancing prediction accuracy.

Table 9 summarizes the average measured and predicted pressure values for both cases.

Table 9. Comparison of results for BMP180 sensor (atmospheric pressure)

Cases	Measured value			Predicted value		
	Min	max	average	min	max	average
1	985.32	989.76	988.24	983.77	986.15	984.80
2	987.42	989.96	988.71	988.22	988.62	988.38

CONCLUSIONS

The proposed system successfully achieved its primary objective: developing an integrated, low-cost solution for environmental data acquisition and predictive analysis with a satisfactory level of accuracy. Among the ARIMA configurations tested, the ARIMA(5,1,0) model yielded the most reliable results, particularly in forecasting humidity and temperature trends.

Regarding sensor performance, the DHT22 sensor demonstrated high reliability for both temperature and humidity measurements, while the BMP180 sensor provided consistent and accurate atmospheric pressure readings. Conversely, the MQ-7 gas sensor exhibited considerable variability, which negatively impacted the accuracy of gas concentration predictions. In both sampling scenarios, predicted gas values were either consistently zero or significantly underestimated, suggesting potential issues related to sensor calibration or sensitivity to environmental noise.

Despite this limitation, the system establishes a solid foundation for real-time environmental monitoring and predictive analytics. Future improvements should focus on refining gas sensor calibration and enhancing the robustness of predictive models for volatile environmental parameters.

ACKNOWLEDGEMENTS

This article was written as part of the authors' activities within the Center for Networking and Career Development in Research in the South-Muntenia Region (CNDCSM), under the project PNRR-III-C9-2022 – I10, contract no. 5/16.11.2022, carried out at Valahia University of Targoviste.

REFERENCES

Aosong Electronics Co., Ltd. (2025). *DHT22 temperature and humidity sensor datasheet*. SparkFun Electronics. [Online], available: https://www.sparkfun.com/datasheets/Sensors/Temperature/DHT22.pdf, accessed on February 22, 2025.

Arduino. (2025). *Arduino Leonardo pinouts*. Arduino Documentation. [Online], available: https://docs.arduino.cc/resources/pinouts/A000057-full-pinout.pdf, accessed on February 22, 2025.

Bosch Sensortec. (2025). *BMP180 digital pressure sensor*. [Online], available: https://pdf1.alldatasheet.com/datasheet-pdf/view/1132068/BOSCH/BMP180.html accessed on February 22, 2025.

Fisher, D. K., & Gould, P. J. (2012). Open-source hardware is a low-cost alternative for scientific instrumentation and research. *Modern Instrumentation*, 1, 8–20. https://doi.org/10.4236/mi.2012.12002

Fuentes, A. (2018). *Hands-on predictive analytics with Python*. Packt Publishing.

Ganghetty, A., Kaur, G., & Malunje, U. S. (2021). Time series prediction of temperature in Pune using seasonal ARIMA model. *International Journal of Engineering Research & Technology*, *10*(11). https://doi.org/10.17577/IJERTV10IS110075

Herrera-Gonzalez, J. L., et al. (2024). Time series (ARIMA) as a tool to predict the temperature-humidity index in the dairy region of the northern desert of Mexico. *Peer J. Environmental Science*, *1*, 1–13. https://doi.org/10.7717/peerj.18744

Kulkarni, S., Bhadane, A., & Gajjar, H. (2023). Raspberry Pi-based weather prediction and analysis of temperature and humidity using ARIMA model. *BioGecko: A Journal for New Zealand Herpetology*, *12*(3), 5525–5533.

Maurizio, D. P. E. (2013). *Data acquisition systems: From fundamentals to applied design*. Springer. DOI:10.1007/978-1-4614-4214-1

Monk, S. (2022). *Programming Arduino: Getting started with sketches* (3rd ed.). McGraw Hill.

Potter, D., & Eren, H. (2012). Instrumentation engineers handbook: Process software and digital networks (Vol. 3, 4th ed., Chapter 19). CRC Press.

Sarma, P., Singh, H. K., & Bezboruah, T. (2018). A real-time data acquisition system for monitoring sensor data. *International Journal of Computer Sciences and Engineering*, *6*, 539–542. https://doi.org/10.26438/ijcse/v6i6.539542

Siahaan, V., & Sianipar, R. H. (2023). *Time-series weather: Forecasting and prediction with Python*. Balige City, North Sumatera.

Singh, H. K., Gogoi, R., & Bezboruah, T. (2009). Design approach for a web-based data acquisition and control system. In *International Conference of Internet Computing* (pp. 16–19).

SparkFun Electronics. (2025). *Technical data: MQ-7 gas sensor*. [Online], available: https://www.sparkfun.com/datasheets/Sensors/Biometric/MQ-7.pdf, accessed on February 22, 2025.

Spyrou, E. D., Tsoulos, I., & Stylios, C. (2022). Applying and comparing LSTM and ARIMA to predict CO levels for a time-series measurements in a port area. *Signals*, *3*(2), 235–248. https://doi.org/10.3390/signals3020015

Tibshirani, R. (2023). Autoregressive integrated moving average models. In *Introduction to time series*. University of California, Berkeley.

Wicaksana, H., Ananda, N., Budiawan, I., Santoso, B., Handoko, R., Maulana, A., Suciarti, S., & Utoro, A. (2022). Air temperature sensor estimation on automatic weather station using ARIMA and MLP. *Ultimatics: Jurnal Teknik Informatika, 14*(2), 103–110. https://doi.org/10.31937/ti.v14i2.2865

Scientific Papers. Series E. Land Reclamation, Earth Observation & Surveying, Environmental Engineering. Vol. XIV, 2025
Print ISSN 2285-6064, CD-ROM ISSN 2285-6072, Online ISSN 2393-5138, ISSN-L 2285-6064

REPURPOSING SAND-WASHING SLUDGE AS A SUSTAINABLE GROWTH MEDIUM FOR NON-FRUIT BEARING PLANT CULTIVATION

Sally SALEHI[1], Farid Gholamreza FAHIMI[2], Masoud Kia DALIRI[2], Ahmad TAVANA[2], Keyvan SAEB[2]

[1]Islamic Azad University, Faculty of Environment, Department of Environmental Science and Engineering, Tonekabon Branch, Tonekabon, Iran, Waste Management Organization of Tehran Municipality, District 15, Tehran, Tehran Province, Iran
[2]Islamic Azad University, Faculty of Environment, Department of Environmental Science and Engineering, Tonekabon Branch, Tonekabon, Iran

Corresponding author emails: fgh.fahimi@gmail.com, dr.mkiadaliri@gmail.com, ahmadtavana@gmail.com, keivansaeb@gmail.com

Abstract

Recycling construction soil and debris is a key strategy for reducing pollution and enhancing economic efficiency. The process of sand production from construction debris, while beneficial, results in the accumulation of dense sludge containing harmful elements in sand-washing machines like EvoWash. This study investigates the potential reuse of mineral-rich sludge from the EvoWash machine for cultivating non-fruit-bearing plants, addressing environmental concerns at the Aabali landfill in Tehran. Eight plant species were selected: Nerium, Spruce, Rose, Eucalyptus, Bitter Olive, Myrtle, Ornamental Pistachio, and Cactus, chosen for their compatibility with the heavy metal content in the sludge and their native presence in Tehran, facilitating reuse without extensive transportation. Comprehensive laboratory analyses identified essential mineral elements in the sludge, indicating its potential for plant growth. Bi-weekly monitoring of plant growth over four months showed that a mixture of sludge and garden soil significantly improved plant development compared to pure sludge or garden soil alone. While certain plants struggled in 100% sludge, the mixed medium yielded superior growth outcomes. The study provides insights into the feasibility of using EvoWash sludge for sustainable plant cultivation, presenting a promising solution for reusing construction debris sludge and aligning with eco-friendly waste management practices. The findings highlight the potential of EvoWash sludge in enhancing soil fertility and supporting plant growth, contributing to sustainable agricultural practices and environmental conservation.

Key words*: Sand-Washing Sludge, Sustainable Growth Medium, Non-Fruit Bearing, Environmental Conservation, EvoWash.*

INTRODUCTION

Recycling of construction soil and debris has long been considered as an effective method to reduce pollution and negative environmental impacts, while also enhancing economic efficiency and job creation. Among the recycling methods, producing sand from construction debris is noteworthy. Although this process reduces many environmental risks and contributes to generating income and returning a significant portion of debris to the cycle, it is not without environmental challenges. The most significant drawback of this process is the accumulation of dense sludge and clay-like sediment at the bottom of the recycled sand-washing machine such as EvoWash. Due to the nature of the recycled raw materials, this sediment contains environmentally harmful elements.

The management of sludge resulting from the EvoWash process after washing recycled sand from construction debris is a critical issue in modern sludge treatment. Tests indicate that this sludge, similar to sewage sludge, is rich in nutrients, especially organic matter, and can be successfully used to improve soil fertility (Roig et al., 2006; Urbaniak et al., 2016) and enhance agricultural productivity (Salehi, 2022; 2023; Sugurbekova et al., 2023; Zhakypbek et al., 2024). However, there are general concerns that the presence of potential pathogenic microorganisms (Bibby & Peccia, 2013; Ye et al., 2011), toxic organic compounds (Clarke & Smith, 2011; Peng et al., 2015; Santos et al., 2009), and heavy metals (Bloemendal et al.,

2008; She et al., 2022; Tiruneh Ababu et al., 2014) may be generated in the sludge, similar to the challenges associated with the use of sludge from the EvoWash process.

Therefore, addressing this sludge appropriately with economically viable and environmentally acceptable methods has become a topic of significant importance (Salehi, 2022; 2023; Xu et al., 2023). The use of sludge in agriculture has been implemented globally, with numerous studies showing positive effects on soil and crop production, including increased nutrient and organic matter content (Mohan et al., 2014; Suhadolc et al., 2010; Wang et al., 2008), improved soil structure and porosity, enhanced cation exchange capacity (Angin & Yaghanoglu, 2011), and enzymatic activity (Siebielec et al., 2018).

However, the quality of sludge from the EvoWash process is generally dependent on the treatment technology and the composition of recycled construction waste in the overall amount of treated water (Eid et al., 2017). Therefore, methods for its use should be developed separately for each sand production facility to prevent environmental damage and pollutant accumulation with sustainable development (Cieślik et al., 2015; Kacprzak et al., 2017; Mohan et al., 2014).

The production of sludge from washing sand by the EvoWash machine in Iran is limited to the disposal and reclamation center for soil and construction debris in Tehran, located in the Aabali landfill. The Aabali landfill, situated at approximately 12°44'35" N latitude and 39°39'51" E longitude, about 25 kilometers east of Tehran, at an altitude of 1700 meters in the Hazar Dareh mountains, has a total area of about 545 hectares (Figure 1). The disposal areas within this complex have different applications based on the types of incoming waste. Over the years, to prevent the loss of construction materials and reduce the amount of buried and released debris, equipment for reclaiming sand from debris has been installed with a nominal capacity of 120,000 tons per year.

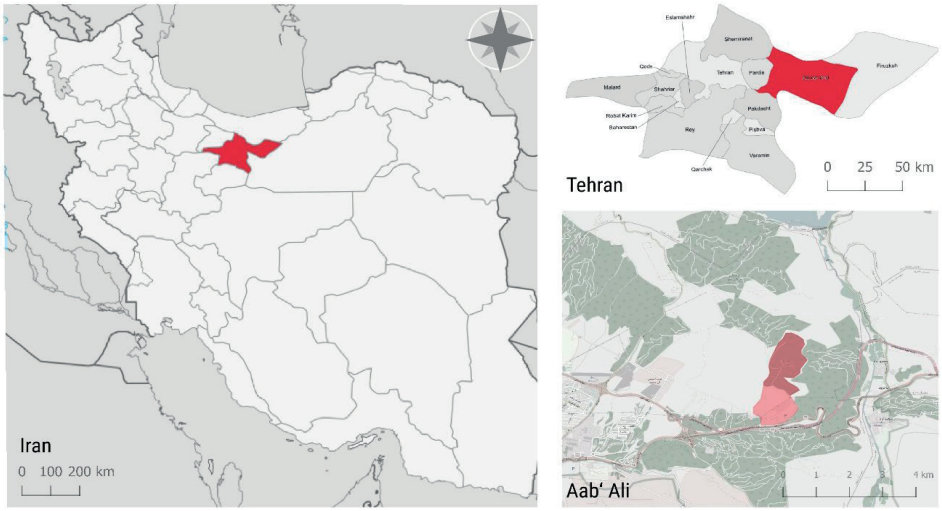


Figure 1. Geographic location of the Aabali disposal and processing center in Tehran

Tehran's Aabali landfill receives a massive influx of approximately 4,000 tons of soil and debris every day. Despite this, the center demonstrates a significant commitment to recycling, processing about 500,000 tons of sand in 2023. This effort resulted in the daily reclamation of roughly 1,370 tons of soil. Investigations indicate that this amount has increased by around 10% compared to 2020, and with the planned expansion of extraction plants in the area, it is predicted to increase by 15% until 2026 (Tehran Municipality, 2023).

A significant problem in sludge management at the Aabali landfill in Tehran is the

accumulation and disposal of sludge within the landfill area. In 2023, after the settling basins for sludge (2 ponds, each with 4,800 m^3 capacity) were filled and sludge overflowed from these basins, approximately 15,000 tons of sludge (as dry solid materials) were left in the area. Currently, there is no strategy for using this buried sludge, and the need for sludge management in the hierarchy of waste, including reducing sewage sludge production (using effective settling and dewatering processes) and finding solutions for use in construction or agriculture, has been emphasized (Salehi, 2022; 2023).

The exploration of sludge for cultivating non-fruit bearing plants has garnered attention, driven by its potential benefits. Concurrently, research has delved into cultivating aquatic plants in metal-laden sludge, envisioning them as potential fertilizers within safe metal concentration limits (Amulya et al., 2023). Furthermore, the adoption of light-emitting diodes (LEDs) in protected horticulture, particularly in Northern Europe, has demonstrated enhanced plant growth by ensuring consistent radiative fluxes across seasons (Paucek et al., 2020).

Despite these promising avenues, the use of sludge for irrigation requires careful consideration of potential risks. In arid regions facing water scarcity, sludge serves as a crucial resource for irrigating vegetable and forage crops (Othman et al., 2021). But sludges, which root in construction debris, contain significantly considerable elements. Hydroponic systems utilizing different sludge types as fertilizer and irrigation water for green plant cultivation have shown promise (Magwaza et al., 2020a; Magwaza et al., 2020b). However, untreated sludge irrigation has been associated with heavy metal accumulation in plants, with iron being a predominant metal in fruits (Ahmed et al., 2022).

The practice of utilizing sludge for irrigation, while economically advantageous, poses substantial health and environmental risks. Sludge, laden with minerals but traces of heavy metals, is notably generated in significant quantities (Ngobeni et al., 2021). Additionally, concerns arise about the fate of endocrine-disrupting compounds (EDCs) in sludge treatment and their potential impact on aquatic wildlife groups (Siegrist et al., 2005).

This pilot study explores the mineral-rich characteristics of sludge from the EvoWash machine for cultivating non-fruit bearing plants, focusing on eight distinct species including Nerium, Spruce, Rose, Eucalyptus, Bitter Olive, Myrtle, Ornamental Pistachio, and Cactus. The sludge derived from the EvoWash sand-washing process is abundant in essential elements like iron, calcium, magnesium, phosphorus, and potassium, making it a valuable resource for plant growth. The choice of these plant species is due to the presence of heavy metals such as lead, mercury, and cadmium in the sludge and the potential human and animal hazards if fruit-bearing plants were planted. Moreover, these selected plant species are native to the study area, allowing for the potential reuse of the sludges without the need for extensive transportation. Transporting these sludges via containers would result in spillage and environmental pollution due to their nature, leading to high costs.

MATERIALS AND METHODS

Identification of sludge from the EvoWash machine Characteristics

The research initiated by identifying the physical and chemical characteristics of sludge from the EvoWash sand-washing machine. This involved analyzing the levels of essential mineral elements such as calcium, magnesium, lead, cadmium, potassium, and more. The data was obtained through comprehensive laboratory tests, including Flame Photometry Method (F.P.M), Standard Methods (St. M.), and pH measurements using St. M. 4500-H+B and St. M. 4500-P-D methods.

Assessment of Soil Fauna Viability

The research focused on soil fauna, particularly earthworms, as biological indicators for soil health. Earthworms were exposed to sludge and a sludge-garden soil mixture, and their movement and survival were observed, providing insights into the ecological compatibility of EvoWash sludge, a crucial consideration for sustainable land use.

Simultaneously, eight selected plant species, including roses, bitter olive, and ornamental pistachio, were cultivated using EvoWash

sludge as the growth medium. Plant growth and health were monitored bi-weekly, with a parallel study involving the same species in pots with 100% garden soil for comparative assessment of EvoWash sludge's efficacy in supporting plant growth.

The selected plants were grown in 15 kg pots with bi-weekly irrigation after surface soil drying, and growth was documented twice a week. After two months, Rose, Bitter Olive, and Ornamental Pistachio exhibited more favorable growth than counterparts in garden soil. Eucalyptus showed limited growth in 100% EvoWash soil, prompting further investigation into a sludge and garden soil mixture. Over four months, all plants in EvoWash-based cultivation displayed superior growth compared to those in garden soil. Although certain plants struggled in 100% EvoWash soil, the introduction of mixed EvoWash and garden soil significantly improved their growth. Overall, after four months, all plants exhibited better growth in the mixed EvoWash and garden soil, indicating its potential as a viable growth medium. This comprehensive approach allowed for a holistic evaluation of EvoWash sludge in both ecological and horticultural contexts Data

Laboratory Studies and Sample Collection

In the field study stage, a total of 30 samples were collected from both old and new sedimentation basins, in packages of 1 and 3 kilograms. Additionally, for the examination of the soil characteristics outside the basins, and the investigation of avalanche soil, excavation, and reservoir water, samples were separately collected from the soil abandoned in the area through channels. Avalanche soil, excavation soil delivered by a container, and water from each reservoir were sampled from various parts and packaged as composite samples. These samples were sent to accredited environmental organization laboratories with Grade 1. The map below shows the location of the sample collection (Figure 2).

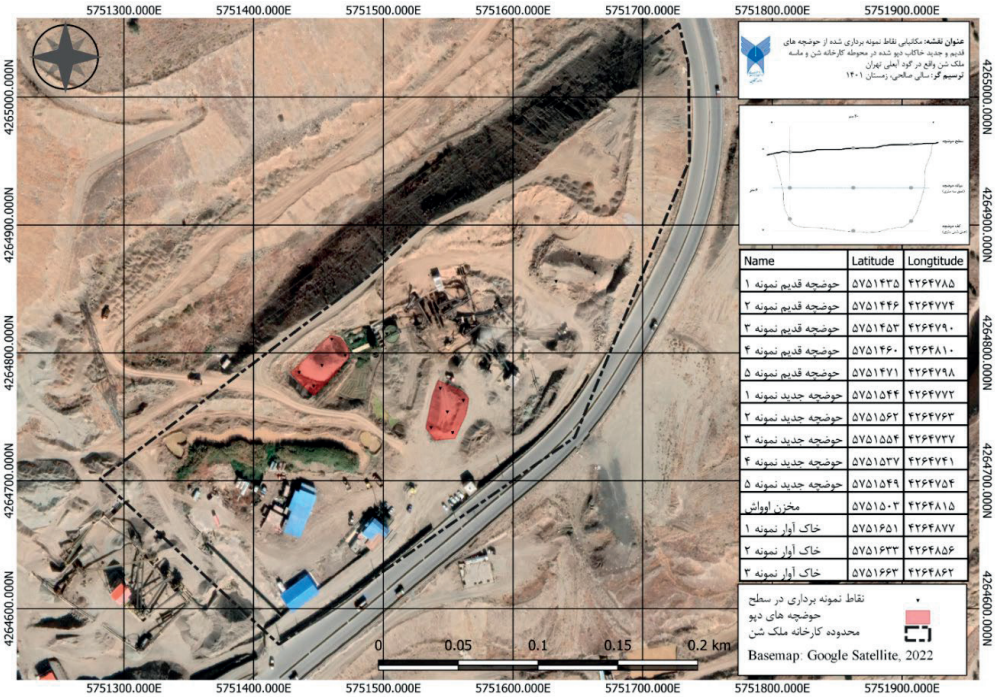


Figure 2. The location of the samples collection

Sampling Method and Volume

After exposure to sunlight, the sedimentation basin undergoes a decrease in volume by losing water and becomes compacted with the new sedimentation basin. The deeper the sedimentation basin is, the less likely it is to increase in volume and change its physicochemical properties after rainfall or snowfall in the region. Therefore, samples for examination must be taken from different depths (basin surface, three-meter depth, and six-meter depth), various points in the basins (old and new), and also from the entrance area soil released by a container and the sedimentation basin itself. Although it should be considered that due to the entry of sedimentation basins from 22 different areas of Tehran municipality with different construction materials and lifetimes, the sedimentation basin from each container has different characteristics. However, with a sufficient number of samples, general information about the sedimentation basin in the area can be obtained.

The sampling method was two-stage systematic (zigzag sampling from corner points of basins) and purposive (aiming to collect samples from different points to achieve general physicochemical characteristics of the sedimentation basin). Considering the size of the study population, nature, and research goal based on the Cochran formula (for a population with an unknown volume and variance) with a 5% error rate, a minimum of 23 samples were required for laboratory studies.

Since the sampling method in this research was two-stage, the surrounding soil soaked with the sludge and the entrance soil by containers were also sampled in the first stage. Although this soil was needed to assess the possibility of reusing the sludge, as transferring the sludge to another center for recycling is costly and may cause environmental pollution due to dust dispersion and the possibility of spillage from transport containers, the feasibility of using the sludge from the EvoWash machine in the Aabali landfill area was examined. Therefore, the available soil for mixing with the sludge must be sourced either from the surrounding area or the input soils to the area. For this reason, these soils were also examined and analyzed in the laboratory and for practical applications.

The samples' volume, according to the laboratory standards, was one kilogram. Due to the possibility of spillage, incorrect sampling, and minimizing errors, three-kilogram samples were prepared in the research area and then divided into smaller packages in the laboratory.

RESULTS AND DISCUSSIONS

In the context of managing and organizing sludge, the first step is to identify the physical and chemical characteristics of the sludge to enable its utilization in various industries and sectors. As this sludge has been used in cultivation plants, the garden chalky soil from the surrounding green spaces has been analyzed accordingly to understand the impacts of changing the level of elements of the soil comparing to the sludge. According to the findings, the results showed an increase in the levels of lead, sodium, ammonia, copper, iron, zinc, arsenic, nickel, and chromium. Additionally, the levels of electrical conductivity, total nitrogen, chloride, nitrite, and nitrate in the sludge have increased, while the levels of calcium, magnesium, potassium, soil acidity, and total phosphorus have decreased (Table 1).

Table 1. Analysis of elemental composition in garden chalky soil versus EvoWash machine sludge at the surface level (0-60 cm depth) in the new basin

	Element	Symbol	Unit	Garden chalky soil	Sludge	Changes	Test
1	Calcium	Ca	mg/kg	1532	356	decrease	F.P.M
2	Magnesium	Mg	mg/kg	252	25	decrease	F.P.M
3	Lead	Pb	mg/kg	12.3	26	increase	St. M. 3110-B
4	Cadmium	Cd	mg/kg	1<	2.5<	increase	St. M. 3110-B

5	Potassium	K	mg/kg	168	6.77	decrease	F.P.M
6	Soil Acidity	pH	-	7.57	7.40	decrease	St. M. 4500-H+B
7	Electrical Conductivity	EC	Ds/m	<1.0	2948.32	increase	St. M. 2510
8	Total Nitrogen	NT	%	0.5	1.2	increase	St. M. 4500-P-D
10	Sodium	Na	mg/kg	74.1	218.06	increase	F.P.M
11	Total Phosphorus	PT	mg/kg	15.7	>0.2	decrease	St. M. 4500-P-D
15	Chloride	CL	mg/kg	74	210	increase	F.P.M
16	Soluble Salts	TDS	Ppm	983	1585.13	increase	St. M. 2540-C
17	Nitrite	NO2	mg/kg	0.9	9.6	increase	St. M. 4500-NO2-B
18	Nitrate	NO3	mg/kg	25	30	increase	St. M. 4500-NO3-B
20	Bicarbonate	HCO3	mg/kg	47	64	increase	St. M. 4B-CO2-D
21	Alkalinity	TAC	meq/L	14.7	20.7	-	St. M. 2320-B
22	Ammonia	NH3	mg/kg	4	6.8	increase	St. M. 4500-NH2-C
25	Copper	CU	mg/kg	9.5	28.20	increase	St. M. 3110-B
27	Iron	Fe	mg/kg	93.2	4932.0	increase	St. M. 3110-B
28	Zinc	Zn	mg/kg	8.3	89.19	increase	St. M. 3110-B
29	Arsenic	As	mg/kg	0.2	25.22	increase	St. M. 3110-B
30	Nickel	Ni	mg/kg	4.73	37.9	increase	St. M. 3110-B
32	Chromium	Cr	mg/kg	4.89	26.40	increase	St. M. 3110-B
33	Mercury	Pb	mg/kg	<0.01	0.54	increase	St. M. 3110-B

Comparison between the garden soil and the sludge in the new basin indicates that most elements in the process of sand extraction and sludge production have changed negatively, considering the aim of the research.

By comparing the sludge at the surface of the new basin with the sludge at the bottom of the old basin, it can be concluded that some elements have increased over time, while others have decreased. This indicates that natural purification of the sludge does not occur over time, and measures should be taken to manage the sludge properly. The table below shows the changes in sludge compared to soil standards after accumulation and settling (Table 2).

Table 2. Evaluation of the lowest observed values for key parameters and elements against relevant standards for construction soil, sludge, and green space soil, as defined by Saed & Tila (2021)

	Element	Symbol	Unit	Sludge at the bottom of the old basin	Differences in accumulation	Standards for wastewater for agricultural irrigation	Standards for green space soil
1	Calcium	Ca	mg/kg	280	decrease	200	400
2	Magnesium	Mg	mg/kg	29	increase	100	40
3	Lead	Pb	mg/kg	24	decrease	50	300
4	Cadmium	Cd	mg/kg	2.5>	-	1	40
5	Potassium	K	mg/kg	5.78	decrease	6	350
6	Soil Acidity	pH	-	7.46	increase	6.5 - 8	More than 7

7	Electrical Conductivity	EC	Ds/m	2648.29	decrease	500-700	3000
8	Total Nitrogen	NT	%	197	increase	More than 2	75
10	Sodium	Na	mg/kg	205.89	decrease	8	200
11	Total Phosphorus	PT	mg/kg	0.2>	-	6	300
15	Chloride	CL	mg/kg	203	decrease	600	250
16	Soluble Salts	TDS	Ppm	1733.15	decrease	500-2000	1000
17	Nitrite	NO2	mg/kg	10	increase	Less than 3	250
18	Nitrate	NO3	mg/kg	18	decrease	Less than 50	250
20	Bicarbonate	HCO3	mg/kg	77	increase	170	200
21	Alkalinity	TAC	meq/L	20.3	decrease	270	-
22	Ammonia	NH3	mg/kg	17	increase	100	20
25	Copper	CU	mg/kg	28.95	increase	100	100
27	Iron	Fe	mg/kg	48560	decrease	2000	20000
28	Zinc	Zn	mg/kg	88.61	decrease	200	200
29	Arsenic	As	mg/kg	21.62	decrease	18	18
30	Nickel	Ni	mg/kg	37.75	decrease	50	50
32	Chromium	Cr	mg/kg	24.55	decrease	100	110
33	Mercury	Pb	mg/kg	1.08	increase	10	50

The comprehensive analysis of parameters and elements against established standards confirms adherence to permissible limits. To optimize plant growth, a recommended mixture of soil amendments should consist of soft soil, gravel, poultry litter ash, biomass ash, and compost. (Kominko et al., 2019).

To further assess the efficacy of sludge from the EvoWash machine in comparison to other growth mediums, a comparative cultivation study was conducted using different substrates; including hundred percent sludge from the EvoWash machine, a mixture of sludge from the EvoWash machine and garden chalky soil (1:1) to reduce sludge density and permeate the structure of the planting substrate, a mixture of sludge from the EvoWash machine, garden chalky soil and compost plus powdered sulfur (to control the pH) (1:1:1) and hundred percent garden chalky soil. The data includes plant height (Figure 3), leaf count (Figure 4) and the presence of branches or buds (Figure 5) at four different time points: four weeks after planting, two months after planting, six months after planting, and one year after planting (Table 3).

Table 3. Evaluation of the growth of investigated plants in different planting substrates

	Medium	First day	After four weeks	After two months	After six months	After one year
Nerium	Sludge	70 cm, 23 leaves, 1 main branch	70 cm, 20 leaves, 1 main branch	73 cm, 9 leaves, 1 main branch, dying	-	-
	Sludge, soil	64 cm, 30 leaves, 1 main branch	65 cm, 30 leaves, 1 main branch	67 cm, 33 leaves, 1 main branch	77 cm, 47 leaves, 1 main branch, 2 side branches	90 cm, 65 leaves, 1 main branch, 5 side branches
	Sludge, soil, compost	25 cm, 10 leaves, 1 main branch	30 cm, 15 leaves, 2 main branches	35 cm, 20 leaves, 3 main branches	40 cm, 25 leaves, 4 main branches	45 cm, 30 leaves, 5 main branches
	Soil	73 cm, 21 leaves, 1 main	73 cm, 23 leaves, 1 main	75 cm, 25 leaves, 1 main	79 cm, 31 leaves, 1 main	82 cm, 52 leaves, 1 main

		branch	branch	branch	branch, 2 side branches	branch
Spruce	Sludge	48 cm, 18 leaves, 1 main branch	48 cm, 18 leaves, 1 main branch	48 cm, 18 leaves, 1 main branch	50 cm, 19 leaves, 1 main branch	51 cm, 20 leaves, 1 main branch
	Sludge, soil	35 cm, 23 leaves, 1 main branch	35 cm, 24 leaves, 1 main branch	36 cm, 24 leaves, 1 main branch	52 cm, 26 leaves, 1 main branch	68 cm, 29 leaves, 1 main branch, budding
	Sludge, soil, compost	40 cm, 15 leaves, 2 branches	45 cm, 20 leaves, 3 branches	50 cm, 25 leaves, 4 branches	55 cm, 30 leaves, 5 branches	60 cm, 35 leaves, 6 branches
	Soil	51 cm, 17 leaves, 1 main branch	51 cm, 17 leaves, 1 main branch	54 cm, 19 leaves, 1 main branch	60 cm, 20 leaves, 1 main branch	71 cm, 23 leaves, 1 main branch, budding
Rose	Sludge	30 cm, 10 leaves, 1 main branch	30 cm, 12 leaves, 1 main branch	32 cm, 12 leaves, 1 main branch, budding	35 cm, 22 leaves, 3 branches	48 cm, 52 leaves, 4 side branches, budding
	Sludge, soil	31 cm, 7 leaves, 1 main branch	32 cm, 10 leaves, 1 main branch	35 cm, 19 leaves, 2 branches	42 cm, 27 leaves, 2 branches, budding	57 cm, 43 leaves, 3 side branches, budding
	Sludge, soil, compost	20 cm, 12 leaves, 1 main branch	25 cm, 17 leaves, 2 branches	30 cm, 22 leaves, 3 branches	35 cm, 27 leaves, 4 branches	40 cm, 32 leaves, 5 branches
	Soil	24 cm, 11 leaves, 1 main branch	24 cm, 11 leaves, 1 main branch	27 cm, 17 leaves, 1 main branch	35 cm, 34 leaves, 1 main branch, budding	42 cm, 56 leaves, 2 side branches, budding
Eucalyptus	Sludge	82 cm, 30 leaves, 3 branches	82 cm, 15 leaves, 3 branches	82 cm, 7 leaves, 3 branches, dying	-	-
	Sludge, soil	85 cm, 39 leaves, 3 branches	87 cm, 41 leaves, 3 branches	88 cm, 44 leaves, 3 branches, budding	94 cm, 52 leaves, 4 branches, budding	130 cm, 93 leaves, 7 branches
	Sludge, soil, compost	50 cm, 20 leaves, 2 branches	60 cm, 25 leaves, 3 branches	70 cm, 30 leaves, 4 branches	80 cm, 35 leaves, 5 branches	90 cm, 40 leaves, 6 branches
	Soil	87 cm, 46 leaves, 5 branches	87 cm, 46 leaves, 5 branches	89 cm, 50 leaves, 5 branches, budding	92 cm, 57 leaves, 6 branches	96 cm, 74 leaves, 8 branches
Bitter olive	Sludge	50 cm, 3 leaves, 1 main branch	50 cm, 3 leaves, 1 main branch	52 cm, 4 leaves, 1 main branch	54 cm, 9 leaves, 1 main branch	57 cm, 17 leaves, 1 main branch
	Sludge, soil	46 cm, 2 leaves, 1 main branch	47 cm, 5 leaves, 1 main branch	50 cm, 14 leaves, 2 main branches	77 cm, 73 leaves, 4 main branches	130 cm, 140 leaves, 7 main branches
	Sludge, soil, compost	30 cm, 18 leaves, 2 branches	35 cm, 23 leaves, 3 branches	40 cm, 28 leaves, 4 branches	45 cm, 33 leaves, 5 branches	50 cm, 38 leaves, 6 branches
	soil	57 cm, 3 leaves, 1 main branch	57 cm, 5 leaves, 1 main branch	60 cm, 13 leaves, 2 main branches	77 cm, 65 leaves, 4 main branches	98 cm, 83 leaves, 6 main branches
Myrtle	Sludge	30 cm, 18 leaves, 1 main branch	30 cm, 17 leaves, 1 main branch	30 cm, 3 leaves, 1 main branch	-	-
	Sludge, soil	35 cm, 12 leaves, 1 main branch	35 cm, 12 leaves, 1 main branch	38 cm, 14 leaves, 1 main branch	48 cm, 21 leaves, 2 main branches	55 cm, 37 leaves, 3 main branches

	Sludge, soil, compost	30 cm, 20 leaves, 2 branches	35 cm, 25 leaves, 3 branches	40 cm, 30 leaves, 4 branches	50 cm, 40 leaves, 5 branches	60 cm, 50 leaves, 6 branches
	Soil	27 cm, 15 leaves, 1 main branch	27 cm, 17 leaves, 1 main branch	30 cm, 34 leaves, 2 main branches	48 cm, 24 leaves, 4 main branches	| 60 cm, 45 leaves, 5 main branches
Ornamental pistachio	Sludge	78 cm, 14 leaves, 1 main, 3 side branches	80 cm, 18 leaves, 1 main, 3 side branches	82 cm, 22 leaves, 1 main, 3 side branches	95 cm, 68 leaves, 1 main, 5 side branches	120 cm, 114 leaves, 1 main, 7 side branches
	Sludge, soil	73 cm, 17 leaves, 1 main, 3 side branches	74 cm, 20 leaves, 1 main, 3 side branches	77 cm, 47 leaves, 1 main, 5 side branches	118 cm, 79 leaves, 1 main, 9 side branches	163 cm, 134 leaves, 1 main, 11 side branches
	Sludge, soil, compost	80 cm, 30 leaves, 3 branches	90 cm, 40 leaves, 4 branches	100 cm, 50 leaves, 5 branches	110 cm, 60 leaves, 6 branches	120 cm, 70 leaves, 7 branches
	soil	75 cm, 14 leaves, 1 main, 4 side branches	75 cm, 20 leaves, 1 main, 4 side branches	78 cm, 43 leaves, 1 main, 5 side branches	120 cm, 83 leaves, 1 main, 9 side branches	165 cm, 146 leaves, 1 main, 12 side branches
Cactus	Sludge	7 cm height, 8 cm width, 1 leaf	7 cm height, 8 cm width, 1 leaf	7 cm height, 8 cm width, 1 leaf	15 cm height, 10 cm width, 2 leaves	30 cm height, 15 cm width, 3 leaves
	Sludge, soil	7 cm height, 8 cm width, 1 leaf	7 cm height, 8 cm width, 1 leaf	7 cm height, 8 cm width, 1 leaf	9 cm height, 8 cm width, 1 leaf	12 cm height, 10 cm width, 2 leaves
	Sludge, soil, compost	10 cm height, 8 cm width, 2 leaves	15 cm height, 10 cm width, 3 leaves	20 cm height, 12 cm width, 4 leaves	25 cm height, 14 cm width, 5 leaves	30 cm height, 16 cm width, 6 leaves
	Soil	7 cm height, 8 cm width, 1 leaf	7 cm height, 8 cm width, 1 leaf	7 cm height, 8 cm width, 1 leaf	7 cm height, 8 cm width, 1 leaf	10 cm height, 10 cm width, 1 leaf

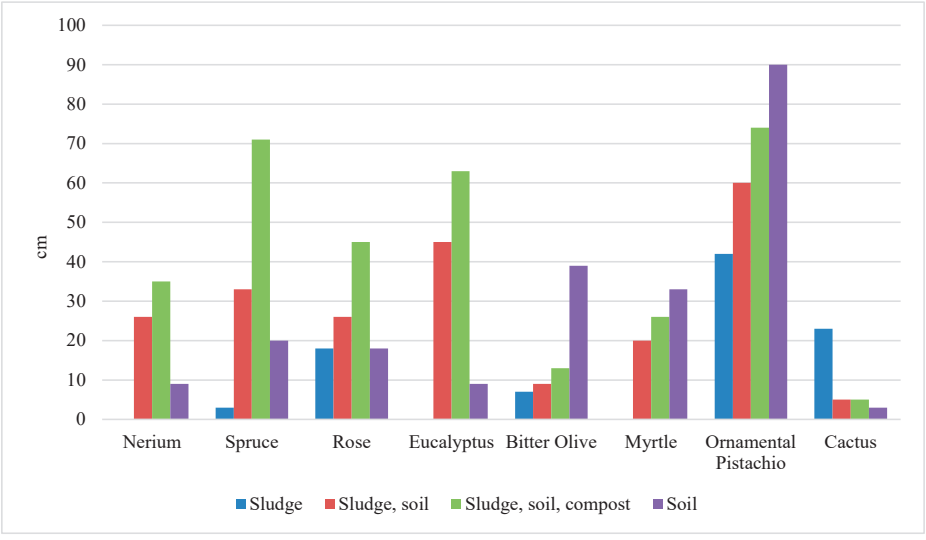


Figure 3. Changes in the growth of selected plant stems throughout the year in different planting substrates

The results of the studies indicate that, in general, all examined plants, except for bitter olive, ornamental pistachio, and cactus, have shown better growth in a mixed sludge (with soil or with soil and compost). Overall, the sludge mixed with soil and compost has proven more conducive to the growth of the examined plants than sludge mixed only with soil. Nerium, eucalyptus, and myrtle plants did not thrive and deteriorated in the pure sludge substrate. Bitter olive, ornamental pistachio, and cactus plants have exhibited better growth in garden soil compared to other substrates. Additionally, cactus plants have shown significantly better and faster growth in the sludge substrate relative to other substrates.

The observed differences in plant growth across different substrates can be attributed to various factors related to the physical, chemical, and biological properties of each substrate. Sludge, particularly when mixed with compost, may provide a richer nutrient profile for plants. This enhanced nutrient availability can contribute to better growth. Moreover, compost, when added to the sludge, increases the organic matter content. Organic matter improves soil structure, water retention, and nutrient availability, fostering favorable conditions for plant growth. It can also enhance aeration and drainage in the substrate. In addition, the addition of soil and compost help balance and buffer pH levels, creating a more suitable environment for plant growth.

On the other side, the presence of beneficial microorganisms in compost positively influences soil health and nutrient cycling, promoting better plant growth. Moreover, the addition of soil can provide a more balanced texture, ensuring proper water movement and root penetration. Cacti, known for thriving in arid conditions, also benefit from the water-retaining properties of sludge while still receiving essential nutrients. However, the physical structure of sludge may impede root development in certain plants, leading to reduced growth and vitality.

On the other hand, the number of leaves in all types of examined plants, except for ornamental pistachio and myrtle has been better and higher in the sludge mixed with soil and compost environment compared to other planting substrates. Regarding ornamental pistachio, the number of leaves in the garden soil substrate has been slightly higher than in other substrates. In the case of cactus plants, both lateral and vertical growth has been greater in the sludge substrate than in other substrates, and the number of new leaves has also been higher (Figure 4).

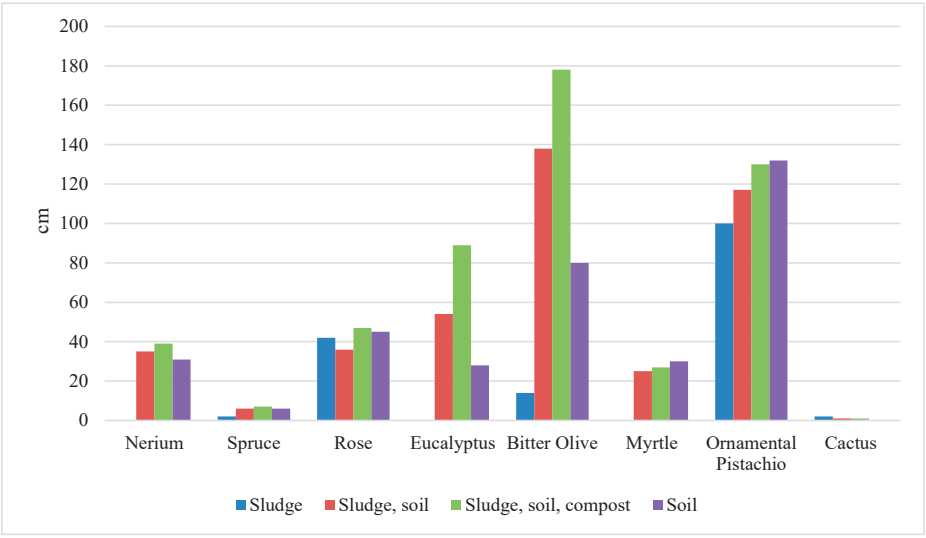


Figure 4. Changes in the leaf count throughout the year in different planting substrates

The highest level of sprouting and new shoots has been observed in the ornamental pistachio plant, which was equal across all three substrates: garden soil, sludge mixed with soil, and sludge mixed with soil and compost. In the next stage, the bitter olive plant exhibited the highest number of sprouts, particularly in the substrate of sludge mixed with soil and compost. Following in order are the narium, eucalyptus, rose, and myrtle plants (Figure 5).

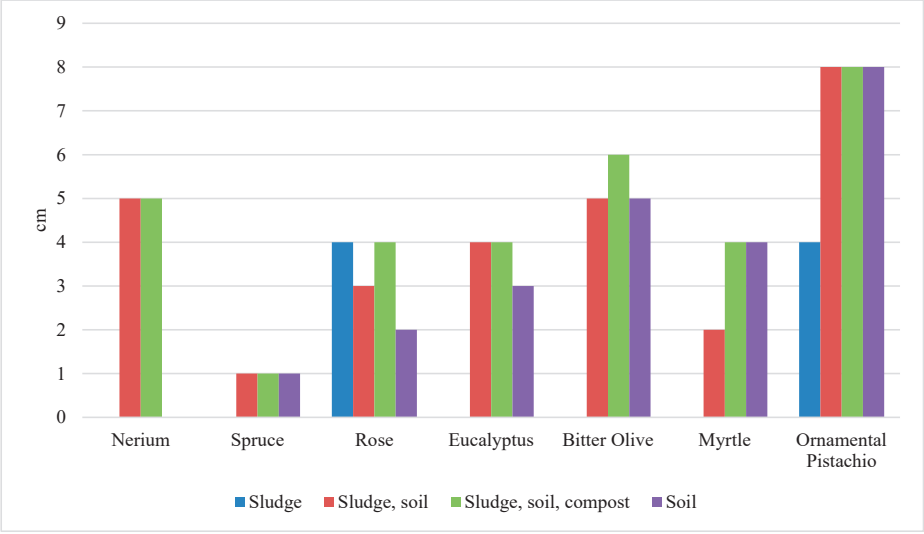


Figure 5. Changes in the branch count throughout the year in different planting substrates

The differences in the growth of various plants in the study can be attributed to several factors related to the composition of the soil and specific requirements of each plant species. The reasons may include nutrient composition, the soil structure, pH level, salinity and soluble salts, moisture content, plant species suitability, time and growth stages, and mineral elements; For instance, Calcium, Magnesium, and Potassium play essential roles in plant growth, including cell structure, enzyme activation, and photosynthesis. The high levels of iron can be detrimental to some plants, and the study mentions variations in iron content in the different soil mixtures. Moreover, essential for root development and flowering, differences in phosphorus levels could impact plant growth. In the following each plant have been analyzed based on the mineral level of its soil nature.

CONCLUSIONS

This pilot study demonstrates the potential of sludge from the EvoWash machine as a viable growth medium for non-fruit-bearing plants. Rich in essential minerals such as iron, calcium, magnesium, phosphorus, and potassium, the sludge showed promise in supporting plant growth, despite concerns regarding heavy metal content. The eight plant species tested - Nerium, Spruce, Rose, Eucalyptus, Bitter Olive, Myrtle, Ornamental Pistachio, and Cactus - exhibited varying degrees of adaptability to the sludge, with most species showing improved growth when the sludge was mixed with garden soil.

The study's findings underscore the importance of optimizing the composition of the sludge and soil mixture to enhance plant growth while mitigating potential risks associated with heavy metal accumulation. Specifically, the incorporation of compost and powdered sulfur significantly improved plant health and growth, suggesting that tailored amendments can address the inherent limitations of using EvoWash sludge as a sole growth medium. Moreover, the successful cultivation of these plants in sludge mixtures not only offers a sustainable solution for managing sludge waste from sand-washing processes but also

contributes to the reclamation of degraded land and the reduction of environmental pollution. By providing a practical method for repurposing construction debris sludge, this research aligns with broader sustainable and eco-friendly practices in waste management and urban agriculture.

Future research should focus on long-term assessments of soil health and plant productivity, exploring a wider range of plant species, and refining sludge treatment processes to further reduce heavy metal content. Additionally, economic analyses of large-scale implementation and the environmental impact of using EvoWash sludge in various agricultural and horticultural contexts would provide valuable insights for policymakers and industry stakeholders. Conducting a more comprehensive elemental analysis of the sludge will provide a deeper understanding of the specific interactions between minerals and their effects on plant growth, focusing on individual plant species to uncover species-specific mineral requirements. Extending the duration of plant monitoring will help assess the long-term effects of sludge application on plant health and productivity, providing insights into the sustainability and durability of the observed growth trends.

Investigating the microbial community dynamics in the soil treated with sludge will reveal how these microorganisms interact with minerals, impacting nutrient availability and uptake by plants. Understanding these interactions can enhance the overall effectiveness of sludge-based fertilization. A thorough toxicity assessment is essential to evaluate potential harmful effects of certain elements, such as lead and cadmium, on both plant health and soil ecosystems, ensuring safe and sustainable agricultural practices.

Considering the broader environmental benefits of sludge utilization in plant cultivation, advanced sludge treatment technologies should be investigated to further refine and enrich the sludge produced by EvoWash machines, enhancing its suitability for plant cultivation while minimizing environmental impacts. Tailoring plant cultivation practices based on the mineral composition of sludge, exploring suitable non-fruit-bearing crops that thrive in specific mineral conditions, and implementing crop rotation strategies will prevent nutrient imbalances and enhance soil fertility.

Integrating sludge utilization into a broader water resource management strategy and exploring the potential of combining treated sludge with water management practices will optimize nutrient availability for plants while reducing the environmental footprint. Engaging local communities in sustainable agricultural practices involving sludge utilization and providing educational programs to raise awareness about the benefits of responsible sludge management, will have a positive impact on both agriculture and the environment. Advocacy for supportive policies that encourage the use of treated sludge in agriculture and collaboration with policymakers to establish guidelines for safe and effective utilization will promote a circular economy approach for sludge resources.

By addressing these aspects in future research and optimizing sludge utilization practices, we can contribute to sustainable agriculture, resource conservation, and environmental stewardship. This study offers a promising pathway for the reuse of mineral-rich sludge in plant cultivation, paving the way for innovative and sustainable practices in urban waste management and green space development.

REFERENCES

Ahmed, D.A.E.-A., Galal, T.M., Al-Yasi, H.M., Hassan, L.M., & Slima, D.F. (2022). Accumulation and translocation of eight trace metals by the different tissues of Abelmoschus esculentus Moench. irrigated with untreated wastewater. *Environmental Science and Pollution Research, 29*(15), 21221-21231. https://doi.org/10.1007/s11356-021-17315-7

Amulya, K., Morris, S., & Lens, P.N.L. (2023). Aquatic biomass as sustainable feedstock for biorefineries. *Biofuels, Bioproducts and Biorefining, 17*(4), 1012-1029. https://doi.org/https://doi.org/10.1002/bbb.2471

Angin, I., & Yaghanoglu, A.V. (2011). Effects of Sewage Sludge Application on Some Physical and Chemical Properties of a Soil Affected by Wind Erosion. *Journal of Agricultural Science and Technology, 13*(5), 757-768. http://jast.modares.ac.ir/article-23-882-en.html

Bibby, K., & Peccia, J. (2013). Identification of Viral Pathogen Diversity in Sewage Sludge by Metagenome Analysis. *Environmental Science & Technology, 47*(4), 1945-1951. https://doi.org/10.1021/es305181x

Bloemendal, J., Liu, X., Sun, Y., & Li, N. (2008). An assessment of magnetic and geochemical indicators of weathering and pedogenesis at two contrasting sites on the Chinese Loess plateau. *Palaeogeography, Palaeoclimatology, Palaeoecology, 257*(1), 152-168. https://doi.org/https://doi.org/10.1016/j.palaeo.2007.09.017

Cieślik, B. M., Namieśnik, J., & Konieczka, P. (2015). Review of sewage sludge management: standards, regulations and analytical methods. *Journal of Cleaner Production, 90*, 1-15. https://doi.org/https://doi.org/10.1016/j.jclepro.2014.11.031

Clarke, B.O., & Smith, S.R. (2011). Review of 'emerging' organic contaminants in biosolids and assessment of international research priorities for the agricultural use of biosolids. *Environment International, 37*(1), 226-247.https://doi.org/https://doi.org/10.1016/j.envint.2010.06.004

Eid, E.M., Alrumman, S.A., El-Bebany, A.F., Hesham, A.E.-L., Taher, M.A., & Fawy, K.F. (2017). The effects of different sewage sludge amendment rates on the heavy metal bioaccumulation, growth and biomass of cucumbers (Cucumis sativus L.). *Environmental Science and Pollution Research, 24*(19), 16371-16382. https://doi.org/10.1007/s11356-017-9289-6

Kacprzak, M., Neczaj, E., Fijałkowski, K., Grobelak, A., Grosser, A., Worwag, M., Singh, B.R. (2017). Sewage sludge disposal strategies for sustainable development. *Environmental Research, 156*, 39-46. https://doi.org/https://doi.org/10.1016/j.envres.2017.03.010

Magwaza, S.T., Magwaza, L.S., Odindo, A.O., Mashilo, J., Mditshwa, A., & Buckley, C. (2020a). Evaluating the feasibility of human excreta-derived material for the production of hydroponically grown tomato plants - Part I: Photosynthetic efficiency, leaf gas exchange and tissue mineral content. *Agricultural Water Management, 234*, 106114. https://doi.org/https://doi.org/10.1016/j.agwat.2020.106114

Magwaza, S.T., Magwaza, L.S., Odindo, A.O., Mditshwa, A., & Buckley, C. (2020b). Partially treated domestic wastewater as a nutrient source for tomatoes (Lycopersicum solanum) grown in a hydroponic system: effect on nutrient absorption and yield. *Heliyon, 6*(12). https://doi.org/10.1016/j.heliyon.2020.e05745

Mohan, G.R., Speth, T.F., Murray, D., & Garland, J.L. (2014). *Municipal Wastewater: A Rediscovered Resource for Sustainable Water Reuse*. In T. Younos & C. A. Grady (Eds.), Potable Water: Emerging Global Problems and Solutions, pp. 153-179. Springer International Publishing. https://doi.org/10.1007/978-3-319-06563-2_6

Ngobeni, P.V., Basitere, M., & Thole, A. (2021). Treatment of poultry slaughterhouse wastewater using electrocoagulation: a review. *Water Practice and Technology, 17*(1), 38-59. https://doi.org/10.2166/wpt.2021.108

Othman, Y.A., Al-Assaf, A., Tadros, M.J., & Albalawneh, A. (2021). Heavy Metals and Microbes Accumulation in Soil and Food Crops Irrigated with Wastewater and the Potential Human Health Risk: A Metadata Analysis. *Water, 13*(23), 3405. https://www.mdpi.com/2073-4441/13/23/3405

Paucek, I., Pennisi, G., Pistillo, A., Appolloni, E., Crepaldi, A., Calegari, B., Gianquinto, G. (2020). Supplementary LED Interlighting Improves Yield and Precocity of Greenhouse Tomatoes in the Mediterranean. *Agronomy, 10*(7), 1002. https://www.mdpi.com/2073-4395/10/7/1002

Peng, C., Lee, J.-W., Sichani, H.T., & Ng, J.C. (2015). Toxic effects of individual and combined effects of BTEX on Euglena gracilis. Journal of Hazardous *Materials, 284*, 10-18. https://doi.org/https://doi.org/10.1016/j.jhazmat.2014.10.024

Roig, A., Cayuela, M.L., & Sánchez-Monedero, M.A. (2006). An overview on olive mill wastes and their valorisation methods. *Waste Management, 26*(9), 960-969. https://doi.org/https://doi.org/10.1016/j.wasman.2005.07.024

Salehi, S. (2022). *Pilot research on the impacts of adding sludge to the process of cultivating plants in the site of Aabali landfill in Tehran* (First edition ed.). Tehran Waste Management Organisation (TWMO).

Salehi, S. (2023). *Pilot research on the impacts of adding sludge to the process of cultivating plants in the site of Aabali landfill in Tehran* (Second edition ed.). Tehran Waste Management Organisation (TWMO).

Santos, J.L., Aparicio, I., Callejón, M., & Alonso, E. (2009). Occurrence of pharmaceutically active compounds during 1-year period in wastewaters from four wastewater treatment plants in Seville (Spain). *Journal of Hazardous Materials, 164*(2), 1509-1516. https://doi.org/https://doi.org/10.1016/j.jhazmat.2008.09.073

She, W., Guo, L., Gao, J., Zhang, C., Wu, S., Jiao, Y., & Zhu, G. (2022). Spatial Distribution of Soil Heavy Metals and Associated Environmental Risks near Major Roads in Southern Tibet, China. International *Journal of Environmental Research and Public Health, 19*(14), 8380. https://www.mdpi.com/1660-4601/19/14/8380

Siebielec, G., Siebielec, S., & Lipski, D. (2018). Long-term impact of sewage sludge, digestate and mineral fertilizers on plant yield and soil biological activity. *Journal of Cleaner Production, 187*, 372-379. https://doi.org/https://doi.org/10.1016/j.jclepro.2018.03.245

Siegrist, H., Joss, A., Ternes, T., & Oehlmann, J. (2005, October 29 - November 2, 2005). Fate of EDCS in wastewater treatment and EU perspective on EDC regulation. *78th annual technical exhibition and conference, Water Environment Federation*, WEFTEC.05®, Washington DC, USA. https://www.dora.lib4ri.ch/eawag/islandora/object/eawag%3A12143

Sugurbekova, G., Nagyzbekkyzy, E., Sarsenova, A., Danlybayeva, G., Anuarbekova, S., Kudaibergenova, R., . . . Moldagulova, N. (2023). Sewage Sludge Management and Application in the Form of Sustainable Fertilizer. *Sustainability, 15*(7), 6112. https://www.mdpi.com/2071-1050/15/7/6112

Suhadolc, M., Schroll, R., Hagn, A., Dörfler, U., Schloter, M., & Lobnik, F. (2010). Single application of sewage sludge – Impact on the quality of an alluvial agricultural soil. *Chemosphere, 81*(11), 1536-1543. https://doi.org/https://doi.org/10.1016/j.chemosphere.2010.08.024

Tehran Municipality (2023). Yearly reports of municipality activities.

Tiruneh Ababu, T., Fadiran Amos, O., & Mtshali Joseph, S. (2014). Evaluation of the risk of heavy metals in sewage sludge intended for agricultural application in Swaziland. *International Journal on Environmental Sciences, 5*(1), 197-216. https://www.indianjournals.com/ijor.aspx?target=ijor:ijes&volume=5&issue=1&article=017

Urbaniak, M., Wyrwicka, A., Zieliński, M., & Mankiewicz-Boczek, J. (2016). Potential for Phytoremediation of PCDD/PCDF-Contaminated Sludge and Sediments Using Cucurbitaceae Plants: A Pilot Study. *Bulletin of Environmental Contamination and Toxicology, 97*(3), 401-406. https://doi.org/10.1007/s00128-016-1868-6

Wang, Y., Xu, Z., Bach, S.J., & McAllister, T.A. (2008). Effects of phlorotannins from Ascophyllum nodosum (brown seaweed) on in vitro ruminal digestion of mixed forage or barley grain. *Animal Feed Science and Technology, 145*(1), 375-395. https://doi.org/https://doi.org/10.1016/j.anifeedsci.2007.03.013

Xu, S., Huang, Z., Huang, J., Wu, S., Dao, Y., Chen, Z., . . . Gong, Q. (2023). Environmental Pollution Assessment of Heavy Metals in Soils and Crops in Xinping Area of Yunnan Province, China. *Applied Sciences, 13*(19), 10810. https://www.mdpi.com/2076-3417/13/19/10810

Ye, C., Shen, Z., Zhang, T., Fan, M., Lei, Y., & Zhang, J. (2011). Long-term joint effect of nutrients and temperature increase on algal growth in Lake Taihu, China. *Journal of Environmental Sciences, 23*(2), 222-227. https://doi.org/https://doi.org/10.1016/S1001-0742(10)60396-8

Zhakypbek, Y., Kossalbayev, B.D., Belkozhayev, A.M., Murat, T., Tursbekov, S., Abdalimov, E., . . . Allakhverdiev, S.I. (2024). Reducing Heavy Metal Contamination in Soil and Water Using Phytoremediation. *Plants, 13*(11), 1534. https://www.mdpi.com/2223-7747/13/11/1534

Scientific Papers. Series E. Land Reclamation, Earth Observation & Surveying, Environmental Engineering. Vol. XIV, 2025
Print ISSN 2285-6064, CD-ROM ISSN 2285-6072, Online ISSN 2393-5138, ISSN-L 2285-6064

VIRTUAL LABS IN ENGINEERING EDUCATION: ENHANCING LEARNING OUTCOMES

Mirela Alina SANDU, Veronica IVANESCU

University of Agronomic Sciences and Veterinary Medicine of Bucharest,
59 Mărăști Blvd, District 1, Bucharest, Romania

Corresponding author email: veronica.ivanescu@fifim.ro

Abstract

This study investigates the integration of virtual laboratories into an undergraduate environmental engineering course through a blended learning approach. Using HybridPraxisLab, a browser-based simulation platform, second-year students engaged in optional virtual modules designed to reinforce theoretical knowledge and procedural skills. Quantitative data collected via a 14-item questionnaire revealed high student satisfaction across accessibility, engagement, and confidence dimensions. Additionally, a significant difference in final laboratory grades was observed between students with high and low virtual engagement, suggesting a positive impact on academic performance. These results support the use of virtual labs as effective and inclusive tools for enhancing learning outcomes in engineering education, especially for part-time or remote learners. The findings highlight the potential of such platforms to supplement traditional instruction and improve readiness for hands-on laboratory tasks.

Key words*: active learning, blended learning, engineering education, student perceptions, virtual laboratories.*

INTRODUCTION

Laboratory-based learning represents a foundational element of engineering education, offering students the opportunity to apply theoretical concepts to real-world scenarios while developing procedural skills and critical thinking (Feisel & Rosa, 2005; Li & Liang, 2024). However, the accessibility of physical laboratories is frequently constrained by logistical, financial, and institutional barriers, such as limited equipment, safety regulations, or scheduling conflicts (Asiksoy, 2023; Balamuralithara & Woods, 2009; Faour & Ayoubi, 2018). These challenges are particularly pronounced in high-enrollment programs or in part-time and distance learning formats (Faour & Ayoubi, 2018; Perales et al., 2019).

To address such limitations, virtual laboratories (VLs) have emerged as flexible, scalable tools that simulate laboratory procedures and allow students to engage with experimental content remotely and safely (Reeves & Crippen, 2021). VLs provide several pedagogical and logistical benefits: they reduce infrastructure costs, increase accessibility, support repeated practice, and minimize environmental and safety risks (Raman et al., 2022). These advantages are especially valuable in applied science and engineering domains where hands-on activities may involve hazardous substances or require specialized equipment that is often unavailable in traditional educational settings (Kapilan et al., 2021; Perales et al., 2019).

When integrated into blended learning models, VLs can enhance student engagement and learning outcomes. Blended approaches combine digital tools with face-to-face instruction, promoting personalized pacing, inclusivity, and active participation (Anjos et al., 2024; Cao, 2023). Within this pedagogical framework, flipped classrooms - where students engage with materials such as simulations or video lectures prior to class - have proven especially effective (Garrison & Vaughan, 2008; Lage et al., 2000). Such formats promote equity in access to learning, regardless of students' geographic location or time constraints (Abdelmoneim et al., 2022; Bonfield et al., 2020; Cao, 2023).

A growing body of evidence supports the effectiveness of VLs in improving conceptual understanding, procedural accuracy, and learner confidence (Abdelmoneim et al., 2022; Asiksoy, 2023; Li & Liang, 2024). VLs have also been linked to reduced student anxiety and improved readiness for physical laboratories, offering a safe environment for experimentation and repetition (Gungor et al., 2022;

Schnieder et al., 2022). During the COVID-19 pandemic, their role was amplified as institutions sought to maintain educational continuity (Kapilan et al., 2021; Schnieder et al., 2022). Beyond emergency use, VLs support inclusive education, particularly for non-traditional, part-time, or remote learners (Abdelmoneim et al., 2022; Bonfield et al., 2020).

Despite the expanding research, most studies on virtual laboratories have focused on domains such as physics, chemistry, or computer science (Faour & Ayoubi, 2018; Reeves & Crippen, 2021). By contrast, their application in environmental engineering - a field that demands interdisciplinary knowledge and specialized equipment - remains relatively underexplored (Wahyudi et al., 2024). Furthermore, few investigations have analyzed how engagement with virtual labs influences academic performance in blended formats that include both full-time and part-time learners (Schnieder et al., 2022).

In this context, the present study explores the use of HybridPraxisLab, a browser-based simulation platform, in an undergraduate Environmental Engineering in Agriculture course at the University of Agronomic Sciences and Veterinary Medicine of Bucharest. The objectives are threefold: (1) to assess students' perceptions of the platform in terms of accessibility, engagement, and confidence; (2) to examine the relationship between virtual lab engagement and academic performance; and (3) to evaluate the potential of virtual labs to enhance traditional laboratory instruction in a sustainable and inclusive manner.

MATERIALS AND METHODS

Study context and participants

This study was conducted at the Faculty of Land Reclamation and Environmental Engineering, within the *Environmental Engineering in Agriculture* undergraduate program at the University of Agronomic Sciences and Veterinary Medicine of Bucharest. The research involved second-year students enrolled in both full-time and part-time (distance learning) formats, who participated voluntarily in a virtual laboratory project aimed at exploring digital tools to enhance engineering education.

A total of 39 students participated: 22 from the full-time program and 17 from the part-time program. All students engaged with the same set of virtual laboratory modules and completed an online questionnaire evaluating their experience. The activity was conducted independently of the standard course curriculum and introduced solely for research purposes. Participation was voluntary and anonymous, and all students provided informed consent prior to inclusion in the study.

Description of the Virtual Lab Platform

Virtual laboratory activities were delivered using HybridPraxisLab, a browser-based educational platform designed to enhance practical skills in environmental engineering through interactive simulation. The platform provides guided access to digital experiments that replicate procedures commonly performed in environmental laboratories. These simulations are consistent with the growing adoption of scenario-based instructional design in online engineering education (Kapilan et al., 2021; Raman et al., 2022).

Each scenario-based module follows a consistent instructional sequence, consisting of: *Theoretical Background*, *Step-by-Step Method*, *Simulation*, *Self-Assessment Quiz*, and *Bibliographic Resources*. This structure supports three key aspects of effective laboratory learning: conceptual understanding, procedural training, and self-reflection (Feisel & Rosa, 2005).

At the time of this study, the platform hosted the following modules:

- Laboratory safety;
- Protocol for sampling and transport of water samples;
- Pipetting: selecting and using micropipettes;
- Acids and bases;
- Determination of pH for different water samples;
- Preparation of solution: from salt to solution;
- Determination of turbidity for different water samples;
- Determination of Chlorides in different water samples;
- Determination of Dissolved Oxygen in water;

- Mass spectrometry: exploring the instrument.

Although these modules were not part of the formal course curriculum, they were made available as optional preparatory tools to help students reinforce theoretical concepts and gain procedural familiarity before participating in physical laboratory sessions. Students received free access to the platform and could explore the simulations at their own pace, outside scheduled class time, using a standard internet connection and personal login credentials. The integration of such open-access and flexible tools has been recognized as a best practice in inclusive engineering education (Abdelmoneim et al., 2022; Bonfield et al., 2020; Schnieder et al., 2022).

Survey design and data collection

To evaluate students' perceptions of the virtual laboratory experience, a structured questionnaire was developed and distributed online after completion of the HybridPraxisLab activities.

The survey was designed to capture feedback across three key dimensions that are commonly highlighted in literature as critical to the perceived value of virtual labs: platform accessibility/ease of use, student engagement, and confidence building (preparation for real labs) (Abdelmoneim et al., 2022; Schnieder et al., 2022). These particular aspects were selected based on prior research indicating their relevance in assessing virtual lab experiences in higher education-namely improving ease of access, enhancing engagement, and boosting students' confidence before hands-on labs (Cao, 2023).

The questionnaire consisted of 14 items, grouped into thematic sections:

- Platform accessibility and usability;
- Student engagement and interest during the virtual lab experience;
- Perceived contribution to understanding and confidence before attending physical labs.

Each item was rated using a 7-point Likert scale, which allows for fine-grained analysis of perception-based data in educational research (Revilla et al., 2014). The full scale used in the questionnaire was as follows:

1 - Strongly disagree;
2 - Disagree;
3 - Slightly disagree;
4 - Neutral;
5 - Slightly agree;
6 - Agree;
7 - Strongly agree.

An additional open-ended question was included to collect qualitative feedback and suggestions for improvement. The combination of closed and open-ended responses reflects best practices in mixed-methods research for exploring learner satisfaction and experience (Reeves & Crippen, 2021).

The survey was distributed anonymously via an online form to all 39 students who participated in the virtual laboratory activities. Participation was voluntary, with no incentives offered. Data collection occurred over a one-week period following the completion of the virtual sessions.

Academic performance evaluation

To complement the perception-based data, this study also examined students' academic performance in the associated laboratory course. The aim was to explore whether engagement with the virtual lab activities was associated with learning outcomes, even though the virtual component was not part of the formal assessment. Similar analytical approaches have been used in engineering education research to evaluate the impact of supplementary digital tools on final course performance (Schnieder et al., 2022).

Final grades from the physical laboratory evaluation were used as the primary indicator of academic performance. These grades reflected students' ability to perform technical procedures, interpret results, and demonstrate understanding of laboratory concepts, as assessed through practical work and written reports.

Although participation in the virtual labs was voluntary and not formally linked to course requirements, students' final laboratory grades were analyzed in relation to their level of engagement with the HybridPraxisLab platform (i.e., number of completed modules). Due to the limited sample size and the exploratory nature of the study, this analysis was descriptive and intended to identify general trends rather than establish causal relationships.

Data analysis

Descriptive statistical methods were used to analyze survey responses and academic performance data. For each Likert-scale item, the mean and standard deviation were calculated, in line with established practices for summarizing perception-based data (Revilla et al., 2014). Survey items were also grouped by dimension to calculate aggregate mean scores for accessibility, engagement, and confidence building, allowing for cross-category comparisons.

In parallel, students' final laboratory grades were analyzed in relation to the number of completed virtual lab modules. As the study was exploratory and based on a relatively small sample (n = 39), the analysis was limited to descriptive comparisons and a Welch's t-test. Inferential analysis was conducted with caution, acknowledging that this does not establish causation but can highlight trends worthy of further investigation (Balamuralithara & Woods, 2009).

All data were processed using Microsoft Excel. No personal identifiers were collected, and all analyses were conducted anonymously to ensure confidentiality. These procedures adhered to standard ethical principles in educational research practice.

RESULTS AND DISCUSSIONS

Survey response rate and overview

Out of the 39 students who participated in the virtual laboratory activities, 36 completed the post-activity survey, resulting in a response rate of 92.3%. The sample included both full-time and part-time students, with no significant difference observed in response behavior between the two groups.

The majority of respondents reported a generally positive experience with the HybridPraxisLab platform. Across all items, responses were well-distributed across the 7-point Likert scale, with only minimal clustering at the extremes. Preliminary review indicated consistently favorable ratings in the areas of ease of use, perceived relevance, and preparation for physical lab work.

The descriptive results of the survey are detailed in the following section, organized by the three evaluated dimensions: accessibility, engagement, and confidence building.

As shown in Figure 1, students rated Confidence Building highest (M = 6.19), followed by Accessibility (M = 6.14) and Engagement (M = 5.98), indicating consistently favorable perceptions across all dimensions.

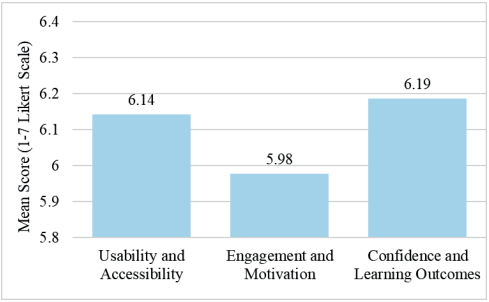


Figure 1. Average scores by survey dimension

Distribution of responses per item

A more detailed analysis of each survey item reveals that students rated the platform consistently high, particularly on items related to clarity of simulation steps, perceived usefulness for understanding lab procedures, and motivational aspects. As shown in Figure 2, the item-wise mean scores ranged between 5.6 and 6.4, reflecting positive reception across all 14 items.

Notably, the highest-rated survey item was *"I would recommend these modules to future students"* (M = 6.36), indicating a strong endorsement of the virtual lab experience. In contrast, the lowest-rated item - *"The design of the simulations encouraged participation"* (M = 5.64) - while still above the neutral midpoint, suggests a potential area for enhancement in terms of simulation interactivity and user engagement features.

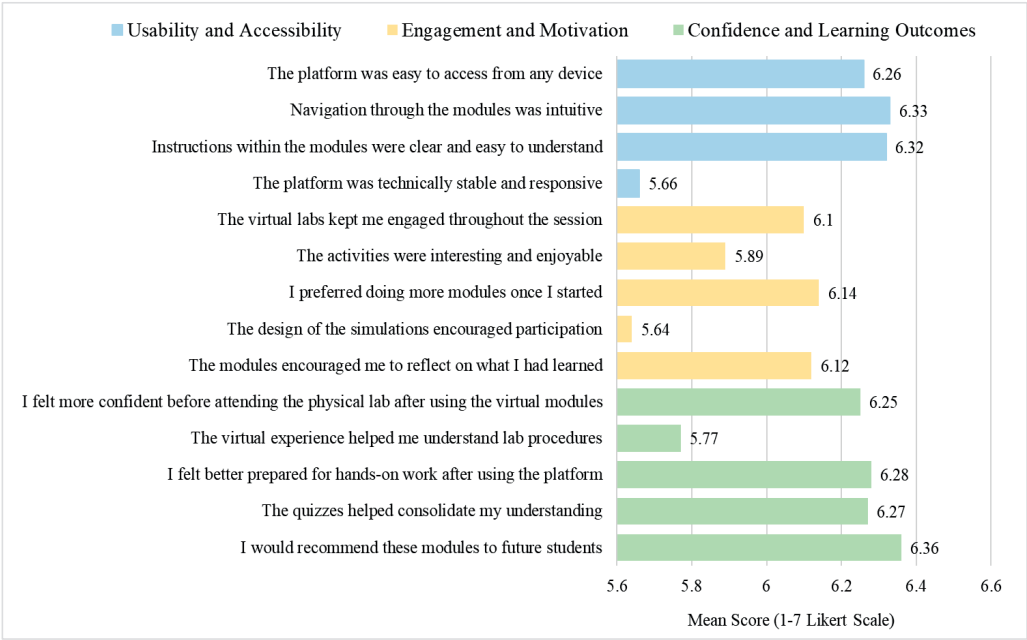


Figure 2. Mean scores on Virtual Lab questionnaire

Qualitative feedback and open-ended responses

Beyond the quantitative data, students were invited to provide open-ended feedback regarding their experience with the virtual lab modules. Out of the 36 respondents, 28 (77.8%) offered qualitative comments. Thematic analysis revealed several recurring patterns:

- **Confidence and preparation**: many students mentioned feeling more confident and better prepared before entering the physical lab session. They appreciated the clarity of procedures and the opportunity to rehearse steps in a safe, self-paced environment (Abdelmoneim et al., 2022; Asiksoy, 2023).
- **Accessibility and flexibility**: respondents frequently highlighted the ease of accessing the simulations from various devices and at their own pace, with part-time students especially valuing this flexibility (Schnieder et al., 2022).
- **Suggestions for improvement**: some students expressed interest in having more modules available, particularly covering additional topics related to sampling and analytical techniques. Others suggested improvements in visual interactivity and feedback mechanisms after quizzes, consistent with observations from prior research (Kapilan et al., 2021).

Selected comments include:

- *"Very well-structured. The simulations made me feel more confident for the real lab."*
- *"I wish more modules were available. I'd be interested in simulations for water analysis."*
- *"Clear and interactive. Helped me understand the pipetting steps in advance."*

Relationship between platform usage and academic performance

To explore whether engagement with the HybridPraxisLab modules had an academic impact, we compared final lab grades between students who completed most of the simulations (≥6 modules) and those who did not.

- **Group A** (n = 19): completed ≥6 virtual modules
  – *Mean final lab grade*: 9.06 (SD = 0.38)
- **Group B** (n = 17): completed <6 modules
  – *Mean final lab grade*: 8.39 (SD = 0.48)

A Welch's t-test indicated that this difference was statistically significant ($t(32.6) = 4.64$, $p < 0.001$), suggesting that greater engagement

with the virtual lab platform was associated with better academic performance. As shown in Figure 3, students with higher virtual lab engagement scored significantly better in the final laboratory assessment. These findings mirror those of Schnieder et al., (2022), who reported improved performance among engineering students using virtual simulations, and with Murillo-Zamorano et al., (2021), who observed similar benefits in gamified digital learning environments.

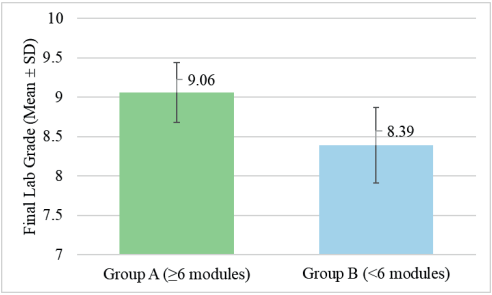


Figure 3. Final laboratory grades by virtual laboratory usage

Summary of findings

Overall, students rated the HybridPraxisLab modules positively across all dimensions. High mean scores (5.64-6.36) indicated strong perceived value, supported by qualitative comments that highlighted increased clarity and preparedness. The flexibility of the platform benefited especially remote and part-time learners, as also shown by Abdelmoneim et al. (2022) and Cao (2023). The statistically significant relationship between platform engagement and academic outcomes reinforces conclusions from broader research in STEM education (Murillo-Zamorano et al., 2021; Schnieder et al., 2022).

Limitations and future research

This study has several limitations that should be acknowledged. First, the sample size was relatively small (N = 36), and all participants were enrolled in a single engineering program at one institution. As such, the findings may not be generalizable across disciplines, academic levels, or institutional contexts.

Second, the virtual lab modules were designed primarily to support preparation for physical lab sessions. While this format proved effective, the study did not evaluate whether simulations could fully replace hands-on labs in a stand-alone virtual setting. Further comparative studies are needed to assess learning outcomes in fully remote versus blended formats.

Third, the evaluation relied primarily on self-reported perceptions and one summative performance metric (final lab grade). Although significant correlations were observed, additionnal data such as practical skill assessments, long-term retention measures, or behavioral analytics (e.g., time spent per module) could provide more nuanced insights into learning effectiveness.

Finally, technical design elements such as the level of interactivity, feedback in quizzes, and simulation realism were not systematically evaluated. Future iterations of the platform would benefit from user-centered design research, incorporating iterative testing and interface improvements based on both student and instructor feedback.

Future research should focus on expanding the range of available modules to cover a broader set of engineering topics and to test the scalability of the platform across larger, more diverse student populations. Additionally, integrating adaptive learning elements or real-time feedback systems could further enhance the effectiveness of virtual laboratory instruction.

CONCLUSIONS

This study investigated the impact of HybridPraxisLab - a virtual laboratory platform - on students' perceptions, engagement, and academic performance within an environmental engineering course. The findings demonstrate consistently positive feedback across all evaluated dimensions: usability and accessibility, engagement and motivation, and confidence and learning outcomes. Students rated all 14 items highly, with mean scores ranging from 5.64 to 6.36 on a 7-point Likert scale, indicating strong acceptance of the virtual modules as effective educational tools.

Qualitative responses further supported these findings. Students emphasized increased confidence before entering the physical lab, greater clarity of procedures, and the value of

self-paced exploration. The virtual format was particularly appreciated by part-time and remote learners, who benefited from its flexibility and accessibility.

Moreover, a statistically significant difference in final lab grades was observed between students who completed most of the modules and those who engaged with the platform less frequently. This suggests a strong association between virtual lab engagement and improved academic outcomes, especially in terms of procedural readiness and conceptual understanding.

The results suggest that virtual labs can:

- Enhance student engagement and motivation through inquiry-based and interactive learning.
- Support procedural readiness and safety awareness before entering the physical lab.
- Reduce access barriers for part-time and remote learners.
- Serve as an effective supplement - not a replacement - for hands-on laboratory experiences.

Given these outcomes, several recommendations emerge for educators and institutions:

1. **Curriculum design**: integrate virtual laboratories as preparatory modules to maximize the effectiveness of in-person sessions.
2. **Assessment strategies**: combine self-assessment tools in virtual modules with in-person evaluations to assess procedural, conceptual, and reflective skills.
3. **Teacher training**: provide instructors with pedagogical and technical support for implementing blended learning approaches.
4. **Equity and accessibility**: expand the availability of virtual labs to support inclusive and flexible learning environments.
5. **Ongoing evaluation**: use learning analytics and regular student feedback to refine content and ensure alignment with course objectives.

While HybridPraxisLab proved to be an asset in this course, further research across other subjects and educational contexts is necessary to fully understand its broader impact. Future work should explore long-term retention, cost-effectiveness, and students' ability to transfer virtual learning experiences to real-world engineering tasks.

In summary, virtual laboratories represent a powerful and scalable tool for fostering active, inclusive, and effective learning in environmental engineering - and beyond. The observed correlation between simulation engagement and lab performance suggests that structured virtual components could be embedded into standard laboratory curricula, particularly as preparatory modules.

To guide future development and institutional decisions, a SWOT analysis of HybridPraxisLab's implementation is presented in Tabel 1.

Tabel 1. SWOT analysis of the HybridPraxisLab's implementation

Strengths	**Weaknesses**
High student satisfaction and engagement	Limited to one course and institution
Improved academic performance and confidence	Not yet validated across disciplines
Flexible access for diverse student profiles	Some modules lack advanced or complex lab procedures
Supports procedural readiness and safety awareness	Not designed as a full replacement for hands-on experimentation
Opportunities	**Threats**
Expansion to other engineering or science domains	Institutional resistance to pedagogical change
Integration with adaptive learning and analytics	Uneven access to infrastructure across student populations
Alignment with blended and inclusive learning policies	Risk of over-reliance in contexts without proper physical labs
Potential for scalable deployment across programs/universities	Platform maintenance and technological dependencies

ACKNOWLEDGEMENTS

This research work was carried out with the support of University of Agronomic Sciences and Veterinary Medicine of Bucharest – Romania, Research Project 1059/15.06.2022, acronym HybridPraxisLab in the competition IPC 2022.

REFERENCES

Abdelmoneim, R., Hassounah, E., & Radwan, E. (2022). Effectiveness of virtual laboratories on developing expert thinking and decision-making skills among female school students in Palestine. *Eurasia Journal of Mathematics, Science and Technology Education*, *18*(12), em2199. https://doi.org/10.29333/ejmste/12708

Anjos, F. E. V. D., Martins, A. D. O., Rodrigues, G. S., Sellitto, M. A., & Silva, D. O. D. (2024). Boosting Engineering Education with Virtual Reality: An Experiment to Enhance Student Knowledge Retention. *Applied System Innovation*, *7*(3), 50. https://doi.org/10.3390/asi7030050

Asiksoy, G. (2023). Effects of Virtual Lab Experiences on Students' Achievement and Perceptions of Learning Physics. *International Journal of Online and Biomedical Engineering (iJOE)*, *19*(11). https://doi.org/10.3991/ijoe.v19i11.39049

Balamuralithara, B., & Woods, P. C. (2009). Virtual laboratories in engineering education: The simulation lab and remote lab. *Computer Applications in Engineering Education*, *17*(1), 108–118. https://doi.org/10.1002/cae.20186

Bonfield, C. A., Salter, M., Longmuir, A., Benson, M., & Adachi, C. (2020). Transformation or evolution?: Education 4.0, teaching and learning in the digital age. *Higher Education Pedagogies*, *5*(1), 223–246. https://doi.org/10.1080/23752696.2020.1816847

Cao, W. (2023). A meta-analysis of effects of blended learning on performance, attitude, achievement, and engagement across different countries. *Frontiers in Psychology*, *14*. https://doi.org/10.3389/fpsyg.2023.1212056

Faour, M. A., & Ayoubi, Z. (2018). The effect of using virtual laboratory on grade 10students' conceptual understanding and their attitudes towards physics. *Journal of Educationin Science, Environment and Health (JESEH)*, *4*(1), 54–68. https://doi.org/10.21891/jeseh.387482

Feisel, L. D., & Rosa, A. J. (2005). The Role of the Laboratory in Undergraduate Engineering Education. *Journal of Engineering Education*, *94*(1), 121–130. https://doi.org/10.1002/j.2168-9830.2005.tb00833.x

Garrison, D. R., & Vaughan, N. D. (2008). *Blended Learning in Higher Education: Framework, Principles, and Guidelines*. Jossey-Bass.

Gungor, A., Avraamidou, L., Kool, D., Lee, M., Eisink, N., Albada, B., Van Der Kolk, K., Tromp, M., & Bitter, J. H. (2022). The Use of Virtual Reality in A Chemistry Lab and Its Impact on Students' Self-Efficacy, Interest, Self-Concept and Laboratory Anxiety. *Eurasia Journal of Mathematics, Science and Technology Education*, *18*(3), em2090. https://doi.org/10.29333/ejmste/11814

Kapilan, N., Vidhya, P., & Gao, X.-Z. (2021). Virtual Laboratory: A Boon to the Mechanical Engineering Education During Covid-19 Pandemic. *Higher Education for the Future*, *8*(1), 31–46. https://doi.org/10.1177/2347631120970757

Lage, M. J., Platt, G. J., & Treglia, M. (2000). Inverting the Classroom: A Gateway to Creating an Inclusive Learning Environment. *The Journal of Economic Education*, *31*(1), 30–43. https://doi.org/10.1080/00220480009596759

Li, J., & Liang, W. (2024). Effectiveness of virtual laboratory in engineering education: A meta-analysis. *PLOS ONE*, *19*(12), e0316269. https://doi.org/10.1371/journal.pone.0316269

Murillo-Zamorano, L. R., López Sánchez, J. Á., Godoy-Caballero, A. L., & Bueno Muñoz, C. (2021). Gamification and active learning in higher education: Is it possible to match digital society, academia and students' interests? *International Journal of Educational Technology in Higher Education*, *18*(1). https://doi.org/10.1186/s41239-021-00249-y

Perales, M., Pedraza, L., & Moreno-Ger, P. (2019, aprilie). Work-In-Progress: Improving Online Higher Education with Virtual and Remote Labs. *2019 IEEE Global Engineering Education Conference (EDUCON)*. 2019 IEEE Global Engineering Education Conference (EDUCON), Dubai, United Arab Emirates. https://doi.org/10.1109/educon.2019.8725272

Raman, R., Achuthan, K., Nair, V. K., & Nedungadi, P. (2022). Virtual Laboratories- A historical review and bibliometric analysis of the past three decades. *Education and Information Technologies*, *27*(8), 11055–11087. https://doi.org/10.1007/s10639-022-11058-9

Reeves, S. M., & Crippen, K. J. (2021). Virtual Laboratories in Undergraduate Science and Engineering Courses: A Systematic Review, 2009-2019. *Journal of Science Education and Technology*, *30*(1), 16–30. https://doi.org/10.1007/s10956-020-09866-0

Revilla, M. A., Saris, W. E., & Krosnick, J. A. (2014). Choosing the Number of Categories in Agree-Disagree Scales. *Sociological Methods & Research*, *43*(1), 73–97. https://doi.org/10.1177/0049124113509605

Schnieder, M., Williams, S., & Ghosh, S. (2022). Comparison of In-Person and Virtual Labs/Tutorials for Engineering Students Using Blended Learning Principles. *Education Sciences*, *12*(3), 153. https://doi.org/10.3390/educsci12030153

Wahyudi, M. N. A., Budiyanto, C. W., Widiastuti, I., Hatta, P., & Bakar, Mohd. S. B. (2024). Understanding Virtual Laboratories in Engineering Education: A Systematic Literature Review. *International Journal of Pedagogy and Teacher Education*, *7*(2), 102. https://doi.org/10.20961/ijpte.v7i2.85271

Scientific Papers. Series E. Land Reclamation, Earth Observation & Surveying, Environmental Engineering. Vol. XIV, 2025
Print ISSN 2285-6064, CD-ROM ISSN 2285-6072, Online ISSN 2393-5138, ISSN-L 2285-6064

THE INFLUENCE OF MUSIC ON PLANT GROWTH IN A SMART GREENHOUSE USING IoT TECHNOLOGY

Cristian STĂNESCU, Gabriel PREDUŞCĂ, Liana Denisa CÎRCIUMĂRESCU

Valahia University of Târgovişte, 13 Sinaia Alley Street, Târgovişte, Romania

Corresponding author email: gabriel.predusca@valahia.ro

Abstract

This paper presents the development and evaluation of an Internet of Things (IoT)-based control system for small-scale greenhouse environments. The core of the system is the Arduino Nano 33 IoT (SAMD21 Cortex-M0, 32-bit), which integrates multiple environmental sensors to monitor temperature, air humidity, soil moisture, and light intensity. Based on user-defined parameters, the system automates plant care actions: activating an LED lighting matrix, powering a ventilation fan, and triggering a water pump for irrigation. System monitoring and control can be performed locally through an LCD interface or remotely via a cloud-based dashboard. Beyond automation, the study investigates the influence of various types of music - such as classical, techno, and meditation - on the germination and growth of lettuce and radish plants. Experimental results indicate that classical and meditation music enhanced plant development, while techno music had a negative effect, despite otherwise optimal environmental conditions. The findings demonstrate the dual potential of IoT systems for smart agriculture: enabling precision environmental control and exploring novel stimuli, such as sound, to support plant growth.

Key words*: IoT, smart greenhouse, Arduino Nano 33 IoT, plant growth, music influence, environmental control, automation.*

INTRODUCTION

Food insecurity in climate-vulnerable regions, such as Kenya, has intensified the need for automated greenhouse systems capable of maintaining stable internal conditions irrespective of external weather fluctuations. This challenge arises from increasingly erratic climatic conditions that inhibit optimal plant development. While conventional greenhouses partially address this by enclosing crops within controlled environments, they often rely heavily on manual oversight to maintain ideal growth parameters. Prior studies have emphasized the significant impact of environmental factors such as light, temperature, and humidity on plant development under greenhouse conditions (Mitova et al., 2021).

Each greenhouse operates within a specific set of environmental parameters, which vary depending on the species being cultivated (Figure 1).

To support healthy plant growth, conditions such as air temperature, humidity, light intensity, and soil moisture must be maintained within tightly controlled thresholds. Addressing both food insecurity and environmental degradation requires integrated, innovative solutions.



Figure 1. Example of a modern large-scale greenhouse

Recent research has therefore focused on low-cost, microcontroller-based systems that automate environmental monitoring and regulation. Gitonga (2020) developed a prototype utilizing sensors, SMS technology, and Bluetooth connectivity to remotely control greenhouse conditions. However, as Natonis (2023) points out, the increasing deployment of IoT devices introduces new challenges in system configuration, network behavior, and device interoperability, requiring robust architecture and management strategies.

The Internet of Things (IoT) paradigm facilitates the development of smart greenhouses that not

only automate internal processes but also allow for remote access and control. While the "Things" aspect focuses on physical devices and user interaction, cloud infrastructure plays a crucial role in processing data and supporting remote communication.

Efficient system design must go beyond enhanced processing power to include scalable architectures that minimize bandwidth consumption and latency. RESTful web services, which operate over the HTTP protocol, can serve as flexible interfaces for these user interactions (Wang, 2017), as illustrated in Figure 2.

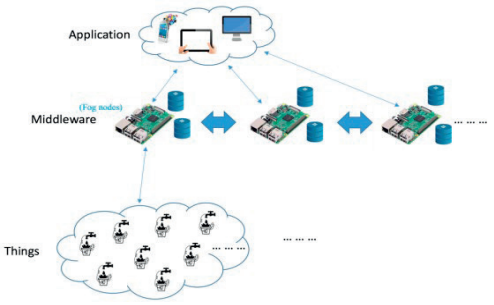


Figure 2. The proposed architecture of the system (Wang, 2017)

Despite these technological advancements, high costs and design complexity have limited the widespread adoption of smart greenhouses. This study proposes the development and testing of an affordable IoT-enabled greenhouse prototype equipped for remote monitoring and environmental automation. In addition to automation, the study explores the use of music as a non-invasive stimulus to enhance plant growth - an emerging area of interest in sustainable agricultural research.

Lai and Wu (2020) found that lettuce seedlings exposed to Gregorian chant, new-age, and waltz music exhibited significant improvements in radicle and hypocotyl elongation, suggesting that certain acoustic frequencies may enhance early plant development. In their experiment involving nine distinct music genres, alfalfa seeds exposed to rock music germinated less effectively, while classical, nature sounds, and waltz promoted germination. Lettuce seedlings responded positively to Gregorian chant, jazz, nature sounds, and new-age music.

This research introduces a user-friendly interface that integrates mobile applications and cloud-based platforms for monitoring and managing greenhouse conditions. By transforming a conventional greenhouse into a smart, responsive system, the study contributes to understanding how IoT automation and acoustic stimuli can jointly promote sustainable, resource-efficient plant growth in controlled environments.

MATERIALS AND METHODS

This section describes the hardware and software components employed in constructing the smart greenhouse prototype. It outlines the configuration of microcontrollers, sensors, actuators, and user interfaces. Additionally, it details the experimental protocol designed to evaluate plant growth under controlled environmental conditions and various musical exposures.

Hardware Components

The smart greenhouse system is built around two primary processing units: the **Arduino Nano 33 IoT** and the **Raspberry Pi 4 Model B**. The Arduino Nano 33 IoT (Figure 3) was chosen for its integrated wireless capabilities and compatibility with the Arduino Cloud platform. During the initial design phase, the Arduino Cloud "Starter Plan" was used to collect sensor data and create a basic dashboard for environmental monitoring. To improve flexibility and system performance, the configuration was later expanded to incorporate a Raspberry Pi.

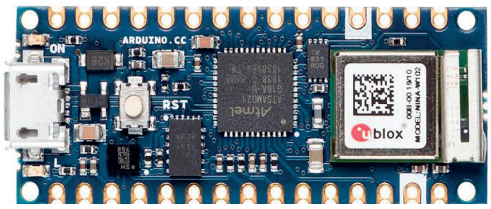


Figure 3. Arduino Nano 33 IoT (Arduino, 2025)

The Raspberry Pi 4 Model B, equipped with 4 GB of RAM, a 16 GB microSD card, built-in Wi-Fi, and a touchscreen display (Figure 4), serves as the local server. This unit manages the graphical interface, local database, and actuator control logic. Its inclusion ensures enhanced system scalability, data security, and offline functionality.



Figure 4. Raspberry Pi 4 Model B (Raspberry Pi, 2025)

The Raspberry Pi 4 Model B, equipped with 4 GB of RAM, a 16 GB microSD card, built-in Wi-Fi, and a touchscreen display (Figure 4), serves as the local server. This unit manages the graphical interface, local database, and actuator control logic. Its inclusion ensures enhanced system scalability, data security, and offline functionality (Table 1).

Sensor Specifications

The smart greenhouse prototype integrates three primary sensors to monitor key environmental parameters essential to plant development:

- *DHT11 (Air Temperature and Humidity Sensor).* This sensor measures ambient temperature and relative humidity. It operates within a temperature range of 0-50°C with ±2°C accuracy, and a humidity range of 20-90% with ±5% accuracy. The DHT11 requires an input voltage of 3.0-5.5 V, communicates through a single digital pin, and consumes between 0.5-2.5 mA during active operation (100-150 µA in standby mode).
- *BMP180 (Barometric Pressure Sensor).* The BMP180 monitors atmospheric pressure and temperature. It operates between 3.3 V and 5 V and communicates via the I²C protocol through the SDA (A4) and SCL (A5) pins. It measures pressure within the 300-1100 hPa range with an accuracy of ±0.12 hPa and has a minimal current consumption of approximately 3 µA. Its compact form factor (14 mm × 12 mm) enables easy integration into embedded systems.
- *Soil Moisture Sensor*. This sensor uses two conductive probes to assess soil moisture by measuring resistance. It operates at 3.3-5 V and provides an analog output signal ranging from 0 (dry) to 1023 (wet), as interpreted by the Arduino's 10-bit ADC.

The environmental parameters were monitored using a set of three sensors: DHT11 for air temperature and humidity, BMP180 for atmospheric pressure, and a soil moisture sensor. A summary of these sensors and their technical specifications is presented in Table 2.

Table 1. Central Computing Units Used in the Smart Greenhouse System

Component	Arduino Nano 33 IoT	Raspberry Pi 4 Model B
Function	Sensor interfacing and real-time control	Local server for control and visualization
Specifications	Wireless, ARM Cortex-M0+ core, integrated Wi-Fi	4 GB RAM, Wi-Fi, touchscreen display
Rationale	Easy wireless setup, Arduino Cloud compatible	Custom UI, local database, higher flexibility

Table 2. Environmental Sensors and Their Technical Specifications

Sensor	**DHT11**		**BMP180**	**Soil**
Parameter	Temperature	Humidity	Pressure	Moisture
Measurement Range	0–50°C	20-90%	300-1100 hPa	0-1023 (ADC)
Accuracy	±2°C	±5%	±0.12 hPa	N/A
Voltage	3-5.5 V	3-5.5 V	3.3-5.5 V	3.3-5.5 V

System Configuration and Components

The physical structure of the system is divided into three functional compartments: the experimental chamber, the control panel, and the water reservoir, as shown in Figure 5.

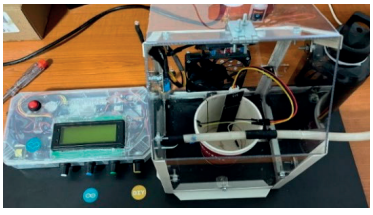


Figure 5. The system setup

- Control panel includes breadboard with all interfacing components:
  - *DS3231 real-time clock (RTC) module* for accurate timestamping of sensor data;
  - *Transistors* to switch actuators (fan, pump, lights);
  - *Potentiometers* to define custom threshold values;
  - *Resistors, jumpers, and wiring* for circuit completion;
- Water tank houses - a submersible pump positioned at its base;
- Ventilation fan - mounted in the main chamber, ensures airflow via small circular vents;

- LED lighting system - 8 UV, 4 red, and 4 sky-blue LEDs simulate daylight spectra to promote photosynthesis.

Experimental Protocol

To investigate the effects of musical stimulation on early-stage plant development, five experimental groups were established. Each group consisted of four Lactuca sativa seedlings (cultivar 'May King'), cultivated under identical environmental conditions inside the smart greenhouse. Musical exposure was administered using a speaker placed at a fixed distance from the seedlings, delivering audio at an average intensity of approximately 65 dB for 3 hours daily over a 9-day period. The auditory conditions applied were:

1. Control group (no music);
2. Techno (aggressive);
3. Classical music;
4. Meditation 432 Hz.

Throughout the experiment, the system continuously logged temperature, humidity, soil moisture, and light intensity. In addition, daily measurements of radicle and hypocotyl length were recorded to assess plant growth dynamics and correlate physiological responses with the respective auditory treatments.

RESULTS AND DISCUSSIONS

Between 2024 and 2025, five experiments were conducted to evaluate the influence of musical stimuli on plant growth within a smart greenhouse prototype.

The tested species included *Lactuca sativa* (cultivars 'May King' and 'Helmut') and *Raphanus sativus* ('Helga'), cultivated under controlled conditions of temperature, humidity, light, and soil moisture.

Each experiment lasted between 7 and 9 days, during which environmental parameters were continuously monitored through an integrated data acquisition system.

The experimental conditions are summarized in Table 3.

Table 3. Experimental setup and conditions

Experiment	**1**	**2**	**3**	**4**	**5**
Species	*L. sativa*	*R. sativus*	*L. sativa*	*L. sativa, R. sativus*	*L. sativa, R. sativus*
Music type	No music	No music	Techno (aggressive)	Classical music	Meditation 432 Hz
Duration	9 days	9 days	9 days	9 days	9 days
Temperature (^{0}C)	Not recorded	20-23	21-24	20-24	23-26
Air humidity (%)	Not recorded	81-84	80-82	82-85	79-84
Soil moisture index	Not recorded	4-5	4-6	4-6	5-6
LED exposure (h/day)	Not recorded	3	3	3	3
Volume (dB)	-	-	~70	~65	~60
Playback	-	-	3 h/day, speaker	3 h/day, speaker	3 h/day, speaker

Plant height – summary by species and experiment

At the conclusion of each experiment, the average plant height was measured to evaluate the effects of musical exposure. Results showed notable differences based on the music type and plant species. The outcomes are presented in Table 4.

Table 4. Average plant height at the end of experiments

Species	**Exp.2 - No music**	**Exp.3 - Techno**	**Exp.4 - Classical**	**Exp.5 - Meditation**
L. sativa	-	2.1 cm	5.7 cm	6.8 cm
R. sativus	6.3 cm	-	6.2 cm	6.5 cm

In the absence of music (Experiment 2), *R. sativus* achieved an average height of 6.3 cm, while lettuce was not included. When exposed to techno music (Experiment 3), *L. sativa* demonstrated significantly stunted growth, averaging only 2.1 cm. In contrast, classical (Experiment 4) and 432 Hz meditation music (Experiment 5) enhanced vertical development in lettuce, with the highest average height recorded under meditation music. *R. sativus* showed more stable growth across treatments, with slight improvements under meditation sound.

Leaf number - summary by species and experiment

Leaf count served as a secondary growth indicator. The average number of leaves per plant is summarized in Table 5.

Table 5. Average number of leaves per plant at the end of experiments

Species	Exp.2 - No music	Exp.3 - Techno	Exp.4 - Classical	Exp.5 - Meditation
L.sativa	-	1-2 leaves	3-4 leaves	4-5 leaves
R. sativus	2-3 leaves	-	3-4 leaves	3-4 leaves

Results indicate a correlation between musical exposure and foliar development. *L. sativa* exposed to techno music developed fewer leaves, while those exposed to classical and meditation music exhibited significant improvements in leaf formation.
R. sativus also showed slightly increased leaf counts under musical conditions compared to the control, with minimal variation between the classical and meditation groups.
These outcomes suggest that harmonic and soothing music may positively influence physiological processes such as photosynthetic efficiency and hormone regulation, contributing to improved plant morphology.

Environmental parameters comparison across experiments

To confirm that observed differences in plant growth were attributable to music rather than environmental variability, average environmental conditions were compared across Experiments 2 through 5. These values are presented in Table 6.

Table 6. Environmental conditions across experiments (average values)

Experiment	Exp.2 - No music	Exp.3 - Techno	Exp.4 - Classical	Exp.5 - Meditation
Temperature (^{0}C)	21.8	22.3	21.9	22.7
Air humidity (%)	82.0	81.5	82.2	81.7
Soil moisture index (0-6)	4.3	4.5	4.4	4.6
Light index (0-10)	1.4	1.6	1.5	1.7

The environmental data confirm that all parameters remained within optimal ranges throughout the trials, with only slight variations. Temperatures were consistently maintained between 21.8°C and 22.7°C, air humidity levels stayed above 80%, and soil moisture remained within the ideal index range of 4 to 5.
Light intensity, though low due to indoor conditions, was supplemented uniformly by a calibrated LED matrix.
These results support the conclusion that differences in plant development are attributable to auditory stimuli rather than uncontrolled environmental factors.

Graphical interpretation of monitored variables

To evaluate the consistency of environmental control and its potential interaction with music exposure, the daily evolution of four key parameters - temperature, air humidity, soil moisture, and light intensity - was graphically analyzed across Experiments 2 to 5. These results are presented in Figures 6 to 9.
Figure 6 shows the daily temperature profiles for the four experiments. Despite minor fluctuations, all temperature values remained within the optimal growth range of 20-26°C. The highest average temperatures were recorded in Experiment 5 (meditation music). However, no thermal stress was observed, indicating that the system maintained an effective microclimate, even with modest variation.

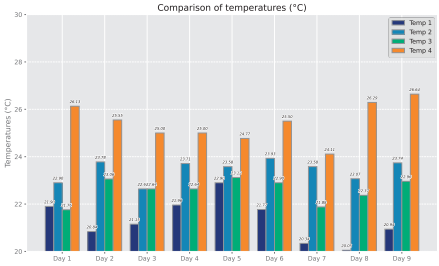


Figure 6. Temperature comparison across experiments

As shown in Figure 7, relative humidity levels remained above 70% throughout all experiments. The most stable and elevated values were recorded during Experiment 4 (classical music), suggesting that the enclosed environment efficiently retained moisture. This stable humidity may have supported the enhanced growth observed under classical music exposure.

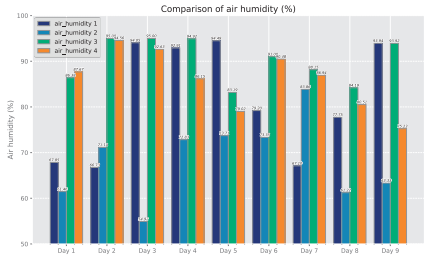


Figure 7. Air humidity comparison

Figure 8 presents soil moisture index trends, with values ranging from 0 (dry) to 6 (high moisture).

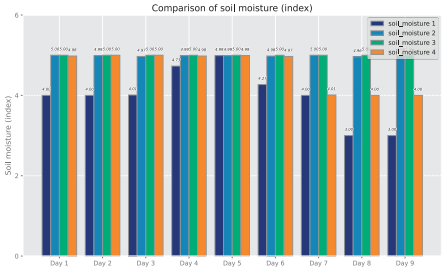


Figure 8. Soil moisture index

Most experiments maintained a consistent range between 3 and 5. Slightly more variability was observed in Experiment 3 (techno music), which may have contributed to the reduced plant growth and germination observed in that group.

Figure 9 depicts natural light levels across experiments, measured on a scale from 0 (complete darkness) to 10 (full daylight). Due to the shaded placement of the setup, natural light intensity remained low (~1.5). However, consistent supplemental lighting from the LED matrix ensured adequate photosynthetic conditions across all trials.

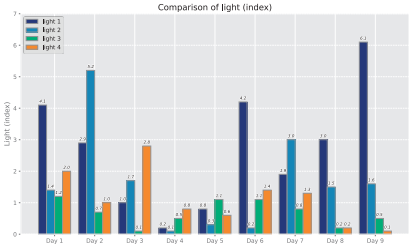


Figure 9. Light index comparison

Final comparative interpretation of prototype versions and music effects

To consolidate the findings, a final comparative analysis was conducted across all prototype versions, including earlier trials without musical treatment (Experiments 1.1 and 1.2) and later ones incorporating music (Experiments 3-6). Environmental variables were compared and visualized in Figures 10 to 14, with corresponding color codes provided in Table 7.

Table 7. Analysis - the legend of colours

Analysis - the legend of colours	
Analysis 1.1	Dark blue
Analysis 1.2	Steel blue
Analysis 3	Mediumseagreen
Analysis 4	Dark orange
Analysis 5	Salmon
Analysis 6	Orchid

All temperature values across experiments remained within the optimal range. Slightly elevated mean temperatures were recorded in Experiments 5 and 6 (meditation and classical music), yet these did not adversely affect plant growth, demonstrating effective thermal regulation by the system (Figure 10).

Experiment 4 (classical music) and Experiment 5 (meditation music) exhibited the most stable and elevated air humidity values (Figure 11).

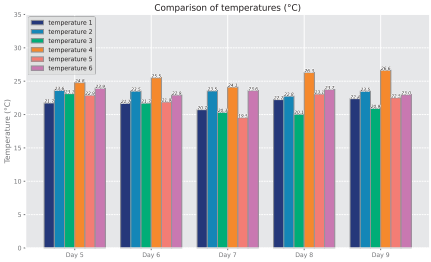


Figure 10. Comparative temperature trends

These findings support the hypothesis that stable humidity levels may contribute to improved germination and plant vigor. Greater variability was observed in Experiments 1.1 and 3 (no music and techno music), potentially correlating with less robust growth.

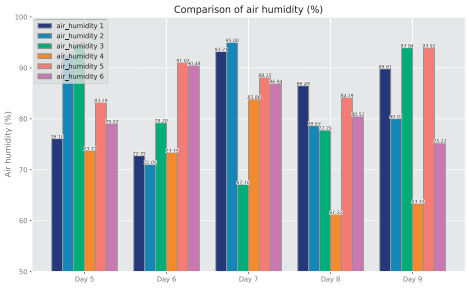


Figure 11. Comparative air humidity trends

Soil moisture remained within optimal levels in most experiments. However, Experiment 3 (techno music) exhibited lower and more fluctuating values, which may have hindered seedling development (Figure 12). This reinforces previous observations of suboptimal plant performance under techno exposure.

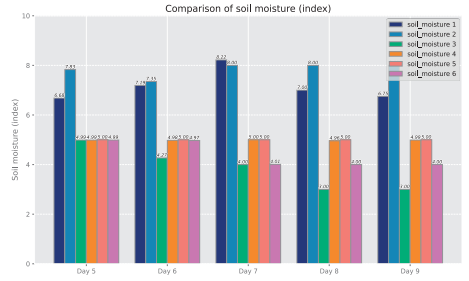


Figure 12. Comparative soil moisture trends

Light levels were consistently low throughout all experiments due to limited natural lighting. The LED matrix effectively compensated for this limitation. Slightly higher light index values were recorded in Experiment 4, possibly due to better placement and reflectivity within the setup (Figure 13).

Atmospheric pressure readings remained relatively stable across all trials (Figure 14). Slight increases were noted in Experiment 5, but no direct influence on plant development was observed. While atmospheric pressure is not typically a manipulated variable in greenhouse conditions, its consistency supports the overall environmental stability of the experimental setup.

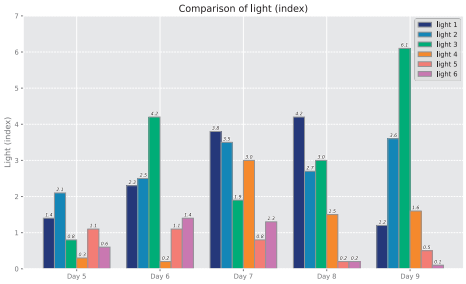


Figure 13. Comparative light intensity

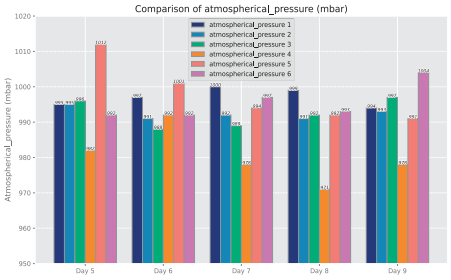


Figure 14. Comparative atmospheric pressure

CONCLUSIONS

The developed smart greenhouse prototype demonstrated effective control over key environmental parameters, outperforming traditional non-automated systems in maintaining stable conditions conducive to plant growth. The integration of sensor-based automation, cloud connectivity, and remote monitoring significantly enhances the system's potential for scalability and full automation in future applications.

Experimental results confirmed that music, particularly classical and meditation genres, served as a notable non-invasive stimulus influencing the physiological development of plants. Lettuce (*Lactuca sativa*) and radish (*Raphanus sativus*) responded positively to harmonic sound treatments, exhibiting increased plant height and greater leaf production under stable environmental conditions.

A detailed analysis of Figures 10-12 revealed a strong interdependency between temperature, air humidity, and soil moisture. Elevated temperatures correlated with increased humidity

- likely due to condensation effects within the enclosure - which in turn helped sustain optimal moisture levels. These dynamics were especially evident in Experiments 4 and 5 (classical and meditation music), where environmental consistency aligned with enhanced plant growth outcomes.

By contrast, Experiments 1.1 and 1.2 (no music) recorded slightly lower values for temperature and humidity, along with less vigorous plant development. This contrast suggests that musical stimulation may play a supportive role in enhancing plant physiological responses, possibly through mechanisms involving hormone regulation or photosynthetic efficiency.

Light intensity, shown in Figure 13, exhibited minimal variation across trials due to the continuous use of an LED lighting matrix. Although natural light contributions were low, consistent artificial lighting maintained photosynthetically active radiation levels sufficient for healthy growth. Observed phototropic behavior, where plants oriented toward the light source, further confirmed its effectiveness.

Atmospheric pressure, illustrated in Figure 14, remained stable across experiments. While no direct relationship was established between pressure fluctuations and plant morphology, its consistency reinforced the environmental control achieved by the prototype. Manipulating this variable for research purposes would require substantial structural modifications and was deemed impractical for small-scale implementations.

Collectively, these findings underscore the complex interplay between environmental variables and plant development. They highlight the value of precision agriculture tools, especially IoT-enabled systems, in advancing sustainable cultivation practices.

Despite its promising results, the study presents several limitations. The small sample size, short experiment duration, and limited variety of music genres constrain the generalizability of the findings. Future research should explore larger-scale prototypes, a broader range of plant species, and more diverse auditory stimuli to deepen our understanding of how environmental and acoustic factors synergistically influence plant development.

ACKNOWLEDGEMENTS

The authors acknowledge the support of the Center for Networking and Career Development in Research in the South-Muntenia Region (CNDCSM), within the framework of project PNRR-III-C9-2022 – I10, contract no. 5/16.11.2022. This work was conducted at Valahia University of Târgoviște as part of ongoing institutional research initiatives.

REFERENCES

Arduino (2025). *Arduino Nano 33 IoT datasheet*. Arduino Docs [Online], available: https://docs.arduino.cc/resources/datasheets/ABX00027-datasheet.pdf accessed on February 22, 2025.

BMP180 Barometric Pressure Sensor Hookup. (2025). SparkFun Electronics [Online], available: https://learn. https://learn.sparkfun.com/tutorials/bmp180-barometric-pressure-sensor-hookup-/all, accessed on February 22, 2025.

Dangi, N. (2017). *Monitoring environmental parameters: Humidity and temperature using Arduino-based microcontroller and sensors* (Bachelor's thesis). Helsinki Metropolia University of Applied Sciences.

Gitonga, N. S. (2020). *Design and fabrication of a greenhouse monitoring and control system based on GSM and Bluetooth* (Bachelor's thesis). Kenyatta University.

Joneus, F., & Ellingsen, A. (2020). *Smart greenhouse: System architecture for remote monitoring and control* (Bachelor's thesis, Computer Engineering). Halmstad University.

Keyestudio (KS0077) (2025). *Soil humidity sensor - Super Learning Kit for Arduino* [Online], available: https://wiki.keyestudio.com/KS0077(78,79)_Super_Learning_Kit_for_Arduino#Project_31:Soil_Humidity_Sensor, accessed on February 22, 2025.

Kurniawan, A. (2020). *Arduino Nano 33 IoT networking*. Apress. https://doi.org/10.1007/978-1-4842-6446-1_4

Lai, Y., & Wu, H. (2020). Effects of different types of music on the germination and seedling growth of alfalfa and lettuce plants. *AGRIVITA Journal of Agricultural Science*, 42(2), 197–204. https://doi.org/10.17503/agrivita.v0i0.2613

Mitova, I., Patamanska, G., & Gigova, A. (2021). Analysis of vegetative and reproductive growth of greenhouse tomatoes cultivated under drip irrigation and fertigation with increasing fertilizer rates. *Scientific Papers. Series E. Land Reclamation, Earth Observation & Surveying, Environmental Engineering*, 10, 152-157.

Natonis, M. M., Manu, L. L. K., Amleni, P. M. C., Nababan, D., Kelen, Y. P. K., & Sucipto, W. (2023). Smart greenhouse design based on Internet of Things (IoT) with microcontroller Arduino Uno. *Jurnal*

Teknik Informatika, 16(1), 35–44. https://doi.org/10.15408/jti.v16i1.30889

Raspberry Pi Foundation (2025). *Raspberry Pi 3 user manual*. https://us.rs-online.com/m/d/4252b1ecd92888dbb9d8a39b536e7bf2.pdf, accessed on February 22, 2025.

Wang, Y. (2017). *IoT device management and configuration* (Master's thesis). University of Saskatchewan, Canada.

Scientific Papers. Series E. Land Reclamation, Earth Observation & Surveying, Environmental Engineering. Vol. XIV, 2025
Print ISSN 2285-6064, CD-ROM ISSN 2285-6072, Online ISSN 2393-5138, ISSN-L 2285-6064

VEGETATION SURVEYS FOR MONITORING CO_2 GEOLOGICAL STORAGE SITES: A CASE STUDY FROM TWO ANALOGUE SITES FROM ROMANIA

Lia STELEA[1, 2], Alexandra-Constanța DUDU[1], Corina AVRAM[1], Gabriel IORDACHE[1], Constantin-Ștefan SAVA[1]

[1]National Institute for Research and Development on Marine Geology and Geoecology – GeoEcoMar, 23-25 Dimitrie Onciul Street, District 2, 024053, Bucharest, Romania
[2]University of Bucharest, 4-12 Regina Elisabeta Blvd, District 3, 030018, Bucharest, Romania

Corresponding author email: lia.stelea@geoecomar.ro

Abstract

Carbon capture and storage (CCS) is a promising solution for reducing carbon emissions, but the risk of CO_2 leakage requires monitoring. As part of project PN 23300404, we aim to develop an environmental monitoring methodology for onshore geological storage sites, evaluating vegetation surveys as a monitoring tool. In 2024, we conducted combined vegetation and geochemical surveys at two sites: Bodoc, an analogue for safe storage, and Băile Lăzărești, an analogue for CO_2 leakage. Using a grid-based sampling approach, we measured soil-flux and concentrations alongside floristic observations. At Bodoc, no significant relationship was observed between CO_2 levels and vegetation state. In contrast, at Băile Lăzărești, areas with high CO_2 concentrations had sparse vegetation and exposed soil, though these features were also present in some low-CO_2 areas due to landscaping. Follow-up surveys are planned for next year to determine the natural variability of the vegetation. Currently, we conclude that vegetation surveys have the potential to be used for leakage identification.

Key words: *CO_2 geological storage, monitoring, vegetation surveys, soil flux, natural analogues.*

INTRODUCTION

The sixth IPCC report (IPCC, 2023) states that the rise in average global temperature measured since preindustrial times is most likely caused by the anthropogenic greenhouse gas (GHG) emissions. Carbon capture and storage is a solution to reduce GHG emissions, recommended by the IPCC as needed, in order to achieve the climate targets (IPCC, 2022). One of the main challenges related to the deployment of this technology is mitigation of potential leakage risk and also assessing its potential impact on ecosystems (West et al., 2005).

The impact of a potential CO_2 seepage from an anthropogenic reservoir on vegetation is relevant considering that this information can be used as an early indicator of leakage (Noble et al., 2012).

Several studies have been made worldwide, based on natural analogues, highlighting the relationship between increased CO_2 concentration in soils, vegetation health and/or substitution of species. The effect of CO_2 can be direct or indirect through pH changes and the remobilisation of nutrients or toxic compounds (Noble et al., 2012). There have been two research directions: the first using controlled leakage sites and the second using natural analogues. The first research direction uses experimental field sites where CO_2 has been injected into soil and documents the effects on the ecosystems. The most important experimental sites are the ZERT site (Keith et al., 2009; Male et al., 2010) and ASGARD site (West et al., 2009). The second research direction is related to natural sites where CO_2 releases are present, such as Germany – Laacher See (Krüger et al., 2009, 2011), Greece – Florina basin (Ziogou et al., 2013), Italy - Latera (Beaubien et al., 2008; Oppermann et al., 2010) Slovenia – Stavešinci (Macek et al., 2005, Pfanz et al., 2007) and the United States – Mammoth Mountain (Bergfeld et al., 2006; Biondi & Fessenden, 1999; McFarland, Waldrop & Haw, 2013).

From previous research it was observed that botanical changes are site and species specific (Noble et al., 2012). Vegetation changes also

depend on factors like soil moisture and pH (Krüger et al., 2011). In general, plants are resistant to an increase in CO_2, with no obvious response at moderate concentrations (Bouma et al., 1997). Plants can show a decrease in height, root respiration and rooting depth (Nobel & Palta, 1989; Vodnik et al., 2006). They can also present yellowing or browning of leaves and other signs of stress following a rapid flux of CO_2 (Pfanz et al, 2011; West et al., 2009). Grasses generally dominate the high CO_2 sites (Beaubien et al., 2008; West et al., 2009). Depending on site, there can be potential bioindicator species like *Polygonum arenastrum* (Krüger et al., 2011), *Polygonum aviculare* (West et al., 2015) and *Minuartia glomerata* (Ziogou et al., 2013). Dead vegetation (e.g. Bergfeld et al., 2006) or the lack of plant cover (Beaubien et al., 2008) can also be indicators.

Romania offers a great potential for this type of studies, since there are many sites that could be used as natural laboratories. Considering this, two natural analogues have been selected as test areas in the framework of a nationally funded research project started in 2023 and aiming to develop an environmental monitoring methodology. The two selected sites are Bodoc (Covasna County), a natural analogue for safe storage and Lăzărești (Harghita County), a natural analogue for leakage of CO_2 in the near environment. On these two sites gas measurements and vegetation surveys have been conducted in September 2024.

MATERIALS AND METHODS

Study areas

Bodoc site corresponds with a carbonated mineral water reservoir. The location used for measurements is on a pasture for cattle on the outskirts of the Bodoc commune along the Borviz brook.

Geologically, the Bodoc area is located at the western limit of the Cretaceous flysch, intensely folded and faulted. The Cretaceous flysch deposits (Sânmartin-Bodoc strata) are composed of an alternation of sandstones, marls, shales and conglomerates. In the deposits of the basement rock there are medium depth aquifers and in the upper side there are post tectonic deposits of the sedimentary cover, with shallow aquifers.

The conglomerate facies, located in a synclinal structure, are strongly affected by tectonic movements (a series of transverse faults), responsible for the migration of mineral waters to the surface (Mutihac, 1990).

Bodoc is known for its mineral waters. On the left bank of Borviz brook there is the well F1 SNAM Talomir (presently in conservation) in Upper Pliocene-Quaternary deposits and on the right bank there is the well F2 SNAM, with oligomineral mineral water (SNAM, 2025).

Băile Lăzărești is situated next to Lăzărești village, within Cozmeni commune, approximately 16 km North-East from Băile Tușnad. It is renowned by highly concentrated carbon dioxide emissions which can exceed 85% in volume (Dudu et al., 2024). From a geological point of view, Băile Lăzărești area is situated on a succession of geological deposits, from the Cretaceous flysch (Sânmartin-Bodoc, Barremian-Albian strata) at the base, to the terrace deposits. The deep geological structure of the area is dominated by a fault system that includes geological complexes, facilitating the migration and distribution of post-volcanic emissions, such as mofettas or mineral water springs (Mutihac, 1990).

Flux and concentration measurements of soil gases

Soil flux and concentration measurements were done using the West Systems portable fluxmeter equipped with CO_2, CH_4 and H_2S sensors. The measurements were done at Bodoc site on two perimeters, one along the brook valley (P4) and one on a pasture for cattle (P3), with a variable sampling distance of 2 or 5 m. In total, 244 points were measured.

At Lăzărești site, gas measurements were done also on two perimeters, one in the area with the most important touristic features (basin, mineral spring and wet mofettas) (P1) and one on a hill recently landscaped on three terraces (P2). The sampling point were 5 m apart. 52 sampling points were measured in total.

Concentration and flux data was processed using FluxRevision software, provided by West Systems.

Vegetation surveys

The quantitative vegetation survey was done in the same place or in the immediate vicinity of the measurement point for gas flux and concentration, in order to correlate the dominance of a given type of vegetation and the concentrations of gases at the soil level at the same place. We used a rectangular quadrant with the sides of 50 cm placed in the points where gas measurements were done.

The interior of every quadrant was digitally photographed with the camera of a Xiaomi Poco M3 mobile phone in order to have a visual record and to analyse the abundance of different categories of vegetation and soil coverage. Digitally, by using the software GIMP 2.6, a grid of 25 points situated at equal distance was created inside the quadrant and the category where each element belongs for each point was selected.

For the quantitative survey there were used 107 points for Bodoc (Figure 1) and 52 points for Băile Lăzărești (Figure 2). Although in Bodoc area there were gas measurements done in 213 points, we chose just some of them for the vegetation survey, for logistic reasons. Also, four points with blurry photographs were eliminated.

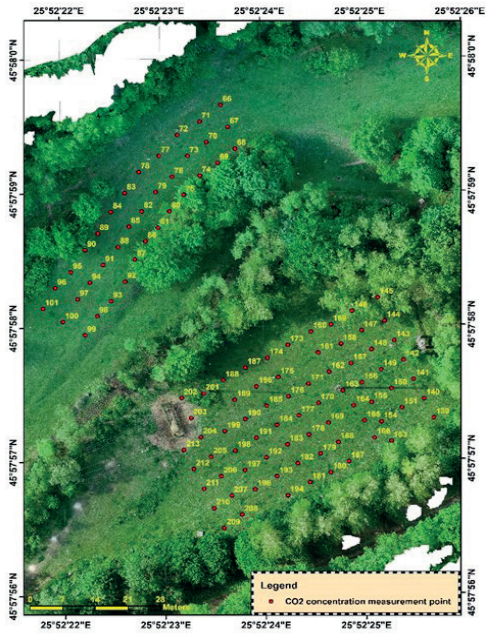


Figure 1. The network of points used at Bodoc for gas measurements and vegetation survey



Figure 2. The network of points used at Băile Lăzărești for gas measurements and vegetation survey

For this survey we intended to do a quantitative evaluation through the presence and dominance of some wide categories of herbaceous or small-sized plants, also considering their apparent state of health. Where possible, the main taxa of herbaceous plants were identified in order to offer us further clues about the character of the plant community.

The most common genera and species were readily identified, while the less common ones were identified using the mobile application iNaturalist (iNaturalist, 2024) through its dedicated function, with its observations georeferenced and made public through the GBIF (GBIF, 2024) network.

The following soil coverage categories were used:

1. dicotyledonous angiosperms (dicots) not known as indicators - healthy organs;
2. monocotyledonous angiosperms (monocots) - healthy organs;
3. herbaceous angiosperms - withered, yellowed, brown or dried organs;
4. mosses;
5. pteridophytes;

6. external (tree leaves, branches, litter etc.) or unidentified (shaded) elements;
7. bare ground;
8. known indicator plants from other studies: *Polygonum sp*., *Minuartia glomerata.*

The criteria according to which the categories 1 and 2 were selected are primarily from literature, where it was concluded that the monocotyledonous angiosperms are generally more frequent than dicotyledonous in areas with high CO_2 (Krüger et al., 2009; Krüger et al., 2011; Noble et al., 2012; West et al., 2009). Category 3 was selected because very high CO_2 emissions can make the plant organs appear yellow or brown (West et al., 2009), or can lead to their death (Bergfeld et al., 2006). Categories 4 and 5 can be dominant in certain locations although literature does not specify whether their presence is related to given CO_2 concentrations. Category 6 is neutral. At the highest level, long-term CO_2 emissions categories 7 or 8 can appear, bare ground or indicator plants. Concerning the latter, the genus *Polygonum* must be mentioned with the species mentioned as indicators in the literature *Polygonum arenastrum* (Krüger et al., 2009) and *Polygonum aviculare* (West et al., 2015), possible other members of the genus, as well as *Minuartia glomerata* (Ziogou et al., 2013), which was not found in the study area. However, the presence of *Polygonum* sp. isn't an unequivocal indication for the presence of high CO_2, being a very common genus present in anthropically disturbed areas.

Using the program Microsoft Excel and the photographs, as well as mapping techniques, we tried to highlight relationships between the percentual composition of soil coverage categories and the flux and concentration of the gases CH_4, CO_2 and H_2S. This was tested for both Bodoc and Băile Lăzărești.

RESULTS AND DISCUSSIONS

Flux and concentration measurements of soil CO_2

Four perimeters for the soil CO_2 concentrations were used: P1 and P2 at Băile Lăzărești, P3 and P4 at Bodoc, all considered separately.

P3 at Bodoc is the pasture for cattle, where the minimum concentration recorded is 413.8 ppm, the average 427 and the maximum is 483.5 ppm. P4 at Bodoc is close to the Borviz brook, with the minimum concentration recorded as 420.4 ppm, the average 438 ppm and maximum as 474 ppm (Figure 3).

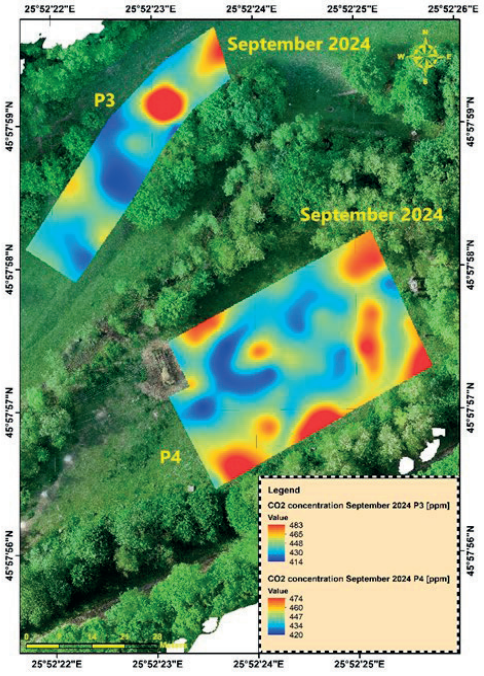


Figure 3. CO_2 concentrations at Bodoc

All these values are close to the background level and do not exceed 500 ppm. On the other hand, Băile Lăzărești have a minimum value of 516.6 ppm in P1 and a maximum measured value of 25863.2 ppm (Figure 4) and an average of 3240 ppm. However, the maximum measured value is not the maximum value for the area, which is probably found in the mofetta set up for tourists close to point 44 (Figure 2).

The perimeter P2 on the hillside has generally above background levels of CO_2, with a minimum of 428.9 ppm, an average of 743.7 ppm and a maximum of 1764.2 ppm (Figure 4).

Vegetation survey at Bodoc

The herbaceous vegetation consists of a cattle pasture in the vicinity of oak forest (Figure 1), with a slight slope in the upper area and flat in the brook area, separated by a slope with ungrazed vegetation. The upper area is shaped like a wide stripe, with the orientation NE-SW.

In the pasture area, the plants are generally no more than 5 cm high from the ground up, due to grazing, except some taxa like *Cirsium arvense*, *Urtica* sp. and *Plantago* sp. Grazing made the species hard to identify. The plants were generally affected by the drought, being withered, yellowed or dried as a result of unusually hot a hot and dry summer and autumn. More vigorous are the plants found close to Borviz brook or in the shade of the surrounding trees and shrubs. The human influence is visible because the upper part bears the traces of a construction's foundation and the lower part, next to the brook, contains several boreholes.

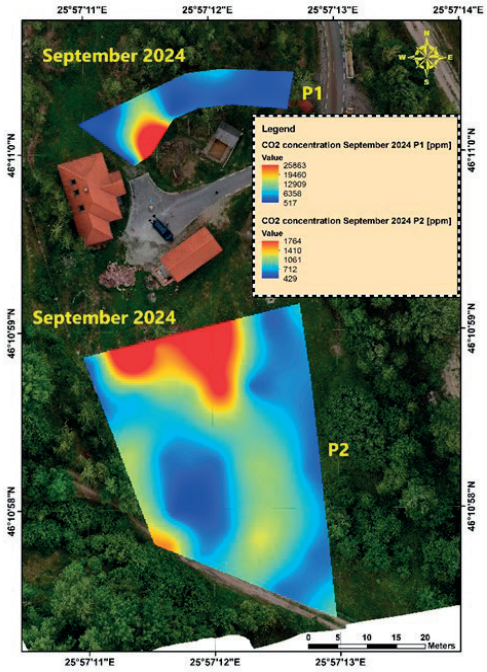


Figure 4. CO_2 concentrations at Băile Lăzărești

Vegetation survey at Băile Lăzărești

The study area has a strong anthropic footprint, being enclosed with a fence and has built structures for balneotherapy and some terracing works. The area has a marked, but not steep slope, with Northern exposure. The herbaceous vegetation doesn't have signs of intervention through grazing or mowing, but can be prevented to grow through treading, mulching or by the presence of balneotherapy constructions (Figure 2). Where present and their growth is not impaired, the herbaceous plants are generally vigorous. Some plants are yellowed in appearance. The trees and shrubs at the site are birches (*Betula pendula*), some small-sized willows (*Salix capraea*) and juniper (*Juniperus communis*).

Mosses are present, without being identified by genus or species. The pteridophytes found are *Lycopodium clavatum*, *Equisetum* sp., *Athyrium filix-femina* and *Pteridium aquilinum*. The dicotyledonous angiosperms are dominated by the families Asteraceae and Fabaceae, especially by the genus *Trifolium*.

Among the monocotyledonous angiosperms dominates the order Poales, with the family Poaceae with the genera *Poa* and *Phleum* and the species *Agrostis capillaris* and *Dactylis glomerata*. We can also find the families Cyperaceae and Juncaceae from the same order.

Comparative analysis

Comparing the two surveys, Bodoc has much more dry or yellowed vegetation compared with Băile Lăzărești, from exposure to the sun and drought probably (Figure 5). The shaded areas have greener plants, especially dicots. From a taxonomical viewpoint, in Băile Lăzărești dominate the monocots, approximately twice as abundant compared to dicots. In Bodoc area healthy monocots and dicots have approximately equal proportions, although the stressed angiosperms tend to be monocots, especially in the sunny areas (Figure 6). Dry or withered angiosperms were generally not identified by class, because they were harder to distinguish. In Băile Lăzărești, the stressed angiosperms (almost completely monocots) are found mostly in balneotherapy and terraced areas (Figure 7). We consider than the effect is probably caused by human activity.

An important mention is the absence of the indicator plants from all photographed quadrants. Although *Polygonum aviculare* was present in both areas, it wasn't found where gas measurements took place, but in the surrounding areas, disturbed by treading.

As neutral elements there are mosses, more frequent in Bodoc, and pteridophytes, more frequent in Băile Lăzărești. Due to the anthropically removed vegetation in Băile Lăzărești, there is a higher percentage of bare ground. In Bodoc, bare ground is present on patches of at most a few centimetres in length.

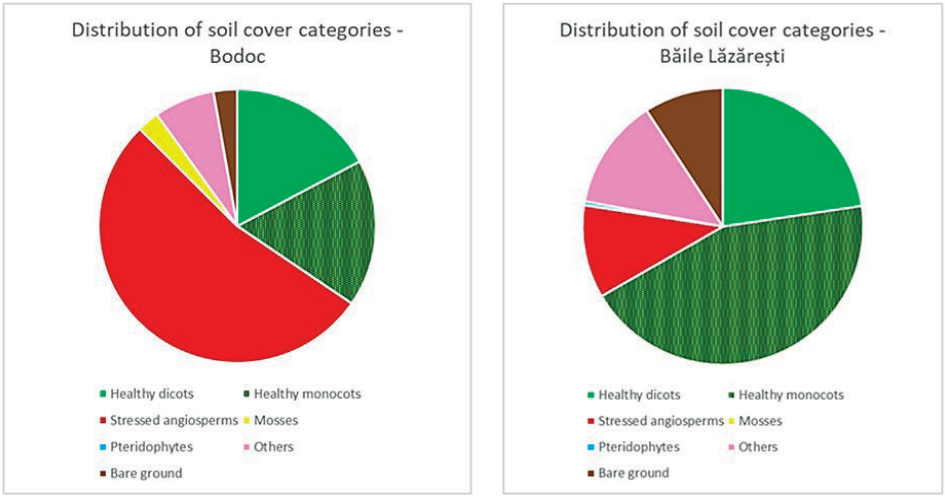


Figure 5. Distribution of soil cover categories at Bodoc and Băile Lăzărești

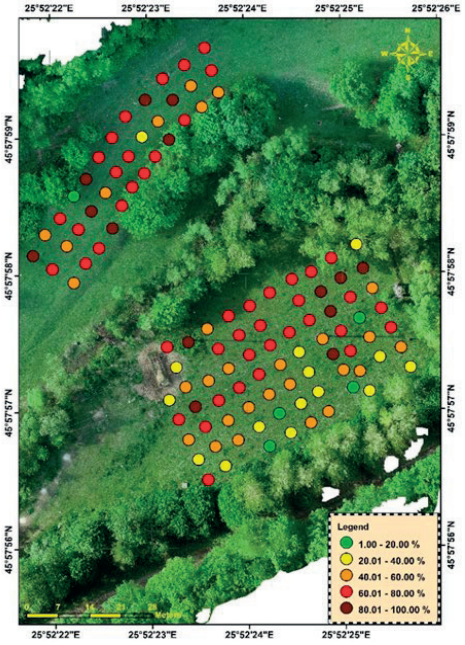


Figure 6. Stressed angiosperms at Bodoc (percentage of total soil coverage)

At Bodoc, most plants found are either stressed or dried. Healthy dicots predominate in the south-western part, which is an area shaded by trees. Healthy monocots seem to be distributed randomly. Increasingly towards the north-west, grows the relative dominance of the monocots over dicots, as well as that of the stressed plants of both classes. The most stressed plants and the most patches of bare ground are found in the upper, North-Western part (Figure 6).

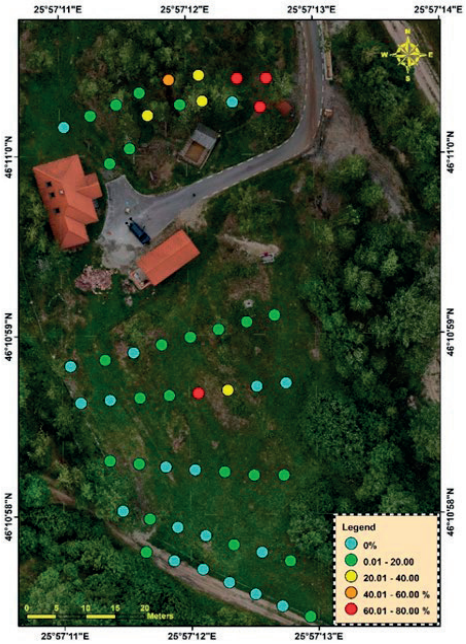


Figure 7. Stressed angiosperms at Băile Lăzărești (percentage of total soil coverage)

For Băile Lăzărești, most plants appear healthy, with a dominance of monocots. The dicots are mostly found in the upper Eastern part, while

the monocots are mostly found to the South-West. The most stressed plants are found in the lower, northernmost area, close to the spa facilities and in the areas where terracing works were done (Figure 7).

The relationship between the vegetation survey and the gas measurements in Bodoc and Băile Lăzărești

For Bodoc, we couldn't highlight the relationships between the composition of soil coverage categories and the higher fluxes or concentrations of CH_4, CO_2 and H_2S. The areas where slightly higher concentrations are present aren't significantly different floristically from the neighbouring areas which have smaller fluxes or concentrations.

For Băile Lăzărești, the points with the highest fluxes and concentrations of CO_2 and other gases are associated with the scanty vegetation, with some dried plants and exposed soil. Plants that are present are predominantly monocots (Poaceae), with some dicots (*Trifolium* sp.). The same soil coverage pattern is present on the stretches of soil where have not been recorded higher concentrations of CO_2 or other gases following the measurements. It is not excluded that those points may indicate intermittent gas sources, but which haven't been captured by measurements.

CONCLUSIONS

The survey represents a preliminary assessment of the herbaceous vegetation from the two studied areas, considering its usage as a bioindicator for carbon dioxide emissions. The selection of the coverage categories was made considering those present in the literature.

The floristic composition of the two areas is too different, thus they cannot be compared among themselves. The Bodoc study area is a cattle pasture, and in the case of Băile Lăzărești, there is an ecosystem without mammalian herbivores, but affected anthropically. Băile Lăzărești has plants of colder climate and higher humidity.

The vegetation succession in Bodoc is not related to the variations in CO_2. In Băile Lăzărești area, on stretches with higher CO_2 flux and concentration, the vegetation is partially absent and the soil is exposed, which could be due to gases, anthropic intervention or a mix of both.

As this is a preliminary study, there is a need for more detailed studies to make a better characterization of the vegetation of the area, using a denser sampling grid and, if possible, identifying all species present.

ACKNOWLEDGEMENTS

The research leading to these results was made within the project PN 23 30 04 04 "Development of an environmental monitoring methodology for potential CO_2 storage sites in Romania (Dezvoltarea unei metodologii de monitorizare de mediu pentru potențialele situri de stocare de CO_2 din România)", financed by the Ministry of Research, Innovation and Digitalization of Romania through the Core Program.

The authors would like to acknowledge and to thank for the support of town halls of Cozmeni and Bodoc, who facilitated the access to the site and the smooth running of the campaigns.

We also thank the anonymous reviewers for all suggestions provided for improving the manuscript.

REFERENCES

Beaubien, S.E., Ciotoli, G., Coombs, P., Dictor, M.C., Kruger, M., Lombardi, S., Pearce, J.M. & West, J.M. (2008). The impact of a naturally occurring CO_2 gas vent on the shallow ecosystem and soil chemistry of a Mediterranean pasture (Latera, Italy). *International Journal of Greenhouse Gas Control 2*(3).

Bergfeld, D., Evans, W.C., Howle, J., & Farrar, C.D. (2006). Carbon dioxide emissions from vegetation-kill zones around the resurgent dome of Long Valley caldera, eastern California, USA. *Journal of Volcanology and Geothermal Research*, *152*(1-2) 140–156.

Biondi, F., & Fessenden, J.E. (1999). Response of lodgepole pine growth to CO_2 degassing at Mammoth Mountain, California. *Ecology*, *80*(7), 2420-2426.

Bouma, T. J., Nielsen, K. L., Eissenstat, D. M. & Lynch, J.P. (1997). Estimating respiration of roots in soil: Interactions with soil CO_2, soil temperature and soil water content. *Plant and Soil*, *195*: 221–232.

Dudu, A.-C., Pavel, A. B., Avram, C., Catianis, I., Iordache, G., Rădulescu, F., Lupașcu, N., Dragoș, A.-G., Dobre, O., Sava, C.S. (2024) Environmental assessment of the area with natural CO_2 emissions in Băile Lăzărești. *Scientific Papers. Series E. Land Reclamation, Earth Observation & Surveying, Environmental Engineering, 13*.

GBIF (2024) https://www.gbif.org/ accessed September 2024

iNaturalist (2024) https://www.inaturalist.org/, accessed September, 2024.

IPCC (2022). Climate Change 2022: Mitigation of Climate Change. Contribution of Working Group III to the Sixth Assessment Report of the Intergovernmental Panel on Climate Change [P.R. Shukla, J. Skea, R. Slade, A. Al Khourdajie, R. van Diemen, D. McCollum, M. Pathak, S. Some, P. Vyas, R. Fradera, M. Belkacemi, A. Hasija, G. Lisboa, S. Luz, J. Malley, (eds.)]. Cambridge University Press, Cambridge, UK and New York, NY, USA. doi: 10.1017/9781009157926.002

IPCC (2023). Sections. In: Climate Change 2023: Synthesis Report. Contribution of Working Groups I, II and III to the Sixth Assessment Report of the Intergovernmental Panel on Climate Change [Core Writing Team, H. Lee and J. Romero (eds.)]. IPCC, Geneva, Switzerland, pp. 35–115, doi: 10.59327/IPCC/AR6-9789291691647

Keith, C.J., Repasky, K.S., Lawrence, Rick L., Jay, S.C., & Carlsten, J.L. (2009) Monitoring effects of a controlled subsurface carbon dioxide release on vegetation using a hyperspectral imager. *International Journal of Greenhouse Gas Control 3*: 626–632.

Krüger, M., West, J., Frerichs, J., Oppermann, B., Dictor, M.C., Jouliand, C., Jones, D., Coombs, P., Green, K., Pearce, J., May, F., Moller, I. (2009). Ecosystem effects of elevated CO_2 concentrations on microbial populations at a terrestrial CO_2 vent at Laacher See, Germany. *Energy Procedia I*: 19331939.

Krüger, M., Jones, D., Frerichs, J., Oppermann, B. I., West, J., Coombs, P., Green, K., Barlow, T., Lister, R., Shaw, R., Strutt, M., & Moller, I. (2011). Effects of elevated CO_2 concentrations on the vegetation and microbial populations at a terrestrial CO_2 vent at Laacher See, Germany. *International Journal of Greenhouse Gas Control*, 5(4), 1093–1098.

Macek, I., Pfanz, H., Francetik, V., Batic, F., & Vodnik, D. (2005). Root respiration response to high CO_2 concentrations in plants from natural CO_2 springs. *Environmental and Experimental Botany*, *54*(1)

Male, E. J., Pickles, W. L., Silver, E. A., Hoffmann, G. D., Lewicki, J., Apple, M., Repasky, K., & Burton, E. A. (2010). Using hyperspectral plant signatures for CO_2 leak detection during the 2008 ZERT CO_2 sequestration field experiment in Bozeman, Montana. *Environmental Earth Sciences*, 60, 251–261.

McFarland, J. W., Waldrop, M. P., & Haw, M. (2013). Extreme CO_2 disturbance and the resilience of soil microbial communities. *Soil Biology and Biochemistry*, 65, 274–286.

Mutihac, V. (1990). *Structura geologică a teritoriului României*. Ed. Tehnică, București.

Nobel, P. S., & Palta, J. A. (1989). Soil O_2 and CO_2 effects on root respiration of cacti. *Plant and Soil*, 120, 263–271.

Noble, R. R. P., Stalker, L., Wakelin, S. A., Pejcic, B., Leybourne, M. I., Hortle, A. L., & Michael, K. (2012). Biological monitoring for carbon capture and storage - A review and potential future developments. *International Journal of Greenhouse Gas Control*, 10, 520–535.

Oppermann, B. I., Michaelis, W., Blumenberg, M., Frerichs, J., Schulz, H. M., Schippers, A., Beaubien, S. E., & Kruger, M. (2010). Soil microbial community changes as a result of long-term exposure to a natural CO_2 vent. *Geochimica et Cosmochimica Acta*, *74*(9), 2697–2716.

Pfanz, H. (2011). Life in dry, terrestrial mofette areas. *IEAGHG Summary Report of the IEGHG Workshop of Natural Releases of CO_2: Building Knowledge for CO_2 Storage Environmental Impact Assessments*, 25–26.

Pfanz, H., Vodnik, D., Wittmann, C., Aschan, G., Batic, F., Turk, B., & Macek, I. (2007). Photosynthetic performance (CO_2-compensation point, carboxylation efficiency, and net photosynthesis) of timothy grass (Phleum pratense L.) is affected by elevated carbon dioxide in post-volcanic mofette areas. *Environmental and Experimental Botany*, *61*(1), 41–48.

SNAM (2025) Deposit presentation. Specialized data on the deposit (in Romanian). *SNAM (National Society for Mineral Waters)*. Retrieved from: https://snam.ro/images/resurse/prezentare-zacamant-talomir-bodoc.pdf . Accessed 20.03.2025.

Vodnik, D., Kastelec, D., Pfanz, H., Macek, I., & Turk, B. (2006). Small-scale spatial variation in soil CO_2 concentration in a natural carbon dioxide spring and some related plant responses. *Geoderma*, *133*(3–4), 309–319.

West, J.M., Jones, D. G., Annunziatellis, A., Barlow, T. S., Beaubien, S.E., Bond, E., Breward, N., Coombs, P., de Angelis, D., Gardner, A., Gemeni, V., Graziani, S., Green, K.A., Gregory, S., Gwosdz, S., Hannis, S., Kirk, K., Koukouzas, N., Kruger, M., Libertini., S., Lister, T.R., Lombardi, S., Metcalfe, R., Pearce, J.M., Smith, K.L., Steven, M.D., Thatcher, K., Ziogou, F. (2015). Comparison of the impacts of elevated CO_2 soil gas concentrations on selected European terrestrial environments. *International Journal of Greenhouse Gas Control 42*: 357–371.

West, J. M., Pearce, J. M., Coombs, P., Ford, J. R., Scheib, C., Colls, J. J., Smith, K. L., & Steven, M. D. (2009). The impact of controlled injection of CO_2 on the soil ecosystem and chemistry of an English lowland pasture. *Energy Procedia*, 1, 1863–1870.

West, J. M., Pearce, J., Bentham, M., & Maul, P. (2005). "Issue Profile: Environmental issues and the geological storage of CO_2." *European Environment 15*: 250–259.

Ziogou, F., Gemeni, V., N. Koukouzas, N., de Angelis, D., Libertini, S., Beaubien, S. E., Lombardi, S., West, J.M., Jones, D.G., Coombs, P., Barlow, T.S., Gwosdz, S., Kruger, M. (2013). Potential environmental impacts of CO_2 leakage from the study of natural analogue sites in Europe. *Energy Procedia* 37: 3521–3528.

Scientific Papers. Series E. Land Reclamation, Earth Observation & Surveying, Environmental Engineering. Vol. XIV, 2025
Print ISSN 2285-6064, CD-ROM ISSN 2285-6072, Online ISSN 2393-5138, ISSN-L 2285-6064

STUDIES SUPPORTING THE DESIGNATION OF A NEW NATURA 2000 SITE: BAHNELE BANCULUI NORD

Sorin ȘTEFĂNUȚ, Florența-Elena HELEPCIUC, Constantin-Ciprian BÎRSAN, Georgiana-Roxana NICOARĂ, Tiberiu SAHLEAN, Gabriela TAMAS, Gabriel-Mihai MARIA, Viorel-Dumitru GAVRIL, Miruna-Maria ȘTEFĂNUȚ, Larisa-Isabela FLORESCU, Mirela-Mădălina MOLDOVEANU, Constanța-Mihaela ION, Ana-Maria MOROȘANU

Institute of Biology Bucharest of the Romanian Academy,
296 Splaiul Independenței, District 6, 060031, Bucharest, Romania

Corresponding author email: florenta.helepciuc@ibiol.ro

Abstract

The Bahnele Bancului peatlands, located in Suceava County, were selected for restoration due to multiple threats, such as habitat degradation, overgrazing, and drainage. The peatland currently faces an unfavourable conservation status, with Picea abies trees, over 80 years old, being the dominant vegetation. By integrating national moss species surveys with ongoing peatland restoration efforts, local research has been significantly supported. Field assessments conducted between 2022 and 2023 revealed valuable species and habitat data. Buxbaumia viridis (Moug. ex Lam. & DC.) Brid. ex Moug. & Nestl., a key moss species that serves as an indicator of well-preserved spruce forests and is protected by the EU Habitats Directive, was identified on the site in June 2022. In addition, priority habitats, such as 91D0 Bog Woodland were observed, with notable species including Sphagnum spp., the rare orchid Epipactis helleborine, and the Carpathian newt (Lissotriton montandoni). These findings have contributed to the completion of the Natura 2000 site designation forms, which include detailed habitat and species data along with a map, highlighting the site's importance for conservation.*

Key words*: bryophytes, threatened species, bog woodland.*

INTRODUCTION

The European network of natural areas, Natura 2000, serves as an umbrella for the long-term conservation of valuable natural habitats in accordance with the Habitats Directive 92/43/EEC, as well as for the protection of threatened flora and fauna species. Peatland habitats play a critical role in environmental preservation and climate change mitigation. Reducing carbon loss in peatlands, which store significantly more carbon than the world's tropical rainforests, means an important reduction in global greenhouse gas emissions (Page & Baird, 2016).

Given their importance and the imperative need to protect these peatland habitats vital for certain species of conservation concern, proposing the inclusion of Bahnele Bancului North (BBN) peatland within the Natura 2000 network represents the most appropriate solution. This will help protect the included Bog Woodland habitat (91D0*) as well as conserve *Buxbaumia viridis* (Moug. ex Lam. & DC.) Brid. ex Moug. & Nestl. (Ștefănuț et al., 2023) and *Lissotriton montandoni* (Carpathian newt) protected species.

According to Steinacker et al. (2019), Bog Woodlands (91D0*) represent the most threatened forest habitats due to their heightened vulnerability to climate change. They advocate for expanding the Natura 2000 network to reduce non-climatic stressors on this habitat, and to support climate change mitigation efforts.

Consistent with the current study, the research conducted by Ștefănuț et al. (2023) provides fundamental support for the proposal to designate new Natura 2000 sites, including BBN peatland. Given that habitat 91D0* is a priority habitat under the EU Habitats Directive (Annex I), also found in the BBN site and hosting moss species such as *B. viridis* and *Sphagnum* spp., and considering Law 49/2011, which ratifies GEO 57/2007 and emphasizes the necessity of designating special conservation areas to ensure their long-term preservation, we prioritized the

BBN peatland proposal under the Natura 2000 framework. Moreover, the solution also supports the EU Biodiversity Strategy for 2030, which calls for strict protection of 10% of the terrestrial area and the preservation of 30% of it by that year (European Commission, 2020) and to reach the Kunming-Montreal Global Biodiversity Framework Target 2 (CBD Secretariat, 2022).

The aim of this study was to assess the BBN site's degradation degree, pinpoint the limiting factors that have impacted the condition of this delicate habitat, outline the methodology employed to efficiently restore the site, and emphasize the importance of implementing legal measures to protect the site by legislation. By adding the BBN peatland to the Natura 2000 network as a Special Area of Conservation (SAC), the main goal is to guarantee its long-term conservation in optimal conditions.

MATERIALS AND METHODS

Site location and description

The BBN peatland is located in the northern region of the Eastern Carpathians and the western part of the Dornelor Depression, southwest of Suceava County. At 898 m a.s.l. elevation, the site's eastern boundary follows the Bancu (Coșnița) stream and the DC 85B communal road (Figures 1 and 2); here, the soil is classified as eutrophic peat. The terrain becomes forested at higher elevations, initially with peaty soil, then developing into a spruce forest with shallow soil, reaching an elevation of up to 970 m a.s.l.

The BBN site's geographical coordinates, covering an area of 18.85 ha, are 47°23'40.743"N 25°11'38.713"E. The BBN site belongs to the North-East administrative region, NUTS level 2 code RO 21, and is entirely located within the Alpine biogeographical region.

This peatland is owned by the Dorna Candrenilor Commune town hall and is not included in the protected natural areas managed by the National Agency for Protected Areas (ANANP).

Evaluation and monitoring activities

In the last years, many efforts have been made by several European countries to adopt national peatland restoration and conservation strategies and ensure their sustainable use. The Institute of Biology of the Romanian Academy Bucharest has also made such efforts between 2022 and 2024. Along with six other sites from the Suceava and Maramureș counties, the BBN peatland was included in the restoration process through the project "*Degraded mires and peatlands restoration of North-East 2 region of Romania (PeatRO3)*" (https://www.ibiol.ro/peatro3/index.htm) funded through EEA Grants mechanisms.

Considering the sensitivity of peatland habitats to biotic and abiotic factors, the evaluation and monitoring activities were designed accordingly. In the first stage, an initial assessment of the peatland conservation status was made, evaluating pressures and threats, vegetation changes, and the indicator species (several taxonomic groups have been inventoried), but also measuring the groundwater level and some environmental variables (water physicochemical parameters, air physical parameters). Subsequently, the monitoring was carried out over the period from 2022 to 2024.

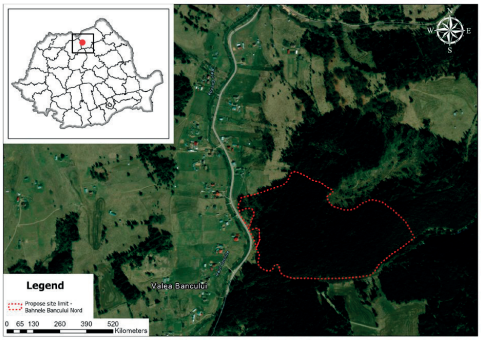


Figure 1. Geographical limits of the BBN proposed site as a SAC, under Natura 2000 network



Figure 2. The site layout next to the DC 85B communal road (drone image) (photo by Bîrsan C.)

The site pressures and threats caused by anthropic and environmental factors were detected throughout the monitoring and restoration period, the codes being assigned according to the European Environment Agency's updated list (2024).
Experts used drones (DJI Mini 2) and cameras to evaluate the vegetation changes and identification keys to assess the indicator species. Field surveys were conducted alongside these methods, allowing experts to identify plant species *in situ*, determine their proportions within the floristic composition, and study the site's conservation value. The nomenclature of plant species follows Sârbu et al. (2013), while habitat types are classified according to the *Interpretation Manual of Natura 2000 Romanian Habitats* (Gafta & Mountford, 2008; Doniță et al., 2005).
The site's water level was measured using five piezometers: four installed in the northern, eastern, southern, and western parts, and the fifth in the site's center. The water level in the five piezometers was recorded at different times during the monitoring process (June 2023, October 2023, April 2024).
The water physicochemical parameters (pH, oxidation-reduction potential− ORP, dissolved oxygen− DO, conductivity, total dissolved solids− TDS, turbidity, and temperature) were measured using the HI9829 multiparameter instrument (Hanna Instruments).
Furthermore, air physical parameters (temperature, relative humidity, and dew point) were measured every 30 minutes using EasyLog EL-USB 2 Data Loggers (DL) placed in two different locations (DL 1: 47°23.754'N 25°11.430'E; DL 2: 47°23.734' N 25°11.455' E).

Reconstruction activities
The restoration activities were determined based on the initial pressure and threats identified.

Barrage construction
In October 2023, a dam with 47°23'45.1"N 25°11'25.2"E coordinates was built to maintain the peatland's optimal hydrological level. The barrage, which measured 40 cm x 300 cm in dimensions, was constructed using natural materials: wooden spikes made from fallen trees on the site, untreated wooden planks, and soil, which were covered with local vegetation (Figure 3).



Figure 3. The barrage built to limit the water flow from the BBN peatland (arrow - the flow direction of the drainage ditch towards DC 85B and the Bancu River)

Water pond construction
To attract some characteristic invertebrates, a 20 sqm water pond (47°23'45.35" N 25°11'25.47" E) with a depth of 50 cm was constructed in September 2022 (Figure 4).



Figure 4. The water pond constructed in BBN peatland

Waste collection
Waste found in different areas of the BBN peatland was collected manually in garbage bags and then transported by the local authorities to specially designed places.

RESULTS AND DISCUSSIONS

Pressures and threats
After the initial evaluation, we found that the BBN peatland has an unfavorable conservation status. This was evidenced by the substantial garbage deposits (Figure 5), low water table caused by drainage through an artificial ditch, which is the main threat in the marshes throughout Europe (Figure 6), overgrazing, and significant vegetation changes with transition to

spruce afforestation (Figure 7), and other pressures and threats (Table 1).



Figure 5. Significant garbage deposits inside BBN



Figure 6. Drainage ditch at the perimeter of the site



Figure 7. Transition of the vegetation to spruce afforestation

Table 1. Main pressures and threats of BBN peatland

Code	Pressure/threat name 2019-2024
PA08	Extensive grazing or undergrazing by livestock
PB01	Conversion to forest from other land uses, or afforestation (excluding drainage)
PB05	Logging without replanting or natural regrowth?
PB23	Physical alteration of water bodies for forestry (including dams)
PE01	Roads, paths, railroads and related infrastructure
PF06	Deposition and treatment of waste/rubbish from built-up areas
PF07	Residential and commercial activities and structures generating pollution to surface or ground waters
PF13	Drainage, land reclamation and conversion of wetlands, marshes, bogs, etc. for built-up areas
PJ01	Temperature changes and extremes due to climate change
PJ03	Changes in precipitation regimes due to climate change

Site's importance: habitats and flora

While the lowest part of the site appears as an eutrophic swamp, as elevation increases, the landscape transitions into a wooded area, first with peaty soil and then into a spruce forest on shallow soil, extending up to an altitude of 970 m.

The marshy area covers approximately 2.28 ha and is characterized by a eutrophic wetland with a shallow peat layer that has not yet been entirely isolated from infiltrating groundwater. Over time, this area may develop into a peat bog if the peat layer becomes sufficiently thick to detach from the influence of mineral-rich infiltration water (Pop, 1960). The plant species recorded in this area include: *Alnus incana* (L.) Moench, *Betula pendula* Roth, *Rhamnus frangula* L., *Salix caprea* L., *Sorbus aucuparia* L., *Caltha palustris* L., *Cirsium palustre* (L.) Scop., *Epilobium palustre* Willd., *Equisetum sylvaticum* L., *Filipendula ulmaria* (L.) Maxim., *Galium palustre* L., *Juncus effusus* L., *Lychnis flos-cuculi* L., *Lycopus europaeus L., Myosotis scorpioides* L., *Potentilla erecta* (L.) Raeusch., *Scirpus sylvaticus* L., *Urtica dioica* L.

The forested area covers 97.72 ha, consisting primarily of coniferous forests. The site is of significant conservation value due to the presence of two habitats of Community

importance: priority habitat **91D0*** Bog woodland that provides habitat for notable moss species such as *B. viridis* and *Sphagnum* spp., and also habitat **9410** Acidophilous Picea forests of the montane to alpine levels (Vaccinio-Piceetea) that hosts several important plant species, including *Sphagnum* spp., *Epipactis helleborine* (L.) Crantz, *Lycopodium annotinum* L., and *Lycopodium clavatum* L.

The **91D0*** Bog woodland habitat covers 1.54 ha of the site and consists primarily of coniferous forests. The tree layer is dominated by spruce (*Picea abies* (L.) H. Karst.), with scattered occurrences of *Pinus sylvestris* L., *Betula pendula*, *Rhamnus frangula*, and *Salix caprea*. In the most oligotrophic areas of the forest, the ground layer is dominated by a thick carpet of Sphagnum moss, often forming dense accumulations at the base of spruce trees. The characteristic moss *Sphagnum squarrosum* Crome exhibited healthy growth and adequate hydration (Figure 8). The understory vegetation is sparse, with only a few recorded species, including *Athyrium filix-femina* (L.) Roth, *Maianthemum bifolium* (L.) F.W.Schmidt, *Vaccinium myrtillus* L., and *Vaccinium vitis-idaea* L. Of particular conservation interest is the presence of *B. viridis*, a species of Community interest, which was observed growing on decomposing fallen logs in various stages of decay.



Figure 8. *Sphagnum squarrosum* in the BBN peatland (photo by Ștefănuț M.M.)

The majority of the investigated area is occupied by the **9410** Acidophilous Picea forests of the montane to alpine levels (Vaccinio-Piceetea) habitat, covering 16.88 ha. The tree layer consists almost exclusively of spruce (*Picea abies*), with occasional occurrences of *Fagus sylvatica* L., and *Sorbus aucuparia.* The shrub layer is poorly developed, with scattered individuals of *Sorbus aucuparia*, *Salix caprea,* and *Sambucus racemosa* L. The herbaceous layer is unevenly distributed, forming patches depending on the amount of light reaching the forest floor. Recorded species include *Oxalis acetosella* L., *Cardamine glanduligera* O.Schwarz, *Campanula abietina* Griseb., *Dryopteris filix-mas* (L.) Schott, *Vaccinium myrtillus, Athyrium filix-femina*, *Maianthemum bifolium, Epipactis helleborine*, *Lycopodium annotinum*, and *Lycopodium clavatum*.

Among the recorded species, *Lycopodium annotinum* and *Lycopodium clavatum* are species of Community interest (Figure 9). They are included in Annex V of the Habitats Directive due to their slow growth and sensitivity to habitat disturbances. These clubmosses are important in forest ecosystems, forming dense mats contributing to soil stabilization and moisture retention. *Epipactis helleborine* is an orchid species listed on the National Red List (Oltean et al., 1994) and included in CITES Appendix II, highlighting its conservation concern.



Figure 9. *Lycopodium clavatum* (left) and *Lycopodium annotinum* (right) (photo by Nicoară G.-R.)

In Romania, according to the European Environmental Agency (EUNIS), 91D0* habitat is already protected in 27 Natura 2000 sites (*Bog Woodland. EUNIS*), while 9410 habitat is protected in 66 Natura 2000 sites (*Acidophilous Picea forests of the montane to alpine levels, Vaccinio-Piceetea, EUNIS*).

Following the inventory of some animal and plant groups, two species protected under the EU Habitats Directive were identified: *B. viridis* and *Lissotriton montandoni* (Carpathian newt).

The Carpathian newt (*Lissotriton montandoni*, Figure 10) was found in April 2024 at the edge of the BBN site (coordinates: 47.396137° N,

25.190248° E), and we only observed one male. Although locally abundant in its distribution range, the species is endemic to the Carpathian Mountains, where it is distributed primarily in the Eastern Carpathians and partially in the Southern Carpathians from 200 to 1900 meters a.s.l. Its terrestrial habitats are represented mainly by moist deciduous, coniferous, or mixed forests, and meadows. Sometimes individuals can be found above the tree line in alpine habitats. The species is mainly affected by the destruction and modification of aquatic breeding habitats. Listed as Least Concern (LC) by the IUCN Red List, the Carpathian newt nevertheless has a descending population trend, although it is protected by the Bern Convention and the Habitats Directive, as well as Laws 13/1993 and 49/2011 in Romania.



Figure 10. *Lissotriton montandoni* in the BBN peatland (Carpathian newt) (photo by Maria G., April 2024)



Figure 11. Mature sporophyte of *Buxbaumia viridis* in the BBN peatland (photo by Ștefănuț S., June 2022)

B. viridis, an important moss species that indicates well-preserved spruce woods, was discovered in the BBN site 91D0* on June 23, 2022 (Ștefănuț et al., 2023). Six individuals were located on a decayed coniferous log at an altitude of 900 m a.s.l., facing west, (47°23'43.8" N 25°11'27.2" E, 895 m a.s.l.) (Ștefănuț et al., 2023) (Figure 11). On April 12, 2024 two individuals were found in the same spot (Figure 12).



Figure 12. Sporophytes of *Buxbaumia viridis* in the BBN peatland (photo by Ștefănuț S., April 2024)

B. viridis is a circumpolar species that is found in Europe, North America, and East Asia. It is also found in Romania in the Alpine bioregion. Sapro-lignical, characteristic of natural and mature spruce forests, *B. viridis* primarily grows on dead wood; however, it can also be rarely found on wood remnants on the ground (Deme et al., 2020; Kropik et al., 2020). It prefers wood in an advanced stage of decay, and it could be found on large fallen trunks and stumps, especially conifers, particularly those close to the streams, because it needs high humidity (Ștefănuț et al., 2023; Puntillo & Puntillo, 2024). However, it has also been found on beech, birch, mountain ash, maple and alder. These special requirements, along with its small size, dioecy, short life span, and low competitiveness with other larger bryophytes, cause its scarcity (Wiklund, 2002). Kropik et al. (2020) state that the climate has the most significant influence on the occurrence of *B. viridis*, with the dead wood quality coming secondarily.

B. viridis has a small size (10-18 cm), with a reduced gametophyte and a well-developed sporophyte, with brown setae that measure 5-10

mm, and a large, green capsule that measures 5-7 mm (Mihăilescu et al., 2015). The upper side of the capsule is slightly flattened, and the cuticle of the capsule exfoliates at maturity. Being an annual, acrocarpous, and dioecious species, *B. viridis* depends on the distance between the male and female bryospores to germinate as well as the existence of a water film that facilitates the antherozoid's progression towards the female (Ștefănuț et al., 2023).

While the gemmae are produced all year round, the juvenile sporophyte individuals start to develop in the fall, and around half of them die before they reach maturity in the summer (Deme & Csiky, 2021); both freezing followed by drought can hinder the development of sporophyte (Dierssen, 2001; Wiklund, 2002). According to Guillet et al. (2021), one of the most important factors influencing the presence of sporophytes− which are regarded as poor competitors (Hola et al., 2014)− may be the humidity. Due to its high-water level and forestation, the BBN peatland offers this protected species an ideal habitat.

Legally protected in Europe by Annex I of the Bern Convention, Annex II of the Habitat-Fauna-Flora Directive *(Directive 92/43/CEE),* and first included in the European List of Bryophytes as a Critically Endangered category - CR (Schumacker and Martiny, 1995)− *B. viridis* was also recently added to the new European Red List's Least Concern group species (Hodgetts et al., 2019). Plášek (2004) suggests that the species needs to be conserved in protected areas designated under the Natura 2000 network.

In a previous study, Ștefănuț et al. (2023) recommended reclassifying the conservation status in Romania of *B. viridis* from Endangered - EN A3c; C1 (Hodgetts and Lockhart, 2020; Ștefănuț & Goia, 2012) to Vulnerable - VU A3c. According to the European Environment Agency EUNIS, *B. viridis* is already protected in about 532 Natura 2000 sites across 18 countries (*Buxbaumia viridis*, *EUNIS*). In Romania, the species is protected in 11 Natura 2000 sites (*Buxbaumia viridis*, *EUNIS*). In the meantime, new reports of this species have been made for both Natura 2000 sites and areas not currently protected, supporting the update of management plans as well as declaring new sites.

The uniqueness and significant conservation value of the site are primarily defined by the presence of two habitats of Community importance (habitat 91D0* Bog Woodland and habitat 9410 Acidophilous Picea forests of the montane to alpine levels) and the occurrence of protected species, specifically *B. viridis* and the endemic *L. montandoni*. The distribution of *B. viridis* is well-documented in the Southern Carpathians, including protected sites, whereas in the Eastern Carpathians, it remains less studied. Consequently, distribution data in this region is scarce, highlighting the need to establish new protected areas in alignment with the EU's Biodiversity Strategy for 2030 (European Commission, 2020).

Restoration efforts - preliminary results

The PeatRO3 project's reconstruction efforts in the BBN peatland were designed to rebalance the ecosystem. One of the main targets was restoring the optimal hydric regime by reducing water loss through the drainage ditches. This goal was achieved by building a barrage across the drainage channel. This measure will encourage the growth of native plant species and limit the emergence of invasive vascular plant species. As a result, the ecosystem can function independently, self-regulate, and develop into an active peat bog that sequesters carbon dioxide through peat production.

The water pond construction aimed to attract invertebrate species such as the protected species *Leucorrhinia pectoralis* (Charpentier, 1825) (Natura 2000). Like other odonates, this species' life cycle depends on a water body, as they lay eggs on the water surface or aquatic vegetation. Dragonfly species can colonize a new water pond in three years after restoration (Elo et al., 2015). In the case of the BBN peatland, if the hydric level increases and remains at an optimum level, the newly formed water ponds can be colonized by *Leucorrhinia pectoralis* (Charpentier, 1825), as a high number of individuals have been reported in the nearby located Pilugani peatland (Manci & Iorgu, 2021).

After waste collection and disposal in September 2022 and October 2023 (25 garbage bags), an informative panel mentioning the restricted activities was placed at the site entrance (Figure 13) to minimize further

garbage accumulation. Besides interdicting garbage disposal, the panel also contains warning messages aimed at restricting other harmful anthropic activities such as grazing and tree cutting. Also, by scanning the QR codes (in Romanian and English) installed on the panel, visitors and local community members can access details about the restoration project, the eco-touristic potential of the site, and additional information on responsible behaviour, thus contributing to the long-term success of habitat preservation.

In their study, Strzelecka et al. (2022) emphasize the importance of a strong link between the residents' relationship with nature and the conservation policies, thus resulting in the need to engage them in various forms of nature stewardship. A better understanding of the residents' bond with nature, an "engagement in" approach through a collaboration that reduces pressures on the habitat (in our case grazing, waste disposal, etc.), will strengthen the connection between nature and the local community, which is directly involved in protecting the site (Restall et al., 2021).



Figure 13. The billboard from the entrance to the site

Monitoring Results - preliminary effects

At the BBN peatland, piezometer data readings indicated optimal hydration, albeit with uneven water distribution across the ecosystem. These variations were influenced by the site topography, the presence of water sources, and the peat`s capacity to retain moisture. Measurements of water level variations from the piezometers undertaken within the site between October 2023 and April 2024 revealed a general increase in hydration with 8, -1, 6.5, -4, and 6 cm, respectively, indicating an improvement in the peatland`s water retention capacity.

Two EasyLog EL-USB 2 Data Loggers (DLs) recorded the meteorological parameters: temperature, humidity, and dew point (Figures 14 and 15). Unlike temperature and dew point, which exhibited constant trends across the two monitoring points (corresponding with normal monthly and seasonal variations), some variations in humidity level were observed. Namely, slight differences were recorded between the humidity of the two site zones, especially in the warmer months. Local environmental factors such as vegetation, water availability, and sun exposure can contribute to these disparities. However, the monthly average humidity levels, which ranged from 74.23% to 98.84% relative humidity, showed that the atmospheric conditions were favourable, with a tendency for higher humidity levels in the southern part of the site.

Variations between the designated points (natural water pond and artificial water pond) were found by *in situ* measurements of water quality parameters using the HI9829 multiparameter instrument (Hanna Instruments) (Table 2).

Table 2. Water parameter values

Parameter	Natural water pond	Artificial water pond
pH	6.69	8.03
ORP (mV)	177.3	-5.5
DO (%)	7.3	3
DO (mg/L)	0.74	0.26
Conductivity (µS/cm)	50	102
TDS (mg/L)	25	49
Turbidity (NTU)	11.4	22.4
Water temperature (°C)	9.39	22.4

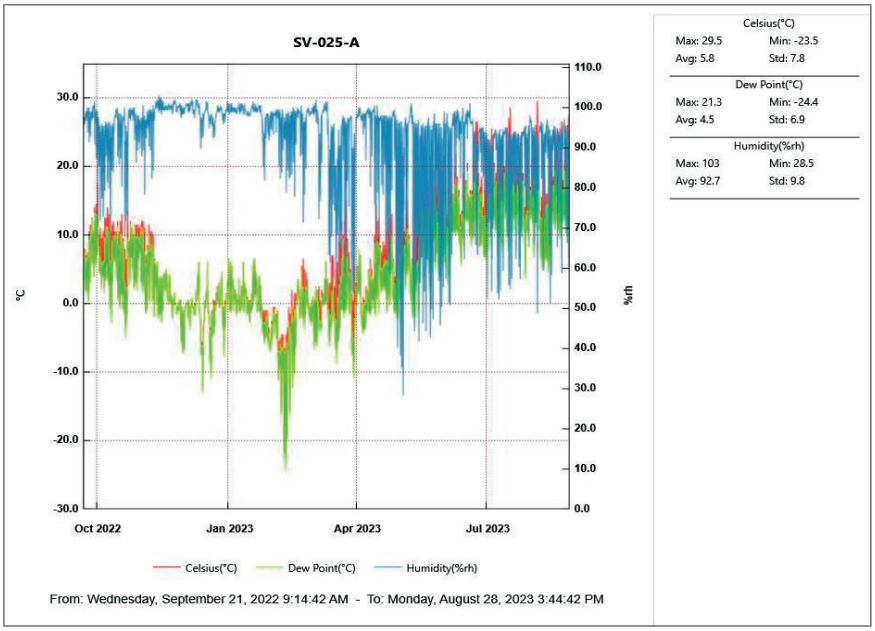


Figure 14. Variations in parameters measured with Data Loggers (September 2022 - August 2023)

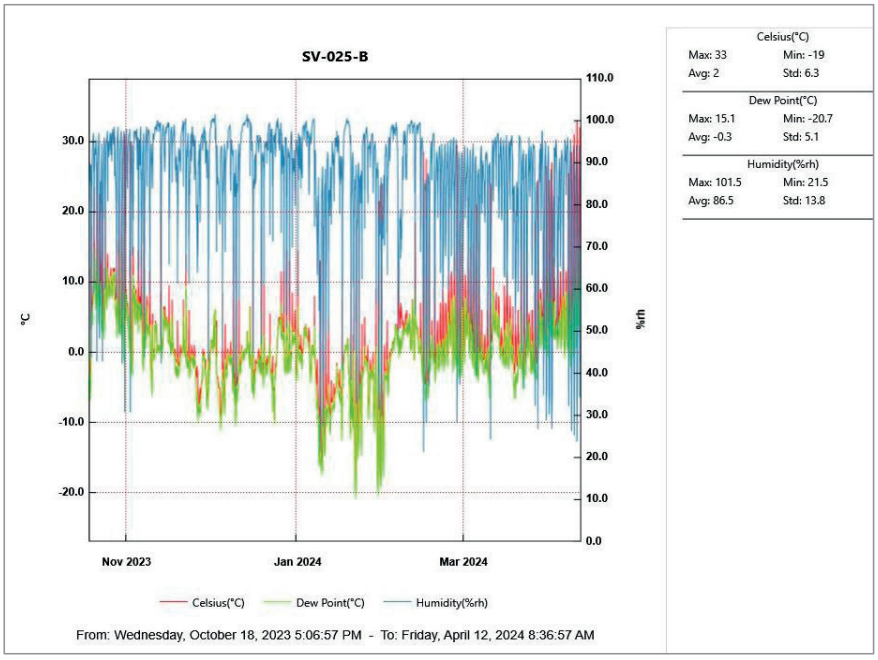


Figure 15. Variations in parameters measured with Data Loggers (October 2023 - April 2024)

The pH values were within the optimal range for both water bodies. Instead, in the natural pond, a positive ORP was recorded, indicating the oxidation of organic materials, whereas the artificial pond had a negative ORP, reflecting reducing reactions. Dissolved oxygen (DO) saturation also differed, measuring 7.30% in the natural pond and 3.00% in the artificial pond,

supporting further chemical processes as indicated by the ORP values. Peat formation occurs through the anaerobic decomposition of organic matter. Due to sediment accumulation, the artificial pond showed higher conductivity, TDS, and turbidity, which led to a reduction in water clarity. Also, water temperature influenced both biological and chemical activities, with lower temperatures slowing these processes and higher temperatures accelerating them.

A better understanding of the restoration process's quality may result from the ongoing improvement and adaptation of the monitoring protocol, guided by methodologies employed in other peatland restoration projects in other countries (Kyrkjeeide et al., 2024). Beyond the national strategies of restoration and conservation of peatlands, in a comparative study, Nordbeck & Hogl (2024) conclude that the European governments are becoming more politically committed to sustainable management of peatlands. Also, maintaining peatlands in good conservation status means a better potential for carbon-storage, an efficient solution for climate change mitigation (IPCC, 2021). Therefore, for the long-term preservation of peatland habitats in our country, a legislative framework must be established supporting these strategies.

CONCLUSIONS

The BBN peatland restoration efforts implemented during the PeatRo3 project led to an overall water table rise, despite the initial unfavourable conservation status.

Ongoing and improved monitoring, alongside the identification of key indicator species will be essential to assess the long-term stability and success of the restoration.

This improvement of the hydric level constitutes a starting point for the development of a legal framework aimed at the conservation and protection of this site.

This study scientifically supports the BBN peatland's designation as a Natura 2000 site, as proposed in April 2024. The primary objective of this designation is to ensure the long-term legal preservation of the protected species, namely *B. viridis* and *L. montandoni,* as well as the priority habitat Bog Woodland (91D0*), with a particular emphasis on their conservation. Furthermore, it advances the broader objective of achieving tangible progress towards the EU's goal of expanding terrestrial protected areas across Europe.

ACKNOWLEDGEMENTS

This research work was carried out from project no. RO1567-IBB03/2024 through the Institute of Biology Bucharest of Romanian Academy and was also financed by the EEA Grants: "Degraded mires and peatlands restoration of North-East 2 region of Romania (PeatRO3)" project.

REFERENCES

Acidophilous Picea forests of the montane to alpine levels, Vaccinio-Piceetea. (n.d.). *EUNIS habitat classification*. https://eunis.eea.europa.eu/habitats/10228 (Accessed on 03.03.2025)

Annex I of the Bern Convention. (n.d.). https://rm.coe.int/168097eb56 (Accessed on 25.02.2025)

Annex II of the Habitat-Fauna-Flora Directive (Directive 92/43/CEE). (n.d.). https://eunis.eea.europa.eu/references/2325/specie (Accessed on 20.02.2025)

Bog Woodland. (n.d.). *EUNIS habitat classification*. https://eunis.eea.europa.eu/habitats/10197#sites (Accessed on 20.02.2025)

Buxbaumia viridis. (n.d.). *EUNIS species profile*. https://eunis.eea.europa.eu/species/2318 (Accessed on 25.02.2025)

CBD Secretariat. (2022). *Kunming-Montreal global biodiversity framework*. https://www.cbd.int/doc/c/e6d3/cd1d/daf663719a03902a9b116c34/cop-15-l-25-en.pdf (Accessed on 06.03.2025)

Deme, J., Csiky, J. (2021). Development and survival of *Buxbaumia viridis* (Moug. ex DC.) Brid. ex Moug. & Nestl. sporophytes in Hungary. *Journal of Bryology, 43*(3), 213–223. https://doi.org/10.1080/03736687.2021.1916169

Deme, J., Erzberger, P., Kovács, D., Tóth, I. Z., & Csiky, J. (2020). *Buxbaumia viridis* (Moug. ex Lam. & DC.) Brid. ex Moug. & Nestl. in Hungary predominantly terricolous and found in managed forests. *Cryptogamie Bryologie, 41*, 89–103. https://doi.org/10.5252/cryptogamie-bryologie2020v41a8

Dierssen, K. (2001). *Distribution, ecological amplitude and phytosociological characterization of European bryophytes*. Bryophytorum Bibliotheca, 56, 289.

Directive Habitats. (1992). Council Directive 92/43/EEC of 21 May 1992 on the conservation of natural habitats and of wild fauna and flora. *Official Journal of the European Communities, 206*, 7–50.

Doniță, N., Popescu, A., Paucă-Comănescu, M., Mihăilescu, S., & Biriș, I. -A. (2005). *Habitatele din România*. București, RO: Editura Tehnică Silvică.

Elo, M., Penttinen, J., & Kotiaho, J. S. (2015). The effect of peatland drainage and restoration on Odonata species richness and abundance. *BMC Ecology, 9*(15), 11. https://doi.org/10.1186/s12898-015-0042-z

European Commission. (2020). *EU Biodiversity Strategy for 2030: Bringing Nature Back into Our Lives*. https://eur-lex.europa.eu/resource.html?uri=cellar:a3c806a6-9ab3-11ea-9d2d-01aa75ed71a1.0001.02/DOC_1&format=PDF (Accessed on 25.02.2025)

European Environment Agency. (2004). *List of conservation measures for the period 2019–2024*. https://cdr.eionet.europa.eu/help/habitats_art17 (Accessed on 25.02.2025)

Gafta, D., & Mountford, J. O. (2008). *Manual de interpretare a habitatelor Natura 2000 din România*. Cluj-Napoca, RO: Risoprint.

Guillet, A., Hugonnot, V., & Pépin, F. (2021). The habitat of the neglected independent protonemal stage of *Buxbaumia viridis*. *Plants, 10*, 83. https://doi.org/10.3390/plants10010083

Hodgetts, N., Cálix, M., Englefield, E., Fettes, N., Criado, M. G., Patin, L., ... & Żarnowiec, J. (2019). *A miniature world in decline: European Red List of Mosses, Liverworts and Hornworts*. Brussels.

Hodgetts, N. G., & Lockhart, N. (2020). *Checklist and country status of European bryophytes – Update*. Irish Wildlife Manuals, No. 123. National Parks and Wildlife Service.

Holá, E., Vrba, J., Linhartová, R., Novozámská, E., Zmrhalová, M., Plášek, V., & Kučera, J. (2014). Thirteen years on the hunt for *Buxbaumia viridis* in the Czech Republic: Still on the tip of the iceberg? *Acta Societatis Botanicorum Poloniae, 83*, 137–145. https://doi.org/10.5586/asbp.2014.015

IPCC. (2021). Annex VII: Glossary. In Matthews, J. B. R., Möller, V., van Diemen, R.,
et al. (Eds.), *Climate Change 2021: The Physical Science Basis*. Cambridge University Press, 2215–2256.

Kropik, M., Zechmeister, H. G., & Moser, D. (2020). Climate variables outstrip deadwood amount: Desiccation as the main trigger for *Buxbaumia viridis* occurrence. *Plants, 10*, 61. https://doi.org/10.3390/plants10010061

Kyrkjeeide, M. O., Jokerud, M., Mehlhoop, A. C., Linn Lunde, M. F., Fandrem, M., & Lyngstad, A. (2024). Peatland restoration in Norway – Evaluation of ongoing monitoring and identification of plant indicators of restoration success. *Nordic Journal of Botany, 4*, e03988. https://doi.org/10.1111/njb.03988

Law 13/1993. (n.d.). https://legislatie.just.ro/Public/DetaliiDocument/3036 (Accessed on 28.02.2025)

Law 49/2011. (n.d.). https://legislatie.just.ro/Public/DetaliiDocumentAfis/127715 (Accessed on 28.02.2025)

Manci, C. O., & Iorgu, E. I. (2021). *Leucorrhinia pectoralis* (Charpentier, 1825), p. 158. In Murariu, D., & Maican, S. (Eds.), *Cartea Roşie a nevertebratelor din România*. Editura Academiei Române.

Mihăilescu, S., Anastiu, P., Popescu, A., et al. (2015). *Ghidul de monitorizare a speciilor de plante de interes comunitar din România*. București, RO: Editura Dobrogea.

Nordbeck, R., & Hogl, K. (2024). National peatland strategies in Europe: Current status, key themes, and challenges. *Regional Environmental Change, 24*, 5. https://doi.org/10.1007/s10113-023-02166-4

Oltean, M., Negrean, G., Popescu, A., et al. (1994). *Lista Roşie a plantelor superioare din România*. Institutul de Biologie, București.

Page, S. E., & Baird, A. J. (2016). Peatlands and global change: Response and resilience. *Annual Review of Environment and Resources, 41*, 35–57. https://doi.org/10.1146/annurev-environ-110615-085520

Plášek, V. (2004). The moss *Buxbaumia viridis* in the Czech part of the Western Carpathians. In Stebel, A., & Ochyra, R. (Eds.), *Bryological Studies in the Western Carpathians* (pp. 37–44). Poznan.

Pop, E. (1960). *Mlaştinile de turbă din Republica Populară Română*. București: Editura Academiei.

Puntillo, D., & Puntillo, M. (2024). Monitoring of *Buxbaumia viridis* in Calabria (southern Italy) with historical overview and some ecological notes. *Borziana, 5*, 5–39.

Restall, B., Conrad, E., & Cop, C. (2021). Connectedness to nature: Mapping the role of protected areas. *Journal of Environmental Management, 293*, 112771. https://doi.org/10.1016/j.jenvman.2021.112771

Sârbu, I., Ștefan, N., & Oprea, A. (2013). *Plante vasculare din România. Determinator ilustrat de teren*. București: Editura Victor B Victor.

Schumacker, R., & Martiny, P. (1995). *Red Data Book of European Bryophytes. Part 2: Threatened Bryophytes in Europe including Macaronesia*. Trondheim: The Committee.

Steinacker, C., Beierkuhnlein, C., & Jaeschke, A. (2019). Assessing the exposure of forest habitat types to projected climate change - Implications for Bavarian protected areas. *Ecology and Evolution, 9*, 14417–14429. https://doi.org/10.1002/ece3.5877

Strzelecka, M., Tusznio, J., Akhshik, A., Rechcinski, M., & Grodzinska-Jurczak, M. (2022). Effects of connection to nature on residents' perceptions of conservation policy justice of Natura 2000. *Conservation Biology, 36*, e13944. https://doi.org/10.1111/cobi.13944

Ștefănuț, S., & Goia, I. (2012). Checklist and red list of bryophytes of Romania. *Nova Hedwigia, 95*, 59–104. https://doi.org/10.1127/0029-5035/2012/0044

Ștefănuț, S., Ion, C. M., Sahlean, T., et al. (2023). Population and conservation status of *Buxbaumia viridis* in Romania. *Plants, 12*, 473. https://doi.org/10.3390/plants12030473

Wiklund, K. (2002). Substratum preference, spore output and temporal variation in sporophyte production of the epixylic moss *Buxbaumia viridis*. *Journal of Bryology, 24*, 187–195. https://doi.org/10.1179/037366802125001358

Scientific Papers. Series E. Land Reclamation, Earth Observation & Surveying, Environmental Engineering. Vol. XIV, 2025
Print ISSN 2285-6064, CD-ROM ISSN 2285-6072, Online ISSN 2393-5138, ISSN-L 2285-6064

PRELIMINARY BIODIVERSITY SURVEY IN A NEWLY PROPOSED SITE OF COMMUNITY IMPORTANCE: THE AVRIG PEAT BOG

Sorin ȘTEFĂNUȚ, Miruna-Maria ȘTEFĂNUȚ, Tiberiu SAHLEAN, Ana-Maria MOROȘANU, Florența-Elena HELEPCIUC, Georgiana-Roxana NICOARĂ, Constantin-Ciprian BÎRSAN, Gabriel-Mihai MARIA, Mihnea VLADIMIRESCU, Anca MANOLE, Constanța-Mihaela ION

Institute of Biology Bucharest of the Romanian Academy,
296 Splaiul Independenței, District 6, 060031, Bucharest, Romania

Corresponding author email: mirunastefanut@gmail.com

Abstract

Peatland habitats are well-known for their function in sequestering carbon, characterized by peat-forming species such as Sphagnum mosses. The Avrig peat bog, located at the foothills of the Făgăraș Mountains in the Olt River basin, is a small site (less than 4 hectares) proposed for designation as a Natura 2000 site. A eutrophic palustrine zone encircles the peat bog`s center oligotrophic zone, dominated by Sphagnum mosses. This area is characterized by the presence of the European-protected priority habitat Active raised bogs (habitat code 7110). We employed a combination of field surveys and aerial investigations to assess the site`s biodiversity and evaluate potential threats. The collected Sphagnum samples were morphologically examined in the laboratory, revealing several species, like Sphagnum medium Limpr., Sphagnum capillifolium (Ehrh.) Hedw. and Sphagnum girgensohnii Russow. The bog also supports rare plant and amphibian species of conservation interest. Targeted management strategies are necessary to mitigate pressures including agricultural runoff, drainage, invasive species, and peat extraction.

Key words*: Sphagnum, peatland restoration, amphibians, rare plant species, Natura 2000, raised bogs.*

INTRODUCTION

Peat bogs are among the most ecologically significant habitats due to their dual role as refugia for endangered species, including glacial relicts, and as natural carbon sinks that accumulate atmospheric CO_2 over millennia. These habitats, particularly in continental regions such as the Făgăraș Mountains' Olt Basin (Sibiu County), are under increasing conservation scrutiny.

In the continental region of Romania, several peat bogs are found in the Făgăraș Mountains' Olt Basin, within the administrative area of Avrig, Sibiu County. Historically, the vascular flora of the Avrig peat bogs has been documented extensively by researchers such as Pop (1937; 1945; 1955; 1960), Șerbănescu (1961; 1964), and Drăgulescu (2003; 2010). Peat stratigraphy and formation processes have been analyzed since the 19th century (Herbich, 1884; Staub, 1884; 1891; Pax, 1908), confirming the Avrig peat bogs as some of the oldest in Romania, with an estimated age of 13,880 ± 90 years (Tanțău et al., 2006; 2009). Notably, the term "Avrig" has been attributed to a specific paleoclimatic cooling phase, dated at 12,360 ± 70 years BP.

Evidence of early anthropogenic influence, dating back 6,000-6,500 years BP, is supported by pollen analyses indicating the presence of cereal crops (Tanțău et al., 2011).

This paper presents the results of the biodiversity and conservation status assessment conducted within the framework of two major restoration projects PeatRO and PeatRO2 - focusing on peat bogs restauration and Natura 2000 site proposals in Romania.

MATERIALS AND METHODS

Among the four peat bogs in Avrig, Sibiu County, previously described by Pop (1960), one was rediscovered in 2016 as part of the PeatRO project. Although the habitat was found in a degraded state, it showed high restoration potential due to the presence of *Sphagnum* species and peatland indicator vascular plants such as *Drosera rotundifolia* L. and *Menyanthes trifoliata* L.

Within the PeatRO2 project - *Degraded Mires and Peatlands Restoration in North-East Romania* (2021-2024), funded by an EEA grant - restoration efforts were carried out, including assessments of vegetation (vascular and bryophyte), faunal composition, and conservation status. We employed a combined qualitative approach, integrating field surveys and drone-based assessments, to evaluate the site's biodiversity, existing pressures, and potential threats. Bryophyte samples were collected and morphologically identified in the laboratory using light microscopy. *Sphagnum* species were classified based on the keys by Plămadă (1998) and Laine et al. (2018), while vascular plants were identified following Ciocârlan (2009). Bryophyte nomenclature adheres to Hodgetts et al. (2020), and vascular plant taxonomy follows *Flora Europaea* with updates from the Euro+Med PlantBase. Plant associations were described in accordance with Sanda et al. (2008a; 2008b).

RESULTS AND DISCUSSIONS

The Avrig peat bog is situated in Sibiu County at 405 m a.s.l. (45.716282°N, 24.400133°E). Ecosystem evaluation during restoration confirmed the presence of species and habitats protected under Council Directive 92/43/EEC (1992). Based on field surveys and drone-based assessments, the area encompassing species and habitats of European interest was delineated. Consequently, the 3.6 h area (Figure 1) was proposed as a new Natura 2000 site, "Mlaștina Avrig" (Avrig Peat bog), aligning with the 2020 Eu State Nature Report emphasis on conservation and biodiversity assessment.

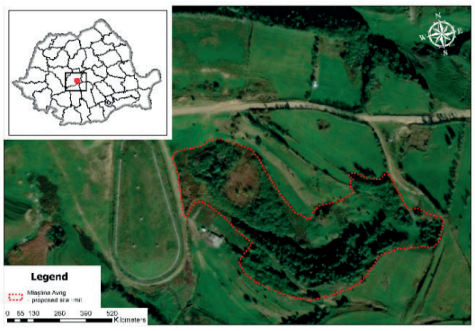


Figure 1. The area of Avrig Peat bog - new NATURA 2000 site proposal

The proposal received official endorsement from Avrig City Hall and the Sibiu Environmental Protection Agency, and has been submitted to the Ministry of Environment, Waters and Forests for final approval. The most ecologically significant area is located at the center of the site - an oligotrophic habitat characterized by acidophilic plant communities and dominated by typical *Sphagnum* species (Figure 2).

This zone corresponds to the EU priority habitat "Active Raised Bogs" (habitat code 7110), covering approximately 1 hectare. The dominant taxa within this habitat belong to the *Sphagnum magellanicum* complex (Figure 3).

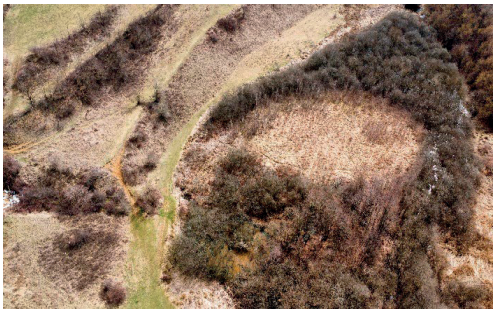


Figure 2. Avrig Peat bog - drone image.
The *Sphagnum* area is an open area surrounded by forest trees (13.03.2025)

Recent taxonomic revisions have limited the distribution of *Sphagnum magellanicum* Brid. to South America, with all previous European occurrences now attributed to either *Sphagnum medium* Limpr. or *S. divinum* Flatberg & K. Hassel (Hassel et al., 2018). Within the Avrig Peat bog, *S. medium* (Figure 4) was recently documented and formally reported as a new record for the Romanian flora (Tomović et al., 2024), highlighting the site's significance for bryological diversity and biogeographical research.

The plant association characterizing this habitat is *Sphagnetum magellanici* (Malcuit, 1929) Kästner et Flösner, 1933. Dominant bryophyte species include *Sphagnum medium* Limpr., *S. divinum* Flatberg & K. Hassel, and *S. palustre* L. (Figure 5). These are accompanied by a diverse assemblage of other *Sphagnum* species, notably *S. angustifolium* (Russow) C.E.O. Jensen (Figures 3 and 6), *S. girgensohnii* Russow, *S. capillifolium* (Ehrh.) Hedw., *S. fallax*

(H. Klinggr.) H. Klinggr. var. *fallax* (Figure 6), and *S. russowii* Warnst. Additional bryophytes recorded include *Polytrichum strictum* Menzies ex Brid. and *Aulacomnium palustre* (Hedw.) Schwägr., further enriching the site's moss flora and underscoring its ecological complexity.



Figure 3. *Sphagnum* species (*S. divinum* - red plants and *S. angustifolium* - geen and yellow plants) from Avrig Peat bog (Photo: Ștefănuț M.-M., 18.11.2022)



Figure 4. *Sphagnum medium* from Avrig Peat bog (Photo: Ștefănuț M.-M., 18.11.2022)



Figure 5. *Sphagnum palustre* from Avrig Peat bog (Photo: Ștefănuț M.-M., 18.11.2022)



Figure 6. *Sphagnum angustifolium* and *Sphagnum palustre* in the bottom right corner (Photo: Ștefănuț M.-M., 18.11.2022)

Among the characteristic vascular plants of peatland ecosystems identified at the site were *Drosera rotundifolia* (Figure 7), *Eriophorum vaginatum* L., and *E. gracile* W.D.J. Koch ex Roth. These species are indicative of acidic, oligotrophic conditions and are commonly associated with well-preserved raised bog habitats.

The site is also ecologically significant due to the presence of the priority habitat *Depressions on peat substrates of the Rhynchosporion* (habitat code 7150). This habitat includes plant assemblages characteristic of the *Sphagno cuspidati–Rhynchosporion albae* Osvald 1923 em. Koch 1926 association. Notable species within this community include *Sphagnum angustifolium*, *S. fallax* var. *fallax*, *Aulacomnium palustre*, *Epipactis palustris* (L.) Crantz, *Eriophorum angustifolium* Honck., *Menyanthes trifoliata* (Figure 8), *Comarum palustre* L. (Figure 9), and *Lysimachia thyrsiflora* L.

The peat bog is encircled by a broad, marshy, eutrophic zone dominated by woody species such as *Salix caprea* L., *Betula pendula* Roth, *Alnus glutinosa* (L.) Gaertn., and *Rhamnus frangula* L. The herbaceous and bryophyte layer comprises a diverse mix, including *Phragmites australis* (Cav.) Trin. ex Steud., *Typha angustifolia* L., *Carex acutiformis* Ehrh., *C. rostrata* Stokes, *Equisetum fluviatile* L., *Thelypteris palustris* Schott, *Alisma plantago-aquatica* L., *Menyanthes trifoliata*, *Caltha palustris* L., *Sphagnum fallax* var. *fallax*, *S. angustifolium*, *S. centrale* C.E.O. Jensen, *Aneura pinguis* (L.) Dumort., *Atrichum*

undulatum (Hedw.) P. Beauv., and *Brachythecium rutabulum* (Hedw.) Schimp.
This zone corresponds to the plant association *Salici cinereae–Sphagnetum recurvi* (Zólyomi 1931) Soó 1954. It is important to note that *Sphagnum recurvum* sensu stricto has recently been confirmed only in the Azores (Dias et al., 2009); in most European contexts, this name refers to a complex comprising *Sphagnum flexuosum* Dozy & Molk., *S. fallax*, and *S. angustifolium* (Hodgetts et al., 2020).



Figure 7. *Drosera rotundifolia* from Avrig Peat bog (Photo: Ștefănuț S., 27.07.2016).



Figure 8. *Menyanthes trifoliata* from Avrig Peat bog (Photo: Ștefănuț S., 27.07.2016)



Figure 9. *Comarum palustre* from Avrig Peat bog

In stagnant water zones within the peatland, an additional carnivorous plant, *Utricularia* sp., was observed, alongside notable herpetofauna of conservation concern. These include the European tree frog (*Hyla arborea*, Linnaeus, 1758) and the European fire-bellied toad (*Bombina variegata*, Linnaeus, 1758), both listed under the annexes of the EU Habitats Directive (Council Directive 92/43/EEC, 1992).
Under the PeatRO2 project, restoration efforts at the Avrig Peat bog targeted the removal of invasive wood vegetation and the mitigation of hydrological degradation.
The overarching goal was to reestablish a favourable water regime, thereby promoting the proliferation of characteristic peatland species while inhibiting the spread of invasive vascular plants.
Restoration activities involved several key interventions:
a) *Hydrological Restoration:* the ecological function of the peatland was enhanced by blocking existing drainage channels to restore natural water retention. During the 2016 assessment (PeatRO project), a drainage channel was identified as a significant source of water loss. In 2023, this channel was blocked by constructing a dam, resulting in a water level increase of approximately 25 cm. This intervention successfully maintained soil moisture even during the severe drought conditions of the 2024 summer and autumn seasons (Figures 10 and 11).
b) *Vegetation Management and Peatland Reconstruction:* the ecological reconstruction of the peatland included the manual removal of invasive woody plant species from its central zone. During the 2016 PeatRO project assessment, this core area was found to be heavily colonized by species such as *Betula pendula*, *Alnus glutinosa*, and *Rhamnus frangula*, whose presence was contributing significantly to water loss through elevated evapotranspiration rates (Figure 12).
As part of the PeatRO2 project, in 2022, the central area of the peatland was cleared of woody plant species (Figure 13). The activity was carried out manually by the project team

members, through careful selection of the cut plants.



Figure 10. Blockage of the drain channel (13.03.2025)



Figure 11. Drone image with the drainage channel and the dam (13.03.2025)



Figure 12. The *Sphagnum* area, invaded by woody plants, before restoration
(Photo Bîrsan C.-C., 18.11.2022)

Several ongoing pressures have been identified at the site, including the illegal dumping of household waste and manure, elevated nitrogen input from potential runoff originating at a nearby sheepfold, recurring wildfires, and the encroachment of invasive plant species.
To address these concerns and ensure long-term ecological stability, the area has been integrated into a monitoring program under the sustainability phase of the PeatRO2 project, which extends from 2024 to 2029. Continued efforts will be essential to maintain the peatland in a favourable hydrological state, safeguarding its ecological functions and biodiversity value.



Figure 13. Drone image with the *Sphagnum* area, after restoration (Photo Ștefănuț S., 13.03.2025)

The restoration activities were promoted on the website of the Institute of Biology Bucharest (IBB) and locally, through discussions with locals, local entrepreneurs and the local administration, and by installing an information board at the entrance to the site (Figure 14). The information board provides two links to the dedicated website (RO and EN) via QR codes.



Figure 14. Information panel installed at the site entrance (Photo: Ștefănuț S., 05.07.2024)

In Romania, peat bog restoration is guided by the National Peat Bog Restoration Strategy, developed in 2017 under the PeatRO project. As part of this initiative, 218 peat bogs were assessed for their biodiversity and conservation status, and 80 were selected for restoration. Among these, the 45 most threatened peat bogs were included in the RO-MEDIU Programme - Environment, Climate Change Adaptation, and Ecosystems - funded through the European Economic Area (EEA) Financial Mechanism. These sites were restored between 16 December 2021 and 30 April 2024.

Under the PeatRO2 project, 12 additional peat bogs in Romania were restored, including the Avrig Peat Bog. The structure of this bog, particularly its central area overgrown with woody vegetation, closely resembles that of Mlaca Tătarilor, the pilot restoration site from the original PeatRO project where the feasibility of peat bog restoration in Romania was first tested. Given that Mlaca Tătarilor, restored over eight years ago, shows promising signs of ecological recovery as of March 2025 (Figure 15), it is likely that the restoration of the Avrig Peat Bog will also result in a better-preserved bog habitat. This aspect supports the conservation of the peatland vegetation, in line with a synthesis of evidence for the effects of such restoring interventions (Taylor et al., 2019) and with the monitoring frameworks and best practices outlined in the European Environment Agency`s 2025 Guidebook for Monitoring and Evaluating Ecosystem-based Adaptation Interventions.



Figure 15. Drone image of the restored Mlaca Tătarilor peat bog, originally rehabilitated in 2016 (Photo: Ștefănuț S., 12 March 2025)

CONCLUSIONS

Peat bogs represent a priority conservation target at the European level, and the restoration actions undertaken by the Institute of Biology Bucharest (IBB) align closely with the objectives outlined in the EU Biodiversity Strategy for 2030. These include expanding the protected area network, enforcing strict protection for high-biodiversity-value sites (covering at least 10% of EU land), and ensuring legal protection of a minimum of 30% of EU territory.

The activities implemented at the Avrig Peat bog not only contribute to achieving these strategic goals but also offer a replicable model for future peatland restoration initiatives. As such, this case study holds significant value for informing Romania's forthcoming national restoration plan, to be finalized by 1 September 2026, under the provisions of EU Regulation 2024/1991. The Avrig Peat bog exemplifies how small-scale restorations can contribute meaningfully to continental biodiversity goals.

ACKNOWLEDGEMENTS

This research work was carried out with the support of the PeatRO2 (RO-ENVIRONMENT-0004) EEA grant. The *Sphagnum* species were identified by Ștefănuț M.-M. in the frame of the Romanian Academy PhD thesis.

REFERENCES

Ciocârlan, V. (2009). *Flora ilustrată a României. Pteridophyta et Spermatophyta* [In Romanian]. București, RO: Editura Ceres.

Council Directive 92/43/EEC. (1992). Council directive 92/43/EEC of 21 May 1992 on the conservation of natural habitats and of wild fauna and flora. *Official Journal of the European Union, L 206*, 7–50. https://eur-lex.europa.eu/legal-content/EN/TXT/?uri=celex%3A31992L0043 Accessed February 2025.

Dias, E., Mendes, C., & Shaw, J. (2009). *Sphagnum recurvum* P. Beauv. on Terceira, Azores, new to Macaronesia-Europe. *Journal of Bryology, 31*, 199–201. https://doi.org/10.1179/174328209X458458

Drăgulescu, C. (2003). *Cormoflora județului Sibiu* [In Romanian]. Brașov, RO: Editura Pelecanus.

Drăgulescu, C. (2010). *Cormoflora județului Sibiu* (2nd ed.) [In Romanian]. Sibiu, RO: Editura Universității „Lucian Blaga" Sibiu.

EU Biodiversity Strategy for 2030 (2020). *Communication from the Commission to the European Parliament, the Council, the European Economic and Social Committee and the Committee of the Regions. EU Biodiversity Strategy for 2030*. https://eur-lex.europa.eu/legal-content/EN/TXT/?uri=celex%3A52020DC0380

European Union. (2024). *Regulation (EU) 2024/1991 of the European Parliament and of the Council of 24 June 2024 on nature restoration and amending Regulation (EU) 2022/869*. *Official Journal of the European Union*. http://data.europa.eu/eli/reg/2024/1991/oj

Euro+Med (2006). *Euro+Med PlantBase – the information resource for Euro-Mediterranean plant diversity*. http://ww2.bgbm.org/EuroPlusMed/. Accessed February 2025.

Guidebook for Monitoring and Evaluating Ecosystem-based Adaptation Interventions. https://climate-adapt.eea.europa.eu/en/metadata/guidances/guideboo

k-for-monitoring-and-evaluating-ecosystem-based-adaptation-interventions Accessed July 2025.

Hassel, K., Kyrkjeeide, M. O., Yousefi, N., Prestø, T., Stenøien, H. K., Shaw, J. A., & Flatberg, K. I. (2018). *Sphagnum divinum* (sp. nov.) and *S. medium* Limpr. and their relationship to *S. magellanicum* Brid. *Journal of Bryology, 40*, 197–222. https://doi.org/10.1080/03736687.2018.1474424

Herbich, F. (1884). Schieferkohlen bei Frek in Siebenbürgen [In German]. *Verhandlungen der kaiserlich-königlichen geologischen Reichsanstalt, 13*, 248–251.

Hodgetts, N.G., Söderström, L., Blockeel, T.L., Caspari, S., Ignatov, M.S., Konstantinova, N.A., Lockhart, N., Papp, B., Schröck, C., Sim-Sim, M., Bell, D., Bell, N.E., Blom, H.H., Bruggeman-Nannenga, M.A., Brugués, M., Enroth, J., Flatberg, K.I., Garilleti, R., Hedenäs, L., Holyoak, D.T., Hugonnot, V., Kariyawasam, I., Köckinger, H., Kučera, J., Lara, F., Porley R.D. (2020). An annotated checklist of bryophytes of Europe, Macaronesia and Cyprus. *Journal of Bryology*, 42(1), 1–116. DOI: 10.1080/03736687.2019.1694329.

Laine, J., Flatberg, K.I., Harju, P., Timonen, T., Minkkinen, K., Laine, A., Tuittila, E.-S., Vasander, H. (2018). *Sphagnum Mosses the stars of european mires*. Helsinki, Finland: Department of Forest Sciences, University of Helsinki, ISBN 10: 951513143X, ISBN 13: 9789515131430.

Pax F. (1908). *Grundzüge der Pflanzenverbreitung in den Karpaten* [In German]. II. Leipzig: Germany, Verlag von Wilhelm Engelmann.

PeatRO, 2015-2017. *Restoration strategies of the deteriorated peatland ecosystems from Romania (PeatRO). Retrieved from https://www.ibiol.ro/peatro/en/index.htm*

PeatRO2, 2021-2024. *Degraded mires and peatlands restoration of North-East 1 region of Romania (PeatRO2). Retrieved from https://www.ibiol.ro/peatro2/index.html*

Plămadă, E. (1998). *Flora briologică a României. Clasa Musci* [In Romanian]. Cluj-Napoca, RO: Editura Presa Universitară Clujeană.

Pop, E. (1937). Semnalări de tinoave şi de plante de mlaştini din România [In Romanian]. *Buletinul Grădinii Botanice şi al Muzeului Botanic de la Universitatea din Cluj, 17*(3-4), 169–181.

Pop, E. (1945). Cercetări privitoare la pădurile diluviale din Transilvania [In Romanian]. *Buletinul Grădinii Botanice şi al Muzeului Botanic de la Universitatea din Cluj, în Timişoara, 25*(1-2), 1–92.

Pop, E. (1955). Mlaştinile noastre de turbă şi problema ocrotirii lor [In Romanian]. *Ocrotirea Naturii. Buletinul Comisiei pentru Ocrotirea Monumentelor Naturii, 1*, 57–105.

Pop, E. (1956). Noi contribuţii cu privire la mlaştinile şi plantele turbicole din R.P.R. [In Romanian]. *Buletin ştiinţific. Secţia de ştiinţe biologice şi ştiinţe agricole (şi) Secţia de geologie şi geografie, 8*(1), 47–68.

Pop, E. (1960). *Mlaştinile de turbă din Republica Populară Română* [In Romanian]. Bucureşti, RO: Editura Academiei.

Report from the Commission to the European Parliament, the Council and the European Economic and Social Committee. The State of Nature in the European Union. Report on the status and trends in 2013 - 2018 of species and habitat types protected by the Birds and Habitats Directives. https://eur-lex.europa.eu/legal-content/EN/TXT/PDF/?uri=CELEX:52020DC0635 Accessed July 2025.

Sanda, V., Öllerer, K., & Burescu, P. (2008a). *Fitocenozele din România. Sintaxonomie, structură, dinamică şi evoluţie* [In Romanian]. Bucureşti, RO: Editura Ars Docendi – Universitatea din Bucureşti.

Sanda, V., Vicol, I., & Ştefănuţ, S. (2008b). *Biodiversitatea ceno-structurală a învelişului vegetal în România* [In Romanian]. Bucureşti, RO: Editura Ars Docendi – Universitatea din Bucureşti.

Schur, F. (1866). *Enumeratio plantarum Transsilvaniae* [In Latin and German]. Viena, Austria.

Staub, M. (1884). Schieferkohlen bei Frek in Siebenbürgen [In German]. *Verhandlungen der kaiserlich-königlichen geologischen Reichsanstalt, 15*, 306–308.

Staub, M. (1891). Die Flora Ungarns in der Eiszeit [In German]. *Földtani Közlöny, 21*, 74–94.

Şerbănescu, I. (1961). Aspecte de vegetaţie din Depresiunea Făgăraşului [In Romanian]. *Comunicările Academiei R.P. Române, 11*(4), 415–420.

Şerbănescu, I. (1964). Cercetări geobotanice în Depresiunea Făgăraşului [In Romanian]. *Anuarul Comitetului Geologie, 36*(2), 311–370.

Tanţău, I., Fărcaş, S., Beldean, C., Geantă, A., Ştefănescu, L. (2011). Late Holocene paleoenvironments and human impact in Făgăraş depression (Southern Transylvania, Romania). *Carpathian Journal of Earth and Environmental Sciences*, *6*(1), 171–178.

Tanţău, I., Reille, M., Beaulieu, J.L., Fărcaş, S., (2006). Late Glacial and Holocene vegetation history in the southern part of Transylvania (Romania) pollen analysis of two sequences from Avrig. *Journal of Quaternary Science*, *21*(1), 49–61.

Tanţău, I., Reille, M., Beldean, C., Fărcaş, S., Beaulieu, J.L. de (2009). Late Glacial vegetation development in the Făgăraşului Depression. *Contribuţii Botanice*, *44*, 141–150.

Taylor, N. G., Grillas, P., Fennessy, M. S., Goodyer, E., Graham, L. L. B., Karofeld, E., Lindsay, R. A., Locky, D. A., Ockendon, N., Rial, A., Ross, S., Smith, R. K., van Diggelen, R., Whinam, J., & Sutherland, W. J. (2019). A Synthesis of Evidence for the Effects of Interventions to Conserve Peatland Vegetation: Overview and Critical Discussion. *Mires and Peat*, *24*, 18.

Tomović, G., Sabovljević, M.S., Stoykov, D., Niketić, M., Boycheva, P., Kaschieva, M., Vidaković, D., Krizmanić, J., Djordjević, V., Krdžić, S., Škondrić, S., Knežević, J., Perić, R., Assyov, B., Jenačković Gocić, D., Raca, I., Šovran, S., Popović, S., Pál Frink, J., Sass-Gyarmati, A., Ştefănuţ, M-M., Sabovljević, A.D. (2024). New records and noteworthy data of plants, algae and fungi in SE Europe and adjacent regions, 18. *Botanica Serbica*, *48*(2), 285–296. https://doi.org/10.2298/BOTSERB2101129

Scientific Papers. Series E. Land Reclamation, Earth Observation & Surveying, Environmental Engineering. Vol. XIV, 2025
Print ISSN 2285-6064, CD-ROM ISSN 2285-6072, Online ISSN 2393-5138, ISSN-L 2285-6064

INDOOR IoT SEEDLING NURSERY DEVELOPMENT

Peter UDVARDY[1], Matyas Csongor KOVACS[1], Levente DIMEN[2]

[1]Óbuda University, Alba Regia Technical Faculty, 45 Budai Street, 8000, Székesfehérvár, Hungary
[2]"1 Decembrie 1918" University of Alba Iulia,
5 Gabriel Bethlen Street, 510009, Alba Iulia, Romania

Corresponding author email: udvardy.peter@uni-obuda.hu

Abstract

In recent years, indoor plant cultivation has become an increasingly popular hobby. However, the natural environment required for optimal plant growth is not universally available, and therefore, it is necessary to replicate the missing environmental factors. Successful cultivation can be greatly enhanced by monitoring and adjusting environmental conditions. By collecting and analysing environmental data, it is possible to set appropriate parameters and optimize the operation of an environmental control system. This system requires sensors and actuators to compensate for environmental deficiencies and automate relevant processes. If the system's parameters are flexible enough, it can support the growth of a wide range of plant species. An effective approach to achieve this flexibility is through an online interface that allows remote access and enables the display of measured data as well as the adjustment of control parameters. A microcontroller-based system can be employed to manage this process. This paper outlines the hardware and software architecture, describes the communication protocols used, and provides an analysis of the system's expected performance.

Key words*: IoT, indoor planting, controlled environment.*

INTRODUCTION

Indoor plant cultivation

There are numerous reasons why individuals may choose to cultivate their own edible plants. While plant cultivation can certainly serve as a fulfilling hobby, extensive research has also demonstrated the positive effects of plants on human well-being. Moreover, various studies explore the specific impacts of different plant species on individuals (Yeo, 2021).

Another significant factor driving home cultivation is the rising cost of food, which is partly attributed to the increasing prices of imported goods. Such price fluctuations are influenced by global events beyond individual control. For instance, rising fuel costs lead to increased transportation expenses, which are ultimately passed on to consumers. In these situations, producing food locally can help reduce household expenditures, thereby mitigating some of the negative financial impacts. Consequently, the practice of growing at least locally suitable edible plants may regain popularity (Arora, 2019).

However, cultivating plants is not always a viable solution. Certain species may not be suitable for open-field cultivation in a given climate due to climate change or their inherent sensitivity to environmental conditions. Some plant varieties are highly susceptible to sudden heavy rainfall, which can damage their yield due to inefficient water distribution. Others struggle with prolonged drought periods, hindering their proper development.

A potential solution is to cultivate plants in controlled or semi-controlled environments, managing their development across various growth stages. Indoor cultivation methods have already gained traction, with industrial-scale operations successfully producing crops such as tomatoes in a cost-effective manner. However, such large-scale solutions are not feasible for the average individual, as not everyone has access to rooftop greenhouses or similar infrastructure. Instead, smaller, more portable, and user-friendly systems could provide a more practical alternative for everyday users (Pehin et al., 2020; Garcia, 2020).

In some cases, full environmental control is not required throughout the plant's entire lifecycle. Certain species only require additional support during specific growth phases, such as the early development stages when they are most

vulnerable. This period typically includes germination and early seedling growth, lasting until the first buds appear. Afterward, some plants become sufficiently resilient to local environmental conditions, allowing for outdoor cultivation until the end of their lifecycle (Leavy & Hossain, 2014).

Environmental control processes must be executed periodically or under specific conditions in response to environmental fluctuations. However, maintaining such conditions requires a level of attention that many individuals, due to their busy schedules, may be unable to provide consistently. Additionally, some people may lack the expertise to recognize when intervention is necessary for optimal plant development. A common example is improper watering - either forgetting to water houseplants entirely or overwatering seedlings to the point of damaging or killing them.

Modern technology enables the automation of processes such as irrigation through the application of appropriate knowledge and tools. Numerous successful experiments and widely implemented systems already regulate or supplement specific environmental factors. Some advanced systems can simultaneously monitor and control multiple parameters, adapting to specific plant needs. However, complexity varies, and some existing solutions are unnecessarily intricate, reducing their efficiency (Palande et al., 2018).

The rise of IoT devices enables real-time monitoring and user adjustments. With intelligent algorithms and proper hardware, these systems can also become self-learning, making them easier to use and more efficient. Given these needs and technological advancements, designing a system that supports individuals in successfully cultivating plants at home presents a valuable and engaging research opportunity. Such a system could significantly improve accessibility and encourage more people to adopt home cultivation practices (Ragaveena et al., 2021).

MATERIALS AND METHODS

Lighting sensor

A wide range of lighting solutions is available for indoor plant cultivation, with their design significantly influenced by specific application requirements. One of the most critical characteristics of lighting fixtures is the electromagnetic wavelength spectrum in which they emit radiation.

For plants, the most suitable wavelengths for photosynthesis and photomorphogenesis - developmental processes influenced by light - are found within the visible light spectrum. Blue light (425-450 nm) and red-orange light (600-700 nm) play a crucial role in plant growth and development. Regarding ultraviolet (UV) radiation, wavelengths below 315 nm are considered harmful, as they can cause structural damage to plant cells.

Different regions of the visible light spectrum have varying effects on plant growth stages. In the early developmental phase, when stem and leaf formation are predominant, the blue wavelength range (400-500 nm) is the most effective, particularly for chlorophyll a absorption. In contrast, during the flowering stage, the red wavelength range (600-700 nm) becomes dominant, as it plays a crucial role in supporting chlorophyll b function (Paradiso & Proietti, 2022). Figure 1 shows the photosynthetic active light spectrum.

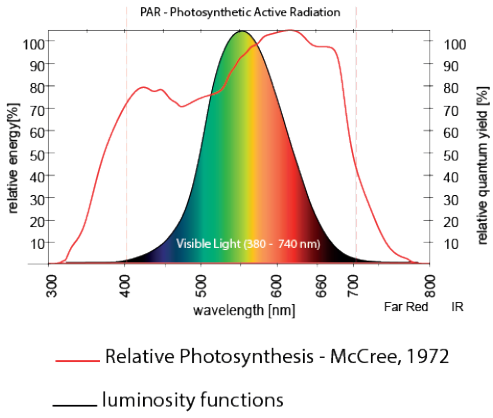


Figure 1. Photosynthetic active light
Source: https://hortione.com/2018/10/lighting-terminology-part-1-par-ppf-ppfd/

For successful indoor plant cultivation, it is essential to use light sources that emit radiation in the most suitable spectrum for each growth stage. During the vegetative phase - when the plant is growing but has not yet entered the flowering stage - the blue wavelength range (400-500 nm) promotes compact and robust

growth. This reduces stem elongation, increases leaf density, and encourages branching, ultimately leading to higher flower production and improved yield (Beszédes et al., 2022).
Various lighting technologies are available for indoor plant cultivation, with LED-based solutions gaining increasing popularity over traditional incandescent bulbs and fluorescent tubes. LEDs are particularly favoured for their high efficiency, long lifespan, and customizable spectral output. In our own cultivation setup, natural light LED strips were used. Although I considered COB (Chip-on-Board) LEDs - known for their higher light intensity and broader coverage - I ultimately opted for lower-power LED strips. These offer easier installation, provide light tailored to the size of the cultivated area and specific plant needs, and require less cooling.

Soil Moisture Sensor

To optimize irrigation, it is essential to determine the moisture content of the soil in which plants are growing. This can be achieved using a capacitive soil moisture sensor, which, when connected to the analog input of an ESP32 microcontroller, represents soil capacitance variations as voltage levels. The capacitance increases proportionally with soil moisture content.
The sensor operates within a supply voltage range of 3.3 V to 5.5 V, allowing it to be powered directly from the 3.3 V output of the microcontroller. The core principle of capacitive sensing is that soil capacitance increases as moisture levels rise. The sensor utilizes a TL555C timer oscillator, which generates periodic square wave signals to charge the sensor. Higher capacitance results in longer charge times, leading to a decrease in the analogue signal read by the microcontroller.
Another approach to soil moisture measurement involves resistive sensors, which determine soil moisture based on electrical resistance. While these sensors are initially more cost-effective and simpler to implement, their major drawback is the oxidation of electrodes in direct contact with the soil, which shortens their lifespan. In contrast, capacitive sensors do not have exposed conductive surfaces in contact with the soil, making them more durable and capable of providing more reliable measurements over time (Mittelbach, 2012).

Other sensors

To determine the intensity of natural light, light-dependent resistors (LDRs) were applied, which vary their resistance based on the amount of incident light. For the measurement setup, I connected the LDR in series with a 10 kΩ resistor, forming a voltage divider. The voltage drop across the divider is measured by the analog input of an ESP32 microcontroller. The voltage value read by the analog input is directly proportional to the intensity of incoming light, enabling continuous monitoring of ambient illumination levels.
The HC-SR04 is an ultrasonic distance sensor widely used in various electronics and robotics projects for accurate and reliable distance measurement. It can be easily integrated with microcontrollers such as Arduino or ESP32 platforms. The HC-SR04 emits ultrasonic waves and detects the reflected signal. By measuring the time taken for the sound waves to travel to an object and return, the sensor calculates the distance between itself and the detected object.
The DHT22 (also known as AM2302) is a digital temperature and humidity sensor commonly used in various electronics and IoT projects for environmental data measurement. It is easy to use, provides accurate readings, and communicates with a microcontroller via a single data line (Yue et al., 2020).

Microcontroller

The ESP32 is more of a family of microcontrollers than a single microcontroller. It offers a wide range of variants that can be selected based on the specific application requirements and essential parameters. For my selection, I had access to three types of ESP32: the ESP32 S3, the ESP32 C6, and the "standard" ESP32 (such as the ESP32-WROOM or ESP32-WROVER modules). These models differ in several important aspects, primarily related to their architecture, functionalities, and intended application areas. The original ESP32 chip is widely available and popular, making it an ideal choice for general IoT projects such as sensor data processing, control tasks, or basic Wi-Fi and Bluetooth applications. It is particularly suitable for low-budget projects due to its cost-

effectiveness while still offering a robust set of features (Maier et al.,2017).

Software

Visual Studio Code, when complemented by PlatformIO, evolves into an open-source integrated development environment (IDE) that supports a wide range of microcontroller types. This integration provides an intuitive, yet professional development environment tailored for embedded systems engineers (https://code.visualstudio.com/).

VS Code is a highly versatile code editor widely adopted in the industry for programming in well-established languages such as Python, C++, C#, and many others. One of the key factors contributing to its widespread success is its open-source nature, which has led to the development of numerous extensions that allow users to tailor the editor to their specific needs. Among these extensions, PlatformIO stands out as a powerful open-source ecosystem designed for IoT system development. It integrates multiple development frameworks, maximizing the number of supported microcontrollers to ensure broad compatibility. The development frameworks supported by PlatformIO include Arduino, ESP-IDF: ESP32, Zephyr OS, Mbed OS, FreeRTOS and LibOpenCM3.

As seen from this list, PlatformIO fully supports ESP32 microcontrollers alongside numerous other platforms. Compared to the original Arduino IDE, the combination of VS Code and PlatformIO offers several advantages. However, due to its broad compatibility and extensive feature set, this platform is inherently more complex and requires a steeper learning curve than the traditional Arduino development environment.

The Arduino Integrated Development Environment (IDE) serves as a primary tool for programming Arduino microcontrollers, providing an intuitive interface for uploading programs to various types of microcontrollers. By default, the IDE offers native support for the Arduino platform.

In addition to its built-in capabilities, the Arduino IDE allows developers to extend its functionality through downloadable extensions, enabling the programming of microcontrollers from other manufacturers. One such extension provides support for ESP32-based microcontrollers, allowing developers to program Espressif-manufactured chips within the same development environment. The selected microcontroller's corresponding compiler processes the source code, ensuring compatibility with the target hardware.

DesignSpark Mechanical is a free, easy-to-use 3D Computer-Aided Design (CAD) software developed by RS Components, built on SpaceClaim technology. It is primarily designed for rapid prototyping, mechanical component and device modeling, and 3D printing projects. The software enables engineers and designers to quickly create and modify complex geometries, making it a valuable tool for product development and iterative design processes (https://www.rs-online.com/designspark/mechanical-software).

RESULTS AND DISCUSSIONS

System development process

In the system, an ESP8266 functioned as the web server and handled data transmission, while an Arduino Mega was responsible for data acquisition from sensors, actuator control, storing operational data in non-volatile memory, and providing a local menu interface to allow data input beyond the web interface.

The primary advantage of the dual-microcontroller system was the increased number of I/O pins, which facilitated the integration of additional sensors. However, based on empirical observations, the system provided more input and output pins than necessary. The ESP32 eliminates the need for two separate microcontrollers sharing tasks and exchanging data internally, thereby simplifying system architecture and reducing communication overhead.

First, the key data points were defined that the device should transmit via the web interface:

- soil moisture content expressed as a percentage, essential for irrigation control;
- threshold soil moisture level at which the system should automatically initiate irrigation;
- the direction of the highest light intensity and the light intensity itself, presented as a percentage. This information helps determine the primary natural light source

based on the system's orientation, which is particularly useful when operating in supplemental lighting mode;
- illumination activation time intervals, displayed in a tabular format;
- the current time according to the ESP32's internal clock;
- sensor scale limits, providing reference points for easier adjustment of new threshold values;
- a graphical representation of system-measured values over a specified time interval.

Next, it is essential to determine which parameters can be modified remotely via the web interface. Based on empirical observations, the following controls provide sufficient flexibility over the system:
- input fields for modifying the lighting activation time intervals;
- action button for changing the lighting operation mode;
- adjustable scaling for sensor measurements: To display sensor readings as percentages, a scale with defined upper and lower limits is required. Users can modify these limits via the web interface for both light intensity detection and soil moisture measurement through dedicated input fields;
- action button for switching the irrigation mode;
- adjustable thresholds for automated irrigation: Users can modify the automatic irrigation threshold via the web interface, as well as specify the "depth" of the water reservoir to define when it should be considered empty. These parameters can be set through dedicated input fields.

Ideally, when the ESP32 receives an empty request to its IP address (i.e., when there is no content following '/' in the URL), it automatically serves the web page to the client. This web page is stored as a string in the ESP32's memory and includes the current data managed within the microcontroller's variables. These data are transmitted along with the entire web page to the client.

When the user fills out a form and clicks the Submit button, the client sends the entered data to the ESP32 using the POST method. The GET method was deliberately avoided, as it appends data to the URL, leading to potential security and usability issues. For instance, data stored in the browser history or saved as a bookmark could be inadvertently reused, resulting in outdated or incorrect information being sent back to the web server. Figure 2 shows the ESP 32 data connection steps.



Figure 2. ESP 32 data connection

The POST method is a more secure and practical alternative, as the transmitted data do not appear in the URL or browsing history. The ESP32 executes the appropriate program function based solely on an action identifier associated with the URL (e.g., /submit1), which handles data reception and processing. After processing is completed, the ESP32 returns either an updated or a reset web page to the client, allowing the user to enter additional data or verify that the intended system changes have been successfully applied. The ESP32 initially stores the form-submitted data in its internal variables. If a change occurs, the data are subsequently saved to external non-volatile memory for long-term storage. Once the HTML code for the web page and the corresponding ESP32 code for serving the web interface are completed, the functionality of the web server can be tested. Figure 3 shows the flowchart of the main project programme.

The ESP32 must be connected to a network. To achieve this, the SSID (wireless network name) and password of the router are provided to the ESP32, allowing it to establish a connection. To determine the IP address assigned to the ESP32 by the router, one can either check the list of connected devices in the router's interface - provided that the router recognizes the ESP32's hostname - or identify the microcontroller using its MAC address. Some routers automatically assign a device name based on the ESP32's identifier, while others do not. For instance, on the router used during development, the ESP32 was assigned the device name ESP-283150. Alternatively, the microcontroller can be identified by retrieving its MAC address through other means.

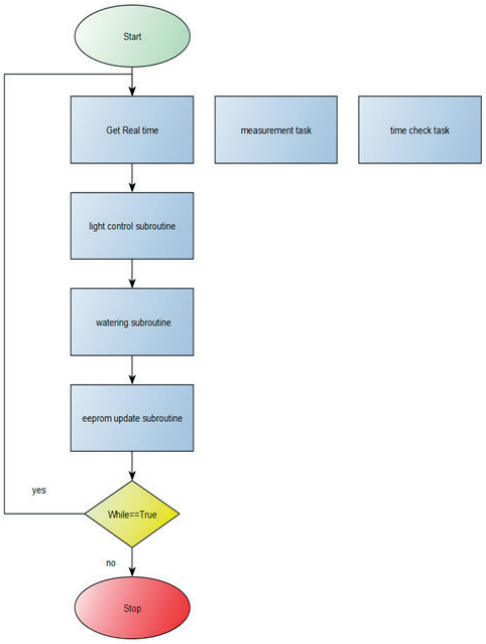


Figure 3. Flowchart of the main programme and tasks

IoT lighting system

The ESP microcontroller performs an hourly check to determine whether a predefined activation time requires the operation of the LED strips and whether a corresponding deactivation time mandates their shutdown.

If these conditions are met, the microcontroller activates the LED strips. The system allows only whole-hour time settings rather than minute-based configurations because the effect of illumination duration is negligible for time intervals smaller than an hour. However, if precise minute-level control becomes necessary, the program can be modified accordingly.

The lighting mode depends on the user-selected operating mode, in Supplementary Lighting Mode the duty cycle of the LED strips' PWM signal is adjusted based on ambient light intensity. This enables the system to optimize illumination by complementing natural light and in Illumination Mode the LED strips operate with a fully saturated PWM signal, meaning they emit continuous maximum brightness. Figure 4 shows how the light sensor reacts to the light intensity and light direction changes.

Due to their low heat emission, the LED strips do not require additional cooling. The generated heat is safely dissipated into the surrounding environment, preventing damage to both the LEDs and the supporting board during operation.

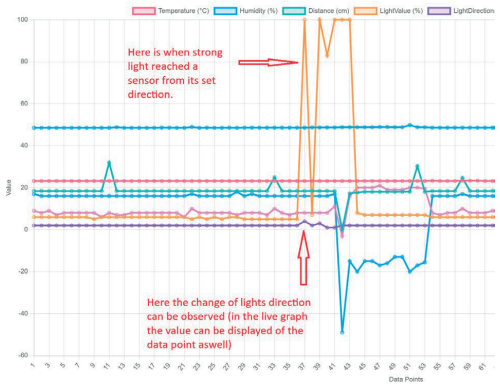


Figure 4. Changes in the light sensor readings/status

Soil moisture

The selected soil moisture sensors provide an output voltage ranging between 1.2 V and 2.8 V based on measurement results. These signals are converted into digital values by the analog input of the ESP32 microcontroller. Since the voltage range of individual sensors may vary slightly, these threshold values can be configured independently.

During the calibration process, the first step is to determine the sensor's output in dry air, which is typically around 3000. Next, by immersing the sensor's soil-contacting portion in water, the lower threshold value is obtained, usually around 1000. After calibration, variations in soil moisture percentage can be accurately tracked, and the sensors provide reliable measurements.

Periodic recalibration may be necessary, for instance, when replacing sensors. The minimum and maximum values of new sensors can be easily set via the web interface. This feature is particularly useful because some newer sensor models, such as the capacitive soil moisture sensor v2.0, operate within a different voltage range (e.g., between 900 and 4000). This flexibility ensures that threshold values can be conveniently adjusted when replacing sensors.

During this process, only automatic irrigation is possible. Before executing irrigation, the system verifies whether there is a sufficient water level in the storage container; otherwise, the pump will not be activated. During irrigation, a

predetermined volume of water is dispensed over a specific time period. The exact amount of water per cycle was determined through experimental testing. For the duration of irrigation, the lighting system is automatically turned off to indicate that irrigation is in progress and to allocate sufficient power to the pump, preventing system overload due to excessive current draw. After the irrigation cycle is completed, the lighting is reactivated if necessary.

If the size of the plant containers changes, it may become necessary to adjust the dispensed water volume or increase the number of irrigation cycles. Currently, these modifications can only be implemented by reprogramming the system. However, in the future, a more flexible and user-friendly solution could be developed if needed.

The system allows for two types of irrigation methods. As the name suggests, in top-down irrigation, water is applied to the soil surface and infiltrates downward under the influence of gravity. This method enables soil moisture sensors to respond immediately to irrigation since water reaches the sensor area more quickly. As a result, the measured moisture level rapidly reaches the predefined upper threshold. After irrigation, the soil moisture level gradually decreases, but the variation is not significant.

Figure 5 shows the flowchart of the irrigation management.

In bottom-up irrigation, water is delivered beneath the plant's soil, requiring it to be absorbed from below. This method is slower because water wicking through the soil takes time, particularly in larger volumes of substrate. Consequently, soil moisture sensors display delayed responses to irrigation. However, this can be advantageous, as it results in more stable moisture readings, avoiding abrupt fluctuations. Due to the slower response time, time-based control is necessary between irrigation cycles to prevent excessive water application. Additionally, this method requires sufficiently large overflow containers beneath the plant holders; otherwise, water may overflow. This issue can be managed by using adequately sized reservoirs. Although alternative solutions exist to prevent overflow, this method has proven to be effective in practice.

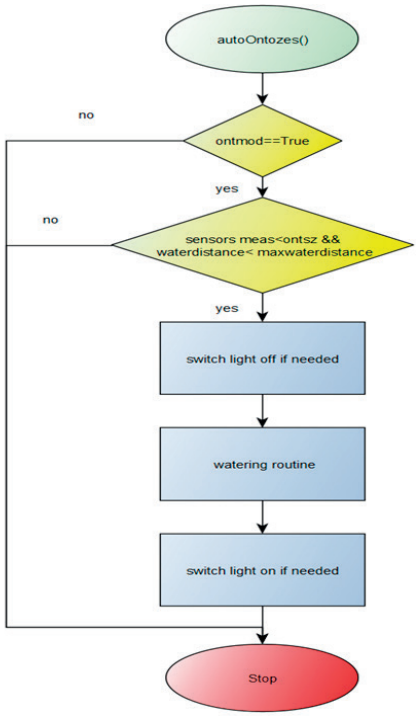


Figure 5. Flowchart of the irrigation management

Figure 6 shows the changes of soil moisture content and the threshold point.

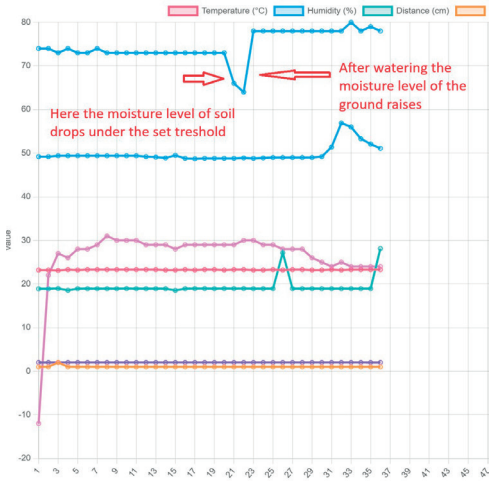


Figure 6. Changes of the moisture sensor status

CONSLUSIONS

The potential for further development of the system is somewhat limited due to the constraints of the ESP32 microcontroller. The primary limitation is its relatively low number of input and output pins. Additionally, certain pins cannot be fully utilized for all functions; for example, some internal resources required for ADC operations are also needed to support Wi-Fi functionality. As a result, ADC2 pins cannot be used as analog inputs within the system.

However, a more complex system could be designed by integrating multiple ESP32-based microcontrollers alongside a central processing unit. In such a configuration, individual units would handle specific tasks while the central unit would collect data via Bluetooth or Wi-Fi and manage the control of actuators based on the gathered information.

Since the LED strips are not fixed to the mounting surface, they can be easily replaced as needed, allowing for the use of strips with different light spectra. It is also possible to install multiple LED strips with varying spectra, and by modifying the program, users could select which strips should be active based on the current growth stage of the plants.

However, a drawback of this approach is that inactive strips do not emit any light, which may reduce the overall illumination output. On the other hand, if full illumination from all four strips is not necessary, and only half of them is sufficient, this can be advantageous. In this way, plants receive a light spectrum more closely aligned with their optimal growth requirements, ultimately improving cultivation quality.

If higher-power light sources, such as COB LEDs, are required, the system can accommodate their control. However, due to their significant heat generation, COB LEDs necessitate the use of large heat sinks to prevent overheating, which could damage the LEDs or substantially reduce their lifespan. For implementation, it is recommended to replace the current base that integrates the electronics and components with a substrate that can also function as a heat sink, as wood is not suitable for this purpose.

By controlling multiple pumps, it would be possible to irrigate the plants in individual seedling containers separately, significantly enhancing the system's flexibility and functionality. The ESP32 microcontroller has enough PWM-capable I/O pins to facilitate this implementation. Furthermore, the system could be improved by incorporating a predefined maximum soil moisture threshold during irrigation, preventing overwatering. This feature would be particularly beneficial for plants sensitive to excessive moisture, allowing the system to support the care of such species as well.

The system can be expanded with a camera module compatible with certain microcontrollers, such as the ESP32-CAM. By integrating an ESP32-CAM, it would be possible to visually monitor the plants, capture images, or even stream real-time video. The captured images could be displayed on the system's web interface, or the stream could be transmitted directly to the user's device. To implement this feature, in addition to the ESP32-CAM, a web server capable of handling video streaming would need to be developed. However, this integration would also increase the system's complexity, as the camera functions as a separate microcontroller unit.

An additional challenge may arise from the fact that transmitting the video stream to the central microcontroller and subsequently to the user client does not necessarily represent the most efficient use of resources. However, such an expansion could significantly enhance the system's functionality and user experience in the future.

Plant growth is influenced by various environmental factors, the monitoring of which can provide valuable insights for system users. For instance, soil temperature measurement can be achieved by integrating an appropriate sensor. However, expanding the current system is necessary, as all available analogue inputs are occupied. One possible solution is to integrate an additional microcontroller to manage the new sensor. Alternatively, a more extensive system redesign could be implemented, such as utilizing sensor modules that transmit data in digital format to the central unit via an interface like I2C. This approach would facilitate the connection of multiple sensors more efficiently.

The enhanced system offers a greater number of useful functionalities compared to its predecessors. Its efficiency has been improved,

and its design has been simplified in certain aspects by utilizing a single microcontroller as its core, rather than two separate units with distinct functions. However, this design choice entails some limitations regarding the system's potential for further expansion. The system facilitates plant growth by automating key developmental processes and collecting data on both the plants and their surrounding environment.

Throughout the period in which the system supports plant growth, valuable data is gathered regarding the direction of optimal lighting exposure and other environmental factors that influence plant development. During the development process, multiple opportunities for further improvement were identified. These enhancements could significantly extend the system's functionality and lifespan while making plant care more convenient and efficient for users.

REFERENCES

Arora, N. K. (2019). Impact of climate change on agriculture production and its sustainable solutions. *Environmental Sustainability, 2*(2), 95–96. https://doi.org/10.1007/s42398-019-00078-w

Beszédes, B., et al. (2022). Artificial lighting experimental environment in agriculture for seed germination. In *Proceedings of AIS 2022 - 17th International Symposium on Applied Informatics and Related Areas* (pp. 77–81). Székesfehérvár: Óbudai Egyetem. ISBN: 9789634493020

Garcia, L. (2020). IoT-based smart irrigation systems: An overview on the recent trends on sensors and IoT systems for irrigation in precision agriculture. *Sensors, 20*(4), 1042. https://doi.org/10.3390/s20041042

Leavy, J., & Hossain, N. (2014). Who wants to farm? Youth aspirations, opportunities and rising food prices. *IDS Working Papers, 2014*(439), 1–44. https://doi.org/10.1111/j.2040-0209.2014.00439.x

Maier, A., et al. (2017). Comparative analysis and practical implementation of the ESP32 microcontroller module for the internet of things. In *2017 Internet Technologies and Applications (ITA)* (pp. 143–148). IEEE. https://doi.org/10.1109/ITECHA.2017.8101926

Mittelbach, H., et al. (2012). Comparison of four soil moisture sensor types under field conditions in Switzerland. *Journal of Hydrology, 430–431*, 39–49. https://doi.org/10.1016/j.jhydrol.2012.01.041

Palande, V., Zaheer, A., & George, K. (2018). Fully automated hydroponic system for indoor plant growth. *Procedia Computer Science, 129*, 482–488. https://doi.org/10.1016/j.procs.2018.03.028

Paradiso, R., & Proietti, S. (2022). Light-quality manipulation to control plant growth and photomorphogenesis in greenhouse horticulture: The state of the art and the opportunities of modern LED systems. *Journal of Plant Growth Regulation, 41*, 742–780. https://doi.org/10.1007/s00344-021-10337-y

Pehin, S. F., et al. (2020). A study on youth aspiration and perception of agriculture and its policy implications. In A. J. Vasile (Ed.), *Handbook of Research on Agricultural Policy, Rural Development, and Entrepreneurship in Contemporary Economies* (pp. 441–453). IGI Global. https://doi.org/10.4018/978-1-5225-9837-4.ch022

Ragaveena, S., et al. (2021). Smart controlled environment agriculture methods: A holistic review. *Reviews in Environmental Science and Bio/Technology, 20*, 887–913. https://doi.org/10.1007/s11157-021-09591-z

Yeo, L. B. (2021). Psychological and physiological benefits of plants in the indoor environment: A mini and in-depth review. *International Journal of Built Environment and Sustainability, 8*(1), 57–67.

Yue, S. J., et al. (2020). IoT based automatic water level and electrical conductivity monitoring system. In *2020 IEEE 8th Conference on Systems, Process and Control (ICSPC)* (pp. 95–100). IEEE. https://doi.org/10.1109/ICSPC50992.2020.9305768

Microsoft (n.d.). *Visual Studio Code*. https://code.visualstudio.com/

RS Components (n.d.). *DesignSpark Mechanical Software*. https://www.rs-online.com/designspark/mechanical-software

Scientific Papers. Series E. Land Reclamation, Earth Observation & Surveying, Environmental Engineering. Vol. XIV, 2025
Print ISSN 2285-6064, CD-ROM ISSN 2285-6072, Online ISSN 2393-5138, ISSN-L 2285-6064

BIBLIOMETRIC ANALYSIS OF SOIL POLLUTION RESEARCH BASED ON WEB OF SCIENCE

Bao-Zhong YUAN

Huazhong Agricultural University, College of Plant Science and Technology,
Wuhan city, Hubei province, PR China

Corresponding author email: yuanbz@mail.hzau.edu.cn

Abstract

This study analyzed 5,166 research and review articles on the topic of soil pollution published up to July 20, 2024, including 72 top-cited papers. The publications, primarily written in English, originated from 129 countries or regions and appeared in 961 journals and five book series. The five most productive journals were Science of the Total Environment (298 articles, 5.77%), Environmental Science and Pollution Research (218, 4.22%), Environmental Pollution (162, 3.14%), Chemosphere (142, 2.75%), and Environmental Monitoring and Assessment (138, 2.67%). The top five contributing countries - China, Spain, the United States, Poland, and India - each published more than 275 papers. Using co-occurrence network visualization with VOSviewer, the keywords were grouped into seven distinct thematic clusters. In addition, the 25 keywords with the strongest citation bursts were identified through CiteSpace analysis. Most of the publications were aligned with three key Sustainable Development Goals: Sustainable Cities and Communities (SDG 11), Zero Hunger (SDG 2), and Climate Action (SDG 13). The findings of this study not only provide a comprehensive overview of the current state of research in soil pollution but also offer valuable guidance for shaping future research directions in this critical environmental field.

Key words: *bibliometric analysis, soil pollution, VOSviewer, CiteSpace, Web of Science.*

INTRODUCTION

Soil, as one of the most fundamental natural resources for human survival, is increasingly threatened by various types of pollutants. Among these, environmental pollution caused by agricultural mulch film residues has become a growing concern, attracting significant research attention in recent years (Wang et al., 2024). Bibliometric analysis has provided valuable insights into the research landscape, trends, and thematic domains within the field of soil micro- and nanoplastics pollution (Liu et al., 2023).

Gao et al. (2022) conducted a comprehensive literature review on the subject of "land pollution" using CiteSpace software, performing both bibliometric analysis and visual presentation. Similarly, Pan et al. (2024) analyzed global trends and the evolution of research hotspots in soil microplastic pollution. Gong et al. (2023) conducted a bibliometric study on global research activities related to micro- and nanoplastic toxicity in earthworms.

Another emerging area of concern is military-related soil pollution, where heavy metal contamination remains the primary issue, as highlighted by Stadler et al. (2022). Du et al. (2022) reviewed influencing factors, threshold derivation, and the application of heavy metal limits in soils using a combined approach of bibliometric analysis and scientific knowledge mapping. Gao et al. (2022) also applied bibliometric techniques to evaluate global research efforts in soil remediation. In a related context, Ajibade et al. (2022) found that incorporating biochar and compost into soils can reduce pollutant uptake by plants and improve soil nutrient content and productivity. As research on soil health has expanded, Liu et al. (2020) performed a bibliometric analysis of publications on soil health from 1999 to 2018. Furthermore, Sun and Yuan (2023) analyzed top-cited papers in the field of soil science, while Yuan and Sun (2023) investigated research trends related to rice and greenhouse gas emissions.

The purpose of the present study is to conduct a bibliometric analysis of global research

output on the topic of "Soil Pollution" using the Web of Science (WoS) Core Collection from Clarivate Analytics. The analysis was carried out using CiteSpace and VOSviewer software to map trends, hotspots, and knowledge structures in the field.

MATERIALS AND METHODS

1. Web of Science

The publication data were retrieved from the Web of Science Core Collection, specifically from the following indexes: the Science Citation Index Expanded (SCIE, 1900–present) and the Social Science Citation Index (SSCI, 2005–present). Additionally, records were collected from the Conference Proceedings Citation Index–Science (CPCI-S, 2015–present) and the Conference Proceedings Citation Index–Social Science & Humanities (CPCI-SSH, 2015–present).

2. Data collection

Data collection was completed on July 20, 2024. The search was conducted using the following topic (TS) keywords: "Soil Pollution", "Agricultural Soil Pollution", "Soil Pollution Assessment", "Soil Pollution Control", "Urban Soil Pollution", and "Water and Soil Pollution". Only documents categorized as articles or review articles were included.

In total, 5,166 records were obtained from the WoS Core Collection. Journal impact factors (both IF 2023 and 5-year IF) were obtained from the *Journal Citation Reports* (JCR 2023), published in June 2024, which contained the most recent available data.

3. VOSviewer and CiteSpace

For bibliometric visualization, VOSviewer version 1.6.20 (van Eck & Waltman, 2023) was used with its default parameter settings. The top 25 keywords with the strongest citation bursts were identified and analyzed using CiteSpace (Basic version 6.3.R1).

RESULTS AND DISCUSSIONS

1. Document type and language of publication

All 5,166 publications analyzed in this study were indexed in the following databases: SCIE (5,111 papers, 98.94%), SSCI (307, 9.94%), CPCI-S (190, 3.68%), and CPCI-SSH (231, 5.83%). Regarding document type, the majority were research articles (4,776 papers, 92.45%), followed by review articles (390 papers, 7.55%) and proceedings papers (190 papers, 3.68%). Most papers were published in English (5,015 papers, 97.08%). Other publication languages included Portuguese (43 papers, 0.83%), French (24 papers, 0.47%), Chinese (19 papers, 0.37%), Spanish (18 papers, 0.35%), German (12 papers, 0.23%), and Polish (11 papers, 0.21%).

2. Publication output

Figure 1 illustrates the temporal distribution of publications on soil pollution research between 1990 and 2024. The highest annual output was recorded in 2022, with 580 papers.

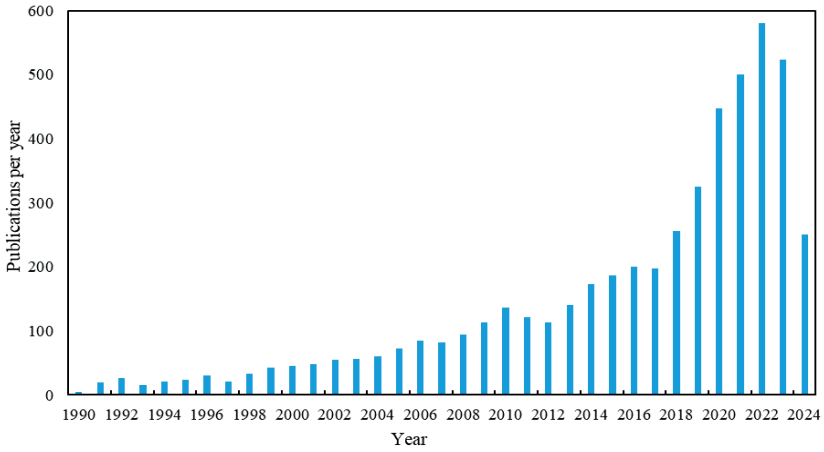


Figure 1. Trends in the quantity of published papers on soil pollution topic research from 1990 to 2024

The number of publications increased steadily over the decades, with 239 papers published between 1990 and 1999, 711 papers from 2000 to 2009, 1,851 papers during 2010 to 2019, and 2,302 papers between 2020 and 2024. An additional 62 papers were published between 1903 and 1989, although this early period is not represented in Figure 1 due to the low volume. Cumulatively, the 5,166 papers have an h-index of 144 and a total citation count of 140,047, resulting in an average of 27.11 citations per paper**.** The earliest identified publication on the topic of soil pollution is titled *"Soil Pollution and Disease in Camps"*, authored by Caldwell in 1903 and published in the *British Medical Journal.*

3. Web of Science categories and research areas

Between 1903 and 2024, publications related to soil pollution were distributed across 152 Web of Science (WoS) subject categories and 97 research areas.

Table 1 presents the top 20 categories and areas based on the number of published papers.

Table 1. Top 20 WoS categories and research areas on soil pollution topic research from 1903 to 2024

Rank	WoS categories				Research areas		
	Categories	No. papers	% total papers		Areas	No. papers	% total papers
1	Environmental Sciences	3,033	58.711			3,166	61.285
2	Soil Science	521	10.085		Agriculture	781	15.118
3	Water Resources	505	9.775		Engineering	648	12.544
4	Engineering Environmental	475	9.195		Water Resources	505	9.775
5	Public Environmental Occupational Health	283	5.478		Chemistry	375	7.259
6	Toxicology	247	4.781		Science Technology Other Topics	317	6.136
7	Geosciences Multidisciplinary	232	4.491		Public Environmental Occupational Health	283	5.478
8	Plant Sciences	224	4.336		Toxicology	247	4.781
9	Agronomy	189	3.659		Geology	243	4.704
10	Green Sustainable Science Technology	177	3.426		Plant Sciences	224	4.336
11	Meteorology Atmospheric Sciences	171	3.31		Meteorology Atmospheric Sciences	171	3.31
12	Chemistry Analytical	158	3.058		Geochemistry Geophysics	126	2.439
13	Ecology	157	3.039		Biotechnology Applied Microbiology	103	1.994
14	Environmental Studies	147	2.846		Materials Science	91	1.762
15	Chemistry Multidisciplinary	139	2.691		Biochemistry Molecular Biology	75	1.452
16	Geochemistry Geophysics	126	2.439		Biodiversity Conservation	63	1.22
17	Multidisciplinary Sciences	121	2.342		Energy Fuels	62	1.2
18	Engineering Chemical	116	2.245		Physics	61	1.181
19	Agriculture Multidisciplinary	104	2.013		Microbiology	54	1.045
20	Biotechnology Applied Microbiology	103	1.994		Food Science Technology	44	0.852

The top five categories included Environmental Sciences (3,033 papers, 58.711%), Soil Science (521 papers, 10.085%), Water Resources (505 papers, 9.775%), Engineering Environmental (475 papers, 9.195%), Public Environmental Occupational Health (283 papers, 5.478%). The top five research areas include Environmental Sciences Ecology (3,166 papers, 61.285%), Agriculture (781 papers, 15.118%), Engineering (648 papers, 12.544%), Water Resources (505 papers, 9.775%), Chemistry (375 papers, 7.259%).

4. Core journals

All 5,166 publications analyzed in this study were published across 961 scientific journals and five book series**.** Table 2 presents the top 20 core journals, each of which has published more than 47 papers on the topic of soil pollution. The table includes data on the number of articles per journal, 2022 impact factor (IF), five-year impact factor, quartile ranking in the highest WoS category (if the journal belongs to multiple), total citations, and average citations per article. The top five journals are *Science of the Total Environment* (298 papers, 5.768%), *Environmental Science and Pollution Research* (218 papers, 4.22%), *Environmental Pollution* (162 papers, 3.136%), *Chemosphere* (142 papers, 2.749%), *Environmental Monitoring and Assessment* (138 papers, 2.671%). Among the top 20

journals, nine were classified in Quartile 1 (Q1), indicating the highest level of scientific impact and visibility. Three journals were ranked in Q2, another three in Q3, two in Q4, while three journals did not have an available impact factor in 2023. When assessed by average citations per article, *Geoderma* ranked highest with 63.6 citations per paper, followed by *Science of the Total Environment* (62.7), *Chemosphere* (59.3), *Environmental Pollution* (56.0), and *Journal of Hazardous Materials* (51.7). Citation network analysis further revealed that 168 journals met the minimum threshold of five published articles in this domain, with 161 of them exhibiting citation interconnections. The resulting network visualization, based on Web of Science data, identified 15 distinct clusters, each represented by a unique color in Figure 2, reflecting the thematic and collaborative structure within the field of soil pollution research.

Table 2. Top 20 core Journals on soil pollution topic research indexed in the WoS

Rank	Journal	TP	Ratio	IF 2023	IF 5year	QC	Citations	Avg. citations
1	*Science of the Total Environment*	298	5.768	8.2	8.6	Q1	18688	62.7
2	*Environmental Science and Pollution Research*	218	4.22	-	-	-	5138	23.6
3	*Environmental Pollution*	162	3.136	7.6	8.3	Q1	9079	56.0
4	*Chemosphere*	142	2.749	8.1	7.7	Q1	8425	59.3
5	*Environmental Monitoring and Assessment*	138	2.671	2.9	3.1	Q3	2855	20.7
6	*Water Air and Soil Pollution*	135	2.613	3.8	3.6	Q2	3256	24.1
7	*Environmental Geochemistry and Health*	105	2.033	3.2	4	Q2	2134	20.3
8	*Journal of Hazardous Materials*	96	1.858	12.2	11.9	Q1	4967	51.7
9	*Sustainability*	91	1.762	3.3	3.6	Q2	953	10.5
10	*Ecotoxicology and Environmental Safety*	79	1.529	6.2	6.3	Q1	2351	29.8
11	*Journal of Soils and Sediments*	79	1.529	2.8	3.3	Q3	1784	22.6
12	*Fresenius Environmental Bulletin*	75	1.452	-	-	-	250	3.3
13	*Environmental Earth Sciences*	71	1.374	2.8	3	Q3	1405	19.8
14	*Eurasian Soil Science*	71	1.374	1.4	1.4	Q4	434	6.1
15	*Journal of Geochemical Exploration*	67	1.297	3.4	3.4	Q1	2622	39.1
16	*Journal of Environmental Management*	62	1.2	8	7.9	Q1	2728	44.0
17	*International Journal of Env. Research and Public Health*	60	1.161	-	-	-	873	14.6
18	*Environmental Research*	53	1.026	7.7	7.5	Q1	1711	32.3
19	*Polish Journal of Environmental Studies*	50	0.968	1.4	1.5	Q4	1369	27.4
20	*Geoderma*	47	0.91	5.6	6.7	Q1	2987	63.6

Note: TP: Total publications; Ratio: Ratio of 5,166 (%); IF 2023: journal impact factor in 2023; IF5 year: journal impact factor of 5 years; QC: Quartile in category.

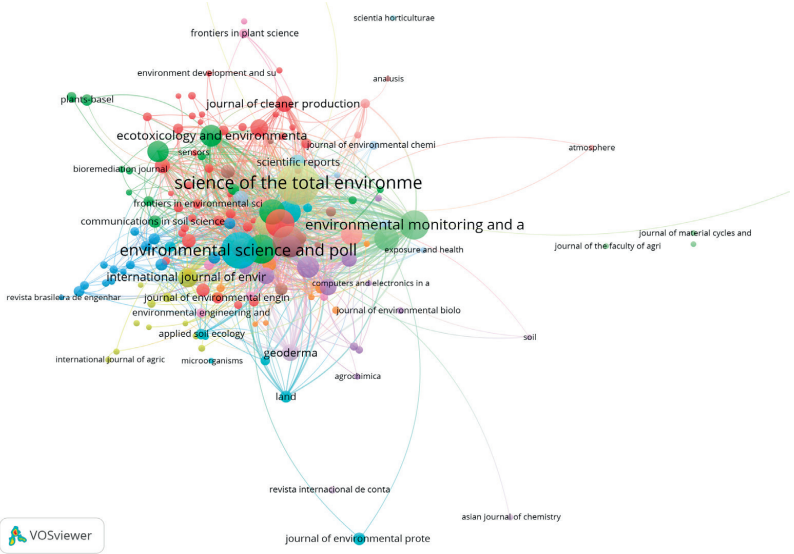


Figure 2. Network visualization maps of citation journals with minimum of 5 publications in the field of soil pollution topic research based on WoS with 161 circles and fifteen clusters

5. Countries/regions co-authorship analysis

A total of 129 countries or regions contributed to the 5,166 publications analyzed in this study.

Table 3 presents the top 20 contributors, each having published at least 90 papers on soil pollution, as indexed in the Web of Science Core Collection. Among these, the leading contributors were the People's Republic of China, Spain, the United States, Poland, and India, each of which produced more than 275 publications.

Out of the 129 participating countries or regions, 91 met the minimum threshold of five publications required for inclusion in the co-authorship network analysis. Of these, 90 demonstrated active collaborative relationships and were interconnected through co-authorship links.

The resulting international collaboration network was visualized and categorized into nine distinct clusters, as shown in Figure 3, illustrating the structural patterns of global cooperation and regional research alliances within the domain of soil pollution.

Table 3. Top 20 countries published papers in the field of soil pollution topic research based on WoS

Rank	Countries/Regions	Records	% of 5,166
1	Peoples R China	1,544	29.888
2	Spain	372	7.201
3	USA	325	6.291
4	Poland	292	5.652
5	India	275	5.323
6	Italy	246	4.762
7	Russia	230	4.452
8	Iran	222	4.297
9	France	214	4.142
10	Brazil	196	3.794
11	Germany	174	3.368
12	Turkey	164	3.175
13	England	130	2.516
14	Pakistan	125	2.42
15	Romania	112	2.168
16	Netherlands	105	2.033
17	Saudi Arabia	97	1.878
18	Czech Republic	94	1.82
19	South Korea	94	1.82
20	Egypt	90	1.742

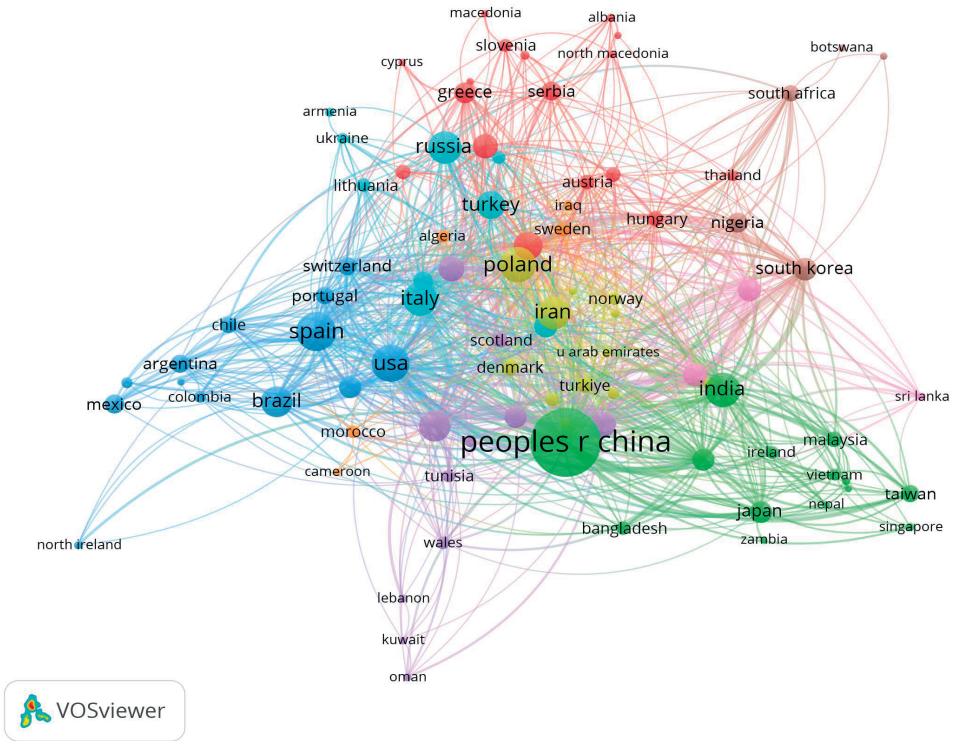


Figure 3. The country co-authorship network map of soil pollution topic research based on WoS with 90 nodes and nine clusters

The co-authorship network, based on publication volume, revealed a structured distribution across nine clusters.

The first cluster (red) comprised seventeen countries or regions, including Germany, Romania, and others. The second cluster (green) included fourteen countries or regions, most notably the People's Republic of China and India. The third cluster (blue) consisted of thirteen countries or regions, such as Spain, the United States, and Brazil.

The fourth cluster (yellow) encompassed twelve countries or regions, including Poland and Iran. The fifth cluster (violet) contained eleven countries or regions, with France, Pakistan, and England among the notable contributors. The sixth cluster (light blue) was composed of ten countries or regions, including Italy, Russia, and Turkey. The seventh cluster (orange) included five countries or regions, such as Sweden and Morocco, while the eighth cluster (pink) also comprised five countries or regions, including South Korea and Nigeria. Lastly, the ninth cluster (brown) consisted of three countries or regions: Saudi Arabia, Egypt, and Sri Lanka.

6. Organizations (Affiliations) co-authorship analysis

According to publication data from the Web of Science, a total of 4,636 organizations contributed to the 5,166 papers analyzed in this study.

Table 4 lists the top 15 organizations, each of which produced more than 49 publications, along with their respective share of the total output and country of origin.

The five most prolific institutions were the Chinese Academy of Sciences (339 publications, 6.56%), the University of Chinese Academy of Sciences (116, 2.25%), the Consejo Superior de Investigaciones Científicas (CSIC) in Spain (100, 1.94%), the Centre National de la Recherche Scientifique (CNRS) in France (98, 1.90%), and the Russian Academy of Sciences (97, 1.88%). Among the top 15 organizations, nine were based in China, two in France, two in Russia, and one in Spain, indicating a strong research presence from institutions in East Asia and Europe in the field of soil pollution.

Table 4. Top 15 organizations publishing papers in the field of soil pollution topic research based on WoS

Rank	Organizations	Records	% of 5,166	Country
1	Chinese Academy of Sciences	339	6.562	China
2	University of Chinese Academy of Sciences CAS	116	2.245	China
3	Consejo Superior De Investigaciones Cientificas CSIC	100	1.936	Spain
4	Centre National De La Recherche Scientifique CNRS	98	1.897	France
5	Russian Academy of Sciences	97	1.878	Russia
6	Egyptian Knowledge Bank EKB	89	1.723	Egypt
7	Zhejiang University	73	1.413	China
8	INRAE	69	1.336	France
9	Nanjing Institute of Soil Science CAS	66	1.278	China
10	Lomonosov Moscow State University	60	1.161	Russia
11	Institute of Geographic Sciences Natural Resources Research CAS	58	1.123	China
12	China University of Geosciences	51	0.987	China
13	Research Center for Eco Environmental Sciences RCEES	51	0.987	China
14	Chinese Academy of Agricultural Sciences	50	0.968	China
15	Northwest A F University China	49	0.949	China

7. All Keywords co-occurrence analysis

Using the full counting method for co-occurrence analysis, a total of 11,242 author keywords were identified. Among these, 584 keywords met the minimum threshold of five occurrences and were grouped into eighteen clusters in the resulting network map visualization. The twenty most frequently co-occurring author keywords - each appearing more than 70 times - were: *soil pollution*, *heavy metals*, *soil*, *heavy metal*, *phytoremediation*, *cadmium*, *soil contamination*, *pollution*, *risk assessment*, *lead*, *trace elements*, *bioremediation*, *spatial distribution*, *ecological risk*, *arsenic*, *soil remediation*, *remediation*, *potentially toxic elements*, *biochar*, and *contamination*. Each author's keywords occurred more than 70 times.

For Keywords Plus, 7,730 terms were identified, of which 931 met the threshold of five occurrences. These were grouped into twelve clusters in the network visualization.

The top twenty Keywords Plus, each occurring more than 202 times, included: *heavy-metals*, *contamination*, *pollution*, *cadmium*, *accumulation*, *lead*, *sediments*, *agricultural soils*, *trace-elements*, *toxicity*, *water*, *spatial-distribution*, *plants*, *zinc*, *copper*, *polycyclic aromatic hydrocarbons*, *growth*, *urban soils*, and *area*. Each keyword plus occurred more than 202 times.

In total, 17,223 unique keywords were identified. Based on increasing thresholds of five, six, seven, and eight occurrences, 1,470, 1,205, 1,023, and 880 keywords met the respective criteria. These were ultimately grouped into seven main clusters, each representing a distinct thematic perspective within the field of soil pollution research, as illustrated in Figure 4.

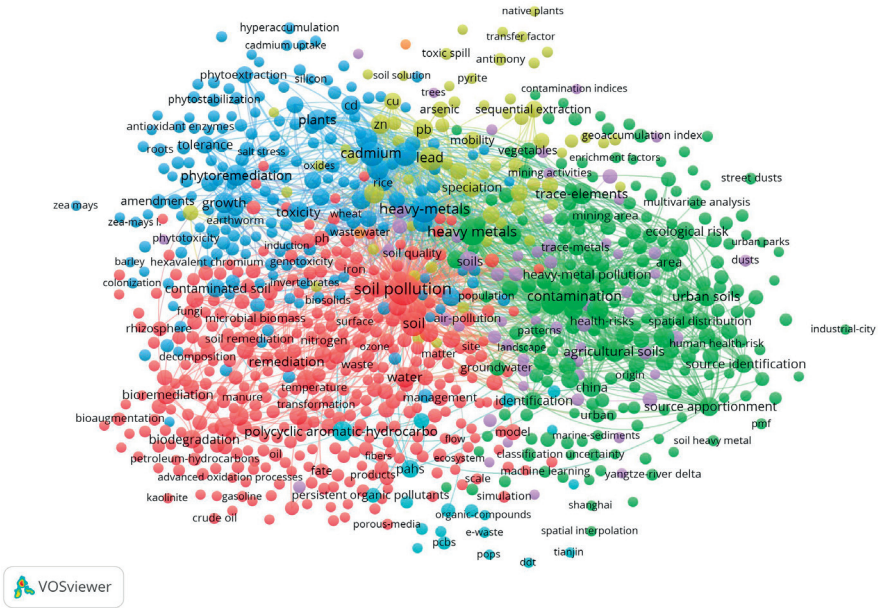


Figure 4. VOSviewer co-occurrence network visualization mapping of most frequently all keywords on soil pollution topic research with seven main clusters. Co-occurrence network of all keywords including author keywords and keywords plus

The top twenty most frequently co-occurring keywords across all sources included: *soil pollution*, *heavy-metals*, *heavy metals*, *contamination*, *pollution*, *soil*, *cadmium*, *lead*, *accumulation*, *sediments*, *agricultural soils*, *zinc*, *trace-elements*, *phytoremediation*, *toxicity*, *copper*, *water*, *remediation*, *plants*, and *spatial-distribution*. Each of these keywords appeared more than 257 times.

The same dataset visualized in Figure 4 was further analyzed by time period and presented as an overlay map in Figure 5. In this temporal visualization, blue-colored nodes represent earlier research topics, while yellow and green nodes indicate more recent areas of focus, highlighting current research fronts.

The seven thematic clusters identified in Figure 4 encompass a broad range of subfields within soil pollution research. These include: (1) soil pollution remediation, (2) soil heavy metal contamination, (3) heavy metal accumulation and phytoremediation, (4) bioavailability and extraction of heavy metals, (5) soil dust and particulate matter impacts on vegetation, (6) polycyclic aromatic hydrocarbons (PAHs), and (7) wastewater and metal toxicity.

The first cluster (red in Figure 4) consists of 347 keywords that met the threshold of eight occurrences and primarily focuses on *soil pollution remediation*. The 20 most frequently used keywords in this cluster include: *soil*

pollution, *soil*, *water*, *remediation*, *adsorption*, *bioremediation*, *removal*, *degradation*, *impact*, *organic matter*, *biodegradation*, *environment*, *quality*, *sorption*, *wastewater*, *biochar*, *diversity*, *sewage sludge*, *management*, and *extraction*, each appearing more than 87 times.

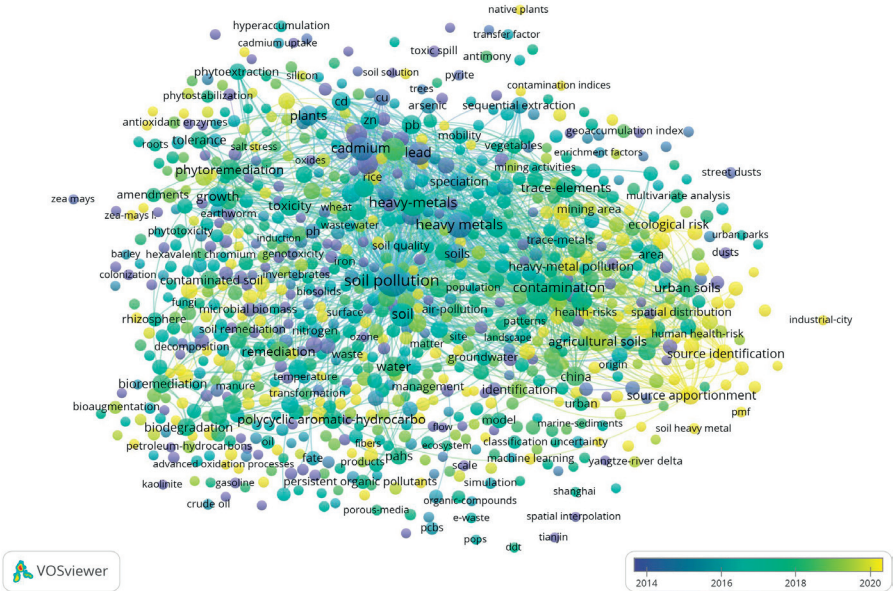


Figure 5. VOSviewer co-occurrence overlay visualization mapping of most frequently all keywords on soil pollution topic research. The years in which specific keywords frequently occur are shown by different colours

The second cluster (green) includes 206 keywords and represents research on *heavy metal contamination of soil*. This was identified as a front-line research theme. The top 22 keywords in this cluster, each with more than 123 occurrences, are: *heavy metals*, *contamination*, *pollution*, *sediments*, *agricultural soils*, *trace elements*, *spatial distribution*, *heavy metal*, *urban soils*, *China*, *area*, *source apportionment*, *heavy-metal pollution*, *ecological risk*, *elements*, *risk assessment*, *soil contamination*, *source identification*, *health risk*, *city*, *risk assessment*, and *identification*.

The third cluster (blue) comprises 183 keywords and centers on *heavy metal accumulation and phytoremediation*. The 21 most frequent terms in this group include: *heavy metals*, *cadmium*, *accumulation*, *zinc*, *phytoremediation*, *toxicity*, *copper*, *plants*, *growth*, *contaminated soils*, *Cd*, *metals, contaminated soil, contaminated soil*, *contaminated soil*, *exposure*, *tolerance*, *bioaccumulation*, *oxidative stress*, *phytoextraction*, *availability*, *plant*, and *chromium*, each occurring more than 84 times.

The fourth cluster (yellow) consists of 65 keywords and addresses *the bioavailability and extraction of various heavy metals*. The top 20 terms - each mentioned more than 35 times - include: *lead*, *Pb*, *bioavailability*, *speciation*, *Zn*, *trace elements*, *mercury*, *Cu*, *mobility*, *sequential extraction*, *fractionation*, *arsenic*, *mine*, *immobilization*, *sequential extraction procedure*, *mine tailings*, *tailings*, *toxic metals*, *manganese*, and *Spain*.

The fifth cluster (violet) comprises 57 keywords and focuses on *the effects of soil dust and particulate matter on vegetation*. The 20 most common keywords include: *soils*, *dust*, *particulate matter*, *vegetation*, *fly ash*, *heavy metal*, *magnetic susceptibility*, *vicinity*, *deposition*, *susceptibility*, *samples*, *particles*, *metal pollution*, *parameters*, *forest soils*, *atmospheric deposition*, *PAH*, *topsoil*, *Turkey*, and *India*, each with more than 20 occurrences.

The sixth cluster (light blue) includes 20 keywords and is centered on *polycyclic aromatic hydrocarbons (PAHs)*. Frequent keywords in this group, each appearing more than eight times, are: *polycyclic aromatic hydrocarbons*, *PAHs*, *persistent organic pollutants*, *polychlorinated biphenyls*, *air*, *organochlorine pesticides*, *PCBs*, *polybrominated diphenyl ethers*, *sites*, *dibenzo-p-dioxins*, *e-waste*, *DDT*, *fluxes*, *organic compounds*, *dry deposition*, *POPs*, *Tianjin*, and several variants of polychlorinated substances.

The seventh cluster (orange) is the smallest, consisting of only two keywords: *wastewater* and *metal toxicity*, each of which appeared more than eight times.

8. Burst of keywords

A keyword burst analysis was conducted using CiteSpace (Basic version 6.2.R6) to identify emerging trends and research hotspots in the field of soil pollution. The analysis focused on the top 25 keywords exhibiting the strongest citation bursts between 1994 and 2024, as shown in Figure 6.

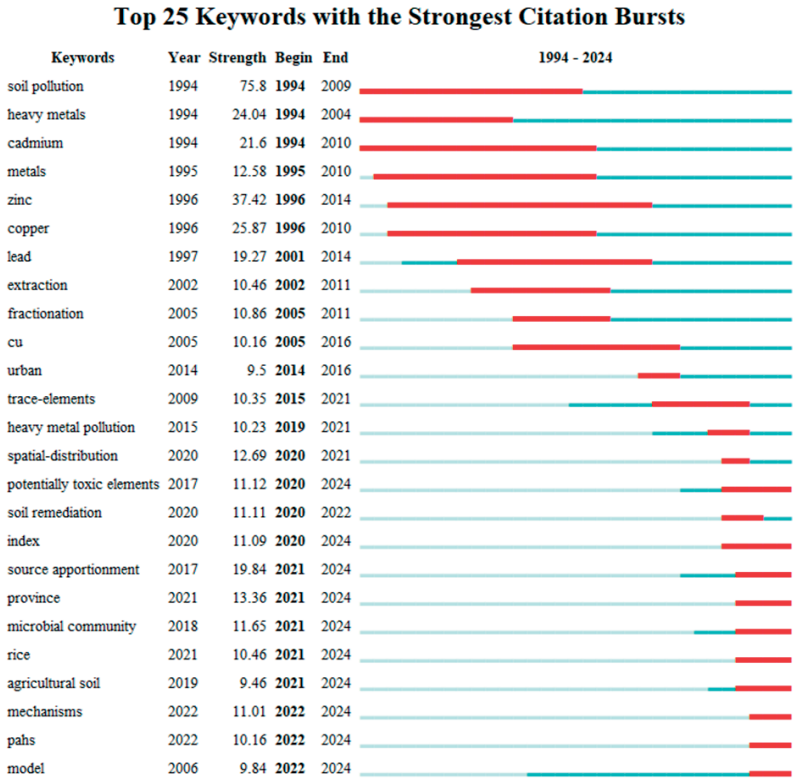


Figure 6. Information about top 25 keywords of soil pollution topic research with the strongest citation bursts from 1994 to 2024 by CiteSpace (6.2.R6). Begin, year when the burst begins; End, year when the burst ends. Red grids indicate the years when a particular term started to be frequently used. A longer the red bar, the keywords have been cited for a longer duration

These keywords - indicative of sudden increases in scholarly attention - include: *soil pollution*, *heavy metals*, *cadmium*, *metals*, *zinc*, *copper*, *lead*, *extraction*, *fractionation*, *Cu*, *urban*, *trace elements*, *heavy metal pollution*, *spatial distribution*, *potentially toxic elements*, *soil remediation*, *index*, *source apportionment*, *province*, *microbial community*, *rice*, *agricultural soil*, *mechanisms*, *PAHs*, and *model*. These terms reflect the evolving focus and interdisciplinary nature of soil pollution research over the past three decades.

9. Top papers based on Essential Science Indicators (ESI)

The analysis of top-cited literature was conducted using the Essential Science Indicators (ESI) database, which was last updated on July 11, 2024, and covers a 10-year and 4-month period from January 1, 2014, to April 30, 2024**.** According to ESI data, a total of 72 top papers were identified, including 72 highly cited papers and one hot paper**.**

These publications span a range of years, with distribution as follows: 2014 (5 papers), 2015 (4), 2016 (2), 2017 (2), 2018 (8), 2019 (6), 2020 (10), 2021 (11), 2022 (10), 2023 (12), and 2024 (2). The journals that published multiple top papers include: *Science of the Total Environment* (14 papers), *Environmental Research* (7), *Journal of Hazardous Materials* (6), *Environmental Pollution* (3), *Journal of Environmental Management* (3), *Chemosphere* (2), *Environment International* (2), *Environmental Science & Technology* (2), *Journal of Water Process Engineering* (2), and *Water, Air, and Soil Pollution* (2).

These findings underscore the prominence of multidisciplinary environmental science journals in disseminating high-impact research on soil pollution.

10. The most frequently cited articles

The annual citations of the eight papers showed an increasing trend after a year of publication (Figure 7). The eight papers were written by Li et al (2014), Duruibe et al (2007), Facchinelli et al (2001), Chen et al (2015), Bläsing and Amelung (2018), Michalak (2006), Goovaerts (1999), Manta et al (2002). From the publication year to July 20, 2024, the total citations for each paper of the most citation eight papers were 2082, 1296, 1117, 1030, 880, 867, 837 and 810 times, and the average citation per year each paper were 189.3, 72.0, 46.5, 103.0, 125.7, 45.6, 32.2 and 35.2 times.

Among the eight articles, the highest average citation paper per year were 189.3 (Li et al, 2014), also includes two papers both Chen et al (2015) and Bläsing and Amelung (2018), which were the top papers (highly cited paper) based on ESI.

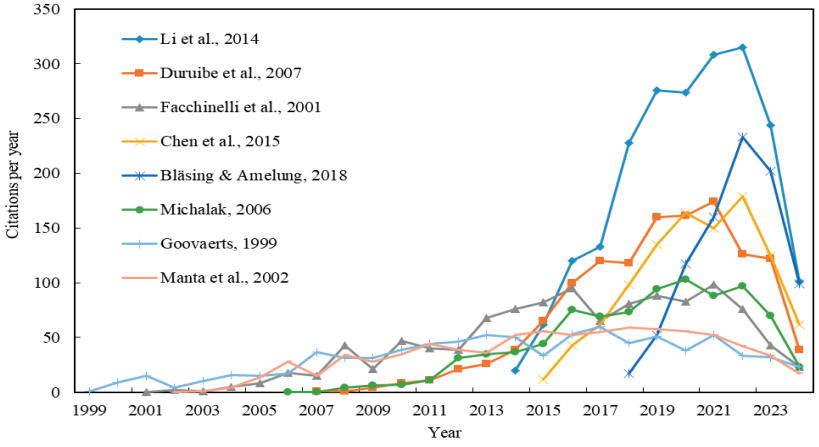


Figure 7. Comparison of the citations per year of the eight papers related to soil pollution topic research from their initial publications to July 20, 2024

11. Sustainable development goals

Table 5 presents the distribution of soil pollution research papers in relation to all Sustainable Development Goals (SDGs).

The analyzed papers addressed thirteen of the Sustainable Development Goals (SDGs), with the highest concentration of research focused on five key goals: SDG 11 – Sustainable Cities and Communities, SDG 2 – Zero Hunger, SDG 13 – Climate Action, SDG 3 – Good Health and Well-Being, and SDG 15 – Life on Land.

Table 5. All Sustainable Development Goals for soil pollution topic research papers

Rank	Sustainable Development Goals	Record Count	% of 5,166
1	11 Sustainable Cities and Communities	2144	41.502
2	02 Zero Hunger	638	12.35
3	13 Climate Action	556	10.763
4	03 Good Health and Well Being	509	9.853
5	15 Life on Land	477	9.233
6	06 Clean Water and Sanitation	443	8.575
7	12 Responsible Consumption and Production	120	2.323
8	14 Life Below Water	120	2.323
9	07 Affordable and Clean Energy	20	0.387
10	01 No Poverty	8	0.155
11	09 Industry Innovation and Infrastructure	8	0.155
12	04 Quality Education	6	0.116
13	16 Peace and Justice Strong Institutions	4	0.077

CONCLUSIONS

This study conducted a comprehensive bibliometric analysis of 5,166 publications related to soil pollution research. The leading journals contributing to this field include *Science of the Total Environment*, *Environmental Science and Pollution Research*, *Environmental Pollution*, *Chemosphere*, and *Environmental Monitoring and Assessment*. In terms of national contributions, the top five publishing countries were the People's Republic of China, Spain, the United States, Poland, and India.

Through co-occurrence network visualization using VOSviewer, author keywords were categorized into seven thematic clusters, highlighting the multidimensional nature of soil pollution research. Additionally, most papers aligned with three key Sustainable Development Goals (SDGs): SDG 11 – Sustainable Cities and Communities, SDG 2 – Zero Hunger, and SDG 13 – Climate Action.

The findings of this analysis not only reflect the current landscape and emerging trends in soil pollution research but also offer valuable insights to guide future investigations and interdisciplinary collaborations in this critical environmental domain.

REFERENCES

Ajibade, S., Nnadozie, E. C., Iwai, C. B., Ghotekar, S., Chang, S. W., Ravindran, B., & Awasthi, M. K. (2022). Biochar-based compost: A bibliometric and visualization analysis. *Bioengineered, 13*(7–12), 15013–15032.

Bläsing, M., & Amelung, W. (2018). Plastics in soil: Analytical methods and possible sources. *Science of the Total Environment, 612*, 422–435.

Caldwell, R. (1903). Soil pollution and disease in camps. *British Medical Journal*, *1903*, 248–249.

Chen, H. Y., Teng, Y. G., Lu, S. J., Wang, Y. Y., & Wang, J. S. (2015). Contamination features and health risk of soil heavy metals in China. *Science of the Total Environment, 512*, 143–153.

Du, Z. L., Lin, D. S., Li, H. F., Li, Y., Chen, H. A., Dou, W. Q., Qin, L., & An, Y. (2022). Bibliometric analysis of the influencing factors, derivation, and application of heavy metal thresholds in soil. *International Journal of Environmental Research and Public Health, 19*(11), 6561.

Duruibe, J. O., Ogwuegbu, M. O. C., & Egwurugwu, J. N. (2007). Heavy metal pollution and human biotoxic effects. *International Journal of the Physical Sciences, 2*(5), 112–118.

Facchinelli, A., Sacchi, E., & Mallen, L. (2001). Multivariate statistical and GIS-based approach to identify heavy metal sources in soils. *Environmental Pollution, 114*(3), 313–324.

Gao, J., Faheem, M., & Yu, X. (2022). Global research on contaminated soil remediation: A bibliometric network analysis. *Land, 11*(9), 1581.

Gao, L., Hu, T. Z., Li, L., Zhou, M. Y., & Zhu, B. Q. (2022). Land pollution research: Progress, challenges, and prospects. *Environmental Research Communications, 4*(11), 112001.

Gong, W. W., Li, H. F., Wang, J. C., Zhou, J. H., Zhao, H. K., Wang, X. X., Qu, H., & Lu, A. X. (2023). Global research activities on micro(nano)plastic toxicity to earthworms. *Toxics, 11*(2), 112.

Goovaerts, P. (1999). Geostatistics in soil science: State-of-the-art and perspectives. *Geoderma, 89*(1–2), 1–45.

Li, Z. Y., Ma, Z. W., van der Kuijp, T. J., Yuan, Z. W., & Huang, L. (2014). A review of soil heavy metal pollution from mines in China: Pollution and health risk assessment. *Science of the Total Environment, 468*, 843–853.

Liu, H. D., Cui, L. Z., Li, T., Schillaci, C., Song, X. F., Pastorino, P., Zou, H. T., Cui, X. Y., Xu, Z. H., & Fantke, P. (2023). Micro- and nanoplastics in soils: Tracing research progression from comprehensive analysis to ecotoxicological effects. *Ecological Indicators, 156*, 111109.

Liu, Y. N., Wu, K. N., & Zhao, R. (2020). Bibliometric analysis of research on soil health from 1999 to 2018. *Journal of Soils and Sediments, 20*(3), 1513–1525.

Manta, D. S., Angelone, M., Bellanca, A., Neri, R., & Sprovieri, M. (2002). Heavy metals in urban soils: A case study from the city of Palermo (Sicily), Italy. *Science of the Total Environment, 300*(1–3), 229–243.

Michalak, A. (2006). Phenolic compounds and their antioxidant activity in plants growing under heavy metal stress. *Polish Journal of Environmental Studies, 15*(4), 523–530.

Pan, B. G., Zhang, F. T., Zhu, X. Q., Huang, L., Wu, Y., Tang, J. Q., & Feng, N. X. (2024). Global trends and hotspots evolution in soil microplastic pollution research: A bibliometric analysis based on the Web of Science. *Ecological Indicators, 161*, 111974.

Stadler, T., Temesi, Á., & Lakner, Z. (2022). Soil chemical pollution and military actions: A bibliometric analysis. *Sustainability, 14*(12), 7138.

Sun, J., & Yuan, B. Z. (2023). Mapping of top papers in the subject category of Soil Science. *COLLNET Journal of Scientometrics and Information Management, 17*(1), 7–22.

Wang, K. S., Jin, T., Wang, B., Yuan, Z. M., Peng, K. W., & Hu, Y. (2024). Evolution of hotspots and research trends in agricultural mulch film research: A bibliometric review. *Frontiers in Environmental Science, 12*, 1394808.

Yuan, B. Z., & Sun, J. (2023). Research trend of rice and greenhouse gases based on Web of Science: A bibliometric analysis. *All Earth, 35*(1), 16–30.



ISSN 2285 – 6064
ISSN-L 2285 – 6064